

TESTING FOR ASSEMBLY RULES ALONG DISTURBANCE GRADIENTS IN A RIPARIAN BROADLEAVED FOREST

DYAKOV, N. R.

*Ecology Department, University of Yambol, 8 Hale, Yambol, Bulgaria
(e-mail: nickydyakov@gmail.com)*

(Received 5th Sep 2018; accepted 12th Nov 2018)

Abstract. Riparian habitats often represent highly disturbed sites with relaxed competitive plant integrations and increased resource supply, which frequently lead to promoted colonization of alien and invasive plant species. Unfortunately, there is a knowledge gap about the assembling mechanisms that govern vegetation structure and composition along disturbance gradients. This study tried to answer the question if riparian vegetation assembling is governed by abiotic or biotic forces, as well as whether the strength and nature of assembling mechanisms change along local disturbance gradients. We used species-based approach in which species data of sampled vegetation were compared with a null model assuming random organization. The resulting variance ratios were regressed on the local flooding and logging disturbance gradients. We found that the studied riparian vegetation is dominated by abiotic assembling rules. Their nature did not change along the two disturbance gradients, but their strength did. It seems that the overwhelming factor that rules the riparian vegetation structure and composition in the area is the periodical flooding from the nearby river. It is most prominent in most frequently flooded habitats, then it slowly decays towards the more distant uplands. Its influence is so powerful that it can overshadow other potential assembling factors, and can promote the establishment of native and exotic (including invasive) species. Perhaps, the biotic filter never plays a significant role in the assembling of this highly disturbed and dynamic vegetation. In order to stop further colonization and to preserve these valuable sites from degradation, additional human-induced disturbances should be completely restricted, and natural ones be kept in its historical range. These findings should not be overlooked in the prospective management activities anymore, but should be incorporated in future action plans. Only then, we can hope that these ecosystems could be conserved at their current state for the upcoming generations.

Keywords: *riparian forest, niche limitation, biotic filter, habitat filter, null model*

Introduction

Riparian habitats often represent areas governed by disturbance and resource supply gradients (Dyakov and Zhelev, 2013). This often leads to relaxed plant competition (Huston and DeAngelis, 1994; Naeem et al., 2000) and decreased resource uptake, which is eventually followed by colonization of alien plant species (Belote et al., 2008; Brown and Peet, 2003; Davis et al., 2000, 2005; Holle and Simberloff, 2005). Eventual invasion can seriously deteriorate these valuable sites (Richardson et al., 2007). In order to properly conserve riparian habitats, it is urgent for these highly disturbed and prone to degradation ecosystems to be studied, and the relative importance of different assembling mechanisms to be well understood.

There are three main groups of processes known to influence vegetation assembly in a given place (Götzenberger et al., 2012; Weiher and Keddy, 2001). Seed dispersal filter is the first one, governed mainly by stochastic forces, determining which species of the regional species pool will reach the site (Eriksson, 1992; Hubbell, 2001). Then come environmental (habitat) and biotic filters, acting more or less simultaneously, they determine which one of the arrived species will survive and establish (Keddy, 1992). Habitat filter sifts the arrived species based on their physiological adaptations to the local environmental conditions (Weiher et al., 1998). Biotic filter sifts the species based on their

ecological adaptations to interact with the already established ones (Wilson et al., 1996a). The outcome of these three groups of assembling mechanisms determines the final structure and composition of vegetation. However, the discussion about the relative contribution of each group is far from over and the topic remains essential in vegetation ecology (Götzenberger et al., 2012).

Riparian vegetation is useful model system to study assembling mechanisms because flooding disturbance creates strong environmental gradient that causes species reassembling, and controls establishment and competition among interacting species. It is partly explicable by vegetation propagule pressure that flooding water brings in these habitats, as well as by flood-induced vegetation scouring and sediment deposition (Brown and Peet, 2003). Together with the moisture gradient, running from the riverbed to the upland, it generates diverse vegetation that could not be easily explained by a single assembling mechanism. It is almost completely unclear if dispersal, abiotic or biotic filters dominate community assembling, or how they interact (Fraaije et al., 2015).

Logging tends to shift species composition and increase overall plant diversity (Belote et al., 2012, 2009; Dyakov and Zhelev, 2013). Vegetation resistance (lack or small shift in plant species composition following disturbance) is known to depend on logging intensity, increasing light availability, and the size of regional species pool (Belote et al., 2012), suggesting that the first years after logging disturbance should be most highly dominated by abiotic assembling processes. Then, after 5-10 (or more years), following the site colonization by similar or other species (including exotic and invasive plants) (Dyakov and Zhelev, 2013) from the regional pool, biotic assembling mechanisms should slowly take over and begin to dominate local vegetation structuring (Belote et al., 2012, 2009; Mouquet et al., 2003).

Different methods can be used to test for assembly rules. The classical one is focused on species' taxonomic identity and diversity – species-based approach. An alternative one uses species' functional traits, inferring that they represent species adaptation to the environment – trait-based approach (Götzenberger et al., 2012). Among the species-based approaches there are two varieties that have been used – species co-occurrence and niche limitation. The first method frequently suffers from ambiguities due to not controlling for environmental heterogeneity (Götzenberger et al., 2012), therefore, the second one is often preferred. When employing it, it is better to be based on species abundances (Wilson et al., 1996b), because abundance is highly variable in almost all plant communities and assembling rules may be visible only in species abundance (Weiher and Keddy, 2001; Wilson and Gitay, 1995).

Since the earliest work on community assembly rules, null models were used to simulate random samples employing mathematical algorithm to redistribute the data of the original ones (Götzenberger et al., 2012; Wilson et al., 1987). For example, evidence for niche limitation can be achieved by comparing the observed variation in species richness or diversity to that of random communities (Palmer and van der Maarel, 1995). Lower than expected variance in species richness indicates niche limitation, though not always (Palmer and van der Maarel, 1995), i.e. the vegetation is structured mainly by biotic interactions. Higher than expected variance means that there is higher environmental heterogeneity, i.e. the vegetation is structured mainly by abiotic assembly rules (Götzenberger et al., 2016). However, there is necessity to “discount most of the effects of the environmental heterogeneity”, which is often accomplished through application of a patch-based null model (Wilson and Gitay, 1995).

This study's objective was to determine if biotic or abiotic rules dominate the vegetation assembling, and if the nature and strength of vegetation assembling rules change along the disturbance gradient? If the vegetation assembling is dominated by abiotic rules, then 1) the observed variation of sampled vegetation will be greater than the null model, or 2) lesser than the null model – if it is assembled by biotic rules. If the vegetation assembling rules do not change along the disturbance gradient, 3) then variance ratio between observed versus expected species frequency and abundance should be constant along the disturbance gradient. It was assumed that the vegetation assembling rules will be dominated by abiotic processes and their strength and nature will not change along the disturbance gradient.

Materials and methods

Study site

The study site is located in the Southeast Bulgaria, Balkan Peninsula and has the following coordinates: 42°13'05" – 42°11'00"N and 26°33'31" – 26°34'59"E (*Fig. 1*). It is a mixed riparian broadleaved forest growing on the right lowland river plain of Tundzha River. The total area is about 470 ha. It is surrounded all-around with agricultural fields. This forest is one of the last remaining spots of uncut semi-natural (there are several well established alien/invasive plant species) forests in the area.

Soils are alluvial. Mean annual temperature of the soil at 2 cm depth is 13 °C. Climate is temperate. Winter is mild, followed by relatively warm spring. Summer is hot, and autumn is very dry. Mean annual temperature is 12 °C. Mean annual rainfall is about 550 mm. Mean annual wind velocity is about 2.5 m/s, mainly from north and northeast direction. Total sunny days annually are around 90. Growing period continues for about seven months.

Studied riparian forest is periodically flooded during late winter and early spring months. The flooding is a result of the melting snow and spring rainfall. It causes high river waters, which inundate extensive agricultural and forested territories downstream. In some years, the flooding continues for months, turning the riparian forest into swamp. Furthermore, during the last 20 years, different parts of the studied forest were logged periodically with low to moderate intensity (up to about 50% canopy reduction).

Field sampling

Sampling design was based on the gradsect approach of Austin and Heyligers (1990). Its advantages are: (1) relatively cheap, (2) highly effective, (3) easy to apply on the field, but requiring experienced workers. The sampling was done in July, 2009. Studied territory was crossed with several transects running from the moistest parts, near the riverbed, to the driest upper lands. The length of different transects was between 500 and 1100 m. Transect starting points were chosen on random basis. Sampling plots were set systematically along transects. Trying to avoid spatial autocorrelation, the minimal distance between the plots was at least 200 m (*Fig. 1*). The sampling plot is a 0.1 ha rectangle – 50 × 20 m (*Fig. 2*). Totally, 42 sample plots were set. The middle line of the rectangle is 50 m long plastic tape. Along the tape, at equal distances of 10 m to each other, five 1 m² subplots – 2 × 0.5 m rectangles were laid. The exact placement of the subplots (whether on the left or right side) was determined randomly. Due to shrub layer thickness in some plots, setting of five subplots was not possible, instead only four were set.

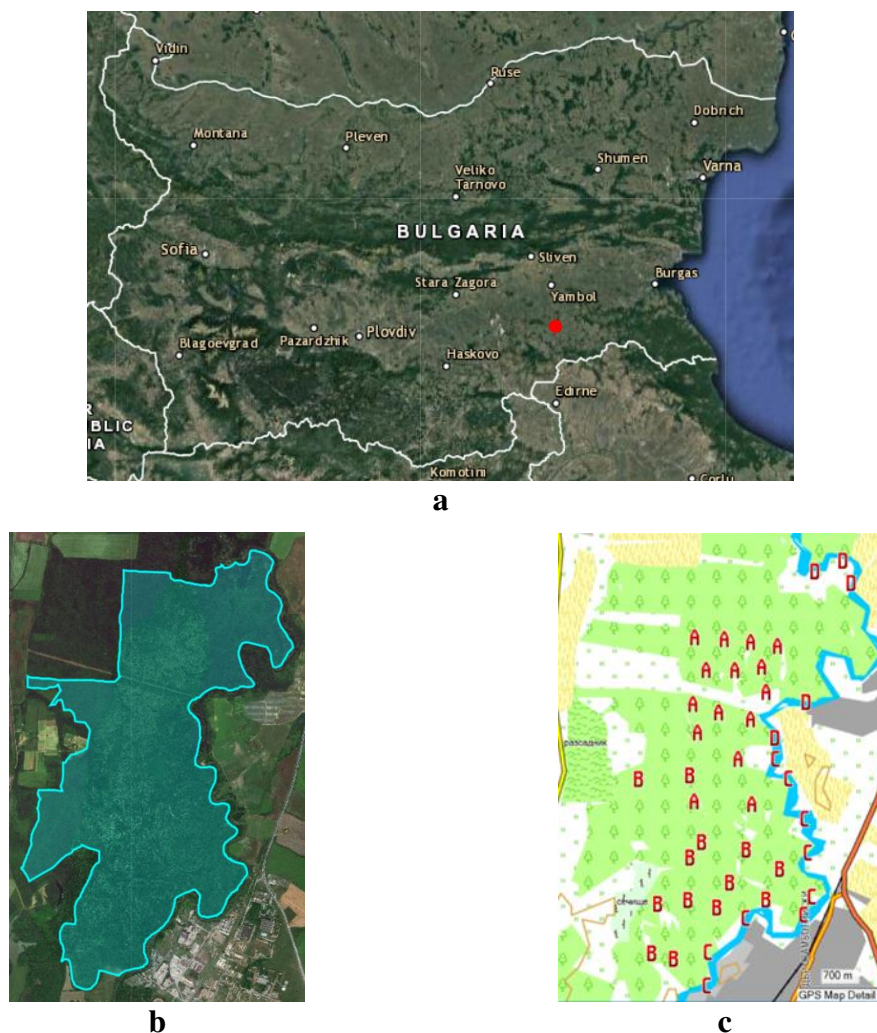


Figure 1. *a.* Overall map of the studied area location depicted as a red dot (above). *b.* Local map with contours of the studied territory (below left). *c.* Spatial distribution of the 42 sampling plots (below right). A = forest communities dominated by *Acer campestre* and *Crataegus monogyna*; B = forest communities dominated by *Ulmus minor*, *Acer campestre* and *Fraxinus oxycarpa*; C = forest communities dominated by *Acer negundo* and *Fraxinus oxycarpa*; D = forest communities dominated by *Acer negundo* (Dyakov and Zhelev, 2013)

As an expression of vegetation abundance in each subplot, species cover was determined visually in percent. Exact distance to the riverbed of all plots was measured on a map. For all samples, years after last logging were calculated using data from forest authority unit. Measured data for total species number, plot cover, tree, shrub, perennial, biennial and annual species number were averaged between the 1 m² subplots. Trying to express the moisture gradient of habitats and to adapt our sampling design to the patch-based model (Wilson and Gitay, 1995), all 208 subplots were grouped into four Sample Pools (SPs) – beginning with the moistest places (SP1), located nearest to the riverbed, and ending with the driest ones (SP4), located furthest from the river channel. Dominant plant species in the four SPs were determined on the basis of their mean subplot cover.

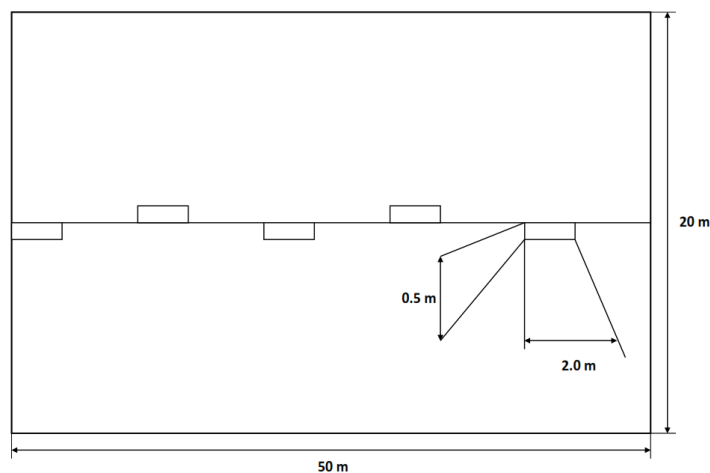


Figure 2. Sampling plot

Statistical analysis

Before using them, all variables were tested for normality with Shapiro-Wilk test (Shapiro and Wilk, 1965). It is generally preferred method for inquiring if a variable is normally distributed (Zar, 2010). As assumed beforehand, they were not normally distributed, therefore, all sample pools were compared for statistically significant differences in medians with Mood test (Mood, 1954; Zar, 2010). β -diversity was measured as a DCA (Detrended Correspondence Analysis) (Hill and Gauch, 1980) gradient length in SD (Standard Deviation) units.

Null model

The test for niche limitation was done using specific randomization for the null model construction. Species \times samples matrix was randomized using the recommended by Götzenberger et al. (2012) “C2” randomization. It randomizes species abundances within samples across all species and keeps fixed species richness and total sample abundance (Götzenberger et al., 2012).

Variance ratios

We have tracked variance ratio change along the two main disturbance gradients (moisture/flooding gradient, expressed as distance to the riverbed, and logging gradient, expressed as years after logging). Ratios are calculated for the frequency and abundance data separately as a ratio between the observed and expected (null model) variables’ variance (Wilson and Gitay, 1995). The two ratios were regressed on the two disturbance gradients and plotted for all species taken together and separated by life forms/guilds (Wilson, 1989). Only trend-lines with maximal R^2 [coefficient of determination or explained variation by the fitted regression (Zar, 2010)] values were retained on the graphs.

Results

The four SPs were compared for differences in the medians for several environmental and vegetation variables shown in *Table 1*. They were dominated by

almost identical tree, shrub and herbaceous species. Only SP1 was dominated by a different tree species – *Acer negundo* – an invasive exotic tree introduced from North America.

Table 1. Comparison of the four SPs by several environmental and vegetation variables

	Sample Pool 1 (n=55)	Sample Pool 2 (n=34)	Sample Pool 3 (n=69)	Sample Pool 4 (n=50)
Distance to riverbed (m)	†8(6-23)a	81(64-142)b	342(294-439)c	655(604-705)d
Years after logging	17(17-17)a	12(10-13)b	12(10-12)b	11(10-12)b
Plot cover (%)/1 m ²	20(11-37)a	27(19-34)a	26(18-32)a	29(20-38)a
Species number/1 m ²	4(4-5)a	8(6-9)b	7(7-8)b	9(7-12)b
H (Shannon-Weiner diversity)	0.719a (0.582-1.012)	1.095b (0.708-1.632)	1.215bc (0.797-1.561)	1.552d (1.161-1.825)
β-diversity	27.36	5.20	7.60	4.10
E (Evenness)	0.529ab (0.430-0.713)	0.613bc (0.388-0.733)	0.642c (0.506-0.720)	0.730d (0.642-0.773)
Tree species/1 m ²	1(1-1)a	2(1-3)ab	2(1-3)b	3(3-3)b
Shrub species/1 m ²	1(1-1)a	1(1-1)a	1(0-1)a	1(0-1)a
Perennial species/1 m ²	2(1-2)a	4(3-4)b	4(3-4)b	5(2-7)b
Annual and biennial species/1 m ²	0.0(0.0-0.3)a	1(0.7-1.0)b	0.8(0.5-0.8)c	0.4(0.2-0.9)abc
Alien species/1 m ²	0.0(0.0-1.0)a	0.0(0.0-0.0)b	0.0(0.0-0.0)b	0.0(0.0-0.0)b
Alien cover/1 m ²	0.0(0.0-0.6)a	0.0(0.0-0.0)b	0.0(0.0-0.0)b	0.0(0.0-0.0)b
Dominant trees	<i>Acer negundo</i>	<i>Ulmus minor</i> <i>Acer campestre</i> <i>Quercus robur</i>	<i>Ulmus minor</i> <i>Acer campestre</i> <i>Fraxinus oxycarpa</i>	<i>Acer campestre</i> <i>Fraxinus oxycarpa</i> <i>Ulmus minor</i>
Dominant shrubs	<i>Rubus canescens</i>	<i>Rubus caesius</i> <i>Rubus canescens</i>	<i>Ligustrum vulgare</i> <i>Rubus canescens</i>	<i>Rubus canescens</i> <i>Ligustrum vulgare</i>
Dominant herbs	<i>Dactylis glomerata</i> <i>Myrrhoides nodosa</i> <i>Urtica dioica</i>	<i>Chaerophyllum byzantinum</i> <i>Chaerophyllum temulentum</i> <i>Urtica dioica</i>	<i>Dactylis glomerata</i> <i>Urtica dioica</i> <i>Chaerophyllum temulentum</i>	<i>Chaerophyllum temulentum</i> <i>Festuca gigantea</i> <i>Dactylis glomerata</i>

†Medians (1st-3rd quartile) are shown. Medians in the rows with distinct letters are significantly different at $P \leq 0.05$ (Mood test)

The four SPs showed significant differences in the distance-to-the-riverbed variable, the annual and biennial species number per 1 m², as well as in diversity and evenness, especially between SP1 and SP3/SP4. SP1 was also significantly different from the other three pools in perennial species number per 1 m². However, the change in species diversity and evenness seemed to happen gradually because the intermediate SPs (SP2 and SP3) showed no significant difference between each other. There were no other significant differences among the last three pools in any other variable. However, another variable that attracts attention is β-diversity length, which is extremely high in the most disturbed SP1. Finally, it should be noticed that SP1 also has significantly higher alien number and cover per 1 m² compared to the rest three SPs.

Flooding gradient

Regression of frequency and abundance variance ratios on flooding gradient is shown in *Figure 3*.

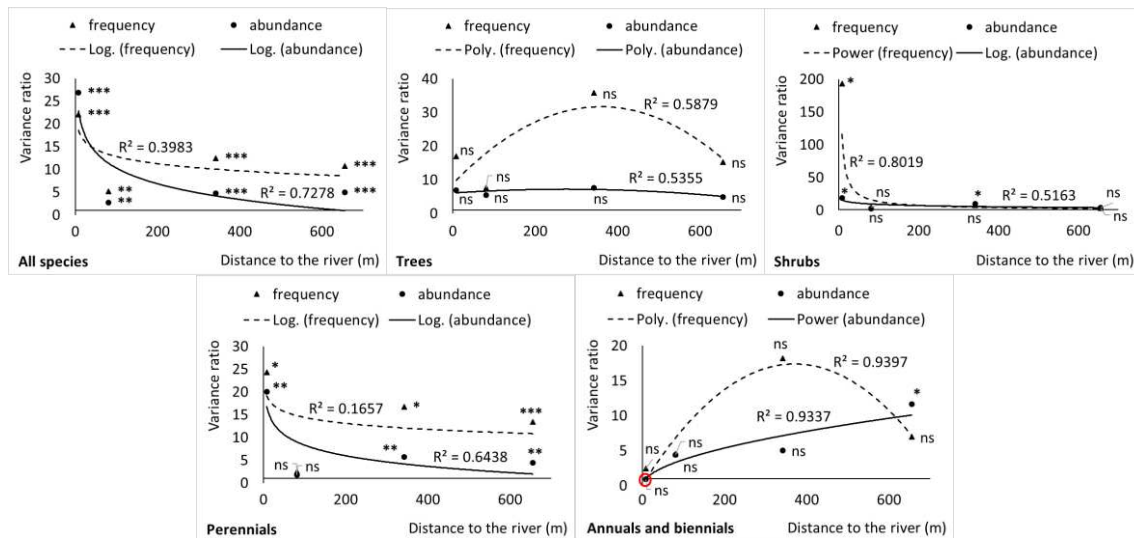


Figure 3. Variance ratio of observed versus expected species frequency and abundance regressed on the distance-to-the-riverbed variable. Only trend-lines with maximal R^2 were kept. The horizontal unbroken line shows the null model value of variance ratio = 1.0. The only case where the ratio was below 1.0 (0.89) is encircled with red circle. The SPs are arranged as in Table 1. * $P < 0.05$; ** $P < 0.01$; *** $P < 0.001$; ns = not significant

The prevailing function that best explained ratio variation was logarithmic. In all cases but one, variance ratios were much greater than 1.0, indicating excessive variance among the observed data. Only for abundance data of annuals and biennials in SP1 we have found variance deficit. Yet, it was statistically not significant (*Fig. 3*). Shrub and perennial species, as well as all species taken together, showed greater variance ratios in the closest to the river habitats (SP1 and SP2), which are also most disturbed. Then, variance ratios gradually declined with the increasing aridity and stability of the environment. Trees, annuals and biennials showed similar trends with maximal ratios in the moderately moist/disturbed habitats, especially for the frequency ratios data.

Logging gradient

The relationship between variance ratios and logging gradient is shown in *Figure 4*. Note that data points do not correspond to SPs as they were arranged in *Figure 3*.

Shrubs, perennials, and all species taken together, showed similar trends for both variance ratios. There is steep increase of ratios with the increasing time after the logging event. The annuals and biennials showed the opposite trend. Trees fall in between, showing hump-shaped trend, especially for the frequency data. However, the overall trend was determined by the perennial life form, likewise in the previous figure too.

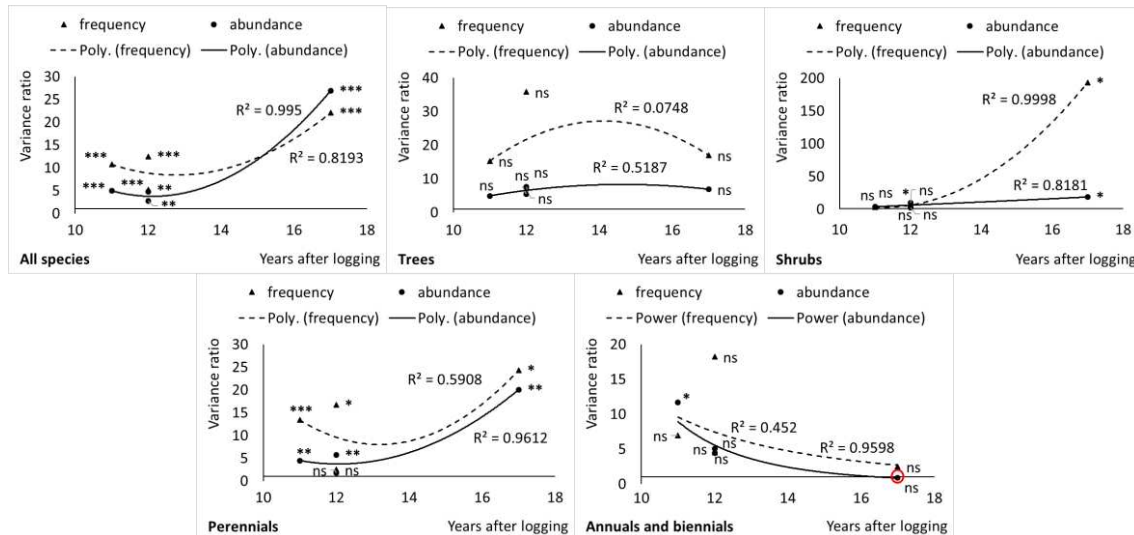


Figure 4. Variance ratio of observed versus expected species frequency and abundance regressed on the years-after-logging variable. Only trend lines with maximal R^2 were kept. The horizontal unbroken line shows the null model value of variance ratio = 1.0. The only case where the ratio was below 1.0 (0.89) is encircled with red circle. The SPs are not arranged as in Figure 1 and Table 1 (see Table 1 for more details). * $P < 0.05$; ** $P < 0.01$; *** $P < 0.001$; ns = not significant

Discussion

This study has found that studied riparian vegetation is dominated by abiotic assembly rules. The nature of assembly rules did not change along the two disturbance gradients, but only their strength did. In other words, our results supported the first of the two alternative hypotheses, i.e. that observed variation of sampled vegetation will be greater, compared to the null model. The third tested hypothesis was partly supported too, i.e. that variance ratio of observed versus expected species frequency and abundance will not change along the disturbance gradients.

There is considerable knowledge gap about how disturbance affects assembly rules. It has been suggested, however, that niche-based assembly rules should be weaker in most disturbed communities (Weiher and Keddy, 2001).

Flooding gradient

This study used a flooding-distance disturbance gradient that runs from the most closely located to the riverbed habitats towards the most distantly located ones, assuming that the former will be most heavily influenced by it (most disturbed), and the later most lightly influenced (least disturbed). Also, trying to overcome habitat heterogeneity, using Wilson and Gitay (1995) patch-based model, all vegetation samples were divided into four sample pools. We found that the most closely located to the riverbed SP1 differs significantly from the other SPs in most vegetation characteristics. For example, species number/1 m², Shannon diversity, perennial species number/1 m², and, finally, alien species number and cover/1 m² distinguish it from the other SPs. However, the more stable habitats had greater native species richness and evenness in contradiction to Cash et al. (2012) (ski-run disturbance). They also had lower β -diversity in agreement with Myers et al. (2015) (fire disturbance). The opposite

trend has been documented for the alien species richness, showing highest values in most disturbed places. Aliens like *Acer negundo* and *Amorpha fruticosa*, for example, dominated the most frequently disturbed communities, located closely to the river channel. Similar trends, in one aspect, have also been found by Brown and Peet (2003), who reported that riparian habitats were richer on native and exotic species compared to upland areas. They tried to explain this trend with the flooding frequency. In a similar conditions to ours, it was also found (Biswas and Mallik, 2010; Fraaije et al., 2015) that species diversity was maximal at the middle parts of the flooding gradient, sharply decreasing towards the moistest and driest ends. Fraaije et al. (2015) explained this trend with the environmental filter, but also stressed that seed dispersal filter was able to overshadow the environmental filter along the flooding gradient. They suggested that the assembling force of seed dispersal should not be overlooked, especially when studying such highly dynamic communities like riparian vegetation.

Although, in our study, environmental filter dominated along the flooding gradient, its structuring force was greater at the most disturbed sites. Not all functional groups, however, conformed to this trend. For example, the trees and annuals/biennials showed almost entirely nonsignificant variance ratios along the flooding gradient in contradiction to Biswas and Mallik (2010). Hence, observed trend cannot be explained by a single assembling mechanism. Described vegetation composition is probably influenced of several assembling mechanisms (Myers et al., 2015). Predominating role of flooding water is obvious. It not only disturbs the riparian vegetation by its scouring effect (Brown and Peet, 2003; Ward, 1998), but also brings great quantities of sediments (Davis et al., 2000; Tabacchi et al., 1998), as well as numerous propagules (Fraaije et al., 2015; Holle and Simberloff, 2005) from the upstream riverine habitats, including many exotic and invasive species' seeds (Dyakov and Zhelev, 2013; Richardson et al., 2007; Stohlgren et al., 1998). Extremely high measures of β -diversity in the most disturbed sites probably reflect the compressed habitat breadths (Myers et al., 2015) of many species due to flooding disturbance, hence relaxing biotic filter and enforcing the role of environmental and seed dispersal filters. The outcome is a highly complex system of variously disturbed sites, with different amounts of available soil resources, and varying degrees of native and exotic species colonization.

Logging gradient

Human-induced disturbance gradient that has been used in the current study is the time-logging gradient. We assumed that the disturbance effect is going to be most severe shortly after logging and will slowly decline with passage of time (Belote et al., 2012). Hence, we expected that the variance ratio of recently logged communities will be much greater than that of earlier-logged ones. However, we did not sample along a real time-logging gradient, but instead we sampled chronosequences, where space replaces time (Christensen and Peet, 1984; Foster and Tilman, 2000), or, with other words, sites with different age since logging were sampled.

What we have found was the opposite of what we expected, i.e. variance ratios increased with passing time since logging, meaning that not only shortly after the logging vegetation assembly was governed by abiotic rules, but also – many (in our case 17) years afterwards. However, there were deviations from this trend. For example, the trees showed maximal ratios 14 years after logging, and the guild of annuals/biennials showed opposite trend – decreasing variance ratios with increasing age since logging. Nevertheless, perennial species had overwhelming role in the general relationship form.

Although using different approaches, there are previous studies investigating the subject of logging effect on vegetation composition (Belote et al., 2008, 2012, 2009; McDonald et al., 2008; Reiners, 1992). For example, Belote et al. (2012) have found that species diversity decreased after 10 years post-logging at their subplot level, which is equal to our sampling unit of 1 m², and well agrees with our results for the time interval between 11-th and 20-th year after logging. However, they also found that community resistance – “the ability of a community to maintain compositional integrity” – declined with increasing timber-harvesting disturbance, which was assumed to be minimal shortly after the logging event, and to increase afterwards. High community resistance could be viewed as analogous to low-variance ratio vegetation, which is governed by biotic assembly rules (for instance, competition). In that case, Belote et al. (2012) findings directly contradict what we have found – generally, increasing variance ratio in the post-logging years.

In another study, Belote et al. (2008) investigated diversity-invasibility relationship of Appalachian oak-dominated forests. They found a positive relationship between native and nonnative species across all scales of observation and levels of disturbance, and positive correlation of post-disturbance native and nonnative richness with disturbance intensity. Again, the first part of these finding agrees with our results that communities shortly after disturbance tend to be richer on native species. However, in our case, the least logged communities showed most nonnative richness. A possible explanation could be that the least logged vegetation in our study was located closest to the riverbed, hence, it was also most heavily invaded by alien species. Perhaps, it is due to the propagule pressure (brought by the flooding water), which is most intensive at the closest-to-riverbed habitats (Brown and Peet, 2003), and known to be able to overcome the stressful abiotic conditions (Holle and Simberloff, 2005). It seems that the flooding gradient with its effect is capable to overshadow the other disturbing forces. Another explanation can be sought in a contingent imperfection of riparian vegetation’s logging history record, coupled with the drawbacks (Bakker et al., 1996) of chronosequence approach that we used. Still, another explanation could be invoked from other unaccounted disturbance sources, such as wild boar (*Sus scrofa*) digging activities (which are profound across the area). They were most intensive in the moistest habitats (author pers. observations), bringing additional extensive soil disturbances, and thus, easing exotic species colonization.

Conclusion

In summary, we have found that the assembling of riparian broadleaved forest under study is governed entirely by abiotic rules. These assembling forces do not change their nature along the local disturbing gradients, but do change only their strength. It seems that the overwhelming factor that rules the riparian vegetation structure and composition is the periodical flooding from nearby river. It is most prominent in most frequently flooded habitats, then slowly decays towards the more distant uplands. Its influence is so powerful that it can overshadow other potential assembling factors, and promote establishment of native and exotic (including invasive) species in the area. Perhaps, biotic filter never plays a significant role in the assembling of this highly disturbed and dynamic vegetation. In order of ceasing further colonization and preserving these valuable sites from degradation, additional human-induced disturbances should be completely restricted, and the natural ones kept in its historical range. These findings

should not be overlooked in the prospective management activities anymore, but incorporated in future management plans. Only then, we can hope that these ecosystems could be conserved at their current state for the upcoming generations.

Acknowledgements. The author is thankful to Petar Zhelev and Suzana Stankulovska for their help on the field.

REFERENCES

- [1] Austin, M. P., Heyligers, P. (1990): New Approach to Vegetation Survey Design: Gradsect Sampling. – In: Margules, C., Austin, M. (eds.) *Nature Conservation: Cost Effective Biological Surveys and Data Analysis*. CSIRO, Canberra, Australia, pp. 31-36.
- [2] Bakker, J. P., Olf, H., Willems, J. H., Zobel, M. (1996): Why do we need permanent plots in the study of long-term vegetation dynamics? – *Journal of Vegetation Science* 7: 147-156.
- [3] Belote, R. T., Jones, R. H., Hood, S. M., Wender, B. W. (2008): Diversity–invasibility across an experimental disturbance gradient in Appalachian forests. – *Ecology* 89: 183-192.
- [4] Belote, R. T., Sanders, N. J., Jones, R. H. (2009): Disturbance alters local–regional richness relationships in Appalachian forests. – *Ecology* 90: 2940-2947.
- [5] Belote, R. T., Jones, R. H., Wieboldt, T. F. (2012): Compositional stability and diversity of vascular plant communities following logging disturbance in Appalachian forests. – *Ecological Applications* 22: 502-516.
- [6] Biswas, S. R., Mallik, A. U. (2010): Disturbance effects on species diversity and functional diversity in riparian and upland plant communities. – *Ecology* 91: 28-35.
- [7] Brown, R. L., Peet, R. K. (2003): Diversity and invasibility of southern Appalachian plant communities. – *Ecology* 84: 32-39.
- [8] Cash, F. B., Conn, A., Coutts, S., Stephen, M., Mason, N. W., Anderson, B. J., Wilson, J. B. (2012): Assembly rules operate only in equilibrium communities: Is it true? – *Austral Ecology* 37: 903-914.
- [9] Christensen, N. L., Peet, R. K. (1984): Convergence during secondary forest succession. – *Journal of Ecology* 72: 25-36.
- [10] Davis, M. A., Grime, J. P., Thompson, K. (2000): Fluctuating resources in plant communities: a general theory of invasibility. – *Journal of Ecology* 88: 528-534.
- [11] Davis, M. A., Thompson, K., Philip Grime, J. (2005): Invasibility: the local mechanism driving community assembly and species diversity. – *Ecography* 28: 696-704.
- [12] Dyakov, N., Zhelev, P. (2013): Alien species invasion and diversity of riparian forest according to environmental gradients and disturbance regime. – *Applied Ecology and Environmental Research* 11: 249-272.
- [13] Eriksson, O. (1992): Evolution of seed dispersal and recruitment in clonal plants. – *Oikos* 63: 439-448.
- [14] Foster, B. L., Tilman, D. (2000): Dynamic and static views of succession: testing the descriptive power of the chronosequence approach. – *Plant Ecology* 146: 1-10.
- [15] Fraaije, R. G. A., ter Braak, C. J. F., Verduyn, B., Verhoeven, J. T. A., Soons, M. B. (2015): Dispersal versus environmental filtering in a dynamic system: drivers of vegetation patterns and diversity along stream riparian gradients. – *Journal of Ecology* 103: 1634-1646.
- [16] Götzenberger, L., Botta-Dukát, Z., Lepš, J., Pärtel, M., Zobel, M., de Bello, F. (2016): Which randomizations detect convergence and divergence in trait-based community assembly? A test of commonly used null models. – *Journal of Vegetation Science* 27: 1275-1287.

- [17] Götzenberger, L., de Bello, F., Bråthen, K. A., Davison, J., Dubuis, A., Guisan, A., Lepš, J., Lindborg, R., Moora, M., Pärtel, M., Pellissier, L., Pottier, J., Vittoz, P., Zobel, K., Zobel, M. (2012): Ecological assembly rules in plant communities—approaches, patterns and prospects. – *Biological Reviews* 87: 111-127.
- [18] Hill, M. O., Gauch, H. G. (1980): Detrended correspondence analysis: an improved ordination technique. – *Vegetatio* 42: 47-58.
- [19] Holle, B. V., Simberloff, D. (2005): Ecological resistance to biological invasion overwhelmed by propagule pressure. – *Ecology* 86: 3212-3218.
- [20] Hubbell, S. P. (2001): *The Unified Neutral Theory of Species Abundance and Diversity*. – Princeton University Press, Princeton, NJ.
- [21] Huston, M. A., DeAngelis, D. L. (1994): Competition and coexistence: the effects of resource transport and supply rates. – *The American Naturalist* 144: 954-977.
- [22] Keddy, P. A. (1992): Assembly and response rules: two goals for predictive community ecology. – *Journal of Vegetation Science* 3: 157-164.
- [23] McDonald, R. I., Motzkin, G., Foster, D. R. (2008): The effect of logging on vegetation composition in Western Massachusetts. – *Forest Ecology and Management* 255: 4021-4031.
- [24] Mood, A. M. (1954): On the asymptotic efficiency of certain nonparametric two-sample tests. – *The Annals of Mathematical Statistics* 25: 514-522.
- [25] Mouquet, N., Munguia, P., Kneitel, J., Miller, T. (2003): Community assembly time and the relationship between local and regional species richness. – *Oikos* 103: 618-626.
- [26] Myers, J. A., Chase, J. M., Crandall, R. M., Jiménez, I. (2015): Disturbance alters beta-diversity but not the relative importance of community assembly mechanisms. – *Journal of Ecology* 103: 1291-1299.
- [27] Naeem, S., Knops, J. M., Tilman, D., Howe, K. M., Kennedy, T., Gale, S. (2000): Plant diversity increases resistance to invasion in the absence of covarying extrinsic factors. – *Oikos* 91: 97-108.
- [28] Palmer, M. W., van der Maarel, E. (1995): Variance in species richness, species association, and niche limitation. – *Oikos* 203-213.
- [29] Reiners, W. A. (1992): Twenty years of ecosystem reorganization following experimental deforestation and regrowth suppression. – *Ecological Monographs* 62: 503-523.
- [30] Richardson, D. M., Holmes, P. M., Esler, K. J., Galatowitsch, S. M., Stromberg, J. C., Kirkman, S. P., Pyšek, P., Hobbs, R. J. (2007): Riparian vegetation: degradation, alien plant invasions, and restoration prospects. – *Diversity and Distributions* 13: 126-139.
- [31] Shapiro, S. S., Wilk, M. B. (1965): An analysis of variance test for normality (complete samples). – *Biometrika* 52: 591-611.
- [32] Stohlgren, T., Bull, K., Otsuki, Y., Villa, C., Lee, M. (1998): Riparian zones as havens for exotic plant species in the central grasslands. – *Plant Ecology* 138: 113-125.
- [33] Tabacchi, E., Correll, D. L., Hauer, R., Pinay, G., Planty-Tabacchi, A.-M., Wissmar, R. C. (1998): Development, maintenance and role of riparian vegetation in the river landscape. – *Freshwater Biology* 40: 497-516.
- [34] Ward, J. V. (1998): Riverine landscapes: biodiversity patterns, disturbance regimes, and aquatic conservation. – *Biological Conservation* 83: 269-278.
- [35] Weiher, E., Keddy, P. (2001): *Ecological Assembly Rules: Perspectives, Advances, Retreats* – Cambridge University Press, Cambridge.
- [36] Weiher, E., Clarke, G. D. P., Keddy, P. A. (1998): Community assembly rules, morphological dispersion, and the coexistence of plant species. – *Oikos* 81: 309-322.
- [37] Wilson, J. B. (1989): A null model of guild proportionality, applied to stratification of a New Zealand temperate rain forest. – *Oecologia* 80: 263-267.
- [38] Wilson, J. B., Gitay, H. (1995): Limitations to species coexistence: evidence for competition from field observations, using a patch model. – *Journal of Vegetation Science* 6: 369-376.

- [39] Wilson, J. B., Gitay, H., Agnew, A. D. (1987): Does niche limitation exist? – *Functional Ecology* 391-397.
- [40] Wilson, J. B., Crawley, M. J., Dodd, M. E., Silvertown, J. (1996a): Evidence for constraint on species coexistence in vegetation of the Park Grass experiment. – *Vegetatio* 124: 183-190.
- [41] Wilson, J. B., Terry, C. E. W., Trueman, I. C., Jones, G., Atkinson, M. D., Crawley, M. J., Dodd, M. E., Silvertown, J. (1996b): Are there assembly rules for plant species abundance? An investigation in relation to soil resources and successional trends. – *Journal of Ecology* 84: 527-538.
- [42] Zar, J. H. (2010): *Biostatistical Analysis*. – Prentice Hall, Upper Saddle River, NJ.

BIOMASS ESTIMATION AND MAPPING OF CAN GIO MANGROVE BIOSPHERE RESERVE IN SOUTH OF VIET NAM USING ALOS-2 PALSAR-2 DATA

LUONG, V. N.^{1*} – TU, T. T.¹ – KHOI, A. L.¹ – HONG, X. T.¹ – HOAN, T. N.² – THUY, T. L. H.²

¹*Space Technology Institute, Vietnam Academy of Science and Technology
18 Hoang Quoc Viet str., Cau Giay dist., Hanoi 100000, Vietnam*

²*Institute of Geography, Vietnam Academy of Science and Technology
18 Hoang Quoc Viet str., Cau Giay dist., Hanoi 100000, Vietnam*

**Corresponding author*

e-mail: nvluong@sti.vast.vn; phone: +84-2437-562-985; Fax: +84-2437-914-622

(Received 24th Jul 2018; accepted 14th Nov 2018)

Abstract. In this study, we used radar data from the ALOS-2 PALSAR-2 satellite to build biomass estimation models and then create a biomass map in Can Gio Mangrove Biosphere Reserve. We used the single variable regression and multivariate regression method, in which 30 sample plots for training model and 15 sample plots for validation model, the coefficient of determination (R^2) and root mean square error (RMSE) were used as metrics for evaluating the biomass estimates. The regression analyses showed that the HV polarization was highly related to the biomass, linear model ($R^2 = 0.74$; RMSE = 28.16), exponential model ($R^2 = 0.69$; RMSE = 28.73), and polynomial model ($R^2 = 0.76$; RMSE = 28.03). However, the HH polarization did not show a high relationship with the above-ground biomass, linear model ($R^2 = 0.42$), exponential model ($R^2 = 0.46$), or polynomial model ($R^2 = 0.42$). We also tried multiple linear regression between the parameters extracted from radar image (HH, HV, and textures) and field biomass. The coefficient of determination (R^2) between the biomass and two independent variables (HH and HV) was 0.79, and RMSE was 29.78. However, the model with the combination of HV variable and eight texture variables provided a better result ($R^2 = 0.81$; RMSE = 27.76), in other word the model could explain 81% variation of forest biomass. This model was used to produce the aboveground biomass map in Can Gio Biosphere Reserve in South of Vietnam.

Keywords: *microwave data, HH polarization, HV polarization, backscattering, textures, model, mangrove ecosystem, Vietnam*

Introduction

Mangroves are unique ecosystems that occur along ocean coastlines throughout the tropics and are the most carbon-rich forests in those regions. The economic potential of mangroves stems from three main sources, namely, forest products, estuarine and near-shore fisheries, and ecotourism (FAO, 1994; Cannicci et al., 2008; Donato et al., 2011; Alongi, 2012).

Climate change has been one of the biggest challenges for most countries in the 21st century. (IPCC, 2001; Raghuvanshi et al., 2008), carbon dioxide (CO_2) is one of a primary interactant of global warming (IPCC, 2011; Rogelj et al., 2016). Forest sequestrate atmospheric (CO_2) in the form of plant biomass during photosynthesis (IPCC, 2003; Drégelyi-Kiss et al., 2008). Mangrove forest has great potential for CO_2 sequestration (Ong et al., 2004; Alongi et al., 2012). Mangrove forests account for only approximately 1% of the world's forests, but for about 10–14% of the CO_2 sequestration. Therefore, if the mangrove ecosystem is destroyed, the resultant amount

of gas emissions could be very high (Cannicci et al., 2008; Drégelyi-Kiss et al., 2008; Alongi, 2012).

In 1943, the mangrove forest area in Vietnam was 408,500 ha. It decreased from 400,000 ha in the 1960s to 73,000 ha in the 1990s, due to the use of herbicides during the Indochina War and conversion of mangroves for agriculture and aquaculture. In 2015, mangrove area increased to 270,000 ha due to government and donor-funded planting efforts and mangrove protection policies (Mai Sy Tuan, 2016).

Mapping and carbon stock data are important in determining conservation priorities for climate change mitigation efforts as well as implementing programs such as REDD + (Hutchison et al., 2014). However, until now, there is still uncertainty about the amount of carbon emissions caused by the loss of mangrove forests because there is insufficient data on carbon stocks in these ecosystems (Donato et al., 2011; Hutchison et al., 2014).

The estimation of forest biomass using remote sensing data has proved to be more advantageous than traditional method, because it has advantages such as technology, space, time and cost (Lu, 2006; Gibbs et al., 2007; Goetz et al., 2011). The main remote sensing data is available as; optical satellite, lidar and radar satellite (Lu, 2006).

Optical satellite data

Studies on the estimation of forest biomass using optical satellite images such as Tucker et al. (1973), Tucker (1977), and Sader et al. (1989) have been of interest since very early to this now-a-day, and are usually about the use of plant indicators such as Normalized Difference Vegetation Index (NDVI) (Hamdan et al., 2013; Kamal et al., 2015; Wicaksono et al., 2016) and Leaf Area Index (LAI) (Wicaksono et al., 2016; Castillo et al., 2017). However, due to disadvantages of optical satellite data such as high saturation, clouds, especially in tropical regions, the applications of these indicators are limited.

Lidar data

Lidar provides an excellent source of data for estimating forest biomass because it has three-dimensional information about forests (Maclean, 1998; Chen, 2013). Hayashi et al. (2015) developed empirical models to estimate aboveground biomass (AGB) and canopy height from the Ice, Cloud, and land Elevation Satellite (ICESat)/Geoscience Laser Altimeter System (GLAS) data in Borneo. However, due to the trade off between cost, high processing capacity, and specialized software, the application of Lidar data for a large geographical area is very limited (Lu, 2006; Chen, 2013; Sinha et al., 2015).

Radar satellite data

Radar data is used for estimation of forest biomass with high potential because this data is not affected much from natural conditions such as at day-night time, cloud cover, other advantages such as temporal availability, large-scale coverage, and lower saturation (Wu, 1987; Gibbs et al., 2007; Le Toan et al., 2011; Sinha et al., 2015). The long-wavelength Synthetic Aperture Radar (SAR) satellite is expected to have much promise for forest biomass map estimates (MacRoberts, 2007; Smith and Brown, 2009; Le Toan et al., 2011). The backscattering value of L-band and P-band SAR data have demonstrated sensitivity to structure, cover, volume, and biomass of the forests penetrating into the branches and stems of trees (Sun et al., 2002; Balzter, 2001; Morel

et al., 2011). A number of previous studies have shown an impressive relationship between the SAR data and biomass (Le Toan et al., 1992; Santos et al., 2010; Peregon et al., 2013).

Several researchers have reported saturation problems of the L-band SAR backscattering over highly varying levels of biomass (Imhoff, 1995; Luckman et al., 1997; Mermoz et al., 2015). However, numerous reports indicate that the L-band SAR backscattering was saturated at around 150–200 Mg/ha (Motohka et al., 2011; Avtar et al., 2013; Le Toan et al., 2013; Ni et al., 2014).

The major SAR techniques for estimates of woody volume and biomass attempted by a number of researchers so far are dual-wavelength SAR interferometry (Balzter, 2001), random volume over-ground model (Hajnsek et al., 2009), water cloud model (Cartus et al., 2012), a combination of forest structure and radiative transfer models (Brolly et al., 2012), and electromagnetic modeling (Mermoz et al., 2015). The models mentioned above are relatively complex and difficult to implement in practice. Only regression correlation models are relatively easy to apply (Le Toan et al., 1992; Englhart et al., 2011; Carreiras et al., 2013; Izuka and Tateish, 2014).

Over the last decade in Viet Nam, there have been several studies using satellite imagery for estimating biomass and forest timber, e.g. Bui et al. (2011) conducted a study on the leaf canopy biomass in Cat Tien National Park, Lam Dong province using ALOS AVNIR 2 image. Huong et al. (2011) used SPOT5 satellite image to estimate woody volume. However, these studies have used only optical image data. Due to the limited ability of optical satellite imagery in the estimation of mangrove forest biomass on the ground, the models constructed in these studies are often complex and have several intermediate steps, thus limiting the application. As an urgent and mandatory requirement from forested countries to participate in climate change adaptation and REDD programs (Saatchi et al., 2011). However, the estimation of biomass from satellite data is very challenging due to the diverse nature of forests, especially tropical forests (Sinha et al., 2015; Kumar et al., 2015).

The purpose of this study was to develop the best model for estimation of mangrove forest biomass and then to create a forest biomass map. In this study, we have used radar data from ALOS-2 PALSAR-2 (The Advanced Land Observing Satellite-2), a Japanese satellite launched in 2014, which operates in L-band radar and collects very high spatial resolution data.

Study area

Can Gio mangrove forest lie entirely in the Can Gio district of Ho Chi Minh city in South of Vietnam. The boundary ranges from Nha Be district in the north to the East Sea in the south and from Dong Nai and Ba Ria-Vung Tau provinces in the east to Long An in the west. The area measures 35 km from north to south and 30 km from east to west (*Fig. 1*).

Topographically, the Can Gio mangrove forest forms a basin with a minimum altitude range of 0 m – 1.5 m, in the northeastern sector of the forest, with downward inclines from the east, south, and west. The climate has two seasons, rainy season from May to October and dry season from November to April.

Plant diversity, about 105 plant species, belonging to 48 genera are found in Can Gio mangrove forest, including *Rhizophora apiculata* constituted the main part of the flora, together with other assemblages of *Bruguiera gymnorrhiza*, *Bruguiera parviflora*,

Ceriops sp., *Kandelia candel*, *Rhizophora mucronata*, *Sonneratia alba*, *Sonneratia ovata*, *Sonneratia caseolaris*, *Avicennia alba*, *A. officinalis*, *A. lanata* (stunted trees in abandoned salt fields), *Aegiceras majus*, *Thespesia populnea*, *Hibiscus tiliaceus*, *Lumnitzera racemosa*, *Xylocarpus granatum*, and *Excoecaria agallocha* (Tuan et al., 2002).

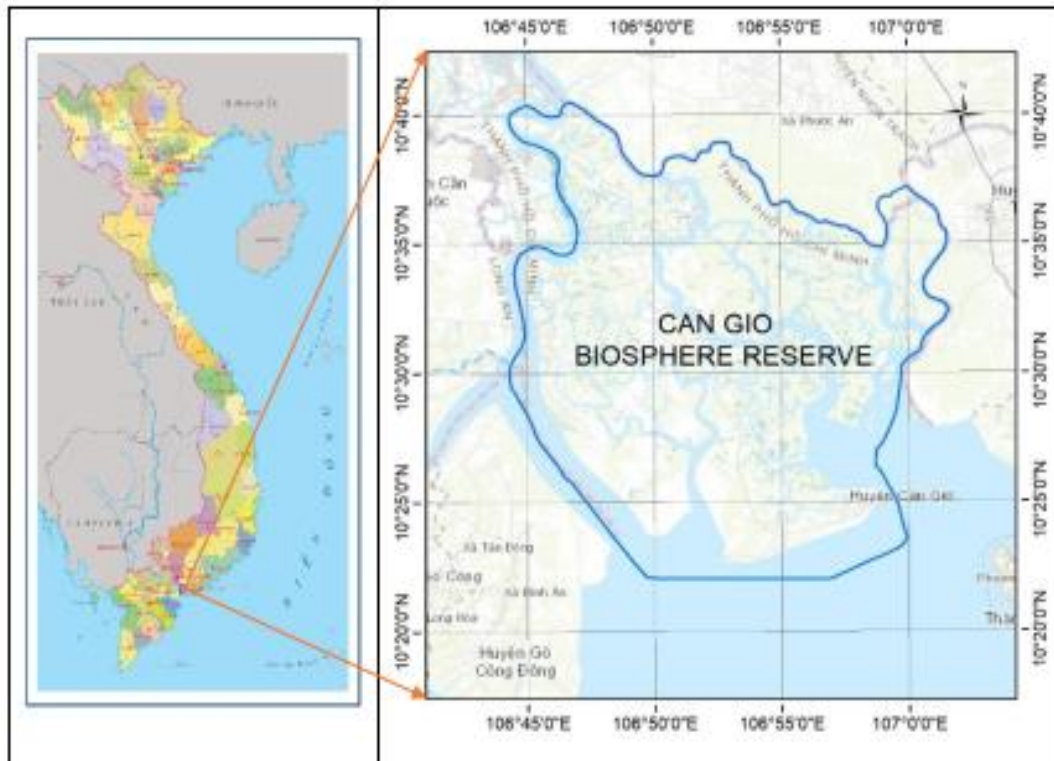


Figure 1. Study area position in Vietnam map (Can Gio Biosphere Reserve)

Methodologies

Selection and processing of satellite data

In this study, we used ALOS-2 PALSAR-2 version 2.1, HH (horizontal transmitting, horizontal receiving) and HV (horizontal transmitting, vertical receiving) polarizations with a pixel resolution of 6.25 m, available as a geometrically corrected product. The digital number (DN) values of the SAR (Synthetic Aperture Radar) images in both the HH and HV polarizations were calibrated by calculating the backscattering intensity using *Equation 1* (JAXA, 2014).

$$\sigma^{\circ} = 10 * \log_{10} DN^2 + CF \quad (\text{Eq.1})$$

where:

σ° is the sigma-naught backscattering intensity in the units of *decibels* (dB).

CF is the calibration factor, which is currently set as -83.

In this study, we also used eight texture values from ALOS-2 PALSAR-2 images, including contrast, correlation, dissimilarity, entropy, homogeneity, mean, second

moment, and variance (Haralick et al., 1973; Anys et al., 1994). The formulas for the texture measurements used in this study are shown in *Equations 2–9*:

$$Contrast = \sum_{n=0}^{N_g-1} n^2 \sum_{\substack{i=1 \\ |i-j|=n}}^{N_g} j \sum_{j=1}^{N_g} p(i, j) \quad (Eq.2)$$

$$Dissimilarity = \sum_{n=0}^{N_g-1} n \sum_{\substack{i=1 \\ |i-j|=n}}^{N_g} j \sum_{j=1}^{N_g} p(i, j)^2 \quad (Eq.3)$$

$$Homogeneity = \sum_i \sum_j \frac{1}{1 + (i - j)^2} p(i, j) \quad (Eq.4)$$

$$SecondMoment = \sum_i j \sum_j \{p(i, j)\}^2 \quad (Eq.5)$$

$$Correlation = \frac{\sum_i j \sum_j (i, j) p(i, j) - \mu_x \mu_y}{\sigma_x \sigma_y} \quad (Eq.6)$$

$$Entropy = \sum_i j \sum_j p(i, j) \log(p(i, j)) \quad (Eq.7)$$

$$Mean = \sum_{i,j=0}^{n-1} i p_{i,j} \quad (Eq.8)$$

$$Variance = \sum_i j \sum_j (i - u)^2 (p(i, j)) \quad (Eq.9)$$

where:

$p(i, j)$ is the normalized co-occurrence matrix such that $\sum (i, j = 0, n - 1, p(i, j)) = 1$
 $\mu_x, \mu_y, \sigma_x, \sigma_y$ are the means and standard deviations of p_x, p_y .

The software used in this study included ENVI versions 5.4, ArcGIS 10.2 for satellite image processing, map editing, and R for statistical analysis. The details of the ALOS-2 PALSAR-2 data used in the research are shown in *Table 1* and *Figure 2*.

Table 1. ALOS-2 PALSAR-2 data used in this research

No.	Scene ID	Observation date	Observation angle	Polarizations	Pixel resolution (m)
1	ALOS2151050200	10 March 2017	36.6°	HH, HV	6.25
2	ALOS2152303410	10 March 2017	36.6°	HH, HV	6.25



Figure 2. ALOS-2 PALSAR-2 data used in this research

Field work

Field surveys are important for collecting in situ data for accurate analysis of satellite-based estimates. We conducted a field survey during April 2017 to collect the ground truth data. In this study, the size of a sample plot is 0.05 ha (20 × 25 m). We measured the diameter at breast height ($D_{1.3cm}$) and tree height (H_m). We also recorded the types of tree species during the field survey by Vietnam’s flora books Pham (2003).

Forty-five sample plots in total are used in this study. We used a random selection method for training (30 sample plots) and validation data (15 sample plots). The inventory data summary is provided in Table 2. The distribution of the sample plot positions is shown in Figure 3.

Table 2. Forest inventory parameters for the training data

Parameter	Training field data				Validation field data			
	Minimum	Maximum	Mean	Standard deviation	Minimum	Maximum	Mean	Standard deviation
Diameter (m)	5.83	17.60	10.16	3.25	7.11	17.60	11.62	2.93
Height (m)	6.34	17.04	12.82	2.92	7.88	17.04	14.34	2.31
Biomass ($Mg \cdot ha^{-1}$)	9.24	254.29	99.20	76.90	11.31	255.42	179.52	67.60

The survey results show that: Dense mangrove forests include dominant species as *Rhizophora apiculata*, *Bruguiera gymnorrhiza*, *Avicennia germinans*, *Sonneratia caseolaris* and *Aegyceras corniculatum*. Open mangrove forests include dominant species as *Rhizophora apiculata*, *Avicennia germinans*, *Ceriops decandra*, *Lumnitzera racemosa*, *Sonneratia caseolaris*, and *Lumnitzera racemosa*. Young forests and scrubs include dominant species as *Ceriops decandra*, *Lumnitzera racemosa*, *Avicennia germinans*, and *Rhizophora apiculata*. The components of mangrove species in study area show in Table 3.

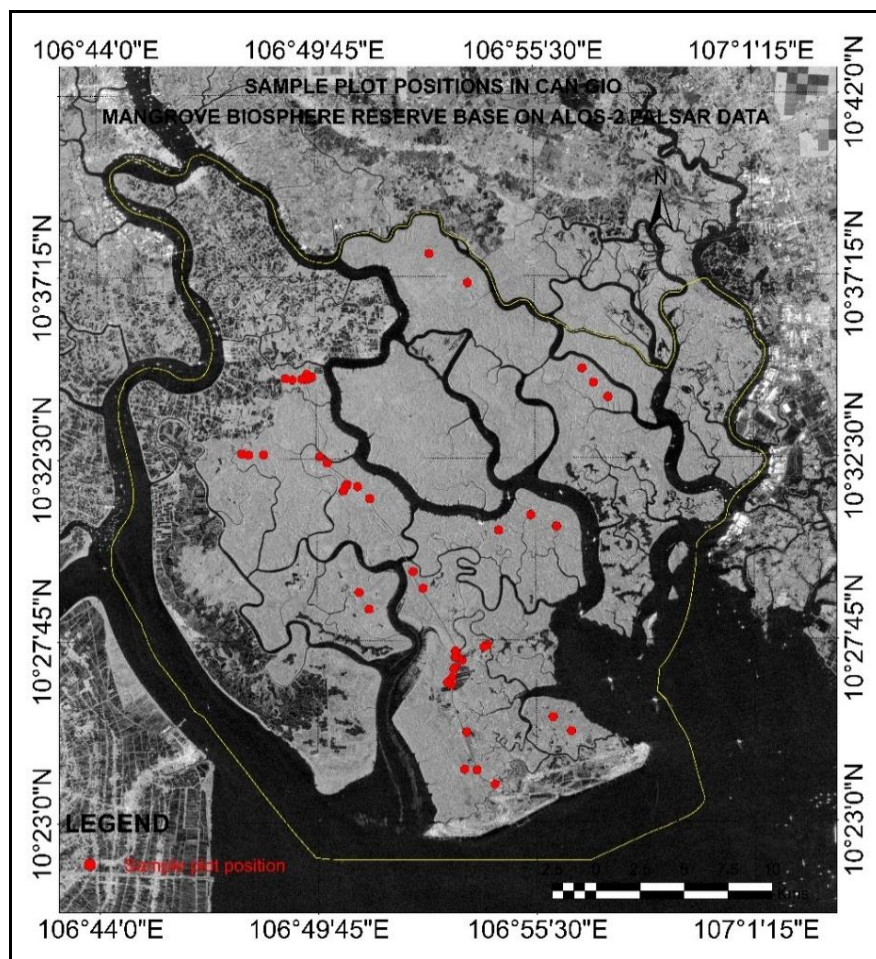


Figure 3. Sample plot position in Can Gio Biosphere Reserve

Table 3. The components of mangrove species in the study area

No.	Forest classes	Sample plot number	Components of mangrove species in the study area by ratio 1/10
1	Dense mangrove forest	15, 17, 19, 20, 37, 39, 40, 42, 44, and 45	7.93 <i>Rhizophora apiculata</i> + 0.95 <i>Bruguiera gymnorrhiza</i> + 0.86 <i>Avicennia decandra</i> + 0.25 <i>Sonneratia caseolaris</i> + 0.01 <i>Aegyceras corniculatum</i>
2	Open mangrove forests	5, 8, 9, 10, 11, 12, 13, 14, 21, 22, 28, 33, 34, 35, 36, 38, 41, and 43	2.91 <i>Rhizophora apiculata</i> + 2.91 <i>Avicennia germinans</i> + 1.58 <i>Ceriops decandra</i> + 1.44 <i>Lumnitzera racemosa</i> + 0.83 <i>Bruguiera parviflora</i> + 0.43 <i>Sonneratia caseomosa</i> + 0.07 <i>Lumnitzera racemosa</i> + 0.03 other species
3	Young forests and scrubs	1, 2, 3, 4, 6, 7, 16, 18, 23, 24, 25, 26, 27, 29, 30, 31, and 32	8.55 <i>Ceriops decandra</i> + 0.70 <i>Lumnitzera racemosa</i> + 0.70 <i>Avicennia germinans</i> + 0.03 <i>Rhizophora apiculata</i> + 0.03 other species

We used allometric equations (*Eq. 10–18*) here to calculate the AGB (Above Ground Biomass) for different mangrove species as well as the main species in the study area’s mangrove forest. The equations are shown in *Table 4*.

Table 4. Allometric equations used for mangroves species

Species	Allometric equations	References	Eq. No.
Rhizophora appiculata	$AGB = 0.235 * D^{2.42} (R^2 = 0.98)$	Ong et al. (2004)	(Eq.10)
Avicennia germinans	$AGB = 0.140 * D^{2.40} (R^2 = 0.97)$	Fromard et al. (1998)	(Eq.11)
Bruguiera gymnorrhiza	$AGB = 0.186 * D^{2.31} (R^2 = 0.99)$	Clough and Scott (1989)	(Eq.12)
Bruguiera parviflora	$AGB = 0.168 * D^{2.42} (R^2 = 0.99)$	Clough and Scott (1989)	(Eq.13)
Xylocarpus granatum	$AGB = 0.0823 * D^{2.59} (R^2 = 0.99)$	Clough and Scott (1989)	(Eq.14)
Ceriops decandra	$AGB = 0.208 * D^{2.36} (R^2 = 0.96)$	Cao (2007)	(Eq.15)
Lumnitzera racemosa	$AGB = 0.74 * D^{2.32} (R^2 = 0.99)$	Trung et al. (2009)	(Eq.16)
Sonneratia caseolaris	$AGB = 0.199 * \rho^{0.90} * D^{2.22} (R^2 = 0.99)$	Komiyama et al. (2005)	(Eq.17)
Common equation	$AGB = 0.25 * \rho * D^{2.592} (R^2 = 0.98)$	Komiyama et al. (2005)	(Eq.18)

In allometric *Equations 10–18*:

- AGB is the aboveground biomass of a tree in kilograms (kg)
- D is the diameter at breast height (1.3 m) in centimeters (cm)
- ρ is the wood density (tons dry matter/m³ fresh volume) (IPCC, 2003)

Results

Training of biomass model

Coefficient of determination (R^2) and root mean square error (RMSE) were used as metrics for evaluating relationships. The results of the relationship between each backscattering intensity (HH, HV polarizations) and biomass value on the basis of the field observation plot were analyzed using the coefficient of determination (R^2). The assessment of these relationships has been shown by regression lines: The HV polarization was highly related to the biomass, according to the linear model ($R^2 = 0.74$; RMSE = 28.16), exponential model ($R^2 = 0.69$; RMSE = 28.73), and polynomial model ($R^2 = 0.76$; RMSE = 28.03); whereas the HH polarization did not show a significant relationship with the aboveground biomass according to the linear, exponential, and polynomial models (R^2 respectively were 0.42, 0.46, and 0.42). The results are shown in *Figure 4*.

We also analyzed multiple linear regression between the parameters extracted (HH, HV, and textures) from the radar image from ALOS-2 PALSAR-2 and field biomass. As shown in *Table 5*, the adjusted coefficient of determination (R^2) between the biomass and two independent variables (HH and HV) was 0.79 and RMSE = 29.48; that of biomass and eight independent variables of textures (contrast, correlation, dissimilation, entropy, homogeneity, mean, second moment, variance) was 0.49. We used a combination of backscattering and textures variables from HH, the result obtained with $R^2 = 0.58$. However, the adjusted coefficient of determination (R^2) for the combination was 0.82 and RMSE = 27.56. The summary of the relationship between the field-measured biomass and ALOS-2 PALSAR-2 data is shown in *Table 5*.

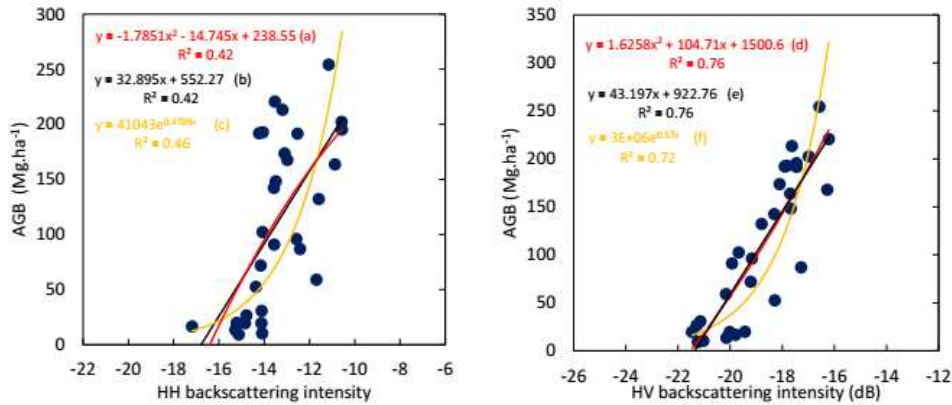


Figure 4. The relationship between biomass and L-band backscattering intensity: (a) Polynomial model (Biomass and HH), (b) Linear model (Biomass and HH), (c) Exponential model (Biomass and HH), (d) Polynomial model (Biomass and HV), (e) Linear model (Biomass and HV), and (f) Exponential model (Biomass and HV)

Table 5. The summary of the relationship between biomass and satellite data

No.	Model	Relationship	Coefficient of determination (R ²)
<i>Single-variable model</i>			
1	Model 1	AGB = 33.121HH + 555.81	0.42
2	Model 2	AGB = 44.318HV + 945.99	0.74
3	Model 3	AGB = 40278e ^{0.4689xHH}	0.46
4	Model 4	AGB = 5E + 06e ^{0.5883xHV}	0.72
5	Model 5	AGB = -2.4301HH ² - 31.429HH + 13	0.42
6	Model 6	AGB = 1.9415HV ² + 118.03HV + 1641.2	0.76
<i>Multil-variable model</i>			
7	Model 7	AGB= 957.79 + 11.58HH + 36.79HV	0.79
8	Model 8	ABG = -16817.86 - 1733.35Contrast + 49.90Correlation + 10249.89Dissimilarity - 254.70Entropy + 16974.67Homogeneity + 23.41Mean - 1084.849SecondMoment + 40.53Variance	0.49
9	Model 9	ABG = 3084.31 + 168.53Contrast + 36.17Correlation - 1090.15Dissimilarity - 89.71Entropy - 1729.60Homogeneity - 17.23Mean - 427.95SecondMoment + 16.09Variance + 39.53HH	0.58
10	Model 10	ABG = -65714.04 - 6726.42Contrast + 2.46Correlation + 40273.92Dissimilarity - 115.77Entropy + 67144.71Homogeneity - 6.04Mean - 432.67SecondMoment + 28.39Variance + 46.61HV	0.81

Validation of biomass model

We have selected training models with R² > 0.7 (high correlated) as validation models. Models 2 (R² = 0.74; RMSE = 28.16), 4 (R² = 0.72; RMSE = 33.64) 6 (R² = 0.75; RMSE = 28.73), 7 (R² = 0.78; RMSE = 29.87), and 10 (R² = 0.81; RMSE = 27.76). The results of the validation model are shown in *Figure 5*.

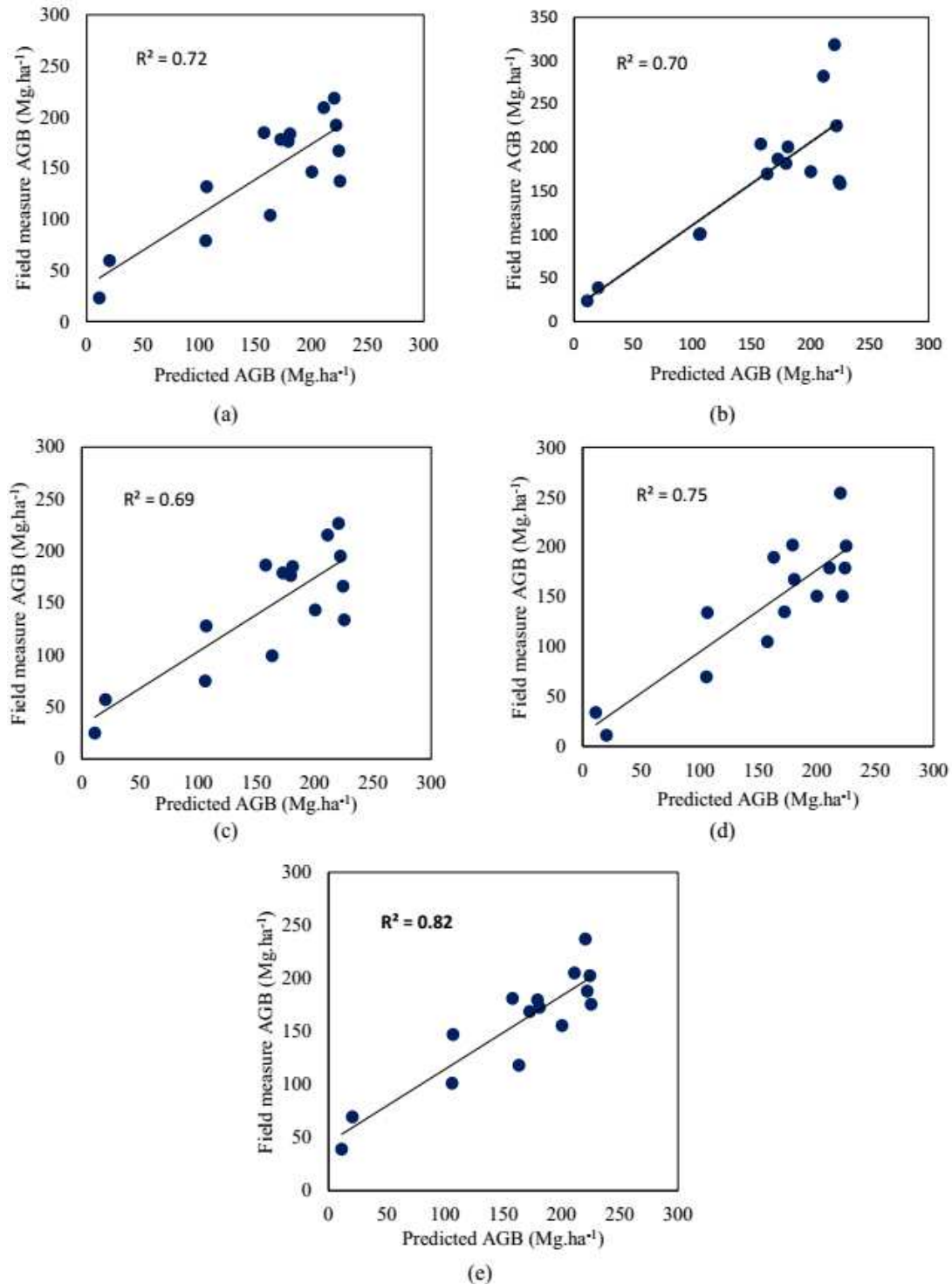


Figure 5. The validation results: (a) Model 2, (b) Model 4, (c) Model 6, (d) Model 7, and (e) Model 10. The 1:1 cross plots between the predicted and ground data are shown

We have found Model 10 to be the best, including training model ($R^2 = 0.81$; RMSE = 27.76) and validation model ($R^2 = 0.82$; RMSE = 27.56), and have selected the Model 10 for map mangrove biomass for Can Gio Biosphere Reserve, Ho Chi Minh, city in South of Vietnam.

Mapping

The model derived by the best combination of the HV backscattering intensity and eight textures from ALOS-2 PALSAR-2 (Model 10) is shown below:

$$\text{Biomass (Mg.ha}^{-1}\text{)} = -65714.04 - 6726.42\text{Contrast} + 2.46\text{Correlation} + 40273.92\text{Dissimilarity} - 115.77\text{Entropy} + 67144.71\text{Homogeneity} - 6.04\text{Mean} - 432.67\text{SecondMoment} + 28.39\text{Variance} + 46.61\text{HV}$$

This model was used to produce the aboveground biomass map in Can Gio Biosphere Reserve, Ho Chi Minh city in South of Vietnam. The results show that very rich mangrove forest is 13843.66 ha (18.45%), rich mangrove forest area is 20188.03 ha (26.90%), medium mangrove forest area is 7517.89 ha (10.02%), poor mangrove forest area is 4648.30 ha (6.19%), bare soil area is 730.30 ha (0.97%), and the water body area is 28120.15 ha (37.47%). More details are shown in *Table 6* and the biomass map is shown in *Figure 6*.

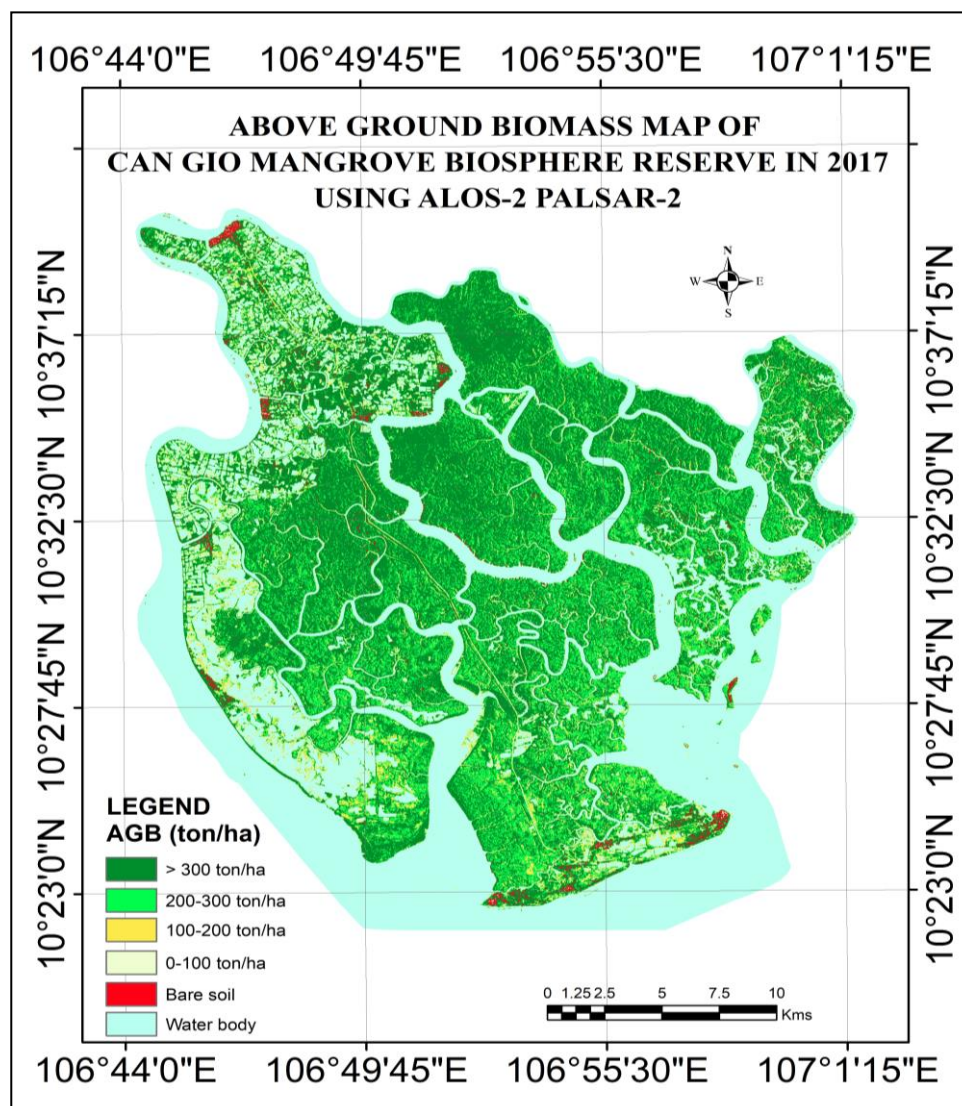


Figure 6. Aboveground biomass map of Can Gio Biosphere Reserve

Table 6. Aboveground biomass distribution of Can Gio Biosphere Reserve

No.	Classes	Biomass level (ton.ha ⁻¹)	Area	
			(ha)	(%)
1	Vey rich forest	>300	13843.66	18.45
2	Rich forest	200-300	20188.03	26.90
3	Medium forest	100-300	7517.89	10.02
4	Poor forest	0-100	4648.73	6.19
5	Bare soil	-	730.30	0.97
6	Water body	-	28120.15	37.47
	Total		75048.76	100.00

Discussion

The sensitivity of the radar signal to the biomass depends on the frequency, polarization, and incidence angle (Le Toan et al., 1992; Dobson et al., 1992; Van Truong et al., 2017). The forest structure is a complex matter; and the radar signal is sensitive to forest's characteristics as well as the horizontal and vertical structure of the forest. The L-band ALOS-2 PALSAR-2 data can penetrate into the forested canopy, and the backscattering is sensitive to the size of branches and tree trunks, which are main component of the forest biomass. The backscattering intensity received by a SAR sensor is characterized by the polarized (horizontal or vertical) combinations of the transmitted and received signals (Anys et al., 1994; Izuka et al., 2015; Kumar et al., 2015). The HH polarization receives the signal reflected straight from an object. Therefore, it is more sensitive to changes in moisture, and thus the HH backscattering intensity varies highly between dry or wet objects. Conversely, the HV polarization receives a signal reflected at a 90 degree angle from an object. In other words, the HV polarization receives a very different signal reflected at a different angle away from the received direction. Forest structures are complex in nature, resulting in volumetric rather than surface scattering. Therefore, HV data is more sensitive to the biomass than HH data. The structural information obtained from the SAR data provides additional information about the forest canopy structure (combination of horizontal and vertical forest structures). Thus, the combination of backscattering and textural parameters from SAR data has improved the model of biomass estimation in this study.

Some literature overviews of satellite data application for biomass estimation have been reviewed by Sinha et al. (2015), Tsitsi et al. (2016), and Kumar and Mutanga (2017). They have concluded that radar satellite data are more potential for biomass estimates especially in the tropical forest region, where forest structures are complex and often covered by clouds. Recent studies have also shown promising results for the estimation of forest biomass using satellite radar data. For example, Basuki et al. (2013) reported R^2 from 0.70 to 0.75 for biomass estimates; Minh et al. (2018) have obtained high correlation ($R^2=0.71$) between the radar signal and in situ biomass, Ghosh and Behera (2018) have estimated aboveground biomass with high accuracy ($R^2 = 0.71$), and Berninger et al. (2018) have also shown high model performance ($R^2 = 0.70-0.76$). Other studies have also obtained high correlation between the mangrove forest biomass and radar data. For example, Pham et al. (2018) got $R^2 = 0.59$ between biomass and radar data, Argamosa et al. (2018) obtained high correlation (R^2 of 0.79) between forest

biomass and radar data. In general, major concerns of the researches are to improve the accuracy of the biomass estimates using satellite data, and our research is not an exception. Nevertheless, major limitation of the SAR system for estimating biomass is that the backscattering intensity becomes saturated when the biomass exceeds a certain critical value, even with the HV backscattering intensity. In this research, the best-validated model showed saturation point around 200–250 Mg.ha⁻¹. Therefore, the model presented in the research is sensitive to the biomass until that biomass value is reached.

Conclusions

In this study, we have developed a methodology for biomass estimation and mapping of mangrove forests. A case study in Can Gio Biosphere Reserve, Vietnam was conducted based on ALOS-2 PALSAR-2 data and field plot data. From the results of this study, we have obtained the following conclusions:

- HV polarization has a better relationship with mangrove forest biomass when compared to HH polarization in the single-variable model.
- Combined HV and HH polarization by multi-variable models have improved relationship to the biomass compared to single-variable models.
- We obtained $R^2 = 0.58$ by the combination of backscattering variables and textures variables (contrast, correlation, dissimilation, entropy, homogeneity, mean, second moment, and variance) using HH polarization. However, by replacing the backscattering and textures variables from HV polarization, the model significantly improved ($R^2 = 0.82$; RMSE = 27.56) the biomass estimates. This best model was used to produce an up-to-date biomass map of Can Gio Biosphere Reserve.
- The saturation in this study was found to be around 200–250 Mg.ha⁻¹. This result was improved compared to previous studies.
- The results showed that very rich mangrove forest is 13843.66 ha (18.45%), rich mangrove forest area is 20188.03 ha (26.90%), medium mangrove forest area is 7517.89 ha (10.02%), and poor mangrove forest area is 4648.30 ha (6.19%).

The estimation of mangrove forest biomass using the satellite data is important for monitoring mangrove biomass changes over time. We recommend monitoring of mangrove biomass changes every two years or at least every five years (according to the forest inventory period of Vietnam), using radar satellite data. Our hope is that the satellite based monitoring of mangrove forests can contribute significantly to the sustainable management of mangrove forests and to the participation on REDD+ programs.

Acknowledgements. The authors are grateful to the VT-UD. 05/17-20 project from National Research Program on Space Science and Technology for financial support to this research. We would like to thank JAXA for sharing ALOS-2 SAR data for this study in the framework of the ALOS Research program, PI No. 1172.

REFERENCES

- [1] Alongi, D. M. (2012): Carbon sequestration in mangrove forests. – *Carbon Management* 3(3): 313-322.
- [2] Anys, H., Bannari, A., He, D. C., Morin, D. (1994): Texture analysis for the mapping of urban areas using airborne MEIS-II images. – *Proceedings of the First International Airborne Remote Sensing Conference and Exhibition, Strasbourg, France, 12-15 September 1994*, pp. 231-245.
- [3] Avtar, R., Suzuki, R., Takeuchi, W., Sawada, H. (2013): PALSAR 50 m mosaic data based national level biomass estimation in Cambodia for implementation of REDD+ Mechanism. – *PloS one* 8(10): e74807.
- [4] Balzter, H. (2001): Forest mapping and monitoring with interferometric synthetic aperture radar (InSAR). – *Progress in Physical Geography* 25(2): 159-177.
- [5] Brolly, M., Woodhouse, I. H. (2012): A “Matchstick Model” of microwave backscatter from a forest. – *Ecological Modelling* 237: 74-87.
- [6] Bui, N. L. H. et al. (2011): Estimating biomass of the canopy of leaves by using satellite data ALOS AVNIR-2. – *National Workshop on GIS Applications, Vietnam, 2011*.
- [7] Cannicci, S., Burrows, D., Fratini, S., Smith, T. J., Offenber, J., Dahdouh-Guebas, F. (2008): Faunal impact on vegetation structure and ecosystem function in mangrove forests: a review. – *Aquatic Botany* 89(2): 186-200.
- [8] Cao, H. B. (2009): Nghiên cứu khả năng hấp thụ CO₂ của quần thể dà quánh (*Ceriops decandra* Dong Hill) tự nhiên tại Khu Dự trữ sinh quyển rừng ngập mặn Cần Giờ, thành phố Hồ Chí Minh (Doctoral dissertation, Trường Đại học Nông Lâm TP. Hồ Chí Minh) (Vietnamese version). Study on the ability of CO₂ absorption of the natural *Ceriops decandra* Dong Hill (Dà quánh) populations in Can Gio Mangrove Biosphere Reserve (Doctoral dissertation, Nong Lam University Ho Chi Minh City) (Translated by Luong, V.N).
- [9] Carreiras, J. M. B., Melo, J. B., Vasconcelos, M. J (2013): Estimating the above-ground biomass in Miombo Savanna woodlands (Mozambique, East Africa) using L-band synthetic aperture radar data. – *Remote Sens.* 5: 1524-1548.
- [10] Cartus, O., Santoro, M., Kellndorfer, J. (2012): Mapping forest aboveground biomass in the Northeastern United States with ALOS PALSAR dual-polarization L-band. – *Remote Sensing of Environment* 124: 466-478.
- [11] Castillo, J. A. A., Apan, A. A., Maraseni, T. N., Salmo III, S. G. (2017): Estimation and mapping of above-ground biomass of mangrove forests and their replacement land uses in the Philippines using Sentinel imagery. – *ISPRS Journal of Photogrammetry and Remote Sensing* 134: 70-85.
- [12] Chen, Q. (2013): Lidar remote sensing of vegetation biomass. – *Remote Sensing of Natural Resources* 399: 399-420.
- [13] Clough, B. F. and Scott, K. (1989): Allometric relationships for estimating aboveground biomass in six mangrove species. – *Forest Ecol. Manage.* 27: 117-127.
- [14] Dobson, M. C., Ulaby, F. T., LeToan, T., Beaudoin, A., Kasischke, E. S., Christensen, N. (1992): Dependence of radar backscatter on coniferous forest biomass. – *IEEE Transactions on Geoscience and remote Sensing* 30(2): 412-415.
- [15] Donato, D. C., Kauffman, J. B., Murdiyarso, D., Kurnianto, S., Stidham, M., Kanninen, M. (2011): Mangroves among the most carbon-rich forests in the tropics. – *Nature Geoscience* 4(5): 293-297.
- [16] Drégelyi-Kiss, Á., Drégelyi-Kiss, G., Hufnagel, L. (2008): Ecosystems as climate controllers–biotic feedbacks (a review). – *Applied Ecology and Environmental Research* 6(2): 111-135.
- [17] Englhart, S., Keuck, V., Siegert, F. (2011): Aboveground biomass retrieval in tropical forests. The potential of combined X- and L-band SAR data use. – *Remote Sens. Environ.* 115: 1260-1271.

- [18] FAO (1994): Mangrove Forest Management Guideline. – Food and Agriculture Organization of the United Nations, Roma.
- [19] Fromard, F., Puig, H., Mougins, E., Marty, G., Betoulle, J. L., Cadamuro, L. 1998: Structure above-ground biomass and dynamics of mangrove ecosystems: new data from French Guiana. – *Oecologia* 115: 39-53.
- [20] Gibbs, H. K., Brown, S., Niles, J. O., Foley, J. A. (2007): Monitoring and estimating tropical forest carbon stocks: making REDD a reality. – *Environmental Research Letters* 2(4): 045023.
- [21] Goetz, S., Dubayah, R. (2011): Advances in remote sensing technology and implications for measuring and monitoring forest carbon stocks and change. – *Carbon Management* 2(3): 231-244.
- [22] Hajnsek, I., Kugler, F., Lee, S. K., Papathanassiou, K. P. (2009): Tropical-forest-parameter estimation by means of Pol-InSAR: The INDREX-II campaign. – *IEEE Trans. Geosci. Remote Sens.* 47: 481-493.
- [23] Hamdan, O., Khairunnisa, M. R., Ammar, A. A., Hasmadi, I. M., Aziz, H. K. (2013): Mangrove carbon stock assessment by optical satellite imagery. – *Journal of Tropical Forest Science* 554-565.
- [24] Haralick, R. M., Shanmugam, K., Dinstein, I. H. (1973): Textural features for image classification. – *IEEE Trans. Syst. Man Cybern.* 6: 610-621.
- [25] Hayashi, M., Saigusa, N., Yamagata, Y., Hirano, T. (2015): Regional forest biomass estimation using ICESat/GLAS spaceborne LiDAR over Borneo. – *Carbon Management* 6(1-2): 19-33.
- [26] Trung, V.P., Hoan, D.H., Sinh, V.L. (2009): Nghiên cứu khả năng tích tụ Carbon của rừng trồng Cóc trắng (*Lumnitzera racemosa* WILLD) tại khu dự trữ sinh quyển rừng ngập mặn Cần Giờ-Thành phố Hồ Chí Minh (Vietnamese version). Study on the ability of carbon storage by *Lumnitzera racemosa* WILLD in Can Gio Mangrove Biosphere Reserve, Ho Chi Minh City (Translated by Luong, V.N).
- [27] Huong, N. T. T. (2011): Áp dụng phương pháp địa thống kê để ước lượng trữ lượng lâm phần dựa vào ảnh vệ tinh SPOT5 (2011). Tạp Chí Nông nghiệp và Phát triển Nông thôn, Kỳ 1, 2 tháng 2 năm 2011 (Vietnamese version). Applying geostatistic to estimate stand forest volume based on SPOT 5 data. – *Journal of Agriculture and Rural Development*, Vol. 1,2, February 2011 (Translated by Luong, V.N).
- [28] Hutchison, J., Manica, A., Swetnam, R., Balmford, A., Spalding, M. (2014): Predicting global patterns in mangrove forest biomass. – *Conservation Letters* 7(3): 233-240.
- [29] Iizuka, K., Tateishi, R. (2015): Estimation of CO₂ sequestration by the forests in Japan by discriminating precise tree age category using remote sensing techniques. – *Remote Sensing* 7(11): 15082-15113.
- [30] Imhoff, M. L. (1995): Radar backscatter and biomass saturation-Ramifications for global biomass inventory. – *IEEE Transactions on Geoscience and Remote Sensing.* 33 (2): 511-518. DOI: 10.1109/36.377953.
- [31] IPCC (2001): Climate Change 2001 IPCC Third Assessment Report. – Intergovernmental Panel on Climate Change Geneva, IPCC Secretariat.
- [32] IPCC (2003): Good Practice Guidance for Land Use, Land-Use Change and Forestry. – IPCC National Greenhouse Gas Inventories Programme Technical Support Unit, Japan.
- [33] JAXA (2014): ALOS-2/Calibration Result of JAXA Standard Products. – Japan Aerospace Exploration Agency, Earth Observation Research Center, Tsukuba, Japan, 2014.
- [34] Kamal, M., Phinn, S., Johansen, K. (2015): Object-based approach for multi-scale mangrove composition mapping using multi-resolution image datasets. – *Remote Sensing* 7(4): 4753-4783.
- [35] Komiyama, A., Pongpan, S., Kato, S. (2005): Common allometric equations for estimating the tree weight of mangroves. – *Journal of Tropical Ecology* 21 (04): 471-477. DOI: 10.1017/ S0266467405002476.

- [36] Kumar, L., Sinha, P., Taylor, S., Alqurashi, A. F. (2015): Review of the use of remote sensing for biomass estimation to support renewable energy generation (2015). – *J. Appl. Remote Sens.* DOI: 10.1117/1.JRS.9.097696.
- [37] Le Toan, T., Beaudoin, A., Riom, J., Guyon, D. (1992): Relating forest biomass to SAR data. – *IEEE Transactions on Geoscience and Remote Sensing* 30(2): 403-411.
- [38] Le Toan, T.; Quegan, S.; Davidson, M. W. J.; Balzter, H.; Paillou, P.; Papathanassiou, K.; Ulander, L. (2011): The BIOMASS mission: mapping global forest biomass to better understand the terrestrial carbon cycle. – *Remote Sens. Environ.* 115: 2850-2860.
- [39] Le Toan, T.; Mermoz, S.; Bouvet, A.; Villard, L. K. C. (2013): Forest Cover Change and Biomass Mapping. – K&C Initiative Report on an International Science Collaboration Led by JAXA, Tokyo, Japan.
- [40] Lu, D. (2006): The potential and challenge of remote sensing-based biomass estimation. – *International Journal of Remote Sensing* 27(7): 1297-1328.
- [41] Luckman, A., Baker, J., Kuplich, M. T., Yanasse, F. C. C., Frery, C. A. (1997): A study of the relationship between radar backscatter and regenerating tropical forest biomass for spaceborne SAR instruments. – *Remote Sens. Environ.* 60: 1-13.
- [42] Maclean, G. A. (1988): Estimation of foliar and woody biomass using an airborne lidar system. – Wisconsin Univ., Madison, WI (USA).
- [43] Mai, S. T. (2016): Mangrove-related policy and institutional framework in Vietnam. – MFF-FAO Final workshop for “Income for Coastal Communities for Mangrove Protection” Project, December 2016.
- [44] McRoberts, R. E., Tomppo, E. O. (2007): Remote sensing support for national forest inventories. – *Remote Sensing of Environment* 110(4): 412-419.
- [45] Mermoz, S., Réjou-Méchain, M., Villard, L., Le Toan, T., Rossi, V., Gourlet-Fleury, S. (2015): Decrease of L-band SAR backscatter with biomass of dense forests. – *Remote Sensing of Environment* 159: 307-317.
- [46] Morel, A. C., Saatchi, S. S., Malhi, Y., Berry, N. J., Banin, L., Burslem, D., Ong, R. C. (2011): Estimating aboveground biomass in forest and oil palm plantation in Sabah, Malaysian Borneo using ALOS PALSAR data. – *For. Ecol. Manag.* 262: 1786-1798.
- [47] Motohka, T., Shimada, M., Isoguchi, O., Ishihara, M. I., Suzuki, S. N. (2011): Relationships between PALSAR backscattering data and forest above ground biomass in Japan. – *Geoscience and Remote Sensing Symposium (IGARSS), 2011 July, IEEE International*, pp. 3518-3521.
- [48] Ni, W., Zhang, Z., Sun, G., Guo, Z., He, Y. (2014): The penetration depth derived from the synthesis of ALOS/PALSAR InSAR data and ASTER GDEM for the mapping of forest biomass. – *Remote Sensing* 6(8): 7303-7319.
- [49] Ong, J. E., Gong, W. K., Wong, C. H. (2004): Allometry and partitioning of the mangrove, *Rhizophora apiculata*. – *Forest Ecology and Management* 188(1-3): 395-408.
- [50] Peregon, A.; Yamagata, Y. (2013): The use of ALOS/PALSAR backscatter to estimate above-ground forest biomass: A case study in Western Siberia. – *Remote Sens. Environ.* 137: 139-146.
- [51] Pham, H. H. (2003): Flora of Viet Nam. Volume 1, 2, 3. – Young Publishing House, Ho Chi Minh City, Vietnam.
- [52] Raghuvanshi, S. P., Raghav, A. K., Chandra, A. (2008): Renewable energy resources for climate change mitigation. – *Applied Ecology and Environmental Research* 6(4): 15-27.
- [53] Rogelj, J., Den Elzen, M., Höhne, N., Fransen, T., Fekete, H., Winkler, H., ... Meinshausen, M. (2016): Paris Agreement climate proposals need a boost to keep warming well below 2 C. – *Nature* 534(7609): 631.
- [54] Saatchi, S. S., Harris, N. L., Brown, S., Lefsky, M., Mitchard, E. T., Salas, W., Petrova, S. (2011): Benchmark map of forest carbon stocks in tropical regions across three continents. – *Proc. Natl. Acad. Sci. USA* 108: 9899-990.

- [55] Sader, S. A., Waide, R. B., Lawrence, W. T., Joyce, A. T. (1989): Tropical forest biomass and successional age class relationships to a vegetation index derived from Landsat TM data. – *Remote Sensing of Environment* 28: 143IN1159-156IN2198.
- [56] Santos, J. R., Lacruz, M. P., Araujo, L. S., Keil, M. (2010): Savanna and tropical rainforest biomass estimation and spatialization using JERS-1 data. – *International Journal of Remote Sensing* 23(7): 1217-1229.
- [57] Sinha, S., Jeganathan, C., Sharma, L. K., Nathawat, M. S. (2015): A review of radar remote sensing for biomass estimation. – *International Journal of Environmental Science and Technology* 12(5): 1779-1792.
- [58] Sun, G., Ranson, K. J., Kharuk, V. I. (2002): Radiometric slope correction for forest biomass estimation from SAR data in the Western Sayani Mountains, Siberia. – *Remote Sensing of Environment* 79(2-3): 279-287.
- [59] Tuan, L. D. et al. (2002): *Can Gio Mangrove Biosphere Reserve*. – Agriculture Publishing House, Ho Chi Minh City.
- [60] Tucker, C. J. (1977): *Use of Near Infrared/Red Radiance Ratios for Estimating Vegetation Biomass and Physiological Status*. – NASA Goddard Space Flight Center, Greenbelt, MD, United States
- [61] Tucker, C. J., Miller, L. D. (1973): *The remote estimation of a grassland canopy: its biomass chlorophyll, leaf water, and underlying soil spectra*. – Technical Report (US International Biological Program Grassland Biome) No 237.
- [62] Van Truong, V., Duong, N. D., Tuan, T. A. (2017): Mapping land cover using multi-temporal sentinel-1A data: A case study in Hanoi. – *Vietnam Journal of Earth Sciences* 39(4): 345-359.
- [63] Wicaksono, P., Danoedoro, P., Hartono, Nehren, U. (2016): Mangrove biomass carbon stock mapping of the Karimunjawa Islands using multispectral remote sensing. – *International Journal of Remote Sensing* 37(1): 26-52.
- [64] Wu, S. T. (1987): Potential application of multipolarization SAR for pine-plantation biomass estimation. – *IEEE Transactions on Geoscience and Remote Sensing* (3): 403-409.

CHARACTERISTIC OF ATMOSPHERIC BTEX CONCENTRATIONS AND THEIR HEALTH IMPLICATIONS IN URBAN ENVIRONMENT

AL-HARBI, M.

*Department of Environmental Technology Management, College of Life Sciences, Kuwait University, P.O. Box 5969, 13060 Safat, Kuwait
e-mail: dr.meshari@ku.edu.kw*

(Received 30th Aug 2018; accepted 8th Nov 2018)

Abstract. The atmospheric concentrations of BTEX (benzene, toluene, ethylbenzene, m,p-xylene and o-xylene) were measured in five different urban cities in Kuwait through the year of 2016. The overall mean of total BTEX in all sites tested in this study was 5.21 $\mu\text{g}/\text{m}^3$ and it was found that the toluene level was the highest in all monitored sites. In terms of seasonal variations, BTEX concentrations were slightly higher in the winter than in the summer. This is plausibly due to higher chemical removal reaction rates of BTEX and to dust storm in the summer that eventually removes BTEX from the atmosphere. The diurnal patterns showed high records of BTEX concentrations in the morning (07:00–8:00 h) and during rush hours (19:00–21:00 h) in the evening, due to high volume of traffic and weak atmospheric dispersion and photochemical reactivity. Low records of BTEX concentrations were detected during midday, probably due to the high rate of photochemical reactions, to the increased mixing depth, to the upshifting of the urban boundary layer, and to the decreased traffic volume. Benzene/Toluene (B/T) and Xylene/ethylbenzene (X/E) ratios suggested that vehicular emissions were the main source of BTEX. Since individual pollutant exposure is associated with cancer risk (CR), BTEX concentrations are far from being safe for the population residing in these urban cities. According to individual hazard quotient (HQ), there is no serious threat of chronic non-cancer health effects in specific target organs for the urban cities population. A quite extensive review of BTEX in atmosphere was presented and it was found that the amount of BTEX in Kuwait was among the lowest compared with that of other cities in the world.

Keywords: *BTEX in ambient air, seasonal and diurnal variations, source apportionment, health risk assessment, spatial distribution*

Introduction

Several epidemiological studies have proven the harmful impacts of volatile organic compounds (VOCs) in urban ambient air. Over the last several decades, importance in determining the VOCs in the atmosphere has increased. VOCs play a vital role in the formation of ozone (Berezina et al., 2017; Olumayede et al., 2014) and photochemical oxidants (Derstroff et al., 2017). Recently many researchers have focused on the VOCs BTEX compounds (benzene, toluene, ethyl benzene and xylene) due to their toxicity and well correlated with each other (Bretón et al., 2017; Baek et al., 2015; Kerchich et al., 2012; Miller et al., 2010, 2009; Hoque et al., 2008).

BTEX can be found in both outdoor and indoor environments (Bolden et al., 2015; Fazlzadehdavilb et al., 2016; Le ha et al., 2017). They are generated from different sources such as vehicles, gasoline evaporation, heating systems, tobacco and aerosols (Xu et al., 2018; Hamid et al., 2017; Gennaro et al., 2015; Environment Australia, 1999). Also, it can be found in used items such as glues, cleaning products, paints, cosmetics and solvents (Holgate et al., 1999). The most important source of benzene for both indoor and outdoor exposure is the traffic (Gennaro et al., 2013; Jo et al., 1999). The concentration of VOCs and BTEX can vary between seasons and year to year due to the effect of source emissions, environmental conditions in the city, vehicle types, flow rates

and speeds of traffic (Buczynska et al., 2015; Borgie et al., 2014; Tager et al., 2009; Truc and Oanh, 2007; Paul et al., 1997).

Several attempts have been made all over the world to identify, quantify and characterize the level of VOCs BTEX in various environments. Lee et al. (2002) studied the concentrations of VOCs in urban atmosphere of Hong Kong. VOCs range was from undetectable to 1396 $\mu\text{g}/\text{m}^3$ and the BTEX were the major constituents, approximately more than 60% in composition of total VOC detected. In another study done by Hinwood et al. (2007), the geometric mean (GM) of daily BTEX concentrations documented for the study population from four Australian cities were benzene 0.80 mg/m^3 , toluene 2.83 mg/m^3 , ethylbenzene 0.49 mg/m^3 and xylenes 2.36 mg/m^3 . Zhang et al. (2012) measured the level of BTEX during autumn, winter, spring, and summer seasons in Beijing, China. The average concentrations of the total measured BTEX during the four seasons were 27.2, 31.9, 23.2, 19.1 $\mu\text{g}/\text{m}^3$, respectively. Miller et al. (2012) studied the BTEX levels in the urban industrial city of Windsor in Canada. The three-year mean concentrations in $\mu\text{g}/\text{m}^3$ were: benzene (0.76), toluene (2.75), ethylbenzene (0.45), o-xylene (0.47), (m-p)-xylene (1.36) and the total mean concentrations of BTEX were 5.64 $\mu\text{g}/\text{m}^3$. Duan et al. (2017) investigated the atmospheric concentrations of BTEX in China and researchers observed that BTEX species were higher in the winter than in the summer and toluene was more abundant compared with BTEX species. Pourfarzi et al. (2016) reported that the BTEX concentrations present in refueling stations in Iran are generally higher than typical outdoor air levels and ethylbenzene has the highest average concentration followed by benzene.

Numerous studies used benzene/ benzene (B/T), toluene/ benzene (T/B), and xylene/ethylbenzene (Σ X/E) ratios as indicatives of emission sources or photochemical age. In one study reported by Wang et al. (2012), benzene to toluene ratio range was 0.4–1.0 in the urban area of Beijing, China. In another study (Liu et al., 2005), the B/T ratio from roadside in Beijing was 0.61. Barletta et al. (2005) concluded that an average B/T value of 0.6 might be used to characterize vehicle emissions. Miller et al. (2012) considered the mobile emission is the major source of toluene to benzene (T/B) ratio, with the highest observed ratio occurring in the summer, the lowest in winter, and fall and spring values fell in between in the city of Windsor in Canada. Similarly, Khoder (2007) found from different areas in Cairo that the average toluene/benzene ratio (T/B) was 2.45 and 2.42 for the urban areas and 1.29 for the rural area, suggesting that motor vehicle emission is the main source of emission. Likewise, xylene/ethylbenzene (Σ X/E) ratio is used as an indicative of photochemical age and in most studies it ranged from 1.1 to 4.8 regardless of the geographic location (Rad et al., 2014; Hsieh et al., 2011; Truc and Oanh, 2007; Ho, et al., 2004). Low X/E ratio suggests an aged air parcel as these species are removed from air via different mechanisms including dispersion, deposition, and chemical reaction. Other studies done by Parra et al. (2006), Smith et al. (2007) and Su et al. (2010) reported significant proportional correlations among the BTEX species. They suggested that the high correlations ($r > 0.74$) between ethylbenzene and the two xylene species means that the species were originating from common sources and the relatively lower correlation coefficients ($r < 0.60$) seen between benzene and the other BTEX species were due to fact that benzene is emitted from vehicles whereas the other species are emitted from both vehicles and industrial activities.

Previous epidemiological studies have related the BTEX levels to several health outcomes. Benzene has been correlated with increased rates of leukemia and solid tumors (Vigliani et al., 1976). Some studies linked benzene from traffic emissions and cancer in members of the community especially children (Nordlinder et al., 1997). Exposure to toluene and xylenes has been associated with adverse effects on the nervous

system, liver and kidneys (ATSDR, 2003; USEPA, 2004). Exposure to ethyl benzene has a negative impact on the respiratory system and the kidneys (ATSDR, 2003; NTP, 1999). Several other studies highlighted the harmful effects of BTEX on human beings as well as the entire ecosystem. Up to the knowledge of the author, this study is the first thorough study investigating diurnal, seasonal, and spatial variations of BTEX level in ambient air of Kuwait. Additionally, source apportionment of atmospheric BTEX and cancer risks and non-cancer effects associated with exposure to atmospheric BTEX were also examined. This study was conducted during the year of 2016 at five representatives and spatially distributed sampling locations in Kuwait. This study is an attempt to control atmospheric concentrations of BTEX in ambient air of Kuwait and reduce their detrimental health outcomes.

Materials and methods

Study area and sampling

The atmospheric concentrations of BTEX (benzene, toluene, ethylbenzene, m,p-xylene and o-xylene) were measured in five different urban cities in Kuwait through the year of 2016. The five representative urban cities in Kuwait selected from south to north were Ali Sabah Al-Salem (Latitude: 29° 17.373'N, Longitude: 48° 9.291'E), Fahaheel (Latitude: 29° 4.818'N, Longitude: 48° 6.969'E), Al-Salam (Latitude: 29° 4.818'N, Longitude: 48° 0.426'E), Saad Al-Abdullah (Latitude: 29° 18.916'N, Longitude: 47° 43.347'E), and Al-Jahra (Latitude: 29° 19.927'N, Longitude: 47° 39.699'E) (*Fig. 1*). Ali Sabah Al-Salem city is situated at the south part of urban development of Kuwait with a population around 50,237 residents. This city is surrounded by main oil refineries (Mina Al-Ahmadi and Mina Abdullah) of the country. Moreover, it is proximate to petrochemical industrial plants such as ammonia, urea, polyethylene polypropylene plants and wastewater treatment plant. The city is also fronting express highway (No.30) that spreads from downtown of Kuwait to the borders of Saudi Arabia. Fahaheel city is located in the south of Kuwait just after Ali Sabah Al-Salem city toward the Kuwait city, and has a population twice that of Ali Sabah Al-Salem city (around 105,000). This area is surrounded by numerous emission sources including three large petroleum refineries, Greater Burgan field, several small, medium, and large petrochemical industrial plants, and the largest highway (Road No.30). Al-Salam city was selected because of its unique location as it is exposed to the many sources of various air pollutants. It lies approximately in the center part of Kuwait and bordered by two large highways (Road No.40 and 50) in the east and west, respectively. In the south, north, and in the middle of the city, there are numerous roads, government establishments, and stores, which are considered as emission sources. Saad Al-Abdullah city is located in the north part of Kuwait and surrounded by several industrial companies and workshops, involved in a wide range of activities such as petro chemical, farms army forces establishments, construction/recycling, insulation and fiber glass, mechanical and chemical plants. Al-Jahra city is situated at the north part of the residential band of Kuwait followed Saad Al-Abdullah city toward boarder between Kuwait and the Kingdom of Saudi Arabia and it is one of the largest populated city with a population of about 490,000 residents. The city is bounded by various small-medium industrial, commercial areas, industrial, powers plant, desalination plants as well as wastewater treatment plants. Additionally, several road network are available in this city including highway# 80, highway# 70, and it is fronting the largest express highway, 6th ring road.



Figure 1. Sampling sites for ground-level BTEX samples collected in Kuwait

Measurements of the atmospheric concentrations of BTEX (benzene, toluene, ethylbenzene, m,p-xylene and o-xylene) were performed from 1st January 2016 until 31st December 2016 on an hourly basis (8760 hourly data were recorded per year for each location), simultaneously in five different urban cities in Kuwait. Measurements of the atmospheric concentrations of BTEX were carried out by HORIBA Air Quality Monitoring Station (AQMS), which are located in the center of the five urban cities in Kuwait. BTEX species were analyzed with automatic sampling throughout all year. Analyzers were calibrated before the start-up and data were crossed checked and

verified. Kuwait is witnessed by two distinct seasons: winter and summer. Summer season extends from April to October and is characterized as hot and humid. While winter season spreads from November to March, and is experienced as cooler with minimal rainfall. Regarding the wind characteristics, the most prevailing wind direction throughout the year is northwesterly winds followed by southeasterly winds, which was observed more often from February to April. Wind speed varied from 2.8 to 5.9 m/s with an average of 4.2 m/s during the studied period.

Exposure and risk assessment

The health risk assessment of BTEX consists of two parts; one quantifies the cancer effects of the chemicals, while the second addresses the non-cancer effects of the chemicals. Cancer risks are expressed as a probability of suffering an adverse effect (cancer) during a life time (assumed to be 70 years). To assess cancer risks, integrated lifetime cancer risk (ILTCR) due to the exposure to BTEX was estimated.

Only those substances that are known or suspected human carcinogens were considered in calculating integrated lifetime cancer risk (ILTCR). Formaldehyde, acetaldehyde, benzene, and ethylbenzene are believed to be carcinogenic (Dutta et al., 2009; Tunsaringkarn et al., 2012; Zhou et al., 2015). For non-carcinogens, hazard quotient (HQ) was used to assess non-cancer effects of BTEX. The daily exposure (E) of an individual by intake process (only inhalation was considered) was calculated from *Equation 1*:

$$E = \frac{C \times I_{ra} \times E_{da}}{B_{wa}} \quad (\text{Eq.1})$$

where the description of the variables used is tabulated below.

Variable	Description	Value	Units
E	Daily exposure		mg/kg-day
C	Concentration of the pollutant		mg/m ³
I _{ra}	Inhalation rate*, adult	0.83*	m ³ /h
E _{da}	Exposure duration, adult	24	hr/day
B _{wa}	Body weight, adult	65	kg

*The value of inhalation rate (adult) is taken from USEPA (1997)

The integrated lifetime cancer risk (ILTCR) was calculated from *Equation 2*:

$$\text{ILTCR} = E \text{ (mg Kg}^{-1} \text{ day}^{-1}) \times \text{SF (mg}^{-1} \text{ Kg day)} \quad (\text{Eq.2})$$

where SF is the carcinogenic potency slope or a slope factor of inhalation unit risk for toxics when the exposure-carcinogenic effect is considered as linear, taking from EPA (<http://www.epa.gov/iris>).

Human health risk estimates for inhalation of non-carcinogens are expressed as hazard quotient (HQ). It is defined as the ratio of yearly average daily received concentration (C_y) and the reference concentration, R_fC (a level below which adverse health effects are not likely to occur). HQ was calculated from *Equation 3*:

$$HQ = \frac{C_y}{RfC} \quad (\text{Eq.3})$$

The reference concentration (RfC) for each pollutant was obtained from EPA (<http://rais.ornl.gov>) and California Office of Environmental Health Hazard Assessment (<http://www.arb.ca.gov/toxics/healthval/acute.pdf>).

Statistical analysis

To evaluate the differences among sites, One-way ANOVA analysis was employed using STATISTICA software. Statistical significance was considered once p-value < 0.05. Statistical Software R programming language, with package open-air version 2.13.2, was utilized for other statistical tests and plotting graphs.

Results and discussion

Diurnal, seasonal, and spatial variations of BTEX concentrations

The atmospheric levels of BTEX in five different urban cities in Kuwait during the year of 2016 were quantified and descriptive statistics are presented in *Table 1*. Among the BTEX compounds, toluene showed the highest concentrations in all sites, with an average varied between $6.96 \pm 2.71 \mu\text{g}/\text{m}^3$ to $14.85 \pm 4.41 \mu\text{g}/\text{m}^3$ followed by MP-Xylene ($1.82 \pm 0.54 - 9.88 \pm 1.22 \mu\text{g}/\text{m}^3$), and o-xylene ($1.00 \pm 0.34 - 9.79 \pm 0.49 \mu\text{g}/\text{m}^3$). Ethylbenzene ($0.78 \pm 0.27 - 8.88 \pm 0.28 \mu\text{g}/\text{m}^3$) and benzene ($2.49 \pm 0.83 - 3.80 \pm 0.33 \mu\text{g}/\text{m}^3$) were present at lower concentrations. The overall mean of total BTEX in all sites tested in this study was $5.21 \mu\text{g}/\text{m}^3$. These observations are consistent with several previous studies where toluene was found the highest in the atmosphere of urban cities (Duan et al., 2017; Hoque et al., 2008; Johnson et al., 2010; Miller et al., 2009; Parra et al., 2006; Smith et al., 2007; Srivastava et al., 2005). Higher concentrations of toluene might be due to human activities such as fuel burning, the use of glues, cleaning products, paints, cosmetics and solvents (Holgate et al., 1999).

The diurnal variations of BTEX concentrations of benzene, toluene, ethylbenzene, and xylene in five different urban cities in Kuwait during the year of 2016 are shown in *Figure 2a-d*. The diurnal variations of BTEX concentrations followed similar arrangement: increased at 07:00–8:00 h, then decreased at 9:00–16:00 h and thereafter increased and reached a peak at 21:00 h, and finally decreased slightly at 1:00–6:00 h. The similar pattern of BTEX species suggested a common source of the pollutants. This BTEX profile is consistent with the diurnal trends found in other urban areas (Alghamdi et al., 2014; Tang et al., 2007; Filella and Peñuelas, 2006; Yang et al., 2005; Ho et al., 2004). High records of BTEX concentrations in the morning (07:00–8:00 h) and during rush hours (19:00–21:00 h) in the evening were due to high volume of traffic, the main contributor of VOC emissions, and other evaporative emissions sources (Martins et al., 2016; Song et al., 2008; Ho et al., 2004; Na et al., 2003;). Additionally, atmospheric dispersion and photochemical reactivity are weak during these periods. Conversely, low records of BTEX concentrations during midday can be possibly attributed to the high intensity of solar radiation that induces photochemical reaction, increases the mixing depth, and shifting up the urban boundary layer. In addition to that, traffic volume in midday decreases and thus the contribution of vehicle-related sources becomes trivial.

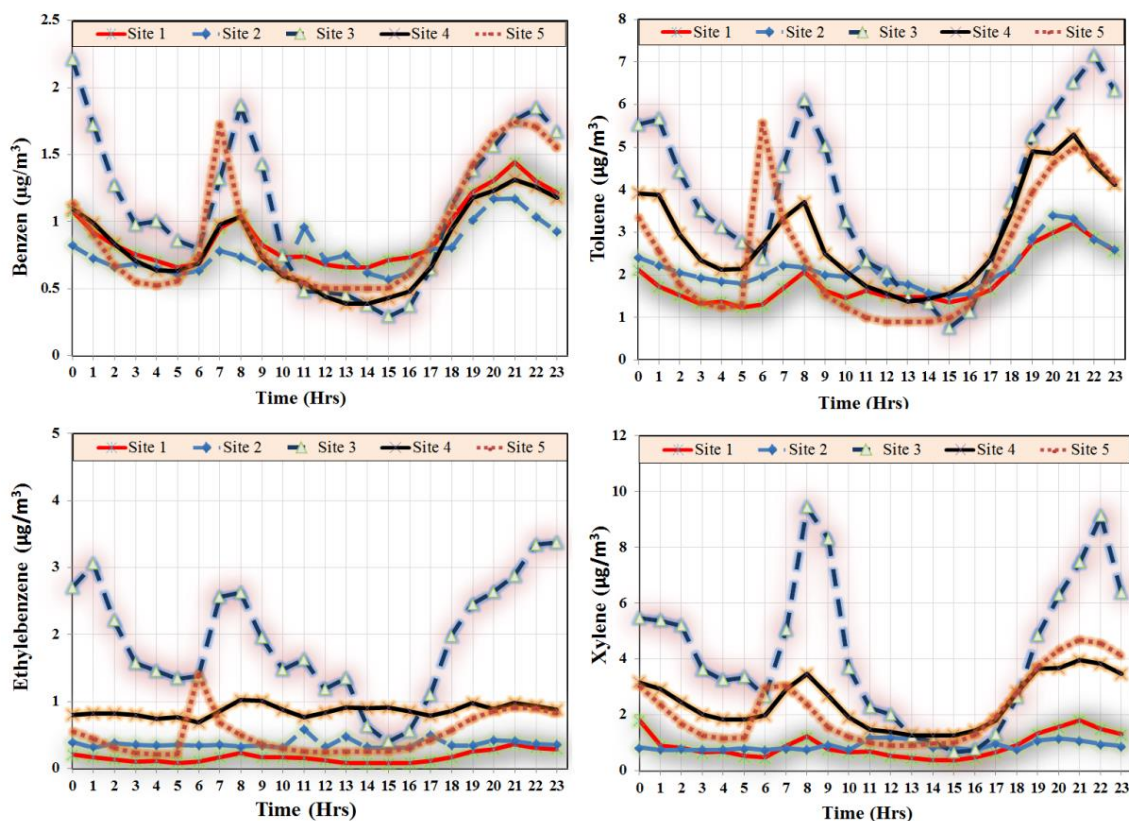


Figure 2. Diurnal BTEX average concentrations at five sites in Kuwait; (a) benzene, (b), toluene, (c) ethyl benzene, and (d) xylene. These data are the average hourly concentrations per year

Table 1. Descriptive statistics of average daily concentration of BTEX in ($\mu\text{g}/\text{m}^3$)

BTEX	Descriptive statistics	Site 1	Site 2	Site 3	Site 4	Site 5
Benzene	Max.	27.1	46.8	109.4	90.3	96.9
	Min.	0.02	0.22	0.005	0.03	0.01
	Ave.	2.49	2.87	3.80	2.58	3.51
	Med.	2.33	1.47	1.59	1.66	1.4
	SD	0.30	0.83	0.43	1.00	0.33
Toluene	Max.	40.9	85.5	171.9	48.30	75.5
	Min.	0.004	0.150	0.038	0.038	0.105
	Ave.	6.96	8.16	14.85	11.09	9.14
	Med.	5.04	1.880	5.716	5.453	3.61
	SD	2.71	3.43	4.41	3.41	2.21
Et-benzene	Max.	29.55	42.73	98.83	44.97	27.32
	Min.	0.004	0.173	0.043	0.043	0.004
	Ave.	0.78	1.60	8.88	3.73	2.12
	Med.	0.30	1.04	3.16	1.65	0.65
	SD	0.27	0.85	0.28	0.51	0.62

MP-Xylene	Max.	64.3	34.2	188.4	128.50	39.4
	Min.	0.009	0.217	0.043	0.043	0.009
	Ave.	1.82	2.82	9.88	6.07	6.67
	Med.	1.4	1.17	0.95	2.56	2.17
	SD	0.54	0.72	1.22	0.66	0.49
O-Xylene	Max.	44.80	35.5	179.20	51.30	35.90
	Min.	0.004	0.173	0.043	0.043	0.004
	Ave.	1.00	1.99	9.79	4.55	3.03
	Med.	0.52	1.39	2.08	2.38	1.04
	SD	0.34	0.94	0.49	0.46	0.18

Site 1: Ali Sabah Al-Salem, Site 2: Al-Fahaheel, Site 3: Al-Salam, Site 4: Saad Al-Abdullah, Site 5: Al-Jahra

Table 2 illustrates the seasonal variations of BTEX between winter and summer months among the five locations. Temperature in Kuwait is usually between 6 °C in winter and 45 °C in the summer. Overall, in all five tested sites, BTEX levels in the winter were higher than that of the summer. Seasonal variation of BTEX level in some sites (site 1, 3, and 5) was statistically significant (p -values < 0.05). Similar observations were also reported in the previous studies where BTEX concentrations in the winter were higher than those in the summer (Baek et al., 1997; Hartwell et al., 1987; Wathne, 1983). Low BTEX concentrations in the summer are possibly due to higher chemical removal reaction rates of BTEX compared with winter months. In the summer, the high temperatures combined with long daytime induces evaporation rate that would eventually promote BTEX dispersion in air. Another plausible reason to the decreasing level of BTEX in the summer is due to the frequent dust storms in Kuwait as in the case of other counties that witness arid and semi-arid climates. These dust storms remove the BTEX from the atmosphere during the summer time and thus reduce their concentrations.

Table 2. Seasonal variations of BTEX between winter and summer months among the five locations. The reading represents average value \pm Standard deviation and units are in $\mu\text{g}/\text{m}^3$

Location/season	Benzene	Toluene	Et-benzene	Σ -Xylene
Site 1				
Winter	2.7 \pm 0.92	9.9 \pm 1.4	0.81 \pm 0.41	3.43 \pm 0.29
Summer	2.3 \pm 0.92	5.5 \pm 1.5	0.04 \pm 0.001	1.98 \pm 0.4
<i>P</i> -value	0.24	0.022*	0.016*	0.018*
Site 2				
Winter	3.8 \pm 0.85	10.9 \pm 5.0	1.66 \pm 0.46	4.0 \pm 0.7
Summer	2.6 \pm 0.92	6.0 \pm 0.86	1.63 \pm 0.84	3.44 \pm 0.8
<i>P</i> -value	0.24	0.26	0.94	0.33
Site 3				
Winter	5.0 \pm 0.85	14.2 \pm 5.8	8.2 \pm 3.5	12.8 \pm 2
Summer	4.4 \pm 1.2	12.01 \pm 4.2	7.2 \pm 2.1	10.5 \pm 1.9
<i>P</i> -value	0.15	0.20	0.12	0.11

Site 4				
Winter	2.96 ± 0.9	12.4 ± 2.4	4.7 ± 3.5	11.8 ± 2.1
Summer	2.22 ± 0.6	9.0 ± 1.9	1.8 ± 0.4	8.4 ± 2.4
P-value	0.16	0.06	0.009*	0.006*
Site 5				
Winter	3.5 ± 3.0	11.7 ± 4.2	2.9 ± 1.9	11.5 ± 1.0
Summer	2.3 ± 2.0	6.0 ± 3.0	0.94 ± 0.73	4.4 ± 3.4
P-value	0.026*	0.026*	0.026*	0.015*

*A p-value of < 0.05 was considered statistically significant. Site 1: Ali Sabah Al-Salem, Site 2: Fahaheel, Site 3: Al-Salam, Site 4: Saad Al-Abdullah, Site 5: Al-Jahra

Atmospheric BTEX levels were also spatially quantified in the five urban sites and results are shown in *Figure 3a-d*. The highest concentrations of BTEX compounds were detected in site 3 whereas the lowest concentrations were found in site 1 (*Fig. 3a-d*). This observation indeed indicates that BTEX compounds originated from similar emission source. Site 3 is surrounded by four main congested highways (40 and 50 roads and 5th and 6th ring roads) and several small roads inside the city. This indeed suggested that vehicle emission might be a prevailing source for BTEX compounds in this study.

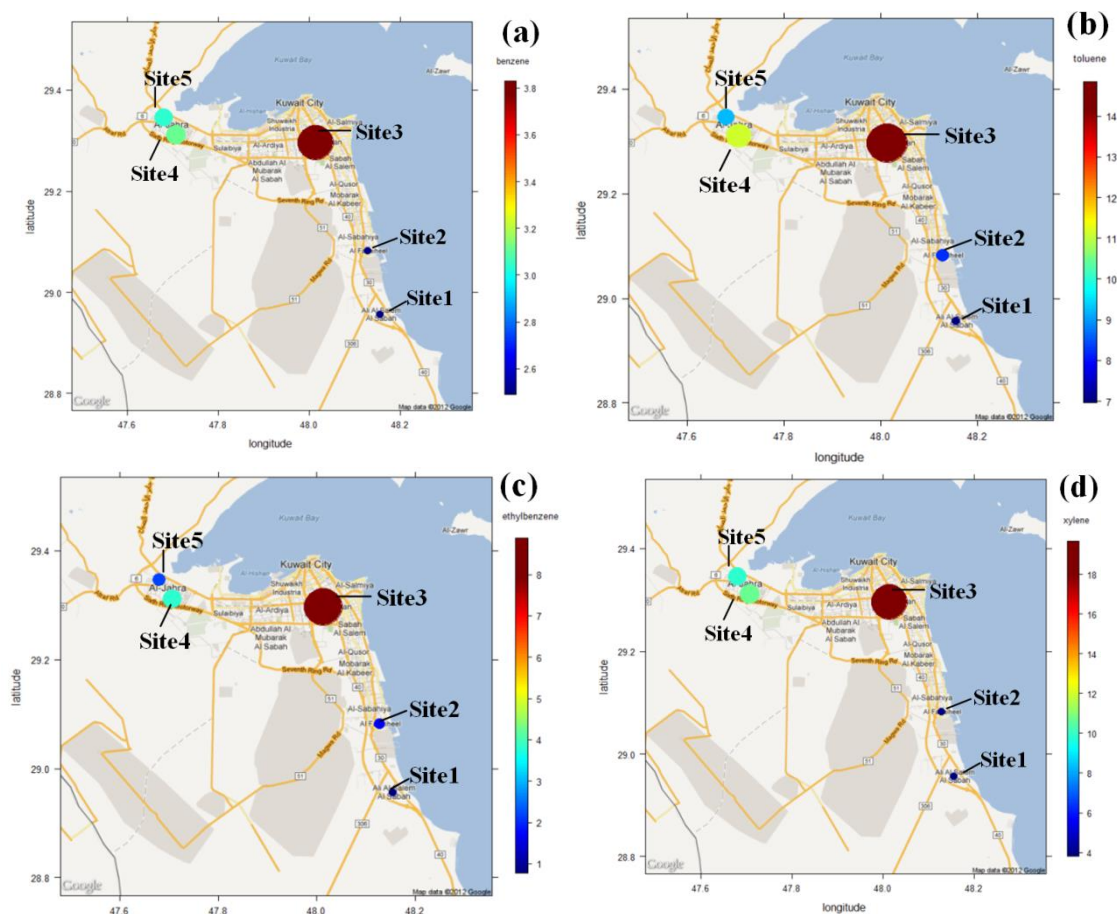
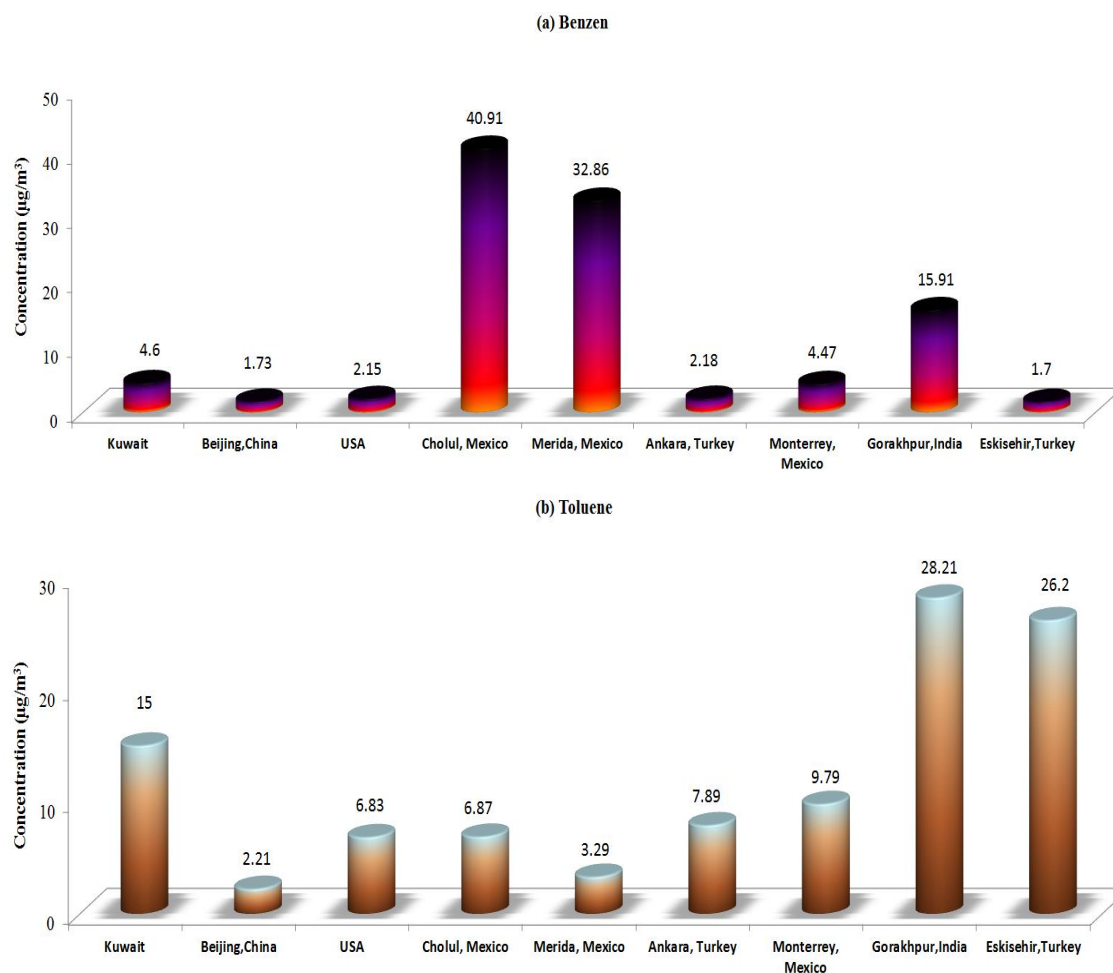


Figure 3. Mean hourly concentrations of (a) benzene, (b) toluene, (c) ethylbenzene, and (d) Σ -xylene. The units are in $\mu\text{g}/\text{m}^3$

Comparison of BTEX levels in Kuwait with other cities in the world

The concentrations of BTEX compounds measured in the five urban cities in this study (Fig. 1) were also compared with those found in other cities over the world (Gao et al., 2018; Bretón et al., 2017; Masih et al., 2016; Menchaca-Torre et al., 2015; Batterman et al., 2014; Demirel et al., 2014; Yurdakul et al., 2013). As shown in Figure 4a, the highest benzene levels were reported in Mexico (Cholul and Merida) (40.91 and 32.86 $\mu\text{g}/\text{m}^3$) and India (Gorakhpur) (15.91 $\mu\text{g}/\text{m}^3$). The average benzene concentration in Kuwait (4.6 $\mu\text{g}/\text{m}^3$) was similar to those in Mexico (Monterrey) (4.47 $\mu\text{g}/\text{m}^3$), Turkey (Ankara) (2.18 $\mu\text{g}/\text{m}^3$), and the USA (2.15 $\mu\text{g}/\text{m}^3$). The lowest levels of benzene were found in China (Beijing) (1.73 $\mu\text{g}/\text{m}^3$) and Turkey (Eskisehir) (1.7 $\mu\text{g}/\text{m}^3$). Toluene level, as shown in Figure 4b, was the highest in India (Gorakhpur) (28.21 $\mu\text{g}/\text{m}^3$) and Turkey (Eskisehir) (26.2 $\mu\text{g}/\text{m}^3$) followed by Kuwait (15 $\mu\text{g}/\text{m}^3$), Mexico (Monterrey) (9.79 $\mu\text{g}/\text{m}^3$), Turkey (Ankara) (7.89 $\mu\text{g}/\text{m}^3$), the USA (6.83 $\mu\text{g}/\text{m}^3$), and the others. The lowest toluene levels were detected in China (Beijing) (2.21 $\mu\text{g}/\text{m}^3$) and Mexico (Merida) (3.29 $\mu\text{g}/\text{m}^3$). For ethylbenzene level, it is clear from Figure 4c that it was the highest in Mexico (Cholul and Merida) (13.87 and 8.29 $\mu\text{g}/\text{m}^3$). The average ethylbenzene concentration in Kuwait (5 $\mu\text{g}/\text{m}^3$) was similar to those in India (Gorakhpur) (3.38 $\mu\text{g}/\text{m}^3$) and the USA (1.28 $\mu\text{g}/\text{m}^3$). Minimum levels of ethylbenzene were found in China (Beijing) (0.38 $\mu\text{g}/\text{m}^3$) and Mexico (Monterrey) (0.43 $\mu\text{g}/\text{m}^3$). Xylene level in different countries is shown in Figure 4d.



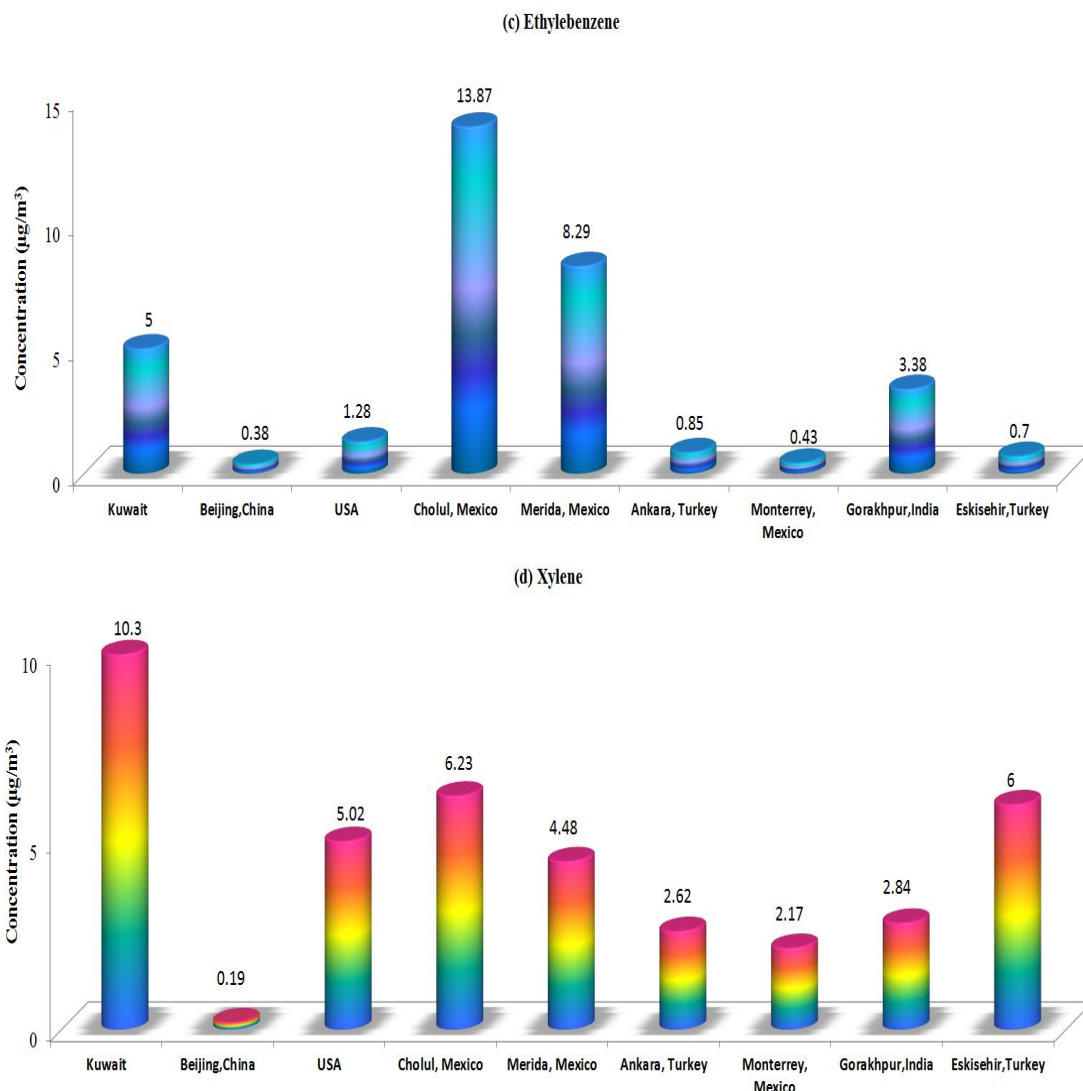


Figure 4. Comparison of BTEX concentrations for fourteen cities including Kuwait: (a) benzene, (b) toluene, (c) ethylbenzene, and (d) xylene (ΣX)

It is important to note that xylene level in Kuwait was reported as Σ (m-o-p) xylene, but in the most recent studies reported in this study, xylene was reported as either o-xylene or p-xylene. Therefore, direct comparison cannot be made and only higher differences in xylene level between countries should be considered. Relatively Kuwait has the highest xylene level ($10 \mu\text{g}/\text{m}^3$) followed by Mexico (Cholul) ($6.23 \mu\text{g}/\text{m}^3$), Turkey (Eskisehir) ($6 \mu\text{g}/\text{m}^3$), and the USA ($5.02 \mu\text{g}/\text{m}^3$). Xylene levels were the lowest in China (Beijing) ($0.19 \mu\text{g}/\text{m}^3$). It is noteworthy to mention that each city has particular region sources and they differ in fuel types, fuel consumption pattern, and meteorological conditions. These factors can significantly influence BTEX level in ambient air and induce differences among cities in different parts of the world.

Benzene/toluene (B/T) ratios

Average benzene-toluene (B/T) ratios were calculated for the five sampling urban cities to differentiate between vehicular emissions and other combustion sources.

Previous studies suggest that the ratio of different aromatic compounds (particularly benzene and toluene) can be useful in identifying VOC sources, and a B/T ratio of around 0.5 has been reported to be characteristic of vehicular emissions (Brocco et al., 1997; Perry and Gee, 1995). In this study, B/T ratio ranged from 0.4 to 0.8, 0.3 to 1.5, 0.3 to 0.4, 0.4 to 0.5, and 0.3 to 0.8 in Ali Sabah Al-Salem, Al-Fahaheel, Al-Salam, Saud Al-Abdullah, and Al-Jahra, respectively. Additionally, average B/T ratios in Ali Sabah Al-Salem, Al-Fahaheel, Al-Salam, Saud Al-Abdullah, and Al-Jahra were 0.5, 0.7, 0.35, 0.45, and 0.45, respectively. Higher average B/T ratio (0.7) was found in Fahaheel compared to other urban cities neighbourhoods, while Al-Salem had low average B/T (0.35) ratio. The high B/T ratio in Al-Fahaheel showed that large additional sources of benzene are emitted, possibly from industrial emissions, as Al-Fahaheel is adjacent to Al-Ahmadi petroleum refinery and other petrochemical industries. Previous studies reported that B/T ratio increases with increasing traffic volume, industrial emissions and other urban sources in denser areas (Lee et al., 2002; Brocco et al., 1997) found that the B/T ratio in the urban area of Rome ranged from 0.3 to 0.5. In Hong Kong B/T ratio was of about 0.2 (Lee et al., 2002) and 0.1 was reported in other Asian cities such as Manila and Bangkok (Gee et al., 1998). In southern Taiwan (Hsieh et al., 2006), the average B/T ratios in Nei-Pu, Ping-Tung, Ping-Nan, Ren-Wu, Lin-Yuan and Nan-Zi were 0.77, 0.59, 0.12, 0.38, 1.67 and 0.34, respectively. Our average (B/T) ratios in the five locations were between 0.35 and 0.7, suggesting vehicular emissions as the main source of VOCs.

Σ -xylene/ethylbenzene (X/E) ratio

In this study, xylene/ethylbenzene (Σ X/E) ratio is used to assess the relative age of the air parcels. Several studies used X/E ratio to evaluate the relative age of the air parcels (Hsieh et al., 2006; Monod et al., 2001; Truc et al., 2007). Conceptually, ethylbenzene is considered a low reactive species whereas xylenes are considered a highly reactive species. Hence, low X/E ratio suggests an aged air parcel. X/E ratios ranged from 2.9 to 11.5, 1.2 to 4.3, 2.2 to 2.6, 1.1 to 5.9, and 4 to 7.6 in Ali Sabah Al-Salem, Al-Fahaheel, Al-Salam, Saud Al-Abdullah, and Al-Jahra, respectively. Recently Rad et al., 2014 reported X/E ratios ranged from 1.13 to 4.95 in Ahvaz metropolitan city, Iran. Hsieh et al., 2011 stated that X/E ratios of five different traffic tunnels in southern Taiwan, where X/E ratios ranging from 2.4 to 12.1. Truc et al. (2007) investigated X/E ratios in three roadsides in Hanoi, Vietnam and X/E ratios ranged from 1.2 to 2.9. In Hong Kong, average values of X/E ratios were from 1.5 to 2.2 (Ho, et al., 2004). Other X/E ratios were also reported for different urban samples, ranging from 1.3 for Tokyo to above 4.8 in Athens (Truc et al., 2007); however, the most common values are between 2.0 and 3.0 (Monod et al., 2001). The X/E ratios found in our study are in the range of reported X/E ratios in the previous studies and therefore the contribution of vehicular emissions is still the foremost source of VOCs. However, this does not eliminate the possibility of other non-traffic sources. The average X/E ratios in Ali Sabah Al-Salem, Al-Fahaheel, Al-Salam, Saud Al-Abdullah, and Al-Jahra were 9.7, 2.6, 2.4, 4.2, and 5.4, respectively. Higher average X/E ratio (9.7) was found in Ali Sabah Al-Salem compared to other urban cities neighbourhoods (averages from 2.4-5.4). Such high value indicates that the freshly emitted xylene in the transportation decayed at different rates to OH-oxidation in the atmosphere. Conversely, the lower X/E ratio (2.4) in Al-Salam implies an aged air parcel.

Exposure and risk assessment

Numerous researchers have reported the detrimental impacts of BTEX on human health as illustrated in the introduction section. Thus, to assess cancer risks and non-cancer effects due to the exposure to measured atmospheric BTEX at the five representative sites (*Fig. 1*), the average daily exposure, individual Hazard Quotient (HQ) and integrated lifetime cancer risk (ILTCR) were estimated and the values are reported in *Table 3*. In term of exposure, toluene was found the highest in all sites compared with other individual components. With respect to sites, residents of site 3 received higher dose of exposure from the pollutants in comparison to other four sites and consequently probability of cancer risk was the highest in site 3.

Table 3. Estimate of individual pollutant exposure, associated non-cancer hazard and cancer risk

Compounds	Site	Yearly average concentration (mg/m ³)	Daily average exposure (mg kg ⁻¹ day ⁻¹)	HQ	ITLCR
Benzene	Site 1	2.49E-03	7.62E-04	8.29E-02	2.20E-05
	Site 2	2.87E-03	8.79E-04	9.56E-02	2.54E-05
	Site 3	3.83E-03	1.17E-03	1.28E-01	3.39E-05
	Site 4	2.58E-03	7.91E-04	8.61E-02	2.29E-05
	Site 5	3.51E-03	1.07E-03	1.17E-01	3.11E-05
Toluene	Site 1	6.96E-03	2.13E-03	1.74E-02	
	Site 2	8.16E-03	2.50E-03	2.04E-02	
	Site 3	1.49E-02	4.55E-03	3.71E-02	
	Site 4	1.11E-02	3.40E-03	2.77E-02	
	Site 5	9.14E-03	2.80E-03	2.28E-02	
Et-Benzene	Site 1	7.80E-04	2.39E-04	7.80E-04	9.23E-07
	Site 2	1.60E-03	4.91E-04	1.60E-03	1.90E-06
	Site 3	8.88E-03	2.72E-03	8.88E-03	1.05E-05
	Site 4	3.73E-03	1.14E-03	3.73E-03	4.41E-06
	Site 5	2.12E-03	6.51E-04	2.12E-03	2.51E-06
m,p-Xylene	Site 1	1.82E-03	5.58E-04	2.60E-03	
	Site 2	2.82E-03	8.63E-04	4.02E-03	
	Site 3	9.88E-03	3.03E-03	1.41E-02	
	Site 4	6.07E-03	1.86E-03	8.67E-03	
	Site 5	6.67E-03	2.04E-03	9.53E-03	
o-Xylene	Site 1	1.99E-03	6.11E-04	2.57E-03	
	Site 2	9.97E-04	3.05E-04	1.28E-03	
	Site 3	9.79E-03	3.00E-03	1.26E-02	
	Site 4	4.55E-03	1.39E-03	5.86E-03	
	Site 5	3.03E-03	9.29E-04	3.91E-03	

Site 1: Ali Sabah Al-Salem, Site 2: Fahaheel, Site 3: Al-Salam, Site 4: Saad Al-Abdullah, Site 5: Al-Jahra

Except ethyl benzene at site 1, estimated ILTCR in all sites, as shown in *Table 3*, exceeded the threshold value of 1E-06, indicating significant risk. The highest estimated

ILTCR for ethyl benzene was 1.05×10^{-5} and was found in site 3. As for benzene, the highest ILTCR value (3.39×10^{-5}) was found in site 3 while the lowest value (2.20×10^{-5}) was found in site 1. It was reported that for benzene exposure of $1 \mu\text{g}/\text{m}^3$, the lifetime risk of chronic leukemia is $4.4\text{--}7.6 \times 10^{-6}$ (Crump, 1994). The calculated cancer risk in this study offers insights that exposure level of BTEX is far from being safe for population residing in these urban cities, with the highest threat in site 3.

According to estimated hazard quotient (HQ), non-cancer effects, it is evident from *Table 3* that individual HQs did not exceed unity for any pollutant. If the $\text{HQ} > 1$, it indicates long term exposure may result in detrimental health effects. Again benzene showed highest HQs in all sites compared with other individual chemicals and site 3 is labelled as the highest susceptible site for non-cancer effects. Based on individual HQs, which did not exceed unity in all sites, it shows no serious threat of chronic non-cancer health effects in specific target organs for the urban cities population.

It is imperative to mention that BTEX were considered as precursors for various atmospheric reactions, which would indeed make their indirect health impact on residents as well as ecosystems still viable. Thus, further control measures are urgently needed for mitigating the emissions of these toxic compounds in Kuwait. In line with the results of this study and previous studies, vehicle emission was identified as a prevailing source for BTEX. Therefore, to mitigate BTEX emission, vehicles numbers driven by individual should be reduced, as cars in Kuwait has exceeded 1.5 million. Additionally, stricter emission standards should be enacted. Furthermore, the current traffic status of prevailing traffic congestion with high pollutant's emission is urgently needed to be improved. These suggestions collectively might effectively reduce BTEX emission into atmosphere and subsequently reduce their health impacts on population.

Conclusions

BTEX compounds were measured during the year 2016 in five different urban cities from Kuwait. It was found that toluene was the most abundant amongst the BTEX compounds, followed by MP-xylene, o-xylene, ethylbenzene and benzene during the period of the study. ΣBTEX showed a seasonal variation, with higher concentrations during the winter than in the summer, probably due to higher chemical removal reaction rates of BTEX and dust storm in the summer that ultimately eliminates the BTEX from the atmosphere. BTEX compounds showed diurnal variations, high records in the morning and during rush hours in the evening, which possibly attributed to weak atmospheric dispersion and photochemical reactivity and high volume of traffic. While decreased concentrations of BTEX were observed during midday, perhaps as a result of decreased traffic volume, shifting up the urban boundary layer, high rate of photochemical reaction, and the increased mixing depth. Benzene/Toluene (B/T) and Xylene/ethylbenzene (X/E) ratios proposed that vehicular emissions were the predominant source of BTEX. The individual hazard quotient (HQ) showed no serious threat of chronic non-cancer health effects in specific target organs for the urban cities population.

Acknowledgements. The authors would like to thank Kuwait University for supporting the completion of this study.

Conflict of interests. The corresponding author states that there is no conflict of interests.

REFERENCES

- [1] Alghamdi, M. A., Khoder, M., Abdelmaksoud, A. S., Harrison, R. M., Hussein, T., Lihavainen, H., Jeelani, H., Goknil, M. H., Shabbaj, I. I., Almeahmadi, A. M., Hyvärinen, A. P., Hämeri, K. (2014): Seasonal and diurnal variations of BTEX and their potential for ozone formation in the urban background atmosphere of the coastal city Jeddah, Saudi Arabia. – *Air Quality, Atmosphere & Health* 7: 467-480.
- [2] ATSDR (2003): Toxicological Profile Information Sheet. – Agency for Toxic Substances and Disease Registry, Department of Health and Human Services, Public Health Service, USA.
- [3] Baek, S. O., Kim, Y. S., Perry, R. (1997): Indoor air quality in homes, offices and restaurants in Korean urban areas—indoor/outdoor relationships. – *Atmos. Environ.* 31: 529-544.
- [4] Baek, S. O., Suvarapu, L. N., Seo, Y. K. (2015): Occurrence and concentrations of toxic VOCs in the ambient air of Gumi, an electronics-industrial city in Korea. – *Sensors* 15: 19102-19123.
- [5] Batterman, S., Su, F.-C., Li, S., Mukherjee, B., Jia, C. (2014): Personal exposure to mixtures of volatile organic compounds: modeling and further analysis of the RIOPA data. – *Resp Rep Health Eff Inst* 181: 3-63.
- [6] Barletta, B., Meinardi, S., Rowland, F. S., Chan, C. Y., Wang, X., Zou, S., Chan, L. Y., Blake, D. R. (2005): Volatile organic compounds in 43 Chinese cities. – *Atmospheric Environment* 39: 5979-5990.
- [7] Berezina, E. V., Moiseenko, K. B., Skorokhod, A. I., Elansky, N. F., Belikov, I. B. (2017): Aromatic volatile organic compounds and their role in ground-level ozone formation in Russia. – *Dokl. Earth Sc.* 474: 599-603.
- [8] Bolden, A. L., Kwiatkowski, C. F., Colborn, T. (2015): New look at BTEX: are ambient levels a problem? – *Environ Sci Technol* 49: 5261-5276.
- [9] Borgie, M., Garat, A., Cazier, F., Delbende, A., Allorge, D., Ledoux, F., Courcot, D., Shirali, P., Dagher, Z. (2014): Traffic-related air pollution. A pilot exposure assessment in Beirut, Lebanon. – *Chemosphere* 96: 122-128.
- [10] Bretón, J. G. C., Bretón, R. M. C., Ucan, F. V., Baeza, C. B., Fuentes, M. L. E., Lara, E. R., Marrón, M. R., Pacheco, J. A. M., Guzmán, A. R., Chi, M. P. U. (2017): Characterization and sources of aromatic hydrocarbons (BTEX) in the atmosphere of two urban sites located in Yucatan Peninsula in Mexico. – *Atmosphere* 8: 107.
- [11] Brocco, D., Fratarcangeli, R., Lepore, L., Petricca, M., Ventrone, I. (1997): Determination of aromatic hydrocarbons in urban air of Rome. – *Atmos. Environ.* 31: 557-566.
- [12] Buczynska, A. J., Krata, A., Stranger, M., Grieken, R. V. (2015): Atmospheric BTEX concentrations in an area with intensive street traffic. – *Atmospheric Environ* 43: 311-318.
- [13] Crump, K. S. (1994): Risk of benzene-induced leukaemia: A sensitivity analysis of the pliofilm cohort with additional follow-up and new exposure estimates. – *Journal of Toxicology and Environmental Health* 42: 219-242.
- [14] Demirel, G., Ozden, O., Döğeroğlu, T., Gaga, EO. (2014): Personal exposure of primary school children to BTEX, NO₂ and Ozone in Eskisehir, Turkey: relationship with Indoor/outdoor concentrations and risk assessment. – *Sci. Total Environ.* 473: 537-548.
- [15] Derstroff, B., Hüser, I., Bourtsoukidis, E., Crowley, J. N., Fischer, H., Gromov, S., Harder, H., Janssen, R. H. H., Kesselmeier, J., Lelieveld, J., Mallik, C., Martinez, M., Novelli, A., Parchatka, U., Phillips, G. J., Sander, R., Sauvage, C., Schuladen, J., Stöner, C., Tomsche, L., Williams, J. (2017): Volatile organic compounds (VOCs) in photochemically aged air from the eastern and western Mediterranean, *Atmos. – Chem. Phys.* 17: 9547-9566. <https://doi.org/10.5194/acp-17-9547-2017>: 2017.
- [16] Duan, X., Li, Y. (2017): Sources and fates of BTEX in the general environment and its distribution in coastal cities of China. – *Journal of Environmental Science and Public Health* 1: 86-106.

- [17] Dutta, C., Som, D., Chatterjee, A., Mukherjee, A. K., Jana, T. K., Sen, S. (2009): Mixing ratios of carbonyls and BTEX in ambient air of Kolkata, India and their associated health risk. – *Environmental Monitoring and Assessment* 148: 97-107.
- [18] Environment Australia (1999): National Pollution Inventory Contextual Information. – Department of the Environment and Heritage, Commonwealth of Australia, Canberra.
- [19] Fazlzadehdavilb, M., Hazrati, S., Rostami, R., Farjaminezhad, M. (2016): Preliminary assessment of BTEX concentrations in indoor air of residential buildings and atmospheric ambient air in Ardabil, Iran. – *Atmospheric Environment* 132: 91-97.
- [20] Filella, I., Peñuelas, J. (2006): Daily, weekly and seasonal relationships among VOCs, NO_x and O₃ in a semi-urban area near Barcelona. – *Journal of Atmospheric Chemistry* 54(2): 189-201.
- [21] Gao, J.; Zhang, J.; Li, H.; Li, L.; Xu, L.; Zhang, Y.; Wang, Z.; Wang, X.; Zhang, W.; Chen, Y.; et al. (2018): Comparative study of volatile organic compounds in ambient air using observed mixing ratios and initial mixing ratios taking chemical loss into account— A case study in a typical urban area in Beijing. – *Sci. Total Environ.* 628: 791-804.
- [22] Gee, I. L., Sollars, C. J. (1998): Ambient air levels of volatile organic compounds in Latin American and Asian cities. – *Chemosphere* 36: 2497-2506.
- [23] Gennaro, G. D., Farella, G., Marzocca, A., Mazzone, A., Tutino, M. (2013): Indoor and outdoor monitoring of volatile organic compounds in school buildings: indicators based on health risk assessment to single out critical issues. – *International Journal of Environmental Research and Public Health* 10: 6273-6291.
- [24] Gennaro, G. D., Dambruoso, P. R., Gilio, A., Marzocca, A., Tutino, M. (2015): Indoor and outdoor volatile organic compounds monitoring in a multi-storey car park. – *Environment Engineering and Management Journal* 14: 1563-1570.
- [25] Hamid, H. H. A., Jumah, N. S., Latif, M. T., Kannan, N. (2017): BTEXs in indoor and outdoor air samples: source apportionment and health risk assessment of benzene. – *Journal of Environmental Science and Public Health* 1: 62-70.
- [26] Hartwell, T. D., Pellizzari, E. D., Perritt, R. L., Whitmore, R. W., Zelon, H. S., Sheldon, L. S., Sparacino, C. M., Wallace, L. (1987): Results from the total exposure assessment methodology (TEAM) study in selected communities in Northern and Southern California. – *Atmos Environ* 21: 1995-2004.
- [27] Hinwood, A. L., Rodriguez, C., Runnion, T., Farrar, D., Murray, F., Horton, A., Glass, D., Sheppard, V., Edwards, J. W., Denison, L., Whitworth, T., Eiser, C., Bulsara, M., Gillett, R. W., Powell, J., Lawson, S., Weeks, I., Galbally, I. (2007): Risk factors for increased BTEX exposure in four Australian cities. – *Chemosphere* 66: 533-541.
- [28] Ho, K. F., Lee, S. C., Guo, H., Tsai, W. Y. (2004): Seasonal and diurnal variations of volatile organic compounds (VOCs) in the atmosphere of Hong Kong. – *Science of the Total Environment* 322(1-3): 155-166.
- [29] Hoque, R. R., Khillare, P. S., Agarwal, T., Shridhar, V., Balachandran, S. (2008): Spatial and temporal variation of BTEX in the urban atmosphere of Delhi, India. – *Science of the Total Environment* 392: 30-40.
- [30] Holgate, S. T., Samet, J. M., Koren, H., Maynard, R. L. (1999): *Air Pollution and Health*. – Academic Press, California, USA.
- [31] Hsieh, L. T., Yang, H. H., Chen, H. W. (2006): Ambient BTEX and MTBE in the neighborhoods of different industrial parks in Southern Taiwan. – *Journal of Hazardous Materials A* 128: 106-115.
- [32] Hsieh, L. T., Wang, Y. F., Yang, H. H., Mi, H. H. (2011): Measurements and correlations of MTBE and BETX in traffic tunnels. – *Aerosol and Air Quality Research*. 11: 763-775.
- [33] Jo, W. K., Park, K. H. (1999): Concentrations of volatile organic compounds in the passenger side and the back seat of automobiles. – *J. Expo. Anal. Environ. Epidemiol.* 9: 217-227.
- [34] Johnson, M. M., Williams, R., Fan, Z., Lin, L., Hudgens, E., Gallagher, J., Vette, A., Neas, L., Ozkaynak, H. (2010): Participant-based monitoring of indoor and outdoor

- nitrogen dioxide, volatile organic compounds, and polycyclic aromatic hydrocarbons among MICA-air households. – *Atmospheric Environment* 44: 4927-4936.
- [35] Kerchich, Y., Kerbachi, R. (2012): Measurement of BTEX (benzene, toluene, ethylbenzene, and xylene) levels at urban and semirural areas of Algiers City using passive air samplers. – *J Air Waste Manag Assoc.* 62: 1370-1379.
- [36] Khoder, M. I. (2007): Ambient levels of volatile organic compounds in the atmosphere of Greater Cairo. – *Atmospheric Environment* 41: 554-566.
- [37] Le Ha, V. T., Vo. Hie, N. T. T., Dung, N. T., Yoneda, M., Vinh, T. H. (2017): Preliminary assessment of BTEX concentrations indoor and outdoor air in residential Homes in Hanoi. – *Vietnam Journal of Science and Technology* 55. 78-84.
- [38] Lee, S. C., Chiu, M. Y., Ho, K. F., Zou, S. C., Wang, X. (2002): Volatile organic compounds (VOCs) in urban atmosphere of Hong Kong. – *Chemosphere* 48: 375-382.
- [39] Liu, Y., Shao, M., Zhang, J., Fu, L. L., Lu, S. H. (2005): Distributions and source apportionment of ambient volatile organic compounds in Beijing City, China. – *Journal of Environmental Science Health Part A Toxic/Hazardous Substances and Environmental Engineering* 40: 1843-1860.
- [40] Martins, E. M., Borba, P. F., Dos Santos, N. E., Dos Reis, P. T., Silveira, R. S., Corrêa, S. M. (2016): The relationship between solvent use and BTEX concentrations in occupational environments. – *Environ Monit Assess* 188: 608-614.
- [41] Masih, A., Lall, A., Taneja, A., Singhvi, R. (2016): Inhalation exposure and related health risks of BTEX in ambient air at different microenvironments of a terai zone in north India. – *Atmospheric Environment* 147 55-66.
- [42] Menchaca-Torre, H. L.; Mercado-Hernandez, R.; Mendoza-Dominguez, A. (2015): Diurnal and seasonal variation of volatile organic compounds in the atmosphere of Monterrey, Mexico. – *Atmos. Pollut. Res.* 6: 1073-1081.
- [43] Miller, L., Xu, X., Luginaah, I. (2009): Spatial variability of volatile organic compounds in Sarnia, Ontario, Canada. – *Journal of Toxicology and Environmental Health, Part A* 72: 610-624.
- [44] Miller, L., Lemke, L. D., Xu, X., Molaroni, S. M., You, H., Wheeler, A. J., Booza, J., Grgicak-Mannion, A., Krajenta, R., Graniero, P., Krouse, H., Lamerato, L., Raymond, D., Reiners Jr., J., Weglicki, L. (2010): Intra-urban correlation and spatial variability of air toxics across an international airshed in Detroit, Michigan (USA) and Windsor, Ontario (Canada). – *Atmospheric Environment* 44: 1162-1174.
- [45] Miller, L., Xu, X., Grgicak-Mannion, A., Brook, J., Wheeler, A. (2012): Multi-season, multi-year concentrations and correlations amongst the BTEX group of VOCs in an urbanized industrial city. – *Atmospheric Environment* 61: 305-315.
- [46] Monod, A., Sive, C. S., Avino, P., Chen, T., Blake, T. R., Rowland, S. (2001): Mono aromatic compounds in ambient air of various sites: a focus on correlations between the xylenes and ethylbenzene. – *Atmos. Environ.* 35: 135-149.
- [47] Na, K., Kim, Y. P., Moon, K. C. (2003): Diurnal characteristics of volatile organic compounds in the Seoul atmosphere. – *Atmos. Environ.* 37: 733-742.
- [48] Nordlinder, R., Jarvholm, B. (1997): Environmental exposure to gasoline and leukemia in children and young adults – an ecology study. – *Int. Arch. Occup. Environ. Health* 70: 57-60.
- [49] NTP (1999): NTP toxicology and carcinogenesis studies of ethyl benzene (CAS No. 100-41-4) in F344/N Rats and B6C3F1 Mice (Inhalation Studies). – *Natl. Toxicol. Program. Tech. Rep. Ser.* 466.
- [50] Olumayede, E. G. (2014): Atmospheric volatile organic compounds and ozone creation potential in an urban center of Southern Nigeria. – *International Journal of Atmospheric Sciences* 2014: 1-7.
- [51] Parra, M. A., González, L., Elustondo, D., Garrigó, J., Bermejo, R., Santamaría, J. M. (2006): Spatial and temporal trends of volatile organic compounds (VOC) in a rural area of northern Spain. – *Science of the Total Environment* 370: 157-167.

- [52] Paul, J. (1997): Improved air quality on Turkish roads: fuels and exhaust gas treatment. – *Environmental Research Forum* 7-8: 145-152.
- [53] Perry, R., Gee, I. L. (1995): Vehicle emissions in relation to fuel composition. – *Science of the Total Environment* 169(1-3): 149-156.
- [54] Pourfarzi, F., Fazlzadeh, M., Hazrati, S. (2016): Benzene, toluene, ethylbenzene and xylene concentrations in atmospheric ambient air of gasoline and CNG refueling stations. – *Air Qual Atmos Health* 9: 403-409.
- [55] Rad, H. D., Babaei, A. A., Goudarzi, G., Angali, K. A., Ramezani, Z., Mohammadi, M. M. (2014): Levels and Sources of BTEX in ambient air of Ahvaz metropolitan city. – *Air Qual Atmos Health* 7: 515-524.
- [56] Smith, L. A., Stock, T. H., Chung, K. C., Mukerjee, S., Liao, X. L., Stallings, C., Afshar, M. (2007): Spatial analysis of volatile organic compounds from a community-based air toxics monitoring network in Deer Park, Texas, USA. – *Environmental Monitoring and Assessment* 128: 369-379.
- [57] Song, Y., Dai, W., Shao, M., Liu, Y., Lu, S. H., Kuster, W. et al. (2008): Comparison of receptor models for source apportionment of volatile organic compounds in Beijing, China. – *Environment Pollution* 156(1): 174-183.
- [58] Srivastava, A., Sengupta, B., Dutta, S. A. (2005): Source apportionment of ambient VOCs in Delhi city. – *Science of the Total Environment* 343: 207-220.
- [59] Su, J. G., Jerret, M., Beckerman, B., Verma, D., AltafArain, M., Kanaroglou, P., Stieb, D., Finkelstein, M., Brook, J. (2010): A land use regression model for predicting ambient volatile organic compound concentrations in Toronto, Canada. – *Atmospheric Environment* 44: 3529-3537.
- [60] Tager, I., Constantini, M., Jerrett, M., Frampton, M. (2009): The HEI critical review of the health effects of traffic-related air pollution. – *Health Effects Institute Annual Meeting*, Portland, OR, May 3-5, 2009.
- [61] Tang, J. H., Chan, L. Y., Chan, C. Y., Li, Y. S., Chang, C. C., Liu, S. C. et al. (2007): Characteristics and diurnal variations of NMHCs at urban, suburban and rural sites in the Pearl River Delta and a remote site in South China. – *Atmospheric Environment* 41(38): 8620-8632.
- [62] Truc, N. T. Q., Oanh, N. (2007): Roadside BTEX and other gaseous air pollutants in relation to emission sources. – *Atmospheric Environment* 41: 7685-7697.
- [63] Tunsaringkarn, T., Prueksasit, T., Kitwattanavong, M., Siritwong, W., Sematong, S., Zupuang, K., Rungsiyothin, A. (2012): Cancer risk analysis of benzene, formaldehyde and acetaldehyde on gasoline station workers. – *Journal of Environmental Engineering and Ecological Science*. <http://dx.doi.org/10.7243/2050-1323-1-1>.
- [64] USEPA (2004): Integrated Risk Information System (IRIS) Substance List Website. – United States Environmental Protection Agency, Office of Research and Development, National Center for Environmental Assessment, USA.
- [65] Vigliani, E. C., Forni, A. (1976): Benzene and leukemia. – *Environ. Res.* 11: 122-127.
- [66] Wang, Y., Ren, X., Ji, D., Zhang, J., Sun, J., Wu, F. (2012): Characterization of volatile organic compounds in the urban area of Beijing from 2000 to 2007. – *Journal of Environmental Sciences* 24: 95-101.
- [67] Wathne, B. M. (1983): Measurement of benzene, toluene and xylenes in urban air. – *Atmos Environ* 17: 1713-1722.
- [68] Xu, B., Chen, X., Xiong, J. (2018): Air quality inside motor vehicles' cabins: A review. – *Indoor and Built Environment* 27: 452-465.
- [69] Yang, K. L., Ting, C. C., Wang, J. L., Wingenter, O. W., Chan, C. C. (2005): Diurnal and seasonal cycles of ozone precursors observed from continuous measurement at an urban site in Taiwan. – *Atmospheric Environment* 39(18): 3221-3230.
- [70] Yurdakul, S.; Civan, M.; Tuncel, G. (2013): Volatile organic compounds in suburban Ankara atmosphere, Turkey: Sources and variability. – *Atmos. Res.* 120-121: 298-311.

- [71] Zhang, Y., Mu1 Y., Liu, J., Mellouki, A. (2012): Levels, sources and health risks of carbonyls and BTEX in the ambient air of Beijing, China. – *Journal of Environmental Sciences* 24: 124-130.
- [72] Zhou, Y., Li, C., Huijbregts, M. A. J., Mumtaz, M. M. (2015): Carcinogenic Air Toxics Exposure and Their Cancer-Related Health Impacts in the United States. – *PLoS ONE* 10(10): e0140013. DOI: 10.1371/journal.pone.0140013.

PLANT SPECIES RICHNESS IN FRAGMENTED AGRICULTURAL LANDSCAPE – META-ANALYSIS

SARAN, E.* – DUSZA-ZWOLIŃSKA, E. – GAMRAT, R.

*Department of Ecology, Environmental Protection and Management, West Pomeranian
University of Technology
al. Piastów 17, 70-310 Szczecin, Poland*

**Corresponding author
e-mail: edyta.saran@zut.edu.pl*

(Received 2nd Oct 2018; accepted 28th Nov 2018)

Abstract. Fragmentation of agricultural landscape is considered as a threat to biodiversity of many important habitats around the world. Change to the use of land causing loss, isolation and degradation of ecosystems, is one of the main subjects of study in the field of ecology and conservation biology. An appropriate and complex analysis of factors shaping species diversity of the objects in fragmented agricultural landscape may contribute to the understanding and limiting the negative impact of this phenomenon on biocenosis. This paper is a meta-analysis in order to determine the applied research methods and a synthetic representation of the impact of landscape fragmentation on various spatial objects. The aim of the study was to analyse the main assumption of The Theory of Island Biogeography which states that with the decrease of the area of objects, their biodiversity will decrease, while their isolation will increase. An attempt was also made to assess the impact of particular factors that may affect the plant species richness in given objects. The meta-analysis was carried out on the basis of selected criteria for 41 scientific articles in European countries. It was assumed that one cannot unequivocally state the correctness of applying this theory to any type of objects. The conducted study indicated that usually the greatest positive influence on phytodiversity has the size of a given patch, while isolation was assigned a negative impact. The review of landscape research confirmed the thesis that the surface and isolation cannot be unambiguously determined to shape biodiversity in the patches.

Keywords: *landscape fragmentation, rural landscape, phytodiversity, patch metrics, landscape metrics*

Introduction

Over the last centuries, the deforestation and transformation of other ecosystems into farming land as well as forestation of empty or unused areas caused changes to biodiversity in the substantial area of Europe (Vellend et al., 2007). By the end of the nineteenth century, traditional farming prevailed, however it changed over years, focusing on cultivation of cereals (Luoto et al., 2003). The development of agriculture has led to the expansion of arable land and fragmentation of natural biocenoses, which in turn is considered the greatest threat to biodiversity (Montis et al., 2017).

Tscharntke et al. (2005) consider that intensification of farming takes place on two spacial scales: local and connected with the landscape (e.g. converting meadows into farming land, applying monocultures or fragmentation of natural habitats), whereby landscape scale reflects local consequences of enhanced farming practices. It is believed that local intensification is most of all the use of agrochemicals, an increase of the area subject to cultivation, shallowing and drying of mid-field ponds, closing outflows of drainage ditches as well as mechanisation of farming (Bratli et al., 2006). However, agricultural landscape does not consist of the cropland, but also of meadows, forest patches, midfield islets, baulks, roadverges, heathland or ponds (Williams et al., 2004;

Aavik and Lira, 2010). Midfield islets and roadverges are considered as small remnant grassland habitats typical for contemporary agriculture landscape (Cousins, 2006).

The patches of natural or semi-natural vegetation preserved till today form the so-called environmental islands, which are a refuge for many species of plants and animals (Bosiacka and Pieńkowski, 2004). In addition, urban and infrastructural expansion, which is the hallmark of the modern world, has an important impact on the landscape (Krausmann et al., 2003; Luo et al., 2015).

In a modern world, whose defining characteristic is increasingly urban and infrastructural expansion, natural environmental processes are subject to successive degradation. For this very reason, optimization of activities with a purpose of rational management of environmental resources and the protection of landscape in the spirit of sustainable development (Irvine et al., 2009) has become one of the important tasks (Degórski, 2015; Wiedmann et al., 2012).

Landscape is defined as an area, perceived by people, whose character results from actions and interactions of environmental or anthropogenic factors, which constitutes an important component of the quality of life of a society, both in urban and rural areas and in the areas with high level of degradation or in areas of high natural values (Chmielewski et al., 2015; Richling and Solon, 2011).

The definitions of landscape used around the world may be systematized by dividing them into two categories: visual (i.e. the idea of a picture) and physical or geographical (Longatti and Dalang, 2007; Richling and Solon, 2011). Landscape within geographical meaning is a part of environment constituting of patches, corridors and matrix. Matrix is understood as a structural component (or a set of similar structural components), most commonly distinguished in the categories of land cover, which: (a) dominates the area of the local landscape (b) its special location is such that it combines all most distant cut-off points of a local landscape, (c) it constitutes the surroundings of the majority of the remaining spacious components of the local landscape (Solon et al., 2015; Pieńkowski and Podlasiński, 2017). Matrix may constitute habitat for some indigenous species (Fisher and Lindenmayer, 2007) and it allows them to move through corridors among patches (Ricketts, 2001). The conditions of the matrix determine the scope of environmental factors, which model the structure and the processes taking place in a given patch. It is thought that the type and the quality of the matrix is essential in determining the abundance and species composition within the objects (Ewers and Didham, 2006). However, in fact, blurring of distinctions between species inhabiting the fragments and the habitat of a matrix is a common occurrence. “The blurring” of species is most common in small objects and on the edges of big patches, which may disrupt the form of a given area and the outline of the isolation effect (Cook et al., 2002).

Landscape fragmentation, in particular rural landscape, is considered one of the main causes of a decrease in plant species diversity, which may in time lead to extinction of many valuable species (Quine and Watts, 2009; Montis et al., 2017; Qi et al., 2017). The division of environment, caused mainly by anthropogenic activities, leads to the creation of small and isolated objects and the separation of ecotone zones on their edges, which disturbs the integrity of these ecosystems (Heinken and Weber, 2013; Lindborg et al., 2014). The consequence of this phenomenon is a disturbance of the process of genetic information exchange among increasingly smaller populations (Ibáñez et al., 2014).

In order to systematize research on fragmentation, many theoretical assumptions and landscape models are analyzed, which may be helpful in a better understanding of

processes taking place in the landscape (Fischer and Lindenmayer, 2007; Fardila et al., 2017). The most widespread is the conceptual model of habitat fragmentation based on The Theory of Island Biogeography (MacArthur and Wilson, 1967). MacArthur and Wilson (1967) were the first to assume, that a decrease in the area of habitats will lead to a decrease of biodiversity, whereas their isolation will increase (Kattan and Murcia, 2003). According to The Theory of Islands Biogeography, an area is the main physical parameter which has a positive influence on biodiversity of a given object. However, so far it has not been established conclusively, to what extent an increase of a patch area or of the number of habitats in a patch, affects the abundance and species diversity. Patch isolation is characteristic for landscape fragmentation, which is said to affect negatively the richness of species as it reduces their dispersion (Karger et al., 2014). This model led to the development of more complex methods of classifying landscapes, such as the patch-corridor-matrix model (Forman and Gordon, 1981) and the landscape mosaic model (Wiens, 1995).

Due to the awareness of the danger connected with landscape fragmentation, there is a lot of research conducted for the purpose of defining its actual impact on plant species diversity (Iida et al., 1995; Haig et al., 2000; Hanski, 2005; Cangolo et al., 2006). There is also research conducted with respect to the influence of environment homogenization on fauna, inclusive of insects (Löffler and Fartmann, 2017), e.g. ants (Dauber et al., 2006), butterflies (Ricketts, 2001), mammals (Vieira et al., 2009), e.g. bats (Fuentes-Montemayor et al., 2013); birds (Carrara et al., 2015), reptiles and amphibians (Watling and Donnelly, 2008). There is also experimental research conducted, in artificially created environment (Cook et al., 2002; Collins et al., 2009; Allan et al., 2015), where the aim of the study is purposeful manipulation of the landscape. In such artificially created conditions, it is often not possible to check some of the features of the particular objects studied, e.g. their shape, degree of replication, site initiation and position on the landscape (Debinski and Holt, 1999). Due to the awareness of negative impact of fragmentation on the richness of species of ecosystems, many habitats are recreated and analysis of the effectiveness of such approach is performed on them. These analyses show positive impact of habitats restitution not only on the biodiversity in objects restored but also in their surroundings (Prach et al., 2015; Conradi and Kollmann, 2016; Waldén et al., 2017).

In this study, the main assumption of The Theory of Island Biogeography was analyzed, based on the example of landscape studies, which states that with the decrease of the area of objects, their biodiversity will decrease, while their isolation will increase. An attempt was also made to assess the impact of particular factors that may affect the plant species richness in given objects, with particular emphasis on the landscape matrix. For this purpose: (1) the research methods used in the implementation of landscape studies were analyzed, (2) the collected information was compared, and (3) the obtained results were synthetically presented. The meta-analysis included papers in the field of ecology and biology conservation, including articles published in 1997 – 2018 in Europe (15 countries, 41 papers).

Materials and methods

For the purpose of analysing the influence of fragmentation on the diversity of plant species and comparing research methods, in December 2017 and in January 2018, a systematic search of the source literature was carried out. The search of papers was

divided into two categories: 1) English- language papers included in ScienceDirect, Wiley Online Library and SpringerLink databases and 2) papers published in selected, Polish scientific topic journals (*Dissertations of Cultural Landscape Commission, Hydrobiology, Polish Journal of Ecology, Water-Environment-Rural Areas, Scientific Papers of the University of Life Sciences in Wroclaw. Agriculture*). The existing Polish databases of papers do not allow a complex search of papers with use of sets of keywords. For this reason the Polish publications were selected based on a review of the journals, whose topics include studies on the structure and functioning of the landscape.

All papers found in the English-language databases were searched for with use of the following keywords (in various configurations): ‘biodiversity’, ‘connectivity’, ‘habitat fragmentation’, ‘habitat loss’, ‘isolation’, ‘landscape fragmentation’, ‘matrix’, ‘small habitats’, ‘species richness’ (*Table 1*). On that basis, the first, preliminary selection of the papers was made. The table below presents all the keywords used and their definitions.

Table 1. Selected keywords and their definitions

Term	Definition	References
Biodiversity	‘the variety of life and its processes; it includes the variety of living organisms, the genetic differences among them, the communities and ecosystems in which they occur, and the ecological and evolutionary processes that keep them functioning, yet ever changing and adapting’	DeLong, 1996 for Noss and Cooperrider, 1994
Connectivity	‘measure of landscape structure; the degree to which the landscape facilitates or impedes movement among resource patches’	Taylor et al., 1993
Habitat fragmentation	‘breaking apart of a large area of habitat into several smaller areas’	Lindenmayer and Fischer, 2006
Habitat loss	‘loss of habitat for a given species from an area, precluding that taxon from persisting there; viz the area becomes nonhabitat for that species’	Lindenmayer and Fischer, 2006
Isolation	‘distance to another patch and areas of patches’ ‘disrupts species distribution patterns and forces dispersing individuals to traverse a matrix habitat that separates suitable habitat fragments from each other; defined by the Euclidean distance between habitat fragments’	Graae, 2000 Ewers and Didham, 2006
Landscape fragmentation	‘landscape characterized by a strong contrast between native vegetation patches and their surrounding matrix’	Mortelliti et al., 2010
Matrix	‘the area between the habitable patches’	Debinski, 2006
Small habitats	‘patches found outside protected areas, such as road verges, shading trees, mid-field islets and cropland set aside’	Lindborg et al., 2014
Species richness	‘the number of different species occurring in some location or under some condition such as pollution’	DeLong, 1996

Selected articles were chosen based on the indication of Fardila et al. (2017), who conducted a detailed meta-analysis in relation to the impact of fragmentation on the species richness of all living organisms. They suggested that there is a need to better integrate studies published in languages other than English with the broader international literature. Fardila et al. (2017) reviewed only papers written in English and as they indicate this might have biased the geographic distribution of the studies they sampled. Therefore, among others, the authors of this paper limited their research to European literature covering only the world of plants, which enabled the described analyses to be carried out. The paper refers not only to English-language works, but also research of Polish scientists was used, enabling preliminary analysis of the existing trend in research on the structure and functioning of the landscape. It is worth noting that access to Polish-language works is quite limited due to the lack of their English translation.

The selection of papers (the Polish ones and those available from the English-language literature databases) was based on the following criteria: in the contents of the paper the landscape had to be defined as agricultural or at least partially connected with agricultural landscape, the study had to involve plant species and must have been conducted in the Western European countries. Experimental research was excluded though, as it presents test results obtained through a purposeful manipulation of the landscape. The authors of the paper wanted to present research findings connected with the objects which are naturally present in the agricultural landscape. Based on the aforementioned criteria, the analysis involved in total 41 studies published between years 1997-2018 in 15 European countries, namely: Austria, Belgium, Denmark, Estonia, Finland, France, the Netherlands, Luxembourg, Germany, Norway, Poland, Portugal, Sweden, Great Britain and Italy.

Each paper analysed was classified in the context of 5 features: 1) type of study, 2) study design (location, patch area, its type and number), 3) source of floristic data (research, inclusive of field research), 4) main metrics (variables involved in the research) and 5) data analysis (own work based on Fardila et al., 2017) (*Figure 1*).

While analysing the “data analysis” category in each paper, it was verified whether the authors included in their research the following items: Geographical Information System (GIS), statistical calculations and the method of defining species richness (the total number of species and the application of biodiversity measurement indices).

The publications were also divided into ten categories connected with the main aims of study related to the influence of a given factor on the richness of plant species: (1) species richness affected by fragmentation; (2) interior and edge, (3) isolation, (4) patch attributes, (5) habitat conditions, (6) landscape structure, (7) dispersion, (8) fragmentation in time, (9) abandonment, (10) plant life-traits, and an additional, eleventh category (11) connected with the conservation of the objects: establishment of conservation and management strategies.

Based on the analysis of the papers selected, the objects characteristic for the agricultural landscape were established as the objects of studies: forest patches, grasslands, mid-field islets, road verges, heathland and ponds. The summary table presents (*Appendix 1*) detailed information about the analyzed articles.

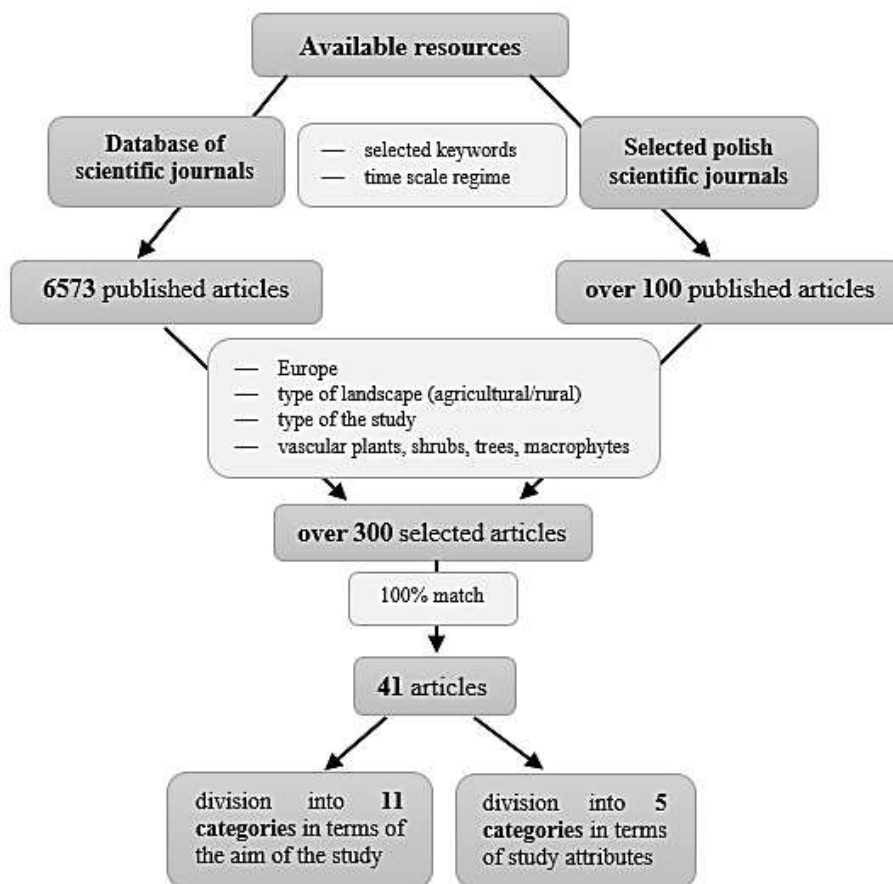


Figure 1. Methodology scheme

Results

Entering various configurations of the selected keywords into the literature databases as chosen resulted in finding the total of 6673 papers published in years 1997-2018. Following that, 41 papers which fulfilled the criteria as presented in “Methods” section were selected. The selected papers were published in 16 scientific journals. The leading ones were: *Journal of Vegetation Science* and *Biological Conservation* (14.6%), whereas *Agriculture, Biodiversity and Conservation*, *Ecography*, *Ecosystems and Environment*, *Forest Ecology and Management* as well as *Landscape Ecology* published three papers each (7.3%) (Appendix 2).

Study design and species data

In all analysed studies the most common method of acquiring information on the species composition of objects studied were field studies (95.1%) carried out mostly in the vegetation period of one year (61.0%). Eight research teams were collecting data on plants over the period of 2 years (19.5%), however, some papers did not contain any information on the length of the studies carried out (16.7%). The analysis of 2 out of 41 papers selected was based on the existing data: survey carried out by the Provincial Government of Drenthe and The Lincolnshire data set (Grashof-Bokdam, 1997; Verheyen et al., 2004, respectively). Some of the research as presented in the studies

was carried out in laboratories, where also the composition and the properties of soil extracted from a studied object were analysed (38.8%) (*Appendix 1*).

The subject of studies in the Western European countries were very diversified objects forming part of the agricultural landscape: grassland patches (20), forest patches (20), midfield islets (5), ponds (4), road verges (3) and heathlands (1) (*Figure 2*). Some of the studies analysed referred to more than one object (14.6%).

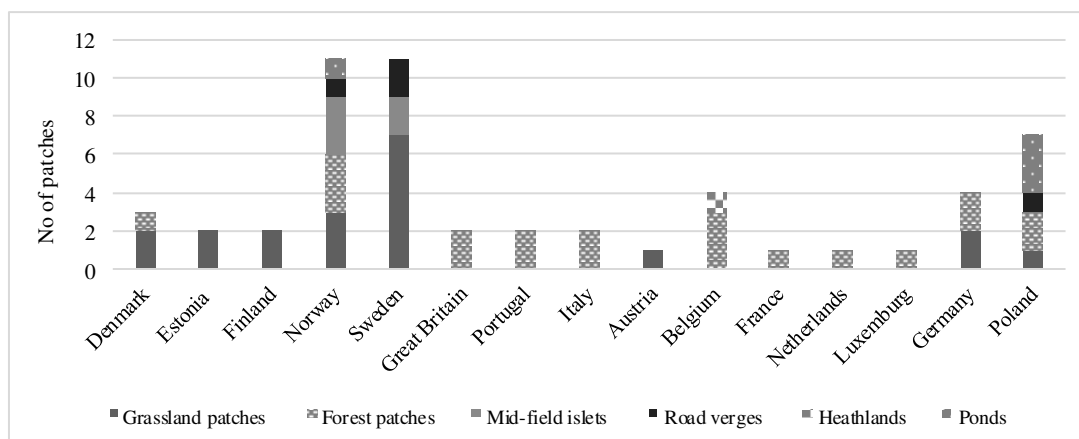


Figure 2. Type and number of the objects studied in 15 European countries

Aim of the studies

The first basic criteria determining the choice of papers for further analysis was the aim of the study (*Table 2*). The topic of all foreign papers as analysed was the determination of the influence of the fragmentation of the habitats and the landscape on the plant species richness of the objects typical for the agricultural landscape. In large part of the studies this thematic scope was defined as the main aim of the study (18 papers constituting 43.9%). In 14 papers, apart from determining the influence of the fragmentation of the habitats and the landscape on the plant species richness, the features of the objects of study (size, shape) were the main factor which motivated the authors to take up and to perform the research (34.1%). Habitat-related factors, the quality and the features of the landscape as well as isolation effect (31.7%, 22.0%, and 19.5%, respectively) constituted also a very important aspect influencing the phytodiversity of the object studied in the scientific papers as analysed. A presentation of the fragmentation of the agricultural landscape over years and the historical context of the development of the landscape was the main aim for 8 research teams (19.5%). Two out of all the studies analysed focused on determining the plant species richness in two zones of a given object: ecotone as a transition area and the interior (4.9%). In few papers it was verified whether plant life-traits, their dispersive abilities and an abandonment had an actual impact on species composition (2.4%, 4.9%, and 2.4%, respectively). The main aim of three studies was a presentation of conservation and management strategy within study points subject to analysis (7.3%). In almost half of the studies (51.2%), the authors presented the rationale for conservation of given objects, even though this were not the main aims of the studies. The following table contains a summary and a presentation of the main aims of the studies analysed.

Table 2. Main features of the analysed studies

Study attributes	References
Fragmentation	Grashof-Bokdam, 1997; Jacquemyn et al., 2001; Dumortier et al., 2002; Kolb and Diekmann, 2004; 2005; Verheyen et al., 2004; Piessens et al., 2005; Bratli et al., 2006; Cousins 2006, Helm et al., 2006; Johansson et al. 2008; Reitalu et al., 2009; Hamre et al., 2010; Gazol et al., 2012; Öckinger et al., 2012; Lindborg et al., 2014; Huber et al., 2017; Buffa et al., 2018
Interior and edge	Grashof-Bokdam, 1997; Vallet et al., 2010
Isolation	Bruun, 2000a, 2000b; Graae, 2000; Krauss et al., 2004; Petit et al., 2004; Cousins, 2006, Cousins et al., 2007; Zulka et al., 2014
Patch attributes	Bruun 2000b; Honnay et al., 1999; Graae, 2000; Jacquemyn et al., 2001; Krauss et al., 2004; Petit et al., 2004; Orłowski and Nowak, 2005, Økland et al., 2006, Cousins et al., 2007; Raatikainen et al., 2009; Lomba et al., 2011; Bosiacka and Pieńkowski, 2012; Lomba et al., 2013; Zulka et al., 2014
Habitat conditions	Bruun, 2000a; Kolb and Diekmann, 2004; Hérault and Honnay, 2005; Cousins, 2006; Löbel et al., 2006; Økland et al., 2006; Raatikainen et al., 2009; Hamre et al., 2010; De Sanctis et al., 2010; Gazol et al., 2012; Zulka et al., 2014; Koszelnik-Leszek et al., 2015; Huber et al., 2017
Landscape structure	Honnay et al., 1999; Krauss et al., 2004; Petit et al., 2004; Hérault and Honnay, 2005; Cousins, 2006; Löbel et al., 2006; Økland et al., 2006; Mathias, 2007; Gazol et al., 2012
Dispersion	Graae, 2000, Orłowski and Nowak, 2005
Fragmentation in time (historical context)	Jacquemyn et al., 2001; Luoto et al., 2003; Bosiacka and Pieńkowski, 2004; Cousins, 2006, Cousins et al., 2007, Johansson et al., 2008; Reitalu et al., 2009; Gamrat et al., 2017
Abandonment	Luoto et al., 2003
Plant life-traits	Hérault and Honnay, 2005
Establishment of conservation and management strategies	Orłowski and Nowak, 2005, Lomba et al., 2011, 2013

Data analysis

Species richness is considered an important measure used for determining biological diversity of a given area. This is mostly due to the simplicity of measuring it in the case of vascular plants. The appraisal and the monitoring of biodiversity may be conducted by reference to various scales: local, landscape, and the macroscale (Ferretti et al., 2006).

The majority of the analysed Western European studies, employed landscape scale (43.9%), which takes into account the influence of matrix on plant species richness.

A little less, 36.6% of studies used local scale as a reference point of their analysis. The least common was macroscale category (19.5%), which takes into account among others climate change aspect, which is line with the overall trend in landscape studies around the world (Opdam and Wascher, 2004; Engler and Guisan, 2009; Keshtkar and Voigt, 2016).

The diversity of species is a measure which takes into account the total species richness and their abundance/density. Patch level approach uses for measuring species richness an α diversity index defining the total number of species in a given area - S . It depends on the area of a given space and the size of a sample. However, in focal patch approach a diversity index - γ , which constitutes a total of variety - α (Whittaker, 1972; Sienkiewicz, 2010) is applied. The most common indices for determining this measure are diversity (H) and evenness indices, Shannon's (E) (Shannon, 1948) and Simpson's (D) (Simpson, 1949) (Gotelli and Chao, 2013). From among 41 European, English-language studies, only 4 used more detailed diversity indices - α or γ . In the remaining 37 papers species richness was defined as the total number of species established in a given area during field studies, through making lists of species and taking phytosociological pictures.

In the majority of papers analysed for the purpose of presenting the location of study points and their area, defining the level of their isolation and the distance between them as well as the fragmentation of given areas over time (90.2%), Geographical Information System (GIS) was used (e.g. Honnay et al., 1999; Dumortier et al., 2002; Bosiacka and Pieńkowski, 2012; Buffa et al., 2018). Most commonly used software for this purpose was ArcGIS package (59.5%) (e.g. Økland et al., 2006). One of the papers used Fragstats (2.4%) (De Sanctis et al., 2010). In a small part of given papers there was not mentioned the name of the software used (10.8%) (e.g. Bruun, 2000b; Raatikainen et al., 2009).

Inclusion of statistical analysis into the research might seem necessary for the purpose of complex presentation of links between a number of factors connected with habitats, the landscape or the environment and the plant species richness. However, in small part of performed studies it was not included (7,3%) (Bosiacka and Pieńkowski, 2004; Koszelnik-Leszek et al., 2015; Gamrat et al., 2017). Studies, which applied statistical analysis in their studies, determined the connection between various factors influencing the plant species richness of the selected objects of study.

Variables involved in research

An analysis of the selected studies showed diversity in the selection of factors which may influence the plant species richness (*Figure 3*). The most commonly studied factor was the area of a given object (63.4%) (e.g. Grashof-Bokdam, 1997; Kolb and Diekmann, 2004; Mathias et al., 2007; Öckinger et al., 2012; Koszelnik-Leszek et al., 2015; Huber et al., 2017). The most important group which determined the scope and the performance of the studies were „landscape metrics” group components (38.5%), with the level of isolation being the most commonly determined value for this category (28.3%) (Graae, 2000; Dumortier et al., 2002; Piessens et al., 2005; Bosiacka and Pieńkowski, 2012). The least commonly established were connections between the plant-related metrics and the species richness (9.6%) (e.g. Brunn, 2000a; Kolb and Diekmann, 2005; Lindborg et al., 2014).

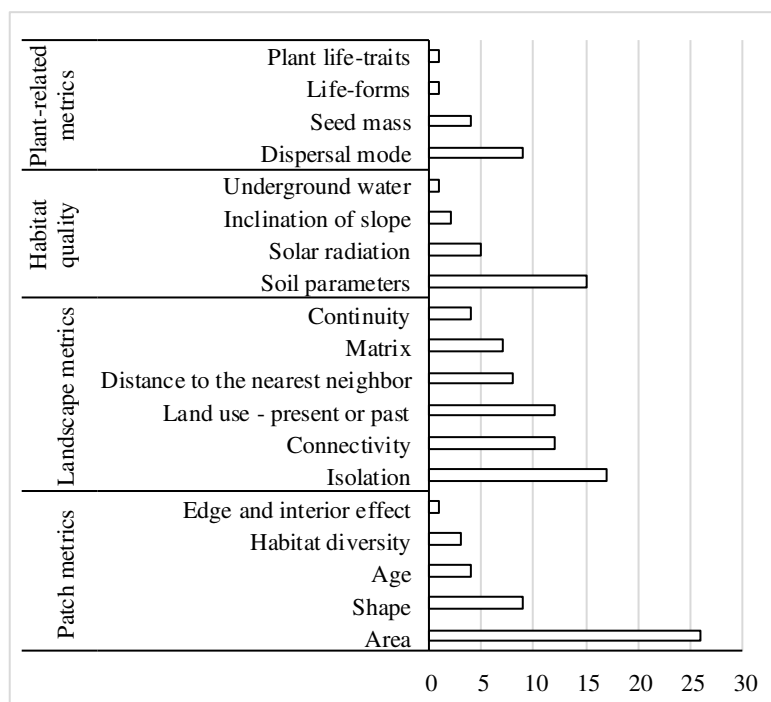


Figure 3. Variables involved in research divided into 4 categories

Factors affecting plant species richness

All the papers included in this analysis considered more than one factor affecting plant species richness. The influence of these factors was categorized for each type of the object studied as: positive, negative and no relevance.

Grassland patches

In the majority of the studies analyzed it was established that the greatest positive influence on plant species richness in grassland patches had the current area of the object (40.0%) (Figure 4) (e.g. Krauss et al., 2004; Cousins et al., 2007; Raatikainen et al., 2009). It was concluded that an increase of an area occupied leads to an increase of a number of plant species present there. The way these objects are used (mowing or animal grazing) (e.g. Luoto et al., 2003; Reitalu et al., 2009; Hamre et al., 2010). and the diversity of habitats also have a positive impact (e.g. Mathias et al., 2007) (25.0%, 20.0%, respectively).

The largest negative impact on species richness may be attributed to objects' isolation (30.0%) (e.g. Raatikainen et al., 2009; Reitalu et al., 2009; which impairs dispersive abilities of species, forcing them to migrate through hostile matrix. Also abandonment of the grassland patches through a withdrawal of any plant care procedures had a negative impact (15.0%) (e.g. Reitalu et al., 2009; Gazol et al., 2012). The analysis of the papers allowed also for determining the factors, which according to the researchers, did not affect species richness. Continuity, current connectivity, landscape history and land-use were considered factors whose values and scope have no impact on plant species richness (10.0%, respectively) (e.g. Johansson et al., 2012).

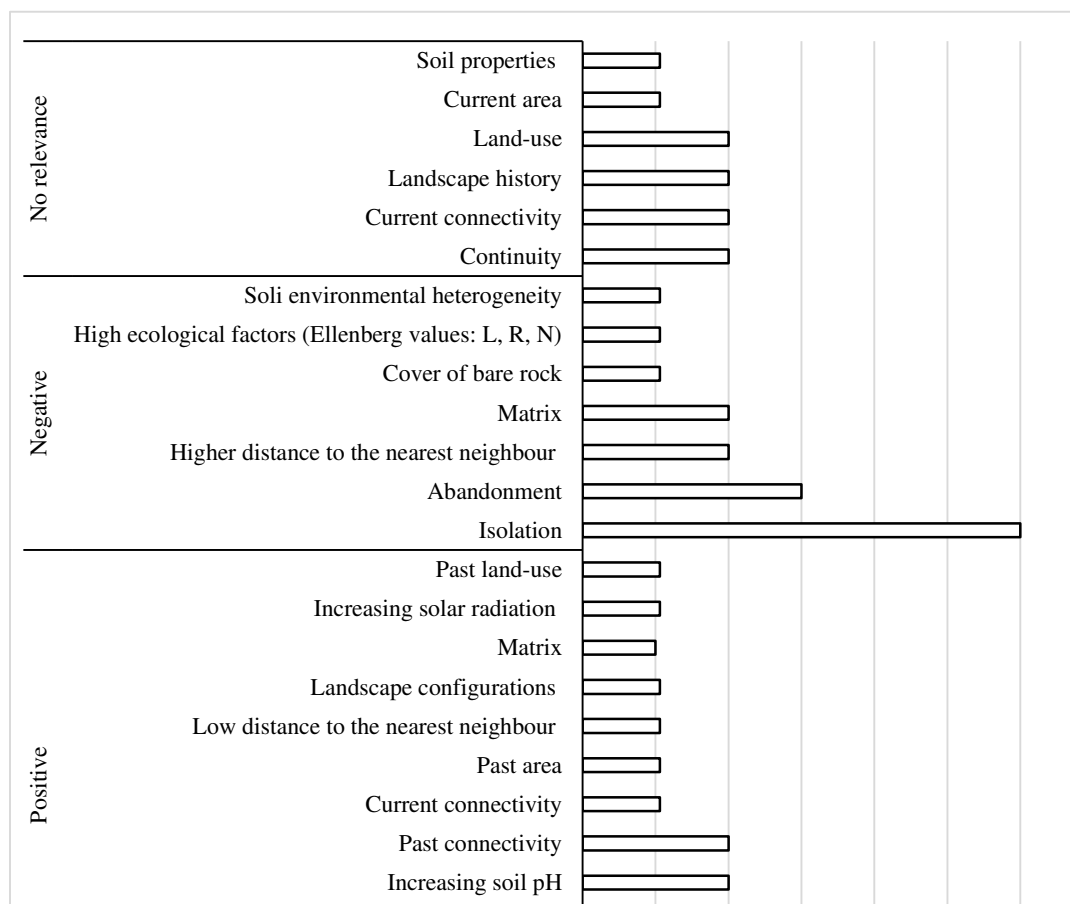


Figure 4. Influence of variables involved in research divided into 3 categories: positive, negative and not affecting plant species richness in grassland patches (L – light value, R – reaction of soil value, N – nitrogen value)

Forest patches

In the case of the forest patches as studied, similarly as in the case of grassland patches, the largest positive influence was attributed by the scientists to their current area (55.0%) (Honnay et al., 1999; Jacquemyn et al., 2001; Verheyen et al., 2004; Kolb and Diekmann, 2004; Buffa et al., 2018). An exception was three studies (15.0%) (Lomba et al., 2011, 2013; Koszelnik-Leszek et al., 2015) in which it was established that there was no significant connection between species richness and the size of objects. One of the factors which were considered favorable for an increase of species richness was also current connectivity – it was concluded that plant species were more common in well-connected patches (Grashof-Bokdam, 1997; Petit et al., 2004; Verheyen et al., 2004; Hérault and Honnay, 2005; Kolb and Diekman, 2005) (25.0%) (Figure 5).

The biggest negative impact was attributed to isolation (25.0%) (e.g. Graae, 2000; Kolb and Diekmann, 2004), whereas ecological values were considered nonaffecting in 10.0% of studies on plant species richness of the selected landscape objects (e.g. Petit et al., 2004).

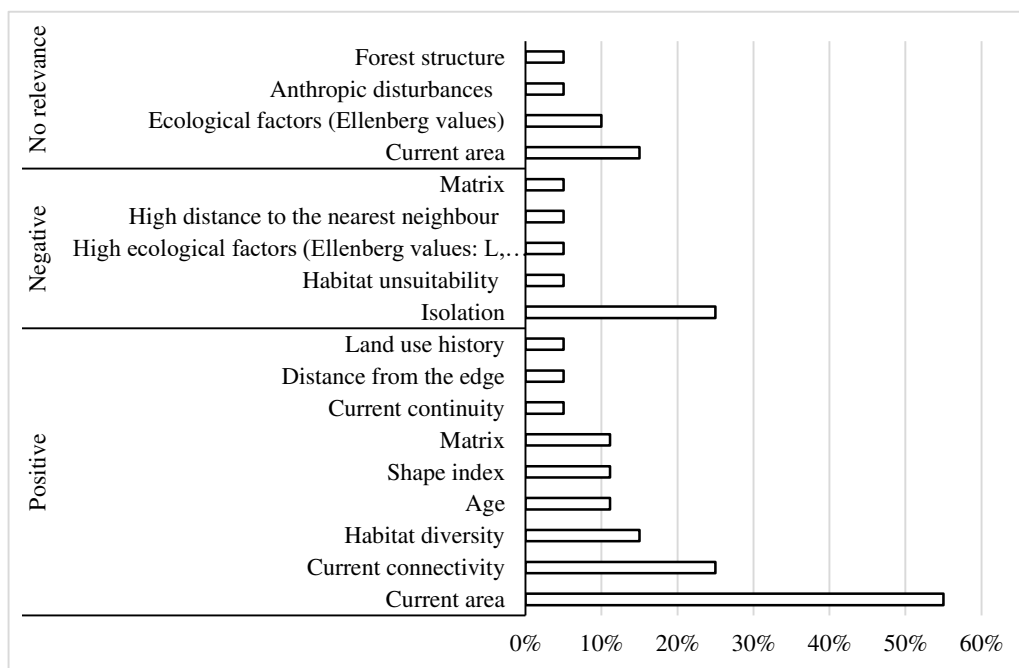


Figure 5. Influence of variables involved in research divided into 3 categories: positive, negative and not affecting plant species richness in forest patches (L – light value, R – reaction of soil value, N – nitrogen value)

Midfield islets

Half of the research teams whose studies comprised midfield islets, considered that the appropriate management of these objects (Cousins, 2006) and their current area (Cousins, 2006) had a positive impact on plant species richness (Figure 6). Habitat diversity of the patches also had positive effect on phytodiversity of these areas (33.3%) (Bratli et al., 2006).

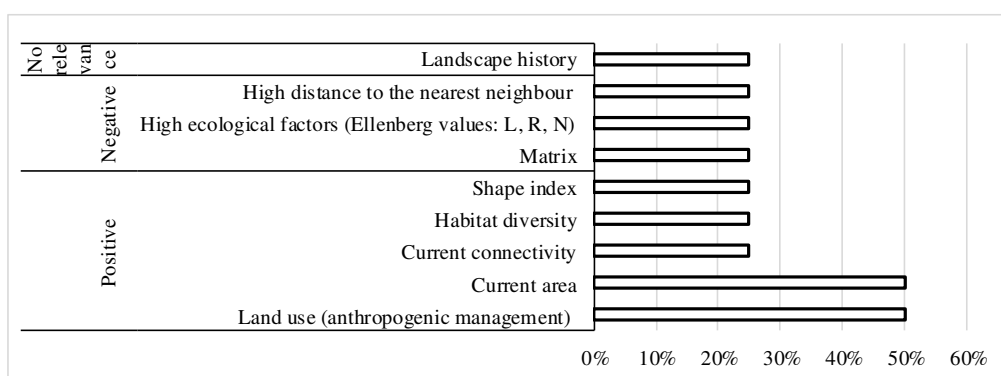


Figure 6. Influence of variables involved in research divided into 3 categories: positive, negative and not affecting plant species richness in midfield islets (L – light value, R – reaction of soil value, N – nitrogen value)

Negative factors were considered to be a long distance to the closest neighbour (Lindborg et al., 2014), matrix and high ecological factors (Økland et al., 2006). Studies performed by Cousins (2006) showed that landscape history is irrelevant for plant species richness.

Road verges

Road verges constituting a mandatory component of every agricultural landscape are positively affected by purposeful human activity – plant-care activities within road verges (e.g. mowing) (50.0%) (Cousins, 2006; Økland et al., 2006) (Figure 7). An important environmental factor which has a positive influence on plant communities is habitat diversity (Gamrat et al., 2017), shape index (Økland et al., 2006), current area (Økland et al., 2006) and the landscape aspect – current connectivity (Cousins, 2006) (25.0% respectively).

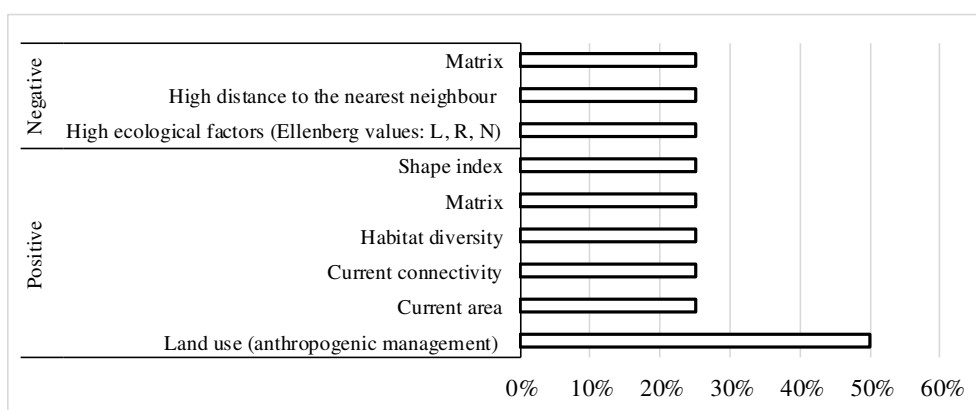


Figure 7. Influence of variables involved in research divided into 2 categories: positive and negative on plant species richness in road verges (L – light value, R – reaction of soil value, N – nitrogen value)

Based on the English-language literature related to road verges, three factors which affect negatively plant species diversity were determined: long distance to the nearest neighbour (Lindborg et al., 2014), which results from the insulation of these objects, high ecological values and the matrix (Økland et al., 2006). Nonaffecting factors were not identified.

Heathlands

Literature on heathlands (Piessens et al., 2005) is sporadic. It was established though that isolation has a negative impact on plant species richness. It was also concluded that current area of the object studied does not affect its phytodiversity.

Ponds

Out of the 41 papers as selected (based on the methodological criteria applied), four research teams included ponds in their studies (Appendix 1). It was determined that floristic diversity is positively affected by the current area and the shape of the objects (Økland et al., 2006; Bosiacka and Pieńkowski, 2012). The matrix (Gamrat et al., 2017)),

high ecological values (Økland et al., 2006) and isolation (Bosiacka and Pieńkowski, 2012) were considered to be negative factors (25.0%, respectively) (Figure 8).

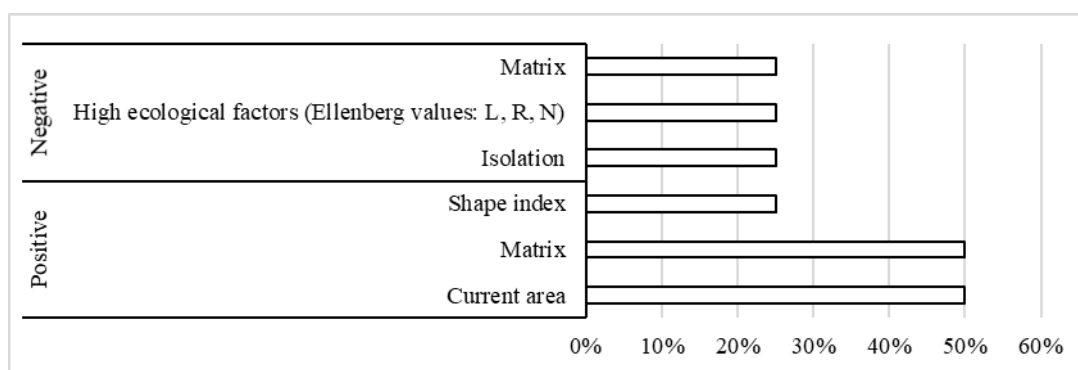


Figure 8. Influence of variables involved in research divided into 2 categories: positive and negative on plant species richness in ponds

In the majority (75.0%), ponds were examined in the area of the north-western part of Poland, which may be due to the fact that these are objects characteristic of the young glacial landscape (Bosiacka and Pieńkowski, 2004).

Discussion

Based on the methodological criteria selected attempts were made to select a group of scientific papers. In the given literature, the methods of evaluating an impact of fragmentation on plant species richness in different spatial objects characteristic for the agricultural landscape in 15 Western European countries were analyzed. The categorization of scientific papers proposed in the methodological part allowed to compare the applied research methodologies and their analysis, as well as to determine the impact of fragmentation of the agricultural landscape on the species richness of the studied objects.

The meta-analysis of scientific articles is undertaken in order to systematize applied research methods in a given field. In this paper, the authors focused on landscape studies taking into account the species richness of plants that can be shaped by many spatial factors. Aim of this paper was to analyze the main assumption of The Theory of Island Biogeography, whose main indicators are the isolation and area of a given object. International research in this subject does not explicitly indicate the possibility of using this theory in relation to various spatial objects in the agricultural landscape. An additional difficulty, indicated by Fardila et al. (2017), is an insufficient number of studies published in a language other than English, included in the international literature of the subject. Therefore, the presented paper presents, in addition to English-language works, the results of research by Polish scientists.

Comparison of all selected articles, indicates that the main types of objects in landscape studies are grasslands (48.8%) and forest patches (48.8%). This differs from the position of Fardila et al. (2017), who reviewed the research on the impact of fragmentation on the species richness of all biotic elements around the world and found that the main subject of researches were forest patches. Less attention was focused on the remaining types of objects. However, it was submitted that the research on

fragmentation should be carried out within various habitat types, because the problem of biodiversity decline affects all ecosystems, not only forest ones (Fardila et al., 2017). Small habitats, such as road verges, shading trees or mid-field islets, are also an important element of the agricultural landscape, raising its value, constituting a refugium and being a source of seed dispersal (Lindborg et al., 2014).

The majority of floral studies of the objects situated in the fragmented agricultural landscape as analyzed was performed in Scandinavian countries – Sweden, Norway, Denmark or Finland (44.4%). From among all studies related to grassland, it was the most common object of studies in these countries (73.4%). It may result from the fact that in the last century a decrease of these areas in Scandinavia by about 90% due to radical changes in their management has been noticed (Eriksson et al., 2002). This led to the need of defining and presenting the negative consequences of the landscape transformation (fragmentation). Biological value of grassland results among others from the fact that it is characterized by very high species density, which often amounts up to even $60 \cdot \text{m}^{-2}$. Furthermore, many species inhabiting grassland are present also in other habitats, constituting their component for example: heathland, road verges, forest patches or small midfield islets surrounded by farm land (Eriksson et al., 2002). It is considered that grassland patches constitute the so called hotspots of diversity being a key factor influencing an increase in biodiversity of the agricultural landscape (Hamre et al., 2010; Habel et al., 2013).

What is worth noting Polish research on grasslands differs from research conducted in other European countries. Above all, there are relatively few of them, and those that are conducted, methodically differ from the European patterns. However, this proportion should change in the coming years, as it is believed that grassland is more prone to degradation due to its spatial location, which allows for an easy change to the way it is used (Fardila et al., 2017). Similarly, as in the case of studies in the remaining European countries, there are few studies performed on small objects with high ecological values such as road verges. As in the case of research in other European countries, in Poland, observations on small but valuable natural objects such as road verges were rarely carried out. The creation of new, even small environmental islands, contributes to inhibiting the extinction of species (Bennet and Saunders, 2011).

Studies on fragmentation of the landscape and habitats are carried out all over the world and involve analyses of flora and fauna. Researchers try not only to define biodiversity of a given area, but also pose a question: how it should be protected and how to manage given objects to be able to prevent homeostasis of ecosystems. Heinken and Weber (2013) claim that fragmentation does not affect in the same way all plant communities and habitats, which makes it more difficult to present or develop one general conservation plan for all ecosystems. Better understanding of fragmentation, achieved due to specialized and complex studies of this process, may help to develop a strategy of conservation of domestic and endangered plant species in isolated objects and identify those which are most susceptible to habitat loss.

Bennet and Saunders (2011) assigned a negative impact on species diversity in the process of habitat degradation to alien species invasion. They consider that proper control and management of objects may be the key importance for maintaining biocenotic balance. Moreover, they suggest that taking appropriate actions not only within isolated patches but also within landscape and macroscale. Additionally, it requires constant control of abiotic factors such as erosion, input of pollutants and anthropogenic pressure connected with recreation aspect.

An analysis of literature allowed a presentation of different approaches to carrying out studies of one area by the same research teams, however with use of different methodology. It was particularly noticeable in the context of studies carried out on Öland island (Sweden) (Löbel et al., 2006; Johansson et al., 2008; Reitalu et al., 2009). Each of the papers presented an influence of a number of different factors (Appendix 1) which may contribute to plant species richness of selected grassland. The selection of a particular factor affected obtained results, which in turn had an influence on the way biodiversity of a given object was perceived. Löbel et al. (2006) concluded that higher pH has a positive impact on phytodiversity of the objects studied. Johansson et al. (2008) considered historical aspects of the use of land to be a positive factor, whereas Reitalu et al. (2009) defined appropriate management of grassland as a positive contributor to plant species richness.

Sjælland island (Denmark) was subject to studies twice (Brunn, 2000a, 2000b), with the aim being the establishment of the influence of isolation and area diversity of the objects on plant species richness. In one of the studies (Brunn, 2000) it was verified additionally whether there is a link between abundance of species and the weight of seeds, and in the second study the author presented forecasts of potential richness and deficit of species (Brunn, 2000a) on the island subject to studies.

Another example of a diversified approach to the selection of factors contributing to biodiversity with respect to the same objects, are studies performed by teams of Lomba et al. (2011, 2013) (Appendix 1). In both studies, different research methodologies with different main assumptions were used. One of the studies focused on presenting forest type (dominant tree species), forest patch spatial attributes (patch area and shape index), and measures of forest management and structure (Lomba et al., 2011) as factors which may potentially affect phytodiversity. In the second one (Lomba et al., 2013) species-area relationship (SARs) was established. SARs is one of the oldest and the best documented research methods, which describes an increase of species richness to area relationship. It may have different forms and it may be explained by different mechanisms (Tessel et al., 2018). However, a selection of factors which may affect phytodiversity made no difference to the results obtained as in both cases it was established that there is no link between current area of forest patches and floristic diversity. Furthermore, in both studies it was established that there is a positive correlation between an increase of species richness and an increase in natural character of forest patches. Whereas shape index, as a physical factor shaping ecotone habitats (Lomba et al., 2011), turned out to be a positive contributor to biodiversity of the whole patches. It is considered that the diversity of the given ecotone with respect to habitats increases with the increase of diversity of the shape of a given object.

Selected scientific articles (especially English-language ones) are characterized by complexity in terms of the analysis of the available subject literature and applied research methodologies. They take into account many factors that can shape the species richness of plants, and check the potential correlations between them, through the use of statistical analysis. In turn, in the research of Polish scientists, the undisputed asset is the detailed field research (phytosociological) related to the acquisition of a large amount of data in the form of phytosociological images and often associated environmental variables. The share of species in the phytosociological picture is usually given in the six-stage combined quantitative scale - coverage (Zarzycki, 2009) proposed by Braun-Blanquet.

The meta-analysis points to the need for scientists to protect the environmental islands as valuable spatial objects. It is recommended to protect larger patches, where there is a low risk of extinction of species characteristic for a given habitat (Krauss et al., 2004; Mathias et al., 2007), or appropriate management of grassland patches (mowing and grazing) (Gazol et al., 2012; Zulka et al., 2014; Huber et al., 2017). In addition, Hamre et al. (2010) also note the need to include historical maps of the studied areas, as they are a useful tool to understand landscape changes over the years, including changes in the spread of plant species and extinction debt. Extinction debt, in ecological terms, is considered to be populations of existing species that are likely to perish as a result of changes in the environment: habitat destruction, climate change or invasion of alien species (Kuussaari et al., 2009).

Summary

The analysis of selected available literature allowed to determine a number of factors affecting the species richness of plants, such as habitat diversity, connectivity, the shape of the object or its management. The conducted study indicates that usually the greatest positive role is assigned to area of a given patch (over 95.0% of the analyzed works including this factor in the research). It allows to conclude that increasing area of habitats and the general number of spatial objects in the landscape may limit the impact of the negative effects of the fragmentation process, which will additionally improve the connectivity. Another analyzed factor affecting the species richness of plants, according to The Theory of Island Biogeography (MacArthur and Wilson, 1967) is isolation. Its negative effect on plant species richness was observed in more than 70.0% of the papers emphasizing this factor in research. The review of landscape research confirmed the thesis that the area and isolation cannot be unambiguously determined to shape biodiversity in the patches. The reason for this may be the diversity of the examined objects, the differentness in the statistical analysis, the insufficient number of field studies, as well as the location of objects in space (geographical aspect).

Fragmentation of the landscape, especially agricultural, is assigned to the negative significance in relation to the preservation of species diversity. As a result of this process, the habitats are reduced, creating isolated patches. They are also often separated by surfaces used by humans, or are adjacent to communities of synanthropic species, adapted to live in a strongly transformed environment. Fragmentation is most often the result of human activity (Kuussaari et al., 2009), directed at the development of agriculture, therefore the task of society, scientists and territorial authorities is to create protection strategies and conduct activities that minimize the negative impact of this process. Not only proper management, but also the creation of new, ever larger objects that are a refuge of biodiversity, can help maintain the homeostasis of endangered ecosystems.

It is suggested to continue, increase the number and refine research into the impact of fragmentation on biodiversity in order to better understand this phenomenon and its effects on the landscape and other elements of the environment. It would be necessary to introduce broader statistical analyzes of biodiversity indicators using, for example, the Shannon and Simpson index for comprehensive research and inference. It should be emphasized that in landscape studies, it is necessary to use geographical information systems (GIS) as a spatial analysis tool to understand and explain the impact of fragmentation on biodiversity.

REFERENCES

- [1] Aavik, T., Lira, J. (2010): Quantifying the effect of organic farming, field boundary type and landscape structure on the vegetation of field boundaries – *Agric. Ecosyst. Environ.* 135: 178-186.
- [2] Allan, E., Manning, P., Alt, F., Binkenstein, J., Blaser, S., Bluthgen, N., Bohm, S., Grassein, F., Holzel, L., Klaus, V. H., Kleinbecker, T., Morris, E. K., Oelmann, Y., Prati, D., Renner, S. C., Rillig, M. S., Schaefer, M., Schloter, M., Schmitt, B., Schoning I., Schrupf M., Solly E., Soraku E., Steckel J., Steffen-Dewenter I., Stempfhuber, B., Tschapka, M., Weiner, C. N., Weisser, W. W., Werner, M., Westphal, C., Wilcke, W., Fischer, M. (2015): Land use intensification alters ecosystem multifunctionality via loss of biodiversity and changes to functional composition – *Ecol. Lett.* 18: 834-843.
- [3] Bennet, A. F., Saunders, D. A. (2011): Habitat fragmentation and landscape change. – In: Sodhi, N.S., Ehrlich, P.R. (eds.) *Conservation biology for all.* Oxford University Press, Oxford: 88-106.
- [4] Bosiacka, B., and Pieńkowski, P. (2004): Analysis of pond transformations and evaluation of the natural values of midfield water bodies in central part of the Nowogard plain – *Woda-Środowisko-Obszary wiejskie* 4(2a): 335-349. (In Polish)
- [5] Bosiacka, B., Pieńkowski, P. (2012): Do biogeographic parameters matter? Plant species richness and distribution of in relations to area and isolation of ponds in NW Polish agricultural landscape – *Hydrobiologia* 689: 79-90.
- [6] Bratli, H., Økland, T., Økland, R. H., Dramstad, W. E., Elven, R., Engan, G., Fjellstad, W., Heegaard, E., Pedersen, O., Solstad, H. (2006): Patterns of variation in vascular plant species richness and composition in SE Norwegian agricultural landscapes – *Agric. Ecosyst. Environ.* 114: 207-286.
- [7] Bruun, H. H. (2000a): Patterns of species richness in dry grassland patches in an agricultural landscape – *Ecography* 23: 641-650.
- [8] Bruun, H. H. (2000b): Deficit in community species richness as explained by area and isolation of sites – *Divers. Distrib.* 6: 129-135.
- [9] Buffa G., del Vecchio, S., Fantinato, E., Milano, V. (2018): Local versus landscape-scale effects of anthropogenic land-use on forest species richness – *Acta Oecol.* 86: 49-56.
- [10] Cangolo, L., Cabido, M., Valladares, G. (2006): Plant species richness in the Chaco Serrano Woodland from central Argentina: Ecological traits and habitat fragmentation effects – *Biol. Conserv.* 132(4): 510-519.
- [11] Carrara, E., Arroyo-Rodríguez, V., Vega-Rivera, J. H., Schondube J.E., de Freitas S.M., Fahrig L. (2015): Impact of landscape composition and configuration on forest specialist and generalist bird species in the fragmented Lacandona rainforest, Mexico – *Biol. Conserv.* 184: 117-126.
- [12] Chmielewski, T. J., Myga-Piątek, U., Solon, J. (2015): Typology of Poland's current landscapes – *Przegląd Geograficzny* 87(3): 377-408. (In Polish)
- [13] Collins, C. D., Holt, R. D., Foster, B. L. (2009): Patch size effects on plant species decline in an experimentally fragmented landscape – *Ecology* 90(9): 2577-2588.
- [14] Conradi, T., Kollmann, J. (2016): Species pools and environmental sorting control different aspects of plant diversity and functional trait composition in recovering grasslands – *J. Ecol.* 104: 1314-1325.
- [15] Cook, W. M., Lane, K. T., Foster, B. L., Holt, R. D. (2002): Island theory, matrix effects and species richness patterns in habitat fragments – *Ecol. Lett.* 5: 619-623.
- [16] Cousins, S. A. O. (2006): Plant species richness in midfield islets and road verges – the effect of landscape fragmentation – *Biol. Conserv.* 127: 500-509.
- [17] Cousins, S. A. O., Ohlson H., Eriksson, O. (2007): Effects of historical and present fragmentation on plant species diversity in semi-natural grasslands in Swedish rural landscapes – *Landscape Ecol.* 22: 723-730.

- [18] Dauber, J., Bengtsson, J., Lenoir, L. (2006): Evaluating effects of habitat loss and land-use continuity on ant species richness in seminatural grassland remnants. –*Conserv. Biol.* 20(4): 1150-1160.
- [19] De Sanctis, M., Alfo, M., Attorre, F., Francesconi, F., Bruno, F. (2010): Effects of habitat configuration and quality on species richness and distribution in fragmented forest patches near Rome – *J. Veg. Sci.* 21: 55-65.
- [20] Debinski, D. M. (2006): Forest fragmentation and matrix effects: the matrix *does* matter – *J. Biogeogr.* 33: 1791-1792.
- [21] Debinski, D. M., Holt, R. D. (1999): A survey and overview of habitat fragmentation experiments – *Conserv. Biol.* 14(2): 342-343.
- [22] Degórski, M. (2015): Polityka krajobrazowa w Polsce: wyzwania i szanse – *Problemy Ekologii Krajobrazu* 60: 13 – 25. (In Polish).
- [23] DeLong, D. C. (1996): Defining biodiversity – *Wildlife Soc. B.* 24(4): 738.
- [24] Dumortier, M., Butaye, J., Jacquemyn, H., Camp, van N., Lust, N., Hermy, M. (2002): Predicting vascular plants species richness of fragmented forests in agricultural landscapes in central Belgium – *Forest. Ecol. Manag.* 158: 85-102.
- [25] Engler, R., Guisan, A. (2009): MigClim: Predicting plant distribution and dispersal in a changing climate – *Divers. Distrib.* 15: 590-601.
- [26] Eriksson, O., Cousins, S. A. O., Bruun, H. H. (2002): Land-use history and fragmentation of traditionally managed grassland in Scandinavia – *J. Veg. Sci.* 13: 743-748.
- [27] Ewers, R. M., Didham, R. K. (2006): Confounding factors in the detection of species responses to habitat fragmentation – *Biol. Rev.* 81: 117-142.
- [28] Fardila, D., Kelly, L. T., Moore, J. L., McCarthy, M. A. (2017): A systematic review reveals changes in where and how we have studied habitat loss and fragmentation over 20 years – *Biol. Conserv.* 212: 130-138.
- [29] Ferretti, M., Bussotti, F., Campitella, G., Canullo, R., Chiarucci, A., Fabbio, G., Petriccione, B. (2006): Biodiversity – its assessment and importance in the Italian programme for the intensive monitoring of forest ecosystems CONECOFOR. – *Ann. Ist. Sper. Selv.* 30(2): 3-16.
- [30] Fischer, J., Lindenmayer, D. B. (2007): Landscape modification and habitat fragmentation: a synthesis – *Global Ecol. Biogeogr.* 16: 265-280.
- [31] Forman, R. T., Gordon, M. (1981): Patches and structural components for a landscape ecology. – *Bioscience* 31: 733-740.
- [32] Fuentes-Montemayor, E., Goulson, D., Cavin, L., Wallace, J. M., Park, K. J. (2013): Fragmented woodlands in agricultural landscapes: The influence of woodland character and landscape context on bats and their insect prey – *Agr. Ecosyst. Environ.* 172: 6-15.
- [33] Gamrat, R., Gałczyńska, M., Kupiec, M. (2017): Diversity of environmental islands in the agricultural landscape of Nowogard and Goleniowska Plains – *Prace Komisji Krajobrazu Kulturowego* 35: 29-42. (In Polish)
- [34] Gazol, A., Tammé, R., Takkis, K., Kasari, L., Saar, L., Helm, A., Pärtel, M. (2012): Landscape and small-scale determinants of grassland species diversity: direct and indirect influences – *Ecography* 35: 944-951.
- [35] Gotelli, N. J., Chao, A. (2013): Measuring and estimating species richness, species diversity, and biotic similarity from sampling data. – In: Levin, S. (ed.) *Encyclopedia of Biodiversity*. Academic Press, Waltham: 195-211.
- [36] Graae, B. J. (2000): The effect of landscape fragmentation and forest continuity on forest floor species in two regions of Denmark – *J. Veg. Sci.* 11: 881-892.
- [37] Grashof-Bokdam, C. (1997): Forest species in agricultural landscape in the Netherlands: Effect of habitat fragmentation – *J. Veg. Sci.* 8: 21-28.
- [38] Habel, J. C., Dengler, J., Janišova, M., Török, P., Wellstein, C., Wiezik, M. (2013): European grassland ecosystems: threatened hotspots of biodiversity – *Biodivers. Conserv.* 22: 2131-2138.

- [39] Haig, A. R., Matthes, U., Larson, D. W. (2000): Effects of natural habitat fragmentation on the species richness, diversity, and composition of cliff vegetation – *Can. J. Botany*. 78(6): 786-797.
- [40] Hamre, L. N., Halvorsen, R., Edvardsen, A., Rydgren, K. (2010): Plant species richness, composition and habitat specificity in a Norwegian agricultural landscape. – *Agric. Ecosyst. Environ.* 138: 189-196.
- [41] Hanski, I. (2005): Landscape fragmentation, biodiversity loss and the societal response. – *EMBO Rep.* 6(5): 388-392.
- [42] Heinken, T., Weber, E. (2013): Consequences of habitat fragmentation for plant species: Do we know enough? – *Perspect. Plant Ecol.* 15: 205-216.
- [43] Helm, A., Hanski, I., Pärtel, M. (2006): Slow response of plant species richness to habitat loss and fragmentation – *Ecol. Lett.* 9: 72-77.
- [44] Hérault, B., Honnay, O. (2005): The relative importance of local, regional and historical factors determining the distribution of plants in fragmented riverine forests: an emergent group approach – *J. Biogeogr.* 32: 2069-2081.
- [45] Honnay, O., Hermy, M., Coppin, P. (1999): Effects of area, age and diversity of forest patches in Belgium on plant species richness, and implications for conservation and reforestation – *Biol. Conserv.* 87: 73-84.
- [46] Huber, S., Huber, B., Stahl, S., Schmid, C., Reisch, C. (2017): Species diversity of remnant calcareous grasslands in south eastern Germany depends on litter cover and landscape structure – *Acta Oecol.* 83: 48-55.
- [47] Ibáñez, I., Katz, D. S., Peltier, D., Wolf, S. M., Connor Barrie, B. T. (2014): Assessing the integrated effects of landscape fragmentation on plants and plant communities: the challenge of multiprocess–multiresponse dynamics – *J. Ecol.* 102: 882-895.
- [48] Iida, S., Nakashizuka, T. (1995): Forest fragmentation and its effect on species diversity in sub-urban coppice forests in Japan – *Forest Ecol. Manag.* 73: 197-210.
- [49] Irvine, K. N., Devine-Wright, P., Payne, S. R., Fuller, R. A., Painter, B., Gaston, K. J. (2009): Green space, soundscape and urban sustainability: an interdisciplinary, empirical study – *Local Environment*. 14(2): 155-172.
- [50] Jacquemyn, H., Butaye, J., Hermy, M. (2001): Forest plant species richness in small, fragmented mixed deciduous forest patches: the role of area, time and dispersal limitation – *J. Biogeogr.* 28: 801-812.
- [51] Johansson, L. J., Hall, K., Prentice, H. C., Ihse, M., Reitalu, T., Sykes, M. T., Kindstrom, M. (2008): Semi-natural grassland continuity, long-term land-use change and plant species richness in an agricultural landscape on Oland, Sweden – *Landscape Urban. Plan.* 84: 200-211.
- [52] Karger, D. N., Weigelt, P., Amoroso, V. B., Darnaedi, D., Hidayat, A., Kreft, H., Kessler, M. (2014): Island biogeography from regional to local scales: evidence for a spatially scaled echo pattern of fern diversity in the Southeast Asian archipelago – *J. Biogeogr.* 41: 250-260.
- [53] Kattan, G. H., Murcia, C. (2003): A review and synthesis of conceptual frameworks for the study of forest fragmentation – *Ecol. Stud.* 162: 183-200.
- [54] Keshtkar, H., Voigt, W. (2016): Potential impacts of climate and landscape fragmentation changes on plant distributions: Coupling multi-temporal satellite imagery with GIS-based cellular automata model – *Ecol. Inform.* 32: 145-155.
- [55] Kolb, A., Diekmann, M. (2004): Effects of environment, habitat configuration and forest continuity on the distribution of forest plant species – *J. Veg. Sci.* 15: 199-208.
- [56] Kolb, A., Diekmann, M. (2005): Effects of life-history traits on responses of plant species to forest fragmentation – *Conserv. Biol.* 19(3): 929-938.
- [57] Koszelnik-Leszek, A., Podlaska, M., Fudali, E., Tomaszewska, K. (2015): Diversity of the midfield forest island's flora in the rural landscape of the south-western Poland in relation to sociological-ecological groups – *Scientific Papers of the University of Life Sciences in Wrocław. Agriculture* 612: 29-55. (In Polish)

- [58] Krauss, J., Klein, A.-M., Stefan-Dewenter, I., Tschardtke, T. (2004): Effects of habitat area, isolation, and landscape diversity on plant species richness of calcareous grasslands – *Biodivers. Conserv.* 13: 1427-1439.
- [59] Krausmann, F., Haberl, H., Schulz, N. B., Erb, K. H., Darge, E., Gaube, V. (2003): Land-use change and socio-economic metabolism in Austria. I: Driving forces of land-use change: 1950–1995 – *Land Use Policy* 20(1): 1-20.
- [60] Kuussaari, M., Bommarco, R., Heikkinen, R. K., Helm, A., Krauss, J., Lindborg, R., Öckinger, E., Pärtel, M., Pino, J., Roda, F., Stefanescu, C., Teder, T., Zobel, M., Steffan-Dewenter, I. (2009): Extinction debt: a challenge for biodiversity conservation – *Trends Ecol. Evol.* 24(10): 564-571.
- [61] Lindborg, R., Plue, J., Andersson, K., Cousins, S. A. O. (2014): Function of small habitat elements for enhancing plant diversity in different agricultural landscapes – *Biol. Conserv.* 169: 206-213.
- [62] Lindenmayer, D. B., Fischer, J. (2006): Tackling the habitat fragmentation panchreston – *Trends Ecol. Evol.* 22(3): 127-132.
- [63] Löffler, F., Fartmann, T. (2017): Effects of landscape and habitat quality on *Orthoptera* assemblages of prealpine calcareous grasslands – *Agric. Ecosyst. Environ.* 248: 71-81.
- [64] Lomba, A., Vaz, A. S., Moreira, F., Honrado, J. P. (2013): Hierarchic species-area relationships and the management of forest habitat islands in intensive farmland – *Forest Ecol. Manag.* 291: 190-198.
- [65] Lomba, A., Vicente, J., Moreira, F., Honrado, J. (2011): Effects of multiple factors on plant diversity of forest fragments in intensive farmland of Northern Portugal – *Forest Ecol. Manag.* 262: 2219-2228.
- [66] Longatti, P., Dalang, T. (2007): The meaning of “landscape” – an exegesis of swiss government texts. – In: Kienast, F., Wildi, O., Ghosh, S. (eds.) *A Changing World. Challenges for Landscape Research*: 35-46.
- [67] Luo, T., Zhang, T., Wang, Z., Gan, Y. (2015): Driving Forces of Landscape Fragmentation due to Urban Transportation Networks: Lessons from Fujian, China – *J. Urban Plann. Dev.* 142(2): 04015013 1- 04015013 13.
- [68] Luoto, M., Rekolainen, S., Aakkula, J., Pykala, J. (2003): Loss of plant species richness and habitat connectivity in grassland associated with agricultural change in Finland – *Ambio* 32(7): 447-452.
- [69] Löbel, S., Dengler, J., Hobohm, C. (2006): Species richness of vascular plants, bryophytes and lichens in dry grasslands: the effects of environment, landscape structure and competition – *Folia Geobot.* 41: 377-393.
- [70] MacArthur, R., Wilson, E. O. (1967): *The theory of island biogeography.* –Princeton University Press, Princeton 203.
- [71] Mathias, Ö., Cousins, S. A. O., Eriksson, O. (2007): Size and heterogeneity rather than landscape context determine plant species richness in semi-natural grasslands – *J. Veg. Sci.* 18: 859-868.
- [72] Montis, de A., Martín, B., Ortega, E., Ledda, A., Serra, V. (2017): Landscape fragmentation in Mediterranean Europe: a comparative approach. –*Land Use Policy* 64: 83-94.
- [73] Mortelliti, A., Amori, G., Boitani, L. (2010): The role of habitat quality in fragmented landscapes: a conceptual overview and prospectus for future research. – *Oecologia* 163: 537-547.
- [74] Öckinger, E., Lindborg, R., Sjödin, N. E., Bommarco, R. (2012): Landscape matrix modifies richness of plants and insects in grassland fragments – *Ecography* 35: 259-267.
- [75] Økland, R. H., Bratli, H., Dramstad, W. E., Edvardsen, A., Engan, G., Fjellstad, W., Heegaard, E., Pedersen, O., Solstad, H. (2006): Scale-dependent importance of environment, land use and landscape structure for species richness and composition of SE Norwegian modern agricultural landscapes – *Landscape Ecol.* 21: 969-987.

- [76] Opdam, P., Wascher, D. (2004): Climate change meets habitat fragmentation: linking landscape and biogeographical scale levels in research and conservation – *Biol. Conserv.* 117(3): 285-297.
- [77] Orłowski, G., Nowak, L. (2005): Species composition of woody vegetation of three types of mid-field woodlots in intensively managed farmland (Wrocław plains, South-Western Poland) – *Pol. J. Ecol.* 53(1): 25-36.
- [78] Petit, S., Griffiths, L., Smart, S. S., Smith, G. M., Stuart, R. C., Wright, S. M. (2004): Effects of area and isolation of woodland patches on herbaceous plant species richness across Great Britain – *Landscape Ecol.* 19: 463-471.
- [79] Pieńkowski, P., Podlasiński, M. (2017): Dominating forms of land covers regards to physical geographical division regions of Poland – *Prace Komisji Krajobrazu Kulturowego* 37: 105-116. (In Polish)
- [80] Piessens, K., Honnay, O., Hermy, M. (2005): The role of fragment area and isolation in the conservation of heathland species – *Biol. Conserv.* 122: 61-69.
- [81] Prach, K., Fajmon, K., Jongepierova, I., Rehounkova, K. (2015): Landscape context in colonization of restored dry grasslands by target species – *Appl. Veg. Sci.* 18: 181-189.
- [82] Qi, K., Fan, Z., Ng, C. N., Wang, X., Xie, Y. (2017): Functional analysis of landscape connectivity at the landscape, component, and patch levels: A case study of Minqing County, Fuzhou City, China – *Appl. Geogr.* 80: 64-77.
- [83] Quine, C.P., Watts, K. (2009): Successful de-fragmentation of woodland by planting in an agricultural landscape? An assessment based on landscape indicators – *J. Environ. Manage.* 90(1): 251-259.
- [84] Raatikainen, K. M., Heikkinen, R. K., Luoto, M. (2009): Relative importance of habitat area, connectivity, management and local factors for vascular plants: spring ephemerals in boreal semi-natural grasslands – *Biodivers. Conserv.* 18: 1067-1085.
- [85] Reitalu, T., Sykes, M. T., Johansson, L. J., Lonn, M., Hall, K., Vandewalle, M., Prentice, H. C. (2009): Small-scale plant species richness and evenness in semi-natural grasslands respond differently to habitat fragmentation – *Biol. Conserv.* 142: 899-908.
- [86] Richling, A., Solon, J. (2011): *Ekologia krajobrazu* – Wyd. Nauk. PWN. Warszawa: 464. (In Polish)
- [87] Ricketts, T. H. (2001): The matrix matters: effective isolation in fragmented landscapes – *Am. Nat.* 158(1): 87-99.
- [88] Shannon, C. E. (1948): A mathematical theory of communication – *The Bell System Technical Journal* 27.
- [89] Sienkiewicz, J. (2010): Concepts of biodiversity – their dimensions and measures in the light of literature – *Ochr. Śr. i Zasobów Nat.* 45: 7-29. (In Polish)
- [90] Simpson, E. H. (1949): Measurement of Diversity – *Nature* 163
- [91] Solon, J., Chmielewski, T., Myga - Piątek, U., Kistowski, M. (2015): Identification and assessment of Polish landscapes - stages and methods of actions within the landscape audit in the administrative regions – *Problemy ekologii krajobrazu* 60: 55-76. (In Polish)
- [92] Taylor, P. D., Fahrig, L., Henein, K., Merriam, G. (1993): Connectivity is a vital element of landscape structure – *Oikos* 68(3): 571-572.
- [93] Tessel, S. M., Palmquist, K. A., Peet, R. K. (2016): Species-Area Relationships. (<http://www.oxfordbibliographies.com/view/document/obo-9780199830060/obo-9780199830060-0147.xml> / accessed on 01.10.2018)
- [94] Tschardtke, T., Klein, A. M., Kruess, A., Dewenter, I. S., Thies, C. (2005): Landscape perspectives on agricultural intensification and biodiversity – ecosystem service management – *Ecol. Lett.* 8: 857-874.
- [95] Vallet, J., Beaujouan, V., Pithon, J., Rozé, F., Daniel, H. (2010): The effects of urban or rural landscape context and distance from the edge on native woodland plant communities – *Biodivers. Conserv.* 19: 3375-3392.
- [96] Vellend, M., Verheyen, K., Flinn, K. M., Jacquemyn, H., Kolb A., van Calster, H., Peterken, G., Graae, B. J., Bellemare, J., Honnay, O., Brunet, J., Wulf, M., Gerhard, F.,

- Hermy, M. (2007): Homogenization of forest plant communities and weakening of species–environment relationships via agricultural land use – *J. Ecol.* 95: 565-573.
- [97] Verheyen, K., Vellend, M., von Calster, H., Peterken, G., Hermy, M. (2004): Metapopulation dynamics in changing landscapes: a new spatially realistic model for forest plants – *Ecology* 85(12): 3302-3312.
- [98] Vieira, M. V., Olifiers, N., Delciellos, A. C., Antunes, V. Z., Bernardo, L. R., Grelle, C. E. V., Cerqueira, R. (2009): Land use vs. fragment size and isolation as determinants of small mammal composition and richness in Atlantic Forest remnants – *Biol. Conserv.* 142: 1191-1200.
- [99] Waldén, E., Öckinger, E., Winsa, M., Lindborg, R. (2017): Effects of landscape composition, species pool and time on grassland specialists in restored semi-natural grasslands – *Biol. Conserv.* 214: 176-183.
- [100] Watling, J. I., Donnelly, M. A. (2008): Species richness and composition of amphibians and reptiles in a fragmented forest landscape in northeastern Bolivia – *Basic Appl. Ecol.* 9: 523-532.
- [101] Whittaker, R. H. (1972): Evolution and measurement of species diversity – *Taxon* 21(2/3): 213.
- [102] Wiedmann, F., Salama, A. M., Thierstein, A. (2012): Urban evolution of the city of Doha: an investigation into the impact of economic transformations on urban structures – *J. Fac. Arch.* 29(2): 35-61.
- [103] Wiens, J. A. (1995): Habitat fragmentation – island vs landscape perspectives on bird conservation – *Ibis* 137: S97-S104.
- [104] Williams, P., Whitfield, M., Biggs, J., Bray, S., Fox, G., Nicolet, P., Sear, D. (2004): Comparative biodiversity of rivers, streams, ditches and ponds in an agricultural landscape in Southern England – *Biol. Conserv.* 115(2): 329-341.
- [105] Zarzycki, J. (2009): Methodological and technical innovation in phytosociological research – *Łąkarstwo w Polsce* 12: 233-247. (In Polish)
- [106] Zulka, K. P., Abensperg-Traun, M., Milasowszky, N., Bieringer, G., Gereben-Krenn, B. A., Holzinger, G., Rabitsch, W., Reischütz, A., Querner, P., Sauberer, N., Schmitzberger, I., Willner, W., Wrška, T., Zechmeister, H. (2014): Species richness in dry grassland patches of eastern Austria: A multi-taxon study on the role of local, landscape and habitat quality variables. – *Agr. Ecosyst. Environ.* 182: 25-36.

APPENDIX**Appendix 1. Juxtaposition of studied area and research methods across different habitat types by various authors. n/i – no information**

Study area				Source of data	Variables involved in research affecting species richness	Data analysis	References
Location	Studied area [ha] 1) landscape 2) patch 3) transect 4) plots/sample	Type of landscape (matrix)	Type/ No of patches				
Austria: Panonian part of eastern Austria	1) n/i 2) 0,05-10,0 3) n/i 4) n/i	agricultural	dry grassland/ 50	field study	size and shape measures, local quality measures, area of extensively used elements, area of linear elements, distance to mainland, area of extensive grassland, area of fallow land, area of short-grass dry grassland, area of short-grass linear elements, landscape heterogeneity	1) GIS, 2) statistical calculations, 3) species richness: No of species	Zulka et al., 2014
Belgium: Flanders, (western part of Belgium and northern part of France)	1) n/i 2) 0,5-5216 3) n/i 4) n/i	agricultural	forest/ 234	field study	area, shape, soli, slope, percentage of ancient and recent forest, isolation, distance to the nearest neighbour	1) GIS, 2) statistical calculations, 3) species richness: No of species	Honnay et al., 1999
Belgium: Vlaams-Brabant	1) 4200 ha 2) n/i 3) n/i 4) n/i	agricultural	forest/ 241	field study	forest age, land use history, age patches, forest area	1) GIS, 2) statistical calculations, 3) species richness: No of species	Jacquemyn et al., 2001
Belgium: Glabbeek	1) n/i 2) 0,1-11,4 3) n/i 4) n/i	agricultural	forest/ 241	field study	pasture exploitation, field exploitation, topographical diversity, isolation, structural diversity, habitat diversity, soil acidity, organic matter, nitrogen of soil, plant available phosphorus, C/N ratio of soil	1) GIS, 2) statistical calculations, 3) species richness: No of species	Dumortier et al., 2002
Belgium: Northwestern part of	1) 70000 ha 2) n/i 3) n/i	agricultural	heathland/ 153	field study	seed longevity index, mean plant height, seed mass, dispersal mode, growth form, self compatibility,	1) GIS, 2) statistical calculations, 3) species richness: No of	Piessens et al., 2005

Flanders, in an area south of Bruges	4) n/i				vegetative spread, seed numer, isolation, light, soil moisture, pH and soil nutrient status, Ellenberg indicators	species	
Denmark: Island Sjaelland	1) ca 40000 ha 2) n/i 3) n/i 4) n/i	agricultural	grassland/ 85	field study	area, isolation, distance to the nearest neighbour, soil pH, potential solar radiation, anlg of slope, seed mass, dispersal structure	1) GIS, 2) statistical calculations, 3) species richness: No of species	Brunn, 2000a
Denmark: Island Sjaelland	1) ca 40000 ha 2) n/i 3) n/i 4) n/i	agricultural	grassland/ 85	field study	area, isolation, distance to the nearest neighbour, soil pH, potential solar radiation, inclination of slope	1) GIS, 2) statistical calculations, 3) species richness: No of species	Brunn, 2000b
Denmark: (i) Hornsherred on Zealand and (ii) Hmmerland in Jutland	1) (i) 48200 (ii) 102900 2) 1-8000 3) n/i 4) n/i	agricultural	forest/ 82	field study	isolation, forest continuity, soli pH, tree species composition and seed dispersal groups, quantity	1) GIS, 2) statistical calculations, 3) species richness: No of species	Graae, 2000
Estonia: Saaremaa, Muhu	1) n/i 2) 1,0-340,0 3) n/i 4) n/i	agricultural	alvar grassland patches, 35	field study	past area, past connectivity, current area, current connectivity	1) GIS, 2) statistical calculations, 3) species richness: No of species	Helm et al., 2006
Estonia: Islands of Saaremaa and Muhu	1) n/i 2) n/i 3) 33 transects: 10x01 m 4) n/i	agricultural	grassland/ 33	field study	soil depth, pH, temperature, moisture and electrical conductivity, relative light availability, shrub cover, historical habitat area connectivity and availability	1) GIS, 2) statistical calculations, 3) species richness: No of species	Gazol et al., 2012
Finland: the Rekijoki river valley	1) n/i 2) <5 ÷ >40 3) n/i 4) n/i	agricultural	grassland/ n/i	field study	patch area, connectivity, solar radiation	1) GIS, 2) statistical calculations, 3) species richness: No of species	Raatikaine n et al., 2009
Finalnd: Somero	1) 10000 ha 2) n/i 3) n/i 4) n/i	agricultural	grassland patches/ 289	field study	habitat connectivity, grazing	1) GIS, 2) statistical calculations, 3) species richness: No of species	Luoto et al., 2003
France: Angers, Nantes	1) n/i 2) ca 1,5 3) n/i	urban/rural	forest/ 10 [5 agr.; 5 urban]	field study	edge effect, distance from the edge and urban–rural context, vegetation structure, light and soil pH, total	1) -, 2) statistical calculations, 3) species richness: No of	Vallet et al., 2010

	4) n/i				species richness, number of forest specialists, forest generalists and non-forest species; Ellenberg	species	
Germany: Northwestern part of the country	1) 36500 ha 2) n/i 3) n/i 4) n/i	agricultural	forest/ 145	field study; check list	abundance of each species, topographic heterogeneity, soil, habitat quality, configuration (area, isolation/buffer, isolation/distance) and continuity	1) GIS, 2) statistical calculations, 3) species richness: No of species	Kolb and Diekmann, 2004
Germany: Göttingen	1) n/i 2) 0,03-5,14 3) n/i 4) n/i	agricultural	calcerous grassland/ 31	field study	area, isolation, landscape diversity	1) -, 2) statistical calculations, 3) species richness: No of species	Krauss et al., 2004
Germany: Southeastern part of the country	1) (i) 2500 (ii) 1000 2) n/i 3) n/i 4) 10 plots: 2x2 m	agricultural	calcerous grasslands/ 18	field study	fragment area, area/perimeter ratio, distance to the nearest calcareous grassland, loss of calcareous grassland, vegetation height (VH), cover of grass (CG), litter (CL), bare soil (BS)	1) GIS, 2) statistical calculations, 3) species richness: No of species	Huber et al., 2017
Germany: Northwestern part of the country	1) 36500 ha 2) >1ha 3) n/i 4) n/i	agricultural	forest/ 145	field study	diaspore mass, seed-bank longevity, dispersal structure, pollination mode, plant height, life span, habitat preference, connectivity, area	1) GIS, 2) statistical analysis, 3) species richness: No of species	Kolb and Diekmann, 2005
Great Britain: (i) uplands, (ii) lowlands	1) n/i 2) mean: (i) 3,1 (ii) 6,8 3) n/i 4) n/i	agricultural	forest/ 308	list of the 120 British Ancient Woodland Indicator species; field study	patch area, shape, isolation, the length of hedgerows and lines of trees in the 1 km square and the area of woodland within 500 m of the vegetation plot, Ellenberg indicator values (pH, light, fertility)	1) GIS, 2) statistical calculations, 3) species richness: No of species	Petit et al., 2004
Great Britain: central Lincolnshire	1) 93000 ha 2) n/i 3) n/i 4) n/i	agricultural	forest/ 326	The Lincolnshire data set (155 species and 326 patches)	life history traits (diaspore production, age of first reproduction, and dispersal mode), presence/absence of age, connectivity, area effects, colonization-extinction rates, diaspore production, age of first reproduction; Ellenberg indicator values	1) -, 2) statistical calculations, 3) species richness: No of species	Verheyen et al., 2004

Italy: Veneto Region	1) n/i 2) 0,08-350 3) n/i 4) 80 plots: 8x8m	urban/ industrial, agricultural	80 georeference d plots.; forest/ 59	field study	human disturbance: 'local scale' and 'landscape scale', distance from the forest edge, size and shape of the patch	1) GIS, 2) statistical calculations, 3) species richness: No of species	Buffa et. al., 2018
Italy: Rome	1) n/i 2) 4,0-37,0 3) n/i 4) n/i	agricultural	forest/ 211	field study	shape, isolation, forest age, habitat quality (chemical properties of the soil, number of additional habitats, forest structure), grazing, surrounding arable land	1) GIS, 2) statistical calculations, 3) species richness: vertical evenness index, Shannon formula	De Sanctis et al., 2010
Luxembourg	1) n/i 2) 0,5-1,22 3) n/i 4) n/i	agricultural	riverine forest/ 153	field study	forest age, depth of the reductive layer, litter thickness, soil productivity (Ellenberg values), soil pH, connectivity, age at first flowering, clonal propagation, dispersal type, germination requirement, life-forms, onset of flowering, mean shoot height, pollination vector, potential mycorrhiza, seed longevity, seed weight, seed production, size and shape	1) GIS, 2) statistical calculations, 3) species richness: No of species	Hérault and Honnay, 2005
Netherlands: Province of Drenthe	1) n/i 2) 0,04-770,9 3) n/i 4) n/i	agricultural	forest/ 312	species data obtained from survey carried out by the Provincial Governme nt of Drenthe	patch area, connectivity, isolation, parameters of soli type and groundwater level	1) GIS, 2) statistical calculations, 3) species richness: No of species	Grashof- Bokdam, 1997
Norway: (i) Vestfold, Østfold, (ii) Akershus, Hedmark and (iii) Oppland	1) n/i 2) mean (i) 0,1972 (ii) 0,0109 (iii) 2,h 3) n/i	agricultural	(i) seminatural/ 160; (ii) midfield islets/ 144; (iii) forest	field study	geographical, area, perimeter, shape index, habitat diversity, land-use, human impact, Ellenberg indicators	1) GIS, 2) statistical calculations, 3) species richness: No of species	Bratli et al., 2006

	4) n/i		245				
Norway: Southeastern part of the country	1) n/i 2) n/i 3) n/i 4) 43 plots: 1,0 ha each	agricultural	grassland/ 282 midfield islets, 144 road verges, 238 forest patches, 254 ponds, 9	field study	area, shape index, landscape heterogeneity, habitat diversity, ecological factors (Ellenberg values: light, moisture, reaction, nitrogen), land-use intensity	1) GIS - ArcView, 2) statistical calculations, 3) species richness: No of species	Økland et al., 2006
Norway: Ornes in Lustrafjorden	1) n/i 2) mean: 0,75 3) n/i 4) n/i	agricultural	semi-natural grassland/ 20; midfield islets/ 18; forest/ 21	field study	patch area, patch perimeter, shape index, canopy height, tree layer cover, shrub layer cover, average Ellenberg moisture, long-term management intensity, agricultural use, presence of wire, presence of boulders, continuity	1) GIS, 2) statistical calculations, 3) species richness: gamma diveristy	Hamre et al., 2010
Poland: Nowogard plains	1) n/i 2) 0,01-1,0 3) n/i 4) n/i	agricultural	ponds/ 53	field study	matrix	1) GIS, 2) -, 3) species richness: No of species	Bosiacka and Pieńkowski , 2004
Poland: Southwestern part of the country	1) n/i 2) 0,03-15,08 3) n/i 4) n/i	agricultural	forest/ 74	field study	area, dispersal mode, origin of the species (native/exotic),	1) GIS, 2) statistical calculations, 3) species richness: No of species	Orłowski and Nowak 2005
Poland: the Szczecin Hills	1) n/i 2) 0,01-1,2 3) n/i 4) n/i	agricultural	ponds/ 50	field study	pond size, isolation, species richness	1) GIS, 2) statistical calculations, 3) species richness: No of species	Bosiacka and Pieńkowski , 2012
Poland: Southwestern part of the country	1) n/i 2) 0,07-15,8 3) n/i 4) n/i	agricultural	forest/ 23	field study	area, shape, matrix	1) -, 2) -, 3) species richness: No of species	Koszelnik- Leszek et al., 2015
Poland: (i) Nowogard and (ii) Goleniów plains	1) (i) 900 (ii) 900 2) n/i 3) n/i 4) n/i	agricultural	ponds/ 13; grasslands/ 4; roadside verges/ 16	field study	habitat quality, neighbourhood (matrix)	1) GIS, 2) -, 3) species richness: No of species	Gamrat et al., 2017
Portugal:	1) n/i	agricultural	forest/ 50	field study	forest type (dominated by pines,	1) GIS,	Lomba et

Metropolitan Area of Porto	2) 0,3-3,0 3) n/i 4) n/i				eucalypts, or both) , patch area, patch shape, diameter at breast height, tree density per hectare, percentage cover of vegetation strata, forest naturalness	2) statistical calculations, 3) species richness: No of species	al., 2011
Portugal: Metropolitan Area of Porto	1) n/i 2) 0,3-3,0 3) n/i 4) n/i	agricultural	forest/ 50	field study	forest type (dominated by pines, eucalypts, or both), area, impact of forest naturalness on species–area relationships	1) GIS, 2) statistical calculations, 3) species richness: No of species	Lomba et al., 2013
Sweden: (i) Island of Selaon (ii) Island of Nynas	1) (i) 2500 (ii) 1000 2) n/i 3) n/i 4) n/i	(i) modern rural, (ii) traditional rural	(i) road verges/ 40; midfield islets/ 176, (ii) road verges/ 40, midfield islets/ 53	field study	isolation, habitat area, past and present land use, landscape context	1) Geographical Information System (GIS), 2) statistical calculations, 3) species richness: number of species	Cousins, 2006
Sweden: Island of Oland	1) n/i 2) n/i 3) n/i 4) 452 sample plots: 2x2 m	agricultural	grassland/ 452 sample plots	field study	soil depth and pH, microtopography, cover of bare rock, cover of vegetation, grazing, mowing, isolation, edge-to-edge distance to the nearest different grassland patch and the connectivity index	1) GIS, 2) statistical calculations, 3) species richness: No of species	Löbel et al., 2006
Sweden: County of Sodermanland	1) n/i 2) 0,42-6,31 3) n/i 4) n/i	agricultural	semi-natural grassland/ 25	field study	area-effects, species density, isolation, patch connectivity, grazing	1) GIS, 2) statistical calculations, 3) species richness: No of species	Cousins et al., 2007
Sweden: Southern part of the country	1) n/i 2) 0,2-18,9 3) n/i 4) n/i	agricultural/ forest	grassland/ 30	field study	area, number of vegetation types, proportion of forest, linear elements, connectivity, historical connectivity	1) GIS, 2) statistical calculations, 3) species richness: No of species	Mathias et al., 2007
Sweden: Island of Oland	1) n/i 2) 0,13-39,91 3) n/i 4) n/i	agricultural	grassland/ 55	field study	grazing intensity, cover of shrubs and trees, the percentages of grassland/ forest/ arable land, geographic position of the vegetation plots: x (East) and y (North), their interaction term	1) GIS, 2) statistical calculations, 3) species richness: Shannon-Wiener index, Shannon evenness	Reitalu et al., 2009

Sweden: Island of Oland	1) n/i 2) n/i 3) n/i 4) 451 plots: 50x50cm	agricultural	grassland/ 98; 451 plots	field study	(East*North) past and present land-use/cover, total habitat area, mean patch size , maximum patch size, patch density, Euclidian nearest neighbour distance, continuity	1) GIS, 2) statistical calculations, 3) species richness: No of species	Johansson et al., 2008
Sweden: the counties of Östergötland and Uppland	1) n/i 2) 1,0-10,0 3) n/i 4) n/i	agricultural/m ixed/ forest	grassland/ 45	field study	patch area, isolation, matrix type	1) GIS, 2) statistical calculations, 3) species richness: No of species	Öckinger et al., 2012
Sweden: (i) Selaön, (ii) Öllösa (iii) Nynäs	1) n/i 2) mean area: (i) 0,0233 ha, (ii) 0,0187 ha, (iii) 0,0299 ha 3) n/i 4) n/i	(i) modern agricultural landscape; (ii) modern forested landscape; (iii) traditional landscape	semi-natural grassland: (i) 20, (ii) 20, (iii) 20; midfield islets: (i) 25, (ii) 25, (iii) 23; road verges: (i) 25, (ii) 22, (iii) 22	field study	canopy height, specific leaf area, seed production, lifespan, clonal propagation, dispersal model	1) GIS, 2) statistical calculations, 3) species richness: beta diversity	Lindborg et al., 2014

Appendix 2. Habitat loss and fragmentation papers by journal

Journal	Total	%Total
Journal of Vegetation Science	5	12.20
Biological Conservation	5	12.20
Agriculture, Ecosystems & Environment	3	7.32
Ecography	3	7.32
Biodiversity and Conservation	3	7.32
Forest Ecology and Management	3	7.32
Landscape Ecology	3	7.32
Acta Oecologica	2	4.88
Journal of Biogeography	2	4.88
A Journal of the Human Environment (AMBIO)	1	2.44
Ecology	1	2.44
Conservation Biology	1	2.44
Ecology Letters	1	2.44
Landscape and Urban Planning	1	2.44
Folia Geobotanica	1	2.44
Diversity and Distributions	1	2.44
Dissertations of Cultural Landscape Commission	1	2.44
Hydrobiologia	1	2.44
Polish Journal of Ecology	1	2.44
Water-Environment-Rural Areas	1	2.44
Scientific Papers of the University of Life Sciences in Wrocław. Agriculture	1	2.44

COMPARATIVE ANALYSIS ON RESPONSES OF VEGETATION PRODUCTIVITY RELATIVE TO DIFFERENT DROUGHT MONITOR PATTERNS IN KARST REGIONS OF SOUTHWESTERN CHINA

ZHOU, Y.¹ – ZHANG, R.^{1,2} – WANG, S. X.^{1*} – WANG, F. T.^{1*} – QI, Y.³

¹*Institute of Remote Sensing and Digital Earth, Chinese Academy of Sciences
Beijing 100101, China*

²*University of Chinese Academy of Sciences, Beijing 100049, China*

³*Gansu Key Laboratory of Arid Climatic Change and Reducing Disaster, Key Laboratory of Arid Climatic Change and Disaster Reduction of CMA, Institute of Arid Meteorology
China Meteorological Administration, Lanzhou 730020, China*

**Corresponding authors*

e-mail: wangsx@radi.ac.cn, wangft@radi.ac.cn

(Received 19th Sep 2018; accepted 22nd Nov 2018)

Abstract. The climate conditions are complex and diverse in Southwest China (SWC), especially the karst area, and the interaction between climate change and terrestrial ecosystems has become complex. Vegetation productivity is an important indicator in terrestrial ecosystems, and can visually reveal the impacts of extreme climate. Drought affects not only the process of photosynthesis directly, but also the changes in vegetation productivity from other forms of interference with photosynthesis. Against this background, we analyzed the time series and spatial distribution characteristics of drought, the temporal and spatial distribution and anomalies of vegetation productivity. For the observation period 2001–2012, we used different drought monitor patterns (including Pa, SPI, SPEI and PDSI) to assess the impact of drought on vegetation productivity (annual NPP and monthly GPP). We mainly want to explore the response of different monitor patterns to vegetation productivity at different stages. NPP exhibited considerable variation during 2001–2012; the droughts in 2009 and 2010 led to NPP reduction by 14.7% and 8.4%, respectively. The NPP is directly proportional to the severity of drought, severe drought had a greater impact on monthly GPP than mild drought, especially for evergreen forests, shrublands, and deciduous forests, while little variation was found for croplands. We compared drought indices-vegetation productivity during the drought season between 2009 and 2010; SPEI has a better correlation with SPI and PDSI. The results demonstrate that SPEI and PDSI are most capable of monitoring the vegetation drought conditions. There will be large differences of the influence on vegetation productivity on different drought levels. Our findings suggested that multi-indices in drought monitoring are needed in order to acquire robust conclusions.

Keywords: *remote sensing, sustainability, patterns, MODIS product, karst mountain area*

Introduction

The Intergovernmental Panel on Climate Change (IPCC) concluded that the climate has changed over the past century and the frequency and intensity of extreme climate events have become more frequent in recent years (Judi et al., 2018). Increase in the frequency and intensity of extreme climatic events (especially meteorological disasters) could have significant impact on vegetation ecosystems (Chen et al., 2012), resulting in lower crop yields, increased loss of forest biomass, higher disease and insect damage (Dai, 2011). Drought is a critical phenomenon of climatic change, and formation

mechanism is more complicated than floods (Dewes et al., 2017). Drought impacts ecosystem mortality, net primary productivity (NPP), gross primary productivity (GPP), and carbon storage worldwide (Zhang et al., 2012; Zhao, 2010). Vegetation productivity is an essential flux in the net ecosystem exchange of CO₂ between the atmosphere and terrestrial ecosystems. It is a key component of the carbon cycle (Piao et al., 2006) and an important indicator for ecosystems. Regional estimates of vegetation productivity are useful for modeling the regional and global carbon cycles. Quantitative estimates of NPP and GPP at a regional level are significant on the global scale for understanding changes in ecosystem structure and function, and predicting terrestrial carbon cycle trends, which determines the sustainable use of natural resources and helps make policy decisions. Previous studies have shown that (Huang et al., 2016) nearly half of the large-scale ecosystem carbon cycle anomalies are caused by drought. With climate change drought events will increase, therefore it is now urgent that we gain a better understanding of the impact of drought on regional carbon ecosystems in forest ecosystems.

Drought indices are a standard for characterizing drought and have been used widely to detect drought intensity, duration, and spatial distribution. Meteorological factors as well as hydrological, soil, crop, irrigation should be considered when monitoring drought, drought characteristics and impacts are very complex. Various drought indices have been developed recently, including the percentage of precipitation anomaly (Pa) (Foley, 1957), the Palmer drought severity index (PDSI) (Palmer, 1965), drought area index (DAI) (Dai et al., 1965), standardized precipitation index (SPI) (McKee et al., 1995), and the standardized precipitation evapotranspiration index (SPEI) (Vicente, 2009). Many scholars use different drought indices to simulate drought and draw a series of results. He et al. (2016) analyzed wheat potential productivity and drought severity during 1962–2010 based on a wheat drought severity index. Wang et al. (2014) used meteorological data from 128 meteorological stations during 1960–2012 based on a standardized precipitation evapotranspiration index to analyze annual variation trends in drought and drought intensity, the frequency of drought events, and the relationship between drought and ENSO events. Wang et al. (2012) used a relative moisture index to analyze the spatial distribution and annual variation in drought frequency and intensity.

Drought monitor patterns of indices have characteristics. Precipitation was considered in Pa and SPI, with simple calculation and flexible time scale. PDSI was a good indicator of soil moisture fluctuations, in which monthly surface temperature was added as input. And precipitation and evapotranspiration were considered in SPEI. These three patterns for monitoring drought are widely used recently.

The resistances of vegetation productivity to drought could estimate the stability of an ecosystem. Understanding the responses of vegetation productivity to drought is very important. Some previous literatures are mainly focused on the effect of meteorological element or single drought monitor patterns on vegetation productivity. Graw et al. (2017) analyzed vegetation productivity and compared precipitation-vegetation dynamics during the drought season in Eastern Cape. Ghali and Nejla (2017) analyze changes of the vegetation productivity and responses to the ongoing drought based on NDVI time series. Zhang et al. (2014) showed the impact of drought on vegetation productivity using PDSI index in the Lower Mekong Basin. Skagen (2018) and Chang et al. (2018) highlighted more significant responses of precipitation and forest structure to drought over a long time scale.

Consequently, the impact of different drought monitor patterns on the vegetation productivity is not completely understood, especially in some local places of karst regions of Southwestern China. In the karst area, evaporation and infiltration of water are particularly serious. Hence, it is necessary to analyze the relationship between drought and vegetation productivity in karst ecosystems.

This work aims to analyze response of vegetation productivity in different patterns of drought indicators in karst regions in order to reveal the process and extent of drought disasters, and understand the impacts of extreme weather events. Despite an existing of literature which has quantified the characteristics of drought change, analyzed the spatial distribution of drought intensity and frequency, and determined its impact on terrestrial vegetation productivity, the influence on vegetation productivity under different patterns of drought indicators has not yet been explicitly addressed. Considering an increasing number of drought events, the analysis of vegetation response to drought events, provides valuable spatial information related to interannual variability. The changes in vegetation productivity are needed for further identification of climate change on carbon budget of regional ecosystem. This will contribute to the explanation of the impact of drought disaster on subtropical and karst mountain ecosystem in SWC.

The objectives of this work were: (i) to characterize and classify drought hazard occurrence based on different patterns of drought indicators during the last 10 years; (ii) to monitor vegetation productivity and analyze NPP anomalies; (iii) to analyze the impact of drought on monthly GPP and compare drought sensitivity with drought index in different drought monitor patterns, and particular different stages of drought occurrence. Vegetation productivity assessment between vegetation condition and detailed analysis on drought impact within different vegetation system were conducted.

Materials and Methods

Study Area

The study area is located at 97°35'~112°06'E, 20°90'~35°31'N, and includes Yunnan, Sichuan, Guizhou, and Guangxi Provinces, and Chongqing City. The "four provinces and one city" cover an area of $113.76 \times 10^4 \text{ km}^2$, which accounts for 11.77% of the total area (*Fig. 1*).

The terrain is complex, and includes the West Sichuan Plateau, the Yunnan-Guizhou Plateau, the Hengduan Mountains, the Sichuan Basin, and the hills of Guangxi. In the region, widespread karst, undulating terrain, barren soil, and the influence of regional climate result in significantly different climate characteristics, in which wide canyons, intensive rivers, and the region's landforms are dominated by plateaus and mountains. The dominant vegetation types include evergreen forest, deciduous forest, mixed forest, shrub, savanna, grassland, cropland and wetland. The region is rich in runoff, rapid water flow, and large droplets, and is the most abundant water resource area in China holding approximately 40% of the country's water resources.

With locating in low latitudes, it is dominated by subtropical monsoon climate with distinct wet and dry conditions. Mean annual precipitation is 1000-1300 mm, with a dry season (from October to April) and rainy season (from May to September). The average annual temperature is 17°C. The spatial and temporal distribution of precipitation is extremely uneven. During the study period, SWC experienced three severe droughts; the first was from September 2006 to December 2007, another was from December

2007 to February 2008, and the most serious was from October 2009 to April 2010, which resulted in a long period of drought over a wide geographic area that had great impact on the country (He et al., 2014). The severe drought event not only significantly affected the daily lives of millions of people but also impacted the terrestrial ecosystem productivity and the carbon cycle in the context of global change.

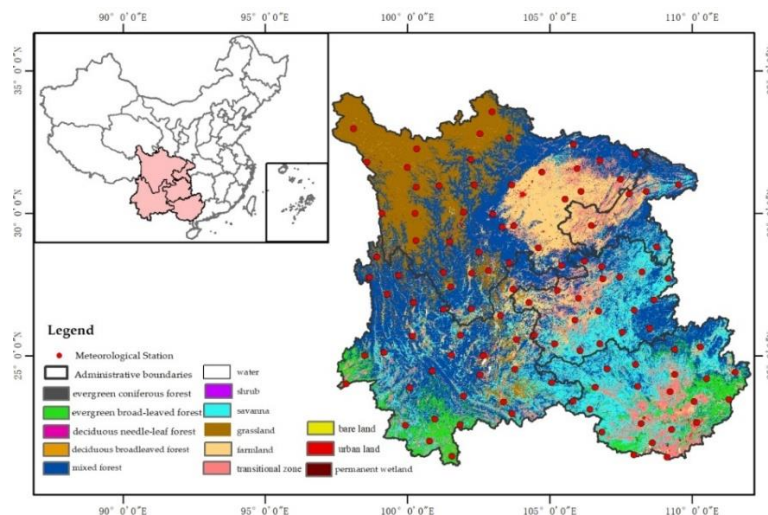


Figure 1. Location of study area and vegetation types. vegetation was obtained from FROM-GLC 2010 land cover product

Data and Methods

In order to illustrate the sensitivity of vegetation productivity under different patterns of drought indicators in karst regions of southwestern China, we analyzed the time series and spatial distribution characteristics of drought in the southwestern region as indicated by three different drought patterns (Tang and Anwaer, 2012). At the same time, data on vegetation productivity was preprocessed using monthly GPP data from MOD17A2H and annual NPP data from MOD17A3H, and used to calculate the monthly GPP and annual NPP, while analyzing the temporal and spatial distribution and anomalies of vegetation productivity. Then, the drought response of different vegetation types to vegetation productivity was considered. Finally, the response of different patterns of drought indicators was obtained.

Meteorological data

To illustrate different drought patterns, the meteorological datasets employed in this study were derived from 112 meteorological observation stations (Fig. 1) in SWC (Chongqing, Sichuan, Guizhou, Yunnan, and Guangxi) over the period 1980 to 2012. Data collected from the National Meteorological Information Center of China Meteorological Administration, included average daily temperature, precipitation, wind speed, sunshine hours, solar radiation, and water vapor pressure among others. The reliability and homogeneity of the monthly meteorological data were controlled and checked by the Chinese Meteorological Administration before its release (Yu et al., 2014). We chose daily mean temperature, daily total precipitation, and water vapor

pressure for this paper, the records were then interpolated to a grid at a resolution of $0.5 \times 0.5^\circ$ (Hutchinson and Xu, 2004) with a smooth thin-plate spline entry method. To fit the calculation of the data with other data, the gridded meteorological datasets were reprojected and resampled to a resolution of 500 M.

Drought indicators

Since the aim of this work is to understand different patterns of drought indicators impacts on vegetation productivity during severe drought events. Drought indices have been used widely to detect drought intensity, duration, and spatial distribution. Drought characteristics and their impacts are very complex. We selected three patterns (includes four indices). Firstly, Pa and SPI indices, which mainly considering the impact of precipitation; secondly, PDSI index, which is an indicator of soil moisture fluctuations, in contrast to Pa and SPI indices that are based solely on precipitation information, PDSI uses both precipitation and temperature as inputs. Thirdly, SPEI index, considering precipitation and evapotranspiration, and retaining the sensitivity of SPI and PDSI to drought events, reflect the intensity, duration of drought and changes in different time scales. These three patterns for monitoring drought are widely used in recent years.

The percentage of precipitation anomaly (Pa)

Pa is a good indicator of precipitation fluctuation, which is the percentage of the anomaly between the precipitation and the average precipitation in the same period (Yao et al., 2018), reflects the deviation and drought conditions of a period of abnormal precipitation (Li and Yang, 2017). As values above -0.5, -0.5 to -0.7, -0.7 to -0.85, -0.85 to -0.95, and below -0.95 represent none, mild, moderate, severe, and extreme drought, respectively.

The Pa was calculated as follows:

$$Pa = \frac{r - \bar{r}}{\bar{r}} \quad (\text{Eq.1})$$

where: r is a certain period of precipitation, \bar{r} is the period of the average annual precipitation. Later, Yang and Li (1994) defined the precipitation anomaly percentage as the water anomaly index Z_i for a given time scale. The formula is:

$$Z_i = \frac{R_i - \frac{1}{n} \sum_{j=1}^n R_{ij}}{\frac{1}{n} \sum_{j=1}^n R_{ij}} \times 100\% \quad (\text{Eq.2})$$

where: R_{ij} is the amount of precipitation in year j month i , n is the number of samples, R_i is the precipitation of month i during the monitoring months, and Z_i is the percentage of precipitation anomaly in month i .

The standardized precipitation index (SPI)

SPI is an indicator of the probability of precipitation occurring during a period (Carbone et al., 2018). In the case of precipitation analysis and drought monitoring and evaluation, the distribution probability Γ is used to describe the change in precipitation.

SPI is obtained by calculating the probability Γ of precipitation distribution in a certain period of time. Then, standardize it to normal. The drought level is then divided by the distribution of the cumulative frequency of standardized precipitation. As values of above -0.5, -0.5 to -1.0, -1.0 to -1.5, -1.5 to -2.0, and below -2.0 represent none, mild, moderate, severe, and extreme drought, respectively. For each pixel, monthly precipitation can be accumulated into different time scales (e.g., 1, 2, 3, 6, 9, 12, and 24 months). The calculation of SPI is as follows:

$$SPI = Sd \frac{t - (C_2 t + C_1)t + C_0}{((d_3 t + d_2)t + d_1)t + 1.0} \quad (\text{Eq.3})$$

where: $t = \sqrt{\ln \frac{1}{G(x)^2}}$, $G(x)$ is the distribution of probability of precipitation associated with the function; x is the precipitation sample value; and s is a positive or negative coefficient of probability density.

- When $G(x) > 0.5$, $G(x) = 1.0 - G(x)$, $s = 1$.
- When $G(x) \leq 0.5$, $G(x)$ is obtained from the distribution function Γ probability density integral formula,

$$G(x) = \frac{1}{\beta \gamma \Gamma(\alpha)} x^{\gamma-1} e^{\gamma-1} d_x, s = -1; x > 0 \quad (\text{Eq.4})$$

where γ and β are the shape and scale parameters of the distribution function; C_0, C_1, C_2 and d_1, d_2, d_3 are the conversion functions of the distribution function Γ to the cumulative frequency, which simplifies the calculation of the approximate solution formula and takes the following values: $C_0 = 2.515517$; $C_1 = 0.802853$; $C_2 = 0.010328$; $d_1 = 1.43278$; $d_2 = 0.189269$; $d_3 = 0.001308$.

The standardized precipitation evapotranspiration index (SPEI)

To calculate SPEI (Zhao et al., 2018), the monthly difference between precipitation (P) and potential evapotranspiration (PET) is used, in which the Thornthwaite method is used to calculate the PET, and monthly temperature as inputs. The difference between P and PET for the month i is calculated as follows:

$$D_i = P_i - PET_i \quad (\text{Eq.5})$$

The D values are aggregated at various time scales:

$$D_n^k = \sum_{i=0}^{k-1} (P_{n-i} - PET_{n-i}), n \geq k \quad (\text{Eq.6})$$

where P is precipitation, PET is the potential evapotranspiration calculated by Thornthwaite method, k is the timescale of the aggregation and n is the calculation number, respectively. D_n^k is based on both the n^{th} climatic water balance and the water balance for the preceding $k-1$ months. The criteria for drought classification based on SPEI is referenced as defined in McKee et al. (1993) and Potopová et al. (2015).

The Palmer Drought Severity Index (PDSI)

PDSI is a good indicator of soil moisture fluctuation (Huang et al., 2012; Angelidis et al., 2012), which is based on the supply and demand concept of the water balance equation (Mika et al., 2005; Heddinghaus, 1991). PDSI is different from the SPI and SPEI, as its time scale is fixed. The index is calculated using precipitation, temperature, and soil parameters. PDSI is calculated as follows:

$$X_i = 0.897X_{i-1} + Z_i/3 \quad (\text{Eq.7})$$

where X_i , X_{i-1} are the current PDSI and previous month's PDSI, respectively. Z_i is the current water abnormality index, which is determined through precipitation. The X_{i-1} term accounts for the effect of duration of drought, while the value of Z is given as follows:

$$Z = dK \quad (\text{Eq.8})$$

$$K = \frac{\overline{ET} + \bar{R}}{\bar{P} + \bar{L}} \quad (\text{Eq.9})$$

where K is the climatic weighing factor, \overline{ET} is the average evapotranspiration, \bar{R} is the average runoff, \bar{P} is the average precipitation, and \bar{L} is the average loss of soil moisture.

Four drought indices can be used to assess the severity degree of droughts, and also we collected 20 cm soil water value (SMV) from some sites during the study period, the monitoring results for each index were compared with the actual data. The category of drought severity was based on the National Standard of the People's Republic of China's "Classification of meteorological drought" (GB/T 20481-2006) and McKee et al. (1993) is shown in *Table 1*.

Table 1. The standard Drought severity category based on drought indices

Drought grade	Non-drought	Mild drought	Moderate drought	Severe drought	Extreme drought
Pa	-0.5<Pa	-0.7<Pa<-0.5	-0.85<Pa<-0.7	-0.95<Pa<-0.85	Pa<-0.95
SPI	-0.5<SPI	-1.0<SPI<-0.5	-1.5<SPI<-1.0	-2.0<SPI<-1.5	SPI<-2.0
SPEI	-0.5<SPEI	-1.0<SPEI<-0.5	-1.5<SPEI<-1.0	-2.0<SPEI<-1.5	SPEI<-2.0
PDSI	-1.0<PDSI	-2.0<PDSI<-1.0	-3.0<PDSI<-2.0	-4.0<PDSI<-3.0	PDSI<-4.0
SMV	0.8<SMV	0.6<SMV<0.8	0.5<SMV<0.6	0.4<SMV<0.5	SMV<0.4

Vegetation productivity datasets

We adopted annual MOD17A3H NPP products and monthly GPP MOD17A2H GPP products from the Numerical Terradynamic Simulation Group (www.ntsug.umt.edu) over the period 2000-2012. The MOD17H (MOD17A2H and MOD17A3H) product provides a description of the Gross and Net Primary Productivity designed for the MODIS sensor aboard the Aqua and Terra platforms. MOD17A2H Version 6 is a GPP product, a cumulative 8-day composite of values with a 500-meter pixel size based on the

LAI/FPAR, which is related to assimilation (Propastin et al., 2012; Leinenkugel et al., 2013). GPP is the amount of carbon absorbed by ecosystems through photosynthesis and is an important component in land-atmosphere CO₂ exchange. MOD17A3H provides annual NPP at a spatial resolution of 500 m, delivered as a gridded Level-4 product in sinusoidal projection. The terrestrial ecosystem NPP is based on data which references the BIOME-BGC model and the light energy utilization model (Jiao et al., 2014; Neumann et al., 2016; Zhang et al., 2008). The products have been recently improved by temporally filling missing and cloud contaminated FPAR/LAI based on the biome parameter look-up table (BPLUT). BPLUT is based on 2839 recently synthesized NPP data which is from the daily Global Modeling, then Assimilation Office (GMAO) meteorological data and the temporal filling of unreliable FPAR greatly improve the accuracy of inputs. To extract the data by mask, the map projection conversion tools and mosaic tools for data projection transformation in MODIS MRT (MODIS Reprojection Tool). We extracted the effective values using the band math tool in ENVI 5.3.

Zhang et al. (2008) indicates that the MOD17 GPP was underestimated (particularly for the cropland) by using measured GPP from eddy covariance flux. As this work mainly analyzed the change of gross primary productivity under different vegetation, the land cover data would be combined with MOD17 parameters. The MOD17 algorithm significantly improved the accuracy of GPP estimates. Neumann et al. (2016) compared MODIS EURO with terrestrial driven NPP, and found that MODIS EURO product provided a consistent, temporally continuous and spatially explicit productivity dataset and was good for elevation. As a result MOD17 products can be used to assess climate change impacts on ecosystems.

Land cover information

We used FROM-GLC2010 land cover product (Ran et al., 2009) at a spatial resolution of 500 m to identify different vegetation types in SWC (<http://data.ess.tsinghua.edu.cn>). This product was based on multi-source land cover classification, considered accuracy of MOD12Q1 land cover product, and used a common classification system (the International Geosphere-Biosphere Programme (IGBP) land-cover classification system). The accuracy of the FROM-GLC 2010 product was validated through comparison with numerous data, including Google Earth, Landsat TM, MODIS land cover, with an overall accuracy of 75% (Yu et al., 2013). These data were used to validate the results of global land surface potential wetland mapping. In the map, vegetation was classified into evergreen broad-leaved forest, evergreen coniferous forest, deciduous broad-leaved forest, deciduous coniferous forest, mixed forest, shrub, savanna, grassland, cropland and wetland. Land cover information was adjusted to improve the accuracy of MOD17 GPP, which provides a consistent, temporally continuous and spatially explicit productivity dataset.

Assessing the impacts of drought on vegetation productivity

The standardized anomaly index (SAI) has been widely employed in the evaluation of precipitation trends (Boczon et al., 2016; Komlan et al., 2017). This index has also been applied effectively to the measurement of NPP anomalies. Here, the NPP simulation value was used to detect monthly NPP anomalies. The effect of drought on the productivity of the vegetation was characterized by the standardized anomaly index (SAI).

$$SAI_{NPP}(n) = [NPP(n) - \overline{NPP}]/(\delta_{NPP}) \quad (\text{Eq.10})$$

where, $SAI_{NPP}(n)$ represents the NPP anomalies, $n=1,2,3,\dots,12$, $NPP(n)$ is the annual NPP, \overline{NPP} is the value of mean NPP, and δ_{NPP} is the standard deviation of the NPP. Abnormal forest productivity is divided into: Normal ($|SAI| \leq A_{Im}$), mildly abnormal ($0.5 < |SAI| \leq A$), moderately abnormal ($1 < |SAI| \leq A_{Ie}$), severely abnormal ($1.5 < |SAI| \leq A$), and extreme anomaly ($|SAI| > 2$). The positive and negative values of SAI represent an increase or decrease in forest productivity, respectively. The larger the absolute value, the more serious the abnormal situation.

To investigate the impact of drought (El-Vilaly et al., 2017) on vegetation productivity (GPP and NPP), we calculated the percentages of drought affected areas ($Pa < -50\%$, $SPI < -0.5$), and then analyzed their correlation with the regional mean NPP among 2001-2012. In order to be consistent with the resolution of NPP and GPP, we resampled Pa, SPI, and meteorological data to 1 km spatial resolution. Then, we calculated the monthly average GPP for the dominant vegetation types and calculated the relative changes of NPP under different drought levels. The purpose is to analyze the response of different vegetation types to different degrees of drought over the study period. To understand the seasonal characteristics of the effects on the vegetation productivity, we calculated monthly mean GPP and compared it with the meteorological anomalies and effects on productivity for different seasons among 12 years. At the same time, we chose the year of abnormal drought (2009-2010) to measure the NPP reduction of different vegetation types.

Results

Drought conditions in Southwest China from 2001 to 2012

We selected daily meteorological data from 1980 to 2012 in SWC, and analyzed the spatial and temporal distribution of drought by calculating drought indicators, Pa, SPI, SPEI and PDSI.

According to drought record, there were three major drought events from 2001 to 2012 (Table 2): June to October 2006; December 2007 to February 2008; and October 2009 to April 2010.

Table 2. Drought events and characteristics from 2001-2012

Drought events	Duration	Mean Precipitation
2006 summer drought	June to October 2006, 5 months	1050 mm
2008 winter drought	December 2007 to February 2008, 3 months	1180 mm
2009 drought	October 2009 to April 2010, 6 months	975 mm

In the summer of 2006, most of the eastern part of SWC suffered the most severe droughts since meteorological records began. The drought continued over a particularly long period and had a wide range of impacts, which led to serious economic loss. In the winter of 2008, drought was widespread in most parts of the southwest and severe drought presented in many areas. The area suffered a once-in-a-century drought from winter 2009 to spring 2010, which lasted for nearly eight months. The affected area is $0.8 \times 10^7 \text{ hm}^2$, approximately 8 million ha. A large number of crops failed, and 25

million people had to cope with less water, resulting in huge economic losses. The following is a detailed explanation of the 2009 drought.

The distribution of the drought indices can be seen in *Fig. 2*. In September and October 2009, the drought began, and drought in eastern Yunnan and central Guizhou was sporadic. From November and December, the drought expanded rapidly, and severe drought occurred in the south of Sichuan, the northwestern Sichuan Basin, and the vast majority of Yunnan. In January and February, the drought was more serious, and heavy drought occurred in the Sichuan Basin, the northwest edge of Yunnan, the southern tropical rainforest fringe, and across Guizhou (excluding the southeastern parts). Drought in most of Chongqing, eastern Sichuan, eastern Guizhou and local areas in Yunnan eased in March, but severe drought occurred in central and eastern Yunnan, south Sichuan, and west Guizhou. The drought came to an end in April. The development of drought reflects the characteristics of “rapid, contiguous, and sequential”.

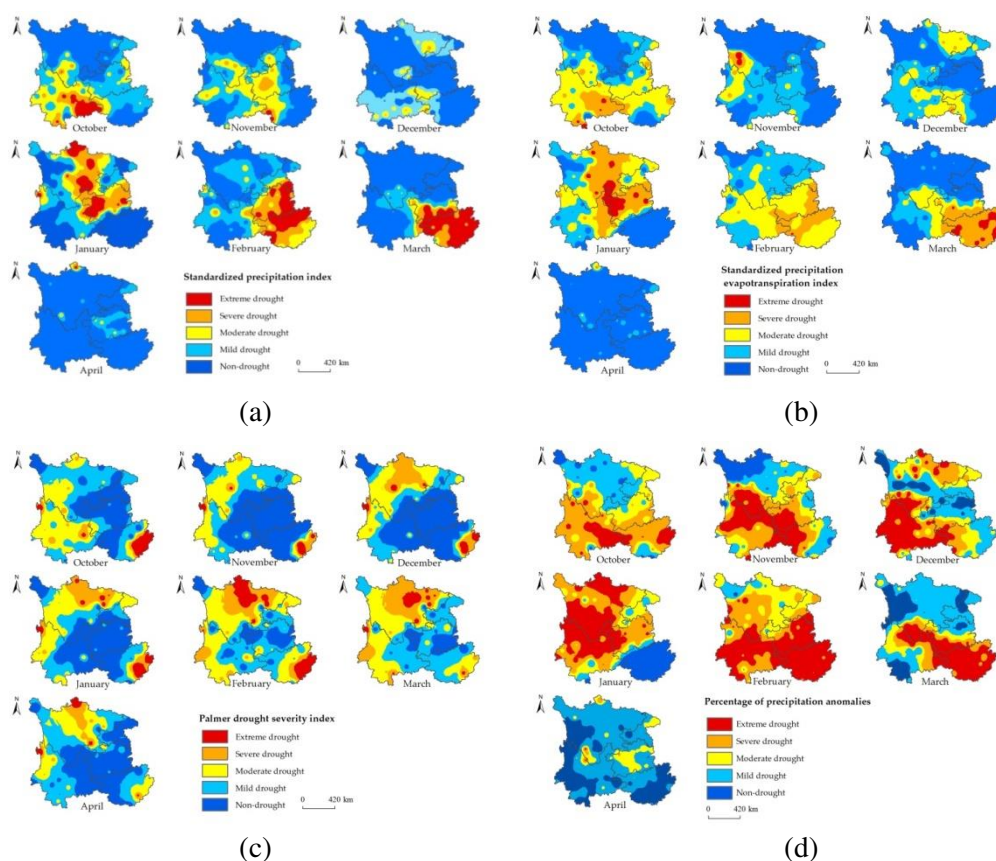


Figure 2. Spatial distribution of drought indices in SWC from October 2009 to April 2010: (a) Pa, (b) SPI, (c) SPEI and (d) PDSI

Each drought monitoring indices has different characteristics. Pa is characterized by a large arid range and contiguous time, and mainly for concentrated in Yunnan, Guangxi. Pa is highly correlated with precipitation. SPI is similar to Pa in spatial distribution and is reduced in scope. The period of drought is mainly concentrated from January to March 2010, the most serious occurred in Guangxi. SPEI characterizes the effect of temperature and surface evapotranspiration, mainly for moderate and severe

drought while, the scope of extreme drought is small. The drought area had further expanded in January 2010. PDSI is different from the SPI and SPEI, as its time scale is fixed, which is a good indicator of soil moisture fluctuation. The severity and extent of the drought have further expanded from January 2010 to March 2010, especially in the central part of Sichuan Province. From the perspective of the entire drought process, winter is more serious.

Correlation between the 20 cm soil moisture value (SMV, from National Meteorological Information Center, <http://data.cma.cn>) and drought indices shows that a significant test of Pearson 0.01 was passed between the drought monitoring indices based on monthly scale and are positively correlated (*Table 3*). SPEI has the highest correlation with SPI, the correlation coefficient is 0.695; the second is SPI and Pa, and the correlation coefficient is 0.683. The correlation between the same monitoring mode and the drought monitoring index is higher, which indicates that the need for drought monitoring based on different patterns. There is a good correlation between the drought index and soil moisture value at the monthly time scale. The correlation between SMV and SPEI is the highest, the correlation coefficient is 0.632. This quantitatively illustrates that SPEI has a better monitoring effect among the several drought indices.

Table 3. The correlations between soil moisture and drought indexes

	SMV	Pa	SPI	SPEI	PDSI
SMV	1.000				
Pa	0.587**	1.000			
SPI	0.591**	0.683**	1.000		
SPEI	0.632**	0.462**	0.695**	1.000	
PDSI	0.616**	0.637**	0.455	0.508**	1.000

Note: * represents 0.05 bilateral significance level; ** represents 0.01 bilateral significance level

After analyzing temperature and precipitation data (*Fig. 3a*), precipitation shortages were observed during 2005-2006 and 2008-2009, while relatively high temperatures were observed for most of 2006 and 2009-2010. In 2009-2010, the annual average temperature was 0.5°C higher than those among 12 years. In addition, the total annual rainfall in 2009 is 10% lower than the average of 12 years. Although the total precipitation in 2010 is close to the long-term average, and the average regional rainfall was only 60% of the 12-year average from September to December 2009. The relationship between precipitation and drought response to vegetation indicated a lag effect.

Relatively extensive and severe droughts occurred in 2004, 2006 and 2009, which affected all SWC regions. Drought indices show the same trend (*Fig. 3b*), reached lower values in 2009. In 2006 and 2009, there was less precipitation and high temperatures, which were conducive to the formation of dry weather conditions. The intensity and extent of drought in 2009 were more severe than those in 2006 and 2008, and the total area affected accounted for 95% of SWC (52% severe drought and 43% mild drought), whereas in 2006, the degree of drought was relatively light, accounting for only 58.7%. Furthermore, the most severely affected region was located in Guangxi, with a mean SPEI was -0.4 in March 2009, lower than the average of the 12-year. This is mainly caused by the simultaneous high temperatures and insufficient precipitation.

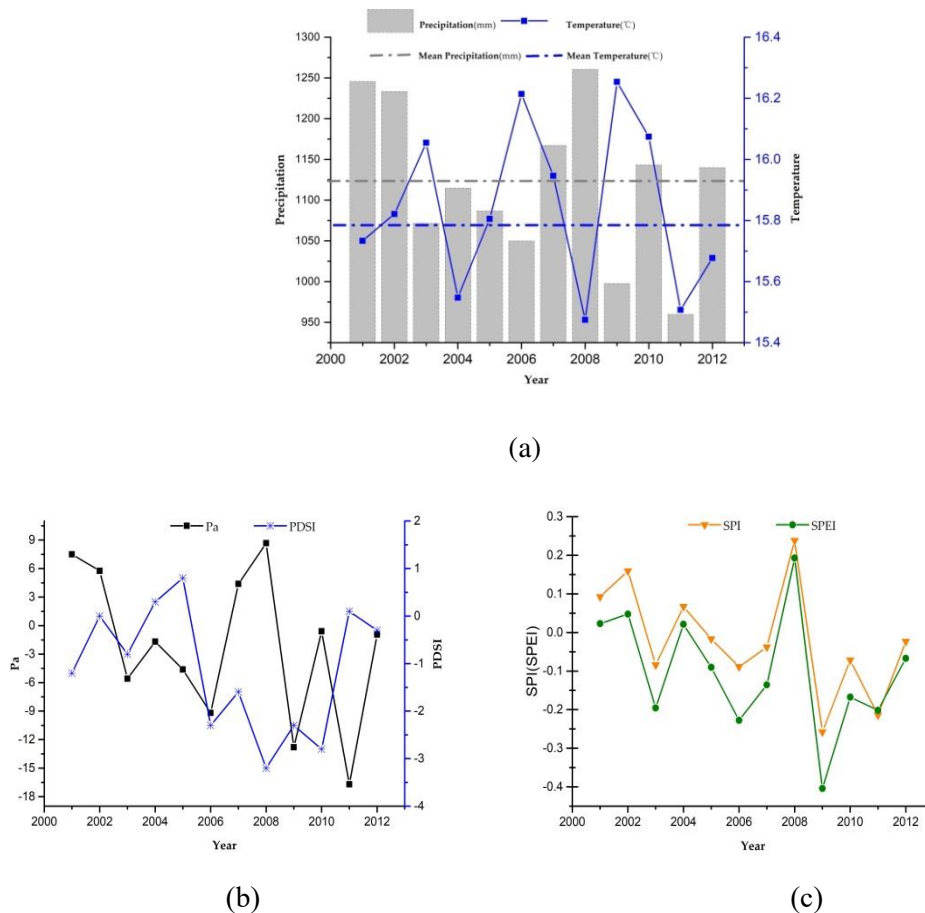


Figure 3. Annual variations for meteorological data and drought indices from 2001 to 2012: (a) precipitation and temperature (b) Pa and PDSI indices (c) SPI and SPEI indices

NPP analysis and Drought impacts on annual NPP

Fig. 4 shows spatial distribution of mean annual NPP from 2001 to 2012, which varied from nearly $142 \text{ g C m}^{-2} \text{ year}^{-1}$ in the western Sichuan region to over $1521 \text{ g C m}^{-2} \text{ year}^{-1}$ in southern Yunnan. Due to the wide variety of vegetation in SWC and the large regional climate differences, the spatial distribution of NPP is uneven and reduces from southeast to northwest; the average occurs in central and southern Guangxi, while the values are higher in eastern and southern Yunnan. Most of middle and eastern Sichuan Province belongs to the Sichuan Basin with its occluded terrain. The temperature is higher than other areas of the same latitude area and it experiences rich precipitation. It is also the most prominent rainy area in China. Hydrothermal conditions are better, NPP is higher, the dominant vegetation type in western Sichuan is grass, and the snowy mountains account for over 30% of the land area. The average NPP here is low. *Fig. 5* shows the annual NPP anomalies during the study period. From *Fig. 2* and *Fig. 5*, it can be seen that the spatial distribution of drought is consistent with the distribution of NPP anomalies. It can be seen from the figure that obvious negative NPP anomalies appeared in the entire region from 2005-2006 and 2009-2010, which was significantly lower than the 12-year average. Compared with other years, the drought situation in these two years is even more serious and extensive (*Fig. 5*). According to

spatial distribution of drought indices (*Fig. 2*), this is also fully illustrated. Particularly it is worth noting that in 2010, a large range of NPP negative anomalies occurred throughout the region.

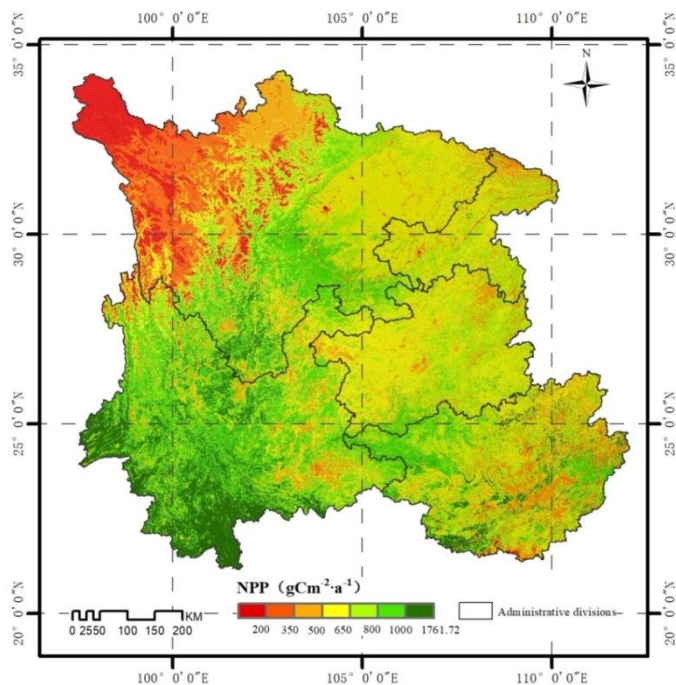


Figure 4. The spatial distribution of mean annual NPP over the 12 years

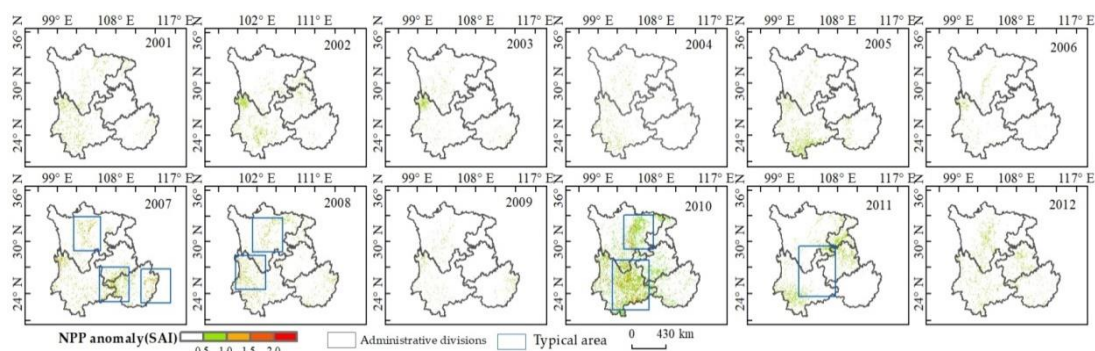


Figure 5. Relative NPP anomalies from the year 2001-2012

Data from other drought years (including 2004, 2006, and 2008) do not indicate a significant reduction in NPP compared with NPP data for 2009 and 2010, which can be explained by the effect level of drought on vegetation productivity. Compared with those in 2005 and 2010, during 2005–2007 and 2008–2010, the percentage of areas that suffered from drought was relatively low, this explains the cause of the NPP anomalies over the 12 years. When the arid area reaches its maximum, the abnormality index (SAI) is the most prominent (*Fig. 6*), which indicated that severe drought has a much greater impact on regional NPP than mild drought. Pei et al. (2013) pointed out that SAI

reaches the maximum when the drought intensity reached peaks. This also fully demonstrates that the views of this work are consistent with previous studies. In years when the drought index did not detect anomalies (e.g., 2001 and 2012) (Fig. 6), the NPP anomalies were mainly caused by floods and other reasons.

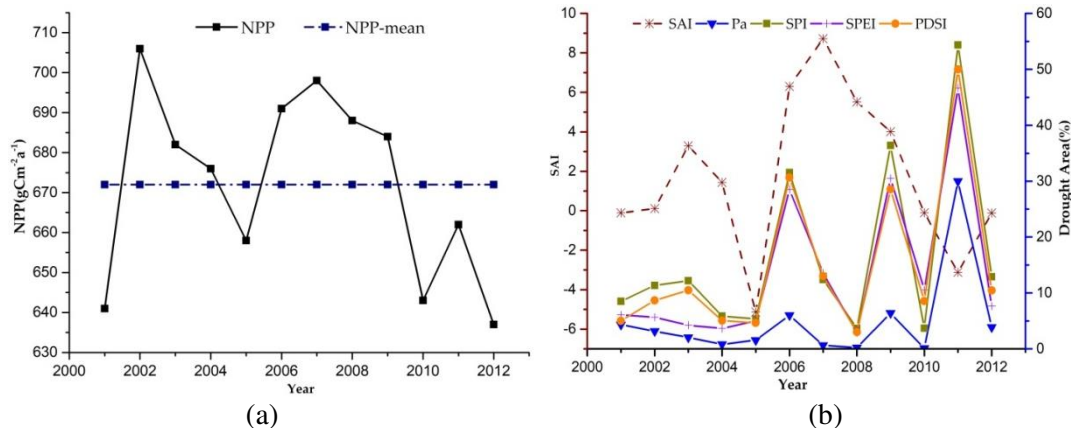


Figure 6. NPP, SAI and drought area of indices from the year 2001-2012 (a) NPP; (b) SAI and drought area of indices

Monthly variations of Drought impact on vegetation productivity

To further analyze the impact of drought on vegetation productivity, we calculated the average monthly vegetation productivity (GPP) and analyzed the impact of drought indices on GPP by different vegetation types during typical drought event (Fig. 7 and Fig. 8). In the study period, 92.3% of the area was hit by severe drought (mild drought), drought mainly occurred in winter and early spring. The drought in 2009 can be traced back to parts of 2008, which is illustrated by the decrease in river water volume in some regions in 2008. The decrease of GPP in 2009 began in October and lasted for four months. Monthly mean GPP ($322.55 \text{ g C m}^{-2}$) reduction continues for a long time, and monthly mean precipitation 93.53 mm, mean temperature 15.8°C . We calculated the average GPP under drought conditions ($\text{Pa} < -0.5$, $\text{SPI} < -0.5$, $\text{SPEI} < -0.5$, $\text{PDSI} < -1.0$) and analyzed the impact of drought indices on GPP production by different vegetation types. The results indicate that drought indices caused reduction in GPP with the order of: $\text{PDSI} < \text{SPEI} < \text{Pa} < \text{SPI}$. From October 2009 to January 2010, the GPP decline from evergreen forest was the greatest (150 g C m^{-2}), followed by shrubland (92 g C m^{-2}) and deciduous forest (103 g C m^{-2}). Since January 2010, drought conditions have eased, vegetation productivity has gradually recovered, and monthly GPP shows a slow rise. In addition, drought has a lagging impact on the productivity of vegetation and GPP is often reflected in the following months. As can be seen from the figure, shrub recovery is the fastest. It can be seen that the changes in the cropland GPP was consistent with the 12-year mean and the decrease was small, which was mainly attributed to human irrigation and other measures. In 2010, the level of drought has eased, and studies show that measures will help alleviate the effects of drought on crops, but they will not prevent the reduction of vegetation. This is also confirmed by the previous research in which the valuation of crop GPP is low.

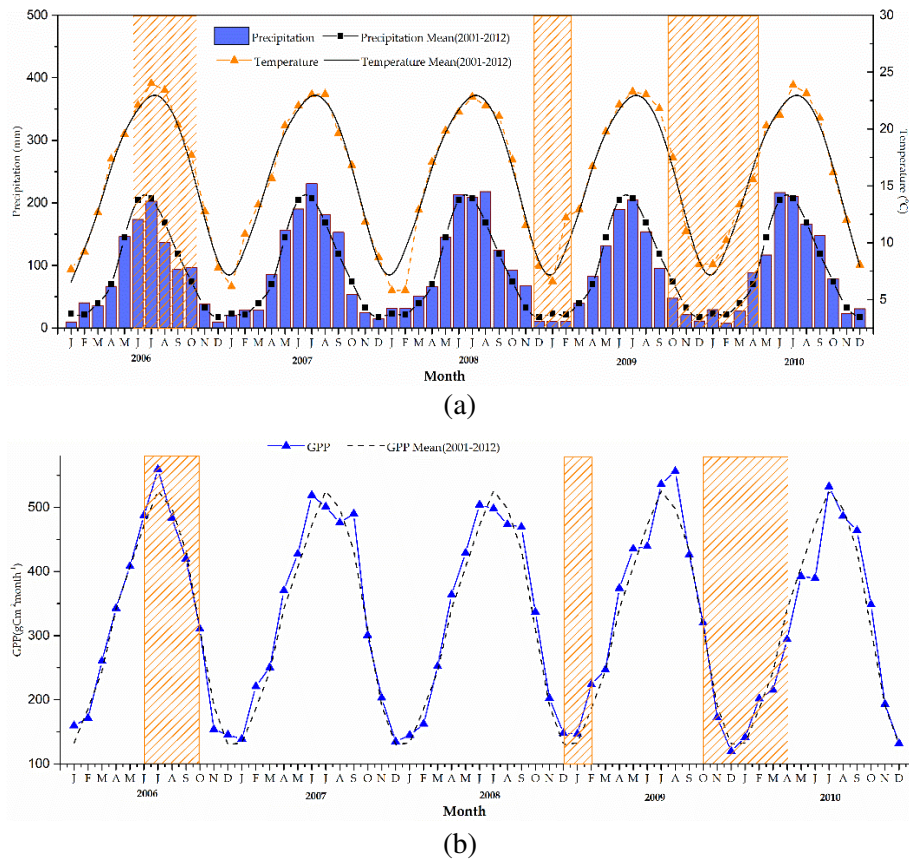


Figure 7. Monthly GPP, temperature, and precipitation averaged in the SWC over drought period, the orange box denotes the drought period experiencing GPP reduction

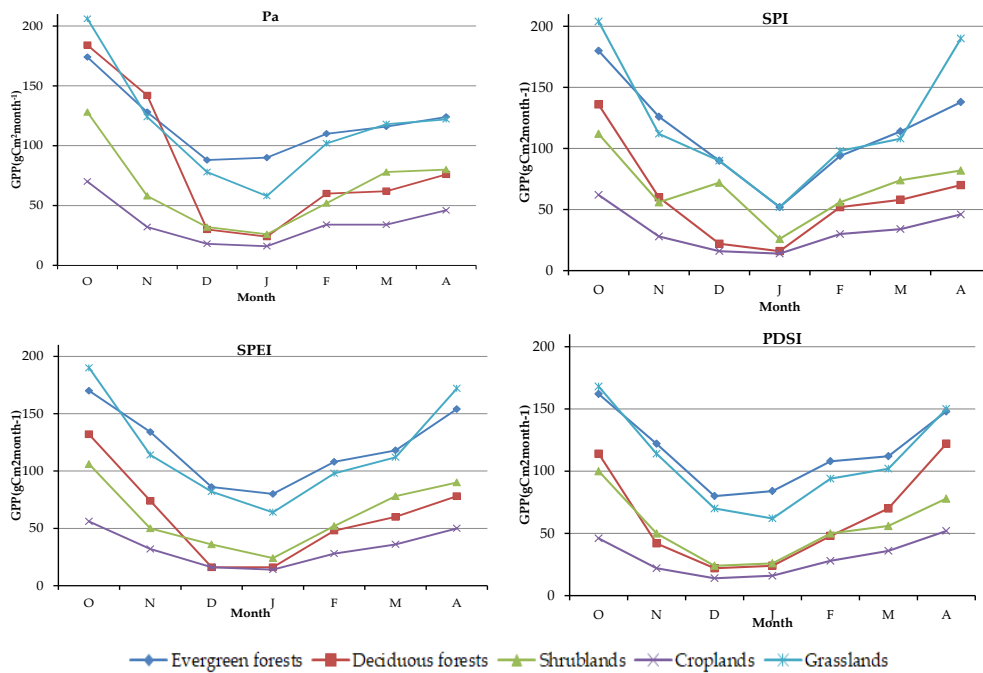


Figure 8. Monthly GPP variations of typical vegetation under drought condition during drought period (from October 2009 to April 2010) in SWC

The response of different drought monitor patterns to vegetation productivity

To understand the relation between vegetation productivity and drought index within monthly scale under each of levels of drought conditions in different monitor patterns. The different indices were compared to GPP during a drought year (2009-2010).

Both SPI and SPEI were found to significantly correlate with monthly GPP under mild drought and extreme drought, with correlation coefficients of 0.745 and 0.752, respectively (*Table 4*). In details, Pa reflects the degree of abnormal rainfall, which shows it fails to make a timely response to drought, and overestimate drought levels. The SPI are stable, which could eliminate the temporal and spatial precipitation differences, and it is sensitive to changes in mild drought. SPI is more relevant to drought and it reflects the different regions and periods of drought well. However, the calculation of SPI only incorporates precipitation data. The other crucial factors (e.g. evapotranspiration and temperature) that can affect the frequency of drought are not included. The process of carbon sinks is complicated as the drought continues to develop. The relation between SPI and GPP is not obvious.

Table 4. *The fitting results between mean monthly GPP and drought indices at different levels*

Drought grade	Fitting equation	Determination coefficient R²	Drought index
Mild drought	$y=0.237x-38.52$	0.745	SPI
Moderate drought	$y=0.342x-61.35$	0.673	SPEI
Severe drought	$y=0.381x+34.63$	0.638	PDSI
Extreme drought	$y=0.565x-45.58$	0.752	SPEI

PDSI is sensitive to GPP in severe droughts and effectively reflects the conditions of water deficit of vegetation. The same pattern was also detected in the correlation between the SPEI and GPP. PDSI and SPEI are more responsive to GPP as the drought continues to develop. It is sure that significant influences of the demand of atmospheric evaporation for vegetation on productivity should be noted. Additionally, the correlations between monthly GPP and drought indices clearly showed that the SPEI and PDSI were most capable of monitoring the vegetation drought conditions in the karst region. The results of this work will provide academic reference for drought ecological risk assessment in the southwestern mountainous areas in China.

Discussion

Drought may affect the production and living of local residents at all levels. There is a contiguous karst area and the most vulnerable ecological ecosystem in Southwestern China, especially on the particular topography and hydrogeological structure. In this work, we analyze vegetation productivity response in different patterns of drought indicators in karst regions in order to reveal the process and extent of drought disasters, and understand the impacts of extreme weather events. We looked at the relationships between vegetation productivity variability and drought indices, and used multiple linear regression analysis to assess the responses to the drought.

Using different patterns of drought indicators, we identified the main impact factors of spatial and temporal patterns of vegetation productivity change. Monthly variations

of drought impact on vegetation productivity indicated that monthly mean GPP reduction continues for a long time, drought has a lagging impact on the vegetation productivity and GPP is often reflected in the following months. This is because the response of vegetation to changes in environmental factors, such as precipitation, temperature, and soil moisture, is a gradual process. In general, spring precipitation and temperature variability seem to be the most significant factors controlling vegetation productivity. Spring drought has the greatest impact on vegetation growth.

In this work, forest management practices such as harvest and thinning were not considered. Forest regrowth after harvest could greatly influence the responses of forest to drought conditions, as these forests have higher productivity. Thereby demanding more water and possibly resulting in water shortage. Therefore, our results might somewhat underestimate drought impacts on vegetation productivity (NPP and GPP). Drought is one of the complex natural hazards, affected by many factors. Climate changes, mainly the precipitation changes and air temperature, play the dominant role. However, other factors such as land use, and CO₂ concentration were not considered to change with time in this study, which could also result in some uncertainties.

Although the vegetation cover in SWC is high, the karst topography is significant and the rock desertification is serious. Restoration of rocky-desertified karst ecosystems is a hot issue in maintaining the sustainability of environments, economy and society in southwestern China. And the correlation between drought indices and vegetation productivity were analyzed, the nonlinear correlations are not considered.

In addition, there are certain uncertainties between MODIS vegetation productivity products and the measured value, which cannot ensure that the simulated value exactly matches the actual situation. These situations can also lead to uncertainty in the analysis. This work provides an example of extreme climate impacts on karst ecosystems and has important implications for global ecology research. The utilization of water resources would be improved by applying ecological restoration technology to effectively prevent soil moisture infiltration in karst areas over the drought season.

The four drought indices belong to different patterns. Pa and SPI indices, which mainly considering the impact of precipitation; PDSI index, which is an indicator of soil moisture fluctuations, in contrast to Pa and SPI indices that are based solely on precipitation, PDSI uses both precipitation and temperature as inputs and was correlated significantly with observed soil moisture data. SPEI, considering precipitation and evapotranspiration, and retaining the sensitivity of SPI and PDSI to drought events, reflect the intensity, duration of drought and changes in different time scales. These three patterns for monitoring drought are widely used in recent years. Using different drought patterns, we identified the main drivers of these spatial and temporal patterns of vegetation productivity change, and these results indicated a close relationship between vegetation and drought events. This is consistent with previous studies that drought responses in productivity across sites, and the results highlight the importance of vegetation recovery.

Conclusions

In this study, we investigated assessments to compare the strengths of different drought indices including Pa, SPI, SPEI, and PDSI in Southwest China. We also analyzed vegetation productivity (annual NPP and monthly GPP). In terms of drought intensity and extent, characteristics were detected in the comparative performances of

Pa, SPI, SPEI and PDSI. Pa showed consistency in the distribution of drought regions, SPI showed a stronger adaptability and better reflected the temporal and spatial variation. SPEI characterized the effect of temperature and surface evapotranspiration, mainly for moderate and severe drought with the small scope of extreme drought. PDSI is a good indicator of soil moisture fluctuation. The spatial distribution of drought is consistent with the distribution of NPP anomaly, and NPP changes of different vegetation types have different characteristics. The level of NPP is directly proportional to the severity of drought. Large reductions in GPP (66.5 g C m^{-2}) were found during both 2009 (14.7%) and 2010 (8.4%) in SWC. The insufficiency of precipitation led to the decrease of NPP from January to April in 2005, and the higher temperature, lower precipitation in 2008-2009 resulted in serious drought. Thus the most severe drought was observed with the largest reduction GPP in 2010. Locations with sparse vegetation have lower productivity. In the region, the GPP of forests, woodlands, and shrub lands exhibited more reductions than that of farmland, which we attribute to irrigation and other measures used by humans. Drought indices caused reduction in GPP with the order of: PDSI < SPEI < Pa < SPI. Our results also suggested relation between vegetation productivity and drought index within monthly scale under each of levels of drought conditions in different monitor patterns, with large differences in the influence of drought conditions on different drought levels. SPEI and PDSI are most capable of monitoring the vegetation drought conditions. Our findings suggested that multi-indices in drought monitoring are needed in order to acquire robust conclusions. The karst area in SWC depend heavily on the very little ecosystem services, especially farming at low elevation, which seem to be the most vulnerable and could collapse due to successive drought events. Further work in this fragile area should focus on improving drought and climate observations and the overall understanding of the expected climate change impact on these fragile and fairly isolated ecosystems in rocky-desertified karst area.

Acknowledgments. This research was funded by the National Key Research and Development Program of China (grant number 2016YFC0803000, 2017YFB0504100), Major Project of High Resolution Earth Observation System (Civil Part) (00-Y30B15-9001-14/16-1) and Youth Innovation Promotion Association of CAS (2015129).

Author Contributions. Z.Y., W.S., W.F. and Q.Y. assisted with the study design and the interpretation of the results; Z.R. designed and wrote the paper.

Conflicts of Interest. The authors declare that they have no conflicts of interest.

REFERENCES

- [1] Angelidis, P., Maris, F., Kotsovinos, N., Hrisanthou, V. (2012): Computation of drought index SPI with alternative distribution function. – *Water Resources Management* 26: 2453-2473.
- [2] Boczon, A., Kowalska, A., Dudzinska, M., Wrobel, M. (2016): Drought in Polish Forests in 2015. – *Polish Journal of Environmental Studies* 25: 1857-1862.
- [3] Carbone, G. J., Lu, J. Y., Brunetti, M. (2018): Estimating uncertainty associated with the standardized precipitation index. – *International Journal of Climatology* 38(4): 607.
- [4] Chang, C. T., Wang, H. C., Huang, C. Y. (2018): Assessment of MODIS-derived indices (2001-2013) to drought across Taiwan's forests. – *International Journal of Biometeorol* 62: 809-822.

- [5] Chen, G. S., Tian, H. Q., Zhang, C., Liu, M. L., Ren, W., Zhu, W. Q., Chappelka, A. H., Prior, S. A., Lockaby, G. B. (2012): Drought in the Southern United States over the 20th century: variability and its impacts on terrestrial ecosystem productivity and carbon storage. – *Climatic Change* 114: 379-397.
- [6] Dai, A. (2011): Drought under global warming: a review. – *Wiley Interdisciplinary Reviews Climate Change* 2: 45.
- [7] Dai, A., Trenberth, K. E., Qian, T. (1965): A global dataset of palmer drought severity index for 1870-2002: relationship with soil moisture and effects of surface warming. – *Journal of Hydrometeorology* 5: 1117-11130.
- [8] Dewes, C. F., Rangwala, I., Barsugli, J. J., Hobbins, M. T., Kumar, S. (2017): Drought risk assessment under climate change is sensitive to methodological choices for the estimation of evaporative demand. – *PLOS ONE* 12(3): 174-196.
- [9] El-Vilaly, M. A. S., Didan, K., Marsh, S. E., van Leeuwen, W. J. D., Crimmins, M. A., Munoz, A. B. (2017): Vegetation productivity responses to drought on tribal lands in the four corners region of the Southwest USA. – *Frontiers of Earth Science* 12: 37-51.
- [10] Foley, J. C. (1957): Droughts in Australia: Review of Records from Earnest Years of Settlement to 1955. – *Australian Bureau of Meteorology, Bulletin No 43*: 128.
- [11] Ghali, M., Nejla, B. A. (2017): Digital technologies and farm productivity: an example from livestock farms. – *EFITA CONGRESS, Montpellier, France*.
- [12] Graw, V., Ghazaryan, G., Dall, K., Delgado Gómez, A., Abdel-Hamid, A., Jordaan, A., Piroška, R., Post, J., Szarzynski, J., Walz, Y., Dubovyk, O. (2017): Drought Dynamics and Vegetation Productivity in Different Land Management Systems of Eastern Cape, South Africa—A Remote Sensing Perspective. – *Sustainability* 9: 1728-1740.
- [13] He, D., Wang, J., Pan, Z. H., Dai, T., Wang, E. L., Zhang, J. P. (2016): Changes in wheat potential productivity and drought severity in Southwest China. – *Theoretical and applied climatology* 130: 477.
- [14] He, D., Wang, J., Dai, T., Feng, L., Zhang, J., Pan, X., Pan, Z. (2014): Impact of climate change on maize potential productivity and the potential productivity gap in Southwest China. – *Journal of Meteorological Research* 28: 1155-1167.
- [15] Heddinghaus, T. R., Sabol, P. (1991): A review of the Palmer Drought Severity Index and where do we go from here. – *Proc. 7th Conf. on Applied Climatology*.
- [16] Huang, G., Zhang, L. F., Wang, Q. L., Guan, J. P. (2012): Precipitation forecasting experiments based on the products of ensemble forecast by using downscaling method. – *Journal of the Meteorological Sciences* 32: 508-514.
- [17] Huang, L., He, B., Chen, A., Wang, H., Liu, J., Lü, A., Chen, Z. (2016): Drought dominates the interannual variability in global terrestrial net primary production by controlling semi-arid ecosystems. – *Scientific Reports* 6: 24639.
- [18] Hutchinson, M. F., Xu, T. (2004): Anusplin Version 4.4, Anuclim Version 6.1. – Fenner School of Environment and Society, Australian National University: Canberra, Australia.
- [19] Jiao, C. C., Yu, G. R., Zhan, X. Y., Zhu, X. J., Chen, Z. (2014): Spatial pattern and regional characteristics of global forest ecosystem net primary productivity. – *Quaternary Sciences* 34: 699-709.
- [20] Judi, D. R., Rakowski, C. L., Waichler, S. R., Feng, Y., Wigmosta, M. S. (2018): Integrated Modeling Approach for the Development of Climate-Informed, Actionable Information. – *Water* 10(6): 775.
- [21] Koudahe, K., Kayode, A. J., Samson, A. O., Adebola, A. A., Djaman, K. (2017): Trend Analysis in Standardized Precipitation Index and Standardized Anomaly Index in the Context of Climate Change in Southern Togo. – *Atmospheric and Climate Sciences* 7(4): 401-423.
- [22] Leinenkugel, P., Kuenzer, C., Dech, S. (2013): Comparison and Enhancement of MODIS Cloud Mask Products for Southeast Asia. – *International Journal of Remote Sensing* 34: 2730-2748.

- [23] Li, Q. F., Yang, G. J. (2017): Temporal Distribution Characteristics of Alpine Precipitation and Their Vertical Differentiation: A Case Study from the Upper Shule River. – *Water* 9: 284-296.
- [24] McKee, T. B., Doesken, N. J., Kleist, J. (1993): The relationship of drought frequency and duration to time scales. – *Proceedings of the 8th Conference on Applied Climatology*, Boston, MA. Am. – Meteorol. Soc. 17(22): 179-183.
- [25] McKee, T. B., Doesken, N. J., Kleist, J. (1995): Drought monitoring with multiple time scales. – *Ninth Conference on Applied Climatology*, American Meteorological Society, Boston, MA: 15-20.
- [26] Mika, J., Horvath, S. Z., Makra, L., Dunkel, Z. (2005): The Palmer Drought Severity Index (PDSI) as an Indicator of Soil Moisture. – *Physics and Chemistry of the Earth* 30: 223-230.
- [27] Neumann, M., Moreno, A., Thurnher, C., Mues, V., Härkönen, S., Mura, M., Bouriaud, O., Lang, M., Cardellini, G., Thivolle-Cazat, A., Bronisz, K., Merganic, J., Alberdi, I., Astrup, R., Mohren, F., Zhao, M., Hasenauer, H. (2016): Creating a Regional MODIS Satellite-Driven Net Primary Production Dataset for European Forests. – *Remote Sensing* 8: 554-572.
- [28] Palmer, W. C. (1965): *Meteorological Drought*. – Washington, DC: US Department of Commerce, Weather Bureau No. 45.
- [29] Pei, F., Li, X., Liu, X., Lao, C. (2013): Assessing the Impacts of Droughts on Net Primary Productivity in China. – *Journal of Environmental Management* 114: 362-371.
- [30] Piao, S., Fang, J., He, J. (2006): Variations in vegetation net primary production in the Qinghai-Xizang Plateau, China, from 1982 to 1999. – *Climatic Change* 74: 253-267.
- [31] Potopová, V., Stěpánek, P., Možný, M., Türkott, L., Soukup, J. (2015): Performance of the standardised precipitation evapotranspiration index at various lags for agricultural drought risk assessment in the Czech Republic. – *Agric. For. Meteorol.* 202: 26-38.
- [32] Propastin, P., Ibrom, A., Knohi, A., Erasmi, S. (2012): Effects of Canopy Photosynthesis Saturation on the Estimation of Gross Primary Productivity from MODIS Data in a Tropical Forest. – *Remote Sensing of Environment* 121: 252-260.
- [33] Ran, Y. H., Li, X., Lu, L. (2009): China Land Cover Classification at 1km Spatial Resolution Based on a Multi-source Data Fusion Approach. – *Advances in earth science* 24: 192.
- [34] Skagen, S. K., Augustine, D. J., Derner, J. D. (2018): Semi-arid grassland bird responses to patch-burn grazing and drought. – *The Journal of Wildlife Management* 82: 445-456.
- [35] Tang, B., Maimaitiming, A. (2012): Research on temporal and spatial distribution characteristics of natural disasters in Tarim Basin during 1949-1990. – *Journal of Arid Land Resources and Environment* 26: 124.
- [36] Vicente-Serrano, S. M., Beguer, A. S., López-Moreno, J. I. (2009): A multiscalar drought index sensitive to global warming: the standardized precipitation evapotranspiration index. – *J Climate* 23(7): 1696-1718.
- [37] Wang, D., Zhang, B., An, M. L., Zhang, T. F., Ji, D. M., Ren, P. G. (2014): Temporal and Spatial Distributions of Drought in Southwest China over the Past 53 years Based on Standardized Precipitation Evapotranspiration Index. – *Journal of natural resources* 29: 1003-1016.
- [38] Wang, M. T., Wang, X., Huang, W. H., Zhang, Y. F., Ma, J. (2012): Temporal and spatial distribution of seasonal drought in Southwest of China based on relative moisture index. – *Transactions of the Chinese Society of Agricultural Engineering (Transactions of the CSAE)* 28: 85-92.
- [39] Yang, Q., Li, Z. Y. (1994): Analysis on the drought index in arid and semi-arid regions. – *Journal of Catastrophology* 9(2): 12-16.
- [40] Yao, N., Li, Y., Lei, T., Peng, L. (2018): Drought evolution, severity and trends in mainland China over 1961-2013. – *Science of the Total Environment* 616: 73.

- [41] Yu, L., Wang, J., Gong, P. (2013): Improving 30 meter global land cover map FROM-GLC with time series MODIS and auxiliary datasets: A segmentation based approach. – *International Journal of Remote Sensing* 34: 5851-5867.
- [42] Yu, M. X., Li, Q. F., Hayes, M. J., Svoboda, M. D., Heim, R. R. (2014): Are droughts becoming more frequent or severe in China based on the standardized precipitation evapotranspiration index: 1951–2010?. – *International Journal of Climatol* 34(3): 545-558.
- [43] Zhang, B. H., Zhang, L., Guo, H. D., Patrick, L., Zhou, Y., Li, L., Shen, Q. (2014): Drought impact on vegetation productivity in the Lower Mekong Basin. – *International Journal of Remote Sensing* 35: 2835-2856.
- [44] Zhang, L., Xiao, J. F., Li, J., Wang, K., Lei, L. P., Guo, H. D. (2012): The 2010 spring drought reduced primary productivity in southwestern China. – *Environmental Research Letters* 7: 45.
- [45] Zhang, Y., Yu, Q., Jiang, J. I. E., Tang, Y. (2008): Calibration of Terra/MODIS gross primary production over an irrigated cropland on the North China Plain and an alpine meadow on the Tibetan Plateau. – *Global Change Biology* 14: 757-767.
- [46] Zhao, M., Running, S. W. (2010): Drought-induced reduction in global terrestrial net primary production from 2000 through 2009. – *Science* 329(5994): 940-943.
- [47] Zhao, A., Zhang, A., Cao, S., Liu, X., Liu, J., Cheng, D. (2018): Responses of vegetation productivity to multi-scale drought in Loess Plateau, China. – *Catena* 163: 165-171.

EVALUATION OF ACUTE TOXICITY AND ANTI-INFLAMMATORY ACTIVITY OF CALLUS EXTRACTS OF *PULICARIA INCISA* (LAM.) DC.

ROUANE, A.^{1,2*} – CHABANE, D.¹ – ARAB, K.²

¹Research Laboratory on Arid Zones (LRZA), Faculty of Biological Sciences, University of Sciences and Technology Houari Boumediene, PB, N°32 El Alia, Bab Ezzouar, 16111 Algiers, Algeria

²Laboratory of Valorization and Conservation of Biological Resources (VALCOR), Department of Biology, Faculty of Sciences, University M'hamed Bougara of Boumerdes, 35000 Boumerdes, Algeria

*Corresponding author

e-mail: rouaneasma@yahoo.fr; phone/fax: +213-21-639-141

(Received 3rd Sep 2018; accepted 5th Nov 2018)

Abstract. This study was aimed to investigate the effect of bioactive molecules of callus infusion of *Pulicaria incisa* (Lam.) DC, by the evaluation of anti-inflammatory activity and acute toxicity. 70% was the higher rate of callus obtained from young capitula cultivated on Murashige and Skoog (1962) (MS) solid medium containing 2.4D 4.10⁻⁵M and KIN 5.10⁻⁶ M for 4 months. A Phytochemical screening based on colorimetric reactions was performed on the callus infusion material. Unlike the absence of primary components (starch, reducing sugars), secondary metabolites such as mucilage, saponins, flavonoids and anthocyanins were revealed. No sign of toxicity was observed by the application of 0.25 to 5 g/kg doses in this investigation, although, a significant anti-inflammatory response was revealed at 5 g/kg compared to that of Diclofenac[®]. The chromatographic analysis (HPLC) detected the presence of 3-hydroxy-4-methoxycinnamic acid the main phenolic acid produced by callus, which could be responsible of the positive anti-inflammatory reaction. These findings suggest that the callus could be an alternative source of bioactive metabolites useful in the human health as an anti-inflammatory source.

Keywords: *Pulicaria incisa* (Lam.) DC., Asteraceae, Tamanrasset, callus infusion, bioactive metabolites, biological effects

Introduction

Pulicaria incisa (Lam.) DC., (Asteraceae) called “Tamayout” or “Ameo” is an endemic aromatic and medicinal herb with golden yellow capitula (flowers) rich in flavonoids and phenolic compounds (Ewais et al., 2014). It is traditionally used by aboriginal people “touaregs” in southern Algeria (Tamanrasset) to treat human pains as flu, fever, coughs, diabetes, palpitations (Maiza, 2008) and also to relieve carminative and anti-inflammatory troubles (Boumaraf et al., 2016). Scientific available studies reported the presence of several metabolites which could have a role in these healing reactions such as sesquiterpene lactones (Ghouila et al., 2009), the flavonoids (Mansour et al., 1990) and the caryophyllene derivatives (San Feliciano et al., 1989). Face to the common use of this aromatic and medicinal plant (PAM) by aboriginal population and healers by its “random-harvesting” without any ecological preservation measurement and the climate changes as rainfall less, soil salinization (Rouane, 2012), the number of “plant feet” is being less and less accessible.

Note that, some of endemic plant species in this Saharan area of Algeria early known for its rich flora are currently disappeared by these problems (Nacer bey et al., 2015). To avoid this current critical situation, tissue culture techniques are being as alternative pathway to obtaining new plant material as callus and cell suspension considered as source for

bioactive component production (Eid and Metwally, 2017). To our knowledge, there is no publication thus on the formation of callus with the secondary metabolites contents before and after callus establishment on this Asteraceae. This manuscript presents the results of the evaluation of a therapeutic power of aqueous extract from callus 4-months by performing chemical screening followed by the determination of the LD₅₀ and the anti-inflammatory activity test on mice.

Materials and methods

Plant material and callus induction

The fresh young-inflorescences of *Pulicaria incisa* Lam. (DC.) were harvested in March 2013, in natural area of Ahaggar Tamanrasset, Latitude: 22° 47' 13" North, Longitude: 5° 31' 38" East, Altitude: 1470 m), recognized according to the plant features by using the flora (Ozenda, 2004) and the book entitled The Hoggar, botanical trip (Sahki and Sahki, 2004), confirmed by the botanists of National Institute of Forest Research "INRF" of Tamanrasset (Tam). The Specimen voucher was deposited in National Herbarium of the Research laboratory of Arid Zones LRZA Herbarium for authentication (N°2-2012 Tam; PAM/LRZA/USTHB).

After isolation, natural capitula of 8 mm diameter were freshly taken, then, sterilized in Mankooza solution (0.01%) for 30 min, well rinsed, thus, immersed in mercuric chloride HgCl₂ (0.01%) for 10 min and rinsed with sterile distilled water 3 times of 5 min each. The capitula were, dried and cultivated on Murashige and Skoog (1962) medium supplemented with 2 mL Morel and Wetmore vitamins (1955), 3% (w/v) sucrose (30 g L⁻¹), 0.8% (w/v) agar (8 g L⁻¹) and different growth regulators combinations and concentrations (*Table 1*). The medium was adjusted to pH 5.8 and autoclaved at 120 °C for 20 min. The cultures were incubated at 27 ± 1°C in total darkness until callus induction and high multiplication. The application of hormone (growth regulators) concentrations and combinations were chosen as treatment to express the morphogenetic capacities of the explants (Chabane, 2007; Rouane, 2012).

Table 1. Different media composition in Auxin-cytokinin concentrations tested

Media	Auxins/Cytokinins (mole/L)				
	2.4D	NAA	IAB	BAP	KIN
Control	None				
M1	5.10 ⁻⁴	-	-	4.10 ⁻⁶	-
M2	3.10 ⁻⁵	-	-	-	5.10 ⁻⁶
M3	4.10 ⁻⁵	-	-	-	5.10 ⁻⁶
M4	-	5.10 ⁻⁶	4.10 ⁻⁶	3.10 ⁻⁴	5.10 ⁻⁶

2.4 D: 2,4-dichlorophenoxyacetic acid, NAA: naphthalene acetic acid, IAB: Indole butyric acid, BAP: 6-benzylaminopurine, KIN: kinetin

Preparation of infusion extracts

Two types of infusion extracts were prepared, in boiled water (for phytochemical screening analysis) and in NaCl (0.9%) for bioactivity tests (anti-inflammatory and acute toxicity).

5 g of each, callus (fresh) and natural capitula (young flowers, air-dried and chopped) were separately soaked in 100 mL of boiled solution for 20 min, then filtered through Wathman filter paper (Cat N°40, 1440-110), the filtrate obtained was used. Note that, natural capitula were only used in phytochemical screening to determine the overall chemical composition of callus obtained by in vitro culture assays.

Animal preparation

Albino mice *Mus musculus* (20-30 g weight intervals, 10-12 weeks-old) under temperature of 22-24 °C, 50% humidity, 12 h photoperiod, fed by pellets scheme and tap water ad libitum were chosen. The Statement of safety was approved by the ethical committee of (CRD-SAIDAL, Algiers).

Biochemical composition

Phytochemical screening

Callus and natural capitula infusions were separately treated with various solvents (Table 2) to detect the different bioactive components by colorimetric or precipitation reactions as shown in Table 2 (Harborne, 1998; Bruneton, 2009).

Table 2. *Phytochemical screening of natural capitula and callus infusion*

Compounds		Chemical reagents	Colorimetric reactions
Primary metabolites	Reducing sugars	Fehling liquor	Orange precipitation
	Starch	Iode (I ₂)	Purple blue
	Glucosides	H ₂ SO ₄	Orange-red-purple
Secondary metabolites	Mucilages	Ethanol	Flaky precipitate
	Flavonoids	HCl + Magnesium chips (Mg) + Isoamelic alcohol	Orange-red
	Anthocyanins	HCl	Red
		Ammonia ½	Blue
	Total tannins	Fe Cl ₃ 5%	Blue black
	Catechic tannins	Stiansy reagent (formol+HCl)	Red
	Saponins	NaOH 0.1 N / HCl 0.1 N	Foam formation
Iridoids	HCl /heating	Blue	

NaOH: sodium hydroxide, HCl: hydrogen chloride, FeCl₃: ferric chloride, H₂SO₄: sulfuric acid

High-performance liquid chromatography analysis (HPLC)

High-performance liquid chromatography (HPLC) was carried out with a Agilent 1100 System, quaternary pump, on-line degasser automatic injector and UV detector with bars of diodes surveyor (DAD), using Hypersil BDS-C18 column (250 × 4.6 mm, 5 µm) at 30 °C. The chromatographic data system was controlled by the mobile phase (acetic acid 0.2%/ACN) for 30 min. The solvent flow rate was 1 mL/min.

Biological activities of callus infusion

The bioactivity determination by two tests (anti-inflammatory and acute toxicity) concerns the application of callus infusion on animal models chosen.

Acute toxicity test

The examination of acute toxicity was performed in oral gavage as prescribed by Litchfield and Wilcoxon (1949). A total of 5 mice (20-30 g) in separated cages of each group; (control group and 5 experimental groups) were fasted 18 h before experiment. An oral gavage of 0.5 mL of callus infusion was administered as follows; 0.25 g/kg, 0.5 g/kg, 1 g/kg, 2 g/kg and 5 g/kg, while the control animals were received the NaCl (0.9%). NaCl expresses the physiological water 0.9% without any risk, was used for the preparation of different extracts (control and treatments) under the same conditions. The mice were monitored from 30 min to 4 h. The body weight variation, general behavioral and toxicity symptoms were noted at least once daily for 14 days (Nana et al., 2011). The DL₅₀ and the maximum dose without effect (MDE) were calculated and compared to the control batch.

Evaluation of carrageenan-induced anti-inflammatory activity

The anti-inflammatory activity of callus extracts of *Pulicaria incisa* was performed using inflammation by edema formation induced by carrageenan on hind-paw of mice (Winter et al., 1962). Four groups of 10 male mice in each (20 to 30 g) were fasted 18 h before the beginning of the experiment. A dose of 0.5 mL was orally given as follows; control group (NaCl 0.9%), experimental groups by callus infusion at 2 g/kg (I), 5 g/kg (II) and Diclofenac[®] at 5 mg/kg (experimental group III). 30 min after each administration, 25 µL of the 1% w/v carrageenan was injected subcutaneously into the plantar aponeurosis of the left hind paw of each mouse. The behavior and responses of all mice were observed and noted (Zhang et al., 2015). Three hours later, the animals were quickly sacrificed. The variation of paw volume of each animal was noted, then, the mean of weight (M) for each group was calculated. The following equations (Eqs. 1–2) were used to calculate the percentages of the edema (%E) and of edema reduction (% E.R) respectively:

$$\% E = \frac{(M LPW - M RPW)}{M RPW} \times 100 \quad (\text{Eq.1})$$

$$\% E.R. = \frac{(\% E PC - \% E PE)}{\% E PC} \times 100 \quad (\text{Eq.2})$$

where: % EPC: percentage of edema of the paw of the control, % EPE: percentage of edema of the paw of the experimental groups, LPW: Left Paw Weight, RPW: Right Paw Weight, M: Mean of weights.

Statistical analysis

The results obtained were analyzed using Statistica Software (6.0). Data were expressed as means ± ESM (or means ± SD), then were subjected to One way analysis of variance (ANOVA) followed by Duncan Multiple Range Test (DMRT) and differences between data means were regarded statistically significant at P < 0.01 and P < 0.05 (Duncan et al., 1977).

Results

Callus induction

This study showed that the young capitula reacted positively onto media tested with 30 to 70% callus induction ratios; M2 (2.4D 3.10^{-5} M/KIN 5.10^{-6} M) with 60% and M3 (2.4D 410^{-5} M/KIN 5.10^{-6} M) with 70% compared to that of M4 (NAA-IAB/BAP-KIN) with 30% (see Fig. 1, Table 3).

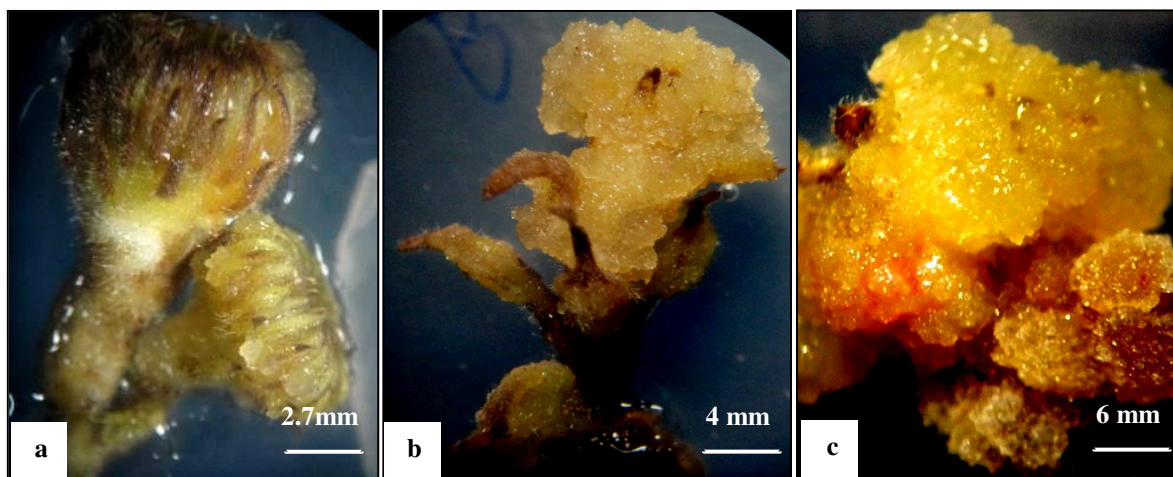


Figure 1. Callus induction and multiplication of capitula explants of *Pulicaria incisa* on culture media (M 3). **a** Induction after 2 weeks, **b** friable callus formation after 4 weeks, **c** callus multiplication after 6 weeks

Nevertheless, no callus was observed onto M1 (2.4D/BAP) even the long maintenance of explants (32 weeks). The M3 is thus, considered the most successful of callus formation in this experiment. The color and morphological aspects of calluses varied with time and the concentrations of growth regulators. All callus masses obtained were friable with variable multiplication degree (low, middle and high) from 40 to 80 mm diameter.

Table 3. Callus induction frequency (%) from *Pulicaria incisa* young capitula after several weeks of culture

Media Aux/Cyto	Call. (%)	Call. col. morph.	Degr. call. form.	W. cult.
Control	0	None	-	32
M1: 2.4D/BAP	0	None	-	32
M2: 2.4 D/KIN	60	Friable, yellowish, whitish to brown	++	2
M3: 2.4 D/KIN	70	Friable, yellowish to whitish brown	+++	2
M4: NAA, IAB/BAP, KIN	30	Friable, whitish to brown	+	6

+: poor, ++: moderate, +++: profuse, Aux/Cyto: (Auxins/Cytokinins) combinations, 2.4 D: 2.4-dichlorophenoxyacetic acid, NAA: naphthalene acetic acid, IAB: indole butyric acid, BAP: 6-benzylaminopurine, KIN: kinetin, Call. (%): Callus percentage, Call. col. morph: Callus color morphology, Degr. call. form: degree of callus formation, W. cult.: weeks of culture

The degree of callus formation expresses the variation of number and diameter of callus mass by capitula with time; +: low with diameter ($d < 40\text{mm}$), ++: middle ($40\text{ mm} < d < 60\text{mm}$), +++: higher ($60\text{mm} < d < 80\text{mm}$). The most important callus mass (diameter, 80 mm) was observed on 2.4D-KIN that on media added of NAA-IAB or BAP-KIN after 4 months.

Biochemical compounds of infusion extracts

Qualitative biochemical composition

The phytochemical screening has mentioned a total absence of primary metabolites (glucosides and starch) with the presence of secondary metabolites.

Table 4 summaries the variation of phytochemical compounds of callus infusion compared to that of natural capitula, callus infusion showed the total absence (-) of primary metabolites (glucosides, reducing sugars, and starch), the presence of secondary metabolites. On the other hand, natural capitula infusion revealed the presence of glucosids, flavonoids, mucilages, tannins, catechical tannins and prints of anthocyanins. Note that, the amount of each varied from a weak (+) to important (+++). The comparison between callus and natural capitula infusion exposed a large amount of mucilage in callus, a middle content in both, of saponins and anthocyanins with a total absence to middle amount of Glucosids, Iridoids and tannins.

Table 4. *Phytochemical composition of callus and natural capitula*

	Compounds	Callus	Natural capitula
Primary metabolites	Starch	-	-
	Reducing sugars	-	-
	Glucosides	-	++
Secondary metabolites	Mucilages	+++	+
	Saponins	++	++
	Flavonoids	+	++
	Anthocyanins	+	+
	Total Tannins	-	++
	Catechic Tannins	-	++
	Iridoids	-	-

-: total absence, +: weak amount, ++: middle amount, +++: important amount

Chromatographic analyses by HPLC

The comparison of samples tested to all standards used revealed a moderate 3-hydroxy-4-methoxycinnamic acid content, considered as the main phenolic acid in callus infusion assay with 3.159% (peak area percent) recorded at $\lambda = 260\text{ nm}$ (see Fig. 2 a, b).

Biological activities evaluation of callus

Oral acute toxicity study and body weight variation

The weighting of all animals recorded an increase of body weight of mice in all control and assays tested with time (see Fig. 3). The callus infusion tested on mice

orally at various doses (0.25 g/kg, 0.5 g/kg, 1 g/kg, 2 g/kg and 5 g/kg) did not toxic, neither mortality was observed after two weeks of application. Note that, 5 g/kg was the maximum dose without effect (MDE) compared to the control batch. Duncan Multiple Range Test (DMRT) revealed a higher significant difference of the body weight between control and all doses tested at 15 days of treatment ($P^{***} < 0.001$).

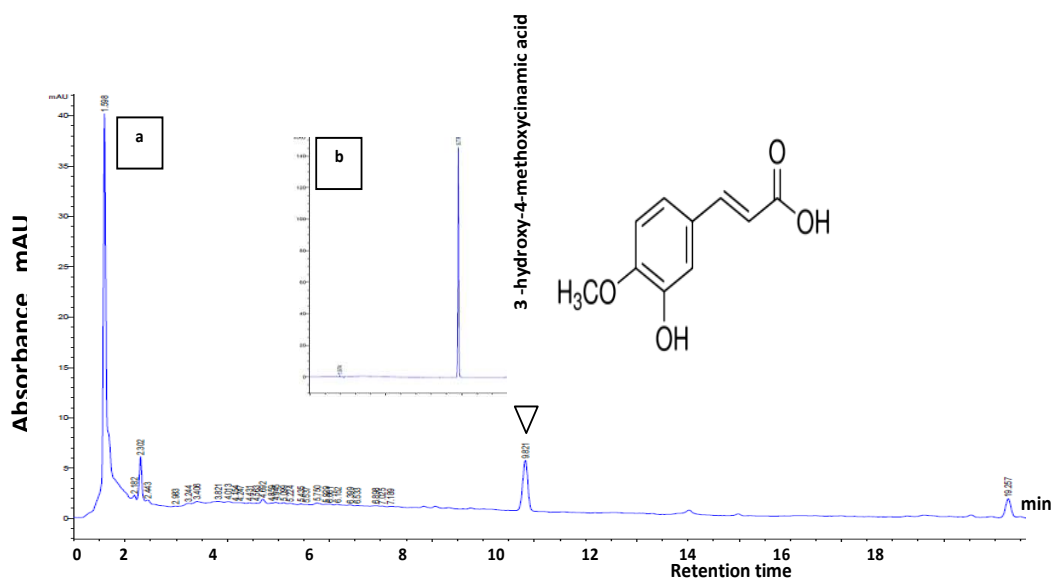


Figure 2. HPLC chromatogram. **a** Callus infusion of *Pulicaria incisa* (Lam.) DC., visualized at $\lambda = 260$ nm; **b** 3-hydroxy-4-methoxycinnamic acid Standard phenolic acid injected in the same conditions

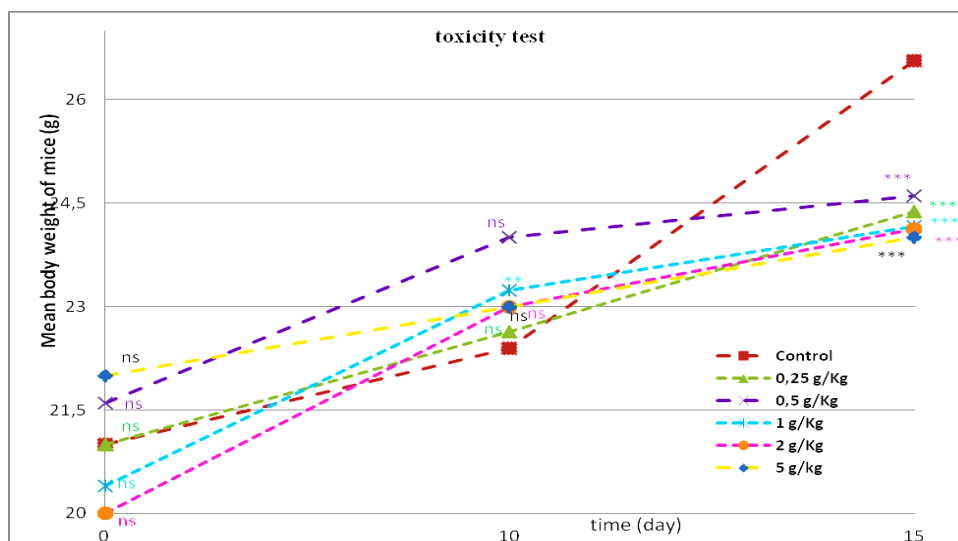


Figure 3. Body weight variation with time of callus infusion treatment compared to the control. Means (means \pm standard error). Duncan Multiple Range Test (DMRT), expressed differences of data means *** indicate a higher significant difference between the control and treatment ($***P < 0.001$), $**P < 0.01$: very significant, ns not significant

Anti-inflammatory activity evaluation

The anti-inflammatory activity of callus infusion was investigated. As shown in Table 5 and Figure 4, the monitored of weight of mice of all groups showed a decrease of the paw edema, of 37.66% (at 2 g/kg), 46.95% (at 5 g/kg) by callus infusion and 40.65% by the Diclofenac[®]. Duncan Multiple Range Test (DMRT) revealed a significant difference between the control compared to experimental group at 5 g/kg dose and the Diclofenac[®] ($P^* < 0.05$).

Table 5. Comparison of edema reactions (edema apparition and reduction) in mice treated with Diclofenac[®] (5 mg/kg) and with callus infusion

Anti-inflammatory test, n = 10					
Doses	Control group NaCl 0.9%	Experimental groups			ANOVA one way
		Callus infusion (I) 2 g/kg	Callus infusion (II) 5 g/kg	Diclofenac [®] (III) 0.005 g/kg	
M. LPW	0.1831 ± 0.007	0.1699±0.004	0.1678±0.0041*	0.1623±0.003*	P 0.027 * $P < 0.05$
M. RPW	0.1263 ± 0.004	0.1327±0.003	0.1355±0.0035	0.1281 ±0.002	P 0.197 $P > 0.05$
% E	45 ± 0.036	28 ± 0.022	24 ± 0.021*	27 ± 0.017*	
% ER	/	37.66	46.95	40.65	

LPW: Left Paw Weight, RPW: Right Paw Weight, %E: percentage of edema, % ER: percentage of edema reduction, Mean± SEM: M Mean; ± SEM: standard error of means, n = 10: total mice in group tested, [®]: Reference, * $P < 0.05$: compared to control, was considered significant by the Duncan Multiple Range Test (DMRT)

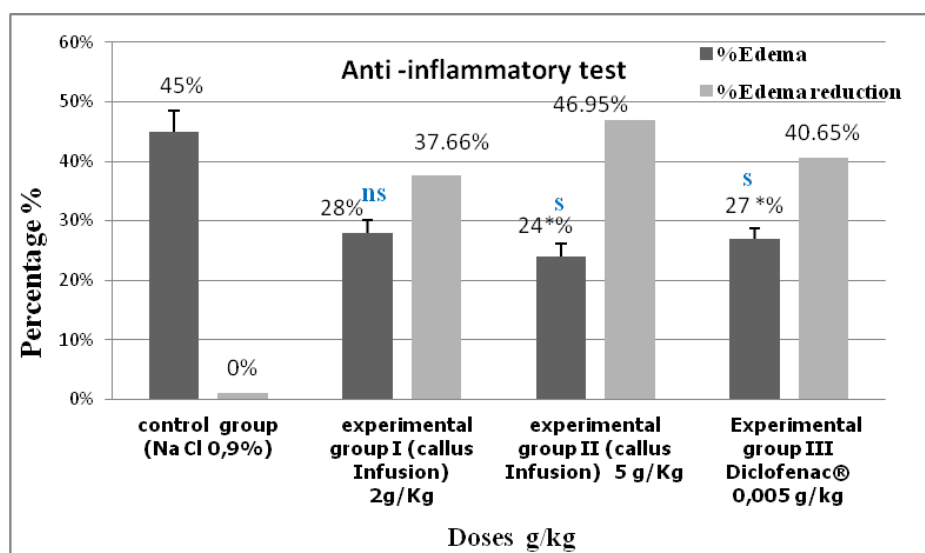


Figure 4. Anti-inflammatory activity evaluation (% mean ± SEM) of callus infusion (2 and 5 g/kg) compared to Diclofenac[®] (5 mg/kg) and control treatment. Means (means ± standard error). The values of Duncan Multiple Range Test (DMRT), expressed with a letter “s” a significant difference between the control compared to experimental group at 5 g/kg dose and the reference (Diclofenac[®]), with $P^* < 0.05$; ns: not significant

Discussion

The influence of different concentrations and combinations of growth regulators on the induction of callus from capitula of *Pulicaria incisa* showed a better response in the medium supplemented with 2,4D and KIN. 70% was the higher callus rate obtained onto 2,4D 4.10^{-5} M and KIN 5.10^{-6} M. The same observations have been noted by Gupta et al. (2015) and Farvardin et al. (2017) who confirmed the effectiveness of 2,4D/KIN in vitro conditions by the best induction and proliferation of callus masses in dicotyledonous plants.

However, capitula cultivated on 2,4D/BAP, did not display any change in their morphological aspects except the total necrotic reaction due to the release of phenolic compounds (Ozyigit et al., 2007); which have generally a negative effect by the inhibition of enzyme functions and the inactivation of explants growth leading browning and darkening of the media (Arnaldos et al., 2001).

Because, the weak amount of anthocyanins in callus is similar to that of capitula, this suggests that dark has no influence upon action of their biogenesis, thus, it is advised to carry out further experiments by exposure of callus under light to boost the biosynthesis process. The same suggestions were previously supposed by Mathur et al. (2010) on callus line of *Panax sikkimensis* Ban. (*Araliaceae*). Also the total absence of starch and reducing sugars indicates that the plant do not synthesize or store starch. That's in agreement with Benhouhou (2005) regarding the presence of "Inulin" in *Pulicaria incisa* Inuleae tribe. However, the highest production of mucilage in callus could be a secondary energy reserve (Langenheim, 2003). Currently, Gupta et al. (2015) advise to harmonize the combinations of growth regulators to ensure the high production of mucilage under in vitro conditions. Further experiments are useful to run cultures under light conditions for the possible high secondary metabolites amounts production.

Regarding the HPLC analysis, 3-Hydroxy-4-methoxycinnamic acid, was appeared to be the main phenolic acid in callus infusion, this result is consistent with the findings of Arafa et al. (2015) and Azeez et al. (2017). These authors have reported that it is the major compound of callus produced under in vitro conditions.

In the current study, the weighting of animals recorded an increase of body weight of mice in all control and assays tested with time; it was expressed by the moderate gaining of weight. Conversely, Jahn and Günzel (1997), also Saad et al. (2016) described the toxicity sign by the weight loss. We consider that, saponins, mucilages, anthocyanins and flavonoids of callus are without any toxic prints on mice (Avachat et al., 2011; Du et al., 2015; Muthukumaran et al., 2017). Note that Hammiche and Maiza (2006) have not scored any toxic effect of *Pulicaria incisa* in the field findings.

The moderate anti-inflammatory activity of the callus infusion registered, could be explained by the presence of 3-hydroxy-4-methoxycinnamic isoferulic acid detected at 260 nm). Our results are in agreement with reports of Shiraki et al. (1998) and Kim et al. (2012), who displayed that the 3-hydroxy-4-methoxycinnamic acid has both antipyretic and anti-inflammatory activities by suppressive of interleukin-alpha compounds production. In addition, the calm state of mice during the experiments was certainly due to the higher amount of mucilage in callus, the polysaccharides, which has softening and anti-inflammatory activities, reducing inflammation (Morrow, 1998; Sindhu et al., 2012). Also, the mucilage richness of callus infusion suggests the soothe effect of inflamed tissues. We suggest that the flavonoids and anthocyanins content in the callus could apply an anti-inflammatory effect. Wiseman et al. (2001) and O'Leary et al. (2004) explained that flavonoids exert multi-level anti-inflammatory properties by

the inhibition of the production of inflammatory cytokines. In parallel, Larrosa et al. (2010) and Havsteen (2002) have reported the synergetic important role of flavonoids and anthocyanins in the protection of veins and capillaries. Moreover, Ez Zoubi et al. (2016) underlined the significant anti-inflammatory effects of flavonoids and mucilage fractions with time on edema especially on cyclooxygenase activity (COX) at the later phase by inhibition. We suppose that saponins of callus infusion act as inhibitors of prostaglandins to increase the anti-inflammatory response.

This study highlighted the successful callus induction using capitula explants and culture conditions chosen, this new material (calluses) provide a higher production of mucilage comparing to mother plant. This overview opens the minds to their use as cell cultures for the production of these active components.

These findings have also successfully showed the effective therapeutic potential of callus to consider in further biological activities. Indeed, the application of callus infusion at (2 and 5 g/kg) on animal models has revealed an interesting anti-inflammatory effect comparing to Diclofenac[®], due to the production of 3-hydroxy-4-methoxycinnamic acid and other components.

Conclusion

This study reports for the first time the callus formation of *Pulicaria incisa* and evaluation of the anti-inflammatory activity due to its biological composition. Based on our results, we have successfully showed an interactive relationship between the pharmacology and the plant biotechnology which could be applying into the large-scale active principles production in the future. In addition, these findings suggest that the callus extracts has a positive oral safety, which is non-toxic, may be useful in human health by anti-inflammatory effects. These effects could be ascribed to phenolic compounds such as 3-hydroxy-4-methoxycinnamic as anti-inflammatory source with markedly reduce edema. Thus, future studies are needed to induce the production of high secondary metabolites amounts in calluses mass, by varying elicitors and medium composition, then, should examine the major components isolated individually after identification by HPLC. The application of this process on other endemic medicinal plants could be more advantageous for metabolites production and brittle plant species preservation independently of current ecological conditions.

Acknowledgements. This study was supported by General Direction of Scientific Research and Technological Development (DGRSDT) with the High Ministry of Research and Study (MESRS) of Algiers. We express our deepest thanks to Pr N. Bouguedoura (LRZA, USTHB), Pr A. Mohammedi (VALCOR) Boumerdes, Dr. K. Azine of Pharmaco-toxicology of CRD Saidal and Z. Bettache of Central Laboratory of Scientific Police (Algiers) for their cooperation.

REFERENCES

- [1] Arafa, N. M., Ibrahim, M. M., Aly, U. I. (2015): Evaluation of total phenolic contents and antioxidant activity of carrot callus extracts as affected by phenylalanine precursor. – *Plant Tissue Culture and Biotechnology* 25: 207-221.
- [2] Arnaldos, T. L., Muñoz, R., Ferrer, M. A., Calderonn, A. A. (2001): Changes in phenol contents during strawberry (*Fragaria ananassa* cv. Chandler) callus culture. – *Physiolgia Plantarum* 113: 315-333.

- [3] Avachat, A. M., Dash, R. R., Shrotriya, S. N. (2011): Recent investigations of plant based natural gums, mucilages and resins in novel drug delivery systems. – Indian Journal of Pharmaceutical Education and Research 45: 86-99.
- [4] Azeez, H., Ibrahim, K., Pop, R., Pamfil, D., Hârța, M., Bobiș, O. (2017): Changes induced by gamma ray irradiation on biomass production and secondary metabolites accumulation in *Hypericum triquetrifolium* Turra callus cultures. – Industrial Crops and Products 108: 183-189.
- [5] Benhouhou, S. A. (2005): Guide to Medicinal Plants in North Africa: *Pulicaria incisa* (Lam.) DC. – IUCN, Malaga, Spain.
- [6] Boumaraf, F. M., Carbone, M., Letizia Ciavatta, M., Benyahia, S., Ameddah, S., Menad, A. Benayache, S., Benayache, F., Gavagninet, M. (2016): Exploring the bioactive terpenoid content of an Algerian plant of the genus *Pulicaria*: the *ent*-Series of *Asteriscunolides*. – Journal of Natural Products 80: 82-89.
- [7] Bruneton, J. (2009): Pharmacognosie, phytochimie, plantes médicinales. – Lavoisier Technique & Documentation. 4^{ème} ed. Paris.
- [8] Chabane, D. (2007): Improvement of date palm (*Phoenix dactylifera* L.) by protoplast fusion of two cultivars Deglet Nour sensitive and Takerboucht resistant to bayoud disease. – Doctorat, USTHB, Algiers, Algeria (in French).
- [9] Du, M., Huang, S., Zhang, J., Wang, J., Hu, L., Jiang, J. (2015): Toxicological test of saponins from *Sapindus mukorossi* Gaerth. – Open Journal of Forestry 5: 749-753.
- [10] Duncan, R. C., Knapp, R. G., Miller, M. C. (1977): Test of Hypotheses in population Means, In: Introductory Biostatistics for Health Sciences. – John Wiley and Son Inc., New York, pp. 71-96.
- [11] Eid, H. H., Metwally, G. F. (2017): Phytochemical and biological study of callus cultures of *Tulbaghia violacea* Harv. Cultivated in Egypt. – Natural Product Research 31: 1717-1724.
- [12] Ewais, E. A., Abd El-Maboud, M. M., Haggag, M. (2014): Studies on chemical constituents and biological activity of *Pulicaria incisa* subsp. *incisa* (Asteraceae). – Report and Opinion 6: 27-33.
- [13] Ez Zoubi, Y., Bousta, D., El Mansouri, L., Boukhira, S., Siham, L., Achour, S., Abdellah, F. (2016): Phytochemical screening, anti-inflammatory activity and acute toxicity of hydro-ethanolic, flavonoid, tannin and mucilage extracts of *Lavandula stoechas* L. from Morocco. – International Journal of Pharmacognosy and Phytochemical Research 8: 31-37.
- [14] Farvardin, A., Ebrahimi, A., Hosseinpour, B., Khosrowshahli, M. (2017): Effects of growth regulators on callus induction and secondary metabolite production in *Cuminum cyminu*. – Natural Product Research 31: 1963-1970.
- [15] Ghouila, H., Beyaoui, A., Jannet, H. B., Hamdi, B., Salah, A. B., Mighri, Z. (2009): Isolation and structure determination of pulicazine, a new sesquiterpene lactone from the Tunisian *Pulicaria laciniata* (Coss. et Kral.) Thell. – Tetrahedron Letters 50: 1563-1565.
- [16] Gupta, M., Kour, B., Kaul, S., Dhar, M. K. (2015): Mucilage synthesis in callus cultures of *Plantago ovata* Forsk. – National Academy Science Letters 38: 103-106.
- [17] Hammiche, V., Maiza, K. (2006): Traditional medicine in Central Sahara: Pharmacopoeia of Tassili N'ajjer. – Journal of Ethnopharmacology 105: 358-367.
- [18] Harborne, J. B. (1998): Phytochemical Methods a Guide to Modern Techniques of Plant Analysis (3rd ed.), Vol 2. – Chapman and Hall, London.
- [19] Havsteen, B. (2002): The bioactivity and medical significance of the flavonoides. – Pharmacology and Therapeutics 96: 67-202.
- [20] Jahn, A. I., Günzel, P. K. H. (1997): The value of spermatology in male reproductive toxicology: do spermatologic examinations in fertility studies provide new and additional information relevant for safety assessment. – Reproductive Toxicology 11: 171-178.
- [21] Kim, E. O., Min, K. J., Kwon, T. K., Um, B. H., Moreau, R. A., Choi, S. W. (2012): Anti-inflammatory activity of hydroxycinnamic acid derivatives isolated from corn bran in

- lipopolysaccharide-stimulated Raw 264.7 macrophages. – Food and Chemical Toxicology 50(5): 1309-1316.
- [22] Langenheim, J. H. (2003): Plant Resins: Chemistry, Evolution, Ecology and Ethnobotany. – Timber Press, Portland, OR, USA.
- [23] Larrosa, M., García-Conesa, M. T., Espín, C., Tomás-Barberán, F. A. (2010): Ellagitannins, ellagic acid and vascular health. – Molecular Aspects of Medicine 31: 513-539.
- [24] Litchfield, J. T., Wilcoxon, F. (1949): A simplified method of evaluating dose-effect experiments. – Journal of Pharmacology and Experimental Therapeutics 96: 99-113.
- [25] Maiza, K. (2008): Pharmacopée traditionnelle saharienne: Sahara algérien. – Thèse de doctorat Ph. D., Université Abou Bakr Belkaid, Algérie.
- [26] Mansour, R. M. A., Ahmed, A. A., Melek, F. R., Saleh, N. A. M. (1990): The flavonoids of *Pulicaria incisa*. – Fitoterapia 61(2): 186-187.
- [27] Mathur, A., Mathur, A. K., Gangwar, A., Yadav, S., Verma, P., Sangwan, R. S. (2010): Anthocyanin production in a callus line of *Panax sikkimensis* Ban. – In Vitro Cellular Developmental Biology - Plant 46: 13-21.
- [28] Morel, G., Wetmore, R. M. (1955): Fern callus tissue culture. – American Journal Botany 38: 141-143.
- [29] Morrow, T. (1998): Herbal Compound for Relief of PMS through Menopausal Symptoms. – US Patent 707.
- [30] Murashige, T., Skoog, F. (1962): A revised medium for rapid growth and bioassays with tobacco tissue cultures. – Physiologia Plantarum 15: 473-497.
- [31] Muthukumar, M., Indu Priyanka, K. R., Bhaskar, S., Kalpana, B., Dinakar, R. (2017): Novel extraction, characterization and pharmaceutical application of okra mucilage (*Abelmoschus esculentus*) as a pharmaceutical excipient. – World Journal of Pharmacy and Pharmaceutical Sciences 6: 321-328.
- [32] Nacer bey, N., Chabane, D., Abdelkrim, H., Aribi, I. (2015): Traditional herbal medicine in Jijel region, Northeast of Algeria. – Advances in Environmental Biology 9: 54-61.
- [33] Nana, H. M., Ngane, R. A., Kuate, J. R., Mogtomo, L. M., Tamokou, J. D., Ndifor, F., Mouokeu, R. S., Ebelle Etame, R. M., AmvamZollo, P. H. (2011): Acute and sub-acute toxicity of the methanolic extract of *Pteleopsis hylo dendron* stem bark. – Journal of Ethnopharmacology 137: 70-76.
- [34] O'Leary, K. A., De Pascual-Teresa, S., Needs, P. W., Bao, Y. P., O'Brien, N. M., Williamson, G. (2004): Effect of flavonoids and vitamin E on cyclooxygenase-2 (COX-2) transcription. – Mutation Research 551: 245-254.
- [35] Ozenda, P. (2004): Flore et végétation du Sahara (3rd ed.). – CNRS, Paris.
- [36] Ozyigit, I. I., Kahraman, M. V., Ercan, O. (2007): Relation between explant age, total phenols and regeneration response in tissue cultured cotton (*Gossypium hirsutum* L.) – African Journal Biotechnology 6: 003-008.
- [37] Rouane, A. (2012): Ethnobotanic, anatomic and phytochemical reactions studies of *Pulicaria incisa* (Lam.) DC., a medicinal plant of Tamanrasset to biotechnological expression. – Magister Thesis, University of Sciences and Technology Houari Boumediene. Algeria (in French).
- [38] Saad, S., Ouafi, S., Chabane, D. (2016): Anti-inflammatory and acute toxicity evaluation of aqueous infusion extract obtained from aerial parts of *Marrubium deserti* de NOÉ growing in Algeria. – African Journal of Traditional Complementary and Alternative Medicines 13: 71-539.
- [39] Sahki, A., Sahki, R. (2004): Le Hoggar: promenade botanique. – Atelier Ésope, Lyon.
- [40] San Feliciano, A., Medarde, M., Gordaliza, M., Del Olmo, E., Del Corral, M. J. M. (1989): Sesquiterpenoids and phenolics of *Pulicaria paludosa*. – Phytochemistry 28: 2717-2721.

- [41] Shiraki, K., Masahiko, K., Kumeda, C. A., Yamamura, J-i., Kamiyama, T. (1998): Antipyretic activity of cinnamyl derivatives and related compounds in influenza virus-infected mice. – *European Journal of Pharmacology* 348: 45-51.
- [42] Sindhu, G., Ratheesh, M., Shyni, G. L., Nambisan, B., Helen, A. (2012): Anti-inflammatory and antioxidative effects of mucilage of *Trigonella foenum graecum* (Fenugreek) on adjuvant induced arthritic rats. – *International Immunopharmacology* 12: 205-211.
- [43] Winter, C. A., Risley, F. A., Nuss, O. W. (1962): Carrageenin induced oedema in hand paw of the rat as assays anti-inflammatory drugs. – *Proceedings of the Society for Experimental Biology and Medicine* 111: 544-547.
- [44] Wiseman, S., Mulder, T., Rietveld, A. (2001): Tea flavonoids: bioavailability in vivo and effects on cell signaling pathways in vitro. – *Antioxidants and Redox Signaling* 3: 1009-1021.
- [45] Zhang, Y., Shu, Z., Yin, L., Ma, L., Wang, X., Fu, X. (2015): Anti-inflammatory and antinociceptive activities of non-alkaloids fractions from *Aconitum flavum* in vivo. – *Revista Brasileira Farmacognosia* 25: 47-52.

UPTAKE KINETICS OF NH_4^+ , NO_3^- AND H_2PO_4^- BY SUBMERGED MACROPHYTES *ELODEA NUTTALLII* (ST. JOHN, 1920) AND *VALLISNERIA NATANS* (JUSSIEU, 1826)

XIONG, H. F.

*Institute of Wetland Resource and Economy, Ezhou polytechnic
Ezhou 436000, Hubei Province, China
(e-mail: xhfeng987@163.com)*

(Received 11th Sep 2018; accepted 27th Nov 2018)

Abstract. The source of lake eutrophication comes from the excessive input of nitrogen and phosphorus and their uncoordinated proportion, while nitrogen and phosphorus are essential elements for the growth of aquatic plants. Using aquatic plants to treat sewage has incomparable advantages compared with chemical and physical methods. It not only makes the whole process is derived for natural behavior, but also improves landscape and avoids new environmental problems. Studying the uptake kinetics of NH_4^+ , NO_3^- and H_2PO_4^- of aquatic plants can help us to select the proper aquatic macrophyte according to the status of eutrophic water. In June 2017, the absorption kinetics of NH_4^+ , NO_3^- and H_2PO_4^- by *Elodea nuttallii* and *Vallisneria natans* under the eutrophication stress were studied in indoor simulation experiments at the plant nutrition laboratory of Huazhong Agricultural University of China. The results showed that the V_{\max} absorbed by NH_4^+ of *Elodea nuttallii* and *Vallisneria natans* at three phosphorus levels decreased with the increase of P concentration. The K_m value increased with the increase of P concentration. On three phosphorus levels, in two plants the V_{\max} of NO_3^- decreased with the increase of P concentration. The K_m value of NO_3^- absorbed by *Elodea nuttallii* at different levels of phosphorus decreased with the increase of P concentration. The K_m of NO_3^- on *Vallisneria natans* increased with the increase of P concentration. The V_{\max} of H_2PO_4^- of *Elodea nuttallii* and *Vallisneria natans* at three nitrogen levels decreased with the increase of N concentration. The K_m value of *Elodea nuttallii* and *Vallisneria natans* at three nitrogen levels increased with the increase of N concentration. In eutrophication environment, the stress of submerged plants will affect their nutrient absorption. The nutritive stress of low N,P increased the absorption potential of N,P. High NP nutrition stress reduced the absorption rate and affinity.

Keywords: aquatic macrophyte, stress, eutrophication, nitrogen and phosphorus, uptake kinetics

Introduction

Lake eutrophication is one of the hot topics in the world today. Nitrogen and phosphorus are two important factors for the eutrophication of freshwater lakes, and they are also the main nutrient elements of plants. The high concentration of nitrogen and phosphorus in water can also cause the imbalance of physiological functions of submerged macrophytes, inhibit their growth and even lead to decline (Cao and Ni, 2004; Been, 2001; Arts, 2002). The latest research shows that the high concentration of nitrogen in lake water is closely related to the degeneration of submerged macrophytes in shallow lakes (Sagrario et al., 2005). High concentration of ammonium nitrogen has attracted much attention due to its physiological stress on aquatic plants (Carr et al., 1997; Xiong et al., 2010; Farnsworth-Lee and Baker, 2000). The direct absorption of nitrogen and phosphorus by plants in water is one of the main mechanisms of eutrophication. At present, the eutrophication management with aquatic plants as the core has become a research hotspot (Huang et al., 2010), especially the restoration of submerged plants, as an important measure to restore the aquatic ecosystem and purify the water eutrophic substances, has attracted more and more attention (Jiang et al., 2004;

Wang et al., 2008). Kinetic method is an effective way to study the characteristics of plant nutrient absorption. The study of nutrient absorption kinetics began in the early 1950s. Epstein and Hagen (1952) first used the kinetic equation of enzymatic reaction to study the absorption of ions by plants. In 1978, Nielsen and Barber (1978) revised the Michaelis-Menten equation and put forward the concept of the lowest equilibrium concentration, so that the equation can quantitatively describe the characteristics of root absorption of nutrients. In terms of research methods, Classen and Barber (1974) first established the exhaustion method in 1974 to obtain various parameters of the kinetic equation, i.e. after hydroponics of plants, the dynamic changes of ion concentration in the culture solution that decrease with time were measured.

On the basis of the kinetic theory of enzymatic reaction, the absorption kinetics of nitrogen and phosphorus in a variety of submerged plants was studied. The mechanism of removing nitrogen and phosphorus from water bodies was further clarified, and the theoretical and practical significance of selecting aquatic plants in the ecological restoration project for the eutrophic water bodies with different nutritional characteristics was carried out (Chang et al., 2008; Han and Yu, 2017).

At present, there are many studies on the absorption kinetics of nitrogen, phosphorus and other nutrient pollutants in submerged plants. The effects of temperature, light and pH on the uptake of nitrogen and phosphorus in aquatic plants were mostly concentrated (Tang et al., 2011; Shen et al., 2006; Jampeetong and Brix, 2009). Liu et al. (2009) have studied the *Potamogeton malaianus* on the absorption kinetics of ammonia nitrogen. Chang and other studies have focused on the absorption kinetics of ammonia nitrogen and nitrate nitrogen by *Jussiaea stipulaceaohwe*, *Elodea nuttallii* and *Eichhornia crassipes* of hyacinth (Chang et al., 2008). Chen et al. (2012) have studied the pollution absorption dynamic of *Hydrilla verticillata* and *Vallisneria asiatica* on nitrogen and phosphorus. Zhang et al. (2013) studied the absorption kinetics of ammonia by *Vallisneria natans* and *Myriophyllum spicatum* under light and dark conditions. The interaction between nitrogen and phosphorus, two important factors of eutrophication in freshwater lakes, has been neglected.

Vallisneria asiatica and *Elodea nuttallii* are common submerged macrophytes in lakes and rivers in the middle and lower reaches of Yangtze River. Their ecological adaptability is wide, their ability to adsorb pollutants is strong, and their community is easy to rebuild. Therefore, in this study, *Elodea nuttallii* and *Vallisneria asiatica* are selected as research object. Studying the effects of nitrogen and phosphorus absorption kinetics under different eutrophic conditions is to provide a theoretical basis for selecting suitable plants for the remediation of water bodies with different pollution levels.

Materials and methods

Experimental materials

Vallisneria asiatica and *Elodea nuttallii* were taken from Liangzi Lake in China (Fig. 1). Each plant was taken about 1000 g. Simulation experiment was completed at the plant nutrition laboratory of Huazhong Agricultural University of China in June 2017. The test was carried out in a glasshouse with a temperature of 22°C-26°C, light intensity of 5000 LX and a relative humidity of 70%-80%. The plants were washed with distilled water and then cultured in 1/8 Hoagland nutrient solution (pH 6.5) for 20 d. Replace the nutrient solutions per 3 d. After water culture for 20 d, the plants with good

growth were selected for nutrient absorption test. Remove plants from the nutrient solution, rinse the plants with deionized water and then transfer to $0.2 \text{ mmol.L}^{-1} \text{ CaSO}_4$ solution. Pre-culture in a greenhouse for 24 h to make it hungry.



Figure 1. Plant sampling point

Absorption test

The experiment set up 3 levels of P, to determine kinetics parameters of NH_4^+ and NO_3^- in two plants under different P stress conditions. The experiment also set 3 levels of N, to determine the kinetic parameters of H_2PO_4^- uptake by two plants under different N stress conditions. The design concentration of NH_4^+ , NO_3^- and H_2PO_4^- as shown in Table 1.

Table 1. The concentration of NH_4^+ , NO_3^- and H_2PO_4^-

	P1	P2	P3		N1	N2	N3
NH_4^+ 1mg.L^{-1}	0.04	0.08	0.5	H_2PO_4^- 0.01mg.L^{-1}	0.4	1.2	3.6
NO_3^- 1mg.L^{-1}	0.04	0.08	0.5				

The absorption kinetics parameters of NH_4^+ , NO_3^- and H_2PO_4^- were determined by conventional exhaustion. The 10 g plants after starvation were moved into the triangular bottle equipped with 250 mL culture solution for absorption experiments. 3 repetitions were set in each absorption test. The experiment was carried out in an artificial climate incubator with a temperature of 25°C , a light intensity of 5000 LX, and a relative humidity of 75%. The absorption liquid samples were taken at 0 h, 1 h, 2 h, 3 h, 4 h, 5 h, 6 h, respectively. After sampling for 1 ml, 1 ml of deionized water was added. The plant was taken out immediately after the sampling was completed. The moisture content on the surface of plants is dried up by filter paper, then measuring fresh weight. The absorption curve was drawn according to the concentration and absorption time of the culture solution. Then the kinetic parameters are obtained according to the absorption curve equation.

Determination method

The concentration of NH_4^+ was determined by indolo blue colorimetry. The concentration of NO_3^- was determined by Ultraviolet spectrophotometry. H_2PO_4^- concentration was determined by molybdate ammonium spectrophotometric method (State Environmental Protection Administration 2002 in Chinese).

Calculation of dynamic parameters

Firstly, the equation of ion consumption curve is obtained. The commonly used equation is univariate quadratic polynomial:

$$Y = a + bX + cX^2 \quad (\text{Eq.1})$$

In the equation, X is the absorption time and Y is the ion concentration. The first derivative of the equation is obtained to obtain a concentration change rate equation:

$$Y' = b + 2cX \quad (\text{Eq.2})$$

Equation 2 is treated as follows: $x \rightarrow 0$, at this time, $y' = b$, thus, the maximum rate of change of concentration is obtained. By considering the volume and root weight of the absorbent liquid and using the formula $V_{\max} = b \times V / \text{fresh weight}$, the maximum absorption rate per unit weight can be obtained. V_{\max} reflects the inherent potential of plants to absorb nutrients. $Y' = 1 / 2b$ is substituted into Equation 2 to find x, and x is replaced by Equation 1 to find Y. Y is the K_m value (concentration of medium at $1 / 2 V_{\max}$). K_m represents the affinity of the absorption system. The small K_m value indicates that the root absorption system has great affinity for this ion.

Method of data analysis

Data processing using double reciprocal transformation of Michaelis Menten dynamic equation (Epstein and Hagen, 1952). Then calculate the kinetic parameters V_{\max} and K_m . The data are processed by double reciprocal transformation by using Michaelis-Menten dynamics equation. The dynamic parameters V_{\max} and K_m are obtained. All the data were processed and analyzed by Excel 2003 software.

Results

The effect of P on the kinetics of absorption of NH_4^+ by two aquatic macrophytes

NH_4^+ absorption concentration of *Elodea nuttallii* and *Vallisneria natans* changes with time, as show in Figure 2. *Elodea* has the fastest absorption rate in the first hour. After 3 h, the absorption rate tends to be stable. The rate of NH_4^+ uptake by 2 water plants decreased with the increase of P concentration. Through the absorption curve of two plants, the ion depletion equation of NH_4^+ was obtained after fitting (Table 2). The kinetic parameters of NH_4^+ in plant absorption were obtained according to the ion depletion equation (Table 3). From Table 3, we can see that the maximum absorption rates of NH_4^+ are $5.055 \text{ ug}^{-1} \cdot \text{g}^{-1} \cdot \text{h}^{-1}$, $5.022 \text{ ug}^{-1} \cdot \text{g}^{-1} \cdot \text{h}^{-1}$ and $4.902 \text{ ug}^{-1} \cdot \text{g}^{-1} \cdot \text{h}^{-1}$, respectively. The maximum absorption rates of NH_4^+ V_{\max} of *Vallisneria natans* are $4.83 \text{ ug}^{-1} \cdot \text{g}^{-1} \cdot \text{h}^{-1}$, $4.57 \text{ ug}^{-1} \cdot \text{g}^{-1} \cdot \text{h}^{-1}$ and $4.33 \text{ ug}^{-1} \cdot \text{g}^{-1} \cdot \text{h}^{-1}$. V_{\max} has a tendency to decrease with the increase of P concentration. The maximum absorption rate V_{\max} of *Elodea nuttallii* to NH_4^+

decreased slightly with the increase of P concentration. The maximum absorption rate V_{\max} of *Vallisneria natans* to NH_4^+ decreases greatly with the increase of P concentration, which is about 5%. The K_m values of NH_4^+ absorbed by *Elodea nuttallii* are $164.8688 \text{ ug.L}^{-1}$, $1206.3271 \text{ ug.L}^{-1}$ and $240.0115 \text{ ug.L}^{-1}$, respectively. K_m values of NH_4^+ uptake by *Elodea nuttallii* under P2 and P3 are 25.15% and 45.58%, which are higher than those under P1, respectively. K_m value of NH_4^+ uptake by *Elodea nuttallii* under P3 condition is 16.33%, which is higher than that under P2 condition. The absorption of NH_4^+ K_m values of *Vallisneria natans* are $176.1859 \text{ ug.L}^{-1}$, $201.9644 \text{ ug.L}^{-1}$ and $215.2731 \text{ ug.L}^{-1}$. K_m values of NH_4^+ uptake by *Vallisneria natans* under P2 and P3 are 14.63% and 22.19%, which are higher than that under P1, respectively. K_m value of NH_4^+ uptake by *Vallisneria natans* under P3 condition is 6.58%, which is higher than that under P2 condition. The K_m value has a tendency to increase with the increase of P concentration.

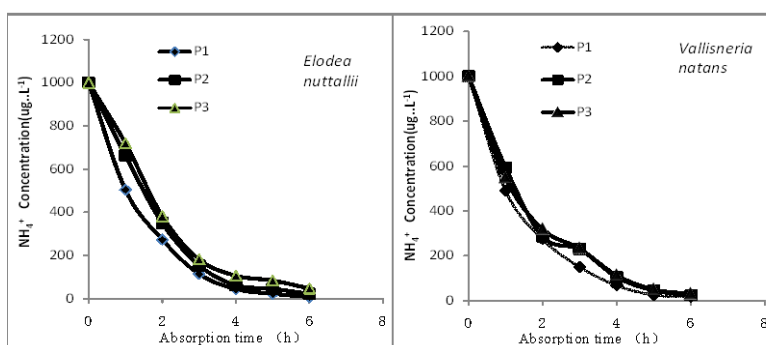


Figure 2. Changes of NH_4^+ concentrations in culture solution for the two aquatic macrophytes P1- 0.04 mg.L^{-1} , P2- 0.08 mg.L^{-1} , P3- 0.5 mg.L^{-1} , $n=3$

Table 2. Equations of NH_4^+ concentration versus uptake time for aquatic macrophytes

	<i>Elodea nuttallii</i>	<i>Vallisneria natans</i>
P1	$y = 70.27x^2 - 504.5x + 844.0$	$y = 66.49x^2 - 483.0x + 834.3$
P2	$y = 68.15x^2 - 507.2x + 914.1$	$y = 60.02x^2 - 457.0x + 864.4$
P3	$y = 64.96x^2 - 490.2x + 933.6$	$y = 57.93x^2 - 443.5x + 851.9$

P1- 0.04 mg.L^{-1} , P2- 0.08 mg.L^{-1} , P3- 0.5 mg.L^{-1} , $n=3$

Table 3. Kinetic parameters of NH_4^+ absorption by the two aquatic macrophytes

Plant species	$V_{\max} (\text{ug}^{-1} \cdot \text{g}^{-1} \cdot \text{h}^{-1})$				$K_m (\text{ug.L}^{-1})$			
	P1	P2	P3	R^2	P1	P2	P3	R^2
<i>Elodea nuttallii</i>	5.045	5.022	4.902	0.9652	164.8688	206.3271	240.0115	0.9832
<i>Vallisneria natans</i>	4.83	4.57	4.33	0.9768	176.1859	201.9644	215.2731	0.9796

P1- 0.04 mg.L^{-1} , P2- 0.08 mg.L^{-1} , P3- 0.5 mg.L^{-1} , $n=3$

The effect of P on the kinetics of absorption of NO_3^- by two aquatic macrophytes

The NO_3^- concentration of *Elodea nuttallii* and *Vallisneria natans* varies with the liquid absorption time, as show in Figure 3. With the prolongation of absorption time, the concentration of NO_3^- in absorption solution decreases. The absorption of NO_3^- by

Vallisneria natans in the first 2 hours is faster than that of *Elodea nuttallii*. Through the absorption curves of the two plants, the ion depletion equation for absorbing NO_3^- is obtained after fitting (Table 4). From Table 5, we know that V_{\max} to NO_3^- of *Elodea nuttallii* are $2.45 \text{ mg}\cdot\text{g}^{-1}\cdot\text{h}^{-1}$, $2.26 \text{ mg}\cdot\text{g}^{-1}\cdot\text{h}^{-1}$ and $1.97 \text{ mg}\cdot\text{g}^{-1}\cdot\text{h}^{-1}$, respectively. V_{\max} of NO_3^- absorbed by *Elodea nuttallii* under P2 and P3 are 7.76% and 19.59%, which are lower than that under P1, respectively.

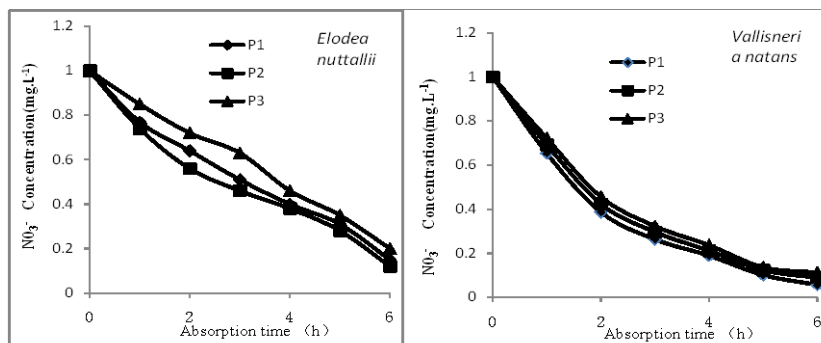


Figure 3. Changes of NO_3^- concentrations in culture solution for the two aquatic macrophytes P1- $0.04 \text{ mg}\cdot\text{L}^{-1}$, P2- $0.08 \text{ mg}\cdot\text{L}^{-1}$, P3- $0.5 \text{ mg}\cdot\text{L}^{-1}$, $n=3$

Table 4. Equations of NO_3^- concentration versus uptake time for aquatic macrophytes

	<i>Elodea nuttallii</i>	<i>Vallisneria natans</i>
P1	$y = 0.019x^2 - 0.245x + 0.929$	$y = 0.052x^2 - 0.417x + 0.890$
P2	$y = 0.023x^2 - 0.266x + 0.907$	$y = 0.050x^2 - 0.407x + 0.909$
P3	$y = 0.009x^2 - 0.197x + 0.962$	$y = 0.048x^2 - 0.396x + 0.923$

P1- $0.04 \text{ mg}\cdot\text{L}^{-1}$, P2- $0.08 \text{ mg}\cdot\text{L}^{-1}$, P3- $0.5 \text{ mg}\cdot\text{L}^{-1}$, $n=3$

Table 5. Kinetic parameters of NO_3^- absorption by the two aquatic macrophytes

Plant species	V_{\max} ($\text{mg}\cdot\text{g}^{-1}\cdot\text{h}^{-1}$)				Km ($\text{mg}\cdot\text{L}^{-1}$)			
	P1	P2	P3	R^2	P1	P2	P3	R^2
<i>Elodea nuttallii</i>	2.45	2.26	1.97	0.981	0.3366	0.3102	0.1534	0.9758
<i>Vallisneria natans</i>	4.17	4.01	3.86	0.969	2631	0.2878	0.3104	0.9699

P1- $0.04 \text{ mg}\cdot\text{L}^{-1}$, P2- $0.08 \text{ mg}\cdot\text{L}^{-1}$, P3- $0.5 \text{ mg}\cdot\text{L}^{-1}$, $n=3$

The V_{\max} of NO_3^- absorbed by *Elodea nuttallii* under P3 condition is 12.83%, which is lower than that under P2 condition. The V_{\max} of NO_3^- on *Vallisneria natans* are $4.17 \text{ mg}\cdot\text{g}^{-1}\cdot\text{h}^{-1}$, $4.01 \text{ mg}\cdot\text{g}^{-1}\cdot\text{h}^{-1}$ and $3.86 \text{ mg}\cdot\text{g}^{-1}\cdot\text{h}^{-1}$. V_{\max} values of NO_3^- absorbed by *Vallisneria natans* under P2 and P3 are 3.83% and 7.43%, which are lower than that under P1, respectively. The V_{\max} value of NO_3^- absorbed by *Vallisneria natans* under P3 condition is 3.74%, which is lower than that under P2 condition. The V_{\max} of the two plants decreased with the increase of P concentration. The Km values of NO_3^- absorbed by *Elodea nuttallii* are $0.3366 \text{ mg}\cdot\text{L}^{-1}$, $0.3102 \text{ mg}\cdot\text{L}^{-1}$ and $0.1534 \text{ mg}\cdot\text{L}^{-1}$, respectively. Km values of NO_3^- absorbed by *Elodea nuttallii* under P2 and P3 are 7.84% and 54.43%, which are lower than that under P1, respectively. The Km value of NO_3^- absorbed by *Elodea nuttallii* under P3 condition is 50.55%, which is lower than that

under P2 condition. The K_m value of *Elodea nuttallii* decreases with the increase of P concentration. The absorption of NO_3^- *Vallisneria natans* K_m values are $0.2631 \text{ mg}\cdot\text{L}^{-1}$, $0.2878 \text{ mg}\cdot\text{L}^{-1}$ and $0.3104 \text{ mg}\cdot\text{L}^{-1}$. K_m values of NO_3^- absorbed by *Vallisneria natans* under P2 and P3 conditions are 9.39% and 17.98%, which are higher than that under P1 conditions, respectively. The K_m value of NO_3^- absorbed by *Vallisneria natans* under P3 condition is 7.85%, which is higher than that under P2 condition. The K_m value of *Vallisneria natans* increases with the concentration of P and the rising trend.

The effect of N on the kinetics of absorption of H_2PO_4^- by two aquatic macrophytes

Figure 4 shows that the ion concentration in solution decrease with the increase of absorption time. Because of plant starvation, the absorption rate of ions is the fastest within 2 h after the start of the experiment. According to Figure 3, the ion depletion equation of two plants is derived (Table 6). Then the kinetic parameters are obtained (Table 7). From Table 7, we know that the maximum absorption rates (V_{\max}) of *Elodea nuttallii* to H_2PO_4^- are $0.29 \text{ mg}\cdot\text{g}^{-1}\cdot\text{h}^{-1}$, $0.25 \text{ mg}\cdot\text{g}^{-1}\cdot\text{h}^{-1}$, and $0.23 \text{ mg}\cdot\text{g}^{-1}\cdot\text{h}^{-1}$, respectively. V_{\max} values of H_2PO_4^- absorbed by *Elodea nuttallii* under P2 and P3 conditions are 13.79% and 20.69%, which are higher than that under P1 conditions, respectively. V_{\max} value of H_2PO_4^- absorbed by *Elodea nuttallii* under P3 condition is 8.0%, which is higher than that under P2 condition. The maximum absorption rates (V_{\max}) of *Vallisneria natans* to H_2PO_4^- are $0.25 \text{ mg}\cdot\text{g}^{-1}\cdot\text{h}^{-1}$, $0.22 \text{ mg}\cdot\text{g}^{-1}\cdot\text{h}^{-1}$, $0.18 \text{ mg}\cdot\text{g}^{-1}\cdot\text{h}^{-1}$. V_{\max} values of H_2PO_4^- absorbed by *Vallisneria natans* under P2 and P3 conditions are 12.0% and 28.00%, which are lower than that under P1 conditions, respectively. V_{\max} value of H_2PO_4^- absorbed by *Vallisneria anatans* under P3 condition is 18.18%, which is lower than that under P2 condition. The V_{\max} of the two plants decreases with the increase of N concentration. The K_m values of H_2PO_4^- absorbed by *Elodea nuttallii* are $0.0132 \text{ mg}\cdot\text{L}^{-1}$, $0.0158 \text{ mg}\cdot\text{L}^{-1}$ and $0.0172 \text{ mg}\cdot\text{L}^{-1}$, respectively. K_m values of H_2PO_4^- absorbed by *Elodea nuttallii* under P2 and P3 are 19.70% and 30.30%, which are higher than that under P1, respectively. K_m value of H_2PO_4^- absorbed by *Elodea nuttallii* under P3 condition is 8.86%, which is higher than that under P2 condition. The K_m values of the absorption of H_2PO_4^- on *Vallisneria natans* are $0.0242 \text{ mg}\cdot\text{L}^{-1}$, $0.0380 \text{ mg}\cdot\text{L}^{-1}$ and $0.0441 \text{ mg}\cdot\text{L}^{-1}$, respectively. The K_m values of H_2PO_4^- absorbed by *Vallisneria natans* under P2 and P3 conditions are 57.02% and 82.23%, which are higher than that under P1 conditions, respectively. The K_m value of H_2PO_4^- absorbed by *Vallisneria natans* under P3 condition is 16.05%, which is higher than that under P2 condition. The K_m value has a tendency to increase with the increase of N concentration.

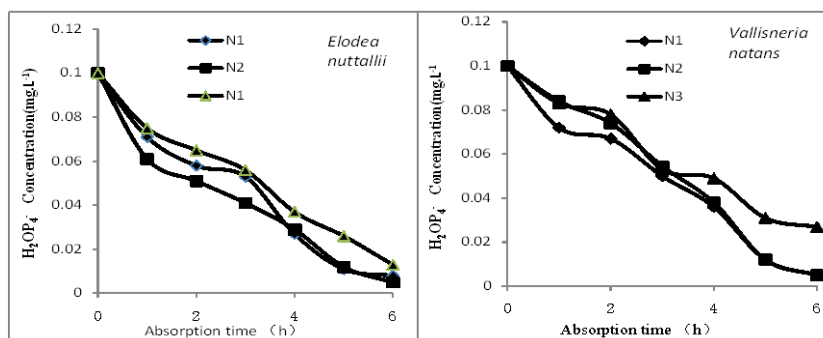


Figure 4. Changes of H_2PO_4^- concentrations in culture solution for the two aquatic macrophytes, N1- $0.4 \text{ mg}\cdot\text{L}^{-1}$, N2- $1.2 \text{ mg}\cdot\text{L}^{-1}$, N3- $3.6 \text{ mg}\cdot\text{L}^{-1}$

Table 6. Equations of H_2PO_4^- concentration versus uptake time for aquatic macrophytes

	<i>Elodea nuttallii</i>	<i>Vallisneria natans</i>
N1	$y = 0.002x^2 - 0.029x + 0.092$	$y = 0.001x^2 - 0.025x + 0.093$
N2	$y = 0.002x^2 - 0.030x + 0.087$	$y = 0.001x^2 - 0.028x + 0.099$
N3	$y = 0.001x^2 - 0.023x + 0.092$	$y = 0.002x^2 - 0.024x + 0.098$

N1-0.4 mg.L⁻¹, N2-1.2 mg.L⁻¹, N3-3.6 mg.L⁻¹

Table 7. Kinetic parameters of H_2PO_4^- absorption by the two aquatic macrophytes

Plant species	V_{\max} (mg ⁻¹ .g ⁻¹ .h ⁻¹)				Km (mg.L ⁻¹)			
	P1	P2	P3	R ²	P1	P2	P3	R ²
<i>Elodea nuttallii</i>	0.29	0.25	0.23	0.955	0.0132	0.0158	0.0172	0.9812
<i>Vallisneria natans</i>	0.25	0.22	0.18	0.969	0.0242	0.038	0.044	0.9798

N1-0.4 mg.L⁻¹, N2-1.2 mg.L⁻¹, N3-3.6 mg.L⁻¹

Discussion

Dynamic parameters Km and V_{\max} can represent the characteristics of aquatic plants absorbing nutrients. The kinetic parameters Km and V_{\max} of nitrogen and phosphorus absorption of submerged plants differ greatly (Chen et al., 2012) and are influenced by environment. Zhang (2012) research found that the V_{\max} and affinity of the *Vallisneria natans* to absorb NH_4^+ were affected by light, temperature and pH. When the temperature is 12°C, the V_{\max} was 0.037 mmol. (g.h)⁻¹ and Km was 0.21 mol.L⁻¹. When the temperature is 12°C, the V_{\max} was 0.208 mmol. (g.h)⁻¹ and Km was 0.61 mol.L⁻¹. Zhang et al. (2013) found that the light intensity had a significant effect on V_{\max} of the *Vallisneria natans* to absorb NH_4^+ . Under the light conditions, the V_{\max} of the *Vallisneria natans* to absorb NH_4^+ was 1.44 times in the dark conditions. Experimental studies have found that the V_{\max} and Km of *Elodea* and *Vallisnerium* for NH_4^+ are affected by the P concentration in the environment. The V_{\max} and affinity of the absorption of NH_4^+ by *Elodea* and *Vallisneria* tend to decrease with the increase of P concentration at the three phosphorus levels. The experimental results showed that the maximum absorption rate and affinity to NH_4^+ of *Elodea nuttallii* and *Vallisneria natans* on the three phosphorus levels decreased with the increase of P concentration. That is to say, with the increase of high P stress, both absorption rate and affinity decrease. The hydrolysate of NH_4^+ is directly passed through cells by free through the way of mountain diffusion, and there are little energy consumption (Runcie et al., 2003; Mehrer and Mohr, 1989). Under severe stress, the cell membrane of plants is destroyed (Xiong et al., 2010). It affects the absorption of NH_4^+ . Plant uptake of P is active transportation, so plants generally don't overeat P. Ma et al. (2008) thinks that the injury of plants under high P stress is mainly manifested in two aspects. One is that high concentration of salt causes excessive osmotic pressure, which leads to water uptake and even loss of water in plant cells. The other one is that excessive salt ions enter the cells, resulting in cell metabolic disorder.

This study found that the V_{\max} of *Elodea nuttallii* and *Vallisneria natans* for NO_3^- decreased with increasing P concentration. The affinity to NO_3^- of *Elodea nuttallii* is decreased with the increase of P concentration under three levels of phosphorus. *Vallisneria natans* affinity for NO_3^- increased with the increase of P concentration.

Zhang (2012) research found that high temperatures severely limit the affinity of *Vallisneria natans* to NO_3^- . Under too low temperature conditions, *Vallisneria natans* showed some inhibition on NO_3^- affinity. The V_{\max} gradually decreases with the increase of illuminance, showing the phenomenon of strong light suppression. NO_3^- uptake by plants is also an active process of absorption. Glutamine synthetase is the first enzyme that has been found to be related to NO_3^- absorption. It is found that under dark conditions, glutamic phthalamine synthetase has higher activity in the roots of large leaf algae (Pregnall, 2004). The uptake of NO_3^- by plants depends on the continuous synthesis of proteins. There may be a transporter between them (Jackson et al., 1973). Ma et al. (2008) studied that when P is high (0.8 mg.L^{-1}), could hardly inhibit or even promote the growth of the three plants within 3 days. It indicates that the tolerance of submerged plants to phosphorus is relatively strong. Under high concentration of phosphorus ribs, there will be no obvious damage to submerged plants in the short term.

Nitrogen and phosphorus are two important essential nutrients for plant growth. Studies (Qian et al., 2005) show that when the nitrogen concentration in the medium is constant, the N/P ratio has a significant influence on the absorption of seaweed P. Similar phenomena have been found in studies on submerged species (Li and Yuan, 2000). This study found that the V_{\max} and affinity to H_2PO_4^- of *Elodea nuttallii* and *Vallisneria natans* decreased with the increase of N concentration. Zhang (2012) research found that the V_{\max} and affinity of the *Vallisneria natans* to absorb H_2PO_4^- were affected by light, temperature and pH. the V_{\max} and affinity of H_2PO_4^- were the strongest under 22°C and $\text{pH}=7$ condition. NP are involved in plant metabolism process, N can promote the absorption of H_2PO_4^- in a certain concentration range. With the increase of N concentration in the solution, the degree of plant stress increased. Thus affecting the absorption of H_2PO_4^- Yan et al. (2007) found that in eutrophic conditions, the increase of ammonia nitrogen concentration would affect the physiological function of *Hydrilla verticillata*. High ammonia nitrogen concentration on *Hydrilla verticillata* is a kind of stress, which can inhibit the growth of plants and even lead to death. Xu et al. (2006) found that when the concentration of ammonia nitrogen is 4 mg, it had a strong stress effect on chlorophyll. Litav and Lehrer (1978) thought that ammonia could cause toxicity to uncoupling of photosynthesis and phosphorylation in chloroplast envelope. Cao and Ni (2007) found that excessive ammonia nitrogen ($> 0.56 \text{ mg.L}^{-1}$) could lead to the degradation of the species of the herb and disrupt the metabolic balance of soluble carbohydrates and free amino acids in plants.

Conclusion

The V_{\max} absorbed by NH_4^+ of *Elodea nuttallii* and *Vallisneria natans* at three phosphorus levels decreased with the increase of P concentration. The K_m value increased with the increase of P concentration. Under the three phosphorus levels, the V_{\max} of NO_3^- in two plants decreased with the increase of P concentration. The K_m value of NO_3^- absorbed by *Elodea nuttallii* at different levels of phosphorus decreased with the increase of P concentration. The K_m of NO_3^- on *Vallisneria natans* increased with the increase of P concentration. The V_{\max} of H_2PO_4^- decreased with the increase of N concentration. The K_m value increased with the increase of N concentration. In eutrophication environment, the stress of submerged plants will affect their nutrient

absorption. The nutritive stress of low N,P increased the absorption potential of N,P. High NP nutrition stress reduced the absorption rate and affinity. This method can be used to screen plants for water ecological restoration in engineering practice, and can also be used as an indicator of plant stress response.

Acknowledgements. This work was financially supported by Hubei science and technology support project (2015BBA151).

REFERENCES

- [1] Arts, G. H. P. (2002): Deterioration of atlantic soft water macrophyte communities by acidification, eutrophication and alkalisation. – *Aquatic Botany* 73: 373-393.
- [2] Been, A., Ni, L. (2001): Effects of water column nutrient enrichment on the growth of *Potamogeton maackianus*. – *Journal of Aquatic Plant Management* 39: 83-87.
- [3] Cao, T., Ni, L. Y. (2004): The response of the antioxidant enzyme in *Ceratophyllum* on inorganic nitrogen increased in water. – *Acta Hydroecologica Sinica* 28(3): 299-302.
- [4] Cao, T., Ni, L. Y. (2007): The role of NH_4^+ toxicity in the decline of the submersed macrophyte *Vallisneria natans* in lakes of the Yangtze River basin. – *China Marine and freshwater Research* 58(6): 581-587.
- [5] Carr, G. M., Duthie, H. C., Taylor, W. D. (1997): Model of aquatic plant productivity: a review of that influence growth. – *Aquatic Botany* 59(3/4): 195-215.
- [6] Chang, H. Q., Li, N., Xu, X. F. (2008): NH_4^+ and NO_3^- uptake kinetics of three aquatic macrophytes. – *Ecology and Environment* 17(2): 511-514.
- [7] Chen, S. Y., Xu, C., Yao, Y. (2012): Uptake Kinetics of Ammonia Nitrate and Phosphorus by Submerged Macrophytes *Hydrilla verticillata* and *Vallisneria natans*. – *Environmental science & Technology* 35(8): 34-36.
- [8] Classen, N., Barber, S. A. (1974): A method for characterizing the relation between nutrient concentration and flux into roots of intact plants. – *Plant Physiol* 54(4): 564-568.
- [9] Epstein, E., Hagen, C. E. (1952): A kinetic study of the absorption of alkaline canons by barley roots. – *Plant Physiology* 27(3): 457-474.
- [10] Farnsworth-Lee, L. A., Baker, L. A. (2000): Conceptual model of aquatic plant decay and ammonia toxicity for shallow lakes. – *Environmental Engineering* 126(3): 199-207.
- [11] Han, L. L., Yu, X. W. (2017): Absorption kinetics of nitrogen and phosphorus in aquatic vegetables in wetland. – *Chinese Journal of Environmental Engineering* 11(5): 2828-2835.
- [12] Huang, L., Wu, N. C., Tang, T. (2010): Enrichment and removal of nutrients in eutrophic water by aquatic macrophytes. – *China Environmental Science* 30(5): 1-6.
- [13] Jackson, W. A., Flesher, D., Hageman, R. H. (1973): Nitrate uptake by dark-grown com seedlings. Some characteristics of apparent induction. – *Plant Physiology* 51: 120-127.
- [14] Jampeetong, A., Brix, H. (2009): Nitrogen nutrition of *Salvinia natans*: effects of inorganic nitrogen form on growth, morphology, nitrate reductase activity and uptake kinetics of ammonium and nitrate. – *Aquatic Botany* 90(1): 67-73.
- [15] Jiang, C. L., Fan, X. Q., Zhang, Y. B. (2004): Adsorption and prevention of secondary pollution of N and P by emergent plants in farmland ditch. – *Journal of China Environmental Science* 24(6): 702-706.
- [16] Li, Q. F., Yuan, Y. X. (2000): Outlook for bioremediation researches on marine aquacultural environment. – *Journal of Fishery Sciences of China* 7(2): 90-92.
- [17] Litav, M., Lehrer, Y. (1978): The effects of ammonium in water on *Potamogeton lucens*. – *Aquat. Bot.* 5: 127-138.
- [18] Liu, F., Li, M., Li, H. L. (2009): A preliminary study under on NH_4^+ -N uptake kinetics of *Potamogeton* different nutrient conditions. – *Journal of Wuhan Botanical Research* 27(1): 98-101.

- [19] Ma, J. M., Jin, T. X., Li, J., Wu, J., Wu, Z. B. (2008): Responses of *Elodea nuttallii*, *Vallisneria natans* and *Potamogeton crispus* to acute stress of phosphorus. – *Acta Hydroecologica Sinica* 32(3): 408-412.
- [20] Mehrer, I., Mohr, H. (1989): Ammonium toxicity description of the syndrome in *Synapis alba* and the search for its causation. – *Physiology Plant* 77(4): 545-554.
- [21] Nielsen, N. E., Barber, S. A. (1978): Differences among genotypes of corn in the kinetics of P uptake. – *Agronomy Journal* 70(5): 695-698.
- [22] Pregnall, A. M. (2004): Effects of aerobic versus anoxic conditions on glutamine sintetase activity in eelgrass (*Zostera marina* L.) roots: regulation of ammonium assimilation potential. – *Journal of Experimental Marine Biology and Ecology* 311(1): 11-24.
- [23] Qian, L. M., Xu, Y. J., Jiao, N. Z. (2005): Effect of nutrient factor on absorption rate of N and P of two species of seaweed. – *Taiwan strait* 24(4): 546-552.
- [24] Runcie, J. W., Ritchie, R. J., Larkum, A. W. D. (2003): Uptake kinetics and assimilation of inorganic nitrogen by *Catenellanipae* and *Ulva lactuca*. – *Aquatic Botany* 76(2): 155-174.
- [25] Sagrario, M. A. G., Jeppesen, E., Goma, J., Sondergaard, M., Jensen, J. P., Lauridsen, T., Landkildehus, F. (2005): Does high nitrogen loading prevent clear-water conditions in shallow lakes at moderately high phosphorus concentrations? – *Freshwater Biology* 50(1): 27-41.
- [26] Shen, G. X., Yao, F., Ni, W. Z. (2006): The kinetics of ammonium and nitrate uptake by duckweed plant. – *Chinese Journal of Soil Science* 37(3): 505-508.
- [27] State Environmental Protection Administration. Water and Wastewater Monitoring Analysis Method. – Fourth Edition. Beijing: China Environmental Science Press. (in Chinese).
- [28] Tang, Y. X., Zheng, J. M., Lou, L. P. (2011): Comparisons of NH_4^+ , NO_3^- and H_2PO_4^- uptake kinetics in three different macrophytes in waterlogged condition. – *Chinese Journal of Eco-Agriculture* 19(3): 614-618.
- [29] Wang, P. F., Wang, C., Wang, X. R. (2008): Purification effects on nitrogen under different concentration and nitrogen conformation transform principles by *Vallisneria spiralis* L. – *Environmental Science* 29: 890-895.
- [30] Xiong, H., Tan, Q., Hu, C. (2010): Structural and metabolic responses of *Ceratophyllum demersum* to eutrophic condition. – *African Journal of Biotechnology* 9(35): 5722-5729.
- [31] Xu, Q. J., Jin, X. C., Wang, X. M. (2006): Effects of Both Single and Combined Pollution of Cd and NH_4^+ on *Hydrilla verticillata* and *Myriophyllum spicatum*. – *Environmental Science* 27(10): 974-978.
- [32] Yan, C. Z., Zeng, A. Y., Jin, X. C. (2007): Physiological effects of ammonia-nitrogen concentrations on *Hydrilla verticillata*. – *Acta Ecologica Sinica* 27(3): 1050-1055.
- [33] Zhang, S. (2012): Nitrogen and Phosphorus Uptake Kinetics of *Vallisneria natans*. – Master degree thesis (in Chinese).
- [34] Zhang, A. W., Cao, T., Zhang, M. (2013): Uptake of ammonium by *Vallisneria natans* and dark regimes *spicatum* under light. – *Journal of Lake Sciences* 25(2): 289-294.

NORFLOXACIN RESISTANT BACTERIAL COMPOSITIONS IN SEDIMENTS OF CHINESE SUBTROPICAL FISH PONDS

MAO, L. T.^{1*} – HUANG, J.¹ – CHEN, Z. G.¹ – MA, X. L.¹ – LIU, H. R.²

¹*School of Life Science, Huizhou University, Huizhou 516007, China*

²*School of Chemistry and Materials Engineering, Huizhou University, Huizhou 516007, China*

**Corresponding author*

e-mail: mlt@hzu.edu.cn; phone: +86-752-252-9555

(Received 12th Sep 2018; accepted 22nd Nov 2018)

Abstract. Antibiotic resistant bacteria are widely spread in environments. However, the compositions of bacteria with antibiotic resistance in subtropical fish pond sediment are still unclear. In present study, to analyze the compositions of norfloxacin resistant bacteria in subtropical fish pond sediments, we selectively cultured the sediment bacteria collected from six subtropical fish ponds located in southern China using the basic medium with 50 µg/ml of norfloxacin, and analyzed their compositions using MiSeq high-throughput sequencing of 16S rRNA gene amplicons. Our results showed that various norfloxacin resistant bacteria existed in the fish pond sediments. And most of them were Gram-negative bacteria. Their spatial distribution was mainly influenced by environmental heterogeneity of the ponds. These results implied that norfloxacin resistance was widespread in Gram-negative bacteria in the fish pond sediments located in southern China. These finding provided reference information to prevent fish infected diseases and to assess the risk of antibiotic resistant bacteria in the fish pond sediments.

Keywords: *antibiotic, bacterial community, environmental heterogeneity, Gram-negative bacteria, high-throughput sequencing*

Introduction

Bacterial pathogens are the major cause of infectious diseases and mortality in wild and farmed fish (Sudheesh et al., 2012). Disease problems constitute that the largest single cause of economic losses in aquaculture (Meyer, 1991). With the rapid growth and intensification of aquaculture, the list of new pathogenic bacterial species isolated from fish has been steadily increasing (Harvell et al., 1999). To control the pathogenic bacteria and enhance fish growth, antibiotics have been widely used in agricultural production over the past decades (Ma et al., 2001; Neela et al., 2015). However, extensive use of antibiotics, especially the overuse of antibiotics in agricultural production, has caused a serious threat of antibiotic resistance (Levy and Marshall, 2004; Goossens et al., 2005; Mathew et al., 2007; Kumarasamy et al., 2010; Laxminarayan et al., 2013). Although the usage of antibiotics in agricultural production is strictly restricted presently, residues of antibiotics in environment and illegal use of antibiotics still cause prevalence of antibiotic resistance, especially in the aquatic systems, such as lakes and fish ponds (Wahid et al., 2014; Moore et al., 2014; Far et al., 2015; Neela et al., 2015; Patil et al., 2016; Yang et al., 2016). In addition, there are many antibiotics used in aquaculture, such as terramycin, also used in clinical trials in China (Ma et al., 2001).

Pond culture is one of the most prevailing culture patterns in China, which is the largest producing area of aquatic products around the world (FAO, 2014; Lu et al., 2015). Sewage discharge and agricultural production cause residues of antibiotics in ponds (Lin et al., 2010; Zhang et al., 2011; Wei et al., 2011; Song et al., 2016; Cheng et

al., 2016). These residues of antibiotics increased the risk of antibiotic resistance. Although the genes of antibiotic resistance in the ponds have been widely investigated (Cheng et al., 2016), and a lot of antibiotic resistance bacteria have been isolated from many ponds (Zhang et al., 2011; Wei et al., 2011; Neela et al., 2015), the compositions of bacteria with antibiotic resistance in the ponds are still unclear.

Screening antibiotic resistant bacteria through culturing by mediums containing antibiotics is commonly used method to study antibiotic resistant bacteria (Kumarasamy et al., 2010; Neela et al., 2015; Li et al., 2017). However, the previous studies mostly focused on signal or few bacterial species. Although high-throughput sequencing technology has been widely used in microbial community analysis (Huang et al., 2018; Ni et al., 2018; Xiang et al., 2018), it is still not to use to investigate composition of antibiotic resistant bacteria in pond sediment.

Norfloxacin is commonly used antibiotic in aquaculture and is frequently detected from various water environments and aquatic animals (Ortiz et al., 1999; Guo and Zhang, 2009; Spongberg et al., 2011; Zhang et al., 2017). To analyze the compositions of antibiotic resistant bacteria in pond sediment, we selectively cultured the sediment bacteria collected from six subtropical fish ponds in southern China using the basic medium containing with norfloxacin and analyzed their compositions using MiSeq high-throughput sequencing of 16S rRNA gene amplicons. Results of the present study provided reference information to prevent fish infective diseases and assess the risk of antibiotic resistance in Chinese subtropical fish ponds.

Materials and methods

Sampling collection and treatment

Sediment samples were collected from 5 fish ponds (GraA, GraF, LatF, GruF, and OreD) located in Yuanzhou Town (113°57' E, 23°07' N) and 1 fish pond (ChiP) located in Huicheng District (114°23' E, 23°05' N) of Huizhou, a subtropical city in southern China on January 22, 2016 (Fig. 1). Fish species farmed in the ponds were showed in Table 1. Three sediment samples were parallelly collected from each pond. Five-point sampling method was used to collect each sediment sample (i.e., five sub-samples were collected at area within 1 m of diameter, and then pooled together with an equal wet weight as one sample).

Table 1. Fish species farmed in the ponds. All fish ponds located in Huizhou, a subtropical city in southern China

Pond name	Pond location	Pond surface area (m ²)	Fish species
GraA	Yuanzhou Town	4,330	Grass carp (<i>Ctenopharyngodon idellus</i>) and tilapia (<i>Tilapia mossambica</i>)
GraF	Yuanzhou Town	3,000	Fries of grass carp
LatF	Yuanzhou Town	3,330	Weever (<i>Lateolabrax japonicus</i>)
GruF	Yuanzhou Town	2,330	Crucian carp (<i>Carassius auratus</i>)
OreD	Yuanzhou Town	4,670	Tilapia (<i>Tilapia mossambica</i>)
ChiP	Huicheng District	5,330	A mixture of multiple fishes

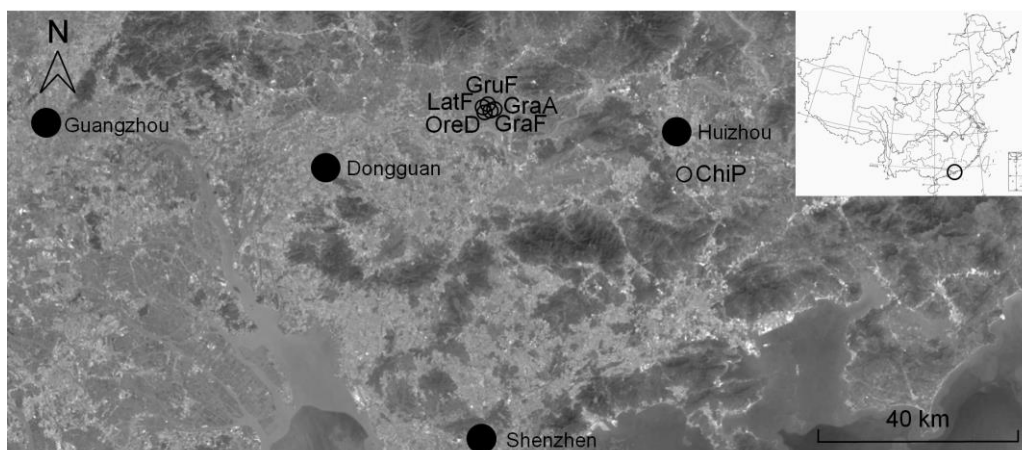


Figure 1. Distribution of sampling ponds. Hollow circles show the sampling ponds, and black spots show the major cities around the sampling ponds

Triplicate 1 g of sediments (wet weight) of each sample were added into conical flask containing 100 ml of the basic medium with 50 µg/ml of norfloxacin referenced a previous report (Ma et al., 2012) and were cultured 24 h at 30 °C in an incubator with 150 r/min. Then the inoculums were centrifugated 10 min at 1200 rpm to concentrate and the suspensions were transferred into 2 ml centrifuge tubes for microbial DNA extraction. The microbial DNA were extracted according to previous description (Fang et al., 2015) and purified using a gel extraction kit (Dingguo, China). DNA concentrations were measured using a Nanodrop 2000 spectrophotometer and diluted to 10 ng/µl for PCR amplification.

PCR amplification and sequencing

V4-V5 hypervariable region of 16S rRNA gene was amplified and sequenced using a MiSeq system, as described previously (Ni et al., 2017; Huang et al., 2018; Xiang et al., 2018). Briefly, the V4-V5 region was amplified using the universal primer pair 515F (5' – GTG YCA GCM GCC GCG GTA – 3') and 909R (5' – CCC CGY CAA TTC MTT TRA GT – 3') with a 12-nucleotide sample-specific barcode included at the 5'-end of the 515F sequence to distinguish samples. PCR was conducted in duplicate with 25-µl reaction mix containing 1 × buffer, 0.25 U of Taq DNA polymerase (Transgen, China), 0.2 mM of each dNTP, 1.0 µM of each primer and 10 ng DNA. The PCR procedure consisted of a pre-denaturation step at 94 °C for 10 min, followed by 30 cycles of 94 °C for 30 s, 56 °C for 30 s and 72 °C for 30 s and a final extension at 72 °C for 10 min. After amplification, the two products of each sample were mixed together and subjected to electrophoresis using a 1.5% agarose gel. The correct band was excised, purified using a gel extraction kit (Axygen, USA), and quantified with the Nanodrop 2000 spectrophotometer. All amplicons were pooled together with an equal molar amount for each sample and sequencing using an Illumina MiSeq system at Guangdong Meilikang Bio-Science, Ltd., China.

Data analysis

The raw sequencing reads were merged using FLASH-1.2.8 software (Magoc and Salzberg, 2011) and per-processed for removing low-quality sequences using QIIME

pipeline version 1.9.0 (Caporaso et al., 2010) as previously described (Ni et al., 2017; Huang et al., 2018; Xiang et al., 2018). Chimera sequences were identified and removed before further analysis using the Uchime algorithm (Edgar et al., 2011). The high-quality sequences were clustered into operational taxonomic units (OTUs) at 97% identity using UPARSE software (Edgar, 2013). Then all samples were randomly resampled to obtain the same number of sequences to overcome the influence of sequencing depth on results. Each OTU was assigned taxonomic information using the RDP classifier (Wang et al., 2007) with Greengenes database gg_13_8.

Principal component analysis (PCA) and non-parametric multivariate analysis of variance (MANOVA) (Anderson, 2001) were used to analyze the difference of microbiota among different groups and were conducted using R 3.5.1 with vegan package (Dixon, 2003). The box plots were drawn to show the relative abundances of significantly different OTUs among groups using STAMP software (Parks et al., 2014). And the statistically significant markers were added to the box plots using and Adobe Illustrator CS5 software according to the post-hoc test results.

All DNA datasets have been submitted to the NCBI Sequence Read Archive database under accession number SRP160514.

Results and discussion

Composition of norfloxacin resistant bacteria in pond sediments

Removing low-quality and chimera sequences, 346,643 high-quality sequences were obtained from the 18 samples. Finally, each sample was randomly resampled 11,000 sequences to further analysis. Except for little sequences ($0.97 \pm 0.38\%$, mean \pm S.E.) could not classified into an explicit phylum, other sequences were classified into 2 Archaea and 65 Bacteria phyla. However, according to previous definition by other researchers (Huang et al., 2018; Xiang et al., 2018), only 15 phyla – Crenarchaeota, Euryarchaeota, Acidobacteria, Actinobacteria, Bacteroidetes, Chlorobi, Chloroflexi, Cyanobacteria, Firmicutes, Nitrospirae, OP8, Planctomycetes, Proteobacteria, Spirochaetes, and Verrucomicrobia – dominated the sediment microbiotas (their relative abundances were more than 1% in at least one sample; *Fig. 2*). They contained up to $98.19 \pm 0.72\%$ of the sequences.

Total of 35,194 OTUs were detected from the 18 sediment microbiotas. However, only 48 OTUs dominated the microbiotas (their relative abundances were more than 1% in at least one sample; *Fig. 3*). They contained up to $67.16 \pm 5.79\%$ of the sequences. Lots of the dominant OTUs were reported as fish and mammal potentially pathogenic bacterial species, such as *Acinetobacter* sp., *Lactococcus* sp., *Escherichia* sp., *Burkholderia* sp., *Streptomyces lanatus*, *Bacteroides* sp., and *Ruminococcus* sp. (Slots and Listgarten, 1988; Kofteridis et al., 2007; Anandham et al., 2010; Fishbain and Peleg, 2010; Sudheesh et al., 2012; Woods and Sokol, 2006; Titécat et al., 2014; Li et al., 2017). And some of them were reported with multi-drug resistance (Li et al., 2017). In addition, potential plant bacterial pathogen *Erwinia* sp. and *Ralstonia* sp. (Swanson et al., 2005; Amin et al., 2011; Kube et al., 2010) also dominated the microbiota. Their norfloxacin resistance increased the bacterial infected risk of fish and plants.

Although norfloxacin is a broad-spectrum antibiotic, especially has a strong bactericidal effect to Gram-negative bacteria, most dominant OTUs were Gram-negative bacteria. This result implied that norfloxacin resistance was widespread in Gram-negative bacteria in the fish pond sediments located at southern China.

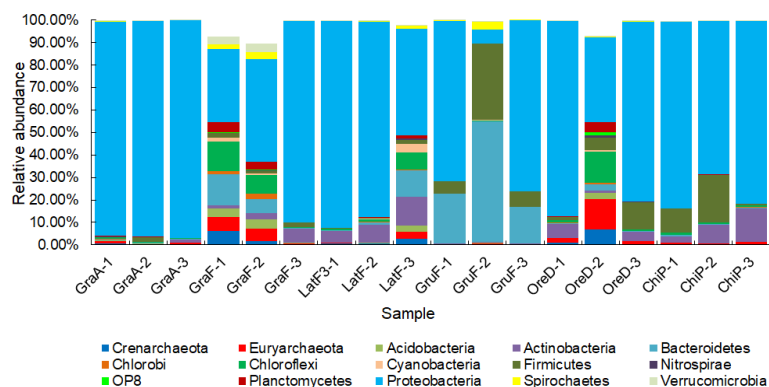


Figure 2. Dominant phyla of norfloxacin resistant bacteria in Chinese subtropical pond sediments. The sediment samples were collected from 5 fish ponds (GraA, GraF, LatF, GruF, and OreD) located at Yuanzhou Town (113°57' E, 23°07' N) and 1 fish pond (ChiP) located at Huicheng District (114°23' E, 23°05' N), in Huizhou, a subtropical city in southern China on January 22, 2016. The pond GraA mainly farmed grass carp (*Ctenopharyngodon idellus*) and tilapia (*Tilapia mossambica*). The pond GraF farmed fries of grass carp. The pond LatF farmed weever (*Lateolabrax japonicus*). The pond GruF farmed fries of crucian carp (*Carassius auratus*). The pond OreD farmed tilapia (*Tilapia mossambica*). The pond ChiP farmed a mixture of multiple fishes

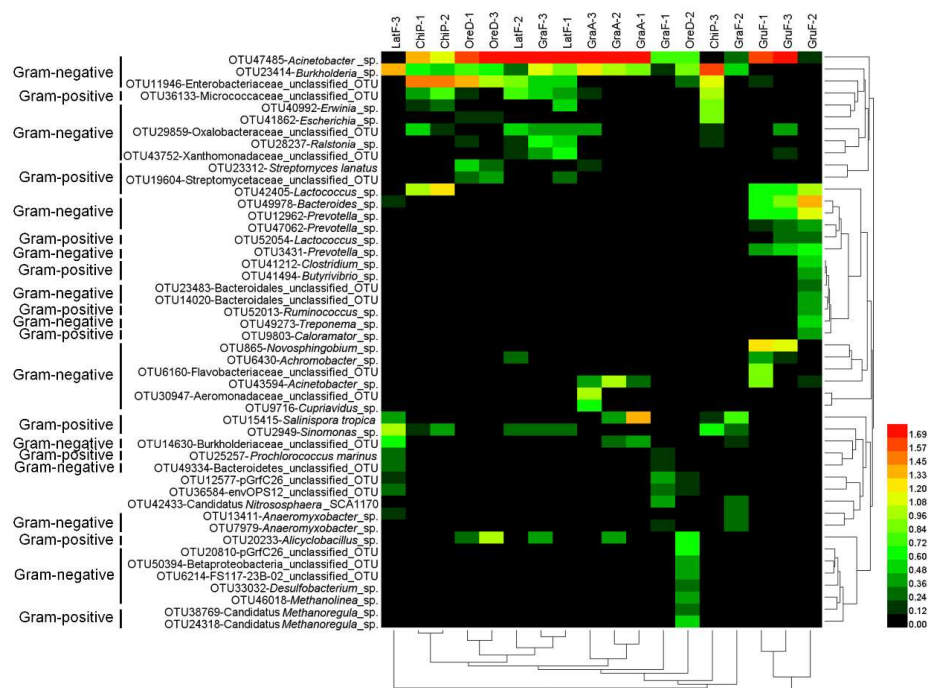


Figure 3. Heat map profile showed dominant OTUs of norfloxacin resistant bacteria in pond sediments. The data was transformed according to the equation $\log_{10}(\text{relative abundance} \times 100 + 1)$ to reduce the magnitude of extremum. The sediment samples were collected from 5 fish ponds (GraA, GraF, LatF, GruF, and OreD) located at Yuanzhou Town (113°57' E, 23°07' N) and 1 fish pond (ChiP) located at Huicheng District (114°23' E, 23°05' N), in Huizhou, a subtropical city in southern China on January 22, 2016. The pond GraF farmed fries of grass carp. The pond LatF farmed weever (*Lateolabrax japonicus*). The pond GruF farmed fries of crucian carp (*Carassius auratus*). The pond OreD farmed tilapia (*Tilapia mossambica*). The pond ChiP farmed a mixture of multiple fishes

Different of norfloxacin resistant bacteria among different ponds

Mechanisms forming and maintaining bacterial bio-diversity are the basic issue of microbial ecology (Ni et al., 2014, 2016; Wu et al., 2017).

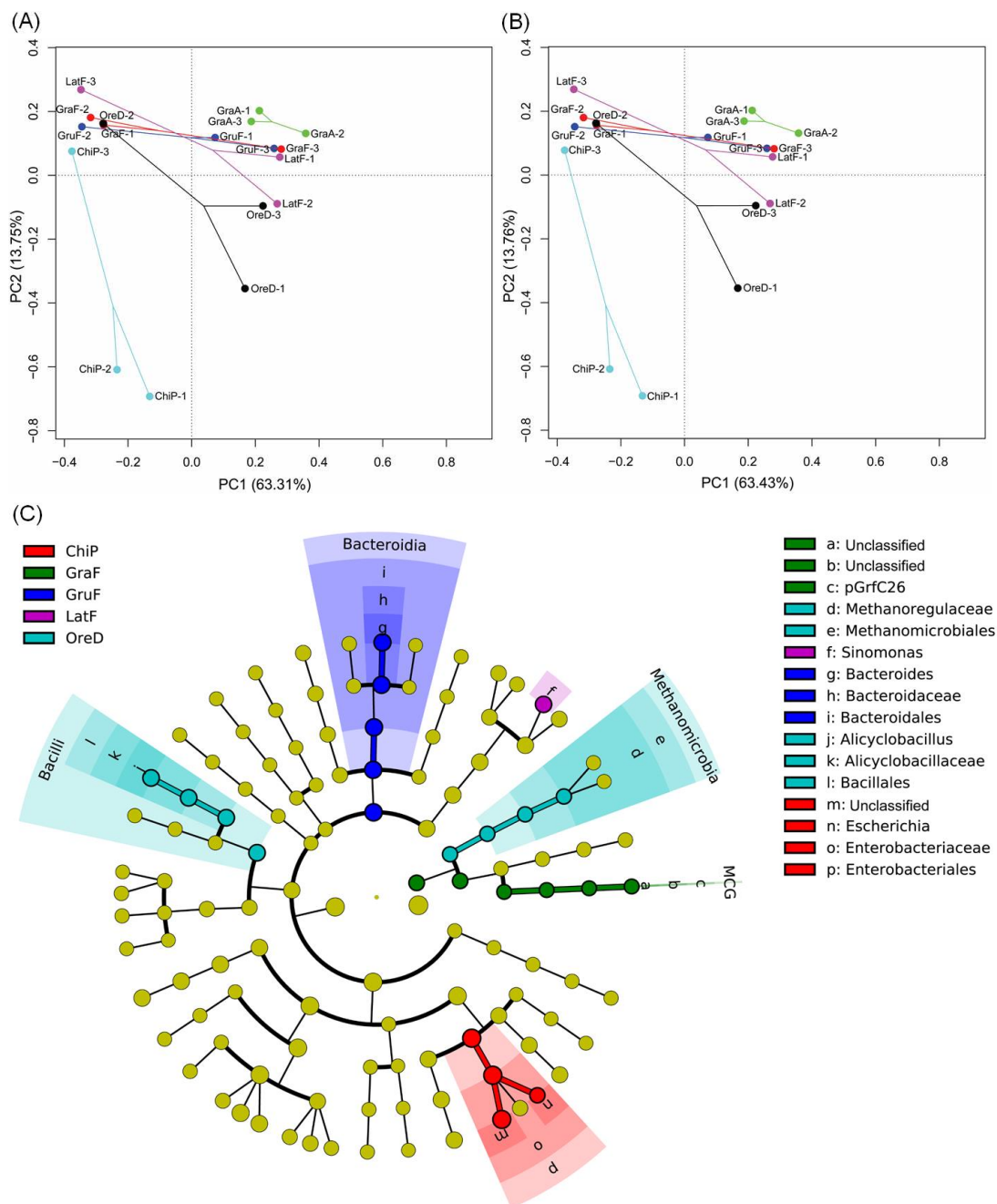


Figure 4. PCA profile based on OTUs (A) and based on dominant OTUs (B), and LEfSe profile based on dominant OTUs (C) showed differences of norfloxacin resistant bacteria in pond sediments. The sediment samples were collected from 5 fish ponds (GraA, GraF, LatF, GruF, and OreD) located at Yuanzhou Town (113°57' E, 23°07' N) and 1 fish pond (ChiP) located at Huicheng District (114°23' E, 23°05' N), in Huizhou, a subtropical city in southern China on January 22, 2016. The pond GraF farmed fries of grass carp. The pond LatF farmed weever (*Lateolabrax japonicus*). The pond GruF farmed fries of crucian carp (*Carassius auratus*). The pond OreD farmed tilapia (*Tilapia mossambica*). The pond ChiP farmed a mixture of multiple fishes

Geographical isolation is one of the primary factors that restrict microbial distribution and emerge a significant distance-decay relationship regarding microbial community similarity (Bell, 2010). However, protesters claim microorganisms are cosmopolitan, and spatial patterns of microbial diversity are driven by environmental heterogeneity (Green and Bohannan, 2006). Our results showed that although significant differences of sediment microbiotas were detected among different ponds both based on the OTU compositions (MANOVA, $F = 1.851$, $p = 0.002$; Fig. 4A) and based on the dominant OTU compositions (MANOVA, $F = 1.926$, $p = 0.016$; Fig. 4B). And *Bacteroides* sp. was significantly enhanced at pond GruF, *Alicyclobacillus* sp. and an unidentified OTUs in family Methanoregulaceae was significantly enhanced at pond OreD, and *Escherichia* sp. and an unidentified OTUs in family Enterobacteriaceae was significantly enhanced at pond Chip (Fig. 4C). However, the microbiotas from the same pond did not cluster together except for those from pond GraA (Fig. 4A and B). These results showed that environmental heterogeneity was the major factor that casted the spatial patterns of microbial diversity.

Conclusion

In conclusion, we firstly investigated the norfloxacin resistant bacteria in fish pond sediments using the method that connected selective culture and high-throughput sequencing. Our results showed norfloxacin resistance was widespread in Gram-negative bacteria, such as *Acinetobacter* sp. and *Burkholderia* sp., in fish pond sediments located at southern China. This increased bacterial infected risk of farmed fish. In addition, mechanisms of these bacteria to resistant to norfloxacin and how to reduce the norfloxacin resistant bacteria are still needed to further study.

Acknowledgements. This work was supported by the Huizhou Science and Technology Planning Project (grant number 2017C0423039, 2016X0419034), and the Major Cultivation Projects of Huizhou University (grant number hzux1201520). The authors thank Dr. Jiajia Ni at Guangdong Meikang BioScience, Inc. for assistance with data analysis and figure preparation.

REFERENCES

- [1] Amin, N. M., Bunawan, H., Redzuan, R. A. et al. (2011): *Erwinia mallotivora* sp., a new pathogen of papaya (*Carica papaya*) in Peninsular Malaysia. – International Journal of Molecular Sciences 12(1): 39-45.
- [2] Anandham, R., Weon, H., Kim, S. et al. (2010): *Acinetobacter brisouii* sp. nov., isolated from a wetland in Korea. – Journal of Microbiology 48(1): 36-39.
- [3] Bell, T. (2010): Experimental tests of the bacterial distance-decay relationship. – ISME Journal 4(11): 1357-1365.
- [4] Caporaso, J. G., Kuczynski, J., Stombaugh, J. et al. (2010): QIIME allows analysis of high-throughput community sequencing data. – Nature Methods 7: 335-336.
- [5] Cheng, W., Li, J., Wu, Y. et al. (2016): Behavior of antibiotics and antibiotic resistance genes in eco-agricultural system: A case study. – Journal of Hazardous Materials 304: 18-25.
- [6] Dixon, P. (2003): VEGAN, a package of R functions for community ecology. – Journal of Vegetation Science 14(6): 927-930.
- [7] Edgar, R. C. (2013): UPARSE: Highly accurate OTU sequences from microbial amplicon reads. – Nature Methods 10: 996-998.

- [8] Edgar, R. C., Haas, B. J., Clemente, J. C. et al. (2011): UCHIME improves sensitivity and speed of chimera detection. – *Bioinformatics* 27: 2194-2200.
- [9] Fang, Y., Xu, M., Chen, X. et al. (2015): Modified pretreatment method for total microbial DNA extraction from contaminated river sediment. – *Frontiers of Environmental Science & Engineering* 9: 444-452.
- [10] FAO (2014): *The State of World Fisheries and Aquaculture 2014*. – Food and Agricultural Organization of the United Nations, New York.
- [11] Far, S. A. H. E., Khalil, R. H., Saad, T. T. et al. (2015): Occurrence, characterization and antibiotic resistance patterns of bacterial communities encountered in mass kills of pond cultured Indian prawn (*Fenneropenaeus indicus*) at Damietta governorate, Egypt. – *International Journal of Fisheries and Aquatic Studies* 2(4): 271-276.
- [12] Fishbain, J., Peleg, A. Y. (2010): Treatment of *Acinetobacter* infections. – *Clinical Infectious Diseases* 51(1): 79-84.
- [13] Green, J., Bohannan, B. J. M. (2006): Spatial scaling of microbial biodiversity. – *Trends in Ecology & Evolution* 21(9): 501-507.
- [14] Goossens, H., Ferech, M., Vander Stichele, R. et al. (2005): Outpatient antibiotic use in Europe and association with resistance: a cross-national database study. – *Lancet* 365(9459): 579-587.
- [15] Guo, H., Zhang, Q. (2009): Residues regulation of norfloxacin in *Ctenopharyngodon idellus*. – *Journal of Aquaculture* 30(10): 24-26.
- [16] Harvell, C. D., Kim, K., Burkholder, J. M. et al. (1999): Emerging marine diseases – climate links and anthropogenic factors. – *Science* 285(5433): 1505-1510.
- [17] Huang, R., Li, T., Ni, J. et al. (2018): Different sex-based responses of gut microbiota during the development of hepatocellular carcinoma in liver-specific *Tsc1*-knockout mice. – *Frontiers in Microbiology* 9: 1008.
- [18] Kofteridis, D. P., Maraki, S., Scoulica, E. et al. (2007): *Streptomyces* pneumonia in an immunocompetent patient: a case report and literature review. – *Diagnostic Microbiology and Infectious Disease* 59(4): 459-462.
- [19] Kube, M., Migdoll, A. M., Gehring, I. et al. (2010): Genome comparison of the epiphytic bacteria *Erwinia billingiae* and *E. tasmaniensis* with the pear pathogen *E. pyrifoliae*. – *BMC Genomics* 11: 393.
- [20] Kumarasamy, K. K., Toleman, M. A., Walsh, T. R. et al. (2010): Emergence of a new antibiotic resistance mechanism in India, Pakistan, and the UK: a molecular, biological, and epidemiological study. – *Lancet Infectious Diseases* 10(9): 597-602.
- [21] Laxminarayan, R., Duse, A., Wattal, C. et al. (2013): Antibiotic resistance – the need for global solution. – *Lancet Infectious Diseases* 13(12): 1057-1098.
- [22] Levy, S. B., Marshall, B. (2004): Antibacterial resistance worldwide: causes, challenges and responses. – *Nature Medicine* 10(12): 122-129.
- [23] Li, J., Cao, J., Wang, X. et al. (2017): *Acinetobacter pittii*, an emerging new multi-drug resistant fish pathogen isolated from diseased blunt snout bream (*Megalobrama amblycephala* Yih) in China. – *Applied Microbiology and Biotechnology* 101(16): 6459-6471.
- [24] Lin, J., Pan, H., Liu, S. et al. (2010): Effects of light and microbial activity on the degradation of two fluoroquinolone antibiotics in pond water and sediment. – *Journal of Environmental Science and Health Part B* 45: 456-465.
- [25] Lu, S., Liao, M., Xie, C. et al. (2015): Seasonal dynamics of ammonia-oxidizing microorganisms in freshwater aquaculture ponds. – *Annals of Microbiology* 65(2): 651-657.
- [26] Ma, G., Qu, Q., Wu, W. et al. (2001): Application of antibiotics in aquaculture. – *Chinese Journal of Fisheries* 14: 73-76.
- [27] Ma, Y., Feng, B., Li, J. et al. (2012): Effects of norfloxacin on the quantity and drug-resistance of bacteria isolated from soil. – *Journal of Traditional Chinese Veterinary Medicine* 31(1): 9-12.

- [28] Magoc, T., Salzberg, S. L. (2011): FLASH: Fast length adjustment of short reads to improve genome assemblies. – *Bioinformatics* 27: 2957-2963.
- [29] Mathew, A. G., Cissell, R., Liamthong, S. (2007): Antibiotic resistance in bacteria associated with food animals: a United States perspective of livestock production. – *Foodborne Pathogens and Disease* 4(2): 115-133.
- [30] Meyer, F. P. (1991): Aquaculture disease and health management. – *Journal of Animal Science* 69(10): 4201-4208.
- [31] Moore, J. E., Huang, J., Yu, P. et al. (2014): High diversity of bacterial pathogens and antibiotic resistance in salmonid fish farm pond water as determined by molecular identification employing 16S rDNA PCR, gene sequencing and total antibiotic susceptibility techniques. – *Ecotoxicology and Environmental Safety* 108: 281-286.
- [32] Neela, F. A., Banu, M. N. A., Rahman, M. A. et al. (2015): Occurrence of antibiotic resistant bacteria in pond water associated with integrated poultry-fish farming in Bangladesh. – *Sains Malaysiana* 44(3): 371-377.
- [33] Ni, J., Yan, Q., Yu, Y. et al. (2014): Fish gut microecosystem: a model for detecting spatial pattern of microorganisms. – *Chinese Journal of Oceanology and Limnology* 32(1): 54-57.
- [34] Ni, J., Xu, M., He, Z. et al. (2016): Novel insight into evolutionary process from average genome size in marine bacterioplanktonic biota. – *Applied Ecology and Environmental Research* 14(2): 65-75.
- [35] Ni, J., Li, X., He, Z. et al. (2017): A novel method to determine the minimum number of sequences required for reliable microbial community analysis. – *Journal of Microbiological Methods* 139: 196-201.
- [36] Ni, J. J., Li, X. J., Chen, F. et al. (2018): Community structure and potential nitrogen metabolisms of subtropical aquaculture pond microbiota. – *Applied Ecology and Environmental Research* (in press).
- [37] Ortiz, J., Vila, M. C., Soriano, G. et al. (1999): Infections caused by *Escherichia coli* resistant to norfloxacin in hospitalized cirrhotic patients. – *Hepatology* 29(4): 1064-1069.
- [38] Parks, D. H., Tyson, G. W., Hugenholtz, P. et al. (2014): STAMP: statistical analysis of taxonomic and functional profiles. – *Bioinformatics* 30(21): 3123-3124.
- [39] Patil, H. J., Benet-Perelberg, A., Naor, A. et al. (2016): Evidence of increased antibiotic resistance in phylogenetically-diverse *Aeromonas* isolates from semi-intensive fish ponds treated with antibiotics. – *Frontiers in Microbiology* 7: 1875.
- [40] Slots, J., Listgarten, M. A. (1988): *Bacteroides gingivalis*, *Bacteroides intermedius* and *Actinobacillus actinomycetemcomitans* in human periodontal diseases. – *Journal of Clinical Periodontology* 15(2): 85-93.
- [41] Song, C., Zhang, C., Fan, L. et al. (2016): Occurrence of antibiotics and their impacts to primary productivity in fishponds around Tai Lake, China. – *Chemosphere* 161: 127-135.
- [42] Spongberg, A. L., Witter, J. D., Acuña, J. et al. (2011): Reconnaissance of selected PPCP compounds in Costa Rican surface waters. – *Water Research* 45: 6709-6717.
- [43] Subasinghe, R. (1997): Fish Health and Quarantine; Review of the State of the World Aquaculture. – FAO Fisheries Circular. Food and Agriculture Organization of the United Nations 886: 45-49.
- [44] Sudheesh, P. S., Al-Ghabshi, A., Al-Mazrooei, N. et al. (2012): Comparative pathogenomics of bacteria causing infectious diseases in fish. – *International Journal of Evolutionary Biology* 2012: 457264.
- [45] Swanson, J. K., Yao, J., Tans-Kersten, J. et al. (2005): Behavior of *Ralstonia solanacearum* race 3 biovar 2 during latent and active infection of geranium. – *Phytopathology* 95(2): 136-143.
- [46] Titécat, M., Wallet, F., Vieillard, M. H. et al. (2014): *Ruminococcus gnavus*: an unusual pathogen in septic arthritis. – *Anaerobe* 30: 159-160.

- [47] Wahid, M. A., Basri, Z. D. M., Halip, A. A. et al. (2014): Antibiotic Resistance Bacteria in Coastal Shrimp Pond Water and Effluent. – In: Hassan, R., Yusoff, M., Alisibramulisi, A. et al. (ed.) InCIEC 2014. Springer, Singapore.
- [48] Wang, Q., Garrity, G. M., Tiedje, J. M. et al. (2007): Naïve Bayesian classifier for rapid assignment of rRNA sequences into the new bacterial taxonomy. – Applied and Environmental Microbiology 73: 5261-5267.
- [49] Wei, R., Ge, F., Huang, S. et al. (2011): Occurrence of veterinary antibiotics in animal wastewater and surface water around farms in Jiangsu province, China. – Chemosphere 82: 1408-1414.
- [50] Woods, D. E., Sokol, P. A. (2006): The Genus Burkholderia. – In: Dworkin, M., Falkow, S., Rosenberg, E. et al. (ed.) The Prokaryotes. Springer, New York.
- [51] Wu, L., Sun, Q., Ni, J. (2017): Not all of the rare operational taxonomic units (OTUs) play the same role in maintaining community stability. – Applied Ecology and Environmental Research 15(1): 105-112.
- [52] Xiang, J., He, T., Wang, P. et al. (2018): Opportunistic pathogens are abundant in the gut of cultured giant spiny frog (*Paa spinosa*). – Aquaculture Research 49: 2033-2041.
- [53] Yang, Y., Cao, X., Lin, H. et al. (2016): Antibiotics and antibiotic resistance genes in sediment of Honghu Lake and east Dongting Lake, China. – Microbial Ecology 72(4): 791-801.
- [54] Zhang, Y. B., Li, Y., Sun, X. L. (2011): Antibiotic resistance of bacteria isolated from shrimp hatcheries and cultural ponds on Donghai Island, China. – Marine Pollution Bulletin 62(11): 2299-2307.
- [55] Zhang, Y., Rong, C., Song, Y. et al. (2017): Oxidation of the antibacterial agent norfloxacin during sodium hypochlorite disinfection of marine culture water. – Chemosphere 182: 245-254.

CUTTINGS GROWTH RESPONSE OF *DALBERGIA SISSOO* (SHISHAM) TO SOIL COMPACTION STRESS

RASHID, M. H. U.^{1,2,3} – ASIF, M.² – FAROOQ, T. H.^{1,2,3} – GAUTAM, N. P.¹ – NAWAZ, M. F.² –
AHMAD, I.² – GILANI, M. M.^{1,2} – WU, P.^{1,3*}

¹*Forestry College, Fujian Agriculture and Forestry University
Fuzhou 350002, Fujian Province, PR China*

²*Department of Forestry and Range Management, University of Agriculture
Faisalabad 38000, Punjab Province, Pakistan*

³*Fujian Provincial Colleges and University Engineering Research Center of Plantation
Sustainable management, Fujian Agriculture and Forestry University
Fuzhou 350002, Fujian Province, PR China*

**Corresponding author*

e-mail: ffwupengfei@126.com, ffwupengfei@fafu.edu.cn; phone: +86-591-8378-0261

(Received 13th Sep 2018; accepted 29th Nov 2018)

Abstract. Because of the intensive use of machinery, soil compaction is a serious concern for soil management authorities worldwide. The use of heavy machinery to perform forestry activities such as logging has increased during the last few decades, which influences the soil ecosystem by inducing soil compaction. The main objective of this study was to observe the morphological growth response of *Dalbergia sissoo* at different compaction levels. Different morphological parameters were recorded including girth/diameter, shoot length, root length, shoot weight, root weight, shoot dry weight, root dry weight, root-shoot ratio, moisture content availability, and biomass production to analyze the effect of soil compaction. As the compaction level increased, the shoot length, root length, root weight to shoot weight ratio, and biomass production decreased. Simultaneously, the bulk density of soil increased as the compaction level increased. Soil compaction produced an overall negative effect on the growth of *D. sissoo*. Different levels of soil compaction significantly affected the physical growth parameters of the plant and reduced growth as soil compaction increased. Based on the results, the plantation of *D. sissoo* without compaction can be a viable option to obtain good quality timber.

Keywords: *biomass production, heavy machinery, morphological growth, soil bulk density, timber*

Introduction

Soil compaction is a significant factor of despoiled land and an important concern for soil management authorities all over the world. It is a serious issue associated with agriculture, forest cropping, wildlife trampling, and land restoration (Arbuckle and Lasley, 2013; Ferrara et al., 2015). The use of heavy equipment in forest management often leads to soil disturbance and compaction, which in turn affects ecosystem resilience and site efficiency (Cambi et al., 2015). This machinery seriously influences the soil ecosystem by rutting the soil, churning the upper soil layer, and soil compaction. Soil compaction can be caused by different harvesting operations that increase the bulk density of the soil (Ampoorter et al., 2012; Nawaz et al., 2013; Jourgholami et al., 2014; Kormanek et al., 2015).

Soil deprivation has become associated with soil compaction in Africa (18 million ha), Asia (10 million ha), Australia (4 million ha), Europe (33 million ha), and a few parts of North America (Silveira et al., 2010). Two main and common conflicts affected by forest management practices are organic matter changes and soil compaction. Due to increase in

soil compaction there will be 24% rise in bulk density, 50% decrease in aeration penetrability, which ultimately leads to lower temperature and moistness of soil. (Tan et al., 2005). At moderate soil compaction levels, 53% of plant species have greater biomass production due to better root-soil interaction, a comparative growth rate increase of 41%, and a total area increase by 35% (Alameda and Villar, 2012). Soil compaction has no interaction with soil microbial properties (SMP), while it has an adverse effect on Nitrogen (N) content (Nawaz et al., 2010). At the same level of compaction, air permeability changes are typically conferred to soil physical properties by the measurement of oxygen diffusion rates (Nawaz et al., 2013).

Dalbergia sissoo is a medium-sized deciduous tree belonging to the family of Papilionaceae. It is a nitrogen-fixing tree and has a great economic value. The successful regeneration of *D. sissoo* depends on minimum competition and plentiful moisture (Singh et al., 2011). It grows in sunlit zones with abundant moisture, as well as in the rich alluvial soil of sandy banks. It is native to Afghanistan, Pakistan, India, Bhutan, and Malaysia and has naturalized in Indonesia, Cyprus, Nigeria and the United States of America (Ahmad et al., 2013). It is generally used in farm forestry and agroforestry projects in Afghanistan, Pakistan, and India. Most of the useful timber produced from *D. sissoo* comes from those countries where it is native, where it is frequently used to make furniture products. It is also used for medicinal purposes and as a fuelwood. The pods of *D. sissoo* contain 2% tannin. Soil fertility for shade-loving crops improves under *D. sissoo*, as dense litter fall decomposes to supplement the soil with phosphorus, organic carbon, and nitrogen (Hossain et al., 2011). It has been recorded that the growth rate of *D. sissoo* in 1 year is 3.7 m and in 10 years about 15 m (Orwa et al., 2009). *Dalbergia sissoo* is an appropriate species for phytoremediation of seleniferous soils (Bitterli et al., 2010).

The purpose of the present study is to examine the response of *D. sissoo* to different soil compaction levels. Heavy machinery in different farm forestry programs produces shear stress on the soil surface (Edlund et al., 2013; Naghdi et al., 2017), and trampling from domestic animals (Ferrara et al., 2015) and vibration from steady heavy traffic can cause deep compaction in the soil (Cambi et al., 2015).

Considering these situations around the world, the present study has been designed to analyze the effect of soil compaction on to the growth of *D. sissoo* cuttings, a species which has already seen some decline and dieback. For this experiment, the *D. sissoo* tree was selected because of its multiple uses, deciduous nature, high timber value, importance for fodder production, good nitrogen-fixing ability, and importance to soil conservation so that it can be successfully grown in different regions with diverse soil textures and soil moisture contents.

Materials and methods

Site description

The experiment was carried out in the research area of the Department of Forestry and Range Management, University of Agriculture Faisalabad, Pakistan (*Fig. 1*). The site lies between Latitude 30.35 °N and 31.47 °N, and Longitude 72.08 °E and 73 °E, at an elevation of 130 to 150 m above sea level. Detailed weather conditions during the course of the experiment are provided in (*Table 1*). Soil physio-chemical properties of the site are provided in (*Table 2*).

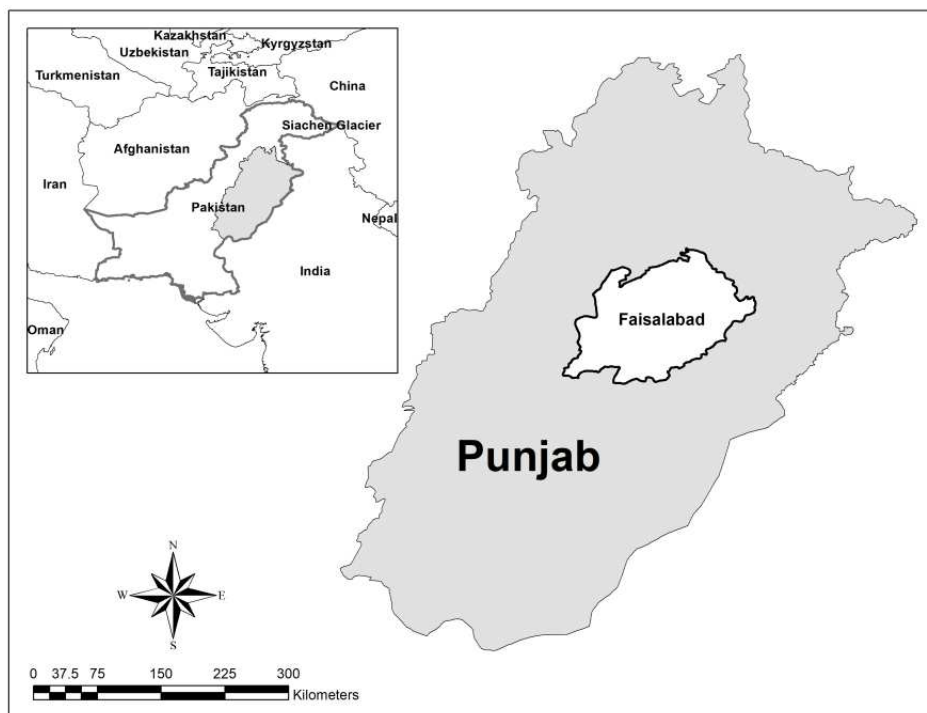


Figure 1. Map of the research site

Table 1. Weather conditions of the study area. (Data taken from the agricultural meteorological cell, University of Agriculture Faisalabad)

Month	Temperature			RH	Rainfall	Sunshine
	Max (°C)	Min (°C)	Avg (°C)	%	mm	hours
April	37.7	20.9	29.3	30.6	28.3	9.2
Avg-10 yrs	32.0	18.8	26.0	46.3	19.7	8.8
May	41.1	26.0	33.5	29.8	10.1	10.4
Avg-10 yrs	38.7	24.4	32.2	29.7	10.2	10.4
June	39.8	27.3	32.8	38.9	41.6	9.38
Avg-10 yrs	40.1	27.5	33.6	39.8	29.9	9.38
July	38.5	38.9	33.7	70.0	117.2	7.0
Avg-10 yrs	37.0	27.6	32.3	58.5	85.8	7.6
August	38.1	28.6	33.4	68.9	66.1	7.9
Avg-10 yrs	36.	26.8	31.4	61.2	50.9	7.6
September	36.7	24.4	30.5	67.7	35.6	8.8
Avg-10 yrs	33.8	22.4	28.1	57.0	47.8	8.3
October	35.0	19.2	27.1	68.2	22.2	7.6
Avg-10 yrs	32.1	19.1	25.5	55.4	10.4	8.05

Table 2. Physical and chemical properties of experimental site

Parameters	Sand (%)	Silt (%)	Clay (%)
0-15 cm	40	45	15
15-30 cm	69	18.5	12.5

Parameters	pH	EC (dS m ⁻¹)	TSS (ppm)	Nitrogen (%)	Phosphorous (ppm)	Potassium (ppm)	Organic matter (%)
0-15 cm	8.0	1.68	1176	0.077	3.9	280	1.54
15-30 cm	8.2	1.35	1236	0.05	9.8	250	0.91

Experimental design

All plots were levelled and aligned by joining their edges. The length of each plot was 4.26 m, width was 1.21 m, the length of boundary pathway was 11.27 m, the length of the middle pathway was 11.58 m, and the width of pathways was 0.76 m (Fig. 2). A manual soil compactor was used to compact the soil and weeding was carried out on regular basis. The beds were prepared, and the experiment was laid out in randomized complete block design (RCBD). For the experiment six treatments were used; T0 (control), T1 (10 beatings with the manual soil compactor), T2 (20 beatings), T3 (30 beatings), T4 (40 beatings), and T5 (50 beatings). The number of replications for each treatment was 12. Beatings were applied with the manual soil compactor (weight, 10 kg) to compact the soil. This was performed by pulling the soil compactor up with the help of rope and then dropping it from a height of 0.6 m on all of the beds (Fig. 3).

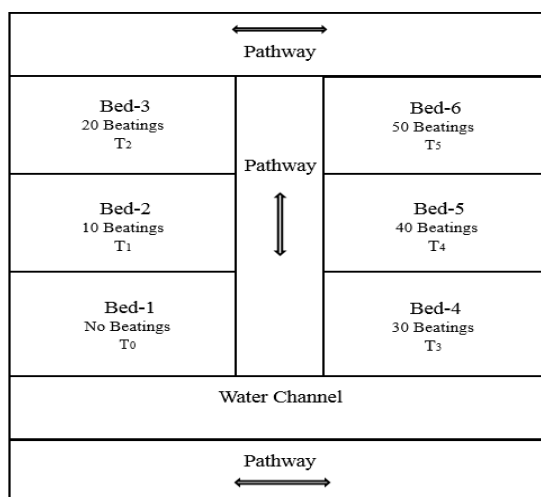


Figure 2. Experimental design

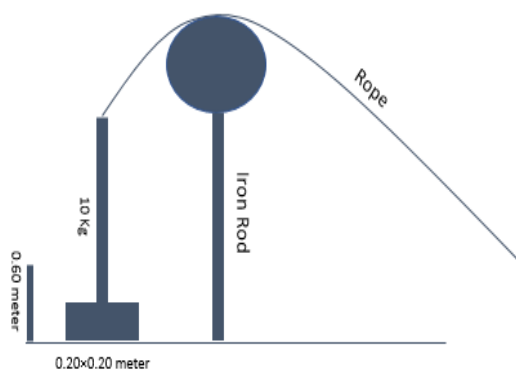


Figure 3. Manual soil compactor used to develop compaction in the soil

Plant sowing and harvesting

Dalbergia sissoo cuttings were collected from the departmental nursery of the University of Agriculture Faisalabad. After compacting the soil, a planting rod was used to transplant the 0.15–0.22 m cuttings into the soil without disturbing the effect of the compaction of the soil. Transplanting was done on the 15th April. A water channel was used to apply irrigation after 3 to 4 days for all of the plots regularly (*Table 3*). The depth of the water channel was 0.45 m and it was 0.76 m wide. During irrigation, water was applied at the surface of the plots. The water absorption rate was very low in highly compacted soil and vice versa. Plants were harvested on the 7th October. Measured plant age was almost 6 months at the time of harvesting. The sampled plants were felled, and the roots were excavated by digging up to the maximum root depth. In the field, the soil was removed from the roots by hand to take the fresh weight. Then the samples were brought to the laboratory for further processing. In the lab, root samples were oven dried for the calculation of biomass production.

Table 3. Different intervals of irrigation during the whole experiment

Date	15-04-16	19-04-16	23-04-16	27-04-16	05-05-16	11-05-16
Irrigation	1 st	2 nd	3 rd	4 th	5 th	6 th
Date	18-05-16	25-05-16	01-06-16	08-06-16	15-06-16	22-06-16
Irrigation	7 th	8 th	9 th	10 th	11 th	12 th
Date	29-06-16	06-07-16	13-07-16	20-07-16	27-07-16	03-08-16
Irrigation	13 th	14 th	15 th	16 th	17 th	18 th
Date	10-08-16	17-08-16	24-08-16	31-08-16	08-09-16	15-09-16
Irrigation	19 th	20 th	21 th	22 th	23 th	24 th
Date	21-09-16	26-09-16	02-10-16			
Irrigation	25 th	26 th	27 th			

Phenological parameters used in the study

Shoot length, root length, shoot fresh weight, root fresh weight, shoot dry weight, root dry weight, root-shoot ratio, biomass production, and moisture content availability were measured. After measuring shoot and root fresh weight of all individual plants, plants were transferred to paper bags and placed in a drying oven (DGH-9202 series thermal electric thermostat drying oven) in order to measure the dry stem and root weight of samples. Stem and root samples were packed in paper bags and dried at 75 °C for 24 h, and then weighed with an electrical balance (electronic scale JJ3000B).

Bulk density was also measured as it is the most frequently used parameter to characterize soil compaction (*Table 4*). Bulk density is difficult to measure in gravelly soils. To measure moisture content availability, the exact fresh weight of samples were taken and then samples were oven dried at 80 °C for 24 h. After oven drying, the dried weight was subtracted from the moist weight and the following equation was used (Jusoh et al., 2011):

$$MC\% = 100 \times \frac{\text{Freshweight} - \text{Dryweight}}{\text{Freshweight}}$$

Table 4. Soil bulk density (BD) of 6 different treatment plots

Beds	Bed-1	Bed-2	Bed-3	Bed-4	Bed-5	Bed-6
Beatings	0	10	20	30	40	50
BD (Mg m ⁻³)	1.3 ± 0.03	1.40 ± 0.05	1.45 ± 0.06	1.55 ± 0.04	1.65 ± 0.08	1.8 ± 0.1

Statistical analysis

One-way ANOVA was used and means that exhibited significant differences were compared with the least significant differences test (LSD). All statistical analyses were conducted using SPSS Statistical Package (SPSS 17.0, SPSS Ins., IL, U.S.A.). Results were statistically analyzed using a P < 0.05 level of significance. Correlation analysis was conducted using the Pearson correlation test (two-tail) to identify relationships between the measured properties

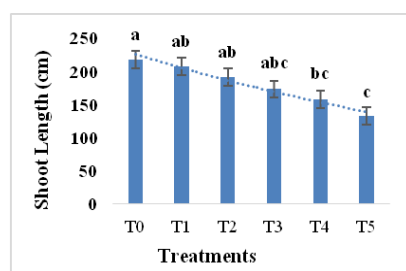
Results

Plant growth

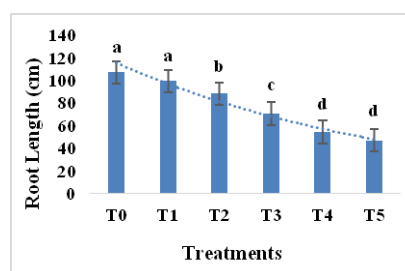
The total length of the shoot was measured with a measuring tape and an average was calculated to express the mean length of the plant. The root length was measured with the help of a meter rod from the base of the plant to the end of the plant and an average was calculated to express the mean root length per replication. According to the ANOVA test, the shoot and root length significantly decreased as compaction level increased, with the results showing significant variation among different compaction levels (Fig. 4a, b).

Biomass distribution pattern

The ANOVA showed variation in *D. sissoo* response at different compaction levels. The shoot and root (both fresh and dry) weight significantly varied with different compaction levels. As depicted in Figure 4c, d, e, and f, the shoot and root weights decreased with increasing compaction, and the root-shoot ratio also showed a decreasing trend with increasing compaction, though this result was not statistically significant (Fig. 5a). In terms of biomass production, ANOVA revealed highly significant variation among compaction levels, with decreasing biomass production with increasing compaction (Fig. 5b).



(a) LSD = 0.0365*



(b) LSD = 0.0001**

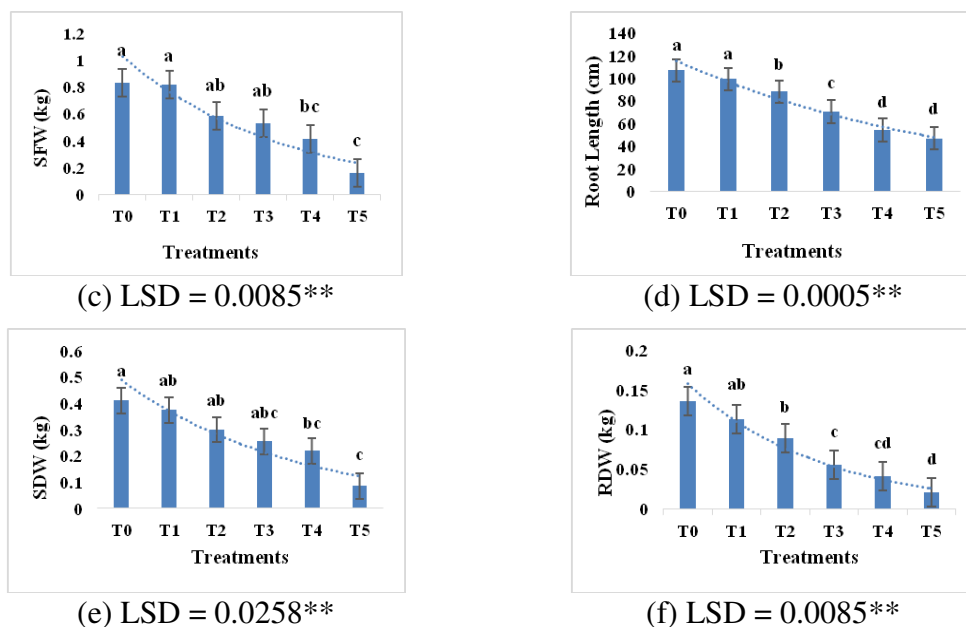


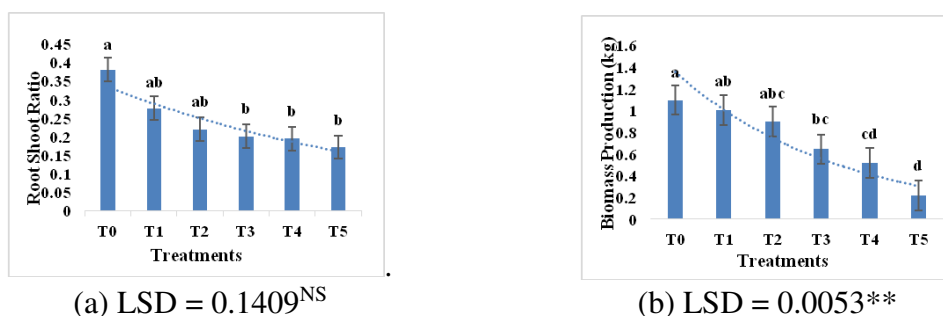
Figure 4. (a) Shoot length, (b) root length, (c) shoot fresh weight, (d) root fresh weight, (e) shoot dry weight, and (f) root dry weight under different soil compaction levels (*significant, **highly significant)

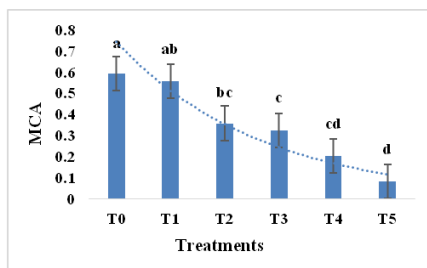
Moisture content availability

Moisture content availability showed a significant difference among compaction levels. The standard error mean at the level of zero compaction (control) was 0.5917, and went on decreasing down to the standard error mean of 0.0820 for the most compacted treatment (Fig. 5c).

Correlation between bulk density, biomass production, and moisture content availability

Bulk density (dry soil mass per unit volume) is the most frequently used parameter to characterize soil compaction, but in swelling and shrinking soils it is recommended to determine the bulk density at the standard moisture content. Bulk density is inversely proportional to shoot and root length, shoot and root dry weight, biomass production, and moisture content availability because bulk density increases with soil compaction, while all the aforementioned traits decrease. Increases in bulk density and soil compaction cause the growth of all these traits to become slow or stunted (Table 5).





(c) LSD = 0.0016**

Figure 5. Variation among root-shoot ratio (a), biomass production (kg) (b), and moisture content availability (kg) (c) under different soil compaction levels (*significant, **highly significant, ^{NS}non-significant)

Table 5. Correlation between bulk density (BD), biomass production (BM), and moisture content availability (MCA). There was significant negative correlation between bulk density and biomass production and moisture content availability. The correlation between biomass production and moisture content availability was significant and positive

Parameters	BD	BM	MCA
Bulk density (BD)	1.0	-0.993**	-0.970**
Biomass production (BM)	-0.993**	1.0	0.965**
Moisture content availability (MCA)	-0.970**	0.965**	1.0

**P < 0.01

Discussion

Cuttings of *D. sissoo* were grown in the natural environment by applying six different compaction treatments. Compaction was done by an iron rod and the effect of compaction on the growth and development of stem and roots was observed. The compaction has a long-lasting effect on soil structure, and occasionally it causes an irreversible damage to plants. Compaction has a negative effect on plant growth and the forest ecosystem (Hartmann et al., 2014). The growth of shoot and roots showed a negative response to compaction in the form of stunted growth. As the compaction level increased from zero to a maximum fifty beatings with the soil compactor, the plant showed a reduced growth response.

Soil compaction severely affected the root system of plants by reducing their ability to access nutrients in the soil, but had a more moderate effect on shoot growth. When soils are highly compacted, the mobility of ions, oxygen, microorganisms, and water in the soil is reduced because macropores turn into micropores which strictly confine the root growth and may also limit shoot growth (Nawaz et al., 2016). The effect of soil compaction on plant growth depends on the soil type and plant species present. Our results showed the shoot weight (dry and fresh) and length decreasing with increased compaction level, in agreement with the results of Alameda and Villar, 2012. Roots have a significant role in nutrient uptake and plant growth. Increased soil compaction can be seen to increase the number of micropores and increase particle distribution (Magagnotti et al., 2012), which has a negative effect on root penetration, root length, and depth of the root. As our results show, the root weight (dry and fresh) and length decreased with increasing compaction, as in the work of Ramalingam et al., 2017.

According to our analysis of variance, compaction level had a significant effect on root weight (fresh and dry). Tracy et al., 2012 found a negative effect of soil compaction on plant growth. Due to compaction, root growth can become stunted and nutrient availability decreases, which has a negative effect on plant biomass production (Kormanek et al., 2015).

If a soil has previously been degraded by salinity, the effect of compaction on the plant growth is compounded. Our statistical analysis showed biomass production (in leaves, stems, and roots) significantly declining as compaction levels increased as Bejarano et al., 2010; and Pérez-Ramos et al., 2010 concluded. For the measurement of soil compaction, water infiltration rate in the soil can be used because the total porosity of the soil decreases due to soil compaction (Bejarano et al., 2010; Arthur et al., 2013). In the same type of soil, the water penetration rate is slower in highly compacted soil as compared with uncompacted soil (Cudzik et al., 2010). Our results showed diminished moisture content availability to plants as compaction levels increased. This, in turn, reduces plant growth (Agherkakli, et al., 2010). Compaction levels in the present study had a significant effect on moisture content availability. Related work indicates that this results in reduced root-shoot ratio (Bengough et al., 2005; Kormanek et al., 2015). In our study, compaction levels had a significant effect on root-shoot ratio.

Conclusions

Different levels of soil compaction significantly affect the morphology and growth of *D. sissoo*, with increased soil compaction reducing growth. We found an overall negative effect of soil compaction on the growth of *D. sissoo*. Consequences of compaction on the soil include increased bulk density. By increasing the accumulation of organic matter, plant growth, and monitoring mechanical operations, we can reduce the problem of soil compaction.

Plantation of *D. sissoo* without compaction is a viable option for good quality timber production. Some other species in this region (e.g. *Eucalyptus camaldulensis*, *Morus alba*, *Acacia nilotica*, and *Bombax ceiba*) are also affected by soil compaction. In future work, we will focus on these species to observe their growth under different soil compaction levels.

Acknowledgments. This research was financially supported by the IFS (grant number D/5279) and the Special Technology Innovation Foundation of Fujian Agriculture and Forestry University (grant number CXZX2016059). We would also like to thank the support of nursery staff of the department of Forestry, University of Agriculture Faisalabad.

Authors contribution. MUHR and MA planned the research. MHUR, MA, IA contributed in field and lab work. Data analysis and interpretation of the results were done by MUHR, THF, MFN and PW. MUHR, and THF wrote the first version of the manuscript. MFN, PW, MMG, NPG and IA provided critical feedback, and all the authors reviewed the final manuscript.

Conflict of interests. Authors declare that there is no conflict of interests.

REFERENCES

- [1] Agherkakli, B., Najafi, A., Sadeghi, S. H. (2010): Ground based operation effects on soil disturbance by steel tracked skidder in a steep slope of forest. – Journal of Forest Science 56(6): 278-284.

- [2] Ahmad, B. I., Khan, R. A., Siddiqui, M. T. (2013): Incidence of dieback disease following fungal inoculations of sexually and asexually propagated shisham (*Dalbergia sissoo*). – Forest Pathology 43(1): 77-82.
- [3] Alameda, D., Villar, R. (2012): Linking root traits to plant physiology and growth in *Fraxinus angustifolia* Vahl. seedlings under soil compaction conditions. – Environmental and Experimental Botany 79: 49-57.
- [4] Ampoorter, E., De Schrijver, A., Van Nevel, L., Hermy, M., Verheyen, K. (2012): Impact of mechanized harvesting on compaction of sandy and clayey forest soils: results of a meta-analysis. – Annals of Forest Science 69(5): 533-542.
- [5] Arbuckle, J. G., Lasley, P. (2013): Iowa Farm and Rural Life Poll. – Summary Report. Iowa State University Extension and Outreach, Ames, IA.
- [6] Arthur, E., Schjønning, P., Moldrup, P., Tuller, M., de Jonge, L. W. (2013): Density and permeability of a loess soil: Long-term organic matter effect and the response to compressive stress. – Geoderma 193: 236-245.
- [7] Bejarano, M. D., Villar, R., Murillo, A. M., Quero, J. L. (2010): Effects of soil compaction and light on growth of *Quercus pyrenaica* Willd. (Fagaceae) seedlings. – Soil and Tillage Research 110(1): 108-114.
- [8] Bengough, A. G., Bransby, M. F., Hans, J., McKenna, S. J., Roberts, T. J., Valentine, T. A. (2005): Root responses to soil physical conditions; growth dynamics from field to cell. – Journal of Experimental Botany 57(2): 437-447.
- [9] Bitterli, C., Bañuelos, G. S., Schulin, R. (2010): Use of transfer factors to characterize uptake of selenium by plants. – Journal of Geochemical Exploration 107(2): 206-216.
- [10] Cambi, M., Certini, G., Neri, F., Marchi, E. (2015): The impact of heavy traffic on forest soils: a review. – Forest Ecology and Management 338: 124-138.
- [11] Cudzik, A., Białczyk, W., Czarnecki, J., Jamroży, K. (2010): Traction properties of the wheel-turfy soil system. – International Agrophysics 24(4): 343-350.
- [12] Edlund, J., Keramati, E., Servin, M. (2013): A long-tracked bogie design for forestry machines on soft and rough terrain. – Journal of Terramechanics 50(2): 73-83.
- [13] Ferrara, C., Barone, P. M., Salvati, L. (2015): Towards a socioeconomic profile for areas vulnerable to soil compaction? A case study in a Mediterranean country. – Geoderma 247: 97-107.
- [14] Hartmann, M., Niklaus, P. A., Zimmermann, S., Schmutz, S., Kremer, J., Abarenkov, K., Frey, B. (2014): Resistance and resilience of the forest soil microbiome to logging-associated compaction. – The ISME Journal 8(1): 226.
- [15] Hossain, M., Siddique, M. R. H., Rahman, M. S., Hossain, M. Z., Hasan, M. M. (2011): Nutrient dynamics associated with leaf litter decomposition of three agroforestry tree species (*Azadirachta indica*, *Dalbergia sissoo*, and *Melia azedarach*) of Bangladesh. – Journal of Forestry Research 22(4): 577.
- [16] Jourgholami, M., Majnounian, B., Abari, M. E. (2014): Effects of tree-length timber skidding on soil compaction in the skid trail in Hyrcanian forest. – Forest Systems 2: 288-293.
- [17] Jusoh, M. A., Abbas, Z., Lee, K. Y., You, K. Y., Norimi, A. M. (2011): Determination of Moisture Content in Mortar at Near Relaxation Frequency 17 GHz. – Measurement Science Review 11: 203-206.
- [18] Kormanek, M., Głab, T., Banach, J., Szewczyk, G. (2015): Effects of soil bulk density on sessile oak *Quercus petraea* Liebl seedlings. – European Journal of Forest Research 134(6): 969-979.
- [19] Magagnotti, N., Spinelli, R., Güldner, O., Erler, J. (2012): Site impact after motor-manual and mechanised thinning in Mediterranean pine plantations. – Biosystems Engineering 113(2): 140-147.
- [20] Naghdi, R., Solgi, A., Zenner, E. K., Najafi, A., Salehi, A., Nikooy, M. (2017): Compaction of forest soils with heavy logging machinery. – Silva 18: 1.

- [21] Nawaz, M. F. (2010): Geochemistry of hydromorphic soils and waters under rice culture and forest-continuous measurements, thermodynamic modelling and kinetics. – Doctoral Dissertation, Université Paul Cézanne-Aix-Marseille III.
- [22] Nawaz, M. F., Bourrie, G., Trolard, F. (2013): Soil compaction impact and modelling. A review. – *Agronomy for Sustainable Development* 33(2): 291-309.
- [23] Nawaz, M. F., Bourrié, G., Trolard, F., Ranger, J., Gul, S., Niazi, N. K. (2016): Early detection of the effects of compaction in forested soils: evidence from selective extraction techniques. – *Journal of Soils and sediments* 16(9): 2223-2233.
- [24] Orwa, C., Mutua, A., Kindt, R., Jamnadass, R., Simons, A. (2009): Agroforestry Database: A Tree Species Reference and Selection Guide Version 4.0. – World Agroforestry Centre ICRAF, Nairobi, KE.
- [25] Pérez-Ramos, I. M., Gómez-Aparicio, L., Villar, R., García, L. V., Maranon, T. (2010): Seedling growth and morphology of three oak species along field resource gradients and seed mass variation: a seedling age-dependent response. – *Journal of Vegetation Science* 21(3): 419-437.
- [26] Ramalingam, P., Kamoshita, A., Deshmukh, V., Yaginuma, S., Uga, Y. (2017): Association between root growth angle and root length density of a near-isogenic line of IR64 rice with DEEPER ROOTING 1 under different levels of soil compaction. – *Plant Production Science* 20(2): 162-175.
- [27] Silveira, M. L., Comerford, N. B., Reddy, K. R., Prenger, J., DeBusk, W. F. (2010): Influence of military land uses on soil carbon dynamics in forest ecosystems of Georgia, USA. – *Ecological Indicators* 10(4): 905-909.
- [28] Singh, B., Yadav, R., Bhatt, B. P. (2011): Effects of mother tree ages, different rooting mediums, light conditions and auxin treatments on rooting behaviour of *Dalbergia sissoo* branch cuttings. – *Journal of Forestry Research* 22(1): 53-57.
- [29] Tan, X., Chang, S. X., Kabzems, R. (2005): Effects of soil compaction and forest floor removal on soil microbial properties and N transformations in a boreal forest long-term soil productivity study. – *Forest Ecology and Management* 217(2-3): 158-170.
- [30] Tracy, S. R., Black, C. R., Roberts, J. A., Sturrock, C., Mairhofer, S., Craigon, J., Mooney, S. J. (2012): Quantifying the impact of soil compaction on root system architecture in tomato (*Solanum lycopersicum*) by X-ray micro-computed tomography. – *Annals of Botany* 110(2): 511-519.

NEW RECORDS OF MACROFUNGI FROM TRABZON PROVINCE (TURKEY)

KELES, A.

Mathematics Van Yüzüncü Yıl University, Education Faculty, Department of Science and Mathematics, Van, Turkey

(e-mail: alikeles61@yahoo.com; phone: +90 432 225 17 01)

(Received 17th Sep 2018; accepted 2nd Jan 2019)

Abstract. This study was based on three macromycete samples collected during field studies carried out to determine the macrofungal biodiversity of Of and Çamburnu districts of Trabzon province (Turkey). As a result of necessary investigations, *Pluteus variabilicolor* Babos (Pluteaceae), *Coprinopsis urticicola* (Berk. & Broome) Redhead, Vilgalys & Moncalvo (Psathyrellaceae) and *Chroogomphus confusus* Y.C. Li & Zhu L. Yang (Gomphidiaceae) were recorded from Turkey for the first time. Brief descriptions and photographs related to macro- and micromorphologies of the species are provided together with their localities, geographical positions, collection date and Genbank number related to genetic sequences.

Keywords: *biodiversity, Basidiomycota, Pluteus, Coprinopsis, Chroogomphus*

Introduction

Due to its excellent flora and climate (Dündar et al., 2016), Turkey is assumed to be very rich in naturally growing macrofungi, and currently comprises about 2,500 macrofungi species more than 85% of which belong to the phylum Basidiomycota (Kaya and Uzun, 2018). The Basidiomycota is a large fungal division with over 30,000 species. Most of the macrofungi such as agarics, bracket fungi, puffballs, earth stars, stinkhorns, boletes, etc., are included in this division. A great majority of the basidiomycota are terrestrial with wind-dispersed spores. Most of them are saprotrophic and are involved in litter and wood decay, but there are also pathogens of trees such as the honey fungus, *Armillaria*. Common woodland mushrooms grow in a mutually symbiotic relationship with the roots of trees, forming ectotrophic mycorrhiza. As saprotrophs, basidiomycetes play a vital role in recycling nutrients but they also cause severe damage as agents of timber decay. Basidiocarps of many mushrooms are edible, and some are grown commercially for food. It is also well known that the basidiocarps of certain mushrooms are poisonous (Webster and Weber, 2007).

During routine field studies in Trabzon province, some macromycete samples were collected and identified as *Pluteus variabilicolor* Babos, *Coprinopsis urticicola* (Berk. & Broome) Redhead, Vilgalys & Moncalvo and *Chroogomphus confusus* Y.C. Li & Zhu L. Yang. Tracing the current literature it is found that almost 2200 basidiomycete taxa have been reported from Turkey, 24, 18 and 2 of which belong to the genera *Pluteus*, *Coprinopsis* and *Chroogomphus* respectively (Sesli and Denchev, 2014; Kaya, 2015; Solak et al., 2015; Akata et al., 2016; Allı et al., 2017; Uzun et al., 2017). But the check-lists on mycobiota of Turkey and recently contributed data (Işık and Türkekul, 2017; Kaya et al., 2016; Keleş and Oruç, 2017; Kaya and Uzun, 2018; Sadullahoğlu and Demirel, 2018; Sesli, 2018, Uzun and Acar, 2018; Uzun and Kaya, 2018; Uzun et al., 2018) reveals *Pluteus variabilicolor*, *Coprinopsis urticicola* and *Chroogomphus confusus* have not been previously reported from Turkey. The study aims to make a contribution to the mycobiota of Turkey by adding new records.

Materials and methods

Macrofungi sampling

Macrofungi samples were collected from Of and Çamburnu districts of Trabzon province in 2012 and 2014 (*Figure 1*). Trabzon province has surface area of 4664 km² and located in eastern Black Sea Region of Turkey, where the annual average temperature is 14.7°C and the average precipitation is 819.6 mm. During field studies, required ecological and morphological characteristic of the samples were noted and they were photographed in their natural habitats. Then the samples were taken to the fungarium. Microscopic investigations were carried out under a Leica DM500 light microscope. Morphological identification of the specimens were carried out with the help of Gierczyk et al. (2014), Li et al. (2009), Migliozi (2011), Desjardin et al. (2015) and Breitenbach and Kränzlin (1991). Using molecular methods, ITS region was investigated to conform the morphological identification. The samples are kept at the fungarium of Van Yüzüncü Yıl University in Van (VANF).

Molecular studies

Total DNA was extracted from dry fungarium materials using a EurX GeneMATRIX Plant & Fungi DNA isolation kit (Poland). The internal transcribed spacer (ITS) regions, including the 5.8S nrDNA were amplified by the polymerase chain reaction (PCR) with the primer pair ITS1-F/ITS4 (White et al., 1990; Gardes and Bruns, 1993). The primer sequences used are given below;

- **ITS1-F** 5' TCCGTAGGTGAACCTGCGG 3'
- **ITS4** 5' TCCTCCGCTTATTGATATGC 3'

The amplification conditions were set as follows: denaturation at 95°C for 5 min, 35 cycles of 45 s at 95°C, 45 s min at 52°C, 60 s at 72°C, and a final extension of 5 min at 72°C. The PCR products were purified using the ExoSAP-IT™ PCR Product Cleanup Reagent and sequenced with an ABI 3730XL DNA analyzer (Applied Biosystems, Foster City, CA) and an BigDye Terminator v3.1 Cycle terminator cycle sequencing kit (Applied Biosystems, Foster City, CA). Consensus sequences were assembled using in BioEdit software, CAP contig.



Figure 1. Species collection locations

Results

Descriptions, photographs of fruiting bodies and images of microcharacters are provided. The taxonomy of the taxa are in accordance with Kirk et al. (2008).

Pluteus variabilicolor Babos

Macroscopic and microscopic features

Pileus 3-6 cm wide, surface smooth and streaked up to half, yellow and central umbo. Lamellae free, rather dense, creamy white. Stipe 2.5-6 × 0.4-0.7 cm, surface smooth, cylindrical, slightly enlarged at the base, striatum length, whitish yellow. Basidia 20-28 × 5.8-8 µm, clavate, 4-spores. Spores 5.4-7.0 × 4.5-5.6 µm, ellipsoid, subglobose, thin-walled. Cheilocystidia 40-48 × 12-15 µm, hyaline, thin-walled, short. Pleurocystidia 65-120 × 19-35 µm (Figure 2).

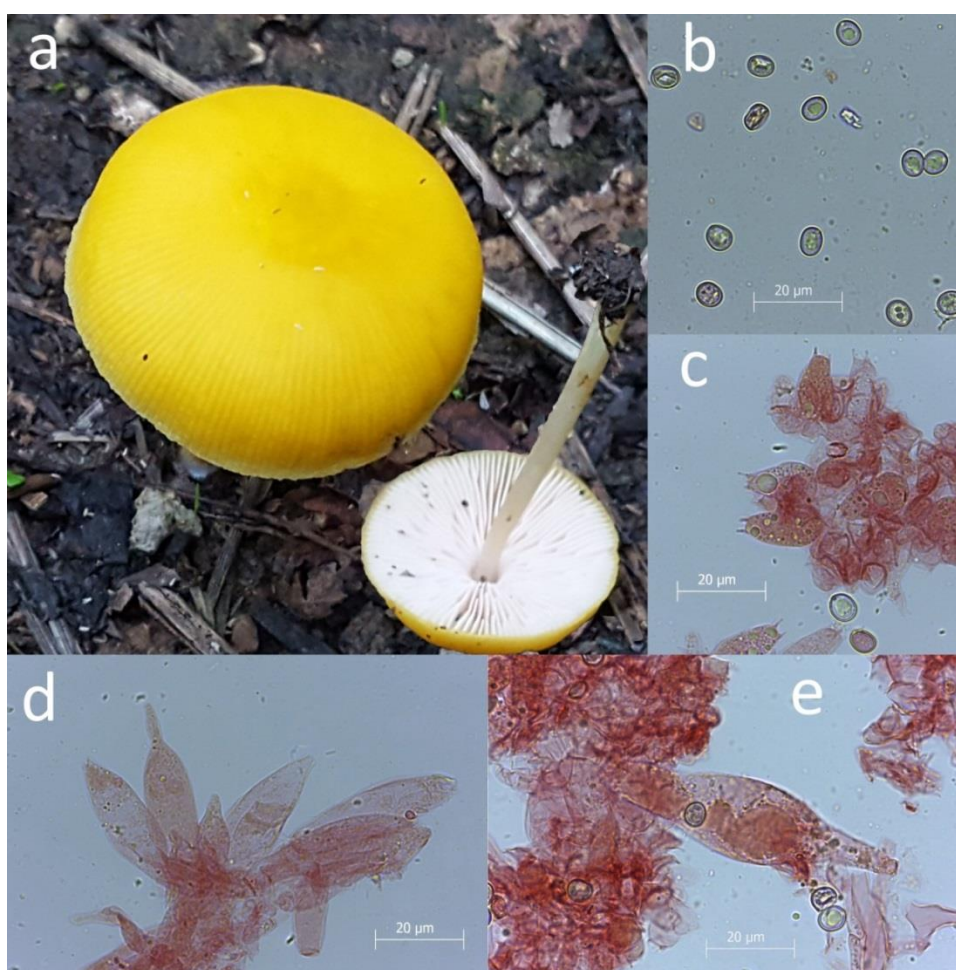


Figure 2. *Pluteus variabilicolor* a) Basidiocarp b) spores c) basidia d) Cheilocystidia e) Pleurocystidia

Specimen examined

Turkey - Trabzon, Of, Ballica neighborhood, under *Corylus* sp. trees, 40°52'845"N, 40°16'849"E, 86 m. 27.08.2015, AK. 2963, Genbank number MH 724931.

***Coprinopsis urticicola* (Berk. & Broome) Redhead, Vilgalys & Moncalvo**

Syn: *Agaricus urticicola* Berk. & Broome, *Coprinopsis urticicola* var. *hawaiiensis* Keirle, Hemmes & Desjardin, *C. urticicola* var. *salicicola* (Uljé & Noordel.) Walley, Verbeken, Kerckh., Keersm., Christiaens, Esprit, Leyman & Van de Kerckh., *C. urticicola* var. *salicicola* (Uljé & Noordel.) Noordel., *C. urticicola* (Berk. & Broome) Redhead, Vilgalys & Moncalvo, *Coprinus brassicae* Peck, *C. urticicola* (Berk. & Broome) Buller, *C. urticicola* var. *salicicola* Uljé & Noordel., *C. urticicola* var. *urticicola* (Berk. & Broome) Buller, *Pilosace urticicola* (Berk. & Broome) Kuntze, *Psathyra urticicola* (Berk. & Broome) Sacc.

Macroscopic and microscopic features

Pileus 0.4-0.8 × 0.2-0.4 cm, ellipsoid when young, then ellipsoid or egg-shaped, pure white. Flesh broken up into small white. Lamellae free, initially white, then greyish-brown and eventually black. Stipe 2-4 × 0.5-0.1 cm, cylindrical, surface smooth, white, slightly clavate base. Basidia 17-26 × 6-9.5 µm, 4-spored. Spores 5.5-8.7 × 4.7-6.2 µm, ellipsoid, pale brown, usually carries a wide germ pore on the base. Cheilocystidia 40-70 × 12-18 µm, globose and ellipsoid. Pleurocystidia 45-80 × 17-30 µm, cylindrical, narrowly conical (*Figure 3*).

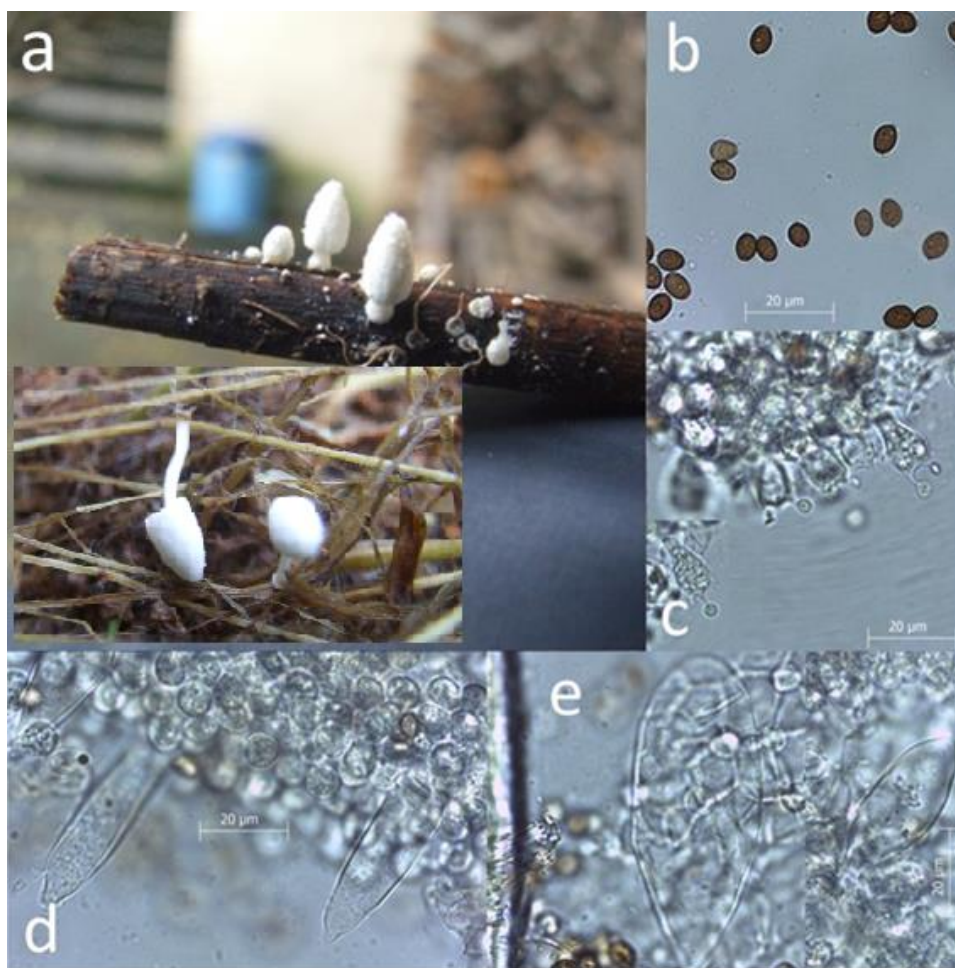


Figure 3. *Coprinopsis urticicola* a) Basidiocarp b) spores c) basidia d) Cheilocystidia e) Pleurocystidia

Specimen examined

Trabzon, Of, Ballica neighborhood, on *Urtica* sp. remains, 40°52'492"N, 40°16'474"E, 121 m 31.07.2012, AK. 2044, Genbank number MH 748639.

Chroogomphus confusus Y.C. Li & Zhu L. Yang

Macroscopic and microscopic features

Pileus 4-8 cm wide, convex, surface smooth and bright, hairless, grayish brown or reddish brown. Lamellae decurrent, greyish orange. Stipe 5-10 × 1-2 cm, subcylindric, yellowish to pale orange. Basidia 38-60 × 9-18 μm, 4-spored. Spores 14-21.6 × 6-7.5 μm, smooth, ellipsoid, dextrinoid and dark gray. Cystidia 110-160 × 18-22 μm, subclavate (*Figure 4*).



Figure 4. *Chroogomphus confusus* a) Basidiocarp b) spores c) basidia d) Cheilocystidia

Specimen examined

Turkey – Trabzon, Çamburnu, around Maritime Faculty, under pine trees, 40°55'390"N, 40°12'596"E, 16m. 29.10.2014, AK. 2871, Genbank number MH 724933.

Discussion

With this study three Basidiomycete taxa, *Pluteus variabilicolor*, *Coprinopsis urticicola* and *Chroogomphus confusus* were reported from Turkey for the first time. General characteristics of all the three taxa are in agreement with those given in literature.

Pluteus variabilicolor was erected by Babos (1978) from Hungary. It is generally characterised by yellowish orange pileus colour when young which turns to light yellow later on. It differs from many other *Pluteus* species by having dimorphic pileipellis and caulocystidial elements (Lezzi et al., 2014). Macro and micromorphological characteristics of *P.* was compared with similar *Pluteus* species in *Table 1*.

Table 1. Comparison of *Pluteus variabilicolor* with similar *Pluteus* species (Vizzini and Ercole, 2011; Kuo, 2015)

Species	<i>P. variabilicolor</i>	<i>P. aurantiorugosus</i>	<i>P. leoninus</i>
Habitat	under <i>Corulus</i> sp. trees	on decaying hardwood	on decaying hardwood
Pileus	3-6 cm	2-5 cm	3-5 cm
Pileus color	lemon yellowish	bright scarlet to orange when young, fading to orangish yellow in age	Gold-yellow with abrown-yellow center
Stipe	2.5-6 × 0.4-0.7 cm	1.5-4 × 0.2-0.4 cm	4-5(9) × 0.2-0.5 cm
Basidia	20-28 × 5.8-8.3 μm	25-30 × 6-8 μm	20-37 × 7.5-10 μm
Spores	5.4-7 × 4.5-5.6 μm	5.5-8 × 4-5 μm	5.5-7 × 5-6 μm
Cheilocystidia	40-48 × 12-15 μm	35-45 × 12.5-22.5 μm	65 × 12 μm
Pleurocystidia	65-120 × 19-35 μm	40-55(60) × 20-23 μm	100 × 28 μm

Coprinopsis urticicola is characterized by its habitat on rotting stems of herbs as well as on fine branchlets, the small fruiting bodies, the branched velar hyphae, and the primarily elliptical spores < 9 μm long (Breitenbach and Kränzlin, 1991). *Coprinopsis urticicola* was compared with morphologically similar species in the following *Table 2*.

Table 2. Comparison of *Coprinopsis urticicola* with closer *Coprinopsis* species (Gierczyk et al., 2011; Amandeep et al., 2012)

Species	<i>C. urticicola</i>	<i>C. vermiculifer</i>	<i>C. gonophylla</i>
Habitat	on herbs remnants	on burnt places or bare, clayey soil	on the sandy and stony meadow
Pileus size	0.4-0.8 × 0.2-0.4 cm	1.4-1.7 cm	up to 0.3 cm
Pileus color	pure white	brownish gray, pileal scales grayish white	Veil white, breaking into patches
Stipe	2-4 × 0.5-0.1 cm	2.5-2.8 cm	6 × 0.1-0.3 cm
Basidia	17-27 × 5.5-10 μm	17-22 × 12-13.6 μm	15-30 × 7-9 μm
Spores	5.6-8.7 × 4.7-6.2 μm	(9.3)10-13.6 × (6.8)7.6-9.3 μm	7.0-8.5 × 6.5-8.0 × 5.5-6.0 μm
Cheilocystidia	40-70 × 12-18 μm	39-59.5 × 27-35.7 μm	40-85 × 25-45 μm
Pleurocystidia	45-80 × 17-30 μm	34-85 × 25.4-37.4 μm	50-120 × 40-20 μm

Chroogomphus confusus has a brownish orange to orange pileus, a nonamyloid pileipellis and reduced amyloidity in the pileal trama (Li et al., 2009). *Chroogomphus confusus* was compared with morphologically similar species in the following Table 3.

Table 3. Comparison of *Chroogomphus confusus* with closer *Chroogomphus* species (Li et al., 2009; Martin et al., 2016; Razaq et al., 2016)

Species	<i>C. confusus</i>	<i>C. mediterraneus</i>	<i>C. rutilus</i>
Habitat	under pine trees	growing under <i>Pinus halepensis</i>	in mixed forests
Pileus size	4-8 cm	2.5-7 (8) cm	2-8 (10) cm
Pileus color	grayish brown or reddish brown	grayish, cream-orange, vinaceous to dingy vinaceous brown	grayish, vinaceous to dingy vinaceous brown
Stipe	5-10 × 1-2 cm	6-10 × 1-2 cm	5-8 (12) × 0.5-1.5 cm
Basidia	38-60 × 9-18 µm	50-60 × 10- 15 µm	40-50 × 12-14 µm
Spores	14-21.6 × 6-7.5 µm	(15.5)16-19(21) × (5.5)6-7.5(8) µm	16.5-19(21) × (5.5)6-8 µm
Cheilocystidia	110-160 × 18-22 µm	(90) 100-175 × 17-21 µm	118-170 × 16-23 µm
Pleurocystidia		(90) 100-175 × 17-21 µm	118-170 × 16-23 µm

Conclusion

Pluteus variabilicolor, *Coprinopsis urticicola* and *Chroogomphus confusus* were given as new records from Turkey, increasing the current taxa numbers of the genera *Pluteus*, *Coprinopsis* and *Chroogomphus*, in Turkey, to 24, 25 and 2 respectively. The current determined taxa number and the current plant biodiversity of Turkey indicate that, macrofungal biodiversity studies should be handled with top priority.

REFERENCES

- [1] Akata, I., Uzun, Y., Kaya, A. (2016): Macrofungal diversity of Zigana Mountain. – *Biological Diversity and Conservation* 9(2): 57-69.
- [2] Allı, H., Çöl, B., Şen, İ. (2017): Macrofungi biodiversity of Kütahya (Turkey) province. – *Biological Diversity and Conservation* 10(1): 133-143.
- [3] Amandeep, K., Atri, N. S., Munruchi, K. (2014): Taxonomic study on coprophilous species of *Coprinopsis* (Psathyrellaceae, Agaricales) from Punjab, India. – *Mycosphere* 5(1): 1-25.
- [4] Babos, M. (1978): *Pluteus* studies, I. (Basidiomycetes, Pluteaceae). – *Annales Historico-Naturales Musei Nationalis Hungarici*, Budapest 70: 93-97.
- [5] Breitenbach, J., Kränzlin, F. (1991): *Fungi of Switzerland*. – Volumes 4. Verlag Mykologia, Lucerne, Switzerland.
- [6] Desjardin, D. E., Wood, M. G., Stevens, F. A. (2015): *California Mushrooms: The Comprehensive Identification Guide*. – Timber Press: Portland, OR. 560 p. USA.
- [7] Dündar, Ö., Demircioğlu, H., Özkaya, O., Dündar, B. (2016): Kültür mantarlarının muhafazası ve kalite özellikleri üzerine yapılan araştırmalar. – *Turkish Journal of Agriculture: Food Science And Technology* 4(3): 150-154.
- [8] Gardes, M., Bruns, T. D. (1993): ITS primers with enhanced specificity for basidiomycetes-application to the identification of mycorrhizae and rusts. – *Molecular Ecology* 2: 113-118.
- [9] Gierczyk, B., Kujawa, A., Pachlewski, T., Szczepkowski, A., Wójtowski, M. (2011): Rare species of the genus *Coprinus* Pers. s. Lato. – *Acta Mycol* 46(1): 27-73.

- [10] Gierczyk, B., Kujawa, A., Szczepkowski, A. (2014): New to Poland species of the broadly defined genus *Coprinus* (Basidiomycota, Agaricomycotina. – *Acta Mycol* 49(2): 159-188.
- [11] Işık, H., Türkekul, İ. (2017): A new record for Turkish mycota from Akdağmadeni (Yozgat) province: *Russula decolorans* (Fr.) Fr. – *Anatolian Journal of Botany* 1: 1-3.
- [12] Kaya, A. (2015): Contributions to the Macrofungal Diversity of Atatürk Dam Lake Basin. – *Turkish Journal of Botany* 39: 162-172.
- [13] Kaya, A., Uzun, Y. (2018): New Contributions to the Turkish Ascomycota. – *Turkish Journal of Botany* 42: 644-652.
- [14] Kaya, A., Uzun, Y., Karacan, İ. H., Yakar, S. (2016): Contributions to Turkish Pyrenomataceae from Gaziantep province. – *Turkish Journal of Botany* 40: 298-307.
- [15] Keleş, A., Oruç, Y. (2017): *Leucocoprinus brebissonii* (Godey) Locq, A New Record for Turkish Mycobiota. – *Anatolian Journal of Botany* 1(2): 49-51.
- [16] Kirk, P. F., Cannon, P. F., Minter, D. W., Stalpers, J. A. (2008): *Dictionary of the Fungi*. – 10th ed. Wallingford, UK: CAB International.
- [17] Kuo, M. (2015): *Pluteus aurantiorugosus*. – MushroomExpert.Com http://www.mushroomexpert.com/pluteus_aurantiorugosus.html.
- [18] Lezzi, T., Vizzini, A., Ercole, E., Migliozi, V., Justo, A. (2014): Phylogenetic and morphological comparison of *Pluteus variabilicolor* and *P. castri* (Basidiomycota, Agaricales). – *Ima Fungus* 5(2): 415-423.
- [19] Li, Y. C., Yang, Z. L., Tolgor, B. (2009): Phylogenetic and biogeographic relationships of *Chroogomphus* species as inferred from molecular and morphological data. – *Fungal Diversity* 38: 85-104.
- [20] Martin, M. P., Siquier, J. L. I., Salom, J. C., Telleria, M. T., Finschow, G. (2016): Barcoding sequences clearly separate *Chroogomphus mediterraneus* (Gomphidiaceae, Boletales) from *C. rutilus*, and allied species. – *Mycoscience* 57(6): 384-392.
- [21] Migliozi, V. (2011): *Pluteus variabilicolor*, specie frequente nella cerreta di Macchiagrande di Manziana (RM). – *Parliamo di Funghi* 19(1): 3-9.
- [22] Razaq, A., Ilyas, S., Khalid, A. N. (2016): Molecular Identification of Chinese *Chroogomphus roseolus* from Pakistani Forests, a Mycorrhizal Fungus, Using ITS-rDNA Marker. – *Pak. J. Agri. Sci.* 53(2): 393-398.
- [23] Sadullahoğlu, C., Demirel, K. (2018): *Flammulina fennae* Bas, A new record from Karz Mountain (Bitlis). – *Anatolian Journal of Botany* 2(1): 19-21.
- [24] Sesli, E. (2018): *Cortinarius* ve *Lyophyllum* Cinslerine Ait Yeni Kayıtlar. – *Mantar Dergisi* 9(1): 18-23.
- [25] Sesli, E., Denchev, C. M. (2014): Checklists of the myxomycetes, larger ascomycetes, and larger basidiomycetes in Turkey. – 6th edn. Mycotaxon, Checklists Online (<http://www.mycotaxon.com/resources/checklists/sesli-v106-checklist.pdf>): 1-136.
- [26] Solak, M. H., Işıoğlu, M., Kalmış, E., Allı, H. (2015): Macrofungi of Turkey, Checklist, Volume II. – Üniversiteliler Ofset, Bornova, İzmir.
- [27] Uzun, Y., Acar, İ. (2018): A New *Inocybe* (Fr.) Fr. Record for Turkish Macrofungi. – *Anatolian Journal of Botany* 2(1): 10-12.
- [28] Uzun, Y., Kaya, A. (2018): *Leucocoprinus cepistipes*, A New Coprinoid Species Record for Turkish Macromycota. – Süleyman Demirel University, Journal of Natural and Applied Sciences 22(1): 60-63.
- [29] Uzun, Y., Acar, İ., Akçay, M. E., Kaya, A. (2017): Contributions to the macrofungi of Bingöl, Turkey. – *Turkish Journal of Botany* 41: 516-534.
- [30] Uzun, Y., Karacan, İ. H., Yakar, S., Kaya, A. (2018): New additions to Turkish Tricholomataceae. – *Anatolian Journal of Botany* 2(2): 65-69.
- [31] Vizzini, A., Ercole, E. (2011): A new annulate *Pluteus* variety from Italy. – *Mycologia*, 103(4): 904-911.

- [32] Webster, J., Weber, R. (2007): *The Fungi*. – Third Edition. Cambridge University Press, The Edinburgh Building, Cambridge CB2 8RU, UK.
- [33] White, T. J., Bruns, T., Lee, S., Taylor, J. (1990): Amplification and direct sequencing of fungal ribosomal RNA genes for phylogenetics. – In: Innis, M. A., Gelfand, D. H., Shinsky, J. J., White, T. J. (eds.) *A Guide to Methods and Applications*. Academic Press.

EFFECT OF DROUGHT STRESS ON CHLOROPHYLL FLUORESCENCE, AND BIOMASS PORTIONING OF *AEGILOPS TAUSCHII* L.

ABBAS, A. – YU, H. – CUI, H. – YU, H. – LI, X.*

*Key Laboratory of Weed and Rodent Biology and Management, Institute of Plant Protection,
Chinese Academy of Agricultural Sciences, Beijing, China*

**Corresponding author*

e-mail: xjli@ippcaas.cn; phone: +86-10-6281-3309

(Received 19th Sep 2018; accepted 26th Nov 2018)

Abstract. *Aegilops tauschii* Coss. is one of the problematic weeds, which competes for resources in wheat crop. Drought stress affects productivity, growth, and development of the crops. A greenhouse experiment was conducted to evaluate the effect of different field capacity levels on biomass partitioning and chlorophyll fluorescence on *Aegilops tauschii* population of China. Dry biomass, plant height, leaf area (LA), leaf area ratio (LAR), specific leaf area (SLA), and the root-shoot ratio (RSR) fluctuated under different field capacity levels and decreased with increasing drought stress level. Maximum dry biomasses, plant height (1.71 g and 15.6 cm) were observed in 70-80% field capacity while the minimum (0.70 g and 12.7 cm) were observed under 10-20% field capacity (FC) level. In root-shoot ratio maximum (0.72 g) was observed in 50-60% field capacity level while minimum (0.60 g) was observed under 10-20% field capacity level. Similarly, in LAR and SLA the maximum values (111.67 cm, 175.45 cm and 433.59 g) were observed in 70-80% field capacity level while the minimum values (68.78 g, 42.02 g and 86.32 g) were recorded under 10-20% field capacity level. Similarly, drought stress also influences the maximum fluorescence (F_m) in the light-adapted state and has an effect on the maximum quantum yield of PSII. Similarly, the trend was observed in qP (photochemical quenching) and qN (non-photochemical quenching) like minimal and maximal fluorescence.

Keywords: *growth biomass, abiotic stress, Aegilops tauschii and field capacity, photosynthetic activity, water stress and mechanism of Aegilops tauschii*

Abbreviations: LA: Leaf area; LAR: Leaf area ratio; SLA: Specific leaf area; Fo: Minimal fluorescence; F_m: Maximum fluorescence; qP: Photochemical quenching; qN: non-photochemical quenching; PSII: Photosystem II

Introduction

Goat grass (*Aegilops tauschii* Coss.) is among one of the noxious exotic weeds (Dudnikov, 2014), with troublesome effect particularly in wheat-growing areas (Zhang et al., 2007). It is native to temperate Asia, tropical Asia and Europe (USDA, 2010). *Aegilops tauschii* was thought to be an aggressive plant that scattered across more than ten provinces (Fig. 1) of China (Wei et al., 2008, 2007; Su et al., 2013). It competes with the main wheat for capturing resources such as nutrients, light, and water. It reduced the crop's yield because it performs better under environmental stress conditions (Curtis and Halford, 2014). Under natural environmental conditions plant faces different types of environmental constraints such as drought stress, salinity stress and temperature stress (Tatrai et al., 2016; Mittler, 2006; Ibanez et al., 2010). Under different abiotic stresses, plants change their physiological, molecular and cellular conditions (Massa et al., 2013). Water is the main component and has an important role in plant growth and development. Roots have an important role among plant parts to uptake the water under drought condition and distribute in whole plant body (Wang et al., 2013).



Figure 1. Geographic zones of *Aegilops tauschii* and red dot indicating the affected provinces

Plant response to limited water is fundamental for implementing crop management strategies (Chaves et al., 2003). Under drought stress levels plants stimulate phenological and biochemical changes which decrease plant growth (Benjamin et al., 2014). Plant growth parameters (plant height, leaf area, dry weight biomass, and chlorophyll fluorescence) are affected under drought condition (Guo et al. (2016). In addition the photosynthetic activity is directly affected under water stress condition (Wu et al., 2010). The crop vulnerability under drought stress depends upon the duration of growth stages, plant species, and stress intensity (Singh et al., 2013). One of the prominent techniques for attaining comprehensive estimates of photosynthetic activities is chlorophyll fluorescence. Chlorophyll fluorescence is an important and fast technique for the examination of photosynthetic activities (Sajbidorova et al., 2015). Plant biochemistry and function of PSII are affected by different abiotic stresses (Yang, 2013). Drought stress significantly effects maximal fluorescence (F_m), maximum fluorescence in the light-adapted state (F'_m), the maximum quantum yield of PSII, photochemical quenching q_P and non-photochemical quenching q_N (Dias and Bruggemann, 2010). Similarly, Cendrero-Mateo et al., 2015 along with Van der Tol et al., 2009 reported that accessibility of light, nutrition, and drought stress manipulate the relationship between photosynthesis, chlorophyll fluorescence, and non-photochemical quenching.

In general, under different abiotic stress conditions chlorophyll fluorescence is a dominant technique for photosynthetic activity (Barbagallo et al., 2003; Proctor et al., 2003; Gottardini et al., 2014). This technique has been used in the study of wheat stress response under different abiotic stress conditions, such as water stress (Eduardo et al., 2002), heat stress (Lu et al., 1999, 2001; Chaerle et al., 2007), cold stress (Rizza et al., 2001; Ying et al., 2002), salt stress (Lu et al., 2003), and nitrogen deficiency (Lu et al., 2001; Shangguan et al., 2000) (Sampol et al., 2003). As we know *Aegilops tauschii* is a rich source of genetic material and perform better under biotic and abiotic stress condition (Assefa and Fehrmann, 2000; Hsam et al., 2001; Colmer et al., 2006).

Some studies investigated the biological characteristic in different crop plant species under different abiotic stresses (Ma et al., 2010). In order to ascertain control strategies for resistant weeds, problem-solving approaches of the species characters should be constructed (Beffa, 2012). Chlorophyll fluorescence was observed on barley leaves when the carbon assimilation was affected (Quick and Horton, 1984). It started an era for stress detection on photosynthesis with chlorophyll fluorescence measurement. In weed science, herbicide stress on Photosystem II (PSII) was used for the dose optimization by measuring photosynthetic efficiency (Kempenaar et al., 2010). Chlorophyll fluorescence was used to quantify the agar-based Syngenta ‘RISQ’ test and detected the herbicide resistance in *Alopecurus myosuroides* depending on the dose response analysis (Kaundun et al., 2011; Wang et al., 2015). Due to the fast-growing habit under the stressful environmental condition, we design an experiment to evaluate the effect of different field capacity levels on biomass partitioning and chlorophyll fluorescence of *Aegilops tauschii*. The objective of this study is to develop a method capable to be used in the field for measuring chlorophyll fluorescence quantum yield of PSII (Fv/Fm) under different water capacity level. The results would contribute to the strategic decision to understand the behavior of *Aegilops tauschii* under different field capacity level.

Materials and method

Plant materials, growth conditions, and stress treatments

A greenhouse experiment was conducted at The Institute of Plant Protection, Chinese Academy of Agricultural Sciences, Beijing, China. *Aegilops tauschii* seeds were collected from five different parts of China. After drying for one week in open sunlight, deformed and damaged seeds were discarded, and apparently healthy seeds were air-dried and then stored at 4 °C. Before sowing seeds were soaked in water for 24 h. A complete randomized design was applied under four replication with four treatments of different field capacity levels (10-20% (D1), 30-40% (D2), 50-60% (D3) and 70-80% (D4). Seeds of similar size were sown in plastic pots (15 cm in diameter and 13 cm in height) with seven seeds per pot in June 2017. Each pot contained similar volumes of sandy loam soil, and hummus in a ratio of 3:1. Initially, pots were watered thoroughly, with soil moisture maintained at about 80–100% field capacity, to ensure the seed germination. Fifteen days after sowing different field capacity levels were maintained in the pots according to the experimental layout and continued until 60 DAS treatment instigation. Soil moisture was measured by using a TDR soil moisture meter (TRIMEPICO, Germany).

Growth parameters

Plant height was measured with a meter rod from the base of the plant to the leaf tip. The height of five chosen plants was measured in each pot and was averaged. Leaf area was measured by a portable leaf meter, and five plants from each pot were selected for further analysis. For recording dry biomass allocation data five plants were removed carefully and washed for the further procedure; the plants were separated into root and shoot put into an oven and dried for 48 h, dry weight was measured with a digital weight balance. Leaf area ratio was determined as follows: total leaf area divided by dry weight biomass. Specific leaf area (SLA) is measured as the ratio of leaf area to dry mass.

Chlorophyll fluorescence

Chlorophyll fluorescence was measured with an imaging-PAM Mini-Series (IMAG-K5, Walz Germany) (Fig. 2) following the procedure described by van Kooten and Snel (1990). Chlorophyll fluorescence imaging-PAMs are highly sensitive research instruments which give quantitative information on the quantum yield of photosynthetic energy conversion. Selected plants of *Aegilops tauschii* were placed in the darkroom for 30 min before measuring the Chlorophyll fluorescence under the different field capacity levels. This imaging-PAM mini-series was used to measure minimum fluorescence (F_o'), maximum fluorescence ($F'm$), the quantum yield of PSII (Φ PSII), photochemical quenching (qP) and non-photochemical quenching (qN). The photochemical quenching (qP) (Eq. 1) and non-photochemical quenching (qN) (Eq. 2) was determined by the following formula shown in Equations 1 and 2.

$$qP = (F'm - F_s) / (F'm - F_0) \quad (\text{Eq.1})$$

$$qN = (F_m - F'm) / F'm \quad (\text{Eq.2})$$

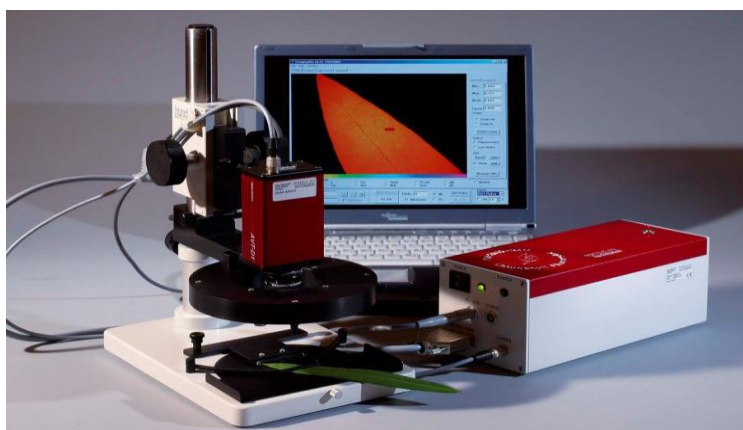


Figure 2. PAM M-series used for chlorophyll fluorescence parameters

Statistical analysis

Statistix 8.1 software (Analytical software, Statistix; Tallahassee, FL, USA, 1985-2003) was used for statistical data extrapolation. Analysis of variance (ANOVA) for plant dry weight biomass, root biomass, and leaf weight biomass was used to find out the effect of treatments and Tukey's honest significance difference (HSD) test was used at 0.05 probabilities to compare the differences among the treatment means. All the results are expressed in standard error (SE) and shown in the figures.

Results

Effect of different field capacity level on growth parameters

Drought stress significantly affects all the parameter under study about biomass partitioning and chlorophyll fluorescence. Chlorophyll fluorescence and growth parameter significantly decreased with increasing drought stress level. Data regarding dry weight biomass of *Aegilops tauschii* under different field capacity level (Table 1)

indicated that dry weight biomass was significantly ($p < 0.05$) influenced by different field capacity level, maximum dry weight biomass (1.71 g) was recorded under 80% field capacity level, and the minimum (0.70 g) was recorded in lower field capacity level (10-20%). The maximum reduction (59%) in dry weight biomass was recorded in (10-20%) field capacity level respectively. In this study, maximum plant height (15.6 cm) was recorded under 70-80% field capacity level while minimum (12.7 cm) was recorded in lower field capacity level. The maximum reduction in plant height (18.5%) was under 10-20% field capacity level. Regarding root-shoot data, the maximum value (0.72 g) was recorded in 70-80% field capacity level while the minimum (0.60) was recorded under 10-20% field capacity level. The reduction with decreasing water field capacity was (16.6%) under 10-20% field capacity level. Regarding leaf area data the maximum (Fig. 3) (111.67 cm) was recorded under 80% field capacity level while the minimum (68.78 cm) was recorded under lower field capacity (10-20%) level. The maximum reduction in leaf area (38%) was recorded through lower field capacity level. Leaf area ratio (LAR) and specific leaf area (SLA) were significantly affected under field capacity levels, the maximum LAR and SLA (175.45 and 433.59) was recorded under 80% field capacity level while the minimum (42.02 and 86.32) was recorded under lower field capacity level (10-20%). The maximum reduction (76% and 80%) in LAR and SLA was recorded through a decreasing field capacity level.

Table 1. Dry weight biomass, plant height, leaf area (cm), leaf area ratio, specific leaf area and root shoot ratio of *Aegilops tauschii* under different field capacity levels

Field capacity	Dry weight	Plant height (cm)	Leaf area	LAR	SLA	R/S ratio
D1	0.70 C	12.7 C	68.78 B	42.02 B	86.32 B	0.60 A
D2	0.98 C	13.5 BC	92.22 AB	77.76 B	147.63 B	0.71 A
D3	1.19 B	15 AB	99.95 A	102.10 B	239.5AB	0.72 A
D4	1.71 A	15.6 A	111.67 A	175.45 A	433.59A	0.68 A

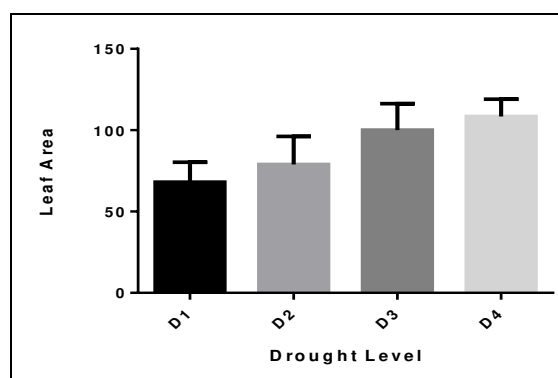


Figure 3. Effect of different capacity levels on leaf area (m^2) of *Aegilops tauschii* L.

Effect of different field capacity levels on chlorophyll fluorescence

Photosynthetic activity (Chlorophyll Fluorescence) was significantly affected under different capacity levels. In different field capacity levels the maximum minimal fluorescence (F_o') was recorded under 20% field capacity and gradually decreased with

increasing field water capacity, and reached a 0.12 value at maximum field capacity (70-80%). Maximal fluorescence (F_m) (Fig. 4b) was recorded (0.32) in 70-80% field capacity and minimum fluorescence (Fig. 4a) (0.20) was recorded under 10-20% field capacity. Under different field capacity levels values of the quantum yield of PSII (F_v/F_m) reaction centre were recorded. Maximum PSII (Fig. 5a) (0.44) was recorded under 70-80% field capacity level while minimum (0.29) was recorded under 10-20% field capacity level. Similarly, trend was observed in effective quantum yield on Photosystem II (Fig. 5b). The photochemical quenching ingenuousness of the center of PSII determines the proportion of energy engrossed by photosystem pigments, which is used for photosynthesis (Van Kooten and Snel, 1990). In addition, the results showed that photochemical quenching qP (Fig. 6a) was increased under 70-80% field capacity and reached a maximum (0.52) and decreased gradually with decreasing field water capacity and reached a minimum (0.39) level. The non-photochemical quenching (qN) (Fig. 6b) is an important mechanism to protect the plant. In non-photochemical quenching $qN = (F_m - F'_m)/F'_m$ directly correlate with field capacity level. An increase in non-photochemical quenching was observed with an increase of field capacity level. Maximum non-photochemical quenching (0.79) was recorded under 70-80% field capacity level and reached a minimum (0.61) at 20% capacity level.

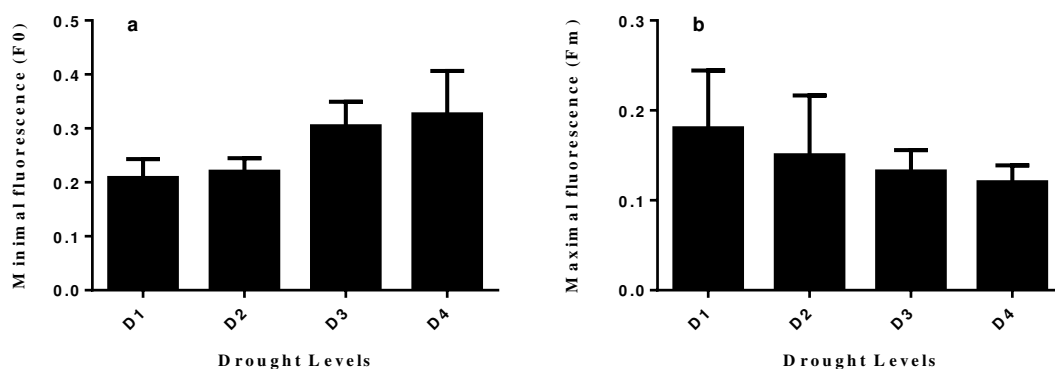


Figure 4. Effect of different capacity levels on minimal fluorescence and maximal fluorescence of *Aegilops tauschii* L. Bars are expressed as \pm SE

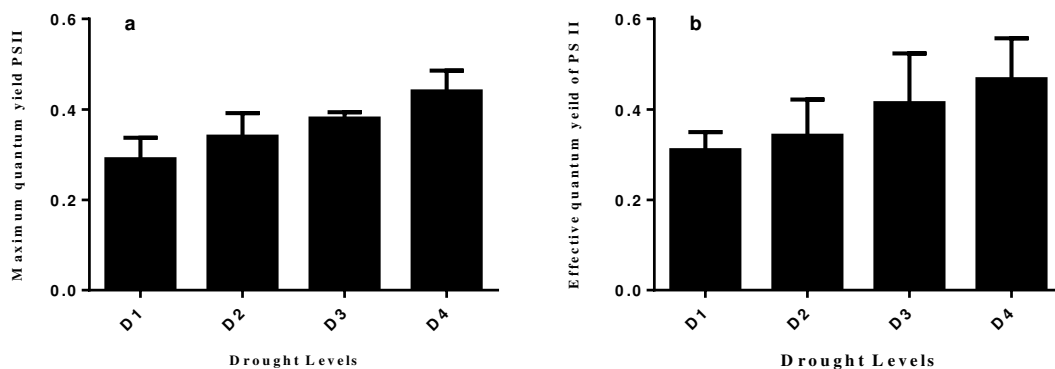


Figure 5. Effect of different capacity levels on the maximum quantum yield on Photosystem II and effective quantum yield on Photosystem II under different field capacity levels

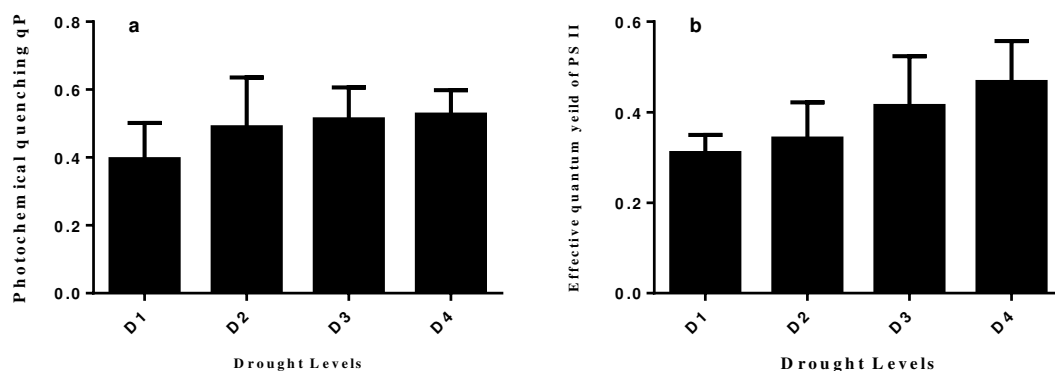


Figure 6. Effect of different capacity levels on photochemical quenching (qP) and non-photochemical quenching (qN) of *Aegilops tauschii* L. Bar are expressed as \pm SE

Under drought stress duration non-photochemical quenching (qN) showed a decline, at 70-80% field capacity a qN value of 0.79 was recorded, which was higher than at 10-20% field capacity (0.61). This showed that the degree of ingenueness of PS II and reaction center under drought stress condition were very low as compared to high field capacity (70-80%), which affect the photosynthetic activity in plants. In our study plant leaves and photosynthetic activity severely damaged under lower field capacity which led to decrease in Fm' , Fv/Fm , $\Phi PSII$, QP , and qN . While *Aegilops tauschii* performed better under drought stress condition.

Discussion

In the present study, we analyzed the effect of different field capacity levels on the biomass partitioning and chlorophyll fluorescence on *Aegilops tauschii*. The plants were irrigated after three days interval. The *Aegilops tauschii* was surviving better under high water stress at 20% field capacity. Under lower field capacity *Aegilops tauschii* shows aggressiveness and perform better. According to the above results, under higher field capacity *Aegilops tauschii* growth is higher than in lower field capacity. This competitive utilization of water in *Aegilops tauschii* in an early stage help to utilize more water content of the soil and initiates more rapid growth as compared to the wheat crop. *Aegilops tauschii* can uptake more water as compared to another crop.

However, lower field capacity level (10-20%) negatively affected the leaves, root, and plant dry biomass of *Aegilops tauschii*. Water is an important component for growth, development, and production (Kabbas et al., 2018). Likewise, Bortolheiro and Silva (2017) and Yamaguchi-Shinozaki and Shinozaki (2006) reported that accessibility and unavailability of proper water seriously affect the biochemical processes, physiology, and morphology of crop plants. Plant growth and biomass allocation are affected under drought stress (Li et al., 2008) and with the variation in availability of water vary the growth and biomass of the plants (Padilla et al., 2009). Chuhan (2013) reported a decrease in biomass production of switch grass under lower field capacity level.

Plants under different drought stress conditions decreased the dry biomass and distorted the biomass allocation from root to leaves. We also conclude that under lower

field capacity dry biomass significantly increases and *Aegilops tauschii* survive better. Similarly, results were found in *Prunus mongolica* in root to shoot ratio under different field capacity levels (Guo et al., 2015; Liu et al., 2017). Similarly, in our study different field capacity levels affected *Aegilops tauschii* growth. Rehimy et al. (2010) said that *Plantago ovata* and *P. psyllium* are significantly affected under drought stress condition. Azevedo (2011) reported under lower field capacity *Carapa guianensis* has maximum growth and biomass. In our study, *Aegilops tauschii* was suppressed under lower field capacity (20 to 40%) level. This may be due to a survival mechanism and growth under different conditions. Under lower water field capacity plant height decreased due to a decline in cell enlargement (Li et al., 2008; Manivannan et al., 2007; Wang et al., 2013). Likewise, Moran and Shower (2005) said that lower field capacity affects or decrease the fresh weight and shoot weight (35% and 35%) of *A. palmeri* S. Continuous water stress affect the smaller leaf of dwarf plants (Haffani et al., 2014).

Under different abiotic stress conditions, chlorophyll fluorescence is an important and common method to determine the leaves photosynthetic activity (Resco et al., 2008). Moreover, Lichteuthaler and Miede (1997) said that plant leaves are sensitive in nature under drought stress condition, decreased the photosynthetic rate at Photosystem II and increased the non-photochemical quenching. In our experiment, lower field capacity greatly affected the chlorophyll fluorescence of *Aegilops tauschii* and considerably decline with a decreasing of field capacity level. The date related to chlorophyll fluorescence of *Aegilops tauschii*. Minimal fluorescence (F_0) increased, while maximal fluorescence (F_m) decreased with increasing field capacity level. This showed that the transportation energy absorbed by Photosystem II partially suppressed the photochemical reaction.

The increase in energy by fluorescence and thermal deactivation loss evidently reduced the photosynthesis energy. Under lower field capacity, photosynthetic activity of *Aegilops tauschii* was damaged that gradually decreased the F_v/F_m value. This showed that the initial reaction of photosynthesis in *Aegilops tauschii* is concealed and the exchange competence of light energy was decreased by inhibiting the potential active center. Chlorophyll fluorescence (F_0) is a powerful component under drought stress condition (Percival and Sheriffs, 2002). The photochemical quenching imitates to an increase in minimal fluorescence and a decrease in maximum fluorescence (F_m) or a ratio of F_v/F_m (Thomas and Turner, 2001). In *Aegilops tauschii*, photochemical quenching and non-photochemical quenching was decreased under lower field capacity level. An important component of Photosystem II is photochemical quenching (q_P) (Li et al., 2013), and protection system under stress condition is non-photochemical quenching (q_N). It showed the proportion of energy absorbed by the PSII pigment but deactivation as a heat (Maxwell and Johnson, 2000). *Aegilops tauschii* photosystem II was significantly damaged due to decreased non-photochemical quenching (q_N) and trapping of heat indulgence potential. This showed that long-term lower water availability affects the photosynthetic process in *Aegilops tauschii* which partially suppressed the photochemical reactions. Similarly, this kind of results have been reported in different crops, such as sugar beet (Sikuku et al., 2010) *Coronilla varia* (Yang et al., 2013) In *P. mongolica* and *L. ruthenicum* (Guo et al., 2015) it was showed that chlorophyll fluorescence parameters are extensively affected under different field capacity levels.

Conclusion

This study revealed the survival mechanism of *Aegilops tauschii* under different field capacity levels. In conclusion, our results showed that lower field capacity affects the biomass partitioning and chlorophyll fluorescence of *Aegilops tauschii*. Furthermore, all growth-related parameters start declining under 20 to 40% field capacity, the growth and survival of *Aegilops tauschii* were adversely affected under higher field capacity of 60 to 80%. Likewise, lower field capacity level damages *Aegilops tauschii* leaves, photosynthetic activity that leads to a decrease in minimal fluorescence (F₀), maximal fluorescence (F_m), and maximum quantum yield of PSII (F_v/F_m), photochemical quenching q_P and non-photochemical quenching q_N, therefore, lower field capacity level severely affects *Aegilops tauschii*.

Acknowledgements. This study was funded by the “National key Research and Development Program of China (2106YFD0300701) and the earmarked fund for China Agriculture Research System (CARS-25).

Conflict of interests. The authors declare that they have no conflict of interests.

REFERENCES

- [1] Assefa, A., Fehrmann, H. (2000): Resistance to wheat leaf rust in *Aegilops tauschii* Coss. and inheritance of resistance in hexaploid wheat. – Genetic Resources and Crop Evolution 47: 135-140.
- [2] Azevedo, G. F. D. C. (2011): Photosynthetic parameters and growth in seedlings of *Bertholletia excelsa* and *Carapa guianensis* in response to pre-acclimations to full sunlight and mild water stress. – Acta Amazonica 44: 67-77.
- [3] Barbagallo, R. P., Oxborough, K., Pallett, K. E., Baker, N. R. (2003): Rapid, noninvasive screening for perturbations of metabolism and plant growth using chlorophyll fluorescence imaging. – Plant Physiology 132: 485-493.
- [4] Beffa, R., Figge, A., Lorentz, L., Hess, M., Laber, B., Ruiz-Santaella, J. P. (2012): Weed resistance diagnostic technologies to detect herbicide resistance in cereal-growing areas. A review. – Julius-Kuhn-Archiv 434: 75-78.
- [5] Benjamin, J. G., Nielsen, D. C., Vigil, H. F., Mikha, M. M., Calderon, F. (2014): Water deficit stress effects on corn (*Zea mays* L.). – Open Journal of Soil Science 4: 151-160.
- [6] Bortolheiro, F. P. A. P., Silva, M. A. (2017): Physiological response and productivity of safflower lines under water deficit and rehydration. – Anais da Academia Brasileira de Ciências 89: 3051-3066.
- [7] Cendrero-Mateo, M. P., Carmo-Silva, A. E., Porcar-Castell, A., Hamerlynck, E. P., Papuga, S. A., Moran, M. S. (2015): Dynamic response of plant chlorophyll fluorescence to light, water, and nutrient availability. – Function of Plant Biology 42: 8-12.
- [8] Chaerle, L., Leinonen, I., Jones, H. G., Straeten, D. V. D. (2007): Monitoring and screening plant populations with combined thermal and chlorophyll fluorescence imaging. – Journal of Experimental Botany 58: 773-784.
- [9] Chauhan, B. S. (2013): Growth response of switchgrass (*Rottboellia cochinchinensis*) to water stress – Weed Science. 61: 98-103.
- [10] Chaves, M. M., Maroco, J. P., Pereira, J. S. (2003): Understanding plant responses to drought from genes to the whole plant. – Functional of Plant Biology 12: 239-264.
- [11] Colmer, T. D., Flowers, T. J., Munns, R. (2006): Use of wild relatives to improve salt tolerance in wheat. – Journal of Experimental Botany 57: 1059-1078.

- [12] Curtis, T., Halford, N. G. (2014): Food security: the challenge of increasing wheat yield and the importance of not compromising food safety. – *Annals of Applied Biology* 164: 354-372.
- [13] Dias, M. C., Bruggemann, W. (2010): Limitations of photosynthesis in *Phaseolus vulgaris* under drought stress: gas exchange, chlorophyll fluorescence, and Calvin cycle enzymes. – *Photosystem* 48: 96-102.
- [14] Dias, M. C., Bruggemann, W. (2010): Limitations of photosynthesis in *Phaseolus vulgaris* under drought stress: gas exchange, chlorophyll fluorescence, and Calvin cycle enzymes. – *Photosystem* 48: 96-102.
- [15] Eduardo Adonias DeSousa, M. D., Ross, H. Albert, B. A., Bernadette Kalman, M. D. (2002): Cognitive impairments in multiple sclerosis: A review. – *American Journal of Alzheimer's Disease & Other Dementias* 17: 23-29.
- [16] Gottardini, E., Cristofori, A., Cristofolini, F., Nali, C., Pellegrini, E., Bussotti, F., Ferretti, M. (2014): Chlorophyll-related indicators are linked to visible ozone symptoms: evidence from a field study on native *Viburnum lantana* L. plants in northern Italy. – *Ecological Indicators* 39: 65-74.
- [17] Guo, Y., Hongyuan, Y., Dongsheng, K, Fang, Y., Donghua, L., Yajuan, Z. (2015). Effects of gradual soil drought stress on the growth, biomass partitioning, and chlorophyll fluorescence of *Prunus mongolica* seedlings. – *Turkish Journal of Biology* 39: 532-539.
- [18] Guo, Y. Y., Yu, H. Y., Kong, D. S., Yan, F., Zhang, Y. J. (2016): Effects of drought stress on growth and chlorophyll fluorescence of *Lycium ruthenicum* Murr. seedlings. – *Photosynthetica* 54(4): 524-531.
- [19] Haffani, S., Mezni, M., Slama, I., Ksontini, M., Chalabi, W. (2014): Plant growth, water relations and proline content of three vetch species under water-limited conditions. – *Grass and Forage Science* 69: 323-333.
- [20] Hsam, S. L. K., Kieffer, R., Zeller, F. J. (2001): The significance of *Aegilops tauschii* glutenin genes on bread-making properties of wheat. – *Cereal Chemistry* 78: 521-525.
- [21] Ibanez, H., Ballester, A., Munoz, R., Jose, Q. M. (2010). Chlororespiration and tolerance to drought, heat and high illumination. – *Journal of Plant Physiology*. 167: 732-738.
- [22] Kaundun, S. S., Hutchings, S. J., Dale, R. P., Bailly, G. C., Glanfield, P. (2011): Syngenta RISQ test: a novel in-season method for detecting resistance to post-emergence ACCase and ALS inhibitor herbicides in grass weeds. – *Weed Research* 51: 284-293.
- [23] Kebabs, S., Benseddik, T., Makhloufi, H., Aid, F. (2018). The physiological and biochemical behavior of *Gleditsia triacanthos* L. Young seedlings under drought stress conditions. – *Notulae Botanicae Horti Agrobotanici* 46: 585-592.
- [24] Kempenaar, C., Lotz, L. A. P., Snel, J. F. H., Smutny, V., Zhang, H. J. (2011): Predicting herbicidal plant mortality with mobile photosynthesis meters. – *Weed Research* 51: 12-22.
- [25] Korten, O. V., Snel, J. (1990): The use of chlorophyll fluorescence nomenclature in plant stress physiology. – *Photosynthesis Research* 25: 147-50.
- [26] Krause, G. H., Weis, E. (1991): Chlorophyll fluorescence and photosynthesis: the basics. – *Annual Review of Plant Physiology and Plant Molecular Biology* 42: 313-349.
- [27] Li, F. L., Bao, W. K., Wu, N., You, C. (2008): Growth biomass partitioning, and water-use efficiency of a leguminous shrub (*Bauhinia faberi* var. *microphylla*) in response to various water availabilities. – *New Forest* 36: 53-65.
- [28] Li, G. L., Wu, H. X., Sun, Y. Q. (2013): The response of chlorophyll fluorescence parameters to drought stress in sugar beet seedlings. – *Russian Journal of Plant Physiol.* 60: 337-342.
- [29] Lichtenthaler, H. K., Miehe, J. A. (1997): Fluorescence imaging as a diagnostic tool for plant stress. – *Trends in Plant Sciences* 2: 316-320.
- [30] Liu, Y., Li, P., Xu, G. C., Xiao, L., Ren, Z. P., Li, Z. B. (2017): Growth, morphological and physiological responses to drought stress in *Bothriochloa ischaemum*. – *Frontier in Plant Science* 8: 230-237.

- [31] Lu, C. M., Vonshak, A. (1999): Characterization of PSII photochemistry in salt-adapted cells of the cyanobacterium *Spirulina platensis*. – *New Phytologist* 141: 231-239.
- [32] Lu, C. M., Zhang, J. H. (1998): Effects of water stress on photosynthesis, chlorophyll fluorescence and photoinhibition in wheat plants. – *Australian Journal of Plant Physiology* 25: 883-892.
- [33] Lu, C. M., Zhang, J. H., Zhang, Q. D., Li, L. B., Kuang, T. Y. (2001): Modification of photosystem II photochemistry in nitrogen deficient maize and wheat plants. – *Journal of Plant Physiology* 158: 1423-1430.
- [34] Lu, C. M., Qiu, N., Wang, B., Zhang, J. H. (2003): Salinity treatment shows no effects on Photosystem II photochemistry but increases the resistance of Photosystem II to heat stress in halophyte *Suaeda salsa*. – *Journal of Plant Physiology* 54: 851-860.
- [35] Ma, J., Ni, X., Shi, H. Y., Liu, W. Z. (2010): Flowering biology of *Amygdalus mongolica*. – *Acta Botanica Boreali-Occidentalia Sinica* 30: 1134-1141.
- [36] Manivannan, P., Jaleel, C. A., Kishorekumar, A., Sankar, B., Somasundaram, R., Sridharan, R., Panneerselvam, R. (2007): Changes in the antioxidant metabolism of *Vigna unguiculata* L. by propiconazole under water deficit stress. – *Colloids and Surfaces B: Biointerfaces* 57: 69-74.
- [37] Massa, A. N., Kevin, L., Buell, R. C. (2013): Abiotic and biotic stress responses in *Solanum tuberosum* group Phureja DM1-3 516 R44 as measured through whole transcriptome Sequencing. – *The Plant Genome* 6: 1-10.
- [38] Maxwell, K., Johnson, G. N. (2000): Chlorophyll fluorescence: a practical guide. – *Journal of Experimental Botany* 51: 659-668.
- [39] Mittler, R. (2006): Abiotic stress the field environment and stress combination. – *Trends in Plant Science* 11: 15-19.
- [40] Moran, P. J., Showler, A. T. (2005): Plant responses to water deficit and shade stresses in pigweed and their influence on feeding and oviposition by the beet armyworm (Lepidoptera: Noctuidae). – *Environmental Entomology* 34: 929-937.
- [41] Percival, G. C., Sheriffs, C. N. (2002): Identification of drought-tolerant woody perennials using chlorophyll fluorescence. – *Journal of Arboriculture* 28: 215-223.
- [42] Padilla, F. M., Ortegab, R., Sanchezab, J., Pugnairea, F. I. (2009): Rethinking species selection for restoration of arid shrublands. – *Cellular and Molecular Life Sciences* 66(1): 173-86.
- [43] Proctor, M. C. F. (2003): Comparative ecophysiological measurements on the light responses, water relations and desiccation tolerance of the filmy ferns *Hymenophyllum wilsonii* Hook and *H. tunbrigense* (L.). – *Annals of Botany* 9: 717-727.
- [44] Quick, W. P., Horton, P. (1984): Studies on the induction of chlorophyll fluorescence in barley protoplasts. Factors affecting the observation of oscillations in the yield of chlorophyll fluorescence and rate of oxygen evolution. – *Proceedings of the Royal Society of London Series B Biological Sciences* 220: 361-370.
- [45] Rahimi, A., Husseini, S. M., Pooryosef, M., Fateh, I. (2010): Variation of leaf water potential, relative water content, and SPAD under gradual drought stress and stress recovery in two medicinal species of *Plantago ovata* and *P. psyllium*. – *Plant Ecophysiology* 2: 53-60.
- [46] Resco, V., Ignace, D. D., Sun, W., Huxman, T. E., Weltzin, J. F., Williams, D. G. (2008): Chlorophyll fluorescence, predawn water potential, and photosynthesis in precipitation pulse-driven ecosystems-implications for ecological studies. – *Functional Ecology* 22: 479-83.
- [47] Rizza, F., Pagani, D., Stanca, A. M., Cattivelli, L. (2001): Use of chlorophyll fluorescence to evaluate the cold acclimation and freezing tolerance of winter and spring oats. – *Plant Breeding* 120: 389-392.
- [48] Sajbidorova, V., Lichtnerova, H., Paganova, V. (2015): The impact of different water regime on chlorophyll fluorescence of *Pyrus pyraeaster* L. *Sorbus domestica* L. – *Acta Universitatis Agriculturae et Silviculturae Mendelianae Brunensis* 63: 1575-1579.

- [49] Sampol, B., Bota, J., Riera, D., Medrano, H., Flexas, J. (2003): Analysis of the virus-induced inhibition of photosynthesis in malmsey grapevines. – *New Phytology* 160: 403-412.
- [50] Shangguan, Z. P., Shao, M. A., Dyckmans, J. (2000): Effects of Nutrition and water deficit on the Net photosynthetic rate and chlorophyll fluorescence in winter wheat. – *Journal of Plant Physiology* 156: 46-51.
- [51] Sikuku, P. A., Netondo, G. W., Onyango, J. C., Mysyimi, D. M. (2010): Chlorophyll fluorescence, protein, and chlorophyll content of three rainfed rice varieties under varying irrigation regimes. – *Journal of Agricultural and Biological Science* 5: 19-25.
- [52] Singh, S. J., Singh, S. K. (2013): Genetic variability analysis in coriander (*Coriandrum sativum* L.). – *Journal of Spices and Aromatic Crops* 22: 81-84.
- [53] Su, Z., Ma, X., Guo, H., Sukiran, N. L., Guo, B., Assmann, S. M., Ma, H. (2013): Flower development under drought stress: Morphological and transcriptomics analyses reveal acute responses and long-term acclimation in *Arabidopsis*. – *Plant Cell* 25: 3785-3807.
- [54] Tatrai, Z. A., Sanoubar, R., Pluhar, Z., Mancarella, S., Orsini, F., Gianquinto, G. (2016): Morphological and physiological plant responses to drought stress in *Thymus citriodorus*. – *International Journal of Agronomy* ID 4165750.
- [55] Thomas, D. S., Turner, D. W. (2001): Banana (*Musa* sp.) leaf gas exchange and chlorophyll fluorescence in response to soil drought, shading, and lamina folding. – *Scientia Horticulturae* 90: 93-108.
- [56] U. S. Department of Agriculture Forest Science, Natural Resource Conservation Service (2010): The Plants Database. – <http://plants.usda.gov>.
- [57] Van, D. T., Verhoef, C. W., Timmermans, J., Verhoef, A., Su, Z. (2009): An integrated model of soil-canopy spectral radiance observations, photosynthesis, fluorescence, temperature, and energy balance. – *Biogeosciences Discussion* 6: 6025-6075.
- [58] Van, K. O., Snel, J. F. H. (1990): The use of chlorophyll nomenclature in plant stress physiology. – *Photosynthesis Research* 25: 147-150.
- [59] Wang, P., Kaiser, Y. I., Menegat, A., Gerhards, R. (2015): Weed PAM: A rapid in-season herbicide resistance detector. – 17th European Weed Research Society Symposium 137: 287-291.
- [60] Wang, W. L., Wan, Y. J., Liu, B., Wang, G. X., Tang, X. Y., Chen, X., Liang, B., Zhuang, W. (2013): Influence of soil gradual drought stress on *Acorus calamus* growth and photosynthetic fluorescence characteristics. – *Acta Ecologica Sinica* 33: 3933-3940.
- [61] Wei, H. T., Li, J., He, X. R. (2007): Genetic diversity of *Aegilops tauschii* revealed by SSR markers. – *Southwest China Journal of Agricultural Sciences* 20: 270-274.
- [62] Wei, H. T., Li, J., Peng, Z. S., Lu, B., Zhao, R., Yang, Z. J. (2008): Relationships of *Aegilops tauschii* revealed by DNA fingerprints: The evidence for agriculture exchange between China and the West. – *Progress in Natural Science* 18: 1525-1531.
- [63] Wu, G. L., Duan, R. Y., Wang, Z. G., Zhang, Z. X., Wu, L. F. (2010): Effects of drought stress and rehydration on chlorophyll fluorescence characteristics in *Fragaria* × *ananassa* Duch. – *Acta Ecologica Sinica* 30: 3941-3946.
- [64] Yamaguchi-Shinozaki, K., Shinozaki, K. (2006): Transcriptional regulatory networks in cellular responses and tolerance to dehydration and cold stresses. – *Annual Review of Plant Biology* 57: 781-803.
- [65] Yang, W. Q., Gu, M. Y., Kou, J. C. (2013): Effect of drought and rewatering on the photosynthesis and chlorophyll fluorescence of *Coronilla varia*. – *Acta Agrestia Sinica* 21: 1130-1135.
- [66] Ying, J., Lee, E. A., Tollenaar, M. (2002): Response of Leaf Photosynthesis during the grain-gilling period of maize to the duration of cold exposure, acclimation, and incident PPFD. – *Crop Science* 42: 1164-1172.
- [67] Zhang, C. X., Li, X. J., Huang, H. J., Wei, S. H. (2007): Alert and prevention of the spreading of *Aegilops tauschii*, the worst weed in a wheat field. – *Acta Phytophylacica Sinica* 34: 103-106 (in Chinese).

THE RELATIONSHIP BETWEEN MINERAL NITROGEN CONTENT AND SOIL PH IN GRASSLAND AND FODDER CROP SOILS

WATROS, A.¹ – LIPIŃSKA, H.² – LIPIŃSKI, W.³ – TKACZYK, P.⁴ – KRZYSZCZAK, J.^{5*} –
BARANOWSKI, P.⁵ – BRODOWSKA, M. S.⁴ – JACKOWSKA, I.⁶

¹*New Chemical Synthesis Institute
Al. Tysiąclecia Państwa Polskiego 13 A, 24-110 Puławy, Poland*

²*Department of Grassland Science and Landscaping, University of Life Sciences in Lublin
ul. Akademicka 15, 20-950 Lublin, Poland*

³*State School of Higher Education in Chełm, ul. Pocztowa 54, 22-100 Chełm, Poland*

⁴*Department of Agricultural and Environmental Chemistry, University of Life Sciences in
Lublin, ul. Akademicka 15, 20-950 Lublin, Poland*

⁵*Institute of Agrophysics Polish Academy of Sciences
ul. Doświadczalna 4, 20-290 Lublin, Poland
(phone: +48 (81) 744 50 61; fax: +48 (81) 744 50 67)*

⁶*Department of Chemistry, University of Life Sciences in Lublin
ul. Akademicka 15, 20-950 Lublin, Poland*

**Corresponding author*

e-mail: jkrzyszczak@ipan.lublin.pl; phone: (81) 744 50 61; fax: (81) 744 50 67

(Received 4th Sep 2018; accepted 28th Nov 2018)

Abstract. This study attempted to evaluate the relationship between mineral nitrogen (N_{\min}) content and soil pH in the 60-90 cm layer of grassland soils relative to other selected agricultural fodder crops. The area of the study uniformly covered the whole territory of Poland. The dependence between N_{\min} content and soil pH was expressed as correlation coefficients, while their significance was evaluated using the one-way non-orthogonal analysis of variance classification. Regardless of sampling date (spring or autumn) and land use (meadow, pasture, hay and pasture or alternate), soil pH had a significant effect on N_{\min} concentration. The correlation between N_{\min} and soil pH in grasslands on mineral soils was positive, regardless of soil sampling date. In turn, in organic soils a negative correlation between pH and N_{\min} content was observed in the spring period, whereas in autumn this trend did not persist and the correlation was positive. On the other hand, in the case of agricultural fodder crops (maize or mixed cereal) N_{\min} content in the 60-90 cm layer and soil pH were found to be positively correlated, regardless of spring or autumn sampling date, with a correlation coefficient higher than 0.9. The obtained results can be used for diminishing environmental hazards.

Keywords: *mineral soils, organic soils, maize, mixed cereals, regression equations*

Introduction

One of the major problems related to agricultural production effectiveness is to control soil acidification through properly conducted liming treatments. Arable soils in Poland are characterized by excessive acidification, which results not only from environmental reasons, but to a large extent from incompetent land use and insufficient use of calcium fertilizers (Filipek and Skowrońska, 2013). The most commonly used

nitrogen fertilizers causing soil acidity increase are ammonium sulphate and urea. Acidified soil prevents proper growth and development of crop plants and due to this yields obtained are much lower than potential ones (Siebielec et al., 2012; Tkaczyk and Bednarek, 2011). Improper identification of this problem can result in application of increased rates of mineral and organic fertilizers and this, in turn, has a very negative environmental impact. It leads not only to degradation of surface and groundwaters, but also to increased greenhouse gas emissions, both as a result of land use intensification and directly due to unfavorable soil pH. However, in the context of sustainable farming a farmer should take into consideration not only the short-term impact of agricultural practices used to increase profit, but also the long-term effect associated with climate change and soil degradation. Only such an approach can lead to the maintenance of farming profitability over the long term, both at the farm level and at the level of the entire region or country, while simultaneously providing environmental protection. It is also important that the soil content of mineral nitrogen (and other macro- and micronutrients) depends, among others, on soil physical and chemical properties, among which pH is one of the more important factors that modify the rate of conversion of this element (Burton and Prosser, 2001; De Boer and Kowalchuk, 2001; Skowron, 2004; Coyne and Frye, 2005). Low soil pH promotes the process of ammonification, while at higher pH the process of nitrification occurs more easily (Sapek, 1999; Kyveryga et al., 2004). With a decrease in soil pH, an increase in the ammonium nitrogen content was noted (with its maximum value at a pH of 3.5), but at the same time a significant decrease in the nitrate nitrogen content. The content of the nitrate form of mineral nitrogen was found to be several times lower in soils with a pH close to 3.5 than in soils characterized by a pH of 7.5 (Skowron, 2004). Due to this, in acidic soils one should expect lower nitrate nitrogen losses caused by leaching, but at the same time worse supply of plants with this nutrient. Proper fertilizer management, which takes into account soil acidification, is possible by using precise agriculture systems that allow the spatial variation of soil physico-chemical properties and the relationships between these properties to be taken account of. Precise agriculture systems are based on both monitoring and environmental research regarding, among others, the effects of soil physical and chemical properties on macro- and micronutrient content in various ecosystems (Tkaczyk et al., 2017; 2018a; 2018b). Such research also allows to make an assessment of the effectiveness of treatments applied by using physical and mathematical models that describe the processes occurring in the soil-plant-atmosphere system (Walczak et al., 1997; Lamorski et al., 2013). Thanks to it, a farmer knows not only what treatments should be carried out in the field and when, but he can also forecast yields and ultimately - estimate profit. The change in local climate conditions due to global climate change is one of the yield-affecting factors that are more difficult to evaluate. Therefore, in this context studies on the impact of climate change on plant production which take into account various climate change scenarios (Pirttioja et al., 2015; Fronzek et al., 2018), coupled with analysis of the effects of adaptation treatments (Ruiz-Ramos et al., 2018; Rodríguez et al., 2018), become extremely important. Soil biological activity (Wnuk et al., 2017; Gleń-Karolczyk et al., 2018; Walkiewicz et al., 2018) and atmospheric conditions should also be included in the factors that determine the direction and rate of soil nitrogen conversion. Thanks to studies on the temporal and spatial variation of meteorological series from various climatic zones (Baranowski et al., 2015; Hoffmann et al., 2017; Krzyszczak et al., 2017a; 2017b; Krzyszczak et al., 2018) and their prediction using statistical methods (Murat et al., 2018), not only can

the impact of climate change on agricultural production be evaluated, but we can also attempt to assess this impact on the soil content of macronutrients (nitrogen).

Changes in the structure of precipitation, both its frequency and intensity, are observed as a result of climate change, which can strongly affect infiltration of mineral nitrogen contained in the soil water solution (Powlson, 1988; Trehan, 1996; Tremblay et al., 2001; Coyne and Frye, 2005) from the subsurface layer deeper into the soil profile. Some studies show that almost half of the mineral nitrogen contained in the 0-30 cm layer can migrate to the deeper layers due to leaching (Soon et al., 2001). Soil nitrogen leaching and penetration into groundwater are an unfavorable phenomenon (Paz and Ramos, 2004) having significant economic, production and environmental consequences (Soon et al., 2001). Monitoring of soil mineral nitrogen has been conducted in Poland for many years (Lipiński, 2010; Fotyma et al., 2010; Regulation, 2002). This study attempted to identify the effects of factors such soil pH and land use on the content of nitrogen in the 60-90 cm soil layer, from which it can migrate to waters. Because soil mineral nitrogen content exhibits high temporal variability (Yu et al., 2003), with its maximum content in the soil during the spring period and the minimum content at the turn of August and September, which is a result of changes in the intensity of nitrification and enhanced nitrogen uptake by plants (Łoginow et al., 1987), therefore the analysis was carried out for two sampling dates – spring and autumn. The study hypothesized that there would be differences in the mineral nitrogen content beyond the reach of the main root system of crop plants in grassland and arable soils depending on selected soil properties and land use. The aim of this study was to evaluate mineral nitrogen content in grassland soils relative to other selected agricultural fodder crops depending on soil pH.

Material and methods

Soil samples analysis

To evaluate soil mineral nitrogen content, soil samples were used which had been collected during environmental investigations conducted by the Regional Chemical and Agricultural Stations in agricultural farms across Poland. Soil samples were taken from 60-90 cm layer using Egner stick of the length of 90 cm, from fields with a total area of not more than 4 ha. Each total sample (with a weight of about 200 g) consisted of 15-20 primary samples collected from an area of not more than 100 m². Samples were collected over the period 2010-2012 at two sampling dates – spring and autumn. Soil sampling in spring were conducted before applying fertilizers in February-April, whereas for sampling in autumn - after harvesting in September-October.

The collected samples were transferred to the Laboratory in tightly sealed containers and they were kept at a constant controlled temperature of -18°C until the mineral nitrogen analysis was performed. The soil samples with natural moisture content (after defrosting) were subjected to extraction with a 1% potassium sulfate solution at a ratio of 1:10. In the extracts obtained, nitrate and ammonium nitrogen content was determined spectrophotometrically using a Skalar San Plus System auto-analyzer (according to the standard PN-R-04028:1997). Mineral nitrogen content, as total nitrate and ammonium nitrogen, was expressed in mg·kg⁻¹ of dry matter of the soil sample (DM). The following parameters were also determined in the examined samples: dry matter content, soil organic carbon (C_{org}) using the Tiurin method (according to PN-ISO 14235:2003), grain-size distribution using the laser method, and pH in 1 mol KCl dm⁻³.

Determination of dry matter was made using the gravimetric method after drying at 105°C (according to PN-ISO 11465:1999). As the extraction of nitrate and ammonium is carried out in a fresh soil sample, obtained results are recalculated to the dry matter content using the empirical coefficient suitable for the soil of specific granulometric composition. Based on the analysis of organic matter and pH, soils were classified as mineral (up to 10%) or organic (over 10%) and were assigned to one of the following five soil pH classes (Pokojska, 2004; Gonet et al., 2015): very acidic soils (pH < 4.5), acidic soils (pH in the range between 4.6 and 5.5), slightly acidic soils (5.6 < pH < 6.5), neutral soils (6.6 < pH < 7.2), and alkaline soils (pH > 7.2).

Sampling sites

Because in the first year the geographical coordinates of the sampling sites were determined, in the next years soil sampling was carried out in the same fields. Determination of geographical coordinates of sampling sites was performed using GPS Pathfinder ProXT by Trimble (Westminster, CO 80021, USA, www.trimble.com). To verify the study hypothesis, the mineral nitrogen content and soil pH in the 60-90 cm layer sampled from soils under grasslands, maize and mixed cereal crops was evaluated (Table 1). The location of soil sampling sites is shown in Fig. 1. In the case of each site where the same crop was grown in successive years of the study, the average nitrogen content for the respective years was calculated. As far as sites located in grasslands are concerned, the same land use was continued throughout the entire study period and the average N_{min} content was evaluated for the period 2010-2012.

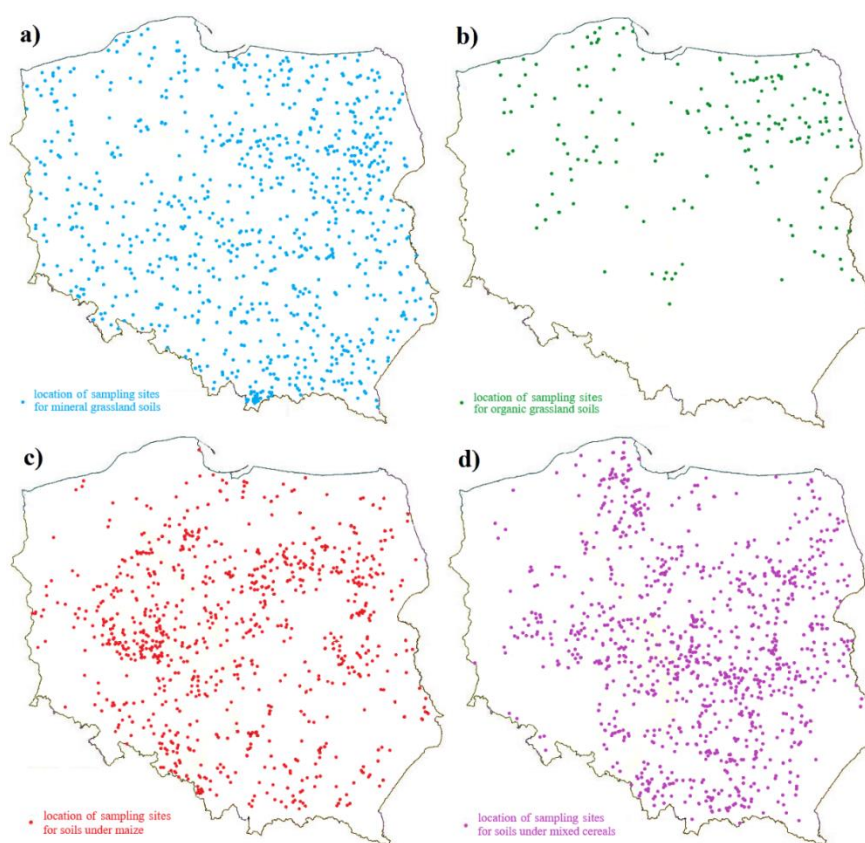


Figure 1. Location of soil sampling sites for a) grasslands on mineral soils; b) grasslands on organic soils; c) maize; d) mixed cereals; in hydrographic areas of Poland

Table 1. Number of analyzed soil samples taken from the 60-90 cm soil layer in grasslands as well as in maize and mixed cereal crops on mineral and organic soils

Crop type/land use		Number of samples
Grasslands on mineral soils	Total	859
	Meadows	521
	Pastures	160
	Hay and pasture	84
	Alternate	98
Grasslands on organic soils	Total	167
	Meadows	111
	Pastures	17
	Hay and pasture	39
	Alternate	0
Maize		826
Mixed cereal		951

Statistical analysis

The mineral nitrogen content in the 60-90 cm layer under the soil surface was evaluated both as an annual average and separately for the spring and autumn dates, depending on the determined pH class and land use. The study results were analyzed using standard statistical methods. By assigning the selected sites to the specific factors, such as type of land use and acidification class, basic descriptive statistics - average value and standard deviations (SD) of mineral nitrogen content were calculated. Relationships between N_{\min} content and a specific factor were characterized by Pearson's correlation coefficients. They were assessed statistically using the one-way non-orthogonal analysis of variance classification with Tukey confidence intervals ($p = 0.05$). In order to predict potential losses, simple regression analysis was performed in the SAS v. 9.1 software and the linear regression coefficients calculated. Obtained linear equations describe the relationship between the soil pH and the N_{\min} content in the 60-90 cm soil layer for varying land use and the type of soil (mineral, organic). The goodness of fit of linear regression was evaluated using determination coefficients (R^2).

Results and discussion

Mineral nitrogen content in the 60-90 cm soil layer was investigated taking into account the pH of mineral and organic soils. Regardless of the percentage of organic matter or land use, the amount of N_{\min} in the evaluated layer was dependent on pH (Fig. 2). Increase of pH leads to changes in resource availability for microbes and alter their community structure, modifying their activity and C-use efficiency (Kennedy et al., 2004; Grover et al., 2017). It was stated by Rousk et al. (2010) that the relative abundance and diversity of bacteria were positively related to pH. This effect impacts mineralisation process, leading to higher N_{\min} content in soils with higher pH. In our case higher N_{\min} content was detected in soils with a pH ranging 5.6-6.5, whereas its least amount in soils showing the highest acidification (pH below 4.5). A similar correlation was also found in the studies of Sapek and Kalińska (2004; 2007) and Sapek (2010). In their opinion, lower acidity reduces the release of the ammonium form of nitrogen and at the same time promotes nitrification and the release of the nitrate form of nitrogen.

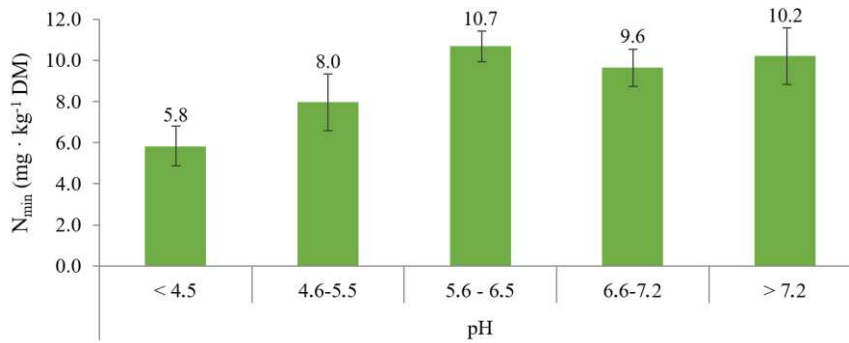


Figure 2. Average mineral nitrogen N_{\min} content in the 60-90 cm soil layer depending on soil pH. DM stands for dry matter of the soil sample

In the present study, the amount of N_{\min} clearly increased with increasing pH of mineral soils, regardless of crops grown, whereas in organic soils the largest amounts of N_{\min} were found in soil with a slightly acidic pH, followed by very acidic and acidic soils (Fig. 3). In soils with a pH above 6.5, the amount of N_{\min} in the 60-90 cm layer decreased. In organic soils significantly larger values of N_{\min} content in the 60-90 cm soil layer were observed, regardless of the land use or soil pH. Mineral nitrogen concentration in a specific soil layer reflects the balance of nitrogen on the one hand supplied with mineral and organic fertilisers, as well as released by microorganisms during mineralisation of organic matter, and on the other hand assimilated by plants, leached, denitrified or immobilised (Wong and Nortcliff, 1995). Recent study by Tian et al. (2017) shows that that both C and N mineralization rates in subsoil are significantly lower than in topsoil and that that net N mineralization in subsoil was limited by low amounts of labile C source (which provides energy) and degradable organic N (which provides material). Therefore, in mineral soils mineralization may be weaker than in organic soils due to limited C content, subsequently leading to significantly lower N_{\min} content in these soils.

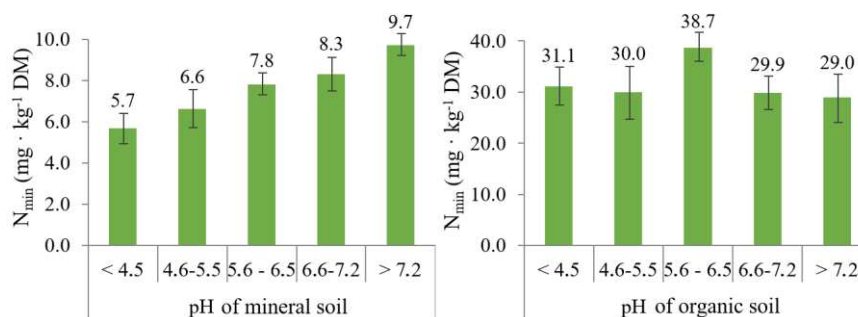


Figure 3. Average mineral nitrogen N_{\min} content in the 60-90 cm layer of mineral and organic soils depending on soil pH. DM stands for dry matter of the soil sample

Generally, the mineral nitrogen content for the specific pH ranges was higher in spring, except for sites with a pH above 7.2 (Fig. 4). This applied to both mineral and organic soils, though as regards the latter ones with a neutral pH, a higher content was also found for the autumn sampling date. In the study of Arbačiauskas et al. (2014) for

Lithuanian agricultural lands the similar tendency was observed for 60-90 cm layer, regardless of different texture of subjected soils or nitrogen fertilisation rates.

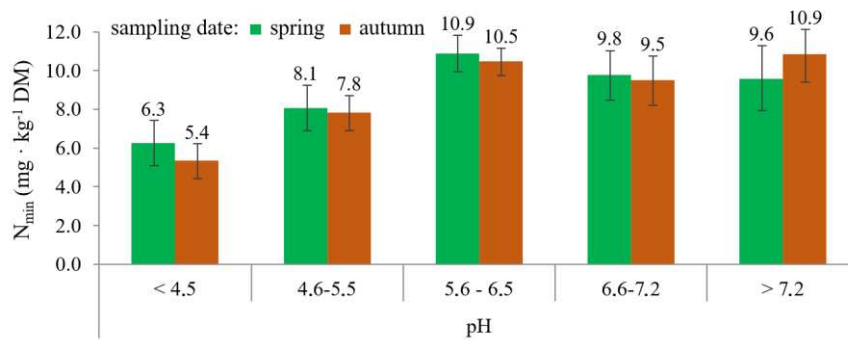


Figure 4. Average mineral nitrogen N_{min} content in the 60-90 cm layer depending on sampling date and soil pH. DM stands for dry matter of the soil sample

The highest mineral nitrogen losses as influenced by pH in mineral soils – as regards its content in the 60-90 cm layer – were observed in soils under maize crops, while slightly lower ones in soils under mixed cereals. In grasslands, this influence was clearly weaker (Fig. 5). Pietrzak et al. (2006) also demonstrated the effect of soil pH on mineral nitrogen leaching in permanent grasslands. They observed the concentration of the ammonium form to be higher by about 1.8 times and the concentration of the nitrate form by about 2.5 times in the soil solutions from limed fields compared to soil extracts from unlimed fields.

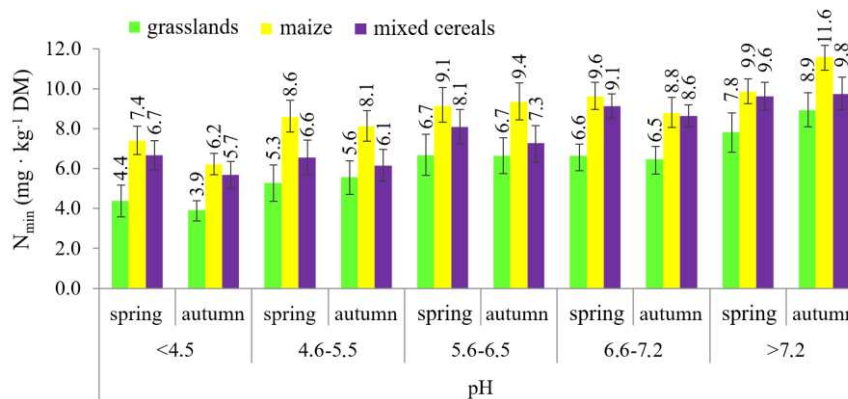


Figure 5. Average mineral nitrogen N_{min} content in the 60-90 cm layer of mineral soils depending on land use, sampling date, and soil pH. DM stands for dry matter of the soil sample

In organic soils, an increase in N_{min} content in the 60-90 cm layer under grasslands was noted both in spring and in autumn, but mostly to a pH of 6.5. Above this value, the amount of N_{min} in the evaluated layer decreased, particularly in spring (Fig. 6).

N_{min} content in soils under grasslands was also modified by a higher soil pH and land use. This applied in particular to meadows (spring and autumn) and also pastures, predominantly at sites with a pH above 6.5, as well as to hay and pasture grasslands with a pH above 5.5 (Fig. 7).

On the other hand, a different situation was observed for N_{\min} content in organic soils – the highest content was found in soils with a slightly acidic pH, primarily in hay and pasture grasslands as well as in pastures. At a higher pH, the N_{\min} content was lower than in more strongly acidified soils (Fig. 8).

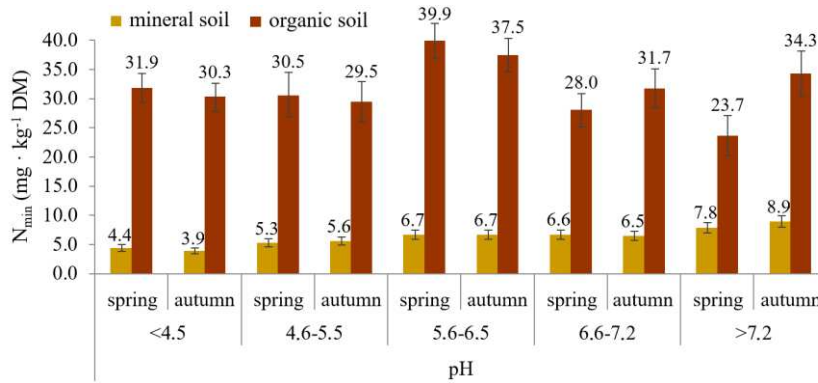


Figure 6. Average mineral nitrogen N_{\min} content in the 60-90 cm layer of mineral and organic soils depending on sampling date and soil pH. DM stands for dry matter of the soil sample

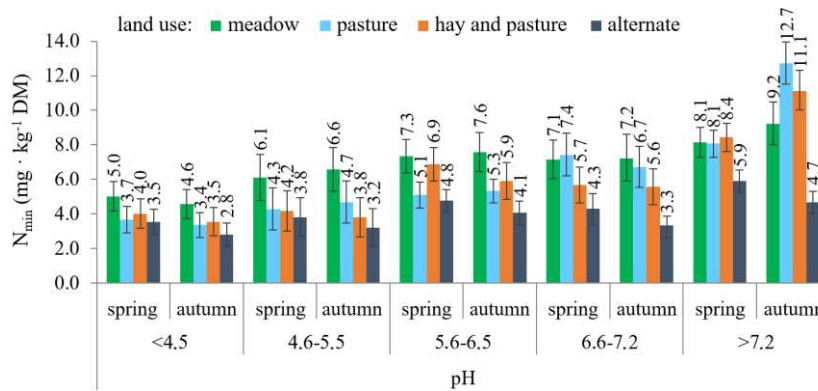


Figure 7. Average mineral nitrogen N_{\min} content in the 60-90 cm layer of mineral soils depending on grassland land use, sampling date, and soil pH. DM stands for dry matter of the soil sample

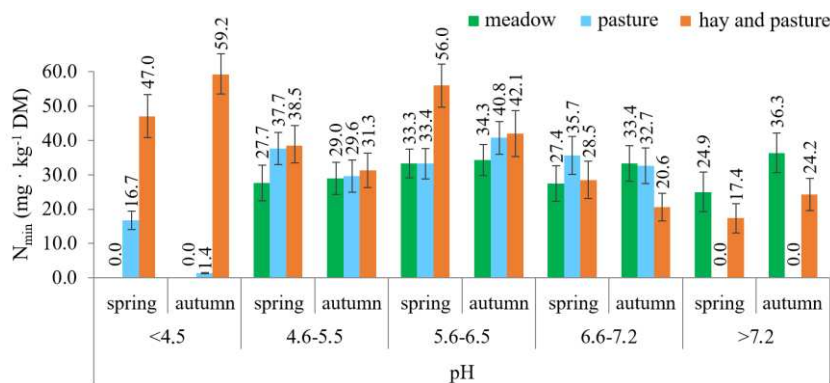


Figure 8. Average mineral nitrogen N_{\min} content in the 60-90 cm layer of organic soils depending on grassland land use, sampling date, and soil pH. DM stands for dry matter of the soil sample

The obtained study results were confirmed statistically (Table 2, Figs. 9-12). A strong positive correlation was shown between soil pH and N_{\min} content in the 60-90 cm layer, predominantly for mineral soils, both in spring and in autumn. During the spring period, organic soils exhibited a negative relationship between soil pH and N_{\min} content, but in autumn this trend did not persist. In spring, in objects with higher pH, a smaller amount of N_{\min} in the 60-90 cm layer was found for organic soils, especially on meadows and hay and pastures. It means that the N_{\min} losses decreased with increasing pH. In organic soils the ammonium form predominated over nitrate form, and the lack of grazing, or partial grazing, contributed to a smaller extent to the amount of N_{\min} coming from animal waste. Sapek (2010) observed that the release of the ammonium nitrogen ($N-NH_4$) was significantly reduced with decrease of the soil acidity. On the other hand, the lower acidity of the soil favored the nitrification and release of nitrate nitrogen ($N-NO_3$). Similar conclusions were drawn by Skowron (2004), who observed that the content of active forms of nitrogen ($N-NH_4$ and $N-NO_3$) in the mineral soils depended highly on their pH. Acidification clearly contributed to the increase in the content of ammonium nitrogen, while the content of nitrate nitrogen increased with increasing pH. In these mineral soils, the nitrate form was also predominant over the ammonium form. But in organic soils this tendency is reversed. In soils under meadow land use, especially permanent grasslands, the sodding process and the way they are used, as well as fertilization, additionally shape the dynamics and course of nitrogen release from the soil.

Table 2. Relationships between soil pH and mineral nitrogen N_{\min} content in the 60-90 cm soil layer expressed in terms of correlation coefficients with a breakdown into both land use and soil sampling date

Land use	Sampling date	
	spring	autumn
Grasslands on mineral soils	0.97*	0.92*
Meadows on mineral soils	0.95*	0.91*
Pastures on mineral soils	0.97*	0.85*
Hay and pasture grasslands on mineral soils	0.87*	0.84*
Alternate grasslands on mineral soils	0.85*	0.80*
Grasslands on organic soils	-0.48*	0.48*
Meadows on organic soils	-0.51*	0.85*
Pastures on organic soils	0.75*	0.78*
Hay and pasture grasslands on organic soils	-0.72*	-0.83*
Maize	0.98*	0.91*
Mixed cereal	0.96*	0.98*
Total soils	0.77*	0.90*
Total mineral soils	0.99*	0.96*
Total organic soils	-0.48*	0.48*
Total soils (on an annual basis)	0.85*	
Total mineral soils (on an annual basis)	0.99*	
Total organic soils (on an annual basis)	-0.17*	

* correlation significant at significance level $p = 0.05$

Additionally, the soil's abundance in organic matter can affect the efficiency of nitrogen mineralization (Sapek, 2010). As demonstrated by Hatch et al. (2002), nitrogen immobilization resulted from the increased activity of soil microorganisms. It should be emphasized that the organic carbon had contradictory influence on the nitrogen release

to the soil solution. The increase of the C_{org} content promotes the binding of nitrogen in the soil and reduces the solubility of its mineral forms. Smaller amounts of nitrate nitrogen may indicate a lower intensity of the nitrification process. In the soils with smaller humus content, the mineralization process is stronger than in the soils with a high content of organic carbon. In the study of Sapek and Kalińska (2004) the amount of N released in the process of mineralization in acid soil was $186.6 \text{ kg N} \cdot \text{ha}^{-1} \cdot \text{year}^{-1}$, whereas in the limed soil it was $164.1 \text{ kg N} \cdot \text{ha}^{-1} \cdot \text{year}^{-1}$. According to the same authors, the mineralization of nitrogen is more intensive in the summer months (May - July), which increases the release of mineral forms during and after the growing season, and results in increased leaching in autumn. Mineralization, as well as leaching, are also impacted by weather conditions, especially by air temperature and precipitation.

In the case of maize and mixed cereal crops, on the other hand, the measurements made both in spring and in autumn confirmed significant positive relationships between pH and N_{min} , with the value of correlation coefficient above 0.9. The highest negative correlation coefficients in spring and autumn were demonstrated for hay and pasture use on organic soils. The calculated coefficients of determination confirmed the significant effect of mineral soil pH on N_{min} content, regardless of sampling date, both in grasslands and in soils under mixed cereal and maize crops. But pH could only slightly modify (by only 24%) the occurrence of nitrogen in the 60-90 cm layer of organic soil.

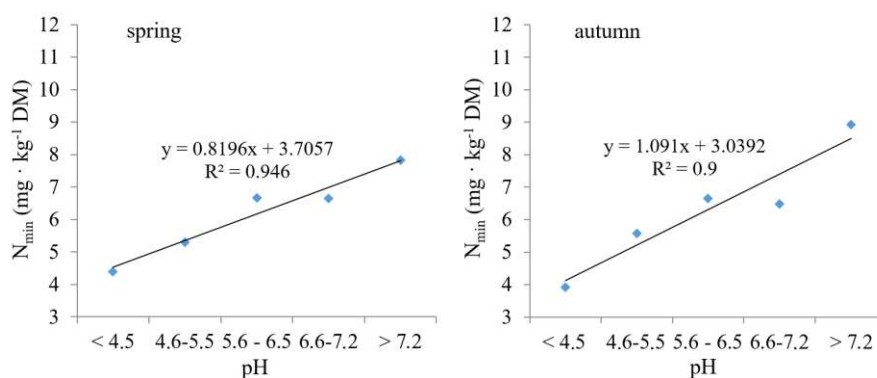


Figure 9. Relationship between soil pH and average mineral nitrogen N_{min} content in the 60-90 cm layer of mineral soils under grasslands for spring and autumn soil sampling dates. DM stands for dry matter of the soil sample

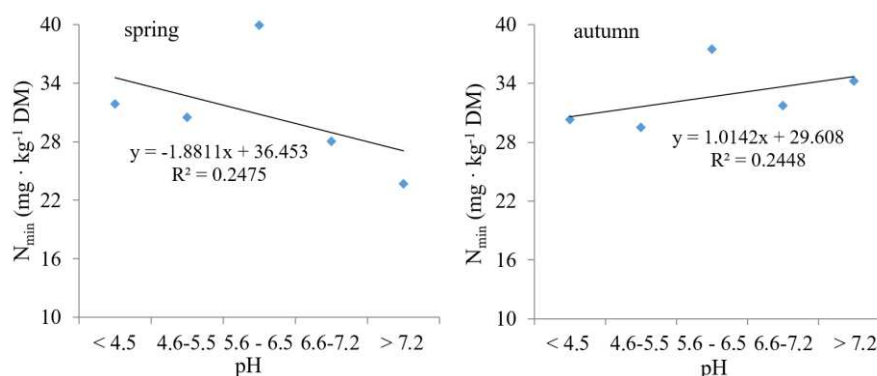


Figure 10. Relationship between soil pH and average mineral nitrogen N_{min} content in the 60-90 cm layer of organic soils under grasslands for spring and autumn soil sampling dates. DM stands for dry matter of the soil sample

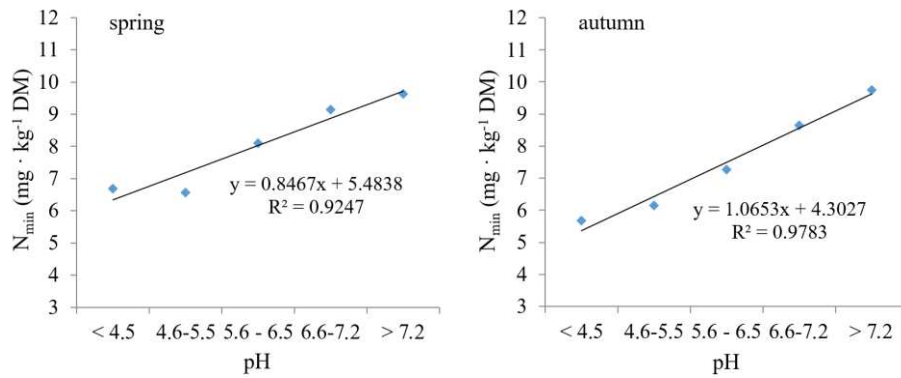


Figure 11. Relationship between soil pH and average mineral nitrogen N_{min} content in the 60-90 cm layer of mineral soils under mixed cereals for spring and autumn soil sampling dates. DM stands for dry matter of the soil sample

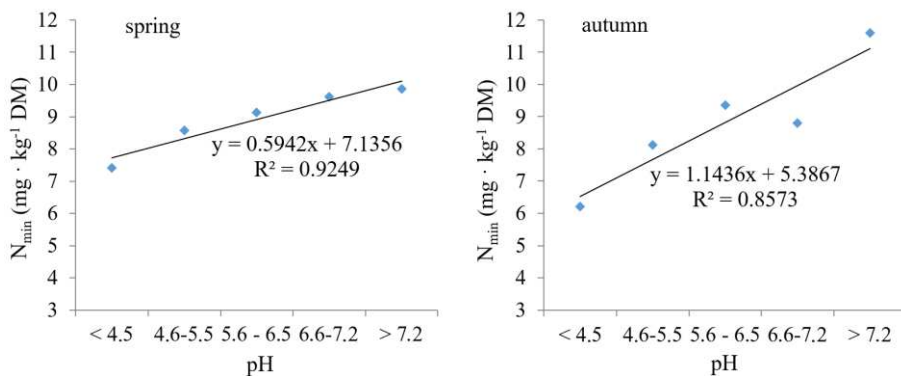


Figure 12. Relationship between soil pH and average mineral nitrogen N_{min} content in the 60-90 cm layer of mineral soils under maize for spring and autumn soil sampling dates. DM stands for dry matter of the soil sample

Conclusions

The results of this study confirm that there is a strong relationship between pH of the studied soils and N_{min} , regardless of soil sampling date, use of the studied soils, or organic carbon content in them. In the case of samples collected in autumn, the correlation coefficient was usually positive and had a lower value than for samples collected in spring, for which, in turn, negative correlations (anticorrelations) were found more frequently. Only organic soils exhibited negative correlations, but at the same time these were one of the lowest correlation coefficients obtained. Mineral soils were characterized by a strongly positive relationship between pH and N_{min} content. Land use did not cause significant differences in this relationship. The obtained results are extremely important from the utilitarian point of view because they can facilitate determining an optimal rate of mineral nitrogen in soils of varying pH. This may lead to reduction of leaching of nitrogen from topsoil and its infiltration to groundwater, as well as its emissions as NO_2 , which is a greenhouse gas with huge contribution to creating the greenhouse effect, and ultimately, to decrease the harmful impact of grasslands and agricultural crops on environment.

Acknowledgements. This paper has been partly financed from the funds of the Polish National Centre for Research and Development within the framework of the project BIO-FERTIL, contract number: BIOSTRATEG3/347464/5/NCBR/2017.

REFERENCES

- [1] Arbačiauskas, J., Staugaitis, G., Vaišvila, Z., Mažvila, J., Adomaitis, T., Šumskis, D., Enė, L. Ž., Lubyte, J., Mažeika, R. (2014): The interdependence of mineral nitrogen content in different soil layers of Lithuanian agricultural lands. – *Žemdirbystė (Agriculture)* 101(2): 133-138. <http://dx.doi.org/10.13080/z-a.2014.101.017>.
- [2] Baranowski, P., Krzyszczak, J., Sławiński, C., Hoffmann, H., Kozyra, J., Nieróbca, A., Siwek, K., Gluza, A. (2015): Multifractal analysis of meteorological time series to assess climate impacts. – *Climate Research* 65: 39-52. <https://doi.org/10.3354/cr01321>.
- [3] Burton, S. A., Prosser, J. I. (2001): Autotrophic ammonia oxidation at low pH through urea hydrolysis. – *Applied and Environmental Microbiology* 67(7): 2952.
- [4] Coyne, M. S., Frye, W. W. (2005): Nitrogen in soil. Cycle. – In: Hillel, D. (ed.) *Encyclopedia of soil in the environment*. Elsevier Ltd., 13-21.
- [5] De Boer, W., Kowalchuk, G. A. (2001): Nitrification in acid soils: micro-organisms and mechanisms. – *Soil Biology and Biochemistry* 33: 853-866.
- [6] Filipek, T., Skowrońska, M. (2013): Current dominant causes and effects of acidification of soils under agricultural use in Poland. – *Acta Agrophysica* 20(2): 283-294. (in Polish).
- [7] Fotyma, M., Kęsik, K., Pietruch, C. (2010): Mineral nitrogen in soils of Poland as an indicator of plants nutrient requirements and soil water cleanness. – *Nawozy i Nawożenie* 38: 4-83. (in Polish).
- [8] Fronzek, S., Pirttioja, N., Carter, T. R., Bindi, M., Hoffmann, H., Palosuo, T., Ruiz-Ramos, M., Tao, F., Trnka, M., Acutis, M., Asseng, S., Baranowski, P., Basso, B., Bodin, P., Buis, S., Cammarano, D., Deligios, P., Destain, M. F., Dumont, B., Ewert, F., Ferrise, R., François, L., Gaiser, T., Hlavinka, P., Jacquemin, I., Kersebaum, K. C., Kollas, C., Krzyszczak, J., Lorite, I. J., Minet, J., Minguez, M. I., Montesino, M., Moriondo, M., Müller, C., Nendel, C., Öztürk, I., Perego, A., Rodríguez, A., Ruane, A. C., Ruget, F., Sanna, M., Semenov, M. A., Sławiński, C., Stratonovitch, P., Supit, I., Waha, K., Wang, E., Wu, L., Zhao, Z., Rötter, R. P. (2018): Classifying multi-model wheat yield impact response surfaces showing sensitivity to temperature and precipitation change. – *Agricultural Systems* 159: 209-224. <https://doi.org/10.1016/j.agsy.2017.08.004>.
- [9] Gleń-Karolczyk, K., Boligłowa, E., Antonkiewicz, J. (2018): Organic fertilization shapes the biodiversity of fungal communities associated with potato dry rot. – *Applied Soil Ecology* 129: 43-51. <https://doi.org/10.1016/j.apsoil.2018.04.012>.
- [10] Gonet, S., Smal, H., Chojnicki, J. (2015): *Chemical properties of soil*. – Soil science. Warszawa, PWN, 201-205. (in Polish),
- [11] Grover, S. P., Butterly, C. R., Wang, X., Tang, C. (2017): The short-term effects of liming on organic carbon mineralisation in two acidic soils as affected by different rates and application depths of lime. – *Biology and Fertility of Soils* 53: 431-443.
- [12] Hatch, D., Goulding, K., Murphy, D. (2002): Nitrogen. – *Agriculture, hydrology and water quality*. CABI Publishing, 7-27.
- [13] Hoffmann, H., Baranowski, P., Krzyszczak, J., Zubik, M., Sławiński, C., Gaiser, T., Ewert, F. (2017): Temporal properties of spatially aggregated meteorological time series. – *Agricultural and Forest Meteorology* 234-235: 247-257. <https://doi.org/10.1016/j.agrformet.2016.12.012>.
- [14] Kennedy, N., Connolly, J., Clipson, N. (2004): Impact of lime, nitrogen and plant species on bacterial community structure in grassland microcosms. – *Environmental Microbiology* 7: 780-788.

- [15] Krzyszczak, J., Baranowski, P., Hoffmann, H., Zubik, M., Sławiński, C. (2017a): Analysis of Climate Dynamics Across a European Transect Using a Multifractal Method. – In: Rojas, I., Pomares, H., Valenzuela, O. (eds.) *Advances in Time Series Analysis and Forecasting: Selected Contributions from ITISE 2016 - Contributions to Statistics*. Springer International Publishing, Cham, 103-116. https://doi.org/10.1007/978-3-319-55789-2_8.
- [16] Krzyszczak, J., Baranowski, P., Zubik, M., Hoffmann, H. (2017b): Temporal scale influence on multifractal properties of agro-meteorological time series. – *Agricultural and Forest Meteorology* 239: 223-235. <https://doi.org/10.1016/j.agrformet.2017.03.015>.
- [17] Krzyszczak, J., Baranowski, P., Zubik, M., Kazandjiev, V., Georgieva, V., Sławiński, C., Siwek, K., Kozyra, J., Nieróbca, A. (2018): Multifractal characterization and comparison of meteorological time series from two climatic zones. – *Theoretical and Applied Climatology* (in press). <http://dx.doi.org/10.1007/s00704-018-2705-0>.
- [18] Kyveryga, P. M., Blackmer, A. M., Ellsworth, J. W., Isla, R. (2004): Soil pH effects on nitrification of fall-applied anhydrous ammonia. – *Soil Science Society of America Journal* 68: 545-551.
- [19] Lamorski, K., Pastuszka, T., Krzyszczak, J., Sławiński, C., Witkowska-Walczak, B. (2013): Soil water dynamic modeling using the physical and support vector machine methods. – *Vadose Zone Journal* 12(4). <https://doi.org/10.2136/vzj2013.05.0085>
- [20] Lipiński, W. (2010): The content of mineral nitrogen in arable soils of nitrate vulnerable zones (NVZ). – *Nawozy i Nawożenie* 38: 111-120.
- [21] Łoginow, W., Janowiak, J., Szychaj-Fabisiak, E. (1987): The variability of the total content of the individual forms of nitrogen in the soil. – *Zeszyty Naukowe ATR Bydgoszcz* 23: 13-24. (in Polish).
- [22] Murat, M., Malinowska, I., Gos, M., Krzyszczak, J. (2018): Forecasting daily meteorological time series using ARIMA and regression models. – *International Agrophysics* 32(2): 253-264. <https://doi.org/10.1515/intag-2017-0007>.
- [23] Paz, J. M., Ramos, C. (2004): Simulation of nitrate leaching for different nitrogen fertilization rates in a region of Valencia (Spain) using a GIS-GLEAMS system. – *Agriculture, Ecosystems & Environment* 103: 59-73.
- [24] Pietrzak, S., Urbaniak, M., Sapek, B. (2006): The assessment of changes of the concentration and leaching of mineral forms of nitrogen in soil solutions. – *Woda-Środowisko-Obszary Wiejskie* 6(17): 51-63. (in Polish).
- [25] Pirttioja, N., Carter, T. R., Fronzek, S., Bindi, M., Hoffmann, H., Palosuo, T., Ruiz-Ramos, M., Tao, F., Trnka, M., Acutis, M., Asseng, S., Baranowski, P., Basso, B., Bodin, P., Buis, S., Cammarano, D., Deligios P., Destain, M. F., Dumont, B., Ewert, F., Ferrise, R., François, L., Gaiser, T., Hlavinka, P., Jacquemin, I., Kersebaum, K. C., Kollas, C., Krzyszczak, J., Lorite, I. J., Minet, J., Minguéz, M. I., Montesino, M., Moriondo, M., Müller, C., Nendel, C., Öztürk, I., Perego, A., Rodríguez, A., Ruane, A. C., Ruget, F., Sanna, M., Semenov, M. A., Sławiński, C., Stratonovitch, P., Supit, I., Waha, K., Wang, E., Wu, L., Zhao, Z., Rötter, R. P. (2015): Temperature and precipitation effects on wheat yield across a European transect: a crop model ensemble analysis using impact response surfaces. – *Climate Research* 65: 87-105. <https://doi.org/10.3354/cr01322>.
- [26] Pokojska, U. (2004): Soil reaction. – *Ecological-soil investigations*. Warszawa, PWN, 198-204. (in Polish).
- [27] Powlson, D. S. (1988): Measuring and minimising losses of fertilizer nitrogen in arable agriculture. – In: Jenkinson, D. S., Smith, K. A. (eds.) *Nitrogen Efficiency in Agricultural Soils*. Elsevier Applied Science, 231-245.
- [28] Regulation (2002): Regulation of the Minister of Environment of 23 December 2002 concerning specific requirements to be met by action programs aimed at reducing runoff of nitrogen from agricultural sources. – *Dz. U. (Journal of Laws) of 2003, No. 4, item 44*.
- [29] Rodríguez, A., Ruiz-Ramos, M., Palosuo, T., Carter, T. R., Fronzek, S., Lorite, I. J., Ferrise, R., Pirttioja, N., Bindi, M., Baranowski, P., Buis, S., Cammarano, D., Chen, Y.,

- Dumont, B., Ewert, F., Gaiser, T., Hlavinka, P., Hoffmann, H., Höhn, J. G., Jurecka, F., Kersebaum, K. C., Krzyszczak, J., Lana, M., Mechiche-Alami, A., Minet, J., Montesino, M., Nendel, C., Porter, J. R., Ruget, F., Semenov, M. A., Steinmetz, Z., Stratonovitch, P., Supit, I., Tao, F., Trnka, M., de Wit, A., Rötter, R. P. (2019): Implications of crop model ensemble size and composition for estimates of adaptation effects and agreement of recommendations. – *Agricultural and Forest Meteorology* 264: 351-362. <https://doi.org/10.1016/j.agrformet.2018.09.018>.
- [30] Rousk, J., Bååth, E., Brookes, P. C., Lauber, C. L., Lozupone, C., Caporaso, J. G., Knight, R., Fierer, N. (2010): Soil bacterial and fungal communities across a pH gradient in an arable soil. – *ISME Journal* 4: 1340-1351. <http://dx.doi.org/10.1038/ismej.2010.58>.
- [31] Ruiz-Ramos, M., Ferrise, R., Rodríguez, A., Lorite, I. J., Bindi, M., Carter, T. R., Fronzek, S., Palosuo, T., Pirttioja, N., Baranowski, P., Buis, S., Cammarano, D., Chen, Y., Dumont, B., Ewert, F., Gaiser, T., Hlavinka, P., Hoffmann, H., Höhn, J. G., Jurecka, F., Kersebaum, K. C., Krzyszczak, J., Lana, M., Mechiche-Alami, A., Minet, J., Montesino, M., Nendel, C., Porter, J. R., Ruget, F., Semenov, M. A., Steinmetz, Z., Stratonovitch, P., Supit, I., Tao, F., Trnka, M., de Wit, A., Rötter, R. P. (2018): Adaptation response surfaces for managing wheat under perturbed climate and CO₂ in a Mediterranean environment. – *Agricultural Systems* 159: 260-274. <https://doi.org/10.1016/j.agsy.2017.01.009>.
- [32] Sapek, B. (1999): Estimation of nitrogen compounds mineralization by the in situ incubation method and the nitrogen balance in the mineral meadow soil. – *Wiadomości IMUZ* 20(1): 39-57. (in Polish).
- [33] Sapek, B. (2010): Nitrogen and phosphorus release from soil organic matter. – *Woda-Środowisko-Obszary Wiejskie* 10, 3(31): 229-256. (in Polish).
- [34] Sapek, B., Kalińska, D. (2004): Mineralization of soil organic nitrogen compounds in the light of long-term grassland experiments in IMUZ. – *Woda-Środowisko-Obszary Wiejskie* 4, 1(10): 183-200. (in Polish).
- [35] Sapek, B., Kalińska, D. (2007): Mineralization of nitrogen and phosphorus compounds in the soil of agriculturally used and not used meadow. – *Roczniki Gleboznawcze* 58(1): 109-120. (in Polish).
- [36] Siebielec, G., Smreczak, B., Klimkowicz-Pawlas, A., Maliszewska-Kordybach, B., Terelak, H., Koza, P., Hryńczuk, B., Łysiak, M., Miturski, T., Gałązka, R., Suszek, B. (2012): Monitoring of chemistry in arable soils in Poland in the years 2010-2012. – *IUNG-PIB w Puławach*: 1-202. (in Polish).
- [37] Skowron, P. (2004): Nitrogen active forms content at differentiated pH soils in laboratory experiment conditions. – *Annales UMCS sec. E* 59(1): 363-368. (in Polish).
- [38] Soon, Y. K., Clayton, G. W., Rice, W. A. (2001): Tillage and previous crop effects on dynamics of nitrogen in a wheat-soil system. – *Agronomy Journal* 93: 842-849.
- [39] Tkaczyk, P., Bednarek, W. (2011): Evaluation of soil reaction (pH) in the Lublin region. – *Acta Agrophysica* 192(18): 173-186. (in Polish).
- [40] Tkaczyk, P., Bednarek, W., Dresler, S., Krzyszczak, J., Baranowski, P., Sławiński, C. (2017): Relationship between assimilable-nutrient content and physicochemical properties of topsoil. – *International Agrophysics* 31(4): 551-562. <https://doi.org/10.1515/intag-2016-0074>.
- [41] Tkaczyk, P., Bednarek, W., Dresler, S., Krzyszczak, J. (2018a): The effect of some soil physicochemical properties and nitrogen fertilisation on winter wheat yield. – *Acta Agrophysica* 25(1): 107-116. <https://doi.org/10.31545/aagr0009>.
- [42] Tkaczyk, P., Bednarek, W., Dresler, S., Krzyszczak, J., Baranowski, P., Brodowska, M. S. (2018b): Content of certain macro and microelements in orchard soils in relation to agronomic categories and reaction of these soils. – *Journal of Elementology* 23(4): 1361-1372. <https://doi.org/10.5601/jelem.2018.23.1.1639>.
- [43] Trehan, S. P. (1996): Immobilisation of ¹⁵NH⁴⁺ in three soils by chemical and biological processes. – *Soil Biology and Biochemistry* 28(8): 1021-1027.

- [44] Tremblay, N., Scharpf, H. C., Weier, U., Laurence, H., Owen, J. (2001): Nitrogen management in field vegetables. A guide to efficient fertilisation. – Agriculture and Agri-Food Canada, 1-63.
- [45] Walczak, R. T., Witkowska-Walczak, B., Baranowski, P. (1997): Soil structure parameters in models of crop growth and yield prediction. Physical submodels. – International Agrophysics 11: 111-127.
- [46] Walkiewicz, A., Brzezińska, M., Bieganowski, A. (2018): Methanotrophs are favored under hypoxia in ammonium-fertilized soils. – Biology and Fertility of Soils 54(7): 861-870. <https://doi.org/10.1007/s00374-018-1302-9>.
- [47] Wnuk, E., Walkiewicz, A., Bieganowski, A. (2017): Methane oxidation in lead-contaminated mineral soils under different moisture levels. – Environmental Science and Pollution Research 24(8-9): 1-9. <https://doi.org/10.1007/s11356-017-0195-8>.
- [48] Wong, M. T. F., Nortcliff, S. (1995): Seasonal fluctuations of native available N and soil management implications. – Fertilizers Research 42: 13-26. <https://doi.org/10.1007/BF00750496>.
- [49] Yu, Z., Kraus, T. E. C., Dahlgren, R. A., Horwath, W. R., Zasoski, R. J. (2003): Mineral and dissolved organic nitrogen dynamics along a soil acidity-fertility gradient. – Soil Science Society of America Journal 67: 878-888.

EXPLORING THE FACTORS IN VISITORS' BEHAVIORAL INTENTIONS – MEDIATION EFFECTS ON PERCEIVED ENVIRONMENTAL INVOLVEMENT AND ECOTOURISM SUPPORT

DING, Z. F.¹ – CAO, B.^{2*}

¹*Public Sports Department, Anshan Normal University, Anshan, Liaoning 114007, China*

²*Physical Education Institute, Shaanxi Normal University, Xi'an, Shaanxi 710119, China*

**Corresponding author*

e-mail: caoben@snnu.edu.cn; phone: +86-186-2967-5612

(Received 18th Sep 2018; accepted 26th Nov 2018)

Abstract. Based on resource-based theory and theory of planned behavior, this study aims to explore potential visitors' behavioral intentions to ecotourism and the interaction relations among variables of perceived environmental involvement, ecotourism support, as the mediators, and behavioral intentions, as the dependent variable. Selecting ecotourism in Sichuan Province for the research, the visitors proceeded to fill the questionnaire survey, from the potential visitors' point of view about ecotourism. A total of 348 valid copies were retrieved for the analysis of parameter estimation. They reveal positive and significant effects of visitors' innovation and interests on perceived environmental involvement, visitors' interests and perceived environmental involvement on support, as well as visitors' perceived environmental involvement and support on behavioral intentions. It is further discovered that "interests" play the key factor in driving the intention of visitors' future selection of ecotourism products. The research results provide suggestions and reference for related units in Sichuan Province developing and promoting ecotourism.

Keywords: *innovation, perceived risk, perceived environmental involvement, support, behavioral intention*

Introduction

Under environmental awareness, a lot of consumers have realized the direct impact of purchase behaviors on ecological problems that customers would consider environmental issues, even purchase products compatible with ecology, and are willing to pay more for environment friendly products (Laroche et al., 2001; Sahakian et al., 2018). Consumers with ecological awareness would try to protect the environment through different methods. Environmental awareness reflects on intangible service consumption, where the promotion of ecotourism or ecotourism is a significant example. Ecotourism stresses on the re-thinking of culture, education, and travel agents about recreation (Hetzer, 1965; Lee, 2014). Sichuan Province that located in the west of China is a province without sea. Coastal areas in China present better development to result in the situation of strong east and weak west. Although local authority has fully invested in the development of ecotourism, information about visitors' requirements for ecotourism is short. The understanding of potential visitors' attitudes towards and behavioral intentions of ecotourism would benefit the successive promotion of ecotourism. The strategic viewpoint of resource-based theory could be the evaluation indicator of tourist spots or the development potential of a tourist spot. Different from traditional travel patterns, ecotourism, as an emerging travel method, is the tourism activity with special interests as

well as an innovative tourism product for visitors. It seems to induce consumers' perceived risk when purchasing ecotourism products, and such factors would possibly affect visitors' perceived environmental involvement, support, and future behavioral intentions. By reviewing past research, the lack of discussions on above variables induces the motivation of this study.

This study, based on resource-based theory and the “belief (perception) → attitude → intention” model (Oliver, 1980), aims to explore potential visitors' behavioral intentions of ecotourism products, construct visitors' innovation, perceived risk, and interests in ecotourism as the antecedents, take perceived environmental involvement and ecotourism support as the mediators, and use behavioral intentions as the dependent variable to discuss the interactive relations among such variables. Selecting Sichuan Province for the research and combining the viewpoint of potential visitors to ecotourism in Sichuan Province, the questionnaire survey is proceeded, and the research results are provided for the development and promotion of ecotourism in Sichuan Province as well as strategic reference for the promotion of ecotourism in other areas.

Literature review

Effects of innovation on perceived environmental involvement and support

There are several synonyms of “ecotourism”. Such synonyms focus on “nature” and are a kind of “nature oriented tourism” mainly starting from the viewpoint of environment and developing and promoting tourism on the premise of “sustainability” (Xu et al., 2017). Overall speaking, ecotourism resources contain natural resources of scenery and wild animals and plants (Lu et al., 2017) as well as humanistic resources of local historical relics and indigenous culture (Xu et al., 2017). Those are core tourism resources for the development of ecotourism.

Innovation refers to the tendency to purchase new products more often and more rapidly than others (Midgley and Dowling, 1978; Wu et al., 2016, 2017). “Product innovation” is frequently applied to tourism and leisure industries. Ecotourism, as the tourism activity with special interests, is the tourism product aiming at consumers who are interested in special spots or activities using natural environment and space for the continuous extension (Xu et al., 2017).

Involvement is the individual inner power to affect consumer behavior in the EKB model (Engel et al., 1995). Chiu et al. (2014) pointed out involvement as invisible motivation, disturbance, or concerns induced by special situations or stimulations to affect the data collection, information processing, and decision making. Support or acceptance is an attitude. Hartini et al. (2017) regarded attitude as the psychological tendency generated through learning; such a tendency was a persistent evaluation of certain subject. Attitude strength is generally considered to be correlated with product involvement and presented with the commitment of attitude. Attitude is obedience and might achieve the level of identity. When a consumer's attitude is implanted in mind and becomes a part of the value system, the attitude might be internalized (Yoon et al., 2001; Lee and Back, 2006; Hartini et al., 2017).

This study stands for regarding consumer innovation as consumer characteristics, similar to personality traits. A visitor would be influenced the consumer behavior because of the characteristic to pursue novelty and uniqueness. Subjective curiosity plays a primary role in people's ecotourism motivation, as a visitor's subjective curiosity about ecotourism would induce the emphasis on the correlation with purchase activity.

Referring to the belief (perception) → attitude → intention model proposed by Oliver (1980) and theory of planned behavior proposed by Ajzen and Fishbein (1980), it is inferred in this study that visitors with higher innovation would enhance the involvement in tourism products. Meanwhile, according to the psychological cognition process of belief (perception) → attitude, it is inferred that visitors with higher innovation would enhance the acceptance of tourism products. Accordingly, H1: visitors' innovation presents direct and positive effects on perceived environmental involvement and H4: visitors' innovation shows direct and positive effects on ecotourism support are proposed in this study.

Effects of perceived risk on perceived environmental involvement and support

Flynn and Goldsmith (1993) pointed out high perceived risk on purchasing new service, implying that new service marketers had to achieve consumer needs for accepting the risk. Involvement is closely related to perceived risk. According to Kapferer and Laurent (1986), consumers, when perceiving high purchase risk, would appear high concerns about the purchase behavior and higher emphasis on the correlation with oneself to present high involvement. In this case, H2: visitors' perceived risk in tourism reveals direct and positive effects on perceived environmental involvement is proposed.

Xu et al. (2017) found out lower intention of consumers to tourism destination with higher perceived risk in safety. According to the psychological cognition process of belief (perception) → attitude, visitors, when perceiving high purchase risk, would appear adverse effects on the acceptance of the tourism product, based on risk averse. For this reason, H5: visitors' perceived risk in tourism shows direct and negative effects on ecotourism support is proposed.

Effects of interest on perceived environmental involvement and support

“Resource-based theory” could be applied to tourism for evaluating tourist spots or the attraction and development potential of a tourist spot, providing core tourism resources for satisfying visitors' interests in the tourism resources and attracting tourists to visit the destination to maintain the persistent competitive advantage (Lu et al., 2017; Wu et al., 2017). Biljana et al. (2002) proposed to measure ecotourists' interests with natural areas, rainforests and native jungles, national parks, lakes and rivers, seaside, world heritage which were not being cultivated and interfered, nature learning, and photography of landscape and wild animals in order to understand visitors' interests in the uniqueness of the nature and to predict and confirm potential ecotourists. Perceived environmental involvement reveals close relations with interests, and interests are the content of perceived environmental involvement (Kapferer and Laurent, 1986; van Voorst and Hellman, 2015). Individual interests in certain affairs rely on individual characteristics. Interests and needs are major individual characteristics to affect the attention. An individual would search (expose) and examine (pay attention to) information related the requirement. Individual interests or involvement in certain brand or product reveal the attention to the brand or product related information. Referring to Oliver (1980) and Ajzen and Fishbein (1980), a consumer with higher interests or preference would appear higher involvement in the product or purchase behaviors. Meanwhile, referring to the psychological cognition process of belief (perception) → attitude, a consumer with higher interests or preference would show beneficial effects on the acceptance of tourism products. It is therefore inferred that H3: visitors' interests in tourism resources present

direct and positive effects on perceived environmental involvement, and H6: visitors' interests in tourism resources reveal direct and positive effects on ecotourism support.

Effects of perceived environmental involvement and support on behavioral intention

Behavioral intention is often used for measuring future behavior. Oliver (1980) proposed the satisfaction decision cognition model that satisfactory evaluation and judgment resulted from purchase behaviors would affect behavioral intention. Zeithaml et al. (1996) argued that service quality would affect behavioral intention, was the indicator to judge successive purchase behaviors, and would result in financial results through behaviors.

As mentioned above, with high involvement, attitudes might be internalized that involvement would affect consumer behaviors. Past research discovered that involvement could effectively explain the changes in overseas tourism product purchase; it implied the correlations among involvement, attitude, and intention (Deery et al., 2017; Clarke and Mahadi, 2017). In this study, involvement is regarded as the dimension of belief, support as attitude, and behavioral intention as intention. According to Oliver's (1980) logic, visitors with higher ecotourism involvement would enhance the ecotourism support and behavioral intentions to ecotourism, and visitors enhance the ecotourism support would also enhance the behavioral intentions to ecotourism. Accordingly, the following hypotheses are established. H7: visitors' perceived environmental involvement appears direct and positive effects on ecotourism support. H8: Visitors' perceived environmental involvement shows direct and positive effects on behavioral intention. H9: Visitors' ecotourism support reveals direct and positive effects on behavioral intention.

Methodology of research

Definition and measurement of variable

The definition and measurement of variables are referred to relevant empirical research. In addition to good reliability and validity of original items, the current situations of ecotourism resources in Sichuan Province and the semantic meanings of items are taken into account. All items are measured with Likert's 7-point scale.

Referring to Flynn and Goldsmith (1993), innovation is defined as visitors' acceptance of novel tourism service. Referring to Kapferer and Laurent (1986), perceived risk is defined as visitors' perceived unfavorable results of new tourism product. Referring to Biljana et al. (2002) and the current situation of tourism resources in Sichuan Province, interest is defined as the attraction of tourism resources to visitors. According to Zaichkowsky (1994), perceived environmental involvement refers to visitors' overall perception of the correlation with purchased ecotourism products. Referring to Yoon et al. (2001), ecotourism support is defined as visitors' acceptance attitude towards ecotourism. Based on the definition of Zeithaml et al. (1996), behavioral intention reveals visitors' continuous and advantageous purchase behaviors to ecotourism in the future.

Participants and procedures

With judgmental sampling, visitors to Sichuan Province are regarded as the research samples in this study. Aiming at visitors returning from Sichuan Province as the object for the questionnaire survey, are preceded at Shuangliu Airport and the high speed rail station. Visitors to Sichuan Province concentrate on peak season that the survey is

preceded during July – November, 2017, to enhance the representativeness by covering the peak season. The numbers of visitors in Sichuan Province is 600 million per year that is statistics data in 2017. A total of 1000 questionnaires were distributed, but 348 valid copies of questionnaire are acquired at last. The basic data of sampled visitors contain mostly female (53.2%) and single (60.5%), average age 24.8, students (43.9%), monthly income about RMB 7000, and first time to Sichuan Province (69.5%). SPSS is further utilized for the structural analysis of samples, exploratory factor analysis, and reliability analysis. According to the observation variables established in this study, the structural equation model (SEM) of causal relations among variable is constructed for testing the research hypotheses.

Results of research

Exploratory factor analysis aims to test the construct validity of dimensions in order to ensure the explanatory power and stability. Six items in innovation (Cronbach's $\alpha = 0.88$), 5 items in perceived environmental involvement (Cronbach's $\alpha = 0.86$), 5 items in support (Cronbach's $\alpha = 0.83$), and 5 items in behavioral intention (Cronbach's $\alpha = 0.91$) are separately extracted 1 dimension. Furthermore, 2 dimensions are extracted from 7 items in perceived risk, namely "psychological risk" (Cronbach's $\alpha = 0.84$) and "real risk" (Cronbach's $\alpha = 0.87$), 3 dimensions are extracted from 16 items in interest, namely "unique landscape resources" (Cronbach's $\alpha = 0.92$), "origin and integrity" (Cronbach's $\alpha = 0.86$), and "folk culture" (Cronbach's $\alpha = 0.81$), according to the factor loadings. The structural equation model (SEM) presents the standard factor loadings $\chi^2 = 227.45$ (df = 209), $\chi^2/df = 1.09$, $p = 0.1345$, GFI = 0.94, AGFI = 0.91, RMR = 0.04, RMSEA = 0.02, CFI = 0.97, NNFI = 0.98, and NFI = 0.96. All the measurements are shown in *Table 1*. Among 9 research hypotheses in this study, 3 paths of innovation → support, perceived risk → perceived environmental involvement, and perceived risk → support do not achieve the significant parameter estimate, while the rest of innovation → perceived environmental involvement, interest → perceived environmental involvement, interest → support, perceived environmental involvement → support, perceived environmental involvement → behavioral intention, and support → behavioral intention reach the significant parameter estimate of 0.01. Overall speaking, 6 out of 9 research hypotheses are supported in this study.

Discussion

This study focuses on ecotourism, the emerging tourism, to discuss visitors' innovation tendency to tourism products, which is regarded as the content of personal traits. From the viewpoint of "resource-based theory" and combining existing natural resources in Sichuan Province, visitors' interests in tourism resources in Sichuan Province are discussed to construct the visitor behavioral intention integration model for further test. The structural equation model constructed in this study shows good fit. *Figure 1* reveals that innovation, interest, and perceived risk are the antecedents of the causal model and would affect successive "perceived environmental involvement (integrated perception) → support (attitude) → behavioral intention". Apparently, the combination of "resource-based theory" with the psychological cognition model of "belief (perception) → attitude → intention" is verified in the research on ecotourism.

Table 1. Measurement of variables

Innovation	Cronbach's α
<p>In my friends circle, I am always the first to visit a new attraction. I am interested in trying out the new tour launched by the travel agency. I love traveling more than others. I know the latest tourist attractions before others. I will consider visiting places where I have never heard before. I know new sightseeing tours more than others.</p>	0.88
<p>Perceived risk</p> <p>I am worried about whether the ecotourism itinerary is dangerous. I will worry about choosing whether to participate in eco-tourism. I am not sure if I will regret to participate in eco-tourism. I will worry that the quality of eco-tourism is not as good as expected. I will worry about the cost of eco-tourism. I am not sure if the ecotourism trip has a special feature.</p>	0.86
<p>Interest</p> <p>Sichuan has a variety of sightseeing resources The scenery of Sichuan is incomparable in its area. The scenery of Sichuan is unique Sichuan has the equivalent of landscape in the world. Sichuan has beautiful mountain views. The geological landscape of Sichuan is amazing. The natural scenery of Sichuan is refreshing. The maintenance of the natural environment in Sichuan is quite perfect. The preservation of the historic culture of Sichuan is quite complete. The landscape of Sichuan maintains the original simplicity and tranquility. The ancient architecture of Sichuan ancient temples and temples preserves the traditional ancient style. The natural environment of Sichuan will not be crowded and messy. Sichuan is rich in native products. Sichuan has a long history of historic buildings and cultural relics.</p>	0.83
<p>Perceived environmental involvement</p> <p>Ecological sightseeing is important to me. Eco-tourism is what makes me feel good. My life is closely related to ecological sightseeing. I am attracted to eco-tourism. Ecotourism is valuable to me.</p>	0.86
<p>Ecotourism support</p> <p>The development of ecological tourism in Sichuan is promising. The development of ecological tourism in Sichuan is advantageous. Sichuan develops ecological tourism is competitive. Developing ecological tourism is beneficial to Sichuan. Developing ecological tourism is worthwhile for Sichuan.</p>	0.83
<p>Behavior intention</p> <p>Even if the cost is high, I will still consider participating in eco-tourism. I am willing to participate in the ecological sightseeing of Sichuan in the future In the future, I will give priority to participating in the ecological sightseeing of Sichuan. I will accept the recommendation of others to participate in the ecological sightseeing of Sichuan. I will recommend to my relatives and friends to participate in the ecological sightseeing of Sichuan.</p>	0.91

$\chi^2 = 227.45$ (df = 209), $\chi^2/df = 1.09$, $p = 0.1345$, GFI = 0.94, AGFI = 0.91, RMR = 0.04, RMSEA = 0.02, CFI = 0.97, NNFI = 0.98, NFI = 0.96

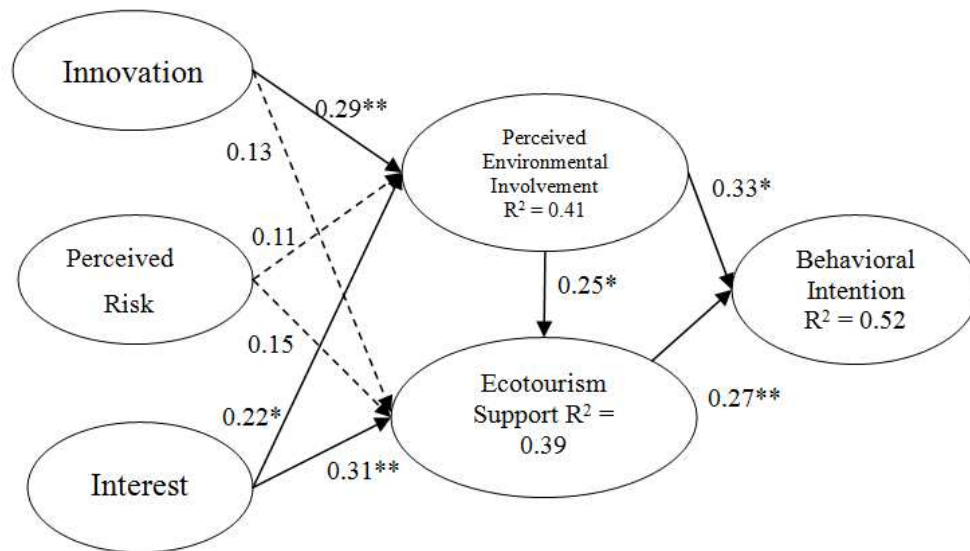


Figure 1. Empirical model

Moreover, the test of standardized parameter estimates in *Figure 1* shows that 6 out of 9 causal paths constructed in this study are supported, where the effects of “perceived risk → perceived environmental involvement” and “perceived risk → support” are insignificant, revealing that visitors’ perceived risk of ecotourism does not influence the intention to the future selection of ecotourism. It is inferred in this study that visitors still present perceived risk on emerging tourism, and the influence might be weaker and insignificant than innovation and interests. In regard to the development of ecotourism, the meaning of management is implied, while the effect of “innovation → support” is not significant, either, possibly because innovation is individual perception which could affect support (attitude) and successive behavioral intention through perceived environmental involvement. It is also proved that “innovation” and “interest” are the antecedents to affect visitors’ future behavioral intention. It supports the ecotourism interest scale proposed by Biljana et al. (2002) to effectively explain visitors’ participation in ecotourism activity as well as to predict and confirm the opinions of potential ecotourists by understanding visitors’ interests in the uniqueness of nature and learning natural environment. Meanwhile, it also corresponds to the findings of Xu et al. (2017) and Hartini et al. (2017) that subjective curiosity plays extremely important role in the people’s ecotourism motivation.

The analysis reveals (*Table 2*) total 5 influence paths of behavioral intention, with the total effect 0.288, where 2 indirect paths driven by “innovation” (innovation → perceived environmental involvement → behavioral intention and innovation → perceived environmental involvement → support → behavioral intention) show the total effect 0.116 (0.096 + 0.02) and 3 indirect paths driven by “interest” (interest → perceived environmental involvement → behavioral intention, interest → perceived environmental involvement → support → behavioral intention, and interest → support → behavioral intention) appear the total effect 0.171 (0.073 + 0.015 + 0.083). In comparison with the effect, the antecedent drive of “interest” is stronger than it of “innovation”. Apparently, “interest” is the key driving factor in visitors’ future selection of ecotourism product. It is worth of relative units’ emphases to develop marketing strategies.

Table 2. Influence path and effect of behavioral intention

Influence path	Influence effect
Innovation → perceived environmental involvement → behavioral intention (0.29×0.33)	0.096
Innovation → perceived environmental involvement → support → behavioral intention ($0.29 \times 0.25 \times 0.27$)	0.02
Interest → perceived environmental involvement → behavioral intention (0.22×0.33)	0.073
Interest → perceived environmental involvement → support → behavioral intention ($0.22 \times 0.25 \times 0.27$)	0.015
Interest → perceived environmental involvement → behavioral intention (0.31×0.27)	0.083
Total effect	0.288

Implications

In comparison with mass tourism, ecotourism is the tourism with innovative concept and has not been popularized. Understanding the behavioral intention of potential visitors to ecotourism is the core objective of a promotion unit. By summing up above analyses and discussions of behavioral intention, the management of marketing practice to promote ecotourism in Sichuan Province is proposed in this study as follows:

(1) *The conservation and maintenance strategies of core tourism resources*

“Interest” is the driving factor in visitors selecting emerging ecotourism products. Research findings show that the origin and integrity of ecology are the key components. Accordingly, the relevant promotion units are suggested to pay attention to core tourism resources, including the maintenance and conservation of natural environment and ancient culture. Traditional and original characters of landscape environment, ancient temples, and architecture and relics should be preserved. It should avoid from losing the original characteristics because of reconstruction and renewal in order to correspond to “nature” emphasized in ecotourism. In addition to the maintenance and conservation of natural and humanistic environment, the marketing and promotion strategies should stress on the natural and humanistic characteristics of “origin and integrity” in Sichuan Province to drive potential visitors’ intention, by inducing the inner interests, to participate in ecotourism in Sichuan Province.

(2) *Innovation strategies for ecotourism products*

“Innovation” is also the driving factor in visitors’ ecotourism product orientation. Research proves that new spots and new itineraries are the key components of innovation. Apparently, factors in potential visitors’ future selection of ecotourism products reflect on individual inner characters. The relevant promotion units are therefore suggested to positively develop new ecotourism spots in Sichuan Province and integrate travel agents to promote ecotourism package tours so as to attract potential visitors of ecotourism by convenient tourism service.

(3) *Development potential and marketing and promotion strategies of ecotourism*

It is discovered in this study that ecotourism is the key component of support, revealing the evaluation of potential visitors to the development of ecotourism in Sichuan Province. Such information could encourage the confidence of relevant promotion units in promoting ecotourism to be the basis to continuously promote and develop ecotourism. What is more, word-of-mouth is the key component of behavioral

intention, showing the importance of “word-of-mouth” and “behavioral loyalty” in the development of ecotourism in Sichuan Province. In this case, relevant promotion units should devote to the overall planning of ecotourism products and the management and promotion of the quality of ecotourism so as to attract potential visitors to participate in ecotourism and implement the promotion of ecotourism through the word-of-mouth and behavioral loyalty.

REFERENCES

- [1] Ajzen, I., Fishbein, M. (1980): *Understanding Attitudes and Predicting Social Behavior*. – Prentice-Hall, Englewood Cliffs, NJ.
- [2] Biljana, J., Cornwell, T. B., Mather, D. (2002): Exploring the usefulness of an ecotourism interest scale. – *Journal of Travel Research* 40(3): 259–269.
- [3] Chen, K. K. (2014): Assessing the effects of customer innovativeness, environmental value and ecological lifestyles on residential solar power systems install intention. – *Energy Policy* 67: 951–961.
- [4] Chiu, Y. T. H., Lee, W. I., Chen, T. H. (2014): Environmentally responsible behavior in ecotourism: antecedents and implications. – *Tourism management* 40: 321–329.
- [5] Clarke, N., Mahadi, N. (2017): Differences between follower and dyadic measures of LMX as mediators of emotional intelligence and employee performance, well-being, and turnover intention. – *European Journal of Work and Organizational Psychology* 26(3): 373–384.
- [6] Deery, S., Walsh, J., Zatzick, C. D., Hayes, A. F. (2017): Exploring the relationship between compressed work hours satisfaction and absenteeism in front-line service work. – *European Journal of Work and Organizational Psychology* 26(1): 42–52.
- [7] Engel, J. F., Blackwell, R. D., Miniard, P. W. (1995): *Consumer Behavior* (8th ed.). – Dryden, Fort Worth, TX.
- [8] Flynn, L. R., Goldsmith, R. E. (1993): Identifying innovators in consumer service markets. – *The Service Industries Journal* 13(3): 97–109.
- [9] Frohlick, S., Johnston, L. (2011): Naturalizing bodies and places: tourism media campaigns and heterosexualities in Costa Rica and New Zealand. – *Annals of Tourism Research* 38(3): 1090–1109.
- [10] Grant, R. M. (1991): The resource-based theory of competitive advantage: implications for strategy formulation. – *California Management Review* 33(3): 114–134.
- [11] Hartini, N., Ariana, A. D., Dewi, T. K., Kurniawan, A. (2017): Improving urban environment through public commitment toward the implementation of clean and healthy living behaviors. – *Psychology Research and Behavior Management* 10: 79–84.
- [12] Hetzer, N. D. (1965): Environment, tourism, culture. – *Links* 1(2): 1–3.
- [13] Kapferer, J. N., Laurent, G. (1986): Consumer involvement profiles: a new practical approach to consumer involvement. – *Journal of Advertising Research* 25(6): 48–56.
- [14] Laroche, M., Bergeron, J., Barbaro-Forleo, G. (2001): Targeting consumers who are willing to pay more for environmentally friendly products. – *The Journal of Consumer Marketing* 18(6): 503–520.
- [15] Lee, C. K., Back, K. J. (2006): Examining structural relationships among perceived impact, benefit, and support for casino development based on 4 years longitudinal data. – *Tourism Management* 27(3): 466–480.
- [16] Lee, R. L. (2014): Travel, liquidity and order in Malaysian Modernity. – *Asian Journal of Social Science* 41(6): 580–599.
- [17] Lu, D., Liu, Y., Lai, I., Yang, L. (2017): Awe: an important emotional experience in sustainable tourism. – *Sustainability* 9(12): 2189. doi.org/10.3390/su9122189.

- [18] Midgley, D., Dowling, G. R. (1978): Innovation: the concept and its measurement. – *Journal of Consumer Research* 4: 229–242.
- [19] Oliver, R. L. (1980): A cognitive model of the antecedents and consequences of satisfaction decisions. – *Journal of Marketing Research* 17(4): 460–469.
- [20] Sahakian, M., Saloma, C., Ganguly, S. (2018): Exploring the role of taste in middle-class household practices. – *Asian Journal of Social Science* 46(3): 304–329.
- [21] van Voorst, R., Hellman, J. (2015): One risk replaces another. – *Asian Journal of Social Science* 43(6): 786–810.
- [22] Wu, T., Tsai, H. T., Tai, Y. N. (2016): Would corporate social responsibility affect consumers' attitudes towards brand and purchase behavior? Buyer-seller guanxi as the moderator. – *Revista de Cercetare si Interventie Sociala* 53: 272–287.
- [23] Wu, T. J., Wu, Y. C. J., Tsai, H. T., Li, Y. B. (2017): Top management teams' characteristics and strategic decision-making: A mediation of risk perceptions and mental model. – *Sustainability* 9: 2265. DOI: 10.3390/su9122265.
- [24] Xu, S., Mingzhu, L., Bu, N., Pan, S. (2017): Regulatory frameworks for ecotourism: An application of total relationship flow management theorems. – *Tourism Management* 61: 321–330.
- [25] Yoon, Y., Gursoy, D., Chen, J. S. (2001): Validating a tourism development theory with structural equation modeling. – *Tourism Management* 22(4): 363–372.
- [26] Zaichkowsky, J. L. (1994): The personal involvement inventory: reduction, revision, and application to advertising. – *Journal of Advertising* 23(4): 59–69.
- [27] Zeithaml, V. A., Berry, L. L., Parasuraman, A. (1996): The behavioral consequences of service quality. – *Journal of Marketing* 60(2): 31–46.

SUSTAINABLE DEVELOPMENT OF GREEN BUILDING BASED ON INTUITIONISTIC FUZZY ANALYTIC HIERARCHY PROCESS

HUANG, Y.^{1,2} – WU, W.² – YANG, S.^{1,2*}

¹*Zhuhai College of Jilin University
Caotang Crescent (Wan), Jinwan District, Zhuhai City 519041, China*

²*Faculty of Innovation and Design, City University of Macau
Avenida Padre Tomás Pereira Taipa, Macau City 999078, China*

**Corresponding author*

e-mail: samyang8747@qq.com; phone/fax: +86-177-6523-4675; fax: +86-853-6523-4675

(Received 18th Sep 2018; accepted 26th Nov 2018)

Abstract. A city is an area highly concentrated in buildings, but is also an important place for energy consumption and waste generation, so the development of buildings with low energy consumption and less pollutant emissions is an important way to achieve energy conservation and emission reduction, and sustainable development of cities in China. On the basis of systematically combing and broadly absorbing the relevant research results of sustainable development and urban greening, and combining with the mathematical methods such as variation coefficient and intuitionistic fuzzy analytic hierarchy process, urban housing buildings are taken as the subject of evaluation. With sustainable development as the evaluation background, the aim of study is to systematically and comprehensively evaluate and analyze the building greening level. Based on the analysis of green building theory and predecessors' research results, the influence of economic, political, technical and other factors on the development of green building in nearly 300 cities in China is analysed. And combined with the actual development examples of Shenzhen City, it is further discussed. It is concluded that the research method used in this paper is correct, and Shenzhen is selected as an example to provide reference for the sustainable development of other cities

Keywords: *sustainable development, Chinese architecture, green building, Shenzhen, greening evaluation methods*

Introduction

As the population grows rapidly, resources are wasted and consumed, the environment is destroyed, and the new concept of sustainable development is gradually formed. More and more people are paying attention to environmental protection, green, health and ecological balance. From experts and scholars to the public are calling for taking good care of the environment, saving resources and avoiding waste, and doing their part and responsibility for the sustainable development of the society. The concept of green building is the important direction of the development of building energy efficiency is an important measure to speed up the change pattern of urban and rural construction in China, is also an important means of sustainable development in our country in the future. It analyze that influence of economic environment, policy environment and technology environment on the basis of difference in the construction of green build, and has a certain research value for the future city green build and the sustainable development of city (Zhu et al., 2016).

Research background and motivation

Since the transformation of human society from agriculture to industrialization, great changes have taken place in production and lifestyle. On the one hand, it has greatly improved people's living conditions, promoted rapid economic growth and enriched human material and cultural life. However, at the same time, human sustainable development is facing new problems, the contradictions among the ecosystem of people and earth, living environment and natural resources are becoming increasingly acute, mainly manifesting in: forest destruction, desertification, global energy crisis, and environmental pollution. These problems have gradually become a hot issue of common concern around the world. As Qiu Baoxing, chairman of the Chinese Academy of Urban Sciences, said, "the most successful thing in China's industrial civilization in the past has also become the biggest obstacle to China's urban green development". Therefore, it is necessary to abandon the extensive development in the thinking of industrial civilization and the rigid mode of mass production in life. Only by abandoning this extensive economic characteristic of seeking economic development by sacrificing the environment can sustainable development be realized from the source. But sustainable development and ecological civilization are not totally denying industrial civilization, but the new stage and new form of self-adjustment and self-development of industrial civilization. They are not overflowing the historical period of industrial civilization. In essence, they are the ecological reconstruction of industrial civilization. They are based on industrial civilization and coordinate the sustainability between the two aspects of economy and environment.

The Eighteenth National Congress of the Communist Party of China included the concept of scientific development in the Party's guiding ideology (Hu, 2018), and clearly put forward that it is necessary to consciously take comprehensive, coordinated and sustainable development as the basic requirements for the in-depth implementation of the concept of scientific development. In 2015, the Fifth Plenary Session of the Eighteenth Central Committee once again sounded the horn of green development (Yang, 2016), and put forward a series of new measures to achieve green development. In 2017, the report of the Nineteenth National Congress pointed out that it is necessary to establish and practice the concept of "green water and green mountains are golden mountains and silver mountains". It pointed out the direction for the construction of ecological civilization and paid great attention to ecological civilization and green development. Under the strong call of the state on sustainable development, green development and ecological civilization (Hu, 2018), all walks of life in the production process are also actively responding.

According to the classification of national economic industries, issued with the approval of the general administration of quality supervision, inspection and quarantine and the standardization administration of China, and implemented on November 1, 2011, construction industry, as one of the important pillar industries, has played a great role in promoting the rapid development of China's economy. But the construction industry has made such an important contribution to our economy, at the same time, the damage to our energy, resources and environment cannot be underestimated. According to the *China Building Energy Consumption Research Report (2017)*, China's total building energy consumption in 2015 accounted for 20% of the total national energy consumption; housing construction consumed 1/3 of the total steel in the whole life cycle, and urban water and construction land also reached 1/3 of the total. In addition, in

terms of building energy consumption, there is a certain proportion of growth every year, and the phenomenon is obvious.

According to the *China Environmental Situation Bulletin 2016* published in June 2017, of the 338 cities in China, the air quality in 254 cities exceeded the standard, accounting for 75.1% of the total cities in the country, while the number of cities meeting the standard was only 24.9%. Although the air quality in China is gradually improving compared with that in 2015, from the ratio of air quality in 338 cities shown in *Figure 1*, it can be seen that, in terms of China's environmental air condition, China is facing more complex and serious environmental quality problems and the task is still very arduous.

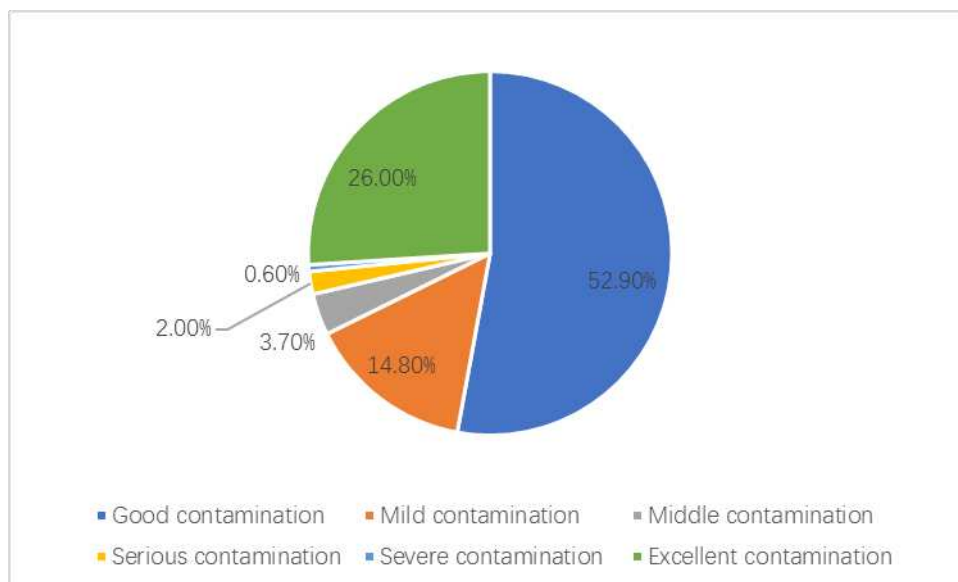


Figure 1. Proportion of environmental air quality in 338 cities of China in 2016, the data comes from *China Environmental Situation Bulletin*

China is in a critical period of new urbanization construction, most cities will be built on a large scale in the future, and the sustainable development of the construction field is related to the sustainable development of the whole society. Therefore, green building is an important development direction of building energy conservation in the future, an important grasp to speed up the transformation of urban and rural construction mode, but also an important means of sustainable development in China's future. The development of green building is affected by all aspects of the city (Yang and Zhou, 2010). It has become an important topic to be discussed urgently what guaranteeing and encouraging measures the city should take to more effectively promote the construction of green building and promote the overall sustainable development of the region (Huang and Shi, 2016).

Materials and methods

Basic theories of sustainable development

With the rapid growth of population, the gradual reduction of resources and the increasing destruction of the environment, the new concept of sustainable development

has gradually come into being. “Some works” have laid a preliminary foundation for the formation of sustainable theory and made a systematical study of the problems faced by the long-term economic development of mankind. They include *Silent Spring* published by Rachel Carson, American marine biologist, in 1962, the report of *Limits to Growth* submitted by a group of 17 people led by Dennis in Massachusetts Institute of Technology in 1972, *Blueprint for Survival* submitted by E. Goldsmith, British ecologist, in 1972 and other works. These reports profoundly analyze the problems in the process of human development and the importance of sustainable development. In 1987, the World Commission on Environment and Development (WECED) submitted *Our Common Future* to the UN General Assembly and formally proposed the concept and model of “sustainable development” (Wuelser and Pohl, 2016). In this investigation report, human development is closely combined with ecological environment and sustainable development is defined as the development of the ability to meet the needs of contemporary people without harming the development needs of future generations.

The proposal of sustainable development is a profound reflection of human beings on the status quo of the ecological environment, which has been unanimously recognized by the international community since its formation (Takahashi, 2017). Its meaning can also be explained from the following four perspectives. From the perspective of economics, sustainable development is to achieve the highest net benefits under the premise of ensuring the rational use of resources and ensuring that the ecological environment is not destroyed (Sharma et al., 2016). From the perspective of sociology, sustainable development is to “improve the quality of human life without exceeding the capacity to maintain ecosystem tolerance”. Human survival and the earth’s carrying capacity and biodiversity achieve harmonious unity and co-existence, which is also mentioned in the *Survival Strategy*. From the perspective of natural ecology, sustainable development is the coordinated balance between natural resources and ecological environment system, and it satisfies the sustainable survival of human beings in an optimal balance state (Aggarwal and Singh, 2018). From the perspective of science and technology, sustainable development is to adopt new technologies and techniques that can save resources and reduce environmental pollution. From the perspective of scientific and technological innovation, it can not only meet the original intention of economic development and social needs (Tao et al., 2009), but also achieve the purpose of sustainable utilization of living environment and natural resources, so as to achieve the coordination of the three (Rahmati et al., 2016).

Since 2006, the total output value of “China’s construction industry” has been continuously increasing, its annual value-added since 2009 has reached 6.5% of GDP, and its position is stable. As an extremely important branch of the construction industry, the consumption of energy, materials, water resources and land occupancy of housing construction industry is even greater in the whole process of production and management (Rodríguez et al., 2016). According to incomplete statistics, about half of the global energy and materials are consumed by the housing construction industry. According to the “*Analysis Report of Market Prospects and Investment Strategic Planning of China’s Intelligent Building Industry*” from 2013 to 2017, the total energy consumption of China’s housing construction is increasing year by year, accounting for nearly 30% of the total energy consumption (Shafie et al., 2017). The whole process of building activities causes rapid deterioration of the ecological environment and heavy energy burdens. Therefore, facing the sustainable development, in the process of building production, saving resources and strengthening the recycling of materials and

waste disposal in the construction process will play an important role in building a “two-oriented society” in China (Baden and Prasad, 2016).

Sustainable development of “housing construction enterprises” should run through the whole process of preparing, planning, design, construction and maintenance after use. Every link from land use, building materials use, production process use and so on will be implemented specifically to save resources and avoid pollution.

Sustainable development and green building

Under the background of the rapid development of global urbanization in the 21st century, the key problem of sustainable development lies in the sustainable development of urban areas (Chong and Wang, 2016). How to transform the concept of sustainable development into urban practice to effectively promote urban sustainable development is undoubtedly a hot topic in sustainable development today. One of the core issues of sustainable development is resources and environment, which is embodied as the mode of energy-saving, environmental protection and ecological development in “urban development” (Wang, 2017). In the past two decades, China’s construction industry has shown explosive growth, but due to the lack of awareness of sustainable development, the construction industry in China has always been a “high energy consumption and high pollution” industry (Shengshi Zhou, 2010).

. According to statistics, the resources consumed in the whole process of building activities (building materials production, construction, use, waste disposal, etc.) ranked first in all industries (Yuan et al., 2017). Sustainable development of construction industry means to integrate the concept of sustainable development into every link of construction, to save energy, reduce pollution, and improve the ecological and environmental benefits of buildings as much as possible. From this point of view, the sustainable development of the construction industry plays an important role in promoting urban sustainable development (Edgren, 2016).

“Green building” is a response to the concept of sustainable development in the field of building, and it is also one of the strategic means to achieve sustainable development in cities. At present, there is no uniform definition of green building in the world. The definition and connotation of green building are defined by the *Green Building Evaluation Criteria* formulated in 2006 – “buildings that can save resources (energy, land, water and materials), protect the environment, reduce pollution, provide people with healthy, applicable and efficient use space, and harmoniously live with nature in the whole life cycle” (Wu et al., 2017). The revised *Green Building Evaluation Criteria (2014)* retains the original definition of green building and adds green civil buildings to residential and public buildings based on office buildings, shopping malls and hotels (Xiu et al., 2017). Green building stresses saving resources, reducing pollution and harmonious coexistence between man and nature (Wu et al., 2016). These concepts are highly consistent with the concept of sustainable development. With the widespread concern of the concept of sustainable development of building in China, the importance of green building development in China’s construction industry has been greatly enhanced.

Evaluation method of green housing construction facing sustainable development

Generally speaking, there are many greening evaluation methods: fuzzy comprehensive evaluation method, neural network evaluation method, fuzzy analytic

hierarchy process, and intuitionistic fuzzy analytic hierarchy process (Alwan et al., 2017). In order to make this greening evaluation more scientific and reasonable, their advantages and disadvantages will be elaborated.

Fuzzy comprehensive evaluation method comes from the application of fuzzy mathematics theory (Pang et al., 2016). Based on membership degree theory, the factors of qualitative evaluation and those factors with fuzzy boundary and difficult to quantify are transformed into quantitative evaluation, and then comprehensive evaluation is made on the things to be evaluated (Brown, 2016). The basic idea of fuzzy comprehensive evaluation method is to establish factor set and comment set firstly; then, after the weight vectors of each evaluation index are determined, the evaluation matrix of each index is expressed by membership degree vector; and then the weights and evaluation matrix are synthetically calculated, and from the first level to the highest level, according to the principle of maximum membership, the final results of fuzzy comprehensive evaluation are obtained (Broman and Robèrt, 2017). This method can transform qualitative indicators into quantitative indicators, which has strong practicability and strong correlation among various evaluation steps, and it is widely used in things or objects restricted by many factors (Baishou and Gao, 2017). However, this method has strong subjectivity in the process of determining the weight of indicators, which makes the evaluation results easy to be affected and its reliability is reduced (Staffordsmith et al., 2017).

“Intuitionistic fuzzy analytic hierarchy process” is an organic combination of “intuitionistic fuzzy set theory” and “analytic hierarchy process”. On the basis of the above “fuzzy analytic hierarchy process” (Zhang et al., 2012), this method adds the information of non-membership degree. Its basic ideas are: to clarify the relationship among the factors of the object to be evaluated, to establish an evaluation hierarchical structure model; to compare the importance of each factor (Kopnina, 2016); to establish an intuitionistic fuzzy complementary judgment matrix (Yang et al., 2012); to test the consistency of the intuitionistic fuzzy complementary judgment matrix; to determine the weights of indicators at all levels; and finally to get the evaluation grade level results. This method is the extension of fuzzy theory. The attitude of support, opposition and neutrality is more fully reflected in the process of weight calculation. It is more in line with people’s subjective judgment thinking and it is the application extension of fuzzy mathematics in the greening evaluation process of housing construction enterprises. It is more flexible and persuasive to deal with the contradiction between forecasting and reality caused by human subjectivity, making the greening evaluation more objective (Kopnina, 2017).

Results

Analysis of factors influencing the greening of housing construction

The domestic and foreign literature on the study of the factors affecting the greening of housing construction can be divided into the following four categories.

Greening concept. What can provide realistic solutions to the disharmonious development between man and nature is called greening concept. As an important pillar industry in social production, housing construction industry is not only the provider of material information, but also its producer. Enterprise’s strategy in environmental protection can directly affect the ecological environment of the place where the enterprise is located.

Greening capability. The foundation of greening capability is the green resources owned by enterprises. There are certain forms and objective existence of resources, but the former is invisible but active. Although the two concepts are different, they are closely related and can be transformed into each other.

Greening environmental benefits. Environmental friendliness is affected by a series of aspects such as efficient utilization of material, resources, and energy and waste disposal. Therefore, low consumption and emission reduction, high efficiency and environmental protection, as well as integration and optimization are the basic direction of the future development of China's housing construction industry.

Greening economic benefits. The greening evaluation of housing construction enterprises is closely related to the factors such as market share, profit growth rate, asset return rate and the proportion of green building development. At the same time, the green economy is also included in the greening evaluation. The collection of these factors is the greening economic benefits, which can also be defined as the dominant benefit of green building.

Through the analysis of the above content, the greening impact factors of green housing construction can be assumed, as shown in *Figure 2*. Greening concept, greening capability, greening environmental benefits and greening economic benefits these four elements work together on the green development of housing construction. At the same time, ideas and capabilities also play a role in promoting environmental and economic benefits; in addition to the interaction between environmental and economic benefits, the two will turn into greening ideas and greening capabilities. In this way, the five of them complement each other and influence each other.

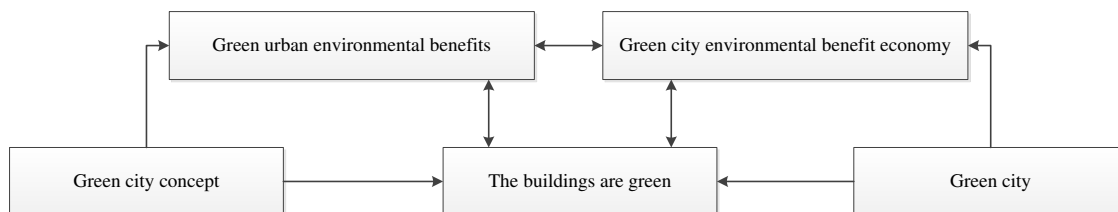


Figure 2. The elements influencing the greening of buildings. The above factors are summarized from the relevant domestic and foreign literature

Establishment of greening evaluation model for housing construction

(1) Building a hierarchical structure model

Through the above analysis and study of the factors affecting the greening of housing construction, the links between the various factors are clarified to stratify and establish a hierarchical structure model, as shown in *Figure 3*.

(2) Establishment of intuitionistic fuzzy complementary judgment matrix

The degree of importance of each factor is two-two compared with that of intuitionistic fuzzy judgment matrix (Yi and Zhao, 2013; *Eq. 1*).

$$A = (a_{ij})_{n \times n} \quad (\text{Eq.1})$$

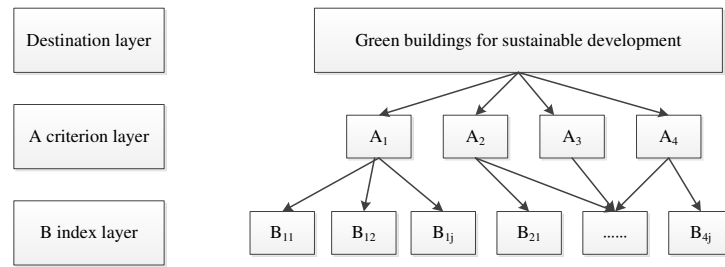


Figure 3. The hierarchical structure model of evaluation, through the above analysis and study of the factors affecting the greening of housing construction

When comparing the importance of the factors, the definition scale as shown in Table 1 is adopted.

Table 1. Definition scale of the importance of the attribute

Evaluation grade	Intuitionistic fuzzy number
Factor i is extremely important than factor j.	(0.90,0.10,0.00)
Factor i is strongly important than factor j.	(0.80,0.15,0.05)
Factor i is obviously important than factor j.	(0.70,0.20,0.10)
Factor i is slightly important than factor j.	(0.60,0.25,0.15)
Factor i is as important as factor j.	(0.50,0.30,0.20)
Factor i is relatively not important than factor j.	(0.40,0.45,0.15)
Factor i is not important than factor j.	(0.30,0.60,0.10)
Factor i is rather important than factor j.	(0.20,0.75,0.05)
Factor i is extremely no more important than factor j.	(0.10,0.90,0.00)

(3) Consistency test of intuitionistic fuzzy complementary judgment matrix

According to the intuitionistic fuzzy complementary judgment matrix established in (2), we need to test its consistency. The following consistency test formula is given (Eq. 2):

$$d(\bar{A}, A) = \frac{1}{2(n-1)(n-2)} \sum_{i=1}^n \sum_{j=1}^n (|\bar{u} - u| + |\bar{v} - v|) \quad (\text{Eq.2})$$

In Equation 2, A refers to the intuitionistic fuzzy judgment matrix obtained from the two-two comparison of indexes in each layer, $A = (a_{ij})_{n \times n}$; \bar{A} suggests the intuitionistic fuzzy consistent judgment matrix calculated through A, $\bar{A} = (\bar{a}_{ij})_{n \times n}$.

(4) Calculation of the weight of judgment matrix

The vector of the first level index is known as: $A = (a_1, a_2, \dots, a_n)$, $a_i = (u_i, v_i) (i = 1, 2, \dots, n)$ is the form of intuitionistic fuzzy numbers, u_i is an indicator of the importance of target decision making, and v_i is the not important degree of indicator to target decision-making. The following formula (Eq. 3) is applied to calculate relative weights.

$$W^T = [W_1 W_2 \dots W_n] = \left[\begin{array}{ccc} \frac{\sum_{j=1}^n a_{1j}}{\sum_{i=1}^n \sum_{j=1}^n a_{ij}} & \frac{\sum_{j=1}^n a_{2j}}{\sum_{i=1}^n \sum_{j=1}^n a_{ij}} & \dots & \frac{\sum_{j=1}^n a_{ij}}{\sum_{i=1}^n \sum_{j=1}^n a_{ij}} \end{array} \right] \quad (\text{Eq.3})$$

(5) Determination of membership matrix R

After judging the indicators $A_i(i = 1,2,3,4)$ on by one, the initial membership matrix R of the index level factor set can be obtained (Eq. 4).

$$R = \begin{bmatrix} r_{11} r_{12} \dots r_{1j} \\ r_{21} r_{22} \dots r_{2j} \\ \dots \\ r_{i1} r_{i2} \dots r_{ij} \end{bmatrix} \quad (\text{Eq.4})$$

In Equation 4, the membership of qualitative index is directly evaluated by experts. Five language variables: “excellent”, “good”, “moderate”, “comparatively poor” and “poor” are set up in the qualitative indexes b_{11} , b_{12} and b_{13} for experts to choose. The method used here is fuzzy statistics, that is, according to the survey results, the frequency of the index occurring in a certain evaluation grade is sued as its membership. In addition, qualitative indicators such as b_4 and b_{16} are evaluated with two language variables “yes” and “no” and are expressed with two scores of 1 and 0, respectively.

As for the determination of the membership degree of quantitative index, triangular fuzzy function is used as the membership function of quantitative index in order to determine its membership degree. The concrete steps of constructing triangular fuzzy function are:

Firstly, collect and determine the value of the same index in different cities and get the maximum value a and the minimum value b of the index as the critical interval $[a, b]$ of the index, and three equidistant points y_1 , y_2 and y_3 are inserted between them. The distance $d = (b-a)/4$ is used to calculate the membership function of the index B_{ij} belonging to grade E_t .

(6) Intuitionistic fuzzy comprehensive evaluation

Finally, the total score is calculated according to the score formula (Eq. 5):

$$S = W \bullet R = (W_1, W_2, W_3, \dots, W_n) \bullet R \quad (\text{Eq.5})$$

It can be specifically evaluated according to Table 2.

Table 2. Green evaluation standard for housing construction enterprises based on sustainable development

	Supper excellent greening city	Excellent greening city	Greening city	Relative greening city	Not identified
Evaluation value	[1,0.8]	[0.8,0.6]	[0.6,0.4]	[0.4,0.2]	[0.2,0]

As can be seen from *Table 2*, if the evaluation value is between 1 and 0.8, it indicates that the city belongs to the super excellent greening city; if the evaluation value is between 0.8 and 0.6, it indicates that the city belongs to the excellent greening city... Evaluate in this way.

Discussion

Discussion of the weight value (W_i) of each criterion

The purpose of this study is to understand the impact of urban economic, policy, social and other environmental differences on green building construction. The development differences of green building in China have been studied before, and then the influence of various environmental factors on the development of green building will be discussed. A number of independent variable data of economic, policy, social and other factors on behalf of the above influencing factors studied are collected and collocated. Through multiple regression analysis, the influencing relationship of independent variable data on the dependent variable data of the development of green building is clarified, and then the multiple regression results are studied and analyzed.

Analysis framework construction

In order to verify the impact factors analyzed above and their corresponding indicators and urban green building construction related impact relationship, a complete analysis framework is drawn up, to achieve the purpose of this study through regression model estimation and test. The analytical framework developed is shown in *Figure 4*.

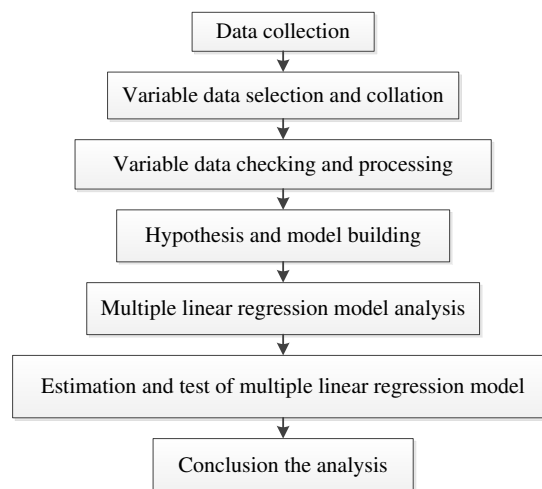


Figure 4. Regression analysis architecture diagram, in order to verify the impact factors analyzed above and their corresponding indicators and urban green building construction related impact relationship

The framework of regression analysis is divided into 7 steps. The first and the second steps are, based on the influencing factors obtained through the above analysis, to preliminarily get the relevant factors, including the number of green building projects as a dependent variable and other influencing factors as independent variables, and to select, collect and process the variable data; the third step is to check the basic data and

conduct default value processing; the fourth step is to set hypothesis and construct preliminary model; the fifth step is to estimate the linear regression model through SPSS software by using independent variable data analysed and collocated, and get the results of the model; the sixth step is to test the model and estimate the model, including the overall explanatory power R², F test, significance P test, regression coefficient and t value test, model residual distribution test, D-W test and Variance-Inflation-Factor testing, and finally, the regression model is obtained; the seventh step is to give a summary of this chapter and explain in detail according to the results of the model. Detailed model analysis steps are discussed in the following section.

Calculation of index weight of building construction greening

According to the steps obtaining weight above, the corresponding comparison matrix is constructed by two-two comparing index level. Comparing the importance of the four first-order indexes with respect to the target layer, the intuitionistic fuzzy judgment matrix is obtained as follows (Eq. 6):

$$A = \begin{bmatrix} 0.5(0.8,0.15) & (0.1,0.9) & (0.7,0.2) \\ (0.15,0.8) & 0.5(0.1,0.9) & (0.6,0.3) \\ (0.9,0.1) & (0.9,0.1) & 0.5(0.9,0.1) \\ (0.2,0.7) & (0.3,0.6) & (0.1,0.9) & 0.5 \end{bmatrix} \tag{Eq.6}$$

To determine the subordinate degree of qualitative indicators, the form of questionnaire survey is adopted and the indicators are evaluated according to the scores of experts. The five language variables of “excellent”, “good”, “medium”, “relative poor” and “poor” are used as the ratings. The leaders and management of the enterprise and a total of 20 experts from the floor and grass-roots staff evaluate the qualitative indicators in the evaluation system from the actual situation of Chinese buildings, and get the expert rating table shown in Table 3.

According to the above findings, the membership degree of a certain index refers to the frequency of occurrence of the index in a certain evaluation grade according to the survey results. Thus, the membership degree of the greening spirit and consciousness, green culture, and perfection and implementation of green system can be obtained, respectively: R₁₁ = (0.8,0.1,0.1,0,0); R₁₂ = (0.6,0.2,0.2,0,0); R₁₃ = (0.7,0.2,0.1,0,0).

Table 3. Expert evaluation from of green qualitative evaluation index of China State Construction

Number	Index evaluation	Excellent	Good	Medium	Relative poor	Poor
b ₁₁	Greening spirit and consciousness	16	2	2	0	0
b ₁₂	Green culture	12	4	4	0	0
b ₁₃	Perfection and implementation of green system	14	4	2	0	0

Model application and case analysis

Exploration and practice of green building development in Shenzhen

As the “first window” of the coastal developed cities and the reform and opening up, Shenzhen’s green building development has created a remarkable “Shenzhen speed” of

economic development. According to statistics, in 2017, “China’s total GDP” was 1600.198 billion yuan, ranking fourth among the mainland cities; the per capita GDP was 149,497 yuan/person, ranking fifth among the mainland cities in China. The economic development situation has long been in the forefront of Chinese cities (Gao and Wang, 2018), laying an economic foundation for the development of “green building industry” in Shenzhen. According to the data, the real estate industry is the main direction (30–50%) of fixed assets investment in Shenzhen in recent years and has maintained a growth trend for many years. The real estate investment volume has increased year by year since 2008. Although the growth rate has declined from 2012, the overall view is that the real estate develops well. The development trend of production is good. The rapid development of the real estate industry has brought some economic benefits to Shenzhen. However, due to the inherent characteristics of resource consumption and pollution emission of construction activities, the real estate industry has been developing in the past with the mode of “high consumption and high discharge”. How to reduce the consumption of natural resources and reduce the damage of the ecological environment in the process of industrial development has become a key research topic.

Under the contradiction of seeking “economic development” and “environmental resources” pressure, green buildings with the characteristics of resource conservation and environmental friendliness are eager to come out. All kinds of signs show that the development of green buildings is one of the necessary ways for the “sustainable economic development” of cities. The Shenzhen Municipal Government attaches great importance to the development of green buildings. At present, it is gradually building a green building construction system with four key points: laws and policies, project demonstration, financial support and technical support, which has contributed to the sustainable development of Shenzhen’s economy, environment and society.

Discussion

Shenzhen green building demonstration area and demonstration project lead construction

(1) The national green building demonstration area – Guangming New Area

“Guangming” New Area is located in the northwest of Shenzhen City, with a total area of 156.1 km². It is one of the “four new cities” put forward by Shenzhen City in 2007 for the development, and is positioned as “ecological high-tech industry new city”. In 2008, the Shenzhen Municipal Government signed an agreement with the Ministry of Housing and Urban-Rural Construction to establish Guangming New Area as a pilot project for the construction of “National Green Building Demonstration Zone” to explore the experience of building green buildings in China. In January 2009, Shenzhen Construction Bureau and Guangming New Area Administrative Committee formulated the *Guangming New Area Green Building Demonstration Project Construction Management Trial Rules* to actively promote the construction of various demonstration projects in Guangming New Area, so as to promote the proportion of green buildings reaching more than 80% in 32 km² green building demonstration areas.

(2) Green building star demonstration project – Longyueju affordable housing

Longyueju affordable housing is located in Longhua New Area of Shenzhen City, adjacent to Shenzhen North Railway Station. It is a large residential area invested by

Shenzhen Municipal Government to solve the housing problems of talented people and low-and-middle-income families. It is one of the “ten livelihood projects” in Shenzhen in 2010, and it is also the largest comprehensive affordable housing project in Shenzhen up to now. Under the requirements of the *12th Five-Year Plan for Building Energy Conservation and Green Building in Shenzhen* and the *Development Plan for Housing Security in Shenzhen (2011-2015)* for the overall green building construction in Shenzhen as well as the energy conservation and emission reduction targets of Longhua New Area and the construction of green building, the affordable housing of Longyueju, as the pilot project for affordable housing that first constructed following green building standard in Shenzhen, has set an example for Shenzhen to build a “green building capital” and a “green building demonstration city” (Fig. 5).

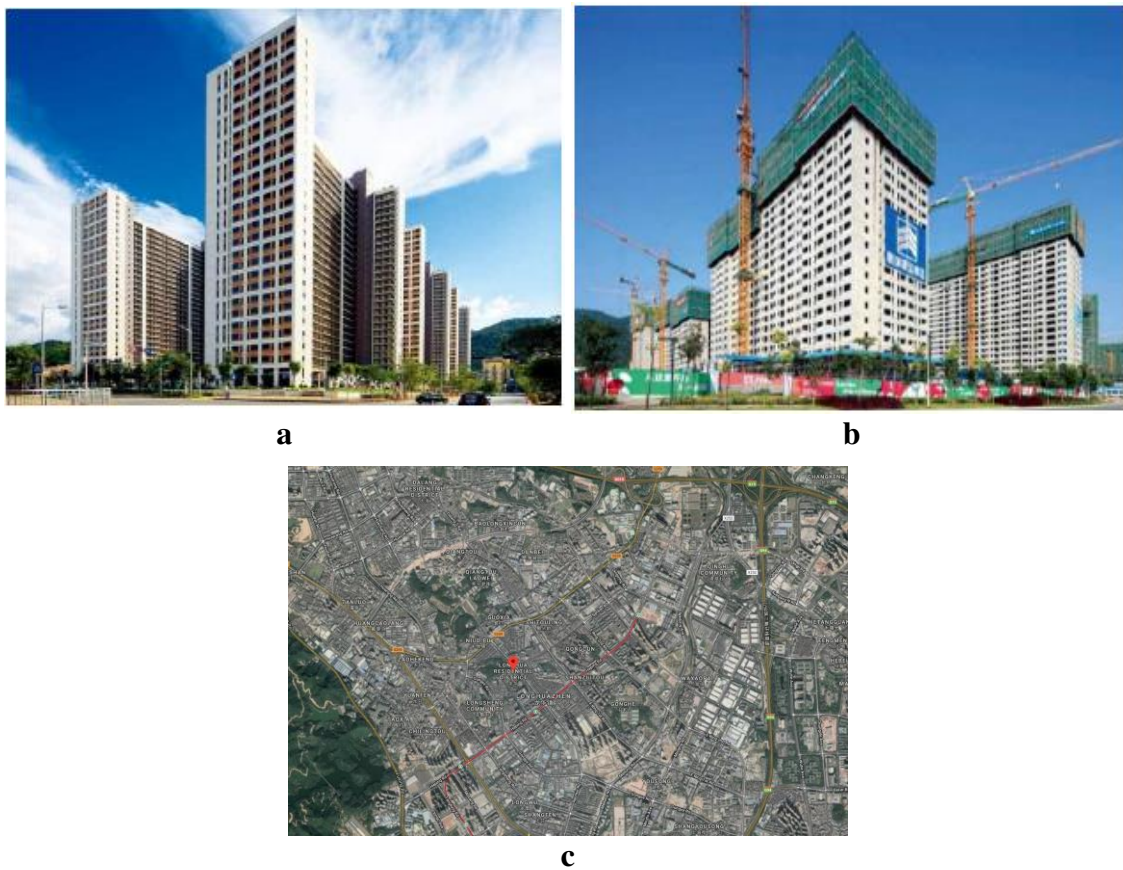


Figure 5. *a.* The real picture of Longyueju, from Baidu image. *b.* Construction process and construction site, from Baidu image. *c.* The location of Longhua New Area, Shenzhen, from Google earth

Conclusion

Based on the above research results of green building development and its influencing factors, the main influencing factors behind the differences of urban green building development in China are analyzed through the multiple regression model of green building influence, and an empirical analysis is made through the experience of Shenzhen green building development. The following conclusions are drawn:

(1) There are great differences between regions and between cities in the overall development of green building projects. At present, the green building market in China is mainly concentrated in the eastern coastal areas, as well as some municipalities directly under the central government and provincial capitals. It suggests that the development of green building in these cities is to some extent jointly affected by the urban economic environment, green building related policy environment and technology environment and other factors;

(2) The greening evaluation system and its evaluation model for sustainable development of housing construction enterprises are established by using intuitionistic fuzzy analytic hierarchy process. The empirical analysis of green evaluation of China Construction Corporation shows that the evaluation system and model established are both effective (Zhu, 2010). It is calculated that the greening level of China Construction Corporation is a super excellent greening grade.

(3) The strong government support has a significant impact on the development of green buildings in cities. Through the empirical study on the development of green buildings in Shenzhen, it is found that the government can effectively promote the development of urban green buildings by adopting a series of relevant laws and policies, combined with incentives, technology promotion, public publicity and other actions. Based on the analysis and summary of the construction experience of Shenzhen green building demonstration zone and demonstration project, the advanced experience of Shenzhen green building development can provide references for policy makers and implementers in other cities.

This paper combines data and theory through analysis method. Intuitionistic fuzzy analytic hierarchy process is an organic combination of intuitionistic fuzzy set theory and analytic hierarchy process. Based on the case of Shenzhen, this paper summarizes the factors affecting the development of green building, and provides methods and paths for future research.

Acknowledgement. Much gratitude is owed to the Zhuhai College of Jilin University for funding this study (Zhuhai College of Jilin University three levels of talent construction project funding ; Project of 100 people project training program for young teachers, Zhuhai College of Jilin University) and providing relevant research assistance.

REFERENCES

- [1] Aggarwal, R., Singh, S. (2018): A hybrid approach for supplier selection based on revised data envelopment analytic hierarchy process. – *International Journal of Operational Research* 31(4): 478-509.
- [2] Alwan, Z., Jones, P., Holgate, P. (2017): Strategic sustainable development in the uk construction industry, through the framework for strategic sustainable development, using building information modelling. – *Journal of Cleaner Production* 140(1): 349-358.
- [3] Baden, D., Prasad, S. (2016): Applying behavioural theory to the challenge of sustainable development: using hairdressers as diffusers of more sustainable hair-care practices. – *Journal of Business Ethics* 133(2): 1-15.
- [4] Broman, G. I., Robèrt, K. H. (2017): A framework for strategic sustainable development. – *Journal of Cleaner Production* 140: 17-31.
- [5] Brown, L. D. (1991): Bridging organizations and sustainable development. – *Human Relations* 44(8): 807-831.

- [6] Chong, H. Y., Wang, X. (2016): The outlook of building information modeling for sustainable development. – *Clean Technologies & Environmental Policy* 18(6): 1-11.
- [7] Edgren, L. (2017): Contemporary Conservation Theory for Sustainable Development of Cultural Heritage Objects. – *International Journal of the Inclusive Museum* 10(1): 1-8.
- [8] Gao, G., Wang, T. (2018): Study on the relationship between the opening of environmental tax and the prevention and control of air pollution in China. – *American Institute of Physics Conference Series* 1944. <https://doi.org/10.1063/1.5029789>.
- [9] Hu, A. (2018): *China's Road and China's Dream*. – Springer Nature, Singapore.
- [10] Huang, X., Shi, X. (2017): Evaluation of supply capacity of food emergency logistics in natural disaster. – *International Conference on Logistics, Informatics and Service Sciences*, 24-27 July 2016. 10.1109/LISS.2016.7854588.
- [11] Kopnina, H. (2016): Victims of unsustainability: a challenge to sustainable development goals. – *International Journal of Sustainable Development & World Ecology* 23(2): 113-121.
- [12] Li, B., Gao, Y. (2015): Application of the improved fuzzy analytic hierarchy process for landslide hazard assessment based on RS and GIS. – *International Conference on Intelligent Earth Observing and Applications (Vol. 9808)*. International Society for Optics and Photonics. DOI: 10.1117/12.2207381.
- [13] Pang, B., Lin, B., Lv, Q., Liu, Y. (2016): The application of fuzzy theory in the evaluation and recruitment of university interpretation teachers. – *International Conference on Natural Computation, Fuzzy Systems and Knowledge Discovery (pp. 1108-1113)*, IEEE.
- [14] Rahmati, O., Pourghasemi, H. R., Zeinivand, H. (2016): Flood susceptibility mapping using frequency ratio and weights-of-evidence models in the Golastan province, Iran. – *Geocarto International* 31(1): 42-70.
- [15] Rodríguez, A., Ortega, F., Concepción, R. (2016): A method for the evaluation of risk in it projects. – *Expert Systems with Applications* 45(C): 273-285.
- [16] Shafiei, M. W. M., Abadi, H., Osman, W. N. (2017): The indicators of green buildings for Malaysian property development industry. – *International Journal of Applied Engineering Research* 12(10): 2182-2189.
- [17] Sharma, R., Fantin, A. R., Prabhu, N., Guan, C., Dattakumar, A. (2016): Digital literacy and knowledge societies. – *Telecommunications Policy* 40(7): 628-643.
- [18] Stafford-Smith, M., Griggs, D., Gaffney, O., Ullah, F., Reyers, B., Kanie, N. et al. (2017): Integration: the key to implementing the sustainable development goals. – *Sustainability Science* 12(6): 911-919.
- [19] Takahashi, I. (1990): AHP applied to binary and ternary comparisons. – *Journal of the Operations Research Society of Japan* 33(3): 199-206.
- [20] Wang, X. (2017): 50. Research on cost benefit index system of green reconstruction based on existing buildings. – *Boletín Técnico* 55(10): 339-346.
- [21] Wu, P., Song, Y., Shou, W., Chi, H., Chong, H. Y., Sutrisna, M. (2017): A comprehensive analysis of the credits obtained by LEED 2009 certified green buildings. – *Renewable & Sustainable Energy Reviews* 68: 370-379.
- [22] Wu, S. R., Fan, P., Chen, J. (2016): Incorporating culture into sustainable development: A cultural sustainability index framework for green buildings. – *Sustainable Development* 24(1): 64-76.
- [23] Wuelser, G., Pohl, C. (2016): How researchers frame scientific contributions to sustainable development: a typology based on grounded theory. – *Sustainability Science* 11(5): 789-800.
- [24] Xiu, Y., Fu, Y., Cui, W. (2017): Research on the sustainable development of china's foreign trade enterprises under the background of the change of the macroeconomic situation of the international economy. – *Journal of Computational & Theoretical Nanoscience* 14(6): 2733-2738.

- [25] Yang, F. (2015): Contemporary construction of ecological civilization: from ecological crisis to ecological governance. – *Chinese Journal of Urban & Environmental Studies* 03(04): 1550030.
- [26] Yang, G., Zhou, Y. (2010): Research on the government incentive of green buildings in China. – *International Conference on Management and Service Science* (pp. 1-5), IEEE.
- [27] Yang, Y., Xu, W., Jing, P. (2012): The fuzzy comprehensive evaluation of financial ecological environment of Kunming. – *International Conference on Information Management, Innovation Management and Industrial Engineering* (Vol. 2, pp. 62-65), IEEE.
- [28] Yuan, Y., Yu, X., Yang, X., Xiao, Y., Xiang, B., Wang, Y. (2017): Bionic building energy efficiency and bionic green architecture: a review. – *Renewable & Sustainable Energy Reviews* 74: 771-787.
- [29] Zhang, C., Li, W., Yang, H. (2012): A new drug risk assessment model of comprehensive hospitals. – *International Conference on Biomedical Engineering and Biotechnology* (pp. 1165-1168), IEEE Computer Society.
- [30] Zhou, S. (2010): The transformation and thinking of management concept in construction industry based on sustainable development. – *International Conference on Management and Service Science* (pp. 1-5), IEEE.
- [31] Zhou, T., Wang, Y. P., Wang, F. (2009): A dynamic assessment of Ecological Footprint and Biocapacity in Guangzhou using RS and GIS. – *Urban Remote Sensing Event* (pp. 1-9), IEEE.
- [32] Zhou, Y., Zhao, X. G. (2013): Safety Management of Oil Depot Based on Fuzzy Analytic Hierarchy Process. – In: *2012 International Conference on Information Technology and Management Science (ICITMS 2012) Proceedings* (pp. 67-72). Springer, Berlin, Heidelberg.
- [33] Zhu, W., Shi, M. (2017): Study on labor relations from the perspective of “The belt and road initiative”. – *International Conference on Logistics, Informatics and Service Sciences*, IEEE.
- [34] Zhu, Y. Y. (2010): Research on the evaluation of customer satisfaction under B2C e-commerce. – *International Conference on Networking and Digital Society* (Vol. 1, pp. 601-604), IEEE.

ECOLOGY ENVIRONMENT RESEARCH ABOUT CARBON EMISSION EFFICIENCY IN CHINA BASED ON A NOVEL SUPER EPSILON-BASED MEASURES (SEBM) MODEL

SONG, A.¹ – YANG, X.² – ZHANG, X.³ – WANG, F.⁴ – HUANG, W.^{1*}

¹*School of Management, Huazhong University of Science and Technology
Wuhan 430074, China*

²*School of Management and Economics, North China University of Water Resources and
Electric Power, Zhengzhou 450045, China*

³*School of Business, Zhengzhou Vocational College of Finance and Taxation
Zhengzhou 450048, China*

⁴*School of Economics and Trade, Zhengzhou Institute of Technology
Zhengzhou 450044, China*

**Corresponding author
e-mail: huangwl@mail.hust.edu.cn*

(Received 18th Sep 2018; accepted 26th Nov 2018)

Abstract. With China's rapid economic development, the carbon emission has become a serious issue and the evaluation of carbon emission efficiency has drawn the attention of academia. Although the Data Envelopment Analysis (DEA) method is widely used in determining carbon emission efficiency, there are many limitations in the traditional DEA mathematical models including the original elements information loss due to the change of the proportion of the elements, too narrow efficiency boundaries, and the existence of undesirable outputs. As a result, a novel super epsilon-based measures (SEBM) carbon emission efficiency evaluation model is expected to overcome the limitations in the traditional carbon emission efficiency determination models, based on which the carbon emission efficiency of China is analyzed from time and spatial dimensions respectively. Finally, contrastive empirical analysis results of SEBM model and other classical DEA models indicate that the former has remarkable superiority over the other models. Based on the experimental results, it is found that China's carbon emission efficiency is inversely proportional to the level of economic development, and carbon emission efficiency values in China have generally increased, which highlights the significance of energy-saving emission reduction policies.

Keywords: *data envelopment analysis (DEA), carbon emission efficiency, super epsilon-based measures (SEBM) model, empirical analysis (EA), model efficiency evaluation*

Introduction

The competition between traditional energy and new energy has been intensifying. Traditional energy does not have the clean and pollution-free features of hydropower, solar energy, wind energy and other new energies (Wang et al., 2016). By contrast, traditional energies such as oil, coal and natural gas still occupy the principal position in global energy (Xu et al., 2014). A major concern of traditional energy sources is that carbon emissions are considered. Since energy conservation and emission reduction regulations were proposed in 2006, carbon emission reduction and carbon emission efficiency improvement are used as metrics by all sectors of society (Roar Adland et al., 2017). The emergence of electric vehicles is caused by industrial circles (Yun et al., 2017). Research on carbon emission efficiency is also on the rise (Henson et al., 2015). China, as the world's largest developing

country, has continuously and rapidly expanded its economy since the late 1980s, maintaining an annual growth rate of more than 9% for over three decades (Wang et al., 2015). China's extensive economic growth is condemned to have high-energy consumption, high carbon emissions and other issues (Wang et al., 2013). Taking carbon emission efficiency as the entry point, this study takes the information from all of the regions in China as data support, conducts innovation research expansion on the most popular carbon emission efficiency model from the academic literature, and comparatively analyses on the carbon emission efficiency model in 29 provinces and cities in China (Liu et al., 2014).

Our study aims to design an SEBM model to evaluate carbon emission efficiency, which can solve the problems which other models cannot solve. There are two streams of relevant literature surrounding this research: the focus issues of carbon emission efficiency in the academic literature and the data envelopment analysis (DEA)-based carbon emission efficiency evaluation models.

Early researchers primarily used the ratio of total carbon emissions together with a select factor as the evaluation index of carbon efficiency, namely, single element carbon efficiency. For example, the carbon emissions efficiency, known as carbon productivity, was defined as the ratio of GDP and the carbon emissions during a select period (Kaya and Yokobori, 1993). Later, carbon index (carbon emissions per unit energy consumption), energy intensity (energy consumption per unit of GDP) and carbon emissions intensity index (CO₂ emissions per unit of GDP) were used as the evaluation index to measure carbon efficiency (Mielnik and Goldemberg, 1999; Ang, 1999; Sun, 2005). In addition, new evaluation indices such as industrialization cumulative per capita emissions, and carbon emissions by per capita per unit GDP were found to better reflect scientific, fair and reasonable principles, so they became more reasonable indices for the measurement of carbon efficiency evaluation (Zhang et al., 2008). Single factor index evaluation carbon efficiency is easy to understand and operate, but there are different opinions about its usefulness, because of the diversity of the measurement index (Zhou et al., 2010). Therefore, many researchers have relied on total factor efficiency to determine carbon emissions. For instance, the carbon emissions efficiency should be integrated into the three contexts of energy consumption, economic development and carbon emissions; so that the evaluation results are comprehensive and rational (Ramanathan, 2002). And slack variables were used to measure the comprehensive performance of carbon emissions of 30 OECD countries during the period of 1998-2002 (Zhou et al., 2006). Furthermore, bidirectional causality between economic growth and energy use and between energy use and carbon emissions (Wang et al., 2016).

In recent years, domestic and foreign researchers have generally used DEA to examine the efficiency of carbon emissions within the framework of the total factor. Ramanathan (2005, 2006) integrated the four indices of CO₂ emissions using DEA, and obtained the CO₂ emissions efficiency of 17 countries in the Middle East and North Africa. Marklund and Samakovlis (2007) estimated the cost of carbon emissions reduction of the European countries by building a distance-direction function based on the DEA. Zhou et al. (2010) measured the carbon emissions efficiency of 18 countries with the highest global CO₂ emissions using MCPI, and constructed a correlation analysis of the influencing factors of carbon emissions efficiency. Wang and Zhou (2012) used the DEA method to measure the carbon emission efficiency of each province in China from 2001 to 2007 and concluded that China's carbon emission efficiency varied. Zhou and Nie used the slack-based measure

(SBM) to quantify the inter-provincial industrial carbon emission efficiency of 30 provinces in China and analyse the similarities and differences (Grinsven et al., 2016).

From the perspective of a carbon emission efficiency model, the academic community relies on DEA to analyze carbon emission efficiency (Niu et al., 2016). The model development process first adopted the CCR-DEA model and then the BCC-DEA model, which examines carbon emission efficiency in constant returns to scale (CRS) and variable returns to scale (VRS) (Cranmer, 2016). After the DEA model developed the SBM and other models to consider the non-expected output, researchers have mostly used the SBM-DEA model or other relevant models supported by it. For example, carbon emission efficiency is calculated using the SBM model; the stochastic frontier analysis or redundancy analysis is used to revise the efficiency value, and the three-stage DEA model of SBM efficiency, Tobit regression or Malmquist index is used to analyze the carbon emission efficiency (Kim, 2016). Alternatively, the SBM from an operational research perspective and statistical regression are combined to examine carbon emission efficiency (Baleentis et al., 2016), but research on the applicability of the model is not comprehensive. Some scholars have proposed the super-efficiency-DEA (SE-DEA) to enlarge the efficiency boundary of carbon emission and effectively eliminate the limitation of the efficiency value boundary of the original DEA model (Szczepańska and Wiśniewska, 2012). Some scholars have partially supplemented the DEA model from the radial direction and non-radial direction angles of the directional distance function. In 2016, a series of significant progress in theory was made: Tone summarised the shortcomings of CRS and SBM models and proposed the epsilon-based measure model (EBM), which solves the problem of the proportional change in factors and the original ratio information of loss efficiency frontier (Andrie and Ursu, 2016). However, the efficiency boundary remained restricted, and the model was still insufficient. In consideration of the advantages and disadvantages of the CCR-BCC-SBM-EBM-SE model, this study proposes the SEBM model (Bretschger and Valente, 2016), which can effectively expand the efficiency of the boundary and solve the factor changes in the same proportion, the original ratio information of factors in the leading edge of loss efficiency and other issues (Shao and Wang, 2016). The current study also provides further theoretical and data support for other scholars in studying carbon emission efficiency.

The article structure is presented as follows: in Section 2, the classical mathematical models in data envelopment analysis (DEA) are presented, including the Charnes, Cooper and Rhodes (CCR) model, the Banker, Charnes and Cooper (BCC) model, the super-efficiency-data envelopment analysis (SE-DEA) model and the epsilon-based measure (EBM) model. Then, a novel super epsilon-based measures (SEBM) model is proposed further in Section 3. Section 4 discusses and analyses the differences in carbon emission efficiency in 29 regions in China from 2004 to 2014, where the characteristics of classical DEA models of CCR, EBM, SE models and the proposed SEBM model are comparatively analyzed from the time and spatial dimension. Section 5 concludes the paper.

Materials and methods: theoretical model establishment

The DEA method is widely used in determining carbon emission efficiency (Xian and Huang, 2016). This section discusses the CCR-DEA, BCC-DEA, SE-DEA, EBM-DEA and SEBM-DEA models from a theoretical perspective. From the variable perspective, the DEA model has an input-oriented angle and an output-oriented angle but no guidance angle (Dzonzi-Undi and Li, 2016; Obeng et al., 2016; Vaidya and

Campbell, 2016). This study only provides the theoretical formula of the three angle models of the SEBM model.

Suppose we have a set of independent homogeneous decision-making units denoted by $DMU_j (j = 1, 2, \dots, n)$. Each observation $DMU_j (j = 1, 2, \dots, n)$ uses m inputs $x_{ij} (i = 1, 2, \dots, m)$ to produce s outputs $y_{rj} (r = 1, 2, \dots, s)$. DMU_o represents one of the n DMUs under evaluation, and x_{io} and y_{ro} are the i^{th} input and r^{th} output for DMU_o , respectively.

CCR model

The technical efficiency of the O^{th} DMU can be calculated by the input-oriented CCR (Charanes et al., 1978) model (Eq.1):

$$\begin{aligned} & \text{Min } \theta_o \\ & \text{subject to } \sum_{j=1}^n x_{ij} \lambda_j \leq \theta_o x_{io}, i = 1, 2, \dots, m, \\ & \sum_{j=1}^n y_{rj} \lambda_j \geq y_{ro}, r = 1, 2, \dots, s, \\ & \lambda_j \geq 0, j = 1, 2, \dots, n. \end{aligned} \tag{Eq.1}$$

where v_i and u_r are the weights assigned to input i ($i = 1, 2, \dots, m$) and output r ($r = 1, 2, \dots, s$), respectively, and λ is the weight multiplier of each DMU. In the above formula, the optimal solution θ_o^* represents the efficiency value $\theta_o^* \in (0, 1]$.

BCC model

The BCC model assumes that the production process belongs to a fixed-scale gain. That is, when the input amount increases in geometric proportion, the output also increases in geometric proportion (Sarkar, 2013). However, the actual production process may also belong to the state of increasing returns to scale or decreasing returns to scale. To analyze the changes in returns to scale of the DMUs, Banker et al. (1984) proposed the BCC model (Eq. 2):

$$\begin{aligned} & \text{Min } \theta_o \\ & \text{subject to } \sum_{j=1}^n x_{ij} \lambda_j \leq \theta_o x_{io}, i = 1, 2, \dots, m, \\ & \sum_{j=1}^n y_{rj} \lambda_j \geq y_{ro}, r = 1, 2, \dots, s, \\ & \sum_{j=1}^n \lambda_j = 1, \\ & \lambda_j \geq 0, j = 1, 2, \dots, n. \end{aligned} \tag{Eq.2}$$

Compared with the CCR model, the constraint $\sum_{j=1}^n \lambda_j = 1$ is added to the BCC model, so that the production scale of the projection point is at the same level as the scale of production being evaluated.

SE-DEA model

If the effective DMUs are too affected by the effect of data on the CCR model, no comparison exists. Andersen and Petersen (1993) removed the assessed DMUs from the efficient boundary and took the remaining DMUs as basis to form a new efficiency boundary and calculate the distance from the removed DMU to the new efficient boundary. Thus, all of the DMUs achieved complete sequencing, that is, the super-efficiency model. The SE-DEA model (Eq. 3) based on the CCR model is expressed as follows:

$$\begin{aligned}
 & \text{Min } \theta_o \\
 & \text{subject to } \sum_{\substack{j=1 \\ j \neq o}}^n x_{ij} \lambda_j \leq \theta_o x_{io}, i = 1, 2, \dots, m, \\
 & \sum_{\substack{j=1 \\ j \neq o}}^n y_{rj} \lambda_j \geq y_{ro}, r = 1, 2, \dots, s, \\
 & \sum_{\substack{j=1 \\ j \neq o}}^n \lambda_j = 1, \\
 & \lambda_j \geq 0, j \neq o.
 \end{aligned} \tag{Eq.3}$$

Banker and Chang (2006) demonstrated that the super-efficiency model is highly susceptible to outliers, and thus, the model could detect the existence of outliers in the dataset. In a number of datasets of effective DMUs, SE-DEA effectively was shown to amplify the efficiency boundary, and many practical problems were analyzed effectively because of the limitation of the previous efficiency boundary. The SE-DEA reveals the potential for these practical applications.

EBM model

In 2010, Tone argued that the same rate reduction of input factor in traditional DEA (CCR) models violates physical truth and that the SBM model has the original ratio information of factors aside from loss efficiency. He proposed the EBM model which overcame the above shortcomings. The model's theoretical formulas are expressed as follows (Eq. 4):

$$\begin{aligned}
 & \gamma^* = \text{Min } \theta_o - \varepsilon^- \sum_{i=1}^m \frac{w_i^- s_i^-}{x_o} \\
 & \text{subject to } \sum_{j=1}^n x_{ij} \lambda_j + s_i^- = \theta_o x_{io}, i = 1, \dots, m, \\
 & \sum_{j=1}^n y_{rj} \lambda_j \geq y_{ro}, r = 1, \dots, s, \\
 & \lambda_j, s_i^- \geq 0, \forall i, j, r.
 \end{aligned} \tag{Eq.4}$$

This formulation indicates that γ^* is obtained as the optimal internally dividing value between the radial θ_o and the non-radial term $\varepsilon^- \sum_{i=1}^m \frac{w_i^- s_i^-}{x_o}$, where s_i^- is the amount

of slack in the i^{th} input, and w_i^- is the i^{th} input weight and satisfies $\sum_{i=1}^m w_i^- = 1 (w_i^- \geq 0, \forall i)$. ε^- is a key parameter in the range of $[0,1]$, and it indicates the importance of the non-radial part in the calculation of the efficiency value. If $\varepsilon^- = 0$, the EBM model will be simplified as the input-oriented CCR model. If $\theta_o = \varepsilon^- = 1$, the EBM model will be transformed into the SBM model. Before calculating the EBM efficiency scores, we should first estimate the value of the core parameters ε^- and w_i^- . We determine ε^- and w_i^- using Pearson's correlation coefficient (Tavana et al., 2013; Tone and Tsutsui, 2010).

Results: the proposed SEBM model

The theoretical analysis and research on the CCR, BCC, SEDEA and EBM models are presented. To overcome these three problems, first, the input efficiency should have the same reduction rate. Second, if too many effective units exist, the actual problems will not be effectively analyzed. Third, the original ratio information of the factor of the leading edge of loss efficiency should be obtained. In this study, the SEBM model is presented, and the theoretical formula of the SEBM model is given in three aspects:

Input-orientation (Eq. 5):

$$\begin{aligned}
 \gamma^* = \text{Min } & \theta_o - \varepsilon^- \sum_{i=1}^m \frac{w_i^- s_i^-}{x_o} \\
 \text{subject to } & \sum_{\substack{j=1 \\ j \neq o}}^n x_{ij} \lambda_j + s_i^- = \theta_o x_{io}, \quad i = 1, \dots, m, \\
 & \sum_{\substack{j=1 \\ j \neq o}}^n y_{rj} \lambda_j \geq y_{ro}, \quad r = 1, \dots, s, \\
 & \sum_{\substack{j=1 \\ j \neq o}}^n \lambda_j = 1, \\
 & \lambda_j, s_i^- \geq 0, \quad \forall i, j, r.
 \end{aligned} \tag{Eq.5}$$

Output-orientation (Eq. 6):

$$\begin{aligned}
 \gamma^* = \text{Min } & \frac{1}{\varphi_o - \varepsilon^+ \sum_{i=1}^s \frac{w_i^+ s_i^+}{x_o}} \\
 \text{subject to } & \sum_{\substack{j=1 \\ j \neq o}}^n x_{ij} \lambda_j \geq x_{io}, \quad i = 1, \dots, q, \\
 & \sum_{\substack{j=1 \\ j \neq o}}^n y_{rj} \lambda_j - s_r^+ = \varphi_o y_{ro}, \quad r = 1, \dots, s, \\
 & \sum_{\substack{j=1 \\ j \neq o}}^n \lambda_j = 1, \\
 & \lambda_j, s_r^+ \geq 0, \quad \forall i, j, r.
 \end{aligned} \tag{Eq.6}$$

In the above model, the reciprocal of γ^* is obtained as the optimal internally dividing value between the radial φ_o and the non-radial term $\varepsilon^+ \sum_{i=1}^m \frac{w_i^- s_i^-}{x_o}$, where s_i^+ is the amount of slack in the i^{th} output, and w_i^+ is the i^{th} output weight and satisfies $\sum_{i=1}^m w_i^+ = 1 (w_i^+ \geq 0, \forall i)$. ε^+ is a key parameter in the range of [0,1]. This indicates the importance of the non-radial part in the calculation of the efficiency value.

Non-orientation (Eq. 7):

$$\gamma^* = \text{Min} \frac{\theta_o - \varepsilon^- \sum_{i=1}^n \frac{w_i^- s_i^-}{x_o}}{\varphi_o - \varepsilon^+ \sum_{i=1}^s \frac{w_i^+ s_i^+}{x_o}}$$

subject to

$$\sum_{\substack{j=1 \\ j \neq o}}^n x_{ij} \lambda_j + s_i^- = \theta_o x_{io}, \quad i = 1, \dots, m,$$

$$\sum_{\substack{j=1 \\ j \neq o}}^n y_{rj} \lambda_j - s_r^+ = \varphi_o y_{ro}, \quad r = 1, \dots, s,$$

$$\sum_{\substack{j=1 \\ j \neq o}}^n \lambda_j = 1,$$

$$\lambda_j, s_i^-, s_r^+ \geq 0, \quad \forall i, j, r.$$

(Eq.7)

The SEBM model effectively solves several problems of the DEA model. Regarding applicability, the expansion of an efficient boundary can be applied in more datasets. SEBM can be applied in an actual situation to remove the ratio change restrictions of the input elements. System errors can be avoided without loss of the original data information.

Discussion: empirical analysis

Data description

In this study, Chinese human capital stock and total energy consumption in 2017 are taken as input factors. Output indicators include GDP and carbon emissions, which are desirable outputs in the CCR/BCC/SE model and are undesirable outputs in the EBM and SEBM models. The input and output data are obtained from the ‘China Statistical Yearbook’ and ‘China Energy Statistical Yearbook’. The basic descriptive statistics of the 29 regions in China are shown in *Table 1*.

Spatial dimension analysis

In this section, we first calculate the optimal value of each DMU using CCR, BCC, SE-DEA, EBM and SEBM models under CRS and VRS. The results are shown in *Tables 2* and *3*, respectively. We then analyze the differences in carbon emission efficiency in 29 regions of China from the spatial dimension. According to the spatial distribution, the efficiency value in the west is the highest, followed by the middle, and the lowest in the east. This finding suggests that the technology and management level

in the west is relatively high. To reflect clearly the regional variability of the four models results, we illustrate them in *Figures 1* and *2*.

Table 1. *Descriptive statistics*

Statistics	Minimum (M)	Maximum (X)	Average value (E)	Standard error	Standard deviation
GDP (billion yuan)	113.52	16413.66	3196.5712	162.21195	2897.19812
Labor force (ten thousand people)	94.10	4500.05	1002.3773	41.45137	740.34507
Capital stock (ten thousand yuan)	178.68	48416.44	7317.7862	421.18654	7522.63220
Total energy consumption (million tons of standard coal)	742.48	38899.25	11990.4673	437.90044	7821.15186
Carbon emission (ton)	343.47	34923.51	9373.4433	381.42376	6812.44625

Table 2. *Carbon emission efficiency in China's provinces: constant returns to scale*

	Regions	CCR-DEA	Ranking	EBM-DEA	Ranking	SE-DEA	Ranking	SEBM-DEA	Ranking
Central regions	Henan	0.482	14	0.577	21	0.482	14	0.577	21
	Hubei	0.425	18	0.609	17	0.425	18	0.609	17
	Hunan	0.545	11	0.785	8	0.545	11	0.785	8
	Jiangxi	0.257	28	0.457	29	0.257	28	0.457	29
	Anhui	0.399	20	0.547	23	0.399	20	0.547	23
	Shanxi	0.923	2	0.890	4	0.938	2	0.891	4
	Jilin	0.472	15	0.554	22	0.472	15	0.554	22
	Heilong jiang	0.505	13	0.644	11	0.505	13	0.644	11
Eastern regions	Beijing	0.206	29	0.651	10	0.206	29	0.651	10
	Tianjin	0.548	9	0.602	18	0.548	9	0.602	18
	Hebei	0.764	6	0.788	7	0.764	6	0.788	7
	Liaoning	0.557	8	0.628	15	0.557	8	0.628	15
	Shanghai	0.329	23	0.497	27	0.329	23	0.497	27
	Jiangsu	0.311	25	0.458	28	0.311	25	0.458	28
	Zhejiang	0.282	27	0.520	25	0.282	27	0.520	25
	Fujian	0.373	22	0.634	12	0.373	22	0.634	12
	Shandong	0.524	12	0.590	19	0.524	12	0.590	19
	Guangdong	0.318	24	0.589	20	0.318	24	0.589	20
	Hainan	0.308	26	0.522	24	0.308	26	0.522	24

Western regions	Inner Mongolia	0.907	3	0.889	5	0.919	3	0.890	5
	Guangxi	0.396	21	0.628	14	0.396	21	0.628	14
	Sichuan	0.857	4	0.989	1	0.868	4	0.991	1
	Guizhou	0.452	16	0.744	9	0.452	16	0.744	9
	Yunnan	0.745	7	0.826	6	0.745	7	0.826	6
	Shaanxi	0.442	17	0.632	13	0.442	17	0.632	13
	Gansu	0.410	19	0.498	26	0.410	19	0.498	26
	Qinghai	0.547	10	0.610	16	0.547	10	0.610	16
	Ningxia	0.842	5	0.983	2	0.842	5	0.985	2
	Xinjiang	0.978	1	0.964	3	0.996	1	0.966	3

Table 3. Carbon emission efficiency in China's provinces: variable returns to scale

	Region	BCC-DEA	Ranking	EBM-DEA	Ranking	SE-DEA	Ranking	SEBM-DEA	Ranking
Central regions	Henan	0.655	11	0.834	12	0.655	11	0.834	12
	Hubei	0.480	21	0.785	14	0.480	21	0.785	14
	Hunan	0.675	10	0.956	8	0.675	10	0.957	8
	Jiangxi	0.278	28	0.512	29	0.278	28	0.512	29
	Anhui	0.406	25	0.640	25	0.406	25	0.640	25
	Shanxi	0.986	1	0.985	4	1.018	3	0.987	5
	Jilin	0.481	20	0.660	23	0.481	20	0.660	23
	Heilong jiang	0.515	18	0.767	16	0.515	18	0.767	16
Eastern regions	Beijing	0.234	29	0.686	21	0.234	29	0.686	21
	Tianjin	0.553	16	0.665	22	0.553	16	0.665	22
	Hebei	0.969	4	0.987	3	0.981	5	0.989	4
	Liaoning	0.740	9	0.820	13	0.740	9	0.820	13
	Shanghai	0.341	27	0.611	27	0.341	27	0.611	27
	Jiangsu	0.489	19	0.764	17	0.489	19	0.764	17
	Zhejiang	0.419	23	0.690	20	0.419	23	0.690	20
	Fujian	0.381	26	0.723	19	0.381	26	0.723	19
	Shandong	0.973	3	0.957	7	0.991	4	0.958	7
	Guangdong	0.571	12	0.912	11	0.571	13	0.914	11
Hainan	0.565	14	0.619	26	0.591	12	0.624	26	
	Region	BCC-DEA	Ranking	EBM-DEA	Ranking	SE-DEA	Ranking	SEBM-DEA	Ranking
Western regions	Inner Mongolia	0.953	6	0.928	9	0.968	6	0.929	9
	Guangxi	0.410	24	0.734	18	0.410	24	0.734	18
	Sichuan	0.955	5	0.995	1	1.023	2	1.003	2
	Guizhou	0.569	13	0.963	6	0.569	14	0.964	6
	Yunnan	0.762	8	0.916	10	0.764	8	0.918	10
	Shaanxi	0.517	17	0.781	15	0.517	17	0.781	15
	Gansu	0.425	22	0.599	28	0.425	22	0.599	28
	Qinghai	0.558	15	0.659	24	0.558	15	0.659	24
	Ningxia	0.929	7	0.992	2	0.960	7	1.003	1
	Xinjiang	0.984	2	0.983	5	1.030	1	0.989	3

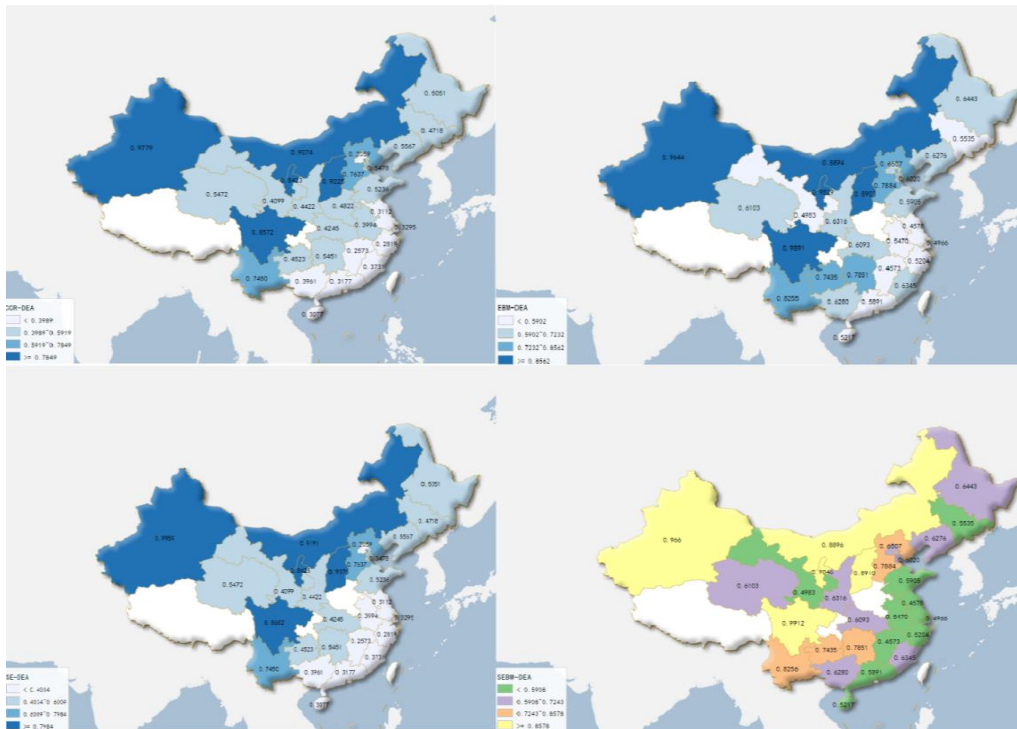


Figure 1. Spatial dimension analysis of carbon emissions efficiency in China from 2004 to 2014: constant returns to scale

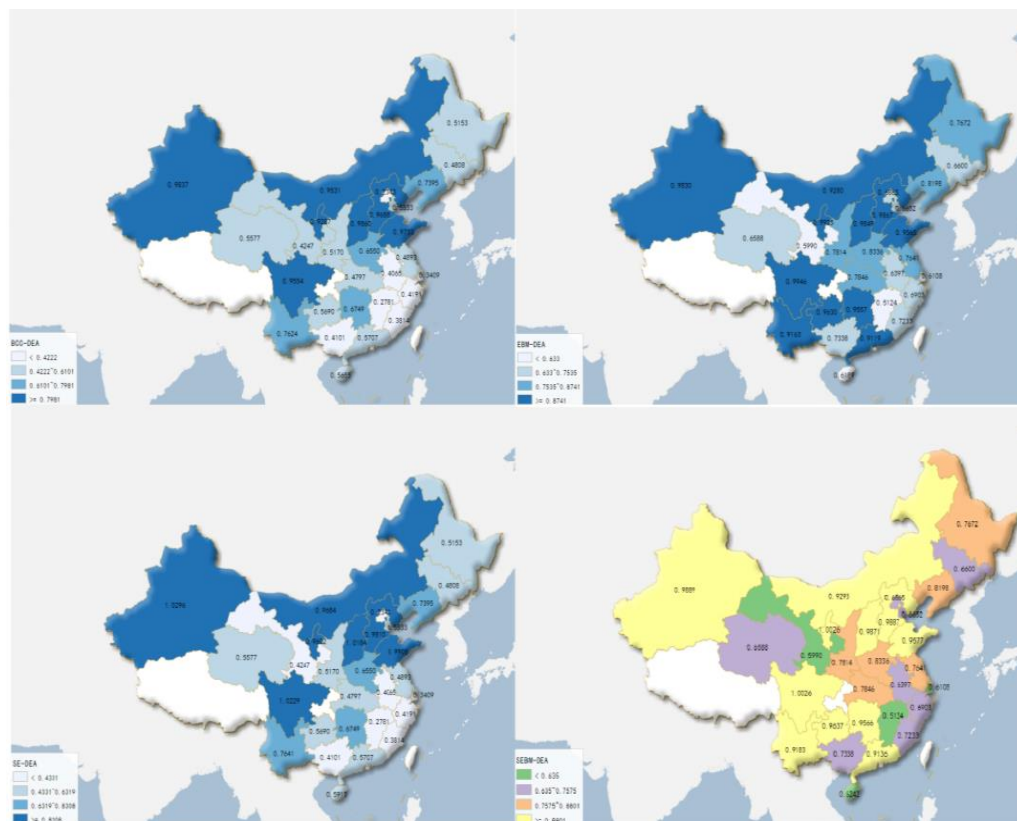


Figure 2. Spatial dimension analysis of carbon emissions efficiency in China from 2004 to 2014: variable return scale

CCR-DEA/BCC-DEA efficiency evaluation

CCR is the most basic DEA model under the CRS angle. Technical efficiency is the production efficiency of the DMU under an optimal scale. However, the DMU is mostly provided with VRS, and thus the BCC model is more suitable in real situations.

As shown in *Tables 2 and 3* and *Figures 1 and 2*, specific to the CCR model, the efficiency values in all provinces are below 1, and the DEA is not valid in all. The carbon emission efficiencies in Xinjiang, Shanxi and Inner Mongolia are above 0.9, which is relatively high. The efficiency values in Jiangxi, Beijing and Zhejiang are below 0.3, which is relatively low. This finding indicates a huge difference in carbon emission efficiency among the different provinces and that the total carbon emission efficiency in China is relatively low. The carbon emission efficiency value in the western region is high, and the efficiency values in six of the ten provinces in the western region are greater than 0.5. The carbon emission efficiency values in the eastern region are the lowest, and the efficiency values in seven of the eleven provinces are less than 0.4. The carbon emission efficiency values in the middle are ranked between those in the west and those in the east. The efficiency values in most of these provinces range from 0.4-0.55.

Specific to the BCC model, the efficiency values in all provinces are below 1. The pure technical efficiency is not valid, but the whole efficiency values are higher than those of the CCR model. The efficiency values in seven provinces are above 0.9, and Shanxi, Xinjiang and Shandong are the top three in efficiency value. The efficiency values in Jiangxi, Beijing and Shanghai are the lowest at below 0.4. In summary, the efficiency values obtained from the BCC model with VRS are applicable in actual situations.

EBM-DEA efficiency evaluation

As the assumed condition of the radial CCR model is too strict, the identified efficiency values usually differ from the actual economy conditions. Therefore, the EBM model combined with radial and non-radial characteristics can effectively solve the problems existing in the CCR model measurement.

From the CRS angle, the comparison of efficiency values of the CCR model and the EBM model shows that the EBM efficiency value is higher than the CCR efficiency value. As shown in *Tables 2 and 3* and *Figures 1 and 2*, Sichuan, Ningxia and Xinjiang are the top three in efficiency values obtained from the EBM model with the efficiency values above 0.9. Jiangxi, Jiangsu and Shanghai are at the bottom three. The ranks decrease compared with the CCR efficiency value. But the efficiency values, which are all above 0.45, increase. This result shows that the EBM model can effectively solve conditions with extreme measurement values in the CCR model with the measurement result closer to the actual economy conditions.

From the VRS angle, BCC efficiency value and EBM efficiency value indicate that the EBM efficiency value is relatively high. Sichuan, Ningxia and Hebei are the top three in efficiency values gained from the EBM model. They all increased compared with BCC efficiency value ranking. Jiangxi, Gansu and Shanghai are the bottom three. Although Shanghai, Jiangxi and Gansu are ranked in a lower position than the BCC efficiency value ranking, all efficiency values approximately increase.

SE-DEA efficiency evaluation

When the traditional DEA model measures and compares the efficiency value, there is a defect that multiple decision-making units of leading surface cannot be further compared and evaluated. However, the SE-DEA model can measure the valid DMUs of the DEA by transmitting the DMUs to the leading surface.

In the CRS angle, with respect to the basic CCR model, the average SE-DEA efficiency value in Shanxi, Inner Mongolia, Xinjiang and Sichuan in 2004–2014 decreases because the DEA in these four provinces is valid for some of the identified years. Therefore, the SE-DEA measures those years in which the leading line for production is reached. For example, as shown in *Tables 2 and 3* and *Figures 1 and 2*, the DEA of Shanxi is valid in 2004, 2005 and 2007. The CCR efficiency value is 1, and the SE-DEA efficiency values are 1.101, 1.024, 1.034 and 1.006, respectively. Therefore, the average SE-DEA efficiency value is completely improved.

In the VRS angle, the SE-DEA efficiency values in Xinjiang, Sichuan and Shanxi are relatively high at 1.030, 1.023 and 1.018, respectively. After the BCC-DEA in these regions becomes valid, further analysis is conducted using the SE-DEA, which evaluates the carbon emission efficiency in various provinces accurately.

SEBM-DEA efficiency evaluation

The SEBM model integrates the advantages of the SE-DEA model and the EBM model and further compares and analyzes the DMUs.

As shown in *Tables 2 and 3* and *Figures 1 and 2*, in the CRS angle, the average SEBM efficiency values in Shanxi, Inner Mongolia, Sichuan and Xinjiang in 2004–2014 increase compared with the EBM efficiency values because the DEA in the five provinces in 2004–2014 is valid in some years. Therefore, the SEBM further analyses the years in which the leading line for production is reached. For example, the DEA of Shanxi in 2004, 2005, 2006 and 2007 is valid, and the EBM efficiency value is 1. The SEBM further measures these four years, and the SEBM efficiency values are 1.003, 1.003, 1.001 and 1.001, respectively. Therefore, the average SEBM efficiency value is improved overall. Compared with the SE-DEA and SEBM efficiency values in the four years, the SEBM efficiency value is lower than the SE-DEA efficiency value, and the differences in the four years are lessened. The SEBM model is not only able to further evaluate valid DMUs but also reduce the problem on extreme values, lessen the differences among efficiency values, and ensure that the measurement results meet the actual economic conditions.

In the VRS angle, the SEBM efficiency values in 12 provinces increases compared with the EBM efficiency value. The SEBM-DEA efficiency value in Sichuan and Ningxia is 1, but the SEBM efficiency value in Sichuan decreases compared with SE-DEA efficiency value. The SEBM efficiency value in Ningxia increases compared with the SE-DEA efficiency value in Sichuan. This result shows that the SEBM efficiency value lessens the differences in the efficiency values in various regions.

Analysis on time dimension

To analyze the results on a large scale, we divide the 29 regions into three categories: eastern, central and western. We utilize the CCR, BCC, SE-EBM and SEBM models to analyze the differences in carbon emission efficiency in the three areas and the whole country from 2004 to 2014. The results are reported in *Tables 4 and 5*. The time trends

of the calculated results in these three areas and the whole country from 2004 to 2014 are reported in *Figures 3 and 4*.

Table 4. Carbon emission efficiency in China's areas: constant returns to scale

Year	CCR-DEA model				EBM-DEA model			
	Central regions	Eastern regions	West regions	The whole country	Central regions	Eastern regions	West regions	The whole country
2006	0.541	0.423	0.692	0.548	0.687	0.609	0.816	0.702
2007	0.551	0.432	0.685	0.552	0.683	0.595	0.814	0.695
2008	0.539	0.436	0.687	0.551	0.666	0.597	0.816	0.692
2009	0.523	0.421	0.671	0.535	0.645	0.584	0.786	0.670
2010	0.512	0.444	0.678	0.544	0.625	0.594	0.777	0.666
2011	0.497	0.426	0.678	0.532	0.609	0.583	0.772	0.655
2012	0.475	0.411	0.656	0.513	0.595	0.581	0.754	0.645
2013	0.410	0.363	0.579	0.450	0.527	0.557	0.692	0.595
2014	0.393	0.345	0.571	0.436	0.537	0.550	0.679	0.591

Year	SE-DEA model				SEBM-DEA model			
	Central regions	Eastern regions	West regions	The whole country	Central regions	Eastern regions	West regions	The whole country
2004	0.544	0.405	0.664	0.533	0.701	0.610	0.817	0.706
2005	0.540	0.414	0.689	0.544	0.689	0.619	0.820	0.708
2006	0.545	0.423	0.700	0.552	0.687	0.609	0.817	0.702
2007	0.552	0.432	0.685	0.552	0.683	0.595	0.814	0.695
2008	0.539	0.436	0.693	0.553	0.666	0.597	0.816	0.692
2009	0.523	0.421	0.671	0.535	0.645	0.584	0.786	0.670
2010	0.512	0.444	0.679	0.544	0.625	0.594	0.777	0.666
2011	0.497	0.426	0.689	0.536	0.609	0.583	0.772	0.655
2012	0.475	0.411	0.656	0.513	0.595	0.581	0.755	0.645
2013	0.410	0.363	0.582	0.451	0.527	0.557	0.692	0.595
2014	0.393	0.345	0.572	0.436	0.537	0.550	0.680	0.591

Table 5. Carbon emission efficiency in China's areas: variable return scale

Year	BCC-DEA model				EBM-DEA model			
	Central regions	Eastern regions	West regions	The whole country	Central regions	Eastern regions	West regions	The whole country
2004	0.551	0.547	0.714	0.605	0.779	0.752	0.853	0.794
2005	0.565	0.573	0.716	0.620	0.776	0.760	0.867	0.801
2006	0.575	0.588	0.725	0.632	0.783	0.765	0.869	0.806
2007	0.587	0.595	0.726	0.638	0.787	0.766	0.877	0.810
2008	0.578	0.586	0.728	0.633	0.789	0.772	0.880	0.814
2009	0.569	0.575	0.713	0.621	0.780	0.766	0.862	0.803
2010	0.579	0.587	0.717	0.630	0.777	0.780	0.863	0.808
2011	0.587	0.577	0.723	0.630	0.777	0.783	0.874	0.813
2012	0.575	0.565	0.717	0.620	0.783	0.790	0.866	0.814
2013	0.497	0.524	0.643	0.558	0.699	0.750	0.808	0.756
2014	0.493	0.519	0.647	0.556	0.709	0.751	0.786	0.752

Year	SE-DEA model				SEBM-DEA model			
	Central regions	Eastern regions	West regions	The whole country	Central regions	Eastern regions	West regions	The whole country
2004	0.564	0.572	0.817	0.654	0.780	0.754	0.870	0.801
2005	0.568	0.573	0.730	0.626	0.776	0.764	0.869	0.803
2006	0.582	0.588	0.735	0.637	0.784	0.765	0.870	0.806
2007	0.597	0.602	0.727	0.644	0.788	0.767	0.877	0.811
2008	0.578	0.587	0.736	0.636	0.789	0.772	0.882	0.814
2009	0.569	0.575	0.713	0.621	0.780	0.766	0.862	0.803
2010	0.579	0.591	0.723	0.633	0.777	0.781	0.864	0.809
2011	0.590	0.583	0.742	0.639	0.778	0.783	0.877	0.814
2012	0.578	0.574	0.723	0.627	0.783	0.791	0.867	0.815
2013	0.497	0.525	0.646	0.559	0.699	0.750	0.809	0.756
2014	0.498	0.522	0.653	0.560	0.709	0.752	0.789	0.753

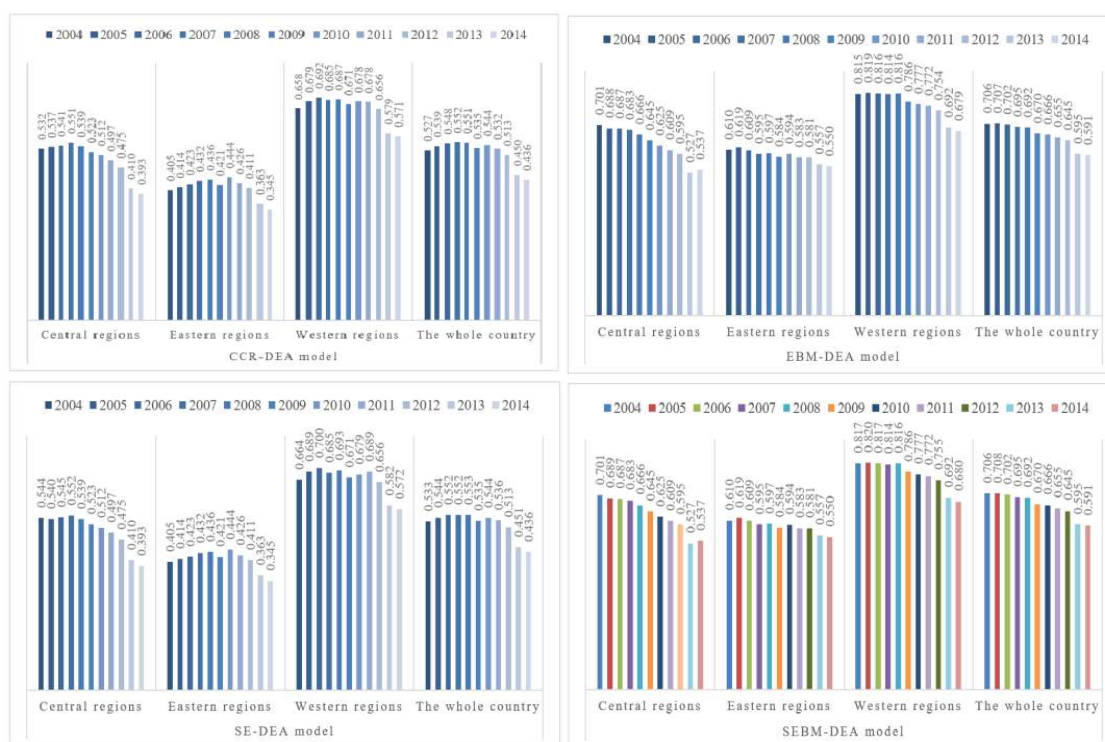


Figure 3. Time dimension analysis of carbon emissions efficiency in China from 2004 to 2014: constant returns to scale

CCR-DEA/BCC-DEA efficiency evaluation

As shown in *Tables 4* and *5* and *Figures 3* and *4*, In the CRS angle, the nationwide carbon emission efficiency value is low at 0.4–0.56. The trends increased, decreased, and then reached a peak of 0.552 in 2007. These trends tend to decrease in an increscent range in 2013. The carbon emission efficiency values are high in the west at above 0.57 and reached its peak in 2006 at 0.692. Then, the values tend to fluctuate and decrease. In the middle area, the efficiency values are 0.4–0.56 and reach its peak at 0.551 in

2007. These values decrease continuously and reach 0.393 in 2014. The efficiency values in the east are the lowest at 0.35–0.45. These values tend to increase and then decrease, reaching a peak at 0.444 in 2010, finally decreasing continuously.

In the VRS angle, the nationwide efficiency value is 0.55–0.64, which is lower than the CCR efficiency value, but still tends to fluctuate and decrease. The value reached its peak at 0.638 in 2007, decreases continuously, and then decreases in an increscent range in 2013. The efficiency value in the west is high at 0.6–0.73. It tended to fluctuate and decrease, and then increase steadily from 2004 to 2008. It started to decrease in 2009 and decreased in an increscent range in 2013. The east follows with an efficiency value of 0.5–0.6, which fluctuated to decrease and then reached its peak at 0.587 in 2007. The efficiency value in the middle area is relatively low but is not much different from that in the east. The value reached its peak at 0.587 in 2011 and decreased in an increscent range in 2013.



Figure 4. Time dimension analysis of carbon emissions efficiency in China from 2004 to 2014: variable return scale

EBM-DEA efficiency evaluation

In the CRS angle, EBM-DEA efficiency values in the east, middle, west and nationwide increase compared with the CCR-DEA efficiency value and tend to decrease steadily. The efficiency value is the highest in the west, followed by the middle, and the lowest in the east. This finding clearly shows that the difference in efficiency values in the east, middle and west gradually decreases and that EBM-DEA can decrease the difference in efficiency values in various regions and years.

The EBM-DEA efficiency value with the VRS angle is higher than the EBM-DEA efficiency value with the CRS angle. In the VRS angle, the difference in EBM-DEA

efficiency values in the east, middle, west and nationwide gradually decreases, and the efficiency values from 2004 to 2012 tended to increase steadily. As shown in *Tables 4* and *5* and *Figures 3* and *4*, the efficiency value is highest in the west (0.77–0.88), followed by the middle (0.7–0.79), and the lowest (0.75–0.79) in the east. In sum, under the VRS angle, the carbon emission efficiency values in the east, middle, west and even nationwide are relatively balanced from 2004 to 2014.

SE-DEA efficiency evaluation

In the CRS angle, the SE-DEA efficiency value in the middle, west and nationwide increases compared with CCR-DEA efficiency value because the partial CCR-DEA efficiency value of some provinces in some years is 1 and the DEA is valid. The SE-DEA model further analyses valid DMUs. As shown in *Tables 4* and *5* and *Figures 3* and *4*, for example, the SE-DEA efficiency value in the middle area in 2004, 2005, 2006 and 2007 was higher than the CCR-DEA efficiency value. The reason for this finding is that the DEA of Shanxi in the middle in 2004, 2005, 2006 and 2007 is valid, and the SE-DEA efficiency values are 1.101, 1.024, 1.034 and 1.006, respectively. Therefore, the average SE-DEA efficiency value in the middle from 2004 to 2007 was higher than the CCR-DEA efficiency value. The carbon emission efficiency value in the middle, east, west and nationwide tends to fluctuate and then decrease. The efficiency value in the west fluctuates greatly, and the carbon emission efficiency value nationwide barely fluctuates.

In the VRS angle, the SE-DEA efficiency values in the east, middle, west and nationwide increase compared with that of the BCC-DEA model. The peak efficiency value in the west appeared in 2004, thus indicating that the SE-DEA further evaluates the DMUs reaching the leading line for production.

SEBM-DEA efficiency evaluation

In the CRS angle, the SEBM-DEA efficiency values in the middle, east, and west and nationwide increase compared with the EBM-DEA efficiency values and tend to decrease year by year. The efficiency value in the west is the highest. Compared with that in the SE-DEA model, the difference in efficiency values in the west, middle and east decrease, and the difference in different regions and years decreases, as well.

In the VRS angle, the efficiency values in the middle, east, west and even nationwide decrease progressively and increase to different extents compared with EBM-DEA efficiency values. With respect to the SE-DEA model, the difference in different regions and years gradually decreases. This finding shows that the SEBM-DEA model integrates the characteristics of EBM-DEA and SE-DEA to evaluate the efficiency value of DMUs more completely than the other models.

Conclusion

First, this study thoroughly analyses the development of a theoretical model for carbon emission efficiency and finds that traditional DEA models, namely, CCR-DEA, BCC-DEA, SE-DEA and EBM-DEA, have some inadequacies. For the CCR/BCC model, the application restriction of efficient boundary is not considered. The problem of factor proportion change synchronization (non-realistic) also exists. The SBM/EBM model is unsuitable for a data cube with more valid cells. The SE-DEA model is

unsuitable for a condition in which the factors of leading surface are not changeable in the same proportion. Therefore, this study proposes the SEBM model, which can effectively solve the above-mentioned problems and contribute to carbon emission efficiency theory using data analysis in China.

Second, we analyze and calculate the carbon emission efficiency in 29 regions of China in 2004–2014 using five models: CCR-DEA, BCC-DEA, SE-DEA, EBM-DEA and SEBM-DEA. The analysis result in spatial dimension shows that China has the highest carbon emission efficiency in the west, average in the middle, and the lowest in the east. Under the CRS angle (in five models), Hebei and Liaoning rank high in the east, Shanxi ranks high in the middle and Xinjiang and Ningxia rank high in the west. Under the VRS angle (in five models), Hebei and Shandong have the highest efficiency in the east, Shanxi has the highest in the middle and Sichuan and Xinjiang are the highest in the west. The analysis result in the time dimension shows that in the CRS and VRS angles, the west has the highest efficiency, followed by the middle, and the east has the lowest. Conversely, in the CRS angle, the east and the west have a huge difference in efficiency. Since 2006, China's carbon emission efficiency values have generally increased, thus indicating that the policy of energy saving and emission reduction is effective in China.

Finally, based on the efficiency values in various regions in China, the environment has been damaged to an extreme degree, carbon emission is too high, carbon emission efficiency is the lowest in the country, and the energy utilization rate is low in the east. These results likely stem from the extensive development of the economy in recent years. Although the economy in the east is developing rapidly, the industrial sector will be further transformed to reduce carbon emission. In the middle regions, development is fast, but with the unreasonable output-input matching, the economic aggregate cannot be guaranteed to expand rapidly, and the carbon emission efficiency cannot be guaranteed to be low. Clearly, the middle regions follow behind the east in terms of economic development. The extensive economy of the west cannot continue while it is developing on a large scale. Moreover, the west should realize that its geographic position is not good and that it should pay more attention to the development of new energy and high value-added economy to develop its economy.

Acknowledgements. This paper was supported by the 2017 Henan water resources safety and clean energy collaborative management innovative technology team and the National Natural Science Foundation of China (71573086).

REFERENCES

- [1] Adland, R., Alger, H., Banyte, J., Jia, H. (2017): Does fuel efficiency pay? Empirical evidence from the drybulk timecharter market revisited. – *Transportation Research Part A: Policy and Practice* 95: 1-12.
- [2] Andersen, P., Petersen, N. C. (1993): A procedure for ranking efficient units in data envelopment analysis. – *Management Science* 39(10): 1261-1264.
- [3] Andrieş, A. M., Ursu, S. G. (2016): Financial crisis and bank efficiency: An empirical study of European banks. – *Economic Research-Ekonomska Istraživanja* 29(1): 485-497.
- [4] Ang, B. W. (1999): Is the energy intensity a less useful indicator than the carbon factor in the study of climate change. – *Energy Policy* 27(5): 943-946.

- [5] Baležentis, T., Li, T., Streimikiene, D., Baležentis, A. (2016): Is the Lithuanian economy approaching the goals of sustainable energy and climate change mitigation? Evidence from DEA-based environmental performance index. – *Journal of Cleaner Production* 116: 23-31.
- [6] Banker, R. D., Charnes, A., Cooper, W. W. (1984): Some models for estimating technical and scale inefficiencies in data envelopment analysis. – *Management Science* 30(9): 1078-1092.
- [7] Bretschger, L., Valente, S. (2016): Productivity gaps and tax policies under asymmetric trade. – *Economics Working Paper Series* 239: 1-37. DOI: 10.3929/ethz-a-010611130.
- [8] Charnes, A., Cooper, W. W., Rhodes, E. (1978): Measuring the efficiency of decision making units. – *European Journal of Operational Research* 2(6): 429-444.
- [9] Cranmer, S. R. (2016): Predictions for dusty mass loss from asteroids during close encounters with solar probe plus. – *Earth, Moon, and Planets* 118(2-3): 51-79.
- [10] Dzonzi-Undi, J., Li, S. (2016): RETRACTED: Safety and environmental inputs investment effect analysis: Empirical study of selected coal mining firms in China. – *Resources Policy* 47: 178-186.
- [11] Grinsven, H. V., Tiktak, A., Rougoor, C. W. (2016): Evaluation of the Dutch implementation of the nitrates directive, the water framework directive and the national emission ceilings directive. – *Njas Wageningen Journal of Life Sciences* 78: 69-84.
- [12] Henson, S. A., Yool, A., Sanders, R. (2015): Variability in efficiency of particulate organic carbon export: A model study. – *Global Biogeochemical Cycles* 29(1): 33-45.
- [13] Kaya, Y., Yokobori, K. (1993): *Global Environment, Energy, and Economic Development*. – United Nations University. Tokyo.
- [14] Kim, J. (2016): Vehicle fuel-efficiency choices, emission externalities, and urban sprawl. – *Economics of Transportation* 5: 24-36.
- [15] Liu, L., Ma, X. Q., Mao, Z. J. (2014): Empirical study on the economic effect of energy conservation and emission reduction in different industrial stages. – *Advanced Materials Research* 962: 1541-1546.
- [16] Marklund, P. O., Samakovlis, E. (2007): What is driving the EU burden-sharing agreement: Efficiency or equity? – *Journal of Environmental Management* 85(2): 317-329.
- [17] Mielnik, O., Goldemberg, J. (1999): The evolution of the “Carbonization Index” in developing countries. – *Energy Policy* 27(05): 307-308.
- [18] National Bureau of Statistics of the People’s Republic of China (2015): *China Statistical Yearbooks 2015*. – NBS, Beijing.
- [19] Niu, S., Jia, Y., Ye, L., Dai, R., Li, N. (2016): Does electricity consumption improve residential living status in less developed regions? An empirical analysis using the quantile regression approach. – *Energy* 95: 550-560.
- [20] Obeng, K., Sakano, R., Naanwaab, C. (2016): Understanding overall output efficiency in public transit systems: The roles of input regulations, perceived budget and input subsidies. – *Transportation Research Part E: Logistics and Transportation Review* 89: 133-150.
- [21] Ramanathan, R. (2002): Combining Indicators of Energy Consumption and CO₂ Emissions: Across-country Comparison. – *International Journal of Global Energy Issues* 17(03): 214-227.
- [22] Ramanathan, R. (2005): An analysis of energy consumption and carbon dioxide emissions in countries of the Middle East and North Africa. – *Energy* 30(15): 2831-2842.
- [23] Ramanathan, R. (2006): A multi-factor efficiency perspective to the relationships among world GDP, energy consumption and carbon dioxide emissions. – *Technological Forecasting & Social Change* 73(5): 483-494.
- [24] Roar, A., Harrison, A., Justina, B., Hai, Y. J. (2017): Does fuel efficiency pay? Empirical evidence from the drybulk timecharter market revisited. – *Transportation Research Part A: Policy and Practice* 95: 1-12.

- [25] Sarkar, S. (2013): Testing weak form efficiency of Indian stock market - an empirical study on BSE. – *IEEE Transactions on Antennas & Propagation* 18(1): 112-114.
- [26] Shao, Y., Wang, S. (2016): Productivity growth and environmental efficiency of the nonferrous metals industry: An empirical study of China. – *Journal of Cleaner Production* 137: 1663-1671.
- [27] Sun, J. W. (2005): The decrease of CO₂ emission intensity is decarbonization at national and global levels. – *Energy Policy* 33(8): 975-978.
- [28] Szczepańska, K., Wiśniewska, M. (2012): Human performance improvement in the health care organizations. Results of empirical study in Poland. – *Foundations of Management* 4(2): 97-108.
- [29] Tavana, M., Mirzagoltabar, H., Mirhedayatian, S. M., Saen, R. F., Azadi, M. (2013): A new network epsilon-based DEA model for supply chain performance evaluation. – *Computers & Industrial Engineering* 66(2): 501-513.
- [30] Tone, K., Tsutsui, M. (2010): An epsilon-based measure of efficiency in DEA—A third pole of technical efficiency. – *European Journal of Operational Research* 207(3): 1554-1563.
- [31] Vaidya, K., Campbell, J. (2016): Multidisciplinary approach to defining public e-procurement and evaluating its impact on procurement efficiency. – *Information Systems Frontiers* 18(2): 333-348.
- [32] Van Grinsven, H. J., Tiktak, A., Rougoor, C. W. (2016): Evaluation of the Dutch implementation of the nitrates directive, the water framework directive and the national emission ceilings directive. – *NJAS-Wageningen Journal of Life Sciences* 78: 69-84.
- [33] Wang, J. T., Cao, Q. F., Chen, T. Y., Wang, X. (2016): An empirical study on the technical efficiency of foreign direct investment in China with environmental constraints. – *The Chinese Economy* 49(2): 94-104.
- [34] Wang, Q., Zhou, P., Zhou, D. (2012): Efficiency measurement with carbon dioxide emissions: the case of China. – *Applied Energy* 90(1): 161-166.
- [35] Wang, Q. W., Zhou, P., Shen, N., Wang, S. S. (2013): Measuring carbon dioxide emission performance in Chinese provinces: a parametric approach. – *Renewable and Sustainable Energy Reviews* 21: 324-330.
- [36] Wang, S., Fang, C., Wang, Y., Huang, Y., Ma, H. (2015): Quantifying the relationship between urban development intensity and carbon dioxide emissions using a panel data analysis. – *Ecological Indicators* 49: 121-131.
- [37] Wang, S., Zhou, C., Li, G., Feng, K. (2016): CO₂, economic growth, and energy consumption in China's provinces: Investigating the spatiotemporal and econometric characteristics of China's CO₂ emissions. – *Ecological Indicators* 69: 184-195.
- [38] Xian, Y., Huang, Z. (2016): Sources of carbon productivity change: A decomposition and disaggregation analysis based on global Luenberger productivity indicator and endogenous directional distance function. – *Ecological Indicators* 66: 545-555.
- [39] Xu, S., Zhang, Z., Si, D. (2014): The study of the operating performance of marine industry in the blue economic zone: An empirical analysis based on DEA and Tobit Model. – *Asian Agricultural Research* 6(6): 16-21.
- [40] Yun, L., Dan, N., Xin, G. Z., Yan, B. L. (2017): Market structure and performance: An empirical study of the Chinese solar cell industry. – *Renewable and Sustainable Energy Reviews* 70: 78-82.
- [41] Zaim, O., Taskin, F. (2000): Environmental efficiency in carbon dioxide emissions in the OECD: A non-parametric approach. – *Journal of Environmental Management* 58(2): 95-107.
- [42] Zhang, Z., Qu, J. S., Zeng, J. J. (2008): A quantitative comparison and analysis on the assessment indicators of greenhouse gases emission. – *Journal of Geographical Sciences* 18(04): 387-399.
- [43] Zhou, P., Ang, B. W., Poh, K. L. (2006): Slacks-based efficiency measures for modeling environmental performance. – *Ecological Economics* 60(1): 111-118.

- [44] Zhou, P., Ang, B. W., Han, J. Y. (2010): Total factor carbon emission performance: a Malmquist index analysis. – *Energy Economics* 32(1): 194-201.
- [45] Zhou, Y., Li, Y. P., Huang, G. H. (2015): Planning sustainable electric-power system with carbon emission abatement through CDM under uncertainty. – *Applied Energy* 140: 350-364.

DETERMINATION OF THE EFFECT OF PLANT GROWTH PROMOTING BACTERIA ON WHEAT (*TRITICUM AESTIVUM* L.) DEVELOPMENT UNDER SALINITY STRESS CONDITIONS

SÖĞÜT, S. – ÇİĞ, F.*

Department of Field Crops, Faculty of Agriculture, Siirt University, Siirt, Turkey

**Corresponding author*

e-mail: fatihcig@hotmail.com; phone: +90-533-777-1140

(Received 20th Sep 2018; accepted 2nd Jan 2019)

Abstract. This study was carried out in Field Crops Department Laboratory of Siirt University, Faculty of Agriculture (Turkey) in 2016. In the study, Ceyhan 99 bread wheat cultivar was used. It was aimed to determine the effect of TV14B *Stenotrophomonas maltophilia* P (phosphate solubilizing bacteria), TV119E *Bacillus*-GC group P (phosphate solubilizing bacteria), TV83D *Bacillus atrophaeus* N (nitrogen fixing bacteria), TV54A *Cellulomonas turbata* N (nitrogen fixing bacteria), TV113C *Kluyvera cryocrescens* NP (nitrogen fixing + phosphate solubilizing bacteria), TV83D *B. atrophaeus* + TV119E *Bacillus*-GC group (binary combination) bacterial strains on development of Ceyhan-99 bread wheat cultivar under salinity stress. The germination rate (%), germination percentage (%), plant height (cm), root length (cm), plant wet weight (g), plant dry weight (g), nitrogen amount in the soil (%) and phosphorus amount in the soil (%) were determined with the test conducted. It is concluded that TV14B *S. maltophilia* P bacteria had positive impacts on plant growth parameters at different salinity concentrations. It was observed that TV119E *Bacillus*-GC group P bacteria, in 100 mM salt concentration, increased plant height, phosphorus in the soil and dry weight parameters. TV83D *B. atrophaeus* N bacteria treatment in 125 mM salt concentration increased root length, phosphorus and nitrogen amount in the soil compared to the control treatment. It was observed that treatments of TV54A *C. turbata* N, TV113C *K. cryocrescens* NP and TV83D *B. atrophaeus* +TV119E *Bacillus*-GC group NP bacteria in different salt concentrations increased both phosphorus and nitrogen amounts in the soil. As a result, these bacteria treatments were considered to alleviate the disadvantages of salinity stress.

Keywords: *biofertilizer, biotic stress, salt concentrations, yield, yield elements*

Introduction

Cereals are the plant group with the highest cultivation and yield amounts. Almost half of the Earth's 1.4 billion hectares of cultivated land is used for cereal cultivation. Cool season cereals are cultivated in 49.5% of the land used for cereal cultivation in the world. The rapid increase in the world population and steady development of living standards made it necessary to obtain higher yields in agricultural production, which is an important source for human nutrition. For this reason, the concept of soil fertility gained importance and became a hot topic. One of the most effective means of increasing the unit area productivity is usage of chemical fertilizers. It is stated that, despite the varying production conditions, share of fertilizers in yield increase is approximately 50% (Aydeniz, 1992). A significant amount of nitrogen and phosphorus is being removed from soil through surface runoff and drainage waters due to incorrect and excessive fertilizer usage (Guttman, 1999). This leads to an increase in the nitrate concentration in drinking water reserves and in leaf vegetables, as well as forage crops, which adversely affects the health of the animals fed with these feed crops (Abdel et al., 1997).

Tough, the bacteria known as biological fertilizer and promoting plant growth gradually increase their place in the studies on production of biological preparations,

with their positive effects on plant growth and systemic resistance (Upadhyay et al., 2014; Ansari and Ahmad, 2018).

Recognition of potential damages given by the chemical inputs, used to increase quality and yield in agricultural production, in the long term resulted in a quest for alternative solutions. Approaches such as “Organic Agriculture”, “Integrated Pest Management” and “Good Agricultural Practices” aim at minimizing the amount of synthetic inputs. Plant Growth Promoting Rhizobacteria (PGPR) are getting more attention in the studies on biological preparations due to their positive effects on plant growth and systemic resistance.

Ceyhan-99 wheat variety by superior adaptability, efficiency and quality is one of the most cultivated varieties of bread wheat in Turkey and has the potential to also be trained in a similar ecological conditions world. There has not been any study on the resistance to salinity with PGPR application before. Therefore, the development of PGPR application with Ceyhan-99 wheat varieties was discussed.

In this study, effects of microorganisms on growth and development of wheat under salinity stress were examined by using nitrogen fixing and phosphate solubilizing bacteria as biological fertilizer elements, in order to avoid the environmental and human health threats posed by inorganic fertilizers (Shrivastava and Kumar, 2015; Hashem et al., 2016).

Literature review

Several studies have been carried out in many countries on the effects of Plant Growth Promoting Rhizobacteria (PGPR) on yield increase (Chen et al., 1996; Luz, 2000; Romero, 2000; Wall, 2000). Although the positive impacts of PGPR on plant development have not been fully explained, it is known that these bacteria can produce plant hormones such as auxin (Jeon et al., 2003; Aslantaş et al., 2007; Sabır, 2013), cytokinin (García de Salamone et al., 2001), gibberellin (Gutiérrez-Mañero et al., 2001) and ethylene (Glick et al., 1995); fixate symbiotic nitrogen (N) (Şahin et al., 2004); dissolve mineral phosphate (P); mineralize organic phosphate and other nutrients (Jeon et al., 2003; Canbolat et al., 2006); show antagonistic impact on pathogens by synthesizing siderophore, antibiotics, enzyme and fungicide compounds or via competition (Dey et al., 2004).

The use of bacteria in agriculture as biofuels or control agents has increased since 1990s. In recent years, the scope of biological fertilization has extended to include free living rhizobacteria usage as plant growth promoter, biological control agent or biofertilizer.

Öztürk et al. (2003) analysed the impacts of inoculating plant growth promoting bacteria on wheat and barley yield at three different nitrogen fertilization levels. It was shown that inoculation of the seeds with *Azospirillum brasilense* Sp246 has significant impacts on the yield and yield elements. It was reported in the study that *Azospirillum brasilense* Sp246 has the potential to be used as biological fertilizer in summer wheat and barley cultivation in organic and good agricultural practices. Çakmakçı et al. (2007) stated that inoculation of *Bacillus* RC01, *Bacillus* M-13, *Bacillus* RC02, *Rhodobacter* RC04, *Paenibacillus* RC05, *Pseudomonas* RC06 and *Bacillus* OSU-142 bacteria isolated from the roots of wheat and barley increases barley root weight by 21.4%, 17.9%, 25.0%, 21.4%, 28.6%, 21.4% and 32.1% and body weight by 39.0%, 30.5%, 28.8%, 32.2%, 54.2%, 32.2% and 47.6%, respectively. They argue that these strains have

significant potential to be used as biological fertilizers. Narula et al. (2005) isolated and identified diazotrophs that fixate nitrogen and produce plant hormones such as azotobacter and used these as biological fertilizers with different nitrogen dosages on wheat and cotton plants under field conditions. They observed significant impacts on wheat using biological inoculants. The researchers showed that the impact of biological inoculants are more visible in the second year, as the inoculator amount is maintained in the soil. Furthermore, when appropriate biological fertilizers are used, 25-30 kg of nitrogen can be saved in wheat cultivation. Salantur et al. (2006) studied the impacts of root bacteria inoculation on growth and yield of summer wheat under greenhouse and field conditions. The results of greenhouse trials showed that the bacteria have positive and significant impact on the number of tillers, plant length, dry matter and protein content of the plant. It was presented that the root bacteria inoculated in wheat increased the growth, kernel yield and N content under field conditions.

Materials and methods

Materials

Wheat (Ceyhan-99)

Ceyhan-99 bread wheat cultivar was used in the study. This cultivar has a height of 90 to 100 cm. The plant is resistant to lodging and has white-spined spike structure. Spikes are upright with medium length. The grains are oval, hard, white colour and thousand grains weight has 42 to 45 g. The cultivar is moderately resistant to winter and drought and its fertilizer reaction and harvesting-threshing ability is good.

Bacteria strains

The bacteria inoculated in wheat are *Stenotrophomonas maltophilia* P (phosphate solubilizing bacteria) TV14B, *Bacillus* sp. P (phosphate solubilizing bacteria) TV119E, *Bacillus atrophaeus* N (nitrogen fixing bacteria) TV83D, *Cellulomonas turbata* N (nitrogen fixing bacteria) TV54A, *Kluyvera cryocrescens* NP (nitrogen fixing + phosphate solubilizing bacteria) TV113C, *B. atrophaeus* + *Bacillus* sp. (binary combination) TV83D + TV119E and they were isolated from Van Lake Basin. The strains were identified in Bacteriology Laboratory of Atatürk University Faculty of Agriculture Department of Field Crops and the impacts of PGPR tested under greenhouse and field conditions.

Soil properties

Some soil properties were determined as neutral in terms of pH, saltless, low in organic matter and lime, insufficient phosphorus, sufficient and more potassium, iron, manganese and copper, deficiency in zinc (Table 1).

Table 1. Some properties of experimental soil

pH	Ec ds/m	Lime CaCO ₃ %	Organic matter %	Phosphorus P ₂ O ₅ kg/da	Potassium K ₂ O kg/da	Fe ppm	Cu ppm	Zn ppm	Mn ppm	Sand %	Clay %	Silt %	Texture
6.87	0.602	0.64	0.90	1.67	114	13.01	1.78	0.60	21.89	41.64	51.32	7.04	L

Methods

Experimentation

The study was carried out in Field Crops Department Laboratory of Faculty of Agriculture Siirt University in Turkey, on factorial design in randomized plots with 3 replications first factor is bacteria application with 6 strains and control level. Second factor was salt concentration with 5 levels. According to the experiment design, there were 3 plants in each pot. Pots used in experiment top diameter: 16.5 cm, base diameter 12.5 cm, height 14 cm and volume 2.1 l features.

The study was carried out under the conditions of 20-24 °C (daily) and 70-50% (daily) humidity. The light was programmed to be 16/8 h light/dark.

Fertilizer application

As control treatment, 200 mg N/kg, 60 mg P₂O₅/kg doses were applied for standard fertilization in 1 kg pots (Alpaslan et al., 1998).

Salt concentrations

Soil salinity and salinity stress usually refers to NaCl (Tort and Türkyılmaz, 2003). Thus, only NaCl was used to create salinity stress. In order to create salinity stress in germination medium, 0, 50, 75, 100 and 125 mM NaCl solutions were applied to the pot soil under field conditions in line with Tüzüner (1990) to create unsalty, slightly salty, salty, very salty and too salty levels, respectively.

Bacterial treatment

In the experiments, bacteria isolated from Van Lake Basin, which are already identified via microbial identification system (MIS) and which have proven PGPR activity under greenhouse and field conditions, were used. The bacteria were cultured in liquid medium and encoded to the seeds. Nutrient broth (NB) and ASHBY medium were used as liquid media for bacteria cultures. The nutrient media was sterilized at 121 °C in autoclave and transferred from solid nutrient medium to the liquid nutrient medium in the sterilized container. The bacteria transferred to the liquid medium were incubated in the shaker at 26 ± 2°C for 2 h. The cultured bacteria were applied to the seeds in 10⁸ cfu/ml concentration (Clark, 1965).

Obtaining the data

The experiment was continued for 6 weeks and following observations and measurements were made in accordance with the methods used by other researchers (Sehirali, 1989; Steiner et al., 1989; Kırtok et al., 1994).

Germination rate (%): the number of seeds germinated in the first four days is determined and calculated as percentage. In order to investigate the effect of wheat on germination rate, the rate of germination was obtained at the end of fourth days.

Germination percentage (%): the percentage of germinated seeds at the end of the 8th day of germination is determined. In order to determine the number of germinated seeds with the application of salt and bacteria, the percentage of germination was determined on the 8th day.

At the end of the 6th week:

Plant length (cm): the distance from the crown to the end of the flag leaf was measured in cm in each plant before the harvest and the average plant length was calculated.

Root length (cm): after the harvest, root of each plant was measured. The longest root was measured in each plant and the root length was found in cm.

Plant wet weight (g): the plants were dried and weighted after being harvested and their roots are cleared from soil.

Plant dry weight (g): the plants were dried in the oven at 65 °C until a fixed weight and weighted.

Nitrogen and phosphorus amount in the soil (%): Nitrogen and phosphorus content of the soil was measured after the harvest according to Kacar (1984).

The study was established to determine the effect of salt and PGPR applications during the first development period of the plant. Therefore, the experiment was ended at the end of the first development period of 6 weeks. Similar studies have been followed in previous studies (Moxley et al., 1978; Timm et al., 1991; Al et al., 2004).

Statistical analysis of the results

Statistical calculations were done in Costat and SPSS software in accordance with the experiment plan. The differences between the averages were determined using Duncan test.

Results

In this study, bacterial treatments were done in pot soils with different NaCl concentrations (0, 50, 75, 100 and 125 mM) to reduce salinity stress for the plants cultivated in these pots and yield parameters are measured after 42 days development period. While the bacteria treatment group was not fertilized, the control group was fertilized at the normal doze (200 mg N/kg, 60 mg P₂O₅/kg) and no bacterial treatment was done.

Germination rate

The highest germination rate value in bacterial treatments was obtained as 95.33% in *B. atrophaeus* + *Bacillus*-GC group treatment at the same time give closely values in, 84.33% for *K. cryocrescens*, 83.67% for *Bacillus*-GC group and Control, 79.33% *C. turbata* and 78.67% for *S. maltophilia*, while the lowest germination rate was obtained as 70.33% for *B. atrophaeus* bacterial treatments (*Table 2*).

In general, it was observed that the germination rate obtained from the salt applications was different and the differences between the values were significant. The germination rate in 0, 50, 75, 100 and 125 mM dosages of salt concentrations were measured as 94.29, 87.38, 81.91, 79.05 and 68.33%, respectively, and these figures were recorded as germination rates. The highest germination rate was obtained as 94.29% in 0 mM salt concentration, while the lowest germination rate was obtained as 68.33% in 125 mM treatment (*Table 3*).

In general, it was observed that the germination rate obtained from bacterial and salt treatments was found statistically significant.

Table 2. Duncan test results for obtaining the data in Ceyhan 99 wheat species inoculated with different bacteria strains

Bacterial treatments	Obtaining the Data							
	Germination rate (%) [*]	Germination percentage (%) ^{ns}	Plant height (cm) [*]	Root length (cm) ^{**}	Plant wet weight (g) [*]	Plant dry weight (g) [*]	Nitrogen amount (%) ^{***}	Phosphorus amount (%) [*]
Control	83.67 ^b	100.0	25.98 ^a	24.53 ^{abc}	0.309 ^a	0.036 ^a	0.052 ^a	5.401 ^a
<i>Stenotrophomonas maltophilia</i> P	78.67 ^{bc}	99.3	24.79 ^{ab}	26.08 ^a	0.300 ^a	0.033 ^{ab}	0.048 ^c	4.928 ^c
<i>Bacillus</i> -GC group P	83.67 ^b	100.0	25.20 ^{ab}	25.07 ^{abc}	0.263 ^b	0.028 ^b	0.052 ^b	5.024 ^b
<i>Bacillus atrophaeus</i> N	70.33 ^c	100.0	24.33 ^b	25.19 ^{ab}	0.250 ^{bc}	0.023 ^c	0.052 ^a	4.539 ^e
<i>Cellulomonas turbata</i> N	79.33 ^{bc}	100.0	24.67 ^b	24.09 ^{bcd}	0.215 ^{cd}	0.017 ^d	0.051 ^{ab}	4.732 ^d
<i>Kluyvera cryocrescens</i> NP	84.33 ^b	99.7	23.41 ^b	22.91 ^d	0.205 ^d	0.016 ^d	0.050 ^b	4.911 ^c
<i>Bacillus atrophaeus</i> + <i>Bacillus</i> -GC group NP	95.33 ^a	100.0	25.33 ^{ab}	23.52 ^{cd}	0.178 ^d	0.015 ^d	0.052 ^a	4.722 ^d
Averages	82.19	99.9	24.82	24.48	0.246	0.024	0.051	4.894

***P < 0.001; **P < 0.01; *P < 0.05; ns non-significant

Table 3. Duncan test results for obtaining the data in Ceyhan 99 wheat species with different salt concentrations

Salt concentrations	Obtaining the Data							
	Germination rate (%) ^{**}	Germination percentage (%) ^{ns}	Plant height (cm) ^{ns}	Root length (cm) [*]	Plant wet weight (g) [*]	Plant dry weight (g) [*]	Nitrogen amount (%) ^{***}	Phosphorus amount (%) [*]
0 mM	94.29 ^a	99.52	25.38	24.38 ^{ab}	0.268 ^a	0.020 ^b	0.054 ^a	5.094 ^a
50 mM	87.38 ^b	99.76	25.26	25.59 ^a	0.258 ^{ab}	0.024 ^{ab}	0.053 ^{ab}	4.826 ^d
75 mM	81.91 ^{cd}	100.00	24.37	24.61 ^{ab}	0.221 ^c	0.024 ^{ab}	0.051 ^{cd}	4.931 ^b
100 mM	79.05 ^c	100.00	24.24	24.26 ^{ab}	0.227 ^{bc}	0.026 ^a	0.050 ^d	4.908 ^c
125mM	68.33 ^d	100.00	24.44	23.57 ^c	0.254 ^{ab}	0.027 ^a	0.052 ^{bc}	4.711 ^e
Averages	82.19	99.86	24.74	24.48	0.246	0.024	0.052	4.894

***P < 0.001; **P < 0.01; *P < 0.05; ns non-significant

Germination percentage

The highest germination percentage value in bacterial treatments was obtained as 100% in *B. atrophaeus* + *Bacillus*-GC group, *Bacillus*-GC group, *B. atrophaeus*, *C. turbata* and Control treatments at the same time give closely values in, 99.7% for *K. cryocrescens*, while the lowest germination percentage was obtained as 99.3% for *S. maltophilia* bacterial treatments (Table 2).

In general, it was observed that the germination percentage obtained from the salt applications was close and the differences between the values were not significant. The germination percentage in 0, 50, 75, 100 and 125 mM dosages of salt concentrations were measured as 99.52, 99.76, 100, 100 and 100%, respectively, and these figures were recorded as germination percentage. The highest germination percentage was obtained as 100% in 75 mM, 100 mM and 125 mM salt concentration, while the lowest germination percentage was obtained as 99.52% in 0 mM treatment (Table 3).

In general, it was observed that the germination percentage obtained from bacterial and salt treatments was found statistically not significant.

Plant height

The highest plant height value in bacterial treatments was obtained as 25.98 cm in control treatment at the same time give closely values in 25.33 cm for *B. atropurpureus* + *Bacillus*-GC group, 25.20 cm for *Bacillus*-GC group and 24.79 for *S. maltophilia*, while the lowest plant height was obtained as 23.41 cm for *K. cryocrescens* bacterial treatments (*Table 2*).

In general, it was observed that the plant height obtained from the salt applications was close and the differences between the values were not significant. The plant heights in 0, 50, 75, 100 and 125 mM dosages of salt concentrations were measured as 25.38 cm, 25.26 cm, 24.37 cm, 24.24 cm and 24.44 cm, respectively, and these figures were recorded as plant heights. The highest plant height was obtained as 25.38 cm in 0 mM salt concentration, while the lowest plant height was obtained as 24.24 cm in 100 mM treatment (*Table 3*).

In general, it was observed that the plant height obtained from the bacterial treatments were found statistically significant.

Root length

The highest root length value in bacterial treatments was obtained as 26.08 cm in *S. maltophilia* treatment besides other values in 25.19 cm for *B. atropurpureus*, 25.07 cm for *Bacillus*-GC group, 24.53 for Control treatment, 24.09 cm for *C. turbata*, 23.52 cm for *B. atropurpureus* + *Bacillus*-GC group while the lowest root length was obtained as 22.91 cm for *K. cryocrescens* bacterial treatments (*Table 2*).

It was observed that the root length obtained from the salt applications was close and the differences between the values were significant. The plant heights in 0, 50, 75, 100 and 125 mM dosages of salt concentrations were measured as 24.38 cm, 25.59 cm, 24.61 cm, 24.26 cm and 23.57 cm, respectively, and these figures were recorded as root length. The highest root length was obtained as 25.59 cm in 50 mM salt concentration, while the lowest root length was obtained as 23.57 cm in 125 mM treatment (*Table 3*).

In general, it was observed that the root length obtained from bacterial and salt treatments was found statistically significant.

Plant wet weight

The highest plant wet weight value in bacterial treatments was obtained as 0.309 g in Control treatment at the same time give closely value in, 0.300 g for *S. maltophilia*, while the lowest plant wet weight was obtained as 0.178 for *B. atropurpureus* + *Bacillus*-GC group bacterial treatments (*Table 2*).

It was observed that the plant wet weight obtained from the salt applications was different and the differences between the values were significant. The plant wet weight in 0, 50, 75, 100 and 125 mM dosages of salt concentrations were measured as 0.268 g, 0.258 g, 0.221 g, 0.227 g and 0.254 g, respectively, and these figures were recorded as plant wet weights. The highest plant wet weight was obtained as 0.268 g in 0 mM salt concentration, while the lowest plant wet weight was obtained as 0.221 g in 75 mM treatment (*Table 3*).

In general, it was observed that the plant wet weight obtained from bacterial and salt treatments was found statistically significant.

Plant dry weight

The highest plant dry weight value in bacterial treatments was obtained as 0.036 g in Control treatment at the same time give closely value in, 0.033 g for *S. maltophilia*, while the lowest plant dry weight was obtained as 0.015 g for *B. atrophaeus* + *Bacillus*-GC group bacterial treatments (Table 2).

It was observed that the plant dry weight obtained from the salt applications was different and the differences between the values were significant. The plant dry weight in 0, 50, 75, 100 and 125 mM dosages of salt concentrations were measured as 0.020 g, 0.024 g, 0.024 g, 0.026 g and 0.027 g, respectively, and these figures were recorded as plant dry weights. The highest plant dry weight was obtained as 0.027 g in 125 mM salt concentration, while the lowest plant dry weight was obtained as 0.020 g in 0 mM treatment (Table 3).

In general, it was observed that the plant dry weight obtained from bacterial and salt treatments was found statistically significant.

Nitrogen amount in the soil

The highest nitrogen amount in the soil was obtained in *B. atrophaeus* bacterial treatment (Table 4). Close figures were obtained in terms of the nitrogen amount in the soil in the other bacterial treatments which were control group and *Bacillus atrophaeus* + *Bacillus*-GC group NP. treatment.

Table 4. Duncan test results for amounts of nitrogen in Ceyhan 99 wheat species inoculated with different bacteria strains in different salt concentrations

Nitrogen amounts*						
Bacteria treatments	Salt concentration					Averages
	0 mM	50 mM	75 mM	100 mM	125 mM	
Control	0.051 ^{c-g}	0.053 ^{b-f}	0.053 ^{b-f}	0.054 ^{a-d}	0.050 ^{d-g}	0.0522 ^A
<i>Stenotrophomonas maltophilia</i> P	0.055 ^{a-e}	0.048 ^{gh}	0.050 ^{c-g}	0.037 ⁱ	0.050 ^{d-g}	0.0480 ^C
<i>Bacillus</i> -GC group NP	0.055 ^{b-g}	0.053 ^{b-g}	0.049 ^{efg}	0.049 ^{efg}	0.053 ^{b-f}	0.0518 ^B
<i>Bacillus atrophaeus</i> N	0.052 ^{b-g}	0.054 ^{a-e}	0.051 ^{c-g}	0.050 ^{d-g}	0.055 ^{a-e}	0.0524 ^A
<i>Cellulomonas turbata</i> N	0.049 ^{efg}	0.053 ^{b-f}	0.049 ^{efg}	0.053 ^{b-f}	0.052 ^{b-g}	0.0512 ^{AB}
<i>Kluyvera cryocrescens</i> NP	0.054 ^{a-e}	0.050 ^{c-g}	0.051 ^{c-g}	0.051 ^{c-g}	0.045 ^h	0.0502 ^B
<i>Bacillus atrophaeus</i> + <i>Bacillus</i> -GC group NP	0.051 ^{c-g}	0.051 ^{c-g}	0.050 ^{d-g}	0.057 ^a	0.052 ^{b-g}	0.0522 ^A
Averages	0.054 ^A	0.053 ^{AB}	0.051 ^{CD}	0.050 ^D	0.052 ^{BC}	

*The statistical analysis was done at p < 0.05 significance level and different letters indicate statistically significant treatments

Phosphorus amount in the soil

The highest phosphorus amount in the soil was measured in the control group and phosphorus figures were obtained differently in bacterial treatments (Table 5).

Table 5. Duncan test results for amount of phosphorus in Ceyhan 99 wheat species inoculated with different bacteria strains in different salt concentrations

Phosphorus amounts***						
Bacteria treatments	Salt concentrations					Averages
	0 mM	50 mM	75 mM	100 mM	125 mM	
Control	5.673	5.210	6.130	5.840	4.150	5.4007 ^A
<i>Stenotrophomonas maltophilia</i> P	5.170	5.670	4.470	4.580	4.750	4.9280 ^C
<i>Bacillus</i> -GC group NP	4.310	4.120	5.573	5.917	5.200	5.0240 ^B
<i>Bacillus atrophaeus</i> N	4.813	4.410	4.473	4.420	4.580	4.5393 ^E
<i>Cellulomonas turbata</i> N	5.380	4.920	4.177	4.533	4.650	4.7320 ^D
<i>Kluyvera cryocrescens</i> NP	5.560	4.703	4.930	4.417	4.943	4.9107 ^C
<i>Bacillus atrophaeus</i> + <i>Bacillus</i> -GC group NP	4.750	4.750	4.760	4.650	4.700	4.7220 ^D
Averages	5.0938 ^A	4.8262 ^D	4.9305 ^B	4.9081 ^C	4.7105 ^E	

***The statistical analysis was done at $p < 0.001$ significance level and different letters indicate statistically significant treatments

Discussion

TV14B *S. maltophilia* P in 0 mM salt concentration increased plant wet weight, nitrogen and phosphorus amounts in the soil and root length parameters. It was observed that this bacterium increased plant dry weight and the amount of phosphorus in the soil in 50 mM salt concentration and increased root length in 75 mM salt concentration.

It was observed that TV119E *Bacillus*-GC group P increased plant height, the amount of phosphorus in the soil and dry weight parameters in 100 mM.

It was determined that TV83D *B. atrophaeus* N bacteria increased root length and the amount of nitrogen in the soil in 0 mM salt concentration and root length, phosphorus and nitrogen amounts in the soil in the control group in 125 mM salt concentration.

TV54A *C. turbata* N bacterial treatment was found to provide increment in root length in 0 mM salt concentration compared to the control group. In 125 mM salt concentration, an increment in the amount of phosphorus and nitrogen in the soil was observed compared to the control treatment.

TV113C *K. cryocrescens* NP bacterial treatment increased the root length in 50 mM salt concentration and increased the amount of phosphorus in the soil in 125 mM salt concentration compared to the control treatment.

TV83D *B. atrophaeus* + TV119E *Bacillus*-GC group NP bacterial treatment was observed to increase germination rate and percentage parameters. An increase was observed in the amount of phosphorus in the soil in 125 mM salt concentration and in the amount of nitrogen in the soil in 100 mM salt concentration.

Aliye et al. (2008) reported that *B. subtilis* strain increased the plant height and weight compared to the control group. It is reported by many researchers (Dokuyucu et al., 1997; Salantur, 2003; Şahin et al., 2004; Salantur et al., 2006; Çakmakçı et al., 2007; Naiman et al., 2009) that bacterial inoculation results in increment in the plant height. The results of this research are in line this finding.

Mayak et al. (2004) used *Achromobacter piechaudii* bacterium, which is isolated from plant root rhizosphere and carries ACC deaminase enzyme, in their study in Israel. The results of the study showed that this bacterium increased wet and dry weights in tomato seedlings in the presence of NaCl over 172 mM.

Jalili et al. (2009) observed an increase in germination of canola seeds under salt stress with PGPR bacterial inoculation, containing ACC deaminase. The findings in our study are similar to those of the researchers.

Çakmakçı et al. (2007), used *Bacillus* OSU-142, *Panibacillus polymyxa*, *Bacillus megaterium*, *Bacillus* M-13, *Bacillus licheniformis*, *Pseudomonas putida* and *Rhodobacter capsulatus* isolates, which can fixate nitrogen, for the development of barley. The researchers reported that some of these isolates can produce indole acetic acid, while some others can solubilize phosphate; and they obtained 28.8 to 54.2% increment in body weight and 17.9 to 32.1% increment in root length. Furthermore, they stated that inoculation of phosphorus solubilizing bacteria is beneficial for the uptake of nitrogen, iron, manganese and copper by the plant.

Soil analysis is done after the harvest and the highest nitrogen amount was obtained in TV83D *B. atropaeus* N bacterial treatment. It was observed that bacterial treatments without fertilizer increased the nitrogen amount in the soil, thus it can be resulted that these bacterial treatments help nitrogen fixation. The amount of nitrogen in the soil measured in the control treatment with inorganic fertilization is close to the bacterial treatments. It can be concluded from *Table 4* that the nitrogen amount accumulated in the soil decreases as the salt concentration increases.

According to soil analysis results, the highest amount of phosphorus was obtained in the control treatment. Bacterial treatments without fertilizer have shown to increase the amount of phosphorus in the soil, which can be concluded as these bacteria can solubilize phosphorus. The amount of nitrogen in the soil measured in the control treatment with inorganic fertilization is close to the bacterial treatments. It can be concluded from *Table 5* that the phosphorus amount accumulated in the soil decreases as the salt concentration increases.

Previous studies showed that PGPRs have different mechanisms such as fixating free nitrogen in the air (Çakmakçı et al., 2007), and solubilizing inorganic phosphate sources (Aslantaş et al., 2007). The results obtained in this research are similar to those findings.

Conclusion

As a result, it is thought that TV14B *S. maltophilia* strain can be an alternative to fertilization in the soil without salinity stress and reduce the problems encountered. On the other hand, TV119E *Bacillus*-GC group strain is thought to alleviate the challenges faced in wheat farming especially in the saline soils.

Furthermore, TV113C *K. cryocrescens*, TV83D *B. atropaeus*, TV54A *C. turbata* and TV83D *B. atropaeus* + TV119E *Bacillus*-GC group bacterial treatments are thought to reduce the adverse effects of salinity stress and increase the nitrogen and phosphorus amounts in the soil.

Selected strains showed good phosphate solubilizing and nitrogen fixing ability. A pot experiment in a greenhouse was conducted in order to investigate the effect of different phosphate solubilizing and nitrogen fixing bacterial species on wheat.

In this study, the bacteria, which have been studied in the laboratory and field conditions, were inoculated. These bacteria have been isolated from their natural environment and have not been studied before. With this result, it is aimed to create a new alternative which cannot be polluting the environment and can be used in sustainable and organic agriculture.

Acknowledgements. This study is Ms. thesis and is supported with the project no 2016- SİÜFEB-24 by Siirt University Coordinator of Scientific Research and Projects.

REFERENCES

- [1] Abdel, M., Khalba, M., Abdel-Klakk, H. M. A., Abdel-Ghani. M. L. (1997): Adverse Environmental of N Fertilizer Abuse. – M. Egypt. Bio-Organik Farming System for Sustainable Agriculture, 20 November–6 December, 1995, Cairo, pp. 50-57.
- [2] Al, I., Dong, Y., Triplett, E. W. (2004): Nitrogen fixation in wheat provided by *Klebsiella pneumoniae* 342. – Mol. Plant Microbe Interact. 17: 1078-1085.
- [3] Aliye, N., Fininsa, C., Hiskias, Y. (2008): Evaluation of rhizosphere bacterial antagonists for their potential to bioprotect potato (*Solanum tuberosum*) against bacterial wilt (*Ralstonia solanacearum*). – *Biological Control* 47: 282-288.
- [4] Alpaslan, M., Güneş, A., İnal, A. (1998): Deneme Tekniği. – Ankara Üniversitesi Ziraat Fakültesi, Yayın No: 1501, Ders Kitabı 455, Ankara.
- [5] Ansari, F. A., Ahmad, I. (2018): Biofilm development, plant growth promoting traits and rhizosphere colonization by *Pseudomonas entomophila* FAP1: A promising PGPR. – Adv. Microbiol. 8(3): 235.
- [6] Aslantaş, R., Çakmakçı, R., Şahin, F. (2007): Effect of plant growth promoting rhizobacteria on young apple tree growth and fruit yield under orchard conditions. – *Scientia Horticulturae* 111: 371-377.
- [7] Aydeniz, A. (1992): Gübreleme ekonomi ilişkileri. – II. Ulusal Gübre Kongresi Tebliğleri, 30 Eylül-4 Ekim, 1991, Ankara, pp. 71-80.
- [8] Çakmakçı, R., Dönmez, M. F., Erdoğan, Ü. (2007): The effect of plant growth promoting rhizobacteria on barley, seedling growth, nutrient uptake, some soil properties and bacterial counts. – *Turkish Journal of Agriculture and Forestry* 31: 189-199.
- [9] Canbolat, M., Bilen, S., Çakmakçı, R., Şahin, F., Aydın, A. (2006): Effect of plant growth promoting rhizobacteria and soil compaction on barley seedling growth, nutrient uptake, soil properties and rhizosphere microflora. – *Biology and Fertility of Soils* 42: 350-357.
- [10] Chen, Y., Mei, R., Lu, S., Liu, L., Klopper, J. W. (1996): The Use of Yield Increasing Bacteria (YIB) as Plant Growth Promoting Rhizobacteria in Chinese Agriculture. – In: Uthkede, R. S., Gupta, W. K. (eds.) *Management of Soil Borne Diseases*. Kalyani Publishers, Ludhiana, pp. 164-184.
- [11] Clark, F. E. (1965): Aerobic Spore Forming Bacteria. – In: Black, C. A. et al. (eds). *Methods of Soil Analysis, Part 2*. American Society of Agronomy, Madison, WI, pp. 1473-1476.
- [12] Dey, R., Pal, K. K., Bhatt, D. M., Chauhan, S. M. (2004): Growth promotion and yield 90 enhancement of peanut (*Arachis hypogaea* L.) by application of plant growth promoting rhizobacteria. – *Microbiological Research* 159: 371-394.
- [13] Dokuyucu, T., Akkaya, A., Kirtok, Y. (1997): Bakteri aşılmasının (*Azospirillum brasiliense* Sp246) ekmeklik buğday (*Triticum aestivum* L.) çesidi Gemini'nin verim

- unsurları üzerine etkisi. – Türkiye II. Tarla Bitkileri Kongresi, 22-25 Eylül 1997, Samsun, pp. 56-60.
- [14] García De Salamone, I. E., Hynes, R. K., Nelson, L. M. (2001): Cytokinin production by plant growth promoting rhizobacteria and selected mutants. – Canadian Journal of Microbiology 47: 404-411.
- [15] Glick, B. R., Karaturović, D. M., Newell, P. C. (1995): A novel procedure for rapid isolation of plant growth promoting pseudomonads. – Canadian Journal of Microbiology 41: 533-536.
- [16] Gutiérrez-Mañero, F. J., Ramos-Solano, B., Probanza, A., Mehouchi, J., Tadeo, F. R., Talon, M. (2001): The plant-growth-promoting rhizobacteria *Bacillus pumilus* and *Bacillus licheniformis* produce high amounts of physiologically active gibberellins. – Physiologia Plantarum 111: 206-211.
- [17] Guttman, B. S. (1999): Biology. – WCB/McGraw-Hill, Iowa. Boston.
- [18] Hashem, A., Abd Allah, E. F., Alqarawi, A. A., Al-Huqail, A. A., Wirth, S., Egamberdieva, D. (2016): The interaction between arbuscular mycorrhizal fungi and endophytic bacteria enhances plant growth of *Acacia gerrardii* under salt stress. – Front Microbiol. 7: 1089.
- [19] Jalili, F., Khavazi, K., Pazira, E., Nejati, A. and Asadi Rahmani, H. (2009): Use of ACC deaminase –containing fluorescent pseudomonads to alleviate effects of salinity on canola (*Brassica napus* L.) growth in germination stage. – Iranian J. Soil Research (Soil Water Sci.) 23(1): 91-105.
- [20] Jeon, J. S., Lee, S. S., Kim, H. Y., Ahn, T. S., Song, H. G. (2003): Plant growth promotion in soil by some inoculated microorganisms. – Journal of Microbiology 41: 271-276.
- [21] Kacar, B. (1984): Bitki besleme uygulama klavuzu. – Ankara Üniversitesi Ziraat Fakültesi Yayınları, Ankara.
- [22] Kırtok, Y. (1984): Tahıllarda biyolojik verim, hasat indeksi ve tane verimi. I. Tarımsal kriter olarak çevre koşullarından etkilenişleri. – Doğa Bilimleri Dergisi 8(1): 96-102.
- [23] Luz, W. C. (2000): Plant growth promoting rhizobacteria in graminicolous crops in Brazil. – Fifth International PGPR Workshop, 29 October–3 November 2000, Cordoba-Argentina.
- [24] Mayak, S., Tirosh, T., Glick, B. R. (2004): Plant growth-promoting bacteria that confer resistance to water stress in tomato and pepper. – Plant Sci. 166: 525-530.
- [25] Moxley, M. G., Berg, W. A., Barrau, E. M. (1978): Salt tolerance of five varieties of wheatgrass during seedling growth. – Journal of Range Management 31(1): 54-55.
- [26] Naiman, A. D., Latronico, A., Salamone, I. E. A. (2009): Inoculation of wheat with *Azospirillum brasilense* and *Pseudomonas fluorescens*: impact on the production and culturable rhizosphere microflora. – European Journal of Soil Biology 45: 44-51.
- [27] Narula, N., Kumar, V., Singh, B., Bhatia, R., Lakshminarayana, K. (2005): Impact of biofertilizers on grain yield in spring wheat under varying fertility conditions and wheat-cotton rotation. – Archives of Agronomy and Soil Science 51(1): 79-89.
- [28] Öztürk, A., Çağlar, Ö., Sahin, F. (2003): Yield response of wheat and barley to inoculation of plant growth promoting rhizobacteria at various levels of nitrogen fertilization. – J. Plant Nutrition Soil Science 166: 262-266.
- [29] Romerio, R. S. (2000): Preliminary results on PGPR research at the Universidade Federal de Viçosa, Brazil. – Fifth International PGPR Workshop, 29 October–3 November 2000, Cordoba-Argentina.
- [30] Sabır, A. (2013): Improvement of grafting efficiency in hard grafting grape berlandieri hybrid rootstocks by plant growth-promoting rhizobacteria (PGPR). – Scientia Horticulturae 164(5): 24-29.
- [31] Salantur, A. (2003): Erzurum Pasinler Ovalarındaki Buğdaygil Bitkilerinin Yetiştigi Topraklardan İzole Edilen Asimbiyotik Bakteri Suşlarının Buğday ve Arpada Gelişme ve

- Verim Üzerine Etkileri (Doktora Tezi, Basılmamış). Atatürk Üniversitesi Fen Bilimleri Enstitüsü, Erzurum.
- [32] Salantur, A., Ozturk, A., Akten, S. (2006): Growth and yield response of spring wheat (*Triticum aestivum* L.) to inoculation with rhizobacteria. – Plant Soil Environment 52(3): 111-118.
- [33] Shrivastava, P., Kumar, R. (2018): Soil salinity: a serious environmental issue and plant growth promoting bacteria as one of the tools for its alleviation. – Saudi. J. Biol. Sci. 22(2): 123-131.
- [34] Steiner, J. J., Grabe, D. F., Tulo, M. (1989): Single and multiple vigor tests for predicting seedling emergence of wheat. – Crop Sci. 29: 782-786.
- [35] Şahin, F., Çakmakçı, R., Kantar, F. (2004): Sugar beet and barley yields in relation to inoculation with N₂-fixing and phosphate solubilizing bacteria. – Plant Soil 265: 123-129.
- [36] Şehirli, S. (1989): Tohumluk ve teknolojisi. – Güneş Tohumculuk Yayınları, Ankara.
- [37] Timm, D. A., Waskom, R. M., Miller, D. R., Nabors, M. W. (1991): Greenhouse evaluation of regenerated spring wheat for enhanced salt tolerance. – Cereal Research Communications 19(4): 451-457.
- [38] Tort, N., Türkyılmaz, B. (2003): Physiological effects of NaCl on two barley (*Hordeum vulgare* L.) cultivars. – Turkish Journal of Field Crops 8: 68-75.
- [39] Tüzüner, A. (1990): Toprak ve su analiz laboratuvarları el kitabı. – Mülga KHGM Yayınları, Ankara.
- [40] Upadhyay, S. K., Singh, J. S., Saxena, A., Singh, D. P. (2014): Impact of PGPR inoculation on growth and antioxidants status of wheat plant under saline condition. – Plant Biol. 14: 605-611.
- [41] Wall, L. G. (2000): Consequences of an Overview on PGPR Work in Argentina: The Field Should Be Wider. – Fifth International PGPR Workshop, 29 October–3 November 2000, Cordoba-Argentina.

ANALYSIS OF THE MORPHO-ANATOMICAL TRAITS OF FOUR MAJOR GARLIC (*ALLIUM SATIVUM* L.) CULTIVARS IN THE PHILIPPINES

RAGAS, R. E. G.^{1*} – PADRON, F. K. J. R.² – RUEDAS, M. Y. A. D.³

¹*Department of Biology and Environmental Science, College of Science, University of the Philippines Cebu, Gorordo Avenue, Lahug, Cebu City, 6000 Cebu, Philippines*

²*Philippine Rice Research Institute, Central Experiment Station, Maligaya, Science City of Muñoz, 3119 Nueva Ecija, Philippines*

³*Occidental Mindoro State College, Quirino Street, San Jose, 5100 Occidental Mindoro, Philippines*

*Corresponding author

e-mail: rragas@up.edu.ph; phone: +63-32-232-8187/ext. 310

(Received 24th Sep 2018; accepted 2nd Jan 2019)

Abstract. Cultivating garlic after the rice season has been increasingly attractive for rice farmers in the Philippines especially in areas where rice production is constrained by water scarcity. In Mindoro, Philippines, garlic cultivars planted include ‘Mindoro White’ (MW), ‘Lubang’ (LB), ‘Batanes White’ (BW), and ‘Ilocos White’ (IW). This study provides an in-depth analysis of major local garlic cultivars for classification and for selection of those with improved adaptation and marketability. For classification, we focused on phenotypic stable traits. Among these traits analyzed, clove weight ($p < 0.001$) and number of bulb leaf sheaths ($p < 0.05$) were significantly different. While there were small differences in their clove number and bulb color, bulb circumference ($p < 0.001$) and weight ($p < 0.01$) were highly significant. BW has the largest bulb circumference (126.50 ± 1.88 mm) and weight (22.38 ± 0.94 g) while MW has the smallest (103.30 ± 1.57 mm) and is lightest (13.78 ± 0.50 g). Bivariate analysis revealed that the highest bulb circumference and weight values of MW population correspond to the lowest values of BW population suggesting that these cultivars are two distinct populations. This was further supported by classical clustering analysis that distinguished them by bulb circumference (87.12%), clove number (76.01%) and number of clove vascular structures (78.27%). Across cultivars, measurements of the epidermal and parenchymal cells significantly differed. Qualitative analysis of the bulb characteristics showed that BW exhibits a regular, multi-fan bulb structure with three layers of large cloves implying market attractiveness while IW’s distinctly tight clove’s skin indicates long storage potential.

Keywords: *allium, bulb morphology, clove anatomy, cluster analysis, post-rice cultivation*

Introduction

Garlic (*Allium sativum* L.) is a monocotyledonous herb that produces a bulb, an aggregate of sheath-covered cloves serving as the main economic organ (Stavelikova, 2008). It is the second most widely cultivated *Allium* distributed from boreal areas to tropic regions (Mhazo et al., 2014). Central Asia is recognized as the *Allium*’s main center of origin which is supported by the discoveries of several primitive garlic types in the northwestern side Tien-Shan Mountains (Kotlinska et al., 1991; Etoh and Simon, 2002; Kamenetsky, 2007) and genetic fingerprinting (Volk et al., 2004; Kamenetsky et al., 2007; Zhao et al., 2011; Jo et al., 2012). It is also the home to the richest genetic diversity of garlic (Kamenetsky et al., 2007).

In the Philippines, regions with Type I climate, characterized by a dry season during November to April, are main producers of garlic. Occidental Mindoro remains the second largest garlic producer, which shares 17% of the country's garlic national production (BAS, 2009). Farmers call it 'white gold' because it is a profitable crop planted in the fallow period after rice. Garlic cultivars usually grown in Mindoro include 'Lubang', 'Mindoro White', 'Batanes White' and 'Ilocos White'.

Morphological and anatomical studies are valuable in the *Allium* genus, since they provide suitable data for diagnosis of different taxa (Stearn, 1980; Fritsch and Friesen, 2002). Morphological traits of garlic are used in evaluating the diversity of garlic collection and classification based on phenotypic characters (Keller, 2002; Volk et al., 2004; Panthee, et al., 2006; Kamenetsky et al., 2007; Volk and Stern, 2009). However, since garlic is highly adaptive to its growth environment (Volk et al., 2004) and to different agroclimatic regions (Mario et al., 2008; Hirata et al., 2016), it is important to evaluate traits that were either influenced or not by growth environment for a reliable classification of cultivars. Moreover, Volk and Stern (2009) reported that clove arrangement, number of cloves, clove weight, clove skin color, and clove skin tightness were stable for each cultivar regardless of production location and conditions whereas those that vary with growth location include bulb traits.

The International Plant Genetic Resources Institute (IPGRI) Descriptor for *Allium* (2001) is the most common scheme used in evaluating and characterizing traits of garlic accessions. In addition, according to Miryeganeh and Movafeghi (2009), the anatomy of scapes and vegetative organs of *Allium* have been used for taxonomical purposes in different hierarchical levels. Most important anatomical studies on *Allium* were focused on the structure of the bulb scales (Fritsch, 1988), leaf (De Mason, 1990; Mathew, 1996), and scape (Miryeganeh and Movafeghi, 2009).

Given that garlic (*A. sativum*) is the only *Allium* that produces cloves, anatomy of clove and its potential use in the classification and delimitation of species of *A. sativum* is important. Hence, this work provides the clove anatomical findings on local garlic cultivars grown in the Philippines and represents some distinctions among cross-sections of cloves. Moreover, this study evaluated stable traits of four major garlic cultivars commonly grown in the Philippines to provide information in classification, market recognition, and identification of production-quality garlic.

Materials and methods

Bulb and clove characteristics

Four major local garlic cultivars were obtained from a garlic grower cooperative in Occidental Mindoro, Philippines (12° 21' 19.2456" N and 121° 3' 37.8324" E) which include 'Mindoro White (MW)', 'Lubang (LB)', 'Batanes White (BW)' and 'Ilocos White (IW)'. These garlic cultivars are the most common garlic planted for commercial production in major garlic provinces in the country. MW accessions are from Mindoro province while LB accessions are originally from the Lubang Island located in the northwest of the northern end of Mindoro (*Fig. 1*). The accessions IW and BW are from the northern provinces of the Philippines specifically in the provinces of Ilocos Norte and Batanes, respectively.

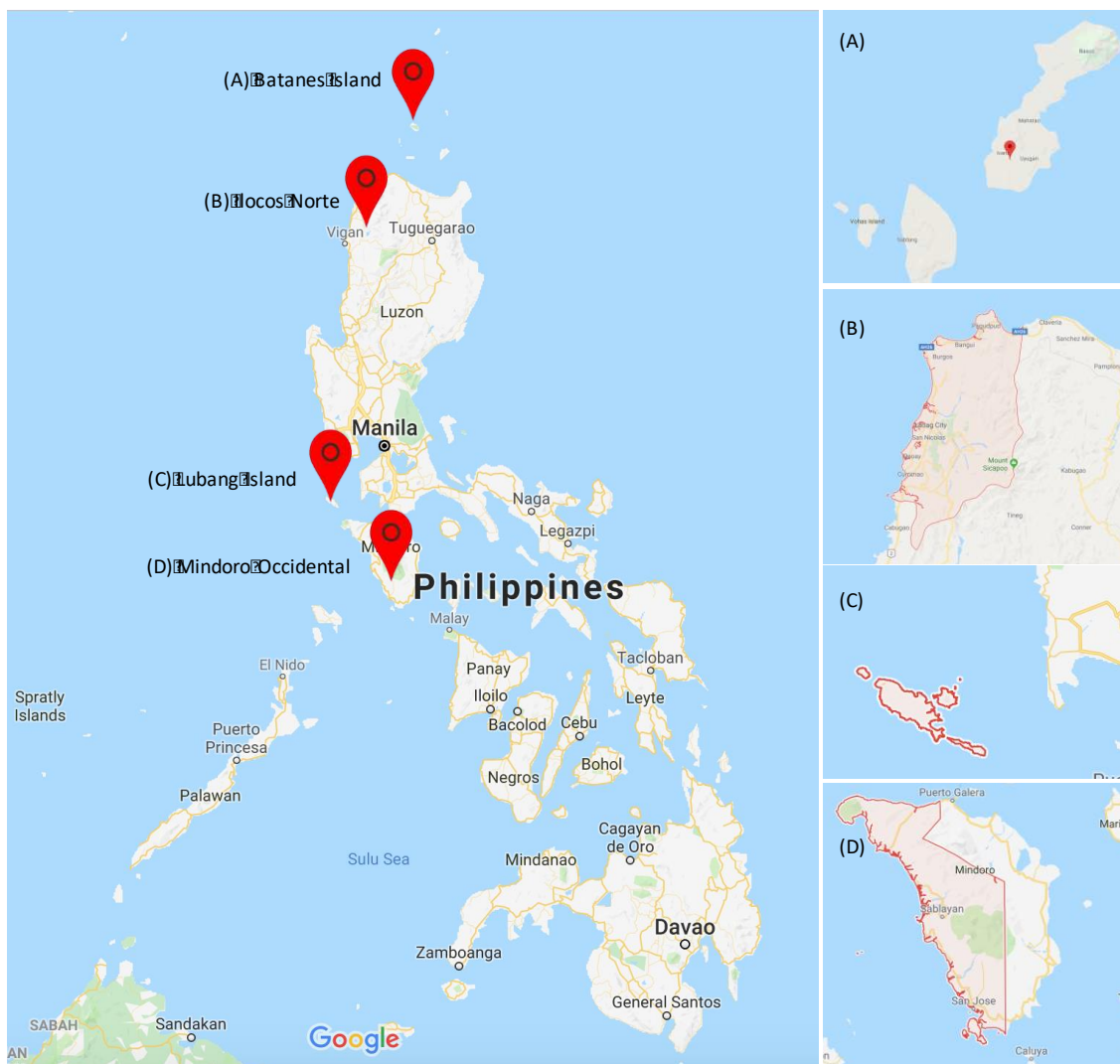


Figure 1. Location map of the origins of the garlic accessions in the Philippines. ‘BW’ in Batanes Island (A), ‘IW’ in Ilocos Norte (B), ‘Lubang’ in Lubang Island (C), and MW in Mindoro Occidental (D). (Google Map, 2018)

For each cultivar, nine bulbs (further categorized into large, medium, and small-sized bulbs, each having three representatives) were randomly selected to which phenotypic traits of the bulb and its cloves were analyzed based on IPGRI Descriptor for *Allium* (2001) (Fig. 2). Phenotypic data of the bulb collected from each cultivar include: sheath color and number, bulb shape, structure type, bulb circumference (mm) and weight (g). For the clove data, analysis on scale color and tightness, clove arrangement within a bulb, number of cloves per bulb, and weight (g) were made. In particular, the sheath and scale color as these are highly subjective, a color chart was used to distinguish intensity of color as indicated in the IPGRI (2001).

Microscopy analysis

The cross-sections of clove samples from each garlic cultivar were prepared and fixed in 70% ethanol for 48 h. Following the methods of Gerlach (1977) as cited by Silva et al. (2015), they were then stained with safranin and fast green to distinguish the

plant cell structures (Fig. 3). Thereafter, the sections were dehydrated through a graded ethanol series and then mounted on glass slide with a cover slip for observation. Each clove section was then examined under a light microscope (Axio Lab.A1, ZEISS, Germany) and dissecting microscope (Olympus, SZ61, Japan) linked to a digital camera. From the resulting images, sizes of the epidermal and parenchyma cells, size and number of rows of the vascular structures, and number of vascular structure per row were analyzed with Image J software (National Institutes of Health, USA).

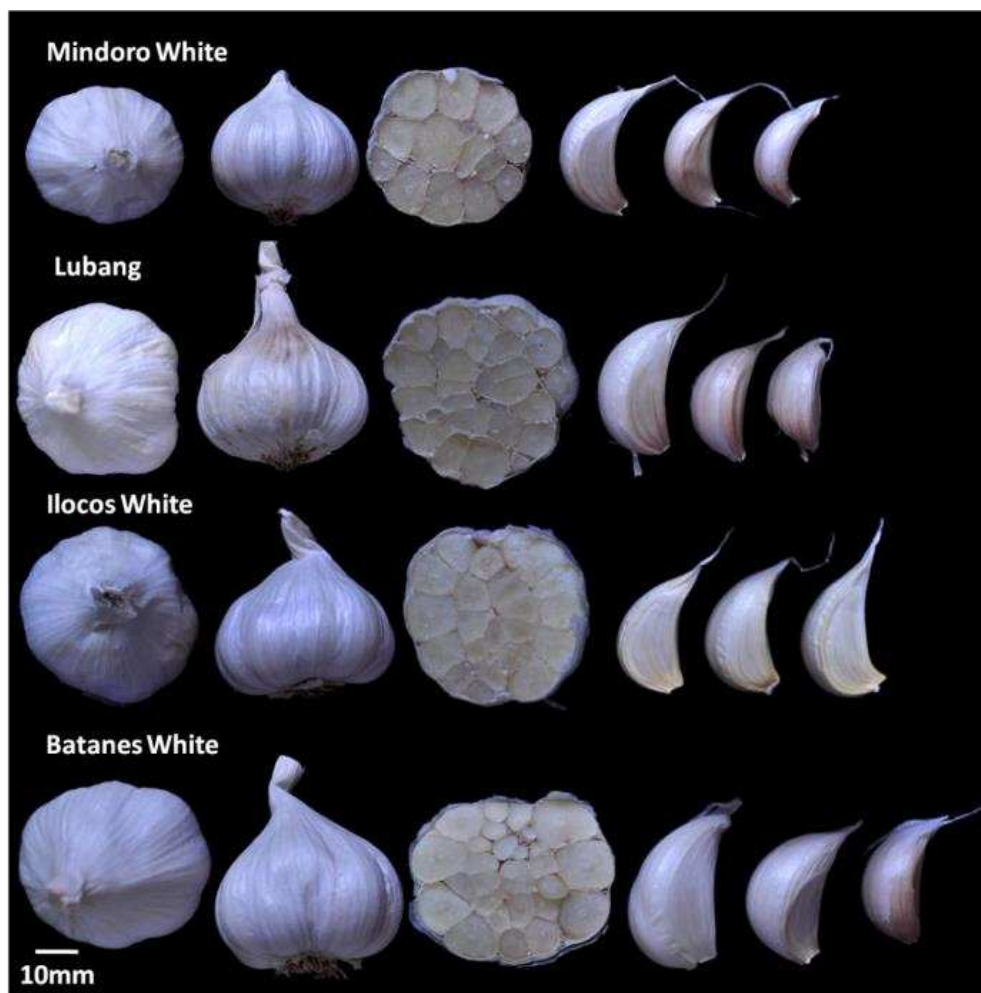


Figure 2. Bulb and clove characteristics of four major local garlic cultivars in the Philippines showing arrangement of cloves and coloration of bulb sheath and clove skin

Statistical analysis

Analysis of variance on quantitative data was performed using R Commander, a package available in R version 3.5.0. Qualitative data was summarized based on careful examinations of bulbs and cloves of each cultivar. Principal component analysis (PCA) was used to detect the characters that are most relevant to distinguish among the cultivars. Clusters of cultivars were formed on the basis of these factors using Classical Clustering Analysis (CCA). The graph representing classification is a dendrogram of similitude with standardized distances representing the closest cultivars in homogeneous groups.

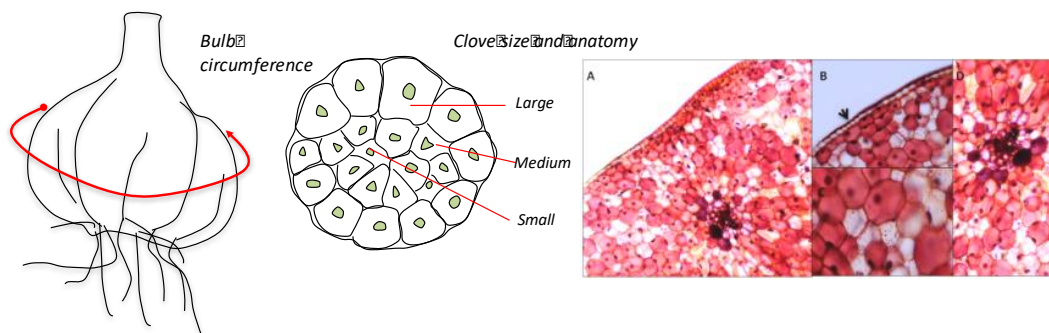


Figure 3. Diagrammatic presentation of parameters measured from bulb and clove characteristics as well as anatomical analysis of garlic cloves using safranin and fast green dyes under light microscope (A) Clove section under LPO (10x), (B) Epidermal cells (arrow head), (C) Normal clove cells with nuclei, (D) Vascular tissue under HPO (40x)

Results

Bulb characteristics

Color and pattern of bulb sheath were similar among cultivars except for LB which had darker sheath and more prominent brown stripes. MW, BW and IW all had white sheath with brown stripes. Similarities on the bulb shape and its structure type were also observed among cultivars. The bulb shape of MW and LB was circular with a prominent basal plate, BW and IW, were broadly ovate with an even (same level as the cloves) basal plate (Table 1). The MW and IW had similar bulb structure type which is regular two-fan groups while LB and BW had regular multi-fan groups. Regular two-fan groups have large outer cloves and small inner cloves while regular multi-fan groups have large outer cloves, medium inner cloves and small innermost cloves.

Table 1. Bulb and clove morphological characteristics of four garlic cultivars grown in the Philippines

Cultivar	Bulb			Clove		
	Sheath color	Shape	Structure type	Scale color	Scale tightness	Arrangement
Mindoro White	White/light brown stripe	Circular, basal plate prominent	Regular two-fan groups	Tan lower and white/pale upper	Loose	2 layers
Lubang	White-tan/moderate brown stripe	Circular, basal plate prominent	Regular multi-fan groups	Brown lower and white/pale upper	Moderate	3 layers
Batanes White	White/light brown stripe	Broadly ovate, basal plate even	Regular multi-fan groups	Light brown/tan lower and white upper	Moderate	3 layers
Ilocos White	White/light brown stripe	Broadly ovate, basal plate even	Regular two-fan groups	Yellowish lower and white/pale upper	Snug	2-3 layers

Significant differences in bulb weight and circumference were observed among four garlic cultivars (Fig. 4). Bulb circumference and weight of 'LB' (122.46 ± 2.20 mm and 18.8 ± 1.16 g) is comparable with IW (119.32 ± 1.26 mm and 19.77 ± 0.76 g). Among the cultivars, BW produced the biggest and heaviest bulb while MW had the smallest

and consequently the lightest. Bulb sheath number, ranges from five to seven with MW having the most number of sheath.

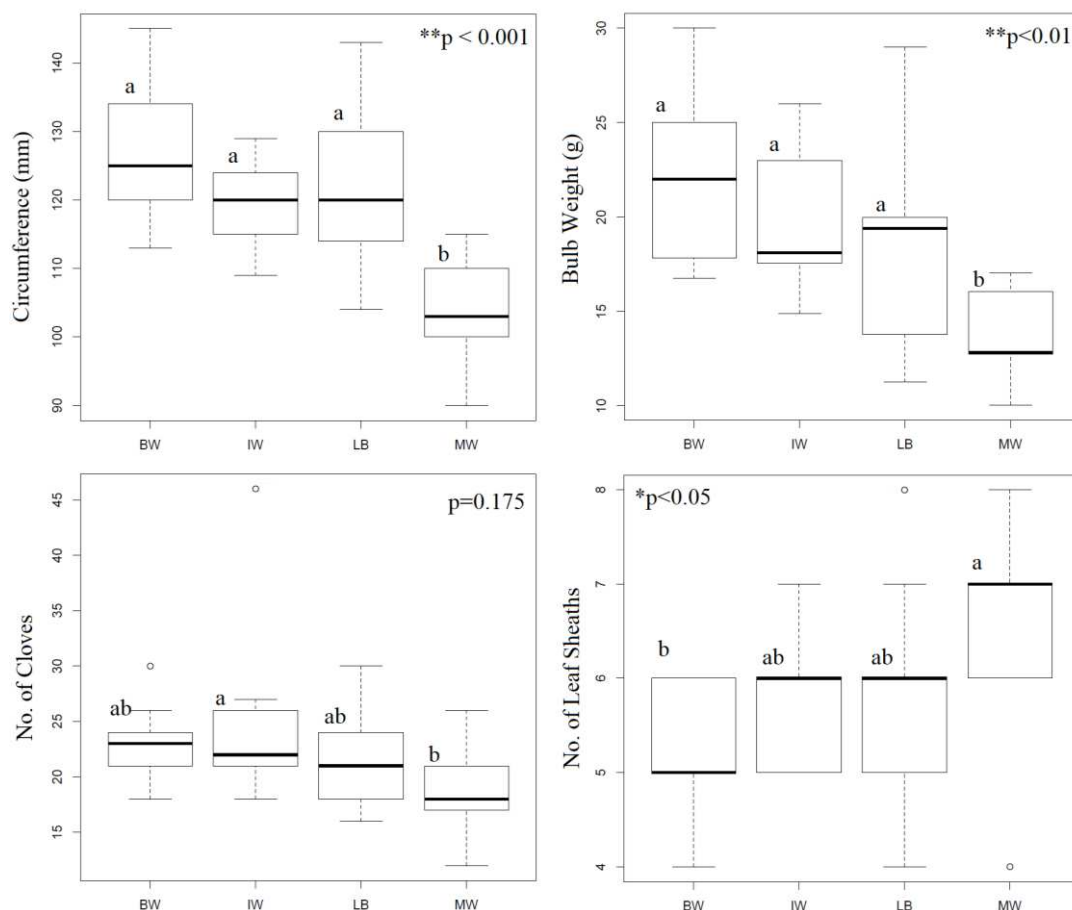


Figure 4. Bulb characteristics of four garlic cultivars in the Philippines. BW = Batanes White, IW = Ilocos White, LB = Lubang, MW = Mindoro White

Bivariate analysis of bulb circumference and weight through 95% confidence ellipse was used to estimate the population of each cultivar (Fig. 5). The results revealed that the common weight and circumference ranges of the four cultivars fall in the 15-18 g and 110-118 mm, respectively. While there exist two distinct cultivars, namely BW and MW, overlapping of bulb characteristics was still observed. The most notable overlap was between the smallest and lightest predicted populations of BW and the largest and heaviest populations of MW. Moreover, the population of IW cultivars was within the boundaries of the BW population, and that the largest bulb characteristic values of IW only reached the median values of BW. The LB, on the other hand, showed a wide range of bulb characteristics. While its bulb circumference and weight were comparably higher than MW and IW, it did not completely share with the BW population. Additionally, LB circumference and weight showed weaker correlation compared with the correlations observed in other cultivars. For instance, the bulb circumference of LB that were on the same circumference range as the other three cultivars weighed on the lower weight range, in fact, LB's largest bulbs were not necessarily heavier than their smaller counterparts from other cultivars.

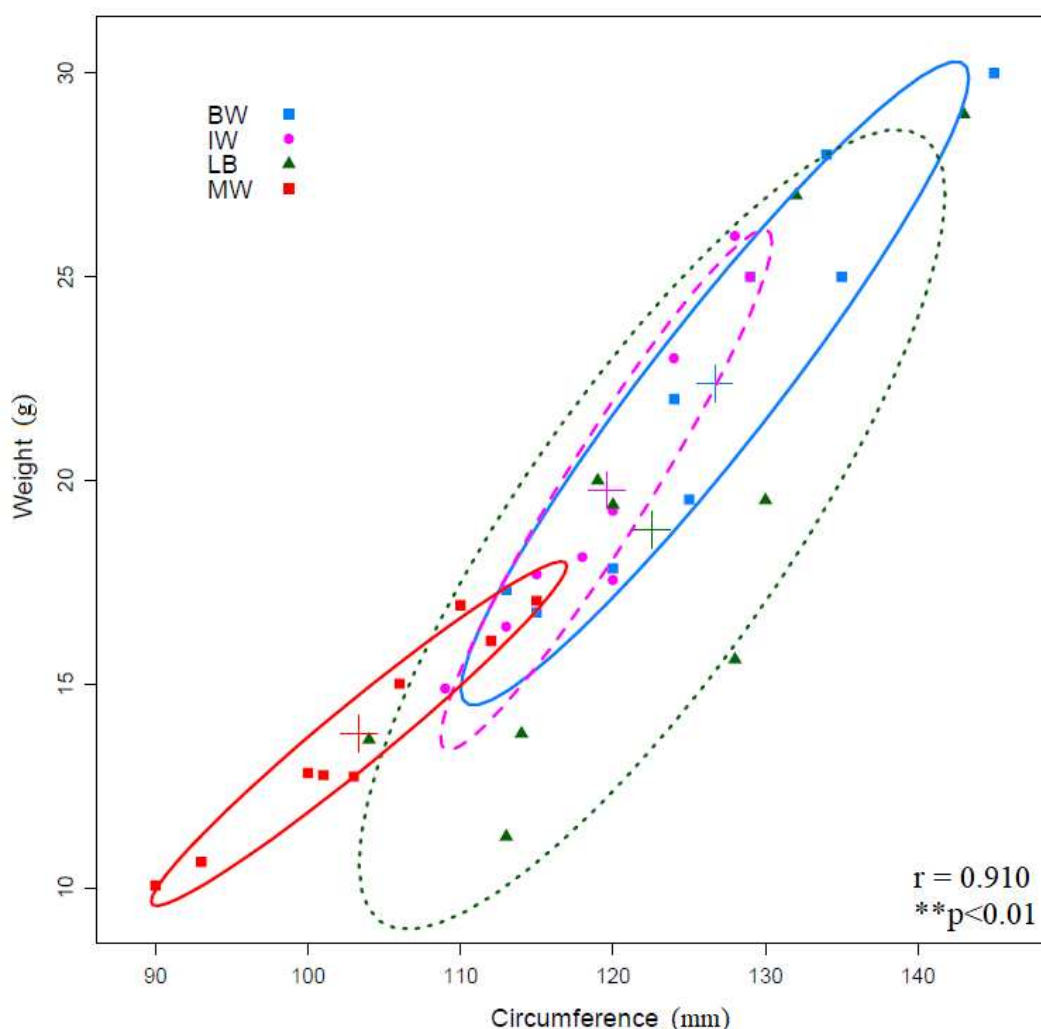


Figure 5. Scatter plot of bulb weight and circumference of four garlic cultivars in the Philippines using 95% confidence ellipse visualization (R Studio). BW = Batanes White, IW = Ilocos White, LB = Lubang, MW = Mindoro White

Clove characteristics

Cultivars were classified according to clove scale color and tightness, number of cloves per bulb, clove arrangement and clove weight (Table 1 and Fig. 4). Two hues of clove skin color were observed among cultivars. Different clove skin colors were also observed varying from tan to yellowish upper part to pale-white lower part. High variability was observed at the lower part of the clove skin and not as much in the upper part. White-pale upper part was observed in all cultivars except for BW which only had a white upper part. For the color of lower part, MW, LB, BW, and IW had tan, brown, light brown-tan, and yellowish, respectively. Clove skin tightness varied from snug to loose (Table 1). Clove arrangement within the bulb varied from two layers as observed in MW, two to three layers in IW, and three layers in BW and LB.

A significant difference in clove weight among garlic cultivars was observed (Fig. 6). The clove weight of MW is significantly different from other cultivars except for LB. Clove number per bulb among cultivars were not significantly different from

each other (Fig. 4). The IW produced the most numerous cloves per bulb while BW had the highest clove weight. The MW produced the fewest cloves and the lightest clove weight (Figs. 4 and 6). It was also observed that the larger the cloves produced, the heavier the bulb.

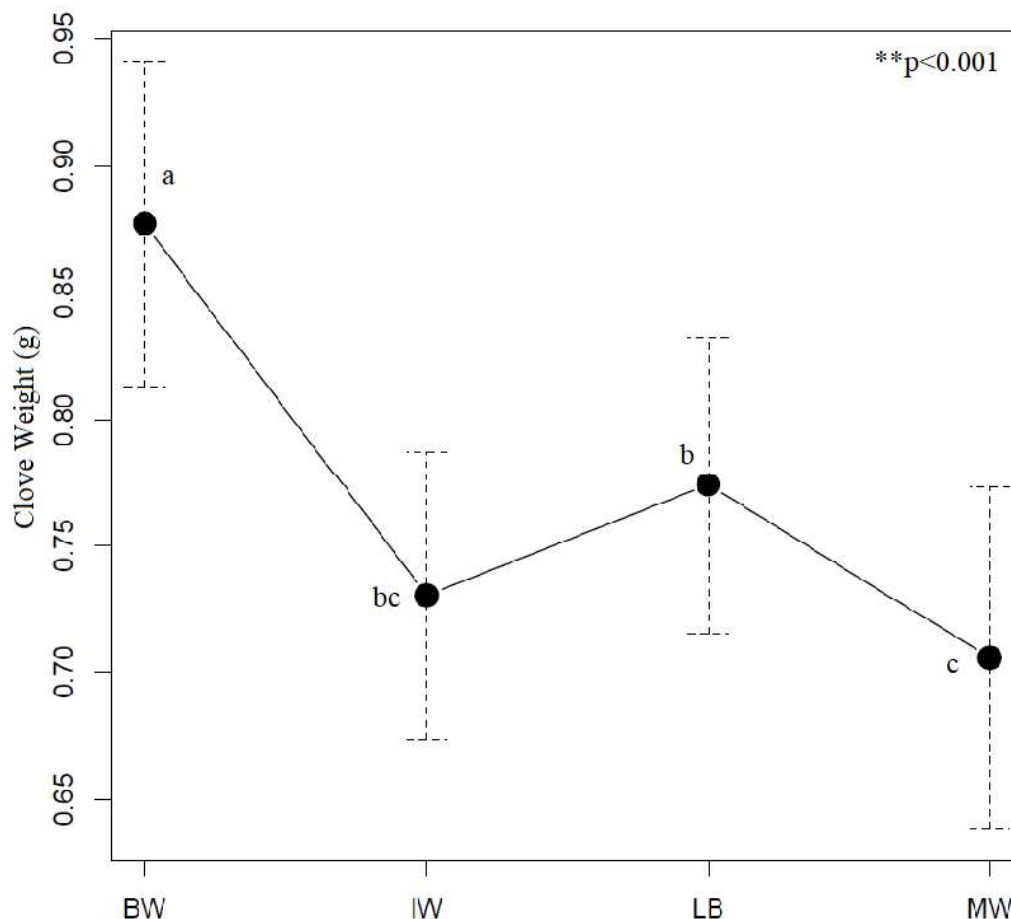


Figure 6. Clove weight of four garlic cultivars in the Philippines. BW = Batanes White, IW = Ilocos White, LB = Lubang, MW = Mindoro White

The dendrogram gave the clustering pattern for the garlic cultivars shown in Figure 7. There were two main clusters; the BW cultivar cluster and the other cultivars. The MW and LB cultivars were classified into the same group, but the IW cultivar was separated into a minor group. The distances between the cultivars ranged from 0.99 to 1.00, suggesting that genetic diversity between the garlic cultivars was moderately high.

Anatomical characterization

Differences in shape of clove's cross-sections were observed. The shape of the clove cross-sections was elliptic-oblong in MW and LB, circular in BW and cuboidal in IW. Across cultivars, epidermis was single layered with a thin cuticle outer covering. Epidermal cells were more or less isodiametric-cuboidal. Minimum width of epidermal cells across cultivars was 0.020 mm. BW had the biggest (width: 0.040 ± 0.002 mm) and thickest (length: 0.035 ± 0.002 mm) layer of epidermal cells among the cultivars (Table 2). Thinnest epidermal cell layer was observed in MW.

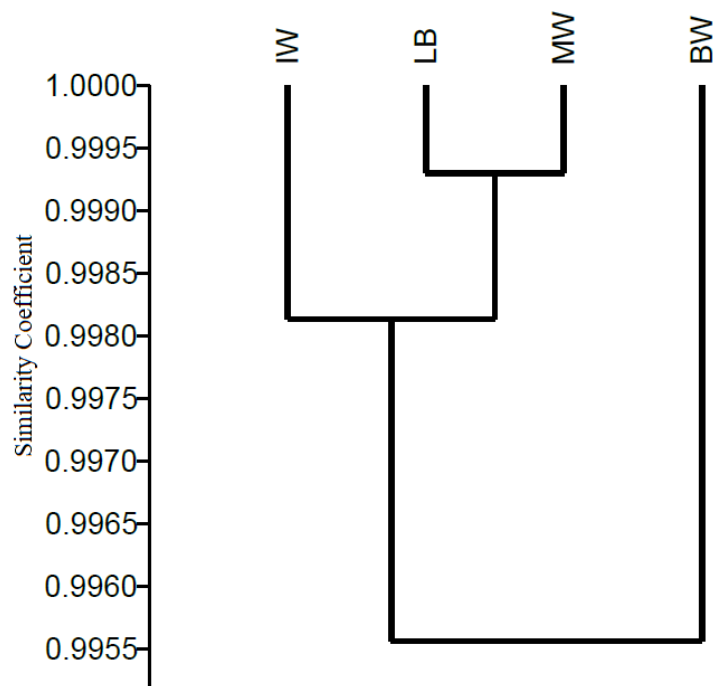


Figure 7. Similarity dendrogram generated by classical cluster analysis (CCA) using PAST 3.15 software showing two major clusters on the basis of morphology and anatomical characters of four garlic (*Allium sativum* L.) accessions in the Philippines. BW = Batanes White, IW = Ilocos White, LB = Lubang, MW = Mindoro White

Table 2. Anatomical characteristics of the cloves of four garlic cultivars grown in the Philippines

Cultivar	Epidermal cell		Parenchymal cell		Vascular structure	
	Width (mm)	Length (mm)	Width (mm)	Length (mm)	Width (mm)	Length (mm)
MW	0.034±0.002	0.019±0.001	0.111±0.004	0.130±0.006	0.167±0.008	0.184±0.019
LB	0.030±0.001	0.028±0.001	0.109±0.005	0.113±0.006	0.152±0.010	0.178±0.014
BW	0.040±0.002	0.035±0.002	0.111±0.005	0.150±0.006	0.183±0.130	0.213±0.014
IW	0.036±0.002	0.029±0.002	0.119±0.005	0.130±0.007	0.149±0.005	0.200±0.014
p-value	0.002	0.000	0.426	0.006	0.049	0.321
LSD (5%)	0.004	0.004	0.013	0.017	0.020	0.029

Values are means ± standard errors

BW = Batanes White, IW = Ilocos White, LB = Lubang, MW = Mindoro White

Parenchymal cells vary from hexagonal to ovoidal. LB had the smallest parenchyma cells while IW (in terms of width) and BW (in terms of length) have the largest (Table 2). Cell staining revealed that parenchyma cells contained compounds but were mostly starch granules. Most of the parenchyma cells of LB contained starch and carbohydrates while only few carbohydrates containing parenchyma cells were observed in MW.

The vascular structures were arranged in a ring like pattern in cortex which is commonly observed in monocots. They were collateral in all cultivars. Furthermore, vascular structures were surrounded with vascular sheaths consisting of some layers of

small parenchyma cells. BW had the largest vascular structure in terms of length and width while LB had the smallest (*Table 2*). One to three layers of vascular structures were observed across cultivars. The BW had the most number of vascular structures (3 layers) per clove while MW (1-2 layers) had the fewest. Width and length of cells of different tissues were not congruent. A cultivar with the highest cell width does not imply that it also had the utmost length.

Multivariate analyses

Classical clustering analysis was used to detect similarities among cultivars using quantitative variables that were statistically significant and all of the qualitative variables. The analysis showed two major groups having BW the least similar (99.56%) cultivar compared with other cultivars, while IW shared 99.80% similarity with a second group, LB and MW. The LB and MW shared the highest similarity (99.93%) among all cultivars (*Fig. 7*).

Cross-validating the results with the PCA, the first three PCA axes described 97.71% of the total variance, thus indicating that these three axes represent the majority of the variation for the morphological and anatomical characteristics. The first axe accounts for 87.12% variability, which is correlated to the bulb circumference and bulb weight. The second axe represents 78.27% of the variation, which represents the characteristics of the vascular structure number within the clove and the third axe separates the cultivars on the basis of their clove number.

Discussion

Variation in both qualitative and quantitative characters was observed in this study. We focused our analysis on bulb and clove traits primarily because they are the economic organs of garlic used in culinary, medicine, and propagation. Bulb weight, in particular, is the parameter which has the most direct impact on garlic yield as it represents the most significant production characteristics and its market value (Moravčević et al., 2017). According to Panthee et al. (2006), variation in qualitative characters are useful for varietal descriptor and variety identification, in contrast to quantitative characters that have direct application in variety improvement programs owing to its agronomic interest.

Bulb circumference and weight of the four cultivars in this study were significantly different with BW being the largest and heaviest bulb, followed by IW, LB and then, MW being the smallest and lightest. The largeness and heaviness of BW could be accounted to the number of cloves and clove weight. The present finding is in accordance with the results of Islam et al. (2007) and Yeshiwas et al. (2018) who reported significant variation for bulb weight due to genotypic difference. Additionally, in India, Rakesh Sharma et al. (2018) found that bulb diameter and weight contributed maximum towards the total variability in their evaluated germplasm. The slight change in order between IW and LB in terms of clove weight could be due to carbohydrates stored in their clove's cells. The cells of LB cloves were anatomically small but had more carbohydrates containing parenchyma cells as revealed after cell staining. Plant cells contain large amount of carbohydrates such as starch, glycogen and cellulose, which are important for energy, structure, storage and increasing biomass (Guertin and Sabatini, 2005). In garlic, carbohydrates play an important role from dormancy and sprouting (Mashayekhi et al., 2016).

Hirata et al. (2016) evaluated garlic diversity based on morphological, physiological and isozyme variation of collected germplasm from Asia including Southeast Asia and reported that all accessions from tropical regions have comparable bulb yield in terms of weight and circumference as well as number and weight of cloves. Menezes-Sobrinho et al. (1999) identified bulb weight and bulb skin color among many characters to have a combination of qualitative and quantitative characters in principal components which are similar to the present study. In this study, cultivars differed in qualitative traits including bulb shape and structure type, and bulb sheath number and color. These traits are considered valuable for market recognition (Volk et al., 2004) because consumers are attracted to colorful, bigger, flavorful and unique types of garlic for different culinary purposes. While BW is easily distinguished as the biggest garlic, LB could be the choice for a colorful garlic due to its unique bulb sheath color. The MW, on the other hand, would be a preferred cultivar for flavor and aroma, which are ascribed to its small bulb size similar to the findings of Medina and Garcia (2007).

With regard to bulb structure type, both LB and BW have a regular multi-fan groups with cloves arranged in three layers within a bulb. This type of garlic is a valuable specimen for propagation as overall bulb yield and quality are influenced, not only by growth location and farmer's management practice (Volk and Stern, 2009), but also by the size and quality of the planting stock (Conci et al., 2003 Melo et al., 2006). Initial planting stock that is of sufficient size and quality yields higher harvests because it can produce bigger bulb circumference and considered as more valuable commercial assets (Castellanos et al., 2004). Each clove can develop a new plant and often, large-sized cloves are utilized as seedlings. Heredia et al. (1997) and Gwandu and Isa (2016) reported that bulb selection based on the number of cloves are partially due to findings that a bulb with few cloves produces large individual seeds, which in turn contributes to a greater bulb yield, but does not imply the use of a greater amount of seed. However, in this study, cultivars that have bulb with many cloves produced larger individual seeds as observed in BW.

Obtaining only three distinct clusters from sampled cultivars indicates that there must be a frequent material flow from one place to another owing to the small geographical region of the Philippines. Garlic is a clonally propagated species, which may reduce variation hence little number of clusters. This observation is congruent to several studies on diversity analysis of garlic germplasm in other countries in which despite large geographical coverage and number of garlic accessions, only a few clusters were derived. For example, Panthee et al. (2006) examined 179 garlic germplasms in Nepal and found only three clusters. Menezes-Sobrinho et al. (1999) characterized 89 garlic germplasms of Brazil and found 13 clusters. Lallemand et al. (1997) evaluated 65 garlic accessions and found six clusters on the basis of morphological characters. Hence, three clusters from a relatively small geographical coverage in the Philippines are reasonable. However, it is noteworthy that local garlic cultivars evaluated in this study have much larger circumference than those reported by Hirata et al. (2016).

Garlic from warm, short-day lowland tropical regions produces poor bulbs as compared with garlic from temperate zones, which produces bigger bulbs, where days are longer and winters are cold (Brewster, 2008). Bulb formation is greatly influenced by photoperiod and temperature (Brewster, 1990). In an attempt to improve garlic bulb size in the tropics, Ragas et al. (2016) studied the effect of night break on phenotypic traits of locally produced and one imported cultivar planted in selected Philippine provinces. They observed that all garlic cultivars produced larger bulbs when exposed

to night break treatment than those in natural sunlight. Interestingly, BW in this study had larger and heavier bulb produced than ‘Taiwan’, the imported accession reported by Ragas et al. (2016). Hence, locally-produced cultivar especially BW has the potential to outperform imported garlic available in the Philippine market.

The shape of the clove’s cross- sections differed among the cultivars studied. However, the shape of the cross-section of cloves and bulbs of LB and MW were relatively similar probably because of the proximity in the geographical origins of these cultivars. The LB cultivars were originally from Lubang, an island, northwest of Mindoro province. However, Batanes, where BW originated, is a province of some distance from the other provinces (Ilocos and Mindoro), which may be the reason for the distinct differences between the BW and the other garlic cultivars studied. In all cultivars examined, the clove epidermis consisted of a single cell layer, which is congruent to the observations of Miryeganeh and Movafeghi (2009) in scape and Mashayekhi and Columbus (2014) in leaf blade structures of *Allium* species. Size of cells in epidermis, ground and vascular tissues differed from one cultivar to the other. Observations on plants suggest that growth and most morphology do not depend on the number of cells or their size within an organ (Walbot, 2012). This matches the result obtained in this study wherein a cultivar with smallest bulb circumference is not the cultivar with the smallest cell size or vice versa. Plant cells have their own adaptations to achieve near normal morphology despite fewer cells or small cell size (Haber and Foard, 1961). For instance, the LB had smaller cell size than MW even if the latter had smaller bulb circumference.

Anatomical characterization of several cross-sections of the clove revealed that cell size is invariable within a given cultivar; therefore, a useful criterion for grouping similar cultivars. On the other hand, the layers and number of vascular structures per layer are inconsistent among cultivars studied implying that it is an important anatomical character for taxonomic classification. These were confirmed in the clustering analysis which detected highest similarities between LB and MW cultivars, both originally from Mindoro province; and the BW consistently remained the least similar with the rest of the cultivars studied.

Conclusion

This study established the morpho-anatomical characterization of major Philippine garlic cultivars by analyzing stable phenotypic traits which are expected to facilitate efficient measure for revealing relationships and detecting morphologically similar garlic cultivars. The results point at one population (BW) that displayed significant bulb traits and suggest that this cultivar could be further improved to match desirable traits of an imported garlic available in the Philippine market. To represent a richer selection base, however, for the needs of culinary and pharmaceutical purposes, it is recommended that future work should consider larger number of germplasm and should be tested at multi-location sites for national variety trial test useful for dissemination to researchers, farmers, and consumers.

Acknowledgements. Authors would like to thank Korean Program for International Agriculture (KOPIA) for the research fund provided. MAGRO and First Christian Cooperative for providing the garlic cultivar samples. Assistance in garlic collection ably supported by Emmanuel G. Ruedas, Jennifer M. Manangkil, and Marcelino L. Marturillas are highly appreciated.

REFERENCES

- [1] Brewster, J. L. (1990): Physiology of Crop Growth and Bulbing. – In: Rabinowitch, H. D., Brewster, J. L. (eds.) Onions and Other Vegetable Alliums. CRC Press, Boca Raton, FL, pp. 53-88.
- [2] Brewster, J. L. (2008): Onions and Other Vegetable Alliums, 2nd ed. – CABI Publishing, Wallingford, Oxfordshire, UK.
- [3] Bureau of Agricultural Statistics (2009): Department of Agriculture Philippines. – https://psa.gov.ph/sites/default/files/commodity_factsheet2009.pdf (accessed 27 November 2017).
- [4] Castellanos, J. Z., Vargas-Tapia, P., Ojodeagua, J. L., Hoyos, G. (2004): Garlic productivity and profitability as affected by seed clove size, planting density and planting method. – Horticultural Science 39(6): 1272-1277.
- [5] Conci, V. C., Canavelli, A., Lunello, P., DiRienzo, J., Nome, S. F., Zumelzu, G., Italia, R. (2003): Yield losses associated with virus-infected garlic plants during five successive years. – Plant Disease 87: 1411-1415. <http://dx.doi.org/10.1094/PDIS.2003.87.12.1411>.
- [6] De Mason, D. A. (1990): Morphology and Anatomy of Allium. – In: Rabinowitch, H. D., Brewster, J. L. (eds.) Onions and Allied Crops (Vol. 1). CRC Press, Boca Raton, FL, pp. 27-51.
- [7] Etoh, T., Simon, P. W. (2002): Diversity, Fertility and Seed Production in Garlic. – In: Rabinowitch, H. D., Currah, L. (eds.) Allium Crop Science: Recent Advances. CAB International, Wallingford, Oxon, pp. 101-117.
- [8] Fritsch, R. M. (1988): The root anatomy of the genus *Allium* L. (*Alliaceae*). – Beiträge zur Biologie der Pflanzen 67: 129-160.
- [9] Fritsch, R. M., Friesen, N. (2002): Evolution, Domestication and Taxonomy. – In: Rabinowitch, H. D., Currah, L. (eds.) Allium Crop Science: Recent Advances. CABI Publishing, Wallingford, Oxfordshire, UK. pp 5-27.
- [10] Gerlach, D. (1977): Botanische Mikrotechnik. – Thieme Verlag, Stuttgart.
- [11] Google (2018): Google map of Mindoro, Philippines. – <https://goo.gl/maps/sz6CY9npRGp> (accessed 9 November 2018).
- [12] Guertin, D., Sabatini, D. (2005): Cell Size Control. – Encyclopedia of Life Sciences, John Wiley & Sons, London, pp. 1-10. DOI: 10.1038/npg.els.0003359.
- [13] Gwandu, H. A., Isa, Y. S. (2016): Effects of clove size and defoliation intensity on the growth and yield of garlic (*Allium sativum* L.) in Sokoto, Nigeria. – International Journal of Research in Engineering and Science 4(9): 37-41.
- [14] Haber, A., Foard, D. (1961): Anatomical analysis of wheat growing without cell division. – American Journal of Botany 4: 438-446.
- [15] Heredia, A., Heredia, E., Laborde, J. A. (1997): Number of cloves per bulb; selection criteria for garlic improvement. II Results with “Taiwan” type. – Acta Horticulturae. 433: 271-277. <https://doi.org/10.17660/ActaHortic.1997.433.26>.
- [16] Hirata, S., Abdelrahman, M., Yamauchi, N., Shigyo, M. (2016): Diversity evaluation based on morphological, physiological and isozyme variation in genetic resources of garlic (*Allium sativum* L.) collected worldwide. – Genes and Genetic Systems 91: 161-173. <https://doi.org/10.1266/ggs.15-00004>.
- [17] IPGRI ECP/GR, AVRDC (2001): Descriptors for Allium (*Allium spp.*) – International Plant Genetic Resources Institute, Rome, European Cooperative Programme for Crop Genetic Resources Networks (ECP/GR). Taipei, Asian Vegetable Research and Development Center, pp. 1-42.
- [18] Islam, M. J., Ak, M., Hossain, M., Khanam F, Majumder, U. K., Rahman, M. M., Rahman, M. S. (2007): Effect of mulching and fertilization on growth and yield of garlic at Dinajpur in Bangladesh. – Asian Journal of Plant Science 6(1): 98-101.

- [19] Jo, M. H., Ham, I. K., Moe, K. T., Kwon, S. W., Lu, F. H., Park, Y. J., Kim, W. S., Won, M. K., Kim, T. I. Lee, E. M. (2012): Classification of genetic variation in garlic (*Allium sativum* L.) using SSR markers. – Australian Journal of Crop Science 6: 625-631.
- [20] Kamenetsky, R. (2007): Garlic: botany and horticulture. – Horticultural Reviews 33: 123-172.
- [21] Kamenetsky, R., Khassanov, F., Rabinowitch, H. D., Auger, J., Kik, C. (2007): Garlic and Aromatic. – Plant Science and Biotechnology 1(1): 1-5.
- [22] Keller, E. R. J. (2002): Cryopreservation of *Allium Sativum* L. (Garlic). – Springer-Verlag, Berlin, pp. 37-47.
- [23] Kotlinska, T., Havranek, P., Navratill, M., Gerasimova, L., Pimakhov, A., Neikov, S. (1991): Collecting onion, garlic and wild species of *Allium* in Central Asia, USSR. FAO/IBGR. – Plant Genetic Resources 83(84): 31-32.
- [24] Lallemand, J., Messian, C. M., Briand, F., Etoh, E. (1997): Delimitation of varietal groups in garlic (*Allium sativum* L.) by morphological, physiological and biochemical characters. (In: Burba, J. L., Galmarini, C. R. (eds.) Proceedings on First International Symposium on Edible Alliaceae.) – Acta Horticulturae 433: 123-129.
- [25] Mario, P. C., Viviana, B. V., Maria, I. G. A. (2008): Low genetic diversity among garlic *Allium sativum* L.) accessions detected using random amplified polymorphic DNA (RAPD). – Chilean Journal Agricultural Research 68(1): 3-12.
- [26] Mashayekhi, K., Mohammadi Chiane, S., Mianabadi, M., Ghaderifar, F., Mousavizadeh, S. J. (2016): Change in carbohydrate and enzymes from harvest to sprouting in garlic. – Food Science Nutrition 4: 370-376. DOI: 10.1002/fsn3.299.
- [27] Mashayekhi, S., Columbus, J. T. (2014): Evolution of leaf blade anatomy in *Allium* (*Amaryllidaceae*) subgenus *Amerallium* with a focus on the North American species. – American Journal of Botany 101(1): 63-85. <https://doi.org/10.3732/ajb.1300053>
- [28] Mathew, B. (1996): A review of *Allium* Sect. *Allium*. – Royal Botanic Gardens, Kew.
- [29] Medina, J. D. Garcia, H. S. (2007): Garlic post-harvest operations. Food and Agricultural Organization. – http://www.fao.org/fileadmin/user_upload/inpho/docs/Post_Harvest_Compndium_-_Garlic.pdf (accessed 24 February 2018).
- [30] Melo, P. D., Resende, R. O., Cordeiro, C. M. T., Buso, J. A., Torres, A. C., Dusi, A. N. (2006): Viral reinfection affecting bulb production in garlic after seven years of cultivation under field conditions. – European Journal of Plant Pathology 116: 95-101. <https://doi.org/10.1007/s10658-006-9042-3>.
- [31] Menezes-Sobrinho, J. A., de Charchar, J. M., Aragao, F. A. S., Menezes-Sobrinho, J. A. (1999): Morphological characterization of garlic germplasm by multivariate analyses of principal components and canonic variables. – Horticultura Brasileira 17: 96-101.
- [32] Mhazo, M. L., Ngwerume, F. C. Masarirambi, M. T. (2014): Garlic (*Allium sativum*) propagation alternatives using bulblets and cloves of different sizes in a semi-arid subtropical environment. – Annual Research and Review in Biology 4(1): 238-235.
- [33] Miryeganeh, M., Movafeghi, A. (2009): Scape anatomy of *Allium* sect. (*Alliaceae*) in Iran. – Journal of Science (University of Tehran) 35(1): 1-5.
- [34] Moravcevic, D., Varga, J., Pavlovic, N., Todorovic, V., Ugrinovic, M. (2017): Production and chemical characteristics of the populations of spring garlic (*Allium sativum* L.) from the Serbian genetic collection. – Emirates Journal of Food and Agriculture 29(3): 227-236. <https://doi.org/https://doi.org/10.9755/ejfa.2016-11-1680>.
- [35] Panthee, D. R., KC, R. B., Regmi, H. N., Subedi, P. P., Bhattarai, S., Dhakal, J. (2006): Diversity analysis of garlic (*Allium sativum* L.) germplasms available in Nepal based on morphological characters. – Genetic Resources and Crop Evolution 53(1): 205-212. <https://doi.org/10.1007/s10722-004-6690-z>.
- [36] Ragas, R. E. G., Guittap, C. F. C., Bongat, F. B., Lee, J. T., Rasco, E. T. (2016): Initial studies on increasing garlic bulb size through night-break treatment in the Philippines. – Acta Horticulturae 1134: 131-137. <https://doi.org/10.17660/ActaHortic.2016.1134.18>

- [37] Rakesh Sharma, V., Malik, S., Kumar, M., Sirohi, A. (2018): Morphological classification of genetic diversity of Garlic (*Allium sativum* L.) germplasm for bulb and yield-related traits using principal component analysis. – International Journal of Current Microbiology and Applied Science 7(6): 2016-2022. <https://doi.org/10.20546/ijcmas.2018.706.238>.
- [38] Silva, T. M., Vilhalva, D. A. A., Moraes, M. G., Figueiredo-Ribeiro, R. C. L. (2015): Anatomy and fructan distribution in vegetative organs of *Dimerostemma vestitum* (Asteraceae) from the campos rupestres. – Anais da Academia Brasileira de Ciencias 87(2): 797-812. <https://doi.org/10.1590/0001-3765201520140214>.
- [39] Stavelikova, H. (2008): Morphological characteristics of garlic (*Allium sativum* L.) genetic resources collection information. – Horticultural Science (Prague) 35(3): 130-135. <https://doi.org/10.17221/661-HORTSCI>.
- [40] Stearn, W. (1980): *Allium* L. – In: Tutin, T., Heywood, W., Burges, N., Moore, D., Valentine, D., Walters, S., Webb, D. (eds.) Flora Europaea, Vol. 5. Cambridge University Press, Cambridge, pp. 49-69.
- [41] Volk, G. M., Stern, D. (2009): Phenotypic characteristics of ten garlic accessions grown at different North American locations. – Horticultural Science 44(5): 1238-1247.
- [42] Volk, G. M., Henk, A. D., Richards, C. M. (2004): Genetic diversity among US garlic clones as detected using AFLP methods. – Journal of American Society for Horticultural Science 129: 559-569.
- [43] Walbot, V. (2012): Thinking inside the wooden box- classic views of cell size control in plants. – BMC Biology 10: 101.
- [44] Yeshiwas, Y., Negash, B., Walle, T., Gelaye, Y., Melke, A., Yissa, K. (2018): Collection and characterization of garlic (*Allium sativum* L.) germplasm for growth and bulb yield at Debre Markos, Ethiopia. – Journal of Horticulture and Forestry 10(3): 17-26. <https://doi.org/10.5897/JHF2017.0500>.
- [45] Zhao, W. G., Chung, J. W., Lee, G. A., Ma, K. H., Kim, H. H., Kim, K. T., Chung, I. M., Lee, J. K., Kim, N. S., Kim, S. M., Park, Y. J. (2011): Molecular genetic diversity and population structure of a selected core set in garlic and its relative using novel SSR markers. – Plant Breeding 130: 46-54. <https://doi.org/10.1111/j.1439-0523.2010.01805.x>.

A BIBLIOMETRIC ANALYSIS OF CONTEMPORARY RESEARCH REGARDING INDUSTRIAL SYMBIOSIS: A PATH TOWARDS URBAN ENVIRONMENTAL RESILIENCE

AKHTAR, N.^{1*} – SAQIB, Z.² – KHAN, M. I.¹ – MARTIN, M. A.⁴ – ATIF, S. B.^{2,3} – ZAMAN, M. H.²

¹*Department of Environmental Science, International Islamic University, Sector H-10, Islamabad 44000, Pakistan*

²*GIS and Eco-Informatics Laboratory, Department of Environmental Science International Islamic University, Sector H-10, Islamabad 44000, Pakistan*

³*Department of Geography, Government College, Asghar Mall, Rawalpindi, Pakistan*

⁴*IVL Swedish Environmental Research Institute, Stockholm, Sweden*

**Corresponding author
e-mail: nadia@iiu.edu.pk*

(Received 27th Sep 2018; accepted 29th Nov 2018)

Abstract. The conceptual framework of industrial symbiosis (IS) is gaining recognition for ensuring the conservation of natural resources and resilience of socio-ecological surroundings. Significant scholastic strides have been made for explaining the conceptual paradigm of IS. The current study relied upon the Bibliometric mapping technique to decipher the contemporary orientations in the recent publications (2007-2017). The findings revealed that China, UK and the USA are the pivot for promoting research interests in the field. The loci of IS research was observed more skewed in favour of economically developed and industrialized countries. The findings of this study also acknowledge a growing propensity towards research collaboration between and among nations.

Keywords: *industrial ecology, bibliometric analysis, ecological sustainability, environmental resilience, applied ecology*

Introduction

Industrial symbiosis (IS) initially emerged as a branch of the industrial ecology (IE). Laybourn and Lombardi (2012) opined that the theoretical framework of IS is based on engaging diverse production activities, through an integrated network to foster eco-innovation and long term cultural changes. This emerging branch of knowledge tries to elaborate the interconnectedness of natural environment and human society (Chertow, 2008). Therefore, an understanding regarding mutualistic relationships among organism help to re-design the process of industrial production for the sustainability of natural resources (Desrochers, 2001; Zhang et al., 2015a). The conceptual framework is gaining acceptance as a pragmatic strategy to improve efficiency in production activities (Laybourn and Lombardi, 2012). These strategies are obligatory and incumbent for ensuring the conservation of natural resources and achieving the goals of social, economic and environmental sustainability.

The paradigm of IS envisaged a framework to engage traditionally disparate industrial activities in a synchronized manner for maximizing advantages. Thus, it emphasizes on physical exchange of materials, energy, water and byproducts through integrated linkages (Chertow, 2000). The traditional modus operandi in this regard was through collaboration and exploring the synergistic possibilities that transpire through

preconceived integrations in a limited geographic proximity. However, with the advancements in theory and practice, the scope of IS now transcends the limitations of physical proximity (Laybourn and Lombardi, 2012).

Significant scholastic efforts have been made for explaining the concept of IS, defining its boundaries, its evolution, progression, practices and different strategies adopted to implement it during the last two decades (Chertow, 2000; Mirata and Pearce, 2006; Baas, 2011; Martin and Eklund, 2011; Laybourn and Lombardi, 2012; Lombardi et al., 2012; Maclachlan, 2013; Marinos-Kouris and Mourtsiadis, 2013; Alfaro and Miller, 2014; Chertow and Park, 2016; Mauthoor, 2017). During this period, the focus of IS research witnessed a number of evolutionary transformations. Chertow and Park (2016) substantiated that the conceptual frameworks of inquiry in IS are changing in response to socio-economic and technological changes. They also perceived that such propensities are quite evident in case studies, mechanism adopted for investigations, proposals designed for investigations and modelling techniques relied upon for analysis in IS studies. In this connection, Paquin and Howard-Grenville (2013) pronounced another aspect of such evolutionary tendencies and termed it a shift from “blind dates” to “arranged marriages”. Elaborating on this, they maintained that many of contemporary developments in the domain of IS research are now being facilitated by either governmental or non-governmental factors. The growing research inclinations in China towards IS are often cited to corroborate such assertions. In this country, the availability of large networks of eco-industrial parks (EIP) facilitated by the China National Demonstration Eco-Industrial Park Program are encouraging scientific publications in the field of IS. The other notable initiatives of similar objectives are National Industrial Symbiosis Program in the United Kingdom (UK) and Resource Efficiency Flagship Initiative in Europe (Laybourn and Lombardi, 2012; Paquin and Howard-Grenville, 2013).

Despite increasing importance and interest in IS, focus on recalling earlier advances in the domain appeared a less explored arena of research. Two important review papers authored by Yu et al. (2014) and Chertow and Park (2016) attempted to comprehensively review the orientations of research in this domain. The former researcher tried to quantitatively map and mention the noticeable strides in this domain from 1997 to 2012, while, the latter focused on the time period from 1997 to 2014. These researchers not only identified the seminal articles but also identified key themes, researchers and journals in this branch of knowledge. These researchers concluded that the field of IS stemmed from and was rooted in IE. Yu et al. (2014) identified five distinctive topical areas in the contemporary IS research i.e. wastewater treatment and management, solid waste management, energy efficiency, self-organization of IS systems, and policy making and evaluation of IS and EIP projects. Whereas, Chertow and Park (2016) sub-divided their assertions into seven categories based on the nature of study: Foundation, Performance, Mechanism, Modeling, Structure, Case Study, and Proposal.

However, both of these studies deployed bibliometric analysis technique for assessments. The Bibliometric or Scientometric mapping (Cobo et al., 2011) approach is a visual technique of informatics. This assessment approach quantitatively displays structural and dynamic aspects of scientific research proclivities for the specified temporal duration (Liu and Gui, 2016). The technique also offers replicable opportunities for quantitative estimations and visual mapping in the domain of ecology (Neff and Corley, 2009; Govindaradjou and John, 2014). These features enable to

understand the noticeable progressions in the field of interest for systematic review and assessments. It empowers the researchers to decipher the impacts of inter-disciplinary imprints on the prevailing mode of investigations. The bibliometric analysis is also considered helpful for postulating about the emerging trajectories in research orientations (Yu et al., 2014). The similar nature of methodologies have been relied upon for analyzing evolutionary developments and contemporary advances in diversified fields of knowledge (Eito-Brun and Rodríguez, 2016; Liu and Gui, 2016; Mishra et al., 2016; Atif et al., 2018).

The current research was designed to assess the contemporary trends regarding IS research by evaluating the recent publications (2012-2017). The study was designed to identify the salient features of the recent research concerning IS. Besides identifying research inclinations, the study will also attempt to provide a snapshot of key research networks and subject areas of recent publications. Thus, the present study will provide an opportunity to synchronize the efforts for environmental sustainability in the present phase of rapid population growth, urbanization and looming industrialization in the developing world.

Material and methods

The Bibliometric or Scientometric mapping technique was relied upon to decipher the contemporary research orientations in the domain of IS. This study deployed co-occurrence analysis technique to identify networks of collaborating organizations, countries, citations and co-authorships. The technique facilitates the representation of the related items with the help of networks maps through nodes and links (Liu and Gui, 2016). The size of the node is a measure of centrality and thus depicts the importance of the impacts (Wasserman and Faust, 1994). The larger nodes served as hubs in the analysis thereby depicting the significance of articles, keywords, and authors.

The technique is considered reliable (Yu et al., 2014) and was deployed to analyse the spatio-temporal trends and to identify intellectual communities engaged with research concerning IS. It was subsequently relied upon for the “keyword co-occurrence analysis test” to understand the emerging developments in the domain of IS studies. *Table 1* succinctly describes the nature and scope of study, data sources and the methodology implemented for data retrieval and assessments of facts.

Data collection and preparation

The current study is a meta-analysis, based upon the bibliographic information, retrieved from Scopus. The study focused on the research published between January 2012 till March 2017 against the search term “industrial symbiosis”. Ostensibly, it seems that the use of a single keyword may compromise the authenticity of findings by excluding the related studies with different nomenclatures but at the same time avoiding digressions. The study carried out by Atif et al. (2018) has successfully experimented this technique. The query returned 398 records, which were further scrutinized for relevance. On this criteria, a total of 395 records (*Appendix-I*) were selected for further processing. The data was refined using Notepad ++ to standardize the variants used in keywords, authors, journals, organizations and country names.

Table 1. Study approach adopted for exploring research productivity trends in IS (2012-17)

Objectives	Questions	Indicators
Spatio-temporal distribution of IS research productivity	How many documents are published annually? Which are the most productive countries? Key institutions involved in IS research	Number of documents published per year Number of publications per country Ranking of key organizations and collaboration network
Identify most productive research communities	Who are the most productive authors? Who are the authors that collaborate? Who are authors that share a common interest?	Ranking of most productive authors by complete count method Co-authorship Analysis Co-citation analysis
Key lines of research	Which are the key subject areas under which IS research is being carried out? What are the key themes of IS research?	Contribution by subject based on Scopus classification Keyword Co-occurrences

Data Analysis

The data for current study was analyzed with the help of Bibexcel (Persson et al., 2009) and bibliographic networks developed in VOS Viewer (Van Eck and Waltman, 2011). Bibexcel was used due to its flexibility, ability to handle a large amount of data and its compatibility with other softwares like Excel, Pajek and VOS Viewer (Mishra et al., 2016). The network data obtained from Bibexcel was further processed in VOS Viewer to develop network maps. The findings were subsequently relied upon for depicting salient characteristics of the selected studies. The bibliometric indicators like annually published articles, country wise publication, top authors, top journals and subject categories were directly obtained from Scopus. The content analysis of the selected publications was carried out to scrutinise the causations responsible for reported orientations in contemporary research regarding IS.

Results

Since the study aims, primarily, to cover all aspects of research concerning IS for the time period from 2012 to 2017, therefore all documents, from all countries and languages available have been thoroughly scrutinized. For this purpose 395 publications, specifically related to “industrial symbiosis” were retrieved from the Scopus database for the selected time interval. These studies were carried out by the authors from 24 countries related with 20 different disciplinary areas. The data retrieved included: articles (262), other documents included conference papers (59), book chapters (28), articles in press (22), review articles (15), conference reviews (4), books (2), editorials (2) and the solitary available note. These articles were published in three languages: English (383), Chinese (10) and German (2).

In this connection, the following top five journals were observed in the forefront i.e. Journal of Cleaner Production (92), Journal of Industrial Ecology (JIE) (43), Resources, Conservation and Recycling (13), Computer Aided Chemical Engineering (11) and Shentai Xuebo Acta Ecologica Sinica (11). These five journals account for 42.7% of the total published documents.

Spatio-temporal distribution of research

The spatio-temporal connotations of these scholastic linkages were also magnified with the help of distribution maps and statistical diagrams. The approach is considered helpful for depicting the scholastic collaborations between and among nations (Liu and Gui, 2016). The topic of IS appeared in literature around 1997, afterward, it grew exponentially with correlation coefficient $r^2 = 0.88$ (Figure 1). The findings in Figure 1 also depicting the research productivity of the previous five years (2012-17) in relation to overall research published since 1997.

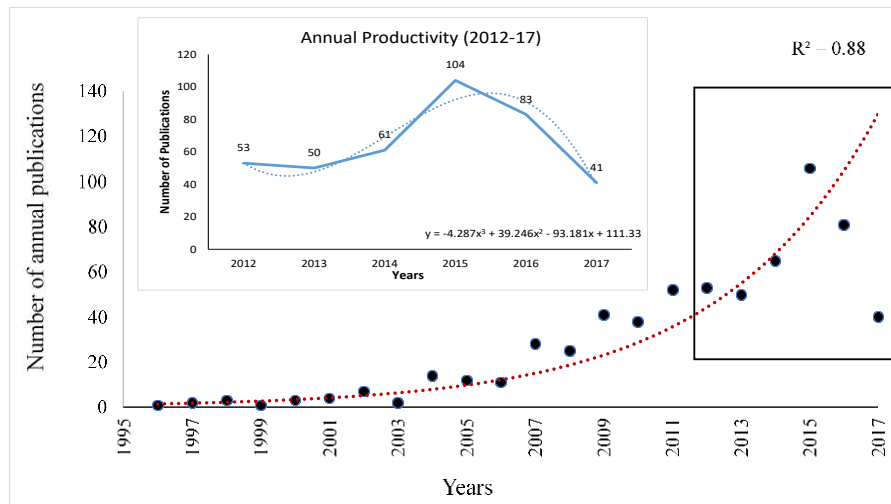


Figure 1. Annual productivity in IS research (1997-2017), while recent fluctuations encompassing the time period (2012-17) have been condensed in the inset

Spatial scope of IS has expanded to 24 countries (Figure 2) during this period and research hubs are mainly located in industrialized contextual settings (Appendix-II) such as China (85), United Kingdom (49) and United States (49). The other countries with significant contributions are Italy (34), Japan (27), Netherlands (21), Philippines (21), Australia (19), Canada (19), and France (19). The findings revealed that about 363 organizations from these countries are involved in IS research. In this connection De-La-Salle University, Manila (22), National Institute for Environmental Studies for Japan (21), University of Surrey, United Kingdom (19), University of Tokyo, Japan (11), Tsinghua University, China (11) and the University of Nottingham, Malaysia (11) are the most prominent contributors towards IS research.

The subsequent co-occurrence frequency analysis depicted a growing tendency towards collaboration between and among different nations. In this regard, the highest scientific collaboration was observed between China and Japan in (17) cases. The participating organizations in these collaborations are the Chinese Academy of Sciences, the National Institute of Environmental Studies (NIES), Japan and Nagoya University, Japan. The researchers such as Liang Dong, Tsuyoshi Fujita affiliated with NIES, Japan and Yong Geng, chief researcher in Chinese Academy of Sciences are, apparently, the most active contributors in this collaboration network. Most of these scientific research collaborations in this network were funded through various programs of Natural Science Foundation of China (11) and Ministry of Environment, Japan (8).

Research Communities

The current study also attempted to identify the most productive authors with respect to a number of publications during the similar time period (2012-2017). The ranking is based on the complete count method. In this scheme of assessments every occurrence of the author is counted provided his name has been mentioned in the list of co-authors in a publication selected for this study. Total citations and h-index were subsequently calculated using the Bibexcel and presented in *Figure 3*.

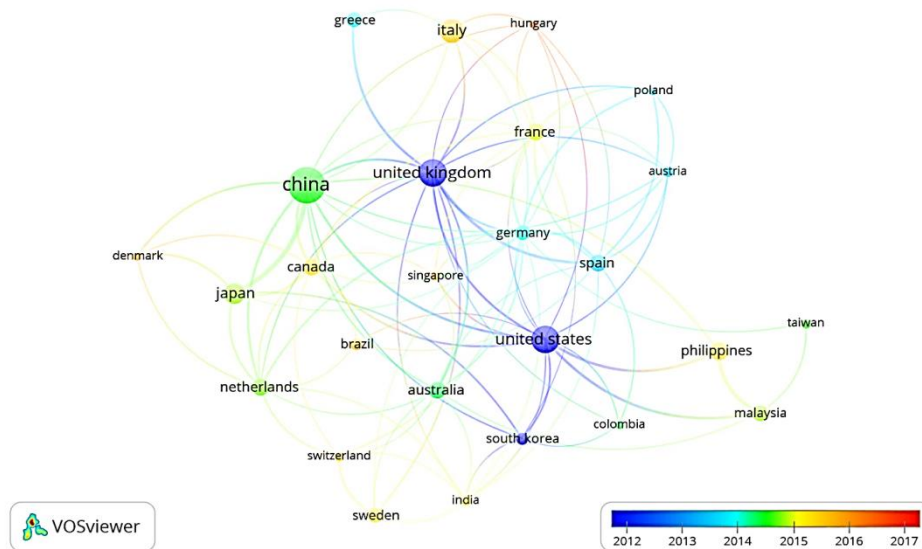


Figure 2. Geographical network of IS research productivity retrieved from corresponding author addresses (2012-17)

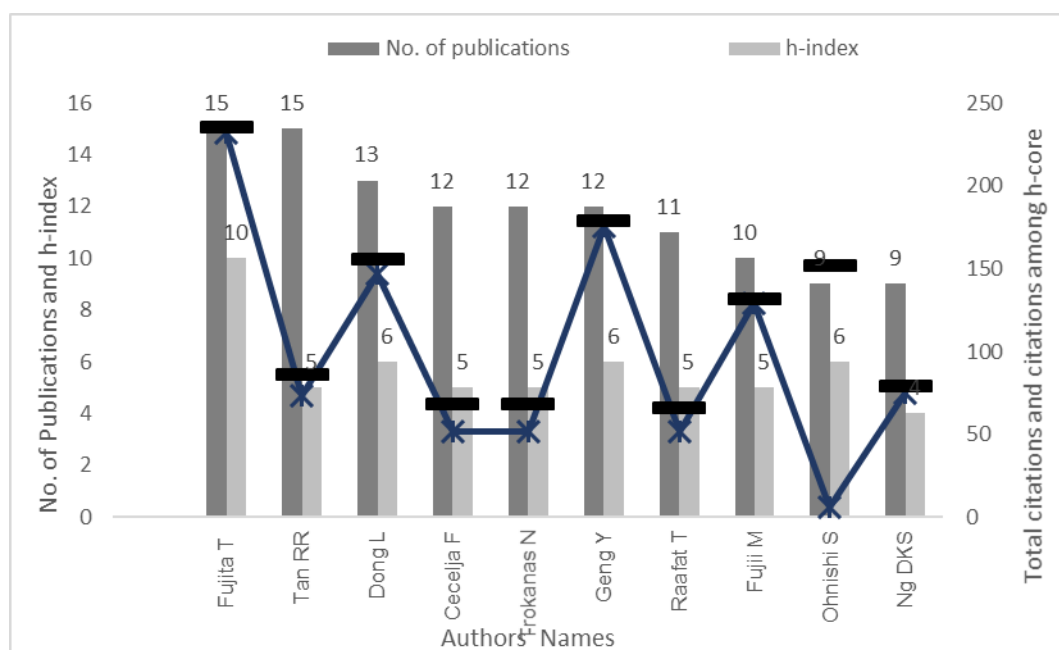


Figure 3. Ten most productive authors based on number of publications and h-index (N=395)

Tsuyoshi Fujita from NIES, Japan and Raymond R. Tan from De La Salle University Philippines were observed as the two most proficient and productive authors with 15 publications apiece. It is pertinent to mention that NIES, Japan (20) and De La Salle University (33) also emerged as the most productive organizations. However, scientific contributions by Tsuyoshi Fujita has received more acknowledgments in terms of citations (235), than Raymond R. Tan (86).

Clusters in research collaborations

The selected publications were analyzed to find out the scale and orientation of contemporary research collaborations. To identify the most productive collaborating authors, a co-authorship network map was developed using VOS viewer (*Figure 4*). The findings have been condensed in *Table 2*. The findings in the table explicitly convey the affiliations of authors, the focus of research and published studies ensuing from these research collaborations.

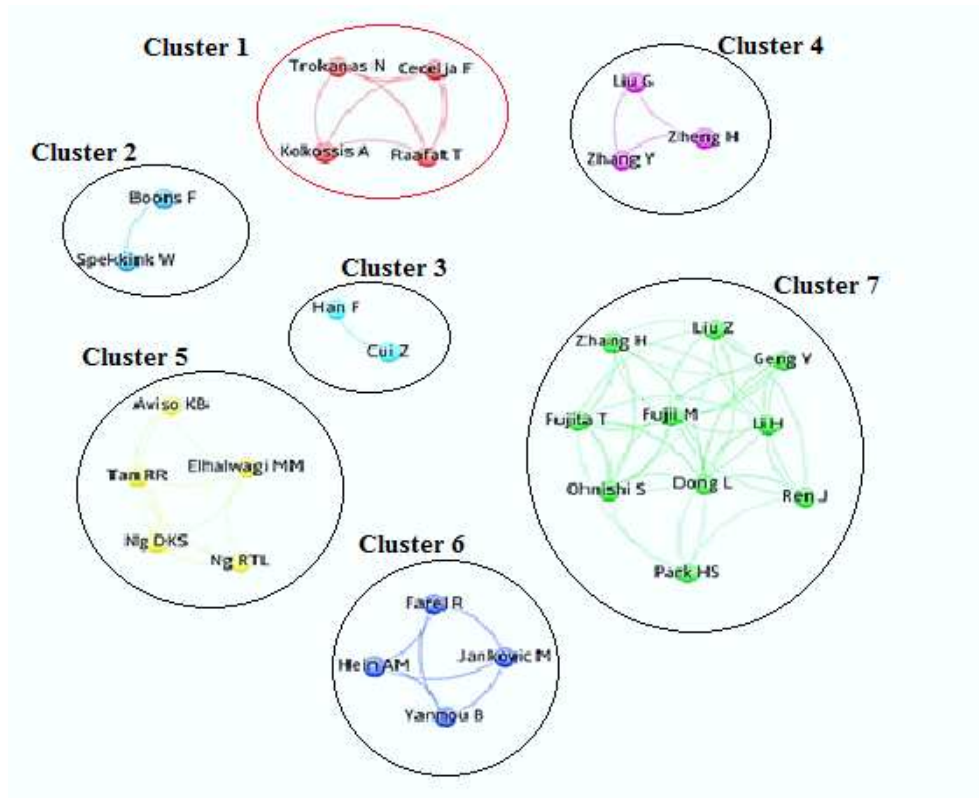


Figure 4. Co-authorship network with seven clusters working on IS

Co-citation analysis

Co-citation analysis technique is also relied upon to understand the conceptual orientations and imprints of contemporary research. The findings of current study in (*Figure 5*) portrayed that Marian Chertow, Yong Geng and Raymond Tan have the significant bearings and followings in the domain of IS research.

Table 2. Co-authorship cluster classification with affiliations and research areas

Cluster Number	Scholars Affiliation	Research Area	Reference Literature
Cluster 1	Center for Process and Information Science, Faculty of Engineering and Physical Science, University of Surrey, UK National Technical University, Athens, Greece	Semantic and ontological approaches for IS	(Trokanas et al., 2012; Trokanas et al., 2014b; Trokanas et al., 2014a; Trokanas et al., 2014c; Trokanas et al., 2015a; Trokanas et al., 2015b)
Cluster 2	Sustainable Consumption Institute, University of Manchester, UK University de los Andes, Bogota, Columbia	IS dynamics and influence of different factors	(Boons et al., 2011; Boons and Spekkink, 2012; Boons et al., 2014; Boons et al., 2015; Boons et al., 2017)
Cluster 3	School of Environmental Science and Engineering, Shandong University, China	IS application in China	(Yu et al., 2015b; Yu et al., 2015c; Yu et al., 2015a)
Cluster 4	State Key Joint Laboratory of Environmental Simulation and Pollution Control, School of Environment, Beijing Normal University, China	Network analysis of IS Systems	(Zhang et al., 2013a; Zhang et al., 2013b; Zhang et al., 2013c; Zhang et al., 2015a; Zhang et al., 2015b; Zhang et al., 2015c; Zhang et al., 2016)
Cluster 5	Center for Engineering and Sustainable Development Research, De La Salle University, Manila, Philippines Department of Chemical and Environmental Engineering, Centre of Excellence for Green Technologies, University of Nottingham, Malaysia Campus. Department of Chemical and Biological Engineering, University of Wisconsin, United States	Fuzzy programming and optimization based IS system and EIP designs	(Ng et al., 2014a; Ng et al., 2014b; Ng et al., 2014c; Tan et al., 2016)
Cluster 6	Laboratoire Genie Industriel, CentraleSupélec, Université Paris-Saclay, France, Paris-Saclay Energy Efficiency (PS2E), France	EIP design architecture and modelling for IS	(Hein et al., 2015a; Hein et al., 2015b; Hein et al., 2016; Hein et al., 2017a; Hein et al., 2017b)
Cluster 7	National Institute for Environmental Studies, Japan National Engineering Laboratory for Hydrometallurgical Cleaner Production Technology, Institute of Process Engineering, Chinese Academy of Sciences, China. Center for Social and Environmental Systems Research, National Institute for Environmental Studies (NIES), Japan Centre for Engineering Operations Management, Department of Technology and Innovation, University of Southern Denmark. School of Environmental Science and Engineering, Shanghai Jiao Tong University, China University of Ulsan, South Korea	Low carbon IS options, environmental and economic benefits of IS for China	(Geng et al., 2009; Dong et al., 2013; Zhang et al., 2013a; Zhang et al., 2013b; Zhang et al., 2013c; Zhang et al., 2015a; Zhang et al., 2015b; Zhang et al., 2015c; Zhang et al., 2016)

Keyword analysis

Keyword co-occurrence maps represent the cognitive structure of a discipline. Atif et al. (2018) opined that the selection of keywords depicts the focus and orientation of the scientific research. For this purpose, the keywords from the publications were retrieved

and processed for analysis. The findings have been illustrated in *Figure 6*. Only such terms as the ones recurring at least five times were mentioned. The strategy was deployed to overcome the excessive noise. *Figure 6* displays an overlay visualization of the keyword co-occurrences. The size of the node reflects frequency, while, the color of the node represents the publishing time period.

The central nodes represent the keywords such as “industrial symbiosis” (277), “industrial ecology” (123), “sustainable development” (77), “industry” (76), and “eco-industrial park” (67). Whereas, the keywords like “waste management” (43), “environmental impacts” (42) “recycling” (41), “economics” (39), “Life cycle assessment” (33) and “carbon” (25) also appeared significantly in the analysis (*Figure 6*).

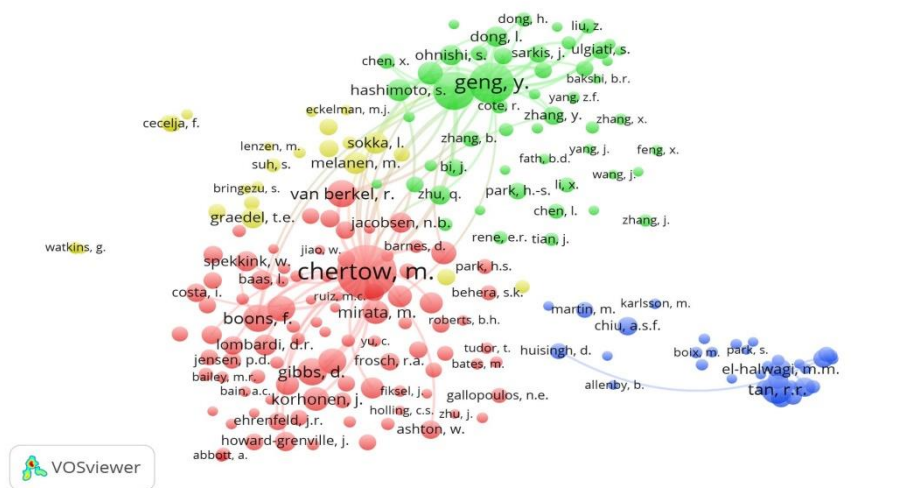


Figure 5. Co-citation network map of cited authors in documents retrieved from Scopus database

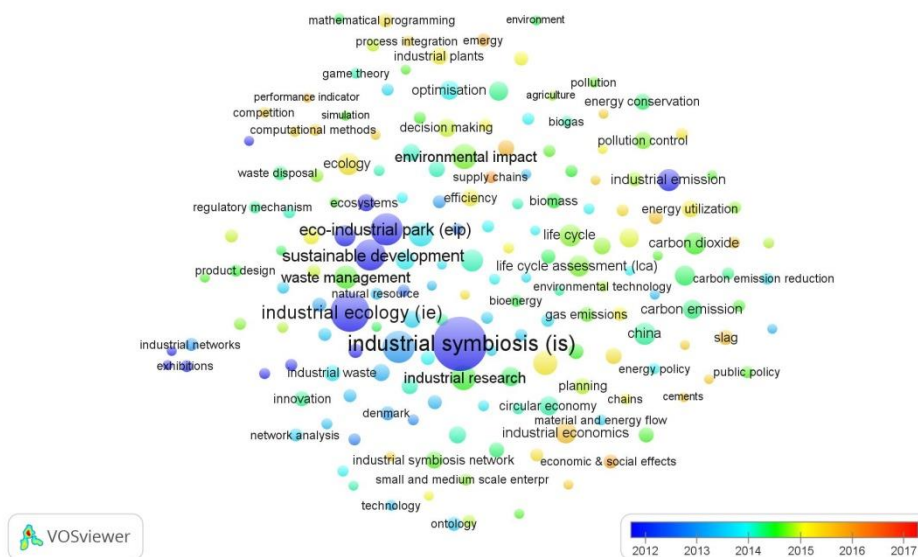


Figure 6. Keyword occurrences in IS related literature for the period 2012-17

Discussion

The resource depletion, accelerating demands for goods and services are compelling the human conscience to strive for environmental and ecological sustainability. The researchers and policy makers are striving to postulate doable measures to achieve these goals. Chertow (2000) proclaimed that in response to these demands the research inclinations towards IS started to gain acceptability from 1997 onwards. The findings of the study in *Figure 1* corroborate and substantiate these assertions. During the span of two decades (1997-2017), IS has evolved from a “signature topic” (Lifset, 2012) in IE to a more systematic, promising and advancing research discipline. As a result, the IS studies are gaining significant attention.

The findings of the study revealed that a large share (34%) of the publications were contributed by two journals, namely Journal of Cleaner Production and Journal of Industrial Ecology (JIE); similar findings were reported by Yu et al. (2014).

The findings in the *Figure 2* also pointed towards growing research collaboration between and among nations, ranging from regional to inter-continental engagements. These findings are in line with the assertions of previous investigations. In this connection, Chertow and Park (2016) and Yu et al. (2014) opined that IS is an advancing interdisciplinary field and rapidly attracting the attention of the research community. In this regard, China from Asia, UK from Europe and USA from the North America were identified as the hub and stimulator for promoting research interests in the field. Whereas, the findings of this study also portrayed that the majority of collaborations are being carried out by developed industrial economies. While the orientation towards IS research was observed in fomenting stages in the southern hemisphere. However, a growing penchant for such cross-country collaborations was also noticed, such as India (7) which is shifting from an agricultural to an industrial economic base.

The research collaborations are needed and encouraged (Iglić et al., 2017) for postulating pragmatic strategies to address the issues from divergent contextual settings. The findings based upon co-authorship analysis help to identify major research groups/collaborations in the field of IS. The findings in *Figure 1* and *Table 2* portrayed the emergence of seven distinctive streams of investigations as an outcome of these research collaborations. The most frequent research collaborations were observed among the researchers from China, Japan, Phillipines and UK. The most productive cluster (07) published (09) papers. This collaboration was observed among researcher from NIES, Japan, Chinese Academy of Sciences, China, University of Southern Denmark and University of Ulsan South Korea. This cluster is also the biggest in terms of number of researchers (10) engaged in collaboration.

The findings of the study (*Figure 5*) substantiate the previous assertions of Yu et al. (2014) that the scholastic contributions of Marian Chertow have more acknowledgment than any other scholar in the domain. The scholar is credited for defining the scope and sphere of this emerging research domain. In this context, Geng et al. (2009) and Tan et al. (2016) were observed as the next most influential scholars, having significant bearings on the emerging paradigm shifts in the field of IS.

The emerging dimensions of industrial symbiosis research were observed more focused on minimizing the impacts of industrial production on environmental, social and economic capitals. These initiatives are incumbent for ensuring the conservation of natural resources and the resilience of socio-ecological surroundings.

Conclusion

The field of Industrial Symbiosis (IS) is gaining acceptance for achieving the objectives through the integration of industrial production systems and collaborative research efforts. The current study revealed growing inclinations towards IS research. The findings portrayed that field is diversifying in scope and gaining acceptance from across the globe.

The outcomes of the study also depicted that industrial economies such as China, UK and USA are spearheading the domain of IS research. The plausible explanation for the growing orientations towards IS research in China can be the premise that the industrial growth remained steadier in this region. The research paradigm in IS are mainly conceived to ensure low carbon emission through research collaboration. The policy makers and researchers in China are stressing and promoting cross-country collaborations. The research paradigms in IS are mainly conceived to ensure low carbon emissions through research collaborations. More focused efforts will be required in the domain of IS to achieve the ultimate goal of clean and green industrial production in the face of mounting pressures from consumer-oriented life-style changes.

Acknowledgements. The financial assistance rendered by Higher Education Commission of Pakistan (HEC, Pakistan) under National Research Program for Universities (NRPU) Project No. 4728 is acknowledged. We are also indebted to anonymous reviewers for their invaluable suggestions to improve the orientation and quality of this manuscript.

REFERENCES

- [1]. Alfaro, J. , Miller, S. (2014): Applying industrial symbiosis to smallholder farms: Modeling a case study in Liberia, West Africa. – *Journal of Industrial Ecology*. 18: 145-154.
- [2]. Atif, S., Saqib, Z., Ali, A., Zaman, M., Akhtar, N., Fatima, H., Atif, M. , Farooqi, S. (2018): Identification of Key-Trends and Evaluation of Contemporary Research Regarding Urban Ecosystem Services: A Path Towards Socio-Ecological Sustainability of Urban Areas. – *APPLIED ECOLOGY AND ENVIRONMENTAL RESEARCH*. 16: 3545-3581.
- [3]. Baas, L. (2011): Planning and uncovering industrial symbiosis: comparing the Rotterdam and Östergötland regions. – *Business Strategy and the Environment*. 20: 428-440.
- [4]. Boons, F., Chertow, M., Park, J., Spekkink, W. , Shi, H. (2017): Industrial symbiosis dynamics and the problem of equivalence: Proposal for a comparative framework. – *Journal of Industrial Ecology*. 21: 938-952.
- [5]. Boons, F. , Spekkink, W. (2012): Levels of institutional capacity and actor expectations about industrial symbiosis: Evidence from the Dutch stimulation program 1999–2004. – *Journal of Industrial Ecology*. 16: 61-69.
- [6]. Boons, F., Spekkink, W., Isenmann, R., Baas, L., Eklund, M., Brullot, S., Deutz, P., Gibbs, D., Massard, G. , Romero Arozamena, E. (2015): Comparing industrial symbiosis in Europe: Towards a conceptual framework and research methodology. –
- [7]. Boons, F., Spekkink, W. , Jiao, W. (2014): A process perspective on industrial symbiosis: Theory, methodology, and application. – *Journal of Industrial Ecology*. 18: 341-355.

- [8]. Boons, F., Spekkink, W. , Mouzakitis, Y. (2011): The dynamics of industrial symbiosis: a proposal for a conceptual framework based upon a comprehensive literature review. – *Journal of Cleaner Production*. 19: 905-911.
- [9]. Chertow, M. , Park, J. (2016). Scholarship and practice in industrial symbiosis: 1989–2014. *Taking stock of industrial ecology*. Springer.
- [10]. Chertow, M. R. (2000): Industrial symbiosis: literature and taxonomy. – *Annual review of energy and the environment*. 25: 313-337.
- [11]. Chertow, M. R. (2008). Industrial ecology in a developing context. *Sustainable development and environmental management*. Springer.
- [12]. Cobo, M. J., López-Herrera, A. G., Herrera-Viedma, E. , Herrera, F. (2011): Science mapping software tools: Review, analysis, and cooperative study among tools. – *Journal of the American Society for Information Science and Technology*. 62: 1382-1402.
- [13]. Desrochers, P. (2001): Cities and industrial symbiosis: Some historical perspectives and policy implications. – *Journal of Industrial Ecology*. 5: 29-44.
- [14]. Dong, L., Fujita, T., Zhang, H., Dai, M., Fujii, M., Ohnishi, S., Geng, Y. , Liu, Z. (2013): Promoting low-carbon city through industrial symbiosis: A case in China by applying HPIMO model. – *Energy policy*. 61: 864-873.
- [15]. Eito-Brun, R. , Rodríguez, M. L. (2016): 50 years of space research in Europe: a bibliometric profile of the European Space Agency (ESA). – *Scientometrics*. 109: 551-576.
- [16]. Geng, Y., Zhang, P., Côté, R. P. , Fujita, T. (2009): Assessment of the national eco-industrial park standard for promoting industrial symbiosis in China. – *Journal of Industrial Ecology*. 13: 15-26.
- [17]. Govindaradjou, S. , John, D. (2014): Quantitative analysis of research trends in a leading ecological journal: bibliometric study during 2003-2012. – *South African Journal of Libraries and Information Science*. 80: 27-40.
- [18]. Hein, A. M., Jankovic, M., Farel, R., Sam, L. I. , Yannou, B. (2015a): Modeling industrial symbiosis using design structure matrices. 17th International Dependency and Structure Modeling Conference, DMS 2015.
- [19]. Hein, A. M., Jankovic, M., Farel, R. , Yannou, B. (2015b): A conceptual framework for eco-industrial parks. ASME 2015 International Design Engineering Technical Conferences and Computers and Information in Engineering Conference. American Society of Mechanical Engineers, V004T005A024-V004T005A024.
- [20]. Hein, A. M., Jankovic, M., Farel, R. , Yannou, B. (2016): A data-and knowledge-driven methodology for generating eco-industrial park architectures. ASME 2016 International Design Engineering Technical Conferences and Computers and Information in Engineering Conference. American Society of Mechanical Engineers, V004T005A002-V004T005A002.
- [21]. Hein, A. M., Jankovic, M., Feng, W., Farel, R., Yune, J. H. , Yannou, B. (2017a): Stakeholder power in industrial symbioses: A stakeholder value network approach. – *Journal of Cleaner Production*. 148: 923-933.
- [22]. Hein, A. M., Yannou, B., Jankovic, M. , Farel, R. (2017b): Towards an Automatized Generation of Rule-Based systems for architecting eco-industrial parks. International Conference on Research into Design. Springer, 691-699.
- [23]. Iglič, H., Doreian, P., Kronegger, L. , Ferligoj, A. (2017): With whom do researchers collaborate and why? – *Scientometrics*. 112: 153-174.
- [24]. Laybourn, P. , Lombardi, D. R. (2012): Industrial symbiosis in European policy. – *Journal of Industrial Ecology*. 16: 11.
- [25]. Lifset, R. (2012): Indications of Progress. – *Journal of Industrial Ecology*. 16: 1-1.
- [26]. Liu, C. , Gui, Q. (2016): Mapping intellectual structures and dynamics of transport geography research: a scientometric overview from 1982 to 2014. – *Scientometrics*. 109: 159-184.

- [27]. Lombardi, D. R., Lyons, D., Shi, H., Agarwal, A. (2012): Industrial symbiosis: testing the boundaries and advancing knowledge. – *Journal of Industrial Ecology*. 16: 2-7.
- [28]. Maclachlan, I. (2013): Kwinana Industrial Area: agglomeration economies and industrial symbiosis on Western Australia's Cockburn Sound. – *Australian Geographer*. 44: 383-400.
- [29]. Marinos-Kouris, D., Mourtsiadis, A. (2013): INDUSTRIAL SYMBIOSIS IN GREECE: A STUDY OF SPATIAL ALLOCATION PATTERNS. – *FRESENIUS ENVIRONMENTAL BULLETIN*. 22: 2174-2181.
- [30]. Martin, M., Eklund, M. (2011): Improving the environmental performance of biofuels with industrial symbiosis. – *Biomass and Bioenergy*. 35: 1747-1755.
- [31]. Mauthoor, S. (2017): Uncovering industrial symbiosis potentials in a small island developing state: The case study of Mauritius. – *Journal of Cleaner Production*. 147: 506-513.
- [32]. Mirata, M., Pearce, R. (2006): Industrial symbiosis in the UK. – *Industrial Ecology and Spaces of Innovation* (Green K and Randles S (eds)). Edward Elgar, Cheltenham, UK. 77-105.
- [33]. Mishra, D., Gunasekaran, A., Papadopoulos, T., Childe, S. J. (2016): Big Data and supply chain management: a review and bibliometric analysis. – *Annals of Operations Research*. 1-24.
- [34]. Neff, M. W., Corley, E. A. (2009): 35 years and 160,000 articles: A bibliometric exploration of the evolution of ecology. – *Scientometrics*. 80: 657-682.
- [35]. Ng, R., Wan, Y., Ng, D., Tan, R. (2014a): Stability analysis of symbiotic bioenergy parks. 17th conference on process integration, modelling and optimisation for energy saving and pollution reduction. 859-864.
- [36]. Ng, R. T., Hassim, M. H., Ng, D. K., Tan, R. R., El-Halwagi, M. M. (2014b). Multi-objective design of industrial symbiosis in palm oil industry. *Computer Aided Chemical Engineering*. Elsevier.
- [37]. Ng, R. T., Ng, D. K., Tan, R. R., El-Halwagi, M. M. (2014c): Disjunctive fuzzy optimisation for planning and synthesis of bioenergy-based industrial symbiosis system. – *Journal of Environmental Chemical Engineering*. 2: 652-664.
- [38]. Paquin, R. L., Howard-Grenville, J. (2013): Blind dates and arranged marriages: Longitudinal processes of network orchestration. – *Organization Studies*. 34: 1623-1653.
- [39]. Persson, O., Danell, R., Schneider, J. W. (2009): How to use Bibexcel for various types of bibliometric analysis. – *Celebrating scholarly communication studies: A Festschrift for Olle Persson at his 60th Birthday*. 5: 9-24.
- [40]. Tan, R. R., Andiappan, V., Wan, Y. K., Ng, R. T., Ng, D. K. (2016): An optimization-based cooperative game approach for systematic allocation of costs and benefits in interplant process integration. – *Chemical Engineering Research and Design*. 106: 43-58.
- [41]. Trokanas, N., Bussemaker, M., Velliou, E., Tokos, H., Cecelja, F. (2015a). BiOnto: An ontology for biomass and biorefining technologies. *Computer Aided Chemical Engineering*. Elsevier.
- [42]. Trokanas, N., Cecelja, F., Raafat, T. (2014a): Semantic input/output matching for waste processing in industrial symbiosis. – *Computers & Chemical Engineering*. 66: 259-268.
- [43]. Trokanas, N., Cecelja, F., Raafat, T. (2014b). Towards a re-usable ontology for waste processing. *Computer Aided Chemical Engineering*. Elsevier.
- [44]. Trokanas, N., Cecelja, F., Raafat, T. (2015b): Semantic approach for pre-assessment of environmental indicators in Industrial Symbiosis. – *Journal of Cleaner Production*. 96: 349-361.

- [45]. Trokanas, N., Cecelja, F., Yu, M. , Raafat, T. (2014c). Optimising environmental performance of symbiotic networks using semantics. *Computer Aided Chemical Engineering*. Elsevier.
- [46]. Trokanas, N., Raafat, T., Cecelja, F., Kokossis, A. , Yang, A. (2012). Semantic formalism for waste and processing technology classifications using ontology models. *Computer aided chemical engineering*. Elsevier.
- [47]. Van Eck, N. J. , Waltman, L. (2011): Text mining and visualization using VOSviewer. – arXiv preprint arXiv:1109.2058.
- [48]. Wasserman, S. , Faust, K. (1994). *Social network analysis: Methods and applications*, - Cambridge university press,
- [49]. Yu, C., Davis, C. , Dijkema, G. P. (2014): Understanding the evolution of industrial symbiosis research: A bibliometric and network analysis (1997–2012). – *Journal of Industrial Ecology*. 18: 280-293.
- [50]. Yu, F., Han, F. , Cui, Z. (2015a): Assessment of life cycle environmental benefits of an industrial symbiosis cluster in China. – *Environmental Science and Pollution Research*. 22: 5511-5518.
- [51]. Yu, F., Han, F. , Cui, Z. (2015b): Evolution of industrial symbiosis in an eco-industrial park in China. – *Journal of Cleaner Production*. 87: 339-347.
- [52]. Yu, F., Han, F. , Cui, Z. (2015c): Reducing carbon emissions through industrial symbiosis: a case study of a large enterprise group in China. – *Journal of Cleaner Production*. 103: 811-818.
- [53]. Zhang, H., Dong, L., Li, H.-Q., Chen, B., Tang, Q. , Fujita, T. (2013a): Investigation of the residual heat recovery and carbon emission mitigation potential in a Chinese steelmaking plant: A hybrid material/energy flow analysis case study. – *Sustainable Energy Technologies and Assessments*. 2: 67-80.
- [54]. Zhang, H., Dong, L., Li, H., Fujita, T., Ohnishi, S. , Tang, Q. (2013b): Analysis of low-carbon industrial symbiosis technology for carbon mitigation in a Chinese iron/steel industrial park: a case study with carbon flow analysis. – *Energy policy*. 61: 1400-1411.
- [55]. Zhang, Y., Zheng, H., Chen, B., Su, M. , Liu, G. (2015a): A review of industrial symbiosis research: theory and methodology. – *Frontiers of Earth Science*. 9: 91-104.
- [56]. Zhang, Y., Zheng, H., Chen, B. , Yang, N. (2013c): Social network analysis and network connectedness analysis for industrial symbiotic systems: model development and case study. – *Frontiers of Earth Science*. 7: 169-181.
- [57]. Zhang, Y., Zheng, H. , Fath, B. D. (2015b): Ecological network analysis of an industrial symbiosis system: a case study of the Shandong Lubei eco-industrial park. – *Ecological Modelling*. 306: 174-184.
- [58]. Zhang, Y., Zheng, H., Shi, H., Yu, X., Liu, G., Su, M., Li, Y. , Chai, Y. (2016): Network analysis of eight industrial symbiosis systems. – *Frontiers of Earth Science*. 10: 352-365.
- [59]. Zhang, Y., Zheng, H., Yang, Z., Liu, G. , Su, M. (2015c): Analysis of the industrial metabolic processes for sulfur in the Lubei (Shandong Province, China) eco-industrial park. – *Journal of Cleaner Production*. 96: 126-138.

APPENDIX

Appendix-I. 395 selected and reviewed articles

Author Name(s)	Title	Source Title	Year	Vol.	Issue	P. Start	P. End	Doi
Zhou X., Zhang H.	Research on industrial symbiosis mode logistics industrial cluster in Shenyang Economic Zone	Proceeding of 2012 International Conference on Information Management, Innovation Management and Industrial Engineering, ICIII 2012	2012	2		489	492	
Romero D., Molina A.	Green virtual enterprise breeding environments: A sustainable industrial development model for a circular economy	IFIP Advances in Information and Communication Technology	2012	380	AICT	427	436	10.1007/978-3-642-32775-9_43
Kopacek B., Schadlbauer S.	Introduction to zero WIN	Electronics Goes Green 2012+, ECG 2012 - Joint International Conference and Exhibition, Proceedings	2012					
Schadlbauer S., Kopacek B., Gallo M., Arnaiz S.	The ZeroWIN production model	Electronics Goes Green 2012+, ECG 2012 - Joint International Conference and Exhibition, Proceedings	2012					
Arranz P., Tarragó J., Vallvé X., Marwede M., Den Boer E., Rothe M., Wüst F., Middendorf A., Cocciantelli J.-M., Lippert M.	Practical demonstrator 'Design for recycling photovoltaic system'	Electronics Goes Green 2012+, ECG 2012 - Joint International Conference and Exhibition, Proceedings	2012					

Author Name(s)	Title	Source Title	Year	Vol.	Issue	P. Start	P. End	Doi
Marwede M., Schischke K., Arranz P., Hickey S., Fitzpatrick C., Ospina J., Yang M., Nissen N.F., Lang K.-D.	Methodology to identify design for recycling measures for high-tech sectors	Electronics Goes Green 2012+, ECG 2012 - Joint International Conference and Exhibition, Proceedings	2012					
Nesbit S., Stano J., Atwater J.W., Casavant T.	Cascading water: Combining GIS and system analysis to maximize water reuse	Canadian Journal of Civil Engineering	2012	39	12	1321	1327	10.1139/cjce-2012-0251
Den Boer E., Williams I., Fitzpatrick C., Arranz P., Dietrich J., Kent A., Tischer A., Durao V., Perthes H., Peagam R., Kopacek B.	Bringing all industrial networks together and next steps	Electronics Goes Green 2012+, ECG 2012 - Joint International Conference and Exhibition, Proceedings	2012					
Li G.	A paradigm of constructing industrial symbiosis and coupling in China's county-region economic sustainable development	Green Technologies and Business Practices: An IT Approach	2012			1	14	10.4018/978-1-4666-1972-2.ch001
Watts C., Binder C.R.	Simulating shocks with the hypercycles model of economic production	iEMSs 2012 - Managing Resources of a Limited Planet: Proceedings of the 6th Biennial Meeting of the International Environmental Modelling and Software Society	2012			2651	2659	
Diwekar U.	Green engineering and sustainability: A systems analysis perspective	Sustainability: Multi-Disciplinary Perspectives	2012			273	309	10.2174/978160805103811201010273

Author Name(s)	Title	Source Title	Year	Vol.	Issue	P. Start	P. End	Doi
Karkanias C., Karagiannidis A., Antonopoulos I.S., Samaras P.	Adopting rational waste management schemes: The case of Preveza municipality	Economics and Policy of Energy and the Environment	2012		3	65	79	
Hiete M., Ludwig J., Schultmann F.	Intercompany Energy Integration: Adaptation of Thermal Pinch Analysis and Allocation of Savings	Journal of Industrial Ecology	2012	16	5	689	698	10.1111/j.1530-9290.2012.00462.x
Wells P., Zapata C.	Renewable Eco-industrial Development: A New Frontier for Industrial Ecology?	Journal of Industrial Ecology	2012	16	5	665	668	10.1111/j.1530-9290.2012.00487.x
Chopra S.S., Khanna V.	Toward a network perspective for understanding resilience and sustainability in industrial symbiotic networks	IEEE International Symposium on Sustainable Systems and Technology	2012					10.1109/ISSST.2012.6227987
Lin K.-N.	Cradle to cradle at CSC: Through integrated recycling system and industrial symbiosis	AISTech - Iron and Steel Technology Conference Proceedings	2012			217	224	
Usón S., Valero A., Agudelo A.	Thermoeconomics and Industrial Symbiosis. Effect of by-product integration in cost assessment	Energy	2012	45	1	43	51	10.1016/j.energy.2012.04.016
Ohnishi S., Fujita T., Chen X., Fujii M.	Econometric analysis of the performance of recycling projects in Japanese Eco-Towns	Journal of Cleaner Production	2012	33		217	225	10.1016/j.jclepro.2012.03.027
Clark J.H., Pfaltzgraff L.	Industrial symbiosis using green chemistry	Technical Proceedings of the 2012 NSTI Nanotechnology Conference and Expo, NSTI-Nanotech 2012	2012			706	707	
Raafat T., Trokanas N., Cecelja F., Kokossis A., Yang A.	Semantically-enabled Formalisation to Support and Automate the Application of Industrial Symbiosis	Computer Aided Chemical Engineering	2012	31		1055	1059	10.1016/B978-0-444-59506-5.50042-0

Author Name(s)	Title	Source Title	Year	Vol.	Issue	P. Start	P. End	Doi
Shi L., Liu G., Guo S.	International comparison and policy recommendation on the development model of industrial symbiosis in China	Shengtai Xuebao/ Acta Ecologica Sinica	2012	32	12	3950	3957	10.5846/stxb201111131724
Shi X., Yang J., Wang R., Zhao L.	An approach for analyzing resources metabolism of industrial ecosystems	Shengtai Xuebao/ Acta Ecologica Sinica	2012	32	7	2012	2024	10.5846/stxb201104180505
Meneghetti A., Nardin G.	Enabling industrial symbiosis by a facilities management optimization approach	Journal of Cleaner Production	2012	35		263	273	10.1016/j.jclepro.2012.06.002
Raafat T., Cecelja F., Yang A., Trokanas N.	Semantic support for industrial symbiosis process	Computer Aided Chemical Engineering	2012	30		452	456	10.1016/B978-0-444-59519-5.50091-5
Trokanas N., Raafat T., Cecelja F., Kokossis A., Yang A.	Semantic Formalism for Waste and Processing Technology Classifications Using Ontology Models	Computer Aided Chemical Engineering	2012	30		167	171	10.1016/B978-0-444-59519-5.50034-4
Behera S.K., Kim J.-H., Lee S.-Y., Suh S., Park H.-S.	Evolution of 'designed' industrial symbiosis networks in the Ulsan Eco-industrial Park: 'Research and development into business' as the enabling framework	Journal of Cleaner Production	2012	29-30		103	112	10.1016/j.jclepro.2012.02.009
Liu L., Zhang B., Bi J., Wei Q., He P.	The greenhouse gas mitigation of industrial parks in China: A case study of Suzhou Industrial Park	Energy Policy	2012	46		301	307	10.1016/j.enpol.2012.03.064
Geißen S.-U., Bennemann H., Horn H., Krull R., Neumann S.	Industrial wastewater treatment and recycling - Potentials and prospects [Industrieabwasserbehandlung und -recycling - Potenziale und Perspektiven]	Chemie-Ingenieur-Technik	2012	84	7	1005	1017	10.1002/cite.201200006
Andrade L.C., Míguez C.G., Gómez M.C.T., Bugallo P.M.B.	Management strategy for hazardous waste from atomised SME: Application to the printing industry	Journal of Cleaner Production	2012	35		214	229	10.1016/j.jclepro.2012.05.014

Author Name(s)	Title	Source Title	Year	Vol.	Issue	P. Start	P. End	Doi
Geng D., Li J., Liu J., Song X.	System analysis of circular economy development in coal mining area	Advanced Materials Research	2012	524-527		2735	2740	10.4028/www.scientific.net/AMR.524-527.2735
Blengini G.A., Busto M., Fantoni M., Fino D.	Eco-efficient waste glass recycling: Integrated waste management and green product development through LCA	Waste Management	2012	32	5	1000	1008	10.1016/j.wasman.2011.10.018
Golev A., Corder G.D.	Developing a classification system for regional resource synergies	Minerals Engineering	2012	29		58	64	10.1016/j.mineng.2011.10.018
Geng Y., Fu J., Sarkis J., Xue B.	Towards a national circular economy indicator system in China: An evaluation and critical analysis	Journal of Cleaner Production	2012	23	1	216	224	10.1016/j.jclepro.2011.07.005
Laybourn P., Lombardi D.R.	Industrial Symbiosis in European Policy: Overview of Recent Progress	Journal of Industrial Ecology	2012	16	1	11	12	10.1111/j.1530-9290.2011.00451.x
Lombardi D.R., Lyons D., Shi H., Agarwal A.	Industrial Symbiosis: Testing the Boundaries and Advancing Knowledge	Journal of Industrial Ecology	2012	16	1	2	7	10.1111/j.1530-9290.2012.00455.x
Paquin R.L., Howard-Grenville J.	The Evolution of Facilitated Industrial Symbiosis	Journal of Industrial Ecology	2012	16	1	83	93	10.1111/j.1530-9290.2011.00437.x
Jensen P.D., Basson L., Hellowell E.E., Leach M.	'Habitat' Suitability Index Mapping for Industrial Symbiosis Planning	Journal of Industrial Ecology	2012	16	1	38	50	10.1111/j.1530-9290.2011.00438.x
Salmi O., Hukkinen J., Heino J., Pajunen N., Wierink M.	Governing the Interplay between Industrial Ecosystems and Environmental Regulation: Heavy Industries in the Gulf of Bothnia in Finland and Sweden	Journal of Industrial Ecology	2012	16	1	119	128	10.1111/j.1530-9290.2011.00403.x
Chertow M., Ehrenfeld J.	Organizing Self-Organizing Systems: Toward a Theory of Industrial Symbiosis	Journal of Industrial Ecology	2012	16	1	13	27	10.1111/j.1530-9290.2011.00450.x
Lombardi D.R., Laybourn P.	Redefining Industrial Symbiosis: Crossing Academic-Practitioner Boundaries	Journal of Industrial Ecology	2012	16	1	28	37	10.1111/j.1530-9290.2011.00444.x

Author Name(s)	Title	Source Title	Year	Vol.	Issue	P. Start	P. End	Doi
Chen X., Fujita T., Ohnishi S., Fujii M., Geng Y.	The Impact of Scale, Recycling Boundary, and Type of Waste on Symbiosis and Recycling: An Empirical Study of Japanese Eco-Towns	Journal of Industrial Ecology	2012	16	1	129	141	10.1111/j.1530-9290.2011.00422.x
Mattila T., Lehtoranta S., Sokka L., Melanen M., Nissinen A.	Methodological Aspects of Applying Life Cycle Assessment to Industrial Symbioses	Journal of Industrial Ecology	2012	16	1	51	60	10.1111/j.1530-9290.2011.00443.x
Ashton W.S., Bain A.C.	Assessing the "Short Mental Distance" in Eco-Industrial Networks	Journal of Industrial Ecology	2012	16	1	70	82	10.1111/j.1530-9290.2011.00453.x
Boons F., Spekkink W.	Levels of Institutional Capacity and Actor Expectations about Industrial Symbiosis: Evidence from the Dutch Stimulation Program 1999-2004	Journal of Industrial Ecology	2012	16	1	61	69	10.1111/j.1530-9290.2011.00432.x
Zhou L., Hu S.-Y., Li Y., Jin Y., Zhang X.	Modeling and Optimization of a Coal-Chemical Eco-industrial System in China	Journal of Industrial Ecology	2012	16	1	105	118	10.1111/j.1530-9290.2012.00447.x
Ferrer G., Cortezia S., Neumann J.M.	Green City: Environmental and Social Responsibility in an Industrial Cluster	Journal of Industrial Ecology	2012	16	1	142	152	10.1111/j.1530-9290.2011.00442.x
Brent G.F., Allen D.J., Eichler B.R., Petrie J.G., Mann J.P., Haynes B.S.	Mineral Carbonation as the Core of an Industrial Symbiosis for Energy-Intensive Minerals Conversion	Journal of Industrial Ecology	2012	16	1	94	104	10.1111/j.1530-9290.2011.00368.x
Liu C., Ma C., Zhang K.	Going beyond the sectoral boundary: A key stage in the development of a regional industrial ecosystem	Journal of Cleaner Production	2012	22	1	42	49	10.1016/j.jclepro.2011.09.022

Author Name(s)	Title	Source Title	Year	Vol.	Issue	P. Start	P. End	Doi
Usón S., Valero A., Valero A., Costa J.	Thermoeconomic fuel impact approach for assessing resources savings in industrial symbiosis: Application to kalundborg ecoindustrial park	Proceedings of the 25th International Conference on Efficiency, Cost, Optimization and Simulation of Energy Conversion Systems and Processes, ECOS 2012	2012	3		346	356	
Valero A., Usón S., Costa J.	Exergy analysis of the industrial symbiosis model in Kalundborg	Proceedings of the 25th International Conference on Efficiency, Cost, Optimization and Simulation of Energy Conversion Systems and Processes, ECOS 2012	2012	1		406	416	
Gregson N., Crang M., Ahamed F.U., Akter N., Ferdous R., Foisal S., Hudson R.	Territorial agglomeration and industrial symbiosis: Sitakunda-Bhatiary, Bangladesh, as a secondary processing complex	Economic Geography	2012	88	1	37	58	10.1111/j.1944-8287.2011.01138.x
Li J., Wang Y., Zhou M.	Application of emergy theory in industrial ecosystem analysis	Advanced Materials Research	2012	361-363		1249	1254	10.4028/www.scientific.net/AMR.361-363.1249
Yang L., Tong L.	Research of typical EIPs based on the social network analysis	Shengtai Xuebao/ Acta Ecologica Sinica	2012	32	13	4236	4245	
Martin M., Svensson N., Fonseca J., Eklund M.	Quantifying the environmental performance of integrated bioethanol and biogas production	Renewable Energy	2013	61		109	116	10.1016/j.renene.2012.09.058
Li G.	A paradigm of constructing industrial symbiosis and coupling in China's county-region economic sustainable development	Sustainable Practices: Concepts, Methodologies, Tools, and Applications	2013	3		1218	1231	10.4018/978-1-4666-4852-4.ch068

Author Name(s)	Title	Source Title	Year	Vol.	Issue	P. Start	P. End	Doi
MacLachlan I.	Kwinana Industrial Area: Agglomeration economies and industrial symbiosis on Western Australia's Cockburn Sound	Australian Geographer	2013	44	4	383	400	10.1080/00049182.2013.852505
Raafat T., Trokanas N., Cecelja F., Bimi X.	An ontological approach towards enabling processing technologies participation in industrial symbiosis	Computers and Chemical Engineering	2013	59		33	46	10.1016/j.compchemeng.2013.03.022
Li J., Gao Y.	Research on eco-industry symbiosis system based on complex network	Proceedings of 2012 3rd International Asia Conference on Industrial Engineering and Management Innovation, IEMI 2012	2013			759	769	10.1007/978-3-642-33012-4-76
Marinos-Kouris D., Mourtsiadis A.	Environmental limits of industrial symbiosis: The case of aluminium eco-industrial network	Fresenius Environmental Bulletin	2013	22	12	3549	3557	
Valero A., Usón S., Torres C., Valero A., Agudelo A., Costa J.	Thermoeconomic tools for the analysis of eco-industrial parks	Energy	2013	62		62	72	10.1016/j.energy.2013.07.014
[No author name available]	IFIP WG 5.7 International Conference on Advances in Production Management Systems, APMS 2012	IFIP Advances in Information and Communication Technology	2013	397	PART 1			
Dong L., Zhang H., Fujita T., Ohnishi S., Li H., Fujii M., Dong H.	Environmental and economic gains of industrial symbiosis for Chinese iron/steel industry: Kawasaki's experience and practice in Liuzhou and Jinan	Journal of Cleaner Production	2013	59		226	238	10.1016/j.jclepro.2013.06.048
Paquin R.L., Howard-Grenville J.	Blind Dates and Arranged Marriages: Longitudinal Processes of Network Orchestration	Organization Studies	2013	34	11	1623	1653	10.1177/0170840612470230

Author Name(s)	Title	Source Title	Year	Vol.	Issue	P. Start	P. End	Doi
Liu G.-F., Chen F.-D.	NISP-based research on the system structure of urban symbiosis network in China	Applied Mechanics and Materials	2013	427-429		2923	2927	10.4028/www.scientific.net/AMM.427-429.2923
Gao X.L., Li R.Q., Li R.	Study on byproducts recycling in eco-industrial parks	Advanced Materials Research	2013	788		288	292	10.4028/www.scientific.net/AMR.788.288
Liao M.-I., Ma H.-W.	The potential environmental gains from industrial symbiosis: Evaluation of CO2 reduction through a crucial by-product	International Journal of Applied Environmental Sciences	2013	8	2	129	136	
Shi X.Q., Li X.N., Yang J.X.	Eco-management benefit analysis of industrial resources from life cycle perspective: A case study of a virtual symbiosis network	Shengtai Xuebao/ Acta Ecologica Sinica	2013	33	19	6398	6410	10.5846/stxb201304180738
Dong L., Fujita T., Zhang H., Dai M., Fujii M., Ohnishi S., Geng Y., Liu Z.	Promoting low-carbon city through industrial symbiosis: A case in China by applying HPIMO model	Energy Policy	2013	61		864	873	10.1016/j.enpol.2013.06.084
Marinos-Kouris D., Mourtsiadis A.	Industrial symbiosis in Greece: A study of spatial allocation patterns	Fresenius Environmental Bulletin	2013	22	7 B	2174	2181	
Zhang H., Dong L., Li H., Fujita T., Ohnishi S., Tang Q.	Analysis of low-carbon industrial symbiosis technology for carbon mitigation in a Chinese iron/steel industrial park: A case study with carbon flow analysis	Energy Policy	2013	61		1400	1411	10.1016/j.enpol.2013.05.066
Gu C., Leveneur S., Estel L., Yassine A.	Industrial symbiosis optimization control model for the exchanges of the material/energy flows in an industrial production park	IFAC Proceedings Volumes (IFAC-PapersOnline)	2013			1015	1020	10.3182/20130619-3-RU-3018.00182
Liu G.-S., Xu S.-Q., Sun Y.-W., Han J.-Y.	Eco-industrial symbiosis network equilibrium model	Beijing Keji Daxue Xuebao/Journal of University of Science and Technology Beijing	2013	35	9	1221	1229	

Author Name(s)	Title	Source Title	Year	Vol.	Issue	P. Start	P. End	Doi
Eckelman M.J., Chertow M.R.	Life cycle energy and environmental benefits of a US industrial symbiosis	International Journal of Life Cycle Assessment	2013	18	8	1524	1532	10.1007/s11367-013-0601-5
Ng R.T.L., Ng D.K.S., Tan R.R.	Systematic approach for synthesis of integrated palm oil processing complex. Part 2: Multiple owners	Industrial and Engineering Chemistry Research	2013	52	30	10221	10235	10.1021/ie400846g
Ng R.T.L., Ng D.K.S.	Systematic approach for synthesis of integrated palm oil processing complex. Part 1: Single owner	Industrial and Engineering Chemistry Research	2013	52	30	10206	10220	10.1021/ie302926q
Xiong W., Wang J., Tang W., Kong W., Zeng Z., Ouyang J., Liu M., Wang G., Huang M., Xiong D.	Establishment of integrative circular agro-ecology system for multiple agricultural industries in Three Gorges Reservoir Area	Nongye Gongcheng Xuebao/Transactions of the Chinese Society of Agricultural Engineering	2013	29	14	203	209	10.3969/j.issn.1002-6819.2013.14.026
Trokanas N., Raafat T., Cecelja F., Kokossis A.	OFIS - Ontological Framework for Industrial Symbiosis	Computer Aided Chemical Engineering	2013	32		523	528	10.1016/B978-0-444-63234-0.50088-9
Zhu J., Ruth M.	Exploring the resilience of industrial ecosystems	Journal of Environmental Management	2013	122		65	75	10.1016/j.jenvman.2013.02.052
Zhang Y., Zheng H., Chen B., Yang N.	Social network analysis and network connectedness analysis for industrial symbiotic systems: Model development and case study	Frontiers of Earth Science	2013	7	2	169	181	10.1007/s11707-012-0349-4
Zhang H., Dong L., Li H.-Q., Chen B., Tang Q., Fujita T.	Investigation of the residual heat recovery and carbon emission mitigation potential in a Chinese steelmaking plant: A hybrid material/energy flow analysis case study	Sustainable Energy Technologies and Assessments	2013	2	1	67	80	10.1016/j.seta.2013.03.003

Author Name(s)	Title	Source Title	Year	Vol.	Issue	P. Start	P. End	Doi
Husgafvel R., Watkins G., Linkosalmi L., Dahl O.	Review of sustainability management initiatives within Finnish forest products industry companies - Translating Eu level steering into proactive initiatives	Resources, Conservation and Recycling	2013	76		1	11	10.1016/j.resconrec.2013.04.006
Pajunen N., Watkins G., Husgafvel R., Heiskanen K., Dahl O.	The challenge to overcome institutional barriers in the development of industrial residue based novel symbiosis products - Experiences from Finnish process industry	Minerals Engineering	2013	46-47		144	156	10.1016/j.mineng.2013.03.008
Hara K., Uwasu M., Yabar H., Zhang H.	Urban development and its impacts on energy and resource consumptions in the Yangtze river delta: Trends and future prospects	Yangtze River: Geography, Pollution and Environmental Implications	2013			121	127	
Boons F.	Ecological Modernization and Industrial Ecology	The Handbook of Global Companies	2013			388	402	10.1002/9781118326152.ch23
Feng L., Di J.H.	A new model of industrial symbiosis optimization	Hydraulic Engineering - Proceedings of the 2012 SREE Conference on Hydraulic Engineering, CHE 2012 and 2nd SREE Workshop on Environment and Safety Engineering, WESE 2012	2013			365	370	
Spekkink W.	Institutional capacity building for industrial symbiosis in the Canal Zone of Zeeland in the Netherlands: A process analysis	Journal of Cleaner Production	2013	52		342	355	10.1016/j.jclepro.2013.02.025

Author Name(s)	Title	Source Title	Year	Vol.	Issue	P. Start	P. End	Doi
Boons F.	Industrial Symbiosis and the Chemical Industry: Between Exploration and Exploitation	Management Principles of Sustainable Industrial Chemistry: Theories, Concepts and Industrial Examples for Achieving Sustainable Chemical Products and Processes from a Non-Technological Viewpoint	2013			131	145	10.1002/9783527649488.ch9
Montastruc L., Boix M., Pibouleau L., Azzaro-Pantel C., Domenech S.	On the flexibility of an eco-industrial park (EIP) for managing industrial water	Journal of Cleaner Production	2013	43		1	11	10.1016/j.jclepro.2012.12.039
Watkins G., Husgafvel R., Pajunen N., Dahl O., Heiskanen K.	Overcoming institutional barriers in the development of novel process industry residue based symbiosis products - Case study at the EU level	Minerals Engineering	2013	41		31	40	10.1016/j.mineng.2012.10.003
Termsinvanich P., Thadaniti S., Wiwattanadate D.	Conceptual model for effective implementation of industrial symbiosis: A case study of Mab-Ta-Phut industrial estate	Mediterranean Journal of Social Sciences	2013	4	1	133	139	10.5901/mjss.2013.v4n1p133
Albino V., Garavelli A.C., Romano V.A.	A Classification of industrial symbiosis networks: A focus on materials and energy recovery	IFIP Advances in Information and Communication Technology	2013	397	PART 1	216	223	10.1007/978-3-642-40352-1_28
Wang G., Feng X., Chu K.H.	A novel approach for stability analysis of industrial symbiosis systems	Journal of Cleaner Production	2013	39		9	16	10.1016/j.jclepro.2012.08.031
Antonopoulos I.S., Zouboulis A.I., Karagiannidis A., Samaras P.	Applying dpsir analysis as a decision support tool for fostering industrial symbiosis concept	Fresenius Environmental Bulletin	2013	22	12 C	3830	3839	

Author Name(s)	Title	Source Title	Year	Vol.	Issue	P. Start	P. End	Doi
Ng W.P.Q., Lam H.L.	Sustainable supply network design through optimisation with clustering technique integration	Chemical Engineering Transactions	2013	35		661	666	10.3303/CET1335110
Rankin W.J.	Towards zero waste production in the minerals and metals sector	TMS Annual Meeting	2013			392	403	
Gu C., Leveueur S., Estel L., Yassine A.	Modeling and optimization of material/energy flow exchanges in an eco-industrial park	Energy Procedia	2013	36		243	252	10.1016/j.egypro.2013.07.028
Mohammed F.A., Yao H.M., OludayoTadé M., Biswas W.	A framework for synergy evaluation and development in heavy industries	Re-Engineering Manufacturing for Sustainability - Proceedings of the 20th CIRP International Conference on Life Cycle Engineering	2013			591	595	
Gu C., Estel L., Yassine A., Leveueur S.	A multiobjective optimization model for designing and optimizing an ecological industrial park	Proceedings - International Conference on Natural Computation	2013			595	600	10.1109/ICNC.2013.6818046
Wood B.M., Jader L.R., Schendel F.J., Hahn N.J., Valentas K.J., Mcnamara P.J., Novak P.M., Heilmann S.M.	Industrial symbiosis: Corn ethanol fermentation, hydrothermal carbonization, and anaerobic digestion	Biotechnology and Bioengineering	2013	110	10	2624	2632	10.1002/bit.24924
Kreiger M.A., Shonnard D.R., Pearce J.M.	Life cycle analysis of silane recycling in amorphous silicon-based solar photovoltaic manufacturing	Resources, Conservation and Recycling	2013	70		44	49	10.1016/j.resconrec.2012.10.002
Jung S., Dodbiba G., Chae S.H., Fujita T.	A novel approach for evaluating the performance of eco-industrial park pilot projects	Journal of Cleaner Production	2013	39		50	59	10.1016/j.jclepro.2012.08.030

Author Name(s)	Title	Source Title	Year	Vol.	Issue	P. Start	P. End	Doi
Mohammed F.A., Biswas W.K., Yao H.M., Tadó M.O.	Assessment of industrial by-product synergies from process engineering and sustainability principles	Progress in Industrial Ecology	2013	8	3	156	165	10.1504/PIE.2013.060663
Romero E., Ruiz M.C.	Framework for applying a complex adaptive system approach to model the operation of eco-industrial parks	Journal of Industrial Ecology	2013	17	5	731	741	10.1111/jiec.12032
Patala S., Hämäläinen S., Jalkala A., Pesonen H.-L.	Towards a broader perspective on the forms of eco-industrial networks	Journal of Cleaner Production	2014	82		166	178	10.1016/j.jclepro.2014.06.059
Giurco D., Prior J., Boydell S.	Industrial ecology and carbon property rights	Journal of Cleaner Production	2014	80		211	223	10.1016/j.jclepro.2014.05.079
Short S.W., Bocken N.M., Barlow C.Y., Chertow M.R.	From refining sugar to growing tomatoes: Industrial ecology and business model evolution short et al. from refining sugar to growing tomatoes	Journal of Industrial Ecology	2014					10.1111/jiec.12171
Yu B., Li X., Shi L., Qian Y.	Quantifying CO2 emission reduction from industrial symbiosis in integrated steel mills in China	Journal of Cleaner Production	2014					10.1016/j.jclepro.2014.08.015
Chopra S.S., Khanna V.	Understanding resilience in industrial symbiosis networks: Insights from network analysis	Journal of Environmental Management	2014	141		86	94	10.1016/j.jenvman.2013.12.038
Schiller F., Penn A.S., Basson L.	Analyzing networks in industrial ecology - A review of Social-Material Network Analyses	Journal of Cleaner Production	2014	76		1	11	10.1016/j.jclepro.2014.03.029
Li W., Cui Z., Han F.	Methods for assessing the energy-saving efficiency of industrial symbiosis in industrial parks	Environmental Science and Pollution Research	2014					10.1007/s11356-014-3327-4
Li W., Cui Z., Han F.	Methods for assessing the energy-saving efficiency of industrial symbiosis in industrial parks	Environmental Science and Pollution Research	2014	22	1	275	285	10.1007/s11356-014-3327-4

Author Name(s)	Title	Source Title	Year	Vol.	Issue	P. Start	P. End	Doi
Trokanas N., Cecelja F., Raafat T.	Semantic input/output matching for waste processing in industrial symbiosis	Computers and Chemical Engineering	2014	66		259	268	10.1016/j.compchemeng.2014.02.010
Cerceau J., Mat N., Junqua G., Lin L., Laforest V., Gonzalez C.	Implementing industrial ecology in port cities: International overview of case studies and cross-case analysis	Journal of Cleaner Production	2014	74		1	16	10.1016/j.jclepro.2014.03.050
Harmsen J.	Novel sustainable industrial processes: From idea to commercial scale implementation	Green Processing and Synthesis	2014	3	3	189	193	10.1515/gps-2013-0102
Jiao W., Boons F.	Toward a research agenda for policy intervention and facilitation to enhance industrial symbiosis based on a comprehensive literature review	Journal of Cleaner Production	2014	67		14	25	10.1016/j.jclepro.2013.12.050
Simboli A., Taddeo R., Morgante A.	Analysing the development of Industrial Symbiosis in a motorcycle local industrial network: The role of contextual factors	Journal of Cleaner Production	2014	66		372	383	10.1016/j.jclepro.2013.11.045
Aviso K.B.	Design of robust water exchange networks for eco- industrial symbiosis	Process Safety and Environmental Protection	2014	92	2	160	170	10.1016/j.psep.2012.12.001
Zhu J., Ruth M.	The development of regional collaboration for resource efficiency: A network perspective on industrial symbiosis	Computers, Environment and Urban Systems	2014	44		37	46	10.1016/j.compenvurbsys.2013.11.001
Zhang B., Wang Z.	Inter-firm collaborations on carbon emission reduction within industrial chains in China: Practices, drivers and effects on firms' performances	Energy Economics	2014	42		115	131	10.1016/j.eneco.2013.12.006
Mirabella N., Castellani V., Sala S.	Current options for the valorization of food manufacturing waste: A review	Journal of Cleaner Production	2014	65		28	41	10.1016/j.jclepro.2013.10.051

Author Name(s)	Title	Source Title	Year	Vol.	Issue	P. Start	P. End	Doi
Gonela V., Zhang J.	Design of the optimal industrial symbiosis system to improve bioethanol production	Journal of Cleaner Production	2014	64		513	534	10.1016/j.jclepro.2013.07.059
Dong L., Gu F., Fujita T., Hayashi Y., Gao J.	Uncovering opportunity of low-carbon city promotion with industrial system innovation: Case study on industrial symbiosis projects in China	Energy Policy	2014	65		388	397	10.1016/j.enpol.2013.10.019
Park H.-S., Behera S.K.	Methodological aspects of applying eco-efficiency indicators to industrial symbiosis networks	Journal of Cleaner Production	2014	64		478	485	10.1016/j.jclepro.2013.08.032
Yu C., De Jong M., Dijkema G.P.J.	Process analysis of eco-industrial park development - The case of Tianjin, China	Journal of Cleaner Production	2014	64		464	477	10.1016/j.jclepro.2013.09.002
Tian J., Liu W., Lai B., Li X., Chen L.	Study of the performance of eco-industrial park development in China	Journal of Cleaner Production	2014	64		486	494	10.1016/j.jclepro.2013.08.005
Liu G.F., Ma Y.T.	Study on by-product synergy and eco-industrial parks in China based on american experience	Applied Mechanics and Materials	2014	472		884	888	10.4028/www.scientific.net/AMM.472.884
Romero E., Ruiz M.C.	Proposal of an agent-based analytical model to convert industrial areas in industrial eco-systems	Science of the Total Environment	2014	468-469		394	405	10.1016/j.scitotenv.2013.08.049
Notarnicola B., Tassielli G., Renzulli P.A.	Potential developments of industrial symbiosis in the Taranto productive district	Pathways to Environmental Sustainability: Methodologies and Experiences	2014			215	224	10.1007/978-3-319-03826-1_21
Teh B.T., Ho C.S., Matsuoka Y., Chau L.W., Gomi K.	Determinant factors of industrial symbiosis: Greening Pasir Gudang industrial park	IOP Conference Series: Earth and Environmental Science	2014	18	1			10.1088/1755-1315/18/1/012162

Author Name(s)	Title	Source Title	Year	Vol.	Issue	P. Start	P. End	Doi
Park J.Y., Park H.-S.	Securing a competitive advantage through industrial symbiosis development: The case of steam networking practices in Ulsan park and park competitive advantage and industrial symbiosis	Journal of Industrial Ecology	2014	18	5	677	683	10.1111/jiec.12158
Deutz P.	Food for thought: Seeking the essence of industrial symbiosis	Pathways to Environmental Sustainability: Methodologies and Experiences	2014			3	11	10.1007/978-3-319-03826-1_1
Trokanas N., Cecelja F., Yu M., Raafat T.	Optimising environmental performance of symbiotic networks using semantics	Computer Aided Chemical Engineering	2014	33		847	852	10.1016/B978-0-444-63456-6.50142-3
Zhang Y., Zheng H., Chen B., Su M., Liu G.	A review of industrial symbiosis research: theory and methodology	Frontiers of Earth Science	2014	9	1	91	104	10.1007/s11707-014-0445-8
Geng Y., Liu Z., Xue B., Dong H., Fujita T., Chiu A.	Emergy-based assessment on industrial symbiosis: a case of Shenyang Economic and Technological Development Zone	Environmental Science and Pollution Research	2014	21	23	13572	13587	10.1007/s11356-014-3287-8
Paquin R.L., Tilleman S.G., Howard-Grenville J.	Is there cash in that trash?: Factors influencing industrial symbiosis exchange initiation and completion	Journal of Industrial Ecology	2014	18	2	268	279	10.1111/jiec.12120
Xu S., Liu G., Lv W., Liu Y.	The nonlinear complementarity model of industrial symbiosis network equilibrium problem	RAIRO - Operations Research	2014	48	4	559	594	10.1051/ro/2014024
Boons F., Spekink W., Jiao W.	A Process Perspective on Industrial Symbiosis: Theory, Methodology, and Application Boons et al. A Process Perspective on Industrial Symbiosis	Journal of Industrial Ecology	2014	18	3	341	355	10.1111/jiec.12116
Trokanas N., Cecelja F., Raafat T.	Towards a re-usable ontology for waste processing	Computer Aided Chemical Engineering	2014	33		841	846	10.1016/B978-0-444-63456-6.50141-1

Author Name(s)	Title	Source Title	Year	Vol.	Issue	P. Start	P. End	Doi
Cutaia L., Morabito R., Barberio G., Mancuso E., Brunori C., Spezzano P., Mione A., Mungiguerra C., Li Rosi O., Cappello F.	The project for the implementation of the industrial symbiosis platform in sicily: The progress after the first year of operation	Pathways to Environmental Sustainability: Methodologies and Experiences	2014			205	214	10.1007/978-3-319-03826-1_20
Golev A., Corder G.D., Giurco D.P.	Industrial symbiosis in gladstone: A decade of progress and future development	Journal of Cleaner Production	2014	84	1	421	429	10.1016/j.jclepro.2013.06.054
Ng R.T.L., Ng D.K.S., Tan R.R., El-Halwagi M.M.	Disjunctive fuzzy optimisation for planning and synthesis of bioenergy-based industrial symbiosis system	Journal of Environmental Chemical Engineering	2014	2	1	652	664	10.1016/j.jece.2013.11.003
Schiller F., Penn A., Druckman A., Basson L., Royston K.	Exploring Space, Exploiting Opportunities: The Case for Analyzing Space in Industrial Ecology Schiller et al. Exploring Space, Exploiting Opportunities	Journal of Industrial Ecology	2014	18	6	792	798	10.1111/jiec.12140
Yu C., Davis C., Dijkema G.P.J.	Understanding the evolution of industrial symbiosis research: A bibliometric and network analysis (1997-2012)	Journal of Industrial Ecology	2014	18	2	280	293	10.1111/jiec.12073
Alfaro J., Miller S.	Applying Industrial Symbiosis to Smallholder Farms: Modeling a Case Study in Liberia, West Africa	Journal of Industrial Ecology	2014	18	1	145	154	10.1111/jiec.12077
Zou Y.-L., Li C.-F., Yao Z.-D., Cao Y.-Y.	AN research on energy management and cooperation performance in eco-industrial symbiosis network	Advanced Materials Research	2014	986-987		211	214	10.4028/www.scientific.net/AMR.986-987.211

Author Name(s)	Title	Source Title	Year	Vol.	Issue	P. Start	P. End	Doi
Ng R.T.L., Hassim M.H., Ng D.K.S., Tan R.R., El-Halwagi M.M.	Multi-objective design of industrial symbiosis in palm oil industry	Computer Aided Chemical Engineering	2014	34		579	584	10.1016/B978-0-444-63433-7.50081-X
Li C., Feng L.	Evolutionary game analysis of the eco-industrial symbiosis network considering externality	Complex Systems and Complexity Science	2014	11	3	58	64	10.13306/j.1672-3813.2014.03.009
Ng R.T.L., Wan Y.K., Ng D.K.S., Tan R.R.	Stability analysis of symbiotic bioenergy parks	Chemical Engineering Transactions	2014	39		859	864	10.3303/CET1439144
Noureldin M.B., Farooq Z., Al-Owaidh M., Al-Saed H.	New systematic approach using combined constraints logic propagation and mathematical programming techniques for energy efficient synthesis of eco-industrial parks	Process Development Division 2014 - Core Programming Area at the 2014 AIChE Annual Meeting	2014			305	307	
Benjamin M.F.D., Tan R.R., Razon L.F.	A methodology for criticality analysis in symbiotic bioenergy parks	Energy Procedia	2014	61		41	44	10.1016/j.egypro.2014.11.901
Ramli A., Mokhtar M., Aziz B.A., Ngah N.A.	The cooperative approach in managing safety issues for Halal industrial parks in Malaysia: Embracing opportunity	Progress in Industrial Ecology	2014	8	4	295	318	10.1504/PIE.2014.066805
Carmen Lenuta T.	Contributions to the foundation of a waste management plan on an area level	International Multidisciplinary Scientific GeoConference Surveying Geology and Mining Ecology Management, SGEM	2014	3	5	95	101	
Short S.W., Bocken N.M.P., Barlow C.Y., Chertow M.R.	From refining sugar to growing tomatoes: Industrial ecology and business model evolution	Journal of Industrial Ecology	2014	18	5	603	618	10.1111/jiec.12171

Author Name(s)	Title	Source Title	Year	Vol.	Issue	P. Start	P. End	Doi
Arranz P., Anzizu M., Pineau A., Marwede M., Den Boer E., Den Boer J., Cocciantelli J.-M., Williams I.D., Obersteiner G., Scherhauser S., Vallvé X.	The development of a resourceefficient photovoltaic system	Proceedings of Institution of Civil Engineers: Waste and Resource Management	2014	167	3	109	122	10.1680/warm.13.00027
Steingrímsson J.G., Seliger G.	Conceptual framework for near-to-site waste cycle design	Procedia CIRP	2014	15		272	277	10.1016/j.procir.2014.06.014
Obersteiner G., Pertl A.	Waste Avoidance Through Industrial Symbiosis [Abfallvermeidung durch industrielle Symbiose]	Osterreichische Wasser- und Abfallwirtschaft	2014	66		417	423	10.1007/s00506-014-0191-x
Dong H., Ohnishi S., Fujita T., Geng Y., Fujii M., Dong L.	Achieving carbon emission reduction through industrial & urban symbiosis: A case of Kawasaki	Energy	2014	64		277	286	10.1016/j.energy.2013.11.005
Noureldin M.B., Farooq Z., Al-Owaidh M., Al-Saed H.	New systematic approach using combined constraints logic propagation and mathematical programming techniques for energy efficient synthesis of eco-industrial parks	Sustainable Engineering Forum 2014 - Core Programming Area at the 2014 AIChE Annual Meeting	2014			351	353	
Li X., Xiao R., Zeng Y., Yao Z.	Vulnerability analysis of symbiotic network in eco-industrial parks	Shengtai Xuebao/ Acta Ecologica Sinica	2014	34	16	4746	4755	10.5846/stxb201212191820
Eckelman M.J., Ashton W., Arakaki Y., Hanaki K., Nagashima S., Malone-Lee L.C.	Island waste management systems: Statistics, challenges, and opportunities for applied industrial ecology	Journal of Industrial Ecology	2014	18	2	306	317	10.1111/jiec.12113
Stubbs W.	Exploration of barriers to mainstreaming industrial ecosystems in Australia	Progress in Industrial Ecology	2014	8	4	319	335	10.1504/PIE.2014.066814

Author Name(s)	Title	Source Title	Year	Vol.	Issue	P. Start	P. End	Doi
Rosano M., Schianetz K.	Measuring sustainability performance in industrial parks: A case study of the Kwinana industrial area	International Journal of Sustainable Development	2014	17	3	261	280	10.1504/IJSD.2014.064181
Wang G., Feng X., Khim Hoong C.	Symbiosis analysis on industrial ecological system	Chinese Journal of Chemical Engineering	2014	22	6	690	698	10.1016/S1004-9541(14)60084-7
Dean C.A., Fath B.D., Chen B.	Indicators for an expanded business operations model to evaluate eco-smart corporate communities	Ecological Indicators	2014	47		137	148	10.1016/j.ecolind.2014.07.010
Campos T.R.T., Fonseca M.V.A., Morais R.M.N.	Reverse logistics: A route that only makes sense when adopting a systemic vision	WIT Transactions on Ecology and the Environment	2014	180		41	52	10.2495/WM140041
Kikuchi Y., Kimura S., Okamoto Y., Koyama M.	A scenario analysis of future energy systems based on an energy flow model represented as functionals of technology options	Applied Energy	2014	132		586	601	10.1016/j.apenergy.2014.07.005
Spekkink W.	Building capacity for sustainable regional industrial systems: An event sequence analysis of developments in the Sloe Area and Canal Zone	Journal of Cleaner Production	2014					10.1016/j.jclepro.2014.08.028
Cecelja F., Trokanas N., Raafat T., Yu M.	Semantic algorithm for Industrial Symbiosis network synthesis	Computers and Chemical Engineering	2015	83		248	266	10.1016/j.compchemeng.2015.04.031
Chen P.-C., Ma H.-W.	Using an Industrial Waste Account to Facilitate National Level Industrial Symbioses by Uncovering the Waste Exchange Potential	Journal of Industrial Ecology	2015	19	6	950	962	10.1111/jiec.12236
Meylan F.D., Moreau V., Erkman S.	CO2 utilization in the perspective of industrial ecology, an overview	Journal of CO2 Utilization	2015	12		101	108	10.1016/j.jcou.2015.05.003
Patrício J., Costa I., Niza S.	Urban material cycle closing - Assessment of industrial waste management in Lisbon region	Journal of Cleaner Production	2015	106		389	399	10.1016/j.jclepro.2014.08.069

Author Name(s)	Title	Source Title	Year	Vol.	Issue	P. Start	P. End	Doi
Kwon G.-R., Woo S.H., Lim S.-R.	Industrial ecology-based strategies to reduce the embodied CO2 of magnesium metal	Resources, Conservation and Recycling	2015	104		206	212	10.1016/j.resconrec.2015.08.008
Spekkink W.	Varieties of industrial symbiosis	International Perspectives on Industrial Ecology	2015			142	156	10.4337/9781781003572.00017
Patchell J.	Intersection of industrial symbiosis and product-based industrial ecologies: Considerations from the Japanese home appliance industry	International Perspectives on Industrial Ecology	2015			175	190	10.4337/9781781003572.00019
Wang Q., Deutz P., Gibbs D.	UK-China collaboration for industrial symbiosis: A multi-level approach to policy transfer analysis	International Perspectives on Industrial Ecology	2015			89	107	10.4337/9781781003572.00014
Olayide O.E.	Industrial ecology, industrial symbiosis and eco-industrial parks in Africa: Issues for sustainable development	International Perspectives on Industrial Ecology	2015			30	45	10.4337/9781781003572.00011
Boons F., Spekkink W., Isenmann R., Baas L., Eklund M., Brullot S., Deutz P., Gibbs D., Massard G., Arozamena E.R., Puente C.R., Verguts V., Davis C., Korevaar G., Costa I., Baumann H.	Comparing industrial symbiosis in Europe: Towards a conceptual framework and research methodology	International Perspectives on Industrial Ecology	2015			69	88	10.4337/9781781003572.00013
Deutz P., Lyons D.I., Bi J.	International perspectives on industrial ecology	International Perspectives on Industrial Ecology	2015			1	249	10.4337/9781781003572

Author Name(s)	Title	Source Title	Year	Vol.	Issue	P. Start	P. End	Doi
Iacondini A., Mencherini U., Passarini F., Vassura I., Fanelli A., Cibotti P.	Feasibility of Industrial Symbiosis in Italy as an Opportunity for Economic Development: Critical Success Factor Analysis, Impact and Constrains of the Specific Italian Regulations	Waste and Biomass Valorization	2015	6	5	865	874	10.1007/s12649-015-9380-5
Madsen J.K., Boisen N., Nielsen L.U., Tackmann L.H.	Industrial Symbiosis Exchanges: Developing a Guideline to Companies	Waste and Biomass Valorization	2015	6	5	855	864	10.1007/s12649-015-9417-9
Zoccola M., Montarsole A., Mossotti R., Patrucco A., Tonin C.	Green Hydrolysis as an Emerging Technology to Turn Wool Waste into Organic Nitrogen Fertilizer	Waste and Biomass Valorization	2015	6	5	891	897	10.1007/s12649-015-9393-0
Lombardi L., Carnevale E., Baclocchi R., Costa G.	Biogas Upgrading by a Combination of Innovative Treatments Based on Carbonation of Waste Incineration Residues	Waste and Biomass Valorization	2015	6	5	791	803	10.1007/s12649-015-9413-0
Earley K.	Industrial symbiosis: Harnessing waste energy and materials for mutual benefit	Renewable Energy Focus	2015	16	4	75	77	10.1016/j.ref.2015.09.011
Atkins M.J., Walmsley M.R.W., Walmsley T.G., Neale J.R.	Integration of biomass conversion technologies and geothermal heat into a model wood processing cluster	Chemical Engineering Transactions	2015	45		169	174	10.3303/CET1545029
Gonela V., Zhang J., Osmani A.	Stochastic optimization of sustainable industrial symbiosis based hybrid generation bioethanol supply chains	Computers and Industrial Engineering	2015	87		40	65	10.1016/j.cie.2015.04.025
Abate S., Lanzafame P., Perathoner S., Centi G.	New Sustainable Model of Biorefineries: Biofactories and Challenges of Integrating Bio- and Solar Refineries	ChemSusChem	2015	8	17	2854	2866	10.1002/cssc.201500277

Author Name(s)	Title	Source Title	Year	Vol.	Issue	P. Start	P. End	Doi
Benjamin M.F.D., Ubando A.T., Razon L.F., Tan R.R.	Analyzing the disruption resilience of bioenergy parks using dynamic inoperability input–output modeling	Environment Systems and Decisions	2015	35	3	351	362	10.1007/s10669-015-9562-5
Zhang Y., Zheng H., Fath B.D.	Ecological network analysis of an industrial symbiosis system: A case study of the Shandong Lubei eco-industrial park	Ecological Modelling	2015	306		174	184	10.1016/j.ecolmodel.2014.05.005
Beloborodko A., Rosa M.	The Use of Performance Indicators for Analysis of Resource Efficiency Measures	Energy Procedia	2015	72		337	344	10.1016/j.egypro.2015.06.049
Yu C., Dijkema G.P.J., de Jong M.	What Makes Eco-Transformation of Industrial Parks Take Off in China?	Journal of Industrial Ecology	2015	19	3	441	456	10.1111/jiec.12185
Lopes M.S.G.	Engineering biological systems toward a sustainable bioeconomy	Journal of Industrial Microbiology and Biotechnology	2015	42	6	813	838	10.1007/s10295-015-1606-9
Rončević B., Fric U.	Researching industrial symbiosis: Challenges and dilemmas	Applied Modelling and Computing in Social Sciences	2015			35	49	10.3726/978-3-653-05821-5
Päivärinne S., Hjelm O., Gustafsson S.	Excess heat supply collaborations within the district heating sector: Drivers and barriers	Journal of Renewable and Sustainable Energy	2015	7	3			10.1063/1.4921759
Li Y., Shi L.	The Resilience of Interdependent Industrial Symbiosis Networks: A Case of Yixing Economic and Technological Development Zone	Journal of Industrial Ecology	2015	19	2	264	273	10.1111/jiec.12267
Chandra-Putra H., Chen J., Andrews C.J.	Eco-Evolutionary Pathways Toward Industrial Cities	Journal of Industrial Ecology	2015	19	2	274	284	10.1111/jiec.12234
Strazza C., Magrassi F., Gallo M., Del Borghi A.	Life Cycle Assessment from food to food: A case study of circular economy from cruise ships to aquaculture	Sustainable Production and Consumption	2015	2		40	51	10.1016/j.spc.2015.06.004

Author Name(s)	Title	Source Title	Year	Vol.	Issue	P. Start	P. End	Doi
Simboli A., Taddeo R., Morgante A.	The potential of Industrial Ecology in agri-food clusters (AFCs): A case study based on valorisation of auxiliary materials	Ecological Economics	2015	111		65	75	10.1016/j.ecolecon.2015.01.005
Bakshi B.R., Ziv G., Lepech M.D.	Techno-ecological synergy: A framework for sustainable engineering	Environmental Science and Technology	2015	49	3	1752	1760	10.1021/es5041442
Lam H.L., How B.S., Hong B.H.	Green supply chain toward sustainable industry development	Assessing and Measuring Environmental Impact and Sustainability	2015			409	449	10.1016/B978-0-12-799968-5.00012-9
Yu F., Han F., Cui Z.	Evolution of industrial symbiosis in an eco-industrial park in China	Journal of Cleaner Production	2015	87	C	339	347	10.1016/j.jclepro.2014.10.058
Chertow M., Park J.	Scholarship and practice in industrial symbiosis: 1989–2014	Taking Stock of Industrial Ecology	2015			87	116	10.1007/978-3-319-20571-7_5
Cecelja F., Raafat T., Trokanas N., Innes S., Smith M., Yang A., Zorgios Y., Korkofygas A., Kokossis A.	E-Symbiosis: Technology-enabled support for Industrial Symbiosis targeting Small and Medium Enterprises and innovation	Journal of Cleaner Production	2015	98		336	352	10.1016/j.jclepro.2014.08.051
Martin M., Svensson N., Eklund M.	Who gets the benefits? An approach for assessing the environmental performance of industrial symbiosis	Journal of Cleaner Production	2015	98		263	271	10.1016/j.jclepro.2013.06.024
Hein A.M., Jankovic M., Farel R., Sam Lei I., Yannou B.	Modeling industrial symbiosis using design structure matrices	Modeling and Managing Complex Systems - Proceedings of the 17th International DSM Conference	2015			209	219	
Paquin R.L., Busch T., Tilleman S.G.	Creating economic and environmental value through industrial symbiosis	Long Range Planning	2015	48	2	95	107	10.1016/j.lrp.2013.11.002

Author Name(s)	Title	Source Title	Year	Vol.	Issue	P. Start	P. End	Doi
Martin M.	Quantifying the environmental performance of an industrial symbiosis network of biofuel producers	Journal of Cleaner Production	2015	102		202	212	10.1016/j.jclepro.2015.04.063
Gaidajis G., Kakanis I.	Examination of industrial symbiosis potential interactions in an industrial area of NE greece	Journal of Engineering Science and Technology Review	2015	8	3	130	135	
Bertels S., Bowen F.	Taking Stock, Looking Ahead: Editors' Introduction to the Inaugural Organization & Environment Review Issue	Organization and Environment	2015	28	1	3	7	10.1177/1086026615576798
Liu C., Côté R.P., Zhang K.	Implementing a three-level approach in industrial symbiosis	Journal of Cleaner Production	2015	87	1	318	327	10.1016/j.jclepro.2014.09.067
Spekkink W.	Building capacity for sustainable regional industrial systems: An event sequence analysis of developments in the Sloe Area and Canal Zone	Journal of Cleaner Production	2015	98		133	144	10.1016/j.jclepro.2014.08.028
Bin S., Zhiquan Y., Jonathan L.S.C., Jiewei D.K., Kurle D., Cerdas F., Herrmann C.	A big data analytics approach to develop industrial symbioses in large cities	Procedia CIRP	2015	29		450	455	10.1016/j.procir.2015.01.066
Aid G., Brandt N., Lysenkova M., Smedberg N.	Looplocal - A heuristic visualization tool to support the strategic facilitation of industrial symbiosis	Journal of Cleaner Production	2015	98		328	335	10.1016/j.jclepro.2014.08.012
Trokanas N., Cecelja F., Raafat T.	Semantic approach for pre-assessment of environmental indicators in Industrial Symbiosis	Journal of Cleaner Production	2015	96		349	361	10.1016/j.jclepro.2013.12.046
Rosa M., Beloborodko A.	A decision support method for development of industrial synergies: Case studies of Latvian brewery and wood-processing industries	Journal of Cleaner Production	2015	105		461	470	10.1016/j.jclepro.2014.09.061

Author Name(s)	Title	Source Title	Year	Vol.	Issue	P. Start	P. End	Doi
Leigh M., Li X.	Industrial ecology, industrial symbiosis and supply chain environmental sustainability: A case study of a large UK distributor	Journal of Cleaner Production	2015	106		632	643	10.1016/j.jclepro.2014.09.022
Trokanas N., Bussemaker M., Velliou E., Tokos H., Cecelja F.	BiOnto: An Ontology for Biomass and Biorefining Technologies	Computer Aided Chemical Engineering	2015	37		959	964	10.1016/B978-0-444-63577-8.50005-X
Chudobiecki J., Wanat L.	Industrial symbiosis and green business parks in the wood-based sector in Poland	Wood Processing and Furniture Manufacturing Challenges on the World Market and Wood-Based Energy Goes Global - Proceedings of Scientific Papers	2015			221	228	
Albino V., Fraccascia L., Savino T.	Industrial Symbiosis for a Sustainable City: Technical, Economical and Organizational Issues	Procedia Engineering	2015	118		950	957	10.1016/j.proeng.2015.08.536
Bailey M., Gadd A.	Quantifying the potential of industrial symbiosis: The LOCIMAP project, with applications in the humber region	Taking Stock of Industrial Ecology	2015			343	357	10.1007/978-3-319-20571-7_19
Yu B., Li X., Shi L., Qian Y.	Quantifying CO2 emission reduction from industrial symbiosis in integrated steel mills in China	Journal of Cleaner Production	2015	103		801	810	10.1016/j.jclepro.2014.08.015
Wu J., Li C., Yang F.	The disposition of chromite ore processing residue (COPR) incorporating industrial symbiosis	Journal of Cleaner Production	2015	95		156	162	10.1016/j.jclepro.2015.02.041
Walls J.L., Paquin R.L.	Organizational Perspectives of Industrial Symbiosis: A Review and Synthesis	Organization and Environment	2015	28	1	32	53	10.1177/1086026615575333

Author Name(s)	Title	Source Title	Year	Vol.	Issue	P. Start	P. End	Doi
Golev A., Corder G.D., Giurco D.P.	Barriers to Industrial Symbiosis: Insights from the Use of a Maturity Grid	Journal of Industrial Ecology	2015	19	1	141	153	10.1111/jiec.12159
Puente M.C.R., Arozamena E.R., Evans S.	Industrial symbiosis opportunities for small and medium sized enterprises: Preliminary study in the Besaya Region (Cantabria, Northern Spain)	Journal of Cleaner Production	2015	87	C	357	374	10.1016/j.jclepro.2014.10.046
Hein A.M., Jankovic M., Farel R., Yannou B.	A conceptual framework for eco-industrial parks	Proceedings of the ASME Design Engineering Technical Conference	2015	4				10.1115/DETC2015-46322
Yu F., Han F., Cui Z.	Reducing carbon emissions through industrial symbiosis: A case study of a large enterprise group in China	Journal of Cleaner Production	2015	103		811	818	10.1016/j.jclepro.2014.05.038
Yu F., Han F., Cui Z.	Assessment of life cycle environmental benefits of an industrial symbiosis cluster in China	Environmental Science and Pollution Research	2015	22	7	5511	5518	10.1007/s11356-014-3712-z
Tsvetkova A., Hellström M., Gustafsson M., Sjöblom J.	Replication of industrial ecosystems: The case of a sustainable biogas-for-traffic solution	Journal of Cleaner Production	2015	98		123	132	10.1016/j.jclepro.2014.08.089
Päivärinne S., Lindahl M.	Exploratory study of combining Integrated Product and Services Offerings with Industrial Symbiosis in order to improve Excess Heat utilization	Procedia CIRP	2015	30		167	172	10.1016/j.procir.2015.02.101
Ammenberg J., Baas L., Eklund M., Feiz R., Helgstrand A., Marshall R.	Improving the CO ₂ performance of cement, part III: The relevance of industrial symbiosis and how to measure its impact	Journal of Cleaner Production	2015	98		145	155	10.1016/j.jclepro.2014.01.086

Author Name(s)	Title	Source Title	Year	Vol.	Issue	P. Start	P. End	Doi
Wen Z., Meng X.	Quantitative assessment of industrial symbiosis for the promotion of circular economy: A case study of the printed circuit boards industry in China's Suzhou New District	Journal of Cleaner Production	2015	90		211	219	10.1016/j.jclepro.2014.03.041
Li H., Dong L., Ren J.	Industrial symbiosis as a countermeasure for resource dependent city: A case study of Guiyang, China	Journal of Cleaner Production	2015	107		252	266	10.1016/j.jclepro.2015.04.089
Kennedy C.A.	Industrial ecology and cities	Taking Stock of Industrial Ecology	2015			69	86	10.1007/978-3-319-20571-7_4
Dong L., Fujita T.	Promotion of low-carbon city through industrial and urban system innovation: Japanese experience and China's practice	World Scientific Reference on Asia and the World Economy	2015			257	279	10.1142/9789814578622_0033
Puente M.C.R., Arozamena E.R., Evans S.	Industrial symbiosis opportunities for small and medium sized enterprises: Preliminary study in the Besaya region (Cantabria, Northern Spain)	Journal of Cleaner Production	2015	87	1	357	374	10.1016/j.jclepro.2014.09.046
Cutaia L., Luciano A., Barberio G., Scaffoni S., Mancuso E., Scagliarino C., La Monica M.	The experience of the first industrial symbiosis platform in Italy	Environmental Engineering and Management Journal	2015	14	7	1521	1533	
Aviso K.B., Chiu A.S.F., Yu K.D.S., Promentilla M.A.B., Razon L.F., Ubando A.T., Sy C.L., Tan R.R.	P-graph for optimising industrial symbiotic networks	Chemical Engineering Transactions	2015	45		1345	1350	10.3303/CET1545225

Author Name(s)	Title	Source Title	Year	Vol.	Issue	P. Start	P. End	Doi
Vardanega R., Prado J.M., Meireles M.A.A.	Adding value to agri-food residues by means of supercritical technology	Journal of Supercritical Fluids	2015	96		217	227	10.1016/j.supflu.2014.09.029
Cerdas F., Kurle D., Andrew S., Thiede S., Herrmann C., Zhiquan Y., Jonathan L.S.C., Bin S., Kara S.	Defining circulation factories - A pathway towards factories of the future	Procedia CIRP	2015	29		627	632	10.1016/j.procir.2015.02.032
Wang H., Xu X., Zhu G.	Landscape changes and a salt production sustainable approach in the state of salt pan area decreasing on the coast of Tianjin, China	Sustainability (Switzerland)	2015	7	8	10078	10097	10.3390/su70810078
Daddi T., Tessitore S., Testa F.	Industrial ecology and eco-industrial development: Case studies from Italy	Progress in Industrial Ecology	2015	9	3	217	233	10.1504/PIE.2015.073414
Deutz P., Ioppolo G.	From theory to practice: Enhancing the potential policy impact of industrial ecology	Sustainability (Switzerland)	2015	7	2	2259	2273	10.3390/su7022259
[No author name available]	Modeling and Managing Complex Systems - Proceedings of the 17th International DSM Conference	Modeling and Managing Complex Systems - Proceedings of the 17th International DSM Conference	2015					
Liu J., Nie X., Zhou C., Shi Y., Liu R.	The design of agri-industrial ecological park: A case study of Zhengzhou national economic-technological development area	Shengtai Xuebao/ Acta Ecologica Sinica	2015	35	14	4891	4896	10.5846/stxb201311242804
Graedel T.E., Lifset R.J.	Industrial ecology's first decade	Taking Stock of Industrial Ecology	2015			3	20	10.1007/978-3-319-20571-7_1
Adiansyah J.S., Rosano M., Vink S., Keir G.	A framework for a sustainable approach to mine tailings management: Disposal strategies	Journal of Cleaner Production	2015	108		1	13	10.1016/j.jclepro.2015.07.139

Author Name(s)	Title	Source Title	Year	Vol.	Issue	P. Start	P. End	Doi
Benjamin M.F., Ubando A., Razon L., Tan R.R.	Analyzing the disruption resilience of microalgal multi- functional Bioenergy systems using dynamic inoperability input-output modeling	Chemical Engineering Transactions	2015	45		1579	1584	10.3303/CET1545264
Johnson J.A.	Dilemmas of 19th-century liberalism among German academic chemists: Shaping a national science policy from Hofmann to Fischer, 1865- 1919	Annals of Science	2015	72	2	224	241	10.1080/00033790.2015.1007525
Mannino I., Ninka E., Turvani M., Chertow M.	The decline of eco-industrial development in Porto Marghera, Italy	Journal of Cleaner Production	2015	100		286	296	10.1016/j.jclepro.2015.03.054
Qu Y., Liu Y., Nayak R.R., Li M.	Sustainable development of eco-industrial parks in China: Effects of managers' environmental awareness on the relationships between practice and performance	Journal of Cleaner Production	2015	87	1	328	338	10.1016/j.jclepro.2014.09.015
Ubando A.T., Culaba A.B., Aviso K.B., Tan R.R., Cuello J.L., Ng D.K.S., El- Halwagi M.M.	Fuzzy mathematical programming approach in the optimal design of an algal bioenergy park	Chemical Engineering Transactions	2015	45		355	360	10.3303/CET1545060
Olsson L., Wetterlund E., Söderström M.	Assessing the climate impact of district heating systems with combined heat and power production and industrial excess heat	Resources, Conservation and Recycling	2015	96		31	39	10.1016/j.resconrec.2015.01.006
Li W., Cui Z., Han F.	Methods for assessing the energy-saving efficiency of industrial symbiosis in industrial parks	Environmental science and pollution research international	2015	22	1	275	285	10.1007/s11356-014-3327-4

Author Name(s)	Title	Source Title	Year	Vol.	Issue	P. Start	P. End	Doi
Feiz R., Ammenberg J., Baas L., Eklund M., Helgstrand A., Marshall R.	Improving the CO ₂ performance of cement, part II: Framework for assessing CO ₂ improvement measures in the cement industry	Journal of Cleaner Production	2015	98		282	291	10.1016/j.jclepro.2014.01.103
Tan R.R., Ng R.T.L., Andiappan V., Wan Y.K., Ng D.K.S.	An optimization-based cooperative game approach for allocation of costs and benefits in interplant process integration	Chemical Engineering Transactions	2015	45		403	408	10.3303/CET1545068
Ferrão P., Lorena A., Ribeiro P.	Industrial ecology and portugal's national waste plans	Taking Stock of Industrial Ecology	2015			275	289	10.1007/978-3-319-20571-7_14
Boix M., Montastruc L., Azzaro-Pantel C., Domenech S.	Optimization methods applied to the design of eco-industrial parks: A literature review	Journal of Cleaner Production	2015	87	1	303	317	10.1016/j.jclepro.2014.09.032
Gregson N., Crang M., Fuller S., Holmes H.	Interrogating the circular economy: the moral economy of resource recovery in the EU	Economy and Society	2015	44	2	218	243	10.1080/03085147.2015.1013353
Noureldin M.M.B., El- Halwagi M.M.	Synthesis of C-H-O Symbiosis Networks	AIChE Journal	2015	61	4	1242	1262	10.1002/aic.14714
Duraccio V., Gnoni M.G., Elia V.	Carbon capture and reuse in an industrial district: A technical and economic feasibility study	Journal of CO ₂ Utilization	2015	10		23	29	10.1016/j.jcou.2015.02.004
Schieb P.-A., Lescieux-Katir H., Thénot M., Clément- Larosière B.	Biorefinery 2030: Future prospects for the bioeconomy	Biorefinery 2030: Future Prospects for the Bioeconomy	2015			1	123	10.1007/978-3-662-47374-0
Ferrell J.C., Shahbazi A.	County government led EIP development using municipal biomass resources for clean energy production, a case study of the Catawba County North Carolina ecocomplex	Progress in Industrial Ecology	2015	9	1	69	81	10.1504/PIE.2015.069835

Author Name(s)	Title	Source Title	Year	Vol.	Issue	P. Start	P. End	Doi
Silva C.M.A., Nielsen C.V., Alves L.M., Martins P.A.F.	Environmentally friendly joining of tubes by their ends	Journal of Cleaner Production	2015	87	1	777	786	10.1016/j.jclepro.2014.09.022
Rao P., Patil Y.	Climate resilience in natural ecosystems in india: Technology adoption and the use of local knowledge processes and systems	Handbook of Climate Change Adaptation	2015			2063	2077	10.1007/978-3-642-38670-1_95
Marinos-Kouris D., Mourtsiadis A.	Environment and recycling: Some comments on the entropy limits	Fresenius Environmental Bulletin	2015	24	3B	1158	1163	
Baas L., Hjelm O.	Support your future today: Enhancing sustainable transitions by experimenting at academic conferences	Journal of Cleaner Production	2015	98		1	7	10.1016/j.jclepro.2015.02.059
Røyne F., Berlin J., Ringström E.	Life cycle perspective in environmental strategy development on the industry cluster level: A case study of five chemical companies	Journal of Cleaner Production	2015	86		125	131	10.1016/j.jclepro.2014.08.016
Lenhart J., Van Vliet B., Mol A.P.J.	New roles for local authorities in a time of climate change: The Rotterdam Energy Approach and Planning as a case of urban symbiosis	Journal of Cleaner Production	2015	107		593	601	10.1016/j.jclepro.2015.05.026
Zhang Y., Zheng H., Yang Z., Liu G., Su M.	Analysis of the industrial metabolic processes for sulfur in the Lubei (Shandong Province, China) eco-industrial park	Journal of Cleaner Production	2015	96		127	138	10.1016/j.jclepro.2014.01.096
Sahakian M.	The social and solidarity economy: Why is it relevant to industrial ecology?	Taking Stock of Industrial Ecology	2015			205	227	10.1007/978-3-319-20571-7_10
Benjamin M.F.D., Tan R.R., Razon L.F.	A methodology for criticality analysis in integrated energy systems	Clean Technologies and Environmental Policy	2015	17	4	935	946	10.1007/s10098-014-0846-0
Maillé M., Frayret J.-M.	Industrial Waste Reuse and By-product Synergy Optimization	Journal of Industrial Ecology	2016	20	6	1284	1294	10.1111/jiec.12403

Author Name(s)	Title	Source Title	Year	Vol.	Issue	P. Start	P. End	Doi
Papathanasoglou A., Panagiotidou M., Valta K., Loizidou M.	RESEARCH ARTICLE: Institutional Barriers and Opportunities for the Implementation of Industrial Symbiosis in Greece	Environmental Practice	2016	18	4	253	259	10.1017/S1466046616000454
Wu J., Wang R., Pu G., Qi H.	Integrated assessment of exergy, energy and carbon dioxide emissions in an iron and steel industrial network	Applied Energy	2016	183		430	444	10.1016/j.apenergy.2016.08.192
Zhang B., Wang Z., Lai K.-H.	Does Industrial Waste Reuse Bring Dual Benefits of Economic Growth and Carbon Emission Reduction?: Evidence of Incorporating the Indirect Effect of Economic Growth in China	Journal of Industrial Ecology	2016	20	6	1306	1319	10.1111/jiec.12375
Ubando A.T., Culaba A.B., Aviso K.B., Tan R.R., Cuello J.L., Ng D.K.S., El-Halwagi M.M.	Fuzzy mixed integer non-linear programming model for the design of an algae-based eco-industrial park with prospective selection of support tenants under product price variability	Journal of Cleaner Production	2016	136		183	196	10.1016/j.jclepro.2016.04.143
Peter Sahay S.S., Dash S.N., Joga Rao H.	Economical benefit through industrial symbiosis: Trash to treasure: A case study in an Indian industrial area	Research Journal of Pharmaceutical, Biological and Chemical Sciences	2016	7	6	932	937	
Wu J., Qi H., Wang R.	Insight into industrial symbiosis and carbon metabolism from the evolution of iron and steel industrial network	Journal of Cleaner Production	2016	135		251	262	10.1016/j.jclepro.2016.06.103
Guo B., Geng Y., Sterr T., Dong L., Liu Y.	Evaluation of promoting industrial symbiosis in a chemical industrial park: A case of Midong	Journal of Cleaner Production	2016	135		995	1008	10.1016/j.jclepro.2016.07.006

Author Name(s)	Title	Source Title	Year	Vol.	Issue	P. Start	P. End	Doi
Pan H., Zhang X., Wang Y., Qi Y., Wu J., Lin L., Peng H., Qi H., Yu X., Zhang Y.	Emergy evaluation of an industrial park in Sichuan Province, China: A modified emergy approach and its application	Journal of Cleaner Production	2016	135		105	118	10.1016/j.jclepro.2016.06.102
Álvarez R., Ruiz-Puente C.	Development of the Tool SymbioSyS to Support the Transition Towards a Circular Economy Based on Industrial Symbiosis Strategies	Waste and Biomass Valorization	2016			1	10	10.1007/s12649-016-9748-1
Taylor C.D., Gully B., Sánchez A.N., Rode E., Agarwal A.S.	Towards materials sustainability through materials stewardship	Sustainability (Switzerland)	2016	8	10			10.3390/su8101001
Atkins M.J., Walmsley M.R.W., Walmsley T.G.	Integration of new processes and geothermal heat into a wood processing cluster	Clean Technologies and Environmental Policy	2016	18	7	2077	2085	10.1007/s10098-016-1171-6
Taddeo R.	Local industrial systems towards the eco-industrial parks: The model of the ecologically equipped industrial areas	Journal of Cleaner Production	2016	131		189	197	10.1016/j.jclepro.2016.05.051
Hodgson E., Ruiz-Molina M.-E., Marazza D., Pogrebnyakova E., Burns C., Higson A., Rehberger M., Hiete M., Gyalai-Korpos M., Lucia L.D., Noël Y., Woods J., Gallagher J.	Horizon scanning the European bio-based economy: a novel approach to the identification of barriers and key policy interventions from stakeholders in multiple sectors and regions	Biofuels, Bioproducts and Biorefining	2016	10	5	508	522	10.1002/bbb.1665
Ren J., Liang H., Dong L., Sun L., Gao Z.	Design for sustainability of industrial symbiosis based on emergy and multi-objective particle swarm optimization	Science of the Total Environment	2016	562		789	801	10.1016/j.scitotenv.2016.04.092

Author Name(s)	Title	Source Title	Year	Vol.	Issue	P. Start	P. End	Doi
Secchi M., Castellani V., Collina E., Mirabella N., Sala S.	Assessing eco-innovations in green chemistry: Life Cycle Assessment (LCA) of a cosmetic product with a bio-based ingredient	Journal of Cleaner Production	2016	129		269	281	10.1016/j.jclepro.2016.04.073
Velenturf A.P.M.	Promoting industrial symbiosis: empirical observations of low-carbon innovations in the Humber region, UK	Journal of Cleaner Production	2016	128		116	130	10.1016/j.jclepro.2015.06.027
Luciano A., Barberio G., Mancuso E., Sbaffoni S., La Monica M., Scagliarino C., Cutaia L.	Potential Improvement of the Methodology for Industrial Symbiosis Implementation at Regional Scale	Waste and Biomass Valorization	2016	7	4	1007	1015	10.1007/s12649-016-9625-y
Velenturf A.P.M., Jensen P.D.	Promoting Industrial Symbiosis: Using the Concept of Proximity to Explore Social Network Development	Journal of Industrial Ecology	2016	20	4	700	709	10.1111/jiec.12315
Renzulli P.A., Notarnicola B., Tassielli G., Arcese G., Di Capua R.	Life cycle assessment of steel produced in an Italian integrated steel mill	Sustainability (Switzerland)	2016	8	8			10.3390/su8080719
Liu Z.-Y., Varbanov P.S., Klemeš J.J., Yong J.Y.	Recent developments in applied thermal engineering: Process integration, heat exchangers, enhanced heat transfer, solar thermal energy, combustion and high temperature processes and thermal process modelling	Applied Thermal Engineering	2016	105		755	762	10.1016/j.applthermaleng.2016.06.183
Päivärinne S., Lindahl M.	Combining Integrated Product and Service Offerings with Industrial Symbiosis – a study of opportunities and challenges	Journal of Cleaner Production	2016	127		240	248	10.1016/j.jclepro.2016.04.026

Author Name(s)	Title	Source Title	Year	Vol.	Issue	P. Start	P. End	Doi
Bacudio L.R., Benjamin M.F.D., Eusebio R.C.P., Holaysan S.A.K., Promentilla M.A.B., Yu K.D.S., Aviso K.B.	Analyzing barriers to implementing industrial symbiosis networks using DEMATEL	Sustainable Production and Consumption	2016	7		57	65	10.1016/j.spc.2016.03.001
Hu Y., Lin J., Cui S., Khanna N.Z.	Measuring Urban Carbon Footprint from Carbon Flows in the Global Supply Chain	Environmental Science and Technology	2016	50	12	6154	6163	10.1021/acs.est.6b00985
Zhang Y., Zheng H., Shi H., Yu X., Liu G., Su M., Li Y., Chai Y.	Network analysis of eight industrial symbiosis systems	Frontiers of Earth Science	2016	10	2	352	365	10.1007/s11707-015-0520-9
Felicio M., Amaral D., Esposto K., Gabarrell Durany X.	Industrial symbiosis indicators to manage eco-industrial parks as dynamic systems	Journal of Cleaner Production	2016	118		54	64	10.1016/j.jclepro.2016.01.031
Kikuchi Y., Kanematsu Y., Ugo M., Hamada Y., Okubo T.	Industrial Symbiosis Centered on a Regional Cogeneration Power Plant Utilizing Available Local Resources: A Case Study of Tanegashima	Journal of Industrial Ecology	2016	20	2	276	288	10.1111/jiec.12347
Kikuchi Y., Kanematsu Y., Sato R., Nakagaki T.	Distributed Cogeneration of Power and Heat within an Energy Management Strategy for Mitigating Fossil Fuel Consumption	Journal of Industrial Ecology	2016	20	2	289	303	10.1111/jiec.12374
Ohnishi S., Fujii M., Ohata M., Rokuta I., Fujita T.	Efficient energy recovery through a combination of waste-to-energy systems for a low-carbon city	Resources, Conservation and Recycling	2016					10.1016/j.resconrec.2016.11.018

Author Name(s)	Title	Source Title	Year	Vol.	Issue	P. Start	P. End	Doi
Liu Z., Adams M., Cote R.P., Geng Y., Li Y.	Comparative study on the pathways of industrial parks towards sustainable development between China and Canada	Resources, Conservation and Recycling	2016					10.1016/j.resconrec.2016.06.012
Kliopova I., Baranauskaite-Fedorova I., Malinauskiene M., Staniškis J.K.	Possibilities of increasing resource efficiency in nitrogen fertilizer production	Clean Technologies and Environmental Policy	2016	18	3	901	914	10.1007/s10098-015-1068-9
Liu G., Hao Y., Zhou Y., Yang Z., Zhang Y., Su M.	China's low-carbon industrial transformation assessment based on Logarithmic Mean Divisia Index model	Resources, Conservation and Recycling	2016	108		156	170	10.1016/j.resconrec.2016.02.002
Ghali M.R., Frayret J.-M., Robert J.-M.	Green social networking: Concept and potential applications to initiate industrial synergies	Journal of Cleaner Production	2016	115		23	35	10.1016/j.jclepro.2015.12.028
Sun L., Li H., Dong L., Fang K., Ren J., Geng Y., Fujii M., Zhang W., Zhang N., Liu Z.	Eco-benefits assessment on urban industrial symbiosis based on material flows analysis and emergy evaluation approach: A case of Liuzhou city, China	Resources, Conservation and Recycling	2016					10.1016/j.resconrec.2016.06.007
Zhe L., Yong G., Hung-Suck P., Huijuan D., Liang D., Tsuyoshi F.	An emergy-based hybrid method for assessing industrial symbiosis of an industrial park	Journal of Cleaner Production	2016	114		132	140	10.1016/j.jclepro.2015.04.132
Shiraki H., Ashina S., Kameyama Y., Hashimoto S., Fujita T.	Analysis of optimal locations for power stations and their impact on industrial symbiosis planning under transition toward low-carbon power sector in Japan	Journal of Cleaner Production	2016	114		81	94	10.1016/j.jclepro.2015.09.079
Park J.M., Park J.Y., Park H.-S.	A review of the National Eco-Industrial Park Development Program in Korea: Progress and achievements in the first phase, 2005-2010	Journal of Cleaner Production	2016	114		33	44	10.1016/j.jclepro.2015.08.115

Author Name(s)	Title	Source Title	Year	Vol.	Issue	P. Start	P. End	Doi
Horváth G.Á., Harazin P.	A framework for an industrial ecological decision support system to foster partnerships between businesses and governments for sustainable development	Journal of Cleaner Production	2016	114		214	223	10.1016/j.jclepro.2015.05.018
Mat N., Cerceau J., Shi L., Park H.-S., Junqua G., Lopez-Ferber M.	Socio-ecological transitions toward low-carbon port cities: Trends, changes and adaptation processes in Asia and Europe	Journal of Cleaner Production	2016	114		362	375	10.1016/j.jclepro.2015.04.058
Sumabat A.K., Lopez N.S., Yu K.D., Hao H., Li R., Geng Y., Chiu A.S.F.	Decomposition analysis of Philippine CO2 emissions from fuel combustion and electricity generation	Applied Energy	2016	164		795	804	10.1016/j.apenergy.2015.12.023
Daddi T., Iraldo F., Frey M., Gallo P., Gianfrate V.	Regional policies and eco-industrial development: The voluntary environmental certification scheme of the eco-industrial parks in Tuscany (Italy)	Journal of Cleaner Production	2016	114		62	70	10.1016/j.jclepro.2015.04.060
Jensen P.D.	The role of geospatial industrial diversity in the facilitation of regional industrial symbiosis	Resources, Conservation and Recycling	2016	107		92	103	10.1016/j.resconrec.2015.11.018
Manara P., Zabaniotou A.	Co-valorization of Crude Glycerol Waste Streams with Conventional and/or Renewable Fuels for Power Generation and Industrial Symbiosis Perspectives	Waste and Biomass Valorization	2016	7	1	135	150	10.1007/s12649-015-9439-3
Tan R.R., Andiappan V., Wan Y.K., Ng R.T.L., Ng D.K.S.	An optimization-based cooperative game approach for systematic allocation of costs and benefits in interplant process integration	Chemical Engineering Research and Design	2016	106		43	58	10.1016/j.cherd.2015.11.009

Author Name(s)	Title	Source Title	Year	Vol.	Issue	P. Start	P. End	Doi
Budzianowski W.M.	A review of potential innovations for production, conditioning and utilization of biogas with multiple-criteria assessment	Renewable and Sustainable Energy Reviews	2016	54		1148	1171	10.1016/j.rser.2015.10.054
Fernandez-Mena H., Nesme T., Pellerin S.	Towards an Agro-Industrial Ecology: A review of nutrient flow modelling and assessment tools in agro-food systems at the local scale	Science of the Total Environment	2016	543		467	479	10.1016/j.scitotenv.2015.11.032
Tiu B.T.C., Cruz D.E.	An MILP model for optimizing water exchanges in eco-industrial parks considering water quality	Resources, Conservation and Recycling	2016					10.1016/j.resconrec.2016.06.005
Iacobescu R.I., Angelopoulos G.N., Jones P.T., Blanpain B., Pontikes Y.	Ladle metallurgy stainless steel slag as a raw material in Ordinary Portland Cement production: A possibility for industrial symbiosis	Journal of Cleaner Production	2016	112		872	881	10.1016/j.jclepro.2015.06.006
Leong Y.T., Lee J.-Y., Chew I.M.L.	Incorporating Timesharing Scheme in Ecoindustrial Multiperiod Chilled and Cooling Water Network Design	Industrial and Engineering Chemistry Research	2016	55	1	197	209	10.1021/acs.iecr.5b02722
Zhao Q., Shi X.Q., Shi L.	A review of the industrial symbiosis network	Shengtai Xuebao/ Acta Ecologica Sinica	2016	36	22	7288	7301	10.5846/stxb201507301598
Albino V., Fraccascia L., Giannoccaro I.	Exploring the role of contracts to support the emergence of self-organized industrial symbiosis networks: An agent-based simulation study	Journal of Cleaner Production	2016	112		4353	4366	10.1016/j.jclepro.2015.06.070
Mantese G.C., De Piere B.A., Amaral D.C.	A procedure to validate industrial symbiosis indicators combining conceptual and empirical validation methods	Advances in Transdisciplinary Engineering	2016	4		166	175	10.3233/978-1-61499-703-0-166
Branson R.	Re-constructing Kalundborg: The reality of bilateral symbiosis and other insights	Journal of Cleaner Production	2016	112		4344	4352	10.1016/j.jclepro.2015.07.069

Author Name(s)	Title	Source Title	Year	Vol.	Issue	P. Start	P. End	Doi
Stratigaki C., Loucopoulos P., Migiakis A., Zorgios Y.	Combining model-driven and capability-driven developments: A case study of industrial symbiosis	CEUR Workshop Proceedings	2016	1753		12	22	
Liu J.R., Yan Y.T., Nie X.R., Yan L.	The application of life cycle assessments to the evaluation of the environmental benefits of industrial symbioses: Research progress and challenges	Shengtai Xuebao/ Acta Ecologica Sinica	2016	36	22	7202	7207	10.5846/stxb201411032156
Boons F., Chertow M., Park J., Spekkink W., Shi H.	Industrial Symbiosis Dynamics and the Problem of Equivalence: Proposal for a Comparative Framework	Journal of Industrial Ecology	2016					10.1111/jiec.12468
Chattopadhyay S., Kumar N., Fine C., Olivetti E.	Industrial symbiosis among small and medium scale enterprises: Case of Muzaffarnagar, India	TMS Annual Meeting	2016			173	177	
Dumoulin F., Wassenaar T., Avadí A., Paillat J.-M.	A Framework for Accurately Informing Facilitated Regional Industrial Symbioses on Environmental Consequences	Journal of Industrial Ecology	2016					10.1111/jiec.12495
[No author name available]	CEUR Workshop Proceedings	CEUR Workshop Proceedings	2016	1753				
Verguts V., Dessein J., Dewulf A., Lauwers L., Werkman R., Termeer C.J.A.M.	Industrial symbiosis as sustainable development strategy: Adding a change perspective	International Journal of Sustainable Development	2016	19	1	15	35	10.1504/IJSD.2016.073650
Lignos G., Stancari S., Bikos S., Kokossis A.	Structural and economic analysis of Industrial Symbiosis networks: a hybrid approach to assess investment opportunities	Computer Aided Chemical Engineering	2016	38		1617	1622	10.1016/B978-0-444-63428-3.50274-5
Holgado M., Morgan D., Evans S.	Exploring the scope of industrial symbiosis: Implications for practitioners	Smart Innovation, Systems and Technologies	2016	52		169	178	10.1007/978-3-319-32098-4_15

Author Name(s)	Title	Source Title	Year	Vol.	Issue	P. Start	P. End	Doi
Hein A.M., Jankovic M., Farel R., Yannou B.	A data- and knowledge-driven methodology for generating ecoindustrial park architectures	Proceedings of the ASME Design Engineering Technical Conference	2016	4				10.1115/DETC2016-59171.pdf
Henkel M., Stratigaki C., Stirna J., Loucopoulos P., Zorgios Y., Migiakis A.	Extending capabilities with context awareness	Lecture Notes in Business Information Processing	2016	249		40	51	10.1007/978-3-319-39564-7_4
Holgado M., Benedetti M., Evans S., Introna V.	Contextualisation in industrial energy symbiosis: Design process for a knowledge repository	Proceedings of the Summer School Francesco Turco	2016			139	144	
Afshari H., Gourlia J.-P., Farel R., Peng Q.	Energy symbioses in eco-industrial parks: Models and perspectives	Proceedings of the ASME Design Engineering Technical Conference	2016	4				10.1115/DETC2016-59965.pdf
Stirna J., Zdravkovic J., Henkel M., Loucopoulos P., Stratigaki C.	Modeling organizational capabilities on a strategic level	Lecture Notes in Business Information Processing	2016	267		257	271	10.1007/978-3-319-48393-1_18
Siskos I., Van Wassenhove L.N.	Synergy Management Services Companies: A New Business Model for Industrial Park Operators	Journal of Industrial Ecology	2016					10.1111/jiec.12472
Afshari H., Farel R., Peng Q.	Need for optimization under uncertainty: Designing flow exchanges in eco-industrial parks	Proceedings of the ASME Design Engineering Technical Conference	2016	4				10.1115/DETC2016-59974.pdf
Mohammed F., Biswas W.K., Yao H., Tadó M.	Identification of an environmentally friendly symbiotic process for the reuse of industrial byproduct - An LCA perspective	Journal of Cleaner Production	2016	112		3376	3387	10.1016/j.jclepro.2015.09.104

Author Name(s)	Title	Source Title	Year	Vol.	Issue	P. Start	P. End	Doi
Husgafvel R., Nordlund H., Heino J., Mäkelä M., Watkins G., Dahl O., Paavola I.-L.	Use of Symbiosis Products from Integrated Pulp and Paper and Carbon Steel Mills: Legal Status and Environmental Burdens	Journal of Industrial Ecology	2016	20	5	1187	1198	10.1111/jiec.12348
Qi Y., Zhu T., Gao S., Wang J.F., Ji Y.J., Zhang M., Bu X.X.	Preliminary exploration of the Chinese industrial park's circularization reform using key material flow analysis	Shengtai Xuebao/ Acta Ecologica Sinica	2016	36	22	7335	7345	10.5846/stxb201508151708
[No author name available]	3rd International Conference on Sustainable Design and Manufacturing, SDM 2016	Smart Innovation, Systems and Technologies	2016	52		1	688	
Kanematsu Y., Oosawa K., Kikuchi Y.	Agriculture	Energy Technology Roadmaps of Japan: Future Energy Systems Based on Feasible Technologies Beyond 2030	2016			405	414	10.1007/978-4-431-55951-1_27
De Souza V., Borsato M., Bloemhof J.	Designing eco-effective reverse logistics networks	Advances in Transdisciplinary Engineering	2016	4		851	860	10.3233/978-1-61499-703-0-851
Leong Y.T., Tan R.R., Aviso K.B., Chew I.M.L.	Fuzzy analytic hierarchy process and targeting for inter-plant chilled and cooling water network synthesis	Journal of Cleaner Production	2016	110		40	53	10.1016/j.jclepro.2015.02.036
Shi L., Chen W.Q.	Industrial ecology in China: Retrospect and prospect	Shengtai Xuebao/ Acta Ecologica Sinica	2016	36	22	7158	7167	10.5846/stxb201611232387
Kikuchi Y., Kanematsu Y., Okubo T.	A computer-aided scenario analysis of national and regional energy systems based on feasible technology options	Computer Aided Chemical Engineering	2016	38		1959	1964	10.1016/B978-0-444-63428-3.50331-3
Yong J.Y., Klemeš J.J., Varbanov P.S., Huisingh D.	Cleaner energy for cleaner production: Modelling, simulation, optimisation and waste management	Journal of Cleaner Production	2016	111		1	16	10.1016/j.jclepro.2015.10.062
Petek J., Glavič P., Kostevšek A.	Total Site Resource Efficiency System	Computer Aided Chemical Engineering	2016	38		2235	2240	10.1016/B978-0-444-63428-3.50377-5

Author Name(s)	Title	Source Title	Year	Vol.	Issue	P. Start	P. End	Doi
Yazan D.M., Romano V.A., Albino V.	The design of industrial symbiosis: An input-output approach	Journal of Cleaner Production	2016					10.1016/j.jclepro.2016.03.160
Kuznetsova E., Zio E., Farel R.	A methodological framework for Eco-Industrial Park design and optimization	Journal of Cleaner Production	2016					10.1016/j.jclepro.2016.03.025
Notarnicola B., Tassielli G., Renzulli P.A.	Industrial symbiosis in the Taranto industrial district: Current level, constraints and potential new synergies	Journal of Cleaner Production	2016					10.1016/j.jclepro.2016.02.056
Szabó S., Bódis K., Kougias I., Moner-Girona M., Jäger-Waldau A., Barton G., Szabó L.	A methodology for maximizing the benefits of solar landfills on closed sites	Renewable and Sustainable Energy Reviews	2017	76		1291	1300	10.1016/j.rser.2017.03.117
Fraccascia L., Giannoccaro I., Albino V.	Rethinking Resilience in Industrial Symbiosis: Conceptualization and Measurements	Ecological Economics	2017	137		148	162	10.1016/j.ecolecon.2017.02.026
Wu J., Guo Y., Li C., Qi H.	The redundancy of an industrial symbiosis network: A case study of a hazardous waste symbiosis network	Journal of Cleaner Production	2017	149		49	59	10.1016/j.jclepro.2017.02.038
Wang D., Li J., Wang Y., Wan K., Song X., Liu Y.	Comparing the vulnerability of different coal industrial symbiosis networks under economic fluctuations	Journal of Cleaner Production	2017	149		636	652	10.1016/j.jclepro.2017.02.137
Desrochers P., Szurmak J.	Long distance trade, locational dynamics and by-product development: Insights from the history of the American cottonseed industry	Sustainability (Switzerland)	2017	9	4			10.3390/su9040579
Sun L., Spekkink W., Cuppen E., Korevaar G.	Coordination of industrial symbiosis through anchoring	Sustainability (Switzerland)	2017	9	4			10.3390/su9040549

Author Name(s)	Title	Source Title	Year	Vol.	Issue	P. Start	P. End	Doi
Hein A.M., Jankovic M., Feng W., Farel R., Yune J.H., Yannou B.	Stakeholder power in industrial symbioses: A stakeholder value network approach	Journal of Cleaner Production	2017	148		923	933	10.1016/j.jclepro.2017.01.136
Sun L., Li H., Dong L., Fang K., Ren J., Geng Y., Fujii M., Zhang W., Zhang N., Liu Z.	Eco-benefits assessment on urban industrial symbiosis based on material flows analysis and emergy evaluation approach: A case of Liuzhou city, China	Resources, Conservation and Recycling	2017	119		78	88	10.1016/j.resconrec.2016.06.007
Tiu B.T.C., Cruz D.E.	An MILP model for optimizing water exchanges in eco-industrial parks considering water quality	Resources, Conservation and Recycling	2017	119		89	96	10.1016/j.resconrec.2016.06.005
Fraccascia L., Giannoccaro I., Albino V.	Efficacy of landfill tax and subsidy policies for the emergence of industrial symbiosis networks: An agent-based simulation study	Sustainability (Switzerland)	2017	9	4			10.3390/su9040521
Gabriel M., Schöggel J.-P., Posch A.	Early front-end innovation decisions for self-organized industrial symbiosis dynamics- A case study on lignin utilization	Sustainability (Switzerland)	2017	9	4			10.3390/su9040515
Saraceni A.V., Resende L.M., de Andrade Júnior P.P., Pontes J.	Pilot testing model to uncover industrial symbiosis in Brazilian industrial clusters	Environmental Science and Pollution Research	2017	24	12	11618	11629	10.1007/s11356-017-8794-y
Daddi T., Nucci B., Iraldo F.	Using Life Cycle Assessment (LCA) to measure the environmental benefits of industrial symbiosis in an industrial cluster of SMEs	Journal of Cleaner Production	2017	147		157	164	10.1016/j.jclepro.2017.01.090
Mauthoor S.	Uncovering industrial symbiosis potentials in a small island developing state: The case study of Mauritius	Journal of Cleaner Production	2017	147		506	513	10.1016/j.jclepro.2017.01.138

Author Name(s)	Title	Source Title	Year	Vol.	Issue	P. Start	P. End	Doi
Liu Z., Adams M., Cote R.P., Geng Y., Chen Q., Liu W., Sun L., Yu X.	Comprehensive development of industrial symbiosis for the response of greenhouse gases emission mitigation: Challenges and opportunities in China	Energy Policy	2017	102		88	95	10.1016/j.enpol.2016.12.013
Serdar M., Biljecki I., Bjegović D.	High-performance concrete incorporating locally available industrial by-products	Journal of Materials in Civil Engineering	2017	29	3			10.1061/(ASCE)MT.1943-5533.0001773
Yedla S., Park H.-S.	Eco-industrial networking for sustainable development: review of issues and development strategies	Clean Technologies and Environmental Policy	2017	19	2	391	402	10.1007/s10098-016-1224-x
Ubando A.T., Aguilar K.D.T.	Fuzzy quadratic programming model for the optimal design of an algal bioenergy park under optimal price markdown percentage	IEEE Region 10 Annual International Conference, Proceedings/TENCON	2017			936	941	10.1109/TENCON.2016.7848142
Leong Y.T., Lee J.-Y., Tan R.R., Foo J.J., Chew I.M.L.	Multi-objective optimization for resource network synthesis in eco-industrial parks using an integrated analytic hierarchy process	Journal of Cleaner Production	2017	143		1268	1283	10.1016/j.jclepro.2016.11.147
Ceglia D., Abreu M.C.S.D., Da Silva Filho J.C.L.	Critical elements for eco-retrofitting a conventional industrial park: Social barriers to be overcome	Journal of Environmental Management	2017	187		375	383	10.1016/j.jenvman.2016.10.064
Winans K., Kendall A., Deng H.	The history and current applications of the circular economy concept	Renewable and Sustainable Energy Reviews	2017	68		825	833	10.1016/j.rser.2016.09.123
Yap N.T., Devlin J.F.	Explaining Industrial Symbiosis Emergence, Development, and Disruption: A Multilevel Analytical Framework	Journal of Industrial Ecology	2017	21	1	6	15	10.1111/jiec.12398

Author Name(s)	Title	Source Title	Year	Vol.	Issue	P. Start	P. End	Doi
Ohnishi S., Dong H., Geng Y., Fujii M., Fujita T.	A comprehensive evaluation on industrial & urban symbiosis by combining MFA, carbon footprint and emergy methods—Case of Kawasaki, Japan	Ecological Indicators	2017	73		315	324	10.1016/j.ecolind.2016.10.016
Taddeo R., Simboli A., Ioppolo G., Morgante A.	Industrial symbiosis, networking and innovation: The potential role of innovation poles	Sustainability (Switzerland)	2017	9	2			10.3390/su9020169
Wang Q., Deutz P., Chen Y.	Building institutional capacity for industrial symbiosis development: A case study of an industrial symbiosis coordination network in China	Journal of Cleaner Production	2017	142		1571	1582	10.1016/j.jclepro.2016.11.146
Zhang C., Romagnoli A., Zhou L., Kraft M.	Knowledge management of eco-industrial park for efficient energy utilization through ontology-based approach	Applied Energy	2017					10.1016/j.apenergy.2017.03.130
Fan Y., Qiao Q., Fang L., Yao Y.	Emergy analysis on industrial symbiosis of an industrial park – A case study of Hefei economic and technological development area	Journal of Cleaner Production	2017	141		791	798	10.1016/j.jclepro.2016.09.159
Sharib S., Halog A.	Enhancing value chains by applying industrial symbiosis concept to the Rubber City in Kedah, Malaysia	Journal of Cleaner Production	2017	141		1095	1108	10.1016/j.jclepro.2016.09.089
Couto Mantese G., Capaldo Amaral D.	Comparison of industrial symbiosis indicators through agent-based modeling	Journal of Cleaner Production	2017	140		1652	1671	10.1016/j.jclepro.2016.09.142
Fraccascia L., Albino V., Garavelli C.A.	Technical efficiency measures of industrial symbiosis networks using enterprise input-output analysis	International Journal of Production Economics	2017	183		273	286	10.1016/j.ijpe.2016.11.003
Tseng M.-L., Bui T.-D.	Identifying eco-innovation in industrial symbiosis under linguistic preferences: A novel hierarchical approach	Journal of Cleaner Production	2017	140		1376	1389	10.1016/j.jclepro.2016.10.014

Author Name(s)	Title	Source Title	Year	Vol.	Issue	P. Start	P. End	Doi
Kim H.-W., Ohnishi S., Fujii M., Fujita T., Park H.-S.	Evaluation and Allocation of Greenhouse Gas Reductions in Industrial Symbiosis	Journal of Industrial Ecology	2017					10.1111/jiec.12539
Halstenberg F.A., Lindow K., Stark R.	Utilization of Product Lifecycle Data from PLM Systems in Platforms for Industrial Symbiosis	Procedia Manufacturing	2017	8		369	376	10.1016/j.promfg.2017.02.047
Dong L., Wang Y., Scipioni A., Park H.-S., Ren J.	Recent progress on innovative urban infrastructures system towards sustainable resource management	Resources, Conservation and Recycling	2017					10.1016/j.resconrec.2017.02.020
Wang X., Shi X.Q.	A review of industrial ecology based on GIS	Shengtai Xuebao/ Acta Ecologica Sinica	2017	37	4	1346	1357	10.5846/stxb201606301326
Oguntoye O., Evans S.	Framing Manufacturing Development in Africa and the Influence of Industrial Sustainability	Procedia Manufacturing	2017	8		75	80	10.1016/j.promfg.2017.02.009
Hein A.M., Yannou B., Jankovic M., Farel R.	Towards an automatized generation of rule-based systems for architecting eco- industrial parks	Smart Innovation, Systems and Technologies	2017	65		691	699	10.1007/978-981-10-3518-0_60
Dias G.M., Ayer N.W., Khosla S., Van Acker R., Young S.B., Whitney S., Hendricks P.	Life cycle perspectives on the sustainability of Ontario greenhouse tomato production: Benchmarking and improvement opportunities	Journal of Cleaner Production	2017	140		831	839	10.1016/j.jclepro.2016.06.039
Medina-González S., Graells M., Guillén-Gosálbez G., España A., Puigjaner L.	Systematic approach for the design of sustainable supply chains under quality uncertainty	Energy Conversion and Management	2017					10.1016/j.enconman.2017.02.060
Malinauskienė M., Kliopova I., Hugi C., Staniškis J.K.	Geostrategic Supply Risk and Economic Importance as Drivers for Implementation of Industrial Ecology Measures in a Nitrogen Fertilizer Production Company	Journal of Industrial Ecology	2017					10.1111/jiec.12561

Author Name(s)	Title	Source Title	Year	Vol.	Issue	P. Start	P. End	Doi
Deutz P., Baxter H., Gibbs D., Mayes W.M., Gomes H.I.	Resource recovery and remediation of highly alkaline residues: A political-industrial ecology approach to building a circular economy	Geoforum	2017					10.1016/j.geoforum.2017.03.021

Appendix-II. Top ten countries in IS research with industrial growth indicators

Countries	No. of Papers	Annual Industrial Growth rate	Industrial production in Price (million US\$)
China	85	6.10%	474,000
USA	49	0.10%	351,600
UK	49	3.10%	38,500
Italy	34	1.80%	39,400
Japan	27	2.00%	138,000
Netherland	21	3.10%	13,100
Philippines	21	7.20%	9,920
Australia	19	-1.60%	369,400
Canada	19	4.80%	22,200
France	19	1.30%	30,900

HOW DO PLANTS RESPOND TO PATCH AREA AND ITS DISTRIBUTION PATTERN IN HORQIN SAND LAND, CHINA

WU, J.^{1,2} – HOU, X. Z.¹ – XU, C. L.³ – LIU, Z. M.^{2*}

¹*Liaoning Ecological Engineering Vocational College, Shenyang 110001, P R China*

²*Institute of Applied Ecology, Chinese Academy of Sciences, Shenyang 110016, P R China*

³*Experimental Forest Farm of Liaoning province, Fushun 113300, P R China*

**Corresponding author*

e-mail: 0227wujing@163.com

(Received 30th Sep 2018; accepted 29th Nov 2018)

Abstract. To elucidate the plant response to habitat fragmentation, 18 interdune lowlands with different sizes in active sand dunes of Horqin Sand Land were selected, and the interdune lowland was considered as fragmented habitat patch. In our study, the effect of patch size on plant distribution pattern was explored and different protocols of species diversity conservation were proposed. Our results showed different plant sensitivities to habitat fragmentation: type I, species are restricted by patch area and distributed regularly in fragments; type II, species are not restricted by patch area, and their distribution is irregular in fragments; type III, species mainly distributed in large fragments; type IV, species mainly distributed in small fragments; type V, species mainly distributed in middle-sized fragments. Exploring the effects of fragmentation habitat size on plant species diversity and its distribution pattern will provide theoretical basis for plant diversity conservation in semi-arid sand dunes.

Keywords: *biodiversity, habitat loss, habitat isolation, patch, landscape*

Introduction

Habitat fragmentation has been considered as one of the major threats to biodiversity (Brunet et al., 2011; Wu et al., 2013; Murphy and Romanuk 2014; Matthews et al., 2014; Ducatez and Shine, 2017). Fragmentation processes often result in "patchy" habitat segments, called patchy habitat. As the degree of fragmentation increases, the original patch is isolated from the highly altered retrogressive landscape and gradually recedes and eventually develops into a biogeographic "habitat islands", producing a range of ecological or biological effects at different levels of population, community, ecosystem and even landscape.

The size, environmental heterogeneity and marginal effects of habitat patches have important effects on species richness and abundance in patches (Benedick et al., 2006; Santos et al., 2008; Leal et al., 2012; Fahrig et al., 2015). Different species have different sensitivity, adaptability and tolerance to landscape fragmentation (Haila, 2002; Hill et al., 2003; Swihart et al., 2003; Kolb et al., 2005; Hudson et al., 2017). The influence of habitat patches such as Qiandao Lake and Three Gorges Reservoir on plant diversity has been reported in China (Ding, 2005). Many studies have focused on the real islands in geography (Halley et al., 2014; Phillips et al., 2018), but less attention has been paid to the ecological effects of habitat patches in the broad sense of biogeography and ecology. As a relatively independent vegetation unit in sand dune ecosystem, the interdune lowlands have unique patch properties in sand dune landscape, which can be regarded as "fragmented habitat islands" in sand dune ecosystem, and play an important role in determining plant diversity and distribution pattern of sand dune ecosystem.

However, the impact of fragmented patch area in the sand dune ecosystems of semi-arid regions (i.e., interdune lowlands) on plant diversity and island accumulation has not been reported.

Therefore, we investigated the plant diversity of interdune lowlands in the active dune ecosystem of the Horqin Sandy land, and conducted regression analysis on the relationship between the relative frequency and abundance of typical species and fragmented island area. This study is aiming to explore the plant diversity protection scheme applicable to different ecological groups and reveal the processes and mechanisms of the impacts of the habitat island on the plant diversity. This study can provide a theoretical basis for biodiversity protection and guides the practice of biodiversity protection in semi-arid areas.

Material and Methods

Study site

The study site is located at Wulanaodu region (42°47'- 43°25' N, 118°38'-120°43' E, 480 m a.s.l.), eastern Inner Mongolia, China (*Figure 1*). The region has a semi-arid climate. The annual average temperature is 6.3°C. The annual average rainfall is ca. 340 mm, most of which is received during June to September. The windy season is from March to May. The growing season starts in late April and ends in late September.

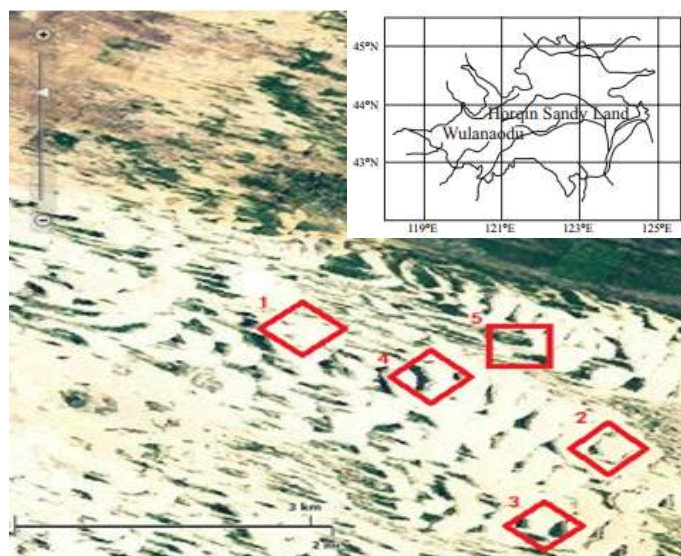


Figure 1. Location map and five sampling sites in Horqin sandy land

The active sand dune areas, 15–35 m in height, are advancing at a speed of ca. 6–7 m year⁻¹, and, following the aforementioned fencing since the 1980s, are permanently closed off from the natural grassland (>600 ha). The natural grassland and the active sand dunes experience the same climatic conditions, i.e. similar rainfall, temperature, humidity etc. The vegetation before the intense grazing period was dominated by perennial grasses, such as *Phragmites communis* and *Calamagrostis epigeios*, whereas after the onset of grazing pasammophilous species, such as *Artemisia wudanica* and *Agriophyllum squarrosum*, became more established.

Experimental procedures

We selected 18 interdune lowlands ranging in size from 0.10 to 5.64 hm² in 2012 (Table 1) (Liu et al., 2003). We used grid sampling at a resolution of 10 × 10 m. We established transects divided into 10-m intervals in each plot, all running in the vertical direction of the prevailing wind, and then selected 1 × 1 m quadrats, 10-m-spaced, along each transect (Wu et al., 2016). The species richness and abundance in the sample were recorded. For bunchgrasses (e.g. *C. squarrosa*), we counted the number of clusters to obtain the abundance, whereas for clonal species (e.g. *S. gordejewii* and *P. communis*) we counted the number of ramets, and for discrete species (e.g. *A. squarrosus*) the number of individuals were counted. The frequency of each species was determined within each plot.

Table 1. Basic information of 18 selected interdune lowlands

Plot number	Geographical coordinates of the center of the interdune lowland	Size (hm ²)	Dam Height (m)
1	42°59.900 N, 119°38.009 E	0.05	25
2	42°59.367 N, 119°38.789 E	0.27	28.5
3	42°58.089 N, 119°38.169 E	0.30	25.5
4	42°58.170 N, 119°37.886 E	0.32	25
5	43°00.964 N, 119°38.887 E	0.60	24
6	42°59.789 N, 119°37.236 E	0.66	25
7	42°59.767 N, 119°37.709 E	0.67	22.5
8	42°59.640 N, 119°37.886 E	1.00	25
9	42°59.805 N, 119°37.964 E	1.35	24.5
10	43°00.001 N, 119°37.870 E	2.27	23
11	42°59.862 N, 119°37.974 E	2.94	19
12	42°59.958 N, 119°37.844 E	3.22	23
13	42°59.442 N, 119°38.749 E	4.35	26.5
14	43°00.336 N, 119°37.609 E	5.01	25
15	42°00.498 N, 119°37.154 E	5.25	24.5
16	42°00.598 N, 119°38.504 E	6.19	26
17	42°00.156 N, 119°38.454 E	6.84	22
18	42°00.453 N, 119°37.231 E	11.3	24.5

Species diversity measure

- Species abundance: number of species within a community.
- Frequency of a species (%) = occurrence of the certain species/number of total samples.
- Abundance of a species (%) = total plants of certain species/ total plants of total species.

Classification of typical plant responses to habitat fragmentation

Based on the differences of typical plant responses to the habitat area, plants were divided into the five categories (Table 2).

Data analysis

All the statistic analysis was conducted in SPSS software. Model selection was based on maximum R², and residual analysis showed that the model fit was adequate.

Statistical significance was determined at $P = 0.05$. We analyzed the relationships between patch area and frequency and relative abundance for 6 type's species.

Table 2. Classification of typical plant responses to habitat fragmentation

Type	Relationship	Distribution
I	Significant	Regular
II	No significant	Irregular
III	Significant	Mainly distributed in large fragments
IV	No significant	Mainly distributed in small fragments
V	No significant	Mainly distributed in middle-sized fragments

Results

Species composition

According to the data of 18 interdune lowlands, there are 114 species belonging to 36 families in the patch habitat of horqin Sandy land. Among them, 25 species belong to *Compositae*, 13 species belong to *Graminae*, 11 species belong to *Leguminosae*, 6 species belong to *Cyperaceae*, 7 species belong to *Chenopodiaceae*, and the remaining 57 species belong to 31 families. Among them, 10 species is Psammophytes, 76 species are meadows plants and 22 species are steppes (Table 3).

Table 3. Species list in the 18 selected patchy habitats

Number	species	General	Ecological group	Life form	Frequency
1	<i>Artemisia halodendron</i>	Compositae	P	SS	0.99
2	<i>Artemisia wudanica</i>		P	SS	1.36
3	<i>Artemisia frigida</i>		P	SS	1.24
4	<i>Inula salsoloides</i>		P	PH	10.7
5	<i>Artemisia gmelinii</i>		LMS	SS	0.33
6	<i>Artemisia lavandulaefolia</i>		LMS	PH	23.5
7	<i>Erigeron acer</i>		LMS	BH	0.06
8	<i>Eupatorium lindleyanum</i>		LMS	PH	0.07
9	<i>Hypochoeris grandiflora</i>		LMS	PH	0.03
10	<i>Inula britannica</i>		LMS	PH	8.78
11	<i>Lactuca indica</i>		LMS	BH	1.06
12	<i>Lactuca tatarica</i>		LMS	PH	5.70
13	<i>Leibnitzia anandria</i>		LMS	PH	6.89
14	<i>Taraxacum mongolicum</i>		LMS	PH	16.7
15	<i>Taraxacum borealisinense</i>		LMS	PH	3.45
16	<i>Carduus nutans</i>		LMS	BH	0.02
17	<i>Cirsium segetum</i>		LMS	PH	0.46
18	<i>Ixeris chinensis</i>		LMS	PH	34.1
19	<i>Scorzonera capito</i>		LMS	PH	0.05
20	<i>Senecio jacobacea</i>		LMS	PH	0.42
21	<i>Sonchus brachyotus</i>		LMS	PH	10.4
22	<i>Serratula cardunculus</i>		LMS	PH	0.04
23	<i>Xanthium sibiricum</i>		LMS	AH	0.07

Number	species	General	Ecological group	Life form	Frequency
24	<i>Heteropappusaltaicus</i>		STS	PH	0.18
25	<i>Agriophyllum squarrosum</i>	Chenopodiaceae	P	AH	0.34
26	<i>Corispermum candelabrum</i>		P	AH	5.77
27	<i>Salix gordejewii</i>	Salicaceae	P	S	34.5
28	<i>Caragana microphylla</i>	Leguminosae	P	S	1.56
29	<i>Hedysarum fruticosum</i>		P	SS	3.76
30	<i>Agrostis clavata</i>	Gramineae	LMS	PH	16.8
31	<i>Arthraxon hispidus</i>		LMS	AH	9.87
32	<i>Calamagrostis epigeios</i>		LMS	PH	46.6
33	<i>Pennisetum alopecuroides</i>		LMS	PH	1.31
34	<i>Phragmites communis</i>		LMS	PH	60.4
35	<i>Miscanthussacchariflorus</i>		LMS	PH	15.6
36	<i>Echinochloa frumentacea</i>		LMS	PH	0.31
37	<i>Septoria mougeotii</i>		LMS	PH	0.02
38	<i>Chloris virgata</i>		LMS	AH	10.8
39	<i>Eragrostis pilosa</i>		LMS	AH	30.2
40	<i>Setaria viridis</i>		LMS	AH	0.98
41	<i>Pennisetum centrasiaticum</i>		LMS	PH	1.67
42	<i>Astragalus adsurgens</i>	Leguminosae	LMS	PH	0.45
43	<i>Glycine soja</i>		LMS	AH	3.06
44	<i>Kummerowia striata</i>		LMS	PH	2.64
45	<i>Melilotus suaveolens</i>		LMS	ABH	0.67
46	<i>Trigonella korshinskyi</i>		LMS	AH	0.01
47	<i>Vicia amoena</i>		LMS	PH	0.34
48	<i>Swainsonia salsula</i>		LMS	SS	1.78
49	<i>Thermopsis lanceolata</i>		LMS	PH	1.83
50	<i>Radix Glycyrrhizae</i>		STS	PH	0.65
51	<i>Bolboschoenus compactus</i>	Cyperaceae	LMS	PH	5.91
52	<i>Bolboschoenus planiculmis</i>		LMS	PH	0.37
53	<i>Carex caespitosa</i>		LMS	PH	10.6
54	<i>Carex duriuscula</i>		LMS	PH	12.3
55	<i>Heleocharis intersita</i>		LMS	PH	0.26
56	<i>Scirpus tabernaemontani</i>		LMS	PH	0.02
57	<i>Populus spp.</i>	Salicaceae	LMS	S	5.76
58	<i>Salix microstachya</i>		LMS	S	31.5
59	<i>Salix mongolica</i>		LMS	S	0.87
60	<i>Alisma orientale</i>	Alismataceae	LMS	PH	0.04
61	<i>Sagittaria trifolia</i>		LMS	PH	0.05
62	<i>Chenopodium acuminatum</i>	Chenopodiaceae	LMS	AH	0.04
63	<i>Chenopodium glaucum</i>		LMS	AH	3.67
64	<i>Bassia dasyphylla</i>		STS	AH	0.34
65	<i>Chenopodium aristatum</i>		STS	AH	0.22
66	<i>Salsola ruthenica</i>		STS	AH	0.12
67	<i>Polygonum hydropiper</i>	Polygonaceae	LMS	PH	0.02
68	<i>Polygonum lapathifolium</i>		LMS	AH	0.01
69	<i>Polygonum thunbergii</i>		LMS	AH	0.01

Number	species	General	Ecological group	Life form	Frequency
70	<i>Polygonum laxmanni</i>		P	PH	0.01
71	<i>Equisetum ramosissimum</i>	Equisetaceae	LMS	PH	0.02
72	<i>Equisetum sylvaticum</i>		LMS	PH	0.02
73	<i>Euphorbia humifusa</i>	Euphorbiaceae	LMS	AH	0.02
74	<i>Gentiana squarrosa</i>	Gentianaceae	LMS	PH	0.02
75	<i>Plantago depressa</i>	Plantaginaceae	LMS	PH	3.09
76	<i>Glaux maritima</i>	Primulaceae	LMS	PH	0.05
77	<i>Halerpestes cymbalaria</i>	Ranunculaceae	LMS	PH	5.93
78	<i>Potentilla discolor</i>	Rosaceae	LMS	PH	1.32
79	<i>Potentilla Chinensis</i>		LMS	PH	1.02
80	<i>Potentilla supina</i>		LMS	PH	0.67
81	<i>Potentilla anserina</i>		LMS	PH	0.66
82	<i>Typha minima</i>	Typhaceae	LMS	PH	1.33
83	<i>Artemisia laciniata</i>	Compositae	STS	PH	1.78
84	<i>Artemisia scoparia</i>		STS	ABH	3.65
85	<i>Artemisia sieversiana</i>		STS	ABH	1.34
86	<i>Heteropappus altaicus</i>		STS	PH	0.34
87	<i>Lespedeza davurica</i>	Leguminosae	STS	SS	10.9
88	<i>Oxytropis ramosissima</i>		STS	PH	0.02
89	<i>Sophora flavescens</i>		STS	PH	1.98
90	<i>Cynanchum sibiricum</i>	Asclepiadaceae	STS	PH	0.31
91	<i>C. chinense</i>		STS	PH	0.01
92	<i>Cleistogenes squarrosa</i>	Gramineae	STS	PH	6.81
93	<i>Galium verum</i>	Rubiaceae	STS	PH	0.28
94	<i>Rubiaschumahhaha</i>		P	PH	0.01
95	<i>Ulmus pumila</i>	Ulmaceae	STS	S	0.05
96	<i>Linaria vulgaris</i>	Scrophulariaceae	LMS	PH	0.01
97	<i>Portulaca oleracea</i>	Portulacaceae	STS	AH	0.05
98	<i>Spiked Loosestrife</i>	Lythraceae	LMS	PH	0.01
99	<i>Lythrum virgatum</i>		LMS	PH	0.01
100	<i>Erodium stephanianum</i>	Geraniaceae	LMS	PH	0.01
101	<i>Allium odorum</i>	Liliaceae	LMS	PH	0.01
102	<i>Asparagus brachyphyllus</i>		LMS	PH	0.01
103	<i>Asparagua dahuricus</i>		LMS	PH	0.01
104	<i>Viola philippica</i>	Violaceae	LMS	PH	0.01
105	<i>Viola prionantha</i>		LMS	PH	0.01
106	<i>Tragus bertesonianus</i>	Rutaceae	STS	PH	0.01
107	<i>Lappula echinata</i>	Boraginaceae	STS	ABH	0.01
108	<i>Radix Arnebiae</i>		STS	PH	0.01
109	<i>Scutellaria baicalensis</i>	Labiatae	STS	PH	0.01
110	<i>Tirbulus terrestris</i>	Zygophyllaceae	LMS	AH	0.01
111	<i>Saposhnikovia divaricata</i>	Umbelliferae	STS	PH	0.01
112	<i>Silene jennisseensis</i>	Caryophyllaceae	STS	PH	0.02
113	<i>Cuscuta chinensis</i>	Convolvulaceae	STS	AH	0.01
114	<i>Betula platyphylla</i>	Betula	LMS	S	0.01

The responses of typical plants to fragmented patch area

Type I (species is restricted by patch area and distributed regularly in fragments)

The frequency and relative abundance of *Artemisia wudanica*, *Phragmites communis* decreased logarithmically. The frequency and relative abundance of *Lespedeza davurica* showed a change of binomial function with the increase of the area of the fragmented habitat, when the area of plaque is around 2 hm², its frequency is lowest, and its relative abundance tends to increase with patch area (*Figure 2*).

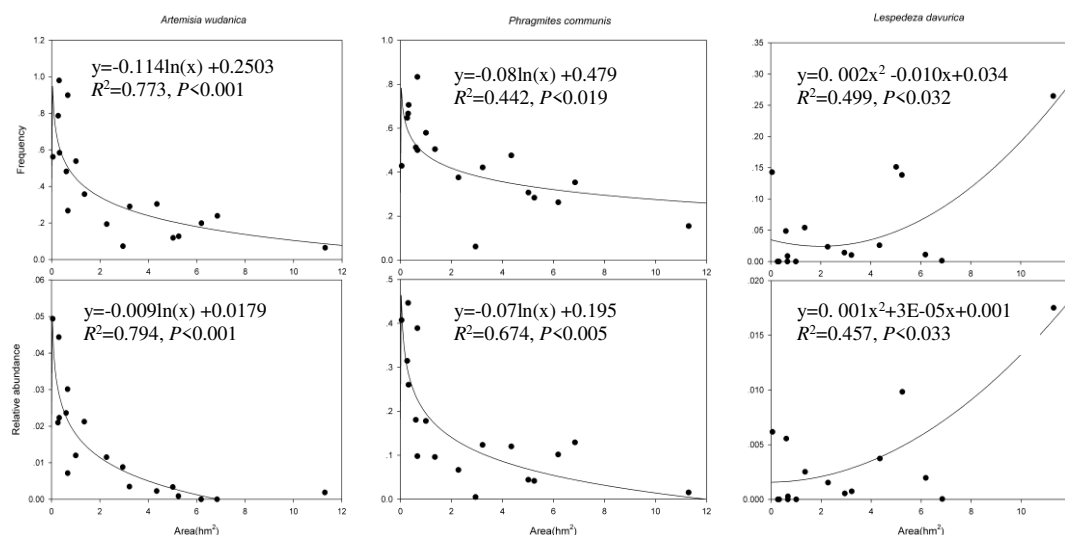


Figure 2. Changes in the frequency and abundance of *Artemisia wudanica*, *Phragmites communis*, *Lespedeza davurica* with increasing interdune lowland size

Type II (species is not restricted by patch area, and their distribution is irregular in fragments)

There was no significant change in the frequency and relative abundance of *Salix gordejewii* with the increase of plaque habitat area. *Salix gordejewii* appeared in different interdune lowlands, and the relative abundance of *Salix gordejewii* decreased with the increase of patch area (*Figure 3*).

Type III (species mainly distributed in large fragments)

The frequency and relative abundance of *Eragrostis pilosai* increased significantly with the increase of patch area, that is, the population size and distribution of *Eragrostis pilosai* declined sharply (*Figure 4*).

Type IV (species mainly distributed in small fragments)

The frequency and relative abundance of *Vicia amoena* showed no significant change with the increase of patch area. *Vicia amoena* is more frequent in small and medium-sized interdune lowlands; the population size of *Vicia amoena* varies little with increased habitat fragmentation (*Figure 5*).

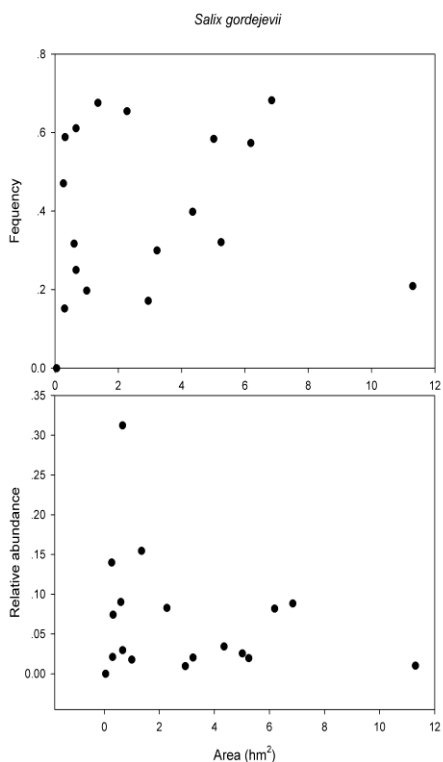


Figure 3. Changes in the frequency and relative abundance of *Salix gordejievii* population with interdune lowland area

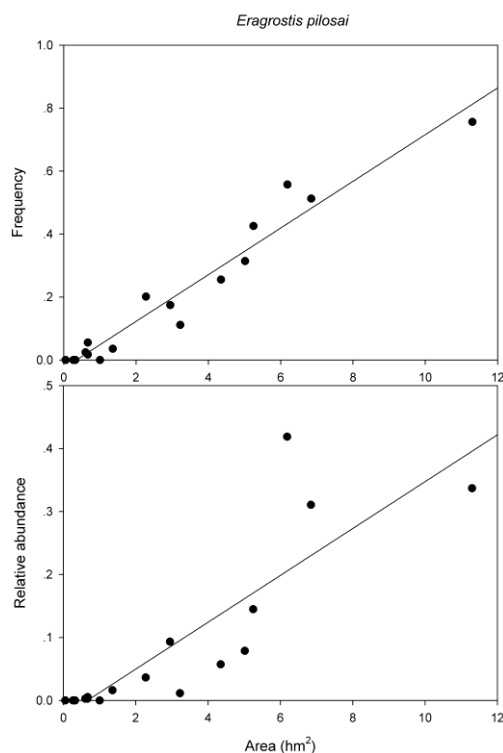


Figure 4. Changes in the frequency and relative abundance of *Eragrostis pilosai* population with interdune lowland area

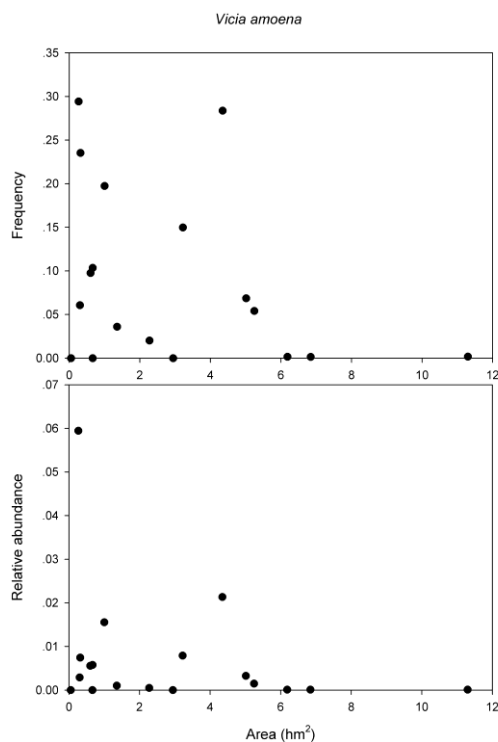


Figure 5. Changes in the frequency and relative abundance of *Vicia amoena* population with interdune lowland area

Type V (species mainly distributed in middle-sized fragments)

The frequency and relative abundance of *Chenopodium aristatum* showed no significant change with the increase of patch area, the frequency of *Chenopodium aristatum* was higher in medium size patch and lower in small and large size patch. The population size of *Chenopodium aristatum* had no significant change with the increase of habitat fragmentation. There was no significant change in the frequency and relative abundance of *Sophora miltiorrhiza* with the increase of patch area, and the size of population was not significant change with the increase of habitat fragmentation (Figure 6).

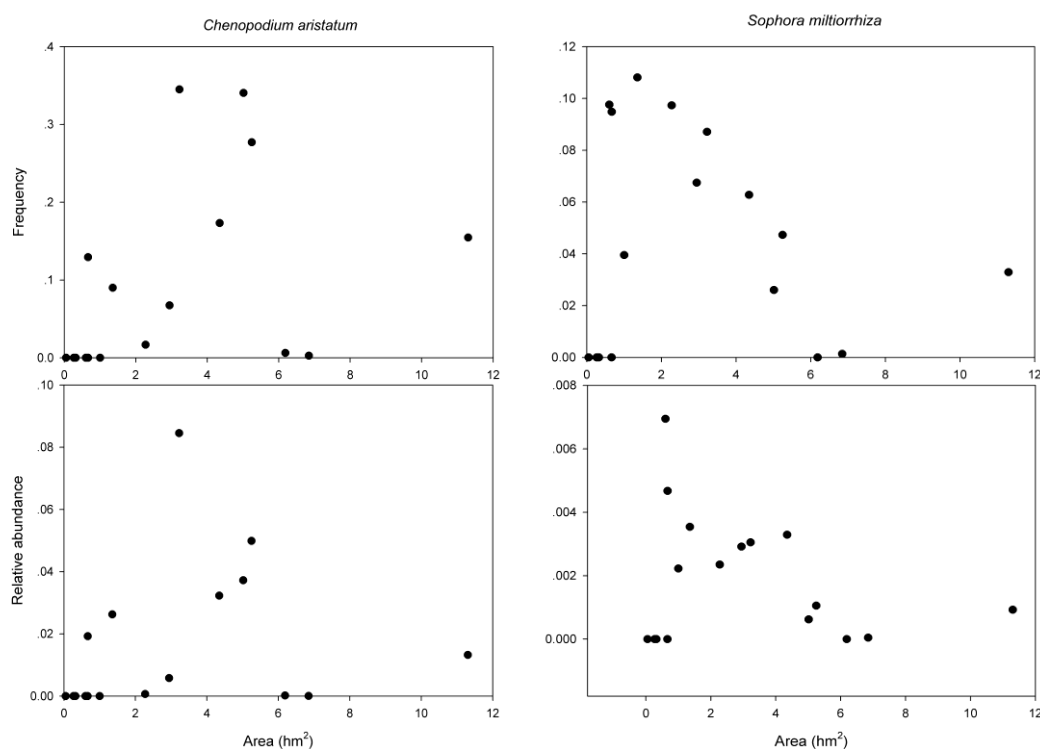


Figure 6. Change in the frequency and relative abundance of *Chenopodium aristatum* and *Sophora miltiorrhiza* with interdune lowland area

Discussion

Contrary to the existing view that species frequency show a negative trend with decreasing fragment area (Hill and Curran, 2003; Echeverría et al., 2007; Kornera and Jeltschb, 2008), our results showed that some species responded positively to habitat fragmentation and the species tolerance to habitat fragmentation was different. The plant-environmental feedback process in the dune system has a significant effect on plant growth and reproduction (Hambäck et al., 2007; Giladi et al., 2014; Winfree et al., 2015). The feedback process of *Artemisia wudanica* to wind erosion is as follows: After *Artemisia wudanica* is blown by the wind, the plant will fall down at a certain wind erosion depth, and the sand blocking area will increase accordingly. The microenvironment of the buried parts of the plants has changed. For example, 1) the soil volume has increased and the soil water content has increased; 2) mycorrhizal fungus activity capacity increased; 3) in the effective use of resources increased in the soil.

These changes have created favorable conditions for the adventitious roots on the sandy branches. In the case of a large number of adventitious roots, the growth of the plant increases, and the ability to block sand increases.

Reeds can appear in meadow grasslands and in the interdune lowlands. On the one hand, they belong to meadows, and on the other hand, they have the ability to adapt to wind sand. Previous studies have concluded that reeds can quickly invade and settle in habitats with intense sand activity due to its strong cloning and reproduction ability, (Liu et al., 2006; Liu et al., 2008). Therefore, in the broken patches of mobile dunes, especially in small areas with intense sand activity (Ma et al., 2010; Zobel et al., 2010; Wu et al., 2013), reeds show the ability to adapt to sandstorm interference (Liu et al., 2007). Reeds can be rapidly expanded from lowland to windward slopes through Rhizome extension and asexual strains. As pioneers, they create suitable habitat conditions for other species to invade, drive new vegetation succession in transition zones, and reduce wind and sand fluidity.

Lespedeza davurica has a persistent soil seed bank and can also ensure its population development under strong interference, while playing an important role in maintaining community diversity and system stability (Li et al., 2006). *Lespedeza davurica* population can expand the adjacent space by increasing the number of branches. The high-density population of *Lespedeza davurica* expands the plant elevation space in the form of lateral branches, that is, transverse space. The low-density population of *Lespedeza davurica* occupied the longitudinal space by increasing its branches, gradually occupied the horizontal space (Li, 2005).

Conclusions

In the practice of species diversity conservation, programmers should be tailored to the sensitivity of the species to habitat fragmentation. For example, with the increase in the area of patches, the frequency and relative diversity of *Artemisia wudanica*, *Phragmites communis*, and *Vicia amoena* are all reduced. Therefore, when protecting *Artemisia wudanica*, *Phragmites communis*, and *Vicia amoena*, the focus should be on protecting small islands. The frequency and relative abundance of *Lespedeza davurica* increase with the increase of patch area. Therefore, when protecting *Lespedeza davurica*, we should focus on a large area of islands; the frequency and relative abundance of *Chenopodium aristatum* and *Sophora flavescens* are higher in the middle area islands, therefore, when protecting *Chenopodium aristatum* and *Sophora flavescens*, the middle area islands should be protected.

Acknowledgments. We thank Jianqiang Qian and Yongming Luo for field assistance. The study was financially supported by the National Natural Science Youth Foundation of China (31600443) and the Liaoning Natural Science Foundation (201800170).

REFERENCES

- [1] Benedick, S., Hill, J. K., Mustaffa, N., Chey, V. K., Maryati, M., Searle, J. B., Schilthuizen, M., Hamer, K. C. (2006): Impacts of rain forest fragmentation on butterflies in northern Borneo: Species richness, turnover and the value of small fragments. – J Appl Ecol 43: 967-977.

- [2] Brunet, J., Valtinat, K., Mayr, L. M., Felton, A., Lindbladh, M., Bruu, H. H. (2011): Understorey succession in post-agricultural oak forests: habitat fragmentation affects forest specialists and generalists differently. – *For. Ecol. Manage.* 262: 1863-1871.
- [3] Ding, L. Z. (2005): Islanding landscape in thousand-island lake region and its effect on plant diversity. – Hangzhou, Zhejiang University.
- [4] Ducatez, S., Shine, R. (2017): Drivers of extinction risk in terrestrial vertebrates. – *Conserv. Lett.* 10: 186-194.
- [5] Echeverría, C., Newton, A. C., Lara, A., Benayas, J. M. R., Coomes, D. A. (2007): Impacts of forest fragmentation on species composition and forest structure in the temperate landscape of southern Chile. – *Global Ecol. Biogeogr.* 16: 426-439.
- [6] Fahrig, L., Girard, J., Duro, D., Pasher, J., Smith, A., Javorek, S., King, D. J., Lindsay, K. E., Mitchell, S. W., Tischendorf, L. (2015): Farmlands with smaller crop fields have higher within-field biodiversity. – *Agric. Ecosyst. Environ.* 200: 219-234.
- [7] Giladi, I., May, F., Ristow, M., Jeltsch, F., Ziv, Y., Triantis, K. (2014): Scale-dependent species–area and species–isolation relationships: a review and a test study from a fragmented semi-arid agro-ecosystem. – *J. Biogeogr.* 41: 1055-1069.
- [8] Haila, Y. (2002): A conceptual genealogy of fragmentation research: From island biogeography to landscape ecology. – *Ecol Appl* 12: 321-334.
- [9] Halley, J. M., Sgardeli, V., Triantis, K. A. (2014): Extinction debt and the species–area relationship: a neutral perspective. – *Global Ecol. Biogeogr.* 23: 113-123.
- [10] Hambäck, P. A., Summerville, K. S., Steffan-Dewenter, I., Krauss, J., Englund, G., Crist, T. (2007): Habitat specialization, body size, and family identity explain lepidopteran density–area relationships in a cross-continental comparison. – *Proc. Natl Acad. Sci. USA.* 104: 8368-8373.
- [11] Hill, J. L., Curran, P. L. (2003): Area, shape and isolation of tropical forest fragments: effects on tree species diversity and implications for conservation. – *J Biogeogr* 30: 1391-1403.
- [12] Hudson, L. N., Newbold, T., Contu, S., Hill, S., Lysenko, I., Palma, A. D., Phillips, H. R. P., Alhusseini, T. I., Bennett, D. J., Bugter, R. J. F., Buscardo, E. (2017): The database of the PREDICTS (Projecting Responses of Ecological Diversity in Changing Terrestrial Systems) project. – *Ecol. Evol.* 7: 145-188.
- [13] Kolb, A., Diekmann, M. (2005): Effects of life-history traits on responses of plant species to forest fragmentation. – *Conserv Biol* 19: 929-938.
- [14] Kornera, K., Jeltsch, F. (2008): Detecting general plant functional type responses in fragmented landscapes using spatially-explicit simulations. – *Ecol. Model.* 210: 287-300.
- [15] Leal, I. R., Filgueiras, B. K., Gomes, J. P., Luciana, B., Bullet, I., Andersen, A. N., Conserv, B. (2012): Effects of habitat fragmentation on ant richness and functional composition in Brazilian Atlantic forest. – *Biodivers. Conserv.* 21(7): 1687-1701.
- [16] Li, L. (2005): Study on germination and growth of *Lespedeza davurica*. – Changchun. Dongbei Normal University.
- [17] Li, X. H., Li, X. L., Jiang, D. M., Liu, Z. M. (2006): Germination strategy and ecological adaptability of *Eragrostis pilosa*. – *J Appl Ecol* 17(4): 607-670. (in Chinese with English abstract).
- [18] Liu, B., Liu, Z. M., Guan, D. X. (2008): Seedling growth variation in response to sand burial in four *Artemisia* species from different habitats in the semi-arid dune field. – *Trees-struct Funct* 22: 41-47.
- [19] Liu, J. G., Ouyang, Z. Y., Pimm, S. L. (2003): Protecting China's Biodiversity. – *Science*, 300: 1240-1241.
- [20] Liu, Z. M., Yan, Q. L., Baskin, C. C., Ma, J. L. (2006): Burial of canopy-stored seeds in the annual psammophyte *Agriophyllum squarrosum* (Chenopodiaceae) and its ecological significance. – *Plant Soil* 288: 71-80.

- [21] Liu, Z. M., Li, X. L., Yan, Q. L., Wu, J. G. (2007): Species richness and vegetation pattern in interdune lowlands of an active dune field in Inner Mongolia, China. – *Biol Conserv.* 140: 29-39.
- [22] Ma, J. L., Liu, Z. M., Zeng, D. H., Liu, B. (2010): Aerial seed bank in *Artemisia* species: how it responds to sand mobility. – *Trees-struct Funct* 24: 435-441.
- [23] Matthews, T. J., Cottee-Jones, H. E. W., Whittaker, R. J. (2014): Habitat fragmentation and the species–area relationship: a focus on total species richness obscures the impact of habitat loss on habitat specialists. – *Divers. Distrib.* 20: 1136-1146.
- [24] Murphy, G. E. P., Romanuk, T. N. (2014): A meta-analysis of declines in local species richness from human disturbances. – *Ecol. Evol.* 4: 91-103.
- [25] Phillips, H. R. P., Halley, J. M., Urbina-Cardona, J. N., Purvis, A. (2018): The effect of fragment area on site-level biodiversity. – *Ecography.* 41: 1220-1231.
- [26] Santos, B. A., Peres, C. A., Oliveira, M. A. (2008): Drastic erosion in functional attributes of tree assemblages in Atlantic forest fragments of northeastern Brazil. – *Biol Conserv* 141: 249-260.
- [27] Swihart, R. K., Gehring, T. M., Kolozsvary, M. B. (2003): Responses of ‘resistant’ vertebrates to habitat loss and fragmentation: The importance of niche breadth and range boundaries. – *Divers Distrib* 9: 1-18.
- [28] Winfree, R., Fox, J., Reilly, J. R., Carveau, D. P. (2015): Abundance of common species, not species richness, drives delivery of a real-world ecosystem service. – *Ecol. Lett.* 18: 626-635.
- [29] Wu, J., Liu, Z. M., Qian, J. Q. (2013): Non-linear effect of habitat fragmentation on plant diversity: Evidence from a sand dune field in a desertified grassland in northeastern China. – *Ecol Eng* 54: 90-96.
- [30] Wu, J., Qian, J. Q., Hou, X. Z., Carlos, A. B., Liu, Z. M., Xing, B. Z. (2016): Spatial variation of plant species richness in a sand dune field of northeastern Inner Mongolia, China. – *J Arid Land* 8: 434-442.
- [31] Zobel, M., Moora, M., Herben, T. (2010): Clonal mobility and its implication for spatio-temporal patterns of plant communities: what do we need to know next? – *Oikos* 119: 802-806.

ESTIMATION OF CONSTRUCTION WASTES BASED ON THE BILL OF QUANTITY IN SOUTH CHINA

LIU, J. K.* – LIU, Y. D. – ZHAO, S. M. – LI, S. M.

*Department of Construction Management, School of Management, Guangzhou University
510006 Guangzhou, People's Republic of China*

**Corresponding author
e-mail: ljkgowell@163.com*

(Received 28th Apr 2018; accepted 5th Oct 2018)

Abstract. In this paper, taking the South China area as an example, a list of construction wastes has been established based on the bill of quantities, and a calculation method for the production of construction waste of new residential projects has been proposed. According to the existing research data, the scrap rate of the main materials is obtained, and the waste production of the newly-built project is estimated, which is 0.326 m³ per unit area. The model in this article estimates the amount of construction waste and promotes the classification and reduction of construction waste at the construction site. It is recommended to adopt source reduction measures, implement a classification system and improve relevant laws and regulations, as well as optimize the waste market. Meanwhile, this model includes waste production budget into bidding, providing reference for improving the management level of domestic construction departments.

Keywords: *construction waste, bill of quantities, waste rate, case analysis*

Introduction

Recently, the process of urbanization has intensified and the old city has gradually improved. Disposal of construction waste has become one of the focuses of domestic and foreign scholars. According to available data, China's annual construction waste accounts for 40% of the total municipal waste (Li, 2007). Taking the example of Guangzhou, a major city in South China (*Fig. 1*), the newly-built construction area was 162,895,600 m² at the end of 2016. The construction of new buildings and the demolition of construction projects in Guangzhou each year produce a large amount of construction waste. The large amount of construction waste and its disastrous effects in China is obvious (Devora Isiordia et al., 2017; Wani et al., 2018; Landowski et al., 2017; Camara et al., 2018; Yang et al., 2017; Fu and Liu, 2017; Pazand and Hezarkhani, 2018). The disposal, reduction, recycling and utilization of construction wastes have aroused public attention while little attention is paid to the output of construction waste in construction activities (Liu and Wang, 2013; Lu et al. 2017; Yuan, 2017; Huang et al., 2018; Alsulaiman and Nizam, 2018). Due to the differences in the types of building structure, construction technology, and management level, as well as the complex and diverse output of construction waste, the calculation is relatively troublesome. In addition, the data analysis method is different from each country and region resulting the waste rate being difficult to be used directly (Li et al., 2016; Sufiya et al., 2018). In addition, it takes much time and manpower to accurately obtain the scrap rate of building materials. Therefore, many scholars reflect the production of construction waste through the ratio of building materials to waste (Fattaet al., 2003; Kofoworola and Gheewala, 2009; Lu et al., 2011; Li et al., 2013a; Chooi et al., 2016; Chuanlei et al., 2018).

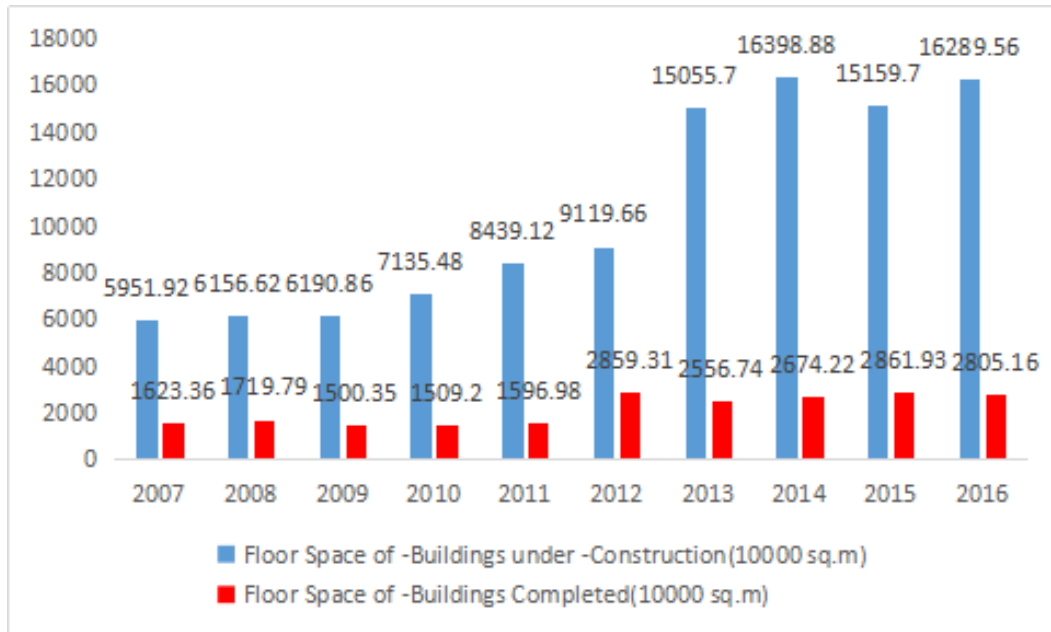


Figure 1. Construction and completion area of Guangzhou City in 2007-2016 (GBS, 2017)

Proper reduction and disposition of construction waste will promote the efficiency of resources and sustainable development of economy and environment, which arouse attention from all countries in the world. The waste disposal and on-site construction management level of the new building is related to the sustainable development of China's construction industry (Liu and Wang, 2011; Adegbuyi et al., 2018). In this paper, taking South China as an example, based on the bill of quantities, the output of new construction waste is analyzed. By estimating the output of waste generated during the construction of a new construction project through bill of quantities, it is possible to more accurately understand the types and output of construction waste, so that the governments and contractors can intuitively know the disposal costs of construction waste. Then the economic benefits of recycling wastes are derived, encouraging contractors to adopt “reduction, recycling and utilization” strategies. Besides, with the bill of quantities, implementation of energy conservation and emission reduction will be more effective.

Literature review

Bossink and Brouwers (1996) conducted on-site observation and weighed five housing buildings, and found that the waste rate of various building materials accounted for 1% to 10% of the purchased materials, and an average 9% of purchased materials became waste. Enshassi's research in Gaza revealed that the material waste rate was about 3.6-11% (Enshassi, 1996; Roslee and Tongkul, 2018). Solís-Guzmán et al. (2009) investigated the scrap rate of materials from 1 to 10 floors of civil residential through the classification of budget. Tam et al. (2007) investigated 19 engineering projects based on work subcontracting and project types, and analyzed the loss of five major building materials. Katz and Baum (2011) surveyed 10 multi-storey civil construction projects on the spot and found that the loss of main building materials was different at

various construction stages, and also found the scrap rates of the main materials at different stages, such as concrete, steel bars, blocks, mortar, tiles, and wood. Through field surveys of 22 new construction projects and questionnaires, Poon et al. (2004) obtained waste rates for various materials during the construction process of government projects and private projects. According to the European waste list, Llatas (2011) divided construction waste into residual waste, packaging waste, earthwork, and hazardous waste. He established an estimation model for construction waste and estimated the output of several major wastes. In Brazil, Pinto and Agopyan (1994) found that waste generated from the construction project accounted for 20%-30% of the material weight in the construction site. Paola et al. (2015) used two models to quantify the weight and volume of several newly-built residential construction wastes, in order to quantify the waste of Mediterranean residential projects which were under construction. It was found that the data between the models were different from the data collected by other projects by an average of 1-10%. Fatta et al. (2003) assumed the average construction waste generation rates in the construction field and estimated the total amount of construction waste in Greece. Based on the construction permit issued by Thailand, Kofoworola and Gheewala (2009) used construction area to estimate the construction waste of the construction and demolition project, and found that the waste generated from the residential project and the non-residential project was 21.38 kg/m² and 18.99 kg/m², respectively. In order to estimate the total amount of waste, Villoria Sáez et al. (2012, 2014) use construction area as a variable to evaluate waste production. Based on the production and composition of waste from the demolition project in the Florida area of Spain, Cochran et al. (2017) obtained estimations of construction waste from residential and non-residential projects. According to the weight estimations, the main components of waste are: concrete accounted for 56%, wood 13%, gypsum board 11%, residual debris 8% and roof coating 7%. Through calculation and investigation, Mah et al. (2016) found that different construction methods would affect the production of construction waste. They also concluded that the production of waste generating from the buildings, which used traditional construction method, was 9.88 t/100 m², the mixed construction method was 3.29 t/100 m², and the demolition project was 104.28 t/100 m². Between 2011 and 2016, the construction and demolition waste in Tehran (Iran Capital) reached 82,645,051 m³, which included 30% of mixed mortar, 19% of concrete, 18% of broken bricks, and 11% of earthworks (Alireza, et al., 2017; Shabi et al., 2018). The waste rate of new construction projects in different Countries (Region) is shown in *Table 1*.

Table 1. Estimation of construction and demolition wastes in different countries (region)

The author	Time	Country (region)	Type of construction project	Construction and demolition waste assessment	Research conclusions
Bossink and Brouwers	1996	Netherlands	Residential project	Weight percentage	About 1-10% of building materials become waste
Amnon et al.	2010	Israel	Residential project	According to the construction phase	One third of the total waste generated during the construction process is caused early in the construction phase

Tam et al.	2007	Hong Kong	Residential and non-residential projects	The consumption rate of the five main building materials	13.18% waste generated in private homes
Pinto et al.	1994	Brazil	Residential project	Weight	The weight of waste accounts for 20-30% of construction materials
Kofoworola et al.	2009	Thailand	Residential and non-residential projects	kg/m ²	Residential: 21.38 kg/m ² Non-residential: 18.99 kg/m ²
Villoria Sáez et al.	2012	Spain	Residential project	m ³ /m ²	Total waste
Cohran et al.	2007	America	Residential and non-residential projects	Weight percentage	Ratio of 8 materials
Solis-Guzmán et al.	2009	Spain	Residential project	m ³ /m ² According to each construction's three waste types	1-10 floor material scrap rate
Llatas	2011	Spain	Residential project	Three types of material scrap rate of m ³ /m ²	0.1388 m ³ /m ²
Paola et al.	2015	Spain	Residential project	Weight and volume	The difference between the waste rate of new construction materials and other projects is 1-10%
Chooi Mei Mah et al.	2016	Malaysia	Residential and non-residential projects	t/100 m ² , effect of different construction methods on waste	Traditional construction method: 9.88 t/100 Mixed construction method 3.29 t/100 m ² Demolition project: 104.28 t/100m ²
Alireza et al.	2017	Iran	Residential and non-residential projects	Questionnaire	From 2011 to 2016, an average of 16, 529, 219 m ³ of construction and demolition waste was generated each year: 30% of mixed mortar, 19% of concrete, 18% of broken bricks, and 11% of earth

In China, some scholars pay attention to the quantitative estimation of construction waste. Wang et al. (2010) conducted investigations on 116 construction areas. Under construction projects throughout the country, they found out that the projects might produce waste at various stages of construction. According to the investigation data on

construction waste from Central China, the amount of materials that have not been converted into structures and turned into scrap accounts for about 1% to 15% of material purchases (Wu et al., 2000; Mahtab et al., 2018). Through interviews and questionnaire, Li et al. (2010, 2013b) obtained the scrap rates and the volume of use of major materials, as well as the amount of waste generated during the demolition of temporary facilities. Then they calculated the output of construction waste per construction area. At the same time, 25 new construction projects were investigated, including 16 residential projects, 2 commercial projects, 4 industrial projects, and 3 public projects. Meanwhile, the characteristics of different types of construction materials waste rates were discovered. Through comparison, the management level of construction waste in domestic construction departments was analyzed. Chen et al. (2012) established a method for estimating urban construction waste production based on building area and construction waste coefficient. Besides, based on quadratic curve regression, exponential trend model, Grey GM (1, 1) model and BP neural network, they established variable-weight combined model to reveal the future of urban construction waste, which based on the principles of forecast effectiveness optimization. Through questionnaires and expert interviews, according to the classification of construction packaging waste and the corresponding indicators in the list of construction quantities, Wang et al. (2017) established a list of construction building packaging waste, and accurately analyzed the sources and the quantitative treatment of construction packaging waste at the construction site. Liu (2013) established an estimation model for construction waste in his doctoral thesis and listed the application of the model in brick-concrete structure. He also estimated that 0.34 m³/m² for waste will be generated by new residential projects. In order to implement the “Opinions of the People’s Government of Henan Province on Strengthening the Management of Urban Construction Waste and Promoting the Utilization of Resources” and regulate the disposal of construction waste in Henan built-up areas, DHURCHP (2016) formulated the “Measures for the Calculation of Construction Waste in Henan Province (interim)”, and determined the content of major components of the waste in each construction area (Tables 2 and 3).

Table 2. The content of main material components in the waste output of the construction unit area (kg/m²)

Classification		Abandoned steel	Waste concrete and sand	Waste brick	Waste glass	Combustible waste	Total
Civil construction	Masonry structure	13.8	894.3	400.8	1.7	25.0	1336
	Reinforced-concrete structure	18.0	1494.7	233.8	1.7	25.0	1773
	Brick and wood structure	1.4	482.2	384.1	1.8	37.2	907
	Steel structure	29.2	651.3	217.1	2.6	7.9	908
Industrial building	Masonry structure	18.4	863.4	267.2	2.0	27.5	1178
	Reinforced-concrete structure	46.8	1163.8	292.3	1.9	37.7	1543
	Brick and wood structure	1.8	512.7	417.5	1.7	32.1	966
	Steel structure	29.2	651.3	217.1	2.6	8.0	908

Table 3. Estimation of wastes from domestic construction and demolition projects

The author	Time	Construction project type/structure	Construction and demolition waste assessment	Research conclusions
Wang et al.	2010	Civil construction	Surveyed 116 civil construction projects across the country	Statistics on the type, quantity, and loss rate of waste that may occur in different construction processes
Wu et al.	2000	Brick masonry, frame and frame - shear wall structure	Statistical survey	The amount of construction waste generated per unit building area of masonry concrete, frame and frame-shear wall structure is 50 to 200 kg/m ² , 45 to 150 kg/m ² , and 40 to 150 kg/m ² , respectively
Li et al.	2013a	Residential project	Interviews and surveys, kg/m ²	The main waste output indicators: concrete 16.2 kg/m ² , brick block 3.4 kg/m ² , ceramic 0.3 kg/m ² , mortar 1.7 kg/m ² , metal 1.9 kg/m ² , timber 7.7 kg/m ²
Chen et al.	2012	Civil and office projects	Urban construction waste production estimation method system based on building area and production and waste coefficient	The total amount of construction waste in Hainan Province grew to 8.135 million tons from 2001 to 2010, with an average annual growth rate of 12.7%
Wang et al.	2017	Residential, commercial, public buildings, etc.	Establish a list of construction packaging wastes based on the bill of quantities and propose a method for the quantitative estimation of construction site packaging wastes at the construction site, through questionnaire surveys and expert interviews	Accurately and comprehensively estimate the amount of packaging waste at the construction site
Liu	2013	Residential project	Establish construction waste inventory and construction waste estimation model through questionnaire	The new residential project generates approximately 0.34 m ³ of waste per m ² of built-up area (considering earthwork)

Methods

Establishment of an estimation model for construction waste

List of the classification of construction wastes

In this study, various aspects of the project manager were examined through questionnaires and personal interviews. Combine existing research and surveys and based on

the project inventory model, each construction waste list has its project code and project name. The compilation of the list is based on the “Code for the Calculation of Construction Quantity of House Construction and Decoration Engineering” (MOHURD, 2013) (Hereinafter referred to as “measurement specification”). Meanwhile, it classifies the list of construction wastes that may be generated during the construction process of the project and divides the list of different levels of construction waste, such as sub-divisions of earthwork, backfill, foundation treatment, foundation pit and slope support, brickwork, steel reinforcement engineering (European Commission, 2008). Due to different construction sites and different construction purposes, the same material type must also be listed separately.

The construction waste sorting list is integrated according to the construction site and construction purpose, which basically involves all the construction site of the entire construction process, and has ensured the integrity and accuracy of the measurement of construction waste. List of construction waste on the construction site is shown in *Table 5*.

Determination of construction waste inventory

In order to determine the quantity of each item that may generate construction waste in the construction process Q_i . This article refers to a list of the quantities of 10 new residential projects in South China (*Table 4*) and categorize the content of the list. Those types of project structures in the list are mainly frame structures and frame shear structures (*Table 5*), which are the basement or multi-story buildings, as well as typical residential projects.

Table 4. *New residential projects in South China*

Project name	Construction area	Structure type	Construction site
Beiliu High School 14# Student Dormitory Project	4160 m ²	Framework	Yulin City, Guangxi Zhuang Autonomous Region
Guilin Banghui Textile Co., Ltd. 2# dormitory building	3065.34 m ²	Brick structure	Guilin City, Guangxi Zhuang Autonomous Region
Luzhai County Elementary Experimental Middle School 3#, 4# Student Dormitory Building	6310 m ²	Framework	Liuzhou City, Guangxi Zhuang Autonomous Region
Rongxian Middle School Student Dormitory Building Project	6435 m ²	Framework	Yulin City, Guangxi Zhuang Autonomous Region
Fusui Middle School 4# student apartment building project	6211.36 m ²	Framework	Chongzuo City, Guangxi Zhuang Autonomous Region
Yixiangyuan Plaza, a residential building	11864.8 m ²	Frame shear wall structure	Huizhou City, Guangdong Province
Guifeng Garden 3# Building	7020.92 m ²	Frame shear structure	Jiangmen City, Guangdong Province
Mai Yousheng Residence Building	3566.88 m ²	Shear wall structure	Dongguan City, Guangdong Province
Mingfa Gaobangxincheng C10# Building	12537.46 m ²	Shear wall structure	Huizhou City, Guangdong Province
No. 4 Student Dormitory of Phase 3 Project of Huizhou Engineering Technology School	5516 m ²	Frame shear wall structure	Huizhou City, Guangdong Province

Table 5. Classification of construction waste rate list

Project number	Project name	Unit	Waste rate (%)
010101002	Excavation of Earth	m ³	88.3
010101	Earthwork		
010103001	Backfill	m ³	67.3
010103002	Residual Disposal	m ³	21
010103	Backfill		
010201009	Deep Mixing Pile	m	3.2
010201016	Grouting Foundation	m, m ³	4
010201	Foundation Treatment		
010202001	Diaphragm Wall	m ³	3.9
010202010	Reinforced concrete Bracing	m ³	3.4
010202	Shoring of Side for Foundation Pit		
010401004	Brick foundation	m ³	3.9
010401003	Solid Brick Wall	m ³	2
010401004	Porous Brick Wall	m ³	7.1
010401009	Solid Brick column	m ³	2
010401	Brick Masonry		
010501001	Bed Course	m ³	3.1
010501003	Independent Foundation	m ³	3.1
010501	Cast-in-place Concrete Foundation		
011301001	Ceiling Plastering	m ²	3.2
011301	Plasterer		
011406001	Paint Coating	m ²	3.1
011406	Plastering Paint		
011701002	External Scaffolding	m ²	5
011701003	Internal Scaffolding	m ²	5
011701	Scaffolding Work		
011702001	Foundation	m ²	5
011702002	Rectangular Column	m ²	5
011702003	Structural Column	m ²	5
011702005	Foundation Beam	m ²	5
011702009	Lintel	m ²	5
011702014	Beam Plate	m ²	5
011702028	Copping	m ²	5
011702	Concrete Formwork and Support		
011201001	Wall General Plastering	m ²	3.2
011201	Wall Plastering		
011201001	Column, Beam Surface General Plastering	m ²	3.2
011201	Column (Beam) Surface Plastering		
010502001	Rectangular Column	m ³	3.1
010502002	Structural Column	m ³	3.1
010502	Cast-in-place Concrete Column		

010503001	Foundation Beam	m ³	3.1
010503005	Lintel	m ³	3.1
010503	Cast-in-place Concrete Beam		
010505001	Beam Plate	m ³	3.1
010505001	Balustrade	m ³	3.2
010505	Cast-in-place Concrete Slab		
010506001	Straight Staircase	m ²	3.2
010506	Cast-in-place Concrete Staircase		
010507001	Apron, Ramp	m ³	3.4
010507005	Handrail, Copping	m ³	3.4
010507007	Gutter (Eave Gutter); Eave Board	m ³	3.3
010507004	Steps	m ³	3.4
010507	Other Cast-in-place Concrete Members		
010515001	Cast-in-place Member Steel Bar	t	2
010515002	Prefabricated Steer Bar	t	2
010515	Reinforcement Work		
030412001	Regular Lamp	Suit	1.3
030412004	Decorative Lighting	Suit	1.3
030412	Lighting Appliance Installation		
030404034	Light Switch	Number	1.5
030404035	Receptacle	Number	1.8
030404	Installation of Control Equipment and Low Voltage Electrical Apparatus		
010901001	Tiled Roof	m ²	3
010901	Tiles, Profiles and Other Roofs		
010902001	Roll Roofing Waterproofing	m ²	3.9
010902002	Roof Coating Waterproof	m ²	0.5
010902	Roof Waterproofing and Other		
011001001	Thermal Insulation Roof	m ²	4.7
011001003	Thermal Insulation Wall	m ²	4.7
011001	Heat, Insulation		
011102003	Block Building Floor	m ²	2
011102	Bonded Floor Surface		
011105003	Block Kick Line	m ²	2
011105	Baseboard Radiator		
011204003	Block Wall Skirt	m ²	2
011204	Wall Block Layer		

Waste rate data from literature Wang et al. (2010), Wu et al. (2000), Li et al. (2010, 2013b), Liu and Wang (2013), Liu et al. (2017). Some data obtained from the book "Standard quantity of Shenzhen building works consumed (2003)" and the investigation data on construction waste from South China

Estimation of construction waste production

In order to calculate the amount of construction waste, determining the bill of quantity that may generate construction waste should be done. During the construction of the project, the construction waste is divided into three categories: packaging waste,

residual waste, and spoil. Packaging waste mainly includes cement packaging bags, containers and other building material packaging bags, etc. Residual waste refers to waste materials produced during the construction of a project, such as floor ash, debris, broken blocks, etc. Spoil is a waste, which is produced during the excavation process. The volume of these three types of construction waste : CW_{Pi} represents the volume of packaging waste; CW_{Ri} represents the volume of residual waste; CW_{Si} is the volume of spoil. The units used to calculate the output of construction waste shall be in accordance with the units specified in the “Specifications for List of Construction Project List Price”. Besides, list uses traditional units, such as m, m², m³, kg or m³/m², etc. According to the known amount of work in construction waste list, the volume of construction waste at the construction site can be calculated by *Equation 1*:

$$CW_{Bi} = \sum CW_{Pi} + \sum CW_{Ri} + \sum CW_{Si} \quad (\text{Eq.1})$$

where CW_{Bi} is the estimated waste production during construction; CW_{Pi} is the production of packaging waste at the construction stage “i”; CW_{Ri} is the output of residual waste during the construction phase “i”; CW_{Si} is the amount of residual soil at the construction stage “i”.

The type and quantity of packaging waste generated during each construction phase is calculated by *Equation 2*:

$$CW_{Pi} = \sum Q_i \times F_P \times F_C \times F_I \quad (\text{Eq.2})$$

where CW_{Pi} is the production of packaging waste at the construction stage “i”; Q_i is the amount of materials used during the construction phase “i”; F_P is packaging and waste factors; F_C is conversion factor; F_I is incremental factor.

The type and amount of residual waste generated during each construction phase is calculated by *Equation 3*:

$$CW_{Ri} = \sum Q_i \times F_P \times F_C \times F_I \quad (\text{Eq.3})$$

where CW_{Ri} is the output of residual waste during the construction phase “i”; Q_i is the amount of materials used during the construction phase “i”; F_P is packaging and waste factor; F_C is conversion factor; F_I is incremental factor.

The type and quantity of spoil produced during each construction phase is calculated by *Equation 4*:

$$CW_{Si} = \sum Q_i \times F_S \times F_C \times F_I \quad (\text{Eq.4})$$

where CW_{Si} indicates the estimation of production of spoil at construction stage “i”; Q_i is the amount of materials used during the construction phase “i”; F_S is soil factor; F_C is conversion factor; F_I is incremental factor.

Cases

Case introduction

This article uses a typical new residential project in South China as a case. In *Table 6*, the selected list items cover most of the construction processes of the house construction and help us to compute the parts of the list that may generate waste more comprehensively. According to formula (2), (3), and (4), the following examples are listed in *Table 6*. The main waste of list item 010505001 “Beamed slabs” is concrete, and the project volume is 907.79 m³, the waste rate is 3.1%. With this data, the waste production calculated by formula (3) is 49.929 m³. This means that 907.79 m³ of concrete is used in the construction of the slabs, which wastes 49.929 m³. Besides, the list subitem 011102003 “Block floor” in the slab surface layer uses 1177 m² tiles to complete the floor laying of the project. This work wastes 28.805 m² of tile material. The amount of material loss for other list items is listed in *Table 6*. According to the list, the amount of concrete discarded is 254.674 m³, floor ash is 331.468 m², and the total volume of comprehensive construction waste is 4497.418 m³. The new employee residential project produces approximately 0.046 m³ of concrete waste per m² of construction area, and 0.060 m² landing ash. The average production of waste per construction area of the new project for this framework is 0.326 m³. In *Table 6*, the most important waste is earthwork, mortar concrete, wood, scrap bricks, etc. (*Figs. 2–3*).

Table 6. Estimation of volume of construction waste that may occur in new construction project

Type: New project application: Staff dormitory floors: 5 Gross building area: 5567.85 m ²								
Building body height: 18.3 m Structure type: Frame structure								
Project number	Project name	Project feature	Unit	Quantities	Factors			Waste production
					F _P /F _R /R _S	F _C	F _I	
010101002	Excavation of earth	Manual excavation within 1.5 m depth, three kinds of soil	m ³	1330	0.01	1	1	13.1
010101	Earthwork							
010103001	Backfill	Excavator backfill	m ³	668.7	0.01	1	1	6.687
010103002	Residual disposal	Hydraulic excavator dipper capacity 1, dump truck to transport soil (within 1 km)	m ³	406	0.01	1	1.2	4.872
010103	Backfill							
010201009	Deep mixing pile	Commercial ordinary concrete, less than 30 m	m	408.9	0.05	1	1.1	22.489
010201016	Grouting foundation	Commercial ordinary concrete C35	m, m ³	44.4	0.06	1	1.1	2.93
010201	Foundation treatment							

010202001	Diaphragm wall	Commercial ordinary concrete C25	m ³	92.5	0.06	1	1.1	6.105
010202010	Reinforced concrete bracing	Commercial ordinary concrete C30	m ³	54	0.06	1	1	3.24
010202	Shoring of side for foundation pit							
010401004	Brick foundation	Perforated brick 240×115×90, cement mortar M7.5	m ³	182.84	0.05	1	1.25	11.428
010401003	Solid brick wall	Concrete brick wall 240×115×90 wall thickness 24 cm, cement mortar M7.5	m ³	368.79	0.04	1	1.25	18.439
010401004	Porous brick wall		m ³	779.12	0.06	1	2	93.494
010401009	Solid brick column	Perforated brick 240×115×90, Cement mortar M7.5	m ³	92.5	0.05	1	1.1	5.088
010401	Brick masonry							
010501001	Bed course	Commercial ordinary concrete C15	m ³	18.34	0.06	1	1	1.01
010501003	Independent foundation	Commercial ordinary concrete C30	m ³	148.85	0.05	1	1	7.443
010501	Cast-in-place concrete foundation							
010502001	Rectangular column	Commercial ordinary concrete C25	m ³	222.13	0.06	1	1.1	14.661
010502002	Structural column		m ³	82.21	0.07	1	1	5.755
010502	Cast-in-place concrete column							
010503001	Foundation beam	Commercial ordinary concrete C25	m ³	66.53	0.06	1	1.1	3.992
010503005	Lintel		m ³	16.58	0.06	1	1.1	1.094
010503	Cast-in-place concrete beam							
010505001	Beam plate	Commercial ordinary concrete C25	m ³	907.79	0.05	1	1.1	49.929
010505001	Balustrade		m ³	4.66	0.06	1	1	0.28
010505	Cast-in-place concrete slab							
010506001	Straight staircase	Commercial ordinary concrete C25	m ²	215.38	0.07	1	1	15.077

010506	Cast-in-place concrete staircase							
010507001	Apron, ramp	Commercial ordinary concrete C20	m ³	93.6	0.05	1	1	4.68
010507005	Handrail, coping	Commercial ordinary concrete C25	m ³	7.38	0.05	1	1	0.369
010507007	Gutter (eave gutter), eave board		m ³	0.4	0.06	1	1	0.024
010507004	Steps	Commercial ordinary concrete C15	m ³	0.9	0.06	1	1	0.054
010507	Other cast-in-place concrete members							
010515001	Cast-in-place member steel bar	Safety of cast-in-place member rebar	t	199.038	0.01	1	1	1.99
010515002	Prefabricated steel bar		t	0.302	0.01	1	1	0.003
010515	Reinforcement work							
010901001	Tiled roof	Western ceramic tile (J tile); Cement mortar 1: 3	m ²	475	0.01	1	1	4.75
010901	Tiles, profiles and other roofs							
010902001	Roll roofing waterproofing	3 thick SBS modified bitumen waterproof membrane with 2 layers	m ²	1194.3	0.01	1	1	11.943
010902002	Roof COATING WATERPROOF	3 thick polymer cement based waterproof coating	m ²	1194.2	0.01	1	1	11.942
010902	Roof waterproofing and other							
011001001	Thermal insulation roof	40 thick extruded poly styrene board (flame retardant type)	m ²	1099.7	0.01	1	1.1	12.097
011001003	Thermal insulation wall	20 thick inorganic insulating mortar	m ²	235.7	0.01	1	1	2.357
011001	Heat, insulation							
011102003	Block building floor	8 thick 350×350 antiskid floor tile	m ²	1177	0.05	1	1	58.85

011102	Bonded floor surface							
011105003	Block kick line	10 thick 600×150 ceramic anti-skid polishing brick, white cement slurry slit	m ²	576.1	0.05	1	1	28.805
011105	Baseboard radiator							
011201001	Wall general plastering	5 thick 1: 0.5: 3 cement lime mortar wood rubbing; 15 thick 1: 16 cement-lime mortar	m ²	8243.1	0.03	0.66	1.1	179.535
011201	Wall plastering							
011201001	Column, beam surface general plastering	15 thick 1: 1: 6 cement-lime mortar; 5 thick 1: 0.5: 3 cement-lime mortar	m ²	1817.1	0.03	0.66	1	35.979
011201	Column (beam) surface plastering							
030412001	Regular lamp	LED light, energy saving ceiling lamp 1*30 W 220 V	Suit	586	0.01	1	1	5.86
030412004	Decorative lighting	Energy saving double tube ceiling fluorescent	Suit	3	0.01	1	1	0.03
030412	Lighting appliance installation							
011301001	Ceiling plastering	5 thick 1: 0.5: 3 cement-lime mortar; 10 thick 1: 1: 4 cement-lime mortar	m ²	4880.2	0.03	0.66	1.2	115.954
011301	Plasterer							
011204003	Block wall skirt	10 thick 400×200 white tile transverse cross seam close seam paving white cement wipe joint	m ²	479.5	0.25	1	1	119.875
011204	Wall block layer							
011702001	Foundation	Plywood form, timbering	m ²	44.4	0.26	1	1	11.544
011702002	Rectangular column		m ²	1817.1	0.25	1	1.1	499.703

011702003	Structural column		m ²	885.6	0.26	1	1	230.256
011702005	Foundation beam		m ²	618.8	0.25	1	1	154.7
011702009	Lintel		m ²	320.6	0.25	1	1	80.15
011702014	Beam plate		m ²	7959.3	0.26	1	1.1	2276.36
011702028	Copping		m ²	186.2	0.25	1	1	46.55
011702	Concrete formwork and support							
011406001	Paint coating	Surface oil white latex paint	m ²	13921.1	0.01	1	1.2	167.053
011406	Plastering paint							
011701002	External scaffolding	Steel tube external scaffold with fastener, double row	m ²	3364.7	0.01	1	1	33.647
011701003	Internal scaffolding	Fastener type steel tube scaffold, single row	m ²	7595.1	0.01	1	1.1	83.546
011701	Scaffolding work							
030404034	Light switch	Triplex switch 10 A 250 V, bottom side 1.3 m clear switch with protective door	No.	438	0.01	1	1	4.38
030404035	Receptacle	Double two three stage five hole concealed socket, 10 A 250 V, underside 0.3 m underground socket with protective door	No.	1147	0.01	1	1	11.47
030404	Installation of control equipment and low voltage electrical apparatus							
Total								4497.418

F_P, F_R, F_S, F_C, F_I are from Llatas (2011)

Case analysis

(1) Result analysis

According to the above analysis and existing research data (Llatas, 2011; Azeem et al., 2018), the proportion of concrete, bricks and blocks, ceramics, mortar, metal, and wood in the construction waste is large (*Fig. 6*). This article establishes a simple construction

waste estimation model. By enumerating the application of the model to a new construction project, the estimation model can use the engineering bill of quantities to estimate the production of new construction waste based on the scrap rate of building materials. Then, through visits of construction site and existing research surveys, the main components and sources of construction waste can also be found. Through research, it has been found that the differences in the scrap rates for different types of building materials are significant.



Figure 2. a. Estimation case of construction waste for new residential projects. **b.** Waste concrete

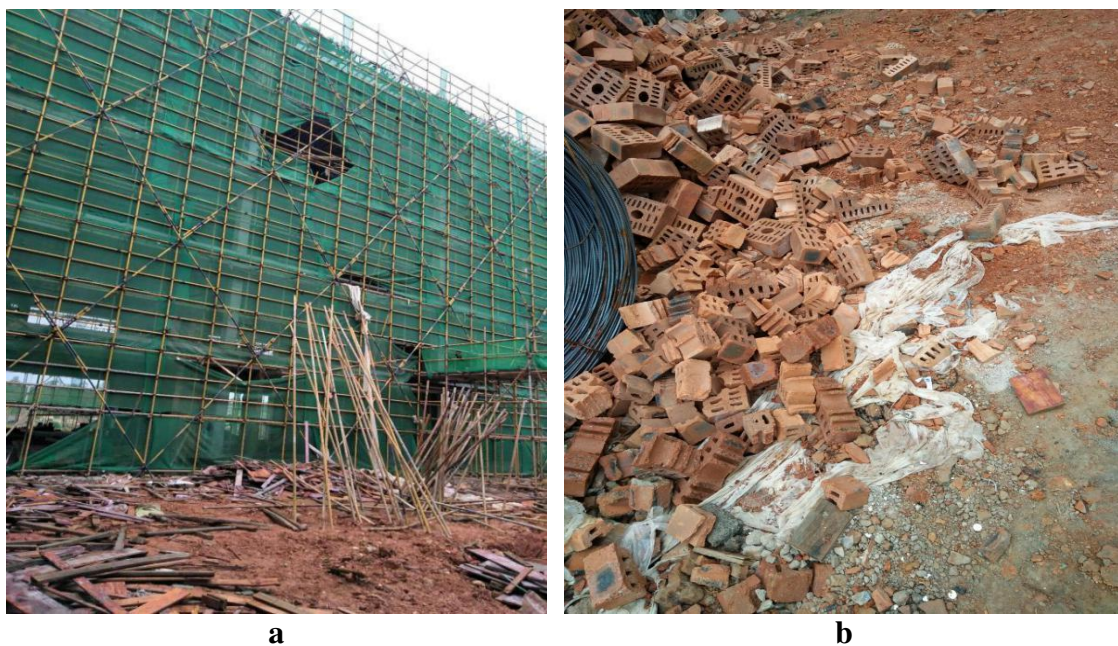


Figure 4. a. Waste wood. **b.** Discarded bricks

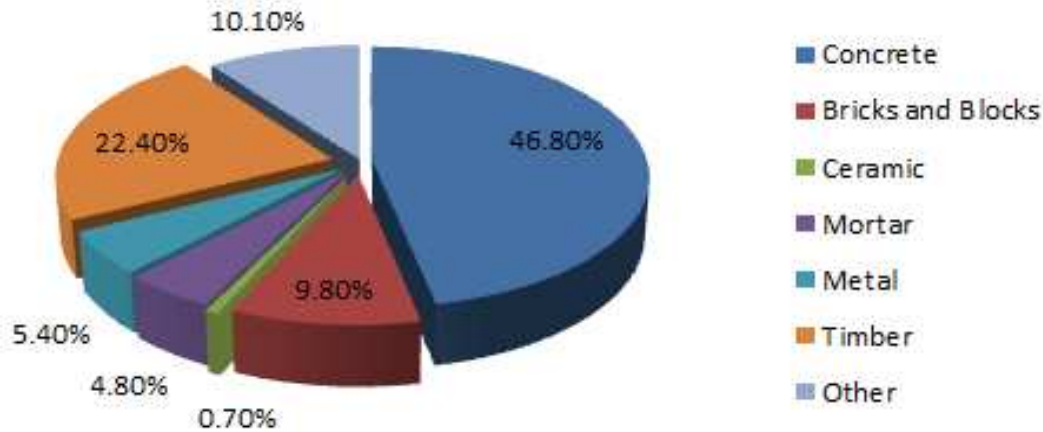


Figure 6. Proportion of production of building waste in newly-built residential buildings with frame structure

(2) Comparison between existing research data

Compare research data from China to that from other countries (Regions), the unit of measurement is different because of the different methods for measuring building waste (Table 7). Compared with existing domestic data, the survey analysis in this article shows that the amount of construction waste generated from new residential projects in South China is lower than our previous research data. Liu and Wang (2013) estimate that a new residential project will generate approximately 0.34 m³ / m² of construction waste per floor area. The production of construction waste from Spanish residential projects surveyed by Llatas (2011) is approximately 0.1388 m³/m², but the results of the surveys in this article show that the average output per construction area of newly built projects is 0.326 m³, which is slightly higher than existing research data abroad. Figure 7 is a histogram of the production of new residential waste in China and other countries. In this figure, the differences between waste production in different countries and different types of structures are clear (in m³/m²).



Figure 7. Histogram of China and other countries residential waste production

Table 7. Production of new residential waste in China and other countries (region)

The Author	Country (region)	Time	Structure type	Waste output
Solis-Guzmán et al.	Spain	2009	Frame structure	0.031 m ³ /m ²
Lin	China Taiwan	2006	Reinforced concrete structure	0.54 m ³ /m ²
Poon et al.	Hong Kong	2001	Frame shear structure	0.175 m ³ /m ²
Liu and Wang	China	2013	Brick concrete structure	0.34 m ³ /m ²
Amnon et al.	Israel	2010	Frame shear structure	0.2 m ³ /m ²
Llatas et al.	Spain	2011	Frame structure	0.1388 m ³ /m ²

(3) Causes analysis

The production of construction waste in developed countries is lower than that in China, since researches started early on construction waste, the waste disposal market is relatively mature and the technology is more advanced in other developing countries. Recently, with the gradual promotion of green construction technology, construction waste has attracted the attention of the domestic construction industries. Then, due to the rapid development of BIM technology, BIM has been used increasingly widespread in the construction industry, reducing rework and material waste. Meanwhile, the use of prefabricated construction components has reduced waste production to some extent (Tam and Hao, 2014; Villoria Sáez et al., 2014; Zho et al., 2018). Besides, the improvement of construction technology, the strengthening management of governments and construction departments, as well as the economic benefits of waste recycling make the production of construction waste show a decreasing trend.

With the rapid development of economy and education, the demands of professionals from all aspects of work have also increased. Due to the gradual promotion of tertiary education, the management level of managerial staff and the professional quality of people have been improved. People's awareness of waste disposal has also been significantly improved at the same time. In addition, the government has gradually strengthened the management of construction waste and increased publicity on the proper management of construction waste, relevant laws and regulations have also been continuously improved. All of the improvement above prompting workers and managers to increase their management awareness about the reduction of construction waste. Therefore, the total amount of construction waste generated during the construction process gradually decreases.

Results and discussion

At present, the total amount of waste generated annually by construction activities in China is still huge, the overall utilization rate is low, and the environmental impact is large. Therefore, effective measures must be adopted to strengthen the management of construction waste. This paper proposes the following aspects to strengthen the reduction management of construction waste.

(1) Reduction of the source of construction waste

In developed countries, the management of construction waste mainly adopts reduction measures from the origin. To fundamentally reduce the production of

construction waste, we must standardize design drawings, reduce design changes, and strengthen the management of construction sites. Besides, it is also necessary to continuously improve construction technology and increase research on new technologies, as well as promote publicity of the management of construction wastes. The design and construction processes are the main sources of waste generation. Only by eliminating the sources of construction waste, can we fundamentally solve the problem of construction waste.

(2) Implementing a classification system

Different structural types of projects should adopt different classification disposal systems. Relevant departments should formulate a waste classification system and require the construction companies to paste the regulations of construction wastes on the construction sites. As for the waste generated at the construction site, it should be classified into inert or hazardous. It is better to transport recycled waste firstly, then recycle waste, and finally transport non-recyclable waste to designated locations for disposal.

(3) Improving related laws and establish supervision and management system

Although many places have issued relevant construction waste disposal systems, there is no clear control over the production of construction waste, and there are no specific requirements for classification, disposal, and reasonable recycling. Therefore, we must further improve the construction waste disposal system and implement supporting management measures. People should aware that it is forbidden to bury recyclable construction waste, and the recycling waste must be sorted, recycled, or stacked according to regulations. Also, relevant departments must use law to punish the companies which disobey the regulation strictly..

(4) Making economic benefits more considerable

China does not pay enough attention to the recycling of construction waste, since there is no good market for the recycling of construction waste, and relevant departments have not seen the considerable benefits of recycling waste. Construction waste is a renewable resource, thus, recycling of construction waste should be developed as an industry. Relevant departments should take active measures to encourage recycling of construction waste.

(5) Including waste production budget in bidding

At present, a large amount of construction waste not only wastes a lot of raw materials, but also causes huge financial losses Including the production budget of construction waste into bids as a requirement for bidding can solve these problems efficiently. For example, the owner can put the requirements for recycling into the bidding documents, then, the contractor should estimate the production of construction waste and the cost of its loss, meanwhile, the contractor shall propose specific measures for waste reduction in the bidding documents and estimate the cost saving from adopting waste reduction measures. This will not only allow owners and contractors to see the considerable economic benefits of building waste, but also encourage contractors to adopt recycling strategies for construction waste during the construction

process to reduce waste production. The waste of construction will be decreased significantly, if the reduction of construction waste is incorporated into the “Tendering and Bidding Law” as a mandatory requirement, and the indicators for various types of construction waste production being identified according to the type of tender projects.

Conclusions

(1) This paper builds an estimation model of construction waste based on bill of quantities and lists new projects in Southern China applying the model. After the analysis of component and production of the construction waste in the project, it can be found that the average output of waste per area of the new construction project is 0.326 m^3 , which is consistent with the situation in the southern regions and is relatively the same as existing research studies. This model is simple and useful, since it uses a bill of quantities to compile a list of construction waste and it can be used in other structural types of projects. By estimating the possible construction waste, the government and the construction departments can see the waste production and economic losses directly, so as to promote and encourage the construction departments to take effective measures to manage the construction waste and improve the management level of on-site construction.

(2) Through the analysis of results, the disposal method of construction waste is discussed. The number of construction waste will be decreased greatly, if taking the reduction of the source of construction waste as the primary measure, establishing a perfect sorting and disposal system and improving relevant regulations and policies, as well as implementing supporting management measures. Besides, it is better to make the economic benefits of recycling construction waste more considerable and improve the management of waste market. Also, including the production budget of construction waste in bidding documents as a bidding requirement is necessary. Finally, if the reduction of construction waste is written into the “Tendering and Bidding Law” as a mandatory requirement and the control indicators for waste production can be identified clearly, the total amount of construction waste will be reduced significantly.

(3) There are some disadvantages of this study. As for the areas of this study, it only covers residential projects, except of commercial, industrial, educational and other public projects. In terms of the construction waste estimation model, the waste lists using to estimate are not enough and not complete. These drawbacks will be improved in future research.

(4) The conclusion of this paper can be used as a reference for construction waste research, especially for developing countries. Many developing countries do not have a European construction waste list standard, but they can measure the amount of waste in conjunction with the local bill of quantities and waste rates.

Acknowledgements. The research was supported by the National Natural Science Foundation of China (71501052), The author would like to acknowledge the valuable suggestions of the editor and three anonymous reviewers.

REFERENCES

- [1] Alireza, A., Tahereh, G., Nader, Y. et al. (2017): 15: 14: Quality and quantity of construction and demolition waste in Tehran. – *Journal of Environmental Health Science & Engineering*. DOI: 10.1186/s40201-017-0276-0.
- [2] Amnon, T., Hadassa, B. (2011): A novel methodology to estimate the evolution of construction waste in construction sites. – *Waste Management* 31: 353-358.
- [3] Bossink, B. A. G., Brouwers, H. J. H. (1996): Construction waste: quantification and source evaluation. *Journal of Construction. – Engineering and Management* 122(1): 55-60.
- [4] Chen, C. L., Yang, J. X., Lv, B., Song, X. L. (2012): Generation estimation and forecasting of urban construction and demolition waste: a case study of Hainan Province. – *Environmental Science & Technology* 35(11): 173-179.
- [5] Cochran, K., Townsend, T., Reinhart, D. et al. (2007): Estimation of regional building-related C&D debris generation and composition: Case study for Florida, US. – *Waste Management* 27(7): 921-931.
- [6] Chooi, M. M., Takeshi, F., Chin, S. H. (2016): Construction and demolition waste generation rates for high-rise buildings in Malaysia. – *Waste Management & Research* 34(12): 1224-1230.
- [7] Camara, E. M., Caramaschi, E. P., Di Dario, F., Petry, A. C. (2018): Short-term changes in two tropical coastal lagoons: effects of sandbar openings on fish assemblages. – *Journal of Coastal Research* 34(1): 90-105.
- [8] Ding, T., Xiao, J. (2014): Estimation of building-related construction and demolition waste in Shanghai. – *Waste Management* 34: 2327-2334.
- [9] Department of Housing and Urban-Rural Construction of Henan Province (DHURCHP). (2016): Measures of Henan Province on Measurement and Accounting of Construction waste. – China Legal Publishing House, Beijing.
- [10] Devora Isiordia, G. E., Robles Lizarraga, A., Fimbres Weihs, G. A., Alvarez Sanchez, J. (2017): Comparison of discharge methods for spill of brines, from a desalination plant in sonora, mexico. – *Revista Internacional De Contaminacion Ambiental* 33(SI): 45-54.
- [11] European Commission (2008): Directive 2008/98/EC on Waste (Waste Framework Directive). – <http://ec.europa.eu/environment/waste/framework> (accessed on May 21, 2014).
- [12] Enshassi, A. (1996): Materials control and waste on building sites. – *Building Research and Information* 24(1): 31-4.
- [13] Pazand, K., Hezarkhani, A. (2018): Predictive Cu porphyry potential mapping using fuzzy modelling in Ahar–Arasbaran zone, Iran. - *Geology, Ecology, and Landscape* 2(4): 229-239.
- [14] Fatta, D., Papadopoulos, A., Avramikos, E., Sgourou, E., Moustakas, K., Kourmoussis, F., Mentzis, A., Loizidou, M. (2003): Generation and management of construction and demolition waste in Greece—an existing challenge. – *Resources, Conservation & Recycling* 40: 81-91.
- [15] Francesco, D. M., Francesco, B., Caterina, M., Stefano, B., Moreno, M. (2016): Quality assessment for recycling aggregates from construction and demolition waste: An image-based approach for particle size estimation. – *Waste Management* 48: 344-352.
- [16] Fu, H., Liu, X. (2017): A study on the impact of environmental education on individuals' behaviors concerning recycled water reuse. – *Eurasia Journal of Mathematics Science and Technology Education* 13(10): 6715-6724.
- [17] Alsulaiman, A., Nizam, A.A. (2018): Evaluation Ability Of Different Barada River *Micrococcus* Spp. Strain To Bioremediation Of Hydrocarbons. -*Journal CleanWAS*, 2(2) : 01-05.
- [18] Guangdong Bureau of Statistics (GBS) (2017): Statistical Yearbook of Guangdong Province. – China Statistical Publishing House, Beijing.

- [19] Huang, B. J., Wang, X. Y., Kua, H. W., Geng, Y., Raimund, B., Ren, J. Z. (2018): Construction and demolition waste management in China through the 3R principle. *Resources, Conservation & Recycling* 129: 36-44.
- [20] Sufiyan, I., Zakariya, R., Yaacob, R. (2018): Delineation Of Flood Risk Zones And 3D Modeling In Terengganu River Catchment Using Gis And Swat. *-Environment & Ecosystem Science*, 2(2): 01-05.
- [21] Jin, R. Y., Li, B., Zhou, T. Y., Wanatowski, D., Piroozfar, P. (2017): An empirical study of perceptions towards construction and demolition waste recycling and reuse in China. – *Resources, Conservation & Recycling* 126: 86-98.
- [22] Katz, A., Baum, H. (2010): A novel methodology to estimate the evolution of construction waste in construction sites. – *Waste Management* 31(2): 351-358.
- [23] Chuanlei, L., Guomin, L., Yuanfei, H., Guojun, W. (2018): Research On Mental Health Status And The Relationship Between Spiritual Belief And Self – Harmony. - *Science Heritage Journal*, 2(2): 16 -20.
- [24] Kofoworola, O. F., Gheewala, S. H. (2009): Estimation of construction waste generation and management in Thailand. – *Waste Management* 29: 731-738.
- [25] Landowski, B., Pajak, M., Zoltowski, B., Muslewski, L. (2017): Method of building a model of operational changes for the marine combustion engine describing the impact of the damages of this engine on the characteristics of its operation process. – *Polish Maritime Research* 24(4): 67-76.
- [26] Adegbuyi, O., Ogunyele, A. C., Akinyemi, O. M. (2018): Petrology and Geochemistry of Basement Gneissic Rocks around Oka-Akoko, Southwestern Nigeria. - *Malaysian Journal of Geosciences*, 2(2): 11-16.
- [27] Li, J. R., Mi, X. M., Ding, Z. K., Wang, J. Y. (2010): Investigation and Analysis on the Output Level of New Construction Waste. – *Construction Economy* 01: 83-86.
- [28] Li, J. R., Ding, Z. K., Mi, X. M., Wang, J. Y. (2013a): Investigation on the Waste Generation of Residential Building Construction. – *Urban Issues* 05: 21-25.
- [29] Li, J. R., Ding, Z. J., Mi, X. M., Wang, J. Y. (2013b): A model for estimating construction waste generation index for building project in China. – *Resources, Conservation & Recycling* 74: 20-26.
- [30] Li, P. (2007): Comprehensive utilization of construction waste to develop recycling economy. – *Special Zone Practice and Theory* 6: 84-91.
- [31] Roslee, R., Tongkul, F. (2018): Engineering Geological Study On The Slope Failure Along The Kimanis To Keningau Highway, Sabah, Malaysia. - *Geological Behavior*, 2(2): 01-09.
- [32] Li, Y. S., Zhang, X. Q., Ding, G. Y., Feng, Z. Q. (2016): Developing a quantitative construction waste estimation model for building construction projects. – *Resources, Conservation and Recycling* 106: 9-20.
- [33] Lin, Z. W. (2006): Model Development for Estimating the Quantity of a Single Buildings Demolition Waste. – National Central University, Taoyuan, Republic of China.
- [34] Shabi, T.H., Islam, A.K.M.M., Hasan, A.K., Juraimi, A.S., Anwar, M.P. (2018): Differential Weed Suppression Ability In Selected Wheat Varieties Of Bangladesh. - *Acta Scientifica Malaysia*, 2(2): 01-07.
- [35] Liu, J. K. (2013): Research on Cost Compensation Model for Construction and Demolition Waste Management. – South China University of Technology, Guangzhou.
- [36] Liu, J. K., Wang, Y. S. (2011): Establishment and application of performance assessment model of waste management in architectural engineering projects in China. – *Journal of Systems Engineering Procedia* 4: 147-155.
- [37] Mahtab, M.H., Ohara, M., Rasmy, M. (2018): The Impact Of Rainfall Variations On Flash Flooding In Haor Areas In Bangladesh. - *Water Conservation and Management*, 2(2): 06-10.

- [38] Liu, J. K., Wang, Y. S. (2013): Cost analysis of construction and demolition waste management: case study of the Pearl River Delta of China. – *Open Construction and Building Technology Journal* 7: 251-257.
- [39] Azeem, N., Arslan, C., Rashid, H., Sattar, A. (2018): Comparative Study Of Hospital Waste Management Practices At Different Health Care Units In District Faisalabad For The Development Of Improvement Strategies. - *Earth Sciences Pakistan*, 2(2): 16-21.
- [40] Liu, J. K., Wang, Y. S., Lin, Y. Y. (2012): A model for quantification of construction waste in new residential buildings in Pearl River Delta of China. – *Open Construction and Building Technology Journal* 6: 398-403.
- [41] Liu, J. K., Pang, Y. S., Wang, D., Zhou, J. W. (2017): An Empirical Investigation of Construction and Demolition Waste Management in China's Pearl River Delta. – In: Chau, K. W. et al. (eds.) *Proceedings of the 21th International Symposium on Advancement of Construction Management and Real Estate*. Springer, Singapore, pp. 197-212.
- [42] Zhu, H., Liu, G., Zhong, D., Zhang, T., Lang, J., Yao, J., Ashraf, M.A. (2018): Diagenetic controls on reservoir quality of tight sandstone: A case study of the upper triassic yanchang formation chang 7 sandstones, ordos basin, China. - *Earth Sciences Research Journal*, 22(2): 129-139.
- [43] Llatas, C. A. (2011): model for quantifying construction waste in projects according to the European waste list. – *Waste Management* 31(6): 1261-1276.
- [44] Lu, W., Yuan, H., Li, J., Hao, J. J. L., Mi, X., Ding, Z. (2011): An empirical investigation of construction and demolition waste generation rates in Shenzhen city, South China. – *Waste Management* 31: 680-687.
- [45] Lu, W. S., Chris, W., Peng, Y., Chen, X., Zhang, X., L. (2017): Estimating and calibrating the amount of building related construction and demolition waste in urban China. – *International Journal of Construction Management* 17: 13-24.
- [46] Ministry of Housing and Urban-Rural Development of the People's Republic of China (MOHURD) (2013): *Specifications of Charging on Bill of Quantities of Construction Projects*. – China Planning Press, Beijing.
- [47] Olugbenga, O. A., Lukumon, O. O., Saheed, O. A., Muhammad, B., Hafiz, A. A., Hakeem, A. O., Omolola, O. A. (2018): Designing out construction waste using BIM technology: Stakeholders' expectations for industry deployment. – *Journal of Cleaner Production* 180: 375-385.
- [48] Paola, V. S., César, P. A., Merino. M. D. R. (2015): New quantification proposal for construction waste generation in new residential constructions. – *Journal of Cleaner Production* 102: 58-65.
- [49] Pinto, T. P., Agopyan, V. (1994): Construction Waste as Raw Materials for Low-Cost Construction Products. – In: Kibert, C. J. (ed.) *Proceedings of the First Conference of CIB TG 16 on Sustainable Construction*. Tampa, Florida, pp. 335-342.
- [50] Poon, C. S., Yu, A. T. W., Jaillon, L. (2004): Reducing building waste at construction sites in Hong Kong. – *Construction Management and Economic* 22: 675-689.
- [51] Solís-Guzmán, J., Marrero, M., Montes-Delgado, M. V., Ramírez-de-Arellano, A. (2009): A Spanish model for quantification and management of construction waste. – *Waste Management* 29: 2542-2548.
- [52] Tam, V. W. Y., Hao, J. L. (2014): Prefabrication as a mean of minimizing construction waste on site. – *Journal International Journal of Construction Management* 14: 113–121.
- [53] Tam, V., W. Y., Shen, L. Y., Tam, C. M. (2007): Assessing the levels of material wastage affected by sub-contracting relationships and projects types with their correlations. – *Building and Environment* 42: 1471-1477.
- [54] The office of Shenzhen Construction Cost Management (2003): *Standard Quantity of Shenzhen Building Works Consumed*. – Publishing House of the Intellectual Property in China, Beijing.

- [55] Villoria Sáez, P., Del Río Merino, M., Porrás-Amores, C. (2012): Estimation of construction and demolition waste volume generation in new residential buildings in Spain. – *Waste Management & Research* 30: 137-146.
- [56] Villoria Sáez, P., Del Río Merino, M., Porrás-Amores, C., González, A. S. A. (2014): Assessing the accumulation of construction waste generation during residential building construction works. – *Resources, Conservation & Recycling* 93: 67-74.
- [57] Wang, G. L., Yu, Z. P., Shen, X. D., Chen, J., Li, C. X. (2010): Kind and amount of castoff in construction site. – *Project Quality* 28(11): 66-71.
- [58] Wang, L., Wang, J. X., Cheng, X. W. (2017): Model for quantification of apparent construction packaging waste. – *Packaging Engineering* 38(15): 231-234.
- [59] Wani, S. A., Najjar, G. R., Akhter, F. (2018): Characterization of available nutrients that influence pear productivity and quality in Jammu & Kashmir, India. – *Journal of Environmental Biology* 39(1): 37-41.
- [60] Won, J. S., Cheng, J. C. P., Lee, G. (2016): Quantification of construction waste prevented by BIM-based design validation: Case studies in South Korea. – *Waste Management* 49: 170-180.
- [61] Wu, H. Y., Duan, H. B., Zheng, L. N., Wang, J. Y., Niu, Y. N., Zhang, G. M. (2016): Demolition waste generation and recycling potentials in a rapidly developing flagship megacity of South China: Prospective scenarios and implications. – *Construction and Building Materials* 113: 1007-1016.
- [62] Wu, X. G., Li, H. Q., Du, T. (2000): Analysis of the quantity and the composition in construction waste. – *J. Huazhong Univ. of Sci. & Tech* 12: 96-97+100.
- [63] Yang, A., Han, Y., Li, S., Xing, H., Pan, Y., Liu, W. (2017): Synthesis and comparison of photocatalytic properties for Bi_2WO_6 nanofibers and hierarchical microspheres. – *Journal of Alloys and Compounds* 695: 915-921.
- [64] Yuan, H. P. (2017): Barriers and countermeasures for managing construction and demolition waste: A case of Shenzhen in China. – *Journal of Cleaner Production* 157: 84-93.
- [65] Zheng, L., Wu, H. Y., Zhang, H., Duan, H. B., Wang, J. Y., Jiang, W. P., Dong, B. Q., Liu, G., Zuo, J., Song, Q. B. (2017): Characterizing the generation and flows of construction and demolition waste in China. – *Construction and Building Materials* 136: 405-413.

THE RELATIONSHIPS BETWEEN ENVIRONMENTAL FACTORS AND SITE INDEX OF ANATOLIAN BLACK PINE (*PINUS NIGRA* ARN. SUBSP. *PALLASIANA* (LAMB.) HOLMBOE) STANDS IN DEMİRCİ (MANİSA) DISTRICT, TURKEY

GÜLSOY, S. * – ÇINAR, T.

Isparta University of Applied Sciences, Faculty of Forestry, 32260 Isparta, Turkey
(phone: +90-505-547-0196; fax: +90-246-211-3948)

*Corresponding author
e-mail: srkgulsoy@gmail.com

(Received 1st Oct 2018; accepted 26th Nov 2018)

Abstract. In this study, the relationships between the productivity of Anatolian black pine forests and the environmental variables were investigated in Demirci (Manisa) district of Turkey. Inventory study was performed on 40 stands totally. Ages and heights for 3 different plus trees in each stand were measured and site (bonitet) index values were calculated according to height at the age of 100 for the black pine. At the first stage, Pearson and Spearman correlation analyses were used to determine binary linear relations between productivity of the species and environmental factors in the district. Multiple regression analysis and regression tree method were performed to obtain the productivity models of the species, respectively. As a result of these analyses, it has been concluded that the lower slopes and flats with a smooth surface at average altitudes of 1000 m-1350 m are the most suitable areas for the productivity of Anatolian black pine in the district. Furthermore, it has been found that litter thickness on the soil is not a clear indicator for the productivity of the species in the natural stands. On the other hand, it has been determined that the north aspect significantly contributes to the productivity of this species in the elevations below 1000 m and all these relationships are especially related with water and nutrition contents in the environment.

Keywords: *Anatolian black pine, climate, ecological modelling, productivity, site conditions*

Introduction

Increasingly growing global population and industrialization result in irregular and uncontrolled exploitation of natural resources. This poses a great threat to all living communities including primarily to forests, which are considered as natural resources. At this stage, it is important to protect, ensure the sustainability and efficient management of forests that are globally crucial. Turkey is comprised of different geographical regions due to its climate, soil properties and topographic structure, and situated at the intersection of three continents and harbours three different phytogeographical regions; therefore, it hosts a very high biological diversity (Demir, 2013; Negiz et al., 2017). This also has reflections on the country's forestlands and allows the presence of many different species especially plant species, reptiles, bird and mammalian animal species, which all lead up to high biological diversity (Davis, 1965-1988; Kabalak and Sert, 2010). Such high biological diversity makes Turkey's forests nationally and globally vital, while it also requires thorough research on forests.

The Earth is covered with forests by 31% (3.9 billion hectare) (Keenan et al., 2015) forests covers 28.6% of the entire land area in Turkey, which accounts for 22.342.935 hectares (Kahriman et al., 2017). As regards the tree species, oak forests cover the largest area with 5.886.195 hectares, which is followed by brutian pine (*Pinus brutia* Ten.) forests with 5.610.215 hectares and black pine (*Pinus nigra* Arn.) with 4.244.921

hectares (Anonim, 2015). Based on this piece of information, it can be suggested that all the abovementioned species play quite an important role for forestry strategies of the country.

Black pine which is one of the dominant species in the forest assets of Turkey is a primary forest tree species that has a very wide distribution area starting from South Europe up to Turkey (Atalay and Efe, 2012). It can be argued that black pine is a typical South European forest tree species that is ecologically and economically important in the abovementioned distribution area. The taxon of this species that is distributed in Turkey is Anatolian black pine (*Pinus nigra* Arn. subsp. *pallasiana* (Lamb.) Holmboe), while it is reported that this taxon has minimum 15 geographical variations due to different climate and topographic condition in its natural distribution areas (Atalay and Efe, 2012). Anatolian black pine is mainly distributed at elevations of 400-1800 m in the Central Black Sea, Western Black Sea, Marmara, Aegean, Mediterranean and Central Anatolia Regions, while the boundaries of its distribution may partially vary depending on different geographical regions. This species is usually distributed up to 1400 m on slopes facing the sea in the highly mountainous areas of the Northern Anatolia region along with the *Picea orientalis* L. and *Abies* species, while it is distributed up to 1800 m along with the *Pinus sylvestris* L. species on the southern slopes of these mountains. Moreover, Anatolian black pine is distributed up to 1800 m on southern drier slopes in the Aegean and Marmara regions, while it establishes forests with *Cedrus libani* A. Rich, *Abies cilicica* Carr. and *Juniperus* species at elevations of 1000-1800 m in the Mediterranean region. This species is known to usually establish forests along with various oak species at elevation of 1200-1600 m in steppes in the Central Anatolia (Bahadır and Kenan, 2010; Atalay and Efe, 2012).

Anatolian black pine is subject to intensive production and management activities in forests at industrial scale especially thanks to its high quality and hard wood (Güller, 2012). It has a high economic return and high contribution to ecological cycle, it is contented with respect to soil requirements, it has a wider range of ecological tolerance compared to many other species and it is one of the species that have the greatest infiltration into steppe areas that have arid and semi-arid climate; therefore, it is commonly preferred for afforestation activities (Güner et al., 2011). It is crucial for Turkey's forestry strategies to obtain productive forests as a result of afforestation with this species. On the other hand, given that the forestlands are still shrinking at global scale, successful afforestation activities to be carried out by countries with their primary forest species are becoming more and more important because it is argued that the existing forests should be preserved or enlarged and degraded forests should be rehabilitated to become more productive with a view to ensuring the sustainability of multidimensional exploitation of forest ecosystems across the world (Faostat, 2014).

Demirci (Manisa) district is one of the important distribution areas of Anatolian black pine in Turkey. It is the second primary tree species with the highest distribution with 15.628 ha after oak species in this locality. There is 37.298 hectare of forestless land and 26.033 hectare of degraded forestland in the district (Anonymous, 2011). It is important at global scale and for the country's forestry strategies to determine the suitability of the concerned forestless lands and degraded forestlands for afforestation with Anatolian black pine for further productivity in the future. Therefore, this study was conducted to identify the areas in this locality that can be potentially productive for Anatolian black pine for rehabilitating degraded forestland to become productive and establishing new forests.

Material and Methods

Study area

The study area was located at 38° 54' - 39° 10' northern latitudes and 28° 24' - 28° eastern longitudes in the Northeast of Manisa province situated within the boundaries of the Aegean Region. According to Köppen-Geiger climate classification, the study area is classified into the sub-climate type of mild winters and very hot summers in the humid mid-latitude climate type with mild winters which is the most common climate type in Turkey (annual average total precipitation is 689 mm) (Öztürk et al., 2017). The district is situated on Menderes (Saruhan – Menteşe) massif. Neogene deposits are the most common deposits in the locality. Kürtköyü formation of the basin starts with Early-Mid Miocene conglomerates while Yeşilköy formation contains sandstone-mudstone alternations. Furthermore, Late Miocene-Early Pliocene aged Adala formation consisting of lime stones lies in the vicinity of Demirci located in this basin. As regards other formations apart from the abovementioned ones, basalt and gyans are also observed on volcanic masses such a andesite, dacite, trachyte and rhyolite (Helvacı, 2015).

Demirci district host various tree species due to its climate and topography. *Pinus brutia* Ten. var. *brutia*, *Pinus nigra* Arn. subsp. *pallasiana* (Lamb.) Holmboe, *Quercus ithaburensis* subsp. *macrolepis*, *Quercus cerris* L. var. *cerris* and *Fagus orientalis* Lipsky that is distributed in a partial area establish natural forests in the district (Anonymous, 2011).

Data collection

The research was conducted within the boundaries of 3 different Forest Sub-Directorates (FSD) (Demirci FSD, Başalan FSD and Akpınar FSD) affiliated to Demirci Management Directorate in Manisa Demirci Locality. Once the stand types of the locality were integrated with the topographic maps, Anatolian black pine stands were mainly located at an elevation of 652 m-1693 m and moderately mountainous and partially high-mountainous regions. The study was conducted in 40 sampling plots each sized 20x20m in this elevation range (Fig. 1).

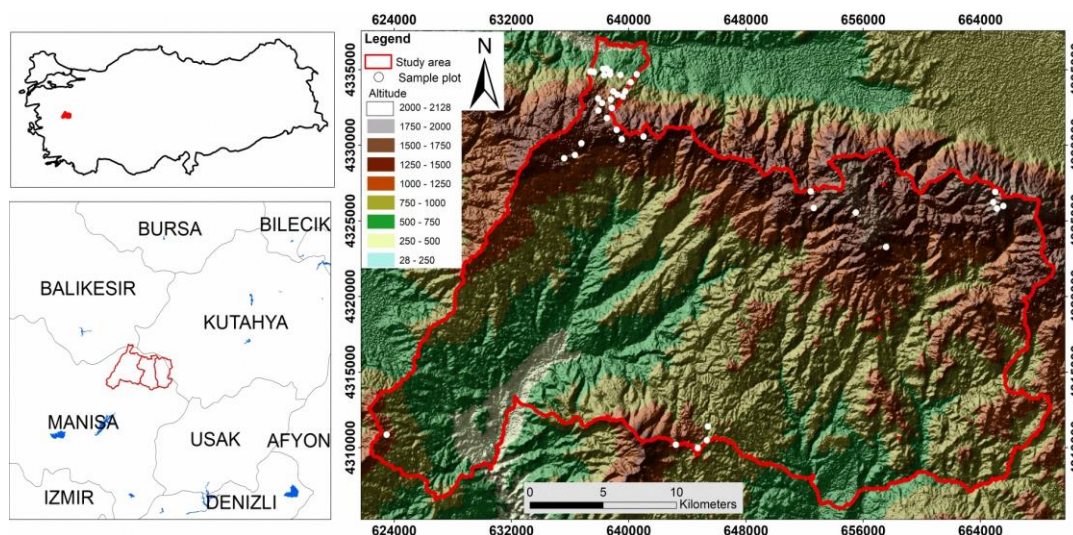


Figure 1. Sampling plot locations on the location map of Demirci (Manisa) district in Turkey

In each sampling plot, minimum 3 plus trees (bonitet trees) with healthy were identified to determine the productivity of the species, their height (m) was measured in planted position with Blume-Leisse equipment and age measurement was made on the core sample taken at breast height (d_{1.30} m) with an increment borer. Elevation was measured at 4 different points that were 20 meters distant from the centre of the sampling plots and perpendicular to the central point and the landform index (McNab, 2010) was calculated using the following formulation:

$$\bar{Z} = ((Z_1 - Z_0) + (Z_2 - Z_0) + \dots + (Z_n - Z_0))/N \quad (\text{Eq.1})$$

In this formulation; \bar{Z} : is landform index value, Z_0 : is the elevation of the central point of the sampling plots (m), Z_1, Z_2, Z_n : refer to the elevation of the edge point of the sampling plot (m) and N : refer to the number of measurements at the edge point of the sampling plots.

With another study during the field surveys, the slope position was determined taking account of the average distance from the upper edge of the hill to the position of the sampling plot and the terrain surface (flat, undulated, concave, convex) was determined through the observations on the plots. Moreover, surface stoniness (%) was determined with iron bar penetration method at 10 points randomly designated inside the sampling plot. After these steps, a soil pit was dug in each sampling plot by which soil depth (m) was determined, while the total litter thickness (cm) was measured from the organic layer of the pit surface. As a result of these inventory studies, the slope degree of the sampling plots ranged from 4° to 61° while Anatolian black pine was distributed on slightly steep lands to very steep lands. The terrain surface of the sampling plots was mainly concave by 32% while the slope position was lower slope with the same percentage. The soil depth in the sampling plots ranged from 32 cm to 120+ cm, while the litter thickness varied from 0.5 cm to 10 cm; furthermore, surface stoniness was 1%-35%. The skeleton content of the soil at a depth of 0-30 cm ranged from 0.5% to 60%.

Soil samples were taken from surface of these pits at a depth of 0-30 cm, through which bedrock formation of the sampling plots were determined. Finally, latitude and longitude degrees of each sampling point were recorded at the mid-point with Global Position Systems (GPS) equipment, and these coordinates were uploaded to the digital maps from which information about some environmental variables was obtained. At this stage, first Digital Elevation Model (DEM) of the study area was developed. Contour maps with a scale of 1/25000 were used to develop the DEM. Elevation (m), slope degree (°), topographic position index (De Reu et al., 2013), topographic roughness index (Cavalli et al., 2013), radiation index (McCune and Keon, 2002) and heat index (Beers, 1966) of the locality were determined using the DEM. The increase in the topographic position index value indicates the mountainous and hilly areas within a scale. Topographic roughness index is an indication of the roughness of the terrain. Radiation index takes values from 0 to 1 and this value is closer to 1 indicates more sunny places. Heat index is a value that reflects the average temperature in the environment as a combination of aspect and slope degree.

Annual average temperature (°C) and annual average precipitation (mm) variables were obtained from the climate maps available in the database at <http://www.worldclim.org> according to the coordinates of the sampling area (Fick and Hijmans, 2017).

At the next stage of the study, soil samples taken from the field to the laboratory were air dried and sieved through 2 mm screen. Then, texture of these soils was analysed using Bouyoucos hydrometer method, soil reaction was analysed using pH-meter with glass electrode in H₂O and 1N KCl solutions, organic carbon content was analysed with Walkley-Black method, total nitrogen content was analysed with semi-micro Kjeldahl method, lime content was analysed with Scheibler calcimeter method (Karaöz, 1989a,b). As a result of these soil analysis, the nitrogen content was found to vary from 0.008% to 0.104%, while the organic matter content ranged from 1.13% to 5.67%, and pH varied from 5.11 to 7.02. The highest lime content was found to be 0.28% while lime was not found in most of the soils.

Finally, all variables classified in different types as categorical, present-absent and constant data were uploaded to Microsoft Excel program and a digital data matrix of environmental variables was obtained. The names of all these variables assessed in this study were coded before the statistical analyses (*Table 1*).

Table 1. Variables used in statistical analyses and their codes

Variables	Code	Variables	Code
Site index	stindx	Soil organic matter content (%)	orgmat
Elevation (m)	elvtm	Soil actual pH	actph
Annual average temperature (°C)	temptr	Soil lime content (%)	limeco
Annual average precipitation (mm)	precipr	Sand (%)	sand
Slope degree (°)	slopdg	Silt (%)	silt
Heat index	heatin	Clay (%)	clay
Topographic position index	tpindx	Soil depth (cm)	soildp
Radiation index	radinx	Undulating hills	undult
Surface stoniness	surfst	Convex land	convex
Landform index	landix	Concave land	conrav
Topographic roughness index	rougix	Flat land	fltnd
Lower slope position	lslope	Schist	schist
Lower middle slope position	lomslp	Talc	talc
Upper middle slope position	upmslp	Gneiss	gneiss
Upper slope position	uslope	Migmatitic gneiss	miggns
Litter thickness (cm)	ltrthc	Hematite	hematt
Soil skeleton (%)	sskelt	Graywacke	graywk
Soil nitrogen (%)	nitrgn		

Statistical analysis

The binary linear relations between the site index of Anatolian black pine and constant environmental variables were assessed with Pearson correlation analysis, while the relationships with categorical environmental variables were assessed with Spearman correlation analysis (Hauke and Kossowski, 2011). In order to determine the representative factor from the variables of sand, dust and clay that were estimated to cause multicollinearity problem due to the high correlation between them in ecological models, principal components analysis was performed (Bro and Smilde, 2014). Finally, in order to model potentially most productive site of Anatolian black pine in the district, stepwise multiple regression analysis (Tabachnik and Fidell, 2012) and regression tree technique (Özkan, 2012) were applied. For statistical analysis, SPSS Version 21.0 and PC-ORD Version 6.0 package software was used.

Results and Discussion

According to the findings of this study, it was understood that the soils were classified into poor and moderate class as regards nitrogen content, poor to rich class in terms of organic matter content, moderately acidic and neutral class with respect to pH degrees, slightly calcareous or non-calcareous class with respect to lime content (Çepel, 1995). In a study conducted in a *Pinus nigra* forest in Sütçüler (Isparta) locality, the organic matter content of the soils was found to range from 0.55% to 13.4%, pH from 5.2 to 7.6 and total lime content from 0.15% to 48.4% (Gülsoy, 2009). In another study conducted in Gölcük (Isparta), nitrogen content of the soils ranged from 0.003% to 0.053%, organic carbon content from 0.042% to 1.071%, and pH from 5.54 to 6.73 in *Pinus nigra* forest (Karatepe, 2004). As generally understood from these studies, the reserves in the soils may vary. This is considered to be the result of the variation in bedrock, climate and geomorphological characteristic of the localities where the studies are conducted. As a matter of fact, it was reported that the existing aspect difference at local scale even beyond different localities might lead to differences in reserve such nitrogen and organic carbon by affecting the litter decomposition rate (Karatepe, 2004).

The soil texture classes were determined with the assessment of soil particles according to sand, dust and clay content using the texture triangle developed the international particle diameter class (Çepel, 1988). The most common soil type in the sampling plot were sandy-loam (52.5%) and loamy sand (27.5%). On the other hand, 6 bedrock types were identified in the study area. The most common bedrock types were migmatite gnays and gnays. In a study conducted in the Aegean Region, it was reported that sandy-loamy soils with high percentage of small-diameter gravel and sand due to quartzite in the red Mediterranean forest soils that were formed on gnays bedrock were dominant (Atalay et al., 1990). Furthermore, these soil were reported to have good drainage and be permeable. Therefore, it could be suggested in this study that the soil types identified in the Anatolian black pine sites were influenced by the gnays bedrock type.

The mean age of plus trees obtained from all sampling plots was found to be 58.5, while the average height was 18.2 m. After the plus trees in the sampling plots of the study were indexed to 100 years, the highest number of sampling plots was found in the site class II (45%) while the lowest number of plots was in site class IV (7.5%), whereas there was no sample in site class V (Kalıpsız, 1963). Pearson correlation analysis was performed to determine the relationship between the site index and independent variable in the form of constant data during the statistical assessment, while Spearman correlation analysis was performed for the environmental variables that were in the form of categorical data.

As a result of these analyses, a statistically significant positive correlation was found with site index and elevation ($r=0.319$), annual average precipitation ($r=0.360$) and flat landform ($r=0.360$); and a statistically significant negative correlation was found with annual average temperature ($r=-0.323$), topographic roughness index ($r=-0.312$) and upper slope position ($r=-0.316$).

At the second stage, in order to model productivity according to the site index values in the Anatolian black pine sites, stepwise multiple regression analysis was performed, and as a result 2 different model were obtained (Table 2).

Out of the models that were obtained, it was found that the 2nd Model (R^2 : 0.281) was more explanatory. In this model, flat landform and lower-middle slope position were the variables that involved in the model. Both of these variables had a positive contribution

to the model. 8 of 40 sampling plots that were studied had flat landform while their average site index value was found to be 30.0 m, while the average site index value was 25.1 in 32 sampling plots with different landforms. Therefore, there was an average difference of 4.9 m, which was reflected to the model. The site index value of lower-middle slope position, which was the other environmental variable in the model, in 10 sampling plots was found to be 28.0 m, whereas the average site index value of the sampling plots with other slope position was 25.5 m. Again the difference of 2.5 m between these values resulted in statistically important difference in the model.

Table 2. Findings of stepwise multiple regression analysis

Models	R ²	p	Model variables		VIF
1	0.186	0.005	Constant	25.13	1.000
			fltInd	4.193	
2	0.281	0.002	Constant	24.191	1.021
		0.033	fltInd	5.424	
			lomslp	3.277	1.021

Although the model obtained here was considered valid, the determination coefficient was very low due to the current R² value. For that reason, Regression tree method was applied at the next stage of the study to model productivity in the Anatolian black pine stands. The tree model obtained as a result of the analysis was statistically important, while the R² value of the model was found to be 0.709 (Fig. 2).

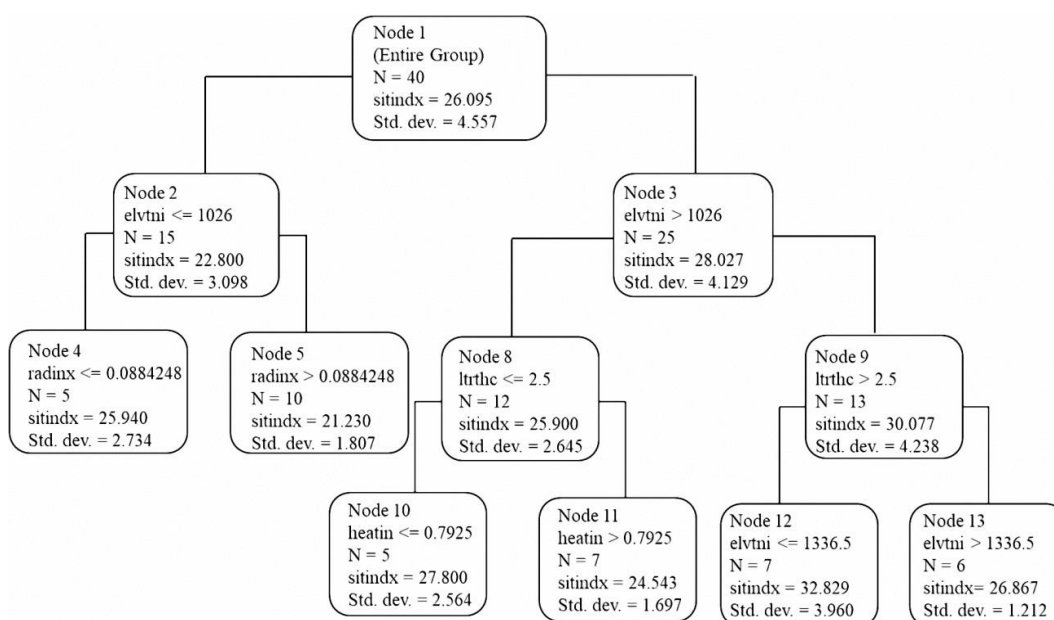


Figure 2. Model dendrogram obtained by regression tree technique

In the tree model, there were 6 different open-ended nodes, the highest contribution to the model was made by elevation (100%), litter thickness (28%), radiation index (20%) and heat index (8%), respectively. In case when the elevation ranged from 1026.0 to 1336.5 m and litter thickness was greater than 2.5 cm in the district, the highest site index value was found (32.8 m). The fact that litter thickness was higher in

areas where Anatolian black pine was productive might initially make one think that the average decomposition was slow, but it indicated that actually productivity should be low. Nevertheless, this is not the case. To clarify this result, organic matter content of sampling plots with a litter thickness of 2.5 cm (3.11%) was compared with the organic matter content of sampling plots with a litter thickness lower than 2.5 cm (3.05%). The assessment made revealed that there was no significant difference between the soils with respect to organic matter content and the soils were humic in both cases (2.1%-4.0%) (Çepel, 1995). This showed that the litter ratio at the top layers of the soil (0-30 cm) in Anatolian black pine stands in the district might not be a precise indicator for the organic matter ratio in the mineral soil part and thus for the productivity of the species.

A holistic evaluation of the findings obtained at this stage would demonstrate that an integrated interpretation of the models with binary linear analyse applied at the first stage was extremely important for the explanation of the concerned relationships. The positive relationship of the productivity of Anatolian black pine with flat landform, elevation and precipitation and the negative relationship with annual average temperature, topographic roughness index and upper slope positions in the binary linear relationships is an important finding that explains the increased productivity of the species in areas where the litter thickness in the model increased. To be clearer, this is considered to be a result of the thickness of the litter that accumulated without any carry-over on flat lands at the most optimum elevation range (around 1000-1350 m) and climate conditions suitable for the productivity of the species or the thickness of the litter that multiplied on lower slopes due to carry-over from the upper and middle slopes. Therefore, it is thought that the primarily dominant environmental factor that influenced the productivity of the species was actually optimum climate condition affected by elevation, while the secondary factor were the condition under which the species used water and nutrient at optimum level under the soil and geomorphological factors that were shaped by lower slope position and flat land as a whole.

These comments are consistent with the studies reporting that productivity increased under optimum climate conditions influenced by elevation and optimum water and nutrient economy conditions affected by slope position in Anatolian black pine stands (Özkan and Gülsoy, 2009; Güner et al., 2011; Özkan, 2013; Gülsoy et al., 2014; Güner et al., 2016). For example, in a study conducted in Dedegül mountain (Beyşehir) locality, climate conditions influenced by elevation, landform position and soil depth were the most dominant environmental factor that affected the productivity of Anatolian black pine just like in this these (Özkan et al., 2008). It was also reported in the study that the species could more easily overcome water deficit in summer period on lower slopes at an elevation of 1600 m – 1800 m and deep soils and thus keep its productivity high. It is possible to interpret the relations in this context through the water and nutrient economy, which are shaped indirectly, in terms of elevation, climate, slope position and soil depth. Moreover, it was reported in another study conducted in Eskişehir (Türkmendağı) locality that elevation was the dominant environmental factor that increased the productivity of the species and the site index increased especially in areas where precipitation increased in the most arid three months in summer period (Oğuzoğlu and Özkan, 2015). In another study conducted in recent years, it has been determined that the productivity of black pine has decreased after the 1970s in the Mediterranean basin, which is one of the most sensitive regions to climate change (Janssen et al., 2018). It is stated that this situation is related to increasing summer temperature and drought in the region as a result of climate change trends in recent

years. Therefore, all these remarks support the argument that the productivity of Anatolian black pine in the locality decreased depending on especially the severity of summer drought. As a matter of fact, there are other studies showing that soil nutrition content and water deficit due to environmental conditions and climate change are the most limiting factors for the productivity of the Anatolian black pine and other some tree species in the Mediterranean Region (Sarris et al., 2007; Piovesan et al., 2008; Güner et al., 2016). In the light of this information, the findings of this study revealed that Anatolian black pine trees at the suitable elevation range and flat land in this locality minimized water deficit by decreasing the evapotranspiration amount at sufficient soil depth and tolerated summer drought on one hand, while on the other hand they exploited nutrients under these conditions at optimum level and kept their productivity dynamic level.

On the other hand, the finding obtained in this study demonstrated that the lowest site index value (21.2 m) was found in areas where the elevation was lower than 1026 m and the radiation index was greater than 0.88. Radiation index closer to 1 pointed to the hottest aspect with the longest sunshine duration (Aertsens et al., 2010). Therefore, the fact that the radiation index was greater than 0.88 especially at lower elevations can be interpreted as areas with the harshest dry summer contrary to the abovementioned remarks and the decreased productivity of the species can be associated with this matter. Indeed, in a study highlighting the importance of aspect in addition to elevation for the productivity of the species, it was recommended that Anatolian black pine should be preferred on slopes at northern aspects with calcschist and dolomitic limestone and inclination greater than 40% and cedar should be preferred on slopes at southern aspects during the afforestation activities to be carried out at an elevation of 1500-2000 m in the Eastern Mediterranean Region (Polat et al., 2014).

Conclusions

Pinus nigra is widely used in afforestation activities and erosion control in Turkey and across the world since it has a wide distribution, tolerates harsh continental climate and habitat conditions and has the highest penetration into steppe compared to the other species, while it is also economically important. In this study, general site conditions and the areas where it can be most potentially productive were determined in Demirci district that is known to be one of the areas where Anatolian black pine, which is the taxon of this species distributed in Turkey, is widely distributed. In conclusion, it is possible to say that the effect of climatic conditions on water and nutrient economy in the environment is a very important factor reflected in the productivity of the species. This implies, indirectly, that climate change will affect the productivity of this species in the future. In this case, depending on the possible climate change scenarios in the future, it is also important to model the areas where this species can be the most productive. On the other hand, considering the wide distribution of this species, it is thought that there is a need for further studies at local scale in both Turkey and the world, through which the ecological requirements of the species can be clarified better and further and appropriate benefit can be obtained at global level.

Acknowledgements. We would like to thank Süleyman Demirel University Scientific Research Projects Coordination Unit for supporting our study under the project number SDÜ-BAPKB-4742-YL1-16.

REFERENCES

- [1] Aertsen, W., Kint, V., Van Orshoven, J., Özkan, K., Muys, B. (2010): Comparison and Ranking of Different Modelling Techniques For Prediction of Site Index in Mediterranean Mountain Forests. – *Ecological Modelling* 221(8): 1119-1130.
- [2] Anonymous (2011): Manisa Demirci Amenejman Planı. – Republic of Turkey General Directorate of Forestry Publications, 35 s., Ankara. (In Turkish).
- [3] Anonymous (2015): Türkiye Orman Varlığı–2015. – Republic of Turkey General Directorate of Forestry Publications, 32 p., Ankara. (In Turkish).
- [4] Atalay, I., Efe, R. (2012): Ecological attributes and distribution of Anatolian black pine [*Pinus nigra* Arnold. subsp. *pallasiana* Lamb. Holmboe] in Turkey. – *Journal of Environmental Biology* 33(2): 509-519.
- [5] Atalay, İ., Sezer, L. İ., Temuçin, E., Işık, Ş., Mutluer, M. (1990): The Factors affecting soil-forming in the Aegean Region. – *Aegean Geographical Journal* 5(1): 32-43.
- [6] Bahadır, M., Emet, K. (2010): The analyse of essential tree species which present main climate types in Turkey, by using GIS. - *Journal of TÜBAV Science* 3(1): 94-105.
- [7] Beers, T. W., Dress, P. E., Wensel, L. C. (1966): Notes and observations: aspect transformation in site productivity research. - *Journal of Forestry* 64: 691-692.
- [8] Bro, R., Smilde, A. K. (2014): Principal component analysis. - *Analytical Methods* 6(9): 2812-2831.
- [9] Cavalli, M., Trevisani, S., Comiti, F., Marchi, L. (2013): Geomorphometric assessment of spatial sediment connectivity in small Alpine catchments. - *Geomorphology* 188: 31-41.
- [10] Çepel, N. (1988): Toprak ilmi: Ders kitabı. - İstanbul University, Faculty of Forestry Publications, Puplication No: 3416-389, 289 p., İstanbul. (In Turkish).
- [11] Çepel, N. (1995): Orman Ekolojisi. - İstanbul University, Faculty of Forestry Publications, Puplication No: 426, 536 p., İstanbul. (In Turkish).
- [12] Davis, P. H. (1965-1988): Flora of Turkey and the East Aegean Islands. - Vols. 1-9. Edinburgh University Press, Edinburgh, UK.
- [13] De Reu, J., Bourgeois, J., Bats, M., Zwertvaegher, A., Gelorini, V., De Smedt, P., Chu W., Antrop, M., De Philippe, M., Finke, P., Van Meirvenne, M., Verniers, J. (2013): Application of the topographic position index to heterogeneous landscapes. - *Geomorphology* 186: 39-49.
- [14] Demir, A. (2013): A rising value in the sustainable development; the Turkey assessment in terms of biodiversity. - *Istanbul Commerce University Journal of Science* 12(24): 67-74.
- [15] Faostat (2014): Food and Agriculture Organization of the United Nations World Statistics website. - Retrieved from <http://faostat.fao.org/site/626/DesktopDefault.aspx?PageID=626#anchor>.
- [16] Fick, S. E., Hijmans, R. J. (2017): WorldClim 2: new 1-km spatial resolution climate surfaces for global land areas. - *International Journal of Climatology* 37(12): 4302-4315.
- [17] Güller, B. (2012): Effects of heat treatment on density, dimensional stability and color of *Pinus nigra* wood. - *African Journal of Biotechnology* 11(9): 2204-2209.
- [18] Gülsoy, S., Süel, H., Özdemir, S., Özkan, K. (2014): Modeling Site Productivity of Anatolian Black Pine Stands in Response to Site Factors in Buldan District, Turkey. - *Pakistan Journal Botany* 46(1): 213-220.
- [19] Güner, Ş. T., Özkan, K., Çömez, A., Çelik, N. (2011): Woody indicator species of probable productive potential areas of Anatolian black pine (*Pinus nigra* subsp. *pallasiana*) in the Inner Anatolia Region. - *Ecology* 20(80): 51-58.
- [20] Güner, Ş. T., Çömez, A., Özkan, K., Karataş, R., Çelik, N. (2016): Modelling the productivity of Anatolian black pine plantations in Turkey. - *Journal of the Faculty of Forestry Istanbul University* 66(1): 159-172.

- [21] Hauke, J., Kossowski, T. (2011): Comparison of values of Pearson's and Spearman's correlation coefficients on the same sets of data. - *Quaestiones Geographicae* 30(2): 87-93.
- [22] Helvacı, C. (2015): Geological features of neogene basins hosting borate deposits: an overview of deposits and future forecast, Turkey. - *Bulletin of the Mineral Research and Exploration* 151: 173-219.
- [23] Janssen, E., Kint, V., Bontemps, J. D., Özkan, K., Mert, A., Köse, N., İçel, B., Muys, B. (2018): Recent growth trends of black pine (*Pinus nigra* JF Arnold) in the eastern mediterranean. - *Forest Ecology and Management* 412: 21-28.
- [24] Kabalak, M., Sert, O. (2010): Notes on four species of click beetles (Coleoptera: Elateridae) from Turkey. - *The Coleopterists Bulletin* 64(2): 160-162.
- [25] Kahriman, A., Sönmez, T., Şahin, A. (2017): Tree volume tables for Calabrian pine in Antalya and Mersin region. - *Kastamonu University Journal of Forestry Faculty* 17(1): 9-22.
- [26] Kalıpsız, A. (1963): Türkiye'de Karaçam (*Pinus nigra* Arnold) Mesçerelerinin Tabii Bünyesi ve Verim Kudreti Üzerine Araştırmalar. - Republic of Turkey, Ministry of Agriculture, General Directorate of Forestry Press 349(8): 48-57, İstanbul. (In Turkish).
- [27] Karaöz, M. Ö. (1989a): Toprakların su ekonomisine ilişkin bazı fiziksel özelliklerinin laboratuvarında belirlenmesi yöntemleri. - *Journal of The Faculty of Forestry Istanbul University* 39(2): 133-144. (In Turkish).
- [28] Karaöz, M. Ö. (1989b): Toprakların bazı kimyasal özelliklerinin (pH, karbonat, tuzluluk, organik madde, total azot, yararlanılabilir fosfor) analiz yöntemleri. - *Journal of The Faculty of Forestry Istanbul University* 39(3): 64-82. (In Turkish).
- [29] Karatepe, Y. (2004): Amount of nitrogen and organic carbon in soil and nitrogen and organic matter in forest floor of black pine (*Pinus nigra* Arn. supsp. *pallasiana* (Lamb.) Holmboe) stands developed in Gölcük (Isparta). - *Turkish Journal of Forestry* 2: 1-16.
- [30] Keenan, R. J., Reams, G. A., Achard, F., De Freitas, J. V., Grainger, A., Lindquist, E. (2015): Dynamics of global forest area: Results from the FAO Global Forest Resources Assessment 2015. - *Forest Ecology and Management* 352: 9-20.
- [31] McCune, B., Keon, D. (2002): Equations for potential annual direct incident radiation and heat load. - *Journal of Vegetation Science* 13: 603-606.
- [32] McNab, W. H. (2010): Effects of landform on site index for two mesophytic tree species in the Appalachian Mountains of North Carolina, USA. - *International Journal of Forestry Research* 2010: 1-7.
- [33] Negiz, M.G., Kurt, E.Ö., Şentürk, Ö. (2017): A case study on the account of species-centered medicinal and aromatic plant species richness in Isparta-Yenişarbademli Region woodlands. - *Turkish Journal of Forestry* 18(4): 282-288.
- [34] Oğuzoğlu, Ş., Özkan, K. (2015): Productivity distribution modelling of Anatolian Black Pine (*Pinus nigra* subsp. *pallasiana* var. *pallasiana*) in the Türkmen Mountain, Eskişehir. - *Biological Diversity and Conservation* 8(2): 134-140.
- [35] Özkan, K. (2012): Modelling ecological data using classification and regression tree technique (CART). - *Turkish Journal of Forestry* 13: 1-4.
- [36] Özkan, K. (2013): Modeling Productivity of Crimean Pine by Using Fuzzy Logic Applications. - *Eurasian Journal of Forest Science* 1(1): 52-60.
- [37] Özkan, K., Gülsoy, S. (2009): Effect of environmental factors on the productivity of Crimean pine (*Pinus nigra* subsp. *pallasiana*) in Sütçüler, Turkey. - *Journal of Environmental Biology* 30(6): 965-970.
- [38] Özkan, K., Gülsoy, S., Mert, A. (2008): Interrelations Between Height Growth and Site Characteristics of *Pinus nigra* Arn. subsp. *pallasiana* (Lamb.) Holmboe. - *Journal The Malaysian Forester* 71: 9-16.
- [39] Öztürk, M. Z., Çetinkaya, G., Aydın, S. (2017): Climate types of Turkey according to Köppen-Geiger climate classification. - *Geography* 35: 17-27.

- [40] Piovesan, G., Biondi, F., Di Filippo, A., Alessandrini, A., Maugeri, M., (2008): Drought driven growth reduction in old beech (*Fagus sylvatica* L.) forests of the central Apennines, Italy. - *Global Change Biology* 14: 1265-1281.
- [41] Polat, S., Polat, O., Kantarcı, M. D., Tüfekçi, S., Aksay, Y. (2014): Relationships between some environmental characteristics and site indices (H38) of Taurus cedar (*Cedrus libani* A. Rich.) and Black pine (*Pinus nigra* Arnold.) afforestation areas in the Kadıncık Basin of Mersin. - *Journal of Forestry Research* 1(1A): 22-37.
- [42] Sarris, D., Christodoulakis, D., Koerner, C., (2007): Recent decline in precipitation and tree growth in the eastern Mediterranean. - *Global Change Biology* 13: 1187-1200.
- [43] Tabachnik, B. G., Fidell, L. S. (2012): *Using multivariate statistics* (6th Edition). - US: Pearson.

RATIONAL PLANNING OF PUBLIC OPEN SPACE BY EXPLORING THE EFFECTS OF ENVIRONMENTAL FACTORS ON HUMAN RECREATION – A CASE STUDY IN SHANGHAI, CHINA

LI, Z.¹ – XIE, C.¹ – LU, H.² – CHE, S.^{1*}

¹*Eco-Planning and Design Lab, School of Agriculture and Biology, Shanghai Jiao Tong University, Shanghai 200240, China*

²*International Education College, Zhengzhou University of Light Industry Zhengzhou 450002, China*

**Corresponding author
e-mail: chsq@sjtu.edu.cn*

(Received 10th Oct 2018; accepted 27th Nov 2018)

Abstract. Along with the urbanization, the rapid increase in urban population has become one of the most important global environmental issues. The natural spaces were continually replaced by built-up areas. There is a growing recognition that public open space (POS) in urban areas could offer many desirable human well-being possibilities by interactions with nature. In the current study, we conducted a survey in POS to investigate residents' recreation features and environmental factors affecting their recreation perceptions. The results show that diversified activity types including both active enjoyment and passive activity were required in urban POS by people in Shanghai, which was different for people from some other countries and cultures. Furthermore, the results have revealed how landscape and environmental factors of POS affect residents' recreation perceptions. Crime situation, quiet atmosphere, and environmental sanitation have been the three most critical variables of POS concerned by people. For the natural environment in POS, even the diversified species of plants were concerned by most residents, the vegetation density received the relatively lowest preference rating. Overall, planning of a large open grassland with tree patches on the edges is desirable in POS, where visitors could not only get close to nature but also some recreational activities could be carried out. All the findings in this study could give insights into the design and management of urban POS that are favorable for natural places and the health of people in urban areas.

Keywords: *architecture & greenery, outdoor spaces, landscape elements, landscape preference, questionnaire, Shanghai*

Introduction

As reported by many previous studies, rapid urbanization caused high concentrations of population and built-up areas in urban areas. The loss of natural spaces in urban areas leads to deterioration of urban residents' health (Peen et al. 2010; Lederbogen et al. 2011). All these resulted in a great need to plan open space for outdoor recreation and connection with nature (Lin et al. 2014; Zhu et al. 2017). A public open space (POS) means one open-access public space, which should be facilely accessed by all people regardless of age, ethnicity, physical limitations or other characteristics (Carmona et al., 2003; Judd, 2010; Hecke et al., 2016). The appearance of POS may be varied, such as urban parks, playgrounds, squares, streets, and vacant lots etc. The functions of POS may also be varied, such as providing the opportunities for leisure, socializing, sports or just simple relaxation (Chiesura, 2004; Laforteza et al., 2009). As essential elements in modern urban design, many studies have confirmed that POS was a cost-effective

contributor for improving public health, relieving urban life stress and creating democratic space (Wang, 2011; Henderson, 2013). The benefits of POS would continue to increase as more people would be concentrated in urban areas (Madanipour et al., 2013).

Considering these benefits, POS were greatly welcomed and required by urban residents (Matsuoka and Kaplan, 2008). It became increasingly important in urban design, especially in some highly urbanized regions where more people concentrated and natural lands were quite poor (Laforteza et al., 2013; Lin et al., 2014). Thus, it puts forward higher requests to both the quantity and quality of POS. There were close relations and intense interactions between people and POS. The activity pattern of residents could be affected by the environmental factors of urban POS (Rishbeth, 2004). Furthermore, the application of POS would also be determined by residents per their characteristics (Peschardt et al., 2012). The attitudes of residents towards POS would be influenced by both the physical conditions of spaces and demographic features of involved people. Thus, both the objective attributes and subjective psychology should be taken into account in POS design (Berg and Koole, 2006; Acar and Sakıcı, 2008; Berg and Winsum-Westra, 2010; Zheng et al., 2011).

Over the past decade, many studies have found that people with different cultural and ethnic backgrounds may use POS in different ways. Urban POS are generally used for active activities including walking, dog walking, sports activities and exercise in some western countries (Agency, 1994; Dunnett et al., 2002). While Gobster found that minority groups in Lincoln Park (Chicago) were more likely to engage in passive social park activities such as picnicking, talking and socialising than were the white people (Gobster, 2002). It was a challenge for urban or landscape professionals to provide an all-purpose POS for people with diverse socio-economic and cultural characteristics. On the other hands, the environmental factors of POS would also affect human perception. People generally tend to prefer the POS with more natural elements such as water, vegetation, etc. (Kaplan, 2001; Chou et al., 2016). It means that the larger proportion of natural patch area may promote urban residents' environmental preference in urban POS (Van den Berg, 2010). However, some studies held the opposing opinions referring to the relationship between landscape environment and human preference. Parsons suggested that ecologically natural landscapes are perceived to be less attractive (Parsons, 1995). Thus, more effort should be made for broadening our knowledge through examining the relationship between environmental factors of POS and human's preferences. It is essential to investigate the perspectives of people on the recreational functions of POS, as well as critical influence variables of POS.

With accelerated urbanization, making humans and natural systems in urban area develop toward the mutually beneficial direction has become one of the most important environmental topics. Considering the fact that Shanghai in China has experienced the largest and rapidest flux of urbanization and many people have moved from rural regions to urban regions (Peng, 2011; Zhang et al., 2013) the population of this city is quite diverse, including immigrants, new and native Shanghai residents. These people are distributed across classes with different demographic and socio-economic characteristics. It is necessary and significant for us to explore the recreation features and landscape perceptions of people on POS at the beginning of 'the Overall Planning of Shanghai (2020-2040)'. It aimed to ensure that as many residents as possible could benefit from POS in Shanghai where natural resources were quite limited and partially taken up by building areas. In this study, the main focuses were the followings: (1)

exploring the interactions between residents and urban POS, understanding how the residents utilized and perceived POS in their daily life; (2) examining the relationship between environmental factors of POS and residents' recreation, which were conducive to explore the most attractive features of POS. The findings in this study may be significant for the planning, design and management of POS. It also provides a methodology for linking environmental design and human preferences, which can be applied not only in Shanghai but also in some other cities with similar situations.

Materials and methods

Ethical approval

This study was approved by the Shanghai Jiao Tong University and Shanghai Urban Planning and Land Resources Bureau. All procedures performed in this study involving human participants were in accordance with the 1964 Helsinki declaration and its later amendments or comparable ethical standards.

Description of the study area

This selected study area was Shanghai, China, 30°82'30"–31°82'70"N and 120°85'20"–121°84'50"E. It was one of the largest cities and most important global economic centres. The total area of Shanghai is 6340.5 km² with a population of 24.2 million (Bureau, 2017). The built-up area is 2408 km², which accounts for 43.6% of the city area. Approximately 50% of the population are distributed in the city centre. Based on the data of sixth national census, most Shanghai residents are aged between 45-60 years old.

Since the large area and population diversity of Shanghai, sample plots were performed. The selected sample plots were distributed across different districts. From the geographic location, the built-up area of Shanghai could be divided into central city, suburban area, and satellite town. According to the development history of the districts in Shanghai, the built-up area could be categorized into five stages: before the founding of the People's Republic of China (before 1949), before the reform and opening-up policy (1949 to 1978), the 1980s, the 1990s, and the early 21st century. In this study, eight representative sample plots with varying socio-economic and environmental characteristics were selected for the investigation, including plots from the central city, suburban area, and satellite town (*Fig. 1, Table 1*).

Table 1. Sample plots in Shanghai

Sample plot	Area (km ²)	Location	Development history	Main function
People's square (PSS)	1.41	Central city	Early 1950s	Traditional center
Ruijin (RJ)	1.72	Central city	Mid-19th century	Historical concession
Xujiahui (XJH)	1.42	Central city	1980s	Commercial sub-center
Caojiadu (CJD)	1.53	Central city	Late 1980s	Residential area
Xinzhuang (XZ)	1.75	Suburb area	Late 1990s	Residential area
Fangsong (FS)	2.36	Satellite town	Early 21st century	Residential area
Laochengxiang (LCX)	1.66	Central city	Before the founding of the People's Republic of China	Special neighborhood
Weifang (WF)	2.09	Central city	1960s	Workers' village

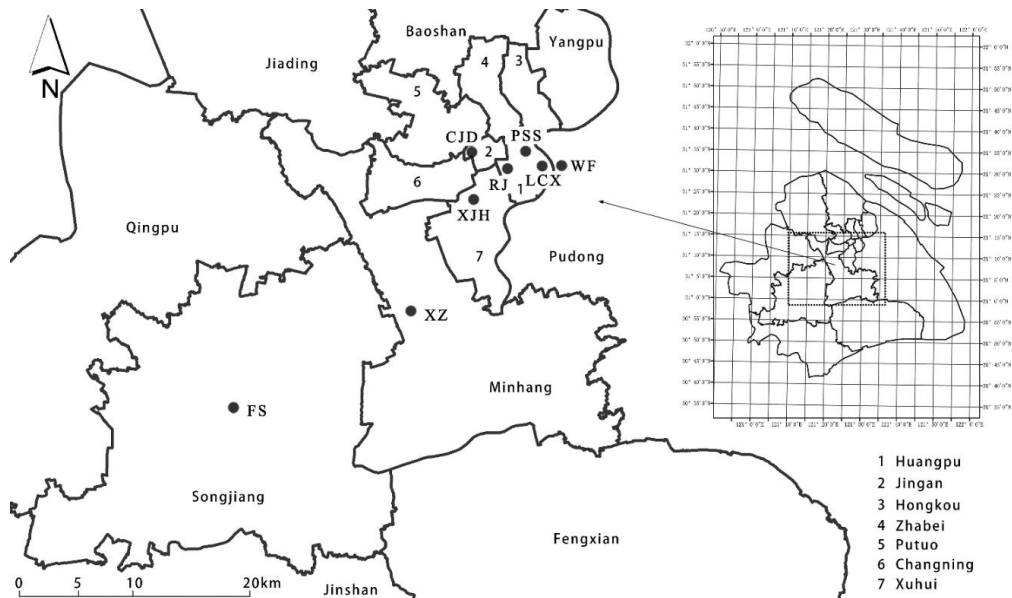


Figure 1. Locations of eight sample plots in Shanghai. (The black circles mean the sample plots)

In each sample plot, all the available POS were pre-investigated and marked on a map. During the pre-investigation towards these POS, all the recreational activity types were identified and recorded. Especially, in each sample plot, the POS that greatly contributed to the recreation of residents were identified as investigation sites, where questionnaire survey could be easily conducted for gathering more residents (Fig. 2). A total of 18 urban parks, 18 playgrounds and squares, and 20 casual streets were selected from the sample plots for further questionnaire survey.



Figure 2. Examples of POS selected in this study. A, B, urban parks; C, squares; D, casual streets

Questionnaire design

The questionnaire was designed, including the following sections: (1) profile of the respondents, including their demographic and socio-economic characteristics (*Table 2*); (2) activity types, providing with multiple choices; (3) degree of recreational demands (single choice; quantifying the demand level on visiting POS for recreation). The quantification was evaluated with a five-point Likert-type scale ranging from 1 (very low demand) to 5 (very high demand); and (4) preferences for characteristics of POS, including the landscape features and attributes. There was a total of 33 variables for describing general features of POS and evaluating the attractiveness to nearby residents (Asa et al., 2009; Tveit, 2009; Sevenant and Antrop, 2010; Zhao, 2012). These variables were designed and characterized based on previous studies (Tveit et al., 2006; Ode et al., 2008; Fry et al., 2009). The attractiveness of each variable to respondents was also scored from 1 (with very weak attraction) to 5 (with very strong attraction). Generally, the questionnaire was designed to collect the information and answer following questions: What were the general characteristics of the POS visitors in Shanghai? What were the recreation features of POS visitors, including recreational activity types and recreational demand level? How the environmental factors of POS would affect residents' behaviour?

Table 2. Demographic and socio-economic characteristics of the respondents

Characteristics	No.	Ratio (%)	Characteristics	No.	Ratio (%)
Gender			Monthly income per capita (RMB)		
Male	572	57.3	<2000	108	10.8
Female	427	42.7	2000–5000	380	38.0
Age			5000–8000	286	28.6
<18 years	94	9.4	>8000	226	22.6
18 years to 44 years	611	61.2	Dwelling location		
45 years to 60 years	117	11.7	Central city	480	48.0
>60 years	177	17.7	Suburb area	342	34.3
Education level			Satellite town	177	17.7
Primary and junior middle school	158	15.8	Household size		
High school and technical school	276	27.6	1	89	8.9
Junior college and bachelor's degree	468	46.8	2	164	16.4
Graduate degree and above	98	9.8	3	406	40.6
			4	197	19.7
			≥5	144	14.4

Questionnaire survey

The questionnaire survey was performed in the selected POS during July 10th to August 16th in 2015 (excluding rainy days). The survey was conducted on a face-to-face basis, which has been considered as the most sociable way to recruit interviewers and collect data (Sheskin, 1985). The questionnaires were randomly distributed to the

residents who visited the selected POS for recreation. During the survey, each POS was visited twice every week (once in weekdays and once in weekend) mainly at two periods (7:00-11:00 and 16:00-19:00). Since it was hot in summer, POS would be visited by relatively more residents for recreation in this period.

Before the survey, the respondents would be informed on the purpose of this investigation, ensuring the confidentiality of their answers. When the participants agreed to fill in questionnaires and checked the box stating their agreement, the interview began. Some respondents were minors, thus their agreement form would be checked by guardians. For minors without stating agreement form guardians could refuse the participation of children by sending us an email after investigation. It was assumed that they agreed to participate without receiving refusal. A total of 1150 questionnaires were delivered and collected on site, with 999 containing complete and valid responses. Only the questionnaires with complete and valid results were included in the following analysis. The field survey was conducted with the assistance of undergraduate and graduate students from the Department of Landscape Architecture of the Shanghai Jiao Tong University.

Data analysis

The relationships between recreation features (including recreation activities and recreational demand degrees) and characteristics of respondents were analysed with a one-way analysis of variance (ANOVA). In addition, the environmental variables of POS affecting residents' recreation perceptions were identified with factor and principal component analyses. All statistical analyses were conducted with SPSS v.18.0 software package (SPSS Inc., USA).

Results

Characteristics of respondents

The demographic and socio-economic characteristics of respondents in this study were analysed and presented (*Table 2*). Respondents between the ages of 18-44 were the most representative group and those less than 18 years were the least representative group. For the gender, the number of male respondents was slightly higher (57.3%) than that of female (42.7%). Following characteristics were also most frequently and typically observed in POS visitors: the educational level was junior college and bachelor' degree (46.8%); the monthly income per capita was 2000-5000 RMB (38.0%) and the household size was 3 persons (40.6%).

Recreation features in relation to characteristics of respondents

Degree of recreational demands

The degree of recreational demands was collected from respondents, which was significantly related to the age, gender, educational level and monthly income of the respondents ($p < 0.01$). For the age, the degree of recreational demands was generally increased with age (*Fig. 3*). The degree of recreational demands was the highest for people above 60 years (4.956). For the gender, the degree of recreational demands reported by female respondents (4.858) was higher than that of by male respondents (4.211). For the educational level, the degree was also increased with higher educational

level. Specifically, the degree of recreational demands was the highest (4.723) for those respondents with a graduate degree and above. Finally, the degree of recreational demands was negatively associated with the monthly income of the respondents. The degree was the highest in respondents with monthly income per capita under 2000 RMB (4.923), while it was the lowest for those with monthly income per capita above 8000 RMB (4.128).

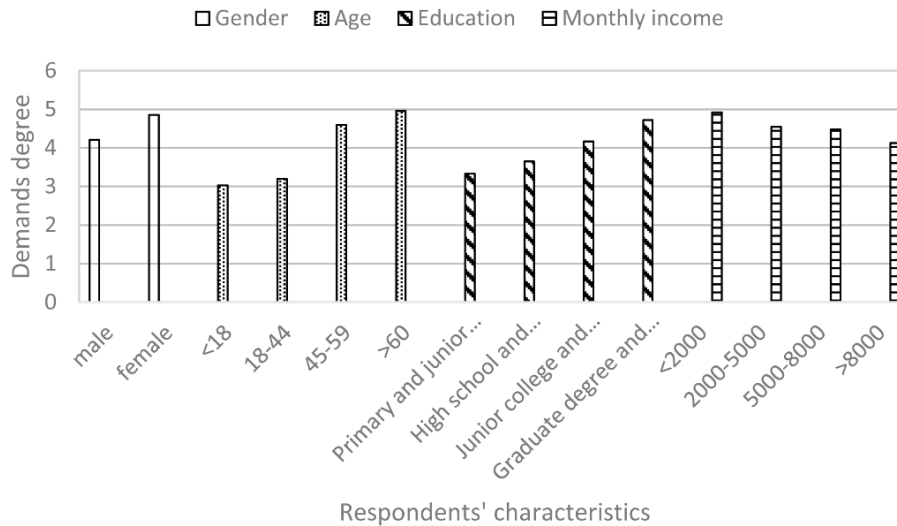


Figure 3. Degree of recreational demands in relation to the characteristics of respondents

Choice of recreational activity types

The preferred recreational activity types in POS were revealed by the questionnaire data (Fig. 4). And respondents' choices of recreational activity types were significantly related to their gender, age, and educational level ($p < 0.01$).

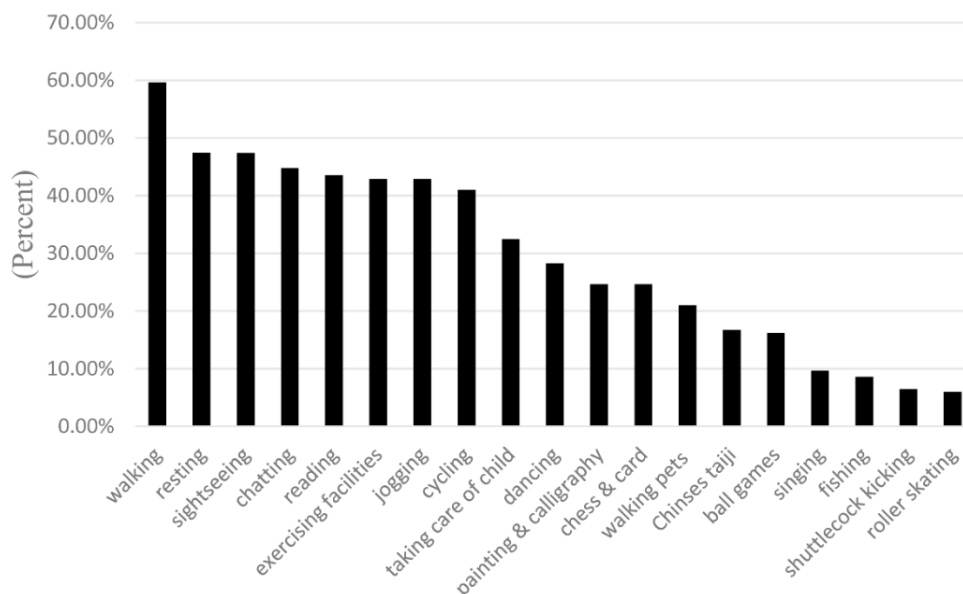


Figure 4. Respondents' preferences to activity types based on the questionnaire

For the gender, sports activities were preferred by male respondents, such as ball games, chess and card, while more quiet and low-intensity activities were preferred by female respondents, such as dancing and sightseeing. The preference of recreational activity types was also varied among respondents with different age. The respondents less than 18 years old preferred to walk, sightsee, read or jog; those aged between 18-44 years old preferred to walk, sightsee, and play ball games; those aged between 45-59 years old preferred to walk, play exercising facilities, rest and sightsee; walk and rest were preferred by those aged above 60 years old. Varied activity types were also observed among respondents with different educational levels. Specifically, the respondents graduated from primary and junior middle school preferred to rest or walk; those who graduated from high school and technical school preferred to walk, sightsee; the respondents with higher education levels preferred to walk, sightsee, rest or jog in POS, including those graduated from junior college and with the degree of bachelor, graduate and above.

Preferences for landscape elements and environmental factors of POS

The six factors were extracted via varimax rotation based on the results of eigenvalue-one criterion. Then the six factors were named per their features (*Table 3*): resources and maintenance, landscape cognitive attributes, facilities, natural environment, safety, and municipal services. Totally 22 variables were included with factor loadings greater than 0.5, while some variables were excluded, including buffets, toilets, signage systems, form and activity duration etc.

From the results in *Table 3*, it showed that crime situation (4.67) was considered as the most essential variable by most respondents, which was followed by quiet atmosphere (4.42) and environmental sanitation (4.41). The attractiveness of urban POS would also be influenced by some other variables, such as accessibility (4.07), diversified species of plants (4.09), air environment (4.30) and microclimate (4.06) etc. The recreational facility (4.01) was ranked as the most critical variable in facilities by respondents and it was followed by the resting facility (3.96).

Discussion

Recreation features of residents in POS

In this study, it was found that recreation features in POS would be varied for residents with different demographic and socio-economic characteristics, which was consistent with some previous studies (Maas et al., 2009). Meanwhile, both the active (walking and exercising) and passive activities (resting and sightseeing) in POS were preferred by the residents of Shanghai, China. Socializing with each other was specially preferred by these residents and they would like the activities such as dancing and singing, chess and card, and Chinese Taiji. While people in some western countries mainly used urban POS for active activities (Agency, 1994; Dunnett et al., 2002), minority groups in Lincoln Park (Chicago) preferred passive social park activities (Gobster, 2002). Compared to that in these countries and cultures, residents' selection of recreation activities in POS of Shanghai was quite different (Dunnett et al., 2002; Gobster, 2002; Özgüner, 2011). This finding may be resulted from the special lifestyles and habits of residents in Shanghai, China.

Table 3. Principal component analysis of the preferences for the landscape elements and attributes in POS

	Average value	Standard deviation	Factor load	Variance (%)	Cronbach's α
Factor 1: Resources and maintenance				10.759	0.825
Diversified species of plants	4.09	0.835	0.686		
Maintenance of infrastructure	3.90	0.940	0.655		
Environmental sanitation	4.41	0.714	0.573		
Unique sites for special needs	3.80	0.935	0.532		
Diversified sites for recreation	3.60	0.907	0.638		
Factor 2: Landscape cognitive attributes				9.244	0.748
Accessibility	4.07	0.995	0.699		
Cultural features	3.55	0.942	0.735		
Coherence	3.67	0.952	0.546		
Diversity	3.50	0.886	0.572		
Factor 3: Facilities				9.101	0.759
Recreational facilities	4.01	0.881	0.792		
Resting facilities	3.96	0.891	0.698		
Landscape structures	3.33	0.927	0.652		
Exercising facilities	3.92	0.885	0.648		
Factor 4: Natural environment				8.722	0.711
Air environment	4.30	0.912	0.805		
Vegetation density	3.90	0.918	0.666		
Microclimate	4.06	0.873	0.766		
Quiet atmosphere	4.42	0.741	0.546		
Factor 5: Safety				6.623	0.651
Patrol	4.35	0.827	0.836		
Crime situation	4.67	0.619	0.621		
Limited open time	3.71	1.009	0.513		
Factor 6: Municipal services				6.343	0.676
Illumination	4.03	0.856	0.735		
Groundwater treatment	4.00	1.140	0.527		

Environmental factors affecting residents' perceptions of POS

According to some previous studies, the feeling of personal safety was one of the main reasons for preventing people from visiting POS for recreation, especially for the women and children (He, 2002; Jorgensen et al., 2002). Consistent with the results of these studies, our study also revealed that crime situation was one of the most critical factors concerned by the residents (4.67). It meant that the feeling of personal safety in POS has still been worried by most people in Shanghai. During our investigation, groups of people complained that tramps and scavengers were frequently observed in the POS which may be scary for women and children. It may also help explain the fewer female respondents in our questionnaire survey, although their degree of

recreational demands was higher than that of male respondents. Meanwhile, both the quiet atmosphere (4.42) and environmental sanitation (4.41) ranked high in preference ratings of POS, which was similar to some previous studies. Gobster found that the cleanliness and maintenance were critical preferences for POS (Gobster, 2002). During our questionnaire survey in these POS, the littering of garbage could be observed which partially indicate the lack of management and maintenance of POS in Shanghai. Furthermore, it is further noted in this study that diversified species of plants (4.09), air environment (4.30) and microclimate (4.06) were also one of the most appealing environmental factors of POS. However, the vegetation density received the lowest preference rating (3.90) in the factor of natural environment (*Table 3*), which suggested that respondents preferred a moderately open vegetation. While plant communities with densely spaced plants are perceived as less attractive and unsafe. This finding confirmed the conclusions of some studies that found a correlation between vegetation density and security considerations in POS (Bjerke et al., 2006; Laing et al., 2009). Gobster observed that humans have strong preferences for landscapes correlated to the vegetation configuration with cleared or grassy understory (Gobster, 1994). While POS with highly dense vegetation are usually perceived as messy, unkempt and unattractive (Hands, 2002).

Good accessibility to POS (4.07) was another preference of respondents. The visiting of residents to POS would be increased after improving the accessibility of POS. Since the POS should be easily accessed by all the people including the elderly and disabled residents, barrier-free access should be provided (Adinolfi et al., 2014). Regarding the facilities, recreational (4.01) and resting facilities (3.96) were intensely preferred by the respondents. This result was also consistent with several previous studies by Dunnnett et al. (2002), Woolley (2006) and Jim and Chen (2006). In all these studies, it was observed that the diversity of recreational facilities and the number of available seats would be closely related to the visiting frequency of people to POS. Kemperman and Timmermans even found that diverse visitors would be attracted by facilities applicable for group activities in POS (Kemperman and Timmermans, 2006).

Some practical implications for POS design

The results have indicated that recreation features in POS were quite different for residents with various characteristics. And considering that the aging population has been greatly increased in Shanghai in China (Institute of finance and trade economics 2010/2011), the recreation features of the elderly should be primarily considered in POS planning and design. For example, the walkways around and across the POS meeting the requirements of walking may be welcomed by elderly residents. In addition, the specific composition of target residents should be analysed and considered. As above mentioned, for residents with different characteristics, the recreation features would be varied, as well as the types of recreational activity. On this basis, the preferences for the POS should be found and the POS must be designed and developed to satisfy these preferences, including recreational facilities, multifunctional space divisions, and special sites etc.

On the other hand, landscape and environment preferences of people would be determined by many specific aspects. The environmental factors of POS could affect residents' perceptions. Even the diversified species of plants were concerned by most residents, the vegetation density received relatively the lowest preference rating. This finding demonstrated that an open space with large continuous grassland and scattered

trees can promote the residents' perceptions of POS when considering the feeling of personal safety. Planning of a large open grassland with tree patches on the edges is desirable in POS, where visitors could not only get close to the nature but also some recreational activities could be carried out. Meanwhile, regular patterns, diverse colors, and cultural elements, such as direction signs, or street furniture, may help diminish the negative effects of dense vegetation on residents' feeling of security. Furthermore, increasing surveillance and patrol could also improve the feeling of personal safety in POS. The quiet atmosphere could be achieved by optimizing the site selection while the sanitation could be maintained by improving management. Finally, the sufficient resting facilities should be provided, such as seats and resting areas. Some good measures enabling improved POS were shown in *Figure 5*.



Figure 5. Optimal measures for improving and modifying POS

Conclusion

Previous studies have stated that urbanization is associated with people's depression, chronic diseases and mental disorders (Peen et al., 2010; Lederbogen et al., 2011). POS in urban area has the potential to significantly contribute to public health, relieving urban life stress and creating democratic space (Henderson, 2013; Tyrväinen et al., 2014). Both the environmental conditions of POS and demographic features of people would influence the recreation attitudes towards POS. The study attempted to bridge the gap between people's recreation features and natural environmental factors in POS. We investigated how the residents utilized and perceived POS in their daily life. The results further reveal how landscape and environmental factors of POS affect residents' recreation perceptions. Even the diversified species of plants were preferred by residents, the vegetation density would influence their perceptions on POS. All the findings we observed in this study could contribute to urban and landscape professionals in POS designing and improvement that focus on a healthy and sustainable urban environment. And the methodology in this study can be applied not only in Shanghai but also in some other cities, which link environmental design and human preferences together.

Acknowledgments. We acknowledge the financial support from the Projects of National Natural Science Foundation of China (NO. 31470702). The authors would like to thank Prof. Jiajun Lou and Hao Xu for providing guidelines of this study, as well as all the members participating in the survey.

Conflict of interests. The authors declare no conflict of interests.

REFERENCES

- [1] Acar, C., Sakıcı, Ç. (2008): Assessing landscape perception of urban rocky habitats. – *Building & Environment* 43(6): 1153-1170.
- [2] Adinolfi, C., Suárez-Cáceres, G. P., Cariñanos, P. (2014): Relation between visitors' behaviour and characteristics of green spaces in the city of Granada, south-eastern Spain. – *Urban Forestry & Urban Greening* 13(3): 534-542.
- [3] Agency, R. P. (1994): *People Using the Royal Parks. Annual Report of Royal Parks Agency.* – University of North London Press, London.
- [4] Asa, O., Gary, F., Tveit, M. S., Pernette, M., David, M. (2009): Indicators of perceived naturalness as drivers of landscape preference. – *Journal of Environmental Management* 90(1): 375-383.
- [5] Berg, A. E. V. D., Koole, S. L. (2006): New wilderness in the Netherlands: An investigation of visual preferences for nature development landscapes. – *Landscape & Urban Planning* 78(4): 362-372.
- [6] Berg, A. E. V. D., Winsum-Westra, M. V. (2010): Manicured, romantic, or wild? The relation between need for structure and preferences for garden styles. – *Urban Forestry & Urban Greening* 9(3): 179-186.
- [7] Bureau, S. M. S. (2017): *Shanghai Statistical Year Book 2017.* – China Statistics Press, Beijing.
- [8] Carmona, M., Heath, T., Oc, T., Tiesdell, S. (2003): *Public Spaces - Urban Spaces: The Dimensions of Urban Design.* – Elsevier, Amsterdam.
- [9] Chiesura, A. (2004): The role of urban parks for the sustainable city. – *Landscape & Urban Planning* 68(1): 129-138.
- [10] Chou, W. Y., Lee, C. H., Chang, C. Y. (2016): Relationship between urban open spaces and humans' health benefits from an ecological perspective: A study in an urban campus. – *Landscape & Ecological Engineering* 12(2): 255-267.
- [11] Dunnett, N., Swanwick, C., Woolley, H. (2002): *Improving Urban Parks, Play Areas and Green Spaces.* – Department for Transport, Local Government and the Regions, London.
- [12] Fry, G., Tveit, M. S., Ode, Å., Velarde, M. D. (2009): The ecology of visual landscapes: Exploring the conceptual common ground of visual and ecological landscape indicators. – *Ecological Indicators* 9(5): 933-947.
- [13] Gobster, P. H. (1994): The urban savanna: reuniting ecological preference and function. – *Restoration Ecology* 12(1): 64-71.
- [14] Gobster, P. H. (2002): Managing urban parks for a racially and ethnically diverse clientele. – *Leisure Sciences* 24(2): 143-159.
- [15] Hands, D. E., (2002): Enhancing visual preference of ecological rehabilitation sites. – *Landscape & Urban Planning* 58(1): 57-70.
- [16] Hecke, L. V., Deforche, B., Dyck, D. V., Bourdeaudhuij, I. D., Veitch, J., Cauwenberg, J. V. (2016): Social and physical environmental factors influencing adolescents' physical activity in urban public open spaces: A qualitative study using walk-along interviews. – *Plos One* 11(5): e0155686.
- [17] Henderson, K. A. (2013): The contributions of leisure and active recreation to health and well-being. – *African Journal for Physical Health Education, Recreation and Dance:*

- Building Livable Communities through the Collaboration of Recreation, Leisure and Tourism Initiatives: Supplement 4(18).
- [18] Institute of Finance and Trade Economics (2010/2011): Report on China's Fiscal Policy. – Institute of Finance and Trade Economics, Beijing.
- [19] Jim, C. Y., Chen, W. Y. (2006): Recreation-amenity use and contingent valuation of urban greenspaces in Guangzhou, China. – *Landscape & Urban Planning* 75(1-2): 81-96.
- [20] Judd, B. H. (2010): Whose public space? International case studies in urban design and development. – *Journal of Urban Design* 16(3): 429-431.
- [21] Kaplan, D. R. (2001): The nature of the view from home: psychological benefits. – *Environment & Behavior* 33(4): 507-542.
- [22] Kemperman, A. D. A. M., Timmermans, H. J. P. (2006): Heterogeneity in urban park use of aging visitors: A latent class analysis. – *Leisure Sciences* 28(1): 57-71.
- [23] Laforteza, R., Carrus, G., Sanesi, G. Davies, C. (2009): Benefits and well-being perceived by people visiting green spaces in periods of heat stress. – *Urban Forestry & Urban Greening* 8(2): 97-108.
- [24] Laforteza, R., Davies, C., Sanesi, G. Konijnendijk, C. C. (2013): Green infrastructure as a tool to support spatial planning in European urban regions. – *iForest - Biogeosciences and Forestry* 6(1): 102-108.
- [25] Lederbogen, F., Kirsch, P., Haddad, L., Streit, F., Tost, H., Schuch, P., Wüst, S., Pruessner, J. C., Rietschel, M., Deuschle, M., Meyer-Lindenberg, A. (2011): City living and urban upbringing affect neural social stress processing in humans. – *Nature* 474(7352): 498.
- [26] Lin, B. B., Fuller, R. A., Bush, R., Gaston, K. J., Shanahan, D. F. (2014): Opportunity or orientation? Who uses urban parks and why. – *Plos One* 9(1): e87422.
- [27] Maas, J., Van Dillen, S. M., Verheij, R. A., Groenewegen, P. P. (2009): Social contacts as a possible mechanism behind the relation between green space and health. – *Health & Place* 15(2): 586-595.
- [28] Madanipour, A., Knierbein, S., Degros, A. (2013): *Public Space and the Challenges of Urban Transformation in Europe*. – Routledge, London.
- [29] Matsuoka, R. H., Kaplan, R. (2008): People needs in the urban landscape: Analysis of landscape and urban planning contributions. – *Landscape & Urban Planning* 84(1): 7-19.
- [30] Ode, Å., Tveit, M. S., Fry, G. (2008): Capturing landscape visual character using indicators: Touching base with landscape aesthetic theory. – *Landscape Research* 33(1): 89-117.
- [31] Özgüner, H. (2011): Cultural differences in attitudes towards urban parks and green spaces. – *Landscape Research* 36(36): 599-620.
- [32] Parsons, R. (1995): Conflict between ecological sustainability and environmental aesthetics: Conundrum, canard or curiosity. – *Landscape & Urban Planning* 32(3): 227-244.
- [33] Peen, J., Schoevers, R. A., Beekman, A. T., Dekker, J., (2010): The current status of urban-rural differences in psychiatric disorders. – *Acta Psychiatr Scand* 121(2): 84-93.
- [34] Peng, X. (2011): China's demographic history and future challenges. – *Science* 333(6042): 581-587.
- [35] Peschardt, K. K., Schipperijn, J., Stigsdotter, U. K. (2012): Use of small public urban green spaces (SPUGS). – *Urban Forestry & Urban Greening* 11(3): 235-244.
- [36] Rishbeth, C. (2004): Ethno-cultural representation in the urban landscape. – *Journal of Urban Design* 9(3): 311-333.
- [37] Sevenant, M., Antrop, M. (2010): The use of latent classes to identify individual differences in the importance of landscape dimensions for aesthetic preference. – *Land Use Policy* 27(3): 827-842.
- [38] Sheskin, I. M. (1985): *Survey Research for Geographers*. – Association of American Geographers, Washington.

- [39] Tveit, M., Ode, Å., Fry, G. (2006): Key concepts in a framework for analysing visual landscape character. – *Landscape Research* 31(3): 229-255.
- [40] Tveit, M. S. (2009): Indicators of visual scale as predictors of landscape preference; a comparison between groups. – *Journal of Environmental Management* 90(9): 2882-2888.
- [41] Tyrväinen, L., Ojala, A., Korpela, K., Lanki, T., Tsunetsugu, Y., Kagawa, T. (2014): The influence of urban green environments on stress relief measures: A field experiment. – *Journal of Environmental Psychology* 38(6): 1-9.
- [42] Van den Berg, A. E., Hartig, T., Staats, H. (2010): Preference for nature in urbanized societies: Stress, restoration, and the pursuit of sustainability. – *Journal of Social Issues* 63(1): 79-96.
- [43] Wang, W., Li, P., Wang, W., Namgung, M. (2011): Exploring determinants of pedestrians' satisfaction with sidewalk environments: Case study in Korea. – *Journal of Urban Planning and Development* 138(2): 166-172.
- [44] Woolley, H. (2006): Freedom of the city: Contemporary issues and policy influences on children and young people's use of public open space in England. – *Children's Geographies* 4(01): 45-59.
- [45] Zhang, H., Chen, B., Sun, Z., Bao, Z. (2013): Landscape perception and recreation needs in urban green space in Fuyang, Hangzhou, China. – *Urban Forestry & Urban Greening* 12(1): 44-52.
- [46] Zhao, J., Wang, R., Cai, Y., Luo, P. (2012): Effects of visual indicators on landscape preferences. – *Journal of Urban Planning and Development* 139(1): 70-78.
- [47] Zheng, B., Zhang, Y., Chen, J. (2011): Preference to home landscape: wildness or neatness? – *Landscape & Urban Planning* 99(1): 1-8.
- [48] Zhu, C., Ji, P., Li, S. (2017): Effects of urban green belts on the air temperature, humidity and air quality. – *Journal of Environmental Engineering & Landscape Management* 25(1): 39-55.

PHYSIOLOGICAL PERFORMANCE OF MAIZE (*ZEA MAYS* L.) UNDER STRESS CONDITIONS OF WATER DEFICIT AND HIGH TEMPERATURE

HAMA, B. M. – MOHAMMED, A. A.*

*Crop Science Department, College of Agricultural Sciences, University of Sulaimani
Sulaimani, Kurdistan Region, Iraq
(e-mail: bekhal.mustafa@univsul.edu.iq; phone: +964-770-190-0487)*

**Corresponding author
e-mail: aram.muhammed@univsul.edu.iq; phone: +964-770-157-6760*

(Received 10th Oct 2018; accepted 29th Nov 2018)

Abstract. The effect of water deficit is usually consistent with the influence of high temperature. In order to evaluate each of the two factors on the physiological performance of six maize (*Zea mays* L.) hybrids independently, two different experiments have been conducted in the field and the greenhouse. Physiological processes in different vegetative growth stages V10, V14, VT and reproductive growth stage R3 were studied. Photosynthetic rate (P_n), transpiration rate (E), and stomatal conductance (g_s) as well as specific leaf area (SLA) were examined. Four different water levels were used, while I_1 was well irrigated, on the other levels water deficit was created, in I_2 in the vegetative growth period, in I_3 in the reproductive growth period and in I_4 at both vegetative and reproductive periods. The rate of photosynthesis of all six hybrids was increased from V10 to R3 under the effect of I_1 , while variations in other physiological performance were correlated with water levels and also with the tolerance potential of maize hybrids. The influence of water deficit treatments combined with the effect of high temperature limited the efficiency of physiological traits especially photosynthesis. The consistency between leaf area and the amount of dry matter that partitioned to the leaves was behaved for maintaining the photosynthetic area under stress condition. The greatest change in the rate of the physiological traits of all hybrids occurred with raising the temperature from T_1 to T_4 in the greenhouse.

Keywords: *growth response, drought stress, heat stress, corn, irrigation levels*

Introduction

Although the maize crop is classified as a C4-plant the rate of development and productivity are profoundly influenced by drought stress and high temperature, especially in certain stages of crop growth (Brandner and Salvucci, 2002; Tester and Bacic, 2005). The crop productivity in arid and semiarid regions is limited by both high temperature and drought during season growth (Dalirie et al., 2010). All physiological processes are affected by severe environmental factors, and because these processes contribute significantly to the source of the provision of growth requirements, there will be a decrease in the biomass accumulation and the process of seed formation and production (Yang and Zhang, 2006; Prasad et al., 2008; Barnabas et al., 2008; Efeoğlu, 2009; Hatfield and Prueger, 2015).

Specific leaf area is an important factor in the estimation of canopy photosynthesis in crop growth and development, where competition between the source and the sinks will occur. Generally, a higher SLA and a high assimilation rate per unit leaf mass seems to be the most important for achieving fast growth. A negative relationship between SLA and plant photosynthesis was found for a set of genotypes from tropical and temperate sources that were early sown in the field due to environmental or genetic influences (Hund et al., 2005).

Temperature is one of the most important environmental factors influencing mitochondrial respiration. Respiration exponentially increases with increasing temperatures from 30–35 or 40 °C, reaching a plateau at 40–50 °C (Prasad et al., 2008). At a temperature above 40 °C the enzymes that carry out photosynthesis lose their shape and functionality, and the photosynthetic rate declines rapidly. Ben-Asher et al. (2008) revealed a gradual decline of about 1 Pn unit per 1 °C increase in temperature, while the highest temperature treatment descended Pn 50–60%. The transpiration rate was increased from 0.25 and 0.36 mm h^{-1} to 0.36 and 0.54 mm h^{-1} under the influence of high temperature.

Drought stress in maize led to a significant decline in net photosynthesis (33.22%), transpiration rate (37.84%), stomatal conductance (25.54%), water use efficiency (50.87%), as compared to well water control (Anjum et al., 2011; Allen and Ort, 2001). Effect of water shortage during different growing stages of maize sustained different extent impact on biomass accumulation, partitioning and kernel yield (Mi et al., 2018). It was reported that drought usually leads to a reduction of important photosynthetic pigments, and deterioration in the photosynthetic apparatus especially the photosystem II reaction centre (Zhang et al., 2013). To prevent excessive water loss and physiological disadvantages, plants regulate transpiration by adjusting the stomatal conductance (Chaves et al., 2002). Crops are generally more sensitive to water deficit and heat stress during reproductive stages of development (Iings et al., 2013). The physiological responses of plants to effect of drought and heat stress, create a strong relationship between the plant water status and temperature, thus making it very hard to separate the contributions of heat and drought stress under field conditions, the impacts of water deficit and heat stress on the processes of crop plant photosynthesis either through the regulation by stomatal closure or decreasing flow of CO_2 into mesophyll tissue (Prasad et al., 2008). The interrelations between SLA and photosynthesis also can be helpful in clarifying differences between photosynthetic rates with different expression dry weight or area bases.

The objective of the study was an investigation of the effect of water deficit and heat stress in combination on the physiological processes Pn , E , and g_s and their impacts on growth performance of a set of maize hybrids under the field condition, where there is water deficit and high temperature and independently in the greenhouse where the only heat stress condition is present.

Materials and methods

The research was conducted in the field and greenhouse of college of Agricultural Sciences\University of Sulaimani\Sulaimani\KRG-Iraq (35° 34' 19" N 45° 22' 1.6" E with altitude of 754 m.a.s.l), during the summer season of 2016 and the spring season of 2017 in order to evaluate growth and development of six maize hybrids through studying of some of the physiological traits under the effect of water deficit and high temperature in the field and only heat stress condition in the green house, the map of the study site is demonstrated in *Figure 1*. A field experiment was conducted in growth condition with the seasonal mean temperature shown in *Table 1*, and only high temperature stress (30, 35, 40, and 45 °C) as (T_1 , T_2 , T_3 , and T_4) in the greenhouse during the growth stages pre-silking and post silking. Six maize hybrids {Medium 791(H_1), Cantabpis(H_2), Btaris(H_3), Fijr 260(H_4), Es-SOLITO 635(H_5) and Dhqan(H_6)} were seeded.

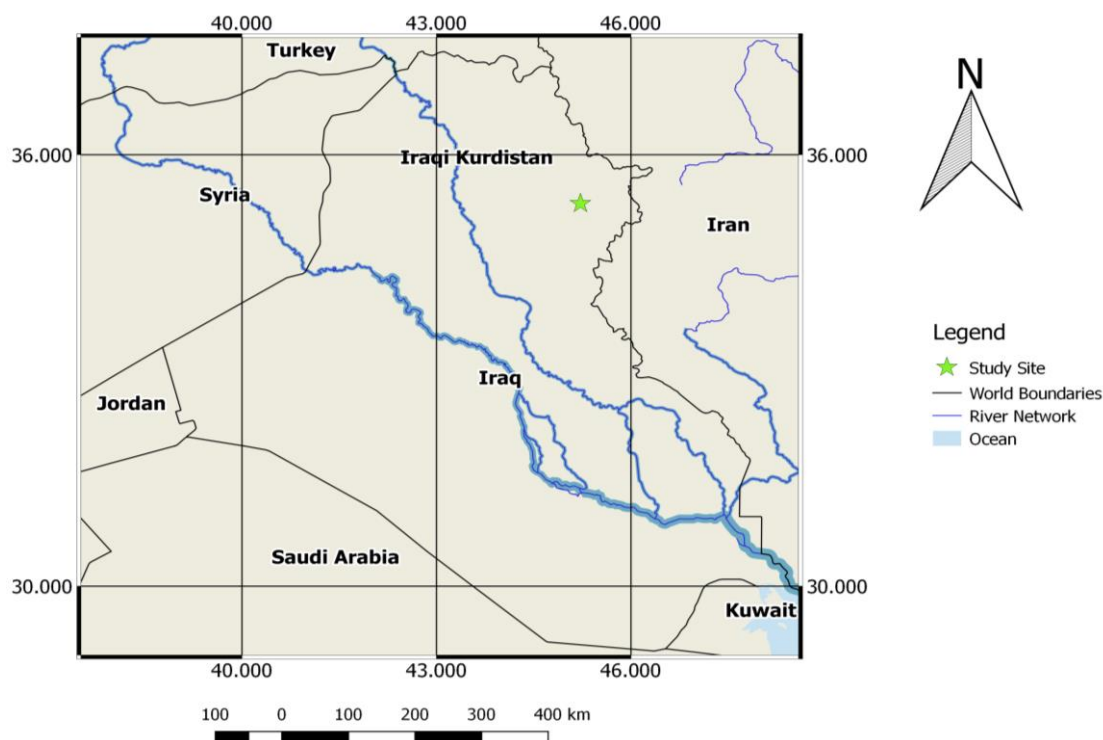


Figure 1. Map of the study site

Table 1. Some meteorological data of the growth season period from July to November, 2016

Growth season period (month)	Precipitation	Air temp. °C		Relative humidity %		ET _o
		AT _{max}	AT _{min}	RH _{max}	RH _{min}	
July	0	43.5	35.4	35.8	22.9	7.9
August	0	45.4	37.2	31.6	20.4	7.6
September	0	38.3	29.8	42	26.2	6.04
October	0.1	31	22.8	45.3	28.5	4.24
November	0.1	23	15.1	46.9	31.2	2.87

Field experiment

The field experiment was laid out as a split plot design with three replicates, the treatments were arranged in which water deficit levels will be in the main plots and the six hybrids were randomly distributed within sub-plots, the plot size was (4 × 10.2) m. Four irrigation treatments were applied during the growing season, which were well irrigation (I₁), deficit irrigation during the vegetative period (I₂), water deficit during reproductive period (I₃), and water deficit during both of vegetative and reproductive growth periods (I₄), water deficit was arranged by breaking one irrigation between each two irrigations. Thermal gravimetric method was used to evaluate accurate availability between field capacity and temporary wilting point to prevent the occurrence of moisture stress in the canopy, so there was no uniformity in the irrigation intervals due to crop requirement and air temperature that directly affected soil moisture content and

reference evapotranspiration (ET_o). The soil available water was determined after calculating the soil water content at field capacity (F.C -33) and wilting point (W.P -1500 kpa) from the models proposed by Karim (1999, *Eqs. 1 and 2*):

$$F.C = 13.28 + 0.397(\text{clay } \%) \quad (\text{Eq.1})$$

$$P.W.P = 4.57 + 0.35(\text{clay } \%) \quad (\text{Eq.2})$$

Where:

F.C = Soil water content at (-33 kpa).

P.W.P = Soil water content at (-1500 kpa)

The irrigation (across the growing season) was applied when the soil moisture content became around 20% to raise the moisture content of the soil to field capacity (30.54%) (*Table 2*).

Table 2. ET_c (amount of applied water) for I₁, I₂, I₃ and I₄ during growing season

Growth stages	Irrigation levels	T _{min}	T _{max}	T _{mean}	ET _o	K _c	ET _c
Initial stage (28 days)	I ₁	35.6	43.63	39.615	8.39	0.7	5.873
	I ₂						
	I ₃						
	I ₄						
Rapid growth stage (46 days)	I ₁	35.62	43.88	39.75	7.62	1.2	9.144
	I ₂						
	I ₃						
	I ₄						
Mid-season stage (45 days)	I ₁	24.72	33.24	28.98	5.65	1.2	6.78
	I ₂						
	I ₃						
	I ₄						
Late-season stage (15 days)	I ₁	17.34	26.13	21.74	4.14	0.6	2.484
	I ₂						
	I ₃						
	I ₄						

The crop was seeded on July 04, 2016, with row spacing of 0.7 m and 0.25 m between plants within a row. In order to prevent the lateral spread of water plots a distance of 2 m between plots was left bare. All of phosphorus fertilizer was applied before sowing time at the rate of 200 kg ha⁻¹, while the nitrogen fertilizer, 200 kg ha⁻¹ as urea in 46% was applied by two doses, at seedling stage and at tasseling. All other agricultural processes were done as required.

The photosynthesis rate (*Pn*) μmol m⁻² s⁻¹, (*E*) mmol m⁻² s⁻¹, and (*gs*) mmol m⁻² s⁻¹, were measured for three different plants, six leaves of each plant were selected from most upper levels of the plants, the physiological parameters were measured at vegetative growth stages (10 leaves) V10 (14 leaves) V14 (tasseling) VT, and reproductive growth stage (around silking) R3 using a portable computerized LCA-4

instrument. In addition the leaf area plant⁻¹ was measured according to the equation {Leaf length (cm) × Leaf width (cm) × 0.74}, the rate of dry matter accumulation and its partitioning to shoot along the season was measured using three different destructive samples (include shoot or plant parts above the soil surface), samples were divided into different parts of the shoot (leaves and stem). Fresh weight of each part was taken and then oven dried till complete dryness at 70 °C and then waited. For calculating the specific leaf area (SLA) Equation 3 was used (Vile et al., 2005):

$$\text{Specific Leaf Area} = \frac{\text{Leaf area/Plant}}{\text{Leaf Weight/Plant}} \text{ (cm/ g)} \quad (\text{Eq.3})$$

Greenhouse experiment

The experiment was carried out in a greenhouse, for evaluating the physiological response of same six maize hybrids to the high temperature stress only, while the irrigation was done as required, in a greenhouse in the College of Agricultural Sciences during the period 01 March to the end of Jun in 2017 with Factorial Complete Randomized Design (CRD) with 3 replications in metal containers (0.7 × 3 × 0.5) m, the used soil was brought from the field experiment of Qlyasan. The greenhouse was divided into two parts by using the insulating section for separating the stress part of experiment from control part that thermally controlled between 25 and 27.5 °C, using Temperature and Humidity data logger, while in the second part temperature stress condition was created at two different growth stages pre-silking and post silking by raising the temperature to 30, 35, 40, and 45 °C gradually from 27.5 °C by raising 2.5 °C every 2 h from 6.00 AM to 8.00 PM in order to determine the physiological response under raised temperatures. Scientific illuminators were used for controlling the illumination inside the greenhouse. Seeds of maize hybrids were sown on 01 of March in metal containers in rows with 0.60 m distance between rows and 0.25 cm within plants. Fertilization and all agricultural processes were performed as required. A portable computerized LCA- 4 instrument was used for measuring the Physiological traits (P_n) $\mu\text{mol m}^{-2} \text{s}^{-1}$, (E) $\text{mmol m}^{-2} \text{s}^{-1}$, and (g_s) $\text{mmol m}^{-2} \text{s}^{-1}$, at the growth stage post-silking for maize hybrids in both conditions. The data from the two experiments were statistically analyzed according to the JMP pro13, XLSTAT 2016, respectively, and the significant differences of the treatment means were compared with an LSD test at < 0.05 (Steel et al., 1997).

Results

Open field experiment

Physiological processes

The process of biomass accumulation is closely related to the performance of physiological processes under the influence of water status and ambient temperature. The significant distinction in the physiological performance of six maize hybrids was noticed under the effect of water deficit stress in different growth stages (Figs. 2, 3, and 4). Increasing photosynthetic rates were observed (Fig. 2) from growth stage (ten leaves) V10 to R₃ under the effect of full irrigation (I₁) and also third level of irrigation (I₃) in vegetative growth only where there was no shortage of water, and Figure 3 refers to a linear decline of transpiration rate with the water deficit levels from I₁ to I₄, while the significant effect of irrigation levels on stomatal conductance was showed in Figure

4, indicating a close relation to soil moisture content that was provided by different irrigation levels.

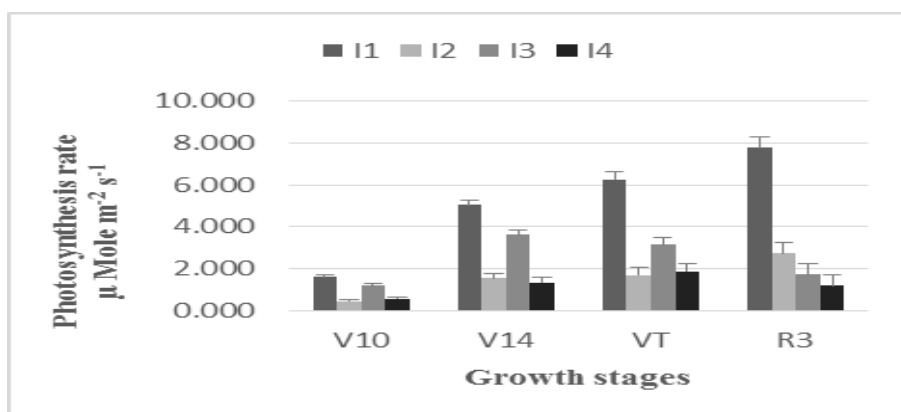


Figure 2. Effect of irrigation levels on the photosynthetic rate (P_n)

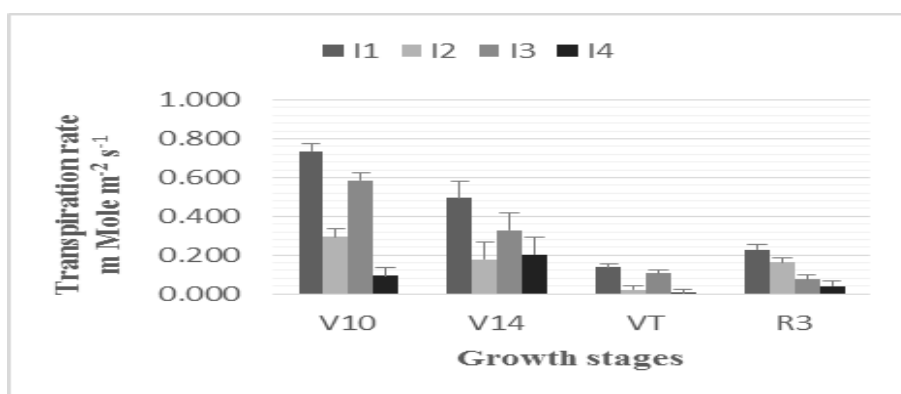


Figure 3. Effect of irrigation levels on the transpiration rate (E)

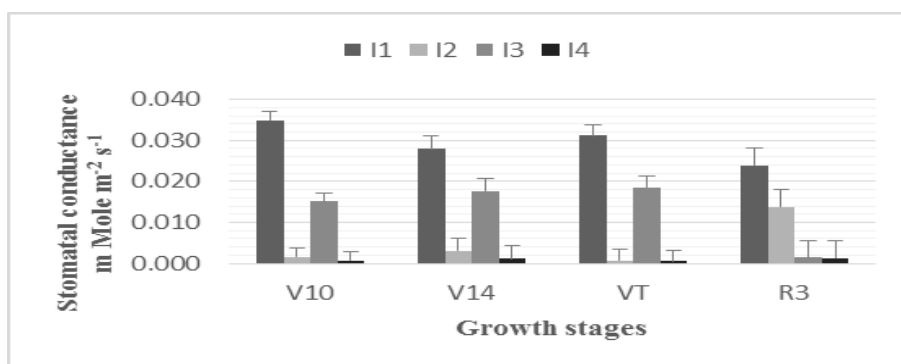


Figure 4. Effect of water deficit levels on the stomatal conductance (g_s)

There were increases in performance of six maize hybrids in photosynthetic rate across different growth stages from early vegetative stages (V10 and V14) to R3 (Fig. 5), while there was a decline in E from vegetative growth V10 to R3 in which plants were at a knee stage (Fig. 6 and 7) and transpiration rates were undertaken with

stomatal conductance of all hybrids with few variations, but the obvious decline was at (tasseling) VT that was considered as a growth stage with greater activity of physiological processes that needs a higher quantity of water. There was a consistent relation between the transpiration rate and stomatal conductance for water balancing attainment.

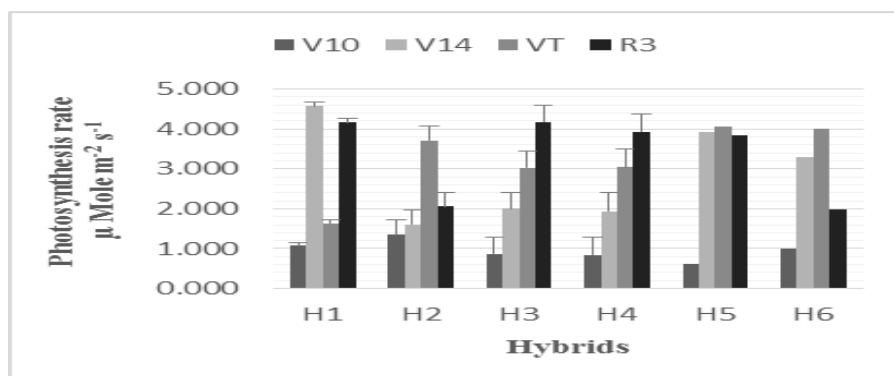


Figure 5. Photosynthetic rate (P_n) of six maize hybrids in different growth stages

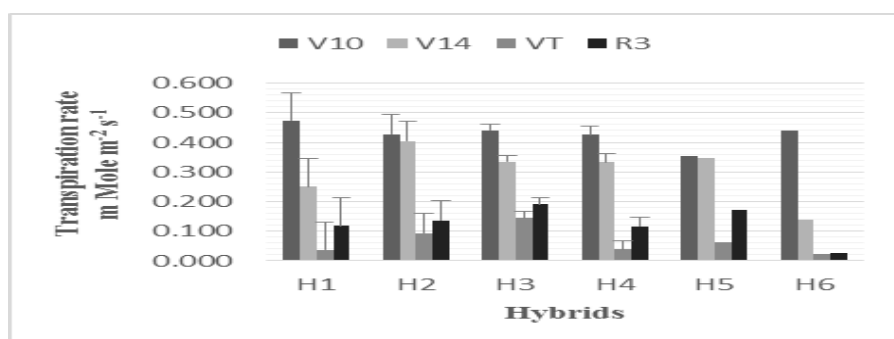


Figure 6. Transpiration rate (E) of six maize hybrids in different growth stages

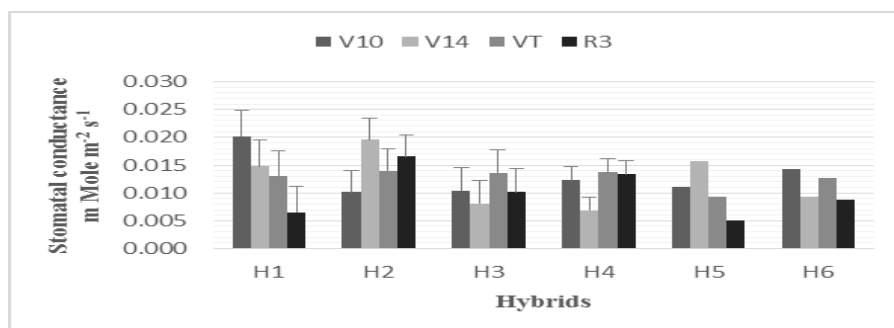


Figure 7. Stomatal conductance (g_s) of maize Hybrids in different growth stages

Specific leaf area (SLA)

The results of specific leaf area which is evidently in relation with leaf area and leaf dry weight are displayed in *Table 3* and *Figure 8*, signalling a significant variation of the impact of irrigation levels. There was a general increase in the SLA at all levels of

water deficit from seedling to the physiological maturity due to plant leaf area development and dry matter accumulation. Plant compatibility between leaf area and the amount of dry matter allocated to the leaves was formed in order to maintain the photosynthetic area under water deficit condition. Maximum SLA was founded to have a significant effect on the 4th level of irrigation from pre-silking stage (31 Aug) to the physiological maturity (180.274, 209.338, 175.899, and 202.567) cm² g⁻¹), while the superiority of third level at dough stage (Oct.16), 189.373 cm² g⁻¹, demonstrated the efficacy of I₃ level during the post silking period, and I₄ level at different stages of the growth season.

Table 3. Effect of water deficit levels in specific leaf area along the growth season

Irrigation treatments	Specific leaf area						
	2-Aug	16-Aug	31-Aug	18-Sep	2-Oct	16-Oct	30-Oct
I ₁	85.344	112.206	137.018	132.140	115.989	102.954	158.718
I ₂	138.269	133.401	134.088	184.854	145.192	165.414	186.696
I ₃	95.010	119.979	141.706	150.237	152.842	189.373	194.988
I ₄	136.350	124.207	180.274	209.338	175.899	171.822	202.567
LSD (P ≤ 0.05)	N.S	N.S	31.852	51.758	22.284	41.256	25.219

The realization of six maize hybrids in SLA was shown significantly in the post-silking period in which the area of photosynthesis represented by leaf area was accomplished according to the tolerance capability of hybrids to perform the effect of water deficit and high temperature in the open field. As shown in *Figure 8* the development of SLA of all hybrids were located during the pre-silking period, showing significant, exceeding of the H₁ (medium 791) hybrid in comparison to other hybrids in the V5 and R3. There was a proportional increase in leaf area and the rate of dry matter accumulation per unit leaf area, the light interception and photosynthesis process is directly related to leaf area during this phase of development. The duration post silking showed more fluctuations in SLA according to genetic differences of six maize hybrids and the severity of water deficit levels. There was significant, exceeding of the medium 791 at R3 with 174.141 cm² g⁻¹, while the Dhqan hybrid showed significant superiority in the later stages of the reproductive period.

Greenhouse experiment

Figures 9 and 10 reveal significant decreasing in photosynthesis as temperature raised from T₁ (30 °C) to T₄ (45 °C), maximum activity of *Pn* was under the effect of T₁ which was 27.5 to 30 °C, and then declined rapidly at (35 °C) T₂, while there was a gradual decline from T₂ to T₃ (40 °C) and the lesser rate of *Pn* was at (45 °C) T₄. Maize hybrid responses to the effect of rising temperature were significant in *Pn* and *E* while stomatal conductance showed non-significant response.

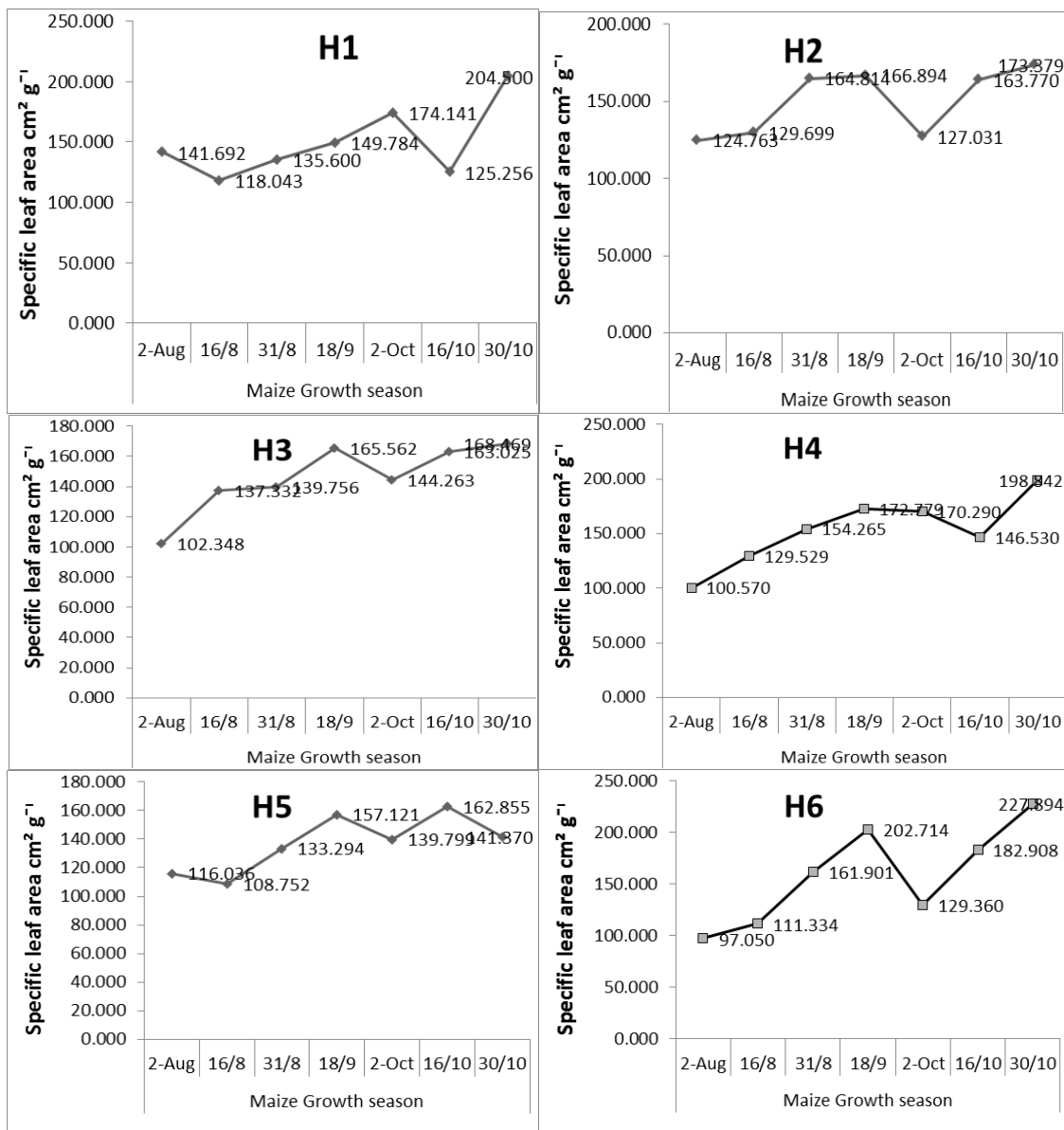


Figure 8. Specific leaf area of six maize hybrids along the growth season

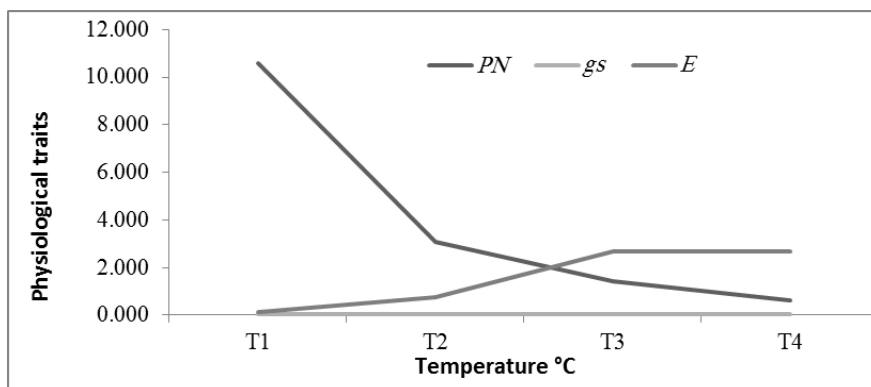


Figure 9. Effect of temperature on physiological traits of maize hybrids in green house

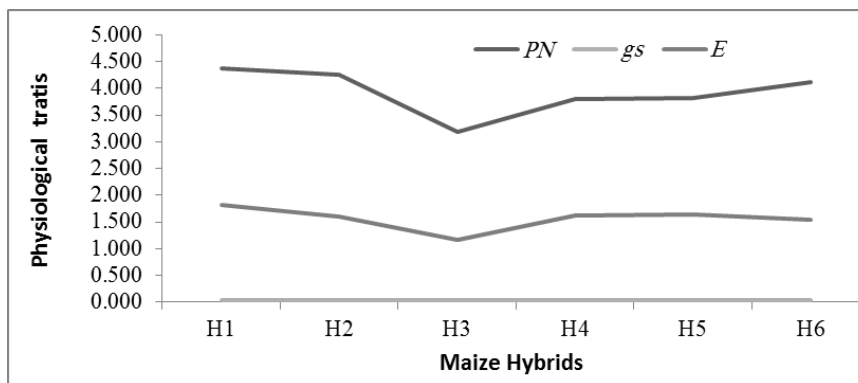


Figure 10. Physiological performances of maize hybrids in green house

The interactions between the effect of temperature levels, and response of maize hybrids demonstrated significant differences in the physiological processes photosynthetic rate, transpiration rate, and stomatal conductance (Figs. 11, 12, and 13), while the highest rate of photosynthetic rate of all hybrids was shown in combination with T₁, the interactions of maize hybrids and T₃ and T₄ showed the maximum rate of transpiration and stomatal conductance.

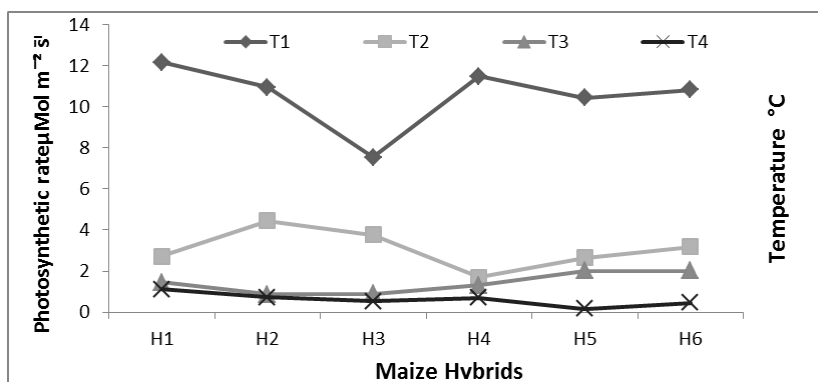


Figure 11. The interactions between maize hybrids and temperature on photosynthetic rate in greenhouse

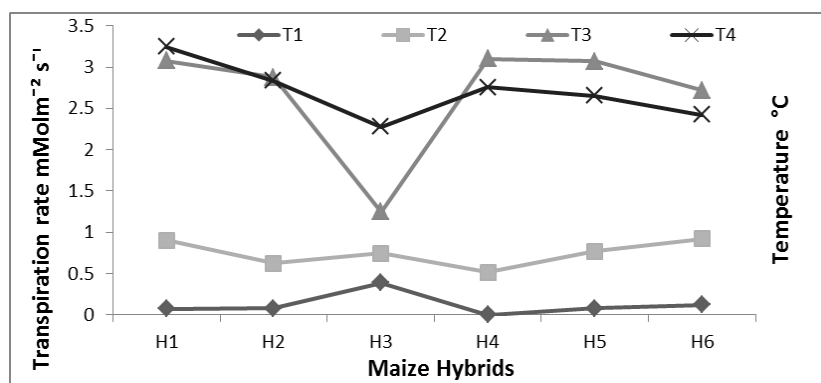


Figure 12. The interactions between maize hybrids and temperature on transpiration rate in the greenhouse

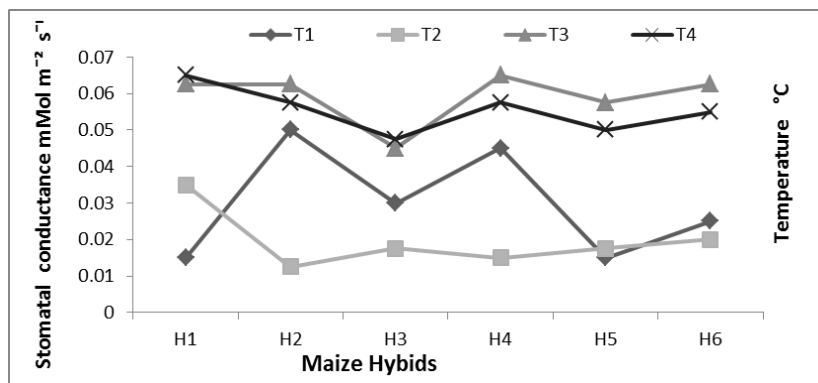
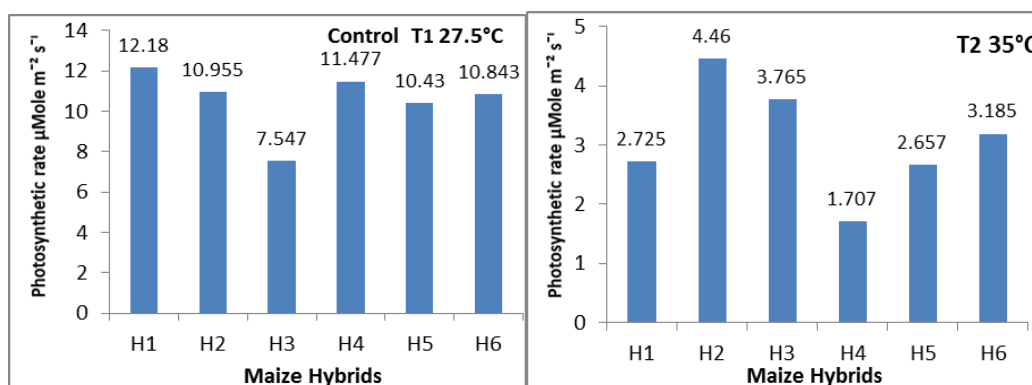


Figure 13. The interactions between maize hybrids and temperature on stomatal conductance in the greenhouse

Comparing the effect of water deficit and heat stress in the field and the single effect of heat stress in greenhouse on the rate of photosynthesis of maize hybrids

The comparison between performance of maize hybrids was achieved at the reproductive growing period because the susceptibility of crops is generally too high to water deficit and heat stress during the reproductive stages of development. The rate of photosynthesis during the growing period around silking (R3) in the greenhouse under control condition (27.5 °C) revealed the highest activity of CO₂ fixation (7.548 – 12.18 μmol m⁻² s⁻¹), displayed by hybrids Medium 791(H₁) and Btaris (H₃) in comparison to stress levels of temperatures T₂ (35 °C), T₃ (40 °C), and T₄ (45 °C) (Fig. 14) the photosynthetic rate of maize hybrids in the open field were higher as well (Fig. 15) in the same growing stage (R3). There was a decline in the *Pn* with rising temperature from 27.5 °C to 35 °C in the greenhouse demonstrated by all hybrids, depressing to lower range (1.707- 4.46 μmol m⁻² s⁻¹) was presented by hybrids Fajir 260 (H₄) and Cantabpis (H₂). There was an additional decline in the rate of photosynthesis with rising temperature from 35 °C to 40 °C and 45 °C.



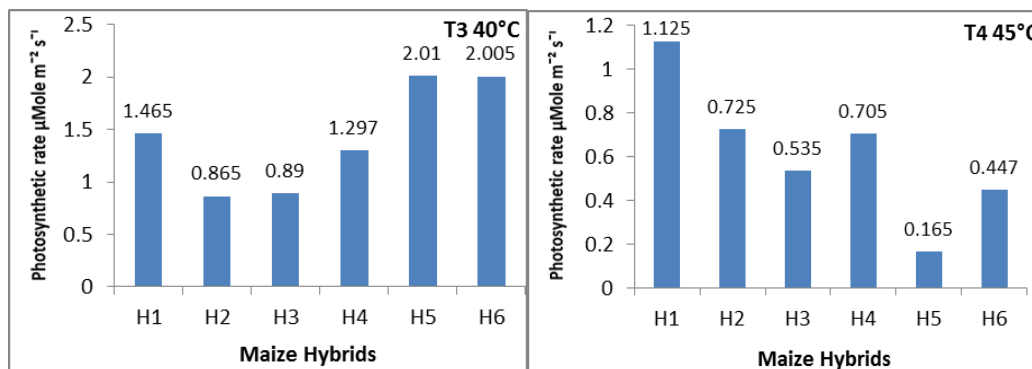


Figure 14. Comparison between *Pn* rate of maize hybrids in the period around silking (R3) under control condition and heat stress treatments T1, T2, and T3 in greenhouse and open field experiments

The rate of *Pn* of all hybrids under the effect of heat stress at 35 °C at a growing stage around silking (R3) showed similarity with *Pn* of all hybrids in the same growing stage in the open field (Fig. 15) in which the air temperature was 38.3 °C (Table 1) and treated with water deficit as well. The similarity between the effect of T₁ (35 °C) on the photosynthetic rate of maize hybrids in the growing stage R3 in the greenhouse and the response of the same hybrids in the same growing stage in the open field may be a clear indication of the effective role of heat stress on physiological process *Pn* in comparison to water deficit. There were differences in the performance of maize hybrids in the greenhouse and the open field due to variation in the tolerance and susceptibility potentials of these hybrids.

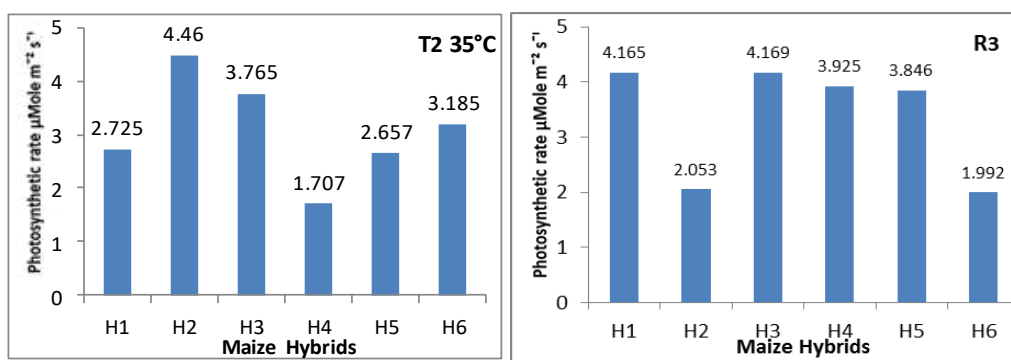


Figure 15. Comparison between *Pn* rate of maize hybrids in the period around silking (R3) under the effect of T2 (35 °C), in the greenhouse and open field experiments

Discussion

Open field experiment

The growth developing from V10 to R3 under the effect of well irrigation and also a third level (I₃) in vegetative growth only (Fig. 2), resulted from an expansion of plant leaf area, while the light interception is directly related to plant leaf area that is considered as increasing in photosynthetic area, which were smaller under the effect of

I₂ and I₄ (Kim et al., 2006; Moosavi, 2012; Lukeba et al., 2013). Maximum rate of *E* was shown under the influence of I₁ and declined at I₂, I₃, and I₄, the higher rates of *E* was in the vegetative stages V10 and V14. These results are in agreement with Ray et al. (2002), Schmidt et al. (2011), Khayatnazhad and Gholamen (2012), Tardieu (2013), Gholipoor et al. (2013) and Liang et al. (2018). The highest rate of (*gs*) was shown under the effect of I₁ in all growth stages and I₃ during the vegetative growth stages with no water deficit, according to the irrigation schedule while the minimum performance of (*gs*) was recorded with I₂ at the pre-tasseling (VT) stage and I₄ across the growth season due to providing a lesser quantity of the crop water requirement under the effect of this level of irrigation (Jeffery et al., 2002; Yu et al., 2016).

Differences in the rate of photosynthesis of maize hybrids in different growth stages may due to the differentiation and plant development that photosynthesis directly affect the rate of dry matter accumulation (Ding et al., 2007; Zhang et al., 2013) especially during the mid age of plants VT around silking toward physiological maturity in which maximum area of plant leaves was produced with exception of the Dihqan hybrid (H₆). This shows a decline in the photosynthetic rate in the later period of post-silking which showed the capability of that hybrid for acclimation to the hot climate at that period, in which the daily air temperature rose to 45 °C that created a condition that can damage photosynthetic pigments and apparatus (Mohammedkhani and Heidari, 2007; Saglam et al., 2014; Ji et al., 2017). The water deficit levels I₂, I₃, and I₄ limited photosynthesis rate of all hybrids, according to the amount of provided water in different growth stages, and also the genetic tolerance of hybrids to the high air temperature that affected gas exchange in these treatments. The greater influence on the physiological traits was with I₂ during the vegetative growth stage and I₃ at reproductive growth and the growth season along with the effect of I₄. The results were in agreement with Del Blanco et al. (2000) and Samarah et al. (2009). However the abiotic stresses, water deficit and heat are usually influenced under the field condition in combination manner, there was a mitigating effect of lower temperature during the beginning of vegetative growth and the later period of the reproductive stage. The effect of the interactions between irrigation level (I₂) and hybrids on the rate of transpiration showed a relative increase in V10 due to lower requirement of plants to water because of smaller size of plants and lower air temperature in that period while there were lower rate of (*E*) at other stages especially at VT in which there was a combination of higher demand of plants to water and higher air temperature. The rate of transpiration was affected by air temperature and physiological resistance of maize hybrids and their adaptation to the low soil water status, similar results were reported by Ray et al. (2002) and Gholipoor et al. (2013). Stomatal conductance (*gs*) showed a lower rate under the influence of the interactions between I₄ level and responses of six maize hybrids, decline in the stomatal conductance and transpiration rate were considered as adaptations to tolerance of plants to dehydration status, in which both stomatal conductance and transpiration rate decrease with a higher water vapor pressure deficit that is resulted under impact of higher air temperature at that period, these results are in line with Bunce (2000), Leakey et al. (2006), Schmidt et al. (2011), Witt et al. (2012) and Kuca and Erekul (2016).

Responses of six maize hybrids to water balance achievement were obviously expressed through the specific leaf area of six maize hybrids in which the leaf characteristics efficiently display the whole plant growth. *Figure 8* displays significant, exceeding of the medium 791 (H₁) hybrid in SLA in comparison to other hybrids on

post silking around R3. The differences in the performance of the hybrid H₁ and other hybrids depend on the genetic capacity for the accomplishment of the consistency between leaf area and potential accumulation of leaf dry matter, smaller leaf dry weight can be compensated by leaf area expansion. While there was general development of SLA of all hybrids during the period of pre-silking, there was a proportional expansion in leaf area and the rate of dry matter accumulation per unit leaf area. The previous studies resulted negative relationships between leaf biomass and photosynthetic rate (Ninemets et al., 2007) which influences the maintenance of plant growth and qualitative aspects of phenology (Vile et al., 2005). The increase in leaf dry weight from the partitioning of more assimilation rate of the leaves resulted in the longevity and maintenance of photosynthetic rate (Westoby et al., 2002). The light interception and photosynthesis process are directly related to leaf area during this stage of growth and development and susceptibility to adverse environmental conditions during one or more phases or stages of phenological development (Hund et al., 2005).

Greenhouse experiment

Since the effects of high temperature and water deficit in the field cannot be studied independently, the responses of maize hybrids to the effect of high temperature were studied in the greenhouse. Physiological responses of six maize hybrids were showing significant variation between the control growth condition and the heat stress condition in the greenhouse because high temperature is considered as a major factor that affect the metabolite activity of plants (Shah et al., 2011; Hatfield and Prueger, 2015). The maximum activity of P_n was under the effect of T₁, and then declined rapidly at T₂ with a 29.2% decrease, but there was gradual decline from T₂ to T₃. There was an increase in the rate of transpiration with increasing the temperature to T₃(40 °C) The plateau state was reached in the rate of E as the temperature continued rising to T₄(45 °C), increasing in transpiration rate may resulted from the necessity of maize plants to cooler conditions under higher temperature to maintain physiological processes but it reached a plateau level from T₃ to T₄ due to water vapor pressure which depend on soil water status and air temperature. These affect the difference between air relative humidity and plant water potential which influence transpiration rate declining (Ray et al., 2002; Taiz and Zeiger, 2006). The direct relationship between P_n and E was shown in response of all maize hybrids except Dihqan hybrid (H₆), while it maintained higher P_n in comparison to Es-SOLITO 635(H₅) but the rate of E was much lower, the potential efficiency of that hybrid may genetically adapted to stress conditions (Leakey et al., 2006; Feng et al., 2014; Obata et al., 2015).

The downhill of the rate of Photosynthesis (P_n) with increasing the effect of heat stress resulted in raising the temperature from the control condition (27.5 °C) to (35 °C) T₁ (40 °C) T₂, and (45 °C) T₃. The maximum rate of CO₂ fixation or photosynthesis displayed by six maize hybrids was under control condition (27.5 °C), which is the optimum extent of temperature for C₄-plant photosynthesis (Steven et al., 2002). The premium rate of P_n under control condition was impaired with the impact of the higher temperature of T₁, T₂, and T₃. The lower average of P_n while the temperature raised to 35 °C demonstrated by all hybrids with discrimination among hybrid responses. There were similar performances of six maize hybrids of photosynthesis averages in the greenhouse and open field during the period around silking (*Fig. 15*). The P_n rate of greenhouse was under heat stress only while, the influence of the combination of water deficit with heat stress was observed in the open field. The results may lead to a more

effective identification of stress factors on the rate of photosynthesis, the effects of heat stress on the metabolic processes and photosynthetic apparatus (Sage and Kubien, 2007). Drought stress allows maintaining of the insufficient growth in plants (Avramova et al., 2015).

Conclusions

The results of the field experiment reveal the direct effect of deficiency of water during the different stages of growth and development of maize. The stress conditions created under the influence of water deficit combined with high temperature more than 40 °C for a long time, predominately during the period of tasseling and silking. A great reduction was generated in the physiological performance, especially photosynthetic rate, which indirectly impact dry matter accumulation and its partitioning of maize, as well the higher rates of *E* was in the vegetative stages V10 and V14. The differences in the physiological performance of the maize hybrids depend on the genetic capacity for the accomplishment of the consistency between leaf area and potential accumulation of leaf dry matter, smaller leaf dry weight can compensate by leaf area expansion. The influence of temperature higher than 35 °C in greenhouse created restriction to the photosynthetic rate of maize hybrids, there were significant decreasing in photosynthesis as temperature raised from 27.5 °C (T₁) to 45 °C (T₄), maximum activity of *Pn* was under the effect of T₁. The relation between *Pn* and *E* was shown in response of all maize hybrids except Dihqan, while it maintained higher *Pn*, the rate of *E* was much lower. The comparison of the effect of temperature as a single factor in the greenhouse and effect of both water deficit and heat stress in the open field revealed greater effect of temperature on photosynthetic rate at reproductive stage R3. Water provided during reproductive stage around silking R3 may mitigate the deleterious effect of high temperature in the field.

REFERENCES

- [1] Allen, D. J., Ort, D. R. (2001): Impact of chilling temperatures on photosynthesis in warm climate plants. – Trends Plant Sci. 6: 36-42.
- [2] Anjum, S. A., Wang, L. C., Farooq, M., Hussain, M., Xue, L. L., Zou, C. M. (2011): Brassinolide application improves the drought tolerance in maize through modulation of enzymatic antioxidants and leaf gas exchange. – Agron. J. & Crop Sci. 197: 177-185.
- [3] Avramova, V., AbdElgawad, H., Zhang, Z., Fotschki, B., Casadevall, R., Vergauwen, L., Knapen, D., Taleisnik, E., Guisez, Y., Asard, H., Beemster, G. T. (2015): Drought Induces Distinct Growth Response, Protection, and Recovery Mechanisms in the Maize Leaf Growth Zone. – Plant Physiology 169:1382–1396.
- [4] Barnabas, B., Jageri, K., Feher, A. (2008): The effect of drought and heat stress on reproductive processes in cereals. – Plant Cell Environ. 31: 11-38.
- [5] Ben-Asher, J., Garcia, A., Hoogenboom, G. (2008): Effect of high temperature on photosynthesis and transpiration of sweet corn (*Zea mays* L. var. rugosa). – Photosynthetica 46(4): 595-603.
- [6] Brandner, S. J. C., Salvucci, M. E. (2002): Sensitivity of Photosynthesis in a C4 Plant, Maize, to Heat Stress. – Plant Physiol. 129: 1773-1780.
- [7] Bunce, A. J. (2000): Responses of stomatal conductance to light, humidity and temperature in winter wheat and barley grown at three concentrations of carbon dioxide in the field. – Glob Change Boil. 4: 371-382.

- [8] Chaves, M. M., Pereira, J. S., Maroco, J., Rodrigues, M. L., Ricardo, C. P. P., Osório, M. L., Carvalho, I., Faria, T., Pinheiro, C. (2002): How plants cope with water stress in the field? Photosynthesis and growth. – *Ann. Bot.* 89: 907-16.
- [9] Dalirie, M., Sharifi, R. S., Farzanea, S. (2010): Evaluation of yield, dry matter accumulation and leaf area index in wheat genotypes as affected by terminal drought stress. – *Not. Bot. Hort. Agrobot. Cluj* 38(1): 182-186.
- [10] Del Blanco, I. A., Rajaram, S., Kronstad, W. E., Reynolds, M. P. (2000): Physiological performance of synthetic hexaploid wheat-derived populations. – *Crop Sci.* 40: 1257-1263.
- [11] Ding, L., Wang, K. J., Jiang, G. M., Liu, M. Z., Gao, L. (2007): Photosynthetic rate and yield formation in different maize hybrids. – *Biol Plantarum.* 51: 165-168.
- [12] Efeoğlu, B. Y., Ekmekçi, N., Çiçek, N. (2009): Physiological responses of three maize cultivars to drought stress and recovery. – *S. Afr. J. Bot.* 75: 34-42.
- [13] Feng, B. Liu, P., Li, G., Dong, S. T., Wang, F. H., Kong, L. A., Zhang, J. W. (2014): Effect of heat stress on the photosynthetic characteristics in flag leaves at the grain-filling stage of different heat-resistant winter wheat varieties. – *Agron. J. & Crop Sci.* 200: 143-155.
- [14] Gholipoor, M., Sinclair, T. R., Raza, M. A. S., Löffler, C., Cooper, M., Messina, C. D. (2013): Maize hybrid variability for transpiration decrease with progressive soil drying. – *Agron. J. & Crop Sci.* 199: 23-29.
- [15] Hatfield, J. L., Prueger, J. H. (2015): Temperature extremes: Effect on plant growth and development. – *Weather and Climate Extremes* 10: 4-10.
- [16] Hund, A., Frascaroli, E., Leipner, J., Jompuk, C., Stamp, P., Fracheboud, Y. (2005): Cold tolerance of the photosynthetic apparatus: pleiotropic relationship between photosynthetic performance and specific leaf area of maize seedlings. – *Molecular Breeding* 16: 321-331.
- [17] Ings, J. A., Mur, L. J., Robson, P. R. H., Bosch, M. (2013): Physiological and growth responses to water deficit in the bioenergy crop *Miscanthus x giganteus*. – *Front Plant Sci.* 4: 00468.
- [18] Jeffery, D., Gesch, R. R., Sinclair, T. R., Allen, L. H., Ray, R. W., Gesch, T. R., Allen, L. (2002): The effect of vapor pressure deficit on maize transpiration response to a drying soil. – *Plant Soil.* 239: 113-121.
- [19] Ji, Y., Zhou, G., Ma, X., Wang, Q., Liu, T. (2017): Variable photosynthetic sensitivity of maize (*Zea mays* L.) to sunlight and temperature during drought development process. – *Plant, Soil and Env.* 63(11): 505-511.
- [20] Karim, T. H. (1999): Models to predict water retention of Iraqi soil. – *J. of the Indian Soc. of Soil Sci.* 47(1): 16-19.
- [21] Khayatnezhad, M., Gholamin, R. (2012): The effect of drought stress on leaf chlorophyll content and stress resistance in maize cultivars (*Zea mays*). – *Afr. J. Microbial. Res.* 6: 2844-2848.
- [22] Kim, S., Sicher, R. C., Bae, H., Gitz, D. C., Baker, J. T., Timlin, J., Reddy, I. (2006): Canopy photosynthesis, evapotranspiration, leaf nitrogen, and transcription profiles of maize in response to CO₂ enrichment. – *Global Change Biol.* 12: 588-600.
- [23] Kuca, Y. O., Erekul, O. (2016): Changes of dry matter, biomass and relative growth rate with different phenological stages of corn. – *Agr. & Agr. Sci. Procedia* 10: 67-75.
- [24] Leakey, A. D., Uribeharrea, B. M., Ainsworth, E. A., Naidu, S. L., Rogers, A., Ort, D. R., Long, S. P. (2006): Photosynthesis, productivity, and yield of maize are not affected by open-air elevation of CO₂ concentration in the absence of drought. – *Plant Physio.* 140: 779-790.
- [25] Liang, Y. P., Gao, Y., Wang, G. S., Si, Z. Y., Shen, X. J., Duan, A. W. (2018): Luxury transpiration of winter wheat and its responses to deficit irrigation in North China Plain. – *Plant Soil Environ.* 64: 361-366.

- [26] Lukeba, J. L., Vumilia, R. K., Nkongolo, K. C. K., Mwabila, M. L., Tsumbu, M. (2013): Growth and leaf area index simulation in maize (*Zea mays* L.) under small-scale farm conditions in a Sub-Saharan African region. – *Am. J. Pl. Sc.* 4: 575-583.
- [27] Mi, N., Cai, F., Zhang, Y., Ji, R., Zhang, S., Wang, Y. (2018): Differential responses of maize yield to drought at vegetative and reproductive stages. – *Plant Soil Environ.* 64(6): 260-267.
- [28] Mohammedkhani, N., Eidari, R. (2007): Effect of water stress on respiration, photosynthetic pigment and water content in two maize cultivars. – *Pak. J. Bot.* 10: 4022-4028.
- [29] Moosavi, S. G. (2012): The effect of water deficit stress and nitrogen fertilizer levels on morphology traits, yield and leaf area index in maize. – *Pak. J. Bot.* 44: 1351-1355.
- [30] Ninemets, N. L., Portsmuth, A., Tena, D., Tobiasi, M., Matesanze, S., Valladares, F. (2007): Do we underestimate the importance of leaf size in plant economics disproportional scaling of support costs within the spectrum of leaf physiognomy. – *Annals of Botany* 100: 283-303.
- [31] Obata, T., Witt, S., Lisek, J., Palacios-Rojas, N., Florez-Sarasa, I., Yousfi, S., Araus, J. L., Cairns, J. E., Fernie, A. R. (2015): Metabolite profiles of maize leaves in drought, heat, and combined stress field trials reveal the relationship between metabolism and grain yield. – *Plant Physio.* 169: 2665-2683.
- [32] Prasad, P. V. V., Staggenborg, S. A., Ristic, Z. (2008): Impacts of Drought and/or Heat Stress on Physiological, Developmental, Growth, and Yield Processes of Crop Plants. – ASA, CSSA, SSSA, Madison, WI.
- [33] Ray, J. D., Gesch, R. W., Sinclair, T. R. Allen, L. H. (2002): The effect of vapor pressure deficit on maize transpiration response to a drying soil. – *Plant Soil.* 239: 113-121.
- [34] Saglam, A., Kadioglu, A., Demralay, M., Terzi. R. (2014): Leaf rolling reduces photosynthetic loss in maize under severe drought. – *Acta Bot.* 73: 315-332.
- [35] Samarah, N. H., Alqudah, A. M., Amayreh, J. A., McAndrews, G. M. (2009): The effect of late-terminal drought stress on yield components of four barley cultivars. – *Agron. J. Crop Sci.* 195: 427-441.
- [36] Schmidt, J. J., Blankenship, E. E., Lindquist, J. L. (2011): Corn and Velvetleaf (*Abutilon theophrasti*) Transpiration in Response to Drying Soil. – *Weed Sci.* 59: 50-54.
- [37] Shah, F., Huang, J., Cui, K., Nie, L., Shah, T., Chen, C., Wang, K. (2011): Impact of high-temperature stress on rice plant and its traits related to tolerance. – *J. Agr Sci.* 10: 1-12.
- [38] Steel, R. G. D., Torrie, J. H., Dickey, D. A. (1997): Principles and Procedures of Statistics: A biometrical approach. 3rd ed. – McGraw Hill Book, Co. Inc., New York, pp. 400-428.
- [39] Steven, J. C., Michael, E. S. (2002): Sensitivity of photosynthesis in a C4 plant, maize, to heat stress. – *Plant Physiology, American Society of Plant Biologists* 129: 1773-1780.
- [40] Taiz, L., Zeiger, E. (2006): *Plant Physiology*. 4th ed. – Sinauer Associates, Inc., Sunderland, MA.
- [41] Tardieu, F. (2013): Plant response to environmental conditions: assessing potential production, water demand, and negative effects of water deficit. – *Front Phys* 18: 00017.
- [42] Tester, M., Bacic, M. (2005): Abiotic stress tolerance in grasses. From model plants to crop plants. – *Plant Physiol* 137: 791-793.
- [43] Vile, D., Garnier, E., Shipley, B., Laurent, G., Navas, M-L, Roumet C, Lavorel S, Díaz, S., Hodgson, J. G., Lloret, F., Midgley, G. F., Poorter, H., Rutherford, M., C., Wilson, P. J., Wright, I. J. (2005): Specific leaf area and dry matter content estimate thickness in laminar leaves. – *Annals of Botany* 96: 1129-1136.
- [44] Westoby, M., Falster, D. S., Moles, A. T., Vesk, P. A., Wright, I. J. (2002): Plant ecological strategies: some leading dimensions of variation between species. – *Annual Review of Ecology and Systematics* 33: 125-159.

- [45] Witta, S., Galiciab, L., Liseca, J., Cairnsc, J., Tiessend, A., Arause, J. L. Palacios-Rojasb, N., Ferniea, A. R. (2012): Metabolic and phenotypic responses of greenhouse-grown maize hybrids to experimentally controlled drought stress. – *Mol Plant* 5: 401-417.
- [46] Yang, J. C., Zhang, J. H. (2006): Grain filling of cereals under soil drying. – *New Phytol.* 169: 223-236.
- [47] Yu, C. L., Hui, D., Deng, Q., Wang, J., Reddy, K. C., Denni, S. (2016): Responses of corn physiology and yield to six agricultural practice over three years in middle Tennessee. – *Scientific Reports* 6: 27504.
- [48] Zhang, X., Huang, G., Zhao, Q. (2013): Differences in maize physiological characteristics, nitrogen accumulation, and yield under different cropping patterns and nitrogen levels. – *Chil. J. Agr. Res.* 74: 326-332.

USE OF DIFFERENT SPECTRAL VEGETATION INDICES TO DETERMINE THE PRESENCE OF MANTLED HOWLER MONKEYS (*ALOUATTA PALLIATA* G.) ON COCOA AGROSYSTEMS (*THEOBROMA CACAO* L.)

SÁNCHEZ-DÍAZ, B.¹ – MATA-ZAYAS, E.¹ – GAMA, L.¹ – RULLAN-SILVA, C.¹ – VIDAL-GARCÍA, F.²
– RINCÓN-RAMÍREZ, J.^{3*}

¹*Universidad Juárez Autónoma de Tabasco, DACBiol, Villahermosa, Tabasco, México*

²*Instituto de Ecología, Xalapa, Veracruz, México*

³*Colegio de Postgraduados, Campus Tabasco, H. Cárdenas, Tabasco, México*

*Corresponding author
e-mail: jrincon@colpos.mx

(Received 12th Oct 2018; accepted 5th Dec 2018)

Abstract. It is important to search for new strategies for biodiversity conservation. Recently, remote sensing has proven its usefulness due to the availability of presence and absence data of select species that can be modeled using different statistical designs. This research gathers data regarding the presence and absence of howler monkeys based on modeling studies, validated by sampling and field surveys. This kind of approach provides useful information that supports decision makers in their conservation efforts. The objective of this research is to identify the most robust spectral vegetation index through statistical analysis using mantled howlers (*Alouatta palliata* G.) as a model species, and different vegetation indices derived from satellite images. We compared certain phenological characteristics of the vegetation (leaf area index, biomass and high chlorophyll content of leaves) in the canopy of cocoa agrosystems (*Theobroma cacao* L.) both with and without howler monkey presence in Tabasco, Mexico. Data on the presence and absence of the species was obtained from agrosystems. Landsat-5 TM images of the agrosystem regions were used to calculate various vegetation indices. Statistical analysis software (SAS) was used to calculate statistically significant differences. A complete random design and two statistical models were applied – standard distances and Student's t-test – to compare the accuracy of vegetation indices. The Ratio Vegetation Index (RVI) had the greatest spectral separability and statistically significant difference on sites with and without the presence of the species in cocoa agrosystems. These indices could be taken as useful variables to predict habitats potentially suitable for the species in support of decision makers, and thus apply conservation efforts for primates.

Keywords: *biodiversity conservation, remote sensing, RVI, satellite images, vegetation phenology*

Introduction

The most promising applications of remote sensing in ecology refer to the fields of climate change, biodiversity conservation and ecosystem dynamics (Benayas, 1993; Turner et al., 2003; Kerr and Ostrovsky, 2003). In that sense, the ecological indicators frequently monitored are the changes in land cover, land use, ecological disturbance and vegetation phenology. Thus, remote sensing is one of the most powerful methods to map abiotic and biotic components of ecosystems (Wang et al., 2008; Rocchini et al., 2013; Avtar et al., 2016). Currently, climate change has a significant effect on all ecosystems leading to a loss of biodiversity regardless of direct human influence (Willis, 2015, Loreto et al., 2017). In this sense, the modeling plays an important role in alerting decision-makers to possible future risks (Bellard et al., 2012). Therefore, using remote sensing technologies helps us understand the possible trends of the

impacts associated with climate change in space and time (Workie and Debella, 2018), and thus, support the development of strategies aiming to reduce those impacts on biodiversity. For example, one environmental characteristic to measure the impacts on vegetation is the plant phenology as a sensitive indicator of climate change and a direct measure of plant vitality (Zhao et al., 2013; Corbane et al., 2015). However, not all phenological changes are associated with climate change (Leong and Roderick, 2015), these could also be caused by pests or fire, among others. The phenological changes of plants can be detected through remote sensing by changes in vegetation spectral index values, to determine the availability of food for some mammals.

Undoubtedly, remote sensing technology is the only economically viable option to provide large-scale, long-term, standardized, full-coverage, high-resolution biodiversity observations (Turner et al., 2003; Skidmore et al., 2015; Lausch et al., 2015; Guo and Liu, 2018). Spectral vegetation indices are metrics derived from remote sensing that can be used to predict potential sites of species presence. These indices are useful to characterize and associate differences between vegetation types with certain phenological characteristics of the canopy, mainly related to vegetation cover parameters such as density, leaf area index and chlorophyll activity (Turner et al., 2015; Skidmore et al., 2015). Spectral reflectance varies with wavelength, healthy vegetation reflects more at certain lengths, especially the Red band (R), and Near Infrared (NIR). When vegetation suffers some kind of stress, such as the presence of pests or drought, the amount of water decreases in the cells. Since the Red band shows active chlorophyll absorption and NIR bands provide information on active chlorophyll reflectance, this difference in the spectral response makes it relatively easy to separate healthy vegetation from other coverings (Jensen, 2007; Genc et al., 2008; Chuvieco, 2016). These can also be used to identify certain changes on healthy vegetation behind cover or to detect differences associated with the presence of some mammal species. In addition, vegetation indices by spectral separability have been widely used in the identification of crops such as oil palm (Anaya and Valencia, 2013; Giraldo, 2017). Remote sensing does not impact biodiversity in a harmful way (Becerra, 2007). Some studies have used satellite images to study species occurrence, such as flamingo populations off Nalabana Island at Chilika Lake, India (Sasamal et al., 2008), emperor penguins on the continental coast of Antarctica (Fretwell et al., 2012), whale pathways through the New Gulf of the Valdes Peninsula in Argentina (Fretwell et al., 2014), gnus, zebras and gazelles in the East of the African Savannah (Yang et al., 2014; Xue et al., 2017), polar bears in the Canadian Arctic (Stapleton et al., 2014), elephant seals in the southern Pacific Ocean (McMahon et al., 2014) and albatrosses in the Bird Island to the west of mainland South Georgia (Fretwell et al., 2017). In this study, satellite images were used to determine the presence of an arboreal species, particularly ones that can be found in significantly transformed habitats, such as primates in cocoa agrosystems. Since the identification of animals in the canopy is difficult due to the resolution of available images, vegetation spectral indices can be used as an indirect tool to detect the monkeys' presence.

Mexico outputs 1.1% of world global cocoa production; and the state of Tabasco contributes 70% of the national production (Córdova-Avalos et al., 2008; Morales et al., 2012). In Tabasco, most of the cocoa plantations are located on Comalcalco, these are between 30 to 40 years old, with an average yield of 94.26 kg/ha (De La Cruz-Landero et al., 2015). The producers that live on their farms in these agrosystems employ family labor, so local knowledge can be valuable to obtain information about

species presence and abundance (Anadón et al., 2009). Mammals such as the mantled howler monkey (*A. palliata*) is one of the few species that inhabit these cocoa farms planted more than 40 years ago (Muñoz et al., 2006; Sánchez-Gutiérrez et al., 2016).

In southeast México, the mantled howler monkey (*A. palliata*) is a species with populations in danger of extinction due to habitat loss, according to Federal Law (Sernapam NOM-059; Jasso-Del Toro et al., 2016). Moreover, the red list of the International Union for the Conservation of Nature (IUCN) considers *A. palliata mexicana* as Critically Endangered. Today, some of these howler monkey populations live in fragmented forests, agrosystems, ecotourism sites and other modified landscapes, being valuable populations for conservation studies (Garber et al., 2015). Due to the change of their original habitats, this species is adapting to exploit small fragments of habitats such as coffee and cocoa agrosystems (Arroyo-Rodríguez and Días, 2010). In Tabasco, Mexico, some studies have reported the presence of howler monkeys in cocoa agrosystems (Vidal-García and Serio-Silva, 2011; Valenzuela-Córdova et al., 2015; Pozo-Montuy and Serio-Silva, 2006; Muñoz et al., 2006).

Howler monkeys consume a diet based on young leaves (suckers) and flowers most of the year, when there is shortage of fruits or seeds (Chaves and Bicca-Marques, 2016). Thus, their displacement during the different seasons of the year is attributed to vegetation phenology, that determines their food availability (Pozo-Montuy and Serio-Silva, 2006; Yiming, 2006). The fact that these monkeys had to adapt to anthropogenic disruption, which lead to the fragmentation and loss of their habitats, and negative effects on vegetation, has important implications regarding their conservation (Pyritz et al., 2010).

The objective of this research was to identify the most robust spectral vegetation index, associating certain phenological characteristics of the vegetation (leaf area index, biomass and high chlorophyll content of leaves), to determine the presence of mantled howler monkeys (*A. palliata*) in the canopy of trees in cocoa agrosystems (*T. cacao*) in Tabasco, Mexico.

Material and methods

Study area

This study was carried out in three different cocoa agrosystems (*Figure 1*), in the town of Comalcalco in the State of Tabasco, Mexico. This is an area of approximately 72,319 ha of which 11,055 ha are cocoa plantations (15.2%) (INEGI, 2012).

Set of satellite data used

A set of available images were reviewed, we looked for non-cloudy images, outside of cocoa pruning period and collected data on monkey presence every time on the same date (or as close as possible). As a result two Landsat-5 TM satellite images were chosen. These images were used on each study site to look for differences among vegetation indices associated with the presence of howler monkeys (*Table 1*). They were taken from the same season, since data from different seasons generated errors related to differences in reflectance values for the same vegetation type due to phenology.

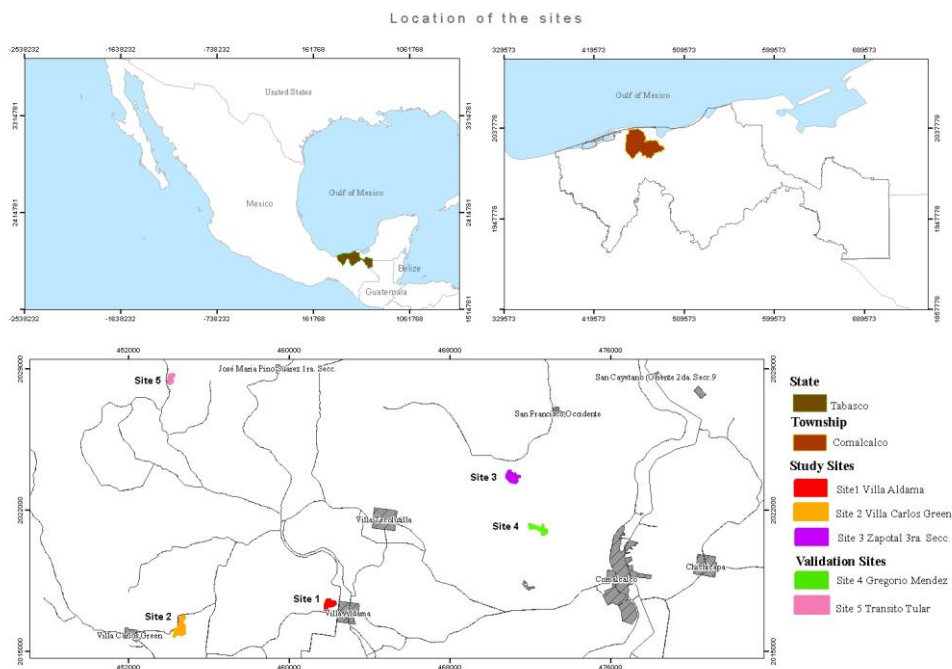


Figure 1. Cocoa agrosystems used as study sites

Table 1. Satellite data used in the study

No.	Satellite	Sensor	Date of Acquisition	Path/Row	Source
1	Landsat-5	TM	02-21-1997	22-47	https://earthexplorer.usgs.gov/
2	Landsat-5	TM	02-28-2011	22-47	https://earthexplorer.usgs.gov/

Presence and absence collection data

A sample of proportions was used to ensure the largest sample size, it is considered as the maximum variance, with a precision of ≤ 0.05 and a reliability of 95%. For security purposes, 9% was added to the sample size obtained. To select the study sites, a survey was sent to 38 cocoa producers during February 2017, along with a compilation of presence and absence records of howler monkeys. Five study sites were selected (cocoa agrosystems) (Figure 2).

To have an estimate of the population structure, data of presence was recorded by direct observation. For each group, information was collected on the number of individuals, sex composition and type of substrate used (tree species).

The Laboratory of Landscape Ecology and Global Change at Juarez Autonomous University of Tabasco has records of howler monkeys on this agrosystems since 2001. On this investigation three different cocoa agrosystems were chosen as study sites: Site 1 (absence-presence) based on the survey, aimed to find in which site the specie was absent in 1997 and present in 2011, Site 2 (Presence-Presence) based on data from personal communication conducted by Valenzuela in June 2016, in which they report that the species has always been present, and Site 3 (Absence-Absence) from the article that published a model made by Vidal-García and Serio-Silva (2011) in which they

report that according to the results of the model, the species has never been present on that site (*Table 2, Figure 3*) (CNES, 2012).



Figure 2. Monkeys in cocoa agrosystems

Table 2. Comparative data within the study sites

Study Sites	Location	Coordinates (UTM)		Remark	Source
		X	Y		
Site 1	Villa Aldama	461830	2017193	Absence-Presence	Survey conducted, 2017 Valenzuela, personal communication, June 2016
Site 2	Villa Carlos G.	454416	2016030	Presence-Presence	Vidal-García and Serio-Silva, 2011
Site 3	Zapotal 3ra. S.	471172	2023367	Absence-Absence	

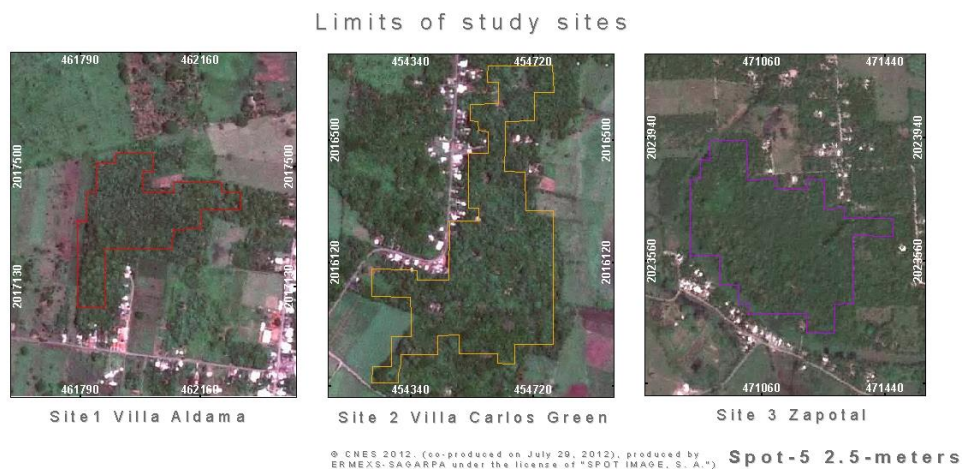


Figure 3. Maps of the study sites

To validate the results, two other cocoa agrosystems were selected: Site 4 (absence-absence) (Vidal-García and Serio-Silva, 2011), and Site 5 (presence-presence) (Valenzuela-Córdova et al., 2015) (Table 3, Figure 4) (CNES, 2012).

Table 3. Comparative data within the validation sites

Study Sites	Location	Coordinates (UTM)		Remark	Source
		X	Y		
Site 4	Gregorio Méndez	472050	2021184	Absence-Absence	Vidal-García and Serio-Silva, 2011
Site 5	Transito Tular	454053	2028453	Presence-Presence	Valenzuela-Córdova et al., 2015

Limits of validation sites



© CNES 2012. (co-produced on July 29, 2012), produced by ERMEXS-SAGARPA under the license of "SPOT IMAGE, S. A." **Spot-5 2.5-meters**

Figure 4. Site maps selected for validation

Pre-processing of satellite images

Images require the correction of possible radiometric and atmospheric distortions in the radiance values that are register by the sensor surveying the earth surface. For geometrical correction, the images were orthorectified using control points for the Landsat-5 TM scenes, using orthophotos at scale 1:15000, through software ArcGIS v 9.2. Radiometric and atmospheric corrections were made with the Idrisi TerrSet software.

Spectral vegetation indices

Nine vegetation indices were calculated for the multispectral images processed. The indices described below were selected based on literature reports that associate them with vegetation characterization.

Normalized Difference Vegetation Index (NDVI)

Normalized Difference Vegetation Index (*Equation 1*) was introduced by Rouse et al. (1974). The combination of its normalized difference formulation and the use of higher chlorophyll absorption and reflection regions make it robust in a wide range of conditions. It is highly correlated to the leaf area index (IAF).

$$NDVI = (NIR - R) / (NIR + R) \quad (\text{Eq.1})$$

Ratio Vegetation Index (RVI)

Ratio Vegetation Index (*Equation 2*) was suggested by Jordan (1969). The ratio of highest reflectivity by absorption of chlorophyll makes it easy to understand and is effective in a wide range of conditions. It has a high correlation with the Leaf Area Index, biomass and high chlorophyll content of leaves.

$$RVI = NIR / R \quad (\text{Eq.2})$$

Soil-Adjusted Vegetation Index (SAVI)

Soil-Adjusted Vegetation Index (*Equations 3*) was proposed by Huete (1988). Minimizes variations induced by the brightness of the soil. L is a correction factor ranging from 0 (for very high vegetation cover) to 1 (for very low vegetation cover). The most commonly used value is L = 0.5, which is for intermediate vegetation cover. It is a modification of the NDVI to explain areas with low vegetation cover (i.e. <40%).

$$SAVI = (NIR - R) / (NIR + R + L) * (1 + L) \quad (\text{Eq.3})$$

Enhanced Vegetation Index (EVI)

Enhanced Vegetation Index (*Equation 4*) was developed by Huete et al. (2002). It is an improvement on NDVI to better take into account soil background and the effects of atmospheric aerosols. The coefficients adopted in the MODIS-EVI algorithm are: L = 1, C1 = 6, C2 = 7.5. EVI requires a blue band and is sensitive to variations in blue band reflection, which limits the consistency of this index through different sensors.

$$EVI = 2.5 * (NIR - R) / (NIR + C1 * R - C2 * B * L) \quad (\text{Eq.4})$$

Second Modified Soil Adjusted Vegetation Index (MSAVI2)

Second Modified Soil Adjusted Vegetation Index (*Equation 5*) was suggested by Qi et al. (1994). Particularly important for areas that have different brightness coefficients of soil. Eliminates the need for user specification of L.

$$MSAVI2 = [2 * NIR + 1 - ((2 * NIR + 1)^2 - 8 * (NIR - R))^{1/2}] / 2 \quad (\text{Eq.5})$$

Transformed Vegetation Index (TVI)

Transformed Vegetation Index (*Equation 6*) was proposed by Deering et al. (1975). This index is designed to eliminate NDVI negative values and stabilize variance.

$$TVI = [\sqrt{NIR - R/NIR + R}] + 0.5 \quad (\text{Eq.6})$$

Perpendicular Vegetation Index (PVI)

Perpendicular Vegetation Index (*Equation 7*) was suggested by Richardson and Wiegand (1977). It uses the perpendicular distance of each pixel to the ground line. Whether the pixel corresponds to soil or vegetation depends on the distance of each pixel from the ground line. By taking into account the reflectivity of the soil, it isolates the information provided by vegetation.

$$PVI = [NIR - a * R - b] / [\sqrt{1 + a^2}] \quad (\text{Eq.7})$$

Modified Soil Adjusted Vegetation Index (MSAVI1)

Modified Soil Adjusted Vegetation Index (*Equation 8*) was suggested by Qi et al. (1994). The vegetation estimate uncertainty is reduced from +2.5% (SAVI) to +1.6% (MSAVI1). It is similar to WdVI in reducing soil noise, but its vegetation index values are higher.

$$MSAVI1 = [NIR - R / NIR + R + L] / (1 + L) \quad (\text{Eq.8})$$

Ashburn Vegetation Index (AVI)

Ashburn Vegetation Index (*Equation 9*) was proposed by Ashburn (1978). A strong influence of the underlying surface and atmosphere. Soil areas are well visible. Is computed following this equation:

$$AVI = 2 * NIR - R \quad (\text{Eq.9})$$

Statistical analysis of vegetation indices

A completely randomized design was used for each of the three study sites, with ten repetitions per vegetation index. The data was analyzed using PROC GLM from SAS. For the analysis of vegetation indices, NDVI, RVI, EVI, TVI, PVI, AVI, SAVI, MSAVI1, and MSAVI2 to determine significant differences between the indices. The multiple comparisons of treatment means were performed by Tukey Test ($\alpha = 0.05$).

Spectral separability analysis

The standard distance was applied to detect changes in vegetation (Kaufman and Remer, 1994) in order to identify the vegetation index with greater spectral separability in relation to the presence or absence of *A. palliata* in cocoa agrosystems (*Equation 10*).

$$M = (\mu_a - \mu_b) / (\sigma_a + \sigma_b) \quad (\text{Eq.10})$$

μ_a, μ_b → Sample means for the presence (a) and absence (b) categories.

σ_a, σ_b → Standard deviation of samples for classes a and b.

If the value of M is greater than one, it indicates good separability.

The study compared the three sites: Site 1 (Absence-Presence), Site 2 (Presence-Presence), and Site 3 (Absence-Absence), in the whole time period between the dates of the satellite images (02-21-1997 and 02-28-2011) recorded by Landsat-5 TM.

Data analysis for independent mean comparison

Parametric statistical tests were carried out to establish significant differences between the values of each index in cocoa agrosystems. Student's T-test was applied for two independent samples.

In this case, two hypotheses were raised:

- H0: There is no significant difference between the vegetation index values for each cocoa agrosystem, so all groups are equal and do not differ from each other.
- H1: There are significant differences between the vegetation index values for each cocoa agrosystem.

The significance level is 5%, i.e. for any probability value (p-value) less than or equal to 0.05 means statistically significant differences. However, if it is greater than 0.05, they are statistically equal.

Validation

A survey with cocoa producers was conducted to validate presence-absence of howler monkeys during the time period of our study (1997 and 2011). We corroborated whether statistically obtaining significant differences in the vegetation indices associated with the presence of howler monkeys in cocoa agrosystems have been due to anthropogenic or natural activities, such as fires, pests or pruning of cocoa.

Index statistics with better spectral separability in the study sites

Records of *A. palliata* were collected to observe presence of the species according to the values obtained from the RVI. There was no land use change at the study sites, so another ten images of Landsat-8 OLI / TIRS were used to complete the seasons of the year for the vegetation phenology analysis (Table 4), From February to April there were dry periods, it was rainy from May to October and, winter storms were detected from November to January. The ArcGis v 9.2 software was used to calculate the maximum and minimum value of the RVI index for each study site by season.

Table 4. Satellite data used to calculate RVI index values in the study sites

No.	Satellite	Sensor	Date of Acquisition	Path/Row	Source
1	Landsat-8	OLI/TIRS	25-01-2016	22-47	https://earthexplorer.usgs.gov/
2	Landsat-8	OLI/TIRS	28-02-2017	22-47	https://earthexplorer.usgs.gov/
3	Landsat-8	OLI/TIRS	08-03-2014	22-47	https://earthexplorer.usgs.gov/
4	Landsat-8	OLI/TIRS	01-04-2017	22-47	https://earthexplorer.usgs.gov/
5	Landsat-8	OLI/TIRS	19-05-2017	22-47	https://earthexplorer.usgs.gov/
6	Landsat-8	OLI/TIRS	25-06-2013	22-47	https://earthexplorer.usgs.gov/
7	Landsat-8	OLI/TIRS	03-07-2016	22-47	https://earthexplorer.usgs.gov/
8	Landsat-8	OLI/TIRS	07-08-2017	22-47	https://earthexplorer.usgs.gov/
9	Landsat-8	OLI/TIRS	03-09-2015	22-47	https://earthexplorer.usgs.gov/
10	Landsat-8	OLI/TIRS	24-12-2015	22-47	https://earthexplorer.usgs.gov/

Results

Description of the study sites and population structure of mantled howler monkeys

From the 38 surveys carried out on cocoa producers, 64% were sites of absence and only 36% recorded the presence of the species. 100% of producers have lived in their cocoa farms for more than 40 years. The owners of the sites with record of absence mentioned that species had never been present. The owners of the sites with record of presence said that species had been seen in the past for more than 30 years in their ranches, this is due to the fact that in the last 50 years 90% of their original habitats have been lost (Pozo-Montuy et al., 2015), and the monkeys took refuge in the cocoa agrosystems. In addition, they pointed out that as long as they are the owners of the farms, they will continue to grow cocoa. However, they warned that new generations could make a change in land use, in addition, because of climate variability, it is expected that a large amount of land suitable for cultivation will be lost due to floods and droughts (Saldarriaga, 2016). Local people attributed the presence of howler monkeys in their ranch to the diversity of fruit trees of which they eat, such as: zapote (*Pouteria sapota*), orange (*Citrus sinensis*), mango (*Mangifera indica*), chestnut (*Artocarpus altilis*), and nance (*Byrsonima crassifolia*), among others, as well as trees that monkeys use as a place of refuge, like: erythrina (*Erythrina poeppigiana*), palo Mulato (*Bursera simaruba*) and rain tree (*Samanea saman*), since they prefer to consume young leaves and ripe fruits due to their protein concentration (Anaya-Lira et al., 2013). However, they mentioned that howler monkeys do not cause any damage to their plantations since monkeys do not eat cocoa. In addition, on the survey sites there are also forest trees, such as: cedro (*Cedrela odorata*), macuilis (*Tabebuia rosea*), and caoba (*Swietenia macrophylla*), among others, that are useful for both people and monkeys (Sanchez-Gutiérrez et al., 2016). Through the survey, the producers stated that between 1997 and 2011 no deforestation has occurred on their land, only pruning takes place at the beginning of the rainy season in May (Matey et al., 2013), so there was no ongoing anthropogenic alteration in the images used from February. They also reported, that they have not had any type of alteration in their vegetation due to any plague or fire. However, climate variability is a proven fact, so they will have different effects in each geographical area or study site (Gallegos, 2017), as the phenology of the plants during flowering is strongly determined by climatic parameters such as temperature and precipitation (Adjalo et al., 2012), which causes variability in different season of the year. In total, 50 individuals of monkeys were recorded among three communities of Comalcalco, in cocoa agrosystems between 30 and 40 years of age (Table 5).

Statistical analysis of vegetation indices

TVI, AVI, PVI and RVI indices are ungrouped because they have statistically significant differences. On the other hand, on "C" group, SAVI and MSAVI1 did not show statistically significant differences between them, and the same is true for group "E" with NDVI, MSAVI2 and EVI. Therefore, an index of each group was chosen: NDVI and SAVI since both are highly correlated with changes in vegetation and leaf area index (Ali et al., 2013) (Table 6).

Table 5. Number of individuals per troop and shade trees in which they were found

Site	Area	Age of cocoa plantation (years)	Main plant species used for shadow	Observed	Number of observed monkey (sex-age-structure)
1	14.36 ha	40	<i>Cedrela odorata</i> <i>Tabebuia rosea</i> <i>Erythrina poeppigiana</i> <i>Pouteria sapota</i> <i>Artocarpus altilis</i>	Presence	25 (3am, 10af, 8j, 4i)
2	28.45 ha	38	<i>Cedrela odorata</i> <i>Tabebuia rosea</i> <i>Bursera simaruba</i> <i>Citrus sinensis</i> <i>Byrsonima crassifolia</i>	Presence	17 (2am, 7af, 4j, 4i)
3	22.31 ha	35	<i>Tabebuia rosea</i> <i>Castilla elástica</i> <i>Swietenia macrophylla</i>	Absence	0
4	15.45 ha	30	<i>Swietenia macrophylla</i> <i>Colubrina arborescens</i> <i>Gliricidia sepium</i>	Absence	0
5	12.21 ha	35	<i>Cedrela odorata</i> <i>Tabebuia rosea</i> <i>Samanea saman</i> <i>Mangifera indica</i>	Presence	8 (1am, 3af, 2j, 2i)

am=adult male
af=adult female
j=juvenile
i=infant

Table 6. Mean comparison in vegetation indices. Mean values grouping on the same letter are not significantly different according to the Tukey test ($p < 0.05$)

t Group	Means	N	Treatment
A	1.11137	10	TVI
B	0.84628	10	AVI
C	0.78736	10	MSAVI1
C	0.76963	10	SAVI
E	0.75599	10	MSAVI2
E	0.73657	10	NDVI
E	0.73415	10	EVI
G	0.59641	10	PVI
H	0.15372	10	RVI

Spectral separability analysis

Values of M greater than one indicate good separability, therefore the index with the best spectral separability was RVI ($M=1.050537248$) compared to the other indices used (Table 7).

Table 7. Spectral separability index (M) for each index and study site

Indices	Site 1	Site 2	Site 3
NDVI	-0.63563823	-1.115936299	-0.540739845
RVI	0.54863390	1.050537248	0.525442761
TVI	-0.61003079	-1.093998335	-0.535439881
PVI	-0.54863463	-1.050525089	-0.525443461
AVI	-0.54863390	-1.050526158	-0.525442761
SAVI	-0.61205795	-1.098791537	-0.53647433

Comparison of means of two populations with *t*-student

The compared values of each index among cocoa agrosystems were: site 1 (Absence-Presence), and site 2 (Presence-Presence), the values obtained where $TT = \pm 2.2622$ and $FT = 3.18$ with $\alpha = 0.05$ show that there is a statistically significant difference, whereas, in site 3 (Absence-Absence), they are statistically equal (Table 8).

Validation

According to the values calculated for the validation, for Site 4 (Absence-Absence) they are statistically equal, and for site 5 (Presence-Presence) there is a statistically significant difference (Table 9).

RVI index statistics in the study sites

The estimation of chlorophyll content using RVI calculated from Landsat-8 OLI/TIRS images for each season per study site is shown in Figure 5. The chlorophyll content ranges were: dry season from 0.39 to 0.22, rainy season from 0.42 to 0.22, and winter storm season between 0.41 and 0.22. Concerning the site where the animals were absent the values were lower with 0.20, 0.21, and 0.22, respectively for each season (Table 10).

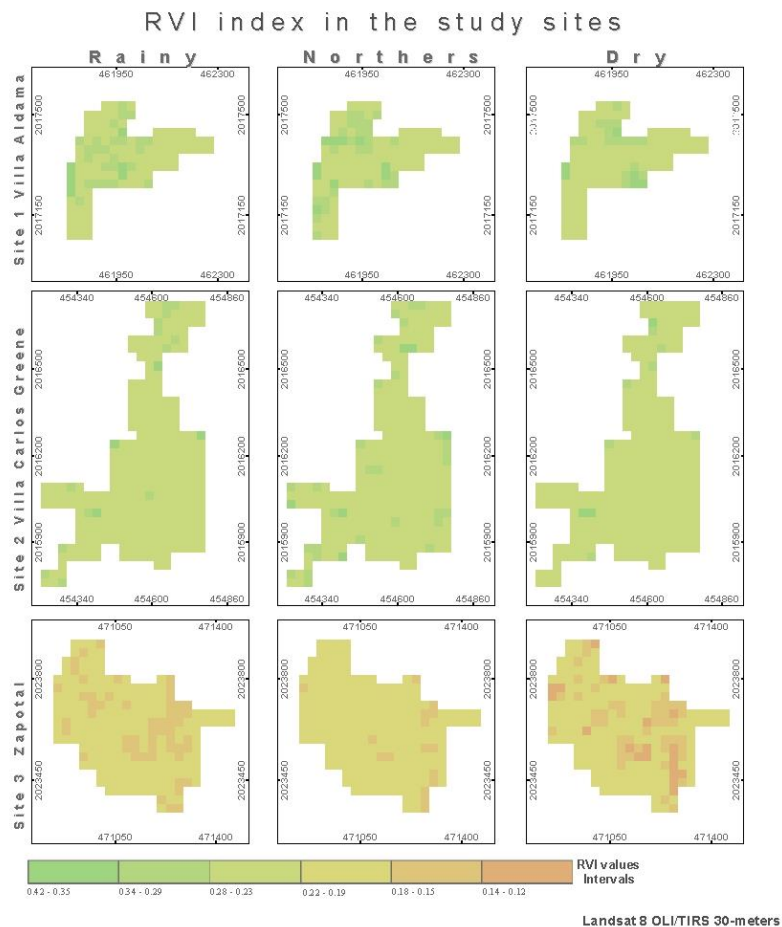


Figure 5. RVI values for the different seasons analyzed

Table 8. Average comparison values for the NDVI, RVI, TVI, PVI, AVI and SAVI indices of LANDSAT-5 TM images

Indices	Site 1		Site 2		Site 3	
	t Value	Value F	t Value	Value r F	t Value	Value F
NDVI	5.94	1.85*	5.04	2.45*	0.90	4.33
RVI	-5.32	2.41*	-4.48	3.15*	-0.66	4.87
TVI	5.70	2.04*	4.90	2.64*	0.81	4.49
PVI	5.25	2.45*	4.52	3.15*	0.66	4.87
AVI	5.32	2.41*	4.52	3.15*	0.44	3.96
SAVI	5.77	2.00*	4.89	2.63*	0.83	4.43

Table 9. Validation values of the mean comparisons

Indices	Site 4		Site 5	
	t Value	Value F	t Value	Value F
NDVI	-0.49	5.19	4.96	1.48*
RVI	2.23	4.09	-4.68	2.18*
TVI	-2.13	5.98	4.87	1.69*
PVI	-1.90	4.35	4.68	2.18*
AVI	-1.86	3.24	4.68	2.18*
SAVI	-2.19	5.30	4.88	1.66*

Table 10. Ranges of RVI relative to the presence and absence of the species

Study site	Seasons	Range of RVI Values
1 (Presence)	Dry	0.35-0.22
	Rainy	0.39-0.24
	Northers	0.38-0.22
2 (Presence)	Dry	0.39-0.23
	Rainy	0.42-0.22
	Northers	0.41-0.23
3 (Absence)	Dry	< 0.20
	Rainy	< 0.21
	Northers	< 0.22

Discussion

Due to fragmentation and habitat loss, primates have been forced to use agrosystems such as cocoa (*Theobroma cacao*) and coffee (*Coffea arabica*) plantations that grow under the shade of trees (Guzmán et al., 2016; Williams-Guillén et al., 2006). These agrosystems can act as the last habitat for species that tolerate a certain level of disturbance (Jasso-Del Toro et al., 2016; Muñoz et al., 2006). In the state of Tabasco, at the municipality of Comalcalco in particular, the mantled howler monkey (*Alouatta palliata Mexicana*), has been observed inhabiting cocoa agrosystems.

This study was carried out at an arboreal environment, between different sites with presence of the howler monkeys in cocoa agrosystems. An indirect method was used, considering the vegetation phenology as a metric to monitor biodiversity from space, as proposed by Skidmore et al. (2015). Through spectral vegetation indices, certain phenological characteristics of plant cover, such as density, leaf area index and

chlorophyll activity were measured (Xue and Su, 2017). The spectral vegetation indices provide insight into habitat quality through vegetation phenology (Bradley and Fleishman, 2008). These metrics allow both calculating and relating healthy vegetation that can be used by monkeys, and can be used as an indicator of food availability to howler monkeys in cocoa agrosystems. Howler monkeys' diet is based on the associated shade trees and do not eat the cocoa fruit, therefore, the vegetation spectral indexes are an important tool to measure certain phenology characteristics from the shaded trees. Food availability will depend on the phenological state of the vegetation, which in this case is associated with the presence of the mantled howler monkey (*A. palliata*).

Similar studies have been conducted to determine the presence of other vertebrates, such as birds and mammals using spectral indices; although, they have been directly observed through the analysis of satellite images in open environments (not arboreal). For instance, flamingo populations (Sasamal et al., 2008), penguins (Fretwell et al., 2012), albatrosses (Fretwell et al., 2017), whales (Fretwell et al., 2014), polar bears (Stapleton et al., 2014), elephant seals (McMahon et al., 2014), gnus, zebras and gazelles (Yang et al., 2014; Xue et al., 2017). These vertebrates have been identified, located and even counted analyzing these satellite images.

This study detected difference between vegetation indices in cocoa agrosystems associated with the presence of mantled howler monkeys. The difference was determined by using the spectral separability of vegetation indices in three study sites. These vegetation indices have hardly been used on arboreal agrosystems. A study to evaluate the correlation between spectral indices to estimate biomass and carbon stock in cocoa and coffee agrosystems indicated that RVI and NDVI show significant differences (Bolfe et al., 2012). However, RVI was considered the best index, since it has a high correlation with leaf area index, biomass and chlorophyll (Coltri et al., 2013; Xu and Su, 2017).

In our research, a statistical analysis was used to identify the most robust spectral vegetation index, associated with the presence of the howler monkey (*A. palliata*) in arboreal environments such as cocoa agrosystems. The RVI index was the one that showed better spectral separability and statistically significant difference. Moreover, the displacement of howler monkeys could be related to the vegetation phenology estimated through the RVI index. The index detects changes on phenology among seasons through the year that can mean changes to food availability (Pozo-Montuy and Serio-Silva, 2006; Ramírez-Orjuela and Sánchez-Dueñas, 2005); although, the NDVI could also be considered as another good indicator of healthy vegetation. Some investigations suggest that there is a significant relation between the high values of NDVI and the presence of species, such as ostriches (*Struthio camelus*; Leyequien et al., 2007) and gnus (*Connochaetes taurinus*; Pettorelli et al., 2011). In the case of primates, the NDVI has been used to model the habitat of the vervet monkey (*Cercopithecus aethiops*) in Africa (Willems et al., 2009). The model indicates that monkeys prefer areas with high NDVI values as an indicator of food availability (green vegetation).

It has been suggested that the use of vegetation spectral signatures can serve as predictors of habitat condition on ecological niche analysis (López-Sandoval et al., 2015), allowing to improve the accuracy of these habitat models (Pettorelli et al., 2014). Nevertheless, some authors consider that these type of spectral signatures have relatively little use (He et al., 2015). The vegetation indices derived from the satellite images of our study area detected differences that can be considered as another variable, which can be used to predict the presence of the species. The different phenological

stages of the vegetation (young leaves and ripe fruits) observed through the RVI index allow associating the presence of the monkeys in search of preferred food and identify their availability during the different seasons of the year. Therefore, these statistically representative indices could also be taken as variables or input parameters to predict habitats potentially suitable for monkeys through an ecological niche model for conservation purposes.

Conclusions

Howler monkeys are a viable subject for carrying out satellite image research in arboreal environments, due to their broad diet. They also had shown the capacity to adapt to small fragments of habitats, and currently have the need to take refuge in environments such as cocoa agrosystems, as the only arboreal habitat available in their vicinity. Their diet is based on the associated (shade) trees of the cocoa agrosystems. Since the monkeys do not eat the cocoa, they are not considered as an undesirable specie in plantations. The vegetation spectral indexes are an important tool to measure certain characteristics in the phenology of the associated trees, since the availability of food depends on the phenological state of the vegetation to a large extent, which in turn is associated with the presence of the mantled howler monkey (*A. palliata*). The vegetation indices derived from the satellite images of our study area detected differences that can be considered as another variable to predict the presence of the species. The different phenological stages of the vegetation (young leaves and ripe fruits) observed through the RVI index allow associating the presence of the monkeys in search of preferred foods and identify their availability during the different seasons of the year. These statistically representative indices could also be taken as variables or input parameters to predict habitats potentially suitable for the presence of the species through an ecological niche model. They can be useful research tools to provide early warning of habitat change and promote timely response in support of decision makers to identify suitable environmental sites, and thus apply conservation efforts for primates and other species.

Acknowledgements. The authors are grateful to the Consejo Nacional de Ciencia y Tecnología de Mexico (CONACYT), for granting the scholarship for the research work.

REFERENCES

- [1] Adjaloo, M. K., Oduro, W., Banful, B. K. (2012): Floral phenology of Upper Amazon cocoa trees: Implications for reproduction and productivity of cocoa. – *ISRN Agronomy*, ID461674: 1-8.
- [2] Ali, M., Montzka, C., Stadler, A., Menz, G., Vereecken, H. (2013): Estimation and validation of leaf area index time series for crops on 5m scale from space. – *Geoscience and Remote Sensing Symposium* 978: 3837-3840.
- [3] Anadón, J. D., Giménez, A., Ballestar, R., Pérez, I. (2009): Evaluation of local ecological knowledge as a method for collecting extensive data on animal abundance. – *Conservation biology* 23(3): 617-625.
- [4] Anaya, J. A., Hernández, G. M. V. (2013): Phenology of the tropical environment in the context of remote sensing. – *Geofocus: Revista Internacional de Ciencia y Tecnología de la Información Geográfica* 13(2): 1578-5157.

- [5] Anaya-Lira, M., Gutiérrez-Olvera, C., Ducoing-Watty, A. M., Cifuentes-Calderón, P., Sánchez-Trocino, M. (2013): Voluntary consumption of fresh food by howler monkeys (*Alouatta palliata* and *A. pigra*) in captivity. – Cuadernos de Investigación UNED 5(1): 151-155.
- [6] Arroyo-Rodríguez, V., Díaz, P. A. D. (2010): Effects of habitat fragmentation and disturbance on howler monkeys: a review. – American Journal of Primatology 72(1): 1-16.
- [7] Ashburn, W. L., Schelbert, H. R., Verba, J. W. (1978): Left ventricular ejection fraction—a review of several radionuclide angiographic approaches using the scintillation camera. – Progress in cardiovascular diseases 20(4): 267-284.
- [8] Avtar, R., Kumar, P., Oono, A., Saraswat, C., Dorji, S., Hlaing, Z. (2016): Potential application of remote sensing in monitoring ecosystem services of forests, mangroves and urban areas. – Geocarto International 32(8): 874-885.
- [9] Becerra, M. R. (2007): Oil palm cultivation and biodiversity. – Boletín El Palmicultor 427: 2.
- [10] Bellard, C., Bertelsmeier, C., Leadley, P., Thuiller, W., Courchamp, F. (2012): Impacts of climate change on the future of biodiversity. – Ecology letters 15(4): 365-377.
- [11] Benayas, J. R. (1993): Perspectives of remote sensing in ecological research. – Revista de teledetección: Revista de la Asociación Española de Teledetección (2): 4.
- [12] Bolfe, É. L., Batistella, M., Ferreira, M. C. (2012): Correlation of spectral variables and aboveground carbon stock of agroforestry systems. – Pesquisa Agropecuária Brasileira 47(9): 1261-1269.
- [13] Bradley, B. A., Fleishman, E. (2008): Can remote sensing of land cover improve species distribution modelling? – Journal of Biogeography 35(7): 1158-1159.
- [14] Chaves, Ó. M., Bicca-Marques, J. C. (2016): Feeding strategies of brown howler monkeys in response to variations in food availability. – PLoS One 11(2): e0145819.
- [15] Chuvieco, E. (2016): Fundamentals of satellite remote sensing: An environmental approach. – CRC press, p468.
- [16] CNES. (2012): (co-produced on July 29, 2012), produced by ERMEX-SAGARPA under the license of "SPOT IMAGE. S.A."
- [17] Coltri, P. P., Zullo, J., do Valle Goncalves, R. R., Romani, L. A. S., Pinto, H. S. (2013): Coffee Crop's Biomass and Carbon Stock Estimation With Usage of High Resolution Satellites Images. – IEEE Journal of Selected Topics in Applied Earth Observations and Remote Sensing 6(3): 1786-1795.
- [18] Corbane, C., Lang, S., Pipkins, K., Alleaume, S., Deshayes, M., Millán, V. E. G., Strasser, T., Borre, J. V., Toon, S., Michael, F. (2015): Remote sensing for mapping natural habitats and their conservation status—New opportunities and challenges. – International Journal of Applied Earth Observation and Geoinformation 37: 7-16.
- [19] Córdova-Avalos, V., Mendoza-Palacios, J. D., Vargas-Villamil, L., Izquierdo-Reyes, F., Ortiz-García, C. F. (2008): Participation of peasant organizations in the commercialization of cacao beans (*Theobroma cacao* L.) in Tabasco, Mexico. – Universidad y ciencia 24(2): 147-158.
- [20] De La Cruz-Landero, E., Córdova-Avalos, V., García-López, E., Bucio-Galindo, A., Jaramillo-Villanueva, J. L. (2015): Agricultural management and socioeconomic characterization of cocoa in Comalcalco, Tabasco. – Foresta veracruzana 17(1): 33-40.
- [21] Deering, D. W., Rouse, J. W., Haas, R. H., Schell, J. A. (1975): Measuring 'forage production' of grazing units from Landsat MSS data. – Proceedings of the 10th International Symposium on Remote Sens. Environ 2: 1169-1178.
- [22] Fretwell, P. T., La Rue, M. A., Morin, P., Kooyman, G. L., Wienecke, B., Ratcliffe, N., Fox, A. J., Fleming, A. H., Porter, C., Trathan, P. N. (2012): An emperor penguin population estimate: the first global, synoptic survey of a species from space. – PLoS One 7(4): e33751.
- [23] Fretwell, P. T., Staniland, I. J., Forcada, J. (2014): Whales from space: counting southern right whales by satellite. – PLoS One 9(2): e88655.

- [24] Fretwell, P. T., Scofield, P., Phillips, R. A. (2017): Using super-high resolution satellite imagery to census threatened albatrosses. – *Ibis* 159(3): 481-490.
- [25] Gallegos, J. A. F. (2017): Climate change indices in the Rio Sabinal basin, Chiapas, Mexico. – *Tecnología y Ciencias del Agua* 8(6): 137-143.
- [26] Garber, P. A., Righini, N., Kowalewski, M. M. (2015): Evidence of alternative dietary syndromes and nutritional goals in the genus *Alouatta*. – In: Kowalewski, M. M., Garber, P. A., Cortés-Ortiz, L., Urbani, B., Youlatos, D. (eds.) *Howler Monkeys*. Springer 4: 85-109.
- [27] Genc, H., Genc, L., Turhan, H., Smith, S. E., Nation, J. L. (2008): Vegetation indices as indicators of damage by the sunn pest (Hemiptera: Scutelleridae) to field grown wheat. – *African Journal of Biotechnology* 7(2): 173-180.
- [28] Giraldo, R. (2017): Study of the Spectral Signatures of Oil Palms Affected with Lethal Wilt, Using Functional Data Statistic Analysis. – *Revista Palmas* 37: 131-139.
- [29] Guo, Q., Liu, J. (2018): Remote sensing has become an indispensable technology for biodiversity research protection and change monitoring. – *Biodiversity Science* 26(8): 785-788.
- [30] Guzmán, A., Link, A., Castillo, J. A., Botero, J. E. (2016): Agroecosystems and primate conservation: Shade coffee as potential habitat for the conservation of Andean night monkeys in the northern Andes. – *Agriculture, Ecosystems & Environment* 215: 57-67.
- [31] He, K. S., Bradley, B. A., Cord, A. F., Rocchini, D., Tuanmu, M. N., Schmidtlein, S., Turner, W., Wegmann, M., Pettorelli, N. (2015): Will remote sensing shape the next generation of species distribution models? – *Remote Sensing in Ecology and Conservation* 1(1): 4-18.
- [32] Huete, A. R. (1988): A soil-adjusted vegetation index (SAVI). – *Remote sensing of environment* 25(3): 295-309.
- [33] Huete, A., Didan, K., Miura, T., Rodriguez, E. P., Gao, X., Ferreira, L. G. (2002): Overview of the radiometric and biophysical performance of the MODIS vegetation indices. – *Remote sensing of Environment* 83(1): 195-213.
- [34] INEGI. National Institute of Statistic and Geography. (2012): *Perspectiva Estadística: Tabasco*. – Instituto Nacional de Estadística y Geografía, Aguascalientes.
- [35] Jasso-Del Toro, C., Márquez-Valdelamar, L., Mondragón-Ceballos, R. (2016): Genetic diversity in Mexican mantled howler monkeys (*Alouatta palliata mexicana*) at the Reserva de la Biosfera Los Tuxtlas (Veracruz, Mexico). – *Revista Mexicana de Biodiversidad* 87(3): 1069-1079.
- [36] Jensen, J. R. (2007): *Remote sensing of the Environment: An Earth Resource Perspective*. – Pearson Prentice Hall. Upper Saddle River, NJ, p592.
- [37] Jordan, C. F. (1969): Derivation of leaf-area index from quality of light on the forest floor. – *Ecology* 50(4): 663-666.
- [38] Kaufman, Y. J., Remer, L. A. (1994): Detection of forests using mid-IR reflectance: an application for aerosol studies. – *IEEE Transactions on Geoscience and Remote Sensing*, 32(3): 672-683.
- [39] Kerr, J. T., Ostrovsky, M. (2003): From space to species: ecological applications for remote sensing. – *Trends in Ecology & Evolution* 18(6): 299-305.
- [40] Lausch, A., Blaschke, T., Haase, D., Herzog, F., Syrbe, R. U., Tischendorf, L., Walz, U. (2015): Understanding and quantifying landscape structure—A review on relevant process characteristics, data models and landscape metrics. – *Ecological Modelling* 295: 31-41.
- [41] Leong, M., Roderick, G. K. (2015): Remote sensing captures varying temporal patterns of vegetation between human-altered and natural landscapes. – *PeerJ* 3: e1141.
- [42] Leyequien, E., Verrelst, J., Slot, M., Schaepman-Strub, G., Heitkönig, I. M., Skidmore, A. (2007): Capturing the fugitive: Applying remote sensing to terrestrial animal distribution and diversity. – *International Journal of Applied Earth Observation and Geoinformation* 9(1): 1-20.

- [43] López-Sandoval, J. A., López-Mata, L., Cruz-Cárdenas, G., Vibrans, H., Vargas, O., Martínez, M. (2015): Modeling of environmental factors that determine the distribution of synanthropic species of *physalis*. – *Botanical Sciences* 93(4): 755-764.
- [44] Loreto, D., Esperón-Rodríguez, M., Barradas, V. L. (2017): The climatic-environmental significance, status and socioeconomic perspective of the grown-shade coffee agroecosystems in the central mountain region of Veracruz, Mexico. – *Investigaciones Geográficas, Boletín del Instituto de Geografía* 92: 87-100.
- [45] Matey, A., Zeledón, L., Orozco Aguilar, L., Chavarría, F., López, A., Deheuvels, O. (2013): Floristic composition and structure of cacao plantations and forest patches in Waslala, Nicaragua. – *Agroforestería en las Américas* Número 49: 61-67.
- [46] McMahon, C. R., Howe, H., van den Hoff, J., Alderman, R., Broolsma, H., Hindell, M. A. (2014): Satellites, the all-seeing eyes in the sky: counting elephant seals from space. – *PloS One* 9(3): e92613.
- [47] Morales, J. D. J., García, A., Méndez, E. (2012): What do you know about Cocoa? – *Revista Mexicana de Ciencias Farmacéuticas* 43(4):79-81.
- [48] Muñoz, D., Estrada, A., Naranjo, E., Ochoa, S. (2006): Foraging ecology of howler monkeys in a cacao (*Theobroma cacao*) plantation in Comalcalco, Mexico. – *American Journal of Primatology* 68(2): 127-142.
- [49] Pettorelli, N., Ryan, S., Mueller, T., Bunnefeld, N., Jędrzejewska, B., Lima, M., Kausrud, K. (2011): The Normalized Difference Vegetation Index (NDVI): unforeseen successes in animal ecology. – *Climate Research* 46(1): 15-27.
- [50] Pettorelli, N., Safi, K., Turner, W. (2014): Satellite remote sensing, biodiversity research and conservation of the future. – *Phil. Trans. R. Soc. B* 369: 20130190.
- [51] Pozo-Montuy, G., Serio-Silva, J. C. (2006): Eating behavior of black howler monkeys (*Alouatta pigra* L) in fragmented habitat in Balacán, Tabasco, Mexico. – *Acta zoológica mexicana* 22(3): 53-66.
- [52] Pozo-Montuy, G., Bravo-Bonilla, A., De la Cruz-Córdova, S., Torres-Flores, R., Cruz-Canuto I., Trejo-Bellido, M., Velázquez-Vázquez, G. (2015): UMA Management Plan in Free Life "The Cocoa Monkey" For the mantled howler monkey (*Alouatta palliata mexicana*). – *Grupo de Biología para la Conservación S de RL de CV* 76: 4-16
- [53] Pyritz, L. W., Büntge, A. B., Herzog, S. K., Kessler, M. (2010): Effects of habitat structure and fragmentation on diversity and abundance of primates in tropical deciduous forests in Bolivia. – *International journal of primatology* 31(5): 796-812.
- [54] Qi, J., Chehbouni, A., Huete, A. R., Kerr, Y. H., Sorooshian, S. (1994): A modified soil adjusted vegetation index. – *Remote Sensing of Environment* 48(2): 119-126.
- [55] Ramírez-Orjuela, C., Sánchez-Dueñas, I. M. (2005): First Census of the Black Howler Monkey (*Alouatta palliata aequatorialis*) in El Chocó Colombian Biogeographic. – *Neotropical Primates* 13(2): 1-7.
- [56] Richardson, A. J., Wiegand, C. L. (1977): Distinguishing vegetation from soil background information. – *Photogrammetric engineering and remote sensing* 43(12): 1541-1552.
- [57] Rocchini, D., Foody, G. M., Nagendra, H., Ricotta, C., Anand, M., He, K. S., Amici, V., Kleinschmit, B., Forster, M., Schmidtlein, S., Feilhaver, H., Ghisla, A., Metz, M., Neteler, M. (2013): Uncertainty in ecosystem mapping by remote sensing. – *Computers & Geosciences*, 50: 128-135.
- [58] Rouse Jr, J., Haas, R. H., Schell, J. A., Deering, D. W. (1974): Monitoring vegetation systems in the Great Plains with ERTS. – *NASA special publication* 351: 309-317.
- [59] Saldarriaga, V. (2016): Effects of temperature variability on productivity and prices of agricultural products: evidence in Peru. – *Inter-American Development Bank* 1091: 9-33
- [60] Sánchez-Gutiérrez, F., Pérez-Flores, J., Obrador-Olan, J. J., Sol-Sánchez, A., Ruiz-Rosado, O. (2016): Tree structure of pruning agroforestry system in Cárdenas, Tabasco, Mexico. – *Revista Mexicana de Ciencias Agrícolas* (14): 2695-2709.

- [61] Sasamal, S. K., Chaudhury, S. B., Samal, R. N., Pattanaik, A. K. (2008): QuickBird spots flamingos off Nalabana Island, Chilika Lake, India. – International Journal of Remote Sensing 29(16): 4865-4870.
- [62] Skidmore, A. K., Pettorelli, N., Coops, N. C., Geller, G. N., Hansen, M., Lucas, R., Schaepman, M. E. (2015): Environmental science: agree on biodiversity metrics to track from space. – Nature 523: 403-405.
- [63] Stapleton, S., LaRue, M., Lecomte, N., Atkinson, S., Garshelis, D., Porter, C., Atwood, T. (2014): Polar bears from space: assessing satellite imagery as a tool to track Arctic wildlife. – PloS One 9(7): e101513.
- [64] Turner, W., Spector, S., Gardiner, N., Fladeland, M., Sterling, E., Steininger, M. (2003): Remote sensing for biodiversity science and conservation. – Trends in ecology & evolution 18(6): 306-314.
- [65] Turner, W., Rondinini, C., Pettorelli, N., Mora, B., Leidner, A. K., Szantoi, Z., Buchanan, G., Dech, S., Dwyer, J., Herold, M., Koh, L. P., Leimgruber, P., Taubenboeck, H., Wegmann, M., Wikelski, M., Woodcock, C. (2015): Free and open-access satellite data are key to biodiversity conservation. – Biological Conservation 182: 173-176.
- [66] Valenzuela-Córdova, B., Mata-Zayas, E. E., Pacheco-Figueroa, C. J., Chávez-Gordillo, E. J., Díaz-López, H. M., Gama, L., Valdez-Leal, J. D. D. (2015): Ecotourism potential of the cacao (*Theobroma cacao* L) farming ecosystem with black howler monkeys (*Alouatta palliata* G) in la Chontalpa, Tabasco. – Agroproductividad 8(5): 3-10.
- [67] Vidal-García, F., Serio-Silva, J. C. (2011): Potential distribution of Mexican primates: modeling the ecological niche with the maximum entropy algorithm. – Primates 52(3): 261-270.
- [68] Wang, Y. Q., Zhou, Y., Wu, Z., Zhang, H., Zhang, J., Jin, Y., Huang, F., Yin, X. (2008): Monitoring landscape dynamics and conditions of natural resources within and adjacent to protected areas. – The International Archives of the Photogrammetry, Remote Sensing and Spatial Information Sciences 37: 1585-1590.
- [69] Willems, E. P., Hill, R. A. (2009): A critical assessment of two species distribution models: a case study of the vervet monkey (*Cercopithecus aethiops*). – Journal of Biogeography 36(12): 2300-2312.
- [70] Williams-Guillén, K., McCann, C., Martínez Sánchez, J. C., Koontz, F. (2006): Resource availability and habitat use by mantled howling monkeys in a Nicaraguan coffee plantation: Can agroforests serve as core habitat for a forest mammal? – Animal Conservation 9(3): 331-338.
- [71] Willis, K. S. (2015): Remote sensing change detection for ecological monitoring in United States protected areas. – Biological Conservation 182: 233-242.
- [72] Workie, T. G., DeBella, H. J. (2018): Climate change and its effects on vegetation phenology across ecoregions of Ethiopia. – Global Ecology and Conservation 13: e00366.
- [73] Xue, J., Su, B. (2017): Significant Remote Sensing Vegetation Indices: A Review of Developments and Applications. – Journal of Sensors 1353691: 1-17.
- [74] Xue, Y., Wang, T., Skidmore, A. K. (2017): Automatic Counting of Large Mammals from Very High Resolution Panchromatic Satellite Imagery. – Remote sensing 9(878): 1-16.
- [75] Yang, Z., Wang, T., Skidmore, A. K., de Leeuw, J., Said, M. Y., Freer, J. (2014): Spotting east African mammals in open savannah from space. – PloS One 9(12): e115989.
- [76] Yiming, L. (2006): Seasonal variation of diet and food availability in a group of Sichuan snub-nosed monkeys in Shennongjia Nature Reserve, China. – American Journal of Primatology: Official Journal of the American Society of Primatologists 68(3): 217-233.
- [77] Zhao, M., Peng, C., Xiang, W., Deng, X., Tian, D., Zhou, X., Yu, G., He, H., Zhao, Z. (2013): Plant phenological modeling and its application in global climate change research: overview and future challenges. – Environmental Reviews 21(1): 1-14.

MODELING AND FORECASTING THE HOUSEHOLD WATER CONSUMPTION IN SAUDI ARABIA

ALMANJAHIE, IBRAHIM M. – CHIKR-ELMEZOUAR, Z.* – BACHIR, A.

*Department of Mathematics, College of Science, King Khalid University
61413 Abha, Saudi Arabia
(phone: +966-17-241-7734; fax: +966-17-241-7637)*

**Corresponding author
e-mail: chikrtime@yahoo.fr*

(Received 1st Oct 2017; accepted 2nd Jan 2019)

Abstract. The demand for water in the kingdom of Saudi Arabia increases due to population growth urbanization, industrialization and the expansion of irrigated agricultural lands. Analyzing the current situation of the water consumption and predicting water demand in the future are essential for the authorities to improve and manage production quantities. The objective of this paper is to find the best model for water consumption in Saudi Arabia and use the fitted model for forecasting. A data for water consumption between January 2010 and July 2017 were analyzed using a multiplicative seasonal autoregressive integrated moving average model (SARIMA). Through our research, we concluded that the best SARIMA model for fitting water consumption in Saudi Arabia is SARIMA (1,0,1) × (1,1,2)₁₂.

Keywords: *water consumption, time series, SARIMA, ACF, PACF, Box-Jenkins*

Introduction

It is widely recognized that the kingdom of Saudi Arabia is one of many countries of the world are entering an era of severe water shortage. Saudi Arabia, with an area of 2.15 million km², is a desert-like country lying in the Middle East in a zone where temperatures are very high in summer and low in winter. The country receives very little of precipitation throughout the year and also does not contain perennial rivers or stable bodies of water. The desert lands throughout the country frequently lose more moisture through evaporation than they receive from precipitation. In fact, more than half of the area of Saudi Arabia is desert. Recently, the arid and water deficit threaten the stability of the country.

The causes of water scarcity are varied; some are natural and others are as a result of human activities. Population growth and the climatic conditions pose a continual challenge and cause the limitation of underground water resources. Also, urbanization, industrialization and the expansion of irrigated agricultural lands have contributed to a dramatic increase in water consumption over the past few decades. Many researchers have discussed the influence of the depletion of underground water resources. They were interested in studying, analyzing and predicting the future demand for water. The journals “Land Economics” and “Water Resources Research” have dedicated much space to this study. Water consumption and demand estimation in developed countries have been at the core of many empirical papers, starting with the work of Gottlieb (1963) and Howe and Lina weaver (1967). Many studies have been made in a large set of countries including Canada (Kulshreshtha, 1996), Denmark (Hansen, 1996), France (Nauges and Thomas, 2000), Spain (Martínez-Espiñeira, 2002), Sweden (Höglund, 1999), and the US (Foster and Beattie, 1979; Agthe and Billings, 1980; Chicoine et al.,

1986; Nieswiadomy and Molina, 1989). Comprehensive reviews of the literature can be found, for examples, in Arbués-Gracia et al. (2003) and Dalhuisen et al. (2003).

Statistical methodologies have been used by many researchers as a tool for understanding and predicting future water demand. Kambale et al. (2016) used autoregressive integrated moving average (ARIMA) model for predicting the climate change scenarios by Inter-Governmental Panel for Climate Change (IPCC) and Indian Network for Climate Change Assessment (INCCA). Hongyan et al. (2017) combined ARIMA model and neural network to propose a prediction model. They used it to predict the 15 years supply and demand for water resources in Shandong Province. Generally, there are many studies dealt with different types of statistical models. We cite, for instance, Cornillon et al. (2008) for principal component analysis (PCA); Rita et al. (2013) and Samsuri et al. (2017) for multiple linear regression model.

In the Kingdom of Saudi Arabia, a general study for the most concise summary of groundwater resources was presented by Al-Ibrahim (1990). He stated that groundwater is the most important source of water in Saudi Arabia. Later, Abushammala and Bawazir (2017) developed an artificial neural network (ANN) model and used it to predict the annual and monthly domestic water demand in Makkah city, Saudi Arabia. Recently, Muhamed et al. (2018) proposed a hybrid model of ANN and ARIMA for predicting the water quality data. They found that the proposed hybrid model is better than the traditional methods and ANN.

None of the previous studies used and discussed the seasonal autoregressive integrated moving average (SARIMA) for predicting water demand in Saudi Arabia. In this paper, we aim to understand the current household water consumption and build a model that will encourage sustainable consumption and conservation of water resources.

A monthly data for the household water consumption in Saudi Arabia will be analyzed and modeled using the SARIMA model. There are two types of this model; additive and multiplicative. For monthly data, an additive model assumes that the difference in the water consumption values between the beginning and middle of each year is approximately the same. For a multiplicative model, the absolute differences in the consumption values are of less interest and importance than the percentage changes. We use the multiplicative SARIMA model since the pattern of the seasonal factor varies with the time series. The monthly water demand model, based on the SARIMA model, is essential for public authorities to improve monthly water production quantities. This study will be utilized for future development programs consideration; especially capital expenditures and water quantities.

The paper is structured as follows: In “Materials and methods” the household water consumption data used in this research is described and the notation of the multiplicative SARIMA model is established. Some models for the data are built and discussed in “Results and discussion”. Also, the best SARIMA model is stated. Finally, “Conclusion” is devoted to the conclusion and recommendation.

Materials and methods

Data collection

Data, for the household water consumption, between January 2010 and July 2017 were obtained from the Ministry of Environment, Water and Agriculture in Saudi Arabia. The data was monthly for the household water consumption, and it is measured in cubic meters (m³) as the water follows through the water meter. The lowest total

water consumption was in February 2010 with $161 \times 10^6 \text{ m}^3$ while the highest was in May 2017 with $285 \times 10^6 \text{ m}^3$. The data values are displayed in the Appendix.

Multiplicative seasonal ARIMA model

The dependence on groundwater supplies often emerges in importance during seasonal lags. Natural phenomena such as temperature also have strong components corresponding to seasons. Because of this, it is appropriate to introduce autoregressive and moving average polynomials that identify with the seasonal lags.

The seasonal autoregressive moving average model, say, ARMA (p, q), takes the form (Eq. 1)

$$\phi_p(B^S)x_t = \theta_q(B^S)\omega_t, \tag{Eq.1}$$

with the following definition. The operators (Eq. 2)

$$\phi_p(B^S)x_t = 1 - \phi_1 B^S - \phi_2 B^{2S} - \dots - \phi_p B^{pS} \tag{Eq.2}$$

and (Eq. 3)

$$\theta_q(B^S) = 1 + \theta_1 B^S + \theta_2 B^{2S} + \dots + \theta_q B^{qS}, \tag{Eq.3}$$

are the seasonal autoregressive operator and the seasonal moving average operator of orders P and Q, respectively, with seasonal period S.

The multiplicative seasonal autoregressive integrated moving average (SARIMA) model of Box Jenkins (Box and Jenkins, 1970) is given by Equation 4:

$$\phi_p(B^S)\varphi(B)\nabla_S^D \nabla^d x_t = \theta_q(B^S)\theta(B)\omega_t, \tag{Eq.4}$$

where ω_t is the usual Gaussian white noise process. The one shorthand notation for the model is

$$\text{ARIMA}(p,d,q) \times (P,D,Q)S$$

With p = non-seasonal AR order, d = non-seasonal differencing, q = non-seasonal MA order, P = seasonal AR order, D = seasonal differencing, Q = seasonal MA order, and S = time span of repeating seasonal pattern. The non-seasonal difference components are $\nabla^d = (1 - B)^d$ and the seasonal is $\nabla_S^D = (1 - B^S)^D$ (Davis, 2005; Dickey et al., 1979). Identification of AR(p)s, MA(Q)s and then an ARMA model is often best done with the ACF and PACF. Table 1 gives a guideline for choosing the best model.

Table 1. Behavior of the ACF and the PACF for the Seasonal ARMA model (Chicoine et al., 1986)

	AR(P)s	MA(Q)s	ARMA (P,Q)s
ACF	Tails off at lags ks, k = 1,2,...	Cuts off after lag Qs	Tails off at lag ks
PACF	Cuts off after lag Ps	Tails off at lags ks k = 1,2...	Tails off at lag ks

Results and discussion

Data exploration

The plot of the household water consumption series is given in *Figure 1*.

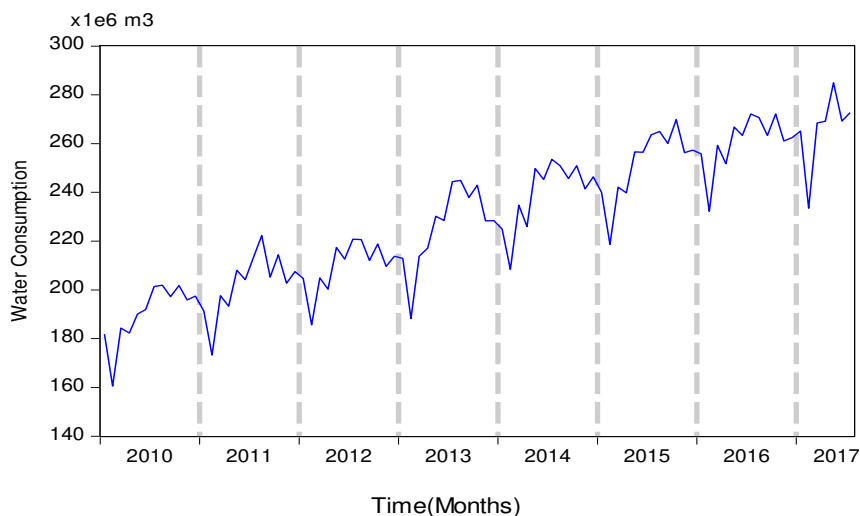


Figure 1. Monthly water consumption in Saudi Arabia between January 2010 and July 2017

From *Figure 1* we can see that there are clear patterns of seasonality. The seasonal variation increases as we move across time. Also, *there is a clearly increasing trend in water consumption over time.*

Building SARIMA model

To build a multiplicative seasonal autoregressive integrated moving average (SARIMA) model based on the Box Jenkins method (Box and Jenkins, 1970), the stages of this method for analyzing time series data are followed: identification, estimation, diagnostic checking and forecasting. For identification, the autocorrelation function (ACF) and partial autocorrelation function (PACF) are used for checking stationarity of the data series and determining if possible the values of p , P , q , Q . *Figures 2 and 3* display the results of ACF and PACF.

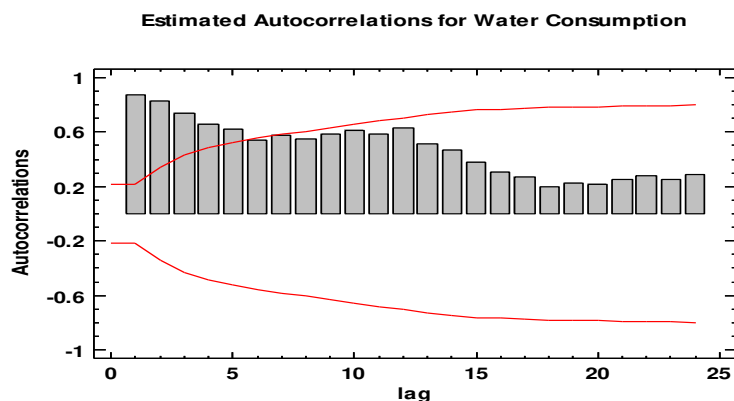


Figure 2. The ACF for the monthly water consumption data in Saudi Arabia between January 2010 and October 2016

The autocorrelations of the water consumption are significant for a large number of seasonal lags, but perhaps the autocorrelations at lags 12 and above are merely due to the propagation of the autocorrelation at lag 1.

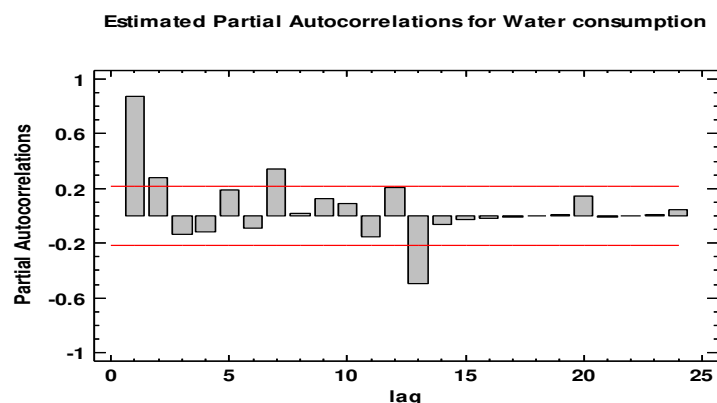


Figure 3. The PACF for the monthly water consumption data in Saudi Arabia between January 2010 and October 2016

Figure 3 shows that there is a spike in the PACF at lags 12, but nothing at seasonal lags in the ACF in Figure 2. This may be suggestive of a seasonal AR(1) term. In the non-seasonal lags, there are three significant spikes in the PACF, suggesting a possible AR(1) term. Note that from Figure 1 it can be seen that the water consumption data needs differencing seasonally, i.e. $D = 1, d = 0$. The pattern in the ACF is not indicative of any simple model. Consequently, this initial analysis suggests that a possible model for this data is an ARIMA(1,0,q)(1,1,Q)[12].

Estimated autocorrelations

The estimated autocorrelations for the monthly water consumption data in Saudi Arabia are shown in Table 2. Table 2 depicts the estimated autocorrelations between values of water consumption at various lags. The lag $k = 1, 2, \dots, 24$ autocorrelation coefficient measures the correlation between values of data at time t and time $t - k$, where $t = 1, 2, \dots, 82$. Also shown are 95.0% probability limits around 0. The lower and upper limits of the 95% probabilities are shown in Figure 2; these limits are computed by $0 \mp z_{\alpha/2} se(\hat{\rho}_k)$, where $z_{\alpha/2} = 1.96$ (at $\alpha = 5\%$) and $se(\hat{\rho}_k)$ is the standard error of the corresponding autocorrelation $\hat{\rho}_k$. If the probability limits at a particular lag do not contain the corresponding autocorrelation, there is a statistically significant correlation at that lag at the 95% confidence level.

Fitting SARIMA model

Choosing the best model will involve obtaining some important values in fitting like the root mean squared error (RMSE), the mean absolute error (MAE), the mean absolute percentage error (MAPE), the mean percentage error (MPE) and Akaike Information Criterion (AIC), which will be compared to their corresponding values when applying the following seasonal ARIMA models:

$$(A) \text{ ARIMA}(1,0,1) \times (1,1,2)_{12},$$

(B) ARIMA(1,1,0) × (1,1,2)₁₂,

(C) ARIMA(2,1,0) × (1,1,2)₁₂,

(D) ARIMA(0,1,2) × (1,1,2)₁₂,

(E) ARIMA(1,1,1) × (1,1,2)₁₂.

Table 2. The estimated autocorrelations between values of data at various lags

Lag	Autocorrelation (r_i)	Std. error (se)	Lower 95.0% Prob. limit	Upper 95.0% Prob. limit
1	0.874044	0.110432	-0.216442	0.216442
2	0.830243	0.175579	-0.34413	0.34413
3	0.73833	0.218267	-0.427796	0.427796
4	0.653835	0.246853	-0.483823	0.483823
5	0.618248	0.267139	-0.523583	0.523583
6	0.539642	0.284052	-0.556734	0.556734
7	0.572324	0.296291	-0.580722	0.580722
8	0.551189	0.30948	-0.60657	0.60657
9	0.584533	0.321228	-0.629597	0.629597
10	0.61312	0.333948	-0.654527	0.654527
11	0.584835	0.347405	-0.680902	0.680902
12	0.63271	0.359211	-0.704041	0.704041
13	0.515042	0.372554	-0.730193	0.730193
14	0.468674	0.381138	-0.747018	0.747018
15	0.377864	0.388103	-0.760669	0.760669
16	0.301906	0.392563	-0.769412	0.769412
17	0.270082	0.395385	-0.774942	0.774942
18	0.198321	0.397628	-0.779339	0.779339
19	0.228487	0.398833	-0.781699	0.781699
20	0.218865	0.400426	-0.784822	0.784822
21	0.251958	0.401882	-0.787676	0.787676
22	0.277167	0.403804	-0.791443	0.791443
23	0.250263	0.406117	-0.795977	0.795977
24	0.29124	0.407994	-0.799655	0.799655

Table 3 represents the comparison results of fitting different models. The model with the lowest value of the Akaike Information Criterion (AIC) is model (A). In addition, the model ARIMA(1,0,1) × (1,1,2)₁₂ has the lowest values in RMSE, MPE and AIC. Therefore, the model ARIMA(1,0,1) × (1,1,2)₁₂ is the best selected model. Table 4 also summarizes the performance of the currently selected model in fitting the historical data. The parameter estimates of the best model are also shown in Table 4.

Table 3. A comparison fitting models

Model	RMSE	MAE	MAPE	MPE	AIC
(A)	2.87793E6	2.20079E6	0.954075	-0.0270854	29.8671
(B)	2.91554E6	2.26702E6	0.978276	0.0428601	29.8687
(C)	2.88255E6	2.1878E6	0.9434	0.0419334	29.8703
(D)	2.89092E6	2.22338E6	0.959992	0.0608748	29.8761
(E)	2.8966E6	2.20382E6	0.952618	0.0371123	29.8800

Table 4. The parameter estimates of ARIMA(1,0,1) × (1,1,2)12

Parameter	Estimate	Std. error	T	P-value
ϕ_1	1.00174	0.001590	629.884	0.000000
θ_1	0.470192	0.108953	4.31553	0.000056
Φ_1	-1.24844	0.106268	-11.748	0.000000
Θ_1	-0.459525	0.128718	-3.57001	0.000678
Θ_2	0.897565	0.115493	7.77157	0.000000

The equation of the ARIMA(1,0,1) × (1,1,2)12 is given as below(Eqs. 5-7). If

$$(1 - \phi_1\beta)(1 - \Phi_1\beta^{12})(1 - \beta^{12})WC_t = (1 - \theta_1\beta)(1 - \Theta_1\beta^{12} - \Theta_2\beta^{24})e_t, \quad (\text{Eq.5})$$

then

$$WC_t = \phi_1WC_{t-1} + (\Phi_1 + 1)WC_{t-12} - \phi_1(\Phi_1 + 1)WC_{t-13} - \Phi_1WC_{t-24} + \phi_1\Phi_1WC_{t-25} + (\theta_1 + \Theta_1)e_{t-12} - (\Theta_2 - \theta_1\Theta_1)e_{t-24} + \theta_1\Theta_2e_{t-36} + e_t, \quad (\text{Eq.6})$$

$$WC_t = 1.00174WC_{t-1} - 0.24844WC_{t-12} + 0.31062WC_{t-13} + 1.24844WC_{t-24} - 1.25061WC_{t-25} + 0.01067e_{t-12} - 1.11363e_{t-24} + 0.21606e_{t-36} + e_t. \quad (\text{Eq.7})$$

Forecasting

We used Equation 7 to forecast data from November 2016 to July 2017; the forecasting results are given in Table 5.

Table 5. Forecasting data from November 2016 to July 2017

Period	Original (m ³)	Forecast (m ³)
11/16	261071635.00	2.63039E8
12/16	262529383.00	2.67532E8
1/17	264786946.00	2.62222E8
2/17	231301561.00	2.39871E8
3/17	268909016.00	2.64531E8
4/17	269628773.00	2.65293E8
5/17	285437797.00	2.79714E8
6/17	269723694.00	2.78574E8
7/17	273197966.00	2.90016E8

The root mean square error between original data and the forecasted data is calculated, that is $RMSE = 7751794.934$.

From *Figure 4* it can be seen that there is a good agreement between the original and forecasted data. Therefore, we conclude that the fitted model, $ARIMA(1,0,1) \times (1,1,2)_{12}$, is appropriate for forecasting.

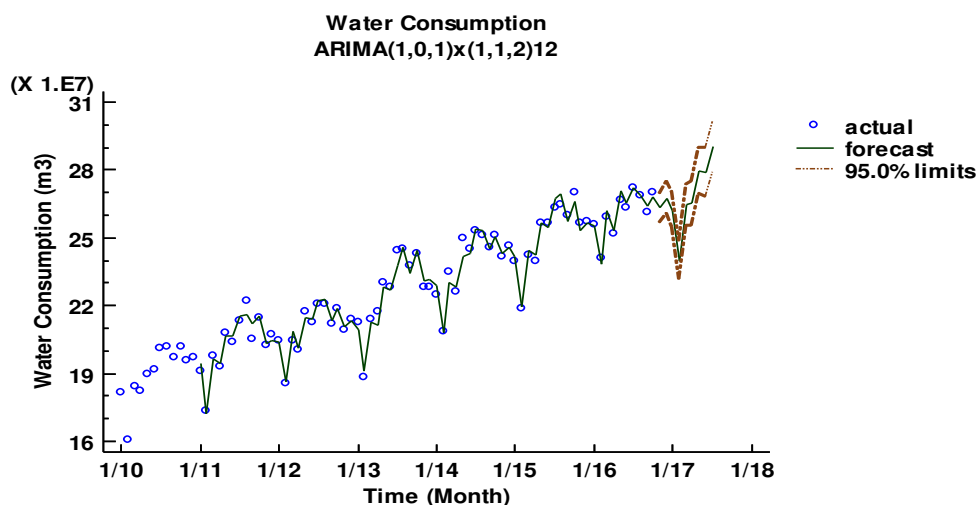


Figure 4. Forecast values based on the SARIMA model (green) and the original values (blue)

Conclusions

This research aimed is to understand current household water consumption by analyzing the current behaviour and water consumption patterns in Saudi Arabia, and to build a model that will encourage sustainable consumption and conservation of water resources. In this paper, we present a different time series model for fitting the monthly household water consumption data in Saudi Arabia between January 2010 and October 2016. Based on the data analyses and comparisons of five SARIMA models, the result indicated that the suitable and effective model for representing the household water consumption data of the time series is the multiplied seasonal model $ARIMA(1,0,1) \times (1,1,2)_{12}$. This model is used then to forecast the monthly water consumption in Saudi Arabia from the period November 2016 to July 2017. The forecasted values show the harmony with its counterparts in the original series values. This result provides a future image of the reality of monthly water demand in Saudi Arabia. Therefore, the officials and decision-makers can adopt the results of this study to face monthly water demand in Saudi Arabia (water scarcity). In particular, the identified multiplicative SARIMA model can be employed by the Ministry of Environment, Water and Agriculture in Saudi Arabia to ensure sustainable water resources management in the basin.

For future study, new modern statistics such as functional time series or fractional time series may be used in analyzing the water consumption data in Saudi Arabia, and the results can be then compared to the SARIMA model and its findings.

Acknowledgements. The authors extend their appreciation to the Deanship of Scientific Research at King Khalid University for funding this work through General Research Project under grant number (G.R.P-58-38).

REFERENCES

- [1] Abushammala, M. F. M., Bawazir, A. K. (2017): Domestic water demand forecasting for Makkah, Saudi Arabia. – *European Water* 58: 481-487.
- [2] Agthe, D. E., Billings, R. B. (1980): Dynamic models of residential water demand. – *Water Resources Research* 16(3): 476-480.
- [3] Al-Ibrahim, A. A. (1990): Water use in Saudi Arabia: problems and policy implications. – *Journal of Water Resources Planning and Management* 116: 375-388.
- [4] Arbués-Gracia, F., García-Valiñas, M. A., Martínez-Espiñeira, R. (2003): Estimation of residential water demand: a state of the art review. – *Journal of Socio-Economics* 32(1): 81-102.
- [5] Box, G. E. P., Jenkins, G. M. (1970): *Time Series Analysis, Forecasting and Control*, 3rd ed. – Prentice Hall, Englewood Cliffs, NJ.
- [6] Chicoine, D. L., Deller, S. C., Ramamurthy, G. (1986): Water demand estimation under block rate pricing: a simultaneous equation approach. – *Water Resources Research* 22(6): 859-863.
- [7] Cornillon, P., Imam, W., Matzner, E. (2008): Forecasting time series using principal component analysis with respect to instrumental variables. – *Computational Statistics and Data Analysis* 52: 1269-1280.
- [8] Dalhuisen, J. M., Florax, R., De Groot, H., Nijkamp, P. (2003): Price and income elasticities of residential water demand: a meta-analysis. – *Land Economics* 79(2): 292-308.
- [9] Davis, W. Y. (2005): Water demand forecast methodology for California water planning area work plan and model review. – Research Report, California Bay-Delta Authority, CA, USA 19: 137-148.
- [10] Dickey, D. A., Fuller, W. A. (1979): Distribution of the estimators for autoregressive time series with unit root. – *Journal of the American Statistical Association* USA 74: 427-431.
- [11] Foster, H. S. J., Beattie, B. R. (1979): Urban residential demand for water in the United States. – *Land Economics* 55(1): 43-58.
- [12] Gottlieb, M. (1963): Urban domestic demand for water in the United States. – *Land Economics* 39(2): 204-210.
- [13] Hamilton, J. D. (1994): *Time Series Analysis*. – Princeton University Press, United State of America, Princeton, NJ.
- [14] Hansen, L. G. (1996): Water and energy price impacts on residential water demand in Copenhagen. – *Land Economics* 72(1): 66-79.
- [15] Höglund, L. (1999): Household demand for water in Sweden, with implications of a potential tax on water use. – *Water Resources Research* 35(12): 3853-3863.
- [16] Hongyan, L., Yuabiao, Z., Zhifeng, C., Zexin, M. (2017): Evaluation and prediction of regional water resources carrying capacity: a case study of Shandong Province. – *Environment and Natural Resources Research* 7(1): 21-33.
- [17] Howe, C. W., Lina weaver, F. P. (1967): The impact of price on residential water demand and its relationship to system design and price structure. – *Water Resources Research* 3(1): 13-32.
- [18] Kambale, J. B., Singh, D. K., Sarangi, A. (2016): impact of climate change on groundwater recharge in a semi-arid region of Northern India. – *Applied Ecology and Environmental Research* 15(1): 335-362.
- [19] Kulshreshtha, S. N. (1996): Residential water demand in Saskatchewan communities: role played by block pricing system in water conservation. – *Canadian Water Resources Journal* 21(2): 139-155.
- [20] Martínez-Espiñeira, R. (2002): Residential water demand in the northwest of Spain. – *Environmental and Resource Economics* 21(2): 161-187.
- [21] Ministry of Environment, Water and Agriculture, Saudi Arabia. – <http://app.mowe.gov.sa/IPS/IPS/Query/InforKSA.aspx?&Min=1&UserId=>

- [22] Muhamad, S., Nurul, H., Mohd, T., Vigneswary, P., Mohd, N., Razak, Z., Suffian, M. D., Idham, K. (2018): Improving the performance of ANN-ARIMA models for predicting water quality in the offshore area of Kuala Terengganu, Malaysia. – *Journal of Sustainability Science and Management* 13(1): 27-37.
- [23] Nauges, C., A. Thomas. (2000): Privately-operated water utilities, municipal price negotiation, and estimation of residential water demand: the case of France. – *Land Economics* 76(1): 68-85.
- [24] Nieswiadomy, M. L., Molina, D. J. (1989): Comparing residential water demand estimates under decreasing and increasing block rates using household data. – *Land Economics* 65(3): 280-289.
- [25] Rita, S., Yony, H., Rubiyanto, Fakhri, A. M., Madzlan, A. (2013): Multiple linear regression (MLR) modeling of wastewater in urban region of southern Malaysia. – *Journal of Sustainability Science and Management* 8(1): 93-102.
- [26] Samsuri, A., Marzuki, I., Si, Y. F. (2017): Multiple linear regression (MLR) models for long term Pm10 concentration forecasting during different monsoon seasons. – *Journal of Sustainability Science and Management* 12(1): 60-69.
- [27] Wei, W. W. S. (2006): *Time Series Analysis: Univariate and Multivariate Methods*, 2nd Edition. – Addison-Wesley, Boston.

APPENDIX

Monthly water consumption data in Saudi Arabia between January 2010 and July 2017 (Ministry of Environment, Water and Agriculture, Saudi Arabia)

Year	Month	Water consumption (m ³)	Year	Month	Water consumption (m ³)
2010	1	181939098	2014	1	224952954
	2	160540706		2	208397220
	3	184361371		3	234749774
	4	182276377		4	225968489
	5	190071038		5	249799599
	6	191941944		6	245316101
	7	201353276		7	253530687
	8	201911967		8	250959716
	9	197210257		9	245723978
	10	201739765		10	250966000
	11	195916912		11	241421651
	12	197488790		12	246410894
2011	1	191445402	2015	1	239995376
	2	173252570		2	218625646
	3	197589877		3	242120060
	4	193327291		4	239764261
	5	208026292		5	256585620
	6	204244441		6	256445988
	7	213421578		7	263626853
	8	222289987		8	265025393
	9	205258673		9	260071576
	10	214452752		10	269842591
	11	202692522		11	256272921

	12	207495739		12	257284729
2012	1	204710434	2016	1	255794090
	2	185681806		2	240752352
	3	204947388		3	259296870
	4	200254874		4	251720038
	5	217412155		5	266836225
	6	212579186		6	263387877
	7	220756924		7	272165315
	8	220619235		8	268817999
	9	212082770		9	261302224
	10	218817360		10	270277919
	11	209670441		11	261071635
	12	213826019		12	262529383
2013	1	212915242	2017	1	264786946
	2	188238373		2	231301561
	3	213767580		3	268909016
	4	217117937		4	269628773
	5	230191686		5	285437797
	6	228494648		6	269723694
	7	244452775		7	273197966
	8	244873159			
	9	237947752			
	10	242969366			
	11	228361039			
	12	228428423			

RESEARCH ON THE EXPRESSION OF SUCROSE SYNTHASE GENE IN SWEET SORGHUM

GAO, H. C.¹ – HUSSAIN, K.² – PANG, H. B.¹ – LI, X. M.¹ – MA, L. J.¹ – WANG, L. L.¹ –
ZHANG, Y. – WU, S. W.³ – LI, Y. Y.^{1*}

¹*College of Life Science, Shenyang Normal University
No. 253 Huanghe North Street, Shenyang, Liaoning 110034, China*

²*Department of Botany, University of Gujrat, HH Campus, Gujrat, Pakistan*

³*College of Science Institute, Shenyang Agricultural University
No. 120 Dongling Road, Shenyang 110866, China*

**Corresponding authors*

e-mail: yueyinglicn@163.com, wusuwen001@126.com

(Received 3rd Oct 2018; accepted 5th Dec 2018)

Abstract. Sucrose synthase is present in all plant tissues. It has an important role in the metabolism of many organizations, especially affecting sucrose metabolism, The higher the gene expression, the higher the sucrose content is. In order to explore the factors affecting the degree of sucrose synthase activity, we selected 10 different varieties of sweet sorghum leaves in different periods and used quantitative PCR (Polymerase Chain Reaction) to determine the cDNA concentration with comparison to a standard curve. In this experiment, the relative expression of the SS gene of HT was compared in different periods. The results showed that there was a difference in the relative expression of the SS gene between different varieties of sweet sorghum.

Keywords: *sweet sorghum, sucrose synthase (SS), RT-PCR, sucrose content, qualitative analyses*

Introduction

Sweet sorghum originated in Africa, it has strong resistance, high photosynthetic rate, high sugar content, wide adaptability, etc (Gao et al., 2017). It is a variant of ordinary grain sorghum (Wu et al., 2014; Zhang et al., 2012), one of the world's important energy plants (Jiang et al., 2012; Vermerris, 2011). In biomass energy systems, it has the name of "the most efficient solar energy converter" because of the high production capacity (Zhao et al., 2015). Sweet sorghum is a drought-tolerant crop. It has a wide range of root systems, strong water absorption. It can absorb moisture from dry soil. Dry areas are, especially non-glycemic areas, not suitable for growing other sugar crops, Sweet sorghum is a salt-tolerant crop which can be planted on a large scale (Yu et al., 2014). It has wide adaptability to soil pH, in the value range of 5.0-8.0 it can be grown normally (Zhao et al., 2015).

Sweet sorghum is the most powerful competitor in the biomass energy system. It is an excellent new renewable energy crop. Its stems and seeds can be pulverized for the production of ethanol, production costs are half of that as corn (Zhan et al., 2003). Therefore, the study of bio-fuel ethanol from sweet sorghum is carried out by the world. (Zhan et al., 2003; Gnansounou et al., 2005). Sweet sorghum is an important sugar crop. The accumulation of sugar in sweet sorghum is mainly based on sucrose. By comparing the gene expression levels of different varieties at different stages, it is found that increasing the sugar content is important. (Ye et al., 2012). In this experiment, the sweet sorghum leaves of 10 varieties were extracted in 4 periods.

Reverse transcription was applied to obtain cDNA. Then real-time fluorescence quantitative technology was used to compare the difference of gene expression in sweet sorghum in different periods and varieties. It is important to understand the law of sugar accumulation in sweet sorghum, the principle of sucrose synthesis, metabolism and regulation. It can also serve as a guide for breeding sweet sorghum varieties with high sugar content, production practices and it also has a good reference for other crops.

Sucrose synthase (SS) is a key enzyme among plant sucrose metabolizing enzymes. Sucrose synthase exists in two forms. In the cytoplasm, sucrose synthase exists in a soluble state and is attached to the cell membrane in an insoluble state, but the former is the main way of existence (Chai et al., 2012), sucrose synthase is present in all plant tissues. It has an important role in the metabolism of many organizations. However, its activity in library tissues is higher than that in photosynthetic tissues. The activity of sucrose synthase is the highest in the tissues and cell walls of some synthetic starches (Xue et al., 2009). In sugar cane, studies have shown that the SS gene has a role in facilitating the unloading of sucrose in the organ during transport (Martin et al., 1993). During the synthesis of sucrose in tomato, SS maintains relatively high activity (Qi et al., 2005). The sucrose metabolic pathway has a dominant position in the sugar metabolism of peach (Zhang et al., 2014). At present, the SS gene has been cloned from plants such as sugar cane (Lingle et al., 2001), Arabidopsis (Chopra et al., 1992), corn, and sugar beet (Hesse et al., 1996).

Compared with conventional PCR technology, real-time PCR technology has high sensitivity, specificity, good repeatability, fast and simple operation, and can be directly used for qualitative analysis and quantitative analysis (Liu, 2011). Real-time fluorescence quantitative technology is a very effective experimental method, which has been widely used in the fields of molecular biology, genetic engineering, medical diagnosis, etc. (Ren et al., 2011). In this experiment, by analyzing the correlation between the SS gene and housekeeping gene expression, the dissolution curves of the two genes are single peaks. It shows that during the PCR amplification process, the reaction specificity is good, quantitatively it is accurate, and there is no non-specific amplification and primer dimer, which is the ideal dissolution curve. It explains that the selected primers can be applied to the relative quantitative analysis and the expression of 10 varieties of sweet sorghum SS gene in 4 growth stages by Comparative Delta-delta Ct method. If other heterogeneous peaks indicate non-specific fluorescence, the quantification is inaccurate and subsequent experiments cannot be performed.

Research design and methods

Plant material

The experimental materials are 10 varieties of sweet sorghum from China, they were provided by Liaoning Academy of Agricultural Sciences, growing in the experimental field under natural conditions and were Jinxi 53, Sweet GL, LTR108, LTR168, HT, collier, M-81E, Rio, Honey, umbrella. 3 repetitions were selected in the four stages of seedling, jointing, heading and maturity. The materials were taken from the sweet sorghum last 2 leaves. The samples were frozen in liquid nitrogen and placed in a -80 °C refrigerator (SANYO, MDF-382E).

Determination of SS activity

The extraction of the enzyme solution is carried out at 0-4 °C, 0.5 g of sorghum leaves was weighed and placed them in a mortar. Enzyme extract and a small amount of quartz sand were added to it. It was ground thoroughly on ice, then transfer to the centrifuge tube, and at 12000 r/min it was centrifuged at 4 °C for 20 min. The supernatant was taken as a crude enzyme solution. 50 µL of the crude enzyme solution was transferred into a test tube and 50 µL HEPES-NaOH buffer (pH 7.5), 20 µL 100 mmol/L UDPG (uridine diphosphate glucose), 20 µL 100 mmol/L fructose, 20 µL 50 mmol/L MgCl₂, were added to it. It was put into a 30 °C water bath for 30 min. 200 µL of 2 mmol/L NaOH was added and a water bath was applied at 100 °C for 10 min. The test tube was cooled in flowing water then hydrochloric acid and resorcinol were added to it and it was shaken well, measured with a spectrophotometer, repeated three times, and averaged.

Total RNA extraction and cDNA synthesis

It was carried out based on the instruction manual of the RNA extraction kit (Promega Z3100). RNA was extracted from the leaves of 10 varieties of sweet sorghum in 4 periods. The diluted RNA samples were added to a clean cuvette, and their absorbance were read with a nucleic acid quantitation meter (ScanDrop 200) at 260, 280 and 230 nm. If A₂₆₀/A₂₈₀ > 1.8, A₂₆₀/A₂₃₀ > 2.0, it proved that the purity of RNA extracted was qualified and can be used in subsequent experiments. RNA mass concentration calculation: RNA µg/µl = A₂₆₀ × 33 × Dilution factor/1000. Then RNA products were detected in 1% agarose gels.

For the synthesis of the first strand of cDNA the RT-PCR (Real-time PCR) kit (TaKaRa RR037A) was used, the reaction system and operation are as follows: The reaction system is 10 µL: 5×PRT Mix 2 µL, RNA template 8 µL. The reverse transcription reaction conditions are as follows: 37 °C 15 min, 85 °C 5 s, Reverse transcription products are stored at -20 °C. Then PCR was used to amplify and detect cDNA: The PCR reaction system is 25 µL: 15.5 µL of dd H₂O, 2.0 µL of 10 × Buffer, 0.5 µL of dNTPs (10 mM), 0.8 µL of Forward Primer (20 µM), 0.8 µL of Reverse Primer (20 µM), 0.5 µL of cDNA, 0.5 µL of Taq enzyme (5 U/µL). The thermal cycles were programmed for an initial denaturation of 3 min at 94 °C, followed by 30 cycles of 30 s at 94 °C, 30 s at 58 °C, and 45 s at 72 °C; and a final 10 min extension at 72 °C. Detection of PCR amplification products was performed by 1% agarose gel electrophoresis.

After electrophoresis on a 0.8% agarose gel at 300 V for 6 min, the clarity and integrity of the RNA bands were visualized on a gel imager.

Design of SS primers

Based on the existing literature, we identify the SS primers (*Table 1*).

Table 1. Primers for SS gene amplification

Primer	Length of primer (bp)	Primer sequence
SS-1 forward primer	19	GTCCCTCAAGACTCCCT
SS-1 reverse primer	19	ATTGGATTGGGCAAAGTAG
Actin-F forward primer	23	ACGGCCTGGATGGCGGTACATG
Actin-R reverse primer	26	GCAGAAGGACGCCTACGTTGGTGAC

Quantitative PCR systems and conditions

The PCR reaction system was 25 μL (TaKaRa RR820A): dd H₂O 15.5 μL , 10 \times Buffer 2.0 μL , dNTPs 0.5 μL (10mM), F-Primer 0.8 μL (20 μM), R-Primer 0.8 μL (20 μM), cDNA 0.5 μL (5 ng/ μL), Taq enzyme 0.5 μL (5 U/ μL). The PCR reaction system is: 94 °C pre-denaturation for 3 min, followed by 30 cycles of 30 s denaturation at 94 °C, 30 s annealing at 58 °C, and 45 s extension at 72 °C, 72 °C extension for 10 min.

Detection of the expression of SS using real-time quantitative PCR

Correlation analyses of SS gene and housekeeping gene expression

In this experiment, the relative quantitative analysis of the target gene was carried out by the Comparative Delta-delta Ct method. The correlation coefficient of the two genes measured by the experiment was required to be greater than 0.98, and the slope of the standard curve of the two genes was less than 0.1 to achieve the use of Comparative Delta. The delta Ct method is used to analyze the standard of data.

Real-time PCR reaction system and conditions

Using the cDNA of 10 sweet sorghum of the same species as a template, the amplification of the target gene and the reference gene was performed, and each sample was set to 3 replicates, and a blank control was set at the same time. The PCR reaction system is 20 μL : 10.0 μL of 2 \times SYBR Premix ExTaq II, 6.0 μL of dd H₂O, 0.8 μL of Forward Primer (20 μM), 0.8 μL of Reverse Primer (20 μM), 0.4 μL of ROX Reference DYE, 2.0 μL of cDNA template (5 ng/ μL). The thermal cycles were programmed for an initial denaturation of 30 s at 95 °C, followed by 40 cycles of 5 s at 95 °C, 20 s at 60 °C, and 30 s at 72 °C.

Data analysis

Processing and analyzing experimental data were performed by using Origin (Origin 8.6) and SPSS (IBM SPSS Statistics 21) software.

Results

Analyses of extraction results of RNA

The extracted sweet sorghum total RNA was detected by agarose gel electrophoresis, and the amplification results from left to right were: JinXi 53, sweet GL, LTR108, LTR168, HT, collier, M-81E, Rio. The strips are clear and bright, indicating that they are both good in integrity and quality during the extraction process and can be used as templates in subsequent experiments.

Detection of cDNA

Using the first strand of cDNA as a template, the target gene SS and the internal reference gene Actin were used as primers for PCR amplification. The strip is clear and bright, It has been proved that the extracted sweet sorghum RNA has been successfully converted into cDNA, and the experiment of the next fluorescent quantitative PCR can be performed.

Qualitative analyses of SS gene expression

Simultaneous amplification of the SS gene and the housekeeping gene by real-time PCR (Corbett, Rotor-Gene-3000) was performed. The amplification curve is shown in *Figures 1–2*. The standard curve is shown in *Figures 3–4*. The correlation coefficient between housekeeping gene and SS gene is greater than 0.98, indicating high correlation. The slope of the standard curve of both genes is less than 0.1. This shows that the next experiment can use the Relative Delta-delta Ct method for relative quantitative analysis.

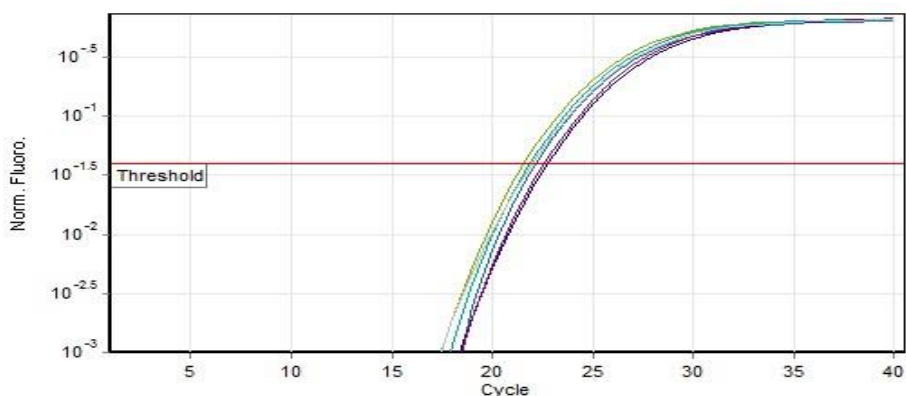


Figure 1. Real-time quantitative PCR amplification of the Actin gene

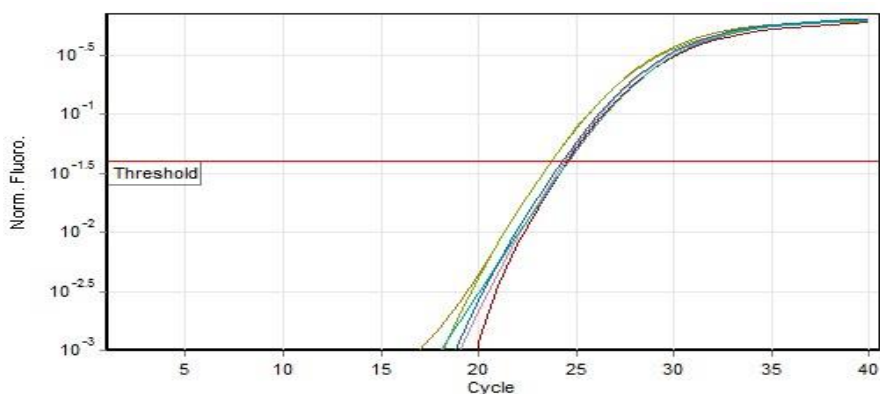


Figure 2. Real-time quantitative PCR amplification of the SS gene

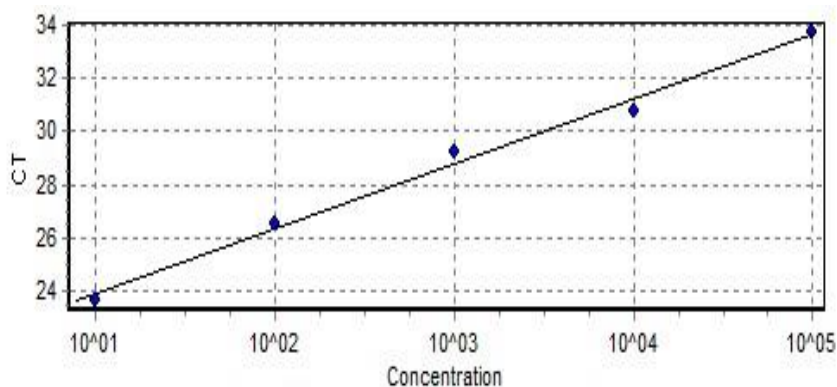


Figure 3. The standard curved of Actin gene

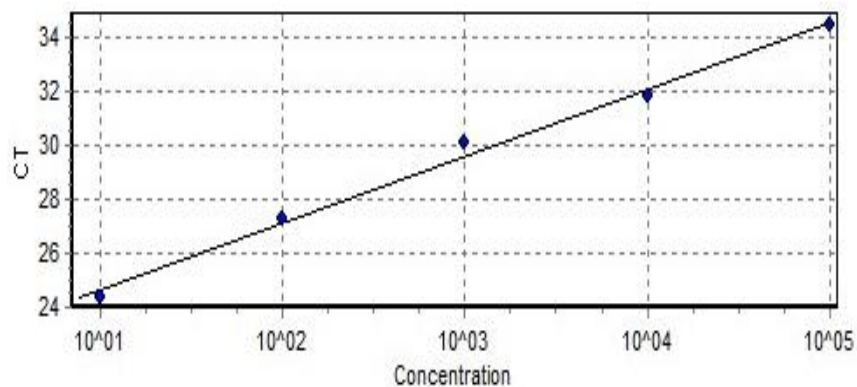


Figure 4. The standard curved of SS gene

Quantitative analyses of SS gene expression

Analysis results of the SS gene and the melting curve of the housekeeping gene are shown in *Figures 5–6*. It can be seen that the melting curve of the SS gene and the housekeeping gene have a single peak. It shows that during the PCR amplification process, the reaction specificity is good and the quantification is accurate. It is an ideal dissolution curve, indicating that the data of the quantitative PCR amplification in this experiment is reliable.

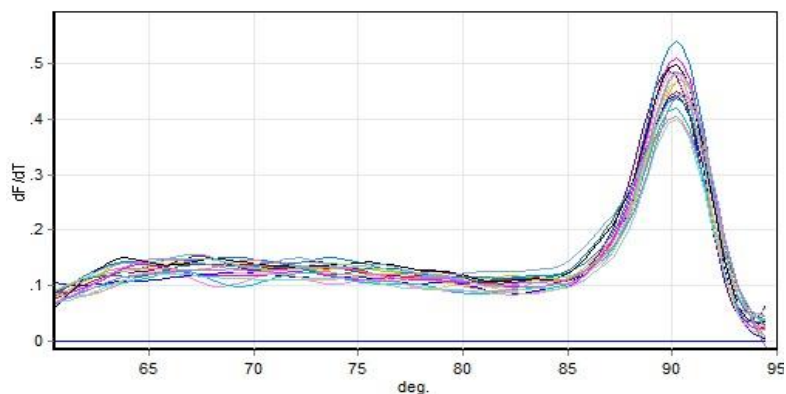


Figure 5. The melting curve of Actin gene

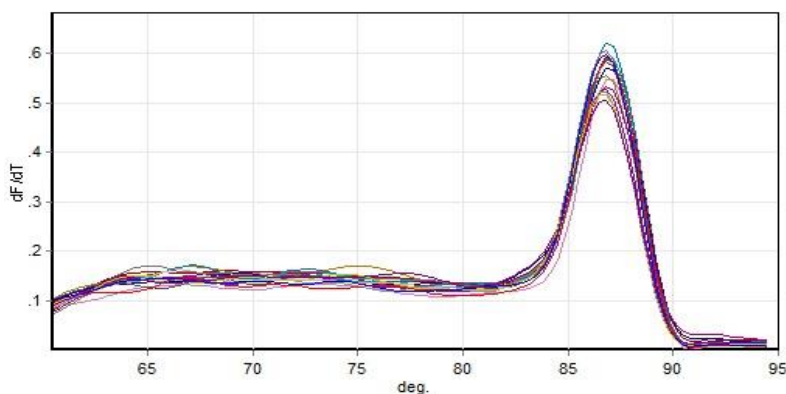


Figure 6. The melting curve of SS gene

Comparative analyses of quantitative expression of SS gene at four stages

Fluorescence quantitative amplification experiments of SS genes in leaves of 10 varieties of sweet sorghum seedlings (Fig. 7), jointing stage (Fig. 8), heading stage (Fig. 9) and maturity (Fig. 10) was carried out then HT was selected as a comparison. Relative quantitative analysis using the Comparative Delta-delta Ct method found that there is a difference in the expression of the relative amounts of sweet sorghum SS in leaves of different varieties at different periods. SS is a key enzyme in sucrose metabolism. Its activity affects the synthesis of sucrose, the higher the expression of SS gene, the higher the content of sucrose.

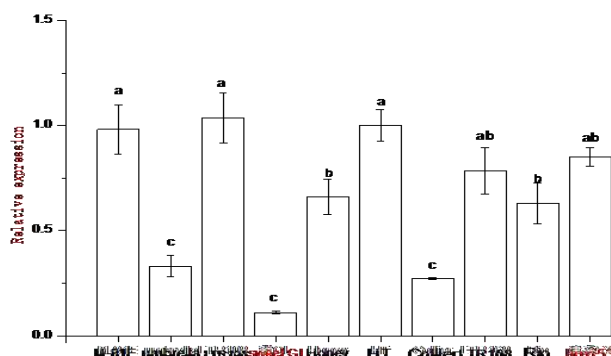


Figure 7. The comparison of different breeds of the SS gene expression in seedling stage

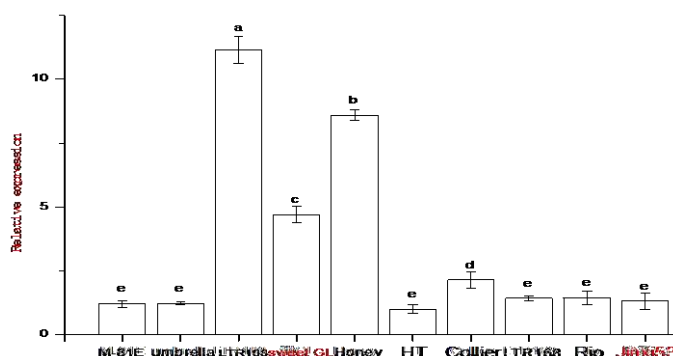


Figure 8. The comparison of different breeds of the SS gene expression in jointing stage

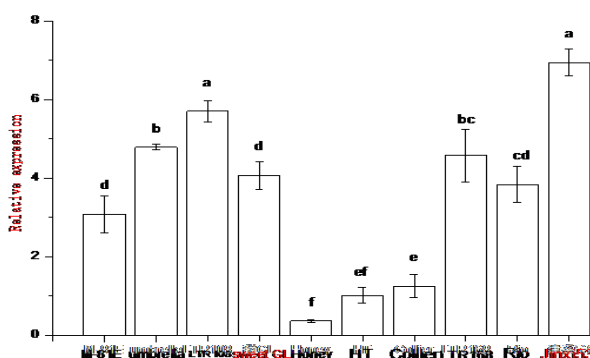


Figure 9. The comparison of different breeds of the SS gene expression in heading stage

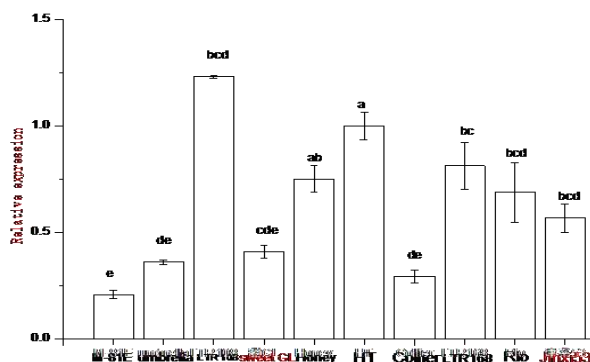


Figure 10. The comparison of different breeds of the SS gene expression in mature stage

Discussion

Sweet sorghum can be used as food, brewing, sugar and a renewable energy resource. It can be used to make ethanol (Cao et al., 2002). The accumulation of sweet sorghum stalk sugar is a very complicated process. In higher plants, sucrose is the main form of carbohydrate transport from photosynthetic source tissues to reservoir tissues. The expression of enzymes involved in its synthesis and decomposition is the main factor affecting sucrose accumulation (An, 2013).

It has many functions, including being able to participate in the synthesis of starch, cellulose and ATP, and mobilizing sucrose into various metabolic pathways, such as structural composition and storage, plant cell metabolism, etc. It is capable of reversibly synthesizing and decomposing sucrose, and regulating plants growth process, etc.

In previous studies, it was found that in the early stage of development of sweet sorghum, the expression of SS was lower, the late increase was obvious, and the heading period was the highest (Yang et al., 2009). In the analysis of SS gene expression in leaves of W452 varieties at different growth stages, the expression level of SS gene in different sweet sorghum varieties showed a trend of increasing first and then decreasing, and the flowering stage reached the highest (Xia et al., 2016).

In this experiment, RNA was extracted from 10 sweet sorghum varieties in 4 periods, and cDNA was reverse transcribed. Then, real-time quantitative PCR was used to compare the difference of SS gene expression between different varieties at different times. By comparison, it was found that the expression of SS gene was different in different periods of the same sweet sorghum variety; while the gene expression of different sweet sorghum varieties in the same period also differed. Taking a certain variety as a control and observing the expression trends of other varieties, it was found that the expression level of LTR108 was the highest in most cases in leaves, the rest of the varieties have different degrees of difference in different periods, so LTR108 varieties should be properly planted. All the varieties in the jointing stage had the highest gene expression, followed by the heading stage and it was the lowest in the seedling stage.

Conclusion

In conclusion, comparison of relative concentrations of SS genes in leaves of 10 varieties of sweet sorghum at different periods, the relative expression levels of SS gene of HT were compared with other 9 varieties in each period. There is a significant

difference in the relative expression of SS gene among different sweet sorghum varieties. The species with the highest relative expression of the SS gene at maturity is the LTR108 variety.

Acknowledgements. The research was partly supported by Major incubating project of Shenyang Normal University.

REFERENCES

- [1] An, Y. R. (2013): Study on the Expression of Sucrose Synthase Gene and Its Relationship with Sugar Content in Sweet Sorghum. – Tianjin Agricultural College, Tianjin.
- [2] Cao, Y. B. (2002): Developing sweet sorghum production and exploring new ways to use energy. – Chinese Seed Industry 1: 28-29.
- [3] Chai, J., Zhang, H., Yao, L. L. (2012): The role of sucrose synthase in plant growth and development. – Life Sciences 24: 81-88.
- [4] Chopra, S., Del-favero, J., Dolferus, R. (1992): Sucrose synthase of Arabidopsis: Genomic cloning and sequence characterization. – Plant Mol Biol 18: 131-134.
- [5] Gao, H. C., Qian, X. D., Bai, L., Pang, H. B., Li, Y. Y. (2017): Comparative study on physiological and biochemical indexes of main cultivated varieties of five kinds of sweet sorghum. – Hubei Agricultural Science 56(19): 3621-3623.
- [6] Gnansounou, E., Dauriat, A., Wyman, C. E. (2005): Refining sweet sorghum to ethanol and sugar: economic tradeoffs in the context of North China. – Bioresource Technology 96: 985-1002.
- [7] Hesse, H., Willmitzer, L. (1996): Expression analysis of a sucrose synthase gene from sugar beet (*Beta vulgaris* L.). – Plant Molecular Biology 30: 863-872.
- [8] Jiang, H., Huang, J., Zhang, Y. H. (2012): Effects of salt stress on antioxidant enzyme activities in sweet sorghum seedlings. – Journal of Shenyang Normal University (Natural Science Edition) 30: 289-292.
- [9] Lingle, S. E., Dyer, J. M. (2001): Cloning and expression of sucrose synthase-1 cDNA from sugarcane. – Journal of Plant Physiology 158: 129-131.
- [10] Liu, C. H. (2011): Research progress and application of real-time fluorescent quantitative PCR technology. – Chinese Practical Medicine 2011: 238-240.
- [11] Martin, T., Frommer, W. B., Salanoubat, M. (1993): Expression of an arabidopsis sucrose synthase gene indicates a role in metabolization of sucrose both during phloem loading and in sink organs. – The Plant Journal for Cell and Molecular Biology 4: 367-377.
- [12] Qi, H. Y., Li, T. L., Liu, H. T. (2005): Study on sugar content and related enzyme activity in different parts of tomato. – Journal of Horticulture 32: 239-243.
- [13] Ren, G. M., Wang, Y. Y. (2007): Research progress of real-time fluorescent quantitative PCR. – Journal of Clinical Medicine Practice 243-245.
- [14] Vermerris, W. (2011): Survey of genomics approaches to improve bioenergy traits in maize, sorghum and sugarcane free access. – Journal of Integrative Plant Biology 53: 105-119.
- [15] Wu, P. H., Li, J. W., DiLi, X. T. (2016): Analysis of main biological characteristics of sweet sorghum exogenous varieties. – Shanxi Agricultural Science 8: 1127-1130.
- [16] Xia, B. X., An, Y. R., Gao, J. M., Luo, F., Chen, X. M., Li, O. J., Wang, F. Y., Shi, D. F., Guan, X. N., Wu, H. Y., Pei, Z. Y. (2016): Correlation between sugar accumulation and expression of sucrose synthase gene in sweet sorghum. – Jiangsu Agricultural Science 44(2): 133-140.
- [17] Xue, W., Cui, J. H., Sun, A. Q. (2009): Correlation between soluble sugar content of sorghum and SS, SPS enzyme activity. – China Agricultural Science and Technology Herald 11: 124-128.

- [18] Yang, M., Li, L. J, Li, L. Y, Wang, B., Chang, J. H., Liu, G. Z. (2009): Correlation analysis between sucrose synthase expression and sucrose accumulation in sweet sorghum. – *Crop Journal* 35(1): 185–189.
- [19] Ye, K., Kuerban, Z., Chen, W. W. (2012): Study on the activity of SS and SPS enzymes of sweet sorghum straw under different sowing periods. – *Xinjiang Agricultural Science* 2012: 1874-1880.
- [20] Yu, H. L., Shi, Z. S., Cong, L. (2014): Comparison of photosynthesis and physiological responses of sweet sorghum and sorghum under drought stress. – *Jiangsu Agricultural Science* 2: 72-75.
- [21] Zhan, X., Wang, D., Tuinstra, M. R. (2003): Ethanol and lactic acid production as affected by sorghum genotype and location. – *Industrial Crops and Products* 18: 245-255.
- [22] Zhang, C. H., Yu, M. L., Ma, R. J. (2014): Dynamic changes of main carbohydrate content and sucrose synthase gene expression level in different developmental stages of peach. – *Jiangsu Journal of Agricultural Sciences* 6: 1456-1463.
- [23] Zhang, S. J., Amej, W., Xue, X. Z. (2014): Analysis of silage quality of maize and sweet sugar sorghum in southern Xinjiang. – *Journal of Grass Industry* 23: 232-240.
- [24] Zhao, H., Zhai, G. W., Zou, G. H. (2015a): Comparison of the changes in the distribution of material accumulation between sweet sorghum and common sorghum. – *Zhejiang Agricultural News* 1: 7-11.
- [25] Zhao, Y. Y., Xu, H., Lu, Z. H. (2015b): Advances in research on energy traits and stress resistance mechanism of sweet sorghum under saline-alkali and drought stress. – *Journal of Jiangxi Agricultural University* 1: 54-59.

IMPACT OF AGRICULTURAL WASTE RETURN ON SOIL GREENHOUSE GAS EMISSIONS

HUANG, D. D.^{1,2} – CAO, G. J.^{1*} – GENG, Y. H.¹ – WANG, L. C.^{3*} – CHEN, X. W.^{2,4} – LIANG, A. Z.^{2,4}

¹*College of Resource and Environment, Jilin Agricultural University
Changchun 130118, China*

²*Key Laboratory of Mollisols Agroecology, Northeast Institute of Geography and Agroecology
Chinese Academy of Sciences, Changchun 130102, China*

³*Institute of Agricultural Resource and Environment, Jilin Academy of Agricultural Sciences
Changchun 130033, China*

⁴*University of Chinese Academy of Sciences, Beijing 100049, China*

**Corresponding authors*

e-mail: cgj72@126.com (Cao, G. J.); wlc1960@163.com (Wang, L. C.)

(Received 12th Oct 2018; accepted 20th Dec 2018)

Abstract. The effects of agricultural waste return on the emissions of greenhouse gases (CO₂, N₂O and CH₄) from corn farmland in the black soil region of Northeast China and its potential to increase temperature were studied to provide a theoretical basis for formulating reduction measures of agricultural greenhouse gas emissions. This study was conducted at the Experimental Station of China Agricultural University in Quanyangou, Lishu County, Siping City, Jilin Province. Static greenhouse gas chromatography was used to monitor soil greenhouse gas fluxes under different fertilization measures, and the different fertilization treatments were analyzed for comprehensive differences in greenhouse effects among corn fields. The results showed that the average CO₂ fluxes and total emissions in response to the straw return treatment were the highest, reaching 388.96 mg·m⁻²·h⁻¹ and 14718.97 kg·hm⁻², respectively, and nitrogen topdressing fertilizer significantly increased CO₂ emissions. With respect to CH₄ emissions, single fertilizer-treated plots had the highest average absorbed flux and total absorption—0.042 mg·m⁻²·h⁻¹ and 1.36 kg·hm⁻², respectively, and with respect to N₂O fluxes, the highest flux and amount were 0.153 mg·m⁻²·h⁻¹ and 5.75 kg·hm⁻², respectively. The global warming potential of the straw *in situ* treatment was significantly higher than that of the other treatments, and the global warming potential of the cattle manure treatment was lower than that of the single chemical fertilizer treatment, but the differences were not significant. Moreover, straw mulch increased CO₂ emissions from black soils, and dry soils were shown to be important sinks of atmospheric CH₄. Combinations of organic and inorganic fertilizers and individual fertilizers can reduce N₂O emissions from soils. Therefore, to achieve higher corn yields and to reduce greenhouse gas emission intensities simultaneously, applications of organic and inorganic fertilizers constitute an ideal soil fertility method in the black soil region of Northeast China.

Keywords: CO₂, N₂O, CH₄, global warming potential, emission intensity

Introduction

With the increasing attention of the international community on climate change, food security and reduced greenhouse gas emissions, research on grain production and reducing greenhouse gas emissions from farmlands has received unprecedented attention from the scientific community (Intergovernmental Panel on Climate Change, 2013). It is estimated that CO₂, CH₄ and N₂O emissions from agriculture account for approximately 12%, 50%, and 60% of the global anthropogenic greenhouse gas emissions, respectively (Ge et al., 2014). The contribution of these three major

greenhouse gases combined to global warming has been reported to be as high as 80% (Yuan et al., 2017). Agricultural activities are one of the major sources of greenhouse gas emissions (Yue et al., 2017). Among them, CH₄ emissions from animal manure have reached 2.86×10⁶ t, and N₂O emissions from animal manure have reached 2.66×10⁵ t, accounting for 28.35% of the total N₂O emissions from agricultural activities; moreover, N₂O emissions from compost account for 5.2% of the N₂O emissions animal manure (National Development and Reform Commission, 2013). Agricultural soils contribute greatly to greenhouse gas emissions (Krobel et al., 2016; Zhang et al., 2017). Fertilization of agricultural soils has a crucial influence on soil greenhouse gas emissions (Cheng et al., 2016; Zhang et al., 2012). Agricultural management techniques such as planting patterns, farming practices, grain filling, and stubble application strongly affect agricultural greenhouse gas emissions. Among all these techniques, fertilization has the greatest impact on greenhouse gas emissions (Qin et al., 2016; Salehi et al., 2017; Zhang et al., 2016a). With the gradual increase in worldwide population, the demand for food will increase, and the amount of greenhouse gas emissions from excessive agricultural activities (such as fertilization) will increase. Thus, the contradiction between food security and greenhouse gas emissions will need to be eliminated; that is, under the premise of ensuring food security, the effective reduction in farmland greenhouse gas emissions will be needed, which is a major problem for the sustainable development of agriculture.

China currently produces the largest agricultural waste output worldwide. The amount of crop straw produced is approximately 650 million tons, and the amount of livestock and poultry manure is approximately 1.73 billion tons (Lozano et al., 2017; Xu et al., 2018; Zhao et al., 2016). These agricultural wastes are not being properly used, which has resulted in a waste of resources and has caused a severe threat to the environment. Researchers in China and abroad have reported that the return of agricultural waste to the field can not only reduce resource waste, reduce the application of chemical fertilizers, improve soil structure, increase soil fertility, and reduce environmental pollution but also affect greenhouse gas emissions by altering soil carbon (C) sequestration potential, which then slows the contribution to global climate change (Epps et al., 2016; Mitran et al., 2016; Zhang et al., 2016). Therefore, replacing some chemical fertilizers with organic fertilizers is an inevitable trend concerning fertilizer applications in the future in China (Ding et al., 2016). This experiment takes corn farmland on black soil in the central part of Jilin Province as a research object and adopts the static box method to study how applications of cow manure, chicken manure, straw and chemical fertilizer under conditions of high organic fertilizer substitution, as well as nitrogen (N), phosphorus (P), potassium (K) and other nutrients, impact greenhouse gas emissions and the warming potential of those emissions. The purpose of this study is to provide a theoretical basis for the resource utilization of agricultural waste and a scientific evaluation of its role in greenhouse gas emissions.

Material and methods

Study site

This experiment was conducted at the Experimental Station of China Agricultural University in Quanyangou, Lishu County, Siping City, Jilin Province, in 2014. The location of the sampling site is given in *Figure 1*. The area had been used to grow monoculture corn under conventional management for more than 10 years, which is

harvested annually, and the soil at the site is black soil. The annual average temperature is 6.5°C, the sunshine duration is 2393-2928 h·year⁻¹, the frost-free period is 115-188 days, and the annual cumulative temperature >10°C is 2900-3100°C. The average annual rainfall is 577 mm and is concentrated mainly in June-August, accounting for approximately 65% of the annual precipitation, and the average annual evaporation is 790-820 mm. The basic physical and chemical properties of the 0-20 cm soil layer are as follows: pH of 6.69, 19.90 g·kg⁻¹ organic matter, 1.26 g·kg⁻¹ total N, 90.72 mg·kg⁻¹ alkaline hydrolysis N, 21.27 mg·kg⁻¹ available P, and 186.18 mg·kg⁻¹ available K.

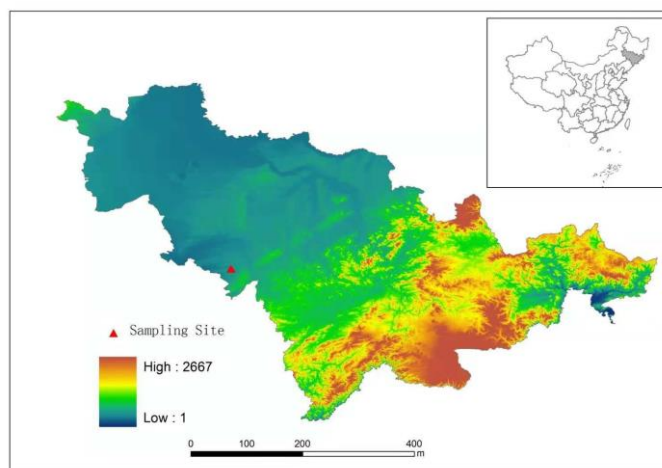


Figure 1. Sampling site

Experimental material

The tested corn variety Liangyu 11 was planted at a ridge spacing of 60 cm, a density of 65000 plants·ha⁻¹ and an intended plant spacing of 25.6 cm. With respect to the tested inorganic fertilizers, N was supplied as urea (46% N), P was supplied as diammonium phosphate (18% N, 46% P₂O₅) or heavy superphosphate (46% P₂O₅), and K was supplied potassium sulfate (K₂O 50%), and agricultural waste included cow manure, chicken manure and corn stalks. The nutrient contents of the different agricultural wastes are shown in *Table 1*.

Table 1. Nutrient contents of different agricultural wastes (w/%)

Organic material	Organic matter	Nitrogen	Phosphorus	Potassium
Cow manure	30.34	1.5	0.96	1.23
Chicken manure	34.38	2.87	1.56	1.68
Corn stalks	58.9	0.72	0.25	1.5

Experimental design

The experiment consisted of 5 treatments, 5 test plots, 3 gas collection boxes placed in each treatment plot, and 3 replicates. Each plot was 76 m², and the area received natural rainfall and no artificial irrigation. This experiment adopts the principle of equal N, P, and K nutrient contents for the experimental design. The N, P, and K contents in the agricultural waste were converted to pure N, pure P, and pure K for analysis. To

generate straw for returning to the field, plants were planted at a density of 65000 plants·hm⁻². One hundred percent of the straw produced was returned to the field, and cow manure and chicken manure were applied to the field at 50% of the total N application rate (240 kg·hm⁻²). The remaining amounts of N, P, and K in the organic fertilizers remained in the treatments, and the nutrient content deficiencies were compensated with chemical fertilizers. In other words, it was ensured that the total N, P and K nutrient components applied to the soil in all fertilization treatments were equal, namely, 240 kg·hm⁻² pure N, 100 kg·hm⁻² P₂O₅ and 120 kg·hm⁻² K₂O. The nitrogen and phosphorus nutrients contained in the straw are insufficient, and the rest is supplemented by chemical fertilizer. The excess potassium in the straw does not need to be supplemented. The five treatments were: CK, no fertilization; S1: single chemical fertilizer application, N 240 kg·hm⁻², P₂O₅ 100 kg·hm⁻², K₂O 120 kg·hm⁻²; S2: straw totally returned to the field, fertilizer nitrogen accounted for nearly 90% of the nitrogen application rate. S3: cow manure returned to the field, the manure nitrogen and chemical fertilizer nitrogen both accounted for 50% of the nitrogen application rate; S4: chicken manure returned to the field, chicken nitrogen and fertilizer nitrogen both accounted for 50% of the nitrogen application rate.

Thirty percent of the N fertilizer application amount was supplied as a basal fertilizer, 40% was applied as topdressing, and 30% was also applied as topdressing. The agricultural wastes as well as the P and potash fertilizers were applied as basal fertilizers at the same time. The specific fertilization schemes are listed in *Table 2*.

On April 27, the agricultural waste was applied to the test plots; it was evenly mixed with the soil to cover the ground surface. On April 28, after mechanical ridging, the surface soil covered the agricultural waste. Manual sowing was conducted on April 29, and the first gas collection was performed on April 30. Fertilization occurred on June 27 and July 28 at the jointing stage and tasseling stages, respectively.

Table 2. Experimental treatment and fertilizer amounts

Treatment	Organic Fertilizer (t·hm ⁻²)	Organic material (kg·hm ⁻²)			Fertilizer (kg·hm ⁻²)		
		Amount of N	Amount of P ₂ O ₅	Amount of K ₂ O	N application rate	P ₂ O ₅ application rate	K ₂ O application rate
CK No fertilization	0	0	0	0	0	0	0
S1 Fertilizer	0	0	0	0	240	100	120
S2 Straw return	12.9	24.38	22.58	135.45	215.62	77.43	0
S3 Cow manure applied to the field	26.67	120	76.8	98.4	120	23.2	21.6
S4 Chicken manure applied to the field	13.29	120	65.22	70.24	120	34.78	49.76

Gas sampling

Greenhouse gas samples were collected using the static box method (Yuan et al., 2017). The gas collection box consisted of stainless steel plates welded together. When gas is collected, water is injected into the gas tank, forming a liquid seal with the gas box lid to ensure that the gas in the tank is closed. Gas samples were collected four times between 9:00 a.m. and 11:00 a.m. for 0, 15, 30, and 45 min, after which 100 ml of

each sample was then pumped into a 100 ml syringe. The sample was subsequently injected into a gas collection bag for storage, which was returned to the laboratory. The temperature inside the box, the soil temperature at a 5 cm depth, the atmospheric temperature, and the atmospheric pressure were recorded to correct the gas mass error caused by the increase in the temperature during the sampling process. The gas sample in the collection bag was ultimately injected into a designated vacuum flask as a sample of the greenhouse gas and sent to the Institute of Applied Ecology, Chinese Academy of Sciences, for testing. The experiment was started on April 29, and the plants were harvested on September 28. The whole growth period was 153 days. Because of the continuous use of basal fertilizers, samples were collected for 7 days, and the N fertilizer topdressings were applied on June 27 and July 28. After continuous sampling for 3 days, the remaining samples were collected once a week. However, due to the large amount of rainfall that occurred on the sample collection day, the gas could not be collected normally, and the gas collection time was delayed. Sampling was performed a total of 29 times. The specific sampling time is shown in *Table 3*.

Table 3. Date and number of sampling

Number	Date	Number	Date	Number	Date
1	Apr.30	11	Jun.4	21	Jul.30
2	May.1	12	Jun.12	22	Jul.31
3	May.3	13	Jun.19	23	Aug.7
4	May.4	14	Jun.28	24	Aug.18
5	May.5	15	Jun.29	25	Aug.27
6	May.6	16	Jun.30	26	Sep.3
7	May.7	17	Jul.7	27	Sep.10
8	May.14	18	Jul.14	28	Sep.17
9	May.21	19	Jul.22	29	Sep.25
10	May.28	20	Jul.29		

Test items and methods

Determination of greenhouse gases (CO₂, N₂O, CH₄): Gas samples were collected from a static chamber, and the contents of the greenhouse gases were determined by gas chromatography. An Agilent gas chromatograph instrument 7890A (Agilent Technologies Co., Ltd, USA) was used, and the CO₂ and CH₄ were determined by a hydrogen flame detector (FID). N₂O was determined using an electron capture detector (ECD). The measurement conditions were as follows: for the FID, the temperature was 300°C, the H₂ gas flow rate was 100 ml·min⁻¹, the practical air flow rate was 200 ml·min⁻¹, and the carrier gas was N₂; for the ECD, the temperature was 330°C, and the carrier gas was N₂ at a flow rate of 2 ml·min⁻¹.

The greenhouse gas emission flux was calculated as

$$F = \rho \cdot h \cdot dc/dt \cdot 273/(273+ T) \quad (\text{Eq.1})$$

where F is the greenhouse gas flux (μg·m⁻²·h⁻¹); ρ is the density of CO₂, N₂O, or CH₄ in the standard state (kg·m⁻³); h is the height of the sampling box (m); dc/dt is the concentration of greenhouse gases in the sampling tank; and T is the average temperature (°C) in the sampling chamber during sampling.

Data analysis

Statistical analyses were carried out using SPSS (version 11.5, SPSS Inc., Chicago, IL, USA), and the treatment means were compared using the least significant difference (LSD) test at a significance level of $P < 0.05$ (Liang et al., 2016).

Results

Atmospheric Temperature, Soil Temperature, and Rainfall During Greenhouse Gas Collection

The environmental conditions on the gas sampling day during the corn growth period in 2014 is shown in *Figure 2*. From April 29 to September 28 (autumn), measurements were taken on a total of 153 days. The atmospheric temperature in the figure is the temperature from 9:00 a.m. to 11:00 a.m. on the collection day. The maximum temperature was 33.03°C , the minimum temperature was 8.00°C , and the average temperature was 22.33°C . The 5 cm belowground temperature represents the mean ground temperature measured by the three gas collection boxes after gas collection on the sampling days; the maximum temperature was 25.33°C , the minimum temperature was 6.23°C , and the average temperature was 18.00°C . During the growth period, the cumulative rainfall was 354.86 mm, and the greatest daily rainfall amounts occurred on June 7 and August 25, which were 38.63 mm and 37.83 mm, respectively.

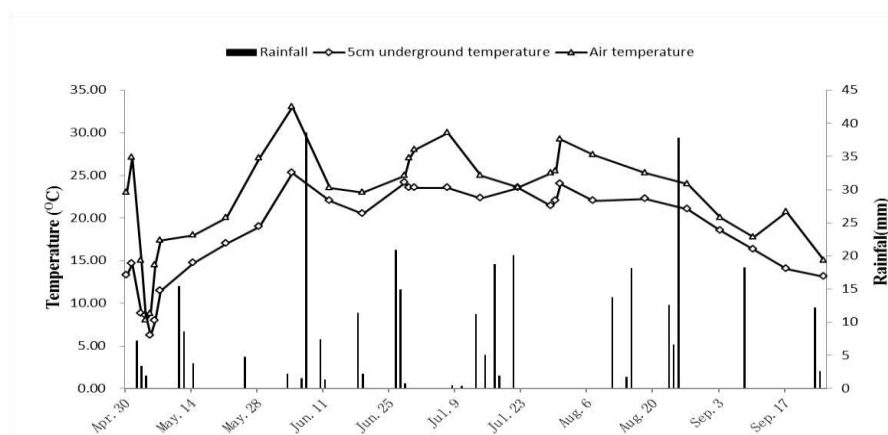


Figure 2. Variation in temperature and rainfall from April 28, 2014, to September 28, 2014

Effects of Agricultural Waste on CO₂ Emission Dynamics

As shown in *Figure 3*, the CO₂ emissions during the whole growth period of corn were essentially the same across all treatments and showed clear seasonal changes; that is, the CO₂ emission flux at the beginning and end of the growth period was relatively low (39.9 to $126.5 \text{ mg}\cdot\text{m}^{-2}\cdot\text{h}^{-1}$). The medium-term emission flux was the highest and peaked at the end of June and at the end of July. Between May 28 and July 31, CO₂ emissions in the control (CK) treatment exceeded $200.00 \text{ mg}\cdot\text{m}^{-2}\cdot\text{h}^{-1}$ and accounted for 81.64% of the total CO₂ emissions during the entire growth period. After each fertilization treatment, the CO₂ emissions increased. Under conditions of equal nutrient concentrations, the average CO₂ flux in each treatment was greater than $200 \text{ mg}\cdot\text{m}^{-2}\cdot\text{h}^{-1}$. Excluding the CK treatment, the other treatments each presented two peaks of CO₂

emissions after N fertilizer was topdressed at the end of June and at the end of July. As shown in *Table 4*, the greatest difference between the average CO₂ emission flux and the total emissions in each treatment was significant, and the average emission flux and total emissions of CO₂ in the straw return treatment (S2) were the highest among the treatments, 0.77% higher (P<0.05) than S1, 8.95% higher (P<0.05) than S3, 3.76% higher (P<0.05) than S4. With the exception of those in the CK treatment, the cumulative CO₂ emissions in the cow manure treatment were the lowest, 3.07% lower (P<0.05) than S1, 9.43% lower (P<0.05) than S2, and 4.49% lower (P<0.05) than S4.

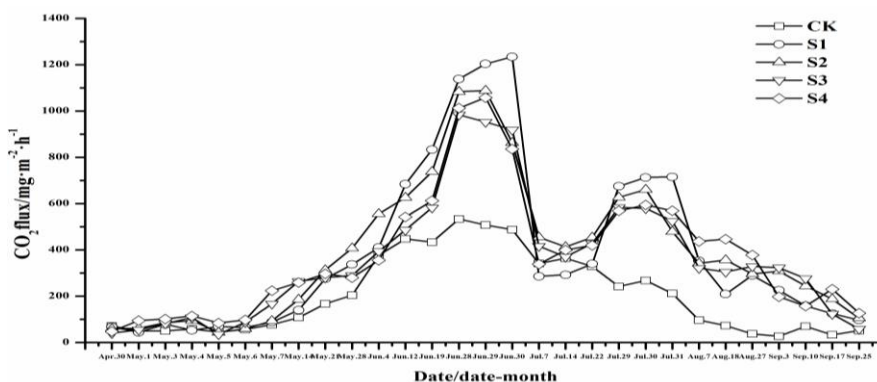


Figure 3. Emission flux of CO₂ under conditions of agricultural waste returned to the field

Table 4. Average emission flux and total cumulative emissions of CO₂, N₂O and CH₄

	Treatment	Average emission flux (mg·m ⁻² ·h ⁻¹)	Cumulative emission flux (kg·hm ⁻²)
CO ₂	CK	200.20d	7538.85e
	S1	385.97b	13753.68c
	S2	388.96a	14718.97a
	S3	357.02c	13330.94d
	S4	374.83b	13957.28b
N ₂ O	CK	0.049c	2.07c
	S1	0.153a	5.75a
	S2	0.139b	5.51b
	S3	0.137b	5.35b
	S4	0.136b	5.21b
CH ₄	CK	-0.035ab	-1.32ab
	S1	-0.042a	-1.36a
	S2	-0.025b	-0.81d
	S3	-0.030b	-1.05c
	S4	-0.034ab	-1.23b

Values followed by the same letter within a column indicate no significant difference at 0.05 level for CO₂, N₂O and CH₄

Effects of Agricultural Waste on the Dynamic Characteristics of N₂O Emissions

The N₂O flux from the farmland during the corn growth period is shown in *Figure 4*. All treatments presented positive values, indicating that dryland soil is a source of N₂O emissions. The figure shows that, in the CK treatment, the N₂O fluctuated widely, ranging from 5.43 μg·m⁻²·h⁻¹ to 116.10 μg·m⁻²·h⁻¹; moreover, the N₂O emissions peaked at 95.38 μg·m⁻²·h⁻¹, 116.10 μg·m⁻²·h⁻¹ and 97.17 μg·m⁻²·h⁻¹ on June 26, July 21 and

August 25, respectively, which may be related to the occurrence of relatively large amounts of rainfall. From June 12 to August 27, the N₂O emissions in the CK treatment exceeded 50.00 μg·m⁻²·h⁻¹, and the average N₂O emission flux in the CK treatment was 49.32 μg·m⁻²·h⁻¹. During the whole growth period, the N₂O emission flux in each fertilizer treatment ranged from 11.90 μg·m⁻²·h⁻¹ to 374.72 μg·m⁻²·h⁻¹. Under conditions of equal N, P and K nutrient contents, the maximum N₂O emissions (374.72 μg·m⁻²·h⁻¹) occurred on June 29 in response to a single application of chemical fertilizer (S1 treatment), most likely due to rainfall that occurred on June 26 and June 27. With respect to the topdressing results, the single fertilizer application (S1) treatment also presented N₂O emission peaks on June 12 and July 30, which may be related to rainfall events that occurred on June 10 and fertilizer applied on July 28. As shown in *Table 4*, the average N₂O emission flux and total emissions between the agricultural waste treatments followed the order of S1>S2>S3>S4, the average emission flux of S1 treatment N₂O is 10.07%, 11.68%, 12.5% higher (P<0.05) than S2, S3 and S4, respectively, the difference between S2, S3 and S4 was not significant; however, the total emissions in S2, S3 and S4 significantly differed from those in S1, and the average N₂O emissions were the highest in the S1 treatment, the cumulative emissions of S1 treatment are 4.35%, 7.48%, 10.36% higher (P<0.05) than S2, S3 and S4, respectively.

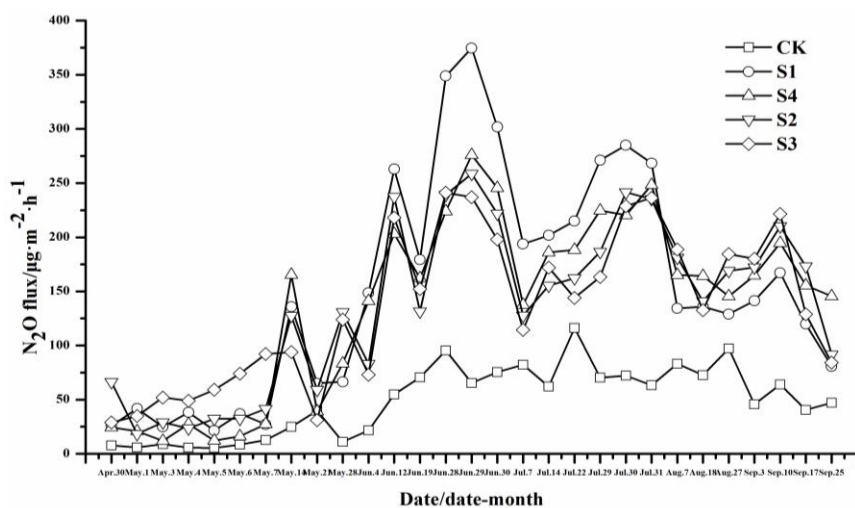


Figure 4. Emission flux of N₂O under conditions of agricultural waste returned to the field

Effects of Agricultural Waste on the Dynamic Change Characteristics of CH₄ Emissions

The CH₄ emission flux in this study is shown in *Figure 5*. The figure shows that each treatment presents a negative value; that is, the atmospheric CH₄ was absorbed by the soil. However, the single application of chemical fertilizer (S1) treatment on August 27 and the 100% straw return (equal to the application of pure N at 215.62 kg·hm⁻²; S2) treatment presented positive values of 15.04 μg·m⁻²·h⁻¹ and 8.80 μg·m⁻²·h⁻¹, respectively. This result may be due to three days of continuous rainfall that occurred from August 23 through August 25; furthermore, the cumulative rainfall of 57.00 mm, soil moisture content, and suitable conditions for methanogens were inhibited. Similarly, the absorption of CH₄ on June 12 fluctuated, which may be related to the rainfall on June 10 and June 11. Two peaks of 117.55 μg·m⁻²·h⁻¹ and 95.02 μg·m⁻²·h⁻¹

occurred on June 29 and July 30, respectively. Under conditions of equal N, P and K, the single application of chemical fertilizer (S1) treatment presented the largest absorption of CH₄ from the atmosphere, and there was no large fluctuation after the S2, S3 or S4 organic and inorganic fertilizer applications. As shown in *Table 4*, the average absorption flux and Cumulative emission flux were in the S1 treatment were significantly higher than those in the three agricultural waste treatments, the average emission flux S1 treatment absorbed 68% more than the S2 treatment (P<0.05), 40% more than the S3 treatment (P<0.05), and 23.53% more than the S4 treatment (P<0.05), the average emission flux difference of the three kinds of agricultural waste is not significant, and comparison among these three agricultural waste treatments, cumulative emission flux were the largest in S4, 51.85% more than S2 (P<0.05) and 17.14% more than S3 (P<0.05), and the differences are significant between S4 and both S2 and S3.

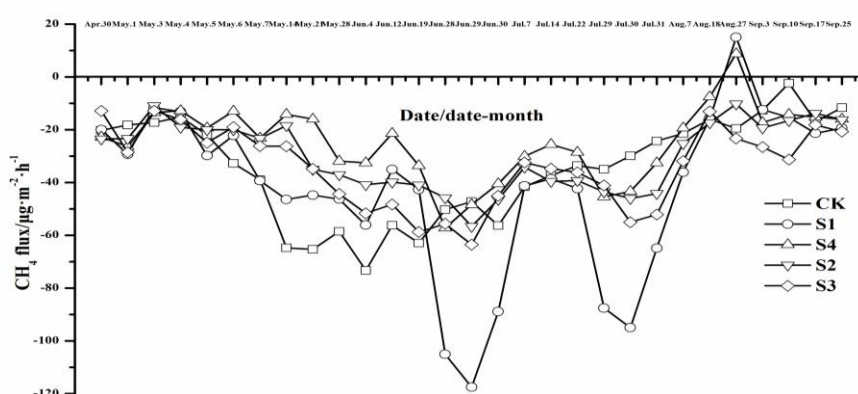


Figure 5. Emission flux of CH₄ under conditions of agricultural waste returned to the field

Impact of Agricultural Waste Disposal on the Global Warming Potential (GWP)

The GWP from corn fields is derived mainly from N₂O emissions, as N₂O is a global greenhouse gas with a dominant warming potential. However, the offset of CH₄ from the GWP of corn fields is only a very small proportion. In this experiment, the fixed C in the soil, which constitutes the offset ratio of the GWP within the corn field, accounts for a large proportion. As shown in *Table 5*, the GWP from the cutting and returning of straw to the field (S2 treatment) was significantly higher than that from the other treatments. In addition, the GWP from returning cow manure to the field (S3) was lower than that from the S1 treatment, which significantly differed from the other treatments. The greenhouse gas emission intensity (GHGI) in the S3 treatment was significantly the lowest among all the treatments.

Table 5. Global warming potential of the different treatments

Treatment	E-CH ₄ CO ₂ (kg·hm ⁻²)	E-N ₂ O CO ₂ (kg·hm ⁻²)	GWP(CH ₄ +N ₂ O) CO ₂ (kg·hm ⁻²)	Emission intensity CO ₂ (kg·hm ⁻²)
CK	-32.925a	616.86e	8122.79d	-
S1	-34a	1713.5a	15433.8b	0.129a
S2	-26.3c	1594.3c	16430.75a	0.114bc
S3	-30.775b	1552.58d	14898.4c	0.111c
S4	-20.2d	1641.98b	15479.09b	0.119b

E-CH₄ and E-N₂O are emissions of CO₂ in terms of CH₄ and N₂O, respectively

Values followed by the same letter within a column indicate no significant difference at 0.05 level

Discussion

Applications of organic fertilizers increase source materials of CO₂ production and thus promote the rate of CO₂ release by soil–crop systems (Zhang et al., 2016b). A relatively high soil organic matter content promotes the growth of soil microbes, increases the bioavailability of soil C pools, and improves soil respiration (Xing et al., 2016). The application of organic fertilizers to agricultural soils is an effective method for increasing soil C pools and slowing the greenhouse effect but also increases the rate of CO₂ release from soil respiration (Li et al., 2013; Yang et al., 2017). The results of the present study show that the highest peak of soil CO₂ emissions in response to farmland fertilization treatment occurs on the 7th day after fertilizer application, at the jointing stage. This finding is due mainly to the combined effects of N topdressing fertilizers, increased rainfall after topdressing, and increased temperatures (Guo et al., 2016). Furthermore, soil CO₂ emission peaks occurred after each topdressing during the corn growing season. These peaks occurred because the application of N fertilizer provides corn and microorganisms with N needed for growth; consequently, root respiration increases, and the soil temperature increases. Moreover, N fertilizer promoted intense activity of soil microorganisms, resulting in a rapid increase in soil CO₂ flux (Afreh et al., 2018; Wang et al., 2016). The CO₂ emission flux of soil treated with organic fertilizer and inorganic fertilizer was significantly higher than that treated without fertilizer (CK). This phenomenon was especially true for the CO₂ emission flux from the treatment in which straw was combined with inorganic fertilizer, which is consistent with previous research results (Ping et al., 2018; Shah et al., 2016). Studies have shown that organic fertilizers have a significant impact on soil emissions. This impact occurs mainly because the application of organic fertilizers improves the physical and chemical properties of soils, increases the accumulation of soil organic matter, and promotes both the activity of soil microorganisms and the growth and vitality of the root system, thus increasing emissions (Nigussie et al., 2017). Applications of crop straw can significantly reduce the soil bulk density and can increase soil porosity, accelerating the release of CO₂ gas that was generated in the soil to the atmosphere; thus, the CO₂ emission flux from straw combined with inorganic fertilizer is greatest.

Soil N₂O is a product of nitrification and denitrification, which are performed by microorganisms. N₂O emissions from farmland are constrained by soil aeration conditions and the concentrations of the reaction substrates. The application of organic fertilizer to farmland provides exogenous C and N to the soil, which is also provided by the decomposition of organic matter. The energy required for the additional organic C affects the activity of soil microbes, which then affects nitrification and denitrification (Shi et al., 2017). The results of the present study show that the peak time of N₂O emissions from farmland soils in each fertilization treatment is consistent with the peak CO₂ emissions from the soil, both of which occurred on the 7th day after topdressing at the jointing stage. This result may be due to the rapid increase in soil N content caused by the N topdressing fertilizer. The average N₂O emissions and total emissions in response to the agricultural wastes were significantly lower than those in response to single fertilizers. This result is because single fertilizers increase crop biomass and then enter soils through rice stalks, roots and other residual biomass to promote soil microbial N activity, which in turn increases N₂O emissions. Moreover, the joint effects of increased rainfall and increased temperature during jointing may have been a factor. Guyader and Maris also concluded that the application of organic fertilizers to treat N₂O

emissions was significantly lower than that of inorganic fertilizers (Guyader et al., 2017; Maris et al., 2016). Giweta also conducted experiments on the long-term fertilization of cultivated red soil and pointed out that the combined application of chemical fertilizers and organic fertilizers could reduce N₂O emissions (Giweta et al., 2017). The substitution of organic fertilizers for chemical fertilizers (at equal N concentrations) can effectively reduce N₂O emissions from dryland fields (Nótás, 2014). Some previous studies have shown that the application of straw and cow manure can increase soil organic matter content, consume soil O₂ concentration, form anaerobic environment, and promote denitrification and increase N₂O emissions (Liu et al., 2008; Lu et al., 2011). However, the results of this study did not significantly increase N₂O emissions, probably due to the application of high C/N organic materials, stimulating soil heterotrophic microbial growth and reproduction, fixing free NH⁴⁺-N in the soil, thereby inhibiting the activity of nitrifying microorganisms in the soil, thus failing to promote N₂O emissions (Recous et al., 1990).

In soils, CH₄ is released mainly by anaerobic methanogens during the process of transmission to the atmosphere, and only a portion of the CH₄ enters the atmosphere (Bansal et al., 2018). Some studies have reported that dryland soils have low CH₄ emissions and that there are many external factors, and dryland soils exhibit good permeability and do not easily produce anaerobic environments; the soil organic matter decomposition rate is high, and soil organic C does not easily accumulate and thus affects CH₄ production. Emissions are therefore considered an important sink of atmospheric CH₄ (Veretennikov et al., 2017). Gao showed that dry soils with good permeability could inhibit the activity of methanogens and lead to lower CH₄ emissions (Gao et al., 2015). The results of the present study showed that, under conditions of equal nutrient concentrations, the characteristics of the different treatments affected the overall absorption and emissions of CH₄; that is, dryland soil serves as an important sink of atmospheric CH₄, and the single fertilizer treatment and straw return treatment presented emissions on August 27, which may be due to the continuous rainfall that occurred from August 23-25. On the 3rd day of rainfall, the soil moisture content increased, making the conditions suitable for methanogens. In this study, the CH₄ emission flux observed under different fertilization treatments has both positive and negative values, and other soils from the cultivated land or grassland (Omonode et al., 2007; Shimizu et al., 2007). The results of this study are consistent. The cumulative emissions during the entire growth period are negative, indicating that soil is the net absorption sink of CH₄. However, some researchers have concluded that the application of organic fertilizers or organic and inorganic fertilizers combined with the application of CH₄ absorption in dry soil (Dong et al., 2005; Yang et al., 2010). In the dryland fields, the effects of the applications of chemical fertilizers and organic fertilizers to soils on the absorption of CH₄ are not consistent, and additional research is needed.

Understanding the contribution of a specific agricultural measure to the greenhouse effect should help in calculating the effects of that measure in combination with others. Due to the different warming effects of the three greenhouse gases, CO₂, CH₄, and N₂O, their impact on global warming is also different. In this paper, the GWP is used to represent the combined effect of the three types of greenhouse gases, that is, to evaluate their comprehensive contribution by calculating the amount of CO₂ emissions equivalent to the cumulative amount of greenhouse gases emitted from the soil (Lin et al., 2016). From the data obtained from this experiment, the calculated GWP of the treatment in which straw was returned to the field was significantly higher than that of

the other treatments, and the lowest GWP was in the treatment in which cattle manure was returned. However, to evaluate the comprehensive greenhouse effects of an agricultural ecosystem, not only must the equivalent CO₂ emissions from greenhouse gas emissions be calculated but also the CO₂ emissions caused by agricultural activities, such as irrigation, machinery and fertilizer applications, must be considered (Song et al., 2013; Sainju et al., 2016). Regarding the three types of agricultural waste treatments in this paper, the soil C sequestration potential and the contribution of different ratios to the greenhouse effect must be further studied.

Conclusion

The results of this study show that the average CO₂ flux and total discharge of the straw return treatment were the highest, reaching 388.96 mg·m⁻²·h⁻¹ and 14718.97 kg·hm⁻², respectively, and the N topdressing fertilizer effects were obvious. With respect to CH₄ emissions, the single fertilizer treatment presented the greatest average absorbed flux and total absorbed amount, which were 0.042 mg·m⁻²·h⁻¹ and 1.36 kg·hm⁻², respectively, and with respect to N₂O fluxes, the highest flux and amount were 0.153 mg·m⁻²·h⁻¹ and 5.75 kg·hm⁻², respectively. The GWP and GHGI of the straw return treatment were significantly higher than those of the other treatments, and the GWP and GHGI of the cattle manure return treatment were significantly lower than those of the other treatments. On the basis of the comprehensive greenhouse effect of the soils and GHGI, it was determined that, compared with the application of chemical fertilizers, the application of the combination of organic and inorganic fertilizers not only reduced the soil's comprehensive greenhouse effect (GWP) but also reduced the GHGI of the soil. Therefore, to achieve increased corn yields and to reduce the GHGI concurrently, the combination of organic and inorganic fertilizer applications (especially those comprising cow manure) represents an ideal soil fertility method in the black soil region of Northeast China.

Acknowledgements. This research was supported by the National Key R&D Program of China (2018YFD030020-3, 2017YFD0300604-2 and 2017YFC0504200); National Natural Science Foundation of China (41430857); Key Research Program of Frontier Sciences, Chinese Academy of Sciences (Grant No. QYZDB-SSW-DQC035); Youth Innovation Promotion Association, Chinese Academy of Sciences (2015183); and “135” project planning of Northeast Institute of Geography and Agroecology, Chinese Academy of Sciences (Y6H2042001).

REFERENCES

- [1] Afreh, D., Zhang, J., Guan, D., Liu, K., Song, Z., Zheng, C. (2018): Long-term fertilization on nitrogen use efficiency and greenhouse gas emissions in a double maize cropping system in subtropical China. – *Soil & Tillage Research* 180: 259-267.
- [2] Bansal, S., Tangen, B., Finocchiaro, R. (2018): Diurnal patterns of methane flux from a seasonal wetland: mechanisms and methodology. – *Wetlands*: 1-11.
- [3] Cheng, G., Zhang, A. F., Wang, X. D., Zhang, W. H., Ke-Qing, D. U. (2016): Assessment of wheat straw and its biochar effects on carbon sink in agricultural ecosystems using "carbon footprint" method. – *Journal of Agro-Environment Science* 35(3): 604-612.

- [4] Ding, M. J., Huang, Y., Yi, W. J., Liu, Y., Chen, Z. S. (2016): Effects of applying organic manure on nitrogen transformation and functional microbes of tobacco-planting soil. – *Southwest China Journal of Agricultural Sciences* 29(5): 1166-1171.
- [5] Dong, Y. H., Ouyang, Z. (2005): Effects of organic manures on CO₂ and CH₄ fluxes of farmland. – *Chinese Journal of Applied Ecology* 16(7): 1303-1307.
- [6] Epps, A. V., Blaney, L. (2016): Antibiotic residues in animal waste: occurrence and degradation in conventional agricultural waste management practices. – *Current Pollution Reports* 2(3): 1-21.
- [7] Gao, D. C., Zhang, L., Liu, Q. (2015): Effects of biochar on CO₂, CH₄, N₂O emission and its environmental benefits in dryland soil. – *Acta Ecologica Sinica* 35(11): 3615-3624.
- [8] Ge, Q. S., Wang, F., Wang, S. W., Cheng, B. B. (2014): Certainty and Uncertainty in Global Warming Studies. – *China Population, Resources and Environment* 24(1): 1-5.
- [9] Giweta, M., Dyck, M. F., Malhi, S. S. (2017): Growing season nitrous oxide emissions from a gray luvisol as a function of long-term fertilization history and crop rotation. – *Canadian Journal of Soil Science* 97(3): 474-486.
- [10] Guo, T. F., Liang, G. Q., Zhou, W., Liu, D. H., Wang, X. B., Sun, J. W. (2016): Effect of fertilizer management on greenhouse gas emission and nutrient status in paddy soil. – *Journal of Plant Nutrition & Fertilizer* 22(2): 337-345.
- [11] Guyader, J., Little, S., Kröbel, R., Benchaar, C., Beauchemin, K. A. (2017): Comparison of greenhouse gas emissions from corn- and barley-based dairy production systems in eastern Canada. – *Agricultural Systems* 152: 38-46.
- [12] IPCC (Intergovernmental Panel on Climate Change) (2013): *Climate change 2013-The physical science basis. – Working group I contribution to the fifth assessment report of the IPCC.* Cambridge, UK: Cambridge University Press.
- [13] Kröbel, R., Bolinder, M. A., Janzen, H. H., Little, S. M., Vandenbygaart, A. J., Kätterer, T. (2016): Canadian farm-level soil carbon change assessment by merging the greenhouse gas model Holos with the introductory carbon balance model (icbm). – *Agricultural Systems* 143: 76-85.
- [14] Li, B., Rong, X. M., Xie, G. X., Zhang, Y. P., Zhou, L., Zhang, Y. (2013): Effect of combined application of organic and inorganic fertilizers on greenhouse gases exchange and comprehensive global warming potential in paddy fields. – *Journal of Soil & Water Conservation* 27(6): 298-304.
- [15] Liang, A. Z., Yang, X. M., Zhang, X. P. (2016): Changes in soil organic carbon stocks under 10-year conservation tillage on a Black soil in Northeast China. – *The Journal of Agricultural Science* 154(8): 1425-1436.
- [16] Lin, L., Gettelman, A., Fu, Q., Xu, Y. (2016): Simulated differences in 21st century aridity due to different scenarios of greenhouse gases and aerosols. – *Climatic Change*: 1-16.
- [17] Liu, E. K., Zhao, B. Q., Li, X. Y. (2008): Biological properties and enzymatic activity of arable soils affected by long-term different fertilization system. – *Journal of Plant Ecology (Chinese Version)* 32(1): 176-182.
- [18] Lozano, F. J., Lozano, R. (2017): Assessing the potential sustainability benefits of agricultural residues: Biomass conversion to syngas for energy generation or to chemicals production. – *Journal of Cleaner Production* 172: 4162-4169.
- [19] Lu, W. T., Jia, Z. K., Zhang, P., Wang, W. (2011): Effects of straw returning on soil labile organic carbon and enzyme activity in semi-arid areas of Southern Ningxia, China. – *Journal of Agro-Environment Science* 30(3): 522-528.
- [20] Maris, S. C., Teira-Esmatges, M. R., Bosch-Serra, A. D., Moreno-García, B., Català, M. M. (2016): Effect of fertilising with pig slurry and chicken manure on greenhouse gas emissions from Mediterranean paddies. – *Science of the Total Environment*: 569-570.
- [21] Mitran, T., Mani, P. K., Basak, N., Mazumder, D., Roy, M. (2016): Long-term manuring and fertilization influence soil inorganic phosphorus transformation vis-à-vis rice yield in a rice-wheat cropping system. – *Archives of Agronomy & Soil Science* 62(1): 1-18.

- [22] National Development and Reform Commission (2013): Second National Communication on Climate Change of The People's Republic of China. – Department of Climate Change, Beijing: China Economic Press: 15-20.
- [23] Nigussie, A., Bruun, S., Kuyper, T. W., De, N. A. (2017): Delayed addition of nitrogen-rich substrates during composting of municipal waste: effects on nitrogen loss, greenhouse gas emissions and compost stability. – *Chemosphere* 166: 352-362.
- [24] Nótás, E. (2014): Effect of N fertilizer forms and soil moisture levels on then gaseous losses. – *Applied Ecology and Environmental Research* 12(2): 589-599.
- [25] Omonode, R. A., Vyn, T. J., Smith, D. R., Hegymegi, P. (2007): Soil carbon dioxide and methane fluxes from long-term tillage systems in continuous corn and corn-soybean rotation. – *Soil & Tillage Research* 95: 182-195.
- [26] Ping, L. I., Lang, M., Miao, L. I., Wei, W., Kai-Kai, L. I. (2018): Short-term effects of different fertilization treatments on greenhouse gas emissions from northeast black soil. – *Environmental Science* 22(2): 337-345.
- [27] Qin, Z., Dunn, J. B., Kwon, H., Mueller, S., Wander, M. M. (2016): Influence of spatially dependent, modeled soil carbon emission factors on life-cycle greenhouse gas emissions of corn and cellulosic ethanol. – *Global Change Biology Bioenergy* 8(6): 1136-1149.
- [28] Recous, S., Mary, B., Faurie, G. (1990): Microbial immobilization of ammonium and nitrate in cultivated soils. – *Soil Biology and Biochemistry* 22(7): 913-922.
- [29] Sainju, U. M. (2016): A global meta-analysis on the impact of management practices on net global warming potential and greenhouse gas intensity from cropland soils. – *Plos One* 11(2): e0148527.
- [30] Salehi, A., Fallah, S., Sourki, A. A. (2017): Organic and inorganic fertilizer effect on soil CO₂ flux, microbial biomass, and growth of *nigella sativa* l. – *International Agrophysics* 31(1): 103-116.
- [31] Shah, A., Lamers, M., Streck, T. (2016): N₂O and CO₂, emissions from south german arable soil after amendment of manures and composts. – *Environmental Earth Sciences* 75(5): 1-12.
- [32] Shi, X., Hu, H. W., Zhubarker, X., Hayden, H., Wang, J., Suter, H. (2017): Nitrifier-induced denitrification is an important source of soil nitrous oxide and can be inhibited by a nitrification inhibitor 3,4-dimethylpyrazole phosphate (dmpp). – *Environmental Microbiology* 19(12): 27-33.
- [33] Shimizu, M., Hatano, R., Arita, T., Kouda, Y., Mori, A. (2013): The effect of fertilizer and manure application on CH₄ and N₂O emissions from managed grassland in Japan. – *Soil Science and Plant Nutrition* 59: 69-86.
- [34] Song, L. N., Zhang, Y. M., Hu, C. S. (2013): Comprehensive analysis of emissions and global warming effects of greenhouse gases in winter-wheat fields in the high-yield agro-region of North China Plain. – *Chinese Journal of Eco-Agriculture* 21(3): 297-307.
- [35] Veretennikova, E. E., Dyukarev, E. A. (2017): Diurnal variations in methane emissions from west siberia peatlands in summer. – *Russian Meteorology & Hydrology* 42(5): 319-326.
- [36] Wang, Z. B., Chen, J., Mao, S. C., Han, Y. C., Chen, F., Zhang, L. F. (2016): Comparison of greenhouse gas emissions of chemical fertilizer types in china's crop production. – *Journal of Cleaner Production* 141: 1267-1274.
- [37] Xing, P. F., Xiao-Sen, W. U., Gao, S. C., Hong-Jie, L. I., Zhao, T. K., Zhou, X. L. (2016): Effects of different fertilization on soil microbial community and functional diversity in maize-wheat crop rotation. – *Journal of Microbiology* 36(1): 22-29.
- [38] Xu, Y. P., Zhu, H. J., Cheng, X. W., Ji, J. (2018): Study on the evolution of agricultural waste recycling industry and multi-industry linkage. – *Journal of Chinese Agriculture Mechanization* 39(4): 90-94.
- [39] Yang, Q. B., Fan, F. L., Wang, W. X. (2010): Effects of different long-term fertilizations on community properties and functions of methanotrophs in dark brown soil. – *Environmental Science* 31(11): 2756-2762.

- [40] Yang, M., Li, Y., Li, Y., Chang, S. X., Yue, T., Fu, W. (2017): Effects of inorganic and organic fertilizers on soil CO₂ efflux and labile organic carbon pools in an intensively managed moso bamboo (*phyllostachys pubescens*) plantation in subtropical China. – *Communications in Soil Science & Plant Analysis* 48(3): 332-344.
- [41] Yuan, J., Sha, Z. M., Hassani, D., Zhao, Z., Cao, L. K. (2017): Assessing environmental impacts of organic and inorganic fertilizer on daily and seasonal greenhouse gases effluxes in rice field. – *Atmospheric Environment* 155: 119-128.
- [42] Yue, W., Dong, H., Zhu, Z., Gerber, P. J., Xin, H., Smith, P. (2017): Mitigating greenhouse gas and ammonia emissions from swine manure management: a system analysis. – *Environmental Science & Technology* 51(8): 4503-4511.
- [43] Zhang, Y. S., Chai, R. S., Fu, L. L. (2012): Greenhouse gas emissions from major agricultural activities in China and corresponding mitigation strategies. – *Journal of Zhejiang University (Agriculture and Life Sciences)* 38(1): 97-107.
- [44] Zhang, Z. S., Cao, C. G., Guo, L. J., Li, C. F. (2016a): Emissions of CH₄, and CO₂, from paddy fields as affected by tillage practices and crop residues in central china. – *Paddy & Water Environment* 14(1): 85-92.
- [45] Zhang, J., Zhang, J., Shen, G., Wang, R., Gao, L., Li, Z., Dai, Y., Meng, G., Xiang, B., Zhang, Z. (2016b): Effects of different types of straw and stalk returning on carbon and nitrogen mineralization in tobacco soil. – *Tobacco Science & Technology* 49(2): 1-6.
- [46] Zhang, K., Zheng, H., Chen, F., Li, R., Yang, M., Ouyang, Z. (2017): Impact of nitrogen fertilization on soil-atmosphere greenhouse gas exchanges in eucalypt plantations with different soil characteristics in southern china. – *Plos One* 12(2): e0172142.
- [47] Zhao, J., Li, Y., Ran, W. (2016): Effects of organic manure partial substitution for chemical fertilizer on crop yield and soil microbiome in a rice-wheat cropping system. – *Journal of Nanjing Agricultural University* 39(4): 594-602.

DETERMINATION OF SEDIMENTATION RATE IN ANZALI LAGOON OF NORTHERN IRAN USING ^{137}Cs TRACER TECHNIQUE

KHALILI VAVDARE, S.¹ – SEDGHI, H.^{2*} – SARRAF, A.³

¹*Department of water resources management, Islamic Azad University, Science and Research Branch, Tehran, Iran
(e-mail: khalilivavdares@gmail.com)*

²*Department of Water Engineering, Science and Research Branch, Islamic Azad University
Tehran, Iran*

³*Department of Civil Engineering, Roudehen Branch, Islamic Azad University, Roudehen, Iran
e-mail: sarraf@riau.ac.ir*

**Corresponding author
e-mail: hsedghi41@gmail.com*

(Received 15th Oct 2018; accepted 2nd Jan 2019)

Abstract. One of the management tools for sediment and erosion control in the different scales from plot to watershed is informing about soil displacement process that can be obtained using fallout radionuclide spectroscopy. In recent decades, use of the radionuclides for determining sedimentation rate was common, among which Cesium (^{137}Cs) is the most often used. In this research, three, 4-meter long sediment cores were collected from the western part of the Anzali Lagoon. The Anzali Lagoon is one of the sediment treated ecosystems in the north of Iran. The level of ^{137}Cs of the sediment samples was measured based on Spectrometry analysis in the Atomic Energy Organization of Iran. The grain size distribution showed that the sediment samples were mainly fine textured (Silt with low plasticity properties). The results represented that the highest amount of the ^{137}Cs was observed in the depth of 2.4-2.7 m, which can be related to the Chernobyl disaster in 1986. An overall sedimentation rate of 8.5 cm yr^{-1} ($=119 \text{ kg m}^{-2} \text{ yr}^{-1}$) was obtained based on the ^{137}Cs calendar of the sediment cores. This sedimentation rate is considerable, and a special arrangement is necessary to save the Lagoon.

Keywords: *core sampler, Anzali Lagoon, sediment color, sediment gradation, sedimentation rate*

Introduction

The Anzali Lagoon with fresh water, located in the southern shore of Caspian Sea (Olah, 1990), is a suitable ecosystem for growing and farming aquatic organisms, so it has crucial importance from different aspects of water resources and ecosystems. The Anzali Wetland is internationally known as an important wetland for migratory birds, and it was registered as a Ramsar site in 1975 (JICA, 2005). In recent years, unfortunately, due to excess import of contaminated wastewater from urban, industrial and agricultural septic system into lagoon, it has faced with the serious risk of heavy metals. These dangerous actions along with entering garbage, water extraction from the lagoon for agricultural purposes, wastewater discharging from fish farms to the lagoon, illegal hunting and fishing, the arrival of non-native species, increase in erosion and sediment transportation of Anzali watershed, sediment deposition and other factors have treated the ecosystem of the lagoon. Because of these risks, the Ramsar Convention has included the Anzali Lagoon into Red List of Ecosystems.

One of the main problems, which existed for long years and was found more in recent years, is sedimentation in the lagoon bottom. The studying on sedimentation rate in a water body such as Anzali Lagoon has a special importance because of the following various reasons. The suspended sediments cause decreasing of dissolved oxygen and declining in the water depth of reservoir by making turbidity in water and filling the lagoon, respectively. In sediments, the benthic and aquatic organism's habitats are damaged, the fish gills is suffered, their spawns is covered and migratory birds' habitats is disordered. By decreasing in the effective volume of the lagoon, water storage capacity will decrease and the water will overflow from that, so the adjacent area may be ponded.

As the sediments are capable to record environmental changes (Sunderland et al., 2008) and contamination entering time, so the determination of sedimentation rate by confident methods is one of the most important purposes in sediment and erosion study. This knowledge can be obtained using fallout radionuclide spectroscopy (Arata et al., 2016). An advantage of radionuclides spectroscopy is the excellence of its accuracy than conventional methods (Schuller et al., 2006). The other advantages of fallout radionuclide methods are capability of evaluation in different scales, short and long terms investigation of erosion, sediment and land use on erosion, cost-free maintenance of samples, sufficiency of a single site visit, usable under different environments and feasibility of its successful application in the world than other usual methods (Jia et al., 2012). In recent years, radiometric dating based on ^{137}Cs and ^{210}Pb has become an important method (Dong et al., 2013) and one of the best approaches has been using of the ^{137}Cs (Zapata, 2002). The ^{137}Cs is the most commonly employed radionuclide in soil (Mabit et al., 2013) that used in a different condition of agriculture and environment throughout the world. The abstraction of this element by the crop is slight and negligible (Wallbrink et al., 2002), but it is strongly adsorbed by clay particles (He and Walling, 1996) and organic matters.

The ^{137}Cs (Cesium 137) is a radioactive element with a relatively long half-life of 30.15 years that have fallout in many countries because of nuclear weapons tests in the 1950s and early 1960s and Chernobyl catastrophic nuclear accident in 1986 (Dong et al., 2013). The regional pattern of the ^{137}Cs deposition showed a range of 160 to 3200 Bq m^{-2} that depended to latitude (García Agudo, 1998). The wide range of the ^{137}Cs was related to atomic actions media in 1952 (Perkins and Thomas, 1980). After the Chernobyl reactor nuclear accident in 1986, for instance, large quantities of ^{137}Cs were released into the atmosphere and a sharp peak in atmospheric fallout occurred (Estrany et al., 2010). Therefore, when a layer has the most of ^{137}Cs radioactivity, this layer will be related to 1986 and sedimentation rate will be determined (Panayotou, 2004; Kotarba et al., 2002).

The ^{137}Cs will form complex with particles and will represent into non-exchangeable form (Ritchie and McHenry, 1990). The ^{137}Cs leaching from soil is low and in general, its migration in the soil by the chemical and biological process is very low and it is translocated in soil just along with colloids particles (Walling and Quine, 1992). Subsequent redistribution of that is mainly caused by physical changes such as erosion and plowing, so it can be used as a suitable mark for estimating soil erosion and sedimentation (Ritchie and McHenry, 1990; Estrany et al., 2010). The depletion of the ^{137}Cs in soil related to reference level will show erosion and relative increase of that will represent deposition of soil.

Considerable efforts have been directed to determine the ages of sediments and erosion by the radionuclide chronology. According to Brown et al. (1981), the results of an experiment using the ^{137}Cs indicated that soil movement in croplands has placed and sediments have quickly adsorbed the ^{137}Cs . The use of the ^{137}Cs technique in Sri Lanka showed that, in the land with different area and utilization, this method has a high capability in estimating of erosion (Champa et al., 2010). A study in Algeria coasts has carried out from 1994 to 2004. For this aim, the ^{210}Pb and ^{137}Cs of sediments have been measured using direct counting in Gama spectrometry detector. The sedimentation rate using a concentration profile of ^{210}Pb and ^{137}Cs and CRS model was obtained 20 to 27 mm yr^{-1} (Nouredine, 2010). The sediment delivery ratio in the black soil region of Northeast China within Hebei catchment was investigated by the distributions of ^{137}Cs , ^{210}Pb , and the grain-size of the sediments, from 1977 to 2007. The overall average deposition rate for the entire period was 22.6 mm yr^{-1} and the precipitation was found to be the main factor affecting the soil erosion of the study area (Dong et al., 2013). Abbaszadeh Afshar et al. (2010) have estimated the rate of soil reformation in the western part of Iran using the ^{137}Cs radionuclide. The result showed that erosion and sedimentation rates were 29.8 and 21.8 $\text{ton ha}^{-1} \text{yr}^{-1}$, respectively. Amini et al. (2012) have investigated the amount of sediment of Holocene in Gorgan gulf and southeastern coast of the Caspian Sea. The average of sediment at the beginning of the Holocene and at the end of that were 2.06 and 5.08 mm yr^{-1} , respectively. The rate of sedimentation in Anzali Lagoon was investigated by Japonica International Cooperation Agency (JICA) and the result showed that the sedimentation rate in around the lagoon was 0 to 6 mm yr^{-1} (JICA, 2005).

A knowledge of sedimentation rates is often useful in planning for dredging operations. The pattern of sedimentation rates can be used to calculate when different areas will require works (Jeter, 1999). On the other hand, the conservation of ecological complex systems and profit from enormous economic, recreational and genetically resources is just subject to study and exact understanding of each wetland. Laboratory analyses of sediment cores can determine the sedimentation rates and the calendar dates associated with various depths within sediments. The aim of this research was an investigation of sediment age of the Anzali Lagoon by the ^{137}Cs to determine entering and displaced sediment rate at there. By understanding its annual rate, this can provide suitable planning for the lagoon conservation and the sediment management.

Materials and Methods

Study area

The Anzali Lagoon is located in the southern shore of Caspian Sea and in the Northern part of Iran between $37^{\circ} 25'$ to $37^{\circ} 32'$ N and $49^{\circ} 15'$ to $49^{\circ} 36'$ E. This water body has high importance for ecosystem because of abundant diversity of plants and animals. In the lagoon watershed with 3740 km^2 area, there are 27 rivers that among them, the top 10 rivers with a higher flow (Table 1) are the main entering rivers to the lagoon. The major volume of sediments into the lagoon is delivered by rivers that flow from upstream. The minimum and maximum mean sea level (MSL) of Anzali watershed are -26 and 3014 m, respectively. The mean annual rainfall of that is 1780 mm, 800 mm higher than evaporation. The climate in the Anzali Wetland watershed is characterized by two distinct types. The lowland area to the north between elevation (El.) -26 m to 500 m is characterized by warm temperatures, high moisture and

abundant rainfall during the summer with a mild climate during the winter. The climate between El. 500 m to 3014 m is noticeably different from the lowland, characterized by cold temperatures, semi-humid conditions, and less rainfall.

Table 1. Mean annual flow for long-term (2002-13) for top 10 rivers of Anzali watershed

River	Mean flow (m ³ s ⁻¹)	River	Mean flow (m ³ s ⁻¹)
Ibrahim	4.03	Pasikhan	18.59
Pirbazar	11.46	Khalkaii	4.45
Siahrud	5.52	Siahmazgi	4.07
Shakhras	10.2	Kolsar	6.41
Masouleh	3.78	Morghak	3.33

In fact, the Anzali lagoon is one of the lakes behind the coast, which once was part of the Caspian Sea. This wetland has expanded a lot in the past but has gradually been filled by delta alluvial deposits of Sefidrud and other rivers in Rasht, Fouman and Masal areas. The area of the Anzali Lagoon during out of wet season is estimated 168 km². The Anzali Lagoon comprises four parts include western part (Abkenar), eastern part (Sheijan), center part (Hendekhale) and the southern part (Siahkishem) (Figure 1). The mean length of that in the east-west direct is about 30 km and in the north-south direct is about 3 km. The depth of the lagoon is in range of 2 m (in Sheijan) to 8 m (in Abkenar). The environment of the Wetland is deteriorating due to the inflow of wastewater, solid waste, and sediment from the upstream.

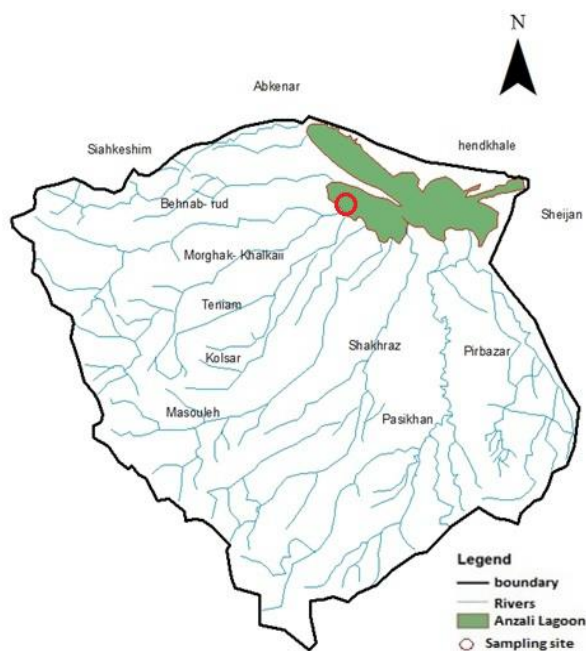


Figure 1. Anzali Lagoon watershed with entering rivers and sampling location

Field sampling

To choose the sampling site and numbers of samples, first, the sediment entering sources situation was checked and then, the locations were determined on the map. After that, based on the local investigations and consideration of limitations, such as

accessing and sampling possibility due to the swampy condition of some sides, three places were chosen in the southern part of the lagoon (Khalkaii River) (*Figure 1*).

To investigate the local sedimentation and the soil layers properties, the sediments were sampled at 3 points in Sep 2016. The sampling was done by a piston core sampler D750. For this purpose, we sampled the sediments of the lagoon, by taking three cores, which were 11 cm in diameter and 4 m in length.

The cores are generally cut across to enable a sedimentary geologist to make a visual study of the sediments, sometimes including grain size measurements. To identify the mechanical and physical characteristics of the soil different layers, mechanical test such as direct-shear and physical tests such as relative density, humidity percent, and grain size distribution were done on sub-samples. The grain size tests was done using sieves with different meshes based on ASTM D6913 and the sediment texture was analyzed using the pipette method. The Munsell Color Chart was also used for identifying the sediment color.

The radionuclide test on all cores is not necessary because of the costs and time consuming labour. A total of 17 samples were selected from the cores horizons based on the sediment color and texture to obtain detailed information on the depositional environment. To determine the sediment age in the sampling location, from first core (BH-1), eight samples were sectioned from 0-0.5, 0.5-1, 1-1.6, 1.6-1.9, 2.2-2.4, 2.4-2.7, 2.9-3.3 and 3.3-4 m. For second core (BH-2), five samples were sectioned from 1.7-2.1, 2.1-2.4, 2.4-3, 3-3.6 and 3.6-4 m. In third core (BH-3), four samples were taken from 1.5-1.8 m, 2-2.8, 3-3.2 m and 3.3-3.5 m. In addition, some portion of the cores were clearly missing (2-2.2 m in BH-1 and 1-1.2, 1.8-2, 2.8-3 and 3.7-4 m in BH-3), which is possibly due to the loss of the sediments during sampling of the cores. In those layers, since the sediments were soft and sandy, they were difficult to sample. Finally, the dried samples were placed in special boxes.

Laboratory measurements

All 17 samples were sent to the Nuclear Science and Technology Laboratory of Iran Atomic Energy Agency. To measure the ^{137}Cs , the Gama ray spectrometer and high pure Germanium detector (HPGe) were used in an energy range of 60 KeV to 3 MeV. To analyze samples, one sample is placed under a detector device, which is connected to a counter computer. After spending 25,000 to 80,000 s, the peak point of the curve is established and on the graph in a channel with 662 Kev, the ^{137}Cs is measured (Kachanoski and Dejong, 1984). The amount of the ^{137}Cs was determined in Becquerel per kg of soil.

For a given depth, the time interval between the deposition date and the core sampling date is equal to the depth divided by the sedimentation rate (Jeter, 1999). This interval is subtracted from the current year in which the core was taken.

Results and discussion

The soil particle-size distribution in *Tables 2, 3 and 4* showed that the sediment samples were mainly fine texture. The soil textures varied substantially. Nevertheless, the main soil texture in the lagoon is clayey silt. In the soil layers of BH-1 from the surface to 4 m depth, there is silt with low plasticity properties (ML). In BH-2, the soil layers of 0-3 m depth and 3-4 m depth were silt with ML and sandy silt with ML, respectively. In BH-3, the soil layers of 0-3 m depth and 3-4 m depth were silt with ML

and clayey silt with ML, respectively. Generally, in the all depths, silt was the major portion of the sediments. Most of the sediments in the Caspian Sea coastal plain are discontinues and displaced sediments that settled in effect of different flow and waves.

Table 2. Soil layers properties in BH-1 core


BH-1			utmX= 352254.05	utmY= 4143541.70		
Layers color	Depth (m)	Layer	Texture	Humidity (%)	LL	PL
blue green	0-1	Silt with low plasticity properties (ML)	Silty sand	41.6		
			Sandy silt			
			Sandy clay silt			
	1-2		Clayey silt with biomass	45.7	45.7	38.8
	2-3		No sampled	47.3		
green			Clayey silt			
	3-4	Sticky silt	45.0	45.0	32.8	
 Sample for Cs-137 test			LL: Liquid limit, PL: Plastic limit			

Table 3. Soil layers properties in BH-2 core


BH-2			utmX= 352444.00	utmY= 4143848.00		
Layers color	Depth (m)	Layer	Texture	Humidity (%)	LL	PL
brown	0-1	Silt with low plasticity properties (ML)	Hard clay	59.7	N.P	N.P
brown			Silty clay			
light brown			Clayey silt			
light green	1-2		Clay and silt with sand	69.2		
light brown			Silty clay			
			Fine sand			
	2-3	Clayey silt	86.5			
		Clayey silt				
		Silty fine sand				
	3-4	Sandy silt with low plasticity properties (ML)	Fine sand and silt	88.0	48.7	33.9
green			Fine sand			
black			Silt and clay with biomass			
			Fine sand			
 Sample for Cs-137 test			LL: Liquid limit, PL: Plastic limit, NP: non plastic			

Figure 2 shows the ¹³⁷Cs concentrations found at different depths in the sediment cores. The increasing trend up to the depth of 2.7 m and then decreasing trend were

observed. The measured ¹³⁷Cs in Figure 2 were shown that the peak of the ¹³⁷Cs radioactivity was in 2.4 to 2.7 m depth, with 9.3 Bq kg⁻¹. If this amount is related to the Chernobyl disaster year (1986), and the soil surface is related to sampling year (2016), the time interval between two events will be 30 years. On the other hand, by considering the middle of 2.4-2.7 m layer, we argue from given data that approximately 255 cm of sediment has been added in the last 30 years. Therefore, the sedimentation rate is determined at 8.5 cm yr⁻¹ (=119 kg m⁻² yr⁻¹ ≈20 million ton km⁻²).

Table 4. Soil layers properties in BH-3 core

BH-3			utmX= 352688.11	utmY= 4143809.84		
Layers color	Depth (m)	Layer	Texture	Humidity (%)	LL	PL
blue-grayish	0-1	Silt with low plasticity properties (ML)	Clayey silt	52.3		
			Silt and fine sand			
	1-2		No sampled	45.0	45.0	36.0
light blue-gray			Clayey silt			
	2-3		No sampled	74.3	46.5	29.7
Light pearl gray			Clayey silt with organic matter			
	3-4	Clayey silt with low plasticity properties (ML)	No sampled	99.0		
light blue			Clayey silt			
dark blue			Clayey silt			
light blue			Clayey silt			
			Non sampled			
	Sample for Cs-137 test		LL: Liquid limit, PL: Plastic limit, NP: non plastic			

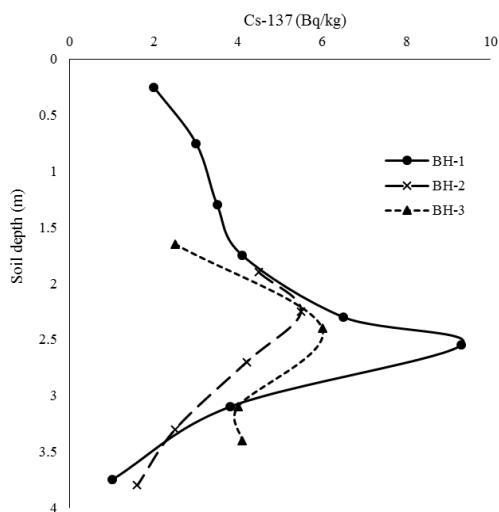


Figure 2. The vertical profiles of Cs-137 concentrations measured in three sediment cores

The depth distributions of the ^{137}Cs activity and the clay percent for the sampled profiles are presented in *Table 5*. The clay particles keep strongly the ^{137}Cs because of surface adsorption of that in soil depth (McCallan et al., 1980). The clay mineral fraction of the sediments acts as an ion exchange media and chemically fixes the cesium in place. Naturally, in an undisturbed soil, increase in soil depth will result an increase in clay percent due to leaching. In the cores (BH-1, BH-2 and BH-3), the clay percent increases with the soil depth, except 2.4-3 and 3.6-4 m in the BH-2. In addition, the ^{137}Cs amount has a direct relation with clay percent and organic matter amount. Therefore, measuring the sediment and erosion amount using the ^{137}Cs in soils with medium or heavy texture will represent a good result.

Table 5. Cs-137 concentration in different depth

Row	Sediment core	Soil depth (m)	Cs-137 (Bq Kg ⁻¹)	Clay (%)
1	BH-1	0.0-0.5	2.0	
2	BH-1	0.5-1.0	3.0	
3	BH-1	1.0-1.6	3.5	
4	BH-3	1.5-1.8	2.5	27.1
5	BH-1	1.6-1.9	4.1	33.4
6	BH-2	1.7-2.0	4.5	37.7
7	BH-2	2.1-2.4	5.5	
8	BH-1	2.2-2.4	6.5	
9	BH-3	2.0-2.8	6.0	
10	BH-1	2.4-2.7	9.3	34.2
11	BH-2	2.4-3.0	4.2	11.1
12	BH-1	2.9-3.3	3.8	33.4
13	BH-3	3.0-3.2	<4	34.2
14	BH-2	3.0-3.6	2.5	
15	BH-3	3.3-3.5	4.1	36.6
16	BH-1	3.5-4.0	1.0	40.9
17	BH-2	3.6-4.0	1.6	10.6

The sedimentation rate of these cores was estimated to be 8.5 cm yr⁻¹. Variation in sedimentation rates was conspicuously evident at depth intervals of approximately 250-350 cm in the core. The profile shows a ^{137}Cs horizon near 400 cm depth (*Figure 3*). This marker (BH-2) can be used to calculate an average sedimentation rate as follows: (400 cm depth / 62 y between 1954 and 2016) equal to 6.5 cm y⁻¹. The profile also shows a ^{137}Cs maximum near 350 cm depth. This marker (BH-3) also can be used to calculate a sedimentation rate: (350 cm depth / 53 y between 1963 and 2016) equal to 5.6 cm y⁻¹. In this case, the same sedimentation rate is calculated from both ways. This is not always the case, however, because events such as unusual floods could occur between the years 1954 and 1963, causing the two calculations to differ.

The total amount of radioactivity deposited on the earth's surface depends on the atmospheric concentration of radioactivity and the amount of rainfall. On the other hand, average siltation rate in lagoons and reservoirs can also be estimated if the ^{137}Cs peak is noticeable in the vertical distribution of this radionuclide in bottom-sediment core samples. As Iran located in the middle of Asia with the approximately 80 mBq cm⁻², it could be inferred that Iran is a normal condition of use of radionuclides and with regard to these cases, it is concerned to utilize this isotope.

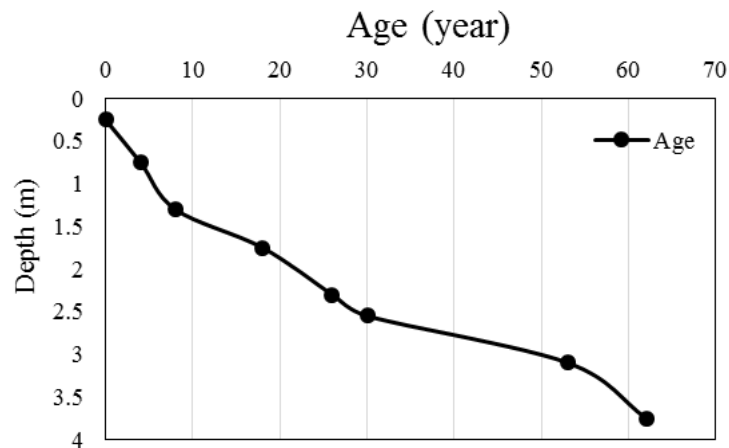


Figure 3. The age of sediment cores by Cs-137 chronolog

Conclusion

To survey sedimentation rate in Anzali Lagoon, Iran, a research was conducted in 2016 by coring from sediment in the southern part of the lagoon. The grain size distribution, liquid limit, and colors of the sediments were determined in soil laboratory. The ^{137}Cs of the samples was also measured in Nuclear Science and Technology Laboratory of Atomic Energy of Iran. The result showed that the sediments were often Silt with low plasticity properties (ML) and green, light brown and blue colors. The highest amount of the ^{137}Cs was observed in 2.4-2.7 m depth, which can be related to 1986 (Chernobyl accident). Therefore, the sedimentation rate was obtained as 8.5 cm yr^{-1} , which is high. The established rates of sediment accumulation confirm that sedimentation conditions in the Anzali Lagoon are fairly intensive and can cause declining in the lagoon water depth. In this regard, the water quality of the lagoon will be affected, which needs to investigate in future works. So, special arrangements should be considered to save the lagoon and protect its value.

REFERENCES

- [1] Abbaszadeh Afshar, F., Ayoubi, S., Jalalian, A. (2010): Soil redistribution rate and its relationship with soil organic carbon and total nitrogen using ^{137}Cs technique in a cultivated complex hill slope in western Iran. – Journal of Environmental Radioactivity 101: 606-614.
- [2] Amini, A., Moussavi, R., Lahijani, H., Mohboubi, A. (2012): Holocene Sedimentation Rate in Gorgan Bay and Adjacent Coasts in Southeast of Caspian Sea. – Journal of Basic and Applied Scientific Research 2(1): 289-297.
- [3] Arata, L., Meusburger, K., Frenkel, E., A'Campo-Neuen, A., Iurian, A., Ketterer, M. E., Mabit, L., Alewell, C. (2016): Modelling Deposition and Erosion rates with Radio Nuclides (MODERN), Part 1: A new conversion model to derive soil redistribution rates from inventories of fallout radionuclides. – Journal of Environmental Radioactivity 162-163: 45-55.
- [4] Brown, R. B., Cutshall, N. H., Kling, G. F. (1981): Agricultural Erosion Indicated by ^{137}Cs Redistribution: I. Levels and distribution of ^{137}Cs activity in soils. – Soil Science Society of America Journal 41: 33-37.

- [5] Champa, K., Dissanayake, A. P., Mahawatte, B. K., Abeynayake, C., Weerasekera, T. S. B. (2010): Use of Cesium-137 technique for the assessment of soil erosion in two selected sites in Uma Oya Catchment in Sri Lanka. – World Congress of Soil Science, Soil Solutions for a Changing World. Brisbane, Australia.
- [6] Dong, Y., Wu, Y., Zhang, T., Yang, W., Liu, B. (2013): The sediment delivery ratio in a small catchment in the black soil region of Northeast China. – International Journal of Sediment Research 28: 111-117.
- [7] Estrany, J., Garcia, C., Walling, D. E. (2010): An investigation of soil erosion and redistribution in a Mediterranean lowland agricultural catchment using Cesium-137. – International Journal of Sediment Research 25(1): 1-16.
- [8] García Agudo, E. (1998): Global distribution of Cs-137 inputs for soil erosion and sedimentation studies. – In: Global distribution of ¹³⁷Cs inputs for soil erosion and sedimentation studies (IAEA-TECDOC--1028). International Atomic Energy Agency (IAEA) 117-121. Vienna, Austria.
- [9] He, Q., Walling, D. E. (1996): Interpreting particle size effects in the adsorption of ¹³⁷Cs and unsupported ²¹⁰Pb by mineral soils and sediments. – Journal of Environmental Radioactivity 30(2): 117-137.
- [10] Jeter, H. W. (1999): Determining the Ages of Recent Sediments Using Measurements of Trace Radioactivity. – Workshop of the Nuclear Regulatory Commission, Region 1, June 1999, in Baltimore, Maryland, USA: 21-28.
- [11] Jia, Y., Wang, Z., Zheng, X., Han, L. (2012): Estimation of soil erosion in the Xihanshui River Basin by using ¹³⁷Cs technique. – International Journal of Sediment Research 27: 486-497.
- [12] JICA. (2005): The Study on Integrated Management for Ecosystem Conservation of the Anzali Wetland in the Islamic Republic of Iran. – Vol 2. Nippon Koei Co.
- [13] Kachanoski, R. G., Dejong, E. (1984): Predicting the temporal relationship between soil Cs-137 and erosion rate. – Journal of Environmental Quality 13(2): 301-304.
- [14] Kotarba, A., Lokas, E., Wachniew, P. (2002): ²¹⁰Pb dating of young Holocene sediments in high-mountains lakes of the Tatra Mountains, Geochronometria. – Journal on Methods and Applications of Absolut's Chronology 21: 73-77.
- [15] Mabit, L., Meusbürger, K., Fulajtar, E., Alewell, C. (2013): The usefulness of ¹³⁷Cs as a tracer for soil erosion assessment: a critical reply to Parsons and Foster. – Earth Sci. Rev 127: 300-307.
- [16] McCallan, M. E., O'Leary, B. M., Rose, C. W. (1980): Redistribution of Caesium-137 by Erosion and Deposition on an Australian Soil. – Australian Journal Soil Resource 18: 119-128.
- [17] Noureddine, A. (2010): Evaluation of the sedimentation rate with ²¹⁰Pb and ¹³⁷Cs using the CRS model and estimation of the total inventory of sediment in the Algerian Coast. – Journal of Oceanography 1(2): 47.
- [18] Olah, J. (1990): Pollution in the Anzali Lagoon catchment preliminary assessment. – FAO, Rome 1-23.
- [19] Panayoto, K. (2004): Geomorphology of the Minnamurra river estuary, southeastern Australia: evolution and management of a barrier estuary. – Ph.D. thesis, School of Geosciences, University of Wollongong.
- [20] Perkins, R. W., Thomas, C. W. (1980): Worldwide fallout. – In: Hanson, W. C. (ed.) Transuranic elements in the environment. USDOE/TIC-22800. US DOE, Washington, DC. 53-82.
- [21] Ritchie, J. C., McHenry, J. R. (1990): Application of radioactive fallout cesium-137 for measuring soil erosion and sediment accumulation rates and patterns: a review. – Journal of environmental quality 19(2): 425-472.
- [22] Schuller, P., Iroumé, A., Walling, D. E., Mancilla, H. B., Castillo, A., Trumper, R. E. (2006): Use of Beryllium-7 to Document Soil Redistribution following Forest Harvest Operations. – Journal of Environmental Quality 35: 1756-1763.

- [23] Sunderland, E. M., Cohen, M. D., Selin, N. E., Chmura, G. L. (2008): Reconciling models and measurements to assess trends in atmospheric mercury deposition. – *Environmental Pollution* 156(2): 526-35.
- [24] Wallbrink, P. J., Belyaev, V., Golosov, V. N., Sidorchuk, A. S., Murray, A. S. (2002): Use of radionuclide, field based and erosion modeling methods for quantifying rates and amounts of soil erosion processes. – CSIRO Land and Water consultancy report.
- [25] Walling, D. E., Quine, T. A. (1992): The use of Cs-137 measurements in soil erosion surveys. Erosion and sediment transport monitoring programs in river basins. – Oslo symposium.
- [26] Zapata, F. (2002): Handbook for the Assessment of Soil Erosion and Sedimentation Using Environmental Radionuclides. – The Netherlands: Kluwer Academic Publishers.

DEVELOPMENT OF AN EFFICIENT REGENERATION SYSTEM VIA SOMATIC EMBRYOGENESIS OBTAINED FROM MATURE EMBRYOS IN SOME GRAIN AND SILAGE SORGHUM CULTIVARS

AVCI, S.

*Eskişehir Osmangazi University, Faculty of Agriculture, Department of Field Crops
Eskişehir, Turkey*

(e-mail: savci@ogu.edu.tr; phone: +00902223242991/4847; fax: +00902223242990)

(Received 15th Oct 2018; accepted 2nd Jan 2019)

Abstract. An effective regeneration system was developed from embryonic callus that was formed by using mature embryos in 6 sorghum cultivars (Gözde 80, Greengo, Leoti, Beydarı, Aldarı and Akdarı). Different auxin (2,4-D and 2,4,5-T) and cytokinin (zeatin and kinetin) combinations on somatic embryogenesis were studied. The highest embryonic callus in all cultivars was derived from cultures in MS medium containing 1 mg/l 2,4-D. The transfer of embryonic callus obtained from medium containing 2,4,5-T + kinetin to the shooting medium (1 or 2 mg/l BA +1.5 mg/l TDZ +1 mg/l IAA) and subsequently rooting medium ($\frac{1}{2}$ MS with 1 mg/l NAA) resulted in a higher shooting and rooting. Different concentrations of BA in the shooting medium did not affect shoot formation. Akdarı and Greengo cultivars produced better callus induction and regeneration than the other cultivars as grain and silage types, respectively. Rooting and surviving rates varied between 10.55-68.37% depending on the growth regulators used at the beginning of culture. Growth and survival rates were increased in plants transferred from high-shoot-rate cultivars to the rooting medium.

Keywords: *sorghum, embryonic callus, 2,4-D, 2,4,5-T, kinetin*

Introduction

Sorghum (*Sorghum bicolor* L. Moench.) is an important cereal like rice, barley, wheat and maize around the World (Ritter et al., 2007; Motlhaodi et al., 2014; Sinha and Kumaravadivel, 2016). It is originated from North Africa and widely grown in tropical and subtropical regions (Dillon et al., 2007). Sorghum is widely used as a food source for human and animal nutrition in the arid and semi-arid regions (Sing and Sing, 1992; Sharma and Ortiz, 2000).

Various reasons such as physiological, morphological and genetic diversity, a wide range of genetic stocks, maps and application of versatile tests through self-fertilization make sorghum important in terms of agriculture, physiological and biotechnological studies (Kong et al., 2000; Hart et al., 2001; Zongo et al., 1993). In cereals, genetic studies performed by gene transfer methods and other biotechnological developments are dependent on the establishment of an effective and repeatable plant regeneration system.

It has been reported that immature embryos are the best explant source in monocots species (Tiidema and Truve, 2004). However, several factors restrict the use of immature embryos for in vitro culture of sorghum; difficulties of donor plants maintenance, problems with isolation and sterilization of immature embryos, unequal production of embryonic callus by different genotypes, and the tendency of good friable embryogenic callus producing genotypes to secrete polyphenols or other inhibitory substances (Rao et al., 1995; Seetharama et al., 2000; Pola et al., 2009).

Although the mature embryos come to the forefront with an unlimited explant source throughout the year, the embryonic callus from mature seeds are difficult and the lack of study performed in cultivated sorghum genotypes is noteworthy. In the previous studies, 2,4-D (2,4-Dichlorophenoxyacetic acid) combined with kinetin provided embryonic callus and regeneration in different sorghum genotypes (Mackinnon et al., 1986; Nirwan and Kothari, 2004; Zhao et al., 2010; Zarif et al., 2013; Hassan et al., 2014). Also, Pola and Mani (2006) stated that 2,4,5-T (2,4,5-Trichlorophenoxyacetic acid) gave the effective embryogenic callus induction from the leaf of sorghum. Pola et al. (2009) investigated that the effect of 2,4-D and 2,4,5-T alone on plant regeneration using mature embryo of sorghum. In this study, the effect of 2,4-D and 2,4,5-T combined with kinetin and zeatin were observed on embryogenic callus induction and regeneration in the mature embryos in grain and silage types of sorghum which have no knowledge about their regeneration capabilities.

Materials and Methods

The study was carried out in Eskişehir Osmangazi University, Faculty of Agriculture, Department of Field Crops, Eskişehir, Turkey. Seeds of Beydarı, Aldarı, Akdarı, Gözde 80, and Leoti cultivars were obtained from the Bati Akdeniz Agricultural Research Institute, and Grengo cultivar provided by May Seed Company. While the grain types (Beydarı, Aldarı and Akdarı) have short plant height, the silage types (Grengo, Gözde 80 and Leoti) are tall and they have the possibility of use regrowth. The grain of Akdarı is white and does not include tannin. These seeds were first allowed in 96% ethanol for 4 min and subsequently 30 min in a 30% bleach solution (Domestos commercial bleach; 4,5% Sodium hypochlorite) for surface sterilization. After sterilization, the seeds were rinsed 5 times with distilled water and then were soaked for 22 h in distilled water at room temperature for easy dissection of embryos from seed. Mature embryos were aseptically dissected from seeds under the stereomicroscope and were cultured scutellum upward on solid MS medium (Murashige and Skoog, 1962) containing growth regulators at different concentrations and combinations. The various levels of 2,4-D and 2,4,5-T (1, 2 and 4 mg/l) and their combinations with 0,5 mg/l kinetin and zeatin were used for callus induction. After callus induction, the calli from 1 mg/l were transferred to media with 1,5 mg/l TDZ (Thidiazuron) and 1 mg/l IAA (3-Indoleacetic acid) combined with 1 and 2 mg/l concentrations of BA (6-Benzylaminopurine) for shoot formation (*Table 1*).

Sucrose (30 g/l) was added to medium and the pH was adjusted to 5.8 and the medium was solidified with 6.5% agar. The medium was autoclaved at 121°C and 1,2 atm pressure for 20 min. All the cultures were incubated in a growth chamber (Panasonic MLR-352H-PA) at 25±1°C, 60% humidity and 16h / 8h photoperiod (long day conditions). The experiment was arranged in three factors in completely randomized design (CRD) with 4 replicates and 5 explants were used in each replicate. First factor was sorghum cultivars, second was auxin types and combinations and third was in auxin concentrations for callus induction while BA concentration was inserted as third factor in shooting and rooting. Arcsine (\sqrt{x}) transformation was applied in percentages data before statistical analysis (Snedecor and Cochran, 1992). Healthy shoots were rooted on 1/2 MS medium containing 1 mg/l NAA (1-Naphthaleneacetic acid). The rooted plantlets were transferred to pots containing peat and vermiculite (4:1) for acclimatization at climate room.

Table 1. The summarise experimental design in a tabular form

Callus induction (mg/l)				Shootin formation (mg/l)			Rooting (mg/l)
2,4-D	2,4,5-T	Kinetin	Zeatin	BA	TDZ	IAA	NAA
1	-	-	-	1	1.5	1	1
	-	-	-	2	1.5	1	1
2	-	-	-				
4	-	-	-				
1	-	0.5	-	1	1.5	1	1
	-	0.5	-	2	1.5	1	1
2	-	0.5	-				
4	-	0.5	-				
1	-	-	0.5	1	1.5	1	1
	-	-	0.5	2	1.5	1	1
2	-	-	0.5				
4	-	-	0.5				
-	1	-	-	1	1.5	1	1
-		-	-	2	1.5	1	1
-	2	-	-				
-	4	-	-				
-	1	0.5	-	1	1.5	1	1
-		0.5	-	2	1.5	1	1
-	2	0.5	-				
-	4	0.5	-				
-	1	-	0.5	1	1.5	1	1
-		-	0.5	2	1.5	1	1
-	2	-	0.5				
-	4	-	0.5				

Results and Discussion

Callus induction

The embryogenic tight and compact calli were obtained from mature embryos as well as non-embryogenic weak and soft calli in dark condition after 4 weeks culture initiation (Figs. 1a and 1b). There were significant differences in the main factors (cultivars, auxin types and combinations and their different doses) and their interactions in terms of callus induction percentage at 1% level. The callus induction from mature embryos in sorghum cultivars ranged from 54.82% to 90.58%, in Leoti and Akdari, respectively (Table 2). It is known that success in callus formation and plant regeneration are largely dependent on the genotype in sorghum (Seetharama et al., 2000; Pola, 2011; Zarif et al., 2013; Hassan et al., 2014). The highest callus induction was obtained from pure doses of the auxins compared to their combinations with kinetin and zeatin. However, combinations of 2,4-D induced more callus formation than combinations of 2,4,5-T. Jogeswar et al. (2007) stated that pure 2,4-D has a crucial importance for embryonic callus initiation in monocotyledon plants. Also, Zhao et al. (2010) observed that 2,4-D alone was sufficient to induce callus formation and the additional kinetin in high concentrations decreased the callus induction in sorghum. Increased doses of auxin affected callus formation negatively and it varied between 74.61% and 56.25% (Table 2). Zhao et al. (2010) found out callus induction obtained from germinating seed of sorghum increased with increasing concentrations of 2,4-D (4 mg/l) in contrast to our study.

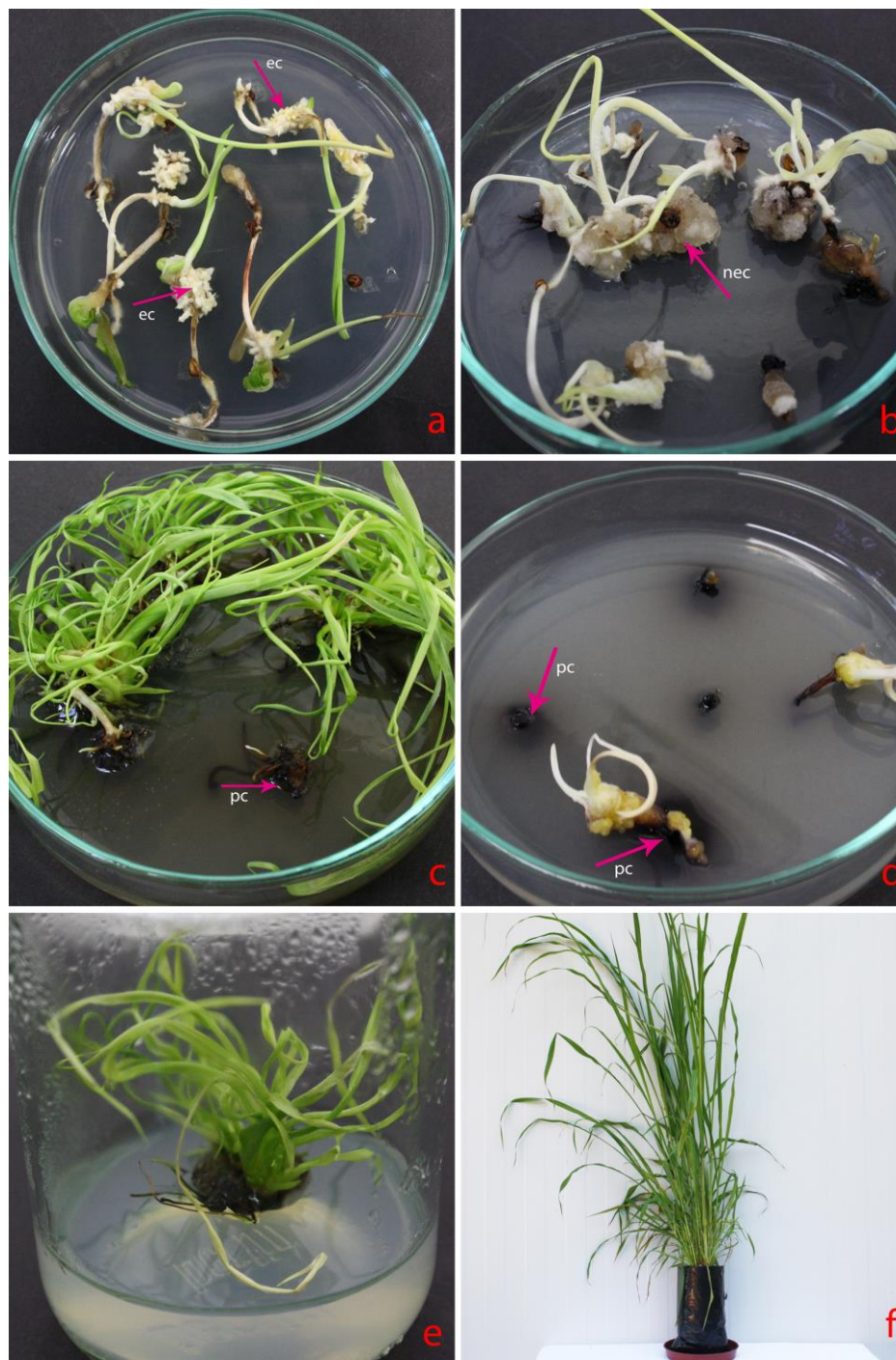


Figure 1. An efficient regeneration system in grain and silage sorghum cultivars. (a) tight and compact embryogenic calli (ec) of Greengo cultivar on callus induction medium (MS supplemented with 1.0 mg/L 2,4,5-T, 0,5 mg/l kinetin) after four week's culture initiation, (b) weak and soft non-embryogenic calli (nec) of Gözde-80 cultivar on callus induction medium (MS supplemented with 1.0 mg/L 2,4,5-T, 0,5 mg/l kinetin), (c) callus regenerating of Greengo on shoot induction medium (MS supplemented with 1,5 mg/l TDZ, 1 mg/l IAA, 1 mg/l BA) after eight week's initiation and phenolic compound (pc) formation during shoot formation, (d) phenolic compound (pc) formation during callus induction of Aldari on callus induction medium (MS supplemented with 1.0 mg/L 2,4-D), (e) rooting of Greengo on root induction medium ($\frac{1}{2}$ MS supplemented with 1 mg/l NAA), (f) acclimatization of Greengo rooting regenerates

In comparison with the study, Zarif et al. (2013) showed that 4 mg/l of 2,4-D was the best concentration in callus induction from seed and immature inflorescence and that the lowest and the highest levels of 2,4-D (1 and 6 mg/l) delayed callus induction. In contrast to these studies, Lu et al. (1983) and Pola et al. (2008) stated that the high 2,4-D concentration in cereals negatively affected the embryonic callus induction in support of our findings. The high-frequency embryogenic calli were also obtained from mature embryos using 2 mg/l of 2,4-D with combined 0.5 mg/l of kinetin by Arulselvi and Krishnaveni (2009).

Table 2. Mean values of callus induction in sorghum cultivars, auxin types and combinations and their doses

Cultivars	Callus induction percentage (%)
Gözde 80	59.62 ^{c*}
Greengo	72.11 ^b
Leoti	59.43 ^{dc}
Beydarı	67.75 ^b
Aldarı	54.82 ^d
Akdarı	90.58 ^a
Auxin types and combinations	
2,4-D	80.08 ^a
2,4-D+Zeatin	69.18 ^{bc}
2,4-D+Kinetin	68.95 ^c
2,4,5-T	74.88 ^b
2,4,5-T+Zeatin	57.75 ^d
2,4,5-T+Kinetin	53.84 ^d
Doses (mg/l)	
1	74.61 ^a
2	69.89 ^b
4	56.25 ^c

*The means shown similar letters are not statistically different at $p \leq 0.05$

Plant regeneration

The shoots and chlorophyll developed 6 weeks after the initiation of culture, and shoot formation was completed within a total of 8 weeks (*Fig. 1c*). The concentrated phenolic compound formation was observed during both callus and shoot induction depending on the genotypes which were negatively affected at the point of regeneration (*Figs. 1c* and *1d*). Nguyen et al. (2007) stated that the most common problem of sorghum tissue culture is the high rate of secretion of phenolic compounds.

To determine the plant regeneration, embryonic calli obtained from 1 mg/l of 2,4-D and 2,4,5-T and their combinations with 0,5 mg/l kinetin and zeatin were used. The best shoot formation was determined in shoot media containing BA regardless of 1 and 2 mg/l (Data not shown). Setting aside the doses of BA, the effects of the genotypes and hormones on plant regeneration were found to be significant (*Table 3*).

Although Akdarı had a high callus induction percentage, the highest number of shoots (2.73 shoots per callus) was obtained with the Greengo cultivar. Also, 2,4,5-T combined with kinetin showed the highest number of shoots (3.39 shoots per callus), while this combination was not effective in callus induction percentage (*Table 3*). Unlike our study, those of Gupta et al. (2006) and Pola et al. (2008) revealed that there was a significant positive correlation between embryonic callus frequency and the number of shoots of sorghum. Shoot number per callus was clearly increased when kinetin was added to medium with 2,4,5-T. Pola et al. (2008) and Hagio (2002) reported

that adding cytokinins (kinetin or 6-benzyladenine) to the callus induction medium resulted in the highest regeneration rate; this supported our findings. Additionally, the use of regeneration medium without growth regulators gave the next highest regeneration rate. Zarif et al. (2013) showed that the addition of kinetin to the culture medium had no effect on the regeneration of sorghum.

Table 3. Mean values of shoot formation in sorghum cultivars, auxin types and combinations

Cultivars	Shoot numbers per callus (number)
Gözde 80	1.52 ^{b*}
Greengo	2.73 ^a
Leoti	1.95 ^b
Beydarı	1.50 ^b
Aldarı	1.13 ^b
Akdarı	1.53 ^b
Auxin types and combinations	
2.4-D	1.82 ^b
2.4-D+Zeatin	0.73 ^c
2.4-D+Kinetin	1.28 ^{bc}
2.4.5-T	2.00 ^b
2.4.5-T+Zeatin	1.40 ^{bc}
2.4.5-T+Kinetin	3.39 ^a

*The means shown similar letters are not statistically different at $p \leq 0.05$

Rooting

The regenerates obtained from the shooting medium were successfully rooted when transferred to the rooting medium containing 1 mg/l NAA (*Fig. 1e*). Also, many previous studies have shown that NAA is successful in the rooting of sorghum (Pola and Mani, 2006; Sai Kishore et al., 2006; Pola et al., 2008). These rooted plants were transferred to a pot containing peat and vermiculite (4:1) and were successfully acclimated to outdoor condition at climate room (*Fig. 1f*). While BA concentration did not affect rooting (data not shown), the rooting percentage of sorghum cultivars and auxin types and combinations showed in significant differences (*Fig. 2*).

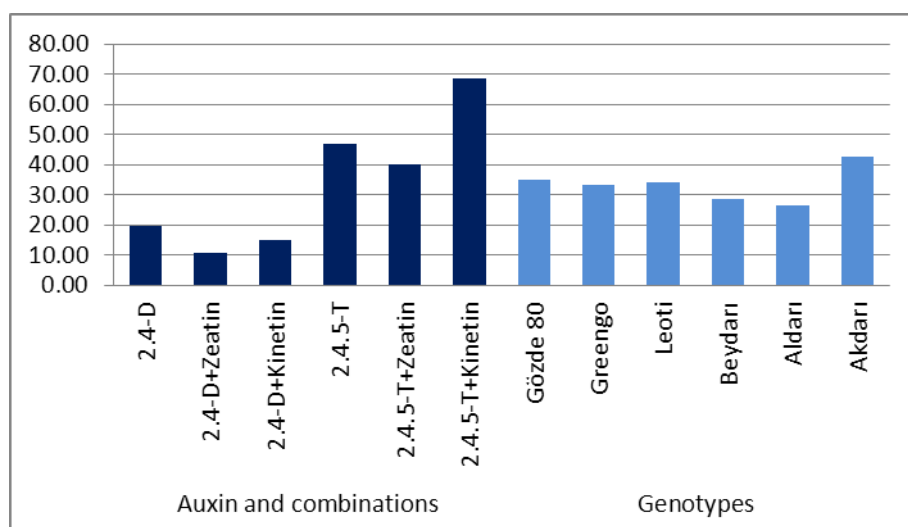


Figure 2. The effects of sorghum cultivars and different auxin types and their combinations on the rooting percentage (%)

The highest rooting percentage was obtained from Akdarı cultivar similar as callus induction percentage. However, silage sorghum cultivars like Greengo giving the highest shooting showed values close to Akdarı. 2,4,5-T and combinations were found to be more effective than 2,4-D and combinations in rooting and subsequent development. The addition of kinetin with the 2,4,5-T to the callus induction medium affected shoot and rooting formation positively despite phenolic compound formation. Simpson et al. (1982) reported that kinetin positively affected the uptake of NO₃ in roots and increased nitrogen content in roots and shoots of wheat. Gupta et al. (2006) stated that kinetin-like cytokinins should be added to the callus formation medium to overcome the genotypic limitations of plant regeneration.

Conclusion

An efficient regeneration system was developed by using mature embryos in sorghum. Akdarı (Tannin-free cultivar) showed the high callus induction and rooting percentages. However, silage cultivars seem to be better in terms of shoot formation and no difference with Akdarı in regard to rooting. While 2,4-D gave better callus induction, 2,4,5-T showed better values of the shoot and rooting formation. The formation of phenolic compounds affected plant regeneration negatively in all cultures. In this study, an efficient regeneration protocol despite the formation of phenolic compounds was developed from mature embryos, an unlimited explant source for tissue culture and gene transfer studies. It was concluded that 1 mg/l 2,4,5-T combined with 0.5 mg/l kinetin should be advised for prolific callus induction and regeneration obtained from somatic embryogenesis by using mature embryos in sorghum.

Acknowledgements. The author thanks Eskişehir Osmangazi University for project support (2014-659).

REFERENCES

- [1] Arulselvi, I. P., Krishnaveni, S. (2009): Effect of hormones, explants and genotypes in *in vitro* culturing of sorghum. – *Journal of Biochemical Technology* 1(4): 96-103.
- [2] Dillon, S. L., Lawrence, P. K., Henry, R. J., Price, H. J. (2007): Sorghum resolved as a distinct genus based on combined ITS1, *ndhF* and *Adh1* analyses. – *Plant Systematics and Evolution* 268(1-4): 29-43.
- [3] Gupta, S., Khanna, V. K., Singh, R., Garg, G. K. (2006): Strategies for overcoming genotypic limitations of *in vitro* regeneration and determination of genetic components of variability of plant regeneration traits in sorghum. – *Plant Cell, Tissue and Organ Culture* 86(3): 379-388.
- [4] Hagio, T. (2002): Adventitious shoot regeneration from immature embryos of sorghum. – *Plant Cell, Tissue and Organ Culture* 68(1): 65-72.
- [5] Hart, G. E., Schertz, K. F., Peng, Y., Syed, N. H. (2001): Genetic mapping of Sorghum bicolor (L.) Moench QTLs that control variation in tillering and other morphological characters. – *Theoretical and Applied Genetics* 103(8): 1232-1242.
- [6] Hassan, L. B., Usman, I. S., Katung, M. D., Bugaje, S. B. (2014): Optimum protocol for shoot formation in karandafi red Sorghum (*Sorghum bicolor* (L.) Moench) through somatic embryogenesis using mature embryo. – *American Journal of Plant Sciences* 5(5): 671-675.
- [7] Jogeswar, G., Ranadheer, D., Anjaiah, V., Kavi Kishor, P. B. (2007): High frequency somatic embryogenesis and regeneration in different genotypes of *Sorghum bicolor* (L.)

- Moench from immature inflorescence explants. – *In Vitro Cellular & Developmental Biology - Plant* 43(2): 159-166.
- [8] Kong, L., Dong, J., Hart, G. (2000): Characteristics, linkage-map positions, and allelic differentiation of Sorghum bicolor (L.) Moench DNA simple-sequence repeats (SSRs). – *Theoretical and Applied Genetics* 101(3): 438-448.
- [9] Lu, C., Vasil, V., Vasil, I. K. (1983): Improved efficiency of somatic embryogenesis and plant regeneration in tissue cultures of maize (*Zea mays* L.). – *Theoretical and Applied Genetics* 66(3-4): 285-289.
- [10] MacKinnon, C., Gunderson, G., Nabors, M. W. (1986): Plant regeneration by somatic embryogenesis from callus cultures of sweet sorghum. – *Plant Cell Reports* 5(5): 349-351.
- [11] Motlhaodi, T., Geleta, M., Bryngelsson, T., Fatih, M., Chite, S., Ortiz, R. (2014): Genetic diversity in ex-situ conserved sorghum accessions of Botswana as estimated by: microsatellite markers. – *Australian Journal of Crop Science* 8(1): 35-43.
- [12] Murashige, T., Skoog, F. (1962): A revised medium for rapid growth and bioassays with tobacco tissue cultures. – *Physiologia Plantarum* 15: 473-497.
- [13] Nguyen, T. V., Thanh Thu, T., Claeys, M., Angenon, G. (2007): Agrobacterium-mediated transformation of sorghum (*Sorghum bicolor* (L.) Moench) using an improved in vitro regeneration system. – *Plant Cell, Tissue and Organ Culture* 91(2): 155-164.
- [14] Nirwan, R. S., Kothari, S. L. (2004): High frequency shoot organogenesis in *Sorghum bicolor* (L.) Moench. – *Journal of Plant Biochemistry and Biotechnology* 13(2): 149-152.
- [15] Pola, S. R., Mani, N. S. (2006): Somatic embryogenesis and plantlet regeneration in *Sorghum bicolor* (L.) Moench, from leaf segments. – *Journal of Cell and Molecular Biology* 5: 99-107.
- [16] Pola, S., Mani, N. S., Ramana, T. (2008): Plant tissue culture studies in *Sorghum bicolor*: immature embryo explants as the source material. – *International journal of plant production* 2(1): 1-14.
- [17] Pola, S., Saradamani, N., Ramana, T. (2009): Mature embryo as a source material for efficient regeneration response in sorghum (*Sorghum bicolor* L. Moench.). – *Sjemenarstvo* 26(3-4): 93-104.
- [18] Pola, S. (2011): Leaf discs as a source material for plant tissue culture studies of *Sorghum bicolor* (L.) Moench. – *Notulae Scientia Biologicae* 3(1): 70-78.
- [19] Rao, A. M., Sree, K. P., Kishor, P. B. K. (1995): Enhanced plant regeneration in grain and sweet sorghum by asparagine, proline and cefotaxime. – *Plant Cell Reports* 15(1-2): 72-75.
- [20] Ritter, K. B., McIntyre, C. L., Godwin, I. D., Jordan, D. R., Chapman, S. C. (2007): An assessment of the genetic relationship between sweet and grain sorghums, within *Sorghum bicolor* ssp. *bicolor* (L.) Moench, using AFLP markers. – *Euphytica* 157(1-2): 161-176.
- [21] Sai Kishore, N., Visarada, K. B., Aravinda Lakshmi, Y., Pashupatinath, E., Rao, S. V., Seetharama, N. (2006): In vitro culture methods in sorghum with shoot tip as the explant material. – *Plant Cell Reports* 25(3): 174-182.
- [22] Seetharama, N., Sairam, R. V., Rani, T. S. (2000): Regeneration of sorghum from shoot tip cultures and field performance of the progeny. – *Plant Cell, Tissue and Organ Culture* 61(2): 169-173.
- [23] Sharma, K. K., Ortiz, R. (2000): Program for the application of genetic transformation for crop improvement in the semi-arid tropics. – *In Vitro Cellular & Developmental Biology - Plant* 36(2): 83-92.
- [24] Simpson, R. J., Lambers, H., Dalling, M. J. (1982): Kinetin application to roots and its effect on uptake, translocation and distribution of nitrogen in wheat (*Triticum aestivum*) grown with a split root system. – *Physiologia Plantarum* 56(4): 430-435.
- [25] Singh, U., Singh, B. (1992): Tropical grain legumes as important human foods. – *Economic Botany* 46(3): 310-321.

- [26] Sinha, S., Kumaravadivel, N. (2016): Understanding genetic diversity of sorghum using quantitative traits. – *Scientifica AI*: 3075023, <http://doi.org/10.1155/2016/3075023>.
- [27] Snedecor, G. W., Cochran, W. C. (1991): *Statistical Methods*. – The Iowa State University Press, Iowa, pp. 593.
- [28] Tiidema, A., Truve, E. (2004): Efficient regeneration of fertile barley plants from callus cultures of several Nordic cultivars. – *Hereditas* 140(3): 171-176.
- [29] Zarif, M., Sadia, B., Kainth, R. A., Khan, I. A. (2013): Genotypes, explants and growth hormones influence the morphogenesis in Pakistani Sorghum (*Sorghum bicolor*): Preliminary field evaluation of sorghum somaclones. – *International Journal of Agriculture and Biology* 15(6): 1157-1162.
- [30] Zhao, L., Liu, S., Song, S. (2010): Optimization of callus induction and plant regeneration from germinating seeds of sweet sorghum (*Sorghum bicolor* Moench). – *African Journal of Biotechnology* 9(16): 2367-2374.
- [31] Zongo, J. D., Gouyon, P. H., Sandmeier, M. (1993): Genetic variability among sorghum accessions from the Sahelian agroecological region of Burkina Faso. – *Biodiversity & Conservation* 2(6): 627-636.

RESPONSIBILITY OF FAT BODIES RELATED TO ENVIRONMENTAL FACTORS ON HONEYBEE (*APIS MELLIFERA* L.) (HYMENOPTERA: APIDAE) STRAINS IN KURDISTAN REGION

RUKHOSH, J. R.^{1*} – TALAL, T. M.² – ABDULBAST, M. A.³

¹College of Agricultural Sciences, University of Sulaimani, Sulaymaniyah, Iraq
(e-mail: Rukhosh1983@yahoo.com)

²College of Agriculture, University of Duhok, Duhok, Iraq
(e-mail: talphys_99@yahoo.com)

³College of Agriculture, Salahaddin University-Erbil, Erbil, Iraq
(e-mail: profabed57@yahoo.com)

*Corresponding author
e-mail: rukhosh.rashed@univsul.edu.iq

(Received 16th Oct 2018; accepted 22nd Dec 2018)

Abstract. This study was carried out from April 2016 to the end of October 2017 including three seasons each year: Spring, early Summer, Summer and Autumn in the apiary of College of Agriculture Science in the University of Sulaimani – Kurdistan Region – Iraq. The results showed the highest rate of unsealed brood area for *Apis mellifera* Native was 1408.500 inch in early Summer 2016 and the lowest rate was 6.250 inch for *Apis mellifera ligustica* in Spring 2017, but the sealed brood area was 5906.500 inch for *Apis mellifera* Native strain in early Summer and the lowest rate was 22.000 inch for *Apis mellifera* Native strain in Autumn 2017. The highest and the lowest rate of Pollen grain area were (1582.750 and 7.290) inch for *Apis mellifera* Native strain in summer 2017 and 2016 respectively. Laboratory test indicated that the fat bodies play an important role in supplying the tissues with essential elements for body activities. Which means those fat bodies function as a reservoir.

Keywords: *Apis mellifera* L., foraging, honey production, nectar, pollen grain

Introduction

Foraging activity and behavior of *Apis mellifera* L. is dependent on many factors working at the same time, and the animals respond to some environmental conditions in a similar manner or method wherever they occur. Foraging for nectar and pollen is a continuous process throughout the year in tropical and sub-tropical regions, where the plants are available. However, the foraging activity of honey bees for pollen are significantly affected by weather conditions and availability of pollen (Neupane and Thapa, 2005). Foraging is one of the distinctive behaviors of honey bee (*Apis mellifera* L.), which links the honey bee colony and the surrounding environment (Abou-Shaara, 2014). It is known that the foraging activity for honeybees begin early in the morning and end in the evening. In some studies, honey bee workers started their foraging activity at 6.17 am in April, in one of the apple orchards (situated in Cheepa) in district Nainital of Kumaon Himalayas, Uttarakhand state of India. This start time however, may also be affected by the region (Joshi and Joshi, 2010). Al-qarni (2006) and Blazyte-Cereskiene et al. (2010) found that temperature has a significant impact on foraging activity, for example high temperature has a negative impact on foraging bees. Additionally, very low temperatures (below 10 °C) can prevent flight. No significant

direct effect of relative humidity was reported on honeybees, including foraging activity (Joshi and Joshi, 2010).

The fat bodies are normally distributed through the body cavity of insects, mostly in the abdomen where they appear as irregular masses of a soft and usually white tissue composed of large, loosely united cells. These cell masses are known collectively as fat body, because the cytoplasm of the cells contains small droplets of oily fat (Snodgrass and Erickson, 2003). The fat bodies can be irregularly distributed in the perivascular space of the abdomen and thorax, surrounding organs (visceral fat body) or in the dorsal and ventral sinus of the abdomen, close to the tegument (parietal fat body), in the head and even in body appendices (Chapman, 1978; Zanini and Caetano, 2003). Ayoub (2011) found that the average dimension of a fat body cell in newly emerged workers ranges between 86.71 and 86.76 μm and in 10-days old workers the average dimension of fat body cells ranges between 89.15 and 89.95 μm , while the average dimensions of fat body cell for foraging workers ranges between 67.33 and 69.05 μm .

Fat body is the main storage agent of the metabolic device of insects and is responsible for the synthesis and supply of hemolymph. Fatty body is made up of cells of the mesodermal origin, which sometimes contain epidermal cells (Oliveira and Cruz-Landim, 2003). Roma et al. (2010) demonstrated that fat body consists of a mass of cells under the epidermis, and in some insects, fat body also surrounds the digestive system and the reproductive system.

The aim of this work is to shed light on the factors related to bee activities, to find out the temperature most sufficient for long journeys (round trips) for each season in the study region, and to determine the adaptability of different bee races to environmental factors in different seasons of the year.

Material and methods

Preparation and arrangement of colonies

This study was carried out from April 2016 to the end of October 2017, and included three seasons per year; Spring, Summer, and Autumn. It was performed in the apiary of College of Agriculture Science in the University of Sulaimany – Iraq. We prepared four colonies of *Apis mellifera carnica*, four colonies of *Apis mellifera ligustica*, and four colonies of *Apis mellifera* Native, taking the following characteristics into account:

The queens were characterized by fertility, similar ages and being uniform in size in each race, therefore all experimental colonies included five frames each homogenous and uniform in activity. For measurements, two Langstroth frames were prepared at first, then it was modified by dividing each frame in to 17 inch in length and 8 inch in wide sections, Holes were inserted into each frame using frame fastening wires (silk), with each unit being one square inch, with a total of 136 units.

The area of the brood, honey and pollen were measured four seasons per year (spring, early summer, late summer and autumn of 2016 and 2017) using the standard Langstroth frame as described above. Also the area of unsealed and sealed broods was measured every 2 weeks until the end of the study. The measurement was taken using a typical frame with the method described by Mustafa (2003) and Targany (2008) (Figs. 1 and 2).



Figure 1. Typical frame

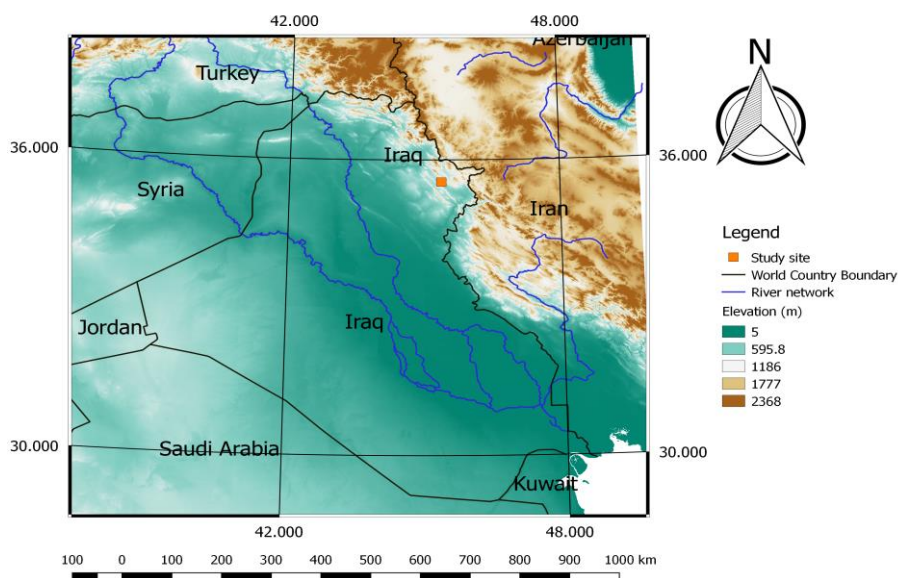


Figure 2. Map of the study site

Labeling of samples

Newly emerged workers were labeled with nail stains of different colors (Snodgrass and Erickson, 2003; Shamdin, 2003; Targany, 2008). One drop of the stain was stamped on the notum, characterized by little hairs, in a position where workers could not clean the label. The preliminary experiment was carried out in the laboratory in order to avoid any side effects of the stains on the viability of these young workers.

Dissection

The workers were fixed on the dissecting tray after the legs and wings were removed, and then were filled with physiological solution. Then the unit was transferred to the dissecting microscope, under which the head was cut off and placed on the filter paper for the measurement.

Workers were cut with a sharp scalpel into two lateral longitudinal slices of the abdomen. These were mounted on the dissecting tray by fine, stainless pins (Mahmoud, 1992; Shamdin, 2003). The workers were kept in a physiological saline with 0.9% w/v of NaCl, 0.9 g per 100 ml distilled water (Pantin, 1964). The fixed workers were dissected under 2x and 4x objective lenses of binocular. After cutting the cuticle and

removing the muscles, the fat bodies were picked up and placed on a clean slide and stained with methylene blue in normal limitation. The binocular dissecting and compound microscope for photographs and measurements was used with an eye piece graticule.

The climatic data

The data of climatic information was taken from Sulaimani General Directorate Meteorology and Seismology.

Statistical analysis

The results were analyzed statistically using factorial RCBD design with triple replicates and performed using the XLSTA program (2016). Duncan's multiple range Test was used to determine the differences between means at P = 0.05.

Result and discussion

Effect of environmental factors on bioactivity of honey bee colonies in spring

Unsealed workers brood area

Table 1 shows the average unsealed workers' brood area in spring. The highest average unsealed brood area of *Apis mellifera ligustica* was dated 14-5-2017 at 1316.250 inch², with an average temperature of 23.75 °C and relative humidity of 38.95%. The average unsealed brood area for *Apis mellifera carnica* and *Apis mellifera* Native were 1188.500 and 1086.500 inch. In the same period and weather conditions the lowest averages were 257.25, 268.75 and 266.500 inch² at 2-4-2016 and 253.000, 257.250 and 260.500 inch² at 2-4-2017 for *A. m. carnica*, *A. m. ligustica* and *A. m. Native* respectively, with an average temperature of 15.75, 16.5 °C and relative humidity of 65.75% respectively.

Table 1. Effect of some honeybee races and environmental factors on unsealed brood area in spring 2016-2017

Period	Honey bee race			Mean	Temperature	Relative humidity %
	<i>Apis mellifera carnica</i>	<i>Apis mellifera ligustica</i>	<i>Apis mellifera Native</i>			
2-4-2016	257.250 j	268.750 ij	266.500 j	264.166	15.75	65.75
16-4-2016	292.250 hij	303.000 hij	295.000 hij	296.750	18.50	61.7
30-4-2016	350.500 gh	356.750 gh	344.750 ghi	350.666	21.50	59.75
14-5-2016	392.500 fg	381.750 g	387.000 fg	387.083	24.50	46
2-4-2017	253.000 j	257.250 j	260.500 j	256.916	16.50	65.75
16-4-2017	487.000 e	477.750 e	456.750 ef	473.833	19.30	63.55
30-4-2017	660.000 d	655.250 d	643.250 d	652.833	21.50	48.5
14-5-2017	1188.500 b	1316.250 a	1086.500 c	1197.083	23.75	38.95
Mean	485.125	385.785	467.531		20.16	56.24375

Different letters mean significant difference (p<0.05) based on Duncan test.

Figure 3 shows the effect of honey bee races on the general average of unsealed brood worker area. These were 485.125, 467.531 and 385.785 inch for *Apis mellifera carnica*, *Apis mellifera* Native and *Apis mellifera ligustica* race respectively. Statistical analysis showed significant differences at level 0.05 among *A. m. ligustica*, *A. m. carnica* and *A. m. Native* at different temperatures and relative humidity. The results agree with Becher et al. (2009) who found that honey bees (*Apis mellifera*) are able to regulate incubation temperatures within a narrow range between 32 and 36 °C. However, this small variation in brood temperature is sufficient to cause significant differences in the behavior of adult bees in agreement with Petz et al. (2004), who found the temperature, in particular, is very important for internal and external activities of honey bee colonies. Maintaining an appropriate degree of temperature from 33 to 36 °C within colonies is very important for honey bees.

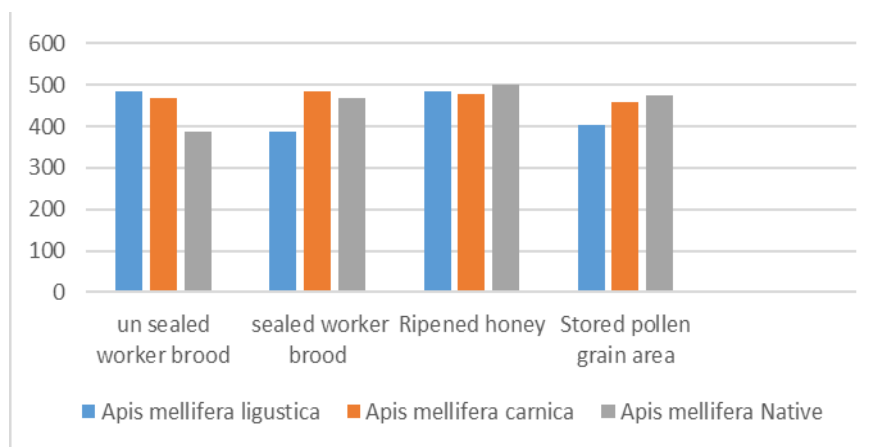


Figure 3. Effect of environmental conditions on the honeybee worker activities in spring

Sealed workers brood area

Table 2 shows the average sealed brood area of the workers in spring. The highest average sealed brood area for *Apis mellifera ligustica* was 1327.750 inch² with an average temperature of 23.75 °C and average relative humidity of 38.95% at 14-5-2017. Comparatively, the average sealed brood area for *Apis mellifera carnica* and *Apis mellifera* Native were 1137.750, 1098.500 inch² respectively during the same period and same weather conditions. Meanwhile, the lowest average of sealed brood was 261.000 inch² for *A. m. ligustica* at 2-4-2016, when the average temperature was 15.75 °C and the relative was humidity 65.75%. At the date of 14-5-2017 the highest general average was 1188.000 inch². Figure 3 shows the effect of the environmental conditions on *A. m. carnica*, *A. m. Native*, and *A. m. ligustica*. The general average of sealed brood area was 508.968, 501.812, and 514.187 inch² respectively. Statistical analysis showed significant differences at level 0.05 between races. According to the results, the sealed worker broods were in high numbers during spring, which is in accordance with Fathy (1997), who found that the results showed that the main peak of brood activity and a high rate of stored pollen were observed in May, and therefore the maximum number of bees was recorded during June and July. However, there is no reciprocal relationship. The lowest level of brood, bee and pollen production occurred during February.

Table 2. Effect of some honeybee races and environmental factors on sealed brood area in the spring season of 2016-2017

Period	Honeybee race			Mean	Temperature	Relative humidity %
	<i>Apis mellifera carnica</i>	<i>Apis mellifera ligustica</i>	<i>Apis mellifera</i> Native			
2-4-2016	274.750 j	261.000 j	297.000 hij	277.583	15.75	65.75
16-4-2016	311.250 ghij	289.250 ij	326.250 ghij	308.916	18.50	61.70
30-4-2016	390.250 efg	342.500 fghij	380.250 efgh	371.000	21.50	59.75
14-5-2016	429.250 e	371.250 efghi	425.250 ef	408.583	24.50	46.00
2-4-2017	277.000 j	267.000 j	296.500 hij	280.166	16.50	65.75
16-4-2017	539.500 d	544.750 d	506.250 d	530.166	19.30	63.55
30-4-2017	712.000 c	710.000 c	684.500 c	702.166	21.50	48.50
14-5-2017	1137.750 b	1327.750 a	1098.500 b	1188.000	23.75	38.95
Mean	508.968	514.187	501.812		20.16	56.24

Different letters mean significant difference ($p < 0.05$) based on Duncan test.

Ripened honey

Table 3 shows the average ripened honey area in spring. The highest average area for *A. m. ligustica* was 1565.750 inch² at 14-5-2017 when the average temperature was 23.75 °C and the relative humidity was 38.95%. The average area for *A. m. carnica* and *A. m. Native* were 1535.750 and 1542.750 inch² during the same period and with the same weather conditions, but the lowest average for the *A. m. carnica* was 215.750 inch² in 2-4-2017 when the average temperature and relative humidity was 16.5 °C and 65.75%. The average of ripened honey area was 476.25, 482.9688 and 499.6875 inch² for *A. m. carnica*, *A. m. ligustica* and *A. m. Native* respectively. The highest general average was 1548.083 inch² at the date of 14-5-2017 and the lowest was 237.166 inch² in 16-4-2016. Figure 3 shows the effect of environmental conditions on *A. m. carnica*, *A. m. ligustica* and *A. m. Native*. The general average of ripened honey area in spring was 476.250, 482.968 and 499.687 inch² respectively. Statistical analysis showed significant differences at level 0.05 among races. According to the results, the amount of honey was high for all races in spring season due to flowering. This matches the findings of Mattu et al. (2012) who studied the times at which foraging starts and stops, the duration of the foraging and length of trips, as well as the number of flowers visited per minute.

Table 3. Effect of some honeybee races and environmental factors on ripened honey area in spring season 2016-2017

Period	Honeybee race			Mean	Temperature	Relative humidity %
	<i>Apis mellifera carnica</i>	<i>Apis mellifera ligustica</i>	<i>Apis mellifera</i> Native			
2-4-2016	236.500 de	234.500 de	273.000 de	248.000	15.75	65.75
16-4-2016	222.250 de	234.250 de	255.000 de	237.166	18.50	61.7
30-4-2016	232.750 de	240.250 de	277.750 d	250.250	21.50	59.75
14-5-2016	228.500 de	252.750 de	268.250 de	249.833	24.50	46.00
2-4-2017	215.750 e	237.000 de	268.750 de	240.500	16.50	65.75
16-4-2017	392.500 c	400.250 c	405.750 c	399.500	19.30	63.55
30-4-2017	746.000 b	699.000 b	706.250 b	717.083	21.50	48.50
14-5-2017	1535.750 a	1565.750 a	1542.750 a	1548.083	23.75	38.95
Mean	476.25	482.968	499.687		20.16	56.24

Different letters mean significant difference ($p < 0.05$) based on Duncan test.

Stored pollen grain area

Table 4 and Figure 3 show the average stored pollen grain area in spring. The highest average area for *A. m. carnica* was 1111.000 inch² at 14-5-2017 when the average temperature was 23.75 °C and the relative humidity was 38.95%. The average area for *A. m. Native* and *A. m. ligustica* were 1088.750 and 972.500 inch² during the same period and the lowest average was 218.750 inch² for *Apis mellifera carnica* at 2-4-2017 when the average temperature and relative humidity was 16.5 °C and 65.75%. The average of stored pollen area was 474.062, 457.687 and 402.416 inch² for *A. m. Native*, *A. m. carnica* and *A. m. ligustica* respectively when the temperature was 20.16 °C and the average relative humidity was 56.24%. The highest general average was 1057.417 inch² at the date of 14-5-2017 and the lowest was 231.583 inch² at 2-4-2016. Statistical analysis showed significant differences at level 0.05 among all three races. The results agree with Neupane and Thapa (2005) who found that the foraging activity of honey bees for pollen are significantly affected by the weather condition and availability of pollen.

Table 4. Effect of some honeybee races and environmental factors on pollen grain area in spring season 2016-2017

Period	Honey bee race			Mean	Temperature	Relative humidity %
	<i>Apis mellifera carnica</i>	<i>Apis mellifera ligustica</i>	<i>Apis mellifera Native</i>			
2-4-2016	221.000 h	216.000 h	257.750 fgh	231.583	15.75	65.75
16-4-2016	241.250 fgh	221.000 h	278.000 fgh	246.750	18.50	61.70
30-4-2016	266.250 fgh	244.250 fgh	297.000 fg	269.166	21.50	59.75
14-5-2016	303.000 ef	269.250 fgh	364.250 e	312.166	24.50	46.00
2-4-2017	218.750 h	230.250 fgh	286.500 fgh	245.166	16.50	65.75
16-4-2017	544.250 d	751.500 c	494.000 d	596.583	19.30	63.55
30-4-2017	756.000 c	751.500C	726.250 c	744.583	21.50	48.50
14-5-2017	1111.000 a	972.500 b	1088.750 a	1057.417	23.750	38.95
Mean	457.687	402.416	474.062		20.162	56.24

Different letters mean significant difference (p<0.05) based on Duncan test.

Effect of environmental factors on bioactivity of honey bee colonies in early summer

Unsealed workers brood area

Table 5 shows the average unsealed workers brood area in early summer. The highest average unsealed brood area for *A. m. Native* at the date of 28-5-2017 was 1408.500 inch² when the average temperature was 26.50 °C and the average relative humidity was 36.50%. The average unsealed brood area for *A. m. carnica* and *A. m. ligustica* were 1333.250 and 1371.750 inch² during the same period and weather conditions, while the lowest average was 132.250 inch² at 9-7-2016 and 767.937, 750.937 and 770.781 inch² at 9-7-2016 for *A. m. carnica*, *A. m. ligustica* and *A. m. Native* respectively, as in shown in Figure 4. Statistical analysis showed significant differences at level 0.05 among studied races. Abou-Shaara et al., (2012) also found

positive correlations between foraging activities and sealed brood area as well as bee numbers.

Table 5. Effect of some honeybee races and environmental factors on unsealed brood area in early summer 2016-2017

Period	Honeybee race			Mean	Temperature	Relative humidity %
	<i>Apis mellifera carnica</i>	<i>Apis mellifera ligustica</i>	<i>Apis mellifera Native</i>			
28/5/2016	438.000 e	413.750 e	439.500 e	430.416	26.75	44.00
11/6/2016	446.500 e	422.250 e	428.750 e	432.500	28.00	35.50
25/6/2016	405.750 e	393.750 e	386.750 e	395.416	30.50	31.75
9/7/2016	138.750 f	133.000 f	132.250 f	134.666	34.50	27.30
28/5/2017	1333.250 ab	1371.750 a	1408.500 a	1371.167	26.50	36.50
11/6/2017	1332.000 ab	1313.500 ab	1229.000 b	1291.500	32.40	30.65
25/6/2017	1019.250 cd	936.500 d	1024.750 cd	993.500	33.50	23.50
9/7/2017	1030.000 cd	1023.000 cd	1116.750 c	1056.583	34.85	22.60
Mean	767.937	750.937	770.781		30.87	31.47

Different letters mean significant difference ($p < 0.05$) based on Duncan test.

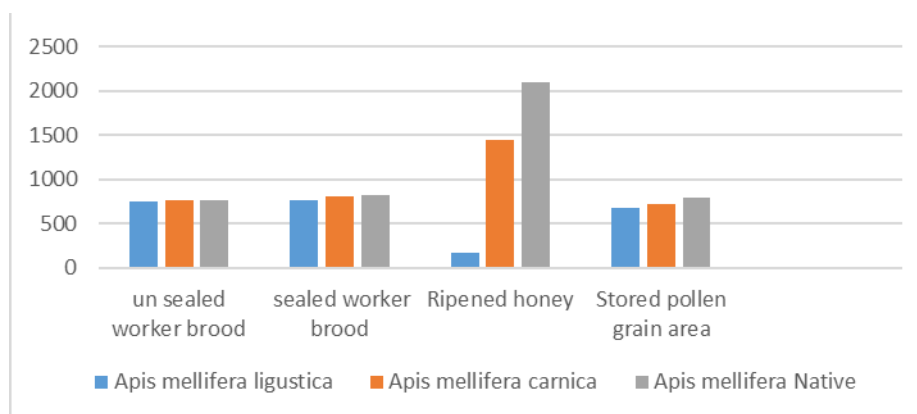


Figure 4. Effect of environmental factors on different the activities of honeybee races in early summer

Sealed workers brood area

Table 6 and Figure 4 show the average sealed brood area of the workers in early summer. The highest average sealed brood area for *A. m. Native* 1514.750 inch² at 28-5-2017 when the average temperature was 26.50 °C and the average relative humidity was 36.50%. The average sealed brood area for *A. m. carnica* and *A. m. ligustica* were 1404.250 and 1319.750 inch² during the same period and weather conditions, while the lowest average of sealed brood was 101.500 inch² for *A. m. Native* at 9-7-2016, when the average temperature and relative humidity were 34.50 °C and 27.30%. The average of sealed workers brood area was 823.843, 803.625 and 770.312 inch² for *A. m. Native*, *A. m. carnica* and *A. m. ligustica* respectively, when the average temperature was 30.87 °C and average relative humidity was 31.47%). The highest general average was

1412.917 inch² in 28-5-2017 and the lowest was 107.000 inch² at 9-7-2016. Statistical analysis showed significant differences at level 0.05 among races. Harbo (2015) found that the bees used a total of 121 grams of honey to produce 1,000 cells of the brood (eggs, larvae, and virgins in the normal brood nest) and about 163 mg of honey to rear the working bees to the virgin stage. In colonies containing incubation of all stages, brood weight was approximately equal to (about 25% less than) the weight of the honey used in its production.

Table 6. Effect of some honeybee races and environmental factors on sealed brood area in early summer 2016-2017

Period	Honeybee race			Mean	Temperature	Relative humidity %
	<i>Apis mellifera carnica</i>	<i>Apis mellifera ligustica</i>	<i>Apis mellifera Native</i>			
Early summer						
28/5/2016	473.250 f	417.750 f	475.250 f	455.416	26.75	44.00
11/6/2016	484.500 f	434.000 f	462.500 f	460.333	28.00	35.50
25/6/2016	459.000 f	412.750 f	438.750 f	436.833	30.50	31.75
9/7/2016	110.000 g	109.500 g	101.500 g	107.000	34.50	27.30
28/5/2017	1404.250 ab	1319.750 b	1514.750 a	1412.917	26.50	36.50
11/6/2017	1389.000 ab	1427.500 ab	1404.250 ab	1406.917	32.40	30.65
25/6/2017	1109.750 cd	1081.750 cde	1143.750 c	1111.750	33.50	23.50
9/7/2017	999.250 de	959.500 e	1050.000 cde	1002.917	34.85	22.60
Mean	803.625	770.312	823.843		30.87	31.47

Different letters mean significant difference (p<0.05) based on Duncan test.

Ripened honey area

Table 7 shows the average ripened honey area in early summer. The highest average area for *A. m. Native* was 5906.500 inch² at 25-6-2017 when the average temperature was 33.50 °C and the relative humidity was 23.50%. In comparison, the average area for *A. m. carnica* and *A. m. ligustica* were 4813.750 and 3781.000 inch² during the same period and weather conditions. The lowest average for *A. m. ligustica* and *A. m. Native* was 243.000 inch² at 9-7-2016 when the average temperature and relative humidity were 34.50 °C and 22.60%. The average of ripened honey area was 2103.000, 1793.156 and 1453.375 inch² for *A. m. Native*, *A. m. carnica* and *A. m. ligustica* respectively as show in Figure 4.

Table 7. Effect of some honeybee races and environmental factors on sealed honey area in early summer 2016-2017

Period	Honey bee race			Mean	Temperature	Relative humidity %
	<i>Apis mellifera carnica</i>	<i>Apis mellifera ligustica</i>	<i>Apis mellifera Native</i>			
Early summer						
28/5/2016	244.250 g	272.000 g	283.250 g	266.500	26.75	44.00
11/6/2016	288.000 g	296.500 g	315.250 g	299.916	28.00	35.50
25/6/2016	288.000 g	316.000 g	324.000 g	309.333	30.50	31.75
9/7/2016	247.000 g	243.000 g	243.000 g	244.333	34.50	27.30
28/5/2017	3143.500 d	2186.000 e	3387.750 cd	2905.750	26.50	36.50

11/6/2017	3785.000 c	2966.750 d	4821.500 b	3857.750	32.40	30.65
25/6/2017	4813.750 b	3781.000 c	5906.500 a	4833.750	33.50	23.50
9/7/2017	1535.750 f	1565.750 f	1542.750 f	1548.083	34.85	22.60
Mean	1793.156	1453.375	2103.000		30.87	31.47

Different letters mean significant difference ($p < 0.05$) based on Duncan test.

The highest general average was 4833.750 inch² in 25-6-2017 and the lowest was 244.333 inch² at 9-7-2016. Statistical analysis showed significant differences at level 0.05 among *A. m. carnica*, *A. m. local* and *A. m. ligustica*. The results agree with Tirado et al. (2013) who indicated that Climate change is associated with a marked disparity in the abundance of honey bees and honey yield. Foraging activities of social insects are affected by climate.

Stored pollen grain area

Table 8 shows the average stored pollen grain area in early summer. The highest average area for *A. m. Native* was 1575.500 inch² at 25-6-2017, when the average temperature was 33.50 °C and relative humidity was 23.50%. The average area for *A. m. carnica* and *A. m. ligustica* were 1401.000 and 1268.750 inch² during the same period and weather conditions. The lowest average was 78.500 inch² for *A. m. Native* at 9-7-2016 when the average temperature and relative humidity were 34.50 °C and 27.30%. The average of stored pollen area was 789.000, 716.281 and 673.906 inch² for *A. m. Native*, *A. m. carnica* and *A. m. ligustica*, with a temperature of 30.87 °C and an average relative humidity of 31.47% as shown in Figure 4. The highest general average was 1415.083 inch² at 25-6-2017 and the lowest was 87.500 inch² at 9-7-2016. Statistical analysis showed significant differences at level 0.05 among *A. m. carnica*, *A. m. Native* and *A. m. ligustica*. The result agree with Mesbah et al. (2017), who showed that the largest quantity of pollen was in August and the summer season, while the lowest was in May and the spring season. Also the highest mean area of brood and honey sealed in trap colonies and without a trap was in September, while the lowest was in May in colonies both with and without traps.

Table 8. Effect of some honeybee races and environmental factors on pollen grain area in early summer 2016-2017

Early summer	<i>Apis mellifera carnica</i>	<i>Apis mellifera ligustica</i>	<i>Apis mellifera Native</i>	Mean	Temperature	Relative humidity %
28/5/2016	332.250 gh	307.500 gh	390.000 g	343.250	26.75	44.00
11/6/2016	352.000 gh	294.500 gh	380.500 g	342.333	28.00	35.50
25/6/2016	303.250 gh	244.250 h	323.000 gh	290.166	30.50	31.75
9/7/2016	86.000 i	97.250 i	78.500 i	87.250	34.50	27.30
28/5/2017	1047.250 ef	967.500 f	979.750 f	998.166	26.50	36.50
11/6/2017	1027.500 ef	982.000 f	1102.500 de	1037.333	32.40	30.65
25/6/2017	1401.000 b	1268.750 c	1575.500 a	1415.083	33.50	23.50
9/7/2017	1181.000 cd	1229.500 c	1482.250 ab	1297.583	34.85	22.60
Mean	716.281	673.906	789.000		30.87	31.47

Different letters mean significant difference ($p < 0.05$) based on Duncan test.

Effect of environmental factors on bioactivity of honey bee colonies in late summer

Unsealed workers brood area

Table 9 shows the average unsealed workers brood area in summer. The highest average unsealed brood area for *A. m. Native* at 23-7-2017 was 920.250 inch² when the average temperature was 32.75 °C and the average relative humidity was 24.15%. The average unsealed brood area for *A. m. carnica* and *A. m. ligustica* was 773.500 and 753.000 inch² during the same period and weather conditions, while the lowest average of unsealed brood area was 86.250 inch² for *A. m. Native* at 6-8-2016 when the average temperature and relative humidity were 43.95 °C and 24.30%. The average of unsealed workers brood area was 382.250, 328.781 and 289.875 inch² for *A. m. Native*, *A. m. carnica* and, *A. m. ligustica* respectively with an average temperature of 36.11 °C and average relative humidity of 27.31% as shows in Figure 5. The highest general average was 815.583 inch² at 23-7-2017 and the lowest was 104.583 inch² at 6-8-2016. Statistical analysis showed significant differences at level 0.05 among *A. m. carnica*, *Apis mellifera* Native and *A. m. ligustica*. Reddy et al. (2012) also found that at the same ambient temperature, outgoing *A. mellifera* foragers and workers who were sampled from the brood nest had a higher chest temperature, much higher than leaving *A. cerana* foragers and brood nest workers. *A. mellifera* colonies also maintained a brood temperature significantly higher than *A. cerana*. Our findings indicate that the larger *A. mellifera* foragers require higher chest temperature to be able to forage in the apiary in Kunming, China.

Table 9. Effect of some honeybee races and environmental factors on unsealed brood area in summer 2016-2017

Summer	Honey bee race			Mean	Temperature	Relative humidity %
Period	<i>Apis mellifera carnica</i>	<i>Apis mellifera ligustica</i>	<i>Apis mellifera Native</i>			
23/7/2016	115.250 g	112.250 g	105.750 g	111.083	34.05	25.85
6/8/2016	115.250 g	112.250 g	86.250 g	104.583	43.95	24.3
20/8/2016	130.250 g	116.500 g	102.250 g	116.333	42.50	26.95
3/9/2016	152.000 g	139.750 g	121.750 g	137.833	34.50	35.7
23/7/2017	773.500 b	753.000 bc	920.250 a	815.583	32.75	24.15
6/8/2017	529.000 d	406.000 e	688.000 c	541	36.70	24.5
20/8/2017	398.750 ef	326.500 f	505.250 d	410.166	34.60	26.44
3/9/2017	416.250 e	352.750 ef	528.500 d	432.5	29.90	30.65
Mean	328.781	289.875	382.250		36.11	27.317

Different letters mean significant difference ($p < 0.05$) based on Duncan test.

Sealed workers brood area

Table 10 and Figure 5 show the average sealed brood area of the workers in summer. The highest average sealed brood area for *A. m. Native* 948.250 inch² at 23-7-2017, when the average temperature was 32.75 °C and the average relative humidity was 24.15%. In comparison, the average sealed brood area for *A. m. carnica* and *A. m. ligustica* were 939.500 and 795.500 inch² during the same period and weather conditions, while the lowest average of sealed brood was 61.250 inch² for *A. m.*

ligustica at 20-8-2016, when the average temperature and relative humidity were 42.50 °C and 26.95% respectively. The average of sealed workers brood area was 397.968, 372.187 and 315.031 inch² for *A. m.* Native, *A. m. carnica* and *A. m. ligustica* respectively, when the average temperature was 36.11 °C and the average relative humidity was 27.31%. The highest general average was 894.41 inch² at 23-7-2017 and the lowest was 62.916 inch² at 20-8-2016. Statistical analysis showed significant differences at level 0.05 among *A. m. carnica*, *A. m.* Native and *A. m. ligustica*. Hossam et al. (2012) and Contreras et al. (2013) also found, that all daily activities and patterns of forager honeybees are under the control and/or change with weather conditions.

Table 10. Effect of some honeybee races and environmental factors on sealed brood area in summer 2016-2017

Summer	Honeybee race			Mean	Temperature	Relative humidity %
Period	<i>Apis mellifera carnica</i>	<i>Apis mellifera ligustica</i>	<i>Apis mellifera local</i>			
23/7/2016	90.250 g	93.000 g	84.500 g	89.250	34.05	25.85
6/8/2016	76.250 g	72.250 g	84.500 g	77.660	43.95	24.30
20/8/2016	61.750 g	61.250 g	65.750 g	62.916	42.50	26.95
3/9/2016	77.000 g	76.500 g	83.500 g	79.000	34.50	35.70
23/7/2017	939.500 a	795.500 b	948.250 a	894.410	32.75	24.15
6/8/2017	710.000 b	560.500 cd	715.750 b	662.080	36.70	24.50
20/8/2017	497.250 def	421.000 f	588.250 cd	502.160	34.60	26.44
3/9/2017	525.500 cde	440.250 ef	613.250 c	526.330	29.90	30.65
Mean	372.187	315.031	397.968		36.11	27.31

Different letters mean significant difference ($p < 0.05$) based on Duncan test.

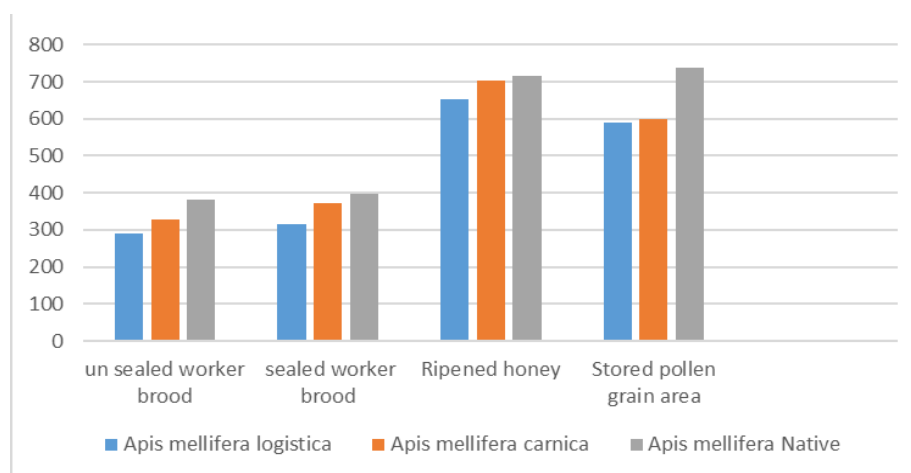


Figure 5. Effect of environmental factors on different the activities of honeybee races in summer

Ripened honey area

Table 11 shows the average ripened honey area in early summer. The highest average area for *A. m.* Native was 1431.000 inch² at 23-7-2017, when the average temperature was 32.75 °C and relative humidity was 24.15%. In comparison, the average area for *A. m.*

carnica and *A. m. ligustica* were 1420.500 and 1370.750 inch² during the same period and weather conditions. The lowest average for *A. m. ligustica* was 257.000 inch² at 23-7-2016, when the average temperature and relative humidity were 34.05 °C and 25.85%. The average of ripened honey area was 715.000, 704.343 and 651.468 inch² for *A. m. Native*, *A. m. carnica* and *A. m. ligustica* respectively as shown in Figure 5. The highest general average was 1290.917 inch² at 6-8-2017 and the lowest was 54.833 inch² at 20-8-2016. Statistical analysis showed significant differences at level 0.05 among races. The results agree with Ali (2011), who found a high foraging rate of Yemeni honeybee in comparison to honey bees in Carniola during June and August and at different times of observation: 6-7 am, 11 to 12 am, and 4 to 5 pm.

Table 11. Effect of some honeybee races and environmental factors on sealed honey area in summer 2016-2017

Summer	Honeybee race			Mean	Temperature	Relative humidity %
Period	<i>Apis mellifera carnica</i>	<i>Apis mellifera ligustica</i>	<i>Apis mellifera Native</i>			
23/7/2016	264.500 d	257.000 d	269.500 d	263.666	34.05	25.85
6/8/2016	275.500 d	271.250 d	275.500 d	274.083	43.95	24.30
20/8/2016	55.000 e	46.000 e	63.500 e	54.833	42.50	26.95
3/9/2016	84.750 e	87.000 e	87.000 e	86.250	34.50	35.70
23/7/2017	1420.5000 a	1370.750 a	1431.000 a	1407.417	32.75	24.15
6/8/2017	1333.250 a	1186.250 b	1353.250 a	1290.917	36.70	24.50
20/8/2017	1165.750 b	1020.000 c	1198.750 b	1128.167	34.60	26.44
3/9/2017	1035.500 c	973.500 c	1041.500 c	1016.833	29.90	30.65
Mean	704.343	651.468	715.000		36.11	27.31

Different letters mean significant difference (p<0.05) based on Duncan test.

Stored pollen grain area

Table 12 and Figure 5 show the average stored pollen grain area in summer. The highest average area for *A. m. Native* was 1582.750 inch² at 23-7-2017, when the average temperature was 32.75 °C and the relative humidity was 24.15%. The average area for *A. m. carnica* and *A. m. ligustica* were 1205.250 and 1191.500 inch² during the same period and with the same weather conditions. In comparison, the lowest average was 7.290 inch² for the *A. m. Native* at 3-9-2016 when the average temperature and relative humidity was 34.50 °C and 35.70%.

Table 12. Effect of some honeybee races and environmental factors on pollen grain area in summer 2016-2017

Summer	Honey bee race			Mean	Temperature	Relative humidity %
Period	<i>Apis mellifera carnica</i>	<i>Apis mellifera ligustica</i>	<i>Apis mellifera Native</i>			
23/7/2016	69.500 ij	86.250 i	60.250 ij	72.000	34.05	25.85
6/8/2016	76.000 ij	62.000 ij	51.750 ij	63.250	43.95	24.30
20/8/2016	55.000 ij	46.000 ij	63.500 ij	54.833	42.50	26.95
3/9/2016	22.500 ij	38.750 ij	7.290 j	22.846	34.50	35.70
23/7/2017	1205.250 de	1191.500 de	1582.750 a	1326.500	32.75	24.15

6/8/2017	1178.250 ef	1163.500 ef	1511.500 b	1284.417	36.70	24.50
20/8/2017	1116.250 fg	1094.000 g	1374.750 c	1195.000	34.60	26.44
3/9/2017	1065.500 gh	1027.000 h	1248.250 d	1113.583	29.90	30.65
Mean	598.531	588.625	737.505		36.11	27.31

Different letters mean significant difference ($p < 0.05$) based on Duncan test.

The average of stored pollen area was 598.531, 588.625 and 737.505 inch² for *A. m. carnica*, *A. m. ligustica* and *A. m. Native* respectively, when the temperature was 36.11 °C and the average relative humidity was 27.31%. The highest general average was 1326.500 inch² at 23-7-2017 and the lowest was 22.846 inch² at 3-9-2016. Statistical analysis showed significant differences at level 0.05 between all races. These results show a low amount of pollen, while Pernal and Currie (2010) found, that in the absence of pollen or with poor pollen quality, colonies of honeybees increase the proportion of pollen foragers without increasing the rate of foraging.

Effect of environmental factors on bioactivity of honey bee colonies in autumn

Unsealed workers brood area

Table 13 shows the average unsealed workers brood area in autumn. The highest average unsealed brood area for *A. m. carnica* at 29-10-2017 was 487.000 inch², when the average temperature was 19.50°C and the average relative humidity was 52.75%. The average unsealed brood area for *A. m. ligustica* and *A. m. Native* was 477.750 and 456.750 inch² during the same period and weather conditions, while the lowest average of unsealed brood area was 18.500 inch² for *A. m. Native* at 29-10-2016 when the average temperature and relative humidity were 22.55 °C and 44.4% respectively.

Table 13. *Effect of some honeybee races and environmental factors on unsealed brood area in autumn 2016-2017*

Autumn	Honey bee race			Mean	Temperature	Relative humidity %
	<i>Apis mellifera carnica</i>	<i>Apis mellifera ligustica</i>	<i>Apis mellifera Native</i>			
17/9/2016	90.250 hijk	133.250 gh	77.000 ijkl	100.166	29.75	38.50
1/10/2016	103.500 ghij	148.250 g	77.000 ijkl	109.583	27.50	40.05
15/10/2016	59.000 ijklm	109.500 ghi	40.000 klm	69.500	24.75	42.00
29/10/2016	30.250 lm	54.500 jklm	18.500 m	34.416	22.55	44.40
17/9/2017	364.250 bc	320.250 cd	473.500 a	386.000	27.45	33.50
1/10/2017	307.500 de	270.750 ef	373.750 b	317.333	22.50	36.75
15/10/2017	253.000 f	257.250 f	260.500 ef	256.916	20.65	40.05
29/10/2017	487.000 a	477.750 a	456.750 a	473.833	19.50	52.75
Mean	211.843	221.437	222.125		24.33	41.00

Different letters mean significant difference ($p < 0.05$) based on Duncan test.

The average of unsealed workers brood area was 222.125, 221.4375 and 211.8438 inch² for *A. m. Native*, *A. m. ligustica* and *A. m. carnica* respectively, when the average temperature was 24.33°C and the average relative humidity was 41.00% as shown in

Figure 6. The highest general average was 473.833 inch² at 29-10-2017 and the lowest was 34.41667 inch² at 29-10-2016. Statistical analysis showed significant differences at level 0.05 among *A. m. carnica*, *A. m. local* and *A. m. ligustica*. The results agree with Taragany (2008), who found that the highest means of the unsealed brood area and sealed brood area can be detected in autumn, when they are fed extra sugar solution and vice versa.

Sealed workers brood area

Table 14 and Figure 6 show the average sealed brood area of the workers in autumn. The highest average sealed brood area for *A. m. Native* 563.000 inch² at 17-9-2017, when the average temperature was 27.45 °C and the average relative humidity was 33.50%. In comparison, the average sealed brood area for *A. m. carnica* and *A. m. ligustica* was 480.500 and 396.500 inch² during the same period and weather conditions, while the lowest average of sealed brood was 22.000 inch² for *A. m. Native* at 29-10-2017, when the average temperature and relative humidity were 19.50 °C and 52.75%. The average of sealed workers brood area was 160.468, 151.437 and 141.625 inch² for *A. m. Native*, *A. m. ligustica* and *A. m. carnica* respectively, when the average temperature was 24.33 °C and the average relative humidity was 41.00%. The highest general average was 480.000 inch² at 17-9-2017 and the lowest was 31.78333 inch² at 15-10-2016. Statistical analysis showed significant differences at level 0.05 among races. These result agree with Harbo (2015), who showed that the average number of adult bees declined steadily from 20 800 in November to 12,000 in March. The brood in the colonies was small before the winter solstice, but soon increased.

Table 14. Effect of some honeybee races and environmental factors on sealed brood area in autumn 2016-2017

Autumn	Honey bee race			Mean	Temperature	Relative humidity %
Period	<i>Apis mellifera carnica</i>	<i>Apis mellifera ligustica</i>	<i>Apis mellifera Native</i>			
17/9/2016	84.750 fg	142.500 e	82.250 fg	103.166	29.75	38.50
1/10/2016	52.750 fg	110.000 ef	52.000 fg	71.583	27.50	40.05
15/10/2016	22.350 g	48.000 fg	25.000 g	31.783	24.75	42.00
29/10/2016	22.750 g	51.000 fg	23.000 g	32.250	22.55	44.40
17/9/2017	480.500 b	396.500 cd	563.000 a	480.000	27.45	33.50
1/10/2017	424.500 c	359.500 d	492.000 b	425.333	22.50	36.75
15/10/2017	22.650 g	54.000 fg	24.500 g	32.383	20.65	40.05
29/10/2017	22.750 g	50.000 fg	22.000 g	32.916	19.50	52.75
Mean	141.625	151.437	160.468		24.33	41.00

Different letters mean significant difference (p<0.05) based on Duncan test.

Ripened honey area

Table 15 shows the average ripened honey area in early summer. The highest average area for *A. m. Native* was 991.500 inch² at 17-9-2017 when the average temperature was 27.45 °C and the relative humidity was 33.50%. The average area for *A. m carnica* and *A. m ligustica* was 957.750 and 917.000 inch² during the same period and weather conditions. In

comparison, the lowest average for *A. m. Native* was 106.750 inch² at 17-9-2016, when the average temperature and relative humidity were 29.75 °C and 38.50%. The average of ripened honey area was 400.437, 387.281 and 383.406 inch² for *A. m. Native*, *A. m. ligustica* and *A. m. carnica* respectively as shown in Figure 6. The highest general average was 955.416 inch² at 17-9-2017 and the lowest was 127.000 inch² at 17-9-2016. Statistical analysis showed significant differences at level 0.05 among *A. m. carnica*, *A. m. Native* and *A. m. ligustica*. Results agree with Bas (2013) who recorded that the highest rate of stored pollen area in autumn was 9.83 inch² when fed with multi- vitamin and vice versa.

Table 15. Effect of some honeybee races and environmental factors on ripened honey area in autumn 2016-2017

Autumn Period	Honey bee race			Mean	Temperature	Relative humidity %
	<i>Apis mellifera carnica</i>	<i>Apis mellifera ligustica</i>	<i>Apis mellifera Native</i>			
17/9/2016	136.500 hi	137.750 hi	106.750 i	127.000	29.75	38.50
1/10/2016	180.000 fghi	177.500 fghi	156.250 ghi	171.250	27.50	40.05
15/10/2016	200.250 efgh	219.250 defg	205.750 efgh	208.416	24.75	42.00
29/10/2016	240.000 def	276.750 de	295.000 d	270.583	22.55	44.40
17/9/2017	957.750 ab	917.000 abc	991.500 a	955.416	27.45	33.50
1/10/2017	912.500 bc	874.000 c	947.500 abc	911.333	22.50	36.75
15/10/2017	200.250 efgh	219.250 defg	205.750 efgh	208.416	20.65	40.05
29/10/2017	240.000 def	276.750 de	295.000 d	270.583	19.50	52.75
Mean	383.406	387.281	400.437		24.33	41.00

Different letters mean significant difference (p<0.05) based on Duncan test.

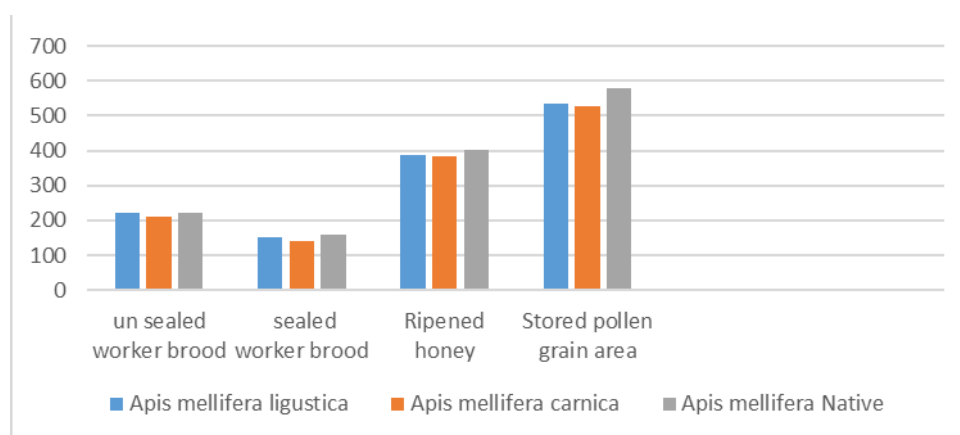


Figure 6. Effect of environmental factors on different the activities of honeybee races in autumn

Stored pollen grain area

Table 16 and Figure 6 show the average stored pollen grain area in autumn. The highest average area for *A. m. Native* was 1196.250 inch² at 17-9-2017, when the average temperature was 27.45 °C and relative humidity was 33.50%. The average area for *A. m. carnica* and *A. m. ligustica* was 1017.250 and 982.500 inch² during the same period and with the same weather conditions. In comparison, the lowest average was

32.000 inch² for *A. m. Native* at 15-10-2016, when the average temperature and relative humidity were 24.75 °C and 42%. The average of stored pollen area was 580.937, 533.812 and 527.250 inch² for *A. m. Native*, *A. m. ligustica* and *A. m. carnica* respectively, when the temperature was 24.33 °C and the average relative humidity was 41.00%. The highest general average was 1065.333 inch² at 17-9-2017 and the lowest was 63.833 inch² at 15-10-2016. Statistical analysis showed significant differences at level 0.05 between all races. The results are in agreement with Tan et al. (2012), who found that *A. cerana* began foraging earlier and at lower temperatures than *A. mellifera* did. *A. cerana* foraging (departures per minute) reached its peak early and at a lower temperature than *A. mellifera* foraging did.

Table 16. Effect of some honeybee races and environmental factors on pollen grain area in autumn 2016-2017

Autumn	Honeybee race			Mean	Temperature	Relative humidity %
	<i>Apis mellifera carnica</i>	<i>Apis mellifera ligustica</i>	<i>Apis mellifera Native</i>			
17/9/2016	109.250 fgh	130.500 f	64.500 ghij	101.416	29.75	38.50
1/10/2016	93.500 fghi	115.750 fg	50.250 ij	86.500	27.50	40.05
15/10/2016	65.250 ghij	94.250 fghi	32.000 j	63.833	24.75	42.00
29/10/2016	87.000 fghi	98.000 fghi	55.750 hij	80.250	22.55	44.40
17/9/2017	1017.250 c	982.500 cd	1196.250 a	1065.333	27.45	33.50
1/10/2017	976.500 cd	952.750 d	1133.750 b	1021.000	22.50	36.75
15/10/2017	978.750 cd	957.750 d	1116.250 b	1017.583	20.65	40.05
29/10/2017	943.000 d	886.500 e	998.750 cd	942.750	19.50	52.75
Mean	533.812	527.250	580.937		24.33	41.00

Different letters mean significant difference (p<0.05) based on Duncan test.

Stages of fat bodies during the life of honey bees

This study also aimed to explain the stages of fat bodies throughout the life of honey bees as shown in *Plate 1*:

- Perivisceral fat bodies in one day old workers appeared with a dense inclusion, dark color and a thick wall with invisible nucleus.
- Perivisceral fat bodies in seven day old workers of *Apis mellifera carnica*: A new generation of fat bodies, slightly larger with vacuolization features inside, and course, thick walls as result of newly emerging in spring.
- Perivisceral fat bodies in fourteen day old worker of *Apis mellifera carnica* in spring: The fat cell was very large, it vacuolated various shapes, and had thick walls, light blue in color.
- Perivisceral fat bodies in twenty one day old worker of *Apis mellifera Native* in spring: The fat bodies were similar to twenty one day old workers of *Apis mellifera ligustica* in spring, but were larger in size.
- Perivisceral fat bodies in twenty eight day old worker of *Apis mellifera Native* in spring: These showed very obvious and clear features, loaded with a dense inclusion, some nucleus and variously shaped, dark purple, vacuolated cells.

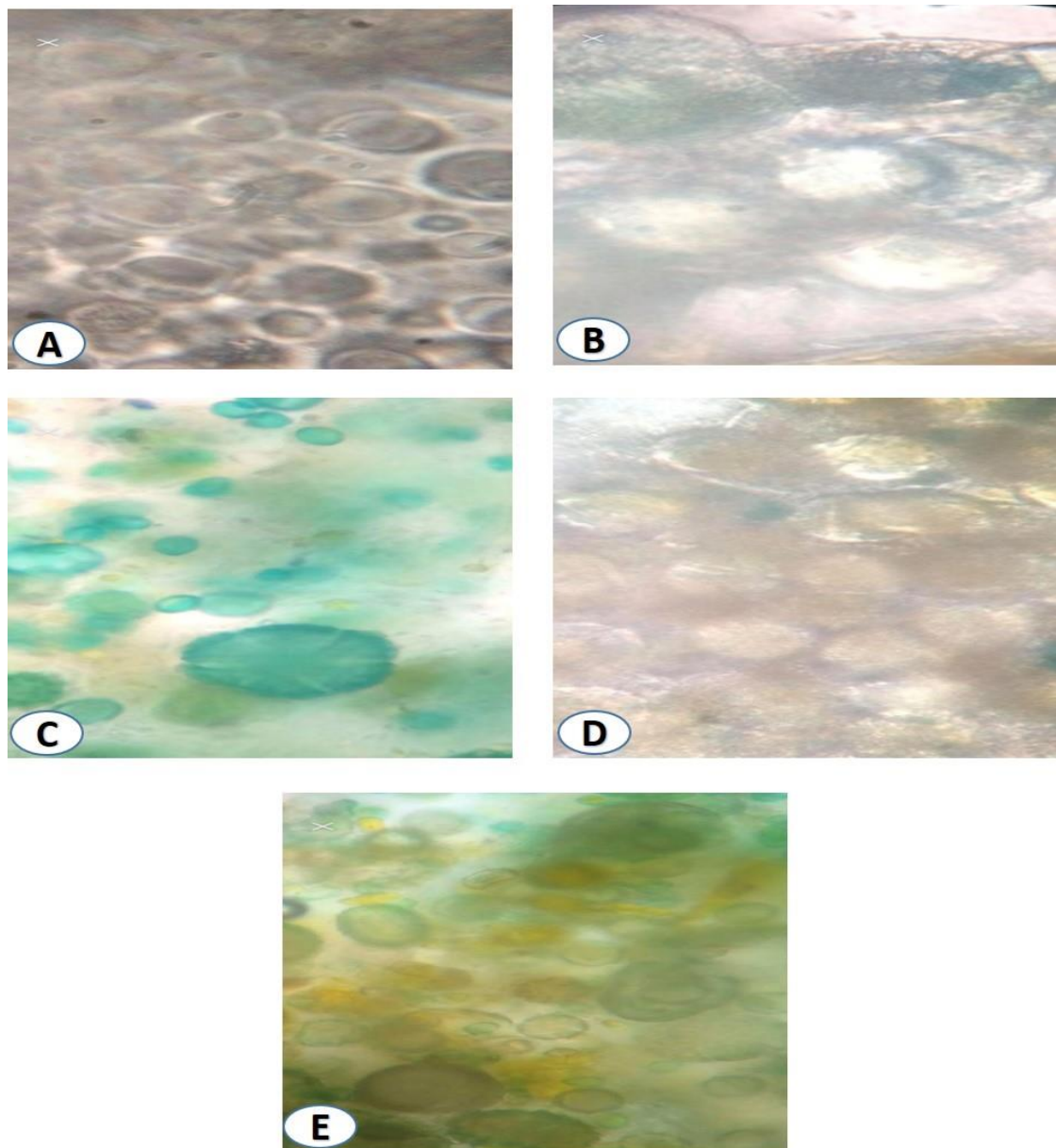


Plate 1. Stages of fat bodies during the life of honey bees (40X)

Conclusion

The results of the field experiment revealed the direct effect of environmental conditions (Temperature and relative humidity) on three races of honeybees. It was conducted for two years in different seasons. Comparing the two races (*Apis mellifera carnica* and *Apis mellifera ligustica*) native to the country with *Apis mellifera* Native during the first year, *Apis mellifera* Native are more affected by environmental factors than the other two races (*Apis mellifera carnica* and *Apis mellifera ligustica*). The results showed the highest rate of unsealed brood area of *Apis mellifera* Native race to be in the early summer of 2016 and the lowest rate of *Apis mellifera ligustica* in spring 2017. The sealed brood area of the *Apis mellifera* Native strain was the highest in early summer, and the lowest rate of *Apis mellifera* Native strain was in autumn 2017. The

highest and the lowest rate of pollen grain area for *Apis mellifera* Native strain were detected in the summer season of 2017 and 2016 respectively. We also studied the fat body difference through the stages of life for honeybees.

The highest and the lowest rate of Pollen grain area were (1582.750 and 7.290) inch for *Apis mellifera* Native strain in summer 2017 and 2016 respectively.

REFERENCES

- [1] Abou-Shaara, H. F. (2012): Notes on water collection by honey bees. – Bee World 89: 50-51.
- [2] Abou-Shaara, H. F. (2014): The foraging behavior of honey bees, *Apis mellifera*. Faculty of Agriculture, Damanhour University, Egypt. – Veterinarni Medicina 59(1): 1-10.
- [3] Ali, M. A. M. (2011): Comparative study for evaluating two honey bee races, *Apis mellifera jementica* (indigenous race) and *Apis mellifera carnica* (carniolan race) in brood production, population development and foraging activity under the environmental conditions of the central region of the Kingdom of Saudi Arabia. – Annals of Agricultural Sciences 56: 127-134.
- [4] Alqarni, A. S. (2006): Tolerance of summer temperature in imported and indigenous honeybee *Apis mellifera* L. Races in central Saudi Arabia. – Saudi Journal of Biological Sciences 13: 123-127.
- [5] Ayoub, Z. N. (2011): Workers ontogeny in queen less or brood less colonies of honey bee (*Apis mellifera* L.). – Ph. D. Thesis. Faculty of Biology and Earth Science, Jagiellonian University, Poland.
- [6] Bas, S. M. A. (2013): A study of the effect of some pollen supplemental food on body organs of honeybee workers and their activities *Apis mellifera* L. (HYMENOPTERA: APIDAE). – M. Sc. Thesis. College of Agriculture, Univ of Dohuk.
- [7] Becher, M. A., Scharpenberg, H., Moritz, R. F. A. (2009): Pupal developmental temperature and behavioral specialization of honeybee workers (*Apis mellifera* L.). – J. Comp. Physiol. A. DOI: 10.1007/s00359-009-0442-7.
- [8] Blazyte-Cereskiene, L., Vaitkeviciene, G., Venskutonyteand, S., Buda, V. (2010): Honey bee foraging in spring oilseed rape crops under high ambient temperature conditions. – Zemdirbyste-Agriculture 97: 61-70.
- [9] Chapman, R. F. (1978): The Insect Structure and Function. – Engl. Univ. Press. Ltd., London, England.
- [10] Contreras, H. L., Goyret, J., Arx, M. v., Pierce, C. T., Bronstein, J. L., Raguso, R. A., Davidowitz, G. (2013): The effect of ambient humidity on the foraging behavior of the hawkmoth *Manduca sexta*. – Journal of Comparative Physiology 199(11): 1053-63.
- [11] Fathy, H. M. (1997): Honey bee colony population in relation to brood rearing and stored pollen. – Archives of Phytopathology and Plant Protection 30(5): 445-452.
- [12] Harbo, J. R. (2015): Effect of brood rearing on honey consumption and the survival of worker honey bees. – Journal of Apicultural Research 32(1): 11-17.
- [13] Hossam, F. A., Ahmad, A. A., Abdelsalam, A. M. (2012): Tolerance of two honey bee races to various temperature and relative humidity gradients. – Environmental and Experimental Biology 10: 133-138.
- [14] Joshi, N. C., Joshi, P. C. (2010): Foraging behaviour of *Apis* spp. on apple flowers in a subtropical environment. – NY Sci. J. 3: 71-76.
- [15] Mahmoud, T. T. (1992): Comparative anatomical and histological study of the heart of four syrphid species (Diptera:syrphidae) in Iraq. – Pak. J. Sci. Ind. Res. 35(5): 182-184.
- [16] Mattu, V. K, Raj, H., Thakur, M. L. (2012): Foraging behavior of honeybees on apple crop and its variation with altitude in Shimla hills of western Himalaya. – International Journal of Science and Nature 3: 296-301.

- [17] Mesbah, H. A. A., El-Sayed, N. A. A., Hassona, N. K., Abdel-Hameed, K. M. A., Abdel-Sattar, H. A. S. (2017): The Common types of pollen grains collected by honey bee workers *Apis mellifera*, L. (Hymenoptera. Apidae) in El-Sabheia Region, Alexandria Governorate, Egypt. – Alexandria Science Exchange Journal: An International Quarterly Journal of Science Agricultural Environments 38(October-December): 913-920.
- [18] Mustafa, A. O. (2003): Effect some of geographic local within Erbil vision in bioactivity of honey bee colonies. – M. Sc. Thesis. College of Agriculture, Salahadin University, Erbil.
- [19] Neupane, K. R., Thapa, R. B. (2005): Alternative to off-season sugar supplement feeding of honey bees. – J. Inst. Agric. Anim. Sci. 26: 77-81.
- [20] Olivera, V. T. P., Cruz-Landim, C. (2003): Morphology and function of insect fat body cells: A review. – Biociencias Proto Algre 11(2): 195-205.
- [21] Pernal, S. F., Currie, R. W. (2010): The influence of pollen quality on foraging behavior in honeybees (*Apis mellifera* L.). – Behavioral Ecology and Sociobiology 51: 53-68.
- [22] Petz, M., Stabentheiner, A., Crailsheim, K. (2004). Respiration of individual honeybee larvae in relation to age and ambient temperature. – J. Compar. Physiol. B 174: 511-518.
- [23] Reddy, P. V. R., Rashmi, T., Varum Rajan, V., Verghese, A. (2012): Foraging activity of honeybee in relation to weather parameters. – Paper presented in 4th National Symposium on Plant Protection in Horticultural Crops, Bangalore, 24-27 April, 2012.
- [24] Roma, G. C., Bueno, O. C., Camargo-Mathias, M. I. (2010): Morpho-physiological analysis of the insect fat body: a review. – Micron 41: 395-401.
- [25] Shamdin, Z. N. (2003): Effect of supplemental protein and vitamins on the development of specific tissues with special concern to their fine structure in relation to the activity of honey bee workers *Apis mellifera* L. (Hymenoptera: Apidae). – M.Sc. Thesis. College of Agriculture, Univ of Dohuk.
- [26] Snodgrass, R. E., Erickson, E. H. (2003): The Hive and Honey Bee: The Anatomy of Honey Bee. – Revised edition by J. M. Graham. Dadant & Sons, Hamilton, Illionis, USA.
- [27] Tan, K., Yang, S., Wang, Z.-W., Radloff, S. E., Oldroyd, B. P. (2012): Differences in foraging and broodnest temperature in the honey bees *Apis cerana* and *A. mellifera*. – Apidologie 43(6): 618-623.
- [28] Targany, Y. M. A. (2008): Effect of rich proteins diet on the activities of honey bee colonies *Apis mellifera* L. (Hymenopter: Apidae). – M.Sc. Thesis. College of Agriculture, Univ of Salahaddin, Erbil.
- [29] Tirado, R., Simon, G., Johnston, P. (2013): Bees in Decline: A Review of Factors That Put Pollinators and Agriculture in Europe at Risk. – Greenpeace Research Laboratories Technical Report (Review). Greenpeace International, Amsterdam, The Netherlands.
- [30] XLSTAT (2017): Data Analysis and Statistical Solution for Microsoft Excel. Addinsoft, Paris, France 2, JMP, Version 12. – SAS Institute Inc., Cary, NC.
- [31] Zanini, D. A., Caetano, F. H. (2003): Ultra structure of the visceral fat body of the Wasp *Michocytarus Cerberus styx*. (Hymenoptera: Vespidae). – Acta Microscopica 12(B): 593.

ELECTRONIC APPENDICES

Appendix 1: Pollen 2016

Appendix 2: Pollen 2017

Appendix 3: Pollen 2016-2017

Appendix 4: Ripened honey 2016

Appendix 5: Ripened honey 2017

Appendix 6: Ripened honey 2016-2017

Appendix 7: Sealed brood 2016

Appendix 8: Sealed brood 2017

Appendix 9: Sealed brood 2016-2017

Appendix 10: Unsealed brood 2016

Appendix 11: Unsealed brood 2017

Appendix 12: Unsealed brood 2016-2017

AN INVESTIGATION OF THE LEAD AND CADMIUM LEVELS OF BLOOD SERUM AND WOOL OF WHITE KARAMAN SHEEP IN THE VAN REGION (TURKEY)

TUNCER, S. S.

Department of Crop and Animal Production, Ozalp Vocational School, Van Yuzuncu Yil University, Van, Turkey

(e-mail: selcukseckintuncer@gmail.com; phone: +90-505-839-8794)

(Received 17th Oct 2018; accepted 5th Dec 2018)

Abstract. This study was conducted to determine heavy metal (lead – Pb and cadmium – Cd) contamination of White Karaman sheep raised in Centrum (industrial area) and Özalp (rural area) districts of Van province in Turkey. Pb and Cd concentrations of blood serum and wool samples were measured with an ICP-OES device at Scientific Research and Implementation Center of Van Yuzuncu Yil University. It was observed that the sheep raised in the Central district of Van had higher levels of Pb and Cd in the blood serum and wool than those of the sheep Özalp district ($p < 0.001$). However, Pb and Cd levels of the sheep were still below the acceptable limits in both districts of Van province. Present findings revealed that pastures of both districts of Van province were safe with regard to food safety and environmental pollution with heavy metals.

Keywords: *heavy metal, blood, wool, sheep*

Introduction

Rapid urbanization and industrialization have made heavy metal emissions a global concern even at quite low concentrations for ecosystems (Rouniosi et al., 2018). Especially the heavy metals of lead (Pb) and cadmium (Cd) pose significant health risks for living organisms. Such heavy metals result in disorders in the central nervous system and in the red blood cell synthesis cause weak bone development, pains in muscles, anaemia and deaths ultimately. Therefore, heavy metal pollution levels should be determined and the risks posed on human and animal health should be put forth (Kaptanoğlu et al., 2014).

Pb and Cd are abundant metals in environment and they are the most toxic metals (Domingo, 1998; Boğa, 2007). Annually 7600 tons Cd and 332000 tons Pb is released to atmosphere through natural phenomena (earthquakes, volcanic eruptions and etc.). On the other hand, 8 times greater Cd and 6 times greater Pb is released to atmosphere through anthropogenic activities (urbanization, industrialization and etc.) (Kahvecioğlu et al., 2004). Such a heavy metal pollution has the greatest impacts on plants. Metal pollution not only influence vegetative organs of the plants, but also have significant effects on generative organs of the plants (Zheljazkov and Nielsen, 1996; Okçu et al., 2009).

Pb exists in nature in organic and inorganic forms. While inorganic form exists in atmosphere in particulate forms, organic Pb generally contaminates nutrients and drinking water (De Jonghe and Adams, 1982; Karademir and Toker, 1995; Okçu et al., 2009). Therefore, organic forms of Pb have greater impacts on living organisms. Meat products and plants grown around the industrial zones or city centers may have Pb levels greater than the normal levels. High-concentration heavy metal intakes of the sheep through pasture plants may pose a high risk of toxicity on animals (Smith et al.,

2010). Lead is not an essential nutrient for soils, generally exist in soils at 15-40 ppm doses and does not pose any health risks on human and plant health under 150 ppm concentration. However, lead concentrations over 300 ppm have potential risks for human health (Dürüst et al., 2004; Öktüren Asri and Sönmez, 2007). Smith et al. (2010) defined 250 µg/l Pb level as the safe upper limit for blood Pb levels.

Cd is relatively rare element and does not exist in pure forms in the nature. It is a significant pollutant since it is toxic at quite low concentrations (Lyons et al., 1996; Okçu et al., 2009). Cd is known with greater toxic impacts on plants (Çatak et al., 2000; Okçu et al., 2009). Accumulation of atmospheric Cd dusts, use of Cd-containing fertilizers and irrigations with wastewater effluents contaminate products consumed by the humans and animals, thus may increase Cd intakes (Jarup and Akesson, 2009; Örün and Yalçın, 2011). Cd levels greater than 3 mg/kg may have toxic impacts on soils and Cd levels over 1 mg/kg in plant dry matter may have toxic impacts on plants (Özbek et al., 1995; Öktüren Asri and Sönmez, 2007). Majority of Cd reaching to soils and plants comes from precipitation of Cd-containing atmospheric dust particles. Dust precipitation around the roads with a high traffic intensity may add about 0.2-1.0 mg/m² Cd to soils annually (Öktüren Asri and Sönmez, 2007). Of the Cd quantities reaching to soils through anthropogenic activities, 54-58% comes from phosphorus fertilizers, 39-41% comes from atmospheric storage and 2-5% comes from sludge and manure treatments (Yost and Miles, 1979).

Turkey with a sheep inventory of 31.507.934 head (TUIK, 2016; Tuncer et al., 2017) is the 7th greatest sheep raiser country of the world (FAO, 2016). The present research site, Van province in Eastern Anatolia Region of Turkey, has the greatest sheep inventory of the country (2.456.493 head) (TUIK, 2016; Tuncer et al., 2017). White Karaman sheep is a race that is widely raised because of very well adapted to the cold and long winter conditions of Eastern Anatolia Region. Therefore, in this study, heavy metal contamination in wool and blood serums of the sheep raised in Van Centrum (industrial area) and Özalp (rural area) districts were investigated and heavy metal contamination was tried to be used as an indicator of food safety and environmental pollution.

Materials and methods

Research site and sampling

Van province is among the 5 province of Turkey with the greatest altitude (Eymirli and Kaya, 2016). Of the present research sites (*Fig. 1*), Central district is located between 38°30'4" N and 43°22'22" E coordinates and Özalp district is located between 38°39'29" N and 43°59'21" E coordinates and the districts have altitudes of 1727 m and 2075 m, respectively. There is one organized industrial zone in Van Central District. It has 1943 workplaces and 7 small industrial sites. Özalp is one of the smallest districts of Van. In addition, the town of Özalp is industrially backward (Bakır, 2016).

As the animal material of the study, 1-2 years old 15 sheep grazed over the pastures of Central and Özalp districts of Van province in August 2018 were used (a total of 30 sheep). Attention was paid as to have the sheep grazed over the same pastures and as to take blood and wool samples in the same day. Blood samples taken from vena jugularis were placed into anticoagulant 10 ml tubes. About 5 g wool samples were taken from neck section of the sheep with steel scissors. Wool samples were placed into clean polyethylene bags and preserved till the analyses. Wool samples were taken close to

skin to eliminate potential differences in heavy metal concentrations in roots and tips (Kurt et al., 2001).



Figure 1. Location of the study areas: A: Van Center, B: Özalp

Analyses on wool and blood samples

Blood samples taken from the sheep were placed into anticoagulant tubes with disposable needles. For laboratory analysis, the devices in Van Yuzuncu Yil University Van Health Vocational School and Veterinary Faculty Laboratories were used. Blood samples were centrifuged at 3500 rpm for 15 min to separate blood serum. Separated serums were transferred to 1.5 ml Eppendorf tubes and preserved at -20°C until the analyses (Karademir, 2007). Wool samples taken from the sheep were washed through 1% Triton-X 100 solution and rinsed through distilled water. Washed samples were then dried in a sterilizator at 100°C for 2 h. Dried samples (100 mg of them) were placed into tubes, supplemented with 1 ml 1/5 nitroperchloric acid mixture and waited for 4 h for dissolution of wool. Dissolved mixture was completed to 10 ml with distilled water. From this mixture, 1 ml was taken for analysis and supplemented with 2 ml distilled water (Kozat, 2006).

Pb and Cd concentrations of blood serum and wool samples were measured with an ICP-OES device at Scientific Research and Implementation Center of Van Yuzuncu Yil University (Alacabey et al., 2017).

Statistical analysis

GLM sub-procedure of SAS 9.4 (2018) statistical software was used for statistical analyses. One-way ANOVA was applied to mean Pb and Cd values of blood serum and wool samples taken from two different regions. Significant means were compared with Duncan's multiple range test. Pearson correlations were calculated between Pb and Cd values of serum and wool samples of each region.

Results and discussion

Pb and Cd levels of blood serum and wool samples collected from Akkaraman sheep at pasture season of Van Central and Özalp districts are respectively provided in

Tables 1 and 2. The greatest Pb and Cd values were observed in blood serum and wool samples of the sheep raised in Central district and the differences from the values of the sheep raised in Özalp district were found to be significant ($p < 0.01$), a finding compatible with the literature (Kahvecioğlu et al., 2004; Rouniosi et al., 2018).

Table 1. Pb and Cd values in blood serum of Akkaraman sheep (mean \pm standard error of the mean)

Area	n	Pb ($\mu\text{g/l}$)	Cd ($\mu\text{g/l}$)
Central	15	49.050 \pm 0.004 ^{a**}	0.375 \pm 0.002 ^{a**}
Özalp	15	47.025 \pm 0.105 ^{b**}	0.150 \pm 0.002 ^{b**}

^{a, b}Different lower cases in the same column represent statistically significant differences

** $p < 0.01$

Table 2. Pb and Cd values of Akkaraman sheep's wool (mean \pm standard error of the mean)

Area	n	Pb ($\mu\text{g/kg}$)	Cd ($\mu\text{g/kg}$)
Central	15	49.375 \pm 0.018 ^{a**}	0.533 \pm 0.068 ^{a**}
Özalp	15	47.725 \pm 0.130 ^{b**}	0.218 \pm 0.013 ^{b**}

^{a, b}Different lower cases in the same column represent statistically significant differences

** $p < 0.01$

Blood serum Pb values of the sheep raised in Central and Özalp districts (49.050 $\mu\text{g/l}$ and 47.025 $\mu\text{g/l}$) (Table 1) were quite below the safe limits (250 $\mu\text{g/l}$). Present values were also quite below the values reported by Villegas et al. (1993) (chronic, 360 $\mu\text{g/l}$) and Braun et al. (1997) (acute, 940 $\mu\text{g/l}$). As compared to the values of the studies carried out at Pb-contaminated sites, present values were again quite lower than the values reported by Smith et al. (2010) (147 $\mu\text{g/l}$) and Swarup et al. (2006) (316 $\mu\text{g/l}$). But, the present values were greater than the values of the same researchers reported for Pb-clean sites (respectively as 26 $\mu\text{g/l}$ and 15 $\mu\text{g/l}$). Similar with the present findings, Liu (2003) reported serum Pb value of the control group as 50 $\mu\text{g/l}$ and Vici1 et al. (2012) reported the same values as between 50 $\mu\text{g/l}$ - 60 $\mu\text{g/l}$. Carrera et al. (2014) reported serum Pb value of the sheep grazed around the mine sites as 67 $\mu\text{g/l}$ and reported the Pb value of the rams as 109 $\mu\text{g/l}$ and such values were greater than the present ones. Pb values of wool samples taken from the sheep raised in Van Central and Özalp districts were found as 49.375 $\mu\text{g/kg}$ and 47.725 $\mu\text{g/kg}$, respectively (Table 2). Present values were quite below the values of Liu (2003) reported for the wool samples of healthy sheep (1010 $\mu\text{g/kg}$) and the sheep grazed over the Pb-contaminated sites (3640 $\mu\text{g/kg}$); the values of Vici1 et al. (2012) reported for the sheep grazed around the mine sites (2070 $\mu\text{g/kg}$) and the sheep grazed far away from the mine sites (1130 $\mu\text{g/kg}$ –1670 $\mu\text{g/kg}$). Present findings revealed that Van Central and Özalp districts could be indicated as clean sites with regard to Pb-contamination.

Present Cd values of blood serums of the sheep raised in Van Central and Özalp districts (0.375 $\mu\text{g/l}$ and 0.150 $\mu\text{g/l}$, respectively) (Table 1) were quite below the values of Barkouch et al. (2008) reported for the sheep grazed around the mine site (3900 $\mu\text{g/l}$) and rural (2900 $\mu\text{g/l}$) sections, the value of Liu (2003) reported for healthy sheep (20 $\mu\text{g/l}$). However, present values were greater than the values reported by Vici1 et al.

(2012) ($<0.015 \mu\text{g/l}$). Cd values of wool samples taken from the sheep raised in Van Central and Özalp districts are provided in *Table 2* ($0.533 \mu\text{g/kg}$ and $0.218 \mu\text{g/kg}$, respectively). As compared to the results of the studies carried out over the clean and contaminated sites, present values were lower than the values reported by Liu (2003) ($2030 \mu\text{g/kg}$ and $370 \mu\text{g/kg}$, respectively), Barkouch et al. (2008) ($110 \mu\text{g/kg}$ and $90 \mu\text{g/kg}$, respectively) and Vıçıl et al. (2012) ($1340 \mu\text{g/kg}$ and $450 \mu\text{g/kg}$ – $3340 \mu\text{g/kg}$). Present findings revealed that blood serum and wool Cd levels of the sheep grazed over the pastures of Van Central and Özalp districts were at low levels, thus it can be stated that there were no-risk of toxicity.

Conclusions

Pb and Cd levels of blood serum and wool samples were higher in sheep raised in Van Central in industrial area than in the sheep raised in Özalp in rural area ($p < 0.001$). However, Pb and Cd values of the sheep in both districts of Van province were below the safe limit values. In brief, toxic levels of heavy metal accumulation (Pb and Cd) were not encountered in blood serum and wool samples of the sheep. Present findings also revealed that pastures in both districts of Van province were safe with regard to food safety and environmental pollution with heavy metals.

Acknowledgements. The final report of this research project was approved by Van Yuzuncu Yil University Animal Research Local Ethic Committee, decision number 2018/12.

REFERENCES

- [1] Alacabey, İ., Kömürçüoğlu, A. U., Alacabey, N. U., Özdek, U., Kul, A. R., Atasoy, N., Yücel, U. M. (2017): Determination of cobalt (Co) level in hair and serum of gas station workers in Van province. – *J Environ Sci Toxicol Food Technol* 11(2): 30-32.
- [2] Bakır, A. (2016): The analysis of the changes in the amounts of heavy metals in different climate conditions in water and mud examples found in the areas where the stream flows to the lake of Van. – MSc Dissertation, Department of Chemistry, University of Van Yuzuncu Yil, Van, Turkey.
- [3] Barkouch, Y., Nocairi, H., Sedki, A., Pineau, A. (2008): Metallic trace elements in blood, wool, kidney and liver of sheep from a mine area of Marrakech-Morocco. – *Environmental Science* 3(1): 15-23.
- [4] Boğa, A. (2007): Properties and effects of heavy metals. – *Arşiv* 16: 218-234.
- [5] Braun, U., Pusterla, N., Ossent, P. (1997): Lead poisoning of calves pastured in the target area of a military shooting range. – *Schweiz Arch Tierheilkd* 139(9): 403-407.
- [6] Carrera, J. P., Mateo, R., Estival, J. R. (2018): Lead (Pb) in sheep exposed to mining pollution: Implications for animal and human health. – *Ecotoxicology and Environmental Safety* 108: 210-216.
- [7] Çatak, E., Güler, Ç., Süleyman, T., Orhan, B. (2000): A statistical study on the effects of Cadmium on some tomato and tobacco genotypes. – *Journal of Balıkesir University Institute of Science and Technology* 2(1): 13-41.
- [8] De Jonghe, W. R. A., Adams, F. C. (1982): Biochemical cycling of organic lead compounds. – *Ecotoxicology* 561-593.
- [9] Domingo, J. L. (1998): Developmental toxicity of metal chelating agents. – *Reproductive Toxicology* 12: 499-510.

- [10] Dürüst, N., Dürüst, Y., Tuğrul, D, Zengin, M. (2004): Heavy metal contents of *Pinus radiata* trees of İzmit (Turkey). – *Asian Journal of Chemistry* 16(2): 1129-1134.
- [11] Eymirli, E. B., Kaya, M. (2016): Branding of High Altitude Products. – Northeast Anatolia Development Agency, Erzurum, Turkey.
- [12] FAO (2016): <http://www.faostat.fao.org>. – Accessed: 25 October 2016.
- [13] Jarup, L., Akesson, A. (2009): Current status of cadmium as an environmental health problem. – *Toxicol Appl Pharmacol* 238(3): 201-208.
- [14] Kahvecioğlu, Ö., Kartal, G., Güven, A., Timur, S. (2004): Environmental effects of metals-I. – *Journal of Metallurgical of UCTEA Chamber of Metallurgical Engineers* 136: 47-53.
- [15] Kaptanoğlu, S., Atasoy, N., Kubilay, Ş., Savran, A., Bakır, A., Yücel, U. F. (2014): Determination of the amount of cadmium in the blood of grazing cattle in the pasture in Van region and investigation of the effects on some specific liver enzymes. – 2nd International Symposium on Environment Morality, Adıyaman, Turkey, pp. 1427-1434.
- [16] Karademir, M., Toker, M. C. (1995): Lead accumulation in the grass and plants growing on some of the crossroads of Ankara from exhaust gases. – 2nd National Ecology and Environment Congress, Ankara, Turkey, pp. 699-711.
- [17] Karademir, B. (2007): Serum Copper and Zinc Levels of Akkaraman and Tuj Sheep According to Age and Sex Under the Winter Condition. – *Kafkas Univ Vet Fak Derg*, 13(1): 55-59.
- [18] Kozat, S. (2006): Importance, necessity and the effects of deficiencies of trace elements in ruminants. – *Journal of Health Sciences of Yuzuncu Yil University* 9(2): 58-67.
- [19] Kurt, D., Denli, O., Kanay, Z, Güzel, C., Ceylan, K. (2001): An investigation of the copper (Cu), zinc (Zn) and selenium (Se) levels of blood serum and the Cu and Zn levels of wool of Akkaraman ewes in the Diyarbakır Region. – *Turk J Vet Anim Sci* 25: 431-436.
- [20] Liu, Z. P. (2003): Lead poisoning combined with cadmium in sheep and horses in the vicinity of non-ferrous metal smelters. – *The Science of the Total Environment* 309(1-3): 117-126.
- [21] Lyons, A.M., Tarazona, J. V., Mothersill, C. (1996): The differential effect of cadmium exposure on the growth and survival of primary and established cells from fish and mammals. – *Cell Biol. Toxicol.* 12: 29-38.
- [22] Okçu, M., Tozlu, E., Kumlay, A. M., Pehlivan, M. (2009): The effects of heavy metals on plants. – *Alinteri* 17: 14-26.
- [23] Öktüren Asri, F., Sönmez, S. (2007): The effect of heavy metal toxicity on plant metabolism. – *Derim* 23(2): 36-45.
- [24] Örün, E., Yalçın, S. S. (2011): Lead, mercury, cadmium: Effects on child health and using hair samples in determination of exposure. – *Ankara University Journal of Environmental Sciences* 3(2): 73-81.
- [25] Özbek, H., Kaya, Z., Gök, M. Kaptan, H. (1995): Soil Science. – Çukurova University Faculty of Agriculture, Publication Number: 73, Adana, Turkey.
- [26] Rouniosi, N., Monavvari, S. M., Abdoli, M. A., Baghdadi, M., Karbassi, A. R. (2018): Optimization process for the removal of heavy metals from aqueous solution using graphene oxide nanosheets and response surface methodology. – *Applied Ecology and Environmental Research* 16(5): 6709-6729.
- [27] SAS (2018): SAS/STAT Software: Hangen and Enhanced. – SAS Inst Inc, USA.
- [28] Smith, K. M., Dagleish, M. P., Abrahams, P. W. (2010): The intake of lead and associated metals by sheep grazing mining-contaminated floodplain pastures in mid-Wales, UK: II. Metal concentrations in blood and wool. – *Science of the Total Environment* 408: 1035-1042.
- [29] Swarup, D., Patra, R. C., Naresh, R., Kumar, P., Shekar, P., Balagangatharathilagar, M. (2006): Lowered blood copper and cobalt contents in goats reared around lead-zinc smelter. – *Small Ruminant Research* 63(3): 309-313.

- [30] TUIK (2016): Turkish Statistical Institute. Livestock Statistics. – <https://biruni.tuik.gov.tr/hayvancilikapp/hayvancilik.zul>. Accessed: 25 March 2016.
- [31] Tuncer, S. S., Sireli, H. D., Dellal, G. (2017): Comparative analysis of various fleece characteristics of Norduz and Zom sheep. – *J Anim Plant Sci* 27(3): 763-770.
- [32] Vıçıl, S., Erdoğan, S., Uygur, V. (2012): Determination of selected essential and toxic element concentrations in soil, plant, sheep blood and wool samples in Akdağmadeni country. – *The Journal of Adana Veterinary Control and Research Institute* 2(2): 15-21.
- [33] Villegas, N. A., Elena, B. O. D., Raymundo, R. A., Dieck, T. A., Reyes, J. L. (1993): Determination of lead in paired samples of blood and synovial fluid of bovines. – *Exp Toxicol Pathol* 45(1): 47-49.
- [34] Yost, K. J., Miles, L. J. (1979): Environmental health assessment for Cadmium: A systems approach. – *J. Environ. Sci. Health* 14(4): 285-311.
- [35] Zheljazkov, V. D. and Nielsen, N. E. (1996): Effect of heavy metals on peppermint and commint. – *Plant and Soil* 178(1): 59-66.

FACTORS AFFECTING THE FARMERS' DECISION ON ARTIFICIAL INSEMINATION: A CASE STUDY OF DIYARBAKIR PROVINCE, TURKEY

AKIN, S. * – KARA, A.

*Department of Agricultural Economics, Faculty of Agriculture, Dicle University
21280, Sur/Diyarbakir, Turkey
(phone: +90-412-241-1000; fax: +90-412-241-1048)*

**Corresponding author
e-mail: sakin@dicle.edu.tr*

(Received 19th Oct 2018; accepted 2nd Jan 2019)

Abstract. The objective of this study was to determine the factors affecting farmers' decision-making on artificial insemination (AI) to improve milk and beef yields of low-yielding local cattle breeds in Diyarbakir province of Turkey. Primary data were obtained from 546 breeders randomly selected among members and non-members of the Cattle Breeders Association of Diyarbakir Province (DCBA) through structured questionnaires completed during face to face farmer interviews. Descriptive statistical analysis and logistic regression methods were used in the analysis of the data. A significant relationship was found between membership status and AI. However, there was no statistically significant difference between DCBA members and non-members on the willingness to apply AI in case of no government support. Government incentives, number of cross- and purebred cattle, and DCBA as the source of information have a positive significant effect on the willingness of the farmers to employ AI, while breeder age, distance from the closest city centre, farm family size, and share of the crop revenue in the total revenue have a negative effect on the adoption of AI.

Keywords: *cattle breeders, artificial insemination, breeder unions membership, logistic regression, Diyarbakir*

Introduction

Historically, artificial insemination (AI) is the first generation of modern reproductive biotechnologies (Thibier, 1990) and has become one of the most important techniques in livestock to achieve genetic improvement. It has widely been used as the most available management practice for cattle breeders, in addition to making high-genetic-merit bulls available to all (Webb, 2003; Bearden et al., 2004).

Besides genetic improvement, prevention of reproductive diseases, and inbreeding control, another advantage of AI is the provision of accurate breeding records; i.e., insemination dates, pregnancy rates, interestrus intervals, and days to first service (Sinishaw, 2004).

Artificial insemination in many countries started with state orientation. For example, In 1987, BRAC (formerly the Bangladesh Rehabilitation Assistance Committee), together with the aid agency Bangladesh Animal Husbandry Department, began to work on a vaccination program that educates money veterinarians from rural communities that will serve farmers in the local environment (BRAC, 2015).

Artificial-insemination practices started in the 1930s in Turkey. After the private sector was authorized to perform AI in 1985, it gained momentum (Gökçen, 1998) and is widely used today (Aksoy et al., 2012).

Livestock support policies have been implemented in different periods with various weights, and there have been important changes in these policies after 2000. During the

period of 2004 and 2008, forage crops, milk-incentive premium, artificial insemination, and calf supports became the most important fostering items (Demir and Yavuz, 2010).

In 2016, of the total milk and meat production in Turkey, the share of Diyarbakir was 2.3% and 0.8%, respectively (TUIK, 2016). The Diyarbakir cattle asset consists mainly of 32.36% low-yielding native breeds, 38.72% crossbreeds, and 28.90% pure breeds (TUIK, 2016). Sustainable and economic animal production depends on the availability of high-yielding cattle breeds and, therefore, quality calves (Yavuz, 2011).

While the number of artificial insemination procedures was more than 40,000 in 2015, it decreased to 7,000 after the abolition of AI support in 2016 in Diyarbakir province (DCBA, 2016).

The purpose of this study was to determine the factors affecting the willingness of cattle breeders to employ AI in Diyarbakir province.

Material and methods

Materials

Diyarbakir province is located at 37° 57' 41 N latitude and 40° 13' 54 E longitude, in the southwest region of Turkey. The primary material of the study was the data obtained from 546 cattle breeder members and non-members of DCBA between the years 2014-2015. In addition, official records of the Diyarbakir Agriculture Provincial Directorate were also used as secondary data (*Fig. 1*).



Figure 1. Map of districts in Diyarbakir province

Methods

The simple random sampling method was used to determine the sample size. To this end, *Equation 1* for finite populations was employed (Çiçek and Erkan, 1996):

$$n = \frac{N \times s^2 \times t^2}{(N - 1) \times D^2 + s^2 \times t^2} \quad (\text{Eq.1})$$

Where:

n = sample size,

s = standard deviation,

t = standard t value at the confidence level considered;

N = size of sampling frame, population, total number of DCMBA members;

D = margin of error as the percentage of population mean.

The parameters used in determination of the sampling size were calculated according to the DCBA records and given in *Table 1*.

Table 1. The parameters used in determination of sample size

Sampling frame	Mean (X)	Standard deviation	Margin of error
2045	15.90	10.62	1.59

Sampling sizes for DCMBA members and non-members were calculated separately at 95% confidence level, by adopting 10% of the population mean as the margin of error. Accordingly, the number of sample size was calculated as follows (*Eq. 2*).

$$n = \frac{2045 \times (10.62)^2 \times (1.96)^2}{(2045 - 1) \times (1.59)^2 + (10.62)^2 \times (1.96)^2} \quad (\text{Eq.2})$$

Considering the possibility of the questionnaires being disregarded due to inconsistent data, the calculated sample size was increased by about 5% and the final sample size reached to 167 for DCBA-member cattle breeders. Surveys were conducted with a total of 546 breeders of which 167 were DCBA members, while the rest (379) had no membership in any union or association.

Descriptive statistical analysis and logistic regression methods were used in the analysis of the data. The former was used to determine the current situation of the farmers, as the latter was adopted to determine the factors associated with the willingness of the cattle breeders to employ AI.

In econometric studies, limited dependent variable regression models are used when the dependent variable is qualitative, indicating two states which refers to the presence or absence of an event. In case of occurrence of an event, the dependent variable takes the value of 1, or zero otherwise. There may be many independent variables describing the dependent variables (Gujarati, 1995; Yavuz, 2001). Three types of methods are used to predict such models. The first is the linear probability method, the second is the logit method, and the third is the probit method.

In this study, the “limited dependent variable” regression model and the logit estimation method were used to determine the factors affecting the willingness of the breeders to employ AI (Gujarati, 1995; Akkaya and Pazarlioğlu, 1998). In the present study, the dependent variable has two outcomes or two categories of responses: 1: adoption of AI and 0: non-adoption of AI. The “logit model” as described above is expressed as follows (*Eq. 3*):

$$P_i = E(Y=1|X_i) = \frac{1}{1 + e^{-(\beta_1 + \beta_2 X_i)}} \quad (\text{Eq.3})$$

For the ease of illustration, the formula could be shown as follows (Eq. 4):

$$P_i = \frac{1}{1 + e^{-Z_i}} \quad (\text{Eq.4})$$

in which (Eq. 5)

$$Z = \beta_1 + \beta_2 X_i \quad (\text{Eq.5})$$

P_i gives information about the explanatory variable (X_i) and i refers to the possibility of the individual making a certain preference. The model can be tested by the LR (k) (likelihood ratio) test with k degrees of freedom.

The marginal or partial effect measures the effect of (x_i) on any one of the independent variables on the mean of the dependent variable y . The marginal effect of an independent x variable is the partial derivative taken with respect to x and is equal to the slope coefficient of the independent variable in the linear regression models. This greatly simplifies analysis in such models. However, interpreting the results of regression analysis can be very difficult in non-linear models such as interactions, categorical variables, or logistic regression, as used in the present study. In such models, it is necessary to see the effect of the independent variables on the dependent variable to interpret the calculated coefficients, in most cases. The calculus and finite difference methods are used in the calculation of the marginal efficiency and the result is not changed in either method, but the finite difference method gives better results in binary variables (Cameron and Trivedi, 2010). In this way, the partial (marginal) effects of independent variables on the dependent variable are calculated according to the finite difference method, in this study. The variables considered in the study were explained in Table 2.

Table 2. Explanations for the variables considered in the study

Breeder age	Age of the respondents in years
Schooling	Education level of the respondents in schooling years
Household size	Number of people in household of the respondent
Distance to the nearest town	Distance of the respondent's village to the nearest town in km
Milk sales	Status of the respondents if he or she sales milk, if yes 1, otherwise 0
Make use of pastures	Status of respondent's making use of pastures (1 = yes; 0 = otherwise)
Barn type	Type of the barn respondent has (if free stall or half open 1; otherwise 0)
<u>Source of agricultural information</u>	
DCBA	If DCBA, 1; otherwise, 0
Neighbours	If neighbours, 1; otherwise, 0
TV	If TV, 1; otherwise, 0
Agricultural agencies	If agricultural agencies, 1; otherwise, 0
Own experience	If respondent's own experience, 1; otherwise, 0
Source of income	If agriculture is the respondent's primary source of income, 1; otherwise 0
Government supports	Status of making use of govt. supports if: yes, 1; otherwise, 0
AI employment	Status of using artificial insemination If yes, 1; otherwise, 0

Prior to the regression analysis, correlation analysis was performed to determine the variables to be included in the regression analysis. The correlation matrix is measured by a large number of variables. It can be explained as variable statistics that combine the variables associated with each other to measure and describe these variables with a single variable, thus reducing the variable and allowing the structure to be measured in this way (Stapleton, 1997).

Results

In the study, the mean age of the respondents was 43.74 and 46.61 years for member and non-member breeders respectively, as illiteracy rate of the two groups of breeders were 45.00% and 57.53% in the same order. The distance to the nearest town was 44.05 and 43.47 km for both groups, respectively (*Tables 3 and 4*).

Table 3. *The demographic structure of the producers*

	Education status					Family size					
	DCBA		Non-members		Total	Person	DCBA		Non-Members		Total
	N	%	N	%	N		N	%	N	%	
Uneducated	76	45.50	218	57.52	294	1-5	63	37.72	107	28.23	216
Primary	69	41.30	129	34.04	198	6-9	81	48.51	166	43.80	322
High	15	9.00	21	5.54	36	10 +	23	13.77	106	27.96	227
University	7	4.20	11	2.90	18	Total	167	100	379	100	546
Total	167	100	379	100	546						

Table 4. *The demographic structure of the producers*

	Non-member breeders					DCBA member breeders				
	N	Min.	Max.	Mean	S _x	N	Min.	Max.	Mean	S _x
Breeder age	378	19	83	46.61	0.674	166	20	83	43.74	0.961
Schooling	379	0	15	2.46	0.161	167	0	15	3.26	0.264
Household size	379	1	19	7.40	0.192	167	1	14	6.31	0.244
Distance to the nearest town	379	15	125	43.47	0.944	167	18	140	60.93	2.429
Milk sales	379	0	1	0.28	0.023	167	0	1	0.41	0.038
Make use of pastures	379	0	1	0.60	0.025	167	0	1	0.87	0.026
Barn type	379	0	1	0.03	0.009	167	0	1	0.05	0.017
<u>Source of agricultural information</u>										
DCBA	379	0	0	0.00	0.000	167	0	1	0.14	0.027
Neighbours	379	0	1	0.13	0.017	167	0	1	0.13	0.026
TV	379	0	1	0.14	0.018	167	0	1	0.15	0.028
Agricultural agencies	379	0	1	0.08	0.014	167	0	1	0.11	0.025
Own experience	379	0	1	0.67	0.024	167	0	1	0.81	0.030
Agriculture as the source of income	379	0	1	0.73	0.023	167	0	1	0.78	0.032
Make use of government supports	379	0	1	0.04	0.010	167	0	1	0.38	0.038
AI employment	379	0	1	0.33	0.024	167	0	1	0.57	0.038

Naturally, it is an expected consequence from an agricultural organization that the members of that organization adopt innovations more than non-members. In the present study, 32.98% of non-member breeders and 57.48% of DCBA member breeders applied artificial insemination. In other words, the practice of artificial insemination was 24.5% higher for DCBA member breeders as compared with non-members (Table 4). Consequently, 96.9 and 81.6% of the DCBA member and non-member breeders have calves from AI, which implies success in AI is higher for DCBA member breeders. Since AI is one of the most reasonable options to increase milk and meat yields in the next generation, breeders were asked whether artificial insemination increases milk yield or not. Of the respondents, 61.5% of DCBA members and 65.6% of non-member breeders agreed that it did. As a matter of fact, in Turkey, AI has been accepted as the most reasonable option for genetic improvement of farm animals to increase milk and beef production, and it has been supported by the governments in different ways (Terin, 2014).

Adoption of new techniques or innovations suggests sustainable behavioural changes without external interventions. Therefore, the breeders were asked whether they would continue to use AI or not in case of a possible government support cut-off. According to the results, 71% and 61% of DCBA member and non-member breeders replied positively to this question (Table 5).

Table 5. Artificial insemination opinions of the breeders

Status of artificial insemination application						Whether or not calves born from artificial insemination					
	No applying		Applying				No		Yes		
	N	%	N	%	Tot.		N	%	N	%	Total
Non-members	254	67.02	125	32.98	379	Non-members	23	18.40	102	81.60	125
DCBA	71	42.52	96	57.48	167	DCBA	3	3.13	93	96.87	96
Opinion whether artificial insemination increases milk yield or not						Status of artificial insemination in case of no support					
	Increased		Not increased				No apply		Apply		
	N	%	N	%	Tot.		N	%	N	%	Total
Non-members	82	65.60	43	34.40	125	Non-Members	49	39.00	76	60.80	125
DCBA	59	61.46	37	38.54	96	DCBA	28	29.00	68	70.80	96
						$X^2 = 2.408, p = 0.121$ (non-significant)					
Causes of not using artificial insemination method											
	1. Reason	2. Reason	3. Reason	Stack total point	%						
Unnecessary	65	0	1	196	35.89						
Low success in native breeds	25	3	0	81	14.83						
Expensive	22	3	0	72	13.18						
No habit	19	2	1	62	11.35						
Having own bull	19	2	0	61	11.17						
Sin	11	4	0	41	7.50						
Lack of knowledge	5	0	1	16	2.93						
No assistance of agr. inst.	2	0	0	6	1.09						
Lack of time	2	0	0	6	1.09						
No assistance of DCBA	1	1	0	5	0.91						
Total				546							

This suggests that a significant behavioural change was achieved with regard to AI employment. However, we may also infer that there was not any behavioural change in about 30% of the respondents. The difference between the two groups was not significant ($P > 0.05$). The reasons for not using AI were non-essentiality, low success rate in local breeds, expensiveness, sinful act, and bull ownership, in respective order (*Table 5*).

According to the results of regression analysis (*Table 7*), breeder age and family size had an insignificant negative effect on the adoption of AI, whereas schooling years, membership in an association, barn type, and use of neighbours as a source of agricultural information had a positive but insignificant effect. Again, distance to the nearest town and proportion of crop revenues in the total farm income had a significant negative effect ($P < 0.01$) on the employment of AI, while milk sales and TV as the source of agricultural information had a significant positive effect on the use of AI at the 90% confidence level. Once more, benefiting from common pastures and the use of agricultural agencies as the sources of information had a significant positive effect ($P < 0.05$) on the adoption of AI, while support payments, cross- and purebred cattle ownership, and the use of DCBA as the source of agricultural information had a strong, positive effect ($P < 0.01$).

When considering the marginal effects of the factors on the adoption of AI, it is obvious (*Table 5*) that the use of DCBA as the source of agricultural information, desire to make use of support payments, use of agricultural agencies as information sources, ownership of cross- or purebred cow, desire to benefit from common pastures, and use of TV as the source of agricultural information increase the possibility of adopting AI by 34.2, 26.5%, 18.1, 17.6, 14.4, 11.9%, respectively. On the other hand, one-unit increments in the distance to the nearest town and in the proportion of crop revenues in the total farm income reduce the likelihood of AI use by 18.9 and 0.03%, respectively.

Discussion

Between 2004 and 2015, all support payments for livestock farmers including AI were made via associations of big- and small-ruminant breeders. Breeders that were members and non-members of DCBA were paid TRY 145 and TRY 92 (USD 32.2 and USD 20.4) per calf from AI, respectively, until 2015. However, the difference between the breeder groups regarding support payments paid per calf disappeared after 2016. All calves from AI or natural insemination cost the same amount of money, and so there are no advantages for DCBA members at all (Anonymous, 2017a).

Age is an important factor affecting the attitudes and behaviors of producers in carrying out agricultural activities (Köksal, 2009). In similar studies on artificial insemination, it has been reported that there is a negative relationship between the age of the producer and the possibility of applying artificial insemination (Sezgin et al., 2008; Sezgin, 2010; Aksoy and Yavuz, 2011; Howley et al., 2012). However, some studies also reported a positive correlation between the age of the producer and artificial insemination (Gençdal et al., 2015; Tambi et al., 1999; Kaaya et al., 2005).

The level of education is closely linked to the developments in the individual's environment and understanding and solving their problems (Yildirim, 1994). Gençdal et al. (2015) determined schooling years to be 4.9 and 4.1 for the farm enterprises that employed and did not employ AI, respectively. In present study, schooling years were calculated to be 3.5 for the respondents preferring AI and 2.1 for those not preferring AI. The difference between the breeder groups regarding schooling years is highly significant ($P < 0.01$).

Table 6. The correlation matrix

	AI	Age	EP	P	D	M*	MS*	BP*	BT*	DCBA*	N*	TV	AA*	OE*	RR*	S*	CPB*
AI	1,00	-0,169**	0,214**	-0,184**	-0,091*	0,230**	0,276**	0,241**	0,03	0,263**	0,110*	0,174**	0,202**	-0,03	-0,177**	0,291**	0,267**
Age	-0,169**	1,00	-0,285**	0,379**	0,03	-0,105*	-0,149**	-0,169**	-0,05	-0,01	0,01	-0,04	-0,04	0,05	0,02	-0,08	-0,108*
EP	0,214**	-0,285**	1,00	-0,203**	-0,04	0,115**	0,164**	0,100*	0,07	0,07	0,128**	0,199**	0,172**	-0,01	-0,129**	0,192**	0,08
P	-0,184**	0,379**	-0,203**	1,00	0,03	-0,139**	-0,164**	-0,120**	-0,03	-0,03	-0,07	-0,216**	-0,01	0,01	0,07	-0,08	-0,08
D	-0,091*	0,03	-0,04	0,03	1,00	0,329**	-0,290**	0,04	-0,05	0,03	0,07	-0,02	0,03	0,178**	0,03	-0,01	0,150**
M*	0,230**	-0,105*	0,115**	-0,139**	0,329**	1,00	0,126**	0,211**	0,05	0,402**	-0,01	0,01	0,142**	0,125**	0,05	0,444**	0,366**
MS*	0,276**	-0,149**	0,164**	-0,164**	-0,290**	0,126**	1,00	0,315**	0,04	0,093*	-0,01	0,06	0,085*	-0,086*	-0,07	0,172**	0,329**
BP*	0,241**	-0,169**	0,100*	-0,120**	0,04	0,211**	0,315**	1,00	-0,03	0,04	0,03	0,06	0,07	0,02	-0,04	0,05	0,447**
BT*	0,03	-0,05	0,07	-0,03	-0,05	0,05	0,04	-0,03	1,00	0,05	0,00	-0,06	-0,02	-0,02	-0,03	0,06	-0,03
DCBA*	0,263**	-0,01	0,07	-0,03	0,03	0,402**	0,093*	0,04	0,05	1,00	0,093*	0,105*	0,151**	-0,06	-0,05	0,391**	0,153**
N*	0,110*	0,01	0,128**	-0,07	0,07	-0,01	-0,01	0,03	0,00	0,093*	1,00	0,365**	0,01	0,07	-0,07	0,04	-0,04
TV*	0,174**	-0,04	0,199**	-0,216**	-0,02	0,01	0,06	0,06	-0,06	0,105*	0,365**	1,00	0,109*	0,06	-0,146**	0,01	-0,04
AA*	0,202**	-0,04	0,172**	-0,01	0,03	0,142**	0,085*	0,07	-0,02	0,151**	0,01	0,109*	1,00	-0,110*	-0,06	0,204**	0,118**
OE*	-0,03	0,05	-0,01	0,01	0,178**	0,125**	-0,086*	0,02	-0,02	-0,06	0,07	0,06	-0,110*	1,00	0,02	-0,05	0,135**
RR*	-0,177**	0,02	-0,129**	0,07	0,03	0,05	-0,07	-0,04	-0,03	-0,05	-0,07	-0,146**	-0,06	0,02	1,00	-0,01	0,01
S*	0,291**	-0,08	0,192**	-0,08	-0,01	0,444**	0,172**	0,05	0,06	0,391**	0,04	0,01	0,204**	-0,05	-0,01	1,00	0,171**
CPB*	0,267**	-0,108*	0,08	-0,08	0,150**	0,366**	0,329**	0,447**	-0,03	0,153**	-0,04	-0,04	0,118**	0,135**	0,01	0,171**	1,00

AI: Application artificial insemination , EP: Education period, P: Population, D: Distance, M: Membership association , MS: Milk sales, BP: Benefitting pasture, BT: Barn type, DCBA: Diyarbakir Cattle Breeders Association, N: Neighbour , AA: Agricultural agencies, TV: television, OE: Own experience, RR: Revenue rate in crop production, S: Support, CPB: Having cross-breed and pure breed

Table 7. Logistic regression analysis results

Independent variables	Coef.	Std Err.	z	p > t	Marginal effect (dy/dx)
Age	-0.013	0.008	-1.48	0.138	-0.003
Education period	0.036	0.034	1.08	0.282	0.008
Population	-0.045	0.318	-1.43	0.154	-0.010
Distance	-0.012	0.005	-2.54	0.011	-0.003
Membership to association*	0.284	0.288	0.99	0.324	0.068
Milk sales*	0.429	0.229	1.88	0.060	0.101
Benefit to pasture*	0.628	0.254	2.47	0.014	0.144
Barn type*	0.091	0.568	0.16	0.872	0.021
DCBA*	1.434	0.500	2.87	0.004	0.342
Neighbour*	0.397	0.270	1.47	0.141	0.096
TV*	0.494	0.267	1.85	0.065	0.119
Agricultural agencies*	0.742	0.309	2.40	0.016	0.181
Own experience*	-0.028	0.249	-0.11	.909	-0.006
Rate in crop production*	-0.780	0.238	-3.28	0.001	-0.189
Support*	1.088	0.349	-3.12	0.002	0.265
Cross and pure breed*	0.768	0.256	3.00	0.003	0.176
_cons	0.176	0.583	-0.30	0.763	

*dy/dx is the discrete change of dependent variable when independent dummy variable shifts from 0 to 1

When we look at the family structure today, we see that the nuclear family structure is common in urban areas whereas the family size increases in rural areas (Anonymous, 2017b). The average family size in rural areas in Diyarbakir is 7.2 persons (Anonymous, 2011). In present study, the average family size was 6.3 persons for the respondents preferring AI and 7.6 persons for the respondent groups ignoring AI. Again, family size was also 6.3 and 7.4 persons for DCBA members and non-members, respectively. Accordingly, a negligible and insignificant relationship between family size and artificial insemination was found in this study, which is in line with the reports of Gençdal et al. (2015), who stated that there was no relationship between AI and family size. As found in this study, a positive and significant relationship between membership and AI was also reported by similar studies, which claimed that membership in an association increased the possibility of AI use (Sezgin, 2010; Aksoy and Denizli, 2012).

In this study, we found that the distance between the breeder's village and the nearest town had a significant negative effect on the likelihood of AI use ($P = 0.011$). A one-unit (1 km) increase in distance will reduce the likelihood of AI use by 0.3%. Similar findings were reported by Gençdal et al. (2015), Aksoy and Yavuz (2011), and Murage and Ilatsia (2011).

Conclusions

The low-yielding local cattle asset and the misperception among breeders that artificial insemination in native breeds is not successful are very important problems to tackle, especially for the breeders with no membership status. However, the main causes

of low success rate in artificial insemination are failure in heat detection in cows, untimely insemination practices and poor semen quality. Nevertheless, the support payments paid for per calf born from artificial insemination were the most important driving force for the success of artificial insemination until 2015. Since the year 2015, the scope of support payments has also covered the calves born from natural insemination. This caused the members of the DCBA to give up the use of artificial insemination.

On the other hand, we can infer from the results that breeders with good relations to agricultural agencies are significantly and positively tended more to employ AI. For that reason, in order to develop the genetic material of the cattle asset of the farms, artificial insemination is an easy and cost effective tool to be considered. However, low conception rate experienced in artificial insemination practices due to untimely applications, failures in heat detection and poor semen quality were the most important reasons for the breeders not to employ artificial insemination. Whereas, support payments paid for the calves born from AI were the main drive for the breeders to prefer AI instead of natural service despite of existing barriers against AI. We can infer from the results that in order to achieve the successful results, more sustainable, robust and long-term policies should be developed and implemented to tackle the existing problems impeding the success of AI.

REFERENCES

- [1] Anonymous (2011): Adrese Dayalı Nüfus Kayıt Sistemi 2010 Yılı Verileri. – <http://tuikapp.tuik.gov.tr/adnksdagitapp/adnks.zul> (06.21.2017).
- [2] Anonymous (2017a): Resmi Gazete. – 26 Eylül 2017 tarihli Hayvansal Destekler Tebliği.
- [3] Anonymous (2017b): Türkiye İstatistik Kurumu İnternet sayfası. – <http://www.tuik.gov.tr> (06.21.2017).
- [4] Akkaya, Ş., Pazarlıoğlu, M. V. (1998): *Econometrics II*. – Erkam Publishers, İstanbul.
- [5] Aksoy, A., Denizli, G. (2012): The evaluation of cattle breeders association's activities in Erzurum province. – *Atatürk Univ. Journal of the Agricultural Faculty* 43: 123-131.
- [6] Aksoy, A., Yavuz, F. (2011): Determination of factors affecting the artificial insemination: East Anatolia Region. – *Atatürk Univ. Journal of the Economic Administrative Sciences Faculty* 5: 33-42.
- [7] Aksoy, A., Terin, M., Keskin, A. (2012): A study on regional impacts of breeding and support policy in dairy cattle sector in Turkey. – *Journal of Agricultural Faculty of Atatürk Univ.* 43: 59-64.
- [8] BRAC (2015): Artificial insemination. Background. – http://www.brac.net/content/brac-artificial-insemination#.VZP43_IVj5w.
- [9] Bearden, H. J., Fuquary, J. W., Willard, S. T. (2004): *Applied Animal Reproduction*. 6th ed. – Mississippi State University, Pearson, Prentice Hall, Upper Saddle River, NJ.
- [10] Cameron, A. C., Trivedi, P. K. (2010): *Microeconometrics Using Stata*. Revised ed. – Stata Press, College Station, TX.
- [11] Çiçek, A., Erkan, O. (1996): *Agricultural Economy Research Sample and Sampling Method*. – Gaziosmanpaşa University Faculty of Agriculture Publishing, Tokat, Turkey.
- [12] Gençdal, F., Terin, M., Yıldırım, İ. (2015): A research on determination of factors affecting the artificial insemination of dairy farms: A case study of Van province of Gevaş district. – *Anadolu J Agr Science* 30: 254-259.
- [13] Gökçen, H. (1998): History of artificial insemination in the world and Turkey. – *Performans Journal*. <http://www.hazimgokcen.net/veterinerlik/dunyada-ve-turkiyede-suni-tohumlamanin> (10.10.2017).

- [14] Gujarati, D. N. (1995): *Basic Econometrics*. – Mc Graw-Hill, USA.
- [15] Howley, P., Donoghue, C. O., Heanue, K. (2012): Factor affecting farmers' adoption of agricultural innovations: a panel data analysis of the use of AI among dairy farmers in Ireland. – *Journal of Agricultural Science* 4: 171-179.
- [16] Murage, A. W., Ilatsia, E. D. (2011): Factors that determine use of breeding services by smallholder dairy farmers in Central Kenya. – *Tropical Animal Health and Production* 43: 199-207.
- [17] Kaaya, H., Bashaasha, B., Mutetikka, D. (2005): Determinants of utilisation of artificial insemination services among Ugandan dairy farmers. – *Science African Crop Science Conference Proceedings* 7: 561-567.
- [18] Köksal, Ö. (2009): *Technical efficiency of alternative farming systems: the case of Greek organic and conventional olive-growing farms*. – PhD Thesis (unpublished), Ankara University, Institute of Science and Technology, Department of Agricultural Economics, Ankara, Turkey.
- [19] Sezgin, A. (2010): *Mass communication in the adoption of animal husbandry innovations Analysis of the impact of vehicles: the example of Erzurum Province*. – *Journal of the Faculty of Veterinary Medicine, Kafkas University* 16: 13-19.
- [20] Sezgin, A., Yurttaş, Z., Yavuz, F. (2008): Impact analysis of the mass media tools on the adoption of the innovations in animal production: the case of Erzurum province. – *Turkish Journal of Agricultural Economics* 14: 75-85.
- [21] Sinishaw, W. (2004): *Study on semen quality and field efficiency of ai bulls kept at the national AI Center*. – M.Sc. Thesis, Addis Ababa University, Faculty of Veterinary Medicine, Debre Zeit.
- [22] Stapleton, C. D. (1997): *Basic Concepts and Procedures of Confirmatory Factor Analysis*. – Paper presented at the Annual Meeting of The Southwest Educational Research Association (Austin, January).
- [23] Tambi, N. E., Mukhebi, W. A. Main, W. O., Solomon, H. M. (1999): Probit analysis of livestock producers' demand for private veterinary services in the high potential agricultural areas of Kenya. – *Agricultural Systems* 59: 163-176.
- [24] Terin, M. (2014): *A research on determination of factors affecting the artificial insemination of dairy farms: a case study of Van province of Gevaş district*. – Doctoral thesis, Science Institute of Sciences, Erzurum.
- [25] Thibier, M. (1990): *New biotechnologies in cattle production*. – *Proceedings of the 7th Congress of the F. A. V. A., 4–7th November, 1990, Pattaya, Thailand*, pp: 513-524.
- [26] Yavuz, F. (2011): *Leader Approach in Rural Development: Case of Erzurum Province*. – *Cattle Breeding Project Hand Book*, 4th ed. Erzurum, Turkey.
- [27] Yıldırım, H. (1994): *A research on professional organization and problems in the agricultural sector of Seyhan and IR districts of Adana province*. – Doctoral thesis, Çukurova Üniversitesi Science Institute of Sciences, Adana.

EFFECTS OF HIGH DIETARY COPPER SUPPLEMENTATION ON THE COPPER ACCUMULATION AND TOTAL COPPER CONTENT IN FATTENING PIGS

ADAMS, S. – YANG, H. – CHE, D.* – JIANG, H.* – QIN, G.

*College of Animal Science and Technology, Jilin Agricultural University
130118 Changchun, China*

**Corresponding authors*

e-mail: hljiang@jlau.edu.cn; phone: +86-186-446-5676; chedongsheng@163.com; phone: +86-136-4431-9554

(Received 27th Oct 2018; accepted 20th Dec 2018)

Abstract. The objective of this current study was to investigate the effects of high dietary copper supplementation on the tissue copper deposition, distribution, and total copper concentration in fattening pigs. A total of 24 (Landrace × Large white × Duroc) pigs with an average initial body weight (BW) of 30 ± 1.05 kg were selected for the current experiment. At the beginning of the experiment, the pigs were randomly divided into four treatment groups with three replicate pens per treatment and two pigs per replicate and arranged in accordance to a completely randomized design based on the BW. The four treatment administered were as follows: 10 mg/kg, 45 mg/kg, 135 mg/kg, and 225 mg/kg of copper. The result indicates that the copper content in the liver, kidney, and heart increased with the increase in dietary copper composition. There was no significant difference in the copper content of the different visceral tissues in the 10 mg/kg treatment group. However, when the copper levels increased to 45 mg/kg and 135 mg/kg, the copper content in the liver was significantly higher than that in the other visceral tissues ($P < 0.05$). At 225 mg/kg dietary copper, there was a significant increase in the copper content of the foreleg muscle. There was no significant difference in copper content of the rib bones, tibia bones, and femur bone marrow copper accumulation between the 10 mg/kg copper and the 45 mg/kg copper fed pigs. In addition, there was no significant difference in the brain, blood, cerebellum, and skin copper content within all the treatment groups. Therefore, dietary copper levels increased with the increase in total copper accumulation in pigs. Hence, higher dietary copper supplementation increased liver, kidney, heart, fur, bones, bone marrow copper accumulation and total copper levels in fattening pigs.

Keywords: *micronutrient, metabolism, bioavailability, visceral tissues, diet, supplementation*

Introduction

Copper is an indispensable micronutrient that forms part of all animal tissues and is required for a variety of biological processes essential for the maintenance of life (Gaetke et al., 2014). It is a co-factor of cellular enzymes, such as catalase, cytochrome oxidase, dopamine-beta-hydroxylase, and peroxidases. The extreme concentrations of copper inhibit sulfhydryl groups on enzymes such as glucose-6-phosphatase and glutathione reductase which protect cells from damage by free radicals (Bremner and Beattie, 1995). The most frequently utilized dietary copper supplement in animals' diet is inorganic copper usually in the form of copper sulphate ($\text{CuSO}_4 \cdot 5\text{H}_2\text{O}$). Copper occurs in the organic forms of chelates, complexes, proteinases, and like other organic trace minerals is often considered as an alternative to inorganic sources in animals diets (Huang et al., 2010). The relative bioavailability estimates of organic copper sources range between 88% and 147% of cupric sulphate in poultry, swine, sheep, and cattle (Baker and Ammerman, 1995). Copper is recognized as a growth-promoting agent in non-ruminant animals but its use at high levels is considered to be detrimental to the

environment (Armstrong et al., 2004; Veum et al., 2004). Diverse concentration and forms of copper have different bioavailabilities and different effects on animals (Guo et al., 2001). For example, copper is widely distributed in different animals' tissues such as the heart, liver, spleen, lungs, kidneys, and other internal organs, at saturated copper concentrations, copper accumulates in the bones. The requirement of copper as a nutrient is low and NRC (1998) recommends three to six milligram per kilogram copper for nursery and grower-finisher pigs. Generally, copper sulphate (125 to 250 mg/kg) is routinely added to nursery pigs diet as a growth promoter and its benefits on feed intake and weight gain have been well documented (Zhao et al., 2014).

However, high dietary copper presents health and environmental concerns when excess copper is excreted in faeces (Kornegay et al., 1997) and accumulated in muscle tissues. The accumulation of copper in animals' tissues and its excretion into soil has implicated to decrease soil productivity and pose both health and environmental threats. It was demonstrated that high dietary copper from inorganic sources antagonises other nutrients utilisation, such as zinc (Zhao et al., 2008) and phosphorus (Banks et al., 2004). As a result of the negative impact of high dietary copper sulphate, the commission of the European Communities regulates maximum allowed total copper in a feed as 170 mg/kg in piglets up to 12 weeks of age and 25 mg/kg in all other pigs. However, the ban on antibiotics usage in some parts of the world has motivated some farmers to still adhere to high copper supplementation in monogastric feeds above the required standards especially in swine nutrition. Hence, we hypothesised that higher copper concentration in swine nutrition may decrease the rate of copper deposition in muscle tissues and organs. The aim of the present study was to investigate the effects of high dietary copper concentrations on tissues and organ copper distribution and deposition in fattening pigs.

Materials and methods

Experimental site and location

This study was performed in the animal breeding station of Jilin Agricultural University located in Changchun city of the Jilin Province in the People's Republic of China. Jilin is found on latitude 43°42' N and longitude 126° 12' E, and Changchun is on latitude 43°88' N and longitude 125°35' E. The annual rainfall ranges between 350-1000 mm (March – August) and dry season between September - February. Winter ranges between November – March with temperatures between -8 °C (17 °F) – -20 °C (-4.6 °F) and summer temperatures between 16°C (61.4°F) and 28 °C (81.2 °F) around May-July.

Experimental design, animals, housing and diet

A total of 24 (Landrace × Large white × Duroc) pigs with an average initial BW of 30 ± 1.05 kg were selected for the current experiment. The experiment was conducted for 87 days including 7 days of pre-feeding trial. At the beginning of the experiment, the pigs were divided into four treatment groups, with three replicate pens per treatment and two pigs per replicate, in accordance with a completely randomized design based on the BW. The copper content in the treatments was formulated based on the national guidelines that stipulated that the body weight of fattening pigs between 30-60 kg should contain ≤ 150 mg/kg copper and body weight above 60 kg should possess ≤

25 mg/kg copper. The four treatment administered were as follows: 10 mg/kg, 45 mg/kg, 135 mg/kg, and 225 mg/kg. The control pigs were fed the basal diet and the experimental pigs were fed the basal diet with the different copper concentrations. Pigs were fed twice daily and provided with 4% of the total body weight. The composition of the basal diet is provided in *Table 1*. The diet was provided in a mash form and formulated in accordance with the (NRC, 1998) nutrients recommendation. The basal diet contains corn-soybean meal as the main raw material and dietary copper was supplemented as copper sulphate (CuSO₄). Water was supplied *ad libitum* throughout the entire experimental period. The pigs were housed in an environmentally-controlled room with an average temperature of 26 °C. The pens were disinfected once a month, cleaned with a broom every day to keep a healthy and hygienic condition, and prevent disease infection among pigs.

Table 1. *Composition of experimental diets and nutrient indexes (%DM basis) prepared using the guidelines of NRC (1998) with corn and soybean as the main energy and protein sources*

Items	30–60 kg	60–120 kg
Ingredients		
Corn	64.5	70.0
Soybean meal	11.0	11.5
Bran	22.0	16.0
Bone meal	1.0	1.0
Limestone	0.4	0.5
Salt	0.4	0.5
Lysine-HCL	0.2	
Trace mineral premix	0.5	0.5
Total	100	100
Calculated nutrient level		
Digestibility energy (MJ/kg)	13.67	13.59
Crude protein (CP)	17.06	15.55
Lysine (Lys)	0.85	0.63
Methionine + Cysteine (Met+Cys)	4.6	4.6
Copper sulphate (CuSO ₄) (mg/kg)	10.00	10.00
Phosphorus (P)	0.65	0.55
Calcium (Ca)	0.64	0.71

Note: per kilogram of premix contains: iron 10000 mg, zinc 1000 mg, manganese 1000 mg, selenium 30 mg, iodine 50 mg, VA2000000IU, VD20000IU vitamin D2000IU, 2000 mg niacin, folic acid, pantothenic acid 2000 mg 30 mg, VK50 mg, riboflavin 250 mg, VB1 200 mg VB12 1000 ug, choline chloride 100 g, antioxidant 20000 mg, biotin 5 mg, VB6100 mg

Organs and tissues sampling

At the end of the feeding trial, three pigs from each group were slaughtered in accordance with the normal farming practice and various organs and tissues were sampled for the determination of copper. The sampling method was as follows: about 20 g of muscle tissues were taken from the forelegs, hind legs, and buttocks and about 0.05 cm² of fur was collected from the back skin of pigs immediately after slaughter.

The abdominal cavity was opened and 10 g of various organs were obtained. The adipose tissues were obtained by taken 20 g of the back muscles of pigs. The femur bone, femur bone marrow, ribs, and bones were collected from pigs for the determination of copper levels.

Blood sampling

Blood samples were taken at the time of slaughtering into separate tubes and heparinized. The samples were immediately transferred to the laboratory where plasma and serum were subsequently separated by centrifuging the whole blood samples at $2500 \times g$ at 4°C for 5 min. The heparinized plasma samples were frozen at -20°C until analysis for copper concentrations.

Chemical analysis

The chemical composition of the diets was analysed by standard methods. Dry matter was determined by drying feed samples at 105°C to constant weight. The crude protein by Kjeldahl and ether extract by Soxhlet fat analysis as described by (AOAC, 2000). The copper concentrations of feed, tissues, organs, faeces, urine, and plasma were analysed by the Flame Atomic Absorption Spectroscopy (Shimadzu Scientific Instruments, Kyoto, Japan) as previously described by (Wu et al., 2015).

Statistical analysis

The data were analysed by one-way analysis of variance (ANOVA) using SPSS version 13.0 (SPSS Inc., Chicago, IL, USA). A probability value of $P \leq 0.05$ was considered to be statistically significant and the multiple comparisons test was performed by LSD method, the test results were estimated as Mean \pm SE.

Results

Copper distribution and deposition in the internal organs

Table 2 shows that among the different tissues and organs analysed from the fattening pigs, the deposition of copper in the liver was higher.

Table 2. Effects of dietary copper levels on different tissues and organs (mg/kg)

Levels	Feed	Liver	Kidney	Heart	Lung	Stomach	Spleen	Pancreas	Lymph nodes
10 mg/kg	10	9.18 \pm 0.16 ^{ab}	8.39 \pm 0.34 ^a	5.84 \pm 0.65 ^{ab}	3.68 \pm 1.63 ^{ab}	1.10 \pm 0.01 ^{ab}	0.95 \pm 0.03 ^{bc}	4.54 \pm 0.95 ^a	4.28 \pm 1.12 ^{abc}
45 mg/kg	45	12.58 \pm 0.14 ^a	10.16 \pm 0.04 ^b	6.30 \pm 0.20 ^b	3.55 \pm 0.78 ^b	2.01 \pm 0.06 ^b	1.94 \pm 0.09 ^b	4.45 \pm 0.98 ^a	4.45 \pm 0.85 ^b
135 mg/kg	135	31.98 \pm 2.20 ^a	13.51 \pm 0.18 ^b	7.64 \pm 0.12 ^c	3.37 \pm 0.05 ^c	2.72 \pm 0.2 ^c	2.68 \pm 0.31 ^c	5.41 \pm 1.76 ^a	3.77 \pm 1.08 ^c
225 mg/kg	225	49.6 \pm 21.37 ^a	20.38 \pm 0.21 ^b	12.49 \pm 0.2 ^b	3.21 \pm 0.65 ^b	3.98 \pm 0.04 ^b	3.88 \pm 0.06 ^b	5.27 \pm 0.96 ^{ab}	3.50 \pm 0.21 ^b

Different letters in the same column the data before are significantly different at the level of $P < 0.05$

We observed that the amount of copper deposition increased with the increase in copper concentration in the feed. The copper content in the liver, kidney, and heart showed an increasing trend with increasing copper levels in the feed. The kidney copper composition in the 225 mg/kg copper sulphate group was approximately 2.5 times higher than that of the kidney copper content in the control group. The lowers copper

accumulation in tissues and organs was registered in pigs supplemented with 10 mg/kg copper. There was no significant difference in copper content in the different visceral tissues at 10 mg/kg group. However, at 45 mg/kg and 135 mg/kg copper content there was a significantly ($P < 0.05$) increase in the liver copper levels compared to other visceral tissues. We observed higher copper levels in the liver followed by the kidneys, heart, spleen, and the pancreas. However, at 225 mg/kg copper levels, there was an increased in liver copper content compared to the kidney copper level. There was a decreased trend in the lungs copper content with the increase in dietary copper levels.

Distribution and accumulation of copper in muscle tissue of fattening pigs

The accumulation of copper in pig muscle tissue and adipose tissue is detailed in *Table 3*. From *Table 3*, there was no significant difference in the copper concentration of pig muscle tissue as the copper content of the feed increases. At 225 mg/kg dietary copper levels, there was a significant increase in the copper content of the foreleg muscle. Although the copper concentration of most muscle tissues increased as the dietary copper content increases, the hind leg muscle observed a slightly decreased in copper content at higher dietary copper levels. Conversely, the copper content of the foreleg muscle was relatively higher than the copper content in the loin and the hip muscle tissues.

Table 3. Dietary copper supplementation on the copper contents in the muscle tissues and fat in pigs fed different copper feeds

Levels	Feed	Foreleg muscle	Hindleg muscle	Loin	Hip muscle	Adipose tissue
10 mg/kg copper	10	0.510±0.004 ^a	0.100±0.144 ^a	0.072±0.09 ^a	0.057±0.003 ^a	0.076±0.005 ^a
45 mg/kg copper	45	0.610±0.050 ^a	0.100±0.017 ^a	0.05±0.026 ^{ab}	0.060±0.020 ^{ab}	0.131±0.021 ^b
135 mg/kg copper	135	0.630±0.070 ^a	0.270±1.091 ^a	0.064±0.05 ^a	0.057±0.120 ^a	0.147±0.364 ^a
225 mg/kg copper	225	0.750±0.020 ^b	0.370±0.585 ^{ab}	0.073±0.034 ^b	0.041±0.065 ^b	0.276±0.420 ^a

Different letters in the same column the data before are significantly different at the level of $P < 0.05$

Distribution and accumulation of copper in porcine bones

From *Table 4* it can be observed that as the content of copper in the feed increases, the accumulation of copper in swine bones also increases.

Table 4. Copper supplementation on the copper content in pigs' bones with different copper feeding doses

Levels	Feed	Rib bone	Tibia bone	Femur bone	Femur bone marrow
10 mg/kg copper	10	4.11±1.05 ^a	4.38±0.83 ^a	4.15±0.02 ^a	0.52±2.96 ^a
45 mg/kg copper	45	5.12±0.25 ^a	4.59±0.68 ^a	18.25± 3.21 ^b	2.52±2.68 ^a
135 mg/kg copper	135	22.28±0.85 ^b	22.13±0.24 ^b	57.36±8.21 ^c	8.32±1.32 ^b
225 mg/kg copper	225	22.45±0.24 ^b	22.22±0.35 ^b	62.32±3.25 ^d	10.25±2.35 ^c

Different letters in the same column the data before are significantly different at the level of $P < 0.05$

The degree of copper accumulation in the tibia bones, rib bones, femur bones, and femur bone marrow varies greatly. However, the degree of copper enrichment in the bone marrow was lower in all the treatment groups. There was no significant difference in the copper levels of the rib bones, tibia bones, and femur bone marrow copper

accumulation between the 10 mg/kg copper and the 45 mg/kg copper fed pigs. The content of copper in the femur bone was significantly higher ($P < 0.05$) than the copper content in the femur bone marrow, ribs, and the tibia bones at 45 mg/kg copper levels. In addition, there was a significant difference in the copper content of the rib bones and the tibia bones at 135 mg/kg copper and 225 mg/kg copper fed pigs. However, the 225 mg/kg treatment groups registered the highest copper content in the tibia bone, femur bone, and femur bone marrow.

Accumulation and distribution of copper in various organs

From *Table 5*, we have observed that as the concentration of copper in the feed gradually increased, the copper content in the pig's brain, cerebellum, blood, skin, and fur shows an increasing trend. The blood and the skin registered the lowest copper accumulation among the treatment groups. There was no significant difference in the brain, blood, cerebellum, and skin copper content within all the treatment groups. However, there was a significant difference in the fur copper content of the 225 mg/kg copper fed pigs in comparison with the control. The fur copper content of the 225 mg/kg copper diet was significantly different from the 135 mg/kg copper diet, but, not significantly different from the 10 mg/kg and 45 mg/kg copper treated groups. Although the copper content of the brain was high, its rate of accumulation was lower compared to the fur.

Table 5. Dietary copper supplementation on the copper content in the brain, skin blood, and fur of pigs fed different copper levels

Treatments	Feed	Brain	Cerebellum	Skin	Blood	Fur
10 mg/kg copper	10	12.137±4.274 ^a	6.794±0.987 ^a	0.039±0.021 ^a	1.604±0.080 ^a	3.791±0.554 ^a
45 mg/kg copper	45	12.037±0.837 ^a	7.255±0.125 ^a	0.059±0.087 ^a	1.684±0.114 ^a	4.474±0.821 ^a
135 mg/kg copper	135	12.261±3.374 ^a	8.321±0.125 ^a	0.071±0.067 ^a	1.890±0.212 ^a	10.560±8.454 ^b
225 mg/kg copper	225	12.354±2.354 ^a	9.321±0.102 ^a	0.084±0.517 ^a	1.684±0.162 ^a	12.540±7.211 ^c

Different letters in the same column the data before are significantly different at the level of $P < 0.05$

Effect of dietary copper levels on the total copper content in pigs

From *Table 6*, we have observed that as the content of copper in the feed increased, the total copper accumulation in the pigs also increased. The total copper content in the 225 mg/kg copper treated group was significantly higher in comparison with the 10 mg/kg, 45 mg/kg, and 135 mg/kg. The copper content in the liver, kidney, femur bone, femur bone marrow, ribs, and fur increased with the increase in copper content of the feed. The copper levels in the muscle tissues, lungs, and other tissues of the fattening pigs body follow a similar trend as other parts of the visceral organs.

Table 6. Effects of dietary copper supplementation on the total copper content in the tissues and organs of pigs

Copper content (mg/kg)	Total copper in tissues and organs of pigs (mg/kg)
10 mg/kg copper	76.501±0.321 ^{Aa}
45 mg/kg copper	102.654±1.880 ^{Aa}
135 mg/kg copper	215.393±1.325 ^{AB}
225 mg/kg copper	256.826±21.201 ^{Bb}

Lowercase letters indicate that there is a significant difference between the data and the control group at the level of ($P < 0.05$). Capital letters indicate that there is a significant difference between the data and the control group at the level of ($P < 0.01$)

Discussion

Dietary supplementation of feed additives has recently gain scientific interest due to the current ban on antibiotics usage as feed supplement in most countries (Adams et al., 2019; Adams et al., 2018a, b; Che et al., 2018). Most animal species have limited access to copper from the environment. The concentration of dietary copper varies greatly because feed materials from different sources have different copper content. The main sources of copper for animals are the food, drinking water, and copper containing supplementations (de Romaña et al., 2011; Tomaszewska et al., 2014). Copper has been used in the formation and maintenance of myelin and is needed for the synthesis of melanin in the eyes, hair, and skin. It is a constituent of cytochrome c oxidase, vital in cellular respiration, and forms a complex relationship with zinc-superoxide dismutase (Letelier et al., 2009; Gaetke et al., 2014). The quantity of copper absorbed from food and water is reasonably low, and the body controls excess amounts of copper by either reducing the absorption or increasing the excretion of copper under normal conditions. The absorption rate of dietary copper is affected by several factors such as sex, age, type of feed, and quantity of copper supplemented (de Romaña et al., 2011). However, the control of internal copper homeostasis prevents the excess accumulation of copper in body tissues and organs (Gaetke et al., 2014). The distribution and accumulation of copper in most tissues of the body have been linked to the total amount of copper supplemented in the diet and the total copper ingested. The supplementation of high copper diets in growing pigs may result in the increased in copper accumulation in organs and excretion in manure, which poses both health and environmental risk (Kornegay and Versteegen, 2001). The excretion of high copper levels in swine manure is reported elsewhere (Yin et al., 2018; Zheng et al., 2018; Liao et al., 2018). Thus, it is important to examine the effects of dietary supplementation of copper on the relative distribution and accumulation of copper in organs and total copper content in fattening pigs.

The present study showed that with the increased in dietary copper levels, there was an increase in the copper content in the tissues and organs of pigs. However, the copper levels in different tissues and organs varied greatly. Similarly, Peña et al. (1999), who indicated that the highest concentration of copper was in the liver, kidneys, brain, heart, and the lowest concentration was in the bones and muscles. The authors indicated that the average copper content in adult animals was three times lower than growing animals. This was due to the high metabolic requirements of copper in growing animals. Also, Bremner and Beattie (1995) indicated that the liver is the main storage site for copper deposition following higher dietary copper consumption and the copper concentrations in a normal adult liver is 18–45 mg copper per gram dry weight. Moreover, the concentration and distribution of copper varied throughout the animal's life. We observed that the total amount of copper retained increased as the copper intake increases, reaching a plateau with dietary copper levels of 225 mg/kg. The accumulation of copper in the liver may increase to concentrations that can affect the normal functioning of the liver causing toxicosis in stress conditions. The adverse accumulation of copper in the liver could lead to liver degradation and damage in situations of Wilson's diseases (Guo et al., 2001; Roberts and Schilsky, 2008). Meanwhile, the blockage of copper absorption by the formation of copper complexes with the intestinal cells and the redistribution of copper in the liver accounts for the use of zinc in the treatment of this Wilson's disease (Bremner and Beattie, 1995). In contrast, Tomaszewska et al. (2014) fed growing rats with 5 mg/kg of organic and inorganic

copper levels per day and observed no copper deposition in the plasma and liver between the control and the experimentally treated group. Yelin et al. (1987), who noted that during liver necrosis, the liver discharges higher concentrations of copper (50 mg/g dry weight) into the blood hence causing rapid accumulation of copper in the erythrocytes and successively causing oxidative injury to the red blood cell.

Conversely, supported by the notion that copper absorption and deposition increased with increasing dietary copper levels (Barceloux and Barceloux, 1999). Copper is an essential trace mineral; little information is available on its absorption in the lungs. The National Research Council in 1977 noted that copper can be absorbed in the lungs due to the manifestation of metal fume fever for the duration of copper volatilization but the occurrence of copper to stimulate metal fume fever was low due to the high temperature requirement for copper volatilization. In this current experiment, we observed significantly decreased in the copper content of the lungs as the concentration of dietary copper levels increases. The reason for the decreased in lungs copper levels at higher dietary copper levels is not established. The absorption of copper in the lymphatic nodes follows similar trend as the absorption of copper in the lungs. The absorption of copper in the stomach depends on several factors such as dietary components, the chemical forms of copper, the interaction of copper with other metals like zinc, selenium, cadmium, and the proportion of the quantity of copper in the stomach (Stern et al., 2007). The absorption of copper in the stomach increased with the increase in dietary copper concentrations. However, the quantity of copper stored in the body does not affect the absorption of copper in the body tissues and the clinical reduction in copper absorption is not affected by the consumption of high concentrations of dietary zinc (Sandström, 2007). The present study indicates that the concentration of copper in the femur bone, femur bone marrow, kidney, and other tissues was much higher than that in muscle tissue. Hence, high dietary copper supplementation does not increase muscle copper deposition.

Conclusion

The result of this study indicated that dietary copper supplementation in the diets of growing pigs increased the copper deposition and accumulation in different body tissues and organs. However, these concentrations of copper were lower in the muscles and other visceral organ. Therefore, indicating that pigs can metabolise higher copper levels above the current standards without significant copper deposition in muscles and other parts.

Acknowledgements. This work was financially supported by the National Key Research and Development Program of China (2017YFD0502104), and the Scientific Project of Jilin Province (20170309003NY & 20180101023JC).

Conflict of interests. The authors declare that there is no conflict of interests.

REFERENCES

- [1] Adams, S., Che, D., Hailong, J., Bao, Z., Rui, H., Danquah, K., Guixin, Q. (2019): Effects of Pulverized Oyster Mushroom (*Pleurotus ostreatus*) on Diarrhea Incidence, Growth Performance, Immunity, and Microbial Composition in Piglets. – *Journal of The Science of Food and Agriculture*. DOI: 10.1002/jsfa.9582.
- [2] Adams, S., Che, D., Hailong, J., Rui, H., Bao, Z., Danquah, K., Guixin, Q. (2018a): Effect of dietary copper levels on the growth performance and nutrient utilization in fattening pigs. – *Indian Journal Animal Research*. DOI: 10.18805/ijar.B-956.
- [3] Adams, S., Che, D., Hailong, J., Han, R., Qin, G., Danquah, K. (2018b): Dietary supplementation of pulverised *Astragalus membranaceus* improved performance, immunity and diarrhoea incidence in weaned piglets. – *Indian Journal Animal Research*. DOI: 10.18805/ijar.B-936.
- [4] AOAC (2000): *Official Methods of Analysis*. – Association of Official Analytical Chemists, Arlington, VA.
- [5] Armstrong, T. A., Cook, D. R., Ward, M. M., Williams, C. M., Spears, J. W. (2004): Effect of dietary copper source (cupric citrate and cupric sulfate) and concentration on growth performance and fecal copper excretion in weanling pigs. – *Journal of Animal Science* 84: 1234-1240.
- [6] Baker, D. H., Ammerman, C. B. (1995): Copper Bioavailability. – In: Ammerman, C., Baker, D., Lewis, A. (eds.) *Bioavailability of Nutrients for Animals*. Academic Press, San Diego, pp. 127-156.
- [7] Banks, K. M., Thompson, K. L., Rush, J. K., Applegate, T. J. (2004): Effects of copper source on phosphorus retention in broiler chicks and laying hens. – *Poultry Science* 83: 990-996.
- [8] Barceloux, D. G., Barceloux, D. (1999): Copper. – *Journal of Toxicology: Clinical Toxicology* 37: 217-230.
- [9] Bremner, I., Beattie, J. H. (1995): Copper and zinc metabolism in health and disease: speciation and interactions. – *Proceedings of the Nutrition Society* 54: 489-499.
- [10] Che, D., Adams, S., Wei, C., Gui-Xin, Q., Atiba, E. M., Hailong, J., 2018. Effects of *Astragalus membranaceus* fiber on growth performance, nutrient digestibility, microbial composition, VFA production, gut pH, and immunity of weaned pigs. – *MicrobiologyOpen* e00712.
- [11] de Romaña, D. L., Olivares, M., Uauy, R., Araya, M. (2011): Risks and benefits of copper in light of new insights of copper homeostasis. – *Journal of Trace Elements in Medicine and Biology* 25: 3-13.
- [12] Gaetke, L. M., Chow-Johnson, H. S., Chow, C. K. (2014): Copper: toxicological relevance and mechanisms. – *Archives of Toxicology* 88: 1929-1938.
- [13] Guo, R., Henry, P. R., Holwerda, R. A., Cao, J., Littell, R. C., Miles, R. D., Ammerman, C. B. (2001): Chemical characteristics and relative bioavailability of supplemental organic copper sources for poultry. – *Journal of Animal Science* 79: 1132-1141.
- [14] Huang, Y., Zhou, T. X., Lee, J. H., Jang, H. D., Park, J. C., Kim, I. H. (2010): Effect of dietary copper sources (cupric sulfate and cupric methionate) and concentrations on performance and fecal characteristics in growing pigs. – *Asian-Australasian Journal of Animal Science* 23: 757.
- [15] Kornegay, E. T., Verstegen, M. W. A. (2001): Swine Nutrition and Pollution and Control. – In: Lewis, A. J., Southern, L. L. (eds.) *Swine Nutrition*. CRC Press, Boca Raton, FL, pp. 609-630.
- [16] Kornegay, E. T., Harper, A. F., Jones, R. D., Boyd, L. J. (1997): Environmental nutrition: nutrient management strategies to reduce nutrient excretion of swine. – *The Professional Animal Scientist* 13: 99-111.
- [17] Letelier, M. E., Faúndez, M., Jara-Sandoval, J., Molina-Berriós, A., Cortés-Troncoso, J., Aracena-Parks, P., Marín-Catalán, R. (2009): Mechanisms underlying the inhibition of

- the cytochrome P450 system by copper ions. – *Journal of Applied Toxicology* 29: 695-702.
- [18] Liao, P., Shu, X., Tang, M., Tan, B., Yin, Y. (2018): Effect of dietary copper source (inorganic vs. chelated) on immune response, mineral status, and fecal mineral excretion in nursery piglets. – *Food and Agricultural Immunology* 29: 548-563.
- [19] National Research Council. (1977): Committee on Medical and Biological Effects of Environmental Pollutants, Arsenic. – National Academy of Sciences, Washington, DC.
- [20] NRC (1998): Nutrient Requirements of Swine. – National Academy Press, Washington, DC.
- [21] Peña, M. M., Lee, J., Thiele, D. (1999): A delicate balance: homeostatic control of copper uptake and distribution. – *Journal of Nutrition* 129: 1251-1260.
- [22] Roberts, E. A., Schilsky, M. L. (2008): Diagnosis and treatment of Wilson disease: An update. – *Journal of Hepatology* 47: 2089-2111.
- [23] Sandström B. (2007): Micronutrient interactions: effects on absorption and bioavailability. – *British Journal of Nutrition* 85: 181-185.
- [24] Stern, B. R., Solioz, M., Krewski, D., Aggett, P., Aw, T. C., Baker, S., Crump, K., Dourson, M., Haber, L., Hertzberg, R., Keen, C., Meek, B., Rudenko, L., Schoeny, R., Slob, W., Starr, T. (2007): Copper and human health: biochemistry, genetics, and strategies for modeling dose-response relationships. – *Journal of Toxicology and Environmental Health* 10: 157-222.
- [25] Tomaszewska, E., Dobrowolski, P., Kwiecień, M., Burmańczuk, N., Badzian, B., Szymańczyk, S., Kurlak, P. (2014): Alterations of liver histomorphology in relation to copper supplementation in inorganic and organic form in growing rats. – *Bulletin of the Veterinary Institute in Pulawy* 58: 479.
- [26] Veum, T. L., Carlson, M. S., Wu, C. W., Bollinger, D. W., Ellersieck, M. R. (2004): Copper proteinate in weanling pig diets for enhancing growth performance and reducing fecal copper excretion compared with copper sulphate. – *Journal of Animal Science* 82: 1062-1070.
- [27] Wu, X. Z., Zhang, T. T., Guo, J. G., Liu, Z., Yang, F. H., Gao, X. H. (2015): Copper bioavailability, blood parameters, and nutrient balance in mink. – *Journal of Animal Science* 93: 176-184.
- [28] Yelin, G., Taff, M. L., Sadowski, G. E. (1987): Copper toxicity following massive ingestion of coins. – *The American Journal of Forensic Medicine and Pathology* 8: 78-85.
- [29] Yin, Y., Gu, J., Wang, X., Tuo, X., Zhang, K., Zhang, L., Guo, A., Zhang, X. (2018): Effects of copper on the composition and diversity of microbial communities in laboratory-scale swine manure composting. – *Canadian Journal of Microbiology* 64: 409-419.
- [30] Zhao, J., Shirley, R. B., Hampton, T. R., Richards, J. D., Harrell, R. J., Dibner, J. J., Vazquez-Anon, M. (2008): Benefits of an organic trace mineral on performance with dietary Cu antagonism in broilers. – *Poultry Science* 87: 52-52.
- [31] Zhao, J., Allee, G., Gerlemann, G., Ma, L., Gracia, M. I., Parker, D., Vazquez-Anon, M., Harrell, R. J. (2014): Effects of a chelated copper as growth promoter on performance and carcass traits in pigs. – *Asian-Australasian Journal of Animal Sciences* 27: 965-973.
- [32] Zheng, P., Pu, B., Yu, B., He, J., Yu, J., Mao, X., Luo, Y., Luo, J., Huang, Z., Luo, C., Wang, S. (2018): The differences between copper sulfate and tribasic copper chloride on growth performance, redox status, deposition in tissues of pigs, and excretion in feces. – *Asian-Australasian Journal of Animal Sciences* 31: 873.

TRANSCRIPTOME PROFILING OF *HALOXYLON AMMODENDRON* SEEDLING AT LOW TEMPERATURE CONDITION

PENG, M. W. – CHANG, Y. L. – WANG, M.* – CHU, G. M.*

*Agricultural College, Shihezi University
Road of North 4th, Shihezi City, Xinjiang 832003, China*

**Corresponding authors
e-mail: wangm1205@163.com, chgmjx@163.com*

(Received 20th Oct 2018; accepted 7th Jan 2019)

Abstract. *Haloxylon ammodendron*, a chenopodiaceae shrub species that mainly distributes in northwest of China, is an ecologically important foundation species and exhibits substantial low-temperature tolerance in the desert area. We employed RNA-Seq technologies to identify genes involved in low temperature, and identified 17995, 15511 and 1550 differentially expressed genes from the comparison of chilling treatment versus control, freezing treatment versus control and freezing treatment versus chilling treatment, respectively. By performing BLAST analysis of these unigenes against public databases, “single-organism metabolic process” and “membrane” were strongly affected at low temperature, and “Plant hormone signal transduction” pathway played an important role in resistance of the plants. In addition, we analyzed transcription factors, and found 499, 453, 55 of them were differentially expressed in these three comparison groups, respectively. A large number of transcription factors were identified at low temperature, and six transcription factors were selected for further expression analysis using qRT-PCR. This study can understand the molecular mechanisms of *Haloxylon ammodendron* at low temperature condition, and also can serve as a valuable resource for relevant research on low-temperature tolerance.

Keywords: *Haloxylon ammodendron*, chilling tolerance, freezing tolerance, transcription factor, illumina

Introduction

Temperature is one of the important environmental factors, and the normal physiological and metabolic activities of plants need suitable temperature. Low temperature restricts the distribution of plants by influencing their germination, growth and development, it can cause adverse effects and even can lead to death (Cai et al., 2011). However, some species have high tolerance to low temperature condition, especially some desert plants that grow in harsh environment. *Haloxylon ammodendron* is mainly distributes in the desert and semi desert areas of the Junggar basin in Xinjiang, China. As the dominant species in the desert area, it has not only ecological value but also economic value. However, the habitat of the Junggar basin is abominable that the maximum temperature is above 40 °C, and the minimum temperature is around -40 °C. It is especially interesting that some desert plants have low temperature germination feature during snow melting in early spring (Huang, 2002; Wang et al., 2006; Huang et al., 2003; Zhang, 2010; Han et al., 2011; Zhou, 2016; Peng, 2018), these desert plants include *H. ammodendron*, *Haloxylon Persicum*, *Anabasis elatior*, *Lepidium apetalum* and *Anabasis aphylla*. Huang research showed that when the early spring temperature rises and the snow melts, which will provide water supply for seed germination, and also provide a favorable environmental foundation for plant breeding (Huang, 2002). Similarly, *Suaeda physophora* can germinate at 10 °C and even at 0 °C from field

observation (Li and Zhang, 2007). In addition, Wang studied proteomics and metabolomics of *H. ammodendron* and *Anabasis aphylla* seedlings under low temperature (Wang, 2018). Therefore, we analyzed the transcription mechanism of *H. ammodendron* at low temperature condition, it will provide valuable resource for relevant research on low-temperature tolerance.

Transcriptional studies, with all the transcriptional information as the research object, analyze the regulatory network of plant bodies from the whole, it can also carry out quantitative and network analysis of individual genes or several genes (Cheng et al., 2015). A scholar had conducted the transcriptome sequencing of *Ammopiptanthus mongolicus*, and obtained a series of annotated genes and differentially expressed genes at low temperature condition, moreover, some metabolic pathways and transcription factors were also studied in order to understand the mechanism of frost resistance (Pang et al., 2013). Some studies presented the whole transcriptome of *Camellia sinensis* and *Sophora moorcroftiana*, and analyzed the change of genes expression during cold acclimation, these information provide a basis for plants to increase tolerance and the ability to adapt to the environment (Wang et al., 2013; Li et al., 2015). Chen et al. identified a large number of cold-responsive genes of *Populus euphratica*, and indicated that the transcription factor, ABA and calcium signal transduction may play an important role at low temperature condition (Chen et al., 2014). Our study presents the transcriptome profile of *H. ammodendron* seedling using Illumina sequencing technology, and yields insights into the molecular mechanisms of *H. ammodendron* seedling at low temperature condition. It could help to explore some genes related to low temperature and improve the understanding of low-temperature tolerance and plant-environment interactions.

Materials and methods

Location of H. ammodendron

H. ammodendron was located on the desert-oasis ecotone spanning an elevation range of 258–265 m in South Junggar Basin, NW China (45°22'43.4"N, 84°50'32.5"E), this is a transitional zone from the oasis to desert (Fig. 1). Geological substrates include aeolian deposits sandy soil and highly eroded diluvial soil. The annual mean temperature varies from 5 to 9 °C, and minimum winter temperature varies from -30 to -41 °C and maximum summer temperatures are 30–40 °C. Snow-melting appears at the end of winter, together with the rainfall that occurs in summer and annual precipitation amounts from 100 mm to 250 mm. Annual potential evaporation is greater than 2000 mm (Wang et al., 2014).

Experimental materials and low temperature treatment

The research material is the seedling of *H. ammodendron*. Experimental seeds were collected in October 2016 from Xinjiang, the southern margin of the Junggar Basin. These seeds were cultured in Petri dish with distilled water. When the length of the seedling is 3 cm, we treated the seedlings with different temperature. Based on the germination characteristics of *H. ammodendron* seeds under the freezing and thawing conditions in early spring (Wang et al., 2006; Huang et al., 2003), and the strong adaptability of the seedlings to environment temperature, we set three temperature treatments, control (20 °C), chilling treatment (3 °C) and freezing treatment (-3 °C),

respectively. Finally, all samples were preserved using liquid N and sent to the Beijing Compass Biotechnology Co., Ltd. to perform high throughput sequencing.

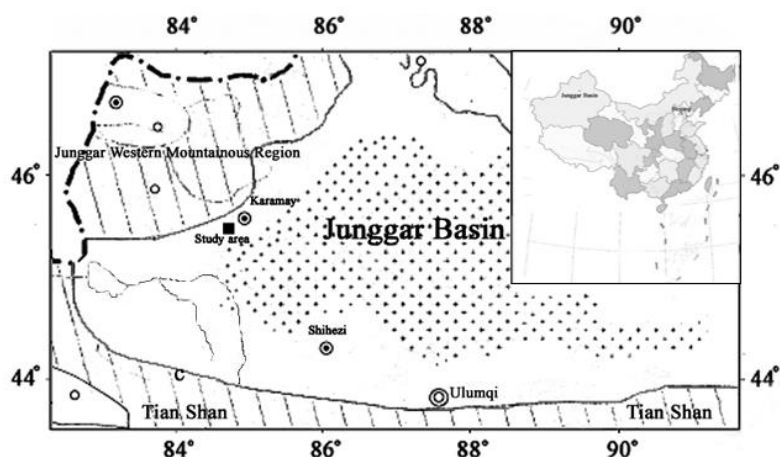


Figure 1. The location map of the Junggar Basin

RNA extraction and cDNA library construction

RNA extracted from control samples and treatment samples was further tested by Agilent 2100 Bioanalyzer (Agilent Technologies, CA, USA). After testing the RNA samples, the eukaryotic mRNA was enriched with magnetic beads containing Oligo (dT). Then join fragmentation buffer to break mRNA into short segments. Using mRNA as template, a base random primer was used to synthesise a chain of cDNA. Then buffer solution was added to synthesise second cDNA chains, after purification, elution, terminal repair, junction sequencing and PCR amplification, the library was finally completed. The sequencing library was sequenced by Illumina Hiseq 2500.

Sequencing, de novo assembly and functional annotation

High quality RNA samples were constructed from the sequencing library. Transcriptome sequencing of the library was carried out using the Illumina Hiseq 2500 high throughput sequencing platform (HiSeq/Miseq), and base calling is used to transform the original image data after sequencing into sequence data, that is the raw reads. Raw reads uses sliding window method to remove redundant sequence, sequence of poor quality, and sequence containing N. After screening, the high quality short sequence (clean reads) is obtained, and the follow-up analysis is carried out by this short sequence.

The high quality short sequence after removing the sequence of the joint, and the low quality at both ends and the low complex sequence was *de novo* assembled by using Trinity (Grabherr et al., 2011; Haas et al., 2009). BLAST software (Avagyan, 2009) is used to transform the transcript sequence into a protein sequence and then function annotation with multiple databases, and functional annotations include Nr, Pfam (Bateman et al., 2000), Swiss-Prot (Consortium, 2015), KOG (Tatusov et al., 2003), Nt, GO (Harris et al., 2004) and KEGG databases. In addition, the software used in NR, NT, Swiss-Prot and KOG database is NCBI blast 2.3.0+. Pfam database is HMMER

package, GO function annotation software is Blast2GO v2.5 (Conesa et al., 2005), and KEGG annotation software is KOBAS 2.1.1 (Xie et al., 2011).

Quantitative real-time PCR analysis

In order to validate the reliability of RNA-Seq and DGE experiment, six transcripts were selected for quantitative qRT-PCR test. Total RNAs were quantified by the NanoDrop ND-2000 (Thermo Scientific) and the RNAs integrity was assessed using agarose gel electrophoresis. While QC of RNA was qualified, in turn to treat RNA of DNaseI, then reverse transcription, cDNA dilution, last PCR by Applied Biosystems 7900HT PCR. After completion of the reaction the data analysis based on the obtained sample Ct value. Relative gene expression levels were calculated using the $2^{-\Delta\Delta C_t}$ (Livaka and Schmittgen, 2001).

Results

Transcriptome sequencing and assembly

Transcriptome sequences are valuable resources. A cDNA library from a seedling of *H. ammodendron* was constructed and sequenced using the Illumina HiSeq2500 platform. Total clean bases generated from each sample exceeded 12G. Total of 40535462 raw reads were generated for the control sample (CK). After removing low-quality reads and trimming off the adapter sequences, 40211335 clean reads were obtained. The Q20 bases percentage and the Q30 bases percentage were 95.40% and 89.26%, respectively. Similar to the control, we obtained 41432865 raw reads and 40994453 clean reads from chilling sample at 3 °C (CA), and obtained 43214542 raw reads and 42973332 clean reads from freezing sample at -3 °C (CB). The Q20 percentage of two samples (CA and CB) were exceeded 94% and Q30 were exceeded 88% (Table 1).

Using Trinity, all the total reads were mixed for further *de novo* assembly, and these produced 437604 transcripts with an N50 of 1268 bp and an average length of 764.78 bp. In addition, all the high-quality reads were assembled into 257695 unigenes with an N50 of 713 bp and an average length of 546.93 bp (Table 2).

Table 1. Sequencing statistics of the *H. ammodendron*

Sample	Raw bases (G)	Clean bases (G)	Raw reads	Clean reads	Q20 (%)	Q30 (%)	GC content (%)
CK	12.16	12.06	40535462	40211335	95.40	89.26	41.68
CA	12.43	12.30	41432865	40994453	95.26	89.02	41.10
CB	12.97	12.89	43214542	42973332	94.99	88.54	41.33

Table 2. Summary statistics of assembly of *H. ammodendron* transcriptome

	Total number	Total assembled bases	N50 (bp)	Average length (bp)
Transcripts	437604	334670343	1268	764.78
Unigenes	257695	140940214	713	546.93

Blast analysis

To predict and analyze the function of the assembled transcripts, non-redundant sequences were submitted to a BLASTx search against the following databases: Nr (NCBI non-redundant protein sequences), Pfam (Protein family), Swiss-Prot (a manually annotated and reviewed protein sequence database), KOG (eukaryotic orthologous groups), Nt (NCBI non-redundant nucleotide sequences), GO (Gene Ontology) and KEGG (Kyoto Encyclopedia of Genes and Genomes). The blast results show that the number of unigenes annotated in the Nr, Pfam, Swiss-Prot, KOG, Nt, GO, KEGG database was 495669 (41.41%), 23 (0.02%), 30748 (25.69%), 29867 (24.95%), 27693 (23.13%), 21179 (17.69%), 45557 (38.06%), respectively (Table 3).

Table 3. Summary statistics of annotation of all unigenes

Database	Nr	PFAM	Swiss-prot	KOG	Nt	GO	KEGG	ALL
Annotated number	49566	23	30748	29867	27693	21179	45557	119682
Annotated percentage (%)	41.41	0.02	25.69	24.95	23.13	17.69	38.06	100

By the Venn diagram, the number of unigenes annotated in Nr and GO databases is large, 10455 and 21179, respectively. The number of unigenes annotated only in KOG and Swiss-prot databases is very few, 708 and 25, respectively. There are 2450 unigenes annotated to the Nt database. A total of 119682 unigenes are annotated, and the number of unigenes annotated to 5 databases was 0 (Fig. 2).

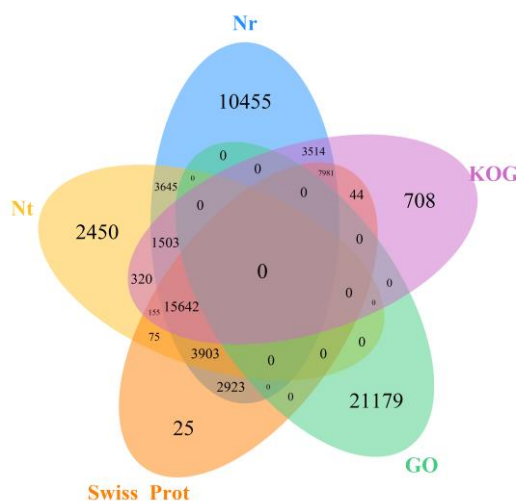


Figure 2. Venn diagram of unigenes were annotated in five databases

Functional annotation of *H. ammodendron* transcriptome sequences

A BLASTx search of protein sequences from the National Center for Biotechnology Information nr database using the unigenes and E-value distribution was performed (Fig. 3A and B), and the resulting E-value distribution revealed that 49.65% of the unigene sequences had top matches. The result shows 80.44% of the unigene sequences matching with specific protein was more than 60% in similarity distribution. To study

the sequence conservation of *H. ammodendron* in other plant species, we analyzed the species distribution of the All-Unigene datasets. The results show that 51.26% of the distinct sequences have top matches with the sequences from *Beta vulgaris subsp. Vulgaris* (51.25%), followed by *Spinacia oleracea* (31.29%), *Vitis vinifera* (1.39%), *Daucus carota subsp. sativus* (0.65%) and other (15.42%) (Fig. 3C).

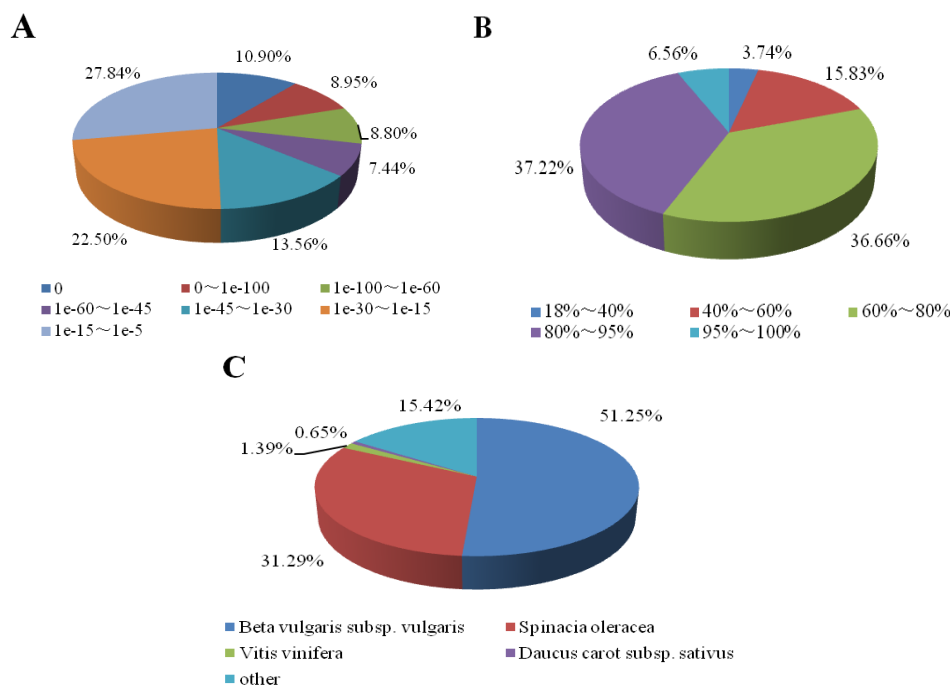


Figure 3. Species distribution of BLASTx results. Unigenes were used in a BLASTx search of the nr database (A) E-value distribution; (B) similarity distribution; (C) species distribution

Gene Ontology (GO) assignments were used to classify the functions of the predicted *H. ammodendron* genes, 21179 (17.69%) unigenes were classified into three major function categories (Biological Process, Cellular Component and Molecular Function). In terms of Biological Processes 14019 unigenes were annotated, the top three GO terms were “single-organism metabolic process” (1531), “cellular protein modification process” (982) and “phosphate-containing compound metabolic process” (880). In terms of cellular components, there are 12639 unigenes were annotated, the top three GO terms were “intrinsic component of membrane” (6109), “intracellular membrane-bounded organelle” (2060) and “membrane” (1332). In terms of molecular function, there are 16176 unigenes were annotated, the top three GO terms were “purine ribonucleoside binding” (3100), “transition metal ion binding” (1507) and “nucleic acid binding” (1399) (Fig. 4).

To assess the integrality of our transcriptome library and effectiveness of the annotation process, we aligned the all-unigenes to the KOG database and 29867 were identified. By classifying the possible functions of these unigenes, they were grouped into 25 functional categories. The clusters related to “general function prediction only” (6584) were the largest group, followed by “signal transduction mechanisms” (3948), “posttranslational modification, protein turnover, chaperones” (3541), and “carbohydrate transport and metabolism” (2052) (Fig. 5).

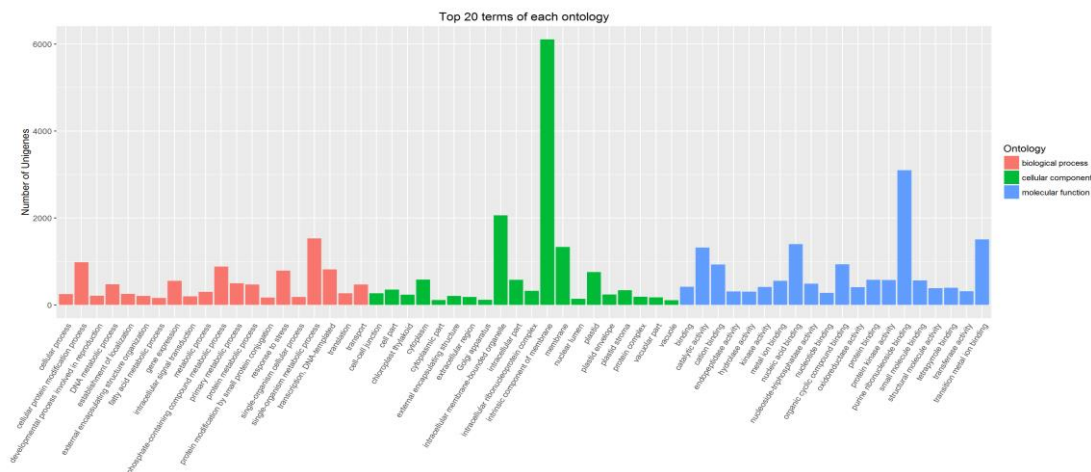


Figure 4. Gene ontology (GO) functional classification of the unigenes

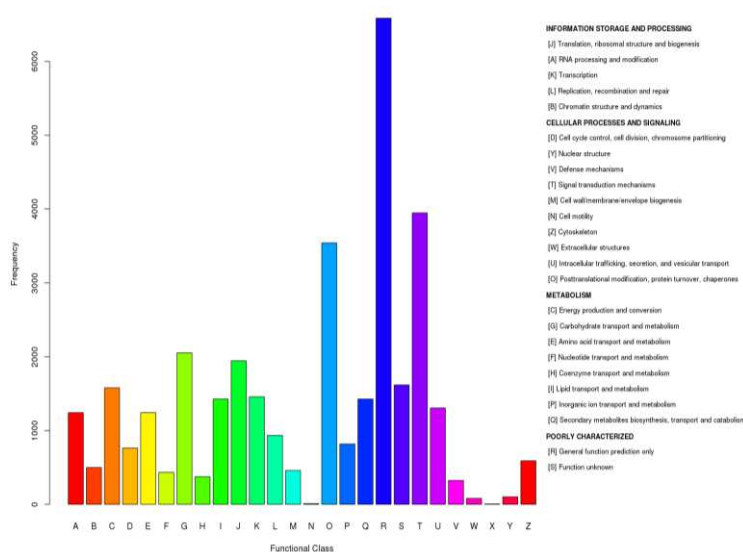


Figure 5. Eukaryotic ortholog groups (KOG) functional classification of the unigenes

To identify the biological pathways in the annotated sequences using the Kyoto Encyclopedia of Genes and Genomes (KEGG), the assembled unigenes were assigned to five specific pathways, including Cellular Processes (A), Environmental Information Processing (B), Genetic Information Processing (C), Metabolism (D), and Organism Systems (E). Metabolism was the category with the greatest number of genes (9561), with carbohydrate metabolism and overview as the two pathways represented by the most genes. 1718 were related to translation, 1507 were related to signal transduction, 1357 were related to folding, sorting and degradation (Fig. 6).

Genes differentially expressed among the samples

To examine the transcript alterations occurring in the germination exposed to low temperature, we used the RPKM method to calculate the expression levels of the unigenes and to identify differentially expressed genes between the types of samples.

The expression of a high number of unigenes was affected at low temperature condition. Only the genes whose expression was identified as being significantly changed with the $FDR < 0.05$ were retained. To analyze the similarities and differences among the low-temperature responsive transcriptome, a hierarchical clustering was prepared to replicates of the control (CK), chilling treatment (CA) and freezing treatment (CB). When the differentially expressed genes were compared under the three conditions, we discovered 17995, 15511 and 1550 genes in the comparisons of CA versus CK, CB versus CK and CB versus CA, respectively. Among these, the genes with significant difference ($|\log_{2}FC| > 1$) are displayed in *Figure 7*.

Functional classification of the differentially expressed genes by gene ontology analysis

To identify the genes that are differentially expressed at low temperature treatment, a functional categorization was carried out by GO analysis. By comparing CA and CK, 17995 differentially expressed genes, including 9286 down-regulated genes and 8709 up-regulated genes, revealed by differentially expressed genes analysis were functionally assigned to the relevant terms in three categories (Biological Process, Cellular Component, and Molecular Function) of the GO database. Among these groups, the terms “single-organism metabolic process”, “membrane”, and “metal ion binding” were dominant in each of the three main categories, respectively (*Fig. A1*). By comparing CB and CK, 15511 differentially expressed genes, including 7915 down-regulated genes and 7596 up-regulated genes, were functionally assigned to the relevant terms. The terms “single-organism metabolic process”, “membrane”, and “catalytic activity” were dominant in each of the three main categories, respectively (*Fig. A2*). By comparing CB and CA, 1550 differentially expressed genes, including 723 down-regulated genes and 827 up-regulated genes, the terms “cellular metabolic process”, “membrane”, and “cation binding” were dominant in each of the three main categories, respectively (*Fig. A3*). “membrane” and “single-organism metabolic process” were mainly terms in the low temperature treatment.

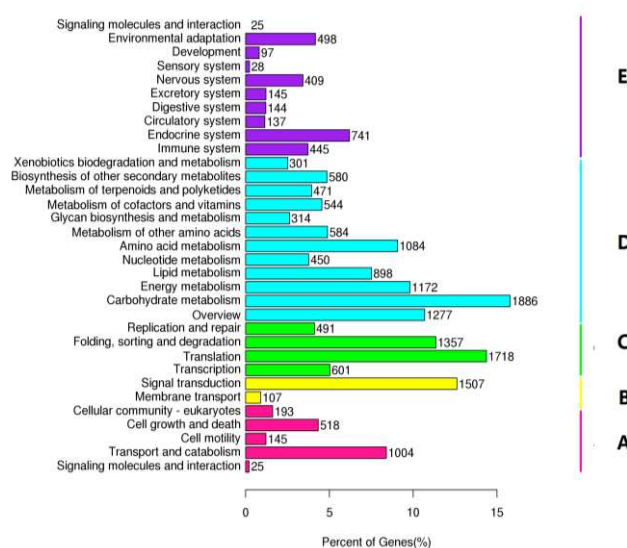


Figure 6. Kyoto Encyclopedia of Genes and Genomes (KEGG) functional classification of the unigenes (A) cellular processes; (B) environmental information processing; (C) genetic information processing; (D) metabolism; (E) organismal systems

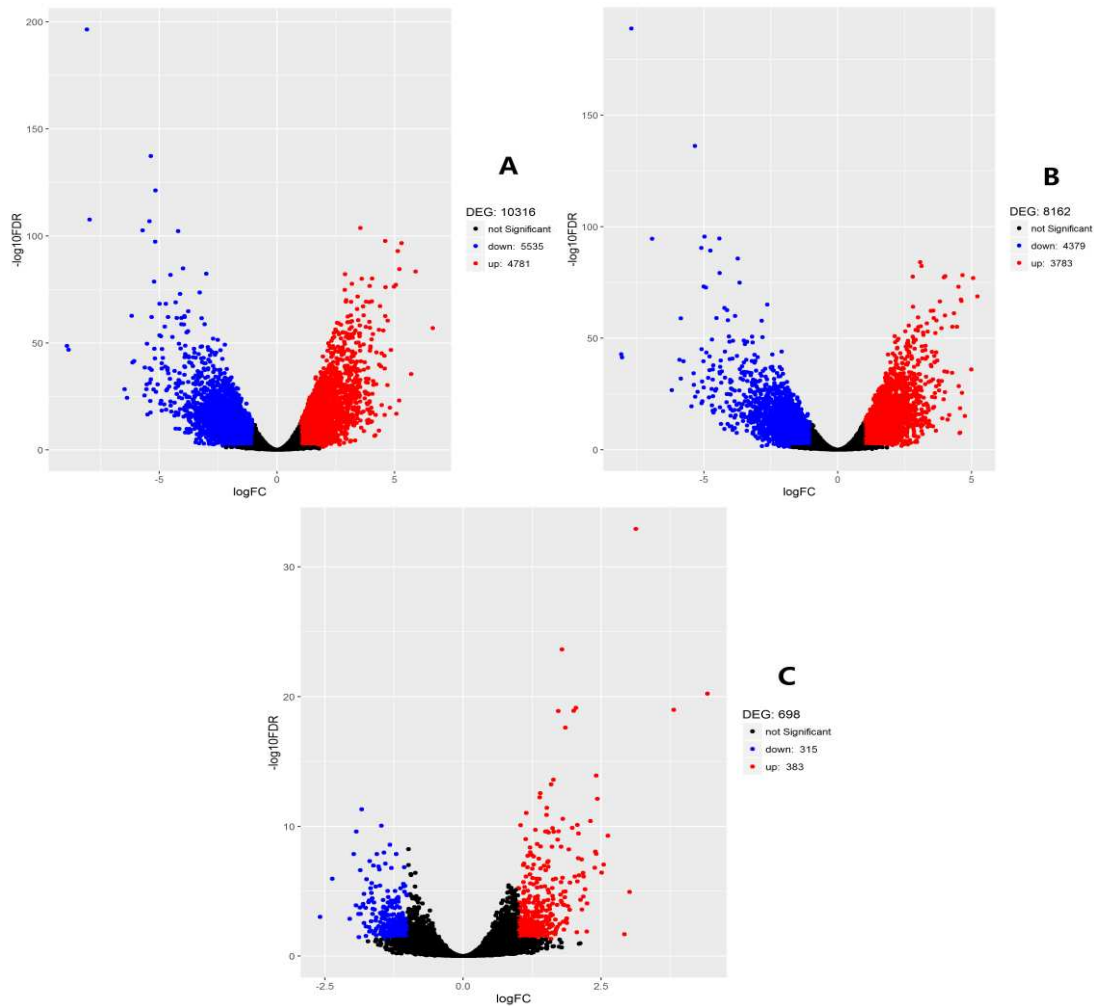


Figure 7. Volcano plot of differentially expressed genes at low temperature condition (A) CA versus CK; (B) CB versus CK; (C) CB versus CA

KEGG pathway analysis of the differentially expressed genes

To determine whether the low temperature responsive genes engaged in specific pathways, the differentially expressed genes were used as objects to search against the KEGG pathway database. The top 10 pathways of the number of differentially expressed genes are counted. By comparing CA with CK, more differentially expressed genes were enriched in this 10 pathway, including 215 differentially expressed genes were related to “Carbon metabolism”, 205 differentially expressed genes were related to “Ribosome”, and 170 differentially expressed genes were related to “Biosynthesis of amino acids”. “Plant hormone signal transduction (131)” and “Amino sugar and nucleotide sugar metabolism (123)” are obviously enriched, and the p-value is $1.51\text{E}-07$ and 0.000946 , respectively (Table 4). By comparing CB with CK, similar to the results of comparing CA with CK, 201 differentially expressed genes were related to “Carbon metabolism”, 166 differentially expressed genes were related to “Ribosome”, and 156 differentially expressed genes were related to “Biosynthesis of amino acids”. “Plant hormone signal transduction (124)” and “Amino sugar and nucleotide sugar metabolism (115)” are obviously enriched, and the p-value is $4.40\text{E}-08$ and 0.000561 , respectively

(Table 5). By comparing CB with CA, 20 differentially expressed genes were related to “Carbon metabolism”, 18 differentially expressed genes were related to “Circadian rhythm-plant”, and 14 differentially expressed genes were related to “Carbon fixation in photosynthetic organisms”. “Circadian rhythm-plant (18)” and “Inositol phosphate metabolism (10)” are obviously enriched, and the p-value is 3.56E-12 and 0.001285, respectively (Table 6).

Table 4. KEGG enrichment analysis of differentially expressed genes between CA and CK

Pathway ID	Pathway	KEGG pathway	Enriched genes	p-value
ko01200	Metabolism	Carbon metabolism	215	0.570662
ko03010	Genetic information Processing	Ribosome	205	0.918432
ko01230	Metabolism	Biosynthesis of amino acids	170	0.965586
ko04141	Genetic information processing	Protein processing in endoplasmic reticulum	149	0.383433
ko04075	Environmental information processing	Plant hormone signal transduction	131	1.51E-07
ko00500	Metabolism	Starch and sucrose metabolism	124	0.831474
ko00520	Metabolism	Amino sugar and nucleotide sugar metabolism	123	0.000946
ko03040	Genetic information processing	Spliceosome	119	0.304011
ko04144	Cellular Processes	Endocytosis	108	0.038656
ko00940	Metabolism	Phenylpropanoid biosynthesis	108	0.254553

Table 5. KEGG enrichment analysis of differentially expressed genes between CB and CK

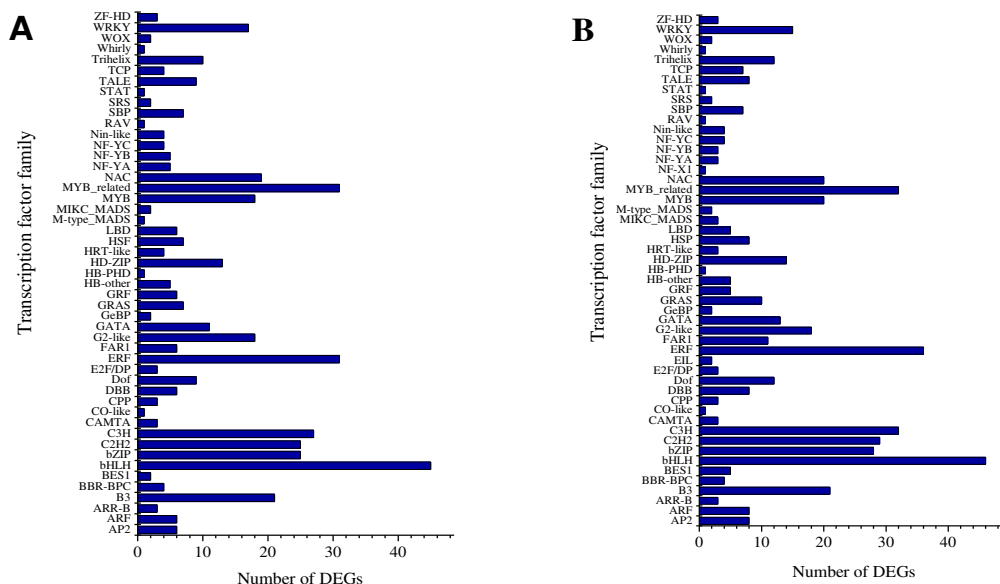
Pathway ID	Pathway	KEGG pathway	Enriched genes	p-value
ko01200	Metabolism	Carbon metabolism	201	0.420369
ko03010	Genetic information processing	Ribosome	166	0.997957
ko01230	Metabolism	Biosynthesis of amino acids	156	0.950114
ko04141	Genetic information processing	Protein processing in endoplasmic reticulum	139	0.285677
ko04075	Environmental information processing	Plant hormone signal transduction	124	4.40E-08
ko00520	Metabolism	Amino sugar and nucleotide sugar metabolism	115	0.000561
ko00500	Metabolism	Starch and sucrose metabolism	112	0.842905
ko00940	Metabolism	Phenylpropanoid biosynthesis	110	0.035962
ko03040	Genetic information processing	Spliceosome	100	0.633846
ko00230	Metabolism	Purine metabolism	95	0.229666

Table 6. KEGG enrichment analysis of differentially expressed genes between CB and CA

Pathway ID	Pathway	KEGG pathway	Enriched genes	p-value
ko01200	Metabolism	Carbon metabolism	20	0.071514
ko04712	Organismal systems	Circadian rhythm - plant	18	3.56E-12
ko00710	Metabolism	Carbon fixation in photosynthetic organisms	14	0.002501
ko04075	Environmental information processing	Plant hormone signal transduction	13	0.002586
ko04141	Genetic information processing	Protein processing in endoplasmic reticulum	13	0.146036
ko00010	Metabolism	Glycolysis/Gluconeogenesis	11	0.105862
ko00562	Metabolism	Inositol phosphate metabolism	10	0.001285
ko00564	Metabolism	Glycerophospholipid metabolism	10	0.009997
ko04626	Organismal systems	Plant-pathogen interaction	9	0.059561
ko04120	Genetic information processing	Ubiquitin mediated proteolysis	9	0.082081

Transcription factors

Transcription factors (TFs) are important upstream regulatory proteins and play significant roles in plant development and tolerance (Chinnusamy et al., 2010). In this study, a total of 1130 unigenes were identified to be involved in transcription. By comparing CA and CK, 499 differentially expressed genes (219 up-regulated and 280 down-regulated) were identified. The largest gene family was the bHLH family, followed by ERF, C3H, MYB-related, C2H2, and bZIP family (Fig. 8A). By comparing CB and CK, 453 differentially expressed genes (197 up-regulated and 256 down-regulated) were identified. The largest gene family was the bHLH family, followed by ERF, C3H, MYB-related, C2H2, and bZIP family (Fig. 8B). By comparing CB and CA, 55 differentially expressed genes (28 up-regulated and 27 down-regulated) were identified. The largest gene family was the WRKY family, followed by MYB-related, bHLH, bZIP, and ERF family (Fig. 8C).



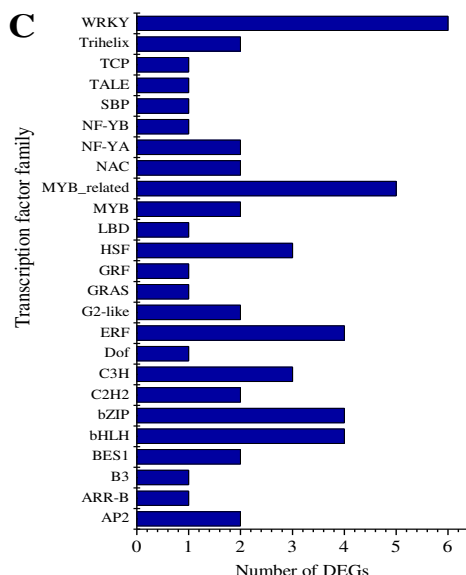


Figure 8. Distribution of differentially expressed genes in transcription factor families (A) CA versus CK; (B) CB versus CK; (C) CB versus CA

Genes expression analysis by qRT-PCR

To confirm the reliability of the RNA-Seq data, real-time quantitative reverse transcription PCR was used to assess the expression level of 6 selected genes which were significantly affected at low temperature. These 6 selected differentially expressed genes are all transcription factors, including bZIP, NAC, HSF, C2H2, LBD and NF-YA, most of them are known to be related to low temperature. Results compared with the sequencing results, although the variation of gene was different, all the unigenes showed consistent expression patterns that were consistent with the RNA-Seq data, indicating that our experimental results were valid (Fig. 9).

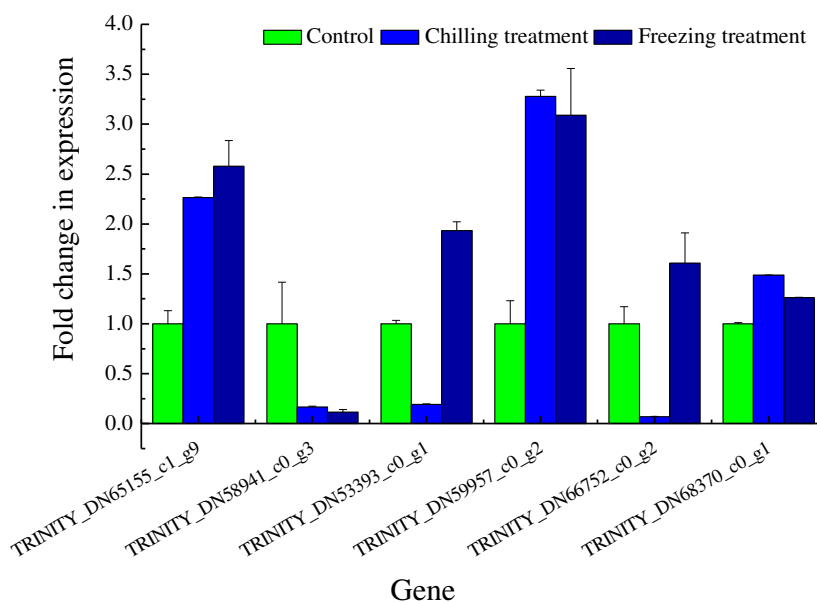


Figure 9. Quantitative real-time PCR analysis of six differentially expressed genes

Discussion

H. ammodendron, as an important component of old Mediterranean flora, is widely spread in the Junggar basin, northeast of the Tarim basin and other desert areas on a range of soil and is a representative psammophytic species (Wang et al., 2014). It is a precious biological resource in the arid desert region. In Junggar basin, most of the desert species can utilize meltwater to germinate in early spring, it is available for better germination and for seedling survival before the desiccation period (Huang et al., 2009). Wang research showed that *H. ammodendron* can germinate when the temperature close to 0 °C (Wang et al., 2006), and Zhang showed that the germination percentage of *H. ammodendron* and *Haloxylon Persicum* were over 80% under 2 °C (Zhang, 2010). In addition, Sun suggested desert seed start to germinate only two days when snow melted at the average daily temperature (day/night) of 3.5 °C (Sun, 2015). Therefore, it is of great significance to study the molecular mechanism of *H. ammodendron* germination at low temperature condition. The cold resistance of plants is a quantitative trait controlled by multiple genes, and a large number of genes are involved in the mechanism of low temperature. *H. ammodendron* has formed a complex mechanism to resist low temperature. When receiving cold signals, some genes are differentially expressed to enhance cold resistance, and some plants will produce a series of reactions, such as morphological level, physiological and biochemical level and molecular level. A transcriptional analysis of *Arabidopsis thaliana* (Norma et al., 2008), wheat (Gulick et al., 2005) and sunflower (Airaki et al., 2012) at low temperature showed that a large number of genes related to photosynthesis were significantly inhibited at low temperature.

By comparing the effects of low temperature on seed germination, we identified 17995, 15511 and 1550 differentially expressed genes in the comparisons of chilling treatment versus control, freezing treatment versus control and freezing treatment versus chilling treatment, respectively. Notably, more genes were differentially expressed under chilling treatment versus control, freezing treatment versus control, indicating that the alteration in gene expression at the cold condition, they will generate a large number of genes to adapt. The number of differentially expressed genes is relatively less under freezing treatment versus chilling treatment, suggesting that chilling treatment and freezing treatment are similar in response to low temperature, and plants are sensitive to low temperature. Moreover, a total of 607 genes overlapped with those of chilling treatment versus control, freezing treatment versus control and freezing treatment versus chilling treatment, indicating a linkage among three comparisons and a progressive biological process. These differentially expressed genes were mapped to each term of the GO database, “single-organism metabolic process” and “membrane” was strongly affected at low temperature condition, and the plasma membrane is believed to be the primary site in response to low temperature signal. Through the analysis of the KEGG pathway, the top 10 pathways were basically same in chilling treatment versus control and freezing treatment versus control, including “Metabolism”, “Environmental Information Processing” and “Genetic Information Processing” pathway. “Plant hormone signal transduction” was significantly enriched in chilling treatment versus control, freezing treatment versus control and freezing treatment versus chilling treatment. A lot of research has proven that plant hormones play an important role in resistance of plants (Nakashima et al., 2014). In this study, 131, 124, 13 differentially expressed genes were found to participate in plant hormone signal transduction.

Membrane systems, which are known to be the primary site of freezing injury in plants, suffer multiple forms of damage caused by freeze-induced cellular dehydration (Kawamura et al., 2003). Membranes must be kept fluid in order to sustain the functional activity of membrane proteins and membranes themselves at low temperature condition (Zhou et al., 2010). An important performance of many plants is to increase unsaturated fatty acids, such as increasing the proportion of oleic acid, linoleic acid and linolenic acid in total fatty acids (Chen et al., 2005). In this study, we identified 3 lipid transfer proteins (LTP) genes and 4 fatty acid desaturase (FAD) genes. Among these, 2 LTP genes and 2 FAD genes were up-regulated, 1 LTP gene and 2 FAD genes were down-regulated at low temperature condition. A series of changes in gene expression will occur in plants, and a large number of genes are induced at low temperature. Some proteins encoded by these genes are so-called anti-freezing proteins (AFPs), including late-embryogenesis-abundant proteins (LEA), the LEA protein functions as an antioxidant, as well as a membrane and protein stabilizer (Tunnacliffe and Wise, 2007). AFPs also include thaumatin-like proteins (TLPs), polygalacturonase-inhibitor proteins (PGIPs), heat-shock proteins (HSPs), etc. Proline is one of the most important organic osmolytes, and participates in the responses to various environmental (Ashraf and Foolad, 2007). The increase of proline is considered as one of the mechanisms of cold resistance, delta-1-pyrroline-5-carboxylate synthase (P5CS) plays a key role in proline biosynthesis, it is involved in osmoregulation and abiotic tolerance in plants (Xia et al., 2014). Szekely shows that P5CS participates in the cold-responsive and shows high expression (Szekely et al., 2008). In our study, we found 1 TLP, 5 PGIPs, 2 LEAs were up-regulated at low temperature, and these genes play an important role to tolerate low temperatures. Contrary to previous research, all genes encoding P5CS were to be significantly down-regulated at low temperature, and this may be the difference displayed by different species.

As an important second messenger, Ca^{2+} was reported play a role in regulating growth processes and cold signaling (Reddy et al., 2011), and it was sensed by proteins of three main classes at low temperature: Ca^{2+} dependent protein kinases (CDPKs), cell adhesion molecule (CaMs) and calcineurin B-like protein (CBL) (Miura and Furumoto, 2013; Boudsocq and Sheen, 2013). A further important pathway is the mitogen-activated protein kinases (MAPKs) cascade (Chinnusamy et al., 2010). Wang et al. showed that CDPKs, calmodulin, CBL, MAPKs were involved in signal transduction upon low temperature in *Camellia sinensis* (Wang et al., 2013). In this study, we identified 4 CDPK genes, 6 MAPK genes, 6 CBL genes and 3 calmodulin genes were up-regulated at low temperature. Yang et al. found that the calcium/calmodulin-regulated receptor kinase (CRLK1) was crucial for cold tolerance in plants (Yang et al., 2010). 1 CRLK1 gene was identified to be up-regulated in this study, meanwhile, we found that 3 CRLK2 were obviously up-regulated at low temperature. Therefore, CRLK2 may be important to tolerate low temperature.

Transcriptional regulation is a key step for plants to adapt the changes of environment, and transcription factors play an important role in the plant. In this study, it was found that many transcription factors have changed at low temperature. Among these TFs, most of the family has been reported to be linked to cold resistance in plants (Rushton et al., 2010; Zhang et al., 2012; Hu et al., 2008; Fode et al., 2008). A large number of transcription factors showed abundant diversity, and some genes in same transcription factor family had both up-regulated and down-regulated genes. The change of expression level of specific transcription factors can greatly affect the ability of

plants to adapt to adversity. The results of this study indicate that low temperature can induce or inhibit the expression of many transcription factors. Among them, bHLH, ERF, C3H, MYB-related, C2H2, and bZIP were the most numerous and significant transcription factor families in chilling treatment versus control and freezing treatment versus control. By comparing freezing treatment and chilling treatment, the lower temperature increased the number of other transcription factor families, which could regulate lower temperature condition. Pang et al. showed that ERF and WRKY transcription factors were up-regulated in seedlings treated at 4 °C for 14 days (Pang et al., 2013). High salt and low temperature could induce the expression of 3 WRKYs genes in grape, indicating that WRKYs was involved in the process of grape resistance to low temperature (Hou et al., 2013). In this study, the ERF (Fold changes from 0.44 to 4.06) and WRKYs (Fold changes from 0.75 to 1.17) of *H. ammodendron* were identified to be up-regulated at low temperatures, these results indicated that they are important regulators of *H. ammodendron* in response to low temperature. Six transcription factors were selected for further expression analysis, and they have been identified by qRT-PCR showing the same trend as our Illumina sequencing.

Conclusions

Haloxylon ammodendron, as one of the dominant species in the desert area of China, has strong low temperature tolerance. In this study, we present a considerable portion of the transcriptome of *H. ammodendron* after low temperature using RNA-seq and differentially expressed gene analyses. Based on the assembled *de novo* transcriptome, a large number of differentially expressed genes were identified, and include many candidate genes involved in low temperature. By performing BLAST analysis of the all unigenes against public databases (Nr, KOG, GO and KEGG), we obtained functional annotations and classifications. Moreover, a large number of transcription factors were identified under low temperature. This represents a fully characterized transcriptome, and provides a valuable resource for genetic and genomic studies in *Haloxylon ammodendron*. It could also help to explore the cold-related genes in improving the understanding of low-temperature tolerance and plant-environment interactions.

Acknowledgements. The research was supported by the Program of the National Natural Science Foundation of China (31570595, 31660194), General Financial Grant of the China Postdoctoral Science Foundation (2017M613253) and Scientific Research Foundation of Shihezi University for Advanced Talents (RCZX201518, RCZX201521).

REFERENCES

- [1] Airaki, M., Leterrier, M., Mateos, R. M., Valderrama, R., Chaki, M., Barroso, J. B. (2012): Metabolism of reactive oxygen species and reactive nitrogen species in pepper (*Capsicum annuum* L.) plants under low temperature stress. – *Plant Cell and Environment* 35(2): 281-295.
- [2] Ashraf, M., Foolad, M. R. (2007): Roles of glycine betaine and proline in improving plant abiotic stress resistance. – *Environmental and Experimental Botany* 59(2): 206-216.
- [3] Avagyan, V. (2009): BLAST+: architecture and applications. – *BMC Bioinformatics* 10(1): 1-9.

- [4] Bateman, A., Birney, E., Cerruti, L., Durbin, R., Eddy, S. R. (2000): The pfam protein families database. – *Nucleic Acids Research* 28(1): 263-266(4).
- [5] Boudsocq, M., Sheen, J. (2013): CDPKs in immune and stress signaling. – *Trends in Plant Science* 18(1): 30-40.
- [6] Cai, H., Tian, S., Liu, C., Dong, H. (2011): Identification of a MYB3R gene involved in drought, salt and cold stress in wheat (*Triticum aestivum* L.). – *Gene* 485(2): 146-152.
- [7] Chen, J., Tian, Q., Pang, T., Jiang, L., Wu, R., Xia, X. (2014): Deep-sequencing transcriptome analysis of low temperature perception in a desert tree, *Populus euphratica*. – *Bmc Genomics* 15(1): 326.
- [8] Chen, N., Guo, S. J., Meng, Q. W. (2005): Relationship between plant chilling tolerance and membrane lipids composition and its advances in researches on molecular biology. – *Biotechnology Bulletin* 21(2): 6-29.
- [9] Cheng, Z. Y., Li, M., Shi, Y., He, P., He, L. L., Li, F. S. (2015): Research of drought-response mechanism in sugarcane by high throughput sequencing-based digital gene expression profiling. – *Molecular Plant Breeding* 13(9): 2018-2028.
- [10] Chinnusamy, V., Zhu, J. K., Sunkar, R. (2010): Gene regulation during cold stress acclimation in plants. – *Plant Stress Tolerance* 639: 39-55.
- [11] Conesa, A., Götz, S., García-Gómez, J. M. (2005): Blast2GO: a universal tool for annotation, visualization and analysis in functional genomics research. – *Bioinformatics* 21(18): 3674-6.
- [12] Consortium, U. P. (2015): UniProt: a hub for protein information. – *Nucleic Acids Research* 43(Database issue): D204-12.
- [13] Fode, B., Siemsen, T., Thurow, C., Weigel, R., Gatz, C. (2008): The Arabidopsis GRAS protein SCL14 interacts with class II TGA transcription factors and is essential for the activation of stress-inducible promoters. – *Plant Cell* 20: 3122-3135.
- [14] Grabherr, M. G., Haas, B. J., Yassour, M., Levin, J. Z., Thompson, D. A., Amit, I. (2011): Full-length transcriptome assembly from rna-seq data without a reference genome. – *Nature Biotechnology* 29(7): 644.
- [15] Gulick, P. J., Drouin, S., Yu, Z., Danyluk, J., Poisson, G., Monroy, A. F. (2005): Transcriptome comparison of winter and spring wheat responding to low temperature. – *Genome* 48(48): 913-923.
- [16] Haas, B. J., Papanicolaou, A., Yassour, M. (2013): De novo transcript sequence reconstruction from RNA-seq using the Trinity platform for reference generation and analysis. – *Nature Protocols* 8(8): 1494-1512.
- [17] Han, J. X., Wei, Y., Yan, C., An, S. Z. (2011): The vivipary characteristic of *Anabasis elatior* and its ecological adaptation. – *Acta Ecologica Sinica* 31(10): 2662-2668.
- [18] Harris, M. A., Clark, J., Ireland, A. (2004): The Gene Ontology (GO) database and informatics resource. – *Nucleic Acids Research* 32(suppl_1): D258-61.
- [19] Hou, L., Wang, W. J., Guo, X. P., Fu, P. N., Liu, X. (2013): Gene cloning and expression analysis of three WRKYs in *Vitis vinifera* L. – *Plant Physiology Journal* 49(3): 289-296.
- [20] Hu, H., You, J., Fang, Y., Zhu, X., Qi, Z., Xiong, L. (2008): Characterization of transcription factor gene SNAC2 conferring cold and salt tolerance in rice. – *Plant Molecular Biology* 67(1-2): 169-181.
- [21] Huang, P. Y. (2002): Non irrigated vegetation and its restoration in Arid Areas. – Beijing: Science Press 123-134.
- [22] Huang, P. Y., Xiang, B., Qi-Jian, L. I., Ze-Hai, X. U. (2009): Relationship between *Haloxylon ammodendron* seedling dynamics and habitat before summer. – *Journal of Desert Research* 29(1): 87-94.
- [23] Huang, Z., Zhang, X., Zheng, G., Gutterman, Y. (2003): Influence of light, temperature, salinity and storage on seed germination of *Haloxylon ammodendron*. – *Journal of Arid Environments* 55(3): 453-464.

- [24] Kawamura, Y., Uemura, M. (2003): Mass spectrometric approach for identifying putative plasma membrane proteins of *Arabidopsis* leaves associated with cold acclimation. – *Plant Journal* 36(2): 141-154.
- [25] Li, H., Yao, W., Fu, Y., Li, S., Guo, Q. (2015): De novo assembly and discovery of genes that are involved in drought tolerance in tibetan *Sophora moorcroftiana*. – *Plos One* 10(1): e111054.
- [26] Li, L., Zhang, X. M. (2007): Germination strategies of two halophytes in salt desert of northwestern china. – *Science in China* 50(1): 115-121.
- [27] Livaka, K. J., Schmittgen, T. D. (2001): Analysis of relative gene expression data using real-time quantitative PCR and the $2^{-\Delta\Delta CT}$ method. – *Methods* 25(4): 402-408.
- [28] Miura, K., Furumoto, T. (2013): Cold signaling and cold response in plants. – *International Journal of Molecular Sciences* 14(3): 5312-5337.
- [29] Nakashima, K., Yamaguchi-Shinozaki, K., Shinozaki, K. (2014): The transcriptional regulatory network in the drought response and its crosstalk in abiotic stress responses including drought, cold, and heat. – *Frontiers in Plant Science* 5(170): 170.
- [30] Norma, P., Esteban, H. H., Luis, F., Di, R. J., Paula, F., Heinz, R. A. (2008): Transcriptomic identification of candidate genes involved in sunflower responses to chilling and salt stresses based on cDNA microarray analysis. – *BMC Plant Biology* 8(1): 11.
- [31] Pang, T., Ye, C. Y., Xia, X., Yin, W. (2013): De novo sequencing and transcriptome analysis of the desert shrub, *Ammopiptanthus mongolicus*, during cold acclimation using Illumina/Solexa. – *BMC Genomics* 14(1): 488-488.
- [32] Peng, M. W., Wang, M., Jiang, P., Chang, Y. L., Chu, G. M. (2018): The impact of low temperature on seed germination of two desert species in Junggar basin of China. – *Applied Ecology And Environmental Research* 16(5): 5771-5780.
- [33] Reddy, A. S., Ali, G. S., Celesnik, H., Day, I. S. (2011): Coping with stresses: roles of calcium-and calcium/calmodulin-regulated gene expression. – *Plant Cell* 23(6): 2010-2032.
- [34] Rushton, P. J., Somssich, I. E., Ringler, P., Shen, Q. J. (2010): WRKY transcription factors. – *Trends in Plant Science* 15(5): 247-258.
- [35] Sun, Y. Y. (2015): Drought Adaptation Characteristics of Plant Seedling Establishment in Junggar Desert. – Shihezi University, Chinese Shihezi.
- [36] Szekely, G., Abraham, E., Cseplo, A., Rigo, G., Zsigmond, L., Csiszar, J., Ayaydin, F. (2008): Duplicated P5CS genes of *Arabidopsis* play distinct roles in stress regulation and developmental control of proline biosynthesis. – *Plant Journal* 53(1): 11-28.
- [37] Tatusov, R. L., Fedorova, N. D., Jackson, J. D. (2003): The COG database: an updated version includes eukaryotes. – *BMC Bioinformatics* 4(1): 41.
- [38] Tunnacliffe, A., Wise, M. J. (2007): The continuing conundrum of the LEA proteins. – *Naturwissenschaften* 94(10): 791-812.
- [39] Wang, M., Zhang, S., Chu, G. (2014): Point pattern analysis of different life stages of *Haloxylon ammodendron* in desert-oasis ecotone of south junggar basin. – *Polish Journal of Environmental Studies* 23(6): 2271-2277.
- [40] Wang, T. T. (2018): Proteomics and metabolomics analysis to cold stress in two desert chenopodiaceae plants seedlings. – Shihezi University, Chinese Shihezi.
- [41] Wang, X. C., Zhao, Q. Y., Ma, C. L., Zhang, Z. H., Cao, H. L., Kong, Y. M. (2013): Global transcriptome profiles of *Camellia sinensis* during cold acclimation. – *BMC Genomics* 14(1): 415-415.
- [42] Wang, X. Y., Wei, Y., Yan, C. (2006): Study on the effects of thermoperiods and fruiting wings on the germination of *Haloxylon ammodendron* seeds. – *Arid Zone Research* 2016(4).
- [43] Xia, Z., Wei, T., Jia, L., Liu, Y. (2014): Co-expression of rice OsP5CS1 and OsP5CS2 genes in transgenic tobacco resulted in elevated proline biosynthesis and enhanced abiotic

- stress tolerance. – Chinese Journal of Applied and Environmental Biology 20(4): 717-722.
- [44] Xie, C., Mao, X., Huang, J., Ding, Y., Wu, J., Dong, S. (2011): Kobas 2.0: a web server for annotation and identification of enriched pathways and diseases. – Nucleic Acids Research 39(Web Server Issue): 316-22.
- [45] Yang, T., Ali, G. S., Yang, L., Du, L., Reddy, A., Poovaiah, B. W. (2010): Calcium/calmodulin-regulated receptor-like kinase CRLK1 interacts with MEKK1 in plants. – Plant Signal Behav 5(8): 991-994.
- [46] Zhang, L., Zhao, G., Jia, J., Liu, X., Kong, X. (2012): Molecular characterization of 60 isolated wheat MYB genes and analysis of their expression during abiotic stress. – Journal of Experimental Botany 63(1): 203-214.
- [47] Zhang, S. J. (2010): Study on Natural Cure of Main Plant Species at Initialized Process in the South Marginal Zone of the Junggar Basin. – Arid Environmental Monitoring 24: 89-93.
- [48] Zhou, Q. (2016): Transcriptome of Seed and DGE Method Research of Seed Low Temperature Germination Period in *Lepidium apetalum* willd. – Xinjiang Normal University, Xinjiang.
- [49] Zhou, Z., Wang, M. J., Zhao, S. T., Hu, J. J., Lu, M. Z. (2010): Changes in freezing tolerance in hybrid poplar caused by up- and down-regulation of PtFAD2 gene expression. – Transgenic Research 19(4): 647-654.

APPENDIX

Figure A1. GO functional classification analysis of differentially expressed genes in CA vs CK

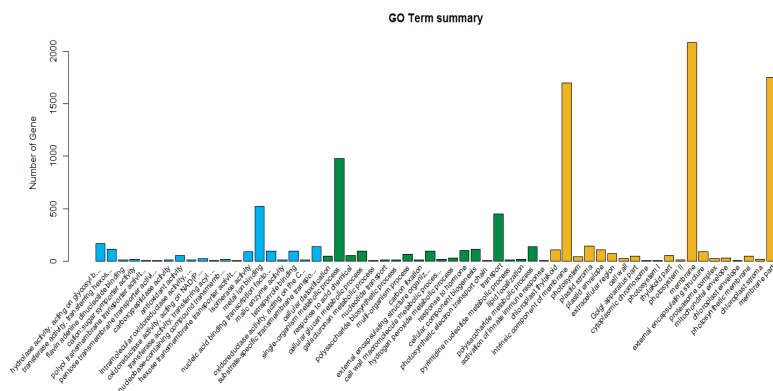
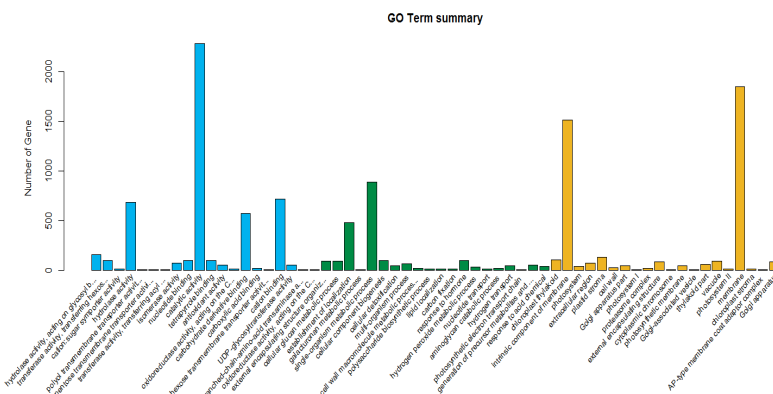


Figure A2. GO functional classification analysis of differentially expressed genes in CB vs CK



EVALUATION OF BREAD WHEAT GENOTYPES IN IRRIGATED AND RAINFED CONDITIONS USING BILOT ANALYSIS

KARAMAN, M.

*Department of Plant Production Technologies, Faculty of Applied Sciences
Mus Alparslan University, Mus, Turkey
(e-mail: karaman2178@hotmail.com; phone: +90-530-600-9136; fax: +90-436-231-2201)*

(Received 23rd Oct 2018; accepted 20th Dec 2018)

Abstract. This study was carried out in 2015-2016 and 2016-2017 seasons under supplemented irrigation (IC) and rainfall conditions (RC) of Diyarbakir in Turkey, was to determine high adaptive yielding with high quality bread wheat genotypes. The obtained data were analyzed using variance and GGE-biplot analysis methods, and the genotypes (G) were evaluated for drought tolerance indices. The average grain yield of two year ranged from 5820 to 6950 kg ha⁻¹ on rainfall conditions and 7880 to 9050 kg ha⁻¹ under supplemented irrigation conditions. The GGE biplot graph showed that G3, G6 and G21 were best genotypes for grain yield. Although G23 did not have the highest grain yield, it was determined that it represented the most stable line. Furthermore, G12 and G16 were determined as suitable genotypes for irrigated conditions and G21 for rainfall condition. It was determined that mean productivity (MP), stress tolerant index (STI), geometric mean productivity (GMP) and harmonic mean (HM) parameters were related with Yp (supplemented irrigation yield) and Ys (rainfall condition yield). Also, yield index (YI), drought resistance index (DRI), yield stability index (YSI) was related with Ys. In the study concluded that the lines G6, G12, G16 and G21 could be candidates for registration.

Keywords: wheat, drought, GGE-biplot, yield components, stability

Introduction

Bread wheat (*Triticum aestivum* L.) is highly adaptable to different ecological areas and has an important role in human nutrition (Dhanda et al., 2004; Nazar et al., 2012). It is reported that the global wheat cultivation is approximately 222.9 million hectares and world wheat production is around 720 million tons by Food Agriculture Organization (FAO, 2015). In Turkey, with a planting area of 7.8 million hectares and production of 22.6 million tons, wheat ranks first in grain production according to Turkish Statistical Institute (TSI, 2015). The rapidly growing world population has made it necessary to increase grain yield per unit area, particularly in light of the gradually reduced agricultural areas. Consumers' expectations concerning the quality of wheat vary; therefore, development of different quality wheat has become a requirement. However, to date, wheat breeding studies have aimed to produce varieties with high grain yield; thus, quality traits desired by the industry and consumers have not been among priority targets. For this reason, wheat imports have increased to meet the high-quality raw material needs of the industry and supply cheap raw materials. In order to keep these imports to a minimum, there is a need to develop new wheat varieties with both the desired quality characteristics and high yield (Erkul, 2006; Yazar et al., 2013).

In Turkey and around the world, wheat cultivation is generally undertaken in rainfed conditions dominated by general drought stress, but in rarer cases, it is also rarely supported by irrigation, which makes it crucial to identify genotypes suitable for both rainfed and irrigated conditions. For this purpose, wheat breeders and agronomists cultivate existing genotypes under both irrigated and rainfed conditions and use the results of these experiments to determine the specific requirements of genotypes based

on mathematical formulas (Farshadfar, 2012; Aktaş, 2017). In studies investigating the tolerability of drought in durum wheat, it is observed that genotypes with low values for yield stability index (YSI), drought resistance index (DRI) and yield index (YI) parameters favor limited watering conditions whereas those with high values harmonic mean (HM), geometric mean productivity (GMP) and mean productivity (MP) values have higher grain yield potential under conditions of no water stress. (Mohammadi et al., 2011; Nouri et al., 2011).

It has been reported that the effect of drought stress on plant growth and grain yield in wheat is dependent on the stage, severity and duration of drought stress, and the main reason for grain yield loss is the negative effect of drought on spike formation and leaf area duration after flowering (Öztürk, 1999). In wheat breeding programs, the selection parameters for varieties suitable for irrigated conditions include grain yield, number of grains per spike, grain weight per spike, and spike per square meter while those for rainfed conditions are plant height, number of spikes per square meter, and spike length (Ozturk and Korkut, 2018).

In this study, genotypes were tested in two different growing seasons under rainfed and irrigated conditions to determine suitable candidates for cultivation in the Southeastern Anatolia Region of Turkey by taking into account the responses of genotypes to these different conditions and the effects on grain yield, quality, yield, and yield components.

Materials and methods

In this study, 20 advanced lines were used as material and five registered varieties intensely cultivated in the Southeastern Anatolia Region in Turkey were utilized as standard (*Table 1*). The experiments were based on a randomized block design with four replications (R), and were conducted in Diyarbakır province, Turkey (37°56' N; 40°15' E; 599 m altitude) under irrigated and rainfed conditions in the 2015-16 and 2016-17 growing seasons (*Figure 1*).

First year, trials were planted on November 11. Harvest was made on June 11 and June 26 in rainfall and irrigation conditions respectively. Second year, trials were planted on November 10. Harvest was made on June 20 and July 01 in rainfall and irrigation conditions respectively. In irrigated trials, the plants were irrigated once at the end of flowering period. It was used 100 mm water per square meter with keel irrigation method. Sowing was performed on parcels of 6 m², 450 seeds per square meter using a sowing machine. Fertilization was under taken with 60 kg ha⁻¹ pure nitrogen (N) and 60 kg ha⁻¹ pure phosphorus (P₂O₅) during sowing and 80 kg ha⁻¹ nitrogen (N) during the tillering period. Harvest was by plot combine harvester. In the area where the experiment was carried out, the soil characteristics were determined as follows: texture = clay, pH = 7.87 (slightly alkaline), organic matter ratio = 0.86 %, salt ratio = 0.32, and lime ratio (CaCO₃) = 8.12 % kg da⁻¹. The total amount of rainfall was 417 mm and 453 mm in the first and second growing seasons of the study (*Table 2*). Both of these values were lower than the long-term average amount of rain (482 mm) (Anonim, 2017). Protein ratio (%) was determination according to (NIR) AACC 39-10 (Anonymous, 1990). Measurement of the spikes per square meter was made over 1 m length and 20 cm width on a row, then multiplied by 5 to calculate the spike number in the area of 1 square meter.

Table 1. Pedigree and Origin of Bread Wheat Genotypes Used in The Study

Genotypes	Symbol	Pedigree	Breeding Institution or Origin
1	G1	Worrakatta/2*Pastor//Danphe #1 Cmsa07m00403s-040ztm-040zty-15ztm-010y-01b-0ymxi11-12\M21sawyt\41	CIMMYT
2	G2	Ka/Nac//Trch/3/Danphe #1 Cmsa07m00445s-040m-0nj-0nj-4y-0b Mxi11-12\M21sawyt\112	CIMMYT
3	G3	Bav92//Irena/Kauz/3/Huites/4/2*Rolf07 Cmss06y00875t-099Topm-099y-099ztm-099y-099m-25wgy-0b Mxi11-12\Msawyt \32	CIMMYT
4	G4	Fret2/Tukuru//Fret2/3/Munia/Chto//Amsel/4/Fret2/Tukuru//Fret2 Cmss06y00878t-099topm-099y-099ztm-099y-099m-17wgy-0b Mxi11-12\Msawyt\33	CIMMYT
Dinç	G5	Check	GAP UTAEM in Turkey
6	G6	Wbl11/Fret2//Pastor*2/3/Murga Cmss06y00937t-099topm-099y-099ztm-099y-099m-10wgy-0b Mxi11-12\Msawyt\44	CIMMYT
7	G7	FrncIn*2/Tecue #1 Cmss07y00941t-099topm-099y-099m-099y-11m-0wgy Mxi11-12\M34eswyt\67	CIMMYT
8	G8	Ceyhan99//Tuj"s"/Onelto See06032	CIMMYT
9	G9	Bav92//Irena/Kauz/3/Huites/4/Doll Cmss05b00188s-099y-099m-099y-099ztm-18wgy-0b	CIMMYT
Pehlivan	G10	Check	TTAEM in Turkey
11	G11	Attila/Bav92//Pastor/3/Attila*2/Pbw65 Cmsa04m00070s-040ztb-040zty-040ztm-040sy-13ztm-04y-0b	CIMMYT
12	G12	Cunningham/4/Sni/Trap#1/3/Kauz*2/Trap//Kauz Cmsa04m00088s-040ztb-040zty-040ztm-040sy-3ztm-01y-0	CIMMYT
13	G13	Sokoll/Excalibur Cmsa04y00612s-25ztp0y-010m-010sy-4m-03y-0b	CIMMYT
14	G14	Wbl11*2/Kkts//Pastor/Kukunacmss05b00525s-099y-099m-099y-099ztm-3wgy-0b	CIMMYT
Aday-12	G15	Check	GAP UTAEM in Turkey
16	G16	Kachu/5/Nac/Th.Ac//3*Pvn/3/Mirlo/Buc/4/2*Pastor Cmss05b00584s-099y-099m-099y-099ztm-8wgy-0b	CIMMYT
17	G17	B.Hashi+B764ta/5/Dove/Inia/4/4777/(2)//Fkn/Gb/3/Pvn See060149-0s-0s-0sd	CIMMYT
18	G18	Krichauff/2*Pastor/4/Milan/Kauz//Prinia/3/Bav92 Cmss06y00337s-040ztp0y-040ztm-040p0y-4ztm-0y-0b	CIMMYT
19	G19	Heilo//Sunco/2*Pastorcmsa06y00492s-040zty-040ztm-040sy-2ztm-0y-0b	CIMMYT
Tekin	G20	Check	GAP UTAEM in Turkey
21	G21	FrncIn/Rolf07cmss06b00013s-0y-099ztm-099y-099m-2wgy-0b	CIMMYT
22	G22	Becard/Kachu Cmss06b00169s-0y-099ztm-099y-099m-28wgy-0b	CIMMYT
23	G23	Rolf07*2/5/Reh/Hare//2*Bcn/3/Croc_1/Ae.Squarrosa (213)//Pgo/4/Huites Cmss06b00704t-099topy-099ztm-099y-099m-23wgy-0b	CIMMYT
24	G24	Usher-16 Crow's/Bow's'-1994/95//Asfoor-5 Icw01-00257-0ap-8ap-0ap/Ots-0ap-12ap-0ap	CIMMYT
Ceyhan-99	G25	Check	DATAE in Turkey

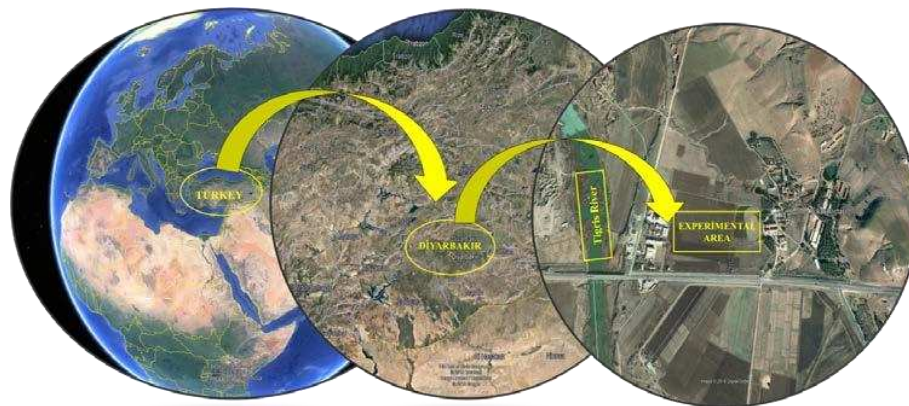


Figure 1. Experimental Area (US Dep of State Geography © 2018 Google image landset/Copernics)

Table 2. Climate data province of 2015-2016 and 2016-2017 wheat growing season in Diyarbakir

Month	Average of Temperature (°C)			Precipitation (mm)		
	2015-2016	2016-2017	Long-Term	2015-2016	2016-2017	Long-Term
September	27.4	24.2	24.8	0.0	5.2	4.1
October	18.4	18.8	17.2	84.2	13.6	34.7
November	9.8	8.2	9.2	10.4	52.0	51.8
December	3.9	2.4	4.0	31.6	135.6	71.4
January	1.1	1.5	1.8	77.2	20.6	68.0
February	7.9	1.5	3.5	69.2	3.8	68.8
March	9.7	9.4	8.5	55.6	90.2	67.3
April	15.7	12.8	13.8	29.0	98.8	68.7
May	19.9	18.8	19.3	41.4	30.6	41.3
June	26.8	26.9	26.3	18.4	2.6	7.9
Total				417.0	453.0	484.0

Drought tolerance parameters were calculated using the following formulas (Equation= 1, 2, 3, 4, 5, 6,7 and 8) developed by previous researchers:

Stress tolerant index (Fernandez, 1992):

$$(STI) = (Y_p * Y_s) / \bar{Y}_p^2 \quad (\text{Eq.1})$$

Tolerance (Hossain et al., 1990):

$$(TOL) = Y_p - Y_s \quad (\text{Eq.2})$$

Geometric Mean Productivity (Fernandez, 1992):

$$(GMP) = \sqrt{(Y_p * Y_s)} \quad (\text{Eq.3})$$

Mean Productivity (Rosielle and Hamblin, 1981):

$$(MP) = (Y_p + Y_s) / 2 \quad (\text{Eq.4})$$

Harmonic Mean (Chakherchaman et al., 2009):

$$(HM) = 2*(Y_p*Y_s)/(Y_p+Y_s) \quad (Eq.5)$$

Yield Stability Index (Bousslama and Schapaugh, 1984):

$$(YSI) = Y_s/Y_p \quad (Eq.6)$$

Yield Index (Gavuzzi et al., 1997):

$$(YI) = Y_s/\bar{Y}_s \quad (Eq.7)$$

Drought Resistance Index (Lan, 1998):

$$(DRI) = Y_s \times (Y_s/Y_p)/\bar{Y}_s \quad (Eq.8)$$

Statistical analysis of data

An analysis of variance (ANOVA) was performed using JMP 5.0 software and genotype by environment interaction (GGE) biplot analysis using GenStat statistical package program 12th Edition (GenStat, 2009). The differences between the averages were examined by a least significant difference (LSD) test ($p < 0.01$ and $p < 0.05$) (Gomez and Gomez, 1984).

Results and discussion

The ANOVA analysis revealed statistically significant differences in the mean grain yield and other quality traits between rainfed (Y_s) and irrigated (Y_p) conditions ($p < 0.01$ and $p < 0.05$) (Table 3).

Grain yield (GY) (kg ha⁻¹)

According to the results of ANOVA, year, genotype and genotype*year were found to have a statistically significant effect ($p < 0.01$) on grain yield in both rainfed and irrigated conditions. The mean grain yield over the two growing seasons was 8520 kg ha⁻¹ and 6080 kg ha⁻¹ for irrigated and rainfed trials, respectively. The highest grain yield was obtained from G12 (9050 kg ha⁻¹) and G16 (9010 kg ha⁻¹) in irrigated trials and G21 (6950 kg ha⁻¹) in rainfed conditions. It has previously been reported that the main factor affecting yield in wheat is the genetic structure of the plant (Gebeyehou et al., 1982). Therefore, genotypes should be evaluated in different environments; i.e., in multiple locations or over different years to determine the grain yield potential. Not only hereditary but also abiotic and biotic stress factors have a role in the variation of genotype responses in different climates and soil structures. High or low levels of precipitation and higher or lower temperatures further increase the effect of GGE (Blum, 1998; Chamurliyski et al., 2015; Kılıç et al., 2018). However, grain yield in wheat is more affected by the distribution of rainfall throughout the growing season, rather than the total amount of precipitation (Çetin et al., 1999).

Table 3. Results of variance analysis

Rainfall Conditions										
Squares Mean										
Resources	DF	GY	HW	TGW	PR	ZS	SPSM	SL	FSPS	GPS
Y	1	163947**	653.6**	1693.46**	15.71**	14413.4**	6042.9**	0.1 ^{ns}	2.0 ^{ns}	189.2*
R[Y]	6	69803.6**	2.9 ^{ns}	0.67 ^{ns}	0.07 ^{ns}	24.5 ^{ns}	112.08 ^{ns}	1.4 ^{ns}	5.6 ^{ns}	12.9*
G	24	233534**	358.7**	643.05**	34.13 ^{ns}	946.54**	7227.7**	69.2**	86.9**	2809.1 ^{ns}
Y*G	24	237439**	67.2 ^{ns}	132.96 ^{ns}	9.72 ^{ns}	946.54**	7529.8**	17.8 ^{ns}	39.3 ^{ns}	2816.1**
CV(%)		6.9	1.9	6.8	7.8	8.6	7.9	7.2	6.2	13.9
Irrigation Conditions										
Squares Mean										
Resources	DF	GY	HW	TGW	PR	ZS	SPSM	SL	FSPS	GPS
Y	1	63937.7**	145.2**	764.8**	0.02 ^{ns}	331.2**	3433.9**	3.9 ^{ns}	20.4 ^{ns}	12.8 ^{ns}
R[Y]	6	8141.8 ^{ns}	0.34 ^{ns}	0.4 ^{ns}	0.02 ^{ns}	11.7 ^{ns}	15.8 ^{ns}	1.4 ^{ns}	4.5 ^{ns}	87.6 ^{ns}
G	24	176936**	139.4**	564.4**	18.9*	1530.9**	6958.6*	34.6**	63.1**	1896.3 ^{ns}
Y*G	24	316624**	6.7 ^{ns}	99.1**	15.6*	297.8**	5772.0 ^{ns}	27.9*	25.5 ^{ns}	1671.5 ^{ns}
CV(%)		4.2	0.5	3.5	4.6	5.8	11.3	7.6	5.4	15.3 ^{ns}

GY: Grain yield, HW: Hectoliter weight, TGW: Thousand grain weight, PR: Protein ratio, ZS: Zeleny sedimentation, SPSM: Number of spikes per square meter, SL: Spike length, FSPS: Number of fertile spikelets per spike, GPS: Number of grains per spike, DF: Degree of freedom, R: Replication, Y: Year, G: Genotype **: Statistically significant at 0.01, *: Statistically significant at 0.05, ns: not significant

Hectoliter weight (HW) (kg hl⁻¹)

ANOVA revealed statistically significant differences between growing seasons and genotypes in terms of mean HW under rainfed and irrigated conditions ($p < 0.01$). Considering the mean values obtained from the two growing seasons, Tekin variety had the highest HW (84.8-81.7 kg hl⁻¹) under both experimental conditions. This trait is influenced by several factors, such as environment, physical properties of grain (e.g., homogeneity and endosperm cavity), and endosperm structure. Studies conducted in this area have reported that HW varies according to hereditary factors (Genç et al., 1993) and different climatic conditions (Ath et al., 1993).

Thousand grain weight (TGW) (g)

According to the two-year average values, the highest TGW values were obtained from the Pehlivan (42.9 g) and Aday-12 (42.7 g) standards in irrigated trials and from the G3 (34.2 g) under rainfed conditions. Flour industrialists attach special importance to TGW since there is a significant positive correlation between this trait and flour yield (Yazar et al., 2013). Despite the consensus on the significant correlation between TGW and quality and grain yield, there are contradictory results concerning the direction of this correlation, with some researchers suggesting that it is positive (Bohac and Cermin, 1969; Knott and Talukdar, 1971) while others reporting a negative correlation (Thorne, 1966). In the current study, TGW was found to have a positive correlation with HW and negative correlation with protein ratio (PR) and zeleny sedimentation (ZS).

Protein ratio (PR) (%)

The mean PR was calculated as 13.1% and 14.5% for irrigated and rainfed conditions, respectively. This indicates that PR is affected by not only environmental conditions but also hereditary factors. While the highest PR belonged to G13 in irrigated conditions, for rainfed trials, no significant difference was observed between the protein ratios of genotypes. In Turkey, it has been reported that protein content of wheat varies ranging between 6 and 22% depending on type, variety, environmental factors, and cultivation conditions (Doğan and Kendal, 2013). These ranges are in agreement with the results obtained in the current study concerning PR. Similarly, in another study conducted in Konya, Turkey, PR in bread wheat was found to vary between 12.62 and 14.16% in rainfed conditions, and 11.53 and 13.85% in irrigated conditions (Şahin et al., 2008; Aydoğan and Soylu, 2017).

Zeleny sedimentation (ZS) (ml)

Year, genotype, and year x genotype interactions had a statistically significant effect on ZS under rainfed and irrigated conditions ($p < 0.01$). Sedimentation is of great importance in determining protein quality in wheat (Peterson et al., 1992). In this study, the highest ZS value was obtained from G6 and G17 genotypes in irrigated conditions and from G6 in rainfed conditions. Ozturk and Aydin (2004) reported the sedimentation values in different environments as 32.2 ml for irrigated, 35.7 for rainfed, 34.0 ml for early water stress, 35.0 ml for late water stress and 37.5 ml for continuous water stress conditions. Compared to their study, we found similar values in irrigated conditions but higher values in rainfed conditions. This is considered to be due to environmental conditions and differences in plant material.

Spikes per square meter (SPSM) (Number)

There were statistically significant differences between years and genotypes in terms of SPSM in both rainfed and irrigated conditions ($p < 0.01$ or $p < 0.05$). The highest number of SPSM was observed in genotype G21 in irrigated trials and G9 in rainfed conditions. Researchers have previously reported that the number of SPSM varies according to sowing norms, variety, sowing time, available water, and climate and soil conditions (Kılıç et al., 2010; Kızıldağ et al., 2016). Although heredity also has a significant role in determining SPSM, this parameter is also influenced by resistance of genotypes to adverse environmental conditions, such as temperature, drought stress, and frost. Studies conducted in various environments suggested that to achieve favorable results concerning grain yield, genotypes having high potential of a greater number of SPSM should be selected (Öztürk and Akten, 1999; Sönmez et al., 1999; Ereku and Köhn, 2006; Karaman, 2017).

Spike length (SL) (cm)

Genotypes G6 and G9 ranked first in terms of SL under irrigated and rainfed conditions, respectively. Aydoğan and Soylu (2017) reported the average SL from their rainfed experiments as 9.75 cm. Similarly, our average measurement of SL was 10.4 cm for rainfed trials; however, we observed that SL was shorter in irrigated conditions (9.9 cm). This may be attributed to genotypes producing more tillers under irrigation.

Fertile spikelet per spike (FSPS) (Number)

FSPS statistically significantly differed between genotypes under irrigated and rainfed conditions ($p < 0.01$). The highest number of FSPS was seen in the Pehlivan variety in irrigated trials whereas for rainfed conditions, many genotypes were included in the same group despite the differences in FSPS. In one of the two previous studies on bread wheat, it was shown that the number of FSPS ranged from 16 to 21 (Genç, 1974), while the other reported no statistically significant difference in this parameter with the values varying between 18.5 and 21.1 (Karaman, 2013).

Grains per spike (GPS) (Number)

According under rainfed conditions, the number of GPS was statistically significantly affected by year ($p < 0.05$) and year*genotype interaction ($p < 0.01$), and the highest value was identified in genotype G9. It has been reported that in wheat, a sufficient amount of nutrients is accumulated in grain after fertilization and greater grain yield is obtained from varieties with a higher number of GPS (Yıldırım et al., 2005). In another study conducted with 14 bread wheat varieties under rainfed conditions in Konya, it was found that the number of GPS ranged from 31.2 to 44.9 and the average of all trials was 37.9 (Aydoğan and Soylu, 2017). In the current study, the average number of GPS was higher (53.5) in rainfed conditions, which may be due to the differences in genotypes and agronomic applications.

Evaluation of yield and other investigated traits using GGE-biplot analysis

It has been reported that GGE biplot analysis is very important because it presents the genotype environmental interaction visually (Kendal, 2015; Sayar, 2017). *Figures 2 to 5* present the results of GGE-biplot analysis of grain yield (*Tables 4 and 5*) and other traits of 25 bread wheat genotypes evaluated in the 2015-16 and 2016-17 growing

seasons under irrigated (IC1, IC2) and rainfed (RC1 and RC2) conditions. The analysis of grain yield revealed that the total variation was 73.38%, of which 44.99% was explained by principal component 1 (PC1) and 28.39% by PC2 (Figure 2 and Figure 3). According to the results of GGE-biplot analysis, the highest grain yield belonged to G3, G6 and G21 in RC1; G3, G7, G11, G21 and G23 in IC1; G1 and Dinç in RC2; and G1, G2, G12 and G16 in IC2. Furthermore, genotypes located closer to the center of the axis had values similar to the experimental mean (Figure 2).

In the biplot graph demonstrating the stability capabilities of genotypes (Figure 3), The G3 line located at the far right of the line dividing the graph has the highest grain yield, and the G6, G7, G21 and G23 lines appear to be more prominent than the remaining genotypes concerning grain yield. Although G23 did not have the highest grain yield, it was determined that it represented the most stable line. Furthermore, based on the results IC1 can be considered as the environment that provided the best conditions for genotypes to demonstrate their potential.

If the angle of the vector was less than 90°, there was a positive correlation between the features, if the angle is more than 90° there is no correlation between features (Yan and Thinker, 2006; Dogan et al., 2016; Oral, 2018). As revealed by the biplot graph showing the correlations between genotype traits under rainfed conditions (Figure 4), GY was positively correlated with SL, FSPS, TGW and HW; and SPSM with ZS, GPS and PR; whereas PR had a negative correlation with TGW and HW. Furthermore, G6 and G21 were more prominent for GY; G8 and Tekin for HW; G3 and Pehlivan for TGW; G6 and G23 for ZS; G9, G11 and G21 for SPSM; G6 and G9 for SL; G6, G8, G11, G14 and Pehlivan for FSPS; and G9 and G11 for GPS.

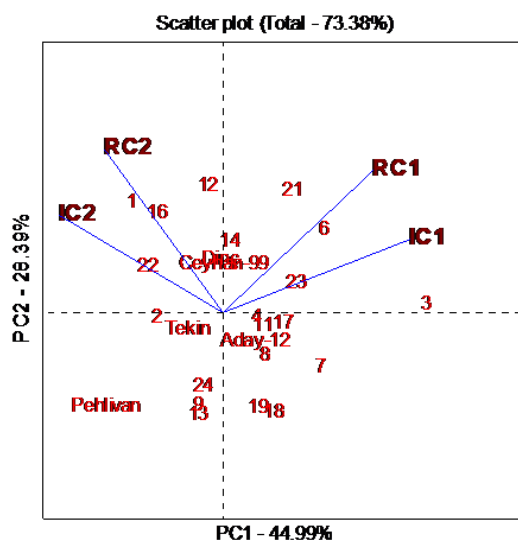


Figure 2. GGE-biplot of grain yield

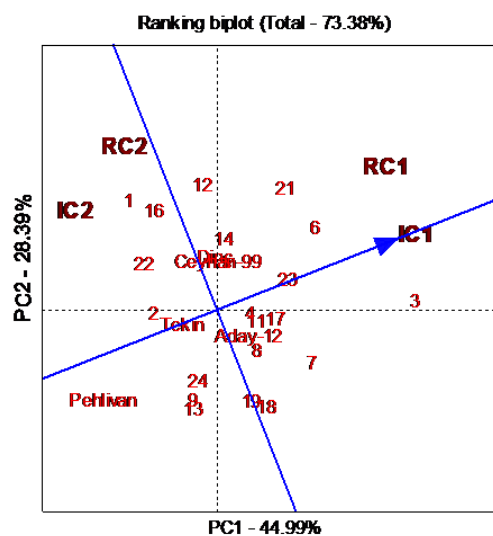


Figure 3. Stability of genotypes in terms of grain yield

For all parameters, the lines closer to the center of the axis showed similar values to the experimental average. According to the biplot graph showing the relationship between the genotype traits under irrigated conditions (Figure 5), there was a significant positive relationship between TGW and SL and FSPS; GY and GPS; SPSM, ZS and PR, and a significant negative correlation between HW, SPSM, PR and ZS. Under these conditions, the most promising genotypes were found to be G3, G12 and G16 for GY;

G18 and Tekin for HW; G8, Pehlivan and Aday-12 for TGW; G13 and G21 for PR; G1, G6, G17 and G23 for ZS; G21 and G24 for SPSM; G4, G6 and G18 for SL; and G6, Pehlivan, Aday-12 and G24 for FSPS; G9 and G23 had values similar to the average.

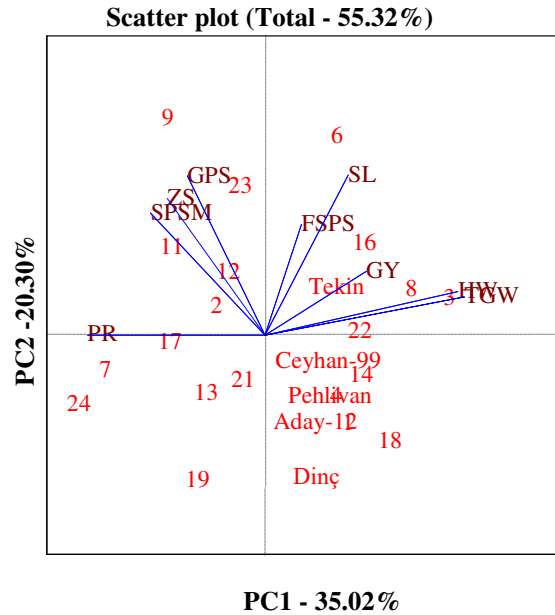


Figure 4. Biplot graph of genotype trait correlations in rainfed conditions

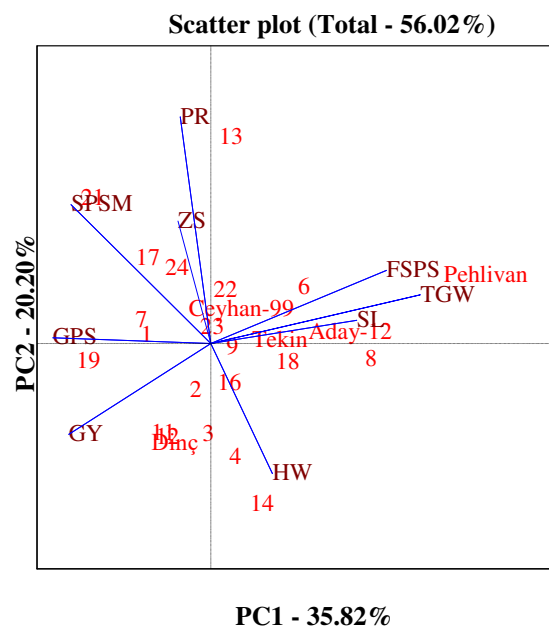


Figure 5. Biplot graph of genotype trait correlations in irrigated conditions

Table 4. The mean grain yield values obtained from the 2015-16 and 2016-17 growing seasons

	2015-16 (kg ha ⁻¹)			2016-17 (kg ha ⁻¹)			Average of two seasons (kg ha ⁻¹)								
	IC1	RC1	% Lost	IC2	RC2	%Lost	IC	RC	% Lost						
G1	7810	f-h	6720	c-e	14	9160	ab	6820	a	26	8480	d-ı	6770	a-c	20
G2	7230	ij	6870	b-d	5	9160	ab	5740	h-l	37	8190	h-j	6300	d-h	23
G3	9600	a	7700	a	20	8230	gh	5170	m	37	8910	ab	6440	c-g	28
G4	8830	bc	6610	c-f	25	8890	a-e	5620	j-m	37	8860	a-c	6110	g-ı	31
Dinç	8540	b-e	6390	c-g	25	8560	c-g	6730	ab	21	8550	c-g	6560	a-f	23
G6	8580	b-e	7810	a	9	8410	e-h	6050	d-j	28	8500	d-ı	6930	ab	18
G7	8940	b	6650	c-f	26	8250	gh	5550	j-m	33	8590	b-f	6100	g-ı	29
G8	7780	gh	6820	b-d	12	7980	h	6130	c-ı	23	7880	j	6480	c-g	18
G9	7920	f-h	5960	f-h	25	8500	d-g	5830	g-l	31	8210	g-j	5890	hı	28
Pehlivan	6830	j	5690	h	17	9040	a-c	5980	e-k	34	7930	j	5830	ı	27
G11	8930	b	6200	d-h	31	8350	f-h	6240	b-h	25	8640	b-f	6220	e-ı	28
G12	8790	b-d	6950	bc	21	9310	a	6370	a-f	32	9050	a	6660	a-d	26
G13	7590	hı	6270	c-h	17	8780	b-f	5400	lm	39	8180	ij	5830	ı	29
G14	8510	b-e	6840	b-d	20	8800	b-f	6380	a-f	27	8650	b-f	6610	a-e	24
Aday-12	8280	d-g	6500	c-g	22	8800	b-f	5720	ı-l	35	8540	c-h	6110	g-ı	28
G16	8650	b-d	6360	c-h	26	9380	a	6540	a-d	30	9010	a	6450	c-g	28
G17	8820	bc	6780	b-d	23	8790	b-f	5500	k-m	37	8800	a-d	6140	f-ı	30
G18	8450	b-e	6250	c-h	26	8370	f-h	5460	k-m	35	8410	e-ı	5860	ı	30
G19	8530	b-e	6070	e-h	29	8430	e-h	5580	j-m	34	8480	d-ı	5820	ı	31
Tekin	7900	f-h	6170	d-h	22	8700	b-g	6300	b-g	28	8300	f-ı	6230	d-ı	25
G21	8930	b	7430	ab	17	8610	c-g	6470	a-e	25	8770	a-d	6950	a	21
G22	7740	hı	6440	c-g	17	8940	a-d	6580	a-c	26	8340	f-ı	6510	b-g	22
G23	8940	b	6940	bc	22	8570	c-g	5930	f-k	31	8750	a-e	6430	c-g	26
G24	8320	c-f	5850	gh	30	8690	b-g	5830	g-l	33	8500	d-ı	5840	ı	31
Ceyhan-99	8070	e-h	6560	c-f	19	8740	b-f	6560	a-d	25	8410	e-ı	6560	a-f	22
Average	8340	a	6590	b	21	8700	a	6020	b	31	8520	a	6080	b	26
Lsd(0.05)	51.9**		69.8**			49.3**		51.5**			12.7**		37.3**		

Letters in the same column from top to bottom are statistically different at the level of $p < 0.01$ or $p < 0.05$. IC1: Irrigated conditions in the first season, IC2: Irrigated conditions in the second season, RC1: Rainfed conditions in the first season, RC2: Rainfed conditions in the second season, IC: Irrigated conditions, RC: Rainfed conditions, **: Statistically significant at 0.01, *: Statistically significant at 0.05

Table 5. The results of the combined analysis of both growing seasons for the investigated parameters and the groups formed

	IC		RC		IC		RC		IC		RC	
	GY		GY		HW		HW		TGW		TGW	
G1	8480	d-1	6770	a-c	82.7	jk	79.8	a-g	37.4	e-h	31.3	b-g
G2	8190	h-j	6300	d-h	83.2	g-j	78.6	e-j	35.9	h-k	28.6	g-j
G3	8910	ab	6440	c-g	83.7	e-g	80.8	a-d	39.9	bc	34.2	a
G4	8860	a-c	6110	g-1	83.3	f-1	79.4	b-h	35.8	h-l	30.2	d-g
Dinç	8550	c-g	6560	a-f	83.8	d-f	79.7	a-g	34.0	l	27.0	ı-k
G6	8500	d-1	6930	ab	84.4	a-d	81.1	a-c	39.8	bc	31.2	c-g
G7	8590	b-f	6100	g-1	81.9	l	74.7	l	36.8	f-1	26.2	jk
G8	7880	j	6480	c-g	84.5	a-c	81.4	ab	40.7	b	33.2	a-c
G9	8210	g-j	5890	hı	83.4	e-1	78.3	g-k	37.1	e-h	28.8	f-j
Pehlivan	7930	j	5830	ı	82.8	jk	79.0	c-ı	42.9	a	34.1	ab
G11	8640	b-f	6220	e-1	83.6	e-h	78.6	e-j	34.5	j-l	26.4	ı-k
G12	9050	a	6660	a-d	82.7	jk	78.4	f-k	36.3	f-j	29.0	f-j
G13	8180	ıj	5830	ı	81.3	mn	76.6	j-l	37.8	d-g	30.2	d-g
G14	8650	b-f	6610	a-e	83.1	h-k	78.9	d-ı	36.7	f-1	28.9	f-j
Aday-12	8540	c-h	6110	g-1	81.5	l-n	76.4	kl	42.7	a	32.0	a-e
G16	9010	a	6450	c-g	83.9	c-e	80.7	a-e	39.9	bc	32.9	a-d
G17	8800	a-d	6140	f-1	83.4	f-1	77.5	h-k	36.1	g-j	26.3	ı-k
G18	8410	e-1	5860	ı	84.6	ab	80.5	a-f	39.5	b-d	31.6	a-f
G19	8480	d-1	5820	ı	84.3	b-d	80.2	a-g	34.2	kl	27.3	h-j
Tekin	8300	f-1	6230	d-1	84.8	a	81.7	a	37.2	e-h	30.1	d-h
G21	8770	a-d	6950	a	81.0	n	77.1	ı-k	36.3	f-j	29.1	f-1
G22	8340	f-1	6510	b-g	82.9	ı-k	80.7	a-e	38.1	c-f	32.1	a-e
G23	8750	a-e	6430	c-g	81.7	lm	77.6	h-k	38.8	b-e	30.5	c-g
G24	8500	d-1	5840	ı	80.2	o	74.7	l	35.0	ı-l	24.4	k
Ceyhan-99	8410	e-1	6560	a-f	82.6	k	79.6	a-h	36.0	g-k	29.2	e-j
Average	8520		6310		83.0		79		37.6		29.8	
Lsd(0.05)	35.5**		43.0**		0.6**		2.1**		1.9**		2.9**	

	IC		RC		IC		RC		IC		RC	
	PR		PR		ZS		ZS		SPSM		SPSM	
G1	13.2	b-e	14.0		38.0	ab	42.3	b-f	104.3	c-e	91.3	j
G2	12.6	d-g	14.7		31.5	g-i	43.5	a-e	113.8	b-e	111.0	b-f
G3	12.8	c-g	13.3		32.8	e-h	39.0	e-g	103.8	c-e	99.0	g-j
G4	12.5	e-g	14.2		30.5	hi	40.0	d-g	104.8	c-e	93.5	ij
Dinç	12.8	c-g	14.2		29.8	ij	38.0	fg	103.8	c-e	101.3	e-j
G6	13.2	b-f	14.4		39.3	a	47.5	a	111.5	b-e	112.5	a-e
G7	13.1	b-f	15.2		35.8	b-d	46.0	a-c	110.8	b-e	105.8	c-h
G8	12.8	c-g	13.7		34.8	d-f	42.3	b-f	101.5	de	105.3	c-i
G9	12.9	b-g	14.8		32.8	e-h	45.0	a-d	112.0	b-e	124.3	a
Pehlivan	13.4	a-d	15.4		32.3	f-i	40.0	d-g	97.0	e	113.3	a-d
G11	12.4	fg	14.4		32.3	f-i	42.8	a-f	112.8	b-e	119.3	ab
G12	13.1	b-f	15.2		30.3	h-j	44.5	a-d	102.3	c-e	109.8	b-g
G13	14.2	a	15.7		36.5	b-d	40.3	d-g	119.8	a-c	101.5	d-j
G14	12.1	g	13.8		24.5	l	36.5	g	107.0	c-e	102.3	d-j
Aday-12	12.9	c-g	14.0		29.8	ij	40.3	d-g	103.3	c-e	103.3	d-i
G16	13.1	b-f	14.2		30.0	ij	42.3	b-f	113.0	b-e	108.5	b-h
G17	13.6	a-c	15.1		39.8	a	45.5	a-c	116.0	b-d	97.0	h-j
G18	13.2	b-f	14.1		31.8	g-i	36.8	g	107.8	c-e	91.0	j
G19	13.3	a-e	14.7		35.3	c-e	45.0	a-d	116.5	b-d	105.8	c-h
Tekin	13.4	a-e	14.7		34.5	d-f	44.5	a-d	108.0	c-e	99.5	f-j
G21	13.8	ab	14.2		34.0	d-g	41.5	c-g	131.8	a	120.3	ab
G22	13.5	a-c	14.8		27.8	jk	38.8	e-g	119.8	bc	108.5	b-h
G23	13.2	b-f	14.8		38.0	ab	46.8	ab	98.3	e	109.3	b-g
G24	13.0	b-g	15.4		26.3	kl	39.3	e-g	127.8	ab	115.3	a-c
Ceyhan-99	13.0	b-f	14.0		37.8	a-c	45.3	a-d	112.8	b-e	111.4	a-g
Average	13.1		14.5		33.0		42.1		110.4		106.4	
Lsd(0.05)	0.9*		Ö.D.		2.7**		5.2**		17.6*		11.9**	

	IC		RC		IC		RC		IC		RC	
	SL		SL		FSPS		FSPS		GPS		GPS	
G1	9.1	e-g	9.5	g-1	17.8	d-f	17.7	cd	55.5	55.3	bc	
G2	8.7	g	9.9	e-1	19.0	b-d	19.5	ab	49.5	56.9	a-c	
G3	10.0	a-e	11.6	a-c	18.0	c-f	18.9	a-c	54.4	56.8	a-c	
G4	10.8	ab	10.5	d-g	18.7	b-e	20.0	a	49.3	51.4	c	
Dinç	9.1	e-g	9.3	h1	18.9	b-d	19.0	a-c	55.9	48.3	cd	
G6	10.9	a	11.7	ab	20.0	ab	20.1	a	52.1	55.2	bc	
G7	9.6	c-g	10.6	c-f	18.1	c-f	17.9	b-d	56.2	53.6	c	
G8	10.3	a-c	10.7	b-e	19.4	a-c	20.5	a	47.7	49.7	cd	
G9	10.4	a-c	11.9	a	18.6	b-f	19.7	a	53.3	66.3	a	
Pehlivan	10.0	a-e	10.4	d-h	20.6	a	20.6	a	39.0	40.1	d	
G11	9.2	d-g	9.3	h1	19.5	a-c	20.3	a	55.7	65.3	ab	
G12	9.7	b-g	10.6	c-g	17.3	ef	19.4	ab	47.1	55.1	bc	
G13	10.0	a-e	10.8	a-e	19.0	b-d	19.8	a	47.4	50.1	cd	
G14	10.3	a-c	10.4	d-g	18.7	b-e	20.6	a	46.7	51.1	c	
Aday-12	10.4	a-c	9.5	g-1	19.9	ab	19.5	ab	55.2	51.9	c	
G16	10.4	a-c	11.2	a-d	18.7	b-e	19.7	a	53.0	56.0	a-c	
G17	10.3	a-c	9.8	e-1	19.2	a-d	19.7	a	60.2	58.5	a-c	
G18	10.7	ab	11.1	a-d	18.9	b-d	18.9	a-c	53.7	50.7	c	
G19	8.9	fg	8.9	1	17.2	f	16.9	d	53.5	50.4	c-d	
Tekin	10.2	a-d	11.1	a-d	18.8	b-d	19.1	a-c	50.1	55.1	bc	
G21	9.6	c-g	9.6	f-1	18.2	c-f	17.6	cd	52.9	51.0	c	
G22	10.0	a-e	11.3	a-d	19.1	a-d	19.1	a-c	53.5	49.8	cd	
G23	9.9	a-f	11.4	a-d	18.9	b-d	20.0	a	56.3	58.7	a-c	
G24	10.3	a-c	10.0	e-h	20.0	ab	19.5	ab	55.4	54.2	c	
Ceyhan-99	9.4	c-g	9.4	f-1	18.9	b-d	19.2	a-c	48.4	47.2	c-d	
Average	9.9		10.4		18.8		19.3		52.1	53.5		
Lsd(0.05)	1.1**		1.1**		1.3**		1.7**		Ö.D	10.6*		

Evaluation of genotypes in terms of drought tolerance

Table 6 presents the drought tolerance parameters of the genotypes based on the average values over the two growing seasons.

Table 6. Two year averages of drought tolerance parameters

	Yp	Ys	TOL	STI	GMP	MP	HM	YSI	YI	DRI
G1	8480	6770	1710	0.79	757.9	763	753	0.80	1.07	0.86
G2	8190	6300	1890	0.71	718.6	725	712	0.77	1.00	0.77
G3	8910	6440	2480	0.79	757.5	768	748	0.72	1.02	0.74
G4	8860	6110	2750	0.75	735.9	749	723	0.69	0.97	0.67
Dinç	8550	6560	1990	0.77	748.8	755	742	0.77	1.04	0.80
G6	8500	6930	1570	0.81	767.2	771	763	0.82	1.10	0.90
G7	8590	6100	2490	0.72	723.9	735	713	0.71	0.97	0.69
G8	7880	6480	1400	0.70	714.3	718	711	0.82	1.03	0.84
G9	8210	5890	2320	0.67	695.7	705	686	0.72	0.93	0.67
Pehlivan	7930	5830	2100	0.64	680.2	688	672	0.73	0.92	0.68
G11	8640	6220	2420	0.74	732.9	743	723	0.72	0.99	0.71
G12	9050	6660	2390	0.83	776.3	785	767	0.74	1.06	0.78
G13	8180	5830	2350	0.66	690.8	701	681	0.71	0.92	0.66
G14	8650	6610	2040	0.79	756.4	763	750	0.76	1.05	0.80
Aday-12	8540	6110	2430	0.72	722.3	732	712	0.72	0.97	0.69
G16	9010	6450	2560	0.80	762.6	773	752	0.72	1.02	0.73
G17	8800	6140	2660	0.75	735.4	747	724	0.70	0.97	0.68
G18	8410	5860	2550	0.68	701.8	713	690	0.70	0.93	0.65
G19	8480	5820	2660	0.68	702.8	715	691	0.69	0.92	0.63
Tekin	8300	6230	2070	0.71	719.3	727	712	0.75	0.99	0.74
G21	8770	6950	1820	0.84	780.5	786	775	0.79	1.10	0.87
G22	8340	6510	1830	0.75	737.0	743	731	0.78	1.03	0.81
G23	8750	6430	2320	0.78	750.6	759	742	0.74	1.02	0.75
G24	8500	5840	2660	0.68	704.7	717	692	0.69	0.93	0.64
Ceyhan-99	8410	6560	1850	0.76	742.7	748	737	0.78	1.04	0.81
Average	8520	6310	2210	0.74	732.7	741	724	0.74	1.0	0.74

Yp: Grain yield in irrigated conditions, Ys: Grain yield in rainfed conditions, TOL: Tolerance, STI: Stress tolerance index, GMP: Geometric mean productivity (GMP), MP: Mean productivity, HM: Harmonic mean, YSI: Yield stability index, YI: Yield index, DRI: Drought resistance index.

Table 6 shows the results of drought tolerant parameters obtained by grain yield formulas under irrigated and rainfed conditions with the highest grain yield being obtained from G12 (9050 kg ha⁻¹) and G21 (6950 kg ha⁻¹), respectively. The tolerance index (TOL) indicates the yield differences between the best and worst conditions for genotypes. The lowest TOL was found in G8 and the highest in G4. G8 with the lowest TOL had higher grain yield than the experimental average for rainfed conditions but did not have better grain yield potential in irrigated conditions compared to other genotypes. Therefore, it can be stated that the performance of some genotypes does not greatly vary in favorable or poor environmental conditions. G4 can be considered as the genotype with the most favorable response to irrigation.

In addition, G17, G19 and G24 with high TOL values were identified as genotypes that had a positive response to irrigation, which significantly increased their yield potential. Although their TOL value was high, G3, G12 and G16 had high grain yields

both rainfed and irrigated conditions. This shows that these genotypes well adapted to both environments. Many researchers have reported that high values of STI, GMP, MP, HM and YI are indicative of the increased drought tolerance of genotypes (Fernandez, 1992; Ramirez and Kelly, 1998; Akçura et al., 2011; Aktaş, 2017).

In the current study, the highest values for these parameters were obtained from G6, G12, G16 and G21, suggesting that these genotypes had good grain yields under both irrigated and rainfed conditions. The remaining two drought parameters investigated in the study were YSI and DRI, which, at low levels, have been shown to indicate drought tolerance (Lan, 1998; Bouslama and Schapaugh, 1984). In the current study, the lowest YSI values belonged to G4 (0.69), G17 (0.70), G18 (0.70), G19 (0.69) and G24 (0.69) and the lowest DRI values were observed in G18 (0.65), G19 (0.63) and G24 (0.64). Anwar et al. (2011) and Aktaş (2017) reported that YI is associated with average yield in conditions presenting with water stress and can therefore be used in drought resistance studies. G6 and G21 were more prominent in terms of YI.

According to the biplot graph demonstrating the status of genotypes in terms of drought parameters and the relationship between these parameters (Figure 6); there was a significant positive relationship between; MP, STI, GMP and HM; YI and grain yield in irrigated conditions; DRI and YI and grain yield in rainfed conditions; and DRI and YSI. The best performing genotypes were found to be G12 and G16 for grain yield in irrigated conditions; G12 and G21 for MP, STI, GMP and HM; G21 for YI and grain yield in rainfed conditions; G6 for DRI and YSI; and G4, G19 and G24 for TOL. Furthermore, the MP, STI, GMP and HM parameters were found to be associated with grain yield in irrigated and rainfed conditions. Whereas YI, DRI and YSI were correlated with grain yield in rainfed conditions.

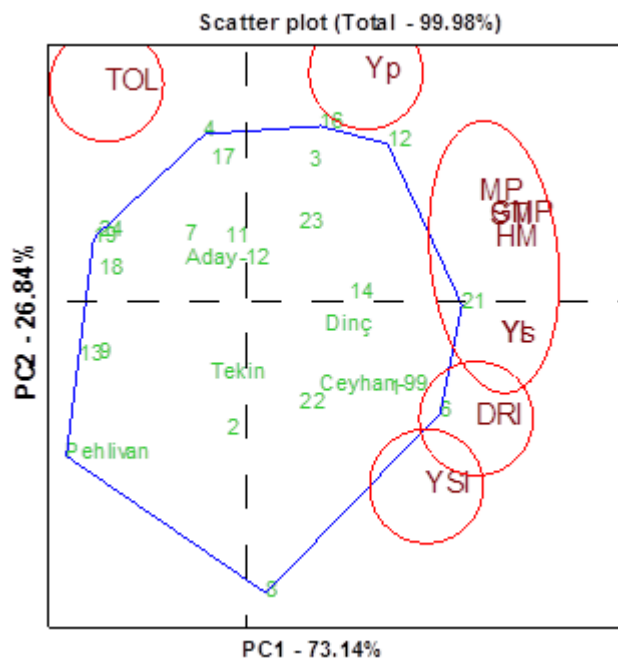


Figure 6. GGE-biplot of the correlation between genotypes and drought tolerance parameters

Conclusion

The results of ANOVA and GGE-biplot analyses of the experiments conducted in two growing seasons under different environmental conditions revealed that the prominent genotypes were G1, Dinç, G6, G12, G14, G21 and Ceyhan-99 for the rainfed conditions and G3, G4, G12, G16, G17, G21 and G23 genotypes for the irrigated conditions. G12 and G21 lines produced favorable results under both rainfed and irrigated conditions, which suggests that these lines better adapt to different climatic conditions than other genotypes. In addition, particularly in rainfed conditions, the G3 line performed better in both yield components (FSPS and SL) and technological quality parameters (TGW and HW). This line (G3) can be used as a parent in breeding studies. Concerning drought parameters, there was a significant positive relationship between MP, STI, GMP and HM, and a significant negative correlation between TOL and YSI. It was also determined that MP, STI, GMP and HM parameters can be used in the selection of genotypes suitable for irrigated and rainfed conditions and YI, DRI and YSI can assist in choosing the best genotypes for rainfed conditions presenting with water stress.

Based on the results of the study, we conclude that G6, G12, G16 and G21 are promising candidate lines for registration.

REFERENCES

- [1] Akçura, M., Partigoç, F., Kaya, Y. (2011): Evaluating of drought stress tolerance based on selection indices in Turkish bread wheat landraces. – *The Journal of Animal & Plant Sciences* 21(4): 700-709.
- [2] Aktas, H. (2017): Türkiye’de yoğun ekim alanına sahip bazı arpa (*hordeum vulgare* L.) çeşitlerinin destek sulamalı ve yağışa dayalı koşullarda değerlendirilmesi. – *Tekirdağ Ziraat Fakültesi Dergisi* 14(03): 86-97.
- [3] Anonim (2017): Diyarbakır Meteoroloji Bölge Müdürlüğü Kayıtları. – <https://www.mgm.gov.tr/Veri-degerlendirme/Il-ve-Ilceler-Istatistik.Asp?=&Diyarbakir>.
- [4] Anonymous (1990): Approved Methods of the American Association of Cereal Chemists. – American Association of Cereal Chemists, Approved Methods Committee, USA.
- [5] Anwar, J., Ghulam, M. S., Makhdoom, H., Javed, A., Mujahid, H., Munir, M. (2011): Drought tolerance indices and their correlation with yield in exotic wheat genotypes. – *Pakistan Journal Botany* 43(3): 1527-1530.
- [6] Atlı, A., Koçak, N., Aktan, M. (1993): Ülkemiz çevre koşullarının kaliteli makarnalık buğday yetiştirmeye uygunluk yönünden değerlendirilmesi. – *Orta Anadolu’da Hububat Tarımının Sorunları ve Çözüm Yolları Sempozyumu*, Konya: 345-351.
- [7] Aydoğan, S., Soylu, S. (2017): Ekmeklik buğday çeşitlerinin verim ve verim öğeleri ile bazı kalite özelliklerinin belirlenmesi. – *Tarla Bitkileri Merkez Araştırma Enstitüsü Dergisi* 26(1): 24-30.
- [8] Blum, A. (1998): *Plant Breeding for Stress Environments*. – CRC Press, Boca Raton, Florida.
- [9] Bohac, J., Cermin, L. (1969): A Study of The Correlation Between Factors Determining The Productivity of Wheat Ears. – *Plant Breed. Abs.* 39(1): 58.
- [10] Bouslama, M., Schapaugh, W. T. (1984): Stress tolerance in soybean. Evaluation of three screening techniques for heat and drought tolerance. – *Crop Science* 24: 933-937.
- [11] Chakherchaman, S. A., Mostafaei, H., Imanparastand, L., Eivazian, M. R. (2009): Evaluation of drought tolerance in lentil advanced genotypes in Ardabil region. – *Iran J. Food Agriculture Environment* 7(3-4): 283-288.

- [12] Chamurliyski, P., Atanasova, D., Penchev, E. (2015): Productivity of foreign common winter wheat cultivars (*Triticum aestivum* L.) under the conditions of dobrudzha region. – Agriculture & Forestry, Podgorica 61(1): 77-83.
- [13] Çetin, Ö., Uygan, D., Boyacı, H., Öğretir, K. (1999): Kışlık buğdayda sulama-azot ve bazı önemli iklim özellikleri arasındaki ilişkiler. – Türkiye III. Tarla Bitkileri Kongresi, Cilt I, 151-156, Adana.
- [14] Dhanda, S. S., Sethi, G. S., Behl, R. K. (2004): Indices of drought tolerance in wheat genotypes at early stages of plant growth. – J. Agronomy & Crop Science 190: 6-12.
- [15] Doğan, Y., Kendal, E. (2013): Diyarbakır koşullarında bazı ekmeklik buğday (*Triticum Aestivum* L.) genotiplerinin tane verimi ve bazı kalite özelliklerinin belirlenmesi. – YYÜ Tarım Bilimleri Dergisi 23(3): 199-208.
- [16] Doğan, Y., Kendal, E., Oral, E. (2016): Identifying of relationship between traits and grain yield in spring Barley by GGE biplot analysis. – Agriculture and Forestry 6(24): 239-252.
- [17] Erekul, O., Köhn, W. (2006): Effect of weather and soil conditions on yield components and bread-making quality of winter wheat (*Triticum aestivum* L.) and winter triticale (*Triticosecale Wittm.*) varieties in North-East Germany. – J. Agronomy and Crop Science 192: 452-464.
- [18] Erkul, E. (2006): Sulamalı koşullarda ileri ekmeklik buğday hatlarının tane verimi ve bazı kalite özelliklerinin belirlenmesi. – ADÜ Ziraat Fakültesi Dergisi 3(1): 27-32.
- [19] FAO. (2015): Food Agriculture Organization. – http://www.fao.org/index_en.htm.
- [20] Farshadfar, E., Jamshid, B., Aghaee, M. (2012): Biplot analysis of drought tolerance indicators in bread wheat landraces of Iran. – International Journal of Agriculture and Crop Sciences. IJACS/2012/4-5/226-233.
- [21] Fernandez, G. C. J. (1992): Effective selection criteria for assessing plant stress tolerance. – Proceedings of The International Symposium on Adaptation of Vegetable And Other Food Crops in Temperature and Water Stress, Taiwan: 257-270.
- [22] Gavuzzi, P., Rizza, F., Palumbo, M., Campaline, R. G., Ricciardiand, G. L., Borghi, B. (1997): Evaluation of field and laboratory predictors of drought and heat tolerance in winter cereals. – Plant Science 77: 523-531.
- [23] Gebeyehou, G., Knott, D. R., Baker, R. J. (1982): Relations among durations of vegetative and grain filling phases, yield components and grain yield in durum wheat cultivars. – CropSci 22: 287-290.
- [24] Genç, İ. (1974): Yerli ve Yabancı Ekmeklik ve Makarnalık Buğday Çeşitlerinde Verim ve Verime Etkili Başlıca Karakterler Üzerinde Araştırmalar. – Çukurova Üniversitesi Ziraat Fakültesi Yayınları, Yayın No: 82. Adana.
- [25] GENSTAT. (2009): GenStat for Windows (12th Edition) Introduction. – VSN International, Hemel Hempstead.
- [26] Gomez, K., Gomez, A. A. (1984): Statistical Procedures for Agricultural Research. – 2nd Edition. John Wiley and Sons. New York. 680 pp.
- [27] Hossain, A. B. S., Sears, A. G., Coxand, T. S., Paulsen, G. M. (1990): Desiccation tolerance and its relationship to assimilate partitioning in winter wheat. – CropScience 30: 622-627.
- [28] Karaman, M. (2013): Investigation of some physiological and morphological parameters in some bread wheat (*triticum aestivum* l.) varieties. – Master Thesis, Dicle University.
- [29] Karaman, M. (2017): Determination of physiological and morphological parameters associated with grain yield and quality traits in durum wheat. – Ph.D. Thesis, Dicle University.
- [30] Kendal, E. (2015): Relationship between chlorophyll and other features in durum wheat (*Triticum turgidum* L. var. durum) using SPAD and biplot analyses. – Journal of Agricultural Science and Technology 17: 1873-1886.

- [31] Kılıç, H., Akar, T., Kendal, E., Sayım, I. (2010): Evaluation of grain yield and quality of barley varieties under rainfed conditions. – African Journal of Biotechnology 9(46): 7825-7830.
- [32] Kılıç, H., Kendal, E., Aktaş, H. (2018): Evaluation of yield and some quality characters of winter barley (*hordeum vulgare* L.) genotypes using biplot analysis. – Agriculture & Forestry 64(3): 101-111. Podgorica.DOI: 10.17707/Agricultural Forest.64.3.09.
- [33] Kızılgöçü, F., Yıldırım, M., Akıncı, C., Albayrak, Ö. (2016): Bazı arpa genotiplerinin Diyarbakır ve Mardin koşullarında verim ve kalite parametrelerinin incelenmesi. – İğdır Üniversitesi Fen Bilimleri Enstitüsü. Dergisi 6(3): 161-169.
- [34] Knott, D. R., Talukdar, B. (1971): Increasing seed weight wheat yield and it's effects on yield components and quality. – Crop Sci. 11(2): 280-283.
- [35] Lan, J. (1998): Comparison of Evaluating Methods for Agronomic Drought resistance in Crops. – Acta Agricultural Boreali-Occidentalis Sinica 7: 85-87.
- [36] Mohammadi, M., Karimizadeh, R., Abdipour, M. (2011): Evaluation of drought tolerance in bread wheat genotypes under dryland and supplemental irrigation conditions. – Australian Journal of Crop Sciences 5(4): 487-493.
- [37] Nazar, H., Ereku, E., Koca, Y. O. (2012): Ekmeklik buğday çeşitlerinin tane verimi ve kalitesi üzerine farklı yaprak gübresi uygulamalarının etkisi. – Adnan Menderes Üniversitesi Ziraat Fakültesi Dergisi 9(2): 5-12.
- [38] Nouri, A., Etmianan, A., Teixeira da Silva, J. A., Mohammadi, R. (2011): Assessment of yield, yield-related traits and drought tolerance of durum wheat genotypes (*Triticum turjidum* var. durum Desf.). – Aust. J. Crop Sci. 5(1): 8-16.
- [39] Oral, E. (2018): Effect of nitrogen fertilization levels on grain yield and yield components in triticale based on AMMI and GGE biplot analysis. – Applied Ecology And Environmental Research 16(4): 4865-4878.
- [40] Öztürk, A., Akten, G. (1999): Some morpho-physiological characters in winter wheat and their effects on grain yield. – Tr. J. of Agriculture and Forestry 23 (Ek sayı 2): 409-422.
- [41] Öztürk, A., Aydın, F. (2004): Effect of water stress at various growth stages on some quality characteristics of winter wheat. – Journal of Agronomy and Crop Science 190(2): 93-99.
- [42] Öztürk, İ., Korkut, K. Z. (2018): Ekmeklik buğday (*Triticumaestivum*L)'ın farklı gelişme dönemlerinde kuraklığın verim ve verim unsurlarına etkisi. – Tekirdağ Ziraat Fakültesi Dergisi 15(2): 128-137.
- [43] Peterson, C. J., Graybosch, R. A., Baenziger, P. S., Grombacher, A. W. (1992): Genotype and environment effects on quality characteristics of hard red winter wheat. – Crop Sci. 32: 98-103.
- [44] Ramirez, P., Kelly, J. D. (1998): Traits Related to Drought Resistance in Common Bean. – Euphytica 99: 127-136.
- [45] Rosielle, A. A., Hamblin, J. (1981): Theoretical aspects of selection for yield in stress and non-stress environment. – Crop Science 21: 943-946.
- [46] Sayar, M. S. (2017): Additive main effects and multiplicative interactions (AMMI) analysis for fresh forage yield in common vetch (*Vicia sativa* L.) genotypes. – Agriculture and Forestry 63(1): 119-127.
- [47] Sönmez, F., Ülker, M., Yılmaz, N., Ege, H., Bürün, B., Apak, R. (1999): Relationship between grain yield and some yield components in Tır wheat. – Tr. J. of Agric. and Forestry 23: 45-52.
- [48] Şahin, M., Göçmen Akçacık, A., Aydoğan, S. (2008): Orta anadolu kuru ve sulmuş koşulları için tescil edilmiş ekmeklik buğday çeşitlerinin verim ve bazı kalite özellikleri yönünden performanslarının belirlenmesi. – Ülkesel Tahıl Sempozyumu. Konya: 390-400.
- [49] Thorne, G. N. (1966): Physiological Aspects of Grain Yield in Cereals. – Growth of Cereals and Grasses. Batter Worths.: 88-106.
- [50] TSI. (2015): Türkiye İstatistik Kurumu. – Bitkisel Üretim İstatistikleri, tuik.gov.tr

- [51] Yan, W., Tinker, N. A. (2006): Biplot analysis of multi-environment trial data. Principles and applications. – Canadian Journal of Plant Science 86: 623-645.
- [52] Yazar, S., Salantur, A., Özdemir, B., Alyamaç, M. E., Kaplan Evlice, E., Pehlivan, A., Akan, K., Aydoğan, S. (2013): Orta anadolu bölgesi ekmeklik buğday ıslah çalışmalarında bazı tarımsal karakterlerin araştırılması. – Tarla Bitkileri Merkez Araştırma Enstitüsü Dergisi 22(1): 32-40.
- [53] Yıldırım, A., Sakin, M. A., Gökmen, S. (2005): Tokat Kazova koşullarında bazı ekmeklik buğday çeşit ve hatlarının verim ve verim unsurları yönünden değerlendirilmesi. – GOÜ. Ziraat Fakültesi Dergisi 22(1): 63-72.

SEED PRIMING WITH ZINC MODULATE GROWTH, PIGMENTS AND YIELD OF CHICKPEA (*Cicer arietinum* L.) UNDER WATER DEFICIT CONDITIONS

MAHMOOD, A.^{1*} – KANWAL, H.¹ – KAUSAR, A.¹ – ILYAS, A.¹ – AKHTER, N.¹ – ILYAS, M.² – NISA, Z.¹ – KHALID, H.¹

¹Department of Botany, GC Women University
Arfa Kareem Road, Block Z Madina Town, Faisalabad City, Punjab Province, Pakistan

²Department of Home Economics, GC Women University
Arfa Kareem Road, Block Z Madina Town, Faisalabad City, Punjab Province, Pakistan

*Corresponding author

e-mail: ammaramahmood772@yahoo.com; phone: +92-334-744-4522

(Received 19th May 2018; accepted 31st Jul 2018)

Abstract. The research was conducted to assess the role of pre-sowing seed treatment with 0.05% ZnSO₄ solution on four varieties of chickpea (*Cicer arietinum* L.) i.e. CM 2008, FG 0902, DO 75-09 and Pb 2008 under three different drought conditions. Seeds primed with distilled water and 0.05% ZnSO₄ solution were sown in plastic pots filled with soil. The osmo-primed seeds were laid in completely randomized design. Drought was maintained in three levels i.e. control 100% FC, 70% FC and 35% FC. After one month of drought treatment 50% plant replicates were sampled for measurement of seed germination characteristics, growth attributes and chlorophyll pigments and left the remaining 50% plants for further growth. Drought was maintained till the crop ripening and at the end yield attributes were recorded. Water deficit stress decreased the germination rate, fresh and dry weight of root and shoot, total chlorophyll, chlorophyll a, chlorophyll b and carotenoid in all chickpea varieties. However, the seed priming with ZnSO₄ improved the growth conditions of the plants. ZnSO₄ seed priming also caused early germination than in non-primed. Overall, the results showed that CM 2008 and FG 0902 chickpea varieties were more drought tolerant than others while there was wide variation among chickpea varieties in response to seed priming with ZnSO₄ solution. Overall, ZnSO₄ seed priming alleviate the drought effect by enhancing the growth condition of plants and in turn the yield of chickpea cultivars.

Keywords: chickpea, drought, seed priming, yield, zinc

Introduction

Cicer arietinum L. is one of the important grain crops of developed and developing countries in terms of food and nutrition. It is included in the major legume plant and is on 3rd place after beans and peas with accounting 10.1 million tons yield production in the world (FAO, 2015). These three pulses (beans, peas, and chickpeas) account for about 70% of global pulse production with chickpea accounting for approximately 17% of the total annually (Muehlbauer and Sarker, 2017). It is a rich source of proteins (23%), carbohydrates (64%) and dietary fibers (19%) and with small amount of cholesterol and fats (Chibbar et al., 2010). Calcium, zinc, magnesium, phosphate, manganese, iron and vitamin K are also present in chickpea (Wood and Grusak, 2007). Water stress is found to be a major growth and yield limiting factor in chickpea around the world (Manjunath and Dhanoji, 2010).

Drought is a period of dry climate conditions which results in water deficit in soil and consequently in plants. Drought areas face below-average rainfall and scarcity of water supply which can last for months to years (Yadav et al., 2006; Toker et al., 2007).

Plants growth and reproduction is negatively affected by low water availability (Chen et al., 2012). In plants, photosynthesis, metabolic pathways and other physiological processes may cease due to intensive drought conditions (Jaleel et al., 2008). Various mineral nutrients depend on moisture of the soil to move through the soil texture and be absorbed by plants (Taiz and Zeiger, 2006). Under water deficit conditions, due to slow mineral diffusion and slow rate of water movement, roots are incapable to absorb several nutrients from the soil (Dubey and Pessaraki, 2001). Plants show different adaptive mechanisms against environmental stresses (Kanwal et al., 2018).

Different macro and micro elements are necessary for normal plant development. In which, micronutrients are chemical compounds required in small quantities but very essential for plant development and growth. Zinc is one of the key micronutrient for plants. Its deficiency in agricultural soils is common in all over the developed and developing countries especially in drought areas (Harris et al., 2007a; Dobermann and Fairhurst, 2000). It is reported that growth and yield of various crops, i.e. maize, wheat, rice etc. is affected by Zn deficiency (Harris et al., 2005, 2007a). The effects of Zn deficiency on plants can be overcome by external application of Zn. It can be applied in the form of fertilizer, spray and priming etc. (Singh, 2007; Farooq et al., 2009). However, seed priming is an easy and cost effective way of Zn application on plants (Salehi Arjmand et al., 2014). It is an extensively used commercial process for many crops that speed up the germination rate and enhances seedling consistency in various crops by triggering the certain physiological processes responsible for seed germination (Halmer, 2003). Seed priming with Zn solution enhanced the seed germination and seedling vigor index in *Hordeum vulgare* (barley) and *Cicer arietinum* (chickpea) as well as results in the maximum economic yield for *Triticum aestivum* (wheat) and *Zea mays* (maize) (Harris et al., 2007c, 2008).

In Pakistan, chickpea is traditionally grown on sandy soils of arid and semi-arid regions. Due to increasing pollution and change in climate water scarcity is a persistent phenomenon in Pakistan and mainly different areas of Baluchistan, Sindh and Southern Punjab are drought affected regions of Pakistan in agricultural point of view. In these regions agriculture and ecosystem are greatly affected by drought conditions (Setter et al., 2001; Reddy et al., 2004). Drought is one of the important limiting factors for chickpea growth and yield in these areas because economic factors and sandy soils do not allow artificial irrigation of chickpea crop. Zn deficiency also prevails in chickpea growing areas of Pakistan (Shah et al., 2007). To overcome the adverse effects of Zn deficiency on plants, seed priming with Zinc Sulphate ($ZnSO_4$) can be an effective way to improve the germination, growth and in turn yield of the crop (Harris et al., 2007b, 2008) and may be helpful in alleviating the adverse effects of drought. However, literature evidenced a little information about influence of $ZnSO_4$ seed priming in enhancing the growth condition and production of chickpea. So, the present study was aimed to assess the role of $ZnSO_4$ seed priming in enhancement of chickpea growth and yield under drought conditions.

Materials and methods

Description of the study site

Experiment was performed in research field area of Government College Women University, Faisalabad, Pakistan with day length of 11 h (light period) night length of 13 h (dark period) in 2015. The experimental time period was started from September

2015 and final yield was harvested in mid of April 2016. The approximate temperature crop faced was 28-34 °C. Geographically research field is located at 31°42' latitude and 73°08' longitude and it is situated at an elevation of 186 meters above sea level. Three drought levels (100-control, 70% and 35% field capacity) were maintained during the whole experiment.

Experimental design and crop establishment

Experiment was laid in completely randomized design and the treatments were analyzed in 4 × 2 × 3 factorial scheme with three replicates, in a total of 72 pots. Four chickpea cultivars (CM 2008, FG 0902, DO 75-09 and Pb 2008) were studied with two different seed priming treatments. The seeds of chickpea collected from Nuclear Institute for Agriculture and Biology (NIAB), Faisalabad, Pakistan. We took four chickpea cultivars, declared as drought resistant by NIAB.

The 72 pots were equally divided in to two sets (each set having 36 pots). One set of 36 pots with seeds primed with ZnSO₄ and other set of 36 pots having seeds primed with distilled water for 12 h. Ten seeds were sown in each plastic pot of 25 cm of diameter and 28 cm length. Each pot was filled with 8 kg of soil mixture with soil + sand + compost in 1:1:1 ratio (*Fig. 1*).

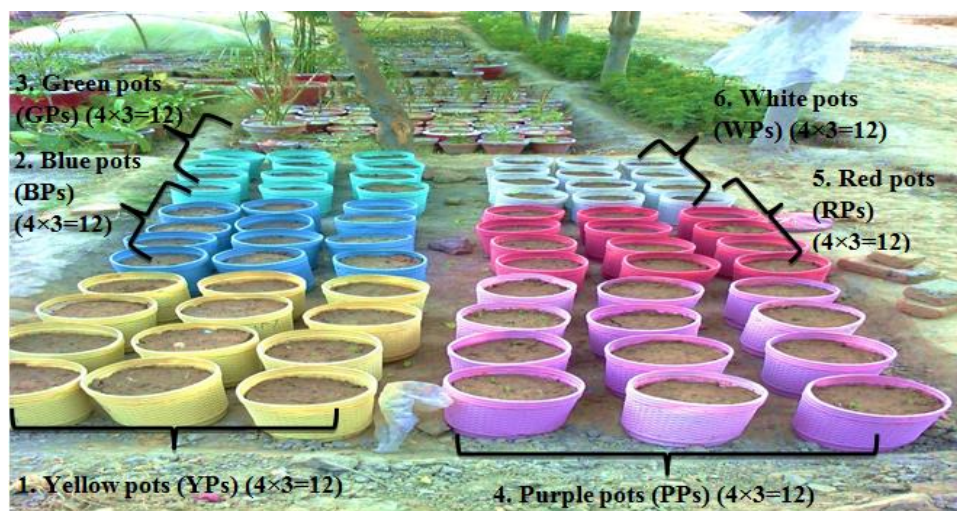


Figure 1. YPs = Controlled (100% FC + distilled water priming) BPs = 70% FC + distilled water priming, GPs = 35% FC + distilled water priming, PPs = 100% FC + ZnSO₄ Priming, RPs = 70% FC + ZnSO₄ Priming, WPs = 35% FC + ZnSO₄ Priming

Field capacity was determined by the estimation of the total moisture contents of the soil by following formula (Khakwani et al., 2012) to maintain the three drought levels.

$$\text{Field Capacity} = \text{saturation percentage} / 2$$

The research area was covered from upper side in order to avoid rainfall water to fall on pots. Thus the drought levels were under controlled conditions.

Observations recorded

After thirty days of germination, data for the following attributes was noted and at the crop ripening yield was recorded.

Seed germination characteristics

The recorded germination attributes include time of germination, number of seeds germinated, percentage germination, rate of germination and seed vigor index. Root and shoot length and fresh and dry weight of seedlings were also measured. These characters were assessed based on formulae (Seyedi et al., 2012; Goodi and Sharifzadeh, 2006) given below:

$$\text{Germination rate} = \frac{\sum ni}{\sum ni di}$$

(ni = number of seeds germinated, di = days of germination)

$$\text{Seed vigor index} = \frac{(\text{Shoot length} + \text{Root length}) \times \% \text{ Germination}}{100}$$

Growth attributes

Fresh shoot weight (FSW) and fresh root weight (FRW) was measured by using electrical balance. Prior to determination of fresh SW and RW, shoots and roots were washed with distilled water and then dried with towel. After that root length (RL) and shoot length (SL) were measured by using ruler. Then sample plants were oven dried for 48 h at 70 °C. After drying the samples their dry shoot weight (DSW) and dry root weight (DRW) were measured by using electrical balance.

Photosynthetic pigments

Chlorophyll pigments including Chlorophyll a, b, Chlorophyll a/b ratio, total chlorophyll content and carotenoids content were measured and calculated according to Lichtenthaler (1987). Concisely, fresh leaves were homogenized with cold acetone (80% v/v), and then centrifuged for 10 minutes at 5,000 rpm × g. The absorbance of each supernatant was read at 663, 645 and 480 nm.

Yield attribute

Yield attributes including number of pods per plant and total yield were recorded.

Statistical analysis

To analyze the data and draw graphs MSTAT and Microsoft Excel were used. MSTAT statistical software was used for the Analysis Of Variance. Wherever, F-test exhibited significant differences between means. Least Significant Differences (LSD) test was applied to compare the means at the 0.05 level of probability (Steel and Torrie, 1996).

Results

In present research, the influences of ZnSO₄ (0.05% w/v) seed priming on four chickpea cultivars were evaluated on the basis of seed germination parameters, growth

attributes, chlorophyll pigments and yield attributes under controlled and drought conditions.

Seed germination parameters

Seed germination characters such as germination percentage, rate of germination and seed vigor index (SVI) gave the minimum values under drought conditions in all chickpea cultivars as compared to control. While, seeds primed with ZnSO₄ exhibited significant (P < .05%) increase in these germination characters as compared to seeds primed with distilled water in all four chickpea cultivars under controlled as well as under drought stress levels. However, CM 2008 and FG 0902 cultivars gave more values of germination percentage, rate of germination and SVI than other cultivars in both conditions i.e. seeds primed with ZnSO₄ and with distilled water (Fig. 2, Table 1).

Table 1. Germination percentage (Ger. %), germination rate (Ger. Rate), seed vigor index (SVI), chlorophyll a (Chl. a), chlorophyll b (Chl. b), chlorophyll a/b ratio (Chl. a/b ratio), total chlorophyll (Total Chl), carotenoids contents of four chickpea cultivars from seeds primed with ZnSO₄ and distilled water and grown in moisture conditions in field capacity and drought stressed

Source of variation	df	Ger. %	Ger. Rate	SVI	Chl. a
Cultivars (Cvs)	3	39.47***	39.47***	92.39***	747.14***
Treatment (T)	1	263.16***	263.16***	312.60***	546.78***
Drought (D)	2	86.63***	86.63***	460.61***	198.58***
Cvs x T	3	4*	4*	8.62***	40.52***
Cvs x D	6	0.74ns	0.74ns	8.03***	88.24***
T x D	2	7.68**	7.68**	26.86***	38.99***
Cvs x T x D	6	0.11ns	0.11ns	0.40ns	9.05***
Error	48	52.78	0.01	53.38	6.16
Source of variation	df	Chl. b	Chl. a/b ratio	Total Chl.	Carotenoids
Cultivars (Cvs)	3	898.22***	369.27***	1023.75***	16.36***
Treatment (T)	1	730.59***	125.42***	1535.86***	57.92***
Drought (D)	2	384.98***	232.71***	226.97***	19.37***
Cvs x T	3	40.57***	5.05**	342.39***	1.08ns
Cvs x D	6	32.76***	60.55***	95.59***	3.26**
T x D	2	15.74***	15.20***	5.89**	8.50***
Cvs x T x D	6	2.22ns	3.33**	4.47**	0.75ns
Error	48	6.22	0.04	0.001	5.87

*, **and *** = significant at 0.05, 0.01, and 0.001 levels, respectively; ns = non-significant; df = degree of freedom

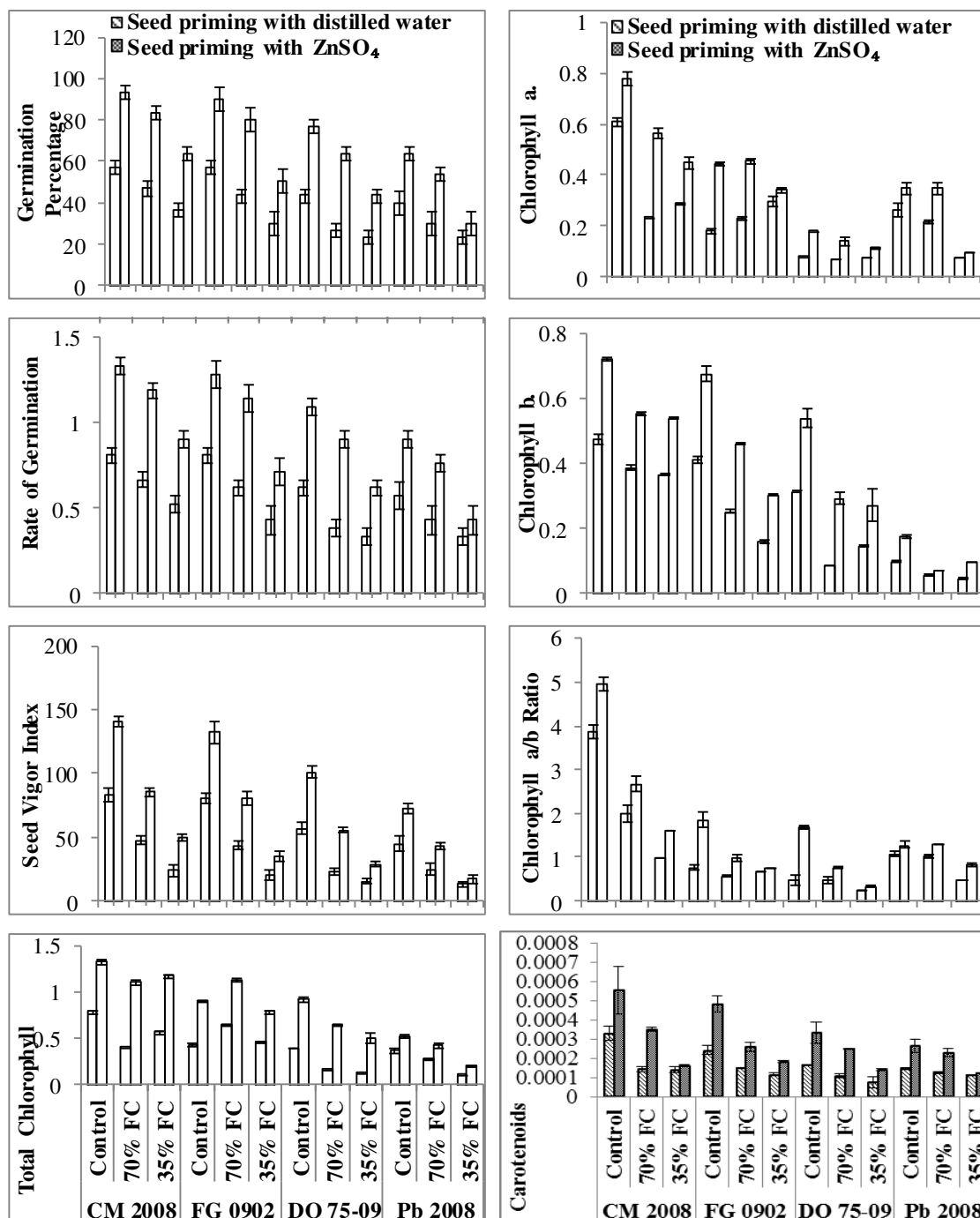


Figure 2. Seed germination and photosynthetic pigments characteristics of four chickpea cultivars raised from seeds primed with ZnSO₄ and distilled water as influenced under drought (Control, 70%FC and 35%FC) stress (Mean \pm S.E.)

Photosynthetic pigments

With increasing drought levels, in all cultivars gave the minimum values of chlorophyll a, chlorophyll b, total chlorophyll content, chlorophyll a/b ratio and carotenoid content was recorded. While, these attributes when measured in plants raised from ZnSO₄ primed seeds of all four cultivars gave more values as compared to distilled

water primed seeds under all three field capacities (100%, 70% and 35% FC). Among all cultivars, Pb 2008 exhibited slight increase in values of Chlorophyll a and Chlorophyll b with ZnSO₄ seed priming treatment at 35% FC and 70% FC respectively. While, DO 75-09 cultivar showed minute increase in the values of carotenoid content at 70% FC and 35% FC with ZnSO₄ seed priming treatment than with distilled water. However, CM 2008 and FG 0902 cultivars showed highly significant ($P < .05\%$) and gave more values in all chlorophyll pigment parameters and carotenoid content with ZnSO₄ seed priming than seeds primed with distilled water at all drought levels than that of other two cultivars (Fig. 2, Table 1).

Growth attributes

Minimum values were recorded in root length (RL) and shoot length (SL), fresh shoot (FSW) and fresh root weight (FRW), dry root (DRW) and dry shoot weight (DSW) under drought stress (70% FC and 35% FC) in all cultivars but seed priming with ZnSO₄ (0.05% w/v) caused a significant ($P < .05\%$) increase in these growth attributes under all levels of field capacities (100%FC, 70%FC and 35%FC) than in plants raised from seeds primed with distilled water. However, CM 2008 and FG 0902 cultivars treated with ZnSO₄ showed higher values of RL and SL as compared to seeds primed with distilled water under all drought conditions (100%, 70% and 35% field capacity) than other two cultivars (Fig. 3, Table 2).

Table 2. Shoot length (SL), root length (RL), shoot fresh weight (SFW), shoot dry weight (SDW), root fresh weight (RFW), root dry weight (RDW), pods per plant and total yield of four chickpea cultivars from seeds primed with ZnSO₄ and distilled water and grown in moisture conditions in field capacity and drought stressed

Source of variation	df	SL	RL	FSW	DSW
Cultivars (Cvs)	3	1285.69***	8338.13***	3396.11***	5559.96***
Treatment (T)	1	1403.62***	2152.22***	2609.36***	7955.87***
Drought (D)	2	2821.98***	94461.47***	29357.39***	123396.04***
Cvs x T	3	11.42***	38.79***	146.55***	118.001***
Cvs x D	6	107.79***	954.26***	22.96***	1000.45***
T x D	2	1.47ns	82.67***	46.97***	466.43***
Cvs x T x D	6	12.09***	74.19***	3.69**	116.49***
Error	48	0.215	0.22	0.02	3.29
Source of variation	df	FRW	DRW	Pods/Plant	Total Yield
Cultivars (Cvs)	3	5660.24***	1143.91***	51.29***	427.75***
Treatment (T)	1	1777.44***	2848.88***	99.19***	1566.97***
Drought (D)	2	33240.3***	3906.86***	33.58***	427.75***
Cvs x T	3	23.45***	292.86***	2.08ns	102.67***
Cvs x D	6	797.87***	155.09***	1.19ns	53.33***
T x D	2	371.18***	484.67***	4*	122.26***
Cvs x T x D	6	30.32***	20.23***	0.56ns	13.70***
Error	48	5.71	1.69	0.67	0.03

*, ** and *** = significant at 0.05, 0.01, and 0.001 levels, respectively; ns = non-significant; df = degree of freedom

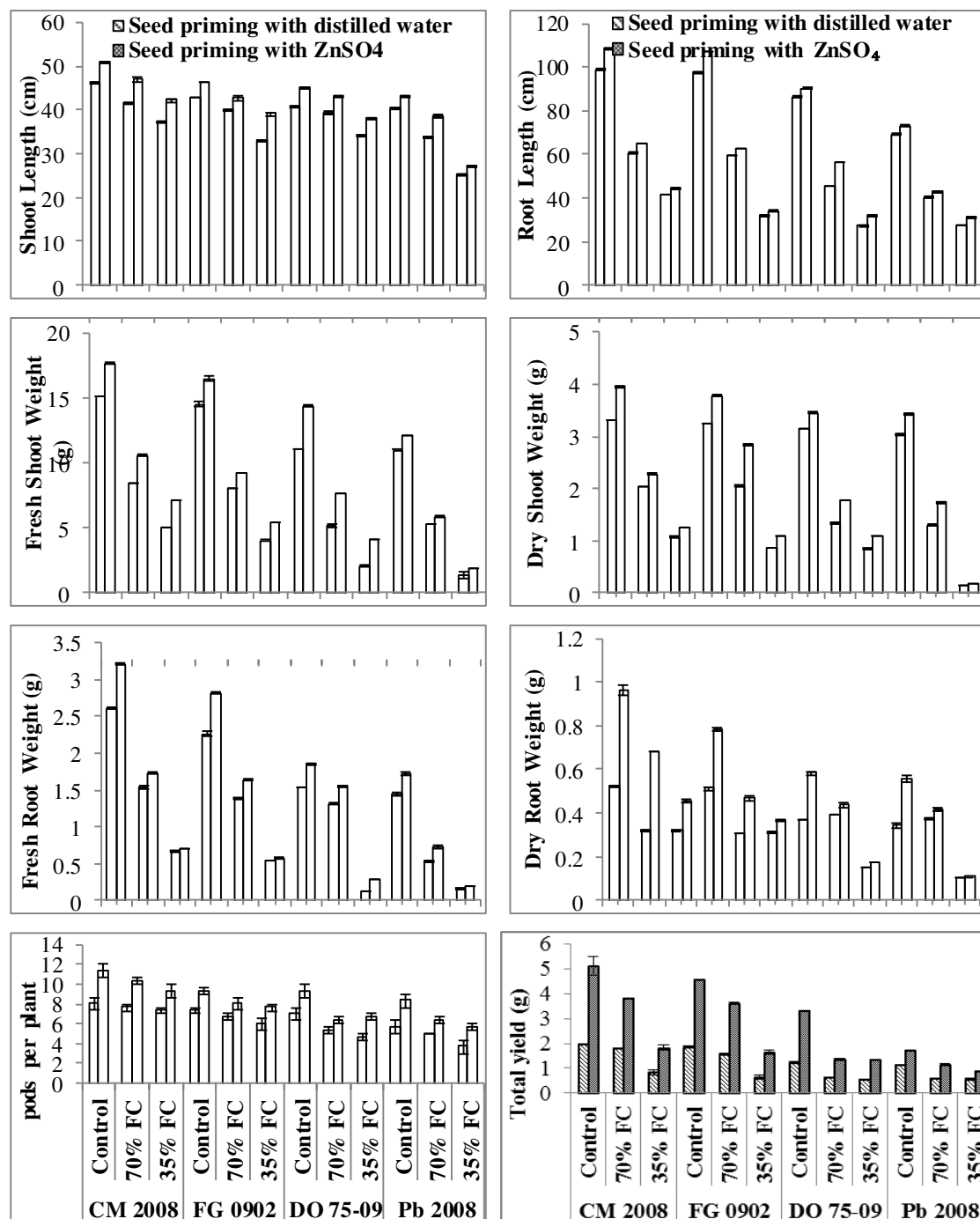


Figure 3. Growth and yield attributes of four chickpea cultivars raised from seeds primed with $ZnSO_4$ and distilled water as influenced under drought (Control, 70%FC and 35%FC) stress (Mean \pm S.E.)

Similarly, CM 2008 and FG 0902 cultivars showed the higher FSW and FRW values of seeds primed with $ZnSO_4$ under all drought levels as compared to seeds primed with distilled water. Seed priming with $ZnSO_4$ caused a slight increase in FSW and FRW of DO 75-09 under controlled and 70% drought condition. But DO 75-09 cultivar showed maxim values under controlled conditions while showed a slight difference of FSW and

FRW in ZnSO₄ primed and distilled water primed seeds under drought of 70% and 35% FC. DSW and DRW were also high significantly ($P < .05\%$) in plants raised from seeds primed with ZnSO₄ of all cultivars under controlled and water deficit conditions than in seeds primed with distilled water.

While, CM 2008 and FG 0902 cultivars showed higher values of DSW and DRW with treatment of ZnSO₄ seed priming under control, 70% FC and 35% FC than in distilled water primed seeds. While, DO 75-09 and Pb 2008 cultivars showed higher values of DSW and DRW under control and 70%FC but there was slight or no change under 35%FC in plants rose from seeds primed with water and ZnSO₄. Overall, CM 2008 and FG 0902 cultivars with ZnSO₄ seed priming treatment showed higher values of these attributes (FSW, FRW, DSW and DRW) than others (Fig. 3, Table 2).

Yield attributes

Yield attributes such as number of pods per plant and yield per plant were significantly ($P < .05\%$) decreased with increasing drought stress levels as compared to control. Whereas, the analysis of data showed that the application of ZnSO₄ (0.05% w/v) as seed priming treatment increased the overall yield of all four cultivars of chickpea under all three field capacities (100%, 70% and 35% field capacity) as compared to plants raised from distilled water primed seeds. However, CM 2008 and FG 0902 chickpea cultivars showed more enhanced yield as compared to other cultivars in plants raised from seeds primed with ZnSO₄ than that of plants raised from distilled water primed seeds under both controlled and water deficit conditions (Fig. 3, Table 2).

Discussion

Pre-sowing seed priming treatment with ZnSO₄ helped the plants to respond positively under different drought levels. Plants take up zinc as a divalent cation (Zn²⁺) from the soil. It is an eloquent nutrient for plant growth and development also functions as a co-factor of various enzymes such as Cu-Zn superoxide dismutase, RNA polymerase, alcohol dehydrogenase, carbonic anhydrase, etc. (Reddy, 2006). It is an important structural, functional and regulatory co-factor of various enzymes which help to enhance the activity of biochemical and physiological mechanisms in plants. Zn is an important component for the metabolism of carbohydrates and auxins, protein synthesis, etc. (Mengel et al., 2001; Broadley et al., 2007).

The results of this research showed that increased levels of drought stress caused decrease in percentage germination, rate of germination and seed vigor index of all chickpea cultivars while ZnSO₄ seed priming treatment enhances the values of all these attributes under all drought levels. The decrease occurred due to low availability of water which eventually resulted in reduction in values of germination attributes. Plant mineral nutrition, yield and growth face deleterious effects of drought stress (Garg et al., 2004; Samarah et al., 2004). Grewal and Williams (2000) reported the influence of Zn along with soil moisture stress on different varieties of *Medicago sativa* L. (alfalfa). They also suggested that alfalfa plants have the ability to tolerate with the excessive moisture stress as well as with water deficit conditions under adequate supply of Zn nutrient. While having a comparison of primed and non-primed seeds Karmore et al. (2015) reported that hydropriming treatment had significant effect on the growth of seedling than non-primed seeds. Slow rate of imbibition could be the cause of decreased seed vigour index in non-primed seeds (Fatemi, 2014). These all findings support the

enhancement of germination characters in present study due to seed priming with ZnSO₄ under all field capacities.

This study revealed that plants grown from ZnSO₄ primed seeds showed increase in values of all growth attributes as compared to developed from seeds primed with distilled water. According to previous research it has been reported that in wheat plants Zn plays an effective role in production of increased dry weight (Imtiaz et al., 2003; Ozkutlu et al., 2006). Arif et al. (2005) and Ali et al. (2007) reported that seed priming treatment with ZnSO₄ caused an increase in plant height. The shoot and root length are fundamental parameters, because roots absorb water and essential nutrients from the soil by having direct contact with it. Whereas, shoot transport the nutrients as well as water to the rest of the plant body. While having comparison with results provided on seed priming effect on growth parameters of maize, it has been revealed that ZnSO₄ seed priming treatment influenced positively shoot and root length of maize and pulses (Ambika and Balakrishnan, 2015).

An increased root length of plants grown from seeds primed with ZnSO₄ as compared to distilled water primed seeds could be the result of extensibility in cell wall of the embryo. Seed priming treatment caused increase in the activity of ROS (reactive oxygen species) scavenging enzymes in order to enhance the plant strength and viability (Ambika and Balakrishnan, 2015). Same researcher also reported that seed priming with ZnSO₄ solution decreased the resistance mechanism of endosperm envelope against growth permitting turgor threshold for germination as compared to non-primed seeds resulting increased shoot and root length. In another study, Harris et al. (2007a) reported that primed seeds show early seed vigour and significantly enhanced shoot and root length, as a result heavier seedlings production occur due to increased activity of α -amylase enzyme.

The results of this study showed that all chickpea cultivars primed with ZnSO₄ gave higher values of all chlorophyll pigment as compared to treated with distilled water under all drought levels. The results presented are the agreement with the findings of Nyachiro et al. (2001), who reported that in six cultivars of wheat the water deficit, caused a significant decrease in the concentration of chlorophyll a and b. it has also been reported that unchanged or decreased chlorophyll content could either be the result of severe drought or prolonged drought conditions (Mafakheri et al., 2010). The absorption of excess energy in the photosynthetic apparatus may be the main cause of ROS in large concentration it could be escaped by degrading the pigments responsible for their absorption (Herbinger et al., 2002). All genotypes showed decreased values of total chlorophyll content but the reduction was very low in tolerant cultivars (Deng et al., 2003) as in CM 2008 and FG 0902 chickpea cultivars in present study.

Carotenoids have a critical role as photoprotective compounds by quenching triplet and singlet oxygen derived from excess light energy, thus limiting membrane damage (Pogson et al., 2006; Tas, 2007). In present study, the higher accumulation of carotenoid in CM 2008 and FG 0902 chickpea cultivars under water stress could result in a positive effect on plant growth by affecting relative water content as reported by Talebi et al. (2013), Franca et al. (2000) and Gunes et al. (2008). However, the more enhanced increase in chlorophyll and carotenoid content in CM 2008 and FG 0902 chickpea cultivars raised from seeds primed with zinc as compared to distilled water primed seeds under control and drought conditions may be due to Zn which functions as a structural, functional and catalytic component of enzymes, proteins and also a co-factor for normal growth and development of biosynthetic pigments (Samreen et al., 2013).

Yield attributes were significantly increased in all chickpea cultivars grown from seeds primed with (0.05% w/v) ZnSO₄ solution as compared to grown from distilled water primed seeds under controlled and drought levels. Drought is one of the greatest yield limiting factors in agriculture (Reddy et al., 2004). Researcher, Harris et al. (2007b) suggested that seed priming with Zn caused a significant increase in weight of grains and total yield. Furthermore, priming treatment induced an increase in grain weight, total yield and plays a fundamental role in availability of Zn as a nutrient in diets of human and animals (Harris et al., 2007b). It is agreement with the results of present research. However, CM 2008 and FG 0902 chickpea cultivars showed more enhanced yield as compared to other cultivars.

Conclusion

From all above discussion, it can be inferred that drought stress adversely affected all the parameters studied in present research such as germination attributes, shoot and root length, shoot and root fresh and dry weights, photosynthetic pigments and yield characteristics were decreased under water deficit conditions in both sets of plants raised from seeds primed with ZnSO₄ (0.05%) solution and with distilled water. However, ZnSO₄ seed priming showed increased values for all mentioned attributes under control as well as under stressed environment in all chickpea cultivars. While, the results of different parameters showed that cultivars CM 2008 and FG 0902 were more tolerant to drought stress as compared to other cultivars. It can be concluded that ZnSO₄ seed priming has positive effect on plant growth and development and could be an effective mean of getting better yield under stressed as well as non-stressed environments. Thus, seed priming treatment of Zn micronutrient can be helpful for researchers to increase the crop resistance against abiotic stresses especially drought stress. However, it is also helpful to increase the yield of crops under drought stress as it increases the root capability to up take water and mineral nutrients from the soil.

Acknowledgements. The first and second authors greatly acknowledge the funding from Higher Education Commission (HEC) of Pakistan as this research work is a part of HEC funded research project entitled “Evaluation of drought tolerance in chickpea (*Cicer arietinum* L.) raised from seeds treated with ZnSO₄” (SRGP 466). The results of this research paper are included as research work of M.Phil studies of Miss. Ammara Mahmood. I would like to acknowledge Miss Amna Mahmood for her help in literature search, Tariq Mahmud Shah for providing seeds of chickpea varieties for study and Ali Noman for guiding me in paper write up.

Author contributions. This work was carried out in collaboration between all authors. ‘Author Ammara Mahmood’ designed the study, wrote the manuscript, managed the field work, practical analysis and wrote the protocol. ‘Author Hina Kanwal’ supervised the whole research work from the beginning to finish and also checked the final draft. ‘Author Noreen Akhter and Aisha Ilyas’ helped in field work and data collection. ‘Author Abida Kausar’ being member of my supervisory committee helped and guided me in laboratory work. ‘Author Madiha Ilyas’ helped to check the nutrient value of yield. ‘Author Zaib UN Nisa’ was paper write up checker. ‘Author Hafsa Khalid’ managed the literature searches. All authors read, checked and approved the final manuscript.

REFERENCES

- [1] Ali, S., Arif, M., Gul, R., Khan, A., Shah, S. S., Ali, I. (2007): Improving maize seed emergence and early seedling growth through water soaking. – Scientific Khyber 19: 173–177.
- [2] Ambika, S., Balakrishnan, K. (2015): Enhancing germination and seedling vigour in cluster bean by organic priming. – Scientific Research and Essays 10: 298–301.
- [3] Arif, M., Ali, S., Shah, A., Javed, N., Rashid, A. (2005): Seed priming maize for improving emergence and seedling growth. – Sarhad Journal of Agriculture 21: 539–543.
- [4] Broadley, M. R., White, P. J., Hammond, J. P., Zelko, I., Lux, A. (2007): Zinc in plants. – New Phytologist 173: 677–702.
- [5] Chen, J., Xu, W., Velten, J., Xin, Z., Stout, J. (2012): Characterization of maize inbred lines for drought and heat tolerance. – Journal of Soil and Water Conservation 67: 354–364.
- [6] Chibbar, R. N., Ambigaipalan, P., Hoover, R. (2010): Molecular diversity in pulse seed starch and complex carbohydrates and its role in human nutrition and health. – Cereal Chemistry Journal 87: 342–352.
- [7] Deng, X., Hu, Z. A., Wang, H. X., Wen, X. G., Kuang, T. Y. (2003): A comparison of photosynthetic apparatus of the detached leaves of the resurrection plant *Boea hygrometrica* with its non-tolerant relative *Chirita heterotrichia* in response to dehydration and rehydration. – Plant Science 165: 851–861.
- [8] Dobermann, A., Fairhurst, T. (2000): Rice: Nutrient Disorders and Nutrient Management. Handbook Series. – Potash and Phosphate Institute (PPI), Potash and Phosphate Institute of Canada (PPIC) and International Rice Research Institute.
- [9] Dubey, R. S., Pessarakli, M. (2001): Physiological Mechanisms of Nitrogen Absorption and Assimilation in Plants under Stressful Conditions. – In: Passarakli, M. (ed.) Handbook of Plant and Crop Physiology (2nd ed.) Marcel Dekker Inc, New York.
- [10] Farooq, M., Basra, S. M. A., Wahid, A., Khaliq, A., Kobayashi, N. (2009): Rice Seed Invigoration. – In: Lichtfouse, E. (ed.) Sustainable Agriculture Reviews. Springer, The Netherlands.
- [11] Fatemi, S. N. (2014): Germination and seedling growth in primed seeds of sunflower under water stress. – Annual Research and Review in Biology 4: 3459–3469.
- [12] Food and Agriculture Organization of the United Nations (FAO) (2007): On-Line Crop Database. – <http://ecocrop.fao.org/ecocrop/srv/en/cropSearchForm>.
- [13] Franca, M. G. C., Thi, A. T. P., Pimental, C., Rossiello, R. O. P., Fodil, Y. Z., Laffray, D. (2000): Differences in growth and water relations among *Phaseolus vulgaris* cultivars in response to induced drought stress. – Environmental and Experimental Botany 43: 227–237.
- [14] Garg, B. K., Burman, U., Kathju, S. (2004): The influence of phosphorus nutrition on the physiological response of moth bean genotypes to drought. – Journal of Plant Nutrition and Soil Science 167: 503–508.
- [15] Goodi, M., Sharifzadeh, F. (2006): Evaluation effect of hydropriming in barley difference cultivars. – Magazine Biaban 11: 99–109.
- [16] Grewal, H. S., Williams, R. (2000): Zinc nutrition affects alfalfa responses to water stress and excessive moisture. – Journal of Plant Nutrition 23: 949–962.
- [17] Gunes, A., Adak, A., Inal, M. S., Bagci, E. G., Cicek, N., Eraslan, F. (2008): Effect of drought stress implemented at pre- or post-anthesis stage some physiological as screening criteria in chickpea cultivars. – Russian Journal of Plant Physiology 55: 59–67.
- [18] Halmer, P. (2003): Methods to Improve Seed Performance. – In: Benech-Arnold, R. L., Sanchez, R. A. (ed.) Seed Physiology, Applications to Agriculture. Food Product Press, New York.
- [19] Harris, D., Rashid, A., Arif, M., Yunas, M. (2005): Alleviating Micronutrient Deficiencies in Alkaline Soils of the North-West Frontier Province of Pakistan: On-Farm

- Seed Priming with Zinc in Wheat and Chickpea. – In: Andersen, P., Tuladhar, J. K., Karki, K. B., Maskey, S. L. (eds.) Micronutrients in South and South East Asia. – ICIMOD, Kathmandu.
- [20] Harris, D., Rashid, A., Miraj, G., Arif, M., Shah, H. (2007a): On-farm seed priming with zinc sulphate solution, a cost-effective way to increase the maize yields of resource poor farmers. – *Field Crops Research* 110: 119–127.
- [21] Harris, D., Rashid, A., Miraj, G., Arif, M. Shah, H. (2007b): Priming seeds with zinc sulphate solution increases yields of maize (*Zea mays* L.) on zinc-deficient soils. – *Field Crops Research* 102: 119–127.
- [22] Harris, D., Rashid, G., Miraj, A., Arif, M., Yunas, M. (2007c): On-farm' seed priming with zinc in chickpea and wheat in Pakistan. – *Plant and Soil* 306: 3–10.
- [23] Harris, D., Rashid, A., Miraj, G., Arif, M. Yunas, M. (2008): On-farm seed priming with zinc in chickpea and wheat in Pakistan. – *Plant and Soil* 306: 03–10.
- [24] Herbinger, K., Tausz, M., Wonisch, A., Soja, G., Sorger, A., Grill, D. (2002): Complex interactive effects of drought and ozone stress on the antioxidant defense systems of two wheat cultivars. – *Plant Physiology and Biochemistry* 40: 691–696.
- [25] Imtiaz, M., Alloway, B. J., Shah, K. H., Siddique, S. H., Memon, M. Y., Aslam, M., Khan, P. (2003): Zinc nutritious of wheat: 1: Growth and zinc uptake. – *Asian Journal of Plant Sciences* 2: 152–155.
- [26] Jaleel, C. A., Manivannan, P., Lakshmanan, G. M. A., Gomathinayagam, M., Panneerselvam, R. (2008): Alterations in morphological parameters and photosynthetic pigment responses of *Catharanthus roseus* under soil water deficits. – *Colloids and Surfaces B: Biointerfaces* 61: 298–303.
- [27] Kanwal, H., Hameed, M., Akhter, N., Ilyas, A., Mahmood, A., Noreen, N. (2018): Ecological and taxonomic significance of root anatomy in some species and cultivars of genus *Canna* L. – *International Journal of Agricultural and Environmental Research* 5(1): 128–137.
- [28] Karmore, V. J. Tomar, G. S. (2015): Effects of seed priming methods on germination and seedling development of winter maize (*Zea mays* L.). – *Advance Research Journal of Crop improvement* 6: 88–93.
- [29] Khakwani, A. A., Dennett, M. D., Munir, M., Baloch, M. S. (2012): Wheat yield response to physiological limitations under water stress condition. – *Journal of Animal and Plant Sciences* 22: 773–780.
- [30] Lichtenthaler, H. K. (1987): Chlorophylls and carotenoids: Pigments of photosynthetic membranes. – *Methods in Enzymology* 148: 350–382.
- [31] Mafakheri, A., Siosemardeh, A., Bahramnejad, B., Struik, P. C., Sohrabi, Y. (2010): Effect of drought stress on yield, proline and chlorophyll contents in three chickpea cultivar. – *Australian Journal of Crop Science* 4: 580–585.
- [32] Mengel, K., Kirkby, E. A., Kosegarten, H., Appel, T. (2001): Principles of Plant Nutrition. – Kluwer Academic Publishers, Dordrecht.
- [33] Manjunath., B. L., Dhanoji, M. M. (2010): Effect of seed hardening with chemicals on drought tolerance traits and yield in chickpea (*Cicer arietinum* L.). – *Journal of Agricultural Science* 3: 186–189.
- [34] Nyachiro, J. M., Briggs, K. G., Hoddinott, J., Johnson-Flanagan, A. M. (2001): Chlorophyll content, chlorophyll fluorescence and water deficit in spring wheat. – *Cereal Research Communications* 29: 135–142.
- [35] Ozkutlu, F., Torun, B., Cakmak, I. (2006): Effect of zinc humate on growth of soybean and wheat in zinc-deficient calcareous soils. – *Communications in Soil Science and Plant Analysis* 37: 2769–2778.
- [36] Pogson, B. J., Rissler, H. M., Frank, H. A. (2006): The Roles of Carotenoid in Energy Quenching. – In: Wydrzynski, T., Satoh, K. (eds.) Photosystem II. The Water/Plastoquinone Oxidoreductase in Photosynthesis. Springer, Dordrecht.

- [37] Reddy, A. R., Chaitanya, K. V., Vivekanandan, M. (2004): Drought induced responses of photosynthesis and antioxidant metabolism in higher plants. – *Journal of Plant Physiology* 161: 1189–1202.
- [38] Reddy, K. J. (2006): Nutrient Stress. – In: Rao, K. V. M., Raghavendra, A. S., Reddy, K. J. (ed.) *Physiology and Molecular Biology of Stress Tolerance in Plants*. Springer, Netherlands.
- [39] Salehi Arjmand, H., Babaei, G. H., Ghorbanpour, M., Sharafi, S. (2014): Effect of zinc coated during storage on the seed quality of barley. – *International Journal of Farming and Allied Sciences* 3: 845–850.
- [40] Samarah, N., Mullen, R., Cianzio, S. (2004): Size distribution and mineral nutrients of soybean seeds in response to drought stress. – *Journal of Plant Nutrition* 27: 815–835.
- [41] Samreen, Humaira, T., Hamidullah, S., Saleem, U., Javid, M. (2013): Zinc effect on growth rate, chlorophyll, protein and mineral contents of hydroponically grown mungbeans plants (*Vigna radiata*). – *Arabian Journal of Chemistry* 10: 1802–1807.
- [42] Setter, T. L., Flannigan, B. A., Melkonian, J. (2001): Loss of kernel set due to water deficit and shade in maize: carbohydrate supplies, abscisic acid, and cytokinins. – *Crop Science* 41: 1530–1540.
- [43] Seyedi, M., Hamzei, J., Fathi, H., Bourbour, A., Dadrasi, V. (2012): Effect of seed priming with zinc sulfate on germination characteristics and seedling growth of chickpea (*Cicer arietinum* L.) under salinity stress. – *International Journal of Agriculture: Research and Review* 2(3): 108-114.
- [44] Shah, N. A., Aujla, K. M., Abbas, M., Mahmood, K. (2007): Economics of chickpea production in the Thal desert of Pakistan. – *Pakistan Journal of Life and Social Sciences* 5: 6–10.
- [45] Singh, M. V. (2007): Efficiency of seed treatment for ameliorating zinc deficiency in crops. – In: *Zinc Crops, Improving Crop Production and Human Health*, 24-26 May, 2007, Istanbul, Turkey.
- [46] Steel, R. G. D., Torrie, J. H., Dickey, D. A. (1996): *Principles and Procedures of Statistics: A Biometrical Approach* (3rd ed.). – McGraw Hill Co, New York, USA.
- [47] Taiz, L., Zeiger, E. (2006): *Plant Physiology* (4th ed.). – Sinauer Associates, Massachusetts.
- [48] Talebi, R., Ensafi, M. H., Baghebani, N., Karami, E., Mohammadi, K. (2013): Physiological responses of chickpea (*Cicer arietinum*) genotypes to drought stress. – *Environmental and Experimental Biology* 11: 9–15.
- [49] Tas, S., Tas, B. (2007): Some physiological responses of drought stress in wheat genotypes with different ploidity in Turkey. – *World Journal of Agricultural Sciences* 3: 178–183.
- [50] Toker, C., Lluch, C., Tejera, N. A., Serraj, R., Siddique, K. H. M. (2007): Abiotic Stresses. – In: Yadav, S. S., Redden, R., Chen, W., Sharma, B. (eds.) *Chickpea Breeding and Management*. CABI, Wallingford.
- [51] Wood, J. A., Grusak, M. A. (2007): Nutritional Value of Chickpea. – In: Yadav, S. S., Redden, R., Chen, W., Sharma, B. (eds.) *Chickpea Breeding and Management*. CABI Publishing, Houston, USA.
- [52] Yadav, S. S., Kumar, J., Yadav, S. K., Singh, S., Yadav, V. S., Turner, N. C., Redden, R. (2006): Evaluation of *Helicoverpa* and drought resistance in desi and kabuli chickpea. – *Plant Genetic Resources* 4: 198–203.

HYDROLOGICAL AND ECOLOGICAL EFFECTS OF CLIMATE CHANGE IN CAOHAİ WATERSHED BASED ON SWAT MODEL

ZHOU, C. W.¹ – YANG, R.^{2*} – YU, L. F.¹ – ZHANG, Y.¹ – YAN, L. B.¹

¹*College of Life Sciences, Guizhou University, Guiyang, Guizhou, China*
(e-mails: C. W. Zhou – changwei.1981@163.com; L. F. Yu – gdyulifei@163.com; L. B. Yan – link_yan@126.com)

²*College of Forestry, Guizhou University, Guiyang, Guizhou, China*

**Corresponding author*
e-mail: yr553017@163.com

(Received 15th Sep 2018; accepted 12th Nov 2018)

Abstract. To understand the impact of meteorological changes on hydrological and water quality in Caohai watershed, Guizhou Province, China, based on the ArcGIS software, the land use map of Caohai watershed in 2017 was used to construct the land use database in the SWAT model, and then the soil database and the default meteorological database were used to establish the SWAT model of the Caohai Dongshan river watershed, the Zhonghe river watershed, the Baima river watershed and the Haizi river watershed. Sixteen climatic scenarios were set to simulate the hydrological response process of Caohai watershed. The results of the model analysis show that the variation of surface runoff and total nitrogen and phosphorus in each watershed is different when the temperature of the watershed rises by 1 °C and the precipitation remains unchanged. Under the same rainfall gradient, the surface runoff decreases with the increase of temperature; under the same temperature gradient, the surface runoff increases with the increase of rainfall, and the change of total nitrogen and phosphorus is more complex, which is related to the soil type and land cover.

Keywords: *hydrological effects, ecological effects, climate change, SWAT model, Caohai*

Introduction

Since the industrial revolution, with the rapid development of the industrial field, the concentration of greenhouse gases such as CO₂ and SO₂ in the atmosphere has increased, resulting in a global greenhouse effect, and the warming of the global climate (Ge et al., 2014). According to climate research in the past 50 years in China, the rate of the average temperature rise is the fastest in the north, and precipitation increases by different degrees in the southwest and west, the middle and lower reaches of the Yangtze river and the southeastern hilly areas. The precipitation increases most significantly in the western watershed, while precipitation decreases in north China, in the south, and in the northeast (Chen et al., 2019; Xiao and Tan, 2018; Zhao et al., 2018; Hu et al., 2013).

The study of water resources by climate change has become one of the most important environmental problems in the 21st century (Solomon, 2007). Climate change affects the water cycle directly or indirectly by influencing regional temperature, precipitation, evaporation, etc. Therefore, the effect of climate change on hydrology is mainly studied by simulating the changes of meteorological factors to predict the effect of the possible increase or decrease of runoff on river watershed water resources (Liu et al., 2008). Vegetation conditions and local climate can interact with each other and climate change. It is an important factor in vegetation growth conditions, and the distribution of vegetation on the ground surface. Growth changes also affect regional

climate (Wang et al., 2014). Specifically, climate affects the growth and distribution of vegetation, and at the same time the height of vegetation. The coverage is different, resulting in reflectance, underlying surface roughness and other surface bars. These differences will change regional climate conditions such as water cycle, Gas-heat cycle and so on. (Shen et al., 2015). The spatial distribution characteristics of vegetation restoration in the Loess Plateau are strip-like and consistent with the agroclimatic region. (He et al., 2015), and the effect of climate on vegetation is delayed (Zhang et al., 2016).

The ecosystem has undergone remarkable changes under the combined influence of climate change and human activities, and the study of the relationship between vegetation and these two has become the focus and core of scholars all over the world (Lu et al., 2017). Based on meteorological data Niu (2013) calculates runoff in and out of the river shutoff watershed for many years. Taking 1983-1987 as the base period, based on the hydrological parameters determined by SWAT-CUP software, a distributed hydrological model is used to simulate the runoff change of the river shutoff watershed.

The annual and seasonal mean temperatures in Guizhou Province have fluctuated and increased in the past 57 years, with an annual average heating rate of 0.13 C/10a. The change of temperature in four seasons is significant, and the trend of change of autumn temperature and winter temperature is obviously higher (Zhu et al., 2018). This study aimed to understand the impact of meteorological changes on hydrological parameters and water quality in Caohai watershed.

Research method

Study area profile

Caohai is located in the eastern part of the Yunnan-Guizhou Plateau, in the northwestern part of Guizhou Province, on the southwest side of Weining Yi Nationality Hui and Miao Autonomous County in the Wumen Mountain (Ha et al., 2017) (N26°49'–26°53', E104°12'–104°18'). It is the largest natural lake and water area on the Guizhou Plateau. The Caohai reserve area is 96 square kilometers, and the water area is 20 km². It belongs to the tropical monsoon humid climate zone. It is characterized by no severe cold in winter, no heat in summer, large daily temperature difference and small annual temperature difference. The average annual temperature is about 10.6, the minimum annual temperature is 1.7 °C, the highest annual temperature is 17.6 °C, the average annual precipitation is 909 mm, the average annual sunshine hours is 1800 h, the frost-free period is 180 days, the dry and wet season are distinct. May-October is the rainy season, the rainfall in this period is accounted for 88% of the precipitation throughout the whole year, from December to March there is only 5% of the total annual rainfall (Zheng et al., 2013; Xia et al., 2016).

Data acquisition

Land use data acquisition

Interpreting the high-definition image data of Caohai watershed (2 m × 2 m) in 2017 for land use classification, the land use types in the study area are divided into six categories, and the land use codes were converted according to the model requirements.

The converted land use codes were AGRL (cultivated land), FRSD (forest land), PAST (grassland), WATR (water area), URML (Construction land), SWRN (unused land).

Soil data acquisition

Based on the HWSO data and the world soil grid map, it is found that there are four main types of soil in the Caohai, namely, HAPLIC LUVISOLS1, HAPLIC LUVISOLS2, WATER BODIES, DUNES & SHIFT.SANDS. The three variables missing in Chinese soil data, namely, SOL_BD of soil moisture density, SOL_AWC of effective water holding, and SOL_K of saturated water conductivity, need to be calculated by using SPAW software.

The method of estimating soil erosion factor K, which was improved by Williams (1983) in EPIC model, is more convenient. Only soil organic carbon and soil particle data were used to estimate K value (Eqs. 1–5).

$$K_{USLE} = f_{csand} \times f_{cl-si} \times f_{orgc} \times f_{hisand} \quad (\text{Eq.1})$$

$$f_{csand} = 0.2 + 0.3 \times e^{[-0.256 \times M_{sand} \times (1 - \frac{M_{silt}}{100})]} \quad (\text{Eq.2})$$

$$f_{cl-si} = \left(\frac{M_{silt}}{M_{clay} + M_{silt}} \right)^{0.3} \quad (\text{Eq.3})$$

$$f_{orgc} = 1 - \frac{0.25 \times orgC}{orgC + e^{(3.72 - 2.95 \times orgC)}} \quad (\text{Eq.4})$$

$$f_{hisand} = 1 - \frac{0.7 \times (1 - \frac{M_{sand}}{100})}{(1 - \frac{M_{sand}}{100}) + e^{[-5.51 + 22.9 \times (1 - \frac{M_{sand}}{100})]}} \quad (\text{Eq.5})$$

In the formula, M_{sand} is the 0.05-2.00 mm sand content, M_{silt} is the 0.002-0.05 mm clay content, M_{clay} is the 0.02 mm powder content, $orgC$ is the organic carbon content.

Acquisition of meteorological data

Based on the meteorological data from SWAT meteorological database, the climate change in the study area is simulated.

Results and analysis

Caohai sub watershed division

Based on the generated river network map, the Caohai watershed was divided into four watersheds, namely Dongshan river watershed, Zhonghe river watershed, Baima river watershed, and Maojiahaizi river watershed. Then, the SWAT model was used to divide the -watersheds of each watershed. In the division of SWAT watershed, lake surface is selected as the outlet of each river watershed, and the specific watershed division of each river watershed is shown in *Figure 1*.

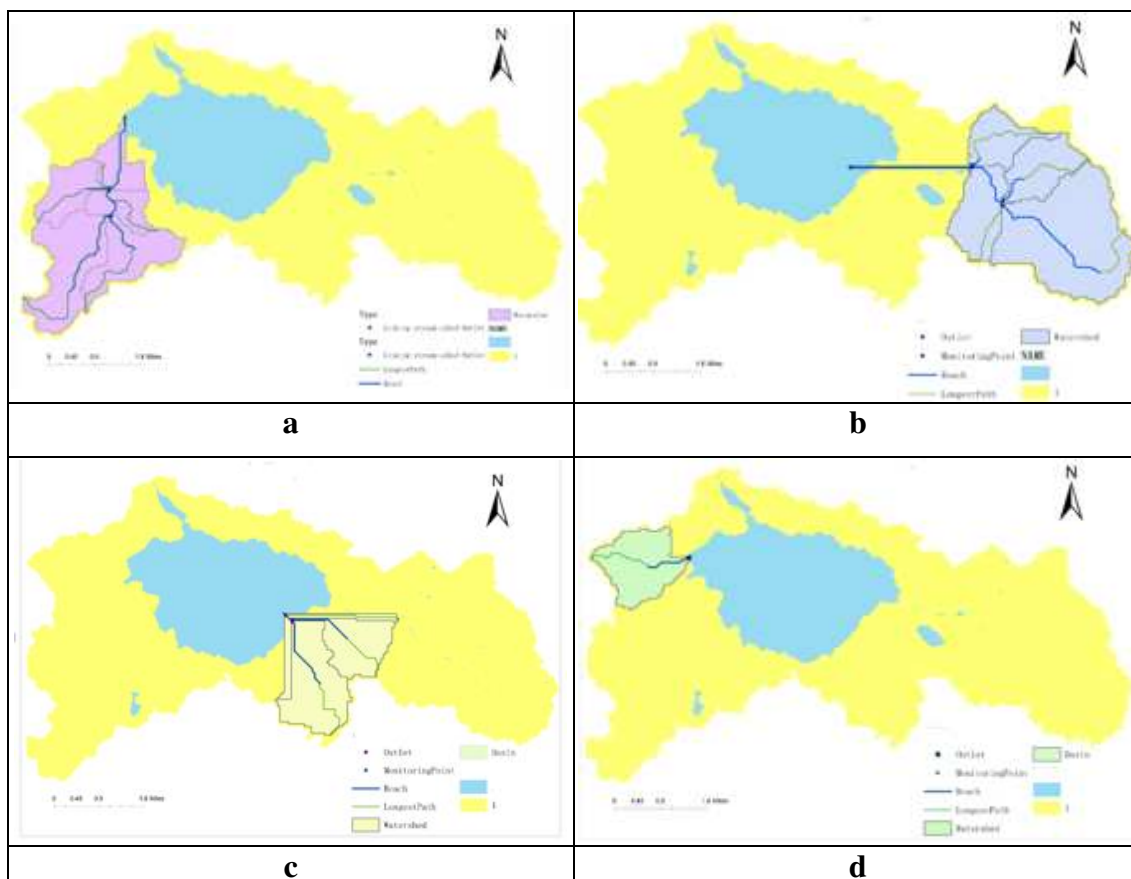


Figure 1. Sub watershed map of the area of the Maojiahaizi river watershed. **a** Dongshan river watershed, **b** Zhonghe river watershed, **c** Baima river watershed, **d** Maojiahaizi river watershed

Analysis of response unit of hydrology to climate change

The meteorological data have an important impact on the water cycle. Most of the rivers flowing into the Caohai are small rivers in the surrounding areas, most of which originate from springs. The supply of water resources in the Caohai is very limited. The reason why the Caohai can basically maintain the natural environment of the lakes and marshes is that the hydrogeological structure of the Caohai is conducive to the storage of surface water and groundwater, and the main recharge of surface water and groundwater in the Caohai area comes from precipitation. In the trend of global warming, meteorological factors will also change. In this paper, the response of hydrology to climate change in the Caohai watershed is carried out by simulating the changes of the temperature and precipitation values. The runoff of a river watershed is changed by local climatic conditions and the underlying conditions of the river watershed. Therefore, this paper analyzes the hydrological response to climate change in the Caohai watershed by changing the influence of temperature and precipitation on the annual average runoff, total nitrogen and total phosphorus of the Caohai.

Assume that the highest and lowest temperatures on the basis of the original were +0 °C, +1 °C, +3 °C, +5 °C, annual precipitation change on the basis of the original were -5%, 0%, +5%, +10%, changing the SWAT model to the highest temperature of the meteorological database (TMPMX), the lowest temperature (TMPMN) and monthly total precipitation (PCPMM) it was used to simulate climate change in Caohai

watershed runoff, and its influence to total nitrogen and phosphorus in the valley. Finally, the annual runoff (total nitrogen and phosphorus) and the percentage of annual runoff (total nitrogen and phosphorus) under unchanged climatic conditions were used to represent the change of annual runoff (b) (total nitrogen and phosphorus).

$$b = \frac{(y_i - y_0)}{y_0} \times 100\% \quad (\text{Eq.6})$$

In *Equation 6*: y_i is the annual average runoff (total nitrogen and phosphorus) (m^3/s) under the i climate scenario, y_0 is the annual average runoff (total nitrogen and phosphorus) (m^3/s) without changing the climate conditions.

Analysis of surface runoff in Caohai watershed under different climate scenarios

Annual runoff data of watershed are derived from surface runoff of watershed during the simulation period (SURFACE RUNOFFQ) in the output summary file (OUTPUT.STD) of SWAT model. The analysis of each watershed is shown in *Tables 1–4*.

In the rows of *Table 1* it can be observed that when the temperature is constant, the rainfall decreases by 5% compared to the original value, the surface runoff decreases by 0.003%, the rainfall increases by 5%, the surface runoff increases by 0.007%, the rainfall increases by 10%, and the surface runoff increases by 0.013%. When the temperature rises by 1 °C, the precipitation decreases by 1.351%, the precipitation decreases by 5%, the surface runoff decreases by 1.371%, the precipitation decreases by 0.02%, the rainfall increases by 5%, the runoff decreases by 1.341%, the rainfall increases by 10%, and the surface runoff decreases by 1.338%.

In the columns of *Table 1* it can be observed that in the case of constant rainfall, if the temperature rises by 1 °C, the surface runoff decreases by 1.351%; if the temperature rises by 3 °C, the surface runoff decreases by 3.711%; if the temperature rises by 5 °C, the surface runoff of the watershed decreases by 5.348%. When the rainfall increased by 5%, the temperature increased by 1 °C, the surface runoff decreased by 3.704%, the temperature increased by 5 °C, and the surface runoff decreased by 5.345%.

Table 1. Runoff change rate under climate change scenarios in Dongshan river watershed

Temperature change	Precipitation change			
	-5%	0%	+5%	+10%
0 °C	-0.003	0.000	0.007	0.013
1 °C	-1.371	-1.351	-1.341	-1.338
3 °C	-3.714	-3.711	-3.704	-3.701
5 °C	-5.352	-5.348	-5.345	-5.342

It can be seen from *Table 2* that when the temperature rises by 0 °C and the precipitation decreases by 5%, the surface runoff in the Zhonghe river watershed reduces by 0.006% compared with the climate-invariant scenario, the rainfall increases by 5%, 10%, and the surface runoff increases by 0.006% and 0.013%. When the temperature rises by 1°C, the rainfall is unchanged, the surface runoff reduces by

1.309%; when the rainfall reduced by 5%, the runoff reduced by 1.324%, which reduced by 0.15% compared with the same temperature and rainfall; The rainfall decreased by 5% and 10%, and the runoff decreased by 1.296% and 1.289 respectively, which was increased by 0.013% and 0.02% compared with the same temperature and rainfall. When the temperature rises by 3°C, the rainfall does not change, the surface runoff reduces by 3.118% compared with the climate constant scenario; when the rainfall reduces by 5%, the surface runoff reduces by 3.125%, when rainfall increased by 5% and 10%, surface runoff decreased by 3.112% and 3.109% respectively, but it increased by 0.006% and 0.009% compared with the same temperature and rainfall, when the temperature rises by 5 °C, the surface runoff decreases by 4.150%, when the rainfall changes by - 5%, +5%, +10%, the surface runoff changes little compared with the same temperature and rainfall.

Table 2. Runoff change rate under climate change scenarios in Zhonghe river watershed

Temperature change	Precipitation change			
	-5%	0%	+5%	+10%
0 °C	-0.006	0.000	0.006	0.013
1 °C	-1.324	-1.309	-1.296	-1.289
3 °C	-3.125	-3.118	-3.112	-3.109
5 °C	-4.762	-4.761	-4.759	-4.756

In the columns of *Table 3* it can be observed that the surface runoff is increasing with the increase of rainfall at the same temperature in the Baima river watershed. In the rows of the table it can be observed that under the same rainfall gradient, with the increase of temperature, the surface runoff shows a trend of decreasing. When the temperature rises by 1 °C, the runoff increases by 0%, and the surface runoff decreases by 1.127% compared with the climate-invariant scenario; When the rainfall decreased by 5%, the surface runoff decreased by 1.138%, which was 0.011% lower than the same temperature precipitation; The rainfall increased by 5% and 10% respectively, and the surface runoff increased by 0.002% and 0.004%, which was 1.129% and 1.131% higher than the same temperature precipitation. When the temperature increased by 3 °C and 5 °C, the rainfall did not change, and the surface runoff decreased by 2.966% and 4.150%.

Table 3. Runoff change rate under climate change scenarios in Baima river watershed

Temperature change	Precipitation change			
	-5%	0%	+5%	+10%
0 °C	-0.002	0.000	0.002	0.004
1 °C	-1.138	-1.127	0.002	0.004
3 °C	-2.968	-2.966	-2.965	-2.964
5 °C	-4.151	-4.150	-4.149	-4.147

In the rows of *Table 4* it can be observed that under the condition of constant temperature, the precipitation decreases by 5% and the surface runoff decreases by 0.002%; the precipitation increases by 5%, the surface runoff increases by 0.002%; the precipitation increases by 10%, and the surface runoff increases by 0.005%.

In the columns of *Table 4* it can be observed that when the temperature increases by 1 °C, 3 °C, 5 °C, and the rainfall is constant, the surface runoff of the Maojiahaizi river watershed reduces by 1.258%, 3.338%, and 4.538%, respectively. At a temperature increase of 1 °C, rainfall decreased by 5%, surface runoff decreased by 1.277%; rainfall increased by 5%, surface runoff decreased by 1.254%; rainfall increased by 10%, and surface runoff decreased by 1.249%.

Table 4. Runoff change rate under climate change scenarios in Maojiahaizi river watershed

Temperature change	Precipitation change			
	-5%	0%	+5%	+10%
0 °C	-0.002	0.000	0.002	0.005
1 °C	-1.277	-1.258	-1.254	-1.249
3 °C	-3.340	-3.338	-3.335	-3.333
5 °C	-4.540	-4.538	-4.537	-4.535

Analysis of changes of total nitrogen and phosphorus in Caohai watershed under different climate scenarios

The total nitrogen quantity data is the sum of organic nitrogen total amount (ORGN_OUT), ammonium nitrogen total amount (NH4_OUT), nitrate total amount (NO3_OUT) and nitrite total amount (NO2_OUT) in SWAT model output channel (.rch) file, and the unit is kg. The total amount of phosphorus is the sum of the total amount of organic phosphorus (ORGP_OUT) and the total amount of mineral phosphorus (MINP_OUT) in channel (.rch) files, and the unit is kg. The change rate of total nitrogen in each watershed is shown in *Tables 5, 7, 9 and 11*, and the rate of change of total phosphorus in *Tables 6, 8, 10 and 12*.

Table 5. Change rate of total nitrogen in Dongshan river watershed

N Temperature change	Precipitation change			
	-0.05%	0%	0.05%	0.1%
0 °C	0	0	-0.154	-0.1472
1 °C	-1.349	-1.5623	-1.5085	-1.5051
3 °C	2.9656	2.7997	2.8078	2.814
5 °C	-8.1034	-8.2702	-8.2645	-8.2569

Table 6. Change rate of total phosphorus in Dongshan watershed

P Temperature change	Precipitation change			
	-0.05%	0%	0.05%	0.1%
0 °C	0	0	-0.033	-0.0224
1 °C	-0.2561	-0.3597	-0.2813	-0.2761
3 °C	0.6959	0.6516	0.658	0.667
5 °C	0.9719	0.9253	0.9331	0.9398

It can be seen from *Table 5*, under the condition of constant temperature, the precipitation decreased by 5%, the total nitrogen content in the Dongshan watershed did not change compared with the precipitation; when the precipitation increases by 5%, the total nitrogen in the watershed decreases by 0.1540%. When the precipitation decreases by 10%, the total nitrogen decreases by 0.1472%, which means a 0.0068% increase compared with the previous gradient. When the temperature increases by 1 °C and the precipitation is constant, the total nitrogen in the watershed decreases by 1.5623%; if the precipitation decreases by 5%, the total nitrogen in the watershed decreases by 1.3490%, the rainfall increases by 5% and 10%, and the total nitrogen in the watershed decreases by 1.5085% and 1.5051 respectively. Under the condition of constant precipitation, when the temperature increased by 1 °C, the total nitrogen decreased by 1.5623%; the temperature increased by 3 °C, the total nitrogen in the watershed increased by 2.9977%; when the temperature increased by 5 °C, the total nitrogen decreased by 8.2702%.

It can be seen from *Table 6* that in the case of a temperature increase of 1 °C, the rainfall does not change, the total phosphorus content in the Dongshan watershed decreases by 0.3597%; the rainfall decreases by 5%, the total phosphorus decreases by 0.2561%; and the precipitation increases by 5%. Total phosphorus decreased by 0.2813%; precipitation increased by 10% and precipitation decreased by 2.761%. In the case of 5% reduction in precipitation, the temperature did not change, the total phosphorus in the watershed did not change; if the temperature increased by 1 °C, the total phosphorus in the watershed decreased by 0.2561%; the temperature increased by 3 °C, 5 °C, the total phosphorus in the watershed increased by 0.6595% and 0.9719%, respectively.

In the rows of *Tables 5* and *6* it can be seen that under the same temperature gradient, with the increase of rainfall, the total nitrogen and total nitrogen in the watershed showed a decreasing trend first and then an increasing one. In the rows, under the same precipitation gradient, with the increase of temperature, the total nitrogen in the watershed decreased first, then increased and then decreased. The total phosphorus in the watershed decreased first and then increased.

It can be seen from *Table 7*, under the condition of constant temperature, the precipitation decreased by 5%, the total nitrogen in the Zhonghe river watershed increased by 6.022%, the precipitation increased by 5%, 10%, and the total nitrogen in the watershed increased by 0.0027% and 0.0177%. Under the condition of constant precipitation, the temperature increased by 1 °C, the total nitrogen in the watershed decreased by 2.4135%; the temperature increased by 3 °C, the total nitrogen increased by 0.0274%; the temperature increased by 5 °C, the total nitrogen decreased by 7.2739%.

Table 7. Change rate of total nitrogen in Zhonghe river watershed

N Temperature change	Precipitation change			
	-5%	0%	5%	10%
0 °C	6.0022	0	0.0027	0.0177
1 °C	-1.7208	-2.4135	-2.2964	-2.2911
3 °C	0.6122	0.0274	0.0388	0.042
5 °C	-6.6919	-7.2739	-7.2753	-7.2763

It can be seen from *Table 8*, under the condition of constant temperature, rainfall decreased by 5%, total phosphorus in the Zhonghe river watershed increased by 10.4262%, rainfall increased by 5%, total phosphorus increased by 0.6644%. Rainfall increased by 10% and total phosphorus increased by 0.6746%. Under the condition of constant precipitation, in the case of a 1 °C temperature rise, total phosphorus in the Zhonghe river watershed decreased by 1.1845%; if the temperature increased 3 °C, the total phosphorus decreased 1.1675%; the rainfall increased by 10% and the total phosphorus decreased by 1.1535.

Table 8. Change rate of total phosphorus in Zhonghe river watershed

P Temperature change	Precipitation change			
	-5%	0%	5%	10%
0 °C	10.4262	0	0.6644	0.6746
1 °C	-1.1399	-1.1845	-1.0791	-1.0778
3 °C	-1.218	-1.1675	-1.1619	-1.1535
5 °C	-0.9862	-0.9346	-0.9367	-0.9335

In the rows of *Tables 7* and *8* it can be observed that under the same temperature gradient, the total nitrogen and total phosphorus in the watershed decreased first and then increased. In the columns it can be seen that under the same precipitation gradient, the total nitrogen in the watershed decreases first and then increases, while the total phosphorus in the watershed decreases first and then increases.

It can be seen from *Table 9*, when the temperature rises by 3 °C, the rainfall decreases by 5%, then increases by 5% and 10%, and the total nitrogen increases by 5.9643%, 5.9486%, 5.9487% and 5.9527% respectively. Under the same precipitation gradient, the precipitation remained unchanged, the temperature increased by 1 °C, 3 °C, and the total nitrogen content in the Baima river watershed increased by 2.9442%, 5.9643%. When the temperature increased 5 °C, the total nitrogen content of the watershed decreased by 11.2602%.

Table 9. Change rate of total nitrogen in Baima river watershed

N Temperature change	Precipitation change			
	-5%	0%	5%	10%
0 °C	0.0182	0	0.0053	0.0099
1 °C	2.9442	2.9124	2.9315	2.934
3 °C	5.9643	5.9486	5.9487	5.9527
5 °C	-11.2602	-11.2805	-11.2789	-11.2776

It can be seen from *Table 10*, when the temperature rises by 5 °C, the rainfall does not change, the total phosphorus content in the Baima river watershed increases by 4.2445%; the rainfall decreases by 5%, the total phosphorus increases by 4.4471%; the rainfall increases by 5%, 10%. The total phosphorus increased by 4.2425% and 4.2473%. Under the condition of constant precipitation, the temperature increases by 1 °C, 3 °C, and 5 °C, and the total phosphorus content in the watershed increases by 0.9561%, 4.0261%, and 4.2445%, respectively.

Table 10. Change rate of total phosphorus in Baima river watershed

P Temperature change	Precipitation change			
	-5	0	5	10
0 °C	0.1993	0	0.0057	0.0185
1 °C	1.2247	0.9561	1.0357	1.0414
3 °C	4.2266	4.0261	4.0309	4.0413
5 °C	4.4471	4.2445	4.2425	4.2473

In the rows of *Tables 9* and *10* it can be seen that the total nitrogen and phosphorus in the watershed decrease first and then increase with the increase of rainfall under the same temperature gradient. In the columns it is shown that with the same precipitation gradient, the total nitrogen increases first and then decreases, while the total phosphorus increases.

It can be seen from *Table 11*, under the condition of constant temperature, if the precipitation decreases by 5%, the total nitrogen in the Maojiahaizi river watershed decreases by 0.0357%, if the precipitation increases by 5% and 10%, the total nitrogen in the watershed increases by 0.0090% and 0.0100%. Under the condition of constant precipitation, if the temperature increased by 1 °C and 3 °C, the total phosphorus content in the watershed increased by 1.3782% and 4.6177%, respectively; if the temperature increased by 5 °C, and the total phosphorus decreased by 12.0781%.

Table 11. Change rate of total nitrogen in Maojiahaizi river watershed

N Temperature change	Precipitation change			
	-5%	0%	5%	10%
0 °C	-0.0357	0	0.009	0.018
1 °C	1.3715	1.3782	1.4056	1.4056
3 °C	4.6284	4.6617	4.665	4.6688
5 °C	-12.1102	-12.0781	-12.0757	-12.0695

It can be seen from *Table 12*, under the condition of constant precipitation, the temperature increases by 1 °C, the total phosphorus content in Haizi river watershed decreases by 0.3844%, the temperature increases by 3 °C, 5 °C, and the total phosphorus content in the watershed increases by 0.7536%, 1.2348. %.

Table 12. Change rate of total phosphorus in Maojiahaizi river watershed

P Temperature change	Precipitation change			
	-5%	0%	5%	10%
0 °C	0.2005	0	0.0088	0.0247
1 °C	-0.1152	-0.3844	-0.2987	-0.2987
3 °C	0.954	0.7536	0.7605	0.7667
5 °C	1.4402	1.2348	1.2495	-1.2836

In the rows of *Tables 11* and *12*, under the same temperature gradient, with the increase of rainfall, the total nitrogen content of Haizi river Watershed increased, and the total phosphorus decreased first and then increased. In the columns, the total nitrogen in the watershed showed a trend of increasing first and then decreasing, and the amount of total phosphorus first decreased and then increased.

Discussion and conclusion

(1) A study on the hydrological response of 16 climate scenarios was carried out for the SWAT model of the Caohai watershed: On the same rainfall gradient, the runoff of the watershed decreases with the increase of temperature, and on the same temperature gradient, the surface runoff of the watershed increases with the increase of rainfall.

(2) Through the analysis of the change of total nitrogen and phosphorus simulated by the model, under the same climate scenario, the change rate of total nitrogen and phosphorus is different in different river watersheds. for example, when precipitation is constant, the temperature increases by 5 °C. Total nitrogen decreased 8.2702% and total phosphorus increased 0.9253% in Dongshan river watershed. The total nitrogen decreased 7.2739% and the total phosphorus decreased 0.9346% in the Zhonghe river watershed; the total nitrogen decreased 11.2805% in the Baima river watershed and the total phosphorus increased 4.2445%; the total nitrogen decreased 12.7081% and the total phosphorus 1.2348% in the Haizi river watershed. In different climate scenarios, the trend of total nitrogen and phosphorus change is different, and the change of nitrogen and phosphorus is related to a series of complex factors such as land cover and soil type of watershed.

Acknowledgements. This work was supported by the Major Project of Guizhou Province (Qian Ke He Major Project Zi [2016]3022-06), the Application Foundation Major Project of Guizhou Province (Qian Ke He JZ Zi [2014] 200211), the Construction Program of Biology First-class Discipline in Guizhou (GNYL [2017] 009), the Key Discipline Construction Project of Ecology in Guizhou Province (Guizhou Degree ZDXK[2016]7)

REFERENCES

- [1] Bao, G., Tan, Z., Bao, Y. et al. (2013): 1982-2006 vegetation cover in Mongolia Plateau spatial-temporal variations of cover. – *Desert of China* 33(3): 918-927.
- [2] Chen, Y., Zhang, R., Wang, Y., Fan, Z., Chen, F. (2019): Climate and hydrological changes indicated by spruce tree ring width in the upper reaches of Nujiang River. *Resources and environment in arid areas*. – 33(1): 126-130.
- [3] Ge, Q., Wang, F., Wang, S., Cheng, B. (2014): Definition and uncertainty of seven questions concerning global warming. – *China Population, Resources and Environment*, 1: 1-6.
- [4] Han, Z., Zhangshui, W., Cao, X. T. (2017): Distribution characteristics of nitrogen and phosphorus and estimation of sediment release flux in Caohai, Guizhou. – *Journal of Ecology* 9: 2501-2506.
- [5] He, Y., Yao, W., Zhang, Y., et al. (2015): Spatial variability of vegetation restoration on the Loess Plateau based on MODIS/NDVI. – *China Soil and Water Conservation Science* 13(2): 63.

- [6] Hu, H., Huang, G., Huang, H. (2013): Analysis of runoff variation and its influencing factors at Tieling Station in Liaohe River Watershed. *Soil and water conservation study.* – 2: 98-102.
- [7] Liu, C., Liu, X., Zheng, H. (2008): Discussion on the impact of climate change on hydrology and water resources. – *Science and Society* 2: 21-27.
- [8] Liu, Z., Shao, Q. Q. (2014): Vegetation cover change in Sanjiang source area and its relationship with gas relationship between phenological factors. – *Study on Soil and Water Conservation* 21(6): 334-339.
- [9] Lu, Q., Wu, S., Zhao, D. Alpine grasses on the Qinghai-Tibet Plateau from 1982 to (2017): Land cover change and its relationship with climate. – *Geographic Science* 37(2): 29-300.
- [10] Niu, L. (2013): *The Impact of Climate and Land Use Change on Runoff Based on SWAT.* – Central China Normal University, Wuhan.
- [11] Shen, M., Piao, S., Jeong, S. J. et al. (2015): Evaporative cooling over the Tibetan Plateau induced by vegetation growth. – *Proceedings of the National Academy of Sciences of the United States of America* 112(30): 9299.
- [12] Solomon, S. D., Qin, M., Manning, Z., Chen, M., Marquis, K. B., Averyt, M. T., Miller, H. L. (2007): IPCC 2007. *Climate Change 2007: The physical science basis. Contribution of Working Group I to the Fourth Assessment Report of the Intergovernmental Panel on Climate Change.* – *Computational Geometry* 2: 1-21.
- [13] Tan, J. (2018): Characteristics and causes of the main mode variation of summer rainfall anomalies in the Yangtze River Basin, Xiao Zhixiang. – *Plateau Meteorology* 5: 1304-1312.
- [14] Wang, Y., Feng, J., Gao, H. (2014): Numerical simulation of the impact of land cover change on regional climate in China. – *Theoretical & Applied Climatology* 115: 141.
- [15] Williams, J. R., Renard, K. G., Dyke, P. T. (1983): EPIC-A New Method for Assessing Erosion's Effect on Soil Productivity. – *Journal of Soil & Water Conservation* 38(5): 381-383.
- [16] Xia, P., Kong, X., Yu, L. (2016): Effects of land use and landscape pattern on nitrogen and phosphorus output in small watershed of Caohai Wetland. – *Journal of Environmental Sciences* 8: 2983-2989.
- [17] Zhang, H., Fang, N., Shi, Z. (2016): Spatiotemporal patterns for the NDVI and its responses to climatic factors in the Loess Plateau, China. – *Acta Ecologica Sinica* 36(13): 3960.
- [18] Zhang, Q., Wang, Q., Zhang, C., et al. (2014): Changes of grassland vegetation coverage and their driving power: take Maqu County, Gannan Tibetan Autonomous Prefecture as an example. – *China's Agricultural Resources Zoning* 35(4): 58-62.
- [19] Zhao, G., Han, Y., Liu, M., Hou, J., Shi, H., Liu, W., Guo, Y., Qiao, Q. (2018): Spatial and temporal characteristics of extreme precipitation events in Henan Province from 1961 to 2013. – *Soil and Water Conservation Research* 25(06): 115-120.
- [20] Zheng, J., Xia, P., Lin, T., Zhou, Y. 2013 . Nitrogen and phosphorus contents and distribution characteristics of farmland ditches in the suburb of Caohai, Guizhou. – *Mountain Agrobiolgy* 3: 224-228.
- [21] Zhu, D., Xiong, K., Dong, X. (2018): Spatial and temporal variation of temperature in Guizhou from 1960 to 2016. – *Study on Soil and Water Conservation* 25(4): 168-173+180.

EXAMINING THE SUITABILITY OF THE HEARTWOOD AND SAPWOOD IN THE WHITE POPLAR TO PULP MAKING IN TERM OF FIBER MORPHOLOGY

MERTOGLU-ELMAS, G.

*Department of Forest Industrial Engineering, Istanbul University-Cerrahpasa
34473 Sariyer, İstanbul, Turkey*

**Corresponding author
e-mail: mertoglug@istanbul.edu.tr*

(Received 28th Sep 2018; accepted 29th Nov 2018)

Abstract. Nowadays, decreasing raw material for the production of pulp from wood has led to search for alternative sources. For this reason, the possibilities of using existing natural species in pulp production are being investigated. White poplar (*Populus alba* L.), which is a widespread naturally-grown in many parts of Turkey, has the potential to be an alternative pulp raw material. In this study, the fiber dimensions of heartwood and sapwood of white poplar were prepared for microscobic measurements. Also, the relationships between fiber dimensions measured were examined with a specific view to fiber morphology to evaluate their suitability for pulp production. The fiber length of heartwood is higher due to having more 5 year-old groups on it. The changes in the fiber diameter of the sapwood and heartwood by the ages usually showed a polynomial course. The age-related changes were increased from min to average values in the fiber wall width of the heartwood. The felting rate of heartwood indicated that a pulp with proportionally more heartwood would yield a paper with better physical properties, especially tear strength. Based on the results the muhlstep ratio of heartwood and sapwood that both woods are suitable for paper production.

Keywords: *fiber dimensions, pulp, Shultze's macerattion method, fiber length, felting power*

Introduction

The demand for forestry resources increases along with the diversity and volume of forestry industrial products. Forests are important sources with biodiversity including species richness and endemic species due to the sustainability and renewability of the wood (Kharkwal et al., 2004; Standavor and Kenderes, 2003). Given easy processing, adaptability to technological developments, aesthetics, high resilience, mechanic and acoustic characteristics of wood, the forests provide one of the most convenient materials for human use (Istek et al., 2010). Suitability for use and quality of the wood largely depend on the growth rate of the tree and its location, which define the formative characteristics as well as its age, diameter, heartwood-sapwood ratio, morphological characteristics (Gultekin, 2014; Bozkurt, 1971; Dogu, 2002; Hernandez, 2013; Bamber, 1987; Cobas et al., 2013; Eroglu and Usta, 2004).

White poplar grows naturally in almost every region of Turkey. This species grows on banks of streams and roads (*Fig. 1*) (Yaltirik and Efe, 1994).

The dimensions of the fiber (length, width and diameter of fiber) and the relationship between the dimensions of the fiber (felting ratio, coefficient of elasticity, runkel ratio, modulus of rigidity and F factor) is important in the determination of the paper strength properties from pulp (Horn, 1978; Seth and Page, 1988; Horn and Setterholm, 1990; Ververis et al., 2004; He et al., 2014). It can be explained by these parameters;

- Fiber length affects paper resistance properties positively.
- Thickness of fiber also has an effect on the strength individual fibers.
- Pulp made up very thin cell wall thickness of fibre gives high strength properties except low tear strength otherwise if pulp from thick fiber particularly. It gives lower strength properties and volumes of papers (Kirci, 2003). The bursting and tensile strength of paper from hardwoods gives morphological effects similar to those made from softwoods (Horn, 1978).

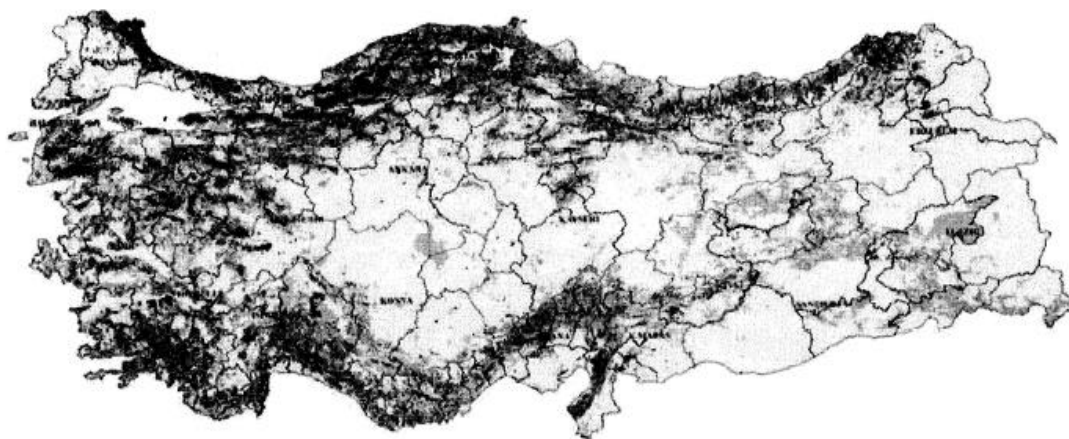


Figure 1. The map of Turkey Forests of presence (Republic of Turkey General Directorate of Forestry, 2018)

Suitability of the wood used as raw material for paper production is evaluated over the resistance characteristics of the pulp through the fiber lengths and the relationships between the dimensions of the fibers. This study aims at investigating the effects of sapwood and heartwood of white poplar wood on suitability in pulp and paper industry thanks to its rather easier and faster growing and shorter maintenance period. The study attempts at determining the suitability for pulp production through determination of the dimensions of the fibers of sapwood and heartwood and its proportion.

Materials and methods

Materials

Naturally grown the white poplar (*Populus alba* L.) samples were supplied from Bahçeköy-Istanbul. The average of the measurements conducted on different positions showed that the tree was approximately 60-62 years old. Age measurements were taken on the disk samples in the form of pie slice. The discs which were obtained at approximately breast height of tree stems (1.30 m) and then were divided into annual ring groups with five-year ages from heartwood to sapwood. Two samples of a thickness of 3 mm were taken from the disks. Each five-year segment of heartwood (H) and sapwood (S) separately was classified and numbered starting from zero. The heartwood had 40 years of rings whereas the sapwood has 20 years of rings. These individual fiber chips were cut and prepared woods as heartwood and sapwood.

Methods

When the suitability of raw materials for paper making is assessed, the relationships between fiber dimensions, fiber length, width, wall thickness and lumen width and fiber dimensions, give important clues about the possibilities presented by the raw material for pulp production. The specimens were subject to morphology analysis. The fiberizing process was performed using the Shultze's macerating method (Mahesh et al., 2015; Chamberlain, 1915). After being washed thoroughly, fibers are blended for 3 min in a mixer. The obtained fiber suspension was strained in a Büchner funnel using a strainer with small holes. Then, the fibers that remained on the strainer were placed in small-sized tubes to be preserved by adding glycerin on them in order to prepare the microscope slides. While preparing the microscope slides, it is essential to pay attention to the cleanliness of lam and lamellae and to the prevention of air bubbles while the sample is being placed on the lam. The mixture that consists of fiber and glycerin is dripped on the lam while being spread in a homogeneous manner, the lamella is placed above it and stabilized with varnish.

They were measured with the aid of a projection microscope by projecting the images on a surface according to Tappi T232 cm-85 (1985) standards. Measured maximum, minimum and mean dimensions of fibers were determined to calculate the relationships between fiber dimension. The criterion used in determining the suitability of fiber morphological properties for pulp production are defined below.

- Elasticity ratio: $(\text{Lumen radius}/\text{fiber width}) \times 100$.
- Felting power: $\text{Fiber length}/\text{fiber width}$.
- Runkel classification: $\text{Fiber membrane width}/\text{lumen radius}$.
- Rigidity coefficient: $(\text{Cell wall thickness}/\text{fiber radius}) \times 100$.
- F-factor: $(\text{Fiber length}/\text{cell wall thickness}) \times 100$.
- Muhlstep classification: $(\text{Cell wall thickness area}/\text{fiber cross-sectional area}) \times 100$.

Statistical analysis

In this study, in order to determine the heartwood and sapwood fiber properties, 50 units of fiber length and 50 units of fiber width and cell wall of samples representing the same population were measured as fiber dimensions and their average was calculated. Hence, Microsoft Office (Excel-2003) was used for analysis and drawing charts. Statistical minimum, maximum, mean (μ) and standard deviation (σ) values of fiber dimension parameters measured as fiber length, fiber width, and cell wall thickness are calculated and their data mean is expressed as $\mu \pm \sigma$ ($n=50$). In most studies, statistical evaluations are mostly done with 30 units of data number (n). This study was conducted with fiber length ($n=50$), fiber width ($n=50$), and cell wall thickness ($n=50$) units of data. Also, Averages of each parameter belonging to the relationships between fiber dimensions (felting power elasticity, rigidity coefficient, Runkel classification, Muhlstep ratio, and F factor) were conducted with the heartwood ($n=8$) and sapwood ($n=4$) age groups.

Results and Discussion

In this study, heartwood and sapwood samples taken from a white poplar were classified as different sections of 5-year periods. A minimum number of 50 measurements were taken for each parameter indicating their fiber lengths, fiber widths and wall thicknesses. Max, min and average values obtained from measurements are given in *Table 1* below.

Table 1. The values fiber dimensions

Species	Length (mm)	Width (μm)	Cell wall thick. (μm)	Reference
Sapwood <i>Populus alba</i>	0.84±0.03(n=200)	24.66±1.74(n=200)	3.68±0.25(n=200)	Current
Heartwood <i>Populus alba</i>	0.86±0.03(n=400)	21.3±1.48(n=400)	3.62±0.27(n=400)	Current
<i>Populus tremula</i>	1.41	26.87	6.06	Alkan et al., 2003
<i>Eucalyptus camaldulensis</i>	0.79	13.82	7.43	Huş et al., 1975
<i>Populus nigra</i>	1.25	27.17	4.98	Alkan et al., 2003
<i>Fagus Orientalis</i>	0.67	17.94	4.64	Akgul and Tozluoglu, 2009
<i>Acer platanoides</i>	0.26	21.35	3.54	Durmaz and Ates, 2016
Heartw. <i>Pinus nigra</i>	1442±245	38.5±4.9	12.5	Istek et al., 2010
Sapw. <i>Pinus nigra</i>	2647±349	44.0±5.9	6.9	Istek et al., 2010

F: Fiber; dia.: Diameter; thick: Thickness

In sapwood of 40-60 years' period, the change between max and min of measurements of fibers with 20 years of annual rings equals to 2.4% for fiber length, 2.3% for fiber width, 9.4% for fiber cell wall thickness and 8.2 % for lumen width (Table 1). In heartwood with 40 years of annual rings, on the other hand, the change between the minimum and maximum measurements of fibers in 0-40 years' period equals to 10% for fiber length, % 12 for fiber width, 12.8% for fiber cell wall thickness and 22.9% for lumen width (Table 1).

The relationships between the fiber length and age of the white poplar heartwood are indicated on the Figs. 2-7.

In the five-year age groups of white poplar heartwood, it is seen that the fiber length reaches its maximum level in the first five-year period and reduces to the minimum level at the last five-years period (Fig. 2).

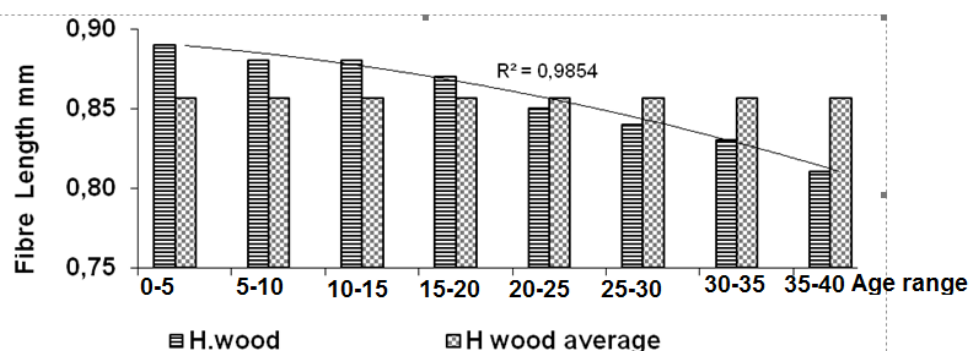


Figure 2. Distribution of the fiber lengths of the white poplar heartwoods' with age

It is thus concluded that the age is inversely proportional to the fiber length of heartwood. When fiber lengths of heartwood are compared with its average by age group, it is seen that the fibers of first fifteen years' age group are significantly longer and the difference start to reduce in the twentieth age group and by the age of twenty-five the average value is higher than the heartwood age groups. The fact that the biomass formation in some species of trees, which have higher fiber length than

sapwood fiber in the first years of heartwood, is consistent with the literature (Istek et al., 2010). Gradual reduction of heartwood from the 20 years' annual rings until 40 years' annual rings might indicate that the fiber quality is reduced towards the pith with a shorter and harder structure.

The width of the sapwood starts from the borders of heartwood and continues up to the bark. It was observed that the fiber length changes of the sapwood, which starts equal to the average at 45 years' period, reduces to the minimum level at 55 years' period and reaches to the maximum level at 50 and 60 years (Fig. 3).

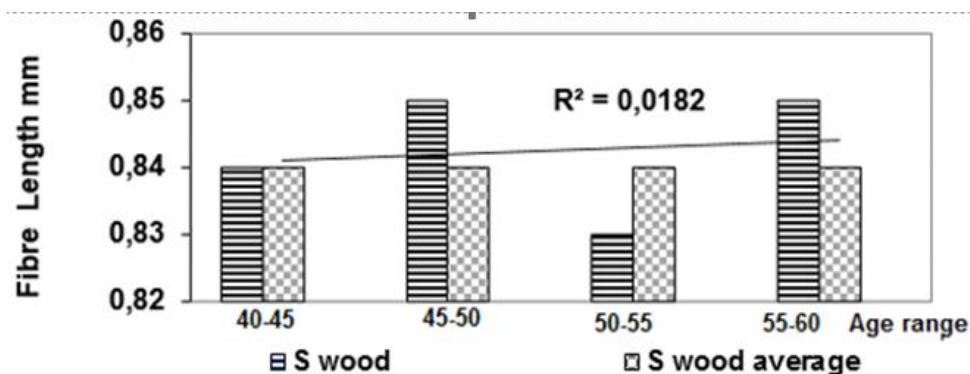


Figure 3. Distribution of the fiber length of the white poplar sapwoods' with age

It is known that the fiber length of the sapwood is generally higher than that of the heartwood. The ratio between the fiber lengths of heartwood and sapwood was found to be 1.02. This difference was caused by the fact that the sampled white poplar was an old tree and that the heartwood had 40 years of annual rings and thus the width of the heartwood is marginally high.

The average fiber lengths of both the heartwood (0.86 ± 0.03) mm ($n=400$) and sapwood (0.84 ± 0.03) mm ($n=200$) of the white poplar were a homogeneous fiber distribution. The fiber length of heartwood and sapwood was typically in the middle classification of the short fiber sequence of hardwood species (0.5-2 mm) (Cobas et al. 2013). These results of the white poplar were higher than those of *F. orientalis*, *Acer platanoides*, *E. camaldulensis* species whereas they remained lower than *Populus tremula* and *Populus nigra* species (Durmaz and Ates, 2016; Huş et al., 1975; Alkan et al., 2003; Akgul and Tozluoglu, 2009).

The fiber width of heartwood of white poplar was observed that the age-dependent changes in the fiber width of the heartwood was high in the formation period of the heartwood whereas, after reducing to the minimum levels, it expands to the levels equal to the average values in the last 35-40 annual rings (Fig. 4).

The ratio between the fiber width of heartwood and sapwood was found to be 0.86 μm . Changes in the width of the sapwood by the ages showed a polynomial course which reaches slightly higher than the average at the earlier years (45 years) and then in the annual rings of 50-55 years reduces to the minimum levels and reaches its maximum level which is slightly higher than the average, during the later years (the annual rings of 60) (Fig. 5).

The fiber width values on average for the heartwood and sapwood were respectively (21.3 ± 1.48) μm ($n=400$) and (24.66 ± 1.74) μm ($n=200$). Although the fiber width of sapwood was wider than that of heartwood, its fiber distribution demonstrated 32 %

more deviation while heartwood demonstrated a more homogeneous distribution (Figs. 4 and 5). The ratio between the fiber lengths of heartwood and sapwood was found to be on average values (0.98). This indicates their fiber lengths are close to each other.

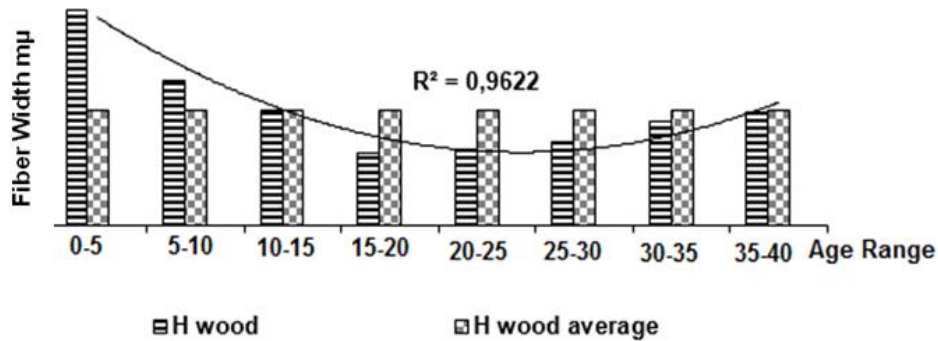


Figure 4. Distribution of the fiber width of the white poplar heartwoods' with age

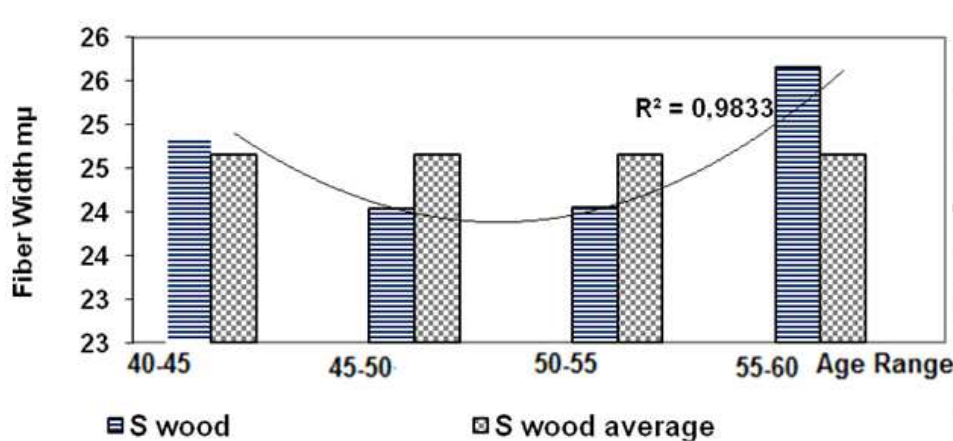


Figure 5. Distribution of the fiber width of the white poplar sapwoods' with age

Cell wall thickness of fibers impact on strength properties of paper. Long-fiber and thin-wall width fibers form non-porous tightly bonded paper which is collapsible and flexible (Akpakpan, 2012; Syed et al., 2016).

The average cell wall thickness of sapwood (3.68 ± 0.25) μm ($n=200$) were thicker than the heartwood (3.62 ± 0.27) μm ($n=400$) of the white poplar that was a more homogeneous fiber distribution (deviation 7.4%).

It was observed that the age-dependent changes in the cell wall thickness of the heartwood is at minimum levels in the first five years whereas it becomes equal to the average value in 10 years annual ring and showed a polynomial relationship course in later years (Fig. 6).

It was further observed that the cell wall thickness sapwood starts well below its average and then gradually increases linearly (Fig. 7).

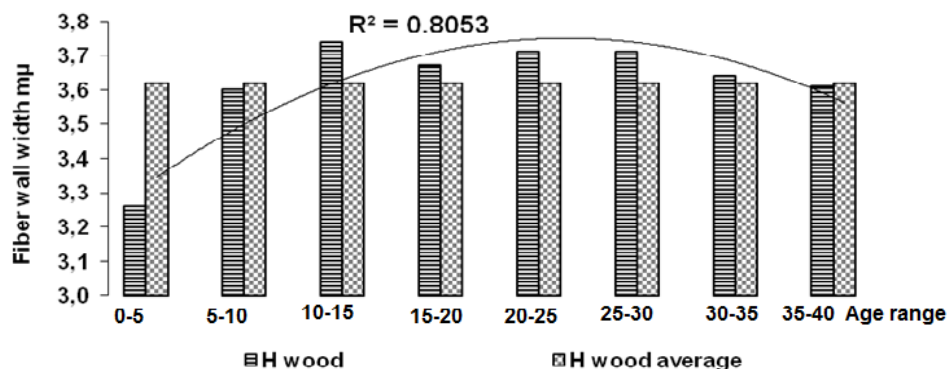


Figure 6. Distribution of the fiber wall width of the white poplar heartwoods' with age

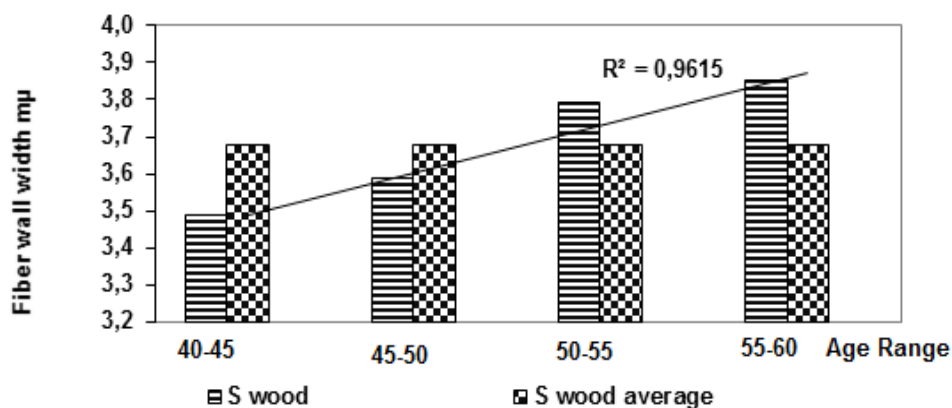


Figure 7. Distribution of the cell wall thickness of the white poplar heartwoods' with age

The relationships between the fiber dimensions

The relationships between the fiber dimensions of the sapwood and heartwood of white poplar were given in the Table 2 and Figs. 8-19.

The felting power (slenderness ratio) is calculated by proportion of the fiber's length to its diameter. The optimum felting power for softwoods is 70. This number is lower for hardwoods (Dutt et al., 2004; Kirci, 2003). It is known that this ratio has a systematic relationship especially with the tear resistance according to the results of physical tests conducted on the paper (Kirci, 2003).

The felting power of heartwood reached minimum 33.2 at 40 years' age and maximum 42.5 at 20 years's age with an average rate of 40.2 (Fig. 8). It was observed that juvenile heartwood has high strength properties at 25 annual ring.

The felting power of white poplar sapwoods' reached minimum 33.13 at 45 years ring and maximum 37.74 at 50 years ring with an average rate of 34.2 (Fig. 9). It was determined that the average felting rate of heartwood (40.2 ± 3.06 ; $n=8$) is 15.2 % higher and a heterogenous distribution than that of sapwood (34.2 ± 2.04 ; $n=4$). When compared with the felting power of hardwoods, the felting rate of white poplar wood is higher than those of hybrid poplar, *Fagus Orientalis*, *Acer platanoides* L. and lower than those of other hardwood species (Table 2) (Akgul and Tozluoglu, 2009; Durmaz and Ates,

2016). Some researchers posit that the resistance properties do not depend merely on the felting rate but also on the cell wall thickness (Ates et al., 2008).

Table 2. The relationships between the fiber dimension of white poplar and some hardwoods

Sample	Felt. Pow.	Elas. Coff.	Runk. ratio	Rig. coeff.	F factor	Muh. Ratio	Reference
Heartwood <i>Populus alba</i>	40.2±3.06	67.84±3.54	0.51±0.07	16.07±1.77	236.7±28.01	56.4±4.81	current
Sapwood <i>Populus alba</i>	34.2±2.04	69.82±1.54	0.4±0.03	15.09±0.77	229±12.50	50.8±2.16	current
Heartwood <i>R. pseudoacacia</i>	54.2	64	0.56	18	-	59.0	Ozdemir et al., 2015
Sapwood <i>R. pseudoacacia</i>	58.1	64.8	0.4	17.6	-	58.0	Ozdemir et al., 2015
<i>Populus nigra</i>	46.0	65.1	0.56	18.3	250.8	57.6	Alkan et al., 2015
<i>E.camaldulensis</i>	57.7	53.8	0.86	23.1	249.1	71.1	Huş et al., 1995
<i>F. Orientalis</i>	59.7	27.6	2.9	37	159.6	93.0	Tank, 1971
<i>F. Orientalis</i>	37.17	48.29	1.1	25.9	140.4	76.7	Akgul and Tozluoglu, 2009
<i>A. platanoides</i>	12.1	71.9	0.76	16.6	141.7	48.4	Durmaz and Ates, 2016

Felt. Pow.: Felting Power; Elas.: Elasticity; Runk: Runkel; Rigid: Rigidity; Muh: Muhlsteph; Coff: Coefficient

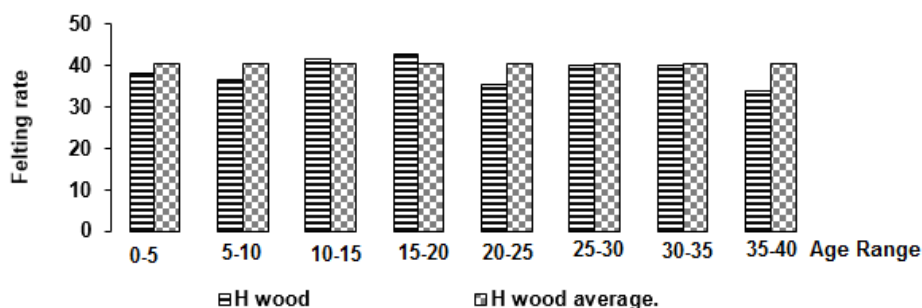


Figure 8. Distribution of the Felting power of the white poplar heartwoods' with age

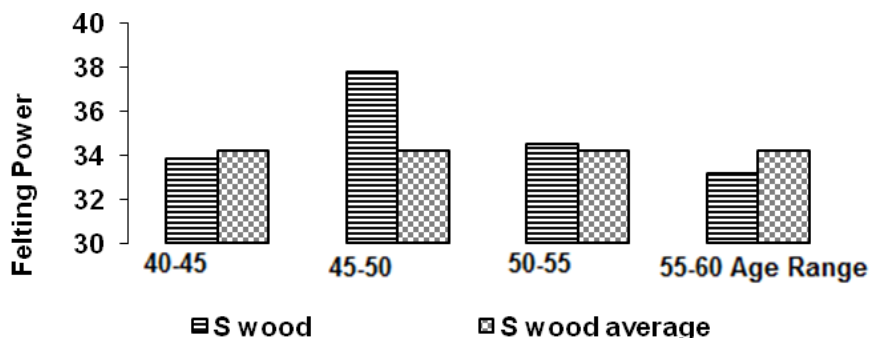


Figure 9. Distribution of the Felting power of the white poplar sapwoods' with age

Coefficient of elasticity (CE) is a ratio that defines the density of the hardwood (Istas et al., 1954). This coefficient calculated as 100 times the ratio of lumen width to fiber diameter, is evaluated under four groups. 1st Group >75, 2nd Group 50<CE<75, 3rd Group 30<CE<50, 4th Group CE<30 (Tank, 1971; Kirci, 2003). This coefficient for heartwood was calculated as around 70 with minimum 64.1, maximum 67.84 and an average of 67.84 ± 3.54 (n=8) in all age groups (Fig. 10). The average of heartwood is within the range of 2nd group and has a density between 0.5-0.55 g.cm⁻³. This indicates that good physical properties will be obtained in paper to be made from such raw material that has fiber dimensions with a thin walled wide lumen.

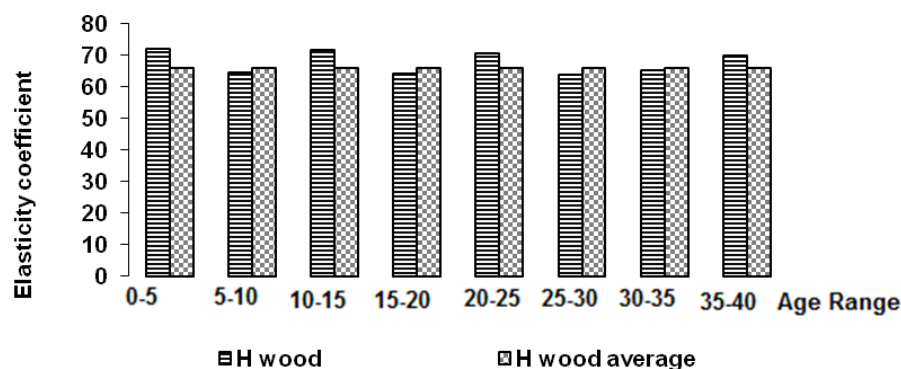


Figure 10. Distribution of the Elasticity coefficient of white poplar heartwoods' with age

The coefficient of elasticity of sapwood is minimum 68.5 in 55 annual ring and maximum 72.0 in 45 annual ring with an average of 69.82 ± 1.54 (n=4) in all annual ring groups (Fig. 11). The elasticity coefficient of the sapwood is higher and a more homogenous distribution than that of heartwood and is within the range of 2nd group with a density above 0.50. It is understood that the sapwood elasticity coefficient has the predicted value (70) for the softwood woods and that the heartwood has a similar value. As a result, it has been shown that the physical properties of the papers to be obtained from white poplar wood raw material will be good and close to the softwood wood. When compared with the elasticity coefficients of hardwood species, the white poplar wood was found to have a value higher than all hardwood species except *Acer platanoides* L. (Table 2) (Durmaz and Ates, 2016).

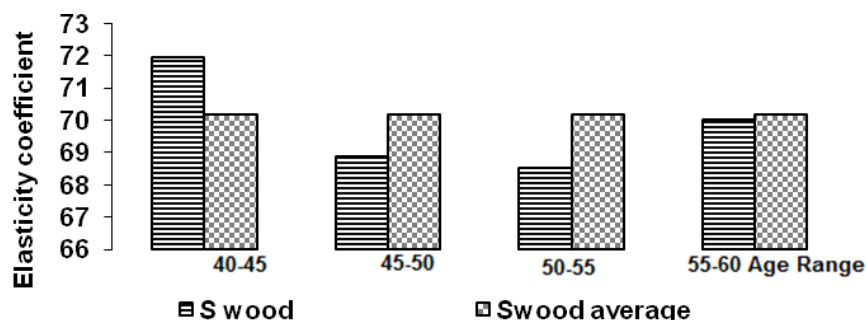


Figure 11. Distribution of the Elasticity coefficient of the white poplar sapwoods' with age

Runkel ratio is calculated by division of double cell wall thickness by the width of lumen. Any ratio lower than 1 indicates that the raw material has fibers with wide lumens and thin cell walls which means that the raw material has desirable properties. At the same time, such a ratio would also indicate that the physical resistance properties of the paper to be produced will be very positive and hence the raw material is suitable for paper production (Eroglu, 1980). The values obtained for the heartwood age groups of this ratio gave a minimum less than 0.4 at 5 years and 15 years and maximum more than 0.5 in the 20 years. Given an average above 0.51 ± 0.07 ($n=8$), the heartwood is suitable for pulp production (Fig. 12) (Eroglu, 1980; Syed et al., 2016).

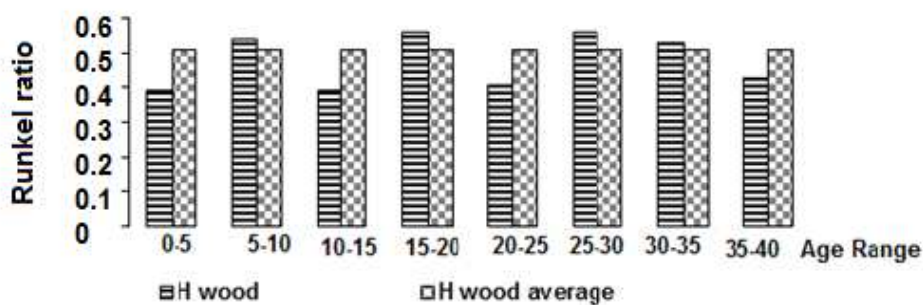


Figure 12. Distribution the Runkel ratio of the white poplar heartwoods' with age

For sapwood age groups, the Runkel ratio was minimum 0.39 at 45 years ring and 0.46 at 60 years ring. With an average ratio of 0.4 ± 0.03 ($n=4$), the Runkel ratio was lower than in sapwood age groups which indicates that the sapwood is suitable for pulp production. It indicated a more homogenous distribution (Fig. 13).

It is determined that the Runkel ratio of heartwood is higher than the value of sapwood. The fact that the wood fiber length is higher than that of the sapwood is the main cause of the positive difference in Runkel ratios. According to the results of white poplar's heartwood and sapwood, it can be said that white poplar wood has a thin cell wall and a sufficient length of fiber, and hence is suitable for pulp production.

The Runkel ratio of the white poplar is similar to that of heartwood and sapwood of *R. pseudoacacia*, *Populus nigra* (Table 2) (Ozdemir et al., 2015; Alkan et al., 2015). It indicates positive resistance and durability properties, except for tear strength.

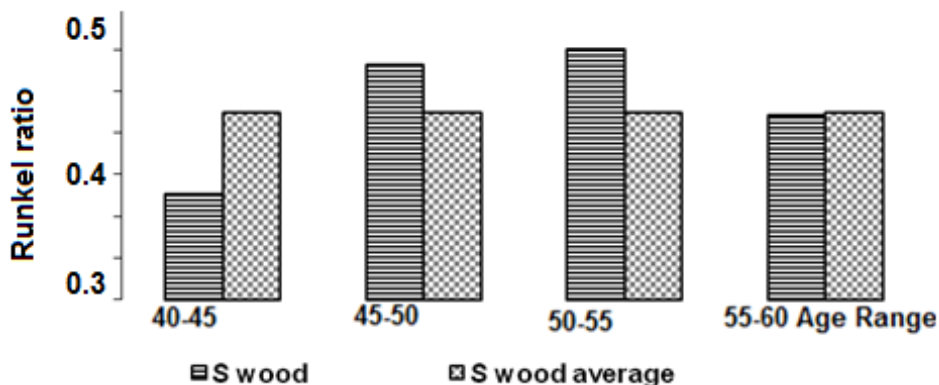


Figure 13. Distribution of the Runkel ratio of the white poplar sapwoods' with age

Muhlstep ratio is related to the cell wall thickness in paper which is calculated as 100 times of the proportion of cell wall area to cross sectional area of fiber and which affects tear and breaking strength of paper. In the heartwood age groups, the Muhlstep ratio was determined minimum 48.2 in first 5 years ring and maximum 56.4 in 20 years ring with an average of 56.4 (Fig. 14).

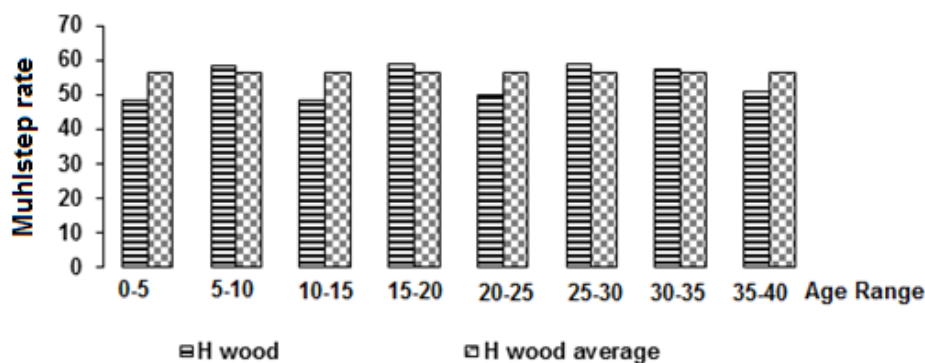


Figure 14. Distribution of the Muhlstep ratio of the white poplar heartwoods' with age

In the sapwood age groups, the Muhlstep ratio was found between 48.3 in 45 years ring and 53.1 in 50-55 years ring with an average of 50.8 which translates into good suitability for pulp production. The results show that the muhlstep ratio of heartwood of white poplar is higher than that of sapwood and that both woods are suitable for paper production (Fig. 15). Based on muhlstep ratio averages of sapwood (50.8 ± 2.16 ; $n=4$) that is more homogenous than heartwood (56.4 ± 4.81 ; $n=8$), the white poplar wood has higher values than *Populus tremula* and *Acer platanoides* L. and lower values than others (Table 2) (Durmaz and Ates, 2016; Alkan et al., 2003).

According to some researchers, this index indicates that use of clones is more suitable in board and corrugated board production rather than paper. Another aspect of papermaking would be blending of long fiber pulp with white poplar. Another, these ratios indicate that white poplar would be more suitable for corrugated board production. Another area of use would be blending in long fiber pulp that contains white poplar.

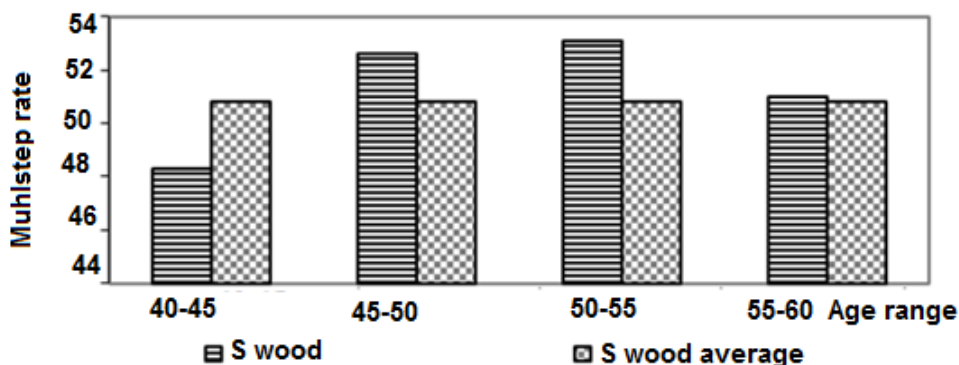


Figure 15. Distribution of the Muhlstep ratio of the white poplar sapwoods' with age

The rigidity coefficient is defined as 100 times of the proportion of cell wall thickness to the fiber diameter and a low rigidity coefficient positively affects the breaking and tears strengths (Bektaş et al., 1999). In the heartwood age groups, the rigidity coefficient was calculated 14.0- 17.9 at 5-20 years' rings and 30 years rings with an average of 16.07 ± 1.77 ($n=8$) (Fig. 16). It was determined that the ratio of the heartwood is lower than other hardwoods species (Table 2).

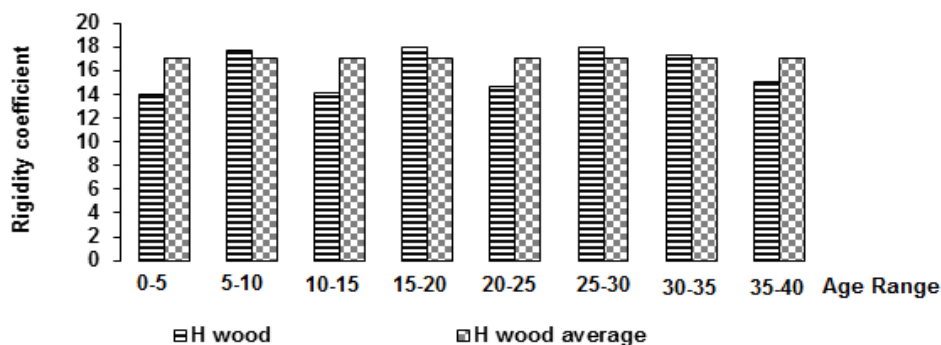


Figure 16. Distribution of the rigidity coefficient of the white poplar heartwoods' with age

In the sapwood age groups, the rigidity coefficient was calculated minimum 14.0 at 45 years ring and maximum 15.8 at 55 years ring with an average of 15.09 ± 0.77 $n=4$ (Fig. 17). It was observed that the rigidity coefficient of the sapwood is higher than that or heartwood. It was also determined that the rigidity coefficient of the heartwood is higher than that of *Populus tremula* and that of sapwood is higher than those of *Populus tremula* and *Acer platanoides* L. (Table 2).

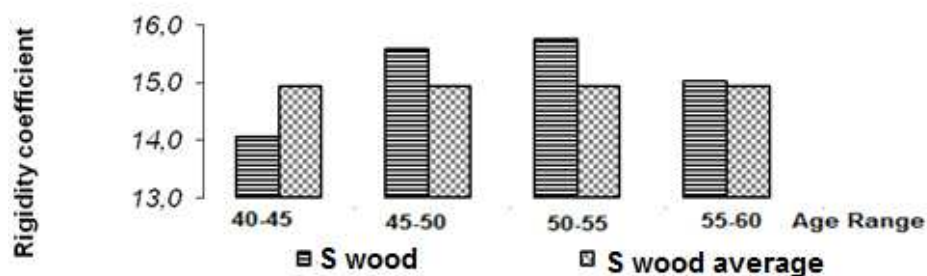


Figure 17. Distribution the rigidity of the white poplar sapwoods' with age

A high coefficient indicates low resistance properties. Ates et al. (2008) confirmed this view in a study on the resistance properties obtained from *P. elongata* (which has a rigidity coefficient of 27.6) through different chemical pulping method. This view is also supported by the fact that the coefficient that shows inverse proportion to rigidity (17.8) elasticity (65) values reflects similar rigidity properties with the elasticity resistance properties of higher limit of second class (Ates et al., 2008).

Given that there is an inverse proportional relationship between the rigidity coefficient (16.07 ± 1.77 ; $n=8$) and elasticity (67.84 ± 3.54 ; $n=8$) of heartwood and between rigidity coefficient (15.09 ± 0.77 ; $n=4$) and elasticity (69.82 ± 1.54 ; $n=4$) of

sapwood of white poplar. The rigidity coefficient of heartwood is larger than that of sapwood, but it has a heterogenous distribution. These woods correspond to second elasticity class, as identified in theoretical calculations, and will yield lower resistance properties. Rigidity coefficient are lower the other hardwoods (Alkan et al., 2015; Durmaz and Ates, 2016; Huş et al., 1995; Ozdemir et al., 2015; Tank, 1971).

The F factor stands for flexibility of the paper and in heartwood annual ring groups, the factor was determined with an average of 236.7 ± 28.01 $n=8$ (Fig. 18).

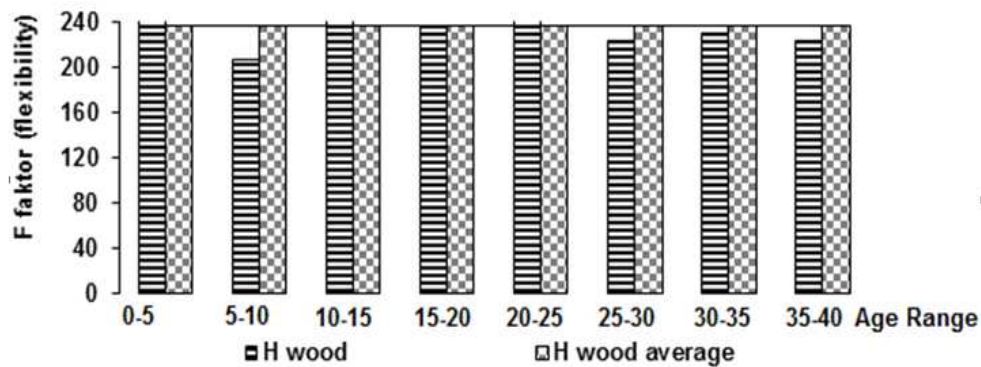


Figure 18. Distribution of the F coefficient of the white poplar heartwoods' with age

F factor (flexibility) indicates the flexibility of the papers to be obtained from the fibers. In sapwood, this factor was found minimum 219 at 55 years ring and maximum 242.3 at 50 years ring with and average of $(229 \pm 12.50; n=4)$. The F factor average of heartwood $(236.7 \pm 28.01; n=8)$ is higher by 3.3% and it has a more homogenous distribution than that of sapwood $(229 \pm 12.50; n=4)$ (Fig. 19). It was observed that these results of the sample were higher than that of *Fagus orientalis* and *A. platanooides* lower than others (Table 2) (Akgul and Tozluoglu, 2009; Tank, 1971; Durmaz and Ates, 2016).

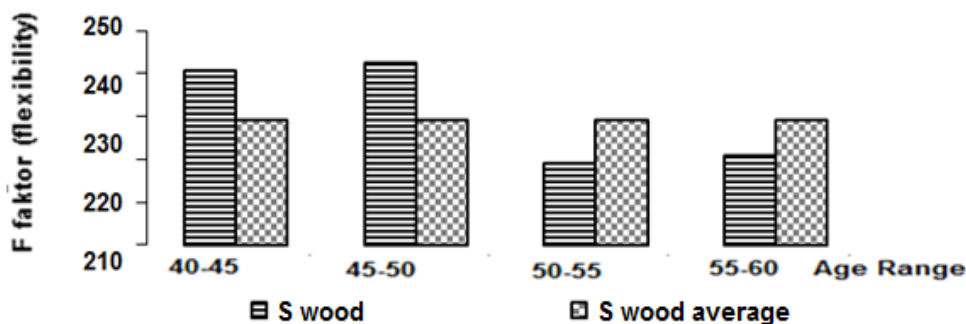


Figure 19. Distribution of the F factory of the white poplar sapwoods with age

The papers obtained from this type of fibers present high flexibility (Akgul and Tozluoglu, 2009). It can be used as the intermediate paper for corrugated board and newspaper, due to low bleaching expenses required due to its light color, in blends with other long fibers for office papers.

Conclusions

The fiber dimensions and relationships between fiber dimension of heartwood and sapwood of white poplar were examined separately for each wood sample by the five-year rings groups with a specific view to fiber morphology to evaluate their suitability for use in pulp production.

1. An inverse correlation was determined between the fiber length of heartwood and its age. Although the fiber length of the sapwood is generally high, it has been found that the fiber length of the white poplar heartwood with 40-year-old annual rings is higher than that of sapwood.
2. Depending on the age of the heartwood, the change in fiber width was found to be high in the formation process of the heartwood and then it was equal to the average value in the last annually rings.
3. The sapwood also showed a polynomial correlation which reaches slightly higher than the average at the earlier years and then reduces to the minimum levels and reaches its maximum level in the process.
4. Although there is a polynomial relationship between the cell wall thickness and age of the heartwood, a linear relationship was determined in the sapwood.
5. The heartwood with high felting ratio has been found to have high tear strength.
6. The flexibility coefficients of sapwood and heartwood have the anticipated values for softwood. It can be stated that the physical properties of the papers obtained from white poplar wood would be similar to those of softwood papers.
7. The Runkel ratios of heartwood and sapwood of white poplar were found be suitable for pulp production due to positive resistance and durability properties, except for tear strength.
8. The Muhlstep ratio indicates that white poplar would be more suitable for corrugated board production. Another area of use would be blending in long fiber pulps that contain white poplar.

REFERENCES

- [1] Akgul, M., Tozluoglu, A. (2009): Some chemical and morphological properties of juvenile woods from beech (*Fagus orientalis* L.) and pine (*Pinus nigra* A.) plantations. – *Trends in Applied Sci Res* 4(2): 116-125. ISSN 1819-3579.
- [2] Akpakpan, A. E., Akpabio, U. D., Obot, I. D. (2012): Evaluation of physicochemical properties and soda pulping of *Nypa fruticans* frond and petiole. – *Elixir Appl.Chem.* 45: 7664-7668.
- [3] Alkan, C., Eroglu, H., Yaman, B. (2003): Fiber morphology of some natural Angiosperme taxa in Turkey. – *Journal of Bartın Forestry Faculty* 5(3): 102-108.
- [4] Ates, S., Yoanghao, N., Akgul, M., Tozluoglu, A. (2008): Characterization and evaluation of *Paulownia elongota* as a raw material for paper production. – *African Journal of Biotech* 7(22): 4153-4158.
- [5] Bamber, R. K. (1987): Sapwood and heartwood. – Forestry Comission of New South Wales, Technical Publication 2.
- [6] Bektaş, I., Tutuş, A., Eroğlu, H. (1999): A study of the suitability of calabrian pine (*Pinus brutia* Ten.) for pulp and paper manufacture. – *Turkish Journal of Agriculture and Forestry* 23(3): 589-597.
- [7] Bozkurt, Y. (1971): Definitions of some important tree species, their technological properties, and their usage. – Istanbul University Publishers 1653(177). Istanbul, Turkey.

- [8] Chamberlain, C. J. (1915): Plant cell physiology: Schultze's macerattion method. – In: Chamberlain, C. J. (ed.) *Methods in Plant Histology*. University of Chicago press, Chicago.
- [9] Cobas, A. C., Felissia, F. E., Monteoliva, S., Area, M. C. (2013): Juvenile poplar refiner pulp. – *BioResources* 8(2): 1646-1656. DOI:10.15376/biores.8.2.1646-1656.
- [10] Dogu, D. (2002): The Factors affecting wood structure. – *Eastern Mediterranean Forestry Research Journal* 8.
- [11] Durmaz, E., Ates, S. (2016): The Comparison of Fibre Morphologies of Growing Some Tree Woods in Turkey Naturally. – *International Forestry Symposium IFS 2016*, pp.771-777.
- [12] Dutt, D., Upadhyaya, J. S., Tyagi, C. H., Malik, R. S. (2004): Studies on pulp and paper making characteristics of some indian non-woody fibrous raw materials-Part II. – *J Sci Ind Res* 63: 58-67.
- [13] Eroglu, H. (1980): Investigating possibilities of obtaining wood pulp from wheat straw by O₂ NaOH method. – Ph.D. Thesis Karadeniz Technical University.
- [14] Eroglu, H., Usta, M. (2004): Technology of production paper and paperboard. – Textbook I, Karadeniz Technical University, Trabzon, Turkey.
- [15] Gultekin, G. (2014): Determination of Chemical, Morphological, Anatomical, Physical and Mechanical Properties of Sapwood and Heartwood of Some Softwood and Hardwood. – Ph.D. Dissertation. University of Kahramanmaraş Sütcü Imam, Kahramanmaras, Turkey.
- [16] He, B., Liu, Y., Ma, L. (2014): Correlation analysis for fiber characteristics and strength properties of softwood kraft pulps from different stages of a bleaching fiber line. – *BioResources* 9(3): 5024-5033. DOI:10.15376/biores.9.3.5024-5033.
- [17] Hernandez, V. (2013): Radiata pine pH and buffering capacity: Effect on age and location in the stem. – *Maderas. Ciencia y tecnología* 15(1): 73-78. DOI: 10.4067/S0718-221X2013005000007.
- [18] Horn, R. A. (1978): Morphology of pulp fiber from hardwoods and influence on paper strength. – US Departman of Forest service. Research paper FPL 312, Forest Product Laboratory Madison, WI.
- [19] Horn, R. A., Setterholm, V. C. (1990): Fiber morphology and new crops. – In: Janick, J., Simon, J. E. (eds.) *Advances in New Crops*. Timber Press, Portland, OR, 270-275.
- [20] Hus, S., Tank, T., Göksel, E. (1975): Türkiye Morphological investiation of Eucalyptus camaldulensis wood and evaluation of medium chemical cellulose in the paper industry. – TUBITAK publications 275. Toag Set. 46. Ankara, Turkey.
- [21] Istas, J. R., Heremans, R., Roekelboom, E. L. (1954): Caracteres generaux de bois feuillus du congo belge en relation avec leur utiliation dans l'industrie des pates a papier: Etude detaillee de quelques essences Gembloux. – INEAC Serie Technique, No 43. 9.
- [22] Istek, A., Gülsoy, S. K., Eroglu, H. (2010): The comparison of fiber properties of sapwood and heartwood of black pine. – In: III.National Karadeniz Forestry Congress, Artvin, Turkey. pp. 1916-1924.
- [23] Kharkwal, G., Mehrotra, P., Rawat, Y. S., Pangtey, Y. P. S. (2004): Comparative study of herb layer diversity in pine forest stands at different altitudes of Central Himalaya. – *Appl. Ecology and Enviro. Res.* 2(2): 15-24.
- [24] Kirci, H. (2003): Pulp Industry. – Lecture notes, Karadeniz Technical University Trabzon, Turkey.
- [25] Mahesh, S., Kumar, P., Ansar, S. A. (2015): A rapid and economical method for the maceration of wood fibers in *Boswellia serrata* Roxb. – *Wood Sci. and Techn. Tropical plant Research* 2(2): 108-111.
- [26] Ozdemir, F., Tutus, A., Bektas, I., Cicekler, M. (2015): Determination of differences in morphology between sapwood and heartwood cells of *Pinus pinea* and *Robinia pseudoacacia*. – *Turkish Journal of Forestry* 16(1): 60-64.

- [27] Republic of Turkey General Directorate of Forestry (2018): The map of Turkey Forests of presence. – Retrieved November 15. <http://ogm.gov.tr>.
- [28] Seth, R. S., Page, D. H. (1988): Fiber properties and tear resistance. – *Tappi J.* 712: 103-107.
- [29] Standavor, T., Kenderes, K. (2003): A review on natural stand dynamics in beechwoods of East Central Europe. – *Appl. Ecology and Enviro. Res.* 1(1–2): 19-46.
- [30] Syed, N. F., Zakaria, M. T., Bujang, J. S. (2016): Fiber Characteristic and papermaking of Seagrass using hand and Blended pulp. – *BioResources* 11(2): 5358-5380.
- [31] Tank, T. (1971): Fibre and cellulose Structure wood of *Fagus orientalis*. – Istanbul University, Journal of Istanbul University Faculty of Forestry, F. Series. A. XXI (2).
- [32] TAPPI Test Methods (1992–1993). – Tappi Press. Atlanta, US.
- [33] Ververis, C., Georghiou, K., Christodoulakis, N., Santas, P., Santas, R. (2004): Fiber dimentions, lignin and cellulose content of various plant material and their suitability for paper production. – *Ind Crops Prod* 19: 245-254.
- [34] Yaltirik, F., Efe, A. (1994): Dendrology. – Lecture Notes, Istanbul University Publishers 3509 (390). Istanbul, Turkey.

IRON OXIDE AND SODIUM HYDROXIDE ELIMINATION OF HEAVY METAL TOXICITY IN WHEAT SEEDLINGS

QIAO, L.* – LIU, H. – HU, C. – HU, L. – DU, H.

College of Life Science and Agronomy, Zhoukou Normal University, Zhoukou 466001, China

**Corresponding author
e-mail: qiaolin2012@126.com*

(Received 15th Sep 2018; accepted 12th Nov 2018)

Abstract. Wheat is an important food crop in China. Iron oxide has a toxic effect on the growth and development of wheat. In this paper, wheat was used as experimental raw material to study the toxicological mechanism of Cr salt on wheat seed germination. To study the effects of hydrogen sulfide (H₂S) on the germination and seedling growth of wheat under Iron oxide salt stress, H₂S donor sodium hydroxide pretreatment could alleviate the inhibition of Iron oxide stress on wheat seed germination and seedling growth could promote the growth of wheat seed germ. It did not significantly promote the growth of radicle. Relief mechanism of sodium sulfide and hydrogen sulfide donor on the growth toxicity of wheat seedlings under Iron oxide salt stress was conducted. The optimum concentration of sodium hydroxide pretreatment was 0.08 mmol/L. At the same time, sodium hydroxide pretreatment reduced the content of superoxide anion and Malondialdehyde (MDA), alleviated the damage of wheat seedlings, and enhanced the stress resistance of wheat seedlings under Iron oxide stress. In summary, H₂S as a signal molecule can mediate the antioxidant response of crop seed germination to Iron oxide stress and can relieve Iron oxide stress-induced oxidative damage to crops. It also can enhance crop resistance under specific circumstances.

Keywords: *Cr salt, sodium hydroxide, heavy metal, toxic mechanism, wheat seeds germination*

Introduction

Almost all green plants on the Earth start from the seed germination, so the germination of seeds plays a crucial role in plant growth and development. Seed plants are usually divided into gymnosperms and angiosperms. Most of the angiosperm seed structure is basically the same, including seed coat, endosperm and embryo in three parts (Aoyama and Okamura, 2010). The seed coat is the outer shell that surrounds the seed and is in the outermost layer of the seed, which protects the embryo and endosperm of the seed pair. The endosperm is an important structure for the storage of nutrients inside the seeds. Before the seeds can be used for photosynthesis, the energy and substances needed for the seed germination process come from the conversion of the energy substances in the endosperm. In some seeds without endosperm, nutrients of the seeds are stored in the cotyledons (Schulze, 1984). The embryo is the most important part of the entire structure of the seed and can be seen as a prototype of the plant before it matures (Awad, 2000; Bauer and Blodau, 2006).

In some researches (Bose and Bhattacharyya, 2008; Howell, 1994), the toxicological effects of four heavy metals (Cu, Cd, Pb and Zn) in soil on wheat seedlings and the dynamic enrichment of heavy metals under the interaction of single and two were systematically studied by dish culture and pot experiments. The micro-damage of heavy metals to wheat seedlings was studied by transmission electron microscopy, and the stress of heavy metals was also discussed. The effects of heavy metal interaction on the physiological characteristics of wheat seedlings and the enrichment characteristics of heavy metals in wheat seedlings were systematically studied in Cenci and Morozzi's

research (Cenci and Morozzi, 1977). The results showed that the interaction had antagonistic effects on wheat growth and physiological indices in varying degrees, among which root elongation was the most important (coefficient of variation was the largest). The effects of elements and their interaction on the enrichment of Cu, Cd and Zn in the interaction combination were above significant level, while the effects on the enrichment of Pb were all very significant level. The enrichment characteristics of heavy metals in wheat plants in different growth periods were systematically analyzed by orthogonal experiment in Hanesch's paper (Hanesch, 2010) and the results showed that the enrichment amount of heavy metals in roots, stems and leaves was greater than that in glume shells and seeds. The result also showed the enrichment amount was significantly correlated with heavy metal stress. Under the interaction of heavy metals, different parts of wheat in different growth stages have different characteristics of heavy metal enrichment. Most of the heavy metal accumulation in different parts of wheat was significantly correlated with the stress of the metal, and the correlation decreased with the growth of wheat.

Oxidative damage destroys the normal physiological environment of the plant. Pretreatment can inhibit the decrease of endogenous content to a certain extent, provide a relatively reducing environment, relieve excessive oxidative environment, and increase the stress resistance of the plant. It can also effectively inhibit the increase of lipid membrane permeability, protect the integrity of lipid membrane, and reduce the induced plasma membrane oxidative damage (Mishra and Gopal, 2008). Treatment can inhibit the decrease of chlorophyll content to a certain extent. The treatment reduced the content of reactive oxygen species and reduced oxidative damage by inducing the increase of active oxygen scavenging enzyme activity in germinating soybean seedlings under drought stress. By increasing the vitality, the activity of increasing iron oxide content in wheat seedlings is reduced, and the content in seedlings is reduced (Singh and Srivastava, 1999). Pre-treatment inhibits the activity to a certain extent, delays the increase of the content, slows the over-oxidation of membrane lipids in the growth process of young wheat seedlings, and protects the stability of the membrane structure, thereby promoting the growth of young seedlings.

Materials and methods

Experimental details and treatments

After the seed undergoes swelling, it enters the stagnant phase of water absorption and the seed enters the internal material activation period. At this stage, the increase of seed respiration, the activation of zymogens and the induction of new enzyme synthesis, proteolysis, synthesis of intracellular macromolecules, etc., require the consumption of a large amount of energy substances. The supply of these energy sources and substances mainly comes from the decomposition of the endosperm or cotyledons. The endosperm is the main storage site for cereals in seeds, of which starch is the main component. Germination of crop seeds is related to many factors, which can be summarized as internal factors and external factors. Internal factors mainly refer to whether the seeds are fully developed and have vitality, whether the seed dormancy is released or not. External factors refer to the external environmental conditions required for the germination of seeds, which play a key role in the normal germination of seeds. Unfavorable external environmental conditions can directly affect the germination of seeds. If these unfavorable factors exceed the normal range of the normal growth and

development of crop seeds, they will not only affect the germination of crop seeds, but also cause damage and even death of crop growth and development.

Experimental material

In general, after sowing, the seeds can germinate normally under suitable temperature conditions, and high temperature and low temperature will affect seed germination. The temperature has an effect on the membrane permeability of the cells and the activity of the hydrolase during the germination of the crop. However, the effects of temperature on seed germination mainly show that the three points are: the highest limit temperature, the lowest limit temperature and the most suitable temperature, of which only the most suitable temperature is the most favorable for seed germination. Optimum germination temperature of crops is related to external conditions. For example, the optimum germination temperature of seeds in warm environment is higher than that in cold regions. The pH value of the soil has a great influence on the seed germination, and the pH value is too high, making the soil strongly alkaline. When seeds are sown in alkaline soil, the seed germination is caused by alkali stress, and strong alkali stress is harmful to the germination of seeds, which can make the seeds burn and cannot germinate normally (*Fig. 1*). The pH value is too low to make the soil acidic, and the seeds of the crop that germinate under the acidic soil will be affected by its physiological metabolism and important osmotic adjustment. Therefore, pH value is also very important for the germination of crop seeds.

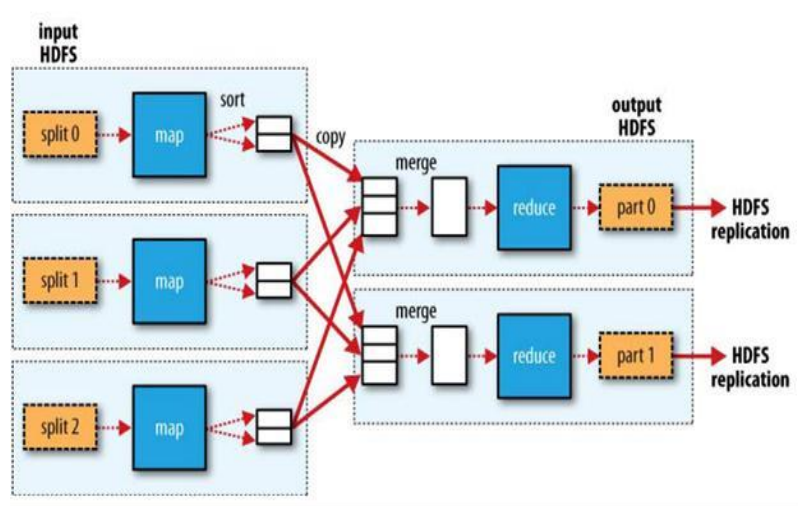


Figure 1. Effect of sodium hydroxide on isozymes of wheat seeds

Treatments

Embryos generally consist of radicles, hypocotyls, germs, and cotyledons. Under suitable external environmental conditions, seeds can grow into new individual plants as they germinate. Germination of seeds is generally considered to be the initial stage of the plant's entire life activity. Seed germination refers to that the seed breaks through the seed coat under suitable environmental conditions and undergoes a series of physiological metabolic changes. It can be roughly divided into three parts, namely the inhalation, activation and seed germination. The swelling effect is a physical change

and is an indispensable step for the germination of the seed. At this stage, the seed absorbs a large amount of water, the seed coat gradually softens, and the air permeability is enhanced. The final moisture content of the seed will reach a threshold value. Generally, the seed threshold of different plants is different. This difference is caused by the different components contained within the seed.

Wheat seed hydrolase activity

At present, heavy metal pollution is a focus of global attention. Due to its characteristics of great harm and difficulty in remediation, many countries attach great importance to it. According to statistics, China's total arable land has been one-fifths contaminated by heavy metals, which has seriously affected the growth and development of crops and the yield and quality of products. One of the stages in the process of plant growth and development during seed germination is most susceptible to external abiotic factors. Once the seeds are germinated, they are subject to heavy metal contamination, which will cause changes in the internal indicators of the seeds. This shows that heavy metals have toxic effects on the germination of plant seeds, but low concentrations of heavy metal ions can stimulate plant growth and development (*Fig. 2*). The seed germination was promoted. On the contrary, when the concentration was higher, the seed germination was inhibited, and the inhibitory effect was obvious with the increase of the concentration.

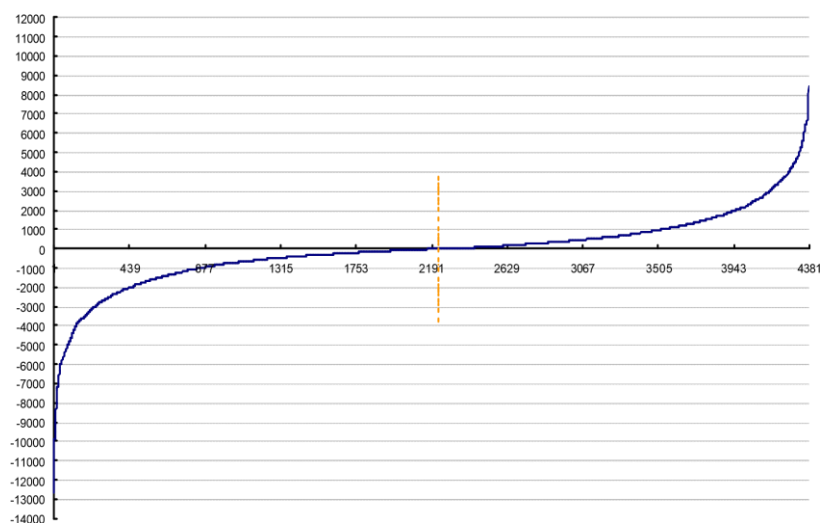


Figure 2. Sulfide content standard curve

Mitigative effects of oxidative damage during germination of wheat seeds

At the same time, it influences various processes of biomechanics such as photosynthesis, respiratory absorption, absorption and transportation of water and nutrition, activity of various enzymes, and transformation, transportation, and accumulation of organic matter. The BOX template in the spatial image processing is to use the pixels to be processed and the eight adjacent pixels around it to average the pixels to remove the pixels that produce mutations. Using this method, the noise of the image can be weakened. It also has some limitations, although the use of BOX template for image processing pays sufficient attention to the use of adjacent pixels, but does not

pay attention to the impact of pixel orientation on the image, so the effect is not ideal when dealing with complex images. Assume that the input sequence is a non-Gaussian, independent and identically distributed stationary process (Eq. 1):

$$C_{Nz} = C_{Nx} \cdot \sum_t s_i^N(t) \quad (\text{Eq.1})$$

The constraints are (Eq. 2):

$$K_x(M, N) = \frac{C_{Mx}}{[C_{Nx}]^{M/N}} \quad (\text{Eq.2})$$

First describe the data model of an OFDM system (Eq. 3):

$$K_1 = L - K_2 + 1, \quad K_2 = \lceil \arg \max_{0 \leq m \leq L - N_c} \sum_{i=m}^{m+N_c-1} |h_i|^2 \rceil - 1 \quad (\text{Eq.3})$$

The received signal vector formed at the receiving end is as follows (Eq. 4):

$$\begin{aligned} \underbrace{\begin{bmatrix} y_{ks+N_c-T+2} \\ \vdots \\ y_{(k+1)s} \end{bmatrix}}_{\mathbf{y}_k} &= \begin{bmatrix} \mathbf{h} & \cdots & 0 \\ \mathbf{O}_{(1)} & \ddots & \vdots \\ 0 & \cdots & \mathbf{h} \end{bmatrix} \cdot \begin{bmatrix} \mathbf{P} & \mathbf{O} & \mathbf{O} \\ \mathbf{O} & \mathbf{P} & \mathbf{O} \\ \mathbf{O} & \mathbf{O} & \mathbf{P} \end{bmatrix} \cdot \begin{bmatrix} \mathbf{I}_{N_c} & \mathbf{O} & \mathbf{O} \\ \mathbf{O} & \mathbf{I}_{N_c} & \mathbf{O} \\ \mathbf{O} & \mathbf{O} & \mathbf{I}_{N_c} \end{bmatrix} \cdot \begin{bmatrix} x_{1:N_c}(k-1) \\ x_{1:N_c}(k) \\ x_{1:N_c}(k-1) \end{bmatrix} + \underbrace{\begin{bmatrix} n_{ks+N_c-T+2} \\ \vdots \\ n_{(k+1)s} \end{bmatrix}}_{\mathbf{n}} \\ &= \mathbf{H} \cdot \mathbf{X} + \mathbf{n} \end{aligned} \quad (\text{Eq.4})$$

Indicates the process of adding a CP (Eq. 5):

$$\mathbf{P} = \begin{bmatrix} \mathbf{O} & \mathbf{I}_{N_c} \\ \mathbf{I}_N & \end{bmatrix} \quad (\text{Eq.5})$$

Its balanced output is shown as (Eq. 6):

$$\begin{bmatrix} z_1(k) \\ \vdots \\ z_N(k) \end{bmatrix} = \begin{bmatrix} D_1 & 0 & \cdots \\ 0 & \ddots & 0 \\ 0 & \cdots & D_N \end{bmatrix} \cdot \mathbf{F}_N \cdot (\mathbf{Y} \cdot \mathbf{w}) \quad (\text{Eq.6})$$

To further reduce complexity (Eq. 7):

$$\mathbf{Y} = \begin{bmatrix} y_{k \cdot s + N_c + 1} & y_{k \cdot s + N_c} & \cdots & y_{k \cdot s + N_c - T + 2} \\ y_{k \cdot s + N_c + 2} & y_{k \cdot s + N_c + 1} & \cdots & y_{k \cdot s + N_c - T + 3} \\ \vdots & \vdots & \ddots & \vdots \\ y_{(k+1) \cdot s} & y_{(k+1) \cdot s - 1} & \cdots & y_{(k+1) \cdot s - T + 1} \end{bmatrix} \quad (\text{Eq.7})$$

There are many types of seeds in nature, and seeds are the reproductive organs of seed plants. The seeds produced by different plants will have large differences in morphology and structure. Seed plants include gymnosperms and angiosperms. Most angiosperms are composed of embryos, endosperm and seed coats.

Statistical analysis

Under the heavy metal stress, the activities of the hydrolase such as amylase and esterase, which are related to seed germination, will change drastically. Amylase, esterase and other hydrolyzing enzymes can hydrolyze macromolecules such as starch and esters into small molecules such as glucose and phosphoric esters and release energy to provide protection for plant seed germination. The stronger the hydrolase activity such as amylase esterase is, the stronger the hydrolyzing power is, and the faster seed germination occurs. Conversely, the weaker the activity is, the weaker the hydrolyzing power is, the energy supply required for seed germination is affected, and the seed germination growth is slow or even inhibited.

Results

Regulation of iron oxides and sodium hydroxide on the antioxidant system of wheat seeds during germination

Iron oxides

From the current research results, it can be seen that higher concentrations of heavy metal ions have a greater impact on the amylase activity of the seed, which severely inhibits the activity of the amylase, thereby impeding the germination of the seed. However, the specific molecular mechanism of heavy metal inhibiting amylase activity is still unclear. In the process of metabolism, it can hydrolyze ester bonds, catalyze the hydrolysis of esters, and provide energy for the germination of plants. In general, the activity of heavy metals on amylase esterase is related to the concentration of heavy metals. High concentrations of heavy metals inhibit the activity of amylase esterase hydrolyzing enzymes, and low concentration treatments have a promoting effect, which corresponds to the morphological indicators of plant seed germination under heavy metal stress (*Fig. 3*).

Therefore, it is speculated that high concentrations of heavy metals may be harmful to the germination of seeds by inhibiting the activity of these hydrolytic enzymes. Finally, the effect of heavy metals on the seed germination is also reflected in the changes of soluble substances, proline content and antioxidant metabolism of the seeds. Generally speaking, under heavy metal stress, plants can increase the osmotic potential of cells through the accumulation of their own organic substances and maintain the normal metabolism of cells. The soluble substances not only participate in the important osmotic adjustment in the plant, but also provide the energy source for the plants and provide the starting material for the synthesis of other organic compounds in the plant.

Sodium hydroxide

Generally speaking, adverse stress has an adverse effect on the growth and development of plants, but under adverse circumstances, the plant's life activities itself will produce a special law to adapt to adversity stress, so that it can better adapt to the

environment. Under stress, the content of stored substances in the seed of the plant will change greatly, generally increasing the content of organic matter such as soluble sugar and soluble protein in the plant. Soluble sugars are involved in the osmotic adjustment of plant cells. The increase of soluble sugar content under stress can increase the osmotic potential of cells and maintain the normal metabolism of cells. The increase of soluble protein content will increase the number of functional proteins in the cells, allowing the plants to better adapt to adversity stress and survive in adverse environments. Therefore, the changes of soluble sugar and soluble protein content can reflect the growth status of the seeds, which is beneficial to improve plant stress resistance (Table 1). In addition, proline is an important substance involved in the seed germination and osmotic adjustment. Under the stress of adversity, the content in the germinating seeds increases rapidly, and its accumulation helps the plants to adapt to adversity, so the content can reflect.

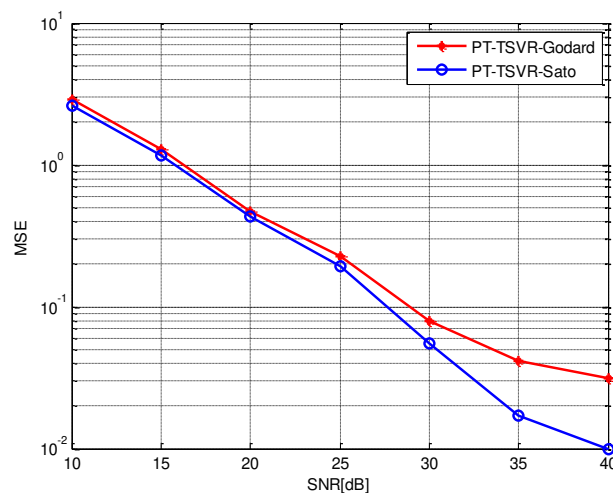


Figure 3. Protein content in wheat seed germination

Table 1. Each category classification result data table

Recall	Precision rate	Average assessment
72.779%	79.091%	75.935%
69.584%	81.954%	75.769%
70.895%	81.285%	76.090%
71.684%	80.059%	75.871%
70.597%	79.761%	75.179%
64.119%	87.931%	76.025%
71.333%	88.000%	79.667%
81.519%	65.692%	73.606%
59.446%	74.441%	66.944%
87.329%	87.671%	87.500%
80.353%	86.246%	63.300%
75.671%	79.429%	77.550%
79.463%	81.750%	80.607%
73.915%	84.825%	79.370%
84.407%	66.922%	75.665%

Discussion

Protein is a macromolecular substance rich in cells, and it is one of the key basic substances in the structure and function of crop seeds. Heavy metal stress can increase the soluble protein content of crop seeds, and then increase the number of functional proteins, which is conducive to the normal metabolic activity of crop seed cells, and increase the resistance of plants to heavy metals. Proline is involved in the key osmotic adjustment of crops. The change of content can reflect the strength of crop resistance. Therefore, the content of proline is used as a physiological indicator of crop stress resistance. Under normal circumstances, the content of proline in crops is relatively low, and the increase of content may be one of the mechanisms of resistance of plants. Smirnoff pointed out that the proline of crops can remove active oxygen accumulated under adverse conditions.

Seed germination is constrained by both internal and external factors, among which internal factors include dormancy and immature seeds, and seed coat restriction and other external factors including light, oxygen, and chemical substances. The minerals in the soil, salt, are crucial for the germination of seeds. However, in recent years, the nutritional structure of the soil has changed due to the destruction of the environment, the lack of water resources, and the abuse of chemical fertilizers. Soil salinization becomes a resource issue and an ecological problem that affects the entire world. The seed germination process starts because photosynthesis cannot be performed. The energy and materials required are supplied by the nutrients stored in the organs. When nutrients are mobilized, they will be converted into easily transportable forms, transported to the most active and fastest growing areas of metabolism, providing energy and carbon skeletons and other substances for a range of physiological activities during germination. Starch and fat are the most common and major storage material for wheat seeds. Although hydrolyzing enzymes such as amylases, etc. are not necessarily required in the germination of wheat seeds, the growth and development of seedlings depends on the activation of storage substances in the endosperm.

In this section, we investigated the changes of amylase isoenzyme activity during the seed germination of wheat under salt stress. Salt stress and aluminum stress have significant toxic effects on the germination of wheat seeds, and they are expressed in the length of radicles, embryos, and the number of radicles and germination rate. Among them, the effect of aluminum stress on radicle growth was particularly obvious. After germination and treatment of wheat seeds, their germination status was significantly relieved, and radicle germination became normal.

Acknowledgements. This work was supported by the National Natural Science Foundation of China (No. 31271627) and Henan Provincial Research Foundation for Science and Technological Breakthroughs, China (Grant No. 152102110106).

REFERENCES

- [1] Aoyama, I., Okamura, H. (2010): Interactive toxic effect and bioconcentration between cadmium and chromium using continuous algal culture. – *Environmental Toxicology* 8: 55-269.
- [2] Awad, F. (2000): Mobilization of heavy metals from contaminated calcareous soils by plant borne, microbial and synthetic chelators and their uptake by wheat plants. – *Journal of Plant Nutrition* 23: 1847-1855.

- [3] Awad, F., Römheld, V. (2000): Mobilization of heavy metals from a contaminated calcareous soil by plant borne and synthetic chelators and its uptake by wheat plants. – *Journal of Plant Nutrition* 23: 1847-1855.
- [4] Bauer, M., Blodau, C. (2006): Mobilization of arsenic by dissolved organic matter from iron oxides, soils and sediments. – *Science of the Total Environment* 354: 179-190.
- [5] Bose, S., Bhattacharyya, A. K. (2008): Heavy metal accumulation in wheat plant grown in soil amended with industrial sludge. – *Chemosphere* 70: 1264-1272.
- [6] Howell, R. J. (1994): Sorption of arsenic by iron oxides and oxyhydroxides in soils. – *Applied Geochemistry* 9: 279-286.
- [7] Cenci, G., Morozzi, G. (1977): Evaluation of the toxic effect of cd^{2+} and cd^{42-} ions on the growth of mixed microbial population of activated sludges. – *Science of the Total Environment* 7: 131-143.
- [8] Clausen, L., Fabricius, I. (2001): Atrazine, isoproturon, mecoprop and bentazone adsorption onto iron oxides. – *Journal of Environmental Quality* 30: 858.
- [9] Debetto, P., Luciani, S. (1988): Toxic effect of chromium on cellular metabolism. – *Science of the Total Environment* 71: 365-377.
- [10] Hagenbuch, I. M., Pinckney, J. L. (2012): Toxic effect of the combined antibiotics ciprofloxacin, lincomycin, and tylosin on two species of marine diatoms. – *Water Research* 46: 5028-5036.
- [11] Hanesch, M. (2010): Raman spectroscopy of iron oxides and (oxy) hydroxides at low laser power and possible applications in environmental magnetic studies. – *Geophysical Journal International* 177: 941-948.
- [12] Lanzky, P. F., Halling-Sä, Rensen, B. (1997). The toxic effect of the antibiotic metronidazole on aquatic organisms. – *Chemosphere* 35: 2553-61.
- [13] Källqvist, T., Meadows, B. S. (1978): The toxic effect of copper on algae and rotifers from a soda lake. – *Water Research* 12: 771-775.
- [14] Mishra, K. B., Gopal, R. (2008): Detection of nickel induced stress using laser-induced fluorescence signatures from leaves of wheat seedlings. – *International Journal of Remote Sensing* 29: 157-173.
- [15] Mittal, S. K., Ratra, R. K. (2000): Toxic effect of metal ions on biochemical oxygen demand. – *Water Research* 34: 147-152.
- [16] Muslu, A., Ergün, N. (2013): Effects of copper and chromium and high temperature on growth, proline and protein content in wheat seedlings. – *Bangladesh Journal of Botany* 42: 105-111.
- [17] Okamura, H., Aoyama, I. (2010): Interactive toxic effect and distribution of heavy metals in phytoplankton. – *Environmental Toxicology* 9: 7-15.
- [18] Prado, A. G. S., Airoidi, C. (2002): The toxic effect on soil microbial activity caused by the free or immobilized pesticide diuron. – *Thermochimica Acta* 394: 155-162.
- [19] Schulze, D. G. (1984): The influence of aluminium on iron oxides: x. properties of al-substituted goethites. – *Clay Minerals* 19: 521-539.
- [20] Schwertmann, H. C. U., Cornell, R. M. (2000): Iron oxides in the laboratory: preparation and characterization. – *Clay Minerals* 27: 393-393.
- [21] Singh, A., Srivastava, V. K. (1999): Toxic effect of synthetic pyrethroid permethrin on the enzyme system of the freshwater fish *Channa striatus*. – *Chemosphere* 39: 1951-1956.
- [22] Tkachenko, A. G. (2004): Mechanisms of protective functions of *escherichia coli*, polyamines against toxic effect of paraquat, which causes superoxide stress. – *Biochemistry* 69: 188-194.

EFFECTS OF DIFFERENT TEMPERATURE CONDITIONS ON YIELD AND PHYSIOLOGICAL PROPERTIES OF RICE (*ORYZA SATIVA* L.)

HE, L. X.^{1,2#} – CHEN, Y. L.^{1#} – ZHANG, T. T.^{1,2#} – ZHENG, A. X.^{1,2#} – CHENG, Y.¹ – DU, P.³ – LAI, R. F.^{1,2} – LU, R. H.¹ – LUO, H. W.^{1,2} – LIU, Y. F.^{1,2} – TANG, X. R.^{1,2*}

¹Department of Crop Science and Technology, College of Agriculture, South China Agricultural University, 510642 Guangzhou, PR China

²Scientific Observing and Experimental Station of Crop Cultivation in South China, Ministry of Agriculture, 510642 Guangzhou, PR China

³Key Laboratory of Key Technology for South Agricultural Machine and Equipment, Ministry of Education, 510642 Guangzhou, PR China

#These author have contributed equally to this work

**Corresponding author*

e-mail: tangxr@scau.edu.cn; phone/fax: +20-8528-0204-618

(Received 3rd Sep 2018; accepted 1st Nov 2018)

Abstract. Temperature is one of the major factors which have a significant effect on plants. This study was carried out to investigate the effect of temperature variation on physio-biochemical characteristics of two rice cultivars i.e., Basmati385 and Xiangyaxiangzhan. A pot experiment with three different treatments of day-night temperature dynamics was carried out in a randomized complete block design with three replications. Treatments included T1: 33 °C/27 °C, T2: 27 °C/21 °C, T3: 21/15 °C under 1200X yellow light intensity and 75% humidity. Results revealed that increase in temperature enhances photosynthesis, the production of photosynthetic pigments, but such increment was higher in Xiangyaxiangzhan than in Basmati385. Furthermore, temperature variably affected protein synthesis, and the activities of enzymatic antioxidants viz., superoxide dismutase (SOD), peroxidases (POD), catalase (CAT) in both cultivars. Moreover, the highest yield was recorded at 27 °C/21 °C for both cultivars and the temperature of 27 °C/21 °C was regarded as the most suitable temperature at filling stage for rice compared with 33 °C/27 °C and 21/15 °C.

Keywords: rice, temperature stress, antioxidant enzyme, chlorophyll content, yield

Introduction

Temperature is a vital ecological variable which determines the growth of plants (Berry and Bjorkman, 2003) and the physiological and plant biochemical reactions such as respiration, protein synthesis and photosynthesis must be carried out under certain temperature conditions. The report of Atkin and Tjoelker (2003) indicated temperature-mediated changes in plant respiration are now accepted as an important component of the biosphere's response to global climate change and temperature is also a major driver of climate change affecting global food production. In spite of the challenges faced due to changing climate, global food production needs to increase by about 70% by 2050, to feed the growing population (Almeselmani et al., 2006). Rice (*Oryza sativa* L.) is the most important cereal feeding more than 3 billion people globally and contributes about 20% to the total calorie intake of humans. Crops are altogether living in specific temperature conditions and influenced by temperature changes. For example, there was a study showing protein synthesis in rapeseed (*Brassica napus*) seedlings could continue at 0 °C

while some polypeptides preferentially accumulate at this temperature, however, synthesis of several others is repressed while many are insensitive to cold treatment (Mezabasso et al., 1986). Each growth stage of each crop has its own temperature requirement for development and normal growth while it could cause prominent effects if crops did not grow in the proper temperature range. Transferring wheats (*Triticum aestivum* L.) from 21/16°C to HT of 36/31°C for intervals of 2 days in the period from head emergence to 10 days after anthesis resulted in grain sterility (Tashiro and Wardlaw, 1990). Temperature higher than 12°C is essential for the growth of normal rice seedling while below 20°C at panicle initiation may cause panicle sterility (Shimono et al., 2007). Moreover, there was a good negative correlation between temperature and oil level in the case of sunflower seeds (Shi et al., 2006a).

Rice is majorly produced and consumed in Asia where it accounts for up to 80% of the caloric requirement (Mahajan et al., 2010). Like other crops, rice which is recognized as a main staple food, also has its own suitable temperature ranges of each growth stages such as germination (16–45 °C), seedling emergence (12–35 °C), rooting (16–35 °C), tillering (9–33 °C), panicle heading (15–30 °C), anthesis (22–35 °C) and ripening (12–30 °C) (Nguyen, 2005). Meanwhile, a previous report demonstrated that temperature higher than 35°C at flowering stage affected rice reproductive growth severely causing spikelet sterility (Matsui et al., 2001). Furthermore, a study showed that the temperature range of 21–26 °C was an optimal range at grain filling stage and temperature higher than 27 °C may cause loss in grain weight (Tashiro and Wardlaw, 1990). In addition, Peng et al. (2004) indicated that yield of grain decreased by 10% for each 1°C increase in growing-season minimum temperature in the dry season. Recently, a report declared that average temperatures from 23 to 29 °C for rice is an optimal temperature range for rice during grain filling stage (Kobata et al., 2018). Moreover, Mo et al. (2016) published a study regarding effects of local climatic conditions and temperature fluctuations on productivity of rice in Guangzhou while suggesting South China should develop some strategies for crop improvement to address them.

There are a lot of physiological processes and biochemical substances which are sensitive to temperature such as photosynthesis, chlorophyll content, protein, reactive oxygen species (ROS) and chlorophyll fluorescence (Kong et al., 2017). For example, temperature at 33 °C in filling stage could cause decrease of chlorophyll content, maximal photochemical efficiency of PS II (F_v/F_m) and the potential photochemical efficiency of PS II (F_v/F_o) (Teng et al., 2008). High growth temperature and CO₂ enrichment decreased the Rubisco content of rice by 22 and 23% (Vu et al., 1997). An examination found that protein concentrations of rice leaves under high temperature at early ripening stage were higher than those of control temperature, but those were slowly decreased with no difference between temperature treatments since at mid ripening stage (Jiyoung et al., 2015).

This study was conducted in Guangdong province (major rice producing province in South China) in order to explore the effect of different temperature conditions on the physiological characteristics of rice leaves at filling stage.

Materials and methods

Experimental details

Seeds of two aromatic rice cultivars i.e., Basmati385 and Xiangyaxiangzhan (widely grown in South China and popular because of their special aroma and enchant flavor)

were used in this study. Pot experiment between June 15th to July 13th in 2018 was conducted at Experimental Research Farm, College of Agriculture, South China Agricultural University, Guangzhou, (23°09'N, 113°22'E and 11 m from mean sea level) China. Before sowing, seeds of both cultivars were soaked in water for 24 h at room temperature and germinated at 37 °C, shade dried and the germinated seeds were sown in PVC trays for nursery while PVC trays were placed in puddled field and covered with a plastic sheet. Then, seedlings were transplanted into soil containing plastic pots (31 cm in diameter and 29 cm in height) in April. The experimental soil contained 24.56% organic matter content, 1.443% total nitrogen; 0.927% total phosphorous, 18.220% total potassium. At heading stage, the pots were translated into phytotron and treated as described below:

T1: 33 °C days and 27 °C nights, under 1200X yellow light intensity and 75% humidity

T2: 27 °C days and 21 °C nights, under 1200X yellow light intensity and 75% humidity

T3: 21 °C days and 15 °C nights, under 1200X yellow light intensity and 75% humidity

There were fourteen pots for each treatment.

Sampling collection

The fresh leaves were sampled from the rice at the end of 7th, 14th, 21st and 28th day after heading stage (translated day, d AH = day after heading stage). Samples were immediately stored at -80°C for biochemical analyses.

Determination of soluble protein and sugar

The soluble protein content of leaves was estimated according to the methods of Bradford (1976). The absorbance was read at 595 nm and expressed as $\mu\text{g g}^{-1}$ FW after reaction with G-250 while contents of soluble sugar was determined by using anthrone-sulfuric acid method (Wang et al., 2015).

Determination of malondialdehyde (MDA) and anti-oxidants responses

The malondialdehyde (MDA) content was measured according the method of Luo et al. (2017). MDA reacted with thiobarbituric acid (TBA) and the absorbance of was recorded at 532 nm, 600 nm, and 450 nm. The content of MDA was calculated as: MDA content ($\mu\text{mol/L}$) = $6.45(\text{OD } 532 - \text{OD } 600) - 0.56\text{OD } 450$ and final result was expressed as $\mu\text{mol g}^{-1}$ FW.

The peroxidase (POD EC1.11.1.7) activity was measured with the method of Luo et al. (2017). The reaction solution included enzyme extract (50 μl) containing 1 ml of 0.3% H_2O_2 , 0.95 ml of 0.2% guaiacol, and 1 ml of 50 mM I^{-1} sodium phosphate buffer (pH 7.0) while the absorbance was read at 470 nm. One POD unit of enzyme activity was defined as the absorbance increase because of guaiacol oxidation by 0.01 (U g^{-1} FW). The superoxide (SOD, EC 1.15.1.1) activity was measured by using nitro blue tetrazolium (NBT) according to Ashraf et al. (2018). 0.05 ml of enzyme extract was added into the reaction mixture containing 1.75 ml of sodium phosphatebuffer (pH 7.8), 0.3 ml of 130 mM I^{-1} methionine buffer, 0.3 ml of 750 $\mu\text{mol l}^{-1}$ NBT buffer, 0.3 ml of 100 $\mu\text{mol l}^{-1}$ EDTA-Na 2 buffer and 0.3 ml of 20 $\mu\text{mol l}^{-1}$ lactoflavin. After reaction, the change in color was measured at 560 nm. One unit of SOD activity is equal to the volume of extract needed to cause 50% inhibition of the color reaction. Catalase (CAT, EC1.11.1.6) activity was estimated with the methods devised by Aebi (1984). An aliquot of enzyme extract (50 μl) was added to the reaction solution containing 1 ml of 0.3% H_2O_2 and 1.95 ml of

sodium phosphate buffer and the absorbance was recorded at 240 nm. One CAT unit of enzyme activity was defined as the absorbance decrease by 0.01 ($\text{U g}^{-1} \text{FW}$).

Determination of chlorophyll contents

The contents of photosynthetic pigment were determined by using 95% alcohol for the extraction (Lichtenthaler, 1987). The absorbance was read at 665 nm, 649 nm, 652 nm and 470 nm. The chlorophyll content was calculated as: chlorophyll a(Ca) (mg/L) = $13.95 \text{ OD}_{665} - 6.88 \text{ OD}_{649}$, chlorophyll b(Cb) (mg/L) = $24.96 \text{ OD}_{649} - 7.32 \text{ OD}_{665}$, total chlorophyll(CT) (mg/L) = $\text{OD}_{652} \times 1000 / 34.5$, carotenoid = $(1000 \text{ OD}_{470} - 2.05 \text{ Ca} - 114.8 \text{ Cb}) / 245$.

Estimation of yield and yield related traits

Rice from six randomly selected pots from each treatment were harvested at maturity stage. Then threshed manually and sun dried (adjusted to ~15% moisture content) to get the grain yield per pot and expressed in grams per hill (g hill^{-1}). Panicle number per pot was determined by counting the panicle numbers of each hill in six different pots in each treatment and averaged. The grains were separated manually from each panicle in order to count total number of grains and filled grains per panicle. 1000-grain weight was recorded by counting six random samples from filled grains, weighed and averaged.

Statistical analyses

This study was managed as a split block design. Data were analyzed using statistical software 'Statistix 8.1' (Analytical Software, Tallahassee, FL, USA) while differences amongst means were separated by using least significant difference (LSD) test at 5% probability level. 'Origin 8.1' (OriginLab Co., Northampton, MA, USA) was used for graphical representation.

Results

Chlorophyll content

As showed in *Figure 1*, there were some differences in chlorophyll contents under different thermostatic conditions. The contents of total chlorophyll, chlorophyll a and chlorophyll b gradually decreased along with the grain filling process. The highest total chlorophyll content was recorded in T1 for both cultivars at 7, 14, 21 days after heading (d AH). Furthermore, the trend for total chlorophyll content at 7 and 14d AH was recorded as: $T1 > T2 > T3$, whereas at 21d AH higher total chlorophyll was recorded in T3 than T2 for Basmati385 while there was no significant difference between the three treatments for Xiangyaxiangzhan. At 28 DAH, there was no significant difference in chlorophyll content of the three treatments for both Basmati385 and Xiangyaxiangzhan. Meanwhile, all values of chlorophyll a and chlorophyll b in both cultivars were remained statistically similar with total chlorophyll.

Anti-oxidant enzyme activities

Different temperature at filling stage affected the anti-oxidative enzyme activities in terms of SOD, POD and CAT (*Fig. 2a-f*). The trend for POD activity was recorded as:

T1 > T2 > T3 at 7 d AH for both cultivars. At 14 d AH, both T1 and T3 remained higher activity of POD than T2 for Basmati whilst the trend of POD activity was recorded as T3 > T2 > T1 for Xiangyaxiangzhan. At 21d AH, the maximum POD activity was recorded in T1 while the minimum value was in T3 for Basmati. However, for Xiangyaxiangzhan, highest POD activity was recorded in T2 and lowest value was in T1. At 28d AH, there was no significant difference of POD activity between T1 and T2 for both cultivars while the value of T3 was remained lowest for Basmati and highest for Xiangyaxiangzhan.

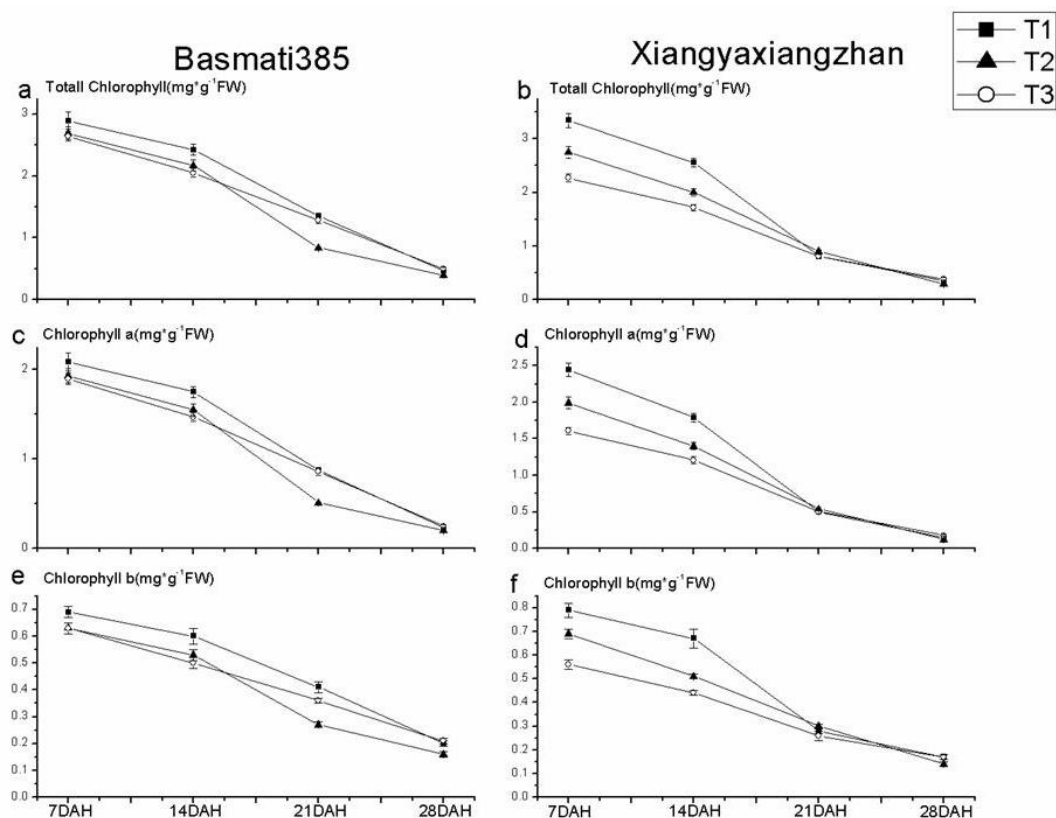


Figure 1. Effect of different temperature conditions at filling stage on chlorophyll content (d AH = days after heading, FW mean fresh weigh, T1 mean T1 treatment (33 °C/27 °C), T2 mean T2 treatment (27 °C/21 °C), T3 mean T3 treatment (21 °C/15 °C), the same as below)

SOD activity was affected differently under different temperature conditions at filling stage. SOD activity in T1 remained at highest level at 7, 14, 21 and 28d AH while the trends at 7, 14, 21d AH were recorded as: T1 > T2 > T3 for both cultivars. At 28d AH, SOD activities of T1 and T2 remained similar while T3 was lower than both T1 and T2 for Basmati. However, there was no significant difference between T2 and T3 whilst the highest value was recorded in T1 for Xiangyaxiangzhan.

The highest CAT activity was recorded in T1 at 7, 14d AH for both cultivars. Meanwhile, the trends for CAT activities at 7, 14d AH were recorded as: T1 > T2 > T3. At 21 DAH, there was no significant difference between T1 and T3 while T2 remained at the lowest level for Basmati while values of three treatments were similar for Xiangyaxiangzhan. Moreover, activities of CAT remained similar in the three treatments at 28d AH for both cultivars.

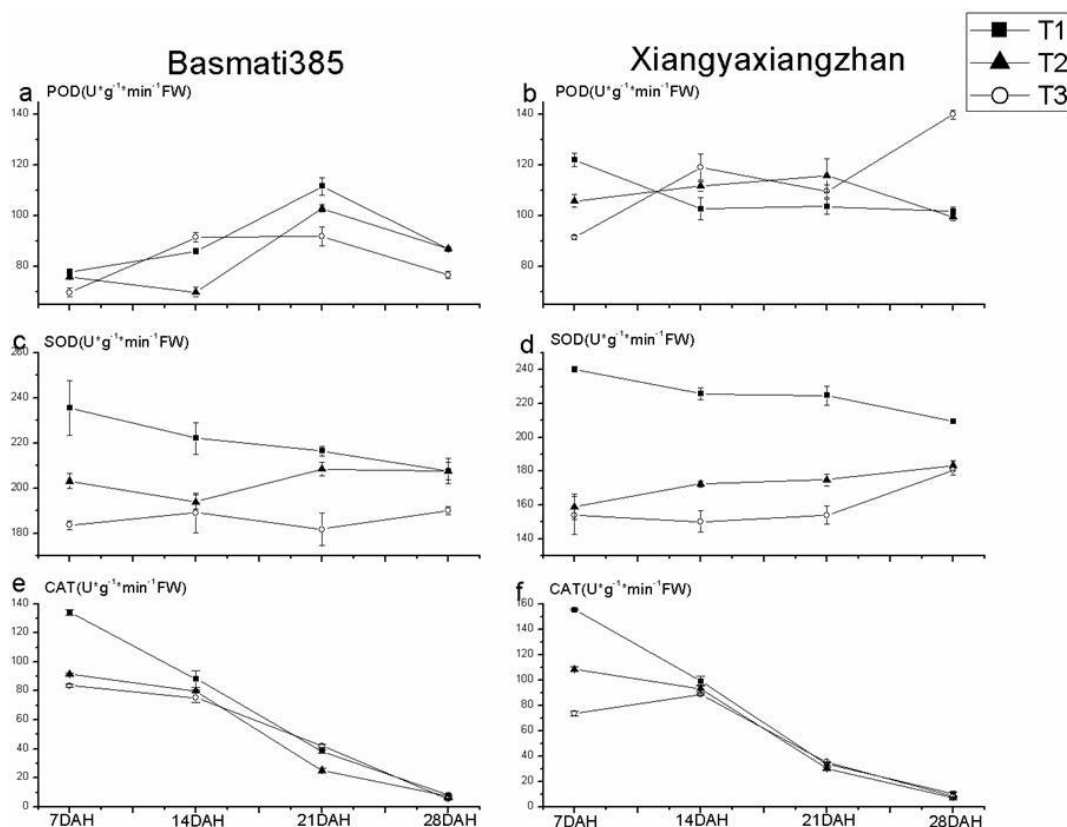


Figure 2. Effect of different temperature conditions at filling stage on anti-oxidant enzyme activities

MDA and soluble protein contents

MDA contents were affected differently under different temperature conditions at filling stage (Table 1). At 7d AH, the trend was recorded as T1 > T3 > T2 for Basmati while T3 > T2 > T1 for Xiangyaxiangzhan. Whereas at 14d AH, CAT activity of T3 was lower than both T1 and T2 for Basmati385 whilst there was no significant difference among T1, T2 and T3 for Xiangyaxiangzhan. At 21d AH, activities of CAT in T1, T2 and T3 remained similar for Basmati385 while value of T1 was lower than both T2 and T3 for Xiangyaxiangzhan. At 28d AH, for Basmati385, values of T1 and T2 remained similar and higher than T3. For Xiangyaxiangzhan maximum was recorded in T1 while there was no significant difference between T2 and T3.

Table 1. Effect of different temperature conditions at filling stage on MDA and soluble protein contents

Cultivar	Treatment	MDA				Soluble protein			
		7DAH	14DAH	21DAH	28DAH	7DAH	14DAH	21DAH	28DAH
Basmati	T1	3.19±0.01a	5.66±0.04a	5.40±0.68a	4.51±0.23a	129.72±2.89a	72.41±9.42b	69.41±1.93a	23.41±0.30b
	T2	2.19±0.06c	5.46±0.02a	5.89±0.10a	3.50±0.18b	130.74±7.71a	111.69±3.98a	47.38±9.22b	33.26±3.15a
	T3	2.68±0.01b	3.28±0.15b	5.51±0.08a	4.66±0.11a	129.78±2.12a	109.84±2.06a	68.04±4.04a	31.10±4.27a
Xiangyaxiangzhan	T1	1.96±0.05c	6.03±0.18a	4.16±0.43b	3.54±0.12a	155.78±3.18a	76.04±5.64b	60.21±1.63b	19.98±1.44b
	T2	2.95±0.05b	6.21±0.30a	6.36±0.22a	2.38±0.13b	133.41±4.94b	71.55±2.18b	59.14±1.28b	20.47±1.49b
	T3	3.42±0.05a	6.24±0.14a	5.94±0.33	2.79±0.03b	109.75±1.77c	115.94±6.67a	67.47±2.21a	4.59±2.55a

Means in the same column followed by different lower case letters for the same variety differ significantly at P < 0.05 by T-test, the same as below

There were some differences on soluble protein content under different temperatures at filling stage (*Table 1*). The content of soluble protein in T1, T2 and T3 were remained similar at 7d AH for Basmati and the trend for Xiangyaxiangzhan was recorded as: T1 > T2 > T3. Minimum content of soluble protein was recorded in T1 at 14d AH for Basmati385 while maximum was observed in T3 for Xiangyaxiangzhan. At 21 d AH, content in T2 was lower than T1 and T3 for Basmati385 while T3 was higher than both T1 and T2 for Xiangyaxiangzhan. At 28d AH, soluble content of T2 and T3 remained similar and higher than T1 for Basmati385. However, for Xiangyaxiangzhan, there was no significant difference between T1 and T2 whilst the maximum was recorded in T3.

Correlation analysis between anti-oxidative enzyme, soluble protein and MDA

As shown in *Table 2*, a significant positive correlation exists between CAT activity and soluble protein content ($r = 0.9128$, $P < 0.01$) and a significant positive correlation between CAT activity and total chlorophyll content ($r = 0.9659$, $P < 0.01$). Besides, the total chlorophyll content and soluble protein content also had a significant positive correlation ($r = 0.9328$, $P < 0.01$).

Table 2. Relationship between anti-oxidative enzymatic activities and MDA

Index	POD	SOD	CAT	MDA	Protein
SOD	-0.2582				
CAT	-0.0921	0.0948			
MDA	0.1330	-0.1259	-0.1517		
Protein	-0.1558	-0.0771	0.9128**	-0.2546	
Total chlorophyll	-0.2332	0.0986	0.9659**	-0.1958	0.9328**

Significant correlations at * $P < 0.05$ and ** $P < 0.01$

Yield and yield related traits

As shown in *Table 3*, for Basmati385, there was no significant difference in panicle number, grains per panicle and 1000-grain weight at different temperatures whilst in grain filling percentage, T2 was higher than both T1 and T3 while there was no significant difference between T1 and T3. Furthermore, the trend of yield was recorded as: T2 > T1 > T3. For Xiangyaxiangzhan, there also was no significant difference in grains per panicle, however, the trend of panicle number was recorded as: T3 > T1 > T2 whilst the highest 1000-grain weight was recorded in T1. Moreover, grain filling percentage of T3 was lower than both T1 and T2 while no significant difference between T1 and T2 and same pattern was found in yield.

Relationship between yield and yield related traits

As shown in *Table 4*, a significant positive correlation exists between yield and grain filling percentage. Panicle number per hill had negative correlation with both 1000-grain weight and grains number per panicle, however, it had a significant positive correlation with panicle number per hill and grain filling percentage. Furthermore, grain filling percentage had negative correlation with grains number per panicle.

Table 3. Effect of different temperature conditions at filling stage on yield and yield related traits

Cultivars	Treatments	Panicle number (hill ⁻¹)	Grains per panicle	Grain filling percentage (%)	1000-grain weight (g)	Yield (g·hill ⁻¹)
Basmati 385	T1	6.67±0.34a	107.83±9.64a	56.51±1.61b	27.65±0.25a	10.51±0.13b
	T2	6.33±0.33a	102.06±1.33a	71.77±6.95a	27.42±0.23a	11.39±0.71a
	T3	6.00±0.34a	92.13±3.66a	57.12±3.14b	27.55±0.10a	9.91±0.13c
Xiangyaxiangzhan	T1	9.33±0.33ab	79.58±5.10a	85.05±2.62a	20.35±0.31a	11.82±0.47a
	T2	7.67±0.67b	87.52±9.18a	87.93±0.44a	19.48±0.05b	11.29±0.30a
	T3	10.5±0.28a	10.11±4.86a	78.90±3.92b	19.74±0.13b	10.38±0.30b

Table 4. Relationship between yield and yield related traits

Index	Panicle number per hill	1000-grain weight	Grain filling percentage	Grains number per panicle
1000-grain weight	-0.8077**			
Grain filling percentage	0.5713*	-0.8152**		
Grains number per panicle	-0.8399**	0.6764**	-0.6577**	
Yield	0.1327	-0.3111	0.6499**	-0.2131

Discussion

Crop production is affected by many factors: sowing, topography, fertilization, and temperature flux. Among all of them, temperature is one of most important part in plant growth and development. For example, high temperature could trigger shortened vegetative phase and steep rise in temperature at the grain filling stage may cause abortion of florets and reduced kernel weight (Alam, 2012) and low temperature could inhibit biomass accumulation of rice seeding and cause the loss of chlorophyll (Bevilacqua et al., 2015). Meanwhile, the Chlorophylls and antioxidant responses are important phenomena in plants which could be affected significantly by temperature. Green plants use light to carry out photosynthesis through chlorophyll, converting carbon dioxide and water into organic compounds that store energy, such as starch, while releasing oxygen. Pigment in the chloroplasts includes two categories: the chlorophyll and carotenoid, chlorophyll including chlorophyll a and chlorophyll b, chloroplast pigments can absorb light energy, but only a few special conditions of chlorophyll a has a role in the conversion of light energy, which means most carotenoids and chlorophyll b pass light energy they absorb to a handful of chlorophyll a, and under special conditions the light energy is transformed into electricity and chemical energy (Haworth et al., 2018; Dalal and Tripathy, 2018). It will be visible, a few special conditions of chlorophyll a has the function of the absorption and conversion of light energy, and most of the chlorophyll a and chlorophyll b all have the function of the absorption and transmission of light (Mauzerall, 1976). At filling stage of rice, 80% of photo assimilate from leaves were absorbed by filling grains (Chen et al., 2005). A previous study showed that there exist a positive correlation between SPAD readings and rice yield (Gholizadeh et al., 2017). Another research (Gilani et al., 2009) also indicated that heat stress cause loss of rice yields by decreasing the chlorophyll content and disturbing cell membrane stability. The study of Peng (2004) and Prasad et al. (2008) also found 14% reduction in leaf photosynthesis due to high

temperature. Besides, Gosavi et al. (2014) found that high temperature could cause decrease of chlorophyll content and increase activities of SOD, POD and CAT because higher activity of antioxidant enzymes might be able to cope with oxidative damage by heat stress under high temperature condition. Furthermore, MDA production is also an important indicator of oxidative stress because of imparting the characteristics of inter- and intracellular membranes (Dash and Mohanty, 2002). In addition, a previous report showed that the protein contents in rice leaves decreased to 53% with an increase in temperature from 28 to 34 °C, while the protein reduction rate was lower (47%) under a further increase in temperature to 40 °C (Gesch et al., 2003). Moreover, there was a decrease of protein content in rice when exposed to 39 °C, compared with average temperature of 32 °C (Tang et al., 2008).

In this study, environment temperature at filling stage affected chlorophyll content significantly for both cultivars. We observed that the total chlorophyll content in flag leaves at 7, 14 DAH increased with the rise of temperature in certain range while content of total chlorophyll decreased gradually after heading stage. Similar trends were also recorded in contents of both chlorophyll a and chlorophyll b (*Fig. 1*). Those results agreed the study of Cai et al. (2015) which indicated that the elevated temperature improved 0.8 SPAD leaf chlorophyll content and leaf area index. The increment of chlorophyll meant a certain range of temperature increase at filling stage could promote leaf chlorophyll synthesis so increase the contents of chlorophyll and even enhance the photosynthesis. The reason may be that the temperature increase in a certain range could enhance the chemical reaction rate inside flag leaves of rice so that the activity of chlorophyll synthase was improved to promote the synthesis of chlorophyll. A similar study was also conducted by Wei and Pan (2008), which found that the nocturnal temperature of the whole growth period significantly affected each period of early rice growth. The higher night temperature is beneficial to the growth of early rice seedling stage and tillering stage, improving the quality of seedling and chlorophyll contents. A previous study (Mohanty et al., 2006) indicated that chloroplast development and chlorophyll biosynthesis were influenced significantly by temperature and light whilst their report implied the presence of both light and heat-inducible elements in their promoters because light and heat-stress stimulated glutamate semi aldehyde aminotransferase and uroporphyrinogen decarboxylase gene (UroD) and gene product abundance. In addition, the contents of total chlorophyll, chlorophyll a and chlorophyll b in T3 remained at a lower level than in both T1 and T2 at 7 and 14 DAH. Those values maybe mean that if the temperature is lower than 22 °C at filling stage it could cause reduction of chlorophyll.

Furthermore, we observed that the activities of POD, SOD and CAT had different responses to temperature at filling stage. Antioxidant enzymes which were including POD, SOD and CAT play an important part in detoxifying active oxygen species while antioxidant enzymes aid cells in removing harmful oxygen species (Pan et al., 2013). At early grouting stage (7DAH), there is no significant difference in POD activity between T1 and T2 while in T3 it remained low. However, POD activity in T3 increased drastically at middle stage and became higher than both T1 and T2. Furthermore, the activities of SOD and CAT in T3 remained lower than in T1 and T2 in a whole filling stage. Those reductions were similar with the study of Bonnacarrère et al. (2011) which found low temperature could reduce activities of antioxidant enzymes or cause a significant change. Both SOD and CAT are essential components of plants oxidative defence system in removal of toxic peroxides. It is mostly universal oxidoreductase that

scavenges H₂O₂ via a two electron transfer producing O₂ and H₂O (Shah et al., 2001). The antioxidant enzymes such as POD, SOD and CAT are effective quenchers of ROS whilst their level may also represent the sensitivity of plants to lipid peroxidation (Imamura et al., 2000). According to the values of our study, the temperature condition lower than 22 °C at filling stage might have formed a cold stress to rice. Meanwhile, highest activities of SOD and CAT were recorded in T1 at both 7 and 14 DAH. The main reason might be the environment temperature of T1 that might already formed a heat stress to rice, however, the stress of this degree cannot do much damage to rice and the plants just need enhancement in the activity of antioxidant enzymes so they can remove the damage mostly. The result of yield confirmed this infer by showing the yield of T2 was higher than T1 in Basmati and in Xiangyaxiangzhan, there was no significant difference between T1 and T2. In addition, the contents of protein also decreased with filling process and it had a significant positive relation with CAT activities. This result agree with Sairam et al. (2000) who found proteins have a significant role in osmo-regulations and in the maintenance of cellular structures when anti-oxidants quench reactive oxygen species (ROS).

Conclusion

In conclusion, a temperature of 33 °C/27 °C at filling stage could enhance the biosynthesis and accumulation of chlorophylls in the early phase. However, 33 °C/27 °C would also create some slight stress resistance to rice. Moreover, a temperature of 21/15 °C not only would reduce the content of chlorophylls but also would lower the activities of anti-oxidative enzyme. Compared with 33 °C/27 °C and 21/15 °C, a temperature of 27 °C/21 °C was regarded as the most suitable temperature at filling stage for rice. In order to reveal the mechanism of chlorophyll synthesis and antioxidant responses under different temperature conditions at filling stage, further research should be done at molecular and physiological level.

Acknowledgements. This study was supported by the National Natural Science Foundation of China (31271646), the National Key R&D Program of China (2016YFD0700301), Graduate Student Overseas Study Program of South China Agricultural University (2017LHPY004), The World Bank Loan Agricultural Pollution Control Project in Guangdong (0724-1510A08N3684), The Technology System of Modern Agricultural Industry in Guangdong (2017 LM1098) and the Student's Platform for Innovation and Entrepreneurship Training Program (201810564029). The authors declare no conflicts of interest.

REFERENCES

- [1] Aebi, H. (1984): Catalase in vitro. – *Methods Enzymol* 105: 121-126.
- [2] Alam, M. Z (2012): *Growth, Yield and Nitrogen Utilization of Barley*. – LAP Lambert Academic Publishing, Riga.
- [3] Almeselmani, M., Deshmukh, P. S., Sairam, R. K., Kushwaha, S. R., Singh, T. P. (2006): Protective role of antioxidant enzymes under high temperature stress. – *Plant Science An International Journal of Experimental Plant Biology* 171: 382-388.
- [4] Ashraf, U., Hussain, S., Akbar, N., Anjum, S. A., Hassan, W., Tang, X. (2018): Water management regimes alter Pb uptake and translocation in fragrant rice. – *Ecotoxicology and Environmental Safety* 149: 128-134.
- [5] Atkin, O. K., Tjoelker, M. G. (2003): Thermal acclimation and the dynamic response of plant respiration to temperature. – *Trends in Plant Science* 8: 343.

- [6] Berry, J., Bjorkman, O. (2003): Photosynthetic response and adaptation to temperature in higher plants. – *Annual Review of Plant Physiology* 31: 491-543.
- [7] Bevilacqua, C. B., Borges, C. T., Venske, E., Almeida, A. D. S., Zimmer, P. D. (2015): Biomass accumulation and chlorophyll content in rice cultivars seedlings under cold stress. – *Scientia Agraria Paranaensis* 14(4): 229-233.
- [8] Bonnacarrère, V., Borsani, O., Díaz, P., Capdevielle, F., Blanco, P., Monza, J. (2011): Response to photooxidative stress induced by cold in japonica rice is genotype dependent. – *Plant Science An International Journal of Experimental Plant Biology* 180: 726.
- [9] Bradford, M. M. (1976): A rapid and sensitive method for the quantitation of microgram quantities of protein utilizing the principle of protein-dye binding. – *Analytical Biochemistry* 72: 248-254.
- [10] Cai, W. W., Wan, Y. F., Tian-Cheng, A. I., You, S. C., Yu-E, L. I., Wang, B. (2015): Impacts of elevated CO₂ concentration and temperature increasing on growth and yield of late rice. – *Chinese Journal of Agrometeorology* 36(6): 717-723.
- [11] Chen, H., Tao, L., Wang, X., Huang, X., Tan, H., Cheng, S., Min, S. (2005): Effect of different irrigation modes during grain filling of rice on translocation and allocation of carbohydrate in rice. – *Scientia Agricultura Sinica* 38(4): 678-683.
- [12] Dalal, V. K., Tripathy, B. C. (2018): Water-stress induced downsizing of light-harvesting antenna complex protects developing rice seedlings from photo-oxidative damage. – *Scientific Reports* 8: 5955.
- [13] Dash, S., Mohanty, N. (2002): Response of seedlings to heat-stress in cultivars of wheat: Growth temperature-dependent differential modulation of photosystem 1 and 2 activity, and foliar antioxidant defense capacity. – *Journal of Plant Physiology* 159: 49-59.
- [14] Gesch, R. W., Kang, I. H., Gallo-Meagher, M., Vu, J. C. V., Boote, K. J., Allen, L. H., Bowes, G. (2003): Rubisco expression in rice leaves is related to genotypic variation of photosynthesis under elevated growth CO₂ and temperature. – *Plant Cell & Environment* 26: 1941-1950.
- [15] Gholizadeh, A., Saberioon, M., Borůvka, L., Wayayok, A., Soom, M. A. M. (2017): Leaf chlorophyll and nitrogen dynamics and their relationship to lowland rice yield for site-specific paddy management. – *Information Processing in Agriculture* 4(4): 259-268.
- [16] Gilani, A. A., Siadat, S. A., Alamisaed, K., Bakhshandeh, A. M., Moradi, F., Seidnejad, M. (2009): Effect of heat stress on grain yield stability, chlorophyll content and cell membrane stability of flag leaf in commercial rice cultivars in Khuzestan. – *Iranian Journal of Crop Science* 11(1): 82-100.
- [17] Gosavi, G. U., Jadhav, A. S., Kale, A. A., Gadakh, S. R., Pawar, B. D., Chimote, V. P. (2014): Effect of heat stress on proline, chlorophyll content, heat shock proteins and antioxidant enzyme activity in sorghum (*Sorghum bicolor*) at seedlings stage. – *Indian Journal of Biotechnology* 13: 356-363.
- [18] Haworth, M., Belcher, C. M., Killi, D., Dewhirst, R. A., Materassi, A., Raschi, A., Centritto, M. (2018): Impaired photosynthesis and increased leaf construction costs may induce floral stress during episodes of global warming over macroevolutionary timescales. – *Scientific Reports* 8: 6206.
- [19] Imamura, S., Yanase, K., Horiguchi, M., Ozaki, M., Wakai, Y. (2000): Changes in antioxidative enzymes in cucumber cotyledons during natural senescence: comparison with those during dark-induced senescence. – *Physiologia Plantarum* 109: 211-216.
- [20] Jiyoung, S., Junhwan, K., Chungkuen, L., Yang, W. H. (2015): Effect of high temperature on leaf physiological changes as chlorophyll composition and photosynthesis rate of rice. – *Korean Journal of Crop Science* 60: 266-272.
- [21] Kobata, T., Palta, J. A., Tanaka, T., Ohnishi, M., Maeda, M., Cedilla, M. K., Barutçular, C. (2018): Responses of grain filling in spring wheat and temperate-zone rice to temperature: Similarities and differences. – *Field Crops Research* 215: 187-199.
- [22] Kong, L., Ashraf, U., Cheng, S., Rao, G., Mo, Z., Tian, H., Pan, S., Tang, X. (2017): Short-term water management at early filling stage improves early-season rice

- performance under high temperature stress in South China. – *European Journal of Agronomy* 90: 117-126.
- [23] Lichtenthaler, H. K. (1987): Chlorophylls and carotenoids: Pigments of photosynthetic biomembranes. – *Methods in Enzymology* 148C: 350-382.
- [24] Luo, H., Zhong, Z., Nie, J., Tang, X. (2017): Effects of ultrasound on physiological characters, yield and quality of rice Yuejingsimiao. – *China Rice* 27(2): 64-67.
- [25] Mahajan, G., Sekhon, N. K., Singh, N., Kaur, R., Sidhu, A. S. (2010): Yield and nitrogen-use efficiency of aromatic rice cultivars in response to nitrogen fertilizer. – *Journal of New Seeds* 11: 356-368.
- [26] Matsui, T., Omasa, K., Horie, T. (2001): The difference in sterility due to high temperatures during the flowering period among Japonica-rice varieties. – *Plant Production Science* 4: 90-93.
- [27] Mauzerall, D. (1976): Chlorophyll and photosynthesis. – *Philosophical Transactions of the Royal Society B Biological Sciences* 273: 287-294.
- [28] Mezabasso, L., Alberdi, M., Raynal, M., Ferrerocadinanos, M. L., Delseny, M. (1986): Changes in protein synthesis in rapeseed (*Brassica napus*) seedlings during a low temperature treatment. – *Plant Physiology* 82: 733-8.
- [29] Mo, Z. W., Pan, S. G., Ashraf, U., Kanu, A. S., Li, W., Wang, Z. M., Duan, M. Y., Tian, H., Kargbo, M. B., Tang, X. R. (2016): Local climate affects growth and grain productivity of precision hill-direct-seeded rice in South China. – *Applied Ecology & Environmental Research* 15: 113-125.
- [30] Mohanty, S., Grimm, B., Tripathy, B. C. (2006): Light and dark modulation of chlorophyll biosynthetic genes in response to temperature. – *Planta* 224: 692.
- [31] Nguyen, N. V. (2005): Global climate changes and rice food security. – *International Rice Commission Newsletter (FAO)* 54: 24-30.
- [32] Pan, S., Rasul, F., Li, W., Tian, H., Mo, Z., Duan, M., Tang, X. (2013): Roles of plant growth regulators on yield, grain qualities and antioxidant enzyme activities in super hybrid rice (*Oryza sativa* L.). – *Rice* 6: 1-10.
- [33] Peng, S., Huang, J., Sheehy, J. E., Laza, R. C., Visperas, R. M., Zhong, X., Centeno, G. S., Khush, G. S., Cassman, K. G. (2004): Rice yields decline with higher night temperature from global warming. – *Proceedings of the National Academy of Sciences of the United States of America* 101: 9971-5.
- [34] Prasad, P. V. V., Staggenborg, S. A., Ristic, Z. (2008): Impacts of Drought and/or Heat Stress on Physiological, Developmental, Growth, and Yield Processes of Crop Plants. – In: Ahuja, L. R., Reddy, V. R., Saseendran, S. A., Qiang, Y. U. (eds.) *Response of Crops to Limited Water: Understanding and Modeling Water Stress Effects on Plant Growth Processes, Advances in Agricultural Systems Modeling 1*. American Society of Agronomy, Madison, WI, pp. 301-355.
- [35] Sairam, R. K., Srivastava, G. C., Saxena, D. C. (2000): Increased antioxidant activity under elevated temperatures: a mechanism of heat stress tolerance in wheat genotypes. – *Biologia Plantarum* 43: 245-251.
- [36] Shah, K., Kumar, R. G., Verma, S., Dubey, R. S. (2001): Effect of cadmium on lipid peroxidation, superoxide anion generation and activities of antioxidant enzymes in growing rice seedlings. – *Plant Science* 161: 1135-1144.
- [37] Shi, Q., Bao, Z., Zhu, Z., Ying, Q., Qian, Q. (2006a): Effects of different treatments of salicylic acid on heat tolerance, chlorophyll fluorescence, and antioxidant enzyme activity in seedlings of *Cucumis sativa* L. – *Plant Growth Regulation* 48: 127-135.
- [38] Shimono, H., Okada, M., Kanda, E., Arakawa, I. (2007): Low temperature-induced sterility in rice: Evidence for the effects of temperature before panicle initiation. – *Field Crops Research* 101: 221-231.
- [39] Tang, R. S., Zheng, J. C., Jin, Z. Q., Zhang, D. D., Huang, Y. H., Chen, L. G. (2008): Possible correlation between high temperature-induced floret sterility and endogenous

- levels of IAA, GAs and ABA in rice (*Oryza sativa* L.). – *Plant Growth Regulation* 54: 37-43.
- [40] Teng, Z. H., Zhi, L., Zong, X. F., Wang, S. G., He, G. H. (2008): Effects of high temperature on chlorophyll fluorescence, active oxygen resistance activity, and grain quality in grain-filling periods in rice plants. – *Acta Agronomica Sinica* 34: 1662-1666.
- [41] Vu, J. C. V., Allen Jr, L. H., Boote, K. J., Bowes, G. (1997): Effects of elevated CO₂ and temperature on photosynthesis and Rubisco in rice and soybean. – *Plant Cell & Environment* 20: 68-76.
- [42] Wang, C. C., Kong, L. L., Mei-Juan, L. I., Tang, X. R., Yao-Dong, D. U., Wang, H. (2015): Effect of water treatments at tillering stage on super rice yield and physiological characteristics. – *Acta Agriculturae Boreali-Sinica* 30(5): 146-152.
- [43] Wei, J. L., Pan, X. H. (2008): Effects of night temperature increase on growth and yield of early season rice. – *Acta Agriculturae Universitatis Jiangxiensis* 30: 427-432.

GAS EXCHANGE PARAMETERS IN RED COVER (*TRIFOLIUM PRATENSE* L.) AND FESTULOLIUM (*FESTULOLIUM BRAUNII* (K. RICHT) A. CAMUS) UNDER DROUGHT STRESS

STANIAK, M.^{1*} – KSIĘŻAK, J.¹ – BOJARSZCZUK, J.¹ – FELEDYN-SZEWCZYK, B.²

¹*Institute of Soil Science and Plant Cultivation – State Research Institute, Department of Forage Crop Production, Czartoryskich 8, 24-100 Puławy, Poland*

²*Institute of Soil Science and Plant Cultivation – State Research Institute, Department of Systems and Economics of Crop Production, Czartoryskich 8, 24-100 Puławy, Poland
(phone: +48-81-478-6790; fax: +48-81-478-6900)*

*Corresponding author
e-mail: staniakm@iung.pulawy.pl

(Received 5th Sep 2018; accepted 26th Nov 2018)

Abstract. Water deficit in the soil is one of the factors that limit the yield of crops, causing great damage to agricultural production. This is the result of genotypic expression as modulated by interaction with the environment. The effect of water deficit on gas exchange parameters of *Festulolium* hybrid and red clover grown in pure stand and in mixture were studied. Two-factor pot experiment was performed in the completely randomized block method, with four replications. Objects were evaluated at two soil moisture levels: well-watered conditions and drought stress. The studies have shown that all the measured parameters were affected by drought stress. Net photosynthetic rate, transpiration rate and stomatal conductance were significantly lower under drought stress than under well-watered conditions in all treatments. Red clover grown in a pure stand responded to stress the most, while *Festulolium* hybrid – the least. It was also found that the highest water use efficiency index (WUE) was observed in *Festulolium* which proves a more economical water management compared to red clover. The mixtures showed smaller yield losses under drought stress compared to red clover grown in pure stand, which indicates their higher suitability to be grown in areas with less rainfall.

Keywords: *photosynthesis, transpiration, stomatal conductance, water-use efficiency*

Introduction

The frequency of extreme climatic events has increased due to global climate change. Environmental stresses are limiting factors for production of important agricultural crops worldwide. According to Li et al. (2011), 25% of the world's agricultural land is under the influence of drought stress, limiting growth, development and productivity of many forage crops. It is argued that breeding of forage species should aim to improve plant strategies to cope with relevant abiotic stresses and optimize growth and phenology to new seasonal variation, and that plant diversity at all levels is a good adaptation strategy (Ergon et al., 2018).

Agriculture is based mainly on rainwater, which is why frequent rainfall is a real threat to agricultural production. Water shortage causes the inhibition of plant growth and development processes as well as disrupts physiological processes, including photosynthesis. It also disrupts the transport and distribution of assimilates (Starck, 2010). Stress leads to disturbance of water balance of the plant, through the decrease of water potential in cells and accumulation of secondary metabolites, which on the one hand, reduce the osmotic potential, but on the other hand, protect the cellular structures. The prolonged stress damages the thylakoid membranes and degradation of lipids

stabilizing protein complexes, which consequently leads to damage to photosystems, mainly PSII. The photosynthetic apparatus exhibits a particular sensitivity to stress factors, which is why it is the first to react to any changes in the environment. Drought inhibits the intensity of photosynthesis, which is probably caused by a decrease in RuBisCo activity and a decrease in diffusion conductivity, which in turn, limits the availability of CO₂ in intercellular spaces (Hura et al., 2007). Under optimal cultivation conditions, the yield of plants depends on the intensity of the photosynthesis and is reduced by the loss of biomass due to respiration process. According to Lawlor (1995), nearly 90% of the accumulated biomass depends on the intensity of the photosynthesis.

The response of individual species to abiotic stresses may vary considerably. First and foremost, this is determined by genetic determinants, but also by a number of external factors, such as: light intensity, temperature, water availability, oxygen and carbon dioxide concentration in the air; and internal factors, such as: leaf structure, chlorophyll content, enzyme activity, or mineral supply (Starck, 2010). From the point of view of yield biology, the plant is resistant to stress, when under unfavourable environmental conditions, it can yield a little less than under optimal conditions (Dziadczyk, 2002). According to Blum (2009), this may be associated with the formation of a larger mass of roots, longer roots, or with the increased root permeability. Olszewska (2008) reported that, the intensity of gas exchange processes also depends on the type of plant cultivation. Compared to monotypic sowing, mixtures are generally less susceptible to adverse environmental conditions due to varied environmental requirements of individual components, different development rhythm, and differences in root system morphology. This makes mixtures yield better and be more reliable in cultivation (Lucero et al., 1999; Hakala and Jauhiainen, 2007).

Red clover (*Trifolium pratense* L.) is an important forage legume to world agriculture because of their environmental and agricultural benefits. It is an assort-lived perennial legume, meaning that it is only productive for two to three years and harvested three to five times a year (OMAFRA, 2011; Tucak et al., 2016). The short persistence of red clover grown in pure stand is mainly due to poor overwintering which can be caused by physical damage, e.g. low temperature and ice cover and pathogens, especially root rot and clover root for which deep snow cover provides ideal conditions (Hakala and Jauhiainen, 2007). Red clover needs at least 500-600 mm of annual precipitation to properly develop, including 300-400 mm during vegetation period (Rojek, 1986). The greatest demand for water is in the period of intensive growth, that is, in the phase of forming main shoots and branches and developing inflorescences. Red clover grows best in a humid, moderately cold climate, under frequent and evenly distributed rainfall during the growing season (OMAFRA, 2011). Several multi-year studies showed that red clover biomass weight was lower in years with less than average precipitation, suggesting that red clover may be susceptible to drought stress. Grasses have high water requirements as well. Their daily demand varies from 0.5 to 3.0 dm³·m⁻², and the amount of water transpired from 1 m² of grass sward per year can amount up to 1000 dm³ (Thomas, 1994). According to Łabędzki (2006), drought during the summer, accompanied by high temperature, can cause a decrease in grass yield by about 30%.

Growing perennial legume-grass mixtures has many benefits. In addition to being valuable, balanced feed for ruminants, mixtures reduce weeds, protect the soil from erosion by rain and wind, increase soil organic matter and soil fertility, improve soil water-holding capacity, and improve to soil structure and yield stability (Gaudin et al.,

2013). Mixtures allow improved resource utilisation and beneficial biological interactions between the crops. Successful mixtures relies on the component crops having complementary rather than competing traits and thus using resources more efficiently than pure crops. They also require smaller doses of mineral nitrogen than grasses grown in pure sowing, due to ability of legumes to fix atmospheric N, utilizing a symbiotic relationship with *Rhizobium trifolii*. Red clover contributes a large amount of naturally produced nitrogen to the soil for use by companion grasses (Queen et al., 2009). It provides them with a unique advantage compared to other plant species. With the increase of energy cost, N-fertiliser has become more expensive, a trend that is expected to continue in the future, which will likely further increase the need of legume production, including red clover (Jensen and Haugaard-Nielsen, 2003).

Knowledge about the physiological and genetic responses of grasses and legumes to drought stress is insufficient. It is predicted that climate change may increase the risk of local droughts, with severe consequences for agricultural practises (Lipiec et al., 2013). This indicates a need to conduct research aimed at recognizing and understanding the responses of various crop species to adverse environmental factors and their possibilities of adapting and acclimatizing to changing conditions. This will allow a bigger use of drought-resistant species resistant, which can effectively use habitat resources and exhibit good water management. High hopes are placed on interspecific and intergeneric hybrids, which combine beneficial traits of parental species in their genomes. They constitute a valuable source of variability for increasing resistance to abiotic and biotic stresses. One of such hybrids is *Festulolium* (*Festulolium braunii* (K. Richt) A. Camus), the effect of the crossing of italian ryegrass (*Lolium multiflorum* Lam.) and meadow fescue (*Festuca pratensis* Huds.) (Østrem et al., 2013). According to Kryszak et al. (2002) *Festulolium* give higher yields by about 20% in comparison to red clover. For this reason, it is used in intensive feed production and sown on arable land and temporary grasslands, both in pure sowing and in mixtures with legumes (Olszewska, 2008). *Festulolium* is one of the most used species in Denmark (Elgersma and Søegaard, 2018).

The aim of the study was to compare gas exchange parameters of *Festulolium* and red clover grown both in pure stands and in mixture under conditions of optimal soil moisture and long-term drought stress.

Materials and methods

Plant material and growth conditions

The research was based on a two-factors pot experiment carried out in 2012-2014, in a greenhouse of the Institute of Soil Science and Plant Cultivation – State Research Institute in Puławy, in Poland [51° 24' 59" N, 21° 58' 9" E] in the completely randomized block method, with four replications. *Festulolium* hybrid cultivar Agula and red clover tetraploid cultivar Bona were grown in pure stands and in mixture (50% grass + 50% legume). Objects were assessed at two soil moisture levels: 70% field water capacity (FWC) as optimum moisture content and 40% FWC as drought stress. Soil moisture content was differentiated 8 weeks after sowing, in the second and third year of growing – 2 weeks after starting of vegetation. In order to maintain the appropriate soil moisture, water losses were made up on a daily basis, to achieve a specified weight of the pot with soil. The treatments were stop after last cut and plants were watered as needed. During the day pots were standing outside and during the night inside the

greenhouse. Temperature of the air in greenhouse was similar to the temperature outside. Average temperature in Puławy, for the years 2012-2014 during vegetation months (IV-X) was respectively: 9.7, 15.2, 17.8, 20.8, 19.0, 13.7, 9.1 °C. In winters pots were in greenhouse, where the lowest temperature did not fall under 0 °C. The pots were cuts every 4-5 weeks in the flowering stage of red clover, on the height of 4-5 cm.

The Mitcherlich pots were filled with 7 kg of lessive soil from arable layer (0-30 cm). It was characterized by a neutral reaction (pH in 1 M KCl 7.4), the available nutrient content of the soil was as follows (mg·100 g⁻¹ soil): phosphorus 24.8, potassium 14.2 and magnesium 2.2.

The seeds were sown in 11 of April 2012, three seeds at 15 points in each pot. After emergence poorly developed seedlings were removed, leaving 8 plants per pot (in mixture – 4 units of *Festulolium* and 4 units of red clover). This proportion lasted over three years. The soil material was fortified with mineral fertilizers at doses (g·pot⁻¹): 0.5 N, 1.0 P, 1.5 K, 0.5 Mg in the form of solutions: NH₄NO₃, KH₂PO₄, K₂SO₄ and MgSO₄ × 7 H₂O before sowing and 0.5 N after each cut of *Festulolium* in pure stand and half of this dose after each cut of mixture. Red clover in pure stand was not fertilized by nitrogen (except of start dose).

Methods and measurements

Gas exchange parameters and dry mass yield (DMY) were evaluated. Physiological plants parameters: net photosynthetic rate (P_N), transpiration rate (E) and stomatal conductance (g_s), were measured with an apparatus CIRAS-2 Portable Photosynthesis System (USA), a 1-2 days before each cut. Leaf gas exchange parameters were measured between 7.00–11.00 am, on the second fully exposed leaf in six replications, at a concentration of 390 ppm CO₂, 1000–1200 PAR [μmol·m⁻²·s⁻¹] and 17–25 °C. Water use efficiency (WUE) was calculated based on the quotient of instantaneous values of photosynthesis and transpiration (P_N/E). Plant material for the research was collected three times during the first growing season, and four times during second and third vegetation year.

The agricultural drought index, determining crop reductions due to water shortage in the soil, was calculated according to the formula (Łabędzki, 2006):

$$YR = 1 - (Y_{re} \cdot Y_p^{-1})$$

where:

YR - agricultural drought index, quantizing the yield reduction,

Y_{re} – yield reduced due soil water deficit,

Y_p – potential yield under optimal soil moisture.

Statistical analysis

The data presented are the mean values from the years 2012-2014, as a result of a similar reaction of the plant examined to different soil moisture uncovered during three study years. The results were statistically analysed with the use of the analysis of variance for the completely randomized design, using Statistica v.10.0 program. Tukey's multiple comparison test was used to compare differences between the means for main effects (factors), while confidence intervals for the means of LSD (α = 0.05) were used to compare the means from the subclasses (interactions).

Results

The effect of the main factors soil moisture (SM) and treatment (T) as well as that of the interactions $SM \times T$ on P_N , E , g_s , WUE were in most cases significant ($p < 0.05$) in all regrowth and average value. Drought stress led to significant decrease in photosynthesis and transpiration rate, stomatal conductance and increased in water use efficiency of red clover and *Festulolium* grown in pure stand and in mixture.

An important factor shaping the level of plant yield is the intensity of leaf gas exchange processes. An analysis of research results showed that red clover and *Festulolium* grown in pure and mixed stand reacted differently to stress. In all the years of research, in the optimal moisture conditions, the red clover cultivated in pure stand assimilated carbon dioxide the most effectively (*Table 1*). Under stress caused by the limit of moisture in the soil, the tested species responded with a significant reduction in the rate of photosynthesis (on average by 12.6% in the first, by 20.1% in the second, and 22.7% in the third year of vegetation). The strongest response to the water deficit in the first and third year of vegetation was noted for red clover cultivated in pure stand, where the average photosynthesis rate decreased by 16.8 and 34.6% respectively, while the red clover cultivated in the mixture demonstrated the highest rate of this process (9.48 and 16.15 $\mu\text{mol CO}_2 \cdot \text{m}^{-2} \cdot \text{s}^{-1}$), compared to the optimally moistened treatments. In the second year of vegetation, the decrease in the rate of photosynthesis under drought stress was the biggest in *Festulolium*. Moreover, this hybrid cultivated in mixture showed significantly higher rate of photosynthesis under drought stress in relations to its cultivation in pure stand. Analysing individual regrowths, it was found that the largest assimilation of carbon dioxide by plants in the first year of vegetation occurred in the third regrowth, while in the second and third year - in the first, second and third regrowth. The calculated values of determination coefficients ($R^2 = 58\%$ in the first, $R^2 = 49\%$ in the second, and $R^2 = 69\%$ in the third year of vegetation) and regression equations showed a significant, positive relationship between the photosynthetic rate and dry mass of the species tested in all years of research (*Fig. 1*). This dependency was directly proportional, which indicates a highly significant influence of the intensity of this process on the yield of the tested species.

A significant variability was recorded in the intensity of water transpiration from the leaf surface in red clover and *Festulolium* grown under limited and optimal soil moisture. In all vegetation years, the highest rate of transpiration was noted for red clover cultivated in pure stand (*Table 2*). Both species responded to water deficiency in soil with a significant reduction in the rate of this process (averagely by 29.5% in the first, 21.2% in the second and 31.5% in the third year of vegetation), compared to the optimally moistened treatments. Species cultivated in pure stand limited the evaporation of water from their leaf surface under stress conditions more than under mixed stand, whereas the smallest difference was found in the *Festulolium* hybrid grown in mixture. A statistical analysis of the results showed a highly significant, positive relationship between the rate of transpiration and the dry mass yield of red clover and *Festulolium* in all the years of the research, as evidenced by high values of determination coefficients ($R^2 = 74\%$, $R^2 = 65\%$ and $R^2 = 87\%$, respectively) (*Fig. 2*).

Under stress conditions, the studied species had significantly lower values of stomatal conductance (on average by 27.8% in the first, by 43.8% in the second, and by 51.6% in the third year of vegetation) compared to optimal conditions (*Table 3*). Irrespective of the method of cultivation and the level of soil moisture, red clover showed higher values of this parameter in the first and third year of vegetation, while

the *Festulolium* hybrid - in the second year of vegetation. Significantly higher values of stomatal conductance, regardless of the level of soil moisture, were recorded in the second and third year of vegetation than in the first. The calculated values of determination coefficients and regression equations showed a significant, positive relationship between stomatal conductance and dry mass yield of red clover and *Festulolium* in all the years of the study ($R^2 = 63\%$, $R^2 = 68\%$ and $R^2 = 87\%$, respectively) (Fig. 3). This dependency was directly proportional, which shows a highly significant effect of this process on the yields of the tested species.

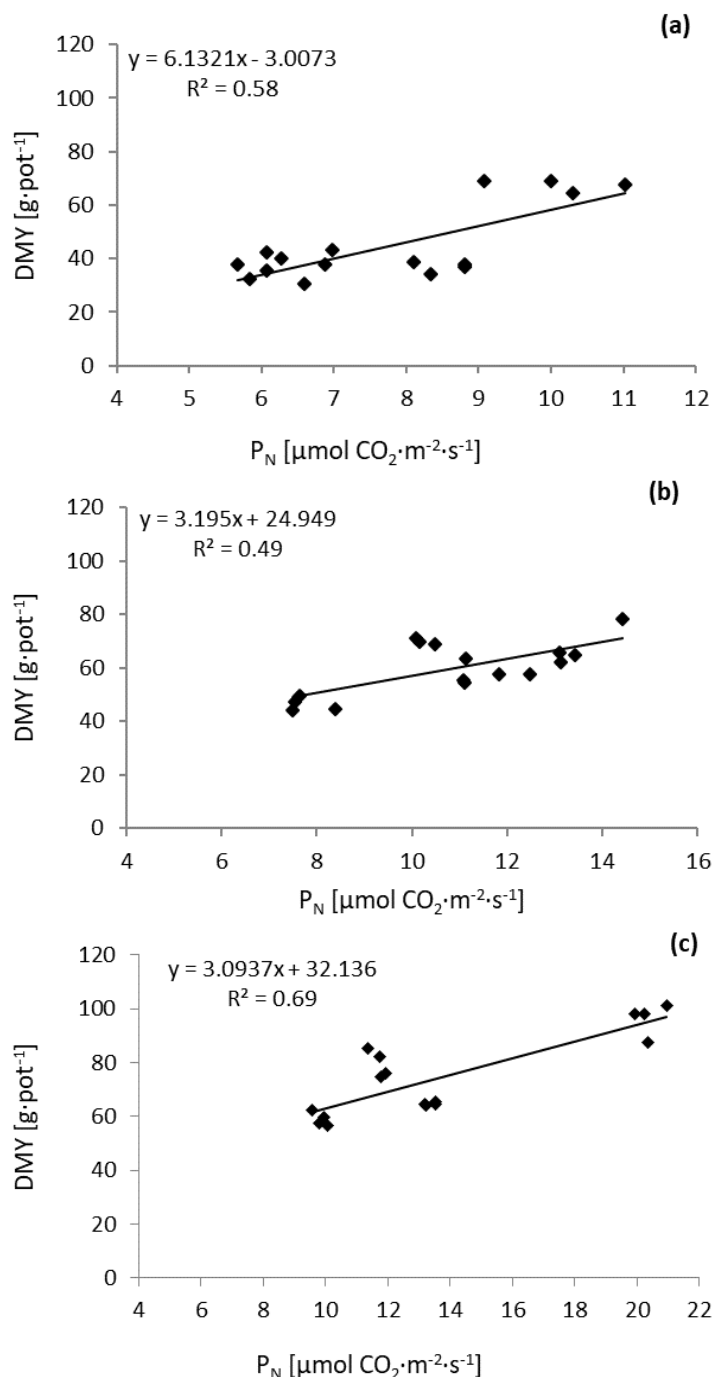


Figure 1. Relationship between net photosynthetic rate (P_N) and dry mass yield (DMY) in the years: 2012 (a), 2013 (b), 2014 (c)

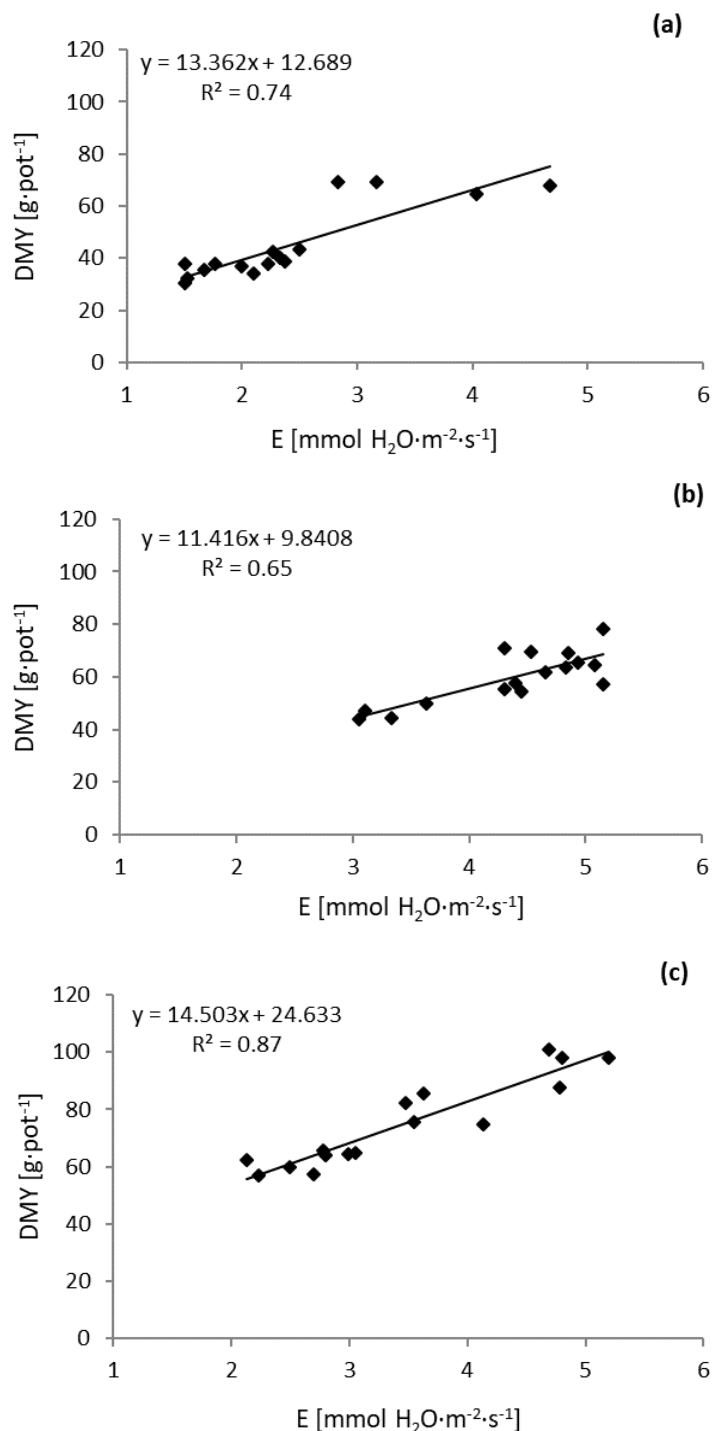


Figure 2. Relationship between transpiration rate (*E*) and dry mass yield (*DMY*) in the years: 2012 (a), 2013 (b), 2014 (c)

Water use efficiency (WUE index) in red clover and *Festulolium* was generally higher under stress conditions caused by water deficit in the soil than under optimal moisture conditions (averagely for treatments by 22.1% in the first, by 5.2% in the second, and by 13.0% in the third year of vegetation) (Table 4). In the first year of vegetation significant differences were found in those species, which were grown in

pure stand, in the third year - in red clover cultivated in a mixture and *Festulolium* in pure stand. In the second year of vegetation, there was no significant difference in the water use efficiency among particular species, the way in their cultivation and the level of soil moisture, but only the tendency to more economical water management for crops grown in long-term drought conditions.

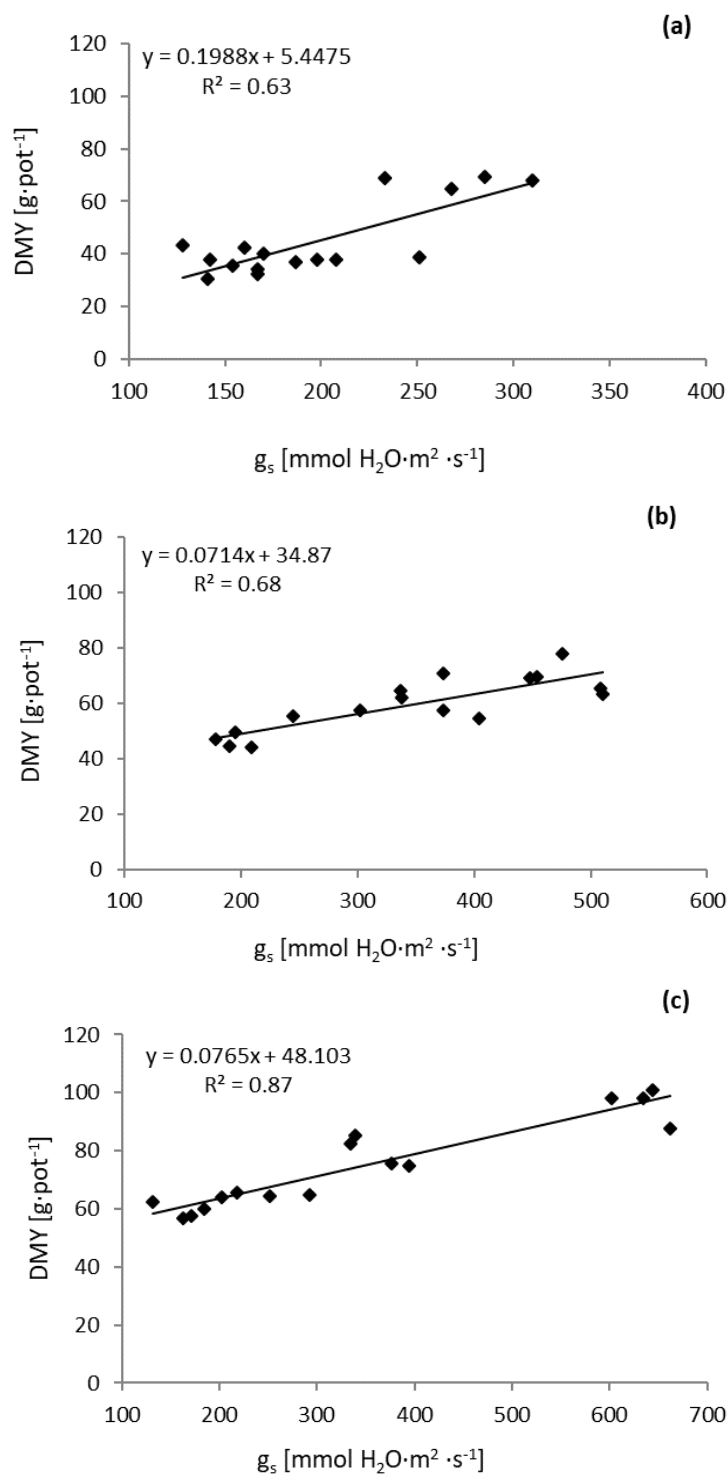


Figure 3. Relationship between stomatal conductance (g_s) and dry mass yield (DMY) in the years: 2012 (a), 2013 (b), 2014 (c)

Table 1. Net photosynthetic rate (P_N) of red clover and *Festulolium* grown in pure stand and in mixture under optimal and drought stress conditions [$\mu\text{mol CO}_2 \text{ m}^{-2} \text{ s}^{-1}$] (mean \pm standard deviation, $n = 6$)

Treatment	I regrowth		II regrowth		III regrowth		IV regrowth		Average ³	
	Soil moisture conditions									
	Optimum	Stress	Optimum	Stress	Optimum	Stress	Optimum	Stress	Optimum	Stress
2012										
Red clover PS ¹	4.62±0.63	3.30±1.11	6.70±2.27	4.33±0.73	19.7±2.26	18.2±1.40	-	-	10.3±1.49	8.60±0.59
Red clover MX ²	7.80±1.86	4.58±1.27	3.98±0.68	3.83±0.76	20.4±2.79	20.0±1.47	-	-	10.7±1.20	9.48±0.99
<i>Festulolium</i> PS	6.83±1.04	6.57±1.26	3.47±0.52	2.50±0.51	9.63±1.92	9.15±1.20	-	-	6.65±0.72	6.07±0.56
<i>Festulolium</i> MX	5.27±0.92	4.98±1.19	2.77±0.63	2.53±0.48	7.00±1.98	5.78±1.12	-	-	5.01±0.71	4.43±0.53
LSD ($\alpha=0.05$)	1.88		1.54		n.s. ⁴				n.s.	
ANOVA summary	f-ratio	p	f-ratio	p	f-ratio	p	-	-	f-ratio	p
Soil moisture SM	13.19	<0.001	10.47	0.002	2.89	0.097	-	-	15.39	<0.001
Treatment T	12.08	<0.001	19.98	<0.001	165.59	<0.001	-	-	93.67	<0.001
SM \times T	3.93	0.015	3.19	0.034	0.26	0.855	-	-	1.15	0.341
2013										
Red clover PS	11.2±2.37	8.92±1.55	15.0±1.64	14.8±0.67	18.7±1.64	13.6±1.12	8.43±0.86	7.05±1.76	13.3±1.03	11.1±1.03
Red clover MX	12.1±2.33	8.70±2.46	6.88±1.00	6.00±0.95	9.73±0.96	9.07±1.37	7.12±1.53	6.00±2.31	8.97±0.67	7.44±0.57
<i>Festulolium</i> PS	9.22±1.69	8.10±1.76	9.27±1.18	9.85±0.89	14.7±1.78	8.63±1.58	7.88±1.09	5.67±1.07	10.3±0.59	8.06±0.93
<i>Festulolium</i> MX	11.9±3.90	10.2±3.78	16.2±4.11	11.4±1.94	16.5±2.62	11.8±2.15	8.57±1.10	6.87±1.62	13.3±0.59	10.1±1.73
LSD ($\alpha=0.05$)	n.s.		2.93		2.68		n.s.		1.49	
ANOVA summary	f-ratio	p	f-ratio	p	f-ratio	p	f-ratio	p	f-ratio	p
Soil moisture SM	7.80	0.008	4.02	0.051	68.28	<0.001	13.90	<0.001	63.72	<0.001
Treatment T	1.78	0.166	72.70	<0.001	34.93	<0.001	2.08	0.118	57.29	<0.001
SM \times T	0.43	0.733	14.28	<0.001	5.65	0.002	0.30	0.823	3.47	0.024
2014										
Red clover PS	22.7±1.22	12.3±1.63	23.2±1.59	15.6±1.40	22.8±0.70	16.0±1.12	12.9±0.97	9.40±1.38	20.4±0.54	13.3±0.25
Red clover MX	20.2±3.44	17.5±1.86	22.7±2.85	15.7±4.44	21.4±1.27	20.9±0.54	11.1±0.96	10.5±2.37	18.8±1.14	16.2±0.55
<i>Festulolium</i> PS	15.2±0.93	12.4±1.08	12.5±1.30	10.8±0.58	11.2±1.25	10.6±0.63	7.83±0.76	5.80±1.44	11.7±0.29	9.91±0.52
<i>Festulolium</i> MX	12.8±1.86	11.7±1.60	11.7±0.72	11.0±1.30	13.7±1.10	9.13±1.00	9.47±0.79	4.77±0.95	11.9±0.61	9.16±0.29
LSD ($\alpha=0.05$)	2.87		3.31		1.54		2.02		0.92	
ANOVA summary	f-ratio	p	f-ratio	p	f-ratio	p	f-ratio	p	f-ratio	p
Soil moisture SM	61.90	<0.001	47.09	<0.001	117.5	<0.001	51.54	<0.001	432.0	<0.001
Treatment T	32.77	<0.001	52.85	<0.001	345.8	<0.001	37.89	<0.001	481.3	<0.001
SM \times T	15.16	<0.001	8.17	<0.001	28.84	<0.001	5.62	0.002	47.56	<0.001

¹PS – species grown in pure stand; ²MX – species grown in mixture; ³average over the three (2012) or four regrowth (2013, 2014); ⁴n.s. – not significant

Table 2. Transpiration rate (*E*) of red clover and *Festulolium* grown in pure stand and in mixture under optimal and drought stress conditions [$\text{mmol H}_2\text{O m}^{-2}\text{s}^{-1}$] (mean \pm standard deviation, $n = 6$)

Treatment	I regrowth		II regrowth		III regrowth		IV regrowth		Average ³	
	Soil moisture conditions									
	Optimum	Stress	Optimum	Stress	Optimum	Stress	Optimum	Stress	Optimum	Stress
2012										
Red clover PS ¹	3.85±0.93	1.38±0.23	4.77±1.36	2.82±0.51	2.40±0.20	1.90±0.26	-	-	3.67±0.69	2.04±0.22
Red clover MX ²	3.63±0.36	2.72±0.89	2.92±0.60	2.27±0.72	2.57±0.38	2.40±0.35	-	-	3.04±0.30	2.46±0.47
<i>Festulolium</i> PS	1.88±0.18	1.68±0.25	3.82±0.56	1.75±0.36	1.58±0.45	1.25±0.24	-	-	2.43±0.24	1.56±0.08
<i>Festulolium</i> MX	1.57±0.51	1.38±0.23	1.87±0.31	2.10±0.37	1.33±0.36	1.07±0.10	-	-	1.59±0.17	1.52±0.06
LSD ($\alpha=0.05$)	0.81		1.05		n.s. ⁴				0.53	
ANOVA summary	f-ratio	p	f-ratio	p	f-ratio	p	-	-	f-ratio	p
Soil moisture SM	37.52	<0.001	31.87	<0.001	12.08	0.001	-	-	62.60	<0.001
Treatment T	25.50	<0.001	14.65	<0.001	44.01	<0.001	-	-	38.94	<0.001
SM \times T	12.17	<0.001	7.86	<0.001	0.59	0.624	-	-	10.76	<0.001
2013										
Red clover PS	3.88±1.01	2.97±0.35	3.92±0.97	3.72±0.85	5.87±0.77	4.97±1.04	7.00±1.46	5.73±1.75	5.17±0.50	4.35±0.35
Red clover MX	4.82±1.75	3.85±1.73	4.13±1.24	2.73±1.40	3.87±0.45	3.15±0.36	4.42±0.84	3.20±1.0	4.31±0.72	3.24±0.39
<i>Festulolium</i> PS	4.30±1.12	2.48±0.62	3.73±0.84	3.47±0.63	5.67±0.56	3.08±0.60	6.05±0.66	4.40±0.51	4.94±0.26	3.36±0.25
<i>Festulolium</i> MX	4.90±1.97	3.47±1.06	5.25±1.01	4.33±0.74	5.40±1.42	5.28±0.59	4.52±0.36	4.38±0.67	5.02±0.48	4.37±0.35
LSD ($\alpha=0.05$)	n.s.		1.54		1.23			n.s.	0.75	
ANOVA summary	f-ratio	p	f-ratio	p	f-ratio	p	f-ratio	p	f-ratio	p
Soil moisture SM	11.56	0.003	17.28	<0.001	27.46	<0.001	13.23	<0.001	74.73	<0.001
Treatment T	1.79	0.061	20.78	<0.001	17.88	<0.001	14.09	<0.001	21.23	<0.001
SM \times T	0.37	0.828	12.38	<0.001	4.07	0.013	1.23	0.310	3.06	0.005
2014										
Red clover PS	4.10±0.33	2.10±0.40	6.37±1.05	3.72±0.36	2.63±0.29	1.73±0.16	6.15±0.66	4.23±0.68	4.81±0.33	2.95±0.12
Red clover MX	2.53±0.52	2.15±0.16	5.92±0.71	3.85±0.72	3.30±0.89	2.83±0.58	5.98±0.67	4.28±0.13	4.44±0.29	3.28±0.24
<i>Festulolium</i> PS	3.08±0.23	2.40±0.26	4.55±0.72	3.70±0.56	2.40±0.78	1.40±0.10	4.48±0.50	2.12±0.47	3.63±0.25	2.41±0.26
<i>Festulolium</i> MX	2.03±0.28	1.77±0.29	4.07±0.24	3.53±0.28	2.13±0.36	1.17±0.21	3.83±0.45	2.47±0.83	3.02±0.18	2.23±0.18
LSD ($\alpha=0.05$)	0.51		0.99		n.s.			n.s.	0.38	
ANOVA summary	f-ratio	p	f-ratio	p	f-ratio	p	f-ratio	p	f-ratio	p
Soil moisture SM	77.10	<0.001	68.12	<0.001	32.09	<0.001	117.20	<0.001	316.7	<0.001
Treatment T	29.67	<0.001	10.40	<0.001	17.62	<0.001	43.58	<0.001	78.14	<0.001
SM \times T	17.65	<0.001	7.32	<0.001	0.71	0.551	1.52	0.223	10.06	<0.001

¹PS – species grown in pure stand; ²MX – species grown in mixture; ³average over the three (2012) or four regrowth (2013, 2014); ⁴n.s. – not significant

Table 3. Stomatal conductance (g_s) of red clover and *Festulolium* grown in pure stand and in mixture under optimal and drought stress conditions [$\text{mmol H}_2\text{O m}^{-2} \text{s}^{-1}$] (mean \pm standard deviation, $n = 6$)

Treatment	I regrowth		II regrowth		III regrowth		IV regrowth		Average ³	
	Soil moisture conditions									
	Optimum	Stress	Optimum	Stress	Optimum	Stress	Optimum	Stress	Optimum	Stress
2012										
Red clover PS ¹	208 \pm 85	47 \pm 9	224 \pm 34	149 \pm 26	398 \pm 55	427 \pm 123	-	-	276 \pm 28	207 \pm 44
Red clover MX ²	132 \pm 28	75 \pm 28	162 \pm 25	166 \pm 20	643 \pm 191	448 \pm 105	-	-	312 \pm 61	230 \pm 36
<i>Festulolium</i> PS	53 \pm 4	40 \pm 10	183 \pm 22	149 \pm 16	349 \pm 161	267 \pm 76	-	-	195 \pm 54	152 \pm 21
<i>Festulolium</i> MX	48 \pm 17	40 \pm 19	153 \pm 24	172 \pm 11	294 \pm 162	216 \pm 40	-	-	165 \pm 57	143 \pm 17
LSD ($\alpha=0.05$)	54.4		36.5		n.s. ⁴				n.s.	
ANOVA summary	f-ratio	p	f-ratio	p	f-ratio	p	-	-	f-ratio	p
Soil moisture SM	34.51	<0.001	10.06	0.003	5.04	0.030	-	-	18.96	<0.001
Treatment T	16.88	<0.001	2.65	0.062	12.47	<0.001	-	-	19.71	<0.001
SM \times T	12.26	<0.001	9.44	<0.001	1.59	0.206	-	-	1.17	0.333
2013										
Red clover PS	529 \pm 113	281 \pm 51	323 \pm 36	296 \pm 106	347 \pm 175	308 \pm 106	424 \pm 210	375 \pm 208	406 \pm 74	315 \pm 62
Red clover MX	406 \pm 242	271 \pm 159	160 \pm 64	81 \pm 27	332 \pm 74	154 \pm 20	527 \pm 84	197 \pm 86	356 \pm 65	176 \pm 26
<i>Festulolium</i> PS	316 \pm 180	203 \pm 72	207 \pm 75	181 \pm 17	564 \pm 82	131 \pm 34	773 \pm 96	285 \pm 71	465 \pm 64	200 \pm 15
<i>Festulolium</i> MX	431 \pm 353	219 \pm 114	412 \pm 28	150 \pm 39	502 \pm 190	373 \pm 136	753 \pm 83	446 \pm 172	525 \pm 109	297 \pm 83
LSD ($\alpha=0.05$)	n.s.		88.0		182.7		214.5		106.2	
ANOVA summary	f-ratio	p	f-ratio	p	f-ratio	p	f-ratio	p	f-ratio	p
Soil moisture SM	10.96	0.002	38.25	<0.001	32.56	<0.001	53.85	<0.001	93.62	<0.001
Treatment T	1.24	0.307	29.02	<0.001	5.48	0.003	7.69	<0.001	9.48	<0.001
SM \times T	0.35	0.786	11.38	<0.001	6.14	0.001	5.17	0.004	3.59	0.022
2014										
Red clover PS	481 \pm 62	146 \pm 31	602 \pm 105	190 \pm 44	785 \pm 96	318 \pm 110	642 \pm 64	323 \pm 112	628 \pm 27	244 \pm 31
Red clover MX	361 \pm 98	198 \pm 26	597 \pm 93	219 \pm 89	795 \pm 142	757 \pm 62	614 \pm 137	284 \pm 52	592 \pm 41	364 \pm 25
<i>Festulolium</i> PS	264 \pm 49	147 \pm 26	313 \pm 96	201 \pm 39	448 \pm 153	191 \pm 39	418 \pm 63	115 \pm 39	361 \pm 38	164 \pm 22
<i>Festulolium</i> MX	292 \pm 55	147 \pm 50	297 \pm 55	198 \pm 34	580 \pm 183	208 \pm 80	348 \pm 43	154 \pm 87	379 \pm 52	177 \pm 23
LSD ($\alpha=0.05$)	84.6		115.8		182.2		n.s.		53.3	
ANOVA summary	f-ratio	p	f-ratio	p	f-ratio	p	f-ratio	p	f-ratio	p
Soil moisture SM	144.60	<0.001	134.32	<0.001	69.40	<0.001	147.16	<0.001	643.46	<0.001
Treatment T	10.28	<0.001	16.17	<0.001	35.23	<0.001	26.08	<0.001	120.86	<0.001
SM \times T	9.75	<0.001	15.06	<0.001	7.34	<0.001	1.79	0.165	19.67	<0.001

¹PS – species grown in pure stand; ²MX – species grown in mixture; ³average over the three (2012) or four regrowth (2013, 2014); ⁴n.s. – not significant

Table 4. Water use efficiency (WUE) of red clover and *Festulolium* grown in pure stand and in mixture under optimal and drought stress conditions [$\mu\text{mol CO}_2\text{md}^{-1}$ of air] (mean \pm standard deviation, $n = 6$)

Treatment	I regrowth		II regrowth		III regrowth		IV regrowth		Average ³	
	Soil moisture conditions									
	Optimum	Stress	Optimum	Stress	Optimum	Stress	Optimum	Stress	Optimum	Stress
2012										
Red clover PS ¹	1.26±0.39	2.45±0.99	1.41±0.27	1.57±0.33	8.23±0.86	9.72±1.51	-	-	2.86±0.37	4.27±0.52
Red clover MX ²	2.16±0.55	1.82±0.76	1.39±0.22	1.77±0.37	8.11±1.48	8.50±1.48	-	-	3.56±0.49	3.92±0.54
<i>Festulolium</i> PS	3.64±0.54	3.90±0.41	0.91±0.11	1.46±0.27	6.43±1.72	7.72±2.60	-	-	2.77±0.45	3.91±0.49
<i>Festulolium</i> MX	3.29±0.57	3.65±0.90	1.49±0.30	1.20±0.05	5.24±0.17	6.12±1.08	-	-	3.11±0.42	2.92±0.32
LSD ($\alpha=0.05$)	n.s. ⁴		0.41		n.s.					0.71
ANOVA summary	f-ratio	p	f-ratio	p	f-ratio	p	-	-	f-ratio	p
Soil moisture SM	3.49	0.069	6.78	0.013	3.73	0.060	-	-	26.23	<0.001
Treatment T	25.68	<0.001	5.13	0.004	13.25	<0.001	-	-	5.45	0.003
SM \times T	2.59	0.066	5.62	0.002	0.53	0.661	-	-	7.65	<0.001
2013										
Red clover PS	3.12±0.45	3.01±0.42	3.85±0.62	3.86±0.61	3.23±0.38	2.87±0.71	1.24±0.20	1.28±0.29	2.62±0.19	2.58±0.12
Red clover MX	2.70±0.68	2.56±0.89	1.72±0.27	2.58±0.97	2.54±0.24	2.88±0.21	1.63±0.37	1.85±0.29	2.11±0.21	2.33±0.35
<i>Festulolium</i> PS	2.55±0.83	3.32±0.51	2.54±0.41	2.89±0.39	2.60±0.24	2.81±0.25	1.31±0.16	1.29±0.15	2.12±0.22	2.40±0.21
<i>Festulolium</i> MX	2.42±0.65	3.01±0.79	2.26±0.68	2.65±0.34	2.87±0.35	2.25±0.47	1.90±0.25	1.58±0.37	2.32±0.24	2.31±0.39
LSD ($\alpha=0.05$)	n.s.		n.s.		0.61		n.s.		n.s.	
ANOVA summary	f-ratio	p	f-ratio	p	f-ratio	p	f-ratio	p	f-ratio	p
Soil moisture SM	2.00	0.164	5.68	0.022	0.85	0.362	0.07	0.795	2.26	0.140
Treatment T	1.04	0.386	19.75	<0.001	3.32	0.029	11.39	<0.001	5.07	0.004
SM \times T	1.43	0.247	1.09	0.363	4.05	0.013	1.95	0.137	1.17	0.334
2014										
Red clover PS	5.55±0.36	5.97±0.97	3.71±0.50	4.21±0.30	8.81±1.26	9.38±1.29	2.12±0.22	2.24±0.24	4.25±0.26	4.54±0.23
Red clover MX	8.13±1.50	8.18±1.01	3.90±0.85	4.04±0.57	6.87±1.75	7.69±1.72	1.86±0.08	2.46±0.60	4.26±0.40	4.95±0.39
<i>Festulolium</i> PS	4.93±0.31	5.20±0.34	2.78±0.29	2.97±0.38	5.06±1.56	7.61±0.99	1.76±0.22	2.75±0.50	3.23±0.20	4.15±0.34
<i>Festulolium</i> MX	6.51±1.76	6.69±0.60	2.89±0.27	3.13±0.46	6.52±0.54	8.09±1.27	2.50±0.37	2.01±0.38	3.96±0.30	4.12±0.25
LSD ($\alpha=0.05$)	n.s.		n.s.		n.s.		0.57		0.47	
ANOVA summary	f-ratio	p	f-ratio	p	f-ratio	p	f-ratio	p	f-ratio	p
Soil moisture SM	0.63	0.431	3.46	0.070	12.38	0.001	8.27	0.006	33.08	<0.001
Treatment T	20.98	<0.001	17.30	<0.001	8.67	<0.001	0.23	0.873	20.57	<0.001
SM \times T	0.07	0.974	0.34	0.800	1.28	0.293	9.15	<0.001	3.94	0.014

¹PS – species grown in pure stand; ²MX – species grown in mixture; ³average over the three (2012) or four regrowth (2013, 2014); ⁴n.s. – not significant

Soil moisture was an important factor shaping the level of dry matter yield of red clover and *Festulolium* cultivated in pure and mixed stands. Regardless of the method of cultivation, both species generally responded with yield reduction under long-term stress (Table 5). The highest decrease in total yield was noted in red clover cultivated in pure stand (PS) - by 34.9% in the first, by 33.7% in the second, and by 22.7% in the third year of vegetation, whereas this decrease was smaller in the mixture (by 10.1, 26.9, and 19.3%, respectively). *Festulolium* hybrid grown in pure stand turned out to be the least sensitive to drought. In the first year of vegetation (1st and 2nd regrowth) and in the second and third year of vegetation (1st regrowth), it showed a higher relative dry matter yield under soil deficit than under optimal water conditions. The reduction in total dry matter yield of red clover and *Festulolium*, expressed as an agricultural drought index (YR), ranged from - 0.061 to 0.349 in the first, from 0.212 to 0.337 in the second, and from 0.104 to 0.227 in the third year of vegetation (Fig. 4). The highest values of the YR index were recorded in the pure stand of red clover, while the smallest – for *Festulolium* hybrid. The yield reduction in mixed crops was on an average level.

Discussion

Water is one of the most important environmental resources determining plant productivity. Plants' response to water deficit is complex. It includes adaptation changes and harmful effects of water stress, as a result of which there occurs disturbance in fundamental life processes. One of the effects of these changes is reduction or inhibition of growth. It results from the reduction of the intensity of gas exchange processes, a decrease in the export of photosynthesis products from leaves to other organs of the plants, and the disruption in transport and distribution of assimilates. Water shortage also inhibits the growth of plants, including leaf blades, which due to their reduced surface, receive less light and absorb less carbon dioxide (Starck, 2010). Our studies showed that red clover and *Festulolium* yielded lower in drought stress conditions. The biggest decline in the total yield was recorded for red clover grown in pure stand (on average by 30.2% for three years), lower in a mixture (by 19.3%), and the smallest in *Festulolium* in pure stand (by 9.5%). Adopting the level of agricultural yield decrease as a criterion of crop resistance to stress, allowed to conclude that *Festulolium* hybrid grown in pure stand was the most resistant to the effects of long-term stress. Red clover grown in pure stand showed the greatest sensitivity to drought, while in the mixture with *Festulolium*, its yield loss was smaller by 10.9%. Similar results were obtained by the authors in studies on the response of alfalfa (*Medicago × varia* Martyn) to water deficit in the soil depending on the type of sowing (Staniak et al., 2018). Under stress conditions, the yield decrease of alfalfa grown in pure stand was by 13% higher compared to the cultivation in a mixture with *Festulolium*. Studies of Küchenmeister et al. (2013) showed that yellow alfalfa (*Medicago falcata* L.), white clover (*Trifolium repens* L.) and birdsfoot trefoil (*Lotus uliginosus* Schkuhr) grown in a mixture with perennial ryegrass (*Lolium perenne* L.) responded to stress with a much lower yield decrease than in pure stand. Tucak et al. (2016) showed high sensibility of red clover grown in pure stand to stressful conditions caused by drought resulted in low yields in 23 cultivars and populations. Also Gaudin et al. (2013) reported about the high sensibility of red clover in pure stand to drought stress. Studies of AbdElgawad et al. (2015) showed that water deficit reduced biomass of legumes (black medic (*Medicago lupulina* L.) and birdsfoot trefoil) and grasses (meadow bluegrass (*Poa pratensis* L.)

and perennial ryegrass) at the dry weight and fresh weight levels, but this effect was stronger in the legumes species.

Table 5. Relative [%] dry mass yield (DMY) of red clover and *Festulolium* grown in pure stand and in mixture under drought stress in relation to optimal conditions

Treatment	Regrowth				Total DMY ³
	I	II	III	IV	
2012					
Red clover PS ¹	61.7	65.7	74.9	-	65.1
<i>Festulolium</i> PS	128.7	106.4	86.9	-	109.5
Red clover + <i>Festulolium</i> MX ²	98.3	83.8	81.9	-	89.9
2013					
Red clover PS ¹	67.0	63.6	63.3	71.8	66.3
<i>Festulolium</i> PS	85.3	81.3	71.3	73.3	79.0
Red clover + <i>Festulolium</i> MX ²	70.1	77.2	67.3	83.5	73.1
2014					
Red clover PS ¹	96.4	75.0	59.1	70.2	77.3
<i>Festulolium</i> PS	103.3	84.8	85.3	84.4	89.6
Red clover + <i>Festulolium</i> MX ²	93.0	80.5	78.6	76.2	83.4
Sum of three years					
Red clover PS ¹	73.0	68.9	64.1	71.1	69.8
<i>Festulolium</i> PS	103.1	90.3	81.6	78.2	90.5
Red clover + <i>Festulolium</i> MX ²	84.2	80.5	74.8	79.9	80.7

¹PS – species grown in pure stand

²MX – species grown in mixture

³Total DMY is the sum of dry mass yield over the three (2012) or four regrowth (2013, 2014)

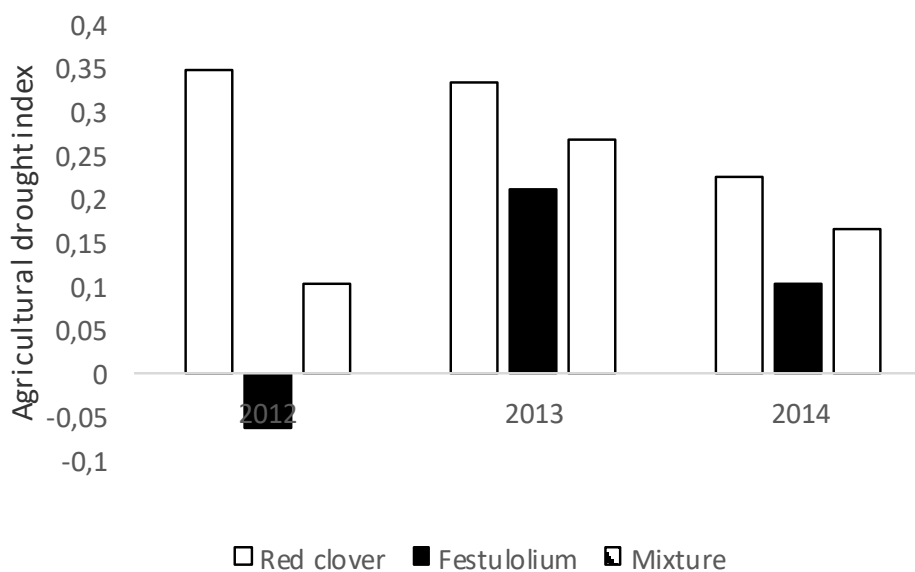


Figure 4. Agricultural drought index for red clover, *Festulolium* and mixture under drought stress conditions

Inhibition of plant growth in drought conditions is a defensive response of plants. Water deficit in the soil affects the reduction of water potential of plant shoots and stimulates the growth of the root. As a result, the plant changes its distribution of assimilates, which in turn causes a lower yield of the aboveground mass (Lucero et al., 1999). According to Lazzarotto et al. (2009) as well as Skinner and Comas (2010) higher resistance in grasses than legumes species to drought could possibly be related to an increased root/shoot ratio under stress conditions, improving water and nutrient use. Lucero et al. (1999) observed that increased soil water deficit decreased root dry matter yield for perennial ryegrass grown in pure stand, but in mixture with white clover root yield decrease was smaller. Many authors underline also that the productivity of mixed crops is influenced by the competition of the plants and their mutual impact on each other. According to Frankow-Lindberg (1986), an intraspecific competition more strongly affects the productivity of red clover, while the interspecific one - of grasses. Hence, growing red clover together with grasses is a very good practice.

Photosynthesis is one of the most stress-sensitive life processes. Factors limiting the photosynthetic activity of plants include: water, carbon dioxide, temperature, and light. The influence of water is not direct, as the water content in chloroplasts is sufficient for photosynthesis. Water, however, strongly affects CO₂ assimilation, as under water deficit, stomata close and CO₂ input gets cut off, which reduces its concentration in the intercellular spaces and hence, photosynthesis is inhibited (Córdobaa et al., 2015). In grasses, a big decrease of photosynthesis can result from the increased participation of photorespiration in gas exchange, which often intensifies under stress, as one of the mechanisms of energy dissipation (Flexas and Medrano, 2002). Our studies have shown that drought stress caused a significant reduction in the rate of photosynthesis and transpiration in the tested plants, regardless of the species and way of cultivation, whereas the highest sensitivity to stress was recorded for red clover grown in pure stand, while the smallest – for hybrid *Festulolium* cultivated in the mixture. Studies of Olszewska (2008) showed a higher rate of photosynthesis and transpiration in *Festulolium* hybrid grown in a mixture with white clover (respectively by 49 and 57%) and birdsfoot trefoil (respectively by 24 and 34%) compared to the pure stand. In turn, the studies AbdElgawad et al. (2015) showed that legumes (black medic and birdsfoot trefoil) exhibit a significantly a higher photosynthesis rate under optimal conditions, but under drought conditions, they limited this process stronger than grasses (perennial ryegrass and meadow bluegrass). According to Dziadczyk (2002), the plant is resistant to stress if it can keep the intensity of the most important life processes on the least changed level in environmental conditions significantly deviating from the optimum.

The survival of plants in drought conditions depends on efficient water management, which is well expressed by water use efficiency index (WUE). It is dependent on the intensity of the photosynthesis and transpiration processes, but also reflects the influence of environmental factors. Our studies have shown that values of WUE index in the tested plant species were higher under stress conditions than under optimal soil moisture in the first and third year of vegetation, especially in the case *Festulolium* hybrids. Studies of Olszewska (2008) showed a significantly higher value of WUE index in *Festulolium* grown in a mixture with white clover and birdsfoot trefoil, but only in the first of the three years of vegetation. This proves that *Festulolium* has a more economical water management and greater resistance to drought stress compared to clover. According to Hall (1990), a high value of WUE index allowed to maintain a high coefficient of crop yields even during drought. In turn, Blum (2009) believes that

WUE index is not associated with drought resistance, as some species resistant to drought show lower WUE values, which is associated with a deeper root system and higher use of water. According to this author, the increase in crop yields under drought conditions is closely connected with the growth and development of the root system, especially at the beginning of the growing season.

Conclusions

The present experiment indicates, that a long-term stress caused by water deficit in the soil significantly reduced the yield of dry mass of red clover and *Festulolium*, regardless of the method of cultivation. Mixtures showed smaller yield losses under drought stress compared to red clover grown in pure stand, which indicates their higher suitability to be grown in areas with less rainfall. Photosynthetic effectiveness of red clover was higher than *Festulolium*, regardless of the level of soil moisture. In terms of long-term drought, the photosynthesis and transpiration rate in the tested species were lower than in the treatments optimally moisturized. Red clover grown in pure stand responded to stress the most, while *Festulolium* hybrid cultivated in the mixture - the least. The water use efficiency index (WUE) of the tested plant species was higher under stress caused by water deficit in the soil than under optimal conditions, whereas significant differences were reported in the first and third year of vegetation. The biggest differences were noted in *Festulolium*, which proves a more economical water management of this hybrid compared to red clover. The selection of crop with high water use efficiency (WUE) traits would be one of the adaptation measures for climate change.

Our studies have shown, that the cultivation of red clover in a mixture with *Festulolium* hybrid is more favorable than in pure stand, especially in areas with less rainfall, due to better yields and higher durability resulting from, i.e. a more efficient water management. It is associated with course of the main physiological processes. Red clover reacted to soil water deficit with a significant decrease of the rate of photosynthesis and transpiration but stronger reaction was observed in pure sowing than in mixture.

Acknowledgements. The studies have been supported by the Polish Ministry of Science and Higher Education within the statutory activity of the Institute of Soil Science and Plant Cultivation – State Research Institute, task 1.01 “Evaluation of resistance to drought stress of *Festulolium braunii* and its mixtures with selected legume species”.

REFERENCES

- [1] AbdElgawad, H., Farfan-Vignolo, E. R., de Vos, D., Asard, H. (2015): Elevated CO₂ mitigates drought and temperature-induced oxidative stress differently in grasses and legumes. – *Plant Science* 231: 1–10.
- [2] Blum, A. (2009): Effective use of water (EUW) and not water-use efficiency (WUE) is the target of crop yield improvement under drought stress. – *Field Crops Research* 112: 119–123.
- [3] Córdoba, J., Molina-Canob, J. L., Pérez, P., Morcuendea, R., Moralejoc, M., Savéd, R., Martínez-Carrasco, R. (2015): Photosynthesis-dependent/independent control of

- stomatal responses to CO₂ in mutant barley with surplus electron transport capacity and reduced SLAH3 anion channel transcript. – *Plant Science* 239: 15–25.
- [4] Dziadczyk, P. (2002): Genetic tolerance to abiotic stress in plants. – *Zeszyty Problemowe Postępów Nauk Rolniczych* 481: 49–60.
- [5] Elgersma, A., Søegaard, K. (2018): Changes in nutritive value and herbage yield during extended growth intervals in grass–legume mixtures: effects of species, maturity at harvest, and relationships between productivity and components of feed quality. – *Grass and Forage Science* 73: 78–93.
- [6] Ergon, A., Seddaiu, G., Korhonen, P., Virkajärvi, P., Bellocchi, G., Jørgensen, M., Østrem, L., Reheul, D., Volaire, F. (2018): How can forage production in Nordic and Mediterranean Europe adapt to the challenges and opportunities arising from climate change? – *European Journal of Agronomy* 92: 97–106.
- [7] Flexas, J., Medrano, H. (2002): Drought-inhibition of photosynthesis in C-3 plants: Stomatal and nonstomatal limitation revisited. – *Annals of Botany* 89: 183–189.
- [8] Frankow-Lindberg, B. E. (1986): Competition in field-sown swards of lucerne or red clover and timothy. – *Swedish Journal of Agricultural Research* 16: 119–128.
- [9] Gaudin, A. C. M., Westra, S., Loucks, C. E. S., Janovieck, K., Martin, R. C., Deen, W. (2013): Improving resilience of northern field crop systems using inter-seeded red clover: a review. – *Agronomy Journal* 3(1): 148–180.
- [10] Hakala, K., Jauhiainen, L. (2007): Yield and nitrogen concentration of above- and below-ground biomasses or red clover cultivars in pure stands and in mixtures with three grass species in northern Europe. – *Grass and Forage Science* 62: 312–321.
- [11] Hall, A. E. (1990): Plant adaptation to hot and dry stresses in relation to horticultural plant breeding. – XXII Inter. Hort. Congr. Plenary lectures S., p. 44–48, Florence, Italy.
- [12] Hura, T., Hura, K., Grzesiak, M., Rzepka, A. (2007): Effect of long-term drought stress on leaf gas exchange and fluorescence parameters in C3 and C4 plants. – *Acta Physiologia Plantarum* 29: 103–113.
- [13] Jensen, E. S., Hauggaard-Nielsen, H. (2003): How can increased use of biological N₂ fixation in agriculture benefit the environment? – *Plant and Soil* 252: 177–186.
- [14] Kryszak, J., Domański, P., Jokś, W. (2002): Use value of *Festulolium braunii* (K. Richter) A. Camus cultivars registered in Poland. – *Grassland Science in Europe* 7: 436–437.
- [15] Küchenmeister, K., Küchenmeister, F., Kayser, M., Wrage-Mönnig, N., Isselstein, J. (2013): Influence of drought stress on nutritive value of perennial forage legumes. – *International Journal of Plant Production* 7(4): 693–710.
- [16] Łabędzki, L. (2006): Droughts and Floods – A Threat to Agriculture. – In: Mioduszewski, W. (ed.) *Water in Agricultural Landscape. Water, Environment, Rural Areas, Poland*.
- [17] Lawlor, D. W. (1995): Photosynthesis, productivity and environment. – *Journal of Experimental Botany* 46: 1449–1461.
- [18] Lazzarotto, P., Calanca, P., Fuhrer, J. (2009): Dynamics of grass-clover mixtures-an analysis of the response to management with the productive grassland simulator (PROGRASS). – *Ecological Modelling* 220: 703–724.
- [19] Li, P., Chen, J., Wu, P. (2011): Agronomic characteristics and grain yield of 30 spring wheat genotypes under drought stress and non-stress conditions. – *Agronomy Journal* 103(6): 1619–1628.
- [20] Lipiec, J., Doussan, C., Nosalewicz, A., Kondracka, K. (2013): Effect of drought and heat stresses on plant growth and yield: a review. – *International Agrophysics* 27: 463–477.
- [21] Lucero, D. W., Grieu, P., Guckert, A. (1999): Effects of water deficit and plant interaction on morphological growth parameters and yield of white clover (*Trifolium repens* L.) and ryegrass (*Lolium perenne* L.) mixtures. – *European Journal of Agronomy* 11: 167–177.

- [22] Olszewska, M. (2008): Gas exchange parameters in *Festulolium braunii* (K. Richt.) A. Camus grown in mixtures with legumes depending on multiple nitrogen rates. – Polish Journal of Natural Science 23(1): 48–72.
- [23] OMAFRA (Ontario Ministry of Agriculture, Food and Rural Affairs) (2011): Red Clover. Cover Crops. – Ontario Ministry of Agriculture, Food and Rural Affairs, Ontario. http://www.omafra.gov.on.ca/english/crops/facts/cover_crops01/redclover.htm (accessed: 31.08.2018).
- [24] Østrem, L., Volden, B., Larsen, A. (2013): Morphology, dry matter yield and phenological characters at different maturity stages of *Festulolium* compared with other grass species. – Acta Agriculture Scandinavica, sec B - Soil and Plant Science 63: 531–542.
- [25] Queen, A., Earl, H., Deen, W. (2009): Light and moisture competition effects on biomass of red clover under-seeded to winter wheat. – Agronomy Journal 101(6): 1511–1521.
- [26] Rojek, S. (1986): Water requirements of papilionaceous plants. – Fragmenta Agronomica 2(10): 3–20.
- [27] Skinner, R. H., Comas, L. H. (2010): Root distribution of temperate forage species subjected to water and nitrogen stress. – Crop Science 50: 2178–2185.
- [28] Staniak, M., Bojarszczuk, J., Książak, J. (2018): Changes in yield, gas exchange parameters, and chemical composition in *Festulolium* and alfalfa grown in pure sowing and in mixture under drought stress. – Acta Agriculture Scandinavica, sec B - Soil Plant Sci. 68(3): 255–263.
- [29] Starck, Z. (2010): Effect of stress conditions on coordination of photosynthetic production and resources allocation. – Postępy Nauk Rolniczych 1: 9–26.
- [30] Thomas, H. (1994): Diversity between and within temperate forage grass species in drought resistance, water use and related physiological responses. – Aspects of Applied Biology 38: 47–55.
- [31] Tucak, M., Popović, S., Čupić, T., Krizmanić, G., Španić, V., Meglič, V., Radović, J. (2016): Assessment of red clover (*Trifolium pratense* L.) productivity in environmental stress. – Poljoprivreda/Agriculture 22(2): 3–9.

RESEARCH ON TEMPORAL AND SPATIAL VARIATION OF HEAT ISLAND EFFECT IN XI'AN, CHINA

GAO, Y.¹ – CHANG, M.^{1,2} – ZHAO, J.^{1*}

¹*College of Architecture, Changan University
No.161 Changan Rd., Yanta Dist., Xi'an 710061, Shaanxi, China*

²*Yuncheng Polytechnic, Yuncheng 0444000, Shanxi, China*

**Corresponding author*

e-mail: gyjemma@163.com/2016041002@chd.edu.cn/478531002@qq.com

(Received 24th Aug 2018; accepted 11th Oct 2018)

Abstract. This paper takes Xi'an, which is a western city in China, experiencing the rapid urbanization, as the research object. It uses 2000 Landsat7 ETM+, 2010 Landsat5 TM and 2016 Landsat8 OLI images as data sources to inverse and normalize surface temperature. Thermal field intensity index (HFI) and urban heat island proportion index (UHPI) were introduced to quantitatively assess the temporal and spatial variation of heat island in Xi'an. Research results demonstrate: (1) From 2000 to 2016, the average temperature in urban areas increased from 32.34 °C in 2006 to 42.45 °C in 2016, with an increase of 10.11 °C in 16 years. (2) From 2000 to 2016, the urban heat island area continuously increased, from 40.59 km² in 2000 to 81.52 km² in 2016, with an increase of about 100.87%. UHPI increased from 0.036 in 2000 to 0.078 in 2016, which indicates the scientific rationality of the index to a certain extent. (3) According to the distribution law, the heat island scope and urban expansion reflect strong time-space consistency. In the 16 years, the distribution pattern of thermal environment changed from “central urban area distribution mode” to “built-up area distribution mode”. (4) From the perspective of the distribution in administrative region, heat island effect was mainly distributed in the old areas such as Lianhu District and Xincheng District in 2000. Due to urban expansion, the phenomenon of “hollow heat island” appeared in 2010. In 2016, heat island effect was distributed in all six areas.

Keywords: *temporal and spatial variation, heat island effect, TM satellite remote sensing image, urbanization, urban thermal environment, Xi'an*

Introduction

While rapid urbanization brings economic development in China, it also brings adverse effects on urban climate, such as abnormal climate changes, intensified urban heat island effects, and frequent occurrence of extreme high temperature events. These problems have seriously threatened people's daily life. Therefore, it is gradually becoming the research focus to quantitatively study the changing trend of urban thermal environment, to discuss the evolution process of urban thermal environment and its influencing factors, and to reveal the formation mechanism and distribution law of urban heat island effect.

Since the remote sensing image has the characteristics of high resolution and wide coverage, domestic and foreign scholars mostly use thermal infrared remote sensing data to study the urban thermal environment. The existing research focuses on the inversion of surface temperature, the interaction between urban thermal environment and surface landscape, the response of urban heat island, the formation mechanism and influencing factors of urban heat island. Research on the quantitative definition and division of the intensity of urban heat island in different years and the law of distribution and evolution, especially on the inland cities in the central and western

regions, is scarce. In terms of research methods, the atmospheric radiation correction method, single window algorithm, split window algorithm and ARCGIS/ENVI software are used to study the urban thermal field. However, most studies use brightness temperature as the main index of thermal environment evaluation, which cannot truly reflect the intensity of urban heat island effect. For example, Qin et al., took Ling County of Shandong Province as an example to compare and analyze the difference between surface temperature and brightness temperature of water body, farmland and village. The average difference was 2.51 °C, 3.52 °C and 5.10 °C respectively (Qin et al., 2004). Ding et al. found that the LST (Land Surface Temperature) of Fuzhou inverted by above three algorithms was about 1.9 °C, 2.9 °C and 5.3 °C higher than the brightness temperature (Ding et al., 2008). In order to accurately analyze the spatial difference of surface heat, the real LST should be retrieved through the satellite thermal infrared data. Brightness temperature for analysis could result in large errors (Tan et al., 2006).

Therefore, in order to accurately analysis the temporal and spatial pattern and evolution of thermal environment in Xi'an in different periods, this paper takes Xi'an as the research object, uses the atmospheric radiation correction method to retrieve the LST of Xi'an urban area in different periods by introducing the thermal field intensity index and the heat island proportion index, hoping to contribute to the research of Xi'an's urban thermal environment.

Research Methods

Introduction to the Research Area

Xi'an City is located at 33.42°N-34.45°N and 107.40°E-109.49°E, in the middle of Guanzhong Plain in China, neighboring Weihe River in the north and Qinling Mountains in the south (*Figure 1*). The territory is about 204 km long from the east to the west and about 116 km wide from the south to the north.

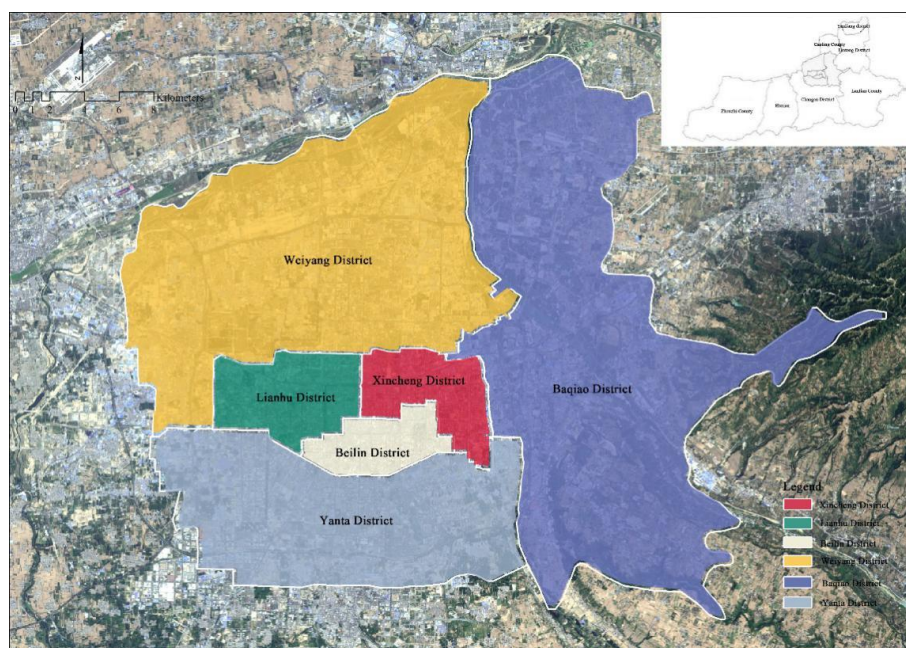


Figure 1. A map of the research area position

The territory is about 204 km long from the east to the west and about 116 km wide from the south to the north. The total area is about 10108 km², of which the urban area is 1066 km². Xi'an is a sub-humid monsoon climate in warm temperate zone. The annual average temperature is about 15.5 °C, and the annual precipitation is about 600 mm. There are 11 districts and 2 counties under the jurisdiction of Xi'an, which are Weiyang District, Xincheng District, Beilin District, Lianhu District, Baqiao District, Yanta District, Yanliang District, Lintong District, Chang'an District, Gaoling District, Hui District, Lantian County and Zhou County. In view of the characteristics of the heat island effect, this paper analyzes the temporal and spatial changes of the heat island in the six districts (Xincheng District, Beilin District, Lianhu District, Yanta District, Baqiao District and Weiyang District) within the third ring of Xi'an.

Research Method

Although the urban heat island effect may occur in all seasons of a year, it has high impact on residents lives in summer. Generally speaking, the four seasons are divided as follows. Spring is from March to May, summer is from June to August, autumn is from September to November, winter is from December to February. Therefore, this paper mainly studies the heat island effect during the summer months (from June to August).

In order to improve the research accuracy, the images with high quality (cloud free and noiseless) and the same or close season were selected. By comparing the image data, the spatial variation of thermal field in Xi'an urban area during the past 16 years was analyzed using the Landsat7 ETM+ on June 29, 2000, Landsat5 TM on June 17, 2010 and Landsat8 OLI on June 17, 2016 (as shown in *Table 1*).

Table 1. A list of remote sensing image data

Year	2000	2010	2016
Time	2000/6/29	2010/6/17	2016/6/17
Satellite	Landsat7 ETM SLC-on	Landsat4-5 TM	Landsat 8 OLI_TIRS
Cloudiness	0.47%	1.87%	0.03%
Strip number	127	127	127
Line number	36	36	36
Longitude	108.8074	108.8074	108.8074
Latitude	34.6108	34.6108	34.6108

At present, there are three main methods for retrieving surface temperature through Landsat TM/ETM thermal infrared data: atmospheric correction method (also known as radiative transfer equation-RTE), single channel algorithm and split window algorithm. By comparing the above three methods, the atmospheric correction method had clear principle, and the process of solving the problem requires only atmospheric profile parameters or abundant atmospheric data to get the surface temperature by software simulation. Although the single window algorithm is simple and accurate compared with atmospheric correction method, it is difficult to obtain multiple kinds of atmospheric parameters that need to be synchronized in the calculation process. The default parameter or standard parameter could lead to large error (Di et al., 2016). Reference 4 retrieved and analyzed the surface temperature by using the above methods. The results showed that when the real time sounding data were available, the root mean

square error of land surface temperature obtained by the atmospheric correction method was the minimum (Huang et al., 2006). Therefore, this paper used the atmospheric correction method to retrieve the surface temperature using ENVI software. The basic principle is as below: First, the influence of atmosphere on surface thermal radiation is estimated. Second, the atmospheric influence is subtracted from the total thermal radiation observed by satellite sensor to obtain the surface thermal radiation intensity. Finally, the thermal radiation intensity is converted to the corresponding surface temperature. The specific method flow is shown in the diagram (Figure 2).

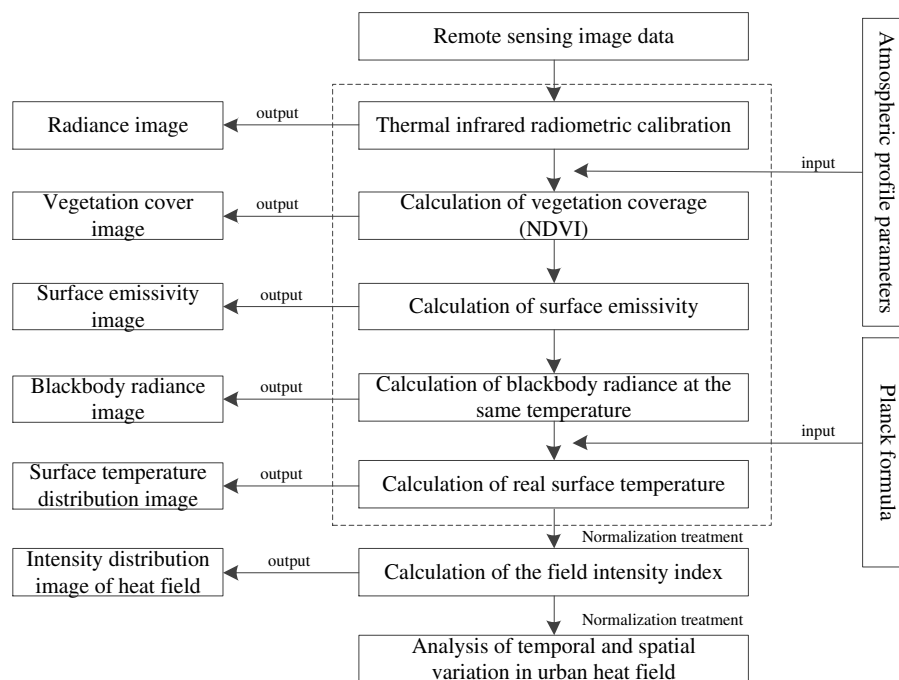


Figure 2. Inversion of surface temperature flow chart by atmospheric correction method

In order to eliminate the influence of the absolute temperature difference in different seasonal phases, this paper introduces the heat field intensity index (abbreviated as HFI) to normalize the surface temperature. HFI can clearly reflect the relative high temperature and low temperature range of the thermal field of the image. And it has the thermal field indication meaning. The expression is as follows (Equation 1):

$$H_i = \frac{T_i - T_{min}}{T_{max} - T_{min}} \quad (\text{Eq.1})$$

where, H_i is the heat field intensity exponent corresponding to the i^{th} pixel, T_i is the surface temperature, T_{min} is the minimum effective surface temperature in image region, and T_{max} is the maximum effective surface temperature in image region. Larger thermal field intensity index indicates that the more likely it is to be in the heat island range. By analyzing a large number of remote sensing images, the thermal intensity index is generally divided into 7 grades (as shown in Table 2): low temperature area, lower temperature area, secondary medium temperature area, medium temperature area, medium high temperature area, high temperature area and ultra-high temperature area,

which can effectively reflect the size of urban heat island.

Table 2. Preliminary division and definition of surface heat field index

Grade	Heat field intensity index	Definition
1	0-0.15	Low temperature area
2	0.15-0.3	Lower temperature area
3	0.3-0.45	Secondary medium temperature area
4	0.45-0.6	Medium temperature area
5	0.7-0.75	Medium high temperature area
6	0.75-0.9	High temperature area
7	0.9-1.0	Ultra-high temperature area

Urban Heat Proportion Index (abbreviated as UHPI) also is introduced in this paper. It can calculate the ratio of the heat island area to region area based on the urban space unit, and puts different weight to indicate the development degree of the heat island in the space unit. This index could more scientifically compare the change of urban heat island between different space units in different years. The larger the index, the more serious the heat island effect. The index has been successively used by the Ministry of Environmental Protection and the Ministry of Housing Urban-Rural Construction as an index to evaluate the urban ecological environment and the urban environmental performance. It has been authorized and widely used in the research on the change of the urban thermal environment. The basic formula is as follows (Equation 2):

$$UHPI = \frac{1}{100m} \sum_i^n w_i p_i \quad (\text{Eq.2})$$

where, UHPI is urban heat proportion index. m is the thermal field intensity grade. i is the temperature grade of suburb higher than urban area. n is the temperature grade of urban area higher than suburb. w_i is the weight of the i^{th} grade, which is the grade value. p_i is the proportion of area at the i grade. In this study, according to the above defined thermal field intensity grade, $m=7$. The three grades of ultra-high temperature area, high temperature area and medium high temperature area are mainly distributed in urban area, which represent the urban heat island area. The temperature in the suburb is mainly below the medium temperature area. Therefore, $n=3$ in this research. The grades of ultra-high temperature area, high temperature area and medium high temperature area are 7, 6 and 5, respectively.

Results and discussion

Dynamic Change of Surface Temperature Retrieval in Xi'an

The remote sensing images in the three periods were processed through the above method, and the 2000-2016 surface temperature distribution diagram is obtained (as shown in the following Figure 3). From the retrieval results of surface temperature in the third periods, it can be seen that the regions with higher temperature are mainly distributed in the built-up area and the area with poor vegetation coverage. From 2010

to 2016, the average temperature and the maximum temperature gradually increased. The temperature ranged from 21.25 °C to 48.03 °C in 2000, and the average temperature was 32.34 °C. In 2010, the range of surface temperature was from 26.27 °C to 51.52 °C, with an average temperature of 38.65 °C. The surface temperature ranged from 24.01 °C to 60.84 °C in 2016, and the average temperature was 42.45 °C. The average temperature increased from 32.34 °C in 2000 to 42.45 °C in 2016, with an increase of 10.11 °C in 16 years (as shown in the following *Figure 4*).

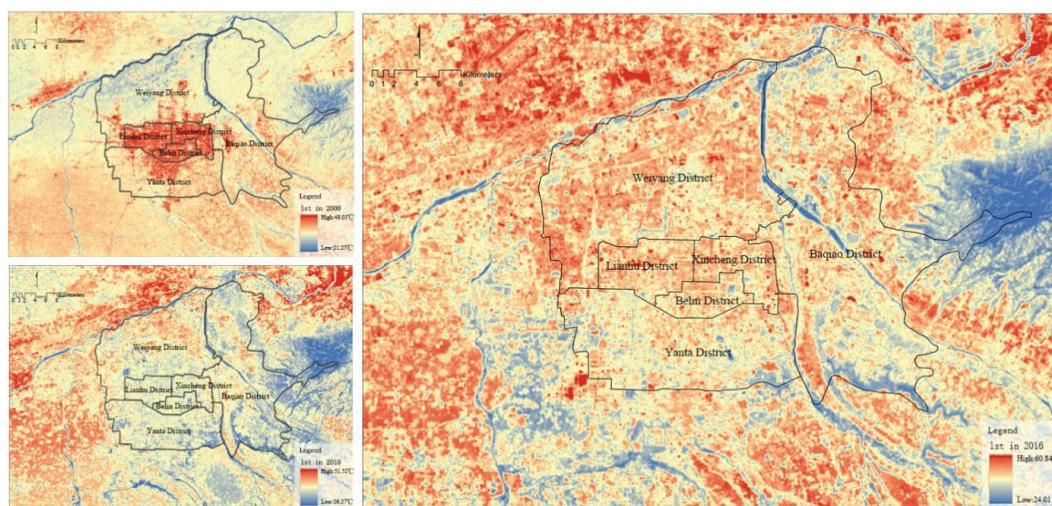


Figure 3. LST distribution from 2000 to 2016

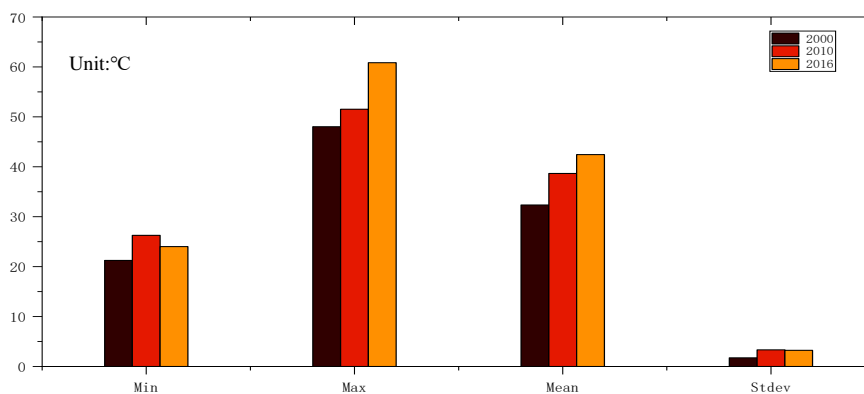


Figure 4. Maximum, minimum, mean and standard deviation of LST from 2000 to 2016

In order to deeply analyze the distribution characteristics of LST in urban area, the surface temperature images of the six districts were extracted through ArcGIS, and the section line was drawn with Bell Tower, the center of city wall in the Ming Dynasty as the benchmark, the south street-north street as the south-north axis, and east avenue-west avenue as the east-west axis (as shown in the *Figures 5, 6 and 7*). It can be seen from the section lines in WE direction and NS direction that the lower LST indicates higher vegetation coverage and lower population density, combining with the corresponding images. Water body and green space have obvious cooling effect on the area. Otherwise, the LST is relatively high. From the perspective of time dimension, the

profile lines of 2000 are all high in the middle and slightly lower on both ends. In 2016, the temperature on both ends increased gradually, and the temperature in some areas were even higher than the middle part. The relative difference of urban thermal environment was reduced, and the thermal environment pattern gradually changed from “distributed central district” to “distributed built-up area”. This indicates that the urban heat island effect and urban expansion show significant temporal and spatial consistency.

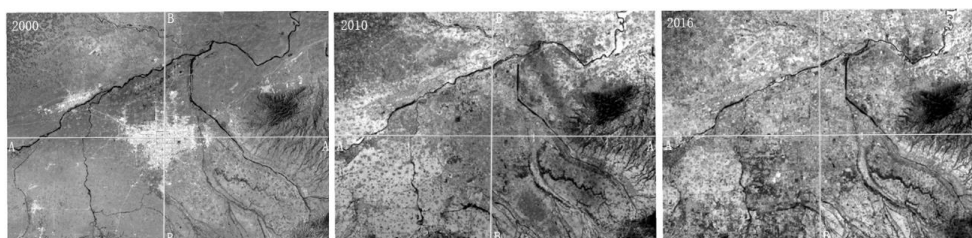


Figure 5. Positions of LST profiles across the study area from 2000 to 2016

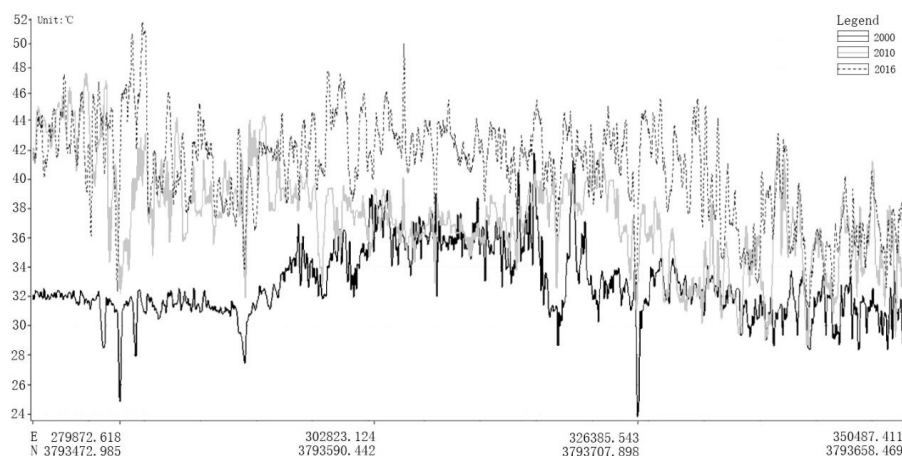


Figure 6. LST distribution of the A-A section across the study area from 2000 to 2016

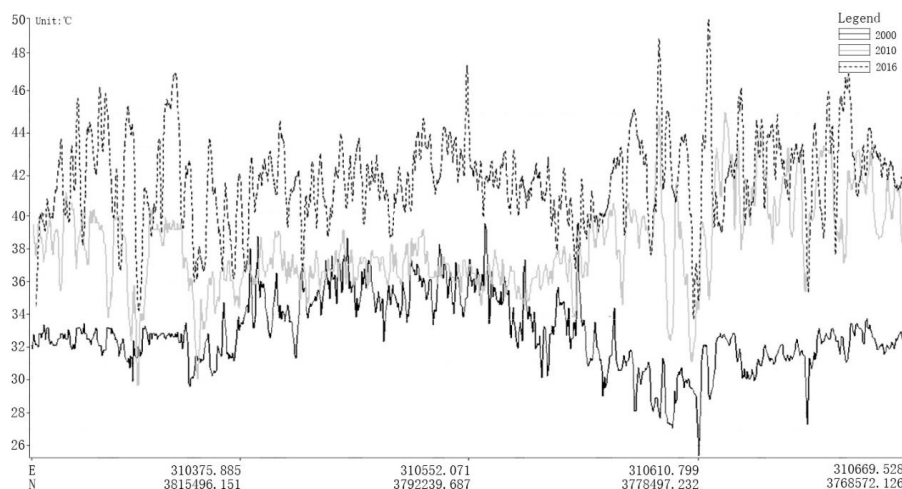


Figure 7. LST distribution of the B-B section across the study area from 2000 to 2016

Spatial Distribution Characteristics of Surface Temperature Grade in Xi'an

As mentioned above, in order to study the temporal variation of urban heat island by using the temperature inversion of different phase images, this paper used the brightness temperature normalization method to reduce the influence of seasonal phase difference. The thermal infrared images of different phases were compared, and the heat field intensity index (HFI) and Urban heat proportion index (UHPI) were introduced to study the change of urban heat island quantitatively. In order to study the urban heat island of Xi'an, the administrative boundary of the six districts of Xi'an City (Xincheng District, Beilin District, Lianhu District, Yanta District, Baqiao District and Weiyang District) was further used to perform the superposition mask operation on the thermal field intensity grade image. The distribution map of urban bright temperature grade was drawn, and the area of different grades was calculated (as shown in *Figures 8, 9* and *Table 2*).

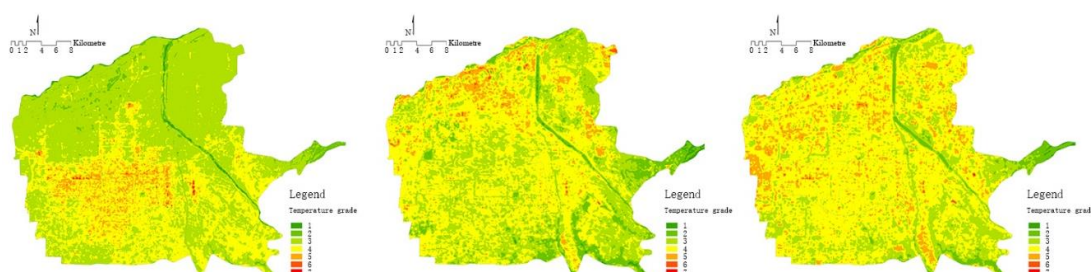


Figure 8. The distribution map of the intensity grade of the heat field in the six districts of Xi'an City

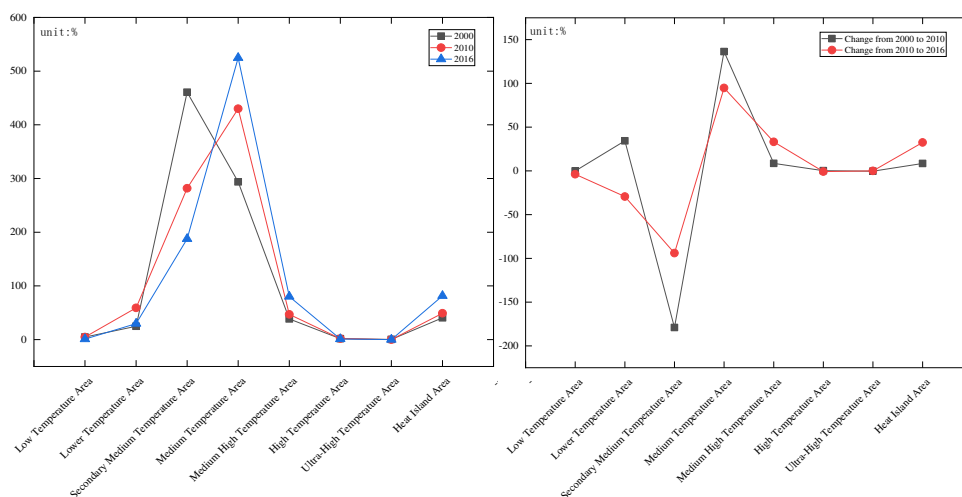


Figure 9. Area distribution map and area change map of six districts in Xi'an

From the qualitative point of view, according to the intensity distribution map of the thermal field in the six districts of Xi'an City, the heat island effect in Xi'an city showed an overall increasing trend from 2000 to 2016. In 2000, the urban heat island effect was concentrated, continuous and distributed in a plane. After 2010, the urban heat island effect was dispersed. The regional heat island aggregation in urban heat island effect was reduced. In 2000, the temperature of Xi'an urban area was obviously higher than

that of the peripheral area, showing the spatial characteristics of decreasing gradually from inside to outside. In 2010, the number and high temperature areas became larger, and the distribution was wider, with obvious characteristics of urban heat island effect. In 2016, the intensity of heat island continuously increased, and the heat island area gradually changed from centralized pattern to decentralized pattern due to the expansion of peripheral cities and the regulating action of vegetation and water body in city. Therefore, strengthening the construction of urban green space and rational planning of water body can further reduce the urban heat island effect in Xi'an.

Table 2. List of intensity area and percentage of thermal field in six districts of Xi'an City

Year	Grade	1	2	3	4	5	6	7
	Grade definition	LTA	L _{er} TA	SMTA	MTA	MHTA	HTA	UHTA
2000	Area	4.78	24.81	460.80	293.68	38.48	1.79	0.32
	Proportion	0.58%	3.01%	55.88%	35.61%	4.67%	0.22%	0.04%
2010	Area	4.69	59.13	281.75	430.06	47.02	2.00	0.01
	Proportion	0.57%	7.17%	34.17%	52.15%	5.70%	0.24%	0.00%
2016	Area	0.89	29.73	187.71	524.82	80.26	1.22	0.04
	Proportion	0.11%	3.61%	22.76%	63.64%	9.73%	0.15%	0.00%
Change from 2000 to 2010	Area	-0.09	34.32	-179.05	136.37	8.54	0.21	-0.30
	Rate of change	-1.93%	138.34%	-38.86%	46.44%	22.19%	11.86%	-95.87%
Change from 2000 to 2016	Area	-3.80	-29.40	-94.04	94.76	33.24	-0.78	0.02
	Rate of change	-81.08%	-49.72%	-33.38%	22.03%	70.69%	-38.96%	179.27%

Remarks: 1) LTA: Low Temperature Area; 2) L_{er}TA: Lower Temperature Area; 3) SMTA: Secondary Medium Temperature Area; 4) MTA: Medium Temperature Area; 5) MHTA: Medium High Temperature Area; 6) HTA: High Temperature Area; 7) UHTA: Ulter-high Temperature Area

From the quantitative point of view, it can be seen from the above table (Table 2) that the area of the medium temperature zone, secondary high temperature zone, high temperature zone and ultra-high temperature zone continuously expanded from 2000 to 2016, and the low temperature zone showed a declining trend. From 2000 to 2010, the area of the secondary high temperature zone and high temperature zone in the six districts in Xi'an has been expanded by 8.54 km² and 0.21 km², with an increase of about 22.19% and 11.86%, respectively. Although the area of the ultra-high temperature zone decreased by 0.30 km², the overall heat island area still increased by 8.45 km² from 2000 to 2010, with an increase of 20.82%. The area of the low temperature zone decreased by 0.09 km², with a decrease of 1.88%. From 2010 to 2016, the area of the secondary high temperature zone and the ultra-high temperature zone increased by 33.23 km² and 0.02 km², with the increase of about 70.69% and 200%. Although the area of high temperature area decreased by 0.77 km², the area of heat island has still expanded by 32.48 km², with an increase of about 39.84%. The area of low temperature zone decreased by 3.80 km², with a decrease of 81.02%. The urban heat island ratio indices of Xi'an City in 2000, 2010 and 2016 were UHPI₂₀₀₀=0.036, UHPI₂₀₁₀=0.050 and UHPI₂₀₁₆=0.078, respectively. This indicates that the heat island effect in the six districts of Xi'an City increased from 2000 to 2016. Obviously, it is further verified that the brightness temperature normalization method, HFI and UHPI can objectively and quantitatively reflect the changes of urban heat island.

Quantitative Analysis of Heat Island effect Boundary Evolution

In order to concretely reflect the spatial distribution of urban heat island in central urban area of Xi'an, ArcGIS software was used to divide the thermal field intensity grade map of the research area combined with administrative boundary to get the value and proportion of each region's geothermal grade area. The detailed statistics are provided in the *Figure 10* and *Table 3* as below.

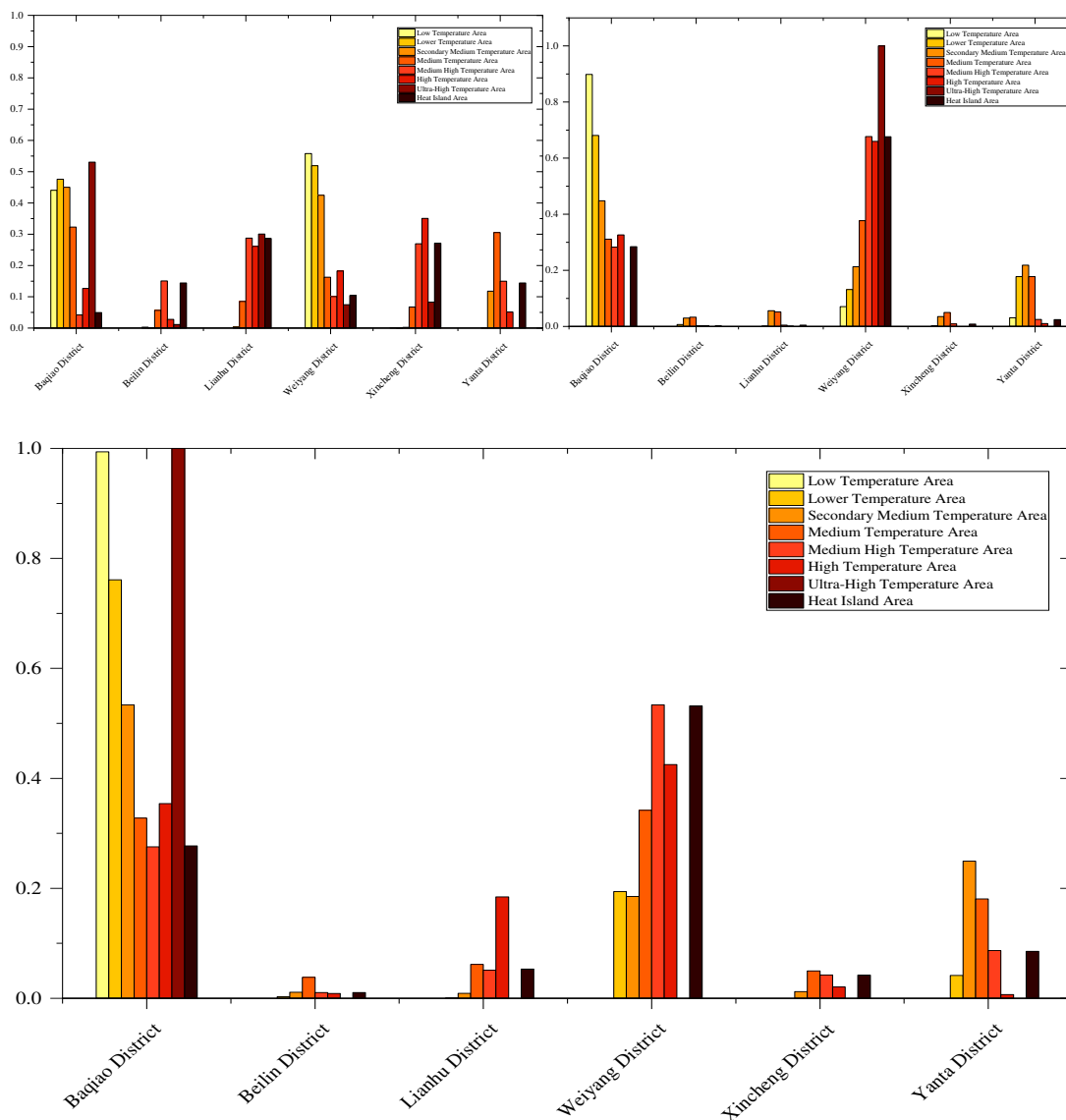


Figure 10. Figure of intensity area ratio of each thermal area in each administrative area of Xi'an from 2000 to 2016

As shown in the *Table 3*, in 2000, the heat island area was mainly concentrated in the densely populated old urban area inside the city wall. The area of heat islands in Lianhu District and Xincheng District is relatively large, accounting for about 28.643% and 27.151% of the total area of heat island, which are followed by Yanta District and Beilin District with the proportions of 14.429% and 14.423%. The proportions of Weiyang District and Baqiao District in low temperature zone, secondary temperature

zone and secondary medium temperature zone are great, which are 55.802% and 44.048%, 51.931% and 47.602%, and 42.477% and 51.931%, respectively. The area of heat island in Weiyang District and Baqiao District occupy large proportions, which were about 67.637% and 28.445% of the total area. The proportion of Baqiao District in the low temperature zone, low temperature zone and secondary medium temperature area is the largest, accounting for 89.852%, 68.089% and 44.783%, respectively. The scope of the heat island further expanded in 2016. However, the intensity grade of local regional heat island in the old urban area decreased and distributed dispersedly. The area proportions of the districts are the same as those in 2010. The proportions of heat island area in Weiyang District and Baqiao District are still larger, but are slightly lower than that in 2010, accounting for 53.167% and 27.706% of the total heat island area. Baqiao District still occupies the largest proportions in the low temperature zone, the lower temperature zone, the secondary modium temperature zone, and slightly increased compared with 2010, accounting for about 99.382%, 76.103% and 53.360%.

Table 3. Table of thermal intensity area in each administrative area of Xi'an from 2000 to 2016

		LTA(km ²)	L _{cr} TA(km ²)	SMTA(km ²)	MTA(km ²)	MHTA(km ²)	HTA(km ²)	UHTA(km ²)	HIA(km ²)
2000	Baqiao District	2.107	11.810	207.527	94.879	1.609	0.226	0.168	2.003
	Beilin District	0.000	0.070	0.543	16.590	5.800	0.050	0.004	5.853
	lianhu District	0.000	0.000	1.690	25.033	11.062	0.467	0.095	11.624
	Weiyang District	2.670	12.884	195.738	47.755	3.879	0.326	0.024	4.228
	Xincheng District	0.007	0.014	1.018	19.759	10.366	0.626	0.026	11.019
	Yanta District	0.000	0.031	54.289	89.667	5.765	0.091	0.000	5.856
2010	Baqiao District	4.216	40.261	126.179	133.723	13.295	0.652	0.000	13.946
	Beilin District	0.000	0.402	8.438	14.128	0.082	0.005	0.000	0.087
	lianhu District	0.000	0.079	15.777	22.266	0.223	0.002	0.000	0.225
	Weiyang District	0.332	7.777	59.917	162.086	31.831	1.318	0.013	33.161
	Xincheng District	0.000	0.103	9.879	21.418	0.418	0.000	0.000	0.418
	Yanta District	0.144	10.509	61.565	76.434	1.171	0.021	0.000	1.191
2016	Baqiao District	0.882	22.628	100.162	172.070	22.115	0.431	0.036	22.583
	Beilin District	0.000	0.088	2.049	20.065	0.842	0.011	0.000	0.853
	lianhu District	0.000	0.010	1.675	32.324	4.113	0.225	0.000	4.337
	Weiyang District	0.005	5.770	34.754	179.406	42.818	0.518	0.000	43.337
	Xincheng District	0.000	0.000	2.275	26.112	3.405	0.025	0.000	3.430
	Yanta District	0.000	1.237	46.796	94.840	6.962	0.008	0.000	6.971

Remarks: 1) LTA: Low Temperature Area; 2) L_{cr}TA: Lower Temperature Area; 3) SMTA: Secondary Medium Temperature Area; 4) MTA: Medium Temperature Area; 5) MHTA: Medium High Temperature Area; 6) HTA: High Temperature Area; 7)UHTA: Ulter-high Temperature Area; 8)HIA: Heat Island Area

In order to clearly and intuitively reveal the distribution of heat island in Xi'an urban area, the thermal field intensity grade map was further processed in ArcGIS, and the

heat island area of urban area from 2000 to 2016 was extracted and visualized (as shown in *Figure 11*). Combined with the actual situation of Xi'an City, in 2000, the urban construction was mainly concentrated in the Second Ring Road, and the population of the region was relatively dense. As a result, the area of heat islands in Lianhu District and Xincheng District was relatively large. In 2010, the heat island area began to appear in the north, west and southwest of the second ring, and the heat island effect within the second ring was weakened. The “hollow heat island” phenomenon occurred. As a result of the large-scale construction of the old urban periphery, there are many new industrial areas, enterprises concentrated areas, stations, commercial districts, and development areas. Due to slow development and factory stagnation, the scope and intensity of the heat island in the eastern region did not increase. Owing to the high vegetation and water coverage of Qujiang River in the southeast, the heat island intensity decreased despite of the development. In 2016, the scope of the heat island was further expanded to the north and the west obviously, showing dispersed distribution, which was resulted from the development and construction of the economic and technological development zone in the northern suburb, the western industrial zone and the high and new technology development zone in recent years. The development in the south and the east was mainly concentrated in the university town and Qujiang New District. There are a large number of parks, large areas of water and good surrounding green conditions, such as: Tang Paradise and Qujiang Ruins Park. As a result, the urban heat island effect is not obvious.

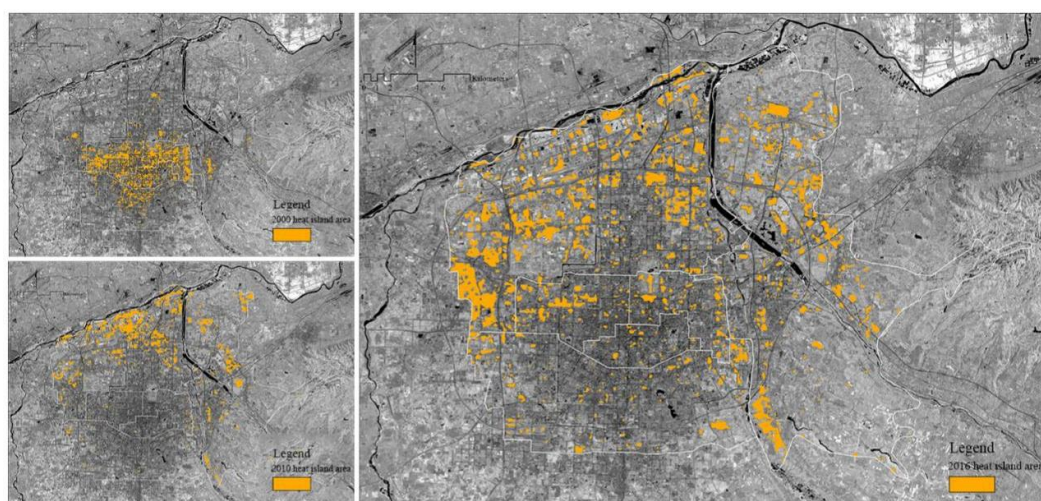


Figure 11. Regional distribution map of Urban Heat Island from 2000 to 2016

Conclusions

(1) According to the surface temperature inversion results, from 2000 to 2016, the average temperature in urban areas increased from 32.34°C in 2000 to 42.45°C in 2016, with an increase of 10.11°C in 16 years. The maximum temperature increased from 48.03°C in 2000 to 60.84°C in 2016. The thermal field profile in 2000 in WE/NS is low in the middle and high at both ends, which indicates obvious heat island effect in old urban area. After 2010, the temperature at both ends in WE/NS direction increased gradually. The temperature of some areas was even higher than that of the old urban area, which indicated that the heat island effect gradually extended to the periphery.

(2) From the perspective of the spatial distribution of surface temperature grade, although the area of ultra-high temperature zone decreased slightly, the area of high temperature area and secondary high temperature area continuously increased, and the overall heat island effect of urban area in Xi'an City increased from 2000 to 2016. To be specific, the area of heat island increased from 40.59 km² in 2000 to 81.52 km² in 2016, with an increase rate of 100.87%. UHPI increased from 0.036 in 2000 to 0.078 in 2016.

(3) As for the distribution law of the heat island effect, from 2000 to 2016, the regional space of the heat island gradually changed from centralized pattern to decentralized pattern. Generally speaking, the area with high vegetation coverage, low building density, greenbelt and water body has lower regional heat island effect. Heat island region shows high temporal and spatial consistency degree with urban expansion. Therefore, urban heat island effect can be alleviated by reasonable planning and transformation.

(4) In term of administrative division, the heat island effect was mainly distributed in the Lianhu District and Xincheng District within the second ring in 2000. After 2010, the heat island effect gradually expanded to the outer four administrative regions, and the "hollow heat island" phenomenon appeared in 2010. In 2016, the heat island effect was distributed in all the six districts, but the area of Weiyang District and Baqiao district occupied large proportions, which were about 53.167% and 27.706%.

Based on the atmospheric correction method, the surface temperature of Xi'an urban area was inverted. HFI and UHPI were introduced to quantitatively evaluate the temporal and spatial variation of the thermal field intensity in Xi'an. The research results have certain reference value for subsequent research. However, due to the lack of synchronous meteorological data when the satellite passes, the atmospheric parameters were calculated by using the atmospheric correction parameter calculator. Meanwhile, with the limited data source, the images of the three periods were collected at different dates, which had certain impact on the results. These limitations will be further improved in the future research work.

Acknowledgements. The research was funded within the project No. 51678058 entitled: "The Influence Mechanism and Control of Urban Space Composition on the Distribution of Suspended Particles", supported by National Natural Science Foundation of China.

REFERENCES

- [1] Balcik, F. (2014): Determining the Impact of Urban Components on Land Surface Temperature of Istanbul by Using Remote Sensing Indices. – *Environ. Monit. Assess.* 186(2): 859-872.
- [2] Chander, G., Markham, B. L., Barsi, J. A. (2007): Revised Landsat-5 thematic mapper radiometric calibration. – *Geoscience & Remote Sensing Letters IEEE* 4(3): 490-494.
- [3] Chen, L., Jiang, R., Xiang, W. (2016): Surface Heat Island in Shanghai and Its Relationship with Urban Development from 1989 to 2013. – *Adv. Meteorol.*: 1-15.
- [4] Di, Y., Zheng, Z., Zhang, B., Yin, H. (2016): Study on Dynamic Evolution Process of the Urban Heat Island in Xi'an. – *Journal Xi'an University of Architecture & Technology (Natural Science Edition)* 48(4): 551-555.
- [5] Ding, F., Xu, H. (2008): Comparison of Three Algorithms for Retrieving Land Surface Temperature from Landsat TM Thermal Infrared Band. – *Journal of Fujian Normal University (Natural Science Edition)* 24(1): 91-96.
- [6] Fan, C., Myint, S., Zheng, B. (2015): Measuring the Spatial Arrangement of Urban

- Vegetation and Its Impacts on Seasonal Surface Temperatures. – *Prog. Phys. Geogr.* 39(2): 199-219.
- [7] Gao, X., Wu, G. X., Du, G. Y., Li, C. P., Shen, H. F. (2015): A Spatio-temporal Changes of Thermal Landscape Pattern Based on a Multifractal Model: a Case Study of Zhengzhou City. – *Acta Ecologica Sinica* 35(20): 6774-6787.
- [8] Grădinaru, S. R., Loja, C. L., Onose, D. A., Gavrilidis, A. A., Patru-Stupariu, I., Kienast, F., Hersperger, A. M. (2015): Land Abandonment As a Precursor of Builtup Development at the Sprawling Periphery of Former Socialist Cities. – *Ecol. Indic.* 57: 305-313.
- [9] Guo, Q., Zhu, Y. (2016): Analyzing the Thermal Environment Simulation for Relieving Heat Island Effect: A Case Study on the City of Xi'an. – *Ecological Economy* 32(3): 161-164.
- [10] He, X., Ye, X., Ma, W., Wang, C. (2017): Study of the Effects of Urban Underlying Surface Changing on the Air Pollution Diffusion in Hangzhou. – *Science Technology and Engineering* 17(11): 122-130.
- [11] Hu, S., Yang, S., Li, W., Zhang, C., Xu, F. (2016): Spatially Nonstationary Relationships Between Urban Residential Land Price and Impact Factors in Wuhan City, China. – *Appl. Geogr.* 68(68): 48-56.
- [12] Huang, M., Xing, X., Wang, P. (2006): Comparison between Three Different Methods of Retrieving Surface Temperature from Landsat TM thermal Infrared Band. – *Arid Land Geography* 29(1): 132-137.
- [13] Jiang, M., Zeng, S., Zeng, J. (2015): Urban Expansion of Tianjin and the Micro Climate Characteristics Evolution-Based on the Urban Thermal Environment Perspective. – *Journal of Arid Land Resources and Environment* 29(9): 159-164.
- [14] Liao, F. H., Wei, Y. D. (2014): Modeling Determinants of Urban Growth in Dongguan, China: A Spatial Logistic Approach. – *Stoch. Environ. Res. Risk Assess.* 28: 801-816.
- [15] Mihai, B., Nistor, C., Simion, G. (2015): Post-Socialist Urban Growth of Bucharest, Romania: A Change Detection Analysis on LANDSAT Imagery (1984–2010). – *Acta Geogr. Slov.* 55(2): 223-234.
- [16] Qin, Z., Li, W., Xu, B., Chen, Z., Liu, J. (2004): The Estimation of Land Surface Emissivity for Landsat TM6. – *Remote Sensing for Land & Resources* 17(3): 28-42.
- [17] Rogan, J., Ziemer, M., Martin, D., Ratick, S., Cuba, N., DeLauer, V. (2013): The Impact of Tree Cover Loss on Land Surface Temperature: A Case Study of Central Massachusetts Using Landsat Thematic Mapper Thermal Data. – *Appl. Geogr.* 45: 49-57.
- [18] Shi, B., Wang, X., Zhao, D. (2017): Numerical Simulation of the Effects of Sky-view Factor on Thermal Environment in Urban Residential Districts. – *Chinese Journal of Applied Mechanics* 34(7): 1181-1186.
- [19] Wang, P., Zhang, J., Lv, R. (2014): Urban Thermal Environment Pattern with Spatial Autocorrelation in Lanzhou. – *Chinese Journal of Ecology* 33(4): 1089-1095.
- [20] Yao, Z., Wei, H., Liu, H., Li, Z. (2013): Statistical Vehicle Specific Power Profiling for Urban Freeways. – *Procedia-Social and Behavioral Sciences* 96: 2927-2938.
- [21] Yin, C., Shi, Y., Wang, H., Wu, J. (2015): Impact of Urban Landscape Form on Thermal Environment at Multi-Spatial Levels. – *Resource and Environment in the Yangtze Basin* 24(1): 97-105.
- [22] Zhang, W., Jiang, J., Zhu, Y. (2015): Spatial-temporal Evolution of Urban Thermal Environment Based on Spatial Statistical Features. – *Chinese Journal of Applied Ecology* 26(6): 1840-1846.
- [23] Zhen, G., Hu, Y., Li, H. (2016): Study of Temporal and Spatial Distribution of Thermal Environment in Wuhan City. – *Science of Survey and Mapping* 41(6): 84-86.
- [24] Zheng, Z. (2013): Statistical analysis of the effects of urbanization on haze days in Beijing area. – *Ecology and Environmental Sciences* 21(8): 1381-1385.

LABORATORY EXPERIMENT ON BIOLOGICAL DECOMPOSITION OF BIOLOGICAL REACTOR LANDFILL

SUN, H. J.* – BIAN, X. Y. – ZHAO, L. H. – QIU, G.

*School of Civil and Architectural Engineering, Liaoning University of Technology
Jinzhou 121001, Liaoning, China*

**Corresponding author
e-mail: sunhongjun_2006@163.com*

(Received 24th Aug 2018; accepted 12th Nov 2018)

Abstract. In order to study the bio-decomposition of bioreactor landfill waste, simulation experiment of different ways of landfill and decomposition stage was conducted. We analyzed decomposition processes of organic matter in different decomposition stages. The landfill can be divided into two types in bioreactor: stratified landfill and non-stratified landfill, each group having four waste decomposition reaction stages. By collecting the reaction gas and leachate in each stage, methane production, pH, moisture content and volatile solids were measured, and the pattern of bio-decomposition was obtained. The results showed that with the gradual deepening of organic matter decomposition in waste, the methane production rate and the pH value of leachate will change greatly. The weight percentage of the biodegradable material gradually decreased and the average moisture content of waste increased from 54.6% to 70.2%. The content of volatile solids in waste decreased from 89% to 51%.

Keywords: *bioreactor landfill, biodegradation, leachate, experimental study, organic matter*

Introduction

Bioreactor landfill speeds up the bio-decomposition of the organic matter through secondary leachate injection and improves the landfill stabilization process. The technology has been widely used in the field. The bioreactor landfill waste's decomposition of organic matter is greatly differs from that of the traditional landfill (Stark and Newman, 2010). Kjeldsen et al. (2002), Chugh (1998) and Ghanem et al. (2001) put forward the changing range of pH 4.7-8.8 in traditional landfill and the pH value was 5.4-8.6 floating in the bioreactor landfill. Olivier and Gourc (2007) and Binder and Bramryd (2001) also pointed out that the pH of waste body changed from 6.5 to 7.6 in the anaerobic decomposition stages. Beaven (2004) and Qian and Koerner (2004) explicitly proposed different moisture content of waste body in the traditional landfill and the bioreactor landfill. Landva et al. (2000) and Clark (2007), Barlaz et al. (2001), Shen (2002) pointed out the change of the organic matter content 5%-75% in the landfill. Kong et al. (2008) put forward creep-decomposition experiment to couple under leachate recharge, Xie et al. (2005) conducted contrast tests of waste compression characteristics and decomposition characteristics under constant load.

In order to research the characteristics of bioreactor landfill waste bio-decomposition a large number of laboratory tests of bioreactor landfill waste bio-decomposition still needs to be conducted. Considering representativeness of the waste sample in laboratory test, all waste samples were collected in Jinzhou Nan-shan Landfill of Liaoning province, China. The samples were fully mixed and test samples were selected when in need. The test samples were divided into two groups; the first group is the direct landfill waste sample, the second group is the layered rubbish sample, which is placed between the soil covering layers. This arrangement can simulate the actual landfill. The landfill was constituted of

four phases, which were aerobic and anaerobic decomposition of waste, methane fermentation and reduced rate methane production. Reaction gases and leachate were collected in each stage. Methane production rate, pH, changes of organic matter in different stages of decomposition, moisture content, volatile solid content and other related indicators were studied. It can be concluded that the biodegradable pattern of the bioreactor landfill waste and decomposition characteristics under different decomposition stages.

Materials and methods

In situ sample collection

Due to the complexity of the components of waste in landfills, the accuracy of geotechnical parameter measurement of waste body is affected by the rubbish sample. Therefore, the conducted garbage is a representative sample which will determine the scientific test result. The samples were collected in Jinzhou Nan-shan Landfill, China (*Fig. 1*). According to the standard methods of geotechnical test, a typical mixed waste sample was obtained. The collected waste sample was mixed several times, and then it was divided into four parts. One part was selected, the other three were discarded. Finally, the selected portion of the waste sample mixed thoroughly again and divided into four parts. One part from the heap was selected and the other three parts were discarded. The selected part of the waste was used in the test.



Figure 1. Waste samples

Test method

In order to study physical characteristics and strength parameters of the waste body under different decomposition stages, the project team developed two sets of laboratory experiments for this test, as it is shown in *Figure 2*. Each reactor corresponded to an experiment and each group included four reactors representing different decomposition stages of waste. The first set of test involved layered waste with no covering by soil layer. The second set of test involved layered waste with soil covering. First of all, the reactor and the gas collecting device and leachate device were connected; the reactor was sealed with o-rings and sealant. A u-shaped pressure gauge was connected by the gas collecting device. The U type pressure gauge providing water pressure difference was observed at 48 h in order to check the seal of the reactor. In the test, the water pressure difference was 2 mm in 12 h and the water pressure difference was 5 mm in 48 h, which meet the sealing performance.



Figure 2. *The diagram of simulation experiment*

The weight of waste was measured before the waste was filled into the reactor (Fig. 3). To guarantee the uniformity of waste, waste was mixed adequately before placed into the bioreactor. Two groups of reactor were filled. The first reactor was directly filled and compacted. In the second reactor an actual processing form of a landfill was simulated. Each layer of landfill was covered by soil.



Figure 3. *Leak test of reactor*

Ensuring that 1500 ml of leachate is produced every day the amount of recharge water poured into the reactor was determined based on the initial water content of the garbage sample, and on the initial moisture content of the test sample. Ensuring that the amount of water is poured into the reactor, the moisture content of the garbage sample reaches 55%. Finally, the reactor was closed, the gas collection device and the leachate collection bag were connected, and the two sets of reactors were set under 28-32 °C (Qiu et al., 2010).

Each reactor was operated under the conditions of a simulated bioreactor to ensure the accuracy and the scientificity of the test by performing the following operation procedure (Qian and Koerner, 2010):

1. Injection of enough amount of water in the reactor to accelerate the production of leachate;
2. Recharging the leachate to the reactor;

- Using activated sludge process, adding anaerobic digestion into the leachate to speed up decomposition of organic matter of waste in the reactor.

The formation samples in different decomposition stages

The waste samples of different decomposition stages were generated under appropriate waste leachate re-circulation and organic matter decomposition conditions by two bio reactors. Each test included four reactors of different decomposition stages. The four decomposition stages were aerobic, anaerobic, methane fermentation and reduced rate methane production phase. Gas, pH value and volatile solids composition in this experiment were used to judge stages of the decomposition of organic matter.

Results and discussion

With the continuous progression of the organic matter degradation step in the garbage sample, the production rate of methane and the pH value of the leachate change greatly. *Figures 4* and *5* showed the statistics of the methane production rate and pH values respectively. In this experiment, leachate was treated by an anaerobic digestion sludge method, and then fed back to the reactor to accelerate the degradation of the organic matter in the reactor. Two sets of tests were conducted on different stages of degradation of garbage samples according to changes in the degradation process. In the first set of tests, the garbage sampling time in the reactor were the 26th day, the 107th day, the 224th day and the 249th day; in the second set of tests, the garbage sampling time in the reactor were the 21st day, the 96th day, the 172nd day and the 234th day. *Figure 4a* shows the yield of methane at different stages of degradation in the first set of experiments, and *Figure 4b* shows the change in pH of the leachate at different steps of degradation in the first set of tests. On the 26th day, the sample went through an anaerobic acidification step, which was phase I. On the 107th day, the methane production rate reached the peak and the pH value was basically neutral. The degradation of the organic matter in the garbage body at this step was very active. This is Phase II; the 224th day sample and the 249th day sample were in the methane production rate reduction stage, that is step III and the maturation step of garbage body degradation, that is step IV, respectively. Using the same method and principle, in the second set of reactors, the extraction time of the samples was 21 days, 96 days, 172 days, and 234 days, respectively. They corresponded to the first step of bio-degradation and the second set of samples, which are Phase II, Phase III and Phase IV. The results are presented in *Figure 5*. The methane production rates in reactors at different decomposition phases are presented in *Table 1*.

Table 1. Methane production in the two different reactors

Decomposition phase	Reactor 1		Reactor 2	
	Time (day)	Methane production (L)	Time (day)	Methane production (L)
Phase I	26	23.38	21	13.67
Phase II	107	194.03	96	231.24
Phase III	224	473.87	172	342.12
Phase IV	249	514.15	234	557.62

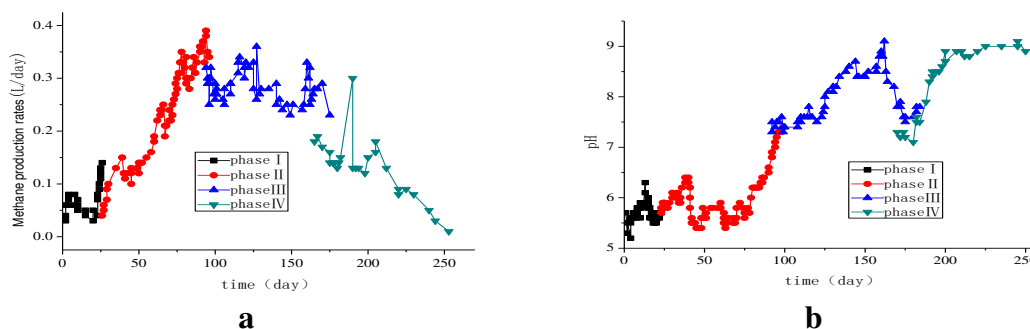


Figure 4. The methane production rate (a) and pH (b) of different decomposition stages of the first test

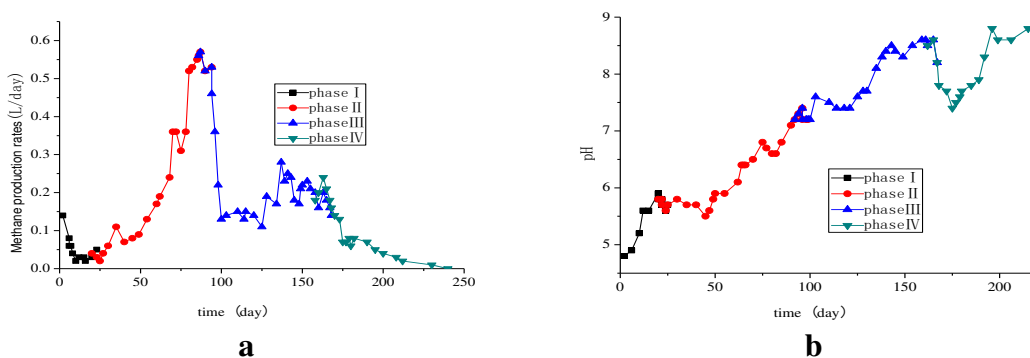


Figure 5. The methane production rate (a) and pH (b) of different decomposition stages of the second test

Change of waste composition in different decomposition stages

The change in weight percentage of waste composition at each phase of decomposition is a big difference. The decomposition of waste reduced the degradable component in waste considerably, while the non degradable component (plastic) remained the same. The rate of decomposition also depended on the type of individual constituent. In *Figure 6* it can be observed that the food wastes were completely consumed by the end of the second phase. On the other hand, only 28% of paper was degraded in this phase. However at the end of the final phase of decomposition the decomposition of paper increased. The paper present in the final phases of decomposition was more like a paste with higher moisture content. This is why a small reduction in the percentage of paper was observed in the final phases of decomposition only. Paper is a major biodegradable waste that has a strong impact on the geotechnical characteristics of waste. As the waste degraded, the percentage of paper decreased, while the percentage of plastic increased. *Figure 6* presents the percentage of paper and plastic at the end of each phase of decomposition.

The results of moisture content analysis

With the progression of the degradation step, the average moisture content of the garbage was also increasing, and the moisture content of the landfill is shown in *Table 2*. In the first set of reactors, the moisture content increased from 58.6% in step I to 64.9% in step

IV. In the second set of reactors, the moisture content increased from 54.6% in step I to 70.2% in step IV. The change of moisture content can help to distinguish the organic matter degradation step of the garbage body. The degradation of the garbage body reduces the void ratio of itself, but it also increases the moisture content.

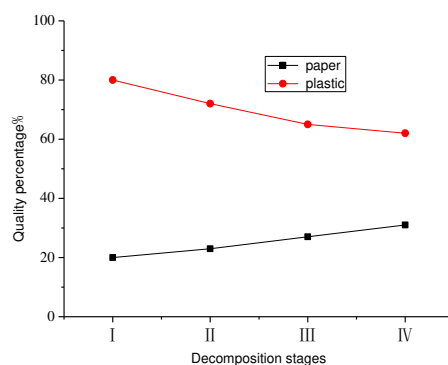


Figure 6. The percentage content of waste paper and plastic in different decomposition stages

Table 2. Moisture content of the solid waste in different degradation stages

Decomposition phase	Reactor 1	Reactor 2
Phase I	58.6	54.6
Phase II	59.2	60.4
Phase III	64.1	68.5
Phase IV	64.9	70.2

The results of volatile solids analysis

After each step of degradation was completed, the percentage of solids in the trash was determined and the results are shown in Figure 7. Leachate recharge has a great influence in the degradation of the garbage sample. With the degradation of the garbage sample, the volatile solid content in the garbage sample is gradually reduced. The percentage of volatile solids showed a big change after each degradation step. In the first set of reactors, the percentage of volatile solids dropped from 94% in Phase I to 41% in Phase IV; in the second set of reactors, the percentage of volatile solids was 89% in Phase I and 51% in Phase IV (Table 3).

Table 3. The percentage content of volatile solids in different degradation stages

Decomposition phase	Reactor 1		Reactor 2	
	Waste decomposition period (d)	The percentage content of volatile solids (%)	Waste decomposition period (d)	The percentage content of volatile solids (%)
Phase I	26	6	21	11
Phase II	107	26	96	22
Phase III	224	38	172	41
Phase IV	249	59	234	49

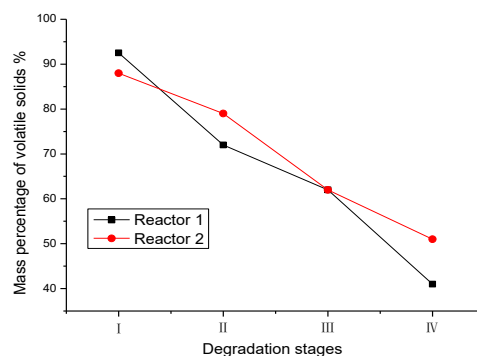


Figure 7. The mass percentage of volatile solids in different degradation stages

Conclusion

A laboratory test instrument of organic matter decomposition of bioreactor landfill has been developed. This instrument has gas and leachate collection device. The test has shown that the equipment's performance is stable. The test was divided into two groups. The first test in the landfill was not layered, without covering soil layer. The second test was layered, and each layer of waste was covered by soil, each test was consisted of four stages of decomposition. With the progression of decomposition stage of waste body's organic matter, the rate of CH₄ and pH of leachate have greatly changed, methane production reached its peak period, and the pH was neutral. The percentage of biodegradable material weight was gradually decreased, but non-biodegradable material remained the same in the process with the progression of the decomposition stage. With the progression of the decomposition stage, the average moisture content of waste body increased, the moisture content raised from 58.6% in Phase I to 64.9% in Phase IV. Similarly in Reactor 2, it increased from 54.6% in Phase I to 70.2% in Phase IV. As the garbage body degrades, the content of volatile solids in the garbage body gradually decreases. The percentage of volatile solids in the first set of reactors decreased from 94% in phase I to 41% in phase IV. As for the second set, the percentage of volatile solids in the reactor dropped from 89% in phase I to 51% in Phase IV.

Acknowledgements. This work was supported and financed by the grant No. 51408290 from National Natural Science Foundation of China.

REFERENCES

- [1] Barlaz, E., Beech, J. F., Matasovic, N. (2001): Discussion of Municipal solid waste slope failure: Waste and foundation soil properties. – J Geotech Geoenviron Eng 127(9): 812-813.
- [2] Beaven, X. (2004): Limit equilibrium analysis of translational failure of landfills under different leachate buildup conditions. – Water Sci Eng 1(1): 44-62.
- [3] Binder, M., Bramryd, T. (2001): Environmental impacts of landfill bioreactor cells in comparison to former landfill techniques. – Water, Air and Soil Pollution 129(1-4): 289-303.
- [4] Chugh, S. (1998): Effect of recirculated leachate volume on MSW degradation. – Waste Manage and Research 16(6): 64-573.

- [5] Clark, J., Augenstein, D., Morck, R. (2007): Bioreactive landfill. – *MSW Management* 10: 53-60.
- [6] Ghanem, I. I., Guowei, G., Jinfu, Z. (2001): Leachate production and disposal of kitchen food solid waste by dry fermentation for biogas generation. – *Renewable Energy* 23(3-4): 673-684.
- [7] Kjeldsen, P., Barlaz, M., Rooker, A. (2002): Present and long-term composition of msw landfill leachate. A review. – *Critical Reviews in Environmental Science and Technology* 32(4): 297-336.
- [8] Kong, X., Sun, X.-L., Zou, D. (2008): Creep-degradation Properties of municipal solid waste in laboratory test. – *Rock and Soil Mechanics* 2(29): 337-341.
- [9] Landva, A. O., Valsangkar, A. J., Pelkey, S. G. (2000): Lateral earth pressure at rest and compressibility of municipal solid waste. – *Canadian Geotechnical Journal* 37(6): 1157-1165.
- [10] Olivier, F., Gourc, J. P. (2007): Hydro-mechanical behavior of municipal solid waste subject to leachate recirculation in a large-scale compression reactor cell. – *Waste Management* 27: 44-58.
- [11] Qian, X., Koerner, R. M. (2004): Effect of apparent cohesion on translational failure analyses of landfills. – *J Geotech Geoenviron Eng* 130(1): 71-80.
- [12] Qian, X., Koerner, R. M. (2010): Modification to translational failure analysis of landfills incorporating seismicity. – *J Geotech Geoenviron Eng* 136(5): 718-727.
- [13] Qiu, G., Liang, L., Sun, H. (2010): Forecasting the settlement of a bioreactor landfill based on gas pressure changes. – *Waste Management & Research* 31(8): 1035-1040.
- [14] Shen, D. S., He, R., Ren, G. P., Traore, I., Feng, X. S. (2002): Effect of leachate recycle and inoculation on microbial characteristics of municipal refuse in landfill bioreactors. – *Journal of Environmental Science* 14(3): 406-412.
- [15] Stark, T. D., Newman, E. J. (2010): Design of a landfill final cover system. – *Geosynthet Int* 17(3): 124-131.
- [16] Xie, Y., Chen, Y., Tang, X. (2005): Development and application of biodegradation-compression test apparatus for municipal solid waste. – *Chinese Journal of Geotechnical Engineering* 5(27): 571-576.

TEMPORAL-SPATIAL DISTRIBUTION CHARACTERISTICS AND ENVIRONMENTAL BACKGROUND OF MIDDLE HOLOCENE SETTLEMENTS ON THE SOUTH COAST OF LAIZHOU BAY, NORTHERN SHANDONG, CHINA

ZOU, C. H. – ZHAO, Q.* – LI, X. M. – GAO, Q.

*School of Water Conservancy and Environment, University of Jinan
Jinan 250022, Shandong Province, China*

**Corresponding author*

e-mail: stu_zhaoq@ujn.edu.cn; phone: +86-135-8910-8827

(Received 29th Sep 2018; accepted 27th Nov 2018)

Abstract. With increasing collaboration between archeology and natural sciences, the interactions between paleocultures and paleoenvironment have received more attention in recent years. In this investigation, the authors used nine radiocarbon dates from five profiles to explore the environmental evolution of the south coast of Laizhou Bay, and investigated the spatial-temporal distributions of archeological sites in the Middle Holocene as well as discussed the relationships between human cultures and environmental changes. The results show that the Neolithic archeological sites were mainly distributed in the flat (slopes $< 4^\circ$) marine plain and alluvial plains with elevations below 29 m, and the quantity and frequency of archeological sites exhibited an early ascending and later descending trend. Multiple data such as those of slope and extent close to the riverside were integrated to indicate that the ability of the ancients to adapt to the environment gradually increased. Further comparison revealed the correlation among Holocene climate change and environmental evolution and the Neolithic cultural development in the study area, which concerns the generally improved living conditions, the development of the primitive culture whereas degeneration coincided with the culture's transition or interruption. The results highlight the geographical factors in the development of prehistoric culture, especially the climatic factors.

Keywords: *the south coast of Laizhou Bay, climate change, settlement distribution, sea level changes*

Introduction

Past Global Changes (PAGES) focused on the coupling between prehistoric human socioeconomic activities and the natural environment. Therefore, the spatial and temporal distribution of archaeological sites and the response of human activities to Holocene climate change have become the central issue of current research on the human-land relationships. Currently, archeologists no longer discuss the rise and fall of civilizations from the perspective of cultural relics but gradually notice the influence of climate and natural environment changes on human activities (Karakasidou, 2005; Kuper and Kröpelin, 2006; Dong et al., 2013; Goude and Fontugne, 2016; Mayke et al., 2013). Since the 1980s, many scholars have used the interdisciplinary studies concerning sedimentary strata, sporopollen analysis and geology, geography and zoology to conduct research on the relationship between paleoenvironment and paleoculture, and they have achieved good research results (Wang et al., 2017; Li et al., 2010; Stanley and Galili, 1996). Research in the field of archeology pays more attention to analyzing the temporal and spatial changes of the distribution of sites and discusses the influence of terrain, landform, slope, sea level and other impact factors on the distribution of sites (Zheng et al., 2018; Demján and Dreslerová, 2016; Guo et al., 2014). Researches showed that prehistoric humans mostly chose terraces and platforms

with superior ecological conditions and rich hydrothermal resources (Dai et al., 2016; An et al., 2015; Tan et al., 2015; Dong et al., 2013; Contreras et al., 2018; Lyndsay et al., 2018; Spencer and Bevan, 2018). However, due to the lack of high-resolution environmental archeological materials, how to precisely define regional human land interactions is remaining a challenging issue.

The Haidai cultural district is centered on the present-day Shandong Province and is among the important cultural lineages of Chinese civilization. In-depth systematic study of the spatial and temporal distribution of this regional archeological site and its environmental background for ancient human activities are of great significance for understanding the origins and processes of Chinese civilization and the interrelationship among environmental evolutions. During the last few decades, research on the climate and environmental evolution of the Neolithic Age in Haidai area has primarily focused on the change of coastline and vegetation in the local area (Yang et al., 2016). Meanwhile, on the basis of paleoclimate and environmental research, some scholars have focused on the impact of sea level fluctuations on paleoculture (Guo et al., 2014). However, those studies have significant imbalances in research areas and outcomes, as well as regional comparative studies and comprehensive analyses. This is not only a shortcoming in the study of paleoclimate and paleoenvironment but also has clearly influenced the understanding of the environmental background of archeological culture in the Neolithic Age. The southern coast of Laizhou Bay is one of the most typical areas of Neolithic cultural sites and is also among the key areas for studying the relationship between ancient cultural sites and environmental evolution. In the last few decades, some intensive research has been conducted on the south coast of Laizhou Bay on the basis of lacustrine-marine facies profile sedimentary information combined with Neolithic archeological data, and has implied the possible cultural impact of paleoclimate variation and the prehistorical human interactions during past global changes. Judian Lake, a lagoon formed by coastal depressions, is the largest ancient lake on the south coast of Laizhou Bay, and the lagoon evolved into a freshwater lake after the Huanghua transgression of the region. Therefore, it is of great significance to study the Judian Lake strata to reveal the paleogeographic environment along the coast of Laizhou Bay. In this study, we analyze the spatial and temporal characteristics of the 142 Neolithic cultural sites on the south coast of Laizhou Bay. Combining earlier reconstructed environmental records and using archeological data with our recent research and experiences, we are now able to delineate a comprehensive picture of the varieties and properties of the Neolithic culture along with the paleoclimatic, paleoenvironmental and paleoecological changes.

Based on the fieldwork, the authors selected two representative profiles in the study area to assist in exploring the features of the Holocene stratum deposition and the process of paleoenvironmental evolution in the study area. Accelerator Mass Spectrometry (AMS) radiocarbon dating methods were used to date samples from the Judian lake (Drilling name abbreviation: JDH) (37°04'25.02"N, 118°43'0.61"E and 3.2 m altitude) and the town of Taitou (Drilling name abbreviation: TTZ) (37°05'21.71"N, 118°39'51.69"E and 7.0 m altitude) profiles for constructing the timescale. All the dating samples were pretreated and measured at Beta dating laboratory in Miami, FL, USA. The Conventional Radiocarbon Ages have all been corrected for total fractionation effects and under the applicable circumstances, the calibration was performed by using 2013 calibration databases (referred to 'cal. BP'). As usual, conventional radiocarbon ages and sigmas are rounded up to the nearest 10

years according to the 1977 International Conference on Radioactive Carbon practice. In addition, we also selected three other profile drills (Drilling name abbreviation: XHK, A1, SWC) in the area and obtained their dating data, which were used to reconstruct the time scale.

The information of 142 archeological sites was collected mainly from the *Atlas of Chinese Cultural Relics: Shandong Section* and other published documents. The chronology of these sites can be classified into four stages based on their cultural sequences and ^{14}C dating data: the HouLi Culture stage (8.5~7.7 cal.ka BP), the Dawenkou Culture stage (6.1~4.6 cal.ka BP), the Longshan Culture stage (4.6~4.0 cal.ka BP) and the Yueshi Culture stage (4.0~3.5 cal.ka BP) (Bureau of National Cultural Relics, 1997). The DEM (Digital Elevation Model) elevation data of the southern coast of Laizhou Bay were collected from the Geospatial Data Cloud website, and the SRTM4.1 DEM data set with a spatial resolution of 30×30 m was also used in this study. Erdas Imagine 9.2 was used to synthesize 4 elevation data maps into a DEM map of the southern coast of Laizhou Bay, which was processed and vectorized in the ArcGIS 10.3 software environment. The ASTM DEM data of 30×30 m horizontal resolution was superimposed with the cultural sites of different periods on the south coast of Laizhou Bay, and the cultural sites of different periods in the area were obtained. The altitudes of archeological sites were obtained by using the 'Extract Values to Points' tool for further analysis.

Study area

The southern coast of Laizhou Bay locates in the north-central region of Shandong Province, China. It covers most of Laizhou County and parts of Guangrao, Shouguang, Changyi and Hanting Counties (*Fig. 1*).

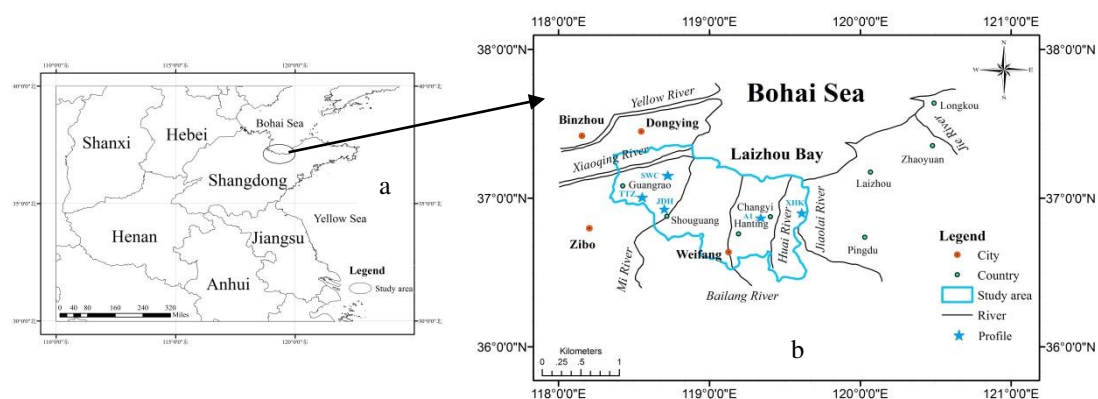


Figure 1. (a) Maps of northern China and surrounding regions showing provincial boundaries and location of Laizhou Bay; (b) geographic sketch of Laizhou Bay and the locations of profiles and sites mentioned in the current study

From the south to the north, the topography of the study area is transformed from aggraded flood plain to alluvial plain, whereas to the Laizhou Bay coast is narrow banded alluvial plain and marine plain. The south coast of the Laizhou Bay exhibits warm temperate continental monsoon climate characterized by warm humid summers and cool, dry winters. The annual average temperature of the study area is 12.2°C , and

the annual average precipitation is 559.5 mm, mainly concentrated in spring and summer. Many short-source rivers (mainly the Xiaoqing River, Mi River, Bailang River, Huai River, Jiaolai River and their branches) constitute an intricate water network in the region.

Results

Dating results

The dating results of nine samples collected from the XHK (Han and Zhang, 2005), the A1 (Liu et al., 2004), the SWC (Guo et al., 2013), the JDH and the TTZ profiles in the study area are shown in *Table 1*. A total of nine radiocarbon dates were obtained and the ages are in stratigraphic order.

Table 1. AMS-¹⁴C ages of the XHK, A1, SWC, JDH and TTZ profiles

Laboratory original code	Depth (m)	Dating method	Dating material	Age (cal.ka BP)	Profile
XHK (4-9 m)	4-9	AMS- ¹⁴ C	Clayey silt	5.530±0.14	XHK
A1-4	4.5	AMS- ¹⁴ C	Clayey silt	5.383±0.064	A1
A1-7	7.6	AMS- ¹⁴ C	Clayey silt	9.826±0.075	A1
SWC-W1	0.75-1	AMS- ¹⁴ C	Clayey silt	5.510±0.07	SWC
SWC-W2	2.25-2.5	AMS- ¹⁴ C	Clayey silt	6.350±0.045	SWC
JDH65	1.29-1.3	AMS- ¹⁴ C	Peat	5.240±0.03	JDH
JDH135	2.69-2.70	AMS- ¹⁴ C	Peat	5.990±0.03	JDH
JDH192	3.83-3.84	AMS- ¹⁴ C	Peat	6.900±0.03	JDH
TTZ	1.61-1.62	AMS- ¹⁴ C	Peat	6.510±0.03	TTZ

Number and elevations of archeological sites

The total number of archeological sites on the southern coast of Laizhou Bay throughout the Neolithic Age is listed in *Table 2*, which shows an early ascending curve and an later descending curve from the 3 Houli sites up to the 27 Dawenkou sites, and an increase to the 101 Longshan sites and finally the 57 sites of the late period of the Yueshi culture. The occurrence frequency of these sites in each period slowly grew from 0.38/100a to 1.8/100a, dramatically increased to 16.83/100a, finally fell to only 2.2/100a (*Table 2*). Accompanied by cultural evolution, the distribution and types of archeological sites in different cultural stages have different changes. In Houli culture stage, the sites have a mostly scattered distribution, and all sites are located on the proluvial platform or alluvial plains near river banks. Different from the previous cultural stage, the sites from the Dawenkou cultural stage mostly appear farther from the river bank and at lower elevations, for example, Wucun, Fujia and Rongzhuang. During the Longshan culture period, the distribution was further expanded. In the western region, there is a trend of a concentrated distribution of dual centers, and the eastern decentralization trend is obvious. It is worth mentioning that a lower elevation archeological site (the Guojingzi site) appeared in the study area during this cultural period, which was the first site found in the northern marine plain. Although the number

of sites in the Yueshi culture stage has decreased significantly, the distribution of landform type and its trend did not change much, and are similar to the previous period.

Table 2. Neolithic cultural sequence and content on the south coast of Laizhou Bay

Archeological culture sequence	¹⁴ C age (ka BP)	Typical sites and contents	Amount/occurrence frequency of the archeological sites (/100a)
Houli Culture	cal. 8.5–7.7	Qianbuxia, Lujiakou and Bianxianwangxi	3/0.38
Dawenkou Culture	cal. 6.1–4.6	Rongzhuang, Dongjia, Wucun, Qianbuxia, and Fujia	27/1.8
Longshan Culture	cal. 4.6–4.0	Lujiakou, Guojingzi and Zhongjia	101/16.83
Yueshi Culture	cal. 4.0–3.5	Xidu and Zhongjia	11/2.2

In the study area, the altitudes of the archeological sites are relatively low, and up to 75% of the sites are distributed in areas below 29 m asl (Table 3). All three Houli culture sites are concentrated in areas with elevations below 39 m asl, and two-thirds of them are distributed in areas with elevations of 10-19 m asl (Fig. 2a).

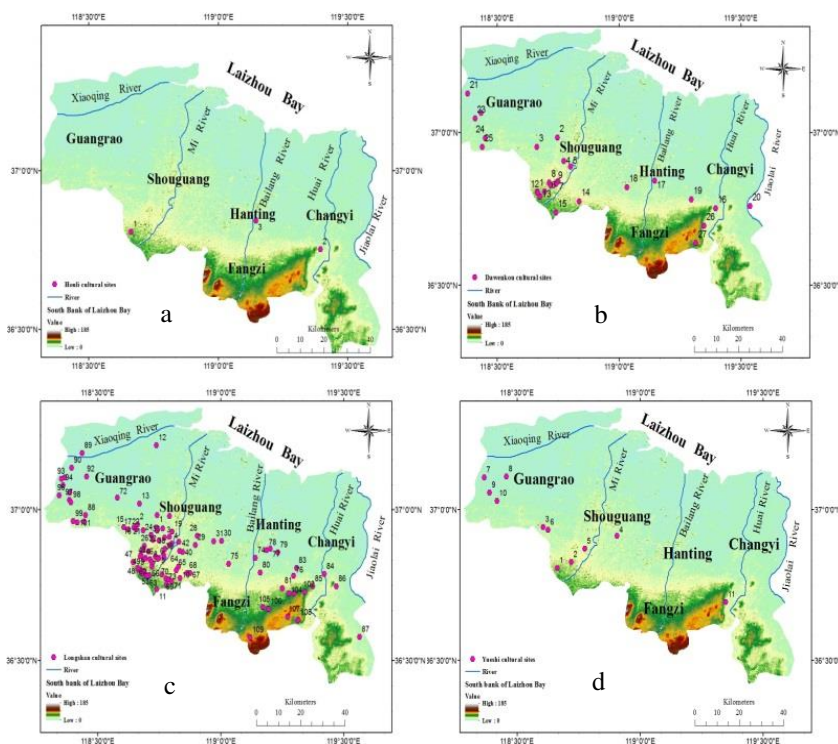


Figure 2. Distribution of archeological sites on the south coast of Laizhou Bay. (a) Houli cultural stage; (b) Dawenkou cultural stage; (c) Longshan cultural stage; (d) Yueshi cultural stage

The number of sites of the Dawenkou culture increases to 27, and the distribution in this stage moves towards high-lying plain with 6 sites above 29 m asl, which represents 22.2% of all the sites of the period (Fig. 2b). During the Longshan cultural stage, the

development of Neolithic Culture accelerated on the southern coast of Laizhou Bay. The number of sites dramatically increased to 101 and their distribution expanded markedly around river banks (Fig. 2c). The percentage of sites above 29 m asl increased by 5.5% from the previous period, but 72.3% of the sites remained in plains with elevations below 29 m asl (Table 3). However, the growing trend in the number of sites was interrupted by a striking decline, and the type of site and spatial agglomeration were greatly reduced in the late Longshan cultural period (~4.0 cal.ka BP). Subsequently, the Yueshi Culture began to develop, but the quantity, scope and distribution density were far less than the previous three cultural stages. There are 9 sites distributed in areas below 29 m asl, which account for 81.2% of all the sites of the Yueshi culture (Fig. 2d).

Table 3. The altitude distribution of the Neolithic cultural sites on the south coast of Laizhou Bay

Classification	Distribution with different altitude				Total
	< 10m asl	10-19m asl	20-29m asl	> 29m asl	
Houli	0	2 66.67%	0	1 33.33%	3
Dawenkou	2 7.41%	12 44.44%	7 25.93%	6 22.22%	27
Longshan	17 16.83%	32 31.68%	24 23.76%	28 27.72%	101
Yueshi	4 36.36%	3 27.27%	2 18.18%	2 18.18%	11

Slope and aspect

The archeological sites of the Houli Culture period are all distributed in an area with a gentle gradient of 2~4°, but there are only three archeological sites for that period and therefore it has no statistical significance. During the Dawenkou Culture period, the archeological sites were mainly distributed in the flat areas with slopes ranging from 0 to 4°, and the cumulative proportion is approximately 89% of the same period. In the gentle slope areas with slopes ranging from 0 to 6°, the distribution of archeological sites shows a trend of decreasing with increasing slope. However, in the 6~8° area, the number of archeological sites is relatively increased, and there are no archaeological sites in the areas above 8°. For the Longshan Culture stage, the archeological sites are also mainly distributed in flat areas with slopes ranging from 0 to 4°, and the cumulative proportion is approximately 86% of the same period. Settlement sites occur within the entire slope distribution, and the number decreases as the slope increases. The distribution trend of archeological sites during the Yueshi period is basically the same as that of the Dawenkou period. The archeological sites are mainly distributed in flat areas with slopes ranging from 0 to 4°, and the cumulative proportion is approximately 91% of the same period. In places with gentle slopes of 0~4°, the distribution of archeological sites shows a trend of decreasing with increasing slopes, but in 6-8° areas, there is a relative increase in the number of archeological sites, and there are no settlements in areas above 8° (Fig. 3).

Viewed from the aspect of archaeological sites, the ancients usually lived on relatively warm aspects such as south, southeast, and southwest aspects, and very few humans lived in the northern aspect. On the habitable aspect, there are fifteen Dawenkou cultural archaeological sites, with a proportion of 55.6%, and 63 archaeological sites from the Longshan Culture period, with a proportion of 62.3%, as

well as 6 archeological sites from the Yueshi Culture period, with a proportion of 54.5%. Among them, the archeological sites from the Longshan Culture period are distributed over various aspects, indicating that the population of the ancients grew on a large scale and their ability to adapt to the environment was enhanced.

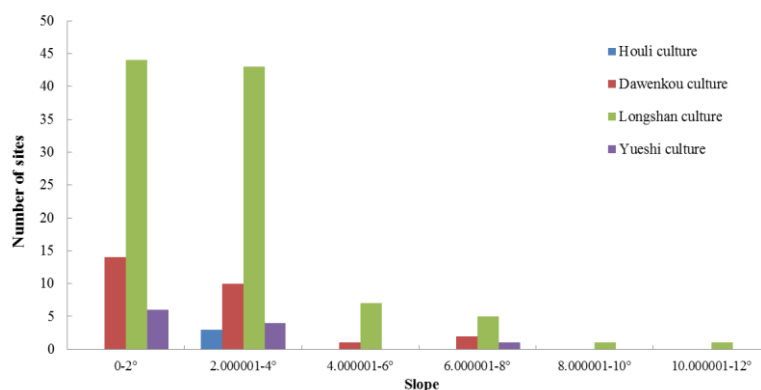


Figure 3. Slope distribution of the middle Holocene archaeological sites

The extent close to riverside

The extent close to riverside reflects the use of water by the ancients. In this investigation, the authors used ArcGIS to establish three river buffer zones of 0-1 km, 1-2 km and 2-3 km based on the present location of the rivers. By calculating the percentage of sites covered by different buffer zones, we can analyze the extent close to riverside of different cultural stages. Somewhat in parallel, the buffer distance 1 km and 3 km showed an overall descending trend for the coverage of the four periods. *Figure 5* lists the coverage by means of proximity analysis and buffer analysis in ArcToolbox. For instance, for the Houli Culture stage, the maximum 1 km coverage is approximately 33.3%, which triples that of the approximately 11.1% for the Dawenkou stage; however, it is merely approximately 9.9% for the Longshan stage and 0% for the Yueshi stage. Similarly, the 3 km coverage in the first three cultural stages changed from 66.7% to 37% and then 26.7%. Although it rose slightly during the Yueshi Culture stage (27.3%), the decline was still larger than that of the previous two cultural stages. From the Houli Culture stage to the Longshan Culture stage, the 1 km and 3 km site coverages were reduced in comparison with the previous period, and the reduction of the four stages were 22.2%, 29.7%, 1.2% and 10.3%, respectively (*Fig. 4*). These results demonstrate that the influence of rivers on the selection of archeological sites has gradually decreased, and the ability of the ancients to adapt to the environment had gradually increased. Due to the small watershed area and limited hydrodynamic forces, the rate of undercutting of rivers is very slow. Therefore, the influence of river undercut on the extent close to riversides is not taken into consideration in this investigation.

Discussion

Environmental changes on the south coast of Laizhou Bay

For the typical continuous natural sedimentary profiles in the same study area, the soil layers at different depths contain information about the evolution of the natural

environment background at different periods. Therefore, analyzing the sedimentary types of soil layers at different depths and combining them with the spatial and temporal distribution characteristics of the sites can help reveal the connection between human civilization development and environmental evolution. According to field surveys and comparative studies concerning strata of typical profiles (Fig. 5), marine deposit and fluvial facies sedimentation occurred on the south coast of Laizhou Bay in the Middle Holocene. The sedimentary lithology can be divided into four layers from top to bottom, and the lithological characteristics of this area are not significantly different (Table 4).

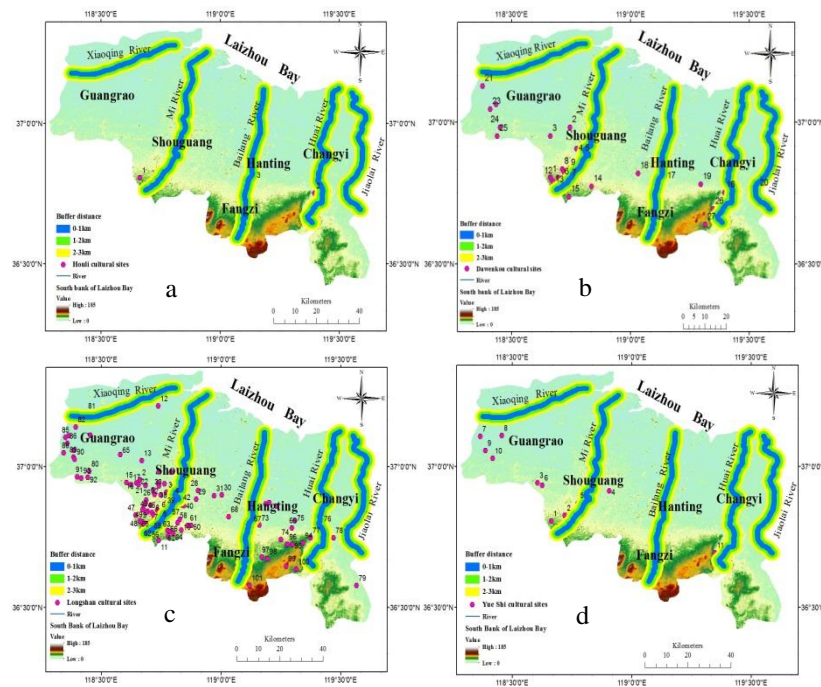


Figure 4. Buffer distance of archeological sites on the south coast of Laizhou Bay. (a) Houli cultural stage; (b) Dawenkou cultural stage; (c) Longshan cultural stage; (d) Yueshi cultural stage

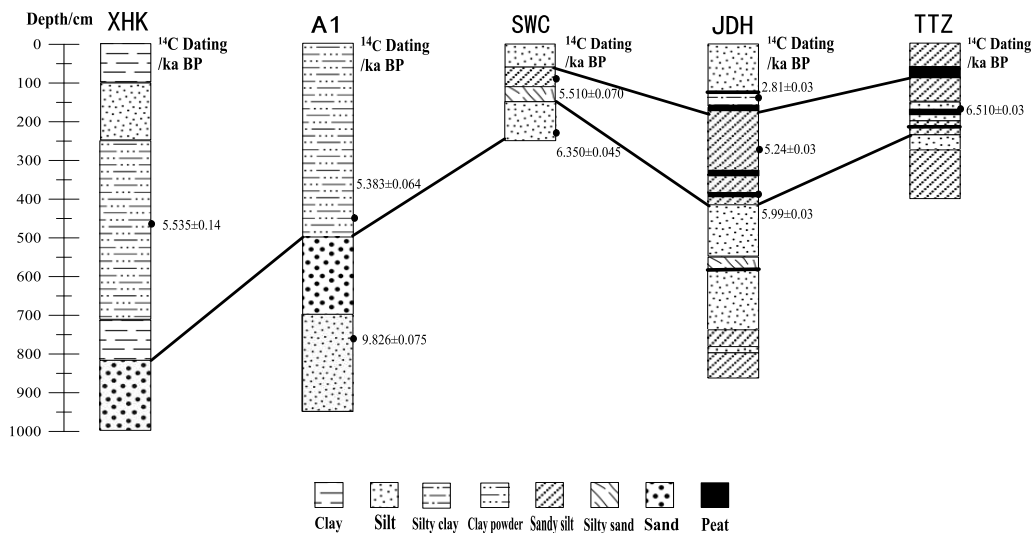


Figure 5. Stratigraphic correlation of typical profiles of the south coast of Laizhou Bay

Table 4. Vertical depositional sequence of sedimentary strata in Judian Lake

Lithology	Buried depth (m)	Sedimentary characteristics	Particle-size parameters				Age (cal.ka BP)
			Mz	KG	SK	QD ϕ	
I. Clay silt and silty clay	0~0.9	The cracks are relatively developed, a large number of plant roots and visible tiny wormholes are sandwiched, and a thin layer of silt is partially attached with mud distribution	5.0-8.3	0.76-1.5	-0.1-0.6	1.5-3.0	
II. Silty sand, sandy silt and silt	0.9~2.5	The color of the upper part is yellowish brown – brown-gray, which occasionally encloses sporadic shells (shell debris), wormholes and plant debris, and the water content is saturated; the lower part is gray-grayish green-grayish black, containing a mud silty clay layer with a high moisture content and a saturated shape	5.1-6.6	0.78-1.54	-0.1-0.6	0.5-1.0	2.81±0.03
III. Clay silt and silty clay	2.5~4.0	The color distribution is horizontally layered, the color changes to gray-grayish green-grayish black, and is rich in organic matter, decaying plant roots, mud and shell debris. The layers are discontinuously distributed with clay silt and silty clay, with brown peat and black clay locally	5.1-6.7	0.74-1.07	0.1-0.6	1.5-2.5	5.24±0.03
IV. Silty sand, sandy silt and silty	4.0~8.6	The color change is yellowish brown-gray–dark gray, and the cracks are relatively developed. The layer generally contains white shells or shell debris, and is concentrated in the lower part	5.4-7.0	0.74-1.16	-0.1-0.6	1.0-1.5	5.99±0.03

By comparison with the TTZ stratum, combined with the results of the XHK, SWC and A1 holes, the Holocene sedimentary facies in the Judian Lake area can be categorized as follows.

(1) The I and II layers in the sedimentary sequence are the Holocene upper continental layers, and they are primarily composed of fluvial facies and lacustrine facies deposits. Layer I and the upper part of layer II are mainly fluvial facies deposits, and the lower part of layer II is mainly lacustrine facies deposits. From the perspective of granularity analysis, the quartile deviation (QD ϕ) value is between 0.5 and 1.0, indicating that the sorting is good to very good; the average grain diameter (Mz) is 5.0~8.3 in a clay – very fine sand – fine silt, and the skewness (SK1), which is between -0.1 and 0.6, is a very positive deviation, and the kurtosis (KG) is between 1.11 and 1.56, which is a narrow kurtosis. The peat layer was subjected to AMS¹⁴C dating, and its age is 2.81 ± 0.03 cal. ka BP. Combined with the lithology analysis of *Table 4*, the sedimentary phase of the I and II layers can be identified as fluvial facies and lacustrine facies deposits according to the lithologic characteristics of sediments and good sorting properties.

(2) The III layer is the marine layer of the Holocene, which is primarily comprised of the lagoon-shallow marine facies. By analyzing the sedimentary strata of JDH, it can be found that there are thick gray, grayish green or grayish black silty clay deposits with a depth of 2.6 m-3.3 m in layer III. Its texture is homogeneous, with horizontal bedding

and light-colored reticulation. It contains more mollusk shells and shell clasts, and has the same sedimentary characteristics as Holocene marine facies. The AMS¹⁴C age of the peat-containing silty clay in the III layer was determined to be 5.24 ± 0.03 cal.ka BP. Meanwhile, the grain size analysis shows that the MZ value ranges from 5.1 to 6.7, belonging to fine silt to ultrafine silt, and the peak state is wide to very wide, the sorting degree is medium-poor, the deviation is positive to extreme positive (*Table 4*). The sediments have extreme kurtosis values, indicating that the sedimentary environment is shallow-lagoon sedimentary environment due to the hydrodynamic conditions of shallow sea and lagoon environment, and the sorting efficiency is poor. The sediments in this area were in a beach environment with good hydrodynamic conditions in the early stage. Combined with the characteristics of the lithologic characteristics and grain size parameters, it can be concluded that the III layer are lagoon-shallow marine facies deposits.

(3) The IV layer is beach shore facies sedimentary environment. The sediments in this layer have normal skewness and peak state values, and the shape of the frequency curve has an almost single peak symmetry (*Table 4*). The grayish-black silt-bearing silty clay was subjected to AMS¹⁴C dating, and its age is 5.99 ± 0.03 cal.ka BP. Compared with the sediments in the third layer, the sorting degree, which is good to medium, becomes better. Because of the strong wave action and reciprocating motion in the beach-shore environment, the sediments are transported and sorted many times, and the fine clay particles are transported far from the shore, resulting in the better sorting degree. The comprehensive analysis of lithological characteristics and grain size characteristics indicates that the beach was in a beach shore sedimentary environment. According to the above-mentioned analysis, the Judian Lake depositional area was a beach-shore facies depositional environment at 5.99 ± 0.03 cal.ka BP, a lagoon-shallow facies depositional environment at 5.24 ± 0.03 cal.ka BP, as well as a continental fluvial facies and lacustrine facies depositional environment at 2.81 ± 0.03 cal.ka BP.

It is generally known that sporopollen are also among the most effective indicators of climate change. Han identified and analyzed the spores and pollens from the profile in Judian Lake sediment area. She found that herbaceous pollens accounted for the absolute predominance, the content was more than 85%. Woody pollens were less than 15%, and there were very few fern spores, the content of which was below 1% (Han and Zhang, 2005). From the Middle Holocene to the Late Holocene, the pollen content of *Quercus* in woody plants was high, and the pollen content of aquatic plants and hydrophytic plants varies from high to low, indicating that the climate shifted from humid to drought at that time. Based on the above-mentioned classification of sedimentary facies, the regularity on the climatic and environmental changes on the south coast of Laizhou Bay from the Middle Holocene to Late Holocene can be summarized as warm and partial wetting environment (early period of the Middle Holocene) - warm and humid environment (late period of the Middle Holocene) - warm and dry environment (late period of the Holocene).

There were also several climate fluctuation events along with the climate change on the southern coast of Laizhou Bay during the Middle Holocene, such as the 7.0 ka BP, 5.5 ka BP, 4.0 ka BP cooling events. The $\delta^{18}\text{O}$ record of Dongge Cave demonstrated the continual increase in monsoon precipitation between 7.2 and 6.0 ka (Dykoski et al., 2005; *Fig. 6a*). Pollen analysis of Judian lake confirmed decreasing temperatures by the relatively increasing concentrations of *Pinus* pollen. *Figure 6d* shows significant cooling at approximately 7.0 ka, which coincided with the wide and shallow cold valley

recorded in the $\delta^{18}\text{O}$ Dunde ice core curve (Yao and Shi, 1992; Fig. 6c). At approximately 5.0 ka, the average $\delta^{18}\text{O}$ values of stalagmites were relatively high despite some fluctuations, indicating a period of decreasing monsoon precipitation during the Middle Holocene (Andersen et al., 2004; Fig. 6a, b). The sporopollen data for the southern coast of Laizhou Bay showed that the forest coverage decreased sharply, while the grassland area expanded, and the forest vegetation was dominated by pine, revealing the climate experienced cooling fluctuation. After 5.0 ka, $\delta^{18}\text{O}$ shifted towards greater values, indicating a decreasing trend in Asian monsoon intensity in the Mid-Late Holocene. This trend became even more prominent at approximately 4.0 ka (Fig. 6a, b). The sporopollen records of this cooling event in the northern Shandong plain showed that the content of algae and ferns increased sharply in the sporopollen pattern, indicating the enlargement of the lake and marsh area. Previous studies have suggested that a flood event occurred in the middle and lower reaches of the Yellow River at approximately 4.0 ka BP, which may caused the south coast of Laizhou Bay once again covered by lakes and marshes, and the aquatic and hydrophytic plants flourished.

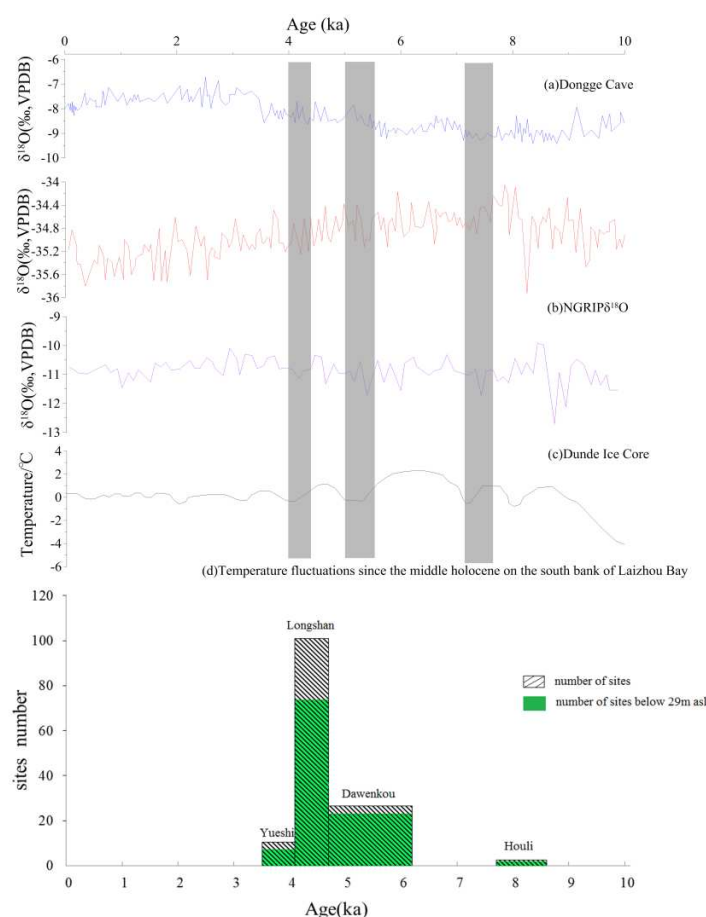


Figure 6. Comparisons between climate records and human settlements in the south coast of Laizhou Bay. (a) The $\delta^{18}\text{O}$ values of stalagmite from Dongge Cave (Dykoski et al., 2005); (b) $\delta^{18}\text{O}$ values from the NGRIP Ice Core (Andersen et al., 2004); (c) $\delta^{18}\text{O}$ values from the Dunde Ice Core (Yao and Shi, 1992); (d) The temperature fluctuation curve since the Middle Holocene; (e) Total number of sites and number of sites below 29 m asl on the south coast of Laizhou Bay (Table 2). The gray shallows show periods of climatic cooling the 7.0 ka BP, 5.5 ka BP, 4.0 ka BP event

Impacts of environmental changes on the development of cultures

The existence and development of prehistoric culture depend on a certain natural environment. The remains of animals and plants found at the settlement sites reflect the influence of the climate environment on the development of prehistoric human culture. Therefore, the representative sites of different cultural stages are selected to summarize the climate and environmental information. *Table 5* shows the corresponding information of the settlement sites on the south coast of Laizhou Bay and paleoenvironment.

Table 5. Correspondence between archeological sites and paleoenvironment on the south coast of Laizhou Bay

Cultural period	Sites	Environmental information	Sources
Houli Culture	Qianbuxia sites	1 The growth of a large number of suitable plants near the ruins of a warm and humid environment; 2 <i>Lamprotula</i> , blue clams and other animal remains are reflected near the Qianbuxia ruins of the forest meadow environment; 3 Suitable climatic conditions, mild and humid; 4 Fishing and hunting activities of ancestors in the riverfront near the sea	(Han and Wu, 1982; Wang and Ning, 2003)
Dawenkou Culture	Qianbuxia sites	1 Increase in dry and cold climate plant specimens and reduction in the wet and warm climate plant specimens; 2 There are numerous aquatic plants and reeds, which indicates that there were abundant water resources	(Kong, 2000)
	Wucun sites	According to the survey, the average annual temperature was 2~4 degrees higher than at present, which was suitable for farmers engaged in farming and fishing	(Jin, 2000)
	Fujia sites	1 The surface of the site is covered by a yellow soil, and the cultural layer is red-brown or gray-brown; 2 The ruins are distributed around the 30-140 m wide puddles of water, suggesting an early drought climate and subsequent humid climate, during which numerous water puddles formed over a long period, residents living in highlands; 3 Millet belonging to the millet agriculture appeared in the ruins	(Kong, 1989)
Longshan Culture	Lujiaokou sites	1 Located on the South Coast of the Laizhou Bay lowland alluvial plain; 2 Fishing activities in the economic life held a certain degree of importance but only in the scope of the river and estuary mouth activities and not in deep ocean operations	(Li et al., 2002; Han, 1985)
	Guojingzi sites	1 The Guojingzi site is located in a shell coast, the shell ¹⁴ C dating is 5.0 cal.ka.BP.; 2 The ruins contain large amounts of plant ash, burned soil and white lumps; 3 There is a small number of hair clams, the remains of which reflect a beach coastline sedimentary environment	(Li et al., 1996; He, 2004)

During 8.5~5.6 ka BP, enjoying a warm and humid climate, superior hydrothermal conditions, high utilization of natural resources and fine living environment, the Neolithic Culture gradually developed. In the Houli Culture stage, hunting and gathering remained the important economic means and humans began to settle down; at the same time, simple millet agriculture emerged. In the early and middle period of Dawenkou Culture, the climate was still warm and humid. With the development of society, the population has increased substantially. The area of settlements expanded, and the proportion of agricultural economy increased. During that period, the number and types of production tools increased. Simultaneously, kiln holes and ceramic wares that were used to store grain have been invented, reflecting the rapid development of agriculture. However, the sites of this period are located on the relatively high elevations of the alluvial platform and alluvial plain. Because of the not fully discharged sea water and warm-humid climate, the study area of the western low-lying alluvial plain and coastal plain often experienced severe flood disasters. Besides, with the harsh environment, it was unsuitable for human settlement.

During 5.6~4.0 ka BP, a series of short cooling events occurred, and the degree of wetness decreased slightly, but the overall climate remained relatively mild, which created the conditions for the development of agriculture and human settlement. Through the evidence of harvesting tools and small-scale rice production found in archaeology, it can be seen that the production tools have been greatly improved. Due to reduced precipitation, the climate was characteristically dry, sea water had withdrawn from the area, the natural environment of the western region of the study area had improved, and human activity appeared. During the late Dawenkou Culture period, the settlement sites became gradually distributed in low-lying areas, in lesser proportion. Regarding the Longshan Culture period, the number and density of archeological sites in the western region increased significantly, and agricultural production also showed great progress. Obviously, the ancient people exhibited better environment adaptability.

At approximately 4.0 ka BP, the climate abruptly changed and the temperature dropped significantly. With the decrease of precipitation, the climate was dry and the environment was unsuitable for human habitation. Accordingly, the Longshan culture suddenly declined. The Yueshi culture appeared later, but the number of archeological sites decreased dramatically, and site areas declined, while the density was also greatly reduced. After 4.0 ka BP, the climate entered the climate fluctuation period, which was accompanied by climate instability, frequent disasters, and poor environmental conditions, resulting in the decline of culture.

Site distribution and seawater intrusion

On the south coast of the Laizhou Bay area, the Holocene sea transgression started from 8.0~7.0 ka BP (He, 2004), and the climate in that period had entered the warm period. With the increase in temperature, the rising water continues to promote the submergence of land, forming a large area of wetlands and waters as well as limiting human activities. There are fewer Houli Cultural archeological sites in this area, which are distributed at elevations above 10 m. Compared with other cultural regions in Shandong Province, settlement sites of the Beixin culture are lacking. Because of the sea transgression, some archeological sites may be submerged.

According to the analysis of *Figure 6e* and *Table 3*, an elevation of 29 m is a special spatial boundary, and there are almost no settlements in areas with elevations above 29 m. The formation of this boundary line is closely related to the transgression during

the Middle Holocene, especially the invasion of the Huanghua transgression. During 8.5~2.5 ka BP, the Huanghua transgression occurred in the plain on the south coast of the Laizhou Bay, and its boundary line extends from Niutou township in the western part of the area to Houzhen-Nancun-Guti-Xiadian in the east and to the front line of Pingduxin river town (Han et al., 1999). To the north of the line, there is a marine plain, which is mainly comprised of silt, muddy silt, muddy marine and coastal sediments, and the distribution of archeological sites almost extended south of the marine plain (south of the Huanghua transgression line). Subsequently, the sea water gradually retreated, and the sea level decreased, while the activities of the ancients gradually expanded to the lower altitudes.

To approximately 6.0 ka BP, because of the Huanghua transgression, the sea level reached its peak (much higher approximately 1-2 m than the modern sea level) and the invasion of sea water forced the ancients to turn to high altitude areas so as to adapt to the changes in the environment (Zhang et al., 2003). The Dawenkou culture is a good indicator of the transgression. The archeological sites are mainly distributed at 10-39 m elevations on the terrace and the alluvial plain to resist disasters from floods. For the low elevation area, there were more stagnant water phenomena, which affected the normal life of the ancients, and were nonconducive to the development of ancient production. Therefore, for the Houli Culture until the middle of the Dawenkou Culture, no archeological sites exist in the 0-9 m low altitude area. During the times of the late Dawenkou culture, seawater began to recede and there was a brief period of cooling, but overall showed warm and humid characteristics suitable for human habitation, and archeological sites at low elevations of 0-9 m began to emerge gradually, while the proportion of which, 7.4%, is relatively small.

After 6.0 ka BP, seawater gradually receded northwards, and the sea level decreased. After the sea retreated, the ancient people's activity range gradually expanded to low altitudes. At the Longshan Culture stage, sea water had basically withdrawn from the area. The climate became dry, and the sea level declining, archeological sites in low-lying areas without ancient settlements in early phases began to gradually appear. It can be seen from the elevation distribution map of Longshan culture site that in the low elevation area of 0-9 m, the number of archeological sites increased obviously, and the proportion increased from 7.4% in the previous period to 16.8%. At the same time, the district found the salt manufacturing site in the Longshan period (Guo Jingzi site), which is located at a low altitude (3 m) near Shouguang city, as a result of the recession in seawater, and the salt-making raw materials used to make salt are very rich, which is conducive to the development of a salt industry according to local conditions (Yan, 2015).

Site distribution with respect to ancient lakes and the ancient channel

The southern coast of Laizhou Bay has historically formed lakes due to seawater intrusion and river diversion, for example, Heizhong Lake and Judian Lake (Fig. 7). On the alluvial plain, which is far from the Xiaoqing River and at a lower elevation, the Dawenkou Culture period archeological sites emerged with a new distribution type, and these archeological sites are located on the southwestern shore of Lake Judian. Up to the Longshan Culture period, the number of settlements in the region increased significantly, and were mainly concentrated on the west coast of the lake area, which showed a circular feature. In 1973, the Chinese Academy of Sciences Institute of Archeology found Lujiakou sites near Biehua lake coast of Lujiakou village, which

belongs to the Dawenkou Culture and Longshan Culture coast. The 4.0 ka BP cooling event reduced the number of Longshan Culture archeological sites, and afterwards the development of Yueshi culture in the lake area also has a settlement site distribution with a proportion of 36.3%. The distribution of the location is unchanged. From the beginning of Dawenkou Culture, the proportion of agricultural economy gradually increased, and the ancient lake provided water and food, which could also be induced by irrigation and fisheries development, improving the quality of life and promoting the progress of human society.

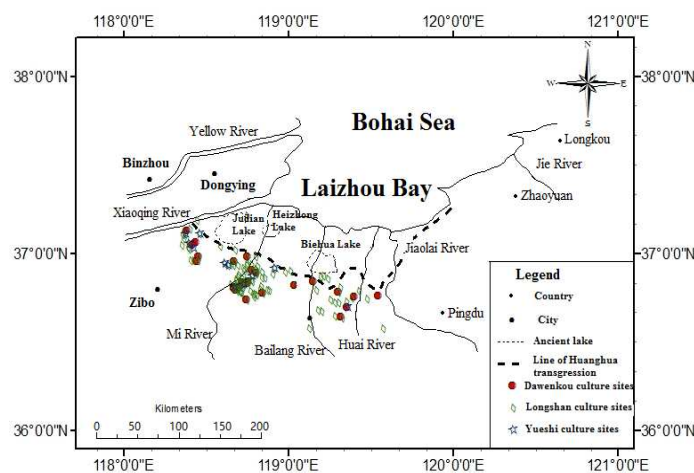


Figure 7. The relationship between settlement sites and Huanghua transgression

There are 25 ancient rivers on the south coast of Laizhou Bay, six of which were formed in the Middle Holocene period, and all of the rivers are located to the west of the river. One of the main river channels has a ^{14}C date of 7.080 ± 96 cal.ka BP, indicating that the ancient river has existed for the past 7 thousand years. Agriculture had begun to appear in the HouLi Culture period, but gathering and hunting continued to constitute a major economic mode. The western part of the Bianxianwangxi site was close to the third ancient river, and with its adequate water resources and convenient fishing and hunting conditions, it became a suitable place to live. The Huanghua transgression induced sea level rise and river diversion, and the river then moved eastward. In that period, the archeological sites were mainly located at the west coast of Mi river. Compared with the Wangxi line sites of the Houli culture period, the position of the site moved relatively eastward. Towards the end of the Mid-Holocene, the sea water gradually retreated from the north, and ancient rivers moved westward. Therefore, the archeological sites of the Longshan Culture period are mainly concentrated in the Mi river, reflecting the characteristics of the ancient people living near the river.

Conclusion

Archeological studies have identified 141 Neolithic cultural sites on the south coast of Laizhou Bay, with a sequence of Houli, Dawenkou, Longshan and Yueshi. Using GIS combined with archeological and geographic data, this paper has presented the spatial-temporal distribution of the Neolithic sites in the study area. Temporally, the total number and frequency of occurrence of archeological sites throughout the

Neolithic Age show an early descending and later ascending curve. From the elevation point of view, the four periods of archeological sites are almost all located in the alluvial plain area below 29 m. Moreover, the formation and development of seawater intrusion, the ancient lake and the ancient river channel all influenced the distribution of the settlement sites; at the same time, human beings have gradually adapted to the environment as it changed, and they utilized resources to develop and progressed according to local conditions. Comparative analysis revealed that the close correlation of the Holocene climate change and environmental evolution with the Neolithic cultural succession indicated that ameliorated conditions generally promoted primitive cultural development, while degeneration coincided with cultural transition or interruption.

Acknowledgements. We would like to express our sincere appreciation to the anonymous reviewers for their suggestions. The work was supported by the special program for the National Natural Science Foundation of China (41471160).

REFERENCES

- [1] An, C. B., Dong, W., Li, H., Zhang, P. Y., Zhao, Y. T., Zhao, X. Y., Yu, S. Y. (2015): Variability of the stable carbon isotope ratio in modern and archaeological millets: evidence from northern China. – *Journal of Archaeological Science* 53: 316-322.
- [2] Andersen, K. K., Azuma, N., Barnola, J. M., Bigler, M., Biscaye, P. (2004): High-resolution record of Northern Hemisphere climate extending into the last interglacial period. – *Nature* 431: 147-151.
- [3] Chen, G. Q. (2013): Study on the Mechanism and Early Warning Evaluation of Seawater Intrusion in Laizhou Bay Area. – East China Normal University, Shanghai.
- [4] Contreras, D., Guiot, J., Suarez, R., Kirman, A. (2018): Reaching the human scale: A spatial and temporal downscaling approach to the archaeological implications of paleoclimate data. – *Journal of Archaeological Science* 93: 54-67.
- [5] Dai, L., Balasse, M., Yuan, J., Zhao, C., Hu, Y., Vigne, J. D. (2016): Cattle and sheep raising and millet growing in the Longshan age in central China: stable isotope investigation at the Xinzhai site. – *Quaternary International* 426: 145-157.
- [6] Demján, D., Dreslerová, D. (2016): Modelling distribution of archaeological settlement evidence based on heterogeneous spatial and temporal data. – *Journal of Archaeological Science* 69: 100-109.
- [7] Dong, G., Jia, X., Elston, R., Chen, F., Li, S., Wang, L. (2013): Spatial and temporal variety of prehistoric human settlement and its influencing factors in the upper Yellow River valley, Qinghai province, China. – *Journal of Archaeological Science* 40(5): 2538-2546.
- [8] Dykoski, C. A., Edwards, R. L., Cheng, H., Yuan, D., Cai, Y., Zhang, M., et al. (2005): A high-resolution, absolute-dated Holocene and deglacial Asian monsoon record from Dongge cave, China. – *Earth & Planetary Science Letters* 233(1): 71-86.
- [9] Goude, G., Fontugne, M. (2016): Carbon and nitrogen isotopic variability in bone collagen during the Neolithic period: influence of environmental factors and diet. – *Journal of Archaeological Science* 70: 117-131.
- [10] Guo, Y., Mo, D., Mao, L., Wang, S., Li, S. C. (2013): The relationship between settlements distribution and environmental changes from the Neolithic to Shang-Zhou periods in north Shandong province. – *Acta Geographica Sinica* 68(4): 559-570.
- [11] Guo, Y., Mo, D., Mao, L., Jin, Y., Guo, W., Mudie, P. J. (2014): Settlement distribution and its relationship with environmental changes from the Paleolithic to Shang-Zhou period in Liyang plain, China. – *Quaternary International* 321(2): 29-36.

- [12] Han, M., Zhang, L. N. (2005): Sedimentary analysis and environmental evolution of Judian lake in the south coastal plain of Laizhou Bay. – *Scientia Geographica Sinica* 25(6): 678-682.
- [13] Han, M., Li, D. G., Zhao, M. H. (1999): Study on the paleo-river course on the southern coast of Laizhou Bay. – *Scientia Geographica Sinica* 19(5): 451-456.
- [14] Han, M., Zhang, L. N. (2005): Sedimentary analysis and environmental evolution of Judian lake in the south coastal plain of Laizhou Bay. – *Scientia Geographica Sinica* 25(6): 678-682.
- [15] Han, R. (1985): Lujiakou Neolithic sites. – *Journal of Archaeological* 3: 313-351.
- [16] Han, Y. S., Wu, H. F. (1982): The origin of underground brines in the coastal plain of Laizhou Bay. – *Geological Review* 28(2): 126-130.
- [17] He, D. L. (2004): Shandong Neolithic environmental archaeology research. – *Oriental Museum* 2: 26-40.
- [18] Jin, G. Y. (2000): The Qianbuxia Site Plant Silicate Body Analysis Report. – Science Press, Beijing.
- [19] Karakasidou, A. (2005): The archaeology of global change: the impact of humans on their environment. – *Choice: Current Reviews for Academic Libraries* 42(5): 894.
- [20] Kong, Q. S. (1989): GuangRao Five Village in Dawenkou Cultural Sites Animal Remains. – Shandong University Press, Jinan.
- [21] Kong, Q. S. (2000): The Qianbuxia Site Excavation Report. – Science Press, Beijing.
- [22] Kuper, R., Kröpelin, S. (2006): Climate-controlled Holocene occupation in the Sahara: motor of Africa's evolution. – *Science* 313(5788): 803-807.
- [23] Li, D. G., Guo, Y. S., Jiang, A. X. (1996): Preliminary study of the Holocene sea transgression and paleo-geo-environmental differences on the southern/northern coast of Shandong Peninsula. – *Acta Oceanologica Sinica* 4(18): 63-71.
- [24] Li, R., Carter, J. A., Xie, S., Zou, S., Gu, Y., Zhu, J. (2010): Phytoliths and microcharcoal at Jinluojia archeological site in middle reaches of Yangtze River indicative of paleoclimate and human activity during the last 3000 years. – *Journal of Archaeological Science* 37(1): 124-132.
- [25] Li, Z. G., Wang, J. G., Liu, G. Q. (2002): The excavation of the Fujia site of Guangrao country of Shandong. – *Archaeological* 9: 36-44.
- [26] Liu, E. F., Zhang, Z. L., Shen, J. (2004): Spore-pollen records of environmental change on the south coast plain of Laizhou bay since the late Pleistocene. – *Journal of Palaeogeography* 6(1): 78-84.
- [27] Lyndsay, M. D., Steven, G. D., Ted, G. (2018): Deposition and pedogenesis of periglacial sediments and buried soils at the Serpentine Hot Springs archaeological site, Seward Peninsula, AK. – *Catena* 170: 204-233.
- [28] Mayke, W., Pavel, T., Dominic, H., Andreas, F., Richard, E., Chen, X. C., Christian, L. (2013): Mapping of the spatial and temporal distribution of archaeological sites of northern China during the Neolithic and Bronze Age. – *Quaternary International* 291: 344-357.
- [29] Spencer, C., Bevan, A. (2018): Settlement location models, archaeological survey data and social change in Bronze Age Crete. – *Journal of Anthropological Archaeology* 52: 71-86.
- [30] Stanley, D. J., Galili, E. (1996): Sediment dispersal along northern Israel coast during the early Holocene: geological and archaeological evidence. – *Marine Geology* 130(1): 11-17.
- [31] Tan, Z., Han, Y., Cao, J., Huang, C. C., An, Z. (2015): Holocene wildfire history and human activity from high-resolution charcoal and elemental black carbon records in the Guanzhong basin of the loess plateau, China. – *Quaternary Science Reviews* 109: 76-87.
- [32] Wang, S. G., Ning, Y. T. (2003): The prospecting report in Houli culture settlements in Shandong Zhangqiu XiaoJing mountain. – *Huaxia Archaeology* 3: 3-11.

- [33] Wang, X., Mo, D., Li, C., Yu, S. Y., Xue, B., Liu, B. (2017): Environmental changes and human activities at a fortified site of the Liangzhu culture in Eastern China: evidence from pollen and charcoal records. – *Quaternary International*. DOI: 10.1016/j.quaint.2017.05.001.
- [34] Yan, S. D. (2015): Salt-making remains of the Longshan age found at the south coast of Laizhou Bay. – *Archaeology* 2015(12): 106-114.
- [35] Yang, S., Li, J., Mao, L., Liu, K. B., Gao, M., Ye, S. (2016): Assessing pollen distribution patterns and provenance based on palynological investigation on surface sediments from Laizhou Bay, China: an aid to palaeoecological interpretation. – *Palaeogeography Palaeoclimatology Palaeoecology* 457: 209-220.
- [36] Yao, T. D., Shi, Y. F. (1992): *Climate and Environment in Megathermal Period of Holocene in China*. – China Ocean Press, Beijing.
- [37] Zhang, W. Y., Han, M., Li, Y. H. (2003): Study on the Cause of Death of Ancient Lakes on the South coast Plain of Laizhou Bay, Shandong Province. – *Paleogeographic Bulletin* 5(2): 224-231.
- [38] Zheng, H. B., Zhou, Y. S., Yang, Q., Hu, Z. J., Ling, G. J., Zhang, J. Z. (2018): Spatial and temporal distribution of Neolithic sites in coastal China: sea level changes, geomorphic evolution and human adaption. – *Science China Earth Sciences* 61(2): 1-11.

RECONSTRUCTION OF TEMPERATURE FOR THE PAST 400 YEARS IN THE SOUTHERN MARGIN OF THE TAKLIMAKAN DESERT BASED ON CARBON ISOTOPE FRACTIONATION OF TAMARIX LEAVES

ZHANG, Z.¹ – ULLAH, I.¹ – WANG, Z.¹ – MA, P.¹ – ZHAO, Y.^{1*} – XIA, X.² – LI, Y.³

¹Hebei Key Laboratory of Environmental Change and Ecological Construction, College of Resources and Environmental Sciences, Hebei Normal University, Shijiazhuang 050024, China

²Xinjiang Institute of Ecology and Geography, Chinese Academy of Sciences
Urumqi 830011, China

³Department of Geography, University of Tennessee, Knoxville, TN 37996, USA

*Corresponding author
e-mail: ecoenvir@163.com

(Received 15th Jun 2018; accepted 2nd Aug 2018)

Abstract. Carbon isotope fractionation is sensitive to the environment factors associated with plant growth; thus, it can be used as a proxy to reconstruct past climate and environmental conditions. We investigated the relationship between carbon isotope signatures ($\delta^{13}\text{C}$) and its fractionation ($\Delta\delta^{13}\text{C}$) of *Tamarix* leaves and a set of climate and environmental factors in the Southern Margin of the Taklimakan Desert (SMTD). A principal component analysis was used to condense these factors as the temperature-, wind-, precipitation-, and humidity-related index, explaining 51.0%, 18.0%, 5.1%, and 4.7% of the total variance, respectively. Combined with the correlation results, temperature is identified as the key growth-limiting factor for *Tamarix* in the SMTD. Specifically, $\delta^{13}\text{C}$ has a statistically significant correlation with the lowest temperature in June (LT_{Jun}) ($r = 0.717$, $p = 0.000$), and $\Delta\delta^{13}\text{C}$ has a statistically significant correlation with the annual mean of the highest temperature (AMHT) ($r = 0.700$, $p = 0.000$). Based on these high correlations, we reconstructed the LT_{Jun} and AMHT records in the past 400 years using $\delta^{13}\text{C}$ and $\Delta\delta^{13}\text{C}$ of *Tamarix* leaves deposited in the *Tamarix* cone. These records revealed a long-term fluctuation in temperature that can be divided into four sub-periods, including the history cold period (1600-1685), history warm period (1686 - 1913), modern cold period (1914-1993), and modern warm period (1994-2010). These records provide useful insight into the paleoclimate and environmental change in this arid region.

Keywords: climate change, environment, key growth-limiting factor

Introduction

Climate and environmental change affect plant carbon isotope signatures ($\delta^{13}\text{C}$) (Seibt et al., 2008), and the carbon isotope fractionation ($\Delta\delta^{13}\text{C}$) is mainly related to the key limiting factors for plant growth (Xu et al., 2015). Temperature and precipitation are the two major growth-limiting factors for the changes in plant carbon isotope signature and fractionation, by affecting its stomata conductance and assimilation rate and altering C:N allocation to carboxylation and leaf structure (Seibt et al., 2008; Liu et al., 2014b). Consequently, $\delta^{13}\text{C}$ and $\Delta\delta^{13}\text{C}$ can be treated as measures of temperature and precipitation (Saurer et al., 1995; Loader et al., 2007; Dodd et al., 2008; Diefendorf et al., 2010), and used as proxies to reconstruct past climate conditions (Dawson and Siegwolf, 2007; Werner et al., 2012). Studies have indicated that precipitation has a negative influence on plant $\delta^{13}\text{C}$ and a positive influence on $\Delta\delta^{13}\text{C}$ (Farquhar et al., 1982; Wang et al., 2003, 2008; Kohn, 2010; Ren et al., 2011). However, the influence of temperature on plant $\delta^{13}\text{C}$

is still unclear (Körner et al., 1988, 1991; Morecroft and Woodward, 1996; Wang et al., 2008, 2013; Gebrekirstos et al., 2009; Diefendorf et al., 2010; Kohn, 2010). This uncertainty is caused by difference of the key growth-limiting factors that affect on plant growth in different regions. The key growth-limiting factors of *Tamarix* growth have been statistically identified in the Southern Margin of the Taklimakan Desert (SMTD), and then the paleoclimate condition is reconstructed based on the relationship between the key growth-limiting factors and meteorological factors.

The Taklimakan Desert is the second largest desert in the world surrounded by the Tianshan Mountain in the north, the Aljin Mountain in the southeast, the Kunlun Mountain in the south, and the Pamir Plateau in the west. It is one of the most arid regions in the world because the high mountains and plateau block the water moist from the Atlantic and Indian oceans. The SMTD is one of the most fragile ecological environment areas in China. *Tamarix* is the major vegetation outside of the oasis that can survive the extremely arid climate in this area. *Tamarix* is mainly distributed on riverbanks, abandoned river channels, and the interlaced zone between desert and oasis. The interaction between wind sand and *Tamarix* forms the *Tamarix* cone, a unique biogeomorphic landform, composing of alternate layers of sand and *Tamarix* twigs and leaves (Xia et al., 2004). Detailed climate records have been derived in this desert area using stable carbon isotope ($\delta^{13}\text{C}$) and its fractionation ($\Delta\delta^{13}\text{C}$) of *Tamarix* leaves from different layers of the *Tamarix* cones (Zhao et al., 2011a, b, 2015a, b, 2016; Zhao, 2012; Sun, 2013; Sun et al., 2013; Guo et al., 2016; Zhang et al., 2017).

In the work reported here, the relationship between carbon isotope ($\delta^{13}\text{C}$) and its fractionation ($\Delta\delta^{13}\text{C}$) signatures and various observed climate factors (1960-2010) were investigated to identify the key growth-limiting factor of *Tamarix* growth. Base on the relationship, the lowest temperature in June (LT_{Jun}) and the annual mean of highest temperature (AMHT) of the past 400 years were reconstructed in the SMTD. This study provides useful insight into the relationship between plant $\delta^{13}\text{C}$, $\Delta\delta^{13}\text{C}$ signatures and climate variables and use $\delta^{13}\text{C}$ and $\Delta\delta^{13}\text{C}$ as proxies to reconstruct paleo-climate and environmental change in arid regions.

Study area

This study was conducted in Andier Meadow (83.82°E, 37.72°N), far from the Minfeng oasis, which belongs to the Hotian Prefecture in the SMTD of Xinjiang Uygur Autonomous Region, China (Fig. 1). The sampling site is located on the edge of the alluvial fan formed by the Andier River, representing a transition zone between the Taklimakan Desert and Kunlun Mountains. This area belongs to the temperate continental and arid desert climate zone. According to the observed data from the Minfeng meteorological station, the mean of annual temperatures is 11.19 °C and relatively constant over the years. The average annual precipitation is 29.4 mm with a relatively large range between 4.0 and 136.9 mm. About 85.4% of the precipitation falls from May to September. The annual average evaporation can reach to 2756 mm.

Data and methods

To minimize the influence of human activity, we investigated a *Tamarix* cone in Andier meadow, more than 100 km away from the Minfeng oasis. We collected the samples layer by layer from top to bottom from June 18th to 20th in 2011. The samples

were collected based on the average thickness when the sedimentary veins are not clear. In total, we collected 106 samples. The freshest leaves of the top layer were dated in 2010.

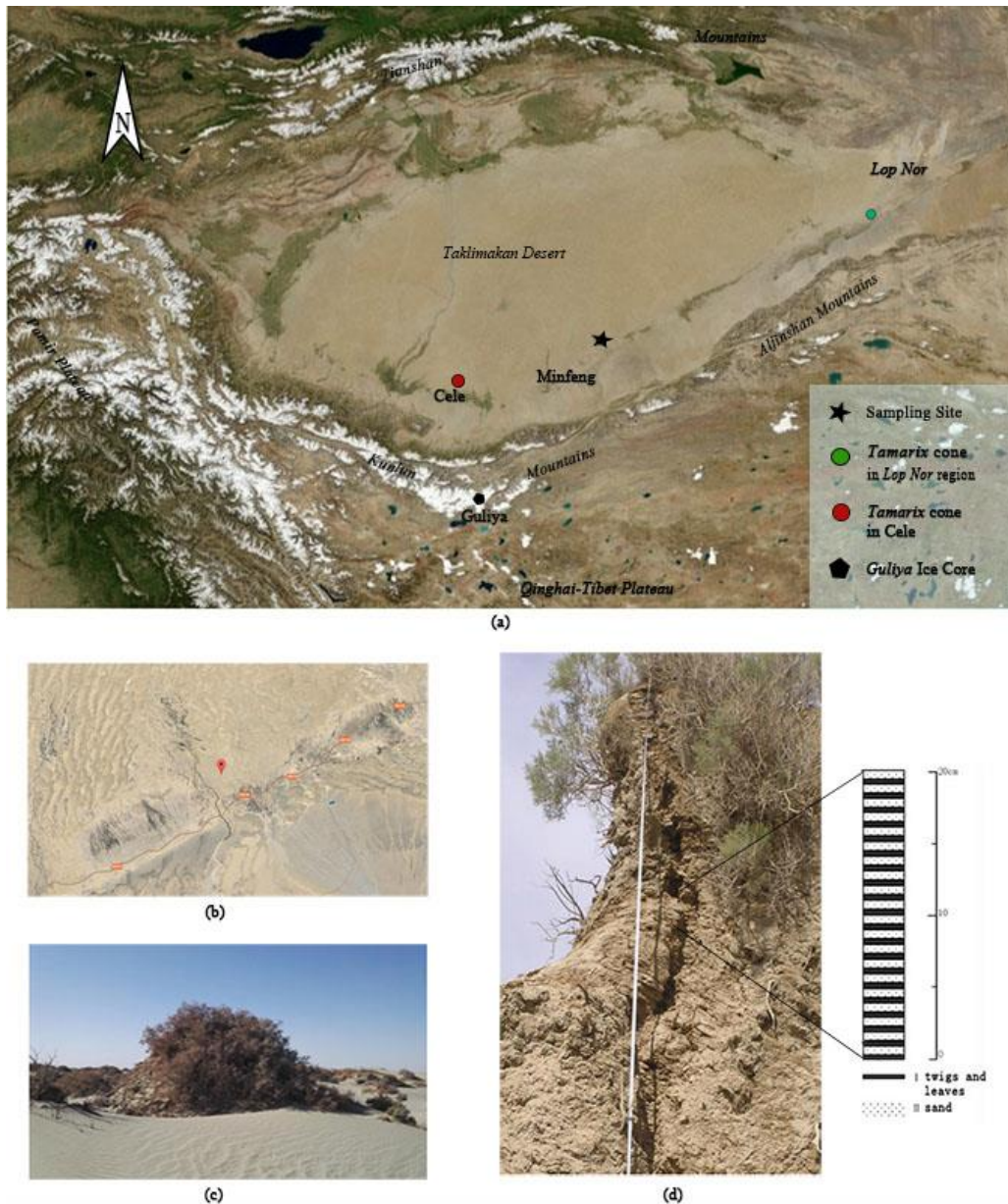


Figure 1. Location of sampling site in Andier meadow of Minfeng County (a, b); a typical *Tamarix* cone (c); a sampling profile of *Tamarix* cone (d)

All samples were pretreated by washing, stoving, grinding, and packing in penetrative bag in the Key Laboratory of Environmental Change and Ecological Construction, Hebei Normal University. The $\delta^{13}\text{C}$ value of each sample was measured in the Nanjing Institute of Geography and Limnology, Chinese Academy of Sciences, based on the Vienna Pee Dee Belemnite (VPDB) standard (the standard error of 0.1‰). Both ^{210}Pb and ^{137}Cs were measured to constrain the age sequence, combined with ^{14}C

dating by the Accelerator Mass Spectrometry Laboratory in Beijing University (Zhao et al., 2015b).

The carbon isotope fractionation ($\Delta\delta^{13}\text{C}$) of *Tamarix* leaves is derived by the following formula (Eq. 1; Farquhar et al., 1984, 1989):

$$\Delta\delta^{13}\text{C} = \frac{\delta^{13}\text{C}_a - \delta^{13}\text{C}_t}{1 + \delta^{13}\text{C}_t/1000} \approx \delta^{13}\text{C}_a - \delta^{13}\text{C}_t \quad (\text{Eq.1})$$

Where $\delta^{13}\text{C}_a$ represents the carbon isotope ratio in atmosphere measured from ice core bubbles or plant $\delta^{13}\text{C}$ value (Friedli et al., 1986; Leavitt and Long, 1989; Mccarroll and Loader, 2004); $\delta^{13}\text{C}_t$ represents the carbon isotope ratio of *Tamarix* leaves.

The climate data were obtained from the Mingfeng meteorological station, close to the sampling site. The data include the monthly and yearly lowest, highest and mean temperature, sunshine duration, precipitation, relative humidity, wind speed, windy days, and sand storms during 1960-2010. These data are divided into three categories: temperature-related, water-related, and wind-related variables.

We first explored the descriptive statistics of $\delta^{13}\text{C}$ and $\Delta\delta^{13}\text{C}$ and then performed bivariate correlation analyses between $\delta^{13}\text{C}$, $\Delta\delta^{13}\text{C}$ and the temperature-related, water-related, wind-related variables. Due to the large number of the variables and their intercorrelations, we applied the principal component analysis to condense the variables into several major components and determine the contributions of different variables to $\delta^{13}\text{C}$ and $\Delta\delta^{13}\text{C}$. The key growth-limiting factors for *Tamarix* were then determined based on their correlations and contributions. We applied the least square regression to establish the relationship between $\delta^{13}\text{C}$ and $\Delta\delta^{13}\text{C}$ and the key growth-limiting factors and use this relationship to reconstruct the variations of these factors in the past. Most of the statistical analyses were performed using IBM SPSS Statistics. The regression was carried out by software, EViews.

Results

$\delta^{13}\text{C}$ and $\Delta\delta^{13}\text{C}$ variations

Based on the chronology established by Zhao et al. (2015b) using ^{14}C , ^{210}Pb and ^{137}Cs dating, we illustrated $\delta^{13}\text{C}$ and $\Delta\delta^{13}\text{C}$ variations for the Mingfeng sampling site in the past 400 years (Fig. 2). The $\delta^{13}\text{C}$ values vary from -26.979‰ to -22.149‰, and the $\Delta\delta^{13}\text{C}$ values fluctuate between 15.397‰ and 20.265‰ with a mean of 18.009‰.

Correlation analysis

We analyzed the correlations between temperature-related variables, including the monthly highest temperature, monthly lowest temperature, monthly mean temperature, annual mean of highest temperatures, annual mean of lowest temperatures, annual mean temperature, monthly sunshine hours and annual cumulative sunshine hours, and $\delta^{13}\text{C}$, $\Delta\delta^{13}\text{C}$. At the 95% confidence level, the significantly related variables were selected and listed in Table 1.

The correlations between $\delta^{13}\text{C}$, $\Delta\delta^{13}\text{C}$ and the water-related variables, such as the monthly precipitation, annual precipitation, monthly mean of air relative humidity, annual mean of air relative humidity, showed that statistically significant correlations ($P < 0.05$) only occur in January ($r = -0.417$, $p = 0.038$) between $\delta^{13}\text{C}$ and precipitation,

and in June ($r = 0.401$, $p = 0.047$) and November ($r = 0.534$, $p = 0.006$) between $\delta^{13}\text{C}$ and air relative humidity. Statistically significant correlations occur in April ($r = 0.445$, $p = 0.026$) between $\Delta\delta^{13}\text{C}$ and precipitation, and in November ($r = -0.579$, $p = 0.002$) between $\Delta\delta^{13}\text{C}$ and air relative humidity only.

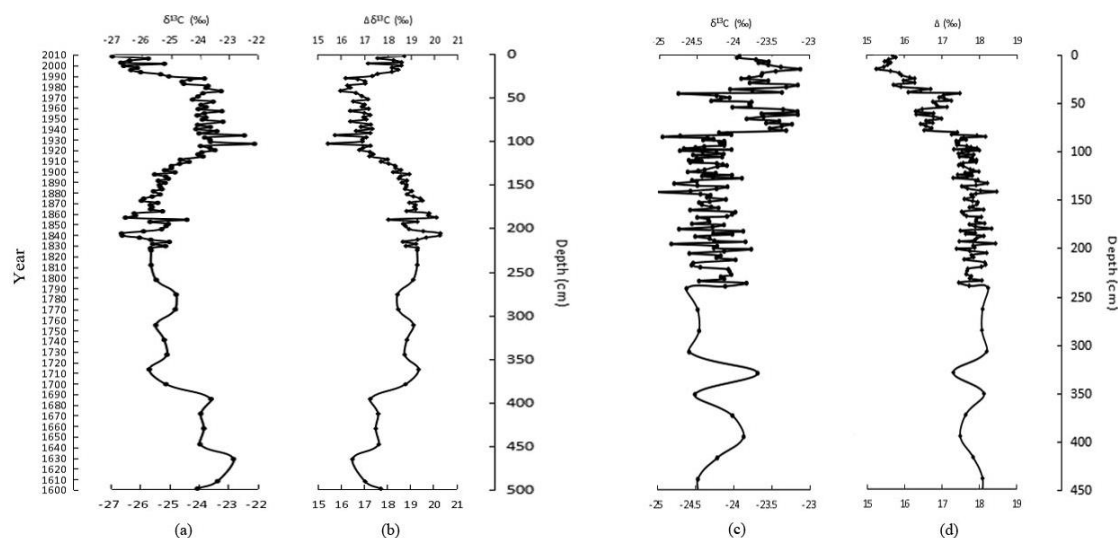


Figure 2. The age sequence of $\delta^{13}\text{C}$ in Minfeng sampling site (a); the age sequence of $\Delta\delta^{13}\text{C}$ in Minfeng sampling site (b); the age sequence of $\delta^{13}\text{C}$ in Cele (Zhang et al., 2017) (c); the age sequence of $\Delta\delta^{13}\text{C}$ in Cele (Zhang et al., 2017) (d)

Table 1. Pearson correlations (r) of temperature-related variables with $\delta^{13}\text{C}$, $\Delta\delta^{13}\text{C}$

Lowest Temperature	$\delta^{13}\text{C}$		$\Delta\delta^{13}\text{C}$	
	r	p	r	p
Lowest temperature in Jan	-0.557	0.004	0.564	0.003
Lowest temperature in Feb	-0.546	0.005	0.575	0.003
Lowest temperature in Mar	-0.537	0.006	0.586	0.002
Lowest temperature in Apr	-0.509	0.009	0.530	0.006
Lowest temperature in May	-0.511	0.009	0.452	0.023
Lowest temperature in Jun	-0.717	0.000	0.626	0.001
Lowest temperature in Jul	-0.602	0.001	0.616	0.001
Lowest temperature in Aug	-0.491	0.013	0.497	0.011
Lowest temperature in Sep	-0.553	0.004	0.566	0.003
Lowest temperature in Oct	-0.557	0.004	0.489	0.013
Lowest temperature in Nov	-0.612	0.001	0.526	0.007
Lowest temperature in Dec	-0.586	0.002	0.495	0.012
Annual mean of lowest temperatures	-0.665	0.000	0.639	0.001
Annual mean of highest temperatures	-0.608	0.001	0.700	0.000
Annual mean temperature	-0.694	0.000	0.671	0.000

The correlations between $\delta^{13}\text{C}$, $\Delta\delta^{13}\text{C}$ and the wind-related variables, such as monthly mean wind speed, annual mean wind speed, monthly windy days, annual

windy days, monthly sand-blowing days, annual sand-blowing days and sandstorm days, were analyzed, and the significantly related variables ($P < 0.05$) were selected and listed in *Table 2*.

Table 2. Pearson correlations (r) of wind-related variables with $\delta^{13}\text{C}$, $\Delta\delta^{13}\text{C}$

	$\Delta^{13}\text{c}$		$\Delta\delta^{13}\text{C}$	
	R	P	R	P
Wind speed in Feb			-0.495	0.012
Wind speed in Mar	0.408	0.043	-0.503	0.010
Wind speed in Apr			-0.494	0.012
Wind speed in May			-0.412	0.041
Wind speed in Jul			-0.415	0.039
Wind speed in Aug	0.433	0.031	-0.415	0.039
Wind speed in Sept	0.656	0.000	-0.629	0.001
Wind speed in Oct	0.528	0.007	-0.593	0.002
Annual wind speed	0.596	0.002	-0.622	0.001

Principal component analysis

Principal component analysis (PCA) carried on the 26 variables related to $\Delta\delta^{13}\text{C}$ for data compression. The KMO (Kaiser-Meyer-Olkin) value (0.496) is poor, however Bartlett's test of sphericity ($P < 0.001$) indicates we can proceed. Based on the rule that the minimum eigenvalue should not be less than 1, four components were extracted from the PCA result (*Table 3*). Eliminating the coefficient less than 0.5, the factor loadings are showed in the rotated component matrix (*Table 4*).

Table 3. Total variance explained

Component		1	2	3	4
Initial eigenvalues	Total	13.258	4.671	1.327	1.223
	% of variance	50.994	17.965	5.103	4.704
	Cumulative %	50.994	68.959	74.062	78.766
Extraction sums of squared loadings	Total	13.258	4.671	1.327	1.223
	% of variance	50.994	17.965	5.103	4.704
	Cumulative %	50.994	68.959	74.062	78.766
Rotation sums of squared loadings	Total	10.639	7.051	1.527	1.261
	% of variance	40.921	27.120	5.875	4.850
	Cumulative %	40.921	68.041	73.916	78.766

Regression analysis

Liner regression analyses were performed to explore the relationship between temperature and $\delta^{13}\text{C}$, $\Delta\delta^{13}\text{C}$, and then regression models were built to reconstruct the paleotemperature. Firstly, based on the correlation ($r = 0.72$, $P = 0.00$) between $\delta^{13}\text{C}$ values and the observed lowest temperature in June (LT_{Jun}), the reconstruction model of LT_{Jun} is (*Eq. 2*):

$$LT_{Jun} = -9.542 - 1.031 * \delta^{13}C$$

Std.Error 5.183 0.209 (Eq.2)
P-value 0.079 0.000

The R^2 of the model is 0.51. We used this equation to reconstruct the LT_{Jun} . *Figure 3a* illustrates the reconstructed lowest temperature in June, and *Figure 3b* shows the comparison between the reconstructed lowest temperature with the observed data from the Minfeng meteorological station.

Table 4. Rotated component matrix^a

	Component			
	1	2	3	4
Lowest temperature in Jan	0.826			
Lowest temperature in Feb	0.797			
Lowest temperature in Mar	0.720			
Lowest temperature in Apr	0.750			
Lowest temperature in May	0.636			
Lowest temperature in Jun	0.795			
Lowest temperature in Jul	0.682			
Lowest temperature in Aug	0.820			
Lowest temperature in Sep	0.873			
Lowest temperature in Oct	0.882			
Lowest temperature in Nov	0.913			
Lowest temperature in Dec	0.875			
Annual mean of lowest temperature	0.967			
Annual mean of highest temperature	0.519			
Annual mean temperature	0.868			
Mean winds peed		0.880		
Wind speed in Feb		0.899		
Wind speed in Mar		0.904		
Wind speed in Apr		0.866		
Wind speed in May		0.936		
Wind speed in Jul		0.929		
Wind speed in Aug		0.656		
Wind speed in Sept		0.685		
Wind speed in Oct		0.736		
Precipitation in Apr				0.847
Air relative humidity in Nov			-0.726	
Lowest temperature in Jan	0.826			
Lowest temperature in Feb	0.797			
Lowest temperature in Mar	0.720			
Lowest temperature in Apr	0.750			

* a. 4 components extracted.

Secondly, based on the highest correlation coefficient ($r = 0.70$, $P = 0.00$) between $\Delta\delta^{13}C$ and the Annual Mean of Highest Temperature (AMHT), which is the highest one

among all temperature-related variables, the relationship between $\Delta\delta^{13}\text{C}$ and AMHT is (Eq. 3):

$$AMHT = 10.274 + 0.556 * \Delta\delta^{13}\text{C}$$

<i>Std.error</i>	2.041	0.118	(Eq.3)
<i>P-value</i>	0.000	0.000	

The R-squared of the model is 0.49. Therefore, we selected AMHT as the representative temperature indicators for the past climate reconstruction. The reconstructed AMHT shows in Figure 3c, the reconstructed data compared with the observed data at Minfeng meteorological station is shown in Figure 3d.

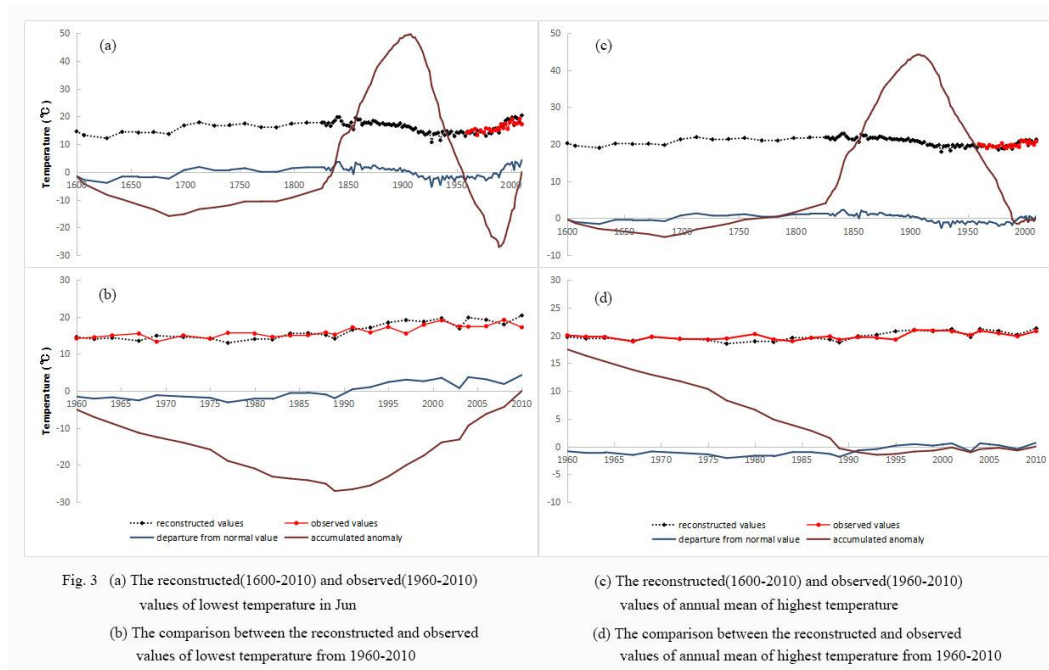


Figure 3. The reconstructed (1600-2010) and observed (1960-2010) values of lowest temperature in Jun (a); the comparison between the reconstructed and observed values of lowest temperature from 1960-2010 (b); the reconstructed (1600-2010) and observed (1960-2010) values of annual mean of highest temperature (c); the comparison between the reconstructed and observed values of annual mean of highest temperature from 1960-2010 (d)

Discussion

Features of the $\delta^{13}\text{C}$

The values of *Tamarix* leaf $\delta^{13}\text{C}$ in the Minfeng sampling site are consistent with the results from Lop Nor (ranging from -24.75‰ to -22.38‰, with a mean of -23.56‰, Xia et al., 2004) and Cele (ranging from -25.008‰ to -23.138‰, with a mean of -24.137‰, Zhang et al., 2017) regions. The $\delta^{13}\text{C}$ signature is heavier than that of arid areas in northern China (Liu et al., 2014a) and broadly in accordance with the $\delta^{13}\text{C}$ composition of C_3 plants in arid environments. The slight difference between the range and average values of $\delta^{13}\text{C}$ in the Minfeng site and values from the Lop Nor and Cele areas is likely due to the difference in climate conditions. Compared with the extremely arid Lop Nor

area (the annual mean precipitation from 1960 to 2010 is 26.83 mm), the climate of Minfeng sites (the annual mean precipitation from 1960 to 2010 is 29.45 mm) is more humid relatively, leading to slightly lower $\delta^{13}\text{C}$ values due to improved water conditions. This finding is similar to other studies (Liu et al., 1997; Sun et al., 2003; Yun, 2010; Zhao, 2012).

Influence of temperature on Tamarix

Temperature is one of the main factors affecting plant growth. The change in temperature may change the plant physiological responses. A declining temperature may result in a reduction in enzyme activity and photosynthetic rate, leading to decreased CO_2 assimilation and a lower growth rate (Beerling, 1994). Several studies have observed an increase in $\Delta\delta^{13}\text{C}$ with decreasing temperature (Mccarroll and Loader, 2004; Treydte et al., 2007; Wang et al., 2013). However, our results show a statistically significant negative correlation between temperature-related variables and $\delta^{13}\text{C}$, and a significantly positive correlation between temperature and $\Delta\delta^{13}\text{C}$. The $\delta^{13}\text{C}$ and $\Delta\delta^{13}\text{C}$ values are correlated with the annual mean of highest temperatures and the lowest temperature in each month. It appears that the higher temperature led to lower $\delta^{13}\text{C}$ values and increased the carbon isotope fractionation. An opposite trend was observed in the Cele site (Zhang et al., 2017), showing some disagreement with our results (Wang et al., 2003; Liu et al., 2007; Shen and Chen, 2000; Zhao et al., 2011b).

Influence of wind speed on Tamarix

Few studies have investigated the effect of wind-related factors on plant growth. In this study, we found that the wind speed is positively related to $\delta^{13}\text{C}$ values and negatively related to $\Delta\delta^{13}\text{C}$ values in *Tamarix* growing seasons, and the correlations between the annual wind speed and $\Delta\delta^{13}\text{C}$ values are more significant than those of $\delta^{13}\text{C}$. The highest correlations are mostly in September, and the correlation between annual mean wind speed and $\Delta\delta^{13}\text{C}$ is -0.622 ($P = 0.001$). These results suggest that the wind speed affects the *Tamarix* growth. The $\delta^{13}\text{C}$ values are much heavier on higher wind speed conditions, and the effect of carbon isotope fractionation is weaker. This may due to the wind from desert is usually hot and dry, which may increase the transpiration and water consumption of *Tamarix*. Therefore, *Tamarix* may reduce stomatal opening status to mitigate water loss. Consequently, the photosynthesis is restrained and the $\delta^{13}\text{C}$ value increases.

Influence of precipitation and relative humidity on Tamarix

Studies have reported the influence of water availability on plant carbon isotope fractionation, and a positive correlation between $\Delta\delta^{13}\text{C}$ and water availability has been observed in most studies (e.g., Wang et al., 2005, 2008; Diefendorf et al., 2010; Kohn, 2010). In our study, a statistically poor negative relationship between the $\delta^{13}\text{C}$ values and the precipitation occurs in January only, and a positive relationship between the $\Delta\delta^{13}\text{C}$ values and the precipitation occurs in April only. We found the relative humidity has a significantly positive correlation with $\delta^{13}\text{C}$ values and negative correlation with $\Delta\delta^{13}\text{C}$ values in November. Different from our study, the $\delta^{13}\text{C}$ values are correlated with precipitation only in February ($r = -0.522$, $p = 0.012$) in the Cele site (Zhang et al., 2017).

These results suggest that the effect of local precipitation and relative humidity is relatively weak on the growth of *Tamarix*. This illustrates that the *Tamarix* growth has been adapted to the arid environment, mainly relies on the groundwater, the annual precipitation of 29.4 mm has little effect on *Tamarix* growth. Our preliminary analysis suggests that more precipitation in January and April, likely correlated with more snow, ice and rainfall on the mountains, may supply more available water for the growth of *Tamarix*, and consequently promote the photosynthetic rate and *Tamarix* growth.

Temperature as the key growth-limiting factor

The results of correlation analysis show that the effect of temperature-related variables on $\delta^{13}\text{C}$, $\Delta\delta^{13}\text{C}$ of *Tamarix* leaves is more significant than those of wind-related and precipitation-related variables. The $\delta^{13}\text{C}$ and $\Delta\delta^{13}\text{C}$ values are highly correlated with temperature-related variables: monthly lowest temperatures, the annual mean of lowest temperatures, the annual mean of highest temperatures and annual mean temperature. The number of wind-related variables is small and that of precipitation- and humidity-related variables is few.

The PCA results show the temperature-related index is the major influence factor on the $\Delta\delta^{13}\text{C}$. The first principal component explained about 51% of the standardized variance, whereas the second principal component accounted for 18%. The first two components explained about 69% of the variance (Table 3). The first component showed strong positive loadings on 15 variables: annual mean temperature, annual mean of lowest temperature, annual mean of highest temperature and all monthly lowest temperatures. The second component shows the positive loadings the 9 wind-related variables only.

The influence of temperature on $\Delta\delta^{13}\text{C}$ has been studied extensively (e.g., Körner et al., 1988, 1991; Morecroft and Woodward, 1996; Wang et al., 2008, 2013; Gebrekirstos et al., 2009; Diefendorf et al., 2010; Kohn, 2010). Our results indicate that the influence of temperature on the *Tamarix* growth is mainly on the carbon isotope fractionation. Thus, the temperature is identified as the key growth-limiting factor for the *Tamarix* growth. Similar results have also been observed by Liu et al. (2014a) and Xu et al. (2015).

Analysis of reconstructed temperature

The lowest temperature in June is significantly associated with the mean value of lowest temperatures in summer ($r = 0.882$, $p = 0.000$), annual mean of lowest temperatures ($r = 0.810$, $p = 0.000$) and the annual mean temperature ($r = 0.746$, $p = 0.000$). So, the reconstructed records of the lowest temperature in June and annual mean of highest temperature represent a long-term temperature fluctuation in the past 410 years (Fig. 3). The mean of LT_{Jun} is 16.08 °C and that of AMHT is 20.58 °C for the full records. According to the departure from the average and the accumulated anomaly, the records can be further divided into the following four sub-periods:

The first period (1600-1685): The departure from normal value of the reconstructed LT_{Jun} and AMHT decreased year after year. The reconstructed LT_{Jun} (the average value is 13.81 °C) and AMHT (the average value is 19.85 °C) below averages. This period is defined as a history cold period.

The second period (1686-1910): The departure from normal value of the reconstructed LT_{Jun} and AMHT rebounded from its lows (1685), and rose fast after

1830. The mean of reconstructed LT_{Jun} is 17.11 °C before 1830, and that rose to 17.37 °C in late 80 years. The mean of AMHT is 21.52 °C. The reconstructed temperatures are warmer than averages. It is defined as the history warm period.

The third period (1911-1993): The departure from normal value of the reconstructed LT_{Jun} and AMHT decreased rapidly till 1993. The mean of reconstructed LT_{Jun} is 14.18 °C and that of AMHT is 19.44 °C, those are cooler than averages until 1993. It is defined as modern cold period.

The fourth period (1994-2010): From 1994, the reconstructed temperatures turned warmer. The mean of reconstructed LT_{Jun} is 18.91 °C and that of AMHT is 20.75 °C. The LT_{Jun} rose more rapidly than AMHT. It is defined as modern warm period.

The mean of observed LT_{Jun} is 15.14 °C and that of AMHT is 19.76 °C from 1960 to 1993, and those from 1994 to 2010 are 19.76 °C and 20.42°C, respectively. The trend of the constructed temperature is accord with those of the observed.

Our reconstructed records are broadly consistent with Zhao et al. (2016) that concluded that the past climate had experienced 4 stages based on TOC, TN and C/N analysis on the same sampling site. In particular, the two of our four periods, 1600-1690 (cool) and 1991-2010 (warm), are consistent with their study, but the other two, 1691-1900 (cool) and 1901-1990 (warm), have the opposite trends. The result shows that it had been warmer before 1912, and then turned cool. This is partly consistent with Zhao et al. (2015a) that reconstructed the climate record of the past 200 years using fossil pollen from the Andier ancient city; the history warm period (1685-1912) is roughly consistent with Guo et al. (2016) that reconstructed the past climate in Cele site based on fossil pollen data, and the history cold period (1600-1685) is consistent with Yao et al.'s (2001) study of the Guliya ice core. The discrepancies between these results may be caused by different materials, precision, or time scale.

Sensitivity of the reconstructed records

The $\delta^{13}C$ and $\Delta\delta^{13}C$ signature of *Tamarix* leaf are sensitive to the climate in the SMTD. The effects of climate on $\delta^{13}C$ and $\Delta\delta^{13}C$ in Minfeng sites are reversed with those in the Cele site and Lop Nor region except for the precipitation. The higher monthly lowest temperature and annual mean of highest temperature promote the *Tamarix* growth in the Minfeng site, whereas limit the *Tamarix* growth in the Cele site (Zhang et al., 2017). The opposite results suggest that the *Tamarix* growth is sensitive to the ecological environment. It may be caused by the difference in their geographical environment. With less population and no reservoir was constructed to adjust the runoff of the Andier river, the Minfeng oasis is smaller than the Cele oasis. Thus, the human interference is relatively lower in the Mingfeng site.

Conclusions

In this paper, we investigated the effects of the climate factors on $\delta^{13}C$ and $\Delta\delta^{13}C$ signatures in the Minfeng site. We found that the effect of temperature is most significant, can contribute to 50% of the carbon isotope fractionation, and is the key growth-limiting factor for the *Tamarix* growth. The wind speed is the second factor affecting on the *Tamarix* growth and it might significantly affect on plant growth in the growing seasons.

The reconstructed records in the lowest temperature in June and annual mean of highest temperature showed that the temperature fluctuated during the past 400 years.

The lowest temperature in June rose more rapidly than the annual mean of highest temperatures in recent decades. Future studies are recommended to investigate the mechanism of the climate factors on the *Tamarix* growth and using multiple proxies to improve the understanding of the past climate change and predict how plants respond to climate change in the future.

Acknowledgements. This research was supported by the National Natural Science Foundation of China (Grant No. 41877448, U1303285) and the Construction Project of Key Disciplines in Colleges and Universities of Hebei Province.

REFERENCES

- [1] Beerling, D. J. (1994): Predicting leaf gas exchange and $\delta^{13}\text{C}$ responses to the past 30000 years of global environmental change. – *New Phytologist* 128(3): 425-433.
- [2] Dawson, T. E., Siegwolf, R. T. W. (2007): Stable isotopes as indicators of ecological change. – Academic Press, San Diego.
- [3] Diefendorf, A. F., Mueller, K. E., Wing, S. L. et al. (2010): Global patterns in leaf ^{13}C discrimination and implications for studies of past and future climate. – *Proceedings of the National Academy of Sciences of the United States of America* 107(13): 5738-5743.
- [4] Dodd, J. P., Patterson, W. P., Holmden, C. et al. (2008): Robotic micromilling of tree-rings: A new tool for obtaining subseasonal environmental isotope records. – *Chemical Geology* 252(1-2): 21-30.
- [5] Farquhar, G. D., Hubick, K. T., Condon, A. G. et al. (1989): Carbon isotope fractionation and plant water-use efficiency. – In: Rundel, P. W., Ehleringer, J. R., Nagy, K. A. (eds.) *Stable isotopes in ecological research*. Springer, New York, pp. 21-40.
- [6] Farquhar, G. D., Richards, R. A. (1984): Isotopic composition of plant carbon correlates with water-use efficiency of wheat genotypes. – *Aust. J. Plant Physiol.* 11(6) 539-552.
- [7] Farquhar, G. D., O'Leary, M. H., Berry, J. A. (1982): On the relationship between carbon isotope discrimination and the intercellular carbon dioxide concentration in leaves. – *Functional Plant Biology* 9(2): 121-137.
- [8] Friedli, H., Lotscher, H., Oeschger, H. et al. (1986): Ice-core record of the $^{13}\text{C}/^{12}\text{C}$ ratio of atmospheric CO_2 in the past two centuries. – *Nature* 324: 237-238.
- [9] Gebrekirstos, A., Worbes, M., Teketay, D. et al. (2009): Stable carbon isotope ratios in tree rings of co-occurring species from semi-arid tropics in Africa: Patterns and climatic signals. – *Global & Planetary Change* 66(3-4): 253-260.
- [10] Guo, F., Zhao, C., Zhao, Y. J. et al. (2016): Pollen assemblages of *Tamarix* cone sedimentary veins and environmental change in the southern margin of Taklimakan Desert for about the last 400 years. – *Acta Palaeontologica Sinica* 55(1): 136-144 (in Chinese).
- [11] Kohn, M. J. (2010): Carbon isotope compositions of terrestrial C_3 plants as indicators of (paleo) ecology and (paleo) climate. – *Proc. Natl. Acad. Sci. U.S.A.* 107: 19691-19695.
- [12] Körner, C., Farquhar, G. D., Roksandic, Z. (1988): A global survey of carbon isotope discrimination in plants from high altitude. – *Oecologia* 74: 623-632.
- [13] Körner, C., Farquhar, G. D., Wong, S. C. (1991): Carbon isotope discrimination by plants follows latitudinal and altitudinal trends. – *Oecologia* 88: 30-40.
- [14] Leavitt, S. W., Long, A. 1989. The atmospheric $\Delta\text{C-13}$ record as derived from 56 Pinyon trees at 14 sites in the southwest United States. – *Radiocarbon* 31(3): 469-474.
- [15] Liu, G. S., Qi, C. M., Lin, X. Y. et al. (1997): Reflection of surface runoff variation by tree-ring in its drainage area. – *Journal of Changchun University of Earth Sciences* 3: 333-336 (in Chinese).

- [16] Liu, X., Su, Q., Li, C., Zhang, Y. et al. (2014a): Responses of carbon isotope ratios of C₃ herbs to humidity index in Northern China. – Turkish Journal of Earth Sciences 23(1): 100-111.
- [17] Liu, X. H., Shao, X. M., Wang, L. L. et al. (2007): Climatic significance of the stable carbon isotope composition of tree-ring cellulose: Comparison of Chinese hemlock (*Tsuga chinensis* Pritz) and alpine pine (*Pinus densata* Mast) in a temperate-moist region of China. – Science in China (D) 7: 1076-1085.
- [18] Liu, X. Z., Zhang, Y., Su, Q. et al. (2014b): Research progress in responses of modern terrestrial plant carbon isotope composition to climate change. – Advances in Earth Science 12: 1341-1354 (in Chinese).
- [19] Loader, N. J., Mccarroll, D., Gagen, M. et al. (2007): Extracting climatic information from stable isotopes in tree rings. – Terrestrial Ecology 1(1): 25-48.
- [20] Mccarroll, D., Loader, N. J. (2004): Stable isotopes in tree rings. – Quaternary Science Reviews 23(7): 771-801.
- [21] Morecroft, M. D., Woodward, F. I. (1996): Experiments on the causes of altitudinal differences in leaf nutrient contents, age and ¹³C of *Alchemilla alpine*. – New Phytol. 134: 471-479.
- [22] Ren, S. J., Yu, G. R. (2011): Carbon isotope composition ($\delta^{13}\text{C}$) of C₃ plants and water use efficiency in china. – Chinese Journal of Plant Ecology 16(5) (in Chinese).
- [23] Saurer, M., Siegenthaler, U., Schweingruber, F. (1995): The climate-carbon isotope relationship in tree rings and the significance of site conditions. – Tellus Series B-Chemical & Physical Meteorology 47(3): 320-330.
- [24] Seibt, U., Rajabi, A., Griffiths, H. et al. (2008): Carbon isotopes and water use efficiency: sense and sensitivity. – Oecologia 155: 441-454.
- [25] Shen, J., Chen, Y. F. (2000): The climatic reconstruction from the tree-ring $\delta^{13}\text{C}$ values of *Cedrus deodara* (Roxb.) Loud. during the past 20 years in Nanjing. – Journal of Plant Resources and Environment 3: 34-37 (in Chinese).
- [26] Sun, B. N., Dilcher, D. L., Beerling, D. J. et al. (2003): Variation in *Ginkgo Biloba* L leaf characters across a climatic gradient in China. – PNAS 12: 7141-7146.
- [27] Sun, Z. Y. (2013): The climate change revealed by the $\delta^{13}\text{C}$ values of *Tamarix* cone sedimentary veins in the south region of Taklimakan Desert. – Hebei Normal University, Shijiazhuang (in Chinese).
- [28] Sun, Z. Y., Zhang, J., Zeng, J. et al. (2013): The modern climate change revealed by the sedimentary veins of *Tamarix* dune in Lop Nor region. – Journal of Arid Land Resources and Environment 27(7): 127-133 (in Chinese).
- [29] Treydte, K., Frank, D., Esper, J. et al. (2007): Signal strength and climate calibration of a European tree-ring isotope network. – Geophys. Res. Lett. 34: 1-6.
- [30] Wang, G., Han, J. M., Liu, D. S. (2003): The carbon isotope composition of C₃ herbaceous plants in loess area of northern China. – Science in China (D) 10: 1070-1076.
- [31] Wang, G., Han, J., Zhou, L. et al. (2005): Carbon isotope ratios of plants and occurrences of C₄ species under different soil moisture regimes in arid region of Northwest China. – Physiologia Plantarum 125(1): 74-81.
- [32] Wang, G., Feng, X., Han, J. et al. (2008): Paleovegetation reconstruction using $\delta^{13}\text{C}$ of soil organic matter. – Biogeosciences 5(2): 1325-1337.
- [33] Wang, G., Li, J., Liu, X. et al. (2013): Variations in carbon isotope ratios of plants across a temperature gradient along the 400 mm isoline of mean annual precipitation in north China and their relevance to paleovegetation reconstruction. – Quaternary Science Reviews 63(1): 83-90.
- [34] Werner, C., Schnyder, H., Cuntz, M. et al. (2012): Progress and challenges in using stable isotopes to trace plant carbon and water relations across scales. – Biogeosciences 9(8): 3083-3111.
- [35] Xia, X. C., Zhao, Y. J., Wang, F. B. et al. (2004): Stratification features of *Tamarix* cone and its possible age significance. – Chinese Science Bulletin 49(14): 1539-1540.

- [36] Xu, M., Wang, G., Li, X. et al. (2015): The key factor limiting plant growth in cold and humid alpine areas also plays a dominant role in plant carbon isotope discrimination. – *Frontiers in Plant Science* (6): 1-9.
- [37] Yao, T. D., Yang, M. X., Kang, X. C. (2001): Comparative study of the climate changes in the past 2000 years by using ice core and tree ring records. – *Quaternary Sciences* 21(6): 514-519.
- [38] Yun, H. B. (2010): Research on the seasonal characteristics of $\delta^{13}\text{C}$, δN and Non-structural carbohydrate of main plants in different ecosystems in the inland of Qinghai-Tibet Plateau. – Northwest Normal University, Xian (in Chinese).
- [39] Zhang, Z. G., Fang, Y., Li, L. et al. (2017): The Reconstruction of the paleotemperature in the southern margin of the Taklimakan Desert based on carbon isotope discrimination of *Tamarix* leaves. – *Applied Ecology and Environmental Research* 15(4): 561-570.
- [40] Zhao, C., Guo, F., Zhao, Y. J. et al. (2015a): Pollen assemblages of *Tamarix* cone and environmental change in Andier ancient city region during the recent 200 years. – *Journal of Arid Land Resources and Environment* 29(11): 158-163 (in Chinese).
- [41] Zhao, Y. (2012): Morphological and physiological responses of *Populus euphratica* leaf to groundwater table variations in the lower reaches of Heihe river. – Lanzhou University, Lanzhou (in Chinese).
- [42] Zhao, Y. J., Wang, X. Y., Xia, X. C. et al. (2011b): The $\delta^{13}\text{C}$ sequence of *Tamarix* cone sedimentary veins and climate reconstruction during last 160 years in Lop Nur region, Xinjiang, China. – *Quaternary Sciences* 31(1): 130-136 (in Chinese).
- [43] Zhao, Y. J., Li, X. F., Xia, X. C. et al. (2011a): C and N contents in organic matter of *Tamarix* dune sedimentary veins and environmental change in Lop Nur region. – *Journal of Arid Land Resources and Environment* 25(4): 149-154 (in Chinese).
- [44] Zhao, Y. J., Liu, H., Che, G. H. et al. (2015b): On age sequence establishment method of *Tamarix* cone sedimentary veins in desert region. – *Arid Zone Research* 32(4): 810-817 (in Chinese).
- [45] Zhao, Y. J., Che, G. H., Liu, H. et al. (2016): C and N content in organic matter of *Tamarix* cone and climatic and environmental change in southern region of Taklimakan Desert. – *Arid Land Geography* 39(3): 461-467 (in Chinese).

CONSIDERATION OF SEASONAL VARIATIONS OF WATER RADIOMETRIC INDICES FOR THE ESTIMATION OF SOIL MOISTURE CONTENT IN ARID ENVIRONMENT IN SAUDI ARABIA

BAHRAWI, J. A. – ELHAG, M.*

*Department of Hydrology and Water Resources Management, Faculty of Meteorology,
Environment & Arid Land Agriculture, King Abdulaziz University
21589 Jeddah, Kingdom of Saudi Arabia*

**Corresponding author
e-mail: melhag@kau.edu.sa*

(Received 11th Aug 2018; accepted 31st Oct 2018)

Abstract. Remote Sensing applications in agricultural practices are comprehensively reliable and cover a multidisciplinary fundamental interest on a local as well as on a regional level. Significantly, vegetation indices are foremost essential remote sensing applications in agricultural activities related to vegetation and/or water, particularly in an arid environment. Adequate water resources management plans are based on better fulfilment of water demand and supply equation. In arid environments, this equation is barely achieved due to water resources limitations. Remote sensing techniques improve the water resources management schemes using five different water radiometric indices of Sentinel-2. Each of them plays a specific role in the quantification of soil/plant water content based on the interpretation of map surface water features and monitors the dynamic of surface water. The study area is located within the main agricultural region of Wadi As-Sirhan, Saudi Arabia. The area is characterized by flourishing agricultural activities. Remote Sensing data acquired by Sentinel-2 proved to be statistically sufficient to estimate soil water content in two different climatic conditions. Statistically, winter estimated indices are a better fit than summer indices. MNDWI and NDWI-2 were best to fit winter soil water content estimations. Meanwhile, RMSE shows no differences between NDWI and NDTI in both climatic conditions.

Keywords: *integrated water resources management, Sentinel-2, soil water content, remote sensing, water radiometric indices*

Introduction

The Kingdom of Saudi Arabia (KSA) has a very low annual precipitation, high temperature, no lakes or flowing rivers and classified as an arid region. Water, therefore, is infrequent and enormously valuable, especially in a country with rapid growth in which the water demands are cumulative. The scarcity of fresh water resources presents the primary difficulty to the existence of biotic life in Saudi Arabia (Elhag, 2016). Generally, the average annual rainfall is closely less than 80 mm, with a sporadic maximum annual rainfall that exceeds 500 mm, particularly in the south-western region (Bahrawi et al., 2016).

Saudi Arabia has experienced an elevated development in all divisions over the last four decades. As a result, a swift intensification in agricultural, industrial and domestic water demands have been perceived. Agriculture is the major water consumption sector as it consumes about 85% of the total national water use (Elhag and Bahrawi, 2014a, 2017a). The government of Saudi Arabia subsidized the agricultural sector during the period 1974-2006 to improve the standard of living in rural areas and to attain self-sufficiency.

Soil water content depends on many parameters that are spatially and temporally variable such as soil type, vegetation cover, crop type, topography, and precipitation. Considering all these variable factors and collecting sufficient measurement data for the account of the spatial variations of the vadose zone soil water content is neither financially nor technically practical (Şen et al., 2017).

Soil water content is the amount of water available for plants uptake at the root zone; coarsely this zone is less than 50 cm of depth (Zhu et al., 2008). Within this thin layer, several important biological and hydrological essential processes take place (Crippen, 1990; Walker, 1999). It is very crucial to monitor this layer to ensure plants survival (Su et al., 1995). Traditional methods of soil water content estimation are usually valid for a small local level like a farm, but it always costs time and effort and is not a sufficient method to estimate spatial and temporal variations of soil water content on a regional scale (Engman, 1991; Wood et al., 1992; Watson et al., 2017).

Remote sensing techniques are now widely used to forecast, monitor and estimate soil water content (Ochsner et al., 2013; Psilovikos and Elhag, 2013). Estimation of soil water content using remote sensing practices is different and generally falls into two groups of methods: 1- passive remote sensing method of estimation and 2- active remote sensing method of estimation (Palecki and Bell, 2013). Both techniques depend on the capability of a certain wavelength to penetrate the root zone and register its reflection (Myneni et al., 1995; Dasgupta, 2007). Short Wave InfraRed (SWIR) wavelength can shallowly penetrate the root zone and SWIR is either registered passively from the sun or actively using Ground Penetration Radar (GPR) systems (Gao, 1996; Moghadas et al., 2013).

Low crop productivity is highly related to the availability of water resources. To optimize the use of limited water resources in arid environments unconventional methods of planning are required (Elhag and Bahrawi, 2017b). Soil water monitoring is a crucial feature of managing water requirements of agricultural fields founded on advanced irrigation techniques (Muñoz-Carpena et al., 2002). The main goal of farmers and decision makers is to keep soil water content within optimized range for better crop production, unsaturated soil, and efficient crop production are challenging (Muñoz-Carpena et al., 2005; Elhag and Bahrawi, 2014b).

Relevant research studies were conducted in similar arid environments. Modified Normalized Difference Water Index was investigated by Zhang and Huai-Liang (2016) to monitor drought condition. Mathieu et al. (1998) were pioneers to study the relationship between laboratory reflectance data and remote sensing data. Other significant scholarly work was conducted by Elhag and Bahrawi (2017b) to assess the hydrological drought indices in other parts of Saudi Arabia.

Several radiometric water indices have been developed within the past few decades. Principally, McFeeters (1996) projected the Normalized Difference Water Index (NDWI). The index utilizes the Green and the Near Infrared bands of remote sensing data. The index was projected to improve the extracted information from the remote sensing data regarding the soil moisture content. Lately, Modified Normalized Difference Water Index (MNDWI) was developed by Xu (2006) to improve the limitations of NDWI, where the Shortwave Infrared was used instead of NIR band. Several academic researches conducted by Xu (2006), Li et al. (2013), Du et al. (2014) and Singh et al. (2015) MNDWI is considered to be a better radiometric water index over NDWI.

Remote sensing techniques provide the tool to estimate soil water content on a large scale in time and in a cost-effective manner (Chauhan, 2003). Irrigation network in the designated area relies on advanced sprinkling irrigation systems. The huge plant water requirement in the study region is supplied from the underlying groundwater aquifer. Spatial correlation between soil water content and vegetation stress may alter the strategy of water management in the study area (Mustafa and Rahman, 2018). Image correction is a preliminary procedure in digital image analysis. Atmospheric and radiometric correction techniques are essential steps. According to Chavez (1996) and Thompson et al. (2018), Atmospheric correction depends on the calibrated radiance value of these offset consents to decide the κ value. The κ decision rule is based specifically on the flying height. The λ^{-K} determines the offset values for the Green, Red and Near Infra-Red band calibration (Beisl et al., 2008). Moreover, radiometric correction is required to harmonize the conducted measurements made with a variety of different satellite sensors under different environmental conditions (Zhu et al., 2015).

The main objective of the current research work is to contemplate the regression correlation between the values of Remotely Sensed water radiometric indices conducted from satellite images and ground truth data. Regression analysis will be considered under seasonal variation from winter to summer to understand the effect of seasonality on the estimation of the water radiometric indices. Therefore, accurate synchronization of ground truth data collection and satellite bypassing were exercised to maximize the use of the irrigational water in the study area.

Materials and methods

Study area

The Wadi As-Sirhan or Sirhan is a valley located in the northwestern part of Saudi Arabia and extends from north-west Saudi Arabia to eastern Jordan (from Lat 30° 45' to 29° 30' N and from Long 37° 50' to 39° 30' E). The Wadi is a high-altitude area with a height of about 500 to 700 meters above sea level, and with a total area of about 9000 km² and a length of more than 300 km, while the width of the valley is between 15 to 50 kilometers (*Fig. 1*). It is in the west-central part of the Sirhan turayf basin and is underlain by Silurian to Miocene-Pliocene sedimentary rocks that are partly covered by volcanic flows. The map area also contains large areas of surficial sand and gravel. Wadi As-Sirhan is characterized by 5 Million Cubic Meter (MCM) annual flow and 18 MCM annual discharge and safe yield of 7-10 MCM/yr (Bahrawi and Elhag, 2016). Hydrogeological investigations in Saudi Arabia demonstrate that groundwater is stored in more than 20 primary and secondary aquifers (Hoetzi, 1995). It has been estimated that the groundwater reserves are about 210,000 m³ of which 17500 m³ is stored in deeper secondary reserves (Al-Rashed and Sherif, 2000). The total volume of groundwater abstracted for irrigation in the designated study area has increased from 23 MCM in 1973 to 2,051 MCM in 2006, while the annual recharge does not exceed 10% (Elhag and Bahrawi, 2014a). The climate in the study area is confined to the semi-arid climate. About 80% of the study area receives less than 100 mm/yr, mostly during the spring months (Şen et al., 2017). The area of Wadi As-Sirhan is characterized by very hot summers, average monthly maximum/minimum in July: 33.9 °C/17.7 °C, and mild winters, average monthly maximum/minimum in January: 14.7 °C/3.8 °C. The calculated annual potential evapotranspiration (ET_o), Penman-Monteith approach (FAO, 1998) for Wadi As-Sirhan is 2,643 mm/yr. The soil of the study area is generally

sandy soil with pH of 6.65 up to 7.4 and with Electric Conductivity EC of 0.031 up to 1.634 ms/cm. There were no significant differences in soil colors either in dry summer soils or wet winter soils. Organic matter content is identified to be low (2.11%). The study area is not covered by natural vegetation. Mainly it is a reclaimed land for crop production. Water radiometric indices interpretation are exercised based on the ratios among the Red, Near Infra-Red and Infra-Red bands of Sentinel-2 over the study area acquired in 2016.

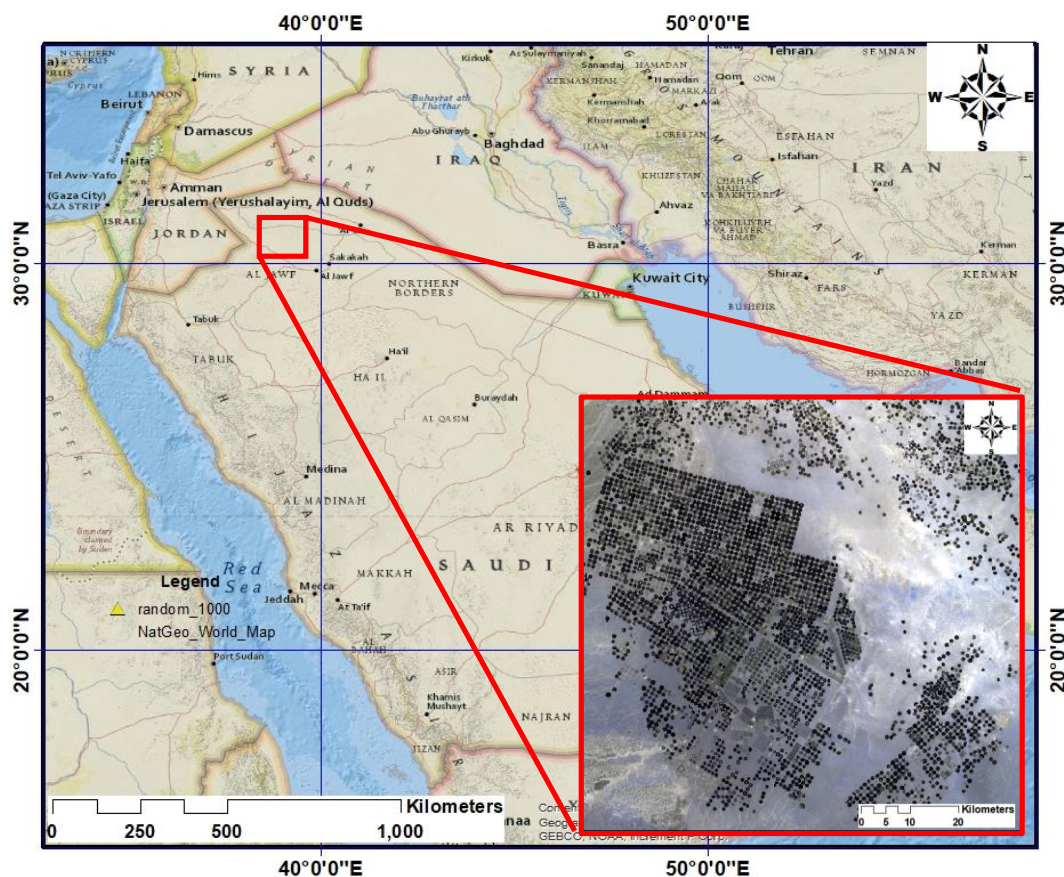


Figure 1. Study area location in false-color composite over a natural color base map

Methodological framework

Dataset and soil sampling

A total number of 150 random soil samples were collected from the cultivated land in Wadi As-Sirhan area with a minimum distance of 1000 m between the location of the samples to avoid data clumping and only bare soil locations were considered, not with crop cover. Soil samples were taken from soil surface level to 10 cm depth then mixed well for soil moisture estimation in triads to obtain the average. Samples were kept in sealed plastic packs and weighed in-situ for accurate estimation of soil moisture content (Elhag and Bahrawi, 2017b). Winter samples were collected in accordance with the bypass of the Sentinel-2 sensor (January 2016), and their locations were marked with wooden sticks for summer data collection (July 2016) as demonstrated in Figure 2. Sentinel-2 images were synchronized to soil samples collection and were downloaded

and processed to represent the winter and the summer seasons correspondingly. Sentinel-2 is made of 12 spectral bands with a 10 m resolution of Visible bands (VI), 20 m resolution of Vegetation Red Edge (VRE) bands and Short-Wave InfraRed (SWIR) bands in addition to 3 bands related to coastal aerosols and water vapor of 60 m resolution. The Remotely Sensed water radiometric indices are conducted from several algorithms that examines basically the VI, VRE, and SWIR bands.

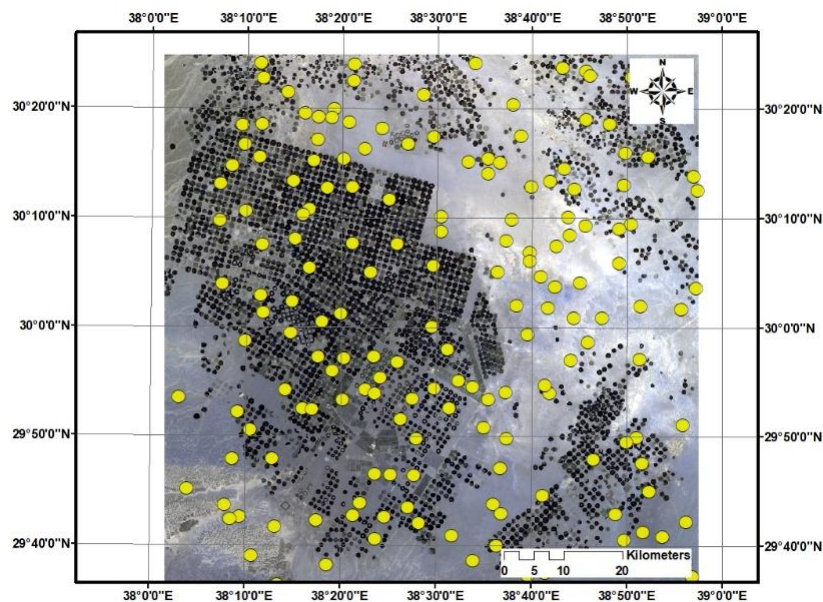


Figure 2. Soil sample location in a false color composition of Sentinel-2

Estimation of soil water content

This study adopted the common gravimetric method of soil water content estimation. The soil water content is expressed either in term of weight or volume. In the current research study, the soil water content is expressed in term of weight as the ratio of the mass between dry soil weight and wet soil weight. Determination of the soil water weight ratio is carried out by drying the soil to a constant weight and calculating the soil sample mass after and before drying. The criterion for drying the soil samples to a constant weight is considered after heat treatment in an oven at temperature between 100–110 °C. Within this range of temperature, it is assured that the water content in the examined samples will be evaporated without any alteration that may occur in the physical or the chemical characteristics of the soil samples. The soil water content in the dry weight approach is calculated following the formula (Eq. 1; Klute, 1986):

$$\theta_d = \frac{\text{wt of wet soil} - \text{wt of dry soil}}{\text{wt of dry soil}} \quad (\text{Eq.1})$$

Soil water content is calculated as the ratio of water mass and the mass of wet soil (θ_w). The alteration from θ_d to θ_w can be calculated as follows (Eq. 2):

$$\theta_d = \frac{\text{wt of water}}{\text{wt of dry soil}} \quad (\text{Eq.2})$$

After manipulation, the water content in wet and dry basis can be expressed as (Eq. 3):

$$\theta_d = \frac{\theta_w}{1-\theta_w} \quad (\text{Eq.3})$$

and (Eq. 4)

$$\theta_w = \frac{\theta_d}{\theta_d+1} \quad (\text{Eq.4})$$

Remote sensing analysis

The amount of water present in leaf internal structure mainly affects the spectral reflectance in the Short-Wave InfraRed (SWIR) interval (ca. 1.2-1.7 μm). The SWIR reflectance is also sensitive to the canopy internal structure. Because the NIR is exaggerated by leaf internal structure and leaf dry matter, but not by the water content, the combination of SWIR and NIR into NDWI calculation removes the leaf dry matter and internal structure and retains the water content. NDWI is less susceptible to atmospheric scattering than NDVI, but it cannot eliminate totally the effects of the background soil reflectance's comparable to NDVI.

The Modified Normalized Difference Water Index (MNDWI) algorithm was developed by (Xu, 2006) to improve the open water features through an efficient elimination of land noise as well as vegetation and soil noise. MNDWI is calculated by Equation 5:

$$MNDWI = \frac{Green - SWIR}{Green + SWIR} \quad (\text{Eq.5})$$

where:

Green is Sentinel-2 Green Band

SWIS is Sentinel-2 Short-Wave InfraRed Band

The Normalized Difference Pond Index (NDPI) was developed by (Lacaux et al., 2007) to distinguish the vegetation cover from its aquatic surroundings. NDPI is calculated by Equation 6:

$$NDPI = \frac{SWIR - Green}{SWIR + Green} \quad (\text{Eq.6})$$

where:

SWIS is Sentinel-2 Short-Wave InfraRed Band

Green is Sentinel-2 Green Band

The Normalized Difference Turbidity Index (NDTI) was developed by (Lacaux et al., 2007) to estimate water turbidity. NDTI is calculated by Equation 7:

$$NDTI = \frac{Red - Green}{Red + Green} \quad (\text{Eq.7})$$

where

Red is Sentinel-2 Red Band

Green is Sentinel-2 Green Band

The Normalized Difference Water Index (NDWI) was found by Gao (1996) Then improved by Ganaie et al. (2013) to measure the liquid water molecules at the Top Of Canopy (TOC) level. NDWI is calculated by *Equation 8*:

$$NDWI = \frac{NIR - SWIR}{NIR + SWIR} \quad (\text{Eq.8})$$

where

NIR is Sentinel-2 Near InfraRed Band

SWIS is Sentinel-2 Short-Wave InfraRed Band

The second Normalized Difference Water Index (NDWI-2) was developed by McFeeters (1996) to detect and measure the surface water extent in addition to the surface water of wetland environments. NDWI-2 is calculated by *Equation 9*:

$$NDWI - 2 = \frac{Green - NIR}{Green + NIR} \quad (\text{Eq.9})$$

where

Green is Sentinel-2 Green Band

NIR is Sentinel-2 Near InfraRed Band

The final step in image data analysis in the current study is data normalization. The above-mentioned Water Radiometric Indices are calculated within a range of -1 to +1. Therefore, Water Radiometric Indices were transformed into the same range of soil water content weights for comparability reasons using Hawkins and Pole (1989) transformation (*Eq. 10*):

$$z = \frac{1}{2} \ln \left(\frac{1+r}{1-r} \right) = \text{arctanh}(r) \quad (\text{Eq.10})$$

where

ln is the natural logarithm function

arctanh is the inverse hyperbolic tangent function

r is the Fisher's z-transformation

Regression analyses

The purpose of the regression analysis is to envisage the regression potentials between soil salinity index from one side and the rest of the hydrological drought indices from the other side. Principle Component Analysis (PCA) is performed to transform a set of likely correlated variables with unlikely correlated variables. Principal components number is less/equal to the variables original number. Following Monahan (2000), PCA fundamental equations are (*Eqs. 11–13*):

First vector $w_{(1)}$ should be answered as follows:

$$w_{(1)} = \arg \max_{\|w\|=1} \{ \sum_i (t_1)_{(i)}^2 \} = \arg \max_{\|w\|=1} \{ \sum_i (x_i \cdot w)^2 \} \quad (\text{Eq.11})$$

The matrix form of the above equation gives the following:

$$w_{(1)} = \arg \max_{\|w\|=1} \{ \|Xw\|^2 \} = \arg \max_{\|w\|=1} \{ w^T X^T Xw \} \quad (\text{Eq.12})$$

$w_{(1)}$ should be answered as follows:

$$w_{(1)} = \arg \max \left\{ \frac{w^T X^T X w}{w^T w} \right\} \quad (\text{Eq.13})$$

Originated $w_{(1)}$ suggests that first component of a data vector $x_{(i)}$ can then be expressed as a score of $tI_{(i)} = x_{(i)} \cdot w_{(1)}$ in the transformed coordinates, or as the corresponding vector in the original variables, $(x_{(i)} \cdot w_{(1)}) w_{(1)}$.

Validation

Validation of Water Radiometric Indices values was carried out using the ground truth data collection. 150 soil samples were analyzed for gravimetric soil water content and plotted against the remotely sensed values. The average accuracy is estimated by a horizontal function of the tested dataset. The average reliability is estimated by a vertical function of the tested dataset. The overall efficiency is estimated the diagonal function of the tested dataset. Following Congalton et al. (1983), a correspondence analysis (CA) was constructed as follows (Eq. 14):

$$CA = \frac{N \sum_{i=1}^r x_{ii} - \sum_{i=1}^r (x_{ij} * x_{ji})}{N^2 - \sum_{i=1}^r (x_{ij} * x_{ji})} \quad (\text{Eq.14})$$

where

r , the number of rows in the error matrix

x_{ii} , the number of observations in row i and column i (the diagonal cells)

x_{i+} , total observations of row i

x_{+i} , total observations of column i

N , a total of observations in the matrix

Results and discussion

Realization of different water radiometric indices was computed succeeding to adequate atmospheric and radiometric corrections. Spatial distribution of the implemented water radiometric indices and their corresponding temporal acquisitions are illustrated in *Figure 3a-e*. The first dataset was comprehended for winter water radiometric indices (January 2016) then six months later (July 2016) the analysis procedures were repeated for the summer dataset (*Fig. 3f-j*).

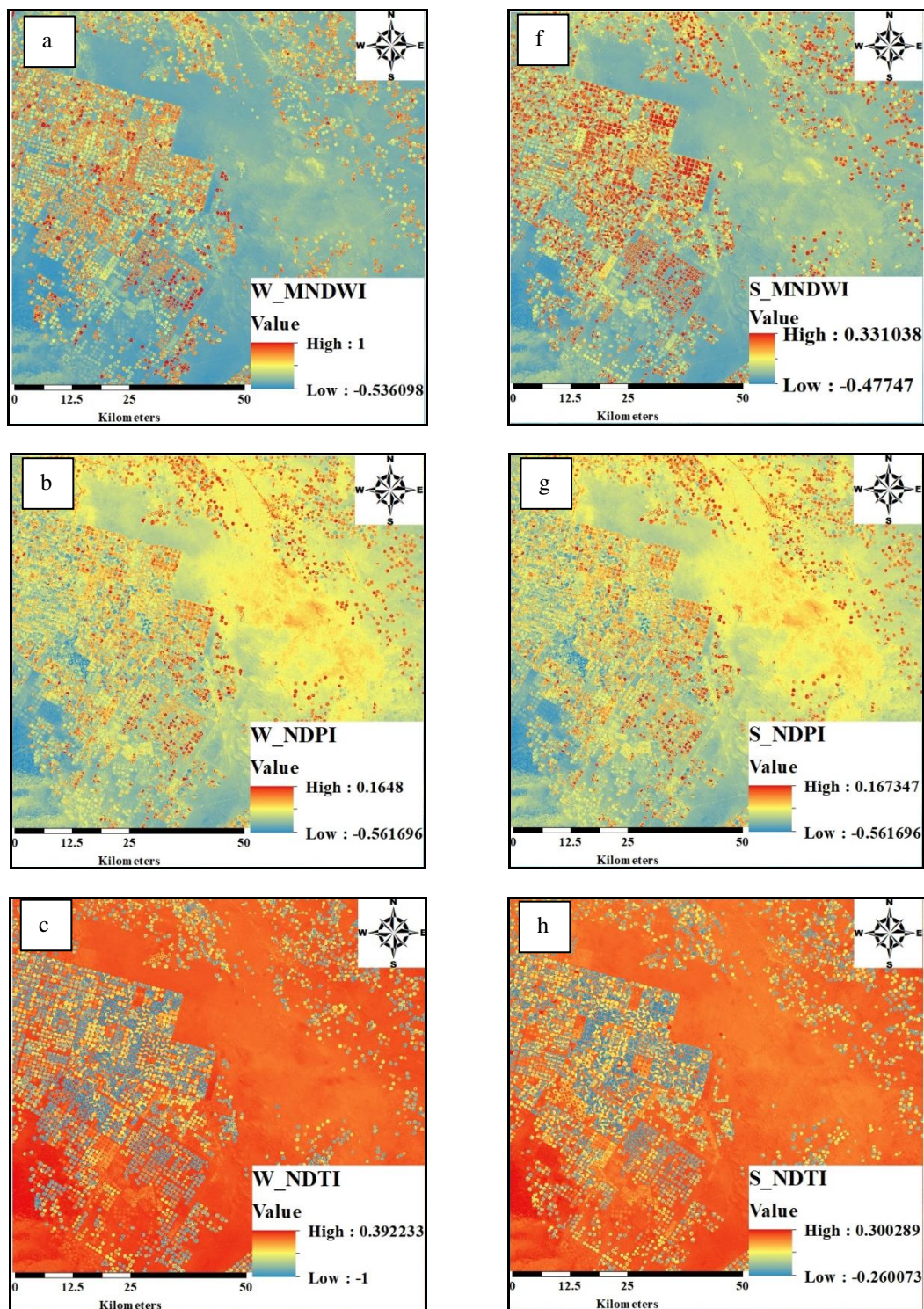
Field data collection and remote sensing techniques were practiced with precise synchronization to optimize the results. Soil water content collected from summer then later winter seasons shows a significant correlation RMSE 0.01. Therefore, the agricultural practice in the designated study area suggests an equivalent amount of the irrigational water utilized in both seasons (Elhag, 2016; Elhag and Bahrawi, 2017b).

Water radiometric indices conducted from remote sensing data showed inconsistency responses between winter and summer seasons (*Table 1* and *Fig. 4a,b*).

The estimated radiometric indices tend to respond preferably in winter rather than summer climatic condition (*Fig. 5a*). MNDWI shows a coherent pattern of estimation in different seasons. Such behavior could be considered as a lack of index sensitivity in the

summer season rather than in the winter season as it agreed with Wang et al. (2013) and Gautam et al. (2015).

NDPI shows an idealistic correlation between the two seasons (*Fig. 5b*). Henceforward, the only foreseen explanation is that there is no ponds formation in the study area and that is why the index cannot differentiate the seasonality dissimilarities. Consequently, NDPI can be exercised all year long with no season preferences (Ji et al., 2009; Dambach et al., 2012).



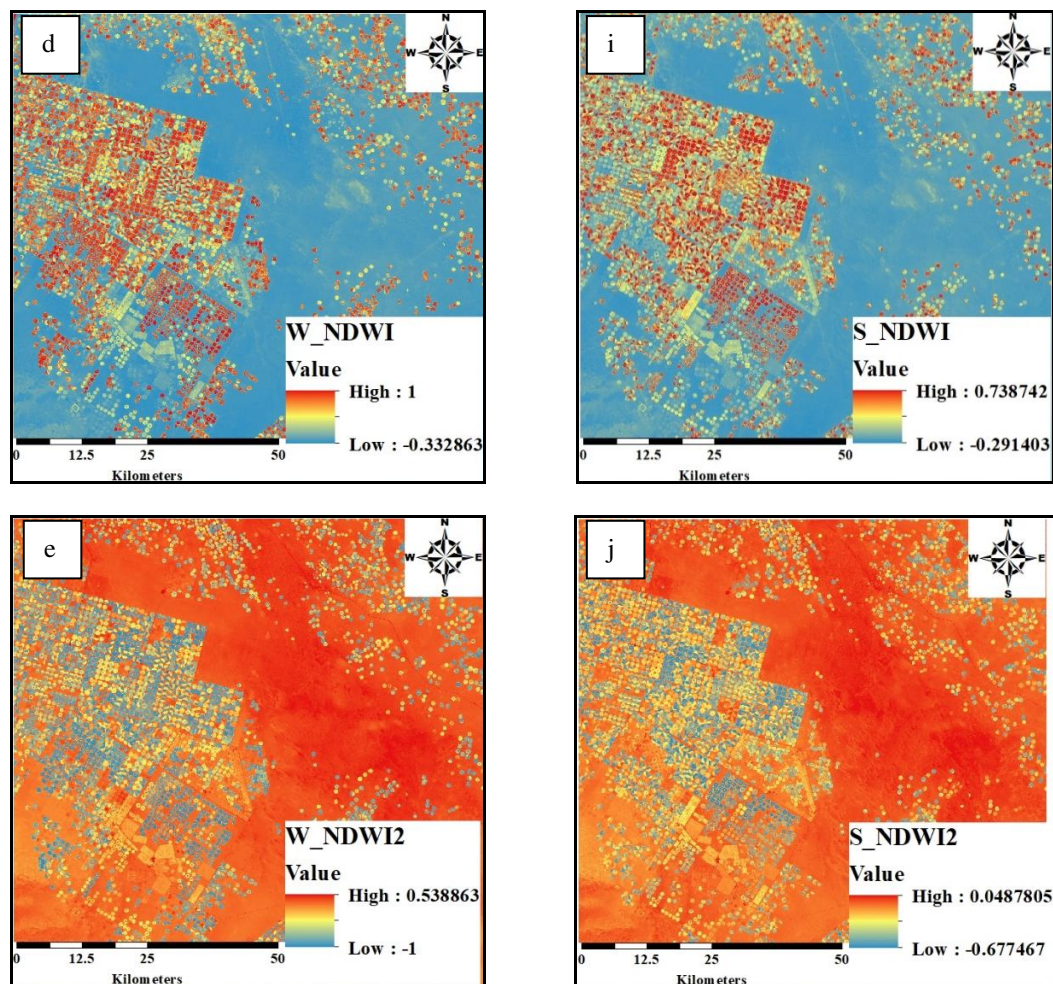


Figure 3. Spatial distribution of five different water radiometric indices in two different seasons (January as a winter season and July as a summer season-2016). **a–e** winter samples (W) and **f–j** summer samples (S)

Table 1. Statistical analysis of the estimated radiometric water indices

	Summer indices			Winter indices		
	R ²	RMSE	Equation	R ²	RMSE	Equation
MNDWI	0.6117	0.08	0.3232x - 0.4061	0.7146	0.06	0.3813x - 0.4643
NDPI	0.9046	0.01	0.1432x - 0.4365	0.9476	0.01	0.1642x - 0.4439
NDTI	0.5397	0.07	0.258x + 0.0287	0.5859	0.08	0.3574x - 0.0029
NDWI	0.4916	0.15	0.5033x - 0.1983	0.5501	0.15	0.6539x - 0.2522
NDWI-2	0.5718	0.07	0.2702x - 0.4212	0.6455	0.07	0.3747x - 0.5051

On the other side, NDTI shows steady correlation along with the seasonal variations (Fig. 5c). NDTI is the only index that showed optimum correlation stability among other radiometric water indices. Accordingly, NDTI behavior is explained by the lack of pure water surfaces and irrigational water is considered as turbid water as it is mixed with soil particles at the surface level as it is confirmed by other scholarly works (Daughtry et al., 2005; Serbin et al., 2009).

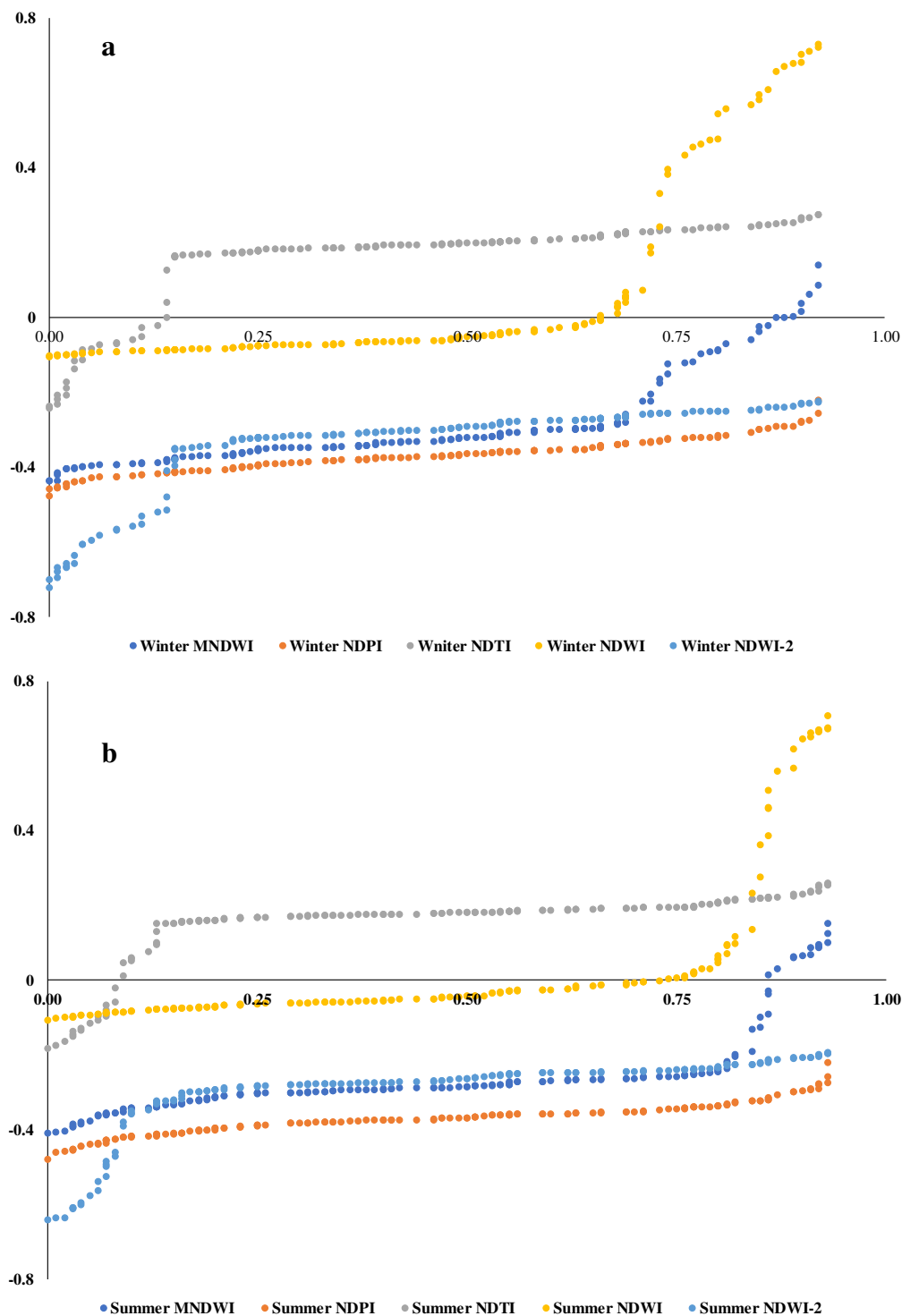
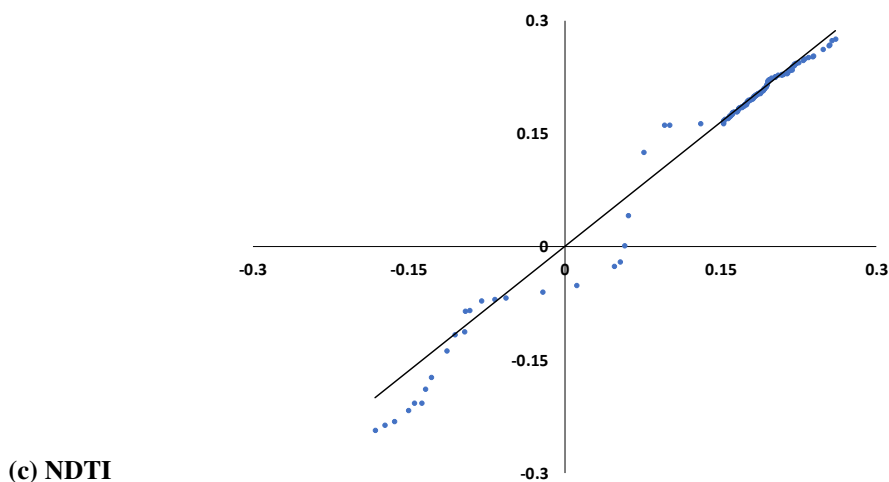
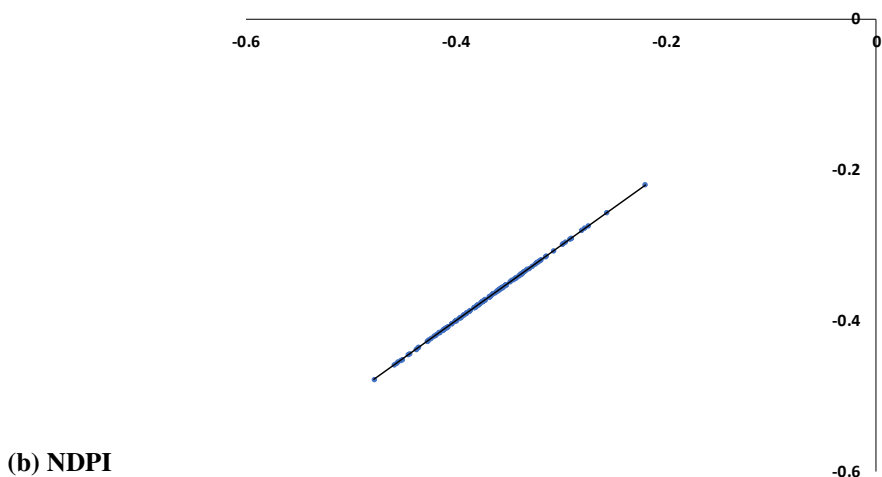
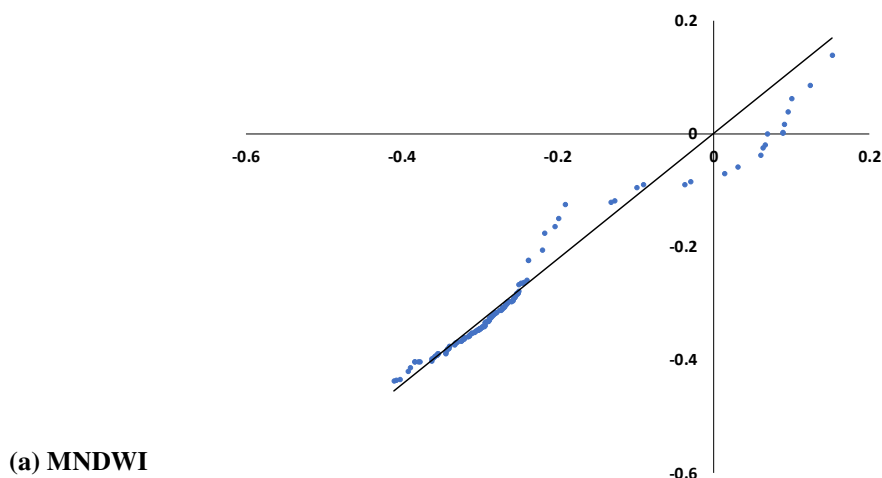


Figure 4. Seasonal variation of the estimated radiometric water indices (**a** for winter and **b** for summer)

Similar behavior to NDTI but with less accuracy is expressed by NDWI. NDWI shows a robust correlation with lower NDWI values rather than with higher values (Fig. 5d). Such results may promote NDWI to be used in winter rather than in summer conditions (Chen, 2006; Gu et al., 2007).

In contrary, the improved index of NDWI was exercised to contradict the sensitivity of the index to the seasonal conditions. NDWI-2 shows significant correlations in summer conditions with no winter condition preferences (Fig. 5e). Therefore, NDWI-2 could be considered as a summer index according to Soti et al. (2009) and Sánchez-Ruiz et al. (2014).



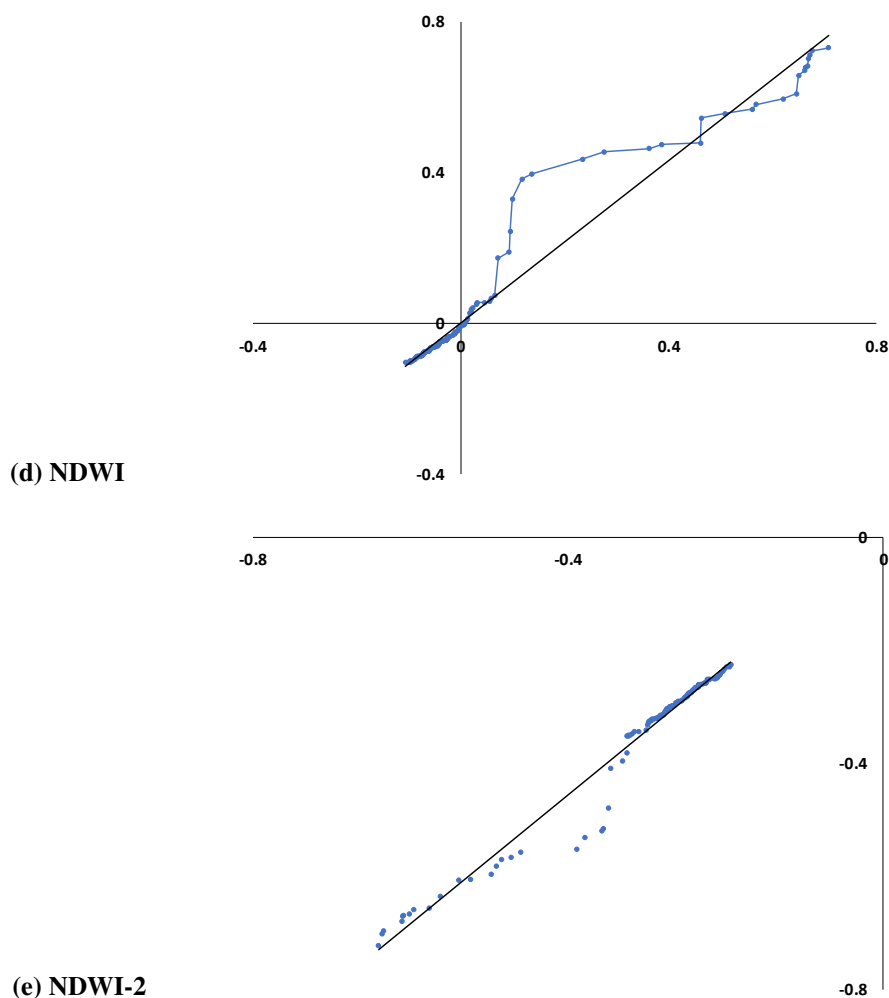


Figure 5. Seasonal radiometric water indices intercorrelation (x-axis is the winter measurements; y-axis is the summer measurements)

Principally, the water radiometric indices used in the current research are varied based on the utilized bands in each rationing. Therefore, categorization of different indices using principal component analysis will help to examine the indices discrepancies (Gidey et al., 2018). *Figure 5* represents the grouping of different indices according to principal component analysis on covariances in both seasons.

Generally, different water radiometric indices fell into two groups in both seasons. The first group contained NDPI and it showed no seasonal variation and kept a neutral behavior. Meanwhile, NDTI from one side and NDWI and MNDWI from the other side showed an alternative behavior across the two seasons (*Fig. 6*). Additionally, NDWI-2 is significantly correlated and grouped together (*Table 2*). Consequently, NDWI-2 is a superposed group (Dehni and Lounis, 2012). Lack of correlation is the main reason of NDTI and NDWI insignificance (*Table 2*). The implemented band length is the driving force of the correlation inconsequentiality between the previously mentioned indices (Lillesand et al., 2014).

The dynamicity of the soil water content dissimilarities proved by the seasonal variations added further complications to designate soil water content in a systematic

uniform perspective. The use of different algorithms based on implementing different combinations and/or ratios of Sentinel-2 bands in the form of water radiometric indices evidenced to be more efficient to overcome water dynamicity problems (Lei et al., 2014; Zhang et al., 2015).

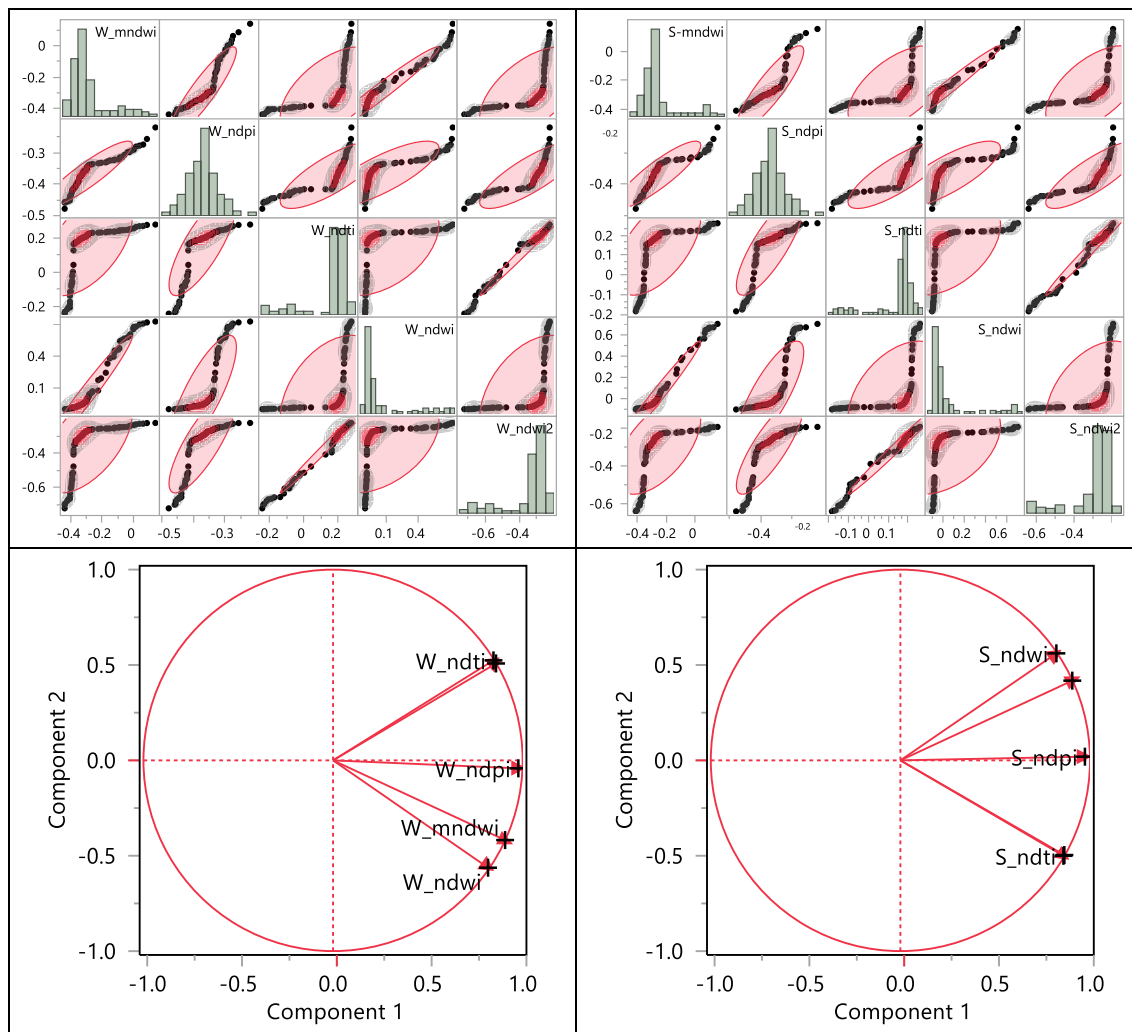


Figure 6. Principal Component Analysis and its correlation matrix of the different water radiometric indices

Table 2. Descriptive statistical analysis and covariant matrix

	W_mndwi	W_ndpi	W_ndti	W_ndwi	W_ndwi2
W_mndwi	1.0000	0.9025	0.5499	0.9766	0.5677
W_ndpi	0.9025	1.0000	0.7874	0.7985	0.8125
W_ndti	0.5499	0.7874	1.0000	0.4068	0.9943
W_ndwi	0.9766	0.7985	0.4068	1.0000	0.4208
W_ndwi2	0.5677	0.8125	0.9943	0.4208	1.0000

	S-mndwi	S_ndpi	S_ndti	S_ndwi	S_ndwi2
S-mndwi	1.0000	0.8796	0.5742	0.9832	0.5787
S_ndpi	0.8796	1.0000	0.8085	0.7919	0.8214
S_ndti	0.5742	0.8085	1.0000	0.4338	0.9917
S_ndwi	0.9832	0.7919	0.4338	1.0000	0.4370
S_ndwi2	0.5787	0.8214	0.9917	0.4370	1.0000

Column	N	DF	Mean	Std dev	Sum	Minimum	Maximum
W_mndwi	150	149	-0.293	0.116	-44.003	-0.437	0.139
W_ndpi	150	149	-0.370	0.043	-55.538	-0.478	-0.219
W_ndti	150	149	0.157	0.121	23.6101	-0.243	0.275
W_ndwi	150	149	0.041	0.228	6.1484	-0.104	0.731
W_ndwi2	150	149	-0.337	0.120	-50.563	-0.722	-0.224

Column	N	DF	Mean	Std dev	Sum	Minimum	Maximum
S-mndwi	150	149	-0.256	0.120	-38.480	-0.410	0.152
S_ndpi	150	149	-0.370	0.043	-55.538	-0.478	-0.219
S_ndti	150	149	0.148	0.102	22.2081	-0.182	0.260
S_ndwi	150	149	0.034	0.208	5.1805	-0.106	0.708
S_ndwi2	150	149	-0.296	0.103	-44.436	-0.640	-0.193

Moreover, higher soil water content was related to the improper and intense irrigation systems which are based on the lack of an operative water resource management plan in the designated study area (Koshal, 2012).

The selection of the profound satellite bands adequate for accurate water radiometric mapping is not systematically comprehensive (Lei et al., 2014; Zhang et al., 2013). Spatial inconsistency and land cover dissimilarities are the main controlling factors of the band sensor selection (Allbed and Kumar, 2013; Zhang et al., 2015). Consequently, the utilized water radiometric indices may have different results in specific areas using different band ratios others than the use of Sentinel-2 as a source of remote sensing data (Drusch et al., 2012; Zhu et al., 2015).

Conclusions

The groundwater resources in the Wadi As-Sirhan are the only water source for the agricultural practices that take place. Therefore, to sustain such agricultural activities in the designated study area an adequate technique of monitoring soil water content is crucial. Remote Sensing data acquired by Sentinel-2 proved to be statistically sufficient to estimate soil water content in two different climatic conditions. The implemented water radiometric indices in the current study can be primarily divided into two groups, climatic condition non-sensitive/ sensitive group. The non-sensitive group contains only the Normalized Difference Pond Index, while the sensitive group contains the rest of the water radiometric indices. Within the second group, there are indices which are less accurate in summer rather than in winter. Modified Normalized Difference Water Index and Normalized Difference Water Index-2 best-fitted winter soil water content estimations. Meanwhile, Normalized Difference Water Index and Normalized Difference Turbidity Index less-fitted winter estimations. However, the Normalized Difference Turbidity Index was statistically proved to be the most defined water radiometric index to estimate soil water content. The current irrigational schemes in Wadi As-Sirhan are not taking into consideration the temporal changes in the climatic conditions, where both summer and winter irrigational schemes are almost the same. Thus, the existing agricultural strategy in Wadi As-Sirhan needs to be revised precisely by the decision makers. Moreover, coherent groundwater resources consumption and soil water content monitoring need to be exercised.

Acknowledgements. This work was supported by the Deanship of Scientific Research (DSR) at King Abdulaziz University, Jeddah, under grant No. (G-192-155-38). The authors, therefore, gratefully acknowledge the DSR technical and financial support.

REFERENCES

- [1] Al-Rashed, M. F., Sherif, M. M. (2000): Water resources in the GCC countries: an overview. – *Water Resources Management* 14: 59-75.
- [2] Allbed, A., Kumar, L. (2013): Soil salinity mapping and monitoring in arid and semi-arid regions using remote sensing technology: a review. – *Advances in Remote Sensing* 2: 373.
- [3] Bahrawi, J. A., Elhag, M. (2016): Simulation of sea level rise and its impacts on the western coastal Area of Saudi Arabia. – *Indian Journal of Geo-Marine Sciences* 45: 54-61.

- [4] Bahrawi, J. A., Elhag, M., Aldhebiani, A. Y., Galal, H. K., Hegazy, A. K., Alghailani, E. (2016): Soil erosion estimation using remote sensing techniques in Wadi Yalamlam Basin, Saudi Arabia. – *Advances in Materials Science and Engineering*. <http://dx.doi.org/10.1155/2016/9585962>.
- [5] Beisl, U, Telaar, J., Schönermark, M. V. (2008): Atmospheric correction, reflectance calibration and BRDF correction for ADS40 image data. – *International Archives of the Photogrammetry, Remote Sensing and Spatial Information Sciences* 37: 7-12.
- [6] Chauhan, N. S. (2003): Spaceborne soil moisture estimation at high resolution: a microwave-optical/IR synergistic approach. – *International Journal of Remote Sensing* 24: 4599-622.
- [7] Chavez, P. S. (1996): Image-based atmospheric corrections-revisited and improved. – *Photogrammetric Engineering and Remote Sensing* 62: 1025-35.
- [8] Chen, Z. (2006): Effects of fire on major forest ecosystem processes: an overview. – *Ying Yong Sheng Tai Xue Bao* 17: 1726-32.
- [9] Congalton, R. G., Oderwald, R. G., Mead, R. A. (1983): Assessing Landsat classification accuracy using discrete multivariate analysis statistical techniques. – *Photogrammetric Engineering and Remote Sensing* 49: 1671-78.
- [10] Crippen, R. E. (1990): Calculating the vegetation index faster. – *Remote Sensing of Environment* 34: 71-73.
- [11] Dambach, P., Machault, V., Lacaux, J.-P., Vignolles, C., Sié, A., Sauerborn, R. (2012): Utilization of combined remote sensing techniques to detect environmental variables influencing malaria vector densities in rural West Africa. – *International Journal of Health Geographics* 11: 8.
- [12] Dasgupta, S. (2007): Remote sensing techniques for vegetation moisture and fire risk estimation. – Ph.D. Dissertation, George Mason University, Virginia, USA.
- [13] Daughtry, C. S. T., Hunt, E. R., Doraiswamy, P. C., McMurtrey, J. E. (2005): Remote sensing the spatial distribution of crop residues. – *Agronomy Journal* 97: 864-71.
- [14] Dehni, A., Lounis, M. (2012): Remote sensing techniques for salt affected soil mapping: application to the Oran region of Algeria. – *Procedia Engineering* 33: 188-98.
- [15] Drusch, M., Del Bello, U., Carlier, S., Colin, O., Fernandez, V., Gascon, F., Hoersch, B., Isola, C., Laberinti, P., Martimort, P. (2012): Sentinel-2: ESAs optical high-resolution mission for GMES operational services. – *Remote Sensing of Environment* 120: 25-36.
- [16] Du, Z., Li, W., Zhou, D., Tian, L., Ling, F., Wang, H., Gui, Y., Sun, B. (2014): Analysis of Landsat-8 OLI imagery for land surface water mapping. – *Remote Sensing Letters* 5: 672-81.
- [17] Elhag, M. (2016): Evaluation of different soil salinity mapping using remote sensing techniques in arid ecosystems, Saudi Arabia. – *Journal of Sensors*. <http://dx.doi.org/10.1155/2016/7596175>.
- [18] Elhag, M., Bahrawi, J. A. (2014a): Conservational use of remote sensing techniques for a novel rainwater harvesting in arid environment. – *Environmental Earth Sciences* 72: 4995-5005.
- [19] Elhag, M., Bahrawi, J. A. (2014b): Potential rainwater harvesting improvement using advanced remote sensing applications. – *Scientific World Journal*. <http://dx.doi.org/10.1155/2014/806959>.
- [20] Elhag, M., Bahrawi, J. A. (2017a): Realization of daily evapotranspiration in arid ecosystems based on remote sensing techniques. – *Geoscientific Instrumentation, Methods and Data Systems* 6: 141.
- [21] Elhag, M., Bahrawi, J. A. (2017b): Soil salinity mapping and hydrological drought indices assessment in arid environments based on remote sensing techniques. – *Geoscientific Instrumentation, Methods and Data Systems* 6: 149.
- [22] Engman, E. T. (1991): Applications of microwave remote sensing of soil moisture for water resources and agriculture. – *Remote Sensing of Environment* 35: 213-26.

- [23] FAO (1998): Guidelines for Computing Crop Water Requirements. – FAO Irrigation and Drainage Paper 56. FAO, Rome.
- [24] Ganaie, H. A., Hashaia, H., Kalota, D. (2013): Delineation of flood prone area using Normalized Difference Water Index (NDWI) and transect method: A case study of Kashmir Valley. – *International Journal of Remote Sensing Applications* 3: 53-58.
- [25] Gao, B.-C. (1996): NDWI—A normalized difference water index for remote sensing of vegetation liquid water from space. – *Remote Sensing of Environment* 58: 257-66.
- [26] Gautam, V .K., Gaurav, P. K., Murugan, P., Annadurai, M. (2015): Assessment of surface water dynamics in Bangalore using WRI, NDWI, MNDWI, supervised classification and KT transformation. – *Aquatic Procedia* 4: 739-46.
- [27] Gidey, E., Dikinya, O., Sebego, R., Segosebe, E., Zenebe, A. (2018): Modeling the spatio-temporal meteorological drought characteristics using the standardized precipitation index (SPI) in Raya and its environs, Northern Ethiopia. – *Earth Systems and Environment*. DOI: 10.1007/s41748-018-0057-7.
- [28] Gu, Y., Brown, J. F., Verdin, J. P. Wardlow, B. (2007): A five-year analysis of MODIS NDVI and NDWI for grassland drought assessment over the central Great Plains of the United States. – *Geophysical Research Letters* 34. <https://doi.org/10.1029/2006GL029127>.
- [29] Hawkins, R. H., Pole, R. A. (1989): Standardization of peak-volume transformations. – *JAWRA Journal of the American Water Resources Association* 25: 377-80.
- [30] Hoetzel, H. (1995): Groundwater recharge in an arid karst area (Saudi Arabia). – *IAHS Publications-Series of Proceedings and Reports-Intern Assoc Hydrological Sciences* 232: 195-210.
- [31] Ji, L., Zhang, L., Wylie, B. (2009): Analysis of dynamic thresholds for the normalized difference water index. – *Photogrammetric Engineering & Remote Sensing* 75: 1307-17.
- [32] Klute, A. (1986): *Methods of Soil Analysis, Part 1. Physical and Mineralogical Properties*. – American Society of Agronomy, Madison, WI.
- [33] Koshal, A. K. (2012): Spectral characteristics of soil salinity areas in parts of South-West Punjab through remote sensing and GIS. – *International Journal of Remote Sensing and GIS* 1: 84-89.
- [34] Lacaux, J. P., Tourre, Y. M., Vignolles, C., Ndione, J. A., Lafaye, M. (2007): Classification of ponds from high-spatial resolution remote sensing: Application to Rift Valley Fever epidemics in Senegal. – *Remote Sensing of Environment* 106: 66-74.
- [35] Lei, L., Tiyip, T., Jiang, H.-N., Kelimu, A. (2014): Study on the soil salinization monitoring based on measured hyperspectral and HSI data. – *Spectroscopy and Spectral Analysis* 34: 1948-53.
- [36] Li, W., Du, Z., Ling, F., Zhou, D., Wang, H., Gui, Y., Sun, B., Zhang, X. (2013): A comparison of land surface water mapping using the normalized difference water index from TM, ETM+ and ALI. – *Remote Sensing* 5: 5530-49.
- [37] Lillesand, T., Kiefer, R. W., Chipman, J. (2014): *Remote sensing and image interpretation*. – John Wiley & Sons, Hoboken.
- [38] Mathieu, R., Pouget, M., Cervelle, B., Escadafal, R. (1998): Relationships between satellite-based radiometric indices simulated using laboratory reflectance data and typical soil color of an arid environment. – *Remote Sensing of Environment* 66: 17-28.
- [39] McFeeters, S. K. (1996): The use of the Normalized Difference Water Index (NDWI) in the delineation of open water features. – *International Journal of Remote Sensing* 17: 1425-32.
- [40] Moghadas, D., Jadoon, K. Z., Vanderborght, J., Lambot, S., Vereecken, H. (2013): Effects of near surface soil moisture profiles during evaporation on far-field ground-penetrating radar data: A numerical study. – *Vadose Zone Journal* 12. DOI: 10.2136/vzj2012.0138.
- [41] Monahan, A. H. (2000): Nonlinear principal component analysis by neural networks: theory and application to the Lorenz system. – *Journal of Climate* 13: 821-35.

- [42] Muñoz-Carpena, R., Li, Y. C., Klassen, W., Dukes, M. D. (2005): Field comparison of tensiometer and granular matrix sensor automatic drip irrigation on tomato. – *HortTechnology* 15: 584-90.
- [43] Muñoz-Carpena, R., Regalado, C. M., Álvarez-Benedi, J., Bartoli, F. (2002): Field evaluation of the new Philip-Dunne permeameter for measuring saturated hydraulic conductivity. – *Soil Science* 167: 9-24.
- [44] Mustafa, A., Rahman, G. (2018): Assessing the spatio-temporal variability of meteorological drought in Jordan. – *Earth Systems and Environment*. DOI: 10.1007/s41748-018-0071-9.
- [45] Myneni, R. B., Hall, F. G., Sellers, P. J., Marshak, A. L. (1995): The interpretation of spectral vegetation indexes. – *IEEE transactions on Geoscience and Remote Sensing* 33: 481-86.
- [46] Ochsner, T. E., Cosh, M. H., Cuenca, R. H., Dorigo, W. A., Draper, C. S., Hagimoto, Y., Kerr, Y. H., Njoku, E. G., Small, E. E., Zreda, M. (2013): State of the art in large-scale soil moisture monitoring. – *Soil Science Society of America Journal* 77: 1888-919.
- [47] Palecki, M. A., Bell, J. E. (2013): US Climate Reference Network soil moisture observations with triple redundancy: Measurement variability. – *Vadose Zone Journal* 12. <https://doi.org/10.2136/vzj2012.0158>.
- [48] Psilovikos, A., Elhag, M. (2013): Forecasting of remotely sensed daily evapotranspiration data over Nile Delta region, Egypt. – *Water Resources Management* 27: 4115-30.
- [49] Sánchez-Ruiz, S., Piles, M., Sánchez, N., Martínez-Fernández, J., Vall-llossera, M., Camps, A. (2014): Combining SMOS with visible and near/shortwave/thermal infrared satellite data for high resolution soil moisture estimates. – *Journal of Hydrology* 516: 273-83.
- [50] Şen, Z., Al-Harithy, S., As-Sefry, S., Almazroui, M. (2017): Aridity and risk calculations in saudi arabian wadis: Wadi Fatimah case. – *Earth Systems and Environment* 1: 26.
- [51] Serbin, G., Hunt, E. R., Daughtry, C. S. T., McCarty, G. W., Doraiswamy, P. C. (2009): An improved ASTER index for remote sensing of crop residue. – *Remote Sensing* 1: 971-91.
- [52] Singh, K. V., Setia, R. Sahoo, S., Prasad, A., Pateriya, B. (2015): Evaluation of NDWI and MNDWI for assessment of waterlogging by integrating digital elevation model and groundwater level. – *Geocarto International* 30: 650-61.
- [53] Soti, V., Tran, A., Bailly, J.-S., Puech, C., Seen, D. L., Bégué, A. (2009): Assessing optical earth observation systems for mapping and monitoring temporary ponds in arid areas. – *International Journal of Applied Earth Observation and Geoinformation* 11: 344-51.
- [54] Su, Z., Troch, P. A., Troch, F. P. De, Nochtergale, L., Cosyn, B. (1995): Preliminary results of soil moisture retrieval from ESAR (EMAC 94) and ERS-1/SAR. Part II: Soil moisture retrieval. – In: *Proceedings of the Second Workshop on Hydrological and Microwave Scattering Modelling for Spatial and Temporal Soil Moisture Mapping from ERS-1 and JERS-1*.
- [55] Thompson, D. R., Natraj, V., Green, R. O., Helmlinger, M. C., Gao, B.-C. Eastwood, M. L. (2018): Optimal estimation for imaging spectrometer atmospheric correction. – *Remote Sensing of Environment* 216: 355-73.
- [56] Walker, J. P. (1999): Estimating soil moisture profile dynamics from near-surface soil moisture measurements and standard meteorological data. – University of Newcastle, New South Wales, Australia.
- [57] Wang, Y., Huang, F., Wei, Y. (2013): Water body extraction from LANDSAT ETM+ image using MNDWI and KT transformation. – In: *Geoinformatics (GEOINFORMATICS), 2013 21st International Conference*, 1-5. IEEE.
- [58] Watson, D. M., Doerr, V. A. J., Banks, S. C., Driscoll, D. A., van der Ree, R., Doerr, E. D., Sunnucks, P. (2017): Monitoring ecological consequences of efforts to restore landscape-scale connectivity. – *Biological Conservation* 206: 201-09.

- [59] Wood, E. F., Lettenmaier, D. P., Zartarian, V. G. (1992): A land-surface hydrology parameterization with subgrid variability for general circulation models. – *Journal of Geophysical Research: Atmospheres* 97: 2717-28.
- [60] Xu, H. (2006): Modification of normalised difference water index (NDWI) to enhance open water features in remotely sensed imagery. – *International Journal of Remote Sensing* 27: 3025-33.
- [61] Zhang, C. W., Tang, J. K., Yu, X. J., Wang, C. L., Mi, S. J. (2013): Quantitative retrieval of soil salt content based on remote sensing in the Yellow River delta. – *Journal of Graduate University of Chinese Academy of Sciences* 30: 220-27.
- [62] Zhang, H.-W., Chen, H.-L. (2016): The application of modified normalized difference water index by leaf area index in the retrieval of regional drought monitoring. – *DEStech Transactions on Engineering and Technology Research*. DOI: 10.5194/isprsarchives-XL-7-W3-141-2015.
- [63] Zhang, T., Zhao, G., Chang, C., Wang, Z., Li, P., An, D., Jia, J. (2015): Information extraction method of soil salinity in typical areas of the yellow river delta based on landsat imagery. – *Agricultural Sciences* 6: 71.
- [64] Zhu, Y., Ren, L., Lu, H. Skaggs, T. H. (2008): Determination of root-zone water storage in a desert woodland using a two-layer moisture balance model. – *IAHS Publication* 322: 246.
- [65] Zhu, Z., Wang, S., Woodcock, C. E. (2015): Improvement and expansion of the Fmask algorithm: cloud, cloud shadow, and snow detection for Landsats 4–7, 8, and Sentinel 2 images. – *Remote Sensing of Environment* 159: 269-77.

THE EFFECT OF POMEGRANATE PEEL AND PISTACHIO HULLS ON PERFORMANCE AND ENTERIC METHANE EMISSIONS IN STRAW-FED LAMBS (*Ovis aries* L.)

YURTSEVEN, S.^{1*} – KAYA, Z.¹ – TAKIM, K.²

¹Faculty of Agriculture, Dept. of Anim. Science, University of Harran, 63000 Şanlıurfa, Turkey

²Faculty of Veterinary Medicine, University of Harran, 63100 Şanlıurfa, Turkey

*Corresponding author

e-mail: syurtseven2001@yahoo.com; phone: +90-414-318-3474; fax: +90-414-318-3274

(Received 10th Sep 2018; accepted 29th Nov 2018)

Abstract. This trial was conducted to determine the effect of pomegranate peel (PP) and pistachio hulls (PH) added to wheat straw (WS) on some performance parameters and production of some greenhouse gases in female *Awassi* lambs (*Ovis aries* L.). This research was conducted in Şanlıurfa province in Southeastern Turkey and it was done at Harran University Faculty of Agriculture. Fifteen lambs were used in a completely randomized design with 52 days periods (45 days of fattening performance and 7 days of gas measurements) and three treatments: control (90% concentrate + 10% WS); PP (90% concentrate + 5% PP + 5% WS); and PH (90% concentrate + 5% PH + 5% WS). Emissions of nitrous oxide (N₂O) and enteric methane (CH₄), and carbon dioxide (CO₂) production were also measured during the last week (7 days). Performance parameters did not change with inclusion of PP and PH in the diet for 0–6 weeks. However, inclusion of PP decreased feed intake during 0–3 weeks. The CO₂ emissions (as g day⁻¹ lamb⁻¹ and g kg⁻¹ dry matter intake) significantly increased in the PP and PH groups, but CH₄ emissions did not significantly change. Total N₂O (g⁻¹ day⁻¹ lamb) emissions from feces were affected by inclusion of PH in the diet. The PH supplementation showed a strong tendency for reducing N₂O emissions from feces of lambs.

Keywords: methane, by-product, manure, sheep, tannin

Introduction

The increase in individual consumption causes the amount of vegetable waste to increase rapidly. An important method of recovery in sustainable vegetable waste management is composting. Another important option is to evaluate wastes such as fruit peel as animal feed. Production of pomegranate and pistachio has increased due to the South Anatolian Project in the Southeastern Anatolia region of Turkey. According to the Turkish Statistics Institution (TUIK, 2016), 144 000 ton of pistachios were produced in Turkey during 2015. Of this, 30% is produced in Şanlıurfa Province, with an average for the last 5 years of 38000–42000 ton/year (TUIK, 2015). In Şanlıurfa, 7 tonnes of soft shells or hulls are produced annually. The pistachio soft hull (PH) is red or burgundy colored and is separated by post-harvest crushing. It is composed of fruit stem, leaf, fruit content, and mesocarp (middle shell) (Shakeri et al., 2014). The PH obtained from the factories also contains some tree leaves.

The PH contains high concentrations of non-structural carbohydrate (36%–40%), moderate concentrations of crude protein (11.4%–13%), 6% fat, and 30%–33.3% neutral detergent fiber - NDF (Shakeri et al., 2013). The PH contains high concentrations of polyphenolic compounds (7.8%) and the halves of these compounds are composed of tannins (Shakeri et al., 2013). Therefore PH cannot enter as only one rough feed in ratio. In Şanlıurfa, 9600 tonnes of pomegranates are produced per year

(TUIK, 2016). Since 48% of the total weight of pomegranate consists of soft crust, 4800 tonnes of these are produced annually. Tannins, which are found in pomegranate seeds and peels (PP) or PH, exhibit inhibitory effects on protein binding and bacterial proliferation and have antimicrobial, antioxidant, and anti-inflammatory effects in digestion both *in vivo* and *in vitro* (Adams et al., 2006; Jayaprakasha et al., 2006; Zarei, 2013).

N₂O is a dangerous greenhouse gas and expected to increase by 35-60% by 2030 with an increase in demand for meat and dairy products (IPCC, 2007). PP or PH containing tannins may improve N utilization efficiency and thereby decrease the N content of manure, which, in turn, may affect N₂O emissions because less N is available to the denitrifying bacteria that use the manure as substrate.

The addition of saponins from PP can thus modify the C and N contents of sheep manure. Sheep (*Ovis aries* L.) produce 8 kg of enteric methane (CH₄) gas per animal per year (Broucek, 2014) and any CH₄ reduction potential due to tannins suppressing CH₄-producing microorganisms in the rumen will be determined *in vivo*. PP and PH can also provide an advantage especially for lowering the higher fiber concentration that comes with the wheat straw. This study will also investigate the potential of PP and PH as forage sources to reduce the use of wheat straw.

Materials and methods

Animal and feed material

The study was conducted between December and November at Sanliurfa province in the Southeast Anatolian Region of Turkey, which lies on 37°9'32.9364 latitude (N) and 38°47'48.8724 longitude (W). Research on animals was conducted according to the institutional committee on animal use. Ethics committee approval was obtained from DOLLVET animal vaccine production center (DOLLVET-HADYEK-2015/01). The experiment was carried out on 6-month-old female Awassi lambs (*Ovis aries* L.) for 52 days: 45 days of fattening performance and 7 days of gas measurements. The total of 15 lambs was divided into three groups (*Table 1*) with five individual compartments of similar individual weight (29.13 ± 3.18 kg) and age (*Fig. 1*).

Table 1. *Experimental groups*

Groups	Concentrate	Forage
1-Control	90 (%)	10 (%) straw
2-Pomegranate peel (PP)	90 (%)	5 (%) straw + 5 (%) pomegranate peel
3-Pistachio hulls (PH) ¹	90 (%)	5 (%) straw + 3 (%) pistachio hulls + 2 (%) pistachio hulls and leaves

¹; PH in the study consists of a mixture of pure pistachio hull and some leafy fraction

The rations were given to the animals as mixed forage and concentrated feed total mixed ration (TMR; *Table 2*). The rate of WS used in the control ration was 10%; PP and PH replaced half of the WS to form the other feeding groups. Dry PP containing some crushed grain was obtained by drying in the sun at 40 °C for 1 week.

The PH used in the study consisted of pure soft burgundy fraction and a small amount of pistachio tree leaves. Dry PP and WS (3–5 cm) were crushed; and the PH was used without treatment (*Table 3*). In order not to stress the lambs, the feeding was

done by adding every morning during the week as a little more than the maximum amount that they could consume daily. At the end of each week, the remaining feed was weighed and subtracted from the feed added for one week and divided into 7 days. Thus, daily feed consumption was found.

Table 2. Contents of total mixed ration (TMR) used in the lamb growth diet in the experiment (g/kg as fed basis)

Feed ingredient	Control	PP ¹	PH
Barley	216.9	216.9	216.9
Corn	266.58	266.58	266.58
Soybean meal	165.78	165.78	165.78
Wheat bran	225	225	225
Limestone	19.44	19.44	19.44
Salt	5.4	5.4	5.4
Vit + min.pre. ²	0.9	0.9	0.9
Wheat straw	100	50	50
PP	0	50	0
PH	0	0	50
Total	1000	1000	1000
Nutrient values (as fed basis)			
Dry matter (%)	89.7	89.4	89.6
ME (Mcal/kg)	2.4	2.4	2.4
Crude protein (%)	16	15.9	15.9
Ether extract (%)	3	3	3
Crude fiber (%)	9.7	9.25	8.4
ADF (%)	11.6	11.8	10.2
NDF (%)	26.8	25.3	24.4
Ash (%)	4.08	4.2	4.1
Calcium (%)	0.87	0.86	0.86
Phosphorus (%)	0.6	0.59	0.59
Sodium (%)	0.31	0.3	0.32
Tannin (mg eq/g) ³	38.25	68.44	79.36
Saponin (mg/g) ³	15.8	54.71	15.6

¹; PP, pomegranate peel; PH, Pistachio hulls. ME, methabolic energy, ²; 1 kg vitamin mineral mixture: 15.000 IU vitamin A, 25 mg Vit E, 4000 IU Vit D3; Trace minerals: Fe: 50 mg, Co: 0.1 mg, Mn: 50 mg, Se: 0.2 mg, I: 0.8 mg, Cu: 10 mg, Zn: 50 mg, ³ ; Dry matter bases

Table 3. Nutritional values of plant byproducts used in the experiment (as fed basis)

	PP ¹	Pistachio hulls	Pistachio hulls and leaves	Wheat straw
Dry matter (%)	91.00	92.00	92.00	91
Crude ash (%)	8.00	9.00	8.50	8.0
Crude protein (%)	5.83	7.03	4.40	8.2
ADF (%)	48.50	20.19	20.6	52
NDF (%)	55.20	24.39	28.2	80

¹; PP, pomegranate peel; ADF, acid detergent fiber; NDF, neutral detergent fiber

CH₄, carbon dioxide (CO₂) and nitrous oxide (N₂O) measurements in respiration chamber

The enteric CH₄ measurement was initiated in lambs adapted to their feed for 45 days. For this purpose, an isolated container (dimensions 2 × 2 × 2 m) with two chambers was turned into a respiration chamber with controlled air inlets and outlets (*Fig. 1*).



Figure 1. Individual compartments and respiration chamber

As there was herd/flock of psychology in the lambs, the rooms were arranged with glass windows. The lambs were able to see each other and reduce stress. In addition, they were left in the room for 24 hours in order to reduce the effect of stress and acclimate to the room environment. Two pipes (as inlet and outlet) were each attached to a fan of approximately 0.25 m³/sec. air supply capacity in each room. The pipes were cylindrical chimneys with a diameter of 10 cm and a length of 30 cm and fresh air was pumped into each room with a fan in the inlet pipe and extracted by another fan in the outlet pipe. Gas emissions were measured by subtracting the concentrations of the gases in the air entering and leaving the chamber.

After the lambs were taken to the room, the fans were activated and the temperature and humidity inside and outside the room were recorded. For each animal, air samples were taken with syringes at least 5–6 times for both inlet and outlet from fan cylinders during daylight and were immediately sealed with an airtight cover. After the end of day light, the sampling was continued and samples were taken every 2 hours. During the gas measurement period, the lambs stayed in the respiratory room with feeders for 23 hours from 08.30 h in the morning until 07:30 h the following morning.

At intervals of 1 h, the rooms were ventilated and the stool and urine of the previous lamb were removed. Gases were identified with gas chromatography (GC) on sampled syringe tubes as ppm for entering and exiting air (SRI Instruments-European Greenhouse GC System® - Germany). A 3-m Hayesep D packed column

was used for CO₂, CH₄, and N₂O diagnosis. Operating conditions for GC: injector temperature was 95°C, column temperature was 85°C, and detector temperature was 320°C–350°C.

Gas concentrations were calculated using the following formula (Petrucci et al., 2010) in the incoming and outgoing air (Eq. 1):

$$CO_2, CH_4, N_2O = \left[C \cdot Ma \frac{P}{RT} V \cdot A \right] \quad (\text{Eq.1})$$

CH₄, CO₂ and N₂O in g/sec, C is fresh air entering the room and gas concentration in the leaving air (ppm), Ma is gas molecular weight (g/mol), P is barometric air pressure (Pa), V is entering and leaving air velocity (m/sec), R is the universal gas constant (8.31 J/molK¹), T is ambient temperature, and A is area of a cross-section of the cylindrical chamber (0.0250 m²).

Chemical analyses

Dry matter, crude ash, and crude protein analyses of feeds used in the trials were performed according to the classical AOAC (1998) procedures. Fiber analyses (acid detergent fiber - ADF and NDF) were performed with an ANKOM Fiber Analyzer according to Van Soest et al. (1991).

Tannin analysis

A standard tannin analysis curve was prepared according to Makkar et al. (1995) and used to calculate tannin contents (Table 4). To prepare the standard curve, 2, 4, 6, 8, 10, and 12 µg/ml pure tannin was placed in the test tubes, 500 µl of Folin Ciocalteu separator was added and mixed for 3 min. After addition of 2500 µl of Na₂CO₃, the tubes were shaken for 60 min, and absorbance measured at 725 nm. The regression equation obtained from reading values revealed tannin concentrations of the feed samples.

The feed samples milled to 1 mm were treated with the condensed tannin (CT) solution. For the CT solution, 0.05 g of FeSO₄ was added to the tube and 0.015 g of ground sample was added. Then 2 ml of 0.55 M butanol–HCl reagent was added to each tube and then mixed with a vortex. The test tube was tightly sealed, kept at 97–100 °C for 1 h, and absorbance values measured at 580 nm (Karaogul, 2011).

Table 4. Determination of condensed tannin value from standard curve

Items	Standard compound	Calibration equation	R ²	LOD/LOQ ³ (µg l ⁻¹)	Q ⁴ (mg equivalent g ⁻¹ dry matter)
Wheat straw	Tannic acid	Y = 0.053x+0.0067	0.98	0–12	35.59 ± 0.74
PP ¹	Tannic acid				103.52 ± 1.65
Pistachio pure hulls	Tannic acid				173.96 ± 2.12
Pistachio hull and leaf (PH) ²	Tannic acid				89.05 ± 0.57

¹ ; PP, pomegranate peel, ² ; PH, consists of pure soft burgundy fraction and a fraction containing a quantity of pistachio tree leaves, ³; LOD/LOQ: Limit of detection/Limit of quantification, ⁴; Quantification

Statistical analyses

Performance data were analyzed in the One-Way ANOVA procedure according to the experimental design of the three-group randomized design and the treatment combinations were compared with the Duncan's test using SPSS. As for gas emission values, the data were statistically analyzed with Levene's test and Shapiro Wilk test for equality of variances and the normality assumption, respectively ($P < 0.05$). Then, these data were analyzed by using Kruskal Wallis H test (SPSS, Version 22, 2013) and presented with median and IQR values (interquartile range) in *Table 5*.

Table 5. Non-parametric results of gas emission values

Groups	Emission (g/day lamb)	Means	Standard deviation	Median	IQR ⁽²⁾	P-value
Control	CH ₄	46.87	26.67	45.26	-	0.21
PP ¹		36.79	13.71	34.06	16.48	
PH ¹		18.72	22.03	11.40	36.36	
Control	CO ₂	514.43	50.9	514.96	412.97	0.04
PP		1079.90	290.6	994.34	924.79	
PH		700.53	91.91	714.25	-	
Control	N ₂ O	186.25	56.84	186.25	-	0.05
PP		182.36	108.42	166.86	206.93	
PH		59.26	21.99	56.25	43.56	

¹; PP, pomegranate peel; PH, pistachio hulls, ²; IQR, interquartile range: quarter value width, the third quadrant and the first quadrant range of an ordered data array

Results

There was no significant difference during the 0-6 week periods of the experiment in terms of the data on the effects of PP and PH additions on feed consumption, live weight change (*Fig. 2*), and feed conversion ratio (*Table 6*).

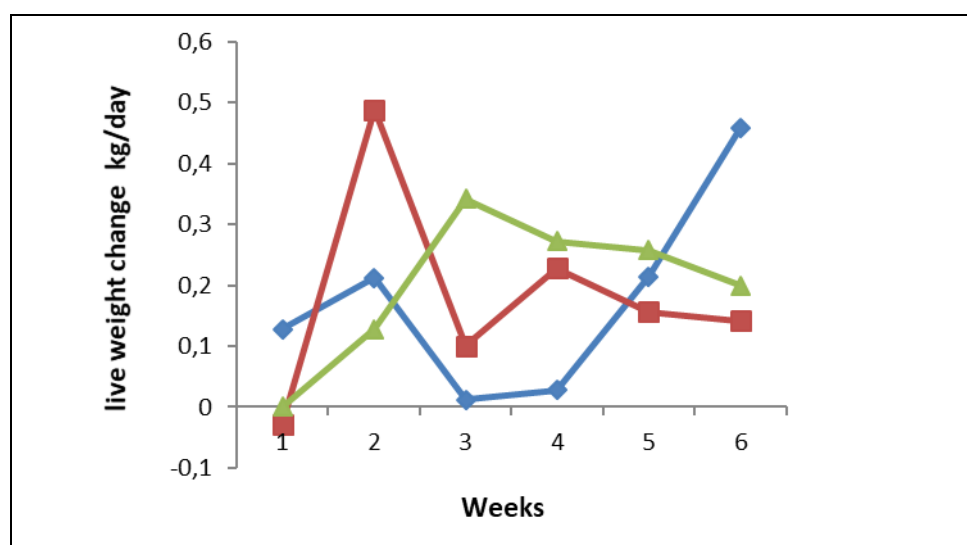


Figure 2. The time dependent changes in live weight gain/change in experimental groups

Table 6. Means of performance data in the experimental groups during the first half and the last half of the trial

	Weeks	Control	PP ¹	PH ²	SEM ³	P-value
Feed consumption (kg/day as fed)	0–3	1.93b ⁴	1.83a	1.93b	0.02	0.02
	3–6	1.90	1.94	1.97	0.03	0.27
	0–6	1.92	1.88	1.95	0.02	0.16
Metabolic energy intake (Mcal/day)	0–3	4.60b	4.41a	4.62b	0.04	0.02
	3–6	4.57	4.62	4.73	0.06	0.25
	0–6	4.61	4.55	4.68	0.05	0.16
Live weight gain (g/day)	0–3	120	220	158	68.8	0.63
	3–6	234	176	244	26.1	0.22
	0–6	213	182	202	29.8	0.81
Feed conversion ratio	0–3	8.19	12.95	15.18	4.59	0.56
	3–6	8.30	13.06	8.40	1.26	0.06
	0–6	9.43	13.9	10.0	1.89	0.37

¹; PP, pomegranate peel, ²; PH, pistachio hulls, ³; SEM, standard error of the mean, ⁴; Different letters show significant differences between the columns in the same row

Except for the first week of the experiment, no significant differences in these performance values were observed. In the first 3 weeks of the experiment ($P < 0.05$), feed consumption was lower in lambs receiving PP (Fig. 3) in terms of trial averages, and similar live weight gains were obtained in all groups ($P > 0.05$).

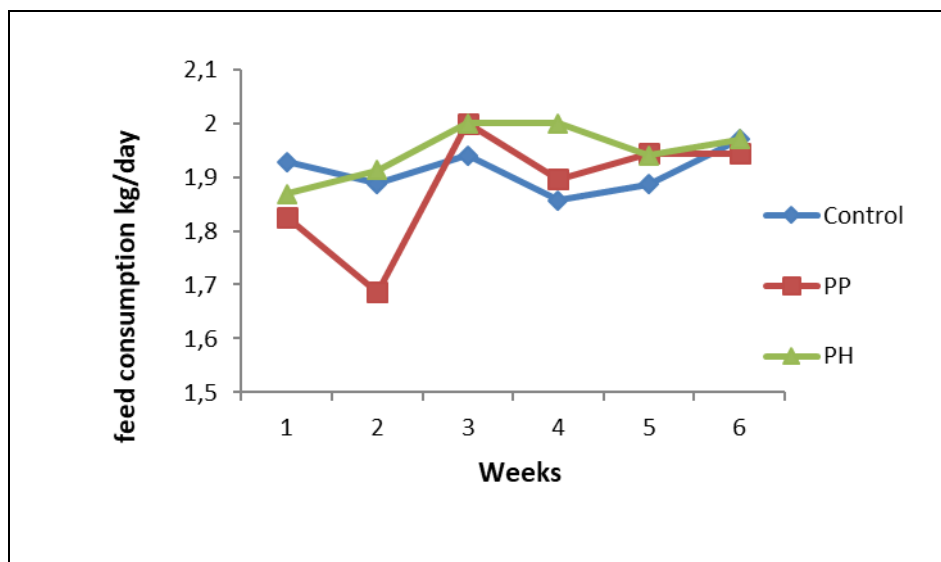


Figure 3. The time dependent changes in feed consumption in experimental groups

Energy consumption was similar throughout the trial in all groups, except during the first weeks ($P < 0.05$). The CH_4 emissions were similar in all groups, but with a decreasing trend for PP and PH groups ($P = 0.07$). However, carbon emissions were higher in the PP and PH groups ($P < 0.05$; Tables 5 and 7). The N_2O emission (g/day lamb¹) in the PH group was lower than in the control and PP group ($P = 0.05$; Fig. 4).

Table 7. Gas emission values according to daily dry matter consumption

	Control	PP ¹	PH ¹	SEM ⁽²⁾	P-value
CH ₄ (g/kg DMI)	24.42	19.74	9.56	5.65	0.07
CO ₂ (g/kg DMI)	268.13a, ³	578.88b	359.31a	70.60	0.03
N ₂ O (g/kg DMI)	100.07b	98.62b	25.97a	34.85	0.03

¹; PP, pomegranate peel; PH, pistachio hulls; DMI, dry matter intake, ²; SEM, standard error of the mean, ³; Different letters show significant differences between the columns in the same row

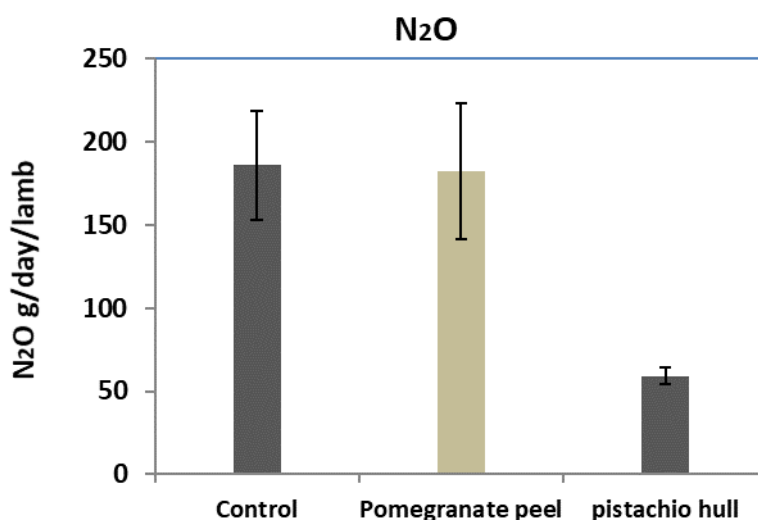


Figure 4. The changes in N₂O emission levels among groups

Discussion

Within the first 3 weeks of the experiment, PP negatively affected feed consumption. This negative effect lasted 3 weeks and became less pronounced during the later weeks of the experiment (*Figs. 2 and 3*) probably due to adaptation to the taste of PP. Provenza (1995) suggests that negative feedback responses diminish over time depending on the negative factor.

The results we obtained were consistent with the results reported by Ghaffari et al. (2014), who feed Afshari and Balouchi male lambs with 30% PH and did not observe any change in feed intake. The CT concentration in some plants did not limit feed consumption at 50 g/kg dry matter (DM) (Barry and McNabb, 1999). However, Bhatta et al. (2002) found that consumption was reduced at CT concentrations above 60 g/kg. In our study, CT at 90.53 g/kg concentrations in the PH groups did not cause a significant decrease in feed consumption except during the first weeks – this may be due to the difference in plant species. Consistent with our findings, Addisu et al (2016) reported that low or moderate concentrations of CT (20–45 mg equivalent/g DM) in feed stuffs did not affect feed consumption. According to Villalba and Provenza (2000), feed consumption of lambs can improve if a low-quality feed is associated with a nutrient. In our study, TMR was preferred in the first 3 weeks in PH groups due to

higher protein concentration of PH than PP. However, it is also possible that the higher saponin content in PP groups may cause fluctuations in feed consumption.

The tendency to similar live weight gain in all groups can be attributed to an internal mechanism related to lambs, but the inclusion of PP as half of the forage had a clear negative effect on the lambs. Abarghuei et al. (2013) suggest that PP contains high concentrations of saponin which reduces protein digestibility due to negative effects on digestion, and decreases feed consumption by reducing the palatability. Compared to PH, the lambs reacted more negatively to the PP, indicating that feeds such as pomegranate are more problematic in terms of taste. Kotsampasi et al. (2014) stated that the addition of PP to the TMR at concentrations of 0, 120, and 240 g/kg did not significantly affect live weight, live weight gain, DM consumption, and feed utilization. Norouzian and Ghiasi (2012) found that PH substituted for up to 30% of forage did not significantly change the performance values of lambs, showed no adverse effects, and could be used a part of forage in lamb fattening. However, PP was tolerated by lambs in later periods of the current study.

The consumption values obtained in our study showed that the CT content of PH was less unappealing for the lambs. According to Sadq et al. (2016), CT has a less reducing effect on digestion and voluntary feed intake. When considering feed consumption, lambs need some time to become accustomed to PH and PP feed. Shabtay et al. (2008) found that fresh PH linearly increased feed consumption and was accompanied by an increased live weight gain – the introduction of tannin-rich PH up to 20% of the ration had positive effects on fattening performance with no harmful effect.

In our study, addition of PP and PH did not significantly affect emissions of enteric CH₄ but there was a declining trend for PP and PH groups in CH₄ emission values when calculated according to kg feed intake ($P = 0.07$). The CH₄ was of enteric origin and CO₂ both enteric and respiratory, because feces in an open environment are not an important source of CH₄ and CO₂. Because of wheat straw's low digestibility, enteric CH₄ production is an important problem but no significant effect of CT in wheat straw-based feeding was observed in our study, and the effects of CT on rumen CH₄ emissions were not clear. The CT generally form complex bonds with ruminal cellulose and reduce hydrogen utilization for methanogenesis (Pinerio-Vazquez et al., 2015).

It is likely that a reduction in WS concentration, the source of cellulose, in the PP and PH groups may have caused the current effect to be hidden. The average daily CH₄ production per animal was 33.5 g over all groups, corresponding to annual CH₄ emission of 12.2 kg per animal. Broucek (2014) found that milk sheep produce 8.4 kg of CH₄ per animal annually, which is lower than that obtained in our study. The difference can be attributed to different breeds used between the studies.

The CO₂ detected may be of both enteric and respiratory origin. The CT can also increase the content of glycoprotein in saliva and stimulate saliva production (Gxasheka et al., 2015). This result shows that high saponin and CT feeds must be chewed more – thus, more O₂ consumption and CO₂ production may have occurred in the PP and PH groups. El Meccawi et al. (2008) found that alfalfa of higher CT content was more effective than *Acacia* in producing body heat. Heat production is an important trigger of high O₂ consumption and CO₂ production in the body.

The N₂O was not of enteric but fecal origin and may be related to possible accumulation of feces in the environment. Every animal kept in the room for 24 h was left with its own external feces. According to this, daily N₂O release per sheep tended to be lower ($P = 0.05$) in the group receiving PH (Fig. 4). Addition of PP and PH

significantly decreased daily N₂O production for kg feed consumption. In this study, CO₂ emission increased in PP and PH groups but decreased N₂O. The global warming potential of N₂O is 298 times stronger than CO₂ and is a greenhouse gas that emerges in animal activities (IPCC, 2007).

The results were promising in terms of nitrogen-based gases. The N₂O production tended to decrease in the PH groups per sheep (*Table 5*) and we had strong indications that N₂O release was related to protein metabolism associated with CT in the rumen and the intestine. We speculate that the lower emissions were due to the lower N content of the feces as a result of greater N binding and inhibition of N transformation. According to Bunglavan and Dutta (2013), 2%–3% CT in the diet may reduce ruminal protein degradation and result in degradation of the tannin–protein complex in the abomasum, and its lower pH (<3.5) may increase the absorption of amino acids in the intestine.

The CT concentration was up to 1% in the PP and PH groups in our study. The results suggested that CT in PH might affect fecal composition by binding proteins in the rumen and so improving protein digestion in the small intestine. The lower emissions from PH were also probably due to the lower contents of mineral N in the manure/feces. An important source of N₂O in feces is ammonia-based nitrogen and it is known that CT decreases ruminal protein dissolution and decreases ammonia concentration. This increases the non-ammonia nitrogen flow in the small intestine (Choi et al., 2012; Naumann et al., 2017).

Conclusion

We found that the use of CT-containing PP and PH feed as half of the wheat straw as roughage feed (WS was 10% in the current study) was a good choice for lamb fattening and production. The CO₂ emissions significantly increased in the PP and PH groups, but they did not effectively reduce the production of enteric CH₄ in the rumen and energy loss through CH₄ for the WS-based feed.

There is significant potential for PH in the fecal emission of nitrogen-based gases. We speculate that the lower emissions were due to the lower N content of the manure as a result of greater N binding and inhibition of N transformation. Thus, some by-products of the food industry have a potential as animal feeds that can reduce N₂O emissions. Reducing the emissions of GHG from ruminants can put such by-products to better use and help in mitigating the adverse impacts of climate change at the same time.

REFERENCES

- [1] Abarghuei, M. J., Rouzbehan, Y., Salem, A. Z. M., Zamiri, M. J. (2013): Nutrient digestion, ruminal fermentation and performance of dairy cows fed pomegranate peel extract. – *Livestock Science* 157: 452-461.
- [2] Adams, L. S., Seeram, N. P., Aggarwal, B. B. (2006): Pomegranate juice, total pomegranate ellagitannins, and punicalagin suppress inflammatory cell signaling in colon cancer cells. – *Journal of Agricultural Food Chemistry* 54: 980-985.
- [3] Addisu, S. (2016): Effect of dietary tannin source feeds on ruminal fermentation and production of cattle; a review. – *Online Journal of Animal and Feed Research* 6(2): 45-56.

- [4] AOAC. Association of Official Analytical Chemistry. (1998): Official methods of analysis 16th ed. – AOAC International. Washington DC. USA.
- [5] Barry, T. N., McNabb, W. C. (1999): The implications of condensed tannins on the nutritive value of temperate forages fed to ruminants. – *British Journal of Nutrition* 81: 263-272.
- [6] Bhatta, R., Shinde, A. K., Vaithyanathan, S., Sankhyan, S. K., Verma, D. L. (2002): Effect of polyethylene glycol-6000 on nutrient intake, digestion and growth of kids browsing *Prosopis cineraria*. – *Animal Feed Science and Technology* 101: 45-54.
- [7] Broucek, J. (2014): Production of Methane Emissions from Ruminant Husbandry: A Review. – *Journal of Environmental Protection and Ecology* 5: 1482-1493.
- [8] Bunglavan, S. J., Dutta, N. (2013): Use of Tannins as Organic Protectants of Proteins in Digestion of Ruminants. – *Livestock Science* 4: 67-77.
- [9] Choi, C. W., Kim, K. H., Chang, S. S., Choi N. J. (2012): Soluble Non-ammonia Nitrogen in Ruminant and Omasal Digesta of Korean Native Steers Supplemented with Soluble Proteins. – *Asian-Australasian Journal Animal Science* 25: 1269-1275.
- [10] El-Meccawi, S., Kam, M., Brosh, A., Degen, A. A. (2008): Heat production and energy balance of sheep and goats fed sole diets of *Acacia saligna* and *Medicago sativa*. – *Small Ruminant Research* 75: 199-203.
- [11] Ghaffari, M. H., Tahmasbi, A. M., Khorvash, M., Naserian, A. A., Vakili, A. R. (2014): Effects of pistachio by-products in replacement of alfalfa hay on ruminal fermentation, blood metabolites, and milk fatty acid composition in Saanen dairy goats fed a diet containing fish oil. – *Journal Applied Animal Research* 42: 186-193.
- [12] Gxasheka, M., Tyasi, T. L., Qin, N., Lyu, Z. C. (2015): An overview of tannins rich plants as alternative supplementation on ruminant animals: A Review. – *International Journal of Agricultural Research and Review* 3: 343-349.
- [13] IPCC. Intergovernmental Panel on Climate Change. (2007): Changes in atmospheric constituents and in radiative forcing. In: *Climate Change 2007: The Physical Science Basis*. – Contribution of Working Group I to the Fourth Assessment Report of the Intergovernmental Panel on Climate Change. Cambridge University Press, Cambridge, UK and New York (Chapter 2).
- [14] Jayaprakasha, G. K., Negi, P. S., Jena, B. S. (2006): Antimicrobial activities of pomegranate. – In: Heber, D., Schulman, R. N., Seeram, N. P. (eds.) *Pomegranates: Ancient Rootsto Modern Medicine* Seeram. CRC Press, Taylor & Francis Group, Boca Raton, FL, USA. p 3-29.
- [15] Karaogul, E. (2011): Extraction and HPLC characterization of some oak species (*Quercus*) roots. – Doctoral Thesis. University of K. Sutcu Imam. K.Maraş, Turkey.
- [16] Kotsampasi, B., Christodoulou, V., Zotos, A. (2014): Effects of dietary pomegranate byproduct silage supplementation on performance, carcass characteristics and meat quality of growing lambs. – *Animal Feed Science and Technology* 197: 92-102.
- [17] Makkar, H. P. S., Blummel, M., Becker, K. (1995): Formation of complexes between polyvinyl pyrrolidones or polyethylene glycols and their implication in gas production and true digestibility in vitro techniques. – *British Journal of Nutrition* 73: 897-913.
- [18] Naumann, H. D., Tedeschi, L. O., Wayne, E. Z., Nichole, F. H. (2017): The role of condensed tannins in ruminant animal production: advances, limitations and future directions. – *Revista Brasileira de Zootecnia* 46: 929-949.
- [19] Norouzian, M. A., Ghiasi S. E. (2012): Carcass Performance And Meat Mineral Content In Balouchi Lamb Fed *Pistachio* By-Products. – *Meat Science* 92: 157-159.
- [20] Petrucci, R. H., Herring, G., Madura, J., Bissonnette, C. (2010): *General Chemistry: Principles and modern applications with mastering chemistry*. – 10th ed. Published by Pearson. Canada.
- [21] Piñeiro-Vázquez, A. T., Canul-Solís, J. R., Alayón-Gamboab, J. A., Chay-Canul, A. J., Ayala-Burgosa, A. J., Aguilar-Pérez, C. F., Solorio-Sánchez, F. J., Ku-Vera, J. C.

- (2015): Potential of condensed tannins for the reduction of emissions of enteric methane and their effect on ruminant productivity. – *Archivos de Medicina Veterinaria* 47: 263-272.
- [22] Provenza, F. D. (1995): Post ingestive feedback as an elementary determinant of food preference and intake in ruminants. – *Journal of Range Management* 48: 2-17.
- [23] Sadq, S. M., Ramzi, D. O. M., Hamasalim, H. K., Ahmed, K. A. (2016): Growth Performance and Digestibility in Karadi Lambs Receiving Different Levels of Pomegranate Peels. – *Open Journal of Animal Sciences* 6: 16-23.
- [24] Shabtay, A., Eitam, H., Tadmor, Y. (2008): Nutritive and antioxidative potential of fresh and stored pomegranate industrial byproduct as novel beef cattle feed. – *Journal of Agricultural Food Chemistry* 56: 10063-10070.
- [25] Shakeri, P., Riasi, A., Alikhani, M. (2013): Effects of feeding pistachio by-products silage on growth performance, serum metabolite and urine characteristics in Holstein male calves. – *Journal of Animal Physiology and Animal Nutrition* 97: 1022-1029.
- [26] Shakeri, P., Riasi, A., Alikhani, M. (2014): Effects of long period feeding *pistachio* by-product silage on chewing activity, nutrient digestibility and ruminal fermentation parameters of Holstein male calves. – *Animal* 8: 1826-1831.
- [27] TUIK. (2015): Turkish Statistical Institute. Crop production statistics in Turkey. – Available at: <<http://tuik.gov.tr>> Accessed on: Feb. 7, 2017.
- [28] TUIK. (2016): Turkish Statistical Institute. Crop production statistics in Turkey. – Available at: <http://www.tuik.gov.tr/PreTablo.do?alt_id=1001> Accessed on: June 28, 2016.
- [29] Van Soest, P. J., Robertson, J. B., Lewis, B. A. (1991): Methods for dietary fiber, neutral detergent fiber and nonstarch polysaccharides in relation to animal nutrition. – *Journal of Dairy Science* 74:583-597.
- [30] Villalba, J. J., Provenza, F. D. (2000): Postingestive feedback from starch influences the ingestive behaviour of sheep consuming wheat straw. – *Applied Animal Behaviour Science* 66: 49-63.
- [31] Zarei, M. (2013): Pomegranate by product (*Punica granatum* L.) in Animal Nutrition. – *International Journal of Research and Reviews in Pharmacy and Applied Science* 3: 685-698.

DETERMINING THE FACTORS AFFECTING RANGELAND SUITABILITY FOR LIVESTOCK AND WILDLIFE GRAZING

FARAZMAND, A.¹ – ARZANI, H.^{2*} – JAVADI, S. A.¹ – SANADGOL, A. A.³

¹*Department of Range Management, Science and Research Branch, Islamic Azad University
Tehran, Iran*

(e-mail: alifarazmand53@yahoo.com; phone: +98-912-271-8331; fax: +98-212-244-6515)

²*Department of Reclamation of Arid and Mountainous Regions, Faculty of Natural Resources,
University of Tehran, Karaj, Iran*

³*Rangeland Research Division, Research Institute of Forests and Rangelands, Tehran, Iran*

**Corresponding author*

e-mail: harzani@ut.ac.ir, phone: +98-263-222-3044; fax: +98-263-222-7765

(Received 7th Jul 2018; accepted 2nd Nov 2018)

Abstract. Rangelands have a significant role in the supply of forage for grazing livestock and wildlife. Therefore, it is necessary to evaluate the rangeland grazing suitability for livestock and wildlife. In this study, the Jeliz Jand Basin was selected. This basin, with an area of 16210.44 ha, lies between longitudes 52° 36' to 50° 52' E and latitudes 35° 44' to 35° 57' N. It is located in north of Firouzkooch city, Tehran Province, Iran, and has a cold semi-arid climate. Data integration was carried out according to the FAO method (1991) using GIS on a scale of 1: 20000. For livestock and wildlife grazing, information on physical factors and vegetation in the form of three sub-models including forage production, water resources and soil sensitivity to erosion was integrated and the final model of rangeland suitability was produced. According to the results, the range suitability for sheep and goats grazing in the study area was determined to be moderate (S2) for 11.3% (1560.3 ha), low (S3) for 80.5% (11148 ha) and unsuitable (N) for 8.3% (1146.5 ha), respectively. Rangeland suitability for cattle grazing in the study area was determined to be high (S1) for 1.7% (228.9 ha), moderate (S2) for 3.6% (498.6%), low (S3) for 0.8% (111 ha) and unsuitable (N) for cattle grazing was 93.9% (13016.9 ha), respectively. Also, about 1491 ha of rangelands were low suitable for wildlife grazing. It is worth mentioning that slope percentage, vegetation composition (presence of class II and III species) and low vegetation cover because of overgrazing and the past land-use conversions were the most important factors limiting rangeland suitability in this Basin. However, it is necessary to reduce the population of cattle and goat, and grazing program should be set up and continued with sheep according to the principles of range management.

Keywords: *rangeland analysis, livestock grazing, multiple use, rangeland suitability, wildlife, GIS, Firoozkooch*

Introduction

Livestock grazing is the major exploitation of rangelands in most developing countries, while rangelands, in addition to livestock production, have other benefits including production of medicinal, industrial, and edible plants, production of nectar and pollen plants, creation of tourism and ecotourism areas, soil conservation, wildlife, hunting, water storage and production, carbon sequestration and so forth that could be resulted in improved income for beneficiaries in the form of multipurpose use (Arzani et al., 2009). These benefits have been emphasized in recent decades to commercialize and economize the exploitation units (Arzani et al., 2016). Because of the high energy expended, livestock grazing on high slopes not only decreases the livestock performance but also increases the risk of erosion and flooding. Livestock grazing in

areas that are susceptible to erosion causes soil degradation and vegetation as well as increased surface area of critical regions. Providing a suitable management plan for rangelands requires identification of its constraints and potential for various types of exploitation. According to FAO (1991), rangeland suitability is defined as the land capability for rangeland exploitation with regard to sustainable land use. Amiri (2008) studied the rangeland suitability of Ghara Aghach rangelands in Esfahan province for livestock grazing and concluded that palatability, species composition and production were the factors limiting grazing suitability in the study area. According to Arzani et al. (2005), steep slope, conversion of rangelands to drylands, early grazing, the rocks susceptible to erosion and low vegetation cover were the most limiting factors in determining rangeland suitability. Toxic plants also reduce rangeland suitability for livestock grazing. Omidvar and Mohtashamnia (2015) also found that among physical and vegetative factors, physical factors such as slope, altitude, distribution of water resources, and precipitation type were more effective in reducing the rangeland suitability as compared with vegetation. According to Arnold and Rodzinsky (1978), this distance depends on vegetation, topography, grazing season, and age of livestock. Gavili et al. (2013) showed that the lack of available forage for livestock due to the low production of desired species as well as low palatability and allowable use were the most important factors in reducing the rangeland suitability of Fereydon Shahr Rangelands of Esfahan. Javadi et al. (2010) considered three sub-models of water resources, soil sensitivity to erosion, and forage production to classify rangeland suitability for goat grazing. According to the results, the rangeland suitability for goat grazing was determined to be S3 for 72.1% and N for 27.9% of the study area, respectively. In Low forage production and the sensitivity of formations to erosion were the most important factors reducing rangeland suitability. Low production and erosion together were identified as limiting factors. In a study conducted by Arzani et al. (2005), physical characteristics and vegetation were introduced as the factors affecting rangeland suitability in Taleghan. Steep slope, conversion of rangelands to drylands, early grazing, the rocks susceptible to erosion, and low vegetation cover were the most limiting factors in determining rangeland suitability. Arzani et al. (2006) studied the range suitability of semi-steppe rangelands in Sabz Kouh, Chahar Mahal Bakhtiari province, and showed the slope was introduced as the main factor in reducing rangeland suitability for livestock grazing. In a study conducted by Mirakhorlou (2000), range condition, trend and capacity were calculated using satellite data, field observations and GIS in Damavand rangelands, and rangeland suitability map was determined for various range improvement methods. Rezaei et al. (2004) investigated soil quality index to assess rangeland suitability for open grazing in Lar Basin. According to Arzani et al. (2006), low forage production, abundant toxic and thorny species around the village and water resources, topography, steep slopes, formations susceptible to erosion, and early cold were among the factors limiting rangeland suitability in Siahrood rangelands, Northeast Tehran. Overall, the factors affecting rangeland suitability are divided into two groups as physical characteristics (slope, the length of range, natural obstacles, sensitivity to erosion, soil stability, water resources, climate, soil properties) and vegetation (production, range condition and trend, capacity, soil cover, and vegetation cover percentage). The present study was aimed to identify the most important factors affecting and limiting rangeland suitability to classify the rangelands of the study area for livestock (sheep, goat, and cattle) and wildlife grazing. Sour et al. (2013) showed the capability of GIS multi criteria evaluation for rangelands suitability assessment. Keno

Terfa and Suryabhadgavan (2015) used Landsat TM 2011 remote sensing satellite images for land-use/land-cover analysis and Multi Criteria Evaluation in a GIS environment to come up with the final suitability map. Ariapour et al. (2013) concluded that using RS and GIS could be useful to water resources suitability of rangeland ecosystems with low cost and high accuracy and speed, if consider standards and criteria of using GIS and RS. According to Rouhi-Moghaddam et al. (2016), in their study area the limiting factors for sheep grazing had been water resources, high slope and vegetation. Rostami et al. (2014) stated that using GIS may lead to the increase in accuracy and speed of implementing plans.

Materials and methods

The Jeliz Jand Basin with an area of 16210.44 ha, lies between longitudes 52° 36' to 50° 52' E and latitudes 35° 44' to 35° 57' N. It is located in north of Firouzkooch city, Tehran Province, Iran (*Fig. 1*). This region has a cold semi-arid climate (modified De-Marton classification). The average annual precipitation is 451.1 mm, and the average annual temperature is 3.1. The current land use in the study area includes range management, dry agriculture, irrigated agriculture, gardens, residential areas, planted forests, and bare lands. Rangelands cover 85.5% of the study area.

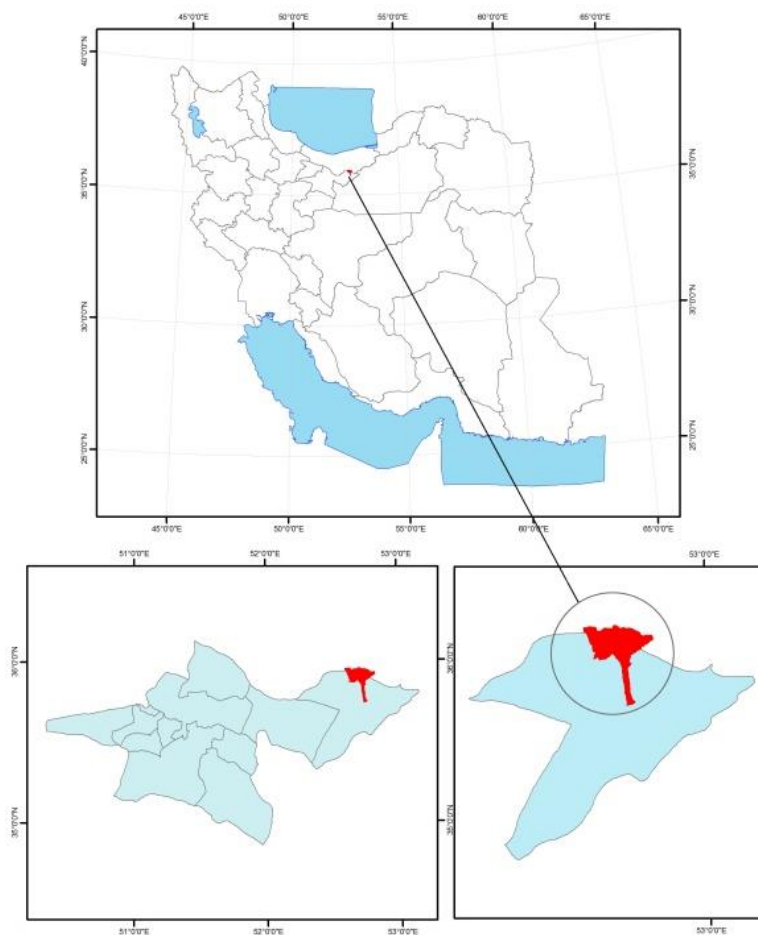


Figure 1. Geographical location of Jeliz Jand in Tehran and Iran

Data integration was carried out according to the FAO method (1991) using GIS on a scale of 1: 20000. Four suitability classes were determined as high (S1), moderate (S2), low (S3), and unsuitable (N). The software MapSource 6.11.6 and ArcGIS 10 were used in this research.

Suitability for livestock (sheep, goat, and cattle) and wildlife grazing

First, the current condition of rangelands was studied. In order to update vegetation data, a vegetation map was developed (*Fig. 2a*). Rangeland types were identified using field observations and GPS. The range condition and range trend were determined using the four-factor method and trend scale method, respectively. *Figure 2b* shows the range allotment map. Forage production was determined by cutting and weighing method. In addition, rangeland capacity, palatability, allowable use, forage quality, livestock type and daily requirement, grazing season, and rangeland area were determined. To determine rangeland suitability for livestock (sheep, goat, cattle) and wildlife grazing, first, three sub-models of soil sensitivity to erosion, water resources and forage production were prepared and finally, these three sub-models were integrated and the final map of rangeland suitability was obtained.

Soil sensitivity to erosion

Soil sensitivity to erosion was determined by MPSIAC method. In this method, nine factors including geology, soil texture, climate, runoff, topography, vegetation, land use, current erosion, and gully erosion were evaluated (*Table 1*).

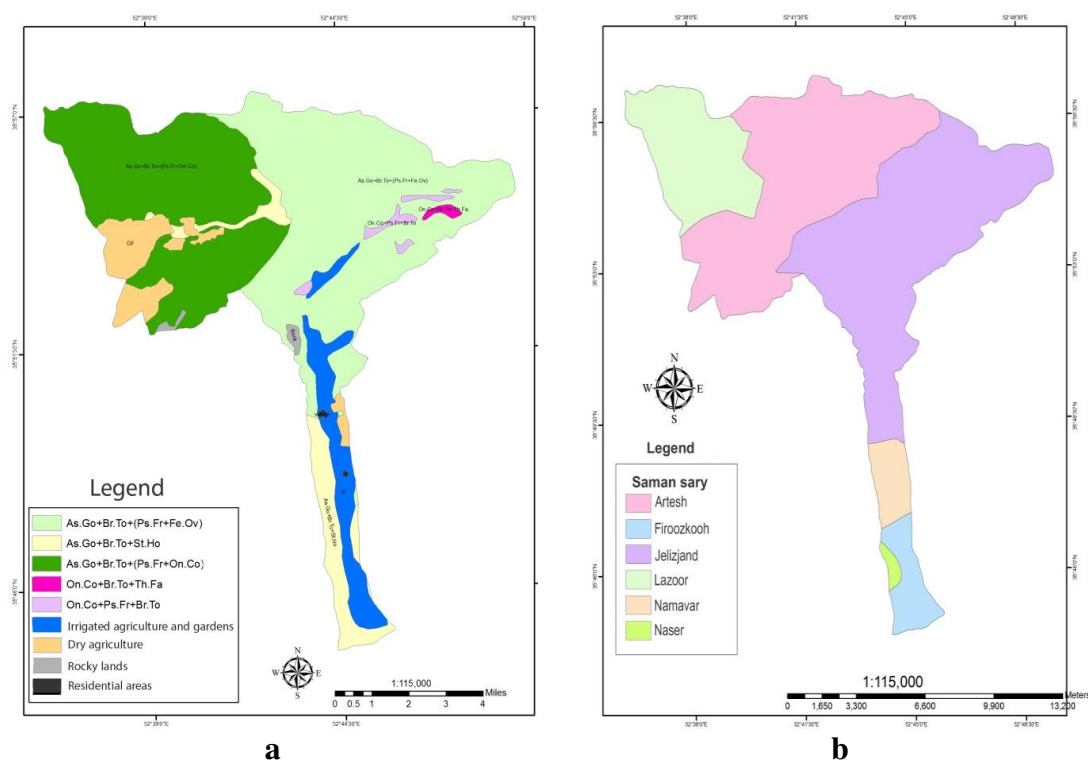


Figure 2. a. Vegetation types map. (The abbreviations indicate the vegetation types of the study area, presented in detail in Table 8). **b.** Range allotment map

Table 1. The area of erosion classes for rangeland suitability classes

Erosion class	I	II	III	IV
Area/h	939/6	5043/5	7872/3	0
Suitability class	S1	S2	S3	N
%	6/78	36/4	56/8	0

Water resources sub-model

The sub-model of water resources includes the slope (Table 2), distance from water resources (Table 3), water quantity, and water quality. Generally, the ability to access water resources depends on maximum distance that livestock can be moved from water resource for grazing.

Table 2. Slope suitability classes for livestock and wildlife

Slope (%)	0-10	11-30	31-70	>70
Sheep and goat	S1	S2	S3	N
Cattle	S1	S2	N	N
Wildlife	N	N	S1	S2

Table 3. Suitability classes for distance from water resources

Suitability Class	S1	S2	S3	N
Distance/km	0- 2	2-4	4-6	6-8

Considering the climatic factors, vegetation characteristics, exploitation season, livestock type, livestock breed, and species composition, the daily water requirement of animal unit in the study area based on forage composition available to animals was considered as 5 liters. Then, the quantity of water was determined in each watering point. The water quantity was determined through comparison of the amount of water available and the amount of water required for livestock (Table 4). The water quality sub model was determined using the factors affecting the quality of drinking water for sheep and its comparison with the water quality in the study area (Tables 5 and 6). Finally, the maps derived from the sub-models were integrated using the limiting factor procedure suggested by (FAO, 1991) and the sub model of water was prepared.

Table 4. Water quantity guide for livestock and wildlife

Available water in the rangeland relative to the livestock requirement(%)	25<	25-50	50-75	75>
Sheep and goat	N	S3	S2	S1
Cattle	N	S3	S2	S1
Wildlife	N	S3	S2	S1

Table 5. Factors affecting the quality of drinking water (Mahdavi, 2003)

Factor	Maximum resistance for sheep and goats
EC (mmhos/cm)	16
Mg (mg/lit)	500
TDS (mg/lit)	12900

Table 6. Total water soluble solids (ppm)

Animal type	Good	Fair	Poor	Limitation
Sheep	1000<	3000-6000	6000 -10000	10000>
goat	1000<	5000-7000	7000 -10000	10000>
Cattle	1000<	5000-7000	7000 -10000	10000>
Wildlife	1000<	3000-6000	6000 -10000	10000>

Forage production and grazing capacity sub model

In order to determine the forage production and the grazing capacity in the vegetation types, firstly, the rate of production of species was harvested by clipping and weighing method in each plot at the end of the vegetative growth stage. Then, the available production in vegetation types for livestock (sheep, goat, and cattle) was calculated by combining the production data with palatability or proper use factor. In order to determine the suitability class of forage production, the ratio of the amount of available production of each vegetation type to its total production was used (*Table 7*). Due to determination of water quantity need for livestock grazing, also, rangeland grazing capacity was calculated for each vegetation type using the amount of forage used for livestock, length of grazing period (105 days), daily animal unit requirement (1.3 kg) and rangeland area.

Table 7. Guidelines for forage production suitability classes by FAO Method (1991)

Row	Available production to total production ratio (%)	Production suitability
1	20>	S1
2	15 -20	S2
3	10 – 15	S3
4	10<	N

Rangeland suitability for wildlife

Rangelands with slopes greater than 70% and rangelands susceptible to erosion, known as protected areas, are recommended for wild goat, goat, ewe, and ram grazing. First, the map of the slopes greater than 70% was prepared with a scale of 1:25000. The map of high and very high susceptibility to erosion was provided using the erosion classes' map. By integrating the maps of susceptibility to erosion, water resources, forage production and slope, the rangeland conservation map was produced, whose land use was wildlife grazing.

Results

According to the results, rangelands comprise 13,855 ha of the study basin, whose slope is below 70% for 12364 ha and above 70% for 1491 ha. The vegetation cover consists of 76 plant species belonging to 21 plant families and five vegetation types. The amount of forage production that could be harvested is 2666.5 tons per year (Table 8).

Table 8. Characteristics of rangeland types on the Jeliz Jand Basin, Firouzkooch

Row	Rangeland types	Area (ha)	Condition	Trend	Available forage kg/ha	Capacity (a.u.m/h)	Grazing capacity (animal unit)
1	<i>Astragalus gossypinus + Bromus tomentellus + Stipa hohenckeriana</i>	1176	Poor	(-)	171/4	4977	-
2	<i>Astragalus gossypinus + Bromus tomentellus + Psathyrostachys fragilis + Festuca</i>	6155	Fair	(-)	208/2	32827	9379
3	<i>Astragalus gossypinus + Bromus tomentellus + (Psathyrostachys fragilis + Onobrychis cornuta)</i>	4832	Good	0	236	29239	8354
4	<i>Onobrychis cornuta + Bromus tomentellus + Thymus fallax Fisch.</i>	57	Fair	(-)	198/2	278	79
5	<i>Onobrychis cornuta + Psathyrostachys fragilis + Bromus tomentellus</i>	179	Fair	(-)	187	826	236
Total	-	12364	-	-	-	-	18048

Soil susceptibility to erosion sub model: According to the results, the rangeland suitability was determined to be good for 6.78% (939.66 ha), moderate for 36.4% (5043.5 ha), and fair for 56.8% (7872.3 ha) of rangelands. Water resources sub-model: An area of 10498 ha of rangelands with a slope below 70% was suitable for sheep and goat common grazing, 600 ha for cattle grazing and 400 ha for wildlife grazing. All rangelands with a slope of over 70% (1491 ha) can only be attributed to wildlife grazing (Table 9). The daily water requirement of a livestock unit weighing 50 g is about 5 l depending on the region, and the water requirement of each livestock unit is equal to 432 l during the grazing season. Water requirement for livestock and wildlife in the area is 9000.4 m³ and the available water is 6070000 m³; therefore, the suitability of the entire area was determined to be S1. There is no limitation in terms of water quality (sheep, goat, cattle, and wildlife) in the study area (S1 class). In terms of water resources distance (sheep, goat, cattle, and wildlife), the suitability of rangelands was determined to be S1 for 12718 ha and S2 for 1137 ha. Rangeland suitability for water resources was determined to be S1 for 3.3% of the study area (461.2 ha), S2 for 26.4% (3652 ha), S3 for 62% (8594.5 ha), and N for 8.3% (1146.5 ha).

Table 9. Slope suitability classes for livestock and wildlife

Slope (%)	0-10	11-30	31-70	70>
Area/ha	2778	4847	5/3873	1491/3
Sheep and goat/ha	2478	4547	5/3473	0
Cattle/ha	300	300	0	0
Wildlife/ha	0	0	400	1491/3

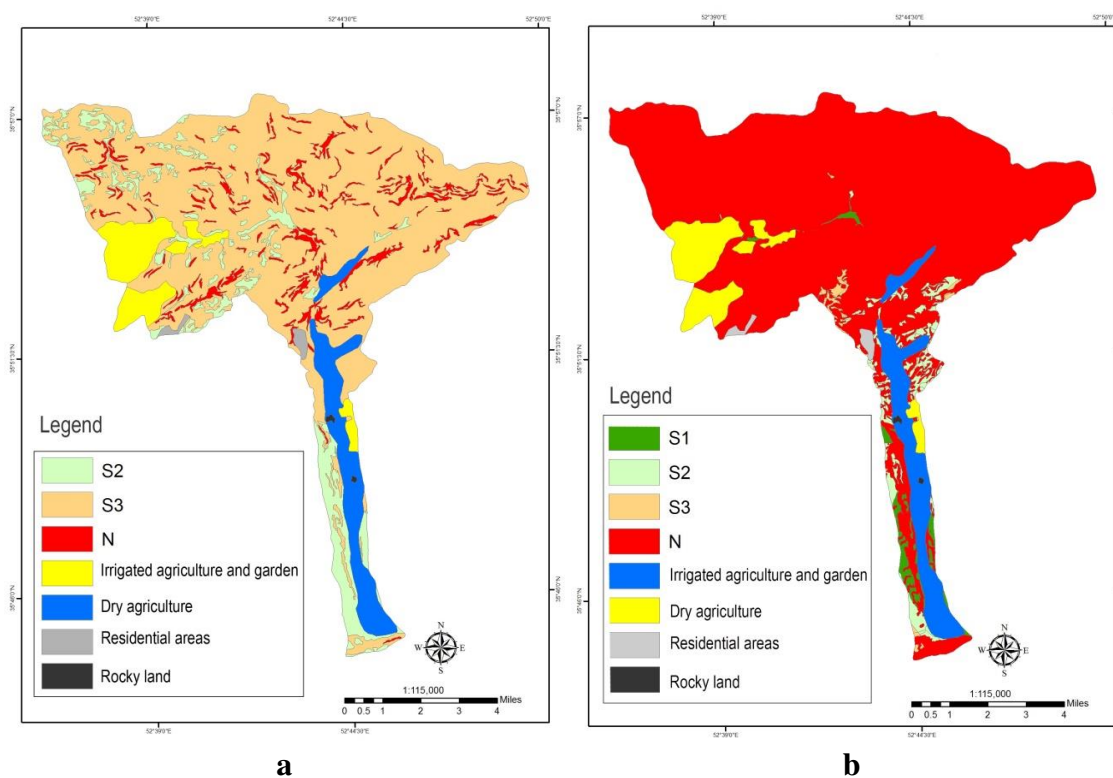
Forage production sub-model:

Available forage production and grazing capacity for livestock and wildlife are presented in (Table 10). Rangeland suitability for forage production was determined to be S2 for 6244 ha (50.36) and S3 for 6154.85 ha (49.64).

Table 10. A comparison of available forage production and grazing capacity between livestock and wildlife

Row	Method parameter	Area (ha)	Available forage (kg)	Grazing capacity (animal unit)
A	Livestock	12398/35	2666697/4	18047
B	Wildlife	1491/3	224467/3	1845/2
C	On slopes that are not suitable for livestock grazing	-	-	-

Final model of rangeland suitability for grazing: the model was obtained from integration of layers including soil susceptibility to erosion, water and forage. According to the results, rangeland suitability for sheep and goat grazing was determined to be S2 for 11.3% (1560.3 ha), S3 for 80.5% (11148 ha), and N for 8.3% (1146.5 ha) (Fig. 3a). Rangeland suitability for cattle grazing was determined to be S1 for 1.7% (228.9 ha), S2 for 3.6% (498.6 ha), S3 for 0.8% (111 ha), and N for 93.9% (13016.9 ha) (Fig. 3b). The suitability of the rangelands for wildlife grazing, where the slope was greater than 70% with an area of 1491 ha, was determined to be S3 (Fig. 3c). The map of common grazing by livestock and wildlife is presented in Fig. 3d.



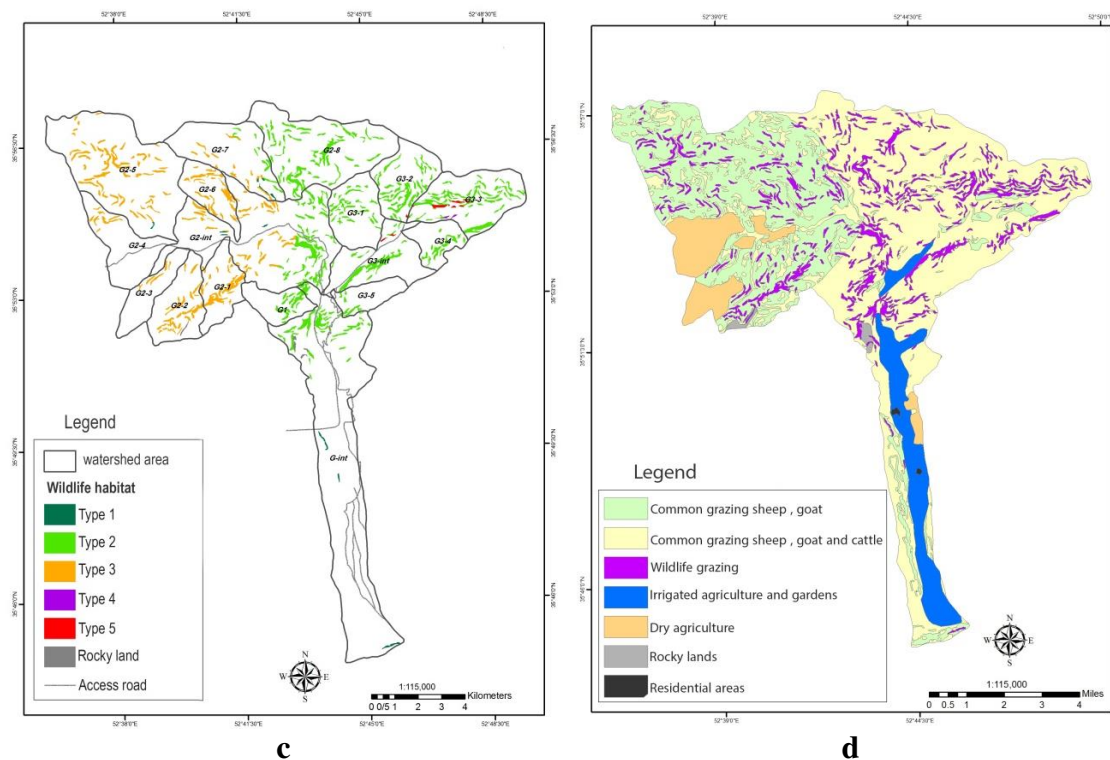


Figure 3. *a.* Rangeland suitability map for sheep and goat grazing, *b.* cattle grazing, *c.* wildlife grazing and *d.* livestock and wildlife common grazing

According to the results, the suitability of the study rangelands for common grazing by livestock and wildlife was determined as follows:

A: 12377 ha of rangelands, where the slope is less than 70%, can be used for common grazing by sheep and goat.

B: 7624 ha of rangelands, where the slope is less than 30%, can be used for common grazing by sheep, goat and cattle.

C: 1491 ha of the study rangelands, where the slope is greater than 70%, can only be grazed by wildlife (*Fig. 3d*).

Discussion

Knowledge of forage production, water resources, and soil sensitivity to erosion is essential to determine rangeland suitability. Palatability, proper use factor are effective for determining , available forage to animals, Amount of production is another factor considered for the production factor. Distance and access to water as well as water quality and quantity are considered for the water resources assessment. The erosion model or rock and soil sensitivity to erosion also include nine factors (geology, climate, soil, runoff, topography, land use, land cover, surface erosion, and river erosion). According to Javadi et al. (2009, 2008, 2006), Arzani et al. (2009, 2017), Alizadeh et al. (2013), Sanaei et al. (2015) and Motamedi and Toopchzadegan (2017), three factors including forage production, water resources and soil susceptibility to erosion were the components of the livestock grazing model. The suitability of most of the lands in the study area was determined to be low (S3) and moderate (S2) for soil susceptibility to

erosion. In a study performed by Alizadeh et al. (2011) in Ghara Aghach, land use, surface cover, runoff and current erosions were respectively introduced as the most important factors affecting the erosion of this basin. The land use type was the most important factor in reducing the rangeland suitability in Roozeh Chai, Urmia (Bani Nemeh, 2003). The negative impacts of overgrazing and early grazing on reduced permeability and increased run off have been reported in several studies (Arzani et al., 2005). In terms of water resources (quantity, quality, and distance from water resources), the suitability of rangeland for most of the lands in the study area was determined to be low and moderate. In the study area, regarding the climatic conditions, the quantity (number of permanent water resources), quality, and distance from water resources, were not limited factors for animal grazing, and all rangeland types were placed in the S1 suitability class. To explain the importance of slope in access to water resources he stated that animals' ability for grazing is reduced by increasing of slope and more energy is consumed. However, the quality and quantity of water resources in the study area caused no limitation. Alizadeh et al. (2011) stated that slope was the most important factor in reducing rangeland suitability in terms of distance from water resources in Semirom region. This result is consistent with our findings in the present study. Gavili et al. (2010) also considered slope as the factor reducing and sometimes limiting rangeland suitability. Therefore, slope has a significant importance in determining rangeland suitability for livestock grazing, so that water penetration is reduced by increasing of slope, resulting in increased run off. On the other hand, the establishment possibility of developed soils decreases on steep slopes and livestock (animal) grazing on steep slopes causes soil movement and difficult plant establishment. In addition, animals spend a lot of energy to move on the steep slopes (for grazing and to reach water sources). Therefore, animal performance is reduced. According to Holchek et al. (2001) and Zhou (1989), the steep slopes (greater than 60% or 75%) are inappropriate for animal grazing. They point out that wildlife graze better than do livestock on steep slopes. In the case of steep slopes, no grazing is recommended and the area should be considered for wildlife and tourism only. The suitability class of most of the rangeland vegetation types was determined to be S2 and S3 for forage production. In the present study, the presence of class II and class III species in the species composition and reduced available forage were the most important factors in reducing the range suitability of the study basin for forage production. All rangelands used by wildlife, with an area of 1491 ha, were classified in the S3 suitability class for forage production. The impact of past uses (conversion of rangelands to dry farming and overgrazing), low vegetation cover, and presence of low-palatability species in the vegetation composition were among the factors reducing rangeland suitability for forage production. Rangeland plowing, in order to develop dry-land cultivation in areas where the annual rainfall provides dryland farming, is one of the factors of rangeland degradation. Such rangelands, having good and deep soil, are among the best rangelands. Grasses and annual forbs produce temporary cover (during the period of the growing season). Therefore, at most times of the year, the soil surface is free of vegetation and exposed to erosion. According to Arzani et al. (2005), rangeland conversion to dry land farming, overgrazing, early grazing, low vegetation cover, and the presence of low palatable species were among the most important factors, limiting rangeland suitability for forage production. Motamedi and Toopchzadegan (2017) stated that in the Hendovan rangelands of Khoy the allowable use, available forage, quantity of water resources, and geology were the most important factors. Accordingly, more

attention need to be paid on designing the guidelines of rangeland suitability for animal grazing and assessing its capability as well as determining the priority of using the vegetation types with the same suitability class. In a study performed by Kit (2000), rangeland suitability was studied in Australia and slope and water resources were identified as the factors limiting rangeland suitability for cattle grazing. In the Qara Aghach rangelands, water resources do not cause limitation on rangeland suitability due to the numerous permanent water resources, while slope is the only factor limiting rangeland suitability in a limited area of the study region. Mfitumukiza (2004) studied the rangeland suitability for cattle grazing in Ga za province, Mozambique, and concluded that among the factors limiting rangeland suitability, the lack of access to water resources, low palatability of species, low forage production, and slope were the most important factors. The results of a study performed by Mostafaei (2015) in the winter rangelands of Hormozgan showed that the suitability of the study rangelands was determined to be unsuitable (N) or low (S3). According to a study performed by Arzani et al. (2006) in the Siahrood region, toxic plants, high slope, temporary water resources and erosion-sensitive formations were the factors limiting rangeland suitability for sheep grazing. High slope and rock and soil sensitivity to erosion were the factors limiting the suitability of rangelands in the Lar area, in order of importance. In the Ardestan area, low production, invasive plants, distance from water resources, exploitation type, and current erosion result in reduced suitability rangeland. In the Bacan plain, slope, distribution of water resources, and the lack of permanent water resources were the factors limiting the suitability of rangelands for sheep grazing. As can be seen, most studies on grazing in rangelands in different climatic regions of the country are consistent with the results of this study. More than 80% of the rangelands of the study area have a low suitability (S3) for sheep grazing. In addition, the rangeland suitability for wildlife grazing was determined to be low (S3). In presenting the grazing suitability model, it should be noted that the factors affecting rangeland suitability will be different due to climatic conditions, vegetation, soil, current exploitation conditions, and topography. Given that the rangelands of the region are currently grazed by sheep, goats, and cattle, it is recommended that sheep grazing could be continued based on grazing program and range management principles. However, the number of cattle and goats should be reduced.

Conclusion

Our results clearly showed that multiple use of rangelands could increase the beneficiaries' income and rangeland sustainable development. However, for future studies, it is necessary to update the methods and socio-economic issues need be taken into consideration.

REFERENCES

- [1] Alizadeh, E., Arzani, H., Azarnivand, H., Mohajeri, A., Kaboli, H. (2011): Range suitability classification for goats using GIS Case Study: Ghareaghach watershed-Semirom. – Iranian journal of Range and Desert Research 18(3): 353-371.
- [2] Amiri, F., Arzani, H., Farah Pour, M., Chai Chi, S., Khajedin, S. J. (2008): Multiple use modal of lands with using GIS (Case study: Ghara aghach basin). – PhD Thesis, Azad Islamic University, Research & Science Unit (in Persian).

- [3] Ariapour, A., Hadidi, M., Karami, K., Amiri, F. (2016): Water resources suitability model by using GIS (case study: Borujerd Rangeland, Sarab Sefid). – *Journal of Rangeland Science* 3(2): 177-188.
- [4] Arnold, G. W., Dudzinsky, M. L. (1978): *Ethology of Free Ranging Domestic Animals*. – Elsevier Scientific Co., Amsterdam, New York.
- [5] Arzani, H. (2009): *Forage Quality and Daily Requirement of Grazing Animal*. – University of Tehran Press, Tehran.
- [6] Arzani, H., Yousefi, S., Jafari, M., Farahpour, M. (2004): Rangeland classification model for sheep grazing using GIS. – *Journal of Environmental Studies* 37: 59-68.
- [7] Arzani, H., Farzam, M., Shams, H., Mohtashamnia, S., Mohseni Fashami, M., Ahmadi, H., Jafari, M., Darvish Sefat, A. A., Shahriari, E. (2005): Rangeland classification model for sheep grazing in the central Alborz, Ardestan and Zagros. – *Journal of Sciences and Technology of Agriculture and Natural Resources* 35: 273.
- [8] Arzani, H., Jankjo, M., Shams, H., Mohtashamnia, S., Fashami, M. A., Ahmadi, H., Jafari, M., Darvishsefat, A. A., Shahriary, E. (2006): A model for classification of range suitability for sheep grazing in Central Alborz, Ardestan and Zagros regions. – *Iranian Journal of Science and Technology of Agriculture and Natural Resources* 10: 273290.
- [9] Arzani, H., Naseri, K. (2007): *Livestock Feeding on Pasture* (translated). – University of Tehran Press, Tehran.
- [10] Arzani, H., Mousavi, S. A., Ajdari, G. (2008): *Classification of Taleghan Rangeland for Multi Purpose Use and Sustainable Management Report*. – Univ. of Tehran, Tehran.
- [11] Arzani, H., Borhani, M., Charesaz, N. (2016): *Global Rangelands, Progress and Prospects* (translated). – Pune Press, Tehran.
- [12] Arzani, H., Beiniyaz, M., Alizadeh, E. (2017): *Model of Extensive Cattle Grazing for Sustainable Use in Rangelands*. – International Conference on Sustainable Development, Canada, Ottawa.
- [13] Bani Nameh, J. (2003): *Land evaluation for land use planning with special attention to sustainable fodder production in the Rouzeh chahi catchments of Orumiyyeh area Iran*. – M.Sc. Thesis International for Geo-information Science and Earth Observation, Enschede, Netherlands.
- [14] Curran, G., Grice, T. (1992): *Poisoning Caused by Plants* – In: Simpson, I. (ed.) *Rangeland Management in Western New South Wales*. NSW Agriculture, Sydney, pp. 102-113.
- [15] Fashtami, M. (2002): *Investigation on range suitability of Lar rangelands using GIS*. – MScThesis, Tarbiat Modares University.
- [16] FAO (1991): *Guidelines: Land Evaluation for Extensive Grazing*. – Soil Bulletin No. 58. FAO, Rome.
- [17] Gavili, E., Vahabi, M., Amiri, F., Arzani, H. (2013): Suitability determination for sheep in rangeland of Ferydounshahr, Isfahan. – *Journal of Range and Watershed Management* 6(4): 595-607.
- [18] Holchek, J. L., Pieper, R. D., Herbel, C. H. (2001): *Range Management. Principles and Practices*. – Prentice Hall, Englewood Cliffs, NJ.
- [19] Javadi, S. A., Asadpour, A., Arzani, H. (2009): Classification of rangeland suitability for goat grazing using GIS (Case study: Baft Jamilabad Range). – *Renewable Natural Resources Research* 1: 13-29.
- [20] Jiao, J., Zou, H., Jia, Y., Wang, N. (2009): Research progress on the effects of soil erosion on vegetation. – *Acta Ecologica Sinica* 29(2): 85-91.
- [21] Keno Terfa, B., Suryabhagavan, K. V. (2015): Rangeland suitability evaluation for livestock production using remote sensing and GIS techniques in Dire District, Southern Ethiopia. – *Global Journal of Science Frontier Research: H₂Environment & Earth Science* 15(1): 11-25.
- [22] Kiet, S. (2000): Expected use GIS map. – *Rangeland* 22(2): 18-20.
- [23] Mahdavi, M. (2002): *Applied Hydrology*. – University of Tehran Press, Tehran.

- [24] Mfitumukiza, D. (2004): Evaluating rangeland potentials for cattle grazing in a mixed farming system. – Master of Science Thesis, Department of Natural Resources, the Netherlands. <http://www.itc.nl/librry/papers2004/msc/nrm/mfitumukiza.pdf>.
- [25] Mir Akhrolou, K. (2000): the use of geographic information systems and remote sensing (GIS, RS) in rangeland management. – Proceedings of Geomatics Conference, Mapping Organization, Tehran, Iran.
- [26] Mostafaei, A. (2014): Economization of rangeland utilization with multiple use in line with sustainable development of the site. – International Conference on Agriculture, Environment and Tourism, Tabriz, Iran.
- [27] Motamedi, J., Toopchizadegan, S. (2017): Evaluation of rangeland suitability for sheep and goats common grazing. – *Journal of Rangeland* 11(1): 27-42.
- [28] Omidvar, E., Mohtashamnia, S. (2014): Rangelands suitability for sheep grazing in semi-steppe rangelands of Tornas Eghlid Fars Province by GIS. – *Renewable Natural Resources Research* 6(2): 65-78.
- [29] Rezaei, S. A., Gilkes, R. J., Tongway, D., Arzani, H. (2004): The use of soil surface properties in rangeland capability assessment through landscape function analysis. – Proc. World Engineers Convention, China.
- [30] Rostami, E., Mehrabe, H., Farahpour, M. (2014): Determining rangeland suitability for sheep grazing using GIS (case study: Sadegh Abad Watershed, Kermanshah Province, Iran). – *Journal of Rangeland Science* 4(4): 319-329.
- [31] Rouhi-Moghaddam, E., Joloro, H., Memarian, H. (2017): Determining range suitability using fuzzy and hierarchical method (case study: Bagheran Birjand Watershed, SouthKhorasan Province, Iran). – *Journal of Rangeland Science* 7(3): 232-241.
- [32] Sanaei, A., Arzani, H., Tavili, A., Farahpour, M. (2015): Assessment of range suitability for sheep grazing according to the MSSG instructions (Case study: Central Taleghan). – *Iranian Journal of Range and Desert Research* 22(2): 275-288.
- [33] Schilling, K. E., Chan, K. S., Liu, H., Zhang, Y. K. (2010): Quantifying the effect of land use land cover change on increasing discharge in the Upper Mississippi River. – *Journal of Hydrology* 387(3-4): 343-345.
- [34] Sour, A., Arzani, H., Feizizadeh, B., Tavili, A., Alizadeh, E. (2013): GIS Multi-Criteria Evolution for Determination of Rangelands Suitability for Goat Grazing in the Middle Taleghan Rangelands. – *International Journal of Agronomy and Plant Production* 4(7): 1499-1510.
- [35] Zhou, Q. (1989): The integration of remote sensing and geographical information systems land resources management in the Australian arid zone. – PhD Thesis, The University of New South Wales Australia.

PHENOLOGICAL PLASTICITY IN *BERBERIS LYCIUM* ROYLE ALONG TEMPORAL AND ALTITUDINAL GRADIENTS

RAHMAN, I. U.^{1,2§} – HART, R.² – AFZAL, A.^{1*} – IQBAL, Z.¹ – ABD_ALLAH, E. F.^{3†} –
ALQARAWI, A. A.³ – IJAZ, F.¹ – ALI, N.¹ – KAUSAR, R.⁴ – MUZAMMIL, S.⁵ – ALZAIN, M. N.
O.⁶ – MAJID, A.¹ – CALIXTO, E. S.⁷

¹*Department of Botany, Hazara University, Mansehra-21300, KP, Pakistan*

²*William L. Brown Center, Missouri Botanical Garden, P.O. Box 299, St. Louis, MO 63166-0299, USA*

³*Department of Plant Production, College of Food & Agricultural Sciences, King Saud University, P.O. Box 2460, Riyadh 11451, Saudi Arabia*

⁴*Department of Environmental Sciences, International Islamic University, Islamabad, Pakistan*

⁵*Department of Biological Sciences, Faculty of Science, King Abdulaziz University, Jeddah 21589, Saudi Arabia*

⁶*Princess Nourah bint Abdulrahman University, College of Science, Biology Department, Riyadh 11451, Saudi Arabia*

⁷*Department of Biology, University of Sao Paulo, SP, Brazil*

**Corresponding author
e-mail: aftabafzalkiani@yahoo.com*

§ORCID ID: 0000-0003-3312-7975; †0000-0002-8509-8953

(Received 24th Jul 2018; accepted 16th Oct 2018)

Abstract. Human influence on the climate change is evident, and the current rate of anthropogenic emissions of greenhouse gases will have widespread impacts on natural ecosystems. Moreover, as global mean temperatures continue to rise; it is pivotal to develop strategies to conserve species and habitats that are vulnerable to climate change. Therefore, the current study assessed the effect of changing climate on fruiting time and phenological plasticity in *Berberis lycium* Royle at Manoor Valley of Northern Pakistan. Further, these changes in fruiting behavior were correlated with temperature changes over the years. Five varying altitudinal sites of Manoor Valley were selected *viz.* Kot, Baila Manoor, Banrhi, Siri and Shamal Pata which range between 1807-2390 m.a.s.l. Observational data on phenological stage of *B. lycium* were recorded in May-October of 2015-17. Ten individuals plant were randomly selected at each altitudinal site and the data recorded. Notable traits were; cover, number of mature fruits and number of immature fruits. GPS was used to record elevation, aspect and position of the plant species and other environmental gradients were measured with the help of weather station. The results were validated using the ordination pattern. Significant changes were observed in all parameters of the species. The results indicated highest gain for bioclimatic variable (bio-9, mean temperature of the driest quarter). The data also indicates that *B. lycium* is highly sensitive to changes in altitude and temperature; it may be adapting to the gradual temperature change over long periods of time by altering the fruiting time or by adjusting to new altitudinal ranges. Furthermore, new phenology patterns and variations of fruiting period in *B. lycium* might be the indication of the raise in global temperature.

Keywords: *ecophysiology, climate change, global warming, phenological patterns, Lesser Himalayas*

Introduction

The world temperature is rising, and thus warming of the climate is unequivocal. Since 1950s, many of the observed changes are unprecedented over decades to millennia and the earth's temperature has risen up to 0.74°C and is likely to increase from 1.8°C to 4°C by 2100 (IPCC, 2007). In recent years, global climate change has threatened environments with increasing global temperatures (IPCC, 2013). This change in climate is occurring due to increased urbanization, and rising concentrations of carbon dioxide stemming from the anthropogenic burning of fossil fuels, which gets trapped into the atmosphere and cause global warming (Bashir and Ahmad, 2017). These changes have the potential to affect species interactions (Walther, 2010). During the postglacial period, species and populations responded to global warming by migrating toward higher latitudes or altitudes, resulting in local extinctions and modifications in species distributions (Petit et al., 2003). However, populations could persist in their current location and withstand environmental stresses if they evolve new adaptive capacities (Lindner et al., 2009). Genetic diversity and phenotypic plasticity are the two key processes that allow plants survival and development under varied environmental regimes (Pigliucci et al., 2006). First, high genetic diversity among and within populations would improve opportunities for rapid adaptation to new environmental stimuli (Hamrick, 2004). Secondly, short-term phenotypic plasticity is a significant means whereby, plants can react and cope with rapid environmental change (Ghalambor et al., 2007). Genetic variability and evolution among organisms at the DNA level is a much-needed resource but takes millions of years. Therefore, under rapid climate change, phenotypic plasticity rather than genetic diversity will likely play a crucial role in allowing plants to persist in their environments (Rehfeldt et al., 2001).

Phenology — the timing of life history stage including the flowering, fruiting, and leaf production of plants — is sensitive to abiotic cues such as day length, temperature and precipitation (Gilman et al., 2010, Cleland et al., 2007). At the same time, biotic factors also influence phenology; plants that are able to respond to seasonal variability are better adopting to maximize the success of their offspring (Hamann, 2004).

It is known that altitude represents a complex gradient along which many environmental variables change concomitantly (Givnish, 1999). Altitudinal gradients are particularly relevant in order to study plant phenological responses to temperature because they provide a wide temperature range over a very short distance. Phenological plasticity is of special importance for species located in mountain habitats since it is much more likely that their offspring will experience a different climate than their parents, if seed dispersal occurs at a relatively short distances up or down the mountain. This change has been widely documented in many studies as evidence of the impact of global climate change on ecosystems, and a considerable amount of studies have focused on temperate as opposed to environments (Sherry et al., 2007). Monitoring changes in the phenology of plants can provide insights as to which plant species are responding to altered climate patterns and is an important indicator as to whether an ecosystem is experiencing a shift. As plant species shift upward in altitude, populations decrease and elevation ranges tend to be smaller than those for temperate species (Colwell et al., 2008).

Flowering and leaf-out phenologies and their responses to climate change have historically been well-studied. In contrast, fruiting phenology responses to climate change have received somewhat less attention, despite the fact that they are critical to reproduction and therefore the persistence and adaptation of populations (Bolmgren and

Lonnberg, 2005). Further, the phenologies of many economically and ethnobotanically important fruits are likely to change with climate change, lending a human dimension to the urgency of studying this life-history stage (Chuine et al. 2004).

Berberis lycium Royle (family: Berberidaceae) is a lesser-known plant, named in English as barberry (Anwar et al., 1979), whereas its fruit is called as “Kashmal” (Usmanghani et al., 1997) and its roots are known as “Darhald” (Nadkarni, 1980). It is native to the Himalayan region of the world and is widely distributed in temperate and semi-temperate areas of Pakistan, India, Afghanistan, Nepal and Bangladesh. In Pakistan, it has historically been recorded as growing in Baluchistan, Khyber Pakhtunkhwa, Punjab and Azad Kashmir at an elevation of 900 to 2900 m (Ali and Khan, 1978). According to the International Union for Conservation of Nature (IUCN), *B. lycium* lies in the vulnerable category (Hamayun et al, 2006). *B. lycium* was reported curing leprosy in Unani system of healthcare. In traditional practices, it is extensively used as medication for several human diseases i.e. broken bones, jaundice, menorrhagia and wounds healing (Singh and Rawat, 2000), acute conjunctivitis, aperient, carminative, colic, ophthalmic inflammation, diarrhea, diuretic, dysentery, expectorant, febrifuge, stomachic and throat infection (Gupta et al., 2015).

The current study was planned to assess phenological plasticity in this important medicinal shrubby plant species along temporal and elevational gradients. In particular we compared contemporary fruiting phenologies to historical norms to elucidate changes over time, and examined environmental conditions along an elevational gradient to link these changes to climate. .

Materials and Methods

Research was undertaken in Manoor Valley, Mansehra, Pakistan (*Fig. 1*). The study area ranges from high subtropical to alpine scrub forest and cold deserts and experiences cloud cover during most of the year. Five varying altitudinal sites were selected for this study on the basis of the species abundance and dominance. These were Kot (1807 m), Baila Manoor (1895 m), Banrhi (2019 m), Siri (2155 m) and Shamal Pata (2390 m).

At each site, elevation was recorded with GPS and aspect with clinometer. During monthly visits throughout the growing season (April–September) 2015–2017, environmental factors (wind speed, temperature, humidity, heat index, dew point, wet bulb and barometric pressure) were measured by handheld weather station (Kestrel weather tracker 4000). For 10 *Berberis lycium* individuals selected randomly during each visit, the cover, the number of immature fruits, and the number of mature fruits were measured.

These data were then compared to phenological patterns of *B. lycium* as characterized in the Flora of Pakistan – a range based on historical specimens collected mostly between 1939 and 1975 – to determine the long-term seasonal change in fruiting behavior.

To characterize the similarity among sites in cover and summer-fruiting phenology we conducted two-way cluster analysis (Bano et al., 2018) based on presence/absence scores in PCORD 5, and a ternary plot (Hammer et al., 2001) based on quantitative values in PAST 3.12. To associate environmental conditions with differences in these response variables among sites, we used Canonical Correspondence Analysis (CCA), based on Bray-Curtis distance measures using CANOCO 5 (Lepš and Šmilauer, 2003).

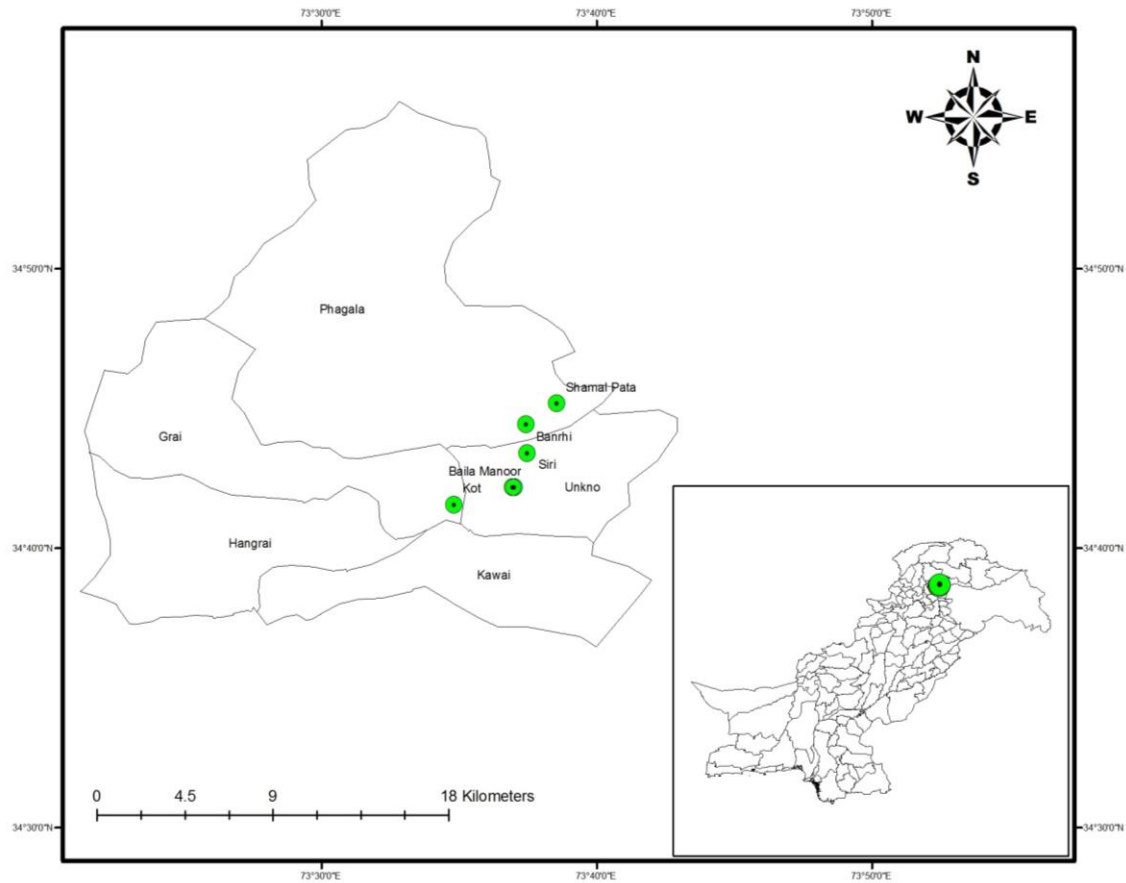


Figure 1. Map of the study area: *Berberis lycium* was studied at five locations (green dots) in Manshehra. The position of Manshehra is given in the inset map at bottom right

Table 1. Means across the growing season of environmental variables measured at different the six localities where *Berberis lycium* was recorded (wind speed averages are given as integers)

Gradients	Localities				
	Kot	Baila Manoor	Banrhi	Siri	Shamal Pata
Altitude (m)	1807	1895	2019	2155	2390
Latitude	N 34°69'282	N 34°70'323	N 34°72'364	N 34°70'317	N 34°75'332
Longitude	E 73°58'045	E 73°61'694	E 73°62'488	E 73°61'600	E 73°64'278
Slope angle	45°	58°	65°	80°	30°
Temperature (°C)	31.3	29.2	25.6	23.7	21
Humidity	47.5	60.3	50.8	68.9	71.9
Heat index	32.5	30.4	24.4	24.4	20.5
Wind speed (m/sec)	1	0	1	0	1
Dew point	18.9	20.3	15.1	17.6	15.7
Wet bulb	22.3	22.2	18.5	19.4	17.3
Barometric pressure	813.5	804.7	792.6	779.3	756.7

Results

Berberis lycium was prominent at Kot, Baila Manoor, Banrhi, Siri and Shamal Pata areas of Manoor Valley, with varying fruiting phenology over geography and season (Fig. 2A-D). Cover of *B. lycium* was directly related to altitude, where higher vegetation cover at lower altitudes was observed (~ 1800 m.a.s.l.).



Figure 2. Phenological conditions of *Berberis lycium* captured at different stations. (A) No fruit at Baila Manoor, (B) mature fruits at Banrhi, (C) mature fruits at Siri, and (D) immature fruiting condition at Shamal Pata

Fruiting exhibited a similar pattern in each year, At the lowest elevation and relatively higher-temperature sites of Kot and Baila Manoor we observed a peak fruiting in spring, with roughly equal quantities of immature and mature spring fruits, while higher elevation sites had not yet begun to fruit in spring (Fig. 3). By summer, fruiting had completed at Kot, and progressively higher sites still retained greater quantities of mature fruits (Fig. 3). Only at the highest site, Shamal Pata, was fruiting still entering its peak in summer (Fig. 3). The ternary plot (Fig. 4) further supports the strong elevational gradient which differentiates sites on the basis of *B. lycium* cover and phenology.

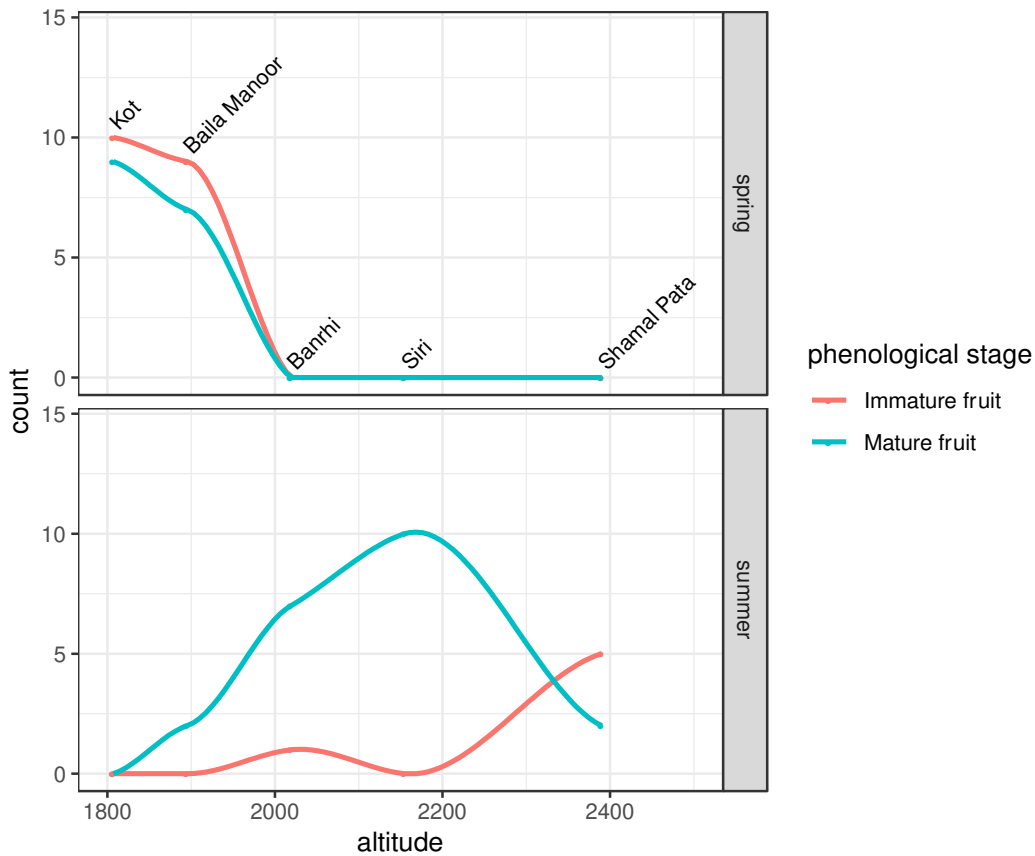


Figure 3. Elevational progression of fruiting phenology: lower elevation sites show peak fruiting in spring while higher sites have not yet begun to fruit; in summer, fruiting is finished at the lower elevation site, peaking at mid-elevations, and has yet to reach its peak at the highest elevation sites

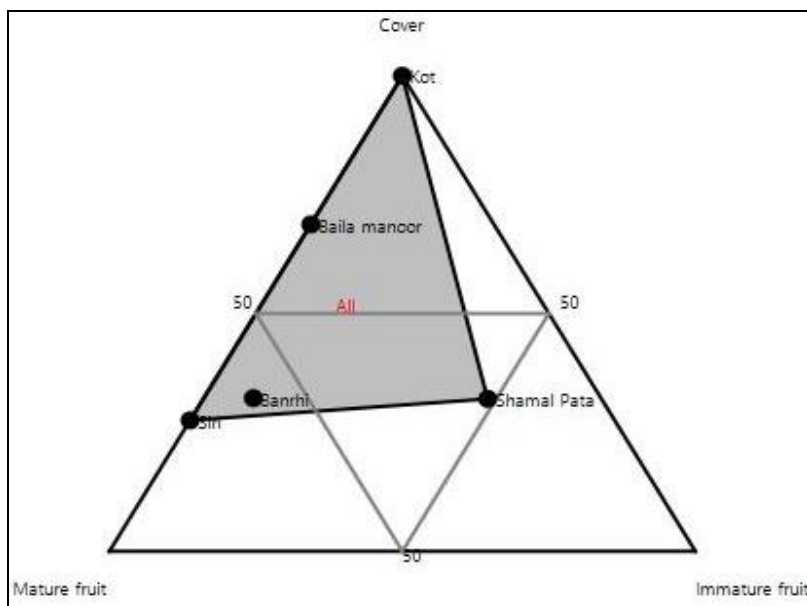


Figure 4. Ternary plot indicating the percentage of all the traits of *Berberis lycium* and its stations

The CCA ordination (Fig. 5) of *Berberis lycium* attributes and environmental gradients showed that different attributes clustered along diverse environmental gradients, which may be summarized as representing the effects of elevation (altitude, temperature, heat index, barometric pressure) and of topography (wind speed, slope). The maximum Eigenvalue was recorded for axis 1 (0.34) followed by axis 2 (0.20). The percentage variance explained for axis 1 and 2 were 62.30% and 100% respectively. The total variation is 0.54 and the explanatory variables account for 100%. The pseudo-canonical correlation for axis 1 and 2 were 1.000 and 1.000. CCA ordination showed that higher values of temperature, barometric pressure, dew point, wet bulb, and heat index were parallel to lower humidity and elevation. Altitude showed negative and significant correlation with temperature, heat index and barometric pressure. Temperature showed positive and significant correlation with heat index and barometric pressure. The maximum strength of gradient was noticed for temperature, barometric pressure, wet bulb, heat index, altitude, density altitude, and slope angle. While minimum environmental gradient strength was observed for humidity, dew point and wind speed. Cover of *Berberis lycium* was significantly higher at the lower elevation sites (Kot and Baila Manoor at 1807-1895 m.a.s.l.). Among the higher sites, the steeper mid-elevation sites of Banrhi and Siri (2019-2155 m.a.s.l.) had the greatest counts of summer mature fruit, while summer immature fruit count was greatest at Shamal Pata (2390 m.a.s.l.), with a relatively shallow slope and high wind speeds (Fig. 5).

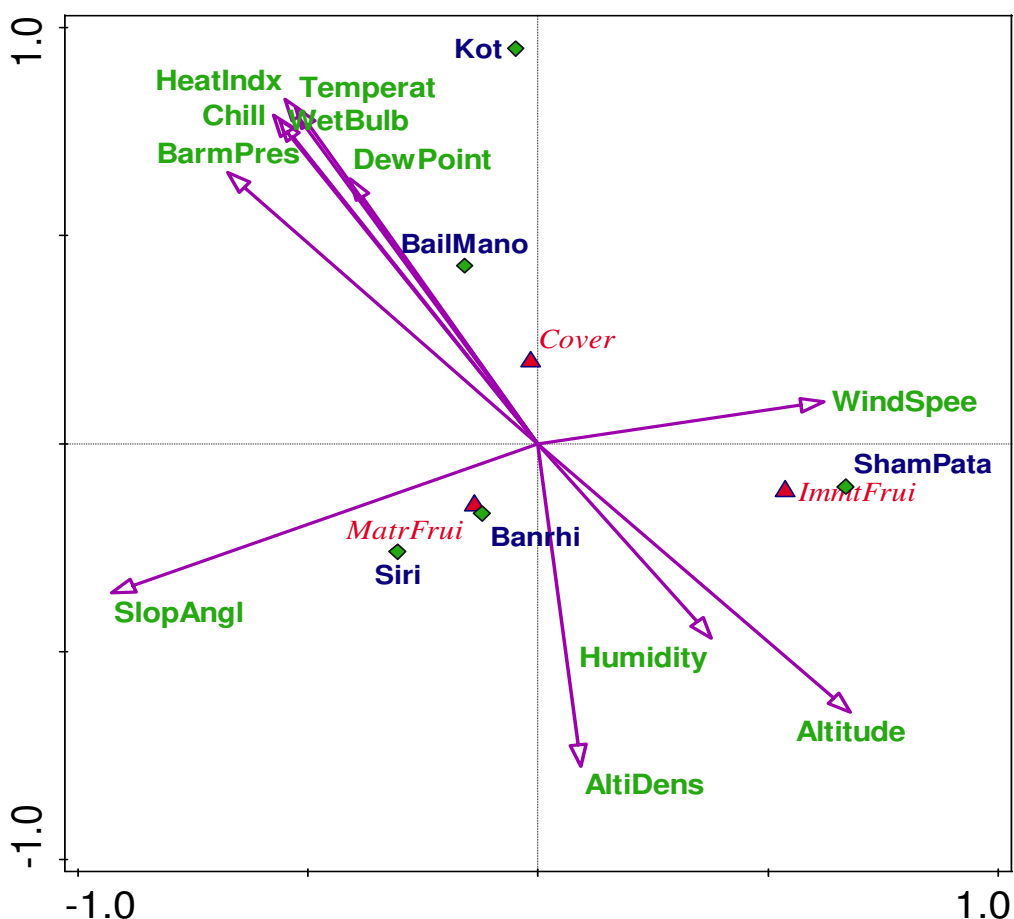


Figure 5. CCA ordination of *Berberis lycium* attributes and stations along different environmental variables

In the Flora of Pakistan, the phenological period of *Berberis lycium* in the area mostly ends by July-August. However, we observe that this phenological period is now only evidenced at the highest altitudes (Shamal pata), while middle and lower elevation sites have completed their fruiting phenology much earlier (in spring, i.e. April-June) (Fig. 6). These higher sites are currently 5.5-10° degrees cooler than the lower sites in average growing season temperature.

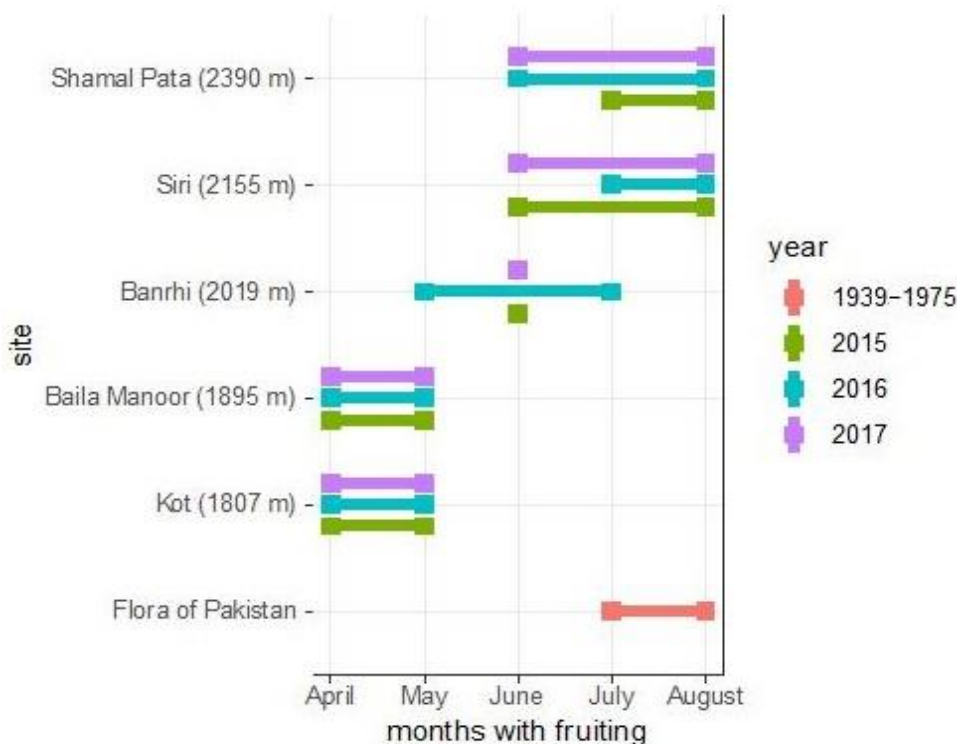


Figure 6. Phenological ranges in five sites monitored 2015–2017 are mostly earlier than phenological ranges recorded in the Flora of Pakistan (1939–1975), with only the highest elevation sites fruiting at comparable times

Discussion

Our results showed phenological variations along the altitudinal gradient, where climatic conditions, especially those related to changes in temperature, had determining roles. The disastrous synchronous effects of climate change and land-use change are evident in Pakistan due to the decline of forest cover (Siddiqui et al., 1999). The recent global data released by NASA and the National Oceanic and Atmospheric Administration (NOAA) suggested that the years this study was conducted (2015–2017) were the hottest recorded, equal or greater to 2° C compared to an 1881–1910 baseline (NASA and NOAA, 2015). Local trends within the far-western Himalaya are more uncertain (Tewari et al. 2017), but there is evidence for warming in the area (Bhutiyani et al., 2010). Some species are very prone to minute changes in the climate as Beigh et al. (2005) pointed out for *Aconitum heterophyllum* in the complex Himalayan region.

The current study predicts similar results as the species will be changing its current habitat and the population density might be significantly affected. Early fruiting behavior was noticed in Kot and Baila Manoor sites, it might be due to the relatively

higher temperatures at these sites. At highest elevation range of this study, immature fruiting condition was on peak, this variability in fruiting phenological pattern might be due to temperature, an important environmental driver, which significantly affects the lifespan of each biotic component of the ecosystem. These results highlight that a particular environmental variable has a great effect on the distribution and dominance of *Berberis lycium* in Manoor Valley. In mountain ecosystems, decrease in population sizes and even extinctions of such species are possible due to the migration of species from their habitat towards higher elevations (Gilman et al., 2010).

Parallel to phenological changes, one of the general trends of species in the Hindu-Kush-Himalayan region, as elsewhere is a change in altitudinal ranges (Song et al., 2004), often in complex response to multiple environmental cues (Tewari et al., 2017). These changes of plant spatial and temporal ranges can result in reorganization of species, leading to the formation of novel communities. Individuals and species as a group deal differently with the variation in abiotic conditions, and thus the likelihood of novel communities' formation higher (Lurgi et al., 2012), with unpredictable consequences (Gilman et al., 2010), and the potential to affect ecosystem resilience (Walther et al., 2010).

In *Berberis lycium*, phenological variations were observed along elevational ranges, and between past and contemporary phenology. The importance of temperature in differentiation the phenology of populations along the elevational gradient suggests that this may also be a key factor in the changes seen over time, although precipitation, land use changes and sampling effort must also be considered (Daru et al 2018). In future work, long-term, cross-taxon monitoring at the level of individual plants could be joined to further research into the historical range and phenology of plant species to better understand how plant communities are responding to changing climatic conditions.

Author's Contributions. IUR conducted the fieldwork, collected data and plant species, FI helped in the herbarium work. AM identified the plants specimens and designed the map. IUR, RH drafted the manuscript and analyzed the data, NA helped in organizing the data. RH, AA and ZI supervised the work. RH, NA and EFA critically reviewed the manuscript. RH and IUR revised the manuscript, AAA, AMNO, ESC, RK and MS helped in revision. All the authors have read and approved the final manuscript.

Acknowledgements. First author would like to thank Higher Education Commission (HEC), Pakistan for granting scholarship under International Research Support Initiative Program (IRSIP) to conduct a research work at Missouri Botanical Garden, USA. The authors would like to extend their sincere appreciation to the Deanship of Scientific Research at King Saud University for its funding to the Research Group number (RG-1435-014).

REFERENCES

- [1] Ali, M. N., Khan, A. A. (1978): Pharmacognostic studies of *Berberis lycium* Royle and its importance as a source of raw material for the manufacture of berberine in Pakistan. – Pakistan Journal of Forestry: p26.
- [2] Anwar, A. K., Ashfaq, M., Nasveen, M. A. (1979): Pharmacognostic Studies of Selected Indigenous Plants of Pakistan. – Pakistan Forest Institute, Peshawar, NWFP, Pakistan.
- [3] Bano, S., Khan, S. M., Alam, J., Alqarawi, A. A., Abd_Allah, E. F., Ahmad, Z., Hashem, A. (2018): Eco-Floristic studies of native plants of the Beer Hills along the Indus River in the districts Haripur and Abbottabad, Pakistan. – Saudi Journal of Biological Sciences 25(4): 801-810.

- [4] Bashir, H., Ahmad, S. S. (2017): Delineation of Catastrophic Effects of Climate Modifications in Pakistan Using GIS and Remote Sensing. – *Universal Journal of Engineering Science* 5(1): 1-4.
- [5] Beigh, S. Y., Nawchoo, I. A., Iqbal, M. (2005): Cultivation and conservation of *Aconitum heterophyllum*: A critically endangered medicinal herb of the Northwest Himalayas. – *Journal Herbs. Spices and Medicinal Plants* 1: 47-56.
- [6] Bhutiyani, M. R., Kale, V. S., Pawar, N. J. (2010): Climate change and the precipitation variations in the northwestern Himalaya: 1866–2006. – *International Journal of Climatology: A Journal of the Royal Meteorological Society* 30(4), 535-548.
- [7] Bolmgren, K., Lonnberg, K. (2005): Herbarium data reveal an association between fleshy fruit type and earlier flowering time. – *International Journal of Plant Sciences* 166: 663-670.
- [8] Chuine, I., Beaubien, E. G. (2001): Phenology is a major determinant of tree species range. – *Ecology Letters* 4: 500-510.
- [9] Cleland, E. E., Chuine, I., Menzel, A., Mooney, H. A., Schwartz, M. D. (2007): Shifting plant phenology in response to global change. – *Trends in Ecology and Evolution* 22(7): 357-365.
- [10] Colwell, R. K., Brehm, G., Cardelús, C. L., Gilman, A. C., Longino, J. T. (2008): Global warming, elevational range shifts, and lowland biotic attrition in the wet tropics. – *Science* 322: 258-261.
- [11] Daru, B. H., Park, D. S., Primack, R. B., Willis, C. G., Barrington, D. S., Whitfield, T. J. S., Seidler, T. G., Sweeney, P. W., Foster, D. R., Ellison, A. M. et al. (2018): Widespread sampling biases in herbaria revealed from large-scale digitization. – *New Phytologist* 217: 939–955.
- [12] Ghalambor, C. K., McKay, J. K., Carroll, S. P., Reznick, D. N. (2007): Adaptive versus non-adaptive phenotypic plasticity and the potential for contemporary adaptation in new environments. – *Functional Ecology* 21: 394-407.
- [13] Gilman, S. E., Urban, M. C., Tewksbury, J., Gilchrist, G. W., Holt, R. D. (2010): A framework for community interactions under climate change. – *Trends in Ecology and Evolution* 25: 325-331.
- [14] Givnish, T. J. (1999): On the causes of gradients in tropical tree diversity. – *Ecology* 876: 193-210.
- [15] Gupta, M., Singh, A., Joshi, H. C. (2015): *Berberis lycium* multipotential medicinal application: An overview. – *International Journal of Chemical Studies* 3(4): 10-13.
- [16] Hamann, A. (2004): Flowering and fruiting phenology of a Philippine submontane rain forest: climatic factors as proximate and ultimate causes. – *Journal of Ecology* 92(1): 24-31.
- [17] Hamayun, M., Khan, S. A., Sohn, E. Y., In-jung, L. (2006): Folk medicinal knowledge and conservation status of some economically valued medicinal plants of District Swat Pakistan. – *Lyonia* 11(2): 101-113.
- [18] Hammer, O., Harper, D. A. T., Ryan, P. D. (2001): PAST: Paleontological Statistics software package for education and data analysis. – *Palaeontologia Electronica* 4(1): 9.
- [19] Hamrick, J. L. (2004): Response of forest trees to global environmental changes. – *Forest Ecology and Management* 197: 323-335.
- [20] Hirzel, A. H., Le Lay, G. (2008): Habitat suitability modelling and niche theory. – *Journal of Applied Ecology* 45: 1372-1381.
- [21] IPCC (Intergovernmental Panel on Climate Change) (2007): Climate change: the physical science basis. Geneva, Switzerland.
- [22] IPCC (Intergovernmental Panel on Climate Change) (2013): IPCC Fifth Assessment Report (AR5). Geneva: WMO, IPCC Secretariat.
- [23] Lepš, J., Šmilauer, P. (2003): Multivariate analysis of ecological data using CANOCO. – Cambridge University Press, New York.

- [24] Lindner, M., Maroschek, M., Netherer, S., Kremer, A., Barbati, A. J. G. G., Seidl, R., Delzon, S., Corona, P., Kolstrom, M., Lexer, M. J. Marchetti, M. (2009): Climate change impacts, adaptative capacity, and vulnerability of European forest ecosystems. – *Forest Ecology and Management* 259: 698-709.
- [25] Lurgi, M., López, B. C., Montoya, J. M. (2012): Novel communities from climate change. – *Philosophical Transactions of the Royal Society B: Biological Sciences* 367: 2913-2922.
- [26] Nadkarni, K. M. (1980): *Indian Material Medica*. – Bombay, India: Popular Parakshan Depot, pp. 180-190.
- [27] NASA, NOAA. (2015): NASA, NOAA Find 2014 Warmest Year in Modern Record. Available in: <<https://www.nasa.gov/press/2015/january/nasa-determines-2014-warmest-year-in-modern-record>> Accessed 15 November 2017.
- [28] Petit, R. J., Aguinagalde, I., De Beaulieu, J. L., Bittkau, C., Brewer, S., Cheddadi, R., Ennos, R. (2003): Glacial refugia: hotspots but not melting pots of genetic diversity. – *Science* 300: 1563-1565.
- [29] Pigliucci, M., Murren, C. J., Schlichting, C. D. (2006): Phenotypic plasticity and evolution by genetic assimilation. – *Journal of Experimental Biology* 209: 2362-2367.
- [30] Rehfeldt, G. E., Wykoff, W. R., Ying, C. C. (2001): Physiologic plasticity, evolution, and impacts of a changing climate on *Pinus contorta*. – *Climatic Change* 50: 355-376.
- [31] Sherry, R. A., Zhou, X., Gu, S., Arnone, J. A., Schimel, D. S., Verburg, P. S., Luo, Y. (2007): Divergence of reproductive phenology under climate warming. – *Proceedings of the National Academy of Sciences* 104(1): 198-202.
- [32] Siddiqui, K. M., Mohammad, I., Ayaz, M. (1999): Forest ecosystem climate change impact assessment and adaptation strategies for Pakistan. – *Climate Research* 12: 195-203.
- [33] Singh, S. K., Rawat, G. S. (2000): *Flora of Great Himalayan National Park*. – Himachal Pradesh, 60-61.
- [34] Song, M., Zhou, C., Ouyang H. (2004): Distributions of dominant tree Species on the Tibetan Plateau under current and future climate scenarios. – *Mountain Research and Development* 24: 166-173.
- [35] Tewari, V. P., Verma, R. K., Von Gadow, K. (2017): Climate change effects in the Western Himalayan ecosystems of India: evidence and strategies. – *Forest Ecosystems* 4(1), 13.
- [36] Usmanghani, K., Saeed, A., Alam, M. T. (1997): *Indusynic medicine*. – Karachi, Pakistan: University of Karachi press, p.120.
- [37] Walther, G. R. (2010): Community and ecosystem responses to recent climate change. – *Philosophical Transactions of the Royal Society B-Biological Sciences* 365: 2019-2024.

ECOLOGICAL AND PHYSIOLOGICAL PERFORMANCE OF WHITE BEAN (*PHASEOLUS VULGARIS* L.) AFFECTED BY ALGAE EXTRACT AND SALICYLIC ACID SPRAYING UNDER WATER DEFICIT STRESS

BEIGZADEH, S.¹ – MALEKI, A.^{1*} – HEYDARI, M. M.¹ – KHOURGAMI, A.² – RANGIN, A.³

¹*Department of Agronomy and Plant Breeding, College of Agriculture, Islamic Azad University Ilam Branch, Ilam, Iran
(e-mail: Sepantasbkf.b686@gmail.com; maleki97@yahoo.com; mirzaeiheydari@yahoo.com)*

²*Department of Agronomy, Khoramabad Branch, Islamic Azad University, Lorestan, Iran
(e-mail: Ali_khorgamy@yahoo.com)*

³*Department of Biology, Islamic Azad University, Ilam Branch, Ilam, Iran
(e-mail: alireza1121sar@gmail.com)*

**Corresponding author
e-mail: maleki97@yahoo.com*

(Received 13th Jul 2018; accepted 31st Oct 2018)

Abstract. In order to investigate the effects of salicylic acid and seaweed extract foliar on photosynthetic pigments of white bean grown under water deficit stress, a split-split plot experiment was conducted based on randomized complete block design with three replicates. The experimental factors consisted of irrigation regimes at three levels, seaweed extract at four levels and salicylic acid foliar application at two levels. In both places of the experiment, application of 150 g.ha⁻¹ seaweed extract along with salicylic acid increased leaf relative water content in plants grown under water deficit stress. The maximum chlorophyll a content (15.15 mg.g⁻¹ FW) was observed when 150 g.ha⁻¹ seaweed extract was applied under no water deficit stress condition. By contrast, the minimum chlorophyll a content (8.34 mg.g⁻¹ FW) was related to 50 g.ha⁻¹ seaweed extract. In addition, the minimum proline content (79 mg.g⁻¹ FW) was found when no salicylic acid foliar was applied under water deficit stress. However, the maximum proline content (123.2 mg.g⁻¹ FW) was obtained when 100 g.ha⁻¹ from seaweed extract was applied under severe water deficit stress. The results indicated that the maximum seed yield (2343.3 kg ha⁻¹) was achieved when 100 g.ha⁻¹ seaweed extract was applied and there was no water deficit stress.

Keywords: *anthocyanin, proline, seed yield, RWC, total chlorophyll*

Introduction

Protein deficiency in diet causes several problems for human health. Besides animal proteins, plant proteins such as legumes are also an important source of proteins. With growing population in the world, protein requirement and consumption of plant resources are increasing. Among various crops, beans are used as one of the most important and valuable sources of plant proteins (Hosseini, 2008) and have been used in human diet for centuries. Beans are a rich source of protein (20-30%) and carbohydrates (50-60%) and a relatively good source of minerals and vitamins (Rehman and Shah, 2004). In most parts of the world, water is a limiting factor for agricultural productions. Drought stress is one of the major threats to successful crop production across the world. Drought stress reduces crop yield by 50% or more (Bai et al., 2006). According to the FAO reports (2010), around 90% of Iran with arid and semi-arid climate conditions is covered with sparse vegetation.

One of the effects of environmental stresses is lipid peroxidation (Bai et al., 2006) and degradation of proteins and nucleic acids (Kovacik et al., 2014).

Salicylic acid is a phenolic compound known as a plant hormone or growth regulator, which plays a key role in defense mechanisms against biotic and abiotic stress factors including drought tolerance. It has a significant role in reducing oxidative damage caused by different stresses in plants and developing an anti-stress mechanism in plant cells. Studies have shown that, under drought stress conditions, salicylic acid improves plant growth, transpiration, stomatal regulation, photosynthesis and ion absorption and transfer (Hayat and Ahmad, 2007). Algae have been used to reduce physiological disturbances caused by mineral deficiency and thus improved grain production and resistance to frost (Sridhar and Rengasamy, 2011). In addition to supplying nitrogen and mineral elements, algae regulate plant growth by releasing plant regulating hormones. The presence of plant hormones such as auxin, gibberellin and cytokinin has been shown in the extract of brown algae. Therefore, application of seaweed extract as a fertilizer, increases the growth and production of plants (Erulan et al., 2009). Inorganic extract of *A. nodosum* contains nitrogen, phosphorus, potassium, calcium, iron, magnesium, zinc, sodium and sulfur. Various types of seaweeds stimulate different responses of plants for example, increase in yield, increase in nutrients uptake, changes in the composition of plant tissues, increase in cold resistance, increase in pathogen resistance and increase in fruits quality and germination rate (Sridhar and Rengasamy, 2011). Seaweed extract is produced by hydrolysis under high pressure, however the process differs from species to species. The final concentration of the extract depends on its use as high concentrations could be harmful for plants. Seaweed extract is suitable for those products in which growth hormones such as IAA, IBA, cytokinins, vitamins and amino acids are used (Kaoaua et al., 2013). This study was conducted to investigate the effects of seaweed extract and salicylic acid on white bean performance, grown under water deficit stress condition.

Materials and Methods

The current study was carried out to investigate the effects of salicylic acid and seaweed extract foliar application on photosynthetic pigments, biochemical characteristics and yield of white bean (*Phaseolus vulgaris* L.) grown under water deficit stress condition in the Agricultural Research Station, Khorramabad, Iran, in 2016 and 2017 growing seasons. The soil characteristics, meteorology data and geographical location of the study site are presented in *Tables 1 and 2*.

The experiments were conducted as a split-split plot experiment based on a randomized complete block design with three replicates. The experimental factors consisted of irrigation regimes (main plots) at three levels, (irrigation after 60 (no water deficit stress), 90 (mild water deficit stress) and 120 mm (severe water deficit stress) evaporation from class A evaporation pan), seaweed extract (*Ascophyllum nodosum*) (sub-plots) at four levels (0, 50, 100 and 150 g.ha⁻¹) and salicylic acid foliar application (sub-sub plots) at two levels (with and without). Chlorophyll a, b and total chlorophyll were measured according to Porra method (Porra, 2002). Anthocyanins and carotenoids were measured based on the methods described by Lichtenthaler and Wellburn (1983). Leaf samples (500 mg) were rest in 5 ml 80% acetone and centrifuged at 13000 rpm at 4 °C for 15 min. The supernatant made up to 10 ml with 80% acetone and used for spectrophotometry.

Table 1. Soil physicochemical properties

Depth	Total N (%)	P(AVO) P.P.M.	K(AVO) P.P.M.	C.E.C. Meq/mg	Neutralized percentage	pH	EC*10	Saturation percentage s.p.	Organic carbon O.C %
0-20	13	9.2	640	30.8	15.2	7.6	0.73	54	1.26
60-20	6	2.8	380	30.2	17.5	7.7	0.49	55	0.63
95-60	3	2.4	240	28.0	24.5	7.8	0.44	52	0.29
125-95	4	2.8	220	28.0	26.0	7.8	0.48	51	0.38

Table 2. Meteorological and geographical properties of the study site

Longitude	Latitude	Altitude	Average annual rainfall	Average temperature	Absolute max temperature	Absolute min temperature
47° 26'	34° 8'	1346 m	538 mm	10.5 °C	41°C	-28.8 °C

Different types of leaf chlorophyll amount were determined based on Arnon (1949) approach. Leaf samples of 0.1 g, from each experimental unit (pots) were obtained from youngest leaves. Samples were grounded and placed in 10 ml of 80% acetone. Resulting extract was centrifuged in 3000 rpm for 10 minutes and the obtained supernatant was placed in cuvette. The absorbance of the solution was recorded by spectrophotometry at 645 and 663 nm wavelengths. Arnon equations were used to estimate the chlorophyll a and b as below:

$$\text{Chlorophyll a (mg/ml)} = [(12/7 \times A_{663}) - (2/69 \times A_{645})] \quad (\text{Eq.1})$$

$$\text{Chlorophyll b (mg/ml)} = [(22/9 \times A_{645}) - (4/68 \times A_{663})] \quad (\text{Eq.2})$$

$$\text{Chlorophyll a+b (mg/ml)} = \text{Chla} + \text{Chlb}) \quad (\text{Eq.3})$$

$$\text{Carotenoid } (\mu\text{g/ml}) = (1000(A_{470}) - 1.8(\text{Chla}) - 85.02(\text{Chlb}))/198 \quad (\text{Eq.4})$$

Proline content was determined using Bates et al. (1973) method. Briefly, 500 ml leaf sample was placed in 10 ml of 3% sulfosalicylic acid and then the homogenate was filtered using filter paper. Then 2 ml of the sample was mixed with 2 ml ninhydrin acid (25.1 g ninhydrin plus 30 ml glacial acetic acid) and 2 ml glacial acetic acid in test tubes. The test tubes were heated at 100 °C for 1 h and then cooled down at 4 °C for 30 min before adding 4 ml toluene. The samples were vortexed and left on the bench for 10 min. The upper layer was used for spectrophotometry at 520 nm. The following equations were used to calculate proline content.

$$\frac{\mu\text{g}}{\text{mL}} \text{ Proline} \times \text{mL toluene} \times \frac{\mu\text{mol}}{115/5\mu\text{g}} \times \frac{5}{\text{sample g}} = \mu\text{mol proline per g fresh sample} \quad (\text{Eq.5})$$

$$\left(\frac{\mu\text{g}}{\text{mL}} \text{ Proline} \times \text{mL toluene}\right) \times \frac{5}{\text{sample g}} = \mu\text{g proline per g fresh sample} \quad (\text{Eq.6})$$

The relative water content was determined using (Diaz-Perez et al., 2006) method. Young leaves were detached and equal leaf discs were prepared and then weighted (fresh weight). The discs were soaked in distilled water for 24 h and weighed again to

determine saturated weight. Finally, the samples were dried in an oven for 48 h to determine dry weight. The relative water content was calculated according to the following equation.

$$\text{RWC} = (\text{FW} - \text{DW}) / (\text{TW} - \text{DW}) * 100 \quad (\text{Eq.7})$$

where: F_w: fresh weight, D_w: dry weight and T_w saturated weight.

Leaf electrolytes leakage was measured according to Flint (1967). Equal leaves were taken and then were cut into discs. The discs were washed using distilled water and then put into tests tubes containing 5 ml deionized distilled water. After 24 h, the electrical conductivity (EC) of the samples was measured using EC meter (Jenway, 4010). To assess the photosynthetic pigments quartz spectrometer cell (UV_160A_SHIMADO model, made in Japan) was used. Electrical conductivity Multi-range (model H18733) was used to measure the EC. The samples were put in the freezer at -20 C for another 24 h and then the EC was measured again. The value of electrical leakage was calculated using the following equation:

$$\frac{Ec_1}{Ec_2} \times 100 \quad (\text{Eq.8})$$

Before exposing data to ANOVA and statistical analysis, SPSS was used to perform test for errors and data normality. Data were analyzed by SPSS as split-plot factorial based on randomized complete block design and Duncan's test was used for mean comparison. Interactive effects of means were signified by Duncan's test by using MSTATC app and MS Excel was used for plots.

Results and Discussion

This study results indicated that the effects of water deficit stress, seaweed extract, and salicylic acid foliar applications were significant on all the studied traits. However, none of the traits were affected by place. Although the interaction between each factor and place was not significant, all interaction between experimental factors was significant. The interaction between place and other experimental factors was only significant on RWC.

Relative Water Content (RWC)

The results showed that main effects of water deficit stress, seaweed extract, and salicylic acid were significant on RWC. Significate interactions are shown in *Table 3*. The results indicated the minimum RWC (36.41%) was due to mild water deficit stress and salicylic foliar application treatment in the first place. In addition, in both sites of the experiment, salicylic acid increased RWC under severe water deficit stress condition and seaweed extract application. Salicylic acid seems to increase the RWC through the ability of the plant to maintain the leaf water potential. It has been reported that spraying salicylic acid during flowering would increase the RWC, osmotic potential and leaf turgidity (Hussain et al., 2008). Ramroudi and Khamar (2013) showed increase of RWC in basil by application of salicylic acid.

Table 3. Analysis of variance on bean traits

Source of variation	df	Carotenoid	Anthocyanin	Total chlorophyll	Chlorophyll a	Chlorophyll b	Electrolyte leakage	RWC	proline	yield
(P) place	1	32.3ns	1995.4ns	20.1ns	0.702ns	10.2ns	4.8ns	160.4ns	45.6ns	985.4ns
(r/P)	4	57.6	410.2	5.7	0.665	2.71	33.8	47.1	76.5	546.4
a	2	437.3**	1434.9ns	208.8**	11.9**	101.7**	1508.2**	2941.5**	567.78**	409.5**
P × a	2	2.5ns	1304.8ns	1.8ns	0.994ns	10.5ns	3.4ns	16.8ns	6.5ns	909.5ns
error	8	3.74	478.6	2.30	0.432	1.60	44.1	22.8	7.87	321.4
b	3	37.4*	1054.5**	194.8**	13.2**	112.6**	693.3**	3138.4**	43.0**	1209.5**
P × b	3	7.38ns	2.147ns	0.039ns	0.182ns	0.053ns	0.113ns	3.5ns	11.34ns	108.5ns
a × b	6	151.0**	121.3**	9.6**	0.493ns	6.6**	74.2**	70.4**	165.5**	231.5**
P × a × b	6	4.59ns	18.99ns	0.163ns	0.103ns	0.048ns	1.4ns	28.2*	6.87ns	430.7ns
error	36	9.64	18.35	1.18	0.395	0.636	6.83	10.9	12.23	187.3
c	1	84.7**	114.7**	49.1**	1.5**	24.0**	123.1**	332.4**	109.4**	654.3**
P × c	1	8.03ns	1.13ns	0.012ns	0.020ns	0.295ns	0.941ns	3.4ns	12.87ns	121.2ns
a × c	2	79.3**	26.3ns	14.2**	0.758*	9.8**	120.5**	81.4**	87.9ns	221.2ns
P × a × c	2	0.313ns	0.102ns	0.404ns	0.018ns	0.218ns	0.021ns	20.3**	1.213ns	108.6ns
b × c	3	124.2**	88.9**	16.4**	7.3**	4.2**	13.4*	21.7**	232.2ns	88.9ns
P × b × c	3	0.866ns	12.4ns	0.164ns	0.136**	0.027ns	0.741ns	4.2ns	2.346ns	78.4ns
a × b × c	6	116.7**	97.8**	5.4**	3.5**	3.1**	8.5ns	51.1**	187.6ns	112.0ns
P × a × b × c	6	2.34ns	11.7ns	0.075ns	0.060ns	0.144ns	0.574ns	21.9**	4.870ns	234.7ns
Error	48	10.71	14.3	0.547	0.212	0.473	4.35	4.4	12.65	67.3
C.V(%)	-	15.5	8.7	4.7	9.7	6.2	9.0	3.7	11.2	12.3

*, ** and ns significant at 5%, 1% and no significant, respectively

Electrolytes leakage

The results (*Table 3*) showed that the maximum electrolyte leakage (38.3%) was related to severe water deficit stress treatment without any foliar application. The minimum value was observed when no water deficit stress was imposed and 150 g ha⁻¹ seaweed extract was applied (*Table 4*). The interaction between water deficit stress and salicylic acid showed that the maximum electrolyte leakage (31.3%) was monitored under severe water deficit stress and salicylic acid foliar application treatments. By contrast, the minimum value (17.3%) was achieved when no water deficit stress was induced but salicylic acid was applied on the plants (*Table 5*). The interaction between seaweed and salicylic acid indicated that the maximum electrolyte leakage (29.3%) was related to control treatment whereas the minimum value (17.2%) was observed when 150 g ha⁻¹ seaweed extract and salicylic acid were applied (*Table 6*).

Table 4. Interaction between water deficit stress and seaweed extract

Treatments		Yield	Proline	Electrolyte leakage
a ₁	b ₁	1902.2bc	79k	21.17cd
	b ₂	2090.6b	79.6h	19.17de
	b ₃	2343.3a	82.2h	16.35fg
	b ₄	2176.6ab	87.6h	16g
a ₂	b ₁	1208.1de	89.5b	28.03b
	b ₂	1408.8d	98.8ef	21.79c
	b ₃	1592.2cd	102.2cde	20.41cde
	b ₄	1790.6c	108.6d	18.29ef
a ₃	b ₁	902.5h	110.5cd	38.28a
	b ₂	1090.3g	121.4d	28.03b
	b ₃	1132.4fg	123.2fg	28.91b
	b ₄	1200.2de	111.2e	21.72c

Means with the same letter are not significantly different from each other (P>0.05 ANOVA followed by DMRT).

Treatment a drought stress at 3 levels.

Treatment of algae b at 4 levels.

Table 5. Interaction between water deficit stress and salicylic acid

Treatments		Electrolyte leakage
a ₁	c ₁	17.29f
	c ₂	19.05e
a ₂	c ₁	23.69c
	c ₂	20.57d
a ₃	c ₁	31.33a
	c ₂	27.14b

Means with the same letter are not significantly different from each other (P>0.05 ANOVA followed by DMRT).

Treatment a drought stress at 3 levels.

Salicylic acid treatment at 2 levels.

Table 6. Interaction between seaweed extract and salicylic acid

Treatments		Electrolyte leakage
b ₁	c ₁	29.27a
	c ₂	29.05a
b ₂	c ₁	23.80b
	c ₂	22.20c
b ₃	c ₁	23.21bc
	c ₂	20.56d
b ₄	c ₁	20.13d
	c ₂	17.22e

Means with the same letter are not significantly different from each other (P>0.05 ANOVA followed by DMRT).

Treatment of algae b at 4 levels.

Salicylic acid treatment at 2 levels.

Under abiotic stresses, such as salinity, drought, high and low temperatures, plants produce reactive oxygen species, molecules which result in oxidative stress through affecting cellular components and plant metabolism. The reactive oxygen species cause considerable damages to the cells lipid membrane and lead to dis-organisation of the lipid matrix (membrane fluidisation), which in turn decrease cell permeability. Therefore, maintaining cell membrane integrity has an important role in increasing stress resistance (Shim et al., 2003). The effect of salicylic acid on plant growth is mainly due to increased cell division in meristem areas and cell growth. Salicylic acid may also impose its effects through other plant hormones (Shakirova et al., 2003).

Chlorophyll a

The results showed that the main effect of water deficit stress, seaweed extract and salicylic acid and some interactions between them were significant on chlorophyll a concentration (*Table 3*). The maximum chlorophyll a concentration (15.15 mg g FW⁻¹) was obtained when 150 g.ha⁻¹ seaweed extract was applied to non-stressed plants. By contrast, the minimum value (8.43 mg g FW⁻¹) was recorded under severe water deficit stress and application of 50 g ha⁻¹ seaweed extract (*Table 7*). In this study, water deficit stress reduced photosynthetic pigments content (chlorophyll and carotenoid). Reduction in photosynthetic pigments under water deficit stress can be attributed to the destruction of chloroplast and photosynthetic apparatus, photo-oxidation of chlorophyll, degradation of precursors of chlorophyll and the suppression of chlorophyll biosynthesis as well as the activation of chlorophyll degrading enzymes and finally hormonal disorders (Orcutt and Nilsen, 2000). However, accumulation of sodium and chloride ions in leaves under salt stress condition also has a negative effect on chlorophyll concentration. Additionally, stress disrupts absorption of certain essential elements such as iron and magnesium, which are essential for chlorophyll synthesis (Neocleous and Vasilakakis, 2007). Lipoxxygenase has been reported as one of the enzymes involved in chlorophyll catabolism, while lipoxxygenase is one of the enzymes involved in lipid peroxidation too (Farooq et al., 2009). Amino acid and seaweed extract foliar application could significantly increase plant height, photosynthetic pigments, potassium content,

phosphorus content, and yield, fresh and dry weight in celery. Seaweed extracts contain large amounts of cytokines, auxins and betaine that increase chlorophyll content of leaves (Shehata et al., 2011).

Table 7. Interaction between water deficit stress, seaweed extract and salicylic acid

Treatments		Carotenoid	Anthocyanin	Total chlorophyll	Chlorophyll b	Chlorophyll a	
a ₁	b ₁	c1	14.65i	39.37fg	12.70mn	3.65klm	9.04ij
		c2	14.26i	33.34i	18.28ef	5.97b	12.26f
	b ₂	c1	19.22defgh	28.34j	15.36hi	5.36cd	9.60i
		c2	27.22ab	40.89efg	17.11g	4.41fghi	12.55f
	b ₃	c1	17.35fghi	48.02cd	18.64ef	5.04de	13.32de
		c2	15.08hi	45.12cde	19.69cd	6.04b	13.42cd
	b ₄	c1	19.67defg	53.42ab	20.33bc	6.10ab	14.05bcd
		c2	16.11ghi	49.29bc	21.30a	5.70bc	15.15a
a ₂	b ₁	c1	23.56bcd	43.27def	11.92n	3.31lm	8.94ij
		c2	24.25bc	40.62efgh	14.90ij	4.25hij	10.68h
	b ₂	c1	29.48a	48cd	13.14lm	4.04ijk	9.61i
		c2	18.11efghi	47.98cd	13.90kl	4.95def	8.79ij
	b ₃	c1	21.03cdef	54.52a	15.99h	4.53efghi	12.00fg
		c2	17.11fghi	48.80c	17.76fg	5.22cd	12.55ef
	b ₄	c1	20.91cdef	56.21c	20.74ab	6.63a	14.20bc
		c2	17.75fghi	55.61a	19.06de	4.38fghi	14.66ab
a ₃	b ₁	c1	22.40cde	39.86fg	12.12n	3.14m	8.75ij
		c2	29.09a	33.67hi	12.77mn	3.73jkl	9.07ij
	b ₂	c1	17.32fghi	39.24fg	12.69mn	4.34fghi	8.43j
		c2	23.55bcd	33.32i	13.08lm	4.37fghi	8.90ij
	b ₃	c1	29.75a	39.85fg	14.42jk	4.76defgh	9.60i
		c2	22.38cde	38.03gh	13.78kl	4.28ghij	9.55i
	b ₄	c1	27.54ab	41.55efg	15.39hi	4.90defgh	11.19gh
		c2	19.53defg	43.57def	15.81hi	4.92def	10.96h

Means with the same letter are not significantly different from each other (P>0.05 ANOVA followed by DMRT).

Treatment a drought stress at 3 levels.

Treatment of algae b at 4 levels.

Salicylic acid treatment at 2 levels.

Chlorophyll b

This study results showed that the main effect of water deficit stress, seaweed extract and salicylic acid and some interactions between them were significant on chlorophyll b concentration (Table 3). The maximum chlorophyll b concentration (6.63 mg g FW⁻¹) was obtained when 150 g ha⁻¹ seaweed extract and salicylic acid were applied on plants grown under mild water deficit stress. By contrast, the minimum value (3.14 mg g FW⁻¹)

¹) was related to severe water deficit stress without seaweed or salicylic acid application (*Table 7*). Salicylic acid application on plants increases chlorophyll (as one of the main components of the photosynthetic apparatus affecting dry weight) and carotenoid content in control and stressed plants, indicating the ability of salicylic acid to improve plant growth. Similarly to the results of this experiment, it has been reported that salicylic acid increased chlorophyll and carotenoid content in barley, wheat, spinach, canola, tomato and pea (El-Tayeb, 2005). Increase in fresh weight, dry weight, root length, stem length and chlorophyll content on the account of seaweed extract has been reported previously (Sridhar and Rengasami, 2011).

Total chlorophyll

The results showed that the main effect of water deficit stress, seaweed extract and salicylic acid and some interactions between them were significant on total chlorophyll concentration (*Table 3*). The maximum total chlorophyll concentration ($21.3 \text{ mg g FW}^{-1}$) was obtained when 150 g.ha^{-1} seaweed extract was applied on plants grown under no water deficit stress. By contrast, the minimum value ($11.9 \text{ mg g FW}^{-1}$) was related to mild water deficit stress without seaweed or salicylic acid application (*Table 7*). Seaweed-based fertilizers improve plants growth by providing more nitrogen, phosphorus, and potassium, as well as supplying micronutrients and secondary metabolites (Karthick et al., 2013). Studies on cucumber, after using seaweed extracts (red and green algae) indicated that fresh and dry weight and leaf area increased probably due to increased nitrogen concentration and improving soil physical conditions through providing more energy for microorganisms helps to improve availability and absorption of mineral nutrients. Increase in yield may also be related to some nutritional elements, especially iron, zinc and manganese in compost and potassium, calcium, magnesium, sulfur, and iron in seaweed extract. These elements can stimulate vegetative growth, chlorophyll biosynthesis, and photosynthesis, which in turn affect flowering and fruit production (Ahmed and Shalaby, 2012).

Anthocyanin

The results indicated that the main effect of water deficit stress, seaweed extract and salicylic acid and some interactions between them were significant on anthocyanin concentration (*Table 3*). The maximum anthocyanin concentration ($56.2 \text{ mmol g FW}^{-1}$) was obtained when 150 g.ha^{-1} seaweed extract and salicylic acid were applied on plants grown under mild water deficit stress. By contrast, the minimum value ($28.3 \text{ mmol g FW}^{-1}$) was related to 50 g.ha^{-1} seaweed extract and salicylic acid treatment on plants grown under no water deficit stress (*Table 7*). Flavonoids, flavones, and anthocyanins have anti-oxidant properties and it has been proven that their production and gene expression increase under stress conditions (Tang et al., 2006). In general, it has been shown that seaweeds affect antioxidant activity and chemical composition of plants grown under environmental stresses (Van Alstyne, et al., 2007).

Carotenoids

The results indicated that the main effect of water deficit stress, seaweed extract and salicylic acid and some interactions between them were significant on carotenoids content (*Table 3*). The maximum carotenoids content ($29.7 \text{ mg g FW}^{-1}$) was obtained when 100 g.ha^{-1} seaweed extract and salicylic acid were applied on plants grown under

severe water deficit stress. By contrast, the minimum value ($14.3 \text{ mg g FW}^{-1}$) was related to non-stressed plants without any seaweed extract or salicylic acid application (Table 7). The induction of carotenoid biosynthesis under stress conditions might be due to their protective role in photosynthetic systems. These pigments are responsible for neutralizing reactive oxygen species and preventing lipid peroxidation and ultimately oxidative stress. Carotenoids release large amounts of energy from photosystems (I) and (II) in the form of heat or chemical reactions which can maintain chloroplast membranes (Koyro, 2006). In a study carried out by Sivasankari et al. (2006), application of 20% seaweed liquid fertilizer (SLF) could increase shoot length, root length, fresh weight, dry weight, chlorophyll, carotenoid, shoots and root protein content, shoots and root amino acids content, alpha amylase and beta amylase activity. The improvement of growth parameters due to salicylic acid might be due to its effect on the photosynthetic apparatus, photosynthesis rate, rubisco enzyme activity, photosynthetic pigments concentration, stomatal conductance, antioxidant defense system, reduction of oxidative stress and ion leakage. An increase in cell membrane integrity, nitrogen metabolism, and mineral nutrition are also mentioned in various studies (El-Tayeb, 2005).

Proline

The results indicated that the main effect of water deficit stress, seaweed extract and salicylic acid and some interactions between them were significant on proline content (Table 3). The minimum proline content (79 mg g FW^{-1}) was obtained when no seaweed extract was applied on plants grown under no water deficit stress. By contrast, the maximum value ($123.2 \text{ mg g FW}^{-1}$) was related to severe water deficit plants treated with 100 g.ha^{-1} seaweed extract (Table 4). In all stress levels, application of 100 or 150 g.ha^{-1} seaweed extract resulted in proline accumulation. Increasing in proline accumulation on the account of a particular treatment, such as seaweed extract, leads to increased resistance to drought stress, followed by higher yields (Koyro, 2006). Water stress cause chlorophyll degradation, and glutamate, which is a precursor of chlorophyll and proline, is transformed into proline, resulting in a reduction in the chlorophyll content (Lawlor and Cornic, 2009). Proline is known as an osmotic regulator that increases in response to salinity stress. One of the most important mechanisms in higher plants grown under salinity conditions is the accumulation of compounds such as proline. Proline accumulation is a primary defense response to maintaining osmotic pressure in cells. It has been reported that proline has a key role in osmotic regulation, protection of cell structures and neutralization of reactive oxygen species as well as malondialdehyde and the ascorbate peroxidase (Ashraf and Foolad, 2007). Another reason to increase the proline content in plants grown under water deficit stress is chlorophyll degradation. As a result, the concentration of these substances increases under stress conditions. In this study, in the plants grown under water deficit stress, the total chlorophyll content decreased whereas proline leaf concentration increased, which is consistent with the above hypothesis.

Seed yield

The results indicated that the main effect of water deficit stress, seaweed extract and salicylic acid and interaction between water deficit stress and seaweed extract was significant on seed yield (Table 3). The maximum seed yield ($2343.3 \text{ kg ha}^{-1}$) was obtained when 100 g ha^{-1} seaweed extract was applied on non-stressed plants. By

contrast, the minimum seed yield ($90.2.5 \text{ kg ha}^{-1}$) was related to severe water deficit plants without seaweed extract application. In all stress levels, application of 100 or 150 g ha^{-1} seaweed extract could increase seed yield. Numerous studies have shown the positive effects of seaweed and biological fertilizers on growth and yield of plants. It is likely that seaweed extract application increases, absorption and storage of nutrients in different parts of the plants, including leaves and stems, which in turn results in increased yield (Ahmad and Khalili, 2006). In addition, it seems that increase in stress, reduces plant growth and nutrient content. Therefore, reduction in vegetative growth due to the reduction of osmotic potential, reproductive growth and finally seed yield is not surprising. Environmental stresses decrease water uptake, transpiration and stomatal closure, which lead to a decrease in growth (Ben-Asher et al., 2006). The results have shown that the application of green and red seaweed extracts and commercial extract of seaweed with compost, improve vegetative growth, dry and fresh weight and yield of cucumber (Ahmed and Shalaby, 2012). Increase in fresh and dry weight might be due to nitrogen availability and improving soil physical properties as well as improved oil microorganisms' activity on the account of seaweed application. Increase in yield may also be related to some nutritional elements, especially iron, zinc and manganese in compost and potassium, calcium, magnesium, sulfur and iron in seaweed extract. These elements can stimulate vegetative growth, chlorophyll biosynthesis and photosynthesis, which in turn affect flowering and fruit production (Ahmed and Shalaby, 2012). Seaweed-based fertilizers improve plant growth through providing more nitrogen, phosphorus and potassium, as well as supplying micronutrients and secondary metabolites. In a study carried out by (Ahmed and Shalaby, 2012) seaweed extract application could increase vegetative growth and fruit yield of cucumber.

Conclusion

Application of salicylic acid and seaweed extract by increasing the activity of anti-oxidant enzymes (including catalase, ascorbate peroxidase and peroxidase) and plant proline, have an important role in the reduction of oxygen radicals (hydroxyl, peroxide hydrogen, and super oxide) that were produced due to water stress. Using salicylic acid and seaweed extract enhance the biosynthesis and protection of photosynthetic pigments under water stress and result in higher chlorophyll concentration. Thus it seems that foliar application of salicylic acid under water stress can promote water saving which is very critical at current situation of water scarcity for agriculture and can mitigate the damages of water stress which may finally result in higher crop yield.

REFERENCES

- [1] Ahmad, A. J., Khalili, M. (2006): Effect of low irrigation on yield and yield components of maize in Miandoab region. – Iranian Journal of Water Research 1(1): 17-28.
- [2] Ahmed, Y. M., Shalaby, E. A. (2012): Effect of Different Seaweed Extracts and Compost on Vegetative Growth, Yield and Fruit Quality of Cucumber. – Journal of Horticultural Science & Ornamental Plants 4(3): 235-240.
- [3] Ashraf, M., Foolad, M. R. (2007): Role of glycine betaine and Proline in Improving Plant Abiotic Stress Resistance. – Environmental and Experimental Botany: 206-216.

- [4] Bai, L. P., Sui, F. G., Ge, T. D., Sun, Z. H., Lu, Y. Y., Zhou, G. S. (2006): Effect of soil drought stress on leaf water status, membrane permeability and enzymatic antioxidant system of maize. – *Soil Science Society of China* 16(3): 326-332.
- [5] Bates, L. S., Waldren, R. P., Teare, I. D. (1973): Rapid determination of free proline for water stress studies. – *Plant and Soil* 39: 205-207.
- [6] Ben-Asher, J., Tsuyuki, I., Bravdo, B. A., Sagih, M. (2006): Irrigation of grapevines with saline water. I. Leaf area index, stomatal conductance, transpiration and photosynthesis. – *Agricultural Water Management* 83: 13-21.
- [7] Diaz-Perez, J. C., Shackel, K. A., Sutter, E. G. (2006): Relative water content. – *Ann of Bot.* 97(1): 85-96.
- [8] El-Tayeb, M. A. (2005): Response of barley grain to the interactive effect of salinity and salicylic acid. – *Plant Growth Regul* 42: 215-224.
- [9] Erulan, V., Thirumaran, G., Soundarapandian, P., Ananthan, G. (2009): Studies on the effect of *Sargassum polycystum* (C. agardh, 1824) extract on the growth and biochemical composition of *Cajanus cajan* (L.) Mill sp. – *American-Eurasian Journal of Agricultural and Environmental Sciences* 6(4): 392-399.
- [10] FAO. (2010): FAOSTAT. Available in <http://faostat.fao.org/> [28 May 2010].
- [11] Farooq, M., Wahid, A., Kobayashi, N., Fujita, D., Basra, S. M. A. (2009): Plant drought stress: effects, mechanisms and management. – *Agronomy for sustainable development* 29(1): 185-212.
- [12] Flint, H. L., Boyce, B. R., Beattie, D. J. (1967): Index of injury drought a useful expression of freezing injury to plant tissues as determined by the electrolytic method. – *Can. J. Plant Sci.* 47: 229-230.
- [13] Hayat, S., Ahmad, A. (2007): *Salicylic Acid: plant hormone*. – Springer, p. 97-99.
- [14] Hosseini, N. M. (2008): *Agriculture and Cereal Production*. – Mashhad University Press (In Persian).
- [15] Hussain, M., Farooq, M., Malik, M. A. (2008): Glycinebetaine and salicylic acid application improves the plant water relations, water use efficiency and yield of sunflower under different planting methods. – *Proceedings of 14th Australian Agronomy Conference, Adelaide, SA, Australia*.
- [16] Kaoaua, M. E., Chernane, H. H., Benaliat, A., Neamallah, L. (2013): Seaweed liquid extracts effect on *salvia officinalis* growth, biochemical compounds and water deficit tolerance. – *African Journal of Biotechnology* 72(28): 4481-4589.
- [17] Karthick, N., Selvakumars, S., Umamaheswari, S. (2013): Effect of three different seaweed liquid fertilizers and a chemical liquid fertilizer on the growth and histopathological parameters of *Eudrilus Eugeniae* (Haplotaxida: Eudrilidae Global). – *Journal of Bio-Science and Biotechnology* 2(2): 253-259.
- [18] Kovacik, J., Klejdus, B., Babula, P., Jarosova, M. (2014): Variation of antioxidants and secondary metabolites in nitrogen-deficient barely plants. – *Journal of Plant Physiology* 171: 260-268.
- [19] Koyro, H. W. (2006): Effect of salinity on growth, photosynthesis, water relations and solute composition of potential cash crop halophyte (*Plantago coronopus* L.). – *Environ Exp Bot* 56: 136-149.
- [20] Lawlor, M. H., Cornic, U. S. (2009): Manganese efficiency and manganese-uptake kinetics of raya (*Brassica juncea*), Weat (*Triticum aestivum*), and oat (*Avena sativa*) grown in nutrient solution and soil. – *J. Plant Nutrition. Soil Sci.* 172: 425-434.
- [21] Lichtenthaler, H. K., Wellburn, A. R. (1983): Determination of total carotenoids and chlorophyll a and b of leaf extract in different solvents. – *Biol. Soc. Trans.* 11: 591-592.
- [22] Neocleous, D., Vasilakakis, M. (2007): Effects of NaCl stress on red raspberry (*Rubus idaeus* L. "Autumn Bliss"). – *Scientia Horticulturae* 112: 282-289.
- [23] Orcutt, D. M., Nilsen, E. T. (2000): *The physiology of plants under stress, soil and biotic factors*. – John Wiley and Sons, New York. pp: 177-235.

- [24] Porra, R. J. (2002): The chequered history of the development and use of simultaneous equations for the accurate determination of chlorophylls a and b. – *Photosynthesis Res.* 73: 149-156.
- [25] Ramroudi, M., Khamar, A. R. (2013): Interaction of salicylic acid spraying and irrigation treatments on some properties of quantitative, qualitative and basal osmotic regulator. – *Journal Applied Research Eco Physiology plants* 1(1): 19-32.
- [26] Rehman, Z. U., Shah, W. H. (2004): Domestic processing effects on some insoluble dietary fiber components of various food legumes. – *Food Chemistry* 87: 613-617.
- [27] Shakirova, F. M., Sakhabutdinova, A. R., Bezrukova, M. V., Fathutdinova, R. A., Fathutdinova, D. R. (2003): Changes in hormonal status of wheat seedlings induced by salicylic acid and salinity. – *Plant Sci* 164: 317-22.
- [28] Shehata, S. M., Abdel-Azem, H. S., El-Yazied, A. A., El-Gizawy A. M. (2011): Effect of foliar spraying with amino acids and seaweed extract on growth chemical constituents, yield and its quality of celeriac plant. – *European Journal of Scientific Research* 58(2): 257-265.
- [29] Shim, I. S., Momose, Y., Yamamoto, A., Kim, D. W., Usui, K. (2003): Inhibition of catalase activity by oxidative stress and its relationship to salicylic acid accumulation in plants. – *Plant Growth Regul* 39: 285-92.
- [30] Sivasankari, S., Venkatesalu, V., Anantharaj, M., Chandrasekaran, M. (2006): Effect of seaweed extracts on the growth and biochemical constituents of *Vigna sinensis*. – *Bioresource Technology* 97: 1745-1751.
- [31] Sridhar, S., Rengasamy, R. (2011): Potential of seaweed liquid fertilizers (SLFS) on some agricultural crop with special reference to protein profile of seedlings. – *International Journal Development Resarch* 7: 55-57.
- [32] Tang, L., Kwon, S. Y., Kim, S. H., Kim, J. S., Choi, J. S., Cho, K. Y., Sung, C. K., Kwak, S. S., Lee, H. S. (2006): Enhanced tolerance of transgenic potato plants expressing both superoxide dismutase and ascorbate peroxidase in chloroplasts against oxidative stress and high temperature. – *Plant Cell Rep.* 25(12): 1380-1386.
- [33] Van Alstyne, K. L., Koellermeier, L., Nelson, T. A. (2007): Spatial variation in dimethylsulfoniopropionate (DMSP) production in *Ulva lactuca* (Chlorophyta) from the Northeast Pacific. – *Marine Biology* 150: 1127-1135.

IMPROVING EFFECT OF EXOGENOUS NICKEL NITRATE APPLICATION ON PHYSIO-BIOCHEMICAL FEATURES, NITROGEN METABOLISM AND EARLY GROWTH OF RICE

ZHANG, T. T.^{1,2#} – HE, L. X.^{1,2#} – ASHRAF, U.^{1,2,3#} – TONG, T. Y.^{1,2#} – CHENG, Y.¹ – SABIR, S.-U.-R.³
– ZHENG, A. X.^{1,2} – LU, R. H.¹ – LAI, R. F.^{1,2} – FENG, H. Y.¹ – TANG, X. R.^{1,2*}

¹*Department of Crop Science and Technology, College of Agriculture, South China Agricultural University, 510642 Guangzhou, PR China*

²*Scientific Observing and Experimental Station of Crop Cultivation in South China, Ministry of Agriculture, 510642 Guangzhou, PR China*

³*Department of Botany, University of Education, Lahore, Faisalabad-Campus, 38000, Punjab, Pakistan*

#These author have contributed equally to this work

**Corresponding author*

e-mail: tangxr@scau.edu.cn; phone/fax: +20-8528-0204-618

(Received 16th Jul 2018; accepted 31st Oct 2018)

Abstract. High Ni²⁺ levels are toxic to plant growth; however, being a micro-nutrient, its application and/or presence in low concentration may improve plant growth. Present study investigated the effects of exogenous Ni application on morpho-physiological attributes of two rice cultivars in China i.e., *Yuxiangyouzhan* and *Meixiangzhan 2*. Nickel was applied exogenously to 11 days old seedlings as Ni(NO₃)₂ in a solution form in the following concentrations: 0.1 mM (Ni1), 0.2 mM (Ni2) and 0.5 mM (Ni3). The seedlings without Ni²⁺ application were taken as control. Results showed that exogenous Ni²⁺ application improved the early growth of seedlings in terms of seedling length, basal diameter, biomass accumulation and seedling index. Substantial improvements were also observed regarding chl a, chl b, total chl contents and carotenoids in plants under Ni²⁺ application compared to CK. Furthermore, all Ni²⁺ treatments decreased the content of Malondialdehyde (MDA). Among all applied concentrations, Ni2 proved better regarding its promotive effects, however further research is needed to explore the molecular basis of Ni-induced modulations in seedlings of both rice cultivars.

Keywords: *chlorophyll; nickel nitrate; rice; seedling; enzymes in nitrogen metabolism; anti-oxidant enzyme*

Introduction

Rapid industrial development, urbanization and other anthropogenic activities are building pools of heavy metals in soils (Nagajyoti et al., 2010). These heavy metals, at an optimum concentration, act as essential micronutrients for the plants and play a beneficial role for plant growth, development and overall productivity.

Similarly, nickel is also recognized as the double-edged element for plants i.e., toxic at high concentrations whilst promotive at low/trace concentrations. However, long term nickel stress could induce significant inhibitory effects on shoots and roots growth, plant height, number of tillers, 1000 grain weight and paddy yield (Nazir and Asghar et al., 2015). Moreover, nickel (Ni²⁺) toxicity caused decline in the activities of antioxidants and induced the accumulation of free proline in both leaves and roots in pea plants (Gajewska and Skłodowska, 2005). Exposure of detached leaves of rice seedlings to NiSO₄ (1 mM) caused remarkable decline in activity of superoxide

dismutase (SOD) and enhanced malondialdehyde (MDA) contents, thus caused leaf senescence (Shi and Zhoum 1998). Rice seedlings exposed to high Ni^{2+} concentrations caused substantial reduction in root and shoot growth along with substantial decline in fresh and dry biomass of rice plants (Rizwan and Imtiaz et al., 2017). A decline in the activities of anti-oxidants e.g., superoxide dismutase (SOD), catalase (CAT) and ascorbate peroxidase (APX) were noted with the increased Ni^{2+} concentrations in paddy leaves.

On the other hand, nickel is an essential element for high plants with a normal range of 0.01-5.00 mg kg^{-1} dry weight (DW) (Welch, 1981); however, such reports are very few. For instance, application of NiCl_2 (1 - 5 $\mu\text{mol L}^{-1}$) can effectively promote vegetative growth of rice seedlings (Wang et al., 1999). It also augmented the chlorophyll content, soluble protein, soluble sugars and peroxidase (POD) activity (Wang and Tian et al., 1999). Its involvement as a non-substitution component of urease seems to be the only proof of its beneficial effect in high plants (Gerendás and Polacco et al., 2015). Fishbein et al. (1997) indicated that Ni^{2+} is a necessary component of plant and bacterial urease which has an important role in catalysing the hydrolysis of urea into ammonia and carbon dioxide in plants. Polacco (1997) reported that soybean cells had an absolute requirement for Ni^{2+} while grown with urea as a sole N source in the presence of citrate. Gerendás et al. (2015) also proved that the nickel deficient paddies showed substantial reduction in growth and urea accumulation owing to the lack of urease activity. Ni-induced improvements in seed germination and early growth in rice mimics its stimulatory effects (Das and Kar et al., 1978; Mishra and Kar, 1974). Furthermore, low concentration of Ni^{2+} can promote the activities of peroxidase and ascorbic acid oxidase in alfalfa leaves and can enhance the disease resistance in crops (Theisen and Blincoe, 1984), nonetheless, the promotive effects of Ni^{2+} in high plants still needs further investigation. Present study investigated the effects of exogenous application of Ni^{2+} at lower concentrations on the physio-biochemical attributes and early growth of rice seedlings with the hypothesis that Ni^{2+} being a trace element could improve the early growth of rice if applied at low concentration.

Materials and methods

Experimental details

Pot experiment, between September to October in 2017, was conducted at Experimental Research Farm, College of Agriculture, South China Agricultural University, Guangzhou, (23°09'N, 113°22'E and 11 m from mean sea level) China.

The experimental soil in Guangzhou was sandy loam with 25.65% of organic matter content, 1.360% total N, 0.956% total P, and 17.460% total K. Before sowing, seeds of two popular rice cultivars i.e., *Meixiangzhan 2* and *Yuxiangyouzhan* were soaked in water for 24 h at room temperature and germinated under moisture conditions. Geminated seeds were sown in plastic pots (31 cm in diameter and 29 cm in height) and allowed to grow for 10 days then Ni^{2+} in the form of $\text{Ni}(\text{NO}_3)_2$ was foliar sprayed with three different concentrations i.e., 0.1, 0.2, and 0.5 mM and regarded as Ni1, Ni2 and Ni3, respectively. Pots without Ni^{2+} application were regarded as control (CK) The measurements were repeated in triplicate and averaged.

Thirty days old seedlings collected from each treatment, except those which were used for the determination of seedling growth, were harvested, washed and immediately stored at -80°C till biochemical analyses (*Fig. 1*).

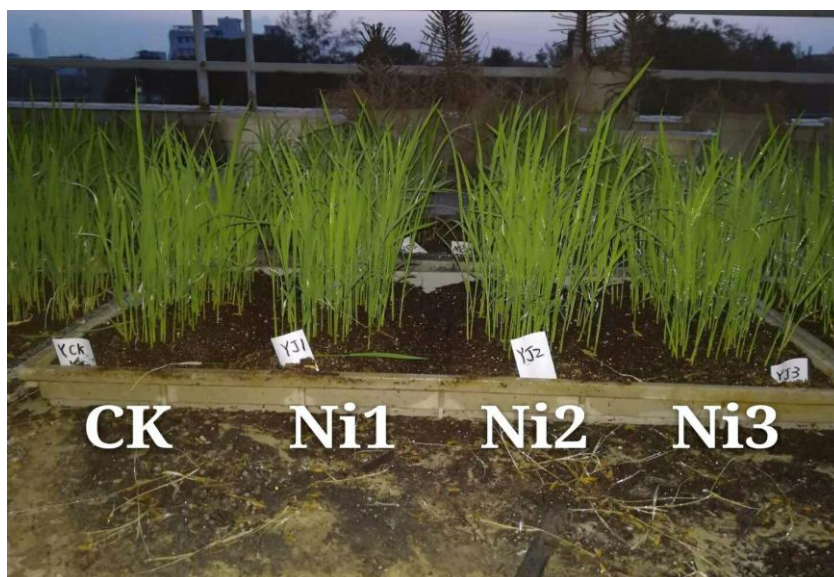


Figure 1. Experimental site

Determination of seedling growth

30 days old 10 seedlings from each treatment were randomly harvested for measuring plant height, basal diameter, dry biomass and seedling index. The seedling index was calculated as:

$$\text{Seedling index} = \text{basal diameter} / \text{plant height} \times \text{dry weight}$$

Determination of soluble protein and malondialdehyde (MDA)

Protein contents were estimated according to Bradford (1976) by using G-250 and expressed as $\mu\text{g g}^{-1}$ FW. Malondialdehyde (MDA) content was measured according to the method of Luo and Zhong et al. (2017) with thiobarbituric acid. MDA reacted with thiobarbituric acid (TBA) and the absorbance was read at 532 nm, 600 nm, and 450 nm. The content of MDA was calculated as: $\text{MDA content } (\mu\text{mol/L}) = 6.45(\text{OD } 532 - \text{OD } 600) - 0.56\text{OD } 450$ and final result was expressed as $\mu\text{mol/g FW}$.

Determination of chlorophyll contents

The fresh leaf samples (0.5 g) were extracted with 95% alcohol and the absorbance was read at 665 nm, 649 nm, 652 nm and 470nm and the chlorophyll contents were estimated according to Arnon (1949).

Determination of anti-oxidants activities

The peroxidase (POD, EC1.11.1.7) activity was measured with the methods of Pan et al. (2013). The reaction solution included enzyme extract (50 μl) containing 1 ml of 0.3% H_2O_2 , 0.95 ml of 0.2% guaiacol, and 1 ml of 50 mM I^{-1} sodium phosphate buffer (pH 7.0). The absorbance was read at 470 nm. One POD unit of enzyme activity was defined as the absorbance increase because of guaiacol oxidation by 0.01 (U/g FW). The superoxide dismutase (SOD, EC 1.15.1.1) activity was measured by using nitro

blue tetrazolium (NBT) according to Pan et al. (2013). enzyme extract (0.05 ml) was added into the reaction mixture containing 1.75 ml of sodium phosphate buffer (pH 7.8), 0.3 ml of 130 mM l^{-1} methionine buffer, 0.3 ml of 750 $\mu\text{mol } l^{-1}$ NBT buffer, 0.3 ml of 100 $\mu\text{mol } l^{-1}$ EDTA-Na 2 buffer and 0.3 ml of 20 $\mu\text{mol } l^{-1}$ lactoflavin. After the reaction, the change in color was measured at 560 nm. One unit of SOD activity is equal to the volume of extract needed to cause 50% inhibition of the color reaction. Catalase (CAT, EC 1.11.1.6) activity was estimated with the methods devised by Aebi (1984). An aliquot of enzyme extract (50 μl) was added to the reaction solution containing 1 ml of 0.3% H_2O_2 and 1.95 ml of sodium phosphate buffer. The absorbance was recorded at 240 nm. One CAT unit of enzyme activity was defined as the absorbance decrease by 0.01 (U/g FW).

Determination of nitrogen metabolism enzymes activities

The activity of nitrate reductase (NR) was measured by using the methods of Sun et al. (2009). One unit of NR activity is defined as NaNO_2 μg formed per gram of fresh samples per hour. The activities of glutamic oxaloacetic transaminase (GOT) were measured by using the methods devised by Ebeid et al. (1981). The aminotransferase activity was expressed by pyruvate formed in 30 min. The activities of glutamine synthetase (GS) and glutamine oxoglutarate aminotransferase (GOGAT) were measured according to Lin and Kao (1996). One unit of GS activity is defined as 1 pmol L-glutamate γ -monohydroxamate formed per min. The reaction mixture (1 ml, pH 8.0) contained 80 pmol Tris-HCl buffer, 40 pmol L-glutamic acid, 8 pmol ATF', 24 pmol MgSO_4 , and 16 pmol NH_2OH . The final pH was 8.0. The reaction was started by addition of the enzyme extract and stopped by adding 2 mL of 2.5% FeCl_2 and 5% trichloroacetic acid in 1.5 M HCl after 30 min incubation at 30 °C. One unit of GOGAT activity is defined as a decrease of 1 OD_{340} per min. The reaction was started by adding L-glutamine immediately following the enzyme preparation. The decline in absorbance was recorded at 340 nm.

Statistical analyses

Data were analyzed using statistical software 'Statistix 8.1' (Analytical Software, Tallahassee, FL, USA) while differences amongst means were separated by using least significant difference (LSD) test at 5% probability level. 'Origin 8.1' (OriginLab Co., Northampton, MA, USA) was used for graphical representation.

Results

Seedling growth

No significant difference was noted in seedling length for *Meixiangzhan 2* and basal diameter for both cultivars among all Ni^{2+} treatments and CK, however seedling length was substantially increased under all Ni^{2+} treatments than CK for *Yuxiangyouzhan 2*. The seedling fresh and dry weight were increased by 19.58-32.23% and 23.08-26.93% (for *Yuxiangyouzhan*) as well as 24.65-32.93% and 29.16-46.88% (for *Meixiangzhan 2*), respectively. Furthermore, the highest seedling index i.e., 1.14 ± 0.03 and 0.78 ± 0.05 was recorded in Ni^{2+} for both *Yuxiangyouzhan* and *Meixiangzhan 2* (Table 1).

Table 1. Effect of Ni²⁺ application on rice seedling quality

Cultivars	Treatment	Seedling length (cm)	Basal diameter (mm)	Fresh weight (mg)	Dry weight (mg)	Seedling index
<i>Yuxiangyouzhan</i>	CK	15.50±0.13b	1.32±0.01a	55.33±2.64b	10.83±1.09b	0.92±0.09b
	Ni1	17.17±0.67a	1.35±0.03a	67.83±5.13a	13.33±0.45a	1.05±0.04ab
	Ni2	16.10±0.49ab	1.34±0.04a	66.17±4.28ab	13.67±0.39a	1.14±0.03a
	Ni3	16.97±0.65ab	1.32±0.02a	73.17±3.27a	13.75±0.44a	1.07±0.03ab
<i>Meixiangzhan 2</i>	CK	15.40±0.92a	1.095±0.02a	47.60±2.88b	8.00±0.29b	0.57±0.02b
	Ni1	17.28±1.21a	1.10±0.07a	61.40±3.55a	11.75±0.14a	0.75±0.01a
	Ni2	15.85±0.76a	1.14±0.03a	62.80±1.76a	10.83±0.67a	0.78±0.05a
	Ni3	16.27±0.95a	1.10±0.07a	59.33±5.25a	10.33±0.93a	0.70±0.06ab

Data in the table are tested with Statistix 8 by LSD (P < 0.05). Values with different small letters in the same line have significant difference

Chlorophyll contents

Exogenous Ni²⁺ application affected the chlorophyll contents significantly. Compared with CK, the contents of chl a were increased by 6.14-20.71% for *Yuxiangyouzhan* and 1.23-8.12% for *Meixiangzhan 2*. The contents of chl b were improved by 10.46-13.5% in Ni2 and Ni3, respectively for *Yuxiangyouzhan* whilst increased by 3.22, 6.66 and 3.79% in Ni1, Ni2 and Ni3 for *Meixiangzhan 2*. Likewise, the total chl contents were increased by 3.97%, 16.33% and 16.96% for *Yuxiangyouzhan* and 2.61%, 7.55% and 2.19% for *Meixiangzhan 2* under Ni1, Ni2 and Ni3, respectively as compared with CK. Furthermore, different nickel applications improved carotenoid contents significantly for both cultivars. For instance, compared with CK, the Ni1, Ni2 and Ni3 resulted in 8.68, 26.40 and 21.88% higher carotenoid contents than CK for *Yuxiangyouzhan* and 3.66, 10.44 and 1.46 higher carotenoid contents for *Meixiangzhan 2*, respectively (Fig. 2).

Nitrogen metabolism enzymes

Overall, all Ni²⁺ treatments regulated the activities of key enzymes involved in nitrogen metabolism (Table 2). The NR activities were increased by 12.27, 18.13 and 10.56% for *Yuxiangyouzhan* and 8.24, 20.03 and 25.56% higher for *Meixiangzhan 2* in Ni1, Ni2 and Ni3, respectively. The activities of GS in all Ni treatments were found statistically similar (P>0.05) for *Yuxiangyouzhan* whereas the highest GS activity was recorded in Ni1 while lowest in Ni3.

Meanwhile, no significant difference was recorded among Ni1, Ni2 and CK for GOGAT activities while lowest GOGAT activity was recorded in Ni3 for *Yuxiangyouzhan*. However, for *Meixiangzhan 2*, 15.12% and 15.15% lower activity of GOGAT was recorded in Ni2 and Ni3 whilst Ni1 remained similar with CK. Compared with control, activities of GOT in Ni1, Ni2 and Ni3 were 1.09, 1.22 and 1.24 fold higher for *Yuxiangyouzhan* while 1.21, 1.16 and 1.02 fold higher for *Meixiangzhan 2*. Moreover, the activities of GPT were improved by 28.74, 51.95 and 29.47% in Ni1, Ni2 and Ni3 for *Yuxiangyouzhan* whilst 49.38, 24.99 and 16.82% for *Meixiangzhan 2*.

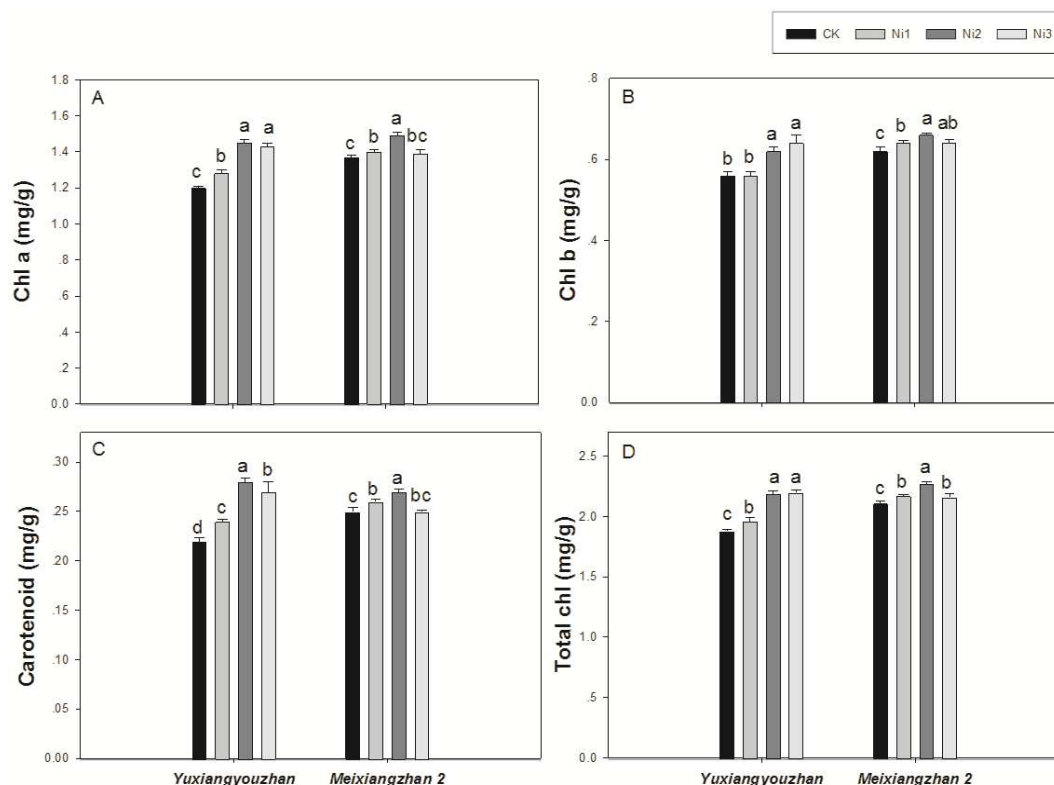


Figure 2. Effect of Ni^{2+} application on chlorophyll content

Table 2. Effect of Ni^{2+} application on nitrogen metabolism

Cultivar	Treatment	NR activity ($\mu\text{g}\cdot\text{g}^{-1}$)	GS activity ($\mu\text{mol}\cdot\text{g}^{-1}\cdot\text{min}^{-1}$)	GOGAT activity ($\mu\text{mol}\cdot\text{g}^{-1}\cdot\text{min}^{-1}$)	GOT activity ($\mu\text{mol}\cdot\text{g}^{-1}\cdot\text{h}^{-1}$)	GPT activity ($\mu\text{mol}\cdot\text{g}^{-1}\cdot\text{h}^{-1}$)
Yuxiangyouzhan	CK	56.74±7.1b	0.36±0.00a	0.30±0.01a	30.59±0.55c	37.36±1.37c
	Ni1	63.71±2.11a	0.34±0.02a	0.34±0.01a	33.58±0.28b	48.10±1.15b
	Ni2	67.03±1.25a	0.37±0.04a	0.32±0.01a	37.18±0.42a	56.77±0.54a
	Ni3	62.74±1.13a	0.37±0.02a	0.24±0.03b	38.00±0.64a	48.37±0.64b
Meixiangzhan 2	CK	58.93±1.23d	0.41±0.02b	0.33±0.01a	34.89±0.59b	42.73±3.00c
	Ni1	63.79±0.68c	0.53±0.06a	0.32±0.01ab	42.36±1.78a	63.83±1.20a
	Ni2	70.74±0.82b	0.38±0.02b	0.28±0.01ab	40.57±0.24a	53.41±0.37b
	Ni3	74.00±1.02a	0.29±0.01c	0.28±0.02b	35.61±0.10b	49.92±0.77

Data in the table are tested with Statistix 8 by LSD ($P < 0.05$). Values with different small letters in the same line have significant difference

MDA contents, osmo-protectants and anti-oxidant responses

Exogenous Ni^{2+} application regulated the anti-oxidative enzymatic activities in terms of SOD, POD and CAT (Table 3). Compared with CK, 8.44 and 8.03% higher POD activities were recorded in Ni1 and Ni3 for *Yuxiangyouzhan* while highest POD activity (21.51% higher than CK) was found for *Meixiangzhan 2* in Ni1. The SOD activities were also increased by 8.68, 9.51 and 27.73% for *Yuxiangyouzhan* whilst 47.58, 29.66 and 27.73% for *Meixiangzhan 2* in Ni1, Ni2 and Ni3 treatments, respectively. Similarly, compared with CK, the CAT activities increased with 13.48, 30.65 and 11.52% in Ni1, Ni2 and Ni3, respectively for *Yuxiangyouzhan* while increased by 16.89 and 19.37% in Ni1 and Ni3, respectively for *Meixiangzhan 2*.

The MDA contents were found significantly lower under all Ni²⁺ treatments than CK for both cultivars. The MDA contents were reduced by 21.96, 26.02, and 35.81% for *Yuxiangyouzhan* and 31.43, 21.54, and 13.34% for *Meixiangzhan 2* in Ni1, Ni2, and Ni3 compared to CK. Furthermore, the protein contents were increased by 20.43 and 13.97% in Ni2 and Ni3, respectively for *Yuxiangyouzhan* while it was 31.74% higher in Ni1 for *Meixiangzhan 2* compared with CK.

Table 3. Effect of Ni²⁺ application on MDA contents, osmo-protectants and anti-oxidant responses

Cultivar	Treatment	Peroxidase activity (U·g ⁻¹ ·min ⁻¹)	Super-oxide dismutase activity (U·g ⁻¹)	Catalase activity (U·g ⁻¹ ·min ⁻¹)	Malondialdehyde content (umol·g ⁻¹)	Soluble protein content (ug·g ⁻¹)
<i>Yuxiangyouzhan</i>	CK	315.94±10.01c	127.61±0.54b	140.42±2.10c	2.52±0.04a	27.14±0.70c
	Ni1	342.60±3.25b	138.69±4.14b	159.35±0.66b	1.97±0.04b	27.32±0.18c
	Ni2	321.63±1.16c	139.74±3.70b	183.46±1.33a	1.87±0.06b	32.68±0.59a
	Ni3	360.90±0.48a	163.00±0.36a	156.60±1.73b	1.619±0.05c	30.93±0.92b
<i>Meixiangzhan 2</i>	CK	345.07±2.38b	106.49±1.21c	117.45±3.85b	2.35±0.05a	25.66±0.85b
	Ni1	419.28±3.66a	157.16±5.58a	137.29±4.07a	1.61±0.00d	33.81±1.63a
	Ni2	342.77±0.76b	138.08±2.46b	114.13±1.32b	1.84±0.05c	25.87±0.29b
	Ni3	341.32±1.22b	137.78±8.59b	140.20±1.73a	2.04±0.05b	23.90±0.26b

Data in the table are tested with Statistix 8 by LSD (P < 0.05). Values with different small letters in the same line have significant difference

Correlation analysis

Significant and positive correlation between seedling index and seedling fresh weight was observed. The same correlation was found among dry weight and activities of both SOD and CAT. Moreover, there also existed a similar correlation between total chlorophyll content and GOT activity (Table 4).

Discussion

Recently, the research on plant micro-nutrition has been given a renowned attention due to its significant effects on plant growth, development and overall crop productivity and grain nutritional qualities as well (Taylor and Harrier, 2001). Previously, Ni²⁺ has been recognized as an essential micronutrient for legumes and possibly all high plants and is a necessary constituent of the enzyme ‘urease’ (Eskew and Welch et al., 1983). In this study, the seedling growth attributes i.e., seedling length, basal diameter, fresh and dry biomass as well as seedling index were substantially improved by exogenous Ni²⁺ application. For example, remarkable improvement was found in height, fresh weight and dry weight under Ni1 treatment for both cultivars while highest value of seedling index was recorded in Ni2 for *Yuxiangyouzhan* and *Meixiangzhan 2* which are 1.74 and 0.78. The values of the seedling index were calculated considering height, dry weight and basal diameter which all are the result of growth and development. Thus, seedling index represents the growth status of seedlings to a certain extent. In this study, Ni²⁺ treatments enhanced the seedling index and it might have indicated that Ni²⁺ application at low concentration is able to improve or stimulate the growth and development of rice seedlings.

Table 4. Relationship among the growth and biochemical parameters

Index	Seedling index	Height	Basal diameter	Fresh weight	Dry weight	Total chl	Chl a	Chl b	POD	SOD	CAT	NR	GS	GOGAT	GOT	GPT
Height	0.362															
Basal diameter	0.933**	0.163														
Fresh weight	0.782*	0.712*	0.569													
Dry weight	0.918**	0.67	0.741*	0.932**												
Total chl	-0.171	0.106	-0.456	0.261	0.042											
Chl a	-0.077	0.11	-0.364	0.31	0.115	0.990**										
Chl b	-0.357	0.069	-0.62	0.13	-0.119	0.966**	0.921**									
POD	-0.46	0.583	-0.643	-0.023	-0.101	0.319	0.246	0.43								
SOD	0.489	0.805*	0.228	0.842**	0.761*	0.353	0.342	0.329	0.407							
CAT	0.862**	0.403	0.756*	0.63	0.822*	-0.133	-0.043	-0.303	-0.274	0.414						
NR	-0.08	0.168	-0.336	0.311	0.115	0.631	0.615	0.637	0.198	0.287	0.026					
GS	-0.254	0.278	-0.353	-0.139	-0.07	0.208	0.187	0.22	0.688	0.221	-0.228	-0.341				
GOGAT	-0.116	-0.042	-0.029	-0.414	-0.179	-0.427	-0.369	-0.496	0.113	-0.499	0.07	-0.28	0.279			
GOT	-0.153	0.43	-0.464	0.323	0.167	0.839**	0.818*	0.824*	0.672	0.57	-0.153	0.452	0.611	-0.215		
GPT	0.058	0.58	-0.283	0.405	0.375	0.648	0.657	0.591	0.679	0.601	0.201	0.519	0.539	0.078	0.0887**	
Protein	0.497	0.533	0.302	0.475	0.632	0.208	0.252	0.094	0.331	0.627	0.554	-0.208	0.648	0.068	0.494	0.628

Previously, it was observed that exposure of plants to 10 μM Ni^{2+} lead to a slight increase in fresh mass while 200 μM Ni^{2+} inhibited shoot growth. It also caused a decline in chlorophyll content, an accumulation of proline hence visible symptoms of Ni toxicity. Nickel deficiency disrupted the ureide catabolism in foliage. It also induced accumulation of xanthine, allantoic acid, ureidoglycolate and citrulline while total ureides, urea concentration and urease activity were reduced (Bai and Reilly et al., 2006). Furthermore, an earlier study found that a Ni-binding protein is necessary for urease activity which is encoded by soybean *Eu3* gene (Freyermuth and Bacanamwo et al., 2000).

Exogenous Ni^{2+} application also enhanced the chl a, chl b, total chl contents and carotenoids. The results of the present study showed that Ni^{2+} treatments increased the content of chl especially $\text{Ni}3$ and $\text{Ni}4$. Highest total chl content was recorded in $\text{Ni}2$ for *Yuxiangyouzhan* and in $\text{Ni}3$ for *Meixiangzhan 2* while $\text{Ni}3$ had highest content of Chl a for both cultivars. Chl a can have an important role in converting light energy into electrical and chemical energy (Asadov et al., 1995). The increment of photosynthetic pigment implied that nickel treatments could enhance the seedling's photosynthesis thus promoting the carbon metabolism and dry matter accumulation rate.

Furthermore, higher activities of NR, GOT and GPT were noted in Ni^{2+} treatments. Nitrate Reductase (NR), glutamic-oxalacetic transaminase (GOT) and glutamate pyruvic (GPT) are key enzymes for nitrogen metabolism in plants. NR, through its catalytic reaction, not only regulates nitrate reduction but also influences the carbon metabolism of photosynthesis (Jamal and Fazli et al., 2006). Deckard et al. grew six corn (*Zea mays* L.) hybrids in field conditions with supplemental N and irrigation. This experiment proved that there exists a positive relation between nitrate reductase activity and grain protein and yield. The increment of enzymatic activities for nitrogen metabolism mean that nickel treatments could enhance nitrogen metabolism inside the seedling. It will, further, promote the uptake of soil nutrients and increase the nitrogen utilization.

In addition, Ni treatments modulated anti-oxidant responses i.e., POD, SOD and CAT. These results corroborated with Silva et al. (2012) who found that Ni played an important role in plant growth and N uptake in crops supplied with urea in calcareous soils. Ni^{2+} deficiency affects plant growth, plant senescence, nitrogen metabolism, iron uptake and disease resistance. Furthermore, Ni^{2+} is absorbed and redistributed in plants via cation and/or metal-ligand complex transport systems. Superoxide dismutase (SOD), peroxidase (POD) and catalase (CAT) collectively build an enzymatic defense system. They synergistically, defend cell membrane system from getting damaged by superoxide free radical. They also inhibit membrane lipid peroxidation and decrease malondialdehyde (MDA) content, in order to reduce damage to the plant cells (Jebara and Jebara et al., 2005). MDA is one of the most important products of membrane lipid peroxidation which can react with free amino acids, phospholipids and may produce ethylene in cellular membranes (Rakwal and Agrawal et al., 2003). So, in the study of plant resistance, physical and physiological aging is a commonly used indicator. MDA content can be a measure of the membrane lipid peroxidation. Thus, it can be used in indirect determination of membrane system damage and plants resistance. Moreover, soluble protein also has a role in osmo-regulation and maintaining cellular structures and functions while anti-oxidants focus on quenching reactive oxygen species (ROS). For instance, SOD is involved in catalyzing the dismutation of superoxide radical whereas POD and CAT are involved in scavenging H_2O_2 (Sairam and Srivastava,

2000). So, antioxidant enzyme activity can reflect the resistance of plants to some extent. The improvements in antioxidant enzyme activity and protein content implied that exogenous application of nickel nitrate could have a 'phytosanitary' effect on rice seedlings thus enhancing their resistance.

Conclusion

The exogenous Ni²⁺ application improved seedling growth and development. It also enhanced the activities of key enzymes involved in nitrogen metabolism and antioxidant defence enzymes. Among Ni²⁺ treatments, Ni₂ proved better than other Ni²⁺ doses for both *Yuxiangyouzhan* and *Meixiangzhan 2*. Even though, application of Ni²⁺ at low concentration could improve the early growth of rice, further investigations are required at physiological and molecular level in order to reveal the exact mechanism of Ni-induced promotive effects in plants. In addition, there are small amount of nitrogen inside nickel nitrate which might affect the result of this study, more research should be carried out with different nickel resources.

Acknowledgements. This study was supported by the National Natural Science Foundation of China (31271646), The World Bank Loan Agricultural Pollution Control Project in Guangdong (0724-1510A08N3684), The Technology System of Modern Agricultural Industry in Guangdong (2017LM1098) and the Innovation and Entrepreneurship Training Program for College Student (201710564005, 201710564012).

REFERENCES

- [1] Aebi, H. (1984): Catalase in vitro. – *Methods Enzymol* 105: 121-126.
- [2] Asadov, A. A., Kotlyarova, N. V., Zulfugarov, I. S. Aliyev, D. A. (1995): Spectral characteristics and orientation of native forms of pigments in the chloroplasts of barley seedlings on continuous and discontinuous illumination. – *Biofizika* 40(2): 245-251.
- [3] Bai, C., Reilly, C. C., Wood, B. W. (2006): Nickel deficiency disrupts metabolism of ureides, amino acids, and organic acids of young pecan foliage. – *Plant Physiology* 140: 433-43.
- [4] Bradford, M. M. (1976): A rapid and sensitive method for the quantitation of microgram quantities of protein utilizing the principle of protein-dye binding. – *Analytical Biochemistry* 72: 248-254.
- [5] Das, P. K., Kar, M., Mishra, D. (1978): Nickel nutrition of plants: I. Effect of nickel on some oxidase activities during rice (*Oryza sativa* L.) seed germination. – *Zeitschrift für Pflanzenphysiologie* 90: 225-233.
- [6] Ebeid, M., Eder, J., Kutáček, M., Piovarči, A. (1981): Transaminase GOT and GPT activity in extirped sprouts of normal and opaque-2 Maize (*Zea mays* L.) seedlings. – *Biologia Plantarum* 23: 345-350.
- [7] Eskew, D. L., Welch, R. M., Cary, E. E. (1983): Nickel: an essential micronutrient for legumes and possibly all higher plants. – *Science* 222: 621-3.
- [8] Freyermuth, S. K., Bacanamwo, M., Polacco, J. C. (2000): The soybean *Eu3* gene encodes an Ni-binding protein necessary for urease activity. – *Plant Journal for Cell Molecular Biology* 21: 53.
- [9] Gajewska, E., Skłodowska, M. (2005): Antioxidative responses and proline level in leaves and roots of pea plants subjected to nickel stress. – *Acta Physiologiae Plantarum* 27: 329-340.

- [10] Gerendás, J., Zhu, Z., Sattelmacher, B. (1998): Influence of N and Ni supply on nitrogen metabolism and urease activity in rice (*Oryza sativa* L.). – *Journal of Experimental Botany* 49: 1545-1554.
- [11] Gerendás, J., Polacco, J. C., Freyermuth, S. K., Sattelmacher, B. (2015): Significance of nickel for plant growth and metabolism. – *Journal of Plant Nutrition and Soil Science = Zeitschrift fuer Pflanzenernaehrung und Bodenkunde* 162: 241-256.
- [12] Jamal, A., Fazli, I. S., Ahmad, S., Abdin, M. Z., Yun, S. J. (2006): Effect of nitrogen and sulphur application on nitrate reductase and ATP-sulphurylase activities in soybean. – *Korean Journal of Crop Science* 51(4): 298-302.
- [13] Jebara, S., Jebara, M., Limam, F., Aouani, M. E. (2005): Changes in ascorbate peroxidase, catalase, guaiacol peroxidase and superoxide dismutase activities in common bean (*Phaseolus vulgaris*) nodules under salt stress. – *Journal of Plant Physiology* 162: 929-936.
- [14] Lin, C. C., Kao, C. H. (1996): Disturbed ammonium assimilation is associated with growth inhibition of roots in rice seedlings caused by NaCl. – *Plant Growth Regulation* 18: 233-238.
- [15] Luo, H., Zhong, Z., Nie, J., Tang, X. (2017): Effects of ultrasound on physiological characters, yield and quality of rice Yuejingsimiao. – *China Rice* 23(2): 64-67.
- [16] Mishra, D., Kar, M. (1974): Nickel in plant growth and metabolism. – *Botanical Review* 40: 395-452.
- [17] Nazir, H., Asghar, H. N., Zahir, Z. A., Akhtar, M. J., Saleem, M. (2015): Judicious use of kinetin to improve growth and yield of rice in nickel contaminated soil. – *International Journal of Phytoremediation* 18: 651.
- [18] Polacco, J. C. (1977): Is nickel a universal component of plant ureases? – *Plant Science Letters* 10: 249-255.
- [19] Rakwal, R., Agrawal, G. K., Kubo, A., Yonekura, M., Tamogami, S., Saji, H., Iwahashi, H. (2003): Defense/stress responses elicited in rice seedlings exposed to the gaseous air pollutant sulfur dioxide. – *Environmental, Experimental Botany* 49: 223-235.
- [20] Rizwan, M., Imtiaz, M., Dai, Z., Mehmood, S., Adeel, M., Liu, J., Tu, S. (2017): Nickel stressed responses of rice in Ni subcellular distribution, antioxidant production, and osmolyte accumulation. – *Environmental Science, Pollution Research International* 2017: 1-12.
- [21] Sairam, R. K., Srivastava, G. C. (2000): Induction of oxidative stress and antioxidant activity by hydrogen peroxide treatment in tolerant and susceptible wheat genotypes. – *Biologia Plantarum* 43: 381-386.
- [22] Shi, G., Zhou, Q. (1998): Effect of nickel on lipid peroxidation in isolated rice leaves. – *Guihaia*.
- [23] Silva, J. A. T. D., Naeem, M., Idrees, M. (2012): Beneficial and toxic effects of nickel in relation to medicinal and aromatic plants. – *Medicinal and Aromatic Plant Science and Biotechnology* 6(Special Issue 1): 94-104.
- [24] Sun, Y. J., Sun, Y. Y., Xu-Yi, L. I., Guo, X., Jun, M. A. (2009): Relationship of nitrogen utilization and activities of key enzymes involved in nitrogen metabolism in rice under water–nitrogen interaction. – *Acta Agronomica Sinica* 35: 2055-2063.
- [25] Taylor, J., Harrier, L. A. (2001): A comparison of development and mineral nutrition of micropropagated *Fragaria x ananassa* cv. Elvira (strawberry) when colonised by nine species of arbuscular mycorrhizal fungi. – *Applied Soil Ecology* 18: 205-215.
- [26] Theisen, M. O., Blincoe, C. (1984): Biochemical form of nickel in alfalfa. – *Journal of Inorganic Biochemistry* 21: 137-146.
- [27] Wang, Y., Tian, T., Fu, H. (1999): Effects of nickel on growth of rice seedling. – *Journal of Central China Normal University* 33: 104-107.
- [28] Welch, R. M. (1981): The biological significance of nickel. – *Journal of Plant Nutrition* 3: 345-356.

QUANTITATIVE RAINFALL ESTIMATION USING WEATHER RADAR BASED ON THE IMPROVED KALMAN FILTER METHOD

RUI, X. P.^{1,2} – QU, X. K.² – YU, X. T.^{3*} – LEI, Q. L.⁴ – FAN, Y. L.²

¹*School of Earth Sciences and Engineering, Hohai University
No. 8 Focheng west Road, Nanjing, Jiangsu 211000, P. R. China*

²*College of Resource and Environment, University of Chinese Academy of Sciences
No. 19(A) Yuquan Road, Shijingshan District, Beijing 100049, P. R. China*

³*School of Traffic and Transportation, Shijiazhuang Tiedao University
17 Northeast, Second Inner Ring, Shijiazhuang, Hebei 050043, P. R. China*

⁴*Institute of Agricultural Resources and Regional Planning, Chinese Academy of Agricultural Sciences/Key Laboratory of Non-point Source Pollution Control, Ministry of Agriculture
No. 12 Zhongguancun South Street, Haidian District, Beijing 100081, P. R. China*

**Corresponding author*

e-mail: yuxt@stdu.edu.cn; phone: +86-0311-87936613

(Received 24th Aug 2018; accepted 11th Oct 2018)

Abstract. To reduce the error of radar rainfall evaluations, an improved Kalman filter (KF) method is used to calibrate the radar quantitative rainfall estimation (QRE). First, the rain gauge rain rate/radar rain rate (G/R) calibration factor model is created in this approach. The prediction and measurement system of the G/R are then established based on the KF. The calibration process of the system parameters and the adaptive estimation process of the system error are introduced to dynamically adjust the KF parameters. Subsequently, the G/R calibration ratio is used to correct the quantitative radar rainfall estimation. The radar and rain gauge hourly rain data of two rain cases in Changchun, China on August 19–20, 2015, and August 6–7, 2016, are used to test the efficiency of the proposed method. The results show that the QRE result based on the KF calibration is better than that without calibration. The average relative errors of the two rain cases decreased from 0.6047 to 0.3557 and 0.2645 and from 0.8052 to 0.3096 and 0.1715 due to the ordinary and improved KFs, respectively. The improved KF is even better than the ordinary KF.

Keywords: *G/R ratio; calibration factors; parameters estimate; state system; adaptive estimation*

Introduction

Radar-based quantitative rainfall estimation with high temporal resolution plays an important role in the monitoring and early warning of meteorological disasters caused by strong convective weather such as storms and floods. Radar-based rainfall estimation commonly uses the empirical relationship model $Z = aI^b$ (where a and b are parameters of the model, Z is the radar reflectivity factor, and I is the rainfall intensity) to estimate the rainfall intensity. However, the radar quantification is affected by factors such as clutter from terrestrial objects, raindrops, and super refraction. In addition, systematic errors of the radar reflectivity values cannot be completely eliminated. The a and b parameters also greatly vary in different areas at the same time or in different rainfall process models, resulting in a relatively large deviation of the radar-based rainfall estimated value and actual rainfall volume (Zheng et al., 2004).

To obtain more accurate radar-based rainfall estimates, the rain gauge rain rate/radar rain rate (G/R; i.e., automatic weather station measurements/weather radar estimates) ratio is generally used to correct the radar estimates. Current methods to obtain G/R mainly include the average calibration method, variational method, and Kalman filter method. The Kalman filter is a linear, unbiased, minimum-variance, recursive filter that is widely applied during the process when precipitation stations and radar are used for the joint rainfall estimation. Ahnert et al. (1986) first proposed to use the Kalman filter as a real-time prediction method of G/R calibration factors and pointed out that this method has advantages such as being able to correct measurement noise, demonstrating estimation errors, and avoiding G/R instability. Subsequently, researchers applied the Kalman filter for the calibration of different types of rainfall or different areas. The studies focused mainly on two areas: (1) Modification of the G/R calibration factor model to be suitable for different types of rainfall and improve the rainfall estimation results using Kalman filter optimization. For example, Chumchean et al. (2006) proposed a $\log_{10}(G/R)$ calibration model that has better filtering effects in areas with fewer precipitation stations. Yahya et al. (2012) comprehensively considered and analyzed the effects of meteorological elements, such as temperature and humidity, on Kalman filter effects and proposed a multi-factor calibration model; and (2) Modification of parameter values used during Kalman filter-based prediction and quantification and improvement of the stability and convergence speed of the Kalman filter algorithm. For example, Yin and Zhang (2005) analyzed the effects of various model parameters on the results and provided suggestions to improve various parameters. Monteiro and Costa (2015) carried out statistical analysis of transfer matrix parameters in the state equation of the prediction formula using rainfall data and obtained better parameters. Xu (2008) and Kim and Yoo (2014) proposed the usage of a self-adaptive filter as a method to estimate model parameters and improve the accuracy of the filter estimation. Zhao et al. (2001) employed a combination of the Kalman filter and variational method to optimize the model parameters and improve the accuracy of radar-based rainfall estimation. In studies in which the Kalman filter was used to calibrate radar-based rainfall estimations, the calibration factor is more associated with fixed rainfall types or the density of precipitation stations; this model is comparatively mature. On the other hand, because the filter algorithm parameters were set as empirical constants, problems occur, such as poor adaptability to different rainfall events or shorter rainfall, decreasing the accuracy of the filter algorithm during calibration. This affects the accuracy of radar-based rainfall estimates, which is one factor that this paper seeks to improve.

This study is based on previous research. The Kalman state parameter model and maximum likelihood estimation are introduced into the ordinary Kalman filter. The state model parameters, state equation, and noise value of the quantitative equation in each step of the Kalman filtering process were corrected to decrease the effects of unreasonable model parameters on the whole filtering process and enhance the stability of the filter algorithm to effectively increase the accuracy of radar-based rainfall estimations.

Study methods

Ordinary Kalman filter algorithm

The Kalman filter algorithm is a process in which two independent estimation equations are established based on a random variable to obtain estimates and appropriate weighting factors are then selected to obtain the weighted average of the two estimates as filter output variables. The G/R calibration factor is used in this paper as the random variable x for the

Kalman filter algorithm.

The Kalman filter algorithm is mainly divided into the prediction and quantification processes. The former uses the estimate of the variable at a previous time to obtain the current a priori estimate. On the other hand, the latter uses the current measurement value to correct the a priori estimate of the previous process and obtain the current posteriori estimate (Liu et al., 2015; Liu et al., 2016; Noh et al., 2014). The specific recursive calculation process was:

Prediction process:

$$\hat{x}_k = A_{k-1}x_{k-1} \quad (\text{Eq.1})$$

$$\hat{P}_k = A_{k-1}P_{k-1}A_{k-1}^T + Q_{k-1} \quad (\text{Eq.2})$$

Quantification process:

$$K_k = \hat{P}_k(\hat{P}_k + R_k + Q_{k-1})^{-1} \quad (\text{Eq.3})$$

$$x_k = \hat{x}_k + K_k(z_k - H\hat{x}_k) \quad (\text{Eq.4})$$

$$P_k = (1 - K_k H)\hat{P}_k \quad (\text{Eq.5})$$

Equation 1 is the state equation. In the equations, \hat{x}_k is the a priori estimate at the time k ; x_{k-1} is the posteriori estimate at time $k-1$; P is the estimated covariance and is one of the results of the filter; and A is the state transition matrix but is in fact a conjectural model of the target state transition, that is, the connection between x_k and x_{k-1} . If *Equation 2* is regarded as first-order linear autoregressive model AT, then A is the coefficient of this model and constant values are normally used.

Equation 3 is the measurement equation, where z_k is the x measured value at time k , that is, the actual G/R ratio; H is the gain of the state variable x_k to the measurement variable z_k ; K is the filter gain matrix, which is an intermediate calculation result of the filter; Q and R are the variances of the state equation and measurement equation, respectively, the mean of which is zero. In the actual calculation process, the Q and R values are usually obtained by analyzing samples from the previous rainfall process, which provides constant Q and R values (Kim and Yoo, 2014; Eldardiry et al., 2015).

Equations 1 to 5 are part of the specific calculation process of the ordinary Kalman filter algorithm. However, in the ordinary Kalman filter algorithm, the transition matrix A in the state equation and the errors of Q and R are assumed to be a priori constant values. This is unreasonable for complex rainfall systems.

Modification of the Kalman filter algorithm

To adapt to the variation characteristics of complex rainfall systems, two improvements were made to the parameters in the Kalman filter algorithm:

(1) The transition matrix A in Equation 1 was assumed to be a temporal variable and the state and measurement equations for the ordinary Kalman filter were established for variable A . The value of A after filtering was substituted into the filter process of the G/R calibration factor to improve the accuracy of the state equation.

(2) Based on the maximum likelihood criterion, real-time estimation and adjustment of Q and R errors was carried out to reflect real-time changes of the system model and enable the Kalman filter to track the system model changes. The derivation process was:

$$R_k = \hat{C}_{vk} + H_k \hat{P}_k H_k^T \quad (\text{Eq.6})$$

$$Q_k = \frac{1}{N} \sum \Delta x_i \Delta x_i^T + P_k - A P_{k-1} A^T \quad (\text{Eq.7})$$

$$\Delta x_k = \hat{x}_k - \hat{x}_{k,k-1} = K_k v_k \quad (\text{Eq.8})$$

$$\hat{C}_{vk} = \frac{1}{N} \sum_{i=k-N+1}^k v_i v_i^T \quad (\text{Eq.9})$$

In the equations, $v_k = z_k - H \hat{x}_k$, N is the width of the smoothing window, \hat{C}_{vk} is expressed as a covariance matrix for the v_k sequence in a smooth window, and R_k and Q_k are the systematic errors of the prediction and measurement, respectively (Maxwell et al., 2018; Monteiro and Costa, 2015).

Model of the improved Kalman filter estimation

This paper set the unfiltered calibration factors as:

$$z_k = \frac{1}{n} \sum_{i=1}^n G_i / R_i \quad (\text{Eq.10})$$

In the equation, n is the total number of automatic weather stations that participated in the calibration, G_i is the rainfall value measured at the weather station at time k , R_i is the radar-based rainfall estimation value at the same location as the weather station obtained from the constructed radar-based rainfall estimation in Subsection: Ordinary Kalman filter algorithm. In Equation 1, the model parameters are: $a = 300$ and $b = 1.4$ (Yang et al., 2015; Marra et al., 2017).

During the Kalman filter algorithm, the parameters at time 0 are: $x_0 = 0$, $P_0 = 0.01$, $Q_0 = 0.25$, and $A_0 = 1$.

Improvement of the Kalman filter algorithm

The Kalman filter algorithm was improved through filter processing of calibration factors, which indirectly adjusted the initial field of the radar-based rainfall estimation and achieved the calibration of radar-based rainfall estimation. The main calculation process was:

(1) Assignment of initial values, $k = 0$ and $k = [0, n]$, where n is the number of hours during which data from radar and automatic weather stations were effectively recorded during rainfall; x is the calibration factor, that is, the G/R prediction value, and x_0 was set as 0; and Q_k and P_k are the systematic errors of the state system and measurement, respectively. At time 0, P_0 and Q_0 were set to 0 and the state transition matrix A was assumed to be 1.

(2) During the prediction process, the right hand side was the prediction process of the state transition matrix A and the left hand side was the prediction process for the calibration factor. In the state equation on the left hand side, the A_{k-1} value was the posteriori estimate of the output from the filtering process based on A at time $k-1$. The a priori estimate of variable x at time k was then obtained based on the left state system. It was assumed that the state transition matrix in the right state equation is always 1, then, the priori estimate of A at time k was obtained.

(3) The radar data at time k were processed based on *Equation 10* and the initial field of the radar-based rainfall estimation at time k was established.

(4) The rainfall data measured by automatic weather stations were inserted and the value of the G/R calibration factor at time k (i.e., Z_k) was calculated based on *Equation 10*. If no valid value exists for the unfiltered calibration factor, the next time was recalculated using a prediction process. If a valid value exists, measurement corrections of the state transition matrix A and calibration factor (variable x) were carried out to solve the Kalman filter equations. During the measurement of these two variables, Q and P have the same value. Finally, the posteriori estimates of the state transition matrix A and calibration factor x at time k were obtained, that is, the best calibration factor x_k at time k . The best calibration factor can be used to correct the initial field of the radar-based rainfall estimation at time k (Thorndahl et al., 2014; Fleming et al., 2017).

(5) If $k < n$, then steps 2–4 are repeated and the best calibration factor can be obtained at every time point.

Figure 1 shows the improved Kalman filter process.

Experiment and analysis

Data and processing

Two rainfall events in the Changchun Area, Jilin Province, China from 1 a.m. on August 19, 2015, to 10 p.m. on August 20 and 5 p.m. on August 6 to 6 a.m. on August 7, were used as study subjects. We used rainfall data from the Changchun weather radar station and encrypted hourly rainfall data from automatic stations. The Changchun weather radar station uses the CINRAD/CC radar series; the weather radar has a spatial resolution of 300 m, temporal resolution of 6 min, detection range of 150 km, and antenna height of 290 m. *Figure 2* shows the distribution of the radar and automatic weather stations; 80% of these stations were used in this experiment, while the remaining weather stations were used for the examination of experimental results.

Radar data were obtained from CAPPI data at a 3 km height. Scanning data of different elevation angles at a certain time were interpolated to the same height as field data of reflectivity factors. At the same time, to eliminate the effects of clutter, data with reflectivities < 15 or > 78 were removed because a reflectivity < 15 is thought to not be able to induce rain, while a reflectivity > 78 might reflect ice–water mixtures and will not induce rainfall (Gou et al., 2014). Spatial and temporal differences exist because the measured values from automatic weather stations represent 1-hour rainfall at a certain

time point and the radar detection values are reflectivity factors. For the uniform comparison, the radar data were processed using the following methods and the weather station as a benchmark.

(1) The polar coordinate data of the radar were converted into a Cartesian coordinate system on a grid plane. The grid and minimum resolution of the polar coordinates of the raw radar data were the same (0.3 km × 0.3 km).

(2) Every 6 minutes, radar-based data were collected and the constant altitude plan position indicator (short for CAPPI) was generated, which was used to estimate the rainfall intensity at that moment based on Equation 1. The calculated rainfall intensities during 1 hour were weighted and summed to generate the radar-based rainfall estimate for 1 hour and establish the initial field of the radar-based rainfall estimation value (Kim et al., 2018).

$$Z = aI^b \tag{Eq.11}$$

In this equation, Z is the reflectivity factor, I is the rainfall intensity, and a and b are model parameters.

(3) Based on the coordinates of the automatic weather stations, the radar-based rainfall estimation field and 12 valid points adjacent to the automatic weather stations were selected. The weighted average of the valid data was used to calculate the radar-based rainfall estimate at the same location of the weather station.

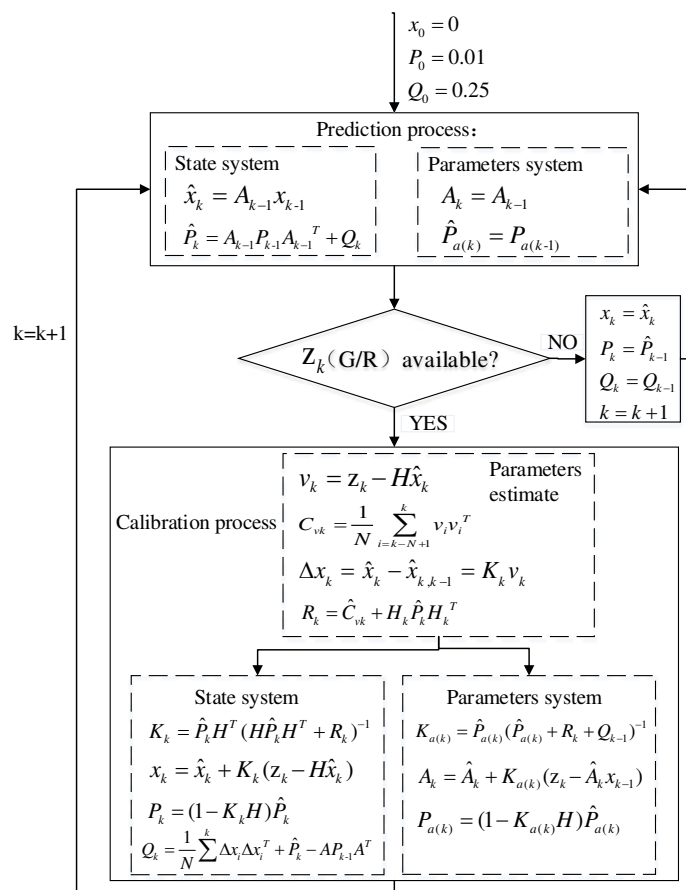


Figure 1. Flow chart of the improved Kalman filter method

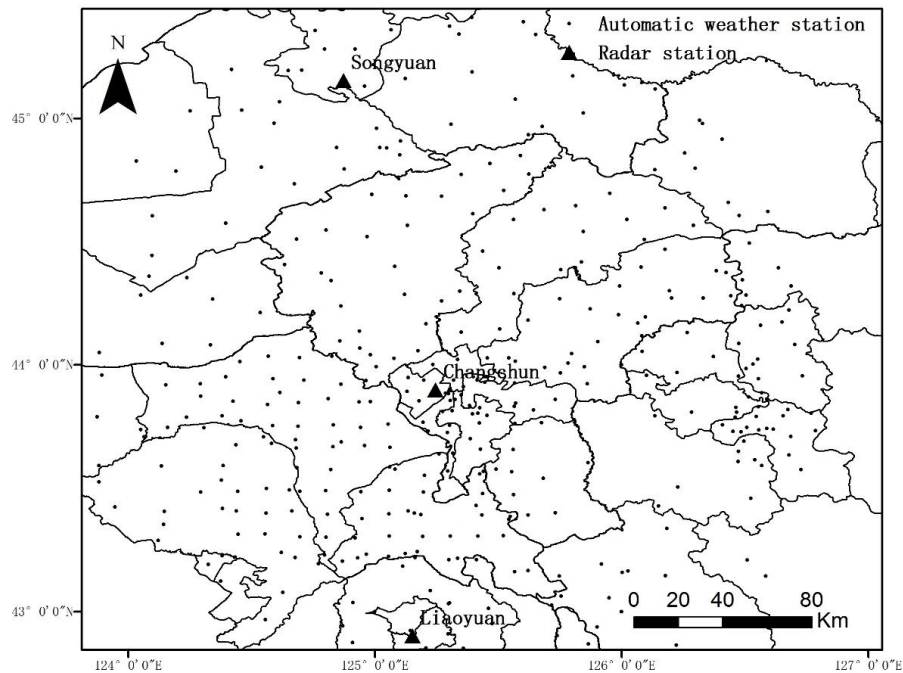


Figure 2. Radar and automatic weather stations

Results of the improved Kalman filter algorithm

G/R ratio

The study area is the effective detection range of the Changchun Radar Base Station. The study area is divided into test area and evaluation areas. In the test area, radar data and data from the automatic weather stations were used to obtain the posteriori estimate of G/R through the Kalman filter method. In the evaluation area, the estimated G/R calibration factor was used for the correction of radar estimates, which were compared with values measured at weather stations in the evaluation area (Cheng and Li, 2013; You et al., 2014; You et al., 2018).

Figure 3 shows that the G/R ratio of the two rainfall events, estimated with the improved Kalman filter, is more consistent with the actual value.

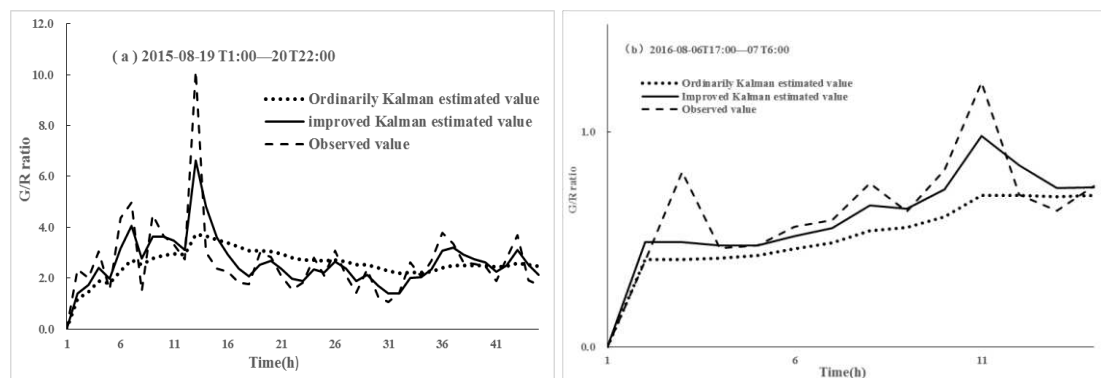


Figure 3. Comparison of the observed G/R ratio and that predicted using the ordinary and improved Kalman filters for the two rainfall events

The improved Kalman filter has a faster convergence speed and strong adaptive ability and the deviation between the estimated value and the actual value of the deviation is small. On the other hand, the G/R ratio estimated with the ordinary Kalman filter shows a greater deviation from the actual value. The convergence speed is slower and the effects of the test sample are larger. The deviation between the estimated and actual values is larger when the time series includes a relatively large value.

Figure 3 also shows that the sample quantity has a greater effect on the Kalman filter. For the ordinary Kalman filter, a rainfall process with a larger sample quantity (Figure 3a) will result in the convergence and gradual stabilization of the filter value; the convergence is very slow in rainfall events with a small sample quantity (Figure 3b). On the other hand, the improved Kalman filter is less affected by the sample quantity, showing a relatively fast convergence speed during both rainfall events. Therefore, the improved Kalman filter has better convergence effects on short rainfall events. Based on the comparison of the estimated and measured values of the two rainfall events (Figure 4), the points of the improved Kalman filter are more clustered, while the points of the ordinary Kalman filter method are more dispersed. The G/R estimate from the improved Kalman filter calibration shows a better correlation with the actual value. The correlation coefficient of the two rainfall events increased from 0.1245 and 0.3721 to 0.7295 and 0.6222, respectively.

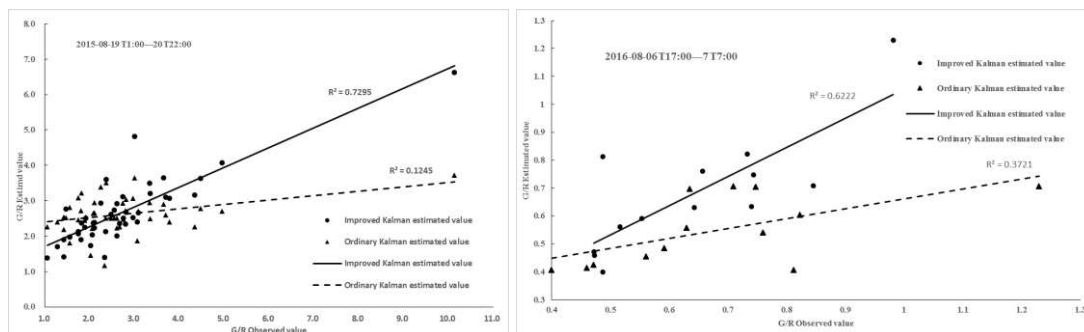


Figure 4. Scatter plots of the observed G/R ratio and that predicted with the ordinary and improved Kalman filters for the two rainfall events

Error analysis

The G/R calibration factor of the two rainfall events was used for the correction of the radar-based rainfall estimates in the evaluation zone. The corrected radar-based rainfall estimate was used for the comparison of the data from the precipitation stations inside the evaluation area (Costa et al., 2016).

Figure 5 shows that, compared with the uncorrected radar-based rainfall estimates, the absolute error of the improved Kalman filter-corrected estimate of hourly radar-based rainfall of the two rainfall events is relatively small, generally in the 0–1 mm range. On the other hand, the absolute error of the ordinary Kalman filter-corrected estimates of hourly radar-based rainfall is ~0–2 mm. Table 1 shows that both Kalman filter methods can solve the poor adaptability of Z–R relationship model parameters and lower radar-based estimates due to errors in the radar estimation system itself. The average relative error of the hourly rainfall during August 19–20, 2015, decreased from 0.6047 to 0.3557 and 0.2645, respectively, with decreases of 41% and 53%. The root-mean-square error decreased from 1.5246 to 0.9794 and 0.6928, respectively. During

the August 6–7, 2016, rainfall event, the average relative error decreased from 0.8052 to 0.3906 and 0.1715, respectively, with decreases of 51% and 85%. The root-mean-square error decreased from 1.3596 to 0.3131 and 0.2163, respectively. This shows that the Kalman filter algorithm could effectively increase the radar-based rainfall estimation accuracy. At the same time, the improved Kalman filter significantly improved the accuracy and stability of the estimates compared with ordinary Kalman filter.

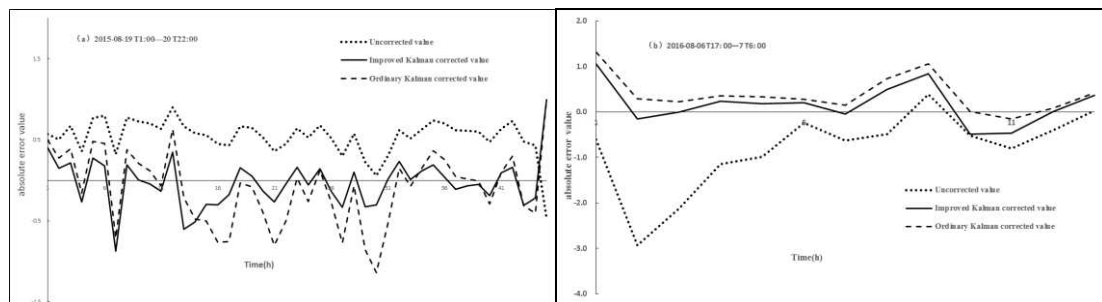


Figure 5. Comparison of the absolute error of different methods for the two rain events

Table 1. Comparison of the error of different methods during two rain events

Method	8-19-2015 1 a.m. to 8-20-2015 10 p.m.		8-6-2016 5 p.m. to 8-7-2016 6 a.m.	
	Average relative error	Root-mean-square error	Average relative error	Root-mean-square error
Radar estimation	0.6047	0.605	0.8052	1.3596
Kalman	0.3557	0.356	0.3906	0.3131
Improved Kalman	0.2645	0.265	0.1715	0.2163

Rainfall distribution

The improved Kalman filter was used to correct the G/R factors for the calibration of the original radar-based rainfall estimate. The improved Kalman filter better calibrates the radar-based rainfall estimate during the two rainfall events than the ordinary Kalman filter. In addition, the comparison of the two rainfall events shows that the calibration effects are better when the rainfall duration in the experiment is longer.

To study the spatial distribution of the rainfall field, a calibration analysis of the rainfall estimate of a certain area at 1–2 a.m. on August 19, 2015 was carried out. Based on the statistical calculations, 52 valid rainfall data points were obtained at 1–2 a.m. on August 19, 2015. Geographical methods were used to interpolate the observed rain gauge values to obtain the surface rainfall distribution (Figure 6a). Figures 6b and 6c show the distribution of the radar-based estimate of rainfall before and after calibration. The radar and rain gauge both show the general range of the rainfall, the centers of the rainfall are relatively notable. However, the radar rain detection centers are smaller than the rainfall range measured by the rain gauges. After correction, the Kalman filter-calibrated radar echo images and the rainfall range obtained from the interpolation of the rain gauges were consistent and could better highlight the rainfall intensity centers. The accurate radar-based rainfall estimation is more conducive for the regional analysis of rainfall in actual applications.

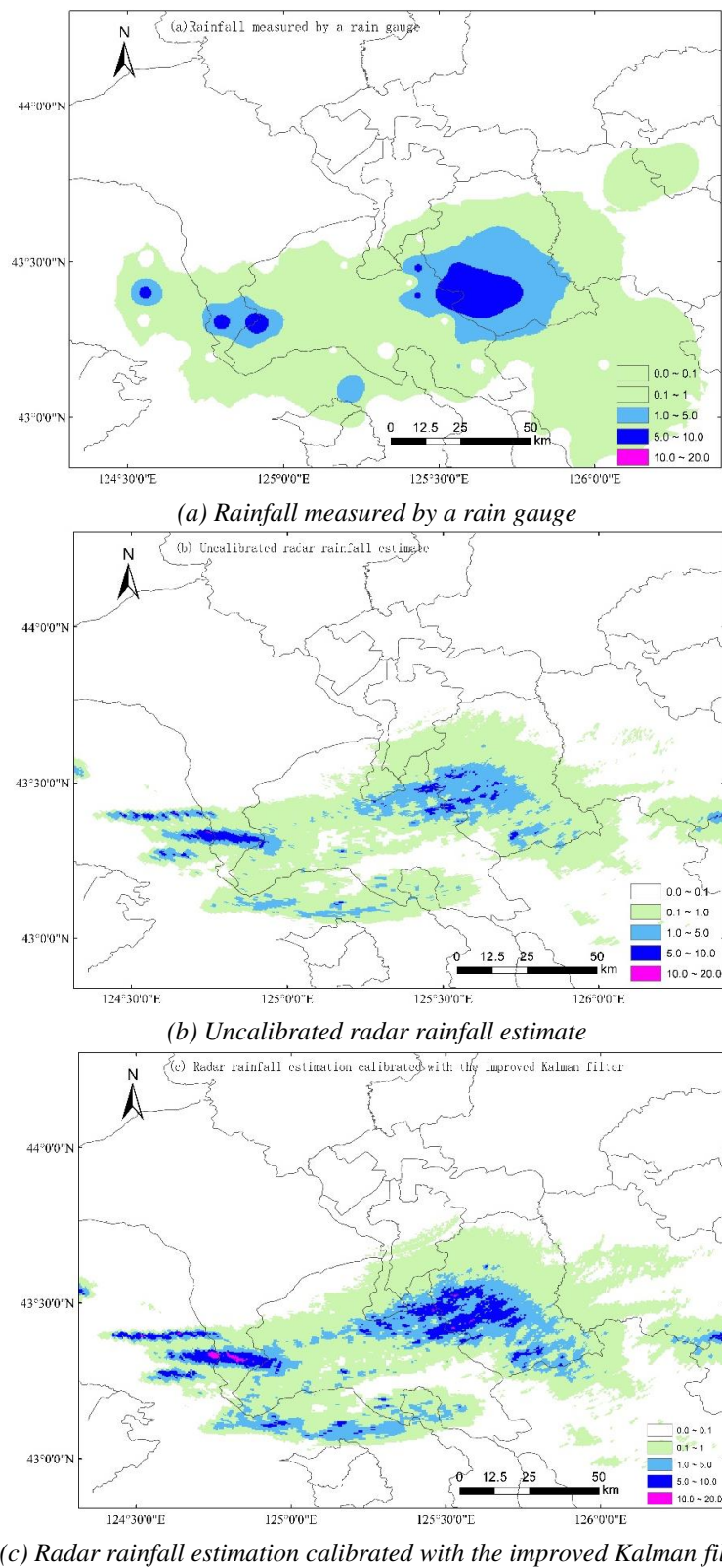


Figure 6. Rainfall distribution estimated by different methods from 1–2 a.m. on August 19, 2015 (unit: mm)

Discussion and conclusion

(1) The G/R calibration model is simultaneously affected by the radar-based rainfall estimation model and measurement factors of automatic rainfall stations. Differences exist in different stages of the rainfall event or different rainfall areas. Kalman filter calibration can result in a smaller variation range for longer rainfall events and tends to be stable, while the variation range of shorter rainfall events is larger and instable. Therefore, better radar-based rainfall estimation results could be obtained during longer rainfall events.

(2) The initial values and setting of model parameters greatly affect the estimation accuracy of the Kalman filter calibration. In contrast to previous studies, such as Zhao et al. (2001) who used empirical constants as model parameters for the Kalman filter, the improved Kalman filter carries out parameter corrections of the state and measurement equations at every step, which decreases the effects of unreasonable model parameters on the whole filtering process and increases the self-adaptive ability of the filter algorithm. During the experiment, the correlation coefficients of the two rainfall events increased from 0.1245 to 0.7295 and from 0.3721 to 0.6222, which increases the accuracy of the G/R calibration factor. This also results in the improvement of the corrected radar-based rainfall estimate.

(3) The G/R ratio from the filter output of the corrected radar-based rainfall estimate was used in this study. The results show that the ordinary Kalman filter could decrease the average relative error from 0.6047 to 0.3557 and from 0.8052 to 0.3096, respectively. On the other hand, the improved Kalman filter could decrease the average relative error from 0.6047 to 0.2645 and from 0.8052 to 0.1715, respectively. Compared with the ordinary Kalman filter method, the improved Kalman filter method can increase the accuracy of radar-based quantitative estimates of regional rainfall. At the same time, after improved Kalman filter calibration, the radar-based estimated field highlights regions with heavy rainfall and that with supplement rainfall that are not measured by automatic weather stations. Compared with other calibration methods for radar-based estimates, such as the dynamic grading method, the proposed Kalman filter does not require large amounts of experimental data for the calculation. At the same time, it is able to provide a filter variance output, which is more conducive for the evaluation and optimization of the calibration system (Hill et al., 2013; Yucel et al., 2015).

As above, the proposed algorithm improves the quality of rainfall estimate effectively, which has a special significance for disasters warning and assesment, such as storm events. However two rainfall events in the Changchun Area in different years were considered in this study. However, the average rainfall is relatively low and there is a lack of validation analysis of different types of rainfall events. To further improve the applicability of the Kalman filter to actual radar-based rainfall estimation, more researches on large amounts of rainfall events are required, and the calibration factors need to be considered into actual rainfall estimate model.

Acknowledgements. The research reported herein was sponsored by the National Key Research and Development Program of China (Grant No. 2017YFB0503605), the Hebei Province Natural Science Fund (Grant No. D2016210008), the National Natural Science Foundation of China (Grant No. 41771478) and the Beijing Natural Science Foundation (Grant No. 8172046).

REFERENCES

- [1] Anhert, P., Krajewski, W. F., Johnson, E. R. (1986): Kalman Filter estimation of radar-rainfall field bias. – In: 23rd Conference On Radar Meteorology. American Meteorological Society, Snowmass, Colorado, U.S.A., pp.33-37.
- [2] Cheng, J. W., Li, J. X. (2013): Design and Implementation of Software Platform to Evaluate Kalman Filter Algorithm. – *Journal of System Simulation* 25(11): 2567-2574.
- [3] Chumchean, S., Seed, A., Sharma, A. (2006): Correcting of real-time radar rainfall bias using a Kalman filtering approach. – *Journal of Hydrology* 317(1-2): 123-137.
- [4] Costa, M., Monteiro, M. (2016). Bias-correction of kalman filter estimators associated to a linear state space model with estimated parameters. – *Journal of Statistical Planning & Inference*, 176: 22-32.
- [5] Eldardiry, H., Habib, E., Zhang, Y. (2015): On the use of radar-based quantitative precipitation estimates for precipitation frequency analysis. – *Journal of Hydrology* 531: 441-453.
- [6] Fleming, C. H., Sheldon, D., Gurarie, E., Fagan, W. F., Lapoint, S., Calabrese, J. M. (2017): Kálmán filters for continuous-time movement models. – *Ecological Informatics*, 40: 8-21.
- [7] Gou, Y. B., Liu, L. P., Yang, J., Wu, C. (2014): Operational application and evaluation of the quantitative precipitation estimates algorithm based on the multi-radar mosaic. – *Acta Meteorologica Sinica* 72(4): 731-748.
- [8] Hill, D. J. (2013): Automated Bayesian quality control of streaming rain gauge data. – *Environmental Modelling & Software* 40(2): 289-301.
- [9] Kim, J., Yoo, C. (2014): Use of a dual Kalman filter for real-time correction of mean field bias of radar rain rate. – *Journal of Hydrology* 519(Part D): 2785-2796.
- [10] Kim, T. J., Kwon, H. H., Lima, C. (2018): A bayesian partial pooling approach to mean field bias correction of weather radar rainfall estimates: application to osungsan weather radar in south korea. – *Journal of Hydrology* 565: 14-26.
- [11] Liu, J., Wang, J., Pan, S., Tang, K., Li, C., Han, D. (2015): A real-time flood forecasting system with dual updating of the nwp rainfall and the river flow. – *Natural Hazards* 77(2): 1161-1182.
- [12] Liu, Q., Yan, C. R., He, W. Q. (2016): Drought Variation and Its Sensitivity Coefficients to Climatic Factors in the Yellow River Basin. – *Chinese Journal of Agrometeorology* 37(6): 623-632.
- [13] Marra, F., Morin, E., Peleg, N., Mei, Y., Anagnostou, E. N. (2017): Intensity-duration-frequency curves from remote sensing rainfall estimates: comparing satellite and weather radar over the eastern mediterranean. – *Hydrology & Earth System Sciences*, 21(5): 2389-2404.
- [14] Maxwell, D. H., Jackson, B. M., Mcgregor, J. (2018): Constraining the ensemble kalman filter for improved streamflow forecasting. – *Journal of Hydrology*, 560: 127-140.
- [15] Monteiro, M., Costa, M. (2015): ‘A comparison between single site modeling and multiple site modeling approaches using Kalman filtering’, in the International Conference on Numerical Analysis and Applied Mathematics 2014. AIP Publishing, Rhodes, Greece, pp. 377-394.
- [16] Noh, S. J., Lim, S., Choi, S. W., Hwang, S. H., Lee, D. R. (2014): Comparison of quantitative precipitation estimation algorithms using dual polarization radar measurements in korea. – *Journal of the Acoustical Society of America* 14(6): 105-116.
- [17] Thorndahl, S., Nielsen, J. E., Rasmussen, M. R. (2014): Bias adjustment and advection interpolation of long-term high resolution radar rainfall series. – *Journal of Hydrology* 508(2): 214-226.
- [18] Xu, Y. (2008): Application of Kalman Filter in Precipitation Estimation by Radar. – *Arid Meteorology* 26(1): 78-82.

- [19] Yahya, S. N. H. S, Tahir, W., Ramli, S., Deni, S. M., Arof, H., Saaid, M. F. M. (2012): Improved estimation of radar rainfall bias over Klang River Basin using a Kalman Filtering approach. – In 2012 IEEE Symposium on Business, Engineering and Industrial Applications. IEEE, Bandung, Indonesia, pp. 368-373.
- [20] Yang, J., Liu, L. P., Zhao, C. C. (2015): Spatial Distribution of Error from the Convective Precipitation Estimation of Radar and Optimization of Z-R Relationship. – *Plateau Meteorology* 34(6): 1785-1796.
- [21] Yin, Z. H., Zhang, P. Y. (2005): Radar Rainfall Calibration by Using the Kalman Filter Method. – *Quarterly Journal of Applied Meteorology* 16(2): 213-219,270.
- [22] You, C., Lee, D., Kang, M. (2014): Rainfall Estimation Using Specific Differential Phase for the First Operational Polarimetric Radar in Korea. – *Advances in Meteorology* 7: 1-10.
- [23] You, C. H., Kang, M. Y., Hwang, Y., Lee, J. J., Jang, M., Lee, D. I. (2018): A statistical approach to radar rainfall estimates using polarimetric variables. – *Atmospheric Research*, 209: 65-75.
- [24] Yucel, I., Onen, A., Yilmaz, K. K., Gochis, D. J. (2015): Calibration and evaluation of a flood forecasting system: utility of numerical weather prediction model, data assimilation and satellite-based rainfall. – *Journal of Hydrology* 523: 49-66.
- [25] Zhao, K., Liu, G. Q., Ge, W. Z. (2001): Precipitation Calibration by Using Kalman Filter to Determine the Coefficients of the Variational Equation. – *Climatic and Environmental Research* 6(2): 180-185.
- [26] Zheng, Y. Y., Xie, Y. F., Wu, L. L., Zhu, H. F., Wang, D. Y. (2004): Comparative Experiment with Several Quantitative Precipitation Estimator Techniques based on Doppler Radar over the Huaihe Valley during Rainy Season. – *Journal of Tropical Meteorology* 20(2): 192-197.

FORMATION MECHANISM OF THE SHELL BEACH IN THE EAST SEA OF BRAZIL – A CASE OF THE ITAPEMA FORMATION IN THE SANTOS BASIN

WAN, L. K. – WU, Y. P.* – JI, Z. F. – WEN, Z. X. – WANG, Z. M. – LI, Z. – QIN, Y. Q. – BIAN, H. G.

Research Institute of Petroleum Exploration & Development of CNPC, Beijing 100083, China

**Corresponding author: Wu Yiping
e-mail: wuyiping01@petrochina.com.cn*

(Received 24th Aug 2018; accepted 11th Oct 2018)

Abstract. Based on the data of the seismic, drilling, cores, logging curves, this paper analyses the seismic reflection structure, drilling lithological, core deposit structure, core and thin section diagenetic porosity and permeability, puts forward the change Changes and cycle characteristics graded phenomenon of sediment grain size of Itapema shell beach in the Santos basin, reveals its formation mechanisms. Results show that the lithology of the Itapema is dominated by coquina, muddy coquina and argillaceous coquina. Bioclastic granule with calcium and bone shell becomes the material base of the shell limestone. Paleogeomorphology controls the shell beach's areal distribution, while lake level changes effect the spatial shifting and evolution law of shell beach. The shell beach could be divided into three sedimentary microfacies: main beach, beach wing, and slope of front-beach. Their distribution depends on the ancient landforms. The main beaches are located on the underwater paleo-uplift and consist of bivalve shell limestones with the developed holes and hillock seismic facies. Beach wings surround the uplifts, composed of muddy shell limestone. The slopes of front-beach are in the transitional area between the underwater paleo-uplift and the depocenter with shaly shell limestone and mudstone. The evolution and migration of the shell beach are influenced by the lake level changes. During HST the bivalve shell beach develops in the east uplifts; During TST the shell beaches shift to the periphery of east uplifts. During LST distribution of the shell beach gradually expands and small scale shell beaches begin to develop in the eastern depression. Therefore the eastern uplifts and the bulge in central and eastern depression can be regarded as favorable shell beach zones. The results of this study are helpful for offshore oil and gas exploration in this area.

Keywords: *coquina, bioclast, ancient uplift, lake level changes, model*

Introduction

As the main battlefield of exploration on both coasts of the Atlantic including the Santos Basin and Campos basin shifts to the deep-water field, values of the pre-salt lacustrine carbonate reservoir in exploration and scientific research become increasingly obvious. The huge lacustrine coquina in Eastern Sea of Brazil is a hot spot for global oil and gas exploration, which has great potential with low research level. Therefore the distribution of high-quality reservoirs is dependent upon the distribution of shell beaches. They are influenced by many factors, such as tectonic action, climate and hydrological conditions. Reservoir parameters including reservoir thickness and properties vary greatly in space and between boreholes. There are significant differences from other well-known biocarbonates (Wang et al., 2016). At the same time, the reservoirs are affected by the shielding effect of overlying salt rock, which results in poor seismic imaging quality and brings about great challenges in reservoir prediction and hydrocarbon exploration (Zhao et al., 2005). In the Eastern Sea of Brazil the formation mechanism of the shell limestone is not studied deeply, the main control

factors are not clear (Liu et al., 2011; Zhu et al., 2017; Thompson et al., 2015; Wright, 2010, 2012; Gomes et al., 2009).

The Santos Basin is located offshore southeast Brazil, on the western coast of the South Atlantic (*Fig. 1*). The Cretaceous strata deposited in the basin can be divided into the Itapema and Barra Velha formations (Wang et al., 2016). The Lower Cretaceous Itapema formation consists of shell beaches deposited in the shallow to semi-deep lacustrine environment (*Fig. 2*).

As an important oil and gas reservoirs, shell limestone has been discovered to account for about 25% of the reserves in East Sea of Brazil. It is of great significance for exploration, such as Libra and Lula oil fields. However, compared to marine carbonate rocks, shell limestone has small sedimentary scope and strong heterogeneity (Guo, 2011), and the degree and depth of research are far behind marine carbonate rocks. The paper takes shell beaches of Santos Basin as an example and analyzes petrological features, then puts forward control factors of the shell beaches and builds up the sedimentary model, which may provide geological basis for oil and gas exploration of the Itapema Formation in the Santos Basin.

Materials and methods

Because the lacustrine carbonate rocks formed in the more restrictive environment than those in the Marine environment, the formation mechanisms of shell beach are so complex that multiple data and methods are needed to reveal its control factors (Guo, 2011). Through analysis of paleotectonics and palaeoclimate, the sedimentary model was established by using core thin sections and seismic data and longing curve.

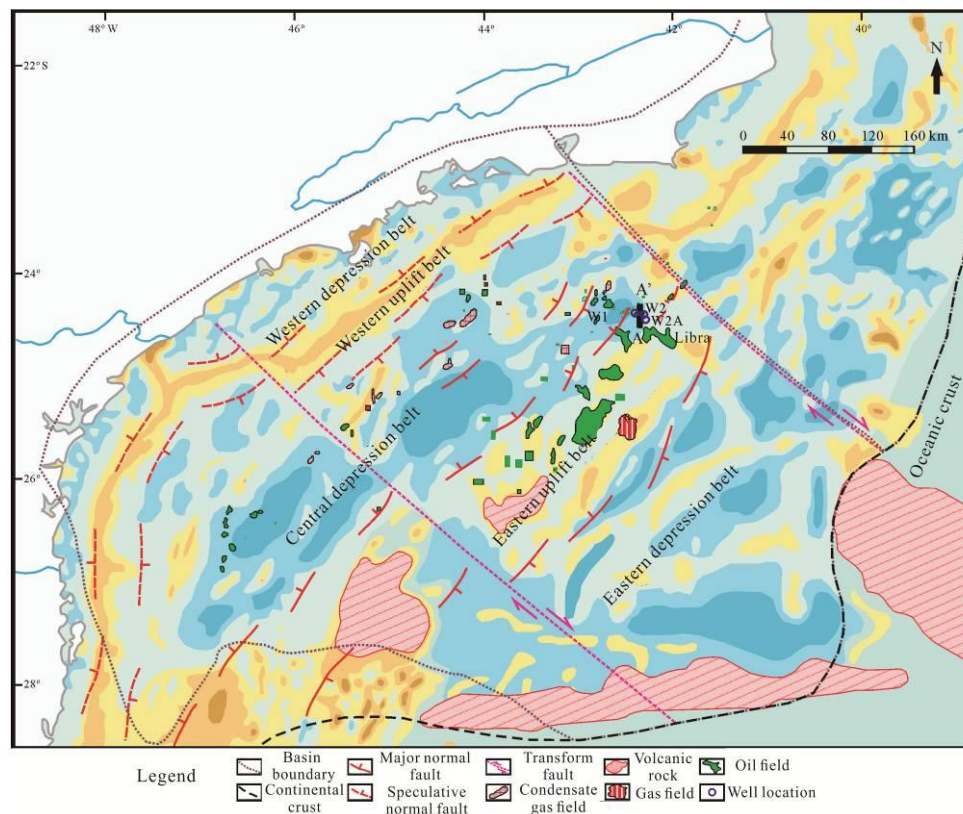


Figure 1. The tectonic setting of Santos Basin

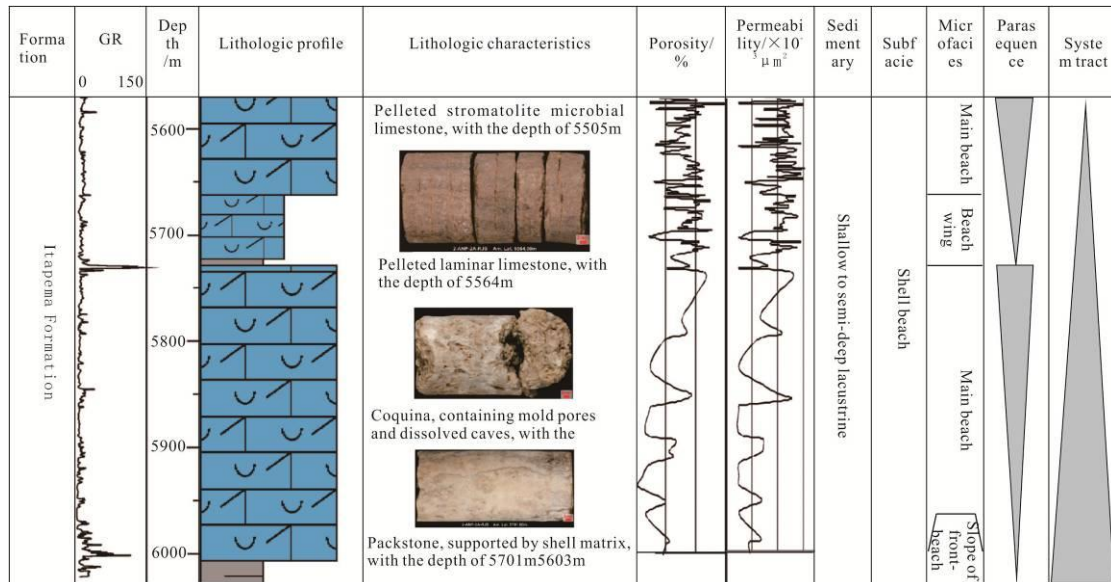


Figure 2. The sedimentary facies of Well W2

Core and microscopic thin section

Shell limestone, also known as Coquina (Zhu et al., 2017), is a tight sedimentary and composed of organic shell and bivalve fossils. The pre-salt coquina on both coasts of the Atlantic refers specifically to the lithologic complex comprised predominately by rigid bivalve shells, secondly by ostracoda and gastropods, and some other carbonate and siliciclastic compositions (Wright, 2012). Core and microscopic thin section observations indicate there are distinct differences in the upper and lower sections of the Itapema and the lithology is divided into coquina, muddy coquina and argillaceous coquina (Fig. 3).

Coquina

Coquina is located in the upper section. Typical coquinas include crystalline limestone, sparry coquina and micritic coquina (Fig. 3a), which are predominately grey brown-colored, moderate- to thick-bedded, blocky, and occasionally laminated. Their thickness is 13-30 m, with larger wave cross-bedding and abundant mold pores and dissolved pores, and contain highly fragmented shells (Hou et al., 2017). The rock is characterized by the strong recrystallization of calcite and is composed of xenomorphic fine crystal-medium crystal calcite from 0.1~0.5 mm. Coquina consists mainly of biogenic carbonate rock supported by 30% to 90% bioclasts, which contain lamellibranch and small amounts of ostracoda and gastropods. The shell bodies are partially broken in a long, flat and messy arrangement. The shell length is much less than 5 mm, and the content varied from 70%~90%. In the upper sedimentary sequence, the content of the shell gradually increases, and the calcite grains gradually get larger. Coquina is one of the most favorable reservoirs in the basin.

Muddy coquina

Muddy coquina develops in the middle section of the cycle with small amounts of mold pores and dissolved pores, can be further divided into muddy sparry coquina and

muddy micritic coquina (*Fig. 3b*), which present mainly grey- to dark grey-colored and moderate- to thin-bedded (Jian et al., 2008). The space between shells is filled with calcite and small amounts of mud (10% to 25%). The cementation of the granule is about 35%. The granule is dominated by double shell clastics with poor separation and distributes with weak orient. Granule content comes up 40~50%. The shell fragment is different extremely with min 0.02 mm and max 3 mm. In general muddy coquina has medium quality of the reservoir.

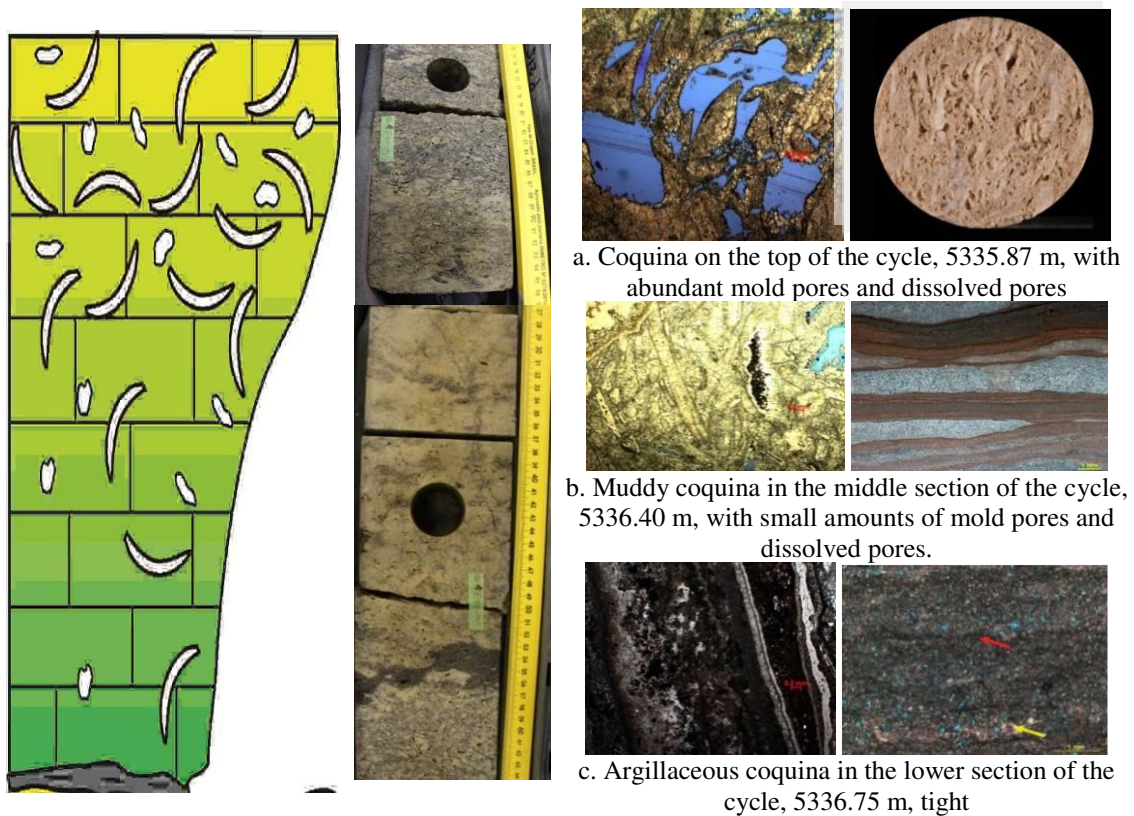


Figure 3. Dominate facies of coquinas of Itapema formation, Santos basin

Argillaceous coquina

Argillaceous coquina located in the lower section of the cycle (*Fig. 3c*), appears dark grey- to grey black-colored, with highly fragmented and directionally arranged shells. Granules are mainly bivalve clastic with disorder arrangement and poor separation, their size 0.2~2 mm, content around 50%. Reservoir space is filled predominately with muds (25–45%), bioclasts are dominated by lamellibranch and contain small amounts of ostracoda, and shells are predominately calcitic and partially aragonitic. There is a small amount of gray-black dung pellets locally with content of less than 5%. Because of tight reservoir they can be defined as poor quality.

Seismic reflection and logging curves

Based on coquina's petrological characteristics, in combination with well logs and seismic facies analysis, the Lower Cretaceous Itapema Formation shell beaches could be divided into 3 microfacies: i.e., main beach, beach wing and slope of front-beach

(Fig. 2). Coquina reservoirs in the study area are within the sedimentary facies belt having unique and distinct seismic reflection features (Fig. 4).

Main beach

The main beach is located in the upper end of the gentle-slope of the shallow lacustrine subfacies, and deemed to be high-energy beach sediments deposited in the freshwater lake basin. The lithology is dominated by coquina, which has the single-layer thickness of 5 m or more (Fig. 2) and contains highly fragmented and densely stacked shells. This type of rock is blocky and relatively pure (Zhao, 2005). Microscopically, the bioclastic shells are generally crystallized and granulated, with no primary structure retained. This indicates that the water-body energy stayed high during the deposition of the main beach, so that shells were entirely broken (Wright, 2012). The main beach is characterized by strong-middle amplitude at peak and high continuity and intermittent clutter on seismic section (Fig. 4), and box-shaped on well log, with low-GR and High-Rt (Fig. 5). In LST (Lowstand System Tract), lowstand delta covers the western uplift belt in the proximity of the high-bulge, bioclastic slump fan was formed on the steep-slope to the lake-side of the margin of the uplift belt, and oolitic beach is present onto the inner gentle-slope at the margin of the uplift belt (Well W3).

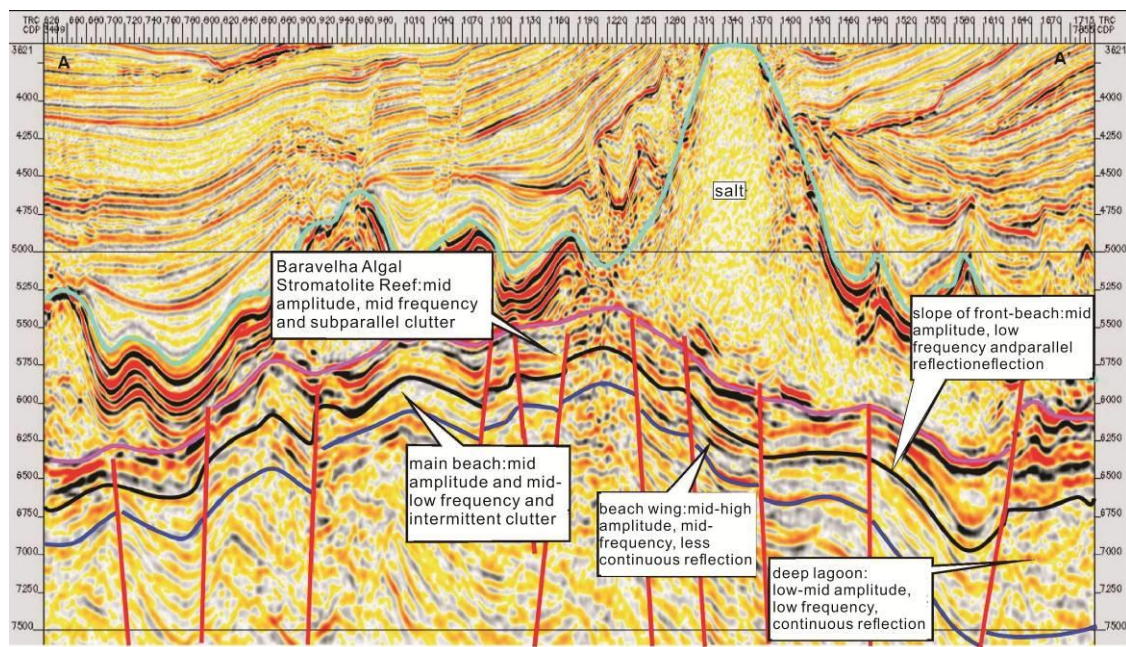


Figure 4. The seismic facies of Itapema formation in the Lower Cretaceous, Santos Basin

Beach wing

The beach wing is present in the periphery of the main beach, and varies in lithology across structural parts. Located to the leeward side, the lithology of the back wing is dominated by limestone, indicating a relatively weak hydrodynamic force. The front wing, which is located to the windward side, and the side wings have the muddy coquina-dominated lithology, which has the single-layer thickness of 2 to 5 m (Fig. 2) and contains relatively intact but disorderly arranged shells, indicating a moderate hydrodynamic force (Zhao et al., 2005; Qin et al., 2014). The beach wing is

characterized by middle-high amplitude at peak and middle frequency and less continuous reflection on seismic section (Fig. 4), and dentate-shaped on well log, with middle-GR and middle-Rt (Fig. 5). In TST (Transgressive System Tract), mollusk was prosperous, and bivalve-dominated organic reefs were developed at different periods (Guo, 2011). These reefs, as revealed by Well W4, have significant cumulative thickness, extend over a short distance in the lateral direction, and transition gradually into the organic reef back beach facies. Well W1 and W2 are drilled near the shoreland, where bioclastic sandy beach facies were formed by bioclasts carried by mixed storms and lake currents, under the influence of the injection of terrigenous clasts and alteration by wave winnowing. When the maximum lake transgression occurs, the limestone-building organisms were inhibited and lacustrine mudstone became dominant.

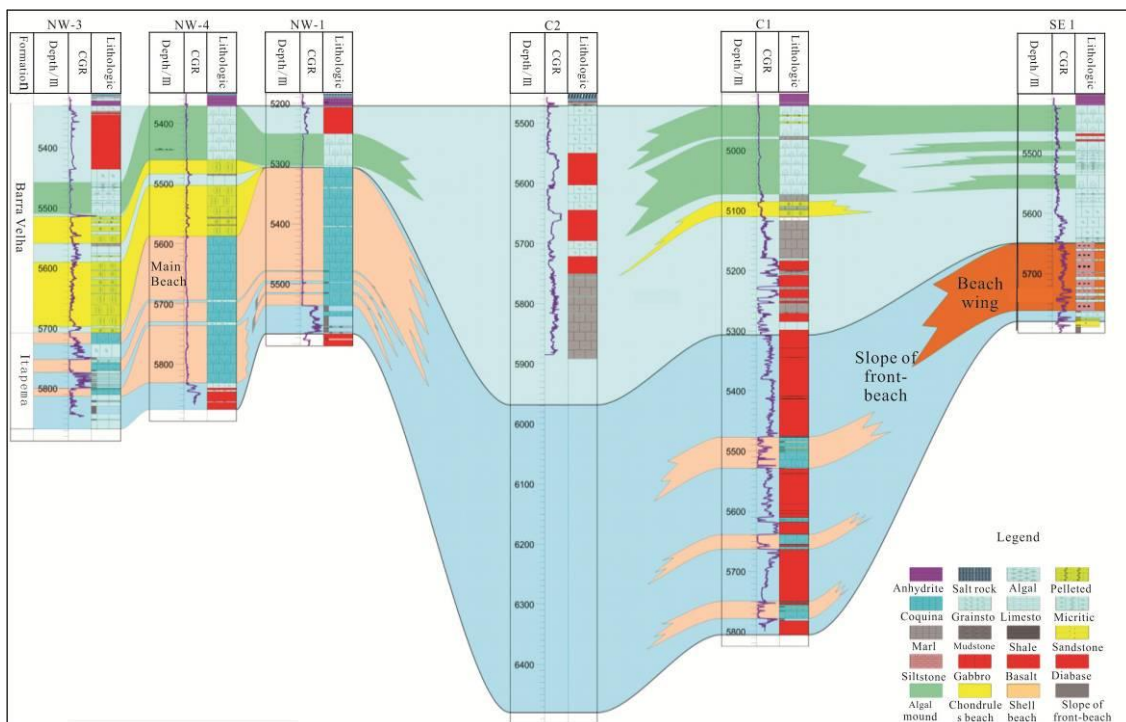


Figure 5. Section across Well NW3, NW4, NW1, C2, C1 and SE1 of Libra block in the Santos Basin

Slope of front-beach

The slope of front-beach is located to the windward side, within the transition zone between the shell beach and the lake basin center. The lithology is dominated by argillaceous coquina, which has the single-layer thickness of 2 m or less and is usually interbedded with dark mudstone. The main beach shell beds are fragmented by wave and then transported by lake wave to the slope of front beach and deposited to form argillaceous coquina, which is not the product of in-situ sedimentation and shares similar sedimentary mechanism with clastic rocks (Liu et al., 2011). Thus, argillaceous coquina contains highly fragmented and directional arranged shell beds (Guo, 2011). The slope of front-beach is characterized by middle amplitude at peak and low frequency and parallel reflection and moderate-strong continuity on seismic section (Fig. 4), and box-shaped and tooth-like on well logs, with low-GR and High-Rt (Fig. 5).

As water level in HST (Highstand System Tract) began to drop gradually, limestone-building organisms (e.g., bivalve) were prosperous once again, the proportion of reef-beach facies bioclastic limestone tended to increase, and the water depth of facies belts generally decreases towards the shoreland.

Results

Study suggests that, the distribution and evolution of the Lower Cretaceous Itapema Formation shell beaches in the Santos Basin are controlled by Calcareous bioclast and paleo-geomorphology and lake level change. Particularly, Calcareous bioclast and paleo-geomorphology controls the shell beach's areal distribution, while sea level change control the spatial shifting and evolution law of shell beach (Liu et al., 2011; Liu and Lv, 2014).

Calcareous bioclast

Shell limestone in study profile is mainly composed of the bivalve shell and rare gastropods and mesomorphic shell, they accidentally contain chara, fish and other biological particles, so bioclastic granule with calcium and bone shell becomes the material base of the shell limestone (*Fig. 3*).

Bivalve shells are main granules of coquina, shell bodies are broken into clastic and are recrystallized, the large wave cross-bedding indicates that the rocks between granules can be sparry cementation. Penecontemporaneous karst reflects the rocks have been exposed soon after the sedimentary (Wright, 2012; Guo, 2011; Hou et al., 2017; Jian et al., 2008). So shell limestone formed in the high energy region between the minimum wave base on the sunny day and the lake level, related to the strong wave transformation and elutriation and cropped up above the lacustrine, shall be deposited in the uplift areas of the shell beach in the shore - shallow lacustrine.

Granules of muddy coquina are given priority to bivalve debris, mainly carbonate sediments with semi-solid or consolidation while the deposition has not been last so long. Then they suffered from waves, currents and storm flow, such as crushing, transportation, abrasion, redeposition. It reflects the strong hydrodynamic conditions. Therefore, it is speculated that muddy coquina may be formed on the medium-high energy environment between the minimum wave base and the maximum wave base on the sunny day, proved to be an integral part of the shell beach.

Granules of argillaceous coquinas derive mainly from bivalve debris with low recrystallization, interstitial fillings contain mainly micritic calcite and clay minerals (Mann and Rigg, 2012), which indicates that the sedimentary water body is deeper, and it has been affected by the weak wave action and incomplete elutriation. On the basis of that Granules of coquinas are transported to the shallow lakes on the low-energy environment and unload quickly in clay, plaster, deposit on the edge of the shell beach. So they may appear between the minimum wave base and the v wave base on the sunny day due to seasonal lake level changes.

Paleo-geomorphology

The tectonic framework of the Santos Basin consists of three depressions and two uplifts. In the basin lacustrine carbonate rocks are generally distributed over the underwater paleo-uplifts (Altenhofen, 2013), which are related to the shell bench.

The main beach is the uplift part of the shell beach with the strongest wave energy and the thickest shell, where the pure shell limestone develops, and is represented by well NW4, NW1 and C1. Beach slope is the edge of the shell beach, far from the center of shell deposition, with weak wave energy and thinner shell, turns into development zone of argillaceous coquinas, represented by well C1 and C2. Sand content is higher close to the edge of the lakeside than that close to half deep lake (Brun and Fort, 2011). The beach wing is the slope part of transiting from the main beach to the beach edge with the strong wave energy, is the mixed development zone of the pure shell and the muddy shell, and represented by well SE-1 (*Fig. 5*).

Due to the screening effect of the western uplift belt, the majority of the terrigenous clasts transported by the rivers flowing into the lake to the west were deposited in the western depression belt. The increase in water depth of the central depression belt allowed for further purification of lake water. As a result of this, the eastern uplift belt became a favorable site for deposition of lacustrine carbonate rock (*Fig. 6*), because it was under a shallow lacustrine environment with moderate water depth and relatively strong wave action, which favors growth of lamellibranch. Thus, the shell beaches, particularly the main beach microfacies, are well developed (*Fig. 5*). In the periphery of the underwater low-bulge, beach wing sediments were formed resulted from the decrease in water energy (Brun and Fort, 2011; Jia et al., 2008). Sedimentation products are dominated by muddy coquina, which contains less shell fragments and interstitial materials. In the transition zone between the underwater low-bulge and the center of the lake basin, which is the transition zone between the shallow lacustrine and the semi-deep lacustrine environments with significant water depth and weakest hydrodynamic force, however, shelly organisms are less likely to grow and it is mainly the slope of front-wing microfacies formed. In the relatively low-lying paleo-gully present between the underwater low-bulges, which has relatively deeper water depth and weaker hydrodynamic force than the low-bulge zone, sediments deposited are similar to the beach wing or slope of front-wing microfacies. In addition, the development of shell beaches is related closely to the second-order paleo-geomorphological highs. All of these evidences reveal that, paleo-geomorphology has significant control on distribution of shell beaches.

Lake level change

The in-depth study of drilling and outcrop data indicates that, the Itapema formation can be roughly considered as a complete lacustrine transgressive cycle (Jia et al., 2008; Zhao et al., 2005), with shell beach sediments formed. Studies show that Itapema Formation mainly develops shell beach deposition in the early and date phases. The scale and evolution of shell beaches are controlled primarily by lake level change (Wang et al., 2016; Hou et al., 2017). Distribution of shell beach is chartered by migrating from northeast to southwest (*Fig. 6*).

During the initial period of lake level rise, the sedimentary environment transitions gradually from the coastal lake to the shallow lake, shell beaches began to form in the low-uplift zone in the center of the lake basin, but with relatively small scale and thickness, and in the uplift zone in the periphery of the lake basin shell beaches were absent due to the frequent exposure to the water surface. Along the shallow lake facies, there are five shell benches, including 45-215, 80-160, 25-145, etc., each of which transformed from the the beach core to the beach slope and to the beach edge, with three zonal pattern spreading (*Fig. 6*).

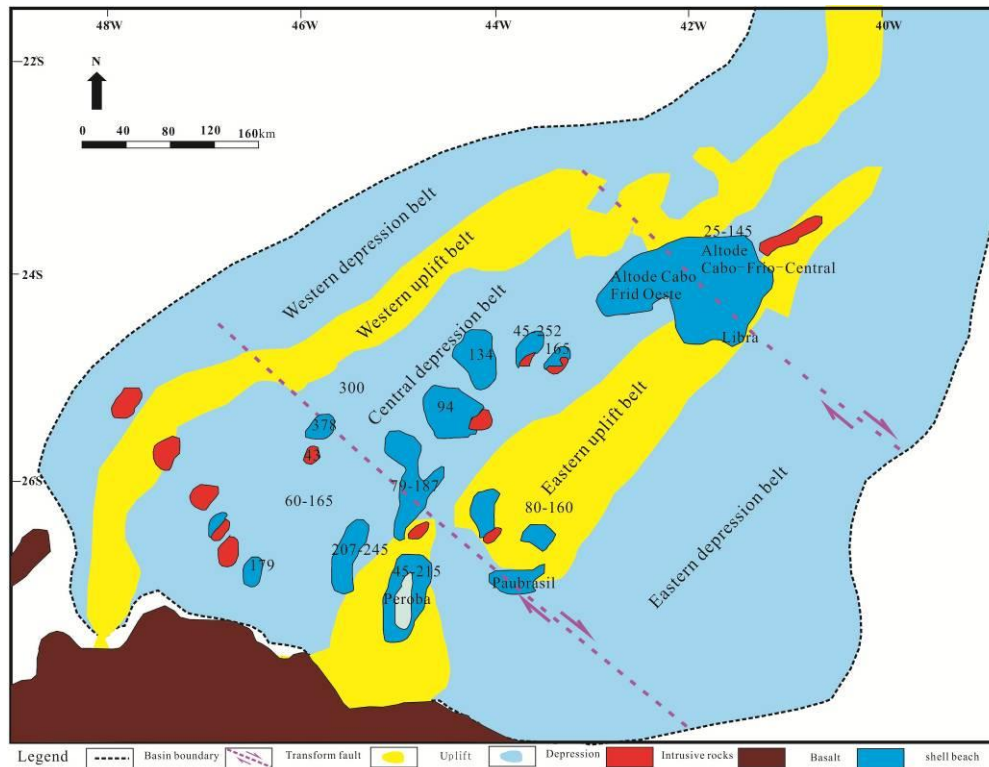


Figure 6. Distribution of shell beach of Itapema formation, Santos basin

During the middle-late period of lake level rise and initial period of lake level fall, lake level rose continually to its maxima, the moderate water depth and availability of abundant lamellibranch permit the shell beaches to form in the underwater uplift zone in the periphery of the lake basin. These shell beaches are commonly thick-bedded and extend over a broad area. In the low-uplift zone in the center of the lake basin (Tellus, 2012), however, the shell beaches are either decreased in scale or vanish due to the increase in water depth.

During the middle-late Itapema period of lake level fall, sedimentary environment transitioned gradually from the shallow lake to the coastal lake, and the influence of outer provenances became increasingly strong. As a result, shell beaches atrophied gradually, were present only in the low-uplift zone in the center of the lake basin and absent in the uplift zone in the periphery of the lake basin (Wang et al., 1981). Along the shallow sea facies some smaller 9 shell beaches developed, including 134-934 and 79-187 (Fig. 6).

The three periods of zonal pattern distribution control developing scope of three types of shell limestone, which has a certain difference in the planar.

Discussion

Based on the study of the seismic reflection structure, drilling lithological, core deposit structure, core and thin section, in combination with the change Changes and cycle characteristics graded phenomenon of sediment grain size of Itapema shell beach in the Santos basin (Garcia et al., 2012), we build the sedimentary model of the Lower Cretaceous Itapema Formation (Fig. 7).

Sedimentary model

In the Santos Basin, the land side of the western uplift zone blocked the majority of terrigenous clasts to the west, and the lake side permits the formation of lake basin marginal platform, due to the influence of reverse synsedimentary faults (Garcia et al., 2012; Modica and Brush, 2004). The fault slope-break belt at the margin of the western high-bulge allows for formation of a coastal lacustrine sedimentary environment, which, with shallow but turbulent water body and strong winnowing effect, favors the sorting of clastic rocks and the development of beach limestones. Accordingly, lake margin, bioclastic sandy beach and bioclastic calcareous beach facies belts were deposited in areas extending from the shoreland to the lake. Lagoon facies belt was formed in the intraplatform low-lying areas on the slope. The fault slope-break belts at the margin of the depression formed a positive high structural setting at the platform margin, where the high-energy and clean shallow lacustrine environment allows for accumulation and prosperity of bivalve and homonemeae organisms. Accordingly, the organic reef facies limestone with a wave-resistance framework was formed, and these reefs are connected and merged to form the linear rim of the platform. In back-reef areas, water body remained turbulent, and bioclasts transported by lake wave altering storms enabled formation of back-organic reef beach and oolitic beach facies belts (Brun and Fort, 2011). In areas outside the fault slope-break belt at the margin of the depression, the slope gradient rose rapidly, and clasts formed by upstream weathering and erosion or storming would accumulate to form bioclastic slump fan.

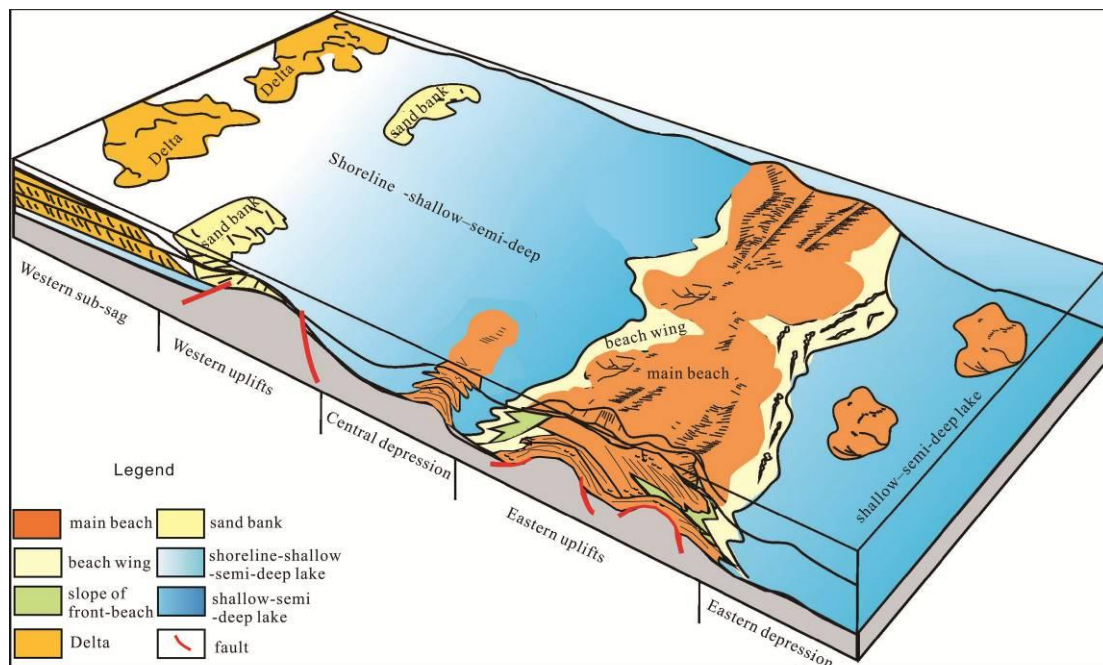


Figure 7. Depositional model diagram of the Itapema Group, Santos basin

Favorable reservoirs

Itapema Formation recorded the maximum lacustrine transgression occurred during the Cretaceous. The main part of the basin was covered by the still-water lake basin sediments and relatively less affected by outer provenances, with exceptional

development of (fan) delta and flooding plain sediments in the periphery of the basin resulted from outer provenances (Xiong et al., 2013). This laid a solid foundation for large-area distribution of shell beaches. Areally, the shell beaches are distributed mainly in the underwater low-bulge belt, surrounding the depocenter. Vertically, the shifting and evolution of shell beaches are controlled primarily by the lake level change: shell beaches shifted gradually towards the shoreland during the lake level rise and towards the lake basin during the lake level fall. Building the sedimentary model has great significance to predicting the distribution of “sweet spot” reservoirs in the Itapema Formation and searching for favorable supplementary blocks (Dorobek, 2008).

Conclusions

(1) The Cretaceous Itapema Coquina in the Santos Basin deposited in shallow to semi-deep lacustrine and is dominated by coquina, muddy coquina and argillaceous coquina. Sedimentary facies of shell beaches are defined as main beach, beach wing and slope of front-beach.

(2) Distribution and evolution of the Lower Cretaceous Itapema shell beaches are controlled by Calcareous bioclast and paleo-geomorphology and lake level change. Particularly, Calcareous bioclast and paleo-geomorphology controls the shell beach's areal distribution, while sea level change control the spatial shifting and evolution law of shell beach.

(3) The vertical evolution of shell beaches is controlled primarily by lake level change. The eastern uplifts and the bulge in central and eastern depression can be regarded as favorable shell beach zones.

Acknowledgements. This project is supported by the National Science and Technology Major Project of China (Grant No. 2016ZX05029).

REFERENCES

- [1] Altenhofen, S. D. (2013): Caracterizao petrografica de deposicoes carbonaticas lacustres do Grupo Lagoa Feia, Bacia de Campos, Brasil. Monografia (Trabalho de Conclusao de Curso). – Universidade Federal do Rio Grande do Sul. Porto Alegre, Brasil.
- [2] Brun, J., Fort, X. (2011): Salt tectonics at passive margins: geology versus models. – *Marine and Petroleum Geology* 28(6): 1123-1145.
- [3] Dorobek, S. L. (2008): Tectonic and Depositional Controls on Syn-Rift Carbonate Platform Sedimentation. – In: Lukasik T. J., Simoj, A. (eds.) *Controls on Carbonate Platform and Reef Development*. SEPM Special Publication 89, Tulsa, Oklahoma, USA, pp. 57-81.
- [4] Garcia, S. F., Letouzey, J., Rudkiewicz, J. et al. (2012): Structural modeling based on sequential restoration of gravitational salt deformation in the Santos Basin (Brazil). – *Marine and Petroleum Geology* 35(1): 337-353.
- [5] Gomes, P. O., Kilsdonk, B., Minken, J. et al. (2009): The outer high of the Santos Basin, southern So Paulo Plateau, Brazil: pre-salt exploration outbreak, paleogeographic setting, and evolution of the syn-rift structures. – AAPG Search and Discovery, Denver, USA.
- [6] Guo, F. (2011): *Carbonate Sedimentology*. – Petroleum Industry Press, Beijing, pp. 224-225.
- [7] Hou, G., Ni, C., Chen, W. et al. (2017): Sedimentary characteristics and factors controlling the Shell Beach in the Da'anzhai member of the Central Sichuan Basin. –

- Journal of Southwest Petroleum University (Science & Technology Edition) 39(1): 25-34.
- [8] Jia, Z., Hong, T., Wang, W. (2008): The building process and influential factors of the stromatolite reefs in the neoproterozoic Jiuliqiao Formation in Huainan region, Anhui. – *Acta Palaeontologica Sinica* 47(1): 47-57.
- [9] Jian, H., Yuan, X. et al. (2008): Analysis on sequence stratigraphy of lacustrine carbonate in the first member of Shahejie Formation in huimin Sag. – *Acta Petrolei Sinica* 29(2): 213-218.
- [10] Liu, S., Hu, X., Li, J. (2011): Great discovery and its significance fro exploration in subsalt reservoir in Santos Basin, Brazil. – *Overseas Exploration* 16(4): 74-81.
- [11] Liu, Z., Lv, M. (2014): Analysis of pre-salt geological characteristics of deepwater basins in South Atlantic Ocean. – *China Petroleum Exploration* 19(6): 63-73.
- [12] Mann, A., Rigg, J. (2012): New geological insights into the Santos Basin. – *Geo ExPro* 9(1): 36-39.
- [13] Modica, C. J., Brush, E. R. (2004): Postrift sequence stratigraphy, paleogeography, and fill history of the deep—water Santos Basin, offshore Southeast Brazil. – *AAPG Bulletin* 88(7): 923-945.
- [14] Qin, Y., Wen, Z., Wang, Z. et al. (2014): Sedimentary characteristics, model and hydrocarbon accumulation of deep water pre-salt carbonate rocks in South Atlantic. – *Earth Science Frontiers* 21(1): 21-31.
- [15] Tellus (2013): Tellus data B/OL. – <http://www.fugro-robertson.com/products/tellusFRL> (2012-12-30).
- [16] Thompson, D. L., Stilwell, J. D., Hall, M. (2015): Lacustrine carbonate reservoirs from Early Cretaceous rift lakes of Western Gondwana: pre-salt coquinas of Brazil and West Africa. – *Gondwana Research* 28(1): 26-51.
- [17] Wang, J. et al. (1981): Diagenesis and digenetic trap of Daanzhai limestone. – *Geochimica* 30: 232-241.
- [18] Wang, Y., Wang, X., Liao, J. et al. (2016): Cretaceous lacustrine algal stromatolite reef characteristics and controlling factors, Santos Basin, Brazil. – *Acta Sedimentologica Sinica* 34(5): 819-829.
- [19] Wright, V. P. (2010): Reservoir architectures in non-marine carbonates (abs.). – AAPG Annual Convention and Exhibition, Houston, Texas, USA, pp. 10-13.
- [20] Wright, V. P. (2012): Lacustrine Carbonates in Rift Settings: The Interaction of Volcanic and Microbial Processes on Carbonate Deposition. *Advances in Carbonate Exploration and Reservoir Analysis*. – Geological Society Special Publication 370, London, pp. 39-47.
- [21] Xiong, L., Li, J., Wu, C. et al. (2013): Tectonic evolution and hydrocarbon accumulation in the Solimoes Basin, Brazil. – *Oil & Gas Geology* 34(3): 363-369.
- [22] Zhao, J., Xia, B., Ji, Y. et al. (2005): Analysis of the high resolution sequence of lacustrine carbonate. – *Acta Sedimentologica Sinica* 23(4): 646-656.
- [23] Zhao, J., Xia, B., Ji, Y. et al. (2005): Analysis of the high resolution sequence of lacustrine carbonate. – *Acta Sedimentologica Sinica* 23(4): 646-656.
- [24] Zhu, S., Wu, K., Lyu, M. et al. (2017): Characteristics and sedimentary model of lacustrine coquina in Campos Basin, Brazil. – *China Offshore Oil and Gas* 29(2): 36-45.

THE INFLUENCE OF ENVIRONMENTAL FACTORS ON *ASPERGILLUS NIGER* GRANITE WEATHERING

WU, Q.^{1,2,3} – HU, H.^{1,2*}

¹*Collaborative Innovation Center of Sustainable Forestry in Southern China of Jiangsu Province, Nanjing Forestry University, 159 Longpan Road, Nanjing, Jiangsu 210037, China*

²*Key Laboratory of Soil and Water Conservation and Ecological Restoration in Jiangsu Province, Nanjing Forestry University, 159 Longpan Road, Nanjing, Jiangsu 210037, China*

³*School of Biological and Food Engineering, Anyang Institute of Technology
Anyang, Henan 455000, China*

**Corresponding author
e-mail: 531208831@qq.com*

(Received 24th Aug 2018; accepted 11th Oct 2018)

Abstract. In order to explore the effects and influence of environmental factors on microbial restoration of waste rock, an efficient rock-weathering strain *Aspergillus niger* XF-1 was isolated from a granite face. Concentrations of SiO₂ in nutrient solution at different temperatures, pH values, generation cycles, and vaccination quantities were measured using shake flask leaching and inductively coupled plasma optical emission spectrometer (ICP-OES) to analyze the grey correlation degree of weathering. The results reveal that the *A. niger* XF-1 strain can be used as a good fungal source for the restoration of degraded habitats in abandoned granite areas, and can also be used to promote the release of more Si elements in granite. Moreover, pH is the dominant factor affecting the weathering of granite by *A. niger*, followed by vaccination quantity and temperature, while generation cycle is the least important factor. The optimum temperature at which granite is weathered by *A. niger* was 28°C, the most appropriate pH value was 3, the most suitable generation was the fifth, and the optimum vaccination quantity was 10⁷ (spore numbers mL⁻¹).

Keywords: *Aspergillus niger*, weathering effect, fermentation, grey correlation degree analysis

Introduction

Granite is one of the most widely distributed rocks globally. In developing countries, abandoned granite mines are often covered with bare rock because of artificial over-exploitation, which has led to severe soil and water loss, sharp declines in plant diversity, deteriorated ecological conditions, and disastrous mine rocky desertification phenomena (Wu et al., 2017a). As natural rocky desertification restoration is almost impossible, appropriate strategies must be developed that can be applied to artificially promote improvements to degraded ecosystems (Qi et al., 2013). One of the most effective ways to do this is to spray a mixture of plant seeds, soil, and nutrients onto exposed mine rock surfaces (Wu et al., 2017b; Borland et al., 2016). In this process, however, when the plants run out the nutrient matrix layer they die and fall off the rock surface and so this does not form a sustainable soil environment (Pratas et al., 2005). Soil formation is therefore a crucial issue to promote plant growth via the fusion of sprayed materials and the rock surface (Barker and Banfield, 1996).

Rock weathering is a key component of soil formation. As part of research in this area, physicochemical weathering effects are often closely studied (Borland et al., 2016; Wang, 2017; Tang et al., 2016; Cheng et al., 2015); previous research by Kevin et al.

led to the conclusion that biological weathering plays a prominent role in certain cases in the presence of biological organisms in the environment (Peng et al., 2015; Li et al., 2015c). The formation of a soil starts from the moment that various organisms begin to develop within loose rock crevices (Williams and Steinbergs, 1959); microbial weathering in this context is one of the most common geological process on Earth, and mainly controls biofilm formation during growth. The organic acids and other metabolites produced during this process mean that one part of rock mineral substances will dissolve (Lian, 2014). Previous work has shown that microbial activity is one of the most important factors in the weathering of rocks and minerals in the biosphere; for example, Bennett et al. noted that the rock weathering performance of microorganisms is related to metabolic by-products, the limited nutrition that can be extracted from special minerals, and growth and development (Bennett et al., 2001). Thus, Si (silicon), Al (aluminum), Fe (ferrum), Mg (magnesium), Ca (calcium), and K (potassium) are dissolved from silicates, aluminosilicates, oxides, phosphates, carbonates, and sulfides during this process (Lian et al., 2008); the various elements that are released also comprise an important nutrient source for plant growth and development. This means that research on microbial weathering rock is one of the important components of ecological environmental restoration, and is therefore of great significance to overall sustainable development.

Bacteria and *fungi* are able to decompose minerals (Chiang et al., 2014; Li et al., 2015c, 2017; Ramos et al., 2014; Song et al., 2015). In another previous study, Castro et al. compared the ability of the bacteria *Pseudomonas*, *Penicillium*, and *Aspergillus* at promoting Zn and Ni dissolution in smithsonite and garnierite and were able to show that the latter was most efficient (Castro et al., 2000). This kind of work was developed by Lian et al. who compared weathering biotite mineral differences between *A. niger* and the glial species *Bacillus*; these workers noted that the weathering effect of the former was better, and also noted that *A. niger* played a leading role in the weathering process of biotite via the secretion of acid metabolites. In this case, *A. niger*-mineral aggregates formed via the extension of hyphae, which then penetrated into microcracks and promoted rock weathering (Dong and Lian, 2014). The original strains *Aspergillus niger* and *Penicillium heteromorphum* PHT were studied by diethylsulfate (DES) induced protoplast mutagenesis and bioleaching of potassium-rich shale (Tang et al., 2011).

Studies on the potassium-releasing effect and influence of *A. niger* on these minerals (Hu et al., 2011) as well as cleaning effects on quartz sands (Song and Lian, 2014) and promotion effect of plant growth (Lü et al., 2015) have also made some progress. To date, however, the influence of *A. niger* on the weathering of granite has not been discussed. *Aspergillus niger* XF-1 is a dominant strain isolated from the granite surface in Suzhou, Jiangsu Province, and has a certain relationship with granite weathering. Therefore, it is of great significance to study the unique functions and ecological effects of lithophytic microorganisms.

For the realization of sustainable development of ecological restoration, we screened the efficient strain to weathering granite, and study the effects of environmental factors on the habitat restoration in abandoned rock mining areas. In current study, an efficient strain of *A. niger* was isolated and purified from the lichen surface of granite rock in this study via preliminary silicon-releasing effect screening. The effect of *A. niger* weathering granite at releasing this mineral was observed under different temperature conditions as well as initial pH values, generation cycles, and vaccination quantities.

Results were then analyzed using the grey correlation analysis method (GCAM) in order to understand the degree of importance and relative function of different factors during the weathering process. This enabled a clear scientific basis to be developed to improve weathering effects, promote the greening of abandoned mine rock slopes, soil formation, and improvements to the overall ecological environment.

Material and methods

Rock samples

Porphyry granite was used as the source rock for this analysis. All experimental rock samples were obtained from an abandoned granite mine on Jinding Mountain, in Wuzhong district, Suzhou, Jiangsu, China (E 120°30', N31°17'). Samples were placed in a sterile kraft bag; lichens were stored in a refrigerator at 4 °C, and the remainder were held in a refrigerator at -20 °C. The fresh rock samples used in this experiment were washed with distilled water, sieved through a 200 mesh after being dried naturally, ground to a particle size < 90 µm, and then autoclaved at 121 °C for 20 min.

Dried samples were then evaluated using x-ray fluorescence (XRF) spectrometry; the elements contained within granite are summarized in *Table 1*. Diffractometer (HX041) analysis showed that the quartz, plagioclase, potassium feldspar, biotite, chlorite or vermiculite accounted for 30-35%, 20-25%, 25-30%, 10-15%, and 5% by mass, respectively.

Table 1. Chemical compositions of the granite used in the experiments

Chemical composition (%)										
SiO ₂	TiO ₂	Al ₂ O ₃	Fe ₂ O ₃	MnO	MgO	CaO	Na ₂ O	K ₂ O	P ₂ O ₅	Others
74.29	0.20	13.54	1.88	0.37	0.28	0.78	3.49	4.78	0.04	0.38

Medium

A potato dextrose agar medium (PDA) was produced by boiling 200 g potato slices for 20 min and then filtering them through eight cotton gauze layers to remove slag. A mixture of 20 g glucose and 20 g agar were then added along with distilled water up to 1,000 ml; this mixture was then heated and stirred well before being sterilized at 121 °C for 20 min.

We also produced a liquid PD culture medium that did not include 20 g agar.

Isolation, purification, and screening of fungal strains

The lichen samples we obtained from rock surfaces were washed many times, remaining fluids were collected and were then oscillated on a shaker at room temperature and 150 rpm for 30 min. A sterile water continuous gradient dilution (i.e., 10⁻⁴, 10⁻⁵, and 10⁻⁶) within a 200 µL suspension was then uniformly coated onto a PDA plate and placed in a constant temperature incubator at 28 °C for between six and seven days. Depending on the subsequent characteristics of the resultant fungal colony, including morphology and color, the strain species was identified and a single colony was selected, purified, and stored at 4 °C in a refrigerator.

We then cultured each strain at 28 °C, 150 rpm for ten days for participation in rock weathering experiments. The strains which significantly released Si were then screened using an inductively coupled plasma optical emission spectrometer plasma emission spectrometer (ICP-OES)(American Vista MXP type); these experiments showed that the XF-1 strain exerted a good weathering effect and so this one was used for the remainder of this analysis.

The experimental strain was identified via its single colony morphological characteristics as well as color, hyphae, conidia, sporangia, and genomic sequence.

The gDNA of the XF-1 strain was extracted using the CTAB method (Wu et al., 2017). In this case, the volume used for the PCR reaction system was 20 L: 2 × PCR reaction mix 10 µL; we also used 1 µL of the forward primer ITS1, 1 µL of the reverse primer ITS4 (10 mmol·L⁻¹), 1 µL of template DNA, and 7 µL of ddH₂O. This mixture enabled us to analyze and identify the gene sequence of 18S rDNA with PCR reaction conditions that comprised predegeneration at 94 °C for 5 min, degeneration at 94 °C for 30 seconds, annealing renaturation at 55 °C for 30 seconds, and elongation at 72 °C for one minute. This procedure was repeated over 30 cycles prior to final elongation at 72 °C for 10 min. Amplification PCR products were then detected via 1% agarose gel electrophoresis, ethidium bromide (EB) staining, and an ultraviolet detector. The purification and sequencing of PCR products was completed by GenScript (Nanjing) Co., Ltd; all sequencing results were submitted to the GenBank database (www.ncbi.nlm.nih.gov) and analyzed using BLAST software.

Spore suspension preparation

The XF-1 strain used in this analysis was cultivated at 28 °C for seven days and was augmented with 5 mL sterile water. Thus, by gently scraping spores on the surface of the agar, a suspension was filled to a 50 mL sterilized triangular bottle, into which several sterile glass ball had been placed in advance, and was then filtered with the sterile absorbent cotton after complete vibration fully. The final residue of this stage was washed three times with sterile water, the filtrate was collected and added to 10 mL with sterile water, and spore suspensions of 10³ mL⁻¹, 10⁵ mL⁻¹, 10⁷ mL⁻¹, 10⁹ mL⁻¹, and 10¹¹ mL⁻¹ were then prepared.

Test design and treatments

Tests were divided into four groups, A, B, C, and D. The aim of the group A test set was to explore the influence of *A. niger* on weathered granite at different temperatures. These experiments comprised 5 g of granite rock powder that placed into a 250 mL triangle bottle, a 100 mL PD medium was then added and pH was adjusted to 7 and the whole mixture was autoclaved at 121 °C for 20 min. Subsequent to cooling to room temperature, 10⁷ mL⁻¹ of 5% *A. niger* spore suspension prepared in advance was then inoculated in a triangular bottle following a sterile operation, and cultivated at 150 rpm and at 5 °C, 15 °C, 28 °C, 32 °C and 37 °C, respectively.

The aim of the group B series of tests was to study the influence of different pH value on weathered granite by *A. niger*. Thus, 5 g of granite rock powder was placed into a 250 mL triangle bottle, 100 mL of PD liquid medium was added, and the pH was adjusted to 3, 5, 7, 9, and 11, respectively. The whole mixture was then autoclaved at 121 °C for 20 min. Subsequent to cooling to room temperature, 10⁷ mL⁻¹ of 5% *A. niger*

spore suspension prepared in advance was then inoculated in a triangular bottle in a sterile manner and cultivated at 28 °C.

The aim of the group C set of tests was to study the influence of different generation cycles on granite weathered by *A. niger*. In this series, 5 g of granite rock powder was placed into a 250 mL triangle bottle, 100 mL of potato sucrose medium was added, the pH was adjusted to 7, and the whole mixture was autoclaved at 121 °C for 20 min. Subsequent to cooling at room temperature, 10⁷ mL⁻¹ of 5% *A. niger* spore suspension from the first, second, third, fourth and fifth generations prepared in advance was inoculated in a triangular bottle in a sterile operation, and cultured at 28 °C and 150 rpm.

The aim of the group D set of tests was to study the influence of different vaccination quantities granite weathered by *A. niger*. In this case, 5 g of granite rock powder was placed into a 250 mL triangle bottle and 100 mL potato sucrose liquid medium was added, the pH was adjusted to 7, and the whole mixture was autoclaved at 121 °C for 20 min. Subsequent to cooling to room temperature, 10³ mL⁻¹, 10⁵ mL⁻¹, 10⁷ mL⁻¹, 10⁹ mL⁻¹, and 10¹¹ mL⁻¹ solutions of 5% *A. niger* spore suspension prepared in advance were inoculated in triangular bottles in a sterile operation and cultivated at 28 °C and 150 rpm.

Each of the group experiments discussed above was repeated in triplicate, with the spore suspension autoclaved at 121 °C for 20 min used for comparisons. On day 30, 5 mL of the fermented liquid from each treatment was taken, centrifuged at 5,000 rpm for 10 min and the resultant supernatant was placed in a 50 mL volumetric flask, filled to a constant volume. We then added 0.05 mL of nitric acid (65%) and SiO₂ sample contents were detected using a plasma ICP-OES.

Scanning electron microscope (SEM) observation of granite

Treated granite residuals were collected and dried at 50 °C. Each sample was then fixed, sprayed with metal, and surface characteristics on day 30 were observed using a SEM (Hitachi-S3400N).

Data analysis

All of the data collected in this study were processed using the software Excel 2010 and variance analyses and significant difference tests were carried out using SPSS 20.0. The influence of different environmental factors on granite weathering by *A. niger* was analyzed using the GCAM, as outlined in this section.

The quantities of SiO₂ released from the various influencing factor treatments were regarded as a reference sequence for the GCAM. Thus, $x_0(k)$ refers to the SiO₂ released from the various treatments, temperature is x_1 , pH is x_2 , generation cycle is x_3 , and vaccination quantity is x_4 ; these values comprised a sequence for comparisons, expressed as x_i ($i = 1, 2, 3, 4$), while $x_i(k)$ denotes treatment data from the influencing factors. Applying the correlation degree formula, the extent of grey correlation between the comparison and reference sequence was then obtained, and this order was arranged in accordance; the influence of comparative sequence (i.e., influencing factors) on the reference sequence was therefore determined by applying the specific calculation steps outlined below.

A. Reference and comparison sequences were determined.

B. The sequence difference of the sequences was calculated via *Equation 1*.

$$\Delta_i(k) = |x_o(k) - x_i(k)| \quad (\text{Eq.1})$$

C. Maximum and minimum differences between two poles were calculated via *Equations 2* and *3*.

$$M = \max_i \max_k \Delta_i(k) \quad (\text{Eq.2})$$

$$m = \min_i \min_k \Delta_i(k) \quad (\text{Eq.3})$$

D. The correlation coefficient between comparison and reference sequences was then determined based on different influencing factors using the transformation data, via *Equation 4*.

$$r_{oi}(k) = \frac{m + \xi M}{\Delta_i(k) + \xi M} \quad (\text{Eq.4})$$

In this expression, ξ denotes the identification coefficient, usually 0.5.
The grey correlation degree was calculated via the *Equation 5*.

$$r_{oi} = \frac{1}{n} \sum_{k=1}^n r_{oi}(k) \quad (\text{Eq.5})$$

In this expression, r_{oi} denotes the grey correlation degree between the comparison sequence, x_i , and the reference sequence, x_o . This calculation process was performed using the grey breeding computer decision system (Li et al., 2016; Gao and Xu, 2016).

Results and discussion

Screening for highly-effective Si-releasing fungi

The amounts of SiO₂ released by fermentation broth of the 18 fungi strains severally cultured for 10 days was determined. Results show that the amount of SiO₂ released by fermentation broth of XF-1 strain (28.44 mg·L⁻¹) was significantly higher than that of other fungi strains and control group (*Fig. 1*). This result indicates that both the growth and metabolism of this fungal strain effectively promotes the dissolution of granite and increases Si release. Strain XF-1 was therefore selected as the target for further study.

Isolation, purification, and identification of strain XF-1

The XF-1 strain possesses well-developed hyphae that are greatly branched and is dark brown with a spherical top capsule. The conidium of this strain is spherical in shape and possesses black or dark brown chrysanthemum-shaped heads produced vertically from specialized hyphae cells with thick and swollen walls (*Fig. 2*). The XF-1 strain was initially judged to be *A. niger* based on these morphological characteristics; further 18S rDNA amplification and sequencing were also performed and these results confirm 99% homology with *A. niger*.

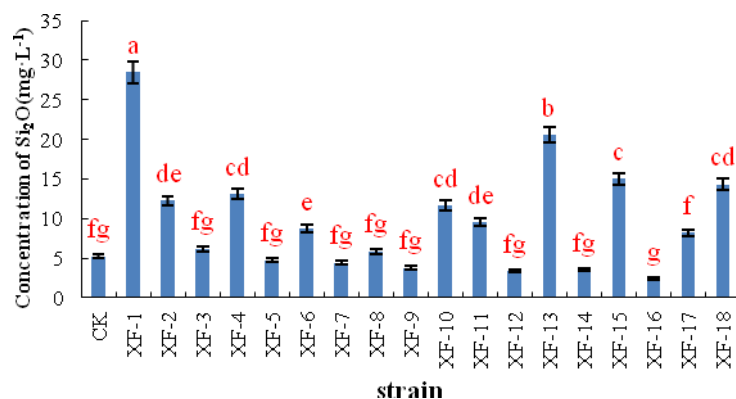


Figure 1. Dissolution action of different fungus strains to granite on day 10. (Standard error bars were marked. Significant differences at 0.05 level were analyzed using Tukey test by SPSS Version 20.0)

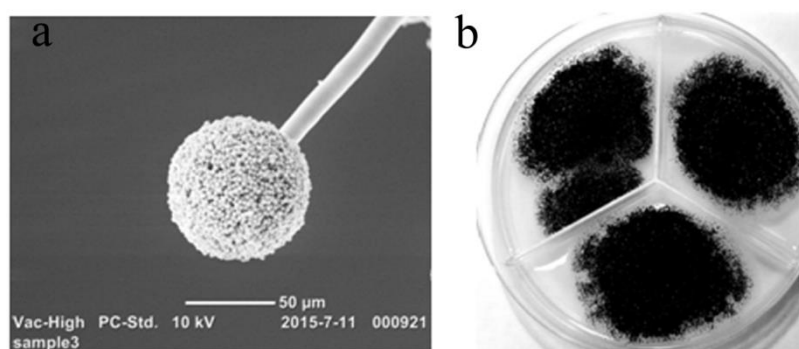


Figure 2. Electron microscopy (SEM) image and colonial morphology of XF-1 strain. **a.** Conidium and conidiophore for XF-1 strain. **b.** Colonial morphology of XF-1 strain on PDA

The influence of environmental factors on Si release from granite

The effects of the four environmental factors considered here (i.e., temperature, pH, generation cycle, and vaccination quantity) on granite weathering by the XF-1 strain are summarized in *Table 2*. Results show that, under experimental conditions with *A. niger*, the SiO₂ content in dissolution was 7.05 times higher on average than the control group (without *A. niger*); these experimental results show that the effect of granite weathering by the XF-1 strain was significantly enhanced compared to the control group (without *A. niger*).

The effects of different culture temperatures on granite weathering

The effects of different culture temperature on granite weathering was significant in this experiment ($p < 0.05$) (*Table 2*). Data show that across all five temperature treatments, the Si-releasing effect of granite weathered by *A. niger* at 28 °C was the highest, significantly better than other treatments ($p < 0.05$) (*Table 2*). Lower, or higher, temperatures that this optimal level were not conducive to granite weathering, a result that is generally consistent with the earlier work of Štyriaková's research on the effects of different temperatures on the weathering of basalt, granite, and gneiss by *Bacillus mucilaginosus* (Štyriaková et al., 2012).

Table 2. Effects of different environmental factors on the weathered granite by *A. niger*

Treatment		Mass concentration of Si (mg·L ⁻¹)	Mass concentration of Si for control (mg·L ⁻¹)	Increased times than control
Temperature (°C)	5	48.86±1.62c	9.06	5.39
	15	71.25±2.91b	9.62	7.41
	28	95.63±1.62a	11.22	8.52
	32	67.89±3.26b	11.84	5.73
	39	50.26±1.89c	12.82	3.92
pH value	3	123.63±4.43a	14.20	8.71
	5	110.86±2.24b	12.42	8.93
	7	95.63±2.54b	11.22	8.52
	9	64.69±1.54c	11.84	5.46
	11	40.32±1.63d	14.04	2.87
Generation cycle	First generation	76.58±3.01d	11.22	6.83
	Second generation	82.56±3.48bc	11.84	6.98
	Third generation	95.63±1.54c	14.02	6.82
	The fourth generation	110.74±3.38ab	13.04	8.49
	The fifth generation	116.59±2.86a	13.42	8.69
Vaccination quantity (spore number·mL ⁻¹)	10 ³	75.78±1.88b	10	7.58
	10 ⁵	88.06±3.03a	11.02	7.99
	10 ⁷	95.63±1.68a	11.22	8.52
	10 ⁹	68.03±1.96bc	10.04	6.78
	10 ¹¹	65.95±1.42c	9.64	6.84
Mean				7.05

Different letters in the same column indicate significant difference in the 5% level

It is noteworthy that the temperatures used in this experiment are related to annual changes in Suzhou, Jiangsu Province, China. The spring and autumn in this region are short, while the summer and winter are long; 5 °C is the lowest average monthly temperature, while 15 °C is the annual mean, 28 °C is the average temperature of the hottest month, 32 °C is the maximum temperature of the hottest month, and 39 °C is the extreme temperature of the region. It is also the case that annual changes of temperature across this region obviously alternate; it has been shown that changes in temperature alternation can easily cause significant damage to a granite body (Ming and Fan, 2017), promoting rock weathering. Thus, the two characteristics of this region, alternate changes in temperature and an average of 28 °C in the hottest month, are both very beneficial to granite weathering.

The effects of pH on granite weathering

We show that different pH values exerted a significant influence on granite weathering effects (Table 2). Results show that at pH value of 3, 5, 7, 9, and 11, the SiO₂ contents of granite dissolved by the XF-1 strain for 30 days resulting in 123.63 mg·L⁻¹, 110.86 mg·L⁻¹, 95.63 mg·L⁻¹, 64.69 mg·L⁻¹, and 40.32 mg·L⁻¹, respectively, fold increases of 8.71, 8.93, 8.52, 5.46, and 2.87 compared to the control (without XF-1 strain). This means that the more acidic the fermentation liquid, the better the Si-release

effect. Indeed, when the pH value was 3, the granite weathering effect was best, significantly different ($p < 0.05$) to weakly acidic, neutral, and alkaline conditions.

In terms of bacterial growth, when the pH value of the fermentation liquid transitioned from acid to alkaline, the number of mycelium pellets formed by *A. niger* was reduced within the cultivation system. In contrast, when the pH value was 9 or 11, most rock powder was not packed, and the SiO₂ content in solution was low; this further illustrates the fact that pH value is advantageous to granite weathering in acidic regions.

Generation cycle effects on granite weathering

We also show that the granite weathering action of different generation cycles was significantly different (Table 2). Data reveal that when the granite was dissolved by the XF-1 strain for 30 days, the SiO₂ content in media from the first, two, three, four, and five generations was 76.58 mg·L⁻¹, 82.56 mg·L⁻¹, 95.63 mg·L⁻¹, 110.74 mg·L⁻¹, and 116.59 mg·L⁻¹, respectively, fold increases of 6.83, 6.98, 6.82, 8.49, and 8.69 times compared to the control (without XF-1 strain). As generation cycle increased, SiO₂ content in granite culture media also gradually increased; indeed, the Si-releasing effect of granite weathered by the XF-1 strain was best in the fifth generation, and there were no significant differences between this generation and the fourth one in terms of weathering effects. Differences between the fifth and other generations were significant ($p < 0.05$); this means that the influence of generation cycle on the weathering effect of granite is likely to increase the activity of *A. niger* in concert with generation cycle.

The effect of vaccination quantity on granite weathering

We show that when granite was dissolved by the XF-1 strain for 30 days in our experiments, the contents of SiO₂ recovered when the vaccination quantity was 10³ mL⁻¹, 10⁵ mL⁻¹, 10⁷ mL⁻¹, 10⁹ mL⁻¹, and 10¹¹ mL⁻¹ were 75.78 mg·L⁻¹, 88.06 mg·L⁻¹, 95.63 mg·L⁻¹, 68.03 mg·L⁻¹, and 69.95 mg·L⁻¹ respectively. These values represent fold increases of 7.58, 7.99, 8.52, 6.78, and 6.84 times those of the control (without XF-1 strain). Data show that the Si-releasing ability of the 10⁷ mL⁻¹ vaccination quantity was the strongest, there was no significant difference between 10⁷ mL⁻¹ and the 10⁵ mL⁻¹ dilutions, but there was a distinct change between the 10⁷ mL⁻¹ and other vaccination quantities ($p < 0.05$). The relationship between vaccination quantity and dissolved SiO₂ content had a clear relationship; when the vaccination quantity increased from 10³ mL⁻¹ to 10⁵ mL⁻¹, the content of dissolved SiO₂ gradually increased, but when the quantity increased to 10⁷ mL⁻¹, dissolved SiO₂ reached its maximum level. Data show that when the vaccination quantity continued to increase, the content of dissolved SiO₂ decreased, a result which indicates that volume of release is closely related to the ability of *A. niger* to weather this rock. The use of an appropriate vaccination quantity might therefore improve the weathering ability of *A. niger*; in a limited space, however, it is clear that the vaccination quantity of microorganisms controls weathering ability. The reasons for this phenomenon might include the fact that the growth of microorganisms is related to nutrient composition, and all the experiments performed here were carried out closed systems where both the pace and nutrition were limited. These systems cannot, therefore, enable sufficient microbial individuals to reproduce, which might have affected their ability to weather granite. This phenomenon is similar, however, to environments in which there is competition between rock surface organisms in natural conditions.

The relationship between environmental factors and A. niger granite weathering

As the environmental factors discussed here all exert a significant on the granite weathering of *A. niger*, it is necessary to determine which are more important. We therefore evaluated the relationship between environmental factors and the weathering action of this bacterium. Data show that, in general, the influence of various factors on granite weathering is non-linear and thus hard to unravel using traditional statistical approaches. Our use of grey relational analysis can overcome this defect (Li et al., 2016; Gao and Xu, 2016); we applied this approach to analyze the relationships between temperature, pH value, vaccination quantity, and generation cycle versus the weathering effects of *A. niger* (Table 3). Our results show that the most important factor influencing the weathering of *A. niger* was pH (x_2), followed by vaccination quantity (x_4), temperature (x_1), and the influence of generation cycle (x_3).

Table 3. Analysis of grey relational degree between different environmental factors and *A. niger* weathered granite

Environmental factor	Temperature (x_1)	pH value (x_2)	Generation cycle (x_3)	Vaccination quantity (x_4)
Grey relational degree	0.56	0.82	0.50	0.63

It is clear that acidolysis is one important way to promote the microbial weathering of minerals (Wu et al., 2018; Welch and Ullman, 1993; Toyama and Terakado, 2015), and comprises both inorganic and organic acids (Lian, 2008). Data show that given the same pH conditions, organic acids are more likely to accelerate the dissolution of minerals than their inorganic counterparts because the former can combine proton exchange with ligand complexes in weathering to form a complex enhancing rock dissolution (Štyriaková et al., 2012). An *A. niger*-granite aggregate was formed on the rock surface in this study to comprise a micro-environment (Fig. 3b); this efficiently enriched organic acids (Zhu et al., 2014; Gadd et al., 2014; Wang et al., 2015), and strengthened the synergetic weathering of organic acids with polysaccharides, hyphae, and adsorbed SiO₂ released to produce a concentration gradient in the fermented liquid, especially oxalic and citric acids. *A. niger* is capable of producing six organic acids: oxalic acid, citric acid, malic acid, tartaric acid, acetic acid and succinic acid, so that the pH of its fermentation liquid is reduced to the lowest value on the 10 d, and the weathering effect of granite is the optimum at this moment (Wu et al., 2018).

This process could therefore be utilized to complete slope ecological restoration, involving the initial adjustment of matrix soil pH values and the use of *A. niger* as a fungal source. The amount of *A. niger* can then be appropriately increased to improve the microbial weathering of granite, and can achieve soil formation, vegetation restoration, and improvements to the ecological environment in the short term.

SEM observations of granite surface changes

A SEM micrograph of granite weathered by *A. niger* on day 30 reveals that this bacterium produced a significant weathering effect (Fig. 3). This image also shows, however, that no obvious dissolution trace was observed on the rock surface without *A. niger* because this active bacterium was absent (Fig. 3a), and there were obvious corrosion traces and a number of mycelia on the granite surface by day 30 (Fig. 3b) (in

this case, the granite surface weathered by *A. niger* at a temperature of 28 °C on day 30 was used as an example). Hyphae interspersed and penetrated the rock surface via cracks and other weak positions, intruded into the interior, produced mechanical damage, loosened the rock structure, increased the contact area, and formed a hyphae-mineral aggregate, making the granite surface rough. This result was previously noted by Lian (2014), Peng et al. (2015), and Toyama and Terakado (2015).

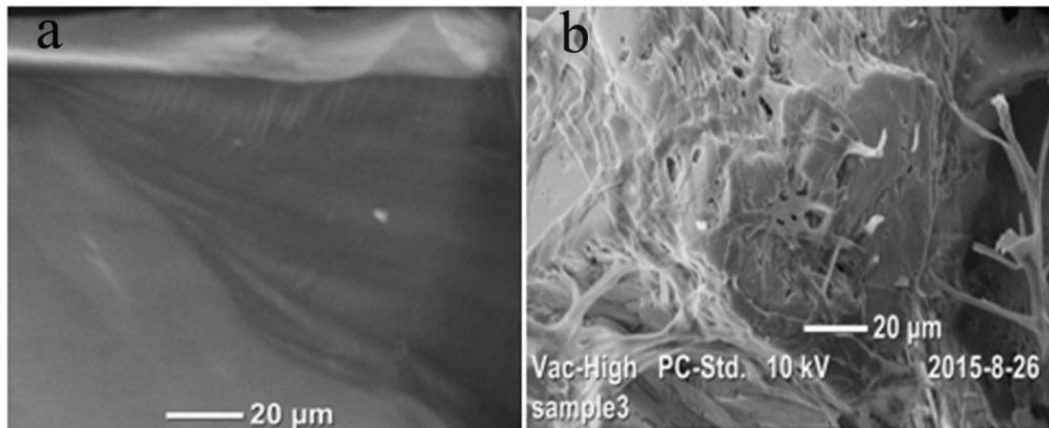


Figure 3. Scanning electron micrograph (SEM) of granite. **a.** The surface of the granite without *A. niger*. **b.** The surface of the granite affected by *A. niger*

Studies have also shown that *A. niger* is widely distributed in soil and comprises an important component of the microbial population. This bacterium is capable of weathering black and micas, common feldspar, phosphate ore, olivine and copper ore tailings (Li, 2015a; Lian, 2008; Sun et al., 2014; Li et al., 2015b, c; Diao et al., 2015; Fomina, 2014), and can corrode P_2O_5 , K_2O and other elements to promote the growth of crops (Dong and Lian, 2014). We show that *A. niger* can also efficiently weather granite in this analysis, and the dissolution quantity of SiO_2 in the fermentation broth on day 30 was 7.05 times more than the control group (without *A. niger*) (Table 2). This result further confirms the acceleration of *A. niger* on granite weathering and corrosion of Si element from the perspective of practice. Si element is not an essential but a beneficial element for plants. Si can make plants with green stems strong, promote root growth, increase plant fruit, improve crop quality, and also make plants resistant to diseases, droughts, insects and lodging. It can also improve soil structure and increase the content of alkali-hydrolysis nitrogen, available potassium and available silicon in soil. In particular, most soils in south China are seriously deficient in silicon in acid soil, and the available silicon content is very low (Chen et al., 2016). Our research results showed that once applied to the remediation of abandoned rock mining areas, XF-1 strain can promote the dissolution of effective silicon in soil, increase the content of available nitrogen, phosphorus and potassium in soil, improve soil nutrient insufficiency, and promote the growth of plants.

A number of issues and obstacles nevertheless remain if *A. niger* is to be used for environmental restoration research. In natural conditions, the pH value that is conducive for the activity of this microbe is very difficult to adjust, while suitable growth temperatures and humidities are also hard to maintain, and the various factors do not worked independently. Therefore, further research is needed to explore these questions.

Conclusions

A XF-1 strain that can weather granite highly effectively was isolated in our experiments from a granite surface. This bacterium was identified as *A. niger* via morphological comparisons and on the basis of 18S rDNA gene sequences. This strain provides a good fungal source that can be used to solve the issue of rapid soil formation on bare rock within abandoned mining areas and also presents a new approach that can be used for the ecological restoration of degraded habitats.

The bacterium *A. niger* exerts an obvious acceleration effect on granite weathering. Our SEM observations reveal the presence of a large number of mycelia and obvious corrosion pits on rock surfaces. In the presence of *A. niger*, the dissolved SiO₂ content was 7.05 times higher on average than just the control (without *A. niger*).

We introduce the use of a GCAM in this experiment to quantitatively assess the degree of influence of each environmental factor on granite weathering by *A. niger* for the first time. Results show that pH is the dominant factor affecting granite weathering by *A. niger*, followed by vaccination quantity and temperature, while the influence of generation cycle was the least important. Data show that when the pH value was 3, the vaccination quantity was 10⁷·mL⁻¹, the fifth generation cycle was used, and the temperature was 28 °C, the best effects were obtained. In cases where temperature and other environmental conditions are suitable for microbial growth, soil formation velocity on exposed rock will be accelerated via microorganisms entering cracks throughout mineral weathering.

Acknowledgements. This research was supported by the positioning research project of Forest Ecosystem of Changjiang River Delta in Jiangsu Province, the Engineering Project ‘Three New’ for Forestry in Jiangsu Province (lysx [2013] 10), a project funded by the Priority Academic Program Development of Jiangsu Higher Education Institutions, the open project of the Key Laboratory of Soil and Water Conservation and Ecological Restoration in Jiangsu Province, and a Fund Project of the Anyang Institute of Technology (YJJ2015011).

REFERENCES

- [1] Barker, W., Banfield, J. (1996): Biologically versus inorganically mediated weathering reactions: relationships between minerals and extracellular microbial polymers in lithobiotic communities. – *Chemical Geology* 132(1-4): 55-69.
- [2] Bennett, P. C., Rogers, J. R., Choi, W. J. et al. (2001): Silicates, silicate weathering, and microbial ecology. – *Geomicrobiology Journal* 18(1): 3-19.
- [3] Borland, H., Amobrosini, V., Indgreen, A. et al. (2016): Building theory at the intersection of ecological sustainability and strategic management. – *Journal of Business Ethics* 135(2): 293-307.
- [4] Castro, I. M., Fietto, J. L. R., Vieira, R. X. et al. (2000): Bioleaching of zinc and nickel from silicates using *Aspergillus niger* cultures. – *Hydrometallurgy* 57(1): 39-49.
- [5] Chen G, Luo, Z. X., Shi, F. Z. et al. (2016): Effect of a new type silicon fertilizer application on yield of two lines hybrid rice. – *Soil and Fertilizer Sciences in China* 55(2): 109-113 (in Chinese).
- [6] Cheng, Y. X., Duan, Y. G., Li, G. H. et al. (2015): Accumulation of freeze-thaw weathering of rock debris flow provenance test study. – *Disaster Science* 30(2): 46-50 (in Chinese).
- [7] Chiang, Y. W., Santos, R. M., Van Audenaerde, A. et al. (2014): Chemoorganotrophic bioleaching of olivine for nickel recovery. – *Minerals* 4(2): 553-564.

- [8] Gadd, G. M., Bahriesfahani, J., Li, Q. W. et al. (2014): Oxalate production by fungi: significance in geomycology, biodeterioration and bioremediation. – *Fungal Biology Reviews* 28(2-3): 36-55.
- [9] Gao, J. J., Xu, G. (2016): Gray correlation analysis of meteorological disasters and crop yield in chongqing. – *Journal of Southwest University (Natural Science Edition)* 38(2): 32-36 (in Chinese).
- [10] Diao, N. N., Li, G. Y., Wang, Y. D. et al. (2015): Bioleaching of copper from high alkaline copper ore tailings with *Aspergillus niger*. – *The Chinese Journal of Process Engineering* 15(1): 132-135 (in Chinese).
- [11] Dong, C. L., Lian, B. (2014): Comparing the bio-weathering effects for biotite by *Bacillus mucilaginosus* and *Aspergillus niger*. – *Bulletin of Mineralogy, Petrology and Geochemistry* 33(6): 772-777 (in Chinese).
- [12] Fomina, M. O. (2014): Variability of coordination complexes of copper accumulated within fungal colony in the presence of copper-containing minerals. – *Biotechnologia Acta* 7(2): 63-69.
- [13] Hu, J., Lian, B., Yu, J. P. et al. (2011): Capability and mechanism of potassium releasing from potassium-bearing minerals by *Aspergillus niger*. – *Bulletin of Mineralogy petrology and Geochemistry* 30(3): 277-285.
- [14] Li, A. G., Song, X. X., Wu, C. X. (2016): The grey correlation analysis between agronomic trait and yield in *Triticum aestivum*. – *Crop Research* 30(1): 18-21 (in Chinese).
- [15] Li, G., Diao, N., Wang, Y. et al. (2015a). Bioleaching of copper from tailings by fermentation broths of *Aspergillus niger* in pellet form. – *Journal of Chemical Industry and Engineering* 66(2): 717-722 (in Chinese).
- [16] Li, H., Cai, L., Yao, Q. Z., Zhou, G. T. (2015b). Fungal involvement in biogeological processes and application to environmental bioremediation. – *Geological Journal of China Universities* 21(3): 382-394 (in Chinese).
- [17] Li, J. F., Zhang, W. J., Lu, J. W. et al. (2015c). Effects of citrate dissolving surface and altering microstructure of biotite. – *Acta Pedologica Sinica* 52(2): 329-335 (in Chinese).
- [18] Li, Y., Li, F. C., Yang, G. et al. (2017): Comparing elements dissolution from biotite bio-weathering by *bacteria* and *fungi*. – *Chinese Journal of Soil Science* 48(1): 86-93 (in Chinese).
- [19] Lian, B. (2014): Research progress of mineral-microbe interactions: a comment for geomicrobiology column. – *Bulletin of Mineralogy, Petrology and Geochemistry* 33(6): 759-763 (in Chinese).
- [20] Lian, B., Chen, Y., Zhu, L. (2008): Progress in the study of the weathering of carbonate rock by microbes. – *Earth Science Frontiers* 15(6): 90-99 (in Chinese).
- [21] Lü, J., Tian, X. H., Yan, H. et al. (2015): Effect of *Aspergillus niger* fermentation liquid on the growth of wheat seedlings in calcareous soil. – *Journal of Northwest A&F University (Natural Sciences Edition)* 43(5): 100-106 (in Chinese).
- [22] Ming, X. F., Fan, C. W. (2017): Effect of freezing-thawing Cycle on the physical and Mechanical properties of granite. – *Science Technology and Engineering* 17(13): 261-265.
- [23] Peng, Y., Song, M., Pedruzzi, I. et al. (2015): K-release and weathering of muscovite by *Cenococcum geophilum*. – *Acta Microbiologica Sinica* 55(3): 282-291.
- [24] Pratas, J., Prasad, M., Freitas, H. et al. (2005): Plants growing in abandoned mines of Portugal are useful for biogeochemical exploration of arsenic, antimony, tungsten and mine reclamation. – *Journal of Geochem Explor* 85(3): 99-107.
- [25] Qi, X., Wang, K., Zhang, C. (2013): Effectiveness of ecological restoration projects in a karst region of southwest China assessed using vegetation succession mapping. – *Ecological Engineering* 54: 245-253.

- [26] Ramos, M. E., Garcia-Palma, S., Rozalen, M. et al. (2014): Kinetics of montmorillonite dissolution: an experimental study of the effect of oxalate. – *Chemical Geology* 363(1): 283-292.
- [27] Song, M., Peng, Y. X., Pedruzzi, I. et al. (2015): Bioweathering and K release of K-bearing minerals by *Penicillium oxalicum*. – *Microbiology China* 42(7): 1410-1417 (in Chinese).
- [28] Song, R. Q., Lian, B. (2014): Effect of *Aspergillus niger* on the impurity removal of quartz sands. – *Bulletin of Mineralogy Petrology and Geochemistry* 33(6): 784-789.
- [29] Štyriaková, I., Štyriak, I., Oberhansli, H. (2012): Rock weathering by indigenous heterotrophic bacteria of *Bacillus* spp. at different temperature: a laboratory experiment. – *Mineralogy and Petrology* 105(3-4): 135-144.
- [30] Sun, D. S., Yin, J. M., Chen, Y. et al. (2014): Effect of crystal structures of potassium-bearing minerals on *Aspergillus niger* growth metabolism and potassium and silicon release. – *Scientia Agricultura Sinica* 47(3): 503-513 (in Chinese).
- [31] Tang, J. T., Pei, X. J., Pei, Z. et al. (2016): Study on rock injured in freeze-thaw cycles. – *Science, Technology and Engineering* 16(27): 101-105 (in Chinese).
- [32] Tang, X. P., Chen, Y., Cao, F. et al. (2014): Breeding of potassium-dissolved Fungi by protoplast mutagenesis and bioleaching potassium-rich shale. – *Journal of Central South University (Science and Technology)* 45(10): 3330-3338 (in Chinese).
- [33] Toyama, K., Terakado, Y. (2015): Differential dissolution technique for the geochemical separation of the calcite and dolomite of dolomitic limestones. – *Geochemical Journal* 49(5): 567-570.
- [34] Wang, R. R., Wang, Q., He, L. Y. et al. (2015): Isolation and the interaction between a mineral-weathering *Rhizobium tropici* Q34 and silicate minerals. – *World Journal of Microbiology and Biotechnology* 31(5): 747-753.
- [35] Wang, S. J. (2017): Effect of humidity change on rock weathering. – *Value Engineering* 36(2): 109-110 (in Chinese).
- [36] Welch, S. A., Ullman, W. J. (1993): The effect of organic acids on plagioclase dissolution rates and stoichiometry. – *Geochimica et Cosmochimica Acta* 57(12): 2725-2736.
- [37] Williams, C. H., Steinbergs, A. (1959): Soil sulphur fractions as chemical indices of available sulphur in some Australian soils. – *Journal of Vacuum Science and Technology* 17(6): 3265-3271.
- [38] Wu, Q. F., Fu, L., Lu, Z. F. (2016): Purification and molecular identification experiments of microbe in soil. – *Journal of Anyang Institute of Technology* 15(4): 27-29 (in Chinese).
- [39] Wu, Y. W., Zhang, J. C., Guo X. P. et al. (2017a): Identification of efficient strain applied to mining rehabilitation and its rock corrosion mechanism: based on boosted regression tree analysis. – *Environmental Science* 38(1): 283-293 (in Chinese).
- [40] Wu, Y. W., Zhang, J. C., Wang, L. J. et al. (2017b): A rock-weathering bacterium isolated from rock surface and its role in ecological restoration on exposed carbonate rocks. – *Ecological Engineering* 101(1): 162-169.
- [41] Wu, Q. F., Hu, H. B., Zhang, X. (2018): Effect of *Aspergillus niger* and its metabolites on weathering of granite. – *Journal of Nanjing Forestry University (Natural Sciences Edition)* 42(1): 81-88 (in Chinese).
- [42] Zhu, Y. G., Duan, G. L., Cheng, B. D. et al. (2014): Mineral weathering and element cycling in soil -microorganism-plant system. – *Science China: Earth Sciences* 1(6): 1107-1116 (in Chinese).

THERMO-HYDRAULIC COUPLED SIMULATION OF IMMISCIBLE CO₂ FLOODING

ZHAO, C. L.^{1,2} – GUO, P.^{1,*} – LONG, F.¹

¹*State Key Laboratory of Oil and Gas Reservoir Geology and Exploitation, Southwest Petroleum University, Chengdu, China*

²*School of Science, Southwest Petroleum University, Chengdu, China*

**Corresponding author*

e-mail: guopingswpi@vip.sina.com

(Received 15th Sep 2018; accepted 12th Nov 2018)

Abstract. As an efficient way to reduce CO₂ in the atmosphere and to extract more hydrocarbons from reservoir, CO₂ flooding is important to reduce environmental and ecological damage by traditional energy. Study on performance of CO₂ in the reservoir and its impact on formation fluids is necessary to oil recovery and to further carbon capture and storage (CCS). In practical, CO₂ is injected into reservoir at low temperature, and both field tests and predictions show that temperature of CO₂ would be lower than that of reservoir while it reaches the target formation, especially for high injection rate. Therefore, further estimation should be conducted to predict how reservoir temperature and properties of fluids are changed during cold CO₂ flooding. In this paper, a mathematical model for non-isothermal immiscible CO₂ flooding is firstly established, then full thermo-hydraulic coupling of the model is simulated on COMSOL by introducing several temperature-dependent and pressure-dependent physical properties of CO₂, oil and rock. The basic reservoir parameters of the model are obtained from one block of Daqing Oilfield, China. Furtherly, effect of CO₂ injection temperature, of CO₂ injection rate and of injector shut-in on reservoir performance is studied. Results show that injection of colder CO₂ causes rapid reduction in reservoir temperature near the injector at the earlier stage. Effect of temperature change is timely shown on physical properties of fluids for full thermo-hydraulic coupling. Oil production rate, oil recovery and production gas-oil ratio all increase as injection temperature increases. Based on a practical situation, this study gives an insight into reservoir performance during cold CO₂ flooding with a numerical method, and it can provide some support for study on temperature change in the reservoir.

Keywords: *immiscible CO₂ EOR, heavy oil, thermo-hydraulic, heat transfer, numerical simulation*

Introduction

Nowadays, settlement of contradiction between environmental protection and growing energy demand is the key to sustainable and high-level development in the future (Ghafoori, et al., 2017; Li, et al., 2017). Although great breakthroughs in green and new energy resources have been continuously achieved, traditional energy like petroleum still dominates the structure. During CO₂ flooding, CO₂ can be stored in the formation for long time after enhancing hydrocarbon recovery, so greenhouse gas emission can be reduced (Zhao, et al., 2014).

In general, temperature contrast between injected CO₂ and oil reservoir is neglected (Smith and Woods, 2011), so it is assumed that oil reservoir is in isothermal situation during injection of CO₂ (Han, et al., 2010). In fact, CO₂ is generally transported and injected at low temperature. For oil reservoir 1500~2000 m below the surface, although CO₂ is in supercritical state at the well bottom after adsorbing heat from formation, it can still be 30~50 K lower than the formation (Li, et al., 2017; Lu and Connell, 2008). A colder region is formed near the injection well (Smith and Woods, 2011). For this temperature contrast, heat transfer happens between CO₂ and formation rock as well as other fluids.

Although a large number of numerical simulations have been focused on temperature change during CO₂ injection, they are mainly about CO₂ geological storage (Li and Laloui, 2016; Shabani and Vilcáez, 2018; Zhang, et al., 2015). Meanwhile, some important physical properties of fluids are assumed as constant in most mathematical models for non-isothermal CO₂ flooding (Binshan, et al., 2012; Elyasi, et al., 2016).

In this paper, physical properties of CO₂, oil viscosity, oil density and CO₂ solubility in oil are considered dependent on temperature and pressure. In this way, thermo-hydraulic coupling during CO₂ flooding is effectively achieved. Then change of phase saturation and reservoir temperature is studied by solving the foregoing model in the COMSOL. Finally, we discuss the effect of CO₂ injection temperature and rate on reservoir performance, and how reservoir behaves after injector being shut down.

Materials and methods

Although miscible CO₂ EOR has high displacement efficiency, CO₂ EOR in some reservoirs can not reach the miscible state for formation conditions, fluid properties and technical factors, such as heavy oil reservoirs (Dyer and Ali, 1989; Kang, et al., 2013; Tran, et al., 2017; Zhou and Yang, 2017). Even so, immiscible CO₂ EOR in heavy oil can also obtain desired displacement efficiency by reducing oil viscosity, swelling oil, decreasing oil-gas interfacial tension, vaporizing and extracting light compositions in the oil (Seyyedsar, et al., 2016).

Based on the study Niu (2010), an immiscible CO₂ EOR mass equation for heavy oil, considering solubility of CO₂ in the oil and not considering chemical reaction, has been adopted. Combined with an energy equation, this new CO₂ EOR mathematical model can realize the coupling of temperature field and porous flow. Temperature (T), pressure (p) and saturation (S_o and S_g) are the primary variables.

Assumptions

This model is established on these assumptions: (1) Oil is heavy oil and is treated as one pseudo composition. (2) CO₂ only dissolves in the oil and vaporization of oil into the gas phase is neglected. (3) No mass transfer between the water phase with oil phase or gas phase. (4) The gas phase only contains CO₂ composition, and the water phase only contains water composition. (5) Capillary effect and diffusion effect are not considered. (6) Molar density of every composition in each phase is a constant. When the fluid is injected into the reservoir at a constant volumetric flow rate, volume of composition i changes for mass transfer between oil and gas phases. This is a common phenomenon in the oil reservoir development by gas injection. For different gas and different displacing pressure, its effect varies. Under relatively low pressure, volumetric flow rate \bar{u}_j of the fluid changes a lot for the dissolution of CO₂ in oil, while, under high pressure, volume of the CO₂ has slight difference before and after dissolving in oil. So the volumetric flow rate \bar{u}_j of the fluid is assumed as a constant during CO₂ flooding in this study.

Mass equation

Firstly, molar density of component i in phase α is given in *Equation 1*:

$$\xi_{i\alpha} = \rho_{i\alpha} / W_i \quad (\text{Eq.1})$$

Then molar density of phase α is shown in *Equation 2*:

$$\xi_{\alpha} = \sum_{i=1}^{N_c} \xi_{i\alpha} \quad (\text{Eq.2})$$

So molar fraction of component i in phase α is calculated by *Equations 3 and 4*:

$$x_{i\alpha} = \frac{\xi_{i\alpha}}{\xi_{\alpha}}, \quad i = 1, 2, \dots, N_c \quad (\text{Eq.3})$$

$$\sum_{i=1}^{N_c} x_{i\alpha} = 1, \quad \sum_{i=1}^{N_c} x_{i\beta} = 1 \quad (\text{Eq.4})$$

where $\xi_{i\alpha}$ is molar density of component i in phase α , mol/m³; ξ_{α} is molar density of phase α , mol/m³; $\rho_{i\alpha}$ is mass density of component i in phase α , kg/m³; W_i is molar mass of component i , kg/mol; $x_{i\alpha}$ is molar fraction of component i in phase α , fraction. The subscript α represents gas phase (g), oil phase (o), and water phase (w); subscripts i represents compositions CO₂ (1), oil (2) and water (3), respectively.

Immiscible CO₂ flooding flow equation which considers CO₂ dissolution in oil can be given as *Equation 5*:

$$\begin{aligned} \frac{\partial}{\partial t} [\phi(S_g \xi_g + S_o \xi_o x_{1o})] + \nabla \cdot (\xi_g \bar{u}_g + \xi_o \bar{u}_o x_{1o}) &= q_1 \\ \frac{\partial}{\partial t} (\phi S_o \xi_o x_{2o}) + \nabla \cdot (\xi_o \bar{u}_o x_{2o}) &= q_2 \\ \frac{\partial}{\partial t} (\phi S_w \xi_w) + \nabla \cdot (\xi_w \bar{u}_w) &= q_3 \end{aligned} \quad (\text{Eq.5})$$

where ϕ is reservoir porosity, fraction; S_{α} phase saturation, %; \bar{u}_{α} is flow velocity of phase α , m/s; ∇ is divergence operator; q_{α} is source or sink of phase α ; x_{1o} and x_{2o} is molar fraction of CO₂ and oil in oil phase respectively, %, $x_{1o} + x_{2o} = 100\%$.

Fraction flow equation is introduced to simplify the model. Firstly, mobility is defined as *Equation 6*:

$$\begin{aligned} \lambda_{\alpha} &= K_{r\alpha} / \mu_{\alpha} \\ \lambda &= \sum_{\alpha=w,o,g} \lambda_{\alpha} \end{aligned} \quad (\text{Eq.6})$$

where λ_{α} is mobility of phase α , m·s/kg; λ is total mobility, m·s/kg; $K_{r\alpha}$ is relative permeability of phase α , fraction; μ_{α} is viscosity of phase α , mPa·s.

Then, fraction of phase α is given in *Equations 7 and 8*:

$$f_{\alpha} = \frac{\lambda_{\alpha}}{\lambda} \quad (\text{Eq.7})$$

$$\sum_{\alpha=w,o,g} f_{\alpha} = 1 \quad (\text{Eq.8})$$

Total flow rate \vec{u} can be expressed as *Equation 9*:

$$\vec{u} = \sum_{\alpha=w,o,g} \vec{u}_{\alpha} \quad (\text{Eq.9})$$

Then (*Eq. 10*),

$$\nabla \cdot \vec{u} = \sum_{\alpha=w,o,g} \nabla \cdot \vec{u}_{\alpha} \quad (\text{Eq.10})$$

Capillary pressure is not considered, so pressure of all the phases is the same, expresses as p . Flow rate of each phase is shown in *Equation 11*:

$$\begin{aligned} \vec{u}_w &= -\frac{\vec{K}K_{rw}}{\mu_w}(\nabla p - \rho_w g \nabla Z) \\ \vec{u}_o &= -\frac{\vec{K}K_{ro}}{\mu_o}(\nabla p - \rho_o g \nabla Z) \\ \vec{u}_g &= -\frac{\vec{K}K_{rg}}{\mu_g}(\nabla p - \rho_g g \nabla Z) \end{aligned} \quad (\text{Eq.11})$$

where \vec{K} is intrinsic permeability tensor, mD; p is pressure, MPa; Z is vertical depth, m; g is gravitational acceleration, m/s²; ρ_{α} is density of phase α , kg/m³.

Relationship of flow rate of each phase and the total one is determined by *Equations 12–14*:

$$\vec{u}_w = f_w \vec{u} \quad (\text{Eq.12})$$

$$\vec{u}_o = f_o \vec{u} \quad (\text{Eq.13})$$

$$\vec{u}_g = f_g \vec{u} \quad (\text{Eq.14})$$

Volumetric fraction of composition i in phase α can be given as *Equation 15*:

$$C_{i\alpha} = \frac{x_{i\alpha} / \xi_{i\alpha}}{\sum_{i=1}^{Nc} x_{i\alpha} / \xi_{i\alpha}} \quad (\text{Eq.15})$$

$c_{i\alpha}$ is volumetric fraction of composition i in phase α , fraction; N_c is number of compositions in the system.

Molar density of phase α is defined as *Equation 16*:

$$\xi_{\alpha} = \left(\sum_{i=1}^{N_c} x_{i\alpha} / \xi_{i\alpha} \right)^{-1} \quad (\text{Eq.16})$$

Combining *Equations 15* and *16*, molar density meets the condition given in *Equation 17*:

$$\xi_{i\alpha} c_{i\alpha} = \xi_{\alpha} x_{i\alpha} \quad (\text{Eq.17})$$

Molar density of each composition in the system is assumed to be constant, so it can be written as *Equation 18*:

$$\begin{aligned} \xi_{1o} &= \xi_{1g} = \xi_1 \\ \xi_{2o} &= \xi_2 \\ \xi_{3w} &= \xi_3 \end{aligned} \quad (\text{Eq.18})$$

Without source or sink, substitution of *Equation 18* into *Equation 5*, mass conservation equations are shown in *Equation 19*:

$$\begin{aligned} \frac{\partial}{\partial t} [\phi(S_g + c_{1o}S_o)] + \nabla \cdot [\vec{u}(f_g + c_{1o}f_o)] &= 0 \\ \frac{\partial}{\partial t} [\phi(1 - c_{1o})S_o] + \nabla \cdot [\vec{u}(1 - c_{1o})f_o] &= 0 \\ \frac{\partial}{\partial t} (\phi S_w) + \nabla \cdot (\vec{u}f_w) &= 0 \end{aligned} \quad (\text{Eq.19})$$

Combining the equations in *Equation 19*, pressure equation can be obtained by *Equation 20*:

$$\nabla \cdot \left[\left(\frac{\vec{K}K_{ro}}{\mu_o} + \frac{\vec{K}K_{rg}}{\mu_g} + \frac{\vec{K}K_{rw}}{\mu_w} \right) \cdot \nabla p \right] = 0 \quad (\text{Eq.20})$$

$K_{r\alpha}$ is determined by *Equation 21*:

$$K_{r\alpha} = S_{\alpha}^2 \quad (\text{Eq.21})$$

Energy equation

Energy equation of three phase flow during immiscible CO₂ EOR is shown in *Equation 22*:

$$\begin{aligned} & \frac{\partial}{\partial t} \{ [\phi(S_o \rho_o C_{po} + S_g \rho_g C_{pg} + S_w \rho_w C_{pw}) + (1-\phi)\rho_s C_{ps}] T \} + \\ & (\bar{u}_o \rho_o C_{po} + \bar{u}_g \rho_g C_{pg} + \bar{u}_w \rho_w C_{pw}) \cdot \nabla T = \\ & \nabla \cdot \{ [\phi(S_o k_o + S_g k_g + S_w k_w) + (1-\phi)k_s] \nabla T \} + (\phi Q_f + (1-\phi)Q_s) \end{aligned} \quad (\text{Eq.22})$$

in which, T is the temperature, K; $C_{p\alpha}$ is the constant pressure heat capacity of phase α , J/(kg·K); k_α is the thermal conductivity of phase α , W/(m·K); k_e is the effective thermal conductivity of reservoir, W/(m·K); k_s is the thermal conductivity of rock in the reservoir, W/(m·K); Q_T is the source or sink of heat in the system, W; Q_f and Q_s are the source or sink of heat in fluid and rock respectively, W.

Auxiliary equations

Saturation constraint equation is given in Equation 23:

$$S_o + S_w + S_g = 1 \quad (\text{Eq.23})$$

Physical properties

In this paper, CO₂ property parameters (density, viscosity, heat capacity and thermal conductivity) are based on the America National Institute of Standards and Technology NIST online database.

Compared with heat capacity and thermal conductivity of CO₂, those of oil change a little with temperature and pressure under reservoir condition, and are set to 0.15 W/(m·K) and 2100.00 J/(kg·K) in this study, respectively. CO₂ solubility in heavy oil is calculated by the correlation developed by Chung et al. (1988), as shown in Equation 24:

$$R_s = \frac{0.178094}{A_1 \gamma^{A_2} (1.8T - 459.67)^{A_7} + A_3 (1.8T - 459.67)^{A_4} e^{[-145.0377 A_5 p + A_6 / (145.0377 p)]}} \quad (\text{Eq.24})$$

where R_s is solubility of CO₂ in oil, m³/m³; $A_1, A_2, A_3, A_4, A_5, A_6, A_7$ are empirical parameters, 0.004934, 4.092, 5.71×10^{-7} , 1.6428, 6.763×10^{-4} , 781.334 and -0.2499, respectively; γ is relative density of oil, and is set to 0.808 in the paper. Viscosity of CO₂-oil system is given by the equation proposed by Lederer (1933) for CO₂ flooding of heavy oil, as given in Equation 25:

$$\ln \mu_m = x_{1o} \ln(\mu_g) + x_{2o} \ln(\mu_o) \quad (\text{Eq.25})$$

where μ_m is viscosity of CO₂-oil system, mPa·s. Welker and Dunlop (1963) presented correlation between oil swelling factor and solubility of CO₂ in oil, as shown in Equation 26:

$$F_s = 1 + 6.233 \times 10^{-5} R_s \quad (\text{Eq.26})$$

where F_s , is swelling factor of oil. Density of heavy CO₂-oil system is calculated by the equation presented by Quail et al. (1988), as given in *Equation 27*:

$$\rho = [B_1 - B_2 T + B_3 p_s] \frac{e^{(-B_4 x_{10})}}{1 + B_5 x_{CH_4}} \quad (\text{Eq.27})$$

where p_s is saturation pressure of oil, MPa; B_1 , B_2 , B_3 , B_4 and B_5 are empirical parameters, 1.1571, 6.534×10^4 , 7.989×10^4 , 3.58×10^3 , 0.05086; x_{CH_4} is molar fraction of CH₄ in oil, %.

In this paper, compressibility of rock is not considered, so its density is a constant. Density of rock is 2640 kg/m³. Isobaric heat capacity of rock is slightly affected by temperature (Eppelbaum, et al., 2014), so it is a constant in this paper 850.00 J/(kg·K). Correlation of thermal conductivity of sandstone with temperature adopts the one established by Kutas (1977), as given in *Equation 28*:

$$k_s = k_{20} - (k_{20} - 1.38072) \left[\exp\left(0.725 \frac{T - 293.15}{T - 143.15}\right) - 1 \right] \quad (\text{Eq.28})$$

where k_{20} is thermal conductivity of rock at 293.15 K, W/(m·K), 3.00 W/(m·K) in this paper; k_s is thermal conductivity of rock at given temperature T, W/(m·K).

Geological model

During CO₂ flow in oil reservoir from the injector to the producer, CO₂ displaces oil ahead (*Fig. 1*), and temperature decreases in the reservoir especially around the injector. An inverted five-spot well pattern is made to perform the CO₂ flooding, as shown in *Figure 2*. Size of the injection-production unit is 144 m × 144 m × 8.3 m (well injector-producer spacing: 100 m). To simulate temperature change in the reservoir more correctly, the model considers heat transfer between reservoir and baserock or caprock. Other input reservoir and CO₂ injection data used in the simulation can be found in *Table 1*, of which the basic parameters of the reservoir are obtained from one block of Daqing Oilfield, China.

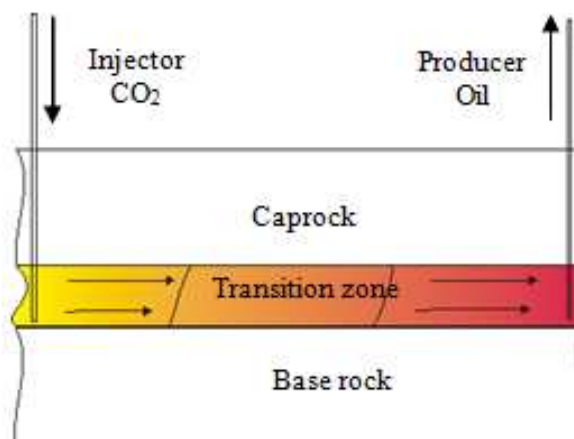


Figure 1. Scheme of CO₂ injection profile in the reservoir

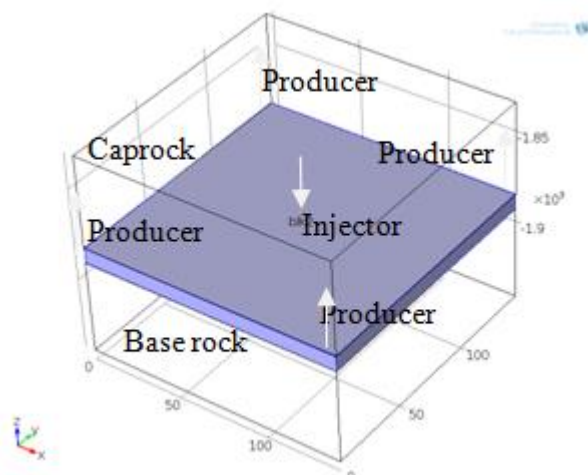


Figure 2. Scheme of inverted five-spot well pattern in the COMSOL

Table 1. Input parameters of non-isothermal CO₂ EOR simulation in inverted five-spot well pattern

Initial formation pressure, MPa	20.50	Oil density in reservoir, kg/m ³	808.80
Average pressure gradient, MPa/100 m	1.12	Oil viscosity in reservoir, mPa·s	2.86
Reservoir temperature, K	358.15	S_{oi} , %	56.60
Average geothermal gradient, K/100 m	4.72	S_{wi} , %	43.40
Middle depth, m	1880.00	Residual oil saturation after CO ₂ flooding S_{or} , %	23.30
Fracture	No	Water saturation after CO ₂ flooding S_{wr} , %	40.00
Porosity, %	12.30	Gas saturation after CO ₂ flooding S_{gr} , %	36.70
K , mD	1.28	Injector-producer spacing, m	100.00
Average sand thickness, m	8.30	CO ₂ injection rate, t/d	5

Results and discussion

Base case

This mathematical model is solved on PDE module of COMSOL, and initial and boundary conditions can be customized on this software. Firstly, base case is simulated with input data shown in *Table 1* for 10 years, to study distribution of oil and gas saturation as well as temperature in the reservoir under continuous injection of CO₂.

Variations of phase saturation (S_g and S_o) distribution in the reservoir

Areal distribution of CO₂ saturation S_g and oil saturation S_o after 0.5 a and 10 a of CO₂ injection are shown in *Figures 3* and *4*, respectively. From these figures, oil is flooded out with continuous injection of CO₂, increasing CO₂ saturation and decreasing oil saturation. The flooding front of CO₂ is not a uniform face, but a flooding transition district which keeps expanding towards the injector.

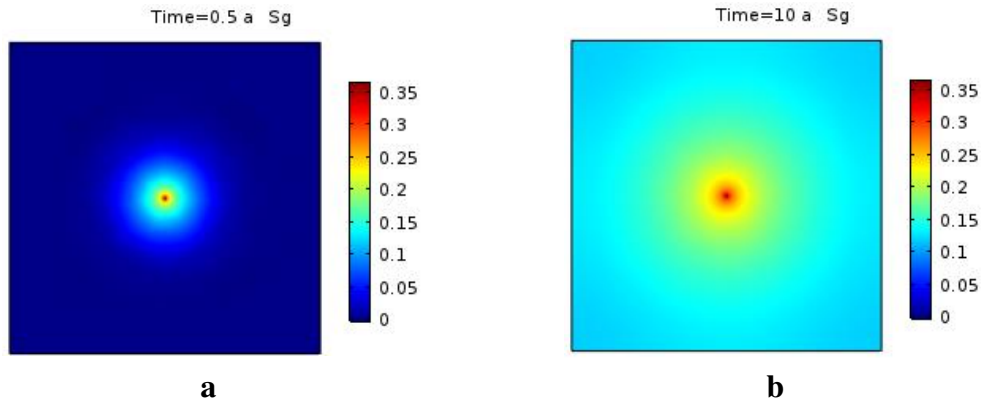


Figure 3. Areal distribution of S_g at (a) 0.5 a, (b) 10 a

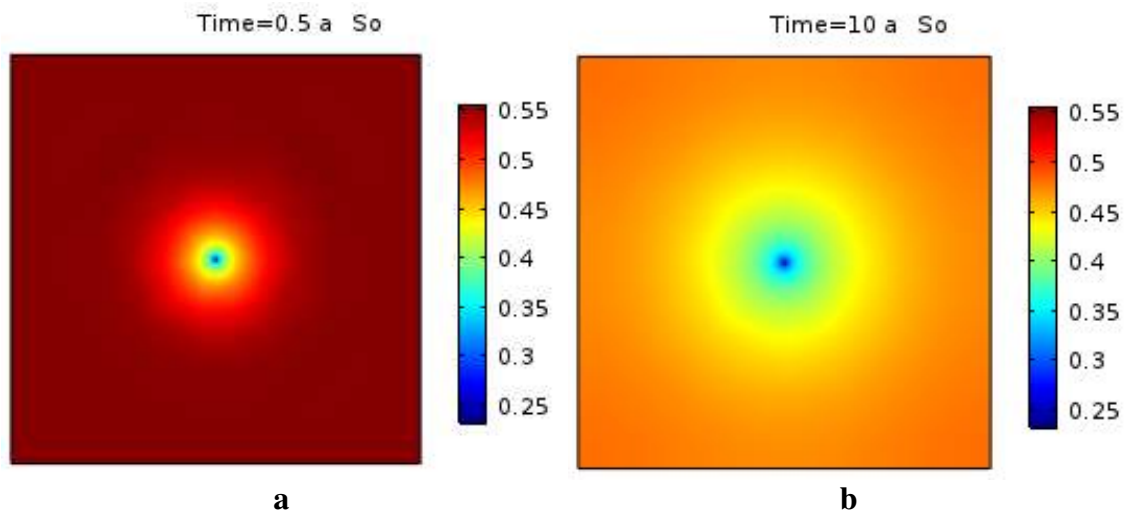


Figure 4. Areal distribution of S_o at (a) 0.5 a, (b) 10 a

To quantify CO₂ and oil saturation during CO₂ injection, S_g and S_o along the injector-producer line after 0.5 a, 2.5 a, 5 a, 7.5 a, and 10 a injection of CO₂ are obtained in Figure 5.

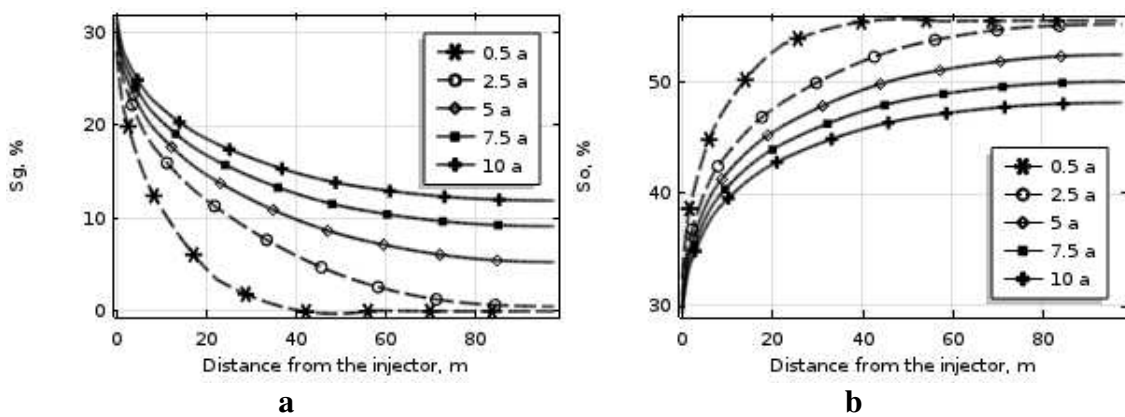


Figure 5. S_g and S_o distributions along the injector-producer line at various times

At the earlier stage (0-2.5 a), large amount of oil is displaced out by CO₂ to the producers, so S_o is decreased quickly near the injector and S_g is increased instead. CO₂ does not break through, and no CO₂ is produced at the producer. For its high saturation, oil still dominates fluids flow in the reservoir. After CO₂ injection for 2.5 a, CO₂ starts to break through in the producer, and it forms a continuous phase in the reservoir. S_o is decreased in the whole reservoir. Although CO₂ can be dissolved in the oil with certain amount, most CO₂ flows in the reservoir as free gas. Compared with oil viscosity, viscosity of CO₂ is very low, so unfavorable mobility ratio is formed in CO₂ flooding. This reduces flow capacity of oil and displacement efficiency. As time goes on, reduction in oil saturation at the same point on the injector-producer line gradually decreases for the same time gap.

Figure 6 shows distribution of flow velocity of CO₂ u_g and oil u_o at the earlier stage (0.5 a) and end (10 a) of CO₂ injection. Direction and quantity of phase velocity are represented by direction and size of the arrows, respectively. The arrow is larger, the velocity is higher. For both phases, velocity on the injector-producer line is the largest velocity among the points on circle around the injector. It gradually decreases away from line on the same circle. At the earlier stage, CO₂ just flows around the injector, while oil is the continuous phase, covering the whole oil reservoir. The point is closer to the injector, u_g is larger. u_o has a reverse changing rule. As CO₂ flooding continuing, more CO₂ is injected into the reservoir, and oil near the injector is flooded towards the producer. S_o in this area reduces, so does its flowing ability. For the expansion of CO₂ in the reservoir, CO₂ on the injector-producer line breaks through in the producer at certain time. Then it forms a continuous phase. Since then, flow resistance of oil increasingly growing, and its relative permeability decreases. This is not favorable for the displacement of oil.

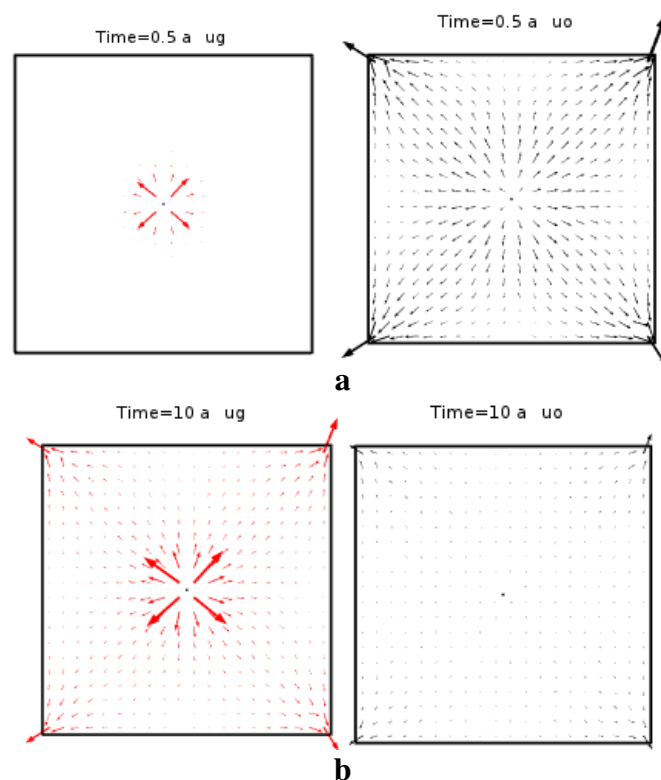


Figure 6. u_g and u_o distribution at (a) 0.5 a and (b) 10 a

Variations of reservoir temperature (T) distribution in the reservoir

Areal distribution of T during injection of CO₂ at 303.15 K for different times is shown in *Figure 7*. T along the injector-producer line is also drawn, as shown in *Figure 8*. From *Figures 7* and *8*, injection of colder CO₂ at the earlier stage causes rapid reduction in T near the injector. As injection continues, change in T slows down, and temperature gradually reaches a stable state after certain time.

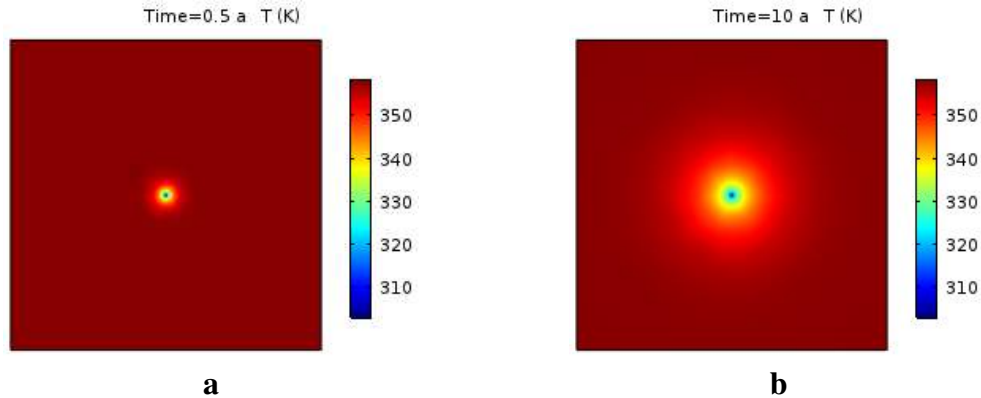


Figure 7. Areal distribution of T at (a) 0.5 a, (b) 10 a

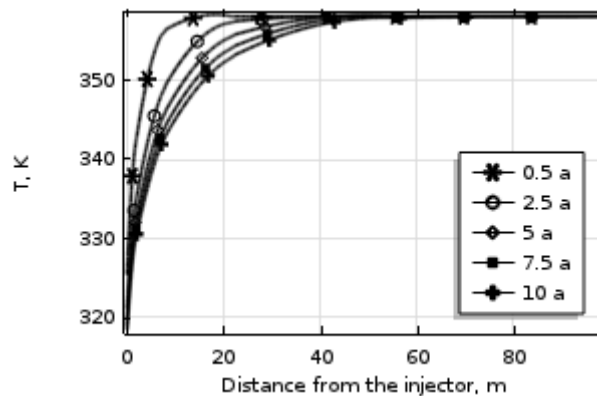


Figure 8. Variation of T along the injector-producer line

From temperature profile along the injector-producer line, as shown in *Figure 9*, we can clearly see that temperature contour line is not vertical, but arc-shaped. As shown in *Figure 10*, after CO₂ is injected into the reservoir at temperature T_{inj} lower than the formation one (T_0), there is a temperature contrast (thermal gradient) between CO₂ and formation. Temperature of CO₂ gradually is increased for heat adsorption from the formation as flowing deep into the reservoir. Formation temperature near the injector is decreased for continuously injected cold CO₂ at the same time. Then, heat in the caprock and base rock is transferred into the oil reservoir timely to offset the temperature drop in formation to some extent. Therefore, temperature changes more quickly in the middle of oil reservoir than that upper or lower zone.

Although fresh CO₂ is continuously injected into the reservoir, it has limited effect on temperature of the whole field. Even so, physical properties and flow conditions

change a lot in the near-wellbore area, so temperature change still has some effect on the CO₂ displacement efficiency.

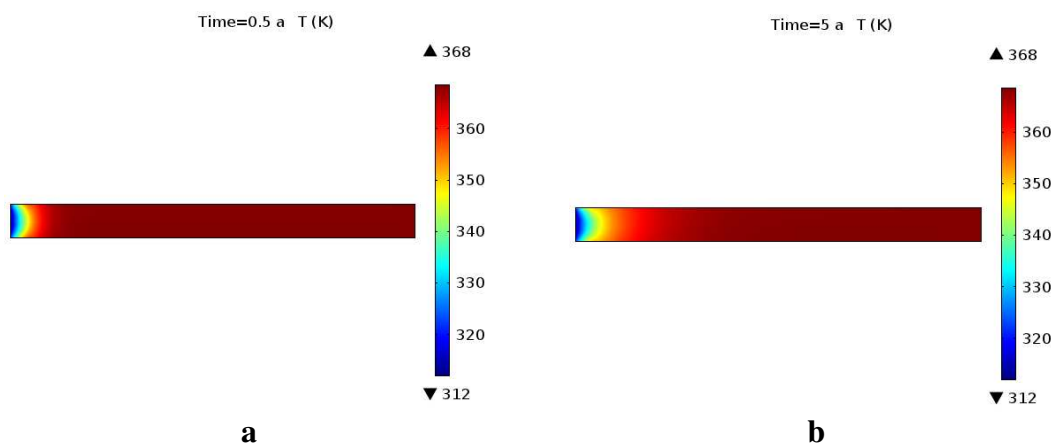


Figure 9. Reservoir temperature (T) profile along the injector-producer line at (a) 0.5 a and (b) 5 a

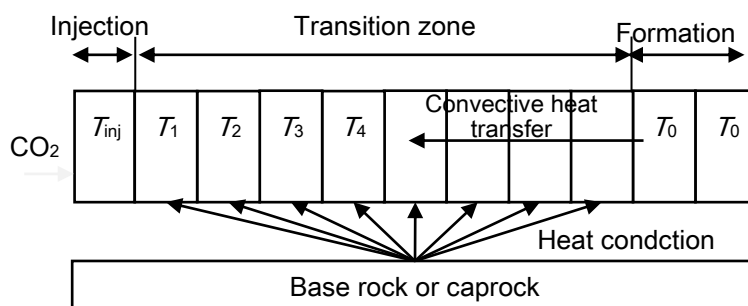


Figure 10. Scheme of heat transfer in the reservoir during low temperature CO₂ injection

Production performance

Oil production rate and production gas-oil ratio (GOR) of different CO₂ injection time are shown in *Figure 11*. It is shown that at the first stage of immiscible CO₂ flooding, there is a slight increase in oil production, and no CO₂ is produced. Then oil production is reduced rapidly and GOR is increased at the same time. At the end of CO₂ injection, oil production is only one third of its maximum and GOR is 50 m³/m³. At beginning, large flowing resistance should be overcome by CO₂ to displace out oil in the pore, and distribution of oil, water and CO₂ in the reservoir are changed quickly. As injection continues, flow condition in the near-wellbore areas is improved to some extent, so does oil production. At 2.5 a, CO₂ starts to breakthrough in the producer and it forms a continuous phase in the formation. Therefore, previous continuous oil is cut into oil droplets or oil threads in some areas, unfavorable for oil flow in the reservoir. CO₂ cannot get miscible with oil in immiscible flooding, and huge viscosity contrast can form unfavorable mobility ratio. As more CO₂ is injected, its flowing resistance is reduced furtherly and more CO₂ is produced from the producer.

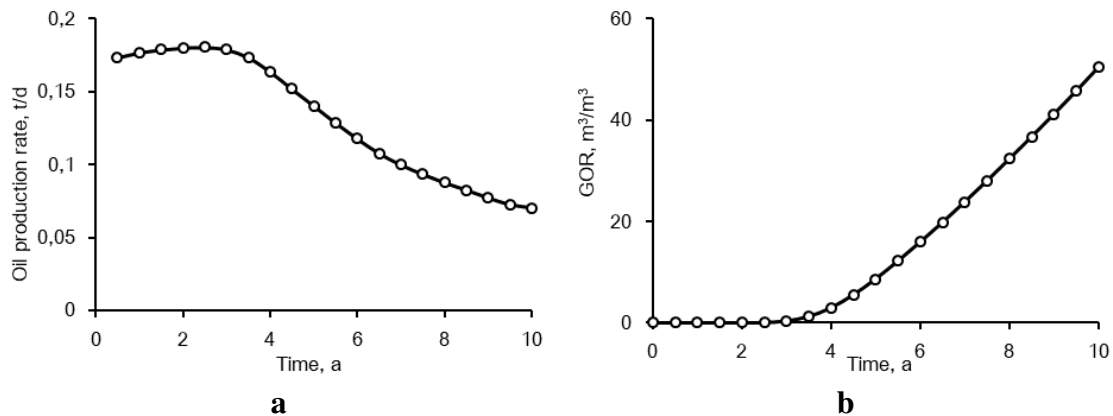


Figure 11. (a) Oil production rate and (b) GOR of five-spot pattern for continuous CO₂ injection

As shown in *Figure 12*, oil recovery increases quickly before CO₂ breakthrough, and grows more slowly thereafter. In this simulation, permeability of the reservoir is extremely low and no fracture is introduced to the model. So producing degree of oil is relatively low. Oil recovery by CO₂ flooding is only about 5% at the end of production.

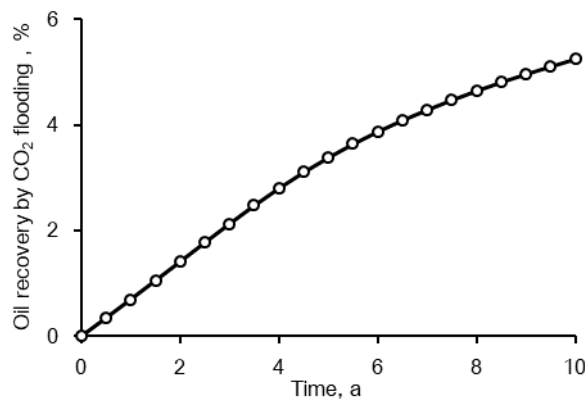


Figure 12. Oil recovery by CO₂ flooding vs time for continuous CO₂ injection

Sensitivity analysis

Effect of CO₂ injection temperature on reservoir behavior

Oil production, GOR and oil recovery during CO₂ injection for CO₂ injection temperature of 303.15 K, 323.15 K and 343.15 K are shown in *Figures 13* and *14*, respectively. As shown in these figures, higher the CO₂ injection temperature, more oil is produced. Under low temperature, oil viscosity, oil density and CO₂ viscosity are increased to some degree in the colder area near the injector, which is not favorable for displacement efficiency of oil by CO₂. CO₂ injection temperature is higher, and the density and viscosity of oil in the near-wellbore area is lower. Under higher temperature, oil can flow more easily, and flowing condition of oil and gas in this area is improved. Oil production, oil recovery and GOR are higher. Therefore, increase in CO₂ injection temperature can reduce the unfavorable effect of injected CO₂ on fluid

flowing capacity in the area around the injector, so more oil displacement efficiency can be achieved.

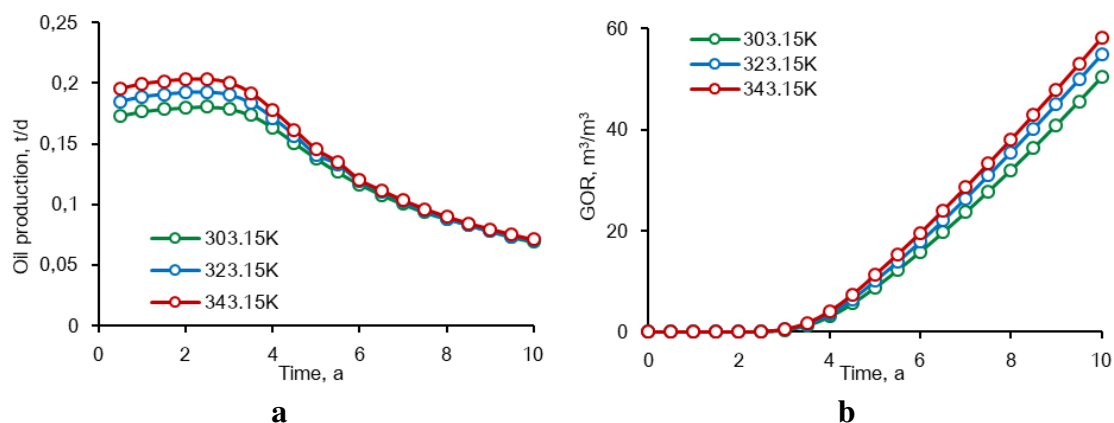


Figure 13. (a) Oil production and (b) GOR with different CO₂ injection temperature

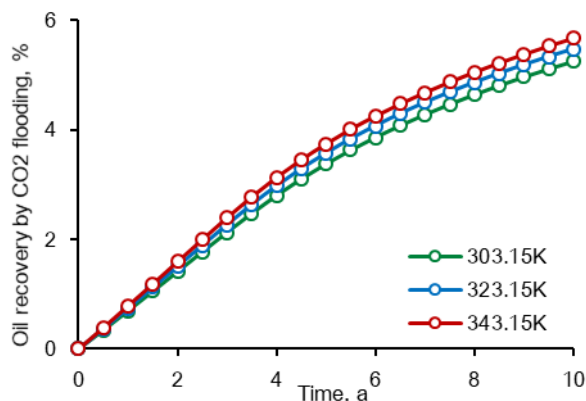


Figure 14. Oil recovery by CO₂ flooding vs time with different CO₂ injection temperature

Effect of CO₂ injection rate on reservoir behavior

Oil production, GOR and oil recovery under different CO₂ injection rate (5.00 t/d, 10.00 t/d and 15.00 t/d) are compared in Figure 15. In Figure 19, oil production is higher for larger CO₂ injection rate, while there is no big difference in oil production after CO₂ breakthrough. As shown in Figure 15, much more CO₂ is produced after breakthrough under higher injection rate, so GOR is much higher. Increase in CO₂ injection rate can improve driving force and displacement efficiency of CO₂, and oil recovery is apparently increased (Fig. 16).

Comparison

Specific data of reservoir temperature and reservoir performance are extremely dependent on reservoir parameters and injection data, so it is unpractical to compare the particular data with those from other study. While the changing rules are consistent with some similar studies, as in the research by Smith and Woods (2011), a thermal front is formed in the reservoir during injection of cold CO₂ and viscosity and density of CO₂ is

increased as its temperature is increased. Moreover, in the 2016 research by Elyasi et al. (2016) shows that temperature change around the injection well can induce thermal strain, which can influence porosity and permeability. More studies show that multi-physical coupling during CO₂ injection exists, and in-depth studies should be focused on this field to obtain high efficiency on CO₂ flooding and CCS. Our ongoing study is also conducted in this direction.

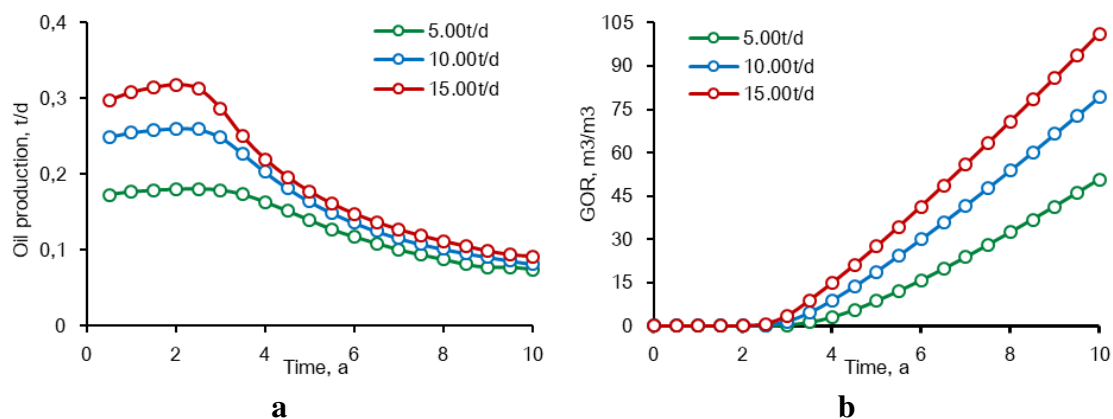


Figure 15. (a) Oil production and (b) GOR with different CO₂ injection rate

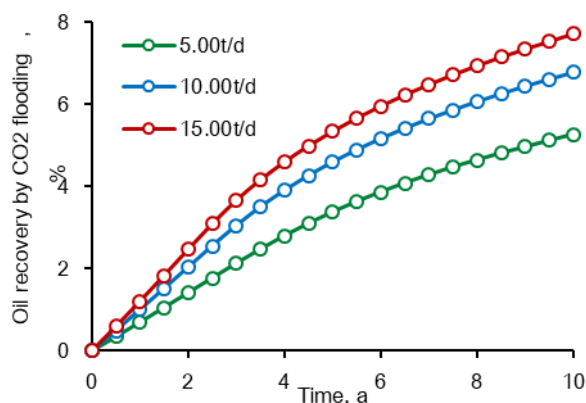


Figure 16. Oil recovery by CO₂ flooding vs time with different CO₂ injection rate

Conclusions

An effective method is developed in this paper to study and predict reservoir temperature and reservoir performance during cold CO₂ flooding. A non-isothermal immiscible CO₂ EOR mathematical model for heavy oil is established by introducing temperature-dependent and pressure-dependent parameters of fluids, then this model is solved and simulated by the Finite Element Method based software COMSOL. The results show that properties of fluids in the reservoir, especially near the injector, and reservoir performance can be influenced by the injection of CO₂ under lower temperature than that of reservoir. Based on this research, more numerical simulations on oil development and production, especially multi-physics coupling, can be realized by combining built-in and user-defined models in COMSOL. Moreover, COMSOL can

be effectively combined with other software, so more complex pore-scale or reservoir-scale multi-physical simulations can be further realized.

Acknowledgements. This work was financially supported by the Open Fund (PLN201830) of State Key Laboratory of Oil and Gas Reservoir Geology and Exploitation (Southwest Petroleum University).

REFERENCES

- [1] Binshan, J., Yu-Shu, W., Jishun, Q., Tailiang, F., Zhiping, L. (2012): Modeling CO₂ miscible flooding for enhanced oil recovery. – *Petroleum Science* 9: 192-198.
- [2] Chung, F. T. H., Jones, R. A., Nguyen, H. T. (1988): Measurements and correlations of the physical properties of CO₂/heavy-crude-oil mixtures. – *SPE Reservoir Engineering* 3: 822-828.
- [3] Dyer, S. B., Ali, S. M. F. (1989): The potential of the immiscible carbon dioxide flooding process for the recovery of heavy oil. – *Technical Meeting/Petroleum Conference of The South Saskatchewan Section*. Regina, Saskatchewan, Canada.
- [4] Elyasi, A., Goshtasbi, K., Hashemolhosseini, H. (2016): A coupled thermo-hydro-mechanical simulation of reservoir CO₂ enhanced oil recovery. – *Energy & Environment* 5: 524-541.
- [5] Eppelbaum, L., Kutasov, I., Pilchin, A. (2014): *Applied Geothermics*. – Springer, Berlin Heidelberg, New Delhi.
- [6] Ghafoori, M., Tabatabaei-Nejad, S. A., Khodapanah, E. (2017): Modeling rock-fluid interactions due to CO₂ injection into sandstone and carbonate aquifer considering salt precipitation and chemical reactions. – *Journal of Natural Gas Science and Engineering* 37: 523-538.
- [7] Han, W. S., Stillman, G. A., Lu, M., Lu, C. (2010): Evaluation of potential nonisothermal processes and heat transport during CO₂ sequestration. – *Journal of Geophysical Research: Solid Earth* 115: 1-23.
- [8] Kang, S., Gao, C., Zhang, S. (2013): Scientific research and field application of CO₂ immiscible flooding in heavy oil recovery. – *SPE Enhanced Oil Recovery Conference*. Kuala Lumpur, Malaysia.
- [9] Kutas, R. I. (1977): Investigation of heat flow in the territory of the Ukraine. – *Tectonophysics* 41: 139-145.
- [10] Lederer, E. L. (1933): Mischungs- und Verdünnungviskosität. – *World Pet. Cong.* 2: 526-528.
- [11] Li, C., Laloui, L. (2016): Coupled multiphase thermo-hydro-mechanical analysis of supercritical CO₂ injection: benchmark for the in Salah surface uplift problem. – *International Journal of Greenhouse Gas Control* 51: 394-408.
- [12] Li, X., Li, G., Wang, H., Tian, S., Song, X., Lu, P., Wang, M. (2017): A unified model for wellbore flow and heat transfer in pure CO₂ injection for geological sequestration, EOR and fracturing operations. – *International Journal of Greenhouse Gas Control* 57: 102-115.
- [13] Lu, M., Connell, L. (2008): Non-isothermal flow of carbon dioxide in injection wells during geological storage. – *International Journal of Greenhouse Gas Control* 2: 248-258.
- [14] Niu, B. (2010): CO₂ flooding in chalk reservoirs-experiments with X-ray computed tomography and reactive transport modelling. – *PhD Thesis*, Technical University of Denmark, pp.27-30.
- [15] Quail, B., Hill, G. A., Jha, K. N. (1988): Correlations of viscosity, gas solubility, and density for Saskatchewan heavy oils. – *Industrial & Engineering Chemistry Research* 27: 519-523.

- [16] Seyyedsar, S. M., Farzaneh, S. A., Sohrabi, M. (2016): Experimental investigation of tertiary CO₂ injection for enhanced heavy oil recovery. – *Journal of Natural Gas Science and Engineering* 34: 1205-1214.
- [17] Shabani, B., Vilcáez, J. (2018): A fast and robust TOUGH2 module to simulate geological CO₂ storage in saline aquifers. – *Computers & Geosciences* 111: 58-66.
- [18] Smith, W. J. R., Woods, A. W. (2011): Some implications of cold CO₂ injection into deep saline aquifers. – *Geophysical Research Letters* 38: 1-6.
- [19] Tran, T. Q. M. D., Neogi, P., Bai, B. (2017): Stability of CO₂ displacement of an immiscible heavy oil in a reservoir. – *SPE Journal* 02: 539-547.
- [20] Welker, J. R., Dunlop, D. D. (1963): Physical properties of carbonate oils. – *Journal of Petroleum Technology* 15: 873-875.
- [21] Zhang, R., Winterfeld, P. H., Yin, X., Xiong, Y., Wu, Y. (2015): Sequentially coupled THMC model for CO₂ geological sequestration into a 2D heterogeneous saline aquifer. – *Journal of Natural Gas Science and Engineering* 27: 579-615.
- [22] Zhao, D. F., Liao, X. W., Yin, D. D. (2014): Evaluation of CO₂ enhanced oil recovery and sequestration potential in low permeability reservoirs, Yanchang Oilfield, China. – *Journal of the Energy Institute* 87: 306-313.
- [23] Zhou, D., Yang, D. (2017): Scaling criteria for waterflooding and immiscible CO₂ flooding in heavy oil reservoirs. – *Journey of Energy Resources Technology* 139.

HYDROLOGICAL AND ECOLOGICAL EFFECT OF CAOHAJ WATERSHED REGULATION PROJECT BASED ON SWAT MODEL

ZHOU, C. W. – YU, L. F.* – ZHOU, Y. – YAN, L. B.

College of Life Sciences, Guizhou University, Guiyang, Guizhou, China
(e-mails: C. W. Zhou – changwei.1981@163.com; Y. Zhou – 812305593@qq.com; L. B. Yan –
link_yan@126.com)

**Corresponding author*
e-mail: gdyulifei@163.com

(Received 15th Sep 2018; accepted 12th Nov 2018)

Abstract. Based on the satellite image of Caohai river watershed in 2017, the land use types of Caohai river watershed were determined by field investigation, which were divided into six categories: farmland, forest land, grassland, water area, construction land and unused land. Based on SWAT model, the non-point source pollution of four regulation projects in Caohai watershed was simulated, and the runoff, sediment, nitrogen and phosphorus of non-point source pollution were analyzed in detail. The results showed that the non-point source pollution in Caohai watershed was light under the four regulation projects. The non-point source pollution is the least under the mode of conversion from farmland to forest land, grassland, water area, construction land and unused land.

Keywords: *Caohai watershed, regulation project, non-point source pollution, SWAT model*

Introduction

The serious water pollution, soil erosion and water resource waste in China make the freshwater resources unable to be fully utilized and aggravate the contradiction between the development of human society and natural resources. Water pollution is divided into point source pollution and non-point source pollution, in which point source pollution has a fixed discharge port (Zang and Gao, 2016), while non-point source pollution is difficult to be treated because of its wide range, complex composition and high uncertainty (Sakaguchia et al., 2014). Relying only on the prevention and control of point source pollution cannot fundamentally solve the water environment problems at the river watershed scale (Wu et al., 2012). The effectiveness of the treatment of point source pollution is often offset by the increase of agricultural non-point source pollution discharge, so that water pollution cannot be well controlled (Luo et al., 2014). In some river watersheds, non-point source pollution has exceeded point source pollution and become the main cause of water environment quality decline (Li et al., 2013; Luo et al., 2014). Therefore, more and more countries are concerned about the role of non-point source pollution in the process of water quality deterioration (Li et al., 2013).

The STANFORD model was introduced. This is the first hydrological model for watershed planning. It has relatively low data requirements and can easily calculate the pollution load (Luo et al., 2014) at the exit of the watershed. Scholars are applying it to the watershed of their own country (Dechmi et al., 2012; Strauch and Volk, 2013), with the rapid development of computer technology and the rapid development of remote sensing technology and geographic information system, the function of non-point source model is increasingly powerful. The most representative and the most promising distributed model with the widest application is SWAT model. The model can discretize

the watershed in many ways, reflect the spatial heterogeneity and hydrophysical process of the watershed (Yuan et al., 2015; Guo et al., 2014), and can better simulate the impact of human activities on the hydrological cycle of the watershed (Zhao et al., 2016; Li et al., 2017).

Fan et al. (2015) described the sources and harms of agricultural non-point source pollution, and introduced the progress of domestic agricultural non-point source pollution prevention measures from the aspects of pollution prevention measures of livestock and poultry breeding, technologies needed for rural sewage treatment, technologies related to control of chemical fertilizers and pesticides, and treatment technologies of rural household waste. In this study, multiple hydrological response unit partitioning method, the minimum threshold means that if land use, soil use or slope is less than this value, then will not be taken into account (Ficklin et al., 2009). The SWAT sensitivity analysis module, which starts with the 2005 edition, is used to determine parameters that have a significant impact on the model for subsequent calibration (Rahman et al., 2015). The sensitivity analysis of the model was performed by LH-OAH analysis method, which is the combination of LH (Latin Hypercube) sampling method and OAT, so it has the advantages of both methods (Zhang et al., 2017).

In recent years, the development of Caohai in Weining County of Guizhou province has also been developing rapidly. At the same time, the area of Caohai wetland is gradually decreasing, people want to survive, birds want to live, the degradation of Weining Caohai wetland, soil erosion is serious, biodiversity is threatened, highlighting the contradiction between protection and development. The unreasonable use of the land type structure in Caohai has led to great problems in the planning of the Caohai regulation project, which has weakened the ecological effects and reduced the biodiversity of the Caohai Lake. The study of the four regulation project in Weining Caohai watershed can not only enrich the use of SWAT model, but also provide a basis for pollution control in national nature reserves, and also provide a strong guarantee for the next step of controlling Caohai watershed. It is of great significance for the rational use of land resources and ecological environment protection in Guizhou Caohai watershed.

Research method

Research area characterization

Caohai (north latitude 26°47'32"–26°52'52", east longitude 104°10'16"–104°20'40") is located in Weining County, western Guizhou Province, China. It is the largest plateau natural freshwater lake in Guizhou. It is also the world's top ten bird watching base. The topographical trend of the Caohai watershed is complex, with the west, south and east sides being higher, and gradually decreasing from the center of the watershed to the north, becoming the direction of the drainage of the Caohai Lake watershed. The grass sea lake watershed is surrounded by plateau melting hills, the terrain is gentle, and the ground is relatively small. From the Caohai Lake watershed, the landform is a plateau hilly watershed, and the ground is undulating (*Fig. 1*).

Caohai belongs to subtropical monsoon humid climate zone. It has no severe cold in winter, no severe heat in summer, large daily temperature difference and small annual temperature difference. The annual average temperature is about 10.6 °C, the annual average minimum temperature is 1.7 °C, the annual average maximum temperature is

17.6 °C, the annual average precipitation is 909 mm, and the average relative humidity is 79%. The average annual sunshine hours are 1800 h, the frost-free period is 180 days, The rainy season is distinct from the dry season. May-October is the rainy season, the rainfall in this period is accounted for 88% of the precipitation throughout the whole year, from December to March there is only 5% of the total annual amount (Zheng et al., 2013; Xia et al., 2016).

Caohai watershed covers an area of 380 km², the lake water area is about 45 km², the altitude is 2173 m, the water depth is about 2 m, the water storage capacity reaches 140 million m³. There are 43 species and 142 genera of aquatic plants in Caohai. Caohai attracts more than 100 species of birds and more than 70 species of rare birds. Among them, the black-necked crane is the most rare migratory bird, which flies here more and more often every year to overwinter therefore, it is becoming the wintering paradise of the black-necked crane (Luo et al., 2017).

The change of water volume in Caohai affects the depth of water and determines the survival space of waterbirds. In recent years, the expansion of county towns has affected the water quality of Caohai. Therefore, it is of great significance to understand the changes of water quality and quantity in the basin for the protection of Hou Dao, represented by black-necked crane.



Figure 1. Topographic map of Caohai watershed

Data preparation for SWAT model construction

According to the Classification Standards for Land Use Status (GB/T21010-2017) and the actual situation of Caohai watershed, the land use types in the research area of Caohai watershed are divided into six categories. As shown in *Table 1*.

Table 1. Distribution characteristics of land use types in the study region

Model coding	Land types	Type code	Area	Percentage of total area
0	Farmland	AGRL	5136.16	53%
1	Forest land	FRST	690.40	7%
2	Grassland	RNGE	820.80	8%
3	Unused land	SWRN	146.24	2%
4	Construction land	URLD	867.20	9%
5	Water area	WATR	2028.16	21%

Soil spatial distribution data from the Institute of Geography of the Chinese Academy of Sciences (1:100,000). The quality of soil data directly affects the effect of model simulation.

Because of the small scope of the Caohai Basin, there is no meteorological station in the study area, so it is difficult to obtain accurate meteorological data of the Caohai Basin. In this study, the climate change in the study area was simulated with the meteorological data from the SWAT meteorological database. Runoff, sediment and other results are generated by the model.

Result and analysis

Output analysis of the Caohai sub watershed

Typical sub watershed division

Under the regulation project of SWAT model, the outlet of Jiahaizi river watershed, Dongshan river watershed, Baima river watershed and Zhonghe river watershed are selected to simulate the output, and the map of the simulated operation of the four sub watersheds is superimposed to get *Figure 2*.

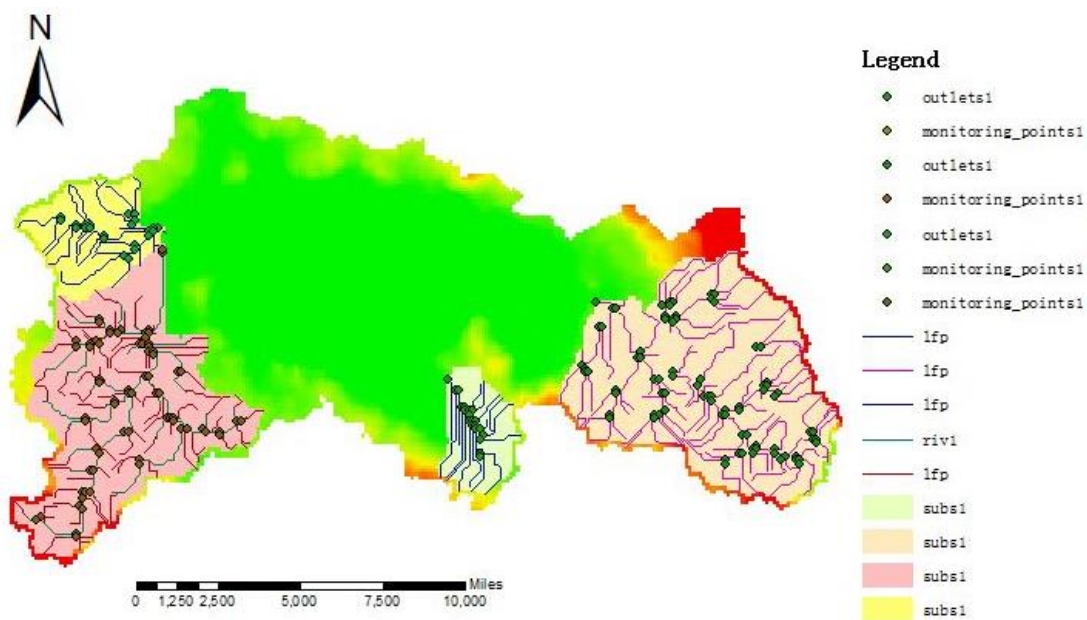


Figure 2. Distribution map of typical sub watershed in Caohai

Watershed runoff analysis

The data of rainfall, runoff, sediment and nutrients in the four river watersheds of the Jiahaizi river watershed, Dongshan river watershed, Baima river watershed and Zhonghe river watershed were analyzed to study the characteristics of pollutants in the whole river watershed, advising on the study of watersheds and the control and management of pollutants.

According to *Figures 3* and *4*, the total rainfall in Caohai watershed in 2017 was 1241, 90 mm, the average rainfall was 103.49 mm, and the most rainfall was in May;

the sum of the four watersheds was 1421.52 mm, the average was 118.46 mm; the sum of the sediments in the four watersheds was 82.80 t/ha, with an average of 6.90 t/ha.

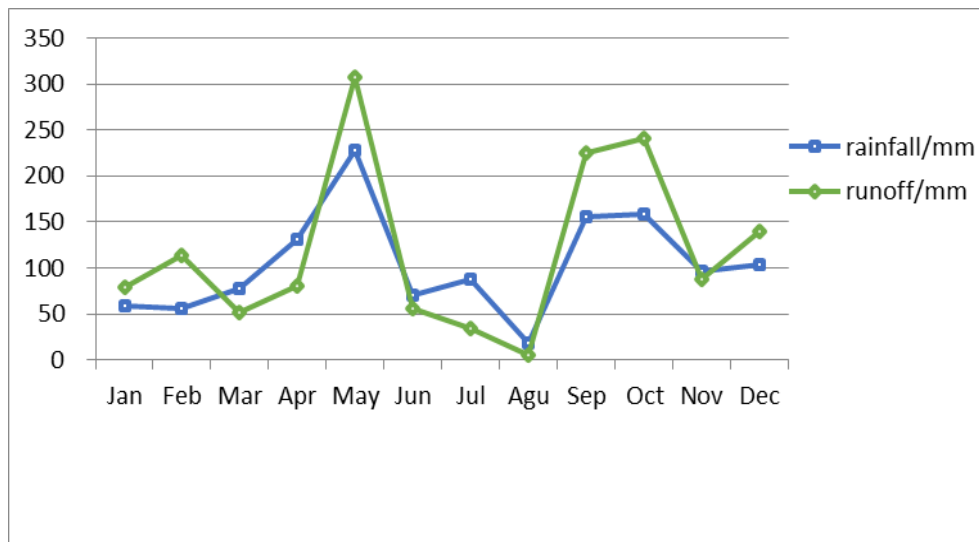


Figure 3. Comparison of monthly precipitation and monthly runoff

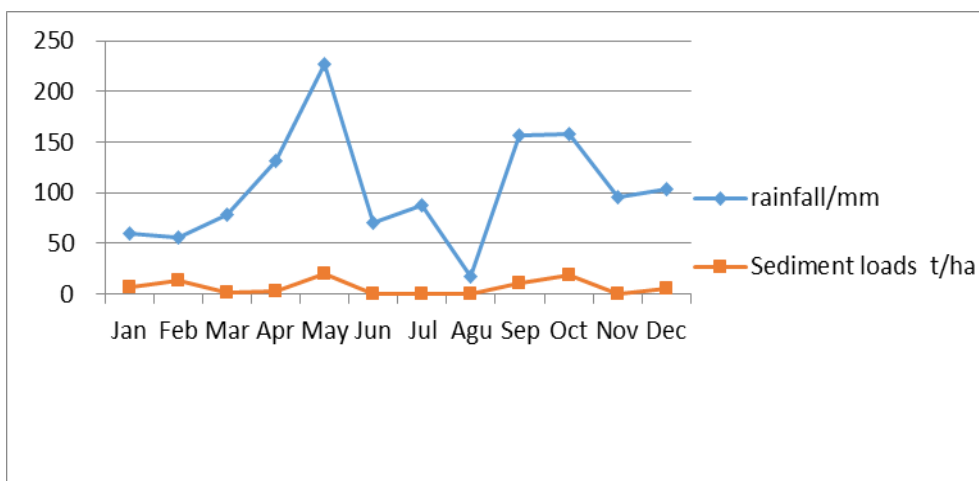


Figure 4. Comparison of monthly precipitation and monthly sediment amount

The precipitation was 227.25 mm in May, in the year with the most rainfall in Caohai watershed. The runoff showed an increasing trend with the increase of precipitation, which indicated that the runoff was related to rainfall, and it was proved that the runoff was related to rainfall, so the simulation reliability of the model was proved. The amount of sediment also increases with the increase of rainfall, which shows that the output of sediment is mainly concentrated in the flood season, and the output of sediment in flood season is the largest. The data also show that it is necessary to control the pollution from non-point sources. In time, we should take advantage of the periods when the output of non-point sources is the highest, such as flood season and the month when the rainfall is the highest, so as to do some preventive measures to reduce the output of non-point source more efficiently.

Analysis of typical pollutants in river watershed

According to *Table 2*, it can be concluded that the total nitrogen (TN) and total phosphorus (TP) in the Jiahaizi river watershed are the least, which is 98.54 kg/ha, 13.49 kg/ha, which indicates that the chemical fertilizer application in the Jiahaizi river watershed is less, and the chemical fertilizer application in the corresponding Baima river watershed is more serious. Total nitrogen content reached 414.16 kg/ha, Total phosphorus content 52.10 kg/ha. It is also obvious that the total phosphorus content in the watershed with higher total nitrogen is also higher, indicating that there is a relationship between the nitrogen and phosphorus content in the soil. According to the situation of total nitrogen and total phosphorus in the four watersheds, it can be seen that the application of chemical fertilizer is more serious in the whole watershed, and corresponding measures should be taken to reduce the application of chemical fertilizer.

Table 2. Contents of TN and TP in four river watershed

Sub watershed name	TN (kg/ha)	TP (kg/ha)
Jiahaizi river watershed	98.54	13.49
Dongshan river watershed	226.57	29.06
Baima river watershed	414.16	52.10
Zhonghe river watershed	353.10	44.14

TN: total nitrogen, TP: total phosphorus

Simulation of the effect of four regulation project on output

Land use of four kinds of regulation project

The comprehensive control of shelterbelt construction and greening measures have improved non-point source pollution. In order to further reduce water pollution and consolidate the comprehensive treatment effect, in response to the national water source protection policy, the implementation of “returning farmland to forests” and “returning farmland to grassland” measures The land use of the four regulation project is shown in *Figure 5*.

After the land use change, the forest land increased by 53% under the mode of farmland changed into forest land, the forest land increased by 9% under the mode of building changed into forest land, the grassland increased by 53% under the mode of farmland changed into grassland, the grassland increased by 9% under the mode of building changed into grassland, and other land use types did not change.

Influence on runoff under four regulation project scenarios

Runoff is the main driving force of non-point source pollution. The change of regional runoff directly affects the change of non-point source pollution load, and runoff is the product of land use conditions. The model simulates the output of runoff and sediment under four regulation projects, as shown in *Table 3*.

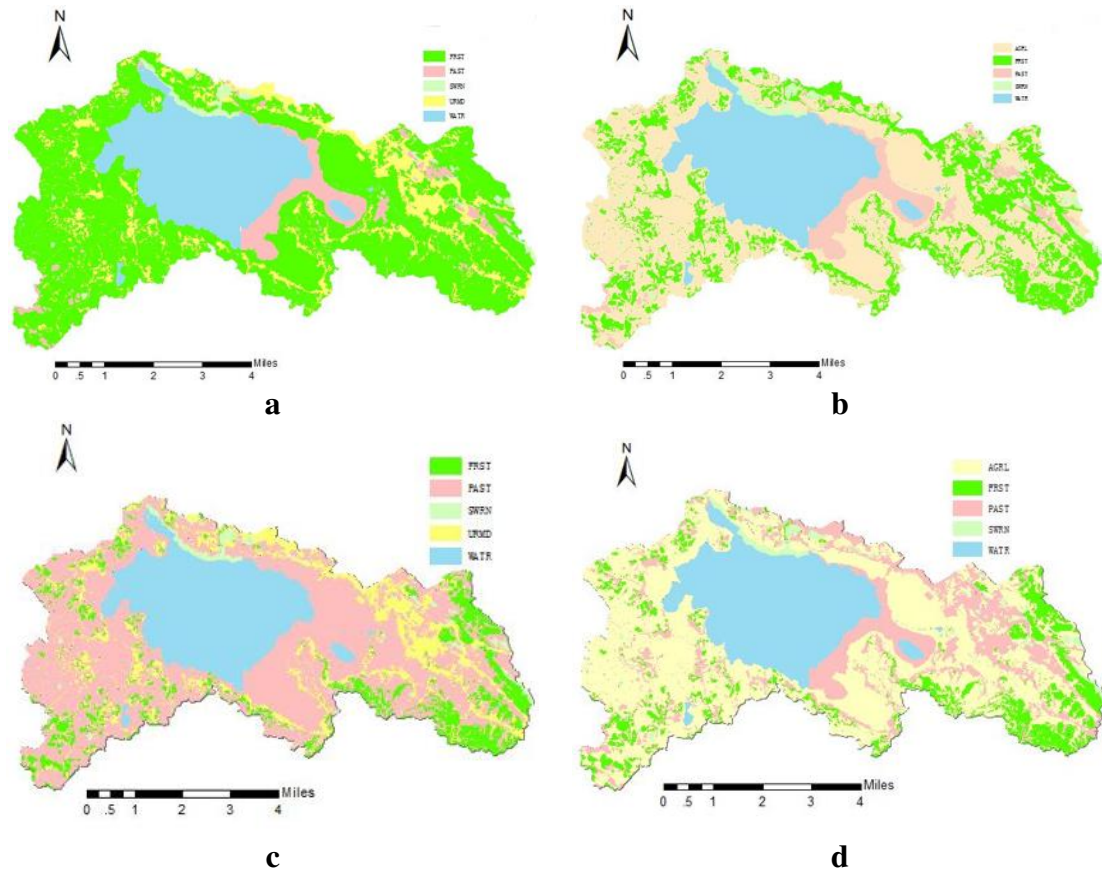


Figure 5. Four regulation modes. **a** Farmland changed into forestland. **b** Building changed into forestland. **c** Farmland changed into grassland. **d** Building changed into grassland

Table 3. Runoff and sediment quantity under regulation project mode

Regulation project mode	Runoff quantity mm	Sediment quantity t/ha
Farmland changed into forestland	289.37	89.47
Building changed into forestland	301.86	97.13
Farmland changed into grassland	321.12	107.26
Building changed into grassland	295.62	94.31

In the case of the same rainfall in 2017, the runoff and sediment volume will vary with the type of land use. When the farmland was changed into forest land mode, the runoff is 289.37 mm, and the sediment volume is 89.47 mm, which is 8% more than the sediment volume in 2017. When the building was changed into forest land mode, the runoff is 301.86 mm, and the sediment volume is 97.13 mm, which is 17.3% more than the sediment volume in 2017. When the farmland was changed into grassland mode, the runoff is 321.12 mm, and the sediment volume is 107.26 mm, which is 29.5% higher than the sediment volume in 2017. When the building was changed into grassland mode, the runoff is 295.62 mm, and the sediment volume is 94.31 mm, which is 13.9% higher than the sediment volume in 2017. At the same time, it can be seen that the runoff of farmland converted to grassland is the largest, and the amount of sediment increases with the increase of runoff.

Influence on four regulation project on typical pollutants

The average annual load of nitrogen and phosphorus can be obtained by simulating the non-point source pollution under the four regulation project, of which the annual load of TN and TP in the base period is the average load of TN and TP in 2017. The total nitrogen and phosphorus loads were obtained by model simulation of the four regulation project, as shown in *Table 4*.

Table 4. Annual load simulation results of TN under regulation project model

Regulation project mode	TN/kg	change rate
Farmland changed into forest land	257.22	-11%
Building changed into forest land	281.14	-3%
Farmland changed into grassland	276.89	-4%
Building changed into grassland	285.65	-1%

In *Table 4*, the nitrogen load of the four regulation modes can be observed, when the farmland was changed into forest land mode, the total nitrogen yield was 257.22 kg, which decreased by 11%. When the building was changed into forest land mode, the total nitrogen yield was 281.14 kg, which decreased by 3%. When the farmland was changed into grassland mode, the total nitrogen yield was 276.89 kg, which decreased by 4%. When the building was changed into grassland mode, the total nitrogen yield was 285.65 kg, which decreased by 1%. It can be concluded that the total nitrogen output is the least when the farmland is transformed into forest land, while the total nitrogen output is the most when the building is transformed into grassland.

Table 5 presents the nitrogen load in the four regulation modes, when the farmland was changed into forest land mode, the total phosphorus output was the least, 27.79 kg, which decreased by 24%. When the building was changed into forest land mode, the total phosphorus output was 32.99 kg, which reduced by 10%. When the farmland was changed into grassland mode, the total phosphorus output was 29.62 kg, which reduced by 19%. When the building was changed into forest land, the total phosphorus output was 34.48 kg, which reduced by 6%.

Table 5. Annual load simulation results of TP under regulation project model

Regulation project mode	TP/kg	Change rate
Farmland changed into forest land	27.79	-24%
Building changed into forest land	32.99	-10%
Farmland changed into grassland	29.62	-19%
Building changed into grassland	34.48	-6%

According to the results, if a series of non-point source pollution control measures are not implemented, the non-point source pollution will be further increased. Therefore, in order to predict the increasing trend of non-point source pollution, it is necessary to strengthen planting and grass planting, return farmland to forest, reduce the application of fertilizers and increase wetlands.

Discussion and conclusion

Four typical sub-watersheds in the Caohai Jiahaizi river watershed, Dongshan river watershed, Baima river watershed and Zhonghe river watershed were selected for SWAT simulation analysis under the four regulation projects. The results showed that the non-point source pollution was less under the four regulation projects, among which the non-point source pollution was less under the conversion of farmland into forest land. Combined with the current situation of land use in the Caohai river watershed, reasonable fertilization should be adopted to reduce non-point source pollution, and a series of greening measures should be adopted, such as planting a variety of shrubs, reducing soil erosion, reducing pollutants into water and increasing wetlands. These treatment schemes have a good effect on controlling non-point source pollution. In order to guarantee the good water quality and improve the water and soil conservation capacity of the Caohai watershed, non-point source pollution should be effectively controlled and the quality of life of the people should be improved.

In order to maintain the water environment health and promote the sustainable development of ecology, economy and society in the Caohai watershed, we should continue to carry out comprehensive water environment improvement in Caohai watershed and invest sufficient manpower and financial resources. Therefore, it is suggested that: first, a mechanism should be established to guarantee the funds for comprehensive remediation of the Caohai watershed to ensure the continuous investment of funds. Second, the mechanism of ecological compensation and protection for water environment in the Caohai river watershed should be established to reverse the long-term lack of systematic planning and protection and reduce the economic burden of ecological construction. Third, it is necessary to establish a mechanism of supervision and inspection for comprehensive regulation of the Caohai river watershed, make the task clear, fulfil responsibility, unify the local departments in thinking, and put watershed management into practice as the responsibility. Fourth, exploring the technical methods according to local conditions and introducing practical and applicable water ecological restoration methods are essential. Fifth, it is necessary to establish a monitoring, dispatching, early warning platform and information sharing mechanism, along with a multi-sector monitoring system, improve the level of comprehensive decision-making management, and achieve sustainable development of the grassland watershed.

Acknowledgements. This work was supported by the Major Project of Guizhou Province (Qian Ke He Major Project Zi [2016]3022-06), the Application Foundation Major Project of Guizhou Province (Qian Ke He JZ Zi [2014] 200211), the Construction Program of Biology First-class Discipline in Guizhou (GNYL [2017] 009), the Key Discipline Construction Project of Ecology in Guizhou Province (Guizhou Degree ZDXK[2016]7)

REFERENCES

- [1] Dechmi, F., Burguete, J., Skhiri, A. (2012): SWAT application in intensive irrigation systems: Modeling, calibration and validation. – *Journal of Hydrology* 470/471: 227-238.

- [2] Fan, L., Zhang, D., Duan, H., Yang, H., Yang, P., Luo, B. (2015): Study on the prevention and control measures of agricultural non-point source pollution in China. – *Environmental Science and Management* 40(11): 85-87.
- [3] Ficklin, D. L., Luo, Y., Luedeling, E. et al. (2009): Climate change sensitivity assessment of a highly agricultural watershed using SWAT. – *Journal of Hydrology* 374(1-2): 16-29.
- [4] Guo, J., Zhang, Z., Wang, S., Strauss, P., Yao, A. (2014): Application of SWAT model to study the impact of land use and climate change on runoff in Chaohe River Basin. – *Journal of Ecology* 34(6): 1559-1567.
- [5] Li, C., Hu, Y., Liu, Z. (2013): Research progress of urban non-point source pollution. – *Journal of Ecology* 32(3): 492-500.
- [6] Li, S., Wei, H., Liu, Y., Ma, W., Gu, Y., Peng, Y., Li, C. (2017): Runoff simulation of Qingshui River Basin in Ningxia under climate and land use change. – *Journal of Ecology* 37(4): 1252-1260.
- [7] Luo, Q., Ren, L., Peng, W. (2014): Non-point source nitrogen and phosphorus load simulation analysis in Liaoning Taizi River Basin. – *China Environmental Science* 34(1): 178-186.
- [8] Luo, Z., Liu, W., Li, Z., Li, X. (2017): Nest site selection of *Tachybaptus ruficollis* in Caohai National Nature Reserve, Guizhou, China Sichuan. – *Journal of Zoology* 36(2): 174-180.
- [9] Rahman, K., Da Silva, A. G., Tejada, E. M., Gobiet, A., Beniston, M., Lehmann, A. (2015): An independent and combined effect analysis of land use and climate change in the upper Rhone River watershed, Switzerland. – *Applied Geography* 63: 264-272.
- [10] Sakaguchia, A., Eguchia, S., Katob, T. et al. (2014): Development and evaluation of a paddy module for improving hydrological simulation in SWAT. – *Agricultural Water Management* 137: 116-122.
- [11] Strauch, M., Volk, M. (2013): SWAT plant growth modification for improved modeling of perennial vegetation in the tropics. – *Ecological Modelling* 269: 98-112.
- [12] Wu, Y. P., Liu, S. G., Chen, J. (2012): Urbanization eases water crisis in China. – *Environmental Development* 2: 141-144.
- [13] Xia, P. H., Kong, X. L., Yu, L. F. (2016): Effects of land-use and landscape pattern on nitrogen and phosphorus exports in Caohai wetland watershed. – *Acta Scientiae Circumstantiae* 36(8): 2983-2989.
- [14] Yang, L., Gao, H. (2016): Research progress of non-point source pollution models at home and abroad. – *Resource Conservation and Environmental Protection* 23(5): 151-155.
- [15] Yuan, Y., Zhang, Z., Meng, J. (2015): Impact of land use and climate change on runoff in Liuxi River Basin based on SWAT model. – *Journal of Applied Ecology* 26(4): 989-998.
- [16] Zhang, L., Karthikeyan, R., Bai, Z. K., Srinivasan, R. (2017): Analysis of streamflow responses to climate variability and land use change in the Loess Plateau Region of China. – *Catena* 154: 1-11.
- [17] Zhao, A.-Z., Zhao, Y.-L., Liu, X., Zhu, X., Pan, Y., Chen, Y. (2016): Study on the impacts of climate change and human activities on blue and green water in the Weihe River Basin. – *Geographical Science* 36(4): 571-579.
- [18] Zheng, J.-N., Xia, P.-H., Lin, T., Zhou, Y. (2013): The contents and distributive characteristics of nitrogen and phosphorus in farmland ditches of the suburban mixed area near to Caohai Natural Reserve, Guizhou. – *Journal of Mountain Agriculture and Biology*.

SIMULATION OF FISH MIGRATION AT DIFFERENT WATER DEPTHS BASED ON BACKPROPAGATION NEURAL NETWORK

LI, R.^{1,2,3} – WU, Z.¹ – LI, L.^{2,3*} – CAI, D.¹ – HUANG, L.^{2,3} – TAO, J.⁴ – LUO, F.⁵ – NORGBEY, E.⁵

¹*College of Life Science and Technology, University of Guangxi, Nanning 530003, China*

²*Guangxi Institute of Water Resources Research, Nanning 530023, China*

³*Guangxi Key Laboratory of Water Engineering Materials and Structures, Nanning 530023, China*

⁴*Harbin Institute of Technology, Harbin 150080, China*

⁵*College of Environment, Hohai University, Nanjing 210098, China*

**Corresponding author
e-mail: LinLsky@163.com*

(Received 26th Sep 2018; accepted 29th Nov 2018)

Abstract. This paper aims to disclose the law of fish migration trajectories at different water depths. For this purpose, the grass carps in a reservoir in southwestern China were taken as the targets, outdoor experiments were performed to monitor their behaviours and environmental factors in the reservoir. Then, the Hydroacoustic Technology, Inc. (HTI) acoustic tracking system and backpropagation neural network (BPNN) were introduced to simulate and analyse the migration of the fish in the natural state. Meanwhile, the vertical distribution of fish was discussed at different temperatures and dissolved oxygen contents. The results show that the BPNN algorithm has a good fitting effect on the planar migration trajectories of the fish, but fails to achieve a desirable fitting result concerning the migration trajectories in the Z direction. Fortunately, the fitting effect of migration trajectories was greatly enhanced by normalization. The fish were distributed differently in spring and summer across the different water depths, under the influence of water temperature and dissolved oxygen content. Overall, the fish obeyed the normal distribution in the vertical direction, and selected water depth mainly based on dissolved oxygen content. The research findings lay a scientific basis for fish resource protection, river ecology assessment and water environment restoration.

Keywords: *backpropagation neural network (BPNN), migration trajectory, simulation analysis, water temperature, dissolved oxygen*

Introduction

Fish are the dominant organisms in aquatic ecosystem. There exists an obvious mutual effect between fish and the water environment. On the one hand, fish are extremely sensitive to the environment of the water body; on the other hand, the water environment is directly affected by fish behaviours. It is generally agreed that ecological safety of the water body can be characterized by the diversity of fish population and variation in fish behaviours, and the fish tend to change their physiological/biochemical responses and swimming behaviours in a changing water environment. Therefore, a clear understanding of fish behaviours helps to protect the water environment and achieve quality and efficient aquaculture.

Much research has been done to reveal the effects of water environment on fish behaviours. Based on the research scope, the existing studies can be roughly divided into small-scale, medium-scale and large-scale ones.

The small-scale research mainly investigates the physiological/biochemical responses of fish to the water environment, including blood circulation, metabolism and immunity (Santana-Garcon et al., 2014), and identifies the correlations between fish body (e.g. length and weight), meat quality and nutritional components and environmental factors like water flow, magnetic field and dissolved oxygen content. The main techniques for small-scale research include field inspections, video imaging, anatomical experiments, etc. For instance, Han et al. (2010) examined the variation in haematological parameters and digestive enzyme activity of carps at four different temperatures, and discovered the significant impact of water temperature on the metabolic status and blood components of the fish.

The medium-scale research focuses on the effects of changing water flow, water quality and magnetic field over fish behaviour. The common approach is to capture the variation in fish behaviours under changing conditions of swimming, foraging and reproduction through water through tests, video imaging, anatomical experiments, acoustic tracking and numerical simulations. For example, Wang et al. (2007) revealed the major impacts of the water habitat parameters, namely, water flow, mean water depth and river width, on the survival and reproduction of fish: the water flow affects the material/energy exchange rate and the spawning activity of fish, while the river depth and width influences the free/collective activity and thus the survival of the fish. Through onsite fish harvesting, Zhang et al. (2008) discovered that water conservancy projects lower the sediment content and turbidity, reduce the biodiversity and fish population, and bring down the dissolved oxygen content and water temperature in the downstream.

The large-scale research aims to identify the responses of fish to the changes in the water body, compare the fish migration and distribution in different habitats, and measure the health of the eco-environment in each habitat. The responses of fish range from foraging to reproduction, and the changes in the water body covers flow, depth, vorticity, temperature, sediment content and dissolved oxygen content. Popular techniques of large-scale research include acoustic tracking, model tests and 3S technology (i.e. GPS (Global Positioning System), RS (Remote Sensing Technology) and GIS (geographic information system)). Below are some of the representative large-scale studies. Guo et al. (2011) measured the discharge, water level, water temperature and sediment content of the Three Gorges Reservoir before and after the first filling, and concluded that the variation in these parameters delays the spawning period, reduces the spawning scale and suppresses the fertilization rate of Chinese sturgeon. Popper et al. (1998) controlled the migration behaviours of fish with underwater acoustic technique like normal sound waves and ultrasound waves, and integrated light, flow field and other factors into the technique.

The previous studies on fish migration behaviours concentrate on modelling and experiments (Haim and Portnov, 2013; Tan et al., 2004; Han et al., 2010; Zhang et al., 1987). In general, the human impacts have been emphasized over the natural impacts on fish behaviours, due to the difficulty in long-term stable monitoring of fish behaviours through existing methods of numerical analysis. Thanks to technological development, there is a shift from the traditional monitoring method (Wang et al., 2007) towards new approaches of fish behaviour monitoring, such as GPS tracking (Guo et al., 2011; Popper and Carlson, 1998), acoustic tracing (Valavanis et al., 2008; Cai and Li, 2012) and computer monitoring (Clark et al., 2004; Mouton et al., 2007).

The traditional monitoring method investigates fish behaviours based on the life history of fish from net fishing, transport tracking to photo taking. The captured data were integrated to derive the locations of fish, and thus the general pattern of fish behaviours. The GPS tacking method originates from the popular technique of GPS positioning. Specifically, a satellite signal receiver is attached to each fish, such that the spatial position of the fish can be determined when the device receives three or more satellite signals at the same time.

The acoustic tracing method tracks fish migration based on the principle of sound propagation and signal reception. Cruz-Font et al. (2012) tacked the migration of lake trout in the US using a novel acoustic telemetry. Pepin and Miller (1993) compared the echo detection data of gill nets and catch samples, and provided new insights into the effect of habitats on fish biomass and distribution. Computer monitoring introduces the latest computer image recognition technology to the real-time monitoring of fish behaviours. However, this approach still faces difficulties and instability in operation.

The HTI acoustic tracking system combines signal reception and acoustic label positioning (Jr and Matarese, 1994; Riding et al., 2009; Monk et al., 2011) into an accurate and efficient way to locate and track fish migration in all kinds of water bodies. Over the years, this system has been widely used to assess the abundance and behaviours of fish in various scenarios of the fishery industry.

Taking grass carps as the targets, this paper carries out outdoor experiments to monitor their behaviours and environmental factors in natural river habitats. Then, the HTI acoustic tracking system and backpropagation neural network (BPNN) were introduced to simulate and analyse the migration of the fish in the natural state. Meanwhile, the vertical distribution of fish was discussed at different temperatures and dissolved oxygen contents. The research findings can provide reference for the later experts to study fish behavior simulation and lay a scientific basis for fish resource protection, river ecology assessment and water environment restoration.

Methodology

Equipment

The main device of our experiments is HTI's model 291 portable acoustic tag reception system, which consists of a laptop, a model 291 portable acoustic tag receiver, a model 492 miniature acoustic tag detector, four 590-series hydrophones, forty 795-series acoustic tags, a Model 490-LP tag programmer, 400 m of 690-series cables, one 115 VAC power line filter, and a set of TagProgrammer/MarkTags/AcousticTag software. The wiring diagram of the system is illustrated in *Figure 1*.

As shown in *Figure 1*, the four hydrophones are arranged on the left side: two at the bottom and two on the surface of the water body; the spacing between each pair of hydrophones is smaller than twice the listening range of a single hydrophone, such that the four hydrophones can work effectively in the hexagon in the figure. The four hydrophones are connected to the model 291 portable acoustic tag receiver. The receiver is linked to the laptop through data lines for data transmission and connected with oscilloscopes for denoising. During the monitoring, pulse signals are sent out by the acoustic tags on the fish, and received and transferred by the group of hydrophones to the tag receiver; then, the signals are denoised by the oscilloscopes before being transmitted to the laptop for storage. The user can perform real-time processing or post-processing of these signals.

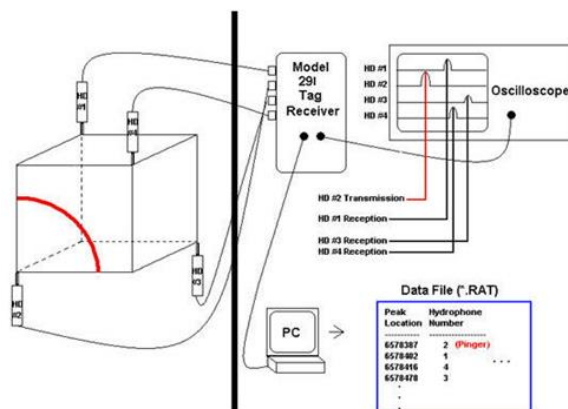


Figure 1. Wiring diagram of HTI's model 291 portable acoustic tag reception system (from HTI manual)

Study area

To study the fish migration trajectory under natural conditions, Tianbao Reservoir (22°52'20"N, 108°14'16"S) in Nanning, China's southwestern Guangxi Autonomous Region, was selected as the study area. Located 5 km away from Nanning, the reservoir is the source of Keli River and a national water park. The reservoir has a water surface area of 73,000 m², a total capacity of 13.6 million m³, and an average water depth of 6.20 m. The dam is a homogeneous earth dam, with the crest width of 5 m, the crest length of 132 m and the maximum height of 32.67 m. The annual water supply is designed to be 2.5 million m³. The location and range of the study area are presented in Figure 2 (He et al., 2018).



Figure 2. Location/range of the study area

Target species

There are 34 species of fish in the water system of Tianbao Reservoir, belonging to 26 genera, 9 families and 4 orders. *Cypriniformes Cyprinidae* are the dominant species. Specifically, *Cypriniformes* take up 67.65% of the total species, *Perciformes* account for 17.65%, *Siluriformes* occupies 11.76%, and *Monopterus albus* makes up 2.94%. The invasive species include *Tilapia nilotica*, *Tilapia mozambiquensis*, *Cirrhinus mrigala*, *Labeo rohita*, and *Clarias gariepinus*. From 2006 to 2007, our research group collected 34 fish samples from Tianbao reservoir, including grass carp, carp, spinibarby fish and crucian carp. Among them, the grass carp (Fig. 3) was selected our experiments. As a target

species, grass carp is the dominant fish in the Tianbao Reservoir, and it is one of the largest species which reported production in China, over 6 million tons per year. It is also a large herbivorous freshwater fish species of the family Cyprinidae native to eastern Asia.



Figure 3. The target species: grass carp

Field experiments

Field experiments were carried out in April (spring) and August (summer), 2011. In each experiment, five 795-series acoustic tags (*Table 1*) were attached to the dorsal fin of five grass carps, denoted as Fish 01–05, respectively. As shown in *Figure 4*, the four hydrophones are arranged at the red, yellow, green and blue positions, respectively. The features of the hydrophone array are listed in *Table 2*. The tagged grass carps were released into the reservoir, and the system started to collect data at one cycle per second. Because the tagged fish need a period for adaptation, the actual sampling cycle was adjusted to 30 s to eliminate the interference of human activities and underwater obstacles. Meanwhile, the water temperature and dissolved oxygen content in spring and summer were also observed.

Table 1. Features of the HTI tags

The tag ID	The tag type	Pulse period (msec)	Pulse delay (msec)	Fish species
TAG-FISH01	S	1000	1	Grass Carp
TAG- FISH02	S	1100	1	Grass Carp
TAG- FISH03	S	1200	1	Grass Carp
TAG- FISH04	S	1300	1	Grass Carp
TAG- FISH05	S	1400	1	Grass Carp

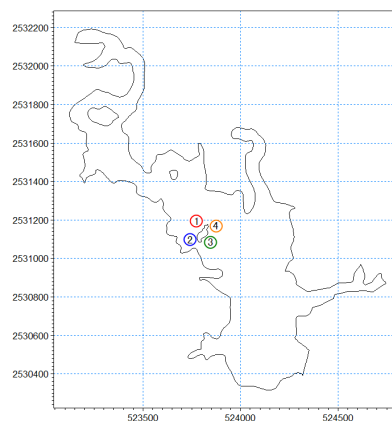


Figure 4. Layout of the hydrophone array

Table 2. Features of the hydrophone array

Hydrophone ID	Type	Coordinates			State	Signal gain	Minimum monitor signal
		X	Y	Z		(dB)	(Volts)
B1	S	523788.69	2531147.64	87.5	R	40	0.1
B2	S	523782.63	2531077.90	91.5	R	40	0.1
B3	B	523833.28	251101.26	87.0	R	40	0.1
B4	B	523830.60	2531151.10	92.0	R	40	0.1

To disclose the law in the migration trajectories of the fish, the hydrological conditions of the reservoir were assumed to be constant. During the experiments, the water level in the reservoir basically stabilized at about 96.45 m (Yellow Sea Height Datum). The monitoring results on migration trajectories are shown in *Figure 5*.



Figure 5. Monitoring results on the migration trajectories of Fish 01–05

BPNN processing

BPNN algorithm

Initialize each weight $w_{ji}(0)$ or threshold $\theta_j(0)$ as a small random value.

Set the training samples: input vectors X_k , $k = 1, 2, \dots, P$; expected outputs: d_k , $k = 1, 2, \dots, P$. Perform 3–5 iterations for each input sample as follows.

Calculate the actual network output and the state of hidden layer neurons (Eq. 1):

$$O_{kj} = f_j \left(\sum w_{ji} o_{ki} + \theta_j \right) \quad (\text{Eq.1})$$

Calculate the training error (Eqs. 2–3):

$$\delta_{kj} = o_{kj} (1 - o_{kj}) (t_{kj} - o_{kj}) \quad (\text{Output layer}) \quad (\text{Eq.2})$$

$$\delta_{kj} = o_{kj} (1 - o_{kj}) \sum_m \delta_{km} w_{mj} \quad (\text{Output layer}) \quad (\text{Eq.3})$$

Find the threshold of modified weights (Eqs. 4–5):

$$w_{ji}(t+1) = w_{ji}(t) + \eta \delta_j o_{ki} + \alpha [w_{ji}(t) - w_{ji}(t-1)] \quad (\text{Eq.4})$$

$$\theta_j(t+1) = \theta_j(t) + \eta \delta_j + \alpha [\theta_j(t) - \theta_j(t-1)] \quad (\text{Eq.5})$$

If k falls in $1-p$, determine if the index meets the accuracy requirement (Eq. 6):

$$E \leq \varepsilon \quad (\text{Eq.6})$$

where ε is the required accuracy.

The BPNN (Hecht-Nielsen, 1988; Macbeth C et al., 1997) has only one hidden layer. The neurons in the input, hidden and output layers can configure themselves.

Normalization

When all samples have positive inputs, the weights of the hidden layer neurons can either increase or decrease at the same time, which slows down the learning speed. To speed up the convergence, it is necessary to normalize the basic unit of measurement before modelling or statistical calculation. The BPNN is trained (probability calculation) and predicted by the statistical probability of samples in events, and normalization is the statistical probability distribution unified between 0 and 1. Through normalization, the mean input of all samples is close to zero or smaller than its mean square error.

Results analysis

BPNN-based simulation of migration trajectories

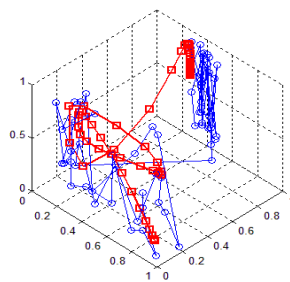
In our research, the migration trajectories of Fish 01–05 were simulated (Eqs. 1–6). The training parameters are given in Table 3. The data on the migration trajectories along the X, Y and Z directions were normalized, and the values were measured before and after the normalization. The correlation coefficients between the measured values and the fitted values (Table 4) before and after the normalization were obtained through simulation and calculation. The measured data and fitted data were normalized and plotted into 3D images from the perspectives of (45, 45) and (-45, -45) (Figs. 6–10). In these images, the blue circle lines stand for the measured data, while the red square lines represent the fitted data.

Table 3. Training parameters

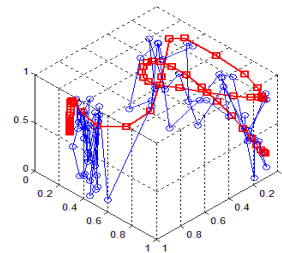
Number	Number of training sessions	Input layer	Hidden layer	Output layer
FISH01	136000	1	7	3
FISH02	132000	1	7	3
FISH03	206000	1	7	3
FISH04	136000	1	7	3
FISH05	136000	1	7	3

Table 4. Correlation coefficient between measured and fitted values before and after normalization

Number	X			Y			Z		
	Before processing	After processing	Increase (%)	Before processing	After processing	Increase (%)	Before processing	After processing	Increase (%)
FISH01	0.8892	0.8923	0.3486	0.9805	0.9913	1.1015	0.3295	0.3764	14.2337
FISH02	0.8871	0.8895	0.2705	0.9798	0.9865	0.6838	0.7958	0.7999	0.5152
FISH03	0.9684	0.9722	0.3924	0.8124	0.8217	1.1448	0.0195	0.0228	16.9231
FISH04	0.8215	0.8324	1.3268	0.8577	0.8611	0.3964	0.3282	0.3560	8.4704
FISH05	0.8417	0.8502	1.0099	0.8724	0.8841	1.3411	0.3534	0.3618	2.3769

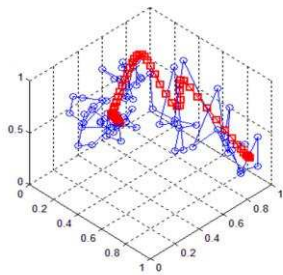


Left view (45, 45)

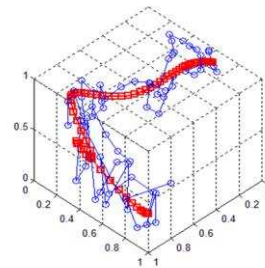


Right view (-45, -45)

Figure 6. Measured and fitted migration trajectories of Fish 01 after normalization

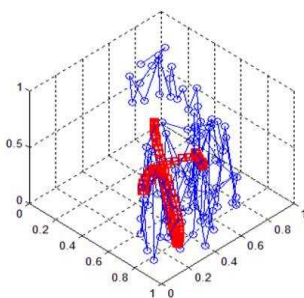


Left view (45, 45)

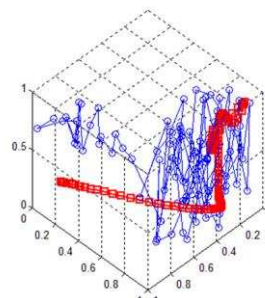


Right view (-45, -45)

Figure 7. Measured and fitted migration trajectories of Fish 02 after normalization



Left view (45, 45)



Right view (-45, -45)

Figure 8. Measured and fitted migration trajectories of Fish 03 after normalization

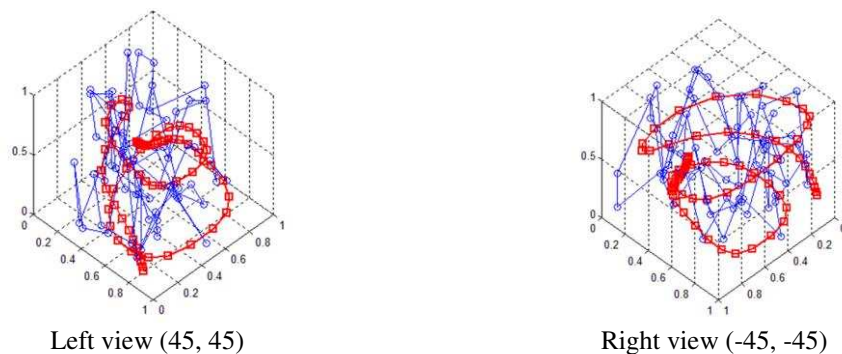


Figure 9. Measured and fitted migration trajectories of Fish 04 after normalization

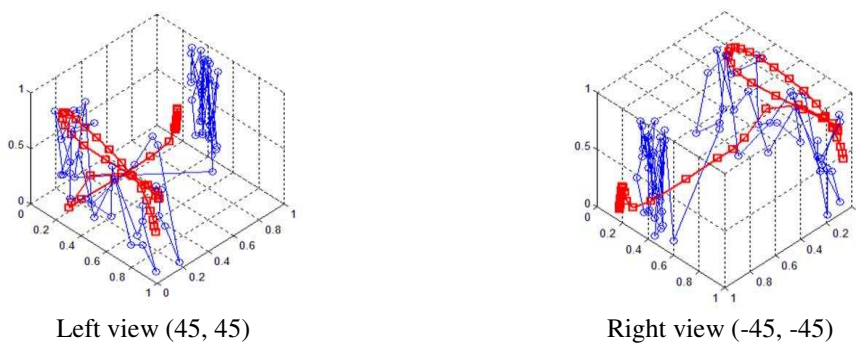


Figure 10. Measured and fitted migration trajectories of Fish 05 after normalization

According to the fitted data, the correlation coefficients in X and Y directions were greater than 0.81. Fish 03 boasted a good fitting performance in the X direction, and Fish 01 and 02 had correlation coefficients above 0.98 in the Y direction. These means the BPNN algorithm has a good fitting effect on the planar migration trajectories of the fish.

In the Z direction, the correlation coefficients of Fish 01, 04 and 05 all fell in 0.32–0.37, while those of Fish 02 and 03 fell out of the range (the correlation coefficient of Fish 03 was as low as 0.01–0.02). Hence, the BPNN algorithm fails to achieve a desirable fitting result concerning the migration trajectories in the Z direction. A possible reason is that the Z values are the absolute elevations of the migrating fish, which cannot reflect the distance to the river bottom. The vertical distance between fish and river bottom is essential to the accurate evaluation of migration trajectories, in addition to the spatial distance between fish and water.

The normalization greatly enhanced the fitting effect of migration trajectories. The correlation coefficients of Fish 01–05 were improved across the board after the 3D images (Fig. 6–10) were considered. Specifically, the correlation coefficients in the X direction increased by 0.27–1.33% and those in the Y direction by 0.40–1.34%. The greatest increase belongs to Fish 04 in the x direction (1.33% from 0.82 to 0.83) and Fish 05 in the y direction (1.34% from 0.87 to 0.88). In the Z direction, the fitting effect of each fish was enhanced obviously except Fish 02. After normalization, the correlation coefficients of Fish 01, 03, 04 and 05 all grew by over 2.30%. Particularly, the correlation coefficient of Fish 03 increased by 16.92% in the Z direction.

Effects of water temperature and dissolved oxygen content on fish behaviours

The growth, metabolism and cranial nerve movement of fish are closely related to the temperature and dissolved oxygen content at different water depths. Here, the behaviours of Fish 01–05 at different water depths were monitored (Table 5) and analysed in April (spring) and August (summer). The analysis shows that the temperature and dissolved oxygen content affected the fish's favourite water depth.

In spring, the average water temperature is 20.97 °C, the average dissolved oxygen concentration is 6.13 mg/L. Neither the water temperature gradient nor the dissolved oxygen content changed significantly across different water depths. Hence, the time that the fish dwelled in each water depth remained basically unchanged (Fig. 11).

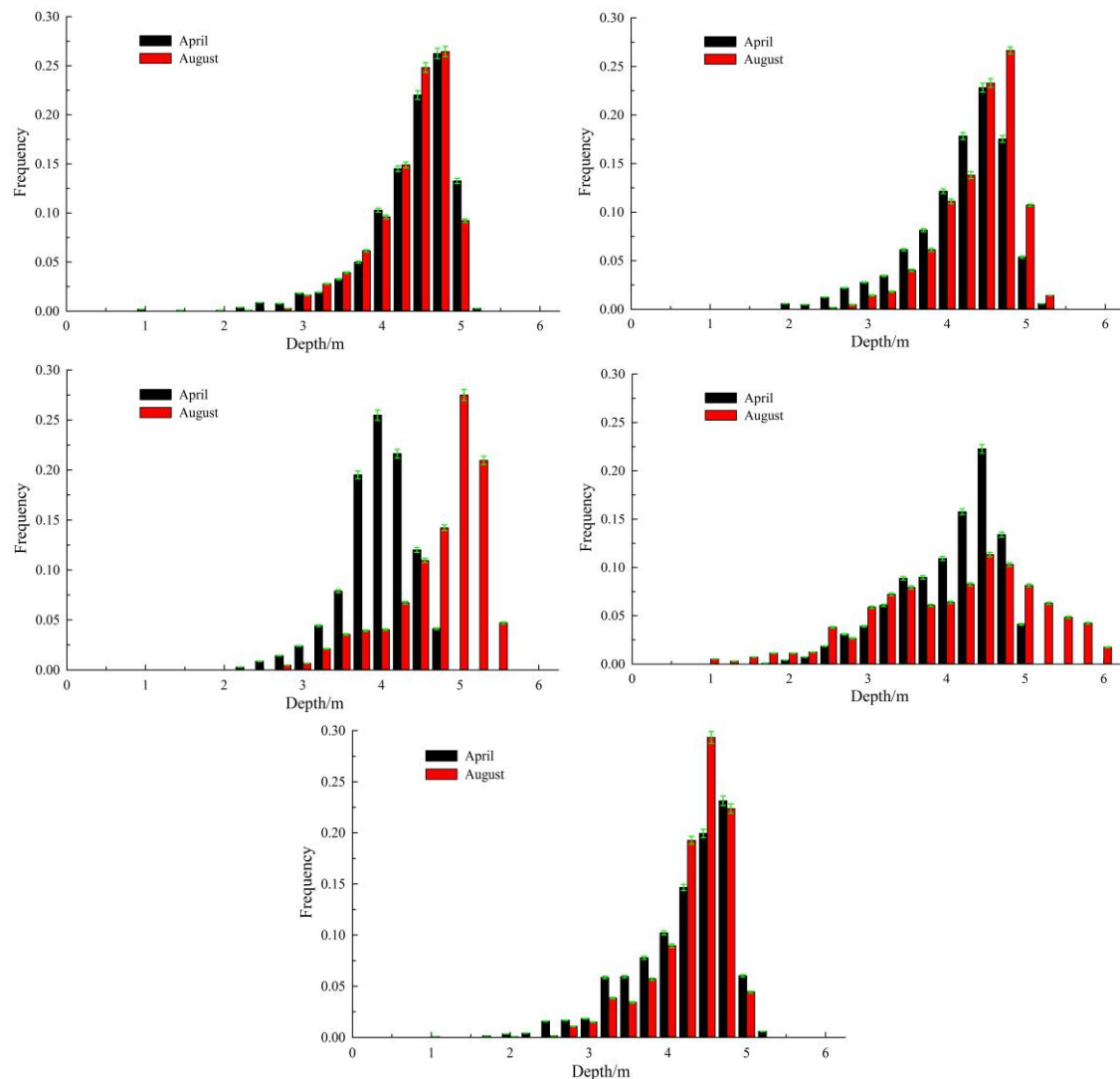


Figure 11. Distribution of fish residence time in different water layers

In summer, the average water temperature is 26.07 °C, the water temperature was much higher than that in spring at all water depths. The surface temperature exceeded the preferred temperature of the fish, and the water temperature declined with the increase of the water depth. On the surface of the reservoir, the amount of phytoplankton and

light intensity remained on a high level. Owing to the long illumination time, the dissolved oxygen content decayed slower in summer than in spring in different water depths. Thus, the fish descended to the depth with the most suitable water temperature and dissolved oxygen content. This is consistent with the research results of Kramer D L (1987).

The dissolved oxygen content plays a decisive role in the fish's selection of water depth (Breitburg, 1994). When the fish were swimming, they tended to choose the optimal depth based on their survival needs. The fish firstly selected the area with the proper content of dissolved oxygen, and then the area with the suitable water temperature. In spring, the fish preferred to stay in the water depth of 3.75–5.00 m, where the temperature was 20 ± 1.00 °C and dissolved oxygen content 5.00–6.00 mg/L; in summer the fish preferred to stay in the water depth of 4.00–5.25 m, where the temperature was 23.30–28.00 °C and the dissolved oxygen content 7.00–8.00 mg/L.

Table 5. Comparison of water depths, water temperatures and dissolved oxygen contents of the fish in spring and summer

Serial number	The prefer depth of the water		Dissolved oxygen concentration		Water temperature	
	Spring	Summer	Spring	Summer	Spring	Summer
FISH01	4.75	4.5	5.859	7.617	21.974	23.972
FISH02	4.5	4.75	6.271	7.460	20.682	25.937
FISH03	4	5	6.493	7.270	19.997	27.901
FISH04	4.5	4.5	6.071	7.617	20.372	26.592
FISH05	4.75	4.5	5.959	7.617	21.862	25.937

Conclusions

Based on the HTI acoustic tracking system and BPNN, this paper simulated and analysed the migration of the fish in the natural state, and the vertical distribution of fish was discussed at different temperatures and dissolved oxygen contents. The research findings can provide reference for the later experts to study fish behavior simulation.

The BPNN algorithm has a good fitting effect on the planar migration trajectories of the fish. However, it failed to achieve a desirable fitting result concerning the migration trajectories in the Z direction, because the Z values, the absolute elevations of the migrating fish, cannot reflect the distance to the river bottom. Fortunately, the fitting effect of migration trajectories were greatly enhanced by normalization.

The fish were distributed differently in spring and summer across the different water depths, under the influence of water temperature and dissolved oxygen content. Overall, the fish obeyed the normal distribution in the vertical direction, and selected water depth mainly based on dissolved oxygen content. When the fish were swimming, they tended to choose the optimal depth based on their survival needs. The fish firstly selected the area with the proper content of dissolved oxygen, and then the area with the suitable water temperature.

Acknowledgements. The work was supported by National Natural Science Foundation of China (NO.51569006 & NO.51409050) , Guangxi Science and Technology Projects (NO.GUIKE

AB17195074), Nanning Science Research and Technology Development Plan (NO.20183045-1) and Guangxi Key Laboratory of Water Engineering Materials and Structures.

REFERENCES

- [1] Breitburg, D. L. (1994): Behavioral response of fish larvae to low dissolved oxygen concentrations in a stratified water column. – *Marine Biology* 120(4): 615-625.
- [2] Cai, D., Li, R. (2012): Research on fish habitat based on acoustic fish tracking system. – *Journal of Convergence Information Technology* 7(23): 195-201.
- [3] Clark, R. D., Christensen, J. D., Caldwell, P. A., Matthews, G. A., Minello, T. J. (2004): A habitat-use model to determine essential fish habitat for juvenile brown shrimp (*Farfantepenaeus aztecus*) in Galveston Bay, Texas. – *Fishery Bulletin* 102(2): 264-77.
- [4] Cruz-Font, L., Shuter, B. J., Blanchfield, P. J. (2012): Tracking lake trout habitat use using a new telemetry approach. – *American Fisheries Society 1 Meeting* 2012.
- [5] Guo, W. X., Wang, H., Xu, J., Xia, Z. (2011): Effects of Three Gorges reservoir on the downstream eco-hydrological regimes during the spawning of important fishes. – *Journal of Hydroelectricity* 30(3): 22-26.
- [6] Haim, A., Portnov, B. A. (2013): Effects of Light Pollution on Animal Daily Rhythms and Seasonality: Ecological Consequences. – *Light Pollution as a New Risk Factor for Human Breast and Prostate Cancers*. – Springer Netherlands, Dordrecht, pp. 71-75.
- [7] Han, J. C., Liu, G. Y., Mei, P. S., Huang, Y. P., Liu, D. F., Chen, Q. W. (2010): Effects of temperature on the hematological indices and digestive enzyme activities of Crucian carp (*Carassius auratus*). – *Journal of Hydroecology* 3(1): 87-92.
- [8] He, L. Z., Feng, M. H., Wang, L. Y. (2018): Analysis on stability of Fengting River dam slope based on three-dimensional finite element. – *Water Conservancy Construction and Management* (6): 20-24.
- [9] Hecht Nielsen, R. (1988): Theory of the backpropagation neural network. – *Neural Networks* 1(1): 445-445.
- [10] Jr, A. W. K, Matarese, A. C. (1994): Status of early life history descriptions of marine teleosts. – *Text* 92(4): 725-36.
- [11] Kramer, D. L. (1987): Dissolved oxygen and fish behavior. – *Environmental Biology of Fishes* 18(2): 81-92.
- [12] Monk, J., Ierodiaconou, D., Bellgrove, A., Harvey, E., Laurenson, L. (2011): Remotely sensed hydroacoustics and observation data for predicting fish habitat suitability. – *Continental Shelf Research* 31(2): S17-S27.
- [13] Mouton, A. M., Schneider, M., Depestele, J., Goethals, P. L. M., Pauw, N. D. (2007): Fish habitat modelling as a tool for river management. – *Ecological Engineering* 29(3): 305-15.
- [14] Macbeth, C., Dai, H. (1997): Effects of learning parameters on learning procedure and performance of a BPNN. – *Neural Networks the Official Journal of the International Neural Network Society* 10(8): 1505.
- [15] Pepin, P., Miller, T. J. (1993): Potential use and abuse of general empirical models of early life history processes in fish. – *Canadian Journal of Fisheries & Aquatic Sciences* 50(6): 1343-45.
- [16] Popper, A. N., Carlson, T. J. (1998): Application of sound and other stimuli to control fish behavior. – *Transactions of the American Fisheries Society* 127(5): 673-07.
- [17] Riding, T. A. C., Dennis, T. E., Stewart, C. L., Walker, M. M., Montgomery, J. C. (2009): Tracking fish using 'buoy-based' GPS telemetry. – *Marine Ecology Progress* 377: 255-62.
- [18] Santana-Garcon, J., Newman, S. J., Harvey, E. S. (2014): Development and validation of a mid-water baited stereo-video technique for investigating pelagic fish assemblages. – *Journal of Experimental Marine Biology & Ecology* 452(1): 82-90.

- [19] Tan, D., Wang, J., Dan, S. (2004): The ratio of flesh to body and analysis on nutritive composition of muscle in *Ancherythroculter nigrocauda*. – *Acta Hydrobiologica Sinica* 28(3): 240-46.
- [20] Valavanis, V. D., Pierce, G. J., Zuur, A. F., Palialexis, A., Saveliev, A., Katara, I., Wang, J. (2008): Modelling of essential fish habitat based on remote sensing, spatial analysis and GIS. – *Hydrobiologia* 612(1): 5-20.
- [21] Wang, Y. R., Li, J., Li, K. F., Rui, J. L. (2007): Hydraulic parameters for the habitat demand of the water-reducing river in hydropower stations. – *Journal of Water Conservancy* 38(1): 107-11.
- [22] Zhang, H., Wei, Q., Yang, G. (2008): Development trend and fishery application of echo sounder. – *Water Conservancy and Fishery* 28(1): 9-13.
- [23] Zhang, Z. R., Xie, R. S., Xiao, L. Y., Wen, S. P. (1987): Effects of magnetic field and magnetic field on the growth of tilapia. – *Journal of Tropical Ocean* 1: 93-95.

LOSS RULES OF TOTAL NITROGEN AND TOTAL PHOSPHORUS IN THE SOILS OF SOUTHWEST MOUNTAINS IN HENAN PROVINCE, CHINA UNDER ARTIFICIAL RAINFALL

WANG, G.^{1*} – LI, Z.² – ZHANG, J.³ – LU, Y.² – CHEN, Z.⁴

¹*Hydrology and Water Resources of Yellow River Scientific Research Institute
Zhengzhou, China*

²*Hydrology and Water Resources Bureau in Henan Province, Zhengzhou, China*

³*Yellow River Henan Bureau, Zhengzhou, China*

⁴*Hydrology and Water Resources Survey Bureau of Nanyang in Henan Province
Nanyang, China*

**Corresponding author
e-mail: zhonggw2020@163.com*

(Received 27th Sep 2018; accepted 28th Nov 2018)

Abstract. To seek a feasible land use structure to control non-point pollution, by indoor artificial rainfall test, total nitrogen (TN) and total phosphorus (TP) as nutrient indexes, five types of soil in southwest of Henan Province were selected to study the nutrient loss rules under six kinds of rainfall intensity. The results were that: (1) the nutrient loss, runoff and sediment yield were accordingly increased with the increase of rainfall intensity in same type of soil. On same rainfall intensity, nutrient loss in the soil of farmland was larger than that in woodland and grassland, the nutrient content in terrace was higher than that in other soil. (2) The nutrient content in silt load was higher than that in bed load out of nutrient enrichment in sediment drain. There was a relationship of power index between nutrient loss and runoff while there was a linear correlation for sediment yield and nutrient loss. (3) The nutrients in farmland mainly went away with sediment erosion while in forest land, TN mainly drained with runoff and TP eroded with sediment. (4) At 0.01 of confidence level, the effect of rainfall intensity on nutrient loss was significant in runoff and sediment; land use types became more significant to TN loss than to TP drain in runoff while it had no prominent effect on the nutrient drain with sediment. Conclusion: It is important to popularize the projects of slope to terrace and grain for green in the region to improve crop yield and reduce non-point source pollution.

Keywords: *artificial rainfall, rainfall intensity, land use type, soil erosion, runoff, nutrients loss*

Introduction

Water pollution is an international problem and agricultural non-point source pollution is its main pollution form (Li and Chen, 2015). The survey showed the non-point source pollution accounted for about two-thirds of total pollution load in the United States and 68% to 83% of which was agricultural non-point source pollution (Li and Hu, 2013). The research found that agricultural non-point source pollution was a major cause of eutrophication of water environment in Denmark (Beibei et al., 2017). The emissions of agricultural non-point pollutant have exceeded the source of industry and life and became the first pollution source inland (Yang et al., 2013). As an important form of non-point source pollution and carrier of transportation, soil erosion is root reason for bringing water bodies pollution, such as lakes, reservoirs, rivers and so on (Li, 2013). The water pollution which is caused by soil erosion had caused economic losses between 2.2 to 7 billion dollars in the USA (Zhou, 2014). Nitrogen and

phosphorus of soil are either the nutrients required by crops or important source of agricultural non-point pollution (Yu et al., 2013). Artificial rainfall method is a common way to study soil erosion in small scale land use manner which not only can test the research results of natural rainfall, but also can make up for the results that cannot be obtained via the natural rainfall in short duration (Wang et al., 2017b; Xi et al., 2014; He et al., 2014).

Danjiangkou Reservoir is water source area of the south-to-north water diversion middle route project, whose water quality is directly related to the stand or fall of the project (Zhang et al., 2018). Soil erosion is serious in upstream of the reservoir due to topography, soil, vegetation, rainfall and human activities, which will lead to regional non-point pollutants boiling up and scope expands unceasingly without control measures, such as chemical fertilizers and pesticides residue, directly affecting water quality of the reservoir (Wang et al., 2017c; Zhang et al., 2015). The research is less on nutrient loss of different land use types in the region up to date. Indoor artificial rainfall experiments are adopted in the study with familiar land use types selected in southwest mountains of Henan Province to explore the rule of nutrients washing away indifferent soil and various rainfall intensity to probe an economical and practical cultivation structure that will be suitable to local ecological environment and conservation of soil and water.

Materials and methods

Test materials and conditions

The experiments were done by slope village and test equipment included five parts: artificial rainfall simulator, trial soil bin, sampling system of runoff and sediment, runoff measurement system and nutrients testing system. Artificial rainfall device was made of steel plate with 2-mm thickness keeping five degrees inclined, total height of which was 1.6 m. The water distributor with uniform pore size was installed above the device and raining height was 1.05 m, rotor flow meter was set up to control rainfall intensity. The soil bin size was 70 cm in length, 40 cm in width and 20 cm in height; runoff exporting size was 30 cm in length, 3 cm in width and 3 cm in height; a basin was placed at the exit of runoff.

The experiments of artificial rainfall had been done during April to August in 2012 in institute of soil and water conservation Chinese Academy of Sciences (CAS) and rainfall intensity was respectively designed as 0.5, 1.0, 1.5, 2.0, 2.5 and 3.0 mm•min⁻¹. After filling the soil into the soil bin, selecting rainfall intensity and turning on the rainfall simulation device, the time was recorded and the samples of water and soil were collected every 10 min when the runoff appeared. 500 ml runoffs were taken out from basin when the rain flowed into the basin settled down for 10 min. After filtering and drying the runoff, the weighed value of the soil was the amount of silt load and the rest of soil in basin was bed load which was collected dried and weighed. After 100 min when the rainfall was stopped and the soil was dug up, another kind of soil was put into the bin to continue the rainfall test in the same rainfall intensity. The tested soil was placed in the container dried naturally and waiting for next rainfall intensity. The nutrients loss of five kinds of soil was tested in sequence under six types of rainfall intensity.

The tested soil was from five land use types in southwest mountains of Henan Province near Danjiangkou Reservoir: timber forest, shrubby grassland, terrace, slope

cropland and waste-grassland. Firstly, sample plots of the five soil types were selected and then those soil types of plough layer keeping original state were collected respectively and carried back to the laboratory. The amounts of soil filled were calculated by the area of soil bin and bulk weight. The soil was compacted once with 2.5 cm thickness soil filled and the surface of soil was loosened before filling the upper soil to prevent the soil delaminating.

Test items and method

The content of total phosphorus (TP) and total nitrogen (TN) need to be tested in the samples of sediment and runoff, tested methods of which are shown in *Table 1*.

Table 1. The test items and methods

Samples	Indexes	Tested methods	Tested standard
Runoff	TN	Alkaline potassium persulfate digestion-UV spectro photometric method	GB 11894-89 (Huan, 2012)
	TP	Ammonium molybdate spectrophotometric method	GB11893-89 (Shen and Li, 2013)
Sediment	TN	Semi-micro Kjeldahl method	GB7173-87 (Mureithi et al., 2014)
	TP	Ammonium molybdate spectrophotometric method	Soil analysis (3 rd edition) (Wang et al., 2016)

Data processing methods

The software of EXCEL, PSS and SAS were used to analyze and study the experimental data, in order to find out the hidden rules in these data.

Results and discussion

The nutrients change in the samples of runoff

In above five kinds of soil, changing rule of TN and TP in runoff was shown in *Figure 1a, b*.

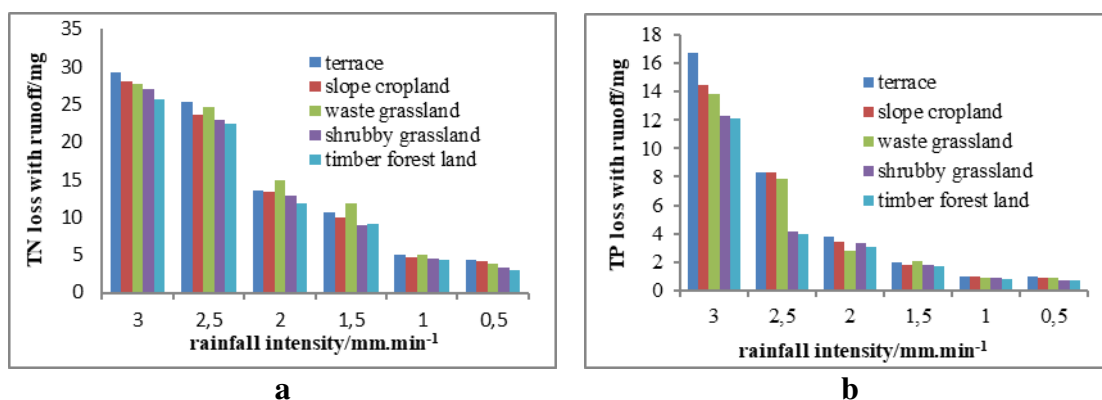


Figure 1. The rule of TN erosion (a) and TP drain (b) in runoff samples

From two figures, the loss of nutrients gradually reduced with runoff decreasing by reduction of rainfall intensity. The larger rainfall intensity was, the more runoff and nutrients loss were in the same type soil. On the whole, nutrients loss in the soils of terrace, hilly land and waste grassland were slightly larger than the one in woodland and shrubby grassland in same rainfall intensity which showed forest land and grassland had a better effect on preventing water and soil losing; the concentration of TP and TN in runoff of terrace was higher than that in other soil, which indicated the engineering of slope to terrace had a very good effect on water conservation.

Farmland (terraces and slope cropland) needed to be ploughed and fertilized when wheat reaped and crop were planted, which caused huge loss of nitrogen and phosphorus on rainfall season especially in the downpour. Large amounts of nitrogen and phosphorus flow into tributaries with runoff and eventually into Danjiangkou Reservoir which seriously threatens water quality of the reservoir. The experiments showed the projects of turn hillsides into terrace and returning farmland to forest and grass had important practical significance, which could reduce soil erosion and non-point source pollution (Wu et al., 2015).

The nutrients change rule in sediment drain

By *Figure 2a, b*, the nutrients loss in sediment drain basically decreased with reduction of rainfall intensity in same soil, and the larger rainfall intensity was, the higher sediment yield and nutrients lost. The loss of TN and TP in farmland soil were respectively 36.2~115.98 times and 10.1~81.4 times of forest and grassland in corresponding rainfall intensity because of better soil structure for the latter, which was in accordance with Tang Jie's research (Tang et al., 2012).

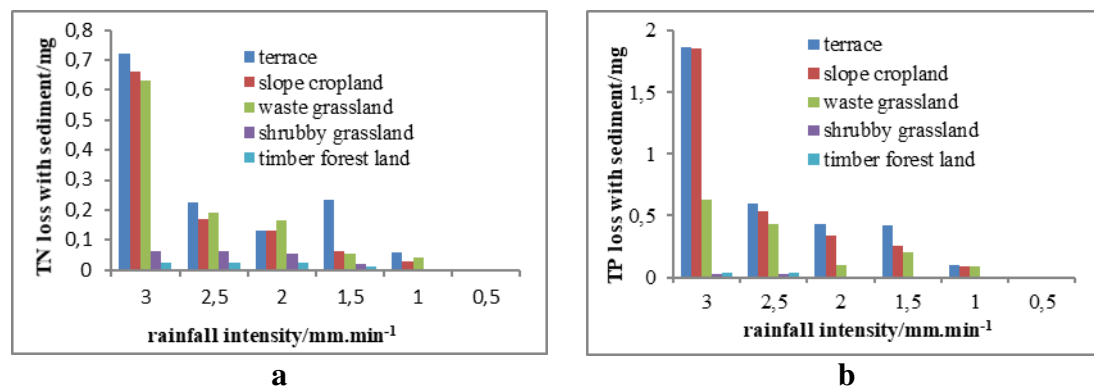


Figure 2. The rule of TN drain (a) and TP drain (b) in sediment samples

Nutrients enrichment in sediment drain

Researches indicated the phenomenon of nutrients enrichment existed in the sediment drain (Guo et al., 2014; Zhang et al., 2015). According to the tested soil, the nutrients enrichment rule in silt load and bed load were shown in *Table 2* (no analysis the enrichment of silt load in timber forest and shrubby grassland due to lower amount). Nutrients content of silt load were higher than the one of bed load in *Table 2*. Nutrients Enrichment rate (NER) means that nutrients content in sediment is divided by the sediment yield, which can characterize the state of nutrients accumulation in sediment.

The soil of arable layer is easy to erode out of human activities and there are more fine grain and compound grain in farmland soil that makes nutrients enrichment more obvious in sediment drain, so the content of TN and TP in silt load is higher than that in bed load.

Table 2. Nutrient enrichment rate in sediment drain

Soil types	NER of bed load		NER of silt load	
	TN	TP	TN	TP
Slope cropland	1.17	1.15	1.76	1.54
Terrace	1.47	1.07	2.43	1.95
Waste-grassland	1.08	1.27	1.23	1.57
Shrubby grassland	1.15	1.53		
Timber forest	1.11	1.19		

Correlativity of nutrients loss and runoff, sediment

The relationship between nutrients loss and runoff

Researches manifested there was an obvious correlativity between surface runoff and non-point source pollution load (Wang et al., 2016, 2017a), and there was a relationship of power exponent between two elements by references (Lv et al., 2015; Shi et al., 2016). In this research, the amount of pollutant output was computed by the following formula:

$$M = \sum Q_i \times C_i$$

In the formula, M is total amount of pollutant output accumulated in each period from the beginning of rainfall; Q_i stands for runoff/sediment drain for period i ; C_i means concentration of pollutant at period i .

According to the formula, there was a significantly positive correlation among the loss of TN, TP and runoff, the fitting equations of which were shown in *Table 3*. M_{TN} expressed total output of TN namely the sum of each period, so was M_{TP} ; Q represented runoff volume.

Table 3. The fitting equations of nutrients loss and runoff

Soil types	Fitting equations	Correlation index
Timber forest	$M_{TN} = 0.2058Q^{1.2016}$	0.9949
Shrubby grassland	$M_{TN} = 0.3793Q^{0.9278}$	0.9998
Waste-grassland	$M_{TN} = 0.2233Q^{1.1995}$	0.9951
Terrace	$M_{TN} = 0.1592Q^{1.2678}$	0.9890
Slope cropland	$M_{TN} = 1.5588Q^{0.7217}$	0.9895
Timber forest	$M_{TP} = 0.1135Q^{1.0921}$	0.9769
Shrubby grassland	$M_{TP} = 0.0034Q^{1.8322}$	0.9643
Waste-grassland	$M_{TP} = 0.0051Q^{1.909}$	0.9885
Terrace	$M_{TP} = 0.0032Q^{1.2678}$	0.9589
Slope cropland	$M_{TP} = 0.0179Q^{0.9172}$	0.9587

The relationship between nutrients loss and sediment drain

The linear regression analysis of nutrients loss and sediment drain was done and the regression equations were shown in *Table 4*. Q was sediment drain and M meant nutrients loss in the table, M_{TN} expressed the loss of TN and M_{TP} represented the drain of TP.

Table 4. The regression equations of nutrients loss and soil erosion

Soil types	Regression equations	Correlation index
Timber forest	$M_{TN} = 0.2065Q + 0.0124$	0.9991
Shrubby grassland	$M_{TN} = 0.2135Q - 0.0003$	0.9934
Waste-grassland	$M_{TN} = 0.3283Q - 0.0271$	0.9907
Terrace	$M_{TN} = 0.2033Q - 0.0002$	0.9979
Slope cropland	$M_{TN} = 0.2219Q - 0.0007$	0.9914
Timber forest	$M_{TP} = 0.5525Q + 0.0524$	0.9955
Shrubby grassland	$M_{TP} = 0.7652Q + 0.0024$	0.9798
Waste-grassland	$M_{TP} = 0.3017Q + 0.0424$	0.9628
Terrace	$M_{TP} = 0.9601Q + 0.0002$	0.9991
Slope cropland	$M_{TP} = 0.554Q + 0.0038$	0.9765

Comparison on nutrients content of runoff and sediment erosion in topsoil

There are two main forms for nutrients drain, one is pollutants which are attracted by soil particles eroding with the soil particles drained, the other is pollutants that are easy soluble in water by leaching into the runoff. In this paper, the nutrients loss ways for slope cropland were shown in *Figure 3a, b*.

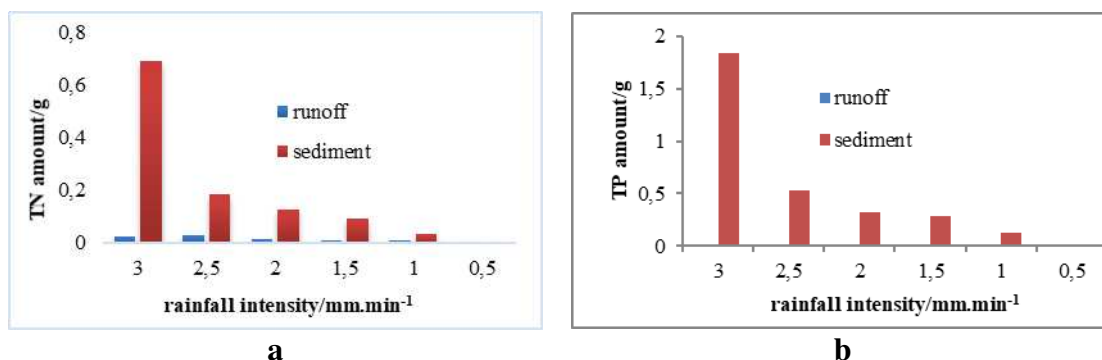


Figure 3. TN (a) and TP (b) amount in runoff and sediment drain in slope cropland

By *Figure 3a, b*, the proportion of nutrients loss with runoff was not large in total nutrients drain and the majority of nutrients were washed away by sediment in slope cropland (namely farmland). TN loss with sediment was far more than that with runoff, the times of them changed between 6.7 with 25.55 because of different rainfall intensity; the times of TP loss with sediment floated from 53.97 to 109.92 compared with that with runoff, which showed nutrients eroded was adsorbed by the fine grain of

soil and carried by sediment drain that was the main way of agricultural non-point source pollution.

Through *Figure 4a, b*, in the soil of timber forest namely woodland, loss of TN with runoff far outweighed that with sediment while the loss of TP mainly disappeared with sediment drain. On same rainfall intensity, TN loss with sediment was 0.13~0.22 times of that with runoff and TP loss with sediment was 1.84~6.6 times of that with runoff.

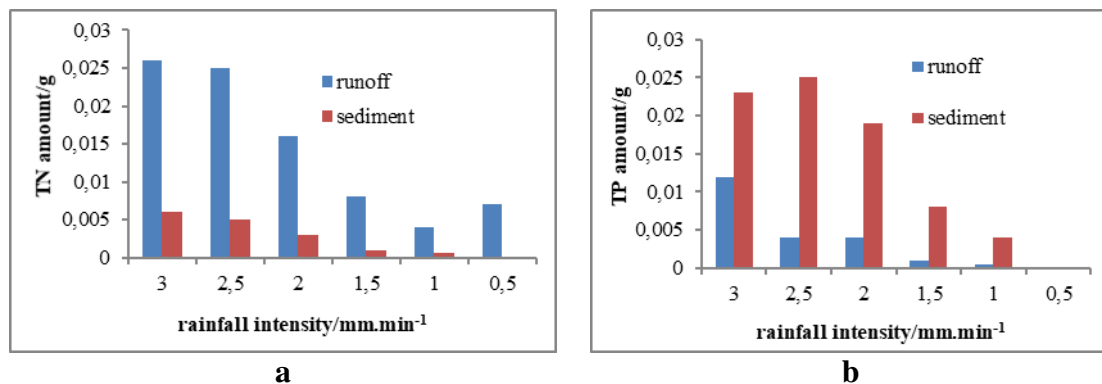


Figure 4. TN (a) and TP (b) amount in runoff and sediment erosion in timber forest

From *Figures 3 and 4*, the nutrients loss with sediment was higher than that with runoff in farmland soil, which was consistent with the results of Wang et al. (2016) and Yao et al. (2013). The loss of TN with sediment was less than that with runoff in forest land and the nutrients loss in woodland was less than the one in farmland. Reason could be from two sides, for one thing, the flow yield was less because of good infiltration in woodland to reduce soil erosion; for another, soil particles eroded were larger carrying little nutrients, which made less nutrients lose with sediment. In addition, gradient influence had not been considered in the experiments, and usually, nutrients loss gradually increased with the increase of slope.

The statistical analysis of land use and rainfall intensity on nutrient loss

Variance analysis of land use and rainfall intensity on the nutrient loss in runoff

Two-factor variance analyses were done by SAS software to study the influence of land use and rainfall intensity on the nutrient loss in runoff, whose results were shown in *Table 5*.

Table 5. Variance analysis of land use and rainfall intensity on TN and TP loss in runoff

Indexes	Source	DF	SS	MS	F value	Pr. >F
TN	Land use types	4	17.893347	4.473337	12.51	<0.0001
	Rainfall intensity	5	2430.826067	486.165213	1360.11	<0.0001
	Error	20	7.148933	0.357447		
	Total	29	2455.868347			
TP	Land use types	4	13.2784867	3.3196217	3.03	0.0419
	Rainfall intensity	5	633.9812567	126.7962513	115.63	<0.0001
	Error	20	21.9315933	1.0965797		
	Total	29	669.31913367			

From *Table 5*, both land use types and rainfall intensity had significant effects on TN loss in runoff whose significant level was $Pr. < 0.0001$. The influence of land use types on TP was slightly significant at 0.05 of confidence level while it was not significant on confidence level of 0.01; there was a significant effect for rainfall intensity on TP loss in runoff whose significant level was $Pr. < 0.0001$.

Variance analysis of land use and rainfall intensity on the nutrient loss in sediment

The variance analysis results of land use and rainfall intensity on TN and TP in sediment were shown in *Table 6*.

Table 6. Variance analysis of land use and rainfall intensity on TN and TP loss in sediment

Indexes	Source	DF	SS	MS	F value	Pr. > F
TN	Land use types	4	0.25713567	0.06428392	3.62	0.0225
	Rainfall intensity	5	0.53330200	0.10666040	6.0	0.0015
	Error	20	0.35557633	0.01777882		
	Total	29	1.14601400			
TP	Land use types	4	1.69064913	0.42266228	3.6	0.0229
	Rainfall intensity	5	2.58242240	0.51648448	4.4	0.0073
	Error	20	2.34732527	0.11736626		
	Total	29	6.62039680			

Based on *Table 6*, land use types had some influence on TN and TP in sediment at 0.05 of confidence level while it had no effect on confidence level of 0.01; rainfall intensity made a significant effect on TN and TP in sediment whose significant level was respectively 0.0015 and 0.0073.

Discussion

The physical properties of soil are the internal factors leading to soil erosion, the degree of soil erosion is usually related to the physical properties of soil itself under certain external forces (Kaya et al., 2016). The above research showed that the soil of timber forest and shrubby grassland could absorb nutrients and reduce soil erosion out of better soil structure; under the same rainfall conditions, the loss of terraced soil in runoff and sediment were all lower than sloping farmland while the concentration of TN and TP were higher than that of other soil, which fully indicated that terrace could store and collect nutrients and achieve on-site infiltration of rainwater.

It is easy to produce soil erosion because of complex topography and abundant rainfall in study area, moreover, Danjiangkou reservoir is water source area of south-to-north water transfer project, its water quality is related to the success of the project. Therefore, it is necessary to adjust the land use structure in the region that restoring steep slope land to forest and grass and changing gentle slope land to terrace, so as to improve crop yield and control soil erosion, non-point agricultural pollution and ensure the water quality safety of the reservoir.

Conclusions

It was studied that the nutrients loss rule of five types of soil in southwest mountains in Henan Province under six kinds of rainfall intensity by artificial rainfall tests and the results were that:

(1) The loss of nutrients, runoff and sediment drain were larger with rainfall intensity increasing in same type soil. On same rainfall intensity, nutrients loss of farmland soil was larger than that in woodland and grassland, the nutrients content in terrace was higher than that in other soil. (2) Due to nutrients enrichment in sediment drain, the nutrients content in silt load was higher than that in bed load. By regression analysis, there was the relationship of power index in nutrients loss and runoff while it was a linear correlation between sediment erosion and nutrients loss. (3) The nutrients in farmland mainly went away with sediment erosion while in forest land, the TN loss with sediment was less than that with runoff and the loss of TP was on the contrary. (4) At 0.01 of confidence degree, there was a significant effect for rainfall intensity on nutrients loss in runoff and sediment; Land use types made a significant influence on the TN loss in runoff but no effect on the TP drain while it had no prominent effect on nutrients loss in sediment.

Above research shows that the land use structure is unreasonable in the region and it is urgent to adjust with returning to forest and grass in steep slope land and turning hillsides to terrace in gentle slope, which can not only improve crop yield, but also control soil erosion and non-point agricultural pollution and ensure water quality safety of the reservoir.

Acknowledgements. The paper was written by the items “Study on Agricultural Non-point Source Pollution in the Water Source Area of Danjiangkou Reservoir Based on Fractal Theory and its Prevention Measures (GG201412)” and funded by the subject “the Risk Assessment of Water Quality and Security System Research for Reservoir Water Source Area in Henan Province (GG201612)”, which applied the detailed data and funding that should be firstly appreciated. And the staff of institute of soil and water conservation CAS paying more efforts to the experiments of artificial simulated rainfall ought to be respected.

REFERENCES

- [1] Beibei, Y., Kai, H., Dezhi, S. et al. (2017): Mapping the scientific research on non-point source pollution: a bibliometric analysis. – *Environmental Science and Pollution Research* 24: 4352-4366.
- [2] Guo, X., Song, F., Gao, Y. et al. (2014): Characteristics of lost sediment and its nutrient enriched effect on three types soil slope under simulated rainfall. – *Journal of Soil and Water Conservation* 28: 23-28.
- [3] He, T., Qin, F., Su, T. et al. (2014): Effect of different cultivation methods on nitrogen and phosphorus losses along with runoff. – *Research of Soil and Water Conservation* 21: 95-103.
- [4] Huan, J. (2012): *Water Quality-Determination of Total Nitrogen-Alkaline Potassium Persulfate Digestion UV Spectrophotometric Method*. – China Environmental Science Press, Beijing.
- [5] Kaya, A., Alemdag, S., Dag, S. et al. (2016): Stability assessment of high-steep cut slope debris on a landslide (Gumushane, NE, Turkey). – *Bulletin of Engineering Geology and the Environment* 75: 89-99.

- [6] Li, Y., Chen, Y. (2015): The path of the prevention legislation in agriculture non-point source water pollution in China under the background of transformation. – *Jiangsu Agricultural Sciences* 43: 441-443.
- [7] Li, Y., Hu, Y. (2013): Strategy of controlling agricultural non-point pollution in Minjiang River basin. – *Journal of Fujian Agricultural and Forestry University (Philosophy and Social Sciences)* 16: 5-8.
- [8] Li, Z. (2013): Review of the current situation and control countermeasures in agricultural non-point source pollution control in China. – *Agricultural Research in the Arid Areas* 31: 207-212.
- [9] Lv, Y., Peng, X., Gao, L. et al. (2015): Characteristics of nitrogen and phosphorus losses through surface runoff on sloping land, red soil hilly region. – *Soils* 47: 297-304.
- [10] Mureithi, S. M., Verdoodt, A., Gachene, C. K. et al. (2014): Impact of enclosure management on soil properties and microbial biomass in a restored semi-arid rangeland, Kenya. – *Journal of Arid Land* 72: 561-570.
- [11] Shen, Y., Li, L. (2013): Modification of ammonium molybdate spectrophotometric method for measurement of dissolved phosphorus. – *Experimental Technology and Management* 30: 56-59.
- [12] Shi, Y., Huang, J., Ni, X. et al. (2016): Effects of fertilization on surface runoff loss of nitrogen and phosphorus from mulberry in the northern Zhejiang Plain, China. – *Agro-Environment and Development* 33: 518-524.
- [13] Tang, J., Liu, C., Yang, W. et al. (2012): Spatial distribution of non-point source pollution in Dahuofang Reservoir catchment based on swat model. – *Scientia Geographica Sinica* 32: 1247-1253.
- [14] Wang, G., Li, Z., Tian, Y. et al. (2016): Effects of rainfall intensity and land use mode on loss of TN and TP in southwest hilly area of Henan Province. – *Yangtze River* 47: 18-22.
- [15] Wang, G., Li, Z., Qu, J. et al. (2017a): Features of soil nutrients loss under different land use in southwest mountainous areas of Henan Province. – *Bulletin of Soil and Water Conservation* 37: 83-88.
- [16] Wang, G., Li, Z., Tian, Y. et al. (2017b): Effects of rainfall intensity and land use on flow volume and sediment yield in Southwest Coteau of Henan Province. – *Engineering Journal of Wuhan University* 50: 182-186.
- [17] Wang, G., Li, Z., Zuo, Q. et al. (2017c): T estimation of agricultural non-point source pollutant loss in catchment areas of Danjiangkou Reservoir. – *Research of Environmental Science* 30: 415-422.
- [18] Wang, Q., Yang, T., Liu, Y. et al. (2016): Review of soil nutrient transport in runoff and its controlling measures. – *Journal of Agricultural Machinery* 47: 67-82.
- [19] Wang, Z., Yang, Y., Ren, R. et al. (2016): Method comparison between ICP-AES and ammonium Molybdate spectrophotometry in determination of total phosphorus in industrial wastewater. – *The Administration and Technique of Environmental Monitoring* 28: 58-61.
- [20] Wu, D., Huang, Z., Xiao, W. et al. (2015): Control of soil nutrient loss of typical reforestation patterns along the three gorges reservoir area. – *Environmental Science* 36: 3825-3831.
- [21] Xi, Y., Tian, W., Li, Y. et al. (2014): Nitrogen and phosphorus runoff losses and loss coefficients in rice-wheat rotation system in Taihu Lake basin. – *Jiangsu Journal of Agricultural Sciences* 30: 534-540.
- [22] Yang, L., Feng, Y., Shi, W. et al. (2013): Review of the advances and development trends in agricultural non-point source pollution control in China. – *Chinese Journal of Eco-Agriculture* 21: 96-101.
- [23] Yao, N., Cheng, Y., Cai, C. (2013): Study on the nitrogen enrichment experiment of purple soil. – *Subtropical Soil and Water Conservation* 25: 14-18.

- [24] Yu, H., Yang, Z., Xiao, R. et al. (2013): Absorption capacity of nitrogen and phosphorus of aquatic plants and harvest management research. – *Acta Prataculturae Sinica* 22: 294-299.
- [25] Zhang, J., Liu, D., Jiang, X. et al. (2015): Research on soil erosion using remote sensing method in Danjiangkou Reservoir – A case study of Shangnan County. – *Journal of Agricultural Resources and Environment* 32: 162-168.
- [26] Zhang, L., Wu, M., Wan, Y. (2018): Study on countermeasures for water quality security of the Danjiangkou Reservoir. – *China Water Resources* 1: 44-47.
- [27] Zhang, Y., Ding, Y., Wang, D. et al. (2015): Effects of slope gradient on yield and particle size distribution of sediment. – *Journal of Soil and Water Conservation* 29: 25-29.
- [28] Zhou, H. (2014): The influence of railway construction on ecological service function and soil erosion problem. – *Technology of Road and Bridge* 14: 204-205.

EFFECTS OF EARLY WATER STRESS ON GRAPEVINE (*VITIS VINIFERA* L.) GROWING IN CV. SYRAH

KORKUTAL, I.^{1*} – BAHAR, E.¹ – CARBONNEAU, A.²

¹*Department of Horticulture, Agricultural Faculty, Namik Kemal University
59030 Tekirdag, Turkey
(phone: +90-282-250-2056)*

²*Agro M, Viticulture-Oenologie (Emeritus), UMR
2 place Viala, F-34060 Montpellier Cedex, France*

**Corresponding author*

e-mail: ikorkutal@nku.edu.tr; phone: +90-282-250-2059

(Received 27th Sep 2018; accepted 14th Nov 2018)

Abstract. Water deficit is a major issue in grapevine production. The purpose of this research was to identify the effects of early water stress on the growing and yield of grapevine. The research was performed in SupAgro/INRA in Montpellier using the ECOTRON System, France. Syrah/SO4 graft combination was used as a plant material. 7 years old and potted grapevines were grown/kept in natural vineyard conditions. A completely randomized block design was used: WS₀ (control) 0; -0.2 MPa, WS₁ -0.2; -0.4 MPa, WS₂ -0.4; -0.6 MPa, and WS₃ -0.6; -0.8 MPa respectively. The limitation of water was started the 15th of May in the 17th E-L stage and ended about the 15th of June in the 27th E-L stage. Analysis of variance was performed on the agronomic data using the MSTAT-C. Means were separated using the LSD test (P < 0.01). It was determined that there was a reduction in vegetative growth. Also the predawn leaf water potential results showed differences between the irrigation levels. These results indicated that the lowest Ψ_{pd} in WS₃ was -0.80 MPa. There was an approximately 55 cm difference determined between the control and other groups in shoot lengths. Besides that the average cluster weight was reduced by about 41% and the yield by about 28% under the early water deficit conditions.

Keywords: *early water deficit, Vitis vinifera L., Syrah cv., vegetative development, yield*

Introduction

Grapevine has been widely used as a model plant to study ecophysiological responses to water stress (Lovisolo et al., 2010). Grapevine growing is traditionally carried out in non-irrigated, extensive agricultural areas in semi-arid regions and dry lands. Abiotic stress, such as drought, reduces the rate of growing and photosynthesis of the grapevine thus limiting leaf functions and changing the source-sink balance. The results showed that berry composition was less sensitive to leaf: fruit ratio than to grapevine water status (Azevedo and Lea, 2011; Etchebarne et al., 2010).

The occurrence of water deficit is clearly important in order to state berry and wine composition. Also the irrigation provided certain wine sensory characteristics (Matthews et al., 1990). Though a late water deficit had no effect on ripening (Matthews and Anderson, 1988). In general, mild water deficits (-0.2 and -0.4 MPa) promoted wine quality in red varieties (Bravdo et al., 1985). Bahar et al. (2011) reported that sudden and extreme water stress results in smaller berries at harvest. On the other hand there is a reduction in the values of 100 berry weight and berry volume.

The effects of different levels of water deficit on growing Syrah berries were examined by Ojeda et al. (2002). Their results showed two types of berry responses to water deficit: an indirect and positive effect on the composition of phenolic compounds

due to the limitation of berry size and a direct action on biosynthesis. The second response can have positive or negative effect the on composition of berries, type of phenolic compounds, application period, and water deficit severity. Otherwise De la Hera Orts et al. (2004) proved that the severe water stress, decreased vigor but also the content of acid and sugar due to photosynthetic activity may be compensated.

Water deficit had inhibition effects (Sadras and Moran, 2012) on reproductive and vegetative growth and changed the vine phenology (Coombe, 1992). Especially water deficit stress has a main effect on grapevine growth and berry development that in conclusion can impact wine quality (Tillet et al., 2011). The results of this study indicated the effects of early water stress levels on vegetative development in cv. Syrah.

Materials and methods

The test was conducted in the 2008 vegetation period by use of Supagro ECOTRON System in Montpellier. Seven years old Syrah / SO4 grafting combination was used as plant material which were planted in 72 L containers, because this cultivar is known as drought tolerant (Schultz, 1996). The test was designed according to a randomized complete block design into four parcels. It has 3 replications and 2 parcel based grapevines and 4 water stress levels [WS₀ (4 L day⁻¹), WS₁ (3 L day⁻¹), WS₂ (2 L day⁻¹), WS₃ (1 L day⁻¹)] (24 grapevines). All vines were equalized by 22 shoots and about 30 clusters. The research was carried out from the second week of May to the second week of June (17th to 27th) (Eichorn and Lorenz, 1977). All plants were re-irrigated and fertilized (6 L day⁻¹) after early water stress period.

Stress groups were designed depending on predawn leaf water potential (Ψ_{pd}) according to Carbonneau (1998), Rogiers et al. (2014), Deloire and Rogiers (2014) WS₀ (Control): 0; -0.2 MPa, WS₁: -0.2; -0.4 MPa; WS₂: -0.4; -0.6 MPa and WS₃: -0.6; -0.8 MPa resp. Predawn leaf water potential (Ψ_{pd}) was measured at tertian days at 03:00 AM by using Scholander Pressure Chamber. Fully expanded leaves are measured (Ψ_{pd}) parcel based (Scholander et al., 1965). The measurement of predawn leaf water potential (PLWP; Ψ_{plwp}), is performed before sunrise, when the stomata of the plant are closed and when the grapevine has been able to equilibrate its water potential with the wettest layer of the soil. PLWP is mainly used for research purposes only. Threshold values for PLWPlwp have been proposed by Carbonneau (1998), which makes it possible to evaluate the degree of water deficit experienced by the plant (Deloire and Rogiers, 2014). Vegetative parameters, such as shoot lengths (cm) in 3 days intervals, shoot elongation rate (cm³ days⁻¹), also average cluster weights (g) and yield (kg per vine) and water potential were measured.

Analysis of variance was performed on the agronomic data using the MSTAT-C statistical software. Means were separated using the LSD test (P < 0.01).

Results and discussion

Phenologic stages

It was determined according to Eichhorn and Lorenz (1977), the phenologic stages and their dates are presented in *Table 1*. and also some climatic data in *Figure 1*. Ojeda et al. (1999) reported that the growing of grapevine in ECOTRON and in the vineyard is coherent. Nevertheless phenologic stages were not affected by the early water stress in Syrah cv.

Table 1. The phenophases according to Eichhorn and Lorenz (1977) in cv. Syrah

Stages E-L	Dates	Phenology
14	14 May	6-7 leaves separated
15	15 May	7-9 leaves separated
16	17 May	10 leaves separated
17*	20 May	Inflorescence full developed
19	22 May	Beginning of flowering
20	23 May	10% caps off
21	24 May	30% caps off
21	28 May	
21	30 May	
23	31 May	50% caps off
23	03 June	
25	04 June	80% caps off
26	05 June	Cap-fall complete
26	06 June	Setting (2 mm)
27**	09 June	Berries pepper corn size (4 mm)
29	13 June	Berries pea size (7 mm)
31	16 June	
33	10 July	Berry touch
35	27 July	Veraison
38	11 September	Harvest

*Beginning of water stress; ** end of water stress

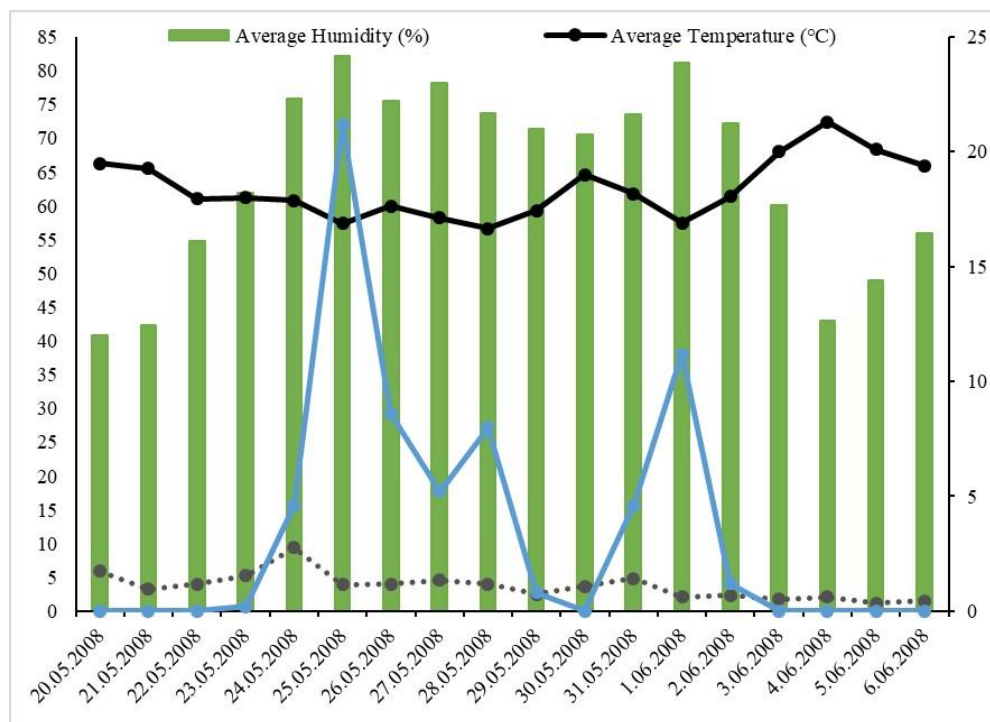


Figure 1. Some climatic data during early water stress

Predawn leaf water potential (MPa) (Ψ_{pd})

Vine water status was measured as Ψ_{pd} and has previously been reported (Bindon et al., 2008). Ψ_{pd} was approximately between 0 and -0.30 MPa in all treatments at the onset of the experiment. A statistically significant difference was found in Ψ_{pd} values in the stress groups. WS₀ was a Control, it was full irrigated during the trial and the Ψ_{pd} values were between -0.21 to -0.29 MPa. In WS₁ Ψ_{pd} values changed to -0.30 to -0.53 MPa. In WS₂ the highest Ψ_{pd} was -0.33 MPa, and the lowest Ψ_{pd} was -0.63 MPa. The lowest Ψ_{pd} in WS₃ was -0.80 MPa. It was seen in Figure 2, that plants were irrigated in the 163 calendar days after bud break there was a linear decrease. Ojeda et al. (2001) notified that the water deficit in early period in cv. Syrah, on the 2nd and on the 40th days after anthesis, Ψ indicated a difference of -0.5 and -0.8 MPa, respectively these results supported our findings.

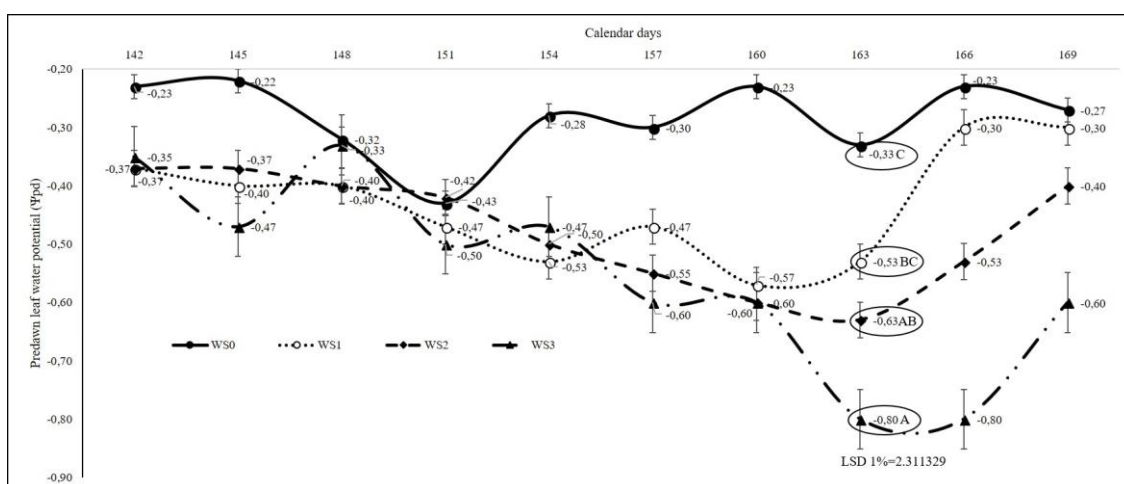


Figure 2. Changes in Ψ_{pd} values during the experiment in Syrah cv.

Vegetative growth

Vegetative growth of Syrah cv. was photographed at different early water stress levels (Fig. 3). In semi-arid environments, early water deficit is therefore a usable tool for controlling vine vigour and canopy (Trigo-Córdoba et al., 2015).

Primary indicator of vine's water deficit is a reduction in leaf and shoot growth (Stevens et al., 1995). Yellow leaves were in plant basal, and also the poor berry set occurred according to the Ψ_{pd} values. Some leaves were detached from the grapevines. In berry set stage, some caps were attached the flowers. This samples were collected on date 18.06.2008 and even on date 28.06.2008. Also, the differences between treatments were detected in berry number per bunch (11.09.2008) same as Korkutal et al. (2011) previously have reported. This difference was seen at harvest when the cluster of Control compared to WS₃ were photographed.

Shoot length (cm)

Just after the third measurement (28 May) there was about 15 cm variation in the control in the stress groups. In the last measurement this was approximately 55 cm's (in the control and in all stress groups). These results are in compliance with the findings of Matthews et al. (1987) who noted an increase in shoot length with irrigation and Korkutal et al. (2011) who reported a 60 cm difference determined in Merlot cv.

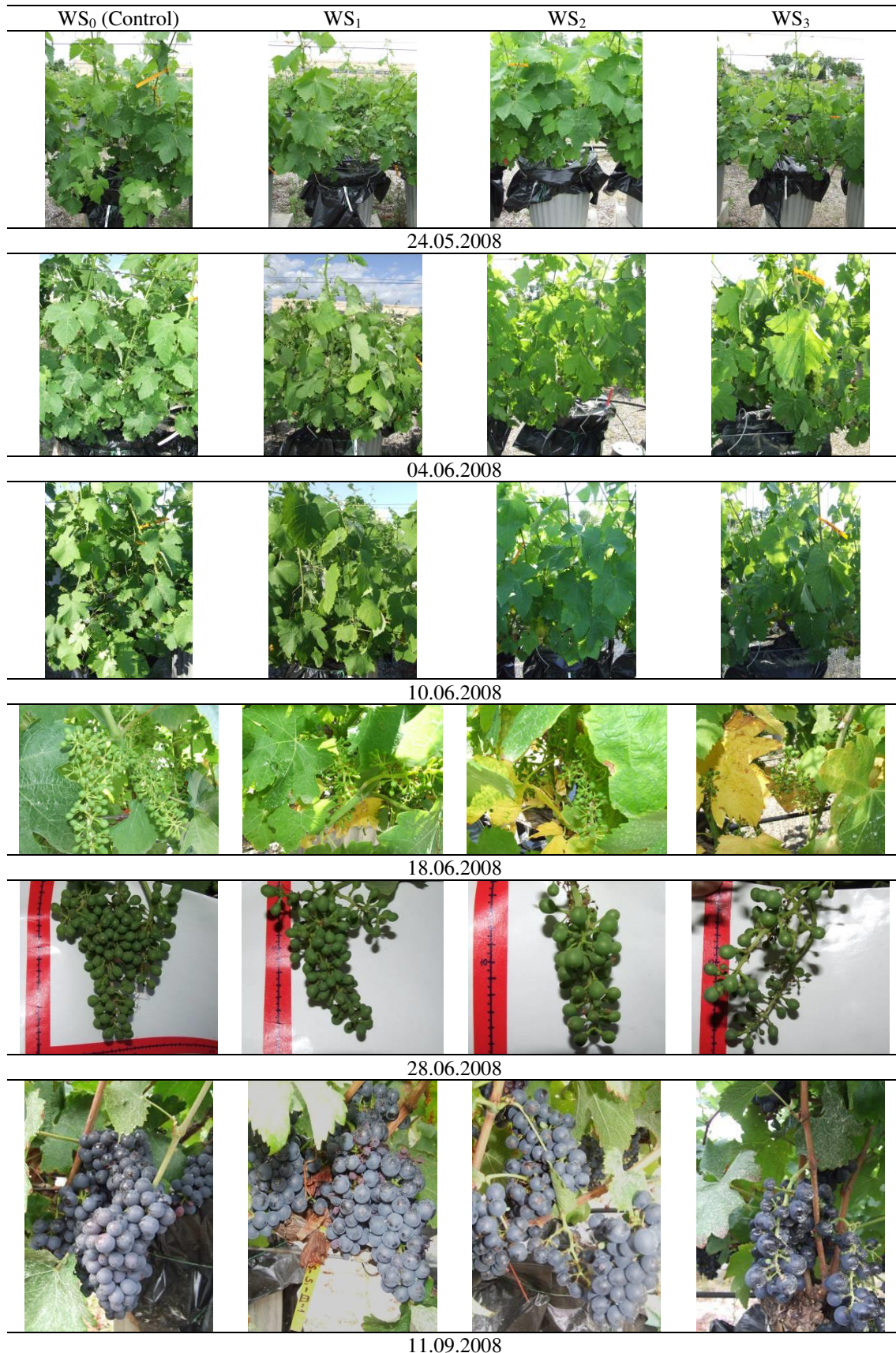


Figure 3. Vegetative growth of Syrah cv. under early water stress condition

The data show that early water deficit has an effect on vegetative growth (Fig. 4). The vine water stress first noticeable symptom is a reduction in shoot growth (Williams, 2010; Keller, 2010). Shoot growth inhibition covers the reduction of internode extension, leaf expansion and tendril elongation (Hardie, 2000) and has been used as a sensitive indicator of grapevine water status (Pellegrino et al., 2005; Lebon et al., 2006). Vegetative growth was reduced because of the early water deficit, our results were in same direction with these researchers.

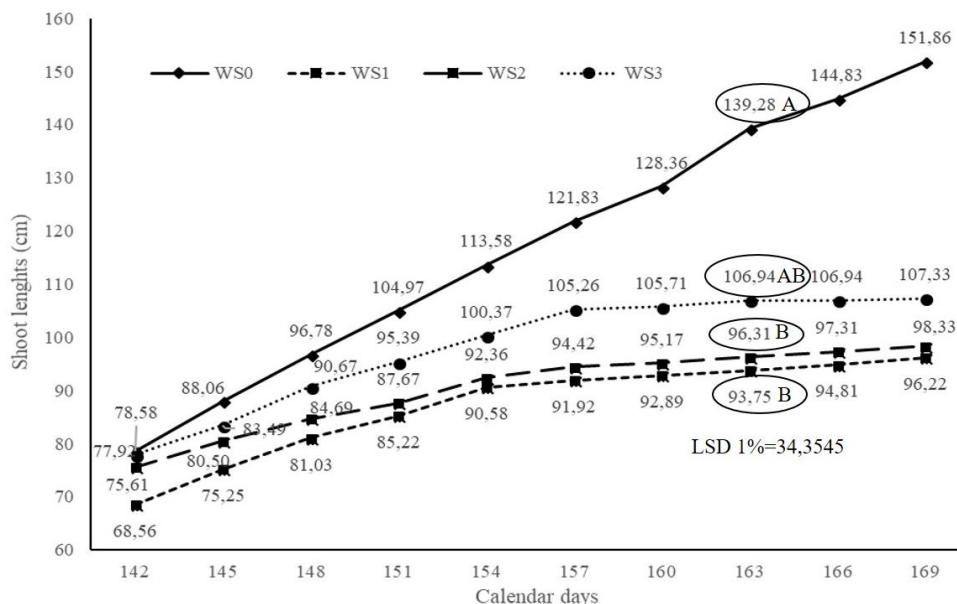


Figure 4. Shoot lengths according to the calendar days in Syrah cv.

Shoot elongation rate (cm 3 days⁻¹)

Water limitation had a decreasing effect on shoot elongation rates (WS₃) (Fig. 5). Severe water deficit reduced shoot growth, changed grape berry composition and promoted ripening, but decrease of yield and berry mass due to excessive exposure was observed by Smart and Coombe (1983) likewise in our findings. When the mean of shoot elongation rates was examined in the stress groups, statistically significant differences (P < 0.01) were determined between the control and other groups.

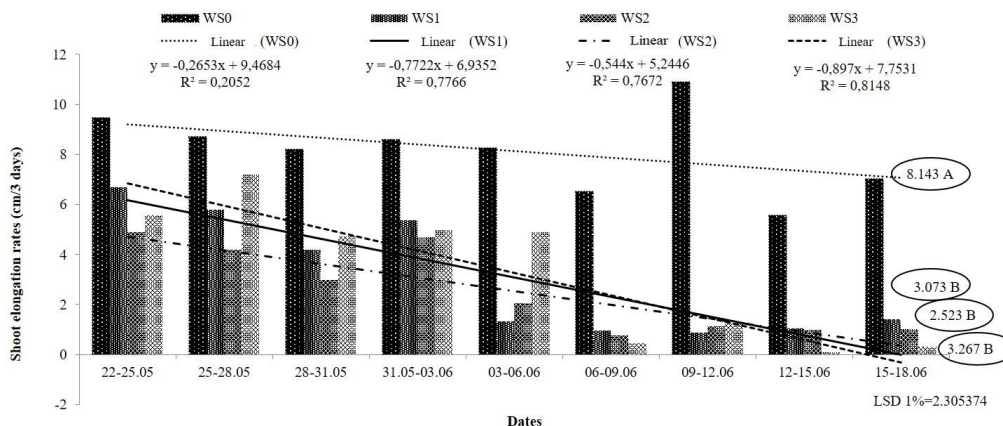


Figure 5. Shoot elongation rates in cv. Syrah

Average cluster weight (g)

Differences in average cluster weight were found due to the stress levels but these were not statistically significant. Control grapevines had the highest average cluster weight 100.93 g and the lowest average cluster weight was measured in WS₃ (59.88 g). Celik (2006) reported Syrah cv. average cluster weight as 200-250 g. Matthews and Anderson (1988) indicated that the inhibition of floral development may be a simultaneous consequence of low water status. Similar results were obtained in our experiment, average cluster weights decreased due to water scarcity. However, in our study because of the early water stress the clusters were smaller and lightweight like Xiao et al. (2018) and Buesa et al. (2017) reported the decrease in berry mass due to water deficit was remarkable (Table 2). Cluster weights decreased about 40.67% compared to control as a result of water stress.

Table 2. Average cluster weights and yield under early water stress

	WS ₀ (Control)	WS ₁	WS ₂	WS ₃
Average cluster weights (g)	102.66	71.97	66.30	59.36
P < 0.01	ns	ns	ns	ns
Yield (kg per vine)	2.84	2.58	2.34	2.05
P < 0.01	ns	ns	ns	ns

ns: non significant

Yield (kg per vine)

In this research yield per grapevine was determined between 2.84 kg per vine and 2.05 kg per vine (Table 2). These results show that early water stress with increasing water stress levels had negative effect on yield (Smart and Coombe, 1983). Yield was reduced about 27.82% compared to control, under early water deficit but these values were not important statistically. This value was also supported by Shellie (2006) and Korkutal et al. (2011), 48% and 50% reduction in yield were determined under irrigation deficit. In addition to these Buesa et al. (2017) argued that in early deficit conditions, yield reduced by 25% compared with that of Control. It should not forgotten be that different deficit irrigation strategies are used to manage the yield (Keller et al., 2016).

Consequently, the period of the water deficit is crucial in specifying berry composition (Matthews et al., 1990). Reducing the irrigation water amount, with the potential to decrease shoot vigour with no yield loss is essential (Dry and Loveys, 1998). As expected, control irrigation resulted in higher yield than the others in our study and in the literature as well (Antolin et al., 2008). Cluster weights and yields were decreased about 40.67% and 27.82%, respectively compared to control. These numeral differences in cluster weight and yield due to the water deficit can be explained by the development of small number but big size grape berries on the rachis.

Conclusion

To sum up our results:

- There was a reduction in vegetative growth.
- The Ψ_{pd} indicated the differences between the irrigation treatments. And the lowest Ψ_{pd} in WS₃ was -0.80 MPa.

- In the last measurement of shoot lengths there was approximately a 55 cm difference between the control and other groups. Corresponding results in shoot elongation rates with water limitation were observed.
- Average cluster weight changed between 59.88 and 100.93 g. Cluster weight was reduced about 40.67% under early water deficit.
- Yield per grapevine was determined between 2.84 kg per vine and 2.05 kg per vine. It was proved that the early water deficit reduced (27.82%) the yield.

Acknowledgements. Our sincere thanks for support belong to LEPSE, Director Thierry Simonneau, and the members of Plant Science Department from LEPSE. They also acknowledge G elle Rolland, Fida Khater (Ph.D. student) and Fatih Gunes Yener who is a *Vinifera* Euromaster student.

REFERENCES

- [1] Antolin, M. C., Santesteban, H., Santa Maria, E., Aguirreolea, J., Sanchez-Diaz, M. (2008): Involvement of abscisic acid and polyamines in berry ripening of *Vitis vinifera* (L.) subjected to water deficit irrigation. – Australian Journal of Grape and Wine Research 14: 123-133. doi.org/10.1111/j.1755-0238.2008.00014.x.
- [2] Azevedo, R. A., Lea, P. J. (2011): Research on abiotic and biotic stress - what next? – Annals of Applied Biology 159: 317-319. doi.org/10.1111/j.1744-7348.2011.00500.x.
- [3] Bahar, E., Carbonneau, A., Korkutal, I. (2011): The effect of extreme water stress on leaf drying limits and possibilities of recovering in three grapevine (*Vitis vinifera* L.) cultivars. – African Journal of Agricultural Research 6(5): 1151-1160. doi.org/10.5897/AJAR11.003.
- [4] Bindon, K., Dry, P., Loveys, B. (2008): The interactive effect of pruning level and irrigation strategy on grape berry ripening and composition in *Vitis vinifera* L. cv. Shiraz. – South African Journal of Enology and Viticulture 29(2): 71-78. DOI: 10.21548/29-2-1439.
- [5] Bravdo, B. A., Hepner, Y., Loinger, C., Tabacman, H. (1985): Effect of irrigation and crop level on growth, yield and wine quality of Cabernet Sauvignon. – American Journal of Enology and Viticulture 6: 132-139.
- [6] Buesa, I., P erez, D., Castel, J., Intrigliolo, D. S., Castel, J. R. (2017): Effect of deficit irrigation on vine performance and grape composition of *Vitis vinifera* L. cv. Muscat of Alexandria. – Australian Journal of Grape and Wine Research 23(2): 251-259. doi.org/10.1111/ajgw.12280.
- [7] Carbonneau, A. (1998): Aspects qualitatifs. – Proceedings 17th World Congress of Vine and Wine, Bratislava, pp. 258-276.
- [8] Coombe, B. G. (1992): Grape Phenology. – In: Coombe, B. G., Dry, P. R. (eds). Viticulture, Vol: 1, Resources in Australia. Winetitles, Underdale, South Australia, pp. 139-153.
- [9]  elik, H. (2006): Grape Cultivar Catalog. – Sunfidan A.  . Mesleki Kitaplar Serisi: 3, Ankara.
- [10] De La Hera Orts, M. L., Martinez-Cutillas, A., Lopez-Roca, J. M., Gomez-Plaza, E. (2004): Effects of moderate irrigation on vegetative growth and productive parameters of Monastrell vines grown in semiarid conditions. – Spanish Journal of Agricultural Research 2: 273-281. DOI: 10.5424/sjar/2004022-81.
- [11] Deloire, A., Rogiers, S. (2014): Monitoring Vine Water Statuses. Part 2: A Detailed Example Using the Pressure Chamber. – Grapevine Management Guide 2014-2015, NSW DPI, Orange, Australia, pp. 15-19.

- [12] Dry, P. R., Loveys, B. R. (1998): Factors influencing grapevine vigour and the potential for control with partial rootzone drying. – Australian Journal of Grape and Wine Research 4: 140-148. doi.org/10.1111/j.1755-0238.1998.tb00143.x.
- [13] Eichhorn, K. W., Lorenz, D. H. (1977): Phaenologische Entwicklungsstadien der Rebe. – Nachrichtenblatt des Deutschen Pflanzenschutzdienstes (Braunschweig) 29: 119-120.
- [14] Etchebarne, F., Ojeda, H., Hunter, J. J. (2010): Leaf:fruit ratio and vine water status effects on Grenache Noir (*Vitis vinifera* L.) berry composition: water sugar, organic acids and cations. – South African Journal of Enology and Viticulture 31(2): 106-115. doi.org/10.21548/31-2-1407.
- [15] Hardie, W. J. (2000): Grapevine biology and adaptation to viticulture. – Australian Journal of Grape and Wine Research 6: 74-81. doi.org/10.1111/j.1755-0238.2000.tb00165.x.
- [16] Keller, M. (2010): The Science of Grapevines: Anatomy and Physiology (1st ed.). – Academic Press, Oxford.
- [17] Keller, M., Romero, P., Gohil, H., Smithyman, R. P., Riley, W. R., Casassa, F., Harberson, J. F. (2016): Deficit irrigation alters grapevine growth, physiology, and fruit microclimate. – American Journal of Enology and Viticulture 67: 426-435. DOI: 10.5344/ajev.2016.16032.
- [18] Korkutal, I., Bahar, E., Carbonneau, A. (2011): Growth and yield responses of cv. Merlot (*Vitis vinifera* L.) to early water stress. – African Journal of Agricultural Research 6(29): 6281-6288. DOI: 10.5897/AJAR11.1893.
- [19] Lebon, E., Pellegrino, A., Louarn, G., Lecoœur, J. (2006): Branch development controls leaf area dynamics in grapevine (*Vitis vinifera* L.) growing in drying soil. – Annals of Botany 98: 175-185. doi: 10.1093/aob/mcl085.
- [20] Lovisolò, C., Perrone, I., Carra, A., Ferrandino, A., Flexas, J., Medrano, H., Schubert, A. (2010): Drought-induced changes in development and function of grapevine (*Vitis* spp.) organs and their hydraulic and non-hydraulic interactions at the whole-plant level: a physiological and molecular update. – Functional Plant Biology 37: 98-116. DOI: 10.1071/FP09191.
- [21] Matthews, M. A., Anderson, M. M. (1988): Fruit ripening in *Vitis vinifera* L: responses to seasonal water deficits. – American Journal of Enology and Viticulture 39(4): 313-320.
- [22] Matthews, M. A., Anderson, M. W., Schultz, H. R. (1987): Phenologic and growth responses to early and late season water deficits in Cabernet franc. – Vitis 26: 147-160.
- [23] Matthews, M. A., Ishii, R., Anderson, M. M., O'Mahony, M. (1990): Dependence of wine sensory attributes on vine water status. – Journal of the Science of Food and Agriculture 51: 321-335. doi.org/10.1002/jsfa.2740510305.
- [24] Ojeda, H., Deloire, A., Carbonneau, A. (2001): Influence of water deficits on grape berry growth. – Vitis 40(3): 141-145.
- [25] Ojeda, H., Deloire, A., Carbonneau, A., Georges, A., Romieu, C. (1999): Berry development of grapevines: Relations between the growth of berries and their DNA content indicate cell multiplication and enlargement. – Vitis 38(4): 145-150.
- [26] Ojeda, H., Andary, C., Kraeva, E., Carbonneau, A., Deloire, A. (2002): Influence of pre- and post-véraison water deficit on synthesis and concentration of skin phenolic compounds during berry growth of *Vitis vinifera* L., cv. Shiraz. – American Journal of Enology and Viticulture 53: 261-267.
- [27] Pellegrino, A., Lebon, E., Simmoneau, T., Wery, J. (2005): Towards a simple indicator of water stress in grapevine (*Vitis vinifera* L.) based on the differential sensitivities of vegetative growth components. – Australian Journal of Grape and Wine Research 11: 306-315. doi.org/10.1111/j.1755-0238.2005.tb00030.x.
- [28] Rogiers, S., Deloire, A., Smith J., Tyerman, S. (2014): Monitoring Vine Water Status. Part 1: Some Physiological Principles. Grapevine Management Guide 2014-2015. NSW DPI, Orange, Australia, pp. 12-14.

- [29] Sadras, V. O., Moran, M. A. (2012): Elevated temperature decouples anthocyanins and sugars in berries of Shiraz and Cabernet Franc. – Australian Journal of Grape and Wine Research 18: 115-122. doi.org/10.1111/j.1755-0238.2012.00180.x.
- [30] Scholander, R. R., Hammel, H. T., Bradstreet, E. D., Hemmielsen, E. A. (1965): Sap pressure in vascular plants. – Science 148: 339-346. DOI: 10.1126/science.148.3668.339.
- [31] Schultz, H. R. (1996): Water relations and photosynthetic responses of two grapevine cultivars of different geographical origin during water stress. – Acta Hort. 427: 251-266. DOI: 10.17660/ActaHortic.1996.427.30.
- [32] Shellie, K. C. (2006): Vine and berry response of Merlot (*Vitis vinifera* L.) to differential water stress. – American Journal of Enology and Viticulture 57: 4.
- [33] Smart, R. E., Coombe, B. G. (1983): Water Relations of Grapevines. – In: Kozłowski, T. T. (ed.). Water Deficits and Plant Growth, Vol. VII, Additional Woody Crop Plants. Academic Press, New York. pp. 137-196.
- [34] Stevens, R. M., Harvey, G., Aspinall, D. (1995): Grapevine growth of shoots and fruit linearly correlate with water stress indices based on root-weighted soil matric potential. – Australian Journal of Grape and Wine Research 1: 58-66. doi.org/10.1111/j.1755-0238.1995.tb00079.x.
- [35] Tillett, R. L., Ergül, A., Albion, R. L., Schlauch, K. A., Cramer, G. R., Cushman, J. C. (2011): Identification of tissue-specific, abiotic stress-responsive gene expression patterns in wine grape (*Vitis vinifera* L.) based on curation and mining of large-scale EST data sets. – BMC Plant Biology 11: 86. DOI: 10.1186/1471-2229-11-86.
- [36] Trigo-Córdoba, E., Bouzas-Cid, Y., Orriols-Fernández, I., Díaz-Losada, E., Mirás-Avalos, J. M. (2015): Influence of cover crop treatments on the performance of a vineyard in a humid region. – Spanish Journal of Agricultural Research 13(4): 1-12. DOI: 10.5424/sjar/2015134-8265.
- [37] Williams, L. E., Grimes, D. W., Phene, C. J. (2010): The effects of applied water at various fractions of measured evapotranspiration on reproductive growth and water productivity of Thompson Seedless grapevines. – Irrigation Science 28: 233-243. DOI 10.1007/s00271-009-0173-0.
- [38] Xiao, Z., Liao, S., Rogiers, S. Y., Sadras, V. O., Tyerman, S. D. (2018): Effect of water stress and elevated temperature on hypoxia and cell death in the mesocarp of Shiraz berries. – Australian Journal of Grape and Wine Research 24(4): 487-497. doi.org/10.1111/ajgw.12363.

PROPOSALS FOR RESOLVING LONG DUE FOREST OWNERSHIP CONFLICTS IN TURKEY (EASTERN BLACK SEA REGION CASE STUDY)

AYAZ, H.^{1*} – INANÇ, S.²

¹*Faculty of Law Department of Public Law, Trabzon University, Trabzon, Turkey*

²*Faculty of Forestry, Artvin Çoruh University, Artvin, Turkey*

**Corresponding author*

e-mail: hayaz@ktu.edu.tr; phone: +90-532-440-8691, +90- 532-480-0207

(Received 2nd Oct 2018; accepted 27th Nov 2018)

Abstract. This paper discusses the principle causes of forest ownership conflicts and the alternative approaches to resolve them. The current forest legislation in Turkey primarily rejects the private forest ownership rights with very limited exceptions. At present, 99.9% of the country's forest is owned by the state. According to the results, the forest property subject to disputes in the Eastern Black Sea Region where the conflicts is most experienced is about 12% of the total forest area. Nearly half of the conflicted area includes the forests registered in the name of individuals in the past. The non-acceptance of private forest property and the nullification of the old-dated private forest property documents have caused both disappointment in people and damages to the forests. Within the scope of the research, land survey and assessments were carried out in the settlements of the Eastern Black Sea Region, and group meetings were held with the local people to determine the causes of the disagreements as well as the requests and expectations of the local people. In addition, the views and proposals of local forest engineers working as state officers in the region were investigated. The results were presented in tables and alternative recommendations were developed based on statistical evaluations. The results indicated that the existing legislation and practices were not considered appropriate by all the forest villagers interviewed and by 75% of the forest engineers working in the regional forestry administration. Legislative changes are inevitable to better protect the forests and minimize the conflicts. The legal property documents given to the people must be valid in forests subject to private property in the historical process. As a solution proposal, private forests located immediately adjacent to and integrated with state forests should be expropriated, but those intermingled within the agricultural and settlement areas should be left to private property provided that sustainability is maintained. The same solution proposal should be valid for the confiscated forests in the course of cadastral works conducted so far.

Keywords: *forest cadastre and ownership, confiscation of forests, private forest ownership, forest protection*

Introduction

The primary focus of the forest policy is to protect forest resources and meet social needs and expectations based on the sustainable management of forests. One of the obstacles to the protection of forests is the uncompleted forest cadastre works. As known, it is impossible to plan and sustainably manage forest resources with unknown ownership, size, location and boundaries. While Turkish forestry initiated planned forestry in the beginning of 20th century, unfortunately the forest cadastral works have not been completed, and forest ownership problems have yet to be resolved. The forest area in Turkey is approximately 23,450,000 ha. Cadastral works have been completed in about 80% of this forest area (GDF, 2016). However, because of the lack of respect for the actual property rights obtained by law in the past in forest areas where cadastral works have been completed, the cadastral process has led to intensive property disputes

and thus forest resources and their sustainability were put under jeopardy. Moreover, cadastral works have often been halted in forest areas where traditionally used and appropriated by villagers.

This would be due to a number of reasons:

(i) Inability to establish a sound basis for forest ownership and frequent changes in ownership policy: In fact, forest ownership is a tool to serve to the purposes of forest policy and should be regulated to achieve the forest policy (Gümüş and Toksoy, 2001). However, Turkish forestry has not been based on such an infrastructure. The Ottoman Empire in the process of demolition has started to see forests as a source of income and manage them for this purpose since 1870. At the same time, the process of granting the rights to private property on the territory of the country has been initiated. In the process, although the transfer of state forests to the private property was banned, private property records also existed on state forests due to many inadequacies. In the first years of the Republic, settlements protruding into the forests continued, part of the forest land was registered in the name of individuals, and some areas were traditionally owned by the people. In the country, legislations acknowledging the forests as a national asset that should belong to the state and intervening the private forest ownership and traditional use have been accepted and implemented since 1937. Any kind of forests subject to private property were nationalized with the recognized legislation and 99.9% of forests were legally owned by the state (Ayaz and Gümüş, 2016).

(ii) The security of utilization and property rights on the forests is an important factor for long-term sustainability (McGinley et al., 2012): Various effects can arise from intervening ownership and the traditional utilization rights. On the one hand, careless exploitation and illegal tree cuts result in forest degradation (Webb et al., 2006; Yachkaschi et al., 2008); on the other, forests are converted to agricultural lands (Poudel et al., 2014) or people compete to get more shares from the resources, causing forests to deteriorate further (Asante et al., 2017). Nationalization of forests in Turkey has led to a significant amount of forest loss. While an average of 31,500 ha of forest area has been burned annually since 1937 (Bilgili, 1998), when official records on forestry began to be kept, approximately 290,000 ha of forest areas were intentionally burned by the public over two years immediately following the nationalization of all forests in 1945 (Çağlar, 1979). Today, a large number of property cases have been filed in courts in the course of sustainable forest cadastre studies. Ironically, people who cannot reach the desired result in the domestic law still continue to utilize the land and carry the cases to the European Court of Human Rights (ECHR). ECHR has concluded that in many of its resolutions, disproportionate interference was imposed on the right to property secured under Article 1 of the Additional Protocol to the Convention, resulting in the repatriation of the country (Ayaz and Inanç, 2009). On the other hand, however, some positive effects of state intervention on forest resources can also be seen. In Ukraine, for example, the majority of forests were in private ownership between 1796 and 1914 during which forest areas fell from 16.2 to 9.7%. However, when forests became nationalized in the later period (1946-1996), the forests increased by about 3 million ha (Nijnik and Kooten, 2000). Furthermore, private forestry initiatives supported by the states in Europe, USA and Japan, where private forests have significant shares, have been successfully performed (Schmithüsen and Hirsch, 2010; Siry et al., 2005; Takahashi et al., 2017; Vangansbeke et al., 2015; Kvarda, 2004; Glück et al., 2010).

(iii) Failure to maintain the completed forest cadastre over time: As a result of the cadastre, state-owned forests by law as well as unclassified forests in accordance with the laws are recorded as state property. While this is the case with official records, most of these forest lands (76%) have continued to be used by former owners after the cadastre (Diktaş et al., 2017). The fact that areas traditionally used and appropriated by the villagers have been registered as state forests led to the halt of cadastral works in some localities due to the resistance of villagers, resulting in the incompleteness of forest boundaries.

(iv) Compromising on illegal behaviors: Studies are underway to see the forests of the country as national asset and register the whole forests as a state property. However, since the 1950s, changes in forest laws have been made and the owned lands that are forests in nature according to universal acceptance were not legally considered as a forest and left to the ownership of people. Furthermore, the lands where the forest cover is destroyed, used for agriculture, collective settlement or animal grazing can be converted to non-forest status and sold out to the invaders, although they are owned by the state. These laws highly threaten forest resources and sustainability and encourage forest destruction.

The issue of forest ownership in the country is problematic due mainly to the legislative arrangements in the first years of the Ottoman Empire and the Republic. In fact, the land used in agriculture in the 1940s was sold to the public by the Treasury. In this process, some forests have been subject to sales even if it is contrary to the legislation. In the settlement units where the forest cadastre has still been carried out, all the lands which is determined to be forest before 1945 were registered as a state forest with all title deed records being invalidated. Moreover, there is no reimbursement for the forests purchased from the state with their cost.

The settlement of the dispute has not been resolved peacefully in order to minimize the infringement of the right. Instead, an approach contradicting the scientific notion was developed in a way that some parts of the forests that are in fact forest land according to international definitions were legally regarded as non-forest areas particularly from 1950 onwards. Thus, forestry legislation has been subject to numerous changes causing an increase in areas that are legally non-forested areas since 1950. Again, since 1970, the forest cover has been gradually destroyed and its land used for agriculture, pasture or collective settlement was taken out of the forest status and sold to the occupiers. As of the end of 2016, nearly 500,000 ha of forest areas were removed from the forest boundaries as their forest cover was illegally destroyed and some of which was sold to the occupiers (Çağlar, 1979).

Ironically, the laws in force encourage the destruction of forests. Specifically, a private forest property with a title deed is not accepted and these places are considered as state forests without paying their owners their costs. However, people who own the state forest areas by destroying them are able to buy those forest lands that they occupy without any justification. This situation has caused an intense reaction of former forest owners on the one hand and threatened the forest resources and their sustainability on the other.

Based on the long due forest ownership problems in the country, the purpose of this study is to enlighten the forest ownership issues over the history and provide proposals to resolve the problems of forest ownership encountered in Turkey by encouraging forest villagers to be a stakeholder and have consent in the process. The results of the study can provide significant contributions to the resolution of forest property problems.

Material and method

The case study area

The case study area covers the provinces of Artvin, Bayburt, Giresun, Gümüşhane, Rize and Trabzon in the Eastern Black Sea Region. Nearly 3.3% of Turkey's population lives in this region (TUİK, 2018). According to General Directorate of Forestry (GDF) records, the total area of the region is 3,870,000 ha, about 40% of which is forested (GDF, 2016). The region is the most challenging area of the country in terms of forest ownership issues that sparked the motivations for selecting the areas as a case study site. To begin with, the case study region is primarily of rugged area with high slopes. Forests, agriculture and settlement areas are intermingled in the region which is subject to scattered settlements. This situation has led to the ownership of the forests surrounding agriculture and settlement areas by the local people. The forests around the villages are sometimes owned by land registry records which are obtained in any way, mostly based on the existence of occupation documents and actual use. The ownership problems in the region have reached to an extent that has caused the lack of performance of forest management planning and implementation processes, impeded forest cadastral works and again led to thousands of property cases to be filed and resolved in the courts. For example, a significant portion of the regional forests (e.g., 12% of the forests of the Maçka State Forest Industry) is excluded from forest management practices due to regional conflicts (social disputes) (Türker et al., 1999). There are some settlements where the forest cadastre has not been completed due to property conflicts in the region. Based on all these rationales, this area was selected for this research. The location of the case study area in Turkey is given in *Figure 1*.

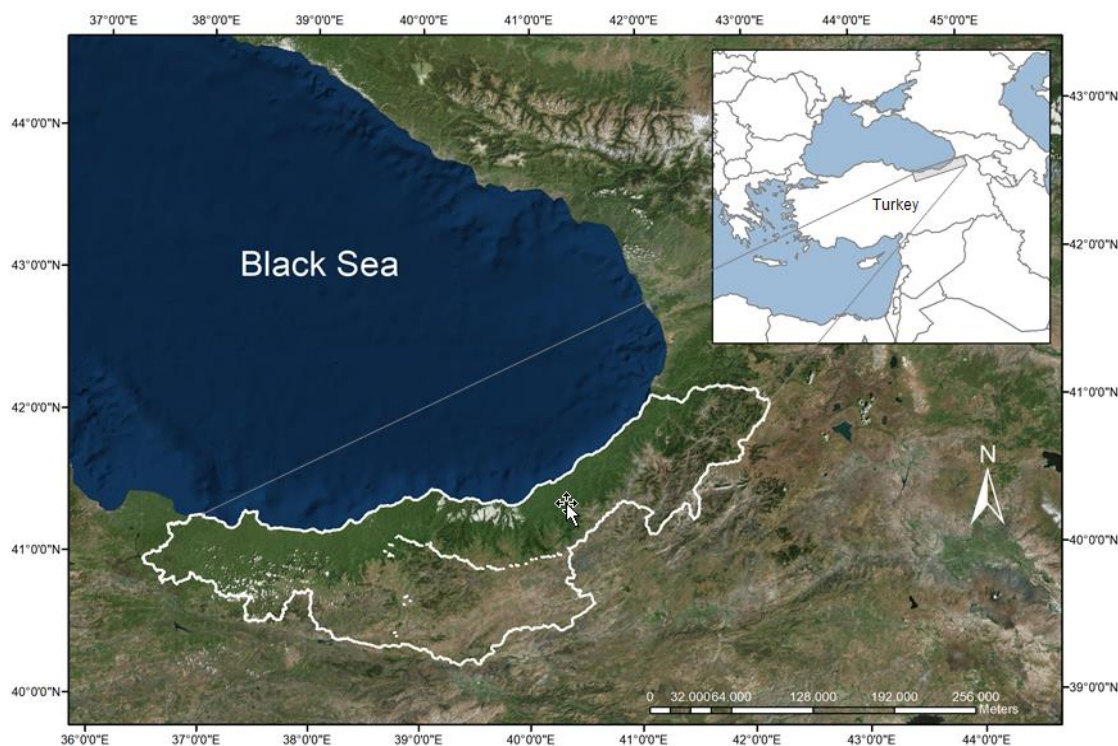


Figure 1. The location of the case study area in Turkey

In the study, first of all, land cadastre records and forest cadastre documents which are primarily kept in forest administration were compiled. Thus, from 1937 onwards, settlement units with finished forest cadastre or forest boundaries established according to different legal arrangements were identified. Later on, information was collected from forest villagers and villages as part of the case study. For this purpose, two villages were selected from each province in the region. In selecting the settlements, the villages among all existing villages where the cadastre works have been established and had the highest number of court cases about property disputes were preferred. In the settlement where the cadastral works have yet to be completed, the forestry officers were interviewed and the sample ones among the villages encountering social conflicts during the implementation of forestry activities were selected. *Table 1* shows the names of the villages subject to field survey and their spatial locations.

Table 1. *The villages where field survey was conducted*

Province	District	Village	Cadastral state
Artvin	Şavşat	Cevizli	Cadastre completed
	Ardanuç	Anaçlı	Cadastre completed
Bayburt	Merkez	Yoncalı	No forest boundaries
	Merkez	Armutlu	Cadastre completed
Giresun	Tirebolu	Belen	Cadastre completed
	Tirebolu	Yaraş	Cadastre completed
Gümüşhane	Center	Süle	No forest boundaries
	Center	Kurtoğlu	Cadastre completed
Ordu	Perşembe	Boğazcık	Cadastre completed
	Perşembe	Kazancılı	Cadastre completed
Rize	Pazar	Bucak	Cadastre completed
	Çamlıhemşin	Topluca	Cadastre completed
Trabzon	Tonya	Iskenderli	No forest boundaries
	Hayrat	Geçit	Cadastre not completed

The villagers in *Table 1* have three distinctive characteristics in terms of cadastre. Forest and land cadastre were completed in 10 villages. The cadastre of the private property was completed in the remaining three villages and the cadastre of state land (forest, rangeland, treasury land etc.) was not completed. In Geçit village, no cadastral work has been conducted.

Sampling method

The second part of the survey is the development and implementation of questionnaire forms to the forest engineers who are the employees of General Directorate of Forestry in the Black Sea region. There are three regional forest directorates (RFD) in the region; namely Artvin, Giresun and Trabzon. A total of 324 forest engineers are employed in all three RFDs. In order to obtain statistical results, it is necessary to know the minimum number of samples. For this purpose, the number of sample size was calculated using a statistically acceptable 95% confidence level and 10% margin of error, assuming that the interviewees had completely different characteristics. According to these acceptances and values, the number of samples is calculated based on the *Equation 1* as follows:

$$n = \frac{F \times t^2 \times P \times Q}{(F \times m^2) + (t^2 \times P \times Q)} \quad (\text{Eq. 1})$$

n: Number of samples

F: Number of forest engineers

t: Confidence level (1.96 for 95% confidence level)

m: Error margin (taken as 10%)

P and Q: Heterogeneity coefficient (-largest value - 0.5 X 0.5)

According to the form, the number of forest engineers required to conduct the survey is 75. In the study, however, a questionnaire was applied to 171 forest engineers working in the region and evaluated. Thirty of the respondents were from Artvin, 66 from Giresun and 75 from Trabzon RFDs.

The identified 14 villages were visited under the scope of the case study and the headman and the villagers who experienced forest ownership problems were interviewed. The underlining reasons of the disputes about the forest status and its property were asked to the villagers during the interview. Some of the plots with conflicts were evaluated in the field. Additionally, some recommendations offered by the villagers about the proposals for resolving the problems were discussed. The questionnaire applied to the regional forest officers consists of 12 questions in total, including the personal characteristics of the respondents and the evaluations on forestry. With the six questions in the first section, the Regional Directorate of Forestry (RDF) that the participants work in; their age, gender, working time, post-graduate training and the position they hold were evaluated. The remaining six questions in the second part identified forestry problems and their views on the forest cadastre. The questionnaire form included blank fillings, multiple choice questions, grading and open-ended questions.

After the face-to-face interview for applying the questionnaire, the results were tabulated and the statistical analysis assessed with the SPSS program (Orhunbilge, 2000; Daşdemir, 2016). The hypothesis that there is no difference between the personal characteristics of interviewed forest engineers and their views and recommendations about forestry problems was tested. Chi-square test was used as a statistical method.

Results

Interviews and investigations in forest villages

After the regional problems related to the forest cadastre and ownership were compiled in the settlement units visited within the scope of the project, those with similar characteristics were brought together and divided into subsections. The main problems identified in this context are listed below, evaluated likewise and discussed in the sections that follow:

- a. The land registry in the private forest properties is not honored and these places are regarded as state forests
- b. The areas used for a long time or with tax-registered documents are also regarded as state forests
- c. Historically non-forest areas that are naturally covered with forest vegetation as they have not been used in recent years are considered as state forests

- d. Different implementations are performed between neighboring settlements in determining forest boundaries
- e. Some of the lands left outside the forest boundaries by the forest engineer in the cadastral commission is subject to the lawsuit by the forest engineers working in the state forest enterprise claiming that they are state forests

a) No respect for land registry records in private forest properties

It is possible to examine this problem in three aspects. The first one of these is the incompatibility of the size and borders of the title deeds with the realities on the ground. As explained introduction, large differences were observed between the amount of land registered and the amount of land owned based on this land register because the measurements were not carried out in the field at the beginning of granting the first title deeds in Ottoman Empire era and there were no maps, drafts and similar other documents to compare to. Sometimes an ownership right for over 50 decare (50,000 m²) areas was claimed based on just a one “Atik Dunam” (nearly 919 m²) with land title registration. As an extreme example, there is only one record in the old title deeds in Bucak Village of Pazar District in Rize Province with a registered area of one Atik Dunam yet the descriptions of the registration boundaries cover the whole village, settlement, agriculture and some forest areas. If this land register definition is respected, it must be assumed that houses belonging to other villagers, agricultural lands and state forests are to be regarded as a single property of a person.

Another problem about the land with old title deeds is the inapplicability of boundaries written on the title deeds to the ground. Specifically, it is impossible to find geographic features, as borders of the land property on the ground, such as border, ridge, creek, path, mountain, rock and a person name indicated in the narration of land registration record. In fact, there are many similar roads, creeks and lines in the same village used to differentiate from each other. Even the geographic directions of the boundaries of the described boundaries were not written in many title deeds. The problems encountered in the application of the title deeds about their amount and the boundaries can also be seen in the legislation. The Constitution and the Forest Law No: 6831 state that forests cannot be possessed with a long term use. The Item No: 20 of the Cadastral Law No: 3402 in effect stating as “*If the boundaries stated in the records and documents that are not based on maps, plans and drawings are suitable for enlargement and changes, the amount indicated on the record is to be respected...*” prohibits the determination of more areas during the cadastral process than the ones recorded in the registration. People holding the old title records are not pleased with these legal regulations.

Another problem experienced in the lands owned by the title deeds in the region is the “*presence of a forest cover*” on the land in 1945. According to the well-known Law No: 4785 dated 1945, which is still in force, the private property lands which were forests in 1945 or considered within the integrity of forests were all nationalized. The serious problem has been brought to today as the nationalization process was “*performed without any action or notification*”. Ironically, there are still many land registry records for private persons for many properties under the scope of nationalization process according to the law. These records could or have not been abandoned because the amount of land subject to nationalization is unknown. Those who have inherited or registered their land registry record about the abovementioned land are still aware of their property which is also respected by their neighbors. In

interviews with forest villagers, it was seen that the old title deeds were regarded as a very credible document and kept with care. In local terms, the “*tribal/signed title deed*” is seen as a strong evidence of the title deeds that contain the sign “*tugra –the sultans signature*” belonging to the sultan of the period. It is a great disappointment that the documents that are thought to be so strong, so long as they are old-dated, are not respected and the records are considered “*invalid*”. Discussion of the amount and the boundaries of the title deeds and only respect for the written area on them are considered with tense reaction.

In the case study area, some of the remnant lands of the Greek emigrants, especially those who migrated through population exchange, were distributed to the Turks coming from Greece and given them the title deeds called an “*exchange title deed*”. However, the immigrants in the country did not stay generally in the Eastern Black Sea Region and sold the land given to them in the local people and moved to the western parts of the country. The remaining agricultural lands from the Greek Cypriots were sold to the public by the Treasury. The title deeds given in this way are referred to as the “*allotment title deed*”. The sizes of these places, which are purchased by paying to the state, are in general compatible with the amount indicated in the title deeds. Many of them have simple cadastral sketches. In the meantime, however, there are forests on some of these sold lands. Essentially, these type of lands sold by the state are regarded as “*nationalized forests*” by the law No: 4785 based on its famous Item stating that the private property lands which were forests in 1945 or considered within the integrity of forests are all subject to nationalization.

The people who had the old dated title deeds at hand, regard those lands as a kind of usurpation of the forests by the state they bought by paying installments until the middle of 1960s. Some people who are opposed to the application complain that “*this law cannot be such an immoral practice imposed on citizens to see the revival of the state*”. The state sells the properties for 20 years in instalments and regards this land as a state property 2-5 years after the sale “*without any action and notification*”. Paradoxically, there has been no actual field work on which land is to be nationalized since 1945 when nationalization process took place. Therefore, the location and the amount of nationalized land is unknown to anyone, including the state. In addition, the costs of the nationalized land sold to the public after the year 1945 were continued to be purchased in instalments. These lands with private property registration change hands by inheritance and subject to trade over the years. In one day over time, cadastral work is conducted and “*this places are nationalized in 1945 as a state forest*” and the records of title deeds are ignored retrospectively. It is quite difficult to explain this process with the rights and justice rules or procedures.

One of the cases of further disappointment is that in 1950 and later years, even the private properties with title deeds that were deemed to be based on the edited maps according to the Title Law No: 766 were regarded as state forests during the forest cadastre work. The justification of the lands as forests is that these places are identified and registered on behalf of individuals contrary to the law, even though it is prohibited to subject the state forests to private property in the Constitution and laws during the registration process of these lands. The forest administration states that the properties which are forests in nature are detected and registered illegally on behalf of individuals and for this reason the title deeds are deemed invalid due to the “*corrupt registry*” process. In anyhow, as a result of the forest cadastre, this land is regarded as a registered

state forest, and since the place has been forest since way before, the property disputes carried to the courts also result in favor of the State.

It is too optimistic to expect landowners to accept this practice. As a matter of fact, forest property and ownership issues in the Eastern Black Sea Region have always been in the agenda. The majority of interviewees state that the state cannot take such an approach. Again, certain number of people think that the forest officers took over their land by changing the legal boundaries of the land. In other words, they are unable to reconcile this practice with the state law, or they think that cadastre employees apply a faulty and biased attitude. For that reason, local people show a hostile attitude towards the state forest officers and worse damage the forests.

The lands with title deeds were taken to the courts after its determination and registration as a state forest without giving any rights to its registered owners. However, judicial decisions resulting mostly in favor of forest administration (it has been determined that this ratio is more than 72% in a survey conducted in the region) cause people to hesitate to file a lawsuit. Since the lost side has to pay for the jurisdictional charges and the other party's proxy fee, not only do they lose the property of the case but also pay the due charges that shake the budget of the low income forestry village (Ayaz, 2004).

b) Regarding the areas used over a long time or with tax-registered documents as state forests

There are tax records that belong to some of the lands owned by individuals. These documents, which legally indicate the use right or possessions of the land, are perceived by the people as if they were documents of ownership. In fact, the local people have accepted the actual use situation of the land, and there is no significant conflict between the villagers. The people request that those land, whether forested or not, be identified on behalf of the occupiers of the areas subject to genuine actual use. In these records, there is a discrepancy between the borders in the field and the amount in the record, similar to the title deeds given in the Ottoman Empire period. Therefore, the fact that these records, which form the basis of the actual use over the forests, are not respected during the cadastre process causes the public to complain about.

On the other hand, the land that has been in private use for many years but with forest trees on is not identified and registered in the name of the user. This also negatively affects the cadastre. Besides, the 70% of individuals' ownership claims is based on the intellectual/use property during the cadastral studies in the region. The invalidity of the long term use rights in forest land is also an important factor in forest cover damages.

Some of the lands are registered as state forests based on a reason that they were forest before and were in integrity with the forests, although some agricultural practices were carried out on them. This situation was perceived by the villagers as an unjustified intervention. The people reacted to the process that the land stayed inactive over many years and the state has not intervened into the process of converting it into an agricultural field, and yet now claims that this area is a state forest after years and takes its ownership. The local people think of the fact that the state is unfair to them as the state gives some lands and houses free to the immigrants and refugees.

c) Historically non-forest areas that are naturally covered with forest vegetation as they have not been used in recent years are considered as state forests

The rural and urban populations in Turkey have continued to increase over time. The rural population has intensively moved to the urban areas particularly after the middle of 1980s. The immigration has also included the forest villages. The population of the forest villages in the country were nearly 15 million around the 1970s that has dropped below 7 million since then (GDF, 2016). In the case study area, the population of the forest villages dropped by 43% from 1970 to the end of 2007 (İnanç, 2010).

After migration from rural areas to the urban and developed areas, some of the land that was used for agriculture, rangeland or grassland was abandoned for itself. Forest vegetation has been developed over time with the contribution of the region's climatic conditions to growth trees on the unused lands. The places that the people had used as agriculture way before were determined as a state forest during the cadastre because they were covered with forest trees. The ownership in the land that was previously owned and constantly used without any controversy by the ancestors was also considered important in terms of the feeling of having "*ancestor heirloom*" by some people in addition to providing some material benefits. There are memories, encountered troubles and shared happiness in those lands. Sometimes there are stone walls, planted, grafted fruit trees that are woven around this area. As a matter of fact, during the visit of the villagers, it was determined that a pear tree exceeding 150 years old in a place where the meadow area and the forest area merged together in the Anaçlı Village of Ardanuç District of Artvin Province and that a few spruce trees together at the same ages were located within the bounded areas as a state forest during the cadastre. The landowner complained that centuries-old fruit trees were not even taken into consideration during the cadastral period and that the land been used for centuries was regarded as a forest.

d) Inconsistencies between different neighboring settlements in determining forest boundaries,

Forest and land cadastre works started in 1939 in the region. However, factors such as tough land conditions, frequent legislative changes and often intervened forest and the non-forest use areas created problems in terms of the cadastral works. Completion of the cadastre in Turkey in an effort to join the European Union was targeted to be finalized particularly with subcontracting the private services. However, quick completion of the cadastre has not provided a solution, but rather triggered serious problems. For example, forest cover has begun to be destroyed in some areas in the region, in addition to filing numerous forest property lawsuits in the courts.

On the other hand, the definition of forests has been frequently changed by legislation in Turkey. Due to these changes, cadastral works have been implemented several times in the same settlement and different applications have been carried out by cadastral delegations who identify forest boundaries. There are some lands in different settlements that are in doubt to account them as forest or non-forest areas. While some cadastral delegations use the choice of forest, some do not regard the properties as a forest in this type of areas. The different applications are also recognized by the local people who complained about the inconsistencies and disparities. This situation was detailed in a study conducted by Ayaz in 2004 (Ayaz, 2004).

e) Some of the lands left outside the forest boundaries are subject to lawsuit

The forest cadastre is conducted by commissions with a member of forest engineers. After the cadastral work has been completed, any natural or legal persons, as a legal right, can file a lawsuit with a claim that the boundaries of the forests have been determined illegally. Among those people are the state forest officials working in GDF. The ironical problem is that the forest boundaries determined by forest engineers working in the state forestry organization is subject to the case in a court by the other forest engineers working in the same state organization. Specifically, a unit in a state forest organization determines the draft boundaries of forest areas and the forest cadastre is carried out according to these boundaries. Afterwards, despite observing the limits of the forests, another unit in the state forest organization can also file a lawsuit for lands outside these boundaries. It is quite cumbersome trying to explain such an absurd situation or process.

One or several forest engineers working in the forestry organization determine the forest borders and other forest engineers again working in the same organizations reject the process afterwards. One of the most complained issues in negotiations with forest villagers is that the employees of the state forest institution have different opinions about the same land base, being forest or non-forest. In addition, the fact that the owners are asked to pay the costs of the judicial charges as well as the consequences of the lost case filed by the state forest officials against the land owners increased the complaints further. Fortunately, the law amendment in 2012 allowed the judicial remedy to be left for payment to the state administration who filed the case which eased a bit the victimization of the people to some extent.

The forest villagers interviewed in the field survey were asked what type of activity they would like to undertake in case they are given the forested areas they claim. Nearly all of the interviewed people stated that they consider it important because these areas have been owned by their ancestors since the beginning. People acknowledge that the claim of ownership has been ongoing for a long time, that these woodlands have a large number of shareholders and that it is unlikely to plan and manage this land. The local people also state that they want to meet their own fuelwood and construction needs freely from this forest. There are also some people who think that they can generate economic income by cutting and selling few trees. Importantly, it has been determined that the villagers do not have knowledge about the sustainable management of forest resources with a plan nor do they have any expectations towards that.

Results of questionnaire applied to forest officers

Forest engineers employed in GDF are directly associated with the problems caused by the conflicts in forest ownership. They conduct the forest cadastre works and are often exposed to an intense reaction by the local people. Most of the private properties are registered as state forest during the cadastral works according to the legislations in effect. Interestingly, nearly 70% of the forest engineers entitled to carry out cadastral works are from different provinces and their families are also adversely affected as a party in forest ownership conflicts. Thus, we tried to identify and evaluate the problems and the possible solutions brought by these forest engineers working within the complex cadastral situation.

The information about the participants such as the regional directorate of forestry employed, age, gender, post-graduate education, employment period and the unit of

work were obtained in the questionnaire. It was also determined that 83% of the forest engineers working in the region were born in the same districts, and the elders of their family lived there. As seen in *Table 2*, approximately 59% of forest engineers working in the region are under 35 years of age.

Table 2. Age of forest engineers in the region

Age	Frequency	Percent	Valid percent	Cumulative percent
0-35	102	59.6	59.6	59.6
36-50	54	31.6	31.6	91.2
51 +	15	8.8	8.8	100.0
TOTAL	171	100.0	100.0	

Approximately 32% of the engineers currently working are between the ages of 36 and 50. Nearly 9% of respondents are aged over 51 years and 16% was female. The proportion of employed forest engineers who have received post-graduate training is around 8%.

The duration of the employment or service was identified to determine the relationship between the working time of the respondents in the forestry organization and their perception on cadastre-ownership issues. According to the results, the average service period of the forest engineers working in Artvin RFD is 7 years, 11.5 years in Giresun RFD and 12.5 years in Trabzon RFD. The average service period is around 11 years when all the regions surveyed are included in the account (*Table 3*).

Table 3. The duration of employment of forest engineers

RDF	Duration of employment (years)	Number of people	Std. Deviation
Artvin	7.30	30	6.007
Giresun	11.59	66	8.975
Trabzon	12.53	75	9.765
Average	11.25	171	9.055

It was decided to determine the current position of the interviewees during the interview. The main purpose here was to determine whether there is a difference in the perception of the forest cadastre problem and the task performed. As shown in *Table 4*, 29% of the interviewees are district forest managers and 32% of them “are engineers in various other branches”. The rate of a forest engineer, who is the head or member of the forest cadastre commission, is about 9%. Approximately 20% of the interviewees are working in the management team such as regional forest manager, assistant regional forest manager, state forest enterprise manager or assistant, branch manager.

The assessment of employed forest engineers about forest stewardship, ownership and cadastre

The information on forest engineers interviewed was compiled and their perceptions on forestry, forest property and cadastre were determined in the same questionnaire. The results obtained are presented in the following sub-sections.

Table 4. *The current position of the forest engineers interviewed*

Job	Frequency	Percent	Valid percent	Cumulative percent
District forest managers	67	39.2	39.2	39.2
Engineers in various other branches	54	31.6	31.6	70.8
Forest cadastre officer	16	9.3	9.3	80.0
Manager	34	19.9	19.9	100.0
TOTAL	171	100.0	100.0	

Surveys were conducted to determine the opinions and solutions proposed by the forest engineers working in the region on forest property issues. Primarily, it was decided to determine the presence/absence and the level of the problem expressed as a general concept. *Table 5* indicates that there are very few who extremely worry that there is an unmanageable problem and those who think there is no problem in the region's forestry. The percentage of those who say that the forestry of the region is not very different from other regions and that the current problems are ordinary is very high (61%). Those who think that the problems are in a worse level than the other regions are considerably high (37%).

Table 5. *The views of forest engineers on forestry problems in the region*

Problem detection	Frequency	Percent	Valid percent	Cumulative percent
1. No problem	2	1.2	1.2	1.2
2. There is a problem at the expected level	104	60.8	60.8	62.0
3. There are quite a few problems	63	36.8	36.8	98.8
4. There is a problem that can not be overcome	2	1.2	1.2	100.0
TOTAL	171	100.0	100.0	

When the distribution of the results within the scope of the three regional forest directorates is examined separately, it is determined that Trabzon RDF employees participated in the “*there are fairly more problems*” opinion higher than Artvin RDF and Giresun RDF did.

Aside from the regular statistics, a deeper statistical analysis was conducted with Chi-square test. As such, the statistical differences between the personal characteristics of interviewed forest engineers and their views and recommendations about forestry problems were examined. The importance and the existence of cadastral and property problems among the forestry related problems experienced in the region were asked. The possible forestry problems were written for them and asked to rank these problems according to their importance. As clearly indicated in *Table 6*, about 65% of the forest engineers surveyed stated that the primary problem in the region was related to cadastre-ownership issues. This is rather an expected result as the most important current agenda in the political arena and the local media is the cadastral property.

One of the most important problems related to forestry in the region appeared to be the protection and sustainable management of forests (22%). In fact, the forest cadastre is the main factor in endangering the sustainability of forests resources because intensive forest damages are frequently encountered with the expectation (fear) that

their lands would be nationalized for forest due to cadastral works. It is therefore possible to relate this problem to the forest cadastre.

Among the forestry problems in the region, the first problem group including afforestation, wood production and forest-community relationships issues, which is considered to be important by us, appeared to be the low level of forestry-related problems. However, the result does not indicate that there is no problem in those challenging areas. The following provides a high level of participation in problem groups in the secondary or lower level as explained on the basis of the data.

Table 6. The list of the problems experienced in forestry activities according to the topics

Forestry issues	Frequency	Percent	Valid percent	Cumulative percent
Afforestation	4	2.3	2.3	2.3
Cadastre-ownership	111	64.9	64.9	67.2
Sustainable protection	38	22.2	22.2	89.4
Business administration	8	4.7	4.7	94.2
Forest-People Relations	10	5.9	5.9	100.0
TOTAL	171	100.0	100.0	

It is useful to put all of the options mentioned as problems in forestry together. In Table 7 the grading of forestry problems by the participants are shown together.

Table 7. Grading of problems experienced in forestry activities according to the issues

Forestry Issues	Importance order (%)				
	I. Degree	II. Degree	III. Degree	IV. Degree	V. Degree
Afforestation	2.3	15.2	21.6	24.6	35.7
Cadastre-ownership	64.9	18.7	9.9	5.8	0.6
Sustainable protection	22.2	37.4	22.2	13.5	4.7
Business administration	4.7	12.9	27.6	30.4	24.6
Forest-people relations	5.9	15.8	18.7	25.7	34.5
TOTAL	100.0	100.0	100.0	100.0	100.0

According to the respondents, the main problem in the field of forestry is the cadastre-ownership problem (Table 7). Approximately 65% regards this problem in the first place and about 18% in the second level. In other words, the cadastral property issue appears to stay in the first two levels (83%). The second most important problem in the field of forestry is expressed as the protection and sustainability of forests. Nearly 60% of the respondents see this problem in the top two levels. The third major problem in the forestry sector arises as forest-community relationships. Those who mark this option in the first two places have a total of 22%. The management of forests including afforestation is not seen as a significant problem by the participants.

According to the results, the most important problem in the field of forestry was the “protection and sustainability” as prioritized it first by Artvin RDF employees statistically different from other RDFs ($p = 0.011$). This problem was found to be more important than the others. In terms of the choice of the “people of the region”, there are differences ($p \leq 0.001$) among the three RDF employees in assessing the sources of the

problems of the forest cadastre and ownership. While Artvin RDF employees consider this issue to be important at 4th level, Giresun RDF employees consider the issue to be important at 2nd level. Unlike the others, Trabzon RDF employees consider the issue to be at 3rd level and less important than the others. There is a significant difference among the RDFs ($p = 0.002$) regarding the “*contradiction of legislation to the expectations*” option, one of the reasons of the forest ownership problem. Artvin and Giresun groups think that the effect of this option is less compared to the Trabzon group.

There was also a significant difference ($p = 0.031$) in terms of the choice of “*practitioner’s inadequacy*” among the causes of the current problem. Giresun RDF staff think that the “*practitioner’s inadequacy*” is a more effective factor than other groups in their problems. Trabzon RDF employees are separated from other groups with the view that this factor is ineffective. Giresun RDF employees recognized this proposal significant at the first level and Artvin RDF employees considered it significant at the second level ($p \leq 0.001$). However, being different from the other RDFs, Trabzon RDF employees stated the proposal not to be implemented. On the other hand, Trabzon RDF employees significantly differ from the other groups ($p = 0.037$) and consider the “*the documents of old ownership should be recognized valid and these forests should be left in the status of private forest property*” option.

The responses of the participants in the survey are tested to identify the differences in terms of sex. The results indicated that male participants were found to be statistically significant ($p = 0.014$) from the other groups with the view that the “*Legal confusion*” option was effective on forest ownership. In addition, while female participants regarded the “*Topographic conditions and land use pattern*” option as one of the effective causes of the problem, male participants significantly differed ($p = 0.015$) from them and did not prefer this option to be effective. The “*effect of changes in land use*” due to out-migration was significantly different ($p = 0.009$) by the women participants.

The effects of the age component on the problem were tested to see the difference in the evaluation of the problem. It was determined that the “*topographic conditions and land use pattern*” choice in the 0-35 age group and over 51 age group was not effective cause in the problem, differing significantly from the middle age group ($p = 0.012$). It has been found that the approach to the problem in terms of the duration of employment is significantly ($.003$) different from those of the others who have been working for 21 years or more. This group believes that the non-rule character of the people of the region is the cause of the problem.

There is a significant relationship between the employment period and “*topographic conditions and land use pattern*”. The 0-10 age group employees differ from the others ($p = 0.040$) and sees the option accelerating the problem further. Employees who worked for 0-10 years and over 21 years significantly differ from others ($p = 0.010$), accepting the idea that completed forest cadastre works “*eases the forest management activities*”. As a solution of the problem, the option “*Implementation without compromise according to current legislation*” was primary accepted by the employees worked in short duration. However, this option was not adopted significantly ($p = 0.010$) as the duration of employees increased and listed at the bottom of alternative list. It was also found that employees over 11 years or more significantly ($p = 0.024$) adopted the view that the “*old property documents should be considered valid and these forests should be left in the status of private forest*”.

Solution proposals for forest property and cadastre problems

The results indicated that the forest property conflicts in the region are seen as a serious problem by the forest engineers working in the forest organization. In this section, opinions and suggestions regarding the source of the problems and their solution proposals are evaluated. The views and the perceptions about the source of the problem of forest ownership in the region are examined. The distribution of the answers given in order of preference in the questionnaire can be seen in *Table 8*.

Table 8. *The main causes of forest property conflicts*

Causes of the problems	Importance level (%)					
	I. degree	II. degree	III. degree	IV. degree	V. degree	VI. degree
Local people	9.4	9.4	15.2	17.5	22.2	26.3
Legal confusion	15.8	21.1	18.7	17.5	17.0	9.9
Geographical conditions and land use pattern	38.0	19.9	21.1	11.7	7.0	2.3
Legislation violates expectations	21.1	26.9	14.6	17.5	14.0	6.4
Effect of change in land use	11.7	15.8	16.4	18.7	19.9	17.0
Inefficiency of practitioners	4.1	7.0	14.0	17.0	19.9	38.0
TOTAL	100.0	100.0	100.0	100.0	100.0	100.0

Among the causes of problems in forest property and cadastre are the actual land use pattern and the topographic structure of the region. The forests in the immediate vicinity have been owned by individuals for many years due to the rugged formation of the region and the intermingled agro-settlement areas with forests. The current legislation sees these areas as illegal and rejects them. The second important reason is that the expectations of the local people were not met. In fact, the forestry legislation in the country was mainly prepared according to the socialist property concept in the 1930s. All forests were seen as state property with very few exceptions. Claims of ownership were often rejected by commissions that practice on behalf of the state and the courts generally decided against the individuals.

The second reason for conflicts in forest ownership was identified as legal confusion. Frequent changes in the legislation on forest cadastre and the property were seen in Turkey. In addition, there are also differences in the recognition of the rights to private property between forestry legislation and general laws such as civil law and the law of debts. Invalidation of old-dated property documents covering forests, the abrogation of property documents based on court decisions and again cancelation of property documents based on court decisions, when forest administration is absent, are all among the important reasons.

The third reason for current conflict is the frequent changes in land use pattern. This finding is based on two different implementations. The first one relates to the existence of previously forested lands yet their forest cover are destroyed and used as agriculture, settlement, pasture and so on. Because these lands are evaluated as forests in old documents (i.e., aerial photographs and topographic maps), they are determined as state forests based on old characteristics of land not the current uses. However, those who use this land illegally demand that their ownership be given to them.

The change in land use is not limited to the destruction of forest areas and conversion to agriculture, settlement or other land uses. The rural population in Turkey has begun to decline particularly since the mid-1980s. As a result, animal breeding in natural lands has been reduced. The decrease in population and number of animals in the countryside resulted in the natural forestation of rangelands and agricultural lands. However, natural forestation of these lands, which were previously used for non-forest purposes, has emerged as a new problem. Since these areas do not generally have property documents like a certificate and mostly owned by the long term usage, they are regarded as a state forest during the cadastral process. This causes conflicts and triggers the reaction of the local people.

In the meantime, the negative attitudes of the people of the region and the inadequacies of practitioners are the least preferred options. The practitioners base the source of the problem on not themselves but on factors external to the people of the region.

Overall, the forest cadastre in the Eastern Black Sea Region was completed at a rate of 15-20% by the beginning of the year 2000. After this date, legislative amendments and arrangements for the coordination of the land cadastre and forest cadastre have facilitated the cadastral work to be accelerated. In the last 20 years, the realization rate of forest cadastre reached 80% level. Although this development seems to be encouraging, there is a doubt about the sustainability of the cadastre to solve the problems. The questions asked and the answers taken to determine the opinions of the respondents in this regard are given in *Table 9*.

Table 9 indicates that nearly 31% thinks that forest cadastre works have positive effects on the implementation of forest management activities. Those who think that the cadastre is not very effective, nevertheless still has benefits, are about 53%. As a result, the overall impression about the importance of the forest cadastre reaches at about 84% rate. Of course, it would be desirable to implement forest management activities in the registered areas of forests. While there is no doubt about this, it is concerned that the conflict of ownership would cause destruction of forests and the lag of forestry activities.

Table 9. *Assessment of whether forest cadastre is beneficial for forestry*

The effects of forest cadastre	Frequency	Percent	V. Percent	Cumulative percent
Forestry work and operations are facilitated	53	31.0	31.0	31.0
Partial positive development in forestry studies	90	52.6	52.6	83.6
There is no effect on forestry studies	12	7.0	7.0	90.6
It disrupts forest-community relations and negatively affects forestry activities	16	9.4	9.4	100.0
TOTAL	171	100.0	100.0	

About 7% thinks that forest cadastre has no positive effects on forestry activities. Those who think that the cadastral works carried out under the current legislation cause too much damages, rather than benefits, to the forests is about 9%.

The opinions of the respondent forest engineers on the implementation of the existing system or the application of alternative methods in the forest cadastre and property determination works were investigated. Furthermore, continuation of the

application of current legislation and alternatives about the change in different ways are also examined. In order to do this, a dialogue meeting was held with the employees in the forest organization in the region before determining alternative approaches that would not threaten forest existence and maintenance. Under this scope, five different alternatives were developed. It is decided to sort six alternatives according to their importance, together with the proposal of the continuation of current application. In addition, a free option is left for those who wish to express free opinions. The results are shown in *Table 10*.

Table 10. *The proposed solutions by the forest engineers*

Options	Order of precedence (%)					
	I. Degree	II. Degree	III. Degree	IV. Degree	V. Degree	VI. Degree
a. According to the current legislation, implementation must be carried out without compromise	25.7	7.0	8.8	4.7	13.5	40.4
b. Ownership of state forests should not be transferred but local governments should be involved	24.0	14.6	14.0	17.0	19.3	11.1
c. The settlement-farming areas should be allowed to be operated by the local people in order to ensure the continuity of the forests that are intertwined	11.7	26.9	21.1	21.6	12.9	5.8
d. Those who belong to the forests that are intertwined with the settlement-agricultural areas should be left in private ownership and measures should be taken to ensure their continuity	19.3	17.5	21.1	19.3	17.0	5.8
e. Old ownership documents should be valid, these forests should be left in the status of private forest	15.2	20.5	13.5	22.2	15.8	12.9
f. All owners, including possession, should be admitted in the forests formed with fast developing tree species (alder for the region etc.), and these areas should be contributed to the continuation and operation as forests	4.1	13.5	21.6	15.2	21.6	24.0
	100.0	100.0	100.0	100.0	100.0	100.0

Approximately 26% of interviewed forest engineers expressed their opinion that forest cadastre should be conducted without any compromise according to the current legislation. The remaining 74% believe that a change in legislation on forest cadastre and ownership is necessary. In view of the preference for options proposed for legislative amendments, approximately 36% (24% + 11.7%) agrees that the forests around the settlements should be managed by the local people in different forms providing opportunities for income, while remaining in state ownership. In places where settlements and agricultural areas are intertwined, about 19% of them desired the private

ownership to be recognized according to old property documents. Regardless of the location of the territory, nearly 15% of the respondents recognize that the property documents of the people be considered valid and these places be given to their former owners during cadastre works. Only 4% of the respondents think that the private ownership of the land covered with fast-growing natural trees, including long term usage, should be given to its owners. Eventually, those who stated that private forest ownership should be recognized reaches 39% in total.

Significant ($p = 0.005$) differences were found in terms of choosing the suggestions for the solution of the problem with the task being performed. While district management chiefs, cadastral unit employees and administrators, who are highly busy with intensive public relations, have expressed the opinion that the current legislation should be changed, the office workers favored primarily the view that the current legislation should be implemented without compromise.

Discussion and conclusion

Conflicts in forest cadastral works have continued since 1936 when the forest ownership work started on a regular basis in Turkey. The problem has not been solved, instead complicated further albeit the legal regulations introduced and implemented several times to solve these conflicts. The frequent amendments to the law do not make the people happy and threaten the sustainability of the forest resources. In the country, the deadlines are frequently renewed and the forests which are destroyed until that time (deadline) are sold to the invaders, or the private forest properties authorized by the cadastral works until the 1960s have not been regarded as forests and left in the hands of titleholders. It is necessary to change this course and introduce a new approach that does not threaten the existence and sustainability of the forest and takes into account the needs and expectations of the people.

Following the establishment of the Republic of Turkey from the mid-1930s until the 1990s, the common approach was that the forests were considered as national assets and thus not subject to private ownership. Furthermore, in this period, including the time of the Ottoman Empire in the country, the trend was that the private ownership of the forest areas was to be handed over to the state ownership as soon as possible (Diker, 1947; Bayraktaroglu, 1968; Çağlar, 1979). Judicial units also adopted this basic approach until the early 2000s, and made the decisions to settle forest ownership disputes in favor of the state. In the meantime, however, it was also suggested that the problem of forest ownership could be solved by uncompromising implementation of existing laws and regulations (Eroğlu, 1999). Since the mid-1990s, various proposals and ideas have been expressed in a way that the needs and expectations of the forest villagers should be taken into consideration in forest management and ownership issues (Gümüş et al., 1998). Alternatively, another group of proposals suggested that certain parts of forests subject to private property should be left under private ownership providing that those forests should be protected and managed as forest resources (Gümüş, 1999; Ayaz, 2004; Meriç, 1999). However, there has been no change in the country's legislation regarding the handover of nationalized forests to their former owners. However, the legal definition of a forest has been changed causing some of the areas not to be considered as forest. The change of forest definition has also caused losses of over 1.2 million ha of forest from 1937 to 2005 due to the removal of degraded forest areas out of the forestry boundaries (Çağlar, Y., 2014).

Approximately 12% of the forests in the case study area is claimed as a private ownership by the people of the region. Nearly half of these ownership claims (47%) is based on cancelled title deeds, while the other part is based on long-term usage (Ayaz, 2004). Forests owned by individuals are mostly small pieces with less than one hectare. The people of the region will be happy if the laws are changed to return these forests to the former owners. Nevertheless, there is no willingness to ensure the sustainable management of these disputed forests. The problems experienced during the handover of forests to the former owners in the Balkan countries may likely be encountered in Turkey due to a number of reasons. These include the existence of small pieces of forests, the feeling that it is not worth trying because there will not be too much economic effect and the lack of expert member in forestry knowledge in family partnerships (Glück et al., 2010). It is unlikely that these forests will be managed efficiently by their owners. As a solution proposal, establishment of forest associations with the private forest owners and the creation of new management approaches are far away alternatives in Turkey (Vangansbeke et al., 2015; Takahashi et al., 2015).

Regarding the proposals of the forest engineers working in state forest organizations in the region, nearly 75% of them calls for an immediate need for legislative changes. Especially managers and the officers in the district forest units and forest cadastral commissions recommend the provision of private forest ownership in wider areas by going through the legislative amendments. Approximately 36% of the interviewed engineers expressed their view that the rules for the property in the legislation should not be changed frequently, but that the local communities would be granted more rights to benefit from these forest resources. There are also some researches suggesting the similar approaches (Koçak, 1999). 19% of respondents agree that private ownership on the fragmented forests in residential areas is quite appropriate. Those who claim ownership of all forests in private property before any preliminary assessment have a 15% share, and the majority of this group has been employees more than 11 years. Only 4% of the respondents think that the forests dominated by fast-growing species such as alder must be subject to private ownership.

When the interviews conducted with the people of the region and the results of the surveys applied to the forest engineers in charge are evaluated together, it can be seen that the majority proposes changes in the current legislation. Otherwise, complaints of local people and forest destruction will continue. The forests in private properties are fragmented with small pieces that cannot be economically managed. In addition, some of the forests that are privately owned are intertwined with the state forests, which would create a serious problem in the future in terms of the integrity of these forests. On the other hand, however, the local people with the forest property do not have the required experience and tendency to manage the forests. There are also many heirs on the subject forests. Based on these ground, handing over the forests to the individuals as a private property would not seem to be an appropriate alternative in terms of forest protection and effective management of forest resources. The option of managing these forests by local governments is also not widely accepted by the parties.

Given the results of the research and the experiences assembled for many years, the problem may be resolved as followings. First of all, the endorsement of legal property documents given to the people in the historical process should be secured by the state particularly in forests subject to private property. Second, the privately owned forests that are integrated with the state forests should be registered as state forest for public benefit with the due costs paid to the owners. With this alternative, the forests would

better be protected and managed in integrity and the former property owners will not be victimized because the costs of their properties will be paid for. Third, the fragmented forests intermingled with the agricultural areas and settlements may be returned to their former owners with the appropriate legislative changes as in the case of countries such as Poland and Ukraine, where the nationalized forest were returned to their owners (Nijnik and Kooten, 2000; Kvarda, 2004) provided that these forests are maintained as is. With this alternative solution proposal, the cadastre-ownership problem can be resolved peacefully without endangering the sustainability of these forests, which are estimated to have a size of 1% or 2% of the region's forest resources. In this way, any forest damages caused by the property disputes can be avoided and technically and scientifically recognized forest areas can also be legally recognized as forests providing legal security to these areas. The same solution proposal is also suggested for the confiscated forests in the course of cadastral works conducted so far. Finally, the results indicated that the existing legislation and practices were not considered appropriate by all the forest villagers interviewed and by 75% of the forest engineers working in the regional forestry administration. Thus, legislative changes are inevitable to better protect the forests and minimize the conflicts.

Acknowledgements. The authors thank, KTUBAP (Black Sea Technical University Scientific Research Found) for the financial support it provided to this project (Project Name: Effects of Forest Cadastre Applications in Eastern Black Sea Region and Alternative Approaches).

REFERENCES

- [1] Asante, W. A., Acheampong, E., Boateng, K., Adda, J. (2017): The implications of land tenure and ownership regimes on sustainable mangrove management and conservation in two Ramsar sites in Ghana. – *Forest Policy and Economics* 85(1): 65-75.
- [2] Ayaz, H. (2004): Turkey Implementation of Law No. 4785 A Study on Forestry and Results (Eastern Black Sea Region Example). – PhD Thesis, KTÜ Institute of Science and Technology, Trabzon, 170 pp.
- [3] Ayaz, H., Gümüş, C. (2016): Forest property in Turkey experienced problems and proposed solutions. – *KAREN Journal of the Institute of Black Sea Studies* 2(2): 212-236.
- [4] Ayaz, H., İnanç, S. (2009): Private Forests in Turkey (Karadere-Kışlak Example). – Congress Book on Socio-Economic Problems in Forestry. SDU, Isparta, pp. 55-64.
- [5] Bayraktaroğlu, H. (1968): Provisions regarding forestry in the Turkish constitution and conditions for their evaluation. – *Journal of the Faculty of Forestry Istanbul University, Series: B* 18(2): 24.
- [6] Bilgili, E. (1998): Forest fires and fire management policies in Turkey. – In proc. FAO Meeting on Public Policies Affecting Forest Fires, FAO Forestry Paper No:138, p 357-362
- [7] Bilmen, Ö. N. (1967): *Law-i Islami and Istilahât-ı Fıkhiyye Kamusu*. – Istanbul.
- [8] Çağlar, Y. (1979): *Forestry Policy in Turkey (Yesterday)*. – Çağlar Printing House, Ankara.
- [9] Çağlar, Y. (2012): *Turkey Forestry History*. – ODTÜ Development Foundation Publishing and Communication AŞ, Ankara.
- [10] Çağlar, Y. (2014): In *Legal Gripper Forests and Forestry*. – Union of Turkish Bar Associations, Ankara.
- [11] Daşdemir, İ. (2016): *Scientific Research Methods* – ISBN:978-605-320-442-8, Nobel Akademik Yayıncılık ve Danışmanlık. 210 pp.

- [12] Diker, M. (1947): *Forestry Yesterday-Today-Tomorrow in Turkey*. – T. C. Ministry of Agriculture, GDF Publications, Ankara.
- [13] Diktaş, N., Gümüş, C., Ayaz, H., Er, U., Sayın, M. A., Gerçek, V., Çolak, N. (2017): *Partial Status of Forests and Partial Forest Management Problems (Trabzon Forest Management Directorate)*. – Research Project (Unpublished), Project No.: 03.8206/2013-(2017): Eastern Black Sea Research Directorate, Trabzon.
- [14] Eroğlu, M., Demirci, A. (1999): *The Importance of Possibility Problem in the Continuity of Our Forest Assets and the Effect of Existing Practices on Solutions*. – Proceedings of the Symposium on Problems of Forest Property in the Eastern Black Sea Region, 8-10 October 1999, Trabzon, pp. 91-99.
- [15] GDF (2016): *Forestry Statistics 2016.rar\ Forestry Statistics 2016\10 Forest cadastre _2016 - RAR Archive*, Unpacked size 10.076.792 bayt. – Access: 07.06.2018.
- [16] GDF (2016): *Forestry Statistics 2016.rar\ Forestry Statistics 2016\1 Forest Presence, 2015 - RAR Archive*, Unpacked size 10.076.792 bayt. – Access: 07.06.2018.
- [17] GDF (2016): *Forestry Statistics 2016.rar\ Forestry Statistics 2016\7 Support for Forest Villagers _2016 - RAR Archive*, Unpacked size 10.076.792 bayt. – Access: 07.06.2018.
- [18] GDF (2016): *Forestry Statistics, 2016. Forestry Statistics 2016 - RAR archive*, unpacked size 10.076.792 bytes. – Access 02.07.2018.
- [19] Glück, P., Avdibegović, M., Čabaravdić, A., Nonić, D., Petrović, N., Posavec, S., Stojanovska, M. (2010): *The preconditions for the formation of private forest owners' interest associations in the Western Balkan Region*. – *Forest Policy and Economics* 12(4): 250-263.
- [20] Gümüş, C. (1999): *Definition of Forest and Forest Regime in Turkey, Law No. 4785*. – Proceedings of the Symposium on Problems of Forest Property in the Eastern Black Sea Region, 8-10 October 1999, Trabzon, pp. 60-76.
- [21] Gümüş, C., Ayaz, H., Batı, M., Hacıhasanoğlu, S. (1998): *Village Forestry Applications in Turkey*. – Proceedings of the Forestry Symposium in the 75th Anniversary of Our Republic, 21-23 October 1998. Istanbul University Publication, Istanbul, pp. 68-77.
- [22] Gümüş, C., Toksoy, D. (2001): *Law No. 4785 over the Years 2000*. – Turkey Foresters Association First National Forestry Congress, March 19-20. 2001. Foresters' Association of Turkey, Ankara, pp. 343-352.
- [23] İnanç, S. (2010): *Investigation of the Impacts of Population Movements on the Forest Presence in Rural Areas (Trabzon Regional Directorate of Forestry)*. – PhD Thesis, KTÜ Institute of Science and Technology, Trabzon.
- [24] İstanbullu, T. (1978): *It Belongs to Someone Else from the State Forest Administration and Operation in Turkey on Research*. – İ. Ü. Forestry Faculty Publications, İstanbul.
- [25] Kvarda, E. (2004): *Non-agricultural forest owners' in Austria-a new type of forest ownership*. – *Forest Policy and Economics* 6: 459-467.
- [26] McGinley, K., Alvarado, R., Cubbage, F., Diaz, D., Donoso, P. J., Jacovine, L. A. G., de Silva, F. L., MacIntyre, C., Zalazar, E. M. (2012): *Regulating the sustainability of forest management in the Americas: cross-country comparisons of forest legislation*. – *Forests* 3: 467-505.
- [27] Meriç, K. (1999): *Forest, Property, Alder and Eastern Black Sea*. – Proceedings of the Symposium on Problems of Forest Property in the Eastern Black Sea Region, 8-10 October 1999, Trabzon, pp. 234-242.
- [28] Nijnik, M., Kooten, G. C. van (2000): *Forestry in the Ukraine: the road ahead?* – *Forest Policy and Economics* 1(2): 139-151.
- [29] Orhunbilge, A. N. (2000): *Sampling Methods and Hypothesis Testing (Review and Expanded Second Edition)*. – Avcıol Printing and Publishing, İstanbul.
- [30] Poudel, M., Thwaites, R., Race, D., Dahal, G. R. (2014): *REDD+ and community forestry: implications for local communities and forest management - a case study from Nepal*. – *International Forestry Review* 16(1): 39-54.

- [31] Schmithüsen, F., Hirsch, F. (2010): Private Forest Ownership in Europe. – Geneva Timber and Forest Study Paper 26. United Nations Food and Agriculture Organization Economic Commission for Europe, Geneva.
- [32] Siry, J. P., Cubbage, F. W., Ahmed, M. R. (2005): Sustainable forest management: global trends and opportunities. – *Forest Policy and Economics* 7: 551-561.
- [33] Takahashi, T., Matsushita, K., de Jong, W. (2017): Factors affecting the creation of modern property ownership of forest commons in Japan: An examination of historical prefectural data. – *Forest Policy and Economics* 74: 62-70.
- [34] TÜİK (2018): <https://www.itspopulation.com>. – Access: 07.06.2018.
- [35] Türker, M. F., Balık, T., Ayaz, H. (1999): The Effects of Social Disputed Forest Areas on Forest Management Activities (Maçka State Forest Company Example). – Proceedings of the Symposium on Forest Property Problems in Eastern Black Sea Region, Trabzon, pp. 251-260.
- [36] Vangansbeke, P., Gorissen, L., Nevens, F., Verheyen, K. (2015): Towards co-ownership in forest management: analysis of a pioneering case 'Bosland' (Flanders, Belgium) through transition lenses. – *Forest Policy and Economics* 50: 98-109.
- [37] Webb, E. L., Shivakoti, G. P. (2006): Forest property rights under nationalized forest management in Bhutan, Sinagpore. – *Environmental Conservation* 33(2): 141-147.
- [38] Yachkaschi, A., Adeli, K., Latifi, H., Mohammadi Samani, K., Seifollahian, M. (2008): Trends in Forest Ownership, Forest Resources Tenure and Institutional Arrangements: Are They Contributing to Better Forest Management and Poverty Reduction? A Case Study from the Islamic Republic of Iran. – Technical Report, FAO, Rome.

FLOATING VETIVER ISLAND (FVI) AND IMPLICATION FOR TREATMENT SYSTEM DESIGN OF POLLUTED RUNNING WATER

KUSIN, F. M.^{1,2*} – HASAN, S. N. M. S.¹ – NORDIN, N. A.¹ – MOHAMAT-YUSUFF, F.^{1,2} – IBRAHIM, Z. Z.¹

¹*Department of Environmental Sciences, Faculty of Environmental Studies, Universiti Putra Malaysia, 43400 UPM Serdang, Selangor, Malaysia*

²*Environmental Forensics Research Unit, Faculty of Environmental Studies, Universiti Putra Malaysia, 43400 UPM Serdang, Selangor, Malaysia*

**Corresponding author*

e-mail: faradiella@upm.edu.my; phone: +60-10-366-6160; fax: +60-38-946-7463

(Received 8th Aug 2018; accepted 5th Oct 2018)

Abstract. Floating Vetiver Island (FVI) system has been investigated in this study as a relatively new technology of artificial wetland treatment. Vetiver grass (*Vetiveria zizanioides*) was used as the treatment vegetation in the FVI owing to its high tolerance to various types of contaminants. Performance of the FVI was tested on actual polluted running water having characterized by a Class III-Class IV river according to water quality index (WQI) classification. Field trial of FVI over a six-week installation demonstrated an improved water quality with significant increase (92%) of dissolved oxygen and great removals of chemical oxygen demand (77%) and nitrate (73%), resulting in 14% increase of the overall WQI. It was proposed that treatment system performance for FVI can be reflected by the number of pontoons (FVIs) and treatment distance required to achieve desired water quality improvement. The calculated pollutant removal rates were incorporated into the estimation of treatment system requirements. Field installation guide for FVI system is also presented along with treatment system maintenance. For such an FVI system, vetiver grass pruning (trimming) at 2-month intervals is recommended for promoting the growth of the plant and for medium- to long-term FVI performance.

Keywords: *pontoons, water quality, treatment design, vetiver grass, pollutant removal*

Introduction

Previous researches have discovered various kinds of artificial wetland treatment systems using plants which are adopted to treat contaminated water such as artificial floating island (AFI), floating treatment wetland (FTW), conventional constructed wetland (CW), floating plant bed system, integrated floating system, integrated ecological floating bed (IEFB) and etc. (Yao et al., 2011; Zhao et al., 2012; Kusin et al., 2014; Chang et al., 2015; Lu et al., 2015; Lynch et al., 2015; Yeh et al., 2015). These artificial wetland treatment technologies produce similar function which is generally for water quality improvement. In this study, floating vetiver island (FVI) using vetiver grass (VG) has been designed and tested for field trial due to high tolerance of VG for contaminant removal in treating polluted water. Vetiver grass (*Vetiveria zizanioides*) has outstanding physiological and morphological features and it is economical and effective in removing pollutants from water (Truong, 2000; Danh et al., 2009; Darajeh et al., 2014; Suelee et al., 2017). Vetiver grass has been used in various water and wastewater treatment applications such as for stormwater, domestic and industrial wastewater treatment including palm oil mill effluent, sewage and mine tailings (Xia et

al., 2000; Shu et al., 2002; Ash and Truong, 2003; Shu and Xia, 2003; Roongtanakiat et al., 2007; Darajeh et al., 2014).

Generally, the removal of pollutants within a floating island system occurs as water passes beneath the floating mat which include uptake of metals and nutrients, contaminant clearing and binding as well as flocculation enrichment of suspended matter by plant roots (Yeh et al., 2015). In most instances, floating island system has been mainly used for purification of polluted water due to its proficiency in removing excess amount of nutrient contents. For instance, application of AFI contributed to reduction in nutrient level such as nitrate, potassium, ammoniacal nitrogen and total suspended solids as a result of nutrient and organic constituent uptakes by plant species which results in alteration of river water quality (Yao et al., 2011; Yeh et al., 2015). Other studies revealed that FTW is significant in removing 10,600 mg of nitrate (N), 428 mg of phosphate (P) and 273 mg of ammonium (AN) per day (Zhang et al., 2015), whilst removals of chemical oxygen demand (COD), total nitrogen (TN) and total phosphorus (TP) are between (24.5% to 37.6%), (34% to 42%) and (36.1% to 81.4%) respectively (Lu et al., 2015). In an example of a polluted river, removal of TN and P was 34% and 68.1%, respectively after one week of floating system installation and nutrient removal continues to increase up to 99% for P after three weeks and 82% for TN after four weeks (Zhao et al., 2012). However, despite being known that floating island system can be a reliable technology in water purification, the challenges remain that of full-scale implementation requirements and selection of appropriate treatment system for site-specific cases.

Notwithstanding this, most of previous studies with regard artificial floating wetland technology have been focusing on the application of such system for treatment of standing or stagnant water such as wetlands, lakes, ponds and on-site drainages (Yeh et al., 2015). However, in this study the FVI system is applied for treatment of polluted running water (i. e. river, stream or canal), which has never been investigated of its potential use. In Malaysia, river water is the main source of raw water and has been extensively used for domestic and agricultural purposes, industrial uses, generation of hydroelectric power, irrigation and other functions within a watershed (Chan, 2012; Othman et al., 2012; Al-Badaii et al., 2013; Cleophas et al., 2013; Kusin et al., 2016). Nevertheless, river water pollution has become a major environmental issue due to various anthropogenic activities from rapid urbanization and inappropriate management attempts (Fulazzaky et al., 2010; Biswas and Tortajada, 2011; Chan, 2012). As a consequence, discharges of several types of pollutants have contaminated the river as well as affecting aquatic organisms. Deteriorating river water quality in Malaysia particularly in the state of Selangor and Federal Territory of Kuala Lumpur has pointed out that attention is needed to treat our rivers for water sustainability in the future (Kusin et al., 2016). Therefore, a potential water treatment system is proposed in this study to purify polluted river to at least achieve a Class II river as required by relevant Malaysian water authorities.

Thus, the objectives of this study are to evaluate pollutant removal efficiency using FVI system in running water for improvement of river water quality and to develop a guideline for FVI design, field installation and estimation of treatment requirements for running water. Performance of the FVI was tested in actual river water and was evaluated of its potential application.

Materials and methods

Study site

A pilot test for assessing treatment efficiency of FVI was performed on actual river water. The river is a relatively small channel with approximately 3 m wide, 0.5 m deep and has flow rate of 0.1 m³/s. It receives domestic discharges within a university campus and nearby residential area having characterized by a Class III-Class IV water based on Water Quality Index (DOE-WQI) classification (*Fig. 1*).

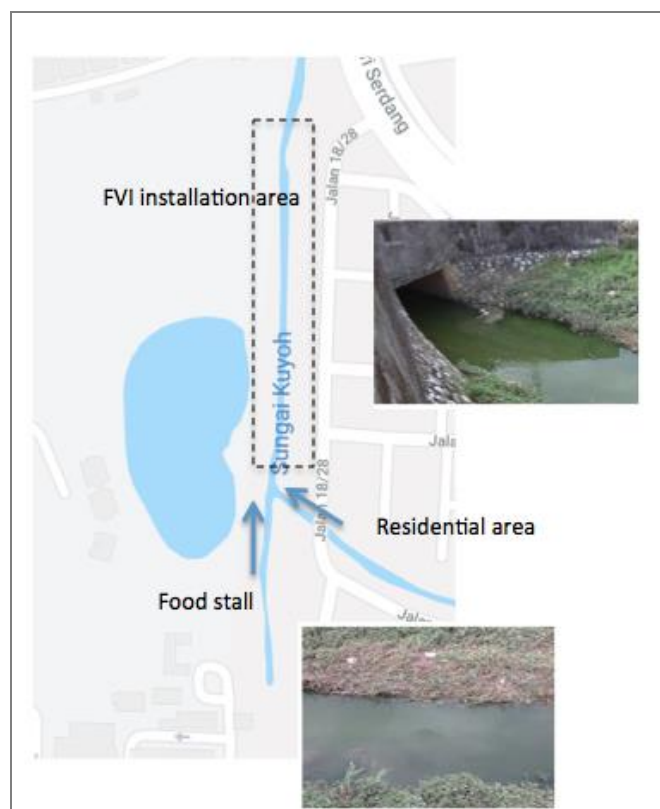


Figure 1. Location of study area

Field deployment of floating vetiver island (FVI)

The FVI was designed for a relatively small river or channel. Fabrication of FVI included the fabrication of floating island mat and VG planting inside the FVI. The FVI were made up of 1 m × 1 m uPVC pipes and synthetic net and were tied using steel band with bolt and nuts so that the net can hold the plants more appropriately (*Fig. 2*). After fabrication, VGs were planted on the floating mat at an amount of 100 tillers per FVI whereby four young tillers were grouped and tied together on the synthetic net to prevent breaking up of the young roots and soils. This was also to avoid VGs from being easily washed away in case of strong river flow (*Fig. 3a*). The VGs were planted evenly over the surface of the FVI to ensure its stability during installation and were placed in water for the growth of the root. Field deployment of FVI was performed through installation of nine FVIs within a distance of 500 m and with different arrangement patterns such as row and diamond planting (*Fig. 3b*). Measured variables for water quality were monitored in six weeks for physicochemical parameters (pH,

temperature, dissolved oxygen (DO), conductivity, total dissolved solids (TDS), turbidity), BOD, COD, TSS, and nutrient contents (nitrate (N), phosphate (P), ammoniacal nitrogen (AN)).

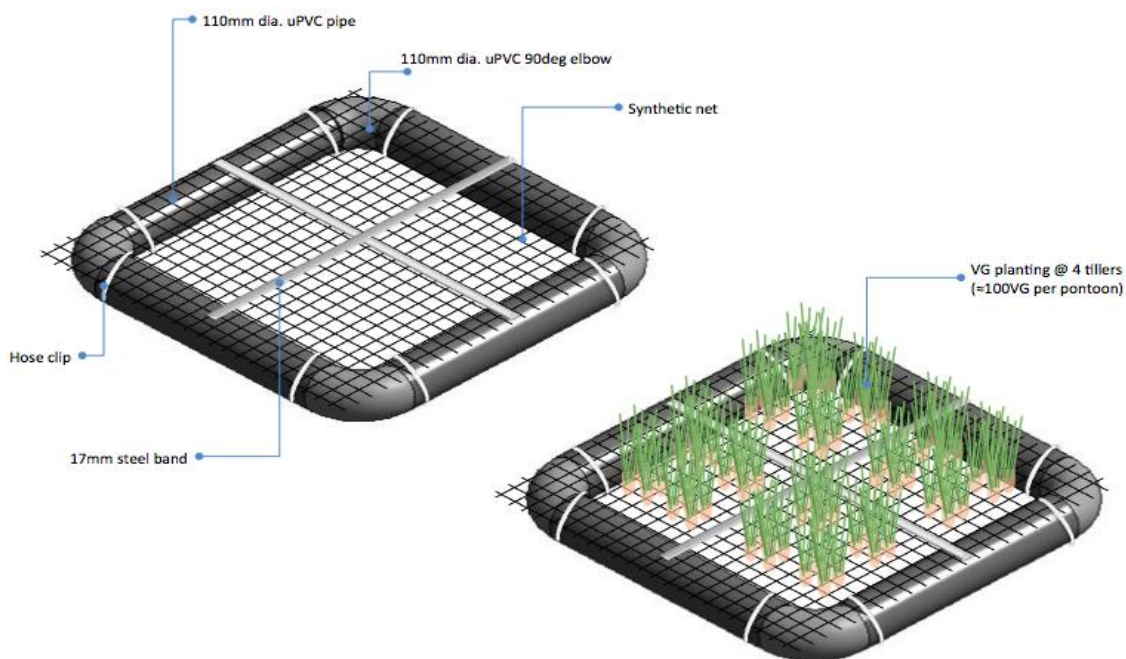


Figure 2. FVI design of 1 m × 1 m in size

Field measurement, sampling and analysis

Measurements of water physicochemical parameters (pH, conductivity, TDS and temperature) were taken using a calibrated Myron L Ultrameter 6P. Turbidity was measured using an Orion Aquafast turbidity meter, while dissolved oxygen was measured using a DO meter. Samples of water for analysis of BOD, COD, TSS, AN, N and P were taken in 1-L polyethylene bottles and were brought back to laboratory for analysis. Laboratory analysis of BOD, COD, TSS, AN, N and P, and the sample preservation were carried out according to standard methods for the examination of water and wastewater (APHA, 2005). Water velocity and water depth were measured using a flow meter with an impeller and were incorporated into the calculation of water flow rate using velocity-area method (Kusin et al., 2012). Sampling and water quality measurements were undertaken on weekly basis (three times a week) at a point before and after the installation of FVI. The water samples were collected at a depth of between 15-20 cm from the surface.

Data analysis

All six water quality parameters (pH, DO, TSS, BOD, COD, AN) required in calculating Water Quality Index (WQI) were determined on-site and also in laboratory. Results obtained were compared with National Water Quality Standards for Malaysia (NWQS) and Malaysian Department of Environment Water Quality Index classification (DOE-WQI) (Table 1). The WQI was calculated using Equation 1 as follows (DOE, 2010):

$$WQI = 0.22SIDO + 0.19SIBOD + 0.16SICOD + 0.15SIAN + 0.16SISS + 0.12SIpH \quad (\text{Eq.1})$$

where SI is the sub-index of each parameters and were obtained from a series of equations.

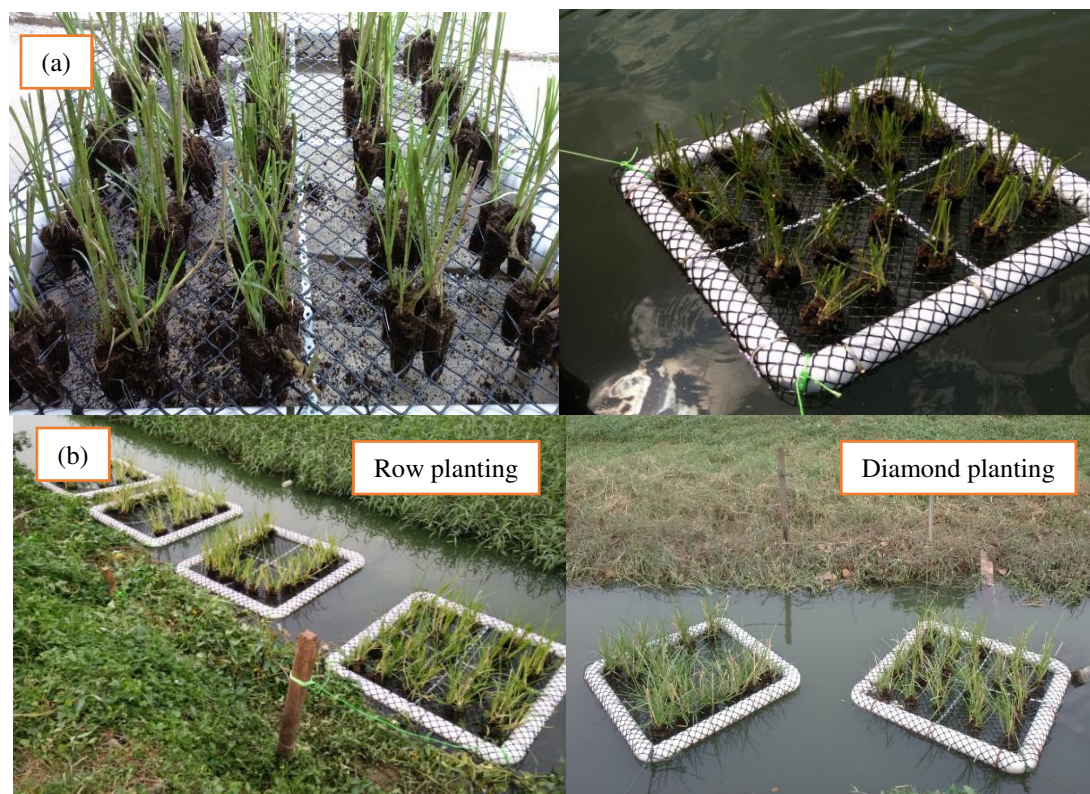


Figure 3. (a) VG planting in the FVI (b) field installation of FVI at site

Table 1. Water quality classification of selected parameters according to National Water Quality Standards (NWQS) for Malaysia (DOE, 2008)

Parameter	Class						
	Unit	I	IIA	IIB	III	IV	V
pH		6.5-8.5	6-9	6-9	5-9	5-9	-
DO	mg/L	7	5-7	5-7	3-5	<3	<1
BOD	mg/L	1	3	3	6	12	>12
COD	mg/L	10	25	25	50	100	>100
TSS	mg/L	25	50	50	150	300	300
AN	mg/L	0.1	0.3	0.3	0.9	2.7	>2.7

Class I	Conservation of natural environment Water supply I – Practically no treatment necessary Fishery I – Very sensitive aquatic species
Class IIA	Water supply II – Conventional treatment required Fishery II – Sensitive aquatic species
Class IIB	Recreational use with body contact
Class III	Water supply III – Extensive treatment required Fishery III – Common of economic value and tolerant species; livestock drinking
Class IV	Irrigation
Class V	None of the above

Statistical analysis

Statistical analysis was performed using SPSS statistical package software version 21. A one-way analysis of variance (ANOVA) was conducted to evaluate the variation in parameter improvement between weeks of observation. Subsequently, a Tukey HSD test was performed for multiple comparison between groups. Statistically significant differences were tested at $p \leq 0.05$.

Results and discussion

Water quality improvement

General trend shows that improvement of water quality was observed throughout field deployment of FVI in the river, whereby the weekly changes of the observed parameters were found to be significantly changing ($p < 0.05$). Results have demonstrated the increase of DO level by 92% (difference from initial value was significant, $p < 0.05$), which was in Class III, while pH was maintained at circum-neutral range within six weeks of FVI installation (*Fig. 4*). DO is an important water quality parameter whereby the high DO level in contaminated water indicates that high amount of oxygen is accessible for the survival of VG and aquatic organisms (Yeh et al., 2015; Zhang et al., 2015). Therefore, application of the FVI has helped in significant increase of DO thus maintaining pH at reasonably good level.

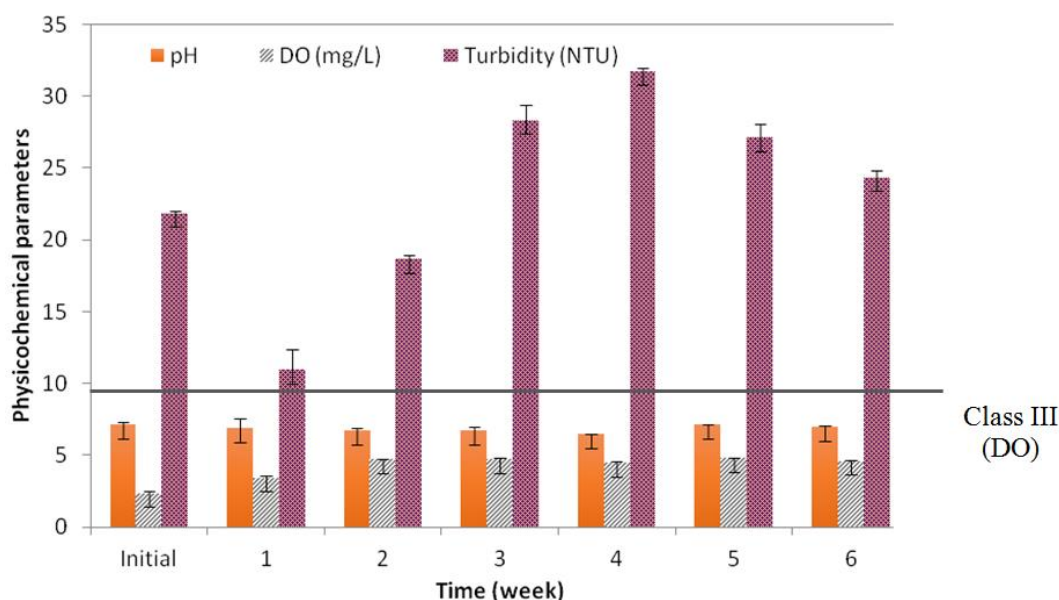


Figure 4. Weekly changes of physicochemical parameters in water after FVI installation

On the other hand, TSS and COD were found significantly decreased ($p < 0.05$) over the installation period (*Fig. 5*), where COD recorded 77% removal in six weeks. Reduction of COD shows that decomposition of organic matter and oxidation of inorganic chemicals such as nitrate and ammonia in water consume less oxygen, which results in adequate oxygen left to support aquatic organisms (Lu et al., 2015). It has been noted that higher removal of organic constituents was due to higher uptake of

contaminants by plant roots and consequently can improve river water quality (Yao et al., 2011; Yeh et al., 2015). Furthermore, fine massive VG root system enhances pollutant removal, which acts as an effective biofilter in trapping both fine and coarse sediment in running water (Truong and Smeal, 2003). This shows that vetiver root has a potential in removing organic constituents in water such as indicated by the amount of TSS, BOD and COD (Xia et al., 2000; Shu, 2003; Darajeh et al., 2014; Zhang et al., 2015).

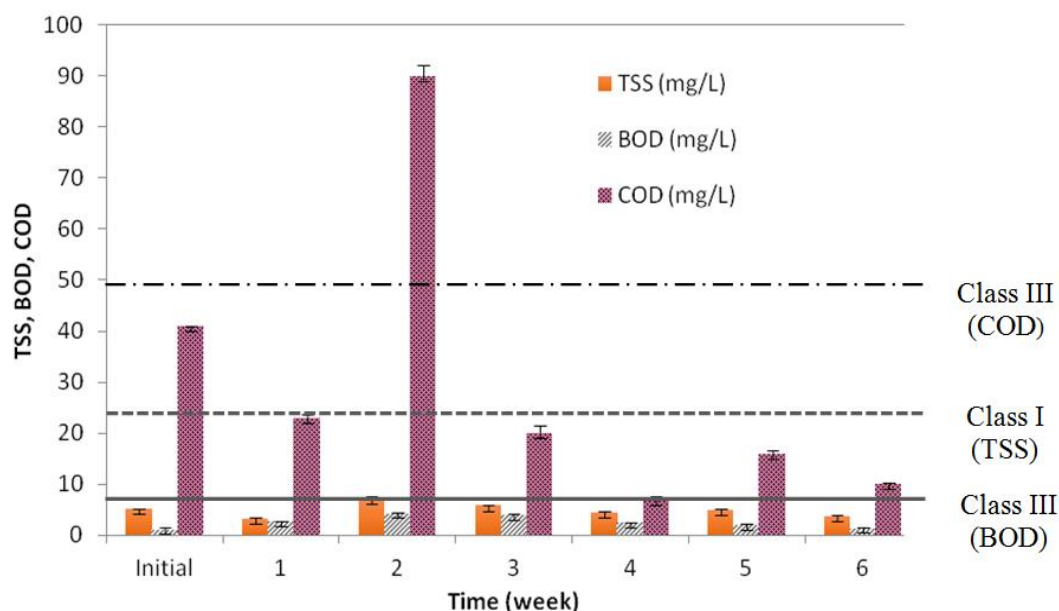


Figure 5. Weekly changes of TSS, BOD and COD of water after FVI installation

Generally, VG plays an important function for nutrient removal by a FVI system in contaminated water. Current findings show that nutrient contents in polluted river, in particular N, P and AN were also found to be significantly decreased (*Fig. 6*). N recorded the highest removal up to 73%, while AN and P showed some reductions, although still persisted at class IV in one month. The findings was in line with previous studies that application of floating islands planted with vegetation indicated high removal of N and P in contaminated water (Xia et al., 2000; Shu, 2003; Yao et al., 2011; Darajeh et al., 2014; Yeh et al., 2015). This is because of stronger absorption of nutrients by vetiver roots for plant growth, which results in higher nutrient removal in water (Truong and Hart, 2001). Notwithstanding this, excess amount of N and P in water bodies may trigger serious pollutants which can cause algal bloom as phytoplankton consume N as their main nutrients (Zhao et al., 2012; Yeh et al., 2015; Zhang et al., 2015). Therefore, removal of nutrient contents by the plants can avoid water eutrophication as well as improving the quality of polluted river. In general, findings suggested that application of FVI has a potential in the purification of the river water especially in removing nitrate and COD, and increasing DO level. Overall, the WQI showed 14% improvement (difference from initial value was significant, $p < 0.05$) after the six-week installation of FVI, although still remained at Class III (*Fig. 7*). Summary of water quality improvement within six weeks of FVI installation is shown in *Table 2*.

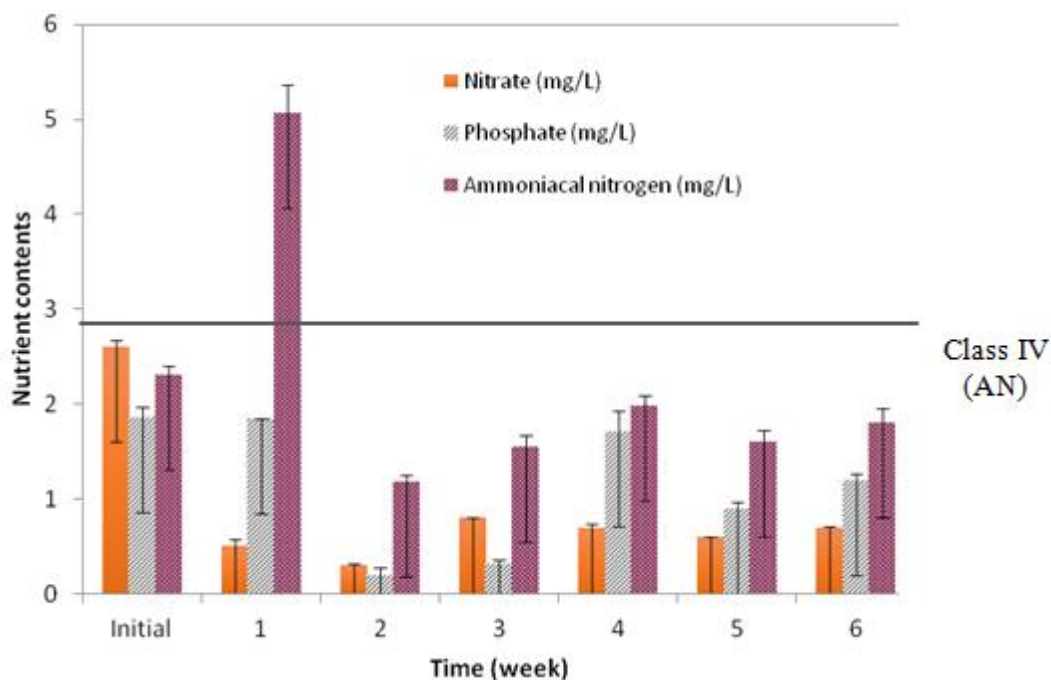


Figure 6. Weekly changes of nutrient contents in water after FVI installation

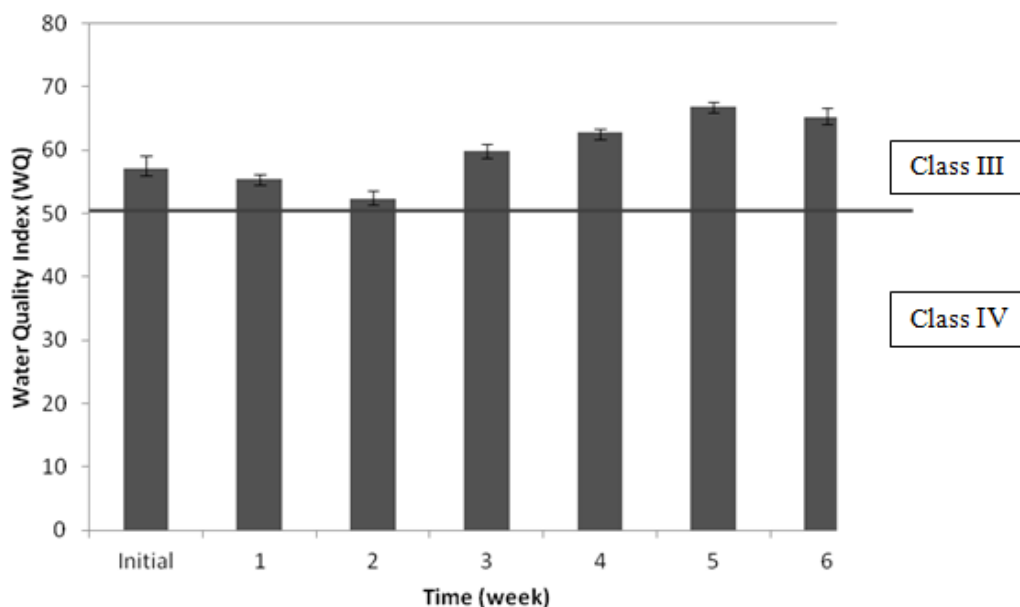


Figure 7. Water Quality Index (WQI) within six weeks of FVI installation

Planting patterns

In general, planting patterns of VG have significant effect on flow resistance across a FVI system. The different planting patterns showed that row planting is more suitable in a small river or stream rather than diamond planting due to more resistance during high flow (Metcalf et al., 2003). However, this is only applicable for a river that receives

relatively low flow of up to 0.1 m³/s. Diamond planting was found to be easily flushed away especially during high flows and heavy rains. This was due to that diamond pattern has less resistance to high flow and was found to be in hydraulic retardance class B (Metcalf et al., 2003). Therefore, three or more FVIs of similar size should be tied together to provide higher stability that can withstand higher flows.

Table 2. Summary of water quality improvement within six weeks of FVI installation

Parameters (mg/L)	Initial	After six weeks
Dissolved oxygen	2.41 (Class III)	4.63 (Class III)
Total suspended solids	5.20 (Class I)	3.80 (Class I)
Chemical oxygen demand	41 (Class III)	10 (Class I)
Nitrate	2.60	0.70
Phosphate	1.86	1.20
Ammoniacal nitrogen	2.30 (Class IV)	1.80 (Class IV)
Water quality index (WQI)	57.00 (Class III)	65.10 (Class III)

Flow rate: 0.06-0.07 m³/s; treatment distance: 0.5 km; river width: 3 m; water depth: 0.5 m; no. of pontoons: 9 (100 tillers each)

*pH remained at circum-neutral range; no improvement of BOD

Implication for FVI treatment system design

In order to calculate effective treatment system requirements (e. g. number of FVI and treatment distance), information on the given flow rate, initial and targeted pollutant concentration are required. The value of the targeted final concentration should have been agreed with relevant regulatory requirements. The estimation was based on the principle of a zero-order kinetics of pollutant removal (Kadlec and Wallace, 2009). Although it was known that some floating wetland treatment systems or AFIs follow a first-order kinetic model for pollutant removal (Wang and Sample, 2013), the model can result in overestimation of treatment system sizing (Kusin et al., 2012). Until further treatment system sizing is developed for floating wetland system, a zero-order kinetics can still predict the required treatment system requirements. According to the zero-order kinetic model, the treatment area required is a function of the pollutant concentration and flow rate divided by the removal rate. In this case the treatment ‘area’ is reflected by the number of floating island system (i. e. no. of pontoons) and treatment distance required. Notwithstanding the proposed design approach above, it is worth noting that when using a zero-order kinetic model several assumptions have been made such as pollutant removal is concentration-independent and under steady-state condition (Kadlec and Wallace, 2009). Even if first-order kinetics is to be adopted, the model on the other hand assumes a plug-flow system which is also rarely the case in real flowing water.

In this study, it is recommended that if the same degree of treatment is received as in the monitored site, a treatment distance of about 3.3 km along with 61 pontoons (FVIs) is required for the same river size in order to achieve a Class II river (i. e. minimum regulatory requirement) (Table 3). Whereas if a Class I river is intended, a treatment distance of 4.8 km is required and with 85 number of pontoons. Note that the estimation of treatment requirements for FVI system here is based on the calculated rates of

pollutant removal in an earlier study (Suelee et al., 2017). A more comprehensive study on the rates of pollutant removal may determine the removal rates more accurately. By using this calculation guide, treatment requirements for other rivers of different sizes and flow rates may then be estimated, however it is subjected to the estimated rate of pollutant removal.

Table 3. Estimation of treatment requirements for FVI system

Design criteria	Treatment requirement	Number of pontoon (FVI)
For 0.1 m ³ /s flow	Requires 1500 m ² treatment 'area' or 750 m ³ of treatment volume	9 (each of 100 no. of VGs)

To achieve Class II river;
(Example from the monitored site of the following characteristics):

Initial parameter concentration (mg/L)	Target concentration (mg/L)	*Treatment 'area' required (m ²)	*Treatment volume required (m ³)
TSS = 5.2	Already Class I	-	-
BOD = 1.21	1	74.11	37.06
COD = 41	25	705.88	352.94
AN = 2.3	0.3	9391.30	4695.65
	Total treatment 'area'/volume required	10171.29	5085.65
	No. of pontoon required	61	
	Treatment distance required	3.3 km	
To achieve Class I river;	Total treatment 'area' required	14214.76	
	No. of pontoon required	85	
	Treatment distance required	4.8 km	

*Treatment requirements are calculated based on the estimated removal rates

Field installation guide for FVI

Specific installation guide for FVI presented here is only applicable for a relatively small river such as the aforementioned system. The river must be clear from invasive plants whilst rubbish/debris must be first trapped from the water flow to avoid damage to FVI and blockage of flow across the river at least 500 m from the FVI system. A concrete structure by the river side is preferable for easy FVI installation and must be provided at a point where flow is stable. FVI of 1 m x 1 m planted with 100 VG tillers can withstand water flow of up to 0.1 m³/s. Non-rusting materials are preferable in the fabrication of FVI such as stainless steel clips, steel bar etc. VG must be planted on the FVI at young age so that the root grows while attaching to the net. VG shoot can be cut

off prior to planting on the FVI to ensure that all tillers are at the same height. This is important to ensure FVI stability whilst the plants are growing on the system.

Treatment system maintenance (vetiver grass pruning)

The shoot of VG should be trimmed (pruning) at 2-month intervals to encourage the growth of the root for efficient pollutant uptake and to lengthen the life cycle of the vetiver grass. Proper pruning of the top crown enhances the efficiency of pollutant uptake by the vetiver system. Based on the observation in an earlier study (Suelee, 2015), pruning should be conducted regularly (e. g. 2-month intervals) by cutting the top crown specifically from the growth point when the plant grows up to 5-6 nodes or when the leaves grow about 50 cm long.

The reason why pruning enhances pollutant uptake by the plant is due to the fact that pruning can promote growing and tillering (Xia, 2003). It was found that as vetiver is a C4 plant (those which photosynthesise following the mechanism of C4 photosynthesis), it requires a large amount of sunshine for its growth and development. Adult vetiver of 150-160 cm high can form shading to the crown's stem and bed, therefore, proper pruning may lessen the shading density and heighten sunshine density in all parts of the plant, especially for improved photosynthesis of the new tillers. Pruning can effectively increase the leaf stomatal conductance and decrease the vapour pressure deficit at some degree, and helpful to the increase of net photosynthetic and transpiration rate (Yin et al., 2015). Xia (2003) suggested that pruning also cuts off pedicels or inhibits the plants from moving into the stage of reproductive growth, which would consume a great deal of water and nutrients owing to flowering and seeding. The old parts when cut off possibly produces stimulation to the plant itself, thus can also improve its growth and tillering.

Long term monitoring

Further monitoring of field FVI system installation can be carried out to observe the changes in water quality parameters at longer time and to evaluate on system design efficiency. This is also important to update on current rates of pollutant removal from such a treatment system. For acquiring more detailed understanding on the pollutant removal rates, the FVI technique can also be installed at other locations e. g. rivers of different flow rates, width and depth, and different ranges of water quality to observe on-site system efficiency more accurately. Monitoring of FVI system after cutting off their shoot at two-month intervals can be useful to observe the effect of plant growth and contaminant uptake.

Conclusions

Findings from field trial of the FVI system have shown that generally water quality is improved as indicated by 14% increase in WQI within six weeks of FVI installation in actual running water. Even though WQI remains at Class III, DO level has significantly increased whilst COD and nitrate were greatly removed. It has been proposed that treatment system performance of FVI can be reflected by the number of pontoons (FVIs) and treatment distance required to achieve desired water quality improvement. Note that also this treatment system design estimation is based on the calculated rates of pollutant removal. Further research may look into the estimation of the intended

removal of pollutants more accurately. Despite this, field installation guide and treatment system maintenance have also been presented such that vetiver grass pruning is very important for medium- to long-term FVI performance.

Acknowledgements. The research was funded by the Humid Tropics Centre (HTC), Department of Irrigation and Drainage (DID), Malaysia. The authors would like to acknowledge Pakar Go Green Sdn. Bhd. for technical guidance and also the Environmental Forensics Research Centre (ENFORCE) Laboratory, Universiti Putra Malaysia for providing laboratory facilities. Special thanks are due to technical staffs of HTC and laboratory staffs of Faculty of Environmental Studies, Universiti Putra Malaysia for their assistance in completing the research.

REFERENCES

- [1] Al-Badaii, F., Othman, M. S., Gasim, M. B. (2013): Water quality assessment of the Semenyih River, Selangor, Malaysia. – *Journal of Chemistry* 1–10. <http://dx.doi.org/10.1155/2013/871056>.
- [2] American Public Health Association (APHA) (2005): *Standard Methods for the Examination of Water and Wastewater*. 19th Ed. – American Water Works Association, Water Environment Federation, Washington DC.
- [3] Ash, R., Truong, P. (2003): The use of vetiver grass wetland for sewerage treatment in Australia. – *Third International Vetiver Conference, Guangzhou, China*.
- [4] Biswas, A. K., Tortajada, C. (2011): Water quality management: an introductory framework. – *International Journal of Water Resources Development* 27(1): 5–11.
- [5] Chan, N. W. (2012): Managing urban rivers and water quality in Malaysia for sustainable water resources. – *Water Resource Development* 28(2): 343–354.
- [6] Chang, Y. H., Wu, B. Y., Lai, C. F. (2015): A study of the ecological benefits of the green energy landscape fountain. – *Ecological Engineering* 75: 128–136.
- [7] Cleophas, F. N., Isidore, F., Lee, K. H., Bidin, K. (2013): Water quality status of Liwagu River, Tambunan, Sabah, Malaysia. – *Journal of Tropical Biology and Conservation* 10: 67–73.
- [8] Danh, L. T., Truong, P., Mammucari, R., Tran, T., Foster, N. (2009): Vetiver grass, *Vetiveria zizanioides*: a choice plant for phytoremediation of heavy metals and organic wastes. – *International Journal of Phytoremediation* 11: 664–691.
- [9] Darajeh, N., Idris, A., Truong, P., Aziz, A. A., Bakar, R. A., Man, H. C. (2014): Phytoremediation potential of vetiver system technology for improving the quality of palm oil mill effluent. – *Advance Material Science and Engineering* 1–10. <http://dx.doi.org/10.1155/2014/683579>.
- [10] Department of Environment (DOE) (2010): *Malaysia Environmental Quality Report 2010*. – DOE, Putrajaya.
- [11] Fulazzaky, M. A., Seong, T. W., Masrin, M. I. M. (2010): Assessment of water quality status for the Selangor River in Malaysia. – *Water, Air and Soil Pollution* 205: 63–77.
- [12] Kadlec, R. H., Wallace, S. D. (2009): *Treatment Wetlands*. 2nd ed. – CRC Press, Boca Raton, Florida.
- [13] Kusin, F. M., Jarvis, A. P., Gandy, C. J. (2012): Hydraulic performance assessment of passive coal mine water treatment systems in the UK. – *Ecological Engineering* 49: 233–243.
- [14] Kusin, F. M., Jarvis, A. P., Gandy, C. J. (2014): Hydraulic performance and iron removal in wetlands and lagoons treating ferruginous coal mine waters. – *Wetlands* 34(3): 555–564.
- [15] Kusin, F. M., Zahar, M. Z. M., Muhammad, S. N., Mohamad, N. D., Madzin, Z., Sharif, S. M. (2016): Hybrid off-river augmentation system as an alternative raw water resource:

- the hydrogeochemistry of abandoned mining pond. – *Environmental Earth Sciences* 75: 230.
- [16] Lu, H. L., Ku, C. R., Chang, Y. H. (2015): Water quality improvement with artificial floating islands. – *Ecological Engineering* 74: 371–375.
- [17] Lynch, J., Fox, L. J., Owen Jr, J. S., Sample, D. J. (2015): Evaluation of commercial floating treatment wetland technologies for nutrient remediation of stormwater. – *Ecological Engineering* 75: 61–69.
- [18] Metcalfe, O., Truong, P., Smith, R. (2003): Hydraulic characteristics of vetiver hedges in deep flows. – Third International Vetiver Conference, Guangzhou, China.
- [19] Othman, F., Eldin, M. E. A., Mohamed, I. (2012): Trend analysis of a tropical urban river water quality in Malaysia. – *Journal of Environmental Monitoring* 14: 3164–3173.
- [20] Roongtanakiat, N., Tangruangkiat, S., Meesat, R. (2007): Utilization of vetiver grass (*Vetiveria zizanioides*) for removal of heavy metals from industrial wastewaters. – *Science Asia* 33: 397–403.
- [21] Shu, W. S. (2003): Exploring the potential utilization of vetiver in treating acid mine drainage (AMD). – Third International Vetiver Conference, Guangzhou, China.
- [22] Shu, W., Xia, H. (2003): Integrated vetiver technique for remediation of heavy metal contamination: potential and practice. – Third International Vetiver Conference, Guangzhou, China.
- [23] Shu, W. S., Xia, H. P., Zhang, Z. Q., Lan, C. Y., Wong, M. H. (2002): Use of vetiver and three other grasses for revegetation of Pb/Zn Mine tailings: Field experiment. – *International Journal of Phytoremediation* 4(1): 47–57.
- [24] Suelee, A. L. (2015): Phytoremediation potential of vetiver grass (*Vetiveria zizniodes*) for water contaminated with selected heavy metal. – Bachelor Thesis, Universiti Putra Malaysia.
- [25] Suelee, A. L., Hasan, S. N. M. S., Kusin, F. M., Mohamat-Yusuff, F., Ibrahim, Z. Z. (2017): Phytoremediation potential of vetiver grass for removal of heavy metal-contaminated water. – *Water, Air & Soil Pollution* 228(4): 158.
- [26] Truong, P. (2000): The global impact of vetiver grass technology on the environment. – Second International Vetiver Conference, Thailand.
- [27] Truong, P., Hart, B. (2001): Vetiver System for Wastewater Treatment. – Technical Bulletin no. 2001/21. Pacific Rim Vetiver Network. Office of the Royal Development Projects Board, Bangkok, Thailand.
- [28] Truong, P., Smeal, C. (2003): Research, Development and Implementation of Vetiver System for Wastewater Treatment: GELITA Australia. – Technical Bulletin no. 2003/3. Pacific Rim Vetiver Network. Office of the Royal Development Projects Board, Bangkok, Thailand.
- [29] Xia, H., Liu, S., Ao, H. (2000): A study on purification and uptake of garbage leachate by vetiver grass. – Second International Vetiver Conference, Thailand.
- [30] Xia, H. P. (2003): Observations and experiments on the multiplication, cultivation and management of vetiver grass conducted in China in the 1950's. – http://www.vetiver.com/CHN_propagation.html.
- [31] Yao, K., Song, S., Zhang, Z., Xu, J., Zhang, R., Liu, J., Cheng, L., Liu, J. (2011): Vegetation characteristics and water purification by artificial floating island. – *African Journal of Biotechnology* 10(82): 19119–19125.
- [32] Yeh, N., Yeh, P., Chang, Y. H. (2015): Artificial floating islands for environmental improvement. – *Renewable and Sustainable Energy Reviews* 47: 616–622.
- [33] Yin, W., Chen, S., Sun, S., Xia, X., Liu, X. (2015): The effects of green pruning on growth the effects of green pruning on growth and physiological characteristics of poplar and physiological characteristics of poplar agroforestry system in China. – Beijing Forest University.

- [34] Zhang, L., Zhao, J., Cui, N., Dai, Y., Kong, L., Wu, J., Cheng, S. (2015): Enhancing the water purification efficiency of a floating treatment wetland using a biofilm carrier. – *Environmental Science and Pollution Research* 1–7.
- [35] Zhao, F., Yang, W., Zeng, Z., Li, H., Yang, X., He, Z., Gu, B., Rafiq, M. T., Peng, H. (2012): Nutrient removal efficiency and biomass production of different bioenergy plants in hypereutrophic water. – *Biomass and Bioenergy* 42: 212–218.

SELECTIVE BIOHERBICIDAL POTENTIAL OF *DELONIX REGIA* ALLELOPATHIC LEAF EXTRACT ON GERMINATION AND SEEDLING GROWTH OF FIELD BINDWEED AND WHEAT

PERVEEN, S.¹ – YOUSAF, M.¹ – MUSHTAQ, M. N.^{2*} – SARWAR, N.³ – KHALIQ, A.⁴ – HASHIM, S.⁵

¹*Department of Chemistry, Government College University, Faisalabad, Pakistan*

²*University of Agriculture Faisalabad, Sub Campus Burewala, Pakistan*

³*Plant Protection Division, Nuclear Institute for Agriculture and Biology, Faisalabad, Pakistan*

⁴*Department of Agronomy, University of Agriculture, Faisalabad, Pakistan*

⁵*Department of Weed Science, University of Agriculture, Peshawar, Pakistan*

**Corresponding author*

e-mail: mnmushtaq@gmail.com

(Received 2nd Sep 2018; accepted 1st Nov 2018)

Abstract. Due to increased risk attached with indiscriminate use of synthetic herbicides, researchers are looking for alternative weed control strategies. Allelopathy is a natural phenomenon that might be exploited for biological weed management in field crops. Allelopathic plant water extracts may provide selective growth inhibition of the weeds. The present studies were conducted to investigate the possible selective phytotoxic effect of *Delonix regia* aqueous, ethyl acetate and lyophilized leaf extract against field bindweed (*Convolvulus arvensis* L.) and wheat (*Triticum aestivum* L.). The results revealed that lower to medium aqueous (2.5 and 5%) and ethyl acetate (50, 500 and 1000 ppm) leaf extract concentrations inhibited field bindweed germination, root length, shoot length and seedling dry biomass by 35-48%, 42-59%, 45-46% and 52-56% respectively, while no significant phytotoxic effect was observed on wheat at these concentrations. It is concluded that lower to medium concentrations of *Delonix regia* leaf extract might be safely utilized for natural control of field bindweed in wheat, reducing reliance upon synthetic herbicides.

Keywords: *allelopathy, biocontrol, Convolvulus arvensis, phytotoxic, Triticum aestivum*

Introduction

Use of synthetic herbicides is an efficient way to control weeds in horticultural and agricultural field crops and herbicide use has been increased many folds in the last few decades. The worldwide consumption of herbicides is about 0.95 million tons per year, which accounts for 47.5% of the total pesticides used (De et al., 2014). Indiscriminate use of herbicides is not only creating herbicide resistant weeds but also posing serious threat to the environment (Polyrakis, 2009). At present, there are 255 herbicide resistant weed species (148 dicots and 107 monocots) reported in 92 crops and 70 countries (Heap, 2018). Moreover, herbicides also contaminate air, soil, surface water, ground water, non-target organisms and herbicide residues in the food has increased risk of human diseases especially in the workers at farm level and/or in agricultural industries (Aktar et al., 2009; Polyrakis, 2009). Therefore, there is a growing public and scientific concern regarding herbicide use and researchers are looking for alternative ways for weed management worldwide.

Higher plants produce secondary metabolites, which are known as allelochemicals, through a phenomenon called allelopathy. The allelochemicals may inhibit growth of the other plants including weeds (Albuquerque et al., 2011). Many plant species have been well documented as allelopathic, producing allelochemicals (Cheng and Cheng, 2015). There are different strategies for using allelopathic plants for weed management. Among the strategies, use of allelopathic plant extracts, as an alternative to synthetic herbicides, is a viable option for managing weeds (Iqbal et al., 2009; Khaliq et al., 2012; Mushtaq et al., 2010).

For effective weed management, allelopathic plant water extracts are required to be selectively phytotoxic against weeds and safe on crops (Haq et al., 2010). However, they might also inhibit germination and growth of crops (Mushtaq et al., 2013). Therefore, it is pertinent to evaluate selective phytotoxic effect of allelopathic plant water extracts against weeds in comparison with crops.

Delonix regia (Boj.) Raf. (flamboyant) is a 10-15 m tall tree native to Madagascar and spread world over in tropical and subtropical regions (Fig. 1). It belongs to biological nitrogen fixing family (Fabaceae) of plants. It is a decorative tree with beautiful flowers and used as shade, shelter, timber, fuel and in apiculture (Orwa et al., 2009). Previously, it has been reported that *Delonix regia* substantially inhibited weeds under its canopy. Aqueous extract of *Delonix regia* inhibited growth of *Centella asiatica* and *Isachne nipponensis* up to 70%. Phytotoxins present in *Delonix regia* were identified as chlorogenic acid, 4-hydroxybenzoic, 3,4-dihydroxybenzoic, 3,5-dinitrobenzoic, L-azetidine-2-carboxylic 3,4-dihydroxybenzaldehyde, 3,4-dihydroxycinnamic and gallic acid (Chou and Leu, 1992).

Field bindweed (*Convolvulus arvensis* L.) is a dicot perennial broadleaf weed which is considered one of the world's top 10 worst weeds by agriculturists and horticulturists (Holm et al., 1977; Skinner et al., 2000). It is an invasive species and problematic weed of many field crops including wheat. Uncontrolled densities of field bindweed may reduce yield of wheat crop by 56%, and it is very difficult to control even with the synthetic herbicides (Black et al., 1994). The present study was conducted to compare phytotoxic protentional and selectivity of *Delonix regia* aqueous, ethyl acetate and lyophilized extracts on germination and early seedling growth of field bindweed and wheat.

Materials and methods

Preparation of extracts

Delonix regia leaves were collected from trees at University of Agriculture, Faisalabad Pakistan. The extraction procedure was modified from previously described (Perveen et al., 2014) unless stated otherwise. The leaves were dried under shade and were ground to fine powder. The aqueous extract was prepared by soaking 10 g leaf powder in 100 ml distilled water. The suspension was placed in an ultrasonic device for 30 min (Sheng et al., 2012). The extract was filtered through two layers of cheesecloth to obtain extract concentration of 10% (10 g/100 ml) and was diluted with distilled water to prepare further aqueous extract dilutions (2.5%, 5% and 7.5%).

For ethyl acetate and lyophilized fractions, 200 ml of acetone was added to 200 ml of 10% *Delonix regia* aqueous leaf extract. After placing at 4 °C for 24 h and filtration with Whatman #1 filter paper, the acetone was allowed to evaporate with a rotary evaporator (BUCHI, Switzerland) under reduced pressure. Aliquots of ethyl acetate

(600 ml) were used to partition the extract 3 times sequentially. Thereafter, ethyl acetate layer was separated, and ethyl acetate was evaporated to obtain the residue. The aqueous phase was lyophilized (freeze-dried) in a Freeze Dryer (Alpha I-5, Christ). Thus, ethyl acetate and lyophilized residue fractions were obtained as 400 and 105 mg respectively. The stock solution of 4000 ppm was prepared by dissolving 100 mg of each residue in 25 ml methanol. The stock solution (4000 ppm) was diluted to prepare 50, 500, 1000 and 2000 ppm extract.



Figure 1. A young plant of *Delonix regia* (flamboyant) at University of Agriculture Faisalabad, Sub Campus Burewala, Pakistan. (Photo by Muhammad Naeem Mushtaq)

Bioassays

Seeds of field bindweed and wheat were surface sterilized with 2% sodium hypochlorite for 2 min and were rinsed with distilled water. Each aqueous extract concentration was added (4 ml) to sterilized petri dishes (9.5 cm) on Whatman #1 filter paper. While, for ethyl acetate and lyophilized fractions, each methanolic extract (2 ml) was added to each petri dish (4.5 cm) except control which received 2 ml of pure methanol. Later, methanol was evaporated and distilled water (2 ml) was added to each petri dish.

Ten seeds were placed on filter paper in each petri dish and the petri dishes were covered and put in a germinator at 24 ± 2 °C with 10/14 h, light/dark. Germination of seeds were noted daily. Root and shoot lengths of field bindweed and wheat were measured 7 days after sowing. The seedlings were dried in an oven at 40°C till constant weight to measure dry weight. Germination index (GI), mean germination time and time to start germination were calculated as reviewed and described earlier (Ranal and Santana, 2006). The GI was calculated as following:

$$GI = \frac{\text{Number of germinated seeds}}{\text{Days of first count}} + \dots + \frac{\text{Number of germinated seeds}}{\text{Days of final count}}$$

Statistical analysis

The data were analyzed by analysis of variance and treatment means were statistically compared using Duncan's Multiple Range Test. The experiments were performed as completely randomized design with 5 replications.

Results

Effect of Delonix regia aqueous leaf extract on germination of field bindweed and wheat

Leaf extract of *Delonix regia* had more inhibitory effect on final germination and germination index and increased mean germination time and time to start germination in field bindweed as compared with wheat (Table 1). At 5% concentration, field bindweed took significantly double time (3.6 days) to start germination, while there was no statistically significant effect on time to start germination for wheat crop as compared with control (Table 1). Germination index and final germination was decreased by 76% and 35% respectively as compared with control in field bindweed at 5% concentration of *Delonix regia* leaf extract. In case of wheat, this medium concentration (5%) did not significantly affect germination index and final germination. At maximum concentration (10%) of *Delonix regia* leaf extract, final germination of field bindweed and wheat was inhibited by 49% and 9% respectively as compared with control (Table 1).

Table 1. *Effect of Delonix regia aqueous leaf extract on germination of field bindweed and wheat*

Leaf extract concentration (%)	Time to start germination (days)		Mean germination time (days)		Germination index		Final germination (%)	
	Field bind weed	Wheat	Field bind weed	Wheat	Field bind weed	Wheat	Field bind weed	Wheat
0	1.80± 0.20c	1.0± 0.0b	3.25± 0.15c	1.90± 0.14b	7.18± 0.3a	11.0± 0.38a	57.30±1.63a	86± 2.45a
2.5	1.80± 0.20c (0)	1.0± 0.0b (0)	3.05± 0.02c (-6)	1.80± 0.13b (-8)	7.1± 0.31a (-1)	11.8± 0.75a (7)	50.60± 1.67b (-12)	88± 1.99a (2)
5.0	3.60± 0.24b (100)	1.0± 0.0b (0)	3.72± 0.20b (14)	1.78± 0.14b (-8)	1.75± 2.3b (-76)	11.2± 0.35a (1)	37.30± 1.63c (-35)	82± 1.99a (-5)
7.5	4.80± 0.20a (167)	1.0± 0.0b (0)	4.80± 0.2a (48)	2.21± 0.19b (14)	0.96± 0.04c (-86)	10.5± 0.58a (-5)	30.60± 1.63d (-47)	84± 2.45a (-2)
10	4.80± 0.20a (167)	1.8± 0.20a (80)	4.92± 0.08a (51)	3.13± 0.07a (61)	1.03± 0.14c (-86)	6.98±0.80b (-36.71)	29.33±1.63d (-49)	78± 3.74b (-9)

Results are presented as mean ± SEM. Means having different letters in the same column are significantly different (P < 0.05) according to Duncan's Multiple Range Test. % increase/decrease as compared with control (0%) is presented in parenthesis, rounded off to nearest whole number

Effect of Delonix regia aqueous leaf extract on early seedling growth of field bindweed and wheat

Aqueous leaf extract of *Delonix regia* inhibited root and shoot length and seedling dry weight of field bindweed more than wheat (Table 2). *Delonix regia* aqueous leaf extract at 5% reduced root and shoot length of field bindweed by 42% and 45%

respectively as compared with control, while root and shoot length of wheat was decreased by only 4% and 5% respectively as compared with control (Table 2). Similarly, seedling dry weight was decreased by 52% in field bindweed as compared with control, while it was statistically at par with control in wheat at 5% leaf extract concentration (Table 2). Highest concentration (10%) further decreased root and shoot length and seedling dry weight of field bindweed and wheat; however, it was less phytotoxic to wheat than field bindweed (Table 2).

Table 2. Effect of *Delonix regia* aqueous leaf extract on seedling growth of field bindweed and wheat

Leaf extract concentration (%)	Root length (cm)		Shoot length (cm)		Seedling dry weight (mg)	
	Field bind weed	Wheat	Field bind weed	Wheat	Field bind weed	Wheat
0	5.08± 0.00a	5.02± 0.02a	5.93± 0.43a	5.3± 0.07b	100± 2.23a	194± 1.88a
2.5	5.04± 0.05a (-1)	4.92± 0.04a (-2)	5.80± 0.04 b (-2)	6± 0.05a (14)	81.80± 0.71b (-18)	191± 3.73a (-2)
5.0	2.93± 0.03b (-42)	4.80± 0.04c (-4)	3.29± 0.05c (-45)	5± 0.07cd (-5)	48.20± 1.65c (-52)	192± 2.56a (-1)
7.5	2.20± 0.00c (-57)	3.83± 0.03d (-24)	2.20± 0.03d (-63)	5± 0.03c (-4)	44.60± 1.96c (-55)	160± 4.09b (-17)
10	1.86± 0.07d (-63)	3.09± 0.03e (-38)	2.22 ± 0.02d (-63)	4.8± 0.05d (-8)	33.60± 1.57d (-66)	125± 2.06c (-36)

Results are presented as mean ± SEM. Means having different letters in the same column are significantly different ($P < 0.05$) according to Duncan's Multiple Range Test. % increase/decrease as compared with control (0%) is presented in parenthesis, rounded off to nearest whole number

Effect of Delonix regia aqueous leaf extract methanolic fractions on germination of field bindweed and wheat

Ethyl acetate and lyophilized methanolic fractions of *Delonix regia* aqueous leaf extract significantly affected time to start germination, mean germination time and germination index in field bindweed, while these germination indices were not significantly affected in wheat (Table 3). At 1000 ppm ethyl acetate fraction, time to start germination and mean germination time of field bindweed was reduced by 30% and 13% respectively as compared with control, while there was no significant reduction in the two germination indices of wheat with application of the same treatment (Table 3). Likewise, germination index and final germination was inhibited by 64% and 48% respectively as compared with control in field bindweed at 1000 ppm ethyl acetate fraction of *Delonix regia*, while germination index and final germination of wheat were not significantly affected at this concentration.

Effect of Delonix regia aqueous leaf extract methanolic fractions on seedling growth of field bindweed and wheat

All concentrations of ethyl acetate and lyophilized fractions of *Delonix regia* leaf extract significantly inhibited root and shoot length and seedling dry weight of field bindweed, while these parameters were only significantly reduced at higher concentrations of leaf extract in wheat (Table 4). At 1000 ppm ethyl acetate fraction, root length, shoot length and seedling dry weight of field bindweed was inhibited by

59%, 46% and 46% respectively as compared with control. Root and shoot length and seedling dry weight was not significantly affected in wheat at 1000 ppm ethyl acetate fraction (Table 4).

Table 3. Effect of *Delonix regia* leaf extract methanolic fractions on germination of field bindweed and wheat

Name of fraction	Concentration (ppm)	Time to start germination (days)		Mean germination time (days)		Germination index		Final germination (%)	
		Field bind weed	Wheat	Field bind weed	Wheat	Field bind weed	Wheat	Field bind weed	Wheat
Control	0	2.0± 0.0cd	1± 0.0 ^{NS}	2.97± 0.20cd	1.43± 0.11 ^{NS}	6.13± 0.60abc	12.5± 0.92 ^{NS}	56.00± 1.63a	96± 2.45a
Ethyl acetate	50	1.60± 0.24d (-20)	1± 0.0 (0)	3.04± 0.10cd (2)	1.64± 0.20 (15)	6.52± 0.55ab (6)	12.97± 1.13 (4)	54.66± 2.49a (-2)	94± 2.45ab (-2)
	500	1.80± 0.20d (-10)	1± 0.0 (0)	2.98± 0.11 cd (0)	1.44± 0.21 (1)	5.70± 0.12abcd (-7)	11.67± 1.16 (-7)	44.00± 1.63 c (-21)	94± 3.20ab (-2)
	1000	2.60± 0.24c (30)	1± 0.0 (0)	3.37± 0.11cd (13)	1.63± 0.19 (14)	2.20± 0.25ef (-64)	13.27± 1.31 (6)	29.33± 1.63d (-48)	94± 2.45ab (-2)
	2000	3.20± 0.20b (60)	1± 0.0 (0)	4.01± 0.21b (35)	1.43± 0.20 (0)	1.83± 0.20ef (-17)	11.10± 1.19 (-11)	25.33± 1.33de (-55)	88± 3.74abc (-8)
	4000	4.20± 0.20a (110)	1± 0.0 (0)	4.57± 0.16a (54)	1.67± 0.10 (17)	1.06± 0.17f (-83)	10.57± 0.63 (-15)	22.66± 1.63e (-60)	80± 4.46c (-17)
Lyophilized	50	1.80± 0.20 d (-10)	1± 0.0 (0)	3.07± 0.12cd (3)	1.33± 0.13 (-7)	6.11± 0.66abc (-0)	11.50± 0.89 (-8)	53.33± 0.11a (-5)	96± 2.45a (0)
	500	2.00± 0.0cd (0)	1± 0.0 (0)	3.18± 0.03cd (7)	1.42± 0.11 (-1)	5.62± 0.18abcd (-8)	12.40± 0.73 (-0.8)	46.66± 0.10bc (-17)	96± 2.45a (0)
	1000	2.20± 0.20cd (10)	1± 0.0 (0)	3.23± 0.20cd (9)	1.64± 0.10 (15)	4.83± 0.51cd (-21)	12.97± 1.03 (4)	46.7± 2.10bc (-4)	92± 3.74ab (-4)
	2000	2.20± 0.37cd (10)	1± 0.0 (0)	3.25± 0.17cd (10)	1.56± 0.17 (9)	4.35± 0.51d (-29)	10.63± 0.90 (-15)	46.66± 2.10bc (-17)	84± 2.45bc (-13)
	4000	2.60± 0.24c (30)	1± 0.0 (0)	3.43± 0.12c (14)	1.87± 0.22 (31)	2.87± 0.72e (-53)	11.90± 1.03 (-5)	29.33± 3.39d (-48)	84± 2.45dc (-13)

Results are presented as mean ± SEM. Means having different letters in the same column are significantly different ($P < 0.05$) according to Duncan's Multiple Range Test. % increase/decrease as compared with control (0%) is presented in parenthesis, rounded off to nearest whole number

Table 4. Effect of *Delonix regia* leaf extract methanolic fractions on seedling growth of field bindweed and wheat

Name of fraction	Concentration (ppm)	Root length (cm)		Shoot length (cm)		Seedling dry weight (mg)	
		Field bind weed	Wheat	Field bind weed	Wheat	Field bind weed	Wheat
Control	0	5.13± 0.02bcd	4.97± 0.06a	5.90± 0.04a	5.09± 0.03ab	105.2± 3.24a	194± 3.29bc
Ethyl acetate	50	5.11± 0.04bcd (-0)	4.89± 0.05a (-2)	5.85± 0.05a (-5)	5.18± 0.02a (2)	85.60± 3.17cd (-19)	201.4± 2.89b (4)
	500	5.09± 0.03cde (-1)	4.91± 0.02a (-1)	5.79± 0.06a (-2)	5.07± 0.03ab (-0)	60.0± 1.97g (-43)	200± 2.37b (3)
	1000	2.20± 0.01 (-59)	4.89± 0.04a (-2)	3.17± 0.03g (-46)	5.02± 0.04abc (-1)	46.20± 2.13h (-56)	201.4± 2.83b (4)
	2000	1.85± 0.04j (-64)	3.31± 0.02b (-33)	2.29± 0.02h (-61)	3.74± 0.06f (-27)	49.0± 1.14h (-53)	129± 1.65g (-34)
	4000	1.19± 0.02k (-77)	2.35± 0.02c (-53)	2.23± 0.01h (-62)	3.17± 0.03g (-38)	32.20± 1.07i (-69)	82.80± 2.37h (-57)
Lyophilized	50	5.33± 0.07a (4)	5.01± 0.03a (1)	5.87± 0.02a (-1)	5.05± 0.03ab (-1)	79.60± 0.98de (-24)	140± 1.39f (-28)
	500	5.28± 0.09ab (3)	4.82± 0.04a (-3)	5.94± 0.05a (1)	4.96± 0.03bc (-3)	71.60± 0.20f (-31)	172± 2.59d (-11)
	1000	4.29± 0.02s (-16)	4.90± 0.02 a (-1)	4.16± 0.02e (-29)	4.99± 0.06bc (-2)	71.40± 2.06ef (-32)	153± 2.80e (-21)
	2000	3.18± 0.02g (-38)	4.73± 0.02a (-5)	4.20± 0.01e (-29)	4.89± 0.03c (-4)	69.60± 0.40f (-34)	126.2± 2.47g (-35)
	4000	2.75± 0.07h (-46)	3.30± 0.02b (-33)	3.52± 0.19f (-40)	4.07± 0.02e (-20)	50.20± 1.46h (-52)	152.2± 4.06e (-22)

Results are presented as mean ± SEM. Means having different letters in the same column are significantly different ($P < 0.05$) according to Duncan's Multiple Range Test. % increase/decrease as compared with control (0%) is presented in parenthesis, rounded off to nearest whole number

Discussion

Aqueous leaf extract and methanolic fractions (ethyl acetate and lyophilized) of *Delonix regia* had differential effect on germination and growth of field bindweed and wheat (Tables 1–4). Lower to medium concentrations of aqueous (2.5 and 5%) and ethyl acetate and lyophilized methanolic fractions (50, 500 and 1000 ppm) of *Delonix regia* significantly inhibited germination and seedling growth of field bindweed, while these concentrations either did not significantly affect the germination and seedling growth of wheat or had very little inhibitory effect on it. Moreover, at lower extract concentrations there was a slight increase in germination and seedling growth of wheat. The slight increase in wheat growth might be due to plant growth promotive effect of allelochemicals on other plant species at lower concentrations (Akhtar et al., 2010; Jamil et al., 2009). Though higher *Delonix regia* leaf extract concentrations were phytotoxic for both field bindweed and wheat; nonetheless, phytotoxicity was very less on wheat as compared with field bindweed. The differential effect of allelopathic plant extracts on other plant species may be exploited to achieve selective phytotoxicity for weed management in field crops (Haq et al., 2010).

In the present study, the inhibitory effect of *Delonix regia* leaf extract may be attributed to variety of allelochemicals (chlorogenic acid, 4-hydroxybenzoic, 3,4-dihydroxybenzoic, 3,5-dinitrobenzoic, L-azetidine-2-carboxylic, 3,4-dihydroxybenzaldehyde, 3,4-dihydroxycinnamic and gallic acid) reported in it (Chou and Leu, 1992). The inhibitory effect of allelochemicals in plant extracts have been well documented (Khaliq et al., 2012; Mushtaq et al., 2010, 2013). The phytotoxic effect of plant extracts is species-specific and concentration-dependent (Haq et al., 2010; Mushtaq et al., 2013). The presence of variety of allelochemicals in plant extract may act in synergistic way to inhibit growth of one plant species while their effect might be neutral or growth promotive on other plant species (Fujita and Kubo, 2003; Inderjit et al., 2002). Though aqueous extract as well as ethyl acetate and lyophilized methanolic fractions showed phytotoxicity in the bioassays; however, aqueous extract and ethyl fraction were more phytotoxic. Aqueous and ethyl acetate allelopathic plant extracts have been reported to have strong phytotoxic effects (Araniti et al., 2013; Mushtaq et al., 2010). Extraction of compounds by both aqueous and organic solvent fractions indicates that *Delonix regia* leaves contain diverse type of allelochemicals belonging to different chemical groups which enhance allelopathic potential of the plant.

Conclusion

Lower to moderate concentrations of *Delonix regia* leaf extract are phytotoxic against field bindweed, while safe on wheat crop. However, further studies may be carried out to evaluate the selective phytotoxic action of *Delonix regia* leaf extract against field bindweed and other weeds in various crops under field conditions. *Delonix regia* is a plant grown in many regions of the world. Its leaves are easily available and may be used to develop eco-friendly and selective bioherbicides in future especially for broad leaf weeds.

REFERENCES

- [1] Akhtar, H., Kausar, A., Akram, M., Cheema, Z. A., Ali, I., Mushtaq, M. N. (2010): Effects of *Dalbergia sissoo* Roxb. leaf extract on some associated crop species of agroforestry. – *Allelopath. J.* 25: 221–226.
- [2] Aktar, M. W., Sengupta, D., Chowdhury, A. (2009): Impact of pesticides use in agriculture: their benefits and hazards. *Interdiscip. – Toxicol.* 2: 1–12.
- [3] Albuquerque, M. B., dos Santos, R. C., Lima, L. M., Melo Filho, P. de A., Nogueira, R. J. M. C., da Câmara, C. A. G., de Rezende Ramos, A. (2011): Allelopathy, an alternative tool to improve cropping systems. A review. – *Agron. Sustain. Dev.* 31: 379–395.
- [4] Araniti, F., Lupini, A., Sorgonà, A., Conforti, F., Marrelli, M., Statti, G. A., Menichini, F., Abenavoli, M. R. (2013): Allelopathic potential of *Artemisia arborescens*: Isolation, identification and quantification of phytotoxic compounds through fractionation-guided bioassays. – *Nat. Prod. Res.* 27: 880–887.
- [5] Black, I. D., Matic, R., Dyson, C. B. (1994): Competitive effects of field bindweed (*Convolvulus arvensis*, L.) in wheat, barley and field peas. – *Plant Prot. Q.* 9: 12–14.
- [6] Cheng, F., Cheng, Z. (2015): Research progress on the use of plant allelopathy in agriculture and the physiological and ecological mechanisms of allelopathy. – *Front. Plant Sci.* 6: 1020.
- [7] Chou, C.-H., Leu, L.-L. (1992): Allelopathic substances and interactions of *Delonix regia* (Boj) Raf. – *J. Chem. Ecol.* 18: 2285–2303.
- [8] De, A., Bose, R., Kumar, A., Mozumdar, S. (2014): Worldwide Pesticide Use. – In: De, A., Bose, R., Kumar, A., Mozumdar, S. (eds.) *Targeted Delivery of Pesticides Using Biodegradable Polymeric Nanoparticles*. Springer India, New Delhi.
- [9] Fujita, K., Kubo, I. (2003): Synergism of polygodial and trans-cinnamic acid on inhibition of root elongation in lettuce seedling growth bioassays. – *J. Chem. Ecol.* 29: 2253–2262.
- [10] Haq, R. A., Hussain, M., Cheema, Z. A., Mushtaq, M. N., Farooq, M. (2010): Mulberry leaf water extract inhibits bermudagrass and promotes wheat growth. – *Weed Biol. Manag.* 10: 234–240.
- [11] Heap, I. (2018): The international survey of herbicide resistant weeds. – <http://www.weedscience.org> (accessed 08.01.2018).
- [12] Holm, L. G., Plucknett, D. L., Pancho, J. V., Herberger, J. P. (1977): *The World's Worst Weeds: Distribution and Biology*. – University Press of Hawaii., Hawaii.
- [13] Inderjit, Streibig, J. C., Olofsdotter, M. (2002): Joint action of phenolic acid mixtures and its significance in allelopathy research. – *Physiol. Plant.* 114: 422–428.
- [14] Iqbal, J., Cheema, Z. A., Mushtaq, M. N. (2009): Allelopathic crop water extracts reduce the herbicide dose for weed control in cotton (*Gossypium Hirsutum*). – *Int. J. Agric. Biol.* 11: 7.
- [15] Jamil, M., Cheema, Z. A., Mushtaq, M. N., Farooq, M., Cheema, M. A. (2009): Alternative control of wild oat and canary grass in wheat fields by allelopathic plant water extracts. – *Agron. Sustain. Dev.* 29: 475–482.
- [16] Khaliq, A., Matloob, A., Aslam, F., Mushtaq, M. N., Khan, M. B. (2012): Toxic action of aqueous wheat straw extract on horse purslane. – *Planta Daninha* 30: 269–278.
- [17] Mushtaq, M., Cheema, Z., Khaliq, A. (2010): Effects of mixture of allelopathic plant aqueous extracts on *Trianthema portulacastrum* L. weed. – *Allelopath. J.* 25: 205–212.
- [18] Mushtaq, M. N., Sunohara, Y., Matsumoto, H. (2013): L-DOPA inhibited the root growth of lettuce by inducing reactive oxygen species generation. – *Weed Biol. Manag.* 13: 129–134.
- [19] Orwa, C., Mutua, A., Kindt, R., Jamnadass, R., Anthony, S. (2009): *Agroforestry database: a tree reference and selection guide version 4.0*. – <http://www.worldagroforestry.org> (accessed 08.05.2018).

- [20] Perveen, S., Yousaf, M., Zahoor, A. F., Rasool, N., Jabber, A. (2014): Extraction, isolation, and identification of various environment friendly components from cock's comb (*Celosia argentea*) leaves for allelopathic potential. – Toxicol. Environ. Chem. 96: 1523–1534.
- [21] Polyrakis, I. T. (2009): Environmental Pollution from Pesticides. – In: Costa, R., Kristbergsson, K. (eds.) Predictive Modelling and Risk Assessment. Springer US, Boston, MA, pp. 201–224.
- [22] Ranal, M. A., Santana, D. G. de (2006): How and why to measure the germination process? – Brazilian J. Bot. 29: 1–11.
- [23] Sheng, Z., Li, J., Li, Y. (2012): Optimization of ultrasonic-assisted extraction of phillyrin from *Forsythia suspensa* using response surface methodology. – J. Med. Plants Res. 6: 1633–1644.
- [24] Skinner, K., Smith, L., Rice, P. (2000): Using noxious weed lists to prioritize targets for developing weed management strategies. – Weed Sci. 48: 640–644.

DETERMINATION OF THE CERTAIN VEGETATION CHARACTERISTICS OF KIZILOVA FOREST PASTURE LOCATED IN THE SOUTH OF TURKEY

BABALIK, A. A.* – YAZICI, N. – FAKIR, H. – DURSUN, I.

*Department of Forest Engineering, Faculty of Forestry, Isparta University of Applied Sciences
32260 Isparta, Turkey
(phone: +90-246-211-3987; fax: +90-246-211-3948)*

**Corresponding author
e-mail: alperbabalik@isparta.edu.tr*

(Received 10th Sep 2018; accepted 27th Nov 2018)

Abstract. Forest pastures are an important resource for Mediterranean countries, providing cheap forage and a reservoir of biodiversity. A case study was conducted of the Kizilova forest pasture (Sutculer) in the Isparta district of Southern Turkey in 2014-2016. The aim of the study is to determine the plant species, plant-covered area, botanical compositions, aboveground biomass, belowground biomass, pasture condition and grazing capacity in a pasture. Vegetation sampling was conducted in spring and autumn (2014-2016). “Line intercept” and “quadrat” methods were used in order to determine the pasture flora of the case study area. The finding was that 106 plant taxa belonged to 23 families, out of which 26 taxa of Asteraceae were determined, while 13 and 11 taxa were determined in Lamiaceae and in Poaceae, respectively. The plant-covered area was found to be nearly 57.7%. The botanical composition of pastures’ taxa is approximately 46.5% Poaceae, 31.2% Fabaceae and 22.3% of other families. The aboveground and belowground biomass productions were calculated as 414.2 kg/da and 745.2 kg/da, respectively. The results indicated that the grazing capacity for an area was on average 153.4 animal units and the average sufficient pasture area per animal unit was 1.3 ha. The case study area of pasture condition was determined as moderate.

Keywords: *above-ground biomass, plant-covered area, botanical composition, grazing capacity, Turkey*

Introduction

Natural vegetation is extremely important for any region. It is a natural structure created by the conditions of that region to protect the soil and the water and to be the nutrition and source of life. Meadow and pasture vegetation, an important part of the natural vegetation cover, hold particular importance as the areas of feed supply that forms the basis of animal production.

A large part of the earth is covered by meadow and pasture areas. These vast areas are resources that are irreplaceable in terms of obtaining animal products, which are the most important source of nutrition for the world’s population.

Meadow and pasture areas constitute 18.8% of the total land area of our country and 37% of the total agricultural land. Meadow and pasture areas were 37.9 million hectares in the 1950s in Turkey, but have dropped to 14.6 million hectares today (Altin et al., 2011). In Turkey, the proportion of areas for planting forage crops within field lands is 11.7% (TSI, 2013). Therefore, meadow and pasture areas are crucial sources of animal feed production. A total of 30% of the hay needed by animals is covered by meadows and pastures, which constitutes about one-fifth of the total area of Turkey (Gokkus, 1994; TSI, 2013). Meadows and pastures supply 68% of the nutrients consumed by our country’s animals in a year as crude protein and 62% of them as starch value (Okatan

and Yuksek, 1997). These figures confirm that meadows and pastures are the main sources of animal nutrition (Erkun, 1999).

The natural pastures in our country are found in highly elevated and rough lands in general. A total of 90% of them are located on grade 6 and 7 lands (Aydin and Uzun, 2002). The hay yield of the pastures in Turkey is about 70 kg/da, which correspond to one-third of the world average (Babalik and Fakir, 2017). Most of the plants that make up the yields of these pastures consist of shrubs and weeds, which animals cannot consume.

The fact that Turkey's natural pastures are in a bad condition today not only adversely affects the stock farming and therefore the country's economy, but also leads to the destruction of land and water resources. As a matter of fact, due to misapplications such as early- and over-grazing, a large proportion of the pastures have lost their natural vegetation cover, and the erosion problem has reached dangerous dimensions. Moreover, grazing in pastures at a density of about 2-3 times higher than the capacities of the pastures has caused a reduction in their productivity (Koc et al., 1994). In order to solve these problems, it is necessary that pastures that are in poor condition be improved immediately in order to produce abundant and good quality forage again. However, the first condition of success in the process of improvement, which aims to enhance any material and its usefulness, is to fully understand the material to be improved. Therefore, various features of pastures in different ecological regions of our country should be studied.

Vegetation analysis aims to quantitatively express the vegetative characteristics of plants in terms of quality and quantity. Although vegetation analysis studies are not very common in our country, plant taxonomy and phytosociology studies have been carried out to determine which plant species exist in pastures. The main purpose of pastures should also be to allow grazing in addition to the protection of soil and water. Thus, the vegetation studies to be carried out in the pastures include the studies to reveal the yield and quality of pasture forage for management (Gokbulak, 2006).

Using vegetation analysis, it is possible to obtain data on information such as the pasture condition, its progress in a positive or negative direction, its grazing intensity in the past, its forage value and effectiveness in terms of grazing, its soil and water conservation characteristics (Gokbulak, 2003), its aesthetic value, the determination of its grazing capacity, and the determination of the effects of drought on vegetation. Moreover, information can be obtained on the dominant plant species and the amount of forage in pastures (Gokbulak, 2006). Indeed, many research studies on this subject have been based on the determination of the floristic composition and ecological characteristics in natural pastures and on the determination of the yield and grazing capacities of pastures.

In Isparta, the total of meadow and pasture areas is 81.719 ha, and 81% of these areas are located on grade 7 lands (Anonymous, 2006). As is the case in our country, the cause of the reduction in the yields of the Isparta pastures is early- and over-grazing. For this reason, some of the pastures have become unable to meet the forage needs of animals (Babalik, 2007).

This study aimed to examine various vegetation features of Kizilova, a forest pasture located in the Sutculer district of Isparta province and to reveal the current situation. The collected data will become the basis for range improvement studies to be carried out in the region and to provide the necessary information about the natural pasture vegetation. Therefore, the study aimed to identify the regional ecological characteristics

that would shed light on the plant species in the Kizilova forest pasture, the extent to which pasture plants cover the soil, the botanical composition, the yield of the pasture, the belowground biomass, the grazing capacity and improvement studies. Moreover, in this study, an attempt was made to reveal what kind of changes would take place based on the protection measures to be taken in the pastures and to determine the benefits that could be achieved by relieving the pressure on forest pastures in the region, where stock farming depended to a great extent on pasture grazing.

Material and Method

Material

Kizilova forest pasture (37°36'06"N - 31°03'52"E), with an area of approximately 200 hectares located within the boundaries of Sutculer district of Isparta province, was selected as the research material (Fig. 1). The pasture area has an average elevation of 1410 meters. It has a general north-west aspect and an average slope of 2% (Fig. 2). It is 92 km from the center of Isparta province.

Kizilova pasture is a type of forest pasture, and the dominant tree species in the forest areas around the pasture area consist of Greek juniper (*Juniperus excelsa* Bieb.) and Turkey oak (*Quercus cerris* L.). Indeed, these two species of trees, especially Greek junipers, hold significant potential for forage in these forest areas, since they do not cover areas very densely in the stands they create.

The research area is located in the transition zone between the Mediterranean climate and the continental climate, and represents the upland zone behind the Mediterranean. According to long-term climate data (1950-2015), the average annual temperature in Sutculer is 12.9°C, and the amount of total annual precipitation is 777.5 mm (TMS, 2016). According to the climate diagram drawn using the Walter method (Walter, 1958), a dry season prevails in the region from the middle of April to the end of October (Fig. 3).

Kizilova forest pasture area defined in the study as the material used continuously for grazing. The research area is located at the C3 cell according to the grid system used in the Flora of Turkey by Davis (1965-1988).

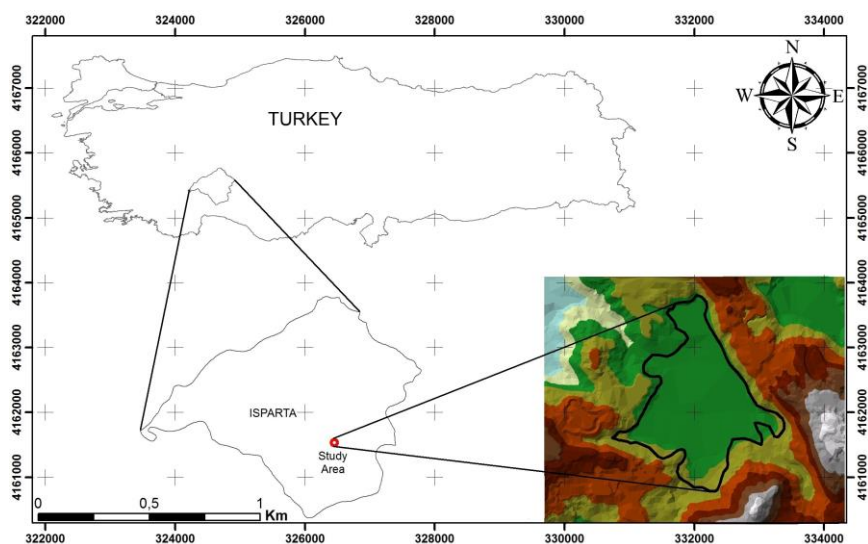


Figure 1. Study area

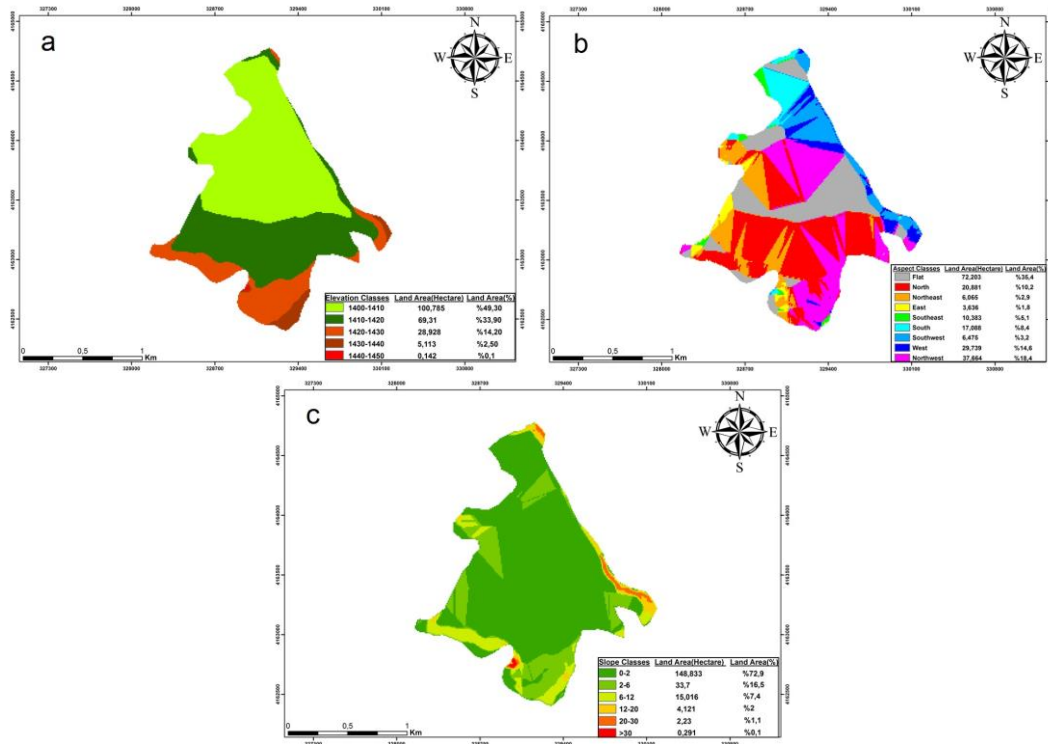


Figure 2. Elevation (a), aspect (b) and slope (c) maps

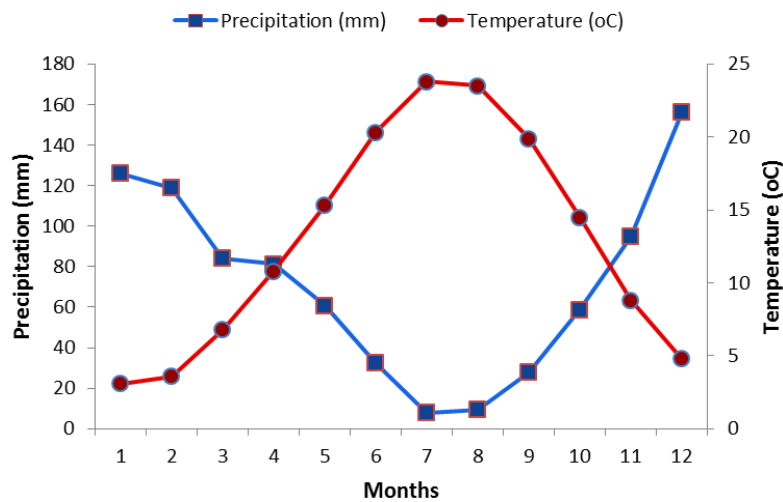


Figure 3. Climate diagram

Method

In order to identify the characteristics of the pasture vegetation in the research area, 10 experimental plots, each measuring 10×5 m², were created and surrounded with barbed wire (Fig. 4). Experimental plots were selected and positioned on a topographical map with a scale of 1:25000 using actual land-use maps, and GIS technology. These experimental plots were randomly distributed to the pasture area,

considering also the variations in the vegetation structure, aspect and altitude. In the measurements carried out in those plots that were closed to grazing, the methods of line intercept (transect) (Babalik, 2004; Dalle et al., 2006; Godinez-Alvarez et al., 2009; Palta and Genc Lermi, 2018) and quadrat (Stohlgren et al., 1995; Wale et al., 2012; Cacan and Kokten, 2014; Babalik and Sarikaya, 2015; Ozgur et al., 2017), which are some of the methods for determining the quantitative characteristics of pasture vegetation, were utilized. The vegetation measurements were carried out in the second half of June and September during both trial years.



Figure 4. A view from the experimental plots

In this study, the following vegetation characteristics of the pasture were determined: plant-covered area, botanical composition, above-ground biomass, belowground biomass, pasture condition and grazing capacity. The line intercept method was used to determine the plant-covered area in pasture (Bilgen and Ozyigit, 2005; Oztas et al., 2003). As per the method, the plant-covered area was calculated by proportioning the intercept areas of plants in the line to the total intercept area (Etchberger and Krausman, 1997). Similarly, the line intercept method was used for determining the botanical composition. For this reason, the plant species were split into three groups: poaceae, fabaceae and other families. Their botanical composition ratio was determined based on the plant-covered area. Above-ground biomass was determined using the quadrat method, and frames of 1x1 m² were used for this purpose. During measurements, the plant material was mown from the soil surface from a height of about 3 cm at the study areas. The mown material was dried in the laboratory at 70°C for 24 hours in the oven. Then they were weighed and the results were calculated in kg/da. The plants were taken for the quadrat measurement for determining the belowground biomass. Then, the remaining roots were taken without harming them, with 20 cm of active roots as a basis (Ozgur et al., 2017). The pasture condition was determined according to the values of plant-covered areas in the pasture.

In addition, 50 disturbed and undisturbed soil samples were taken, with five samples from each of the experimental plots in the research area in June 2015. Texture classes,

organic matter quantities, electrical conductivities, lime amounts, bulk density, pH values and macro plant nutritional elements of these samples were determined in the laboratory. In order to determine soil properties, samples were collected from experimental plots within a depth of 0-20 cm. Soil samples were oven-dried at 105°C, grounded and passed through a 2-mm sieve and each sample was weighed and analyzed. In this context, the particle size distribution of the soil was determined based on the Bouyoucos hydrometer method (Bouyoucos, 1962). The soil texture was defined based on the international particle size distribution classes (Gulcur, 1974). The concentration of soil organic matter was determined by wet combustion described in the Walkley-Black method (Nelson and Sommer, 1996). The electrical conductivity (EC) in 1:5 soil/water suspension was determined by the EC meter (Rhoades, 1982). Amounts of lime were determined by the pressure calcimeter method (Loeppert and Suarez, 1996). Bulk density was determined by the core method (Blake and Hartge, 1986). The pH level was identified in 1:2.5 soil/water suspension by the pH meter (Rowell, 1994; Kantarci, 2000). Macro plant nutritional elements of the soil samples were measured using a Shimadzu 6600 atomic absorption equipment (Gulcur, 1974).

Statistical methods (the variance analysis and the Duncan multiple comparison test) were used to evaluate the data obtained as a result of the measurements carried out in the field and the analyses done in the laboratory. Significance or insignificance of the differences between findings were also revealed. SPSS 20.0 package program was used to evaluate the obtained data (SPSS Inc., 2011).

Results and Discussion

Based on the analyses of the soil samples taken from the 10 experimental plots that were created in the pasture area, it was found that the pasture area soil was composed of 43% clay, 34% sand and 23% dust, classifying the soil as a texture type of "Clay Soil". The amount of organic matter was moderate, at 3.78%. The average amount of lime was 1.55%, the electrical conductivity was 46.64 $\mu\text{s}/\text{cm}$, the bulk density was 1.263 g/cm^3 and the amount of nitrogen was 0.229%. The soil reaction was neutral with a pH of 6.6. Regarding the macro nutritional elements of the soil samples, no evidence was found to restrict the plant development to a severe extent. The dispersion ratio of the soil samples was determined to be 24.6%. In this respect, the pasture soil was susceptible to erosion in general.

The average plant-covered area (PCA) value of the pasture area was determined to be 57.65%. Plant-covered area values (Bakoglu and Koc, 2002), which have quite an important influence on the protection of soil against erosion, showed differences according to the plots of measurements (*Fig. 5*).

According to the results of the variance analysis, there was a significant difference between the plots in terms of the plant-covered area at a level of .1% ($F=27.133$). Some ecological and topographical features (soil properties, aspect, altitude, etc.) are thought to be factors in the occurrence of these differences.

Based on the result of the t test carried out in terms of the plant-covered area according to seasons, there was no significant difference between the seasons ($t=6.535$). However, it was found that the plant-covered area measured in the summer season (60.00%) was higher than the plant-covered area measured in the fall season (55.30%) (*Fig. 6*).

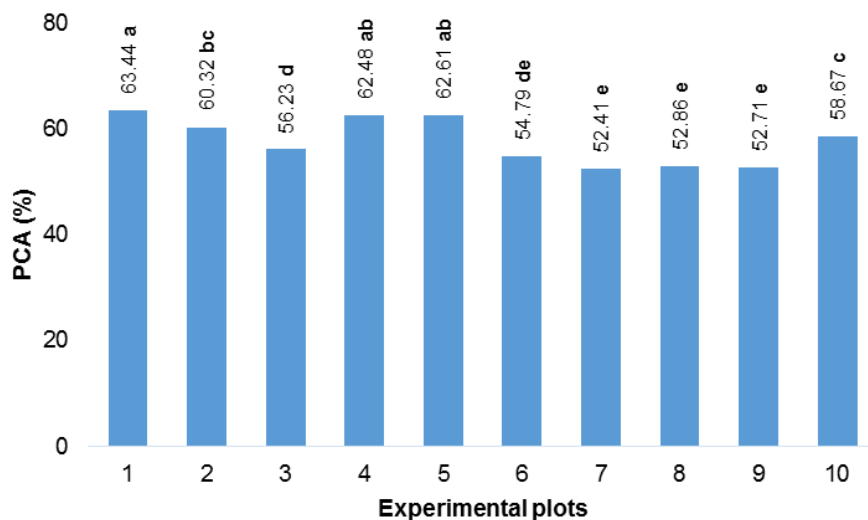


Figure 5. Plant covered area according to the plots

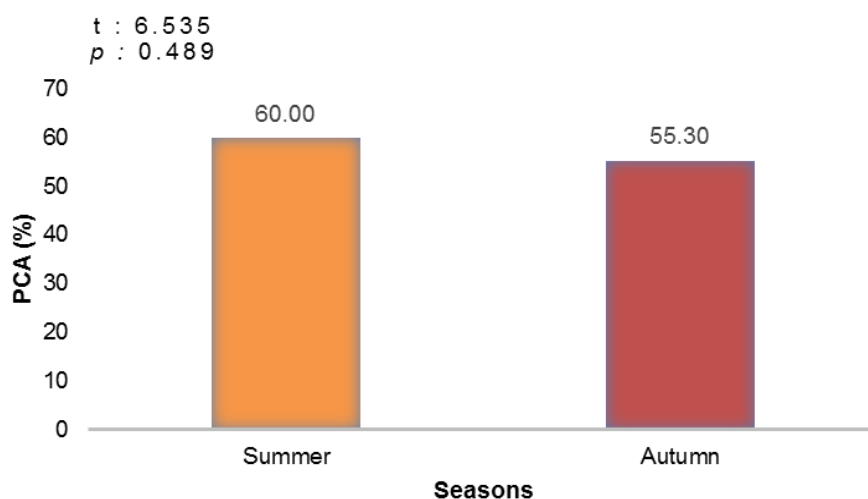


Figure 6. Plant covered area according to seasons

According to the PCA in the pasture, in terms of botanical composition, the rates of Poaceae, Fabaceae, and the other families were 46.47%, 31.17%, and 22.36%, respectively. The Poaceae family showed the highest rate of involvement in the botanical composition in the pasture area, followed by the Fabaceae family and the other families (Fig. 7). Gur and Sen (2016) found similar results in their studies.

In general, the amount of the above-ground biomass (AGB) was 414.2 kg/da in Kizilova pasture. During the summer measurements in June, the above-ground biomass was 451.2 kg/da, which was reduced to 377.2 kg/da during the fall measurements in September.

Based on the variance analysis results regarding the amount of above-ground biomass in the plots, there was a statistically significant difference between the plots (F=23.379) (p<.001) (Fig. 8).

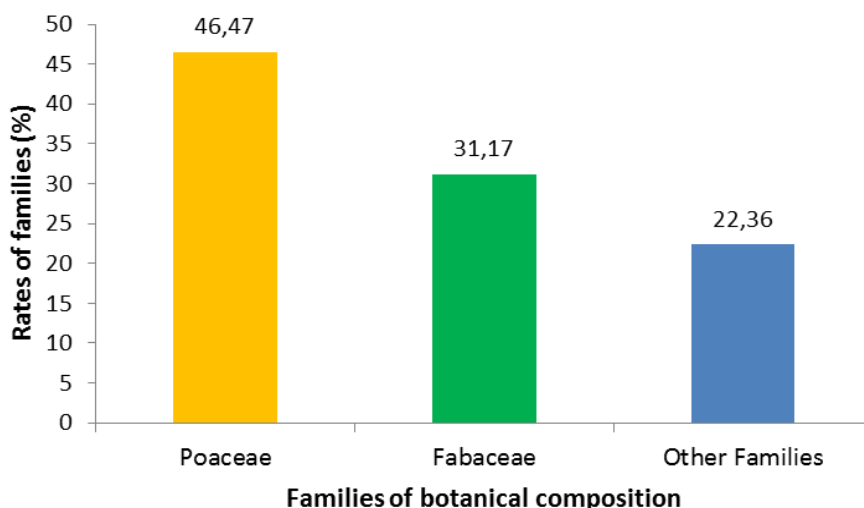


Figure 7. The rate of the families in the botanical composition

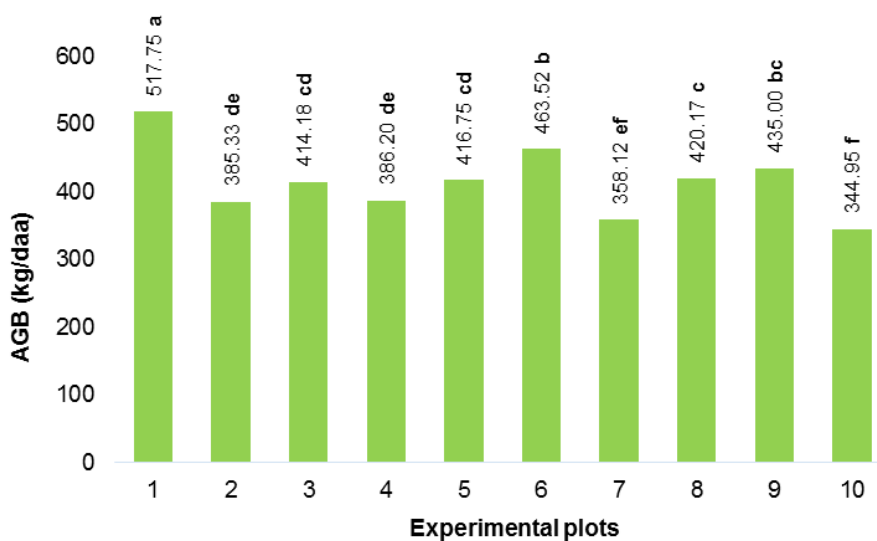


Figure 8. Above-ground biomass according to the plots

There was no significant difference between the seasons based on the t-test ($t=9.438$) in terms of the amount of the above-ground biomass. The amount of above-ground biomass measured in summer season was 451.20 kg/da and the fall season was 377.20 kg/da (Table 1).

Table 1. Families distribution of the above-ground biomass according to seasons

Measurement time	Summer	Fall	Average
Above-ground biomass (kg/da)	451.2	377.2	414.2
Poaceae	208.35	171.1	189.7
Fabaceae	139.7	113.2	126.5
Other families	103.15	92.9	98.0

Regarding the amount of above-ground biomass according to seasons, a decrease was observed in the fall compared to the summer in all three families (*Table 1*). The factor was that precipitation during September and October was less than that during the spring months, and the higher temperature in the pasture area caused the amount of the above-ground biomass to be lower in autumn than in summer. In addition, plants lost components such as branches and leaves in the autumn.

In general, the amount of belowground biomass (BGB) was 745.2 kg/da in Kizilova pasture. During the measurements in June, the belowground biomass was 808.1 kg/da, which was reduced to 682.3 kg/da during the fall measurements in September.

According to the results of the variance analysis of the belowground biomass according to the plots (*Fig. 9*), there was a significant difference between the plots ($F=71.981$) ($p<.001$).

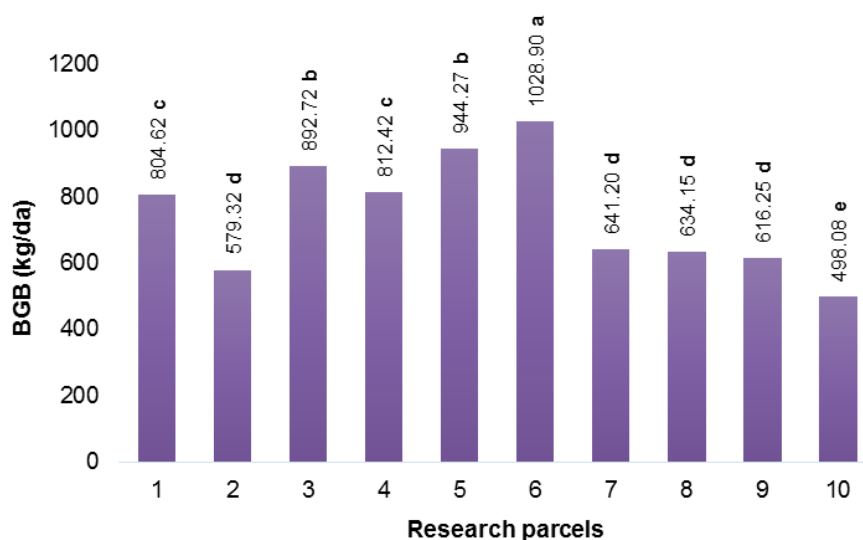


Figure 9. Belowground biomass according to the plots

There was no significant difference between the seasons based on the t test ($t=4.946$) in terms of the amount of the belowground biomass. The amount of belowground biomass measured in summer season was 808.11 kg/da and the fall season was 682.28 kg/da.

The quality level of the pasture in the study area was identified as 4.11, and the pasture condition was “moderate.” However, the quality level of the pasture was very close to poor. This situation is caused as a result of the botanical composition. As Gillen et al. (1991) found, the pressure of overgrazing and poor use results in great damage to the vegetation cover, which naturally leads to a decrease in the quality of the pasture.

Based on the vegetation observations, approximately 170 days between the beginning of grazing (mid-May) and the end of grazing (early November) were determined as the “grazing period” for Kizilova pasture.

The grazing capacity of Kizilova forest pasture was determined to be 153.4 animal units, the unit area grazing capacity was 0.8 animal units, and the pasture size needed for 1 animal unit was determined to be 1.3 ha.

Conclusion and Recommendations

This study was carried out in the Kizilova forest pasture of the Sutculer district of Isparta province to identify the condition of our pastures. The plant-covered area in the research area was 57.65%. A total of 106 plant taxa belonging to 23 families were identified. Families with the most taxa were identified as the Asteraceae, Lamiaceae and Poaceae families, respectively. The botanical composition of the pasture area was 46.47% Poaceae, 31.17% Fabaceae and 22.36% other families. Moreover, the average above-ground biomass was determined as 414.2 kg/da and the belowground biomass as 745.2 kg/da. Based on this, the grazing capacity of the pasture area was determined to be 153.4 animal units, while the pasture area needed for 1 animal unit was calculated as 1.3 ha.

The following suggestions can be made based on the results obtained in this study. Firstly, overgrazing takes place almost all year round in the pasture area. Stray horse flocks play a significant role in overgrazing. Another important problem is early grazing. This has damaged the pasture at an extreme level and caused considerable decline in vegetation quality. There are various signs of erosion in the pasture area. Nevertheless, no factors that would limit plant development at a significant level in the physical and chemical properties of soil samples were found. In this case, it may be possible to restore the pastures to the desired level and to prevent erosion by establishing certain protective measures.

Among the 106 plant taxa in the pasture, 85 were of families other than Poaceae and Fabaceae forage crops. These families consist of plants that are not preferred by animals. In order to increase the proportion of Poaceae and Fabaceae forage crops in the botanical composition, the grazing should be carefully planned, and the grazing capacity must be observed during grazing season.

In order to sustain pastures, they must be used in accordance with the grazing capacity. In addition, both villagers and shepherds should be trained, and villagers should be encouraged to plant forage crops in agriculture areas outside pastures. However, it would be possible to improve the quality of the pasture condition from the “moderate” level to the “good” level by ensuring that animals graze uniformly and by using methods such as fertilization. Moreover, the excessive size of horse flocks that graze in a haphazard manner must be addressed. These are all necessary in order to improve and sustain the pasture area in order to reap optimum benefits.

Acknowledgements. This study was a part of TUBITAK-3001 project. We express our sincere appreciation to The Scientific and Technological Research Council of Turkey (TUBITAK) for their financial support by project which numbered as 114O703.

REFERENCES

- [1] Altin, M., Gokkus, A., Koc, A. (2011): Meadow and pasture management. – Ministry of Agriculture and Rural Affairs, General Directorate of Agricultural Production and Development Volume 1, 331p., Ankara.
- [2] Anonymous (2006): Isparta environmental status report. – Isparta Governorship, Provincial Directorate of Environment and Forestry 450p., Isparta.
- [3] Aydin, I., Uzun, F. (2002): Meadow-Range Management and Breeding. – Ondokuz Mayıs University Faculty of Agriculture Textbooks No: 9, 313p., Samsun.

- [4] Babalik, A. A. (2004): Surface cover measurement methods in meadows and ranges. – Suleyman Demirel Faculty of Forestry Journal A(1): 50-72, Isparta.
- [5] Babalik, A. A. (2007): A research on determination of plant covered area and grazing capacity on the Davraz mountain Kozagaci highland range. – Suleyman Demirel University, J. Fac. For. A(1): 12-19, Isparta.
- [6] Babalik, A. A., Sarıkaya, H. (2015): A research on the hay yield and botanical composition of the Zengi rangeland in Isparta. – Turkish Journal of Forestry 16(2): 96-101.
- [7] Babalik, A. A., Fakir, H. (2017): Comparison of vegetation properties on the protected and grazed rangeland areas: the case of Kocapinar rangeland. – Journal of Forestry 18(3): 207-211.
- [8] Bakoglu, A., Koc, A. (2002): The comparison of some soil and plant of characteristic in grazed and protected range sites: I. Comparison of plant cover characteristic. – Firat University Journal of Science and Engineering 14(1): 37-47.
- [9] Bilgen, M., Ozyigit, Y. (2005): Determination of vegetation characteristics of some rangelands in Korkuteli and Elmali. – Akdeniz University Journal of Agricultural Faculty 18(2): 261-266.
- [10] Blake, G. R., Hartge, K. H. (1986): Bulk Density and Particle Density. – In: Klute, A. (ed.) Methods of Soil Analysis. SSSA Book Series: 5, Madison, 363-381.
- [11] Bouyoucos, G. J. (1962): Hydrometer method improved for making particle size analyses of soils. – Agronomy Journal, 54(5): 464-465.
- [12] Cacan, E., Kokten, K. (2014): Research on the yield herbage and grazing capacity of a range in Cicekyayla village, central district Bingol. – Turkish Journal of Agricultural and Natural Sciences Special Issue (2): 1727-1733.
- [13] Dalle, G., Maass, B. L., Isselstein, J. (2006): Rangeland condition and trend in the semi-arid Borana lowlands, southern Oromia, Ethiopia. – African Journal of Range and Forage Science 23(1): 49-58.
- [14] Davis, P. H. (1965-1988): Flora of Turkey and The East Aegean Islands. – University Press, Edinburgh, Vol.: 1-10.
- [15] Erkun, V. (1999): The importance and historical development of grassland-rangelands: rangeland pasture law practice handbook. – Ministry of Agriculture and Rural Affairs General Directorate of Agricultural Research and Policies, Ankara.
- [16] Etchberger, R. C., Krausman, P. R. (1997): Evaluation of Five Methods for Measuring Desert Vegetation Source. – Wildlife Society Bulletin 25(3): 604-609.
- [17] Gillen, R. L., Mccollum, F. T., Hodges, M. E., Brumer, J. E., Tate, K. W. (1991): Plant community responses to short duration grazing in Tallgrass prairie. – Journal of Range Management 44: 124-128.
- [18] Godinez-Alvarez, H., Herrick, J. E., Mattocks, M., Toledo, D., Van Zee, J. (2009): Comparison of three vegetation monitoring methods their relative utility for ecological assessment and monitoring. – Ecological Indicators 9: 1001-1008.
- [19] Gokbulak, F. (2003): Selected physical properties of heavily trampled soils livestock trails. – Journal of the Faculty of Forestry Istanbul University, Series: A, 53(1): 39-40.
- [20] Gokbulak, F. (2006): Vegetation analysis methods. – Lecture Notes of Master Degree, Istanbul University Graduate School of Applied and Natural Sciences, 98p., İstanbul.
- [21] Gokkus, A. (1994): The place and importance of grassland-rangelands and forage plants in roughage production of Turkey. – Ataturk University Journal of Agriculture Faculty 25: 250-261., Erzurum.
- [22] Gulcur, F. (1974): Physical and chemical soil analysis methods. – Istanbul University Faculty of Forestry Publications, No: 201, Istanbul, Turkey.
- [23] Gür, M., Şen, C. (2016): Some characteristics of legume and grass species determined in a natural rangeland of Thrace region. – Journal of Tekirdag Agricultural Faculty 13(1): 61-69.

- [24] Kantarci, M. D. (2000): Soil science. – Istanbul University Faculty of Forestry Publications, No: 462, Istanbul, Turkey.
- [25] Koc, A., Gokkus, A., Serin, Y. (1994): Situation of Turkey's grassland- rangelands and the importance for erosion. – *Journey of Ecology Environment* 13: 36-41.
- [26] Loeppert, R. H., Suarez, D. L. (1996): Carbonate and Gypsum. – In: Sparks, D. L., Page, A. L., Helmke, P. A., Loeppert, R. H. (eds.) *Methods of Soil Analysis Part 3 – Chemical Methods*. SSSA Book Ser. 5.3. SSSA, ASA, Madison, WI. p. 437-474.
- [27] Nelson, D. W., Sommer, L. E. (1996): Total carbon, organic carbon and organic matter. – In: Sparks, D. L., Page, A. L., Helmke, P. A., Loeppert, R. H. (eds.) *Methods of Soil Analysis Part 3 – Chemical Methods*. SSSA Book Ser. 5.3. SSSA, ASA, Madison, WI. p. 961-1010.
- [28] Okatan, A., Yuksek, T. (1997): Studies on growing of sainfoin excessive grazed grassland parcel (*Onobrychis viciifolia* Scop.) and yield potential. – Turkey 2. Field Crops Congress, Ondokuz Mayıs University Faculty of Agriculture, 22-25 September 1997, 492-498., Samsun.
- [29] Ozgur, F., Karagul, R., Ozcan, M. (2017): Changes in plant composition and forage production in relation to elevations in the rangelands of Alanya province. – *Journal of Forestry* 13(1): 18-27.
- [30] Oztas, T., Koc, A., Comakli, B. (2003): Changes in vegetation and soil properties along a slope on overgrazed and eroded rangelands. – *Journal of Arid Environments* 55: 93-100.
- [31] Palta, S., Genc Lermi, A. (2018): Comparison of some characteristics of protected and non-protected natural rangelands: a case study of Bartın. – *Academic Research Book on Agriculture, Forestry and Aquaculture, Forest Engineering Studies*. ISBN: 978-605-288-401-0, Gece Kitapligi, Bizim Buro Matbaa, Issue: 37-55, Ankara.
- [32] Rhoades, J. D. (1982): Soluble Salts. – In: Page, A. L. (ed.) *Methods of Soil Analysis. Part 2: Chemical and Microbiological Properties*, pp. 149-157. SSSA, Madison, USA.
- [33] Rowell, D. L. (1994): *Soil science: Methods and applications*. – Longman Scientific and Technical, Singapore.
- [34] Stohlgren, T. J., Falkner, M. B., Schell, L. D. (1995): A modified-whittaker nested vegetation sampling method. – *Vegetatio* 117: 113-121.
- [35] SPSS Inc. (2011): *IBM SPSS Statistics 20 Core System User's Guide*. – Chicago, IL, USA.
- [36] TMS (2016): Isparta province Sutculer district climate datas. – Ministry of Forestry and Water Affairs, Turkish State Meteorological Service, Ankara.
- [37] TSI (2013): *Agricultural statistics*. – T. R. Premiership Turkish Statistical Institute. www.tuik.gov.tr Accessed in June 2016.
- [38] Wale, H. A., Bekele, T., Dalle, G. (2012): Floristic diversity, regeneration status, and vegetation structure of woodlands in Metema area, Amhara National Regional State, Northwestern Ethiopia. – *Journal of Forestry Research* 23(3): 391-398.
- [39] Walter, H. (1958): Climadiagram used essentially to detect of drought times. – *Journal of the Faculty of Forestry Istanbul University, Series: B, Volume: 8, Issue: 2, Istanbul*. Translator: Selman Uslu.

EVALUATION OF SOME *TRICHODERMA* SPECIES IN BIOLOGICAL CONTROL OF POTATO DRY ROT CAUSED BY *FUSARIUM SAMBUCINUM* FUECKEL ISOLATES

AYDIN, M. H.

Department of Plant Protection, Faculty of Agriculture, Siirt University, Siirt, Turkey
(e-mail: hadiaydin@siirt.edu.tr; phone: +90-536-599-9794)

(Received 11th Sep 2018; accepted 22nd Nov 2018)

Abstract. *Fusarium* dry rot of potato is a major disease caused by several *Fusarium* species, and *Fusarium sambucinum* Fuckel is considered to be the most aggressive species in worldwide, including Turkey. Biological control based on the use of microorganisms to suppress tuber diseases offers an attractive alternative that has gained great attention due to the significant potential. Several fungal biocontrol agents have been used in plant disease control, and *Trichoderma* group has been reported as effective against tuber pathogens such as *F. sambucinum*. This study was carried out under *in vitro* and *in vivo* conditions. During *in vitro* conditions, the effects of fifteen *Trichoderma* isolates (*T. asperellum* ÖT1; *T. viride* VG18; *T. viride* VG19; *T. harzianum* TZ16, *T. harzianum* LO52; *T. gamsii* VG47; *T. gamsii* VG48; *T. virens* KB31; *T. strigosum* LO43, *T. strigosum* LO8; *T. neokoningii* A15; *T. atroviride* VG3; *T. tomentosum* VG2; *T. Inhamatum* KEB12; *T. hamatum* ÖT16) were studied against three isolates of *F. sambucinum* (Fs2, Fs3 and Fs4) in PDA medium by using duel culture technique in incubation at 22 ± 24 °C. The most effective isolates were *T. virens* KB31, *T. gamsii* VG47, *T. hamatum* ÖT16, *T. asperellum* ÖT1, *T. harzianum* LO52, *T. atroviride* VG3, respectively. During *in vivo* conditions, potato tubers, CV. Desire were wounded and inoculated with 1 ml of *Trichoderma* isolates suspensions (10⁷ spores mL⁻¹), 24 h prior inoculation by *F. Sambucinum*. Reduction rate of dry rot in tubers was recorded during 5-6 weeks of incubation at 20-24 °C to compare with control treatments. Tuber dry rot was reduced by the antagonistic fungal isolates with different rates. The most effective isolates were *T. viride* VG18, *T. asperellum* ÖT1, *T. harzianum* TZ16, *T. virens* KB31 and *T. inhamatum* KEB12, respectively. Potato tubers were also treated with commercial seed fungicides named Celest-Max[®] (Fludioxonil, SC 100 g/l) and Quadris[®] (Azoxystrobin, SC 250 g/l). The results revealed that Fludioxonil treatments were more effective compared to Azoxystrobin treatments and the biological control agents.

Keywords: potato dry rot, *Fusarium sambucinum*, virulence, *Trichoderma* sp., biocontrol

Introduction

Potato dry rot disease is one of the major diseases of potato tubers (*Solanum tuberosum* L.) both in storage and planting. The rate of tubers infected in storage reaches up to 60%. Yield losses attributed to dry rot in field is almost 25% (Hanson et al., 1996; Stevenson et al., 2001). Primary causes of potato dry root disease are several species of *Fusarium* such as *F. sambucinum* Fuckel, *F. solani* (Mart.) Sacc, *F. avenaceum* (Fr.) Sacc, *F. culmorum* (W.G. Sm.) Sacc, and *F. oxysporum* Schltdl (Boyd., 1972; Nelson et al., 1981, 1983; Hanson et al., 1996; Eken et al., 2000; Borca and Carmen, 2013; Stefańczyk et al., 2016; Aydın et al., 2016). Chemical control strategy sometimes may not be quite effective and economical against dry rot in potato. Therefore, alternative methods are needed to control the plant diseases. *Trichoderma* is known as the most widely used antagonists in biological control.

Current study was carried out with a total of 15 isolates and ten *Trichoderma* species. The efficacy of *Trichoderma* species against 3 isolates of *F. sambucinum* (Fs2, Fs3, Fs4) was investigated by duel culture in nutrient media and tuber application methods. Thus, some effective antagonists have been identified. According to our information,

this is the first study on biological control using a large number of *Trichoderma* species against dry rot disease of potato.

Review of literature

Fusarium sambucinum Fuckel - teleomorph *Giberella pulicaris* most (Fr.) Sacc. is one of the most common and aggressive species found in potato tubers throughout the world (Boyd, 1972; Secor and Salas, 2001; Choiseul et al., 2001; Cullen et al., 2005; Sun et al., 2008; Eken et al., 2000; Aydın et al., 2016; Peters et al., 2008). This pathogen also produces trichothecene toxins which are secondary metabolites and cause various problems on humans and animals (Senter et al., 1991).

Fungi is mostly transported by tubers. However, *Fusarium* species such as *F. sambucinum* are common in most potato grown soils and can survive as resistant spores free in soil for a long time (Adams and Lapwood, 1983; Secor and Salas, 2001; Carnegie et al., 1998).

The disease can temporarily be suppressed by some postharvest applications to the tubers. However, when tubers exposed to the pathogen in soil, no measures can be taken. Previous studies indicated that fungicide applications during postharvest period cause resistance to *F. sambucinum* after a while and thus they may not be efficient enough (Hide et al., 1992; Desjardins, 1995; Peters et al., 2001; Gonzalez et al., 2002; Daami-Remadi et al., 2006; Gachango et al., 2012). A large number of studies have been conducted to identify cultivars resistant to dry rot disease of potato caused by *F. sambucinum*, but commercial potato cultivars are often susceptible to this disease (Schisler et al., 1997; Jellis, 1975; Langerfeld, 1979; Hooker, 1981; Jellis and Starling, 1983; Wastie et al., 1989; Ayed et al., 2006b; Aydın and İnal, 2018). Therefore, effective tuber treatments along with other applications prior to planting or during storage may reduce the severity of dry rot disease.

Several studies have been carried out on biological control of plant pathogens. The studies showed that *Trichoderma* species can be used as biological control agents against pathogens in soil microflora, especially in plant roots and tubers (Boosalis, 1964; Wilhelm, 1973; Lockwood, 1977; Cook and Baker, 1983; Whipps et al., 1993; Elad, 2000; Harman et al., 2004; Chaube et al., 2002; Aydın and Turhan, 2009). The role of *Trichoderma* species in biological control can be explained by interactions of biological control mechanisms such as antibiosis, hyperparasitism and competition (Kredics et al., 2003). When *Trichoderma* species are applied to tuberous plants, they colonize on newly formed organs of plants (tubers, roots and stolons) during the production season and maintain their activities (Harman, 2000; Howell, 2003; Aydın and Turhan, 2013). Some studies have reported that *Trichoderma* species can successfully control important tuber and soilborne phytopathogenic fungi such as *F. sambucinum* and *Rhizoctonia solani* Kuhn (Chet and Baker, 1981; Elad et al., 1980; Bell et al., 1982; Manczinger et al., 2002; Aydın and Turhan, 2013). A large number of studies have been conducted to investigate the effects of *Trichoderma* species on dry rot disease of potato caused by *F. sambucinum*. Some of these studies are; *T. viride* Pers. (Sadfi et al., 2001; Ayed et al., 2006a); *T. harzianum* Rifai. (Cherif et al., 2001; Ru and Di., 2012. Wharton and Kirk, 2014) *T. harzianum*, *T. viride* (Daami-Remadi et al., 2006); *Trichoderma* spp. (Schisler et al., 1998); *T. longibrachiatum* Rifai, *T. atroviride* Bissett., *T. virens* (*G. virens*) J.H., Mill., Giddens & A.A Foster (Ru and Di., 2012). The studies generally reported suppressing the dry rot disease of potato at certain rates.

Material and methods

Microorganisms

Pathogen

Three isolates of *F. Sambicunum* (Fs2, Fs3, Fs4) used in the study were obtained from the isolate collection of Phytopathology laboratory in the Department of Plant Protection, Faculty of Agriculture at Siirt University, Turkey. The isolates were isolated from potatoes with signs of dry rot disease. Identifications were performed by classical and DNA based technics, and pathogenicity of the isolates have been previously determined (Aydın et al., 2016; Aydın and İnal, 2018). Before being used in studies, clean tubers were contaminated with the isolates and isolates were re-isolated. Thus, the virulence of the isolates was protected. Isolates purified with single spore culture and stored at +4 °C were used in the study after culturing for 15 days in the dark at 15 °C in Potato Dextrose Agar (PDA, 38 g and 1 L completed with sterile water).

Antagonists

Trichoderma species (Table 1) were selected from isolate collection of Phytopathology laboratory in the Faculty of Agriculture at Siirt University. These isolates were previously isolated from soils in different regions of Turkey and identified both based on colony and conodial morphology (Aydın and Turhan, 2009). Isolates were stored at + 4 °C in oblique agar tubes containing PDA and used in the study after culturing in Potato Dextrose Agar (PDA) medium for 15 days at 24 °C (12 h dark, 12 h light).

Potato cultivars

The potato variety, cv. DESIRE® known to be sensitive to *F. Sambucinum* was used in the study (Aydın and İnal, 2018). The certified tubers weighing 80-100 g and 50-60 mm in diameter, which were not contaminated with any disease, were obtained from a field harvested in the same year.

Antagonism in vitro (duel culture)

Three isolates of *F. sambicunum* (Fs2, Fs3, Fs4) and *Trichoderma* species were grown on PDA and discs with a diameter of 8 mm were taken from the margins using a cork borer. The discs were planted (duel culture techniques) on the opposite side of the plate at equal distance from the periphery. The planting process was performed at the same time to each petri dish containing 20 ml of PDA medium in dotted form. Experiments were performed in an incubator at 22-24 °C. The study was conducted in 6 replications.

The evaluation time was determined based on the time that the pathogen colony was first fully covered by an antagonist. The mycoparasitic activity considering the rate and intensity of *F. sambicunum* colonization by the antagonist was evaluated according to the scale suggested by Turhan (1990) (Table 1).

Inoculation ad tuber treatment

The tubers were thoroughly washed in tap water and then kept in 5% sodium hypochlorite (NaOCI) for 5 min prior to the treatments. They were washed twice in

sterile water and allowed to dry on the drying paper for one day. Colonies taken from 7 to 10-day cultures of *F. sambucinum* isolates were placed into the 8 mm deep and 8 mm diameter holes drilled by an appropriate knife in the mid-belly of tubers. Water was added to the antagonistic *Trichoderma* grown in the PDA for a week, then scraped with a spatula, transferred to a double layer cheesecloth, and the spores were separated from the medium. The density of spore was counted with a haemocytometer slide in a microscope and adjusted to 1×10^6 spores ml^{-1} . Carboxy methyl cellulose in an amount of 0.05% was added to the spore suspensions to strengthen the adhesion, and three drops of Tween 20 were added to ensure uniform distribution of spores in the suspension. Finally, the suspensions were kept in a shaker for 15 min. to maintain the homogeneity. Twenty-four hours after placing the *F. sambucinum* colony into the tubers, 1 ml of the prepared suspensions was added to the drilled holes, and the holes were covered with the tissues taken from the potatoes. Only sterile water and PDA parts were used for the untreated tubers. For comparison purposes, fungicides such as Celestine-Max® (Fludioxonil, 100 g L^{-1} , Syngenta Crop Protection Inc.) registered against *Rhizoctonia solani* of potato in Turkey and Quadris® (Azoxystrobin, 250 g L^{-1} , Syngenta Crop Protection Inc.) usually licensed to the late blight disease caused by *Phytophthora infestans* in potatoes and vegetables were used. Fungicides were mixed with water at the indicated doses (20 ml L^{-1} for Fludioxonil and 75 ml 100 L^{-1} for Azoxystrobin) and 1 ml was added into each hole drilled in tubers.

The treatments of experiment were 1) no treatment (Negative control), 2) treated only with *F. sambucinum* isolates (Fs2, Fs3, Fs4) (Positive control), 3) treated with *Trichoderma* species and pathogen isolates, and finally 4) treated with fungicides. All three tubers were considered as units and the experiment was set up with four replications in a randomized plot design. The tubers over a humidified cloth on a large plastic tray were placed in a climate cabinet set at 15-20 °C. The experiments were conducted in the laboratories of Plant Protection Department, Faculty of Agriculture, Siirt University, Turkey.

Evaluation of tuber treatments

The tubers were cut longitudinally after 5 weeks of incubation; width (w) and depth (d) were measured, the penetration value was calculated using *Equation 1* developed by Lapwood et al. (1984).

$$\text{Penetration (mm): } [w/2 + (d-6)]/2 \quad (\text{Eq.1})$$

The percent (%) effect of the treatments was evaluated according to the Abbott formula (*Eq. 2*), by comparing the values of positive control after computing the average values of each application.

$$\text{Effect of applications (\%): } \frac{X - Y}{X} \times 100 \quad (\text{Eq.2})$$

where:

x: Mean disease severity in positive control plots (%)

y: Mean disease severity in treated plots (%)

Statistical analysis of the experiment was carried out by “JMP 8” statistical software (SAS Institute Inc.) and the differences among treatments were grouped by the LSD (LS Means Differences Student’s t) test

Results

Efficiency of antagonists in vitro

The effects of *Trichoderma* species on *F. sambucinum* isolates (Fs2, Fs3 and Fs4) were presented in *Table 1*. Antagonists and pathogen isolates were cross-planted in dotted form at the same time on the PDA medium. The assessment was based on appearance of the first antagonist that completely covered the pathogen colony in the petri dish. This antagonist was considered to be a very strong hyperparasitic and the others were assessed according to the scale given in *Table 1*. The most efficient antagonists for *F. sambucinum* Fs1 were *T. atroviride* VG3, *T. gamsii* VG47, *T. hamatum* ÖT16 and *T. viride* VG18, respectively. The antagonists for *F. sambucinum* Fs2 were *T. atroviride* VG3, *T. hamatum* ÖT16, *T. gamsii* VG47 and *T. viride* VG18, and those for *F. sambucinum* Fs3 were *T. atroviride* VG3, *T. gamsii* VG47, *T. strigosum* LO43, *T. viride* VG18 and *T. hamatum* ÖT16, respectively. Weakly developed antagonist isolates on three *F. sambucinum* isolates were *T. tomentosum* VG2, *T. neokoningii* A15 and *T. strigosum* LO8, respectively (*Table 1*).

Table 1. Effects of in-vitro antagonists on *F. sambucinum* isolates (Fs2, Fs3, Fs4)

Antagonists	<i>F. sambucinum</i> Fs1	<i>F. sambucinum</i> Fs2	<i>F. sambucinum</i> Fs3
<i>T. hamatum</i> ÖT16	VSH*	VSH	VSH
<i>T. virens</i> KB31	H***	H	H
<i>T. viride</i> VG19	SH**	H	SH
<i>T. viride</i> VG18	SH	VSH*	SH
<i>T. harzianum</i> LO52	SH	SH	SH
<i>T. harzianum</i> TUZ16	H	SH	H
<i>T. strigosum</i> LO8	H	H	H
<i>T. inhamatum</i> KEB12	SH	SH	H
<i>T. asperellum</i> ÖT1	SH	VSH	SH
<i>T. gamsii</i> VG47	VSH	SH	SH
<i>T. tomentosum</i> VG2	H	H	WH****
<i>T. neokoningii</i> A15	H	H	WH
<i>T. atroviride</i> VG3	VSH	VSH	VSH
<i>T. strigosum</i> LO43	H	SH	SH
<i>T. gamsii</i> VG48	VSH	VSH	VSH

VSH*: Very strong mycoparasitism: Antagonist completely covers the colony of the pathogen
SH**: Strong mycoparasitism: Antagonist shows a strong improvement over the pathogen colony
H***: Moderate mycoparasitism: The development of the antagonist on the pathogen colony is easily discernible
WH****: Poor mycoparasitism: Very poor development of antagonist on the pathogen colony is noticed

Trichoderma isolates showed hyperparasitic character and inhibited the pathogen colony by growing over them (Table 1). Some antagonist isolates have also completely covered the pathogen isolates and they have demonstrated very strong hyperparasitic (VSH) features (Table 1). Some *Trichoderma* isolates showed very strong hyperparasitic (VSH) or strong hyperparasitic (SH) features, while some isolates were only moderately hyperparasitic (H) and they were less effective. The efficiency of antagonists showing strong hyperparasitic features were approximately close to each other against three isolates of *F. sambucinum* (Fs1, Fs2, Fs3). For example, *T. atroviride* VG3, *T. gamsii* VG47, *T. gamsii* VG48 and *T. hamatum* ET16 antagonists were the fastest and the most effective mycoparasites against three isolates of the pathogen. Images of antagonist growth on *F. sambucinum* isolates in PDA medium according to the duel culture method were shown Figure 1.

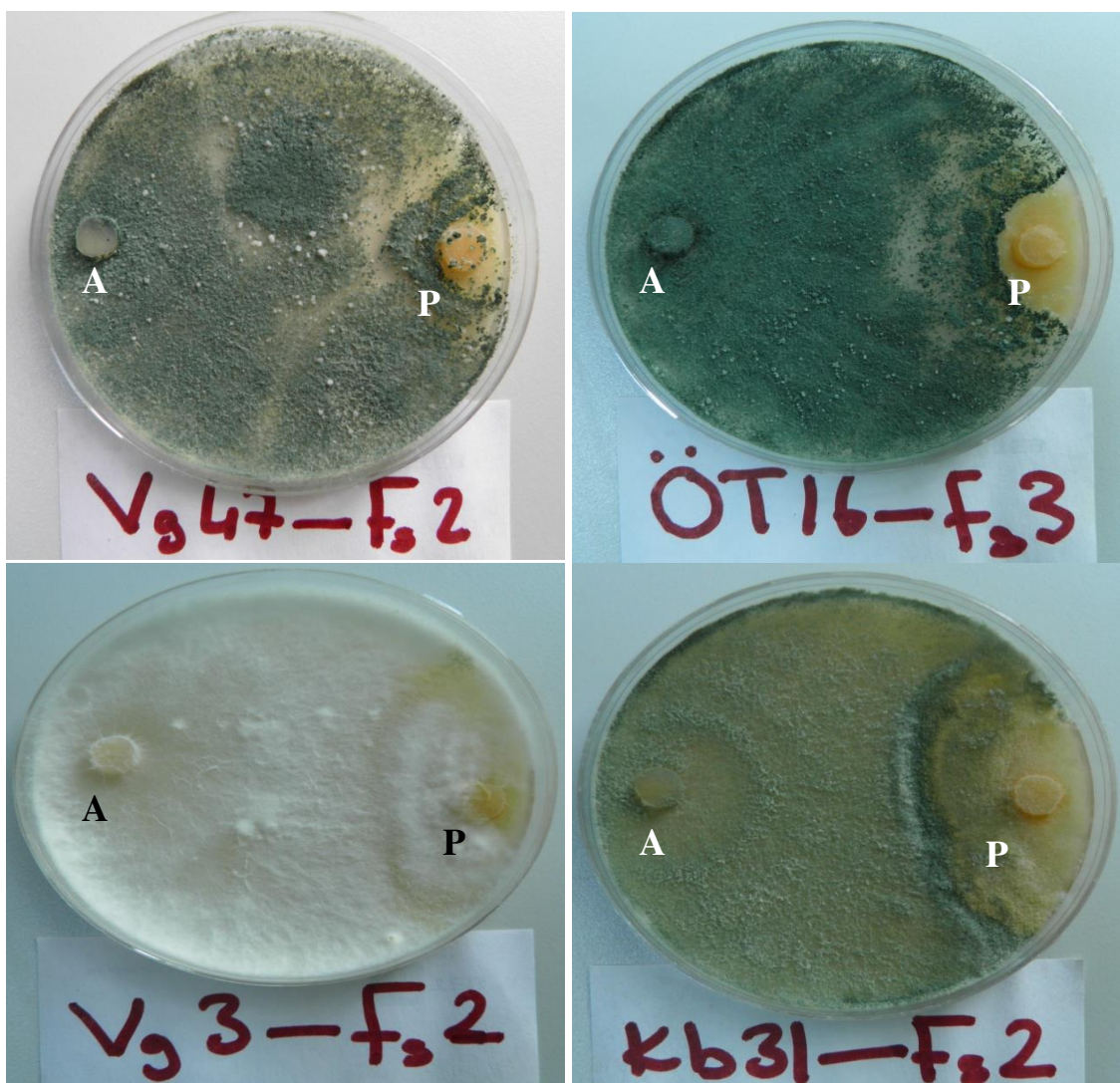


Figure 1. Images of some antagonist growth on *F. sambucinum* isolates in PDA medium according to the duel culture method [*T. gamsii* VG47- *F. sambucinum* 2 (VSH: Very strong mycoparasitism); *T. hamatum* ÖT16 - *F. sambucinum* 3 (VSH: Very strong mycoparasitism); *T. atroviride* VG3- *F. sambucinum* 2 (VSH: Very strong mycoparasitism); *T. virens* KB31- *F. sambucinum* 2 (H: Moderate mycoparasitism); A: Antagonist, P: Pathogen

Evaluation of tuber applications

The efficacy of *Trichoderma* species on tubers against *F. sambucinum* isolates (Fs2, Fs3, Fs4) was presented in Table 2.

Table 2. The extent of suppressing (mm) and grouping of *F. sambucinum* isolates (Fs2, Fs3, Fs4) on potato tubers of some fungicides and *Trichoderma* species

No	Treatments	<i>F.sambucinum</i> Fs2	<i>F.sambucinum</i> Fs3	<i>F.sambucinum</i> Fs4	Mean
1	<i>T. hamatum</i> ÖT16	11.50 kt	12.63 jm	16.06 fg	13.40 c
2	<i>T. virens</i> KB31	11.50 kt	9.06 vx	11.06 mu	10.54 fg
3	<i>T. viride</i> VG19	10.94 mu	13.75 hj	15.50 fh	13.40 c
4	<i>T. viride</i> VG18	12.50 jn	11.56 ks	17.13 ef	13.73 bc
5	<i>T. harzianum</i> LO52	10.13 rw	9.31 ux	10.81 nv	10.08 gh
6	<i>T. harzianum</i> TUZ16	9.38 u	8.50 wy	10.50 pv	9.46 h
7	<i>T. strigosum</i> LO8	12.31 jo	12.88 il	19.00 bd	14.73 b
8	<i>T. inhamatum</i> KEB12	9.75 tx	9.31 ux	10.69 ov	9.92 gh
9	<i>T. asperellum</i> ÖT1	11.06 mu	12.00 jp	17.88 ce	13.64 c
10	<i>T. gamsii</i> VG47	11.75 kr	10.13 rw	13.00 ik	11.63 de
11	<i>T. tomentosum</i> VG2	10.69 ov	8.19 xy	11.81 kr	10.23 gh
12	<i>T. neokonigii</i> A15	9.88 sx	15.56 fg	17.25 df	14.23 bc
13	<i>T. atroviride</i> VG3	11.50 kt	8.44 wy	11.94 kq	10.63 eg
14	<i>T. strigosum</i> LO43	11.88 kr	11.19 lt	18.06 ce	13.71 bc
15	<i>T. gamsii</i> VG48	11.31 kt	10.19 qw	12.88 il	11.46 df
16	Fludioxonil	3.69 z	4.69 z	7.00 y	5.12 i
17	Azoxystrobin	10.44 pv	10.63 ov	14.56 gı	11.87 d
18	Control (+)	19.13 bc	20.06 b	23.81 a	21.00 a
19	Control (-)	0.00	0.00	0.00	0.00
Mean		11.07 b	11.00 b	14.39 a	12.16
CV%		10.56			
LSD _{0,05}		Treatment; 1.03**	Fs; 0.42**	Treatment x Fs 1.79**	

**P < 0.01. Levels not connected by same letter are significantly different

The effects of fungicides and isolates of *Trichoderma* on *F. sambucinum* isolates showed significant differences in terms of individual and mean values (P < 0.01). The differences between the treatments were grouped by the LSD (LSMeans Differences Student's t) test (Table 2). The disease was observed at all tubers in replications inoculated with Fs2, Fs3, and Fs4 isolates of *F. sambucinum* and treated with antagonists and certain fungicides. However, the levels of influence were different. The disease severity in the positive control of Fs2, Fs3 and Fs4 isolates was the highest and it was 19.13, 20.06 and 23.81, respectively. Fludioxonil, a fungicide, was the most inhibitory treatment (3.69, 4.69 and 7 mm) on growth of all three isolates investigated (Fs2, Fs3 and Fs4). The inhibitory effect of Azoxystrobin followed the Fludioxonil as 10.44, 10.63 and 14.56 mm. The most effective of *Trichoderma* species on Fs2 isolate was *T. harzianum* TUZ16 with 9.38 mm. *T. tomentosum* VG2 was effective on Fs3 isolate with 8.19 mm and *T. harzianum* TUZ16 was effective on Fs4 isolate with 10.50 mm. Fludioxonil was the most inhibitory fungicide on growth of all three isolates with an average of 5.12 mm. Average growth of isolates with Azoxystrobin treatment was 11.87. *Trichoderma harzianum* TUZ16 (9.46 mm) was the most inhibitory species of

Trichoderma species and followed by *T. inhamatum* (9.92 mm). Mean values of disease severity with *T. neokoningii* A15, *T. strigosum* LO43, *T. asperellum* ÖT1, *T. hamatum* ÖT16, *T. viride* VG19 and *T. viride* VG18 treatments were 14.23, 13.71, 13.64, 13.40, 13.40 and 13.73, respectively and placed in a separate group. Therefore, *T. Strigosum* LO8 (14.73) and *T. neokoningii* A15 (14.23) were the least effective species. The effect of treatments in preventing the disease was given in *Figure 2*.

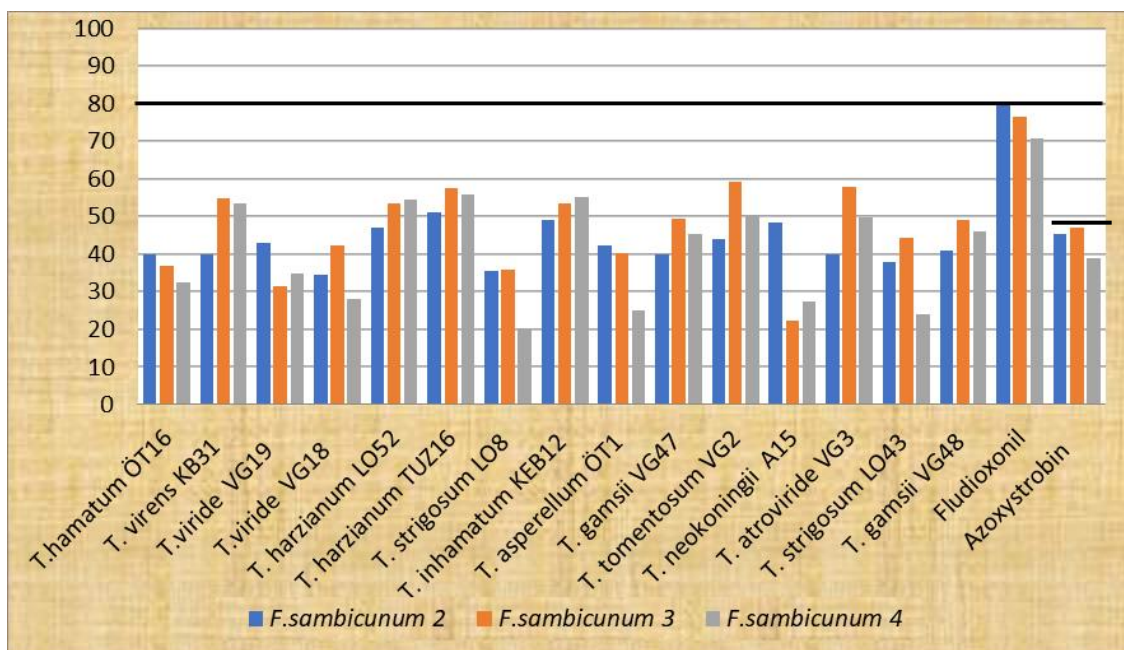


Figure 2. Effects of antagonists and fungicides on the prevention of disease in experiments with *F. sambucinum* Fs2, Fs3, and Fs4 infected isolates

The influence ratio of treatments, comparing the positive control, ranged from 20.20 to 80.71%. Average of the most effective treatments against three isolates of the pathogen was 75.97% for Fludioxonil, 54.82% for *T. harzianum* TUZ16, 49.21% for *T. inhamatum* KEB12, 51.73% for *T. harzianum* LO52, 51.22% for *T. tomentosum* VG2 and 49.21% for *T. atroviride* VG3, respectively. The appearances of some tubers cut in the evaluation phase after the treatments were shown in *Figure 3*.

Following the evaluation, the tissue pieces were taken from pathologically contaminated tubers that had been treated and had not been treated, and they were left to grow on the PDA medium. The growth of pathogen and *Trichoderma* species were observed.

Discussion

This study has been carried out in two phases. In the first phase, the interaction of pathogens and antagonists was measured in the PDA medium. In the second phase, the activity of antagonists was investigated with three isolates of pathogen in potato tubers. Fifteen isolates, 10 of which were *Trichoderma* species, were used in the study. Majority of these species have been reported as the first isolation in Turkey (Aydin and Turhan, 2009). Therefore, this type of *Trichoderma* was the first time studied against

dry rot disease of potato caused by *F. Sambucinum*. According to our information, some *Trichoderma* species such as *T. gamsii* have been studied the first time against this pathogen in potato. Previous studies were mostly conducted with *T. harzianum*, *T. viride* and *T. virens* (Daami-Remadi et al., 2006; Sadfi et al., 2001; Ayed et al., 2006a; Cherif et al., 2001; Ru and Di., 2012; Wharton and Kirk, 2014).



Figure 3. Appearance of disease developments in potato tubers, treated with antagonist and *F. sambucinum* isolates. Above: *T. harzianum* TUZ16- *F. sambucinum* 3 (the most inhibitory antagonist); *T. inhamatum* KEB12- *F. sambucinum* 4 (strong inhibitory antagonist). Below: *T. viride* VG18- *F. sambucinum* 4 (least inhibitory antagonist); *T. neokoningii* A15- *F. sambucinum* 4 (least inhibitory antagonist)

The results showed that some *Trichoderma* species reduced the dry rot disease that occurs in the tubers. The results of our study are in good agreement with some of previous studies. Daami-Remadi et al. (2006) reported that *T. harzianum* and *T. viride* control the disease at a certain rate. The efficiency of isolates from the same species on pathogen was close to each other both in nutrient medium and tubers. For example, *T. harzianum* TUZ16 and *T. harzianum* LO52 isolates obtained from different ecologies had SH and H values in the in vitro study (Table 1). The tuber study revealed that these two isolates of *T. harzianum* were effective in the penetration that ranged from 10.08 to 9.46 mm and at a rate between 54.82 and 51.73%, respectively. The results indicated the differences between the species in activity against the pathogen, but the difference was little in *Trichoderma* isolates of the same species. The efficiency of *T. hamatum* ÖT16, *T. viride* VG18, *T. viride* VG19 and *T. asperellum* ÖT1 isolates against pathogen isolates was high (SH and VSH) in duel cultures and PDA medium due to the mycoparasitism, antibiotic and enzyme production. However, this effect has not sufficiently occurred in vivo conditions. The opposite situation can also occur. A *Trichoderma* isolate that is not sufficiently successful in laboratory conditions may act in vivo. Temperature and some other environmental factors play a great deal of influence on the antagonist activity. This may not adversely affect the biocontrol activity of *Trichoderma* species; but it may reduce the effectiveness over time.

However, the most suitable environment to sustain the activity of a *Trichoderma* species should have similar temperature, moisture and nutrient values to the environment that the species isolated (Samuels, 2006).

T. gamsii VG47, *T. gamsii* VG48 and *T. atrovide* VG3 were successful in preventing the pathogen in both experiments. Our findings are in agreement with the previous studies (Cherif et al., 2001; Ru and Di, 2012; Wharton and Kirk, 2014). The results suggest that these antagonists have high compliance ability under various conditions. Establishment of field experiments with high performance isolates found in this study may lead to better results in terms of biological control against *F. Sambucinum*.

The efficacy of antagonists on the three isolates of *F. sambucinum* (Fs1, Fs2, Fs3) was not significantly different. The results of all experiments showed that the behavior of antagonists affecting the different isolates of pathogen was not significantly different.

After the evaluation, the tissues treated have been taken from the potatoes and planted on the PDA medium. In particular, *Trichoderma* species effective on pathogen were re-isolated (Fig. 4). This shows settling of antagonists into the tissue and continuing their activity. *Trichoderma* species have been reported to colonize and maintain their activity throughout the production season in various organs of plants (tubers, roots and stolons) (Harman, 2000; Howell, 2003; Aydın and Turhan, 2013).

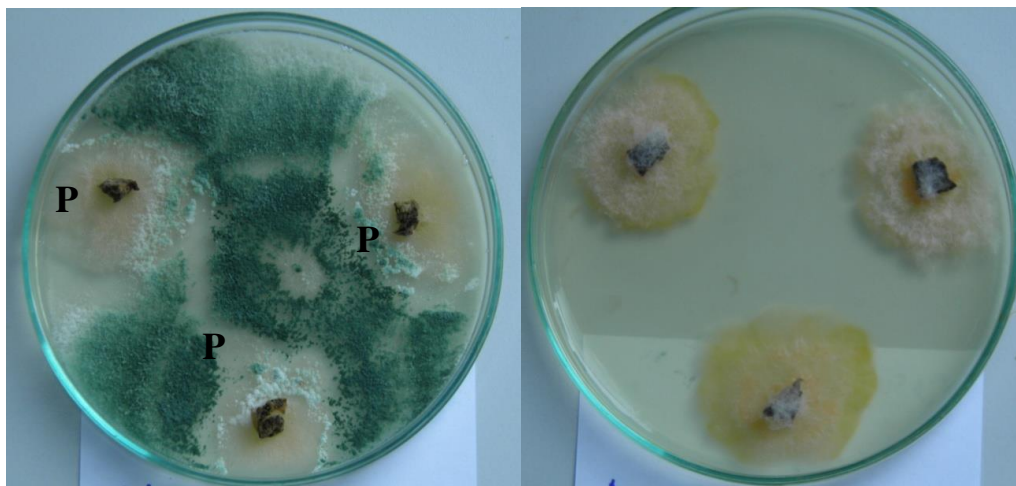


Figure 4. Fungus developing in potato tissues after evaluation. On the left: *T. harzianum* LO52 re-isolation in a treated tuber with green colour. On the right: re-isolation image of *F. sambucinum* in pathogen with salmon colour-infected tuber). A: Antagonist, P: Pathogen

The fungicides with fludioxonil and azoxystrobin effective substances were used in the study. Fludioxonil has been identified as the most effective treatment. The activity of azoxystrobin was found to be low. Fludioxonil is effectively used against *Rhizoctonia solani*, another important tuberous disease of potatoes (Aydın and Turhan, 2009; Aydın et al., 2011). The fludioxonil has also been reported reducing the severity of dry rot disease of potatoes (Al- Mughrabi, 2010).

In contrast to previous studies, multiple isolates which were different from each other in terms of virulence were used in this study. Some *Trichoderma* species have demonstrated efficiency on all pathogen isolates in almost equal proportions.

Conclusion

Dry rot disease caused by *F. sambucinum* is known an economically important field and a postharvest disease throughout the world. Biological control has recently gained great attention and shown significant potential to control the dry rot disease. The use of some *Trichoderma* such as *T. viride* VG18, *T. asperellum* ÖT1, *T. harzianum* TZ16, *T. virens* KB31 and *T. inhamatum* KEB12 successfully suppressed the dry rot in potatoes at different rates. The efficacies of some *Trichoderma* species and Fludioxonil treatments in preventing dry rot disease were higher compared to Azoxystrobin fungicide. The results obtained in this study showed that the use of *Trichoderma* isolates is an important approach in controlling the dry rot caused by *F. sambucinum* on potato tuber.

REFERENCES

- [1] Adams, M. J., Lapwood, D. H. (1983): Transmission of *Fusarium solani* var. *coeruleum* and *F. sulphureum* from seed potatoes to progeny tubers in the field. – Ann. Appl. Biol. 103: 411-417.
- [2] Al-Mughrabi, K. I. (2010): Biological control of *Fusarium* dry rot and other potato tuber diseases using *Pseudomonas fluorescens* and *Enterobacter cloacae*. – Biological Control 53: 280-284.
- [3] Aydın, M. H., Turhan, G. (2009): Studies on Determination of Fungal Antagonists of *Rhizoctonia solani*. – Anadolu J. of AARI 19(2): 49-72.
- [4] Aydın, M. H., Turhan, G. (2013): The Efficacy of *Trichoderma* Species against *Rhizoctonia solani* in Potato and Their Integration with Some Fungicides. – Anadolu J. of AARI 23(1): 12-30.
- [5] Aydın, M. H., İnal, B. (2018): Comparative susceptibility of some commercial potato cultivars to *Fusarium sambucinum* and *F. solani* isolates causing tuber dry rot. – Applied Ecology and Environmental Research 16(4): 4879-4892.
- [6] Aydın, M. H., Turhan, G., Göre, E. (2011): Determination of some antagonists efficiency on the viability and the formation of sclerotia of *Rhizoctonia solani* on potato tubers. – Anadolu J. of AARI 21(2): 29-38.
- [7] Aydın, M. H., Pala, F., Kaplan, C. (2016): Potato tuber sprout rot caused by *Fusarium sambucinum* in Turkey. – Scientific Papers. Series A. Agronomy 59: 189-193.
- [8] Ayed, F., Daami-Remadi, M., Jabnoun-Khiareddine, H., Hibar, K., El Mahjoub, M. (2006a): Potato Vascular *Fusarium* wilt in Tunisia: incidence and biocontrol by *Trichoderma* spp. – Plant Pathol. J. 5: 92-98.
- [9] Ayed, F., Daami-Remadi, M., Jabnoun-Khiareddine, H., El Mahjoub, M. (2006b): Effect of potato cultivars on incidence of *Fusarium oxysporum* f. sp. *tuberosi* and its transmission to progeny tubers. – Journal of Agronomy 5: 430-434.
- [10] Bell, D. K., Weels, H. D., Markham, C. R. (1982): In vitro antagonism of *Trichoderma* species against six fungal plant pathogens. – Phytopathology 72: 379-382.
- [11] Boosalis, M. G. (1964): Hyperparasitism. – Annual Review of Phytopathology 2: 363-376.
- [12] Borca, I. D., Carmen, E. P. (2013): Studies regarding the morphological identification of *Fusarium sambucinum* Fuckel isolated from potato tubers. – ProEnvironment 6: 59-63.
- [13] Carnegie, S. F., Cameron, A. M., Lindsay, D. A., Sharp, E., Nevison, I. M. (1998): The effect of treating seed potato tubers with benzimidazole, imidazole and phenylpyrrole fungicides on the control of rot and skin blemish diseases. – Ann. Appl. Biol. 133: 343-363.
- [14] Boyd, A. E. W. (1972): Potato storage diseases. – Rev. Plant Pathol. 51: 297-321.

- [15] Chaube, H. S., Mishra, D. S., Varshney, S., Singh, U. S. (2002): Biological control of plant pathogens by fungal antagonistic: Historical background, present status and future prospects. – *Annu. Rev. Plant Pathol.* 2: 1-42.
- [16] Cherif, M., Omri, N., Hajlaoui, M. R., Mhamdi, M., Boubaker, A. (2001): Effect of some fungicides on *Fusarium roseum* var. *sambucinum* causing potato tuber dry rot and on *Trichoderma* antagonists. – *Annales de l'INRAT* 74: 131-149.
- [17] Chet, I., Baker, R. (1981): Isolation and biocontrol potential of *Trichoderma hamatum* from soil naturally suppressive to *Rhizoctonia solani*. – *Phytopathology* 71: 286-290.
- [18] Choiseul, J., Allen, L., Carnegie, S.F., Darling, D. (2001): Fungi Causing Tuber Rots of Seed Potatoes in Storage. – In: Hay, R. K. M. (ed.) *Scientific Review 1997–2000*. Scottish Agricultural Science Agency, Edinburgh, UK, pp. 46-8.
- [19] Cook, R. J., Baker, K. F. (1983): *The Nature and Practice of Biological Control of Plant Pathogens*. – APS, SZ Paul, Minnesota.
- [20] Cullen, D. W., Toth, I. K., Pitkin, Y., Boonham, N., Walsh, K., Barker, I., Lees, A. K. (2005): Use of quantitative molecular diagnostic assays to investigate *Fusarium* dry rot in potato stocks and soil. – *Phytopathology* 95: 1462-1471.
- [21] Daami-Remadi, M., Ayed, F., Jabnoun-Khiareddine, H., Hibar, K., El Mahjoub, M. (2006): Comparative susceptibility of some local potato cultivars to four *Fusarium* species causing tuber dry rot in Tunisia. – *Journal of Plant Sciences* 1(4): 306-314.
- [22] Desjardins, A. E. (1995): Population structure of *Gibberella pulicaris* (anamorph *Fusarium sambucinum*) from potato tuber dry rot in North America and Europe. – *Am. Potato J.* 72: 145-156.
- [23] Eken, C., Demirci, E., Sahin, F. (2000): Pathogenicity of the fungi determined on tubers from potato storages in Erzurum, Turkey. – *Journal of Turkish Phytopathology* 29: 61-69.
- [24] Elad, Y. (2000): Biological control foliar pathogens by means of *Trichoderma harzianum* and potential modes of action. – *Crop Protect.* 19: 709-714.
- [25] Elad, Y., Chet, I., Katan, J. (1980): *Trichoderma harzianum* a biocontrol agent effective against *Sclerotium rolfsii* and *Rhizoctonia solani*. – *Phytopathology* 70: 119-121.
- [26] Gachango, E., Kirk, W., Wharton, P. S., Schafer, R. (2012): Evaluation and comparison of biocontrol and conventional fungicides for control of postharvest potato tuber diseases. – *Biol. Control* 63: 115-120.
- [27] Gonzalez, C. F., Provin, E. M., Zhu, L., Ebbale, D. J. (2002): Independent and synergistic activity of synthetic peptides against thiabendazole-resistant *Fusarium sambucinum*. – *Phytopathology* 92: 917-924.
- [28] Hanson, L. E., Schwager, S. J., Loria, R. (1996): Sensitivity to thiabendazole in *Fusarium* species associated with dry rot of potato. – *Phytopathology* 86: 378-384.
- [29] Harman, G. E. (2000): Myths and dogmas of biocontrol. Changes in perceptions derived from research on *Trichoderma harzianum* T-22. – *Plant Dis.* 84: 377-393.
- [30] Harman, G. E., Howell, C. R., Viterbo, A., Chet, I., Lorito, I. M. (2004): *Trichoderma* species - Opportunistic, avirulent plant symbionts. – *Nature Rev.* 2: 43-56.
- [31] Hide, G. A., Read, P. J., Hall, S. M. (1992): Resistance to thiabendazole in *Fusarium* species isolated from potato tubers affected by dry rot. – *Plant Pathol.* 41:745-748.
- [32] Hooker, W. J. (1983): *Compendium of Potato Diseases*. – American Phytopathological Society, Minnesota, USA.
- [33] Howell, C. R. (2003): Mechanisms employed by *Trichoderma* species in the biological control of plant diseases: the history and evolution of current concepts. – *Plant Dis.* 87: 4-10.
- [34] Jellis, G. J. (1975): Screening potato clones for resistance to dry rot (*Fusarium solani* var. *coeruleurn*). – *Annals of Applied Biology* 81: 417-418.
- [35] Jellis, G. J., Starling, N. C. (1983): Resistance to powdery dry rot (*Fusarium sulphureum*) in potato tubers. – *Potato Research* 26: 295-301.
- [36] Kredics, L., Antal, Z., Manczinger, L., Szekeres, A., Kevei, F., Nagy, E. (2003): *Trichoderma* strains with biocontrol potential. – *Food Technol. Biotechnol.* 41(1) 37-42.

- [37] Langerfeld, L. (1979): Prüfung des Resistenzverhaltens von kar-toffelsorten gegenüber *Fusarium coeruleum* (Lib.) Sacc. – Potato Res. 22: 107-122.
- [38] Lapwood, D. H., Read, P. J., Spokes, J. (1984): Methods for assessing the susceptibility of potato tubers of different cultivars to rotting by *Erwinia carotovora* subsp. *atroseptica* and *carotovora*. – Plant Pathology 33: 13-20.
- [39] Lockwood, J. L. (1977): Fungistasis in soil. – Biol. Rev. 52: 1-43.
- [40] Manczinger, L., Antal, Z., Kredics, L. (2002): Ecophysiology and breeding of ycoparacitic *Trichoderma* strains (a review). – Acta Microbiologica et Immunologica Hungarica 49: 1-14.
- [41] Nelson, P. E., Toussoun, T. A., Cook, R. J. (1981): *Fusarium: Diseases, Biology and Taxonomy*. – The Pennsylvania State University Press, University Park, Pennsylvania.
- [42] Nelson, P. E., Toussoun, T. A., Marsas, W. F. U. (1983): *Fusarium* species. An Illustrated Manual for Identification. – The Pennsylvania State Univ. Press, University Park, Pennsylvania.
- [43] Peters, J. C., Lees, A. K., Cullen, D. W., Sullivan, L., Stroud, G. P., Cunnington, A. C. (2008): Characterization of *Fusarium* spp. responsible for causing dry rot of potato in Great Britain. – Plant Pathology 57: 262-271.
- [44] Peters, R. D., Macdonald, I. K., MacIsaac, K. A., Woodworth, S. (2001): First report of thiabendazole-resistant isolates of *Fusarium sambucinum* infecting stored potatoes in Nova Scotia. – Canada Plant Disease 85: 1030.
- [45] Ru, Z., Di, W. (2012): *Trichoderma* spp. from rhizosphere soil and their antagonism against *Fusarium sambucinum*. – African Journal of Biotechnology 11(18): 4180-4186.
- [46] Sadfi, N., Cherif, M., Fliss, I., Boudabbous, A., Antoun, H. (2001): Evaluation of *Bacillus* isolates from salty soils and *Bacillus thuringiensis* strains for the biocontrol of *Fusarium* dry rot of potato tubers. – Journal of Plant Pathology 83: 101-118.
- [47] Samuels, G. J. (2006): *Trichoderma*: Systematics, the sexual state, and ecology. – Phytopathology 96(2): 195-206.
- [48] Schisler, D. A., Slininger, P. J., Bothast, R. J. (1997): Effects of antagonists cell concentration and two-strain mixtures on biological control of *Fusarium* dry rot of potatoes. – Phytopathology 87: 177-183.
- [49] Schisler, D. A., Burkhead, K. D., Slininger, P. J., Bothast, R. J. (1998): Selection, Characterization and Use of Microbial Antagonists for the Control of *Fusarium* Dry Rot of Potatoes. – In: Boland, G. J., Kuykendall, L. D. (eds.) Plant-Microbe Interactions and Biological Control. Marcel Dekker, New York, pp: 199-221.
- [50] Secor, G. A., Sales, B. (2001): *Fusarium* Dry Rot and *Fusarium* Wilt. – In: Stevenson, W. R. et al. (eds.) Compendium of Potato Diseases. 2nd ed. The American Phytopathological Society, St. Paul, MN, pp. 23-25.
- [51] Senter, L. H., Sanson, D. R., Corley, D. G., Tempesta, M. S., Rottinghaus, A. A., Rottinghaus, G. E. (1991): Cytotoxicity of trichothecene mycotoxins isolated from *Fusarium sporotrichioides* (MC-72083) and *Fusarium sambucinum* in baby hamster kidney (BHK-21) cells. – Mycopathology 113: 127-131.
- [52] Stefańczyk, E., Sobkowiak, S., Brylińska, M., Śliwka, J. (2016): Diversity of *Fusarium* spp. associated with dry rot of potato tubers in Poland. – Eur J Plant Pathol. 145: 871-884.
- [53] Stevenson, W. R., Loria, R., Franc, G. D., Weingartner, D. P. (2001): Compendium of Potato Diseases. – APS Press, St. Paul, Minnesota, USA.
- [54] Sun, X. J, BI, Y., Li, Y. C. Han, R. F., Yong-Hong, G. E. (2008): Postharvest chitosan treatment induces resistance in potato against *Fusarium sulphureum*. – Agric. Sci. China 7(5): 615-621.
- [55] Turhan, G. (1990): Further hyperparasites of *Rhizoctonia solani* Kühn as promising candidates for biological control. – Zeitschrift für Pflanzenkrankheiten und Pflanzenschutz 97: 208-215.

- [56] Wastie, R. L., Stewart, H. E., Brown, J. (1989): Comparative susceptibility of some potato cultivars to dry rot caused by *Fusarium sulphurum* and *Fusarium solani* var. *coeruleum*. – Potato Research 32: 49-55.
- [57] Wharton, P. S., Kirk, W. W. (2014): Evaluation of biological seed treatments in combination with management practices for the control of *Fusarium* dry rot of potato. – Biological Control 73: 23-30.
- [58] Whipps, J. M., McQuilken, M. P., Budge, S. P. (1993): Use of fungal antagonists for biocontrol of damping-off and *Sclerotinia* disease. – Pestic. Sci. 37: 309-313.
- [59] Wilhelm, M. S. (1973): Principles of biological control of soil-borne plant disease. – Soil Biol. Biochem. 5: 729-737.

PROTEOME ANALYSIS OF MILK THISTLE (*SILYBUM MARIANUM* L.) CELL SUSPENSION CULTURES IN RESPONSE TO METHYL JASMONATE AND YEAST EXTRACT ELICITORS

POURJABAR, A.¹ – AZIMI, M. R.^{1*} – MOSTAFAIE, A.² – KAHRIZI, D.³ – CHEGHAMIRZA, K.³

¹*Department of Agronomy and Plant Breeding, Faculty of Agriculture, University of Zanjan
Zanjan, Iran
(e-mail: atefeh58@yahoo.com, azimi@znu.ac.ir)*

²*Medical Biology Research Center, Kermanshah University of Medical Sciences
Kermanshah, Iran
(e-mail: amostafaie@kums.ac.ir)*

³*Department of Agronomy and Plant Breeding, Razi University, Kermanshah, Iran
(e-mail: cheghamirza@razi.ac.ir, dkahrizi@razi.ac.ir)*

**Corresponding author
e-mail: atefeh58@yahoo.com*

(Received 28th Jul 2018; accepted 28th Sep 2018)

Abstract. Elicitors cause biosynthesis and accumulation of secondary metabolites by inducing defense responses. In this study, we treated the cell suspension cultures of *Silybum marianum* L. with MeJA (methyl jasmonate) (100 μ M) and YE (yeast extract) (0.1 w/v) as elicitors and measured the content of Silymarin accumulation by HPLC (High Performance Liquid Chromatography). Accumulation of Silymarin significantly increased after 48 h of MeJA and YE application. In order to investigate the effect of abiotic (MeJA) and biotic (YE) stresses on expression of proteins in *S. marianum* cell suspension cultures, we employed high resolution two-dimensional gel electrophoresis coupled with MALDI-TOF-TOF (matrix assisted laser desorption ionization time of flight) mass spectrometry. At least, 249 protein spots showed reproducible and significant changes in the gel. Spots were up or down regulated upon MeJA and YE treatments. Ten protein spots were identified using MALDI-TOF-TOF-MS. The identified proteins belong to different functional categories. The proteins were classified based on carbohydrate metabolism (spots 6 and 22), Nitrogen metabolism (spot 20), storage protein (spot 29), transport process (spot 12), protein modification and chaperones (spot 8), pathogenesis related (spot 1 and 2) and secondary metabolism (spot 3 and 53). The potential role of these proteins in the biosynthetic pathway of flavonoids and the finding of proteins in non-sequenced plants such as *S. marianum* requires further research.

Keywords: *elicitor, HPLC, silymarin, MALDI-TOF-TOF mass spectrometry, two-dimensional gel electrophoresis*

Abbreviations: MeJA, methyl jasmonate; JA, jasmonic acid; YE, yeast extract; MALDI-TOF/TOF, matrix assisted laser desorption ionization time of flight; SLM, silymarin; 2-DE, two-dimensional gel electrophoresis; IEF, isoelectric focusing; IPG strip, immobilized pH gradient strip; SDS-PAGE, sodium dodecyl sulfate-poly acrylamide gel electrophoresis; IgG, immune globulin G; MS, mass spectrometry; CBB, coomassie brilliant blue

Introduction

Silybum marianum L. Gaertn. is an annual or biennial plant of the Asteraceae family (Karkanis et al., 2011). Silymarin (SLM) is a complex mixture of flavonolignans, including, silybin (SB), isosilybin (ISB), silychristin (SCN), silydianin (SDN) and taxifolin (TAX), which is isolated from the milk thistle plant.

Silibinin is the main active component of silymarin (60-70%) (Kroll et al., 2007). Silymarin has been most widely utilized to treat liver, spleen and gall bladder disorders. Silymarin also has anti-cancer, chemopreventive, cardioprotective, neuroactive and neuroprotective activities (Fraschini et al., 2002; Murphy et al., 2000; Lorenz et al., 1984; Bahmani et al., 2015).

Plant cell culture technologies including Hairy roots, callus and cell suspension culture could be an alternative for the production of flavonolignans. Production of silymarin in cell cultures is low in comparison to the whole fruit (0.05–0.4% dry weight vs. 1–3% in fruits) (Cacho et al., 1999; Sánchez-Sampedro et al., 2005a; Sánchez-Sampedro et al., 2005b), in this regard, several approaches have been made to stimulate the productivity of flavonolignans in plant cell cultures. Elicitation is one of the most effective techniques for the large-scale production of secondary metabolites in *in vitro* cultures and for a better understanding of their biosynthesis (El-Garhy et al., 2016; Rahnama et al., 2008). Elicitors enhance the yield of secondary metabolites in cell cultures by regulating the rates of biosynthesis and accumulation (AbouZid, 2012; Barz et al., 1990; Hasanloo et al., 2014; Rahnama et al., 2008).

Jasmonic acid (JA) and its methyl ester, methyl jasmonate (MeJA), have been reported to play an important role in signal transduction processes that regulate defense responses in plants, and enhance the production of secondary metabolites in cell cultures (Wang et al., 2015), i.e. rosmarinic acid in *Coleus blumei* (Szabo et al., 1999), or hypericin in *Hypericum perforatum* (Walker et al., 2002). Methyl jasmonate (MeJA), alone or in combination with yeast extract (YE), strongly promote the accumulation of silymarin (Elwekeel et al., 2012a; Elwekeel et al., 2012b; Sánchez-Sampedro et al., 2008). Treatment of cell suspension culture of *S. marianum* with YE elicitor improved production and release of silymarin into the culture medium to a level of about 3-fold higher than that of the control (Sánchez-Sampedro et al., 2005a).

Most proteomic studies regarding secondary metabolites production have been performed with elicited cell cultures. For instance, polyphenolic biosynthesis, stilbenoid in grapevine (Martinez-Esteso et al., 2011), flavonolignan in *S. marianum* (Corchete and Bru, 2013) have been analyzed at proteome level under the induction of elicitors, such as chitosan, cyclodextrins, methyl jasmonate or yeast extract. In the study by Corchete and Bru (2013), proteome alterations were analyzed in *S. marianum* cell cultures elicited with methyl jasmonate and methyl B cyclodextrin. They identified 19 differentially expressed proteins which belong to a few categories, including metabolism, stress and defense responses and transport processes. Gharechahi et al. (2013) studied proteins from *S. marianum* hairy roots exposed to MeJA and identified expressed proteins involved in various mechanisms like energy production, translocation and secondary metabolism.

In the present study, we performed a proteomic analysis to assay the events occurring in *S. marianum* cell cultures elicited with MeJA and YE. Analysis of protein extracts by the high resolution 2-DE technique coupled with MALDI-TOF/TOF identified several proteins up or down regulated in response to elicitor treatments. Our aim was to investigate the changes of protein pattern and identify proteins in cell suspension cultures of *S. marianum* elicited with MeJA and YE and discussed their putative role in the flavonolignan accumulation.

Materials and Methods

Plant material and cell cultures

This research had been conducted in the Medical Biology Research Center, Kermanshah University of Medical Sciences, Kermanshah, Iran. The seeds of milk thistle (Budakalasz cultivar) from Pakan bazr company, were immersed for 24 h in distilled water, sterilized by ethanol 70% (w/v) for 2-3 min then sterilized by dipping in sodium hypochlorite 2.5% (w/v), Tween 20, 0.1% (v/v), and rinsed exhaustively with sterile distilled water. The seeds were cultured in Murashige and Skoog (MS) medium without growth regulator and incubated in dark condition at 26 ± 1 °C. After germination of seeds, plants were transferred to light. Cell cultures of *S. marianum* were developed from cotyledon and hypocotyl explants from 3-month old callus in MS liquid medium, supplemented with 30 g/L sucrose, 2 mg/L 2,4-dichlorophenoxyacetic acid and 2 mg/L kinitin at pH 5.8 (Pourjabar et al., 2012). Cultures were incubated in the dark at 25 °C and shaken at 90 rpm in darkness. Suspensions were subcultured every 2 weeks in the same medium and were maintained in 250 ml Erlenmeyer flasks with 50 ml of medium.

Culture treatments and elicitation

Suspensions were treated with 2 elicitors methyl jasmonate and YE: Methyl jasmonate (100 µM, final concentration) prepared as a filter-sterilized stock solution in ethanol and yeast extract (0.1% w/v) was dissolved in distilled water and then autoclaved (Sánchez-Sampedro et al., 2005a; Sánchez-Sampedro et al., 2005b). The control was the cell culture in same medium without adding any elicitor. Treatments were done 3 days after transfer, when cells had already started division. All culture experiments were performed in triplicate.

Flavonolignan analysis

One grams of cells were ground in liquid nitrogen and homogenized with 15 ml of 80% methanol. The homogenate was filtered and dried in vacuo below at 60 °C. The dry residue was resuspended in 3 ml distilled water, extracted twice with 6 ml pure ethyl acetate, the extracts were dried in vacuo at 60 °C and redissolved in 1 ml of methanol and kept at 4 °C in darkness (Hasanloo et al., 2008; Pourjabar et al., 2012). The content of flavonoids was determined by HPLC system according to the method of (Hasanloo et al., 2008) on a Knauer liquid chromatography equipped with a Knauer injector with a 20 µl loop, a Nucleosil C18 5 µ (250 × 4.6 mm) column, Knauer K2600A UV detector and Chromgate software for peak integration. The elution time and flow rate were 30 min and 1 ml min⁻¹, respectively and peaks were detected at 288 nm.

Protein extraction

After 48 h elicitation with MeJA (100 µM) and YE (0.1% w/v), control and treated cell suspension cultures were harvested separately. Proteins were extracted according to the method of (Yang et al., 2006) with some modifications. Five grams of cells were ground in liquid nitrogen. To remove DNA, 10 µl DNaseI (2 mg/ml) and 10 µl of 100X Reaction Buffer per ml (100X Reaction Buffer: 100 mM Tris-HCl (pH 7.5), 500 mM MgCl₂, 13 mM CaCl₂) was added and the mixture was incubated at 37 °C for 30 min. Then 2 ml pre-cooled homogenization buffer, 125 mM Tris-HCl (pH 7.5), 250 mM sucrose, 10 mM EDTA, 1 mM phenylmethylsulfonyl fluoride (PMSF) and 1 mM

dithiothreitol (DTT) and 1% Triton X-100 were added and incubated for 1 h. Thereafter, the homogenate was centrifuged at 13500 g for 20 min at 4 °C. The supernatant was mixed with 1/5 volume of cold 50% trichloroacetic acid (TCA) and kept in freezer -20 °C overnight. Then, the mixture was centrifuged at 13500 g for 20 min at 4 °C and the supernatant was discarded. The pellet was washed three times (each 20 min) with cooled acetone containing a 0.5% 2-Mercapto ethanol, centrifuged and completely dried. Pellet was resuspended in lysis buffer (8 M Urea, 2 M Thiourea, 4% CHAPS, 2% IPG buffer pH 4-7 (Bio-Rad), DTT 80 mM and protease inhibitor in 40 mM Tris-Base) and mix for 1 h in a rotator so as to enhance protein solubilization. Finally, the samples were centrifuged at 13500 × g at 4 °C for 10 min. Protein concentration was measured by Bradford assay using IgG as standard (Bradford, 1976).

Two-dimensional gel electrophoresis (2-DE)

Two-dimensional gel electrophoresis (2-DE) was performed according to the method of Mostafaie et al. (2011). Briefly, the IPG strips [pH 4-7, 18 cm length, General electric (GE)] were rehydrated at room temperature overnight in 360 µl rehydration solution (8 M urea, 4% CHAPS, 80 mM DTT, 2% IPG buffers (pH 4-7), 40 mM Tris-Base and 0.002% bromophenol blue) in a reswelling tray (General electric). Isoelectric Focusing (IEF) was performed at 20 °C on an IPGphor Unit (GE Healthcare/Amersham Biosciences) using the following settings: 2 h 500 V, 2 h 3000 V and finally 7 h 8000 V until an accumulated voltage of 54000 V was achieved. For second dimension, focused strips were equilibrated twice, 15 min in 5 ml equilibration solution (50 mM Tris-HCl buffer, pH 8.8, 6 M urea, 30% glycerol, 2% SDS, 1% DTT and 0.002% bromophenol blue) and then 15 min in the same solution containing 2.5% iodoacetamide instead of DTT. The second dimension was performed in 15% separation and 5% stacking gels. Protein spots in 2-DE gels were visualized by Coomassie Brilliant Blue (CBB) R- 350 according to the manufacturer's instructions (Görg et al., 2007; Mostafaie et al., 2011). Three gels for each sample were run and finally a total of eighteen gels were analyzed.

Image analysis

The gels were scanned at a resolution of 300 dots per inch using GS-800 densitometer (Bio-Rad) and were analyzed using the Melanie 6 software. Spot detection, protein quantification and spot pairing were carried out based on Melanie 6 default setting and spot pairs were investigated visually. The molecular masses of proteins on gels were determined by co electrophoresis of standard protein markers and pI of the proteins were determined by migration of the protein spots on 18 cm L (pH 4-7) IPG strips (Mostafaie et al., 2011). One 2-dimensional gel per sample was run for three biologically independent replicates, then percent volume (%vol) of each spot was extracted and analyzed by one way ANOVA test ($p < 0.05$). Only those spots that were present on all three replicate gels and had 1.5-fold changes were selected. Some differentially-expressed protein spots were selected as candidate proteins for MALDI-TOF-TOF analysis.

Protein identification and database search

Differentially-expressed spots were manually excised from preparative Coomassie blue-stained gels. Analysis was carried out by the Proteomics Laboratory; University of York, U.K., using MALDI-TOF-TOF mass spectrometry. Tryptic digestion was

performed after reduction with DTE and S-carbamidomethylation with iodoacetamide. Gel pieces were washed two times with 50% (v:v) aqueous acetonitrile containing 25 mM ammonium bicarbonate, then once with acetonitrile and dried in a vacuum concentrator for 20 min. Sequencing-grade, modified porcine trypsin (Promega) was dissolved in the 50 mM acetic acid supplied by the manufacturer, then diluted 5 times by adding 25 mM ammonium bicarbonate to give a final trypsin concentration of 0.02 µg/µl. Gel pieces were rehydrated by adding 10 µl of trypsin solution, and after 5 min, adequate 25 mM ammonium bicarbonate solution was added to cover the gel pieces.

Digests were incubated overnight at 37 °C. A 1 µl aliquot of each peptide mixture was applied directly to the ground steel MALDI target plate, immediately followed by an equal volume of a freshly-prepared 5 mg/ml solution of 4-hydroxy- α -cyano-cinnamic acid (Sigma) in 50% aqueous (v:v) acetonitrile containing 0.1%, trifluoroacetic acid (v:v). Positive-ion MALDI mass spectra were obtained using a Bruker ultraflex III in reflectron mode, equipped with a Nd:YAG smart beam laser. MS spectra were acquired over a mass range of m/z 800-5000. Final mass spectra were externally calibrated against an adjacent spot containing 6 peptides (des-Arg1-Bradykinin, 904.681; Angiotensin I, 1296.685; Glu1-Fibrinopeptide B, 1750.677; ACTH (1-17 clip), 2093.086; ACTH (18-39 clip), 2465.198; ACTH (7-38 clip), 3657.929.). Monoisotopic masses were obtained using a SNAP averagine algorithm (C 4.9384, N 1.3577, O 1.4773, S 0.0417, H 7.7583) and a S/N threshold of 2.

For each spot, the ten strongest peaks of interest, with a S/N greater than 30, were selected for MS/MS fragmentation. Fragmentation was performed in LIFT mode without the introduction of a collision gas. The default calibration was used for MS/MS spectra, which were baseline-subtracted and smoothed (Savitsky-Golay, width 0.15 m/z, cycles 4); monoisotopic peak detection used a SNAP averagine algorithm (C 4.9384, N 1.3577, O 1.4773, S 0.0417, H 7.7583) with a minimum S/N of 6. Bruker flexAnalysis software (version 3.3) was used to perform the spectral processing and peak list generation for both the MS and MS/MS spectra.

Tandem mass spectral data were submitted to database searching using a locally-running copy of the Mascot program (Matrix Science Ltd., version 2.6.1), through the Bruker BioTools interface (version 3.2). Search criteria included: Enzyme, Trypsin; Fixed modifications, Carbamidomethyl (C); Variable modifications, Oxidation (M); Peptide tolerance, 100 ppm; MS/MS tolerance, 0.5 Da; Instrument, MALDI-TOF-TOF (The version and size of the database can be obtained from the Mascot result page) (Hashemitabar et al., 2014).

Statistical analyses

Statistical analysis was carried out with SPSS (Version 16) software using one-way ANOVA test. All analytical values represent the means of three biological replications. Duncan's post hoc test was used for mean comparison ($p < 0.05$).

Results

Effect of elicitor on biosynthesis of SLM

To assay the effect of MeJA elicitation on SLM production, cell suspension cultures of *S. marianum* in the active growth phase were challenged with 100 µM MeJA and YE (0.1% w/v) separately. Result of this experiment showed that SLM content of the MeJA

treated and YE treated cell cultures increased significantly after 48 h. Comparison between means showed that, there was no significant difference between the cell culture derived from cotyledon and hypocotyl in terms of silymarin content ($p < 0.05$). MeJA and YE treatment after 48 h increased the amount of silymarin production to 1.23 and 1.11 folds respectively in comparison to the control (*Fig. 1*). The highest amount of silymarin was obtained in cell suspension cultures treated with MeJA.

Proteome analysis

In order to investigate the changes in protein pattern in cell suspensions treated with elicitors compared to the control, we performed proteomics analysis of cell suspension cultures. We collected protein samples from control, MeJA treated and YE treated cell suspension cultures at 48 h after subculture, when they showed significant alteration in SLM content. A comparison between all the groups, control, MeJA and YE in both cell cultures derived from cotyledon and hypocotyl calli, leads to the detection of at least 249 protein spots (*Figs. 2 and 3*). One way ANOVA ($p < 0.05$) analysis showed that abundance of 40 protein spots were up or down regulated by at least 1.5 fold after MeJA and YE treatment. Out of the 40 candidate spots, 10 protein spots, which were seen on preparative CBB-stained gel, were selected and manually excised and analyzed by MALDI-TOF-TOF. *Table 1* shows the list of the identified proteins with their respective spot number, theoretical and experimental pI and molecular weight, percent of sequence coverage, protein name and accession number. The accession number was derived from NCBI protein database search and used to search the corresponding protein in uniprot database.

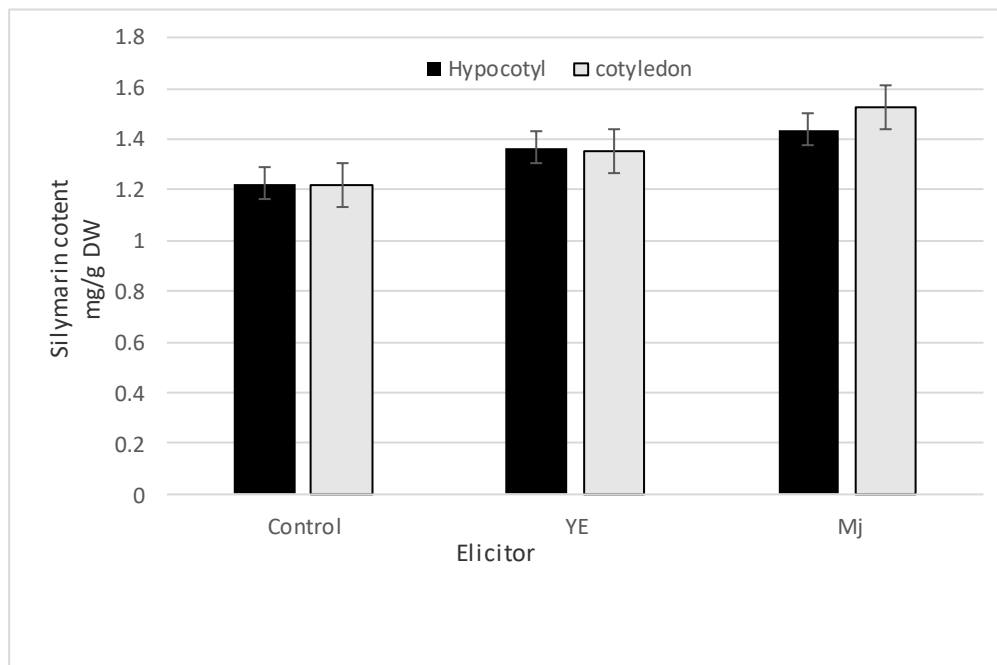


Figure 1. SLM contents of *S. marianum* cell suspension cultures after MeJA and YE treatment at 48 hours after transfer of cell cultures. The values represent the average of three replicate experiments \pm SD. ($*p < 0.05$)

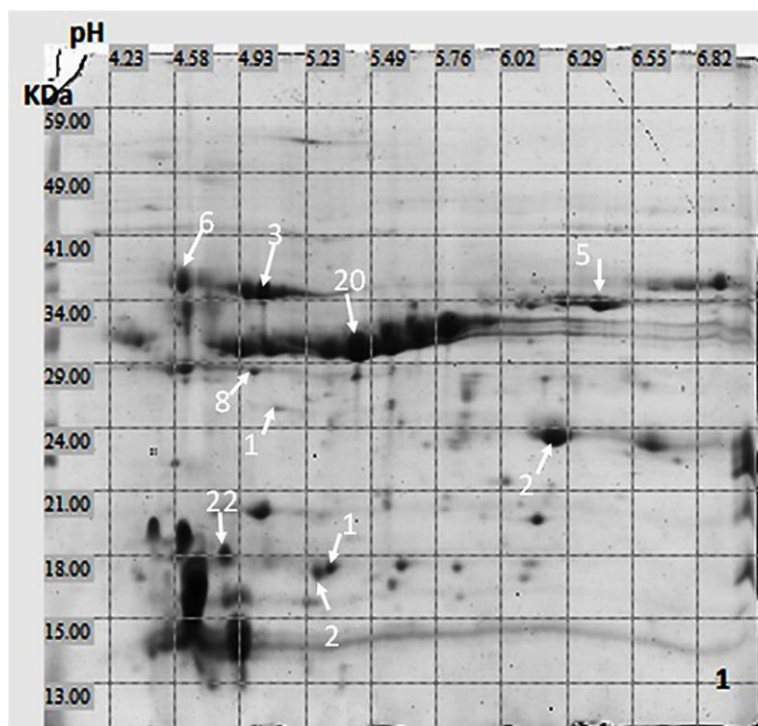


Figure 2. Two-dimensional gel electrophoresis maps of cell suspension cultures. Total protein extract was separated in 18 cm IPG strip (pH 4-7) for the first dimension and 15% SDS-PAGE for the second dimension. The position of the identified proteins is shown in gel

Table 1. Proteins differentially expressed in elicited cell cultures of *Silybum marianum*

Spot No. ^a	Accession No. ^b	Protein name	Mw ^c (calc/theo) (Da)	Pi ^d (calc/theo)	Species	Coverage (%)
1	Q8LNX9	Pathogenesis-related protein	17/17	5.1/5.28	<i>Zinnia violacea</i> (Garden zinnia)	47
2	CAC43324	Pathogenesis-related protein	17/19	5.08/5.33	<i>Zinnia elegans</i>	30
3	AAM97498	O-methyltransferase	35/38	5.58/5.07	<i>Catharanthus roseus</i>	38
6	P48496	Triosephosphate isomerase, chloroplastic	36/34	6.45/4.65	<i>Spinacia oleracea</i> (Spinach)	60
8	AAN07899	20S Proteasome subunit alpha type	28/29	5.07/5.01	<i>Nicotiana benthamiana</i>	35
12	Q40520	Ras-related protein Rab11C	24/18	5.4/5.12	<i>Nicotiana tabacum</i> (Common tobacco)	51
20	O04999	Glutamine synthetase	39/30	5/5.7	<i>Medicago truncatu</i>	40
29	KVII2372.1	11-S seed storage protein	45/30	7.01/6.47	<i>Catharanthus roseus</i>	6
53	CAJ84723	Peroxidase	35/39	7.63/6.68	<i>Catharanthus roseus</i>	54

a Number corresponds to spot ID on gels

b accession number in www.uniprot

c Theoretical and calculated molecular weight

d Theoretical and calculated pI

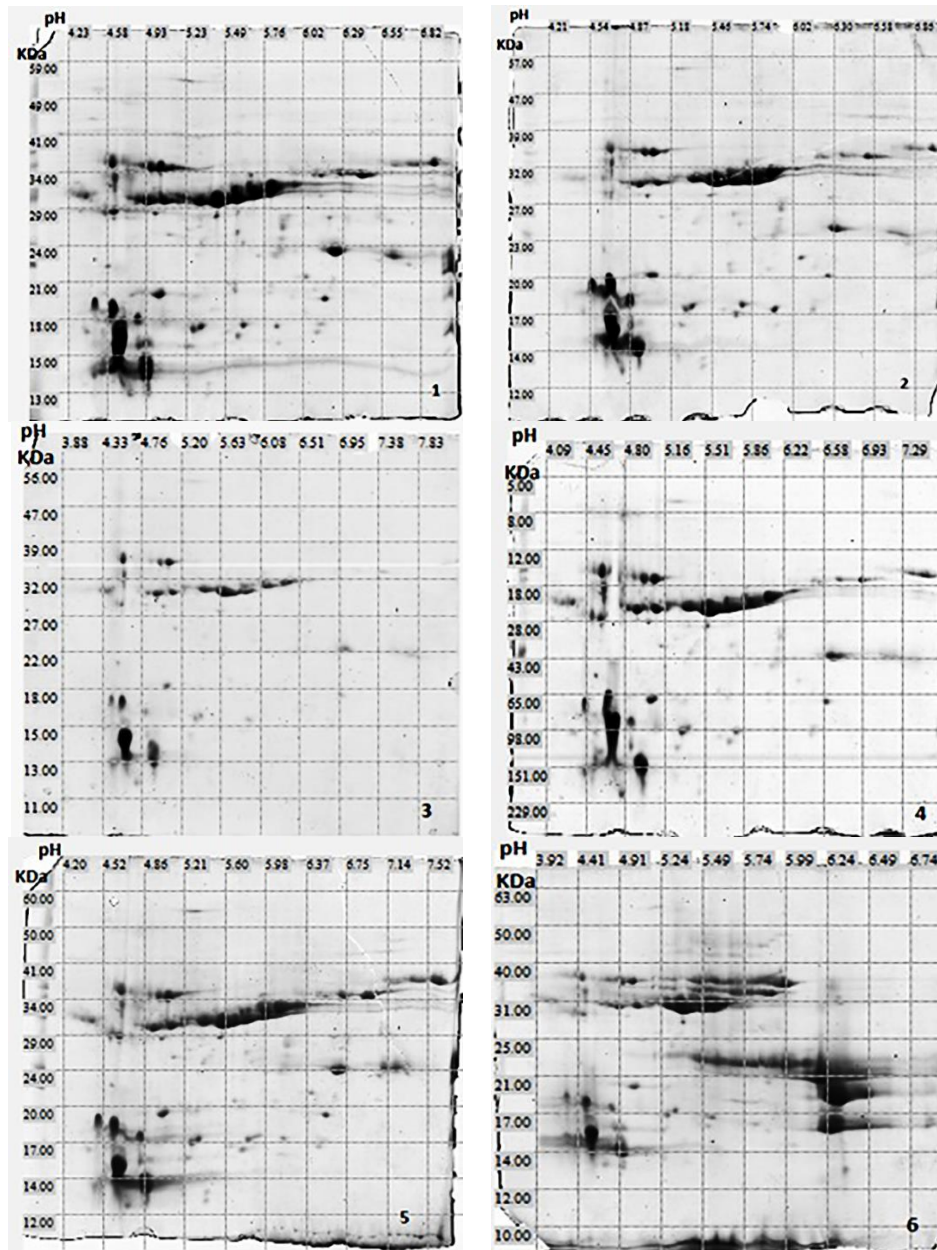


Figure 3. Two-dimensional gel electrophoresis maps of cell suspension cultures 48 h after MeJA and Ye application and controls. 1- Cell suspension cultures Hypocotyl derived (control). 2- Cell suspension cultures Cotyledon derived (control). 3- Hypocotyl cell suspension cultures treated with MeJA. 4- Cotyledon cell suspension culture treated with MeJA. 5- Hypocotyl cell suspension cultures treated with YE. 6- Cotyledon cell suspension culture treated with YE

These 10 identified spots were up or down regulated after elicitation with MeJA and YE compared with control and these proteins differentially accumulated in cell suspensions derived from cotyledons and hypocotyl explants (Fig. 4). Fig. 4 shows the mean expression levels (mean percent volumes) of the differentially expressed spots on a 2-DE gel of proteins extracted from cell suspension cultures 48 h after MeJA and YE application. The expression levels of the identified spots which showed significant changes are presented in Fig. 4. Expression of proteins was even different in cell

suspensions derived from cotyledons and hypocotyl explants. The identified proteins belong to different functional categories (*Table 1*). The proteins were classified based on carbohydrate metabolism (spots 6 and 22), Nitrogen metabolism (spot 20), storage protein (spot 29), transport process (spot 12), protein modification and chaperones (spot 8), pathogenesis related (spots 1 and 2) and secondary metabolism (spots 3 and 53).

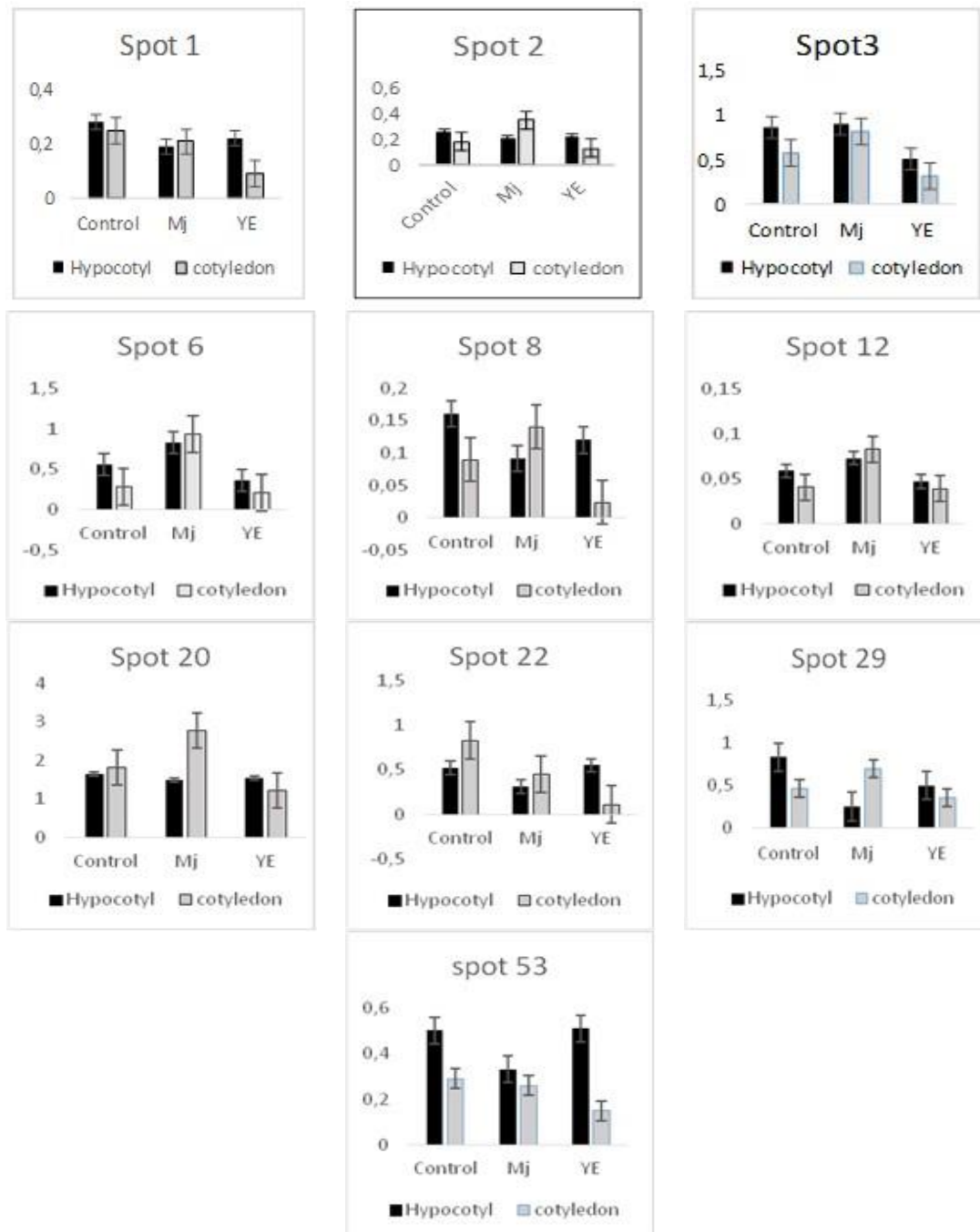


Figure 4. The mean expression levels (mean percent volumes) of the differentially expressed proteins are shown ($p < 0.05$). The values represent the average of three replicate experiments \pm SD. Y axes is the mean expression levels (mean percent volumes) of spots

Two identified proteins belong to carbohydrate metabolism (spots 6 and 22). Accumulation of these protein increased in the presence of MeJA. Alcohol dehydrogenase 2 (spot 22) and Triosephosphate isomerase, chloroplastic (spot 6) decreased in 48 h after treatment with YE (Fig. 4). Glutamine synthetase (GS, spot 20) was found to decrease. Cytosolic glutamine synthetase is encoded by a small family of genes that are well conserved across plant species. Members of the cytosolic glutamine synthetase gene family are regulated in response to plant nitrogen status, as well as to environmental cues, such as nitrogen availability and biotic/abiotic stresses.

Spot 12 (Ras-related protein Rab11C like protein of the Rab family), was upregulated by MeJA and YE elicitors (spot 12, Ras-related protein, up-regulated in all treatments). Rab proteins form the largest section of the Ras superfamily of small GTPases. Spots 1 and 2 were identified as Pathogenesis-related (PR) proteins. Those were up regulated after MeJA and YE treatment in cotyledon cell cultures. We observed the changes in the accumulation of this proteins, (Peroxidase (spot 53) and flavonoid O-methyltransferase (spot 3). It was possible to observe an increase in the accumulation of the protein peroxidase (spot 53) in the YE application in hypocotyl cell cultures and flavonoid O-methyltransferase (spot 3) in hypocotyl cell cultures after MeJA treatment. These two spots (3 and 53) were differentially accumulated in hypocotyl and cotyledon cell cultures after MeJA and YE treatments (Fig. 4).

Discussion

In this study, we investigated the effect of MeJA and YE elicitors on the accumulation of silymarin and protein profile in cell suspension cultures of milk thistle and we observed the changes in the protein levels in response to elicitation. We observed that, exposure of cell suspension cultures to MeJA and YE resulted in SLM accumulation after 48 h incubation. The results of our experiments showed that the use of MeJA and YE increased SLM accumulation in cell suspension cultures, but there was no significant difference between cell cultures derived from hypocotyl and cotyledon explants. This increase is related to the role of the elicitors in stimulating the biosynthesis of flavonoids in the cell suspension cultures. In other research studies, MeJA has been shown to enhance the production of SLM in cell cultures of *S. marianum* (Sánchez-Sampedro et al., 2005a), rosmarinic acid in *Lithospermum erythrorhizon* cell suspension cultures (Ogata et al., 2004), Resveratrol production in *Vitis vinifera* (Tassoni et al., 2005), Flavonoids in *Hypericum perforatum* (Wang et al., 2015), Phenylpropanoid and Isoflavonoid in *Medicago truncatula* cell cultures (Fargat et al., 2008) and azadirachtin in hairy root cultures of *Azadirachta indica* A. (Satdive et al., 2007).

Some stresses, such as osmotic stress, wounding, drought, and exposure to elicitors, which include chitins, oligosaccharides, oligogalaturonides can induce JA signaling (Turner et al., 2002) and cause endogenous Jasmonic acid (JA) accumulation (Gharechahi et al., 2013). JA and its more active derivative, methyl jasmonate (MeJA) cause biosynthesis and accumulation of secondary metabolites by inducing defense responses (Gharechahi et al., 2013; Reymond and Farmer, 1998; Truman et al., 2007). Induction of secondary metabolite accumulation is an important stress response that depends on jasmonates as a regulatory signal (Blechert et al., 1995; Gundlach et al., 1992). Treatment of cell suspension cultures of *Rauvolfia canescens* and *Eschscholtzia californica* to a yeast cell wall elicitor leads to the rapid transient induction of

endogenous jasmonic acid and methyl jasmonate (Gundlach et al., 1992). Jasmonate signaling pathway was supposed to be involved in the yeast extract induced production of silymarin. This arises by increase in lipoxygenase activity and linoleic acid content (Khalili et al., 2009).

These 10 identified spots showed different expression levels of the identified spots (Fig. 2). Proteins were found to be up and down regulated upon MeJA and YE treatment, even the expression of proteins in cell cultures derived from hypocotyl and cotyledon explants was different. Changes in expression of identified proteins in cell suspension cultures derived from Hypocotyl and cotyledon explants may be due to the differentiation and differently expressed proteins in the various plant tissues (cotyledons and hypocotyl), and this requires more research.

Some of the identified proteins in this study are involved in the general metabolism of the plants, including these spots (6, 8, 22, 29 and 20). The induction of stress and proteins related to defense, seen in this study, is associated with the role of the elicitors in plant defense. Change in expression levels of PR proteins was also demonstrated in this study. Spots 1 and 2 were identified as a Pathogenesis-related (PR) protein. It was up regulated after MeJA and YE treatment in cotyledon cell cultures. PR proteins are expressed in plants in response to many biotic and abiotic stresses (Reymond and Farmer, 1998).

A Ras-related protein Rab11C like protein of the Rab family, was upregulated by the two elicitor treatments (spot 12, Ras-related protein, up-regulated in all treatments). Rab proteins form the largest section of the Ras superfamily of small GTPases. The Rab family proteins involved in vesicular transport processes and secretion of secondary metabolites in plants (Nielsen et al., 2008). This is a good result to follow in future research.

We observed changes in the accumulation of the proteins flavonoid O-methyltransferase (spot 3) and peroxidase1 (spot 53). These proteins are involved in secondary metabolism. Regarding *S. marianum* as the non-model plant, an important challenge preventing the detection of specific proteins involved in secondary metabolism is the lack of fully sequenced genomes in non-model plants. Highly conserved proteins can be identified by sequence homology to *Arabidopsis thaliana* and other plant species (Bhattacharyya et al., 2012). Alternatively, specific EST databases have been made to identify proteins (Desgagné-Penix et al., 2010).

In this study, the proteomic approach has identified some of the events that have occurred in cell suspensions cultures of *S. marianum*. This is the basis for future research on *S. marianum* non-sequenced medicinal plant at molecular level. Much of the information obtained in comprehensive proteomic analysis can be achieved by mRNA sequencing at a lower cost and better range coverage. mRNA sequencing along with the proteomics method can be used for further research on secondary metabolism (Martínez-Esteso et al., 2015; Zubarev, 2013).

Conclusion

The results of this study showed that MeJA and YE elicitors caused significant increase in SLM content and activated defense-related proteins, proteins related to the transport mechanism with Extra cellular accumulation and secondary metabolism. The mechanism underlining the fact that metabolic pathways regulate defense response and accumulation of metabolites are largely unknown; however, investigation on analysis of

proteins, and measurement of secondary metabolic will be essential for clear understanding of the pathway especially non-model species such as *S. marianum*. In summary, results shown in this study provide valuable basic information of the cell proteome of *S. marianum* that resulted due to enhanced accumulation of silymarin, and offers interesting possibilities for future research.

Acknowledgements. The authors would like to thank the Medical Biology Research Center (Kermanshah University of Medical Sciences, Kermanshah, Iran) for their support in this research.

REFERENCES

- [1] AbouZid, S. (2012): Silymarin, natural flavonolignans from milk thistle. – In: Phytochemicals-A Global Perspective of Their Role in Nutrition and Health. InTech.
- [2] Bahmani, M., Shirzad, H., Rafieian, S., Rafieian-Kopaei, M. (2015): *Silybum marianum*: beyond hepatoprotection. – Journal of evidence-based complementary & alternative medicine 20(4): 292-301.
- [3] Barz, W., Beimen, A., Drager, B., Jaques, U., Otto, C. H., Super, E., Upmeier, B. (1990): Turnover and storage of secondary products in cell cultures. Oxford University Press.
- [4] Bhattacharyya, D., Sinha, R., Ghanta, S., Chakraborty, A., Hazra, S., Chattopadhyay, S. (2012): Proteins differentially expressed in elicited cell suspension culture of *Podophyllum hexandrum* with enhanced podophyllotoxin content. – Proteome science 10(1): 34.
- [5] Blechert, S., Brodschelm, W., Hölder, S., Kammerer, L., Kutschan, T. M., Mueller, M. J., Zenk, M. H. (1995): The octadecanoic pathway: signal molecules for the regulation of secondary pathways. – Proceedings of the National Academy of Sciences 92(10): 4099-4105.
- [6] Bradford, M. M. (1976): A rapid and sensitive method for the quantitation of microgram quantities of protein utilizing the principle of protein-dye binding. – Analytical biochemistry 72(1-2): 248-254.
- [7] Cacho, M., Morán, M., Corchete, P., Fernández-Tárrago, J. (1999): Influence of medium composition on the accumulation of flavonolignans in cultured cells of (*Silybum marianum* L.) Gaertn. – Plant science 144(2): 63-68.
- [8] Corchete, P., Bru, R. (2013): Proteome alterations monitored by DIGE analysis in *Silybum marianum* cell cultures elicited with methyl jasmonate and methyl B cyclodextrin. – Journal of proteomics 85: 99-108.
- [9] Desgagné-Penix, I., Khan, M. F., Schriemer, D. C., Cram, D., Nowak, J., Facchini, P. J. (2010): Integration of deep transcriptome and proteome analyses reveals the components of alkaloid metabolism in opium poppy cell cultures. – BMC plant biology 10(1): 252.
- [10] El-Garhy, H. A., Khattab, S., Moustafa, M. M., Ali, R. A., Azeiz, A. Z. A., Elhalwagi, A., El Sherif, F. (2016): Silybin content and overexpression of chalcone synthase genes in (*Silybum marianum* L.) plants under abiotic elicitation. – Plant physiology and biochemistry 108: 191-202.
- [11] Elwekeel, A., AbouZid, S., Sokkar, N., Elfishway, A. (2012a): Studies on flavanolignans from cultured cells of *Silybum marianum*. – Acta physiologiae plantarum 34(4): 1445-1449.
- [12] Elwekeel, A., Elfishway, A., AbouZid, S. (2012b): Enhanced accumulation of flavonolignans in *Silybum marianum* cultured roots by methyl jasmonate. – Phytochemistry Letters 5(2): 393-396.
- [13] Farag, M. A., Huhman, D. V., Dixon, R. A., Sumner, L. W. (2008): Metabolomics reveals novel pathways and differential mechanistic and elicitor-specific responses in

- phenylpropanoid and isoflavonoid biosynthesis in *Medicago truncatula* cell cultures. – *Plant physiology* 146(2): 387-402.
- [14] Fraschini, F., Demartini, G., Esposti, D. (2002): Pharmacology of silymarin. – *Clinical drug investigation* 22(1): 51-65.
- [15] Gharechahi, J., Khalili, M., Hasanloo, T., Salekdeh, G. H. (2013): An integrated proteomic approach to decipher the effect of methyl jasmonate elicitation on the proteome of *Silybum marianum* L. hairy roots. – *Plant physiology and biochemistry* 70: 115-122.
- [16] Görg, A., Klaus, A., Lück, C., Weiland, F., Weiss, W. (2007): Two-dimensional electrophoresis with immobilized pH gradients for proteome analysis. – *A laboratory manual*.
- [17] Gundlach, H., Müller, M. J., Kutchan, T. M., Zenk, M. H. (1992): Jasmonic acid is a signal transducer in elicitor-induced plant cell cultures. – *Proceedings of the National Academy of Sciences* 89(6): 2389-2393.
- [18] Hasanloo, T., Khavari-Nejad, R. A., Majidi, E., Ardakani, M. S. (2008): Flavonolignan production in cell suspension culture of *Silybum marianum*. – *Pharmaceutical biology* 46(12): 876-882.
- [19] Hasanloo, T., Eskandari, S., Najafi, F. (2014): Chitosan (middle-viscous) as an effective elicitor for silymarin production in *Silybum marianum* hairy root cultures. – *Research Journal of Pharmacognosy* 1(1): 9-13.
- [20] Hashemitabar, M., Bahmanzadeh, M., Mostafaie, A., Orazizadeh, M., Farimani, M., Nikbakht, R. (2014): A proteomic analysis of human follicular fluid: comparison between younger and older women with normal FSH levels. – *International journal of molecular sciences* 15(10): 17518-17540.
- [21] Karkanis, A., Bilalis, D., Efthimiadou, A. (2011): Cultivation of milk thistle (*Silybum marianum* L. Gaertn.), a medicinal weed. – *Industrial Crops and Products* 34(1): 825-830.
- [22] Khalili, M., Hasanloo, T., Tabar, K. S. K., Rahnama, H. (2009): Influence of exogenous salicylic acid on flavonolignans and lipoxygenase activity in the hairy root cultures of *Silybum marianum*. – *Cell biology international* 33(9): 988-994.
- [23] Kroll, D. J., Shaw, H. S., Oberlies, N. H. (2007): Milk thistle nomenclature: why it matters in cancer research and pharmacokinetic studies. – *Integrative cancer therapies* 6(2): 110-119.
- [24] Lorenz, D., Lückner, P. W., Mennicke, W. H., Wetzelsberger, N. (1984): Pharmacokinetic studies with silymarin in human serum and bile. – *Methods and findings in experimental and clinical pharmacology* 6(10): 655-661.
- [25] Martínez-Esteso, M. J., Selles-Marchart, S., Vera-Urbina, J. C., Pedreno, M. A., Bru-Martínez, R. (2011): DIGE analysis of proteome changes accompanying large resveratrol production by grapevine (*Vitis vinifera* cv. Gamay) cell cultures in response to methyl- β -cyclodextrin and methyl jasmonate elicitors. – *Journal of proteomics* 74(8): 1421-1436.
- [26] Martínez-Esteso, M. J., Martínez-Márquez, A., Sellés-Marchart, S., Morante-Carriel, J. A., Bru-Martínez, R. (2015): The role of proteomics in progressing insights into plant secondary metabolism. – *Frontiers in plant science* 6: 504.
- [27] Mostafaie, A., Yari, K., Kiani, S. (2011): A comparative evaluation of rehydration and cuploading sample application for modified twodimensional gel electrophoresis of human serum proteins using immobilized pH gradient. – *African journal of biotechnology* 10(55): 11711-11715.
- [28] Murphy, J. M., Caban, M., Kemper, K. J. (2000): Milk thistle (*Silybum marianum*). – *Longwood Herbal Task Force*.
- [29] Nielsen, E., Cheung, A. Y., Ueda, T. (2008): The regulatory RAB and ARF GTPases for vesicular trafficking. – *Plant Physiology* 147(4): 1516-1526.
- [30] Ogata, A., Tsuruga, A., Matsuno, M., Mizukami, H. (2004): Elicitor-induced rosmarinic acid biosynthesis in *Lithospermum erythrorhizon* cell suspension cultures: Activities of

- rosmarinic acid synthase and the final two cytochrome P450-catalyzed hydroxylations. – *Plant biotechnology* 21(5): 393-396.
- [31] Pourjabar, A., Mohammadi, S. A., Ghahramanzadeh, R., Salimi, G. (2012): Effect of Genotype, Explant Type and Growth Regulators on The Accumulation of Flavonoides of *Silybum marianum* L. in In vitro Culture. – *World Academy of Science, Engineering and Technology, International Journal of Biological, Biomolecular, Agricultural, Food and Biotechnological Engineering* 6(7): 514-516.
- [32] Rahnama, H., Hasanloo, T., Shams, M. R., Sepehrifar, R. (2008): Silymarin production by hairy root culture of *Silybum marianum* L. Gaertn. – *Iranian Journal of Biotechnology* 6(2): 113-118.
- [33] Reymond, P., Farmer, E. E. (1998): Jasmonate and salicylate as global signals for defense gene expression. – *Current opinion in plant biology* 1(5): 404-411.
- [34] Sánchez-Sampedro, M. A., Fernández-Tárrago, J., Corchete, P. (2005a). Yeast extract and methyl jasmonate-induced silymarin production in cell cultures of (*Silybum marianum* L.) Gaertn. – *Journal of biotechnology* 119(1): 60-69.
- [35] Sánchez-Sampedro, M. A., Fernández-Tárrago, J., Corchete, P. (2005b): Enhanced silymarin accumulation is related to calcium deprivation in cell suspension cultures of (*Silybum marianum* L.) Gaertn. – *Journal of plant physiology* 162(10): 1177-1182.
- [36] Sánchez-Sampedro, M. A., Fernández-Tárrago, J., Corchete, P. (2008): Some common signal transduction events are not necessary for the elicitor-induced accumulation of silymarin in cell cultures of *Silybum marianum*. – *Journal of plant physiology* 165(14): 1466-1473.
- [37] Satdive, R. K., Fulzele, D. P., Eapen, S. (2007): Enhanced production of azadirachtin by hairy root cultures of *Azadirachta indica* A. Juss by elicitation and media optimization. – *Journal of biotechnology* 128(2): 281-289.
- [38] Szabo, E., Thelen, A., Petersen, M. (1999): Fungal elicitor preparations and methyl jasmonate enhance rosmarinic acid accumulation in suspension cultures of *Coleus blumei*. – *Plant Cell Reports* 18(6): 485-489.
- [39] Tassoni, A., Fornalè, S., Franceschetti, M., Musiani, F., Michael, A. J., Perry, B., Bagni, N. (2005): Jasmonates and Na-orthovanadate promote resveratrol production in *Vitis vinifera* cv. Barbera cell cultures. – *New Phytologist* 166(3): 895-905.
- [40] Truman, W., Bennett, M. H., Kubigsteltig, I., Turnbull, C., Grant, M. (2007): Arabidopsis systemic immunity uses conserved defense signaling pathways and is mediated by jasmonates. – *Proceedings of the national academy of sciences* 104(3): 1075-1080.
- [41] Turner, J. G., Ellis, C., Devoto, A. (2002): The jasmonate signal pathway. – *The Plant Cell* 14(suppl 1): S153-S164.
- [42] Walker, T. S., Bais, H. P., Vivanco, J. M. (2002): Jasmonic acid-induced hypericin production in cell suspension cultures of *Hypericum perforatum* L. (St. John's wort). – *Phytochemistry* 60(3): 289-293.
- [43] Wang, J., Qian, J., Yao, L., Lu, Y. (2015): Enhanced production of flavonoids by methyl jasmonate elicitation in cell suspension culture of *Hypericum perforatum*. – *Bioresources and Bioprocessing* 2(1): 5.
- [44] Yang, P., Shen, S., Kuang, T. (2006): Comparative Analysis of the Endosperm Proteins Separated by 2-D Electrophoresis for Two Cultivars of Hybrid Rice (*Oryza sativa* L.). – *Journal of Integrative Plant Biology* 48(9): 1028-1033.
- [45] Zubarev, R. A. (2013): The challenge of the proteome dynamic range and its implications for in-depth proteomics. – *Proteomics*. 13(5): 723-726.

COMPARATIVE STUDY OF BION AND SALICYLIC ACID APPLIED THROUGH FOLIAR AND SEEDLING ROOT DIPPING IN TOMATO AGAINST *ALTERNARIA SOLANI*

ASLAM, M.^{1*} – HABIB, A.¹ – SAHI, S. T.¹ – KHAN, R. R.²

¹Department of Plant Pathology, University of Agriculture, Faisalabad, Pakistan

²Department of Entomology, University of Agriculture, Faisalabad, Pakistan

*Corresponding author
e-mail: mustansar_aslam@live.com

(Received 31st Aug 2018; accepted 5th Nov 2018)

Abstract. *Alternaria solani* is a destructive pathogen to the tomato crop causing heavy losses. The present work was designed during 2015-16 to evaluate the efficacy of Bion and salicylic acid as early blight disease suppressors as well as their use as plant activators under greenhouse conditions. The current study was carried out at field area of Plant Pathology University of Agriculture Faisalabad. Foliar and seedling root dipping application of Bion and salicylic acid (125 ppm and 2 mM) not only reduced the disease severity but also enhanced the plant growth. Maximum disease severity was observed in infected control while minimum disease severity was observed in case of Bion with foliar application in both years. A remarkable increase was observed in Chlorophyll a, b, root fresh/dry weight, photosynthetic rate, shoot fresh/dry weight and growth attributes when *A. solani* inoculated tomato plants were treated with foliar sprays of Bion. A significant healing to cell membrane was observed to reduce the electrolyte leakage in case of Bion and SA application through foliar spray in inoculated plants. Total soluble carbohydrates and total soluble protein contents are increased when Bion was applied through foliar application as compared to seedling root dipping. Increasing trend was observed in 2nd year of study. It is concluded that foliar application of Bion could be more effective in managing the *Alternaria solani* as well as in enhancing the growth and yield of tomato.

Keywords: *Bion*, physiology, yield, photosynthetic rate, seedling root dipping

Introduction

Tomato (*Lycopersicon esculentum* L.) is a member of family Solanaceae and ranked as 2nd most important vegetable crop around the globe (FAO, 2013). Different pathogens like fungus, nematode, bacteria and virus cause different diseases in the tomato crop. Presently, more than 200 tomato diseases are known worldwide among them *Alternaria solani* causing early blight of tomato is the most destructive of field crops (Chaerani and Voorrips, 2006; Abada et al., 2008) that causes yield and quality reduction of the tomato crop. *A. solani* causes the infections on leaves, petiole fruits, twigs and stem that lead to the defoliation, premature fruit drop and drying of twigs which finally decrease the yield. High humidity and high temperature favor the disease and at fruiting stage fruits are more susceptible to the blight infections (Momel and Pemezny, 2006). Chemicals are used either as protection or as a curative agent for controlling early blight of tomato. The used chemicals found to be severely toxic and cause an augmented hazard for the atmosphere in the circumstance of improper usage or handling (Oostendorp et al., 2001). Systemic acquired resistance in plants has been studied in many different pathosystem for nearly a century (Oka et al., 2000). An unconventional to classic chemical plant protection technique is to induce systemic acquired resistance effects. People globally are conscious about environmental hazards

due to use of costly and toxic chemicals. The increasing public awareness about these problems has stimulated research on the use of biological control agents and development of commercial bio products. To save the nature and the environment, organic amendments and plant extracts are needed to be explored (Hafiz, 2009). SAR can be triggered by some chemicals, including salicylic acid (SA) and its synthetic analogues, such as acibenzolar- S-methyl (ASM), a derivative of the benzo 1,2,3 thiadiazole-7-carbothioic acid-S-methyl ester (BTH). Acibenzolar-S-methyl (ASM, Actigard® or Bion®, Syngenta Crop Protection, Inc., Greensboro, NC) is a plant activator inducing systemic acquired resistance (SAR) to confer protection against a broad spectrum of plant pathogens (Meller Harel et al., 2014; Takeshita et al., 2013). In itself, ASM has no antimicrobial effect, but has been reported to protect several plant species against broad spectrum of pathogens including viral, bacterial and fungal diseases (Tripathi and Pappu, 2015). In tomato and cucumber lower concentration of salicylic acid showed a considerable increase in yield attributes (Larque-Saavedra and Martin-Mex, 2007). According to Shakirova et al. (2003) salicylic acid has a positive effect on growth, physiology and yield because of its influence on other plant hormones. Bion significantly increased the yield in case of moderately resistant tomato cultivars (Pradhanang et al., 2005). Bin does not show any negative effect on yield when tomato plants grow under optimal conditions from transplanting to harvest (Romero et al., 2001). The present study was designed with the aim to evaluate the effect of Bion and salicylic acid against *Alternaria solani* in tomato. In addition their mode of application and their role as plant elicitor to improve physiology, biochemical and yield attributes of tomato plant were also checked.

Materials and methods

Role of Bion and salicylic acid treatments on disease severity (%) caused by Alternaria solani

This experiment was carried out by selecting a test cultivar (Prescot) due to its high potential for yield, taken from Ayub Agricultural Research Institute Faisalabad. Tomato plants of test cultivar were sown in the greenhouse of Plant Pathology university of Agriculture Faisalabad. Conditions maintained at 25 ± 2 °C during the day time and 20 ± 2 °C at night. The tomato seeds were sown in trays containing commercial peat and vermiculite (1:1) and seedlings were transplanted after 8 weeks into 30 cm diameter pots filled with the mixture of sandy loam soil mixed with compost (1:1). Watering was done twice a week with tap water up to the pot holding capacity. After 30 days of transplanting, *A. solani* suspension was applied (100 ml/plant) at the rate of (5×10^6 conidia/ml) on tomato plants using an atomizer. Bion and salicylic acid (SA) was dissolved in distilled water to give 125 ppm and 2 mM, respectively, and applied to whole plants at the rate of 50 ml for each plant two days prior to inoculation. For seedling root dipping, before transplanting roots of seedlings were dipped in Bion and SA solutions (above mentioned doses) for one hour and transferred to pots. After treatment application, plants were kept in a greenhouse as mentioned earlier. For controls, healthy and diseased control was maintained, which were inoculated or uninoculated but treated with water. This study was carried out under Complete Randomized Design (CRD) and repeated twice under greenhouse conditions in 2015 and 2016. Each pot planted with three seedlings. Three replicates were used, and each

replicate consisted of four pots. Four treatment groups were made (control, control+ *A. solani*, Bion+ *A. solani* and SA+*A. solani*). The disease severity was recorded according to the rating scale of 0 to 9 (Mayee and Datar, 1986).

Effect of Bion and salicylic acid treatments on physiology, biochemical and yield attributes of tomato plants

This part of experiment was planned to check the effect of Bion and salicylic acid (SA) on physiology, growth, biochemical and yield attributes of tomato plants. Tomato plants were sown in pots in greenhouse conditions. There were six treatment groups as follows: (1) plant without any treatment (healthy control) (2) plant inoculated with *A. solani* (20 ml/plant containing 5×10^6 conidia/ml) (3) plants treated with Bion (4) plants treated with SA (5) plants inoculated with *A. solani* and treated with Bion (6) plant inoculated with *A. solani* and treated with SA. After treatment plants were kept in the greenhouse. Plant height, number of flowers/ plant, photosynthetic rate (PR) and number of fruits/plant were calculated over 50 days of transplanting while the yield was measured at the end of the experiment. This experiment was conducted in three way factorial lay out under the CRD.

Biochemical and physiological attributes

The method used for the quantitative determination of chlorophyll was that of (Vernon and Selly, 1966). The optical density of the plant extract was measured using spectrophotometer (Jenway, 6100 UK microprocessor controlled visible range) of two wave lengths (649 and 665 nm). These are maximum absorption ranges of chlorophyll (a) and (b). The concentrations of chlorophyll (a), (b) and total chlorophyll in plant tissue were measured by using the equations mentioned by Vernon and Selly (1966; Eqs. 1 and 2).

$$\text{Chlorophyll a (mg L}^{-1}\text{)} = 12.7A_{663} - 2.69 A_{645} \quad (\text{Eq.1})$$

$$\text{Chlorophyll b (mg L}^{-1}\text{)} = 20.11A_{649} - 5.18 A_{665} \quad (\text{Eq.2})$$

By adding chlorophyll a and chlorophyll b total chlorophyll was calculated.

The electrolyte leakage percentage was calculated according to the protocol given by Shi et al. (2006). Photosynthetic rate of the top leaf of every plant was recorded with the help of IRGA (Infrared Gas Analyzer) (model, LCA-4; Analytical Development Company, Hoddesdon, England). During data recording, leaf chamber molar gas flow rate $248 \mu\text{mol s}^{-1}$, ambient CO_2 conc. (Cref) was $352 \mu\text{mol mol}^{-1}$, ambient pressure (P) 98.01 kPa, molar flow of air/leaf area $221.06 \text{ mol m}^{-2} \text{ s}^{-1}$, PAR was maximum up to $1050 \mu\text{mol m}^{-2} \text{ s}^{-1}$ and leaf chamber volume gas flow rate (v) 380 mL/min. Total carbohydrates (mg/g) in dry leaves were calorimetrically calculated by following the method given by (Dubois et al., 1956). Protein contents in dry leaves were measured by following the method described by Bradford (1976).

Growth and yield attributes

55 days after transplanting, plants from each treatment were harvested and data on plant growth variables, including plant height, root fresh weight, shoot fresh weight, root dry weight and shoot dry weight and number of flowers/plant and yield was

determined using standard protocols. Plant height was measured with the help of meter rod. Roots were separated from soil and rinsed with tap water to remove free soil then gently blotted to remove free moisture. To determine the dry weight plant material was dried at 70°C for 48 h in a dry oven. The number of flowers in lower, middle and upper clusters of five randomly selected tomato plants was counted and the mean values were computed and used for further analysis. The number of fruits in lower, middle and upper clusters of five randomly selected tomato plants was counted and the mean values were computed and used for further analysis. The yield/plant was taken at the end of the experiment.

Statistical analysis

The data analysis was done in three way factorial arrangement under CRD through computer software statstix 8.1 using Fisher's analysis of variance technique and means of treatment were compared by least significance difference (LSD) test at 5% probability level (Steel et al., 1997).

Results

Techniques to enhance the resistance against the disease

Bion and salicylic acid applied through foliar and seedling root dipping application methods significantly ($p \leq 0.05$) reduced the disease severity in tomato plants (Table 1).

Table 1. Influence of resistance inducers applied through various methods on disease severity (%)

Factors	Disease severity (%)
Method (M)	
Foliar application	30.69 B
Seedling root dipping	35.24 A
Year (Y)	
2015	34.62 A
2016	31.31 B
Treatments (T)	
Healthy control	32.96 B
Infected control	64.50 A
BION	10.96 D
Salicylic acid	23.44 C
LSD (M)	2.23
LSD (Y)	1.11
LSD (T)	1.58
LSD (M × T)	NS
LSD (M×Y)	NS
LSD (T×Y)	NS
LSD (M×T×Y)	NS

Any two means sharing same letters are not significant at $p \leq 0.05$. ** = Highly Significant at $p \leq 0.01$; * significant at $p \leq 0.05$; NS = non significant

Maximum decrease in disease severity was noticed in the case of Bion applied through foliar application as compared to infected and healthy control and salicylic acid (SA) treated plants. Increasing trend was observed in 2nd year of study (Table 1). Regarding interactive effect all the interactions showed non-significant behavior for the disease severity.

Growth attributes

All resistance inducers significantly ($p \leq 0.05$) affected the growth attributes of tomato during both years of study (Table 2). Statistically significant increase was observed in all growth attributes in inoculated plants as compared to un-inoculated plants. Maximum fresh and dry biomass of roots and shoots was observed in Bion treated inoculated plants with foliar application followed by seedling root dipping method during both years of study as compared to control. Regarding different treatments following increasing order was observed Bion + *A. solani* > BION > SA + *A. solani* > SA > Control + *A. solani* > Control in all the studied attributes. Positive response of all the growth attributes was observed during 2nd year of study. Regarding interactive effect of treatments \times method \times year all the factors showed non-significant results except root fresh weight (Fig. 1). However, M \times T showed significant differences ($p \leq 0.05$) for all growth attributes except shoot fresh weight. Regarding the M \times Y both root fresh weight and shoot dry weight showed significant variation. All the growth attributes showed non-significant variation for the interactive effect of T \times Y (Table 2).

Table 2. Influence of resistance inducers applied through various methods on growth attributes of tomato plant

Factors	Root fresh weight	Root dry weight	Shoot fresh weight	Shoot dry weight
	Plant ⁻¹ (g)			
Method (M)				
Foliar application	4.05 A	0.60 A	25.70 A	4.50 A
Seedling root dipping	3.70 B	0.43 B	22.96 B	4.16 B
Year (Y)				
2015	3.92 A	0.55 A	25.50 A	4.38 A
2016	3.82 B	0.49 B	23.15 B	4.28 B
Treatments (T)				
Control	3.08 F	0.30 F	19.26 F	2.97 F
Control + <i>A. solani</i>	3.26 E	0.40 E	21.43 E	4.00 E
BION	4.56 B	0.64 B	27.42 B	4.90 B
Salicylic acid	3.39 D	0.51 D	23.21 D	4.38 D
BION + <i>A. solani</i>	5.03 A	0.68 A	29.40 A	5.11 A
Salicylic acid + <i>A. solani</i>	3.92 C	0.58 C	25.25 C	4.62 C
LSD (M)	0.21	0.12	2.15	0.02
LSD (Y)	0.07	0.03	1.23	0.02
LSD (T)	0.12	0.02	1.50	0.03
LSD M \times T	**	**	NS	**
LSD M\timesY	**	NS	NS	**
LSD T\timesY	NS	NS	NS	NS
LSD M\timesT\timesY	**	NS	NS	NS

Any two means sharing same letters are not significant at $p \leq 0.05$. ** = highly significant at $p \leq 0.01$; * significant at $p \leq 0.05$; NS = non significant

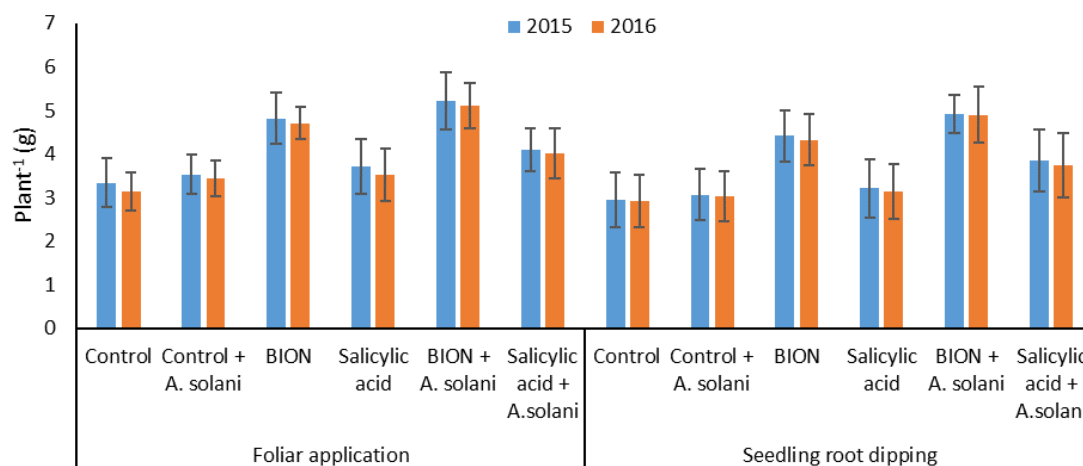


Figure 1. Interactive effect of year \times chemicals \times application methods on root fresh weight as influenced by the different resistance inducers

Physiological attributes

Bion and salicylic acid significantly ($p \leq 0.05$) affected the physiological attributes of tomato during both years of study (Table 3).

Table 3. Influence of resistance inducers applied through various methods on physiological attributes of tomato

Factors	Chlorophyll a (mg L ⁻¹)	Chlorophyll b (mg L ⁻¹)	Total chlorophyll	Electrolyte leakage (%)	Photosynthetic rate ($\mu\text{mol m}^{-2} \text{s}^{-1}$)
Method (M)					
Foliar application	0.57 A	0.18 A	0.75 A	6.58 B	4.62 A
Seedling root dipping	0.51 B	0.15 B	0.66 B	6.69 A	4.47 B
Year (Y)					
2015	0.56 A	0.17	0.73 A	6.84 A	4.69 A
2016	0.52 B	0.16	0.68 B	6.43 B	4.40 B
Treatments (T)					
Control	0.34 E	0.10 F	0.45 F	7.36 B	3.48 F
Control + <i>A. solani</i>	0.46 D	0.13 E	0.59 E	7.88 A	3.65 E
BION	0.66 B	0.20 B	0.87 B	6.83 C	5.45 B
Salicylic acid	0.48 D	0.15 D	0.63 D	6.65 D	4.07 D
BION + <i>A. solani</i>	0.72 A	0.22 A	0.95 A	5.95 E	6.04 A
Salicylic acid + <i>A. solani</i>	0.56 C	0.17 C	0.73 C	5.16 F	4.57 C
LSD (M)	0.03	0.02	0.06	0.05	0.11
LSD (Y)	0.02	NS	0.04	0.23	0.21
LSD (T)	0.04	0.02	0.05	0.11	0.13
LSD M \times T	NS	NS	NS	**	**
LSD M \times Y	NS	NS	NS	**	**
LSD T \times Y	NS	NS	NS	NS	**
LSD M \times T \times Y	NS	NS	NS	NS	*

Any two means within a column sharing same letters are not significant at $p \leq 0.05$. * = significant at $p \leq 0.05$; ** highly significant at $p \leq 0.05$; NS = non significant

Statistically significant increase was observed in photosynthetic rate ($\mu\text{mol m}^{-2} \text{s}^{-1}$) in inoculated plants as compared to un-inoculated plants. The maximum photosynthetic rate (PR) was observed in Bion treated-inoculated plants during both years of study. While minimum PR was noticed in infected control in both years. Regarding different treatments following increasing order was observed Bion + *A. solani* > BION > SA + *A. solani* > SA > Control + *A. solani* > Control in all the studied attributes. Positive response of all the growth attributes was observed during 2nd year of study. Maximum chlorophyll *a*, *b* and total chlorophyll were observed in Bion treated inoculated plant with foliar application followed by seedling root dipping method during both years of study (Table 3). Decreasing trend for the physiological attributes was observed during 2nd year of study except chlorophyll *b* which showed non-significant behavior in case of years (Table 3). In case of electrolyte leakage (EL) opposite behavior during both years of study. Maximum EL was noticed in infected control in both years. Regarding different treatments following decreasing order was observed for different treatments like Control < Bion + *A. solani* < BION < SA + *A. solani* < SA < Control + *A. solani*. Increasing trend in EL was observed during 2nd year of study (Table 3).

Regarding interactive effect of treatments \times method \times year all the factors showed non-significant results except photosynthetic rate (Fig. 2). However, M \times T showed significant differences ($p \leq 0.05$) for EL and PR. Regarding the M \times Y both PR and EL showed significant variation. All the physiological attributes showed non-significant variation for the interactive effect of T \times Y except PR (Table 2).

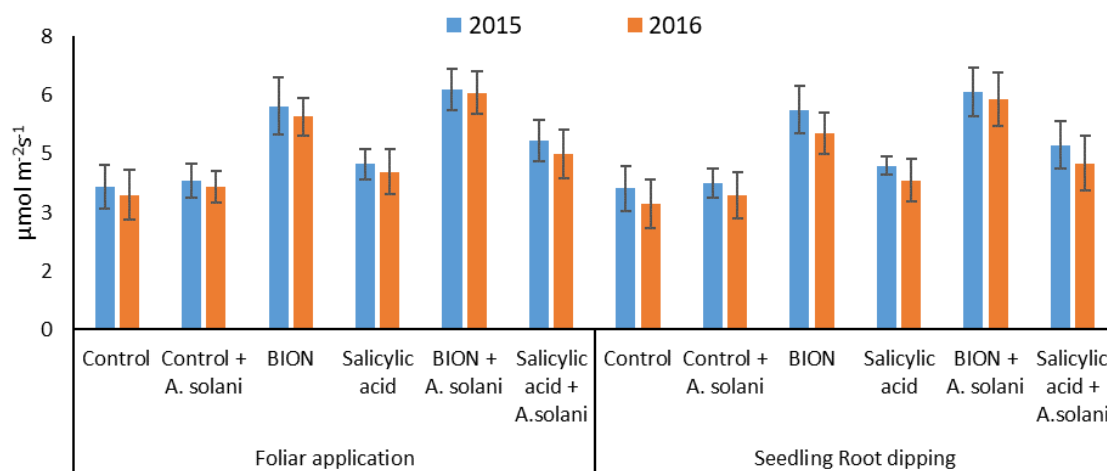


Figure 2. Interactive effect of application methods \times chemicals \times years on photosynthetic rate as influenced by the different resistance inducers

Biochemical attributes

Significant increase was observed in total soluble carbohydrate (TSC), total soluble protein (TSP) of tomato after the application of Bion and SA during both years of study (Table 4). Maximum TSC and TSP were observed in Bion treated inoculated plant with foliar application followed by seedling root dipping method during both years of study (Table 4). Regarding interactive effect of treatments \times method \times year and M \times T all the factors showed non-significant results (Table 4). Regarding the M \times Y only TSP showed

significant variation. While interactive effect of T×Y both TSC and TSP showed significant variation (Figs. 3 and 4).

Table 4. Influence of resistance inducers applied through various methods on TSC, TSP of tomato

Factors	Total soluble carbohydrate (mg/g of dry leaves)	Total soluble protein (mg/g of dry leaves)
Method (M)		
Foliar application	212.50 A	37.820 A
Seedling root dipping	206.31 B	33.806 B
Year (Y)		
2015	211.26 A	36.599 A
2016	207.54 B	35.027 B
Treatments (T)		
Control	186.60 F	29.124 F
Control + <i>A. solani</i>	192.51 E	31.863 E
BION	233.90 B	39.907 B
Salicylic acid	197.87 D	34.877 D
BION + <i>A. solani</i>	241.81 A	42.287 A
Salicylic acid + <i>A. solani</i>	203.72 C	36.820 C
LSD (M)	2.33	2.98
LSD (Y)	2.22	1.11
LSD (T)	4.11	1.93
LSD (M × T)	NS	NS
LSD (M×Y)	NS	**
LSD (T×Y)	**	**
LSD (M×T×Y)	NS	NS

Any two means within a column sharing same letters are not significant at $p \leq 0.05$. * = significant at $p \leq 0.05$; ** highly significant at $p \leq 0.05$; NS = non significant

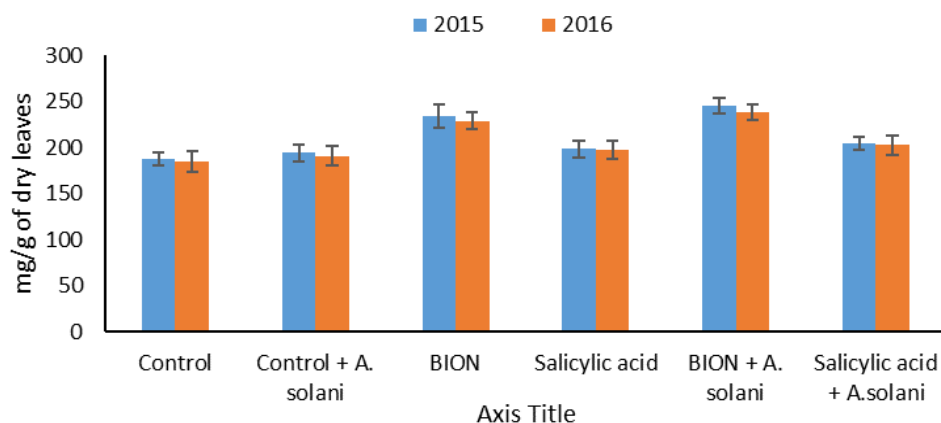


Figure 3. Interactive effect of chemicals × years on total soluble carbohydrates as influenced by the different resistance inducers

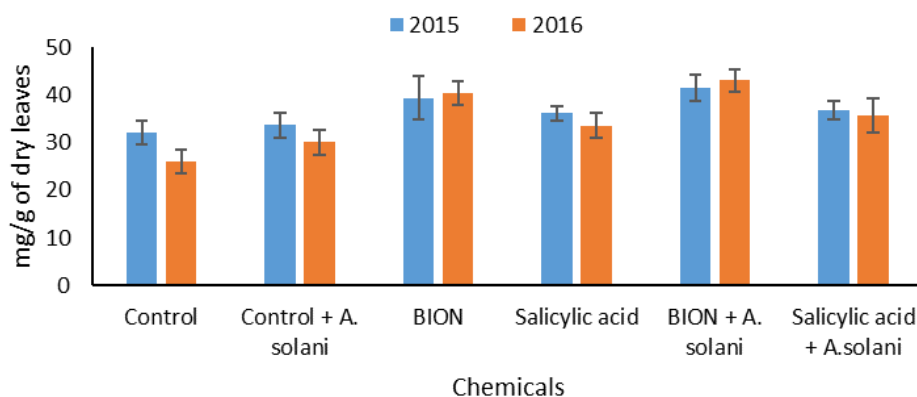


Figure 4. Interactive effect of chemicals \times years on total soluble proteins as influenced by the different resistance inducers

Yield attributes

Bion and salicylic acid significantly ($p \leq 0.05$) influenced the yield attributes (plant height, number of flowers/plant, number of fruits and yield/plant) of tomato during both years of study except plant height and number of fruits, they showed non-significant response regarding years (Table 5). Significant increase was observed in yield attributes in Bion treated inoculated plants through as compared to un-inoculated plants. Maximum plant height, number of flowers/plant, fruit weight and yield/plant were witnessed in Bion treated inoculated plant with foliar application followed by seedling root dipping method as compared to SA and control. For the interactive effect of chemical \times method not a single interaction was found significant regarding yield attributes. Regarding interactive effect of treatments \times method \times year all the factors showed non-significant results (Table 5). However, M \times T also showed non-significant differences ($p \leq 0.05$) for the factors. Regarding the M \times Y all yield attributes showed significant variation except number of flowers per plant. Yield per plant showed significant variation for the interactive effect of T \times Y (Fig. 5).

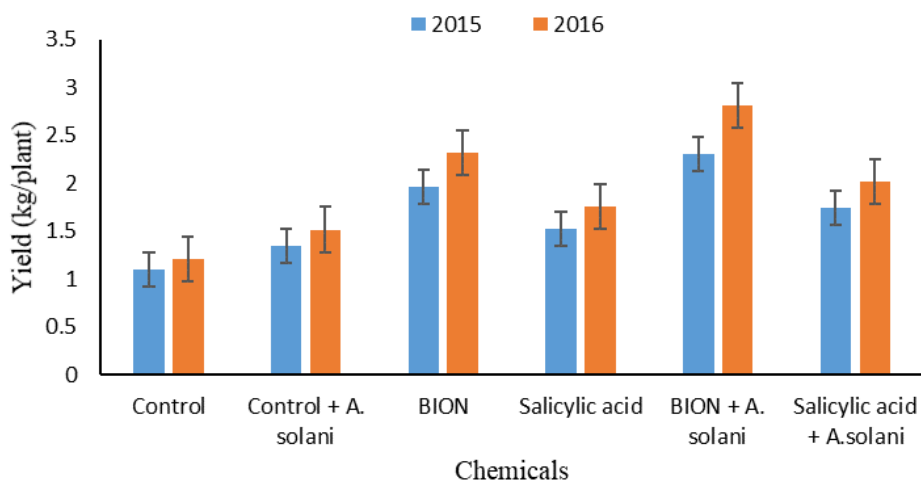


Figure 5. Interactive effect of chemicals \times years on yield/plant as influenced by the different resistance inducers

Table 5. Influence of resistance inducers applied through various methods on yield attributes of tomato

Factors	Plant height (cm)	Number of fruits/plant	Number of flowers/plant	Yield/plant (kg)
Method (M)				
Foliar application	94.30 A	78.44 A	10.44 A	1.90 A
Seedling root dipping	89.16 B	73.63 B	8.836 B	1.68 B
Year (Y)				
2015	92.22	76.89 A	9.53	1.93 A
2016	91.24	75.19 B	9.75	1.65 B
Treatments (T)				
Control	68.50 F	61.96 F	6.75	1.15 F
Control + <i>A. solani</i>	77.31 E	66.07 E	8.39	1.42 E
BION	106.57 B	85.67 B	10.87	2.13 B
Salicylic acid	87.81 D	69.98 D	9.78	1.63 D
BION + <i>A. solani</i>	115.69 A	92.03 A	12.21	2.55 A
Salicylic acid + <i>A. solani</i>	94.51 C	80.52 C	9.82	1.87 C
LSD (M)	1.17	3.78	0.77	0.16
LSD (Y)	NS	1.10	NS	0.20
LSD (T)	2.04	1.92	NS	0.09
LSD M × T	NS	NS	NS	NS
LSD M×Y	**	**	NS	**
LSD T×Y	NS	NS	NS	**
LSD M×T×Y	NS	NS	NS	NS

Any two means within a column sharing same letters are not significant at $p \leq 0.05$. * = significant at $p \leq 0.05$; ** highly significant at $p \leq 0.05$; NS = non significant

Discussion

In the current study, foliar application of Bion and salicylic acid (SA) minimized the severity of early blight disease symptoms of tomato, during 2015-16, as compared to seedling root dipping method and increasing trend was observed in 2016. These results might be due to protection through Bion that gives quick expression of defense related genes (Bokshi et al., 2003; Buzi et al., 2004). Bion activates SAR mechanism and produces a large number of antimicrobial toxins (Govindappa et al., 2010; Nianlai et al., 2010). Foliar application was found better than seedling root dipping method, this result might be due to SAR signal transduction was difficult to trigger resistance in distant parts of the plants. These results coincide with Scarponi et al. (2000) who found Bion effective in triggering resistance in tomato plants against different pathogens: *Pseudomonas syringae* pv. tomato, bacterial canker (Soylu et al., 2003) and Cucumber mosaic virus (Anfoka, 2000). Results further supported by the work of Achuo et al. (2004) in which they found Bion flooding or foliar application induced resistance in tomato against *B. cinerea* has been found effective.

The result of the present study for both years indicated that Bion caused a significant increase in growth attributes under disease conditions as compared to SA and infected control. These results are might be due to SA which is a plant activator and initiates flowering in plants, increases life span of flower, control ions uptake by roots and

stomatal conductivity (Bhupinder et al., 2003). Bion is a functional analogue of SA and it works just like salicylic acid (Faize and Faize, 2018). Significant increase in all growth parameters and yield (Plant height, number of flowers/plant, roots and shoots fresh and dry weights and fruit yield) was observed in tomato plants treated with Bion followed by salicylic acid and diseased control. The results are in harmony with the findings of Szepesi (2005) in which he described that toxin production by the pathogen might be a reason of the decreased fresh weight of infected tomato shoots, which affected the potassium uptake and stomatal utilities that lead to uncontrolled transpiration and rapid water loss and ultimately plant wilting occurred. However, reduction in shoot dry weight may be due to higher respiration rate and destruction of cell membrane (Orcutt and Nilsen, 2000).

However, application of Bion remarkably increased total chlorophyll contents in inoculated leaves as compared to untreated inoculated control. Results of the current study are consistent with work of Solntsev et al. (2005) who stated that the resistance inducers directly affect the pigment formation and boost the photosynthetic mechanism that results in vigorous growth of the wheat plant. Our findings are in agreement with Nafie and Mazen (2008) they described an increase in chlorophyll contents in soybean leaves triggered by Bion against stem rot disease. *Alternaria solani* infection is responsible of decrease in chlorophyll contents and carotenoids in tomato leaves it might be due to discharge of toxins that leading to oxidative burst resulting in programmed cell death (Howlett, 2006).

In the present study, Bion has increased the photosynthetic rate in inoculated plant as compared to untreated inoculated plants (disease control). These results are might be due to increased action of Rubisco and PEP carboxylase under stress (Popova et al., 2003) and that of CA. The resistance inducers boost up the chlorophyll contents in plants so it might be another reason of high photosynthetic rate.

Our findings showed that Bion and SA application considerably decreased the EL % as compared to diseased control. Electrolyte leakage percent (ELP) depicts the amount of injury to the cell membrane. ELP in diseased plants increased markedly up to 2 times as compared to healthy ones. This phenomenon explains that fungal infection badly ruptures the membrane and reduces the membrane stability, it might be due to the correlation between components of the cell and the amount that oozed out. These results are verified by Hamada and Hashem (2003) they found salicylic acid and Thiamin effective against wheat root rot. These findings verify the efficacy of Bion and SA in improving the cell membrane damage through lessening the fungal infection and also these chemicals induce resistance in tomato plant against fungal pathogens. It may be due to Bion application reduced ELP by making membrane stability better, as revealed from our study data also supported by Agarwal et al. (2005) they conducted a study and found abscisic acid and SA effective against oxidative stress in wheat crop.

Application of resistance inducers increased yield per plant and fruit per plant during both years. Results of present study are consistent with Firoz and Hossain (2000) who conducted an experiment in which they sprayed Bion before a week of ear initiation in rice and observed increase in yield. Hossain et al. (2011) also observed higher grain yield of rice by applying Bion as a foliar spray of rice. Similarly, Pradhanang et al. (2005) documented during bacterial wilt field studies, Bion application enhanced the resistance and also significantly increased the yield of tomato genotypes which were moderately resistant to the bacterial wilt pathogen. Bion application enhanced the yield in optimally grown tomato plants that were free of bacterial spot (Romero et al., 2001).

The maximum number of flower branch/plant and number of fruits/plant was obtained with Bion through foliar application. The maximum TSC and TSP were recorded with Bion with foliar application followed by SA and infected control. Montasser et al. (2012) Carbohydrates in leaves were significantly decreased in TYLCV isolates infected of tested plant cultivars as compared to healthy ones; this may be due to the defense effect of the plant against the virus infection where the strategy altered from defensive to survival as described by Khalil et al. (2014). These results are in harmony with the findings of Radwan et al. (2007), Gupta et al. (2010). Chandra et al. (2007) described that SA and Bion application increased TSS and TSP of cowpea plants.

Conclusion

Our results indicated that Bion could be eco-friendly and cost effective strategy against *Alternaria solani* in integrated disease management programs. Foliar application of Bion provided better efficiency than seedling root dipping to manage *A. solani*, but still further research is needed under field condition for the confirmation of method success in tomato crop.

REFERENCES

- [1] Abada, K. A., Mostafa, S. H., Mervat, R. (2008): Effect of some chemical salts on suppressing the infection by early blight disease of tomato. – Egyptian Journal of Applied Science 23: 47-58.
- [2] Achuo, E. A., Audenaert, K. M., Eziane, H., Höfte, M. (2004): The salicylic acid dependent defense pathway is effective against different pathogens in tomato and tobacco. – Plant Pathology 53(1): 65-72.
- [3] Agarwal, S., Sairam, R. K., Srivastava, G. C., Meena, R. C. (2005): Changes in antioxidant enzymes activity and oxidative stress by abscisic acid and salicylic acid in wheat genotypes. – Biologia Plantarum 49: 541-550.
- [4] Anfoka, G. H. (2000): Benzo-(1,2,3)-thiadiazole-7-carbothioic acid S-methyl ester induces systemic resistance in tomato (*Lycopersicon esculentum* Mill cv. Vollendung) to Cucumber mosaic virus. – Crop Protection 19(6): 401-405.
- [5] Bhupinder, S., Usha, K. (2003): Salicylic acid induced physiological and biochemical changes in wheat seedlings under water stress. – Plant Growth Regulation 39(2): 137-141.
- [6] Bokshi, A. I., Morris, S. C., Deverall, B. J. (2003): Effects of Benzothiadiazole and acetylsalicylic acid on β -1-3-glucanase activity and disease resistance in potato. – Plant Pathology. 52(1): 22-7.
- [7] Bradford, M. M. (1976): A rapid and sensitive method for the quantization of microgram quantities of protein utilizing the principle of protein-dye binding. – Analytical Biochemistry 72: 248-254.
- [8] Buzi, A., Chilosi, G., Magro, P. (2004): Induction of resistance in melon seedlings against soil borne fungal pathogens by gaseous treatments with methyl jasmonate and ethylene. – Journal of Phytopathology 152(8-9): 491-497.
- [9] Chaerani, R., Voorrips, R. E. (2006): Tomato early blight (*Alternaria solani*): the pathogen, genetics, and breeding for resistance. – Journal of General Plant Pathology 72(6): 335-347.
- [10] Chandra, A., Anand, A., Dubey, A. (2007): Effect of salicylic acid on morphological and biochemical attributes in cowpea. – Journal of Environmental Biology 28(2): 193-196.

- [11] Dubois, M., Gilles, K. A., Hamilton, J. K., Rebers, P. A., Smith, F. (1956): Colorimetric method for determination of sugar and related substances. – *Analytical Chemistry* 28(3): 350-356.
- [12] Faize, L., Faize, M. (2018): Functional analogues of salicylic acid and their use in crop protection. – *Agronomy* 8(1): 5.
- [13] FAO (2013): Food and Agriculture Organization, United Nations. – <http://faostat.fao.org>.
- [14] Firoz, M. J., Hossain, I. (2000): Induction of resistance to rice against some major diseases with increasing grain yield. – *Bangladesh Journal of Seed Science and Technology* 4(1-2): 37-40.
- [15] Govindappa, M., Lokesh, S., Rai, V. R., Nail, V. R., Raju, S. G. (2010): Induction of systemic resistance and management of safflower *Macrophomina phaseolina* root rot disease by bio control agents. – *Archives of Phytopathology and Plant Protection* 43(1-3): 26-40.
- [16] Gupta, U. P., Srivastava, M., Gupta, U. (2010): Influence of soybean mosaic virus infection on carbohydrate content in nodule of soybean (*Glycine max* L. Merr.). – *International Journal of Virology* 6: 240-245.
- [17] Hafiz, T. B. (2009): Integrated Approach for the Management of Purple Blotch of Onion caused by *Alternaria porri*. – PhD thesis Department of Plant Pathology Sher-e-Bangla Agriculture University Dhaka.
- [18] Hamada, A. M., Hashem, M. (2003): Thiamin and salicylic acid as biological alternatives for control wheat root-rot. – *Egyptian Journal of Agricultural Research* 1: 369-385.
- [19] Hossain, I., Dey, P., Hossain, M. Z. (2011): Efficacy of Bion, Amistar and Tilt in controlling brown spot and narrow brown spot of rice cv. BR11 (Mukta). – *Journal of the Bangladesh Agricultural University* 9(2): 201-204.
- [20] Howlett, B. J. (2006): Secondary metabolite toxins and nutrition of plant pathogenic fungi. – *Current Opinion in Plant Biology* 9: 371-375.
- [21] Khalil, R. R., Bassiouny, F. M., El-DougDoug, K. A., Abo-Elmaty, S., Yousef, M. S. (2014): A dramatic physiological and anatomical changes of tomato plants infecting with tomato yellow leaf curl geminivirus. – *International Journal of Agricultural Sustainability* 10: 1213-1229.
- [22] Larque-Saavedra, A., Martin-Mex, R. (2007): Effect of Salicylic Acid on the Bio-Productivity of Plants. – In: Hayat, S., Ahmad, A. (eds.) *Salicylic Acid. A Plant Hormone*. Springer Publishers, Dordrecht.
- [23] Mayee, C. D., Datar, V. V. (1986): *Phytopathometry Technical Bulletin-1*. – Marathwad Agriculture University, Parabhani, India.
- [24] Meller Harel, Y., Haile Mehari, Z., Rav-David, D., Elad, Y. (2014): Systemic resistance to gray mold induced in tomato by benzothiadiazole and *Trichoderma harzianum* T39. – *Phytopathology* 104: 150-157.
- [25] Momol, T., Pernezny, K. (2006): Florida plant disease management guide: tomato. University of Florida IFAS – <http://edis.ifas.ufl.edu/pdf/PG/PG05990.pdf>.
- [26] Montasser, M. S., Al-own, F. D., Haneif, A. M., Afzal, M. (2012): Effect of Tomato yellow leaf curl bigeminivirus (TYLCV) infection on tomato cell ultrastructure and physiology. – *Canadian Journal of Plant Pathology* 34(1): 114-125.
- [27] Nafie, E., Mazen, M. M. (2008): Chemical induced resistance against brown stem rot in soybean: The effect of benzothiadiazole. – *Journal of Applied Sciences Research* 4: 2046-2064.
- [28] Nianlai, C., Qiao, H., Ping, C., XiaoYing, N., Rui, W. (2010): Effects of BTH, SA and SiO₂ treatment on disease resistance and leaf HRGP and lignin contents of melon seedlings. – *Scientia Agricultura Sinica* 43(3): 535-541.
- [29] Oka, Y., Koltai, H., Bar-Eyal, M., Mor, M., Sharon, E., Chet, I., Spiegel, Y. (2000): New strategies for the control of plant parasitic nematodes. – *Pest Management Science* 56(11): 983-988.

- [30] Oostendorp, M., Kunz, W., Dietrich, B., Staub, T. (2001): Induced disease resistance in plants by chemicals. – *European Journal of Plant Pathology* 107: 19-28.
- [31] Orcutt, D. M., Nilsen, E. T. (2000): Influence of Plant Phytopathogens on Host Physiology. – In: Orcutt, D. M, Nilsen, E. T. (eds.) *The Physiology of Plants under Stress: Soil and Biotic Factors*. John Wiley and Sons, Inc., USA, pp. 239-236.
- [32] Popova, L., Ananiewa, E., Hristova, V., Christov, K., Georgieva, K., Alexieva, V., Stoinova, Z. H. (2003): Salicylic acid and methyl jasmonate induced protection on photosynthesis to paraquat oxidative stress. – *Bulgarian Journal of Plant Physiology (Special Issue)*: 133-152.
- [33] Pradhanang, P. M., Ji, P., Momol, M. T., Olson, S. M., Mayfield, J. L., Jones, J. B. (2005): Application of acibenzolar-S-methyl enhances host resistance in tomato against *Ralstonia solanacearum*. – *Plant Disease* 89(9): 989-993.
- [34] Radwan, D. E. M., Fayez, K. A., Mahmoud, S. Y., Hamad, A., Lu, G. (2007): Physiological and metabolic changes of Cucurbita pepo leaves in response to zucchini yellow mosaic virus (ZYMV) infection and salicylic acid treatments. – *Plant Physiology and Biochemistry* 45(6-7): 480-489.
- [35] Romero, A. M., Kousik, C. S., Ritchie, D. F. (2001): Resistance to bacterial spot in bell pepper induced by acibenzolar-S-methyl. – *Plant Disease* 85(2): 189-194.
- [36] Scarponi, L., Buonaurio, R., Bertona, A. (2000): Persistence of acibenzolar-S-methyl and SAR induction in tomato and pepper plants. – *Proceedings of the 5th Congress of the European Foundation for Plant Pathology. Biodiversity in Plant Pathology*. 18-22 September, Taormina (Italy).
- [37] Shakirova, F. M., Sakhabutdinova, A. R., Bezrukova, M. V., Fathudinova, R. A., Fathutdinova, D. R. (2003): Changes in hormonal status of wheat seedlings induced by Salicylic acid and salinity. – *Plant Science* 164: 317-322.
- [38] Shi, Q., Bao, Z., Zhu, Z., Ying, Q., Qian, Q. (2006): Effects of different treatments of salicylic acid on heat tolerance, chlorophyll fluorescence, and antioxidant enzyme activity in seedlings of *Cucumis sativa* L. – *Plant Growth Regulation* 48(2): 127-135.
- [39] Solntsev, M. K., Franstev, V. V., Karavaev, V. A., Yurina, T. P., Yurina, E. V. (2005): Thermo luminescence of wheat leaves with the plant activator Bion. – *Modern fungicides and antifungal compounds IV: 14th International Reinhardsbrunn Symposium; Friedrichroda, Thuringia, Germany, April, pp. 25-29*.
- [40] Soyulu, S., Baysal, O., Soyulu, E. M. (2003): Induction of disease resistance by the plant activator, acibenzolar-S-methyl (ASM), against bacterial canker (*Clavibacter michiganensis* subsp. *michiganensis*) in tomato seedlings. – *Plant Science* 165: 1069-1075.
- [41] Steel, R. G. D., Torrie, J. H., Dickey, D. A. (1997): *Principles and Procedures of Statistics. A Biometrical Approach*. – McGraw Hill Co., New York, pp. 178-182.
- [42] Szepesi, Á. (2005): Role of salicylic acid pre-treatment on the acclimation of tomato plants to salt-and osmotic stress. – *Acta Biologica Szegediensis* 49(1-2): 123-125.
- [43] Takeshita, M., Okuda, M., Okuda, S., Hyodo, A., Hamano, K., Furuya, N., Tsuchiya, K. (2013): Induction of antiviral responses by acibenzolar-S-methyl against cucurbit chlorotic yellows virus in melon. – *Phytopathology* 103: 960-965.
- [44] Tripathi, D., Pappu, H. R. (2015): Evaluation of acibenzolar-S-methyl-induced resistance against iris yellow spot tospovirus. – *European Journal of Plant Pathology* 142(4): 855-864.
- [45] Vernon, L. P., Selly, G. R. (1966): *The Chlorophylls*. – Academic Press, New York and London.

A RELATIONSHIP BETWEEN ECONOMIC PERFORMANCE AND AIR POLLUTION OF A SCIENCE PARK: A CASE STUDY OF HSINCHU SCIENCE PARK IN TAIWAN

HUANG, S. Z.¹ – CHAU, K. Y.^{2*} – SHEN, H. Z.^{3*} – LI, J.⁴

¹*School of Economics and Management, Guangdong University of Petrochemical Technology
Maoming, China*

²*Faculty of International Tourism and Management, City University of Macau, Macau, China*

³*College of Chemical Engineering, Huaqiao University, Xiamen, China*

⁴*School of Business, Macau University of Science and Technology, Macau, China*

**Corresponding author*

*e-mail: gavinchau@cityu.mo; hzhshen@hqu.edu.cn
(phone: +853-8590-2518; fax: +853-8590-2518)*

(Received 4th Sep 2018; accepted 15th Oct 2018)

Abstract. Rapid economic development has caused serious air pollution which threatens human health. Science parks play an important role in economic development, however their air pollutants deteriorate the ambient air quality. This study investigates the relationship between the economic performance and air pollution of Hsinchu Science Park in Taiwan, which is the biggest production base of semi-conductors and other relevant high-tech industries. The total business turnover and annual average concentrations of sulfur dioxide (SO₂), ozone (O₃), nitrogen oxide (NO_x), carbon monoxide (CO) and particle matter with aerodynamic diameter less than 10 μm (PM₁₀) of Hsinchu Science Park from 1993 to 2012 were employed for the analysis. Vector Auto Regression (VAR) model was used to analyze the relationship between economic performance and air pollution for Hsinchu Science Park. The results indicated that there was a close, long-term and stable relationship between economic performance and air pollution concentrations in Hsinchu Science Park. A significant hysteresis effect of the economic performance was observed on the O₃ and CO concentrations, while a weak hysteresis effect of that was revealed on the SO₂, NO_x and PM₁₀ concentrations. The increasing emissions of O₃ and CO resulted from the production expansion. By contrast, SO₂, NO_x, PM₁₀ were not affected by the growth of economic performance of Hsinchu Science Park.

Keywords: *total business turnover, air pollutions, VAR simulation, impulse response function*

Introduction

Science park, also named as Technology park, is an industrial area planned and developed by governments with a purpose to find a cluster of companies and manufacturers that focus on research and development (R&D) for promoting high-tech industry (Huang et al., 2016). The first science park in the world was the Stanford Research Park in the U.S.A. founded in 1951, which has created better environment for high-tech industrialization. Even if many science parks around the world claimed to have low pollution and low consumption (Huang et al., 2016), they emitted pollutants in reality that posed a great environmental risk on local or neighbored area, however less attentions were attracted from the government, non-governmental organizations (NGOs) and the public. In addition, pollution emission is an important index to evaluate whether

a science park is truly representative of high-tech industry. (Chein et al., 2005). Therefore, it is urgent to investigate the relationship between economic development and air pollution for science parks.

Hsinchu Science Park was built in the north of Taiwan and managed by the Ministry of Science and Technology (MOST), the coordinates are 24.7829 N, 121.0058 E (as seen in *Figure 1*). By the end of 2016, Hsinchu Science Park has assembled 485 high-tech manufacturers which are classified into various industries such as semi-conductors, computers, communications, optoelectronics, precision machinery, biotechnology. The realized total turnover reached 1000 billion NTD which accounted for 12% of Taiwan's GDP. It is ranked as one of the fastest growing parks globally by the SIT SELECTION (U.S.A). However, Hsinchu Science Park suffered from air pollutions such as PM₁₀, SO₂, NO_x, and volatile organic compounds (VOCs) which were attributed to defective air pollution equipment during the economic and technological innovations (Alastuey et al., 2016; Cesari et al., 2016; Huang et al., 2008; Schwarz et al., 2016; Tsai et al., 2011). Conflicts between local residents and governments have also broken out in the past years such as in the Daqi Village, a neighbor of Hsinchu Science Park, which suffered from fugitive foul odor in 1999 and arsenic pollution in 2007.



Figure 1. Location of Hsinchu Science Park in Taiwan

Previous research studies regarding the relationship between economic development and air pollution often focused on a large region, such as a country, a province, and a city. A relatively smaller area, such as a science park, is seldom explored by empirical model. In summary, this study aims to explore the relationship between economic performance and air pollution of Hsinchu Science Park by using Vector Auto Regression (VAR) model, which has been widely applied for the analysis of the relationship (Li et al., 2009; Narayan et al., 2008; Nasir and Rehman, 2011; Peng and Bao, 2006). This study not only investigated the relationship between the economic performance with the air pollution, but also adopted impulse response function to analyze it for a long period of 24 years. Also, it was evaluated whether Hsinchu Science Park was an environmentally friendly unit or not by using the VAR model. The

conclusion could also be supplied as a scientific reference for the governments to make informed decisions.

Methods

Definition of variables

The performance, as one of the subjects, is an important indicator of competitiveness. The performance of science parks is a comprehensive system containing various subset factors such as economic performance, innovation performance, and management performance. The total business turnover is a common indicator to evaluate the economic performance (Huang et al., 2016; Wu et al., 2006) which equals to the subtraction of accumulation of deductible items (the sum of bill collection, sales of fixed assets, sales of wastes, income of interests, presentation of gifts) from the net revenue of manufacturers in a science park (the sum of sales in the declaration, total of receipt notes, sales return and discounts, and sales adjustment of previous period). Whether a science park is successful or not is mainly evaluated by its contributions to the growth of regional GDP and economics. Thus, the total business turnover of manufacturers in Hsinchu Science Park was adopted as the only output variable to represent the park performance. The effect of different industries on the economic performance could be neglected in this study because the total business turnover was collected from overall industries in Hsinchu Science Park (Chu et al., 2004; Huang et al., 2016).

Because of the complexity of air pollution species, SO₂, O₃, NO_x, CO, PM₁₀ which were emitted from the coal-fired power station, the exhaust of motor vehicles etc., were selected according to the Pollutant Standard Index (PSI) in Taiwan and their corresponding concentrations were used as the indices of air pollution. They were adopted as the independent variables for investigating the effect of air pollution on the park performance as shown in *Table 1*.

Table 1. Pollutant concentrations and vice pollution index value table for Taiwan

Pollutants	PM ₁₀	SO ₂	CO	O ₃	NO _x	
PSI value and their impact on health	Statistical methods	24 Hour average	24 Hour average	24 Hour maximum 8-hour average	24 Hour maximum value of the hour	24 Hour maximum value of the hour
	Unit	µg/m ³	ppb	ppm	ppb	ppb
	PSI					
Good	50	50	30	4.5	60	-
Moderate	100	150	140	9	120	-
Unhealthy	200	350	300	15	200	600
Very Unhealthy	300	420	600	30	400	1200
Hazardous	400	500	800	40	500	1600
	500	600	1000	50	600	2000

The total business turnover was gathered from the official website of Hsinchu Science Park and the concentrations of SO₂, O₃, NO_x, CO, PM₁₀ were from statistical database of EPA's air quality webpage. The annual total business turnover and annual average concentrations of SO₂, O₃, NO_x, CO, PM₁₀ were collected during the years from 1993 to 2016 since management system and statistical techniques were not completely established until 1992. The Long-term data would ensure the reliability of the causality inference (Alastuey et al., 2016; Pokorná et al., 2018; Rindfleisch et al., 2008).

Establishment of the model

VAR model is good at predicting interrelated time series systems and analyzing long term dynamic impact of stochastic disturbance on variables, and beneficial for understanding various economic shocks on economic variables, with advantages of preventing missing of important variables, and diminishing errors of endogenous variables (Lütkepohl, 1993). This study established impulse response function proposed by Sims (1980) using VAR model to analyze long-term impact of the economic performance on the shock of air pollutions of SO₂, O₃, NO_x, CO and PM₁₀ in Hsinchu Science Park as seen in *Equation 1*:

$$\begin{aligned}
 P_t = & B_0 + \sum_{p=1}^k \theta_{11p} (P_{t-p}) \\
 & + \sum_{p=1}^k \theta_{12p} (SO_{2\ t-p}) \\
 & + \sum_{p=1}^k \theta_{13p} (O_{3\ t-p}) \\
 & + \sum_{p=1}^k \theta_{14p} (NO_{2\ t-p}) \\
 & + \sum_{p=1}^k \theta_{15p} (CO_{\ t-p}) \\
 & + \sum_{p=1}^k \theta_{16p} (PM_{10\ t-p}) + \varepsilon_{1t} \quad (\text{Eq.1})
 \end{aligned}$$

where dependent variable **P** is the economic performance of Hsinchu Science Park (100 Million TWD); **SO₂** is the concentration of sulfur dioxide (ppb), **O₃** is the concentration of ozone (ppb), **NO_x** is the concentration of nitrogen dioxide (ppb), **CO** is the concentration of carbon monoxide (ppm), **PM₁₀** is the concentration of PM₁₀ (µg/m³); **B₀** is the estimated coefficient, t is time, and ε is a constant error.

The Linear regression equation was analyzed using EViews 6.0 program. Descriptive

statistics, analysis of stability and cointegration test were performed respectively. At last, it was analyzed that impulse response functions of the impact of economic performance on air pollutions of **SO₂**, **O₃**, **NO_x**, **CO**, **PM₁₀** and continuity impact.

Results and discussions

Descriptive statistics

Descriptive statistics analyzed the means and standard deviations of variables as shown in *Table 2*. The correlation coefficient matrix shows the economic performance was significantly correlated with **O₃**, and showed a relatively significant correlation with **SO₂**, **O₃** and **PM₁₀**. The result of Hausman test is 17.98, random probability is significant, and DW (Durbin Watson stat) is 1.67. The result of regression analysis shows that R² is 0.79, and the random effect of variables is significant. Meanwhile, by calculating the AR (Vector Regression) characteristic polynomial, it is found that reciprocals of characteristic polynomial are smaller than 1, and located within the unit circle (as shown in *Figure 2*). The result suggests that the variables are stable for the economic system which consisted of the economic performance of Hsinchu Science Park and air pollution concentrations of **SO₂**, **O₃**, **NO_x**, **CO** and **PM₁₀**. And therefore it is verified that the established model was stable.

Table 2. Means, standard deviations, and correlations of variables

Variables	Mean	S.D.	P	SO ₂	O ₃	NO _x	CO	PM ₁₀
1 P	7543.83	3467.65	1					
2 SO ₂	4.72	2.87	-.47*	1				
3 O ₃	22.56	6.41	.76**	-.19	1			
4 NO _x	18.64	2.47	.17	-.01	-.15	1		
5 CO	.53	.056	-.17	-.24	-.25	.24	1	
6 PM ₁₀	50.23	5.92	-.56*	.47*	-.68**	.28	.01	1

Notes: * p-value < 0.05; ** p-value < 0.01

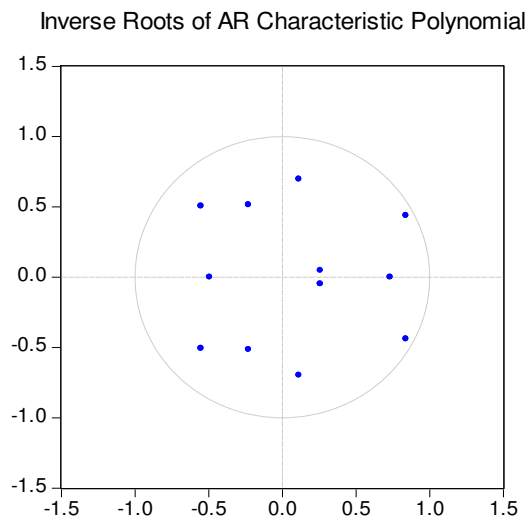


Figure 2. Inverse roots of AR characteristic polynomial

Variable balance test

This study tests the stability of the variables by Augmented Dickey Fuller Test (ADFT) proposed by Said and Dickey (Said and Dickey, 1984). The optimal lag period was determined by using the minimum criterion of Akaike Information Criterion (AIC) to ensure autocorrelation of residuals (Enders, 2004). The results showed that the horizontal sequence of **P**, **PM₁₀** and **O₃** was not stable at a significance level of 0.05, but it became stable through first order difference. Each variable of the equation was used as an independent variable after the lag of second order as shown in *Table 3*.

Table 3. Results of unit root test

Variable	Test type (c, T, d)	ADF statistics	t statistical value	Adjoint probability P	Conclusion
P	(c, T, 1)	-1.710267	-3.574244	0.4105	Instable
D (P)	(c, 0, 1)	-5.266976***	-2.971853	0.0006	Stable
SO ₂	(c, 0, 0)	-20.65626***	-3.029970	0.0000	Stable
O ₃	(c, 0, 0)	-2.856286	-3.040391	0.0704	Instable
D(O ₃)	(c, 0, 1)	-5.399642***	-3.040391	0.0004	Stable
NO _x	(c, 0, 0)	-4.377785***	-3.029970	0.0032	Stable
CO	(c, 0, 0)	-3.247647**	-3.029970	0.0328	Stable
PM ₁₀	(c, 0, 0)	-1.817124	-3.029970	0.3614	Instable
D (PM ₁₀)	(c, 0, 1)	-3.313729**	-3.040391	0.0296	Stable

Note: (c, T, d) separately stand for intercept, time trend and lag order of the equation in the test; the lag order is determined by using SC minimum error criteria; D (X) is X's first order difference; “*”, “**” and “***” mean refusal of null hypothesis at significance level of 10%, 5%, and 1%

The time series of individual variables was not stable. Thus, the cointegration test proposed by Johansen (1995) was used to identify whether there were underlying stable time series and long-term balanced relationship between these unstable variables with the linearity. The results were substituted into the cointegration *Equation 1* and thus evolved in *Equation 2*:

$$P_t = +549.1754SO_2 - 612.5936 O_3 - 612.5936 NO_x + 1634.7140 CO \quad (\text{Eq.2})$$

(288.46) (26.8743) (74.2233) (3453.37)

Given cointegration *Equation 2* and *Figure 2*, the economic performance **P** of

Hsinchu Science Park had a long-term relationship with SO_2 , O_3 , NO_x and CO , while its relationship with PM_{10} was weak enough to ignore. It was a significant positive correlation of P with SO_2 and CO . In other words, when SO_2 and CO increase in Hsinchu Science Park, the economic performance of P increases. While it was a significant negative correlation between P with O_3 and NO_x , suggesting when O_3 and NO_x increase, P decreases.

VAR's impulse response function analysis

The VAR's impulse response function is the sum of a standard deviation, stochastic disturbance term to impact another current, and future values of various variables. It simulates the dynamic interaction among the variables (Enders, 2004). The object of this study is to investigate the response to the independent variable P within the system to the air pollution concentrations in different periods, and the contribution of air pollution concentrations to P . As seen in *Figure 3*, the horizontal axis is the hysteresis effect period of the shock with a maximum of 10 periods. The vertical axis is the impulse response function of a dependent variable to an independent variable. The blue solid line is the dynamic path of the impulse response function, and the two red dotted lines are confidence intervals which are twice the standard deviation.

As shown in *Figure 3(a)*, economic performance has a positive response to performance. It drops to the lowest point in the fourth period, and then gradually converges to zero line, meaning that the effect of investment on the future economic performance was promoting its growth in the first two periods and then the effect gradually decreased to zero. This trend reflects that the economic performance of Hsinchu Science Park targets at the processing and exports and few enterprises make continuous investments to improve the business environment in the science park. *Figure 3(b)* shows the impulse response of the economic performance to SO_2 . After a positive shock is given to SO_2 in the current period, the response function drops to the lowest point in the second period, and then converges gradually. This means there is no significant impact on SO_2 by the growth of economic performance of Hsinchu Science Park in the whole current. *Figure 3(c)* shows the impulse response function of economic performance of Hsinchu Science Park to NO_x . After a positive shock is given to NO_x in this current period, the response reaches the lowest point of the negative response in the third period, and converges gradually from the beginning of the fourth period. This also indicates that there is no significant impact on NO_x by the growth of the economic performance in the current period. *Figure 3(d)* shows an impulse response function of economic performance to PM_{10} . The response nearly approaches zero line in the first and second period, and drops to the negative response at the beginning of the third period. It converges gradually on the fifth period reaching a negative point. This indicates that the economic performance of the science park has no significant impact on PM_{10} in the current period. In view of air pollutant sources, SO_2 is mainly emitted from thermal power plants, steel plants and petrochemical plants, while NO_x and PM_{10} are from the exhaust of vehicles, thermal plants, nitric acid making plants and municipal waste incineration plants in Taiwan (Tsai et al., 2011). On the other hand, the majority of these pollutants were more possibly from the neighboring areas or even further areas such as the mainland of China and Northeast Asia through overseas transportation (Chou et al., 2008; Chou et al., 2010; Shaw et al., 2004). The results are in agreement with the fact that Hsinchu Science Parks excludes these heavy industries to build and operate. Stringent control procedures have been formulated and conducted, and the air

pollution have also been effectively supervised by environmental management of the science park. Thus, it concludes that Hsinchu Science Park is environmentally friendly. The impulse response function of economic performance to O_3 is shown in *Figure 3(e)*. After a positive shock is given to O_3 in the current period, a negative response at the beginning climbs to the highest point of positive response in the third period, and drops to the lowest point in the fifth period, and then converges to zero gradually.

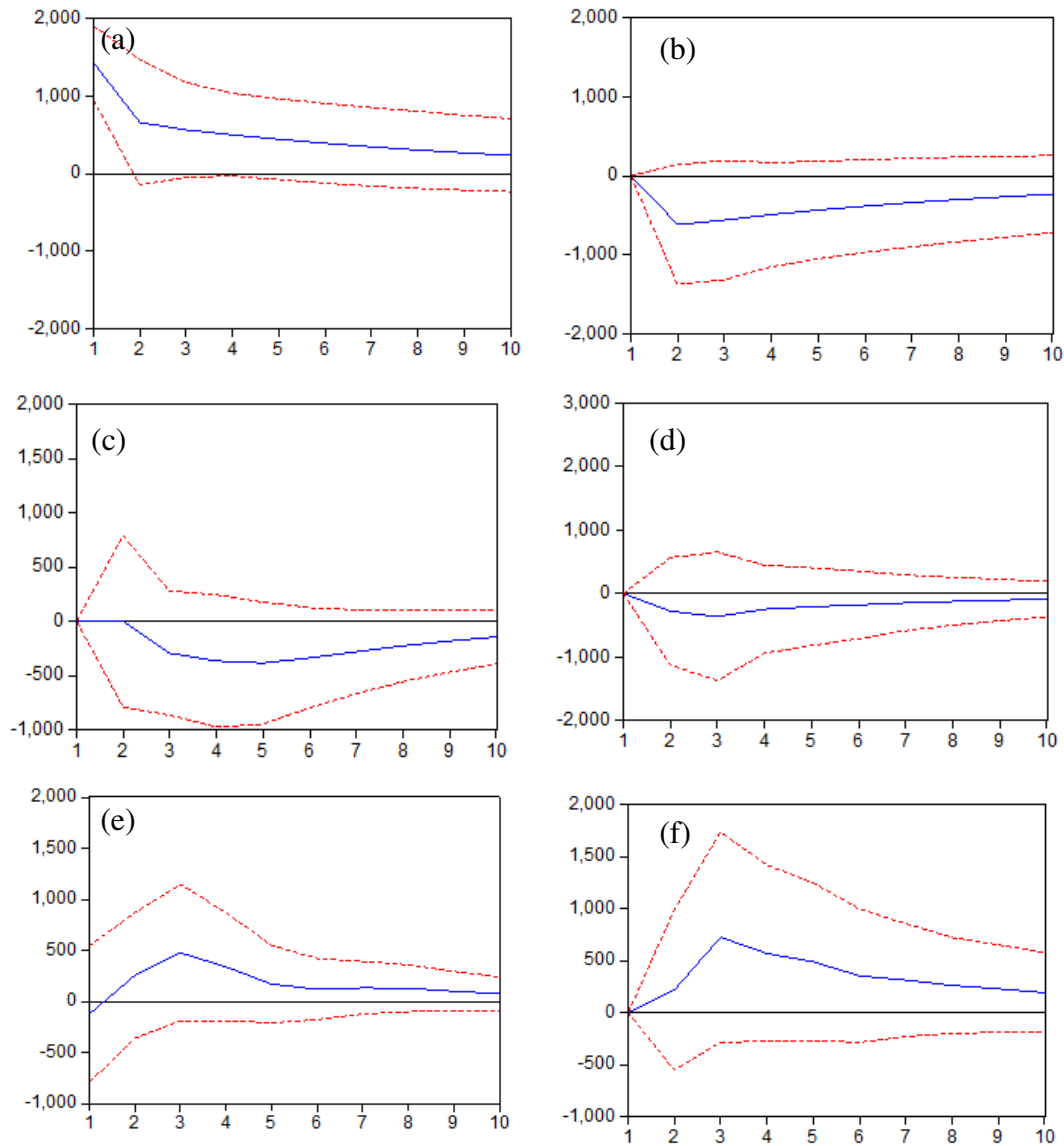


Figure 3. The impulse response function of dependent variables to independent one (a) Response of P to P , (b) Responses of P to SO_2 , (c) Response of P to NO_x , (d) Response of P to PM_{10} , (e) Responses of P to O_3 , and (f) Response of P to CO

This indicates that there is a significant impact of the economic performance growth on O_3 in the current period. The impulse response function of economic performance to CO is shown in *Figure 3(f)*. The impulse response rises to the highest point of positive response in the third period, and drops to the lowest point, and then converges gradually

to zero line. This indicates that there is a significant impact of the growth of economic performance on CO in the current period. When the economic performance improved, more products would be produced and then the input of energy and raw materials increased. More O₃ and CO were emitted during the enlarged production process. There are two main sources of O₃ pollution in Hsinchu Science Park. Firstly, O₃ as a secondary pollutant results from the photo-oxidation between O₂ and the emitted NMHCs (non-methane hydrocarbons) which are emitted in large amounts in various processes of the high-tech industry, such as wafer process, welding, etching, image process, and chemical washing in IC, photo electricity and biotech industries (Price et al., 2004). The other source is the diffusion of O₃ as the primary pollutant in the advanced oxidation water-treatment system where high concentration of O₃ is present (Went et al., 2009). CO comes from the exhaust of vehicles because road logistics is a main transportation in Hsinchu Science Park with a tremendous amount of logistics caused by economic development.

Suggestions

Many countries are activated to develop green economy and green industry in the world. The World Trade Organization (WTO) has exceptional clauses on environmental protection, which imposes green tax on exported goods because the pressure of environmental protection from the international society becomes more and more intense. In this context, low-carbon science parks have been promoted to facilitate the development of low carbon economy, which is beneficial for sustainable development (Gearty, 2008).

The governments should formulate tax systems to promote green economy. A green tax system can be established by using tax leverage to solve prisoner's dilemma between environment and economic development. Moreover, they should formulate incentives and subsidy systems for clean production which shift pollution control towards overall pollution prevention, as well as actively guide enterprise to implement carbon tradition and establish carbon investigation system.

Science parks should be planned and managed based on the concept of sustainable development. The science park management should also shift from end-of-pipe treatment to pollution prevention, conduct evaluation of environmental impact, obtain pollutants discharge license, and implement centralized disposal of waste in accordance with the national and local regulations or standards to prevent air pollution.

The enterprises in science parks should promote green sustainable economic development through R&D, management system, and green technologies. They need to develop green and energy-efficient products. Enterprises should also establish ISO14000, clean production, energy management, green supply chain and environment management system. These measures can reduce expenses in pollution prevention, save raw material or products, improve efficiency and quality of production, and prevent occupational disease.

Research limitations

Because of limitations of data sources, this study has some limitations. Firstly, different industries caused the variation of air pollutions concentrated. Secondly, the air pollution species caused by high-tech enterprises were not considered in this study. These should be considered in future research.

Conclusion

This study investigated the relationship between the economic performance and air pollution of **SO₂**, **O₃**, **NO_x**, **CO**, **PM₁₀** in Hsinchu Science Park from 1993 to 2012. VAR's impulse response function was used to analyze the effect of the science park performance on **SO₂**, **O₃**, **NO_x**, **CO** and **PM₁₀**. The results showed that the park performance has a tight, long-term and stable relationship with air pollution. The park performance is negatively correlated to **SO₂**, **NO_x** and **PM₁₀**. The hysteresis effect of the park performance could be neglected on **SO₂**, **NO_x** and **PM₁₀** as they are not emitted from Hsinchu Science Park but from overseas transportation possibly. On the other hand, the performance is correlated positively to **O₃** and **CO**. The hysteresis effect of the park performance on **O₃** and **CO** is significant, due to the large emission from the production process and transportation in Hsinchu Science Park. Since science parks cause air pollution, the government should encourage enterprises to develop better R&D capabilities to reduce pollution and energy consumption. Meanwhile, the enterprises should develop environmental protection mechanisms actively.

Acknowledgements. This study was supported by “Guangdong Social Science Planning Project” (GD17XGL15).

REFERENCES

- [1] Alastuey, A., Querol, X., Aas, W., Lucarelli, F., Perez, N., Moreno, T., Cavalli, F., Areskoug, H., Balan, V., Catrambone, M., Ceburnis, D., Cerro, J. C., Conil, S., Gevorgyan, L., Hueglin, C., Imre, K., Jaffrezo, J. L., Leeson, S. R., Mihalopoulos, N., Mitosinkova, M., O'Dowd, C. D., Pey, J., Putaud, J. P., Riffault, V., Ripoll, A., Sciare, J., Sellegri, K., Spindler, G., Yttri, K. E. (2016): Geochemistry of PM10 over Europe during EMEP Intensive Measurement Periods in Summer 2012 and Winter 2013. – *Atmos. Chem. Phys.* 16:6107-6129. <https://doi.org/10.5194/acp-16-6107-2016>
- [2] Cesari, D., Donato, A., Conte, M., Merico, E., Giangreco, A., Giangreco, F., Contini, D. (2016): An inter-comparison of PM2.5 at urban and urban background sites: chemical characterization and source apportionment. – *Atmospheric Research* 174-175: 106-119.
- [3] Chein, H. M., Hsu, Y. D., Aggarwal, S. G., Chen, T. M., Huang, C. C. (2005): Evaluation of arsenical emission from semiconductor and opto-electronics facilities in Hsinchu Taiwan. – *Atmospheric Environmental* 40(10): 1901-1907.
- [4] Chien, C. F., Chen, C. P., Lin, K. Y. (2013): An investigation of planning a research park in Hsinchu science park area. – *Journal of Management & Systems* 20(2): 227-255.
- [5] Chou, C. C.-K., Lee, C. T., Cheng, M. T., Yuan, C. S., Chen, S. J., Wu, Y. L., Hsu, W. C., Lung, S. C., Hsu, S. C., Lin, C. Y., Liu, S. C. (2010): Seasonal Variations and Spatial Distribution of Carbonaceous Aerosols in Taiwan. – *Atmos. Chem. Phys. Discuss* 10: 9563-9578.
- [6] Chou, Charles C. K., Lee, C. T., Yuan, C. S., Hsu, W. C., Lin, C. Y., Hsu, S. C., Liu, S. C. (2008): Implications of the Chemical Transformation of Asian Outflow Aerosols for the Long-range Transport of Inorganic Nitrogen Species. – *Atmos. Environ* 42(32): 7508-7519.
- [7] Chu, P. Y., Tzeng, G. H., Teng, M. J., Chiu, H. (2004): A multivariate analysis of the relationship among market share, growth and profitability--The case of the science-based industrial park. – *Sun Yat-Sen Management Review* 12(3): 507-533.
- [8] Enders, W. (2004): *Applied econometric time series* (2 ed.). – Wiley: New Jersey.
- [9] Gearty, M. (2008): Achieving carbon reduction. – *Journal of Corporate Citizenship* 30:81-94.
- [10] Huang, S. Z., Wu, T. J., Tsai, H. T. (2016): Hysteresis effects of R&D expenditures and patents on firm performance: An empirical study of Hsinchu Science Park in Taiwan. –

- Filomat 30(15): 4265-4278.
- [11] Huang, W. M., Lee, W. M., Wu, C. C. (2008): GHG emissions, GDP growth and the Kyoto Protocol: A revisit of Environmental Kuznets Curve hypothesis. – *Energy Policy* 36(1): 239-247.
- [12] Johansen, S. (1995): *Likelihood-Based Inference in Cointegrated Vector Autoregressive Model*. – Oxford: Oxford University Press.
- [13] Li, L., Zhu, J. S., Gao, R. X. (2009): The study on relationship between economic growth and environmental pollution in chongqing base on VAR model. – *Journal of Southwest University* 31(11): 92-96.
- [14] Lütkepohl, H. (1993): *Introduction to Multiple Time Series Analysis*. – Springer-Verlag.
- [15] Narayan, P. K., Narayan, S., Prasad, A. (2008): A structural VAR analysis of electricity consumption and real GDP: Evidence from the G7 countries. – *Energy Policy* 36(7): 2765-2769.
- [16] Nasir, M., Rehman, F. U. (2011): Environmental Kuznets Curve for carbon emissions in Pakistan: An empirical investigation. – *Energy Policy* 39 (3): 1857-1864.
- [17] Peng, S. J., Bao, Q. (2006): Economic growth and environmental pollution: an empirical analysis based on China's time series data (1985~2003). – *Contemporary Finance & Economics* 2006 (7): 5-12.
- [18] Pokorná, P., Schwarz, J., Krejci, R., Swietlicki, E., Havránek, V. (2018): Comparison of PM_{2.5} chemical composition and sources at a rural background site in Central Europe between 1993/1994/1995 and 2009/2010: Effect of legislative regulations and economic transformation on the air quality. – *Environmental Pollution* 241: 841-851.
- [19] Price, H. U., Jaffe, D. A., Cooper, O. R., Doskey, P. Y. (2004): Photochemistry, ozone production, and dilution during long-range transport episodes from Eurasia to the northwest United States. – *Journal of Geophysical Research-Atmospheres* 109 (23): doi:10.1029/2003JD004400.
- [20] Rindfleisch, A., Malter, A. J., Ganesan, S., Moorman, C. (2008): Cross-sectional versus longitudinal survey research: Concepts, findings, and guidelines. – *Journal of Marketing Research* 45(3): 261-279.
- [21] Said, S. E., Dickey, D. A. (1984): Testing for unit roots in autoregressive-moving average models of unknown order. – *Biometrika* 71: 599-607.
- [22] Schwarz, J., Cusack, M., Karban, J., Chalupnickova, E., Havranek, V., Smolík, J., Zdimal, V. (2016): PM_{2.5} chemical composition at a rural background site in central Europe, including correlation and air mass back trajectory analysis. – *Atmospheric Research* 176-177: 108-120.
- [23] Shaw, C. L., Lee, C. T., Cheng, M. T., Yuan, C. S., Wu, Y. L., Chen, S. J., Lin, P. H., Lin, C. Y., Lung, S. C., Chou, C. C., Liu, T. H., Hsu, S. C., Chang, C. C. (2004): Impacts of Long-Range Transport on Air Pollutants in Taiwan. – *Journal of Arid Land Resources and Environment* 18(1): 203-210.
- [24] Sims, C. A. (1980): Macroeconomics and reality. – *Econometrica* 48: 1-48.
- [25] Tsai, H. H., Yuan, C. S., Hung, C. H., Lin, Y. C. (2011): Physicochemical Properties of PM_{2.5} and PM_{2.5-10} at Inland and Offshore Sites over Southeastern Coastal Region of Taiwan Strait. – *Aerosol and Air Quality Research* 11: 663-677.
- [26] Tsai, H. H., Yuan, C. S., Hung, C. H., Lin, C., Lin, Y. C. (2011): Influence of Sea-Land Breezes on the Temporal Distribution of Atmospheric Aerosols over Coastal Region. – *Journal of Air and Waste Management Association* 61: 358-376.
- [27] Went, E. C., Rosario-Ortiz, F. L., Snyder, S. A. (2009): Effect of ozone exposure on the oxidation of trace organic contaminants in waste water. – *Water Research* 43 (4): 1005-1014.
- [28] Wu, W. Y., Tsai, H. J., Chang, K. Y., Lai, M. K. (2006): Assessment of intellectual capital management in Taiwanese IC design companies: Using DEA and the malmquist productivity index. – *R&D Management* 36(5): 531-547.

ANTIMICROBIAL ACTIVITY OF *MORINGA OLEIFERA* AGAINST MULTIDRUG-RESISTANT *STAPHYLOCOCCUS AUREUS* ISOLATED FROM RAW MILK

TIRADO-TORRES, D.¹ – CHAN-KEB, C. A.² – PÉREZ-BALÁN, R. A.² – AKE-CANCHÉ, B.² –
GÓMEZ-SOLANO, M. I. – ARAGÓN-GASTÉLUM, J. L.² – GÓMEZ-LÓPEZ, I.³ – AGUIRRE-CRESPO,
F. J.² – LÓPEZ-RAMOS, M. C.² – GUTIÉRREZ-ALCÁNTARA, E. J.*

¹*Departamento de Ingeniería Civil, División de Ingenierías, Campus Guanajuato, Universidad
de Guanajuato, Av. Juárez N° 77, Col. Centro, Guanajuato, Gto., México*

²*Facultad de Ciencias Químico-Biológica, Universidad Autónoma de Campeche Av. Agustín
Melgar S/N, Buena Vista, CP: 24039 Campeche, Cam., México*

³*Centro Nacional de Metrología, Querétaro, México*

*Corresponding author
e-mail: ejgutier@uacam.mx

(Received 11th Sep 2018; accepted 28th Nov 2018)

Abstract. The objective of the study was to evaluate the antimicrobial activity of aqueous and ethanolic *Moringa oleifera* leaf, stem and seed extracts against multidrug-resistant *Staphylococcus aureus* strains isolated from raw milk in Hidalgo Mexico in 2017. The conventional method was used to identify and isolate *S. aureus*. All isolates were screened for antibiotic sensitivity to 12 antibiotics using the disk-diffusion method, in order to select twenty multidrug-resistant strains. The antimicrobial activity of the *M. oleifera* leaf, stem and seed extracts (aqueous and ethanolic) was tested using the disk-diffusion agar method, with penicillin used as a positive control. Sixty-five *S. aureus* strains were isolated from 56% of the raw milk sample, with an average count of 4.5×10^5 CFU/ml, this is considered as a potential public health risk. All the *S. aureus* strains exhibited resistance to at least two antibiotics. Sixty-five strains exhibited resistance to penicillin and ampicillin. In contrast, all showed sensitivity to ciprofloxacin. Ethanol extract exhibited a higher degree of antimicrobial activity compared to the aqueous extracts and penicillin. This reveals that the leaves, stems and seeds of *M. oleifera* could be an alternative for the control of infections caused by *S. aureus* in humans and cows with mastitis.

Keywords: *foodborne pathogens, natural antimicrobial, bacteria, resistance, antibiotics*

Introduction

Raw milk is an ideal growth medium for different microorganisms, as it is considered a vehicle for *Staphylococcus aureus* (*S. aureus*) infection in humans (Zecconi and Hahn, 2000). This foodborne pathogen is considered as one of the world's leading causes of disease outbreaks related to food consumption and is responsible for a variety of manifestations and diseases (Jamali et al., 2014). Although the precise number of Staphylococcal infections outbreaks is unknown in Mexico, previous studies have indicated that raw milk and dairy products manufactured from raw milk play an important role in outbreaks in humans (Rania et al., 2013; Basanisi et al., 2017). The contamination of milk and milk products with this pathogenic bacteria is mainly caused by the processing and handling of cows with mastitis in unhygienic environments (Thaker et al., 2013).

In Mexico, the production of bovine milk reached 11,707,494 tons in 2016, of which, 14,973 tons was produced in the municipality of Francisco I. Madero (SAGARPA,

2016). As *S. aureus* is capable of acquiring antibiotic resistance determinants, its isolates often exhibit resistance to multiple classes of antimicrobial agents (Rybak and Laplante, 2005). Multiresistant *S. aureus* emerged decades ago due to the widespread and often inappropriate use of antibiotics in livestock (Mehli et al., 2017). The trend of rising antibiotic resistance continues despite the restrictions imposed on its use, both clinically and in food production (EFSA, 2009; NFSA, 2018). Resistant bacteria can be transmitted to humans through food, particularly that of animal origin and/or consumed raw (Phillips et al., 2004), and is a growing public health problem.

Increasing antibiotic resistance in pathogenic bacteria has led to growing demand for alternative safe and natural antimicrobials. The focus is currently on biologically active components isolated from plant species, such as *Moringa oleifera* (*M. oleifera*) (Arora and Onsare, 2014), used in food or herbal medicine, as these may provide a new source of antibacterial compounds (Gutiérrez-Alcántara et al., 2015).

M. oleifera is reported to have an antimicrobial effect on pathogenic bacteria (Brilhante et al., 2015; Peixoto et al., 2011; Viera et al., 2010). The antimicrobial properties of *M. oleifera* have been attributed to different parts of the plant, such as the leaves, seeds, pods and stems (Ferreira et al., 2011; Arora et al., 2013). In addition, studies conducted on this plant have revealed promising anti-inflammatory (Ezeamuzie et al., 1996), pro-coagulant (Nkurunziza et al., 2009), flocculant (in water treatments) (Beltrán-Heredia and Sánchez-Martín, 2009), detoxifying, immune boosting, and anti-parasitic activity (Thilza et al., 2010), for the treatment of diarrhea and skin infections (Farooq et al., 2012). Moreover, it is rich in nutrients and has been used in different products such as oils, foods, condiments and medicine (Viera et al., 2010). However, less extensive research has been conducted on the antimicrobial effects of *M. oleifera* on multidrug resistant pathogenic strains. Currently there are no studies focused on analyzing the effect of the leaf, seed and stems together of *M. oleifera*, previously good results have been observed separately (Brilhante et al., 2015; Lar et al., 2011). The objective of the present study was to evaluate the antimicrobial activity of aqueous and ethanolic *M. oleifera* leaf, stem and seed extracts against multidrug-resistant *S. aureus* strains isolated from raw milk.

Materials and methods

Collection of samples

A total of 100 bulk-tank milk samples (one liter per sample) were collected from between April and August 2017 from 4 farms located in the municipality of Francisco I. Madero, Mexico (Figure 1). One farm was located within the Universidad Politécnica de Francisco y Madero (UPFIM), while the other three farms were located approximately 3.5 km from the university. The four farms (A-B-C-D) had less than 7 Holstein cows each and the age ranged between 2-2.5 years.

The samples were placed in sterilized bags under aseptic conditions and transported in an icebox to the laboratory, where they were then analyzed no more than one hour after their purchase from the dairy farms.

Isolation and detection

The bacteriological method used for identifying and isolating *S. aureus* was performed according to Mehli et al. (2017), in which 10 mL of raw milk was aseptically

removed from each sample, placed in bags containing 90 mL of sterile peptone water (1.0 g bacteriological peptone and 8.5 g L⁻¹ sodium chloride) (Bioxon, the State of Mexico, Mexico), and homogenized manually for 2 min. Ten-fold dilutions were made using sterile peptone water, after which the appropriate dilutions (0.1 mL) were spread on Baird-Parker agar supplemented with 1% egg yolk tellurite emulsion (Bioxon, Estado de Mexico, Mexico). The plates were placed in an incubator (Labtech LIB-150M, USA) for 24-48 h at 37°C.

Suggestive colonies of *S. aureus* (black, shining, and convex, with a 1.0-1.5 mm diameter and surrounded by a clear zone) were selected for seeding in tubes containing Brain Heart Infusion (Bioxon, the State of Mexico, Mexico), which were then incubated for 35°C for 24 h. The presumptive strains of *S. aureus* were confirmed using coagulase, catalase, DNase, acetoin production and maltose fermentation tests (Saka and Terzi, 2018). All strains were also tested for the presence of staphylococcal enterotoxin using a commercial ELISA test kit (3M Tecra Code: FSA1156, New South Wales, Australia). The confirmed *S. aureus* strains were then preserved at 3-5°C for subsequent study.

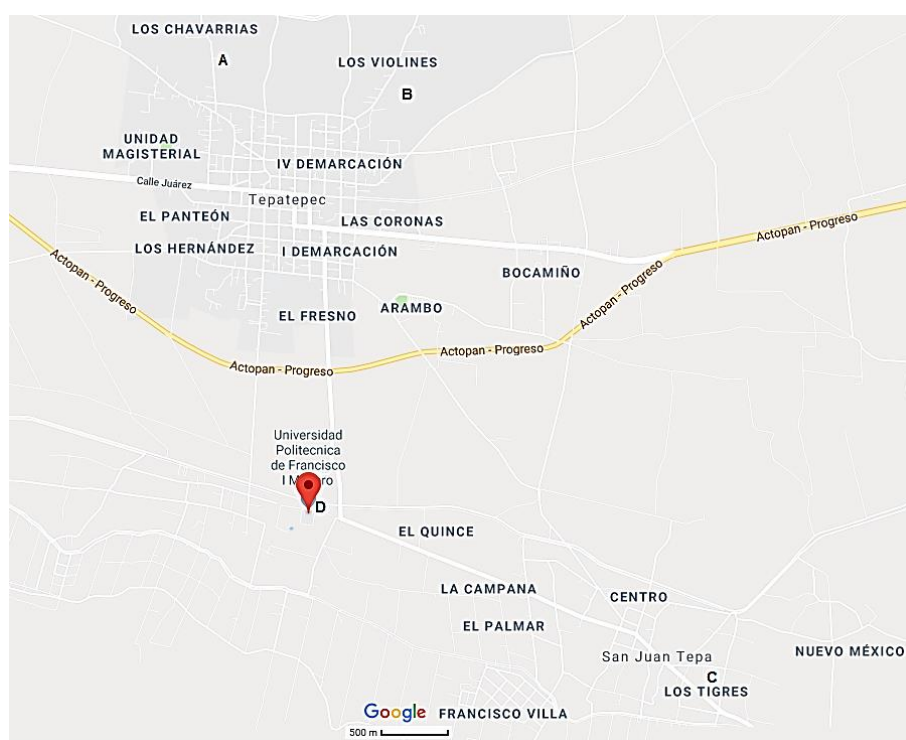


Figure 1. Location of the study areas

Antibiotic susceptibility testing

All *S. aureus* isolates were screened for antibiotic sensitivity to 12 different antibiotics using the disk-diffusion method on Muller-Hinton agar (Oxoid) with commercially available disks (Oxoid) in accordance with the Clinical and Laboratory Standards Institute (CLSI, 2014). The following antimicrobial agents were tested: ampicillin (10µg/mL); cefalotin (30 µg/mL); cefotaxim (30 µg/mL); ciprofloxacin (5 µg/mL); clindamycin (30 µg/mL); dicloxacillin (1 µg/mL); erythromycin (15 µg/mL); gentamicin (10 µg/mL); penicillin (10 IU); tetracycline (30 µg/mL); trimethoprim/sulfamethoxazole (25 µg/mL); and, vancomycin (30 µg/mL). The results

were evaluated after incubation at 35°C for 24 h, while the interpretations of antibiotic resistance were based on CLSI criteria (CLSI, 2014). For quality control, a reference strain of *S. aureus* (ATCC 25923) was used in the study.

Plant material and extract preparation

The extracts were obtained from *M. oleifera* specimens grown in Acapulco, the state of Guerrero, Mexico, and provided by the Universidad Autónoma de Guerrero. The age of the plant was two years.

The fresh leaves, stems and seeds were collected only once in May of 2017, they were cleaned and washed with water and dried in a heated chamber (Cole Parmer 399553-20, I, USA) at 40°C/24 h.

The *M. oleifera* extracts were produced following a previously described method (Gutiérrez-Alcántara et al., 2015; Cruz-Gálvez et al., 2013). Briefly, all the materials were pulverized using an electric blender (Oster BPST02-B00-013, Mexico). About 100 g of the powdered materials (leaves, stems and seeds) were weighed and placed in sterile glass flasks, after which 900 mL of 70% v/v ethanol was added. The flasks were sealed and stored at room temperature for 7 days.

The extracts were filtered through Whatman No. 1 filter paper, with the ethanol extract then evaporated to dryness under reduced pressure using a rotary evaporator (BÜCHI, Vacuum AQ3 176 Controller V-800; Flawil, Switzerland) at 40°C, leaving only the concentrated extract of the constituents of the powdered materials.

To prepare the aqueous extract, 100 g of the powdered materials (leaves, stems and seeds) was placed in a sterile glass flask, to which 900 mL of sterile distilled water was added. This was then heated to boiling point for 10 min and cooled to room temperature. The water was eliminated from the concentrate as described above, with the dried extracts then stored in sterile plastic bags at room temperature until use.

Preparation of the extract solution

A solution was prepared from each aqueous and ethanolic *M. oleifera* extract concentrate (produced from 5 g leaves, stems and seeds), using 100 ml of distilled water (final extract concentration: 50 mg mL⁻¹). *S. aureus* ATCC 25923 strain was used as a quality control.

Inoculum preparation and inoculation. The antibacterial activity of *M. oleifera* leaf, stem and seed extracts was tested using the disk-diffusion agar method, as previously described (Gutiérrez-Alcántara et al., 2016), although with some modifications (it changed the Trypticase Soy Agar agar for a Muller Hinton and penicillin was used as a positive control). Briefly, antibiotic-resistant *S. aureus* strains isolated from raw milk were inoculated in tubes containing 3 mL trypticase soy broth (TSB, Bioxon, the State of Mexico, Mexico) and incubated at 35°C for 24 h. The cultures were washed with sterile isotonic saline solution (0.85% NaCl) via centrifuge at 3500 rpm for 20 min, with the pellets then resuspended in sterile peptone water at approximately 10⁹ CFU/mL. A decimal dilution of these washed cultures was produced using isotonic saline solution to achieve a final approximate concentration of 8 log CFU/mL. A 100 µL suspension was taken from the first dilution of each washed bacterial culture, inoculated on Mueller Hinton plates and extended over the agar (Bioxon, Estado de Mexico, Mexico). Filter paper (Whatman No. 5) disks were placed on the surface of each agar plate. Aliquots (10 µL) of each extract were then placed on each disk (final dose per disc: 1 mg extract), with isotonic saline solution used as a negative control and penicillin as a

positive control. Each test was replicated three times. The plates were incubated for 24 h at 35°C, and then examined for the presence of bacterial inhibition zones around the disk. The diameter (mm) of any resulting inhibition zones was measured and the average diameter values were calculated for each extract.

Statistical analysis

Diameter of *S. aureus* growth was measured and expressed as means of percentage growth inhibition of three replicates. Significant differences were calculated using statistica 8 program (StatSoft, Inc., Tulsa, version 8).

Results and discussion

Prevalence of *S. Aureus*

Sixty-five *S. aureus* strains were identified and isolated from 56% (Table 1) of the raw milk sample, with an average count of 4.5×10^5 CFU/ml. More than one staphylococci colony per plate were evaluated from only eight of the samples. Farm A presented 16 positive samples, while the Farm D presented 11 positive samples (the UPFIM farm).

Table 1. Prevalence of *Salmonella* in the sample of the farms

Farm	Positive samples	Prevalence %
A (n=25)	16	64
B (n=25)	13	52
C (n=25)	16	64
D (n=25)	11	44
Total (n=100)	56	56%

The average *S. aureus* counts obtained in this research exceed the number of bacteria necessary (1.0×10^5 CFU/mL) to produce sufficient enterotoxin in order to induce foodborne intoxication (Cupakova et al., 2012). Moreover, they increase the probability of the production of staphylococcal toxins that are resistant to both the boiling process carried out in homes when raw milk is bought and pasteurization processes (Tebaldi et al., 2008). The isolates obtained in this study should be considered as a potential public health risk, as this pathogen may enter the food chain.

The *S. aureus* frequency observed in the raw milk samples (56%) coincides with the high *S. aureus* frequency reported in raw milk and dairy products in Greece and the USA (57.8% and 62%, respectively) (Papadopoulos et al., 2018; Haran et al., 2012). Furthermore, the results of this study are higher than those reported in Brazil by Fagundes et al. (2010) who observed a 7.3% frequency in raw milk samples, 6.7% in samples taken from individual cows, and 10.8% from bulk tank milk. In Italy, observed a 12.9% frequency in milk samples and dairy products (Basanisi et al., 2016). Riva et al. (2015) found that the prevalence of *S. aureus* was 9.1% in raw milk, while Normanno et al. (2007) reported a 17% contamination rate in milk and dairy products.

It should be noted both that other studies have reported prevalence rates of 66-86.1% (Saka and Terzi, 2018; Rania et al., 2013; Freitas et al., 2015; Rola et al., 2015), and that other authors have also reported the prevalence (13% and 30%) of this pathogen in

pasteurized milk (Akindolire et al., 2015; De Oliveira et al., 2011). The presence of these bacteria, after pasteurization, can be attributed to either the inefficacy of the thermal process or post-process contamination.

S. aureus is usually considered as a major cause of mastitis (Jamali et al., 2015). Certainly, many factors, such as improper bulk tank cleaning, dirty udders, an infected cow, dirty establishments and inappropriate hygiene conditions during milking, storage and manufacturing, are responsible for variations in the prevalence of *S. aureus* in dairy products, including milk (Roberson et al., 1998). For this reason, it is necessary to monitor animals state of health and improve hygienic conditions for milking, washing and the systematic disinfection of plants (Basanisi et al., 2017).

Antimicrobial susceptibility

All the *S. aureus* strains isolated from the raw milk exhibited resistance to at least two antibiotics. Sixty-five strains exhibited resistance to penicillin and ampicillin, followed by dicloxacillin. In contrast, all showed sensitivity to ciprofloxacin, while fifty-nine strains were sensitive to erythromycin (Table 2), fifty-three were sensitive to vancomycin, and fifty-three to tetracycline. The strains showed similar profile resistant to tetracycline and erythromycin, this may be possible because they act on protein synthesis. Ten strains presented intermediate resistance to cefotaxim. Similarly fourteen strains of *S. aureus* presented intermediate resistance to cefalotin and clindamycin despite being from different groups.

Table 2. Counts for *S. aureus* strains exhibiting resistance (R), intermediate resistance (I), or sensitivity (S) to 12 antibiotics

Antibiotic	R	I	S
Ampicillin	65*	0	0
Penicillin	65	0	0
Dicloxacillin	40	20	5
Cefotaxim	32	10	23
Cefalotin	31	14	20
Clindamycin	29	14	22
Gentamicin	28	12	25
Trimethoprim/Sulfamethoxazole	20	15	30
Vancomycin	9	3	53
Tetracycline	8	1	56
Erythromycin	5	1	59
Ciprofloxacin	0	0	65

*strain counts

The results of this study are similar to those obtained from research conducted in China (Yang et al., 2016), in which *S. aureus* strains isolated from bovine mastitis cases were resistant to penicillin (84.09%). In Greece, the most frequently observed resistance was to penicillin (99.3%) (Papadopoulos et al., 2018), while Jamali et al. (2015) observed resistance to penicillin (47.4 %) in strains isolated from raw milk and dairy products. The high percentage of *S. aureus* that is resistant to penicillin could be due to the widespread administration of this antimicrobial to control and treat infections found

in dairy farms (Jamali et al., 2013). Lowy (2003) reported that staphylococcal resistance to penicillin is mediated by β -lactamase, an extracellular enzyme which is synthesized when *S. aureus* is exposed to β -lactam antibiotics.

Resistance to ampicillin was high in all strains (100%), which is in accordance with the natural resistance of *S. aureus* β -lactams induced by exposure to penicillins (Fish et al., 1995). Other studies have shown resistance to ampicillin (Bernardo et al., 2005; Chudobova et al., 2015; Thaker et al., 2013). The results obtained here for ciprofloxacin coincide with a study in which *S. aureus* strains isolated from raw milk and dairy products were sensitive to ciprofloxacin (100%) (Jamali et al., 2015); moreover, Papadopoulos et al. (2018) reported that 97.09% of strains were sensitive to this antibiotic. In addition, strains isolated from clinical cases, raw milk and dairy product in both Mexico and India have been reported to be resistant to ciprofloxacin (Miranda-Novales, 2011; Thaker et al., 2013). Vancomycin-sensitive *S. aureus* has been isolated in Turkey and China (Rağbetli et al., 2016; Yang et al., 2016), while nine strains resistant to vancomycin were found in this study. This resistance is due to the acquisition of the van gene, which is transferred via a plasmid (Bustos-Martínez et al., 2006).

Strains of *S. aureus* that are resistant to erythromycin and tetracyclines but sensitive to gentamycin have been isolated from retail meat in Denmark (Tang et al., 2017), a profile which is different to that observed in the present study for *S. aureus* strains isolated from raw milk samples.

In-vitro antimicrobial activity of M. oleifera

The testing, conducted in this study, of the effect of the leaves, stems and seeds of *M. oleifera* on the twenty antibiotic-resistant *S. aureus* strains isolated from raw milk (previously selected for being multiresistant to 12 antibiotics) revealed that all the strains were sensitive to the two extracts (Table 3).

Table 3. Average diameter values of *M. oleifera* extract produced with two solvents versus antibiotic-resistant *S. aureus* strains and control strains

Strains	Zones of inhibition (Diameter in mm)		
	Ethanollic extract	Aqueous extract	Penicillin
1	24 ± 02	23 ± 04	10 ± 0.2
2	25 ± 03	22 ± 04	10 ± 0.2
3	25 ± 02	23 ± 02	11 ± 0.1
4	25 ± 01	23 ± 01	10 ± 0.2
5	25 ± 02	23 ± 08	11 ± 0.2
6	25 ± 02	21 ± 04	11 ± 0.2
7	25 ± 1.0	23 ± 01	11 ± 0.1
8	24 ± 02	23 ± 06	10 ± 0.2
9	25 ± 02	22 ± 04	9 ± 0.2
10	25 ± 02	23 ± 03	9 ± 0.2
11	25 ± 03	23 ± 03	10 ± 0.3
12	25 ± 02	21 ± 01	10 ± 0.2
13	25 ± 03	23 ± 06	10 ± 0.2
14	25 ± 02	23 ± 08	10 ± 0.2
15	24 ± 02	21 ± 06	11 ± 0.2
16	25 ± 02	23 ± 06	11 ± 0.1
17	25 ± 02	23 ± 04	10 ± 0.2
18	25 ± 01	22 ± 02	11 ± 0.2
19	24 ± 02	23 ± 02	10 ± 0.2
20	25 ± 02	21 ± 02	10 ± 0.2
*SA	25 ± 02	22 ± 02	10 ± 0.2

* SA (*S. aureus* ATCC 25923)

The ethanolic extract presented the highest inhibitory effect against isolates from raw milk with halos of inhibition of 24.83 mm (mean). The mean of the halos of inhibition for the aqueous extract was 22.17 mm, while the penicillin presented halos of inhibition of 9.77 mm, and the halos of inhibition for the control strains were similar to the halos for the multiresistant strain. The strains 1, 8 and 18 showed similar diameters with the extracts used, while the control strain showed similar diameters with the strain 2.

In addition, penicillin, ethanol and aqueous extract showed highly significant difference ($p < 0.0001$).

Currently there are no studies focused on analyzing the effect of the leaf, seed and stems together of *M. oleifera*, previously good results have been observed separately (Brilhante et al., 2015; Lar et al., 2011).

The halos of inhibition found in this study (21-25 mm) coincide with a research in which *M. oleifera* seeds were studied for antimicrobial activity against *Bacillus subtilis*, *Salmonella typhimurium*, *Enterobacter aerogenes*, *Pseudomonas aeruginosa*, *Escherichia coli*, *Vibrio cholerae* and *S. aureus* (Ruttarattanamongkol and Petrasch, 2015). The above mentioned research found that *S. aureus* presented the maximum inhibition zone of 20.67 and 24.67 mm. In contrast Peixoto et al. (2011) observed inhibition halos of up to 35 mm when challenging *S. aureus* with aqueous and ethanolic *M. oleifera* leaf extracts, but they also showed halos de inhibicion de 21-25 mm against *Vibrio parahaemolyticus* and *Enterococcus*. Some authors have attributed the antibacterial effect of the leaves to the presence of saponine, tannic, phenolic and alkaloid phytoconstituents (Doughari et al., 2007).

Working on the same plant species, Bukar et al. (2010) demonstrated the antibacterial activity of ethanolic extract of its seed, via the agar well diffusion method, against *S. aureus*, *Salmonella typhi* and *E. coli*. The activity of the two extracts was compared to a standard antibiotic (penicillin), as this antibiotic showed low efficiency in the previously isolated resistance profiles for the *S. aureus* strains. However, the two *M. oleifera* stem, leaf and seed extracts (ethanolic and aqueous) exhibited higher antibacterial activity compared to penicillin.

The ethanolic extract has been shown to present antimicrobial properties against *S. aureus*, with the findings of this research differing from Brilhante et al. (2015) who reported low antimicrobial effectiveness in ethanol extracts of *M. oleifera* pods, leaves, stems and seeds against *Vibrio spp.* strains, as well as no effect against *E. coli*. Furthermore, the results of the present study concur with those reported previously by other researchers in an evaluation of the antimicrobial effect of *M. oleifera* seed extracts against non-antibiotic resistant *S. aureus* (Viera et al., 2010; Ruttarattanamongkol and Petrasch, 2015).

The aqueous extract used in the present study presented inhibition halos of 22.17 mm, which concurs with the results reported previously by research which evaluated the antimicrobial effect of aqueous *M. oleifera* seed extract against *S. aureus*, *Vibrio cholerae* and *E. coli* isolated from shrimp samples, observing inhibition halos of 19-25 mm (Viera et al., 2010).

While Lar et al. (2011) reported that the aqueous extract of *M. oleifera* seeds had no effect on *E. coli*, *Shigella flexneri* and *S. typhi*, appreciable antimicrobial activity was demonstrated by ethanolic seed extract on the same bacteria.

Similarly Kalpana et al. (2013) found antimicrobial activity using ethanolic extract of leaves of *M. oleifera* against *S. aureus* with diameters of 10-15 mm.

The antimicrobial activity of *M. oleifera* has been attributed to antimicrobial peptides and bioactive compounds (Prasad and Elumalai, 2011). Wang et al. (2016) state that 4-(α -L-rhamnopyranosyloxy) benzyl isothiocyanate, methyl N-4-(α -L-rhamnopyranosyloxy) benzyl carbamate, and 4-(β -D-glucopyranosyl-1 \rightarrow 4- α -L-rhamnopyranosyloxy)-benzyl thiocarboxamide are the three compounds of *M. oleifera* seed that present potent antibacterial activity against some pathogens.

Specifically, the compound 4-(α -L-rhamnopyranosyloxy) benzyl isothiocyanate was found to inhibit the growth of *S. aureus* (Galuppo et al., 2013).

Almost all parts of the *M. oleifera* plant have an antimicrobial effect. In a previous study, Zaffer et al. (2014) found that the aqueous extract of *M. oleifera* bark presented high activity against *S. aureus*, while Devi et al. (2011) demonstrated the antibacterial activity of methanolic *M. oleifera* bark extract against *Bacillus spp.* and *S. aureus*.

In India, Devendra et al. (2011) demonstrated that chloroform *M. oleifera* leaf extract inhibits the growth of *S. aureus* and *Streptococcus pyogenes*, with halos of inhibition of 6.2 and 6.0 mm, these diameters were lowest than ours. Nevertheless, Moyo et al. (2012) used water extract of *M. oleifera* and they did not show any antimicrobial activity against *S. aureus*, this differ with our results. Our findings also differ with that report by Singh et al. (2013), who reported that the ethanolic and aqueous extracts had low activity against the same pathogen.

It has also been shown that the *M. oleifera* flower has an antimicrobial effect against strains of *V. cholerae* and *E. coli* (Brilhante et al., 2015), an antibacterial property of *M. oleifera* flowers that has been attributed to a substance called pterygospermin (Anwar et al., 2007). Many studies have suggested that different crude extracts obtained from different *M. oleifera* tissues present antibacterial activities against both Gram-negative and Gram-positive bacteria (Wang et al., 2016; Bukar et al., 2010; Brilhante et al., 2015; Peixoto et al., 2011). Differences in polarity among the various solvents (methanol, ethanol, chloroform, water, petroleum ether, and ethyl acetate) may be responsible for the differences in the solubility of plant active principles, hence the variation in the degree of antimicrobial activity (Patel et al., 2018).

This study has shown that *S. aureus* strains resistant to multiple antibiotics are commonly found in the raw milk sold in the municipality of Francisco I. Madero, constituting a serious public health risk for the region's population. The most effective antibiotics against *S. aureus* were found to be ciprofloxacin, erythromycin and tetracycline.

The indiscriminate use of antibiotics for prophylactic and other therapeutic purposes could be the reason for the increased antimicrobial resistance of *S. aureus*.

Ethanol extract exhibited a higher degree of antimicrobial activity compared to the aqueous extracts and penicillin. This reveals that the leaves, stems and seeds of *M. oleifera* could be an alternative for the control of infections caused by *S. aureus* in humans and cows with mastitis.

Future studies will need to evaluate the antibacterial effect of *M. oleifera* leaf, stem and seed extract against other multidrug resistant-strains, such as *E.coli*, *Salmonella*, *Shigella*, *Listeria monocytogenes*, and *V. cholerae*.

Acknowledgements. The authors are grateful to the Universidad Politécnica de Francisco I. Madero for the financial support provided to this study.

REFERENCES

- [1] Akindolire, M. A., Babalola, O. O., Ateba, C. N. (2015): Detection of Antibiotic Resistant *Staphylococcus aureus* from Milk: A Public Health Implication. – *Int J Environ Res Public Health* 12(9): 10254-10275.
- [2] Anwar, F., Latif, S., Ashraf, M., Gilani, A. H. (2007): *Moringa oleifera*: a food plant with multiple medicinal uses. – *Phytother Res* 21(1): 17-25.
- [3] Arora, D. S., Onsare, J. G. (2014): In vitro antimicrobial evaluation and phytoconstituents of *moringa oleifera* pod husks. – *Ind Crops Prod* 52(1): 125-135.
- [4] Arora, D. S., Onsare, J. M., Kuar, H. (2013): Bioprospecting of *Moringa* (Moringaceae): microbiological perspective. – *J Pharmacogn Phytochem* 1(6): 193-215.
- [5] Basanisi, M. G., La Bella, G., Nobili, G., Franconieri, I., La Salandra, G. (2017): Genotyping of methicillin-resistant *Staphylococcus aureus* (MRSA) isolated from milk and dairy products in South Italy. – *Food Microbiol* 62: 141-146.
- [6] Beltrán-Heredía, J., Sánchez-Martín, J. (2009): Improvement of water treatment pilot plant with *Moringa oleifera* extract as flocculant agent. – *Environ Technol* 30(6): 525-534.
- [7] Bernardo, W. L., Boriollo, M. F., Gonçalves, R. B., Höfling, J. F. (2005): *Staphylococcus aureus* ampicillin-resistant from the odontological clinic environment. – *Rev Inst Med Trop Sao Paulo* 47(1): 19-24.
- [8] Brilhante, R. S. N., Sales, J. A., De Souza Sampaio, C. M., Barbosa, F. G., De Araújo, N. P. M., De Melo Guedes, G. M. (2015): *Vibrio* spp. from *Macrobrachium amazonicum* prawn farming are inhibited by *Moringa oleifera* Extracts. – *Asian Pac J Trop Me* 8(11): 919-922.
- [9] Bukar, A., Uba, A., Oyeyi, I. (2010): Antimicrobial profile of *Moringa Oleifera* Lam. Extracts against some foodborne microorganisms. – *Bayero Journal of Pure and Applied Sciences* 3(1): 43-48.
- [10] Bustos-Martínez, J. A., Hamdan-Partida, A., Gutiérrez-Cárdenas, M. (2006): *Staphylococcus aureus*: la reemergencia de un patógeno en la comunidad. – *Rev Biomed* 17: 287-305.
- [11] Chudobova, D., Dostalova, S., Blazkova, I., Michalek, P., Ruttkay-Nedecky, B., Sklenar M. (2014): Effect of Ampicillin, Streptomycin, Penicillin and Tetracycline on Metal Resistant and Non-Resistant *Staphylococcus aureus*. – *Int J Environ Res Public Health* 11(3): 3233-3255.
- [12] CLSI. (Clinical and Laboratory Standards Institute) (2014): Performance Standards for Antimicrobial Susceptibility Testing. Nineteen Informational Supplement. – M100-S19 Wayne, Pa, USA.
- [13] CLSI. (Clinical and Laboratory Standards Institute) (2014): Performance Standards for Antimicrobial Susceptibility Testing. Twenty-four Informational Supplement. – Tech. Rep. M100-S24. Wayne, Pa, USA.
- [14] Cruz-Gálvez, A. M., Gómez-Aldapa, C. A., Villagomez-Ibarra, J. R., Chavarría-Hernández, N., Rodríguez-Baños, J., Rangel-Vargas, E., Castro-Rosas, J. (2013): Antibacterial effect against foodborne bacteria of plants used in traditional medicine in central Mexico: Studies in vitro and in raw beef. – *Food Con* 32: 289-295.
- [15] Cupakova, S., Pospisilova, M., Karpiskova, R., Janstova, B., Vorlova, L. (2012): Microbiological quality and safety of goat's milk from one farm. – *Acta Univ Agric Fac Agron* 60(6): 33-38.
- [16] De Oliveira, L. P., Soares, B. L. S., Silva, V. C., Cirqueira, M. G. (2011): Study of *Staphylococcus aureus* in raw and pasteurized milk consumed in the Reconcavo area of the State of Bahia, Brazil. – *J Food Process Technol* 2(6): 1-5.
- [17] Devendra, B. N., Srinivas, N., Talluri, V. S. S. L. P., Latha, P. S. (2011): Antimicrobial activity of *Moringa oleifera* Lam., leaf extract, against selected bacterial and fungal strains. – *International Journal of Pharma and Bio Sciences* 2(3): 13-18.

- [18] Devi, G. S., Priya, V., Abiramasundari, P., Jeyanthi, P. G. (2011): Antibacterial activity of the leaves, bark, seed and flesh of *Moringa oleifera*. – *Int J Phar Sci and Res* 2(8): 2045-2049.
- [19] Doughari, J., Pukuma, M., De, N. (2007): Antibacterial effects of *Balanites aegyptiaca* L. Drel. and *Moringa oleifera* Lam. On *Salmonella typhi*. – *African Journal of Biotechnology* 6(19): 2212-2215.
- [20] EFSA. European Food Safety Authority (2009): Joint scientific report of ECDC, EFSA and EMEA on meticillin resistant *Staphylococcus aureus* (MRSA) in livestock, companion animals and foods. – EFSA-Q-2009-00612. EFSA Scientific Report 301: 1-10.
- [21] Ezeamuzie, I. C., Ambakederemo, A. W., Shode, F. O., Ekwebelem, S. C. (1996): Antiinflammatory effects of *Moringa oleifera* root extract. – *Pharm Biol* 34(3): 207-212.
- [22] Fagundes, H., Barchesi, L., Filho, A. N., Ferreira, M. L., Fernandes Oliveira, C. A. (2010): Occurrence of *Staphylococcus aureus* in raw milk produced in dairy farms in São Paulo state, Brazil. – *Braz J Microbiol* 41(2): 376-380.
- [23] Farooq, F., Rai, M., Tiwari, A., Khan, A. A., Farooq, S. (2012): Medicinal properties of *Moringa oleifera*: An overview of promising healer. – *J Med Plants Res* 6(27): 4368-4374.
- [24] Ferreira, R. S., Napoleão, T. H., Santos, A. F. S., Sá, R. A., Carneiro-da-Cunha, M. G., Morais, M. M. (2011): Coagulant and antibacterial activities of the water-soluble seed lectin from *Moringa oleifera*. – *Lett Appl Microbiol* 53(2): 186-192.
- [25] Fish, D. N., Piscitelli, S. C., Danziger, L. H. (1995): Development of resistance during antimicrobial therapy: a review of antibiotic classes and patient characteristics in 173 studies. – *Pharmacotherapy* 15(3): 279-291.
- [26] Freitas, J. A., Oliveira, J. P., Galinda, G. A. R. (2005): Avaliação da qualidade higiênico sanitária do leite exposto ao consumo na região metropolitana de Belém-PA. – *Rev Inst Adolfo Lutz* 64(2): 212-218.
- [27] Galuppo, M., Nicola, G. R., Iori, R., Dell'Utri, P., Bramanti, P. (2013): Antibacterial activity of glucomoringin bioactivated with myrosinase against two important pathogens affecting the health of long-term patients in hospitals. – *Molecules* 18(11): 14340-14348.
- [28] Gutiérrez-Alcántara, E. J., Rangel-Vargas, E., Gómez-Aldapa, C. A., Falfan-Cortes, R. N., Rodríguez-Marín, M. L., Godínez-Oviedo, A. (2015): Antibacterial effect of roselle extracts (*Hibiscus sabdariffa*), sodium hypochlorite and acetic acid against multidrug-resistant *Salmonella* strains isolated from tomatoes. – *Lett Appl Microbiol* 62: 177-184.
- [29] Gutiérrez-Alcántara, E. J., Gómez-Aldapa, C. A., Román-Gutiérrez, A. D., Rangel-Vargas, E., González-Olivares, L. G., Castro-Rosas, J. (2016): Antimicrobial activity of roselle *Hibiscus sabdariffa* calyx extracts on culture media and carrots against multidrug-resistant *salmonella* strains isolated from raw carrots. – *J Food Saf* 35(4): 450-458.
- [30] Haran, K. P., Godden, S. M., Boxrud, D., Jawahir, S., Bender, J. B., Sreevatsan, S. (2012): Prevalence and characterization of *Staphylococcus aureus*, including methicillin-resistant *Staphylococcus aureus*, isolated from bulk tank milk from Minnesota dairy farms. – *J Clin Microbiol* 50(3): 688-695.
- [31] Jamali, H., Radmehr, B., Thong, K. L. (2013): Prevalence, characterisation, and antimicrobial resistance of *Listeria* species and *Listeria monocytogenes* isolates from raw milk in farm bulk tanks. – *Food Cont* 34(1): 121-125.
- [32] Jamali, H., Radmehr, B., Ismail, S. (2014): Prevalence and antibiotic resistance of *Staphylococcus aureus* isolated from bovine clinical mastitis. – *Journal of Dairy Science* 97: 2226-2230.
- [33] Jamali, H., Paydar, M., Radmehr, B., Ismail, S., Dadrasnia, A. (2015): Prevalence and antimicrobial resistance of *Staphylococcus aureus* isolated from raw milk and dairy products. – *Food Cont* 54: 383-388.

- [34] Kalpana, S., Moorthi, S., Sushila kumari. (2013): Antimicrobial activity of different extracts of leaf of *Moringa oleifera* (Lam) against gram positive and gram negative bacteria. – *Int. J. Curr. Microbiol. App. Sci* 2(12): 514-518.
- [35] Lar, P. M., Ojile, E. E., Dashe, E., Oluoma, J. N. (2011): Antibacterial activity of *Moringa oleifera* seed extracts on some gram negative bacterial isolates. – *African journal of natural sciences* 14: 57-62.
- [36] Lowy, F. D. (2003): Antimicrobial resistance: the example of *Staphylococcus aureus*. – *J Clin Invest* 111(9): 1265-1273.
- [37] Mehli, L., Hoel, S., Thomassen, G. M. B., Jakobsen, A. N., Karlsen, H. (2017): The prevalence, genetic diversity and antibiotic resistance of *Staphylococcus aureus* in milk, whey, and cheese from artisan farm Dairies. – *International Dairy Journal* 65: 20-27.
- [38] Miranda-Novales, M. G. (2011): Antimicrobial resistance in *Staphylococcus aureus* in Mexico. – *Bol Med Hosp Infant Mex* 68(4): 242-249.
- [39] Moyo, B., Masika, P. J., Muchenje, V. (2012): Antimicrobial activities of *Moringa oleifera* Lam leaf extracts. – *African Journal of biotechnology* 11(11): 2797-2802.
- [40] NFSA. (2018): MRSA funnet hos storfe i Rogaland. Oslo, Norway: Norwegian Food Safety Authority (Accessed 23 march 2018). – http://www.mattilsynet.no/dyr_og_dyrehold/produksjonsdyr/storfe/mrsa_funnet_hos_storfe_i_rogaland.20524.
- [41] Nkurunziza, T., Nduwayezu, J. B., Banadda, E. N., Nhapi, I. (2009): The effect of turbidity levels and *Moringa oleifera* concentration on the effectiveness of coagulation in water treatment. – *Water Sci technol* 59(8): 1551-1558.
- [42] Normanno, G., La Salandra, G., Dambrosio, A., Quaglia, N. C., Corrente, M., Parisi, A. (2007): Occurrence, characterization and antimicrobial resistance of enterotoxigenic *Staphylococcus aureus* isolated from meat and dairy products. – *Int J Food Microbiol* 115(3): 290-296.
- [43] Padla, E. P., Solis, L. T., Levida, R. M., Shen, C. C., Ragasa, C. Y. (2012): Antimicrobial isothiocyanates from the seeds of *Moringa oleifera* Lam. – *Z Naturforsch C* 67(11-12): 557-564.
- [44] Papadopoulos, P., Papadopoulos, T., Angelidis, A. S., Boukouvala, E., Zdragas, A., Papa, A. (2018): Prevalence of *Staphylococcus aureus* and of methicillin-resistant *S. aureus* (MRSA) along the production chain of dairy products in north-western Greece. – *Food Microbiol* 69: 43-50.
- [45] Patel, N., Mohan, J. S. S. (2018): Antimicrobial Activity and Phytochemical Analysis of *Moringa oleifera* Lam. Crude Extracts Against Selected Bacterial and Fungal Strains. – *International Journal of Pharmacognosy and Phytochemical Research* 10(2): 68-79.
- [46] Peixoto, J. R., Silva, G. C., Costa, R. A., De Sousa, F. J. R., Vieira, G. H., Filho, A. A. (2011): In vitro antibacterial effect of aqueous and ethanolic *Moringa* leaf extracts. – *Asian Pac J Trop Med* 4(3): 201-204.
- [47] Phillips, I., Casewell, M., Cox, T., De Groot, B., Friis, C., Jones, R. (2004): Does the use of antibiotics in food animals pose a risk to human health? A critical review of published data. – *J Antimicrob Chemother* 53(1): 28-52.
- [48] Prasad, T. N., Elumalai, E. K. (2016): Biofabrication of Ag nanoparticles using *Moringa oleifera* leaf extract and their antimicrobial activity. – *Asian Pac J Trop Biomed* 2011 1(6): 439-442.
- [49] Rağbetli, C., Parlak, M., Bayram, Y., Guducuoglu, H., Ceylan, N. (2016): Evaluation of Antimicrobial Resistance in *Staphylococcus aureus* Isolates by Years. – *Interdiscip Perspect Infect Dis*: 1-4.
- [50] Rania, M. K., Mohamed, A. B., Salah, F. A. A. E. A. (2013): MRSA detection in raw milk, some dairy products and hands of dairy workers in Egypt, a mini-survey. – *Food Cont* 33: 49-53.
- [51] Riva, A., Borghi, E., Cirasola, D., Colmegna, S., Borgo, F., Amato, E. (2015): Methicillin-Resistant *Staphylococcus aureus* in Raw Milk: Prevalence, SCCmec Typing,

- Enterotoxin Characterization, and Antimicrobial Resistance Patterns. – J Food Prot 78(6): 1142-1146.
- [52] Roberson, J. R., Fox, L. K., Hancock, D. D., Gay, J. M., Besser, T. E. (1998): Sources of intramammary infections from *Staphylococcus aureus* in dairy heifers at first parturition. – J Dairy Sci 81(3): 687-693.
- [53] Rola, J. G., Sosnowski, M., Ostrowska, M., Osek, J. (2015): Prevalence and antimicrobial resistance of coagulase-positive staphylococci isolated from raw goat milk. – Small Rum Res 123: 124-128.
- [54] Ruttarattanamongkol, K., Petrasch, A. (2015): Antimicrobial activities of *Moringa oleifera* seed and seed oil residue and oxidative stability of its cold pressed oil compared with extra virgin olive oil. – Songklanakarin J Sci Technol 37(5): 587-594.
- [55] Rybak, M. J., Laplante, K. L. (2005): Community-associated methicillin-resistant *Staphylococcus aureus*: a review. – Pharmacotherapy 25(1): 74-85.
- [56] SAGARPA. (Secretaria de agricultura, Ganadería, recursos naturales, Pesca y Alimentación) (2016): Producción anual. SIAP. Servicio de Información Agroalimentaria y pesquera. – Available at: http://infosiap.siap.gob.mx/anpecuario_siapx_gobmx/indexmpio.jsp. Accessed may 5, 2018.
- [57] Saka, E., Terzi, G. G. (2018): Detection of Enterotoxin Genes and Methicillin-Resistance in *Staphylococcus aureus* isolated from Water Buffalo Milk and Dairy Products. – J Food Sci 83(6): 1716-1722.
- [58] Tang, Y., Larsen, J., Kjeldgaard, J., Andersen, P. S., Skov, R., Ingmer, H. (2017): Methicillin-resistant and susceptible *Staphylococcus aureus* from retail meat in Denmark. – Int J Food Microbiol 249: 72-76.
- [59] Tebaldi, V. M. R., Oliveira, T. L. C., Boari, C. A., Piccoli, R. H. (2008): Isolamento de coliformes, estafilococos e enterococos de leite cru provenientes de tanques de refrigeração por expansão comunitários: identificação, ação lipolítica e proteolítica. – Ciênc Tecnol Aliment Campinas 28(3): 753-760.
- [60] Thaker, H. C., Brahmhatt, M. N., Nayak, J. B. (2013): Isolation and identification of *Staphylococcus aureus* from milk and milk products and their drug resistance patterns in Anand, Gujarat. – Vet World 6(1): 10-13.
- [61] Thilza, I. B., Sanni, S., Zakari, A. I., Sanni, F. S., Muhammed, T., Musa, B. J. (2010): In vitro antimicrobial of water extract of *Moringa oleifera* leaf stalk on bacterial normally implicated in eye disease. – Acad Aren 2(6): 80-83.
- [62] Viera, G. H., Mourão, J. A., Angelo, A. M., Costa, R. A., Vieira, R. H. (2010): Antibacterial effect (in vitro) of *Moringa oleifera* and *Annona muricata* against Gram positive and Gram negative bacteria. – Rev Inst Med Trop Sao Paulo 52(3): 129-132.
- [63] Wang, L., Chen, X., Wu, A. (2016): Mini review on Antimicrobial Activity and Bioactive Compounds of *Moringa oleifera*. – Med Chem 6(9): 578-582.
- [64] Yang, F., Wang, Q., Wang, X., Wang, L., Li, X., Luo, J. (2016): Genetic characterization of antimicrobial resistance in *Staphylococcus aureus* isolated from bovine mastitis cases in Northwest China. – Journal of Integrative Agriculture 15(12): 2842-2847.
- [65] Zaffer, M., Ahmad, S., Sharma, R., Mahajan, S., Gupta, A., Agnihotri, R. K. (2014): Antibacterial activity of bark extracts of *Moringa oleifera* Lam. against some selected bacteria. – Pak J Pharm Sci 27(6): 1857-1862.
- [66] Zecconi, A., Hahn, G. (2000): *Staphylococcus aureus* in raw milk and human health risk. – Bull. IDF 345: 15-18.

EVALUATION SYSTEM AND SPATIAL DISTRIBUTION PATTERN OF ECOLOGICAL CITY CONSTRUCTION – BASED ON DPSIR- TOPSIS MODEL

SHI, S.-X.* – TONG, P.-S.

*College of Public Management, Fujian Agriculture and Forestry University
350002 Fuzhou, Fujian Province, China
(e-mail: hku128sh@yeah.net – P.-S. Tong)*

**Corresponding author
e-mail: fjssx666@163.com*

Both authors contributed equally to this work.

(Received 15th Sep 2018; accepted 12th Nov 2018)

Abstract. Ecological city construction plays a major role in achieving a sustainable and healthy city development. To facilitate the deep understanding of ecological city development condition and its construction process, the following studies were carried out in this paper: a comprehensive evaluation index system was firstly established based on DPSIR-TOPSIS model. The paper then went on to examine the spatial distribution status of ecological city construction according to the clustering results of coordination degree. Obstacle parameter analysis was conducted using obstacle degree model to study ecological construction level in 34 ecological cities. The result showed that: the ecological construction condition of a city in central and coastal area stayed at high level; Good coupling coordination degree among the five factors of DPSIR was found in The Pearl River Delta and The Yangtze River Delta; Driving force and Impact systems that highly affect city ecological construction in western and northern area, while ecological construction in cities like Lanzhou and Xining approached to the state of preliminary coordination. In general, ecological city construction in China is showing a constant improvement. However, cities of high-level coordination are still short-numbered.

Keywords: *ecological city, DPSIR-TOPSIS model, obstacle degree, coordinating degree, spatial pattern distribution*

Introduction

Since the opening up policy, urbanization has been greatly advanced by industrial agglomeration, urban expansion and population migration. In 2012, the urbanization rate reached over 50% for the first time and figure increased over 57.35% in 2016 (Xia et al., 2018). The urbanization has brought in the fast economic development, and at the same time resulted in many environmental and social problems. For instance, non-renewable resources are consumed in a fast speed, domestic and industrial water is massively discharged to the nature, resources and public facilities allocated to percapita is inefficient due to huge growth of population. These problems not only hinder the path of achieving a sustainable social and economic development, but also are against the main concept of building a “wild China”. As the 19th CPC National Congress has promoted the “*Ecological Civilization*” being the main body of China’s economic development, “Wild China” becomes a cause of shared future of mankind. According to statistics, China urbanization rate in the coming ten decades will continue growing. Hence, how to pursue a steady approach to promote urbanization under the “ecological civilization” theme, integrate it into the whole process of urbanization, and achieve the coordinated development between ecological construction and economic & social

development are the practical problems worth attention. This paper is to conduct the evaluation, regional disparity and obstacle degree over 34 cities on their ecological construction, hoping it could contribute to the cause of ecological city construction.

Literature review

Since the industrial revolution, ecological construction has been a common concern of most countries and international organizations. Scholars all over the world have actively carried out theoretical and practical research on this concept and introduced it into ecological cities, following the United Nations presented it in the report of the Man and the Biosphere Program. The earliest “ecology” refers to the living state of biomes in the biosphere (Ghiselin, 1974). Later, the British scholar Tansler (Huang and Zeng, 2015) proposed the “ecosystem”, that is, the biological and ecological environment form a unity in nature. Foreign scholars have not stated the concept of eco-city clearly. However, in a broad sense, eco-city refers to the establishment of social relations based on ecological principles, including social harmony, economic development, and superior natural environment, so that the resource environment can be utilized and recyclable. The eco-city in the narrow sense refers to the design and planning of the city according to the ecology principle, to establish a harmonious, efficient and sustainable ecological society. In this regard, countries have made a lot of achievements in ecological environment construction, such as green politics in the United States, eco-industrial parks in Japan. Based on the current urban development, the meaning of eco-city is enriching constantly. Different countries have drawn up appropriate development routes for their own situations, approaching green cities, but they still have a certain distance from eco-cities. In contrast, domestic scholars have focused on the connotation of “ecological civilization” based on the macro environment and then implemented it into the construction dimension of specific eco-cities. Among them, the macroscopic view involves the relationship between ecological civilization and nature (Gu et al., 2013), the relationship between ecological civilization and modern civilization (Shen, 2013), the relationship between the construction of ecological civilization and the development of the times (Zeng, 2017). The concrete implementation includes the urban ecological environment construction, economic construction, system construction, science and technology construction. Marx (Yu, 2005) once proposed that the socialist society is a harmonious and unified society between man and nature, and ecological civilization is the product of the development of industrial civilization to a certain stage, as an important component of human civilization. Therefore, the construction of ecological civilization is inseparable from the sustainable development of economy and society, and the eco-city is a new vision of the future city.

In recent years, theories and practices of ecological city construction have been under constant development. At the end of 2013, the Central Economic Working Conference had made a clear policy of “fully inserting the concept and principal of ecologic civilization into the development of urbanization to pursue an ecologically characterized urbanization cause”, making the ecological construction a significant policy for the cause of urbanization (Bi et al., 2017). Ecological city construction therefore, will be the important development direction in future urbanization. Yanitsky (1982) pointed out that the basic character of ecological city should be a city of: prosperous economic status, civilized, environmentally beautiful, technology and nature in great harmonious. Kline et al. (2009) indicated that ecological city is a city of economic safety, where

human and nature are harmoniously combined, people's living standard in high level and governments highly responsible to their people etc. In 1992, Rio Declaration promoted that humankind possesses the right of living a naturally coordinated, healthy and rich life. And this is in consistent with the top goal of ecological city construction, i.e. meeting people's basic life requirement and improving their living standard. The development bodies therefore, shall pursuit a human-oriented development concept though city development. Public participation plays a critical role in ecological city construction (Mi and Peng, 2014), and it shall be guaranteed by government policies (Zhao and Wang, 2015). A well management system, the economic, social and cultural innovation are key factors for ecological city construction (Zhang, 2015). It cannot develop well without a complete management system and co-effort of multiple parties on all aspects (Li, 2008). In 2015, President Xi Jinping initiated a series of city environmental improving polices based on the actual development condition of the country. In 2016, measures and policies on pursuing a sustainable and healthy city development were brought out on the basis of "Five Development Concepts". With China's address on ecological civilization and judging from scholar's in-depth studies, it becomes clear that it is not efficient if only focus the study on policy making, party participation etc., it is also important to formulate an appropriate evaluation index system to identify the existing problems and regional disparity. An et al. (2017) conducted such study by describing fragile factors influencing ecological city construction by means of fragility measurement; Zhang and Zhang (2015) built up an evaluation index system based on ecological city connotations, while Cheng and Ning (2014) built up the system from social-ecologic view suggested by experts. Ren et al., (2016) formulated a 3D model of ecological city planning, where the author used measuring method to make comparison to analyze the ecological cities of better development property.

Theoretical and practical studies have been broadly taken by scholars' home and abroad and great achievements have been made. As the previous studies mainly focused on micro body participation in macro policy making, the evaluation index system thus formulated are subjective and the vision is somewhat narrowed. In this paper, and evaluation index system were established based on DPSIR concept model, with TOSPIS method as the evaluation method. Obstacle factors of each city were described using the obstacle degree model. The results and suggestions were then given as reference, hoping it could be the helpful material in sustainable city development and wild China cause.

Ecological city construction evaluation index system based on DPSIR-TOPSIS model

DPSIR model

This paper introduced DPSIR model to evaluate different level of ecological city construction. DPSIR model is developed from the PSR model from Organization for Economic Co-operation and Development (OECD) of European Environment Agency (EEA). It refers to five factors influencing the ecological city construction, i.e. Driving force, Pressure, State, Impact and Response, reflection the causation of "What, why and how". In DPSIR model, Driving force is a dynamic factor for ecological city construction; Pressure refers to human activities affecting the ecological environment, a direct pressure factor affecting the ecological environment; State means the condition of

ecological environment under the above pressure, i.e. the ecological construction level; Impact refers to the ecological construction requirement under a certain system and its impact; Response means the effective measures and policies adopted for ecological development. DPSIR is a causal framework for describing the interactions between humankind and ecological city construction. This framework, due to its clear, hierarchy and objective structure, lays a theoretic foundation for establishing ecological city evaluation system.

Determination of evaluation indexes

Evaluation indexes are selected mainly on the basis of DPSIR-TOPSIS model. It follows a principal of scientific, independent, operational and subjectively & objectively combined. The system is demonstrated in three-layer structures: criteria, key elements, and index (see table 1).

Table 1. Evaluation index system

Criteria	Index	Code	Property	Weight
Driving force 0. 2224	GDP growth rate (%)	C1	positive	0. 0556
	GDP per capita (yuan)	C2	positive	0. 0556
	Urban per capita disposable income (yuan)	C3	positive	0. 0557
	Added value of the tertiary industry (%)	C4	positive	0. 0555
Pressure 0. 2777	Energy consumption per unit GDP (ton of standard coal/million yuan)	C5	negative	0. 0555
	Water Consumption per unit GDP (ton/million yuan)	C6	negative	0. 0556
	Generation of industrial solid waste per unit GDP (ton/million yuan)	C7	negative	0. 0555
	Industrial waste water emission per unit GDP (ton/million yuan)	C8	negative	0. 0555
	CO2 emissions per unit GDP (ton/ million yuan)	C9	negative	0. 0556
States 0. 1665	Park/green space area per capita (m ²)	C10	positive	0. 0556
	Greening coverage in built-up area (%)	C11	positive	0. 0554
	Government fiscal expenditure on environment (%)	C12	positive	0. 0555
Impact 0. 1666	The Engel's coefficient for urban residents (%)	C13	negative	0. 0555
	Rate of good ambient air quality (%)	C14	negative	0. 0555
	Regional environmental noise registration (dB)	C15	negative	0. 0556
Response 0.1668	Comprehensive utilization of industrial solid waste (%)	C16	positive	0. 0556
	Treatment rate of domestic sewage (%)	C17	positive	0. 0556
	Sewage treated & household refuse (%)	C18	positive	0. 0557

Determination of index weights

Dimensionless method

As each index data differs in nature and measurement units, an entropy method is applied to obtain the objective weights, the formula is shown below:

To be applied when the index is positive (*Eq. 1*):

$$X_{ij} = \frac{X_{ij} - X_j^{\min}}{X_j^{\max} - X_j^{\min}} \quad (\text{Eq.1})$$

To be applied when the index is negative (Eq. 2):

$$X_{ij} = \frac{X_j^{\max} - X_{ij}}{X_j^{\max} - X_j^{\min}} \quad (\text{Eq.2})$$

To be applied when the index is moderate (Eq. 3):

$$X_{ij} = 1 - \frac{|X_{ij} - d_i|}{\max |X_{ij} - d_i|} \quad (\text{Eq.3})$$

where d_i is the fixed standard value.

Determination of entropy weights

Entropy weight is an objective weight method. The weight of each index is firstly calculated according to information entropy, among which the irrational weights will be modified though entropy method, thus obtaining a considerably objective index weights. The specific steps are shown below:

(1) Certain indexes are translated after standardization (Eq. 4):

$$X_{ij} = H + X_{ij} \quad (\text{Eq.4})$$

H in normal cases is 1.

(2) The variation coefficient of index j (Eq. 5):

$$g_i = 1 - e_i \quad (\text{Eq.5})$$

(3) The index weight of item j (Eq. 6):

$$W_i = \frac{g_i}{\sum_{i=1}^p g_i} \quad (\text{Eq.6})$$

Evaluation method

TOPSIS model

TOPSIS model was firstly brought out by Hwang and Yoon in 1981. It is a technique for order preference by similarity to ideal solution among the limited evaluation subjects. The order preference is carried out by calculating the optimal value and the worst value of the subjects. The result of the evaluated subject more close to the optimal value and farthest to the worst value is considered the optimal subject, vice versa. This method can best utilize the original data and is applicable for analyzing data of large quantity and extensive distribution. The specific steps are as follows:

(1) Positive ideal solution (Eq. 7):

$$Y^+ = (y_j^+) = y(\max) \quad (\text{Eq.7})$$

Negative ideal solution (Eq. 8):

$$Y^- = (y_j^-) = y(\min) \quad (\text{Eq.8})$$

(2) Calculate respectively the distance between different evaluation index vectors and positive S1 and negative S2 (Eq. 9):

$$S^+ = \sqrt{\sum_{j=1}^{30} (y_{1j} + y_j)^2} \quad S^- = \sqrt{\sum_{j=1}^{30} (y_{1j} - y_j)^2} \quad (\text{Eq.9})$$

(3) Calculate the similarity of different indexes (Eq. 10):

$$C_1 = \frac{S_1^-}{S_1^- + S_1^+} \quad (\text{Eq.10})$$

Similarly, calculate the relative similarity of each year and each sub-system. The lower the S^+ value, the closer the evaluation index to the ideal situation, the better the ecological development state it demonstrates; The lower the S^- , the closer the index to the negative ideal situation, the lower the ecologic development level; The bigger the C_j , the higher level of ecological city construction in the year of j. Based on practical situation of 34 cities, this paper classified the development level of these cities into four category using equal apace method and in accordance with similarity value of C_j . The four categories are: excellent (0.6-0.7); well (0.5-0.6); normal (0.4-0.5); worse (below 0.4).

Obstacle degree model

After measuring the construction level of 34 eco-cities in China from 2011 to 2015, this paper used time series as the standard to select two endpoints on the time axis, 2011 and 2015 as the research object. Then the status of China's eco-city construction at two extreme time points was compared, with a further analysis of each indicator. We introduced a contribution value D_{ij} , deviation degree E_{ij} , obstacle degree to identify the obstacle factors.

The specific steps are (Eqs.11 and 12):

$$D_{ij} = W_{ij} \times W_i E_{ij} = 1 - X_{ij} \quad (\text{Eq.11})$$

$$P_{ij} = \frac{D_{ij} \times E_{ij}}{\sum_{i=1}^m (D_{ij} \times E_{ij})} \quad (\text{Eq.12})$$

where, W_{ij} is the index weight j in criteria layer i, W_i is the index weight of criteria i where the index j is located. X_{ij} is the standardized value of individual index, obstacle degree ($P_{ij}P_{ij}$) is the value of obstacle degree of classified and individual index of year j.

Coupling coordination model

Coupling is a physics concept which refers to two or more systems or motion modes join up by various interactions. The coupling reaches high level when the factors of each system are in positive interaction, vice versa. The specific steps are:

- (1) Calculate the evaluation index by linearity weighted method (Eq. 13):

$$U = \sum_{i=1}^m W_{ij}, \quad U = (B_i, D_i, E_i, H_i, G_i) \quad (\text{Eq.13})$$

where, B_i , D_i , E_i , H_i , G_i are the comprehensive indexes of driving force sub-system, pressure sub-system, state sub-system, impact and response sub-system.

- (2) Through coupling coordination model, the coupling formula for ecological city construction is (Eq. 14):

$$C = \left\{ \frac{S_1 \times S_2 \times S_3 \times S_4 \times S_5}{\left[\frac{S_1 + S_2 + S_3 + S_4 + S_5}{5} \right]} \right\} \quad (\text{Eq.14})$$

where, C is coupling. If $c = 1$, it comes to the optimal coupling state. Factors within the system develops randomly if $c = 0$.

Coupling coordination reflects the coordination condition among different systems, which is the in-depth analysis of coupling, the formula is (Eq. 15):

$$D = \sqrt{C \times T} \quad (\text{Eq.15})$$

where, D is the coupling coordination and T is the comprehensive coordination index.

Ecological city construction evaluation and spatial pattern evolution based on DPSIR-TOPSI

Data source

The paper studies in 2011 and 2015, and its statistical data come from China Statistical Yearbook, China City Statistical Yearbook, and etc. Specific research methods using entropy method, TOPSIS method, the introduction of obstacle degree and coupling degree model, and through clustering method and ARGIS to carry on the spatial pattern distribution of the results.

Eco-construction evaluation analysis based on DPSIR-TOPSIS model

Evaluation results and analysis of ecological city construction (see Table 2)

Evaluation analysis

It is shown from table 1 that the ecological construction level of each city showed an uprising trend. Judging from the change trend, the sub-system of driving force in 2015 went closely to the ideal solution compared with the year of 2011. Specifically, the sub-system of driving force in cities of higher economic level, such as Beijing and Shanghai, approached to the ideal value. In regards to the Pressure change trend, sub-

system of Pressure in Beijing and Shanghai in 2015 decreased by 0.16% and 0.14% respectively compared with the year 2011, showing an increase in environmental pressure. Judging from S+ value of State sub-system and Impact subsystem, the change trend showed that northwest cities had better performance in this two aspects. For instance, Nanjing and Beijing had better performance in sub-system of Impact while other cities are in poor condition. Change trend of Impact sub-system value S- showed the same result as the trend of S+, that is, almost reach the ideal solution. Comprehensively, the result showed as follows: sub-system of Pressure > sub-system of Response > sub-system of Driving force > sub-system of Impact > sub-system of State (see Fig. 1).

Table 2. Topsis evaluate value

City	2011 Years							2015 Years						
	Driving	Pressure	State	Impact	Response	E-V	Ranks	Driving	Pressure	State	Impact	Response	E-V	Ranks
Shenzhen	0.520	0.954	0.498	0.570	0.966	0.623	6	0.804	0.972	0.294	0.571	0.998	0.661	1
Beijing	0.654	0.983	0.534	0.759	0.694	0.641	3	0.820	0.86	0.374	0.711	0.932	0.652	2
Guangzhou	0.785	0.913	0.422	0.847	0.875	0.660	1	0.844	0.982	0.179	0.601	0.997	0.650	3
Nanjing	0.613	0.713	0.452	0.724	0.778	0.582	11	0.733	0.887	0.253	0.699	0.987	0.637	4
Zhuhai	0.468	0.768	0.936	0.741	0.937	0.645	2	0.575	0.804	0.384	0.672	0.994	0.610	5
Xiamen	0.694	0.705	0.260	0.690	0.968	0.598	10	0.467	0.815	0.483	0.634	0.988	0.607	6
Hangzhou	0.541	0.883	0.141	0.365	0.983	0.568	16	0.780	0.946	0.136	0.221	0.982	0.598	7
Harbin	0.187	0.949	0.165	0.624	0.365	0.51	26	0.199	0.995	0.408	0.491	0.996	0.595	8
Jinan	0.414	0.926	0.191	0.89	0.942	0.616	8	0.472	0.969	0.098	0.517	0.997	0.595	9
Shanghai	0.579	0.703	0.123	0.733	0.998	0.580	12	0.746	0.473	0.034	0.598	0.982	0.532	10
Changsha	0.497	0.932	0.089	0.889	0.992	0.620	7	0.528	0.941	0.034	0.716	0.984	0.591	11
Hohhot	0.576	0.756	0.519	0.906	0.364	0.569	15	0.640	0.887	0.225	0.826	0.616	0.585	12
Shenyang	0.32	0.973	0.356	0.918	0.928	0.633	4	0.168	0.989	0.673	0.185	0.981	0.584	13
Haikou	0.357	0.795	0.406	0.481	0.919	0.565	18	0.405	0.845	0.144	0.616	0.990	0.583	14
Changchun	0.203	0.914	0.13	0.985	0.729	0.566	17	0.111	0.900	0.485	0.580	0.997	0.580	15
Chongqing	0.277	0.755	0.567	0.641	0.910	0.551	19	0.275	0.919	0.347	0.641	0.972	0.578	16
Urumchi	0.350	0.369	0.524	0.551	0.412	0.465	32	0.568	0.836	0.066	0.557	0.961	0.567	17
Chengdu	0.418	0.967	0.328	0.749	0.972	0.626	5	0.277	0.961	0.122	0.366	0.995	0.565	18
Hefei	0.315	0.929	0.403	0.354	0.593	0.534	21	0.309	0.931	0.149	0.453	0.981	0.565	19
Fuzhou	0.323	0.907	0.257	0.534	0.984	0.578	13	0.35	0.888	0.108	0.576	0.969	0.564	20
Nanchang	0.174	0.811	0.209	0.913	0.987	0.571	14	0.263	0.898	0.056	0.74	0.999	0.562	21
Zhengzhou	0.254	0.830	0.065	0.660	0.743	0.508	28	0.329	0.931	0.371	0.316	0.949	0.558	22
Xian	0.396	0.924	0.076	0.687	0.741	0.547	20	0.182	0.973	0.095	0.482	0.983	0.558	23
Wuhan	0.363	0.718	0.134	0.306	0.887	0.509	27	0.455	0.905	0.051	0.272	0.995	0.555	24
Tianjin	0.667	0.898	0.141	0.710	0.948	0.613	9	0.475	0.855	0.025	0.445	0.982	0.551	25
Shijiazhuang	0.107	0.406	0.563	0.798	0.995	0.529	22	0.108	0.568	0.600	0.755	0.994	0.550	26
Lanzhou	0.244	0.345	0.08	0.082	0.719	0.396	34	0.244	0.829	0.601	0.56	0.587	0.536	27
Lanning	0.195	0.618	0.321	0.890	0.293	0.479	31	0.179	0.756	0.223	0.586	0.932	0.536	28
Kunming	0.268	0.541	0.495	0.890	0.462	0.516	24	0.271	0.648	0.225	0.904	0.641	0.530	29
Guiyang	0.400	0.450	0.267	0.534	0.704	0.484	30	0.447	0.772	0.158	0.481	0.745	0.525	30
Shantou	0.074	0.780	0.380	0.437	0.963	0.514	25	0.096	0.844	0.307	0.395	0.976	0.518	31
Taiyuan	0.142	0.686	0.202	0.865	0.505	0.496	29	0.32	0.823	0.132	0.641	0.439	0.501	32
Yinchuan	0.128	0.325	0.534	0.887	0.948	0.517	23	0.166	0.538	0.383	0.714	0.711	0.496	33
Xining	0.203	0.401	0.279	0.579	0.642	0.451	33	0.256	0.423	0.377	0.546	0.848	0.488	34

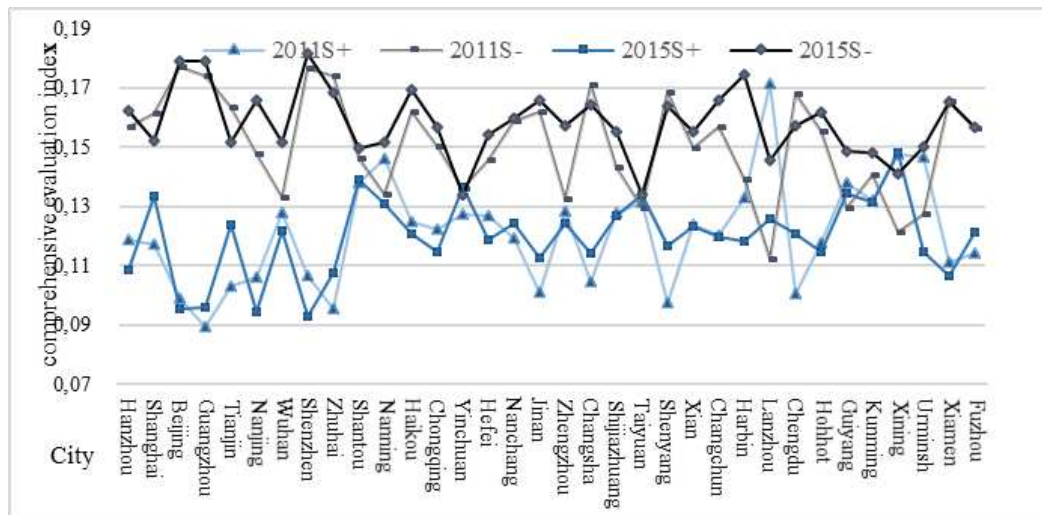


Figure 1. Changes of evaluation index approaching the ideal solution

Eco-environmental carrying capacity of each DPSIR sub-system

Compared with the year 2011, sub-system performance of DPSIR in 2015 were shown as follows (see Fig. 2):

The sub-system of driving force of each city in 2015 showed an uprising trend in general. Cities of high economic level like Shanghai, Beijing, Nanjing and Shenzhen shared bigger proportion, among which Beijing yielded a 23.9% year-on-year growth. On the other hand, subsystem of driving force in northern cities like Shenyang, Xi'an, Changchun experienced a downward trend, among which Xi'an experienced a year-on-year decrease of 21%. Sub-system of pressure in 2015 was in a stage of fluctuation. Beijing, Shanghai and Tianjin went downward by 12.26%, 23.1% and 4.24% respectively, whose performance is still better than low-level economic cities in northwest and southwest regions. Lanzhou and Guiyang showed a significant growth. Lanzhou experienced a year-on-year growth of 48.42% but was still lower than average level judging from its place in the ranking list. Sub-system of pressure in Xiamen increased by 11.2%. The figures suggested that, during ecological construction, super-huge cities still have a lot of work to do in coping with problems like environmental pressure, sustainability issue on their pursuit of the fast economic growth. The State sub-system of each city in year 2015 showed a downward trend, among which Guangzhou decreased by 24.32%. Beijing, Guangzhou, Nanjing and other cities with high economic development showed an excessive encroachment of green land, the maintenance work was unattended and the planning is not in a reasonable condition. Hohhot, Taiyuan and other cities, due to their self-condition and slow economic growth, had a slow pace in green city construction. In 2015, the sub-system of Impact showed more of growth than decrease among cities. Large increase was still mainly shown in northeast cities and cities in Yangtze River Delta. In recent years, although China has been addressing the issue of keeping a good ambient air quality rate, treatment on issues like air pollution, noise control is still less effective. The sub-system of Response in 2015 showed a pleasant trend in general. However, there are also a decrease found in cities like Yinchuan, Lanzhou and Taiyuan with figure reaching over 20%. Due to low awareness of comprehensive utilization of wastes, defective ecologic mechanism and

low-level technological competence, the comprehensive utilization rate of solid waste is hard to reach its best performance in northwest cities.

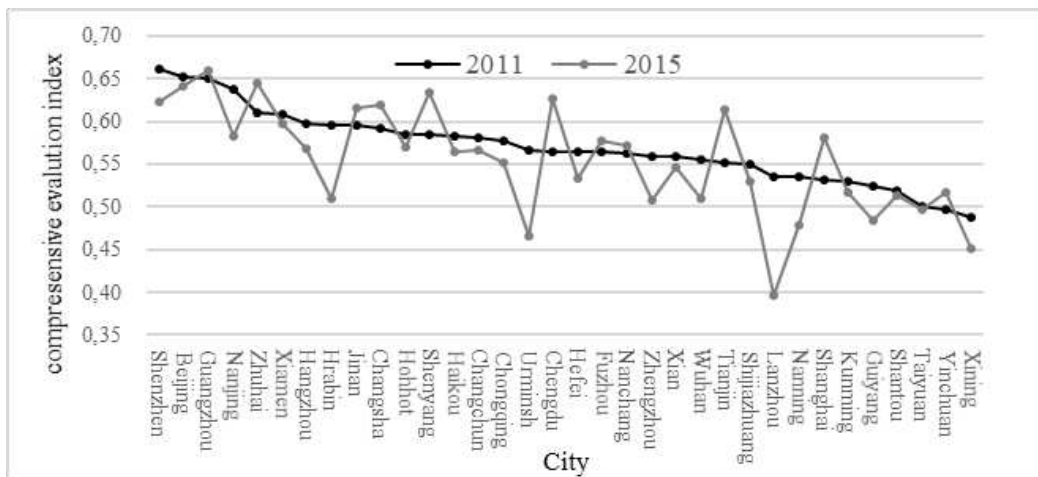


Figure 2. Similarity status among cities in 2011 and 2015

Table 2 and Figure 2 revealed a rank change in 2015 compared with 2011. The rank in some cities like Beijing, Nanjing, Xiamen, Hangzhou went upward, whose rank in 2011 was shown better than central and western cities. Kunming, Shantou, Xining, Yinchuan, Taiyuan and some other northwest cities in 2015 went downward, ranking lower in both 2011 and 2015 and showing a slow ecological construction pace. Fig. 3a suggested a four ecological city construction type. The first type were the cities with best ecological city construction. Examples were Guangzhou, Shenzhen Jinan. The second type was vastly distributed. Bad performance was found in northwest cities like Urumchi, Lanzhou, Xining, clustering into the third and the fourth type. Fig. 3b showed a city rank change in 2015. Among them, Guangdong had three cities listed in the first type. Xiamen and Nanjing upgraded into the first type. Beijing showed no change in the rank. Shenyang, Jinan with other cities clustered into the second type-cities of good ecological construction performance. Yinchuan stationed into the third type in 2015, while Urumchi, Taiyuan, Lanzhou experienced a certain growth in ecological city construction and went up to the second type from the third and the fourth type. In general, ecological construction in each city showed a steady step forward (see Fig. 3).

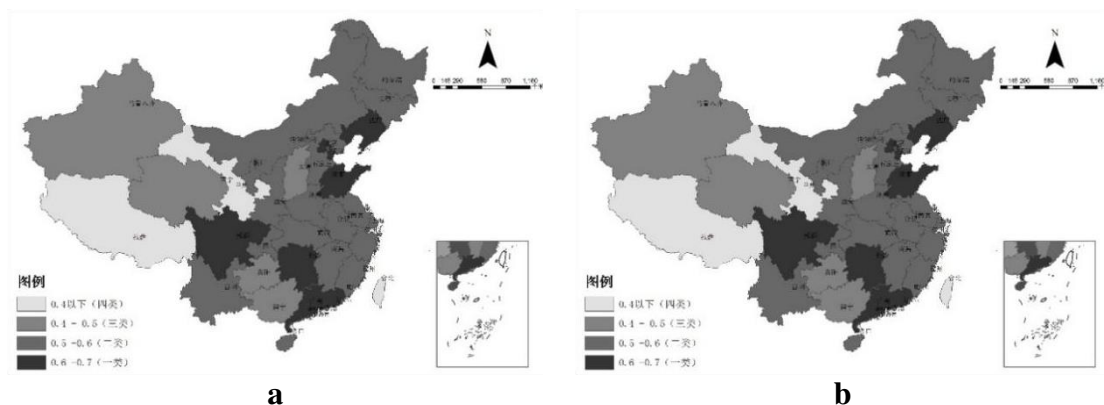


Figure 3. Cluster result of similarity in a 2011 and b 2015

Obstacle degree analysis

Judging from the frequency of the obstacle factors, 8 indexes are frequently occurred as obstacle factors in 2011 and 2015(see table 3). Among these, the added value of the tertiary industry and GDP per capita were two main factors affecting many cities. Rate of good ambient air quality, industrial waste, water emission per unit GDP and park/green space area per capita appeared in cities of good economic performance like Shanghai, Hangzhou and Shenzhen. The respective responding criteria layer of the 8 factors are Driving force sub-system, Pressure sub-system and State sub-system, among which the obstacle factor of State sub-system showed the highest frequency. The eastern and central ecological city was influenced most by this system.

Table 3. Times of index in cities

Index	City							
Rate of good ambient air quality	Hangzhou	Shenzhen						
Added value of the tertiary industry	Hangzhou Tianjin Shanghai	Shanghai Nanjing	Wuhan Zhuhai	Chengdu	Hefei Zhengzhou	Changsha Shenyang	Changchun Xiamen	Shijiazhuang
Generation of industrial solid waste per unit GDP	Shanghai	Xiamen						
Park/green space area per capita	Shanghai	Xian						
Water Consumption per unit GDP	Nanjing	Zhuhai	Nanning	Nanchang	Shijiazhuang			
GDP per capita	Shantou Nanning	Haikou Hefei	Xian Chengdu	Guiyang Kunming	Xian	Harbin		
Greening coverage in built-up area	Hohhot	Guangzhou	Shenzhen	Jinan				
Government fiscal expenditure on environment	Guangzhou	Wuhan	Changsha	Chengdu	Fuzhou			

It indicated the changes of obstacle degree of each sub-system among cities in sample period (see Fig. 4). The values and changes showed that, in general, the sub-system of State and Impact experienced a downward trend. The sub-system of Driving force, Response and Pressure on the other hand went upward during fluctuation. Compared with 2011, changes in 2015 were: Higher obstacle degree was found in the sub-system of Driving force and Pressure; obstacle degree of Pressure sub-system experienced a large increase in cities like Hangzhou, Shanghai, Beijing, Guangzhou and Tianjin. The increase of obstacle degree of response sub-system, such as in Xiamen, Fuzhou and Shanghai, was insignificant. The State sub-system was lower than the Impact subsystem but was still the main obstacle factor both in 2011 and 2015.

In general, the obstacle degree of Response and Impact sub-system were relatively insignificant. The ranking order is shown below: Judging from the rank, in the year of 2011: Driving force sub-system > State sub-system > Pressure sub-system > Impact sub-system > Response sub-system. In the year of 2015: Pressure sub-system > Driving force sub-system > State sub-system > Impact sub-system > Response sub-system.

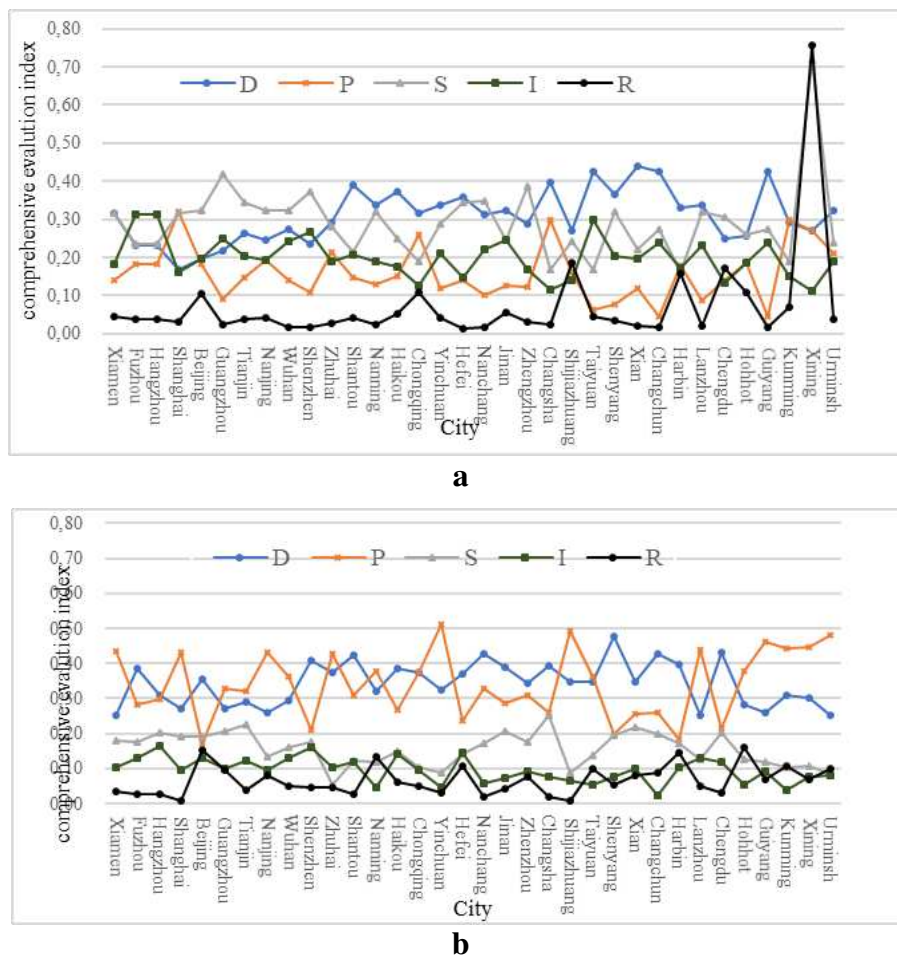


Figure 4. Changes in obstacle degree of each sub-system in **a** 2011 and **b** 2015

Spatial change of coupling coordination distribution

From these changes it can be seen that: high level coupling coordination are stably distributed in provinces of Pearl River Delta and Yangtze River Delta area. In 2011, Beijing, Guangzhou, Zhuhai and Shenzhen ranked the highest in coupling coordination, followed by Xiamen and Nanjing. Beijing, Guangzhou and Shenzhen took the lead in ecological construction by driving force and pressure sector, while Xiamen and Nanjing had State and Impact sub-system as their leading points. Cities with low coupling coordination were found in Lanzhou, Xining, Urumchi, and Guiyang-- mainly those cities in central and western provinces. These cities were commonly found lack of distinct system and are general in low-level performance. The construction of each system in northeast provinces showed a medium level performance and high degree of coordination. During the Five-year economic construction period, cities in eastern China region, such as Hangzhou and Nanjing, made a great achievement on sub-system of Driving force and State, developing faster than other regions. The State sub-system however, was relatively backward. Under the fast economic development background, western China region in general showed a medium-level coupling dis-coordination in 2011 due to their weak self-condition and slow economic development. Generally, the coupling coordination in central and western region under the “economic new normal” went upward in 2015 (see *Figs. 5 and 6*).

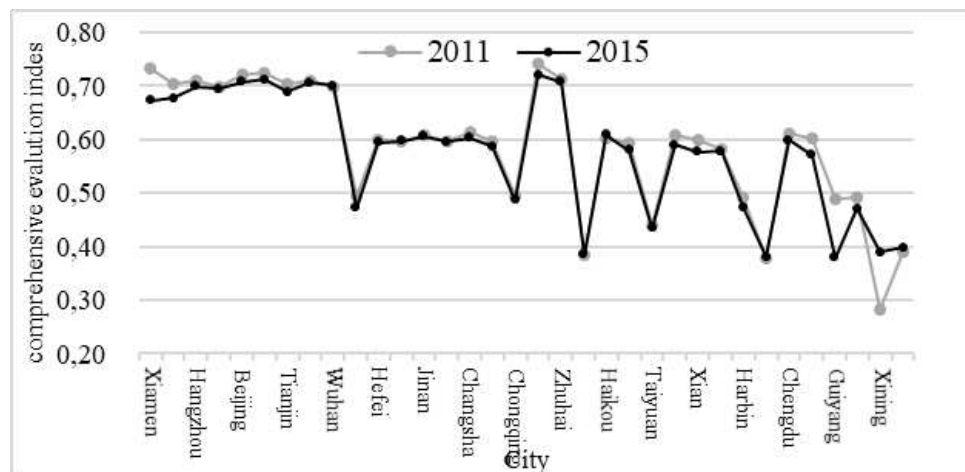


Figure 5. Coupling coordination in 2011 and 2015

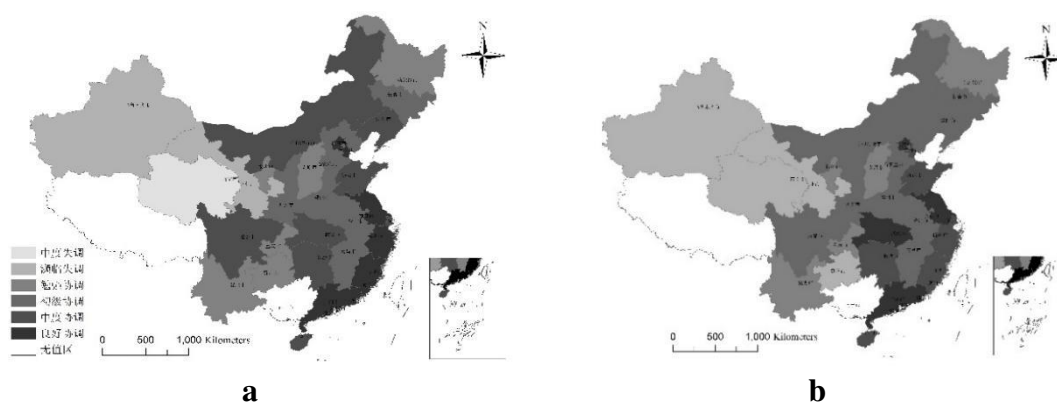


Figure 6. Coupling coordination status in a 2011 and b 2015

Revolution of ecological city construction pattern

This paper adopted a cluster analyzing method to evaluate the coordination scores of each sub-system in 2011 and 2015. The result showed that: cities of the first category in 2011 were represented by Hefei, Xi'an, Shijiazhuang; some cities showed a more distinct score in State and Impact sub-system but low score in coordination, which was represented by Haikou; cities in the second category, represented by Shanghai, Shenzhen, revealed higher scores in Driving force sub-system and coordination but lower score in Pressure sub-system. Cities in the third category represented by Shantou, Urumchi and Lanzhou revealed low score in all five sub-systems and poor coordination; Yinchuan, Chongqing, Harbin and Kunming were in the fourth category and Xining was the only city in the fifth category.

The cluster classification went through certain minor changes in 2015: the first four categories remained in the same condition; Xining from the fifth category went up to the third category, showing a relief in bad coordination. Coordination status in some cities like Fuzhou and Hangzhou changed from medium coordinated to lightly coordinated, showing a decrease in coordination. Shenzhen, Zhuhai and Guangzhou remained the medium coordination. No big change occurred in other cities (see Fig. 7).

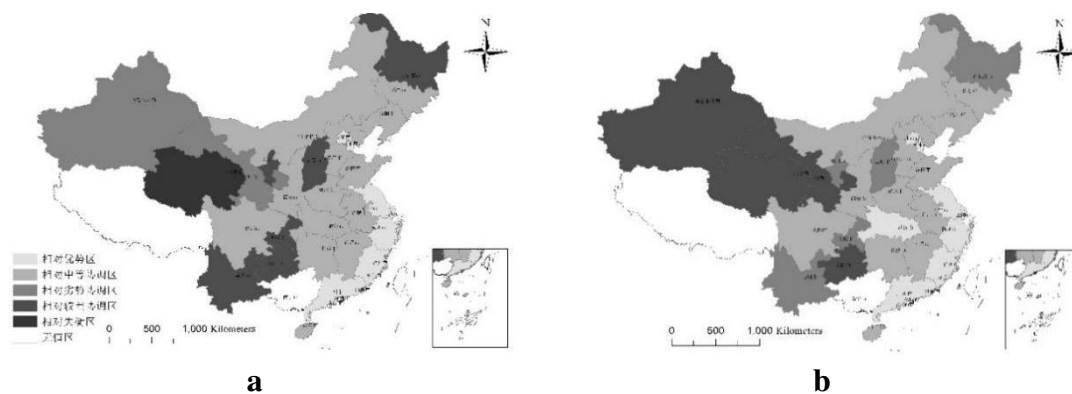


Figure 7. Cluster results in **a** 2011 and **b** 2015

Conclusion and outlook

At the macro level, the construction of China's eco-city has begun to take shape, constructing a localized eco-city model from multiple dimensions such as politics, economy and ecology gradually under the background of the global ecological movement. From the perspective of self-construction, there is still a big gap in the goal of China's eco-city construction from a high level of coordinated development. In comparison, cities with higher economic development have better ecological construction like Beijing, Shanghai, Nanjing, Guangzhou, from the comprehensive evaluation index under the DPSIR model, and vice versa. This is mainly due to the fact that many cities in the initial stage of construction give priority to developing the economy, ignoring ecological damage and environmental pollution. As the economy evolves to a considerable level, it will focus on environmental problems again. They improve their ecological environment by increasing technical and financial resources to rebuild ecological cities. Hence, the central and western regions with poor economic development are still in the game stage of economic development and ecological construction.

The ecological city construction in China still has far way to go in achieving a high-level coordinated development. In regional development, addresses shall be made to develop the strong sub-systems based on practical condition and at the same time paying attention to the other sub-system construction. In general, the statistics revealed a low-pace development of State and Impact sub-system. State sub-system construction in central and eastern region showed a particular weakness waiting to be highly addressed. Northwest regions, on the other hand, shall develop their sub-system of Driving force and at the same time paying attention to issues like resource and environmental pressure and green space per capita etc, so that the effective coordination with sub-system of Response can be achieved. The comprehensive evaluation results showed a general upward rise in each city's ecological construction, reflecting that the condition was getting good. The similarity value among cities showed the good performance of Driving force sub-system and Pressure sub-system in cities with better economic development but bad performance in cities with low economic development. The changes of obstacle degree showed that driving force sub-system and pressure sub-system were the main obstacles hindering the ecological city construction in western and northern region, while State sub-system remained as the main obstacle in central and eastern region. From the statistical changes of the applied model, it can be seen that

ecological city construction in southeast coastal area showed a better performance, while low construction level was found in cities of northwest, southwest and northeast region.

By establishing an evaluation index system based on DPSIR conceptual model, and by carrying out an empirical study using the method of similarity analysis, obstacle degree study and coupling coordination degree model, a relatively comprehensive analysis on city ecological construction level and spatial distribution pattern in China was accomplished. However, further studies are still expected. For instance, although indexes of the evaluation system are carefully selected and it is proved to be representative, mathematical approach and model construction can be further improved. In addition, this study mainly conducted a time-span evaluation on the overall changes and changes of each individual factor concerning ecological city construction, discussions around future development, management approach, inter-province cross-sectional study under the same time scale shall be further conducted. Moreover, studies on ecological city governance shall be fully carried out based on solid knowledge background of ecological city construction process.

Acknowledgements. The work was supported by the China Postdoctoral Science Foundation funded project (2015M571973), National Natural Science Foundation of Fujian Province (2017J01787) and Social Science Planning Project of Fujian Province (FJ2015B194).

REFERENCES

- [1] An, S. W., Wan, S. M., Li, X. J. (2017): Assessment of urban fragility and risk control--a case study of Henan Province. – *Economic Geography* 37(5): 81-86.
- [2] Bi, G. H., Yang, Q. Y., Liu, S. (2017): The coupling and coordinated development of ecological civilization construction and urbanization in China province. – *Economic Geography* 37(1): 50-58.
- [3] Cheng, L., Ning, L. X. (2014): Evaluation of social progress indicators in Baotou eco-city construction. – *Journal of Arid Land Resources and Environment* 28(11):12-16.
- [4] Ghiselin, M. T. (1974): A radical solution to the species problem. – *Systematic Zoology* 23: 536-544
- [5] Gu, S. Z., Hu, Y. J., Zhou, H. (2013): The scientific connotation and basic path of the construction of ecological civilization. – *Resources Science* 35(1): 2-13.
- [6] Huang, Q., Zeng, Y. (2015): Research progress on promoting the construction of ecological civilization in China. – *China Population Resources and Environment* 25(2): 111-120.
- [7] Kline, S. J., Rosenberg. N. (2009): An Overview of Innovation. – In: Rosenberg, N. (ed.) *Studies on Science and the Innovation Process: Selected Works of Nathan Rosenberg*. World Scientific Publishing Co., Singapore.
- [8] Li, X. (2008): Research on ecological civilization and ecological city. – *Urban Studies* 24(S1): 218-225.
- [9] Mi, K., Peng. Y. (2014): An analysis of the index system and application of ecological cities abroad. – *China Population, Resources and Environment* 24(S3): 129-134.
- [10] Ren, H., Du, Y. J., Chen, Y. Q., Ren, P. Y., Huang, H. F. (2016): Three-dimensional evaluation model of eco-city planning scheme from distance measure. – *Science & Technology Progress and Policy* 33(16): 81-85.
- [11] Shen, Q. J. (2013): Study on new urbanization based on ecological civilization. – *Urban Planning Forum* (1): 29-36.

- [12] Xiao, P. Y., Yang, L. Y., Song, Y. (2018): Comprehensive evaluation of urbanization quality in China and its temporal and spatial characteristics. – *China's Population Resources and Environment* 28(9): 112-122.
- [13] Yanitsky, O. (1982): Towards an eco-city: problems of integrating knowledge with practice. – *International Social Science Journal* 34(3): 469-480.
- [14] Yu, K. P. (2005): Scientific outlook on development and ecological civilization. – *Marxism & Reality* (4): 4-5.
- [15] Zeng, Z. H. (2017): Research on the innovation system of China's new type of urbanization inclusive system. – *Urban Studies* 24(5): 1-7.
- [16] Zhang, Z. G., Zhang, X. J. (2015): Study on the system frame construction of ecological city-taking Guangzhou as an example. – *Science and Technology Management Research* 35(21): 245-249.
- [17] Zhang, L. (2015): Comparison and transformation of urban renewal governance model under "new normal". – *Urban Studies* 22(12): 57-62.
- [18] Zhao, G. J., Wang, H. F. (2015): Study on the generation process of low-carbon eco-City. – *Journal of Hebei University of Economics and Trade* 36(6): 77-81.

STUDY ON THE COUPLING RELATIONSHIP BETWEEN ECONOMIC SYSTEM AND WATER ENVIRONMENTAL SYSTEM IN BEIJING BASED ON STRUCTURAL EQUATION MODEL

CHEN, M.^{1,2*} – CHEN, H. Q.³

¹*Ginling College, Nanjing Normal University, Nanjing 210024, China*

²*Gulf Coast Research & Education Center, University of Florida, Wimauma 33598, USA*

³*School of Urban Planning, Yancheng Teachers University, Yancheng 224007, China*

**Corresponding author*

e-mail: Chenming.1008@163.com

(Received 20th Sep 2018; accepted 26th Nov 2018)

Abstract. To study the relationship between the economic system and the water environmental system in Beijing, China, this article brought in the concept of “system coupling”, and calculated their coupling degree using the co-coordination model. Specifically, the economic system consists of population and economic development subsystems; the water environmental system consists of water supply and water environmental carrying capacity subsystems. A total of twelve components were chosen, including population, water consumption per ten thousand Yuan GDP, etc. Besides, the Structural Equation Model (SEM) was innovatively used to analyze the micro-coupling paths among the subsystems. Finally, we drew conclusions from the coupling state perspective and coupling paths perspective, respectively. From the macroscopic point of view, there are complex interactions between the economic system and water environmental system in Beijing, and their coupling degree will increase with the optimization of economic structure and advancement in technologies. From the microscopic point of view, there are also complex interactions among the four subsystems in Beijing. Especially, the water supply subsystem has a certain degree of promotion effect on the other three subsystems.

Keywords: *system coupling, micro-coupling paths, coordination degree analysis, structural equation model, pressure-state-response model*

Introduction

The relationship between environment and economy has been a hot topic in academic circles for a long time (Corinne, 2014; Douai et al., 2012; Spach, 2011). As most researches focus on the environmental Kuznets curve and Eco-economic system, few types of research emphasize the concept of water environment (Van der Ploeg and Withagen, 2013; Aldy, 2005). In recent years, some scholars have researched into the relationship between the urban economic system and the water environmental system, and they concluded that the economic system and the water environmental system are the important components of the urban system (Flores et al., 2014; Ahmed et al., 2016; Apergis and Ozturk, 2015). On one hand, well-functioned economic system facilitates socioeconomic development, as well as brings about water pollution; on the other hand, water environmental system provides the water resources necessary for industry production and daily life. In addition, facing the pressure from water pollution, it is responsible for water purification and decontamination (Ben Jebli et al., 2016).

In this article, Beijing city is the research area as it is the largest city in the north of China. Based on the above-mentioned research results, the Beijing’s urban system is composed of an economic system and a water environment system. To study the

coupling degree between the economic system and the water environmental system, we first divided these systems into four subsystems, each of which consists of several sections. The economic system consists of population and economic development subsystems. The population subsystem consists of gross population section, natural population growth rate section and urbanization rate section; the economic development subsystem consists of GDP section, water supply investment section and water consumption per ten thousand Yuan GDP section. The population subsystem provides the labor force capital necessary for the good function of economic development subsystem, which will in turn benefit the population subsystem. The water environmental system consists of water supply and water environmental carrying capacity subsystems. The water supply subsystem consists of the total amount of water supply for the whole year, water consumption for industry and water consumption for daily life; the water environmental carrying capacity subsystem consists of centralized processing rate of sewage, daily sewage treatment capacity and quantity of waste water effluent (Kanjilal and Ghosh, 2013; Chen and Xu, 2013). The water supply subsystem provides the water resources necessary for the functioning of the social economy, and the water environment carrying capacity subsystem absorbs the waste water and sewage caused by economic activities. In general, the economic system and water environmental system couple with each other and have complex interactions. *Figure 1* is the economic & water environmental system structure diagram of Beijing (Coscieme et al., 2016). This article aims to explore the complicated interplay between the economic system and the water environment system in Beijing, so as to find out practical and theoretical significance.

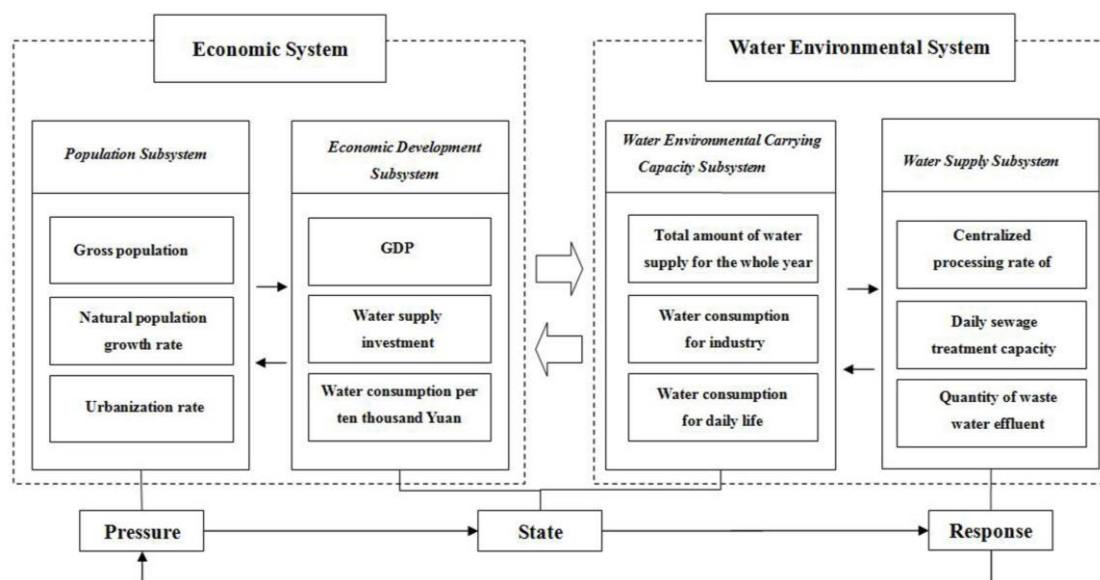


Figure 1. The economic & water environmental system structure diagram of Beijing

Material and methods

Data collection

Beijing is the capital of China, and it is the largest city in the north of the country. Located in the north of the North China Plain (E 115.7 ° -117.4 °, N 39.4 ° -41.6 °),

Beijing has the jurisdiction over 16 counties, with a total area of 16410.54 km² and the total population of 2170.5 million (2017). Affected by a typical temperate continental climate Beijing has an average annual precipitation of 585 mm, and about 76% of the precipitation concentrated in the summer (June, July and August, 2017) (Fig. 2). The GDP of Beijing in 2015 is 229.66 billion Yuan (Lin et al., 2014). Compared with its developed economy, the water resources of this city are relatively scarce. The total water resources is 2.676 billion m³ (2015), per capita water resources is only 123 m³. Apparently, there is a certain contradiction between economic development and water resources supply (Xia et al., 2012).

The distribution of water system in Beijing is shown in Figure 2. It can be seen that 7 major river systems are in the Beijing area.



Figure 2. Distribution of water system in Beijing

In this article, all initial data were obtained from the *Beijing Statistical Yearbook 1997-2013* and *Beijing Water Resources Bulletin 1997-2013*. The total 12 components of economic system and water environmental system in Beijing are shown in Table 1.

Table 1. Components of economic system and water environmental system in Beijing

System	Subsystem	Component	Symbol	Unit
Economic system	Population subsystem	Gross population	X ₁	Ten thousand people
		Natural population growth rate	X ₂	%
		Urbanization rate	X ₃	%
	Economic development subsystem	GDP	X ₄	100 million yuan
		Water supply investment	X ₅	100 million yuan/year
		Water consumption per ten thousand yuan	X ₆	m ³
Water environmental system	Water supply subsystem	Total amount of water supply for the whole year	Y ₁	100 million m ³ /year
		Water consumption for industry	Y ₂	100 million m ³ /year
		Water consumption for daily life	Y ₃	100 million m ³ /year
	Water environment carrying capacity subsystem	Centralized processing rate of sewage	Y ₄	%
		Daily sewage treatment capacity	Y ₅	10 thousand m ³ /day
		Quantity of waste water effluent	Y ₆	10 thousand m ³ /year

Coupling coordination model

Data pre-processing

Data were processed using the maximum difference normalization method. Evaluation indexes include: output index (Eq. 1), input index (Eq. 2).

$$X'_{ij} = \frac{X_{ij} - \min(X_j)}{\max(X_j) - \min(X_j)} \quad (\text{Eq.1})$$

$$X'_{ij} = \frac{\max(X_j) - X_{ij}}{\max(X_j) - \min(X_j)} \quad (\text{Eq.2})$$

where $i = 1, 2, \dots, N$ refers to years, $j = 1, 2, \dots, N$ refers to parameters, X_{ij} represents original values of the parameters, X'_{ij} represents the value after standardization, $\max(X_j)$ and $\min(X_j)$ are the maximum value and minimum value of the parameter, respectively.

Determining index weight using mean square deviation method

The coefficient of variation CV_j was introduced into the mean square deviation method to determine index weight. The calculation methods of CV_j is shown in Equations 3 and 4 show calculation process of weighted value.

$$CV_j = \frac{\sigma_j}{\bar{X}_j} \quad (\text{Eq.3})$$

$$W_j = \frac{CV_j}{\sum_{j=1}^n CV_j} \quad (\text{Eq.4})$$

where CV_j represents the coefficient of variation, σ_j represents the standard deviation of the j th parameter, \bar{X}_j and W_j represent mean value and weighted value, respectively.

Calculating comprehensive index between economic system and water environmental system

The comprehensive indexes of economic system $f(x)$ and water environmental system $g(y)$ were obtained by multiplying the standardized value of parameters and their corresponding weights. The calculation methods of $f(x)$ and $g(y)$ are shown in Equations 5 and 6, respectively.

$$f(x) = \sum_{i=1}^m X'_{ij} W_x \quad (\text{Eq.5})$$

$$g(y) = \sum_{i=1}^n Y'_{ij} W_y \quad (\text{Eq.6})$$

It should be noted that the standardized value of parameters (X'_{ij} , Y'_{ij}) eliminate the influence of the units. Their corresponding weights (\bar{X}_j , W_j) are expressed as the form of rate. Therefore, $f(x)$ and $g(y)$ show no units in Equations 5 and 6.

Coordination degree analysis

The coordination degree reflects how uniform the development of different components within a system is, and it can be described as

$$C = \left\{ \frac{f(x) \times g(y)}{\left[\frac{f(x) + g(y)}{2} \right]^2} \right\}^k \quad (\text{Eq.7})$$

$$T = \alpha f(x) + \beta g(y) \quad (\text{Eq.8})$$

$$D = \sqrt{C \times T} \quad (\text{Eq.9})$$

In the above equations (Eqs. 7–9), C represents the coordination degree, k represents accommodation coefficient (let $k = 2$ in this study), T represents comprehensive evaluation index of economic system and water environmental system. α and β are undetermined coefficients, in this study, let $\alpha = \beta = 0.5$ as they are equally important. D is the coordinated development coefficient (Ozturk and Al-Mulali, 2015; Ozturk and Uddin, 2012).

Structural equation model

Model principle

Structural equation model is a multivariate statistical analysis method to validate the relationship between independent and dependent variables. Apart from reflecting the relationship among latent variables, it can also explore the relationship between latent variables and observed variables. Latent variables are those that can not be measured accurately and directly, they can be measured with some observed variables indirectly. The structural equation model consists of the measurement section and the structural section.

The measurement model (Eqs. 10 and 11) describes the relationship between latent variables and observed variables, while the structural model (Eq. 12) reflects the relationship among latent variables.

$$x = \Lambda_x \xi + \delta \quad (\text{Eq.10})$$

$$y = \Lambda_y \eta + \varepsilon \quad (\text{Eq.11})$$

$$\eta = B\eta + \Gamma \xi + \zeta \quad (\text{Eq.12})$$

where x represents exogenous variables observed vector; ξ represents exogenous latent variable vector; Λ_x represents the relationship between exogenous variables and exogenous latent variables, and Λ_x is the factor loading matrix of exogenous variables observed in the exogenous latent variables; δ represents the residuals vector exogenous observable variables; y is the endogenous observable variable to the amount; η is the endogenous latent variable vector; Λ_y represents relationship between observation

variables and latent variables; ε is the residuals vector of endogenous variables observed; B and Γ are the path coefficient relation matrix, B is endogenous latent variables, Γ effects of exogenous latent variables for the endogenous latent variable values; ζ is the error term of structure equation (Rahman et al., 2016).

Model assumptions

In this study, the Structural Equation Model of Beijing Economic & Water Environment System was built based on the following assumptions:

H1: The water supply subsystem has an impact on the population subsystem; H2: The water supply subsystem has an impact on the economic development subsystem; H3: The water supply subsystem has an impact on the water environmental carrying capacity subsystem; H4: The population subsystem has an impact on the economic development subsystem; H5: The population subsystem has an impact on the water environmental carrying capacity subsystem; H6: The economic development subsystem has an impact on the water environmental carrying capacity subsystem (Su et al., 200).

Based on the above assumptions, the initial conceptual model of economic & water environmental system in Beijing is shown in *Figure 3*.

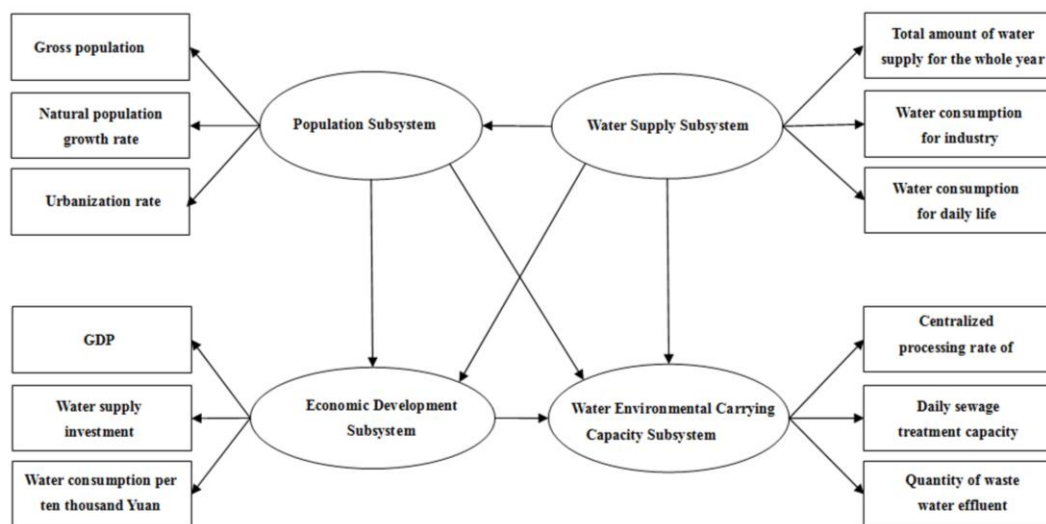


Figure 3. The initial conceptual model of economic & water environmental system in Beijing

Model test

(1) Reliability test

Reliability refers to the degree of consistency (stability) of measurement results. The currently used method is Cronbach's α reliability coefficient. Cronbach's α reliability coefficient is currently the most widely used method. Cronbach proposed this new reliability test method in 1951. This method compares the results of any item in the measurement tool with all other items and makes the internal consistency of the scale more cautious. The equation is as follows (Eq. 13):

$$\alpha = \frac{k}{k-1} \left(1 - \frac{\sum S_i^2}{S_T^2} \right) \quad (\text{Eq.13})$$

where k is the total number of items in the scale, S_i^2 is the variance within the score of the i -th question, and S^2_T is the variance of the total score of all items. It can be seen from Equation 13 that the α coefficient evaluates the consistency between the scores of each item in the scale and belongs to the internal consistency coefficient. In general, the reliability coefficient of the total scale is preferably above 0.8, acceptable between 0.7 and 0.8; the reliability coefficient of the subscale is preferably above 0.7, and 0.6~0.7 is acceptable. If the Cronbach's α coefficient is below 0.6, the Structural Equation Model (SEM) should be corrected (Baek and Kim, 2013; Xiao et al., 2014).

(2) Goodness of fit evaluation

The goodness of fit of the model refers to the degree of consistency between the theoretical hypothesis model and the observed data. According to the principle of parameter estimation of the structural equation model, it refers to the covariance matrix $\Sigma(\theta)$ and the sample covariance matrix S generated in the estimation. Proximity, a viable model should make the difference between S and $\Sigma(\theta)$ as small as possible.

In general, the commonly used fitting evaluation index has the following three categories: (1) Absolute Indices; (2) Relative/Incremental Indices; (3) Parsimony Indices (Chai et al., 2011; Costanza et al., 2013). The classification results of fitting evaluation index are shown in Table 2.

Table 2. The classification results of fitting evaluation index of structural equation model

Index name	Statistic of test	Explanation of terms	Form of expression	Standard or critical value of fit
Absolute fit indices	χ^2 / df	Likelihood – ratio χ^2	$-2\ln(\frac{L}{L_0}) = -2(\ln L_1 - \ln L_0) = (N-1)F_{ML} \sim \chi^2(\frac{1}{2}q(q+1)-k)$	<3
	GFI	Goodness of index	$GFI_{GLS} = 1 - \frac{tr[1 - \hat{\Sigma}(\theta)S^{-1}]^2}{q}$	>0.9
	RMR	Root mean residual	$RMR = \sqrt{\frac{2\sum\sum(s_{ij} - \hat{\sigma}_{ij})}{(p+q)(p+q+1)}}$	<0.05
	RMSEA	Root mean square error of approximation	$F_0 = \max\{\frac{\hat{F} - df}{N-1}, 0\}$	<0.08
Relative fit indices	NFI	Normed fit index	$NFI = \frac{F_b - F_m}{F_b} = \frac{\chi_b^2 - \chi_m^2}{\chi_b^2}$	0.9 < NFI < 1
	TLI	Tacker-Lewis index	$TLI = NNFI = \frac{\frac{\chi_b^2}{df_b} - \frac{\chi_m^2}{df_m}}{\frac{\chi_b^2}{df_b} - 1}$	0.9 < TLI < 1
	CFI	Comparative fit index	$CFI = 1 - \frac{\tau_m}{\tau_b}$	0.9 < CFI < 1
Parsimonious fit indices	AIC	Akaike information criterion	$AIC = \chi^2 + 2k$	The smaller, the better
	CAIC	Continuous Akaike information criterion	$CAIC = \chi^2 + (\ln N)k$	The smaller, the better

Results

The results of the coordinate coordination model

Based on the coupling coordination degree model built above, we input the related data from 1997 to 2013 into *Equations 1–9* mentioned above to calculate the coupling degree, and the results are shown in *Table 3*.

Table 3. *The results of the coordinated development of economic and water environmental systems in Beijing (1997-2013)*

Year	The comprehensive indexes of economic system $f(x)$	The comprehensive indexes of water environmental system $g(y)$	Coordinated development coefficient D
1997	0.1177	0.2268	0.0072
1998	0.1196	0.2185	0.0071
1999	0.1625	0.2331	0.0120
2000	0.1966	0.3357	0.0239
2001	0.1861	0.4104	0.0277
2002	0.2379	0.5014	0.0504
2003	0.2168	0.5069	0.0444
2004	0.3532	0.5891	0.1102
2005	0.3797	0.6968	0.1501
2006	0.4336	0.7053	0.1859
2007	0.6539	0.7400	0.3649
2008	0.6603	0.7370	0.3685
2009	0.7057	0.7607	0.4231
2010	0.6723	0.7610	0.3937
2011	0.8801	0.7607	0.5894
2012	0.9094	0.7684	0.6266
2013	0.9829	0.7657	0.7011

According to the results of data processing in *Table 3*, the trend of the coordinated development coefficient of economic and water environmental systems in Beijing is plotted (*Fig. 4*).

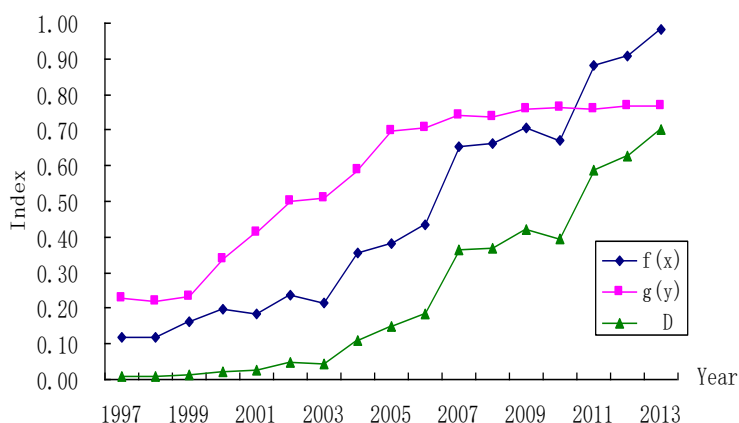


Figure 4. *The coordinated development coefficient of the economic system and the water environmental system of Beijing (1997-2013)*

It can be seen from *Figure 4* that during 1997 to 2013, the economic system composite index increased from 0.1177 in 1997 to the highest value of 0.9829 in 2013. The lowest value of water environment index appeared in 1998, the index value was 0.2185, while the highest value was 0.7684 appeared in 2012. In general, the relationship between Beijing's socio-economic and its protection of the coordinated development of the water environment was good. The degree of coordination between them showed an overall upward trend, and the degree of coupling increased continuously. The coefficient of coordinated development of the economic system and the water environmental system of Beijing increased from the lowest value of 0.0071 in 1998 to the highest value of 0.7011 in 2013.

The results of the structural equation model

Assumptions test

In this paper, Cronbach's α was used to measure the intrinsic reliability of the data, when $\alpha > 0.8$, it shows that the data has good reliability (Baveye et al., 2013). The results of α were obtained by Statistical Product and Service Solutions (SPSS) software with the data of 12 indicators from 1997 to 2013 of Beijing (*Table 4*).

Table 4. *The results of Cronbach's α of structural equation model in Beijing (1997-2013)*

Latent variable	The number of variables	Cronbach's α	Reliability judgment
Population subsystem	3	0.956	Yes
Economic development subsystem	3	0.933	Yes
Water supply subsystem	3	0.851	Yes
Water environment carrying capacity subsystem	3	0.982	Yes

Calculation of structural equation model

The 12 indicators data (from 1997 to 2013 of Beijing) were put into the Structural Equation Model (SEM), and the Maximum Likelihood Estimate method were used to estimate the model parameters by AMOS 7.0 software (*Table 5*). On this basis, the paths of the model were corrected according to M.I prompt value and the actual situation. Finally, the results of the mode were shown by *Figure 5*.

Table 5. *The summary table of overall model fit test in confirmatory factor analysis of structural equation model in Beijing (1997-2013)*

Index name	Statistic of test	Standard or critical value of fit	Test result	Model fit judgment
Absolute fit indices	χ^2/df	<3	2.01	Yes
	GFI	>0.9	0.906	Yes
	RMR	<0.05	0.044	Yes
	RMSEA	<0.08	0.076	Yes
Relative fit indices	NFI	0.9<NFI<1	0.962	Yes
	TLI	0.9<TLI<1	0.954	Yes
	CFI	0.9<CFI <1	0.949	Yes
Parsimonious fit indices	AIC	The smaller, the better	292.17	Yes
	CAIC	The smaller, the better	245.33	Yes

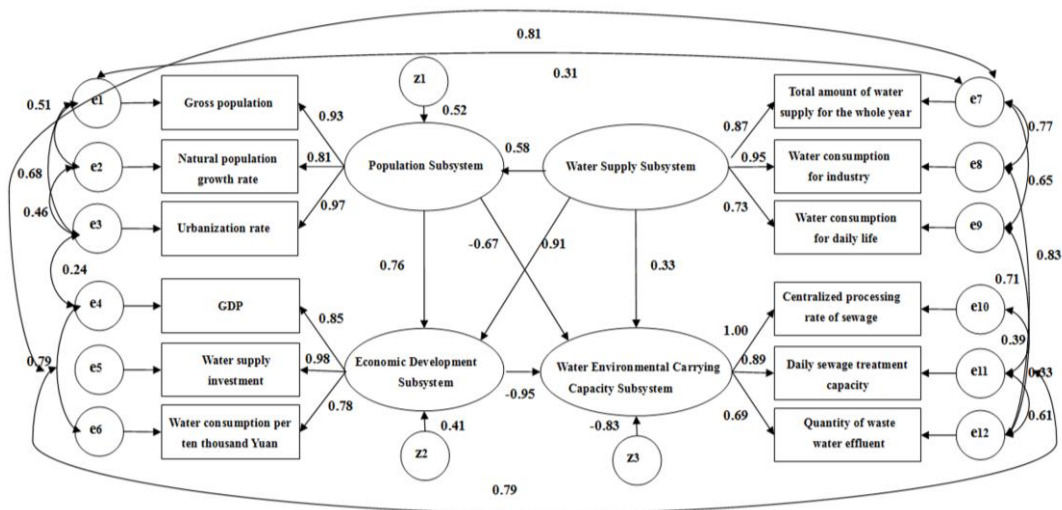


Figure 5. The standardized coefficient model of economic & water environmental system in Beijing

According to the results shown in *Table 5*, it can be found that the basic fitness index of the structural equation model, such as GFI, NFI, AIC all meet the test standard. The results also show that the modified model supports the initial hypothesis, and it has a good fitting effect (Spash, 2011).

The population subsystem has a strong positive influence on the economic development subsystem, and its path coefficient is 0.76. It shows that when the amount of population increases 1 unit, the corresponding amount of economic development will increase 0.76 units. The population subsystem has a strong negative impact on the water environmental carrying capacity subsystem, and its path coefficient is -0.62. It shows that when the amount of population increases 1 unit, the corresponding amount of water environmental carrying capacity will decrease -0.62 units. The water supply subsystem has a significant positive effect on the economic development subsystem, and its path coefficient is 0.91. Thus, when the value of water supply increases 1 unit, the corresponding amount of economic development will increase 0.91 units. The economic development subsystem has a significant negative effect on the water environmental carrying capacity subsystem, and its path coefficient is -0.98. Thus, when the amount of economic development increases 1 unit, the corresponding amount of water environmental carrying capacity will decrease 0.98 units. The water supply subsystem has a weak positive influence on the population subsystem, and its path coefficient is 0.48. It shows that when the amount of water supply increases 1 unit, the corresponding amount of economic development will increase 0.48 units. The water supply subsystem has a weak positive influence on the water environmental carrying capacity subsystem, and its path coefficient is 0.32. It shows that when the amount of water supply increases 1 unit, the corresponding amount of water environmental carrying capacity will increase 0.32 units.

Discussion

In the existing research on system coupling theory, the research involving economic system and environmental system often pays attention to the coupling relationship

between macroeconomics and the whole environment. Representative scholars of this research area include Jiang, H., He, J., Wu, Y. and Zhang, Z. Their research rarely focuses on a refinement of the water environment (Jiang and He, 2010; Panayotou, 1995). In this article, we try to focus on the water environment system and highlighted the characteristics of the water environment system. In terms of specific research content: most scholars have not researched the coupling system from multiple perspectives. For example, Liu, Y., Li, R., Song, X. only measure the coupling state of the system, and then evaluate the coupling effect of the system. There is a lack of in-depth study of the micro-coupling paths (Wu et al., 1996; Dinda, 2004). A few scholars' research involves micro-coupling paths by mechanism model only (Liu et al., 2005; Zuo and Chen, 2001). And the lack of mathematical analysis of specific coupling paths is a common shortcoming in their researches. In contrast, this article explores the system coupling law from the two perspectives of macroscopic state and microscopic paths. The detailed discussions are as follows:

Discussion of coupling state

In this paper, we try to divide the coupling state between the economic system and water environmental system in Beijing from 1997 to 2013 into 5 different stages. According to the classification criteria, the coordinated development coefficient of the economic system and water environmental system in Beijing from 1997 to 2013 is divided into stages as shown in *Table 6* (Chen and Xu, 2014).

Table 6. *The classification standard of coordinated development coefficient*

Coordinated development coefficient (D)	Standard
$0 \leq D \leq 0.1$	Serious uncoordinated stage
$0.1 < D \leq 0.3$	Uncoordinated stage
$0.3 < D \leq 0.5$	Basic coordinated stage
$0.5 < D \leq 0.7$	Good coordinated stage
$0.7 < D \leq 1$	High quality coordinated stage

(1) Serious uncoordinated stage (1997-2003). In the past, the development of water conservancy in Beijing has been neglected due to the high attention paid to economic growth and urbanization by the State and the Beijing Municipal Government. The city's weak sewage treatment caused serious water pollution. Therefore, the coordinated development coefficient of the economic system and the water environmental system in Beijing was so low in a very long period of time, this period was the serious uncoordinated stage.

(2) Uncoordinated stage (2004-2006). In 2004, with the success of China's accession to the WTO and the accelerated adjustment of the national economic structure, Beijing's economic development also ushered in a new opportunity to optimize the economic structure. It eliminated high water consumption and high pollution industries. At the same time, Beijing increased the investment in water pollution control, its water pollution treatment capacity also increased to a certain extent. However, due to the lack of investment in water resources, sewage discharge still increased. The coordinated development coefficient of the economic system and the water environmental system in Beijing was in the uncoordinated stage.

(3) Basic coordinated stage (2007-2010). After 2007, with the Beijing Olympic Games approaching, the environmental protection of Beijing was imminent. The investment in the field of water environmental protection increased rapidly, and the adjustment of the industrial structure was also further accelerated. Beijing has introduced a large number of advanced sewage treatment technology, thus the daily sewage treatment capacity and sewage treatment rate have been greatly improved. During this period, the coordinated development coefficient of the economic system and the water environmental system in Beijing was in the basic coordinated stage.

(4) Good coordinated stage (2011-2012). From 2011 to 2012, the construction of energy-saving economy in Beijing was increasingly perfect. During this period, Beijing's per capita GDP continued to increase, and investment in water supply increased a lot, while the industrial water consumption and domestic water consumption remained basically unchanged. The degree of coordination between the Beijing economic system and the water environmental system was further improved, and it was in a good coordination stage.

(5) High quality coordinated stage (2013). In 2013, the scientific concept of development has been subjected to more attention by all walks of life. Beijing's economic level of urbanization, per capita GDP and many other indicators reached the maximum in recent years. At the same time, Beijing's water pollution treatment capacity continued to improve, industrial water, domestic water demand was stable. The coordination degree between the Beijing economic system and the water environmental system reached the optimal state and was in the stage of high-quality coordination.

Discussion of coupling paths

(1) Coupling paths of population subsystem

The population subsystem has a positive impact on the economic development subsystem, and the population subsystem has a negative impact on the water environmental carrying subsystem. The reason is that, the Beijing's economic & water environmental system is a Pressure-State-Response (P-S-R) system. In this whole system, the population subsystem belongs to the "Pressure Part" (P), the economic development subsystem belongs to the "State Part" (S), and the water environmental carrying subsystem belongs to the "Response Part" (R). The "Pressure Part" (P) promotes the "State Part" (S), which is positively affected, while the "Response Part" (R) has a feedback effect on the "Pressure Part" (P), showing a negative influence. Population growth means the growth of labor and the expansion of the market, thus providing the driving force for economic development. In contrast, the domestic sewage generated by population growth has no serious burden on the water environment. That is, the contribution of population growth to economic development is greater than the burden on the water environment. Therefore, the absolute value of the path coefficient is $0.76 > 0.67$.

(2) Coupling paths of economic development subsystem

The economic development subsystem has a negative impact on the water environment carrying subsystem. The reason is that, the Beijing's economic & water environmental system is a Pressure-State-Response (P-S-R) system. The economic development subsystem belongs to the "State Part" (S), while the water environmental carrying subsystem belongs to the "Response Part" (R). The "Response Part" (R) has a

feedback effect on the “State Part”(S), showing a negative influence. Thus, if the shortage of water supply appears, it will hinder economic development.

(3) Coupling paths of water supply subsystem

The water supply subsystem has a positive impact on the population subsystem, and the water supply subsystem has a positive impact on the economic development subsystem. Meanwhile, the water supply subsystem has a positive impact on the water environment carrying subsystem. The same reason is that, the Beijing’s economic & water environmental system is a Pressure-State-Response (P-S-R) system. In this whole system, the population subsystem belongs to the “Pressure Part”(P), the economic development subsystem and water supply subsystem belong to the “State Part”(S), and the water environmental carrying subsystem belongs to the “Response Part”(R). The “State Part”(S) has a feedback effect on the “Pressure Part”(P), showing a negative influence. The “Pressure Part”(P) promotes the “State Part”(S), which is positively affected. And the “State Part”(S) also promotes the “State Part”(S), which is positively affected. Therefore, all three coupled paths show positive effects. Moreover, the water resources of the water supply subsystem can provide the necessary resource elements for economic development firstly (Barrieu and Fehr, 2014; Wesseh and Lin, 2013). Obviously, the abundant water resources and the developed economy work together to create a livable environment, on the basis of which to promote population growth. It cannot be ignored that abundant water supply can also reduce the pollution of the water environment. Therefore, the contribution of water supply to economic development is greater than the promotion of population growth, and the improvement of water supply to water environment pollution is less than the promotion of population growth. Thus, the result of the absolute value of the path coefficient shows $0.91 > 0.58 > 0.33$.

(4) Coupling paths of water environmental carrying subsystem

The coupling paths of water environmental carrying subsystem are embodied in the above 3 coupling paths. Thus, the coupling path of water environmental carrying subsystem will not be discussed again in this paragraph.

Conclusions

(1) From the macroscopic point of view, the economic system and water environmental system couple with each other and have complex interactions. With the optimizing of economic structure and advancing in technologies, the coupling degree would increase between the two systems.

At the early development stage of Beijing, more emphasis was placed on the increase in economy, leading to unbalanced development with heavy pollution and higher energy consumption, and causing great pollution to the ecology, especially to the water environment. In this stage, the economic system and the water environment system had lower coupling degree. With the optimization of the economic structure and the development of energy-saving economy, development in a scientific and sustainable way is more and more valued, and the coupling degree is getting higher while the development is getting more balanced.

(2) From the microscopic point of view, there are complex coupling paths among the population subsystem, economic development subsystem, water supply system and

water environmental carrying capacity subsystem. Besides, these four subsystems influence each other.

The water supply subsystem has a certain degree of promotion effect to the other three subsystems, thus the city's development can be promoted effectively through improving the level of water supply. Similarly, the population subsystem plays a critical role in promoting the economic development subsystem. Thus it can be concluded that accelerating urbanization is an effective way to promote economic development. On the contrary, the water environmental carrying capacity subsystem is strongly obstructed by the economic development subsystem and the population subsystem. Therefore, the development of the city should be in accordance with its corresponding water environment carrying capacity.

Acknowledgements. This research is supported by (1) National Natural Science Foundation of China (No: 51279058 & No: 41471456); (2) The Major Program of University Natural Science Foundation of Jiangsu Province (No: 14KJA170006); (3) The Joined PhD student program funded by China Scholarship Council (No: 201506710057).

REFERENCES

- [1] Ahmed, A., Uddin, G. S., Sohag, K. (2016): Biomass energy, technological progress and the environmental Kuznets curve: evidence from selected European countries. – *Biomass Bioenergy* 90: 202–208.
- [2] Aldy, J. E. (2005): An environmental Kuznets curve analysis of US state-level carbon dioxide emissions. – *J. Environ Dev.* 14: 48–72.
- [3] Apergis, N., Ozturk, I. (2015): Testing environmental Kuznets hypothesis in asian countries. – *Ecol. Indic.* 52: 16–22.
- [4] Arouri, M. E. H., Ben Youssef, A., M'henni, H., Rault, C. (2012): Empirical analysis of the EKC hypothesis for sulfur dioxide emissions in selected Middle East and North African countries. – *J Energy Dev.* 37: 207–26.
- [5] Baek, J., Kim, H. S. (2013): Is economic growth good or bad for the environment? Empirical evidence from Korea. – *Energy Econ.* 36: 744–749.
- [6] Barriue P, Fehr, M. (2014) Market-consistent modeling for cap-and-trade schemes and application to option pricing. – *Operations Res.* 62: 234–49.
- [7] Baveye, P. C., Baveye, J., Gowdy, J. (2013): Monetary valuation of ecosystem services: it matters to get the timeline right. – *Ecol. Econ.* 95: 231–235.
- [8] Ben Jebli, M., Youssef, S. B., Ozturk, I. (2016): Testing environmental Kuznets curve hypothesis: the role of renewable and non-renewable energy consumption and trade in OECD countries. – *Ecol. Indic.* 60: 824–831.
- [9] Chai, S, Yan, J, Yang, J. (2011): Coupling and coordination degree of economic growth and environmental pollution levels in Shanxi Province. – *Journal of Arid Land Resources and Environment* 25(1): 130–135.
- [10] Chen, M., Xu, C. (2013): Study on water pollution causes and prevention of Jiangsu rural areas. – *Journal of Chemical and Pharmaceutical Research* 5(12): 532–536.
- [11] Chen, M., Xu, C. (2014) Study of urban economic and environmental system coordinated development measure – take Nantong City as the example. – *International Journal of Applied Environmental Sciences* 9(4): 1603–1613.
- [12] Corinne, G. (2014): Beyond environmental and ecological economics: Proposal for an economic sociology of the environment. – *Ecol. Econ.* 105: 240–254.

- [13] Coscieme, L., Pulselli, F. M., Niccolucci, V., Patrizi, N., Sutton, P. C. (2016): Accounting for “land-grabbing” from a biocapacity viewpoint. – *Sci. Total Environ.* 539: 551–559.
- [14] Costanza, R., Alperovitz, G., Daly, H., Farley, J., Franco, C., Jackson, T., Kubiszewski, I., Schor, J., Victor, P. (2013): *Building a Sustainable and Desirable Economy-in-Society-in-Nature*. – ANU E Press, Canberra, Australia.
- [15] Dinda, S. (2004): Environmental Kuznets curve hypothesis: A survey. – *Ecological Economics* 49(4): 431–455.
- [16] Douai, A., Mearman, A., Negru, I. (2012): Prospects for a heterodox economics of the environment and sustainability. – *Camb. J. Econ.* 36: 1019–1032.
- [17] Flores, C. A., Flores-Lagunes, A., Kapetanakis, D. (2014): Lessons from quantile panel estimation of the environmental Kuznets curve. – *Econom Rev.* 33: 815–53.
- [18] Jiang, H., He, J. (2010): The dynamic coupling of coordinated development between regional economic and ecological environment systems based on Jiangsu province. – *Soft Sciences* 24(3): 63–68.
- [19] Kanjilal, K., Ghosh, S. (2013): Environmental Kuznet’s curve for India: evidence from tests for cointegration with unknown structural breaks. – *Energy Policy* 56: 509–515.
- [20] Lin, B., Moubarak, M., Ouyang, X. (2014): Carbon dioxide emissions and growth of the manufacturing sector: evidence for China. – *Energy* 76: 830–837.
- [21] Liu, Y., Li, R., Song, X. (2005) Grey associative analysis of regional urbanization and eco-environment coupling in China. – *Acta Geographica Sinica* 60(2): 237–247.
- [22] Ozturk, I., Al-Mulali, U. (2015): Investigating the validity of the environmental Kuznets curve hypothesis in Cambodia. – *Ecol. Indic.* 57: 324–330.
- [23] Ozturk, I., Uddin, G. S. (2012): Causality among carbon emissions, energy consumption and growth in India. – *Econ. Res.* 25(3): 752–775.
- [24] Panayotou, T. (1995): *Environment Degradation at Different Stages of Economic Development Livelihoods in the Third World*. – Macmillan Press, London.
- [25] Rahman, M. S., Noman, A. H. M., Shahari, F., Aslam, M., Gee, C. S., Isa, C. R., Pervin, S. (2016): Efficient energy consumption in industrial sectors and its effect on environment: a comparative analysis between G8 and Southeast Asian emerging economies. – *Energy* 97: 82–89.
- [26] Spash, C. L. (2011): Social ecological economics: understanding the past to see the future. – *Am. J. Econ. Sociol.* 70(2): 340–375.
- [27] Stern, D. I. (2001) Is there an environmental Kuznets curve for sulfur? – *Journal of Environmental Economics and Management* 1(1): 162–178.
- [28] Su, X., Wang, J., Guo, M., Jiang, Z., Li, H., Niu, Y. (2010): Coupling relationship of agricultural eco-economic system in Wuqi County based on structural equation model. – *Chinese Journal of Applied Ecology* 21(4): 937–944.
- [29] Van der Ploeg, R., Withagen, C. (2013): Green growth, green paradox and the global economic crisis. – *Environ. Innov. Soc. Transit.* 6: 116–119.
- [30] Wesseh, P. K. Jr., Lin, B. (2013) Owusu-Appiah, M. Delving into Liberia’s energy economy: technical change, inter-factor and inter-fuel substitution. – *Renew. Sustain. Energy Rev.* 24: 122–30.
- [31] Wu, Y., Zhang, Z., Lang, D. (1996): The forecasting model of environment-economy coordinated degree and its application. – *Journal of Nanjing University: Natural Sciences* 32(3): 466–472.
- [32] Xia, Z., Wang, J., Yao, W., Lu, M. (2012): Coupling relationship between agricultural industry and resources in the loess hilly region on the background of conservation of water and soil-Based on the perspective of farmers-behavior. – *Chinese Journal of Eco-Agriculture* 20(3): 369–377.
- [33] Xiao, X., Xie, D., Ni, J. (2014): Coupling state of agricultural eco-economic system under emission mitigation and sink enhancement of non-point source pollution – A case

- study of Zhong County in the Three Gorges Reservoir Region. – Chinese Journal of Eco-Agriculture 22(1): 111–119.
- [34] Zuo, Q, Chen, X. (2001) Dynamic model of coupling system for social-economy and eco-environment. – Shanghai Environmental Sciences 20(12): 592–594.

WHETHER ENERGY PRODUCTION CAN GET OUT OF THE ENVIRONMENTAL TRAP? A CASE STUDY FOR REGIONAL ENERGY SECTORS IN ZHEJIANG PROVINCE, CHINA

WANG, K.^{1,2*} – ZHANG, H. Q.^{1,2} – ZHANG, C. J.³

¹*Business School, Hohai University, 211100 Nanjing, China*

²*Institute for Planning and Decision Research, Hohai University, 211100 Nanjing, China*

³*Postdoctoral Workstation of Business Administration, Hohai University
211100 Nanjing, China*

**Corresponding author*

e-mail: wangkai_hhubs@hhu.edu.cn

(Received 25th Sep 2018; accepted 27th Nov 2018)

Abstract. Energy production in Zhejiang Province is facing huge pressure from environmental emissions, while energy production has recently been in surplus. The aim of this paper was to measure the energy efficiency of Zhejiang, from the perspective of industrial and environmental influence factors and the undesirable environmental outputs were considered respectively. We used the principal component analysis model to achieve accurate dimension reduction of input parameters and applied the slack-based model to analyze the environmental energy efficiency of each decision-making units, eleven prefecture-level cities of Zhejiang from 2005 to 2015. Conceptually, this paper classified the status of environmental energy efficiency into four types: High Level, Decreasing Trend, Improving Trend, and Deteriorating Trend. Empirically, the environmental energy efficiency of Zhejiang was more influenced by pure technical efficiency, and scale efficiency had less effect on technical efficiency. Consequently, Hangzhou reached the effective level and Zhoushan was close to that level, while the situation of energy production overcapacity and environmental pollution reduction of the remaining nine decision-making units have not been substantially improved in recent years.

Keywords: *principal component, data envelopment analysis, environmental energy efficiency, undesirable environmental outputs, case study, sustainable policy*

Abbreviations:

The following abbreviations are used in this manuscript:

PCA	Principal Component Analysis	SE	Scale Efficiency
DEA	Data Envelopment Analysis	PTE	Pure Technical Efficiency
SBM	Slack-based Model	CRS	Constant Returns to Scale
DMU	Decision-making Unit	VRS	Variable Returns to Scale
TE	Technical Efficiency	RTS	Returns to Scale

Introduction

With the rapid development of the economy and the low efficiency of energy use, the tarp of environmental quality degradation caused by excessive consumption of energy has increasingly become a bottleneck restricting the sustainable development of Chinese economy (Li et al., 2017; Geng and Doberstein, 2008). In the process of rapid economic development, the improvement of energy use efficiency can greatly alleviate the energy resources depletion and improve the environmental welfare level of energy use (Färe et al., 2007). Thus, improving energy efficiency is increasingly concerned by Chinese governments and energy producers. Zhejiang Province is one of the regions with the highest level of economic development in China. It has a high degree of

industrialization and a large amount of energy consumption. With rapid advancement of industrialization and the rapid economic growth, the total amount of pollution emissions from energy production is still at a high level. In 2015, the Zhejiang total industrial wastewater discharge amounted to 1.47 billion tons, with a total of 2.68 trillion cubic meters of industrial air emissions, and 46.78 million tons of industrial solid waste (Statistics, 2015).

The aim of this research was to understand the extent of efficiency and the optimization potential of the regional energy sectors in the Zhejiang Province of China by using the principal component analysis (PCA) and data envelopment analysis (DEA). In this research, we focused on the evaluation concerning whether the energy decisions were economically efficient, such as the energy facilities investment, the cost of energy generating and transmitting and energy consumption. Especially, we measured the energy efficiency and its impact factors at an industrial and environmental level for Zhejiang Province in view of undesirable environmental outputs including the industrial waste water, solid industrial waste, and industrial waste gas. Meanwhile, two methodologies were suggested in this study as basic paths for assessing the energy efficiency, namely principal component analysis combined with DEA (PCA–DEA), which were used to improve discrimination power.

The energy consumption structure of China, which is dominated by mineral fuels, has led to an increasingly serious problem of environmental pollution (Cao et al., 2012; Shi et al., 2011). Thus, a series of previous studies have focused on the environmental performance of China. Typically, China is currently facing many serious challenges, such as strong energy demands, energy shortages and substantial energy consumption (Chen and Gong, 2017; Gillingham et al., 2009), which are related to the traditional evaluations about the economic concepts, such as energy cost and revenue. However, undesirable output factors generated from energy consumption, especially in the mineral fuels oriented energy industries, should be added to the researching framework of energy efficiency, likewise the process of the official evaluation of environmental performance (Cao et al., 2012; Zhao et al., 2016b). In 1997, the International Energy Agency (IEA) published the first *Energy Efficiency Report*, and updated it every year (Agency, 2013, 2014). The parameters obtained in that report can be used to estimate the energy efficiency across various economic activities, and the parameters were selected from micro-enterprises, industry levels, and macro-policies. Policymakers can increase energy consumption based on economic output growth or reduce energy consumption according to reduced economic output for improving energy efficiency.

Zhejiang is located on the southeast coast of China, and it is south of the Yangtze River Delta. It has 11 prefecture-level cities under its jurisdiction, and GDP in 2015 reached 4.3 trillion yuan, up 8.0% over the previous year, accounting for 6.2% of the national total (Provincial Bureau of Statistical of Zhejiang, 2015). Thus, it is one of the most economically viable provinces in China. In 2015, the Zhejiang total discharge of industrial wastewater, industrial air emission and industrial solid waste, represent a decrease of 1.36%, 0.43%, and 0.46% as compared to 2014 (Statistics, 2014, 2015). Although the environmental burden brought by industrial production has slightly reduced, the total amount of undesirable environmental outputs in terms of absolute numbers is still large. Meanwhile, in 2015, the recently added power supply capacity in Zhejiang was about 7.00 million kilowatts. The total electricity consumption in Zhejiang was 355.39 billion kWh, up 1.4% over the same period of last year. The maximum power consumption of the electricity load was 58.50 million kilowatts, an

increase of only 760,000 kilowatts, and only 11% of the newly added power supply (Provincial Bureau of Statistical of Zhejiang, 2015), which highlighted the overcapacity situation of power generation. Energy production in Zhejiang is not only facing huge pressure from environmental emissions, but also in surplus. Thus, the energy efficiency of Zhejiang has become a subject worth studying. Incorporating undesirable environmental outputs into energy efficiency studies can help us find out which undesirable environmental outputs affect energy efficiency in the province and provide research data for Zhejiang to enhance its energy efficiency by saving energy and reducing emissions. The map of Zhejiang Province is shown in *Figure 1*.



Figure 1. Zhejiang Province of China, by eleven prefecture-level cities

Performance measurement is used to evaluate the performance of decision-making units (DMUs), and it is also a multicriteria decision-making (MCDM) problem (Chang and Lee, 2012). Because stochastic frontier analysis (SFA) (Kumbhakar and Lovell, 2000) and data envelopment analysis (Banker et al., 1984; Charnes et al., 1978) as two kinds of MCDM tools were put forward first, they have been applied to performance measurement for efficiency analysis as effective tools. However, Wang (2003) analyzed that the error existing in the DEA mathematic models can lead to the output efficiency frontier being distorted, while the date used in the DEA is subject to statistical deviation. In addition, due to the DEA techniques ratio between the inputs and outputs of each DMU via a weighting method, the efficiency estimates of a DMU are biased when a slack variable analysis of DEA is calculated.

To deal with the shortages of DEA, Adler and Golany (2001, 2002) proposed a methodology that produces uncorrelated linear combinations of original inputs and outputs to improve discrimination in DEA with minimal loss of information by using principal components. This kind of measuring tool assumes that the separation of variables standing for similar themes such as fixed-asset investment and energy resource input, and the removal of principal components with little or no explanatory power improves the categorization of efficient and inefficient DMUs. Fu and Ou (2013) combined principal PCA and DEA to enhance the efficiency of DMUs more accurately in evaluating the energy performance of Taiwanese Bureau cases. Ghosh and Jintanapakanont (2004) used PCA to understand the latent structure of critical risk factors in Thailand. Due to the fact that the explanatory power of DEA is relatively weak when analyzing several DMUs, Adler and Yazhemy (2010) further concluded that PCA-DEA outperformed PCA variable reduction by comparing their discrimination performance in a simulation exercise. Thus, the literature review showed that the integration of DEA with PCA technology could obtain more stable estimation results when compared to single MCDM oriented methods. Therefore, this research attempted to combine DEA with PCA to construct a performance analysis model for energy efficiency of the Zhejiang Province, China.

In the process of the industrialization of China, when evaluating the production activities of regional energy sectors, researchers mainly considered the capital, labor, economic output and other parameters, focusing on the enterprise, industry, or regional economic level (Cao et al., 2012; Chen and Gong, 2017; Wang et al., 2016; Zha et al., 2016; Zhang et al., 2016; Zhao et al., 2016a). Studies such as that conducted by Yang and Zhao (2009) revealed that the department of manufacturing was the main hampering factor of the total-factor energy efficiency of Zhejiang Province from 1990–2007. Wu (2008) and Qiang et al. (2005) calculated the coal consumption rate of heating and energy investment efficiency of the Northern Zhejiang Province and proposed potential energy saving assignments. These research works performed to date only considered economic output and ignored hazardous impacts on the environment in the process of energy efficiency evaluations, therefore the research results were incompatible with reality. Thus, how to coordinate the future energy development with environmental protection and consider the doubt requirement of economy and cleanliness are great subjects. In addition, with the promotion of energy efficiency policies and intensified environmental conditions, the energy and environmental efficiency of the evaluation requirements are becoming higher. Therefore, when analyzing energy efficiency, the industry or region should be considered as non-energy inputs and undesired output factors including a series of emissions of pollutants. Thus, it is necessary and urgent to fill the gaps for the energy efficiency analysis of Zhejiang Province by considering the undesirable output factors of energy consumption through the integration of DEA with PCA methods.

Based on the above consideration, we aimed to measure the energy efficiency and its impact factors at an industrial and environmental level of Zhejiang Province, while considering undesirable environmental outputs including industrial waste water, solid industrial waste, and industrial waste gas by using the integration method that combined PCA with DEA.

Methodology

We considered that there are n independent regions denoted by DMU_j ($j = 1, 2, \dots, n$). In the process of production, each DMU uses m non-energy inputs x_{ij} ($i = 1, 2, \dots, m$) and k energy inputs x_{pj} ($p = 1, 2, \dots, k$) to produce s desirable outputs y_{rj} ($r = 1, 2, \dots, s$) and t undesirable outputs v_{qj} ($q = 1, 2, \dots, t$).

Environmental Production Technology

The basic thought of environmental production technology is that the general production process can produce some undesirable outputs such as waste water, solid industrial waste, and industrial waste gas. Thus, to minimize the undesirable outputs, it is necessary to arrange certain resources such as environmental protection equipment and manpower, which may lead to the production of desirable outputs in the process of the energy production (Faere et al., 1989; Färe et al., 2007). In this research, we supposed that the energy production process uses capital (C), labor (L), and energy resources (E) as input factors to produce desirable outputs (Y) and undesirable outputs (V). Thus, the environmental production technology function can be described as follows:

$$T = \{(C, L, E, Y, V), \text{ s.t. } (C, L, E) \text{ can produce } (Y, V)\} \quad (\text{Eq.1})$$

Based on the variable assumptions above, we further specified the environmental production technology for n DMUs as *Equation 2*, and the detailed environmental production technology function can be modeled as below:

$$T = \left(\begin{array}{l} (C, L, E, Y, V) \text{ s.t. } \sum_1^j \lambda_j C_p, C, \sum_1^j \lambda_j L_p, L, \sum_1^j \lambda_j E_p, E, \\ \sum_1^j \lambda_j Y_r, \dots, C, \sum_1^j \lambda_j V_q, V, \lambda_j \dots 0, j = 1, 2, \dots, n \end{array} \right) \quad (\text{Eq.2})$$

where λ_j is the weight variable that is utilized to construct a convex combination enveloping all DMUs; and j denotes the total number of DMUs.

Principal Component Analysis Model for Variable Reduction

Principal component analysis (PCA) is a widely used tool for multivariate analysis to achieve accurate dimension reduction by extracting a few, but not all, of the principal components (PCs). PCA can be used to describe most of the variations in the original multivariate data with the least loss of information (Adler and Yazhensky, 2010). Through the mathematic tool of linear transformation, PCA can decompose correlated variables into uncorrelated PCs under the system of the given dataset. After obtaining the extracted PCs, these calculated PCs are estimated as the projections on the eigenvectors of the covariance or correlation matrix of this dataset (Fu and Ou, 2013). Normally, after the formation of the new composite parameters, the PCs of the parameters need to reflect the original parameters of more than 80% information, and the new parameters are independent. If the requirements for independence are not met, then the new parameters need to be analyzed for principal component analysis until they meet all the conditions (Jolliffe and Ian, 2005).

Suppose that there are n independent regions, denoted by X_i ($i = 1, 2, \dots, n$), and each region has m standardized variables on different factors, which are connected with the

input-factors and output factors, marked as X_j ($j = 1, 2, \dots, m$). Thus, the standardized variables matrix can be presented in *Equation 3*.

$$X = \begin{bmatrix} x_{11} & x_{12} & \cdots & x_{1m} \\ x_{21} & x_{22} & \cdots & x_{2m} \\ \vdots & \vdots & \vdots & \vdots \\ x_{n1} & x_{n2} & \cdots & x_{nm} \end{bmatrix} = (X_1, X_2, \dots, X_m) \quad (\text{Eq.3})$$

Based on the standardized variables matrix shown above, the PCA is the process of transferring the original standardized variables into a new systematic variables dataset. To present the relationships between the original standardized variable and PCs, we supposed there were t PCs, denoted as f_c ($c = 1, 2, \dots, t$, $t \leq m$). The equations set can be described as follows:

$$\begin{cases} f_1 = \theta_{11}x_1 + \theta_{12}x_2 + \cdots + \theta_{1m}x_m \\ f_2 = \theta_{21}x_1 + \theta_{22}x_2 + \cdots + \theta_{2m}x_m \\ \vdots \\ f_t = \theta_{t1}x_1 + \theta_{t2}x_2 + \cdots + \theta_{tm}x_m \end{cases} \quad (\text{Eq.4})$$

By using the matrix, *Equation 4* can be presented as follows:

$$F = AX \quad (\text{Eq.5})$$

$$\text{s.t. } F = \begin{bmatrix} f_1 \\ f_2 \\ \dots \\ f_t \end{bmatrix}, \quad A = \begin{bmatrix} \theta_{11} & \theta_{12} & \cdots & \theta_{1m} \\ \theta_{21} & \theta_{22} & \cdots & \theta_{2m} \\ \vdots & \vdots & \vdots & \vdots \\ \theta_{t1} & \theta_{t2} & \cdots & \theta_{tm} \end{bmatrix}, \quad X = \begin{bmatrix} X_1 \\ X_2 \\ \dots \\ X_m \end{bmatrix} \quad (\text{Eq.6})$$

Normally, *Equations 4 and 5* should meet the following conditions:

- (i) There is no correlation between f_i and f_j ($i \neq j$ and $i, j = 1, 2, \dots, t$), ie, $\text{cov}(f_i, f_j) = 0$.
- (ii) f_1 is the largest variance of x_1, x_2, \dots, x_m in all linear combinations. f_2 is the largest variance of x_1, x_2, \dots, x_m in all linear combinations, and there is no correlation between f_1 and f_2 . f_c ($c \leq t$) is the largest variance of x_1, x_2, \dots, x_m in all linear combinations, and there is no correlation between f_1, f_2, \dots, f_c .
- (iii) The coefficient matrix A is an orthogonal matrix.

After satisfying the above conditions, f_1, f_2, \dots, f_c are the principal components of the variables x_1, x_2, \dots, x_m . If the first few PCs of the variance and the proportion of the total variance is greater or equal to 85%, we can use the new variable f_1, f_2, \dots, f_c , instead of the original variable x_1, x_2, \dots, x_m . Thus, the PCA can retain most of the original variable information.

Slack-based Model for Economic-Environmental Energy Efficiency

In the radial DEA model, the measurement of inefficiency degree only includes the proportion of all input-output reductions. For the inefficient DMU, the difference

between its current state and a strong effective target not only includes the proportionally improved portion, but also the slack movement. However, the slack movement is not reflected in the measurement of efficiency in the radial model. With this consideration, Tone (2001, 2002) proposed the Slack-based Model (SBM) and solved the inefficiency calculated by the measurement of radial model did not include the slack movement. The equation of SBM can be shown as follow:

$$\begin{aligned} \min \rho &= \frac{1 - \frac{1}{m} \sum_{i=1}^m s_i^- / x_{ik}}{1 + \frac{1}{q} \sum_{r=1}^q s_r^+ / y_{rk}} \\ \text{s.t. } X\lambda + s^- &= x_k \\ X\lambda - s^+ &= x_k \\ \lambda, s^-, s^+ &\dots 0 \end{aligned} \quad (\text{Eq.7})$$

where the SBM model uses ρ as the efficiency value of the DMU, and measures the inefficiency from both inputs and outputs, which is the reason why it is called the non-oriented model. $x_{ik} \neq 0$ ($i = 1, 2, \dots, m$), $y_{rk} \neq 0$ ($r = 1, 2, \dots, q$). The inefficiency of inputs and outputs can be presented as *Equation 8*. If the efficiency value ρ of the SBM model is 1, this indicates that the evaluated DMU has a strong efficiency. The projection of DUM can be shown by *Equation 9*.

$$1 - \frac{1}{m} \sum_{i=1}^m s_i^- / x_{ik}, 1 + \frac{1}{q} \sum_{r=1}^q s_r^+ / y_{rk} \quad (\text{Eq.8})$$

$$\hat{x}_k = x_k - s^-, \hat{y}_k = y_k + s^+ \quad (\text{Eq.9})$$

Empirical Analysis

In this section, we first selected three kinds of parameters as inputs as well as desirable and undesirable output factors to evaluate the energy efficiency of Zhejiang Province. Second, we used the PCA model to achieve accurate dimension reduction of input factors, which included two kinds of parameters: non-energy inputs and energy inputs factors. Third, we applied the SBM-DEA model to analyze the energy efficiency of each DMU for eleven prefecture-level cities of Zhejiang Province from 2005 to 2015. In addition, to evaluate the energy efficiency abatement potential of each city in Zhejiang Province, the average energy efficiency parameters of each city from 2014 to 2015 were applied so as to analyze the space-time distribution by using a GIS visualization method and the PCA-BEA model. Finally, we estimated the energy efficiency optimization potential through the projection analysis connected with each DMU.

Variable Selection

This research selected non-energy inputs and energy inputs as input factors and categorized the output factors into desirable outputs and undesirable outputs. Based on

the methods of measuring traditional energy efficiency used by Fu and Ou (2013) and Ghosh and Jintanapakanont (2004), we selected five parameters as input factors, non-energy inputs, and energy puts. The non-energy inputs included labor and investment of fixed assets. The energy inputs were coal, oil, and natural gas, which are industry consumption oriented and the unit was converted to the standard coal equivalent. Particularly, in order to estimate the environmental energy efficiency of each DMU, we added three undesirable output factors such as waste gas, solid waste, and waste water into the variable list. Furthermore, we chose GDP as a desirable output factor. The variables of inputs and outputs are shown in *Table 1*.

Table 1. *The variables of inputs and outputs*

Parameter	Units	Abbr. ^b	Data Sources
Non-energy inputs	Labor	10-thousand persons	Labor
	Investment of fixed assets	100 million RMB yuan	IFA
Energy inputs	Coal (Industry Consumption)	10-thousand tons of SCE ^a	Coal
	Oil (Industry Consumption)	10-thousand tons of SCE	Oil
	Natural gas (Industry Consumption)	10-thousand tons of SCE	NG
Desirable output	Gross Domestic Product	100-million RMB yuan	GDP
Undesirable outputs	Waste gas	10-thousand tons	WG
	Solid wastes	10-thousand tons	SW
	Waste water	10-thousand tons	WW

^a SCE denotes standard coal equivalent

^b Abbr. will be used in this research paper

Data Collection and Treatment

In the Zhejiang Province of China, there are eleven prefecture-level cities, the capital Hangzhou (HgZ), Ningbo (NB), Jiaying (JX), Huzhou (HuZ), Shaoxing (SX), Zhoushan (ZS), Wenzhou (WZ), Jinhua (JH), Quzhou (QZ), Taizhou (TZ), and Lishui (LS). The data estimated in this research were collected from the *Zhejiang Statistics Year Book* and *Zhejiang Environment Statistical Yearbook*. In general, Chinese national statistical agencies publish economic, social and environmental statistics for the previous year. Thus, the data required for this research period (2005-2015) comes from the statistical yearbooks published by the official statistical agencies from 2006 to 2016. The sources of the data is presented in *Table 1*. In order to avoid the data interference caused by the time value of price, we converted the GDP and investment of fixed assets under the interest basement of 2015. The descriptive statistics of the dataset are shown in *Table 2*.

Both the variables of inputs and outputs shown in *Table 2* fall into two categories: non-energy inputs and energy inputs, desirable output and undesirable outputs. First, the non-energy inputs and desirable output, Labor, Fixed-Asset Investment (IFA), and GDP of each city were obtained directly from the *Zhejiang Statistics Year Book*. Second, all kinds of energy consumption factors were converted into standard coal equivalents based on the conversion factors from physical units to coal equivalents obtained from

the *China Energy Statistical Yearbook*. Third, to estimate the environmental effect of the undesirable outputs, we chose waste gas, solid waste, and waste water, which are pollutants produced by the energy production activities and obtained from the *Zhejiang Environment Statistical Yearbook*, as output factors. In particular, based on the logical relationships between the inputs and outputs, we took the data of the undesirable outputs and transformed them into another series of parameters, WG^* , SW^* , WW^* , which are the inverse of each other and can be described as follows:

$$WG^* = WG^{-1}, SW^* = SW^{-1}, WW^* = WW^{-1} \quad (\text{Eq.10})$$

Table 2. The descriptive statistics of the dataset

Year ^a	Inputs					Outputs				
	Non-energy inputs		Energy inputs ^b			Dd.output ^c	Undesirable outputs			
	Labor	IFA	Coal	Oil	NG		GDP	WG	SW	WW
2006	Max	55.84	130.61	222.76	3.82	0.22	335.20	196.58	66.04	4,257.38
	Min	512.21	1,502.77	2,287.05	39.27	2.24	3,441.51	2,018.29	678.02	43,710.67
	Mean	290.39	673.50	949.38	16.30	0.93	1,428.61	837.82	281.45	18,144.82
	Std. dev.	155.99	454.08	674.25	11.58	0.66	1,014.60	595.02	199.89	12,886.43
2009	Max	65.95	279.19	283.66	6.89	0.35	533.26	279.48	91.73	4,772.79
	Min	597.47	2,291.65	2,712.17	65.87	3.34	5,098.66	2,672.22	877.06	45,634.05
	Mean	315.72	965.94	1,099.19	26.70	1.35	2,066.39	1,083.00	355.46	18,494.64
	Std. dev.	169.64	652.66	787.50	19.13	0.97	1,480.45	775.91	254.66	13,250.30
2012	Max	72.90	471.98	317.85	4.98	0.97	853.18	395.57	111.99	4,324.99
	Min	644.43	3,722.75	2,906.62	45.56	8.85	7,802.01	3,617.38	1,024.07	39,550.43
	Mean	332.13	1,548.84	1,171.96	18.37	3.57	3,145.81	1,458.55	412.91	15,946.91
	Std. dev.	188.99	1,030.52	846.07	13.26	2.58	2,271.04	1,052.96	298.09	11,512.50
2015	Max	74.50	751.52	315.98	7.20	1.41	1,092.85	539.15	133.14	2,202.16
	Min	663.03	5,556.32	2,905.87	66.24	13.00	10,050.21	6,268.99	1,155.41	33,807.05
	Mean	336.97	2,419.92	1,131.27	25.79	5.06	3,912.58	2,440.23	407.81	13,395.75
	Std. dev.	192.46	1,538.06	830.96	18.94	3.72	2,873.93	1,752.86	299.09	10,000.96

^a The research duration is from 2005 to 2015. Due to the limited space, this statistic table only shows the descriptive statistics of the research duration typically. For more details, please contact the author to obtain the data for Zhejiang Province from 2015 to 2015; ^b The units of the energy input factors is converted into standard coal equivalent according to the *Table 1*; ^c *D.d outputs* are the abbreviation of *Desirable outputs*

As the input and output data have different dimensions, the amount of the data varied greatly, thus the original data can be transformed to eliminate the dimensional influence, and this method allows the input and output data to be in a positive range. The data transformed processing method can be shown as follows:

$$\begin{cases} x'_{ij} = 0.1 + \frac{x_{ij} - \min_j \{x_{ij}\}}{\max_j \{x_{ij}\} - \min_j \{x_{ij}\}} \\ x'_{pj} = 0.1 + \frac{x_{pj} - \min_j \{x_{pj}\}}{\max_j \{x_{pj}\} - \min_j \{x_{pj}\}} \\ y'_{rj} = 0.1 + \frac{y_{rj} - \min_j \{y_{rj}\}}{\max_j \{y_{rj}\} - \min_j \{y_{rj}\}} \\ v'_{qj} = 0.1 + \frac{v_{qj} - \min_j \{v_{qj}\}}{\max_j \{v_{qj}\} - \min_j \{v_{qj}\}} \end{cases} \quad (\text{Eq.11})$$

where the m non-energy inputs x_{ij} ($i = 1, 2, \dots, m$) and k energy inputs x_{pj} ($p = 1, 2, \dots, k$) produce s desirable outputs y_{rj} ($r = 1, 2, \dots, s$), and t undesirable outputs v_{qj} ($q = 1, 2, \dots, t$). The transformed inputs are $x^*_{ij} \in [0.1, 1]$, $x^*_{pj} \in [0.1, 1]$, and the transformed outputs are $y^*_{rj} \in [0.1, 1]$, $v^*_{qj} \in [0.1, 1]$.

Comprehensive Analysis of Environmental Energy Efficiency

In this section, nine parameters of energy and environment of Zhejiang Province were selected. First, the PCA was used to eliminate the overlapping information among the input parameters and generate the corresponding principal components. Second, based on the PCA-DEA model, we calculated the environmental energy efficiency of 11 DMUs. Third, according to the analysis results, this section focuses on the evaluation of the comprehensive technical efficiency (TE), pure technical efficiency (PTE), and scale efficiency (SE) of the environmental energy in the cities of Zhejiang Province. In addition, based on the energy efficiency data, we obtained the potential of improvement concerning environmental energy efficiency of each city. Finally, based on the efficiency adjustment, this paper provides an explanation of the different development trends of environmental energy efficiency in each DMU, and puts forward suggestions for improvement.

Evaluation of Environmental Energy Efficiency

We used the PCA-DEA model to quantitatively estimate the environmental energy performance of Zhejiang Province from 2005 to 2015. This study found that in the 11 years since 2005, the average level of environmental energy efficiency in the 11 cities in Zhejiang Province showed a pyramid shape. First, the comprehensive performance of environmental energy in Hangzhou, Zhoushan, and Lishui was higher than 0.800, accounting for 27% of the total number of cities. Second, the comprehensive performance levels of Jinhua, Taizhou, Jiaxing, Wenzhou, and Shaoxing were relatively low, in fact below the level of 0.500, accounting for 45% of the total number of cities. Finally, Quzhou, Huzhou, and Ningbo were at an intermediate stage of overall efficiency at above 0.50, but below 0.80, accounting for 27% of the total number of cities, same as the number of first-class cities with excellent overall efficiency in Zhejiang Province. The technical efficiency (TE) of each DMU from 2005 to 2015 is shown in *Table 3*.

From the perspective of the overall efficiency of the city distribution, there was a difference in the amount between cities at the front of efficiency and cities that did not reach the most efficient. As the capital of Zhejiang Province, the input-output status of Hangzhou constitutes to be the frontier of environmental energy performance. Although

Zhoushan and Lishui have not achieved optimal status, the average TE in 11 years was higher than 0.80 and the potential for environment and energy performance improvement was relatively less. Compared to the first three cities, the TE of Quzhou, Huzhou, and Ningbo were relatively poor, and energy production activities on the environment had a greater direct and indirect impact. In particular, it should be noted that the average comprehensive performance of five cities in Zhejiang Province was below 0.50.

Table 3. The technical efficiency score of each DMUs (2005–2015)

DMUs ^a	2005	2006	2007	2008	2009	2010	2011	2012	2013	2014	2015	Mean
Hangzhou	1.00	1.00	1.00	1.00	1.00	1.00	1.00	1.00	1.00	1.00	1.00	1.00***
Zhoushan	1.00	0.61	1.00	1.00	1.00	1.00	1.00	1.00	1.00	1.00	1.00	0.96***
Lishui	0.91	1.00	0.86	0.87	0.90	0.91	0.90	0.90	0.88	0.90	0.54	0.87***
Quzhou	0.80	0.60	0.77	0.79	0.78	0.80	0.78	0.81	0.81	0.84	0.27	0.73
Huzhou	0.57	0.44	0.57	0.57	0.59	0.62	0.63	0.63	0.63	0.63	0.42	0.57
Ningbo	0.50	0.42	0.51	0.50	0.51	0.59	0.73	0.56	0.58	0.54	0.39	0.53
Jinhua	0.43	0.33	0.44	0.45	0.46	0.48	0.48	0.48	0.48	0.48	0.57	0.46*
Taizhou	0.40	0.37	0.40	0.40	0.43	0.44	0.45	0.47	0.47	0.47	0.62	0.45*
Jiaxing	0.41	0.32	0.42	0.42	0.44	0.46	0.46	0.46	0.47	0.47	0.27	0.42*
Wenzhou	0.41	0.31	0.40	0.41	0.43	0.45	0.42	0.43	0.43	0.43	0.42	0.41*
Shaoxing	0.39	0.30	0.39	0.39	0.40	0.42	0.42	0.43	0.43	0.43	0.31	0.39*

^a The city ranking is in descending order of *Mean*

*The average score of technical efficiency below the 0.500

*** The average score of technical efficiency better than 0.800

Despite historical reasons such as the crude made energy production mode, the lack of environmental protection concept and the relative backwardness of energy production technology, the average TE of the overall 11 years was relatively low. However, we should pay more attention to the fact that in 2015, the TE of four cities, including Quzhou, Huzhou, Ningbo, Jiaxing, , remained below 0.50. Thus, Zhejiang Province still faces great challenges in improving energy efficiency, and at least eight cities (excluding Hangzhou, Zhoushan, and Lishui) have certain potential for improvement. The overall environmental and energy performance of 11 cities in Zhejiang Province from 2005 to 2015 are shown in *Figure 2*.

Based on the efficiency score changing tendency from 2005 to 2015 within 11 cities from *Figure 2*, we choose the score of 0.50 as the average level. The performance score from less than 0.50 to greater than 0.50 is considered to be a performance improvement, whereas performance is considered a deterioration. Thus, we can clearly know about the environmental energy performance trend of 11 cities in Zhejiang Province, including the technical efficiency (TE), pure technical efficiency (PTE), and scale efficiency (SE), which are presented in *Table 4*.

The trend of environmental performance in 11 cities can be divided into four categories. The first category is High Level, which means the overall efficiency is maintained at 1.00 for the whole research period. Such cities include Hangzhou and Zhoushan. The second category is Decreasing Trend, which means that the overall historical efficiency showed a state of greater than 0.50, but the declining tendency was

less than 0.50 in recent years. Such cities include Lishui, Quzhou, Huzhou, and Ningbo. The third type of city is the Improving Trend, where the overall efficiency of such cities is gradually improving. In recent years, the improvement has been remarkable and above 0.50. Such cities include Jinhua and Taizhou. In the fourth category, Deteriorating Trend, the overall technical efficiency of such cities has been at a long-term low level and shows a deteriorating trend. Such cities include Jiaxing, Wenzhou, and Shaoxing. The tendency of these four types, on the one hand, made us realize that the environmental energy performance among cities in Zhejiang Province is at different levels, and on the other hand, there are some commonalities between the regions, which can provide a research path for finding common influencing factors between the regions.

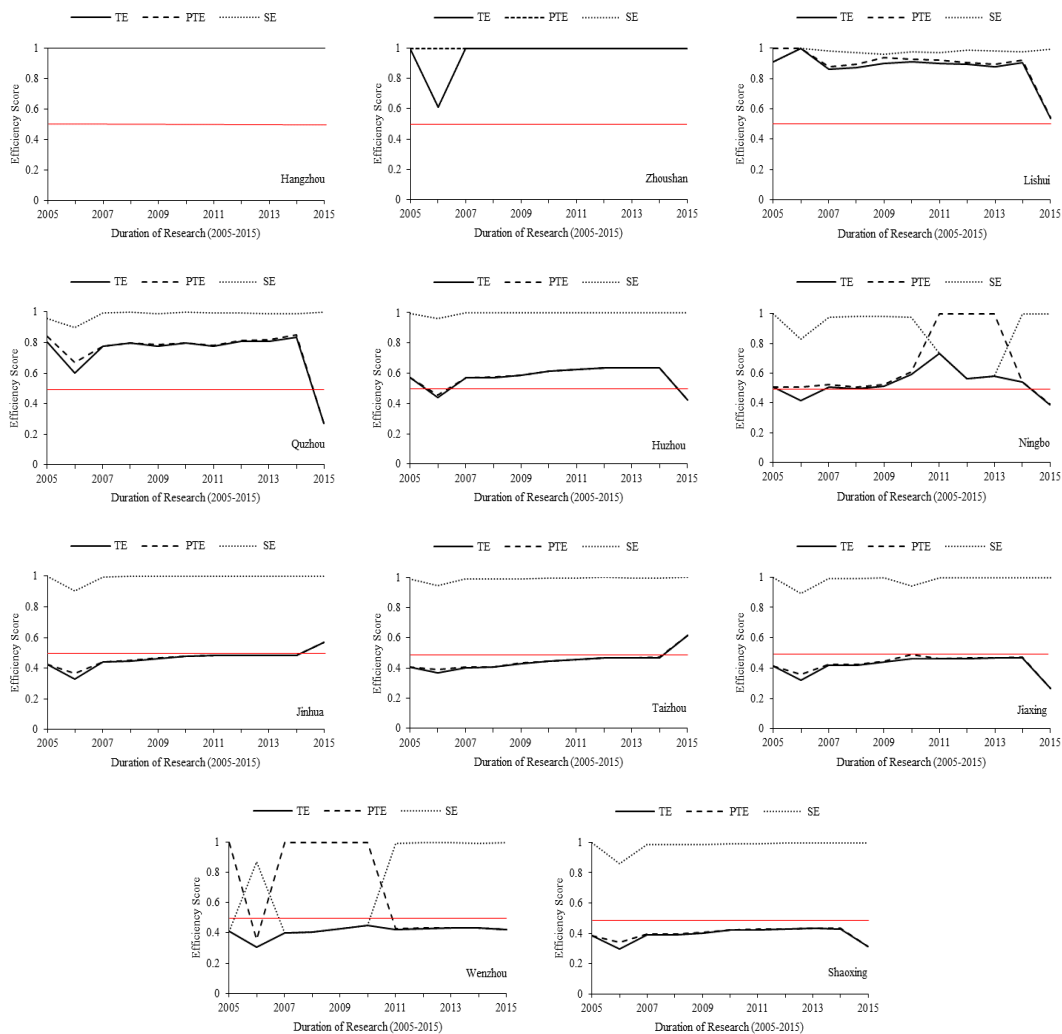



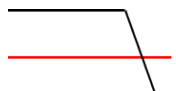
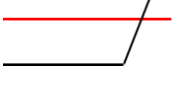
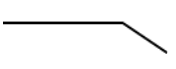
Figure 2. Efficiency score of eleven prefecture-level cities of Zhejiang Province (2005–2015)

^a The red line (—) of each graph shows the level of efficiency score is 0.50

^b The graph of Hangzhou shows both the TE, PTE and SE are 1.00. The graph of Zhoushan, the TE and PTE of 2006 are 0.61, thus the line of TE and PTE are combined with each, which is the same situation for Huzhou, Jinhua, Taizhou, and Shaoxing

^c Technical efficiency (TE), Pure technical efficiency (PTE), Scale efficiency (SE)

Table 4. Four types of environmental energy efficiency tendency (Zhejiang Province Experience)

No.	Tendency Description	DMUs Included	Count	Tendency Graph
1	High Level. The TE of DMUs maintains the level of 1.00. If there have been a relatively small number of lower levels in history, the type of the DUM also can be classified as High Level.	Hangzhou; Zhoushan	2	
2	Decreasing Trend. There has been a middle level (better than 0.05) of TE in history, but the TE of DMUs started to decreasing and be lower than 0.50 recently can be classified as this type.	Lishui; Quzhou; Huzhou; Ningbo	4	
3	Improving Trend. Although the TE of DMUs were lower than 0.50, the TE started to improve and better than 0.50 recently can be classified as this type.	Jinhua; Taizhou	2	
4	Deteriorating Trend. The TE of DMUs maintains the low level, which is always lower than 0.50 and can not be shown the improving tendency in the recent research duration (2013-2015) can be classified as this type.	Jiaxing; Wenzhou; Shaoxing	3	

^a The red line (—) of each graph shows the level of efficiency score is 0.50

Space Distribution of Environmental Energy Efficiency

For the slack-based model, the returns to scale of energy production technology is variable (Variable return to scale, VRS). Thus, the efficiency value obtained from the VRS model is just the technical efficiency. The scale efficiency value can be separated by comparing and calculating the efficiency values of both the CRS and VRS, and the calculation method can be shown as follows:

$$SE = TE/PTE \quad (\text{Eq.12})$$

We averaged the environmental energy efficiency data of Zhejiang Province in 2014 and 2015, and presented the geographical distribution of comprehensive energy efficiency, pure technical efficiency, and scale efficiency in Zhejiang Province by using GPS technology. Hangzhou and Zhoushan are at the forefront of environmental energy efficiency, followed by Lishui City. However, the technical efficiency scores of Jiaxing, Shaoxing, Ningbo, Wenzhou are under 0.5, and worse than cities marked green. Based on the logical relationship between integrated energy efficiency, purely technical efficiency, and economies of scale (*Equation 9*), we found that due to the small number differences of SE between the eleven cities, and the insensitive impact on TE, the comprehensive efficiency was more affected by the PTE, which makes the TE and PTE closer to the data distribution structure. In addition, the economies of scale of Hangzhou and Zhoushan are in a constant state, while the economies of scale of other cities are in a decreasing state. This shows that the marginal efficiency of environmental energy brought by the increase of the scale of energy equipment decreases, and the improvement of energy and environmental efficiency should be

studied from the perspective of upgrading PTE. The spatial distribution of the environmental energy efficiency of the 2014 and 2015 average level for Zhejiang Province is shown in *Figure 3*.

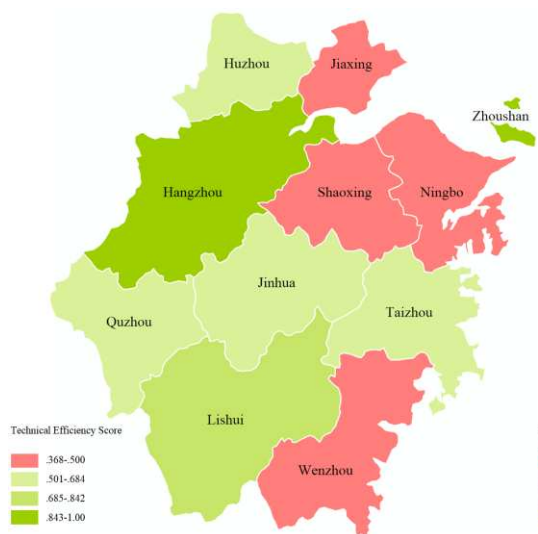


Figure 3.1. TE of each DMU (2014–2015 Average)

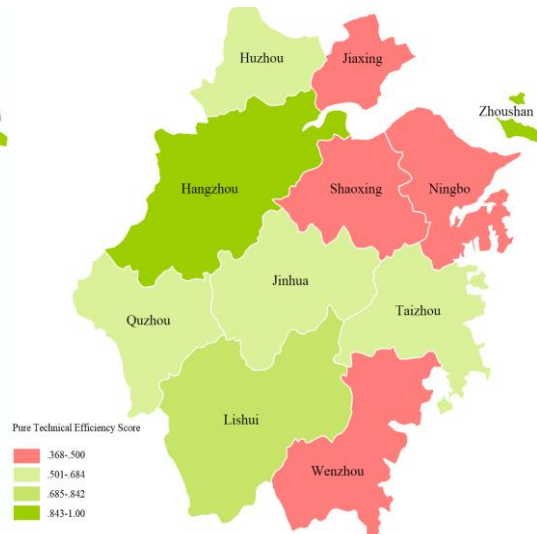


Figure 3.2. PTE of each DMU (2014–2015 Average)

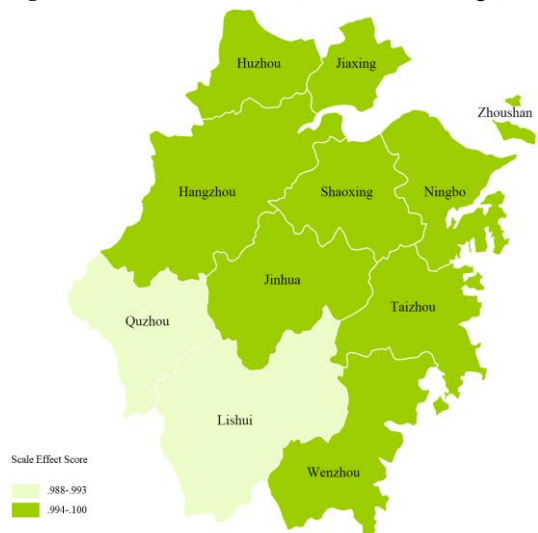


Figure 3.3. SE of each DMU (2014–2015 Average)

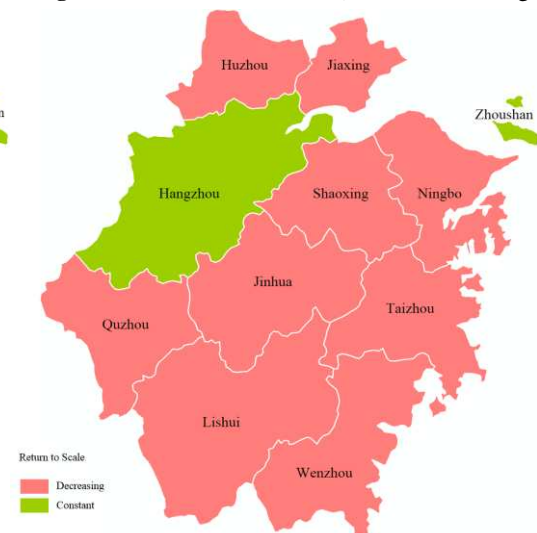


Figure 3.4. RTS of each DMU (2014–2015 Average)

Figure 3. The Space distribution of environmental energy efficiency for Zhejiang (2014–2015 Average). ^a Technical efficiency (TE), Pure technical efficiency (PTE), Scale efficiency (SE)

Estimation of Environmental Energy Efficiency Optimization Potential

DMUs with strong environmental energy performance make up the efficiency frontier and have become an improved reference for non-effective DMUs. Hangzhou and Zhoushan had a strong and effective environment energy performance with input and output factors in a balanced and effective state, which provides a performance reference for other cities to improve their environmental efficiency. The SBM-DEA is a non-radial improvement DEA model and we provided the slack movement and projection per city. Since this paper used a non-dimensional data processing approach,

all production technology elements had values between 0.10 and 1.00 (see *Equation 8* for details). Although non-dimension eliminates the inconsistency between variables, it does not affect the research on environmental energy efficiency improvement, and the proportion between slack movement and projection (see *Table 5*).

Table 5. The slack movement and projection of each DMU in 2015 (Zhejiang Province)

DMUs	CRS Score	Slack Movement of Inputs					Slack Movement of Outputs			
		Non-energy inputs		Energy inputs			Dd.output ^a	Undesirable outputs		
		Labor	IFA	Coal	Oil	NG	GDP	WG	SW	WW
Hangzhou	1.00***	0.00 (1.000) ^b	0.00 (1.00)	0.00 (1.00)	0.00 (1.00)	0.00 (1.00)	0.00 (1.00)	0.00 (0.74)	0.00 (0.60)	0.00 (1.00)
Zoushan	0.96***	0.00 (0.10)	0.00 (0.18)	0.10 (0.10)	0.00 (0.10)	0.00 (0.10)	0.00 (0.10)	0.01 (0.10)	0.00 (0.10)	0.00 (0.10)
Lishui	0.87	0.00 (0.21)	0.00 (0.10)	0.01 (0.10)	0.01 (0.10)	0.00 (0.10)	0.00 (0.10)	0.01 (0.14)	0.01 (0.14)	0.02 (0.21)
Quzhou	0.73	0.00 (0.20)	0.00 (0.13)	0.01 (0.11)	0.01 (0.11)	0.00 (0.01)	0.00 (0.11)	0.11 (0.39)	0.10 (0.48)	0.18 (0.43)
Huzhou	0.57	0.01 (0.28)	0.01 (0.23)	0.01 (0.21)	0.02 (0.21)	0.00 (0.21)	0.00 (0.21)	0.12 (0.49)	0.39 (0.56)	0.16 (0.45)
Ningbo	0.53	0.00 (0.84)	0.00 (0.88)	0.30 (0.87)	0.21 (0.87)	0.01 (0.87)	0.00 (0.87)	0.11 (1.00)	0.13 (1.00)	0.10 (0.54)
Jinhua	0.46	0.00 (0.561)	0.00 (0.33)	0.01 (0.36)	0.17 (0.36)	0.00 (0.36)	0.00 (0.36)	0.01 (0.24)	0.03 (0.20)	0.01 (0.27)
Taizhou	0.45	0.14 (0.53)	0.00 (0.36)	0.12 (0.37)	0.03 (0.37)	0.00 (0.38)	0.00 (0.37)	0.15 (0.38)	0.15 (0.38)	0.12 (0.34)
Jiaxing	0.42	0.00 (0.53)	0.00 (0.47)	0.01 (0.37)	0.08 (0.37)	0.01 (0.37)	0.00 (0.37)	0.03 (0.40)	0.02 (0.49)	0.01 (0.72)
Wenzhou	0.41	0.11 (0.52)	0.14 (0.51)	0.21 (0.49)	0.19 (0.49)	0.00 (0.49)	0.00 (0.49)	0.01 (0.75)	0.53 (0.79)	0.28 (0.49)
Shaoxing	0.39	0.00 (0.56)	0.00 (0.48)	0.03 (0.48)	0.11 (0.48)	0.01 (0.48)	0.00 (0.48)	0.02 (0.29)	0.12 (0.33)	0.34 (0.86)

^a *D.d outputs* are the abbreviation of *Desirable outputs*

^b Inside the “()” is the Projection Value for each variable factors. All the values have been dimensioned

^c Strong efficient of DMUs will be noted as ***, and the slack movement of each variables will be 0.00

(1) Efficiency Improvement from the Perspective of Environmental Energy Efficiency Distribution Structure in DMUs

According to the research ideas provided by environmental production theory, we selected nine variables between input and output, and highlighted the negative output variables brought by energy production to the environment. For Hangzhou and Zhoushan, energy production not only contributed to GDP in an effective manner, but also had a negative impact on the environment in an effective state. There was a certain degree of improvement necessary for Zhoushan for the input factor for energy production, and the negative output of waste gas.

(2) Efficiency Improvement from the Perspective of Input Factor

There was a big difference between the non-energy inputs and energy input factors in the improvement level. According to the information mentioned above, the economies of scale of cities are generally high. Since the contribution of energy infrastructure to environmental energy performance improvement contribution is limited, the labor and energy infrastructure investment in fixed assets is not sensitive to improving

environmental efficiency. However, the input structure of energy resources is more sensitive to the improvement of environmental energy performance. Coal and oil are helpful for reducing environmental pollution and improving environmental energy efficiency.

(3) Efficiency Improvement from the Perspective of the Output Factor

There is a positive interaction between energy input and national economic development. Compared with the energy production waste gas, the improved demand of solid waste and waste water is greater, which should arouse the attention of environmental managers.

Discussion

SBM-DEA is a non-radial improvement DEA model (Gang, 2014) and we provided the slack movement and projection per city. For the energy input structure, Hangzhou and Zhoushan as the frontier environmental energy efficiency had their input and output factors in a balanced and effective state, which provided a performance reference for other cities to improve in terms of environmental efficiency. Cities, where environmental energy performance did not reach an effective level, have more room for improvement in coal and oil than in natural gas. This shows that reducing coal and oil inputs and increasing the share of clean energy in the energy mix are instructive for improving environmental and energy performance in Zhejiang Province. This result agreed with the study of Zhengge and Leike (2011) which found that increasing the proportion of clean energy in energy consumption has a significant impact on improving energy environmental performance.

Technical efficiency can be divided into pure technical efficiency and scale efficiency (Gang, 2014). However, environmental energy performance of Zhejiang Province is more influenced by pure technical efficiency, and scale efficiency has less effect on technical efficiency because the scale efficiency of 80% of cities is effective and the difference in scale efficiency is small in space. Especially, the low efficiency of pure technology suggests that energy consumption and production methods need to be adjusted, such as improving power generation technology and reducing the proportion of coal used (Watanabe and Tanaka, 2007). There is a clear difference in pure technical efficiency between eastern and western of Zhejiang Province. Cities with low efficiency of pure technology are mostly distributed on the eastern coast of Zhejiang, while the situation in western and central Zhejiang is relatively modest. Especially, Hangzhou as the capital of Zhejiang has remained in an effective state of pure technical efficiency over the years. Hong and Baofu (2015) suggest the spatial differences in energy performance are influenced by industrial agglomeration distribution and government regulation. Due to the imbalance of economic and technological development in space, energy production enterprises will make different decisions on the choice of energy resources and production methods based on cost considerations (Yeh et al., 2010).

General evolution of economies of scale in production shows that the production efficiency will go through three stages in succession, namely, increasing scale benefits, constant scale benefits, and decreasing scale benefits (Gans et al., 2011). Hangzhou and Zhoushan are in the stage of constant scale benefits, while other cities are in the stage of decreasing scale benefits. Xu (2015) suggest that in 2015, the energy production industry of Shandong Province, one of the Chinese eastern coastal provinces, mostly use

coal as a thermoelectric energy source. 55% of these power plants are small thermal power, which is defined as the generating capacity is below 5.0×10^4 kW and these power plants form decreasing scale benefits in the energy production. However, Zhoushan has abundant wind energy resources, accounting for 1/3 of the province's wind energy resources. The wind power, as a kind of clean energy source, installed capacity of Zhoushan is 9.78×10^4 kW in 2013, accounting for 26.6% of the total installed capacity within Zhejiang Province (Haichun et al., 2013). Thus, our research evidenced the view again by showing significant decreasing scale benefits in the energy production industry of Chinese eastern coastal cities.

Conclusion

This paper studied the environmental energy efficiency of Zhejiang Province from 2005 to 2015. We added the undesirable outputs of energy production as one of the most important factors to study the output efficiency. To improve discrimination in DEA with minimal loss of information, we used dimensionality reduction, a methodology that produces uncorrelated linear combinations of original inputs and outputs. Besides, we obtained the energy performance parameters of 11 cities in Zhejiang Province for 11 years, which include technical efficiency, pure technical efficiency and scale efficiency, projection value and slack movement of each variable by SBM model.

Eleven prefecture-level environmental energy performance trends in the city could be divided into four categories: High Level, Decreasing Trend, Improving Trend, and Deteriorating Trend. These trends were more influenced by pure technical efficiency, while scale efficiency had less effect on technical efficiency. Hangzhou reached the effective level and Zhoushan was close to it, while the remaining urban environmental energy performance did not reach the effective level. From the changing tendencies of environment energy performance, the performance level of Hangzhou and Zhoushan remained in an effective status, while Jinhua and Taizhou showed a gradual improvement trend, and the remaining cities showed signs of deterioration or no improvement in environmental energy efficiency. In particular, the inflection points of this trend change existed more in 2014 and 2015, and the statistics on energy production overcapacity and environmental pollution in Zhejiang Province have not been substantially improved in recent years. Therefore, the government should vigorously strengthen the policy supervision and adjust energy consumption structure in the energy resources investment. At the same time, energy producer should accelerate technological innovation, and coordinate the development of energy and environmental protection to improve the environmental energy efficiency of high energy-consumption industries.

Acknowledgements. This study was supported by the Postgraduate Research and Practice Innovation Program of Jiangsu Province (No. KYCX17_0512), the Foundation of the Humanities and Social Science Research of the Ministry of Education (No. 17YJC790194) and the China Scholarship Council (No. 201806710133).

Author contributions. Kai Wang and Hengquan Zhang designed the research. Kai Wang performed the research, collected, analyzed the data and wrote the manuscript. Kai Wang edited the manuscript and Chenjun Zhang provided the guidance during research.

REFERENCES

- [1] Adler, N., Golany, B. (2001): Evaluation of deregulated airline networks using data envelopment analysis combined with principal component analysis with an application to Western Europe. – *European Journal of Operational Research* 132: 260-273.
- [2] Adler, N., Golany, B. (2002): Including principal component weights to improve discrimination in data envelopment analysis. – *Journal of the Operational Research Society* 53: 985-991.
- [3] Adler, N., Yazhemsky, E. (2010): Improving discrimination in data envelopment analysis: PCA–DEA or variable reduction. – *European Journal of Operational Research* 202: 273-284.
- [4] Banker, R. D., Charnes, A., Cooper, W. W. (1984): Some models for estimating technological and scale inefficiencies in Data Envelopment Analysis. – *Management Science* 30(9): 1031-1142.
- [5] Cao, J., Ho, M. S., Jorgenson, D. (2012): An Integrated Assessment of the Economic Costs and Environmental Benefits of Pollution and Carbon Control. – In: Aoki, M., Wu, J. (eds.) *The Chinese Economy*. International Economic Association Series. Palgrave Macmillan, London.
- [6] Chang, P. T., Lee, J. H. (2012): A fuzzy DEA and knapsack formulation integrated model for project selection. – *Computers & Operations Research* 39: 112-125.
- [7] Charnes, A., Cooper, W. W., Rhodes, E. (1978): Measuring the efficiency of decision making units. – *European Journal of Operational Research* 2: 429-444.
- [8] Chen, X., Gong, Z. (2017): DEA Efficiency of Energy Consumption in China's Manufacturing Sectors with Environmental Regulation Policy Constraints. – *Sustainability* 9: 210.
- [9] Faere, R., Grosskopf, S., Lovell, C. A. K., Pasurka, C. (1989): Multilateral Productivity Comparisons When Some Outputs are Undesirable: A Nonparametric Approach. – *Review of Economics & Statistics* 71: 90-98.
- [10] Färe, R., Grosskopf, S., Pasurka Jr, C. A. (2007): Environmental production functions and environmental directional distance functions. – *Energy* 32(7): 1055-1066.
- [11] Färe, R., Grosskopf, S., Pasurka Jr, C. A. (2007): Pollution abatement activities and traditional productivity. – *Ecological Economics*, 62(3-4): 673-682.
- [12] Fu, H. P., Ou, J. R. (2013): Combining PCA With DEA to Improve the Evaluation of Project Performance Data: A Taiwanese Bureau of Energy Case Study. – *Project Management Journal* 44: 94-106.
- [13] Gang, C. (2014): *Data Envelopment Analysis: Methods and MaxDEA Software*. – Intellectual Property Publishing House.
- [14] Gans, J., King, S., Stonecash, R., Mankiw, N. G. (2011): *Principles of economics*. – Cengage Learning, Australia.
- [15] Geng, Y., Doberstein, B. (2008): Developing the circular economy in China: Challenges and opportunities for achieving 'leapfrog development'. – *International Journal of Sustainable Development and World Ecology* 15: 231-239.
- [16] Ghosh, S., Jintanapanont, J. (2004): Identifying and assessing the critical risk factors in an underground rail project in Thailand: a factor analysis approach. – *International Journal of Project Management* 22: 633-643.
- [17] Gillingham, K., Newell, R. G., Palmer, K. (2009): Energy Efficiency Economics and Policy. – *Annual Review of Resource Economics* 1: 597-619.
- [18] Haichun, Z., Xiaofen, Y., Zhaodong S., Huisheng, F., Eding, L. (2013): Present situation and development suggestions of new energy development and application in the new district of Zhoushan islands. – *Sino-Globay Energy* 18(1): 101-106.
- [19] Hong, J., Baofu, Z. (2015): Deconstruction, spatial patterns and coupling between energy efficiency and industrial structure in China. – *Resources Science* 37(1): 152-162.

- [20] International Energy Agency (IEA) (2013): Market Report Series Energy Efficiency 2013. – IEA Publications. Available online: https://www.iea.org/publications/freepublications/publication/EEMR2013_free.pdf.
- [21] International Energy Agency (IEA) (2014): Market Report Series Energy Efficiency 2014. – IEA Publications. Available online: <https://www.iea.org/Textbase/npsum/EEMR2014SUM.pdf>.
- [22] Jolliffe, I. (2011): Principal component analysis. – In: International encyclopedia of statistical science. Springer, Berlin, Heidelberg.
- [23] Kumbhakar, S. C., Lovell, C. K. (2003): Stochastic frontier analysis. – Cambridge University Press.
- [24] Li, H., Dong, L., Xie, Y. T., Fang, M. (2017): Low-carbon benefit of industrial symbiosis from a scope-3 perspective: a case study in China. – Applied Ecology and Environmental Research 15(3): 135-153.
- [25] National Bureau of Statistical of China (2006-2016): Energy Statistical Yearbook (2006-2016). – China Statistics Press.
- [26] Provincial Bureau of Statistical of Zhejiang (2006-2016): Zhejiang Statistics Year Book (2006–2016). – China Statistics Press.
- [27] Qiang, J. I., Qiang, L. I., Song, H. K., Mosenthal, P. (2005): Research on energy efficiency resources potential and efficiency power plant in Jiangsu. – Power Demand Side Management.
- [28] Shi, M., Ma, G., Shi, Y. (2011): How much real cost has China paid for its economic growth. – Sustainability Science 6: 135.
- [29] Statistics, Z.P.B.o. (2014): Zhejiang Nature Resources and Statistical Yearbook on Environment. – China Statistics Press.
- [30] Statistics, Z.P.B.o. (2015): Zhejiang Nature Resources and Statistical Yearbook on Environment. – China Statistics Press.
- [31] Tone, K. (2001): A slacks-based measure of efficiency in data envelopment analysis. – European Journal of Operational Research 130: 498-509.
- [32] Tone, K. (2002): A slacks-based measure of super-efficiency in data envelopment analysis. – European Journal of Operational Research 143: 32-41.
- [33] Wang, S. (2003): Adaptive non-parametric efficiency frontier analysis: a neural-network-based model. – Computers & Operations Research 30: 279-295.
- [34] Wang, X., Han, L., Yin, L. (2016): Environmental Efficiency and Its Determinants for Manufacturing in China. – Sustainability 9: 47.
- [35] Watanabe, M., Tanaka, K. (2007): Efficiency analysis of Chinese industry: a directional distance function approach. – Energy Policy 35(12): 6323-6331.
- [36] Wu, C. (2008): Economy Analysis of Architecture Energy Efficiency in Northern Jiangsu Province. – Science & Technology Information.
- [37] Xu, D. (2015): Study of power efficiency based on PCA-DEA. – The Dissertation for master's degree. University of Science and Technology of China.
- [38] Yang, Z. Y., Zhao, Y. (2009): An Analysis on Changes and Influencing Factors of Total-factor Energy Efficiency in Jiangsu. – China Soft Science 18: 1792-1800.
- [39] Yeh, T. L., Chen, T. Y., Lai, P. Y. (2010): A comparative study of energy utilization efficiency between Taiwan and China. – Energy Policy 38(5): 2386-2394.
- [40] Zha, Y., Zhao, L., Bian, Y. (2016): Measuring regional efficiency of energy and carbon dioxide emissions in China: A chance constrained DEA approach. – Computers & Operations Research 66: 351-361.
- [41] Zhang, M., Song, Y., Li, P., Li, H. (2016): Study on affecting factors of residential energy consumption in urban and rural Jiangsu. – Renewable & Sustainable Energy Reviews 53: 330-337.
- [42] Zhao, L., Zha, Y., Liang, N., Liang, L. (2016a): Data envelopment analysis for unified efficiency evaluation: an assessment of regional industries in China. – Journal of Cleaner Production 113: 695-704.

- [43] Zhao, L., Zha, Y., Wei, K., Liang, L. (2016b): A target-based method for energy saving and carbon emissions reduction in China based on environmental data envelopment analysis. – *Annals of Operations Research*.
- [44] Zhengge, T., Leike, L. (2011): Efficiency evaluation of industrial sectors in China accounting for the energy and environment factors based on provincial data by a SBM approach. – *Economic Review* 2: 55-65.

INFLUENCE OF CHANGES IN DISSOLVED OXYGEN CONTENT ON FISH BEHAVIORAL TRAJECTORIES DURING WATER EUTROPHICATION

HUANG, Y. Q.^{1,2,3} – CAI, D. S.^{1,3*} – LI, M. Q.¹ – WU, T. H.² – WU, P. G.^{1,3} – LI, L.^{1,3}

¹College of Civil Engineering and Architecture, Guangxi University, 530004 Nanning, China

²Guangxi Key Laboratory of Environmental Pollution Control Theory and Technology, Guilin University of Technology, 541004 Guilin, China

³Guangxi Water & Power Design Institute, 530023 Nanning, China

*Corresponding author
e-mail: caidesuo@vip.163.com

(Received 30th Sep 2018; accepted 29th Nov 2018)

Abstract. Fish is an important organism in the water and its living environment are a unified whole, interrelating and influencing each other. Changes in fish behavioral trajectories can directly reflect the deterioration degree of water. When the cyanobacteria in the water consume a lot of oxygen during reproduction, death and decomposition, which makes the dissolved oxygen content rapidly decrease, the fish swimming trajectory changes significantly and responds accordingly. In this paper, acoustic tag tracking technology was used to study the swimming ability of fish by simulating the eutrophication process in a simulating natural ecosystems tank and obtain its three-dimensional trajectory to determine the dissolved oxygen threshold when fish behavior changed. The variation regularity of fish behavioral trajectories was investigated with the change of dissolved oxygen content during water eutrophication. The experimental results showed that the individual behavioral response of adult carp was unobvious in the process of oligotropher to light eutropher, but at the state of middle and hyper eutropher was obvious. When the dissolved oxygen is 0.5 mg/L, adult carp began to breathe hard and float on the water surface. When the dissolved oxygen content dropped to 0.2 mg/L, adult carp began to die. During the process of dissolved oxygen content decreasing, the swimming trajectory of adult was convergent in space while they migrated from the bottom of water to surface in the direction of longitudinal water depth, and the swimming speed was slower and slower. Regression analysis was used to analyze the correlation between individual behavioral trajectories of adult carp and dissolved oxygen content. The results indicated that the swimming trajectory of water depth was highly negatively correlated with dissolved oxygen content. The swimming speed of adult carp and dissolved oxygen content had a strong negative correlation. The significant changes in the individual behavioral trajectories of adult carp indicated the environment of water has changed. It was suggested that dissolved oxygen content, which affected the changes of fish behavior, and individual behavioral trajectories of fish as a biological indicator were used to evaluate the water ecological restoration effect and ecological health status of water. It can more accurately reflect the current status of the aquatic ecosystem.

Keywords: *acoustic signal monitoring technology, individual behavioral trajectories of fish, the dissolved oxygen threshold, correlation, water eutrophication*

Introduction

It caused algae and other plankton in water to rapidly multiply, died and decomposed when massive pollutants containing nitrogen and phosphorus nutrients were discharged. Especially in the period from June to September of each year, the water temperature rises and the light intensity increases. It is suitable for cyanobacterial cell division, growth and consumption of a large amount of oxygen, which causes the dissolved oxygen content in water to decrease rapidly. At this time, it is difficult for the

cyanobacteria to complete the normal metabolic process. Then, it is decomposed by microorganisms and decayed. Water quality deteriorated. Aquatic organisms and fish began to die. It was known as “ecological cancer” (Gong, 2006).

The oxygen in the water is mainly derived from air and photosynthesis of aquatic plants, which directly affects the living environment of aquatic organisms. As an important aquatic organism in water, fish relies on obtaining oxygen from water to carry out various physiological activities, and its behavior has a certain relationship with the change of dissolved oxygen content in the water. When the water environment changes, the fish needs to consume a certain amount of energy to adapt the new environment whose energy source needs to be maintained by the dissolved oxygen in the water. Once the water lacks of oxygen, the changes of fish's physiological characteristic and behavior were showed firstly. Fish floated on the water surface and died.

Fish locates on the top of the food chain as an advanced group of aquatic organisms. It can objectively reflect the biological state of water environment, which is a good representation. So, fish is a living “monitor” for water pollution. There are dozens of fishes monitoring materials such as carp, grass carp, silver carp, bighead carp and crucian distributed in most of lakes and reservoirs. Many reports mentioned that carp (*Cyprinus carpio*) was used as a monitoring indicator species to study the effects of changes in water environment on their physiology and behavior. For example, Sakalli studied the effects of sewage treatment plant effluents on hepatic and intestinal biomarkers in common carp (Sakalli et al., 2018). The effects of water-borne lead on the swimming capability and metabolism of juvenile grass carp, critical swimming speed and oxygen consumption rate were measured in water with four concentrations of Pb^{2+} (Zhu et al., 2018).

At present, the monitoring methods of fish behavior used mainly video, image observation and computer simulation technology. Kang et al. used two cameras for tracking the fish behavior in three dimensional data. The 3D data were analyzed for fish behavior such as, swimming speed and surfacing behavior (Kang et al., 2009). Huang et al. studied the behavioral responses of zebrafish under the combination effects of cypermethrin and deltamethrin, a set of motion activities were monitored and analyzed using a computer-imaging technique (Huang et al., 2009). Behavioral variations of fish populations are difficult to measure quantitatively. To quantify such measurements, Vassilis et al. developed a low-cost computer vision system to analyze small fish populations' behavioral variations in aquaculture tanks (Papadakis et al., 2012).

It can obtain the fish swimming behavior characteristics including fish movement speed and acceleration, which relate to water quality by using the computer vision technology in fish movement behavior monitoring (Zhou, 2009; Zhang, 2012; Huang et al., 2017; Yan et al., 2018). It can record the behaviors of fish population to achieve online monitoring and early warning of water quality by using computer vision and video tracking technology (Liao, 2012; Huang, 2014). Image processing technology was combined with computer programming to process the fish motion video. It could simulate the fish trajectories, directly draw the fish's motion trajectories on the video image and realized the real-time tracking (Jiang, 2015).

Although video, image observation and computer simulation techniques are usually used to analyze fish behavior, but the data processing is very difficult and the error is big. It is difficult to obtain quantitative indicators of fish behavioral trajectories. In recent years, acoustic monitoring technology has been gradually applied to fish resource detection and behavior monitoring. Acoustic tracking technology has gradually become

the most important means to monitor the behavior of aquatic animals. For example, it can get the fish swimming speed, migration times, residence time, the changes of habitat and spawning grounds during fish migration by this technology to fish migration monitoring (Steig and Johnston, 2010; Skalski et al., 2012; Pinnix et al., 2013; Teo et al., 2013). Acoustic tag tracking technology was used to obtain fish behavioral trajectories, some physical and mathematical models were established (Cai and Li, 2012; Romine et al., 2014). Acoustic tag tracking technology is used to evaluate the behavior, survival and behavior changes of fish in the ecosystem (Everson et al., 2013; Schultz et al., 2015; Hollo et al., 2017).

In summary, it can see that the acoustic tag tracking technology is mainly used in fish habits, migration, fish stock, fish species protection and habitat restoration. There are few reports on the application of fish behavioral trajectories to the ecological environment. Therefore, in this study, acoustic tag tracking technology was used to study the swimming ability of fish by simulating the eutrophication process in a simulating natural ecosystems tank, and obtain its three-dimensional trajectory to determine the dissolved oxygen threshold when fish behavior changed. The correlation between fish individual behavioral trajectories and dissolved oxygen content was analyzed, which provided a reliable reference for evaluation of ecological restoration effect and ecological health status of water.

Materials and methods

Water eutrophication simulation experimental tank

Water eutrophication status of lakes and reservoirs can be divided into three types: oligotrophy, mesotrophy and eutrophy (Xu and Jiang, 2009). Experiment was carried out by simulating these three eutrophic statuses of natural waters. The length, width, height of simulation experimental tank is 3m×1m×1m; water depth is 0.75m; the thickness of tank substrate is 0.15cm. The tank substrate is consisted of lake sediment, aquatic plants and common aquatic organisms such as fish, shrimp, crabs, snails and loach (*Fig. 1*). The tank was equipped with diving light for simulating lighting, residual chlorine device and water level meters. The water used in the simulated experimental tank is tap water. The concentration of residual chlorine is reduced by aeration to less than 0.02 ppm which is harmless to fish.



Figure 1. *Experimental tank and ecological structure community taken from lake*

Experimental fish selection and domestication

In this experiment, five healthy and lively adult carps with a length of 15cm-20cm and a body weight of about 0.5kg-1.0kg was selected. Five activated acoustic tags were activated and transplanted to these fishes (*Fig. 2*). The transmission frequencies of five tags are set from 3100Hz to 3500Hz. It means that the tags emit an acoustic signal every 3 seconds. After these fishes were domesticated in the tank for one month to adapt the water environment, the simulation experiment of water eutrophication began. At this time, the water was in the oligotrophic stage.

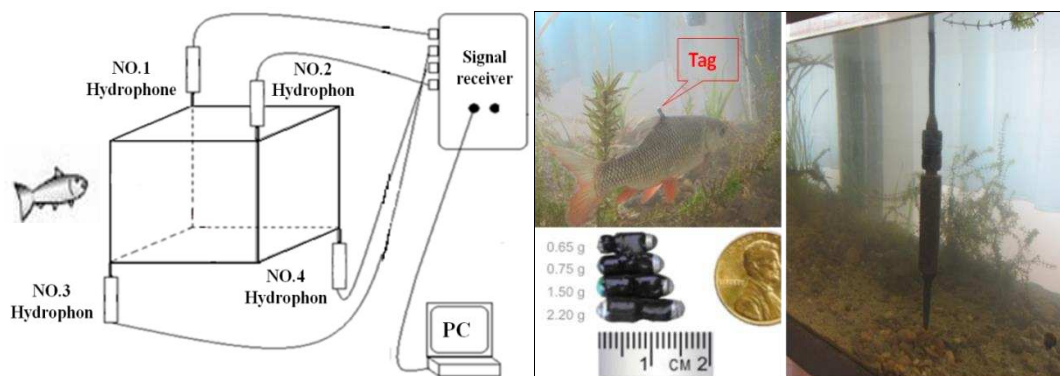


Figure 2. Principle of fish behavioral trajectories monitoring

Experimental method

Preparation of nitrogen and phosphorus nutrient solution

According to water volume in the tank, an appropriate amount of ammonium phosphate was prepared into nitrogen and phosphorus nutrient. The pH value in nutrient solution was reduced after aerating for 48 hours. The nitrogen and phosphorus nutrient solution has pH of 6.85, conductivity of 1354.6 $\mu\text{s}/\text{cm}$, ammonia nitrogen concentration of 180.0 mg/L, total phosphorus concentration of 120.0 mg/L, and total nitrogen concentration of 202.8 mg/L.

Discharge of nitrogen and phosphorus nutrient solution

Nitrogen and phosphorus nutrients were discharged according to the evaluation criteria and classification of lake and reservoir in the Technical Regulations for Surface Water Resources Quality Assessment, Lake (reservoir) Eutrophication Evaluation Method and Grading Technical Regulations (China National Environmental Monitoring Center) and the US Environmental Protection Agency (USEPA) (Zhai et al., 2009).

The nitrogen and phosphorus nutrient solution are discharged in a steady flow of $0.10 \times 10^{-6} \text{ m}^3/\text{s}$, and increased or decreased the amount of solution in the water according to the consumption. It makes the water environment in different nutritional state. Different ecological behavior of fish at each stage is monitored in particular when the environment is in the critical nutritional state. The process of the effect of oxygen consumption on fish behavior during the water eutrophication is shown in *Fig. 3*.

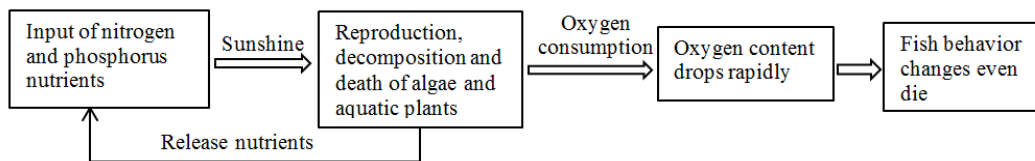


Figure 3. The process of water eutrophication simulation

Monitoring methods and techniques

The methods of water quality monitoring

Water quality monitoring uses two methods: online monitoring and sampling analysis. Water quality monitoring indicators include total phosphorus, total nitrogen, chlorophyll-a, potassium permanganate index, transparency and dissolved oxygen content, which affect water eutrophication and the living environment of fish. Chlorophyll-a, transparency and dissolved oxygen content were monitored by algae detector (Model algae-wader), turbidity meter (Model 2100Q) and dissolved oxygen meter (Model multi 3410). Total phosphorus, total nitrogen and potassium permanganate indexes were sampled and analyzed according to the standard methods.

Fish behavior trajectory monitoring technology

The fish behavior track is monitored by acoustic signal technology, which uses four hydrophones to receive the sound waves transmitting from the acoustic tags transplanted to the fishes. The raw signal is transmitted to PC terminal for signal processing through the data lines (Fig. 2). Two-dimensional or three-dimensional behavioral trajectories of fish can be obtained after denoise processing by PC. Thereby, 2D and 3D behavioral trajectories of fish can be monitored in real-time. The individual behavioral trajectories of fishes are monitored by HTI Model 291 acoustic tag system.

Experimental data processing method

According to the transmission frequency of tag signal, a swimming trajectory point of fish is obtained every three seconds. So a set of data has 1200 trajectory points, which automatically save every one hour. The time of experiment was from February to October 2018 (nine months). The swimming trajectory points of one fish were 7.776×10^4 . After data cleaning such as de-noising and abnormal data elimination, the track points have about 5×10^4 . In this study, some representative data were processed and analyzed.

Regression analysis is one method of data mining, which was used to determine the quantitative relationship between two or more variables (Wu, 2017). In order to find the correlation between dissolved oxygen content and fish behavioral trajectories from these huge experimental data, the method was used in the paper.

Correlation analysis refers to the relationship between a variable x and another variable y , and the quantitative description of x and y . To determine the correlation between the two variables, a bivariate correlation analysis can be used. The correlation coefficient, this statistical indicator, is used to reflect the correlation and the degree of closeness between two variables. It is calculated by product-moment correlation. Therefore, the correlation coefficient is also called linear correlation coefficient or

product difference correlation coefficient, which is represented by the symbol “r”. The range of “r” value is between -1 and +1.

It is used to measure the linear relationship between two variables. It is positive correlation when “r” is more than 0, while it is negative correlation when “r” is less than 0. The two variables are irrelevant correlation when “r” is 0. The more greater of absolute value of “r”, the higher correlation of two variables. According to the absolute value of "r" can be divided into: $0.8 < r < 1.0$ is extremely strong correlated, $0.6 < r < 0.8$ is strongly correlated, $0.4 < r < 0.6$ is moderately correlated, $0.2 < r < 0.4$ is weakly correlated, $0.0 < r < 0.2$ is extremely weakly correlated or not correlated.

SPSS 22.0 analysis software is used to process the data. The correlation coefficient is calculated according to the statistical formula of Pearson correlation coefficient (Zhang, 2003; Wu, 2017):

$$r = \frac{\sum xy - \frac{\sum x \sum y}{N}}{\sqrt{\sum x^2 - \frac{(\sum x)^2}{N}} \sqrt{\sum y^2 - \frac{(\sum y)^2}{N}}} \quad (\text{Eq.1})$$

Analysis of experimental results

Changes in water quality indicators during water eutrophication

Some water quality indicators such as total phosphorus, total nitrogen, chlorophyll-a, permanganate index, transparency and dissolved oxygen were monitored in the process of water eutrophication. The changes of indicators at each stage are shown in *Table 1*.

Table 1. Monitoring results of water quality indicators in the process of eutrophication

Nutritional status classification	Monitoring time	Total phosphorus (mg/L)	Total nitrogen (mg/L)	Chlorophyll-a (mg/L)	Permanganate index (mg/L)	Transparency (m)	Dissolved oxygen (mg/L)
Oligotropher	Feb., 2018	0.003	0.025	0.0015	0.35	7.50	6.0-7.5
Mesotropher	From Mar. to Apr., 2018	0.045	0.46	0.0073	2.86	2.75	4.0-6.0
Light eutropher	From May. to Jun., 2018	0.13	1.12	0.022	8.12	0.48	2.0-4.0
Middle eutropher	From Jul. to Aug., 2018	0.45	5.65	0.125	24.8	0.36	0.5-2.0
Hyper eutropher	From Sep. to Oct., 2018	1.45	16.8	1.33	55.3	0.15	<0.5

Analysis of changes in fish behavioral trajectories during water eutrophication

Fish had a short-term avoidance behavior from pollution sources during the emission of nitrogen and phosphorus nutrients solution. When the concentration of water quality factors in the water environment was balanced, the fish returned to the original behavioral trajectories. It indicated that the fish is sensitive to the change in water environment, but their adaptability is relatively strong. The monitoring results show that the behavioral trajectories of fish in three stages (oligotropher, mesotropher and eutropher) are quite different (*Fig. 4*). At the oligotrophic stage, the fish swam back and forth, and their behavioral trajectories were wide range; the behavioral trajectories of

fish at mesotrophic stage was characterized by preference for activities in a certain area, and the behavioral response was relatively slow; in the eutrophic stage, the fish basically gathered somewhere and didn't move. It indicated that with the change of pollutant concentration in water, the fish had avoidance behavior, they swam slowly because of hypoxia, and their response to external disturbance was not sensitive.

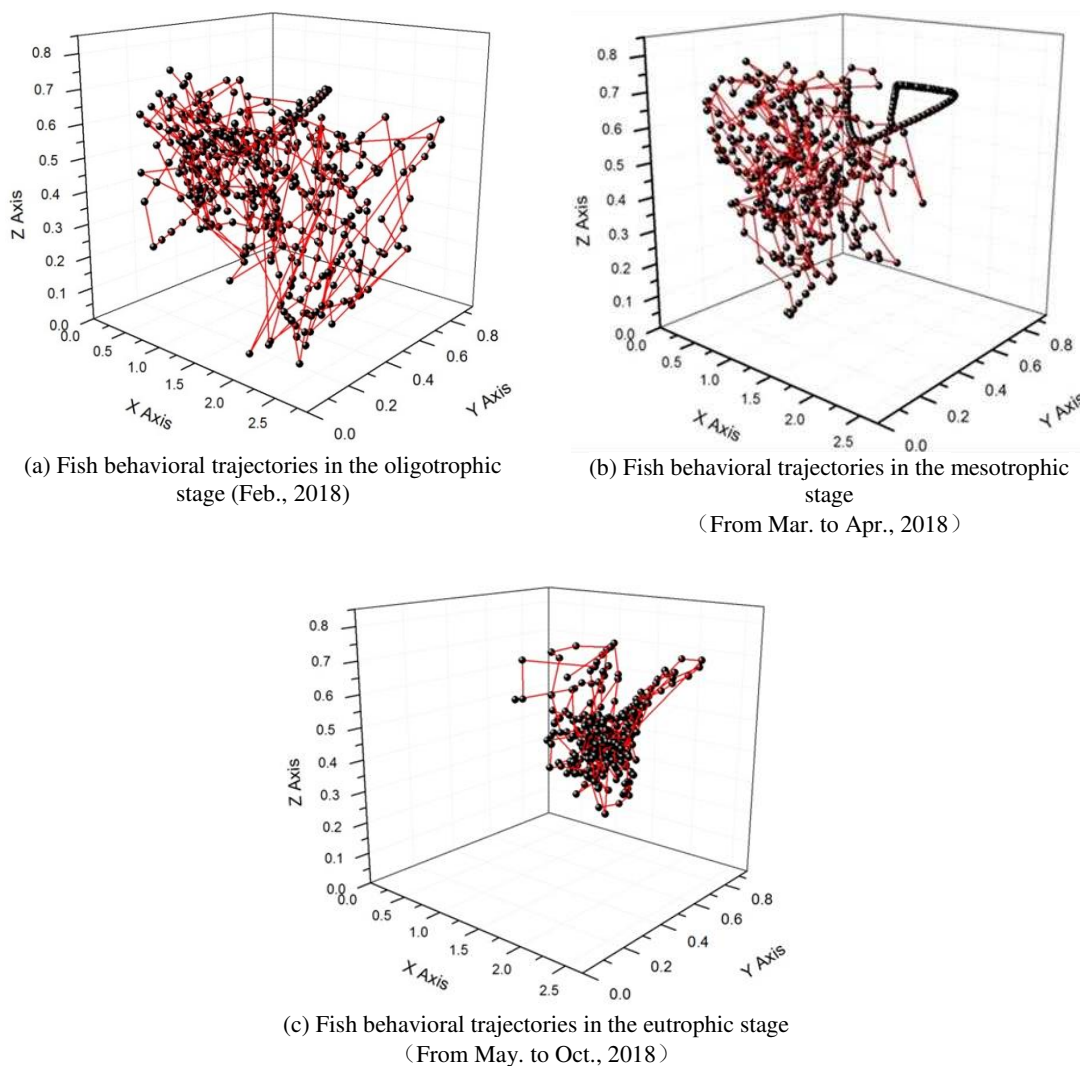
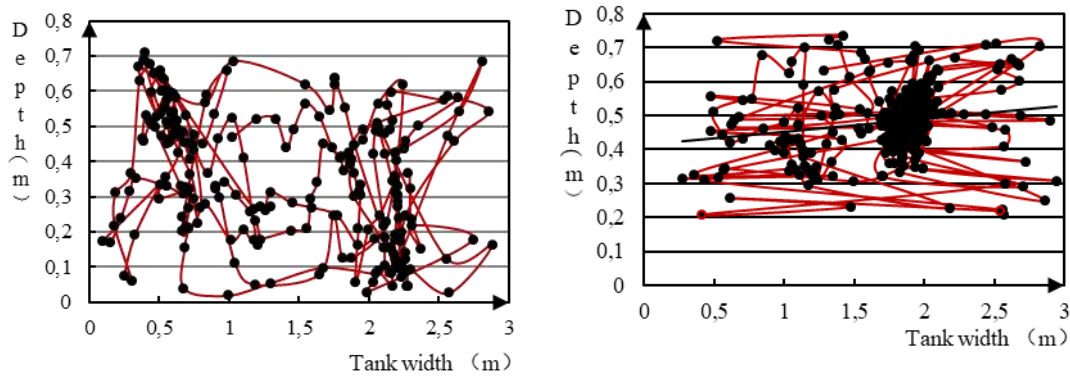


Figure 4. Three-dimensional behavioral trajectories of carp during water eutrophication

Influence of dissolved oxygen content change on fish behavioral trajectories

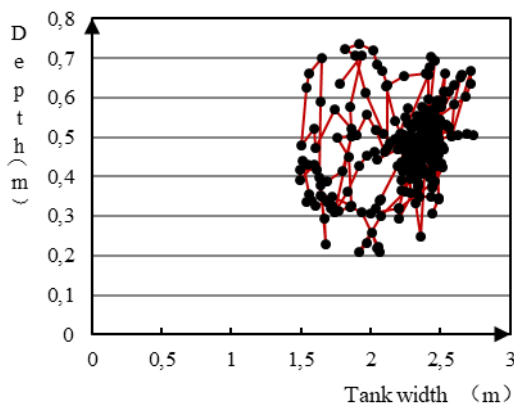
The decrease of dissolved oxygen content not only affects the activity of aquatic organisms, but also indirectly controls the degradation of cyanobacterial toxins. The behavior of fish will also change, and the behavioral responses expressing in various nutrient stages are significantly different. The performance is as follows:

- 1) The dissolved oxygen content was 6.0 mg/L to 7.5 mg/L in oligotrophic stage. At this stage, the carp behavioral trajectories were scattered. They swam back and forth in the water according to their living habits and preferences (*Fig. 5a*).

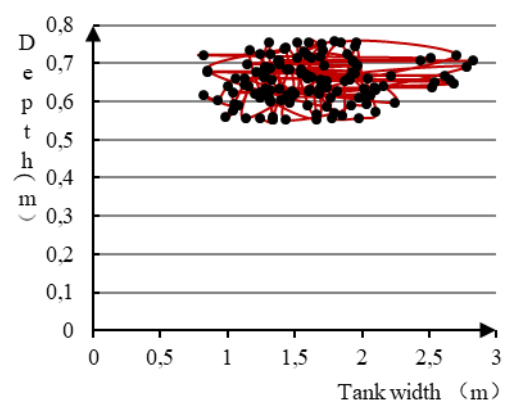


(a) Dissolved oxygen content was 6.0-7.0 mg/L

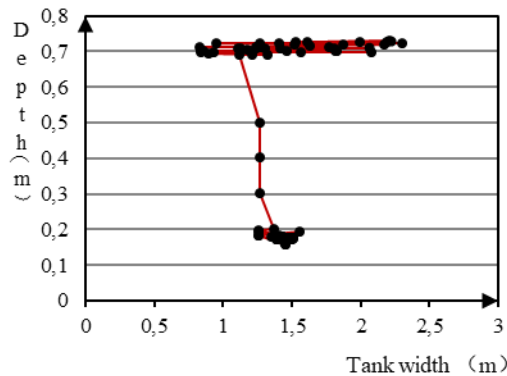
(b) Dissolved oxygen content was 4.0-5.0 mg/L



(c) Dissolved oxygen content was 2.0-3.0 mg/L



(d) Dissolved oxygen content was 0.5-1.0 mg/L



(e) Dissolved oxygen content is less than 0.5 mg/L

Figure 5. Two-dimensional behavioral trajectories in the change process of dissolved oxygen content in water

2) The dissolved oxygen content was 4.0 mg/L-6.0 mg/L in mesotrophic stage. The carp showed short-term avoidance behavior and gathered in one place (Fig. 5b). After a period of adaptation to the water environment, the original trajectories were restored. When the dissolved oxygen content dropped to 4.0 mg/L, their respiratory rate began to increase.

- 3) The dissolved oxygen content was 2.0 mg/L to 4.0 mg/L in light eutrophic stage. The carp was far from the source of pollution and stayed at a certain place for a long time (Fig. 5c). They reacted slowly to external disturbances. When dissolved oxygen content was reduced to 2.0 mg/L, carp breathe faster and excreted a sticky adhesive for self-protection. Occasionally, the head of carp floated on the water surface at a 45-degree angle, and then they dived into the water.
- 4) The dissolved oxygen content was 0.5 mg/L-2.0 mg/L in middle eutrophic stage. The behavioral trajectories of carp were concentrated on 15 cm under the water surface (Fig. 5d). They were characterized by hypoxic asphyxia, shortness of breath, and not scared by external interference. When the dissolved oxygen content was 1.5 mg/L, the carp swam slowly and frequently floated on the water surface at a 45-degree angle.
- 5) The dissolved oxygen content was less than 0.5 mg/L in hyper eutrophic stage. At this time, the carp had a rapid breathing rate, the gill began to turn purple, and they floated on the water surface for a long time (Fig. 5e). The carp swam slowly, and then began to settle down into the water bottom after 48 hours. They died when the dissolved oxygen value was 0.2 mg/L.

Threshold of dissolved oxygen content when fish behavioral trajectories changed

The experimental results showed that the rapid decline of dissolved oxygen content in water was the main factor of behavior change of fish during the process of water eutrophication. The threshold of dissolved oxygen for adult carp started to breathe hard and float was 1.5 mg/L. When dissolved oxygen content dropped to 0.2 mg/L, the carp began to turn over and even died.

Effect of dissolved oxygen content on the swimming speed of carp

During the process of water eutrophication, the changes of dissolved oxygen content not only led to the change of carp trajectory, but also directly affected the swimming speed of carp. The average swimming speed of carp at the oligotrophic and mesotrophic stage was 0.4-0.5 m/s, which was sensitive to external disturbances and vulnerable to scare. At the light and middle eutrophic stage, the swimming speed of carp was 0.2-0.3 m/s, and at that time the carp had no response to external disturbances. The carp often swam slowly on the water surface and the swimming speed was less than 0.2 m/s at the hyper eutrophic stage.

Correlation analysis between individual behavioral trajectories of carp and dissolved oxygen content in the water

Analysis of correlation between behavioral trajectories in depth and dissolved oxygen content

According to the correlation analysis results, the correlation coefficient between behavioral trajectories at water depth and dissolved oxygen content was -0.979 (Table 2). It indicated that there was an extremely strong negative correlation between two variables, and they were significantly related at 0.01 levels (bilateral).

By data analysis, the carp behavioral trajectories at water depth had a linear negative correlation with the dissolved oxygen content. During the process of decreasing dissolved oxygen content, the trajectories of adult carp were convergent in space. In the direction of water depth, behavioral trajectories migrated from the water bottom to surface.

Table 2. Correlation analysis between fish habitat preference at water depth and dissolved oxygen content

Name	Items	Dissolved oxygen content	Fish habitat preference at water depth
Dissolved oxygen content	Pearson correlation	1	-.979**
	Significant (bilateral)	— —	.004
	N	5	5
Fish habitat preference at water depth	Pearson correlation	-.979**	1
	Significant (bilateral)	.004	— —
	N	5	5

** Significantly correlated at 0.01 levels (bilateral)

According to data of carp swimming preference, the fitting curve accords with the polynomial regression analysis type. The relationship between the position preference of carp in depth and the dissolved oxygen content was shown in Fig. 6. The formula of the fitting relationship was:

$$H = -0.0022d^3 + 0.0294d^2 - 0.1523d + 0.7601 \quad (\text{Eq.2})$$

$$R^2 = 0.9979 \quad (\text{Eq.3})$$

In the formula, “H” is the behavioral trajectories in depth and its unit is meter; “d” is the dissolved oxygen content and its unit is mg/L. R^2 is the decision coefficient, which is the square of the correlation coefficient. R^2 is 0.9979.

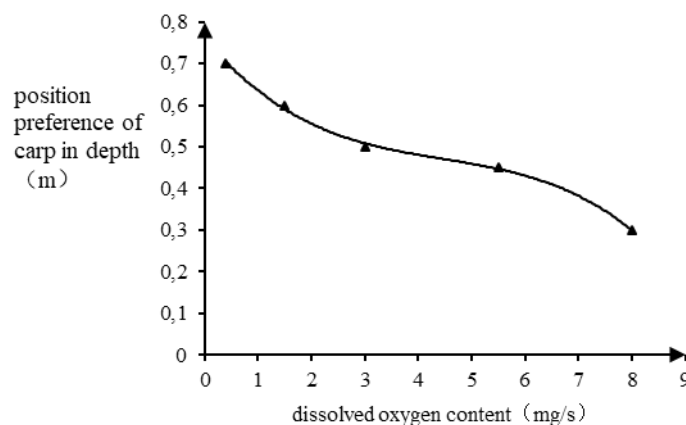


Figure 6. The relationship between the position preferences of carp in depth and the dissolved oxygen content

Analysis of correlation between fish swimming speed and dissolved oxygen content

According to the correlation analysis results of SPSS 22.0 analysis software, the correlation coefficient between carp swimming speed and dissolved oxygen content was 0.987 (Table 3). It indicated that there was an extremely strong correlation between the two variables, which was significantly correlated at 0.01 levels (bilateral).

Table 3. Analysis of the correlation between swimming speed of carp and dissolved oxygen content

Name	Items	Dissolved oxygen content	Swimming speed of carp
Dissolved oxygen content	Pearson correlation	1	.987**
	Significant (bilateral)	—	.002
	N	5	5
Swimming speed of carp	Pearson correlation	.987**	1
	Significant (bilateral)	.002	—
	N	5	5

** Significantly correlated at 0.01 level (bilateral)

From the relationship between the swimming speed of carp and the dissolved oxygen content (Fig. 7), the curve fitting of two variables was polynomial regression analysis type. On the basis of correlation analysis, the formula of linear fitting relationship was:

$$V = -0.0017d^2 + 0.0562d + 0.1201 \quad (\text{Eq.4})$$

$$R^2 = 0.982 \quad (\text{Eq.5})$$

In the formula, “V” is swimming speed of carp and its unit is m/s; “d” is the dissolved oxygen content and its unit is mg/L. R^2 is 0.982.

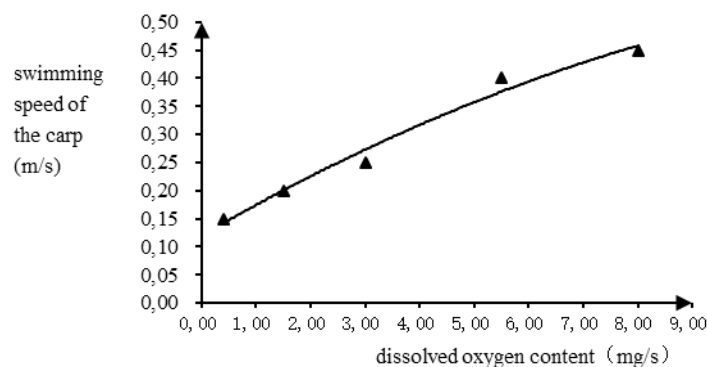


Figure 7. The relationship between the swimming speed of carp and the dissolved oxygen content

It can be seen from the above analysis that the swimming speed of adult carp was highly correlated with dissolved oxygen content. The greater dissolved oxygen content declined, the more adult carp prefer to swim to water surface, and the slower swimming speed. The obvious changes in the individual behavioral trajectories of fish indicated the variation of water quality. Therefore, the effective evaluation of environmental quality of water body was realized by monitoring fish individual behavior trajectories.

Causes Analysis of decreasing of dissolved oxygen content in the process of water eutrophication

The amount of dissolved oxygen content in water is an important factor affecting the growth and reproduction of aquatic plants and organisms. The dissolved oxygen content mainly derives from oxygen releasing from the photosynthesis of aquatic plants and the air. When the water is contaminated by organic pollutants especially, the anaerobic bacteria will multiply and consume oxygen in the water. At this time, the water quality will be deteriorated due to the organic matter decay and decomposition if the oxygen in water is not supplemented in time. In the process of water eutrophication, the continuous reduction of dissolved oxygen content in water is the main factor for fish to change behavior. The main reasons are as follows:

- 1) The effect of water temperature and pressure on dissolved oxygen. The dissolved oxygen content in the water will decrease as the water temperature increases, and vice versa. The decrease of air pressure will reduce the solubility of oxygen and result in hypoxia in water.
- 2) The respiration of phytoplankton and aquatic organisms, oxygen demand in sediment, and oxygenation of nitrogen compounds will consume oxygen in the water. In addition, in the process of water eutrophication, algae and plankton will rapidly propagate and cover the water surface, which prevents the oxygen in the air from entering the water, and also hinders the formation of photosynthesis in aquatic plants. Therefore, oxygen in the water cannot be replenished, causing water quality deterioration.
- 3) There is a lot of organic matter in the water. The decomposition process of organic matters under the action of aerobic bacteria usually consumes a large amount of oxygen. Therefore, in the process of water eutrophication, the reproduction and death of algae and plankton will consume a large amount of oxygen and result in hypoxia.
- 4) Oxidation of inorganic substances. The oxidation will consume a large amount of oxygen when inorganic substance such as hydrogen sulfide or nitrite is present in the water.
- 5) A large number of aquatic organisms die because of oxygen deficiency during the state of hyper eutropher. They sink into the bottom of lake after death and are decomposed by the microorganism. There's less oxygen in the water because micro-organism consume a large amount of oxygen during the decomposition.

Conclusion

At present, most of the evaluation indicators of water eutrophication status only contain the total phosphorus, total nitrogen, chlorophyll-a, permanganate index and transparency in water, but ignore the demand for dissolved oxygen in aquatic plants and aquatic organisms. Through experimental research, it was found that in the process of water eutrophication, the influence of these evaluation indicators on the changes of fish ecological behavior was not obvious. However, the level of dissolved oxygen was the main factor that directly led to the changes of fish behavioral trajectories and even death.

Therefore, from the perspective of aquatic eco-environmental factors and fish ecological behavior, it is suggested that add the dissolved oxygen and individual fish behavioral trajectories as biological indicators based on the original water

eutrophication evaluation system to evaluate the water ecological restoration effect and ecological health status. It can more effectively evaluate the current status of the water ecological environment. The topic will be carried out as follow-up study in the future.

Acknowledgements. This research was financially supported by Research on Fish Individual Behavior Monitoring Technology and its Application in Fish Way and Reservoir Engineering (Grant No. 201405) and Guangxi Science and Technology Plan Project Funding (Grant No. Guike AD18126007).

REFERENCES

- [1] Cai, D., Li, R. (2012): Research on Fish Habitat Based on Acoustic Fish Tracking System. – *Journal of Convergence Information Technology* 7(23): 195-201.
- [2] Dai, H., Chang, Z., Yu, N. (2015): Introduction to data mining. – Tsinghua University Press.
- [3] Everson, I., Taabu-Munyahob, A., Kayandac, R. (2013): Acoustic estimates of commercial fish species in Lake Victoria: moving towards eco system-based fisheries management. – *Fish Res* 139: 65-75.
- [4] Gong, L. (2006): The studies on the effects of suspended sand on the algal growth in the eutrophic water of the Three Gorges Reservoir. – Southwest University.
- [5] Hollo, T, Watson, B. M., Johnston, S. V., Devlin, R. H. (2017): Behaviour of growth hormone transgenic coho salmon *Oncorhynchus kisutch* in marine mesocosms assessed by acoustic tag telemetry. – *Journal of Fish Biology* 90(4): 1660-1667.
- [6] Huang, Y. (2014): Research on early-warning of water quality by monitoring behavioral responses of zebrafish (*Danio rerio*) to acute stress. – Xian University of Architecture and Technology.
- [7] Huang, Y., Zhang, J., Han, X., Huang, T. (2009): Vision-based real-time monitoring on the behavior of fish school. – *Acta Scientiae Circumstantiate* (2): 398-403.
- [8] Huang, Y., Chen, X., Yuan, F. (2017): The video monitoring system of water quality based on stress behavior analysis. – *Fish Journal of Xiamen University (Natural Science)* 56(4): 584-589.
- [9] Jiang, D. (2015): Fish motion tracing technology using video images. – *Journal of Zhejiang Ocean University (Natural Science)* 34(2): 112-118.
- [10] Kang, I. J., Moroishi, J., Nakamura, A. (2009): Biological Monitoring for Detection of Toxic Chemicals in Water by the Swimming Behavior of Small Freshwater Fish. – *J. Fac. Agr, Kyushu Univ.* 54(1): 209-214.
- [11] Liao, Y. (2012): The fish early-warning technique of water quality based on computer vision. – Ningbo University.
- [12] Luo, W., Li, H., Mu, H. (2009): Water Environment Protection. – China Water & Power Press.
- [13] Papadakis, V. M., Papadakis, I. E., Lamprianidou, F., Glaropoulos, A., Kentouri, M. (2012): A computer-vision system and methodology for the analysis of fish behavior. – *Aquacultural Engineering* 46: 53-59.
- [14] Pinnix, W. D., Nelson, P. A., Stutzer, G. (2013): Residence time and habitat use of coho salmon in Humboldt Bay, California: an acoustic telemetry study. – *Environ Biol Fish* 96: 315-323.
- [15] Romine, J. G., Perry, R. W., Johnston, S. V. (2014): Identifying When Tagged Fishes have been Consumed by Piscivorous Predators: Application of Multivariate Mixture Models to Movement Parameters of Telemetered Fishes. – *Animal Biotelemetry*, 2(1): 3.
- [16] Sakalli, S., Giang, P. T., Burkina, V. (2018): The effects of sewage treatment plant effluents on hepatic and intestinal biomarkers in common carp (*Cyprinus carpio*). – *Science of The Total Environment* 635: 1160-1169.

- [17] Schultz, A., Kumagai, K., Bridges, B. (2015): Methods to Evaluate Gut Evacuation Rates and Predation Using Acoustic Telemetry in the Tracy Fish Collection Facility Primary Channel. – *Animal Biotelemetry* 3(1): 13.
- [18] Skalski, J. R., Steig, T. W., Hemstrom, S. L. (2012): Assessing compliance with fish survival standards: A case study at Rock Island Dam, Washington. – *Environmental Science & Policy* 18: 45-51.
- [19] Steig, T. W., Johnston, S. V. (2010): Behavioral results from acoustically tagged fish using innovative techniques for analyzing three-dimensional data. – *Oceans 2010 MTS/IEEE Seattle*, 20-23 Sept. 2010.
- [20] Teo, S. L. H., Sandstrom, P. T., Chapman, E. D., Null, R. E., Brown, K., Klimley, A. P., Block, B. A. (2013): Archival and acoustic tags reveal the post-spawning migrations, diving behavior, and thermal habitat of hatchery-origin Sacramento River steelhead kelts (*Oncorhynchus mykiss*). – *Environ Biol Fish* 96: 175-187.
- [21] Wu, S. (2017): A practical tutorial on data mining. – Beijing: Tsinghua University Press.
- [22] Xu, Z., Jiang, Y. (2009): Lake Eutrophication Assessment: Comprehensive Water Quality Identification Index. – *Journal of Tongji University (Natural Science)* 37(8): 1044-1048.
- [23] Yan, P., Tan, J., Gao, Z., Dai, H., Shi, X., Huang, T. (2018): The analysis of fish movement behavior in vertical slot fishway based on video tracking. – *Acta Hydrobiologica Sinica* 42(2): 250-254.
- [24] Zhang, W. (2012): Research on key technologies of video online monitoring of fish behavior. – Zhejiang University of Technology.
- [25] Zhou, H. (2009): Research on computer vision—based fish movement behavior monitoring system. – Zhejiang University of Technology.
- [26] Zhu, Y. J., Liu, Y., Hu, C. Y. (2018): Swimming behavior and metabolism responses of juvenile grass carp under the exposure of water-borne lead (Pb²⁺). – *Chinese Journal of Ecology* 37(5): 1426-1431.

RESPONSES OF SOIL FACTORS TO NUTRIENT INPUTS UNDER DIFFERENT FARMLAND USES

MA, X.^{1,2,3} – WU, H.³ – CHEN, H.⁴ – SUN, R.⁵ – YANG, X.³ – QIAO, W.¹ – FANG, B.^{1*}

¹*School of Geography Science, Nanjing Normal University, Nanjing 210023, China*

²*Institute of Geographical Sciences, Henan Academy of Sciences
Henan Province, Zhengzhou 450052, China*

³*Huzhou City Environmental Monitoring Center Station, Huzhou 313000, China*

⁴*Education in Qingfeng County, Puyang City, Henan Province, Puyang 457300, China*

⁵*Puyang City Environmental Monitoring Center Station, Puyang 457343, China*

**Corresponding author
e-mail: wenyang731@163.com*

(Received 12th Oct 2018; accepted 19th Nov 2018)

Abstract. To understand the responses of changes of soil factors to nutrient inputs under different farmland uses, we analysed soil test data from different crop land uses before and after harvest in combination with the farmers' survey over the cultivation years in Pujiang County, Zhejiang Province, China. The results showed that the inputs of the crop nutrients and the levels of soil nutrients were significantly correlated on the regional scale. Farmers' fertilisation habits resulted in an excess of phosphorous and potassium in the soil, potentially leading to environmental pollution. The excessive investment of nitrogen and phosphate may have decreased the farmland soil's pH value. For vegetable crops, no significant correlation between the crop nutrient and the levels of soil nutrients was found. This might be due to the randomness of nutrient inputs mainly driven by economic interests. We suggest that soil tests be carried out to help improve nutrient management in Pujiang County, especially for non-cereal and oil crops.

Keywords: *farmland use, soil fertility factor, nutrient inputs, soil factor response, Pujiang County, China*

Introduction

Rapid urbanisation and industrialisation in China have increased the need for cultivated land protection (Cai, 2000). In recent years, the quantity of cultivated land in China has decreased while the quality of the land has degraded (Zhang and Wang, 2000; Gao et al., 2000; Chen et al., 2012; Cai et al., 2004a), characterised by soil erosion, pollution, and a decline in soil fertility. In many areas, excessive nutrient input, such as chemical fertilisers, has not only depleted resources but also caused environmental pollution and negatively affected farmland soil quality (Kou et al., 2004; Gao et al., 2009; Domanski et al., 2001). Zhang analysed the economics of crop fertilisation in Shandong province and concluded that the economic benefit was disconnected from resource efficiency in current crop production (Zhang and Ma, 2000; Liang et al., 2000; Benhl et al., 1991). After investigating Dongfeng County's fertiliser input, output, and economic benefit for a few years, Yu pointed out that the policy of diminishing returns of fertiliser did not change people's minds. When the fertiliser input exceeded a certain limit, both the benefit of the fertiliser and the output of crop will be reduced (Yu et al., 2004; Bruland and Richardson, 2005). Using a small watershed as a unit, Guo analysed

the fertiliser input, the accumulation of soil NO₃-N, and its influence on the gully region of the Loess Plateau. The results showed that the input of chemical fertiliser was an important support and guarantee factor for the adjustment of land use structure in the basin. Fertilizers have increased the area planted with food crops, and the area of non-food land has begun to decrease and that the land use structure had further stretched the fertiliser input (Guo et al., 2003a; Guo et al., 2003b; Li et al., 2008; Zhao et al., 2009; Cai et al., 2004b; Lu, 1998). The research on the relationship between the grain yield of wheat and maize and the fertiliser input in the Huanghuaihai plain showed a serious imbalance in the application of chemical fertiliser for current crop production; the application of chemical fertiliser was no longer the main measure for increasing the output. Reasonable coordination and improvement of the fertiliser utilisation rate was an important measure of energy efficiency (Wu et al., 2003; Lu et al., 2004; Wang et al., 2004). All of these studies have revealed low efficiency in utilising fertilisers for production in China. However, there is an explanation for the relationship between the spatial effects of nutrient inputs and the soil factor in the planting period, according to the test data. On the basis of the soil test data from different types of land use for crop planting in combination with the farmers' survey data for many years, this study presents the nutrient input effects on the soil factors of different types of land use in the planting period. The results can be useful for the rational investment of different nutrients and the proper adjustment of planting structures in different regions.

Materials and methods

Research area

Zhejiang Province is located on the southeast coast of China, and Pujiang County is located in the middle of Zhejiang Province (east longitude 119°42'–120°07', north latitude 29°21'–29°41'), on the rim of the Jinqiu Basin. It is the source of the Puyang and Huyuan Rivers. The whole land area is 907.6637 km² (east to west 39.25 km wide, north to south 36.5 km long). The northwest mountainous area and Pujiang Basin are two types of landscapes in Pujiang County. The northwestern mountainous area belongs to a hilly ground landform that is mainly lofty and is composed of low hills. Pujiang Basin belongs to the Jinqiu hilly basin landform, which is mainly flat farmland, downland, and low hills. The landforms in Pujiang County can be divided into three classes based on height and agricultural use: flatland (elevation lower than 150 m), mid-level district (elevation between 150 m and 500 m), and mid-low mountain area (elevation higher than 500 m) (*Figure 1*). The landscape accords with the seven mountains, two rivers, and one field terrain featured in eastern China. Pujiang County is a subtropical zone with a monsoon climate, distinct seasons, a moderate temperature, sufficient light, and abundant rainfall and natural resources.

In the agricultural land adjacent to the Puyang and Huyuan Rivers, three microclimate belts are formed: the Pujiang Basin, with a small warm and rainy area (area I); the Huyuan River Valley, with a mild and rainy area (area II); and a low, mountains, cool and rainy area (area III; *Figure 1*). The climatic characteristics are shown in *Table 1*.

The regional economic development level in Pujiang County is slightly higher than the national average. Rapid industrial expansion added unprecedented challenges to cultivated land protection. The optimisation of regional resources is becoming an imminent problem.

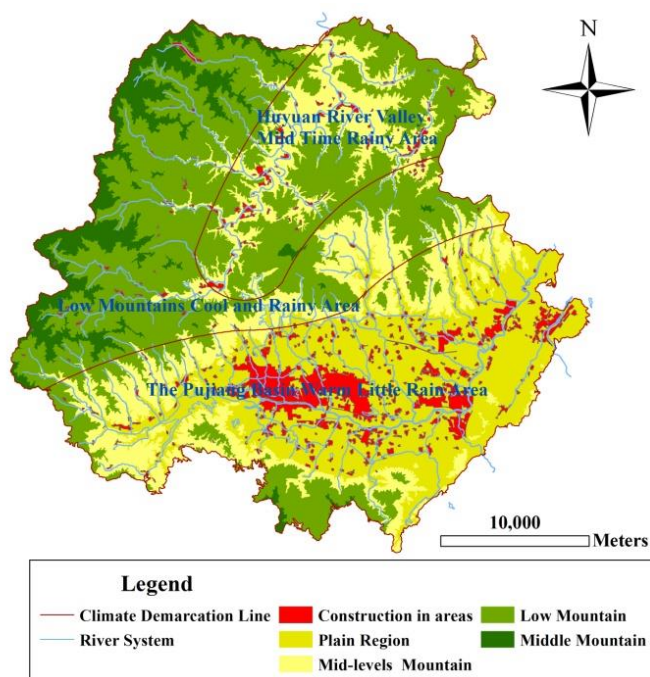


Figure 1. Geographical features of Pujiang County

Table 1. Main soil characteristics of the agricultural climate in Pujiang

Area	Elevation (m)	Average temperature (°C)	Annual rainfall (mm)	>=10°C accumulated temperature	Soil
I	70–300	16–17	1250–1400	4900–5200	Alluvial plain: loamy, paddy soil
II	28–500	15–16	1400–1500	4600–4900	Colluvial valley: clayey, paddy soil
III	500–1200	13.5–15	1500–1577	3900–4600	Hillock: clayey, red soil

Study methods

Household survey

Investigation method

We use a combination of stratified sampling and PPS sampling to chose 107 representative farmers for interviews. The farmers were selected using the method of point, line, and surface. The surface covered a wide range of area. We divided the county into three parts (plain district, mountain district, and low mountain district), and we gave consideration to each village or town in the county. In the meantime, we also considered crop varieties, planting areas, climate differences, typical products, and major industries to balance all these factors. We used a highway as the first line, a pond or ditch as the second line, and a mountain road as the third line. For the point, we considered three classes of crop production levels in addition to the crop variations. The distribution of the survey point is shown in *Figure 2*. The investigational interviews were conducted by professionals of local agricultural technology in the villages or towns, along with university professors and graduate students. These interviewers used a unified, standard door-to-door survey to interview selected crop growers.

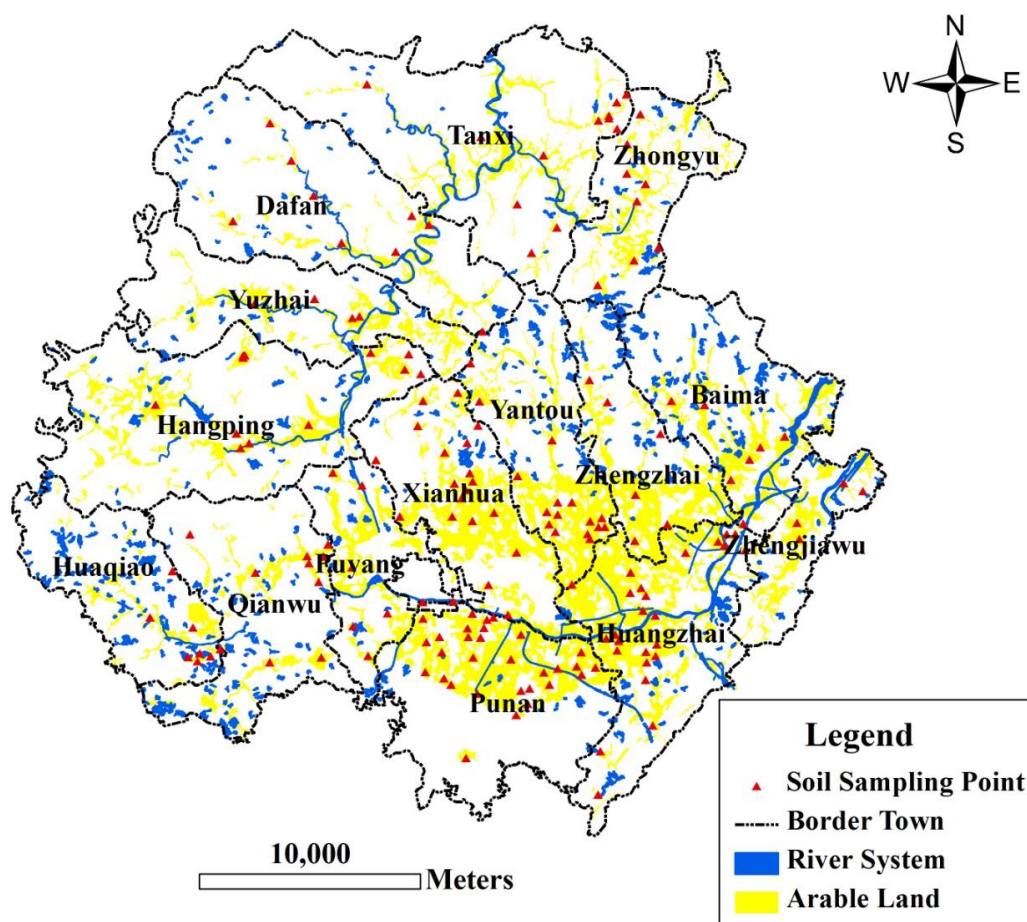


Figure 2. Distribution of sampling points

Investigation content

We designed a detailed questionnaire before the investigation. The main contents included: 1) The status of the use of land, existing problems in agricultural production, crop species, crop yields, the price of agricultural products, the situation of crop growth, and the disasters that occurred in the last 5 years. These data serve to evaluate different benefits of the use of land. 2) Basic information on the farming field, such as terrain conditions, geographical location, and soil properties. These data set the fundamental factors for the spatial analysis of the patterns of land use. 3) Crop management techniques: land consolidation, machine use, inputs and practice methods for all kinds of fertilisers and inputs, the use of various pesticides, and the production and efficiency of agriculture. These data can be used to analyse the relationship between soil nutrients, spatial change, and land usage.

Sampling test and analysis

The sampling point layout

The cultivated land in Pujiang Basin was concentrated in the northwest, along both sides of HuYuanjiang. On the 0~20 cm soil layer of each cultivated land sampling unit, the appropriate layout method is determined according to the shape and size of the unit,

that is, the rectangular block adopts the "S" method, and the approximate square block adopts the "X" method or the checkerboard layout. For areas with complex soil types and topographical conditions, the sampling density is appropriately increased for the dominant crop or cash crop planting area.

The location and altitude of the sample space were determined by a differential GPS instrument, and the surrounding landscape information, farming system and production capacity were investigated and recorded. After thoroughly mixing the collected soils, a 1.5 kg soil sample bag was taken by the quarter method for analysis. We chose a total of 173 sampling points from 107 household fields using a topographic map and a present map of land use in combination with on-the-spot investigation. There was a total of 57 pieces of rice (including rapeseed), 33 pieces of grapes, 32 pieces of vegetables, 21 pieces of peach plum and other pieces totalling 30. Every point layout is shown in *Figure 2*.

Soil sampling method

(1) Sampling time: The first sampling time was before sowing (March 3–12, 2018, a total of 10 days), and the second time for sampling was after harvest and before fertilisation (from November 25 to December 4, 2018, a total of 10 days). The sampling time was integrated with the features of seasonal characteristics and farming activities in the region. The same sampling plots were used for the two sampling periods.

(2) Sampling site and depth: The sampling depth was determined according to the topsoil thickness, usually between 0 and 20 cm.

(3) Sampling method and quantity: We adopted the method of multi-point, mixed-soil sampling, and each mixed agricultural soil sample consisted of 20 sites. First, we tried to make the depth and weight of each sampling point as uniform as possible. The upper and lower proportions of the soil samples were basically the same. We avoided using metal utensils and rubber products during the handling and storage process, because it will pollute the sample. The weight of each composite sample was about 1 kg.

Analysis and testing method

The method of diffusion and absorption was summarised by Lu, the pH value of the soil was determined by pH meter. The soil organic matter was determined by the weight acid method-concentrated sulfuric acid external heating method. The whole N was semi-micro-Kelvin method, and the whole P was Na OH melting-molybdenum anti-colorimetric method. Using Na OH melt-flame photometry, the alkali solution N is alkali diffusion method, the effective P is Na HCO₃ extraction - molybdenum antimony colorimetric method, and the quick effect K is NH₄OAc extraction - flame photometry. We tested and analysed the samples according to the analytical method in line with national standards (Lu, 2000; Liu and Wu). We performed correlation analysis between geographical elements, and the correlation coefficient was determined between the calculation and test.

Correlation analysis method

Correlation analysis is used to reveal the intimate degree of interrelations between geographical elements by calculating and testing the correlation coefficient.

Calculation of correlation coefficient

If we have a series of n measurements of X and Y written as x_i and y_i , where $i = 1, 2, \dots, n$, then the correlation coefficient between them is defined as

$$r_{xy} = \frac{\sum_{i=1}^n (x_i - \bar{x})(y_i - \bar{y})}{\sqrt{\sum_{i=1}^n (x_i - \bar{x})^2 \sum_{i=1}^n (y_i - \bar{y})^2}} \quad (\text{Eq.1})$$

where \bar{x} and \bar{y} are the sample means of X and Y (i.e. $\bar{X} = \frac{1}{n} \sum_{i=1}^n X_i$, $\bar{Y} = \frac{1}{n} \sum_{i=1}^n Y_i$), r_{xy} is the correlation coefficient between X and Y , which is a statistical indicator calculated to show their degree of correlation. Its value lies in the range $[-1, 1]$, with a positive value indicating positive correlation and a negative value indicating negative correlation. The nearer the absolute value of r_{xy} approximates to 1, the closer X and Y are; the closer it approximates to 0, the less correlated they are.

Correlation coefficient test

The correlation coefficient test checks the correlation coefficient against a threshold with a given confidence level. The formula is shown as the following: $P\{|r| > r_\alpha\} = \alpha$ where α means different levels of confidence. If the absolute value of r is greater than the threshold r_α with the confidence level α , X and Y are uncorrelated.

The results of the study and analysis

Statistical analysis results

Results of nutrient input for different crops nutrient inputs

By the means of statistics, calculation, empirical correction, and the abnormal value reject of N , P , and K investment in a county, getting the final results of the corresponding N , P , and K average amounts of different crops per hectare, the results are shown in *Table 2*.

Crop distribution within the region

The structure of the planting crop is normally determined by the traditional market, economics, and technical skills in the region. The survey results in Pujiang showed a stable crop structure. In the towns of Huangyan, Yantou, and Zhengzhai, the main crop is grapes, which occupies 18.53 km^2 . For the Qianwu village and Puyang Street, the main crops are vegetables, and these areas are mainly located on both sides of the Yangjiang River, which supplies plentiful water and has a short distance to the city. The acreage for these areas is 7.49 km^2 .

With a high altitude and great variation of temperature, Hang Ping town is the main production area for mountain vegetables. The planting area is 7.49 km^2 . For food crops,

most families are self-sufficient, and the general area for food crops is about 6.67 km², as shown in *Figure 3*.

Table 2. Mean inputs of N, P, and K for different crops

Nutrient	Grain and oil crop (kg/ha)					Grapes and other fruit (kg/ha)					Vegetables (kg/ha)
	rice	rapeseed	sorghum	corn	wheat	grape	watermelon	sugar	pear	peach plum	vegetables
N	200	100	45	145	210	430	387	290	350	130	450
P	18	11	60	20	40	105	189	120	180	30	210
k	60	20	25	65	25	200	178	125	154	35	160

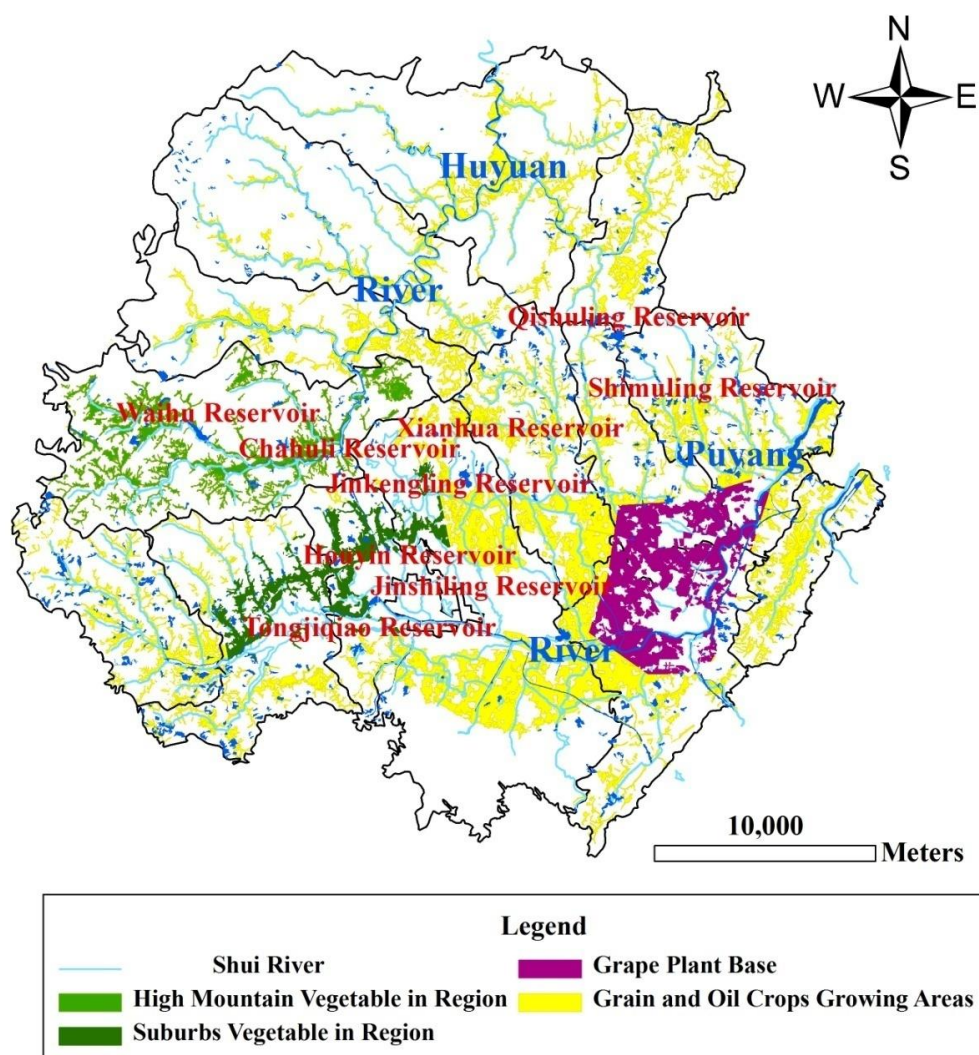


Figure 3. Crop planting areas

The statistical results of soil factors

The change of soil factors

We observed small variations (between -6% and 6%) in soil pH and organic matter

content in different land uses. The fruit land had the highest variation in pH, with a positive correlation with elevation. The pH of vegetable soils, however, was negatively related to elevation. The content of the alkali solution of nitrogen and rapidly available phosphorus and potassium in the soil varied greatly (26.49% ~ 78%) between the two sampling time points, and the mean values of data collected during the second sampling were generally higher than those of the first sampling period (Figure 4).

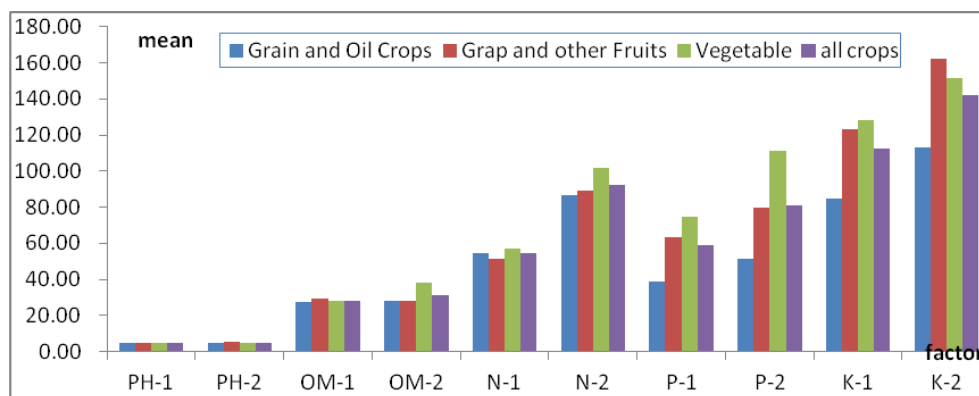


Figure 4. Values of pH and nutrient content in soil before and after different crop plantings (Note: The abscissa is a different soil element, ph-1 and ph-2 itself has no unit, OM-1 OM-2 N-1 N-2 P-1 P-2 K-1 K-2, the units was g/kg. The ordinate represents the amount of change in elements, the units is %)

Nutrient inputs and other factors of crop production had little effect on soil pH and organic matter between the two sampling periods. This might be related to the physical and chemical properties of the soil pH and organic matter themselves. According to the survey, chemical fertiliser was the main nutrient input for vegetable production, and excessive nitrogen fertiliser input resulted in a diminishing pH value. However, although the nutrient input in areas of fruit production was greater than needed, the soil pH did not decrease, but increased slightly, probably because alkaline, organic fertiliser was the dominant type used in these areas. The N, P, and K inputs were mainly from chemical fertilisers, which could be rapidly released in the soil in a short time, resulting in a rapid increase of available nitrogen, phosphorus, and potassium. Combining this with the P, N, and K investments in different crops, we concluded that the greater the amount of nutrient input, the lower the nutrient utilisation efficiency.

The change in soil factor coefficients of variation

The variation coefficient of variation (CV) reflects the variation degree of soil factors of different crops. Generally, $0.01 \leq CV \leq 0.16$ is weak variability, $0.16 < CV \leq 0.50$ is moderate variability, and $CV > 0.50$ is strong variability (López-Granados et al., 2002). For different crops, the CV of the soil pH at the two sampled time points was between 0.09 and 0.13, indicating that the pH value was relatively stable with weak variability. External factors, such as land use types, and the variation of production factors had little effect on the pH value. The CV value of organic matter in the soil varied between 0.26 and 0.31, which is in the moderate intensity range. The certain variation between the two sampling times showed the variations among farmers due to differences in geographical environment, planting structure, and soil organic matter content.

According to the general rule of the change of soil organic matter, in the short term, the value should not appear with so much variation; the reasons for this phenomenon may be closely related to the growing areas' distances from the water source and the farmers' nutrient inputs and their type. Our results indicated that an area with a short distance to water and more N inputs had greater variation in the soil's organic matter content.

Because of an abundant water supply at an early stage, the soil with grapes had an obvious change in soil organic matter content, while the soil with other fruits required less water, which meant its organic matter content did not change as greatly as in the soil with grapes. Therefore, the long distance from the water supply and the greater dispersion of organic matter in the soil resulted in a greater variation in CV values. The CV values indicated that all the crops' soil had little change in alkali solution N before and after planting, but the average value of the soil's alkali-hydrolysable nitrogen increased after harvest. This increase was accompanied by a greater standard deviation, suggesting a greater variation in the soil's available nitrogen. This principle was apparently applicable to the soils with grains, oil crops, and vegetable crops. However, the CV values were reduced, implying that the two crop N inputs might have a certain convergence, which was also in line with the results of the survey. The CV values of grapes and other fruit crops increased after harvest, which might be related to the use of different fruit species and the differences in nutrient inputs. The CV values of the soil's available phosphorus were greater than any other soil factor before planting. This illustrated a close relationship between the amount of rapidly available phosphorus content and the inherent soil properties. After harvest, except for the CV values of vegetables (maybe due to a smaller average increase in available phosphorus than with the other crops), the CV values of all the other crops decreased, probably due to the value of the average is increasing. This also implied that the P input had a strong relationship with the traditional inertia. The CV values of potassium and phosphorus were similar, although not identical. The differences might cause increased differences in input. The average content of potassium increased, and the CV value also increased (Table 3).

Table 3. Soil pH and variation coefficients of soil nutrients

Crop type	PH -1	PH -2	Organic material-1	Organic material-2	Available nitrogen-1	Available nitrogen-2	Rapidly available phosphorus-1	Rapidly available phosphorus-2	Rapidly available potassium-1	Rapidly available potassium-2
Cereals and oil crops	0.11	0.10	0.26	0.22	0.19	0.16	0.87	0.73	0.45	0.48
Grapes and other fruits	0.12	0.13	0.22	0.31	0.18	0.24	0.60	0.48	0.35	0.35
Vegetables	0.10	0.09	0.19	0.24	0.18	0.16	0.45	0.49	0.47	0.45
All crops	0.11	0.12	0.23	0.26	0.19	0.19	0.69	0.62	0.45	0.56

Correlation analysis and test of soil factor for different values

To further explore the relationship between soil factors and nutrient inputs, we used the coefficient method of SPSS Pearson correlation and double sides of significant testing to calculate and test the correlations between N, P, and K input values and soil pH value, organic matter, alkali solution nitrogen, rapidly available phosphorus, and rapidly available potassium change value (Equation 1).

The results showed a strong negative correlation between D-YJ and D-pH, indicating that the value of reduced soil pH was beneficial to the formation of organic soil matter

(Table 4). A significant positive correlation was found between D-YJ and D-JJN ($p < 0.01$), suggesting that the formation of organic matter was closely related to N value, while related data showed that the content of P and K had no correlation with the formation of organic matter. N input had a strong correlation with P and K inputs. However, the survey indicated that P and K inputs were not significant because compound fertilisers were widely applied. From the data, we found that the correlations of D-JJN and D-SXP reached an extremely significant level, but no significant correlation was found between D-JJN and D-SXK. This might be due to crop consistency, absorption capacity on N and P, or that N and P leached into the soil or became volatile to the atmosphere. This also suggests that the ability of crop absorption and the atmosphere and soil's total loss of N and P are basically the same. For N and K, however, crop absorption and loss were quite different.

Table 4. Soil factor index value and N, P, K correlation analysis

	D-PH	D-YJ	D-JJN	D-SXP	D-SXK	N input	P input	K input
D-PH	1	-.205**	-.097	-.168*	.058	.199**	.069	.145
D-YJ	-.205**	1	.263**	.084	-.083	.032	-.035	-.092
D-JJN	-.097	.263**	1	.172*	.080	.293**	.174*	.144
D-SXP	-.168*	.084	.172*	1	.232**	.017	.446**	.218**
D-SXK	.058	-.083	.080	.232**	1	.174*	.173*	.329**
N input	.199**	.032	.293**	.017	.174*	1	.508**	.707**
P input	.069	-.035	.174*	.446**	.173*	.508**	1	.771**
K input	.145	-.092	.144	.218**	.329**	.707**	.771**	1

Note: (1) * indicates that through the bilateral significant test, the correlation coefficient is significant at the level of $\alpha = 0.05$; ** indicates that through the bilateral significant test, the correlation coefficient is significant at the level of $\alpha = 0.01$, the same as below.

(2) D- represents the differences of the two sampling periods' test results of a factor; D-PH represents the difference in the soil's pH content value; YJ represents the soil's organic matter; JJN represents alkali solution N; SXP represents rapidly available phosphorus; SXK represents rapidly available potassium; "investment" represents the amount of a factor that farmers have used, such as "N investment" on behalf of farmers' input of pure N; and N, P, and K respectively represent the pure N, P, and K inputs, the same as below

Correlation analysis of grain and oil crop soil factor and investment factor difference

For food crops, in the experiment period, N, P, and K inputs showed significant correlations, especially between P and K (Table 5), suggesting that the compound fertiliser application pattern had a strong performance in the grain crop.

Table 5. Correlation analysis between the changes in grain and oil crop soil factors and N, P, and K inputs

	D-PH	D-YJ	D-JJN	D-SXP	D-SXK	N input	P input	K input
D-PH	1	-.150	.042	-.010	.114	-.201	.112	.155
D-YJ	-.150	1	.093	.009	-.016	.200	-.096	-.159
D-JJN	.042	.093	1	.229	.005	.422**	.302*	.241*
D-SXP	-.010	.009	.229	1	.266*	.245*	.522**	.325**
D-SXK	.114	-.016	.005	.266*	1	.004	.129	.405**
N input	-.201	.200	.422**	.245*	.004	1	.382**	.387**

P input	.112	-.096	.302*	.522**	.129	.382**	1	.806**
K input	.155	-.159	.241*	.325**	.405**	.387**	.806**	1

Additionally, a strong correlation was shown between rapidly available phosphorus and rapidly available potassium, and no correlation was shown among the other factors (Table 5). This might be due to a strong correlation between P input and K input. In addition, the rate of utilisation of phosphorus and potassium for grain crops might be consistent, implying that the ability for grain crop in utilizing nitrogen might be entirely different. The data from the survey also reflected that the rate of fertilisation was quite different for various species of food crops from dry to paddy land; the N fertiliser rate was high in crops such as rice and low or even non-existent in crops such as legumes and sorghum. The survey results could be well validated by these data.

Correlation analysis of the impact of different soil factors and their inputs on grapes and other fruit crops

For the fruit crops, the differences in soil factors resulted in different characteristics for food crops before and after harvest:

(1) A significant correlation was found between D-JJN and D-YJ (Table 6), demonstrating that the reduced N was closely related to the formation of organic matter, or excessive inputs of N had a stimulating effect on the formation of organic matter. This conclusion was consistent with the conclusion of related research (Liu et al., 1996; Hang et al., 2007).

Table 6. Correlation analysis between the changes of soil factors and N, P, and K inputs

	D-PH	D-YJ	D-JJN	D-SXP	D-SXK	N input	P input	K input
D-PH	1	-.322**	-.195	-.080	-.106	.007	.089	.106
D-YJ	-.322**	1	.434**	.108	-.066	.204	.095	.046
D-JJN	-.195	.434**	1	.143	.140	.380**	.049	.024
D-SXP	-.080	.108	.143	1	.218	-.012	.552**	.171
D-SXK	-.106	-.066	.140	.218	1	.133	.193	.418**
N input	.007	.204	.380**	-.012	.133	1	.553**	.694**
P input	.089	.095	.049	.552**	.193	.553**	1	.724**
K input	.106	.046	.024	.171	.418**	.694**	.724**	1

(2) There was also a significant negative correlation between D-YJ and D-pH (Table 6), suggesting that increased organic matter reduces soil's pH value. This further implies that too much input of N might lead to a decreased soil pH. It can also explain why the values of soil pH in the tested 183 soil samples were all below 6. This also accords with the analysis of the Techno GIN model (Fang and Wang, 2005, 2007; Fang et al., 2012). Excessive input of N was very common in Pujiang crop production, especially in the economic crop production.

(3) The correlations among the increments of soil nutrient factors are weak or even non-existent (see Table 6). This further explains that different crops' nutrient utilisation abilities are also different, and the interactions of crop types and the crop living environment have a decisive influence on crop nutrient usage.

(4) There was evident correlation between N input and the increase of soil alkali solution N content, and similar correlations existed between P input and the increase of

the soil's rapidly available P content, and between K input and the increase of the soil's rapidly available K content.

Correlation analysis of vegetable soil differences and input factors

For vegetable crops, the relationships between the changes of soil factors and input factors were different from those described above before and after harvest. A strong correlation was not shown among input and the growth of soil extractable content, or soil variability, which was contrary to the general phenomenon: soil nutrient factors are closely related to nutrient inputs. However, according to the survey results, cropping patterns might have impacted this phenomenon because of large-scale cultivation and cultivation freedom. Except for the large-scale cultivation, which was relatively consistent, crop growers were free to cultivate the land in vastly different manners. For example, nitrogen input could be as high as 892 kg/ha or as low as 75 kg/ha. The second difference in vegetable nutrient utilisation was the strong negative correlation between D-SXP and D-PH. In the combined survey results, the reasons for this phenomenon might be differences in P input. For example, vegetables, especially eggplant and peppers, need stem support, and therefore require more P input. Consequently, an excessive use of calcium phosphate monobasic reduced the soil pH value. N, P, and K changes in vegetables did not show any correlation (Table 7), suggesting a great variation in nutrient utilisation rates and capacities among different vegetable crops.

Table 7. Analysis of changes in vegetable soil factors and correlations with N, P, and K inputs

	D-PH	D-YJ	D-JN	D-SXP	D-K	N input	P input	K input
D-PH	1	.228	-.241	-.362*	.113	.141	-.092	-.152
D-YJ	.228	1	.095	.174	-.134	-.032	-.082	-.184
D-JN	-.241	.095	1	.112	-.013	.014	.046	.081
D-SXP	-.362*	.174	.112	1	.286	.002	.168	.092
D-K	.113	-.134	-.013	.286	1	.134	.175	.142
N input	.141	-.032	.014	.002	.134	1	.837**	.823**
P input	-.092	-.082	.046	.168	.175	.837**	1	.942**
K input	-.152	-.184	.081	.092	.142	.823**	.942**	1

Conclusions and discussion

Conclusion

For most crops, the crop nutrient input and soil nutrient factor showed an extremely significant correlation in the regional range. Therefore, this relationship may be used to judge the rate of utilisation of adequate nutrients and to develop a quantified scheme to rationalise agricultural nutrient inputs and reduce environmental impact.

From the significant relationship between regional crop nutrient input and soil factors, we can conclude that compound fertiliser may be conducive to improving soil structure, but it leads to a large excess of phosphorus and potassium. Therefore, the acceleration of efficient soil testing engineering may be helpful to promote reasonable and targeted farmland fertilisation.

An excessive investment of nitrogen and phosphate can lead to the reduction of farmland soil's pH value. This may be the direct reason that all the soils in Pujiang County farmland showed a pH value lower than 6. Therefore, better management of nitrogen and phosphate fertilisation may significantly improve the quality of farmland soil. There is no significant correlation between the indicators of vegetable samples. The results of the survey reveal that the vegetable nutrient input is mainly driven by the economic interests of vegetable growers. This may have led to some random behaviours. We believe it is important to pay attention to the crop environment that may impact people's lives and daily diet.

Because of the limitations of real-world conditions, we did not repeat tests on all the sampling points. However, this does not diminish the importance of the study, which reveals problems in agricultural practice. More credible results may require additional investigation to provide more evidence and arguments. This will be the direction of our future efforts. However, whether soil testing and site-specific nutrient management can be used to shift the emphasis from food crops to economic crops is still debatable, because it may require a change of policy to create an incentive for crop growers.

Deficiency

We applied the correlation analysis and field research to study the response of soil factors to nutrient input under different cultivated land use patterns. It was concluded that compound fertilizer may be beneficial to improve soil structure. Excessive input of nitrogen and phosphorus will result in farmland soil pH reduce. The conclusions obtained are basically consistent with others, however, due to limited research time and other reasons, the paper still has some shortcomings to be further improved.

(1) The number of samples is not rich enough. Although it can meet the needs of the research, it may affect the accuracy of the correlation analysis. The subsequent research will increase the sample size appropriately.

(2) The paper mainly analyzes the structural factors such as soil properties and topography. The research on random factors such as farming and management is mainly through reading the literature and combining with field observations. Considering the validity of the survey data, in this paper, the application of the survey data is not sufficient, and there are still improvements to the mechanism revealing. In the follow-up study, attention will be paid to strengthening the quantitative analysis of the influence of structural and random factors.

REFERENCES

- [1] Benhl, D. K., Biswas, C. R., Kalkat, J. S. (1991): Nitrate distribution and accumulation in an Uslochrept soil profile in a long term fertilizer experiment. – *Fert. Res* 28: 173-177.
- [2] Bruland, G. L., Richardson, C. J. (2005): Spatial variability of soil properties in created, restored, and paired natural wetlands. – *Soil Science Society of America Journal* 69(1): 273-284. (In Chinese).
- [3] Cai, Y. L. (2000): Problems of farmland conservation in the rapid growth of china's economy. – *Resources Science* 22(3): 24-28. (In Chinese).
- [4] Cai, X. B., Zhang, Y. Q., Qian, C. (2004a): Effects of different fertilizing manners on the fertility characteristics of the degraded soil in central Tibet. – *Acta Ecologica Sinica* 24(1): 75-83. (In Chinese).

- [5] Cai, X. B., Qian, C., Peng, Y. L. (2004b): Fertility and restoration of degraded soil in central tibet. – *Acta Pedologica Sinica* 04: 603-611. (In Chinese).
- [6] Chen, C., Lq, Y., Liu, J. F. (2012): Analysis and Control Measures of the Environmental Impact by Heavy Fertilizer Use. – *South-to-North Water Transfers and Water Science & Technology* 10(A01): 102-104. (In Chinese).
- [7] Domanski, G., Kuzyakov, Y., Siniakina, S. V., Stahr, K. (2001): Carbon flows in the rhizosphere of ryegrass (*Lolium perenne*). – *Plant Nutr Soil Sci.* 164: 381-387.
- [8] Fang, B., Wang G. (2005): Analysis of crop nutrition limiting factors by TechnoGIN in Pujiang County of Zhejiang Province. – *Journal of Zhejiang University (Agric. & Life Sci.)* 31(4): 417-522. (In Chinese).
- [9] Fang, B., Wang G. (2007): Research on harmonious growth of eco-economy and agricultural N input. – *Acta Ecologica Sinica* 27(1): 214-219. (In Chinese).
- [10] Fang, B., Wu, J. F., Ni, S. X. (2012): Correlation analysis of spatial variability of Soil available nitrogen and household nitrogen inputs at Pujiang County. – *Acta Ecologica Sinica* 32(20): 6489-6500. (In Chinese).
- [11] Gao, X. Z., Ma, W. Q., Cui, Y. (2000): Changes of soil nutrient contents and input of nutrients in arable of China. – *Plant Nutrition and Fertilizer Science* 6(4): 363-369. (In Chinese).
- [12] Gao, H. Y., Guo, S. L., Liu, W. Z. (2009): Soil respiration and carbon fractions in winter wheat cropping system under fertilization practices in arid-highland of the Loess Plateau. – *Acta Ecologica Sinica* 05: 2551-2559. (In Chinese).
- [13] Guo, S. L., Hao, M. D., Dang, T. H. (2003a): N03--N accumulation and its affecting factors in small watershed in gully region of Loess Plateau. – *Journal of Natural Resources* 01: 37-43. (In Chinese).
- [14] Guo, S. L., Zhou, Y. D., Zhang, W. J. (2003b): Effects of Long-term Application of Chemical Fertilizer on Food Production and Soil Quality Attributes. – *Research of Soil and Water Conservation* 01: 16-22. (In Chinese).
- [15] Hang, G. X., Zhou, G. S., Xu, Z. Z. (2007): Spatial heterogeneity of soil respiration and contribution of root respiration in a maize (*Zea mays* L.) agricultural field. – *Acta Ecologica Sinica* 27(12): 5254-5251.
- [16] Kou, C. L., Ju, X. T., Gao, Q. (2004): Effects of fertilization on soil quality in two different cropping systems. – *Acta Ecologica Sinica* 11: 2548-2555. (In Chinese).
- [17] Li, H., Qiu, J. J., Wang, L. G. (2008): Characterization of farmland soil respiration and modeling analysis of contribution of root respiration. – *Transactions of the CSAE* 24(4): 14-20.
- [18] Liang, G. Q., Lin, B., Lin, J. X., Rong, X. N. (2000): Effect of long-term fertilization on the forms of nitrogen in calcareous fluvo-aquic soil. – *Plant Nutrition and Fertilizer Science* 01: 3-10. (In Chinese).
- [19] Liu, Y., Wu, H. (1997). The People's Republic national standards, soil quality-Determination of lead, cadmium graphite furnace atomic absorption spectrophotometry. – The People's Republic of national quality inspection and quarantine prison release. (In Chinese).
- [20] Liu, X. L., Gao, Z., Liu, C. H. (1996): Effect of combined application of organic manure and fertilizers on crop yield and soil fertility in a located experiment. – *Acta Pedologica Sinica* 33(2): 138-147. (In Chinese).
- [21] López-Granados, F., Jurado-Expósito, M., Atenciano, S., García-Ferrer, A., de la Orden, M. S., García-Torres, L. (2002): Spatial variability of agricultural soil parameters in southern Spain. – *Plant and Soil* 246: 97-105.
- [22] Lu, R. K. (1998): Principle and Apply Fertilizer of Soil-Plant Nutrition. – Beijing: Chemical Industry Press 120-165. (In Chinese).
- [23] Lu, Y. (2000): Soil agricultural chemical analysis method. – Beijing: Agricultural Sciencetech Press. (In Chinese).

- [24] Lu, A. X., Zhao, Y. L., Wang, J. H. (2004): Distribution characteristics of nitrogen and phosphorus in agricultural soil profiles under different landuse. – *Acta Ecologica Sinica* 04: 603-611. (In Chinese).
- [25] Wang, H. Y., Zhou, J. M., Chen, X. Q., Du, C. W. (2004): Interaction of NPK fertilizers during their transformation in soils III. Transformations of monocalcium phosphate. – *Pedosphere* 14(3): 379-385.
- [26] Wu, L. F., Chen, F., Ouyang, Z. (2003): The relationship between grain output and fertilizer input in wheat-corn cropping area of the Huang-Huai-Hai plain. – *Plant Nutrition and Fertilizing Science* 9(3): 257-263. (In Chinese).
- [27] Yu, Z. M., Li, P., Kang, S. D. (2004): An investigation of fertilizer for output and efficiency and scientific fertilization suggestion in Dong Feng County. – *Journal of Jilin Agricultural Sciences* 03: 62-67. (In Chinese).
- [28] Zhang, F. S., Ma, W. Q. (2000): The Relationship between Fertilizer Input Level and Nutrient Use Efficiency. – *Soil and Environmental Sciences* 02: 154-157. (In Chinese).
- [29] Zhang, T. L., Wang, X. X. (2000): Development and orientation of research work on soil degradation. – *Journal of Natural Resources* 03: 280-284. (In Chinese).
- [30] Zhao, Y. Y., Xie, Y. S., Hao, M. D. (2009): Effect of fertilization on fertility and nitrate accumulation of black loessial soil of dry land in Loess Plateau. – *Plant Nutrition and Fertilizer Science* 06: 1273-1279. (In Chinese).

HYDROGEN SULFIDE ACCUMULATION FACTORS IN COAL MINE OF SOUTHEASTERN MARGIN OF JUNGGAR BASIN IN CHINA

DENG, Q.^{1,2,3*} – WEI, J.^{2,4} – LI, H.² – WANG, Y.² – WU, X.² – LIU, M.^{1,2}

¹*State Key Laboratory Cultivation Base for Gas Geology and Gas Control, Henan Polytechnic University, 454003 Jiaozuo, P. R. China*

²*School of Safety Science and Engineering, Henan Polytechnic University
454003 Jiaozuo, P. R. China*

³*Collaborative Innovation Center of Coal Safety Production of Henan Province
454003 Jiaozuo, P. R. China*

⁴*Key Laboratory of Public Security Management Technology, Shandong Management University, 250357 Jinan, China*

**Corresponding author*

e-mail: dengqigen@hpu.edu.cn; phone: +86-391-398-6252; fax: +86-391-398-7881

(Received 12th Oct 2018; accepted 19th Nov 2018)

Abstract. Hydrogen sulfide provides an abundance anomaly in many coal mines (districts) in southeastern margin of Junggar basin in China. There are three sets of source rocks in this area, where the coal bearing strata mainly involve low metamorphic bituminous coals of the Xishan formation and the Badaowan formation with less than 45°C geotemperature, which is beneficial to the propagation of Sulfate-Reducing Bacteria. The average Sulfate-Reducing Bacteria value of samples is 791 grams / sample. Along with the runoff direction, the salinity and pH value of groundwater gradually increase. And the hydrochemical types of groundwater are evolved into HCO₃-SO₄-Cl-Na by HCO₃-Ca-Na and HCO₃-SO₄-Na-Ca, with the main components of NaHCO₃. In a reducing environment and with the hydrocarbon abundance, the bacterial sulfate reduction is prone to occur and H₂S is likely to form. Meanwhile, the better pore types of the reservoir are mainly the intergranular pore and intragranular dissolved pore. The average porosity of each coal seam is about 8.5% / porosity values are medium, the average permeability is (5.36×10⁻³~11.6×10⁻³) um² / permeability values are low. The top and bottom slates of coal seam are mainly composed of fine clastic rock and low permeability barrier with the characteristics of good sealing ability. All of this provides a wide space for the reservoir of H₂S, under the action of groove type subsidence structure, uplift type relief structures and the hydrodynamic control of methane. Two types of H₂S accumulation mode of northward monoclinic and imbricated fan-shaped were formed in specific geological condition.

Keywords: hydrogen sulfide (H₂S), control factors, accumulation model, underground water, regional structure

Introduction

Many mining areas in the southeastern margin of the Junggar basin are abundant anomaly with H₂S, resulting in many casualties (Deng et al., 2017). The accumulation model of H₂S in regional coal mines is explored to study the formation, accumulation, and preservation of H₂S in the area in order to provide geology-geochemical basis for occurrence characteristics and prevention of H₂S in coal rock. At present, domestic and foreign scholars have conducted many researches on the H₂S accumulation model in oil and gas from the aspects of regional structure, reservoir characteristics, sedimentary

systems, etc. (Zhu et al., 2006; Fei et al., 2010; Fu et al., 2006; Cai et al., 2009). However, there are few studies on the accumulation mode of H₂S in coal mine. The purpose of this study is to find the controlling factors of hydrogen sulfide occurrence in this region and provide the research basis for the treatment and the genesis of hydrogen sulfide.

Methods

Collect data according to drilling data, seismic interpretation data, engineering geology, etc. Analyze features of regional geological, sedimentary and structural evolution. Identify regional features and hydrogen sulfide distribution status.

According to the regional geological characteristics, combined with the nature of hydrogen sulfide reservoir, underground water activities in coal mine and chemical characteristics of underground water (hot spring), the storage conditions of hydrogen sulfide gas and the control factors of abnormal enrichment were identified.

Structural geological background

The southeastern margin of Junggar basin lies between the Santun river and the Sigong river in Fukang county. Located in the middle-east section of the Urumchi front depression, its structural division belongs to the front depression area of south margin of Junggar basin with the formation of north steep slope (dip angle of 70~80°) and the shape of the southern latitude (dip angle 40~50°) (Qin, 1987). Regional distribution ranges from Liuhuanguo in the east to Shuimogou and Sigong River in the west via Toutun river, Xishan coal mine and north of Urumchi city. The regional geology conditions is summarized in *Figure 1*.

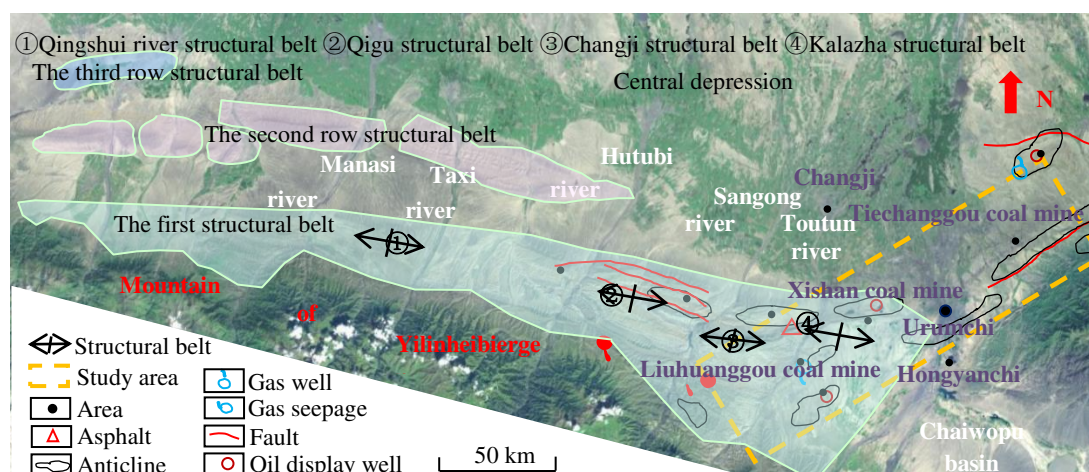


Figure 1. Regional geology conditions

The low-metamorphic bituminous coal was mainly developed in Xishanyao formation (J_{2x}) and Badaowan formation (J_{1b}) of early-middle Jurassic (Tian and Yang, 2011) in this district. The Badaowan formation contains 8~50 layers of coal seams with 8~12 layers of minable coal seams and its total thickness of 14.9~22.8 m. Xishanyao formation contains 3~57 layers of coal seams with 12~20 layers of minable coal seams and its total thickness of 35.6~145.8 m.

Formation mode of H₂S

H₂S can be generated through biochemical degradation of early peat accumulation, bacterial sulfate reduction (BSR) in peat accumulation period and at the stage of coal formation, thermochemical sulfate reduction (TSR) during coal evolution, thermal decomposition sulfides (TDS) and magma (volcanic eruption) activity (Liu et al., 2012; Machel, 2001; Worden et al., 1995).

This region have formed 3 sets of effective source rocks of the Lower Cretaceous Tugulu Group, Middle and Lower Jurassic Period (Badaowan formation and Xishanyao formation) and Middle Permian (Guo et al., 2013). The intensity of source rocks gas-generation in the Middle Permian can reach to $5.0 \times 10^8 \sim 40.0 \times 10^8 \text{ m}^3/\text{km}^2$. The average organic carbon content of dark mudstone in source rocks in the Middle-Lower Jurassic is 15.51%. And the average organic carbon content in coal is as high as 64.49%. The source rocks isopaches of Lower Jurassic is shown in *Figure 2*, in which the organic matrix of Xishanyao formation, mainly composed of 0-II humus, is in a low mature-mature stage. The abundant source rocks provide a solid material basis for the production of H₂S.

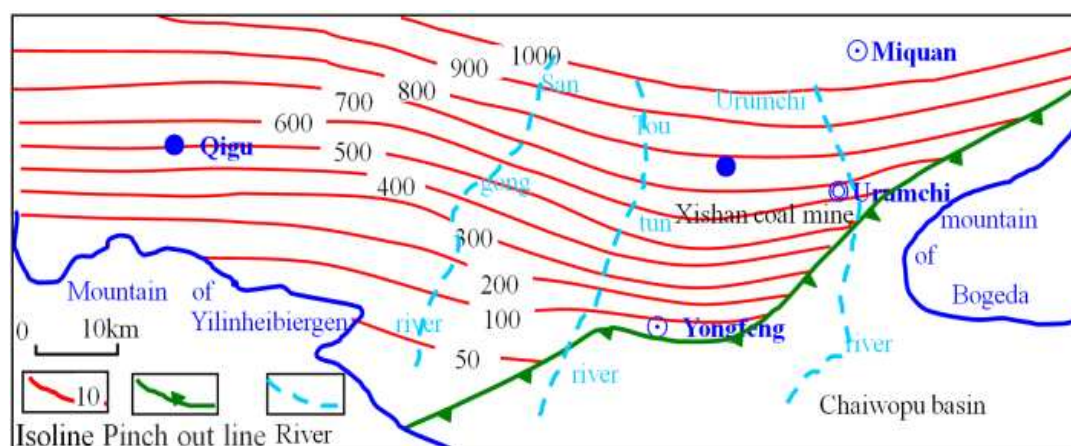


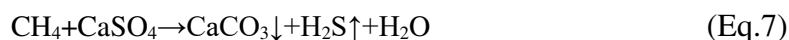
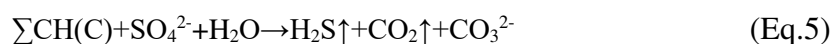
Figure 2. Source rocks isopaches of Lower Jurassic

In southern region, the melted snow and ice on the peak of Yilinheibieren Mountain and Bogeda Mountain flow along the direction of runoff. During its infiltration and runoff, the water dissolves and lixiviates with the anorthite and albite, which is likely to occur chemical reactions, as shown in *Equations 1-4*. Under strong drought evaporation, it may form the high salinity waters type of HCO₃-Ca-Na, HCO₃-SO₄-Na-Ca and HCO₃-SO₄-Cl-Na-K.

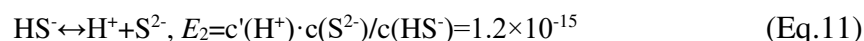
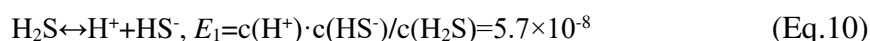
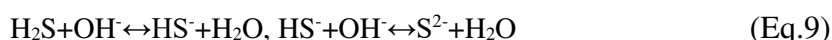


Most of coal seams are low rank coal with the shallow buried depth in the region. And in the coal and rock formations, the microbial activity is more common. From the sampling depth of 254~750 m in each mine, the measured number of Sulfate-Reducing Bacteria (SRB) was (100~3500) /g·samples with an average of 791 /g·samples. In the Xiaolongkou coal mine, the measured number of SRBs was 3500 /g·samples at 312 m below the well. The number of SRBs was 528 /g·samples at 750 m below in the Xishan coal mine and the number of SRBs was 650 /g·samples at 209.5 m below in the Beishan coal mine. It shows that the current depth of mining is conducive to the proliferation of SRB (Deng et al., 2018).

The groundwater environment of coal mine in the region is well-sealed. In the reducing environment, the influence of SRB and the sufficient hydrocarbon organic matter ($\Sigma\text{CH}, \text{C}$), BSR may occur (Headd and Engel, 2013), and then H_2S is formed. Its possible reactions are showed in *Equations 5-8*.



A series of BSR actions will promote calcium ions in water to form calcium carbonate crystals, which are conducive to the positive direction of the reaction. From the south to the north in the coal mine of the area, the cation of Ca^{2+} decreases from 57.8% to 21.2% of deep confined water, which confirms the above reaction process. The underground (spring) water in the area mostly is alkaline water, and the H_2S is soluble in water, so there may be two ionization balance formulas shown in *Equations 9-11*.



In above equations, the E_1, E_2 is an ionization equilibrium constant of H_2S and HS^- . $c(\text{H}^+)$, $c(\text{HS}^-)$ is the concentration of H^+ and HS^- , which is ionization produced by H_2S . $c(\text{H}_2\text{S})$ is the H_2S concentration of unionized. $c'(\text{H}^+)$, $c(\text{S}^{2-})$ is the concentration of H^+ and S^{2-} , which is ionization produced by HS^- . According to the *Equation 10* and *Equation 11*, a relationship between molar ratio of three form sulfur with pH value in the aqueous solution can be drawn, shown in *Figure 3*. So, with the rising of sulfide (H_2S) content, the concentration of HS^- increases respectively, and so does the concentration of OH^- with the hydrolysis of HS^- , namely, the increase of pH value can also promote the further ionization or dissolution of H_2S , further then the solution of H_2S prompts the continuous increase of content of S^{2-} . Thereby, the formation water in this region goes into a cyclic process in which the amount of sulfide content (H_2S) raises continuously and a process in which the pH value will rise slowly.

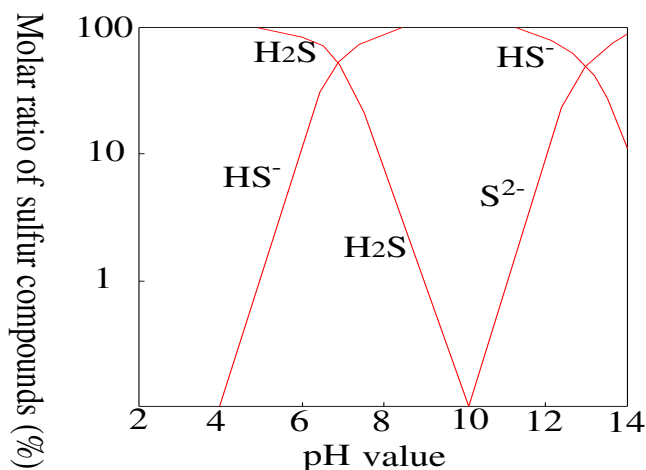


Figure 3. The relationship between molar ratio of sulfur with pH value

After recharging the surface water (ice and snow), the groundwater flows centripetally from the south to the north and gradually flows into the deep. At the same time, the poor continuity of the surrounding rock sand body leads to the slow or stagnant of the underground water in the coal bearing area. Therefore, up-escaping H_2S was blocked in the coal rock. Meanwhile, the slow motion of groundwater carrying H_2S to deep migration is blocked, which results in H_2S abundant enrichment in the coal rock and water. In the vicinity of the fault, the formation water is blocked and the water containing H_2S is exposed to the surface. The formation mode of H_2S in the region is shown in Figure 4.

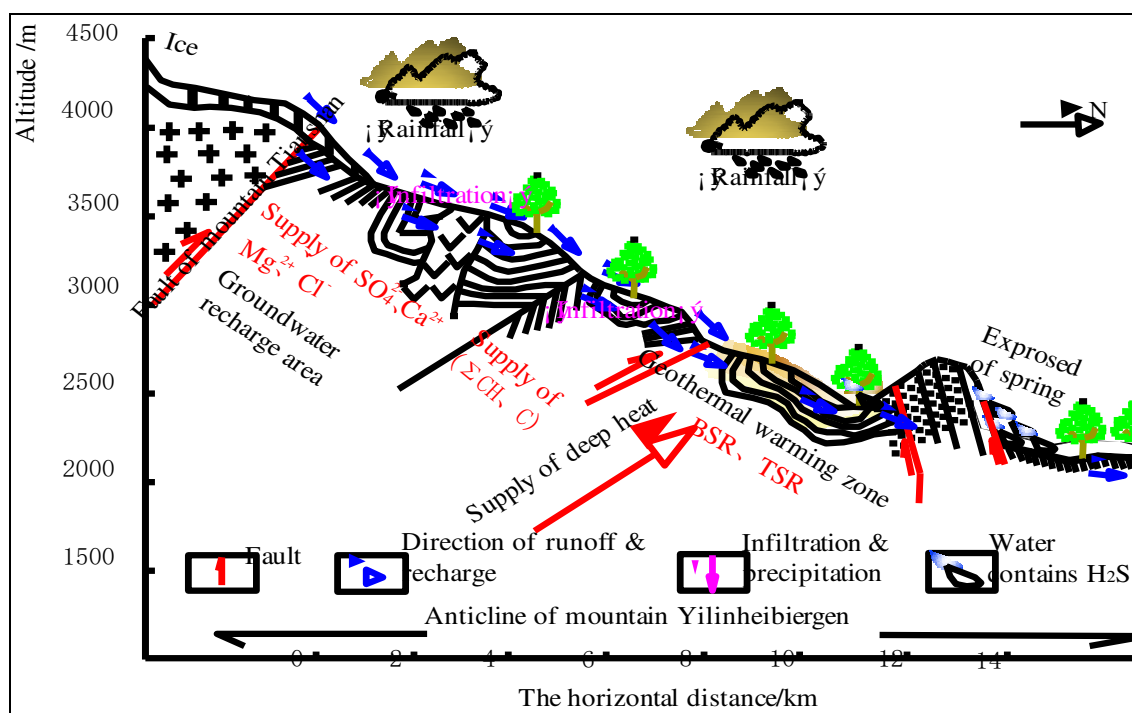


Figure 4. Formation mode of H_2S in study area

Control factors of H₂S accumulation

Control effect of regional structure on H₂S accumulation

Palaeotectus and neotectonics are two main factors controlling H₂S distribution and reservoir (Zhu et al., 2006; Cai et al., 2009). The southeastern margin of Junggar basin, as the succession of depression structure of Mesozoic and Cenozoic, experienced polycyclic tectonic, deposited a thick deposit of source reservoir cap assemblage, created many sets of H₂S-friendly source reservoir cap assemblage, and formed a variety of favorable gas traps. The foreland thrust belt structure leads to the strong extrusion, the universal development of the reverse fault, the coexistence of the anticline and the fractures or the cut from the fractures, which is inductive to the preservation of H₂S. Due to the compression and torsion of the Himalayan movement, the closed-architectural structure of the study area was mainly characterized by broken anticline traps and broken nose traps with the main features of more layers, larger areas, and higher closure. There are many inversion tectonic movements in the region, and the anticline formed by reverse structure is directly covered by the sag of H₂S in the raw storage, which is beneficial to the preservation of H₂S. The long-term faults caused by various tectonic movements provide the necessary access and extensive storage space for H₂S migration, which is beneficial to the reservoir of H₂S.

Regional tectonic movement controls the distribution of H₂S reservoir. The development of structure has created many favorable traps of gas. Abundant source rocks have provided a solid material foundation for the formation of H₂S. The depression structure has created favorable geological conditions for H₂S reservoir. Therefore, the region has a good configuration relationship in the space of H₂S generation, migration and enrichment conditions (source reservoir cap assemblage).

Control effect of the development of caprock on H₂S accumulation

The performance of the caprock in the study area is relatively stable and there are three sets of favorable reservoir and caprock combinations. In each layer, shore-lacustrine, fluvial and delta facies are widely developed, and there widely exist sandstone, siltstone and alluvial fan conglomerate, glutenite and other coarse detrital deposits. Among them, the Mesozoic coal source is the main source rock, with the basic feature of self-generated self-storage combination. In the Sangonghe formation, the Xishanyao formation and the Toutunhe formation of Jurassic, the reservoir lithology is a proven good reservoir which mainly are fine sandstone and quartz feldspar lithic sandstone and mixed sandstone. The porosity of each coal seam in the south of Changji is 0.21~16.42% and the average is 8.41%. The permeability is between $0.22 \times 10^{-3} \sim 23.2 \times 10^{-3} \text{ um}^2$, the average is $11.6 \times 10^{-3} \text{ um}^2$. The porosity of each coal seam in the Liuhuanguo mining area is 4.12~15.91% and the average is 8.71% and the average permeability is $2.12 \times 10^{-3} \text{ um}^2$. The average porosity of each coal seam in the east of the Urumchi river is 8.51%, the average permeability is $5.36 \times 10^{-3} \text{ um}^2$ and the physical characteristics of the regional reservoir are shown in *Table 1* (Deng, 2015; Deng et al., 2017) The reservoir is mainly composed of intergranular pores and intragranular dissolved pores with the characteristics of medium porosity and low permeability reservoir, fractured pore type and the low cap rock permeability. It is clear that the regional medium - good reservoir has a wide range of distribution, which provides a broad favorable space for the reservoir of H₂S.

Table 1. Reservoir bed properties of foreland thrust belt in study area

Horizon	Lithology	Average thickness (m)	Porosity (%)	Permeability (10^{-3}um^2)
Tugulu group (K ₁ tg)	Mainly with purple red, gray green mudstone and siltstone	449~1525	6.60	18.86
Kalazha formation (J ₃ k)	Gray, yellow massive gray wacke, siltstone are cross bedding	50~750	16.12	122.30
Qigu formation (J ₃ q)	Brown red, purple red mudstone with purple red, gray green sandy mudstone and tuff	183~824	9.53	15.38
Toutunhe formation (J ₂ t)	Variegated sandy mudstone, sandstone and fine conglomerate	210~804	10.49	57.51
Xishanyao formation (J ₂ x)	Grey green, yellow, black & gray fine sandstone, siltstone, sandstone and coal seam	380~1080	7.91	0.16
Sangonghe formation (J ₁ s)	Gray, gray yellow, green mudstone, sandstone, a small number of thin coal seams	565~782	8.31	5.13
Badaowan formation (J ₁ b)	Sandstone, siltstone, mudstone and thin coal seam	245~850	9.00	3.25
Xiaoquangou group (T ₂₊₃ xq)	miscellaneous sand, muddy debris, and the lower part of coarse clastic rock and miscellaneous sandstone	500~1000	5.95	0.15

According to the observation and data collection of the fracture from the original coal seam, the fissure development characteristics of the original coal seam are shown in *Table 2* (Deng, 2015; Deng et al., 2017). The fracture of coal seam mostly is primary structure. The distribution of fracture density is up to (50~250) /m with the good openness and connectedness of the fracture. Most of them are not filled with minerals, which increase the permeability of coal seams. Hence, it provides a favorable space for the migration and storage of H₂S in coal seams.

Table 2. Fractured situation of raw coalbed in area

Observation point	Type of coal and rock	Fracture group	Fracture frequency	Length (cm)	High (cm)
Xishan	Bright and semi bright coal	Main fissure	18strip/10cm	>10.0	4~7
		Secondary fissure	6strip/10cm		<1
Dapugou	Bright coal	Main fissure	25strip/15cm	>10.0	2~5
		Secondary fissure	22strip/8cm		0.2~4.0
Shengli	Semi bright coal	Main fissure	7strip/10cm 9strip/10cm	27.0	3~8
Qianshui river mining area	Bright coal	Main fissure	15strip/15cm	25.0	>10
		Secondary fissure	22strip/10cm	0.3~3.0	<1
	Semi bright coal	Main fissure	10strip/10cm	>10.0	1~4
		Secondary fissure	8strip/10cm		<1

It is known that the development of the coal and rock type from bright to semi bright, half dark and dim in microfissures gradually diminishes. The coal seams in the region are mainly bright coal and semi-bright coal, indicating that regional coal reservoirs are conducive to the accumulation of H₂S in coal reservoirs.

The lithology combination of the coal seam roof and bottom is classified into two categories. The first type is coarse clastic rock, including conglomerate, coarse sandstone and medium sandstone. The second type is fine clastic rock, including siltstone, mudstone, and shale. According to the classification method mentioned above, the results of the lithology of the roof and floor of the main coal seams in the region are shown in *Figure 5*.

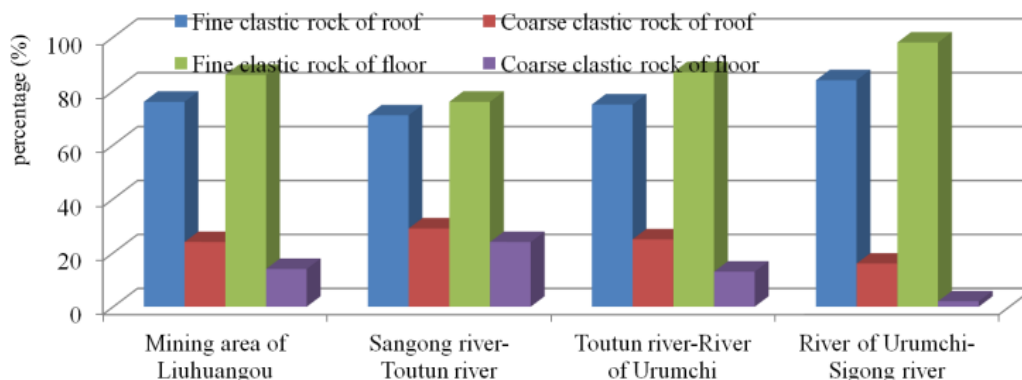


Figure 5. Proportions schematic of roof and floor lithological in regional coal seam

It is shown that the ratio of top and bottom microclastic rock accounts for over 67.2%, and the bottom plate from the Urumchi river to Sigong river reaches 98.1%. In the Toutun river area and the Liuhuanguo mining area, the proportion of roof clastics are 75.4% and 76.2%, respectively and the ratio of clastic rock are 87.0% and 86.3% in the bottom plateau. It is known that the roof and bottom slate of the coal seam mainly composed of microclastic rock is a low permeability barrier layer with poor permeability and good sealing condition. Therefore, the combination of the roof and bottom slate in the regional of Jurassic coal seam is an effective combination of source reservoir cap assemblage of H₂S.

Control effect of buried depth and ground temperature on H₂S accumulation

The contents of hydrogen sulfide and gas were determined by sampling in different buried coal seam of Xishan coal mine in 2013. When the coal seam depth is less than 350 m, the content of gas and H₂S is generally small in each coal mine. When the buried depth is less than 420 m, the methane concentration in the gas components is generally less than 80%. When the buried depth is more than 420 m, the methane fraction of the gas is more than 80%, indicating that the depth of the coal seam gas weathering zone is about 420 m. When the buried depth of coal seam is more than 650 m, the content of gas and H₂S increases rapidly. With the increase of buried depth of coal seam, the gas content of coal seam becomes better, the component of methane rises and the content of H₂S becomes larger. It shows that the content of H₂S has a positive correlation with the buried depth.

Barker and Pawlewicz established the relationship between the maximum paleo temperature and the vitrinite reflectance of coal (Barker and Pawlewicz, 1986):

$$\ln R_0 = 0.0078 * T_{\max} - 1.2 \quad (\text{Eq.12})$$

In the formula, R_0 is the vitrinite reflectivity of coal, T_{\max} is the maximum paleo temperature. The isoline of the region R_0 distribution feature is shown in *Figure 6*. It can be deduced that the maximum paleo-geo-temperature range of the coal formation stage is approximately between 80.0 °C and 110.0 °C.

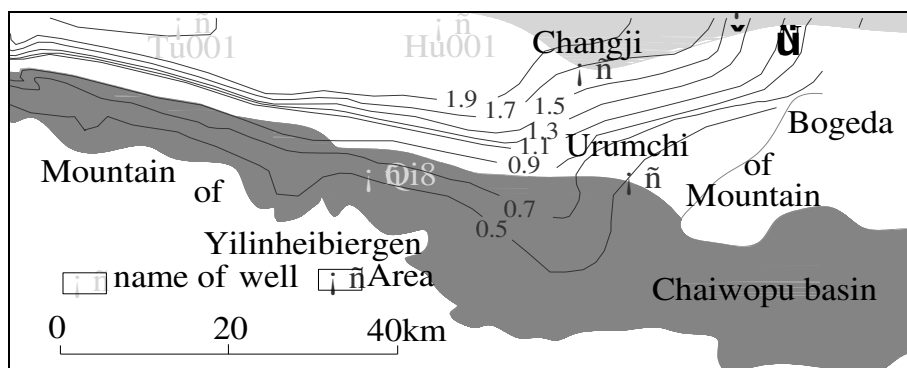


Figure 6. Choropleth of vitrinite reflectance of coal

The current geotemperature gradient in the region is (1.4~2.0) °C/100m (Guo, 2010; Wang et al., 2000). It can be inferred that the temperature distribution of the 3000 m coal rock layer in the current depth is shown in *Figure 7*. The depth of coal seam buried at present is generally 200~1500 m and the geotemperature is less than 45 °C, which is beneficial to the reproduction of SRB.

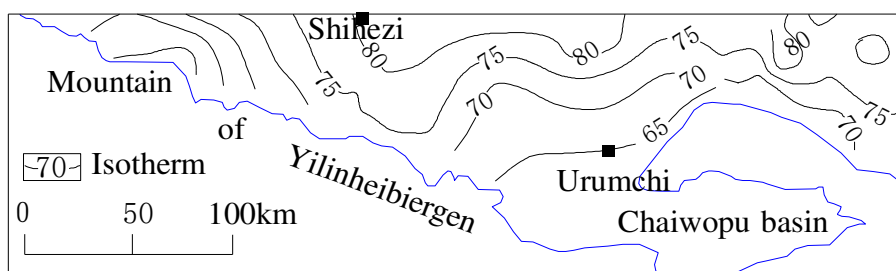


Figure 7. Contours of temperature in 3000 m depth of Junggar basin

Control effect of groundwater on H₂S accumulation

The attitude of water storage structure in the front of the piedmont is influenced by neotectonic. The activity of groundwater affects the enrichment and migration of H₂S. The basement of the regional plain mainly consists of two kinds of groove settlement and uplift, as shown in *Figure 8*. In the piedmont depression or fault zone, a huge sand-gravel layer (aquifer) was accumulated in the Quaternary Period. And above and below the coal-bearing strata of Xishanyao formation, there are good water-retaining layers. The water converges into the basin depression under the action of gravity, resulting in a stagnant and closed state of the groundwater in the coal reservoir within the zone. The H₂S is sealed and stored under the effect of hydrodynamic sealing and gas control.

The salinity of underground water of regional coal mine is between 1.2 g/L and 7.1 g/L with the feature of weak alkaline. In Toutunhe basin, along the runoff direction, the hydrochemical types of groundwater are evolved into HCO₃-SO₄-Cl-Na by HCO₃-Ca-

Na and $\text{HCO}_3\text{-SO}_4\text{-Na-Ca}$, with the main components of NaHCO_3 . Salinity and hardness increase from low to high, salinity rapidly from less than 1.0 g/L to more than 7.0 g/L; and the pH, from 8.1 to 9.3 (Duan et al., 2007; Tian et al., 2017; Li et al., 2016; Chen et al., 2013). The chemical characteristics of the groundwater in each coal mine (area) from the south to north basin are shown in *Table 3* (Deng, 2015; Deng et al., 2017). NaHCO_3 type-water often indicates stable water environment. Water formed under the environmental conditions of the mainland is also a sign of oil in the oil and gas fields and one of the important symbols of reducing environment, which indicates that the underground aquifers are in a reducing environment in the region.

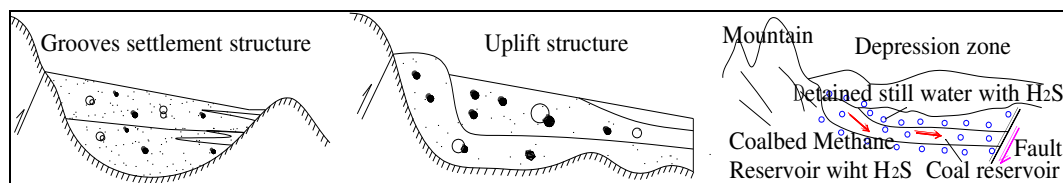


Figure 8. Changes schematic of piedmont base and hydrodynamic action of coal bed methane

Table 3. Groundwater chemical characteristics

Mining area	Daxigou area	Qianshui river area	Liuhuanggou mining area	Xishan coal mine
Hydrochemical type	$\text{SO}_4\text{-Cl-HCO}_3\text{-Ca}$	$\text{SO}_4\text{-Cl-Na}$	$\text{SO}_4\text{-Cl-K+Na}$	$\text{Cl-SO}_4\text{-K+Na}$
Salinity(g/L)	1.1	1.6	3.5	6.2
H_2S content (mg/L)	7.89~25.32	9.26~51.29	23.89~69.45	41.89~259.63
pH	8.3	8.5	8.5	9.0

Accumulation model of H_2S

Geological structure controls the source reservoir cap assemblage of hydrogen sulfide. Under special geological conditions, two types of H_2S accumulation patterns are formed in the region of the northward monoclinic and the imbricated fan-shaped.

H_2S accumulation model of northward monoclinic

The north single oblique H_2S accumulation model is widely distributed in the east of Urumchi. Hydrogen sulfide accumulation is mostly controlled by hydrogeological conditions. The monoclinic south-wing collects the water from rivers and glaciers. The environment of the detention zone of well sealed, the high degree of groundwater salinity and the poor water flow is conducive to the proliferation of SRB. On the water vapor (solid) interface, the occurrence of BSR action forms H_2S , then it is dissolved into water or diffused into the gas, and it migrates with the flow of water to the deep part of the coal bedrock (Cross et al., 2004; Krouse et al., 1988; Cody et al., 2000; Wei et al., 2014). Meanwhile, the poor continuity of the surrounding rock sand-body causes the slowness or the stagnant of the groundwater of the coal-bearing areas. Therefore, the H_2S diffusing upward in coal rock will be blocked. At the same time, the slowness of groundwater carries H_2S to the deep part and H_2S will be blocked, resulting in anomalous enrichment of H_2S in coal rock and water (Zhu et al., 2010; Zhu et al., 2014; Dai et al., 2004; Qiao et al., 2005). The H_2S accumulation model of northward monoclinic is shown in *Figure 9*.

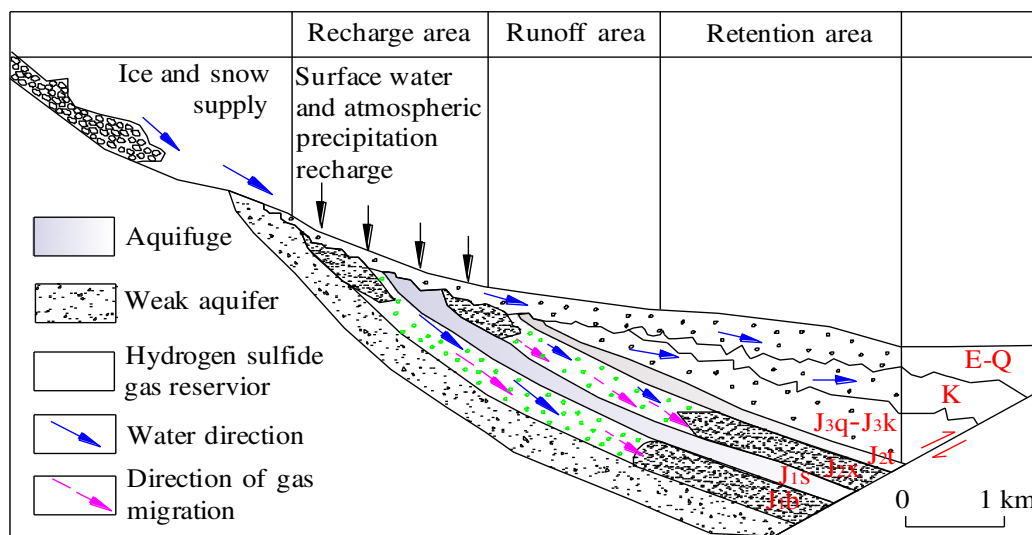


Figure 9. *H₂S accumulation model of northward monoclinic*

H₂S accumulation mode of imbricate type

The imbricate pattern of H₂S accumulation mainly occurs in the Xishan coal mine area of west Urumchi. The area is affected by Urumchi -Miquan strike slip fault, which develops trust nappe structure belt. It is a kind of fracture where one side of the fracture breaks perpendicular to the fracture surface. The most obvious structural feature is echelon anticline distribution, which is in a strong, imbricate pattern (Fan et al., 2012; Wang et al., 2013; Deng et al., 2002; Xu et al., 2001; Qu et al., 2009; Fang et al., 2006). It is shown in *Figure 10*.

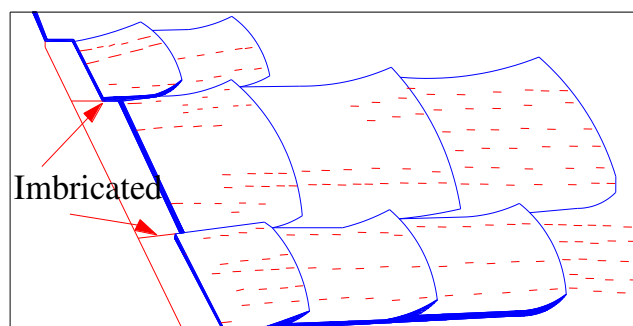


Figure 10. *The schematic diagram of imbrication*

The H₂S is produced by the action of BSR. Part of H₂S meets the metal ions and reacts with them and form a new product. Part of H₂S is integrated into the water, which moves slowly to the deep and forms hydrosulphuric acid so that the water is rich in H₂S. Part of H₂S is mixed into the gas of coal and rock strata, vertical or longitudinal migration along the gas source fracture to the depression part, resulting in an abnormal H₂S enrichment in coal rock strata. Most of the regional faults are relatively independent structural systems and are mainly thrust faults. The H₂S accumulates of imbricated fan-shaped is shown in *Figure 11*.

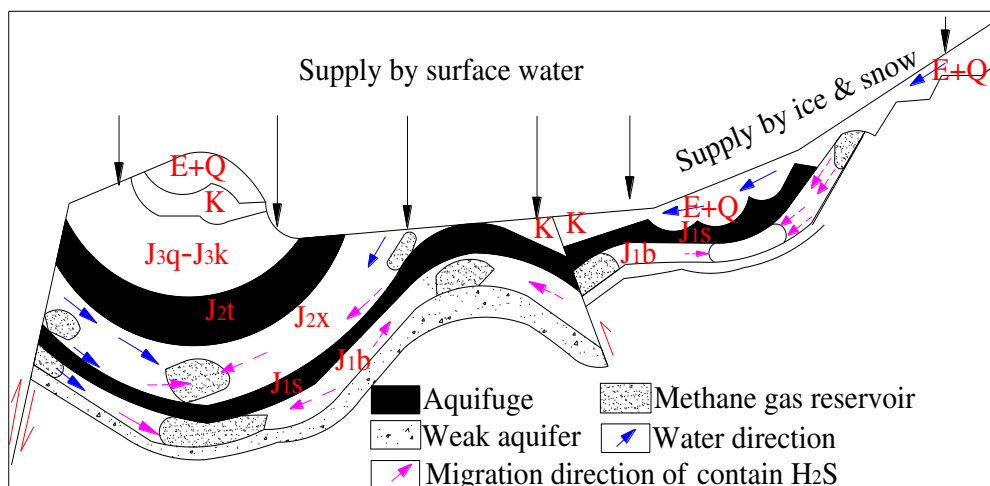


Figure 11. *H₂S accumulation model of imbricated fan-shaped*

Discussion

BSR, TSR and magmatic activity are the main genetic types of hydrogen sulfide in coal mine. The genetic recognition pattern of hydrogen sulfide in coal mine can be established according to the characteristics of coal environment, coal rock thermal evolution history and gas composition.

The depth of coal seam buried at present is generally 200~1500 m and the geotemperature is less than 45 °C, which is beneficial to the reproduction of SRB. Along with the runoff direction, the salinity and pH value of groundwater gradually increase.

According to the characteristics of reservoir lithology, chemical characteristics of groundwater, temperature of coal-series strata, analysis of gas component, bacterial detection of SRB, the BSR is prone to occur and is likely to form the H₂S. However, coal fire in this region has a long history and part of H₂S may be produced by the burning of coal-series strata, which needs further identification.

Conclusion

The hydrogen sulfide are abundant anomaly in many coal mines (districts) in southeastern margin of Junggar basin in China. There are three sets of source rocks in the Tugulu formation of Lower Cretaceous, Middle-Lower Jurassic and Middle Permian in the region. Most of the buried depth of coal seams are 200~1500 m and the temperature of the formation is less than 45 °C, which is beneficial to the propagation of SRB. The average SRB value of samples is 791 grams / sample. Along the runoff direction, the salinity and pH value of groundwater gradually increase. And the hydrochemical types of groundwater are evolved into HCO₃-SO₄-Cl-Na by HCO₃-Ca-Na and HCO₃-SO₄-Na-Ca, with the main components of NaHCO₃. In a reducing environment and the rich hydrocarbon, the BSR is prone to occur and is likely to form the H₂S.

In the region, as the succession of depression structure of Mesozoic and Cenozoic, experienced polycyclic tectonic, deposited a thick deposit of source reservoir cap assemblage, created many sets of H₂S-friendly source reservoir cap assemblage, and formed a variety of favorable gas traps. Meanwhile, the better pore types of the

reservoir are mainly the intergranular pore and intragranular dissolved pore, which is a reservoir of medium porosity and low permeability. The top and bottom slate of coal seam are mainly composed of fine clastic rock and low permeability barrier with the characteristics of good sealing ability. Which provides a wide space for the reservoir of H₂S, under the action of groove type subsidence structure, uplift type relief structures and the hydrodynamic control methane.

Under special geological conditions, there are two types of H₂S accumulation modes which are the northward monoclinic and the imbricated fan-shaped.

Acknowledgements. This work was supported by “National Natural Science Foundation of China (51774116, U1504403)”, “Scientific and Technological Project of Department of Science & Technology of Henan Province (182102210320, 19B620001)” and “Postdoctoral Research Fund of Henan Province (2017)”. In the study process, the authors are also grateful to Professor Mingju Liu of Henan Polytechnic University for his ardent guidance and help.

REFERENCES

- [1] Barker, C. E., Pawlewicz, M. J. (1986): The correlation of vitrinite reflectance with maximum temperature in humic organic matter. – *Paleogeothermics. Lecture Notes in Earth Sciences. Springer Berlin Heidelberg* 5: 79-93.
- [2] Cai, C. F., Li, K., Ma, A., Zhang, C., Xu, Z., Worden, R. H., Wu, G., Zhang, B., Chen, L. (2009): Distinguishing the Cambrian source rock from the Upper Ordovician: evidence from sulfur isotopes and biomarkers in the Tarim basin. – *Organic Geochemistry* 40(7): 755-768.
- [3] Chen, Y., Wang, X. T., Fang, S. H. (2013): Hydrodynamic characteristics of hydrocarbon accumulation in E_{1-2Z} of Huo-Tu structural belt, southern Junggar Basin, NW China. – *Journal of China University of Petroleum* 37(03): 30-36,43.
- [4] Cody, J. D., Hutcheon, I. E., Krouse, H. R. (2000): Fluid flow, mixing and the origin of CO₂ and H₂S by bacterial sulphate reduction in the Mannville Group, Southern Alberta, Canada. *Marine.Petroleum. – Fuel & Energy Abstracts* 41(2): 84.
- [5] Cross, M. M., Manning, D. A. C., Bottrell, S. H., Worden, R. H. (2004): Thermochemical sulfate reduction (TSR): experimental determination of reaction kinetics and implications of the observed reaction rates for petroleum reservoirs. – *Organic Geochemistry* 35(4): 393-404.
- [6] Dai, J. X., Hu, J. Y., Jia, C. Z. (2004): Suggestions for scientific and safety exploration and development of high hydrogen sulfide natural gas fields. – *Petroleum exploration and development* 31(2): 1-4.
- [7] Deng, Q. D., Zhang, P. Z., Ran, Y. K. (2002): Basic characteristics of China's activities. – *Chinese science* 32(12): 1021-1030.
- [8] Deng, Q. G (2015): The study of genesis modes and enrichment control factors of hydrogen sulfide in Jurassic coal seam within the midst of southern margin of Junggar basin. – Henan Polytechnic University, China.
- [9] Deng, Q. G., Liu, M. J., Cui, X. F., Wen, J. (2017): A study of hydrogen sulfide genesis in coal mine of southeastern margin of Junggar Basin. – *Earth Science Frontiers* 24(5): 395-401.
- [10] Deng, Q., Wu, X., Wang, Y., Liu, M. (2018): Activity characteristics of sulfate reducing bacteria and formation mechanism of hydrogen sulfide. – *Applied Ecology and Environmental Research* 16(5): 6369-6383.
- [11] Duan, L., Wang, W. K., Cao, Y. Q. (2007): Hydrochemical characteristics and formation of groundwater in the middle section of the north foot of the Tianshan Mountain. – *Journal of Arid Land Resources and Environment* 21(9): 29-34.

- [12] Fan, G. X., Li, Z., Yang, D. S. (2012): Study on tectonic evolution of Qigu fault zoning belt. – *Journal of Southwest Petroleum University* 34(3): 9-17.
- [13] Fang, S. H., Jia, C. Z., Guo, Z. J. (2006): Re-recognition of the Permian Basin Attributes in the Zhuner Basin and Its Tectonic Significance. – *Geoscience front* 13(3): 108-121.
- [14] Fei, G. A., Zhu, G. Y., Zhang, Y. C. (2010): Global distribution hydrogen sulphide-bearing natural gas and the major factors controlling its formation. – *Earth Science Frontiers* 17(1): 350-360.
- [15] Fu, X. H., Wang, W. F., Yue, J. H. (2006): Genesis analyses of H₂S gas abnormality in gas of Bayi coalmine in Zaozhuang. – *Journal of China Coal Society* 31(2): 206-210.
- [16] Guo, P. Y. (2010): Characteristics of geothermal field of deep mine heat damage control in China. – *China University of Mining & Technology, Beijing*.
- [17] Guo, J. G., Wang, X. L., Pang, X. Q. (2013): Evaluaton and hydrocarbon expulsion characteristics of the Middle-Lower Jurassic source rock in the southern margin of Junggar basin. – *Journal of China University of Mining & Technology* 42(4): 595-605.
- [18] Headd, B., Engel, A. S. (2013): Evidence for niche partitioning revealed by the distribution of sulfur oxidation genes collected from areas of a terrestrial sulfide spring with differing geochemical conditions. – *Appl Environ Microbiol* 79(4): 1171-1182.
- [19] Krouse, H. R., Viau, C. A., Eliuk, L. S., Ueda, A., Halas, S. (1988): Chemical and isotopic evidence of thermochemical sulfate reduction by light hydrocarbon gases in deep carbonate reservoirs. – *Nature* 333: 415-419.
- [20] Li, Y., Cao, D., Wei, Y., Wang, A., Zhang, Q., Wu, P. (2016): Middle to low rank coalbed methane accumulation and reservoiring in the southern margin of Junggar Basin. – *ACTA PETROLEI SINICA* 37(12): 1472-1482.
- [21] Liu, M. J., Deng, Q. G., Zhao, F. J. (2012): Origin of hydrogen sulfide in coal seams in China. – *Safety Science* 50(4): 668-673.
- [22] Machel, H. G. (2001): Bacterial and thermochemical sulfate reduction in diagenetic settings old and new insights. – *Sedimentary Geology* 140(1-2): 143-175.
- [23] Qiao, X. Y., Wang, W. K., Chen, Y. (2005): Characteristics of water storage structure and water cycle in the northern foot of Tianshan Mountains. – *Journal of Earth Sciences and Environment* 27(3): 33-37.
- [24] Qin, S. B. (1987): Geotectonic problems in the southern margin of the Junggar Basin. – *Xinjiang Petroleum Geology* 02: 6-13.
- [25] Qu, G. S., Ma, X. J., Chen, X. F. (2009): On the Structure and Evolution of the Junggar Basin. – *Xinjiang Petroleum Geology* 30(1): 1-6.
- [26] Tian, J. J., Yang, S. G. (2011): Sequence strata and coal accumulation of lower and middle Jurassic formation from southern margin of Junggar Basin, Sinkiang, China. – *Journal of China Coal Society* 36(1): 58-64.
- [27] Tian, X. R., Zhuo, Q. G., Zhang, J., (2017): Sealing capacity of the Tugulu Group and its significance for hydrocarbon accumulation in the lower play in the southern Junggar Basin, northwest China. – *Oil & Gas Geology* 38(02): 334-344.
- [28] Wang, S. J., Hu S. B., Wang, J. Y. (2000): The Characteristics of Heat Flow and Geothermal Field in Junggar Basin. – *Chinese Journal of Geophysics* 43(6): 816-824.
- [29] Wang, T. B., Jia, D., Wei, D. T. (2013): Mesozoic positive and negative structural analysis of the southern margin of the Junggar Basin. – *Geological science* 48(1): 176-190.
- [30] Wei, J. J., Deng, Q. G., Liu, M. J. (2014): Hydrogen sulfide prevention and treatment technology research of coal mine. – *Coal technology* 33(10): 269-272.
- [31] Worden, R. H., Smalley, P. C., Oxtoby, N. H. (1995): Gas souring by thermochemical sulfate reduction at 140 °C. – *AAPG Bulletin* 79(6): 854-863.
- [32] Xu, Y., Liu, F. T., Liu, J. H. (2001): Deep Characteristics of the Collision Zone in Western China and Its Dynamic Significance. – *Journal of Geophysics* 44(1): 40-47.

- [33] Zhu, G. Y., Zhang, Y. C., Ma, Y. S., (2006): Effectiveness thermochemical sulfate reduction on oil and gas industry a H₂S formation accelerating development of the secondary pores in reservoirs. – *Earth Science Frontiers* 13(3): 141-149.
- [34] Zhu, G. Y., Zhang, S. C., Zhang, B. (2010): Marine carbonate reservoir types and accumulation patterns in the central and western regions of China. – *Journal of Petroleum* 31(6): 871-878.
- [35] Zhu, G. Y., Fei, A. G., Zhao, J. (2014): Characteristics and Mechanism of Sulfur Isotope Fractionation of TSR Genesis H₂S. – *Journal of Rock* 30(12): 3772-3786.

AN EVOLUTIONARY GAME STUDY ON IMPLEMENTATION OF ENERGY EFFICIENCY POWER PLANTS BETWEEN GOVERNMENT AND ENTERPRISE CONSIDERING CARBON EMISSION RIGHT TRADING

ZHU, Y. P.^{1*} – FENG, W.¹ – FAN, L. Z.²

¹Management School, Nanchang University, Nanchang, Jiangxi Province 330031, China
(e-mail: vivienne_fw@163.com – W. Feng)

²Management School, Anhui University, Hefei, Anhui Province, 230601, China
(e-mail: 843458904@qq.com)

*Corresponding author
e-mail: zhuyipingnet@ncu.edu.cn

(Received 13th Sep 2018; accepted 28th Nov 2018)

Abstract. EPP (energy efficiency power plant) is a kind of “virtual power plant”, pointing to reduce power consumption and carbon emission by a series of energy-saving measures in a region. The benefits and strategies of government and enterprises influence the effect of implementing EPP, and game analysis is an effective method to analyze this matter. In this paper, an evolutionary game model between government and enterprise implementing EPP considering carbon emission right trading is built, and the model’s stability and evolution paths are analyzed; then Matlab software is used to simulate the impact from sensitivity of some important parameters; at last a calculation example are carried out to analyze the influence on the game equilibrium from government’s rewards and penalties, and a code by VC++ is programmed to achieve the solution of this case study. The results of sensitivity analysis and calculation example are consistent. Suggestion and advice are given respectively to optimize the outcome of the game in each part of above work. We hope the work in this paper is beneficial to formulate a reasonable guide mechanism of EPP, including good government policy orientation, enterprise implementing strategy and reasonable carbon trading strategy, so as to create a good development environment for EPP.
Keywords: *evolutionary game, energy efficiency, demand side management, suggestions, Matlab, vc++*

Introduction

Background

Along with the accelerated process of industrialization and urbanization, a large amount of fossil energy has been consumed, which has caused enormous damage to the environment. The DSM (demand side management) aims to improve energy efficiency, save energy and reduce emissions and protect the environment. EPP (Energy efficiency power plant) is the latest form of DSM. Compared with decentralized demand-side management measures, EPPs have the characteristics of large scale, low financing cost and remarkable energy saving effect. The energy saving measures of EPP include green lighting, high-efficiency motors, frequency conversion governor, energy-saving transformers, high-efficiency household appliances, refrigeration and heating equipment as well as interruptible load. Over the past 10 years, the development of EPP has achieved abundant energy conservation and emission reduction effects and formed a certain scale. For example, the State Grid Energy Research Institute of China counts that the generation capacity of EPP is 640.7 billion kWh in China of 2011-2015, and estimates 2016-2020 is 1.3254 trillion kWh. It can reach 1.9661 trillion kWh during the

period of 2010-2020, equivalent to a reduction of 22,598 kWh in generation capacity and nearly 57 billion USD in investment compared with the conventional power plants (Du et al., 2015).

However, in the implementation process of EPP, enterprises believe that the implementation of EPP will lead to increased costs, and they are not enthusiastic about investing in EPP. The government lacks effective supervision means and incentive mechanism; Public awareness of EPP is not clear. Above problems seriously restrict the development of EPP. The reasons for the above problems lie in that the interests of the major participants are different from each other. If the interests of a single party are taken as the starting point, the optimal decision-making schemes of each party cannot be coordinated and unified, or even conflict, resulting in the failure of EPP implementation. Ultimately there is a lack of scientific game study on implementing EPP, which is also the problem to be solved in this paper.

Literature review

Thus to solve above problems, low carbon investment game analysis is a hot research topic. The game analysis in low carbon environment comes firstly from supply chain research. Du et al. (2015) conducted a game-theoretical analysis and Du et al. (2017) gave low-carbon supply policies for supply chain management. Li et al. (2017) examined the influences of different game structures on the optimal decisions and performance of a low-carbon closed-loop supply chain (CLSC) with price and carbon emission level dependent market demands. Liu et al. (2017) investigated the emission reduction performance for supply chain members in both single-channel and exclusive dual-channel cases. Other researches of supply chain focus on the low-carbon product selection (Meng et al., 2018; Xiao et al., 2018; He et al., 2018) carbon emission reduction (Wang et al., 2018; Zhou and Ye, 2018) and low-carbon strategies (Zu al., 2018)

Followed by the supply chain is the game analysis between participants in low-carbon investment. Luo et al. (2016) developed a Stackelberg-like model to game-theoretically analyze the decentralized decisions of the manufacturer and retailer. Gu et al. (2017) established the evolutionary game model between government and highway logistics enterprises. Wu et al. (2017) used game-based learning theory for reference and built an evolutionary model of low-carbon strategies based on the game between the government and enterprises in the context of a complex network. Zhao et al. (2017) developed the unit root test and the run test to analyze the carbon emission market of four representative cities in China. Chen et al. (2018) examined the role of co-opetition in low-carbon manufacturing.

While the above literatures do not specify what kind of low carbon behavior, so many literatures turn to discuss some kind of specific low-carbon objects, such as solar energy adoption (Varun and Ariane, 2017), low-carbon green oil port (Fan et al., 2012a, b). However, there is a lack of game study on implementing EPPs.

Purpose of the study

While the above researches of low-carbon investment generalizes low-carbon investment of enterprise into low-carbon production, low-carbon behavior, and energy conservation and emission reduction vaguely, but not into what kind of low-carbon behavior specifically, which cannot provide more specific game strategies. There are

some literature mainly discussing the integrated resource planning (Zhu et al., 2017) and energy efficiency (Wang et al., 2015, 2016) of EPP, but we seldom find researches discussing game analysis about implementing EPP. As game analysis between the government and enterprises are the most important subject (Fan et al., 2017; Cao et al., 2016), thus the low-carbon investment to the implementation of EPP is specified, the evolutionary game model of government and enterprise under the background of implementing EPP is established, and the model's stability and evolution paths are analyzed by model derivation, Matlab software and vc++ programs.

Materials and methods

Theoretical basis

Introduction to evolutionary game theory

The combination of dynamic evolution and game analysis constitutes the basis of evolutionary game theory. Evolutionary game theory is based on the limited rationality of participants and it considers that the behavior adjustment of participants is a dynamic process (Ratul, 2012). The whole system is constantly moving to the equilibrium state. When there are multiple equilibrium systems, the equilibrium state of the system is realized, which is determined by the evolutionary path of the initial state and evolution of the system.

Game behavior analysis of implementing EPP

In low-carbon economy, the government is the main body to constraint the resources and environment, which gives guidance and adjustment for enterprise implementing EPP and gives supports from the aspects of laws, regulations and policies. Enterprises are the main body to implement EPP, so they should not only undertake the important task of saving electricity, reducing emissions and protecting the environment, but also take the responsibility for enhancing the competitiveness of their products and ensuring sustainable development of themselves. Because government and enterprises pursue different goals, there is a fierce game in the process of implementing EPP inevitably. Both sides need to adjust their own game strategy according to the other side's, so as to maximize the utility and reach the game equilibrium. Therefore, the best strategy to implement EPP must be the result of multiple games and rational choices between government and enterprises.

The purpose of constructing the game model of the government and enterprise implementing EPP is to help government adopt a reasonable guidance and management mechanism, and help enterprise adopt reasonable implementing measures, which will ultimately contribute to the development of the EPPs.

Building of the evolutionary game model

Hypotheses

(1) Participants in the game

The participants in this game are both local government and enterprises implementing EPP, and both have limited rational characteristics.

(2) Behavioral strategies

The set of government's strategy is {H-Strict supervision, L-Lax regulation}. "Strict supervision" refers to the strict implementation of carbon emission reduction policies by local governments, timely accounting for the carbon emission of enterprises and urging enterprises to comply with carbon emission reduction constraints, in this paper, the way is namely implementing EPP.

The set of enterprise's strategy is {A-implementing EPP, N-not implementing EPP}. "Implementing EPP" refers that enterprises chose to implement EPP to fulfill their duties of supervision and carbon accounting. "Not implementing EPP" refers that enterprises for some reasons do not choose to implement EPP and result in excessive emissions.

So this game contains four pure policy strategies combinations, namely {H-Strict supervision, A-implementing EPP}, {H-Strict supervision, N-not implementing EPP}, {L-Lax regulation, A-implementing EPP} and {L-Lax regulation, N-not implementing EPP}.

(3) Parameter assumptions and their implications

① Suppose the government allocated to the enterprise in a specific period of time of carbon emission quotas as D , at present D is generally determined by historical average level of carbon emissions in carbon trading market, and free distribution is predominate. When the enterprise emissions are not excessive, the carbon emission is D_A . When the enterprise has excessive emissions, the carbon emission is D_N . Obviously $D_A \leq D \leq D_N$.

② The implementation of EPP can save power energy, assuming that the implementation cost of saving a unit (kWh) power is c_0 , the electric price per unit is e , and carbon emission reduction of unit power is d . Set $a = (e - c_0) / d$, then a can be understood as the capacity benefit of unit carbon emission.

③ Assume that the regulatory costs of strict supervision by local governments are C_{gH} , costs of lax supervision are C_{gL} , obviously $C_{gH} \geq C_{gL}$.

④ Suppose that when enterprises' carbon emissions are within the quota, the government can gain profit P_g from the emission reduction, which is related to the emission reduction quantity $D - D_A$, including the reduction of environmental damage caused by enterprise emission reduction, environmental improvement, and the increase of public satisfaction to the government. Enterprises can benefit P_c from emissions cuts, associated with emission reduction $D - D_A$ by implementing EPPs, including social image and reputation improvement, and more government policy support.

⑤ When enterprises carbon emissions are excess, the government will impose fines F on enterprises, which is related to the excess emission $D_N - D$. The fines include both cash penalty and crackdown on those enterprises.

⑥ Assumed that the excessive emissions of enterprises will also bring losses V to local governments, related to the excess emission of enterprises. V includes the damage to the environment by excessive carbon emissions from the enterprise, public dissatisfaction with the government due to environmental variation, and punishment from the higher level government.

Table 1 shows the above parameters and their definitions.

Table 1. Main parameters in the model and their definitions

Parameter	Definition	Parameter	Definition
D	Carbon emission allowances	c_0	EPP implementation cost of saving a unit (kWh) power
D_A	Carbon emission when enterprise adopts strategy A	e	Electric price per unit
D_N	Carbon emission when enterprise adopts strategy N	d	Carbon emission reduction per unit power
C_{gH}	Regulatory costs of strict supervision	P_g	Profit of government when carbon emissions are within the quota
C_{gL}	Regulatory costs of lax supervision	P_c	Profit of enterprise when carbon emissions are within the quota
F	Fines on excessive carbon emissions	V	Losses to local governments by excessive emissions of enterprises

The evolutionary game model

Assuming carbon price (p) per unit is an exogenous variable, determined by the market. When the carbon emissions of an enterprise do not exceed the quota, the income derived from the sale of carbon emission rights will be P_A , $P_A = p(D - D_A)$. When the enterprise emissions are excess, it will be required to purchase the carbon emission right, and the cost is P_N , $P_N = p(D_N - D)$. Assuming that enterprises can meet their emissions targets by purchasing carbon credits from others, local governments will not have to bear the losses (V) because the total amount of carbon quotas in the whole society is stable. The income function of local government and enterprises under different strategies can be obtained in Table 2 (x and y are the probability).

Table 2. The game payment matrix of local government and enterprises (consideration of carbon emission trading)

	Strategies	The enterprise	
		A-implementing EPP (y)	N-not implementing EPP (1-y)
Local government	H-Strict supervision (x)	$P_g - C_{gh}, aD_A + P_c + P_A$	$-C_{gh}, aD_N - P_N$
	L-Lax regulation (1 - x)	$P_g - C_{gl}, aD_A + P_c + P_A$	$-C_{gl} - V, aD_N$

It can be seen that local government's expected benefits ($\pi_g(H)$ and $\pi_g(L)$) of strategy H and L (i.e., strict supervision and lax supervision) and the average expected groups earnings (\bar{U}_g) of local government are as below (Eqs. 1–3):

$$\pi_g(H) = y\pi_g(H, A) + (1 - y)\pi_g(H, N) = y(P_g - F + V) + F - V - C_{gh} \quad (\text{Eq.1})$$

$$\pi_g(L) = y\pi_g(L, A) + (1 - y)\pi_g(L, N) = y(P_g + V) - V - C_{gl} \quad (\text{Eq.2})$$

$$\bar{U}_g = x\pi_g(H) + (1-x)\pi_g(L) \quad (\text{Eq.3})$$

So the replicated dynamic equation for the local government is (Eq. 4):

$$F(x) = dx/dt = x[\pi_g(H) - \bar{U}_g] = x(1-x)(-Vy + V - \Delta C) \quad (\text{Eq.4})$$

Similarly, the enterprises' expected benefits ($\pi_c(A)$ and $\pi_c(N)$) of strategy A and N (i.e., implement EPP or not) and the average expected groups earnings (\bar{U}_c) of enterprise are (Eqs. 5–7):

$$\pi_c(A) = x\pi_c(H, A) + (1-y)\pi_c(L, A) = aD_A + P_c + P_A \quad (\text{Eq.5})$$

$$\pi_c(N) = x\pi_c(H, N) + (1-x)\pi_c(L, N) = -P_Nx + aD_N \quad (\text{Eq.6})$$

$$\bar{U}_c = y\pi_c(A) + (1-y)\pi_c(N) \quad (\text{Eq.7})$$

The replicated dynamic equation for the enterprise is (Eq. 8):

$$F(y) = dy/dt = y[\pi_c(a) - \bar{U}_c] = y(1-y)(P_Nx + P_c + P_A - a\Delta D) \quad (\text{Eq.8})$$

Set $F(x)=0$, two possible stable state points can be obtained: $x_1=0, x_2=1$ and (Eq 9)

$$y^* = 1 - \Delta C / V \quad (\text{Eq.9})$$

Set $F(y)=0$, two possible stable state points also can be obtained: $y_1=0, y_2=1$ and (Eq. 10)

$$x^* = (a\Delta D - P_c - P_A) / P_N \quad (\text{Eq.10})$$

So, (0,0), (1,0), (0,1), (1,1) are the equilibrium points of evolutionary game system. When $V > \Delta C, 0 < y^* < 1$; When $0 < a\Delta D - P_c - P_A < P_N, 0 < x^* < 1$; Then (x^*, y^*) is also the equilibrium point. Therefore, there are totally five equilibrium points.

Model stability analysis and evolution paths

This part will analyze Jacobian matrix's determinant and trace of the equilibrium points.

Four propositions (1)-(4) are given:

- (1) When $a\Delta D < P_c + P_A$, the evolutionary stability strategy of game system is (L, A) ;

- (2) When $R < \Delta C, \alpha\Delta D - P_c > 0$, the evolutionary stability strategy of game system is (L, N) ;
 (3) When $R > \Delta C, \alpha\Delta D > R + P_c$, the evolutionary stability strategy of game system is (H, N) ;
 (4) When $R > \Delta C, 0 < \alpha\Delta D - P_c < R$, there is no evolutionary stability strategy in the game system.

Below is the prove process:

In the carbon trade situation, the Jacobian matrix of this game system is (Eq. 11):

$$\begin{bmatrix} (1-2x)(-Vy+V-\Delta C) & -Vx(1-x) \\ P_N y(1-y) & (1-2y)(P_N x + P_c + P_A - a\Delta D) \end{bmatrix} \quad (\text{Eq.11})$$

Jacobian matrix's determinant and trace of every equilibrium point can be shown in Table 3.

Table 3. Jacobian matrix's determinant and trace of every equilibrium point

Equilibrium point	det J	tr J
(0,0)	$(V - \Delta C)(P_c + P_A - a\Delta D)$	$V - \Delta C + P_c + P_A - a\Delta D$
(0,1)	$\Delta C(P_c + P_A - a\Delta D)$	$a\Delta D - P_c - P_A - \Delta C$
(1,0)	$(\Delta C - V)(P_N x + P_c + P_A - a\Delta D)$	$\Delta C - V + P_N + P_c + P_A - a\Delta D$
(1,1)	$\Delta C(a\Delta D - P_N - P_c - P_A)$	$\Delta C + a\Delta D - P_N - P_c - P_A$
(x^*, y^*)	$\Delta C(\Delta C - V)(P_N x + P_c + P_A - a\Delta D)(P_c + P_A - a\Delta D) / VP_N$	0

There are six situations (a)-(f) for the parameters in this game:

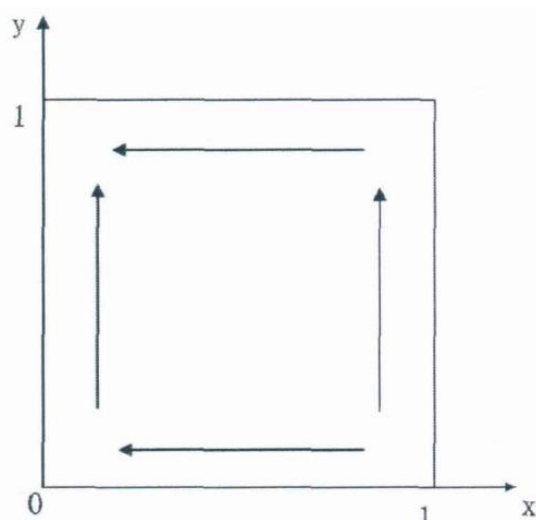
- (a) $V < \Delta C, a\Delta D < P_c + P_A$;
 (b) $V < \Delta C, P_c + P_A < a\Delta D < P_c + P_A + P_N$;
 (c) $V < \Delta C, a\Delta D > P_c + P_A + P_N$;
 (d) $V > \Delta C, a\Delta D < P_c + P_A$;
 (e) $V > \Delta C, P_c + P_A < a\Delta D < P_c + P_A + P_N$;
 (f) $V > \Delta C, a\Delta D > P_c + P_A + P_N$.

Analyzing the Jacobian matrix of every equilibrium point in each situation, local stability of equilibrium point in each situation can be shown in Table 4.

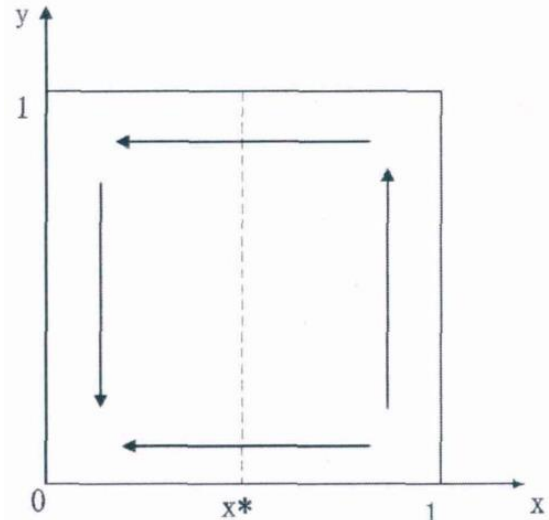
Based on Table 4, the system evolution phase diagram of each situation in Figure 1 can be shown as Figure 1, thus the propositions (1)-(4) can be proved.

Table 4. Local stability of equilibrium point in each situation (considering carbon trading)

Equilibrium point	Situation No. 1			Situation No. 2		
	det J	$tr j$	Stability	det J	$tr j$	Stability
(0,0)	-	Uncertain	Saddle point	+	-	ESS
(0,1)	+	-	ESS	-	Uncertain	Saddle point
(1,0)	+	+	Unstable	-	Uncertain	Saddle point
(1,1)	-	Uncertain	Saddle point	+	+	Unstable
(x^*, y^*)	Unequilibrium point			Unequilibrium point		
Equilibrium point	Situation No.3			Situation No.4		
	det J	$tr j$	Stability	det J	$tr j$	Stability
(0,0)	+	-	ESS	+	+	Unstable
(0,1)	-	-	Saddle point	+	-	ESS
(1,0)	+	+	Unstable	-	+	Saddle point
(1,1)	-	+	Saddle point	-	-	Saddle point
(x^*, y^*)	Unequilibrium point			Unequilibrium point		
Equilibrium point	Situation No.5			Situation No.6		
	det J	$tr j$	Stability	det J	$tr j$	Stability
(0,0)	-	Uncertain	Saddle point	-	-	Saddle point
(0,1)	-	Uncertain	Saddle point	-	+	Saddle point
(1,0)	-	Uncertain	Saddle point	+	-	ESS
(1,1)	-	Uncertain	Saddle point	+	+	Unstable
(x^*, y^*)	-	0		Unequilibrium point		



Situation No.1



Situation No.2

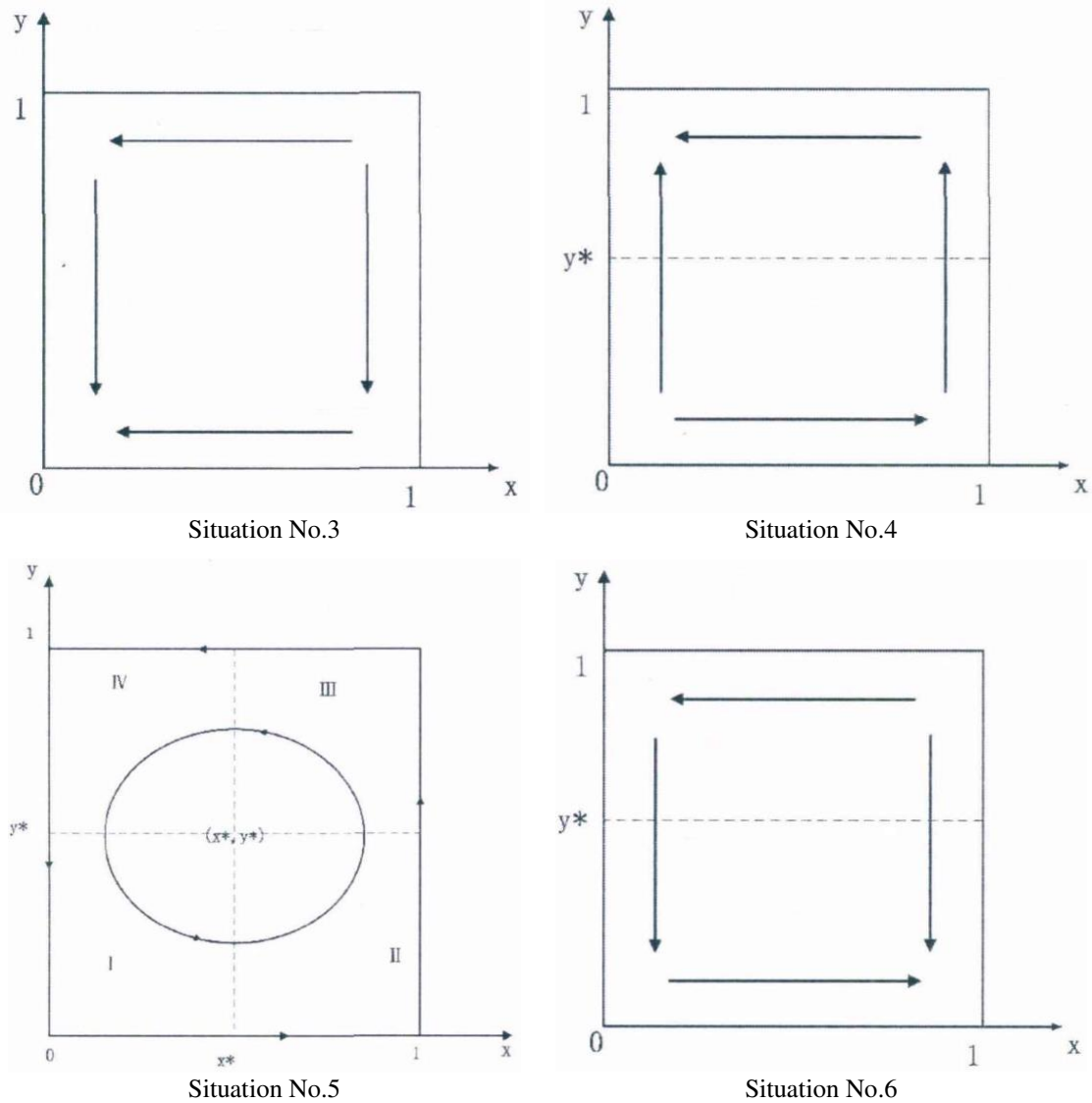


Figure 1. The system evolution phase diagram in each situation

Results

Model result analysis

The following conclusions can be summarized through the model construction and system evolution phase diagram.

(1) When $a\Delta D < P_c + P_A$, the evolutionary stability strategy of game system is $\{L, A\}$. Point (0,1) is the only evolutionary stable point, no matter what the initial state is, the system always converges to (0,1). This suggests that the local government can only have the best interest by opting for lax regulation. The evolution of the system will converge to strategy $\{L, A\}$. This is the stable state the local government would like to see under the carbon emission trading mechanism, namely, under the conditions of lax supervision, the enterprises can consciously implement EPP.

(2) When $V < \Delta C, P_c + P_A < a\Delta D < P_c + P_A + P_N$, the evolutionary stability strategy of game system is $\{L, N\}$. Point (0,0) is the only evolutionary stable point, no matter what

the initial state is, the system always converges to (0,0). It is not willing to be seen by local government. The government can reduce $a\Delta D$ or increase P_c, P_A, P_N to promote the two stages gradually to the situation (1). The concrete measures include properly lower power price e , improve the carbon trading price p , increase earnings to enterprise by intensifying propaganda and support to the enterprise implementing EPP.

(3) When $V > \Delta C, 0 < a\Delta D - P_c - P_A < P_N$, there is no evolutionary stabilization strategy in game system. The evolution trend of the system depends on the initial state of the game between the two groups in *Figure 1*.

(4) When $V > \Delta C, a\Delta D > P_c + P_A + P_N$, the evolutionary stability strategy of game system is $\{H, N\}$. Point (1,0) is the only evolutionary stable point, no matter what the initial state is, the system always converges to (1,0). This moment the loss to local government in lax supervision is more than the regulatory scrutiny when strict supervision, but the earnings to the enterprise by excessive emissions outstrip the benefits of observing carbon emissions constraints.

Parameter sensitivity analysis result

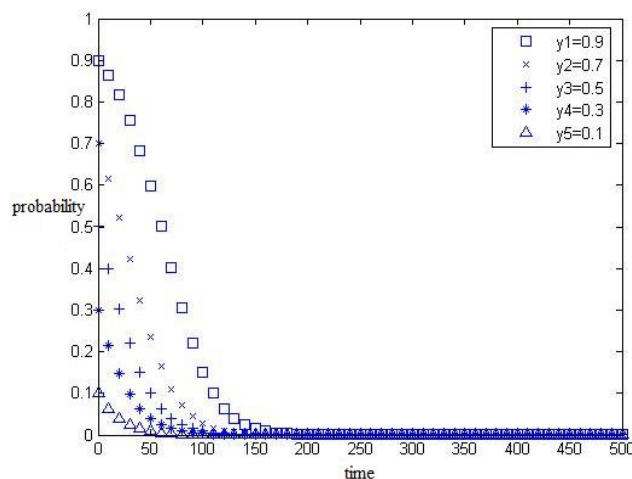
This part will use Matlab software to simulate the impact on the stability of game equilibrium results from some important parameters in the game model.

First the six variables $V, \Delta C, P_N, P_c, P_A, \Delta D$ in the replicated dynamic equation (Eq. 4) and Equation 8 are set as constants, then the impact on the probability y of enterprises implementing EPP from the probability x of government regulation is analyzed.

(1) When $x = 0.2$, replicated dynamic equation is simulated in Matlab, and the evolution result graph of y taking different values is shown in *Figure 2a*.

(2) When $x = 0.8$, replicated dynamic equation is simulated in Matlab, and the evolution result graph of y taking different values is shown in *Figure 2b*.

Figure 2 shows that government's regulatory attitude will have a great impact on the game result. When the government supervises with low probability, the probability of enterprise implementing EPP will gradually decrease and eventually converge to 0. When the government regulates with high probability, the probability of enterprise implementing EPP will gradually increase and eventually converge to 1.



a

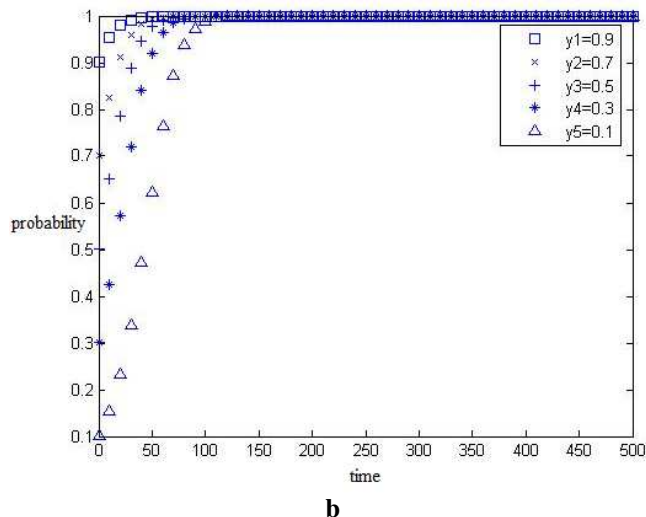


Figure 2. Evolution result graph of y taking different values when $x = 0.2$ and $x = 0.8$

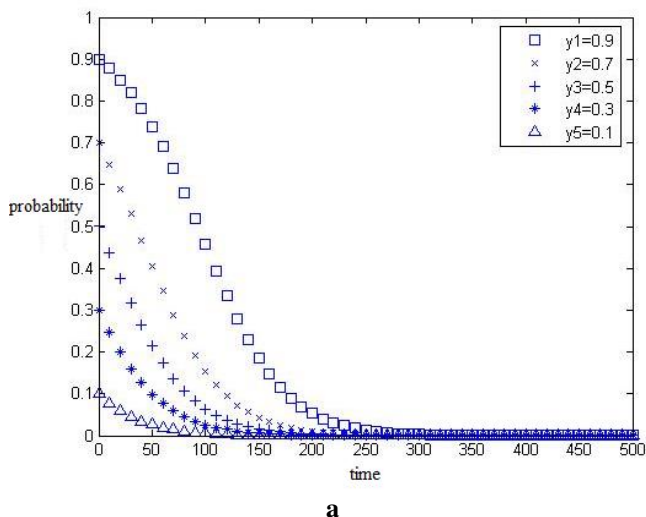
In the second part the impact on the probability y of enterprises implement EPP from the fines F on excessive carbon emissions will be analyzed, and $x = 0.5$ will be set to weaken the impact of government supervision on enterprises.

(1) When $F = 0.2$, replicated dynamic equation is simulated in Matlab, and the evolution result graph of y taking different values is shown in *Figure 3a*.

(2) When $F = 0.5$, replicated dynamic equation is simulated in Matlab, and the evolution result graph of y taking different values is shown in *Figure 3b*.

Figure 3 indicates the punishment strength of the government has a positive influence on the game balance. If the government chooses a large scale of punishments, it will encourage enterprises to actively implement EPP, so that the game equilibrium will evolve towards the ideal direction. If the amount of penalty for not implementing EPP is very low, it cannot affect enterprises effectively.

In the last part the impact on the probability x of local government's supervision from P_g (profit of government when carbon emissions are within the quota) is analyzed, and $y = 0.5$ is set to weaken the impact of enterprises' decision on implementing EPP.



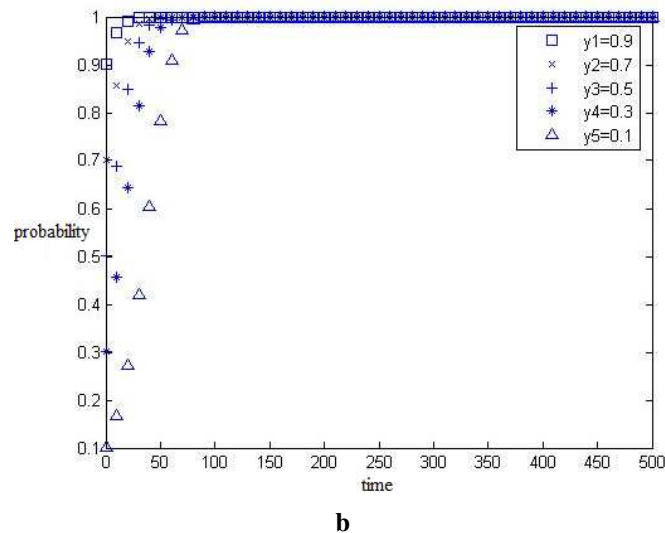


Figure 3. Evolution result graph of y taking different values when $F = 0.2$ and $F = 0.5$

(1) When $P_g = 0.1$, replicated dynamic equation is simulated in Matlab, and the evolution result graph of y taking different values is shown in *Figure 4a*.

(2) When $P_g = 0.6$, replicated dynamic equation is simulated in Matlab, and the evolution result graph of y taking different values is shown in *Figure 4b*.

When social positive reward value is high, regardless of the initial probability x of decision on supervision, after a long period x will gradually increase and in the long term converges to 1. This indicates that when the public has a strong awareness of environmental protection and energy conservation, and recognizes the importance of implementing EPP, the public will urge government to actively regulate enterprises that do not implement EPP, at last promoting the development of EPP.

Calculation example analysis

To verify that the model results are valid or not, this part will use a calculation example to analyze the influence on the game equilibrium from government's rewards and penalties to the enterprise implementing EPP. A case of EPP projects in Hebei Province, China is taken as sample. In this part, three kind of original data are collected in different ways:

(1) The basic information and data of the EPP project, such as project name, investment amount, annual power saving, annual carbon emission, equipment life and other information come from Hebei Demand Side Center (HBDSM).

(2) The common parameters, such as electricity market price, carbon price, rate of interest, rate of depreciation and other data are referred to recent data released by authorities.

(3) To other data needed in this calculation of the EPP project, such as gains and losses for the government when implementing EPP or not, the cost of government regulation, the carbon emission quota that the enterprise is allocated, and other data which are not easy to get, these data are assumed at a reasonable level.

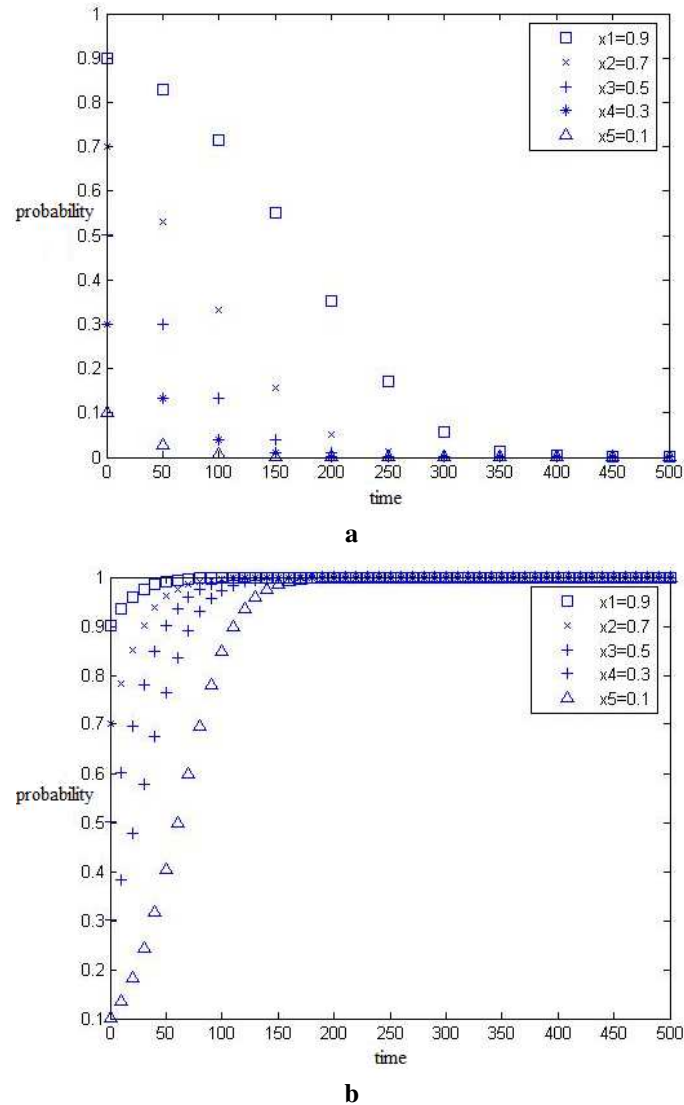


Figure 4. Evolution result graph of x taking different values when $P_g=0.1$ and $P_g=0.6$

Table 4 shows some important parameters in this calculation example.

Table 4. The values of main parameters in the calculation example

Parameter	Unit	Value
Annual power saving (Q)	kWh	$6.325 \cdot 10^5$
c_0	dollar/ kWh	0.042
e	dollar /kWh	0.057
D	kg	4,000,000
C_{gH}	dollar	2,800
C_{gL}	dollar	5,700
Average life of equipment of EPP project (T)	year	18
Annual loan rate (r)	-	5.6%

Assuming the government will reward enterprises according to the power saved by EPP, and the size of the reward is a certain proportion (r_c) of the power saved.

The other parameter is r_p , and the government will punish enterprises according to carbon emission beyond the quota, namely, the size of the penalty is a certain proportion (r_p) of carbon emission beyond the quota.

The impact on the game equilibrium and evolution direction from government's different strategies (mainly r_c and r_p) is analyzed. Because the data in this study are complex and there are multifarious index operation, so vc++ (version 6.0) is used to construct a program to achieve the solution of this case study, and the results are shown in *Table 5*.

Table 5. The strategy probability and expected profit U of government and enterprise under different r_c and r_p

r_c	r_p	x	y	\bar{U}_g (USD)	\bar{U}_c (USD)
0.1	0.1	0.4839	0.3518	3385	51571
0.11	0.1	0.4864	0.3391	3443	51462
0.12	0.1	0.4092	0.3273	3496	51361
0.13	0.1	0.4929	0.3163	3546	51267
0.14	0.1	0.4968	0.3060	3593	51097
0.15	0.1	0.5075	0.2963	3637	51097
0.1	0.11	0.4554	0.2723	3385	51677
0.1	0.12	0.4301	0.2016	5512	51771
0.1	0.13	0.4074	0.1383	6408	51855
0.1	0.14	0.3870	0.0814	7213	51931
0.1	0.15	0.3686	0.0299	7943	51999
0.11	0.11	0.4399	0.2630	4527	51571
0.12	0.12	0.4032	0.1890	5479	51571
0.13	0.13	0.3722	0.1263	6284	51571
0.14	0.14	0.3456	0.0727	6974	51571
0.15	0.15	0.3226	0.0261	7572	51571

According to *Table 5*, when the government adopts the strategy of high reward and light penalty (increase the value of r_c and keep r_p steady), the value of x raises and the value of y decreases progressively, the government's expected profit raises and the enterprise's decreases progressively; When the government adopts the strategy of light reward and heavy penalty (keep r_c steady, increase the value of r_p), both x and y decreases progressively, both expected profit of government and enterprise raises progressively; When the government adopts the strategy of high reward and heavy penalty (increase the value of r_c and r_p), both x and y decreases progressively, the government's expected profit raises and the enterprise's keeps steady. Combined with the expectation of system evolution direction (1, 1)/ strategy {H,A}, compared the three different kinds of incentive strategy, strategy {light reward, heavy penalty} and strategy

{high reward, heavy penalty} are both dominant strategies. While the government and enterprise have a higher expected profit in strategy {high reward, heavy penalty}.

Discussion

In this paper three important contents are put forward:

Firstly, an evolutionary game model between government and enterprise on implementing EPP considering carbon emission right trading is proposed, and the model's stability and evolution paths are analyzed.

Secondly, Matlab software is used to simulate the impact from sensitivity of some important parameters (the probability x of government regulation, fines F on excessive carbon emissions, and the profit of government when carbon emissions are within the quota).

Finally, a calculation example is carried out to analyze the influence on the game equilibrium from government's rewards and penalties. And `vc++` is used to write a program (seen *Appendix*) to achieve the solution of this case study.

Compared to literatures (Du et al., 2015; Xiao et al., 2018) about the game study of low-carbon investment, low-carbon investment is translated into implementation of EPP, and specific research conclusions and specific recommendations are given; Compared to literatures (Wang et al., 2018; Zhou and Ye, 2018) about the game study of carbon emission, besides the carbon emission energy savings are considered as one of the benefits of implementing EPP; Compared to literatures (Zu et al., 2018) about the study of differential game, evolutionary game analysis is focused on and the model's stability and evolution paths are analyzed; Compared to literatures (Gu et al., 2017; Wu et al., 2017) about the evolutionary game study of low carbon, the sensitivity of some important parameters is simulated and the influence on the game equilibrium from government's rewards and penalties by a calculation example are analyzed, which is consistent with the evolutionary model's conclusion.

Conclusion and suggestion

Conclusion

(1) The evolutionary game process and stability strategy of local governments and power generation enterprises are systematically analyzed under the carbon emission trading mechanism. The research found that when the expected increase earnings from enterprise's excess emissions are less than the sum of indirect profit from the carbon emission constraint and the sale of surplus carbon allowance income, excess emissions are not tempting for enterprises implementing EEP, the strategy of enterprises implementing EEP will tend to not excessive emissions, and local governments will choose a strategy of loose regulation. When the loss caused by loose local government supervision exceeds the extra cost of the strict supervision, and the expected increased earnings in excess emission from enterprises implementing EEP is greater than the sum of the income from the carbon emission constraint and the sales of the carbon allowance, and less than the sum of income from the carbon emission constrain, income from the sale of carbon allowances and purchase of carbon allowances in excess emissions, the game between local governments and enterprises implementing EEP shows a periodic behavior pattern.

(2) The different influences of the typical variables on the evolution process of the game are discussed through simulation. It is found that whether the regulatory action chosen by government is positive has a significant impact on the decision-making of the enterprise. The appropriate reward and punishment mechanism of the government will guide the enterprises to choose to product with a low-carbon production methods. And the public's low carbon awareness will also have a positive impact on the government's choice of regulatory actions.

Suggestion

The impact of different initial states and different factors on enterprises emission reduction strategies was analyzed, and policy recommendations were made for local governments. This paper proposes that local governments can promote carbon emissions from enterprises implementing EEP within carbon allowance. The measures that can be taken are to increase incentives for actively complying with carbon-constrained emission reduction enterprises, to appropriately increase the carbon emission trading price of the carbon market, to reduce the cost difference between strict and loose local government supervision, and to strengthen the supervision of the government by public. In the end, the control objectives of the total amount of social carbon emissions will be achieved.

Acknowledgements. This paper is a periodic result of "humanities and social science project of year 2018 for high schools in Jiangxi province, China" (No. TQ18108).

REFERENCES

- [1] Cao, J., Zhang, X. M., Zhou, G. G. (2016): Supply chain coordination with revenue-sharing contracts considering carbon emissions and governmental policy making. – *Environmental Progress & Sustainable Energy* 35(2): 479-488.
- [2] Du, S. F., Zhu, J., Jiao, H. F. et al. (2015): Game-theoretical analysis for supply chain with consumer preference to low carbon. – *International Journal of Production Research* 53(12): 3753-3768.
- [3] Du, S. F., Hu, L., Wang, L. (2017): Low-carbon supply policies and supply chain performance with carbon concerned demand. – *Annals of Operations Research* 255(1-2): 569-590.
- [4] Fan, H. M., Dong, G. S., Zhang, X. N. et al. (2012a): The research on the cooperation and coordination game in constructing low-carbon green oil port. – *Low Carbon Economy* 03(01). DOI: 10.4236/lce.2012.31003.
- [5] Fan, H. M., Dong, G. S., Zhang, X. N. et al. (2012b): The cooperation and coordination game of constructing low-carbon green oil port. – *Applied Mechanics and Materials* 1802(178). <https://doi.org/10.4028/www.scientific.net/AMM.178-181.1036>.
- [6] Fan, R. G., Dong, L. L. et al. (2017): Study on the optimal supervision strategy of government low-carbon subsidy and the corresponding efficiency and stability in the small-world network context. – *Journal of Cleaner Production* 168: 536-550.
- [7] Gu, L. Q., Xi, L. L., Wen, S. L. (2017): Exploration on the low-carbon strategy based on the evolutionary game between the government and highway logistics enterprises. – *Agro Food Industry Hi-Tech* 28(1): 1796-1800.
- [8] He, L. F., Zhang, X., Wang, Q. P. et al. (2018): Game theoretic analysis of supply chain based on mean-variance approach under cap-and-trade policy. – *Advances in Production Engineering & Management* 13(3): 333-344.

- [9] Li, H., Wang, C. X., Xu, L. et al. (2017): Pricing, carbon emission reduction, collection decision, and coordination in a low-carbon closed-loop supply chain. – *Journal of Renewable and Sustainable Energy* 9(6). <https://doi.org/10.1063/1.4991668>.
- [10] Liu, B., Li, T., Tsai, S. B. (2017): Low carbon strategy analysis of competing supply chains with different power structures. – *Sustainability* 9(5): 1-21.
- [11] Luo, Z., Chen, X., Wang, X. J. (2016): The role of co-opetition in low carbon manufacturing. – *European Journal of Operational Research* 253(2): 392-403.
- [12] Meng, X. G., Yao, Z., Nie, J. J. et al. (2018): Low-carbon product selection with carbon tax and competition: effects of the power structure. – *International Journal of Production Economics* 200: 224-230.
- [13] Rai, V., Beck, A. L. (2017): Play and learn: serious games in breaking informational barriers in residential solar energy adoption in the United States. – *Energy Research & Social Science* 27: 70-77.
- [14] Ratul, L. (2012): Evolutionary game theory: an exposition. – *Indian Growth and Development Review* 5(2): 203-213.
- [15] Wang, J. M., Zhu, Y. P., Li, Y. K. (2015): EPP energy efficiency calculation and influencing factor analysis: cases in China. – *Mathematical Problems in Engineering*. <http://dx.doi.org/10.1155/2015/986562>.
- [16] Wang, J. M., Ge, X. J. et al. (2016): Management index systems and energy efficiency diagnosis model for power plant: cases in China. – *Mathematical Problems in Engineering*. <http://dx.doi.org/10.1155/2016/8159871>.
- [17] Wang, X. Y., Xue, M. G., Xing, L. (2018): Analysis of carbon emission reduction in a dual-channel supply chain with cap-and-trade regulation and low-carbon preference. – *Sustainability* 10(3): 1-18.
- [18] Wu, B., Liu, P. F., Xu, X. F. (2017): An evolutionary analysis of low-carbon strategies based on the government-enterprise game in the complex network context. – *Journal of Cleaner Production* 141: 168-179.
- [19] Xiao, W. X., Du, G., Zhang, Y. Y. et al. (2018): Coordinated optimization of low-carbon product family and its manufacturing process design by a bilevel game-theoretic model. – *Journal of Cleaner Production* 184: 754-773.
- [20] Zhao, X. G., Wu, L., Li, A. (2017): Research on the efficiency of carbon trading market in China. – *Renewable and Sustainable Energy Reviews* 79: 1-8.
- [21] Zhou, Y. J., Ye, X. (2018): Differential game model of joint emission reduction strategies and contract design in a dual-channel supply chain. – *Journal of Cleaner Production* 190: 592-607.
- [22] Zhu, Y. P., Hu, Y., Zhang, F. L. (2017): Progressive IRP models for power resources including EPP. – *Mathematical Problems in Engineering*. <https://doi.org/10.1155/2017/2520346>.
- [23] Zu, Y. F., Chen, L. H., Fan, Y. (2018): Research on low-carbon strategies in supply chain with environmental regulations based on differential game. – *Journal of Cleaner Production* 177: 527-546.

APPENDIX

The vc++ source program of the case study

```
①”stdafx.h”  
//stdafx.h: include file for standard system include files,  
//or project specific include files that are used frequently, but  
//are changed infrequently  
#ifndef AFX_STDAFX_H_E360AEIC_F4F9_47B6_9668_14C5744ABE57_INCLUDED_  
#define AFX_STDAFX_H_E360AEIC_F4F9_47B6_9668_14C5744ABE57_INCLUDED_
```

```
#ifMSCVER>1000
#pragma once
#endif // _MSC_VER>1000
#define VC.EXTRALEAN //Exclude rarely-used stuff from Windows headers
#include<afxwin.h> //MFC core and standard components
#include<afxext.h> //MFC extensions
#include<afxdisp.h> //MFC Automation classes
#include<afxdtctl.h> //MFC support for Internet Explorer 4 Common Controls
#ifndef _AFX_NO_AFXCMN_SUPPORT
#include<afxcmn.h> //MFC support for Windows Common Controls
#endif//_AFX_NO_AFXCMN_SUPPORT
//{{AFXinsert_location;}}
//Microsoft VisualC++ will insert additional declarations immediately before the previous line.
#endif//!defined(AFX_STDAFX_H__E360AEIC_F4F9_47B6_9668J4C5744ABE57_INCLUDE_)
②"MathCal.h"
//MathCal.h: main header file for the MATHCAL application
#if!defined(AFX_MATHCAL_H_CD30B733_E51D_4400_9343^BB9BB45A03F8_INCIUDED_)
#define AFX_MATHCAL_H_CD30B733_E5ID_4400_9343_BB9BB45A03F8_INCLUDED_
#endif
#pragma once
#endif // _MSC_VER>1000
#pragma once
#endif // _MSC_VER>1000
#ifndef _AFXWIN_H_
#error include 'stdafx.h' before including this file for PCH
#endif
#include"resource.h"//main symbols
////////////////////////////////////
//CMathCalApp:
//See MathCal.cpp for the implementation of this class
Class CMathCalApp: public CWinApp
{
public:
    CMathCalApp();
// Overrides
//ClassWizard generated virtual function overrides
//{{AFX_VIRTUAL(CMathCaApp)
public:
virtual BOOL InitInstance();
//}}AFX_VIRTUAL
//Implementation
//{{AFX_MSG(CMachCa1App)
//NOTE-the ClassWizard will add and remove member functions here.
//DO NOT EDIT what you see in these blocks of generated code!
//}}JAFX_MSG
    DECLARE.MESSACE_MAP()
};
//{{AFX_INSERT_LOCATION}}

③"MathCalDlg.h"
//MathCalDlg.h:header file
#if!defined(AFX_MATHCALDIG_H_A121E96A_618E_4F51_AED0_C3CF42F246E_INCLUDED_)
#define AFX_MATHCALDLG_H_A121E96A_616E_4F51_AH?_C3CF4E2F246E_INCLUDED_
#endif
#pragma once
#endif//JiSC.VER>1000
////////////////////////////////////
//CMathCalDlg dialog
Class CMathCalDlg: public CDiaiog
//Construction
```

```
public:
#CMathCalDlg(CWnd*pParent*NULL);//standard constructor
//DialogData
//{{AFX.DATA(CMathCalDlg)
enua{IDD=IDO.MATHCAL.DIALOG};
CRichEditCtrl.edit.res;
    Float m_c0;
    Float m_c1;
    Float m_c2;
    Float m_Cc;
    Float m_cp;
    Float m_gsms;
    Float m.lambda;
    Float m.Q;
    Float m_dH;
    Float m_qT;
    Float m_r;
    Float n_rc;
    Float m_rg;
    Float n_rp;
    Float m_T;
    Float m.?;
    Float m_p;
    Float m.Sg;
//}}AFX_DATA
//Class Wizard generated virtual function overrides
//{{AFX.VIRIVAL(CMathCalDlg)
protected:
virtual void Do Data Exchange (CDataExchange*pDX);//DDX/DDVsupport
//}}AFX_VIRTUAL
//Implementation
protected:
HICON m.hlcon;
//Generated message map functions
//{{AFX.MSG(CHathCalDlg)
Virtual BOOL OnlnitDialog();
afx.msg void OnSysCoauoand(UNIT nID,LPARAM IParam);
afx.msg void OnPaintO;
afx.msg HCfRSOROnQueryDraglcon0;
afx.msg void OnButtonCal0;
afx.msg void OnButtonExit0;
//}}AFX.MSG
DECLARE_MESSAGE_MAP()
private:
    float m_pi_g_s;
    float m_pi_g_ns;
    float m_u_g;
    float m_y;
    float Bj_ijo_h;
    float B_pi_l;
    float m_u_m;
    float m_x;
);
//{{AFX.INSERT.LOCATION}}
//MicrosoftVisualC**wil linsert additional declarations immediately before the previous line,
#ifdef APX_MATHCALDLG_H_____A12IE96A.618E_4P51_AD0_C3CF4E2F246E__INCL
UDED_
```

```
④'MatbCalDlg.cpp'  
#include"stdafx.h"  
#include'UathCal.h"  
#include'MatbCalDlg.h'  
#include<stdio.h>  
#include<math.h>  
#include<stdlib.h>  
#ifdef.DEBUG  
#defineneeDEBUG..VEW  
#undefTHIS.FILE  
staticcharTH1S.FILEC3=_FILE_;  
#endif  
//CAboutDlgdialogusedforAppAbout  
Class CAboutDlg:publicCDialog  
{  
public:  
CAboutDlg():  
//DialogData  
//{{AFX.DATA(CAbOUtDlg)  
enua{IDONOT.ABOUTBOX1:  
//)AFX.DATA  
//Class Wizard generated virtual function overrides  
//{{AFX.VIRTUAL(CAboutDlg)  
protected:  
virtual void Do Data Exchange(CDataExchangepDX)//DDX/DDVsupport  
//MAFX.VIRTUAL  
//Implementation  
protected:  
HIAFX.MSG(CAboutDlg)  
//)AFX.MSG  
DECLARE.MESSAGE.MAP()  
CAboutDlg::CAboutDlgO:CDi?log(CAbCMjxDlg::IDD)  
//KAFX.DATA.IKIT(CAboutDlg)  
//HAFX.DATA.IKIT  
Void AboutDlg::Do Data Exchange (CDataExchange*pDX)  
{  
CDialog::DoDaiaExchange(pDX):  
//{{AFX.DATA.MAP(CAboutDlg)  
//)AFX.DATA.MAP  
}  
BEGIN_MESSAGE_MAP(CAboutDlg,CDialog)  
//{i:AFX_MSG_MAP(CAboutDlg)  
//No message handlers  
"}AFX_MSG_MAP  
END_MESSAGE_MAP()  
//CMathCalDlgdialog  
CMathCalDlg::CMathCalDlg(Cffnd*pParent/*=NULL*/)  
:CDialog(CMathCalDlg::IDD,pParent)  
{  
//{{AFX_DATA_INIT(CMathCalDlg)  
M_cO=60000;  
M_cl=0.3108f;  
m_c2=0.296f;  
m_Cc=50000;  
m_cp=1.Of;  
m_gaimna=0.8f;  
m_lambda=0.04f;  
m_Q=632500000.0;
```



```
m_qH=284600000.0;
ra_qL=221300000.0;
m_qT=253000000.0;
m_r=0.0275f;
m_rc=1.0f;
m_rg=1.0f;
m_rp=1.0f;
m_T=18;
m_w=0_042f;
m_p=0.416f;
m_Sg=0.0f;
//}}AFX_DATA_INIT
//NotthatLoadIcondoesnotrequireasubsequentDestroyIconinWin32
m_hIcon=AfxGetApp()->LoadIcon(IDR_MAINFRAME);
m_pi_g_s=0;
m_pi_g_ns=0;
m_u_g=0;
m_y=0;
m_pi_m_h=0;
m_pi_m_l=0;
m_u_m=0;
m_x=0;
m_Sg=0.0f;
}
Void CMathCalDlg::DoDataExchange(CDataExchange*pDX)
{
    CDialog::DoDataExchange(pDX);
    //{{AFX_DATA_MAP(CMathCalDlg)
    DDX_Control(pDX,IDC_RICHEDIT_RES,m_edit_res);
    DDX_Text(pDX,IDC_EDIT_c0,m_c0);
    DDX_Text(pDX,IDC_EDIT_c1,m_c1);
    DDX_Text(pDX,IDC_EDIT_c2,m_c2);
    DDX_Text(pDX,IDC_EDIT_Cc,m_Cc);
    //DDX_Text(pDX,IDC_EDIT_cp,m_cp);
    DDX_Text(pDX,IDC_EDIT_gaimna,m_gamma);
    //DDX_Text(pDX,IDC_EDIT_lambda,m_lambda);
    DDX_Text(pDX,IDC_EDIT_Q,m_Q);
    DDX_Text(pDX,IDC_EDIT_qH,m_qH);
    DDX_Text(pDX,IDC_EDIT_qL,m_qL);
    DDX_Text(pDX,IDC_EDIT_qT,m_qT);
    DDX_Text(pDX,IDC_EDIT_r,m_r);
    DDX_Text(pDX,IDC_EDIT_rc,m_rc);
    //DDX_Text(pDX,IDC_EDIT_rg,m_rg);
    DDX_Text(pDX,IDC_EDIT_rp,m_rp);
    DDX_Text(pDX,IDC_EDIT_T,m_T);
    DDX_Text(pDX,IDC_EDIT_w,m_w);
    DDX_Text(pDX,IDC_EDIT_p,m_p);
    DDX_Text(pDX,IDC_EDIT_Sg,m_Sg);
    //}}AFX_DATA_MAP
}
BEGIN_MESSAGE_MAP(CMathCalDlg,CDialog)
    //{{AFX_MSG_MAP(CMathCalDlg)
    ON_WM_SYSCOMMAND()
    ON_WM_PAINT()
    ON_WM_QUERYDRAGICON()
    ON_BN_CLICKED(IDC_BUTTON_CALC,OnButtonCal)
    ON_BN_CLICKED(IDC_BUTTON_EXIT,OnButtonExit)
    //}}AFX_MSG_MAP
```

```
END — MESSAGE_MAPO
//CMathCalDlgmessagehandlers
BOOLCMathCalDlg::OnInitDialog()
{
    CDialog::OnInitDialog();
    //Add"About..."menu item to system menu.
    //IDM_ABOUTBOX must be in the system command range.

    ASSERT((IDM_ABOUTBOX&0xFFFO)==IDM_ABOUTBOX);
    ASSERT(IDM_ABOUTBOX<0xF000);
    CMenu*pSysMenu=GetSystemMenu(FALSE);
    if(pSysMenu!=NULL)
    {
        CStringstrAboutMenu;
        strAboutMenu.LoadString(IDS_ABOUTBOX);
        if(!strAboutMenu.IsEmpty())
        {
            pSysMenu->AppendMenu(MF_SEPARATOR);
            pSysMenu->AppendMenu(MF_STRING,IDM_ABOUTBOX,strAboutMenu);
        }
    }
    //Set the icon for this dialog. The frame work does this automatically
    //when the application's main window is not a dialog
    SetIcon(m_hIcon,TRUE); //Setbigicon
    SetIcon(m_hIcon,FALSE); //Setsmallicon
    //TODO:Add extra initialization here
    typedef int(WINAPI*SKINH_ATTACHEX)(LPCTSTRstrSkinFile,LPCTSTRstrPassword);
    SKINH_ATTACHEXpFunc=(SKINH_ATTACHEX)::GetProcAddress(::LoadLibrary("skinWSkinH.dll"
    O,"SkinH_AttachEx"));
    if(pFunc)
    {
        pFunc(_T(skin\royale.she'), NULL);
    }
    else
    {
        MessageBox(_T("The repository loading failed!"), _T("lack SkinH.dll") );
    }
    returnTRUE;//returnTRUEunlessyousetthefocustocontrol
}
voidCMathCalDlg::OnSysCommand(UINTnID,LPARAMIParam)
{
    if((nID&0xFFFO)==IDM_ABOUTBOX)
    {
        CAboutDlg dlgAbout;
        dlgAbout.DoModal();
    }
    else
    {
        CDialog::OnSysCommand(nID,IParam);
    }
}
//If you add a minimize button to your dialog, you will need the code below
//to draw the icon. For MFC applications using the document/view model,
//this is automatically done for you by the framework.
voidCMathCalDlg::OnPaint()
{
    if(IsIconic())
    {
```

```
CPaintDCdc(this);//device context for painting
SendMessage(ffM_ICONERASEBKGD, (WPARAM)dc.GetSafeHdc(),0);
//Center icon in client rectangle
intcxlcon=GetSystemMetrics(SM_CXICON);
intcylcon=GetSystemMetrics(SM_CYICON);
CRectrect;
GetClientRect(&rect);
intx=(rect.Width0-cxlcon+1)/2;
inty=(rect.Height0-cylcon+1)/2;
//Drawtheicon
dc.DrawIcon(x, y, m_hicon);
}
else
{
CDialog::OnPaint0;
}
}
//The system calls this to obtain the cursor to display while the user drags
//the minimized window.
HCURSORCMathCalDlg::OnQueryDragIcon()
{
return(HCURSOR)m_hIcon;
}
Void CMathCalDlg::OnButtonCal0
{
//TODO:Addyourcontrolnotificationhandlercodehere
UpdateData();
floatsum_ert=0;//surae"-rt
int i;
for(i=1;i<=m_T;++i)
{
sum_ert+=1.0/exp(m_r*i);
}
//CString msg;
//m_y
m_y=(m_Cc-m_c0-sum_ert*(2*m_gamma-m_rp)*(m_qT-m_qL)/
(sum_ert*(-m_rc*m_qH-(m_rp-m_rc)*m_qT+m_rp*m_qL));
//msg.Format("%f, %f, %f", (m_Cc-m_c0-sum_ert*(m_cp+2*m_gamma-m_rg-
m_rp)*(m_qT-m_qL)),
//sum_ert*(m_rg-m_rc)*ra_qH-(2*m_rg'fm_rp-m_rc-m_cp)*m_qT-(m_rg+rn_rp+in_cp)^qL),
//m_y);
//MessageBox(msg);
//m_x
m_x=(m_c2+m_w+m_Sg-m_c1)*(m_qL-m_qH)/(m_rc*m_qH+(m_rp-m_rc)*m_qT-m_rp*m_qL);
//m_pi_g_s
m_pi_g_s=m_y*sum_ert*((m-gamma-m-rc)*m_qH-(m_rp-m_rc)*m_qT+(m_rp-
m_gamma)*m_qL)+
sum_ert*(m_rp-m_gamma)*(m_qT-m_qL)-m_Cc;
//m_pi_g_ns
m_pi_g_ns=m_y*sum_ert*m_gamma*(m_qH-m_qL)-m_c0-sum_ert*m_gainma*(m_qT-ni_qL);
//m_u_g
m_u_g=m_x*m_pi_g_s+(1-m_x)*m_pi_g_ns;
//m_pi_m_h
m_pi_m_h=m_x*sum_ert*m_rc*(m_qH-m_qT)+sum_ert*((m_p-m_c2-m_w)+
(m_c2+m_w+m_Sg-m_c1)*m_qH);
```

```
//m_pi - m_l = m - x * sum_ert * m - rp 本(m - qL - m_qT) + sum - ert * ((m_p - m_c2 -  
m_w) * iD_Q + (m_c2 + m_w + m_Sg - m_cl) * m_qL);  
//m_ujn  
m_u_m = m_h + (1 - m_y) * m_j; i_m_l;  
CHARFORMAT cf;  
//edit control  
//initialize font and color  
ZeroMemory(&cf, sizeof(CHARFORMAT));  
cf.cbSize = sizeof(CHARFORMAT);  
cf.dwMask = CFM_BOLD | CFM_COLOR | CFM_FACE |  
CFM_ITALIC | CFM_SIZE | CFM_UNDERLINE;  
cf.dwEffects = 0;  
cf.crTextColor = RGB(20, 30, 120); //text color  
strcpy(cf.szFaceName, _T("Times New Roman")); //set font  
m_edit_res.SetDefaultCharFormat(cf);  
CString str;  
str.Format("pi_g_s: %f  
\\npi_g_ns: %f \\n u_g: %f \\n y: %f \\n pi_m_h: %f \\n pi_m_l: %f \\n u_m: %f \\n x: %f",  
m_pi_g_s, m_pi_g_ns, m_u_g, m_y, m_pi_m_h, m_u_m, m_x);  
m_edit_res.SetWindowText(str);  
}  
Void CMathCalDlg::OnButtonExit0  
{  
//TODO: Add your control notification handler code here  
SendMessage(WM_CLOSE, 0, 0);  
}
```

EFFECT OF SOIL PROPERTIES ON THE DIVERSITY AND DISTRIBUTION OF WEEDS IN CITRUS FARMS IN ARID REGION

AL-QAHTANI, S. M.

*Department of Biology, University College of Taymma, University of Tabuk
Tabuk 71491, Saudi Arabia*

(e-mail: salghtani@ut.edu.sa, salghtani18@gmail.com; phone: +96-654-545-7641)

(Received 14th Sep 2018; accepted 12th Nov 2018)

Abstract. The weed diversity and distribution in agroecosystems can be controlled by environmental variables. In this study, soil physical and chemical variables were investigated in three citrus farms located in the northern part of Saudi Arabia. A total of 12 soil physical and chemical variables were measured. Among the studied variables, only organic matter (OM), pH, phosphorus (P), calcium (Ca), bicarbonate (HCO_3) and sulphate (SO_4) were significantly different (one-way ANOVA at $P < 0.05$) among the three studied citrus farms. The regression model ($\text{Adj-R}^2 = 0.416$, $P=0.024$) showed that the organic matter (OM), calcium (Ca) and carbonate (CO_3) significantly affect the species richness of weeds. The multivariate model of CCA explained 68.64% of the variation of the taxonomic composition of weeds in citrus farms. It also revealed strong effect of soil texture (sand %), carbonate (CO_3), pH and sulphate (SO_4) on weed diversity and distribution. It was concluded that the soil physical and chemical properties are strong explanatory variables of the distribution of weeds in agroecosystems.

Keywords: *agroecosystem, ecology, weeds, environmental variables, Saudi Arabia*

Introduction

The problem of the weed invasion in the agroecosystems is considered as one of the most persistent problems threatening the agricultural productivity (Ramirez et al., 2018). The weeds are known as pests as they interfere with plant growth and potentially compete with the crops for light, water and nutrients (Chaudhary and Akram, 1987; Qasem and Hill, 1995; Storkey, 2006; Gomaa, 2012; Wang et al., 2013; Onen et al., 2018; Salehian et al., 2018). The invasion mechanisms of these weeds are still not fully understood. This is due to the complex interaction of weeds with the ecological and environmental settings in the agricultural ecosystem. However, many weed species exhibits remarkable adaptability to various environmental conditions (Onen et al., 2018; Salehian et al., 2018). Interestingly, there are evident reports that allelochemicals secreted by the weeds eventually influence crop germination, growth and survival (Shah and Khan, 2006; Jabeen and Ahmed, 2009; Onen et al., 2018). Therefore, economic loss in agricultural production due to invasion of weeds in agricultural landscape is evident (Aldrich, 1984; Akobundu et al., 1987; Swanton et al., 1993; Khedr and Hegazy, 1998; Fayed et al., 1999; Al-Qahtani, 2018).

It is acceptable fact that the diversity and abundance of weeds in agricultural ecosystems are strongly correlated to the environmental conditions of the soil (Derksen et al., 1994; Andersson and Milberg, 1998; Thomas and Frick, 1993; Fried et al., 2008; Pinke et al., 2010; Ramirez et al., 2018). Furthermore, the diversity of weeds is also associated with variation in the crop cultivation practices and seasonality (El-Demerdash et al., 1997; Andersson and Milberg, 1998; Andreasen and Skovgaard, 2009).

There is a high number of studies that addressed the interaction between plant diversity and the physical and chemical variables of the soil in different parts of the world including arid and semi-arid ecosystems particularly in Saudi Arabia (for instances see Al-Mutairi, 2017). However, most of these available studies focused on natural ecosystems and scarcely concentrated on agroecosystems. Several studies investigated the influence of soil's properties on diversity and distribution of plants such as Al-Mutairi (2017), Al-Masaudi et al. (2018) and Al-Robai et al. (2018). Despite the importance of weeds diversity and abundance in agricultural ecosystems, scarce number of studies were conducted in this context especially those tackled the influence of environmental conditions on the diversity of weeds (but see Al-Yemeny, 1999; Sher and Al-Yemeny, 2011). Most of the available studies aimed to describe the richness and abundance of weeds (see Gomaa, 2012, 2017). Similarly, Chaudhary et al. (1981) and Chaudhary and Akram (1987) provided a comprehensive study of weeds and their ecological and biological habitats in Saudi Arabia. In addition, similar studies were carried out at local scale. Shaltout and El-Halawany (1992) and El-Halawany and Shaltout (1993) studied the diversity patterns of weeds in the date palm farms of Al-Hassa Oasis in the eastern part of Saudi Arabia. Moreover, Al-Yemeny (1999), Sher and Al-Yemeny (2011) and Gazar (2011) described the diversity and taxonomic composition of weeds communities in dates palm orchards in the central part of Saudi Arabia.

The problem of weeds in citrus farms is threatening the production as it is associated with deterioration in fruits' quality and reduced productivity of the citrus trees. According to Al-Qahtani (2018), the common weed species reported in citrus farms in the northern part of Saudi Arabia are *Aizoon canariense*, *Artemisia seiberi*, *Morettia parviflora*, *Oxalis corniculata*, *Setaria viridis* and *Salsola imbricata*. In the same context, Gomaa (2017) reported that the common weed species in citrus farms are *Plantago lagopus*, *Cynodon dactylon*, *Imperata cylindrica* and *Convolvulus arvensis*. There are few common techniques to control weeds in citrus farms. However, these methods/techniques should be accompanied with proper ecological studies to better understand the biology and ecology of these invasive plant species (Al-Qahtani, 2018).

The information about the influence of soil's physical and chemical variables on diversity and distribution of weeds in citrus farms in arid region is incomplete. The study of Gomaa (2017) aimed to describe the species composition and diversity patterns of weeds in citrus farms without any significant efforts to address the possible effects of environmental variables. Therefore, the present study aims to investigate the influence of soil physical and chemical variables on diversity and distribution of weeds in citrus farms in Taymma (Saudi Arabia). This can be considered as pioneering effort to address the possible effect of environmental variables on diversity and distribution of weeds in agroecosystem of arid region (Saudi Arabia).

Materials and methods

Study site

Saudi Arabia has a large area of approximately 2 million km² and that constitutes a nearly 65% of the total area of the Arabian Peninsula. Terrestrial ecosystems are the predominant habitats which mainly consist of desert. The arid climate characterized with low annual precipitation (0-200 mm/year) and fluctuation in temperature regimes in different seasons (Al-Nafie, 2008; El-Sheikh et al., 2013).

The study was conducted in three citrus farms located in Taymma of Tabuk region (Fig. 1). The climate of this region is arid and the temperature ranges from 0 °C in the winter to almost 50 °C during summer. The average annual precipitation is very low which can be less than 150 mm/year. Three citrus farms were selected based on possible accessibility (coordinates 27°34'37.5"N 38°33'48.4"E, 27°32'58.4"N 38°33'59.6"E, 27°34'59.4"N 38°33'33.5"E). The agricultural practices and manures are conventional and no special techniques/methods are applied by farmers. During the cultivation, few pesticides are applied to control mites as well as other insects (e.g. systemic pesticides). Prior permission to carry out the study in those farms was obtained from the owners. The three selected farms (sites) named; Site A, Site B and Site C experience similar regimes and agricultural practices. According to the statements from the farms owners, there was no control/management effort of these weeds in the studied sites.

Surveying the weeds communities

The weeds species were surveyed in the studied sites during the spring of 2018. At each citrus farm, weed species were observed and recorded using the commonly used techniques of 10 × 10 m stands in five randomly selected sites. The species data was recorded as presence/absence data. The specific taxonomical keys of Chaudhary et al. (1981), Chaudhary (2001) and Collenette (1999) which are the main keys of plant species in Saudi Arabia were used to identify the reported weed species.

Soil physical and chemical properties

The physical and chemical variables of the soil in the selected sites were measured. In each site, five soil samples were collected at depth from 0 to 30 cm randomly in March-May 2018. The collected samples were transferred into polyethylene bags and then labelled appropriately. Thereafter, the samples were transferred immediately to the laboratory. Then, extracts of the soil samples were prepared with distilled water at ratio of 1 to 5 following the procedures described previously in Al-Mutairi (2017). The percent of sand (%), conductivity (EC) and pH were measured accordingly. In addition, the soil samples were analyzed for phosphorus (P), Organic Matter (OM), Potassium (K), Sodium (Na), Calcium (Ca), Carbonate (CO₃), Bicarbonate (HCO₃), Sulphate (SO₄) and Chloride (Cl) following the standard methods and techniques as described earlier by Jacson (1965) and Allen et al. (1986).

Statistical analysis

All the statistical analyses were conducted using R program (version 12.4.1). The soil physical and chemical variables were analyzed descriptively for mean and standard error (SE). The one-way ANOVA was used to compare means of soil properties among the studied sites at $P < 0.05$. The function *lm* included in *vegan* package was used to determine the effects of soil variables on species richness. The adjusted regression coefficient (Adj-R²) and significance level (P value) of the regression model were calculated. However, the multivariate analysis of Canonical Correspondence Analysis (CCA) was applied to examine the relationship between species distribution and the soil physical and chemical variables using the function *cca* in *vegan* package. The amount of species variation explained by the soil variables was calculated and expressed as the total variation explained (TVE) is defined as the sum of all eigenvalues divided by the total inertia (Ohmann and Spies, 1998).



Figure 1. Map showing the location of Taymma (Tabuk region), Saudi Arabia. Geographical coordinates of the three selected farms are 27°34'37.5"N 38°33'48.4"E, 27°32'58.4"N 38°33'59.6"E and 27°34'59.4"N 38°33'33.5"E

Results

The studied physical and chemical variables of the soil in the three citrus farms showed remarkable variability. The mean values of the studied soil physical and chemical variables are shown in *Table 1*. The organic matter (OM), pH, phosphorus (P), calcium (Ca), bicarbonate (HCO₃) and sulphate (SO₄) were significantly different (one-way ANOVA at P < 0.05) among the three studied farms.

Table 1. Soil physical and chemical variables (mean ± SE) in citrus farms of Taymma (Tabuk, Saudi Arabia). The one-way ANOVA results show the mean comparison of the soil variables among the three studied sites. The significant values at P < 0.05 are indicated with asterisk

Variable	Site A	Site B	Site C	ANOVA F _{2,14}
Geographical coordinates	27°34'37.5"N 38°33'48.4"E	27°32'58.4"N 38°33'59.6"E	27°34'59.4"N 38°33'33.5"E	-
Organic Matter (OM) (%)	0.480±0.515	2.756±2.203	3.064±1.456	4.127*
Electronic conductivity (EC) (ms/cm)	1288.400±234.884	1387.800±70.645	1370.800±272.343	0.316
pH	7.32±0.279	7.386±0.245	7.904±0.188	6.034*
Potassium (K) (mg/l)	0.570±0.143	0.480±0.087	0.348±0.173	3.223
Sodium (Na) (mg/l)	1.872±0.383	2.158±0.417	2.012±0.131	0.908
Phosphorus (P) (mg/l)	13.600±1.817	22.400±6.656	10.200±2.280	11.261*
Calcium (Ca) (mg/l)	0.115±0.017	0.160±0.051	0.106±0.044	3.641*
Carbonate (CO ₃) (mg/l)	0.094±0.101	0.082±0.056	0.012±0.027	2.095
Bicarbonate (HCO ₃) (mg/l)	2.240±0.225	1.898±0.159	1.340±0.209	25.783*
Sulphate (SO ₄) (mg/l)	7.574±0.864	3.594±0.562	5.880±0.885	32.428*
Chloride (Cl) (mg/l)	0.346±0.280	0.174±0.082	0.140±0.131	1.786
Sand (%)	83.154±1.385	81.886±4.286	77.528±6.956	1.902

In this study, a total of 36 weed species belong to 20 families were reported from three citrus farms in Taymma (Tabuk, Saudi Arabia; see *Appendix*). The linear regression model was applied to investigate the relationship between species richness (total number of species) and the soil physical and chemical variables. The regression model was significant and the adjusted regression coefficient ($\text{Adj-R}^2 = 0.416$, $F_{2,12} = 7.32$ and $P = 0.024$). Organic matter (OM), calcium (Ca) and carbonate (CO_3) were the most important variables that showed significant relationship with weeds species richness.

The multivariate analysis of canonical correspondence analysis (CCA) was employed to determine the relationship between soil variables and distribution of weeds in citrus farms. *Figure 2* exhibited the triplot of CCA. The total inertia of the CCA model was 3.077 and the sum of canonical eigenvalues was 2.112. The amount of variation explained by the canonical eigenvalues can be calculated as the “total variance explained (TVE)”. Here, the TVE was 68.64%. This implies moderately, yet strong relationship between variation in the soil variables and distribution of weeds in citrus agroecosystem.

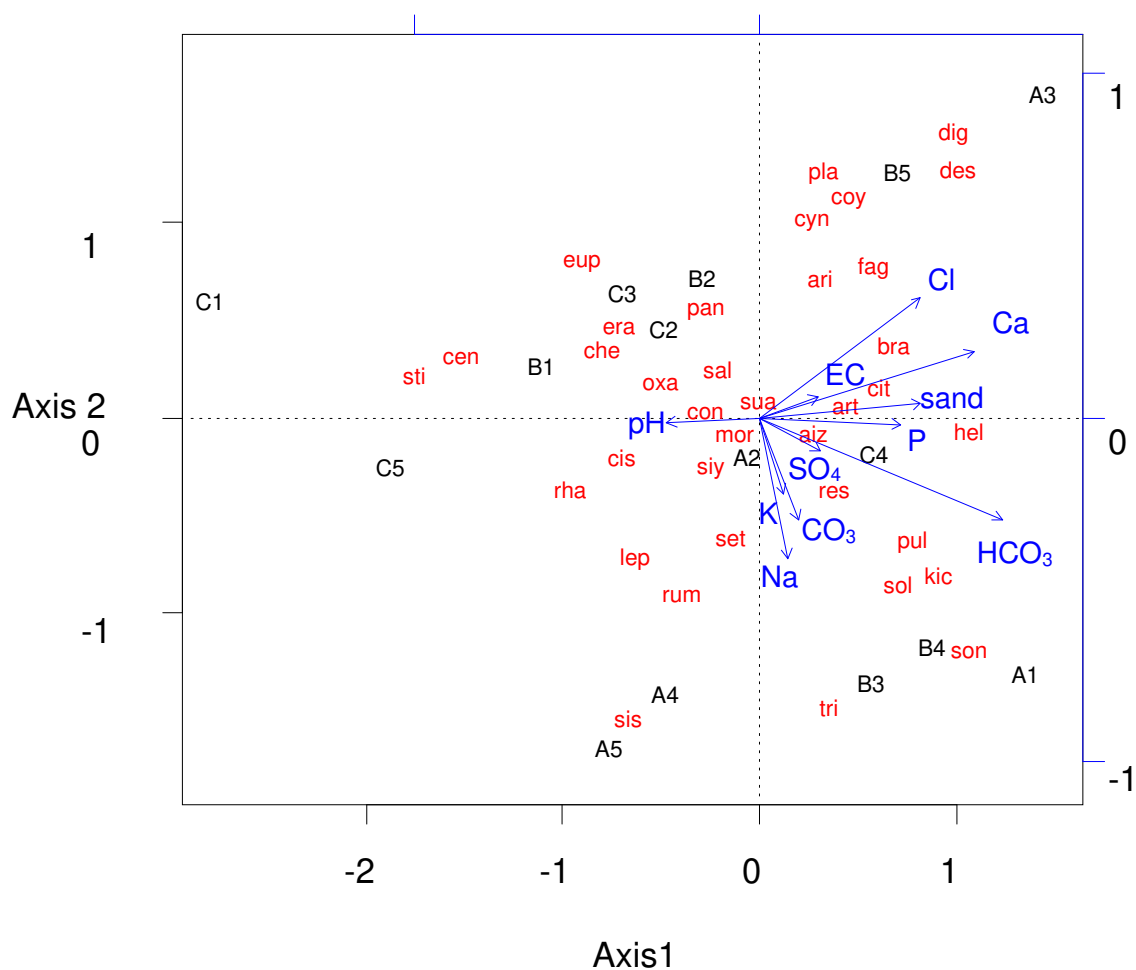


Figure 2. Triplot of Canonical Correspondence Analysis (CCA) showing the correlation between soil physical and chemical variables and distribution of weeds in citrus farm of Taymma (Tabuk, Saudi Arabia). The first three letters of genus names are provided in the figure (see *Appendix* for full names). The organic matter (OM) was removed from the CCA plot as the eigenvalue was less than 0.1

Discussion

There is a relatively high diversity of weed species in citrus farms in this study as a total of 36 species were recorded. The total number of weeds species reported in this study was lesser than what have been reported in similar studies but different agroecosystems such as dates palm and olive orchards of al-Jouf (71 species, Gomaa, 2012), dates palm of Al-hassa (118 species, El-Halawany and Shaltout, 1993) and central part of Saudi Arabia (55 species, Gazer, 2011). However, this was higher compared to the study of Gomaa (2017) who reported 33 weed species in citrus farms in the northern part of Saudi Arabia.

The soil physical and environmental variables showed remarkable variability among the studied farms. The variables of organic matter, pH, phosphorus, carbonate, bicarbonate and sulphate were significantly different among the studied sites. This is in agreement with the study of Al-Mutairi (2017) who reported that organic matter, soil pH and calcium were significantly different among four studied sites in Tabuk region. This possible variation may be due to differences in the soil contents, and texture. The microhabitat of plants in agroecosystems is also affected by other possible factors such as the microflora in the soil especially microbial communities (Zak et al., 2003). Furthermore, the application of different fertilizers would surely result in significant variation in the organic matter contents.

However, Fried et al. (2008) found that the soil pH and soil texture are the most important factors structuring the weed communities in temperate region (France). On the other hand, some studies highlighted the agricultural practices are the main driver for diversity and abundance of weeds in agroecosystems (Rauber et al., 2018).

The species richness of weeds in citrus farms showed to be affected mainly by organic matter (OM), calcium (Ca) and carbonate (CO₃) of the soil as indicated by the adjusted regression coefficient of the linear regression model (Adj-R² = 0.416). Despite, a total of 12 environmental variables were included in the analysis, only the above three variables were significant in the regression model. The possible justification is that the environmental variables are not the only factors controlling the weeds communities in citrus farms as reported on other agroecosystems (see Rauber et al., 2018). Other biotic interaction may contribute in structuring the weeds communities in agroecosystems. These assumptions are supported by the fact that approximately 20-60% of variation in plant communities can be merely explained by environmental variables. The remaining unexplained variation can be related to other spatial and biological factors (Galal and Fahmy, 2012).

The multivariate analysis of canonical correspondence analysis is a reliable technique to reveal the complex relationship between species and environmental variables. In this study, the total variance explained (TVE) percentage was implied that the selected variables had the strength to explain the variation in the weed taxonomic composition in citrus farms (TVE = 68.64%). This amount of TVE is comparable with what have been reported in arid region (e.g Al-Mutairi, 2017). Soil texture (i.e. sand %), carbonate, bicarbonate, pH and sulphate should to be strong drivers controlling the structure of weed communities in citrus farms of Taymma. In general, this is in agreement with previous reports from arid and semi-arid ecosystems (Shaltout and El-Sheikh, 1993; Shaltout et al., 1994; Al-Sodany, 1998; Al-Mutairi, 2017).

Conclusion

To conclude, the present study revealed that soil physical and chemical variables evidently affect the diversity and distribution of weeds in citrus farms in arid region at the northern part of Saudi Arabia. The species richness of weeds in citrus farms was significantly influenced by organic matter, calcium and carbonate contents in the soil. The CCA model showed strong effect of soil texture, carbonate, bicarbonate, pH and sulphate variables on distribution of weeds in agroecosystem. This reflects variation in the preference of weed species towards different environmental variables. It is suggested that further studies should be carried out in this region to better understanding of the invasion mechanisms of weeds in agricultural landscape. This certainly will improve the future management practices of weeds and minimize the agricultural production loss due to manifestation of weeds.

Acknowledgements. I would like to express my sincere gratitude to the farms' owners for facilitating the data collection. This study was supported by the Research Grant (S-1439-0043) provided by The Deanship of Scientific Research, University of Tabuk.

REFERENCES

- [1] Akobundu, I. O., Moreno, R., Pineda, L., Bustamante, M., Maldonado, A., Pareja, M., Martínez, O., Pareja, M., Fión, L., Pareja, M. (1987): *Weed Science in the Tropics: Principles and Practices*. – Asociación Guatemalteca de Manejo Integrado de Plagas, Guatemala (Guatemala).
- [2] Aldrich, R. J. (1984): *Weed-crop ecology: principles in weed management*. – Breton Publishers, N. Scituate, MA.
- [3] Al-Masaudi, A. A., Al-Zahrani, H., Al Toukhy, A., Alsamadany, H. (2018): Plant species distribution and their relation to soil properties in Wadi Elip South Western area in Saudi Arabia. – *Advances in Environmental Biology* 12: 5-9.
- [4] Al-Mutairi, K. A. (2017): Influence of soil physical and chemical variables on species composition and richness of plants in the arid region of Tabuk, Saudi Arabia. – *Ekológia (Bratislava)* 36: 112-120.
- [5] Al-Qahtani, S. M. (2018): Diversity of weeds species in citrus farms of Taymma (Tabuk, Saudi Arabia): Implication for invasive species ecology. – *Bioscience, Biotechnology Research Asia* 15(3): 619-625.
- [6] Al-Robai, S. A., Mohamed, H. A., Ahmed, A. A., Al-Khulaidi, A. W. A. (2018): Effects of elevation gradients and soil components on the vegetation density and species diversity of Alabna escarpment, southwestern Saudi Arabia. – *Acta Ecologica Sinica*. DOI: 10.1016/j.chnaes.2018.09.008.
- [7] Al-Sodany, Y. M. (1998): *Vegetation analysis of canals, drains and lakes of northern part of Nile Delta Region*. – Ph.D. Thesis, Faculty of Science, Tanta University, Egypt.
- [8] Al-Yemeny, M. N. (1999): A check list of weeds in Al-kharj area of Saudi Arabia. – *Pakistan Journal of Biology*, 2: 7-13.
- [9] Allen, S. (1986): *Chemical Analysis*. – Blackwell Scientific Publications, Oxford.
- [10] AlNafie, A. H. (2008): *Phytogeography of Saudi Arabia*. – *Saudi Journal of Biological Science* 15(1): 159-176.
- [11] Andersson, T. N., Milberg, P. (1998): Weed flora and the relative importance of site, crop, crop rotation, and nitrogen. – *Weed Science* 46(1): 30-38.
- [12] Andreasen, C. Skovgaard, I. M. (2009): Crop and soil factors of importance for the distribution of plant species on arable fields in Denmark. – *Agriculture, Ecosystems & Environment* 133: 61-67.

- [13] Chaudhary, S. A. (2001): Flora of the Kingdom of Saudi Arabia. – Ministry of Agriculture and Water, Riyadh.
- [14] Chaudhary, S. A., Akram, M. (1987): Weeds of Saudi Arabia and the Arabian Peninsula. – Regional Agriculture and Water Research Centre, Ministry of Agriculture and Water, Riyadh, Saudi Arabia.
- [15] Chaudhary, S., Parker, C. Kasasian, L. (1981): Weeds of central, southern and eastern Arabian Peninsula. – International Journal of Pest Management 27: 181-190.
- [16] Collentette, S. (1999): Wild Flowers of Saudi Arabia. – National Commission for Wildlife Conservation and Development, Riyadh.
- [17] Derksen, D. A., Thomas, A. G., Lafond, G. P., Loepky, H. A., Swanton, C. J. (1994): Impact of agronomic practices on weed communities: fallow within tillage systems. – Weed Science 41(3): 184-194.
- [18] El-Demerdash, M., Hosni, H., Al-Ashri, N. (1997): Distribution of the weed communities in the North East Nile Delta, Egypt. – Feddes Repertorium 108: 219-232.
- [19] El-Halawany, E., Shaltout, K. (1992): Weed flora of date palm orchards in Eastern Saudi Arabia. – Journal of King Saud University 5: 25-37.
- [20] El-Sheikh, M. A., Thomas, J., Alatar, A. A., Hegazy, A. K., Abbady, G. A., Alfarhan, A. H., Okla, M. I. (2013): Vegetation of Thumamah Nature Park: a managed arid land site in Saudi Arabia. – Rendiconti Lincei 24(4): 349-367.
- [21] Fayed, M., El-Geddawi, I., El-Zeni, M. (1999): Influence of weed interference on growth, yield and quality of sugar beet. – Egyptian Journal of Agricultural Research (Egypt) 77(3): 1251-1263.
- [22] Fried, G., Norton, L. R., Reboud, X. (2008): Environmental and management factors determining weed species composition and diversity in France. – Agriculture, Ecosystems & Environment 128: 68-76.
- [23] Galal, T. M., Fahmy, A. G. (2012): Plant diversity and community structure of Wadi Gimal protected area, Red Sea Coast of Egypt. – African Journal of Ecology 50(3): 266-276.
- [24] Gazer, M. (2011): Vegetation composition and floristical diversity in date palm orchards of Central Saudi Arabia. – Acta Botanica Hungarica 53: 111-126.
- [25] Gomaa, N. H. (2017): Floristic Composition of Weed Vegetation in Citrus Orchards in Aljouf Region, Kingdom of Saudi Arabia. – Journal of Bio-Molecular Sciences 5(1): 15-23.
- [26] Gomaa, N. H. (2012): Composition and diversity of weed communities in Al-Jouf province, northern Saudi Arabia. – Saudi Journal of Biological Sciences 19: 369-376.
- [27] Jabeen, N., Ahmed, M. (2009): Possible allelopathic effects of three different weeds on germination and growth of maize (*Zea mays*) cultivars. – Pakistan Journal of Botany 41: 1677-1683.
- [28] Jacson, M. (1965): Soil Chemical Analysis. – Constable Ltd Co, London.
- [29] Khedr, A. H. A., Hegazy, A. K. (1998): Ecology of the rampant weed *Nymphaea lotus* L. Willdenow in natural and ricefield habitats of the Nile delta, Egypt. – Hydrobiologia 386: 119-129.
- [30] Ohmann, J. L., Spies, T. A. (1998): Regional gradient analysis and spatial pattern of woody plant communities of Oregon forests. – Ecological Monographs 68(2): 151-182.
- [31] Onen, H., Akdeniz, M., Farooq, S., Hussain, M., Ozaşlan, C. (2018): Weed flora of citrus orchards and factors affecting its distribution in western Mediterranean region of Turkey. – Planta Daninha 36: e018172126.
- [32] Pinke, G., Pál, R., Botta-Dukát, Z. (2010): Effects of environmental factors on weed species composition of cereal and stubble fields in western Hungary. – Central European Journal of Biology 5: 283-292.
- [33] Qasem, J., Hill, T. (1995): Growth, development and nutrient accumulation in *Senecio vulgaris* L. and *Chenopodium album* L. – Weed Research 35: 187-196.

- [34] Ramirez, A. H. M., Futch, S. H., Jhala, A. J., Abit, M. J. M., Megh, S. (2018): Weed management practices and herbicide resistance in weeds in Florida citrus. – Philippine Journal of Crop Science 43: 1-8.
- [35] Rauber, R. B., Demaría, M. R., Jobbágy, E. G., Arroyo, D. N., Poggio, S. L. (2018): Weed communities in semiarid rainfed croplands of Central Argentina: comparison between corn (*Zea mays*) and soybean (*Glycine max*) crops. – Weed Science 66: 368-378.
- [36] Salehian, H., Mohammadzadeh, M. (2018): Weed ecology is affected by succession in differently aged gardens of *Citrus sinensis* and *C. reticulata*. – Rendiconti Lincei. Scienze Fisiche e Naturali 29: 35-41.
- [37] Shah, G., Khan, M. (2006): Checklist of noxious weeds of District Mansehra, Pakistan. – Pakistan Journal of Weed Science Research 12: 213-219.
- [38] Shaltout, K. H., El Halawany, E. (1992): Weed communities of date palm in Eastern Arabia. – Qatar University Science Journal 12: 105-11.
- [39] Shaltout, K., El-Din, A. S., El-Sheikh, M. (1994): Species richness and phenology of vegetation along irrigation canals and drains in the Nile Delta, Egypt. – Vegetatio 112(1): 35-43.
- [40] Sher, H., Al-Yemeny, M. N. (2011): Ecological investigation of the weed flora in arable and non arable lands of Al-kharj Area, Saudi Arabia. – African Journal of Agricultural Research 6: 901-906.
- [41] Storkey, J. (2006): A functional group approach to the management of UK arable weeds to support biological diversity. – Weed Research 46: 513-522.
- [42] Swanton, C., Harker, K., Anderson, R. (1993): Crop losses due to weeds in Canada. – Weed Technology 7(2): 537-542.
- [43] Thomas, A. G., Frick, B. L. (1993): Influence of tillage systems on weed abundance in southwestern Ontario. – Weed Technology 7(3): 699-705.
- [44] Wang, Y., Yang, X., Shi, Z. (2013): The formation of the patterns of desert shrub communities on the Western Ordos Plateau, China: the roles of seed dispersal and sand burial. – PloS one 8(7): e69970.
- [45] Zak, D. R., Holmes, W. E., White, D. C., Peacock, A. D., Tilman, D. (2003): Plant diversity, soil microbial communities, and ecosystem function: are there any links? – Ecology 84(8): 2042-2050.

APPENDIX

List of recorded weeds species from Tabuk, Saudi Arabia by Saelm M. Al-Qahtani

Latin name	Family	Life Form	Chorotype
<i>Aizoon canariense</i>	Aizoaceae	Herb	Somalia-Masai
<i>Aristida adscensionis</i>	Poaceae	Perennial grass	Saharo-Arabian
<i>Artemisia seiberi</i>	Asteraceae	Subshrub	Irano-Turanian
<i>Brassica tournefortii</i>	Brassicaceae	Herb	Mediterranean-Saharo-Arabian
<i>Cenchrus ciliaris</i>	Gramineae	Perennial grass	Tropical African
<i>Chenopodium murale</i>	Chenopodiaceae	Herb	Paleotropic
<i>Citrullus colocynthis</i>	Cucurbitaceae	Herb	Saharo-Arabian
<i>Citrus sinensis</i>	Rutaceae	Shrub	Chinese
<i>Convolvulus arvensis</i>	Convolvulaceae	Subshrub	Tropical
<i>Conyza bonariensis</i>	Asteraceae	Herb	American
<i>Cynodon dactylon</i>	Poaceae	Perennial grass	Tropical
<i>Desmostachya bipinnata</i>	Poaceae	Perennial grass	Saharo Arabian-Somalia Masai
<i>Digera muricata</i>	Amaranthaceae	Herb	Paleotropic
<i>Eragrostis barrelieri</i>	Poaceae	Perennial grass	Mediterranean-Saharo Arabian

<i>Euphorbia peplis</i>	Euphorbiaceae	Herb	Mediterranean-Euro Siberian-Irano-Turanian
<i>Fagonia bruguieri</i>	Zygophyllaceae	Subshrub	Saharo Arabian
<i>Heliotropium bacciferum</i>	Boraginaceae	Subshrub	Saharo Arabian-Somalia Masai
<i>Kickxia aegyptiaca</i>	Scrophulariaceae	Subshrub	Saharo Arabian
<i>Lepidium africanum</i>	Brassicaceae	Herb	Tropical African
<i>Morettia parviflora</i>	Brassicaceae	Subshrub	Samalia Masai
<i>Oxalis corniculata</i>	Oxalidaceae	Subshrub	Tropical
<i>Panicum coloratum</i>	Poaceae	Perennial grass	American
<i>Plantago lanceolata</i>	Plantaginaceae	Herb	Mediterranean-Euro Siberian-Irano-Turanian
<i>Pulicaria undulata</i>	Asteraceae	Subshrub	Saharo Arabian-Somalia Masai
<i>Reseda muricata</i>	Resedaceae	Herb	Saharo Arabian
<i>Rhanterium epapposum</i>	Asteraceae	Subshrub	Saharo Arabian
<i>Rumex dentatus</i>	Polygonaceae	Subshrub	Mediterranean-Euro Siberian-Irano-Turanian
<i>Salsola imbricata</i>	Chenopodiaceae	Subshrub	Saharo Arabian
<i>Setaria viridis</i>	Poaceae	Annual grass	Mediterranean-Euro Siberian-Irano-Turanian
<i>Sisymbrium erysimoides</i>	Brassicaceae	Herb	Saharo Arabian-Mediterranean
<i>Sisymbrium irio</i>	Brassicaceae	Herb	Mediterranean-Euro Siberian-Irano-Turanian
<i>Solanum nigrum</i>	Solanaceae	Herb	Mediterranean-Saharo Arabian
<i>Sonchus oleraceus</i>	Asteraceae	Herb	Mediterranean-Euro Siberian-Irano-Turanian
<i>Stipagrostis plumosa</i>	Poaceae	Perennial grass	Saharo Arabian-Irano Turanian
<i>Suaeda vermiculata</i>	Chenopodiaceae	Subshrub	Saharo Arabian
<i>Trigonella anguina</i>	Leguminosae	Herb	Saharo Arabian

REMEDICATION OF ARSENIC CONTAMINATED WATER BY A NOVEL CARBOXYMETHYL CELLULOSE BENTONITE ADSORBENT

MILJKOVIC, M. V.^{1*} – MOMCILOVIC, M.² – STANKOVIC, M.³ – CIRKOVIC, B.⁴ – LAKETIC, D.⁵ –
NIKOLIC, G.⁶ – VUJOVIC, M.¹

¹*Department of Pharmacy, Faculty of Medicine, University of Niš
Bulevar dr Zorana Đinđića 81, 18000 Niš, Serbia
(phone: +381-18-422-6644)*

²*“Vinča” Institute of Nuclear Sciences, University of Belgrade
P. O. Box 522, 11001 Belgrade, Serbia
(phone: +381-11-340-8101)*

³*Department of Chemistry, Faculty of Science and Mathematics, University of Niš
Višegradska 33, 18000 Niš, Serbia
(phone: +381-18-223-430)*

⁴*Faculty of Agriculture, University of Priština
Kopaonička St. bb, 38219 Kosovska Mitrovica – Lesak, Serbia
(phone: +381-28-88-261)*

⁵*Faculty of Sport and Physical Education, University of Priština
Dositja Obradovića bb, 38218 Leposavić, Serbia
(phone: +381-28-84-701)*

⁶*Faculty of Technology, University of Niš, Bulevar Oslobođenja 124, 16000 Leskovac, Serbia
(phone: +381-16-247-203)*

**Corresponding author*

e-mail: vojkanmm_serbia@yahoo.com; phone: +381-64-308-0893

(Received 28th Aug 2018; accepted 22nd Nov 2018)

Abstract. Suitability of bentonite clay modified with sodium carboxymethyl cellulose (Na-CMC) for the removal of arsenic(III) ions from aqueous solution was tested in batch adsorption studies and complemented by theoretical modeling with Langmuir, Freundlich and Temkin isotherm models. The effects of various factors, such as the initial adsorbate concentrations, pH, and temperature of the solutions were investigated in series of experiments. FTIR analysis was used to detect functional groups typical for cellulose and bentonite. Scanning electron microscope was used to analyze the surface morphology of the composites. It was established that the removal process was fast in the beginning and adsorption equilibrium was attained in around 20 minutes with good fittings to both Langmuir and Freundlich model. Maximum adsorption capacity (Q_{max}) obtained from experiments was 9.4 mg/g. No influence of solution pH and temperature on the sorption was noticed. The series of conducted experiments showed that synthesized composites are suitable for the removal of arsenic from wastewaters by adsorption as efficient and low-cost technique.

Keywords: *pollution, waste waters, composite, isotherm model, sorption capacity*

Introduction and literature review

Water contamination by arsenic salts is regarded as a critical issue in growing environmental pollution due to arsenic's toxicity, its abundance and difficulties to

remove it from contaminated sources. For several decades, arsenic is the contaminant of priority interest by the European Union (Council of the European Communities, 1976) and by the Environmental Protection Agency of the United States (EPA) (Environmental Protection Agency, 1982). Arsenic gets at water bodies from natural deposits, smelters, glass industry, electronic waste, mining, combustion of fossil fuels, orchards where arsenical pesticides were used, disposal of chemical wastes, etc. (Mar et al., 2013; Pandey, 2017). It causes serious diseases, such as cancer, neurological disorder, nausea, hyperkeratosis, muscular weakness, and others (Pandey, 2017). US EPA has established a maximum contaminant level (MCL) for arsenic of 0.010 mg/l in drinking water (U.S. Environmental Agency, 2018).

There are many methods for arsenic removal from water sources, such as chemical precipitation, coagulation and flocculation, ion exchange, adsorption, electro deposition, advanced oxidation, membrane filtration, etc. Adsorption seems to be one of the best techniques for this purpose since it is known for its high-removal efficiency, profitability, simplicity, easier and sludge-free operations, and the possibility to recycle (Mar et al., 2013). Numerous materials have been used as adsorbents, such as activated carbon, fly ash, clays, muds, various oxides, polymeric resins, biomaterials, composites, etc. In the last three years, many novel adsorbents have been reported for efficient arsenic removal including zeolitic imidazolate framework-8 (ZIF-8) (Liua et al., 2018), graphene oxide@iron aluminium oxide composite (Majia et al., 2018), α -FeOOH decorated graphene oxide-carbon nanotubes aerogel (Fu et al., 2017), magnetite sub-microparticles (Mejia-Sentillan et al., 2018), cerium loaded cellulose nanocomposite (Santra and Sarkar, 2016), iron oxyhydroxide on the root powder (Lin et al., 2018), etc. There is a pronounced tendency that adsorbents should be more economic. For these reasons, the most desired adsorbents originate from the various by-products and low-cost raw materials locally available in huge amounts.

Sodium carboxymethyl cellulose (Na-CMC) is a white granular powder that is colorless, odorless, non-toxic and water soluble. It is used as thickening agent, emulsion stabilizer, or suspending agent in the food industry but it is also often found in water-based paints, detergents, and paper products. As a typical polymeric derivative of cellulose, it contains carboxylate anion and hydroxyl functional groups (Yan et al., 2014) which are responsible for good complexation ability for some metal ions, such as Cu^{2+} , Cd^{2+} , Co^{2+} , Zn^{2+} , Ni^{2+} and Pb^{2+} (Petrox et al., 2002). Up to our best knowledge, there are no reported studies about arsenic removal by carboxymethyl cellulose.

Herein, we present study based on the removal of As^{3+} ions from aqueous model solutions by acid activated bentonite clay impregnated with Na-CMC as an adsorbent in the batch system. Sorptive features of powdered adsorbent were estimated by analyzing the impact of varying complex experimental conditions and employing theoretical modeling of adsorption. The goal of the work was to elucidate the mechanism of As removal and correlation between structural, functional and sorptive properties of Na-CMC-bentonite composite.

Material and methods

Preparation of Na-CMC-bentonite composite (adsorbent)

Three bentonite clay based adsorbents containing 1, 3, and 5% of Na-CMC were synthesized in our laboratory at Department of Chemistry, Faculty of Science and Mathematics, University of Niš, Serbia. Na-CMC was purchased from Weifang Lude

Chemical Co., Shandong, China. Bentonite was used in experiments as an adsorbent in native form (natural clay, purchased from “Riznica Prirode”, Serbia). 15 grams of bentonite clay was suspended in 300 ml of deionized water and mixed with 0.15 (1%), 0.45 (3%) or 0.75 (5%) g of Na-CMC in order to achieve desired weight ratio. Suspensions were agitated on a magnetic stirrer at 90 °C for 2 h. During stirring, 5 ml of concentrated HCl was added in drops. Prior to adding acid, pH of the suspension was 9.2 while after adding pH dropped down to 1.35. Probes were left to cure overnight and then filtered by vacuum with constant rinsing by using deionized water. Rinsing was carried out until negative reaction for chlorides. Modified clay was dried overnight at 110 °C, crushed and used in experiments. Composites were designated as: GI (1% Na-CMC), GII (3% Na-CMC), and GIII (5% Na-CMC).

Characterization of adsorbent

FTIR spectrometer BOMEM MB-100 (Hartmann & Braun, Canada) with detector DTGS/KBr was used for recording FTIR spectra in a spectral range from 4000 to 400 cm^{-1} with the resolution of 4 cm^{-1} . Morphology of the samples was analyzed by the scanning electron microscope JSM-5300 (Jeol, Japan). For SEM analysis, composite samples were prepared by using instrument JFC-1100E ION SPUTTER for sputtering gold particles for better conductivity. Samples were recorded at magnifications of 1000, 2000, and 5000 times. For EDS analysis which revealed the presence of chemical elements, detector Linx Analytical QX 2000b was used on the same microscope.

Adsorption experiments

Adsorption experiments were carried out in a batch system by contacting mass of 1 g of adsorbent and arsenic solutions of concentrations from 10 to 200 mg/l for 20 minutes. Suspensions were agitated by magnetic stirrer at defined temperature and filtered through quantitative filter paper. The residual concentrations of arsenic in solutions were determined by ICP-OES spectrometer iCAP 6000 (Thermo Fisher Scientific). In order to investigate the influence of experimental conditions on the removal process, initial arsenic concentration, temperature and pH value were considered. Adsorption capacity, Q (mg/g) was determined by the *Equation 1*:

$$Q = \frac{(C_0 - C)V}{m} \quad (\text{Eq.1})$$

where C_0 is the initial concentration of arsenic ions, V is the volume of the solution, m is the mass of bentonite composite and C is the residual concentration of arsenic ions at the equilibrium. Previously it was established that contacting time of 20 min was enough to reach equilibrium of the process.

Effect of solution pH was investigated at values 1, 3, 5, 7 and 9 by stirring 100 mg/l arsenic solution with 1 g of the adsorbent for 20 minutes. After this time, suspensions were filtered and analyzed for remaining arsenic. In order to examine the impact of different temperatures on the sorption process, the same procedure was followed at 20, 30, 40, 50, and 60 °C.

For all analyses, the stock solution of arsenic (1 g/l) was prepared by a diluting proper amount of arsenic (III) nitrate in deionized water.

According to manufacturers specification, bentonite clay has the chemical composition presented in *Table 1*. Along with dominant ratios of silicon and aluminum

oxides, oxides of potassium, iron, titanium and calcium are also present. These “heteroatoms” are responsible for numerous structural deformations in the clay structure, especially those related to forming non-stoichiometric moiety filled with vacancies and charges compensated with suitable ions. Such defects are prone to electrostatic interactions with grafting or doping agents, and among the rest for forming thin films with proper modifiers. In this case, carboxymethyl cellulose is used for this purpose and with the goal to introduce reactive hydroxyl groups which are proven to be responsible for complexation with some metals.

Table 1. Chemical composition of bentonite

Oxide	SiO ₂	Al ₂ O ₃	K ₂ O	Fe ₂ O ₃	TiO ₂	MgO	CaO
Mass ratio (%)	67.81	24.73	3.25	1.89	1.06	0.93	0.33

Three theoretical isotherm models were used to analyze the sorption data. Each model is briefly described below. Langmuir isotherm is usually used to describe monolayer adsorption where all reactive sites on the sorbent’s surface are energetically homogenous. Here no lateral interaction and steric hindrance between the adsorbed molecules is assumed. This model is in its linearized form represented by *Equation 2*:

$$\frac{c_e}{q_e} = \frac{1}{q_{\max} K_L} + \frac{1}{q_{\max}} c_e \quad (\text{Eq.2})$$

where K_L is Langmuir equilibrium constant (l/mg), and Q_{\max} (mg/g) is maximum adsorption capacity. The useful feature of Langmuir isotherm is separation factor, R_L defined by *Equation 3*:

$$R_L = \frac{1}{1 + K_L c_0} \quad (\text{Eq.3})$$

The value of the R_L defines the types of isotherms as unfavorable ($R_L > 1$), linear ($R_L = 1$), irreversible ($R_L = 0$), and favorable $0 < R_L < 1$ (Karagoz et al., 2008).

Freundlich isotherm best describes adsorption onto heterogeneous surfaces which is the opposite to Langmuir’s model. This implies that each molecule of the sorbate is bound at the surface with the different binding energy. It means that stronger binding sites are occupied first and then the binding strength decreases for the rest of the available sites. *Equation 4* defines Freundlich model as:

$$\ln q_e = \ln K_F + \frac{1}{n} \ln c_e \quad (\text{Eq.4})$$

where K_F ((mg/g) (dm³/mg)^{1/n}) is Freundlich constant and $1/n$ is the heterogeneity factor (Haghseresht and Lu, 1998).

Temkin isotherm model considers that adsorption takes place through indirect adsorbate-adsorbate interactions. The linearized form of equation (*Eq. 5*) is given as:

$$q_e = B \ln K_t + B \ln c_e \quad (\text{Eq.5})$$

where K_t (dm^3/mg) is the equilibrium binding constant corresponding to the maximum binding energy and constant $B=RT/b$ represents the heat of adsorption, while $1/b$ indicates the adsorption potential of the adsorbent (Hameed and Ahmad, 2009).

Linear fitting of experimental data was carried out by using software Origin 8.0. For each isotherm model, corresponding values were plotted and fitted by applying option Analysis/Fitting/Fit linear. All sorption parameters were calculated from the parameters which apply to the slope and the intercept of the linear form of isotherm equation.

Results and discussion

Characterization of adsorbents

Scanning electron microscopy

The SEM micrographs of native bentonite clay and carboxymethyl cellulose bentonite based composite are given in *Figures 1 and 2*, respectively.

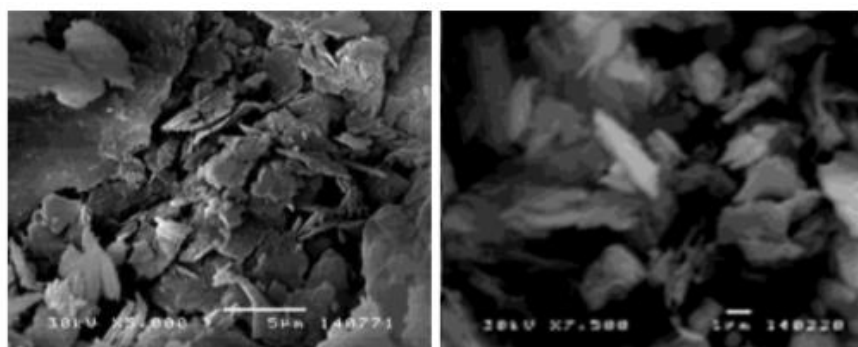


Figure 1. SEM micrographs of native bentonite at magnifications of a) 5000x and b) 7500x

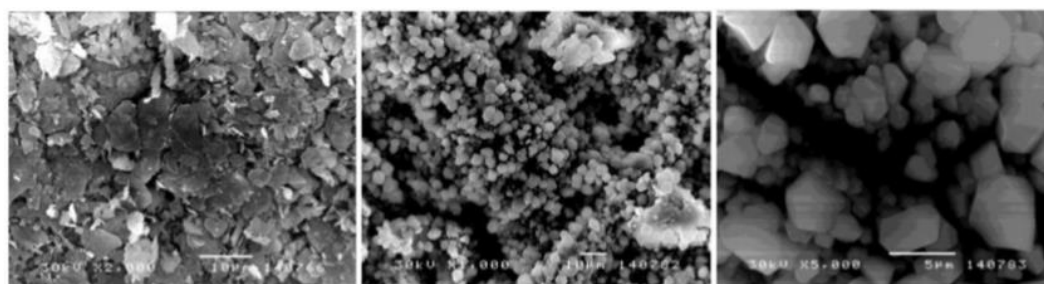


Figure 2. SEM micrographs of carboxymethyl cellulose bentonite based composite with a) 1% b) 3% and c) 5% of modifier

Laminar crystals noticed at magnifications of 5000x are typical for bentonite clays (*Fig. 1*). These particles arranged in a layered manner form the aggregates with diameters of 5 μm on average. Composites with carboxymethyl cellulose show smaller structure changes since thicker crystals are noticed with the higher degree of agglomeration especially in case of the sample where 3% of modifier is applied (*Fig. 2*). Fine grains instead of the dominant laminar structure are attributed to forming of the sticky organic film at the surface of the clay particles.

The SEM-EDS analysis shows that predominant elements in unmodified clay are: Fe, Al, Si, and O. In samples GI, GII and GIII aluminum is the most dominant, due to leaching of Fe during the synthesis of composites.

FTIR spectral analysis

Fourier-transform infrared spectra of native bentonite clay and modified composites which include various ratios of carboxymethyl cellulose are given in *Figure 3*. Two distinctive peaks in bentonite spectrum corresponding to OH stretching vibrations which originate from the Al–Al–OH stretches are observed at 3625 cm^{-1} . The wide peak at 3400 cm^{-1} belongs to the OH stretching of H-bonded water. The bend at 1330 cm^{-1} is due to Si–O bending vibrations. This peak is noticed in native bentonite and GI composite. For samples GII and GIII noticeably weaker peaks for all functional groups are present. For the sample GI, the peaks at 2926 and 2854 cm^{-1} are from C–H vibrations coming from carboxymethyl cellulose. The additional bend corresponding to Al–Al–OH is observed at 925 cm^{-1} . A peak around 800 cm^{-1} with the inflexion at 780 cm^{-1} corresponds to quartz. Carboxymethyl cellulose confirms typical peaks for hydroxyl groups, C–H vibrations and nothing more of interest.

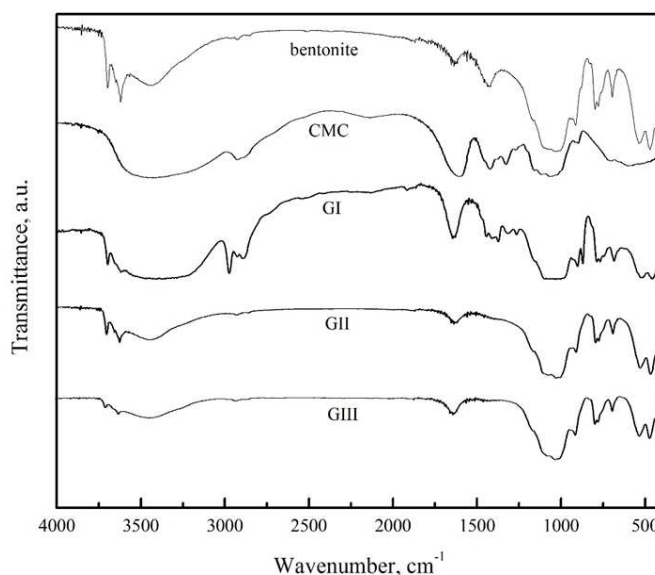


Figure 3. FTIR spectra of native bentonite clay, carboxymethyl cellulose and corresponding composites

Adsorption experiments

Removal degree of arsenic is represented by the *Figure 4*. It is seen that removal degree for the different initial concentrations and for all composites is in the range from 85 to 94%.

In order to analyze the equilibrium condition of arsenic adsorption onto prepared adsorbents three theoretical isotherm models were applied including Langmuir, Freundlich, and Temkin model. Parameters of these models were estimated with the aid of the linear fitting in Origin 8.0 (OriginLab Corporation, USA). Results of the fitting are given in *Figure 5*.

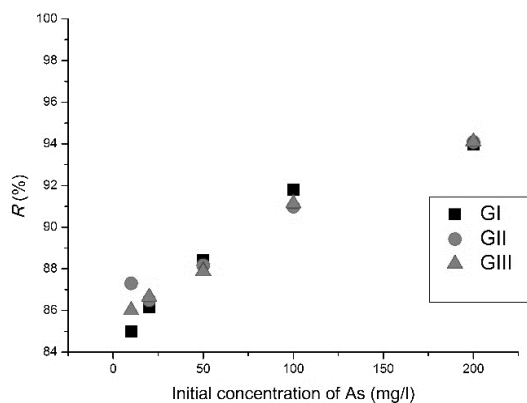


Figure 4. Removal degree of As onto bentonite composites

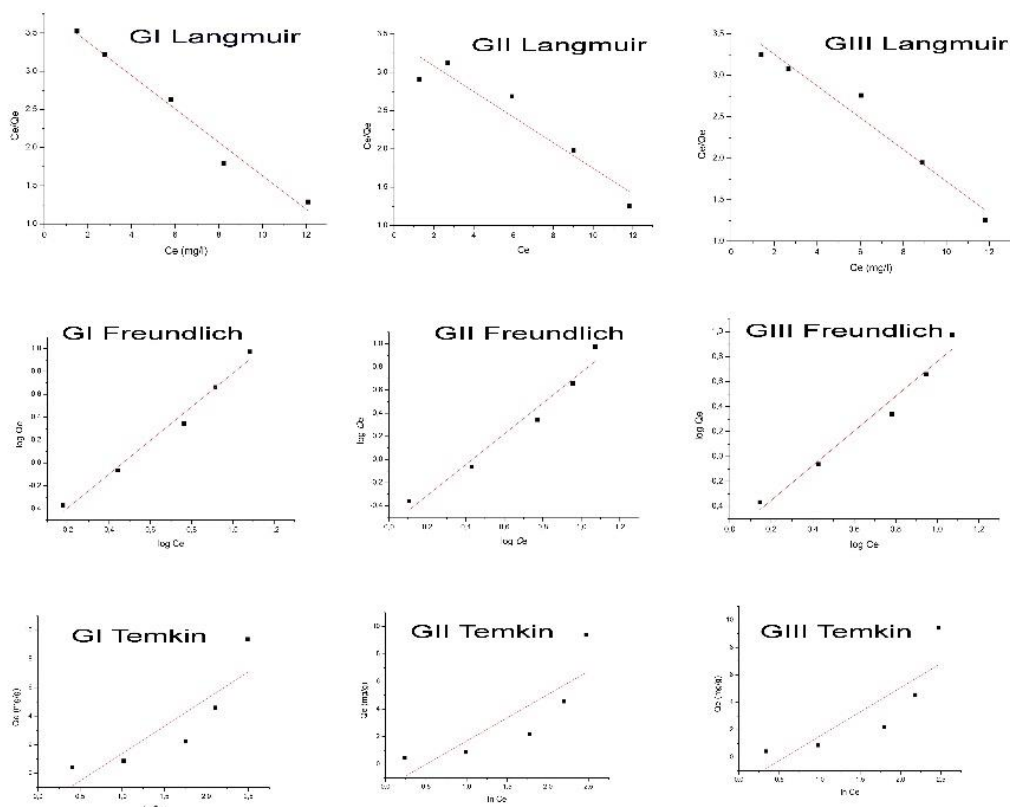


Figure 5. Linear fitting to Langmuir, Freundlich and Temkin isotherm model

Parameters which apply to the slope and the intercept of the linear form of isotherm equation were used for calculation of sorption parameters which are presented in Table 2. It is noticed that Freundlich model fitted well for all three composites, followed by Langmuir and Temkin model. Freundlich model assumes multilayer adsorption and heterogeneity of the process. This model was reported to be the most suitable also in the case of arsenic adsorption onto mesoporous bismuth-impregnated aluminum oxide

although the process was studied by using the lab-scale column (Zhu et al., 2018). In addition, experimental results were also fit well with this model in case of arsenic adsorption onto alum sludge (Jeon et al., 2018). However, there is a hint which distrusts this model as physically relevant. Namely, strong interactions between the adsorbate and adsorbent are observed when the reciprocal Freundlich constant (n) is above 1, as in our case. This basically indicates an unsuitable adsorption process (Komy et al., 2014; Lee et al., 2010). Such statement is in contrast to results attained in this study where with current experimental set-up removal degree was 85% or higher (Fig. 4).

Table 2. Equilibrium model parameters for adsorption of arsenic onto bentonite based adsorbents

Equilibrium model	Parameter	Composite GI	Composite GII	Composite GIII
Langmuir	K_L (l/mg)	0.056	0.05	0.052
	q_{max} (mg/g)	4.56	5.88	5.26
	R_L	0.019	0.017	0.018
	R^2	0.972	0.876	0.948
Freundlich	K_F (l/g)	0.21	0.27	0.23
	n	0.68	0.76	0.72
	R^2	0.981	0.956	0.964
Temkin	A	0.53	0.61	0.56
	b (J/mol)	650.6	733.4	700.2
	R^2	0.686	0.608	0.625

Langmuir model is less suitable to interpret experimental data. Although fair values for correlation coefficients were obtained, estimated values for maximum adsorption capacities for GI, GII, and GIII (4.56, 5.88, 5.26 mg/g, respectively) are far below the experimentally obtained ones (9.4 mg/g for all three composites). The low values of K_L indicate a poor affinity and thus weak bonding of arsenic to the surface of composites at examined conditions. Value for R_L in Langmuir model shows favorable adsorption for all composites.

From Figure 6 it is seen that pH value of solutions has no impact on the removal efficiency of arsenic since adsorption capacities for all three composites differ on the second decimal.

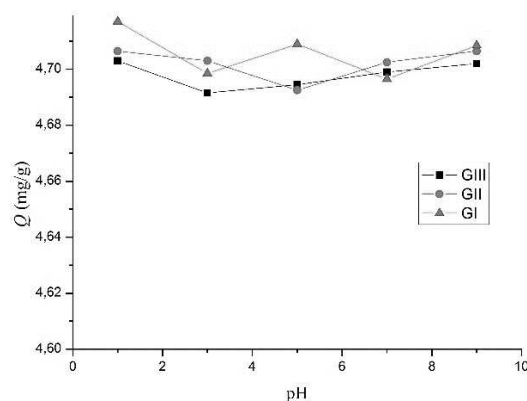


Figure 6. Effect of pH on arsenic adsorption onto bentonite composites

This result is most probably related to the nature of interactions between arsenic ion present in the suspension and electrostatic neutrality of the composites. In case if there is no non-compensated charge on the adsorbent surface the nature of sorptive binding of the As ions are not influenced by electrostatic forces. Hence, the purely physical process takes place. It is conducted by the spontaneous orientation of sorbed ions on the reactive centers of the adsorbent by weak physical forces. However, it is the fact that the number of these sites (for the employed experimental conditions) is not small and it is certainly enough to adsorb great majority of adsorbate.

Another topic which explains the nature of As binding to the porous structure of all three composites is the analysis of temperature impact on the sorption process. From *Figure 7* it can be seen that there are almost no differences in adsorption capacity at different temperatures. To conclude, there is no meaningful influence of thermal energy on the binding of As ions onto surfaces of the composites. It is also in favor of the assumption that arsenic ionic species are bound to the surface of the adsorbent by the weak physical forces and excessive energy does not result in better sorption.

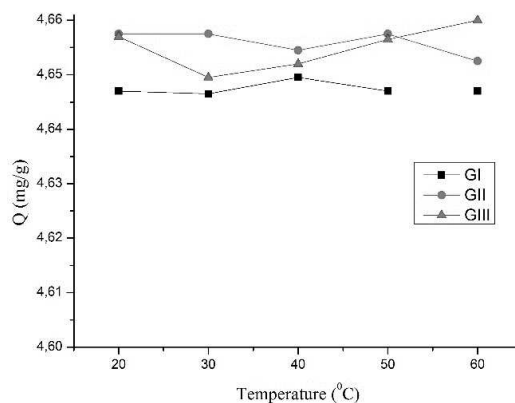


Figure 7. Effect of temperature on arsenic adsorption onto bentonite composites

In order to rate sorptive potential for As(III) removal by Na-CMC-bentonite composite, *Table 3* given below lists achieved maximum adsorption capacities (Q_{max}) obtained from various sorbents in defined experimental conditions.

From *Table 3* one can conclude that significant scientific effort is dedicated to arsenic removal from aqueous media since it is already established that arsenic is very persistent and ubiquitous pollutant. In *Table 3* are presented low cost sorbents obtained from materials that are cheap and abundant. Interesting material is Fe(III)-loaded cellulose which gave twice higher sorption capacity than our material. However, one should bear in mind that we used sodium salt and not the pure cellulose and we certainly lowered the price of the final product by forming a composite which involves the very cheap and easily available bentonite clay. Generally, it is noticed that Na-CMC-bentonite composite achieved moderate success in the sorption of arsenic from solutions. However, if one considers the fact that this composite was produced easily and in short period of time, by using low cost ingredients which are locally available in large amounts, certain feasibility of its production on large scale and applications for treating contaminated water sources could make sense especially in terms of economic profitability.

Table 3. Comparison of As^{3+} maximum adsorption capacities (Q_{max}) for various sorbents

Biosorbent	Experimental conditions	Q_{max} ($mg\ g^{-1}$)	Source
Iron-impregnated chitosan	$C_i=1.007\ mg/l$; $pH=8$	6.48	Ref. ⁵
Fe-sericite composite beads	$C_i=5-25\ mg/l$; $m_{ads}=0.12\ g$; 200 rpm, 12h, $pH=6.82$	9.02	Ref. ¹¹
Synthetic iron sulphide	$pH=6.5$	0.2	Ref. ²⁷
Fe(III)-loaded cellulose	$pH=9$	18.0	Ref. ²⁰
Commercial adsorbents (goethite)	$pH=7.5$	10.1	Ref. ¹²
Commercial adsorbents (mesoporous alumina)	$pH=7$	47.2	Ref. ¹²
Tea fungal biomass	$pH=7.2$; $C_i=1.3\ mg/l$	1.11	Ref. ²¹
Atlantic Cod fish scale	$pH=4$	0,027	Ref. ²⁵
Hydrous ferric oxide incorporated diatomite	$pH=7$	267	Ref. ⁸
Chitosan extracted from shrimp waste	$pH=4,5,6$; $t=30-90\ min$; dosage= $2,3,4\ mg/l$; $C_i=200, 300, 400\ mg/l$	1.3	Ref. ²
Perilla leaf biochar	$pH=3-10$; dosage= $1\ g/l$; $C_i=0.05-7.0\ mg/l$;	3.8 – 11.01	Ref. ²²
Na-CMC-bentonite	$C_i=10-200$	9.4	This study

In contrast to compared studies listed in *Table 3*, Na-CMC bentonite clay composite is material which is very easy and practical for common day practice since it can be employed with no additional adjusting of the pH of the suspension and contacting time is around 20 minutes. This is considered as the main advantage of this sorbent. In addition, preparation of this composite material is fast, safe and involves no harmful ingredients or complicated synthetic procedures.

Conclusion

Composite adsorbents obtained by modification of bentonite showed significant sorptive potential for removal of arsenic(III) ions from water sources. The maximum adsorption capacity, experimentally obtained from isotherm studies, equals 9.4 mg/g. The adsorption process is considered to be fast since the equilibrium is fully attained in only 20 minutes. Good fitting to Freundlich isotherm model pointed out to complex processes at the boundary of the phases liquid-solid which involve multilayer adsorption with different energies of bindings between adsorbate and adsorbent. In the case of presented experimental set-up, high removal degree was attained. This pronounced great affinity of the Na-CMC-bentonite composites towards the dissolved arsenic ions. Bearing in mind low cost of the raw materials which were used to produce this adsorbent, the simplicity of the synthesis and expressed removal feasibility of As^{3+} , this comparative study conveys direct stimulus for practical applications of this composite material and their further examinations in associated frameworks.

Acknowledgements. This study was financially supported by the Ministry of Education, Science and Technological Development of Republic of Serbia through the Project TR34012.

REFERENCES

- [1] Council of the European Communities. (1976): Council Directive 76/464/EEC of 4 May 1976 on pollution caused by certain dangerous substances discharged into the aquatic environment of the community. CELEX-EUR Off. J. L 129, 23e29, 18 May 1976.
- [2] Dehghani, M. H., Maroosi, M., Heidarinejad, Z. (2018): Experimental dataset on adsorption of Arsenic from aqueous solution using Chitosan extracted from shrimp waste; optimization by response surface methodology with central composite design. – Data Brief 20: 1415-1421.
- [3] Environmental Protection Agency. (1982): Code of Federal Regulations, Title 40 e Protection of Environment, Part 423, Appendix A e List of 126 Priority Pollutants. (<https://www3.epa.gov/region1/npdes/permits/generic/prioritypollutants.pdf>). (accessed February 05, 2018).
- [4] Fu, D., He, Z., Su, S., Xu, B., Liu, Y., Zhao, Y. (2017): Fabrication of α -FeOOH decorated graphene oxide-carbon nanotubes aerogel and its application in adsorption of arsenic species. – J. Colloid Interface Sci. 505: 105-114.
- [5] Ganga, D. D., Deng, B., Lin, L. (2010): As(III) removal using an iron-impregnated chitosan sorbent. – J. Hazard. Mater. 182: 156-161.
- [6] Haghseresht, F., Lu, G. (1998): Adsorption characteristics of phenolic compounds onto coal reject-derived adsorbents. – Energy Fuels. 12: 1100-1107.
- [7] Hameed, B. H., Ahmad, A. A. (2009): Batch adsorption of methylene blue from aqueous solution by garlic peel, an agricultural waste biomass. – J. Hazard. Mater. 164: 870-875.
- [8] Jang, M., Min, S. H., Park, J. K., Tlachac, E. J. (2007): Hydrous ferric oxide incorporated diatomite for remediation of arsenic contaminated groundwater. – Environ. Sci. Technol. 41: 3322-3328.
- [9] Jeon, E. K., Ryu, S., Park, S. W., Wang, L., Tsang, D. C. W., Baek, K. (2018): Enhanced adsorption of arsenic onto alum sludge modified by calcination. – J. Clean. Prod. 176: 54-62.
- [10] Karagoz, S., Tay, T., Ucar, S., Erdem, M. (2008): Activated carbons from waste biomass by sulfuric acid activation and their use on methylene blue adsorption. – Bioresour. Technol. 99: 6214-6222.
- [11] Kim, J., Lee, C., Lee, S. M., Lalmunsiana, Jung, J. (2018): Chemical and toxicological assessment of arsenic sorption onto Fe-sericite composite powder and beads. – Ecotoxicol. Environ. Safety 147: 80-85.
- [12] Kim, Y., Kim, C., Choi, I., Rengaraj, S., Yi, J. (2004): Arsenic removal using mesoporous alumina prepared via a templating method. – Environ. Sci. Technol. 38: 924-931.
- [13] Komy, Z. R., Shaker, A. M., Heggy, S. E. M., El-Sayed, M. A. E. (2014): Kinetic study for copper adsorption onto soil minerals in the absence and presence of humic acid. – Chemosphere 99: 117-124.
- [14] Lee, S. M., Kim, W. G., Laldawngliana, C., Tiwari, D. (2010): Removal behavior of surface modified sand for Cd(II) and Cr(VI) from aqueous solutions. – J. Chem. Eng. Data 55: 3089-3094.
- [15] Lin, S., Yang, H., Na, Z., Lin, K. (2018): A novel biodegradable arsenic adsorbent by immobilization of iron oxyhydroxide (FeOOH) on the root powder of long-root *Eichhornia crassipes*. – Chemosphere 192: 258-266.
- [16] Liua, B., Jiand, M., Wanga, H., Zhange, G., Liua, R., Zhangd, X., Qu, J. (2018): Comparing adsorption of arsenic and antimony from single-solute and bi-solute aqueous systems onto ZIF-8. – Colloids Surf. A. 538: 164-172.
- [17] Majia, S., Ghosha, A., Gupta, K., Ghosha, A., Ghorai, U., Santrab, A., Sasikumara, P., Ghosh, U. C. (2018): Efficiency evaluation of arsenic(III) adsorption of novel graphene oxide@ironaluminium oxide composite for the contaminated water purification. – Sep. Purif. Technol. doi: <https://doi.org/10.1016/j.seppur.2018.01.021>.

- [18] Mar, K. K., Karnawati, D., Sarto, Putra, D. P. E., Igarashi, T., Tabelin, C. B. (2013): Comparison of arsenic adsorption on lignite, bentonite, shale, and iron sand from Indonesia. – *Procedia Earth Planet. Sci.* 6: 242-250.
- [19] Mejia-Santillan, M. E., Pariona, N., Bravo-C, J., Herrera-Trejo, M., Montejo-Alvaro, F., Zarate, A., Perry, D. L., Mtz-Enriquez, A. I. (2018): Physical and arsenic adsorption properties of maghemite and magnetite sub-microparticles. – *J. Magn. Magn. Mater.* 451: 594-601.
- [20] Muñoz, J. A., Gonzalo, A., Valiente, M. (2002): Arsenic adsorption by Fe(III) loaded open celled cellulose sponge. Thermodynamic and selectivity aspects. – *Environ. Sci. Technol.* 36: 3405-3411.
- [21] Murugesan, G. S., Sathishkumar, M., Swaminathan, K. (2006): Arsenic removal from groundwater by pretreated waste tea fungal biomass. – *Bioresour. Technol.* 97(3): 483-487.
- [22] Niazi, N. K., Bibi, I., Shahid, M., Ok, Y. S., Burton, E. D., Wang, H., Shaheen, S. M., Rinklebe, J., Lüttge, A. (2018): Arsenic removal by perilla leaf biochar in aqueous solutions and groundwater: An integrated spectroscopic and microscopic examination. – *Environmental Pollution* 232: 31-41.
- [23] Pandey, S. (2017): A comprehensive review on recent developments in bentonite-based materials used as adsorbents for wastewater treatment. – *J. Mol. Liq.* 241: 1091-1113.
- [24] Petrox, S., Nenov, V., Vasilev, S. (2002): Divalent heavy metal removal from water by complexation-ultrafiltration. – In: *Proceedings of the 5th International Conference on membranes in drinking and industrial water production, Mulheim, Ruhr, Germany, 2002*, pp. 245-252.
- [25] Rahaman, M. S., Basu, A., Islam, M. R. (2008): The removal of As (III) and As (V) from aqueous solutions by waste materials. – *Bioresour. Technol.* 99: 2815-2823.
- [26] Santra, D., Sarkar, M. (2016) Optimization of process variables and mechanism of arsenic (V) adsorption onto cellulose nanocomposite. – *J. Mol. Liq.* 224: 290-302.
- [27] Teclu, D., Tivchev, G., Laing, M., Wallis, M. (2008): Bioremoval of arsenic species from contaminated waters by sulphate-reducing bacteria. – *Water Res.* 42: 4885-4893.
- [28] U.S. Environmental Agency. (2018): Chemical Contaminant Rules. (Available at: <https://www.epa.gov/dwreginfo/chemical-contaminant-rules>) (accessed February 05, 2018).
- [29] Yan, X., Zhang, Y., Zhu, K., Gao, Y., Zhang, D., Chen, G., Wang, C., Wei, Y. (2014): Enhanced electrochemical properties of TiO₂(B) nanoribbons using the styrene butadiene rubber and sodium carboxyl methyl cellulose water binder. – *J. Power Sources.* 246: 95-102.
- [30] Zhu, N., Qiao, J., Ye, Y., Yan, T. (2018): Synthesis of mesoporous bismuth-impregnated aluminum oxide for arsenic removal: Adsorption mechanism study and application to a lab-scale column. – *J. Environ. Manage.* 211: 73-82.

ALTITUDINAL GRADIENTS AND FOREST EDGE EFFECT ON SOIL ORGANIC CARBON IN CHINESE FIR (*CUNNINGHAMIA LANCEOLATA*): A STUDY FROM SOUTHEASTERN CHINA

SAEED, S.¹ – SUN, Y.^{1*} – BECKLINE, M.¹ – CHEN, L.¹ – LAI, Z.¹ – MANNAN, A.^{2,3} – AHMAD, A.² – SHAH, S.² – AMIR, M.² – ULLAH, T.⁴ – KHAN, A.⁵ – AKBAR, F.⁶

¹*State Forestry Administration, Key Laboratory for Forest Resources and Environmental Management, Beijing Forestry University, Beijing, China*

²*School of Forestry, Beijing Forestry University, Beijing, China*

³*Punjab Forest Department Government of Punjab, Lahore 54000, Pakistan*

⁴*School of Nature Conservation, Beijing Forestry University, Beijing, China*

⁵*School of Soil and Water Conservation, Beijing Forestry University, Beijing 100083, China*

⁶*Centre for Biotechnology and Microbiology, University of Swat, Swat, Pakistan*

**Corresponding author*

e-mail: sunyj@bjfu.edu.cn; phone: +86-136-4129-8528

(Received 19th Sep 2018; accepted 26th Nov 2018)

Abstract. In forest ecosystems, soil organic matter facilitates carbon sequestration and serves as a sink for atmospheric CO₂. Carbon in forest soils plays an important role in mitigating global climate change. Soil carbon density was measured at three depths (0-20, 20-40, and 40-60 cm) in four different elevation classes sites at the forest exterior and forest interior in the sub-tropical forests of southeastern China. Results showed that soil organic carbon (SOC) varied between 46.48 and 83.12 Mg ha⁻¹ at forest exterior and 50.18 and 90.68 Mg ha⁻¹ at forest interior in different elevation classes. A significant increasing trend in soil organic carbon was found with an increase in elevation at both forest exterior and forest interior. Similarly, a positive correlation between soil organic carbon and elevation was observed at forest exterior (R² = 0.87, P = 0.0001) and forest interior (R² = 0.93, P = 0.0001). The percentages of soil carbon at 0-20, 20-40, and 40-60 cm depths at forest exterior and forest interior were 47.24-52.76, 47.23-52.77, and 46.95-53.05% respectively. Soil bulk density was directly related to soil depth and inversely related to elevation at forest exterior and forest interior. Overall the mean SOC at forest exterior and forest interior was 60.83 Mg ha⁻¹ and 68.20 Mg ha⁻¹ respectively. The study showed that there is a 5.7% difference in soil carbon density between forest exterior and forest interior which highlights the fact that ignoring edge effects may lead to overestimation of soil carbon density. Therefore, we suggest the establishment of permanent sample plots sites at the forest exterior and forest interior and recommend regular periodic surveys of soil for accurate forest soil carbon measurement.

Keywords: *forest edge effects, elevation gradients, soil carbon, soil bulk density, sub-tropical forest*

Introduction

At the global scale, the estimated amount of soil organic carbon (SOC) is about three times that of carbon which resides within vegetation and twice that of atmospheric carbon (Li et al., 2016; Smith et al., 2008). Therefore, small fluctuations in SOC pools may influence global carbon budgets and atmospheric CO₂ concentrations (Du et al., 2014; Li et al., 2016). Generally, increases in SOC mostly result from biomass carbon being transferred to the soil through decomposition (Shaheen et al., 2017). Hence, SOC is primarily balance by carbon input from vegetation production and output through decomposition (Singh et al.,

2011). These SOC production and decomposition processes are usually a measure of soil climate, disturbance and texture as well as land use, hydrology, and topography (Singh and Rawat, 2013). Moreover, altitudinal gradients and climatic variables (precipitation and temperature) could also affect the carbon pool (He et al., 2016).

The forest covers are recognized as the largest and most effective carbon sinks among terrestrial ecosystems and help to mitigate global climate change (Amir et al, 2018; Beckline et al., 2018; Dar and Somaiah, 2015; Mannan et al, 2018; Saeed et al., 2016). Among these forest ecosystems, mountain forest ecosystems have an important role in the global carbon cycle (Gower, 2003) and store about 26% of the total terrestrial ecosystem's carbon (Garten Jr and Hanson, 2006). In addition, forests at high altitudes are known to store more SOC compared to similar forests located at lower altitudes (Charan et al., 2012; Wei et al., 2013; Zhu et al., 2010).

Forest logging, including when under legal forest management, can create edge-like conditions inside the forest (Barros and Fearnside, 2016). Forest edge refers to the limit of continuous canopy or boundary in canopy composition and which is substantially different from the corresponding forest interior (Harper et al., 2005; Remy et al., 2016). Forest edges exhibit different microclimatic conditions such as light, temperature, wind, and soil moisture to the corresponding forest interior. These microclimatic differences enable the forest edges to capture relatively more atmospheric carbon than the forest interior (Remy et al., 2016). Several other studies have shown that microclimatic and edaphic conditions are generally different between forest edges and forest interior zones (Burke and Nol, 1998; Camargo and Kapos, 1995; Davies-Colley et al., 2000; Delgado et al., 2007; Didham and Lawton, 1999; Gehlhausen et al., 2000; Jose et al., 1996; Kapos, 1989; Pohlman et al., 2009; Rodrigues, 1998; Williams-Linera et al., 1998). These studies showed that edges experience faster wind speed, higher soil and air temperature, lower soil and air humidity and vapor pressure, than the interior of a forest. Although in a forest ecosystem the effects of an edge on soil carbon have been broadly studied, little literature is available regarding the edge effect on soil carbon along an altitudinal gradients, especially in China.

China has a unique soil carbon distribution due to its diverse climatic profile ranging from subtropical to alpine, and from humid to arid and desert conditions (Yang et al., 2007). In China, most of the research work has been focused on the evaluation of forest biomass carbon stored in China's forests and storage of other forests ecosystem components, such as SOC, has rarely been reported (Li et al., 2004; Yu et al., 2010). Compared to the periodic National Forest Inventory (NFI), soil surveys are less frequently conducted in the country, hence the lack of national soil carbon data (Peng et al., 2016; Yang et al., 2014). This lack of sufficient soil carbon data limits the accurate evaluation of soil carbon in China (Pan et al., 2011; Yang et al., 2007; Yu et al., 2010). However, based on soil data from field surveys and global data sets from 1980, soil carbon density in the 0-100 cm soil depth in China's forests were estimated at 115.90–193.55 Mg C ha⁻¹ (Li et al., 2004; Xianli et al., 2004; Yang et al., 2007; Yu et al., 2007), while Peng et al. (2016) have estimated 136.11–153.16 Mg C ha⁻¹. These variations in soil carbon reflect a lack of contemporary measurements of forests soil carbon. Similarly, no reliable information is available regarding the effect of edges on soil carbon in China's forest. Therefore, this study estimates SOC and bulk density along forest edges and forest interior, at different altitudes in the sub-tropical forest of China's southeast Fujian province. The results show there is a variation in soil carbon and bulk density at forest edges and forest interior at different elevations.

Materials and methods

Study area

The field surveys were conducted in the Jiangle county in China's southeastern Fujian Province, 117° 05'–117° 40'E and 26° 26'–27° 04'N. The area exhibits a humid tropical climate and the frost-free period usually spreads over 287 days. The area receives an average 1699 mm precipitation annually, while the average yearly temperature is 18.7 °C. The soil type is red, fertile, moist and loamy. The woodland cover of the forest farm is 1887 km², making-up over 83.9% of its geographical area. The main tree species are Chinese Fir (*Cunninghamia lanceolata*), Moso bamboo (*Phyllostachys pubescens*), and Masson pine (*Pinus massoniana*) with the most dominant being Chinese Fir. (Guangyi et al., 2017; Hao et al., 2015; Liping et al., 2018). The shrub layer includes species such as Chinese fringe flower (*Loropetalum chinense*), Rough pellionia (*Pellionia scabra*), Chinese sweetspire (*Itea chinensis*) and Rubus (*Rubus reflexus*) while the herb layer mostly comprises Chinese hicropteris (*Diplazium chinense*), Herba sarcandrae (*Sarcandra glabra*), Parasitic Cyclosorus (*Cyclosorus parasiticus*), and Common lophatherum (*Lophatherum gracile*).

Soil sample treatment and analysis

Field surveys were carried out between April and July 2017 in the study area to collect soil samples covering elevations gradient ranging from 40 m to 1203 m above sea level (a.s.l) (Fig. 1).

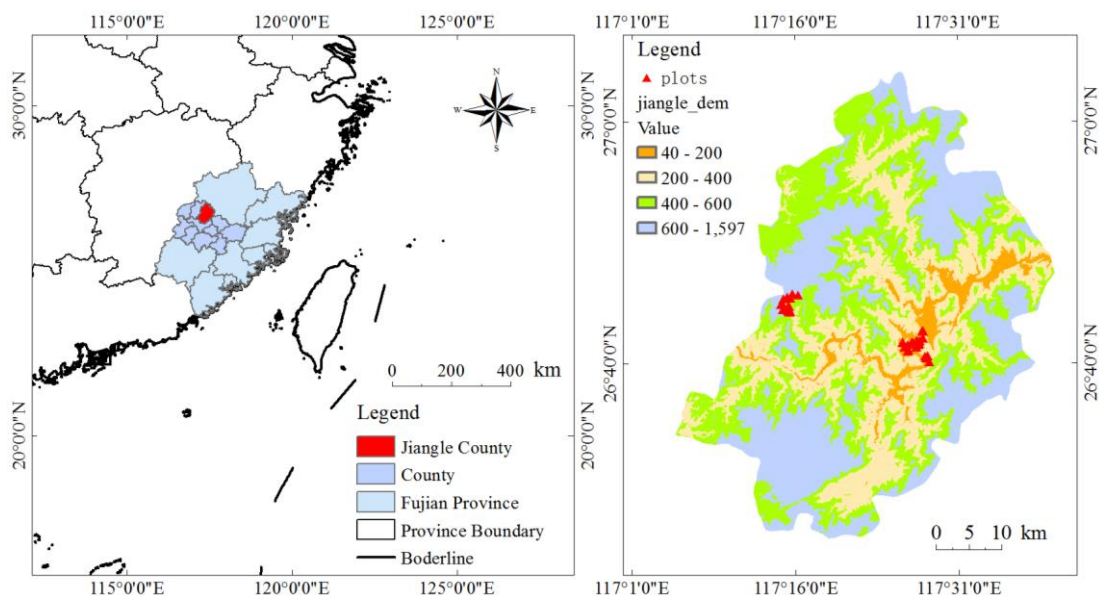


Figure 1. The map and location of the study site

The site characteristics of *Cunninghamia lanceolata* forest at different elevation are given in Table 1. The area was divided into 4 elevation classes (EC) and the elevation difference of each class was 200 m (a.s.l). In each EC, 4 sample plots were taken at forest edges and 4 at forest interior. The forest interior plots were laid out at 60 m distance from the forest edges. The sizes of sample plots ranged between 400 and 600 m². The soil samples were collected from three sub plots of (1 × 1 m) within each

plot of 400 to 600 m² at varying depths. The samples were collected at three depth increments in the center of the subplot (that is, of 0-20, 20-40 and 40-60 cm, respectively). The soil samples were collected using a soil auger (Soil auger, Shangyu Hongguanf instrument and Equipment Co., Ltd., China) and soil core of an identified volume of 100 cm³.

Table 1. Characteristics of the *Cunninghamia lanceolata* forest at different elevation classes in Jiangle County, Fujian Province. Different super scripts in each column represent significant difference ($n = 8, p \leq 0.0001, \text{Alpha} = 0.05$. TTB = total tree biomass)

Classes	Diameter range (cm)	Stem density (Mg ha ⁻¹)	Basal area (m ² ha ⁻¹)	TTB (Mg ha ⁻¹)
1	4-44	1683.33±249.76 ^a	40.09±11.17 ^d	180.94±68.18 ^d
2	4-38	1716.67±232.99 ^a	64.83±12.57 ^c	319.77±80.62 ^c
3	6-42	1447.92±239.78 ^b	94.58±15.39 ^b	511.43±108.73 ^b
4	8-50	1289.58±265.61 ^b	127.69±5.86 ^a	732.13±55.15 ^a
Mean	27	1534.38±294.88	81.80±35.13	436.07±224.16

The collected samples were weighed and packed in labeled bags. Then the samples were transferred to the Southern Forest, Experimental Base of Beijing Forestry University Sanming Jiangle for further analysis. The samples were first air-dried (Shel Lab Gravity Convection Laboratory Oven SGO3) and then the soil bulk density (g cm⁻³) was measured for each soil sample. These air-dried samples were manually ground with a pestle and passed through a 0.50 mm sieve for the determination of SOC as described by (Lu, 1999).

Analysis of soil carbon

To find out the soil carbon of each collected soil sample, the sub samples (1 g) were taken from the labeled sample and analyzed in the laboratory using the oxidizable organic carbon method of (Walkley and Black, 1934). A measure of the soil carbon in Mg ha⁻¹ was obtained by calculating the soil bulk density of each sample according to Equation 1.

$$BD = MS (g)/VC (cm^3) \quad (\text{Eq.1})$$

where BD = Soil bulk density (g cm⁻³), MS = Weight of the soil sample (g) and VC = Volume of the core (cm³)

The soil organic carbon (Mg ha⁻¹) was calculated from the relationship of the soil bulk density, soil organic carbon and depth increment using Equation 2 (Ahmad and Nizami, 2015; Pearson et al., 2007).

$$\text{Soil Carbon (Mg ha}^{-1}\text{)} = BD (g \text{ cm}^{-3}\text{)} \times SOC (\%) \times TH (cm) \times 100 \quad (\text{Eq.2})$$

where TH = Thickness of horizon (cm)

The difference between the soil carbon at the forest interior and forest edges was obtained using Equation 3.

$$SCD = SC (in) - SC (ex) \quad (\text{Eq.3})$$

where SCD = Soil carbon difference (Mg ha^{-1}), SC (in) = Soil carbon at forest interior (Mg ha^{-1}), SC (ex) = Soil carbon at forest exterior (Mg ha^{-1}).

Statistical analysis

MS Excel for Windows 10 was used to analyze soil carbon data. The relationship between SOC and elevation at the forest exterior and forest interior was examined with linear regression (Sigma Plot version 12.5). Similarly, the relationship of soil carbon and bulk density with respect to soil depth was also studied using linear regression (Sigma Plot version 12.5). To test the differences in soil carbon and bulk density at various depths (0–20, 20–40, 40–60), an Analysis of Variance (ANOVA) and Least significant difference (LSD) were performed on the data from forest edges and forest interior. The differences were considered statistically significant at $P < 0.05$. Statistix version 8.1 (Analytical Software, 2005) was used for these analyses. Sigma Plot version 12.5 was used to analyze the relationship between bulk density and elevation at forest exterior and forest interior at various depths.

Results

Soil organic carbon density

The mean soil carbon density up to 0-60 cm depth at the forest exterior and forest interior was 60.83 Mg ha^{-1} and 68.20 Mg ha^{-1} respectively. SOC density increased significantly ($P < 0.05$) with increasing elevation (Fig. 2) and decreased with increasing soil depth in all the EC at both the forest exterior and forest interior. The mean SOC at forest edges and forest interior at 0-20 cm depth was 21.41 and 23.91 Mg ha^{-1} . Similarly, at 20-40 cm and 40-60 cm soil depths the mean SOC at forest exterior and forest interior were 20.24 , 22.61 , and 19.18 , 21.67 Mg ha^{-1} respectively Table 2.

Table 2. Soil organic carbon in different depths at forest exterior and forest interior in Jiangle County, Fujian Province. Different super scripts in each column represent significant difference ($n = 8$, $p \leq 0.0001$, Alpha = 0.05)

Forest exterior (SOC Mg ha^{-1})			
Classes	Depth 1 (0-20 cm)	Depth 2 (20-40 cm)	Depth 3 (40-60 cm)
1	$16.21 \pm 0.20^{\text{no}}$	$15.50 \pm 0.29^{\text{op}}$	$14.77 \pm 0.38^{\text{p}}$
2	$18.42 \pm 0.89^{\text{jkl}}$	$17.72 \pm 0.70^{\text{klm}}$	$16.84 \pm 0.70^{\text{mn}}$
3	$21.76 \pm 1.11^{\text{g}}$	$20.06 \pm 1.38^{\text{hi}}$	$18.92 \pm 1.43^{\text{ijk}}$
4	$29.25 \pm 1.49^{\text{b}}$	$27.68 \pm 1.68^{\text{c}}$	$26.20 \pm 2.03^{\text{d}}$
Mean	$21.41 \pm 5.70^{\text{e}}$	$20.24 \pm 5.30^{\text{d}}$	$19.18 \pm 4.97^{\text{e}}$
Forest interior (SOC Mg ha^{-1})			
1	$17.65 \pm 0.71^{\text{lm}}$	$16.55 \pm 0.63^{\text{mno}}$	$15.98 \pm 0.59^{\text{nop}}$
2	$20.22 \pm 0.77^{\text{h}}$	$19.27 \pm 0.79^{\text{hij}}$	$18.40 \pm 0.78^{\text{jkl}}$
3	$26.47 \pm 2.28^{\text{cd}}$	$24.45 \pm 2.52^{\text{e}}$	$23.11 \pm 2.25^{\text{f}}$
4	$31.31 \pm 0.31^{\text{a}}$	$30.18 \pm 0.40^{\text{ab}}$	$29.20 \pm 0.63^{\text{b}}$
Mean	$23.91 \pm 6.17^{\text{a}}$	$22.61 \pm 6.01^{\text{b}}$	$21.67 \pm 5.83^{\text{c}}$

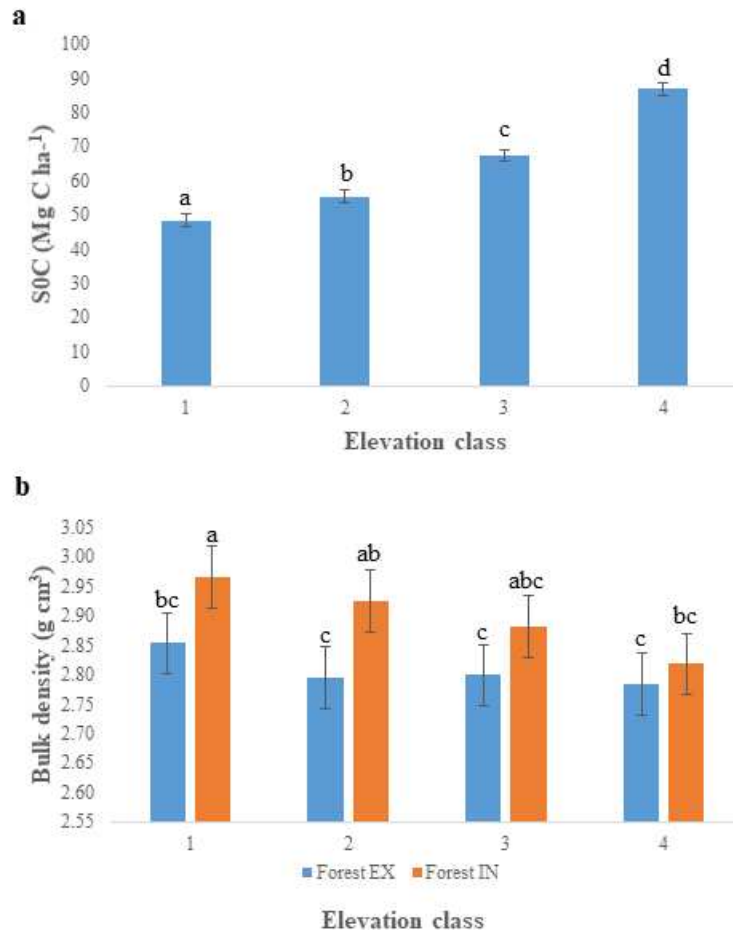


Figure 2. (a) Soil organic carbon in different elevation classes, $p \leq 0.0001$, Alpha = 0.05 (letter on the bars shows significant differences between the soil carbon density across the elevation classes) and (b) Soil bulk density (g/cm^3) in different elevation classes at forest exterior and forest interior, $p \leq 0.0001$, Alpha = 0.05 (letter on the bars shows significant differences between the soil bulk density along the elevation classes at forest exterior and forest interior)

The percentages of soil carbon density at 0-20, 20-40, and 40-60 cm depths at forest exterior and forest interior were 47.24-52.76, 47.23-52.77, and 46.95-53.05% respectively. The highest percentage of soil carbon (34.2%) was observed at 0-20 cm depth in EC 4 at the forest exterior, whereas the lowest (18.5%) was observed in EC 1 at the forest interior. At a depth of 20-40 cm, the highest percentage (34.2%) of soil carbon was observed in EC 4 at the forest exterior, while the lowest (18.3%) was observed in EC 1 at the forest interior. Similarly, at 40-60 cm, the highest soil carbon was in EC 4 (34.1%) at the forest exterior whereas the lowest soil carbon was observed in EC 1 (18.4%) at the forest interior. The correlation analysis highlighted a very positive correlation between elevation between SOC and elevation at the forest exterior ($R^2 = 0.87$, $P = 0.0001$) and forest interior ($R^2 = 0.93$, $P = 0.0001$).

Soil bulk density

The soil bulk densities (BD) at different ECs at forest exterior and forest interior are given in *Figure 2b*. Soil bulk density among the ECs at forest exterior ranged between $2.78 \text{ g}/\text{cm}^3$ at EC 4 to $2.85 \text{ g}/\text{cm}^3$ at EC 1. The mean soil bulk density at forest exterior

was 2.81 g/cm³. The estimated soil BD at the forest interior ranged from 2.82 g/cm³ at EC 4 to 2.96 g/cm³ at EC 1, while the mean soil bulk density at the forest interior was 2.90 g/cm³. The bulk density showed a significant increase ($P < 0.05$) with an increasing in soil depth in all ECs at both the forest exterior and forest interior. Soil bulk density showed significant variation at different depths across all the ECs at forest exterior and forest interior (Fig. 3b). The elevation and soil bulk density were highly negative correlation for different depths. Soil carbon was inversely related to soil bulk density; as soil carbon experienced a decrease with an increase in soil bulk density and vice versa in all ECs at both the forest exterior and forest interior. Similarly, a decreasing trend was observed in the soil bulk density with an increase in elevation.

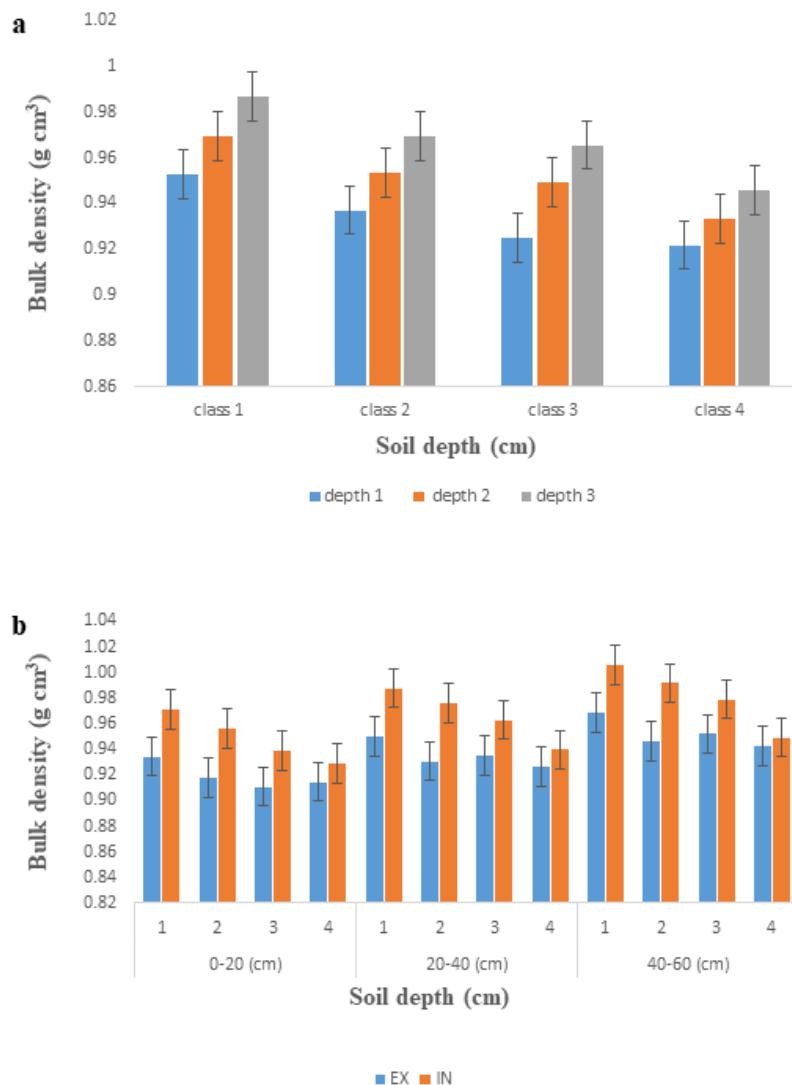


Figure 3. (a) Soil bulk density (g/cm³) in different elevation classes at various depths, $p \leq 0.0001$, Alpha = 0.05 and (b) Soil bulk density (g/cm³) in different depths at forest exterior and forest interior, $p \leq 0.0001$, Alpha = 0.05

Overall the results showed that there are significant ($P < 0.05$) differences in soil carbon in all the EC (Fig. 2). The highest percentage of soil carbon was in EC 4 (33.7%) whereas lowest was in EC 1 (18.7%). Similarly, the percentage of soil carbon

at forest exterior and forest interior in EC 1 was (19.1-18.4%), EC 2 (21.8-21.2%), EC 3 (25-27.1%), and EC 4 (34.2-33.2%), respectively.

Discussion

The present study investigated the variations in the SOC and bulk density at the forest exterior and forest interior across different EC in the Jiangle county of southeastern China. Soil carbon increased with increasing elevation at both forest exterior and forest interior and more SOC was found at the forest interior when compared to the forest exterior. Soil carbon increased with an increase in precipitation and decreased with increasing in temperature (Jobbágy and Jackson, 2000). A significant positive relationship between soil carbon and elevation was observed at both forest exterior ($R^2 = 0.87$, $P = 0.0001$) and forest interior ($R^2 = 0.93$, $P = 0.0001$; *Fig. 4*).

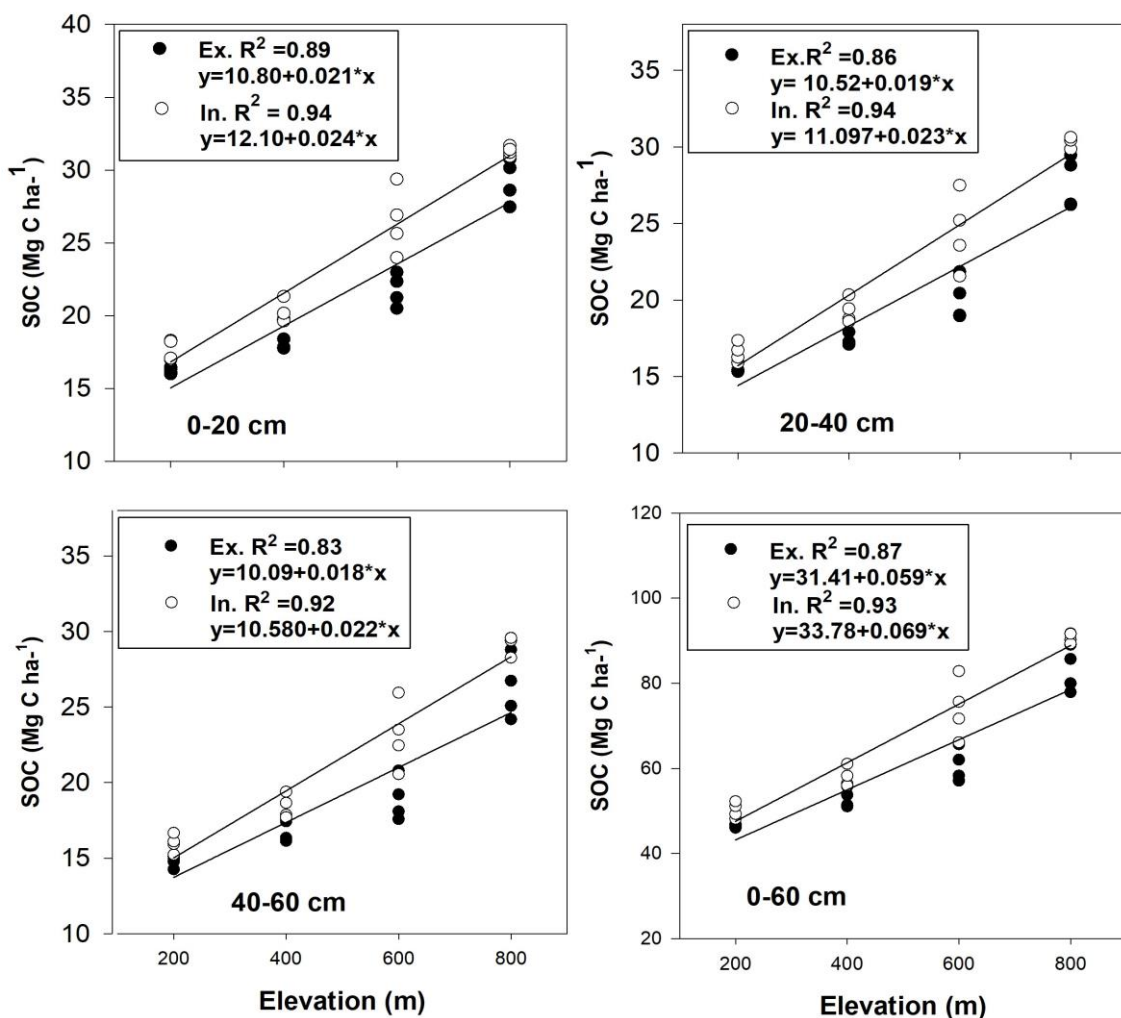


Figure 4. Relationship between elevation and soil organic carbon at forest exterior (Ex) and forest interior (In)

These disparities may be due to the lower temperatures and higher rates of precipitation found at higher elevation. According to Jobbágy and Jackson (2000), Yang et al. (2007)

and Zhu et al. (2010) these differences are due to the distribution of shallower root systems along hilly ecosystems (Jobbágy and Jackson, 2000; Yang et al., 2007; Zhu et al., 2010). Previous research has also reported an increasing trend of soil carbon density with an increase in elevation (Charan et al., 2012; Gupta and Sharma, 2013; Wei et al., 2013; Zhang et al., 2011; Zhu et al., 2010). There was less soil carbon at lower elevations than at higher elevations at both forest exterior and forest interior (*Fig. 4* and *Table 2*). Hence, soils at lower elevations hold significantly lower carbon when compared to soils at higher elevations at both the forest exterior and forest interior. This lower carbon may be attributed to the occurrence of less detritus on the forest floor due to an increase in tree diameter along the elevation gradient. An increase in tree diameter also increases competition among tree species. As a result, there is an increase in the natural shedding of lower branches, hence more deadwood material is present on the forest floor, and consequently more carbon (Charan et al., 2012; Gupta and Sharma, 2013; Wei et al., 2013; Zhang et al., 2011). Furthermore, our results pointed to an overall difference of 5.7% in soil carbon at the forest exterior and forest interior. In comparison, these findings are not consistent with previous findings (Remy et al., 2016), which showed more soil carbon at forest edges as compared to forest interior. However, some of the findings revealed a slight non-significant increase in carbon at forest edges compared to the interior (Barros and Fearnside, 2016). This variation and discrepancy in soil carbon could also be attributed to disturbance and edge-related factors arising from the combined effects of natural and human actions such as winds, floods, farming, roads, streams, and logging (Chaplin-Kramer et al., 2015). In the study area, potentially influential edge related factors include the presence of farmlands, roads, streams, canopy gaps and logging operations. These edge-related factors reduce the soil carbon mainly through soil compaction and soil erosion due to heavy rains and flooding.

A decrease was observed in SOC density with an increase in soil depth in all the ECs at both forest exterior and forest interior *Table 2*. Similar findings were reported by Jobbágy and Jackson (2000) and Dar and Somaiah (2015). This decreasing trend of soil carbon with increasing soil depth may be due to slower soil carbon cycling soil carbon at increased depths and compaction (Dar and Somaiah, 2015; Paul et al., 1997; Trumbore, 2000).

Soil bulk density

In this study we observed a decrease in the soil bulk density with the increasing in elevation at both the forest exterior and forest interior. A negative correlation was observed between soil bulk density at 0-60 cm depth and elevation at forest exterior ($R^2 = 0.10$, $P = 0.0001$) and forest interior ($R^2 = 0.42$, $P = 0.0001$) in all the ECs (*Fig. 5*). Dar and Somaiah (2015) and Sharma et al. (2010) have also reported the similar relationship between elevation and soil bulk density. The soil organic matter and soil bulk density were inversely proportional. The lower bulk density in soil indicates a higher degree of soil organic matter, good granulation, aeration and higher infiltration (Dar and Somaiah, 2015). Our results also endorse the above explanation.

The present study also indicates that the higher soil bulk density results in lower soil carbon at lower elevation than at higher elevation at both forest exterior and forest interior. In this study, soil bulk density showed an increase with an increased in soil depth in all EC at both the forest exterior and forest interior. This may be due to higher bulk density at greater soil depths in the forest floor, as well as with mixing of minerals in the soil (Schulp et al., 2008).

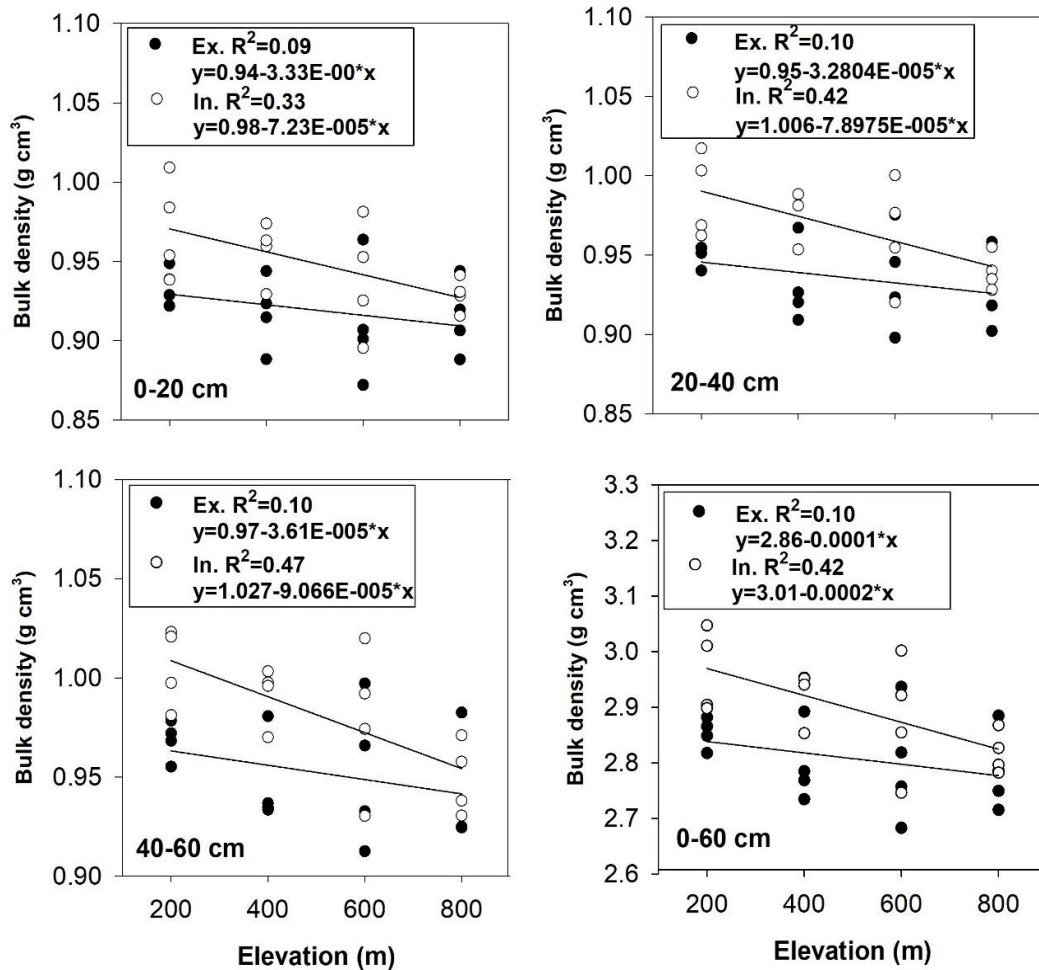


Figure 5. Relationship between soil bulk density and elevation at forest exterior (Ex) and forest interior (In)

Conclusion

Soil carbon density increased significantly with increasing elevation and decreased with increasing soil depth at both forest exterior and forest interior. Forest soil carbon assessment is critical for policy makers when modeling climate scenarios. However, evidence shows that ignoring edge effects may not account for forest soil carbon precisely. Our results showed that the forest interior stored more soil carbon than the forest edge. The magnitude of the edge effect means that ignoring edge effects overestimates carbon stock by 5.7%. These outcomes suggest that edge effects should be given proper consideration during soil carbon accounting.

Acknowledgements. This study was supported by the National Natural Science Foundation of China (31870620) and the 948 Project of State Forestry Administration of China (2015-4-31).

REFERENCES

- [1] Ahmad, A., Nizami, S. M. (2015): Carbon stocks of different land uses in the Kumrat valley, Hindu Kush Region of Pakistan. – *Journal of Forestry Research* 26(1): 57-64.

- [2] Amir, M., Liu, X., Ahmad, A., Saeed, S., Mannan, A., Atif Muneer, M. (2018): Patterns of Biomass and Carbon Allocation across Chronosequence of Chir Pine (*Pinus roxburghii*) Forest in Pakistan: Inventory-Based Estimate. – *Advances in Meteorology* Article ID 3095891, 8 pages, <https://doi.org/10.1155/2018/3095891>
- [3] Barros, H. S., Fearnside, P. M. (2016): Soil carbon stock changes due to edge effects in central Amazon forest fragments. – *Forest Ecology and Management* 379: 30-36.
- [4] Beckline, M., Yujun, S., Etongo, D., Saeed, S., Mukete, N., Richard, T. (2018): Cameroon must focus on SDGs in its economic development plans. – *Environment: Science and Policy for Sustainable Development* 60(2): 25-32.
- [5] Burke, D. M., Nol, E. (1998): Edge and fragment size effects on the vegetation of deciduous forests in Ontario, Canada. – *Natural Areas Journal* 18(1): 45-53.
- [6] Camargo, J., Kapos, V. (1995): Complex edge effects on soil moisture and microclimate in central Amazonian forest. – *Journal of Tropical Ecology* 11(2): 205-221.
- [7] Chaplin-Kramer, R., Ramler, I., Sharp, R., Haddad, N. M., Gerber, J. S., West, P. C., Mandle, L., Engstrom, P., Baccini, A., Sim, S. (2015): Degradation in carbon stocks near tropical forest edges. – *Nature Communications* 6: 10158.
- [8] Charan, G., Bharti, V. K., Jadhav, S., Kumar, S., Angchok, D., Acharya, S., Kumar, P., Srivastava, R. (2012): Altitudinal variations in soil carbon storage and distribution patterns in cold desert high altitude microclimate of India. – *African Journal of Agricultural Research* 7(47): 6313-6319.
- [9] Dar, J. A., Somaiah, S. (2015): Altitudinal variation of soil organic carbon stocks in temperate forests of Kashmir Himalayas, India. – *Environmental Monitoring and Assessment* 187(2): 11.
- [10] Davies-Colley, R. J., Payne, G., Van Elswijk, M. (2000): Microclimate gradients across a forest edge. – *New Zealand Journal of Ecology* 1: 11-121.
- [11] Delgado, J. D., Arroyo, N. L., Arévalo, J. R., Fernández-Palacios, J. M. (2007): Edge effects of roads on temperature, light, canopy cover, and canopy height in laurel and pine forests (Tenerife, Canary Islands). – *Landscape and Urban planning* 81(4): 328-340.
- [12] Didham, R. K., Lawton, J. H. (1999): Edge structure determines the magnitude of changes in microclimate and vegetation structure in tropical forest fragments. – *Biotropica* 31(1): 17-30.
- [13] Du, B., Kang, H., Pumpanen, J., Zhu, P., Yin, S., Zou, Q., Wang, Z., Kong, F., Liu, C. (2014): Soil organic carbon stock and chemical composition along an altitude gradient in the Lushan Mountain, subtropical China. – *Ecological Research* 29(3): 433-439.
- [14] Garten Jr, C. T., Hanson, P. J. (2006): Measured forest soil C stocks and estimated turnover times along an elevation gradient. – *Geoderma* 136(1-2): 342-352.
- [15] Gehlhausen, S. M., Schwartz, M. W., Augspurger, C. K. (2000): Vegetation and microclimatic edge effects in two mixed-mesophytic forest fragments. – *Plant Ecology* 147(1): 21-35.
- [16] Gower, S. T. (2003): Patterns and mechanisms of the forest carbon cycle. – *Annual Review of Environment and Resources* 28(1): 169-204.
- [17] Guangyi, M., Yujun, S., Saeed, S. (2017): Models for Predicting the Biomass of *Cunninghamialanceolata* Trees and Stands in Southeastern China. – *Plos One* 12(1): e0169747.
- [18] Gupta, M., Sharma, S. (2013): Sequestered organic carbon status in the soils under grassland in Uttarakhand State, India. – *Applied Ecology and Environmental Sciences* 1(1): 7-9.
- [19] Hao, X., Yujun, S., Xinjie, W., Jin, W., Yao, F. (2015): Linear mixed-effects models to describe individual tree crown width for China-fir in Fujian province, southeast China. – *PloS One* 10(4): e0122257.
- [20] Harper, K. A., Macdonald, S. E., Burton, P. J., Chen, J., Brosofske, K. D., Saunders, S. C., Euskirchen, E. S., Roberts, D., Jaiteh, M. S., Esseen, P. A. (2005): Edge influence on

- forest structure and composition in fragmented landscapes. – *Conservation Biology* 19(3): 768-782.
- [21] He, X., Hou, E., Liu, Y., Wen, D. (2016): Altitudinal patterns and controls of plant and soil nutrient concentrations and stoichiometry in subtropical China. – *Scientific Reports* 6: 24261.
- [22] Jobbágy, E. G., Jackson, R. B. (2000): The vertical distribution of soil organic carbon and its relation to climate and vegetation. – *Ecological Applications* 10(2): 423-436.
- [23] Jose, S., Gillespie, A. R., George, S. J., Kumar, B. M. (1996): Vegetation responses along edge-to-interior gradients in a high altitude tropical forest in peninsular India. – *Forest Ecology and Management* 87(1): 51-62.
- [24] Kapos, V. (1989): Effects of isolation on the water status of forest patches in the Brazilian Amazon. – *Journal of Tropical Ecology* 5(2): 173-185.
- [25] Li, K., Wang, S., Cao, M. (2004): Vegetation and soil carbon storage in China. – *Science in China Series D Earth Sciences - English Edition* 47(1): 49-57.
- [26] Li, L., Vogel, J., He, Z., Zou, X., Ruan, H., Huang, W., Wang, J., Bianchi, T. S. (2016): Association of soil aggregation with the distribution and quality of organic carbon in soil along an elevation gradient on Wuyi Mountain in China. – *PloS One* 11(3): e0150898.
- [27] Liping, C., Yujun, S., Saeed, S. (2018): Monitoring and predicting land use and land cover changes using remote sensing and GIS techniques—A case study of a hilly area, Jiangle, China. – *PloS One* 13(7): e0200493.
- [28] Lu, R. (1999): *Analytical Methods of Soil Agrochemistry*. – China Agricultural Science and Technology Publishing House, Beijing, pp. 18-99.
- [29] Mannan, A., Feng, Z., Ahmad, A., Liu, J., Saeed, S., Mukete, B. (2018): Carbon dynamics with land use change in Margallah Hills National Park, Islamabad (Pakistan) from 1990 to 2017. – *Applied Ecology and Environmental Research* 16(3):3197-3214.
- [30] Pan, Y., Birdsey, R. A., Fang, J., Houghton, R., Kauppi, P. E., Kurz, W. A., Phillips, O. L., Shvidenko, A., Lewis, S. L., Canadell, J. G. (2011): A large and persistent carbon sink in the world's forests. – *Science* 333(6045): 988-993.
- [31] Paul, E., Follett, R., Leavitt, S., Halvorson, A., Peterson, G., Lyon, D. (1997): Radiocarbon dating for determination of soil organic matter pool sizes and dynamics. – *Soil Science Society of America Journal* 61(4): 1058-1067.
- [32] Pearson, T. R., Brown, S. L., Birdsey, R. A. (2007): *Measurement Guidelines for the Sequestration of Forest Carbon*. – USDA Forest Service, Newton Square, PA.
- [33] Peng, S., Wen, D., He, N., Yu, G., Ma, A., Wang, Q. (2016): Carbon storage in China's forest ecosystems: estimation by different integrative methods. – *Ecology and Evolution* 6(10): 3129-3145.
- [34] Pohlman, C. L., Turton, S. M., Goosem, M. (2009): Temporal variation in microclimatic edge effects near powerlines, highways and streams in Australian tropical rainforest. – *Agricultural and Forest Meteorology* 149(1): 84-95.
- [35] Remy, E., Wuyts, K., Boeckx, P., Ginzburg, S., Gundersen, P., Demey, A., Van Den Bulcke, J., Van Acker, J., Verheyen, K. (2016): Strong gradients in nitrogen and carbon stocks at temperate forest edges. – *Forest Ecology and Management* 376: 45-58.
- [36] Rodrigues, E. (1998): *Edge Effects on the Regeneration of Forest Fragments in South Brazil*. – PhD Thesis, Department of Organismic and Evolutionary Biology, Harvard University, Cambridge, MA.
- [37] Saeed, S., Ashraf, M. I., Ahmad, A., Rahman, Z. (2016): The Bela Forest ecosystem of District Jhelum. A potential carbon sink. – *Pakistan Journal of Botany* 48(1): 121-129.
- [38] Schulp, C. J., Nabuurs, G.-J., Verburg, P. H., de Waal, R. W. (2008): Effect of tree species on carbon stocks in forest floor and mineral soil and implications for soil carbon inventories. – *Forest Ecology and Management* 256(3): 482-490.
- [39] Shaheen, H., Saeed, Y., Abbasi, M., Khaliq, A. (2017): Soil carbon stocks along an altitudinal gradient in different land-use categories in Lesser Himalayan foothills of Kashmir. – *Eurasian soil science* 50(4): 432-437.

- [40] Sharma, C., Gairola, S., Ghildiyal, S., Suyal, S. (2010): Physical properties of soils in relation to forest composition in moist temperate valley slopes of the Central Western Himalaya. – *Journal of Forest and Environmental Science* 26(2): 117-129.
- [41] Singh, H., Kumar, M., Sheikh, M. A., Bhat, J. A. (2011): Forest composition and soil carbon stock in oak and pine forests along altitudinal gradients. – *Indian Journal of Ecology* 38(special issue): 68-71.
- [42] Singh, P. P., Rawat, Y. (2013): Altitude wise variation in soil carbon stock in Western Himalaya. – *New York Science Journal* 6(8): 140-145.
- [43] Smith, P., Fang, C., Dawson, J. J., Moncrieff, J. B. (2008): Impact of global warming on soil organic carbon. – *Advances in Agronomy* 97: 1-43.
- [44] Trumbore, S. (2000): Age of soil organic matter and soil respiration: radiocarbon constraints on belowground C dynamics. – *Ecological Applications* 10(2): 399-411.
- [45] Walkley, A., Black, I. A. (1934): An examination of the Degtjareff method for determining soil organic matter, and a proposed modification of the chromic acid titration method. – *Soil Science* 37(1): 29-38.
- [46] Wei, Y., Li, M., Chen, H., Lewis, B. J., Yu, D., Zhou, L., Zhou, W., Fang, X., Zhao, W., Dai, L. (2013): Variation in carbon storage and its distribution by stand age and forest type in boreal and temperate forests in northeastern China. – *PloS One* 8(8): e72201.
- [47] Williams-Linera, G., Dominguez-Gastelu, V., Garcia-Zurita, M. (1998): Microenvironment and floristics of different edges in a fragmented tropical rainforest. – *Conservation Biology* 12(5): 1091-1102.
- [48] Xianli, X., Bo, S., Huizhen, Z. (2004): Organic carbon density and storage in soils of China and spatial analysis. – *Acta Pedologica Sinica* 41(1): 35-43.
- [49] Yang, Y., Mohammat, A., Feng, J., Zhou, R., Fang, J. (2007): Storage, patterns and environmental controls of soil organic carbon in China. – *Biogeochemistry* 84(2): 131-141.
- [50] Yang, Y., Li, P., Ding, J., Zhao, X., Ma, W., Ji, C., Fang, J. (2014): Increased topsoil carbon stock across China's forests. – *Global Change Biology* 20(8): 2687-2696.
- [51] Yu, D., Shi, X., Wang, H., Sun, W., Chen, J., Liu, Q., Zhao, Y. (2007): Regional patterns of soil organic carbon stocks in China. – *Journal of Environmental Management* 85(3): 680-689.
- [52] Yu, G., Li, X., Wang, Q., Li, S. (2010): Carbon storage and its spatial pattern of terrestrial ecosystem in China. – *Journal of Resources and Ecology* 1(2): 97-109.
- [53] Zhang, M., Zhang, X.-K., Liang, W.-J., Jiang, Y., Guan-Hua, D., Xu-Gao, W., Shi-Jie, H. (2011): Distribution of soil organic carbon fractions along the altitudinal gradient in Changbai Mountain, China. – *Pedosphere* 21(5): 615-620.
- [54] Zhu, B., Wang, X., Fang, J., Piao, S., Shen, H., Zhao, S., Peng, C. (2010): Altitudinal changes in carbon storage of temperate forests on Mt Changbai, Northeast China. – *Journal of Plant Research* 123(4): 439-452.

DETERMINATION FOREST ROAD ROUTES VIA GIS-BASED SPATIAL MULTI-CRITERION DECISION METHODS

ÇALIŞKAN, E.^{1*} – BEDİROĞLU, Ş.² – YILDIRIM, V.²

¹*Department of Forest Engineering, Faculty of Forestry, Karadeniz Technical University
61080 Trabzon, Turkey*

²*Faculty of Engineering, Karadeniz Technical University, 61080 Trabzon, Turkey*

**Corresponding author
e-mail: caliskan@ktu.edu.tr*

(Received 20th Sep 2018; accepted 28th Nov 2018)

Abstract. Forest road route determination is a complex process in which a number of variables should be analyzed simultaneously and it is one of the most important process steps for forest road projects. For this purpose, the factors that are effective on forest road routes should be primarily determined. The effects of each factor should be determined as a weighting coefficient and they should be evaluated and analyzed as a whole. Since the factors with impact on forest road routes are considered a necessity, the management of intense spatial data sets emerges. The analysis of such intense data sets and obtaining quick and accurate results are possible by way of decision support systems known as Geographic Information Systems (GIS). In this study, forest road route determination was carried out using a decision-support system called FOROR (Forest Road Route) developed by us which is a raster-based system, based on GIS technologies. FOROR software is an application that combines GIS and MCDM principles. Manuel provides long-term analysis and benchmarking. Visual Studio and Developer for ArcGIS had been used for creating FOROR. ArcPy, Python programming language had been used at FOROR. In this context, the factors that are effective on forest road routes were determined after which the necessary geographic data layers were identified based on these factors which were then classified according to the standards. For this application, Analytical Hierarchy Process (AHP), Simple Additive Weighting (SAW), Fuzzy Overlay, Promethee and TOPSIS methods of Multi-Criteria Decision Methods (MCDM) were used. Study area is located at Black Sea region of Turkey. Analyses were performed using five different methods for the determination of forest routes; five different routes were found accordingly and these routes were compared to each other as well as to the existing road. The advantages provided by MCDM with support of Geographic Information System for forest road route determination were put forth as a result of the study.

Keywords: *forest road route, spatial multi-criteria decision making, AHP, SAW, TOPSIS, Promethee, Fuzzy Overlay, GIS*

Introduction

Forest roads are among the most important infrastructure facilities for forestry operations which are also renewable natural resources. Forestry operations include forest road design and slope stability, analysis of harvesting systems for economic efficiency and site protection, planning and scheduling of harvests in addition to transportation systems. It is necessary to establish a road route which will enable the achieving of targets in order to plan forestry operations within the frame of sustainability concept. There are numerous studies in which GIS has been used for route determination. GIS is essential in trail route planning with an objective of applying and evaluating a GIS-based methodology for determining optimal recreational trail routes using key information items (Chiou et al., 2010). There is a need for development of spatial data infrastructure that improves the access to reliable information for sustainable management of the forest

and its wildlife resources (Nino et al., 2017; Arpacık et al., 2017). A significant issue in the field of object modeling is proper representation of objects in the real world within a geographical information system (GIS) environment (Sadeghi-Niaraki et al., 2011). However, the number of criteria and approaches that have been adopted in these studies vary significantly. While only a single criterion, such as landslide, is taken into consideration in some studies, others evaluate several criteria simultaneously. Selection was made in some studies among the alternatives created by evaluating the effects of the proposed road, whereas in others the area where the road will be built was evaluated in terms of several criteria after which the best alternatives were attempted to be designed.

Spatial planning of urban forest development can be carried out more easily and quickly within GIS (Narulita et al., 2016). Conventional road planning methods based on topographic maps do not allow forest engineers to create a sufficient number of road alternatives (Chung and Sessions, 2001). If the alternatives are not evaluated in the process of choosing the optimum route, the engineers cannot guarantee that the selected route is the best which minimizes the environmental effects around the route. Chen and Koprowski (2016) have made a good study for saving the habitat and ecosystem. Environmental factors must be taken into consideration as a geodatabase for saving the ecosystem. The terms that environmental factors correspond to are; rivers, lakes, protected areas, soil quality and natural resources. Rapaport and Snickars (1998) carried out a study in which they determined a road route that minimizes the environmental effects with a low-cost while enabling enables transportation in the shortest period of time by way of GIS techniques. Lee and Stucky (1998) developed an algorithm for finding the lowest-cost road route depending on the topography factor and tested it via field work. Sadek et al. (1999) carried out a study in which a GIS platform was developed that brings together the content necessary for the multi-criteria evaluation of route alternatives.

A number of computer-assisted and GIS-based models have been developed in recent years for determining the forest road routes automatically. TRACER (Akay and Sessions, 2005) and PEGGER, ROUTES (Rogers, 2005; Reutebuch, 1988) can be mentioned. Several scientific studies were carried out in Turkey in which computer software (Demir, 2007; Demir and Öztürk, 2004) and GIS methods (Altunel, 2000; Gümüş and Erdaş, 2000; Gümüş, 2008; Akay et al., 2008) were utilized. Yu et al. (2003) developed an algorithm to determine road routes by using raster-based GIS abilities. This algorithm provides solutions which can be used for determining the locations of art structures such as bridges and tunnels along the route.

Forest road location knowledge is coupled with planning models and decision-making tools implemented in geographic information systems (Sačkov et al., 2014). Saha et al. (2005) determined the optimum road route in areas under landslide danger in Himalayas using a GIS-based method. In this study, landslide danger zones, land use, drainage conditions (drainage intensity, creek frequency etc.) and lithological structure were taken into consideration in determination of the road route. Sadeghi-Niaraki et al. (2011) aimed to create a model for determining the best possible road route in a road network by using GIS technologies. They formed a model using Analytical Hierarchy Process (AHP) method and adding variables such as velocity, time weather, address information and road type to the road network model. The defined variables were combined by using the resistance model method in AHP. The variables were subject to sensitivity analysis in the final stage and the developed model was tested using a raster-based GIS model with Multi-Criteria Decision Making (MCDM) methods for determining the optimum

transportation route with the minimum cost for heavy vehicles (Choi et al., 2014). He created the model with a fuzzy logic which was formed by using multiple criteria (velocity, water mass, material size, curve, visibility, distance, road, maintenance etc.) simultaneously so that it can evaluate the total weight of the movements of heavy vehicles.

MCDM methods are interactive and flexible tools for the analysis of complexity among the alternatives which contain different environmental and socio-economic factors. Combining GIS and MCDM techniques provides convenience to the users in determining the various alternatives of criteria and objects with multiple and complex structures. Some researchers have been performing road network analyses using GIS-based road structure and MCDM by considering factors such as wood volume, slope, soil condition as well as the distance between existing forest roads, soil type, geology, hydrography, elevation and tree type in addition to environmental factors (Sadek et al., 1999; Hosseini and Solaymani, 2006; Jusoff, 2008; Mohammadi Samani et al., 2010; Hayati et al., 2012; Çalışkan, 2013; Stergios et al., 2015).

There has been a rapid increase in the interest towards and research on GIS based MCDM methods in recent years. MCDM is a routine activity that is common to individuals and organizations. Selection of the suitable route in planning of forest roads is a complex engineering problem depending on various factors. In this respect, utilization of GIS technologies and spatial multi-criteria decision making methods (MCDM) are required.

It was observed as a result of examining the existing forest road projects that the building cost is higher than the budget of the project due to incorrect route determination, the that environmental effects exceed acceptable limits and that geologically unfavorable areas are being used. As far as GIS is concerned, it significantly simplifies the vehicle routing optimization process, representing, visualizing efficiently and conveniently the obtained results and reducing costs (Zsigraiova et al., 2013). Therefore, in terms of optimum management of resources, forming a GIS-based, and effective route determination model for the forest roads in Turkey is of significant importance. No study has been carried out in Turkey for determining the forest routes which considers the whole major factors (slope, geological structure, rivers, lakes, protected areas, soil quality and natural resources) using raster-based advanced GIS as well as MCDM techniques with special extensions for.

Forest road route determination in this study was carried out dynamically using a raster-based decision-support system. An ArcGIS extension called FOROR (Forest Road Route) was developed for this purpose based on GIS technologies. In this respect, the primary factors with impacts on the forest road route along with the necessary geographic data layers were determined and classified according to the standards. For this application, Analytical Hierarchy Process (AHP), Simple Additive Weighting (SAW), Fuzzy Overlay, Promethee and TOPSIS methods of MCDM were used. Lack of these works is this, we could not see any model considering 5 different MCDM techniques at same extension. Analyses were carried out using five different methods for determining the the forest route as a result of which five different routes were found which were then compared among each other as well as with the existing road.

The purpose of this study is to test multi-criteria decision-making methods in determining forest roads. Five different MCDM methods have been automatically tested by means of special GIS software. Thus, new road routes that are economically feasible and sensitive to the environment have been determined.

Material and Methods

Study Area

Trabzon Province is situated between longitude $39^{\circ} 7' 30''$ and $40^{\circ} 30'$ E and latitude $40^{\circ} 30'$ to $41^{\circ} 7' N$ in central Eastern Black Sea region of Turkey (Figure 1). Eastern Black Sea region and also the city of Trabzon is green-field and has a great tree diversity due to rainy climate. There are many different stands at Trabzon and in case study area chosen. Determining an optimum route for a road in this area is a challenge. The location of the study area has been shown in Fig. 1.

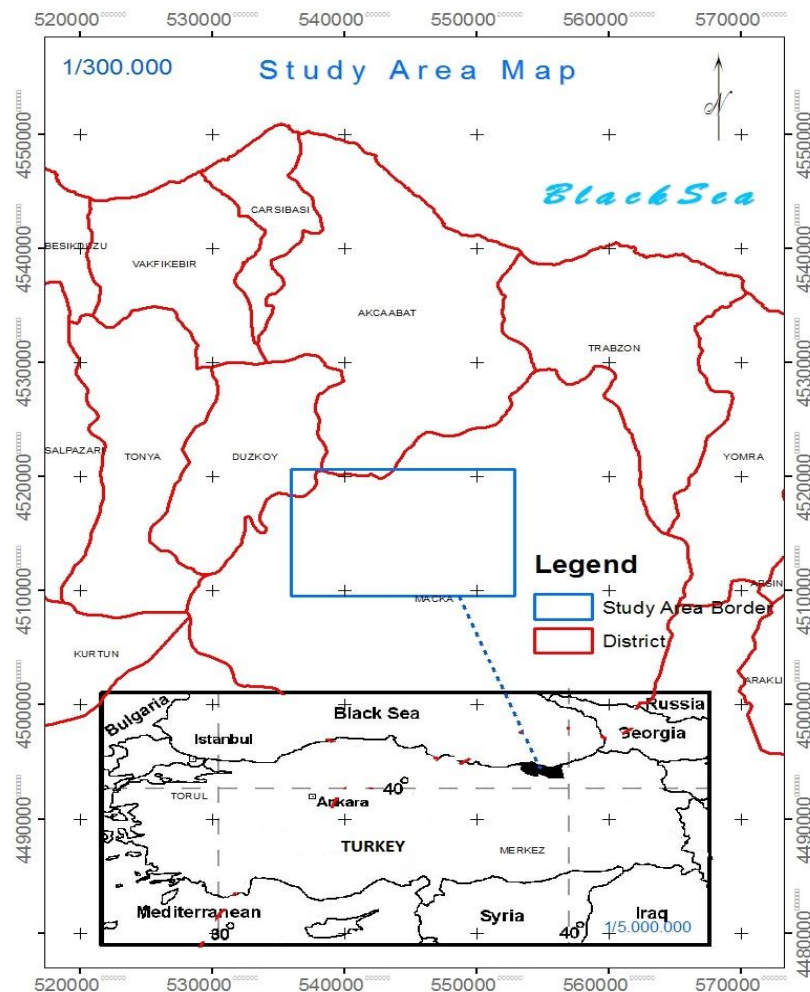


Figure 1. Location of the study area

The process steps for the application in this study has been shown and explained briefly in Fig. 2. The first step was determining factors and sub-factors and determining the weights of factors as analysis criteria. These factors were assigned from academic studies, context sensitive application projects and interviews with experts on this area. These factors and sub-factors and their weights shall be explained briefly in the next section of this paper. The next step was generating a spatial database coherent with factor and sub-factors. The spatial datasets were then analyzed using our special Forest

Road Route (FOROR) extension running at ArcGIS/ArcMap software. Finally, the acquired results were compared and relevant information was provided in the form of tables and verbal discussions.

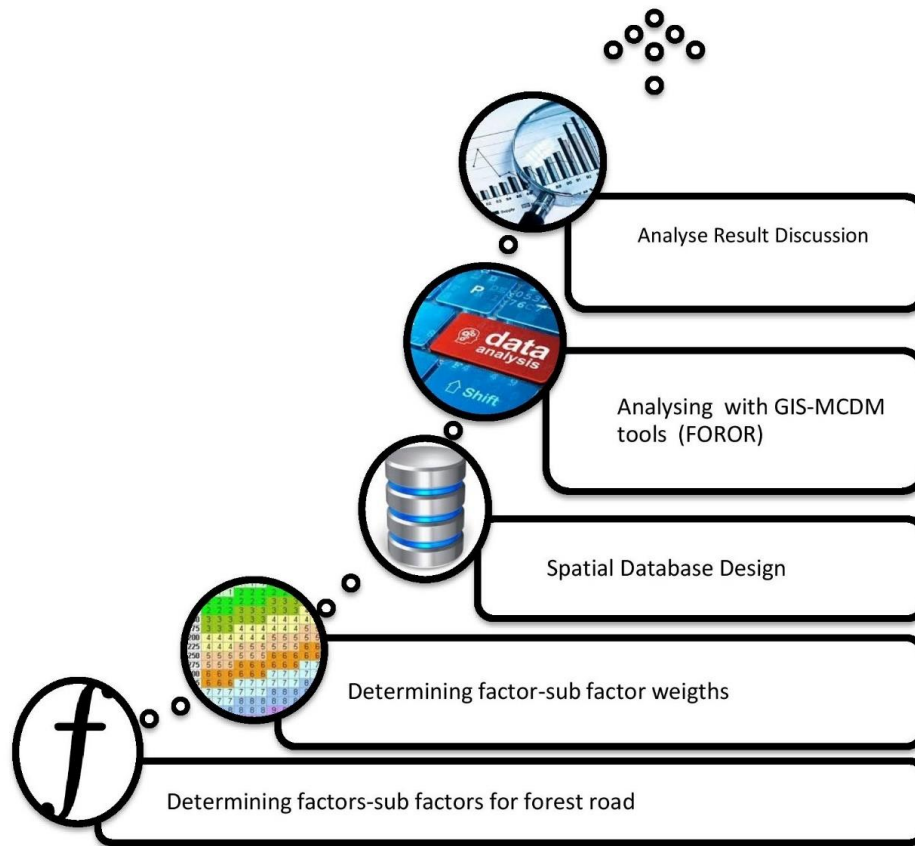


Figure 2. Graphical representation of the workflow

Factors, sub factor and their weights

MCDM is a comprehensive technique and the determination of factor, sub-factor weights was a challenging problem. There are many various approaches in literature for determining weights. The weights were determined in this study by way of interviews with academicians, private sector and forest engineering staff working at similar route determination areas. The objective of the interviews carried out was to get a personal idea of professionals working at route determination studies. Interviews were carried out with 15 academicians working on similar areas such as, geomatics, forestry, civil engineering etc. There was a total of 8 private sector employees to whom we applied for interviews. In addition, 11 forest engineers working at government organizations participated in our interview. Finally, the weights were compared with the relevant studies in literature as a result of which it was put forth that there are no statistically significant differences between our weights and the weights used in various previous studies. Some of these comparison studies are: Bagli, 2011; Kiker et al., 2009; Malczewski, 2007; Malczewski, 1999; Joerin et al., 2001. The weights of factors and sub-factors are given in *Table 1*. Sub-factor weights were indicated directly and factor

weight at SAW order for generating relative rank idea in researcher’s mind between factors. Detailed weights of each factors in AHP, TOPSIS, Promethee or Fuzzy Overlay can be seen in *Table 2*.

Table 1. Factors, sub factor weights

CRITERIA	(Factor) PASS	(Sub Factor) Weight	SAW Order (Rank)
Avalanche	Pass	9	6
Erosion	0-250 meters	-	5
Rivers	100 meters	9	2
	200 meters	7	
	300 meters	5	
	400 meters	3	
	500 meters	1	
Protected areas	Pass	Restricted	8
Natural resources	250 meters	9	9
*Soil	4. degree	5	3
	6. degree	3	
	7. degree	2	
Geology	Kru 1-2-3	1	4
	Gama 2-3	7	
	Jlh-Jkr	5	
	Alv	4	
Land cover	Meadow	1	7
	Nut	7	
	Dry-agric.	5	
	Forest	3	
	Settlement	Restricted	Restricted
Slope	0-5	1	1
	5,01-10	3	
	10,01-20	5	
	20,01-30	7	
	30,01-40	9	
	40,01-90	9	

*Soil type is shown with numbers from 1 to 9. 1 is the best quality soil for agriculture or other usages, other side 9 is poor quality soil. All the geographic dataset was taken from related governmental resources and then reorganized. “SAW” order is rank of each factor in SAW MCDM technique. Pass means definition of intersection between each route and related factor’s geographic dataset

A comparison difference index (CDI) formula applicable for all MCDM methods as a self-technique for comparing evaluations was generated. First of all, it can be seen as a complicated formula but it is too easy to use and calculate. Calculation formula for comparing final routes is given below;

$$CDI = \sum \{ [1 - (y/2z)] * x * t \} \quad (Eq.1)$$

where, *x*: Pass Value due to related factor in meters (line polygon intersection value), *y*: SAW rank in number, *z*: Total factor count, *t*: Sub factor point (determined with interview).

Designing Geodatabase

A geographic database was created in ESRI ArcGIS 10.3 software and projected to Universal Transverse Marketer (UTM) projection, zone 36N. Maps were rectified, digitized, projected and imported to the geographic database.

An accurate and updated geodatabase was created consisting of geographic layers within factors. Geographic layers were redesigned flowingly due to sub-factors included in the factors. These geodatabase layers were; rivers, ways, slope, soil type, geology, erosion, avalanche, natural resource, protected areas and land cover map of area. Some of these geographic layers have been shown in *Fig. 3*.

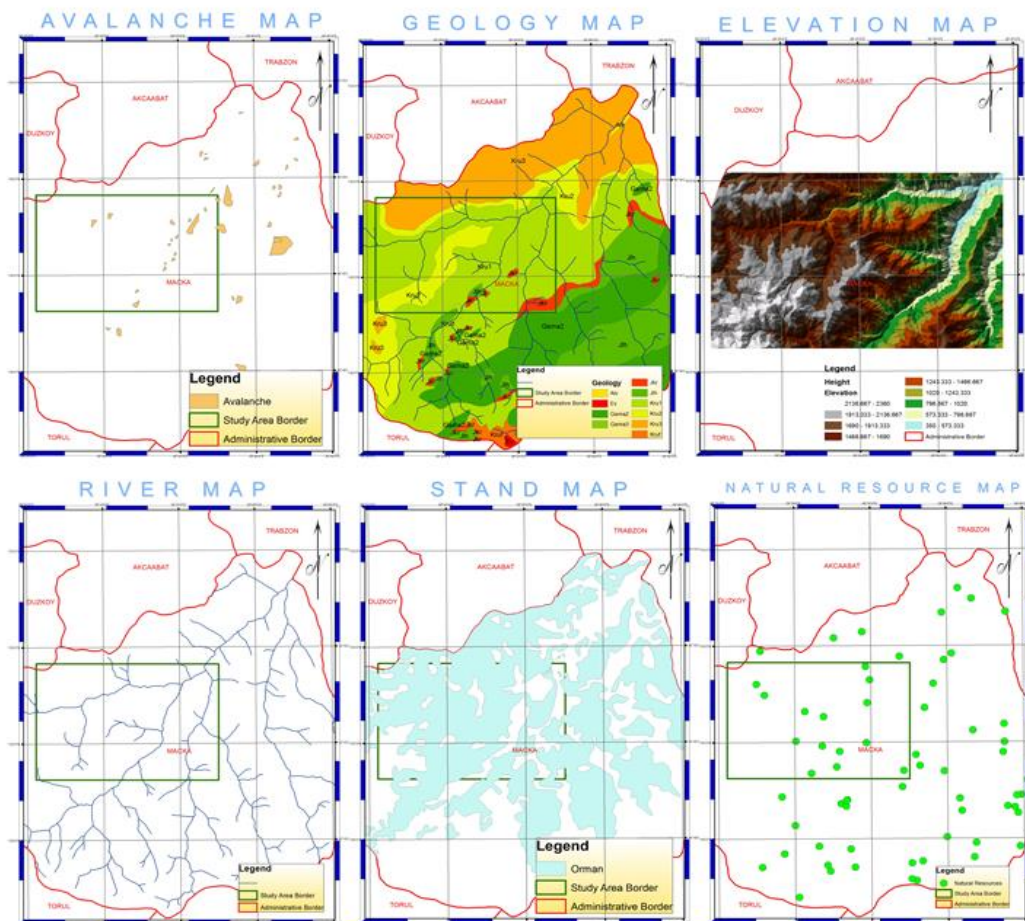


Figure 3. Maps of some geographic layers in Geodatabase

Methodology

The methodology of this paper was based on the principles GIS and MCDM. Common MCDM rules and formulae have been used for calculating factor and sub-factor weights with our special GIS extension (FOROR) (Çalışkan et al., 2016). The calculated factor and sub-factors were then included as part of the GIS analysis processes. GIS analysis processes were interpolating heights and building TIN, ring-buffer for river, way etc. point or polyline data and then merging them with the study area border, interpolating some sample data (like population) with Kriging or Invert

Distance Weighting (IDW) as geostatistical coherent interpolation techniques and reorganizing polygon data before applying raster to vector conversation. Kriging interpolation is generally used for population interpolations, estimations. On the other hand, IDW is used for analysis such as pollution or density clustering analysis. Finally, all the geospatial dataset prepared in vector format was clipped to the study area border which was then converted to raster format in equivalent pixel values for calculating the accumulated cost surface. A conversion to raster format was performed using a cell size of 30x30 m. Cost distance-cost path algorithms were applied to accumulated surfaces and optimum routes were found. There are various algorithms such as Berry, Dijkstra etc. The Cost Distance function creates an output raster in which each cell is assigned the accumulative cost to the closest source cell. The algorithm utilizes the node/link cell representation. Summary explanations and mathematical formulae have been given below this section as well as results of some GIS analyses shown with figures. Our extension includes 5 MCDM same methods. We can apply 5 different calculations for the same geodatabase. Five different methods have been given below.

Multicriteria Techniques

There are 5 well known MCDM techniques used in this study; which are TOPSIS, SAW, Fuzzy Overlay, AHP and Promethee. These techniques have different mathematical formulae and verbal definitions. In this section, their formulae have been acquired from academic studies with less verbal definitions because they have long process steps.

TOPSIS Method

TOPSIS is generated by Yoon and Hwang in 1980 and uses common approaches of ELECTRE method. TOPSIS includes six step processes.

- Step 1: Creating performance decision matrix.

$$A_{ij} = \begin{bmatrix} a_{11} & a_{12} & \dots & a_{1n} \\ a_{21} & a_{22} & \dots & a_{2n} \\ \cdot & & & \cdot \\ \cdot & & & \cdot \\ \cdot & & & \cdot \\ a_{m1} & a_{m2} & \dots & a_{mn} \end{bmatrix} \quad (\text{Eq.2})$$

- Step 2: Calculating the normalized decision matrix (R_{ij}). r_{ij} here is normalized value.

$$r_{ij} = \frac{a_{ij}}{\sqrt{\sum_{i=1}^m a_{ij}^2}} \quad (\text{Eq.3})$$

$i=1, 2, \dots, m; j=1, 2, \dots, n.$

R matrix is obtained as the formula below:

$$R_{ij} = \begin{bmatrix} r_{11} & r_{12} & \dots & r_{1n} \\ r_{21} & r_{22} & \dots & r_{2n} \\ \cdot & & & \cdot \\ \cdot & & & \cdot \\ \cdot & & & \cdot \\ r_{m1} & r_{m2} & \dots & r_{mn} \end{bmatrix} \quad (\text{Eq.4})$$

- Step 3: Calculating the weighted normalized decision matrix. The weighted normalized value V_{ij} is calculated as follows:

$$V_{ij} = \begin{bmatrix} w_1 r_{11} & w_2 r_{12} & \dots & w_n r_{1n} \\ w_1 r_{21} & w_2 r_{22} & \dots & w_n r_{2n} \\ \cdot & & & \cdot \\ \cdot & & & \cdot \\ \cdot & & & \cdot \\ w_1 r_{m1} & w_2 r_{m2} & \dots & w_n r_{mn} \end{bmatrix} = (R_{ij} \times V_{n \times n}) \quad (\text{Eq.5})$$

- Step 4: Ideal (A^*) and Negative ideal (A^-) Solutions.

$$A^* = \left\{ (\max_i v_{ij} | j \in J), (\min_i v_{ij} | j \in J') \right\} \quad (\text{Eq.6})$$

$$A^- = \left\{ (\min_i v_{ij} | j \in J), (\max_i v_{ij} | j \in J') \right\} \quad (\text{Eq.7})$$

- Step 5: Calculating separation measures with Euclidian distance.

$$S_i^* = \sqrt{\sum_{j=1}^n (v_{ij} - v_j^+)^2} \quad (\text{Eq.8})$$

$$S_i^- = \sqrt{\sum_{j=1}^n (v_{ij} - v_j^-)^2} \quad (\text{Eq.9})$$

$i=1,2,\dots,m$ and $j=1,2,\dots,n$.

- Step 6 (Last Step): Calculating proximity to ideal solution.

$$C_i^* = \frac{S_i^-}{S_i^- + S_i^*} \quad (\text{Eq.10})$$

Here, C_i^* is given a value between $0 \leq C_i^* \leq 1$ and $C_i^* = 1$ indicating the proximity of the related decision points to the ideal solution, $C_i^* = 0$ decision points' negative proximity to ideal solution (Yaralioglu, 2004). The factor and sub-factor weights were calculated using TOPSIS.

SAW Method

The mathematic formulation of the method was described by an equation and a simple formula (Kontos et al. 2005);

$$V_i = \sum_{j=1}^n w_j v_{ij} \quad (\text{Eq.11})$$

where, V_i is the suitability index for the area i , w_j is the relative importance weight of criterion j , v_{ij} is the grading value of area i under criterion j , n is the total number of criteria. The factor and sub-factor weights were calculated using SAW (Yildirim et al., 2017).

Fuzzy Overlay Method

The equation using fuzzy Gaussian function can be given as:

$$\mu x = e - f1 * x - f2 \quad (\text{Eq.12})$$

where, the inputs to the equation $f1$ and $f2$ are the spread and the midpoint, respectively (Baidya et al, 2014). The factor and sub-factor weights were calculated using Fuzzy overlay.

AHP Method

AHP is a multi-objective, multi-criteria decision-making approach, which enables the decision maker to arrive at a scale of preference drawn from a set of alternatives. It helps decision makers find out the best suits their goal and their understanding of a complex problem with multiple conflicting and subjective criteria (Ezzabadi et al., 2015; Saaty, 1980). The factor and sub-factor weights were calculated using AHP.

$$A_i P A_j \rightarrow a_{ij} > 1 \quad (\text{Eq.13})$$

$$A_i I A_j \rightarrow a_{ij} = 1 \quad (\text{Eq.14})$$

$$a_{ij} = 1/a_{ji} \quad (\text{Eq.15})$$

$$a_{ij} = 1 \quad (\text{Eq.16})$$

$$(A - \lambda_{\max} I) \times w = 0 \quad (\text{Eq.17})$$

$$a_{ij} = a_{ik} \times a_{kj} \quad (\text{Eq.18})$$

$$w_p = W_p \times W_{p-1} \times \dots \times W_3 \times w_2 \quad (\text{Eq.19})$$

AHP provides measures of inconsistency as a function of the deviation between λ_{max} and n . Finally, global priorities at each node of the hierarchy were calculated by weighting the local priorities with the weights of the corresponding parent nodes. When w_{k-1} is the vector of global priorities (weights) of the elements in the level $(k-1)$, W_k is the matrix of local priorities of the level k with respect to elements of level $(k-1)$. The global priorities at the level k are given by $w_k = W_k \times w_{k-1}$. Since local and global priorities are the same at the second level ($w_1 = [1]$), the global priorities at level p can be computed using Equation (Yildirim et al., 2017). The factor and sub-factor weights were calculated using AHP.

Promethee Method

First of all, a particular preference function need to be determined ($P_j(a,b)$) in order to translate deviation between the evaluations of two alternatives (a and b) on a specific criterion (g_j) into a preference degree ranging from 0 to 1. Preference scores of alternatives on a certain criteria are derived from $(f_j(a)-f_j(b))$, as shown in Equation 20 (Murat et al., 2015).

$$P_j(a,b) = G_j \{f_j(a) - f_j(b)\} \quad (\text{Eq.20})$$

Relative importance (weights) of each criterion needs to be assigned. Within this content, an overall preference index ($\pi(a,b)$) can be computed via taking all the criteria into account (see Equation 21). This preference index is based on the positive $\phi^+(a)$ and negative $\phi^-(a)$ preference flows for each alternative, which measures how an alternative (a) is outranking (see Equation 22) or outranked (see Equation 23) by the other alternatives. The difference between these preference flows is represented as the net preference flow $\phi(a)$ (see Equation 24) (Murat et al., 2015).

$$\pi(a,b) = \sum_{j=1}^k w_j P_j(a,b) \quad (\text{Eq.21})$$

$$\phi^+(a) = \frac{1}{n-1} \sum_b \pi(a,b) \quad (\text{Eq.22})$$

$$\phi^-(a) = \frac{1}{n-1} \sum_b \pi(b,a) \quad (\text{Eq.23})$$

$$\phi(a) = \phi^+(a) - \phi^-(a) \quad (\text{Eq.24})$$

The positive preference flow $\phi^+(a_i)$ quantifies how a given action (a_i) is globally preferred to all the other actions while the negative preference flow $\phi^-(a_i)$ quantifies how a given action (a_i) is globally preferred by all the other actions. An ideal action would have a positive preference flow equal to 1 and a negative preference flow equal to 0. The two preference flows induce two generally different complete rankings on the set of actions. The first one is obtained by ranking the actions according to the decreasing values of their positive flow scores. The second one is obtained by ranking the actions according to the increasing values of their negative flow scores. The

Promethee I partial ranking is defined as the intersection of these two rankings. As a consequence, an action (a_i) will be as good as another action (a_j) if;

$$\varphi^-(a_i) \geq \varphi^-(a_j) \text{ and } \varphi^+(a_i) \leq \varphi^+(a_j) \quad (\text{Eq.25})$$

The factor and sub-factor weights were calculated using Promethee (Toinard et al., 2015).

Creating forest road route determination extension tool

A new GIS and MCDM extension has been developed for ArcMap 10.3 for the purposes of accelerating the process steps, minimizing human-user mistakes and adding special custom-defined algorithms. Microsoft Visual Studio and ArcGIS SDK (Software Developer Kit) for Python were used with ArcObject libraries. This extension named FOROR is a comprehensive tool that automates all analyses and discussion steps (Çalışkan et al., 2016). After the vector based GIS files are opened in addition to giving factor and sub factor weights, it just remains to choose the analysis patterns pre-defined on the tool. The tool consists of all related GIS functions such as Vector-Raster conversion, GIS Analysis (Buffer, Intersect, Overlay etc.), Kriging-IDW Interpolations, Accumulated Cost Surface Calculation and finding optimum routes with Cost Distance Cost Path Algorithms. The extension needs a .mxd file containing related geographic dataset in vector format. You are then directed to enter quantities of your factor, sub-factor weights, points and other related information. TOPSIS, SAW, PROMETHEE, AHP and FUZZY OVERLAY algorithms and mathematical formulas also included into extension.

Sensitivity Analysis

Sensitivity analysis was used to examine the sensitivity of the routes subject to changes in variable weights. This is useful in circumstances where uncertainties exist with regard to the definition of the importance of different route-related variables. In many cases, it is also important to know how the results will change if the weights are changed (Sadeghi-Niaraki et al., 2011). Sensitivity analysis allows the determination of the level of accuracy required for a parameter to make the model sufficiently useful and valid. There are many different sensitivity techniques in literature if MCDM calculations and GIS analysis are sensitive to any changes of parameters. Changing factors, sub-factors or changing order of criteria are well known and commonly used techniques.

Results and Discussion

By applying the described methodology, we obtained the relevant data for all five variants of the forest road route; analyzed, evaluated and compared them after which we selected the one that best suits the methods. GIS based MCDM analyses were applied on geodatabase using our case-sensitive extension (FOROR). Buffer analysis, interpolations, normalizations and vector-raster conversions were carried out automatically for the given factor, sub-factor points and other values. Analysis steps have been shown briefly in *Figure 2* (Workflow Diagram) and the relevant steps were explained in previous sections. The result maps and related tables generated by the

extension are shown automatically in this section. *Figures 4, 5, 6, 7, 8* show the resulting forest road route generated for each MCDM technique and the current forest road used at the field. Each MCDM result route has different flows but at first sight AHP and TOPSIS have closed flows on the map since their mathematical formulas and algorithms are similar.

All factors which affect forest road routes will not, of course, have equal effects on each route. Therefore, in the factor weights and sub-criteria weights should be determined in order to take this variation into account. In the context of this study, it was considered that AHP, TOPSIS, SAW, Promethee and Fuzzy overlay methods from the Multi-Criteria Decision Making (MCDM) methods are suitable after which the weights of the factor and sub-criteria were determined.

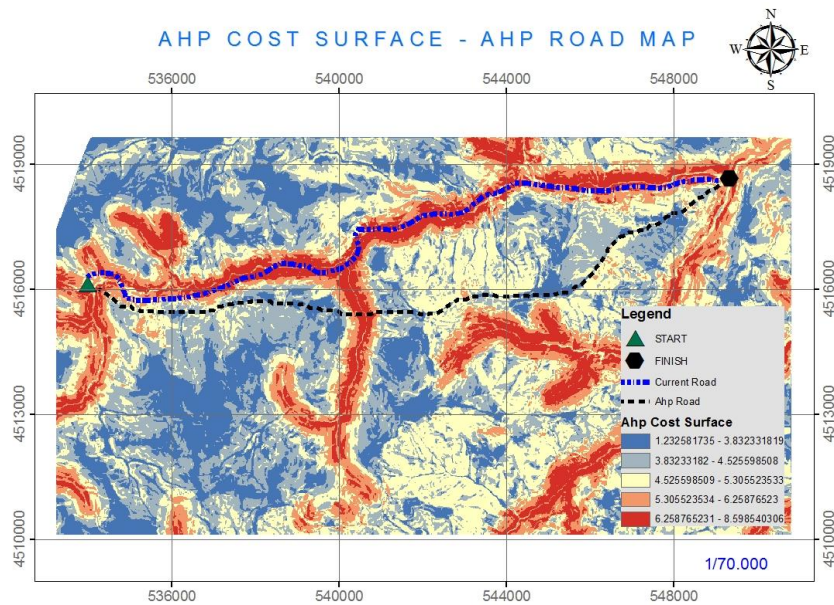


Figure 4. AHP cost surface, AHP route and current route

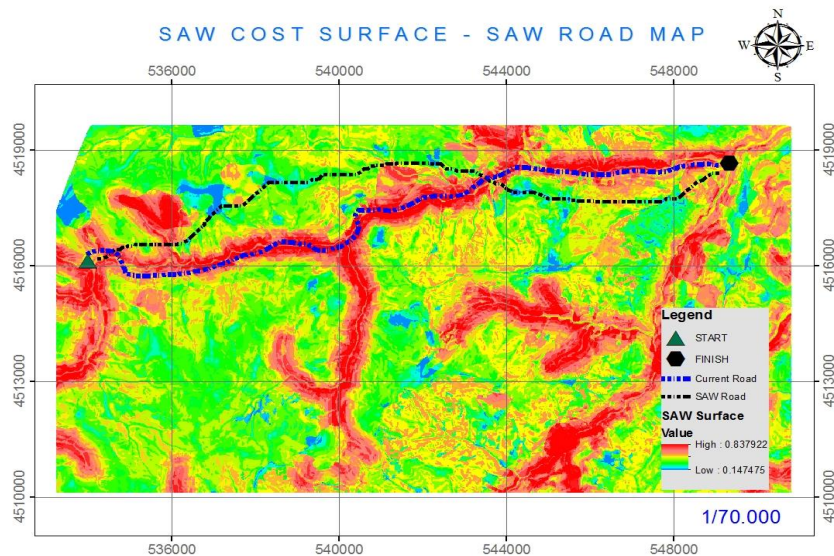


Figure 5. SAW cost surface, SAW route and current route

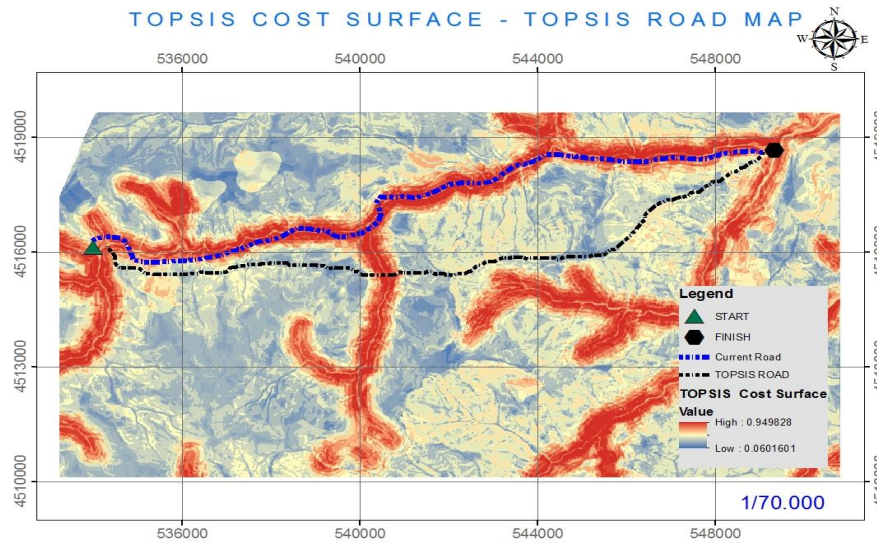


Figure 6. TOPSIS cost surface, TOPSIS route and current route

This paper puts forth a comprehensive method for comparing the most frequently used MCDM techniques and GIS with an automatic model in a case study on forest road route determination. 5 different forest road routes were determined following GIS based MCDM analysis. The manner of approach for discussing which method is suitable and effective for similar linear projects might be by the way of discussing each route respectively in terms of advantageous and disadvantageous results. In this section; one side we have discussed which MCDM technique gives the best offer and other side investigated, if our model is sensitive and acceptable in general.

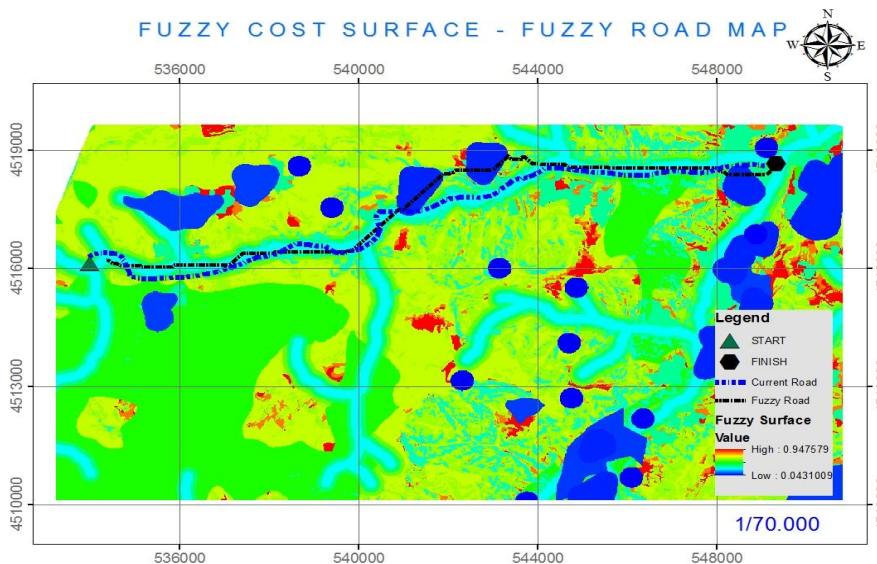


Figure 7. FUZZY cost surface, FUZZY route and current route

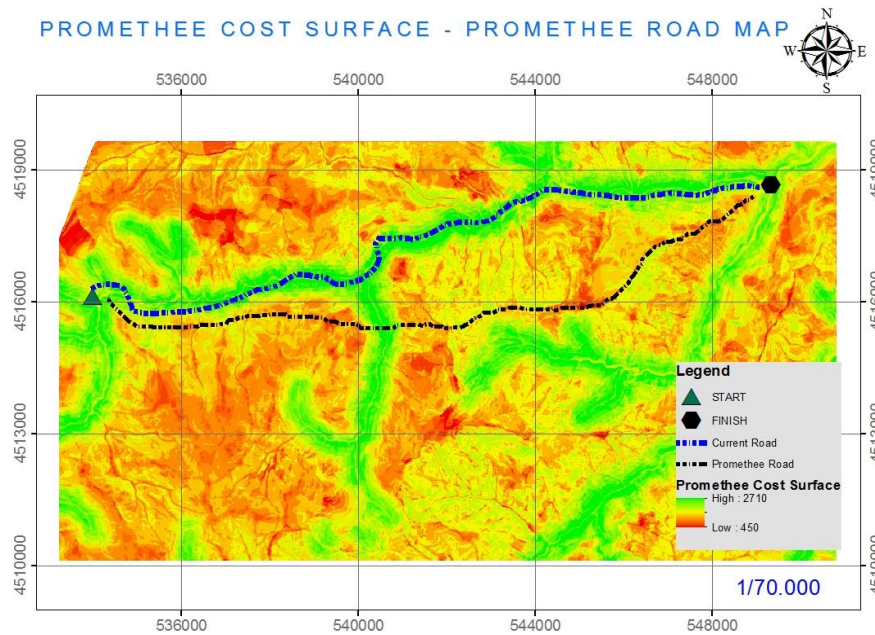


Figure 8. Promethee cost surface, Promethee route and current route

Table 2 shows these five generated forest road routes and the current road discussing in terms of coherency with given criteria (factor, sub-factor) weights. Values in Table 2 are quantity of intersection between route and related factor's geographic dataset. This Table summarizes 6 different routes (Promethee, TOPSIS, AHP, SAW, Fuzzy Overlay and Current Forest Road) as the suitability with given criteria before analysis. When we first consider Table 2, it can clearly be seen that Promethee is advantageous with regard to others. Promethee is advantageous in terms of given criteria's such as Avalanche, River and others. When all the criteria considered totally Promethee is the best method for this study.

No significant difference was observed between the total lengths of the result. The roads were calculated there isn't a big difference between generated 5 roads and current road. TOPSIS route is 16862 m, SAW route is 16156 m, Promethee route is 16420 m, FUZZY route is 16288 m, AHP route is 16828 m and current route is 17138 m.

According to (Eq.1) formula, Promethee is the most effective method with a total CDI score of 175532,50 while the score of the Current Route was 331870,70 which was the worst. Other CDI scores are: TOPSIS- 182319, 3; AHP- 184552,8; SAW- 203678,2; FUZZY-316363,4. Therefore, the effectiveness ranking of MCDM techniques for Forest route determination can be listed as Promethee, TOPSIS, AHP, SAW and Fuzzy overlay according to our studies.

On the other hand, the selected GIS methods yielded sufficient per formation with regard to determining the optimum forest road route. Cost distance-cost path algorithms gives the best route on accumulated cost surface which is based on the case that all five forest road routes are more advantageous than the current forest road (Table 2). Calculation on raster pixels is the correct method on behalf of modelling the complete area in within the study borders. Also reclassifying all factor layers in same pixel resolution (30*30 meter in this application) has solved problems in the process of accumulated cost surface calculation.

Table 2. Comparison of MCDM techniques from final forest roads

Criteria	PASS	Current Road (meters)	AHP (meters)	FUZZY (meters)	TOPSIS (meters)	SAW (meters)	Promethee (meters)
Avalanche	PASS	502,29	848,34	3025,22	855,66	1652,26	353,56
Erosion	0-250 m	-	-	-	-	-	-
Rivers	100 m	10005,78	301,46	11277,72	308,33	885,77	223,79
	200 m	6155,96	449,96	491,93	341,75	618,06	310,86
	300 m	945,91	462,29	510,83	456,17	682,04	327,25
	400 m	31,14	519,07	568,09	627,94	767,18	389,63
	500 m	-	1928,65	971,54	1682,81	928,26	1368,22
Protected Areas	PASS	-	-	-	-	-	-
Natural Resources	250 m	-	367,71	-	335,71	-	367,70
Soil	4	-	-	-	-	21,82	-
	6	3275,46	3702,48	3072,55	3589,77	2206,11	3549,07
	7	13863,23	13139,96	13230,47	13286,94	14298,04	12886,01
Geology	Kru1-2-3	17138,69	16842,43	16303,03	16876,71	16526,37	15745,45
	Gama	-	-	-	-	-	-
	Jlh	-	-	-	-	-	-
Land Cover	Meadow	1296,74	1469,41	1681,25	1384,67	1784,55	1411,76
	Nut	543,43	1728,37	2757,49	1604,11	4272,88	1377,08
	Dry-Agric.	3824,57	455,36	2077,77	336,56	847,65	329,64
	Forest Settlement	11473,96	13189,30	9786,53	13551,36	9621,30	13316,60
	-	-	-	-	-	-	-
Slope	0-5	167,99	909,22	316,16	1006,99	431,51	986,48
	5,01-10	446,92	1901,29	440,49	2037,97	1209,57	2050,40
	10,01-20	1346,33	6447,21	2052,63	6694,03	5991,98	6040,23
	20,01-30	4246,06	6266,39	2743,58	5796,59	6712,39	5958,70
	30,01-40	6265,64	1246,09	6140,66	1268,89	1861,39	1280,10
	40,01-90	4665,75	72,23	4609,51	72,23	319,19	119,17
Total Lenth		17138	16828	16288	16862	16156	16420

Forest road planning with the lowest total construction costs is not always the best solution from an environmental point of view (Liu and Sessions, 1993; Dean, 1997; Chung and Sessions, 2001; Aruga, 2005; Akay, 2006; Hayati et al., 2012). In order to choose the best variant, it is necessary to take into account several criteria (Abdi et al., 2009; Gümüş, 2017).

As a result, an example sensitivity analysis for Promethee forest road route and cost surface was evaluated for this analysis. A python script was generated for this addition

to our extension, FOROR. The function of the script is recalculation of the raster files by changing their weights with percent increase or decreases independent from each other. The sensitivity analysis shows that our GIS analysis is sensitive for 9 factors out of 10. The reason why the 1 factor (Protected Areas) is not sensitive is that there are a few protected areas on the field and this does not affect the analysis results significantly. *Figures 9-10* show how the cost surface is changing when we change weights.

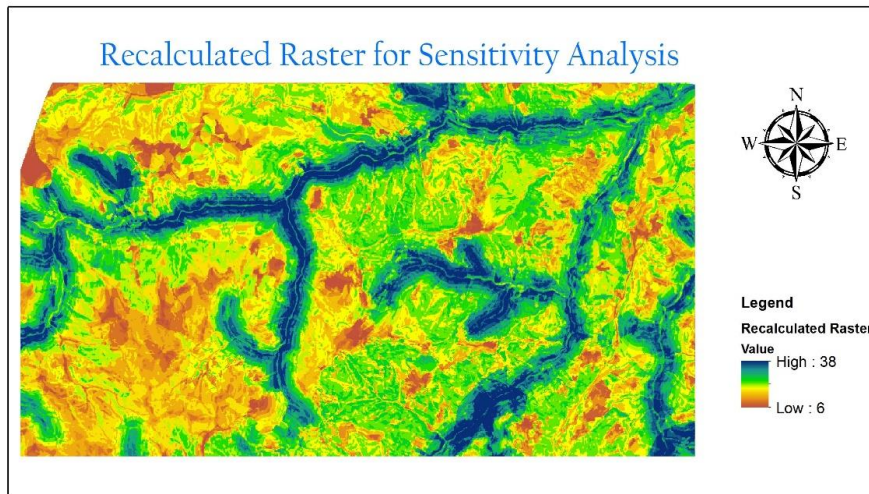


Figure 9. Cost surfaces showing recalculated surface for sensitivity analysis

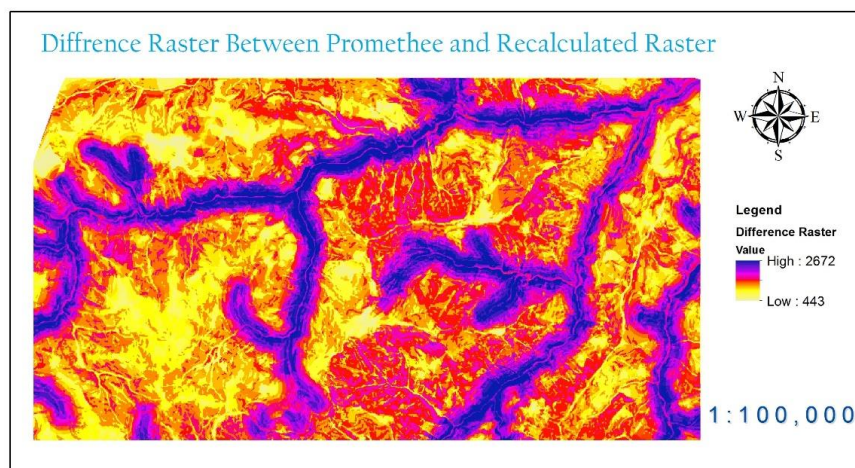


Figure 10. Cost surfaces showing difference between normal and recalculated surface

Conclusion

In this study, forest road route determination was dynamically realized using a raster-based decision-support system based on GIS technologies developed by us, namely FOROR. The major factors which affect the forest road route and necessary geographic data layers were determined accordingly and were then classified according to the standards. For this application, Analytical Hierarchy Process (AHP), Simple Addition

Weighting (SAW), Fuzzy Overlay, Promethee and TOPSIS methods of Spatial Multi-Criteria Decision Methods (MCDM) were used. Analyses were performed using five different methods for the determination of forest routes which were then compared to each other as well as to the existing road.

Forest road route determination is a complex process because of these fields consist various environmental factors. Other sides there are many different aspects for choosing route, if the model is acted upon private sector just economic factors are significant other side aspect of academicians and environmental care groups focused on environmental factors. In this model we considered all of these different aspects and generated an optimum model both environment and economy saving.

Firstly, total length and low-high slope passes of route affects the economic efficiency and then other factors are considered for environmental caring. Clear results at *Table 2* shows are saving environment, but for this purpose low slope area passes are decreased a bit. These new generated routes are balanced optimum routes, with considering all the aspects related to study area.

This paper shown that, using GIS based MCDM gives the best solution for forest road route determination. Especially Promethee resulted best offer, and it is likely to be the best method coherent with GIS. Creating context-specific extensions besides using GIS software is good solution for solving these complicated multidiscipline problems. Our extension FOROR put forth a good performance in analysis and when the results were compared. It has automated too many processes additionally minimizing human mistakes.

The combination of the methodologies used in this study and the forest road route criteria identified by the experts are suggested for future work in forest road routes in other regions.

REFERENCES

- [1] Abdi, E., Majnounian, B., Darvishsefat, A., Mashayekhi, Z., Session, J. (2009): A GIS-MCE based model for forest road planning. – *Journal of Forest Science* 55(4): 171-176.
- [2] Akay, A. E., Sessions, J. (2005): Applying The Decision Support System, TRACER, to Forest Road Design. – *Western Journal of Applied Forestry* 20(3): 184-191.
- [3] Akay, A. E. (2006): Minimizing total costs of forest roads with computer-aided design model. – *Sadhana- Academy Proceedings in Engineering Sciences* 31(5): 621-633.
- [4] Akay, A. E., Erdas, O., Reis, M., Yuksel, A. (2008): Estimating Sediment Yield from a Forest Road Network by Using a Sediment Prediction Model and GIS Techniques. – *Build. Environ.* 43: 687-695.
- [5] Altunel, A. O. (2000): Ormancılık Uygulamalarının Coğrafi Bilgi Sistemi ile Entegrasyonu (Forest application with GIS PhD.Thesis). – *Yayımlanmamış Doktora Tezi. İ.Ü.Fen Bilimleri Enstitüsü.*
- [6] Arpacik, A., Sari A., Başkaya Ş. (2017): For the Future: Sustainable Wildlife Reserve Management in Turkey. – *International Journal of Sciences: Basic and Applied Research (IJSBAR)*, vol.36: 250-261.
- [7] Aruga, K. (2005): Tabu search optimization of horizontal ve vertical alignments of forest roads. – *Journal of Forestry Research* 10: 275-284.
- [8] Bagli, S., Geneletti, D., Orsi, F. (2011): Routing of power lines through least-cost path analysis and multicriteria evaluation to minimise environmental impacts. – *Environmental Impact Assessment Review* 31: 234-239. <https://doi.org/10.1016/j.eiar.2010.10.003>.

- [9] Baidya, P., Chutia, D., Sudhakar, S., Goswami, C., Goswami, J., Saikhom, V., Singh, P., Sarma, K. (2014): Effectiveness of Fuzzy Overlay Function for Multi-Criteria Spatial Modeling-A Case Study on Preparation of Land Resources Map for Mawsynram Block of East Khasi Hills District of Meghalaya, India. – *Journal of Geographic Information System* 6: 605-612.
- [10] Chen, H. L., Koprowski, J. L. (2016): Barrier effects of roads on an endangered forest obligate: influences of traffic, road edges, and gaps. – *Biological Conservation*, Volume 199: 33-40.
- [11] Chiou, C., Tsai, W., Leung, Y. (2010): A GIS-dynamic segmentation approach to planning travel routes on forest trail networks in Central Taiwan. – *Landscape and Urban Planning*, Volume 97, Issue 4.
- [12] Choi, Y., Park, H. D., Sunwoo, C., Clarke, K. C. (2014): Multi-Criteria Evaluation And Least Cost Path Analysis For Optimal Haulage Routing Of Dump Trucks In Large Scale Open-Pit Mines. – *International Journal of Geographical Information Science*, 23:12: 1541-1567.
- [13] Chung, W., Sessions, J. (2001): Designing a forest road network using heuristic optimization techniques. – *Council Engineering (COFE) Conference Proceedings: "Appalachian Hardwoods: Managing Change"* Snowshoe, July 15-18.
- [14] Çalışkan, E. (2013): Planning of forest road network and analysis in mountainous area. – *Life Sci Journal* 10(2): 2456-2465.
- [15] Çalışkan, E., Yıldırım, V., Bediroğlu, Ş. (2016): Foror- A Gİs Based Spatial Multiple Criteria Decision Support Tool For Forest Road Route In Steep Terrain. – 1st International Symposium of Forest Engineering and Technologies, 02-04 June, Bursa, Turkey.
- [16] Christian, T., Ravier, T., Cerin, C., Ngoko, Y. (2015): The Promethee Method for Cloud Brokering with Trust and Assurance Criteria. – 2015 IEEE.
- [17] Dean, D. (1997): Finding optimal routes for networks of harvest site access roads using GIS-based techniques. – *Canadian Journal of Forest Research* 27: 11-22.
- [18] Demir, M. (2007): Impacts, Management and Functional Planning Criterion of Forest Road Network System in Turkey. – *Transport. Res. A-Pol.* 41: 56-68.
- [19] Demir, M., Öztürk, T. (2004): A Research on Forest Road Planning and Projecting by Inroads Software in Bolu Region of Turkey. – *American Journal of Applied Sciences* 1(4): 295-301.
- [20] Ezzabadi, J. H., Saryazdi, M. D., Mostafaeipour, A. (2015): Implementing Fuzzy Logic and AHP into the EFQM model for performance improvement. – *Appl. Soft Comput.* 36, (November 2015), 165-176. DOI=<http://dx.doi.org/10.1016/j.asoc.2015.06.051>.
- [21] Gümüş, S., Erdaş, O. (2000): Orman Yol Geçkilerinin Belirlenmesinde Coğrafi Bilgi Sistemlerinden Yararlanma İmkanları Üzerine Bir Araştırma (Forest road planning with GIS). – *Turkish J. Agric. For.* 24: 611-619.
- [22] Gumus, S., Acar, H. H., Toksoy, D. (2008): Functional forest road network planning by consideration of environmental impact assessment for wood harvesting. – *Environ Monit Assess* 142: 109-116.
- [23] Gumus, S. (2017): An Evaluation of Stakeholder Perception Differences in Forest Road Assessment Factors Using the Analytic Hierarchy Process (AHP), *Forests*, 8(5), 165.
- [24] Hayati, E., Majnounian, B., Abdi, E., Sessions, J., Makhdoum, M. (2013): An expert-based approach to forest road network planning by combining Delphi and spatial multi-criteria evaluation. – *Environmental Monitoring and Assessment*, Springer Publications, 185(2): 1767-1776.
- [25] Hosseini, S. A., Solaymani, K. (2006): Investigation of effective factors for path tracing using GIS in Kheyroud forest (Iran-Mazadaran province). – *Pakistan Journal of Biological Sciences* 9(11): 2055-2061.

- [26] Joerin, F., Thériault M., Musy, A. (2001): Using GIS and outranking multicriteria analysis for land-use suitability assessment. – *International Journal of Geographical Information Science* 15(2): 153-174. DOI: 10.1080/13658810051030487.
- [27] Jusoff, K. (2008): Construction of new forest roads in Malaysia using a GIS-based decision support system. – *Computer and Information Science* 1(3): 48-59.
- [28] Kiker, G. A., Bridges, T. S., Varghese, A., Seager, T. P., Linkov, I. (2005): Application of multicriteria decision analysis in environmental decision making. – *Integr Environ Assess Manag.* 1: 95-108. doi:10.1897/IEAM_2004a-015.1.
- [29] Kontos, D. T., Komilis, D. P., Halvadakis, C. P. (2005): Siting MSW landfills with a spatial multi criteria analysis methodology. – *Waste Management* 25: 818-832.
- [30] Lee, J., Stucky, D. (1998): On Applying Viewshed Analysis for Determining Least-Cost Paths on Digital Elevation Models. – *International Journal Geographical Information Science* 12(8): 891-905.
- [31] Liu, K., Sessions, J. (1993): Preliminary planning of roads using digital terrain models. – *Journal of Forest Engineering* 4: 27-32.
- [32] Malczewski, J. (1999): GIS and multicriteria decision analysis. – New York: John Wiley and Sons.
- [33] Malczewski, J. (2006): GIS-based multicriteria decision analysis: a survey of the literature. – *International Journal of Geographical Information Science* 20(7): 703-726. DOI: 10.1080/13658810600661508.
- [34] Mohammadi Samani, K., Hosseiny, S. A., Lotfalian, M., Najafi, A. (2010): Planning road network in mountain forests using GIS and analytic hierarchical process (AHP). – *Caspian Journal of Environmental Sciences* 8(2): 151-162.
- [35] Murat, S., Kazan, H., Coskun, S. S. (2015): An Application for Measuring Performance Quality of Schools by Using the Promethee Multi-Criteria Decision Making Method. – *World Conference on Technology, Innovation and Entrepreneurship*.
- [36] Narulita, S., Fitriany Zain, A. F. M., Prasetyo, L. B. (2016): Geographic Information System (GIS) Application on Urban Forest Development in Bandung City. – *Procedia Environmental Sciences* 33: 279-289.
- [37] Nino, K., Mamo, Y., Mengesha, G., Kibret, K. S. (2017): GIS based ecotourism potential assessment in Munessa Shashemene Concession Forest and its surrounding area, Ethiopia. – *Applied Geography* 82: 48-58.
- [38] Rapaport, E., Smckars, F. (1998): GIS-based road location in Sweden: a case study to minimize environmental damage, building costs and travel time. – In: Stilwell, J., Geertman, S., Openshaw, S. (eds.) *Geographical Information and Planning*: 135-153. Springer, Heidelberg.
- [39] Reutebuch, S. (1988): ROUTES: A Computer Program for Preliminary Route Location. – U.D.o.A. PNRS, Forest Service. PNW-GTR-216.
- [40] Rogers, L. (2005): Automating contour-based route projection for preliminary forest road designs using GIS. – [MS Thesis.] Washington, University of Washington: 87p.
- [41] Saha, A. K., Arora, M. K., Gupta, R. P., Virdi, M. L., Csaplovics, E. (2005): GIS-based route planning in landslide-prone areas. – *International Journal of Geographical Information Science* 19(10): 1149-1175.
- [42] Saaty, T. L. (1980): *The analytic hierarchy process*. – New York: McGraw-Hill. 269p.
- [43] Sačkov, I., Smrec̃ek, R., Tuc̃ek, J. (2014): Forest transportation survey based on airborne laser scanning data and GIS analyses. – *GISci. Remote Sens.* 51(1): 83-98.
- [44] Sadeghi-Niaraki, A., Varshosaz, M., Kim, K., Jung, J. J. (2011): Real World Representation of a Road Network for RoutePlanning in GIS. – *Expert Syst. Appl.* 38(10): 11999-12008.
- [45] Sadek, S., Berdan, M., Kaysi, I. (1999): GIS platform multi- criteria evaluation of route alignments. – *Journal of Transportation Engineering* 125(2): 144-151.
- [46] Stergios, T., Stavros, S., Fani, S., Athanassios, S., Dirk, J., Olga, C. (2015): Mapping the optimal forest road network based on the multicriteria evaluation technique: the case

- study of Mediterranean Island of Thassos in Greece. – *Environ Monit Assess* 187: 687. DOI 10.1007/s10661-015-4876-9.
- [47] Toinard, C., Ravier, T., Cérin, C., Ngoko, Y. (2015): The Promethee Method for Cloud Brokering with Trust and Assurance Criteria. – *Proceedings- 2015 IEEE 29th International Parallel and Distributed Processing Symposium Workshops*, 2015: 1109-1118.
- [48] Yaraloğlu, K. (2004): *Uygulamada Karar Destek Yöntemleri (Application of Multi criteri decision method)*. – İlkem Ofset, İzmir, 2004.
- [49] Yildirim, V., Yomralioglu, T., Nisanci, R., Çolak, E., Bediroğlu, Ş., Saralioglu, E. (2017): A spatial multicriteria decision-making method for natural gas transmission pipeline routing. – *Structure and Infrastructure Engineering*, 2016.
- [50] Yoon, K., Hwang, C. L. (1980): *Multiple Attribute Decision Making Methods and Applications: A State of the Art Survey*. – Berlin: Springer Verlag.
- [51] Yu, C., Lee, J., Stasiuk, M. J. M. (2003): Extensions to Least-Cost Path Algorithms for Roadway Planning. – *International Journal of Geographic Information Science* 17(4): 361-376.
- [52] Zsigraiova, Z., Semiao, V., Beijoco, F. (2013): Operation costs and pollutant emissions reduction by definition of new collection scheduling and optimization of MSW collection routes using GIS: The case study of Barreiro, Portugal. – *Waste Management* 33(4): 793-806.

ECOLOGICAL AND ECONOMIC FEASIBILITY ANALYSIS OF IRRIGATION ENGINEERING PROJECTS

CHEN, D.^{1,3} – LI, X. C.¹ – LUO, Z. H.^{2,3*} – CHEN, J.¹

¹*Key Laboratory of Efficient Irrigation-Drainage and Agricultural Soil-Water Environment in Southern China (Ministry of Education), College of Agricultural Engineering, Hohai University, Nanjing 210098, Jiangsu Province, P. R. China*

²*College of Resources and Environmental Sciences, Nanjing Agricultural University Nanjing 210095, Jiangsu Province, P. R. China*

³*Department of Agricultural and Biological Engineering, The University of Florida Gainesville 32611, USA*

**Corresponding author*

e-mail: lzhu@njau.edu.cn; phone: +86-25-8439-5815

(Received 22nd Sep 2018; accepted 22nd Nov 2018)

Abstract. Irrigation improvement has been identified as an important adaptation strategy for the food and water security under climate change. Ecological and economic feasibility analysis of irrigation improvement projects is of vital importance to ensure the high investment efficiency and the sustainability of irrigation development. This study integrated energy, economic and sensitivity analysis methods into a combined analysis. A case study on a small-scale irrigation project in plain areas of Jiangsu Province in China illustrated the methodology. The results indicated that different calculation results were obtained by using energy and economic analysis methods, respectively. The conventional monetary-based analysis method could underestimate or overestimate the assessment indicators. Energy as an eco-centric method could neglect the economic utility, human preference and demand. Economic analysis and energy accounting as the complementary valuation methods should be jointly used to provide better insights into the environmental and economic effects of irrigation improvement projects.

Keywords: *water scarcity, eco-efficiency, energy, benefit-cost ratio, sustainability*

Introduction

Debate about global water scarcity and food security has intensified in recent times (Steduto et al., 2017). Irrigation stabilizes crop production, improves crop quality, reduces rural poverty, and allows for diversification in farm production (Zhu et al., 2013). Yet continued increase in demand for water by non-agricultural uses have put irrigation water demand under greater scrutiny and threatened food security (Hanjra and Qureshi, 2010). Investments in irrigation infrastructure and management can minimize the impact of water scarcity and partially meet water demand for food production (Falkenmark and Molden, 2008). Irrigation improvement has been identified as an important adaptation strategy for the food and water security under climate change (Chen et al., 2014b, c). As the most populous country in the world, China faces the same challenges for food and water security (Peng, 2011; Zhu et al., 2013). The amount of water used for agriculture accounts for more than 62% of the total water use in China; the average efficiency of irrigation water use is 0.50, and the amount of available water per m² for the arable land is only 2 m³ (Wang, 2012). Hence, the Chinese government issued its first national outline for agricultural water-saving development (2012–2020) in December 2012. The irrigated area will increase from 6.17E + 11 m² in

2012 to $6.67E + 11 \text{ m}^2$ in 2020, and the efficiency of irrigation water use will rise from 0.50 in 2012 to 0.55 in 2020 (Chen et al., 2013). The investment in agricultural water-saving and irrigation improvement projects are expected to increase greatly in the near future. Scientific analysis of these projects is of vital importance in order to ensure high investment efficiency and the sustainability of irrigation systems.

A variety of methods have been developed to assess irrigation improvement projects, such as discount cash flow analysis, cost and benefit analysis, cost recovery analysis, and real option analysis, optimization methods, the analytic hierarchy process, linear programming, indicator systems, and synthetic evaluation approaches (Chen et al., 2011, 2014b; Abou El-Hassan et al., 2015). Yet these methods focus on the economic values or the monetization of non-economic values of material and resource uses. Natural, social and economic conditions are primary factors in the feasibility analysis of irrigation improvement projects. It is therefore essential to consider both the economic efficiency and the environmental sustainability of project implementation.

Emergy, based on the thermodynamic theory, measures both the free environmental and purchased inputs in the common unit of solar emergy (Chen et al., 2016). It is defined as the available energy of one kind that is used up in transformations directly and indirectly to make a product or service (Odum, 1996). It could put all products of nature, technology, and the economy on a common basis of the prior work required and embodied water (Buenfil, 2001). It has been proven to be a suitable parameter or index to assess the sustainability of water-related projects (Brown and McClanahan, 1996; Kang and Park, 2002; Martin, 2002; Chen et al., 2009, 2011, 2012, 2013, 2014b, 2016; Lv and Wu, 2009; Brown et al., 2010; Pulselli et al., 2011; Arbault et al., 2013; Díaz-Delgado et al., 2014). However, emergy as an eco-centric method could neglect the economic utility, human preference and demand. Conventional economic analysis is also needed as a complementary method for the emergy evaluation of projects. Therefore, this study uses both emergy and economic analysis methods to provide better insights into the feasibility of irrigation improvement projects.

The main objectives of this study are to (1) develop policy decision-making tools for feasibility analysis of irrigation improvement projects, (2) present a comparative analysis of evaluation results using emergy and economic analysis methods, and (3) discuss the related problems and recommendations in policy decisions and project management. The remainder of this paper is organized into the following sections. Section 2 presents a brief overview of the study area and the methods, including the emergy analysis method, the economic analysis method and the sensitivity analysis method. Results are presented and discussed in Section 3. Section 4 concludes by summarizing the main results and pointing to some suggestions based on the emergy and economic evaluations.

Materials and methods

Study area

The study area is located in Taixing City of the Jiangsu Province, China ($31^{\circ}55'N$, $119^{\circ}38'E$). It is in the subtropical monsoon climate zone. The annual average temperature is $14.9^{\circ}C$. Sunshine occurs on an average of nearly 2125 h a year. The frost-free period is about 220 days. The average annual precipitation is 1027 mm, but it rains mainly in the period from June to September. It is located in the plain areas with a seasonal water shortage characteristic. Thus, irrigation is essential for the agricultural

production especially in dry years. Irrigation is accomplished by pumping water from the local river, mainly extracting water from the lower Yangtze River in dry seasons. The irrigation system in this case consisted of a pumping station and earth canals. The pumping station was originally constructed in the 1980s and ran at 56% efficiency in recent years. Due to the seepage in sandy soil, the water conveyance efficiency in earth canal system (the ratio between the water delivered to a farm or field and that diverted from the irrigation water source) was only 5%. Hence an irrigation improvement project was done to upgrade the irrigation system with a new pumping station and concrete-lined canals. Increasing both water efficiency and agricultural production were the main objectives of this project. In this study, this project is subjected to both emergy and economic analyses to evaluate its feasibility. The main data and materials originate from the planning and design report of this project and field survey data. Field survey involves local data collection, unstructured interviews on farmers, field measurements and sample analyses. Policies and practices information about planning, construction and management of irrigation projects are mainly from local department of water resources. Statistical data in agricultural production are mainly from local department of agriculture. The interviews offered some questions in relation to the topics, including operation of the old irrigation system, situation of water supply and demand, inputs and outputs in irrigated farming, and viewpoints on the irrigation improvement project. Data about operation time, electricity consumption and volume of water supply of the pumping station were obtained from the managers and supervisors in the village. Field measurements were mainly conducted on the area and size of the pumping station and canals. Sample analyses of earthworks and construction materials were performed by the local quality monitoring station of construction projects.

Emergy analysis method

Emergy analysis is a top-down systems approach. Its general methodology can be found in detail in the original work (Odum, 1996), and in a series of emergy folios (Odum, 2000; Odum et al., 2000; Brown and Bardi, 2001; Brandt-Williams, 2002). Emergy analysis can identify and compare the contribution of natural resources and ecosystem services to a production process in the common unit of solar emergy. The unit of emergy is the solar emjoule or emergy joule (abbreviated sej) (Odum, 1996). Using the unit of emergy (sej), any resource, material and energy can be put on a common basis by expressing each of them in the emjoules of solar energy that is required to produce them. The costs and benefits of irrigation projects can be calculated and compared based on the emergy theory. The primary costs of this project can be divided into: the costs of construction, e.g. materials, machinery costs and installation services; and the operation and maintenance costs. The benefits include: the benefits of saving water and energy due to increasing water use efficiency; the benefit of arable land increase if concrete-lined canals reduce the canal width; and the benefit of agricultural yield increase due to the improved water-supply and farming conditions. By multiplying these items in Joules (or directly from its mass) by specific transformities, the solar emergy of each cost and benefit can be calculated. Values of transformities are mainly derived from previous studies of emergy evaluations. The global emergy baseline of reference used here is $9.44 \text{ E} + 24 \text{ sej/year}$.

To evaluate the feasibility and eco-efficiency of projects, a composite index named the emergy cost-benefit ratio (*EmCBR*) is proposed based on the conventional cost-benefit analysis, using *Equation 1* (Chen et al., 2011).

$$EmCBR = \frac{B + RV}{C} \quad (\text{Eq.1})$$

where C is the energy cost of the project; B is its energy benefit; and RV is its residual value of the fixed assets. RV , approximated 10% of the construction cost, is the value this project should have at the end of its useful life. This irrigation project was assumed to have a 30-year life span under the effective maintenance and management. Thus, each item was divided by 30 to present data on a yearly basis. A value $EmCBR = 1.0$ is the lowest value for which the project is feasible. Based on the life cycle theory, projects with $EmCBR$ greater than 1.0 are sustainable (Chen et al., 2011, 2014a).

Economic analysis method

The cost-benefit analysis is used in this study to measure the positive or negative consequences of irrigation projects. The costs and benefits of this project are accounted in monetary units. Three indicators are selected to help the economic feasibility analysis:

Net present value (NPV)

NPV is the sum of discounted net benefits: the difference amount between cash inflows and cash outflows, in *Equation 2*. If the NPV of a project is positive, it may be accepted. However, if its NPV is negative, the project should be rejected.

$$NPV = \sum_{t=1}^n (CI - CO)_t (1 + i_0)^{-t} \quad (\text{Eq.2})$$

where CI is the cash inflows, CO is the cash outflows, t is the time of the cash flow, $(CI - CO)_t$ is the net cash flow at time t , and i_0 is the basic discount rate. 7% or 12% are recommended as the basic discount rate for the water conservancy projects in China.

Internal rate of return (IRR)

IRR is the discount rate that makes the net present value of all cash flows from a project equal to zero, in *Equation 3*. The higher a project's IRR , the more desirable it is to undertake the project.

$$\sum_{t=1}^n (CI - CO)_t (1 + IRR)^{-t} = 0 \quad (\text{Eq.3})$$

Benefit-cost ratio (BCR)

BCR is the ratio of the benefits of a project relative to its costs, in *Equation 4*. All benefits and costs should be expressed in discounted present values. Projects with a BCR greater than 1 have positive net benefits. The higher the BCR , the more profitable will be the investment on projects.

$$BCR = \frac{\sum_{t=1}^n B_t (1 + i_0)^{-t}}{\sum_{t=1}^n C_t (1 + i_0)^{-t}} \quad (\text{Eq.4})$$

where B_t is the benefit at time t , C_t is the costs at time t .

Sensitivity analysis method

The above energy and economic methods might lead to uncertainty, due to their extensive calculations and data. Sensitivity analysis could be used to test the robustness of the results by these two methods in the presence of uncertainty (Chen et al., 2014c). Through increasing or decreasing the costs or benefits in a certain proportion, a sensitivity analysis was performed in this study to assess the effects of variations on the results.

Results and discussion

The energy flows of the irrigation project were calculated and presented in *Table 1*. The energy input structure was then calculated and contrasted. The major cost was the Construction (I) in terms of energy, 93.4% of the total cost. The Operation and maintenance (II) only made up 6.6% of the total energy cost. The major specific costs associated with the irrigation project in terms of energy were soil (37.94%), brick (19.88%) and stone (16.95%). These major inputs are raw materials, which are generally underestimated in conventional economic analysis based on monetary units. For example, the soil loss for the earthwork of pumping station and irrigation canals involved two kinds: the net loss of topsoil and other soil lost from land. The current unit cost of earthwork is lower (1.8 \$/m³ for manual work or 0.9 \$/m³ for mechanical work) than its true value (Chen et al., 2011). The most important benefits were irrigation water saving and rice yield increase in terms of energy: 55.12% and 39.33% of the total benefit, respectively. These data also confirmed that the main objectives of this project were to increase the water efficiency and agricultural production. However, the calculated *EmCBR* of the irrigation project is 0.54, showing a low efficiency in terms of energy evaluation.

As shown in *Table 2*, the values of *NPV* were greater than 0 and those of *BCR* were greater than 1, whenever the basic discount rate (i_0) was 7% or 12%. The values of *IRR* were also higher than i_0 . These data indicated that the benefits of this project outweighed the costs, further demonstrating that this project was economically feasible.

By increasing or decreasing the benefits or costs in the certain ranges, changes in *EmCBR*, *NPV*, *IRR* and *BCR* were documented in *Tables 3* and *4*. The data showed that the results of energy and economic analyses, to some extent, were not sensitive to the benefits or costs. It also indicated the robustness of the results using these two methods.

Considering the key indicators, the economic benefit cost ratio of this project was 2.05 ($i_0 = 7\%$) and 1.39 ($i_0 = 12\%$) in *Table 2*, greater than both 0.54 using energy analysis in *Table 1* and 1.0. The ratios resulted in the opposite conclusion on the project feasibility analysis using energy and conventional economic analysis methods respectively. The possible reasons include the differences in the accounting units, the estimate of environmental costs, the selection of accounting items and the calculation

process. Conventional cost-benefit analysis could be used to demonstrate economic feasibility and compare investment opportunities in terms of the time-varying value of money (Chen et al., 2011). Yet some natural resources and environmental impacts could be well appraised in monetary units. The emergy analysis method can measure different forms of energy and resources, including free environmental and purchased inputs, using the unified basis of solar emergy (Chen et al., 2014b). It is also not affected by inflation. A previous study on the emergy evaluation perspectives of an improvement project proposal in a large irrigation district showed the similar assessment results with the values of *EmCBR* (0.97) and *BCR* (1.28), but it has not presented the process of economic analysis and conducted the sensitivity analysis of results (Chen et al., 2011). The emergy theory and method was also used to evaluate the process of water abstraction, distribution and use for irrigated agriculture, which helped the different understanding of the relationship between irrigation projects and agricultural development (Chen et al., 2013). An evaluation of irrigation water in an irrigation system showed the different transformities and emergy values of water in different processes, which provided various water values on the emergy concept (Chen et al., 2014b). An evaluation of three irrigation agricultural systems depicted the emergy contribution of irrigation water rather than the economic contribution (Chen et al., 2014c). These studies confirmed that the emergy theory and method had the merit of objective assessment of natural and environmental resources supporting human activities in terms of the biophysical account of emergy, different from the conventional monetary-based analysis. This method also provided fresh insights into the sustainability analysis of irrigation development. Yet emergy has also suffered a lot of resistance and criticism, such as theoretical arguments, problems of transformity calculations, accounting procedures, co-products or splits treatment, uncertainty, and sensitivity (Hau and Bakshi, 2004; Sciubba and Ulgiati, 2005; Ingwersen, 2010; Rugani and Benetto, 2012). Emergy evaluation is an often-used holistic approach with a uniform unit of measure for quantification or valuation of ecosystem goods and services. However, economic analysis is currently the dominant value measurement system. The application of emergy evaluation in real production and management systems is still limited without the results of economic analysis (Lu et al., 2009). Economic analysis and emergy accounting are complementary valuation methods (Lu et al., 2009; Zhang et al., 2011; Chen et al., 2014c). Integrating the two methodologies into a combined analysis can provide better insight into the environmental and economic effects of irrigated projects. Therefore, the values of *EmCBR*, *NPV*, *IRR* and *BCR* should be served as the feasibility analysis indicators of the projects. A project, only with *EmCBR* and *BCR* greater than 1, *NPV* greater than 0, and *IRR* higher than the basic discount rate (i_0), is considered to be feasible. Moreover, it is of vital importance to select accounting items of the costs and benefits considering the potential environmental and ecological impacts of a project, no matter which method is used in the feasibility analysis of irrigation improvement projects. Lacks of major accounting items can lead to unreliable results of the feasibility analysis, which will negatively affect scientific decision-making in irrigation development. For instance, concrete-lined irrigation canals can reduce seepage during water conveyance, but concrete works might weaken the ecosystem services of unlined canals. Yet it remains difficult to incorporate these ecological effects into the feasibility analysis of projects, due to the valuation complexity needed further studies.

Table 1. Emergy analysis table of the irrigation project (all values are on a yearly basis)

No.	Item	Units	Raw data	Solar transformity (sei/unit)	Solar emergy (sej/year)	Em-value (Em\$)
Emergy costs					3.70E+17	1.09E+05
I. Construction						
1	Soil	g	1.40E+08	1.00E+09	1.40E+17	4.15E+04
2	Cement	g	1.14E+07	3.04E+09	3.46E+16	1.02E+04
3	Sand	g	3.03E+07	1.00E+09	3.03E+16	8.96E+03
4	Stone	g	3.73E+07	1.68E+09	6.27E+16	1.86E+04
5	Steel	g	6.67E+04	6.94E+09	4.63E+14	1.37E+02
6	Brick	g	2.00E+07	3.68E+09	7.36E+16	2.18E+04
7	Labor	\$	4.77E+02	3.38E+12	1.61E+15	4.77E+02
8	Machinery	\$	3.46E+02	3.38E+12	1.17E+15	3.46E+02
9	Temporary works	\$	3.31E+01	3.38E+12	1.12E+14	3.31E+01
10	Construction management	\$	2.03E+02	3.38E+12	6.85E+14	2.03E+02
II. Operation and maintenance						
11	Electricity	J	5.97E+10	1.59E+05	9.49E+15	2.81E+03
12	Labor	\$	3.06E+03	3.38E+12	1.03E+16	3.06E+03
13	Maintenance	\$	1.36E+03	3.38E+12	4.61E+15	1.36E+03
Emergy benefits					1.65E+17	4.89E+04
14	Irrigation water saving	m ³	1.04E+05	8.80E+11	9.11E+16	2.69E+04
15	Energy saving	J	2.83E+10	1.60E+05	4.53E+15	1.34E+03
16	Arable land increase	J	5.59E+10	8.30E+04	4.64E+15	1.37E+03
17	Rice yield increase	J	7.83E+11	8.30E+04	6.50E+16	1.92E+04
Residual value of the fixed assets						
18	Residual value of the fixed assets				3.46E+16	1.02E+04
EmCBR					0.54	

Data sources and calculations are given in the *Appendix*. The raw data are from the planning and design report of this project and field survey. The method of energy transformation refers to (Odum, 1996). Solar transformity is the unit emergy value (sej/g, sej/J, sej/\$), which is the emergy required to generate one unit of output. Transformities are from (Odum, 1996; Chen et al., 2014b). Accounting items with raw data are multiplied by transformities to obtain emergy values (sej/year) and divided by emergy/money ratios to obtain emdollars (Em\$). *EmCBR* is the emergy cost-benefit ratio, referring to *Equation 1*

Table 2. Economic analysis table of the irrigation project

Ratios	Values	
i_0 (%)	7	12
NPV (10 ⁴ Yuan)	50.10	17.19
IRR (%)	18	18
BCR	2.05	1.39

Data and calculations of costs and benefits are in monetary units rather than the unit of energy, referring to the similar processes in the Appendix. i_0 is the basic discount rate (7% or 12% in China). Net present value (NPV) is the sum of discounted net benefits, referring to Equation 2. Internal rate of return (IRR) is the discount rate that makes the net present value of all cash flows from a project equal to zero, referring to Equation 3. Benefit-cost ratio (BCR) is the ratio of the benefits of a project relative to its costs, referring to Equation 4

Table 3. Sensitivity analysis results on the values of EmCBR

	+50%	+20%	+10%	-10%	-20%	-50%
Changes in energy costs	0.27	0.34	0.37	0.45	0.51	0.82
Changes in energy benefits	0.61	0.49	0.45	0.37	0.33	0.20

EmCBR is the energy cost-benefit ratio, referring to Equation 1. Through increasing or decreasing the energy costs or benefits in a certain proportion, the values of EmCBR are obtained to assess the effects of variations on the results

Table 4. Sensitivity analysis results using the economic analysis method ($i_0 = 7\%$)

		NPV (10 ⁴ Yuan)	IRR (%)	BCR
Cost changes	+50%	27.24	11	1.48
	+20%	41.57	14	1.85
	+10%	45.32	16	1.86
	0	50.10	18	2.05
	-10%	54.87	20	2.28
	-20%	60.67	22	2.77
	-50%	75.01	37	4.43
Benefit changes	+50%	100.57	27	3.32
	+20%	70.90	21	2.66
	+10%	59.88	20	2.25
	0	50.10	18	2.05
	-10%	40.31	16	1.84
	-20%	31.34	14	1.77
	-50%	1.68	7	1.11

Net present value (NPV), internal rate of return (IRR) and benefit-cost ratio (BCR) refer to Equations 2, 3 and 4, respectively. The values of NPV, IRR and BCR are obtained through increasing or decreasing the costs or benefits in a certain proportion, to conduct sensitivity analysis.

An integrated feasibility analysis contributes to the objective and rational understanding of the strengths and weaknesses of irrigation engineering projects. However, to date China remains a traditional idea of focusing on irrigation engineering

technology and constructions and ignoring project management. Scientific decision making of project proposal might not be paid much attention at specific periods. For instance, since 2008 Global Financial Crisis, massive water conservancy projects have been rapidly planned and constructed. To assure the successful delivery of these projects, the life cycle of projects including the phases of planning, design, procurement, construction and operation should be considered into the sustainability assessment. Outcomes of policy decisions in ecological and economic terms could be also identified and valued into the development of a decision making tool. In addition, a sustainable mechanism in the political system is needed for achieve the objectives of projects, incorporating ecological and economic analysis in policy decision-making. More energy evaluations and economic analyses should be conducted on irrigation improvement project proposals and the corresponding agricultural systems from the perspectives of environmental, social, political and economical aspects. These actions can provide adequate guidelines for the sustainability of irrigation and agricultural development.

Conclusions

It is of vital importance to evaluate the feasibility of irrigation improvement projects to ensure the high efficiency in the investments and the sustainability of irrigation systems. The comparative analysis of the results of evaluation using different methods will help to make the scientific decision. Emergy analysis, as an effective tool different from conventional economic analysis, highlights the role of the natural and environmental resources supporting human activities from the view of sustainable development. In this study the emergy analysis method was used to evaluate the feasibility of a small-scale irrigation project in plain areas of Jiangsu Province in China. An economic analysis was also conducted on this project for comparisons. The results indicated that different calculation results and conclusions were obtained by using the two methods respectively. The conventional monetary-based analysis method could underestimate or overestimate the assessment indicators. Yet emergy as an eco-centric method could neglect the economic utility, human preference and demand. Economic analysis and emergy accounting as the complementary valuation methods should be jointly used to provide better insights into the environmental and economic effects of irrigation improvement projects. Selection of accounting items of the costs and benefits should also receive great attention for the feasibility analysis of projects, considering more environmental and ecological impacts. The policy decision-making incorporating ecological and economic analyses can help achieve the objectives of irrigation improvement projects.

Acknowledgements. This research is supported by the National Key Research and Development Program of China (2017YFC040320502), the Fundamental Research Funds for the Central Universities (2018B12414), Australian Research Council for Discovery Project Grant (DP170104138) and a Project Funded by the Priority Academic Program Development of Jiangsu Higher Education Institutions (PAPD). We thank the anonymous reviewers and the editors for their constructive comments, which helped us to improve the manuscript.

REFERENCES

- [1] Abou El-Hassan, W., El-Kassar, G., Fujimaki, H., Kitamura, Y., Khater, A. (2015): Assessment of cost-effective alternatives for improving irrigation systems in the Nile Delta. – *Irrig Drain* 64: 454-463.
- [2] Arbault, D., Rugani, B., Tiruta-Barna, L., Benetto, E. (2013): Emergy evaluation of water treatment processes. – *Ecol Eng* 60: 172-182.
- [3] Brandt-Williams, S. L. (2002): Handbook of Emergy Evaluation. Folio# 4. Emergy of Florida Agriculture (2nd printing). – Center for Environmental Policy, Environmental Engineering Sciences, University of Florida, Gainesville.
- [4] Brown, M., Bardi, E. (2001): Handbook of Emergy Evaluation. Folio# 3: Emergy of Ecosystems. – Center for Environmental Policy, University of Florida, Gainesville.
- [5] Brown, M. T., McClanahan, T. (1996): Emergy analysis perspectives of Thailand and Mekong River dam proposals. – *Ecol Model* 91: 105-130.
- [6] Brown, M. T., Martínez, A., Uche, J. (2010): Emergy analysis applied to the estimation of the recovery of costs for water services under the European Water Framework Directive. – *Ecol Model* 221: 2123-2132.
- [7] Buenfil, A. A. (2001): Emergy Evaluation of Water. – Department of Environmental Engineering Sciences. University of Florida, Gainesville, USA.
- [8] Chen, D., Chen, J., Luo, Z. H., Lv, Z. W. (2009): Emergy evaluation of the natural value of water resources in Chinese rivers. – *Environ Manage* 44: 288-297.
- [9] Chen, D., Webber, M., Chen, J., Luo, Z. H. (2011): Emergy evaluation perspectives of an irrigation improvement project proposal in China. – *Ecological Economics* 70: 2154-2162.
- [10] Chen, D., Chen, J., Luo, Z. H. (2012): Communications on emergy indices of regional water ecological-economic system. – *Ecol Eng* 46: 116-117.
- [11] Chen, D., Luo, Z. H., Chen, J., Kong, J., She, D. L. (2013): Emergy evaluation of a production and utilization process of irrigation water in China. – *The Scientific World Journal* 2013: Article ID 438317.
- [12] Chen, D., Luo, Z. H., Chen, J. (2014a): Discussion of methodology for assessing the sustainability of metro systems based on emergy analysis. – *J Manage Eng* 30: 131-133.
- [13] Chen, D., Luo, Z. H., Webber, M., Chen, J., Wang, W. G. (2014b): Emergy evaluation of a pumping irrigation water production system in China. – *Front. Earth Sci.* 8: 131-141.
- [14] Chen, D., Luo, Z. H., Webber, M., Chen, J., Wang, W. G. (2014c): Emergy evaluation of the contribution of irrigation water, and its utilization, in three agricultural systems in China. – *Front. Earth Sci.* 8: 325-337.
- [15] Chen, D., Liu, Z., Luo, Z. H., Webber, M., Chen, J. (2016): Bibliometric and visualized analysis of emergy research. – *Ecol Eng* 90: 285-293.
- [16] Díaz-Delgado, C., Fonseca, C. R., Esteller, M. V., Guerra-Cobián, V. H., Fall, C. (2014): The establishment of integrated water resources management based on emergy accounting. – *Ecol Eng* 63: 72-87.
- [17] Falkenmark, M., Molden, D. (2008): Wake up to realities of river basin closure. – *Water Resources Development* 24: 201-215.
- [18] Hanjra, M. A., Qureshi, M. E. (2010): Global water crisis and future food security in an era of climate change. – *Food Policy* 35: 365-377.
- [19] Hau, J. L., Bakshi, B. R. (2004): Promise and problems of emergy analysis. – *Ecol Model* 178: 215-225.
- [20] Ingwersen, W. W. (2010): Uncertainty characterization for emergy values. – *Ecol Model* 221: 445-452.
- [21] Kang, D., Park, S. S. (2002): Emergy evaluation perspectives of a multipurpose dam proposal in Korea. – *Journal of Environmental Management* 66: 293-306.
- [22] Lu, H. F., Kang, W. L., Campbell, D. E., Ren, H., Tan, Y. W., Feng, R. X., Luo, J. T., Chen, F. P. (2009): Emergy and economic evaluations of four fruit production systems on

- reclaimed wetlands surrounding the Pearl River Estuary, China. – *Ecol Eng* 35: 1743-1757.
- [23] Lv, C. M., Wu, Z. N. (2009): Emergy analysis of regional water ecological–economic system. – *Ecol Eng* 35: 703-710.
- [24] Martin, J. F. (2002): Emergy valuation of diversions of river water to marshes in the Mississippi River Delta. – *Ecol Eng* 18: 265-286.
- [25] Odum, H. T. (1996): *Environmental accounting: emergy and environmental decision making*. – John Wiley & Sons, New York, USA.
- [26] Odum, H. T. (2000): *Handbook of Emergy Evaluation. Folio# 2, Emergy of Global Processes*. Handbook of Emergy Evaluation. – Center for Environmental Policy, Environmental Engineering Sciences, University of Florida, Gainesville.
- [27] Odum, H. T., Brown, M. T., Brandt-Williams, S. (2000): *Handbook of Emergy Evaluation. Folio# 1: Introduction and Global Budget*. – Center for Environmental Policy, Environmental Engineering Sciences, University of Florida, Gainesville.
- [28] Peng, S. (2011): Water resources strategy and agricultural development in China. – *J Exp Bot* 62: 1709-1713.
- [29] Pulselli, F. M., Patrizi, N., Focardi, S. (2011): Calculation of the unit emergy value of water in an Italian watershed. – *Ecol Model* 222: 2929-2938.
- [30] Rugani, B., Benetto, E. (2012): Improvements to emergy evaluations by using life cycle assessment. – *Environmental Science & Technology* 46: 4701-4712.
- [31] Sciubba, E., Ulgiati, S. (2005): Emergy and exergy analyses: Complementary methods or irreducible ideological options? – *Emergy* 30: 1953-1988.
- [32] Steduto, P., Hoogeveen, J., Winpenny, J., Burke, J. (2017): *Coping with Water Scarcity: an Action Framework for Agriculture and Food Security*. – Food and Agriculture Organization of the United Nations, Rome, Italy.
- [33] Wang, A. G. (2012): *The Interpretation of the National Outline for Agricultural Water-Saving Development in China (2012-2020)*. – The Ministry of Water Resources of China (MWR), Beijing.
- [34] Zhang, L., Ulgiati, S., Yang, Z., Chen, B. (2011): Emergy evaluation and economic analysis of three wetland fish farming systems in Nansi Lake area, China. – *Journal of Environmental Management* 92: 683-694.
- [35] Zhu, X., Li, Y., Li, M., Pan, Y., Shi, P. (2013): Agricultural irrigation in China. – *J Soil Water Conserv* 68: 147A-154A.

APPENDIX

Footnotes to Table 1

1 Soil

Soil losses (earthworks) for construction of the irrigation pumping station = 60 m³

Soil losses (earthworks) for construction of irrigation canals = 1500 m³

Soil density in the case study = 2.7 × 10⁶ g/m³

Total weight = (60 m³ + 1500 m³) × (2.7 × 10⁶ g/m³) / (30 years) = 1.40 × 10⁸ g/year

2 Cement

Cements for construction of the irrigation pumping station = 25 t

Cements for construction of irrigation canals = 316.8 t

Total weight = (25 t + 316.8 t) × (1.0 × 10⁶ g/t) / (30 years) = 1.14 × 10⁷ g/year

3 Sand

Sands for construction of the irrigation pumping station = 80 t

Sands for construction of irrigation canals = 829 t

$$\text{Total weight} = (80 \text{ t} + 829 \text{ t}) \times (1.0 \times 10^6 \text{ g/t}) / (30 \text{ years}) = 3.03 \times 10^7 \text{ g/year}$$

4 Stone

Stones for construction of the irrigation pumping station = 90 t

Stones for construction of irrigation canals = 1030 t

$$\text{Total weight} = (90 \text{ t} + 1030 \text{ t}) \times (1.0 \times 10^6 \text{ g/t}) / (30 \text{ years}) = 3.73 \times 10^7 \text{ g/year}$$

5 Steel

Steels for construction of the irrigation pumping station = 2 t

$$\text{Total weight} = (2 \text{ t}) \times (1.0 \times 10^6 \text{ g/t}) / (30 \text{ years}) = 6.67 \times 10^4 \text{ g/year}$$

6 Brick

Amount of bricks for construction of the irrigation pumping station = 4000

Amount of bricks for construction of irrigation canals = 160000

Standard size of a brick = 240 mm × 1150 mm × 530 mm

$$\text{Total weight} = (4000 + 160000) \times (240 \text{ mm} \times 1150 \text{ mm} \times 530 \text{ mm}) \times (1.0 \text{E} + 09) \times (2.5 \times 10^6 \text{ g/m}^3) / (30 \text{ years}) = 2.0 \times 10^7 \text{ g/year}$$

7 Labor

Labor costs for construction of the irrigation pumping station = 1716.6 \$

Labor costs for construction of irrigation canals = 12580.0 \$

$$\text{Yearly costs} = (1716.6 \text{ \$} + 12580.0 \text{ \$}) / (30 \text{ years}) = 477 \text{ \$/year}$$

8 Machinery

Costs for three sets of pumps and other machineries used in 30 years = 10367.3 \$

$$\text{Yearly costs} = (10367.3 \text{ \$}) / (30 \text{ years}) = 346 \text{ \$/year}$$

9 Temporary works

Temporary works for construction of the irrigation pumping station = 992 \$

$$\text{Yearly costs} = (992 \text{ \$}) / (30 \text{ years}) = 33.1 \text{ \$/year}$$

10 Construction management

Costs for construction management and production preparation = 6090 \$

$$\text{Yearly costs} = (6090 \text{ \$}) / (30 \text{ years}) = 203 \text{ \$/year}$$

11 Electricity

Volume of pumped water per year = $5.97 \times 10^5 \text{ m}^3$

$$\text{Electricity for pumping water} = (5.97 \times 10^5 \text{ m}^3) / (792 \text{ m}^3/\text{h}) \times (22 \text{ kW}) \times [3.6 \times 10^6 \text{ J}/(\text{kW} \cdot \text{h})] = 5.97 \times 10^{10} \text{ J/year}$$

12 Labor

Labor costs for operation = 3060 \$/year

13 Maintenance

Maintenance costs for the irrigation pumping station = 253 \$/year

Maintenance costs for irrigation canals = 1110 \$/year

$$\text{Yearly costs} = (253 \text{ \$/year} + 1110 \text{ \$/year}) = 1363 \text{ \$/year}$$

14 Irrigation water saving

Decrease of annual irrigation water quotas per area (667 m^2) for this project = 115 m^3

$$\text{Volume of irrigation water saving} = (115 \text{ m}^3) / (667 \text{ m}^2) \times (900 \times 667 \text{ m}^2) = 1.04 \times 10^5 \text{ m}^3/\text{year}$$

15 Energy saving

Decrease of annual electricity consumption for this project = 7857 kW·h

$$\text{Energy saving} = 7857 \text{ kW} \cdot \text{h} \times [3.6 \times 10^6 \text{ J}/(\text{kW} \cdot \text{h})] = 2.83 \times 10^{10} \text{ J/year}$$

16 Arable land increase

Increased area = 6003 m^2

Yield per unit = 643 g/m^2 (assumed to be that of rice)

$$\text{Total energy} = (6003 \text{ m}^2) \times (643 \text{ g/m}^2) \times (1.45 \times 10^4 \text{ J/g}) = 5.59 \times 10^{10} \text{ J/year}$$

17 Rice yield increase

Increased yield per unit = 90 g/m²

Total energy = (90 g/m²) × (900 × 667 m²) × (1.45 × 10⁴ J/g) = 7.83 × 10¹¹ J/year

18 Residual value of the fixed assets

Total energy (assumed to be 10% of the energy costs of construction) = 3.46 × 10⁷ sej/year × 10% = 3.46 × 10⁶ sej/year

DESIGNING A MODEL FOR PROMOTING HEALTHY CROP FARMING IN KERMANSHAH PROVINCE IN IRAN

MOAREF, M. – POURSAAED, A. R.* – ESHRAGHI SAMANI, R. – CHAHAR SOGHI AMIN, H.

*Department of Agriculture Extension and Education, Ilam Branch, Islamic Azad University
Ilam, Iran*

**Corresponding author*

e-mail: a_poursaeed@yahoo.com; phone: +98-912-065-5719

(Received 22nd Sep 2018; accepted 27th Nov 2018)

Abstract. One of the major concerns of Third World countries is environment and human health protection. Excessive use of chemical inputs in farming endangers the environment and human health. Farming healthy or organic crops is considered as a solution to this problem. In this regard, the present quantitative research aims to design a model to promote healthy crop farming among Kermanshah province farmers. By reviewing of the literature of research and using the extended model of planned behavior, the research variables were identified and by applying slight changes and adding the contextual factors for it, it was selected as conceptual model of research. Descriptive-correlational design was used to validate the variables of healthy crop farming. A total number of 400 beneficiaries in Kermanshah province were selected by multi-stage proportional sampling method in seven cities. The data collection period was from 2017 to 2018. Validity of the researcher-made questionnaire was confirmed by a panel of experts and a measurement model confirmed Validity and reliability of the questions. Data analysis in descriptive statistics section was performed using Spss 23 and Smartpls 3 software. Results of structural equations confirmed the effect of contextual factors, attitude, perceived behavior control, and moral norm in healthy crop farming promotion. Also, using multigroup Analysis by Smart PLS software, demographic factors as moderator constructs were investigated in the path between intent and healthy cropping behavior. The results showed that: Path between intention and behavior was moderated by gender, education, and participation in the extension classes.

Keywords: *sustainable agriculture; organic product; healthy crop farming in Iran; extended Planned Behavior model; Immunotoxicity*

Introduction

Based on the implementing regulations of section B of article (61) of Fourth Development Plan Law in Iran, a healthy crop refers to a crop, which is free from any toxic and pollutant elements or compounds, or produced with the allowed level of these compounds. Based on this definition, it can be stated that the crop can be the result of applying the organic (bio-farming) production guidelines and methods. In this case, it would be free from toxic and pollutant elements and compounds, so they would be called organic crop. They can be also produced as a result of applying other production guidelines and methods and toxic and pollutant elements and compounds are used less than allowed value. Organic agriculture is a human and environmentally friendly production system which abolishes the use of chemical inputs completely or as much as possible (Lampkin and Pade, 1994) and is oriented towards re-establishing the natural balance that has been upset as a result of faulty applications (Lampkin, 1990) . Healthy crop farming is a growing global trend, which encourages proper behavioral policies (UN, 2014). Fertilizers and pesticides were used widely in both small and large scale farms in the past days. In the conventional agriculture, fertilizers were used widely without considering the outcomes and pollutants and the toxins produced, leading to many problems (Chakrabarty et al., 2014), for example, the accumulation of more than

2 million tons of toxins in the ecosystem (Pesticide Action Network, 2009), leaving negative effect on environmental health and human health, both farmer and consumer (Costa et al., 2011). The aim of this policy is proper use of land, reduced use of fertilizers and toxins (Owens et al., 2010). To achieve this goal requires encouraging the farmers for healthy and organic crop farming (Yanakittkul and Aungvaravong, 2017). In line with increasing population, providing the food needed by the human community faces with serious restrictions. This has forced the farmers to use various chemical pesticides to increase their crop yield and combat with plant pests. The use of toxins and chemical fertilizers endangers the life of human beings growingly and affects their health (Haddadi et al., 2017). Chemical inputs were used excessively and uncontrollably to increase the yield of agricultural crops, so that the production of various chemicals increased by 340 times during the 1940 to early 1980s, and billions of tons of substances were released to environment. Different epidemiological studies over several decades have indicated the relationship between overuse of different types of pesticides and the incidence of diseases such as allergies, food poisoning and cancers such as lymph, pancreas, breast, intestine, prostate, thyroid cancers in humans. For example, the ratio of gastrointestinal cancers among American citizens was 1 to 20 in 1950s, but its risk has doubled nowadays, with a ratio of 1 to 8. In this regard, the results of studies on the affected population suggest a high level of pesticides in a patient's cancerous organ compared to healthy people (Hayat et al., 2011).

Problem statement

Various studies have been conducted on the use of organic crops (Donahue, 2017; Mohamad et al., 2014) around the world, but much research has not been conducted on production and motivation of farmers to culture more healthy crops. It is estimated that the annual rate of agricultural consumption to increase by 9 billion people with an increase of 1.1% in 2050 (Alexandratos and Bruinsma, 2012). Population growth and increasing demand for food have led humans to use the technologies in farmlands to achieve more crops (Zhao et al, 2007). Uncontrolled use of agricultural chemical inputs in farms has been an example of human developments. While these chemical inputs have a significant effect on increased food production (Malek Saeedi, 2007), uncontrolled use of fertilizers and chemical pesticides with the hope of more crops and benefits has caused pollution and environmental degradation, and most importantly, loss of human health (Hosseini and Ajoudani, 2012). The use of chemical pesticides has increased so much that World Health Organization reported the Iran's health rank 123 among all countries of the world in 2007, which its main cause was malnutrition and non-observing the principles of optimum use of chemical fertilizers in farms and toxins and hormones of pests and their effects and compounds in agricultural crops. However, this trend has been slightly improved, so that the Iran's rank increased by 30 and reached to 93 in 2016 (World Health Organization, 2016). It is frequently stated that due to imbalance in the control of agricultural waste, fertilizers and pesticides enter the rivers and threaten the life of many people in the country. The use of fertilizer in the agricultural sector is very high in Iran, so that its rate is 4.5 million tons per day, which 87% of it belongs to urea-phosphorus. It should be noted that government subsidizes 800 billion annually for fertilizers and pesticides, which is hazardous for the community (Razavi et al., 2013). One of the major challenges of producing healthy food in Iran is the proper use of pesticides and fertilizers. Organic farming is one of the essential measures in order to achieve the healthy food. Razavi et al (2017) cites Ansari's

(2016) «Based on studies conducted on domestic farming crops, some residuals of chemical fertilizers and toxins have been observed in 63% of them ». With more than 900 thousand hectares of agricultural land, Kermanshah province produces more than 4 million tons of crops per year. Based on the statistics of Agriculture - Jihad in 2016, 87,363 tons (commercial product) of chemical fertilizers have been sold to the beneficiaries through the agricultural - Jihad organization of Kermanshah province (Agricultural Statistics in Iran, 2016), but according to interviews with engineers of this organization, the amount of used fertilizer has reached 120,000 tons this year ,about 130 kg/ha, which its rate has increased compared to past years. This shows that farmers use chemical inputs illegally and out of range on their land. Jihad Agriculture management programs of this province have targeted the production of healthy crops. Several steps have been taken by this organization over the past years, such as recruiting plant protection experts observing the vegetable sector crops. In addition, to achieve 10% of vegetable crops has been targeted in the form of healthy crops in this province (Agricultural Jihad Management of Kermanshah province, 2016). In line with increased adaptation capacities, the dissemination of environmental technologies and social communication can play significant role in promoting the production of healthy crops. Thus, providing proper model for promoting the healthy crop farming behavior leading to improved food security is an essential. This issue is being investigated in this study. This study aims to answer this question: what are the main variables of the healthy crop model and what are their effects on healthy crop farming and what is the level and direction of the effect of model variables on healthy crop farming model.

Review of literature

In a research entitled "Application of the planned behavior analysis theory in adopting organic farming ", Yadavar et al. (2018) concluded that the weight of the perceived behavior control construct was the highest in adopting organic farming. In a research on the "proposed model of organic farming of rice in rural areas of Gilan and Mazandaran provinces", Razavi et al (2017) concluded that the main barriers to organic farming were the lack of government's financial support of farmer, lack of information and knowledge on organic farming. In their research entitled "The conceptual framework presented for studying the behavior of organic farming farmers", Yanakittkul and Aungvaravong (2017) concluded that attitude, behavioral control, farmer risk-taking, government and university supportive policies in changing the farmers' behavior from conventional farming to organic farming is effective. In their research, they used the pattern of planned behavior change. In a research entitled "adaptation of organic farming of fruits and vegetables as an opportunity in Syrian farmers: application of theory of planned behavior and structural equation modeling", Issa and Hamm (2017) concluded that attitude, behavior control, and subjective norm had a significant effect on intention and behavior. The highest effect on behavior was applied by variable of intention.

Sandughi et al. (2016) conducted a study entitled "evaluation of knowledge, attitude and performance of cucumber and tomato greenhouse owners in Isfahan city in the production of healthy crops". Structural equation modeling was used to examine the causal relationships between variables. The research results showed that the knowledge of greenhouse owners with regard to selecting the proper fertilizer and pesticide is not enough and most statistical samples believed that excessive use of pesticides and fertilizers would endanger human health and the environment, but observing the

protection principles related to proper use of the pesticides and fertilizers was at weak level. Moreover, small space of greenhouses, greenhouse economic weaknesses, low literacy and lack of knowledge on other methods of combat with pests led to the selection of the fastest and least risky pest control method. Thus, planning to enhance the knowledge of greenhouse owners on fertilizer selection and pest control methods as well as improving the conditions for marketing healthy crops is essential.

Sandughi and Raheli (2016) conducted a research entitled "development of a planned behavior model for explaining the intention to produce organic crops among the greenhouse owners in Isfahan with using moral norm variable". To examine the causal relationship between the variables, structural equation model theory of planned behavior (TPB) were used. Results suggest that the attitude variable in the TPB model can explain 37% of the variations in the greenhouse owners' intention to produce organic crops, and based on the extended theory of planned behavior (ETPB), the variables of attitude and moral norms are able to explain 58% of the variations in the intention to produce organic crops. Moreover, the results of both models showed that perceived behavior control (control of beliefs) had no significant effect on prediction of greenhouse owners' intentions. The research results suggest that both theories have the potential of predicting the greenhouses' intentions, but adding moral norms to the TPB model as an additional predictor significantly increased the predictive power of the standard model. Therefore, designing intervention programs based on enhancing the attitudes and moral norms in greenhouse owners is recommended to encourage them to produce organic crops. In a study entitled "examining the farmers' willingness and behavior toward using integrated management of pests using Theory of Planned Behavior", Molaei et al. (2016) concluded that the intention variable has a strong and significant effect on predictive behavior and power. Using hierarchical regression, the variables of subjective and moral norms predicted 49.5% of the willingness variable. In their research entitled "the use of the theory of planned behavior to identify the basic and key ideas of Brazilian herders in using natural pasture, Borges et al (2016) showed a significant and positive relationship between farmers' attitudes and their intentions toward improvement of the grasslands

In a research entitled "recognizing organic farming in Kenya using a logical approach", Van-Hulst and Posthumus (2016) concluded that perceived behavior control and attitude and play an important role in adopting organic farming practices through supporting the intention and change of farmers' mentality.

In a research entitled "Explaining the farmer's water conservation behavior using the extended theory of planned behavior: Case Study in Alashtar City", Rahimi Feyzabad et al (2015) concluded that three variables of attitude, moral norms and self-identity affect the intentions of individuals on water conservation. In addition, water conservation behavior is significantly explained by perceived behavior control and intentions.

Taqipour et al. (2015) evaluated the behavior of farmers for membership in Water Users Associations (WUAs) based on the theory of planned behavior in Iran. The research results showed that the two variables of predictive behavior control and orientation had a direct and significant effect on farmers' behavior for membership in WUAs. In their research entitled "Conventional Activation Model: examining the performance and pride predicted in environmental professional behavior", Onwezen et al., (2013) moral norm is a moral commitment sense and predicts the behavior of the individuals.

In a research entitled "Developing an Environmental Behavior Model of Farmers in Shiraz City", Menatizadeh and Zamani (2012) found that two variables of moral norm and subjective norm have the most effect on farmers' intentions for environmental behaviors. Finally, the variables of environmental behavior intention, tangible control of behavior, social subjective norms and environmental attitudes have respectively the highest effect on farmers' environmental behaviors. Abedi Sarvestani (2012) in his research entitled "Environmental attitude and behavior of student of Gorgan University of agricultural sciences and natural resources" showed that there is no significant relationship between attitudes and environmental behaviors, in other words, attitude alone cannot be the correct predictor of behavior, in this research, scholar used planned behavior model for theoretical framework of research.

The results of the research conducted by Okoedo-Okojie and Aphunu (2011) showed that despite the low literacy level of farmers, they had high level of knowledge on the areas of plant nutrition, the adoption and use of chemical fertilizers was high. However, adoption is affected by lack of access to fertilizers, cost, lack of capital and other cases. In addition, access to credit facilities, increased promotion, education and scientific demonstration of practical nutrition technologies are required for improving and changing the status in using the fertilizer. In their research entitled "Knowledge of the members of the rural community: the attitudes towards the safe use of pesticides", Karanamurti et al. (2011) argue that poor management practices with regard to safe use of pesticides is due to lack of knowledge and education. These problems can be solved by promotion organization and holding education and extension classes. In a research entitled "Barriers of organic farming: A case study of Babol city in Iran", Sharifi et al. (2010) found that organic farming requires changes in conventional farming and these changes are not easily possible for the farmer and there are barriers for farmers in this regard. The largest barriers include production, natural, knowledge and attitude, infrastructure, organizational and economic barriers. Attitude and knowledge barriers included lack of interest and willingness to produce these crops, lack of adequate information and education, and a few number of studies in this area and organizational barriers included government's support of organic crops, lack of paying loan for farmers by government. In their research entitled "The views of adolescents and nutritional selection behaviors in terms of environmental effects of food production methods: the use of a psychological model," Bissonnette and Contento (2001) stated that the moral norms are a perceived commitment affecting both intention and behavior.

In a meta-analysis of 185 studies conducted on targeted behavior and planned behavior theories under the title of "The effect of theory of planned behavior", Armitag and Conner (2001) conducted that in order to increase the predictive power of behavior, these theories should be extended and new variables should be added. They proposed variables such as moral norms and descriptive norms.

Conceptual model

The theory of planned behavior is appropriate for organic farming behavior for three reasons. First, adopting organic farming by the farmer required accurate planning. Second, when a farmer resists adopting farming there is behavioral control. Third, adopting healthy farming by farmer faces some technical and social restrictions (Yanakittkul and Aungvaravong, 2017). Two targeted or rational behavior (presented by Fishbaine and Ajzen, 1975) and planned behavior theories (presented by Ajzen 1985) have been used since past to explain human behaviors. With development of

environmental problems over the recent decades, the need to examine environmental behaviors has become important in these theories. Many studies have been conducted to explain behaviors such as environmental protection activities (Fielding, 2008); food habits, and horticulture (Lautenschlager and Smith, 2007), the ways for regenerating the forest (Karppinen, 2005) and the use of healthy foods (Vermeir and Verbeke, 2008) through these theories (Manti Zadeh and Zamani, 2012). Many critics of the theory of planned behavior believe that this theory introduces only one new variable into the model, while evidence suggests that with introducing more variables, its predictive power can be increased. In this regard, Ajzan (1991) argues that this theory can accept new predictor variables. The extended model of planned behavior has been designed by adding the moral variable to the planned behavior model (Figure 1) and it refers to individual opinions on what is right to do or what is wrong to do (Simsekoğlu and Lajunen, 2008). The moral norm has been reported as perceived commitment affecting the intention and behavior. According this explanation Conceptual model of study was drawn (Fig. 2).

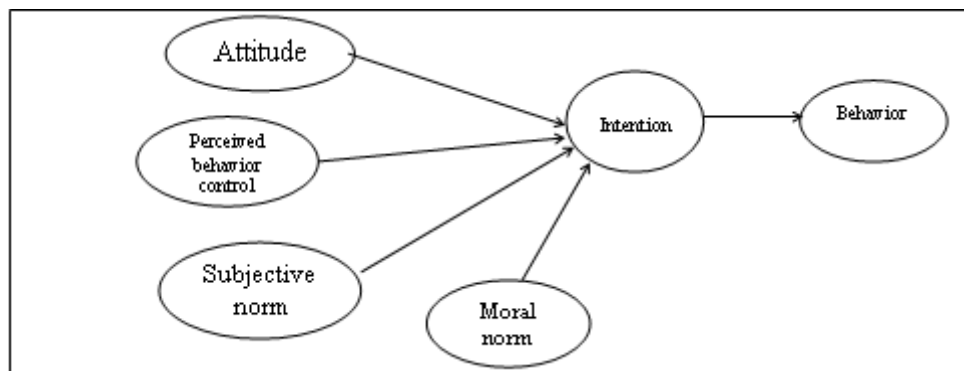


Figure 1. Extended model of planned behavior

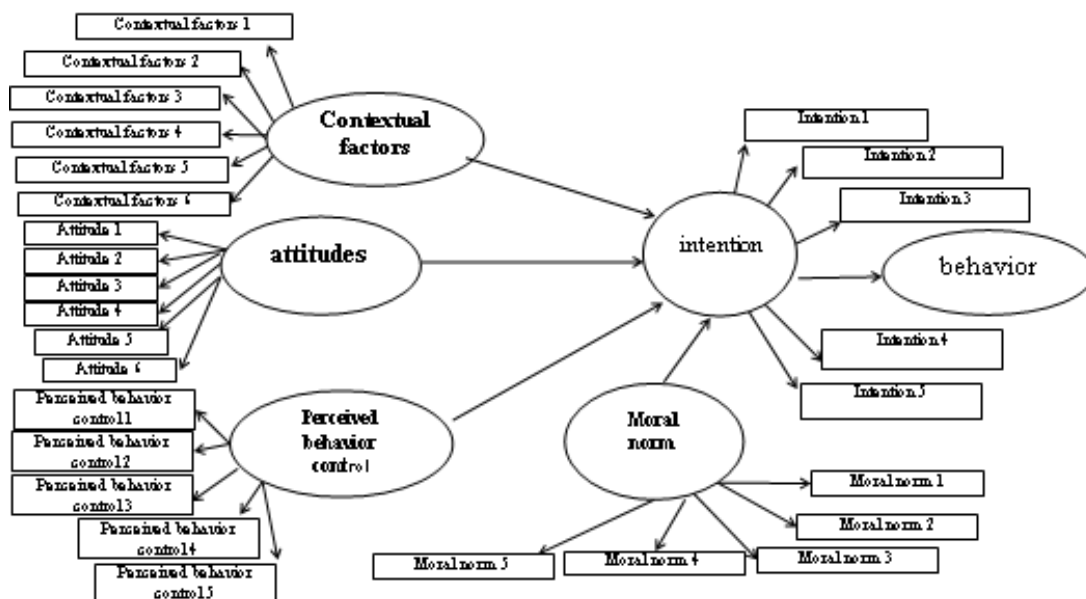


Figure 2. Conceptual model of study

With accurately searching in scientific databases, journals and scientific journals, theses, books, etc., and reviewing of research literature and using the extended model of planned behavior, we achieved the research variables. The research variables included: healthy farming behavior as dependent variable, intention as dependent, independent, moderator variable. Independent variable included: attitude: it means the level of one's valuation or positive or negative feelings to an issue. Perceived behavior control: it refers to one's perception of the difficulty or ease of the process. Moral norm: There is much evidence to introduce the moral norm variable into theory of planned behavior. Adding moral norms is important to perceive the behaviors interpreted as moral (Kaiser, 2006). Contextual factors: it includes government support and Farming Promotion and Education Department support. Demographic characteristics were considered as moderator construct.

Novelty of present study Compared with other research on this topic, are possible to add the contextual factors to the developed planned behavioral model, and measuring its effect on intention and healthy crop behavior, Considering demographic factors as a moderating variable and determining the moderator of this variable, the path between intent and behavior and Using SmartPLS software to determine the relationships between research variables.

Materials and Methods

The research orientation or research paradigm is quantitative. The present study is survey and applied in terms of objective. It is also descriptive in data collection. In order to evaluate the effect of each of the variables of the healthy farming model on behavior, structural equation modeling based on variance was used. The research population included 80304 Kermanshah province beneficiaries (Statistics Center of Agricultural Jihad, Kermanshah Province, 2017). Accordingly, research population was considered to be 25351 people. Using Cochran formula, the sample size was determined to be 385 people. Giving the dynamics of research population and lack of access to some of them, the response rate to the questionnaire might be low. To overcome this problem, 400 questionnaires were distributed among the beneficiaries by multi-stage cluster sampling method.

The data collection tool in this research was a researcher-developed questionnaire with closed questions, scored in the 5-point Likert scale from very low, moderate, high and very high (*Tab. 1*). The validity of the questions was measured through a panel of experts and its reliability was measured by using Cronbach's alpha coefficient. After collecting, refining, encoding and entering the data in this research, they were analyzed in two sections of descriptive and inferential statistics using SPSS 23 and smart PLS 3 software. In the inferential statistics section, structural equation modeling analysis was used through Partial least squares (PLS).

Research hypotheses

- The contextual factors have a positive and significant effect on the intention and behavior of healthy crop farming in Kermanshah province.
- Attitude has a positive and significant effect on the intention and behavior of healthy crop farming in Kermanshah province.

- Perceived behavior control has a positive and significant effect on the intention and behavior of healthy crop farming in Kermanshah province.
- Moral norms have a positive and significant effect on the on the intention and behavior of healthy crop farming in Kermanshah province.
- Intention has a positive and significant effect on healthy crop farming
- Demographic factors moderated path between intention and behavior.

Table 1. Researcher-developed research questionnaire

Index	Questions
Behavior	<p>1- I use organic fertilizers to improve my farm's soil.</p> <p>2- I always read and observe the guidelines for the use of chemicals and pesticides.</p> <p>3- I use biologic methods such as the use of lady beetle to combat with pests.</p> <p>4- To combat with pests and diseases in the land, I use traditional methods such as crop rotation.</p> <p>5- I prefer to kill the diseased or pestilent plants in the land rather than using chemical pesticides.</p> <p>6- At all stages of planting and harvesting, I try not to use fertilizers and chemicals.</p>
Intention	<p>1- I would like to produce crops that do not harm consumers.</p> <p>2- I am interested in producing crops that do not harm the environment.</p> <p>3- I am trying hard to produce healthy crops in my area</p> <p>4- I am interested in producing crops that do not jeopardize future generation resources.</p> <p>5- In the next few years, I am the main producer of healthy crops in the region.</p>
Attitude	<p>1- The production of healthy crops is a good idea for the preservation of the environment and the health of human beings.</p> <p>2- I am concerned with the consumption of agricultural crops that are produced using chemicals.</p> <p>3- If I have land and facilities for farming healthy crops, I will try to produce healthy crops.</p> <p>4- I think that the benefits of producing more healthy crops are more than that of unhealthy crops.</p> <p>5- I prefer production of healthy crops among various farming models</p> <p>6 – I am satisfied with production of healthy crops in land</p> <p>7- production of healthy or organic crops is a proper farming model for farmers of the region</p>
Perceived behavior control	<p>1- Planting and harvesting of the healthy crops is feasible for me</p> <p>2- I have adequate ability to produce the healthy crops in land</p> <p>3- I have high skill in managing and control of healthy crops lands</p> <p>4- it is easy for me to prepare facilities, resources, and equipment required for production of healthy crops</p> <p>5- I can find customer for my healthy crops at the shortest time and with the lowest cost.</p>
Moral norm	<p>1- It is not morally accepted to use chemical fertilizers excessively</p> <p>2- I am morally committed to use chemical fertilizers at the allowed level</p> <p>3- production of chemical crops violates the principles related to relation between human and nature</p> <p>4- farmers are obliged to respect the animals and nature by production of healthy crops</p> <p>5- Production of chemical crops is not morally and legally accepted.</p> <p>6- the use of chemicals violates the nature rules</p> <p>7- I am feeling responsibility in optimal use of chemical fertilizers.</p>
Contextual factors	<p>1- media (TV and radio) provide proper promotional programs for promoting the healthy crops</p> <p>2- government appreciate the farmers using the healthy crops annually</p>

3- government provides adequate subsidiary and facilities for production of healthy crops
4-people welcome healthy crops produced by farmers
5-Governments ensures the healthy crops against the pests and diseases
6- fruit and vegetables squares prefer healthy crops to un-healthy crops

Results

In this section, descriptive statistics was first used to describe demographic factors. Then, inferential statistics was used to evaluate the relationships between the independent and dependent variables of the research. For this purpose, structural equation modeling (SEM), (evaluation of measurement model and structural model) was used.

Based on the results, the mean age of the farmers was 31.72 years with a standard deviation of 11.39 years, so that they were in the range of 15 to 65 years and 299 (75.3%) of the studied farmers were living in Kermanshah and majority of them were male and only 24.7% of them were female. 25.6% of the farmers in Kermanshah province had the highest frequency with diploma education and only 4 (1%) member of them had the least frequency of illiteracy. In addition, 33.7 percent of the farmers examined in Kermanshah province reported that they had an income of between 250 to 330 USD per month, and 1.6 percent with the lowest frequency reported that they have income of more than 416 USD per month. Average farmers income in Kermanshah province is 225 USD. In addition, 310 (78.9%) of the studied farmers in Kermanshah province did not attend in the educational-extension courses on healthy (organic) crop farming, while only 21.1% (83 people) of them attended in these educational-promotional courses.

Inferential statistics

Using structural equation modeling approach, the healthy crops farming model in Kermanshah province is validated.

Structural equation modeling

In this section, the hypotheses are evaluated in the form of a conceptual model proposed by research in two sections of measurement model and structural model using structural equation modeling with partial least squares approach and application SmartPLS software.

The effect of intention on farmer's behavior on healthy crops farming

In this analysis, the latent variables of the research including farmers' behavior with six markers (B1-B6) and farmers' intentions with five markers (I1-I5) entered the SmartPLS 3 software.

Evaluation of the measurement model the effect of intention on farmers' behavior

In order to examine the goodness of fit index, validity and reliability of the measurement model the effect of intention on the farmers' behavior with regard to healthy crop farming, confirmatory factor analysis was used. Goodness of fit indices (Table 2), summary of results (Table 3) and correlation coefficients (Table 4) are presented below.

Table 2. Fit indices measurement model the effect of intention on farmers' behavior

Fit index	SRMR	D_LS	D_G	NFI	RMS_Theta
Proposed value	<0.10	>0.05	>0.05	>0.80	≤0.12
Estimated value	0.69	0.318	0.091	0.98	0.10

Model fit: The research results showed that the indices of the goodness fit of the mentioned model had appropriate value (2). Thus, data were statistically fit to the factor structure and the theoretical contextual of the two latent variables of the research.

One-dimensional markers: The results presented in Table 3 show that the standardized load factor (λ) of all selected markers is high for all above-mentioned constructs (higher than 0.5) and they were statistically significant at the error level of 1% ($P < 0.01$). These results provided adequate evidence to confirm that the selected markers are one-dimensional for the measurement model the effect of intention on farmers' behavior. Hence, it can be stated that these markers have been selected properly for each of the relevant constructs.

Composite reliability: The results presented in Table 3 showed that the composite reliability (CR) of all research constructs was more than 0.60 and their Cronbach's alpha coefficient was higher than 0.70. Hence, all latent variables (constructs) of the research measurement model had a good reliability.

Table 3. Summary of the results of evaluation measurement model the effect of intention on farmers' behavior. **Significant at the error level of 1%

Latent variables	Marker	λ	t	CR	AVE	α
Farmers' behavior	B1	0.74	30.02**	0.86	0.51	0.80
	B2	0.63	16.33**			
	B3	0.73	27.82**			
	B4	0.63	16.87**			
	B5	0.71	24.39**			
	B6	0.78	36.41**			
Farmers intention	I1	0.79	35.74**	0.87	0.59	0.82
	I2	0.79	35.75**			
	I3	0.78	29.28**			
	I4	0.79	35.04**			
	I5	0.66	18.55**			

Convergent validity: The results presented in Table 3 show that the average of variance extracted (AVE) for all research constructs was more than 0.50 Thus, all the constructs of the research model had good convergent validity.

Diagnostic validity: according to the results presented in Table 4, it was found that the average of variance extracted for each of the research constructs ($0.77 < AVE < 0.78$) was higher than the correlation between the constructs ($r = 0.76$). This result showed that the selected markers for each construct share a high percentage of the common

variance of that construct compared to other constructs in the research model, so the diagnostic validity of the constructs in the research measurement model was confirmed.

Table 4. AVE and correlation coefficients. Note: the numbers of table diagonal elements are average of variance extracted and elements below the table diameter are correlation coefficients between the constructs

Latent variables	1	2
1-behavior	0.78	
2- intention	0.76	0.77

According to the results, it can be stated that the proposed measurement model to examine the effect on farmers' intention on their behavior with regard to healthy crop farming with two main latent variables was the proper model for the research analyses.

Evaluation of structural model the effect of intention on behavior of farmers

After confirming the measurement model the effect of farmers' intention on their behavior with regard to healthy crop farming using confirmatory factor analysis, path analysis method (structural model evaluation) was used in order to test the hypothesis in the form of conceptual framework proposed for the research. The model of the research in the standard mode (Figure 3) and the summary of the results (Table 4) derived from the evaluation of the structural model of the effect farmers' intention on their behavior, are presented below.

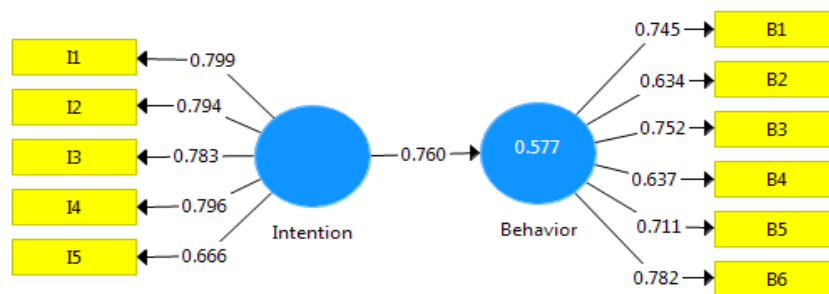


Figure 3. Structural model of the effect of intention on behavior in standard mode.

Path coefficient (γ): the results of Table 5 showed that the path coefficient of intention and behavior of farmers with regard to healthy crop farming was 0.76 and significant at the 1% error level. Thus, with probability of 99%, it can be stated that intention has a positive and significant effect on farmers' behavior with regard to healthy crop farming.

Table 5. Summary of the results of the evaluation of the structural model of the effect of intention on behavior of farmers. **significance at the error level of 1%

Latent variables		Direct effect		Indirect effect		Total effect		F ²	R ²
Indigenous	Exogenous	γ	t	γ	t	γ	t		
behavior	Intention	0.76	33.83**	-	-	0.76	33.83**	0.76	0.57

Coefficient of determination (R²): The results of Table 5 showed that the coefficient of determination of the latent variable of farmers' behavior with regard to

healthy crop farming was 0.57. Thus, it can be stated that 57% of the variations in the variance of framers' behavior with regard to healthy crop farming is predicted by their intentions, which is a significant and high percentage.

Effect size (F2): Based on the Cohen scale, the latent variable of intention to healthy crop farming has a very strong effect on farmers' behavior on healthy crop farming.

Effect of attitude on farmers' behavior on healthy crop farming

In this analysis, the latent variables of the research including farmers' behavior with six cods (B1-B6) and farmers' intentions with five cods (I1-I5) and attitude with seven cods (A1-A7) entered the SmartPLS 3 software.

Evaluation of Measurement Model of Attitude Effect on Farmers' Behavior

In order to examine the fit, validity and reliability of the measurement model the effect of attitude on the behavior of farmers with regard to healthy crops farming, confirmatory factor analysis was used. After eliminating the marker 5 (A5) of the model measurement effect of attitude of farmers on their behavior with regard to healthy crop farming reached to optimized fit. Goodness of fit indices (Table 6), summary of results (Table 7), and correlation coefficient (Table 8) are presented below.

Table 6. Fit indices of model measurement of the effect farmers' attitude on their behavior

Fit index	SRMR	D_LS	D_G	NFI	RMS_Theta
Proposed value	<0.10	>0.05	>0.05	>0.80	≤0.12
Estimated value	0.065	0.647	0.183	0.96	0.09

Model fit: The research results showed that the goodness of fit indices measurement model the effect of farmers' attitude on their behavior had appropriate value (Table 6). Thus, data were statistically fit to the factor structure and the theoretical contextual of the three latent variables of the research.

Table 7. Summary of the results of evaluation measurement model the effect of the farmers' attitude on their behavior. **significance at the error level of 1%

Latent variables	marker	λ	t	CR	AVE	α
Farmers' behavior	B1	0.74	31.38**	0.86	0.51	0.80
	B2	0.63	17.61**			
	B3	0.75	26.81**			
	B4	0.64	18.55**			
	B5	0.70	23.69**			
	B6	0.78	36.13**			
Farmers' intention	I1	0.79	35.89**	0.87	0.59	0.82
	I2	0.78	35.28**			
	I3	0.78	30.80**			
	I4	0.80	37.76**			
	I5	0.67	19.97**			
Farmers attitude	A1	0.69	19.68**	0.87	0.52	0.82
	A2	0.75	25.95**			

	A3	0.81	40.53**			
	A4	0.71	22.90**			
	A6	0.67	18.58**			
	A7	0.68	21.70**			

One-dimensional markers: The results presented in *Table 7* show that the standardized load factor (λ) of all selected markers is high for all above-mentioned constructs (higher than 0.5) and they were statistically significant at the error level of 1% ($P < 0.01$). These results provided adequate evidence to confirm that the selected markers are one-dimensional for the models of measurement effect of farmers' attitude on their behavior. Hence, it can be stated that these markers have been selected properly for each of the relevant constructs.

Composite reliability: The results presented in *Table 7* showed that the composite reliability (CR) of all research constructs was more than 0.60 and their Cronbach's alpha coefficient was higher than 0.70. Hence, all latent variables (constructs) of the research measurement model had a good reliability.

Convergent validity: The results presented in *Table 7* showed that the average of variance extracted (AVE) for all research constructs was more than 0.50. Thus, all the constructs of the research model had good convergent validity.

Table 8. AVE and correlation coefficients. Note: the numbers of table diagonal elements are average of variance extracted and elements below the table diameter are correlation coefficients among the constructs.

<i>Latent variables</i>	<i>1</i>	<i>2</i>	<i>3</i>
<i>1-behaviour</i>	0.78		
<i>2-attitude</i>	0.52	0.76	
<i>3-intention</i>	0.75	0.56	0.77

Diagnostic validity: according to the results presented in *Table 8*, it was found that the average of variance extracted for each of the research constructs ($0.77 < AVE < 0.78$) was higher than the correlation between the constructs ($0.52 < r < 0.75$). This result showed that the selected markers for each construct share a high percentage of the common variance of that construct compared to other constructs in the research model, so the diagnostic validity of the constructs in the research measurement model was confirmed.

According to the results, it can be stated that the proposed measurement model to examine the effect on farmers' attitude on their behavior with regard to healthy crop farming with three main latent variables was the proper model for the research analyses.

Evaluation of structural model effect of attitude on farmers behavior

After confirming the model of measurement effect of farmers' attitude on their behavior with regard to healthy crop farming using confirmatory factor analysis, path analysis method (structural model evaluation) was used in order to test the hypothesis in the form of conceptual framework proposed for the research. The model of the research path with representation of factors loads in the standard mode (*Figure 4*) and the

summary of the results (Table 9) derived from the evaluation of the structural model effect of the farmers' attitude on their behavior are presented below.

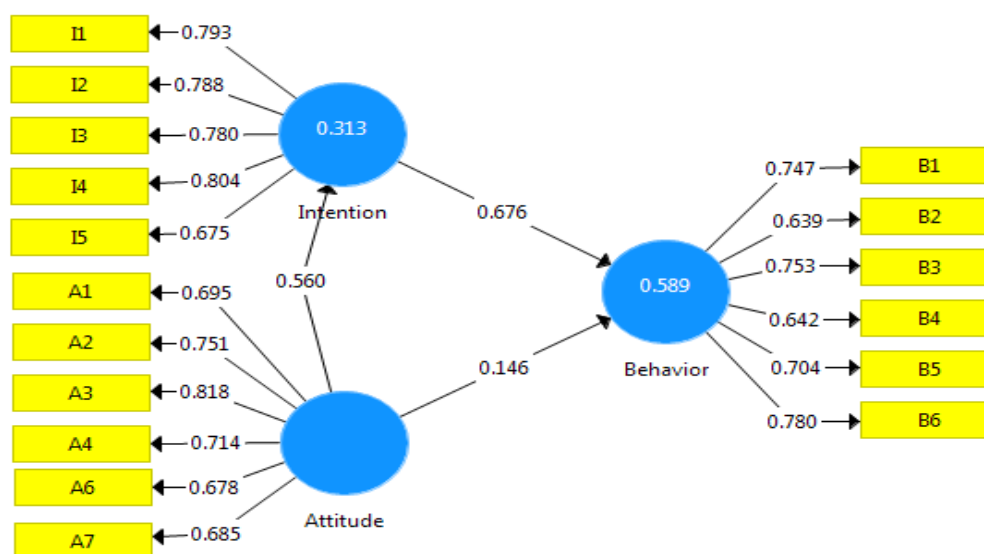


Figure 4. Structural model of the effect of attitude on behavior of farmers with regard to healthy crop farming.

Path coefficient (γ): the results of Table 9 showed that the direct effect of latent variable of attitude on farmers behavior with regard to healthy crop farming was 0.14 and significant at the 1% error level and the indirect effect of the latent variable of attitude on farmers behavior was 0.38 and significant at the level of 1%. In addition, the total effect of latent variable of farmers' attitude on their behaviors was 0.52, which is significant at the level of 1%. Thus, with probability of 99%, it can be stated that attitude has a positive and significant effect on farmers' behavior with regard to healthy crop farming.

Table 9. Summary of the results of the evaluation of the structural model of the effect of attitude on behavior of farmers. **Significance at the error level of 1%

Latent variables		Direct effect		Indirect effect		Total effect		F ²	R ²
Indigenous	Exogenous	γ	t	γ	t	γ	t		
Behavior	attitude	0.14	3.24**	0.38	10.75**	0.52	12.50**	0.03	0.59

Coefficient of determination (R²): The results of Table 9 showed that the coefficient of determination the latent variable of farmers' behavior with regard to healthy crop farming was 0.59. Thus, it can be stated that 59% of the variations in the variance of framers' behavior with regard to healthy crop farming is predicted by the latent variables of intention and attitude, which is a significant and high percentage.

Effect size (F²): Based on the Cohen scale, the variable of attitude has a moderate effect on farmers' behavior on healthy crop farming in Kermanshah province.

The effect of perceived behavior control on farmers' behavior of healthy crop farming

In this analysis, the latent variables of the research including farmers' behavior with six markers (B1-B6) and farmers' intentions with five markers (I1-I5) and perceived behavior control along with five markers (PBC-PBC5) entered the SmartPLS 3 software.

Evaluation model of measurement effect of perceived behavior control on farmers' behavior

In order to examine the fit, validity and reliability of the model measurement the effect of perceived behavior control on the farmers' behavior with regard to healthy crop farming, confirmatory factor analysis was used. Goodness of fit indices (Table 10), summary of results (Table 11) and correlation coefficients (Table 12) are presented below.

Table 10. Fit indices of model of measurement of the effect of perceived behavior control on farmers' behavior

Fit index	SRMR	D_LS	D_G	NFI	RMS_Theta
Proposed value	<0.10	>0.05	>0.05	>0.80	≤0.12
Estimated value	0.061	0.504	0.196	0.97	0.10

Model fit: The research results showed that the goodness of fit indices model of measurement the effect of perceived behavior control of farmers' behavior had appropriate value (Table 10). Thus, data were statistically fit to the factor structure and the theoretical contextual of the three latent variables of the research.

One-dimensional markers: The results presented in Table 11 showed that the standardized load factor (λ) of all selected markers is high for all above-mentioned constructs (higher than 0.5) and they were statistically significant at the error level of 1% ($P < 0.01$). These results provided adequate evidence to confirm that the selected markers are one-dimensional for the models measurement the effect of perceived behavior control on their behavior. Hence, it can be stated that these markers have been selected properly for each of the relevant constructs.

Composite reliability: The results presented in Table 11 showed that the composite reliability (CR) of all research constructs was more than 0.60 and their Cronbach's alpha coefficient was higher than 0.70. Hence, all latent variables (constructs) of the research measurement model had a good reliability.

Table 11. Summary of the results evaluation the model of measurement, the effect of perceived behavior control on farmers' behavior. **Significant at the error level of 1%

Latent variables	Marker	λ	t	CR	AVE	α
Farmers' behavior	B1	0.74	30.68**	0.86	0.51	0.80
	B2	0.63	18.07**			
	B3	0.75	30.07**			
	B4	0.63	17.12**			
	B5	0.70	26.76**			
	B6	0.78	37.62**			
Farmers' intention	I1	0.79	37.04**	0.87	0.59	0.82

<i>Perceived behavior control</i>	<i>I2</i>	0.79	37.33**	0.92	0.70	0.89
	<i>I3</i>	0.78	33.19**			
	<i>I4</i>	0.80	35.83**			
	<i>I5</i>	0.67	19.13**			
	<i>PBC1</i>	0.81	40.01**			
	<i>PBC2</i>	0.83	41.63**			
	<i>PBC3</i>	0.81	37.11**			
	<i>PBC4</i>	0.83	43.38**			
	<i>PBC5</i>	0.88	68.90**			

Convergent validity: The results presented in *Table 11* showed that the average of variance extracted (AVE) for all research constructs was more than 50. Thus, all the constructs of the research model had good convergent validity.

Diagnostic validity: according to the results presented in *Table 12*, it was found that the average of variance extracted for each of the research constructs ($0.77 < AVE < 0.84$) was higher than the correlation between the constructs ($0.49 < r < 0.75$). This result showed that the selected markers for each construct share a high percentage the common variance of that construct compared to other constructs in the research model, so the diagnostic validity of the constructs in the research measurement model was confirmed.

Table 12. AVE and correlation coefficients. Note: the numbers of table diagonal elements are average of variance extracted and elements below the table diameter are correlation coefficients among the construct

<i>Latent variables</i>	<i>1</i>	<i>2</i>	<i>3</i>
<i>1-behaviour</i>	0.78		
<i>2-intention</i>	0.75	0.77	
<i>3-perceived behavior control</i>	0.53	0.49	0.84

According to the results, it can be stated that the proposed measurement model to examine the effect on perceived behavior control on farmers' behavior with regard to healthy crop farming with three main latent variables was the proper model for the research analyses.

Evaluation structural model the effect of perceived behavior control on farmers' behavior

After confirming the model of measurement of the effect of perceived behavior control on farmers' behavior with regard to healthy crop farming using confirmatory factor analysis, path analysis method (structural model evaluation) was used in order to test the hypothesis in the form of conceptual framework proposed for the research. The model of the research with representation of factors loads in the standard mode (*Figure 5*) and the summary of the results (*Table 13*) derived from the evaluation of the

structural model of the effect of perceived behavior control on farmers' behavior are presented below.

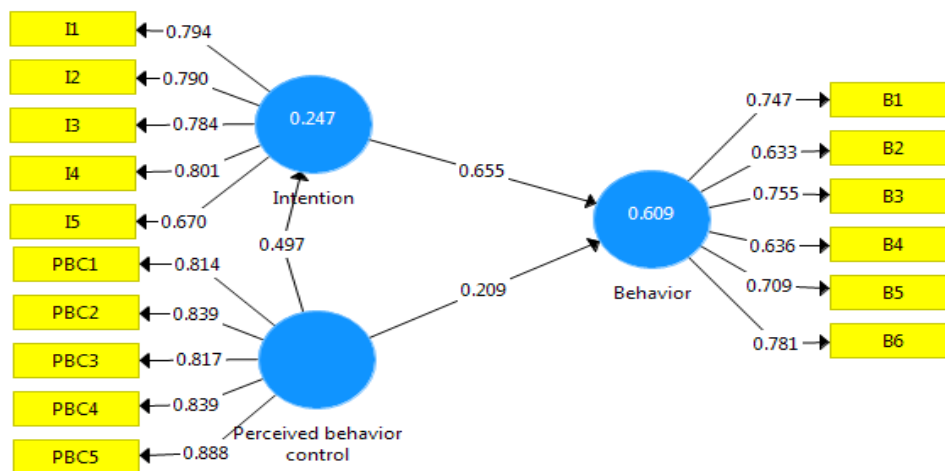


Figure 5. Structural model of the effect of perceived behavior control on cultivation of healthy crops behavior

Path coefficient (γ): the results of *Table 13* showed that the direct effect of latent variable of perceived behavior control on farmers' behavior with regard to healthy crop farming was 0.21 and significant at the 1% error level and the indirect effect of the latent variable of perceived behavior control on farmers' behavior was 0.32 and significant at the level of 1%. In addition, the total effect of latent variable of perceived behavior control on the farmers' behavior was 0.53, which is significant at the level of 1%. Thus, with probability of 99%, it can be stated that perceived behavior control has a positive and significant effect on farmers' behavior with regard to healthy crop farming in Kermanshah city.

Table 13. Summary of the results the evaluation of the structural model the effect of perceived behavior control on farmers' behavior. **Significance at the error level of 1%

Latent variables		Direct effect		Indirect effect		Total effect		F ²	R ²
Indigenous	Exogenous	γ	t	γ	t	γ	t		
behavior	perceived behavior control	0.21	5.05**	0.32	10.23**	0.53	13.47**	0.08	0.61

Coefficient of determination (R²): The results of *Table 13* showed that the coefficient of determination the latent variable of farmers' behavior with regard to healthy crop farming was 0.61. Thus, it can be stated that 61% of the variations in the variance of framers' behavior with regard to healthy crop farming is predicted by the latent variables of intention and perceived behavior control, which is a significant and high percentage.

Effect size (F²): Based on the Cohen scale, the variable of perceived behavior control has a moderate effect on farmers' behavior on healthy crop farming.

The effect of moral norms on farmers' behavior with regard to healthy crop farming

In this analysis, the latent variables of the research including farmers' behavior with six markers (B1-B6) and farmers' intention with five markers (I1-I5) and moral norms with five markers (ES1-ES7) entered the SmartPLS 3 software.

Evaluation measurement model of effect of moral norms on farmers' behavior

In order to examine the fit, validity and reliability of the model of measurement the effect of moral norms on the farmers' behavior with regard to healthy crop farming, confirmatory factor analysis was used. After eliminating two markers EN4 and EN7 of the measurement model, the model of measurement of the effect of moral norms on behavior of farmers with regard to healthy crop farming reached to optimal fit.

Goodness of fit indices (Table 14), summary of results (Table 15) and correlation coefficients (Table 16) are presented below.

Table 14. Fit indices model of measurement the effect of moral norms on farmers' behavior

<i>Fit index</i>	<i>SRMR</i>	<i>D_LS</i>	<i>D_G</i>	<i>NFI</i>	<i>RMS_Theta</i>
<i>Proposed value</i>	<0.10	>0.05	>0.05	>0.80	≤0.12
<i>Estimated value</i>	0.074	0.743	0.225	0.92	0.11

Model fit: The research results showed that the goodness of fit indices the model of measurement the effect of moral norms on farmers' behavior, had appropriate value (Table 14). Thus, data were statistically fit to the factor structure and the theoretical contextual of the three latent variables of the research.

One-dimensional markers: The results presented in Table 15 showed that the standardized load factor (λ) of all selected markers is high for all above-mentioned constructs (higher than 0.5) and they were statistically significant at the error level of 1% ($P < 0.01$). These results provided adequate evidence to confirm that the selected markers are one-dimensional for the models of measurement of the effect of moral norms on farmers' behavior. Hence, it can be stated that these markers have been selected properly for each of the relevant constructs.

Table 15. Summary of the results of evaluation the measurement model of effect moral norms on farmers' behavior. **significance at the error level of 1%

<i>Latent variables</i>	<i>marker</i>	λ	<i>t</i>	<i>CR</i>	<i>AVE</i>	<i>α</i>
<i>Farmers' behavior</i>	<i>B1</i>	0.74	30.11**	0.86	0.51	0.80
	<i>B2</i>	0.63	17.30**			
	<i>B3</i>	0.75	29.57**			
	<i>B4</i>	0.63	17.17**			
	<i>B5</i>	0.70	24.90**			
	<i>B6</i>	0.78	37.40**			
<i>Farmers' intention</i>	<i>I1</i>	0.80	36.11**	0.87	0.59	0.82
	<i>I2</i>	0.79	37.11**			
	<i>I3</i>	0.77	31.11**			
	<i>I4</i>	0.79	35.68**			
	<i>I5</i>	0.66	19.12**			
<i>Moral norms</i>	<i>En1</i>	0.81	36.13**	0.85	0.54	0.79
	<i>En2</i>	0.81	32.26**			
	<i>En3</i>	0.77	22.11**			
	<i>En5</i>	0.67	16.27**			
	<i>En6</i>	0.59	10.79**			

Composite reliability: The results presented in *Table 15* showed that the composite reliability (CR) of all research constructs was more than 0.60 and their Cronbach's alpha coefficient was higher than 0.70. Hence, all latent variables (constructs) of the research measurement model had a good reliability.

Convergent validity: The results presented in *Table 15* showed that the average of variance extracted (AVE) for all research constructs was more than 50. Thus, all the constructs of the research model had good convergent validity.

Table 16. AVE and correlation coefficients. Note: the numbers of table diagonal elements are average of variance extracted and elements below the table diameter are correlation coefficients among the construct

<i>Latent variables</i>	<i>1</i>	<i>2</i>	<i>3</i>
<i>1-behaviour</i>	0.78		
<i>2-intention</i>	0.75	0.77	
<i>3-moral norms</i>	0.37	0.40	0.78

Diagnostic validity: according to the results presented in *Table 16*, it was found that the average of variance extracted for each of the research constructs ($0.77 < AVE < 0.78$) was higher than the correlation between the constructs ($0.37 < r < 0.75$). This result showed that the selected markers for each construct share a high percentage of the common variance of that construct compared to other constructs in the research model, so the diagnostic validity of the constructs in the research measurement model was confirmed.

According to the results, it can be stated that the proposed measurement model to examine the effect on moral norms on farmers' behavior with regard to healthy crop farming with three main latent variables was the proper model for the research analyses.

Evaluation of structural model the effect of moral norms on farmers' behavior

After confirming the model of measurement the effect of moral norms on farmers' behavior with regard to healthy crop farming using confirmatory factor analysis, path analysis method (structural model evaluation) was used in order to test the hypothesis in the form of conceptual framework proposed for the research. The model of the research path with representation of factors loads in the standard mode (*Figure 5*) and the summary of the results (*Table 13*) derived from the evaluation of the structural model the effect of the perceived behavior control on farmers' behavior are presented below.

Path coefficient (γ): the results of *Table 17* showed that the direct effect of latent variable of moral norms on farmers' behavior with regard to healthy crop farming was 0.07 and significant at the 5% error level and the indirect effect of the latent variable of moral norms on farmers' behavior was 0.30 and significant at the level of 1%. In addition, the total effect of latent variable of moral norms on the farmers' behavior was 0.36, which is significant at the level of 1%. Thus, with probability of 99%, it can be stated that the latent variable of moral norms has a positive and significant effect on farmers' behavior with regard to healthy crop farming in Kermanshah city.

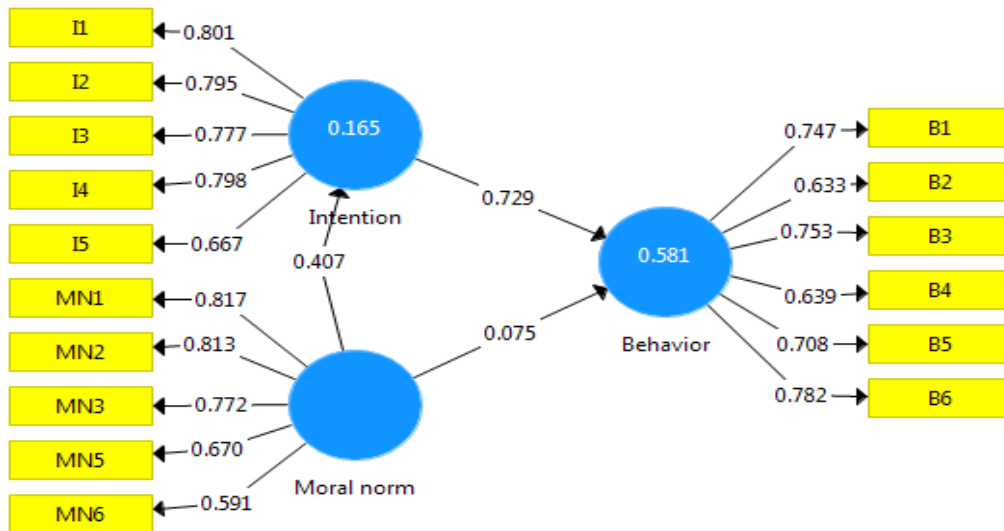


Figure 5. Structural model the effect of moral norms on farmers' behavior with regard to healthy crop farming in standard model

Table 17. Summary of the results the evaluation of the structural model the effect of moral norms on farmers' behavior. **Significance at the error level of 1% and *significance at the level of 5%

Latent variables		Direct effect		Indirect effect		Total effect		F ²	R ²
Indigenous	Exogenous	γ	t	γ	t	γ	t		
behavior	Moral norms	0.07	1.99*	0.30	8.68**	0.36	8.34**	0.01	0.58

Coefficient of determination (R²): The results of *Table 17* showed that the coefficient of determination of the latent variable of farmers' behavior with regard to healthy crop farming was 0.58. Thus, it can be stated that 58% of the variations in the variance of farmers' behavior with regard to healthy crop farming is predicted by the latent variables of intention and moral norms, which is a significant and high percentage.

Effect size (F²): Based on the Cohen scale, the variable of moral norms has a weak effect on farmers' behavior on healthy crop farming.

The effect of contextual factors on farmers' behavior with regard to healthy crop farming

In this analysis, the latent variables of the research including farmers' behavior with six markers (B1-B6) and farmers' intentions with five markers (I1-I5) and contextual factors with six markers (C1-C7) entered the SmartPLS 3 software.

Evaluation of the measurement model effect of contextual factors on farmers' behavior

In order to examine the fit, validity and reliability the measurement model of the effect of contextual factors on the behavior of farmers with regard to healthy crops farming, confirmatory factor analysis was used. Goodness of fit indices (*Table 18*), summary of results (*Table 19*), and correlation coefficient (*Table 20*) are presented below.

Table 18. Fit indices measurement model of the effect of contextual factors on farmers' behavior

Fit index	SRMR	D_LS	D_G	NFI	RMS_Theta
Proposed value	<0.10	>0.05	>0.05	>0.80	≤0.12
Estimated value	0.066	0.663	0.213	0.94	0.10

Model fit: The research results showed that the goodness of fit indices the model of measurement the effect of contextual factors on their behavior had appropriate value (18). Thus, data were statistically fit to the factor structure and the theoretical contextual of the three latent variables of the research.

Table 19. Summary of the results of evaluation measurement model the effect of contextual factors on farmers' behavior. **Significance at the error level of 1%

Latent variables	marker	λ	t	CR	AVE	α
Farmers' behavior	B1	0.74	32.13**	0.86	0.51	0.80
	B2	0.63	17.50**			
	B3	0.75	27.07**			
	B4	0.64	18.49**			
	B5	0.70	24.33**			
	B6	0.78	36.86**			
Farmers' intention	I1	0.79	35.39**	0.87	0.59	0.82
	I2	0.79	35.30**			
	I3	0.77	29.16**			
	I4	0.79	38.76**			
	I5	0.67	18.57**			
Contextual factors	C1	0.74	20.44**	0.88	0.55	0.84
	C2	0.82	34.65**			
	C3	0.75	20.03**			
	C4	0.72	18.16**			
	C5	0.71	17.09**			
	C6	0.68	13.88**			

One-dimensional markers: The results presented in *Table 19* showed that the standardized load factor (λ) of all selected markers is high for all above-mentioned constructs (higher than 0.5) and they were statistically significant at the error level of 1% ($P < 0.01$). These results provided adequate evidence to confirm that the selected markers are one-dimensional for the models of measurement of the effect of underlying factors on farmers' behavior. Hence, it can be stated that these markers have been selected properly for each of the relevant constructs.

-Composite reliability: The results presented in *Table 19* showed that the composite reliability (CR) of all research constructs was more than 0.60 and their Cronbach's alpha coefficient was higher than 0.70. Hence, all latent variables (constructs) of the research measurement model had a good reliability.

- Convergent validity: The results presented in *Table 19* showed that the average of variance extracted (AVE) for all research constructs was more than 50. Thus, all the constructs of the research model had good convergent validity.

Table 20. AVE and correlation coefficients. Note: the numbers of table diagonal elements are average of variance extracted and elements below the table diameter are correlation coefficients among the constructs

Latent variables	1	2	3
1-behaviour	0.78		
2-intention	0.75	0.77	
3-contextual factors	0.28	0.26	0.78

Diagnostic validity: according to the results presented in *Table 20*, it was found that the average of variance extracted for each of the research constructs ($0.77 < AVE < 0.78$) was higher than the correlation between the constructs ($0.26 < r < 0.75$). This result showed that the selected markers for each construct share a high percentage of the common variance of that construct compared to other constructs in the research model, so the diagnostic validity of the constructs in the research measurement model was confirmed. According to the results, it can be stated that the proposed measurement model to examine the effect on contextual factors on farmers' behavior with regard to healthy crop farming with three main latent variables was the proper model for the research analyses.

Evaluation of structural model" the effect of contextual factors on behavior of farmers

After confirming measurement model the effect of contextual factors on farmers' behavior with regard to healthy crop farming using confirmatory factor analysis, path analysis method (structural model evaluation) was used in order to test the hypothesis in the form of conceptual framework proposed for the research. The model of the research with representation of factors loads in the significance mode (*Figure 6*) and the summary of the results (*Table 21*) derived from the evaluation the structural model the effect of contextual factors on farmers' behavior are presented below.

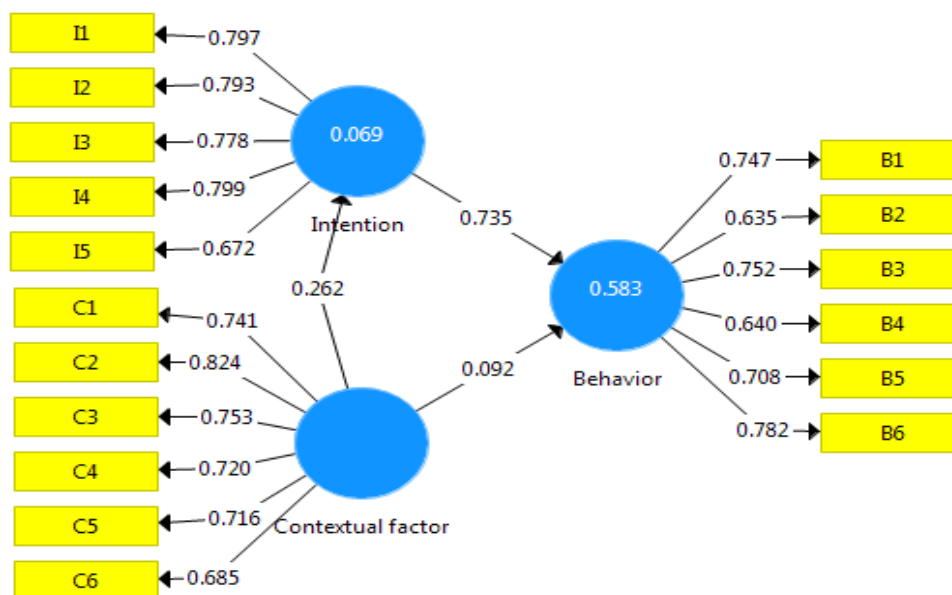


Figure 6. Structural model the effect of contextual factors on behavior of farmers in standard model

Path coefficient (γ): the results of *Table 21* showed that the direct effect of latent variable of contextual factors on behavior of farmers with regard to healthy crop farming was 0.09 and significant at the 1% error level and the indirect effect of the latent variable of contextual factors on behavior of farmers was 0.19 and significant at the level of 1%. In addition, the total effect of latent variable of contextual factors on farmers' behaviors was 0.36, which is significant at the level of 1%. Thus, with probability of 99%, it can be stated that contextual factors has a positive and significant effect on farmers' behavior with regard to healthy crop farming.

Table 21. Summary of the results of the evaluation of the structural model of the effect of contextual factors on behavior of farmers. **Significance at the error level of 1% and *significance at the error level of 5%

Latent variables		Direct effect		Indirect effect		Total effect		F ²	R ²
Indigenous	Exogenous	γ	t	γ	t	γ	t		
behavior	Contextual factors	0.09	2.82**	0.19	5.41**	0.28	6.08**	0.02	0.58

Coefficient of determination (R²): The results of *Table 21* showed that the coefficient of determination of the latent variable of farmers' behavior with regard to healthy crop farming was 0.58. Thus, it can be stated that 58% of the variations in the variance of framers' behavior with regard to healthy crop farming is predicted by the latent variables of intention and contextual factors, which is a significant and high percentage.

Effect size (F₂): Based on the Cohen scale, the variable of contextual factors has a weak effect on farmers' behavior on healthy crop . According the results Healthy crop farming model in Kermanshah province was drawn (*Fig. 7*).

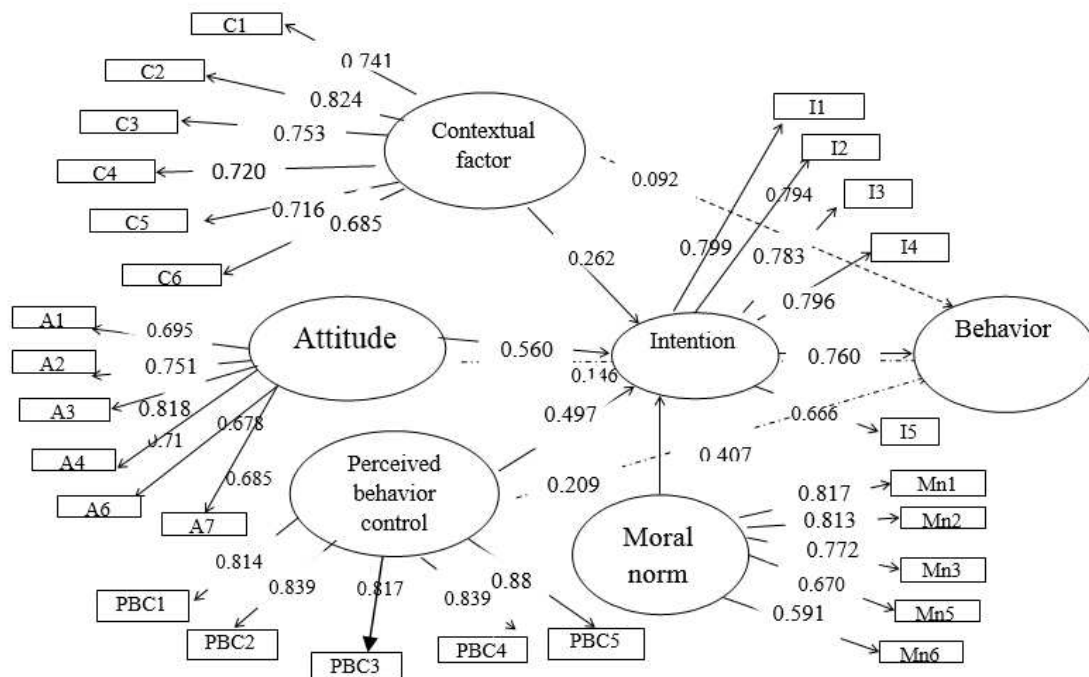


Figure 7. Healthy crop farming model in Kermanshah province

Multigroup analysis

In this analysis, demographic characteristics were considered as moderator construct. Accordingly, multigroup analysis path coefficient of intent and farmer behavior in Kermanshah province with modulation of demographic characteristics were performed in SmartPLS software version 3. Result show that : Among the various demographic characteristics, only the effects of gender variables, education level (basic and higher), participation in educational-extension classes were able to modify the path coefficient of the effect of intention on farmers' behavior regarding the cultivation of healthy products in Kermanshah province. The gender variable had a significant effect on the path between intention and behavior, so that according to the path coefficient between two groups (male and female), it was found that the effect of intention to cultivate a healthy product to behavior of healthy crops in female Beneficiary was greater than that of man (Table 22). The educational variable has a significant statistical effect on the path between intention and behavior. So, based on the path coefficient between the two basic and high levels education, it was shown that the effect on the healthy farming behavior of the beneficiary with higher education is higher than those with basic education (Table 23). The variable of participation in extension-education had a significant effect on the path between intention and the farming behavior of healthy crops. So, based on the path coefficient between the two groups of participants and non-participants, it was determined that the effect of healthy farming intention on healthy cropping behavior in the beneficiary who participated in the classes is more than the other beneficiary. In other words, participation in education - extension classes has led those who have the intention to cultivate healthy crops to be more productive for healthy crop cultivation (Table 24).

Table 22. Effect of intention on farmers' behavior with gender moderating. *Significantly at a level of five percent error

path	Group path coefficient		Difference of path coefficients	t	P-Value
	female	male			
Intention → behavior	0.80	0.69	0.11*	1.99*	0.048

Table 23. Effect of intention on farmers' behavior with a moderating level of education. *Significantly at a level of one percent error

path	Group path coefficient		Difference of path coefficients	t	P-Value
	basic	higher			
Intention → behavior	0.66	0.81	0.15*	2.50*	0.004

Table 24. Effect of intention on the behavior of farmers with the moderation of participation in the educational-extension class. *Significantly at a level of five percent error

path	Group path coefficient		Difference of path coefficients	t	P-Value
	Yes	No			
Intention → behavior	0.84	0.71	0.13*	2.14*	0.032

Discussion and conclusion

The objective of this research was to design a model for promoting healthy crop farming in Kermanshah province in Iran. For this purpose, we thoroughly reviewed the literature on the healthy and organic crop farming and the models of behavior promotion, and barriers and problems in healthy and organic crop farming. Finally, by analyzing the present models, the theory of extended planned behavior was selected as the base model. Based on the results of the research, the most important variables affecting the healthy crop farming behavior in Kermanshah province are contextual variables, attitude, perceived behavior control, moral norms, and intentions. Based on the results of the research and the effect size of the pls analysis, the intention had the most effect, the attitudes and perceived behavioral control variables, the moderate effect, and the contextual factors and moral norms had a weak effect on the healthy crop farming behavior. The results showed that the path coefficient of intention and farmers' behavior with regard to healthy farming was 0.76 and significant at 1% error level. Thus, with a probability of 99%, it can be stated that intention has a positive and significant effect on farmers' behavior with regard to healthy crop farming. The coefficient of determination of the latent variable of farmers' behavior with regard to healthy crop farming was obtained 0.57. Thus, it can be stated that 57% of variations in variance in farmers' behavior with regard to healthy crop farming is predicted by their intentions, which is significant and high percentage. This result is consistent with the results of the study conducted by Molaei et al. (2015), Menatizadeh et al. (2012).

The model of the measurement of the effect of attitude on farmers' behavior with regard to healthy crop farming was confirmed by confirmatory factor analysis. The output of PLS showed that the direct effect of latent variable of attitude on farmers' behavior with regard to healthy crop farming was 0.14 which was significant at the 1% error level and indirect effect of latent variable of attitude on farmers' behavior was 0.38, which was significant at 1% error level. In addition, total effect of latent variable of attitude on behaviors' farmers was 0.52, which was significant at 1% error level. Thus, with a probability of 99%, it can be stated that the latent variable of attitude toward healthy crop farming has a positive and significant effect on farmers' behavior in Kermanshah Province with regard to healthy crop farming. It is consistent with the results of the studies conducted by Sandughi and Raheli (2016), Rahimi Feiz Abad et al (2015), Yanakittkul and Aungvaravong (2017), Issa and Hamm (2017), But with the result of Abedi Sarvestani's research (2011), is inconsistent.

After confirming the model of measurement of the effect of perceived behavior control on farmers' behavior with regard to healthy crop farming using confirmatory factor analysis, the results of path analysis showed that direct effect of the perceived behavior control on farmers' behavior with regard to healthy crop farming was 0.21, which was significant at 1% error level and indirect effect of latent variable of perceived behavior control on farmers' behavior was 0.32, which was significant at 1% error level and total effect of perceived behavior control on farmers' behavior was 0.53, which was significant at 1% error level. Thus, with a 99% probability, it can be stated that the latent variable of perceived behavior control has a positive and significant effect on the farmers' behavior in Kermanshah province with regard to healthy crop farming, which is consistent with the results of the research conducted by Yadavar et al. (2018), Issa and Hamm (2017), Van-Hulst and Posthumus (2016), Taqipour et al. (2015), but these results are not in line with those of Sandughi and Raheli (2016) on lack of effect of the behavior control variable on behavior.

After confirming the model of measurement of the effect of moral norms on farmers' behavior with regard to healthy crop farming using confirmatory factor analysis, the results of path analysis showed that the direct effect of latent variable of moral norms on farmers' behavior with regard to healthy crop farming was 0.07, which was significant at the error level of 5% and in indirect effect of the latent variable of moral norms on farmers' behavior was 30%, which was significant at 1% error. In addition, total effect of latent variable of moral norms on farmers' behavior was 0.36, which was significant at the error level of 1%. Thus, with a probability of 99%, it can be stated that the latent variable of moral norms has a positive and significant effect on the behavior of farmers in Kermanshah province with regard to healthy crop farming. This result is in line with results of research conducted by Menatizadeh and Zamani (2012), Rahimi Feiz Abad et al (2015), Sandughi and Raheli (2016), Onwezen et al. (2013), Bissonnette and Contento (2001), Armitag and Conner (2001).

After confirming the model of measurement of the effect of the contextual factors on farmers' behavior with regard to healthy crop farming using confirmatory factor analysis, the results of their path analysis showed that the direct effect of latent variable of contextual factors on farmers' behavior h was significant at 1% error level and the the indirect effect of the latent variable of contextual factors on farmers' behavior was 0.19, which was significant at 1% error level. In addition, total effect of latent variable of the contextual factors on farmers' behavior was 0.36 which was significant at 1% error level. Thus, with a probability of 99%, it can be stated that the latent variable of the contextual factors has a positive and significant effect on the behavior of farmers in Kermanshah province with regard to healthy crop farming. It is in line with the results of the research conducted by Razavi et al. (2017), Okoedo-Okojie and Aphunu (2011), Karunamoorthi, et al., 2011, Sharifi et al (2010). Based on the results obtained, all research hypotheses are confirmed .The result of multigroup analysis show that: Women, exploiters who have participated in extension classes, and those with higher education ,more than others, convert healthy crops cultivation intentions into healthy crop cultivations behavior. In Iran, there has been no research on the moderator of demographic factors in the path between intent and behavior in healthy crop cultivation, which could be one of the research achievements.

Recommendations

Due to the destructive effects of farmers' behavior, examining the bio-friendly behaviors seems to be an essential. Healthy crop farming was considered as a protective behavior in this research. In this regard, the theory of planned behavior was used.

Farmer's attitude is an important factor, which should be considered. The farmer's attitude is more affected by the environment and the community in which he lives. Thus, the farmers' communication with family members, friends and neighbors and experienced farmers can be useful in creating a positive attitude. Jihad agriculture facilitator can be effective in meeting this important need. Economic profitability also leads to creation of positive attitude toward healthy crop farming. Using the results of the test method, farmer can realize that organic farming in the long run would lead to profit and it is fulfilled through support of other experienced farmers, friends, and Jihad agriculture promoters.

The contextual factors are other variables affecting the intention and behavior of healthy crop farming including government support and Jihad agriculture support and promotion organization. With holding of more promotional classes and making farmers

aware of healthy crop practices, the promotion organization can take steps in achieving this goal. By designing appropriate strategies, such as subsidizing and insurance, government can encourage the farmers to farm healthy crops. In addition, by using mass media such as radio and television, and mental stimulation of the people and creating empathy with farmers, it can force the farmers to protect natural resources and less use of chemical inputs.

The variable of moral norm is an important factor affecting the intentions of healthy crop farming. In Islam, the protection of human health is considered as moral norm. Thus, any non-protective behavior by a person who endangers the health of a person means resistance against the creator (Balali et al., 2009). In Islamic countries like Iran, moral commitments can be created among farmers and beneficiaries with regard to human health and the environment protection through religious beliefs. In this regard, religious leaders can develop positive moral feelings toward protecting the environment from religious aspects among people.

The perceived behavior control variable has significant effect on the intention and behavior of healthy crop farming. One's perception of self affects the intentions and behavior of healthy crop farming, for example, if a person believes that he has intrinsically high power and ability in finding a suitable market for selling his crops and doing proper agricultural practices in land, his intention and behavior would affect his intention and behavior in adopting healthy crop farming. Increasing self-efficacy in a farmer depends on the type of training and messages provided by coworkers and agriculture promoters for farmer.

REFERENCES

- [1] Abedi Sarvestani, A. (2012): Environmental attitude and behavior of student of Gorgan University of agricultural sciences and natural resources. – Iranian agricultural extension and education journal 7(2).
- [2] Agricultural Statistics in Iran (2016): Ministry of Agricultural – Jihad, Department of Planning and Economics, Center for Information and Communication Technology 2.
- [3] Ajzen, I. (1991): The theory of planned behavior. – Organizational behavior and human decision processes 50(2):179-211.
- [4] Ajzen, I. (1985): From intentions to actions: A theory of planned behavior. – In: Kuhl, J., Beckmann, J. (Eds.) Action-control: From cognition to behavior. Heidelberg: Springer 1: 1-39.
- [5] Alexandratos, N., Bruinsma, J. (2012): World agriculture towards 2030/2050: the 2012 revision. – ESA Work 3.
- [6] Ansari, Sh. (2016): [Sanctions: The main cause of entrancing poisons to the country (Persian)] [Internet]. Retrieved from <http://khabardown.ir/news/id/669371>.
- [7] Armitage, C. J., Conner, M. (2001): Efficacy of the Theory of planned behavior. – Organizational behavior and human decision processes 50(2): 179-211.
- [8] Balali, M. R., Keulartz, J., Korthals, M. (2009): Reflexive water management in arid regions: the case of Iran. – Journal of Environmental Values 18(1): 91-112.
- [9] Bissonnette, M. M., Contento, L. R. (2001): Adolescents' perspectives and food choice behaviors in terms of the environmental impacts of food production practices: Application of a psychosocial model. – Journal of Nutrition Education 33(2): 72–82.
- [10] Borges, J. A. R., Tauer, L. W., Lansink, A. G. J. M. (2016): Using the theory of planned behavior to identify key beliefs underlying Brazilian cattle farmers' intention to use improved natural grassland: A MIMIC modelling approach. – Land Use Policy 55: 193-203.

- [11] Chakrabarty, T., Akter, S., Saifullah, A. S. M., Sheikh, M. S., Bhowmick, A. C. (2014): Use of fertilizer and pesticide for crop production in agrarian area of Tangail District, Bangladesh. – *Environment and Ecology Research* 2(6): 253-261.
- [12] Costaa, C, García-Lestónb, J., Costaa, S., Coelho, P., Silva, A., Pingarilho, Mc., Valdiglesiasb, D., Francesca Matteid, V., Dall’Armid, V., Bonassid, S., Laffonb, B., Snawdere, J., Teixeiraa, J. (2014): Is organic farming safer to farmers’ health? A comparison between organic and traditional farming. – *Toxicology Letters* 230(2):166-76. doi: 10.1016/j.toxlet.2014.02.011. Epub 2014 Feb 24.
- [13] Donahue, M. (2017): *Theory of Planned Behavior Analysis and Organic Food Consumption of American Consumers*. – Walden Dissertations and Doctoral Studies. Walden University.
- [14] Educational Workshop for Organic Crops in Jihad Agriculture in Kermanshah Province (2016): Kermanshah Province Agriculture Jihad.
- [15] Fielding, K., S., McDonald, R., Louis, W. R. (2008): Theory of planned behavior, identify and intention to engage in environmental activism. – *Environmental psychology* 28(4): 318-326.
- [16] Fishbein, M, Ajzen, I., (1975): *Belief, attitude, intention and behavior: An introduction to theory and research*. – Reading Mass: Addison-Wesley.
- [17] Haddadi, Sh., Yazdani, S., Saleh, A. (2017): Investigating the factors affecting farmers' willingness for organic farming of cucumber in Alborz Province. – *Iranian Journal of Agricultural Economics and Development* 2-48(3): 369-378.
- [18] Hayati, B., Pish Bahar, A., Hagju, M. (2011): Evaluation of the factors determining consumers' willingness for extra payment pesticide-free fruits and vegetables in Marand. – *The Economics of Agricultural Development Journal* 4: 469-479.
- [19] Heckman, J. (2006): A history of organic farming: Transitions from Sir Albert Howard's War in the Soil to USDA National Organic Program. – *Renewable Agriculture and Food Systems* 21(3): 143-150.
- [20] Hosseini, J., Ajoudani, Z. (2012): Affective Factors in Adopting Organic Farming in Iran. – *Scholars Research Library Annals of Biological Research* 3 (1):601-608.
- [21] Issa, I., Hamm, U. (2017): Adoption of Organic Farming as an Opportunity for Syrian Farmers of Fresh Fruit and Vegetables: An Application of the Theory of Planned Behaviour and Structural Equation Modelling. – *Sustainability journal* 9(11). doi: 10.3390/su9112024.
- [22] Kaiser, F., G. (2006): A moral extension of the theory of planned behavior: Norms and anticipated feelings of regret in conservationism. – *Journal of Personality and Individual Differences* 41(1): 71-81.
- [23] Karppinen, H. (2005): Forest owners choice of reforestation method: application of the theory of planned behavior. – *Forest policy and economics* 7(3):393-409.
- [24] Karunamoorthi, K., Mohammed, A., Jamel, Z. (2011): Peasant association members knowledge, attitude practices towards safe use of pesticide management. – *American Journal of Industrial Medicine* 54: 965-970.
- [25] Lampkin, N. H. (1990): *Organic farming*. – Ipswich: Farming Press.
- [26] Lampkin, N. H., Pade, S. (1994): *The Economics of organic farming: An international perspective* – CAB International, UK.
- [27] Lautenschlager, L., Smith, C. (2007): Understanding gardening and dietary habits among youth garden program participants using the Theory of planned behavior. – *Appetite* 49(11): 122-130.
- [28] Malek Saedi, H. (2007): *Effective factors on the knowledge and attitudes of Jihad Agriculture experts in Fars and Khuzestan provinces toward organic agriculture*. – Master Thesis, Ahwaz Faculty of Agriculture.
- [29] Menatizedeh, M., Zamani, G. H. (2012): Development of environmental behavior model of farmers of Shiraz, Iran. – *Journal of Agricultural Science Promotion and Education* 8(2).

- [30] Mohamad, S. S., Rusdi, S. D., Hashim, N. H. (2014): Organic Food Consumption Among Urban Consumers: Preliminary Results. – *Social and Behavioral Sciences* 130: 509-514.
- [31] Molaei, Kh., Ajili, A., Mohammadzadeh, S., Yazdanpanah M., Foruzani M. (2015): Investigating the tendency and behavior of farmers towards using integrated pest management using the extended theory of planned behavior. – *Journal of Agricultural Promotion and Education Research* 8(2), Summer 2013.
- [32] Okoedo-Okojie, D. U., Aphunu, A. (2011): Assessment of Farmers' Attitude towards the Use of Chemical Fertilizers in Northern Agricultural Zone of Delta State, Nigeria. – *Scholar Research Library. Applied Science Research* 3(1): 363-369.
- [33] Onwezen, M. C., Antonides, G., Bartels, J. (2013): The norm activation model: An exploration of the functions of anticipated pride and guilt in pro-environmental behavior. – *Journal of economic psychology* 39: 141-153.
- [34] Owens, K., Feldman, J., Kepner, J. (2010): Wide range of diseases linked to pesticides. *Pesticides and You – A Quarterly Publication of Beyond Pesticides* 30(2): 13-21. Retrieved from: <http://beyondpesticides.org/health/pid-database>.
- [35] Pesticide Action Network (2009): PAN pesticides database. – Retrieved from: http://pesticideinfo.org/search_use.jsp.
- [36] Rahimi Feiz Abad, F., Yazdanpanah, M., Foruzani, M., Mohammadzadeh, S., Burton, R. (2015): Explaining the farmer's water protection behavior using the extended theory of planned behavior: Case Study of Alashtar City. – *Journal of Agricultural Science Promotion and Education* 12(2), 2016.
- [37] Razavi, H., Pourtaheri, M., Rokneddin Eftekhari, A. (2017): Proposed model for organic farming of rice in rural areas of Gilan and Mazandaran Provinces. – *Rural Research Quarterly* 8(3): 372-387.
- [38] Razavi, H., Pourtaheri, M., Rokneddin Eftekhari, A. (2013): Designing an organic farming model for rice (Case study: Mazandaran and Gilan). – Ph.D thesis of Tarbiat Modares University.
- [39] Sandughi, A., Raheli, H. (2016): Development of a planned behavior model for explaining the intention of producing organic crops among greenhouse farmers in Isfahan, with a variable of moral norm. – *Iranian Research and Development Department* 47(4): 961-974.
- [40] Sandughi, A., Yousefi, A., Amini, A. (2016): Evaluation of knowledge, attitude and practice of cucumbers and tomatoes greenhouse owners in Isfahan City. – In: *The Production of Healthy Crop. Journal of Greenhouse Crop Science and Technology* 7(3): 155-167.
- [41] Sharifi, O., Sadati, A., Rostami, F., Sadati, A. G., Mohammadi, Y., Taher, P. (2010): Barriers to conversion to organic farming: A case study in Babol County in Iran. – *African Journal of Agricultural Research* 5(16): 2260-2267.
- [42] Simsekoğlu, Ö., Lajunen, T. (2008): Social psychology of seat belt use: A comparison of theory of planned behavior and health belief model. – *Transportation Research Part F: Traffic Psychology and Behavior* 11(3): 181–191.
- [43] Taqipour, M., Abbas, E., Chizari, M. (2015): Farmers' Behavior toward Membership in Water User Associations (WUAs) in Iran: Applying the Theory of Planned Behavior. – *European Online Journal of Natural and Social Sciences* 4(2): 336-350.
- [44] United Nations (2014): Population ageing and sustainable management. – *Population Division Department of Economic and Social Affairs* 4 1e4 – Retrieved from: <http://un.org/esa/population>.
- [45] Van-Hulst F. J., Posthumus, H. (2016): Understanding non- adoption of conservation agriculture in Kenya using the reasoned action approach. – *Land Use Policy* 56: 303-314.
- [46] Vermeir, I., Verbeke, W. (2008): Sustainable food consumption among young adults in Belgium: Theory of planned behavior and the role of confidence and values. – *Ecological Economics* 64(3): 542-553.

- [47] WHO (2016): World Health Organization's Ranking of the World's Health. http://www.who.int/gho/publications/world_health_statistics/2016/Annex_B/en.-Pesticide action Network UK.(2014).
- [48] Yadavar, H., Zarifiyan, S., Nami, M. (2018): Applying the behavior analysis theory to organic farming adaptation. – *Journal of Agricultural Science and Sustainable Production* 28(1): 169-183.
- [49] Yanakittkul, P., Aungvaravong, C. (2017): Proposed conceptual framework for studying the organic farmer behaviors. – *Kasetsart Journal of Social Sciences*. <http://dx.doi.org/10.1016/j.kjss.2017.09.001>. Available online 28 September 2017.
- [50] Zhao, J., Luo, Q., Deng, H., Yan, Y. (2007): Opportunities and challenges of sustainable agricultural development in China. – *Philosophical Transactions of the Royal Society B: Biological Sciences* 363(1492): 893–904. doi: <http://dx.doi.org/10.1098/rstb.2007.2190>

THE EFFECTS OF RILL EROSION ON UNPAVED FOREST ROAD

VAROL, T.^{1*} – ERTUĞRUL, M.¹ – ÖZEL, H. B.¹ – EMIR, T.¹ – ÇETİN, M.²

¹*Department of Forest Engineering, Faculty of Forestry, Bartın University, Bartın, Turkey
(phone: +90-378-223-5171)*

²*Department of Landscape Architecture, Faculty of Engineering and Architecture, Kastamonu University, Kastamonu, Turkey
(phone: +90-360-280-2920)*

**Corresponding author
e-mail: tvarol@bartin.edu.tr; phone: +90-378-223-5171*

(Received 25th Sep 2018; accepted 26th Nov 2018)

Abstract. This research aims to investigate the degree of rill erosion and its relationship with the factors effective on rill volume on unpaved forest roads in Bartın Province in Turkey. For this purpose, measurements were made at 380 sample locations on different regions of the forest roads in Arıt and Hasankadı sub-districts. The measurements were performed on 4 years old unpaved forest roads. Among the road surface (RS), road cut (RC), sidecast fill (SCF) and skid trail (ST) road sections, RS and ST ranked as the first two sections with the highest segment length. Segment length is characterized as the most effective field factor on erosion, which further increased the rill volume by the combined effect of increasing slope, in this research. According to the stepwise (forward-backward) regression analysis results, inclusion of both segment length and slope parameters in the RS, SCF and RC equations supports this finding. The correlation of all road sections (RS, SCF, RC, ST) with the segment length are 0.84, 0.63, 0.75 and 0.83, respectively, and the correlation with the slope are 0.55, 0.73, 0.57 and 0.64, respectively. As a result of the slope-based categorization of the relationship between segment lengths and rill volume for the road sections, R² values were found to increase up to 0.88 for RS, 0.78 for SCF, 0.94 for RC and 0.88 for ST. The rill volume at short and steep roads can be lower than the rill volume at long and low-slope roads. Therefore, we calculated the rill volumes per unit road segment area. As a result of application of equations based on shear stress and stream power sediment transport capacity theory, RMSE values with very low mean error were obtained. In further related studies, drainage areas in addition to segment lengths and slope should also be taken into account to determine the positive and negative effects in evaluation of rill erosion amounts. Also, similar studies should be performed on other basins having a larger number of unpaved forest roads as a means to extend the applicability of the obtained findings.

Keywords: *soil loss, road erosion, sediment sources, hydrological constituents, unpaved road*

Introduction

Unpaved forest roads cover a relatively tiny area of a basin, though they have a major effect on numerous hydrological and geomorphic processes in a given basin and they act as a primary sediment source, which make them an interesting subject for various research (Megahan, 1987; Luce and Wemple, 2001; Ramos-Scharron and MacDonald, 2005; Cao et al., 2011, 2014, 2015). The combined effect of soil compaction resulting in reduced infiltration capacity of road surface and the vehicle-induced increase in the sediment yield leads to an increase in surface runoff (Sidle et al., 1985; Ziegler et al., 2000; Croke and Mockler, 2001; Gucinsky et al., 2001; Dougherty et al., 2004; Xu et al., 2007; Eisenbies et al., 2007; Cao et al., 2011; McGroody et al., 2013). This formation occurs even to a greater extent than mass movements (Ketcheson et al., 1999). It has been reported in studies performed in various locations (Australia, China, England, Ghana, Kenya, Kuwait, Malaysia, New Zealand, Norway, Poland, The

United States, Tunisia etc.) that, forestlands feature lower erosion whereas unpaved forest roads exhibit significantly higher erosion (Dunne, 1979; Reid and Dunne, 1984; Kumapley, 1987; Fahey and Coker, 1989; Burroughs et al., 1991; Froehlich, 1991; Douglas, 1993; Grayson et al., 1993; Froehlich and Walling, 1997; Fransen et al., 2001; Xu et al., 2009; Posthumus et al., 2011; Tommervik et al., 2012; Foster et al., 2012; Al-Awadhi, 2013; Desprats et al., 2013; Leh et al., 2013). In this regard, evaluation of the sediment yield of unpaved forest roads gains an increasing importance.

As a result of the higher erosion rates on unpaved forest roads compared to open-channel flow areas or areas with heavy vegetation (such as agriculture and pasture areas), data specific to such areas have been used in estimation of road-induced sediment in the last fifty years (Ramos-Scharron and MacDonald, 2007; Croke et al., 1999). Particularly, conducting an effective land planning requires a good understanding of road-induced erosion and sediment production process. River monitoring, sediment determination methods and road erosion models are widely used to estimate the road-induced erosion. Silt fences, installed on road sites, provide useful information at coarse grained (such as sand and gravel) roads, but they do not provide precise information in determination of fine sediment yields (Ramos-Scharron and MacDonald, 2007). Besides their convenience, monitoring methods are more costly.

SEDMODL2 (Road Sediment Delivery Model), WARSEM (Washington Road Surface Erosion Model), CULSED, USLE (Universal Soil Loss Equation) and its modifications, and ROADMOD are the test based models; whereas WEPP (The Water Erosion Prediction Project) and KINEROS2 (Kinematic Runoff and Erosion Model) are physical models used in estimation of sediment yield (Dube et al., 2004; Cochrane et al., 2007; Elliot et al., 2009; Fu et al., 2010; Cao et al., 2011; Varol, 2015, 2016). Considering the statistical relationship between the observation-driven results derived from experimental models and dependent variables, the use of these models in diverse studies becomes a challenge due to their field-specific nature (Merritt et al., 2003). Physical models are mainly based on hydrological reactions and these models simulate infiltration and run-off routines. Case-based models, on the other hand, estimate the sediment yield produced as a result of a single rainfall or run-off event, thus simulating the erosion. Moreover, experimental models are continuous, whereas physical models are case-based models.

As reported in the studies performed on unpaved forest roads in Turkey; sediment yields vary between 0 - 2.715 tons on gravel-surfaced road sections, and between 1.476 - 28.667 tons on asphalt roads. Spatial sediment yield varies between 0.0004 t/m² and 0.0199 t/m² on gravel surfaced grounds, and between 0.0051 t/m² and 0.0636 t/m² on asphalt roads (Akay et al., 2008). In addition to the afore-stated studies quantitative works on soil erosion characteristics of unpaved roads are also required (Xu et al., 2009; Varol, 2016). Investigation of erosion characteristics is particularly required for steep unpaved forest roads that receive large amounts of rain such as those in Karadeniz Region. GPS aided road surveys and GIS methodology have been commonly used in investigation of road-induced erosion characteristics as these are closely associated with road types and spatial variables. In this regard, the present research was conducted at Arit and Hasankadı Sub-district Directorates of Bartın Forestry Directorate with a view to: (1) define the amount and spatial distribution of road erosion, (2) clarify the relationship between the road segments' erosion characteristics and the effective factors, and (3) propose equations that can be used in estimation of erosion.

Material and method

Study area

The erosion estimation studies for unpaved forest roads were performed in Arit ($32^{\circ} 24' 20''$ - $32^{\circ} 44' 50''$ east longitudes and $41^{\circ} 33' 90''$ - $41^{\circ} 45' 70''$ north latitudes) and Hasankadı ($41^{\circ} 17' 48''$ - $41^{\circ} 22' 35''$ north latitudes and $32^{\circ} 16' 48''$ - $32^{\circ} 29' 06''$ east longitudes) sub-district directorates of Bartın Forest Directorate in Turkey (Fig. 1). The region is dry and hot in summers (Csa) (Varol and Ertugrul, 2015) with a mean yearly temperature of 12.8°C , and annual precipitation is 1044.5 mm (1965-2017). The total rainfall in 2017 in which the study was carried out was 1209.3 mm above the average of 1965-2017 period. In 2017, the highest monthly rainfall amounted to 242.7 mm in August. The sample unpaved forest road locations surrounded with forestlands in both sub-districts are located in basins with about 17.4 ($14.6 + 2.8$) km^2 acreage and their altitudes above sea level vary between 750 and 1200 m. Both road sections are in Kilimli formation and they are composed of Cretaceous aged bedrock sandstone-carbonate sand-stone. In the study area, agricultural and settlement areas in Arit sub-district cover the largest area (7.74 km^2) which are followed by fertile (6.14 km^2) and rough (0.7 km^2) forestlands and forest soil. Hasankadı sub-district is completely composed of fertile forestlands (2.87 km^2).

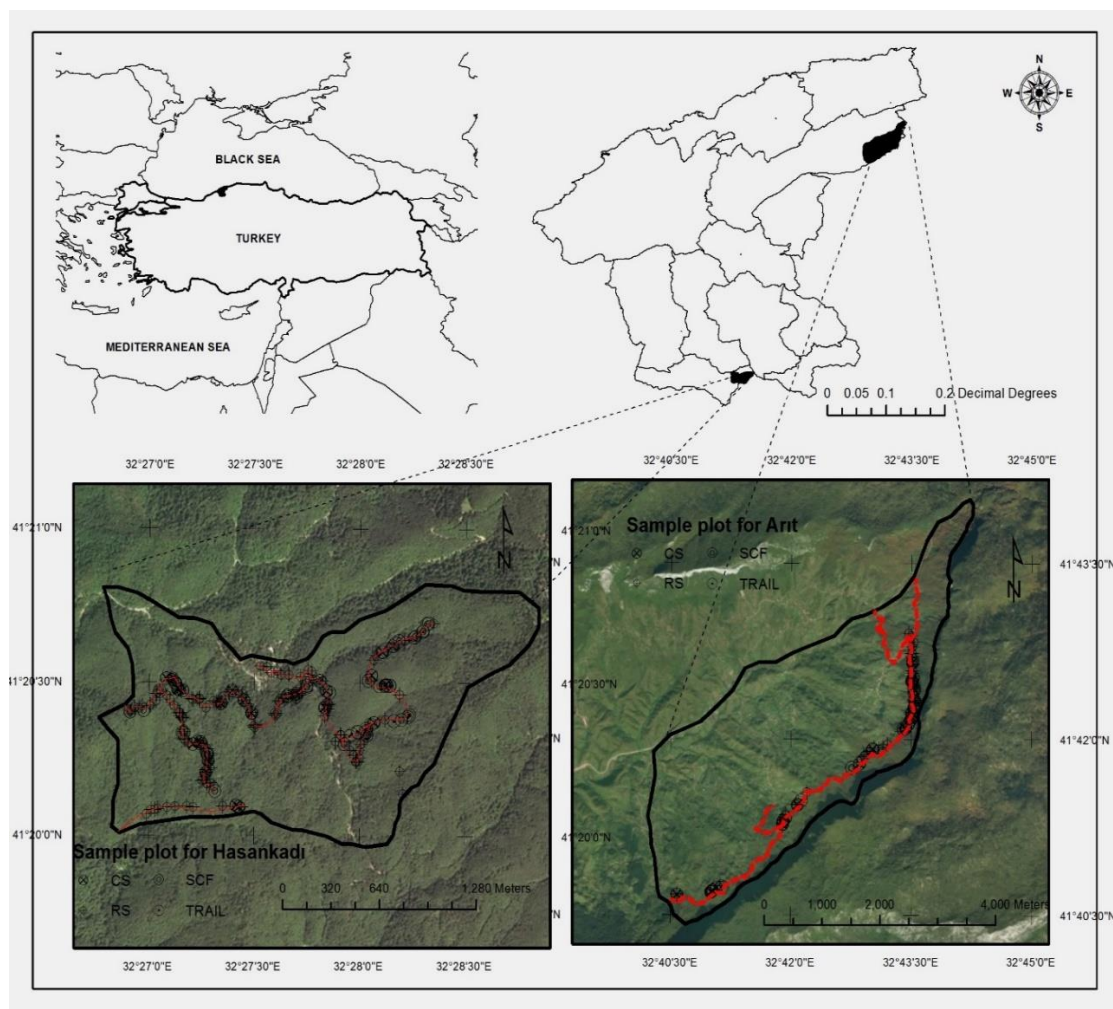


Figure 1. The location of study area

Road network

A forest road consists of a series of hydrological constituents such as road surface (RS), road cut (RC) and sidecast fill (SCF) (Fig. 2). Road surface represents the unpaved surface of the road on which vehicles move, road cut represents the straightly or curvedly cut profile of the slope of the road, and sidecast fill defines the aggregates right under the road that forms during road construction. No vegetation is observed on the road cut sections that have an average height of 2-5 meters and the sidecast fill sections that have straight profiles. Segment lengths observed in the study area vary between 5.0-285.7 m for road cut segment, 3.5-477.3 m for road surface, 2.9-99.6 m for sidecast fill, and 2.2-102.4 m for skid trails.

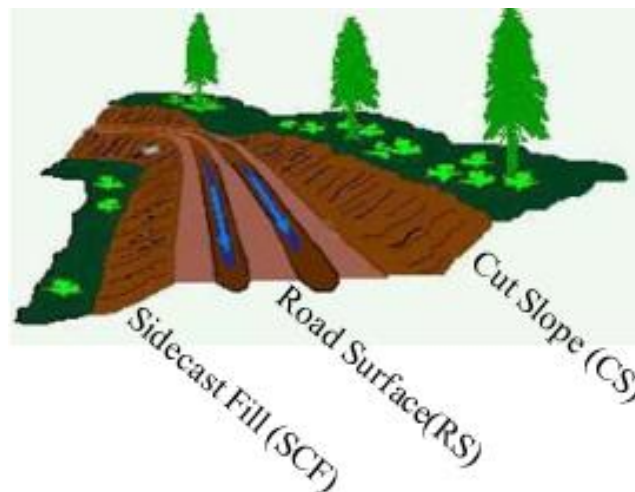


Figure 2. Components of a road (Elliot et al., 2009)

The total forest road length of Arıt sub-district is 148610 m, and that of Hasankadı sub-district is 115700 m. All forest roads in Arıt sub-district are B-type secondary forest roads (The platform width is 3-5 m, ditch width is 0.50-1 m, total width of 3.5-6 m, the minimum curve radius is 12 m, maximum slope 12%, which are generally unpaved roads. The annual amount of product to be transported on these roads is less than 25000 m³) and only 3% are paved forest roads. Those in Hasankadı sub-district are also B-type secondary forest roads and 30% are paved forest roads. Accordingly, the roads in both sub-districts are largely void of road pavement to bear the vehicle loads. These roads have been used for transportation purposes by local residents in addition to forestry and agricultural activities. These roads do not have any surface cover. Compacting is materialized by the vehicles used in agricultural and forestry activities. The newly constructed roads in the road network plan were manually digitized and involved in the network plan. The road surface, road cut and sidecast fill sections of the study area were constructed four years before 2017, skid trail sections were constructed ten years ago. In parallel to the increasing run-off followed by rainfall, surfaces of unpaved forest roads lead to increasing sediment transport. Sediment transport occurs at higher rates at rills that form on the road segments (RS, RC, SCF) (Fig. 3). Therefore, rill formations on each road segments have been subject to examination in this research. In general, a road segment is characterized with the road length between two nodes (Tanimoto, 1999; MacDonald et al., 2001).



Figure 3. Unpaved road segment samples. *a* Sediment transport along the rills that form on the road segment. *b* Highly eroded road surface. *c* Erosion on the node where two road segments intersect

A road segment can be terminated by intersection of the node with another road or an artificial boundary, or it can start and end by a change in road characteristics (such as slope, exposure, etc.). A road segment can be defined as a section of the road with an independent drainage area (Cao et al., 2014). During the road measurements, the start and end points of road segments in addition to the segment lengths and variations in slope were determined via GPS. The characteristics of the road network and road segments on which the measurements were performed are shown in *Table 1*.

Table 1. Characteristics of the road network and road segments in the study area

Road type and segments	Road network's characteristics			Road segments' characteristics			
	Total length (km)	Mean width (m)	Road density (km/km ²)	Count	Mean length (m)	Ratio of rilled segment (%)	Mean slope (%)
RS	14.7	6.11	0.84	206	60.89	40.85	9.42
SCF	14.7	5.94	0.84	48	24.66	50.61	37.62
CS	14.7	6.13	0.84	79	45.80	9.66	35.41
ST	1.9	6.00	0.11	47	28.97	68.86	29.65

RS: Road surface, SCF: Sidecast fill, RC: Road cut, ST: Skid trail

Data

The length, width and depth of rills on each specified road segment were measured by a measuring tape. The slope of rills and the road were measured by a clinometer. Intersecting rills were measured up to the point of junction with the main rill. As a means for an accurate estimation of the erosion on road segments, width and depth measurements were performed at three meter intervals. Measurements were conducted on a total of 427 rills at road surface, road cut, sidecast fill and skid trail sections.

The statistical evaluation of the relationship between slope and length of road segments, which are the effective factors on the amount of road-induced erosion, and erosion was carried out using ANOVA (one-way analysis of variance), Pearson correlation analysis, and RMSE (the root mean square error). ANOVA was used to make a comparison of rill volumes and road segments, Pearson was used for correlation analysis and evaluation of the relationship between the effective factors and road-induced erosion, and RMSE was used to evaluate the efficiency of the estimation models for soil erosion. RMSE is defined with the following *Equation 1* (Bhuyan et al., 2002).

$$RMSE = \sqrt{\frac{\sum_{i=1}^n (O_i - P_i)^2}{n}} \quad (\text{Eq.1})$$

In *Equation 1*, O_i and P_i denotes the observed and estimated values, and n denotes the sum of each value pair. Smaller RMSE values indicate higher consistency between the estimated and the observed values.

Results and discussion

Road segments and rill characteristics

Significantly high ratio of rill were encountered on the skid trail and the road segments other than RC (*Table 1*). Ratio of rill depending on the road length were found as 40.85%, 50.61% and 68.86% respectively for RS, SCF and ST. The results show that, logging roads are subject to higher erosion than RS, and SCF despite being less frequently used and being subject to higher compaction. In general, the slope values of eroded road sections were found to be higher than the average values.

Although the determined erosion rates were higher for RS, erosion values per unit area (km) were found to be close to each other for RS and ST. The underlying reason

for RS's making the biggest contribution to road-induced sediment formation is its having the highest segment length, which results in the highest surface area. Formation of 227 rills on RSs (*Table 2*) supports this finding. Vehicle-induced disintegration of the road surface material also contributes to this situation. Despite the similar average widths of RS and ST at the sampling locations, the difference in the lengths of the two road segments affect rill formation and the resulting rill volume in favor of RS. A difference was also detected between RS and the other road segments after the ANOVA test ($p < 5.31 \cdot 10^{-7}$). In terms of the average rill lengths, RS and ST took the first two places, which further indicated that these road segments produced the highest amount of sediment (*Table 2*). This is mainly attributable to the higher distances at which run-off accumulation and repetition occurs for the mentioned road segments. Among the rill characteristics such as slope, length and volume, the latter two have been found to be more effective on sediment yield. The rill slope for RS is statistically significantly lower than the other road segments ($p < 2 \cdot 10^{-16}$). High sediment yield despite low slope value can be ascribed to the lower erosion strength of the surface material for RS; and higher erosion strength for SCF, RC and ST which are impaired to a lesser degree.

Table 2. Rill characteristics for different road segments

Road section	Rill count	Total rill volume (m ³)	Soil loss per km (m ³ km ⁻¹)	Maximum rill volume (m ³)	Average rill characteristics		
					Length (m)	Volume (m ³)	Rill slope (%)
RS	227	97.56	6.64	5.60	19.22a	0.47a	5.84a
SCF	65	10.52	0.71	3.32	12.48a	0.22b	44.81b
RC	85	3.20	0.22	0.17	4.42b	0.04b	35.68b
ST	50	11.53	6.11	1.68	19.95c	0.24b	29.65c

RS: Road surface, SCF: Sidecast fill, RC: Road cut, ST: Skid trail

The factors that affect rill erosion

Unpaved forest roads exhibit the highest sediment yield values in all forestlands (Akay et al., 2008; Binkley and Brown, 1993; McClelland et al., 1999; Reid and Dunne, 1984). The sediment yield produced on the surface of the road is dependent on the traffic intensity, the surface type of the road, material characteristics, dimensions and the slope (Lang et al., 2018; Rhee et al., 2018; Erdem et al., 2018). Accordingly, the factors such as road, segment and rill lengths, rill volume, segment area and the slope of road segments were examined for determination of sediment yield from road segments and investigation of the relationships between the obtained data. These data are also used in several erosion models such as SEDMODL, FROSAM (The Forest Road Sediment Assessment Methodology), WARSEM, ROADMOD (Seutloali et al., 2015; Morgan and Nearing, 2016; Safari et al., 2016; Rose, 2017).

When the determined rill volumes were subjected to Pearson correlation test with the slope, segment length and segment area values, varying levels of significant relationships were found between the total rill volume and the stated variables for all road segments. The highest correlation among these variables was found between rill volume and segment length for all road segments (RS: $p < 2.2 \cdot 10^{-16}$ and $r = 0.84$, SCF: $p = 1.767 \cdot 10^{-6}$ and $r = 0.68$, RC: $p = 2.22 \cdot 10^{-15}$ and $r = 0.75$, ST: $p = 1.299 \cdot 10^{-11}$ and $r = 0.80$) (*Table 3*).

Table 3. Relationship between rill volume and segment length, segment area variables

Road section	Segment length	Segment area
RS	$p < 2.2 \cdot 10^{-16}$; $r = 0.84$; $t = 22.593$; $df = 204$	$p < 2.2 \cdot 10^{-16}$; $r = 0.66$; $t = 12.666$; $df = 204$
SCF	$p = 1.77 \cdot 10^{-6}$; $r = 0.63$; $t = 5.473$; $df = 46$	$p = 3.03 \cdot 10^{-7}$; $r = 0.66$; $t = 5.986$; $df = 46$
RC	$p = 2.22 \cdot 10^{-5}$; $r = 0.75$; $t = 9.892$; $df = 77$	$p = 1.78 \cdot 10^{-15}$; $r = 0.75$; $t = 9.954$; $df = 77$
ST	$p = 1.30 \cdot 10^{-11}$; $r = 0.80$; $t = 8.992$; $df = 45$	$p = 7.24 \cdot 10^{-13}$; $r = 0.83$; $t = 9.895$; $df = 45$

RS: Road surface, SCF: Sidecast fill, RC: Road cut, ST: Skid trail

The equations obtained after a collective evaluation of the variables such as slope, segment length and segment area with stepwise regression analysis (forward-backward) and resulting p and R² values are as follows (Eqs. 2–5):

For RS:

$$E = 1.11 L + 2.09 S - 24.03 \quad (p < 0.001; R^2 = 0.753) \quad (\text{Eq.2})$$

For SCF:

$$E = 0.13 S + 0.25 L - 8.45 \quad (p < 0.001; R^2 = 0.433) \quad (\text{Eq.3})$$

For RC:

$$E = 0.02 S + 0.02 L + 0.23 \quad (p < 0.001; R^2 = 0.632) \quad (\text{Eq.4})$$

For ST:

$$E = 0.29 L + 0.34 \quad (p < 0.001; R^2 = 0.642) \quad (\text{Eq.5})$$

P values are lower than 0.001 in all equations. In the equations, E is rill volume, S is slope, and L is segment length. As inferred from the equations, the combined effect of the increase in segment length and the increase in slope results in increased erosion. Similar results were also reported by Qin et al. (2018), Zhang et al. (2017), and Navarro-Hevia (2016).

As the road widths within the study area are either identical or very close to each other, the effective factor for rill volume in the segment area is the segment length. Therefore, the Pearson coefficients obtained for each road segment were similar for segment length and segment area. Moreover, as shown in Table 3, segment length and segment area yield similar results for SCF, RC and ST, whereas a higher correlation is obtained with segment length for RS. Stepwise regression Equations 2, 3 and 4 obtained for each road segment show that, slope and segment length together yield higher correlation values. Therefore, the increase in segment area, which is in parallel to the increase in segment length, results in increased rill volume. Also, after a slope-based categorization of the road segments, the findings for erosion estimation increased significantly (Fig. 4). A wide scale of high slope values was observed for SCF, RC and ST, whereas the slope values of RS varied between 2-11% as per the standards for B-

type side roads. As a result of the narrow range of the slope values and similar erosion amounts corresponding to the slopes lower than 5%, the “RS < 5%” graph given in *Figure 4* exhibits a steeper slope as compared to the other graphs. This result is also indicative of the geometric increase in erosion amounts that occur on the road surface with increasing slope.

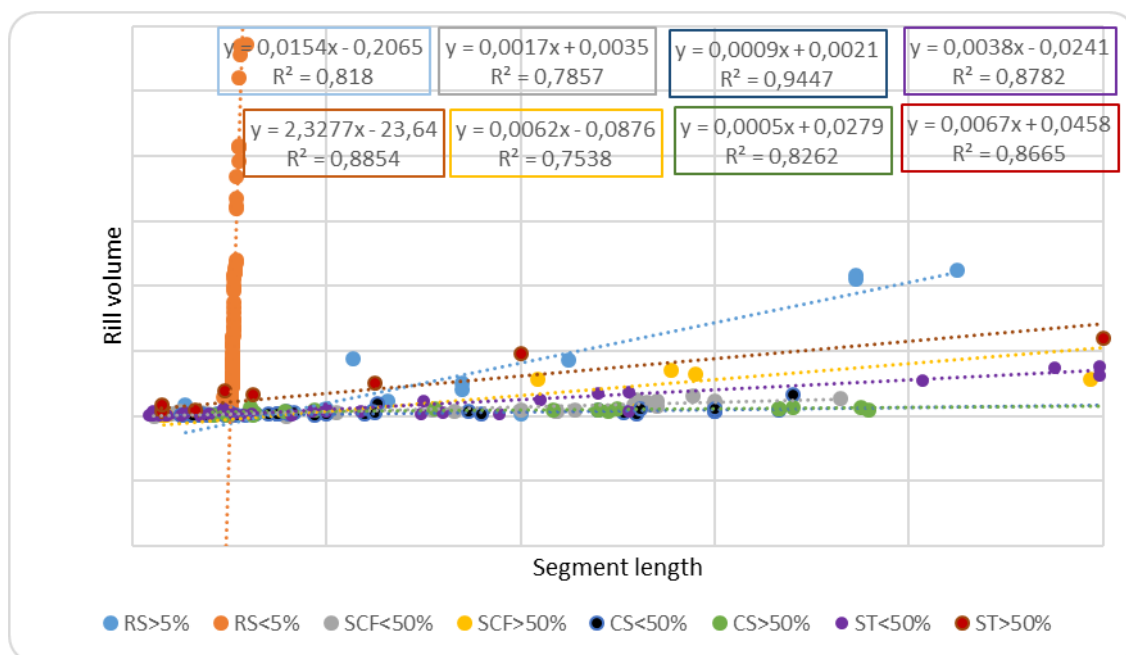


Figure 4. Rill volumes depending on segment lengths which are categorized by their slope

As also stated by Cao et al. (2014, 2015), rill volumes on short and steep road segments may be sometimes lower than those on low slope road segments. Accordingly, we also evaluated the rill volumes per unit segment area. According to the results of the correlation analysis between rill volumes per unit area and slope, the medium level correlation between slope and rill volume for RS and ST increased to a higher level (*Table 4*). As for SCF, the high level of correlation remained at a high level with a higher coefficient. On the contrary, the correlation level for RC with short and low slopes dropped to weak from medium, thus the effect of the slope factor on rill erosion is more evident for RS and ST. It is also revealed by the literature findings (Seutloali and Beckedahl, 2015; Anochie-Boateng et al., 2017; Safari et al., 2016; Thomaz and Ramos-Scharron, 2015; Yousefi et al., 2016) that, slope has a positive effect in the increase of rill erosion.

Table 4. Correlation of total and unit rill volumes for each road segment with slope

Road section	Rill Volume (m ³)	Unit Rill Volume (m ³ /m ²)
RS	$p < 2.2 \cdot 10^{-16}$; $r = 0.55$; $t = 22.593$; $df = 204$	$p < 2.20 \cdot 10^{-16}$; $r = 0.81$; $t = 22.984$; $df = 204$
SCF	$p = 3.67 \cdot 10^{-9}$; $r = 0.73$; $t = 7.316$; $df = 46$	$p = 1.33 \cdot 10^{-15}$; $r = 0.77$; $t = 11.869$; $df = 46$
RC	$p = 5.12 \cdot 10^{-8}$; $r = 0.57$; $t = 6.039$; $df = 77$	$p = 6.56 \cdot 10^{-5}$; $r = 0.43$; $t = 4.222$; $df = 77$
ST	$p = 9.60 \cdot 10^{-7}$; $r = 0.64$; $t = 5.670$; $df = 45$	$p = 1.71 \cdot 10^{-13}$; $r = 0.84$; $t = 10.357$; $df = 45$

RS: Road surface, SCF: Sidecast fill, RC: Road cut, ST: Skid trail

In forestry, as the length of forest roads towards consumption centers increase, the length of inclined distances also increases. This in turn results in increased road-induced erosion risk and sediment yield. This situation is shown for each road segment in *Figure 4* that gives the correlation between segment length and rill volume for each slope category. *Table 5* gives the equations used in previous studies for estimation of erosion on unpaved forest roads. Variables such as L, S, $L^{1/2}$, S^2 , LS, LS^2 , $L^{1/2}S^2$ are used in these equations, which indicate that, segment length and slope are the right variables for estimation of rill erosion. As also shown in *Table 5*, the regression equations involving LS and LS^2 variables yielded the best results.

Table 5. Comparison of the models and statistical results of segment length and slope-based rill erosion estimation studies with the research data

Model	R ²	Reference	Model	R ²
E=aL+b	0.131	Luce et al. (1999)	E=0.02L+0.97	0.052***
E=aS-b	0.160*	Cao et al. (2014)	E=0.11S-0.38	0.221***
E=aL ^{1/2} -b	0.790**	Cao et al. (2014)	E=0.64L ^{1/2} -1.23	0.089***
E=aS ² +b	0.494** 0.110*	Luce et al. (1999) Cao et al. (2014)	E=1.38 10 ⁻³ S ² -0.13	0.449***
E=aLS+b	0.580*** 0.180**	Luce et al. (1999) Madej (2001)	E=7.61 10 ⁻⁴ LS+0.66	0.244***
E=aLS ² +b	0.658***	Luce et al. (1999)	E=9.56 10 ⁻⁶ LS ² +0.62	0.498***
E=aL ^{1/2} S+b	0.600**	Luce et al. (1999)	E=0.01L ^{1/2} S+0.13	0.288***
E=aL ^{1/2} S ² +b	0.629**	Luce et al. (1999)	E=1.28 10 ⁻⁴ L ^{1/2} S ² +0.41	0.515***
E=aL+bS+c	0.543**	Luce et al. (1999)	E=2 10 ⁻³ L+0.11S-0.41	0.221***
E=aL+bS ² +c	0.577***	Luce et al. (1999)	E=-3.71 10 ⁻³ L+1.40 10 ⁻³ S ² +0.21	0.450***
E=aL+bLS ² +c	0.662***	Luce et al. (1999)	E=-2.45 10 ⁻² L+1.13 10 ⁻⁵ LS ² +1.17	0.535***
E=aS+bLS ² +c	0.658***	Luce et al. (1999)	E=-1.35 10 ⁻² S+1.01 10 ⁻⁵ LS ² +0.82	0.499***
E=aS ² +bLS ² +c	0.659***	Luce et al. (1999)	E=5.03 10 ⁻⁴ S ² +6.71 10 ⁻⁶ LS ² +0.37	0.513***
E=aLS ^{1.5} +b	0.840***	Scharron (2010)	E=9.38 10 ⁻⁵ LS ^{1.5} +0.59	0.378***
E=-aLS ^{0.13} +b	0.830**	Scharron (2010)	E=0.02LS ^{0.13} +0.93	0.067***

a, b, c: Coefficients, L: Segment length, S: Slope

As indicated by the results, more accurate findings are obtained through use of the values determined for unit area. The relationships between the maximum and average rill volumes and slope for each road segment are shown in *Figure 5*. Maximum values for all road sections except RC shows high correlation. Erosion estimations were performed using shear stress values and stream power sediment transport capacity theory and the results are shown in *Table 5*. These values were obtained using the data received from all road segments. The resulting findings for each road segment are given in *Table 6*, and the RMSE results of these models are expected to provide higher accuracy in erosion estimations.

Road length, slope and drainage area are the factors that affect erosion. Eroded volume is directly associated with road length which affects soil erosion on road segments by the combined effect of slope. L (segment length) and S (slope) variables together yield better results than single independent variables. This is clearly verified by *Equations 2, 3, 4* and *5*, and the equations given in *Table 6*. The models shown in *Table 6* involve the variables L, S and LS^2 . These models yielded their best results for

RC, which features the shortest segment length, hence the lowest effectiveness. The models specified for RS and ST, which have similar segment lengths, exhibit similar mean error values.

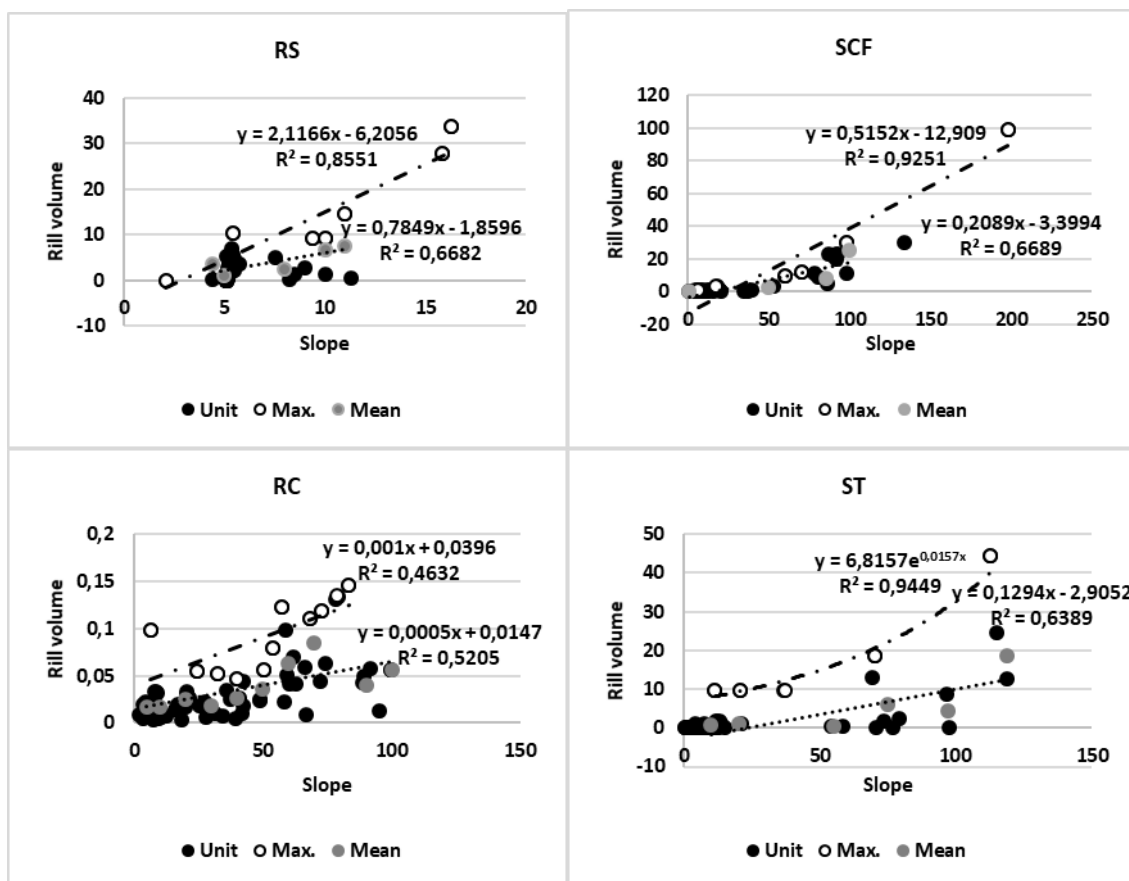


Figure 5. Maximum and average values of rill volumes as a function of slope

Table 6. Comparison of erosion models for road segments given in Table 5

Road section	Model	RMSE
RS	$E = 0.04 L + 0.001 LS^2 + 0.86$	0.16
SCF	$E = 1.71 \cdot 10^{-3} S^2 + 4.25 \cdot 10^{-6} LS^2 - 5.48 \cdot 10^{-2}$	0.32
RC	$E = 8.36 \cdot 10^{-4} S - 1.44 \cdot 10^{-8} LS^2 + 8.62 \cdot 10^{-3}$	0.03
ST	$E = 3.6 \cdot 10^{-3} L + 2.86 \cdot 10^{-7} LS^2 + 4.80 \cdot 10^{-2}$	0.18
TOTAL	$E = -2.45 \cdot 10^{-2} L + 1.13 \cdot 10^{-5} LS^2 + 1.17$	1.45

RS: Road surface, SCF: Sidecast fill, RC: Road cut, ST: Skid trail, L: Segment length, S: Slope

Conclusion

In this study, rill erosion characteristics of different segments of unpaved forest roads were investigated in Arit and Hasankadı Forest sub-districts of Bartın Forestry Directorate. According to the research results, the highest soil erosion rate occurs on road surface, which is followed by sidecast fill and skid trail with similar values, and the lowest erosion rate is observed on skid trail Segment length and the slope of the road

are the factors that affect erosion. As also reported in several other studies, more accurate statistical results are obtained via combined evaluation of segment length and slope. The findings of similar studies also indicate that better results can be obtained through inclusion of drainage area as a variable into the regression equations in estimation of rill erosion. On the other hand, drainage area slightly increases the accuracy of estimation equations particularly for unpaved forest roads. Inclined area had a negative effect on the observed road erosion especially on main roads. For such purposes, drainage area as a variable was excluded from the regression analysis as it is barely associated with the factors that affect road-induced erosion, although it resulted in 5, 10 and 8% increases in correlations for different types of forest roads. This brings about the necessity for evaluation of drainage areas' positive and negative contributions in addition to segment length and slope in future studies on determination of rill erosion. Also, similar studies should be performed on basins with more unpaved forest roads to widen the application extent of the findings obtained. In addition to the erosion rates on unpaved forest road segments, the sediment yield of other sections should also be determined for building road erosion models for basins.

REFERENCES

- [1] Al-Awadhi, J. M. (2013): A case assessment of the mechanisms involved in human-induced land degradation in northeastern Kuwait. – *Land Degradation & Development* 24(1): 2-11.
- [2] Akay, A. E., Erdas, O., Reis, M., Yuksel, A. (2008): Estimating sediment yield from a forest road network by using a sediment prediction model and GIS techniques. – *Building and Environment* 43(5): 687-695.
- [3] Anochie-Boateng, J. K., Sampson, L., Agyekum, P., Ampadu, K. O. (2017): Life-cycle cost comparison of alternative surfacing for steep slopes on low-volume roads in Ghana. – 8th Africa Transportation Technology Transfer Conference, Livingstone, Zambia, 8-10 May 2017.
- [4] Bhuyan, S. J., Kalita, P. K., Janssen, K. A., Barnes, P. L. (2002): Soil loss predictions with three erosion simulation models. – *Environmental Modelling & Software* 17(2): 135-144.
- [5] Binkley, D., Brown, T. C. (1993): Forest practices as nonpoint sources of pollution in North America. – *Journal of the American Water Resources Association* 29(5): 729-740.
- [6] Burroughs, E. R., Foltz, R. B., Robichaud, P. R. (1991): United states forest service research on sediment production from forest roads and timber harvest areas. – *Proceedings of the 10th World Forestry Congress, Paris 2*: 187-193.
- [7] Cao, L., Zhang, K., Liang, Y. (2014): Factors affecting rill erosion of unpaved loess roads in China. – *Earth Surface Processes and Landforms* 39(13): 1812-1821.
- [8] Cao, L., Zhang, K., Dai, H., Liang, Y. (2015): Modeling interrill erosion on unpaved roads in the Loess Plateau of China. – *Land Degradation & Development* 26(8): 825-832.
- [9] Cao, L. X., Zhang, K. L., Dai, H. L., Guo, Z. L. (2011): Modeling soil detachment on unpaved road surfaces on the Loess Plateau. – *Transactions of the ASABE* 54(4): 1377-1384.
- [10] Cochrane, T. A., Egli, M., Phillips, C., Acharya, G. (2007): Development of a forest road erosion calculation GIS tool for forest road planning and design. – *International Congress on Modelling and Simulation: Land, Water & Environmental Management: Integrating Systems for Sustainability*. Christchurch. New-Zealand. p. 1273-1279.

- [11] Croke, J., Mockler, S. (2001): Gully initiation and road-to-stream linkage in a forested catchment, southeastern Australia. – *Earth Surface Processes and Landforms* 26(2): 205-217.
- [12] Croke, J., Hairsine, P., Fogarty, P. (1999): Sediment transport, redistribution and storage on logged forest hillslopes in south-eastern Australia. – *Hydrological Processes* 13(17): 2705-2720.
- [13] Desprats, J. F., Raclot, D., Rousseau, M., Cerdan, O., Garcin, M., Le Bissonnais, Y., ... Monfort-Climent, D. (2013): Mapping linear erosion features using high and very high resolution satellite imagery. – *Land Degradation & Development* 24(1): 22-32.
- [14] Dougherty, W. J., Fleming, N. K., Cox, J. W., Chittleborough, D. J. (2004): Phosphorus transfer in surface runoff from intensive pasture systems at various scales. – *Journal of Environmental Quality* 33(6): 1973-1988.
- [15] Douglas, I. (1993): Impact of roads and compacted ground on post-logging sediment yield in a small drainage basin, Sabah, Malaysia. – *IAHS Publ.* 216: 213-221.
- [16] Dubé, K., Megahan, W. F., McCalmon, M. (2004): Washington Road Surface Erosion Model. – State of Washington Department of Natural Resources, Olympia.
- [17] Dunne, T. (1979): Sediment yield and land use in tropical catchments. – *Journal of Hydrology* 42(3-4): 281-300.
- [18] Eisenbies, M. H., Aust, W. M., Burger, J. A., Adams, M. B. (2007): Forest operations, extreme flooding events, and considerations for hydrologic modeling in the Appalachians—A review. – *Forest Ecology and Management* 242(2-3): 77-98.
- [19] Elliot, W. J., Foltz, R. B., Robichaud, P. R. (2009): Recent Findings Related to Measuring and Modeling Forest Road Erosion. – In: Anderssen, R. S., Braddock, R. D., Newham, L. T. H. (eds.) *Proc. of the 18th World IMACS/MODSIM Congress on International Congress on Modelling and Simulation*. Cairns, Australia.
- [20] Erdem, R., Enez, K., Demir, M., Sariyildiz, T. (2018): Slope effect on the sediment production of forest roads in Kastamonu of Turkey. – *Fresenius Environmental Bulletin* 27(4): 2019-2025.
- [21] Fahey, B. D., Coker, R. J. (1989): Forest road erosion in the granite terrain of southwest Nelson, New Zealand. – *Journal of Hydrology (New Zealand)* 123-141.
- [22] Foster, I. D., Rowntree, K. M., Boardman, J., Mighall, T. M. (2012): Changing sediment yield and sediment dynamics in the Karoo uplands, South Africa; post-European impacts. – *Land Degradation & Development* 23(6): 508-522.
- [23] Fransen, P. J., Phillips, C. J., Fahey, B. D. (2001): Forest road erosion in New Zealand: overview. – *Earth Surface Processes and Landforms* 26(2): 165-174.
- [24] Froehlich, W. (1991): Sediment Production from Unmetalled Road Surfaces. – In: Peters, N. E., Walling, D. E. (eds.) *Sediment and Stream Water Quality in a Changing Environment: Trends and Explanation*. Proceedings of Vienna Symposium, August 1991, pp. 21-30. IAHS Press, Wallingford, UK.
- [25] Froehlich, W., Walling, D. E. (1997): The role of unmetalled roads as a sediment source in the fluvial systems of the Polish Flysch Carpathians. – *IAHS Publication* 245: 159-168.
- [26] Fu, B., Newham, L. T., Ramos-Scharron, C. E. (2010): A review of surface erosion and sediment delivery models for unsealed roads. – *Environmental Modelling & Software* 25(1): 1-14.
- [27] Grayson, R. B., Haydon, S. R., Jayasuriya, M. D. A., Finlayson, B. L. (1993): Water quality in mountain ash forests—separating the impacts of roads from those of logging operations. – *Journal of Hydrology* 150(2-4): 459-480.
- [28] Gucinski H, Furniss, M. J., Ziemer, R. R., Brookes, M. H. (2001): Forest roads: A synthesis of scientific information. – General Technical Report PNW-GTR-509. USDA Forest Service: Portland, OR.
- [29] Ketcheson, G. L., Megahan, W. F., King, J. G. (1999): “R1-R4” and “BOISED” sediment prediction model tests using forest roads in granitics. – *Journal of the American Water Resources Association* 35(1): 83-98.

- [30] Kumapley, N. K. (1987): Erosion of Unsurfaced Earth and Gravel Roads. – In: Proceedings of 9th Regional Conference for Africa on Soil Mechanics and Foundation Engineering, pp. 397-404.
- [31] Lang, A. J., Aust, W. M., Bolding, M. C., McGuire, K. J., Schilling, E. B. (2018): Best Management Practices Influence Sediment Delivery from Road Stream Crossings to Mountain and Piedmont Streams. – *Forest Science* 64(6): 682-695.
- [32] Leh, M., Bajwa, S., Chaubey, I. (2013): Impact of land use change on erosion risk: an integrated remote sensing, geographic information system and modeling methodology. – *Land Degradation & Development* 24(5): 409-421.
- [33] Luce, C. H., Black, T. A. (1999): Sediment production from forest roads in western Oregon. – *Water Resources Research* 35(8): 2561-2570.
- [34] Luce, C. H., Wemple, B. C. (2001): Introduction to special issue on hydrologic and geomorphic effects of forest roads. – *Earth Surface Processes and Landforms* 26(2): 111-113.
- [35] MacDonald, L. H., Sampson, R. W., Anderson, D. M. (2001): Runoff and road erosion at the plot and road segment scales, St John, US Virgin Islands. – *Earth Surface Processes and Landforms: The Journal of the British Geomorphological Research Group* 26(3): 251-272.
- [36] Madej, M. A. (2001): Erosion and sediment delivery following removal of forest roads. – *Earth Surface Processes and Landforms: The Journal of the British Geomorphological Research Group* 26(2): 175-190.
- [37] McClelland, D., Foltz, R., Falter, C., Wilson, W., Cundy, T., Schuster, R., ... Heinemann, R. (1999): Relative effects on a low-volume road system of landslides resulting from episodic storms in northern Idaho. – *Transportation Research Record: Journal of the Transportation Research Board* (1652): 235-243.
- [38] McGroddy, M., Lawrence, D., Schneider, L., Rogan, J., Zager, I., Schmook, B. (2013): Damage patterns after Hurricane Dean in the southern Yucatán: Has human activity resulted in more resilient forests? – *Forest Ecology and Management* 310: 812-820.
- [39] Megahan, W. F. (1987): Effects of Forest Roads on Watershed Function in Mountainous Areas. – In: Balasubramaniam, A. S. et al. (eds). *Environmental Geotechnics and Problematic Soils and Rocks*. Balkema Publishing, Rotterdam, pp. 335-347.
- [40] Merritt, W. S., Letcher, R. A., Jakeman, A. J. (2003): A review of erosion and sediment transport models. – *Environmental Modelling & Software* 18(8-9): 761-799.
- [41] Morgan, R. P. C., Nearing, M. (Eds.). (2016): *Handbook of Erosion Modelling*. – John Wiley & Sons, Chichester, UK.
- [42] Navarro-Hevia, J., Lima-Farias, T. R., de Araújo, J. C., Osorio-Peláez, C., Pando, V. (2016): Soil erosion in steep road cut slopes in Palencia (Spain). – *Land Degradation & Development* 27(2): 190-199.
- [43] Qin, W., Guo, Q., Cao, W., Yin, Z., Yan, Q., Shan, Z., Zheng, F. (2018): A new RUSLE slope length factor and its application to soil erosion assessment in a Loess Plateau watershed. – *Soil and Tillage Research* 182: 10-24.
- [44] Posthumus, H., Deeks, L. K., Fenn, I., Rickson, R. J. (2011): Soil conservation in two English catchments: linking soil management with policies. – *Land Degradation & Development* 22(1): 97-110.
- [45] Ramos-Scharrón, C. E., MacDonald, L. H. (2005): Measurement and prediction of sediment production from unpaved roads, St John, US Virgin Islands. – *Earth Surface Processes and Landforms* 30(10): 1283-1304.
- [46] Ramos-Scharrón, C. E., MacDonald, L. H. (2007): Measurement and prediction of natural and anthropogenic sediment sources, St. John, US Virgin Islands. – *Catena* 71(2): 250-266.
- [47] Scharrón, C. E. R. (2010): Sediment production from unpaved roads in a sub-tropical dry setting—Southwestern Puerto Rico. – *Catena* 82(3): 146-158.

- [48] Reid, L. M., Dunne, T. (1984): Sediment production from forest road surfaces. – *Water Resources Research* 20(11): 1753-1761.
- [49] Rhee, H., Fridley, J., Page-Dumroese, D. (2018): Traffic-induced changes and processes in forest road aggregate particle-size distributions. – *Forests* 9(4): 181.
- [50] Rose, C. W. (2017): Research Progress on Soil Erosion Processes and a Basis for Soil Conservation Practices. – In: Lal, R. (ed.) *Soil Erosion Research Methods*. Routledge, London, pp. 159-180.
- [51] Safari, A., Kavian, A., Parsakhoo, A., Saleh, I., Jordán, A. (2016): Impact of different parts of skid trails on runoff and soil erosion in the Hyrcanian forest (northern Iran). – *Geoderma* 263: 161-167.
- [52] Seutloali, K. E., Beckedahl, H. R. (2015): A review of road-related soil erosion: an assessment of causes, evaluation techniques and available control measures. – *Earth Sciences Research Journal* 19(1): 73-80.
- [53] Sidle, R. C., Pearce, A. J., O'Loughlin, C. L. (1985): *Hillslope Stability and Land Use*. – Water Resources Monograph Series No. 11. American Geophysical Union, Washington, DC.
- [54] Tanimoto, S. (1999): U.S. Patent No. 5,893,898. – U.S. Patent and Trademark Office, Washington, DC.
- [55] Thomaz, E. L., Ramos-Scharrón, C. E. (2015): Rill length and plot-scale effects on the hydrogeomorphologic response of gravelly roadbeds. – *Earth Surface Processes and Landforms* 40(15): 2041-2048.
- [56] Tømmervik, H., Johansen, B., Høgda, K. A., Strann, K. B. (2012): High-resolution satellite imagery for detection of tracks and vegetation damage caused by all-terrain vehicles (ATVs) in Northern Norway. – *Land Degradation & Development* 23(1): 43-52.
- [57] Varol, T. (2015): Comparison of the models used in the calculation of surface erosion in unpaved forest roads. – *Precise Forestry Symposium on Production*, 4-6 June, Ilgaz-Kastamonu/Turkey, Proceedings Book, pp. 434-450.
- [58] Varol, T. (2016): Runoff and soil erosion on unpaved forest road. – *FETEC-2016, 1st International Symposium of Forest Engineering and Technologies*, 02-04 June, Bursa/Turkey, Proceedings Book, pp. 254-264.
- [59] Varol, T., Ertuğrul, M. (2015): Climate change and Forest Fire Trend in the Aegean and Mediterranean Regions of Turkey. – *Fresenius Environmental Bulletin* 24(10B): 3436-3444.
- [60] Xu, X. X., Ju, T. J., Zheng, S. Q. (2007): Field study on biological road erosion in loess hilly region. – *Journal of Agro-Environment Science* 26(3): 934-938.
- [61] Xu, X. L., Liu, W., Kong, Y. P., Zhang, K. L., Yu, B., Chen, J. D. (2009): Runoff and water erosion on road side-slopes: Effects of rainfall characteristics and slope length. – *Transportation Research Part D: Transport and Environment* 14(7): 497-501.
- [62] Yousefi, S., Moradi, H., Boll, J., Schönbrodt-Stitt, S. (2016): Effects of road construction on soil degradation and nutrient transport in Caspian Hyrcanian mixed forests. – *Geoderma* 284: 103-112.
- [63] Zhang, X. C., Nearing, M. A., Garbrecht, J. D. (2017): Gaining insights into interrill erosion processes using rare earth element tracers. – *Geoderma* 299: 63-72.
- [64] Ziegler, A. D., Sutherland, R. A., Giambelluca, T. W. (2000): Partitioning total erosion on unpaved roads into splash and hydraulic components: The roles of interstorm surface preparation and dynamic erodibility. – *Water Resources Research* 36(9): 2787-2791.

MORPHOLOGICAL AND MOLECULAR CHARACTERIZATION OF LOCAL COMMON BEAN (*PHASEOLUS VULGARIS* L.) GENOTYPES

EKBIÇ, E.* – HASANCAOĞLU, E. M.

*Department of Horticulture, Agricultural Faculty, Ordu University, 52200 Ordu, Turkey
(phone: +90-452-226-5200/ext.:6238; fax: +90-452-234-6632)*

**Corresponding author
e-mail: ercanekbic@gmail.com*

(Received 26th Sep 2018; accepted 26th Nov 2018)

Abstract. This study was conducted for morphological and molecular characterization of 33 common bean genotypes collected from Ordu province in Turkey. Genetic relationships among the local common bean genotypes were also identified. In presented genotypes, 3 phenological and 22 morphological characteristics were investigated. The first flower and the first beans were formed 43.42 and 48.55 days after sowing time respectively. The first fresh bean harvest was realized 67.85 days after the sowing time. Pod lengths and pod widths of the genotypes varied between 10.93 and 23.23 cm (average 14.76 cm) and 9.39-22.73 mm (average 15.22 mm) respectively. The first 3 dimensions (PC1, PC2 and PC3) of principal component analysis on morphological data explained 72.27% of total variation. Seed main color, seed secondary color, pod color, pod cross-section and stringiness were prominent characteristics in screening of common bean genotypes. Of the SSR primers, SSR-IAC116 yielded the greatest PIC value (0.82) and it was followed by BMD-45-AIA (0.77) and PV ag004 (0.72) primers. The primers had a mean number of alleles per locus of 2.55. The BM210 had the greatest number of polymorphic alleles per locus (6 alleles). Cluster analysis, composed from molecular data, revealed 3 main groups. The genotypes G14 and G17 were placed alone in the first and second groups and the rest were clustered in the third group. The similarity index values among 33 local common bean genotypes varied between 0.34 and 0.97. The genotypes G04 and G22 were identified as the closest genotypes with a genetic similarity coefficient of 0.97.

Keywords: *genetic resources, diversity, SSR, PCA, polymorphism*

Introduction

Common bean (*Phaseolus vulgaris* L.) is an annual herbaceous vegetable and is a member of *Phaseolus* genus of legumes (*Fabaceae*) family. About 90% of culture common beans is constituted by *Phaseolus vulgaris* L. species of *Phaseolus* genus. There are two gene centers of beans as of Central America (Mesoamerica) and South America (Andean) (Gepts, 2008). There is no precise information about the entry time of the beans to Turkey. However, it is thought that beans entered from Europe to Anatolia 250-300 years ago (Eşiyok, 2012). Bean is produced as the main crop in several regions of Turkey and cultivated as the second crop especially in coastal regions. Ordu province is located in Central and Eastern Black Sea regions and fresh green beans are produced over 478 ha land area with an annual production of 2.870 tons (TÜİK, 2017). Agricultural cultivation and biodiversity have been tightly associated for thousands years and it is still an ongoing process (Lockwood, 1999; Norris, 2008). Turkey with current geographical position and ecological conditions is an origin and diversity center of several plants. Such a diversity resulted from the history since Turkey is among the oldest civilizations. However, natural resource diversity and richness of Turkey is continuously decreasing because of some factors such as rapid

increase in population, environmental pollution, widespread of newly released cultivars and natural disasters (Özgen et al., 1995). From such threatening factors especially high cultivar dynamism in vegetable crops have led farmers to leave local cultivars and use hybrid cultivars instead (Bellon et al., 2015). To encourage the farmers for agro-ecologic, organic and sustainable farming is the most preservative approach for such a rich biodiversity (Altieri, 1999; Finegan and Nasi, 2004; Crowder et al., 2010). Plant genetic resources are composed of local genotypes, their wild relatives, old cultivars and lines with fully-identified genetic characteristics. Local genotypes (landraces) are populations generated through natural or artificial selections for years. Just as commercial cultivars, these populations are stable, high-yield and uniform populations with low adaptation capacities for the regions other than their origin (Zeven, 1998). Besides, biotic and abiotic stress tolerance and some nutritional quality traits of local genotypes are indispensable for plant breeders (Dwivedi et al., 2016). Therefore, preservation and appraisal of local genotypes are the issues of top priority (Negri et al., 2009). Genetic richness has a significant place in plant breeding. Thus, morphologic characterization and DNA-based definition of landraces or populations and put forth of relativity degrees are significant issues in breeding studies. Due to landraces or local genotypes have a large genetic bases, such as resistance to pests and diseases and carrying genes related to several quality attributes, they constitute a significant gene source for preservation of the potential of the population they belonged to. Some genotypes even have significant quality attributes desired by the consumers and such consumers generally pay more for these products (Negri and Tosti, 2002; Galvan et al., 2006). Although common bean is originated from Central America, it is quite well-adapted to ecological conditions of Black Sea region. The region has a quite large genetic variation since local farmers have been mixed-sowing the genotypes they used for years. Morphological differences are used to put forth such a broad diversity. Morphological characterization in essence is an evolutionary method basically focusing on traditional identification of evolutionary and pedigree relations. Using morphological measurements in diversity assessment for phenotypic and agronomic traits such as flower color, growth habit, yield potential, plant height, stress tolerance etc., have limitations, because such morphological traits are governed quantitatively and under environmental influence (Skroch and Nienhuis, 1995). However, the genetic analyses carried out with DNA markers are independent from environment effect. Such analyses are also more informative and quite available for characterization of genetic materials. For genetic characterization of common bean genotypes, restriction fragment length polymorphisms (RFLP) (Velasquez and Gepts, 1994), random amplified polymorphic DNA (RAPD) (Mavromatis et al., 2010; Bukhari et al., 2015), retrotransposon-based interprimer binding sites (iPBSs) (Nemli et al., 2015) and simple sequence repeated (SSR) (Yu et al., 2000; Gaitán-Solís et al., 2002; Blair et al., 2011; Khaidizar et al., 2012) marker techniques were used. Simple sequence repeated markers, also called as microsatellite, are commonly encountered in several loci of a genome (Tautz and Renz, 1984) and these markers were successfully used in genetic characterizations of the common beans (Gomez et al., 2005; Blair et al., 2006; Buso et al., 2006; Sarikamis et al., 2009; Khaidizar et al., 2012; Ulukapı and Onus, 2013). This study was carried out to determine the genetic diversity between 33 local common bean genotypes collected from Ordu province by morphological and molecular characterization. Research findings were expected to have great contributions for definition of a common bean

genetic pool of Ordu province, for preservation of local common bean genotypes and for further breeding studies to be carried out on common beans.

Materials and methods

As the material of the study, 33 bean genotypes collected from different towns of Ordu province in Turkey were used (*Fig. 1; Table 1*).

The seeds were sown in 14-liter pots containing 3:1 (v/v) peat:perlite mixture. Each pot had 3 plants, and 6 plants were used for observations for each genotype.

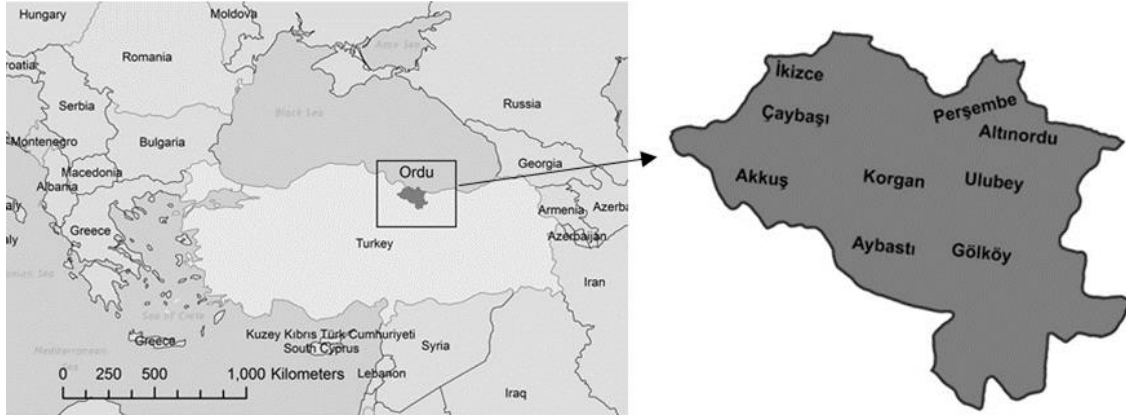


Figure 1. Location of the common bean genotypes sampling

Table 1. Coordinates of collected common bean genotypes

Genotype	Location	Latitude (North)	Longitude (East)	Altitude (m)	Genotype	Location	Latitude (North)	Longitude (East)	Altitude (m)
G01	Altınordu	40.945°	37.916°	89	G18	Çaybaşı	41.029°	37.083°	523
G02	Altınordu	40.945°	37.929°	50	G19	Çaybaşı	41.017°	37.080°	509
G03	Altınordu	40.948°	37.917°	85	G20	Akkuş	40.792°	37.007°	1243
G04	Altınordu	40.937°	37.895°	68	G21	Akkuş	40.793°	37.020°	1262
G05	Altınordu	40.968°	37.858°	160	G22	Akkuş	40.804°	37.037°	1223
G06	Altınordu	40.965°	37.869°	106	G23	Akkuş	40.713°	37.036°	951
G07	Altınordu	40.957°	37.885°	83	G24	Akkuş	40.709°	37.000°	1045
G08	Altınordu	40.943°	37.882°	134	G25	Akkuş	40.882°	37.066°	1122
G09	Perşembe	41.055°	37.777°	13	G26	İkizce	41.057°	37.086°	141
G10	Perşembe	41.116°	37.759°	25	G27	Aybastı	40.669°	37.423°	978
G11	Perşembe	41.033°	37.788°	250	G28	Aybastı	40.671°	37.413°	749
G12	Ulubey	40.887°	37.785°	447	G29	Aybastı	40.672°	37.397°	698
G13	Altınordu	40.968°	37.959°	49	G30	Aybastı	40.680°	37.428°	911
G14	Altınordu	40.961°	37.967°	159	G31	Aybastı	40.686°	37.446°	1048
G15	Gök köy	40.749°	37.676°	796	G32	Aybastı	40.714°	37.411°	775
G16	Korgan	40.826°	37.335°	678	G33	Aybastı	40.696°	37.399°	802
G17	Çaybaşı	41.034°	37.104°	289					

Morphological observations

Local common bean genotypes were evaluated for the time elapsed from sowing time to the first bloom (Flo, day), the first pod formation time (PF, day), the first fresh bean harvest time (GPH, day), pod length (PL, cm), pod width (PW, mm), leaf length (LL, cm), leaf width (LW, cm), terminal leaflet length (TLL, cm), terminal leaflet width (TLW), leaf color (LC), seed length (SL, mm), seed width (SWi, mm), 100 seed weight (SWe, g), pod cross-section (PCS), pod roughness (PR), stringiness (S), shape of distal part (beak, B), pod color (PC), pod secondary color (PSC), pod curvature level (PCL), seed clarity (SC), main seed color (MSC), secondary seed color (SSC) and distribution of secondary color on the seed (DSSC) characteristics in accordance with the standards specified in Genchev and Kiryakov (2005).

Molecular characterization

The BM146, BM210, Bmd-45-AIA, Bmd-8, DROUGH1, PH10B11, PH7B3, PV aaat001, PV ag004, PV at007, PV at008, PV atcc001, PV atcc003, PV atct001, PV gaaat001, SSR-IAC26, SSR-IAC63 and SSR-IAC116 primers selected among the ones used by Ulukapı and Onus (2013) were used for molecular characterization of present common bean genotypes. DNA isolation was performed by using CTAB (cetyl trimethyl ammonium bromide) method in accordance with the protocol of Haymes (1996). DNA concentrations were diluted with TE solution (10 mM Tris, 1 mM EDTA, pH 8.0) to 5 ng/μl. PCR reactions were performed in LongGene A300 Fast thermal cycler in a total volume of 15 μl generated through addition of 7.5 μl PCR Master Mix (Dreamtaq Green Master Mix), 1 μl forward primer (10 pmol), 1 μl reverse primer (10 pmol), 2.5 μl ddH₂O and 3 μl DNA. PCR amplifications were performed in accordance with the protocol of Khaidizar et al., (2012). Amplification conditions were set as; pre-denaturation at 94 °C for 3 min, 2 cycles at 94 °C for 30 s, at 37 °C for 60 s, at 72 °C for 2 min, 2 cycles at 94 °C for 30 s, at 50 °C for 60 s, at 72 °C for 2 min, 41 cycles at 93 °C for 30 s, at 50 °C for 60 s, at 72 °C for 2 min and finally at 72 °C for 5 min. Resultant SSR-PCR products were run in 3% agarose (Fisher BioReagents) gel containing 1x TAE (Tris-Acetic acid-EDTA) solution in SCIE-PLAS (Hu20) electrophoresis unit. Electrophoresis process was performed at 90 Watt and 300 mA current rates for 4 hours. Agarose gel was stained with ethidium bromide (10 mg/ml) for 20 min and imaged under UV transilluminator (Syngene-Ingenius). Bands in resultant gel images were scored as 1 (present) and 0 (absent) and binary data matrices were generated for data analyses.

Statistical analysis

Descriptive statistics for morphological data were calculated with SPSS v.22.0 statistical software, principal component analysis for qualitative phenotypic data was performed with the aid of Past3 software. Polymorphism information content (PIC) values of SSR primers were calculated with the aid of the following modified by Anderson et al. (1993):

$$PIC_i = 1 - \sum_{j=1}^n P_{ij}^2$$

where p_{ij} is the frequency of the j^{th} allele for marker i and summation extends over n alleles. Molecular data were analyzed via Dice module of NTSYSpc v.2.02 (Rolf, 2000) software. Cluster analysis was performed by using UPGMA (un-weighted pair group method with arithmetic mean) (Sneath and Sokal, 1973) and a correlation matrix was generated then.

Results and discussion

Morphological characterization of bean genotypes

With regard to type of growth, 93.93% of the genotypes were climbing type (31 genotypes) and 6.07% showed dwarf growing habit (G09, G24). Sözen et al. (2014) carried out a study with 85 bean genotypes and identified 12 genotypes (14.1%) as dwarf, 42 genotypes (49.4%) as semi-dwarf and 31 genotypes (36.5%) as climbing type. Descriptive statistics for quantitative pod and leaf characteristics and phenological observations of the local bean genotypes are provided in *Table 2*. Mean flowering time of the local genotypes apart from the sowing time was 43.42 days. The earliest flowering was observed in G09, G15, G21, G26 and G27 genotypes with 41 days and the latest flowering was observed in G07 with 55 days. The earliest genotype formed the first pod in 46 days and the latest genotypes formed the first pod in 59 days. Mean the first pod formation time was 48.55 days. The first fresh pod harvest was performed in 58 days in early genotypes (G01, G24, G26, G27 and G32) and in 85 days in late genotype (G07). Pod lengths varied between 10.93 and 23.23 cm. The shortest pod was observed in G09 genotype with 10.93 cm and the longest pod was observed in G33 genotype with 23.23 cm. Pod widths varied between 9.39 and 22.73 mm. The lowest pod width value was obtained in G14 genotype with 9.39 mm and the largest pod was obtained in G25 genotype with 22.73 mm as was seen in *Table 2*. Variation coefficients for tip leaf length, tip leaf width, side leaf length and side leaf width were respectively calculated as 15.67, 13.93, 14.49 and 13.43%. Kar et al. (2005) assessed earliness, yield and quality attributes of 4 determinate and 5 pole-type bean cultivars under unheated greenhouse conditions. Researchers reported the earliest flowering time as 58 days for determinate cultivars and 59 days for pole-type cultivars and reported the first pod harvest times as between 63 and 68 days. Erdiñç et al. (2013) reported the earliest flowering time as 42 days, the latest flowering time as 77 days, the first pod harvest time as 68 days and the latest pod harvest time as 127 days in different common bean genotypes. In another genetic characterization study carried out with 300 common bean genotypes in Honduras, the first flowering times were reported as between 31 and 37 days (Meza et al., 2013). Akbulut et al. (2013) carried out a study with 12 bean genotypes grown in Burdur province and reported the first pod formation time as between 46 and 68 days. In similar previous studies carried out with common beans in Turkey, pod lengths were reported as between 7.48 and 13.8 cm and pod widths as between 7 and 25 mm (Düzdemir, 1998; Madakbaşı et al., 2004).

Seed characteristics evaluations of local bean genotypes are provided in *Table 3*. 100 seed weights varied between 29.67 and 66.40 g. The lowest seed weight value was observed in G14 and the highest seed weight value was obtained from G06 genotype. The greatest variation was observed in seed thickness (16.91%) and it was followed by seed weight (14.85), seed length (9.56%) and seed width (7.62%). Piergiiovanni et al. (2006) reported that seed variation of the common bean germplasm in Abruzzo and Lazio (Italy) was low and 100-seed weight varied between 32.9 and 91.4 g.

Table 2. Descriptive statistics data obtained from some plant growing and leaf characteristics

	Flo (day)	PF (day)	GPH (day)	PL (cm)	PW (mm)	TLL (cm)	TLW (cm)	LL (cm)	LW (cm)
Mean	43.42	48.55	67.85	14.76	15.22	14.88	10.89	14.05	10.24
Minimum	41.00	46.00	58.00	10.93	9.39	10.71	8.53	10.91	8.04
Maximum	55.00	59.00	85.00	23.23	22.73	23.77	17.75	21.48	16.25
Std. dev.	2.93	2.59	6.01	2.88	2.98	2.33	1.52	2.04	1.37
CV %	6.74	5.33	8.85	19.54	19.55	15.67	13.93	14.49	13.43

Std. dev.: standard deviation; CV: coefficient of variation

Table 3. Descriptive statistics data obtained from the seed characteristics

	100 SWe (g)	SL (mm)	SWi (mm)	ST (mm)
Mean	49.07	14.09	8.21	6.52
Minimum	29.67	11.70	6.22	5.04
Maximum	66.40	16.28	9.30	10.42
Std. dev.	2.19	1.34	0.62	1.10
CV %	14.88	9.56	7.62	16.91

Std. dev.: standard deviation; CV: coefficient of variation

Principal component analysis (PCA)

Results of principal component analysis for 12 qualitative characteristics of bean genotypes are provided in *Table 4*. PC 1 (41.97%), PC 2 (21.37%) and PC 3 (8.93%) axes explained 72.27% of total variation among the genotypes. On PC 1 axis, seed main color with a variation coefficient of 0.95 was the primary attribute, the most distinctively indicating the variation among the genotypes. On PC 2 axis, pod secondary color (0.80) and seed secondary color (0.75) were the most distinctive characteristics. On PC 3 axis, pod cross-section (0.82) and stringiness (0.61) were the most distinctive characteristics effecting the variation among the genotypes. Lima et al. (2012) reported that first two principle components explained about 34% of the total variation on common bean genotypes. Meza et al. (2013) indicated that first tree principle components explained 34.18% of total variation and reported the first flowering time, ripened pod color and pod harvest time as the most distinctive characteristics.

Molecular characterization

The 18 SSR markers used in molecular characterizations generated a total of 63 alleles and 46 of them (73%) were polymorphic among the common bean genotypes. Number of alleles per locus varied between 2 and 6 (average 2.55 alleles per locus) (*Fig. 2*). While PBM210, PV aat001 and PV ag004 SSR primers yielded the greatest number of alleles per locus, the greatest number of polymorphic alleles per locus (6 alleles) was observed in BM210 primer. Polymorphism information content (PIC) of the primers varied between 0.06 and 0.82 (*Fig. 3*). The greatest PIC value (0.82) was obtained from SSR-IAC116 primer.

Table 4. Eigenvectors of the first three dimensions of PCA

Characters	PC 1	PC 2	PC 3
Pod cross section	-0.06	0.11	0.82
Pod roughness	-0.32	0.57	0.10
Stringiness	0.22	0.25	0.61
Shape of distal part (beak)	-0.03	-0.26	-0.38
Pod color	-0.31	-0.02	0.22
Pod secondary color	-0.34	0.80	-0.03
Pod degree of curvature	0.26	-0.11	0.49
Seed clarity in pods	-0.27	0.27	0.06
Leaf color	-0.27	0.06	0.23
Seed main color	0.95	0.30	-0.03
Seed secondary color	-0.55	0.75	-0.08
Distribution of seed secondary color	-0.57	0.54	-0.11
Individual variance %	41.97	21.37	8.93
Cumulative variance (PC1 + PC2 + PC3): 72.27%			

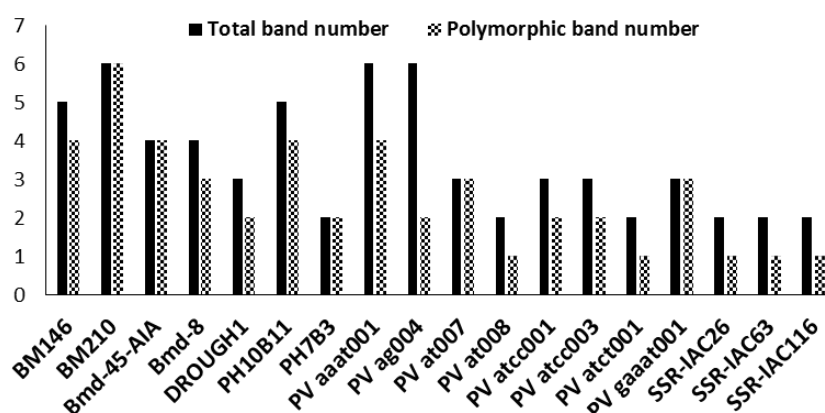


Figure 2. Total number and polymorphic band numbers revealed by SSR primers in common bean genotypes

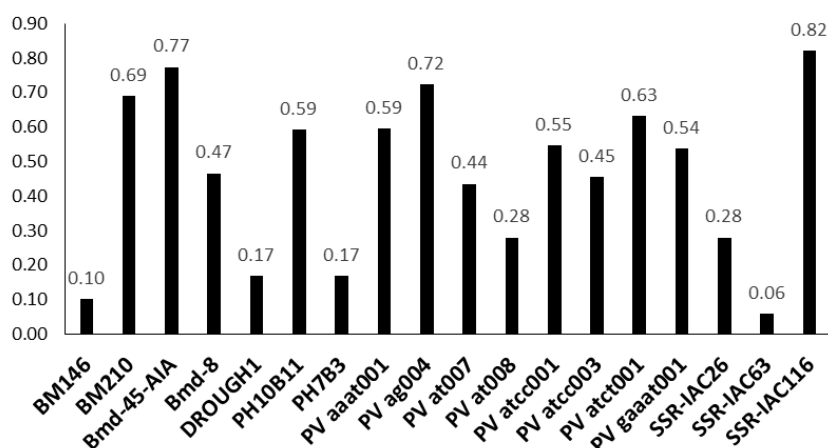


Figure 3. Polymorphism information content of SSR primers in common bean genotypes

Lioli et al. (2005) carried out a diversification study with 33 local common bean genotypes using 14 SSR primers and reported number of alleles per locus as between 2 and 11. Sarıkamış et al. (2009) used 12 SSR primers in a genetic diversity study for 30 common bean genotypes and identified 10 SSR primers as polymorphic. Researchers obtained 45 polymorphic alleles from 10 SSR primers and reported number of alleles per locus as between 2 and 10. Khaidizar et al. (2012) identified bean genotypes collected from Northern Anatolia with the aid of 30 SSR primers and obtained 72 alleles from these SSR primers. Ulukapı and Onus (2013) indicated 73% polymorphism ratio for 22 SSR primers and reported PIC values as between 0.047 and 0.373. Buah et al. (2017) used 6 SSR primers for bean genotypes and obtained 41 alleles (average 7.8 alleles per locus). De Luca et al. (2018) used microsatellite markers for Italian local bean genotypes and reported PIC values as between 0.315 and 0.928.

Genetic relationships between local common bean genotypes

Results obtained from PCR reactions revealed that similarity index among bean genotypes varied between 0.34 and 0.97 (Table 5). A dendrogram was generated with SSR primers (Fig. 4) and bean genotypes were separated into 3 main groups in this dendrogram.

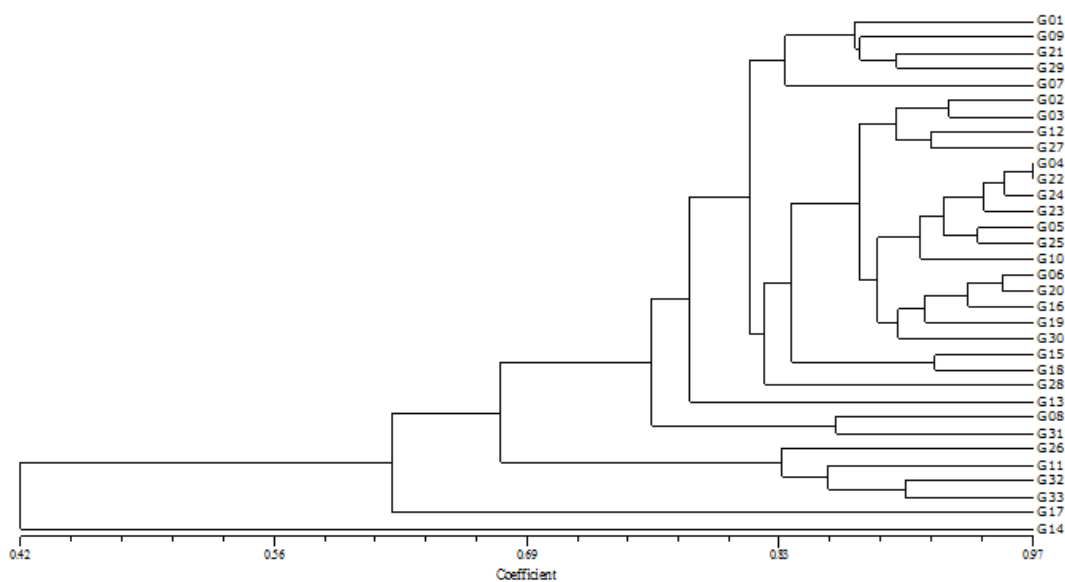


Figure 4. UPGMA dendrogram based on SSR markers

The genotype G14 collected from Altınordu town of Ordu and the genotype G17 collected from Çaybaşı town of Ordu were alone placed in the first and second group of the dendrogram. The difference of G14 and G17 genotypes were also quite distinctive in principal coordinate scatter plot (Fig. 5). All the other genotypes were clustered in the third group. The genotypes G04 and G22 collected from Altınordu and Akkuş towns of Ordu province were the closest genotypes with a genetic similarity index of 0.97. Cluster analysis did not yield town-based geographical separation of the genotypes. Such a case was because local bean producers generally produce their own seeds and

seeds of a locality are served to different local markets. Khaidizar et al. (2012) reported genetic similarity coefficient between the bean genotypes collected from Erzurum and Bayburt provinces as between 0.211 and 0.796 and gathered bean genotypes under two main groups. Ulukapı and Onus (2013) used SSR primers for characterization of 39 bean genotypes and reported genetic similarity coefficients as between 0.52 and 0.98. Researchers gathered bean genotypes under two main groups of a dendrogram. Bukhari et al. (2015) carried out a characterization study with 45 bean genotypes and separated bean genotypes into 7 main groups and reported genetic similarity coefficients as between 0.56 and 0.92.

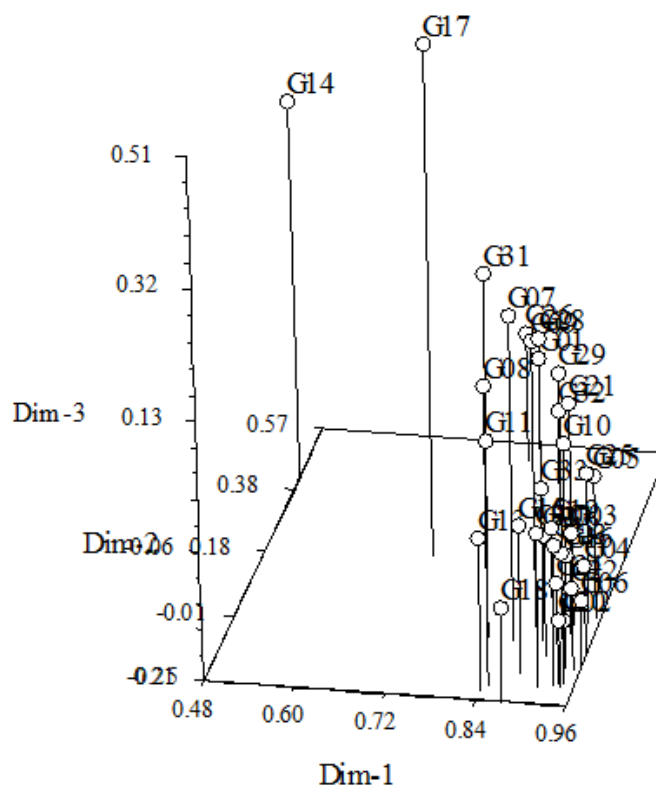


Figure 5. Scatterplot illustration drawn using SSR data

Conclusion

Genetic variations in a gene pool constitute basic sources for breeders. Hereditary characteristics of the materials in this genetic pool should be identified with proper methods and genetic relations among them should be put forth. Such efforts play a significant role in meeting farmer needs. Present local common bean genotypes grown in Central Black Sea region exhibited differences in seed color, pod color and pod stringiness. Molecular characterizations by SSR markers used in this study did not revealed distinctive groups or geographical separations with regard to morphological characteristics. Bean genotypes of Ordu province had a genetic similarity of between 34 and 97%. Such a broad genetic variation may have significant contributions in developing new common bean cultivars.

Acknowledgements. This study was financed by Ordu University with Project Code: TF1438.

Table 5. Genetic similarity matrix between 33 common bean local accessions based on SSR markers

	G01	G02	G03	G04	G05	G06	G07	G08	G09	G10	G11	G12	G13	G14	G15	G16	G17	G18	G19	G20	G21	G22	G23	G24	G25	G26	G27	G28	G29	G30	G31	G32	G33		
G01	1.00																																		
G02	0.82	1.00																																	
G03	0.80	0.93	1.00																																
G04	0.77	0.90	0.91	1.00																															
G05	0.82	0.88	0.90	0.96	1.00																														
G06	0.83	0.93	0.91	0.94	0.93	1.00																													
G07	0.85	0.75	0.79	0.77	0.81	0.79	1.00																												
G08	0.78	0.75	0.76	0.77	0.75	0.84	0.81	1.00																											
G09	0.87	0.79	0.75	0.81	0.84	0.80	0.87	0.72	1.00																										
G10	0.82	0.83	0.87	0.94	0.92	0.90	0.81	0.81	0.86	1.00																									
G11	0.62	0.66	0.69	0.64	0.68	0.67	0.59	0.54	0.57	0.59	1.00																								
G12	0.86	0.92	0.91	0.88	0.86	0.91	0.82	0.79	0.81	0.87	0.57	1.00																							
G13	0.73	0.79	0.81	0.81	0.76	0.84	0.72	0.71	0.72	0.79	0.49	0.86	1.00																						
G14	0.43	0.41	0.42	0.40	0.45	0.37	0.34	0.36	0.37	0.40	0.43	0.44	0.40	1.00																					
G15	0.75	0.85	0.80	0.87	0.85	0.80	0.74	0.74	0.77	0.84	0.58	0.86	0.70	0.43	1.00																				
G16	0.82	0.87	0.92	0.92	0.90	0.95	0.85	0.81	0.81	0.92	0.67	0.90	0.85	0.35	0.81	1.00																			
G17	0.67	0.57	0.67	0.64	0.69	0.58	0.73	0.62	0.70	0.68	0.48	0.61	0.59	0.44	0.58	0.64	1.00																		
G18	0.68	0.83	0.77	0.88	0.83	0.84	0.67	0.75	0.70	0.81	0.54	0.83	0.74	0.41	0.92	0.81	0.49	1.00																	
G19	0.80	0.84	0.85	0.89	0.87	0.92	0.83	0.86	0.75	0.85	0.68	0.85	0.75	0.36	0.85	0.92	0.59	0.86	1.00																
G20	0.82	0.91	0.90	0.93	0.88	0.96	0.78	0.82	0.77	0.86	0.61	0.92	0.85	0.36	0.85	0.92	0.57	0.89	0.90	1.00															
G21	0.86	0.83	0.84	0.88	0.92	0.88	0.82	0.75	0.88	0.90	0.61	0.87	0.75	0.44	0.79	0.87	0.70	0.80	0.81	0.86	1.00														
G22	0.81	0.93	0.88	0.97	0.93	0.94	0.73	0.77	0.83	0.91	0.60	0.88	0.81	0.40	0.87	0.89	0.60	0.88	0.86	0.93	0.88	1.00													
G23	0.78	0.88	0.86	0.96	0.91	0.92	0.74	0.81	0.80	0.94	0.60	0.89	0.82	0.43	0.88	0.89	0.60	0.89	0.85	0.91	0.86	0.96	1.00												
G24	0.80	0.93	0.85	0.94	0.90	0.91	0.72	0.76	0.82	0.87	0.55	0.91	0.79	0.42	0.89	0.87	0.58	0.90	0.85	0.93	0.88	0.97	0.92	1.00											
G25	0.79	0.88	0.93	0.96	0.94	0.90	0.78	0.79	0.81	0.89	0.68	0.86	0.76	0.45	0.85	0.87	0.69	0.83	0.87	0.88	0.86	0.93	0.91	0.90	1.00										
G26	0.69	0.69	0.72	0.74	0.77	0.70	0.60	0.56	0.68	0.68	0.83	0.64	0.53	0.53	0.63	0.67	0.60	0.60	0.68	0.68	0.75	0.70	0.67	0.69	0.77	1.00									
G27	0.87	0.87	0.89	0.86	0.87	0.89	0.79	0.75	0.79	0.85	0.63	0.92	0.85	0.46	0.79	0.86	0.56	0.79	0.79	0.87	0.85	0.86	0.89	0.82	0.84	0.64	1.00								
G28	0.81	0.75	0.80	0.87	0.85	0.83	0.77	0.82	0.80	0.89	0.58	0.79	0.73	0.43	0.78	0.82	0.71	0.79	0.84	0.82	0.83	0.84	0.85	0.83	0.89	0.73	0.76	1.00							
G29	0.89	0.79	0.80	0.87	0.89	0.87	0.81	0.78	0.87	0.89	0.58	0.86	0.77	0.49	0.78	0.86	0.67	0.79	0.84	0.85	0.90	0.87	0.88	0.87	0.85	0.73	0.87	0.85	1.00						
G30	0.84	0.87	0.82	0.86	0.84	0.92	0.83	0.84	0.82	0.84	0.57	0.92	0.79	0.37	0.80	0.88	0.56	0.81	0.89	0.90	0.81	0.86	0.87	0.89	0.84	0.64	0.82	0.84	0.87	1.00					
G31	0.68	0.70	0.72	0.76	0.74	0.75	0.71	0.86	0.71	0.80	0.55	0.71	0.65	0.45	0.77	0.72	0.70	0.78	0.82	0.74	0.75	0.76	0.81	0.75	0.78	0.63	0.65	0.81	0.77	0.75	1.00				
G32	0.72	0.78	0.75	0.79	0.82	0.79	0.64	0.61	0.74	0.74	0.85	0.71	0.62	0.50	0.67	0.71	0.61	0.67	0.71	0.74	0.80	0.78	0.76	0.75	0.79	0.87	0.71	0.72	0.75	0.71	0.67	1.00			
G33	0.72	0.80	0.77	0.76	0.79	0.78	0.71	0.61	0.74	0.71	0.87	0.71	0.66	0.38	0.67	0.77	0.58	0.61	0.74	0.73	0.74	0.75	0.70	0.71	0.76	0.80	0.71	0.66	0.69	0.71	0.60	0.90	1.00		

REFERENCES

- [1] Akbulut, B., Karakurt, Y., Tonguç, M. (2013): Fasulye (*Phaseolus vulgaris* L.) genotiplerinin moleküler karakterizasyonu. – Mediterranean Agricultural Sciences 26(2): 105-108.
- [2] Altieri, M. A. (1999): The ecological role of biodiversity in agroecosystems. – Agriculture, Ecosystems and Environment 74(1-3): 19-31.
- [3] Anderson, J. A., Churchill, G., Autrique, J., Tanksley, S., Sorrells, M. (1993): Optimizing parental selection for genetic linkage maps. – Genome 36(1): 181-186.
- [4] Bellon, M. R., Gotor, E., Caracciolo, F. (2015): Conserving landraces and improving livelihoods: how to assess the success of on-farm conservation projects? – International Journal of Agricultural Sustainability 13: 167-182.
- [5] Blair, M. W., Hurtado, N., Chavarro, C. M., Muñoz-Torres, M. C., Giraldo, M. C., Pedraza, F., Tomkins, J., Wing, R. (2011): Gene-based SSR markers for common bean (*Phaseolus vulgaris* L.) derived from root and leaf tissue ESTs: an integration of the BMC series. – BMC Plant Biology 11: 50.
- [6] Blair, M. W., Giraldo, M. C., Buendia, H. F., Tovar, E., Duque, M. C., Beebe, S. E. (2006): Microsatellite marker diversity in common bean (*Phaseolus vulgaris* L.). – Theoretical Applied and Genetics 113: 100-109.
- [7] Buah, S., Buruchara, R., Okori, P. (2017): Molecular characterisation of common bean (*Phaseolus vulgaris* L.) accessions from Southwestern Uganda reveal high levels of genetic diversity. – Genetic Resources and Crop Evolution 64(8): 1985-1998.
- [8] Bukhari, A., Bhat, M., Ahmad, M., Saleem, N. (2015): Examination of genetic diversity in common bean (*Phaseolus vulgaris* L.) using random amplified polymorphic DNA (RAPD) markers. – African Journal of Biotechnology 14(6): 451-458.
- [9] Buso, G. S. C., Amaral, Z. P. S., Brondani, R. P. V., Ferreira, M. E. (2006): Primer note: microsatellite markers for the common bean *Phaseolus vulgaris*. – Molecular Ecology Notes 6: 252-254.
- [10] Crowder, D. W., Northfield, T. D., Strand, M. R., Snyder, W. E. (2010): Organic agriculture promotes evenness and natural pest control. – Nature 466(7302): 109-112.
- [11] De Luca, D., Cennamo, P., Del Guacchio, E., Di Novella, R., Caputo, P. (2018): Conservation and genetic characterisation of common bean landraces from Cilento region (southern Italy): high differentiation in spite of low genetic diversity. – Genetica 146(1): 29-44.
- [12] Düzdemir, O. (1998): Kuru Fasulye (*Phaseolus vulgaris* L.) Genotiplerinde Verim ve Diğer Bazı Özellikler Üzerine Bir Araştırma. Yüksek Lisans Tezi, – GOÜ. Fen Bilimleri Enstitüsü, Tokat.
- [13] Dwiedi, S. L., Ceccarelli, S., Blair, M. W., Upadhyaya, H. D., Are, A. K., Ortiz, R. (2016): Landrace germplasm for improving yield and abiotic stress adaptation. – Trends in Plant Science 21(1): 31-42.
- [14] Erdiñç, Ç., Türkmen, Ö., Şensoy, S. (2013): Türkiye'nin bazı fasulye genotiplerinin çeşitli bitkisel özelliklerinin belirlenmesi. – Yüzüncü Yıl Üniversitesi Tarım Bilimleri Dergisi 23(2): 112-125.
- [15] Eşiyok, D. (2012): Kışlık ve Yazlık Sebze Yetiştiriciliği. – Meta Basım Matbaacılık Hizmetleri, İzmir.
- [16] Finegan, B., Nasi, R. (2004): The Biodiversity and Conservation Potential of Shifting Cultivation Landscapes. Agroforestry and Biodiversity Conservation in Tropical Landscapes. – Island Press, Washington, DC, pp. 153-197.
- [17] Gaitán-Solís, E., Duque, M., Edwards, K., Tohme, J. (2002): Microsatellite repeats in common bean (*Phaseolus vulgaris*). – Crop Science 42(6): 2128-2136.
- [18] Galvan, M., Menendez-Sevillano, M., De Ron, A., Santalla, M., Balatti, P. A. (2006): Genetic diversity among wild common beans from northwestern Argentina based on

- morpho-agronomic and RAPD data. – *Genetic Resources and Crop Evolution* 53(5): 891-900.
- [19] Genchev, D., Kiryakov, I. (2005): Color Scales for Identification Characters of Common Bean (*Phaseolus vulgaris* L.). – Dobroudja Agricultural Institute-General, Toshevo.
- [20] Gepts, P. (2008): Tropical Environments, Biodiversity, and the Origin of Crops. – In: Moonre, P., Ming, R. (eds.) *Genomics of Tropical Crop Plants*, Springer, New York, pp: 1-20.
- [21] Gomez, O. J., Blair, M. W., Frankow-Lindberg, B. E., Gullberg, U. (2005): Comparative study of common bean (*Phaseolus vulgaris* L.) landraces conserved ex situ in genebanks and in situ by farmers. – *Genetic Resources and Crop Evolution* 52: 371-380.
- [22] Haymes, K. M. (1996): Mini-prep method suitable for a plant breeding program. – *Plant Molecular Biology Reporter* 14(3): 280-284.
- [23] Kar, H., Balkaya, A., Apaydın, A. (2005): Samsun ekolojik koşullarında ilk turfanda taze fasulye yetiştiriciliğinde bazı çeşitlerin performanslarının belirlenmesi üzerinde bir araştırma. – *GOÜ Ziraat Fakültesi Dergisi* 22(1): 1-7.
- [24] Khaidizar, M. I., Haliloglu, K., Elkoca, E., Aydın, M., Kantar, F. (2012): Genetic diversity of common bean (*Phaseolus vulgaris* L.) landraces grown in northeast Anatolia of Turkey assessed with simple sequence repeat markers. – *Turkish Journal of Field Crops* 17(2): 145-150.
- [25] Lima, M. S., Carneiro, J. E. S., Carneiro, P. C. S., Pereira, C. S., Vieira, R. F. Cecon, P. R. (2012): Characterization of genetic variability among common bean genotypes by morphological descriptors. – *Crop Breeding and Applied Biotechnology* 12(1): 76-84.
- [26] Lockwood, J. A. (1999); *Agriculture and biodiversity: Finding our place in this world.* – *Agriculture and Human Values* 16: 365-379.
- [27] Madakbaş, S. Y., Kar, H., Küçükumuzlu, B. (2004): Çarşamba Ovası'nda Bazı Bodur Taze Fasulye Çeşitlerinin Verimliliklerinin Belirlenmesi. – *GOÜ Ziraat Fakültesi Dergisi* 21(2): 1-6.
- [28] Mavromatis, A., Arvanitoyannis, S., Korkovelos, A., Giakountis, A., Chatzitheodorou, V., Goulas, C. (2010): Genetic diversity among common bean (*Phaseolus vulgaris* L.) Greek landraces and commercial cultivars: nutritional components, RAPD and morphological markers. – *Spanish Journal of Agricultural Research* (4): 986-994.
- [29] Meza, N., Rosas, J. C., Martín, J. P., Ortiz, J. M. (2013): Biodiversity of common bean (*Phaseolus vulgaris* L.) in Honduras. evidenced by morphological characterization. – *Genetic Resources and Crop Evolution* 60(4): 1329-1336.
- [30] Negri, V., Maxted, N., Vetelainen, M. (2009): European Landrace Conservation: An Introduction. – In: Vetelainen, M., Negri, V., Maxted, N. (eds.) *European Landraces: On-Farm Conservation, Management and Use*. ECP GR, Rome, Italy.
- [31] Negri, V., Tosti, N. (2002): *Phaseolus* genetic diversity maintained on-farm in central Italy. – *Genetic Resources and Crop Evolution* 49(5): 511-520.
- [32] Nemli, S., Kianoosh, T., Tanyolac, M. B. (2015): Genetic diversity and population structure of common bean (*Phaseolus vulgaris* L.) accessions through retrotransposon-based interprimer binding sites (iPBSs) markers. – *Turkish Journal of Agriculture and Forestry* 39(6): 940-948.
- [33] Norris, K. (2008): Agriculture and biodiversity conservation: opportunity knocks. – *Conservation Letters* 1(1): 2-11.
- [34] Özgen, M., Adak, M., Karagöz, A., Ulukan, H. (1995): Bitkisel Gen Kaynaklarının Koruma ve Kullanımı. – *Türkiye Ziraat Mühendisliği IV Teknik Kongresi* 1: 309-344.
- [35] Piergiovanni, A. R., Taranto, G., Losavio, F. P., Pignone, D. (2006): Common bean (*Phaseolus vulgaris*) landraces from Abruzzo and Lazio regions (Central Italy). – *Genetic Resources and Crop Evolution* 53(2): 313-322.
- [36] Rohlf, F. J. (2000): *NTSYS-pc, Numerical Taxonomy and Multivariate Analysis System, Version 2.1.* – Exeter Software, New York.

- [37] Sarikamis, G., Yasar, F., Bakir, M., Kazan, K., Ergul, A. (2009): Genetic characterization of green bean (*Phaseolus vulgaris*) genotypes from eastern Turkey. – Genetics and Molecular Research 8(3): 880-887.
- [38] Skroch, P., Nienhuis, J. (1995): Qualitative and quantitative characterization of RAPD variation among snap bean (*Phaseolus vulgaris*) genotypes. – Theoretical and Applied Genetics 91(6-7): 1078-1085.
- [39] Sneath, P. H. A., Sokal, R. R. (1973): Numerical Taxonomy: The Principles and Practice of Numerical Classification. – WH Freeman, San Francisco, pp. 573.
- [40] Tautz, D., Renz, M. (1984): Simple sequences are ubiquitous repetitive components of eukaryotic genomes. – Nucleic Acids Research 12: 4127-4138.
- [41] TÜİK (2017): Turkish Statistical Institute data base. – Access date: 20/02/2018.
- [42] Ulukapı, K., Onus, A. N. (2013): Selekte Edilmiş Bazı Yerel Taze Fasulye (*Phaseolus vulgaris* L.) Genotiplerinin Moleküler Karakterizasyonu. – Tarım Bilimleri Dergisi 18: 277-286.
- [43] Velasquez, V. L. B., Gepts, P. (1994): RFLP diversity of common bean (*Phaseolus vulgaris*) in its centres of origin. – Genome 37(2): 256-263.
- [44] Yu, K., Park, S., Poysa, V., Gepts, P. (2000): Integration of simple sequence repeat (SSR) markers into a molecular linkage map of common bean (*Phaseolus vulgaris* L.). – Journal of Heredity 91(6): 429-434.
- [45] Zeven, A. C. (1998): Landraces: a review of definitions and classifications. – Euphytica 104: 127-139.

ESTIMATION AND PREDICTION OF THE SOIL EROSION RISK INFLUENCED BY THE URBANIZATION PROCESS WITHIN A COUNTY IN HILLY AREA OF SOUTHEAST CHINA, USING RUSLE AND CLUEs MODEL

FAN, J.¹ – YAN, L.^{1*} – WU, L.¹ – ZHANG, P.¹ – ZHANG, G.²

¹*College of Life Sciences, Zhejiang University, Zhejiang, Hangzhou 310058, PR China
(e-mail: fanji_990@hotmail.com – J. Fan)*

²*Center for Geographic Information Systems, Georgia Institute of Technology
Atlanta, GA 30308, USA*

**Corresponding author*

e-mail: yanlj@zju.edu.cn; phone: +86-186-5811-1761, +86-571-8820-6605

(Received 28th Sep 2018; accepted 27th Nov 2018)

Abstract. Soil erosion by water is a well-known environmental problem. Urbanization is a worldwide trend, leading to a drastic change of land use forms in local areas, and change in soil erosion risks. This research analyzed the soil erosion risks in the past two decades of Zhuji County, which is located in hilly area of Southeast China and is experiencing fast urbanization process, to evaluate the influence of the urbanization on soil erosion using Revised Universal Soil Loss Equation (RUSLE). Land use maps were developed by using CLUEs (the Conversion and Land Use and its Effect at Small regional extent) model to estimate the soil erosion risk in 3 different urbanization scenarios of 2020. The results showed that, during 1984 to 2009, as the percentage of the urban and built-up area increased from 0.43% to 10.95%, though the extreme erosion value did not have a clear trend, from 1984 to 2004, the percentage of area with soil erosion risk higher than medium level kept increasing from 3.23% to 6.34%, the percentage of area with tolerable soil erosion risk was decreasing from 71.57% to 67.58%. The scenario analysis showed that the change of the urban and built-up area would change the soil erosion risk significantly, especially the high and severe level erosion risk. Higher than medium level soil erosion risk is 7.49% in Scenario 1 with 15.33% urban and built-up area, 8.63% in Scenario 2 with 18.86% urban and built-up area, and 13.07% in Scenario 3 with 25% urban and built-up area. And the buffer zone analysis of a highway in the county also showed that the soil erosion risk correlated with the size of urban and built-up area. These results indicated that Zhuji County needs to pay more attention when urbanize in hilly area since it leads to more severe erosion risk without prevention measurements. And policies should balance the preservation of the agriculture land and the potential soil erosion risk during urbanization process.

Keywords: *land use, scenario, urbanization*

Introduction

Urbanization is a major trend all over the world. According to the world urbanization prospects, the population in the urban area was growing in a high speed. Until 2017, approximately 55% of the world population were urban residents. And United Nations estimated the urban percentage will reach 68% till 2050 (United Nations, 2018). Compared to developed regions, the rate of urbanization is even higher in developing regions. As one of the developing countries with big population and rapid growth, China has experienced drastic urbanization in recent two decades driven by the economic revolution. According to China statistic yearbook, 57.35% of the population was urban until 2016 and in the next 30 years, the urbanization speed will remain at a high level.

As is well recognized, rapid urbanization brings huge pressure on the natural resources and environment (Chen, 2007; Barbera et al., 2010; Akhalkatsi et al., 2017; Op de Hipt et

al., 2018), including soil. Soil is an important resource to human beings, which is not only the foundation of the terrestrial ecosystems, but also an indispensable part of biogeochemical cycles. Soil is considered as a non-renewable resource in hundred-year horizon, which means when soil is eroded, it is hard to recovered. In this aspect, soil conservation is a critical issue during rapid urbanization.

According to the previous researches, urbanization would influence the soil erosion in several aspects as follows. (1) Construction sites would scattered in the city area during the process of urbanization, not only in the central city, but also in the extended areas near farmland or in the hilly area, such as the construction of the road and the places along the road (De Oña et al., 2009; Trenouth and Gharabaghi, 2015). (2) Urbanization always companies with increased proportion of impervious surface. Though after the impervious surface is built, the erosion risk in the area it covered will be lower, the peripheral area in the watershed, however, would be confronted with more serious erosion risk because of the larger amount of runoff than before (Arnold and Gibbons, 1996; White and Greer, 2006; Biggs et al., 2010). (3) Urbanization also dramatically changes the land use types in the area. The main process is the increase of building land, and the decrease of agriculture land and forest. Agriculture land is occupying forest while building land is invading agriculture land. Sometimes, agriculture reclamation will occur at slope land, which leads to higher risk of soil erosion than plain area (Podmanicky et al., 2011; García-Ruiz, 2010). The change of the land use pattern can also change the hydrology process in the area, which is an important factor to soil erosion (White and Greer, 2006; Zhang et al., 2018; Boongaling et al., 2018).

Zhejiang province is a southeast coastal province of China, belonging to the Yangtze River Delta. This area has experienced the most rapid development in China during recent years. In the next three decades, the speed of urbanization will remain at a high rate. To reduce soil erosion, studying the impact pattern and estimating the erosion risk in different developing scenarios would be necessary.

RUSLE (Revised Universal Soil Loss Equation) is a widely applied model in estimating the average soil erosion amount per year (Ouyang et al., 2010; Thomas et al., 2018; Napoli et al., 2016). RUSLE was originally developed to estimate soil erosion amount at field scale (Renard et al., 1991). As the development of the GIS (Geographic Information System), RUSLE is gradually applied on soil erosion prediction and assessing the soil erosion risk at large scale, such as catchment or watershed (Park et al., 2011; Ostovari et al., 2017). Since RUSLE was a field scale model, lots of previous research devoted to adapt it to a large scale, especially in adjusting the algorithm of L and S factors (Van Remortel et al., 2001; Lewis et al., 2005; Qin et al., 2018). In this research, soil erosion risk was assessed by RUSLE. And the algorithm of LS factor was adjusted based on the research area's condition.

Some efforts have been done in soil erosion within regional and large watershed scales (Basile et al., 2010; Beskow et al., 2009; Boix-Fayos et al., 2009; Chen et al., 2017), but there is still few study done in county scale, especially in the coastal area of Southeast China. Soil erosion is usually studied in natural catchment or watershed. However, studying on an administrative area basis would be more meaningful in China for local policy makers to understand the impact of erosion in the whole region and take effective prevention measurements. In this research, a whole county was chosen as the study area.

The main objectives of this research have two folds. (1) Analyze the impact of urbanization in past 2 decades on the soil erosion risk in Zhuji County; (2) By scenario analysis, estimate the soil erosion risk with different urbanization intensities in the next 10

years, and analyze the government policies' influence. This research will be useful to understand the impact of further development in the urbanizing areas and how to take effective prevention measurements, and can also provide guidance on erosion control for other less urbanized area in China.

Methodology

Study area

Zhuji County is located in the middle of Zhejiang province in the coastal area of Southeast China (*Fig. 1*). The center of the county is located at 29.72N and 120.23E, covering 2311 km² area. The county belongs to Puyang River watershed, and has a typical subtropical monsoon climate characterized as hot and dry summer due to the subtropical anticyclone and generally cold and humid winter. The average precipitation and annual temperature are 1373.6 mm/year and 16.3°C, respectively. There are 27 administrative districts (villages and towns) in the county. In the past three decades since Chinese economic reform, Zhuji County has undergone a fast society and economic development. The population (and GDP (Gross Domestic Product)) increased from 0.94 million (248.35 million RMB (Renminbi)) in 1978 to 1.18 million (109906 million RMB) by 2016 (Statistical Bureau of Zhuji City, 2017). And the built-up area in the county expanded rapidly.

Soil characteristic

According to the general survey of soil (GSCC (General Soil Classification of China) system), there are 66 soil species in total in the study area. Red soil and paddy soil are dominant in this area (which in ST system belongs to Ultisols and Inceptisols. (OSD OSSD, 1998; Deckers et al., 2006), which occupied 50.9% and 29.8% of the area respectively. And there is approximately 5.5% yellow soil (Alfisols), 5.1% purplish soil (Inceptisols) and 5.8% regosol. The soil map of the area is shown in *Figure 4* (a. K factor).

Topography

The study area is located at the juncture of two hills. The east and west of the county is enclosure by hills, and between hills there is a valley plain of the Puyang River. The east hills, Kuaiji hills, divide the Puyang River watershed and Cao'e River watershed, while the west hills, Longmen hills, divide the Puyang River watershed and Fuchun River watershed. The elevation of whole area is declined from north to south with the highest place at 1194.6 m. The topography data were obtained from the DEM data which were from International Scientific & Technical Data Mirror Site with the resolution of 30 m.

RS data preparing

A 73-km²-reservoir in the county started to construct from 2013; it influenced the landscape and the local river system largely. So that we acquired the data until 2013, and sieved the data with cloud less than 5%, and the time step was set to 5 to 10 years in order to examine the effect of urbanization. As a result, the data from 1984 to 2009 were chosen as the research data.

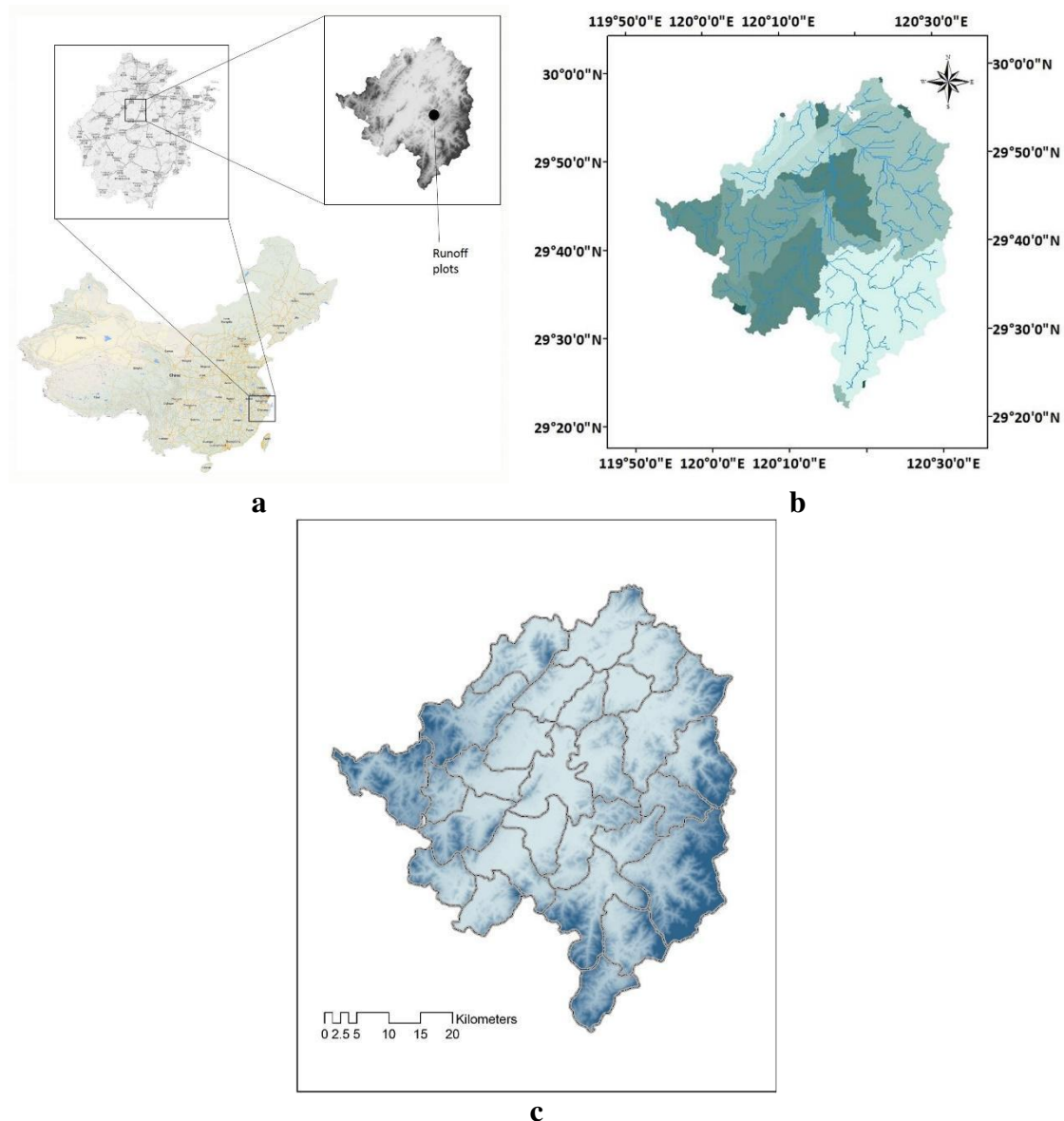


Figure 1. *a* Location of the study area, *b* the watersheds in the area, *c* administrative division of the area

Land use/cover data were classified from Landsat MMS image of the county for 1984, TM images for 1994, and ETM images for 2004 and 2009, all of which were obtained from Geospatial Data Cloud site, Computer Network Information Center, Chinese Academy of Sciences (<http://www.gscloud.cn>). The resolution was 30 m for TM and ETM images, and 80 m for MMS image. In this research, the land use types were mainly classified following Anderson level 1, which includes 1) Urban (including urban and built-up area), 2) Forest, 3) Agriculture (paddy land) 4) Agriculture (crop land), 5) bare land, and 6) water. As a result, there are 6 land use types in total in this study.

The reference land use data were land-use map of 1987 with scale of 1:300,000, map of 1991 with scale of 1:100,000, and map of 2005 with scale of 1:100,000. The classified results were also calibrated and revised by field verification. To verify the

results, we randomly picked 50 points within the study area on the map, and went to the field to check the land use type. The correct number is 46 out of 50.

RUSLE

The Revised Universal Soil Loss Equation (RUSLE) is a widely used empirical model for soil erosion estimation. It was originally proposed by Wischmeier and Smith (1965; Renard et al., 1991) in USA, known as universal soil loss equation (USLE). Since USLE was mainly based on the data from short and gentle slopes, it could not be applied in basins or watershed with complicated environments. Renard et al. (1997) improved the model to RUSLE by modifying the algorithm of factors, especially rainfall-runoff erosivity factor (R factor), slope length and steepness factor (LS factor), and cover-management factor (C factor). The equation of the RUSLE is as follows (Eq. 1):

$$A = R \times K \times LS \times C \times P \quad (\text{Eq.1})$$

where A is average soil erosion amount per year ($\text{Mg ha}^{-1} \text{ year}^{-1}$), R is the rainfall-runoff erosivity factor ($\text{MJ mm ha}^{-1} \text{ year}^{-1}$), K is the soil erodibility factor ($\text{Mg h}^a \text{ MJ}^{-1} \text{ mm}^{-1}$), LS is topography factor (L is slope length factor and S is slope steepness factor), C is cover-management factor, and P is support practice factor.

R factor

R factor is used to quantify the rain-drop strike energy per year in the equation. There are several different algorithms to calculate R factor in using data in different precision, such as rain intensity in 30 min, precipitation amount per day, or precipitation amount per month. In this research, we used the model developed by Xinbo et al. (2001) in the same area (in Zhejiang Province) to calculate the R factor. The model uses daily data of precipitation amount while considering the difference of rainfall intensity among different seasons in one year. The equation is as follows (Eq. 2):

$$R_j = a \left[1 + b \sin \left(\frac{\pi}{12} (j - 1) \right) \right] \sum_{k=1}^N P_k \quad P_k > P_0 \quad (\text{Eq.2})$$

where R_j is the R value of the j month; P_k is the precipitation of the k day in the j month; P_0 is the threshold of precipitation value, only P_k larger than P_0 is calculated in the equation, in this research, the value of P_0 is 12.7 mm; a, b are parameters, according to Xinbo et al. (2001), based on the precipitation data from 1987 to 2000, a is 0.0043, b is 48.13. R value of the whole year is the sum of every month's R value.

Rainfall in the study area was interpolated from 19 rain gauge stations scattered in the Zhejiang Province in which 2 rain gauge stations were in the study area. The interpolation was conducted in using ordinary kriging method with spherical semivariogram model.

The result is as *Figure 4c*.

K factor

K factor is the indicator of the resistance of the soil to erosion by rainfall and runoff. It is mainly related to the physical properties of the soil, such as the particle

composition, the porosity, and ratio of organic matter content. In this research, K factor was calculated using the equation developed by Sharpley and Williams (1990) in the Erosion-production impact calculator model (EPIC). The calculate equation is as follows (Eq. 3):

$$K = \frac{\frac{1}{7.6} (0.2 + 0.3 \cdot \exp(-0.0256SAN(1 - \frac{SIL}{100}))) (\frac{SIL}{CLA+SIL})^{0.3} (1.0 - \frac{0.25OM}{OM+\exp(3.72-2.95OM)}) (1.0 - \frac{0.7SN}{SN+\exp(-5.51+22.9SN)})}{1} \quad (\text{Eq.3})$$

where $SN = 1.0 - SAN / 100$; SAN, SIL, CLA, and OM are the percentage of sand, silt, clay and organic matter in the soil, respectively.

The data required to calculate K factor is obtained from the digital soil map of China, with the map scale 1:1,000,000. The result is as *Figure 4a*.

LS factor

LS factor is the indicator of the topography effect on soil loss. L factor quantifies the slope length effect while S factor quantifies the effect of the slope steepness.

S factor (Eqs. 4-6) is use the algorithm developed by McCool et al. (1987) and revised by Liu et al. (1994):

$$S = 10 \times \sin\theta + 0.03 \quad \theta < 9\% \quad (\text{Eq.4})$$

$$S = 16 \times \sin\theta - 0.50 \quad \theta \geq 9\% \quad (\text{Eq.5})$$

$$S = 21.91 \times \sin\theta - 0.96 \quad \theta \geq 14\% \quad (\text{Eq.6})$$

where θ is the slope gradient (%).

L factor was calculated by the method proposed by Desmet and Govers (1996), in which the L factor of one grid was determined by the contribute area of it (the grids surrounding it), the equation is as follows (Eq. 7):

$$L_{i,j} = \frac{(A_{i,j-in} + D^2)^{m+1} - A_{i,j-in}^{m+1}}{D^2 \times \chi_{i,j}^m \times 22.13^m} \quad (\text{Eq.7})$$

where $L_{i,j}$ is the L factor of grid(i,j), $A_{i,j-in}$ is the effective area which flow into grid(i,j), D is the length of the grid, $\chi_{i,j}$ is the coefficient of grid(i, j), the equation of $\chi_{i,j}$ is as follows (Eq. 8):

$$\chi_{i,j} = \sin(\theta_{i,j}) + \cos(\theta_{i,j}) \quad (\text{Eq.8})$$

where $\theta_{i,j}$ is the slope of grid(i, j), m is the slope length coefficient in original algorithm of L factor of RUSLE, the equation of m is as follows (Eqs. 9-10):

$$m = \frac{\beta}{\beta + 1} \quad (\text{Eq.9})$$

$$\beta = \frac{(\frac{\sin\theta}{0.0896})}{3.0 \times (\sin\theta)^{0.8} + 0.56} \quad (\text{Eq.10})$$

where $\theta_{i,j}$ is the slope of grid(i, j).

The algorithm was written in python for the ArcGIS. The result is as *Figure 4b*.

C factor

C factor is the surface coverage factor, which is used to describe the effect of surface coverage on the erosion. According to the definition, the value of C factor mainly depends on the size of the vegetation which control soil erosion, and it relates to the surface area's status, including surface roughness, the amount of contained water and the plant characteristics. The value of C factor ranges from 0 to 1. Smoother the surface is, less the cover vegetation, closer the value is to 1 and vice versa.

The C factor calculation in this research was mainly based on the land-use type, referencing the value based on the research of Yang et al. (2003), as shown in *Table 1*.

Table 1. Value of C factor and P factor for the land-use types

	C factor	P factor
Water	0.01	1
Urban and built-up	0.2	1
Forest	0.006	1
Paddy land	0.1	0.5
Cropland	0.5	0.5
Bareland	0.35	1

P factor

The support practice factor P represents the impact of support practice, such as contour hedgerows and stripping cropping, on average annual soil erosion. Different soil erosion prevention policy has a different P value. The more effective the practice is, the closer the P value is to 0, and vice versa. At the same time, different land-use type also has a different P value. Due to limited available data, P value in this research was mostly determined by land-use type, which also is a common practice in the research using RUSLE. P value was calculated also based on the value suggested by Yang et al. (2003; *Table 1*).

The result of CP factor is as *Figure 4d*.

CLUEs

Land use transition

To set scenarios and predict the future soil erosion, the Conversion and Land Use and its Effect (CLUE) model was used here to simulate the land use type in certain scenarios. CLUE model is a dynamic model to predict the future land use type with a

spatial allocation module and a non-spatial land-use demand module (Verburg et al., 2002).

Demand module

Land use demand module is a relatively independent part in the CLUE model (Batisani and Yarnal, 2009). It calculates the change of areas for all land use type in an aggregate level. There are various alternative models for the demand module, ranging from extrapolation to social-economic model. In this research, grey model was chosen to extrapolate the future demand of all the land-use type. It is a method to do trend extrapolation. Compare to the least square method, grey model (GM(1, 1)), which based on the grey system theory (Kayacan et al., 2010), would generate a trend line with a gentler gradient. The detail of GM(1, 1) can be found in previous studies such as Kayacan et al. (2010).

Demand prediction was based on the continuous 11-year (from 2000 to 2010) interpreted RS data. There are 7 land-use types in total, including water, forest, paddy land, crop land, urban and built-up land, and bare land. The area of each type was calculated by multiplying the calculated percentage with the total area of Zhuji County.

Model variables selection

Land-use map of 2001 was reclassified into 7 maps with 7 land-use types, respectively, and 2001 was set as the initial year. Each land-use type was a dependent variable in step-wise logistic regression. In this research, we selected 10 explanatory independent variables for the 7 land-use types based on the previous researches (Table 2; Podmanicky et al., 2011; Verburg et al., 2002; Batisani and Yarnal, 2009). However, in the binary logistic regression analysis, the 5th factor, the distance from CBD, the beta value was too small (less than 10^{-7}). As a result, it was deleted from the factors. Beta values and constants for CLUE model are shown in Table 3.

The variables for each land-use type and the result of logistic regression are shown in Table 3.

Table 2. Total explanatory variables of land-use types

No.	Variables	Unit
1	GDP	Yuan/km ²
2	Population density	Inhabitants/km ²
3	Distance from river	m
4	Distance from road	m
5	Distance from CBD	m
6	Slope	Degree
7	Elevation	m
8	Aspect	Derived from DEM (8 directions)
9	Soil organic content	%
10	Area	*

*Category variable

Table 3. Beta value for variables of each land-use type

Variables No.	Water	Urban and built-up	Forest	Paddy land	Cropland	Bare land
1	-	-0.0093	0.0075	-0.0133	0.0019	0.0152
2	-0.0005	-0.0003	0.0004	0.0005	-0.0006	0.0005
3	-	-0.0001	0.0001	-0.0002	0.0000	-
4	-0.0001	-0.0002	0.0001	-0.0001	0.0000	-0.0001
6	0.0039	0.0059	-0.0072	0.0096	0.0024	0.0041
7	0.0005	-0.0005	0.0010	-0.0016	-0.0009	0.0012
8	-	0.0003	-0.0002	0.0002	-0.0001	-0.0007
9	0.0296	-0.0616	0.0443	-0.0119	-0.0221	0.0208
10	-0.0153	-0.0350	0.0307	-0.0508	-0.0038	0.0327
Constant	-3.6301	-0.8707	-0.7393	-1.5464	-0.9422	-7.3565

The variable No. is as shown in Table 2

Scenario setting

According to RUSLE, soil erosion risk is mainly determined by topography, soil erodibility, precipitation in the area, land use/cover types and management measures. Since the natural conditions hardly change in a short period, in this research, only land use types were recognized as the reason cause the changing of the erosion risk.

In order to assess the soil erosion risk in the 2020, the following scenarios were set:

- Scenario 1: the county develops as the land-use planning of 2006-2020. According to the planning, the built-up area will be less than 15.33%.
- Scenario 2: the county develops as the current trend, which is simulated by GM(1,1). The built-up area will occupy 18.86% of the whole county in this scenario.
- Scenario 3: the county will not control the city development; the built-up area will reach 25% till 2020.

In these scenarios, R factor was calculated using the data of 2009, C and P factor were calculated depending on the land use types in different scenarios.

Verification

The data of 2013 was chosen to verify the prediction of CLUEs model. Scenario 1 was chosen to be the data to compare. The results of 2013 simulated in CLUEs is shown as Figure 2a, and the interpreted data is shown as Figure 2b. We randomly pick 500 points at same locations in these two figures in ArcGIS, and compare the values. The result shows the correct rate is 87.2% (436/500).

Analysis of the impact of highway

In this research, we selected a highway started building in 1999 and completed in 2004 to study the impact of road on erosion. The location of the highway was shown in Figure 3. Buffer zone analysis was used to analyze the influence of the highway on

erosion risk. To examine the influence distance of the highway, 20 buffer zones were set, from 60 m to 1200 m with step of 60 m.

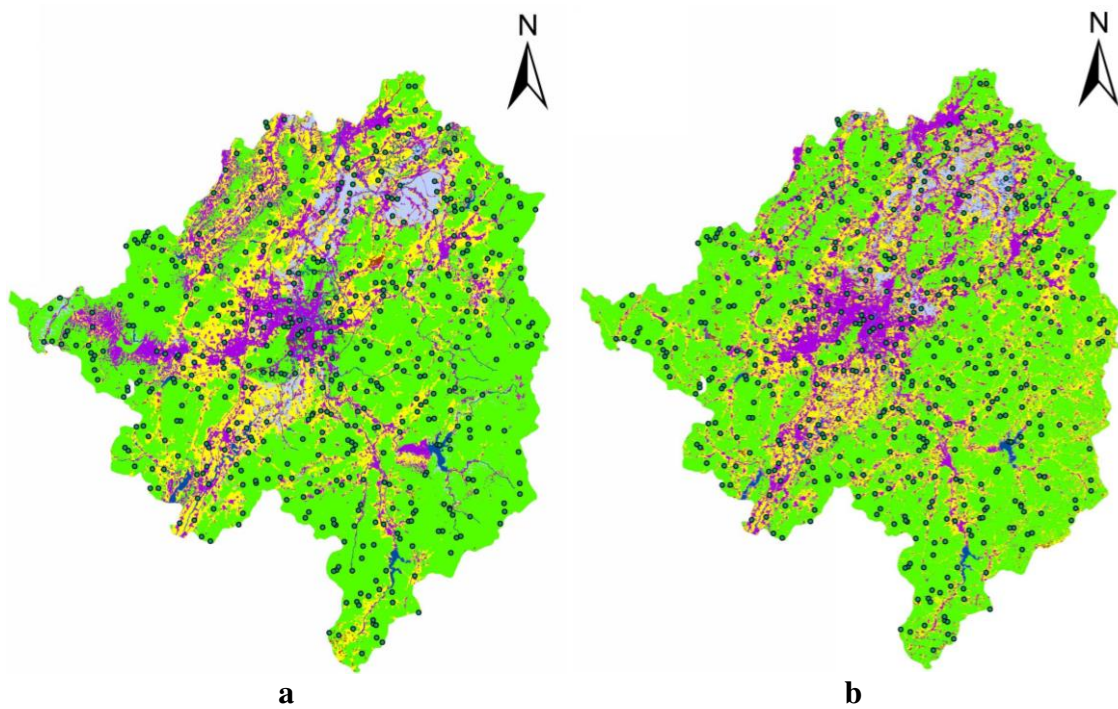


Figure 2. Compare of the simulation and interpreted land use type of 2013. *a* Simulation, *b* interpreted

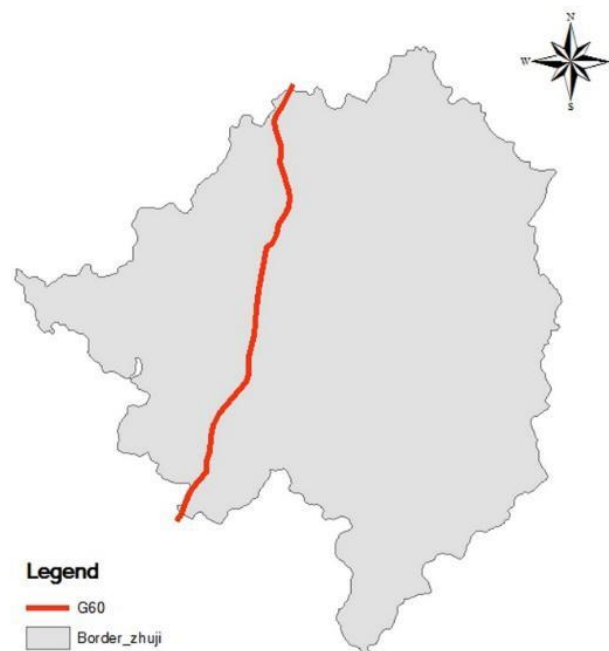
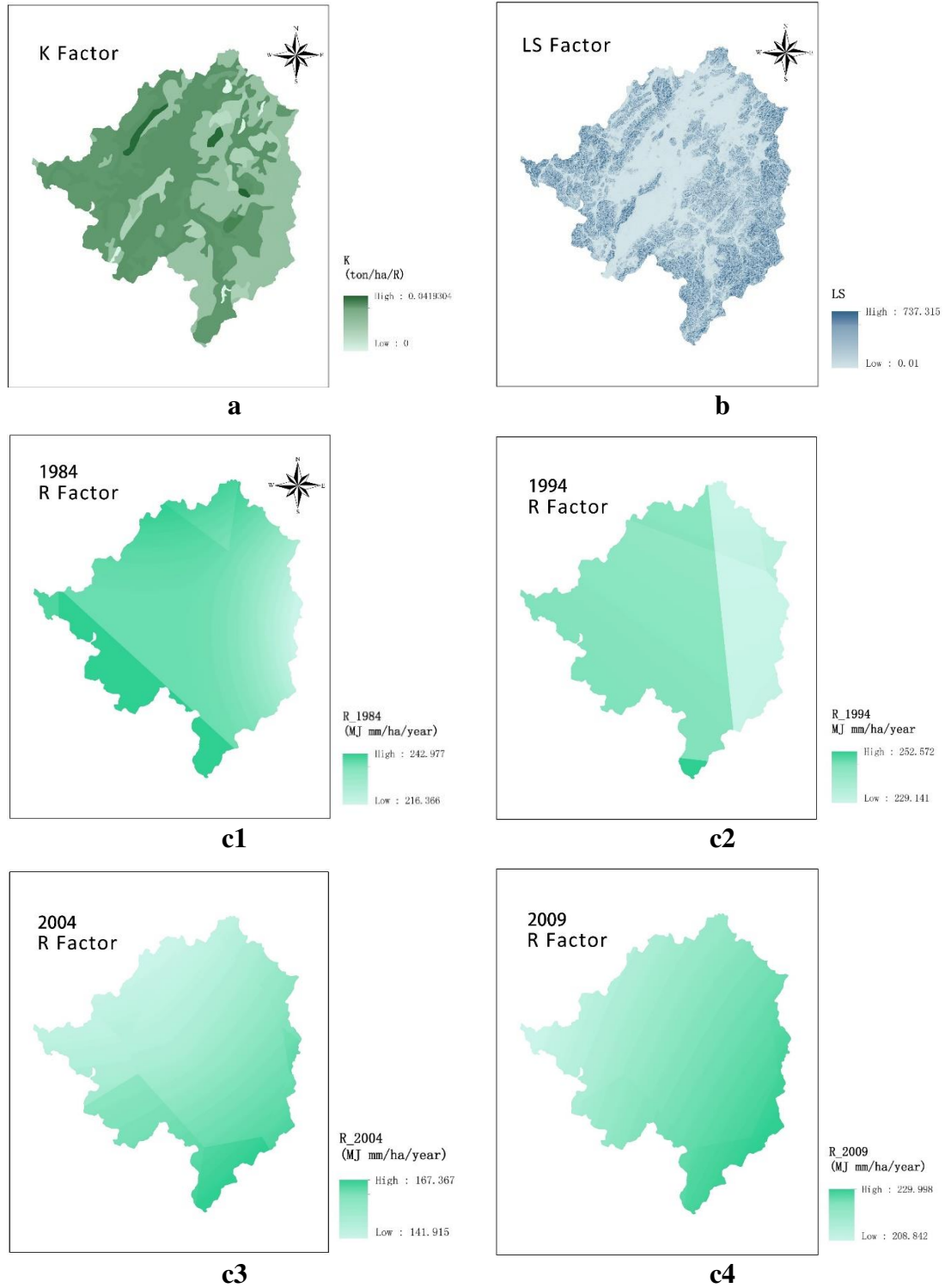


Figure 3. The location of the highway G60

Results

The results of RUSLE factors

Figure 4 shows the results of the factors of RUSLE.



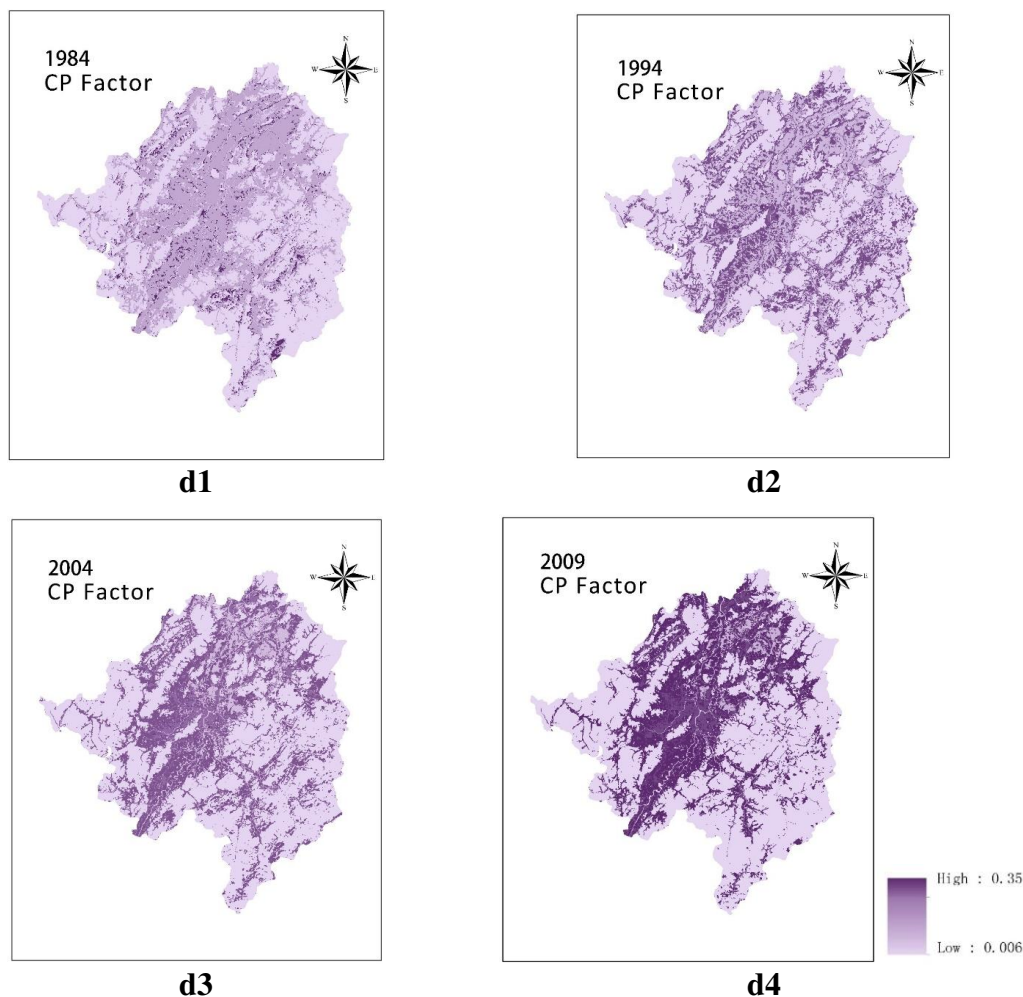


Figure 4. The factors for RUSLE. **a** K factor; **b** LS factor; **c1-4** R factor for 4 years; **d1-4** CP factor for 4 years

Soil erosion change over 1984-2009

Figure 5 shows the result of RUSLE of four different years: 1984, 1994, 2004 and 2009. The maps show the erosion amount of each grid with area of 0.09 ha per grid. Compare to the map of 1984, there are more erosion in 1994, 2004 and 2009. And the maximum erosion amount per grid is highest in 1994 ($938.43 \text{ ton hm}^{-2} \text{ a}^{-1}$). Erosion amount was increasing from 1984 to 1994 in the southeast part of the county, and increasing from 2004 to 2009 in the northwest part of the county.

The change of erosion risk over 1984-2009

The results in Figure 5 was calculated using rainfall data of correspondent year. However, the total rainfall was different from year to year with 2004 being the year with extremely low level (Fig. 4c). To eliminate the difference introduced by rainfall, the rainfall data of 2009, which was close to the average value of past 25 years from 1984-2009, was used to calculate the erosion risk for all years. The result was shown in Figure 6. The erosion risk was divided into 5 ranks based on the erosion amount:

tolerable (less than 1 ton/ha/year), low (1-10 ton/ha/year), medium (10-50 ton/ha/year), high (50-100 ton/ha/year) and severe (more than 100 ton/ha/year).

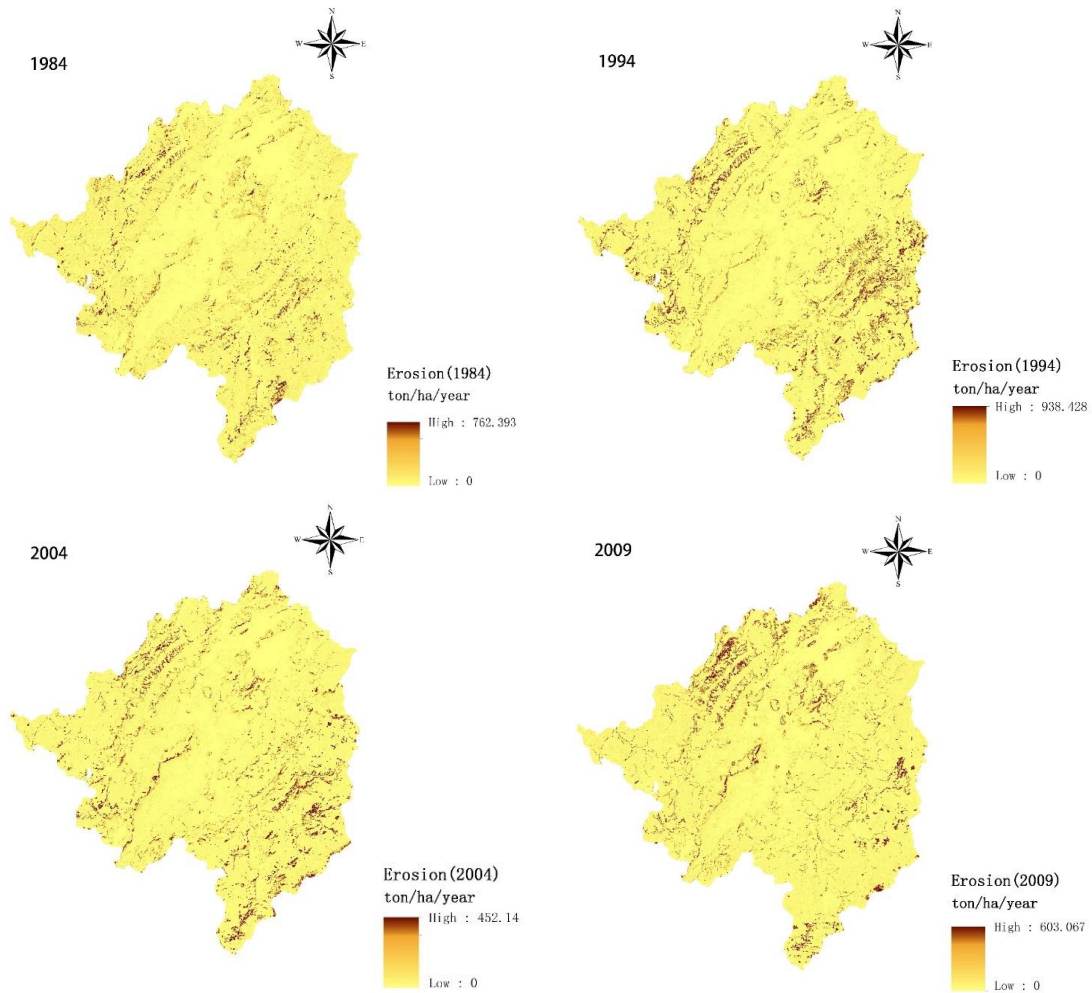
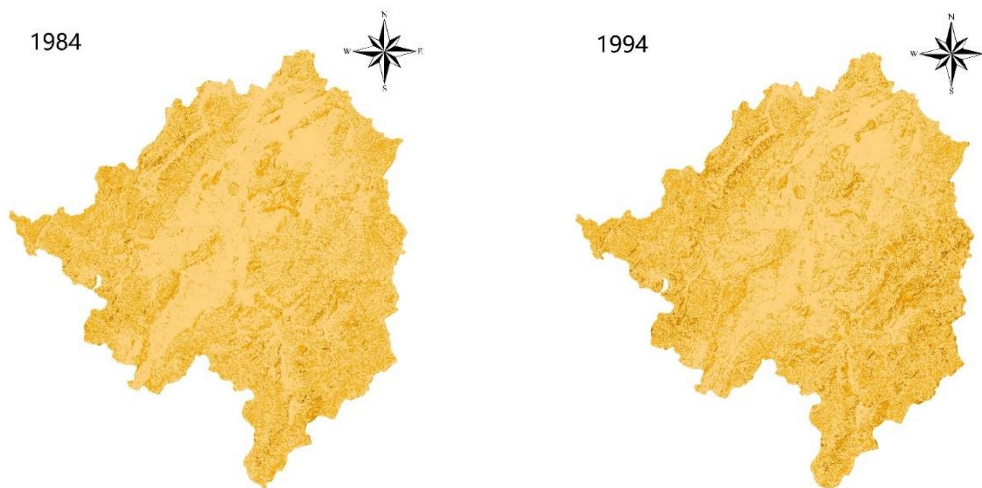


Figure 5. Soil erosion risk in 1984, 1994, 2004 and 2009 (with actual precipitation data)



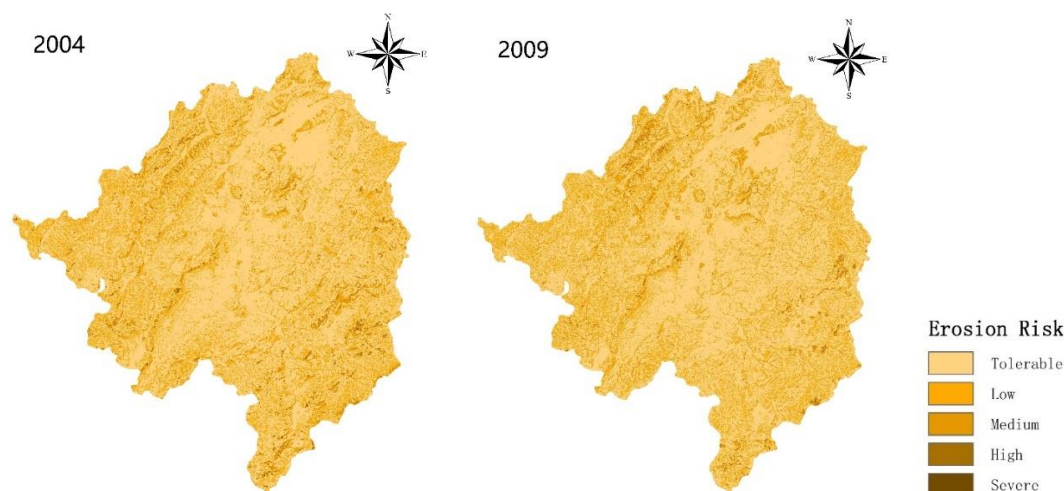


Figure 6. Soil erosion risk in 1984, 1994, 2004 and 2009 (with precipitation data of 2009)

As is shown in *Table 4*, area with tolerable and severe erosion risk was decreasing, while area with low erosion risk was increasing. And the change of the area with medium and high erosion risk shows no clear trend.

Table 4. Soil erosion risk level and the max value

Year	Tolerable	Low	Medium	High	Severe	Max value (ton hm ⁻² a ⁻¹)
1984	71.57%	25.20%	2.74%	0.41%	0.08%	777.69
1994	68.12%	25.02%	5.78%	0.90%	0.18%	819.74
2004	68.01%	25.61%	5.37%	0.88%	0.13%	620.59
2009	67.58%	26.09%	5.32%	0.92%	0.10%	603.07

Scenario analysis

The land use maps from 2009 to 2020 were simulated using CLUEs model, and 2020-year-landuse maps in 3 different scenarios were shown in *Figure 7*. Due to the government restriction on turning cropland and paddy land into urban and built-up land, and with a big proportion of forest in study area, the urban and built-up land was mainly transformed from forest in all these 3 scenarios. The plain in the middle of the county was mostly occupied by agriculture land. As a result, the urban and built-up land was hardly increased in the middle. As shown in *Figure 7*, during the simulation period from 2009-2020, the urban and built-up land increased around lakes at the southeast and the west of the county, as well as the small plain located at the northwest area.

Since the topography in locations of newly urbanization part is mainly hills with high-value LS factor, once the vegetation is removed, the erosion risk will increase largely. *Figure 8* shows the erosion risk under 3 different scenarios. Comparing the result of 3 scenarios, it is obvious that the erosion risk is mainly increased at the newly urbanized area, especially for the increase of the risk at high and severe level. *Table 5* shows the data which compares the ratios of the erosion risk levels in 2009 and different

scenarios. It is clearly that as the area of the urban and built-up land increase, the ratios of high and severe soil erosion risk levels increase, and area with medium erosion risk decreases. The trend appears slightly different with the data in period from 1984 to 2009.

Table 5. Percentages of soil erosion risk levels and the max erosion risk values

	Tolerable	Low	Medium	High	Severe	Max value (ton hm ⁻² a ⁻¹)
2009	67.58%	26.09%	5.32%	0.92%	0.10%	603.07
Scenario_1	67.92%	24.59%	6.20%	1.09%	0.20%	833.87
Scenario_2	66.99%	24.38%	7.09%	1.30%	0.24%	933.24
Scenario_3	62.80%	24.12%	10.69%	2.00%	0.38%	936.31

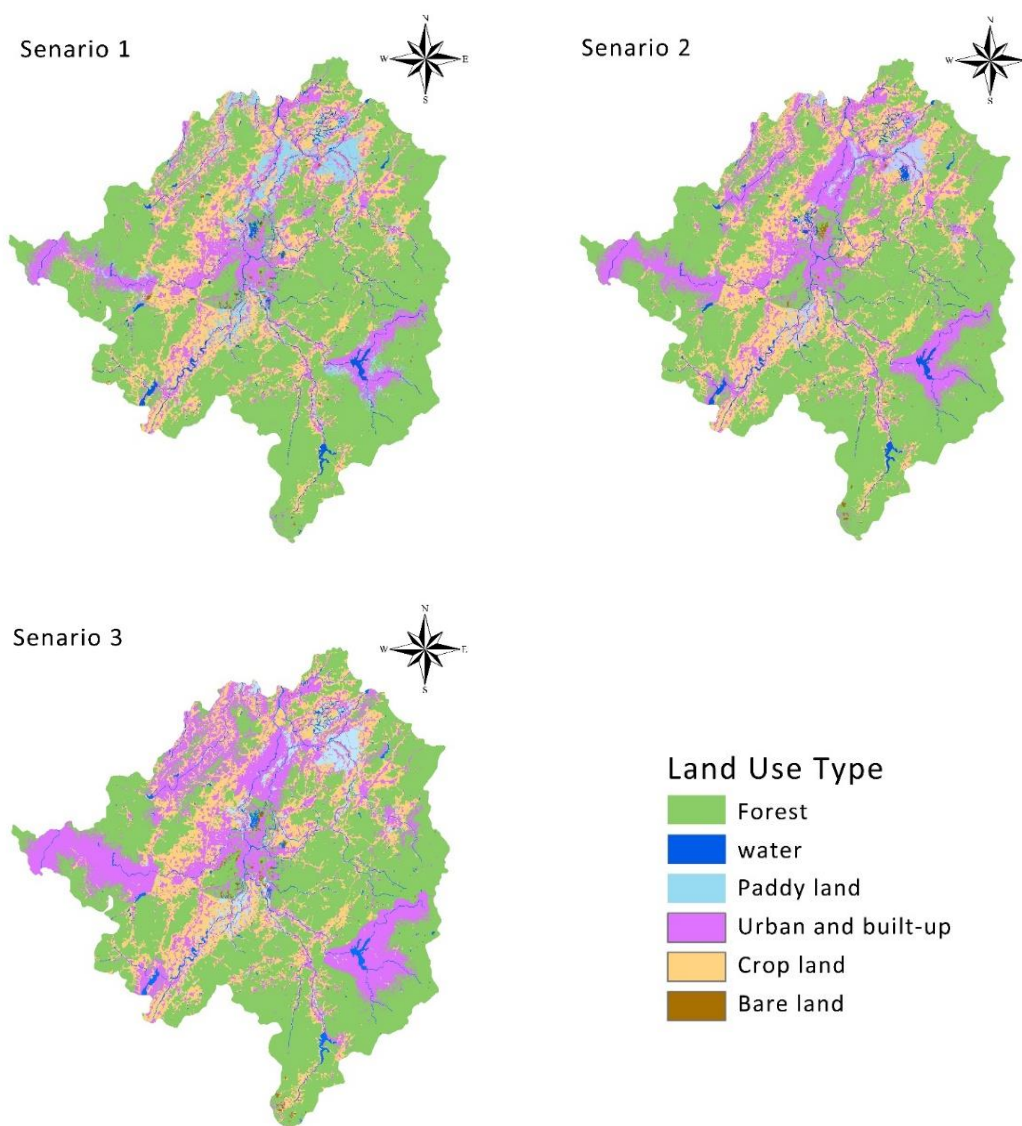


Figure 7. Land use type of 3 scenarios in 2020

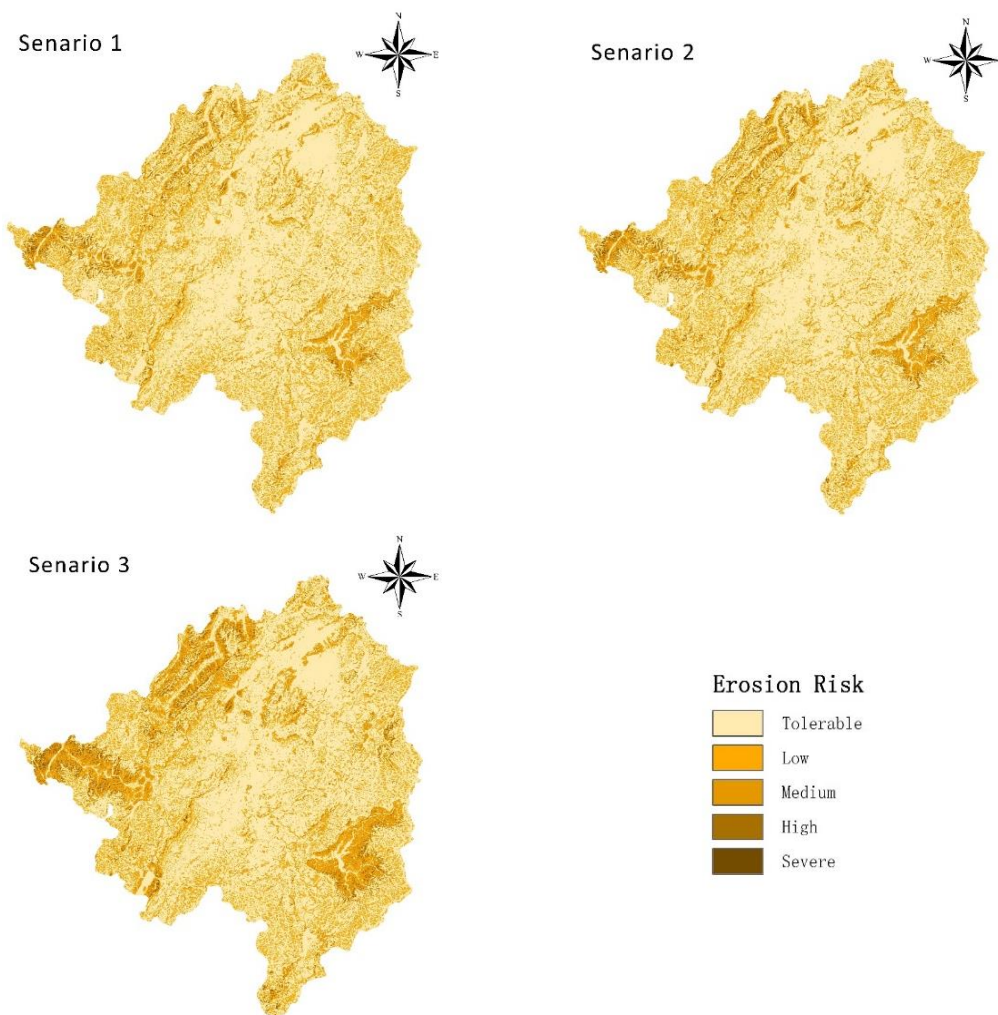


Figure 8. Soil erosion risk of 3 scenarios in 2020

Discussion

Relationship between erosion and built-up area

Wolman (1967) pointed out that during the construction period, the erosion amount would increase in situ, and reach to a higher value than that at the condition with natural vegetation cover. Biggs et al. (2010) studied the urban border from 1938 to 2002, and suggested that even a long period after urban and built-up, the area would be still with a high erosion rate. White and Greer (2006) had studied the relationship between urbanization and the hydrology in the watershed in California. The result showed that the runoff volume was increasing during urbanization, both for annual average and dry-season runoff volume, and the peak value was increasing as well. It indicates that the increase of impermeable surface area would affect the regional hydrological process. And the erosion would be affected by the change of the hydrology.

The process of the urbanization during 1984 to 2009 in Zhuji county is shown as *Figure 9*. Because the middle and north of the county are mainly plains, the urbanization in those areas was faster than the rest of the county. From 1984 to 2009, the total urban and built-up area was increasing from 0.43% (1984) to 10.95% (2009).

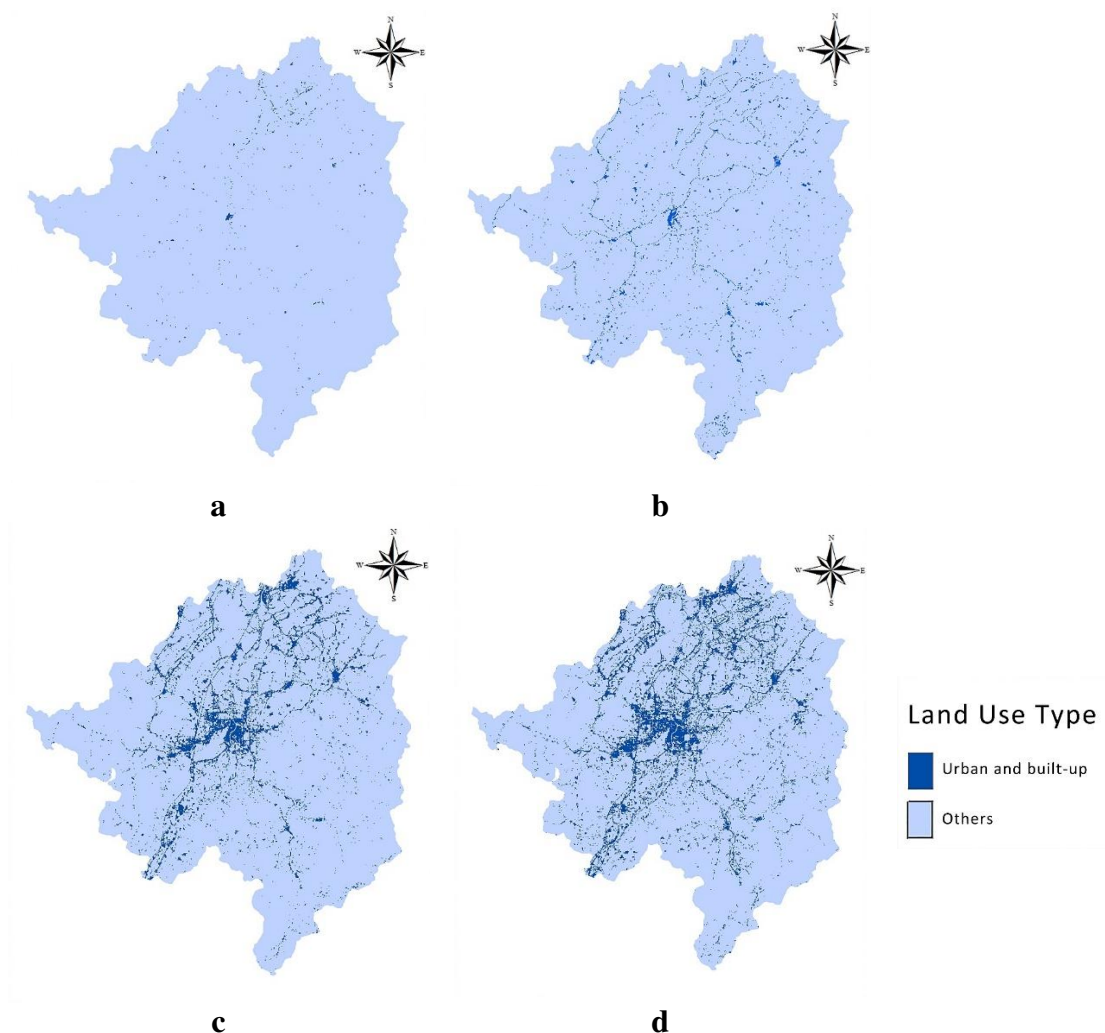


Figure 9. The process of urbanization from 1984 to 2009. **a** 1984, **b** 1994, **c** 2004, **d** 2009

As shown in *Figure 6*, during 1984 to 1994, the erosion risk increased in the southeast of the county since the percentage of cropland transformed by forest was increasing in this district. With further economic development, the ratio of agriculture in the GDP gradually decreased, leading to more cropland transformed back to forest in the Southeast. As a result, the erosion risk was decreasing in the southeast from 1994 to 2009. In 2009, the erosion risk in the southeast hilly area was obviously lower than that of 1994. In contrast, the erosion risk in the north and northwest was higher than that of 1984, driven by the drastic urbanization from 1984-2009 in these areas.

Table 4 shows that the area with tolerable erosion risk level was decreasing from 1984-2009, while the area of low erosion risk level was increasing. In stages perspective, from 1984 to 1994, the area with erosion risk level above medium was increasing sharply; from 1994 to 2009, the area with low erosion risk was increasing, while the area with tolerable erosion risk was decreasing.

Analyzed by the CP value, as the increasing of forest area and decreasing of agriculture area, the erosion risk should be decreasing in the whole area of Zhuji county. However, the data shows that the area with low erosion risk was increasing, though the maximum erosion risk value is decreasing. It indicated that the urbanize process mainly

invade forest area, and though the decreasing area of the agriculture land partly transformed to forest, the other part transformed to urban and built-up area, all of these lead to the rising of the erosion risk in the whole area. *Table 6* shows that the area with severe erosion risk level in urban and built-up area is increasing, while it in crop land is decreasing from 1994 to 2009.

The scenario analysis shows that, the ratios of areas with high and severe erosion levels are increasing with the ratio of the built-up area, as well as the extreme value of the erosion risk. However, the changing trends are different between scenario analysis from 2010 to 2020 and real data from 1984 to 2009. This is probably because of the different way of land use change. During the 1986 to 2009, the urban and built-up land was increased mainly on the plain in the middle of the county, transforming from agriculture land including crop land and paddy land. In the simulation period from 2010 to 2020, driven by the policy of prohibition in occupying the agriculture land, the urban and built-up land is mainly transformed from forest located in the hilly area in the west and the east parts of the county, which lead to the various value of the LS factor in the calculation.

Table 6. Land-use types with severe erosion risk level

Land use type	Areas of Land use type (hm ²)			
	1984	1994	2004	2009
Paddy land	1.8	0	0	0
Cropland	1346.4	4062.6	3586.5	1749.6
Urban and built-up	0	53.1	120.6	266.4
Bare land	486	53.1	227.7	206.1

Because the study area was located in the south-eastern part of China, the precipitation is plentiful for the growth of plant, which will decrease the soil erosion risk. The erosion risk is low in the area as a total. The trend from 1984 to 2009 is mainly showed in the decrease of the tolerable soil erosion risk level. Combining the data of the scenario analysis, the tolerable soil erosion risk area is decreasing during the urban area is increasing (*Fig. 10*).

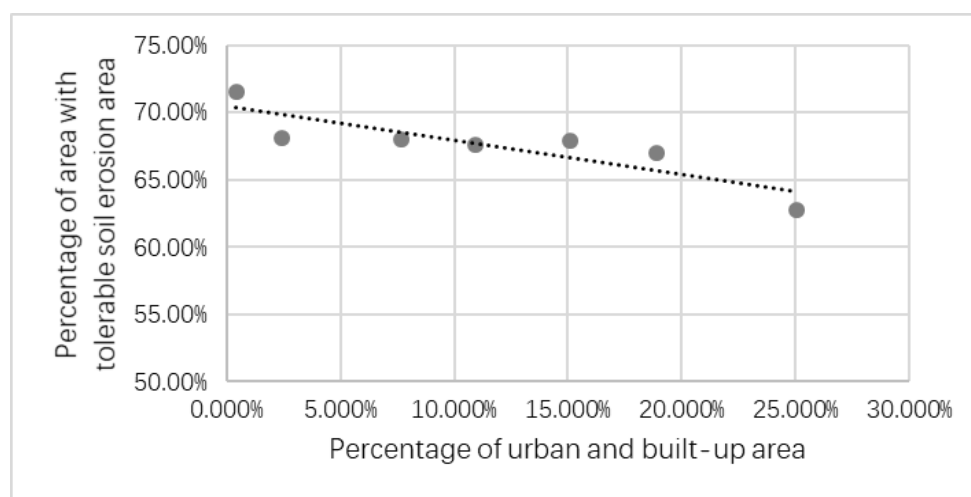


Figure 10. The relationship between tolerable soil erosion area and urban and built-up area

The effect of the highway

Roads are an indispensable part of urbanization. It also influences erosion seriously. Building road will influence the stability of the soil on side slope (Grace III, 1999). The construction sites with unpaved road surface as well as the cut areas are the sources of the erosion (Kalainesan et al., 2009). The spoil deposits of the road construction would also cause severe soil erosion (Dong et al., 2012). The increase of the impervious surface and runoff through the culvert of the highway will increase the erosion risk. Meanwhile, the urban and built-up area and human activities usually increase along the road, which will further increase the erosion risk.

As the *Figure 11* shows, the overall trends of erosion risk along the distance from the highway in tolerable, low and medium level were almost kept the same for 1999, 2004 and 2009. However, overall tolerable level % was highest in 1999, while the low and medium level increased in 2004 and 2009. The trends of high and severe erosion risk levels were different between before and after the highway construction, especially for the severe level. As *Figure 11e* shows, the severe level percentage in 2004 was much higher compared to that of 1999 before the road construction, and the percentage began to decrease when the distance from the highway reached 540 m. The curve of the high erosion risk level shows the similar trend and becomes stable when the distance meets 540 m.

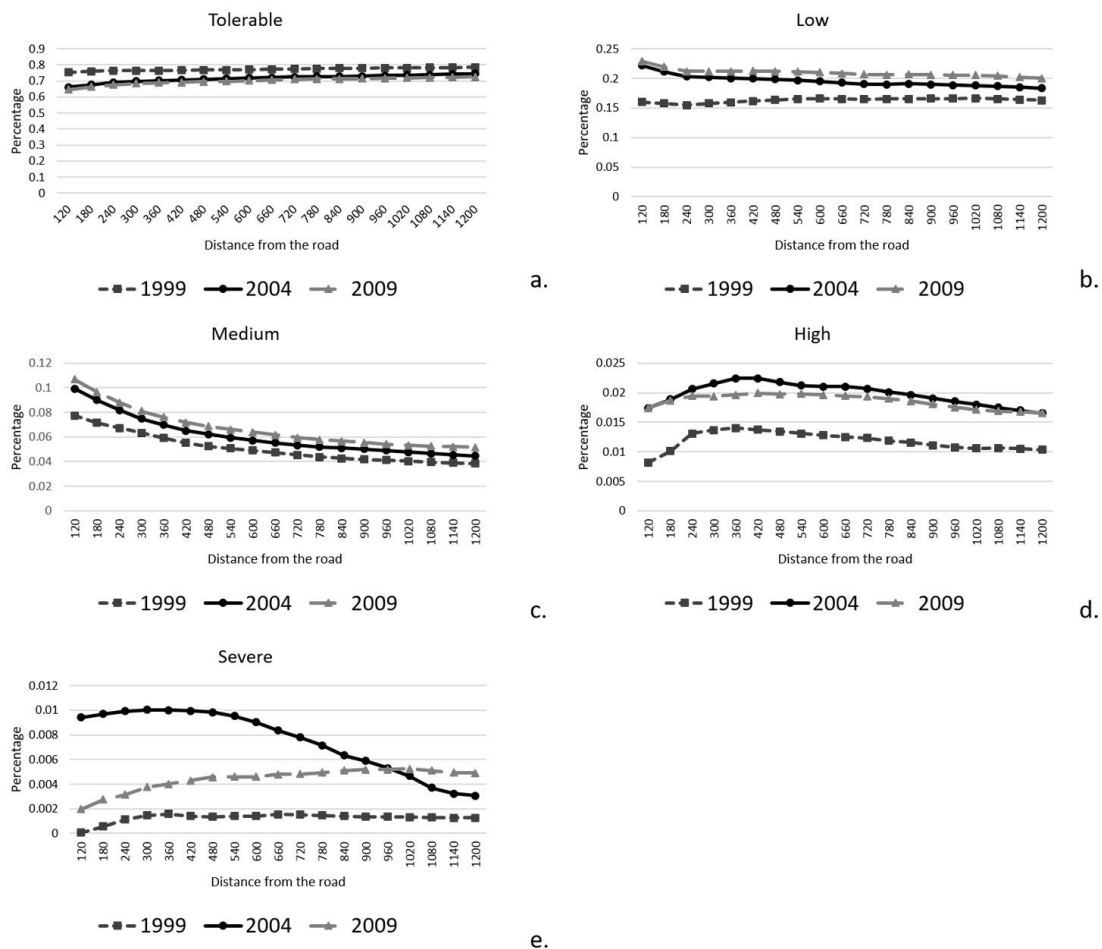


Figure 11. The erosion risk in different buffer zones of highway G60. **a** Tolerable level; **b** low level; **c** medium level; **d** high level; **e** severe level

Meanwhile, the construction of road would accelerate the economic development nearby and increase the urban and built-up area percentage, which could potentially further increase the erosion risk. As the data in 2009 shown, 5 years after the highway completed, erosion risk became more severe than that in 1999 as a whole. In detail, compare to 1999, the percentage of tolerable level decreased, but all the other levels increased, which means the road effect on soil erosion continued after the construction completed.

Figure 12 shows the percentage of the urban and built-up land in the buffer zones in 1999, 2003 and 2009. It indicates that the urban and built-up area increased after the highway was completed. After the highway constructed, the percentage of the urban and built-up area became stable when the distance from the road farther than 420 m.

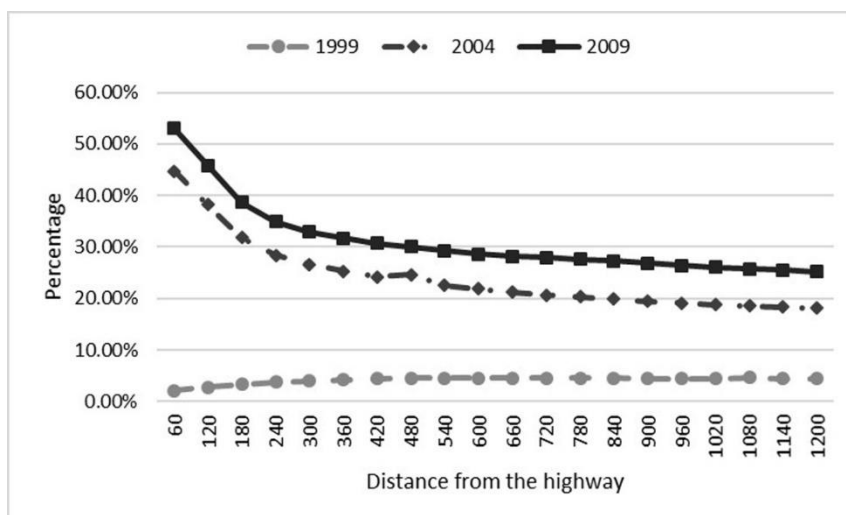


Figure 12. The percentage of the urban and built-up area in the buffer zones

Effect of hydrology change

Urbanization will also change the land use pattern in the catchment. The increased impervious surface and the drainage network will influence the hydrology in the peri urban area significantly (Rodriguez et al., 2013). And peak surface runoff values will increase with the urban and built-up area. Hammer (1972) found that the runoff value in the cross-sectional area in Piedmont Pennsylvania was 3.8 times larger than those in rural area. And naturally, the hydrology change affects the sediment yield and changes the erosion risk (Henshaw and Booth, 2000).

Simulating the hydrology change by urbanization is a key step to estimate the soil erosion risk. RUSLE was used in this research is because of its convenience in acquiring data as well as it has been already widely applied in the world. In this research, the process of the hydrology was mainly simulated by the algorithm of L factor combined with the change of land use types.

We also monitored the hydrological change at the main river (Puyang River) in the study area to examine the effect of the hydrological change on the erosion during the urbanization (from 2000 to 2010) (Fig. 13). Chart b in Figure 13 shows that before 2005 the maximum daily runoff was roughly in the same trend as the maximum daily rainfall. But after 2006, the pattern did not hold any more. Even maximum daily rainfall

was low, the maximum daily runoff still kept in a high level. And the relationship between annual runoff and erosion is also similar to daily data. Compared to the data in 2005, though the annual runoff decreased in 2006, the annual erosion increased.

According to the previous studies (Rodriguez et al., 2013; Hammer, 1972; Henshaw and Booth, 2000), as the urbanization proceeding, the surface runoff should be increasing, however, the data does not show this trend clearly. This maybe because of the location of the monitor station. The station is located in the centre of the county, which is the centre of the urbanization area, it cannot show the change of the runoff and erosion in whole watershed.

Because hydrological change caused by the change of impervious surface was not fully simulated here and the micro topography changed by constructions was kind of hided by the 30-m resolution, the effect of the urban and built-up area increasing was still not fully estimated. It should be studied in future research.

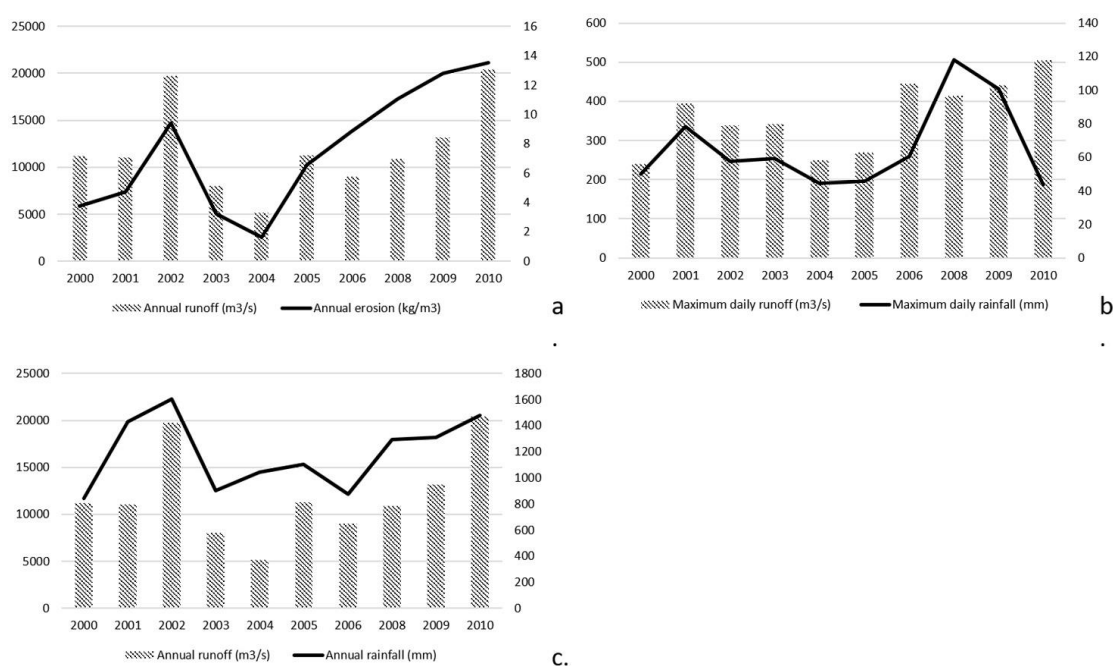


Figure 13. Rainfall and runoff. **a** annual runoff and annual erosion; **b** maximum daily runoff and maximum daily rainfall; **c** annual runoff and annual rainfall; **d** the percentage of the urban and built-up area

Conclusion

This research used the RS data to analyze the land use types from 1984 to 2009 of Zhuji County, estimate the erosion risk by RUSLE, and found the area with high and severe erosion risk was increasing (from 3.23% to 6.34%) and the area with tolerable soil erosion risk was decreasing (from 71.57% to 67.58%) while the built-up area was increasing from 0.43% to 10.95%.

Comparing the 3 scenarios in 2020 which simulated by CLUE model, we found that Scenario 1, because of the least urban and built-up area (15.33%), has the lowest erosion risk. Since the simulation considering the government policy to protect the agriculture land particularly, the urban and built-up area was mainly transformed from forest in hilly area during the simulation. Transforming forest into urban and built-up

area lead to a higher the erosion risk than urbanizing in plain area. And the analysis of the highway impact also showed that the soil erosion risk positively correlated with the urban and built-up area. The result indicates that controlling the urban area can help manage the erosion risk. Considering the erosion risk, if people have to expand the urban and built-up area, the plain would be a better choice than the hilly area. How to balance the erosion risk and the preservation of agriculture land needs to be further studied.

In this research, the effect of hydrology change was mainly simulated by the algorithm of L factor combined with the land use types (CP factor), which reflect the effect of the impervious surface area change. However, the micro topography changed by constructions was not considered here. It needs further research for more accurate estimation.

Acknowledgements. The remote sensing data set is provided by Geospatial Data Cloud site, Computer Network Information Center, Chinese Academy of Sciences. (<http://www.gscloud.cn>). Thanks to the local apartment of land and resources for the reference land use data and the erosion data. A special expression of gratitude goes to the different counterparts for their support such as nuclear agricultural science research institute, Zhejiang University and Shaoxing academy of agricultural sciences. Finally, we would like to thank the reviewers for their comments on this paper.

REFERENCES

- [1] Akhalkatsi, M., Otte, A., Togonidze, N., Bragvadze, T., Asanidze, Z., Arabuli, G., Chikhelidze, N., Mazanishvili, L. (2017): Agrobiodiversity and genetic erosion of crop varieties and plant resources in the Central Great Caucasus. – *Annals of Agrarian Science* 15(1): 11-16.
- [2] Arnold, C. L., Gibbons, C. J. (1996): Impervious surface coverage: the emergence of a key environmental indicator. – *Journal of the American Planning Association* 62(2): 243-258.
- [3] Barbera, E., Curro, C., Valenti, G. (2010): A hyperbolic model for the effects of urbanization on air pollution. – *Applied Mathematical Modelling* 34(8): 2192-2202.
- [4] Basile, P. A., Riccardi, G. A., Zimmermann, E. D., Stenta, H. R. (2010): Simulation of erosion-deposition processes at basin scale by a physically-based mathematical model. – *International Journal of Sediment Research* 25(2): 91-109.
- [5] Batisani, N., Yarnal, B. (2009): Urban expansion in Centre County, Pennsylvania: spatial dynamics and landscape transformations. – *Applied Geography* 29(2): 235-249.
- [6] Beskow, S., Mello, C. R., Norton, L. D., Curi, N., Viola, M. R., Avanzi, J. C. (2009): Soil erosion prediction in the Grande River Basin, Brazil using distributed modeling. – *Catena* 79(1): 49-59.
- [7] Biggs, T. W., Atkinson, E., Powell, R., Ojeda-Revah, L. (2010): Land cover following rapid urbanization on the US–Mexico border: implications for conceptual models of urban watershed processes. – *Landscape and Urban Planning* 96(2): 78-87.
- [8] Boix-Fayos, C., de Vente, J., Albaladejo, J., Martínez-Mena, M. (2009): Soil carbon erosion and stock as affected by land use changes at the catchment scale in Mediterranean ecosystems. – *Agriculture, Ecosystems & Environment* 133(1-2): 75-85.
- [9] Boongaling, C. G. K., Faustino-Eslava, D. V., Lansigan, F. P. (2018): Modeling land use change impacts on hydrology and the use of landscape metrics as tools for watershed management: The case of an ungauged catchment in the Philippines. – *Land Use Policy* 72: 116-128.

- [10] Chen, H., Oguchi, T., Wu, P. (2017): Assessment for soil loss by using a scheme of alternative sub-models based on the RUSLE in a Karst Basin of Southwest China. – *Journal of Integrative Agriculture* 16(2): 377-388.
- [11] Chen, J. (2007): Rapid urbanization in China: A real challenge to soil protection and food security. – *Catena* 69(1): 1-15.
- [12] De Oña, J., Osorio, F., Garcia, P. A. (2009): Assessing the effects of using compost-sludge mixtures to reduce erosion in road embankments. – *Journal of Hazardous Materials* 164(2-3): 1257-1265.
- [13] Deckers, J., Driessen, P., Nachtergaele, F., Spaargaren, O. (2006): World Reference Base for Soil Resources. – In: Lal, R. (ed.) *Encyclopedia of Soil Science*. 2nd Ed. CRC Press, Boca Raton, FL, pp. 1918-1923.
- [14] Desmet, P., Govers, G. (1996): A GIS procedure for automatically calculating the USLE LS factor on topographically complex landscape units. – *Journal of Soil and Water Conservation* 51(5): 427-433.
- [15] Dong, J., Zhang, K., Guo, Z. (2012): Runoff and soil erosion from highway construction spoil deposits: A rainfall simulation study. – *Transportation Research Part D: Transport and Environment* 17(1): 8-14.
- [16] García-Ruiz, J. M. (2010): The effects of land uses on soil erosion in Spain: A review. – *Catena* 81(1): 1-11.
- [17] Grace III, J. M. (1999): Erosion control techniques on forest road cutslopes and fillslopes in North Alabama. – *Transportation Research Record: Journal of the Transportation Research Board* 1652(1): 227-234.
- [18] Guo, X., Wang, Z., Ru-liang, Z. (2001): Study on temporal distribution of rainfall erosivity and daily rainfall erosivity model in red soil area of Zhejiang (in Chinese). – *Journal of Soil and Water Conservation* 15(3): 35-37.
- [19] Hammer, T. R. (1972): Stream channel enlargement due to urbanization. – *Water Resources Research* 8(6): 1530-1540.
- [20] Henshaw, P. C., Booth, D. B. (2000): Natural restabilization of stream channels in urban watersheds. – *JAWRA Journal of the American Water Resources Association* 36(6): 1219-1236.
- [21] Kalainesan, S., Neufeld, R. D., Quimpo, R., Yodnane, P. (2009): Sedimentation basin performance at highway construction sites. – *Journal of Environmental Management* 90(2): 838-849.
- [22] Kayacan, E., Ulutas, B., Kaynak, O. (2010): Grey system theory-based models in time series prediction. – *Expert Systems with Applications* 37(2): 1784-1789.
- [23] Lewis, L. A., Verstraeten, G., Zhu, H. (2005): RUSLE applied in a GIS framework: Calculating the LS factor and deriving homogeneous patches for estimating soil loss. – *International Journal of Geographical Information Science* 19(7): 809-829.
- [24] Liu, B., Nearing, M., Risse, L. (1994): Slope gradient effects on soil loss for steep slopes. – *Transactions of the ASAE* 37(6): 1835-1840.
- [25] McCool, D., Brown, L., Foster, G., Mutchler, C., Meyer, L. (1987): Revised slope steepness factor for the Universal Soil Loss Equation. – *Transactions of the ASAE* 30(5): 1387-1396.
- [26] Napoli, M., Cecchi, S., Orlandini, S., Mugnai, G., Zanchi, C. A. (2016): Simulation of field-measured soil loss in Mediterranean hilly areas (Chianti, Italy) with RUSLE. – *Catena* 145(246-256).
- [27] Op de Hipt, F., Diekkrüger, B., Steup, G., Yira, Y., Hoffmann, T., Rode, M. (2018): Modeling the impact of climate change on water resources and soil erosion in a tropical catchment in Burkina Faso, West Africa. – *Catena* 163(63-77).
- [28] OSD OSSD (1998): *Keys to Soil Taxonomy*.
- [29] Ostovari, Y., Ghorbani-Dashtaki, S., Bahrami, H. A., Naderi, M., Dematte, J. A. M. (2017): Soil loss estimation using RUSLE model, GIS and remote sensing techniques: a

- case study from the Dembecha Watershed, Northwestern Ethiopia. – *Geoderma Regional* 11: 28-36.
- [30] Ouyang, W., Hao, F., Skidmore, A. K., Toxopeus, A. G. (2010): Soil erosion and sediment yield and their relationships with vegetation cover in upper stream of the Yellow River. – *Science of The Total Environment* 409(2): 396-403.
- [31] Park, S., Oh, C., Jeon, S., Jung, H., Choi, C. (2011): Soil erosion risk in Korean watersheds, assessed using the revised universal soil loss equation. – *Journal of Hydrology* 399(3-4): 263-273.
- [32] Podmanicky, L., Balázs, K., Belényesi, M., Centeri, C., Kristóf, D., Kohlheb, N. (2011): Modelling soil quality changes in Europe. An impact assessment of land use change on soil quality in Europe. – *Ecological Indicators* 11(1): 4-15.
- [33] Qin, W., Guo, Q., Cao, W., Yin, Z., Yan, Q., Shan, Z., Zheng, F. (2018): A new RUSLE slope length factor and its application to soil erosion assessment in a Loess Plateau watershed. – *Soil and Tillage Research* 182(10-24).
- [34] Renard, K. G., Foster, G. R., Weesies, G. A., Porter, J. P. (1991): RUSLE: Revised universal soil loss equation. – *Journal of Soil and Water Conservation* 46(1): 30-33.
- [35] Renard, K. G., Foster, G. R., Weesies, G. A., McCool, D., Yoder, D. (1997): Predicting Soil Erosion by Water: A Guide to Conservation Planning with the Revised Universal Soil Loss Equation (RUSLE). *Agriculture Handbook* 703. – USDA, Washington.
- [36] Rodriguez, F., Bocher, E., Chancibault, K. (2013): Terrain representation impact on periurban catchment morphological properties. – *Journal of Hydrology* 485(0): 54-67.
- [37] Sharpley, A. N., Williams, J. R. (1990): EPIC-erosion/productivity impact calculator: 1. Model documentation. – *Technical Bulletin-United States Department of Agriculture* 1768 Pt 1.
- [38] Stastical Bureal of Zhuji City (2017): *Statistical Bulletin of National Economic and Social Development of Zhuji City*. – National Bureau of Statistics of China, Beijing.
- [39] Thomas, J., Joseph, S., Thirvikramji, K. P. (2018): Estimation of soil erosion in a rain shadow river basin in the southern Western Ghats, India using RUSLE and transport limited sediment delivery function. – *International Soil and Water Conservation Research* 6(2): 111-122.
- [40] Trenouth, W. R., Gharabaghi, B. (2015): Event-based design tool for construction site erosion and sediment controls. – *Journal of Hydrology* 528(790-795).
- [41] United Nations (2018): *World Urbanization Prospects, the 2017 Revision*. – Population Division D O E A S A, United Nations, New York.
- [42] Van Remortel, R. D., Hamilton, M. E., Hickey, R. J. (2001): Estimating the LS factor for RUSLE through iterative slope length processing of digital elevation data within ArcInfo grid. – *Cartography* 30(1): 27-35.
- [43] Verburg, P. H., Soepboer, W., Veldkamp, A., Limpiada, R., Espaldon, V., Mastura, S. S. (2002): Modeling the spatial dynamics of regional land use: the CLUE-S model. – *Environmental Management* 30(3): 391-405.
- [44] White, M. D., Greer, K. A. (2006): The effects of watershed urbanization on the stream hydrology and riparian vegetation of Los Peñasquitos Creek, California. – *Landscape and Urban Planning* 74(2): 125-138.
- [45] Wolman, M. G. (1967): A cycle of sedimentation and erosion in urban river channels. – *Geografiska Annaler Series A Physical Geography* 49(2): 385-395.
- [46] Yang, D., Kanae, S., Oki, T., Koike, T., Musiake, K. (2003): Global potential soil erosion with reference to land use and climate changes. – *Hydrological Processes* 17(14): 2913-2928.
- [47] Zhang, L., Nan, Z., Yu, W., Zhao, Y., Xu, Y. (2018): Comparison of baseline period choices for separating climate and land use/land cover change impacts on watershed hydrology using distributed hydrological models. – *Science of the Total Environment* 622-623: 1016-1028.

SPIDER COMMUNITIES AFFECTED BY EXCLUSION NETS

PAJAČ ŽIVKOVIĆ, I.¹ – LEMIC, D.^{1*} – SAMU, F.² – KOS, T.³ – BARIĆ, B.¹

¹*Department of Agricultural Zoology, Faculty of Agriculture, University of Zagreb
Svetošimunska 25, 10000 Zagreb, Croatia*

²*Plant Protection Institute, Centre for Agricultural Research, Hungarian Academy of Science
H-1525 Budapest, Hungary*

³*Department of Ecology, Agronomy and Aquaculture, University of Zadar, Zadar, Croatia*

**Corresponding author*

e-mail: dlemic@agr.hr; phone: +385-1-239-3649

(Received 30th Sep 2018; accepted 22nd Nov 2018)

Abstract. Spiders are one of the most abundant natural enemies in apple orchards and have an important role in the biological control of harmful arthropods. Recently, coloured shade nets were introduced into management practices to improve the utilization of solar radiation by fruit trees and to exclude pest species. While the coloured netting in apple orchards had a positive effect on fruits, the secondary aim of our research was to analyse the influence the nets had on spider diversity and species composition. In this study we sampled the ground dwelling spider assemblage by pitfall trapping and identified spiders to species. Traps were placed under trees covered by four types of exclusion photo selective nets and uncovered (control) trees in an untreated experimental plot of an apple orchard. In total 456 individuals belonging to 13 families and 26 species of spiders were collected. Two wolf spider (*Araneae*, *Lycosidae*) species dominated the assemblages; *Trochosa robusta* (Simon, 1876) and *Hogna radiata* (Latreille, 1819) comprised 45% of the total adult catch. Spider abundance showed a declining trend over season in all treatments. Most importantly, there was no difference either between the abundance, species richness or the species composition of spiders in the treatments. The study strongly indicates that insect exclusion nets have no negative effect on ground dwelling spider assemblages.

Keywords: *Araneae, shade nets, apple orchard, Trochosa robusta, Hogna radiata*

Introduction

For sustainable agricultural systems, self-regulation of insect pests by predatory arthropods is considered to be crucial in preventing insect pest outbreaks (Kromp, 1999). Spiders, as one of the most abundant natural enemies in apple orchards, have an important role in the natural control of harmful arthropods in pome production (Pekár and Kocourek, 2004). However, the intensity of the management practices can seriously limit the positive effect of spiders and other beneficial organisms on pests that they control. Intensively managed agricultural areas are treated on a regular basis by different agrochemicals, but even a small number of synthetic, broad- spectrum insecticide applications can severely reduce spider abundance and diversity in apple orchards and the time required for recovery may be lengthy (Miliczky et al., 2000). While in low-intensity apple production (e.g. self-sustainable ecological systems) spiders play a key role in the regulation of lepidopteran pests (Nyffeler and Benz, 1987), in intensive apple production spiders can regulate only some secondary pest populations below economically damaging levels, but usually cannot efficiently regulate the primary, key pest populations (e.g. codling moth (*Cydia pomonella* L.)) (Cross et al., 2015).

Integrated apple production is based on the application of environmentally and toxicologically acceptable treatments with an emphasis on the use of ecologically

favourable control methods. The preservation of natural enemies of secondary pests is a crucial part of successful integrated pest management (IPM) and all affective control methods should only be minimally harmful or completely harmless to these important natural enemies (Cross et al., 2015). By reducing the insecticide applications diversity and species composition of ground dwelling arthropods can be improved (Cole et al., 2005). Like some other beneficial insects (e.g. ground beetles), spiders serve as bio-indicators of the stability of sustainable agro-ecosystems (Dennis et al., 1997, 1998 cit. Cole et al., 2005). The diversity and species composition of European epigeic spider fauna was intensively studied in IPM apple production orchards and up to 37 species were found (Bogya and Markó, 1999; Bogya et al., 1999; Pekár, 1999).

Management intensity at other scales also influences natural enemy populations. Batáry et al. (2012) studied the effects of landscape scale management intensity and agroecosystem type on the biodiversity of spiders and other arthropods. They found that management intensity affected several functional groups positively, including hunting spiders, and lower landscape scale management intensity also increased species richness spiders. The diversity of spiders is also affected by habitat heterogeneity. It is known that in areas of ecological infrastructure (e.g. flowering field margins and border strips, hedges, ditches and stone walls) a positive effect on the arthropod complex is found (Franin, 2016) as they enhance the diversity of the fauna in IPM systems (Boller et al., 2004). A study by Bousekou and Kherbouche-Abrus (2017) demonstrated that there are diverse and stable spider communities at the edges of wheat crops that could be related to the diversified flora offering different microhabitats and ecological niches to cater to the varied habitat requirement of multiple spider species (Bousekou and Kherbouche-Abrus, 2017).

Smaller scale alternative management practices can also greatly improve the efficiency of biological control. In recent times a new approach used involves the use of coloured shade nets (ColorNets) that improve the utilization of solar radiation by fruit trees (Shahak et al., 2004). The coloured netting in apple orchard has a positive effects on flowering, fruit-set, fruit size, colour and internal quality, in addition to non-specific reduction of water stress, superficial damage and sunburn (Shahak et al., 2004). Such systems usually also include anti-hail nets and these can inadvertently act as insect exclusion netting systems too. The beneficial effects of netting structures against Lepidoptera species (e.g. codling moth) has been proven in several studies (Tasin et al., 2008; Sauphanor et al., 2012; Pajač et al., 2016). Dedicated exclusion nets are designed to control a single pest species, although other pests might also be controlled, depending on the mesh size used (Chouinard et al., 2017). Since the netting structures form a physical barrier to the entry of insect pests, it potentially also serves as a barrier to beneficial insects and allied forms such as spiders that inhabit agroecosystems (Pajač et al., 2016). The main objective of the present research is to analyse the possible effects of the exclusion nets on spider diversity and species composition in an IPM apple orchard.

Materials and methods

Study area

The study was conducted during the vegetation period of 2015 in an apple orchard, situated in the northwest part of Croatia (46°9'47"N, 15°52'52"E). This area is characterized by a continental-humid climate of warm, rainy summers and cold winters (Penzar and Penzar, 2000). The elevation is 282 m, the average annual precipitation is

850 mm and the average annual temperature is 11 °C (HMD, 2017). The soil in the research area is typical pseudogley (IUSS Working Group WRB, 2015). In the plantation of 3600 m² apple cultivars of 'Braeburn', 'Idared', 'Golden Delicious', 'Granny Smith' and 'Jonagold' were grown following standard IPM practices. IPM in practice, involves using several control measures based on knowledge of the crop, pests and associated natural enemies to avoid crop loss and minimize harmful effects on the environment. In this apple orchard IPM involves: identifying pests; identifying the natural enemies of pests' monitoring both and tolerating higher levels of pests; using a treatment threshold to decide when control is needed; managing weeds by mulching treatments between rows several times in the season; and follow-up to see how well control measures work and if further action is needed. Experiments took place in the central part of the orchard planted with cv. 'Braeburn'. During the research period, insecticide treatments were not applied to the experimental site. The orchard was surrounded by agricultural fields (arable lands and grasslands).

Experimental design

Four types of exclusion photo selective nets (Agritenax nets and Stop Drosophila Normal net) were placed randomly in three replicates in the experimental area of the orchard (*Fig. 1*). The size of a single net was 6 × 6 m. Three rows of trees served as spatial replicates of the treatment. In each row there were four randomly selected neighbouring apple trees completely covered with nets and an uncovered control. Pitfall traps were placed beneath each experimental tree (distance between trees were 10 m), in the case of netted trees, inside the enclosed area. Agritenax nets (Tenax S.r.l., Italy) were used with a set mesh size of 2.4 × 4.8 mm but in different colours (white, red and yellow). Stop Drosophila Normal net (Artes Politecnica, Italy) had a pearl colour and a 0.9 × 1 mm mesh size. While exclusion nets are designed to control a pest species, no pest should be under the nets at the beginning of investigation period. So, before setting up nets in May 2015, existing arthropod fauna on apple trees was eliminated by applying neonicotinoid insecticide thiacloprid (Calypso® 480 SC, Bayer CropScience). Exclusion nets were set up at petal fall and were removed after the harvest of apple fruits as is standard practice.

Spider sampling

Spiders were collected during the summer and autumn (from July 1st until October 15th, 2015). Pitfalls were polythene pots (Ø = 10 cm wide and h = 20 cm) half filled with salted water (20% solution) for preservation. Fifteen pitfall traps (twelve under covered and three under uncovered trees) were set in the IPM orchard. Traps were inspected on a weekly basis (from week 28 to week 42) and spiders were transferred to 70% ethanol pending identification to species.

Data analysis

A preliminary analysis of adult abundance and species richness data included inspection of data distribution and variation by replicate and date. Overall catches were very similar in all three replicates, but spider abundance showed a marked seasonal decline in all treatments over the sampling dates. Since spider catches were relatively low per pitfall per sampling date, the final data analysis of abundance and richness was carried out on data pooled across replicates but analysed by date. Abundance data were

log transformed and then analysed using a linear model that included treatment as fixed factor and sampling date as continuous covariate. The same model structure was applied for species richness in a generalized linear model with Poisson distribution and log link function. To understand whether species composition was affected by the treatments we applied detrended correspondence analysis (DCA). For this ordination analysis data was pooled across sampling dates but was kept separate by replicate.

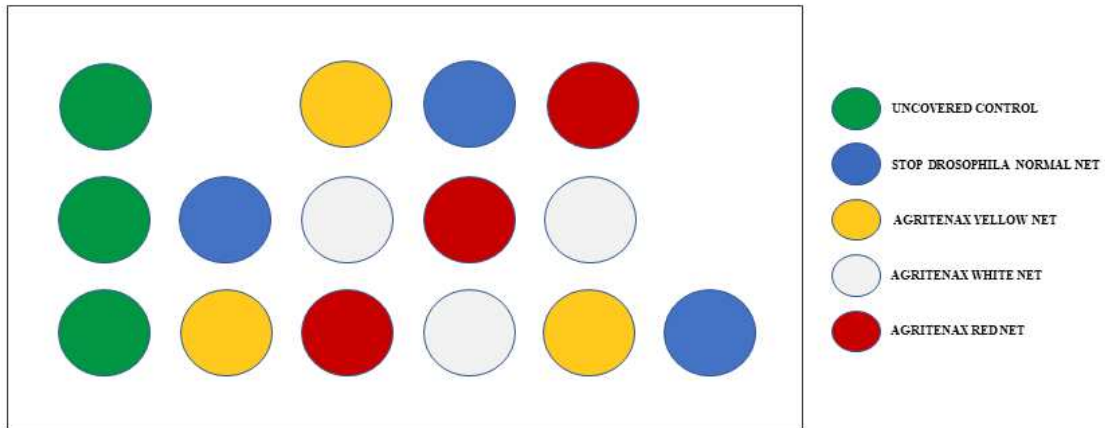


Figure 1. Schematic representation of experimental design

Results and discussion

Approximatley 456 individuals belonging to 26 species and 13 families of spiders were collected (*Table 1*). Spider abundance showed a natural declining trend over season (*Fig. 2*) (effect of date: $F = 43.83$, d.f. = 1, 65, $P < 0.0001$); however, the rate of decline was not significantly different across treatments (effect of date x treatment: $F = 1.01$, d.f. = 4, 65, $P = 0.41$).

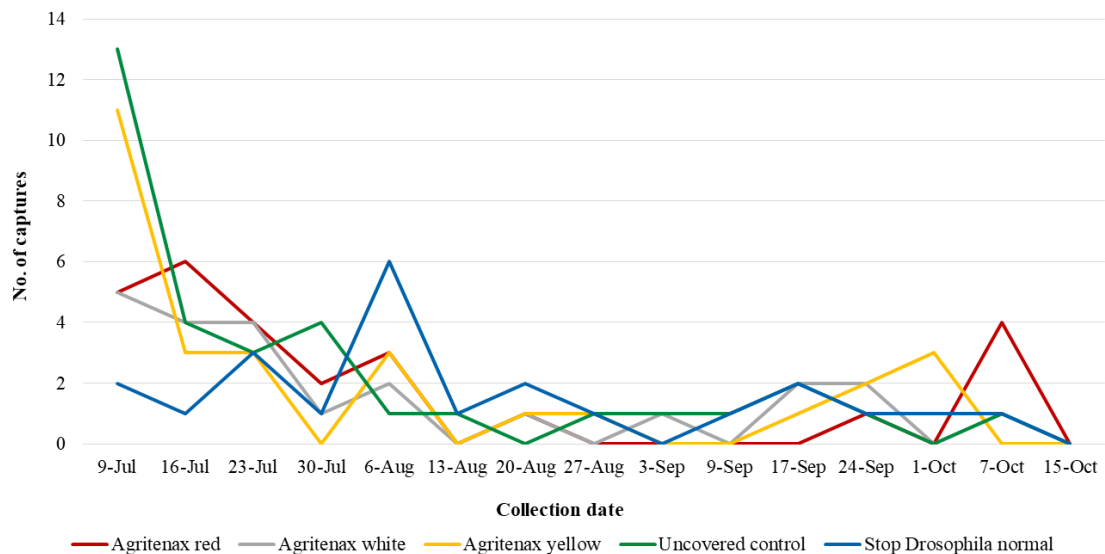


Figure 2. Seasonal distribution of spider species during 2015 in IPM apple orchard under different exclusion nets and on uncovered control

Table 1. The list of spider species and captures in IPM apple orchard

Family	Species	A.w.*	A.r.	S.D.n.	A.y.	U.c.
Agelenidae	<i>Agelena labyrinthica</i> (Clerck, 1757)				1	
	<i>Allagelena gracilens</i> (Koch, 1841)			1		
Dysderidae	<i>Dysdera erythrina</i> (Walckenaer, 1802)		2	1	1	2
Gnaphosidae	<i>Drassodes lapidosus</i> (Walckenaer, 1802)	1				
	<i>Drassyllus pumilus</i> (Koch, 1839)				1	1
	<i>Zelotes aurantiacus</i> (Miller, 1967)		1	1		
	<i>Zelotes longipes</i> (Koch, 1866)	3		2	2	4
Hahniidae	<i>Cryphoeca silvicola</i> (Koch, 1834)	2	1		1	2
Linyphiidae	<i>Centromerus sylvaticus</i> (Blackwall, 1841)			1		
	<i>Diplostyla concolor</i> (Wider, 1834)		1	2		
	<i>Stemonyphantes lineatus</i> (Linnaeus, 1758)			1		
	<i>Tenuiphantes flavipes</i> (Blackwall, 1854)	1				
Liocranidae	<i>Liocranoeca striata</i> (Kulczynski, 1882)	2			1	1
Lycosidae	<i>Alopecosa pulverulenta</i> (Clerck, 1757)		1			1
	<i>Hogna radiata</i> (Latreille, 1819)	2	10	3	3	11
	<i>Pardosa agrestis</i> (Westring, 1861)		1		1	1
	<i>Pardosa hortensis</i> (Thorell, 1872)		2		1	
	<i>Pardosa palustris</i> (Linnaeus, 1758)					2
	<i>Trochosa robusta</i> (Simon, 1876)	6	5	8	6	5
	<i>Xerolycosa miniata</i> (Koch, 1834)				1	
Philodromidae	<i>Philodromus cespitum</i> (Walckenaer, 1802)					1
Phrurolithidae	<i>Phrurolithus festivus</i> (Koch, 1835)	1		1		1
Tetragnathidae	<i>Pachygnatha degeeri</i> (Sundevall, 1830)	3		1	5	
Theridiidae	<i>Enoplognatha thoracica</i> (Hahn, 1833)		1		1	
Thomisidae	<i>Zodarion rubidum</i> (Simon, 1914)	1			3	
Zodariidae	<i>Zodarion rubidum</i> (Simon, 1914)		1	1		

*Net type: A.w. - Agritenax white; A.r. - Agritenax red; S.D.N. - Stop Drosophila normal; A.y. - Agritenax yellow; U.c. - Uncovered control

There was no difference between the abundance of spiders between treatments (effect of treatment: $F = 1.23$, d.f. = 4, 65, $P = 0.31$; Fig. 3a) which indicates that netting structures did not have a negative effect on spider communities. A contrast analysis that compared all net treatments with the control (contrast effect: $F = 3.08$, d.f. = 1, 65, $P = 0.084$) showed that there was a tendency for net treatments to harbour more spiders than the un-netted control. Since the exclusion nets can change environmental variables (e.g. temperature, humidity, light and etc.) (Brkljača et al., 2016; Fruk et al., 2016) it is evident that these changes also positively affected spider fauna and could possible improve the habitat requirements for spiders.

When considering species richness, two wolf spider (Araneae, Lycosidae) species *Trochosa robusta* (Simon, 1876) and *Hogna radiata* (Latreille, 1819) comprised 45% of the total adult catch, and these were the only two species that were found in all treatments. With the exception of the red net treatment, all other treatments included 2-3 unique species, mostly unique species that were recorded from one treatment only

(Table 1). Despite of variation in the low frequency species, the number of species recorded in the treatments fell within the narrow range of 10-14 species. The Poisson model indicated that there was no effect of the applied nets on species richness (effect of treatment: $\chi^2 = 0.18$; d.f. = 1; $P = 0.99$; Fig. 3b).

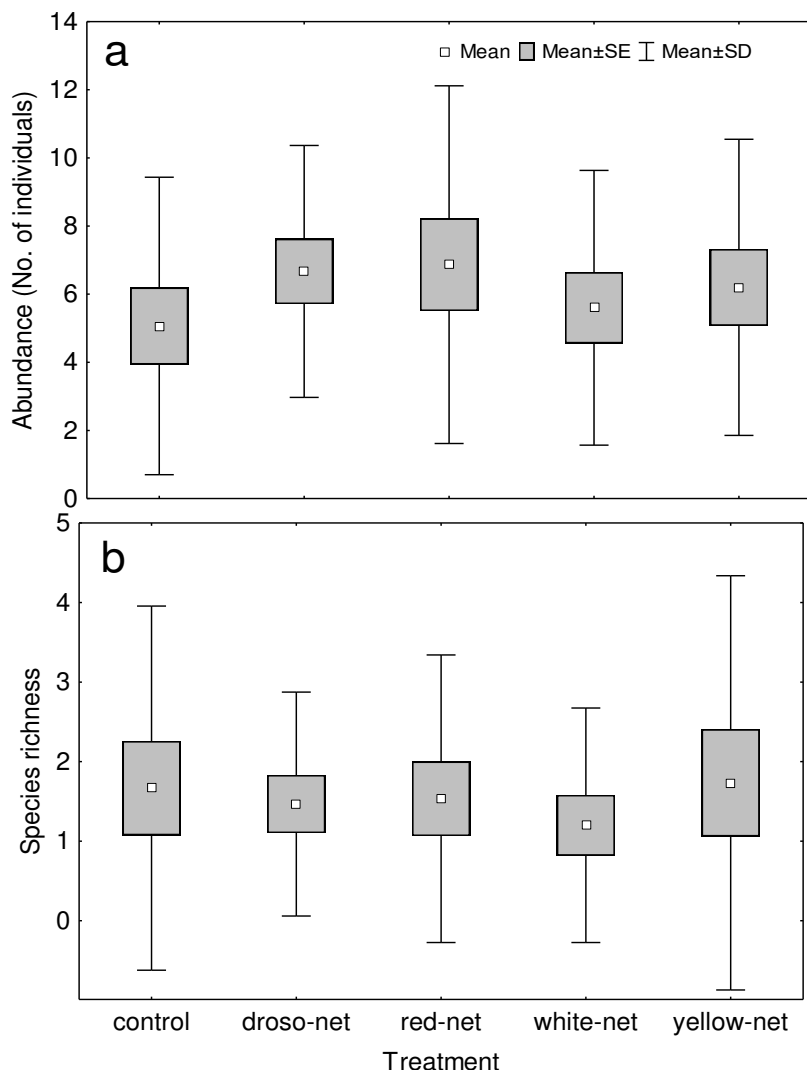


Figure 3. Abundance (a) and species richness (b) of spiders per treatment (number of individuals and species caught, respectively)

Ordination analysis was used to visualise how net treatments influenced spider species composition and assemblages. The first two axes of the applied DCA only cumulatively explained 27% of the total variation in the data (Eigenvalues of axes 1 and 2, respectively: 0.46, 0.33). The ordination plot indicated that there was no separation either by treatment or by the three planting rows (replicates), in which the replicates were placed (Fig. 4).

The composition and diversity of the species recorded corresponded with similar investigations of the spider fauna in apple orchards (Bogya and Markó, 1999), as the assemblage was dominated by species from the Lycosidae and Gnaphosidae families. These predominantly ground dwelling species can have an important synergistic effect

on canopy dwelling natural enemies, as they may prey on dislodged and migrating pests (Dainese et al., 2017). By implementing netting structures as a relatively new mechanical and environmentally friendly method into agricultural management practices we can improve the microclimate conditions for the development of spiders (e.g. important pest species predators) that can help us in regulating the populations of harmful insects in fruit production. This work was the first of its kind in Croatia investigating spider diversity in an agroecological system will serve us as important baseline information for further future research.

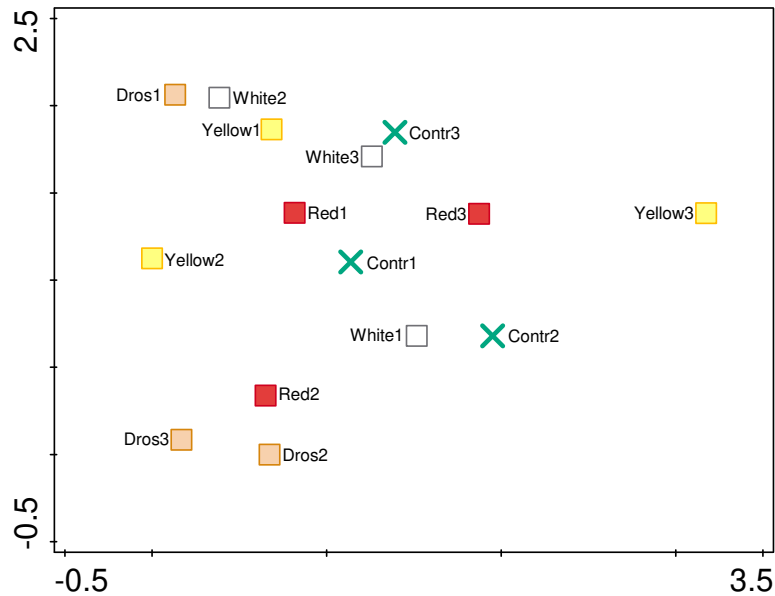


Figure 4. DCA ordination plot of spider assemblages in individual netted and control trees over the whole sampling period

The study showed that insect exclusion nets had no negative effect on beneficial spider assemblages and there was even a tendency for nets to promote their abundance, indicating that netting systems favour spider species that inhabit orchards. Considering that this alternative, environmentally friendly management approach excludes pest species and at the same time has no negative effect on the natural enemy complex, the present study provides data to support the ongoing use of pest exclusion netting in apple orchard production systems.

Conclusions

Spiders have not received much attention by researchers in Croatia, despite their ability to be used as bioindicators in agricultural systems. In this study we demonstrated the diversity of spider community assemblages from apple orchards in northwest Croatia, where 456 individuals belonging to 26 species and 13 families of spiders were collected. There was no difference between the abundance of spiders between treatments which indicated that the exclusion nets favour species composition and richness and their implementation into the practice can possibly improve the agricultural habitat for these beneficial species in the production of apples.

Acknowledgements. This experiment was made in the frame of research project aimed to develop automatic system for detection pest and beneficial insect populations living in above ground biotypes (LIFE13 ENV/HU/001092). The research was done on the experimental plot of research project aimed to increase the fruit quality due to the effects of differently coloured photo selective anti-hail nets (LIFE13 ENV/HR/000580) in orchards. The authors would like to thank family Fruk which owns an orchard and Project Coordinator Tomislav Jemrić who allowed experiment to be carried out. Authors thank Dr Katarina Mikac for comments and English editing that significantly improved the manuscript.

REFERENCES

- [1] Batáry, P., Holzschuh, A., Orci, K. M., Samu, F., Tschardtke, T. (2012): Responses of plant, insect and spider biodiversity to local and landscape scale management in cereal crops and grasslands. – *Agriculture, Ecosystems & Environment* 146(1): 130-136.
- [2] Bogya, S., Markó, V. (1999): Effect of pest management systems on ground-dwelling spider assemblages in an apple orchard in Hungary. – *Agriculture, Ecosystems & Environment* 73: 7-18.
- [3] Bogya, S., Markó, V., Szinetár, Cs. (1999): Comparison of pome fruit orchard inhabiting spider assemblages at different geographical scales. – *Agricultural and Forest Entomology* 1: 261-269.
- [4] Boller, E. F., Avilla, J., Joerg, E., Malavolta, C., Wijnands, F. G., Esbjerg, P. (2004): *Integrated Production: Principles and Technical Guidelines*. 3rd edition. – IOBC/WPRS Bulletin 27(2): 1-12.
- [5] Bouseksou, S., Kherbouche-Abrous, O. (2017): Accessing on biodiversity of Aranea (Arachnida, Arthropoda) in wheat field at Mitidja region (Algeria). – *Proceedings of 52nd Croatian & 12th International Symposium on Agriculture*, Dubrovnik, Croatia, pp. 45-50.
- [6] Brkljača, M., Rumora, J., Vuković, M., Jemrić, T. (2016): The Effect of photoselective nets on fruit quality of apple cv. ‘Cripps Pink’. – *Agric. Conspec. Sci.* 2: 87-90.
- [7] Chouinard, G., Veilleux, J., Pelletier, F., Larose, M., Phillion, V., Cormier, D. (2017): Impact of exclusion netting row covers on arthropod presence and crop damage to ‘Honeycrisp’ apple trees in North America: A five-year study. – *Crop Protection* 98: 248-254.
- [8] Cole, L. J., McCracken, D. I., Downie, I. S., Dennis, P., Foster, G. N., Waterhouse, A., Murphy, K. J., Griffen, A. L., Kennedy, M. P. (2005): Comparing the effects of farming practices on ground beetle (Coleoptera: Carabidae) and spider (Araneae) assemblages on Scottish farmland. – *Biodiversity & Conservation* 14: 441-460.
- [9] Cross, J., Fountain, M., Markó, V., Nagy, C. (2015): Arthropod ecosystem services in apple orchards and their economic benefits. – *Ecological Entomology* 40: 82-96.
- [10] Dainese, M., Schneider, G., Krauss, J., Steffan-Dewenter, I. (2017): Complementarity among natural enemies enhances pest suppression. – *Scientific Reports* 7: 8172.
- [11] Franin, K. (2016): True bugs fauna (Insecta: Heteroptera) in ecological infrastructure of vineyard. – *Doctoral Thesis*, University of Zagreb, Faculty of Agriculture.
- [12] Fruk, G., Fruk, M., Vuković, M., Buhin, J., Jatoi, M. A., Jemrić, T. (2016): Colouration of apple cv. ‘Braeburn’ grown under anti-hail nets in Croatia. – *Acta Horticult. Regiotec.* 19: 1-4.
- [13] HMD (Croatian Meteorological Society) (2017): <http://www.meteohmd.hr/hr/aktualnosti/meteoroloska-postaja-krapina,103.html>. – Accessed on 15. 09. 2017.
- [14] IUSS Working Group WRB. (2015): *World Reference Base for Soil Resources 2014, update 2015. International Soil Classification System for Naming Soils and Creating Legends for Soil Maps*. – *World Soil Resources Reports No. 106*. FAO, Rome.

- [15] Kromp, B. (1999): Carabid beetles in sustainable agriculture: a review on pest control efficacy, cultivation impacts and enhancement. – *Agriculture, Ecosystems and Environment* 74: 187-228.
- [16] Miliczky, E. R., Calkins, C. O., Horton, D. R. (2000): Spider abundance and diversity in apple orchards under three insect pest management programs in Washington State, U.S.A. – *Agricultural and Forest Entomology* 2: 203-215.
- [17] Nyffeler, M., Benz, G. (1987): Spiders in natural pest control: a review. – *Journal of Applied Entomology* 103: 321-339.
- [18] Pajač Živković, I., Jemrić, T., Fruk, M., Buhin, J., Barić, B. (2016): Influence of different netting structures on codling moth and apple fruit damages in Northwest Croatia. – *Agriculturae Conspectus Scientificus* 81(2): 99-102.
- [19] Pekár, S., Kocourek, F. (2004): Spiders (Araneae) in the biological and integrated pest management of apple in the Czech Republic. – *JEN* 128(8): 561-566.
- [20] Pekár, S. (1999): Side-effect of integrated pest management and conventional spraying on the composition of epigeic spiders and harvestmen in an apple orchard (Araneae, Opiliones). – *Journal of Applied Entomology* 123: 115-120.
- [21] Penzar, I., Penzar, B. (2000): *Agrometeorologija*. – Školska knjiga, Zagreb (in Croatian).
- [22] Sauphanor, B., Severac, G., Maugin, S., Toubon, J. F., Capowiez, Y. (2012): Exclusion netting may alter reproduction of the codling moth (*Cydia pomonella*) and prevent associated fruit damage to apple orchards. – *Entomologia Experimentalis et Applicata* 145: 134-142.
- [23] Shahak, Y., Gussakovsky, E. E., Cohen, Y., Lurie, S., Stern, R., Kfir, S., Naor, A., Atzmon, I., Doron, I., Greenblat-Avron, Y. (2004): A new approach for light manipulation in fruit trees. – *Acta Horticulturae* 636: 609-616.
- [24] Tasin, M., Demaria, D., Ryne, C., Cesano, A., Galliano, A., Anfora, G., Ioriatti, C., Alma, A. (2008): Effect of anti-hail nets on *Cydia pomonella* behavior in apple orchards. – *Entomologia Experimentalis et Applicata* 129(1): 32-36.

ROLE OF PHYCOREMEDIATION FOR NUTRIENT REMOVAL FROM WASTEWATERS: A REVIEW

EMPARAN, Q.¹ – HARUN, R.^{1*} – DANQUAH, M. K.²

¹*Department of Chemical and Environmental Engineering, Faculty of Engineering
Universiti Putra Malaysia, 43400 Serdang, Malaysia*

²*Department of Chemical and Petroleum Engineering, Curtin University
98009 Miri, Sarawak, Malaysia*

**Corresponding author*

e-mail: mh_razif@upm.edu.my; phone: +60389466289; fax: +60386567120

(Received 26th Sep 2018; accepted 22nd Nov 2018)

Abstract. The presence of high concentrations of chemical oxygen demand (COD), biochemical oxygen demand (BOD) and nutrients in wastewater generated industrially or domestically has resulted in significant water pollution situations and subsequently is leading to adverse health problems. Algae have been used in various applications in environmental biotechnology especially for phycoremediation as a tertiary wastewater treatment strategy through assimilation of high concentration of nitrogen and phosphorus for their growth, thus reducing potential eutrophication problems. This article discusses the role of phycoremediation to remove COD, BOD and nutrients from wastewater. The mechanism for nutrient removal from wastewater, challenges to process development and current commercial-scale algae-based wastewater treatment are reviewed too. It appears that phycoremediation plays a vital role to treat wastewaters efficiently.

Keywords: *microalgae, wastewater pollution, COD, BOD, efficiency*

Introduction

In the last few decades, the rapid population growth, industrial revolution, and urbanization have led to various forms of environmental pollution. The disposal of untreated wastewater (e.g. industrial, municipal, palm oil mill effluent, amongst others) directly into water bodies such as rivers, lakes, and oceans is considered a simple and cheap discharge method in communities where wastewater disposal is not well regulated (Chan et al., 2009). This contributes significantly to water shortage. In addition, the potential of high concentrations of toxic pollutants moves into human and animal food chain could result in significant health problems (Barakat, 2011).

The quality of water will degrade when untreated wastewater discharged into the receiving water body (e.g. rivers, streams, lakes) and lead to the problem of clean water for human consumption. Besides that, the discharged of wastewater containing the excessive amount of nutrients (e.g. nitrogen, phosphorus) into the receiving water body can also lead to another problem like eutrophication resulted in the depletion of oxygen level in the water (Lau et al., 1997). Generally, phosphorus in the form of orthophosphates is known as the limiting nutrient in the freshwater system. However, runoff wastewater containing extremely concentration of phosphorus can lead to the eutrophication (Cai et al., 2013). The abnormally low level of oxygen in the water body can harm aquatic life by inducing the reduction of aquatic animals (e.g. fishes, prawns, among others) and microorganisms (e.g. bacteria, fungi, algae) population (Sperling and Chernicharo, 2005).

According to Driscoll et al. (2003) and Smith (2003), the eutrophication in fresh and coastal or marine ecosystems also leads to some problems such as water discoloration and foaming and increasing in blooms of toxic algal species and their biomass, mortality rate of aquatic species, sedimentation of organic particles as well as decreasing in water transparency.

Nitrate occurs naturally in water; however, it is undesirable substance in public water because of its high concentration in drinking water may either cause serious health problems like methemoglobinemia (blue-baby syndrome) or source of nitrosamines after its reduction to nitrite (Schoeman and Steyn, 2003; Abdel-Raouf et al., 2012). According to Abdel-Raouf et al. (2012) also stated that the purpose of removing phosphate from wastewater is to protect water from eutrophication.

Treated wastewaters obtained from conventional treatments remain undesirable for discharge because of their characteristics still not able to meet the standards set by local authorities (Loh et al., 2013). Therefore, more effective treatment technologies are required in order to reduce the exposure of toxic chemicals to natural ecosystems. The use of microalgae to treat wastewater and hazardous contaminants is currently of global interest due to the effective photosynthetic uptake of high concentrations of minerals, ionogens, and organics by microalgae, and the capacity to simultaneously utilize carbon dioxide (CO₂) (Mohan et al., 2001; Zeng et al., 2012). Microalgae cells have the ability to remove nutrients such as phosphorus, nitrogen, ammonium as well as heavy metals in wastewater (Phang and Ong, 1988; Aziz and Ng, 1992; Sydney et al., 2011; Abdel-Raouf et al., 2012). A life cycle economic assessment has shown that, for microalgae cultivation, the growth media formulation and composition contribute significantly to the operating cost and is a major consideration for scale-up design (Clarens et al., 2009; Lam and Lee, 2011). Hence there is the need to look into cheaper nutrients sources, and wastewaters containing the right nutrients compositions could be a viable alternative. This will also reduce the cost of microalgae biomass generation for the production of biofuels, animal feed, and essential oils amongst others. Meanwhile, the microalgae biomass production after treatment of heavy metal from wastewaters can be used as a potential feedstock for biochar, charcoal, biofuel and biogas production (Safonova et al., 2004; Chinnasamy et al., 2010; Poo et al., 2018). Therefore, the aims of this paper are to comprehensively review the current use of both free cells and immobilized algae in treating wastewaters to obtain some new ideas to deal with wastewaters without having a negative effect on the environment.

Microalgae and macroalgae

Algae are aquatic plant-like organisms (phytoplankton) with various shapes. They lack roots, stems, and leaves, with cell walls made of cellulose. Algae cells are divided into macroalgae and microalgae. Macroalgae are multicellular organisms with size up to several meters while microalgae are small organisms (unicellular) with their size in the range 0.2-100 µm (Bhatt et al., 2014).

Sharma et al. (2011) categorized microalgae into several groups: (i) prokaryotic blue-green (cyanobacteria); (ii) eukaryotic green (*Chlorophyceae*); (iii) eukaryotic brown (*Phaeophyceae*); (iv) eukaryotic red (*Rhodophyceae*); and (v) eukaryotic diatoms (*Bacillariophyceae*) as shown in *Table 1*.

According to Brennan and Owende (2010) and Mata et al. (2010), algae are photosynthetic prokaryotic or eukaryotic microorganisms that can grow rapidly and

have the ability to adapt to harsh environments due to their unicellular or simple multicellular structure. They are thallophytes containing chlorophyll as their main photosynthetic pigment. In fact, microalgae have more effective access to carbon dioxide, water (H₂O) and nutrients due to their simple cellular structure compared to terrestrial plants. As a result, they are known to have very high carbon capturing and photosynthetic efficiencies with the ability to convert solar energy into useful biomass and reduce CO₂ concentrations in the atmosphere more efficiently than terrestrial plants (Packer, 2009; Kumar et al., 2013).

Table 1. Classification of microalgae and related species (Packer, 2009)

Algae group	Microalgae species
Prokaryotic blue-green (<i>Cyanobacteria</i>)	<i>Arthrospira, Gloeocapsa, Microcystis, Oscillatoria</i> , etc.
Eukaryotic green (<i>Chlorophyceae</i>)	<i>Botryococcus, Chlamydomonas, Chlorella, Scenedesmus</i> , etc.
Eukaryotic brown (<i>Phaeophyceae</i>)	<i>Dinobryon, Mallomonas, Ochromonas, Synura, Uroglena</i> etc.
Eukaryotic red (<i>Rhodophyceae</i>)	<i>Porphyridium</i>
Eukaryotic diatoms (<i>Bacillariophyceae</i>)	<i>Asterionella, Cyclotella, Fragilaria, Surirella</i> , etc.

Metabolism of microalgae

Generally, the growth of microalgae biomass depends on carbon source and photons to perform photosynthesis (Costa and de Morais, 2013). Microalgae can modify their internal structure by both biochemical and physiological acclimations. Externally, they can also excrete various compounds to other cells, supply nutrients or limit the growth of competitors.

Autotrophic microalgae use inorganic compounds and sunlight as a carbon and energy source. In the presence of light, these autotrophic microalgae are referred to as photoautotrophic since they use light photons as an energy source to generate chemical energy by photosynthesis (Amaro et al., 2011). During photosynthesis by autotrophic algae, CO₂ and water are converted into carbohydrate (glucose) and further metabolized to yield energy which drives the formation of adenosine triphosphate (ATP) from adenosine diphosphate (ADP). The energy in ATP is then used to drive various processes in the cells, and in doing so is converted back to ADP ready to pick up more energy to enable growth (Brennan and Owende, 2010). Heterotrophic microalgae use solely organic compounds and exogenous nutrients as a source of carbon and energy for growth in dark conditions (Amaro et al., 2011). According to Huang et al. (2010), cultivation of heterotrophic microalgae overcomes problems associated with limited light photons that affect the attainment of high cells densities during photosynthesis. Some microalgae are mixotrophic, with the capacity to exist as autotrophic or heterotrophic depending on the concentration of organic compound and also the availability of light (Chojnacka and Noworyta, 2004).

Phycoremediation

Microalgae have been used in various applications of environmental biotechnology especially for bioremediation (e.g. phycoremediation). Bioremediation is the part of environmental biotechnology that uses a biological process to treat contaminants (Boopathy, 2000). Gani et al. (2015a), Rao et al. (2011), and Olguin (2003) defined phycoremediation as the use of algae to remove or transform pollutants, including nutrients and toxic chemicals from wastewater and CO₂ from waste air together with biomass production. Wastewaters treatment by microalgae can be performed in the form of suspended free-cells culture and immobilized cells. The suspended free-cells culture is the condition of microalgae living cells move independently within the bottles containing medium under a condition to ensure uniform cells distribution (Katarzyna et al., 2015). Meanwhile, the immobilized cells is the condition of microalgae living cells be prevented from flow freely from its original location to all parts of the medium. This approach can be performed by keeping the microalgae living cells in the carriers such as NaCS-PDMDAAC capsules (Zeng et al., 2012), alginate (Sumithrabhai et al., 2016) and chitosan beads (Fierro et al., 2008).

The use of suspended free-microalgae cells culture to treat wastewater was first studied by Oswald et al. (1957). The process involves the removal of nitrogen and phosphorus from wastewater whilst simultaneously providing oxygen (O₂) for aerobic bacteria coexisting in the culture. Biologically treating wastewater using microalgae is a reliable process due to the high photosynthetic efficiency and growth rates. Furthermore, microalgae have effective nutrient uptake capacity with the potential to achieve great removal of nitrogen and phosphorus as well as heavy metals from wastewater (Hernandez et al., 2006; Hameed, 2007; Sengar et al., 2011; Abdel-Raouf et al., 2012).

Microalgae require significant amounts of phosphorus and nitrogen for proteins synthesis (45-60% microalgae dry weight), nucleic acids and phospholipids for their growth (Rao et al., 2011). In this respect, nutrient removal using microalgae presents major prospects for tertiary wastewater treatment aimed at removing ammonia, nitrate, and phosphate (Rawat et al., 2011; Abdel-Raouf et al., 2012; Gani et al., 2015b). After nutrient uptake by microalgae during wastewater treatment, the purified water can be decanted to harvest the free cells microalgae (Abdel-Raouf et al., 2012).

Phycoremediation has been used in various applications: (i) removal of nutrients from organic matter-rich wastewater; (ii) removal of nutrients and xenobiotic compounds using algae-derived sorbents; (iii) treatment of heavy metal-rich wastewater; (iv) sequestration of CO₂; (v) transformation and degradation of xenobiotic; and (vi) detection of toxic compounds using algae-based biosensors. Application of phycoremediation for wastewater treatment has significant benefits (Eroglu et al., 2012; Sivakumar and Rajendran, 2013; Whangchenchom et al., 2014; Gani et al., 2015a). The following are key characteristics of the process.

- i. It is cost-effective, eco-friendly and safe.
- ii. Microalgae used are non-pathogenic photosynthetic organisms and produce non-toxic substances.
- iii. It efficiently reduces nutrient load and leads to a reduction in total dissolved solid.
- iv. It detoxifies and removes pollutants (e.g. heavy metals) from toxic waste-rich sludge more effectively than conventional chemical treatment technologies.

- v. It increases dissolved oxygen (DO) levels via photosynthetic activity.
- vi. Microalgae use CO₂ fixation from the atmosphere as a source of carbon for growth thus reduce greenhouse gasses (GHG).
- vii. Production of high-value products derived from nutrient-rich microalgae biomass for bio-fertilizer production and as feed for animals and aquaculture.
- viii. Simple operation and maintenance.
- ix. Construction and operation costs are cheaper than mechanical treatment plants such as activated sludge and sequencing batch reactors.
- x. Sustainable treatment solution with significant potential for energy and nutrient recovery.

Figure 1 shows the schematics of mixed microbial community-based treatment of wastewater exploiting the metabolic relationship between microalgae and bacteria. First, the bacteria proliferate and produce CO₂ for microalgae growth. The CO₂ is used by the microalgae during photosynthesis in the presence of light to produce O₂ which is assimilated by the bacteria for growth. According to Sharma and Khan (2013), microalgae produce oxygen from water as a by-product of photosynthesis and bacteria use the oxygen to oxidize organic compounds. During photosynthesis, the end product of bio-oxidation of organic compounds namely, carbon dioxide, is further fixed into cells carbon by microalgae. As a result, the pollutants level in wastewater are reduced to undetectable or acceptable limits set by local authorities.

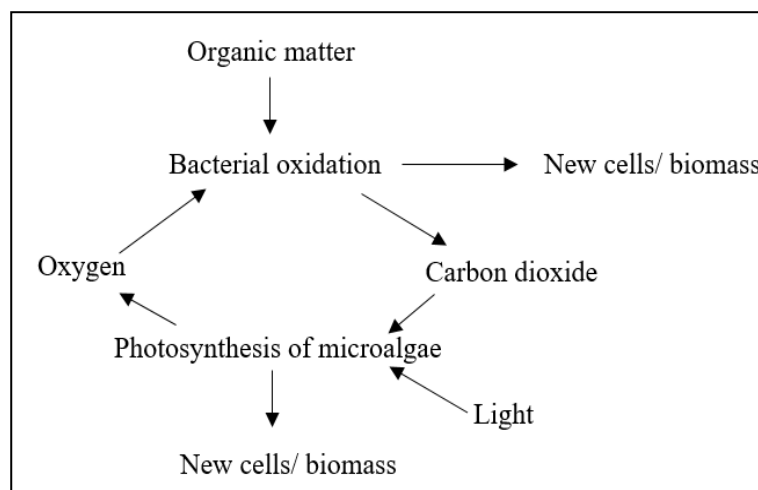


Figure 1. BOD removal through the photosynthetic oxygenation approach (Gani et al., 2015a)

Generally, the generated microalgae biomass from wastewater treatment process is used for agriculture (fertilizer and soil conditioners) and biofuels industries (Eroglu et al., 2012). In this respect, the cultivation of microalgae using wastewater serves a dual role of pollutants load reduction and production of various valuable products.

Mechanisms of carbon, nitrogen and phosphorus removal in phycoremediation

Elements like carbon, nitrogen, phosphorus and, sulfur together with small amounts of trace metals (e.g. sodium, calcium, iron etc.) are required for algae growth. Amongst

these elements, uptake of nitrogen and phosphorus is critical for algal growth (Cai et al., 2013).

Autotrophic microalgae fix carbon (in the form of CO_2) biologically from the atmosphere by photosynthesis. Microalgae can also use carbon in the form of soluble carbonates for their growth, either by direct uptake or conversion of carbonate to free CO_2 through a carboanhydrase activity (Cai et al., 2013).

Nitrogen in wastewater is present in the form of NH_4^+ (ammonia), NO_2^- (nitrite) and NO_3^- (nitrate) (Hadiyanto et al., 2013). The conversion of inorganic nitrogen into organic forms can be carried out by eukaryotic microalgae via assimilation (Cai et al., 2013). *Figure 2* shows the steps involved in the conversion of inorganic nitrogen into organic forms. Firstly, translocation of inorganic nitrogen takes places across the plasma membrane of the algae cells with subsequent reduction to nitrate and nitrite by nitrate and nitrite reductase, respectively. The next step is the conversion of ammonium into amino acids (glutamine). Nitrate reductase utilizes the reduced form of nicotinamide adenine dinucleotide (NADH) to transfer two electrons in the reaction for the conversion of nitrate into nitrite. Next, nitrite is further reduced to ammonium by nitrite reductase and ferredoxin (Fd) to transfer six electrons in the reaction. All inorganic forms of nitrogen are reduced to ammonium before being incorporated into amino acids within the intracellular fluid. Finally, glutamine synthase using glutamate (Glu) and adenosine triphosphate (ATP) facilitates the incorporation ammonium into amino acids (glutamine) (Cai et al., 2013).

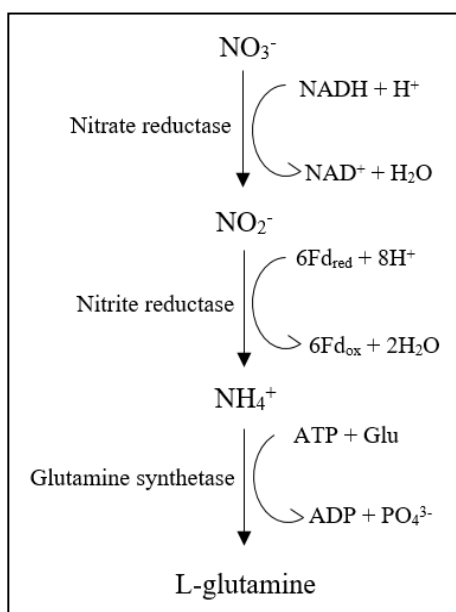


Figure 2. Schematic of the conversion of inorganic nitrogen to its organic form via assimilation (Cai et al., 2013)

The phosphorus present in lipids, nucleic acids, and proteins as well as intermediates of carbohydrate metabolism is a result of phosphorus uptake. Inorganic phosphorus in the form of phosphates plays a crucial role in the growth of algae cells and also their energy metabolism. According to Martínez et al. (1999), algae metabolism relies mostly on inorganic phosphorus in the forms of hydrogen phosphate (HPO_4^{2-}) and dihydrogen

phosphate (H_2PO_4) which is then incorporated into organic compounds through a phosphorylation process involving the production of ADP-derived ATP together with energy input. The oxidation of respiratory substrates, electron transport system of mitochondria, or light (photosynthesis) is all sources of energy input. Phosphates are transferred across the plasma membrane of the algal cells for utilization.

The nitrate and phosphate in the wastewater are adsorbed through the matrix pore surface of microcapsules membrane. After that, the uptake and assimilation of nitrate and phosphate ion by immobilized microalgae cells for growth occur and result in the reduction of N and P content in wastewater and further improves the quality of wastewater for discharge (Zeng et al., 2012).

Selection of microalgae species for phycoremediation

The selection of microalgae species for wastewater treatment is a critical consideration. According to Shi et al. (2007) and Olguin (2003), the selection of microalgae species for wastewater treatment should consider its robustness against wastewater pollutants, the capability to grow well (high growth rates), and their efficiency in assimilating nutrient from wastewater. A lot of studies focusing on various species of microalgae cultivated in wastewater for the removal of nitrogen and phosphorus have been reported. *Scenedesmus*, *Chlorella*, and *Botryococcus* are commonly used microalgae for removing nutrients (nitrogen and phosphorus), COD and BOD as shown in Table 2.

Table 2. Comparison of phycoremediation efficiency by different microalgae species (suspended free-cells microalgae cultures) grown in the various wastewater effluent

Microalgae species	Source of the wastewater (ww)	Parameter	Removal efficiency (%)	Ref.
<i>Chlorella</i> sp.	Synthetic aquaculture wastewater	COD	COD = 15%	Udom et al., (2013)
		TN	TN = 91%	
		NH_4^+	NH_4^+ = 100%	
		TP	TP = 93%	
<i>Chlorella</i> sp.	Domestic wastewater before the primary settling	COD	COD = 50.90%	Wang et al., (2010)
		TN	TN = 68.40%	
		NH_4^+	NH_4^+ = 82.40%	
		PO_4^{3-}	PO_4^{3-} = 83.20%	
<i>Chlorella vulgaris</i>	Sewage wastewater collected from the treatment plant	BOD	BOD = 70%	Abou-Shanab et al., (2013)
		COD	COD = 66%	
		TN	TN = 71%	
		TP	TP = 67%	
	Treated piggery wastewater	TN	TN = 49%	Abou-Shanab et al., (2013)
		TP	TP = 18%	
	Sewage wastewater collected from the various drains	BOD	BOD = 98.70%	Ahmad et al., (2013)
		COD	COD = 98.30%	
TKN		TKN = 93.10%		
NO_3^-		NO_3^- = 98.30%		
TP		TP = 98%		

Microalgae species	Source of the wastewater (ww)	Parameter	Removal efficiency (%)	Ref.
		PO ₄ ⁺	PO ₄ ⁺ = 98.60%	
	Drainage solution from the commercial green production	TN	TN = 20.70%	Hultberg et al., (2013)
		TP	TP = 99.70%	
	Sewage wastewater collected from the treatment plant	BOD	BOD = 70.91%	Kshirsagar, (2013)
		COD	COD = 80.64%	
		NO ₃	NO ₃ = 78.08%	
		PO ₄ ⁺	PO ₄ ⁺ = 79.66%	
	Sewage wastewater collected from the 2 nd clarifier treatment plant	NO ₃ ⁻	NO ₃ ⁻ = 99%	Su et al., (2012)
		NO ₂ ⁻	NO ₂ ⁻ = 99%	
		NH ₄ ⁺	NH ₄ ⁺ = 99%	
		PO ₄ ³⁻	PO ₄ ³⁻ = 99%	
	Sewage wastewater collected from the primary settling tank	NH ₄ ⁺	NH ₄ ⁺ = 50%	Lau et al., (1997)
		PO ₄ ³⁻	PO ₄ ³⁻ = 50%	
	Synthetic sewage	NO ₃ ⁻	NO ₃ ⁻ = 87%	Eroglu et al., (2012)
	Leather processing collected from the manufacturing facility	BOD	BOD = 22%	Rao et al., (2011)
		COD	COD = 38%	
		TKN	TKN = 73%	
		NO ₃ ⁻	NO ₃ ⁻ = 91.49%	
		NO ₂ ⁻	NO ₂ ⁻ = 89%	
		NH ₄ ⁺	NH ₄ ⁺ = 80%	
		PO ₄	PO ₄ = 94%	
	Textile wastewater (garment factory) collected from the holding tank	COD	COD = 62.30%	Lim et al., (2010)
		NH ₄ ⁺	NH ₄ ⁺ = 45.10%	
		PO ₄ ⁺	PO ₄ ⁺ = 33.30%	
	Chemical (based products) wastewater collected from the Periyor	NO ₃ ⁻	NO ₃ ⁻ = 84%	Dominic et al., (2009)
		NO ₂ ⁻	NO ₂ ⁻ = 100%	
		PO ₄ ³⁻	PO ₄ ³⁻ = 69.23%	
	Sewage wastewater	COD	COD = 78%	Kumar et al., (2018)
		NO ₃ ⁻	NO ₃ ⁻ = 75%	
<i>Chlorella sakina</i>	Tannery wastewater	NO ₃ ⁻	NO ₃ ⁻ = 9.11%	Jaysudha and Sampathkumar, (2014)
		NH ₄ ⁺	NH ₄ ⁺ = 62.04%	
		PO ₄ ³⁻	PO ₄ ³⁻ = 81.94%	
<i>Chlorella pyrenoidosa</i>	Dairy wastewater collected from the farm	BOD	BOD = 88%	Yadavalli et al., (2013)
		COD	COD = 85%	
		NH ₄ ⁺	NH ₄ ⁺ = 98%	
		PO ₄ ³⁻	PO ₄ ³⁻ = 98%	
<i>Chlorella zofingiensis</i>	Piggery wastewater collected from the private farm	COD	COD = 79.84%	Zhu et al., (2013)
		TN	TN = 82.70%	
		TP	TP = 98.17%	

Microalgae species	Source of the wastewater (ww)	Parameter	Removal efficiency (%)	Ref.
<i>Chlorella minutissima</i>	Primary treated domestic wastewater	BOD	BOD = 95%	Sharma and Khan, (2013)
		COD	COD = 90%	
		NO ₃ ⁻	NO ₃ ⁻ = 91.49%	
		NH ₄ ⁺	NH ₄ ⁺ = 90%	
		PO ₄ ³⁻	PO ₄ ³⁻ = 74.27%	
<i>Chlorella sorokoniana</i>	Synthetic municipal wastewater	PO ₄ ³⁻	PO ₄ ³⁻ = 69%	Hernandez et al., (2006)
	Municipal wastewater collected from the aerobic activated sludge	PO ₄ ³⁻	PO ₄ ³⁻ = 72%	
<i>Chlorella sp.</i>	Mixed wastewaters from piggery and winery	TN	TN = 89%	Ganeshkumar et al., (2018)
		TP	TP = 49%	
<i>Chlamydomonas sp.</i>	POME collected from the facultative pond	COD	COD = 29.13%	Ding et al., (2016)
		TN	TN = 72.97%	
		NH ₄ ⁺	NH ₄ ⁺ = 100%	
		TP	TP = 63.53%	
<i>Scenedesmus sp.</i>	Noodle processing - MLSS (aeration tank)	COD	COD = 71.85%	Whangchencho m et al., (2014)
	Noodle processing - effluent (final sedimentation tanks)	COD	COD = 39.89%	
	Primary treated domestic wastewater	NH ₄	NH ₄ = 90%	Sharma and Khan, (2013)
	Synthetic 2f medium with 44 mg/L nitrate and 6 mg/L phosphate	NO ₃ ⁻	NO ₃ ⁻ = 20%	Fierro et al., (2008)
		PO ₄ ³⁻	PO ₄ ³⁻ = 30%	
<i>Scenedesmus obliquus</i>	Treated piggery wastewater	TN	TN = 58%	Abou-Shanab et al., (2013)
		TP	TP = 24%	
		TN	TN = 60%	Jimenez-Perez et al., (2004)
		NO ₃ ⁻	NO ₃ ⁻ = 84%	
		NH ₄ ⁺	NH ₄ ⁺ = 57%	
		TP	TP = 83%	
	Synthetic brewery effluent	COD	COD = 57.50%	Mata et al., (2012)
		TN	TN = 20.80%	
<i>Scenedesmus acutus</i>	Municipal wastewater effluent was collected from the conventional activated sludge plant	COD	COD = 77.30%	Sacristán de Alva et al., (2013)
		NO ₃ ⁻	NO ₃ ⁻ = 71.10%	
		NH ₄ ⁺	NH ₄ ⁺ = 93.60%	
		PO ₄ ³⁻	PO ₄ ³⁻ = 66.20%	
<i>Scenedesmus quadricauda</i>	Domestic wastewater collected from the sewage wastewater treatment plant	BOD	BOD = 89.21%	Kshirsagar, (2013)
		COD	COD = 70.97%	
		NO ₃ ⁻	NO ₃ ⁻ = 70.32%	
		PO ₄ ³⁻	PO ₄ ³⁻ = 81.34%	
<i>Scenedesmus rubescens</i>	Municipal wastewater collected from the secondary treatment plant	TP	TP = 11.40%	Aravantinou et al., (2013)
	Sewage wastewater collected from the 2 nd clarifier treatment plant	NO ₃ ⁻	NO ₃ ⁻ = 99%	Su et al., (2012)
		NO ₂ ⁻	NO ₂ ⁻ = 99%	
		NH ₄ ⁺	NH ₄ ⁺ = 99%	
		PO ₄ ³⁻	PO ₄ ³⁻ = 99%	
<i>Scenedesmus</i>	POME	BOD	BOD =	Rajkumar and

Microalgae species	Source of the wastewater (ww)	Parameter	Removal efficiency (%)	Ref.
<i>dimorphus</i>			71.50%	Takriff, (2015)
		COD	COD = 79%	
		TN	TN = 87.50%	
		NH ₄	NH ₄ = 88.50%	
		TP	TP = 92.50%	
<i>Chlamydomonas incerta</i>	POME	COD	COD = 3.8%	Kamyab et al., (2017)
		NO ₃ ⁻	NO ₃ ⁻ = 12.5%	
		NH ₃ ⁻	NH ₃ ⁻ = 3.7%	
		PO ₄	PO ₄ = 70%	Kamyab et al., (2015)
		COD	COD = 67.35%	
<i>Chlamydomonas mexicana</i>	Treated piggery wastewater	TN	TN = 62%	Abou-Shanab et al., (2013)
		TP	TP = 30%	
<i>Chlamydomonas polypyrenoideum</i>	Dairy wastewater collected from the oxidation pond	NO ₃ ⁻	NO ₃ ⁻ = 90%	Kothari et al., (2013)
		NO ₂ ⁻	NO ₂ ⁻ = 74%	
		NH ₄ ⁺	NH ₄ ⁺ = 90%	
		PO ₄ ³⁻	PO ₄ ³⁻ = 70%	
<i>Chlamydomonas reinhardtii</i>	Sewage wastewater collected from the 2 nd clarifier treatment plant	NO ₃ ⁻	NO ₃ ⁻ = 99%	Su et al., (2012)
		NO ₂ ⁻	NO ₂ ⁻ = 99%	
		NH ₄ ⁺	NH ₄ ⁺ = 99%	
<i>Chlamydomonas sp.</i>	Leachates	NH ₄ ⁺	NH ₄ ⁺ = 70%	Paskuliakova et al., (2018a)
		NH ₄ ⁺	NH ₄ ⁺ = 83%	Paskuliakova et al., (2018b)
<i>Botryococcus sp.</i>	Diary wastewater collected from the goat breeding farm	BOD	BOD = 73.30%	Gani et al., (2015c)
		COD	COD = 48.80%	
		TN	TN = 48.28%	
		PO ₄ ³⁻	PO ₄ ³⁻ = 62.71%	
	Greywater from the residential area	BOD	BOD = 82%	Gani et al., (2015b)
		COD	COD = 88%	
		TN	TN = 52%	
		PO ₄ ³⁻	PO ₄ ³⁻ = 37.50%	
<i>Botryococcus braunii</i>	Domestic wastewater collected from the Adyar river	BOD	BOD = 66.67%	Raj, (2015)
		COD	COD = 71.21%	
		NH ₄ ⁺	NH ₄ ⁺ = 82.94%	
	Greywater collected from the hostel	TP	TP = 97.59%	Gokulan et al., (2013)
		BOD	BOD = 76.13%	
		COD	COD = 91.32%	
		NO ₃ ⁻	NO ₃ ⁻ = 69.58%	
		NH ₄ ⁺	NH ₄ ⁺ = 97.82%	
	Municipal wastewater collected from the primary settling tank	NO ₃ ⁻	NO ₃ ⁻ = 60.31%	Can et al., (2013)
		NO ₂ ⁻	NO ₂ ⁻ = 53.50%	

Microalgae species	Source of the wastewater (ww)	Parameter	Removal efficiency (%)	Ref.
		NH ₄ ⁺	NH ₄ ⁺ = 100%	
		PO ₄ ³⁻	PO ₄ ³⁻ = 99%	
<i>Oscillatoria</i> sp.	Municipal wastewater collected from the Pune Corporation	NO ₃ ⁻	NO ₃ ⁻ = 97%	Azarpira et al., (2014)
		PO ₄ ³⁻	PO ₄ ³⁻ = 93%	
<i>Nostoc commune</i>		NO ₃ ⁻	NO ₃ ⁻ = 96%	
		PO ₄ ³⁻	PO ₄ ³⁻ = 84%	
<i>Nostoc</i> sp.	Primary treated domestic wastewater	NO ₃ ⁻	NO ₃ ⁻ = 45.68%	Sharma and Khan, (2013)
		NH ₄ ⁺	NH ₄ ⁺ = 90%	
	Dairy wastewater collected from the treatment plant	BOD	BOD = 40.44%	Kotteswari et al., (2012)
	PO ₄ ³⁻	PO ₄ ³⁻ = 21.08%		
<i>Desmodesmus</i> sp.	Sewage wastewater collected from the facultative lagoon treatment plant Synthetic industrial wastewater	TN	TN = 80%	Komolafe et al., (2014)
		PO ₄ ³⁻	PO ₄ ³⁻ = 38.70%	
		TP	TP = 94%	Rugnini et al., (2018)
<i>Tetraselmis suecica</i>	Aquaculture wastewater collected from the fish farm	TN	TN = 95.70%	Michels et al., (2014)
		TP	TP = 99.70%	
<i>Tetraselmis chuii</i>	Aquaculture – recirculation aquaculture system (RAS)	TN	TN = 69.50%	Sirakov and Velichkova, (2014)
		NO ₂ ⁻	NO ₂ ⁻ = 79.17%	
		PO ₄ ³⁻	PO ₄ ³⁻ = 64.70%	
<i>Neochloris vigensis</i>	Municipal wastewater collected from the secondary treatment plant	TP	TP = 53.40%	Aravantinou et al., (2013)
<i>Chlorococcum spec.</i>		TP	TP = 25.10%	
<i>Spirulina</i> sp.	Synthetic dairy wastewater	BOD	BOD = 81%	Sumithrabhai et al., (2016)
		COD	COD = 83%	
		TN	TN = 77%	
		TP	TP = 69%	
	Dairy wastewater collected from the factory	COD	COD = 77%	Ahmed, (2014)
		NO ₃ ⁻	NO ₃ ⁻ = 80%	
		PO ₄ ³⁻	PO ₄ ³⁻ = 72%	
	POME collected from the anaerobic fourth pond	COD	COD = 50%	Hadiyanto et al., (2014)
		TN	TN = 40%	
TP		TP = 40%		
<i>Spirulina platensis</i>	POME collected from the anaerobic fourth pond	COD	COD = 50.79%	Hadiyanto et al., (2013)
		TN	TN = 96.50%	
		TP	TP = 85.92%	
	POME	BOD	BOD = 78.30%	Rajkumar and Takriff, (2015)
		COD	COD = 84.90%	
		TN	TN = 91%	
NH ₄ -N		NH ₄ -N = 93.80%		
	TP	TP = 96.80%		
<i>Auxenochlorella protothecoides</i>	Municipal wastewater collected from the treatment plant	COD	COD = 88.99%	Zhou et al., (2012)

Microalgae species	Source of the wastewater (ww)	Parameter	Removal efficiency (%)	Ref.
		TN	TN = 59.70%	
		TP	TP = 81.52%	
<i>Oocystis</i> sp.	Fish processing wastewater collected from the fish farm	COD	COD = 71.10%	Riano et al., (2011)
		NH ₄ ⁺	NH ₄ ⁺ = 95%	
		TP	TP = 74.10	
<i>Euglena viridis</i>	Sewage wastewater collected from the drain opens into river, Yamuna	BOD	BOD = 96.20%	Sengar et al., (2011)
<i>Gloeocapsa gelatinosa</i>		COD	COD = 82%	
<i>Synedra affinis</i>		NO ₃ ⁻	NO ₃ ⁻ = 100%	
		NO ₂ ⁻	NO ₂ ⁻ = 100%	
		PO ₄ ³⁻	PO ₄ ³⁻ = 100%	
<i>Gloeocapsa gelatinosa</i>	Chemical (based products) wastewater collected from the Periyor	NO ₃ ⁻	NO ₃ ⁻ = 80.90%	Dominic et al., (2009)
<i>Synechocystis salina</i>		NO ₂ ⁻	NO ₂ ⁻ = 100%	
		PO ₄ ³⁻	PO ₄ ³⁻ = 75%	
		NO ₃ ⁻	NO ₃ ⁻ = 82.50%	
		NO ₂ ⁻	NO ₂ ⁻ = 96.23%	
	PO ₄ ³⁻	PO ₄ ³⁻ = 64.52		
<i>Pithopora</i> sp.	Thermal wastewater collected from the power station	BOD	BOD = 88.23%	Murugesan and Dhamotharan, (2009)
		COD	COD = 87.75%	
		NO ₃ ⁻	NO ₃ ⁻ = 23.07%	
		PO ₄ ³⁻	PO ₄ ³⁻ = 89.37%	
<i>Nannochloris oculata</i>	Aquaculture wastewater -recirculation aquaculture system (RAS)	TN	TN = 78.40%	Sirakov and Velichkova, (2014)
		NO ₂ ⁻	NO ₂ ⁻ = 84.38%	
		PO ₄ ³⁻	PO ₄ ³⁻ = 14.70%	
<i>Characium</i> sp.	POME collected from the anaerobic pond	COD	COD = 45.41%	Selvam et al., (2015)
		TN	TN = 88.60%	
		NH ₃ ⁻	NH ₃ ⁻ = 90.35%	
		NH ₄ ⁺	NH ₄ ⁺ = 87%	
		TP	TP = 99.5.0%	
		PO ₄ ³⁻	PO ₄ ³⁻ = 99.10%	
Micro algal mixture	POME collected from the final pond	COD	COD = 71.16%	Kamyab et al., (2014)
	Textile wastewater	TN	TN = 70.10%	Huy et al., (2018)
		TP	TP = 100%	
	Urban wastewater	BOD	BOD = 51%	Marella et al., (2018)
		COD	COD = 91%	
		TN	TN = 95.10%	
		TP	TP = 88.9%	
Algal-bacterial culture	Municipal wastewater collected from the 2 nd clarifier treatment plant	COD	COD = 98.2%	Su et al., (2011)
		TKN	TKN = 88.3%	
		PO ₄ ³⁻	PO ₄ ³⁻ = 64.8%	

Microalgae species	Source of the wastewater (ww)	Parameter	Removal efficiency (%)	Ref.
	Synthetic wastewater	COD	COD = 65.62%	Ji et al., (2018)
		TN	TN = 21.56%	
		TP	TP = 70.82%	
	Municipal wastewater	TN	TN = 83%	Delgadillo-Mirquez et al., (2016)
TP		TP = 100%		
Algal biofilm	Artificial municipal wastewater	TP	TP = 97%	Sukačova et al., (2015)

Application of phycoremediation in treating wastewater using suspended-free cells of microalgae

Microorganisms especially microalgae have received significant attention in wastewater treatment. This is due to their capability to take up and assimilate plant nutrients, pesticides, organic and inorganic pollutants in their unicellular structure (Sahu, 2014). According to Pittman et al. (2011), a lot of microalgae species thrive in wastewater containing high concentration of nitrogen and phosphorus and use them as a vital source of energy for their growth. This leads to significant uptake and reduction of nutrient concentrations.

Cultivation of microalgae in wastewater treatment system offers several advantages. The process is simple, economical and sustainable. Zhou et al. (2012) reported that growing microalgae in wastewater is probably the most promising approach to reduce costs of production in term of nutrients and clean water supply. Furthermore, Rawat et al. (2011) reported that readily available municipal wastewater can be used as a growth media to cultivate microalgae together with the added benefits of bioremediation (e.g. phycoremediation).

Chlorella sp. reduced COD (15%), total nitrogen (TN) (91%), ammonium (NH₄⁺) (100%) and total phosphorus (TP) (93%) from synthetic aquaculture for 22 days (Komolafe et al., 2014). It has been shown that *C. vulgaris* grown in sewage wastewater accomplished removal of BOD (98.70%), COD (98.30%), total kjeldahl nitrogen (TKN) (93.10%), nitrate (NO₃⁻) (98.30%), TP (98%) and (phosphate) PO₄³⁻ (98.60%) (Wang et al., 2010). As Whangchenchom et al., (2014) reported that *Scenedesmus sp.* was capable of removing 73.37% of COD from wastewaters in Thailand. Suspended free-cell of *Scenedesmus sp.*, cultivated in synthetic 2f medium reduced NO₃⁻ and PO₄³⁻ by 20% and 30%, respectively (Fierro et al., 2008). Removal of TN, NO₃⁻, NH₄⁺, and TP from piggery wastewater using *Scenedesmus obliquus* was achieved at 60, 84, 57 and 83%, respectively (Ji et al., 2013). Sacristán de Alva et al., (2013) and Su et al. (2012) used others strains of *Scenedesmus* species to treat wastewater. High removal of NO₃⁻, (nitrite) NO₂⁻, NH₄⁺, and PO₄³⁻ were achieved as compared to Kothari et al. (2013) using *Chlamydomonas polypyrenoideum*. Gokulan et al. (2013) evaluated the nutrients removal efficiency of *Botryococcus braunii* in greywater samples collected from a hostel. They reported that *B. braunii* removed 76.13%, 91.32%, 69.58%, 97.82%, 97.59% of BOD, COD, NO₃⁻, NH₄⁺ and TP, respectively. Ganeshkumar et al. (2018) studied the potential of *Chlorella sp.* to treat mixed wastewater from piggery and winery in India. The treatment process was conducted for 10 days in at 23°C in an orbital shaker. The initial concentration of TN and TP of 284 mg/L and 11 mg/L was

reduced to 30.22 mg/L and 4.78 mg/L, respectively. Therefore, the study achieved good removal of TN and TP up to 89.36% and 56.56%, respectively. The removal efficiency of nutrients, COD and BOD from various wastewaters for other studies were summarized in *Table 2*.

It can be summarized that the phycoremediation technology has the ability to remove nutrients from wastewaters up to certain removal efficiency. However, the removal efficiency of nutrients depends on the types of wastewaters and microalgae species to be treated and be used as bioremediation agent, respectively. Besides that, some microalgae species shown great removal efficiency of nitrogen removal from wastewaters. An explanation for this was due to the role of nitrogen to build microalgae cells through anabolism pathway. Protein, chlorophyll, amino acids and also genetic materials are major made up of nitrogen (McElwee et al., 2006). Thus, the phycoremediation process has a potential to reduce the nitrogen to the lowest concentration from wastewaters.

Rock minerals, soil erosion and animal waste decomposition are the natural sources of phosphorus in the aquatic system. Phosphorus removal from wastewaters is vital to avoid eutrophication problem. This problem could be achieved through phycoremediation process which exhibited great removal efficiency of phosphorus as shown in *Table 2*. *Table 2* also shows the phycoremediation process for various wastewaters using different types of microalgae species.

Algae immobilization

De-Bashan and Bashan (2010) defined immobilized cells as living cells by which natural or artificial methods have been used to restrict independent movement from its original position to all part of an aqueous phase. Immobilization of microalgae in polymers can overcome problems associated with biomass harvesting from suspended free-cells cultivated in wastewater. Although solid-liquid separation technologies such as centrifugation and filtration can be used to separate free cells. There are several types of immobilization: (i) covalent coupling (ii) affinity immobilization (iii) adsorption (iv) confinement in liquid-liquid emulsion (v) capture behind semi-permeable membrane; and (vi) entrapment in polymers (Malik, 2002; Eroglu et al., 2015). They can be further categorized into “passive” (immobilization onto natural or synthetic gel-like carriers) and “active” (using flocculants, chemical attachment, and gel encapsulation) (Moreno-Garrido, 2008).

Immobilization of microalgae by entrapment using gel polymers is the most common method in wastewater treatment applications (Eroglu et al., 2015). There is a physical separation between the microorganisms and the treated wastewater in polymeric immobilization, and this is similar to biofiltration. The microalgae cells are immobilized and entrapped alive in the polymer gel matrix. The gel pores are smaller in size than the microalgae. The wastewater fluid flows through the pores of the polymer and sustains microalgae metabolism and growth (Cohen, 2001). The wastewater diffuses through the polymer pores, resulting in uptake of nutrients by the entrapped microalgae cells. Compared to suspended free-cells microalgae cultures cells, the following are some advantages of immobilized microalgae in treating wastewater: (i) provides stability to the photobioreactor (PBR) system design (ii) enhance operational stability (iii) easy to regenerate immobilized microalgae (iv) avoids cell washout (v) facilitates the cultivation of microalgae and easy of harvesting of their biomass (vi) high and rapid

uptake of nutrient plus shorter retention time (vii) allows bioprocess with better light utilization efficiency per area and higher cell densities (viii) yields significant metabolite concentrations (ix) high tolerance against harsh environments like extreme pH, temperature, ultraviolet radiation and toxic compounds (x) protects aging cultures against the harmful effects of photoinhibition (xi) protects microalgae cells from being consumed by wild zooplankton (xii) enhances the capacity of biosorption and bioactivity of the biomass; and (xiii) allow immobilization of more than one microorganism (usually microalgae co-immobilized with bacteria species) (de-Bashan and Bashan, 2010; Eroglu et al., 2015; Vasilieva et al., 2016).

Successful entrapment allows microalgae cells to move freely within the space of beads with the optimal pore size that facilitates diffusion of wastewater and metabolic products into and/or out of the polymer system (Malik, 2002). According to Eroglu et al. (2015), the dual effect of enhanced photosynthetic rate and ionic exchange between the nutrient ions and the immobilized matrix results in efficient removal of nutrients from wastewater. Anionic gels (such as carrageenan and alginate) and cationic gels (such as chitosan) adsorb cations (e.g. NH_4^+) and anions (PO_4^{3-} , NO_3^- , NO_2^-) with high efficiency. In addition, PO_4^{3-} is removed efficiently from wastewater via precipitation by calcium ions of alginate or chitosan gels.

Immobilizing materials or carriers can be put into two categories; synthetic and natural polymer (Eroglu et al., 2015; Vasilieva et al., 2016). Examples of synthetic polymers for wastewater treatment include polyacrylamide, polyurethane, polyvinyl, polypropylene, and polystyrene, polysulfone, epoxy resins, and filter papers. Natural polymers can be derived from plant polysaccharides. These include agar, cellulose, alginate, carrageenan, and chitosan. The immobilizing materials possess hydrophilic properties for enhanced diffusion of wastewater into the beads.

Natural polymers such as alginate, carrageenan, and chitosan are the most commonly used immobilizing materials in wastewater treatment (Shi et al., 2007; Zhang et al., 2008; Moreno-Garrido, 2008; Eroglu et al., 2015; Sumithrabhai et al., 2016), and this due to the following advantages. They are (i) non-toxic, easy to process, and cost-effective; (ii) transparent and permeable; (iii) hydrophilic and have higher nutrient/product diffusion rates than synthetic polymers; (iv) more environmentally friendly and produces less hazardous waste following treatment; and (v) bio-compatible. The use of these natural polymers in wastewater treatment also poses some disadvantages. They are (i) less stable as they dissolve slightly in highly contaminated wastewater; (ii) do not retain their polymeric structure in the presence of high concentration of phosphate and some cations (e.g. calcium and magnesium); and (iii) susceptible to microbial degradation. However, the degradation of the natural polymer in highly contaminated wastewater can be minimized by the composite assembly of polymers. For example, the stability of carrageenan gels can be enhanced by mixing the carrageenan with polyacrylamide (Eroglu et al., 2015).

There is a generic method for immobilizing microalgae onto polymers. Briefly, the microbial suspension is mixed with the macromolecular monomers of the selected polymer (e.g. alginate, carrageenan, chitosan solution) to form polymeric gels (e.g. spherical beads produced via the small orifice of syringe) after solidification. The monomers cross-link to each other with di- and multi-valent cations such as calcium chloride to produce polymers with entrapped microbes within the matrix. Generally, as the concentration of monomers and cross-linking agents' increases, the mechanical strength of the polymer increases, resulting in pore size reduction (de-Bashan and

Bashan, 2010). Table 3 shows the removal efficiency of pollutants from wastewater using different immobilizing materials.

Table 3. Comparison of phycoremediation efficiency by immobilized algae grown in the various wastewaters

Microalgae Species	Immobilizing material	Source of the wastewater	Parameter	Removal efficiency (%)	Ref.	
<i>Chlorella vulgaris</i>	Chitosan nanofiber mats	Synthetic sewage effluent	NO ₃ ⁻	NO ₃ ⁻ = 87%	Eroglu et al., (2012)	
	Twin-layer system	Synthetic secondary wastewater	NO ₃ ⁻	NO ₃ ⁻ = 93%	Shi et al., (2007)	
			NH ₄ ⁺	NH ₄ ⁺ = 94%		
			PO ₄ ³⁻	PO ₄ ³⁻ = 89%		
	Calcium alginate beads	Domestic primary treated wastewater	NO ₃ ⁻	NO ₃ ⁻ = 96.40%	Hameed, (2007)	
			NH ₄ ⁺	NH ₄ ⁺ = 100%		
	Carrageenan beads	Sewage wastewater collected from the primary settling tank	NH ₄ ⁺	NH ₄ ⁺ = 95%	Lau et al., (1997)	
			PO ₄ ³⁻	PO ₄ ³⁻ = 99%		
	<i>Chlorella vulgaris</i> and <i>Azospirillum brasilense</i>	Alginate beads	Municipal wastewater collected from the stream of wastewater after the initial aerobic activated sludge treatment	NO ₃ ⁻	NO ₃ ⁻ = 15%	De-Bashan et al., (2004)
				NH ₄ ⁺	NH ₄ ⁺ = 100%	
PO ₄ ³⁻	PO ₄ ³⁻ = 36%					
<i>Chlorella sorokiniana</i> and <i>Azospirillum brasilense</i>			PO ₄ ³⁻	PO ₄ ³⁻ = 72%	Hernandez et al., (2006)	
<i>Chlorella pyrenoidosa</i> and activated sludge	Polyvinyl alcohol (PVA) – sulfate gel	Synthetic wastewater	NO ₃ ⁻	NO ₃ ⁻ = 80%	Huang and Wang, (2003)	
			PO ₄ ³⁻	PO ₄ ³⁻ = 88%		
<i>Chlorella salina</i>	Sodium alginate beads	Tannery wastewater	NO ₃ ⁻	NO ₃ = 98.71%	Jaysudha and Sampathku mar, (2014)	
			NH ₄ ⁺	NH ₄ = 98.54%		
PO ₄ ³⁻			PO ₄ = 99.39%			
<i>Spirulina maxima</i>		Synthetic dairy effluent	BOD	BOD = 81.05%	Sumithrabhai et al., (2016)	
			COD	COD = 82.86%		
			NO ₃ ⁻	NO ₃ ⁻ = 77%		
			PO ₄ ³⁻	PO ₄ ³⁻ = 69.05%		
<i>Scenedesmus rubescens</i>	Twin-layer system	Synthetic secondary wastewater	NO ₃ ⁻	NO ₃ ⁻ = 95%	Shi et al., (2007)	
			NH ₄ ⁺	NH ₄ ⁺ = 96%		
			PO ₄ ³⁻	PO ₄ ³⁻ = 89%		
<i>Scenedesmus</i>	Chitosan	Synthetic 2f medium with 44	NO ₃ ⁻	NO ₃ ⁻ = 96%	Shi et al., (2007)	

Microalgae Species	Immobilizing material	Source of the wastewater	Parameter	Removal efficiency (%)	Ref.
sp.	beads	mg/L nitrate and 6 mg/L phosphate	PO ₄ ³⁻	PO ₄ ³⁻ = 94%	(2008)
	Sodium alginate sheets	Domestic secondary effluent	NH ₄ ⁺	NH ₄ ⁺ = 100%	Zhang et al. (2008)
			PO ₄ ³⁻	PO ₄ ³⁻ = 100%	

Factors affecting nutrients removal from wastewater in immobilized systems

There are several factors that influence nutrients removal from wastewater in immobilized systems. These include the thickness of immobilized media, concentration of microalgae, and amount of beads.

The thickness of immobilized media

Zhang et al. (2008) investigated the effect of the thickness of *Scenedesmus sp.* immobilized gel on the uptake of nitrogen and phosphorus. They found out that gel thickness up to 3 mm is removed nutrients efficiently with higher algal biomass. Another studied by Hameed (2007) reported that small size beads with about 2.8 mm in diameter demonstrated higher removal efficiency for nitrate and phosphate than others beads (4 and 6 mm in diameter) in 48 h. Low thickness media facilitate convective transport of nutrients between the gel media and the nutrient environment.

The concentration of immobilized algae

Too high cell density in gel results in low removal efficiency (Zhang et al., 2008). Sodium alginate sheets (3 mm thickness) which containing microalgae with 2×10^8 cells achieved higher nutrient removal compared to other sheets with 1.33×10^8 and 3×10^8 cell counts. Compared to low (3.5×10^5 cells) and high (3.10×10^6 cells/bead) cell stocking, calcium alginate beads containing microalgae cells (1.5×10^6 cells/bead) demonstrated a greater capacity to effectively remove NH₄⁺ and PO₄³⁻ from primary treated domestic wastewater (Hameed, 2007). They revealed that increasing cells stocking in beads causes leakage problems and affects the removal efficiency of target pollutants from wastewater. According to Jimenez-Perez et al. (2004), super-concentrated cells stockings may restrict to some extent the nutrient diffusion through the gel pores.

The quantity of beads in wastewater

The removal of target pollutants from wastewater is influenced by the quantity of beads containing algae cells used in the wastewater treatment process. A more effective removal of nitrate and phosphate from wastewater was achieved by 11 beads of algae than 16, 32, and 64 beads (Hameed, 2007). Tam and Wong (2000) accomplished a great removal of NH₄⁺ and PO₄³⁻ from synthetic primary treated domestic wastewater within 24 h in bioreactors having an optimal algal bead concentration of 12 beads/mL equivalent to 1:3 algal beads: wastewater v/v. NH₄⁺ removal was significantly lower with 15 beads/mL algal concentration. They discussed that excessive increase in the quantity of beads results in high-density beads structure that hinders light penetration into cells and subsequently enhances self-shading effects, which limits the metabolic activities of microalgae. Moreover, the high concentration of beads results in the

settling of beads at the bottom of the reactor due to ineffective air distribution to fluidize them.

Current commercial-scale in wastewater treatment systems using suspended free-cells of microalgae

There are several companies used algae for wastewater treatment practices worldwide for the commercial and industrial application. The companies that involve in algae-based energy (biogas) and fuel (biofuel and biodiesel) research are Algae Enterprises (Australia), Aquanos Energy Ltd. (Israel) and Fcc Aqualia (Spain). Adequate mass cultivation and harvesting of algae for algae biomass in wastewater is important to the aforementioned companies to achieve commercial viability. This is because the biomass can be used as feedstock for any biogas, biofuel, biodiesel or biofertilizer. According to the Website of these companies, they have developed different systems to treat wastewater using algae.

Algae Enterprises collaborated with the main shareholder, namely Sustainability Ventures Group have developed a technology, known as Photoluminescent Algae System (PAS) comprises of thin plastics embedded with fluorescent dyes in Australia (<http://www.algaeenterprises.com/wastewater-treatment>). Based on this system, the growth of algae is improved by fine-tuning the colors and wavelengths of incoming abundant sunlight that reaches the algae inside. This sustainable technology uses algae to remove pollutants including excessive nutrients from dairy wastewater in the presence of sunlight. In addition, this technology also integrates with the anaerobic digester to generate electricity through anaerobic digestion of harvested algae biomass to produce biogas with methane as the main component which can be used as a renewable source. Nutrient-rich residue materials (fertilizer product) resulting from the biogas generation are used for agriculture to produce even more algae. Meanwhile, the treated waste streams are recycled for irrigation and other purposes on the dairy farm.

Aquonos Energy Ltd developed a novel algae-based wastewater treatment system in Israel (https://finder.startupnationcentral.org/company_page/aquanos). The Aquanos system is characterized by lower energy consumption than conventional wastewater treatment system. Basically, this system consists of three distinct but interrelated processes namely, anaerobic treatment, aerobic treatment and separation of solid (algae) from treated effluent. The first stage is the anaerobic treatment of the incoming wastewater. The purpose of anaerobic treatment is to reduce the organic load to the downstream aerobic processes and at the same time to produce biogas for energy recovery as well as to produce CO₂. The second stage is the aerobic treatment of anaerobic effluent which takes place in the fix film aerobic system. The aerobic system is aerated by a stream of oxygen-rich algae which are grown in the separate raceway pond. Based on this system, the algae are grown in the raceway pond to produce high dissolved oxygen in the liquid. Then, this liquid recirculates through the fix film system supplying oxygen for bacterial decomposition of organic pollutants. At the end of the process, namely solid separation stage is where the excessive algae and excessive biomass are separated from treated effluent. The treated effluent is discharged into the environment and reused for agriculture, while the excessive biomass is returned to the anaerobic stage to produce additional biogas. The end product is high-quality effluent produce using less energy than the conventional system as well as resource harvesting through the production of high quality and high-level algae by-product.

Fcc Aqualia in Spain partnered with University of Southampton (England), BDI (Austria), Frounhofer Society (German), HyGear (Netherlands) and Volkswagen (German) companies under All-Gas project for developing a new pond system to cultivate algae using nutrients present in the wastewater at wastewater treatment plant to produce biodiesel and biogas (methane) made from biomass to power vehicles (<https://www.power-technology.com/uncategorised/news/aqualias-biofuel-project-produces-first-algae-biomass-in-spain/>). Basically, they have two different processes of the sequential order under this project, namely All-Gas Alternative 1 (post lipid extraction) and All-Gas Alternative 2 (pre lipid extraction) to obtain biodiesel, biomethane, and biogas. For All-Gas Alternative 1, the incoming raw wastewater is pre-treated and the effluent is discharged into raceway pond containing algae culture. After that, the dense algae culture is harvested and the treated wastewater is discharged to the environment, while the harvested algae biomass undergoes the anaerobic process in anaerobic digester. The biogas is produced during anaerobic treatment and the further undergo pre-treatment and upgrading process to obtain pure methane and CO₂, respectively. The biomethane are stored in the refueling station, while the CO₂ is supplied to the algae culture grown in the aforementioned raceway pond to promote high growth rate and yield of algae. In addition, the remaining residue after anaerobic treatment in anaerobic digester undergoes dewatering method to concentrate prior to the extraction process to produce biodiesel and biofertilizer (remain residue). The All-Gas Alternative 2 has the same process of sequential order as All-Gas Alternative 1 but the lipid extraction process occurs directly upon harvesting. They produce approximately 200000 L of biodiesel and 600000 m³ of biomethane per year from approximately 3000 kg of dry algae with 20 percent of oil content after grown in ponds of 10 hectares. They claim that the Volkswagen vehicles that have been power using algae-based biogas emit zero emissions. The European Commission contributed about 12 million euro (\$15.9 million USD) for this project with the target of at least 10% renewable energy used in their transport sectors by 2020. So far, there is none company use immobilized algae to treat wastewaters commercially.

Wastewater treatment challenges using suspended free-cells of microalgae

To date, limited investments have been pushed into the development of commercial-scale algal wastewater treatment plant, and this has been the result of technical challenges relating to scale-up feasibility, harvesting, and dewatering of biomass. Practical application of current emerging technologies is still in its infancy, with most of the technologies validated only at the laboratory scale.

Most algae are cultivated in closed PBRs for phycoremediation and biomass production (Kamarudin et al., 2015; Lage et al., 2018). The expensive culture system with high capital cost and energy requirements for mixing and gas exchange together with the cost of harvesting to achieve feasible algal solid concentration has constrained the integration of microalgal system with wastewater treatment at large-scale levels. This can partially be addressed through the use of other systems such as open raceway pond. However, environmental factors such as temperature fluctuation, weather influence, and light penetration can affect the efficiency of phycoremediation and productivity of biomass.

Algae require sufficient amount of CO₂ for growth. Thus, low-cost approach using flue gas from power plants as carbon source can be applied. However, the high

concentration of substances like nitrogen oxide, sulfur oxide, and heavy metals presents in the flue gas causes the medium very acidic for algae cultivation. As a result, algae cultivation is prone to contamination and inhibition, resulting in low wastewater treatment efficiency and low biomass production. Therefore, the flue gas can be pre-treated to minimize contamination before exposure to the microalgae cells. The pre-treatment process could significantly increase the total operation cost.

Kamarudin et al. (2015) propose the following for consideration in algal POME treatment: (i) pre-treatment of wastewater to remove growth inhibitors; (ii) feasible and economical method for algae cultivation and biomass harvesting; and (iii) selection of suitable microalgae strains.

High concentration of nutrients such as ammonium can inhibit the growth of algae and lead to poor wastewater treatment efficiency. According to Cai et al. (2013), nitrogen in the form of ammonium is the most preferred source for effective and rapid growth of algae due to effective redox reaction during nitrogen assimilation and the less energy requirement for the reaction to occur.

The selection of suitable algae for effective phycoremediation and CO₂ fixation is critical to the process development as microalgae cells have different tolerance to the range of pollutants, CO₂ concentration, and also the culture condition. According to Choul-gyun (2002), algal strain such *Chlorella kessleri* is capable of removing various concentration of nitrogen up to 1400 mg/L indicating that this algal strain has a high tolerance to nitrogen.

Numerous studies have been conducted by researchers around the world on the application of algae for phycoremediation and biomass production for sustainable bio-products production. With further research and development targeted at addressing some of the above-mentioned challenges, commercial-scale wastewater treatment using algae can be achieved.

Wastewater treatment challenges using immobilized microalgae

There are some challenges with the use of polymer immobilized microalgae systems according to Cai et al. (2013). These are (i) the capability of the system to remove pollutants present in wastewater effectively; (ii) cost of polymer and subsequent immobilization process; (iii) chemical forces and interactions between the immobilization matrix and the cell wall may result in abiotic stresses (iv) limited diffusion of substrate or fluid like wastewater, metabolic products, oxygen and CO₂ to and from the cells in the polymeric matrix; (v) sufficient light penetration into the polymer matrix containing algal cells; and (vi) the metabolism of microalgae is affected by its confinement in a limited space. However, these issues can be addressed by combining optimized immobilization matrices with smart bioreactor designs.

Conclusion

Effective wastewater treatment is vital in order to improve the quality of wastewaters effluent which must be met the regulations standards set by local authorities before discharge. Thus, the use of suspended free-cells microalgae culture emerges as a viable option in future and can be explored to treat wastewaters containing nutrients sources with simultaneous CO₂ capture which are required for growth and support microalgae cultivation. For that reason, the use of biochemical abilities of suspended free-cells

microalgae culture is a popular approach to be used as a tertiary treatment in conventional wastewater treatment which can remove nutrient and BOD efficiently in the engineered system like high rate algal ponds. Most recent studies have highlighted the various advantages of immobilized microalgae in carriers as compared to suspended free-cells microalgae culture for removal of nutrients, BOD and COD from wastewaters. For instance, application of immobilized algae to treat wastewaters capable to reduce the cost of all process by circumventing the need for downstream processes using dewatering and harvesting methods to separate the biomass and treated effluent. In contrast, a very costly dewatering and harvesting methods are required to obtain biomass derived from free-cells microalgae culture due to their dilute nature and small in size. Therefore, the immobilized microalgae in capsules not only ease the harvesting process but also increase the efficiency of wastewaters treatment with CO₂ sequestration and bioproduct generation derived from microalgae biomass. The removal of nutrient, BOD and COD from wastewaters using immobilized microalgae cells has been one of the major interesting research subjects carried out by researchers globally due to its environment-friendly approach for sustainable development in the future.

Acknowledgements. The authors thank the support of any parties involved in this project especially Universiti Putra Malaysia for providing the equipment and research facilities to conduct this project. The financial contribution provided by MyBrain15 Scheme is acknowledged.

REFERENCES

- [1] Abdel-Raouf, N., Al-Homaidan, A. A., Ibraheem, I. B. M. (2012): Microalgae and wastewater treatment. – *Saudi Journal of Biological Sciences* 19(3): 257-275.
- [2] Abou-Shanab, R. A. I., Ji, M. K., Kim, H. C., Paeng, K. J., Jeon, K. J. (2013): Microalgal species growing on piggery wastewater as a valuable candidate for nutrient removal and biodiesel production. – *Journal of Environmental Management* 115: 257-264.
- [3] Ahmad, F., Khan, A. U., Yasar, A. (2013): Comparative Phycoremediation of Sewage Water by Various Species of Algae. – *Proceedings of the Pakistan Academy of Sciences* 50(2): 131-139.
- [4] Ahmed, S. G. K. A. (2014): Dairy Wastewater Treatment Using Microalgae in Karbala City, Iraq. – *International Journal of Environment, Ecology, Family and Urban Studies (IJEEFUS)* 4(2): 13-22.
- [5] Amaro, H. M., Guedes, A. C., Malcata, F. X. (2011): Advances and Perspectives in Using Microalgae to Produce Biodiesel. – *Applied Energy* 88(10): 3402-3410.
- [6] Aravantinou, A. F., Theodorakopoulos, M. A., Manariotis, I. D. (2013): Selection of microalgae for wastewater treatment and potential lipids production. – *Bioresource Technology* 147: 130-134.
- [7] Azarpira, H., Behdarvand, P., Dhumal, K., Pondhe, G. (2014): Potential use of cyanobacteria species in phycoremediation of municipal wastewater. – *International Journal of Bioscience* 4(4): 105-111.
- [8] Aziz, M. A., Ng, W. J. (1992): Feasibility of wastewater treatment using the activated-algae process. – *Bioresource Technology* 40(3): 205-208.
- [9] Barakat, M. A. (2011): New Trends in Removing Heavy Metals from Industrial Wastewater. – *Arabian Journal of Chemistry* 4(4): 361-377.
- [10] Bhatt, N. C., Panwar, A., Bisht, T. S., Tamta, S. (2014): Coupling of algal biofuel production with wastewater. – *Scientific World Journal* : 1-10.
- [11] Boopathy, R. (2000): Factors limiting bioremediation technologies. – *Bioresource Technology* 74(1): 63-67.

- [12] Brennan, L., Owende, P. (2010): Biofuels from Microalgae-A Review of Technologies for Production, Processing, and Extractions of Biofuels and Co-Products. – *Renewable and Sustainable Energy Reviews* 14(2): 557-577.
- [13] Cai, T., Park, S. Y., Li, Y. (2013): Nutrient Recovery from Wastewater Streams by Microalgae: Status and Prospects. – *Renewable and Sustainable Energy Reviews* 19: 360-369.
- [14] Can, S. S., Demir, V., Korkmaz, S. A., Can, E. (2013): Treatment of domestic waste water with *Botryococcus braunii* (*Chlorophyceae*). – *Journal Of Food Agriculture And Environment* 11(October): 3-5.
- [15] Chan, Y. J., Chong, M. F., Law, C. L., Hassell, D. G. (2009): A Review on Anaerobic–Aerobic Treatment of Industrial and Municipal Wastewater. – *Chemical Engineering Journal* 155(1-2): 1-18.
- [16] Chinnasamy, S., Bhatnagar, A., Hunt, R. W., Das, K. C. (2010): Microalgae cultivation in a wastewater dominated by carpet mill effluents for biofuel applications. – *Bioresour. Technol.* 101: 3097-3105.
- [17] Chojnacka, K., Noworyta, A. (2004): Evaluation of *Spirulina sp.* growth in photoautotrophic, heterotrophic and mixotrophic cultures. – *Enzyme and Microbial Technology* 34(5): 461-465.
- [18] Choul-gyun, L., Lee, K. (2002): Nitrogen Removal from Wastewaters by Microalgae Without Consuming Organic Carbon Sources. – *J. Microbiol. Biotechnol* 12: 979-985.
- [19] Clarens, A. F., Ressureccion, E. P., White, M. A., Colosi, L. M. (2009): Environmental life cycle comparison of algae to other bioenergy feedstocks. – *Environmental Science and Technology* 44(5): 1813-1819.
- [20] Cohen, Y. (2001): Biofiltration - The treatment of fluids by microorganisms immobilized into the filter bedding material: a review. – *Bioresource Technology* 77(3): 257-274.
- [21] Costa, J. A. V., de Morais, M. G. (2013): An Open Pond System for Microalgal Cultivation. – In: Pandey, A., Lee, D. J., Chisti, Y., Soccol, C. Y. (eds.) *Biofuels from Algae*, Elsevier B.V., San diego.
- [22] De-Bashan, L. E., Hernandez, J. P., Morey, T., Bashan, Y. (2004): Microalgae growth-promoting bacteria as “helpers” for microalgae: A novel approach for removing ammonium and phosphorus from municipal wastewater. – *Water Research* 38(2): 466-474.
- [23] De-Bashan, L. E., Bashan, Y. (2010): Immobilized microalgae for removing pollutants: Review of practical aspects. – *Bioresource Technology* 101(6): 1611-1627.
- [24] Delgadillo-Mirquez, L., Lopes, F., Taidi, B., Pareau, D. (2016): Nitrogen and phosphate removal from wastewater with a mixed microalgae and bacteria culture. – *Biotechnology Reports* 11: 18-26.
- [25] Ding, G. T, Yaakob, Z., Takriff, M. S., Salihon, J., Abd Rahaman, M. S. (2016): Biomass Production and Nutrients Removal by a Newly-Isolated Microalgal Strain *Chlamydomonas sp.* in Palm Oil Mill Effluent (POME). – *International Journal of Hydrogen Energy* 41(8): 4888-4895.
- [26] Dominic, V., Murali, S., Nisha, M. (2009): Phycoremediation efficiency of three microalgae *Chlorella vulgaris*, *Synechocytis salina* and *Gloeocapsa gelatinosa*. – *SB Academic Review* 16(1-2): 138-146.
- [27] Driscoll, C. T., Whitall, D., Aber, J., Boyer, E., Castro, M., Cronan, C., Goodale, C., Groffman, P., Hopkinson, C., Lambert, K., Lawrence, G., Ollinger, S. (2003): Nitrogen Pollution in the Northeastern United States: Sources, Effects, and Management Options. – *BioScience* 53(4): 357-374.
- [28] Eroglu, E., Agarwal, V., Bradshaw, M., Chen, X., Smith, S. M., Raston, C. L., Swaminathan Iyer, K. (2012): Nitrate Removal from Liquid Effluents Using Microalgae Immobilized on Chitosan Nanofiber Mats. – *Green Chemistry* 14(10): 2682.
- [29] Eroglu, E., Smith, S. M., Raston, C. L. (2015): Application of Various Immobilization Techniques for Algal Bioprocesses. – In: Moheimani, N. R., McHenry, M. P., de Boer,

- K., Bahri, P. (eds.) Biomass and Biofuels from Microalgae, Springer International Publishing, Murdoch.
- [30] Fierro, S., del Pilar Sánchez-Saavedra, M., Copalcúa, C. (2008): Nitrate and phosphate removal by chitosan immobilized *Scenedesmus*. – Bioresource Technology 99(5): 1274-1279.
- [31] Ganeshkumar, V., Subashchandrabose, S. R., Dharmarajan, R., Venkateswarlu, K., Naidu, R., Megharaj, M. (2018): Use of mixed wastewaters from piggery and winery for nutrient removal and lipid production by *Chlorella sp.* MM3. – Bioresource Technology 256(February): 254-258.
- [32] Gani, P., Sunar, N. M., Latiff, A. A., Kamaludin, N. S., Parjo, U. K., Emparan, Q. (2015a): Experimental Study for Phycoremediation of *Botryococcus sp.* on Greywater. – Applied Mechanics and Materials 773-774: 1312-1317.
- [33] Gani, P., Sunar, N. M., Latiff, A. A., Joo, I. T. K., Parjo, U. K., Emparan, Q., Er, C. M. (2015b): Phycoremediation of Dairy Wastewater by Using Green Microalgae: *Botryococcus sp.* – Applied Mechanics and Materials 773-774: 1318-1323.
- [34] Gani, P., Sunar, N. M., Matias-peralta, H., Latiff, A. A. A., Kalthsom, U. K., Razak, A. R. A. (2015c): Phycoremediation of Wastewaters and Potential Hydrocarbon from Microalgae: A Review. – Advances in Environmental Biology 9(20):1-8.
- [35] Gokulan, R., Sathish, N., Praveen Kumar, R. (2013): Treatment of grey water using hydrocarbon producing *Botryococcus braunii*. – International Journal of ChemTech Research 5(3): 1390-1392.
- [36] Hadiyanto, H., Christwardana, M., Soetrisnanto, D. (2013): Phytoremediations of Palm Mill Effluent (POME) by Using Aquatic Plants and Mircoalgae for Biomass Production. – Journal of Environmental Science and Technology 6(2): 79-90.
- [37] Hadiyanto, H., Soetrisnanto, D., Christwardhana, M. (2014): Phytoremediation of Palm Oil Mill Effluent Using Pistia Stratiotes Plant and Algae. – International Journal of Engineering (IJE) 27(12): 1809-1814.
- [38] Hameed, M. S. A. (2007): Effect of algal density in bead, bead size and bead concentrations on wastewater nutrient removal. – African Journal of Biotechnology 6(May): 1185-1191.
- [39] Hernandez, J. P., De-Bashan, L. E., Bashan, Y. (2006): Starvation enhances phosphorus removal from wastewater by the microalga *Chlorella spp.* co-immobilized with *Azospirillum brasilense*. – Enzyme and Microbial Technology 38(1-2): 190-198.
- [40] https://finder.startupnationcentral.org/company_page/aquanos.
- [41] <http://www.algaeenterprises.com/wastewater-treatment>.
- [42] <https://www.power-technology.com/uncategorised/newsaqualias-biofuel-project-produces-first-algae-biomass-in-spain>.
- [43] Huang, G., Wang, Y. (2003): Nitrate and Phosphate Removal by Co-immobilized *Chlorella pyrenoidosa* and Activated Sludge at Different pH Values. – Water Qual. Res. J. Canada 38(3): 541-551.
- [44] Huang, G., Chen, F., Wei, D., Zhang, X., Chen, G. (2010): Biodiesel production by microalgal biotechnology. – Applied Energy 87(1): 38-46.
- [45] Hultberg, M., Carlsson, A. S., Gustafsson, S. (2013): Treatment of drainage solution from hydroponic greenhouse production with microalgae. – Bioresource Technology 136: 401-406.
- [46] Huy, M., Kumar, G., Kim, H. W., Kim, S. H. (2018): Photoautotrophic cultivation of mixed microalgae consortia using various organic waste streams towards remediation and resource recovery. – Bioresource Technology 247(June): 576-581.
- [47] Jaysudha, S., Sampathkumar, P. (2014): Nutrient removal from tannery by free and immobilized cells of marine microalgae *Chlorella salina*. – International Journal of Environmental Biology 4(1): 21-26.
- [48] Ji, M., Abou-Shanab, R. A. I., Hwang, J., Timmes, T. C., Kim, H., Oh, Y., Jeon, B. (2013): Removal of Nitrogen and Phosphorus from Piggery Wastewater Effluent Using

- the Green Microalga *Scenedesmus obliquus*. – Journal of Environmental Engineering 139(9): 1198-1205.
- [49] Ji, X., Jiang, M., Zhang, J., Jiang, X., Zheng, Z. (2018): The interactions of algae-bacteria symbiotic system and its effects on nutrients removal from synthetic wastewater. – Bioresource Technology 247(July): 44-50.
- [50] Jimenez-Perez, M. V., Sanchez-Castillo, P., Romera, O., Fernandez-Moreno, D., Perez-Martinez, C. (2004): Growth and nutrient removal in free and immobilized planktonic green algae isolated from pig manure. – Enzyme and Microbial Technology 34(5): 392-398.
- [51] Kamarudin, K. F., Tao, D. G., Yaakob, Z., Takriff, M. S., Rahaman, M. S. A., Salihon, J. (2015): A Review on Wastewater Treatment and Microalgal By-Product Production with a Prospect of Palm Oil Mill Effluent (POME) Utilization for Algae. – Der Pharma Chemica 7(7): 73-89.
- [52] Kamyab, H., Din, M. F. M., Lee, C. T., Ponraj, M., Soltani, M., Mohamad, S. E., Roudi, A. M. (2014): Micro-macro Algal Mixture as a Promising Agent for Treating POME Discharge and Its Potential Use as Animal Feed Stock Enhancer. – Journal Teknologi (Sciences and Engineering) 68(5): 1-4.
- [53] Kamyab, H., Din, M. F. M., Keyvanfar, A., Majid, M. Z. A., Talaiekhosani, A., Shafaghat, A., Lee, C. T., Shiun, L. J., Ismail, H. H. (2015): Efficiency of Microalgae *Chlamydomonas* on the Removal of Pollutants from Palm Oil Mill Effluent (POME). – Energy Procedia 75: 2400-2408.
- [54] Kamyab, H., Chelliapan, S., Din, M. F. M., Shahbazian-Yassar, R., Rezanian, S., Khademi, T., Kumar, A., Azimi, M. (2017): Evaluation of *Lemma Minor* and *Chlamydomonas* to Treat Palm Oil Mill Effluent and Fertilizer Production. – Journal of Water Process Engineering 17(May): 229-236.
- [55] Katarzyna, L., Sai, G., Avijeet Singh, O. (2015): Non-enclosure methods for non-suspended microalgae cultivation: Literature review and research needs. – Renewable and Sustainable Energy Reviews 42: 1418-1427. <https://doi.org/10.1016/j.rser.2014.11.029>.
- [56] Komolafe, O., Velasquez Orta, S. B., Monje-Ramirez, I., Noguez, I. Y. Y., Harvey, A. P., Ledesma, M. T. O. (2014): Biodiesel Production from Indigenous Microalgae Grown in Wastewater. – Bioresource Technology 154(November): 297-304.
- [57] Kothari, R., Prasad, R., Kumar, V., Singh, D. P. (2013): Production of biodiesel from microalgae *Chlamydomonas polypyrenoideum* grown on dairy industry wastewater. – Bioresource Technology 144: 499-503.
- [58] Kotteswari, M., Murugesan, S., Rk, R. (2012): Phycoremediation of Dairy Effluent by using the Microalgae *Nostoc sp.* – International Journal of Environmental Research and Development 2(1): 35-43.
- [59] Kshirsagar, D. A. (2013): Bioremediation of Wastewater By Using Microalgae : an Experimental Study. – International Journal of Life Science Biotechnology and Pharma Research 2(3): 339-346.
- [60] Kumar, M., Sharma, M. P., Dwivedi, G. (2013): Algae Oil as Future Energy Source in Indian Perspective. – International Journal of Renewable Energy Research 3(4): 913-921.
- [61] Kumar, P. K., Krishna, S. V., Verma, K., Pooja, K., Bhagawan, D., Himabindu, V. (2018): Phycoremediation of sewage wastewater and industrial flue gases for biomass generation from microalgae. – South African Journal of Chemical Engineering 25: 133-146.
- [62] Lage, S., Gojkovic, Z., Funk, C., Gentili, F. (2018): Algal Biomass from Wastewater and Flue Gases as a Source of Bioenergy. – Energies 11(3): 664.
- [63] Lam, M. K., Lee, K. T. (2011): Renewable and sustainable bioenergies production from palm oil mill effluent (POME): Win-win strategies toward better environmental protection. – Biotechnology Advances 29(1): 124-141.

- [64] Lau, P. S., Tam, N. F. Y., Wong, Y. S. (1997): Wastewater Nutrients (N and P) Removal by Carrageenan and Alginate Immobilized *Chlorella vulgaris*. – Environmental Technology 18(9): 945-951.
- [65] Lim, S. L., Chu, W. L., Phang, S. M. (2010): Use of *Chlorella vulgaris* for bioremediation of textile wastewater. – Bioresource Technology 101(19): 7314-7322.
- [66] Loh, S. K., Lai, M. E., Ngatiman, M. (2013): Zero Discharge Treatment Technology of Palm Oil Mill Effluent. – Journal of Oil Palm Research 25(3): 273-281.
- [67] Malik, N. (2002): Biotechnological potential of immobilised algae for wastewater N, P and metal removal: a review. – BioMetals 15: 377-390.
- [68] Marella, T. K., Parine, N. R., Tiwari, A. (2018): Potential of diatom consortium developed by nutrient enrichment for biodiesel production and simultaneous nutrient removal from waste water. – Saudi Journal of Biological Sciences 25(4): 704-709.
- [69] Martínez, M. E., Jiménez, J. M., El Yousfi, F. (1999): Influence of phosphorus concentration and temperature on growth and phosphorus uptake by the microalga *Scenedesmus obliquus*. – Bioresource Technology 67(3): 233-240.
- [70] Mata, T. M., Martins, A. A., Caetano, N. S. (2010): Microalgae for Biodiesel Production and Other Applications: A Review. – Renewable and Sustainable Energy Reviews 14(1): 217-232.
- [71] Mata, T. M., Melo, A. C. Simões, M., Caetano, N. S. (2012): Parametric study of a brewery effluent treatment by microalgae *Scenedesmus obliquus*. – Bioresource Technology 107(January): 151-158.
- [72] McElwee, K., Baker, J., Clair, D. (2006): Pond Fertilization: Ecological Approach and Practical Application. – John Wiley & Sons.
- [73] Michels, M. H. A., Vaskoska, M., Vermuë, M. H., Wijffels, R. H. (2014): Growth of *Tetraselmis Suecica* in a Tubular Photobioreactor on Wastewater from a Fish Farm. – Water Research 65: 290-296.
- [74] Mohan, N., Balasubramanian, N., Subramanian, V. (2001): Electrochemical treatment of simulated textile effluent. – Chemical Engineering and Technology 24(7): 749-753.
- [75] Moreno-Garrido, I. (2008): Microalgae immobilization: Current techniques and uses. – Bioresource Technology 99(10): 3949-3964.
- [76] Murugesan, S., Dharmotharan, R. (2009): Bioremediation of thermal wastewater by *Pithophora sp.* – Current World Environment 4(1): 137-142.
- [77] Olguin, E. J. (2003): Phycoremediation: Key issues for cost-effective nutrient removal processes. – Biotechnology Advances 1(2): 81-91.
- [78] Oswald, W. J., Gotaas, H. B., Golueke, C. G., Kellen, W. R., Gloyna, E. F., Hermann, E. R. (1957): Algae in Waste Treatment. – Sewage and Industrial Wastes 29(54): 437-457.
- [79] Packer, M. (2009): Algal capture of carbon dioxide; biomass generation as a tool for greenhouse gas mitigation with reference to New Zealand energy strategy and policy. – Energy Policy 37(9): 3428-3437.
- [80] Paskuliakova, A., McGowan, T., Tonry, S., Touzet, N. (2018a): Microalgal bioremediation of nitrogenous compounds in landfill leachate - The importance of micronutrient balance in the treatment of leachates of variable composition. – Algal Research 32: 162-171.
- [81] Paskuliakova, A., McGowan, T., Tonry, S., Touzet, N. (2018b): Phycoremediation of landfill leachate with the chlorophyte *Chlamydomonas sp.* SW15aRL and evaluation of toxicity pre and post treatment. – Ecotoxicology and Environmental Safety 147: 622-630.
- [82] Phang, S. M., Ong, K. C. (1988): Algal Biomass Production in Digested Palm Oil Mill Effluent. – Biological Wastes 25: 77-191.
- [83] Pittman, J. K., Dean, A. P., Osundeko, O. (2011): The potential of sustainable algal biofuel production using wastewater resources. – Bioresource Technology 102(1): 17-25.
- [84] Poo, K., Son, E., Chang, J., Ren, X., Choi, Y., Chae, K. (2018): Biochars derived from wasted marine macro-algae (*Saccharina japonica* and *Sargassum fusiforme*) and their

- potential for heavy metal removal in aqueous solution. – J. Environ. Manage. 206: 364-372.
- [85] Raj, A. S. (2015): *Botryococcus braunii* as a Phycoremediation Tool for the Domestic Waste Water Recycling from Cooum River, Chennai, India. – Journal of Bioremediation & Biodegradation 6(3): 1-9.
- [86] Rajkumar, R., Takriff, M. S. (2015): Nutrient Removal from Anaerobically Treated Palm Oil Mill Effluent by *Spirulina Platensis* and *Scenedesmus Dimorphus*. – Der Pharmacia Lettre 7(7): 416-421.
- [87] Rao, P., Kumar, R. R., Raghavan, B., Sivasubramanian, V. (2011): Application of phycoremediation technology in the treatment of wastewater from a leather-processing chemical manufacturing facility. – Water SA 37(1): 7-14.
- [88] Rawat, I., Kumar, R. R., Mutanda, T., Bux, F. (2011): Dual Role of Microalgae: Phycoremediation of Domestic Wastewater and Biomass Production for Sustainable Biofuels Production. – Applied Energy 88(10): 3411-3424.
- [89] Riano, B., Molinuevo, B., Garcia-Gonzalez, M. C. (2011): Treatment of fish processing wastewater with microalgae-containing microbiota. – Bioresource Technology 102(23): 10829-10833.
- [90] Rugnini, L., Costa, G., Congestri, R., Antonaroli, S., Sanità di Toppi, L., Bruno, L. (2018): Phosphorus and metal removal combined with lipid production by the green microalga *Desmodesmus sp.*: An integrated approach. – Plant Physiology and Biochemistry 125: 45-51.
- [91] Sacristán de Alva, M., Luna-Pabello, V. M., Cadena, E., Ortíz, E. (2013): Green Microalga *Scenedesmus Acutus* Grown on Municipal Wastewater to Couple Nutrient Removal with Lipid Accumulation for Biodiesel Production. – Bioresource Technology 146: 744-748.
- [92] Safonova, B. E., Kvitko, K. V., Iankevitch, M. I., Surgko, L. F., Afti, I. A., Reisser, W., (2004): Biotreatment of Industrial Wastewater by Selected Algal-Bacterial Consortia. – Microb. Enhanc. Oil Recover.: 347-353.
- [93] Sahu, O. (2014): Reduction of Heavy Metals from Waste Water by Wetland. – International Letters of Natural Sciences 7: 35-43.
- [94] Schoeman, J. J., Steyn, A. (2003): Nitrate removal with reverse osmosis in a rural area in South Africa. – Desalination 155: 15-26.
- [95] Selvam, T. B. T., Renganathan, R., Takriff, M. S. (2015): Nutrient Removal of POME Using POME Isolated Microalgae Strain. – Advanced Materials Research 1113: 364-369.
- [96] Sengar, R. M., Singh, K. K., Singh, S. (2011): Application of phycoremediation technology in the treatment of sewage water to reduce pollution load. – Indian journal Science Resource 2(4): 33-39.
- [97] Sharma, G., Khan, S. (2013): Bioremediation of Sewage Wastewater Using Selective Algae for Manure Production. – International Journal of Environmental Engineering and Management 4(6): 573-580.
- [98] Sharma, Y. C., Singh, B., Korstad, J. (2011): A critical review on recent methods used for economically viable and eco-friendly development of microalgae as a potential feedstock for synthesis of biodiesel. – Green Chemistry 13(11): 2993-3006.
- [99] Shi, J., Podola, B., Melkonian, M. (2007): Removal of nitrogen and phosphorus from wastewater using microalgae immobilized on twin layers: An experimental study. – Journal of Applied Phycology 19(5): 417-423.
- [100] Sirakov, I. N., Velichkova, K. N. (2014): Bioremediation of wastewater originate from aquaculture and biomass production from microalgae species - *Nannochloropsis oculata* and *Tetraselmis chuii*. – Bulgarian Journal of Agricultural Science 20(1): 66-72.
- [101] Sivakumar, R., Rajendran, S. (2013): Role of Algae in Commercial Environment. – International Research Journal of Environment Sciences 2(12): 81-83.
- [102] Smith, V. (2003): Eutrophication of freshwater and coastal marine ecosystems a global problem. – Environmental Science and Pollution Research 10(2): 126-139.

- [103] Sperling, M. V., Chernicharo, C. A. D. L. (2005): Biological Wastewater Treatment in Warm Climate Regions. – IWA Publishing.
- [104] Su, Y., Mennerich, A., Urban, B. (2011): Municipal wastewater treatment and biomass accumulation with a wastewater-born and settleable algal-bacterial culture. – Water Research 45(11): 3351-3358.
- [105] Su, Y., Mennerich, A., Urban, B. (2012): Comparison of nutrient removal capacity and biomass settleability of four high-potential microalgal species. – Bioresource Technology 124: 157-162.
- [106] Sukačová, K., Trtílek, M., Rataj, T. (2015): Phosphorus removal using a microalgal biofilm in a new biofilm photobioreactor for tertiary wastewater treatment. – Water Research 71: 55-63.
- [107] Sumithrabhai, K., Thirumarimurugan, M., Sivakumar, V. M., Sujatha, S. (2016): Expedient Study on Treatment of Dairy Effluent in Fluidized Bed Reactor Using Immobilized Microalgae. – International Journal of Advanced Engineering Technology 7(2): 231-235.
- [108] Sydney, E. B., da Silva, T. E., Tokarski, A., Novak, A. C., de Carvalho, J. C., Woiciehowski, A. L., Larroche, C., Soccol, C. R. (2011): Screening of microalgae with potential for biodiesel production and nutrient removal from treated domestic sewage. – Applied Energy 88(10): 3291-3294.
- [109] Tam, N. F. Y., Wong, Y. S. (2000): Effect of immobilized microalgal bead concentrations on wastewater nutrient removal. – Environmental Pollution 107(1): 145-151.
- [110] Udom, I., Zaribaf, B. H., Halfhide, T., Gillie, B., Dalrymple, O., Zhang, Q., Ergas, S. J. (2013): Harvesting microalgae grown on wastewater. – Bioresource Technology 139: 101-106.
- [111] Vasilieva, S. G., Lobakova, E. S., Lukyanov, A. A., Solovchenko, A. E. (2016): Immobilized Microalgae in Biotechnology. – Moscow University Biological Sciences Bulletin 71(3): 170-176.
- [112] Wang, L., Min, M., Li, Y., Chen, P., Chen, Y., Liu, Y., Wang, Y., Ruan, R. (2010): Cultivation of green algae *Chlorella sp.* in different wastewaters from municipal wastewater treatment plant. – Applied Biochemistry and Biotechnology 162(4): 1174-1186.
- [113] Whangchenchom, W., Chiemchaisri, W., Tapaneeyaworawong, P., Powtongsook, S. (2014): Wastewater from instant noodle factory as the whole nutrients source for the microalga *Scenedesmus sp.* Cultivation. – Environmental Engineering Research 19(3): 283-287.
- [114] Yadavalli, R., Heggors, G. R. V. N., Rao, G., Naga, V. (2013): Two Stage Treatment of Dairy Effluent Using Immobilized *Chlorella Pyrenoidosa*. – Journal of environmental health science & engineering 11(1): 36.
- [115] Zeng, X., Danquah, M. K., Zheng, C. R., Chen, X. D., Lu, Y. (2012): NaCS-PDMDAAC immobilized autotrophic cultivation of *Chlorella sp.* for wastewater nitrogen and phosphate removal. – Chemical Engineering Journal 187: 185-192.
- [116] Zhang, E., Wang, B., Wang, Q., Zhang, S., Zhao, B. (2008): Ammonia-nitrogen and orthophosphate removal by immobilized *Scenedesmus sp.* isolated from municipal wastewater for potential use in tertiary treatment. – Bioresource Technology 99(9): 3787-3793.
- [117] Zhou, W., Li, Y., Min, M., Hu, B., Zhang, H., Ma, X., Li, L., Cheng, Y., Chen, P., Ruan, R. (2012): Growing Wastewater-born Microalga Auxeno *Chlorella Protothecoides* UMN280 on Concentrated Municipal Wastewater for Simultaneous Nutrient Removal and Energy Feedstock Production. – Applied Energy 98: 433-440.
- [118] Zhu, L., Wang, Z., Shu, Q., Takala, J., Hiltunen, E., Feng, P., Yuan, Z. (2013): Nutrient removal and biodiesel production by integration of freshwater algae cultivation with piggy wastewater treatment. – Water Research 47(13): 4294-4302.

AN EARLY EMBRYO MODEL OF STERLET (*ACIPENSER RUTHENUS*) FOR THE ASSESSMENT OF LEAD EFFECTS

CRISTINA, R. T.* – BAROGA, M. – GROZEA, A. – MIHAILOV, S. A. – SIRB, N. M. – DUMITRESCU, E. –
MUSELIN, F.

*Banat's University of Agriculture and Veterinary Medicine „King Michael I of Romania” from
Timisoara (BUAVMT), 119, Calea Aradului, 300645 Timisoara, Romania*

**Corresponding author*

Romeo Teodor Cristina, DVM, PhD. BUAVMT

e-mail: rtcristina@yahoo.com, romeocristina@usab-tm.ro; phone/fax: +40-256-277-140

(Received 5th Apr 2018; accepted 27th Nov 2018)

Abstract. The objective of the study was to devise a 96 h test of sterlet embryos (*Acipenser ruthenus*) in order to evaluate if this species is suitable for water pollution investigation as an evaluation tool. Replicate concentrations of lead acetate were selected from 400, 200, 100 and 50 µgL⁻¹. Each mirror-aquarium was filled with 10 L of lead acetate dilutions, excluding the control, the free sterlet embryos were inserted as follows: 50 / aquarium, i.e. 100 / concentration and control group). The fish were examined at time 0, then at: 12, 24, 48, 72 and 96 hours, every change in behavior or in the body somatic was statistically analyzed, according to ANOVA (significant when $p < 0.05$, or less). Evaluation revealed significant connection among the embryos length ($p < 0.05$), weight ($p = 0.01$; $p < 0.01$) and the dead embryos proved the deleterious feature of lead at 400 and 200 µgL⁻¹. The main critical points were: the delayed resorption of the yolk sac; deformed tail; undeveloped eyes; massive haemorrhages; atypical / altered pigmentation and exitus observed at 12 h. Although *A. ruthenus* is not considered as a standard subject in the pollution assays, it was observed that, changes can be applied for early fish stages as a parallel to other accepted tests.

Keywords: *acute risk-assay, free-embryos, heavy metals, sterlet*

Introduction

It is known that the group of vertebrates that respond without delay if the environment is polluted, as a result of the anthropogenic activities, is the fish. Pollutants of freshwater sources, through their risk potential, can affect the human and animal health. Plentiful risk-assays, guides and standards being conceived, validated, and applied today (ASTM, 1988).

In eco-toxicology and bio-medical field fish adults and those early stages are helpfully handled, in order to test various substances, from industrial pollutants to medicinal active substances (Braunbeck et al., 2005).

However, the benefit of using acute toxicity tests for fish is represented by the applicability to a wide range of substances, this methodology is also used to compare the sensitivity to other aquatic species (Schirmer et al., 2008; Bakos et al., 2013).

The advance of the toxicity tests is bringing new evidence about the toxicological effects upon various fish species and those evolutive stages. Thus, the acute embryo tests are useful because it offers a simply accessible low-cost choice, which can give accurate outcomes (McKim, 1977; Embry et al., 2010; Rácz et al., 2012).

The early-stages provide rapid results and can enable a large number of repetitions in a short time period, consequently increasing the availability and reproducibility of the results (Luckenbach et al., 2001; Lammer et al., 2009).

In this intention, zebrafish (*Danio rerio*) was originally tested, due to the numerous benefits provided compared to other species of lab animals currently used in experiments (Chakraborty et al., 2009; De Oliveira, 2009; Hill et al., 2005; Kovács et al., 2015; McGrath and Li, 2008; Mosneang et al., 2014, 2015a; Scholz et al., 2008).

Our prior observations had revealed similarities between zebrafish and another species, the pikeperch (*Sander lucioperca*) (Mosneang et al., 2015b), this reinforcing the confidence that also other fish species could be successfully used in such kind of experiments. In this respect, we had started an initial study in Romania on the sterlet (*Acipenser ruthenus*, Class: *Actinopterygii*; Order: *Acipenseriformes*; Family: *Acipenseridae*) a valuable species from the sturgeon family (Reinartz, 2017).

An important reason of why *Acipenser ruthenus* was chosen for this study was, on the one hand, its nutritional importance (meat and caviar being highly appreciated), and on the other hand, the fact that this species is threatened with extinction in many countries of the Danube basin and Central Europe where sturgeon has been included on the IUCN red list as "vulnerable". (Gessner et al., 2010).

In the case of *Acipenseridae* sp. effects of heavy metals have been hypothesized / proven as possible / contributing factors for decline of sturgeon population anywhere in the world. Until now studies were done using the acute (96-h) and chronic toxicity tests for: copper (Cu), cadmium (Cd), zinc (Zn), and lead (Pb), in a family member of *A. ruthenus*, namely the white sturgeon (*Acipenser transmontanus*) enlisted also as threatened species in Canada and the United States (Calfee et al., 2014; Little et al., 2012, 2014; Vardy et al., 2014; Wang et al., 2014).

Lead as toxic marker, represents one of the most confirmed threats of the aquatic environment due to its deleterial potential on the fish species, including here the sturgeons, from hatching problems and embryos' malformation (Osman et al., 2007), metabolic imbalance, feeding alterations (Weber, 1996) and high mortality levels of juveniles (Hariharan et al., 2016).

In sturgeons lead and other aquatic pollutants certainly accumulate (Little et al., 2014; Raskovic et al., 2015; Subotic et al., 2013) affecting the spermatozoa quality (Linhartova et al., 2015) or generating adverse behavioral changes (Vardy et al., 2014; Wang et al., 2014).

In this aim, our reason was to provide information regarding the lead activity on sterlet embryos exposed to four different lead concentrations, in a static 96 hours acute toxicity test. The test was conceived as a simply replicable procedure, in the light of the known related methodologies and as a notable laboratory instrument for the contamination monitoring (OECD Test No. 203; OECD Test No. 210; OECD Test No. 236).

Material and Methods

OECD Tests No. 236 and 210 were adopted: 2013, acute risk-assays, were adapted for early stages of *A. ruthenus*. Our interest was to identify all the signs dependable with the lead acetate exposure, including here: general behavior, anatomical and morphological features and the survival rate at different concentrations of lead.

The Test Substance and Concentrations

The methodology for determining the acute toxicity substances in early stage or adult fish requires knowledge of the physico-chemical properties of the investigated

substances, for the selection of the most appropriate test method (e.g. static, semi-static, or with continuous flow), in order to preserve the constant concentration of the test substance. In our study, the test substance was lead which was formed by solubilization of lead acetate ($C_8H_{12}O_8Pb$) Lead acetate (or Lead (IV) Acetate, $\geq 99.99\%$) is a trace metal basis and the most soluble salt in water. This is the reason for using this salt in our in vitro study (and also by the majority of researchers in this research topic). In our test the pure lead concentration was essential and it is known that 1 mg of lead acetate contains 54.622% pure lead (Merck, Germany). Also all methodologies for OECD tests are using lead acetate. To cover the problems that could arise from testing metal toxicity without testing the chemical composition of the test waters we respected the requirements of Meyer et al. (2012), and serial dilutions were performed (Meyer et al., 2012; PubChem – SID 24864770).

For study duplicate concentrations from $400 \mu\text{gL}^{-1}$ (400 ppb), $200 \mu\text{gL}^{-1}$ (200 ppb), $100 \mu\text{gL}^{-1}$ (100 ppb) and respectively $50 \mu\text{gL}^{-1}$ (50 ppb) (representing the admitted limit for drinking water in the EU) were chosen (Directive 98/83/EC) (Table 1).

Table 1. Obtainment of lead acetate experimental concentrations

Dilution in duplicate	
1 g of lead acetate contains 54.622% pure lead	
Concentration / Lead acetate / pure Lead	Successive dilutions
400 ppb ($400 \mu\text{gL}^{-1}$) 12.4 mg lead acetate in 20 L water	In 20 L initial and from this successively:
200 ppb ($200 \mu\text{gL}^{-1}$) or 6.2 mg lead acetate in 20 L water	1:1 dilution to 20 L
100 ppb ($100 \mu\text{gL}^{-1}$) or 3.6 mg lead acetate in 20 L water	1:1 dilution to 20 L
50 ppb ($50 \mu\text{gL}^{-1}$) or 1.8 mg lead acetate in 20 L water	1:1 dilution to 20 L

After dilutions, no perceptible precipitates were present in none of the used dilutions. The water used for the experimental and control groups was a microbiologic pure bottled water (Aqua Carpatica, Romania), with a natural oligomineral content and with a balanced pH (7.0 to 7.2). This water is certified in Romania as being free of nitrates and nitrites and with no potentially dangerous concentrations (e.g. chlorine, heavy metals and other potentially harmful substances). To kill any microbiologic content, water was sterilized by ultraviolet (UV) radiation, at 254 nm, for 10 minutes / five litre flasks. Consequently, water containing lead at the appropriate test concentrations was introduced into the test aquariums for 3 hours prior to the introduction of fish' early stages, to properly incorporate and stabilize the temperature at 18°C (which is the optimum growth temperature for the early stages of *A. ruthenus*).

The Experimental Methodology

Experimental Aquariums and Free Embryos of *Acipenser ruthenus*

The experimental aquariums and the juvenile sterlet sturgeon were provided by the Department of Fisheries from the Faculty of Animal Science Timisoara, Romania the parents being reared in Recirculating Aquaculture System (RAS). The artificial

reproduction, egg incubation, and initial rearing of the free embryos were carried out in agreement with accepted methodologies for *A. ruthenus* (Chebanov and Galich, 2011).

The obtained sterlet free embryos were healthy, without somatic visible defects. Since this study started using hatched free embryos at two days of age (knowing that natural mortality in day one can reach approximately 50%). Feeding was not necessary for the entire study period, knowing that the *A. ruthenus* free embryos start to feed commonly at 6 to 7 days of life, after their yolk-sac is absorbed (Chebanov and Galich, 2011).

During the study, the free embryos were kept in mirror glass aquariums of ten-liter capacity (two spaces / one concentration), with the embryos maintained for 96 hours in a static system, exposed to different lead test solutions.

Since the sturgeon early stages are extremely vulnerable organisms, the best possible maintenance was vital to be reproduced, to avoid the modification of the authentic experimental results. The room temperature was maintained at 18°C, and the temperature in the aquariums, verified at each two hours was maintained at 18 ±1.2°C. To preserve the optimum parameters, the room temperature registration was provided with a thermostat and freshening was assured with an air-conditioning system. In accordance with the measures necessary for testing and knowing that at this stage, sturgeon embryos are initially negatively phototactic, the daily photoperiod was maintained at 10 h light / 14 h dark, the temperature and the oxygen requirements, were appropriate for sturgeon early stages (air saturation provided oxygen levels; at 2-2.5 mgO₂L⁻¹, and the temperature to not fluctuated more than ±1.2°C). The dissolved oxygen value was within the normal range from the first treatment day to the last, because the aeration introduction in each of the aquarium filters ensured the optimum level of oxygen above 70% to correspond with the aeration rate (Chebanov and Galich, 2011).

The samples were carried out in pairs (groups A and B) and each mirror-aquarium was filled with 10 L of water. After the acclimation period, the free embryos were inserted: 50 larvae / aquarium, i.e. 100 larvae / concentration as follows: E1A, E1B / 400 µgL⁻¹; E2A, E2B / 200 µgL⁻¹; E3A, E3B / 100 µgL⁻¹; E4A and E4B / 50 µgL⁻¹. The control group (C) consisted of 100 healthy larvae.

The Free Embryos Examination

Sterlet free embryo specimens were monitored at the examination time 0 and then, at 12, 24, 48, 72, and 96 hours (one hour / read). From the start of each examination, every behavioral change or alteration in the somatic body was noted. The measurements included the individual weighing, the total length, pre-anal length, and total height of the larva, and these were carried out according to the scheme shown in *Figure 1*.

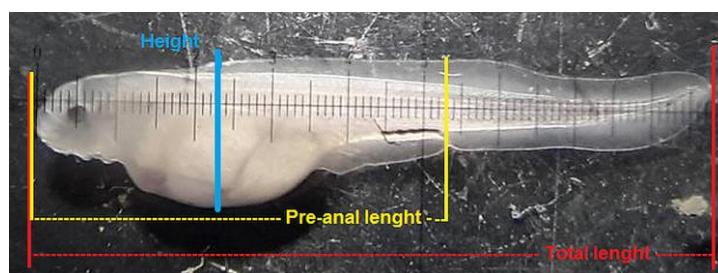


Figure 1. Scheme of starlet sturgeon free embryo measurement

At the onset of the study, at day two after hatching, the initial measured average length of a sterlet free embryo was of 9.7 mm (all embryos being normal, showing small eyes, nose openings, well developed fin folds and yolk sac) and the individual body weight ranging from 0.191 to 0.195 g. The main toxicity critical points were observed in conformity with the OECD instructions, presented in *Table 2*.

Table 2. Critical toxicity points according to OECD guidelines [OECD Tests No. 210 and 236: 2013]

Crt. no.	Larvae somatic / behavioral changes
1.	Tail undetachment
2.	Arrhythmic heartbeat
3.	Edema or haemorrhages in thoracic cavity
4.	Magnification of thoracic cavity / fluid accumulation
5.	Body pigmentation
6.	Tail in: V, L or S letter shape or unfinished growth
7.	Immobility / severe altered mobility / slow / rapid - alternative mobility
8.	Swimming: vertically or like propeller
9.	A larva is considered dead if, it weren't gill movements observed and if touching the caudal peduncle would not have registered any reaction

Fish Anesthesia and Euthanasia

To examine with minimal possible aggression, the vital and somatic changes, the temporary immobilization and afterwards, the free embryos euthanasia was carried out with tricaine mesylate (*syn.* Metacaine; Tricaine, MS-222; Fiquel) (Merck, Germany) the substance accepted both in the EU and in the US for fish anesthesia / euthanasia. The substance (a white powder) was diluted to a concentration of 100 mgL⁻¹ (as anesthetic) and 500 mgL⁻¹ (as euthanasiant), for a contact period from 2 to 10 minutes (Science Direct Topics: Tricaine mesylate).

Instrumentation

The somatic changes of fish were observed under a Kruss model Optronic GmbH (Germany) microscope, using the 10× objective (WF10× / 20), and the weight was assessed using a Sohn GmbH electronic balance (Kern ABJ 220-4M with 0.01 mg error). The pH, oxygen, and the water temperature were measured using a Hach HQ40D, portable analyzer, (Hach Products, Germany) (*Figure 2*).



Figure 2. Portable analyzer, (Hach Products, Germany) used for measurements and research aquariums

Statistical Analysis

The statistical values were analyzed as the mean (\bar{x}), variance (s), CV (critical value), average (S_x and $S_x \%$), mean \pm SEM (mean's middle error), and were graphically expressed through the GraphPad Prism 6.0 for Windows (GraphPad, San Diego USA). For the evaluation of differences between the groups, the two-way ANOVA, with the t -test and respectively Bonferroni's multiple comparison test correction were conducted, the statistical difference being set at $p < 0.05$ or lower.

Results and Discussion

During the sterlet testing, two strong critical points were initially identified:

a) The attempt of the sterlet larvae to escape upon introduction into the tanks containing the highest concentration ($400 \mu\text{gL}^{-1}$).

b) The negative response of the sterlet larvae to swim and move after descending to the bottom of the aquarium, followed by the subsequent appearance of various behavioral disorders.

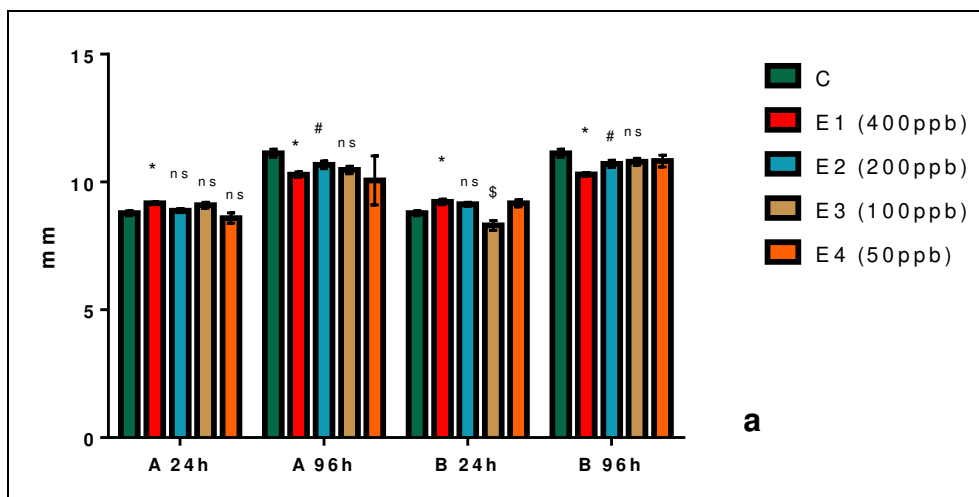
Sterlet larvae maximum mortality was observed at lead concentrations of 400 and $200 \mu\text{gL}^{-1}$. The first dead larvae were detected after 12 hours of lead exposure, with the peak at 72-96 hours interval.

The main changes considered as critical points identified by us, which is evidence of the deleterious activity of lead including: delayed resorption of the yolk sac, deformed / modified tail, undeveloped eyes, massive haemorrhages (cardiac / pericardial / peritoneal / general), abnormal / altered pigmentation and exitus.

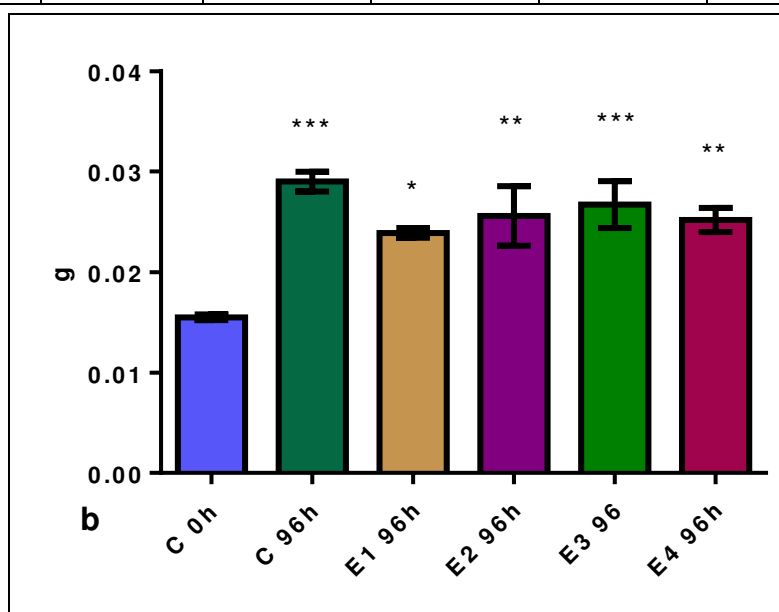
Under the microscope, tail undetachment was also observed; the acute toxicity to the studied larvae being emphasized by the lack of tail posting, oversized abdomen, bleeding heart and / or absence of regular heartbeats. Compared with the control, the results disclosed different, but significant, statistical values registered for the average length parameters measured at 24 and 96 hours and for the main weight parameters at moment 0 and 96 hours per the experimental concentrations. Statistical evaluation revealed a significant association among the influence of lead to the length ($*p < 0.05$) and weight ($**p = 0.01$; $***p < 0.01$) parameters and respectively the number of dead sterlet larvae at the same concentration proving the deleterious activity of lead (*Figure 3*).

Analyzing comparatively with healthy larvae, the consequences of contact with the experimental solutions were observed mainly after 12 hours of exposure to lead. The main behavioral alterations were fast and erratic movements of larvae to the 400 and $200 \mu\text{gL}^{-1}$ concentrations, manifested by corkscrew and circular type motions, irregular contractions, and stationary side position on the aquarium bottom. These low swimming performances were amplified over the course of the experiment and included heart haemorrhages, distended abdomen, and tail in a V, L, or S shape etc. (*Figure 4*).

The greatest percentage of dead larvae was found after 96 hours in the case of the E1A / 1B and E2A / 2B treatments. In terms of the experimental parameters, the measured pH values were between 7.1 and 7.3 and the thermal curve was maintained into the comfort zone of the larvae until the final day of the test (18 to 19.2°C) (*Figure 5*).



Group (n=10)	C	E1 (400ppb)	E2 (200ppb)	E3 (100ppb)	E4 (50ppb)
	X±SEM	X±SEM	X±SEM	X±SEM	X±SEM
A 24h	8.78±0.10	9.17±0.05*	8.88±0.08 ^{ns}	9.09±0.12 ^{ns}	8.59±0.20 ^{ns}
A 96h	11.12±0.16	10.29±0.11*	10.67±0.15 [#]	10.47±0.15 ^{ns}	10.06±0.96
B 24h	8.78±0.10	9.22±0.11*	9.13±0.08 ^{ns}	8.30±0.19 [§]	9.17±0.14
B 96h	11.12±0.16	10.30±0.07*	10.71±0.14 [#]	10.79±0.14 ^{ns}	10.82±0.23



Group (n = 10)	X±SEM	SD	Lower 95% CI	Upper 95% CI
C 0h	0.0155±0.000279	0.000882	0.01487	0.01613
C 96h	0.02901±0.000987***	0.003122	0.02678	0.03124
E1 96h	0.0239±0.0005*	0.00158	0.02277	0.02503
E2 96h	0.02558±0.002969**	0.009388	0.01886	0.0323
E3 96h	0.02673±0.002337***	0.007389	0.02144	0.03202
E4 96h	0.02519±0.001191**	0.003766	0.0225	0.02788

Figure 3. The evolution of the average length parameters at various lead concentrations at 24 and 96 hours of exposure (a) and the significance of the weight parameters at various lead concentrations at day 0 and 96 h of exposure (b)

Where: * $p < 0.05$; ** $p = 0.01$; *** $p < 0.01$; # comparative to Control $p < 0.05$; ns = not significant

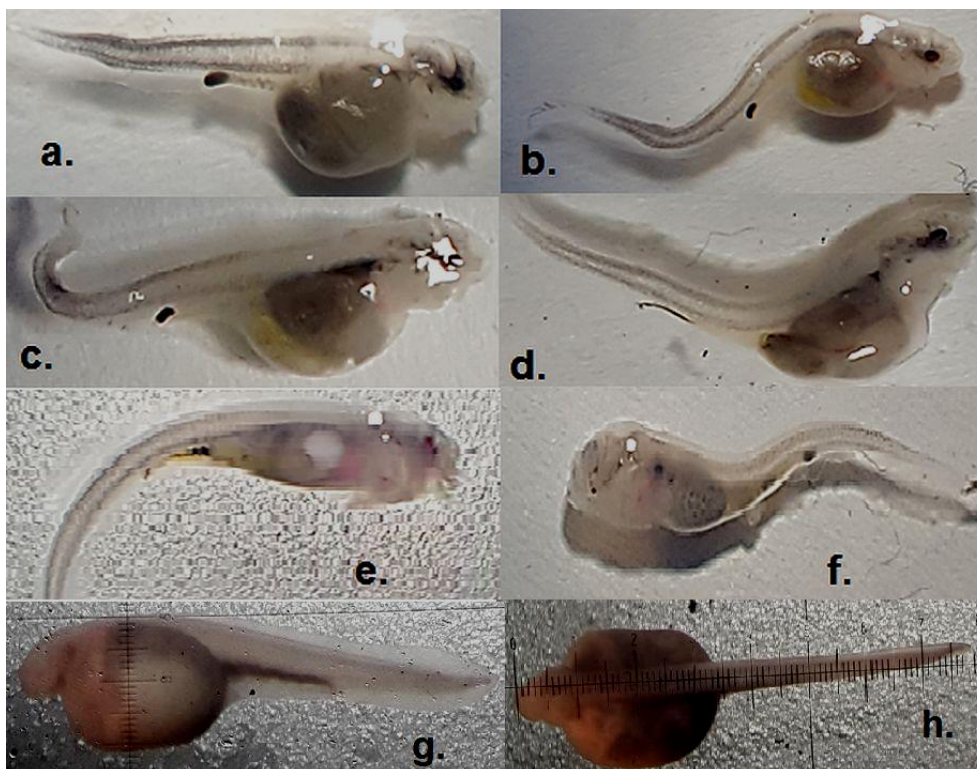


Figure 4. Structural abnormal features observed in starlet larvae exposed to lead: (a) delayed resorption of the yolk sac; (b) “S” shape deformed tail; (c) hook shape tail; (d) “V” shape spinal column; (e) less intense pigmentation, generalized hemorrhages; (f) scoliosis, undeveloped eyes; comparative: healthy larve and scale (lateral (g) and dorsal (h))

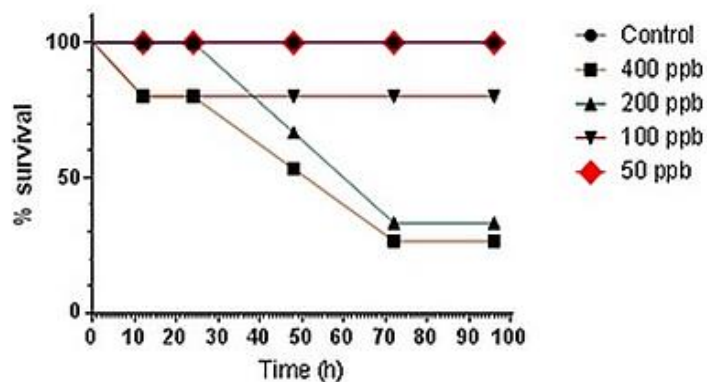


Figure 5. The survival rate / lead concentration during the test period

Initial studies have shown that fish are sensitive enough to detect pollutants in waters both in acute and long-term studies. More and more researchers are utilizing embryo and larval toxicity tests as alternatives to the adult fish acute or chronic toxicity tests, as these are reliable tools to assess the toxicity potential (Embry et al., 2010; Chakraborty et al., 2009; Scholz et al., 2008).

In this aim, in the last decade, studies on this topic were largely diversified, including here different species of sterlet sturgeon, bringing useful information, primarily related

to the fields of environmental, aquatic, and reproductive toxicology for the species *Acipenser transmontanus* (Calfee et al., 2014; Little et al., 2012, 2014; Vardy et al., 2014; Wang et al., 2014), the data for *Acipenser ruthenus* are much more sparse (Raskovic et al., 2015; Linhartova et al., 2015).

We observed that the acute toxicity effects of miscellaneous sources, such as heavy metals (in our case), but also effluents, contaminants etc., is highlighted in the registered anatomical and ethological changes of sturgeon early stages (Calfee et al., 2014; Little et al., 2012). This is noteworthy, as it is a strong motivation why these fish categories are used in recent pollution hazard and risk assessments including here sturgeons (Vardy et al., 2014; Raskovic et al., 2015).

As a research alternative, we agree with authors who have assessed that fish could be completely complementary to rodents or other mammals (especially in toxicology and drug research) (Schirmer et al., 2008; Embry et al., 2010; Chakraborty et al., 2009; De Oliveira, 2009) and we appreciate that with the development of present sterlet *in vitro* model, investigators will be able to replace and offer significant results about water toxicity which will be valuable also to vertebrate research. Based on this observation we noted also that sterlet sturgeon have appropriate features to conditions of temperate climate, making them a suitable candidate, as alternative for zebrafish embryos and larvae, in some specific experiments (eco-tox, embrionar, pollution) in this climate.

As a limitation, it should be pointed out that many aquatic toxicity experiments which have been published have the same shortcomings as the present study, with chemical exposures reported as expected concentrations actually without much more accurate measuring responses. But even if, the studied exposures to lead are not entirely well-known, this work demonstrates that the sterlet sturgeon could credibly be added to the list of the suitable organisms for toxicity tests.

The presence of the mentioned behavioral alterations (considered as critical control points and practically identical with those found in zebrafish), identified for the sterlet early stages are sustaining the results obtained, and consider the sterlet sturgeon as a possible new fish species that could be added to the already recognized and internationally accepted fish species (e.g. zebrafish, medaka, fathead minnow or trout) for the acute tests in the environmental toxicology.

In the favour of this, the analysis of biological damages in conjunction with other endpoints (mortality, external factors etc.) could help to the better interpretation of the effects of lead and could easily be extrapolated to other heavy metals (on sturgeon or other fish species to understand their populational decline), which means early identification of bioaccumulation present in this species (Raskovic et al., 2015; Noel et al., 2013; Waszak and Dabrowska, 2009).

It is also important to mention, that the methodology extrapolation to sturgeons is needed, given the notable scientific and economical importance of these unique natural resource, considered as a central, species in countries where the habitat of this species is located (Reinartz, 2017; Subotic et al., 2013).

The use of *Acipenser ruthenus* early developmental stages is beneficial, since fish embryos and larvae are exempt from animal protection laws. According to the European welfare regulations, this test is categorized as *in vitro* testing, and thus is not subjected to the animal protection legislation situation that, in our point of view, can be easily extrapolated to any fish larvae and further studies on different species (Directive 2010/63/EU).

Conclusions

We consider that this method could be developed as an alternative assay, though the sterlet sturgeon (*Acipenser ruthenus*) is not yet considered as a standard in the assays for toxicology or pollution.

Data obtained could be useful to determine the critical concentration of a single or multiple contaminants that may cause sizeable consequences as environmental pollutants.

Acknowledgements. This study was conducted using the support and infrastructure of the project "Dezvoltarea infrastructurii de cercetare, educație și servicii în domeniile medicinei veterinare și tehnologiilor inovative pentru RO 05", code SMIS-CSNR 2669. Many thanks for Dr. Judit Házi for the valuable comments.

Conflict of Interests. The authors declare no conflict of interests.

REFERENCES

- [1] ASTM (American Society for Testing and Materials) ASTM E1241-05. (1988): Standard Guide for Conducting Early Life-Stage Toxicity Tests with Fishes. – Available at: <https://www.astm.org/Standards/E1241.htm> (Accessed 12.12.2017).
- [2] Bakos, K., Kovács, R., Staszny, Á., Sipos, D., Urbányi, B., Müller, F., Csenki, Zs., Kovács, B. (2013): Developmental toxicity and estrogenic potency of zearalenone in zebrafish (*Danio rerio*). – *Aquatic Toxicology* 136-137: 13-21.
- [3] Braunbeck, T., Böettcher, M., Hollert, H., Kosmehl, T., Lammer, E., Leist, E., Rudolf, M., Seitz, N. (2005): Towards an alternative for the acute fish LC50 test in chemical assessment: the fish embryo toxicity test goes multi-species - an update. – *ALTEX* 22: 87-103. (PMID: 15953964).
- [4] Calfee, R. D., Little, E. E., Puglis, H. J., Scott, E., Brumbaugh, W. G., Mebane, C. A. (2014): Acute sensitivity of white sturgeon (*Acipenser transmontanus*) and rainbow trout (*Oncorhynchus mykiss*) to copper, cadmium, or zinc in water-only laboratory exposures. – *Environmental Toxicology and Chemistry* 33: 2259-2272. Available at: <http://dx.doi.org/10.1002/etc.2684>.
- [5] Chakraborty, C., Hsu, C. H., Wen, Z. H., Lin, C. S., Agoramorthy, G. (2009): Zebrafish: a complete animal model for in vivo drug discovery and development. – *Current Drug Metabolism* 10: 116-124. (PMID:19275547).
- [6] Chebanov, M. S., Galich, E. V. (2011): Sturgeon Hatchery Manual. – FAO Fisheries and Aquaculture Technical Paper. No. 558, ISSN 2070-7010, Ankara, Turkey. Available at: <http://www.fao.org/docrep/017/i2144e/i2144e.pdf> (Accessed 12.12.2017).
- [7] De Oliveira, R. (2009): Zebrafish early life-stages and adults as a tool for ecotoxicology assessment. – Dissertation Biology Department, University of Aveiro, Portugal. Available at: <https://ria.ua.pt/bitstream/10773/8838/1/6237.pdf> (Accessed 12.12.2017).
- [8] Directive 2010/63/EU of the European Parliament and of the Council of 22 September 2010 on the Protection of Animals Used for Scientific Purposes. – Available at: <http://eurlex.europa.eu/LexUriServ/LexUriServ.do?uri=OJ:L:2010:276:0033:0079:en:PDF> (Accessed 12.12.2017).
- [9] Directive 98/83/EC of 3 November 1998 on the quality of water intended for human consumption. – OJ L 330, 5.12.1998, p. 32-54. Available at: <http://eurlex.europa.eu/legal-content/EN/TXT/PDF/?uri=CELEX:31998L0083&from=EN> (Accessed 12.12.2017).
- [10] Embry, R. M., Belanger, S. E., Braunbeck, T. A., Galay-Burgos, M., Halder, M., Hinton, D. E., Léonard, M. A., Lillicrap, A., Norberg-King, T., Whale, G. (2010): The fish

- embryo toxicity test as an animal alternative method in hazard and risk assessment and scientific research. – *Aquatic Toxicology* 97: 79-87. Available at: <https://doi.org/10.1016/j.aquatox.2009.12.008>.
- [11] Gessner, J., Freyhof, J., Kottelat, M. (2010): *Acipenser ruthenus*. – The IUCN Red List of Threatened Species 2010: e.T227A13039007. <http://dx.doi.org/10.2305/IUCN.UK.2010-1.RLTS.T227A13039007.en>.
- [12] Hariharan, G., Purvaja, R., Rame, R. (2016): Environmental safety level of lead (Pb) pertaining to toxic effects on grey mullet (*Mugil cephalus*) and Tiger perch (*Terapon jarbua*). – *Environmental Toxicology* 31: 24-43. (<http://dx.doi.org/10.1002/tox.22019>)
- [13] Hill, A. J., Teraoka, H., Heideman, W., Peterson, R. E. (2005): Zebrafish as a model vertebrate for investigating chemical toxicity. – *Toxicology Science* 86: 6-19. Available at: <https://doi.org/10.1093/toxsci/kfi110>.
- [14] Kovács, R., Csenki, Zs., Bakos, K., Urbányi, B., Horváth, Á., Garaj-Vrhovac, V., Gajski, G., Geric, M., Negreira, N., de Alda, L., Barceló, D., Heath, E., Kosjek, T., Zegura, B., Novak, M., Zajc, I., Baebler, S., Rotter, A., Ramsak, Z., Filipic, M. (2015): Assessment of toxicity and genotoxicity of low doses of 5-fluorouracil in zebrafish (*Danio rerio*) two-generation study. – *Water Research* 77: 201-212.
- [15] Lammer, E., Carr, G. J., Wendler, K., Rawlings, J. M., Belanger, S. E., Braunbeck, T. (2009): Is the fish embryo toxicity test (FET) with the zebrafish (*Danio rerio*) a potential alternative for the fish acute toxicity test? – *Comparative Biochemistry and Physiology Part C Toxicology and Pharmacology* 149: 196-209. Available at: <https://doi.org/10.1016/j.cbpc.2008.11.006>.
- [16] Linhartova, P., Gazo, I., Shaliutina-Kolesova, A., Hulak, M., Kaspar, V. (2015): Effects of tetrabrombisphenol A on DNA integrity, oxidative stress, and sterlet (*Acipenser ruthenus*) spermatozoa quality variables. – *Environmental Toxicology* 30: 735. Available at: <http://dx.doi.org/10.1002/tox.21953>.
- [17] Little, E. E., Calfee, R. D., Linder, G. (2012): Toxicity of Copper to Early-life Stage Kootenai River White Sturgeon, Columbia River White Sturgeon, and Rainbow Trout. – *Archives of Environmental Contamination and Toxicology* 63: 400-408. Available at: <http://dx.doi.org/10.1007/s00244-012-9782-3>.
- [18] Little, E. E., Calfee, R. D., Linder, G. (2014): Toxicity of smelter slag-contaminated sediments from Upper Lake Roosevelt and associated metals to early life stage White Sturgeon (*Acipenser transmontanus* Richardson, 1836). – *Journal of Applied Ichthyology* 30: 1497-1507. Available at: <http://dx.doi.org/10.1111/jai.12565>.
- [19] Luckenbach, T., Kilian, M., Tribskorn, R., Oberemm, A. (2001): Fish early life stage tests as a tool to assess embryotoxic potentials in small streams. – *Journal of Aquatic Ecosystem Stress and Recovery* 8: 355-370. Available at: <https://doi.org/10.1023/A:1012976809450>.
- [20] McGrath, P., Li, C. Q. (2008): Zebrafish: a predictive model for assessing drug-induced toxicity. – *Drug Discovery Today* 13: 394-401. Available at: <https://doi.org/10.1016/j.drudis.2008.03.002>.
- [21] McKim, J. M. (1977): Evaluation of tests with early life stages of fish for predicting long-term toxicity. – *Journal of the Fisheries Research Board of Canada* 34: 1148-1154. Available at: <https://doi.org/10.1139/f77-172>.
- [22] Meyer, J. S., Adams, W. J., Deforest, D. K., Dwyer, R. L., Gensemer, R. W., Gorsuch, J. W., Johnston, R. K., Santore, R. C., Van Genderen, E. (2012): Water chemistry matters in metal-toxicity papers. – *Environmental Toxicology and Chemistry* 31: 689-690. Available at: <http://dx.doi.org/10.1002/etc.1773>.
- [23] Moşneang, C. L., Dumitrescu, E., Muselin, F., Ciulan, V., Grozea, A., Cristina, R. T. (2015a): Use of zebra fish eggs as early indicators of aquatic environmental pollution. – *Polish Journal of Environmental Studies* 24: 2079-2085. Available at: <https://doi.org/10.15244/pjoes/58649>.

- [24] Moşneang, C. L., Grozea, A., Dumitrescu, E., Muselin, F., Cristina, R. T. (2015b): A correlation between two different species of fish embryos used in a freshwater qualitative pollution test. – *Romanian Biotechnology Letters* 20: 10352-10357. Retrieved from <http://www.rombio.eu/rbl2vol20/21.pdf>.
- [25] Moşneang, C. L., Grozea, A., Oprescu, I., Dumitrescu, E., Muselin, F., Gál, D., Cristina, R. T. (2014): Assessment of 2,4-difluoroaniline aquatic toxicity using a zebra fish (*Danio rerio*) model. – *Thai Journal of Veterinary Medicine* 44: 445-452. Retrieved from <http://www.tci-thaijo.org/index.php/tjvm/article/view/25818>.
- [26] Noel, L., Chekri, R., Millour, S., Merlo, M., Leblanc, J. C., Guerin, T. (2013): Distribution and relationships of As, Cd, Pb and Hg in freshwater fish from five French fishing areas. – *Chemosphere*, 90: 1900-1910. Available at: <https://doi.org/10.1016/j.chemosphere.2012.10.015>.
- [27] OECD Test No. 203. Adopted: 17 July 1992, Updated: 10 December 2009. Fish, Acute Toxicity Test. – *Guidelines for the Testing of Chemicals, Section 2. Effects on Biotic Systems*. 1992. (<http://dx.doi.org/10.1787/9789264069961-en>).
- [28] OECD Test No. 210. Adopted: 26 July 2013. Guidelines for the Testing of Chemicals Fish, Early-life Stage Toxicity - Fish, Early-life Stage Toxicity Test. – 2013. (<http://dx.doi.org/10.1787/9789264203785-en>).
- [29] OECD Test No. 236. Adopted: 26 July 2013. Fish Embryo Acute Toxicity (FET) Test. – 2013. (<http://dx.doi.org/10.1787/9789264203709-en>).
- [30] Osman, A. G., Wuertz, S., Mekkawy, I. A., Exner, H. J., Kirschbaum, F. (2007): Lead induced malformations in embryos of the African catfish *Clarias gariepinus* (Burchell, 1822). – *Environmental Toxicology* 22: 375-389. (<http://dx.doi.org/10.1002/tox.20272>)
- [31] PubChem, Open Chemistry Database (2017): SID 24864770: Lead (IV) acetate. Available at: <https://pubchem.ncbi.nlm.nih.gov/substance/24864770#section=Top> (Accessed 12.12.2017.)
- [32] Rác, G., Csenki, Zs., Kovács, R., Hegyi, Á., Baksa, F., Sujbert, L., Zsákovics, I., Kis, R., Gustafson, R., Urbányi, B., Szende, B. (2012): Subacute Toxicity Assessment of Water Disinfection Byproducts on Zebrafish. – *Pathol. Oncol. Res.* 18: 579-584. Available at: <http://dx.doi.org/10.1007/s12253-011-9479-3>.
- [33] Raskovic, B., Poleksic, V., Visnjic-Jeftic, Z., Skoric, S., Gacic, Z., Djikanovic, V., Jaric, I., Lenhardt, M. (2015): Use of histopathology and elemental accumulation in different organs of two benthophagous fish species as indicators of river pollution. – *Environmental Toxicology* 30: 1153-1161. Available at: <http://dx.doi.org/10.1002/tox.21988>.
- [34] Reinartz, R. (2017): Sturgeons in the Danube River Biology, Status, Conservation. – Retrieved from <http://www.dstf.eu/assets/Uploads/documents/Sturgeons-in-the-Danube-RiverReinartz2002.pdf> (Accessed 12.12.2017).
- [35] Schirmer, K., Tanneberger, K., Kramer, N. I., Volker, D., Scholz, S., Hafner, C., Lee, L. E., Bols, N. C., Hermens, J. L. (2008): Developing a list of reference chemicals for testing alternatives to whole fish toxicity tests. – *Aquatic Toxicology* 90: 128-137. Available at: <https://doi.org/10.1016/j.aquatox.2008.08.005>.
- [36] Scholz, S., Fischer, S., Gündel, U., Küster, E., Luckenbach, T., Voelker, D. (2008): The zebrafish embryo model in environmental risk assessment-applications beyond acute toxicity testing. – *Environmental Science and Pollution Research International* 15: 394-404. Available at: <https://doi.org/10.1007/s11356-008-0018-z>.
- [37] Science Direct Topics. Tricaine mesylate - an overview. Tricaine mesylate (MS-222). – Available at: <http://www.sciencedirect.com/topics/medicine-and-dentistry/tricaine-mesylate> (Accessed 12.12.2017).
- [38] Subotic, S., Spasic, S., Visnjic-Jeftic, Z., Hegedis, A., Krpo-Cetkovic, J., Mickovic, B., Skorić, S., Lenhardt, M. (2013): Heavy metal and trace element bioaccumulation in target tissues of four edible fish species from the Danube River (Serbia). – *Ecotoxicology and Environmental Safety* 98: 196-202. (<https://doi.org/10.1016/j.ecoenv.2013.08.020>).

- [39] Vardy, D. W., Santore, R. C., Ryan, A. C., Giesy, J. P., Hecker, M. (2014): Acute toxicity of copper, lead, cadmium, and zinc to early life stages of white sturgeon (*Acipenser transmontanus*) in laboratory and Columbia River water. – *Environmental Science and Pollution Research* 21: 8176-8187. (<http://dx.doi.org/10.1007/s11356-014-2754-6>).
- [40] Wang, N., Ingersoll, C. G., Dorman, R. A., Brumbaugh, W. G., Mebane, C. A., Kunz, J. L., Hardesty, D. K. (2014): Chronic sensitivity of White sturgeon (*Acipenser transmontanus*) and rainbow trout (*Oncorhynchus mykiss*) to cadmium, copper, lead, or zinc in laboratory water-only exposures. – *Environmental Toxicology and Chemistry* 33: 2246-2258. (<http://dx.doi.org/10.1002/etc.2641>).
- [41] Waszak, I., Dabrowska, H. (2009): Persistent organic pollutants in two fish species of Percidae and sediment from the Sulejowski reservoir in central Poland. – *Chemosphere*, 75: 1135-1143. (<https://doi.org/10.1016/j.chemosphere.2009.03.001>).
- [42] Weber, D. N. (1996): Lead-induced metabolic imbalances and feeding alterations in juvenile fathead minnows (*Pimephales promelas*). – *Environmental Toxicology* 11: 45-51. ([http://dx.doi.org/10.1002/\(SICI\)1098-2256\(1996\)11:1<45::AID-TOX7>3.0.CO;2-9](http://dx.doi.org/10.1002/(SICI)1098-2256(1996)11:1<45::AID-TOX7>3.0.CO;2-9)).

AN ASSESSMENT OF THE GENETIC DIVERSITY IN SELECTED WHEAT LINES USING MOLECULAR MARKERS AND PCA-BASED CLUSTER ANALYSIS

ALI, Y.^{1*} – KHAN, M. A.¹ – HUSSAIN, M.² – ATIQ, M.¹ – AHMAD, J. N.³

¹Department of Plant Pathology, University of Agriculture Faisalabad, Faisalabad, Pakistan

²Plant Pathology Research Institute, Ayub Agricultural Research Institute, Faisalabad, Pakistan

³Department of Entomology, University of Agriculture Faisalabad, Faisalabad, Pakistan

*Corresponding author

e-mail: yasirklasra.uca@gmail.com

(Received 7th Jul 2018; accepted 20th Sep 2018)

Abstract. A comprehensive germplasm evaluation study of wheat elite lines was conducted at Wheat Research Institute Faisalabad-Pakistan to identify new sources of leaf, stripe and stem rust resistance and high yield potential during crop seasons 2015-2017. The parent lines were selected on the basis of phenotypic characteristics and slow rusting history for race non-specific resistance genes by the selection of desirable parents used in filial generation (F1-F5). In primary evaluation, 112 lines were selected on the basis of rust reaction and high phenotypic uniformity for further testing against rust resistance and high yield potential. Among these, 32 lines exhibited *Lr34/Yr18*, 22 lines showed *Lr46/Yr29*, and 30 lines indicated the combination of *Sr2/Yr30*. Principal component analysis (PCA) based cluster analysis exhibited that, cluster I and III had clear separation compared to cluster II, IV and V. It was concluded that seven elite lines i.e. V-70003, V-70034, V-70054, V-70070, V-70085, V-70103 and V-70104 exhibited both the linkages of three slow rusting genes (*Lr34/Yr18*, *Lr46/Yr29* and *Sr2/Yr30*) and high yield characteristics and are expected to contribute toward food security at national and global levels.

Keywords: *breeding, grain yield, rust resistance, SSR markers, Triticum aestivum*

Introduction

Wheat (*Triticum aestivum* L.) along with maize and rice is a strategic crop for worldwide food security. The estimated global wheat production for the year 2015-2016 is 734.2 MT which is slightly higher than the demand of 716.2 MT (FAO, 2016). The demand for wheat continues to rise at an annual rate of 1.6% and some estimates indicate that 60% more wheat will be needed by 2050 (FAO, 2016).

Wheat is mainly hit by three types of rusts stripe/yellow, leaf/brown and stem/black that reduce its produce (Roelfs et al., 1992). Evolution of two high temperature tolerant yellow rust races caused severe epidemics in main wheat growing regions of the world since 2000 (Hovmoller et al., 2008). Recent identification of various virulent races of Ug99 i.e. TTKSK, TTKSF, TTKSF+, TTKSP, PTKST and three virulent brown rust races CCPS, MCDS and FBPT are significant threat to wheat production worldwide necessitating integrated and collaborative management strategies of the diseases (Terefe et al., 2014; Pretorius et al., 2015; Patpour et al., 2016).

In Pakistan yellow and leaf rust have been a constant risk to its sustainable production. The reason behind rapid collapse of the assortments is associated to the evolution of new virulent races in assortment due to race specific genes of presentation. The recent and last trend of genomic fight in wheat assortment is “resistance based on preservative effects of accumulation of race non-specific genes” (Singh et al., 1998).

The race non-specific yellow and leaf rust resistance appearing in several assortments is based on durable genes that have additive effects (Singh et al., 2005). The economic, most effective, environmentally friendly, and easy to use method to reduce losses caused by the rusts is cultivation of resistant assortments (Cheng and Chen, 2014; Kalappanavar et al., 2008). In current era of scientific research main focus is to achieve race non-specific slow rusting resistance by combining several minor or adult plant genes (Singh et al., 2000).

Continuous breeding results in narrow genetic variation in gene pool of wheat advance lines and also lead to problems regarding adaptation as well as biotic and abiotic stresses (Zhang et al., 2005). Highest genetic variation among parentage is necessary to achieve transgressive segregation (Joshi et al., 2004). Selection of genetically different parentage through breeding results in maximum variation in progenies. Therefore, there is an urgent need to exploit the existing elite lines to evolve high yielding lines that have extensive adoptability under changing meteorological conditions (Baranwal et al., 2012). The use of molecular markers for the assessment of genetic variation is receiving much attention. Many wheat researchers have studied the genetic diversity in bread wheat using different molecular markers such as RFLPs (Kim and Ward, 2000), ISSRs (Nagaoka and Ogihara, 1997), STS (Chen et al., 1994), AFLPs (Burkhamer et al., 1998) and RAPDs (Joshi and Nguyen, 1993). Though, the most of these molecular marker systems (Devos and Gale, 1992) exhibit a low level of genetic diversity in the selected wheat lines, especially among cultivated lines/cultivars.

The simple sequence repeats (SSRs), also termed as microsatellites, have been proposed as the most-suitable markers for the evaluation of diversity and genetic variation among wheat cultivars/lines, as they are chromosome-specific, multiallelic and consistently distributed along chromosomes (Roder et al., 1998). The SSRs markers have been applied widely for genetic stability of gene bank accessions (Borner et al., 2000), marker-assisted selection in wheat (Huang et al., 2000), identifying QTLs (Kandel et al., 2017), and tagging resistance genes (Mutari et al., 2018). Such molecular markers have also demonstrated a high level of genetic diversity among diploid species (Hammer et al., 2000). Such markers also revealed a high level of polymorphism among diploid species (Hammer et al., 2000), in the accessions of tetraploid wild wheat *Triticum dicoccoides* (Fahima et al., 2002), and as well as in hexaploid wheat varieties (Stachel et al., 2000; Prasad et al., 2000). Cluster and principal component analyses are main genomic diversity tools having comparative differences with each other. PCA based cluster analysis is robust technique to assess family linkage (Mellingers, 1972). Hence, the main goal of present study were to evaluate (1) wheat advanced lines having race non-specific rust resistance through DNA molecular markers (2) high yielding lines through cluster and Principal component analyses.

Materials and methods

For genetic evaluation plant material comprised 855 wheat elite lines (F6 generation) of 45 diverse crosses based on 8-10 year wheat rust history and high yield characteristics (*Table 1*) were selected from gene pool of Wheat Research Institute Faisalabad. The trial was sown during 2nd week of November, 2015-2016 at Wheat Research Institute (WRI) Faisalabad through hand drill following augmented design with single replication split with 9 blocks having five plots per block containing 19 genotypes with one check (Morocco). Each plot comprises of 20 rows 2.5 m long and

25 cm apart. Morocco was inoculated using spraying, dusting and hypodermal needle injection methods twice during month of January and February to develop high rust inoculum pressure (Roelfs, 1988). Disease severity percentage and field response were observed following modified Cobb's scale (*Table 2*) for five consecutive observations after every 7 days interval when morocco became 50-60% susceptible.

Table 1. Detail of parents used in crossing

S/N	Name of line/cultivar	Leaf rust resistance status	Stripe rust resistance status	Acceptable yield kg ha ⁻¹	Maximum yield kg ha ⁻¹
1	INQ.91	Moderately resistant	Moderately resistant	4800	6700
2	WBLLI	Resistant	Resistant	4250	6850
3	AS-2002	Moderately resistant	Susceptible	4550	6655
4	FSD.08	Partially resistant	Moderately resistant	4453	6650
5	AUQAB 2000*2/LAKTA-1	Resistant	Resistant	4775	6900
6	V-87094	Partially resistant	Partially resistant	4850	6900
7	V-09014	Slow rusting	Susceptible	4700	6850
9	SH.88/PAK.81	Partially Resistant	Resistant	4611	6800
10	SHAFQAQ-06	Partially resistant	Partially resistant	4100	6400
11	MILAN/KAUZ	Resistant	Susceptible	4011	6100
12	BABAX	Partially resistant	Partially resistant	4100	6700
13	ALTAR	Moderately resistant	Resistant	4310	6850
14	MAYA 74'S'/MON'S'	Susceptible	Partially resistant	4300	6500
15	MAYA/PVN	Resistant	Resistant	4011	6430
17	PB96/V87094//MH97	Moderately resistant	Resistant	4204	6100
18	TRAP#1	Resistant	Resistant	4500	6600
19	SH88/2*ATTILA	Moderately resistant	Moderately susceptible	4800	6700
20	CNDO/R143	Resistant	Resistant	4250	6850
21	SERI.1B	Moderately resistant	Susceptible	4550	6655
22	PBW343*2/KUKUNA	Partially resistant	Moderately resistant	4453	6650
23	C80.1/3*BATAVIA	Susceptible	Resistant	4475	6800
24	WH576	Partially resistant	Partially resistant	4750	6700
25	PASTOR	Resistant	Resistant	3800	6450
26	MEXI_2	Partially resistant	Partially resistant	4200	6600
27	KRONSTADF2004	Moderately resistant	Resistant	4310	6760
28	ROLF07*2/KIRITATI	Susceptible	Partially resistant	4200	6650
29	KIRITATI	Resistant	Resistant	4050	6050
30	WAXWING	Slow rusting	Susceptible	4000	6150

The genotypes recorded to be resistant through primary evaluation (112) along with five checks were subjected to further screening for rusts resistance and high yield potential at WRI Faisalabad during second week of November, 2016-2017. The genotypes were planted by Norvigion in experimental area of Wheat Research Institute in Augmented design. Each test entry was planted in a plot (six rows of five meter

length). In order to facilitate development of rust epidemics two rows of Morocco were planted around each side of experimental material. Artificial inoculation of experimental material was done in the morning from first week of January to end of February using spraying, dusting and hypodermal needle injection method (Rao et al., 1989), twice a week until a heavy inoculum develops (Roelfs et al., 1992). The applied inoculum consisted of yellow (80E85) and mixture of leaf rust (PHTTL, PGRTB, KSR/JS, TKTPR and TKTRN) races collected from Murree, Kaghan and Faisalabad. High humidity was maintained by frequent irrigations.

Table 2. Disease rating scale used for rust resistance/susceptibility of wheat elite lines

Reaction	Code	Symptoms
Immune	0	No visible infection
Resistant	R	Visible necrotic or chlorosis with or without uredia
Moderately resistant	MR	Small uredia surrounded by necrotic areas
Mixed (intermediate)	M	Small uredia present surrounded by necrotic areas as well as medium uredia with no necrosis but possible some distinct chlorosis
Moderately susceptible	MS	Medium uredia with no necrosis but possible some distinct chlorosis
Moderately susceptible-susceptible	MSS	Medium uredia with no necrosis but possible some distinct chlorosis as well as large uredia with little or chlorosis present
Susceptible	S	Large uredia are present with little or no chlorosis

Cobb's scale (Peterson et al., 1948)

Molecular evaluation and yield testing of 112 selected wheat advance lines through molecular marker and PCA based cluster analysis

The putatively selected 112 wheat advance lines through primary evaluation were further assayed to molecular characterization to identify race non-specific resistance genes *Lr34/Yr18*, *Lr46/Yr29* and *Sr2/Yr30* using a set of 3 DNA molecular markers viz. X-barc-352, XWMC-44, and Xgwm-533 respectively (William et al., 2003; Suenaga et al., 2003; Hussain et al., 2015). This present study work was carried out at Integrated Genomics Cellular Developmental and Biotechnology Laboratory, Post Graduate Agricultural Research Station (PARS) Campus, University of Agriculture Faisalabad.

DNA extraction and quantification

The fresh leaf samples from 30 day-old seedling were collected from the Wheat Research Institute Faisalabad. After tagging, samples were washed with purified water and frozen immediately in liquid nitrogen (LN₂) chamber available in PARS campus University of Agriculture-Faisalabad and stored at -80 °C in deep freeze for DNA extraction by using Cetyl Trimethyl Ammonium Bromide (CTAB) method (Bansal et al., 2014). Leaves were crushed in CTAB buffer to release DNA from the cell. Samples were incubated in water bath at 65 °C for 25–30 min. Tubes were centrifuge at 4000 rpm for 5 min and the upper aqueous phase was transferred to new tubes. Chloroform: isoamyl alcohol (24:1 v/v) (300-500 µl) was added and vortex 4-5 times to mix the contents properly. For further purification other reagents such as RNase and NaCl were also added and centrifuged for 5 min at 14000 rpm and supernatant was transferred to fresh tubes. DNA was precipitated by adding (500 µl) of chilled isopropanol in the tubes and let it at -20 °C for 25-30 min. The tubes were then

centrifuged at 14000 rpm for 15 min to precipitate the DNA. The DNA pellet was washed 2-3 times with 500 µl of 70% ethanol and air dried before re-suspension in 20-30 µl ddH₂O. The DNA concentration was measured by spectrophotometer. An aliquot of sample was diluted in water (1/80th or 1/100th) and its absorbance was measured at 260 nm using a UV spectrophotometer.

PCR-marker assay

PCR amplifications were performed in a total volume of 25 µl containing 50-100 ng/µl of genomic DNA, 2.5 µl of 10X PCR buffer with 2.5 mM (2 µl) of MgCl₂, 0.5 of 10 mM dNTPs, 0.5 µl each forward and reverse primer, 1U of Taq DNA polymerase and 17 µl of ddH₂O (Ahmad et al., 2017). Reagents were purchased from Invitrogen (USA). PCR was performed using the Eppendorf Mastercycler, Germany. The amplification parameters used for all primer sets i.e. X-barc-352, Xwmc-44 and Xgwm-533 restricted to specific durable resistance genes are presented in *Table 3*.

Table 3. Amplification parameters used for all primer sets linked to their specific durable resistance genes

Resistance genes	Primers	Cycle condition
<i>Lr34/Yr18</i>	X-barc-352	94 °C 5 min, 38 cycles (94°C 30 s, 60°C 30 s-1 min, 72 °C 30 s), 72 °C 5 min
<i>Lr46/Yr29</i>	Xwmc-44	94 °C 5 min, 45 cycles (94 °C 1 min, 55 °C 1 min, 72 °C 2 min), 72 °C 10 min
<i>Sr2/Yr30</i>	Xwm-533	94 °C 5 min, 45 cycles (94 °C 1 min, 60 °C 1 min, 72 °C 2 min), 72 °C 10 min

Electrophoresis

After PCR amplification, electrophoresis was carried out on the Syngene gel documentation system USA for SSR markers (Hussain et al., 2015). An amount of 1.5 g high resolution agarose gel was weighted in the electric balance and dissolved in 100 mL 1 X TAE buffer (acetic acid pH = 7.8; Sodium acetate 2 mM; EDTA 10 mM; Tris HCL 40 mM) in a conical flask. It was heated for about 2-3 min by keeping it in oven and then left to cool under running tap water and mixed gently after adding 2 µl ethidium bromide (fluorescent dye) in this solution. The prepared solution was poured slowly into the gel tank. The combs of required size and teeth were inserted in it and leave it for 10-15 min to allow polymerization of gel. After polymerization, the 1XTAE buffer was poured into the gel tank to submerge the gel to 3-6 mm depth. The first well was loaded with 1 Kb ladder molecular weight marker (Promega) as a size standard. Appropriate amounts of about 8 µL of each PCR samples were loaded into the other wells. The gel tank was closed and the gel was run for 30 min by providing 50 to 100 V current to intercalate ethidium bromide in gel. After electrophoresis, the amplified products were visualized under ultraviolet transilluminator and gel pictures were obtained using Gene Snap version 7.6.03 of Syngene gel documentation system USA.

Yield testing of selected advanced lines on the basis of their genetic traits

For yield testing, data of other genetic traits such as plant height (cm), spike length (cm), the number of spikelet per spike, yield (kg ha⁻¹), thousand grain weight (gram)

and protein percentage of all the 112 selected advanced lines along with five checks were recorded. The combined data of grain yield and its components were then subjected to analysis to estimate mean, standard error, range, simple correlation and variance. All variables traits were analyzed by PCA based cluster analyses using software program Statistica v. 10 and SPSS v.12. Cluster analysis identifies parameters which are further classified into a number of clusters following Ward's methods (Ali et al., 2008). The lines in each cluster were also analyzed for simple statistics. To show variation pattern among lines Euclidean distance were calculated and their relationship was shown in the scattered diagram.

Results

The current study was planned to achieve durable-type resistance by accumulating designated slow rusting race non-specific genes with high yield characteristics of wheat advance lines. The plant material was selected from 855 heads rows of 45 crosses planted at Wheat Research Institute Faisalabad, during crop 2015-2016, only 112 lines were selected on the basis of grain color, shape, high phenotypic uniformity and rust reactions (Table 4).

Table 4. Selection of single head crosses from F6 generation of 45 crosses during 2015-2016

Sr. #	Name of crosses	Tested entries	Selected entries
1	CHENAB2000/INQ.91/5/WBLL1*2/4/SNI/TRAP#1/3/KAUZ*2/TRAP//KAUZ	19	3
2	AS-2002/5/FRET2*2/4/SNI/TRAP#1/3/KAUZ*2/TRAP//KAL	19	1
3	FSD.08/6/BABAX/3/FASAN/Y//KAUZ/4/BABAX/5/LU 26/HD2179	19	4
4	KAUZ//ALTAR84/AOS/3/MILAN/KAUZ/4/HUITES/5/KAUZ//ALTAR	19	8
5	SH.88/PAK.81//MH.97//OTUS/TOBA97	19	3
6	SH.88/PAK.81//MH.97//CUMHURIYET/NE	19	3
7	OASIS/5*ANGRA//INQ.91///MILAN/S87230//BABAX	19	4
8	TRM//MAYA 74'S'MON'S'/3/INQ.91/4/PBW343	19	7
9	87094/ERA//PAK-81/2*V-87094/3/SHAFaq-06/4/MAYA/PVN	19	5
10	PFAU/MILAN/5/CHEN/A.SQ(TAUS)//BCN/3/VEE#7/BOW/4/PASTOR/6/QINGHAIBRI/WBLLI//BRBT2	19	3
11	INQALAB 91*2/KUKUNA//KIRITATI//V-09014	19	3
12	AUQAB 2000*2/LAKTA-1	19	4
13	FSD.08/6/BABAX/3/FASAN/Y//KAUZ/4/BABAX/5/LU26/HD2179/7/PB.96/87094//MH.97	19	6
14	TAM200/Tui/6/PVN/CRC422/ANA/5/BOW//CROW/BUC/PVN/3/YR/YR/4/TRAP#1/7/*21NQ-91	19	2
15	INQ/AUQAB/3/SH.88/90A204//MH.97	19	1
16	SH88/WEAVER/3/DWL5023/SNB//SNB	19	1
17	SH88/WEAVER/6/LU26/HD2179/5/BABAX/3/MANGO/VEE#10//PRL/4/BABAX	19	0
18	KAUZ//ALTAR84/AOS/3/PASTOR/4/TILHI/7/CNO79//PF70354/MUS/3/PASTOR/4/BAV92/5/FRET2/KUKUNA//FRET2/6/MILAN/KAUZ//PRINIA/3/BAV92	19	0
19	SH88/2*ATTILA/6/ACHTAR*3//KANZ/KS8585/4/MILAN/KAUZ//PRINIA/3/BAV92/5/MILAN/KAUZ//PRINIA/3/BAV92	19	2

20	CNDO/R143//ENTE/MEXI_2/3/AEGILOPSSQUARROSA(TAUS)/4/W EAVER/5/PICUS/6/TROST/7/TACUPETO F2001/8/OASIS/KAUZ//4*BCN/3/2*PASTOR	19	3
21	CNDO/R143//ENTE/MEXI_2/3/AEGILOPSSQUARROSA(TAUS)/4/W EAVER/5/PICUS/6/TROST/7/TACUPETO F2001/8/CROW'S'/NAC//BO W'S'	19	9
22	PFAU/SERI.1B//AMAD/3/INQALAB91*2/KUKUNA/4/WBLL1*2/KUR UKU/5/PVN/YACO/3/KAUZ*2/TRAP// KAUZ	19	3
23	HUW234+LR34/PRINIA//PBW343*2/KUKUNA/3/ROLF07/4/SNI/TRA P#1/3/KAUZ*2/TRAP//KAUZ	19	0
24	PRL/2*PASTOR//PBW343*2/KUKUNA/4/CAR422/ANA//TRAP#1/3/K AUZ*2/TRAP//KAUZ	19	0
25	C80.1/3*BATAVIA//2*WBLL1/3/PBW343*2/KUKUNA/4/KAUZ / SITE	19	3
26	INQALAB 91*2/KONK//INQALAB 91*2/KUKUNA/3/INQ- 91*2/TUKURU	19	1
27	WHEAR/KRONSTAD F2004/3/CROW'S'/NAC//BOW'S'	19	1
28	WHEAR/KRONSTADF2004/3/PB96/V87094//MH97	19	1
29	FRT/SA42/3/PB96/87094//MH-97	19	1
30	WHEAR/KRONSTAD F2004//KAUZ / SITE	19	7
31	PFAU/MILAN//PBW343*2/TUKURU/3/T.DICOCCON P194625/A.SQ (372)//TUL....	19	1
32	PFAU/MILAN//PBW343*2/TUKURU/3/NR381	19	1
33	CROC_1/AE.SQUARROSA(205)//KAUZ/3/ATTILA/4/BOW/PRL//BUC /3/WH576/5/AMSEL/ATTILA//INQ.91/PEW'S'	19	3
34	CROC_1/AE.SQUARROSA (205)//KAUZ/3/PASTOR/4/THELIN/5/INQ/AUQAB	19	5
35	MINO/898.97/4/INIA66/7C//MAYA/3/PCI/TRM	19	1
36	CHONTE//PBW343*2/KUKUNA/3/CHENAB2000/INQ.91	19	0
37	CHONTE//PBW343*2/KUKUNA/INQ.91*2/TUKURU/3/T.DICOCCOM /P194624/AE.SQ (409)//BCN/4/2*INQ.91/2*/....	19	1
38	PB96/87094/MH-97/3/AMSEL/ATTILA//INQ.91/PEW'S'	19	0
39	PB96/87094//MH-97/3/MILAN/S87230//BABAX	19	1
40	LU26/HD2179//TTR'S'/JUN'S'/3/HP1744//4/MILAN/S87230//BABAX	19	0
41	CNDO/R143//ENTE/MEXI_2/3/AEGILOPSSQUARROSA(TAUS)/4/W EAVER/5/IRENA/6/LERKE/7/TAN/PEW//SARA/3/CBRD	19	5
42	PBW343*2/KUKUNA//KRONSTADF2004/3/PBW343*2/KUKUNA/4/C HENAB2000/INQ.91	19	1
43	PBW343*2/KUKUNA//KRONSTADF2004/3/PBW343*2/KUKUNA/4/C HENAB2000/INQ.91	19	1
44	ATTILA*2//CHIL/BUC*2/3/KUKUNA/4/WAXWING*2/TUKURU	19	1
45	ROLF07*2/KIRITATI/3/SW8688//PBW343*2/KUKUNA	19	2
Total		855	112

All 112 selected wheat elite lines were further characterized on the basis of amplification of SSR molecular markers X-Barc352, Xwmc-44 and Xgwm-533 (Table 5). Among these lines, 32 lines exhibited *Lr34/Yr18*, 22 lines showed *Lr46/Yr29*, and 30 lines indicated the combination of *Sr2/Yr3*. Molecular marker X-barc-352 indicated association to *Lr34/Yr18* which was present on chromosomal loci 1BL. Only

24 advanced lines were amplified by polymerase chain reaction (PCR) in which 19 genotypes were resistant and five advanced lines i.e. V-70001, V-70005, V-70006, V-70008, V-70009 and V-70010 were found susceptible (*Fig. 1*).

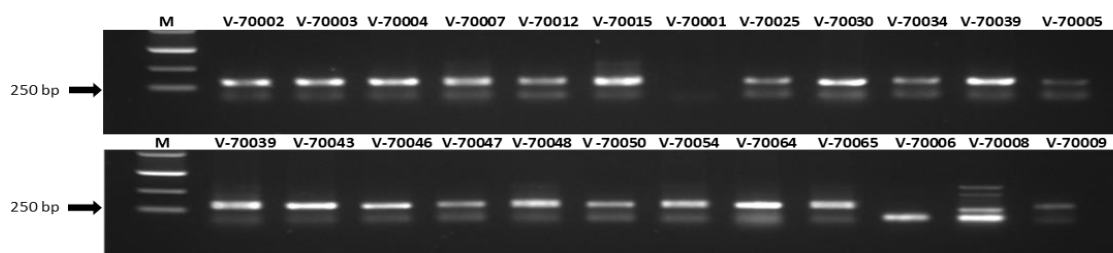


Figure 1. PCR amplification profile of 24 advanced lines for SSR marker X-barc 352 linked to *Lr34/Yr18*; M = 1 Kb DNA Ladder Marker

Table 5. Detail of selected elite lines showing combination of three designated slow rust, race non-specific resistance genes

Plant material		Genotypic markers		
V. Code	Name of genotypes	<i>Lr34/Yr18</i> (X-barc-352)	<i>Lr46/Yr29</i> (XWMC-44)	<i>Sr2/Yr30</i> (Xgwm-533)
70002	CHENAB2000/INQ.91/5/WBLL1*2/4/SNI/TRAP #1/3/KAUZ*2/TRAP//KAUZ PB-36259-0A-0A-0A-9A-0A	+	-	+
70003	CHENAB2000/INQ.91/5/WBLL1*2/4/SNI/TRAP #1/3/KAUZ*2/TRAP//KAUZ PB-36259-0A-0A-0A-12A-0A	+	+	+
70004	AS2002/5/FRET2*2/4/SNI/TRAP#1/3/KAUZ*2/T RAP//KAL PB-36109-0A-0A-0A-7A-0A	+	-	+
70007	FSD.08/6/BABAX/3/FASAN/Y//KAUZ/4/BABA X/5/LU 26/HD2179 PB-36121-0A-0A-0A-8A-0A	+	+	-
70012	KAUZ//ALTAR84/AOS/3/MILAN/KAUZ/4/HUI TES/5/KAUZ//ALTAR84/AOS/3/MILAN/KAUZ/ 4/HUITES PB-36189-0A-0A-0A-5A-0A	+	-	+
70014	KAUZ//ALTAR84/AOS/3/MILAN/KAUZ/4/HUI TES/5/KAUZ//ALTAR84/AOS/3/MILAN/KAUZ/ 4/HUITES PB-36189-0A-0A-0A-15A-0A	-	+	+
70015	KAUZ//ALTAR84/AOS/3/MILAN/KAUZ/4/HUI TES/5/KAUZ//ALTAR84/AOS/3/MILAN/KAUZ/ 4/HUITES PB-36189-0A-0A-0A-17A-0A	+	+	-
70025	OASIS/5*ANGRA//INQ.91//MILAN/S87230//BA BAX PB-36286-0A-0A-0A-8A-0A	+	-	+
70030	TRM//MAYA74'S'/MON'S'/3/INQ.91/4/PBW 343 PB-36360-0A-0A-0A-11A-0A	+	-	+

70033	TRM//MAYA74'S'/MON'S'/3/INQ.91/4/PBW 343 PB-36360-0A-0A-0A-19A-0A	-	+	+
70034	87094/ERA//PAK- 81/2*V87094/3/SHAFQA06/4/MAYA/PVN PB-36369-0A-0A-0A-11A-0A	+	+	+
70039	PFAU/MILAN/5/CHEN/A.SQ(TAUS)//BCN/3/VE E#7/BOW/4/PASTOR/6/QINGHAIBRI/WBLLI// BRBT2 PB-36377-0A-0A-0A-3A-0A	+	+	+
70043	INQALAB91*2/KUKUNA//KIRITATI///V-09014 PB-36447-0A-0A-0A-14A-0A	+	-	+
70046	AUQAB 2000*2/LAKTA-1 PB.37077-0A-0A-0A-8A-0A	+	-	+
70047	AUQAB 2000*2/LAKTA-1 PB.37077-0A-0A-0A-14A-0A	+	+	-
70048	AUQAB 2000*2/LAKTA-1 PB.37077-0A-0A-0A-19A-0A	+	+	-
70050	FSD.08/6/BABAX/3/FASAN/Y//KAUZ/4/BABA X/5/LU 26/HD2179/7/PB.96/87094//MH.97 PB.37082-0A-0A-0A-9A-0A	+	-	+
70054	FSD.08/6/BABAX/3/FASAN/Y//KAUZ/4/BABA X/5/LU26/HD217 9/7/PB.96/87094//MH.97 PB.37082-0A-0A-0A-19A-0A	+	+	+
70061	SH88/2*ATTILA/6/ACHTAR*3//KANZ/KS8585/ 4/MILAN/KAUZ//PRINIA/3/BAV92/5/MILAN/K AUZ//PRINIA/3/BAV92 PB No. 36821-0A-0A-0K-8A-0A	-	+	+
70064	CNDO/R143//ENTE/MEXI_2/3/AEGILOPSSQU ARROSA(TAUS)/4/WEAVER/5/PICUS/6/TROS T/7/TACUPETOF2001/8/OASIS/KAUZ//4*BCN /3/2*PASTOR PB No. 36829-0A-0A-0K-15A-0A	+	+	+
70065	CNDO/R143//ENTE/MEXI_2/3/AEGILOPSSQU ARROSA(TAUS)/4/WEAVER/5/PICUS/6/TROS T/7/TACUPETOF2001/8/CROW'S'/NAC//BOW'S' PB No. 36830-0A-0A-0K-1A-0A	+	-	+
70070	CNDO/R143//ENTE/MEXI_2/3/AEGILOPSSQU ARROSA(TAUS)/4/WEAVER/5/PICUS/6/TROS T/7/TACUPETOF2001/8/CROW'S'/NAC//BOW'S' PB No. 36830-0A-0A-0K-12A-0A	+	+	+
70072	CNDO/R143//ENTE/MEXI_2/3/AEGILOPSSQU ARROSA(TAUS)/4/WEAVER/5/PICUS/6/TROS T/7/TACUPETOF2001/8/CROW'S'/NAC//BOW'S' PB No. 36830-0A-0A-0K-14A-0A	+	-	+
70076	PFAU/SERI.1B//AMAD/3/INQALAB91*2/KUKU NA/4/WBLL1*2/KURUKU/5/PVN/YACO/3/KA UZ*2/TRAP//KAUZ PB No. 36836-0A-0A-0K-10A-0A	+	+	+
70084	WHEAR/KRONSTADF2004//KAUZ/SITE PB No. 36880-0A-0A-0K-1A-0A	+	-	+
70085	WHEAR/KRONSTADF2004//KAUZ/SITE PB No. 36880-0A-0A-0K-11A-0A	+	+	+

70086	WHEAR/KRONSTADF2004//KAUZ/SITE PB No. 36880-0A-0A-0K-12A-0A	+	-	+
70087	WHEAR/KRONSTADF2004//KAUZ/SITE PB No. 36880-0A-0A-0K-13A-0A	+	+	-
70088	WHEAR/KRONSTADF2004//KAUZ/SITE PB No. 36880-0A-0A-0K-15A-0A	-	+	+
70092	PFAU/MILAN//PBW343*2/TUKURU/3/NR381 PB No. 36885-0A-0A-0K-13A-0A	+	-	+
70096	CROC_1/AE.SQUARROSA(205)//KAUZ/3/PAST OR/4/THELIN/5/INQ/AUQAB PB No. 36893-0A-0A-0K-3A-0A	-	+	+
70098	CROC_1/AE.SQUARROSA(205)//KAUZ/3/PAST OR/4/THELIN/5/INQ/AUQAB PB No. 36893-0A-0A-0K-5A-0A	+	-	+
70101	MINO/898.97/4/INIA66/7C//MAYA/3/PCI/TRM PB No. 36894-0A-0A-0K-15A-0A	+	-	+
70103	CNDO/R143//ENTE/MEXI_2/3/AEGILOPSSQU ARROSA(TAUS)/4/WEAVER/5/IRENA/6/LERK E/7/TAN/PEW//SARA/3/CBRD PB No. 36976-0A-0A-0K-4A-0A	+	+	+
70104	CNDO/R143//ENTE/MEXI_2/3/AEGILOPSSQU ARROSA(TAUS)/4/WEAVER/5/IRENA/6/LERK E/7/TAN/PEW//SARA/3/CBRD PB No. 36976-0A-0A-0K-10A-0A	+	+	+
70107	CNDO/R143//ENTE/MEXI_2/3/AEGILOPSSQU ARROSA(TAUS)/4/WEAVER/5/IRENA/6/LERK E/7/TAN/PEW//SARA/3/CBRD PB No. 36976-0A-0A-0K-18A-0A	+	+	-
70108	PBW343*2/KUKUNA//KRONSTADF2004/3/PB W343*2/KUKUNA/4/CHENAB2000/INQ.91 PB No. 36978-0A-0A-0K-8A-0A	+	+	-

+ sign shows the presence of rust resistance genes in wheat genotypes while
- sign shows absence of rust resistance genes in wheat genotypes

SSR marker Xwmc-44 exhibited linkage to *Lr46/Yr29* leaf and stripe rust resistance gene located on chromosome arm 7B. Its bands showed the amplification in the range of 242 bp. Eight elite lines were resistant while 16 advanced lines like V-70011, V-70012, V-70013, V-70014, V-70016, V-70017, V-70018, V-70019, V-70020, V-70021, V-70022, V-70023, V-70024, V-70026, V-70027 and V-70028 were found susceptible with *Lr46/Yr29* and the amplification of only 24 elite lines by polymerase chain reaction has been demonstrated (Fig. 2). PCR-based diagnostic marker XGWM-533 was linked to *Sr2/Yr30* stem and stripe rust resistance gene. *Sr2/Yr30* was exist on chromosomal loci 3BS. All advanced lines indicated the presence of this gene with the band size of 120 bp. Twenty four lines amplified by PCR showed that 13 lines were resistant while 11 genotypes i.e. V-70007, V-70015, V-70029, V-70031, V-70032, V-70035, V-70036, V-70037, V-70038, V-70040 and V-70041 were found susceptible (Fig. 3).

From this investigation it was concluded that among 112 advanced lines, only 10 lines V-70003, V-70034, V-70039, V-70054, V-70064, V-70070, V-70076, V-70085, V-70103 and V-70104 demonstrated the association of 3 designated slow rusting/race non-specific genes. This is very significant linkage, as it gives resistance against all 3 types of rust i.e. stripe, leaf and stem rust. Similarly, 15 genotypes Viz. V-70002, V-

70004, V-70012, V-70025, V-70030, V-70043, V-70046, V-70050, V-70065, V-70072, V-70084, V-70086, V-70092, V-70098 and V-70101 exhibited the linkage of *Lr34/Yr18* and *Sr2/Yr30*. Linkage of *Lr46/Yr29* and *Sr2/Yr30* was indicated in 5 lines viz. V-70014, V-70033, V-70061, V-70088, V-70096 and the association of *Lr34/Yr18* and *Lr46/Yr29* was identified in 7 lines including V-7007, V-70015, V-70047, V-70048, V-70087, V-70107, and V-70108. All these brilliant advanced lines having durable type resistance along with low values of area under disease progress curve may be used in future hybridization schemes to enhance level of resistance in the adapted wheat cultivars of Pakistan (Inqilab-91, Uqab-2000, AS-2002, Seher-2006 and Fareed-06 etc).

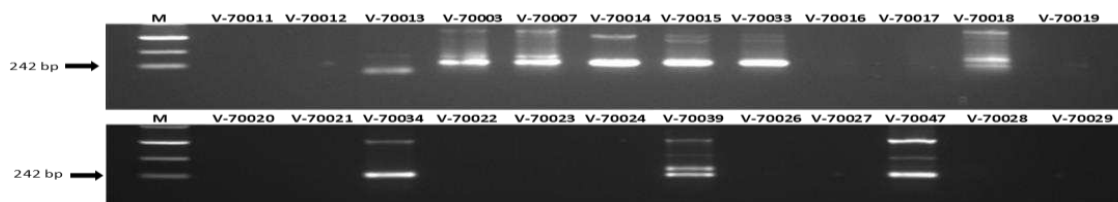


Figure 2. PCR amplification profile of 24 advanced lines for SSR marker XWMC-44 linked to *Lr46/Yr29*; M = 1 Kb DNA Ladder Marker



Figure 3. PCR amplification profile of 24 advanced lines for SSR marker XGWM-533 linked to *Sr2/Yr30*; M = 1 Kb DNA Ladder Marker

Yield testing of selected wheat elite lines on the basis of their genetic traits

Basic statistics for all parameter is described in *Table 6* showed a considerable variability among germplasm that were under study. Medium to high variance was determined for plant height (cm), thousand grain weight, number of spikelet per spike and grain yield (kg ha^{-1}) while small variance was determined for spike length (cm) and protein percentage.

Correlation analyses

A matrix of correlation coefficient among grain yield and its component was determined (*Table 7*). Results indicated that plant height exhibited significant correlation with protein (%) while highly significant correlation with spike length. Thousand grain weight exhibited significant relationship with number of spikelet per spike. A highly significant correlation was observed between grain yield (kg/ha^{-1}) and 1000 grain weight indicating the need of more emphasis on these parameters to increase yield in wheat.

Table 6. Basic statistics for 6 quantitative variables of 112 advance lines along with five checks

Sr. no	Parameters	Mean ± S.D.	Minimum value	Maximum value	Variance
1.	PH (cm) ^a	106.479 ± 7.1192	86.000	124.000	50.70
2.	GY (Kg/ ha ⁻¹) ^b	3762.829 ± 609.2895	2469.000	4800.000	371233.7
3.	P (%) ^c	11.430 ± 0.8742	9.400	13.600	0.8
4.	TGW (g) ^d	36.921 ± 3.5343	30.000	45.000	12.5
5.	SL (cm) ^e	9.392 ± 1.1790	6.980	12.920	1.4
6.	SSP ^f	45.458 ± 4.8649	36.430	55.980	23.7

^aPlant height (cm); ^bGrain yield (Kg ha⁻¹); ^cProtein (%); ^d1000 grain weight (g); ^eSpike length (cm); ^fNumber of spikelet per spike

Table 7. Correlation coefficient (r) matrix for estimated six parameters of genotypes

Parameters	X1	X2	X3	X4	X5	X6
PH (cm) (X1)	1.000					
GY (kg/ha ⁻¹) (X2)	0.077 0.406	1.000				
P (%) (X3)	0.193* 0.037	0.152 0.102	1.000			
TGW (g) (X4)	0.044 0.638	0.252** 0.006	0.062 0.504	1.000		
SL (cm) (X5)	0.256** 0.005	0.074 0.429	0.226* 0.014	0.170 0.067	1.000	
SSP (X6)	0.098 0.296	0.079 0.396	0.054 0.565	0.205* 0.026	0.482** 0.000	1.000

Upper values indicated Pearson's correlation coefficient. Lower values indicated level of significance at 5% probability. * = significant (P < 0.05); ** = highly significant (P < 0.01). Abbreviations as in Table 6

Cluster analysis categorized 112 wheat lines along with five checks into 5 clusters (Table 8; Fig. 4). Distribution pattern of all the genotypes into various clusters exhibited the presence of considerable genetic variability among the genotypes for most of the traits studied. Association among these cluster members showed that clusters V, IV and II showed maximum, while cluster I and III indicated minimum mean values for most of the traits respectively (Table 9). Results confirmed that all genotypes formed in cluster V under trial condition exhibited highest mean values for all traits. After testing under different environmental conditions, all 13 lines of cluster V except V-70078 due to lack of resistance genes (Table 5) could be used for their direct release as variety. Furthermore, all these outstanding lines might be used in hybridization programs to develop rust resistance and high yield varieties.

Six PCs (PC1-PC6) were made from original statistical data revealing 98% of total variation (Table 10). Out of six principal components three PCs (PC1-PC3) have Eigen value greater than 1, accounted for individual variance values of 30.93, 18.44, and 17.84% with 67.21% of cumulative variation of grain yield respectively. The first two PCs were plotted on PC axis 1 and 2 that showed high variability in the existing wheat lines and checks (Fig. 5). Traits with largest absolute values closer to unity within the

PC1 influence the clustering more than those with lower absolute values closer to zero (Chahal and Gosal, 2002). Therefore, in this investigation, differentiation of the advanced lines into different cluster was due to the cumulative effect of a number of traits rather than the contribution of specific few characters. All traits in PC1 showed negative component value whereas, grain yield (kg/ha^{-1}) exhibited great effect in second Principal Component (PC2). Traits having relatively higher value in the PC3 like number of spikelet per spike, thousand grain weight and spike length had more contribution to the total variation and they were the ones that most differentiated the clusters. Plant height (cm), grain yield (kg/ha^{-1}) thousand grain weight (g) in the PC4, plant height (cm), protein (%), thousand grain weight (g) in PC5, spike length (cm), grain yield (kg/ha^{-1}) and thousand grain weight (g) in PC5 were the major contributors to each Principal Components (PC). The current investigation confirmed that advanced wheat lines exhibited wide range of variations for the traits studies and it also proposed that ample prospects for genetic improvement of wheat genotypes through selection directly from bread wheat genotypes and conservation of the germplasm for future utilization.

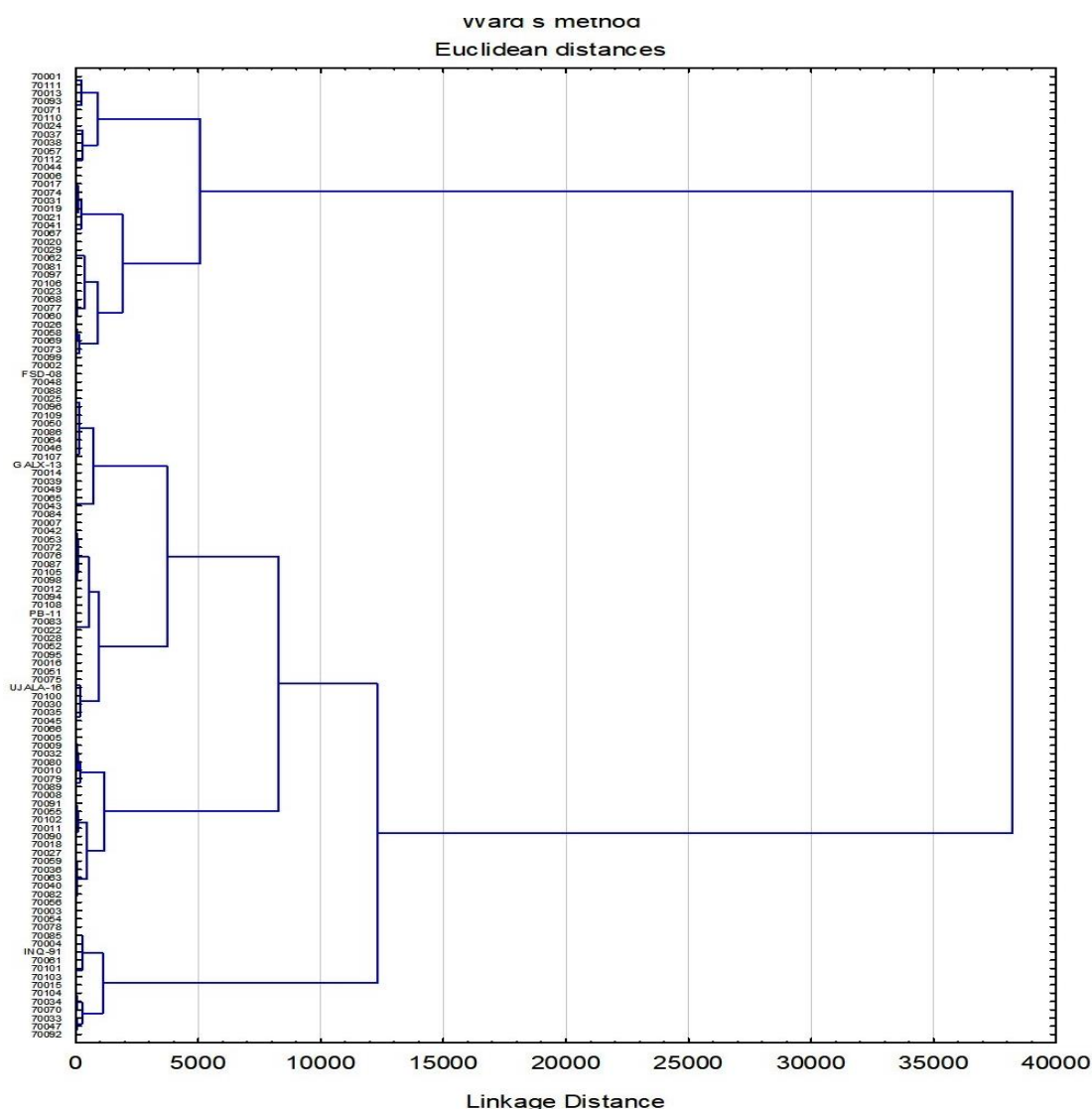


Figure 4. Cluster diagram of 112 advance lines and varieties based on sic traits under study

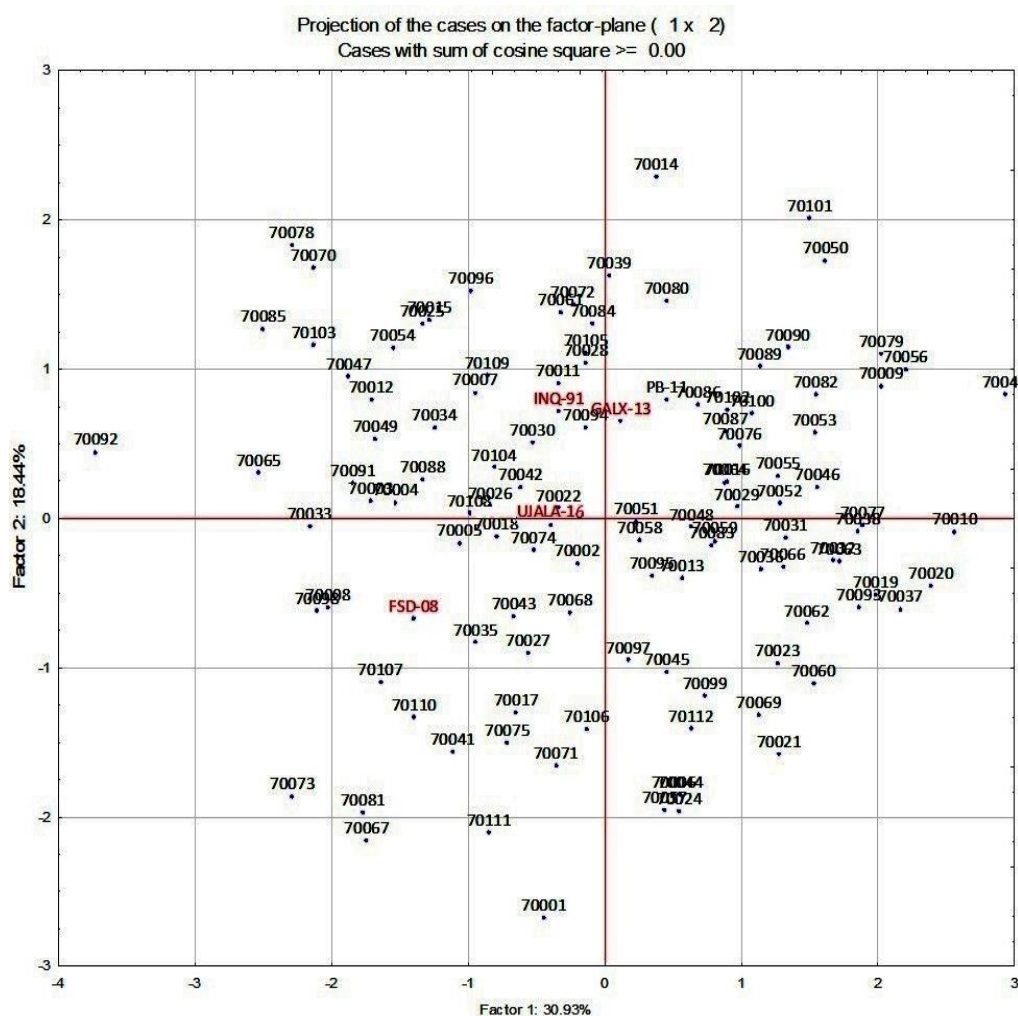


Figure 5. Scattered diagram of first two PCs (Factor 1 as PC1 and Factor 2 as PC2)

Discussion

PCR-based DNA markers associated with genes controlling target economic traits have significant role to attain sustained wheat production. Molecular marker-trait combinations give an effective alternative to phenotyping for selecting varieties that have linkage of desirable genes in breeding populations.

Here we used three SSR markers XGWM-533, XWMC-44 and X-barc-352 for effective marker assisted selection of *Sr2/Yr30*, *Lr46/Yr29* and *Lr34/Yr18* in selected wheat elite lines. This investigation exhibited, among all tested genotypes only 10 advanced lines showed a tight linkage to *Sr2/Yr30*, *Lr46/Yr29* and *Lr34/Yr18* having durable type resistance under the severe disease epidemics. According to Singh and Bowden (2011), resistance near immunity can be achieved by combining 4-5 race non-specific resistance genes in a cultivar. Though, slow level of resistance can be attained by combining 2 to 3 race non-specific/minor genes in a genotype (Lagudah et al., 2009). International Maize and Wheat Improvement Centre (CIMMYT) and Ayub Agriculture Research Institute (AARI) planned a technique of combining race non-specific resistance genes alone or in linkage with some other genes to control recently evolved strains of wheat rust (Rehman et al., 2013).

Table 8. Five cluster grouping wheat lines based on six parameters under study

Cluster	Frequency	Cluster membership
I	22	V-70005, V-70009, V-70010, V-70011, V-70018, V-70026, V-70027, V-70032, V-70036, V-70040, V-70056, V-70058, V-70059, V-70063, V-70069, V-70073, V-70079, V-70080, V-70082, V-70089, V-70090 and V-70099
II	29	V-70007, V-70008, V-70012, V-70016, V-70022, V-70028, V-70030, V-70035, V-70042, V-70045, V-70051, V-70052, V-70053, V-70055, V-70066, V-70072, V-70075, V-70076, V-70083, V-70087, V-70091, V-70094, V-70095, V-70100, V-70102, V-70105, V-70108, UJALA-16 and PB-11
III	30	V-70001, V-70006, V-70013, V-70017, V-70019, V-70020, V-70021, V-70023, V-70024, V-70029, V-70031, V-70037, V-70038, V-70041, V-70044, V-70057, V-70060, V-70062, V-70067, V-70068, V-70071, V-70074, V-70077, V-70081, V-70093, V-70097, V-70106, V-70110, V-70111 and V-70112
IV	21	V-70002, V-70014, V-70025, V-70033, V-70039, V-70043, V-70046, V-70048, V-70049, V-70050, V-70064, V-70065, V-70084, V-70086, V-70088, V-70096, V-70098, V-70107, V-70109, GALX-13 and FSD-08
V	15	V-70003, V-70004, V-70015, V-70034, V-70047, V-70054, V-70061, V-70070, V-70078, V-70085, V-70092, V-70101, V-70103, V-70104 and INQ-91

Table 9. Mean and standard deviation for five clusters based on six parameters under study

Traits	Mean ± SD				
	Cluster – I	Cluster – II	Cluster – III	Cluster – IV	Cluster – V
PH (cm)	104.55±9.64	106.41±5.17	106.33±7.88	106.81±6.49	109.27±4.92
GY (g)	3583.3±148.9	3969.0±92.0	2911.2±235.0	4246.7±72.8	4653.5±100.0
P (%)	11.21±0.96	11.39±0.76	11.40±0.90	11.34±0.96	12.00±0.59
TGW (g)	36.62±3.81	36.62±3.46	35.80±2.64	37.48±3.83	39.41±3.51
SL (cm)	8.73±1.10	9.29±0.88	9.50±1.41	9.69±1.02	9.93±1.16
SSP	43.46±4.55	45.18±4.72	45.55±4.96	46.58±5.09	47.18±4.58

Abbreviations as in Table 6

Table 10. Eigen values, percent individual variance and percent cumulative variance for 6 characters studied on 112 advanced wheat lines along with five checks

Parameters	PC1	PC2	PC3	PC4	PC5	PC6
PH (cm)	-0.47	-0.33	-0.47	0.65	0.04	-0.12
GY (kg ha⁻¹)	-0.40	0.71	-0.25	0.047	-0.53	0.05
P (%)	-0.46	-0.06	-0.64	-0.56	0.21	-0.14
TGW (g)	-0.49	0.59	0.24	0.16	0.57	0.01
SL (cm)	-0.77	-0.34	0.18	-0.10	-0.06	0.49
SSP	-0.67	-0.19	0.53	-0.11	-0.19	-0.43
Eigen value	1.85	1.11	1.07	0.79	0.70	0.47
Individual variance (%)	30.93	18.44	17.84	13.25	11.68	7.85
Cumulative variance (%)	30.93	49.37	67.21	80.46	92.14	98.00

Abbreviations as in Table 6

These genotypes are important source of rust protection with high yield potential. The resistance in determined genotypes seems to be durable in nature. The race specific resistance controlled by the parent lines was vulnerable as the single line V-70001 exhibited severe disease outbreaks ranging from 50-60% in the disease screening plots. Combination form these parent lines against common stripe and leaf rust races proved very effective with lower disease severity in the country (Hussain et al., 2006).

Many new released cultivars have been banned for general cultivation only because of disease vulnerability against novel stripe and leaf rust races (Khan et al., 2002). Combining 2-3 or more genes in a wheat genotype for race non-specific resistance has remained the main emphasis of researchers to combat the changing nature of novel virulent races (Roelfs, 1988). To contest this problem, DNA molecular marker technique was used for improving rust resistance through combining various race non-specific resistance genes in selected wheat lines. Genotypes possessing slow rust linkage illustrated lower area under disease progress curve at adult-plant stage have durable resistance as also indicated by various researchers (Bariana et al., 2001; Singh et al., 2005; Singh and Bowden, 2011). Because the race non-specific resistance like partial and durable rust resistance is polygenic as observed elsewhere, therefore, it remains effective for longer time period, even if the pathogen change its virulence pattern through mutation or recombination (Dehghani and Moghaddam, 2004). Thus, in present study, genotypes having low rust intensity could be considered as durable lines carrying high level of rust resistance to *Sr2*, *Lr46*, and *Lr34* virulences, that might be used in future hybridization schemes to protect crop stability. For its relative ease, productivity and specificity, many researchers have examined the robustness of these molecular markers to identify the occurrence of stripe and leaf rust resistance in wheat germplasm (Dakouri et al., 2013; Lagudah et al., 2006; Mustafa et al., 2013).

In order to evaluate, maintain and use advanced lines effectively it is necessary to study the extent of genetic variability available. Morphological characterization has been successfully used for determination of genetic variability and variety development (Fufa et al., 2005). Analysis of genetic variability through cluster and PCA analyses among germplasm collection help in sorting and core collection of genotype that used for specific breeding purpose (Muhammadi and Prasana, 2003). The cluster analysis classified lines into clusters that showed high intra cluster homogeneity and inter cluster heterogeneity (Jaynes et al., 2003). Considering the significant correlation between grain yield and thousand grain weight and also that the average values of these two parameters for Cluster V are greater than the average of all elite lines. Member of this cluster may be used to increase yield in breeding schemes. The results of this investigation are in line with the findings of Leilah and Al-Khateeb (2005), Ali et al. (2008), Hendawy et al. (2011), and Hristov et al. (2011) who demonstrated the significant correlation between grain yield and other quantitative variables. Spike length and plant height were positively correlated. Same was observed in case of thousand grain weight and number of spikelet per spike i.e. as it decreased the grain yield (kg ha^{-1}) also decrease and as it increased the grain yield also increase (Kamyab et al., 2009).

The principal component analysis showed that, all six PCs had 98% of total variation in the data (Hailegiorgis et al., 2011). Principal component and cluster analyses allowed natural clustering of wheat germplasm. Accordingly, the various measurement methods can be properly used for clustering of wheat germplasm (Kraic et al., 2009). Thus results demonstrated that PCA based cluster analyses is more precise indicator of difference among wheat advance lines than cluster analyses not based on PCA.

However, increased yield potential is stated goal for researchers. Progress in yield characteristics results from the progressive accumulation of minor genes possessing high yield potential (Ajmal et al., 2013). In present investigation, 32 lines showed the linkage of *Lr34/Yr18*, 22 lines demonstrated *Lr46/Yr29* and 30 lines exhibited the linkage of *Sr2/Yr30*. Determining the existence of *Sr2*, *Lr46*, and *Lr34* genes in current elite lines is useful to predict field response. The stability of these selected elite lines helps decision in selecting parentage for future hybridization and to develop new varieties with improved yellow and leaf rust resistance. Thus, the scheme of combining race non-specific genes through breeding is the best way to attain durable resistance in wheat germplasm under continuously changing virulence pattern in the country.

Conclusion

The advanced lines V-70003, V-70034, V-70039, V-70054, V-70064, V-70070, V-70076, V-70085, V-70103 and V-70104 exhibited the combination of all three slow rusting genes (*Lr34/Yr18*, *Lr46/Yr29* and *Sr2/Yr30*). In principal component analysis was demonstrated that six principal components PC1, PC2, PC3, PC4, PC5 and PC6 accounted for 98.00% of the total variation. The first two principal components PC1 and PC2 with values of 30.93 and 18.44%, respectively, contributed more to the total variation indicating hybridization breeding program can be initiated by the selection of genotypes from the PC1 and PC2. Among all traits evaluated plant height (cm), Plant height (cm), grain yield (kg ha⁻¹), protein (%), thousand grain weight (g), spike length (cm), and number of spikelet per spike in each principal component contributed more to the total genetic variations. In conclusion, the crosses between advanced lines selected from cluster-V are expected to produce better genetic recombination and segregation in their progenies. Therefore, these advanced lines need to be crossed and selected to develop high yielding pure line variety.

Acknowledgements. The authors dedicated this research manuscript to Dr. Makhdoom Hussain, Director Wheat Research Institute AARI, Faisalabad for providing research facilities at Wheat Research Experimental Area, Faisalabad.

REFERENCES

- [1] Ahmad, J. N., Ahmad, S. J., Aslam, M., Ahmad, M. A., Contaldo, N., Paltrinieri, S., Bertaccini, A. (2017): Molecular and biologic characterization of a phytoplasma associated with Brassica campestris phyllody disease in Punjab province, Pakistan. – European Journal of Plant Pathology 149(1): 117-125.
- [2] Ajmal, S., Minhasi, N. M., Hamdani, A., Shakiri, A., Zubair, M., Ahmad, Z. (2013): Multivariate analysis of genetic divergence in wheat (*Triticum aestivum*) germplasm. – Pakistan Journal of Botany 45(5): 1643-1648.
- [3] Ali, Y., Atta, B. M., Akhter, J., Monneveux, P., Lateef, Z. (2008): Genetic variability, association and diversity studies in wheat (*Triticum aestivum* L.) germplasm. – Pakistan Journal of Botany 40(5): 2087-2097.
- [4] Bansal, U. K., Kazi, A. G., Singh, B., Hare, R. A., Bariana, H. S. (2014): Mapping of durable stripe rust resistance in a durum wheat cultivar Wollaroi. – Molecular Breeding 33: 51-59.

- [5] Baranwal, D. K., Mishra, V. K., Vishwakarma, M. K., Yadav, P. S., Arun, B. (2012): Studies on genetic variability, correlation and path analysis for yield and yield contributing traits in wheat (*T. aestivum* L. em Thell.). – Plant Arch 12(1): 99-104.
- [6] Bariana, H. S., Hayden, M. J., Ahmed, N. U., Bell, J. A., Sharp, P. J., McIntosh, R. A. (2001): Mapping of durable adult plant and seedling resistances to stripe rust and stem rust diseases in wheat. – Australian Journal of Agricultural Research 52: 1247-1255.
- [7] Borner, A., Chebotar, S., Korzun, V. (2000): Molecular characterization of the genetic integrity of wheat (*Triticum aestivum* L.) germplasm after long-term maintenance. – Theoretical and Applied Genetics 100: 494-497.
- [8] Burkhamer, R. L., Lanning, S. P., Martens, R. J., Martin, J. M., Talbert, L. E. (1998): Predicting progeny variance from parental divergence in hard red spring wheat. – Crop Science 38: 243-248.
- [9] Chahal, G. S., Gosal, S. S. (2002): Principles and Procedures of Plant Breeding: Biotechnology and Conventional Approaches. – Alpha Science International, Oxford, UK.
- [10] Chen, H. B., Martin, J. M., Lavin, M., Talbert, L. E. (1994): Genetic diversity in hard red spring wheat based on sequence-tagged-site PCR markers. – Crop Science 34: 162-1632.
- [11] Cheng, P., Chen X. M. (2014): Virulence and molecular analyses support asexual reproduction of *Puccinia striiformis* f. sp. *tritici* in the U. S. Pacific Northwest. – Phytopathology 104: 1208-1220.
- [12] Dakouri, A., McCallum, B. D., Radovanovic, N., Cloutier, S. (2013): Molecular and phenotypic characterization of seedling and adult plant leaf rust resistance in a world wheat collection. – Molecular Breeding 32: 663-677.
- [13] Dehghani, H., Moghaddam, M. (2004): Genetic analysis of the latent period of stripe rust in wheat seedlings. – Journal of Phytopathology 152: 325-330.
- [14] Devos, K. M., Gale, M. D. (1992): The use of random amplified polymorphic DNA markers in wheat. – Theoretical and Applied Genetics 84: 567-572.
- [15] Fahima, T., Röder, M. S., Wendehake, K., Kirzhner, V. M., Nevo, E. (2002): Microsatellite polymorphism in natural populations of wild emmer wheat, *Triticum dicoccoides*, in Israel. – Theoretical and Applied Genetics 104: 17-29.
- [16] FAO (2016): What is Conservation Agriculture? – <http://www.fao.org/ag/ca/la.htm> 1. FAO, Rome.
- [17] Fufa, H., Baenizger, P. S., Beecher, B. S., Dweikat, I., Graybosch, R., Eskridge, A. K. M. (2005): Comparison of phenotypic and molecular-based classifications of hard red winter wheat cultivars. – Euphytica 145: 133-146.
- [18] Hailegiorgis, D., Mesfin, M., Genet, T. (2011): Genetic Divergence Analysis on Some Bread Wheat Genotypes Grown in Ethiopia. – Journal of Central European Agriculture 12: 344-352.
- [19] Hammer, K., Filatenko, A. A., Korzun, V. (2000): Microsatellite markers: a new tool for distinguishing diploid wheat species. – Genetic Resources and Crop Evolution 47: 497-505.
- [20] Hendawy, S. E., Sakagami, J. I., Hu, Y., Schmidhalter, U. (2011): Screening Egyptian wheat genotypes for salt tolerance at early growth stages. – International Journal of Plant Breeding 5(3): 1735-8043.
- [21] Hovmoller, M. S., Amor, H., Yahyaoui, E. A., Annemarie, F. J. (2008): Rapid global spread two aggressive strains of a wheat rust fungus. – Molecular Ecology 17(17): 3818-3826.
- [22] Hristov, N., Mladenov, N., Spika, A. K., Jeromela, A. M., Jockovic, B., Jacimovic, G. (2011): Effect of environment and genetic factors on the correlation and stability of grain yield components in wheat. – Genetika 43(1): 141-152.
- [23] Huang, X. Q., Hsam, S. L. K., Zeller, F. J., Wenzel, G., Mohler, V. (2000): Molecular mapping of the wheat powdery mildew resistance gene *Pm24* and marker validation for molecular breeding. – Theoretical and Applied Genetics 101: 407-414.

- [24] Hussain, M., Ayub, N., Khan, S. M., Khan, M. A., Muhammad, F., Hussain, M. (2006): Pyramiding rust resistance and high yield in bread wheat. – *Pakistan Journal of Phytopathology* 18: 11-21.
- [25] Hussain, M., Khan, M. A., Hussain, M., Javed, N., Khaliq, I. (2015): Application of phenotypic and molecular markers to combine genes for durable resistance against rust virulences and high yield potential in wheat. – *Internal Journal Agriculture and Biology* 17: 421-430.
- [26] Jaynes, D. B., Kaspar, T. C., Colvin, T. S., James, D. E. (2003): Cluster analysis of spatiotemporal corn yield pattern in an Iowa field. – *Agronomy Journal* 95: 574-586.
- [27] Joshi, A. K., Kumar, S., Chand, R., Ortiz-Ferrara, G. (2004): Inheritance of resistance to spot blotch caused by *Bipolaris sorokiniana* in spring wheat. – *Plant Breeding* 123: 213-219.
- [28] Joshi, C. P., Nguyen, H. T. (1993): RAPD (random amplified polymorphic DNA) analysis based intervarietal genetic relationships among hexaploid wheats. – *Plant Science* 93: 95-103.
- [29] Kalappanavar, I. K., Patidar, R. K., Srikant, K. (2008): Management strategies of leaf rust of wheat caused by *Puccinia recondita* f. Sp. *Triticicrob. Ex. Desm.* – *Karnataka Journal of Agricultural Sciences* 21(1): 61-64.
- [30] Kamyab, M., Hassani, H., Tohidinejad, E. (2009): Agronomic behavior of a new cereal (Tritipyrum: AABBEBEb) compared with modern Triticale and Iranian bread wheat cultivars. – *Plant Ecophysiology* 150: 69-80.
- [31] Kandel, J. S., Krishnan, V., Jiwan, D., Chen, X., Skinner, D. Z., See, D. R. (2017): Mapping genes for resistance to stripe rust in spring wheat landrace PI 480035. – *PloS One* 12(5): p.e0177898.
- [32] Khan, M. A., Hussain, M., Hussain, M. (2002): Wheat leaf rust (*Puccinia recondita*) occurrence and shifts in its virulence in Punjab and NWFP. – *Pakistan Journal of Phytopathology* 14: 1-6.
- [33] Kim, H. S., Ward, R. W. (2000): Patterns of RFLP-based genetic diversity in germplasm pools of common wheat with different geographical or breeding program origins. – *Euphytica* 115: 197-208.
- [34] Kraic, F., Mocák, J., Roháčik, T., Sokolovičová, J. (2009): Chemometric characterization and classification of new wheat genotypes. – *Nova Biotechnol* 9: 101-106.
- [35] Lagudah, E. S., McFadden, H., Singh, R. P., Huerta-Espino, J., Bariana, H. S., Spielmeyer, W. (2006): Molecular genetic characterisation of the *Lr34/Yr18* slow rusting resistance gene region in wheat. – *Theoretical and Applied Genetics* 114: 21-30.
- [36] Lagudah, E. S., Krattinger, S. G., Herrera-Foessel, S., Singh, R. P., Huerta-Espino, J., Spielmeyer, W., Brown-Guedira, G., Selter, L. L., Keller, B. (2009): Gene-specific markers for the wheat gene *Lr34/Yr18/Pm38* which confers resistance to multiple fungal pathogens. – *Theoretical and Applied Genetics* 119: 889-898.
- [37] Leilah, A. A., Al-Khateeb, S. A. (2005): Statistical analysis of wheat yield under drought conditions. – *Elsevier* 61: 483-496.
- [38] Mellingers, J. S. (1972): Measures of genetic similarity and genetic distance. – *Studies in Genetics VII Univ Tex Publ.* 27(13): 145-153.
- [39] Muhammadi, S. A., Prasanna, B. M. (2003): Analysis of genetic diversity in crop plants- Salient statistical tools and considerations. – *Crop Science* 43: 1234-1248.
- [40] Mustafa, G., Alam, M. M., Khan, S. U., Naveed, M., Mumtaz, A. S. (2013): Leaf rust resistance in semi dwarf wheat cultivars: a conspectus of post green revolution period in Pakistan. – *Pakistan Journal of Botany* 45: 415-422.
- [41] Mutari, B., Udupa, S. M., Mavindidze, P., Mutengwa, C. S. (2018): Detection of rust resistance in selected Zimbabwean and ICARDA bread wheat (*Triticum aestivum*) germplasm using conventional and molecular techniques. – *South African Journal of Plant and Soil* 35(2): 101-10.
- [42] Nagaoka, T., Ogihara, Y. (1997): Applicability of inter-simple sequence repeat polymorphisms in wheat for use as DNA markers in comparison to RFLP and RAPD markers. – *Theoretical and Applied Genetics* 94: 597-602.

- [43] Patpour, M., Hovmoller, M., Justesen, A., Newcomb, M., Olivera, P., Jin, Y., Szabo, L., Hodson, D., Shahin, A., Wanyera, R. (2016): Emergence of virulence to SrTmp in the Ug99 race group of wheat stem rust, *Puccinia graminis* f. sp. *tritici*, in Africa. – *Frontier in Plant Science* 7: 34-45.
- [44] Peterson, R. F., Campbell, A. B., Hannah, A. E. (1948): A diagrammatic scale for estimating rust severity on leaves and stems of cereals. – *Canadian Journal of Genetics and Cytology* 26: 496-500.
- [45] Prasad, M., Varshney, R. K., Roy, J. K., Balyan, H. S., Gupta, P. K. (2000): The use of microsatellites for detecting DNA polymorphism, genotype identification and genetic diversity in wheat. – *Theoretical and Applied Genetics* 100: 584-592.
- [46] Pretorius, Z., Visser, B., Terefe, T., Herselman, L., Prins, R., Soko, T., Siwale, J., Mutari, B., Selinga, T., Hodson, D. (2015): Races of *Puccinia triticina* detected on wheat in Zimbabwe, Zambia and Malawi and regional germplasm responses. – *Australian Journal of Plant Pathology* 44: 217-224.
- [47] Rao, S. K. V., Snow, J. P., Berggren, G. T. (1989): Effect of growth stages and initial inoculum level on leaf rust development and yield losses caused by *Puccinia recondita* f. sp. *tritici*. – *Journal of Phytopathology* 127: 200-210.
- [48] Rehman, A. U., Sajjad, M., Khan, S. H., Ahmad, N. (2013): Prospects of wheat breeding for durable resistance against brown, yellow and black rust fungi. – *International Journal of Agriculture and Biology* 15: 1209-1220.
- [49] Roder, M. S., Korzun, V., Gill, B. S., Ganal, M. W. (1998): The physical mapping of microsatellite markers in wheat. – *Genome* 41: 278-283.
- [50] Roelfs, A. P. (1988): Genetic control of phenotypes in wheat stemrust. – *Annual Review of Phytopathology* 26: 351-367.
- [51] Roelfs, A. P., Singh, R. P., Saari, E. E. (1992): *Rust Diseases of Wheat: Concepts and Methods of Disease Management*. – CIMMYT, D. F., Mexico.
- [52] Singh, R. P., Mujeeb-Kazi, A., Huerta-Espino, J. (1998): Lr46: a gene conferring slow rusting resistance to leaf rust in wheat. – *Phytopathology* 88(9): 890-894.
- [53] Singh, R. P., Huerta-Espino, J., Rajaram, S. (2000): Achieving near-immunity to leaf rust and stripe rust in wheat by combining slow rusting resistance genes. – *Acta Phytopathologica et Entomologica Hungarica* 35: 133-139.
- [54] Singh, R. P., Huerta-Espino, J., William, H. M. (2005): Genetics and breeding for durable resistance to leaf and stripe rusts in wheat. – *Turkish Journal of Agriculture and Forestry* 29: 121-127.
- [55] Singh, S., Bowden, R. L. (2011): Molecular mapping of adult-plant race-specific leaf rust resistance gene Lr12 in bread wheat. – *Molecular Breeding* 28: 137-142.
- [56] Stachel, M., Lelley, T., Grausgruber, H., Vollmann. (2000): Application of microsatellites in wheat (*Triticum aestivum* L.) for studying genetic differentiation caused by selection for adaptation and use. – *Theoretical and Applied Genetics* 100: 242-248.
- [57] Suenaga, K., Singh, R. P., Huerta-Espino, J. and William, H. M. (2003): Microsatellite markers for genes *Lr34/Yr18* and other quantitative trait loci for leaf rust and stripe rust resistance in bread wheat. – *Phytopathology* 93: 881-890.
- [58] Terefe, T. G., Visser, B., Herselman, L., Selinga, T., Pretorius, Z. A. (2014): First report of *Puccinia triticina* (leaf rust) race FBPT on wheat in South Africa. – *Plant Disease* 98: 101-109.
- [59] William, H. M., Singh, R. P., Huerta-Espino, J., Ortiz-Islas, S., Hoisington, D. (2003): Molecular Marker mapping of leaf rust resistance gene *Lr46* and its association with stripe rust gene *Yr29* in wheat. – *Phytopathology* 93: 153-159.
- [60] Zhang, P., Dreisigacker, S., Melchinger, A. E., Reif, J. C., Ginkel, M. V., Kazi, A., Hoisington, D., Warburton, M. L. (2005): Quantifying novel sequence variation and selective advantage in synthetic hexaploid wheats and their backcross-derived lines Using SSR markers. – *Molecular Breeding* 15: 1-10.

IMPACT OF ORGANIC AND CONVENTIONAL FARMING PRACTICES ON SOIL QUALITY: A GLOBAL REVIEW

SHEORAN, H. S.^{1*} – KAKAR, R.² – KUMAR, N.³ – SEEMA¹

¹*Department of Soil Science, CCS Haryana Agricultural University
Hisar-125004, Haryana, India*

²*Haryana Space Applications Centre, CCS HAU Campus, Hisar-125004, Haryana, India*

³*Department of Agronomy, CCS Haryana Agricultural University
Hisar-125004, Haryana, India*

**Corresponding author
e-mail: sheoranhardeep2008@gmail.com*

(Received 10th Jul 2018; accepted 20th Dec 2018)

Abstract. As world population grows, the demand for food production increases ultimately creating a huge pressure on our shrinking natural resources. With this increased demand for food researches have realized that conventional farming would neither be able to increase productivity nor would be able to improve the soil quality and there is a need for an alternative farming practice to conserve our environment while sustaining the natural resources. Among the alternative practices, organic farming, which is very popular, aims at reducing the use of synthetic fertilizers and pesticides in order to improve production and ecosystem health. The aim of our paper is to compare the long term effects of conventional and the alternative organic farming practices on soil quality and crop productivity as they are considered to be two major indices that measure agricultural sustainability on long term basis. Therefore, many studies around the world are evaluating the organic farming practices as an alternative was found to be superior in their physical, chemical and biological properties than their conventional counterparts. In addition, the studies showed that the organic farming practices are economically viable in the long term for both crop productivity and environmental sustainability.

Keywords: *management practices, soil properties, microbial communities and soil quality*

Introduction

“Soil: A living and life-giving natural resource, dynamic natural body on the surface of the earth in which plants grow, composed of mineral and organic materials and living forms.” N. C. Brady

The world's populations currently is increasing at an exponential rate and as the demand for food production increases, tremendous pressure and demands are going to be positioned on our natural resources like soil. Conventional methods of farming largely include the use of high dose of synthetic fertilizers and agrochemicals with heavy reliance on tillage practices which will continue to be the customary method of fabrication and the penalty will be reflected in terms of diminished soil quality, affecting the soil's ability of crop production (Gomiero et al., 2011). In contrast, organic farming attempts to mimic or follow natural processes that tend to improve soil and plant health while preserving soil and water resources (Gomiero et al., 2011). These intensive farming practices have resulted in a decline in soil organic matter affecting the soil physical, chemical and biological properties. The declining soil quality due to reduced level of organic matter is imposing a serious threat to sustainability of present agricultural systems which are completely relying on agro-chemicals and high energy

inputs. These inputs have an enormous deleterious impact on soil and water, causing degradation in form of erosion, alkalinity, salinity, acidification, water logging, macro and micronutrients deficiencies that ultimately affect soil quality and crop productivity (Lopes et al., 2011). In addition, excessive use of fertilizers and pesticides causes the accumulation of toxic elements that are resistant to degradation in the soil. It is well established that overall, conventional farming leads to degradation of soils, and certainly going to create problems in achieving the target of sustainability in terms of agricultural production. These challenges questioning to sustainability are going to be accelerated by affecting natural weather phenomenon such as longer periods of drought, which may be attributed to climate change (Montgomery, 2007a). Further, leaching losses of nitrate cause eutrophication of surface waters and contamination of groundwater. Moreover, when soil applied pesticides fails to reach the target, they affect adjacent ecosystems through leaching or aerial drift affecting the diversity and abundance of non targeted microorganisms causing negative effects on ecosystem processes and trophic interactions (Pimentel and Edwards, 1982). There is growing realization among agricultural scientists that though the conventional farming practices have led to achieve the target of self sufficiency (increased food production) but it was at the cost of quality of food, deterioration in environment and degradation of natural resources. Therefore, there is a growing concern about the environmental, economic and social effects of chemical-dependent conventional farming system that have led the scientific community to seek alternative systems that may make agriculture more sustainable and profitable.

Though, agricultural practices are of numerous types and based on the farming techniques they can be generalized as organic, sustainable or conventional. Organic farming aims to thrive plenty of crops, without inclusion of synthetic fertilizers or growth regulators, while sustaining soil quality. This can be called as a traditional method of farming that completely relies on ecosystem services, maintains the integrity of the soils while attaining potential yields (Willer and Lernoud, 2013). Organic farming relies on on-farm techniques of crop rotation, use of organic manures such as vermicompost, farmyard manure (FYM) etc., however, noticeable changes in soil properties could occur only after several years of continuous adoption of these practices. The real picture of overall sustainability with organic farming practices, however, continues to face many challenges. For instance, the Rodale Institute Farming System trial is a well-received study that started in 1981 and has continued to the present (Rothamsted Research, 2005). The experimental trials represent a holistic comparison of the effects of the conventional and organic farming practices soil health, and the study also analyzed the crop yields, economic and energy inputs, and human health and clearly indicated that organic farming was found to be superior in every aspect over conventional system of management (*Fig. 1*).

Due to the many different factors determining crop productivity and soil health, there is a need for much more extensive research on the subject. Therefore, goal of writing this review paper was to use reliable, long-term research that made specific assessments of the two generalized types of farming and then compare the results.

Review of work done

The pertinent literature on the evaluation of soil quality under different land management practices has been reviewed under the following heads:

Soil physical properties

- Bulk density
- Infiltration rate
- Aggregate size distribution
- Moisture retention characteristic

Soil chemical properties

- pH, EC, CaCO₃
- Soil organic carbon and its fractions
- Available N, P, K and micronutrients

Soil biological properties

- Microbial biomass carbon
- Microbial population and enzymatic activities

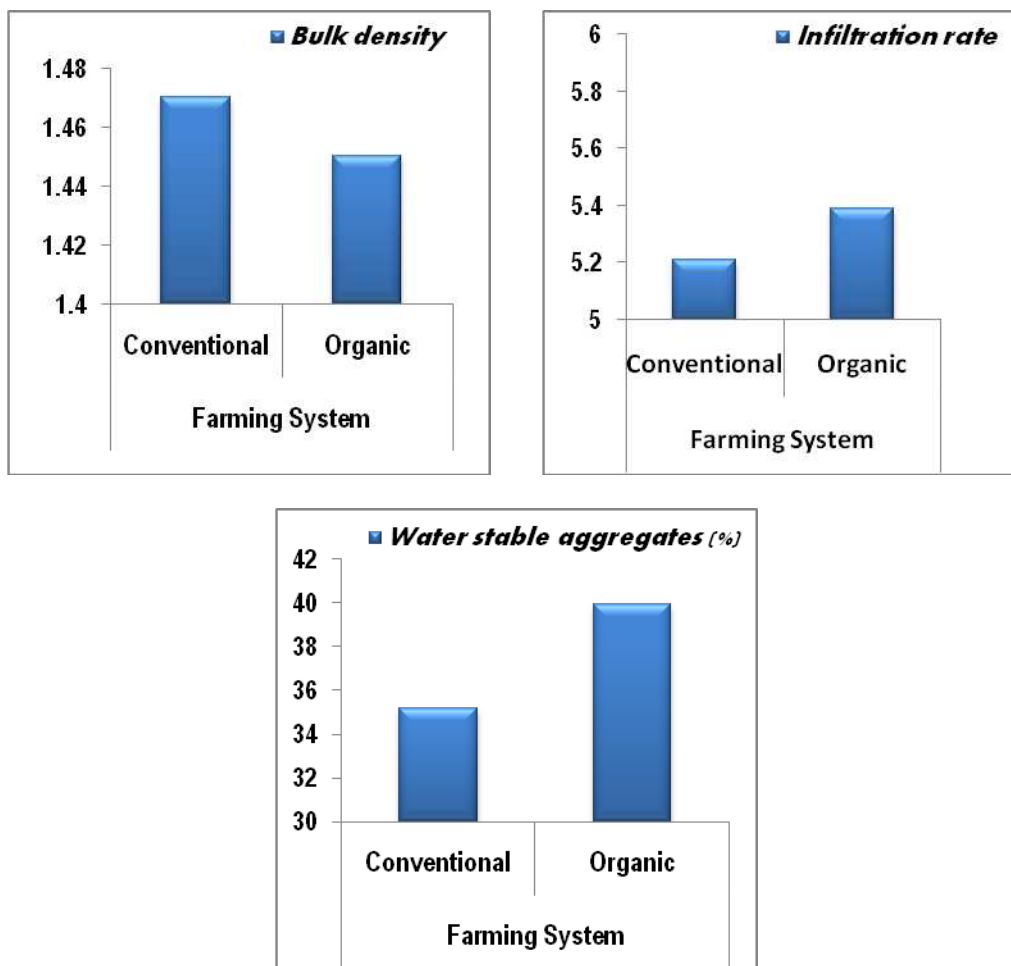


Figure 1. The bulk density, infiltration rate and WSA of soils under organic and conventional farming system (Sheoran, 2018)

Soil physical properties

Bulk density

The literature available on the effect of organic farming on soil bulk density is controversial. Some of the long-term trails have shown no significant difference in bulk

density (Rothamsted Research, 2005) between organically and conventionally managed soils while other have reported reduction in bulk density (Shepherd et al., 2002; Chen et al., 2011; Hati and Bandyopadhyay, 2011). The continuous application of organic material reduces compaction, bulk density and penetration resistance (Chen et al., 2011) and provides more favorable physical properties than in the conventional fertilized systems in surface soil. Quist et al. (2006) studied the influence of alternative and conventional management practices on soil physical and hydraulic properties and reported that bulk density in the surface layer was 3% lower under alternative management practices (1.39 Mg m^{-3}) than under conventional practices (1.43 Mg m^{-3}). Sihi et al. (2017) studied soil health in organic versus conventional farming of basmati rice (*Oryza sativa*) in North India and reported lower bulk density (1.26 and 1.31 Mg m^{-3} in organic and conventional farming, respectively) under organic farming. Similar results were also reported by Suja et al. (2017) in Taro (*Colocasia esculenta* (L.) Schott).

Infiltration rate

The land-use pattern and the land-management i.e., conventional and organic farming, both have different impacts on the infiltration capacity and water storage of the soils. Continuous application of organic matter helps in improving soil structure and subsequently alteration in pore size distribution. Levick (1992) found significantly higher water infiltration, porosity, organic carbon and soil respiration, and lower bulk density and penetration resistance in bio-dynamically farmed than the conventionally farmed soils. High inputs of fertilizers and the use of heavy machinery leads to soil compaction and loss of soil biological activity while organic farming system produces a sustainable soil structure with high biological activity which enhances water infiltration and soil water-holding capacity (Poudel et al., 2001; Quist et al., 2006; Jenkins et al., 2011; Williams et al., 2017). Furthermore, the biological activities supported by organic farming have plenty of bio-pores which in turn enhance water infiltration rates into the soil (Schnug and Haneklaus, 2002). Organic farming system is more useful for earthworm populations as compared to the conventional system resulting into greater number and biomass of earthworms which produce more “biopores” in the soil, and hence creates higher infiltration capacity (Schnug et al., 2004). Fueki et al. (2012) carried out a study to clarify the differences in physical aspects (water permeability and macropores) between organically and conventionally managed soils and reported that the infiltration rate was 6-10 times higher in organic soils than in conventionally managed soils, owing to larger macropores in organic management. Similar results were published by Das et al. (2015) for north-east India reporting the infiltration rate of 3.18 cm hr^{-1} in the conventional to 17.69 cm hr^{-1} in the organic fields.

Aggregate size distribution

The effect of organic farming on aggregate stability in apple (*Malus domestica*) orchard was assessed by Chung (2007) in relation to conventional farming and results revealed that organic farming produced greater aggregation in $>2 \text{ mm}$ size and increased aggregate stability. Zhao et al. (2017) studied the stability and size distribution of soil aggregates under different land uses and measured as mean weight diameter, the percentage of water-stable aggregate and the percentage of each size fraction. The study suggested that land use affected the stability and size distribution of

soil aggregates through the integration of soil organic matter and types of land use. Greater organic matter buildup in organic fields is critical to increase soil aggregate stability (Papadopoulos et al., 2006; Thuries et al., 2001; Sihi et al., 2017). In a study in Switzerland analyzing both biodynamic and organic plots compared to conventional (Fließbach et al., 2007) it was found that significantly higher aggregate stability and water infiltration rates occurs within the organically managed fields, however, a number of European studies found no difference between conventional and organic (Petersen et al., 1997). Higher aggregate stability was measured in organic than in conventional farming systems (Siegrist et al., 1998). Soil aggregate stability was strongly correlated with earthworm activity which was found to be higher under organic than under conventional management (Mader et al., 2002). Organic farming with animal manure has been shown to increase water-stable aggregates compared with conventional farming with inorganic fertilizers (Pulleman et al., 2004).

Moisture retention characteristic

Water retention and transport capacity of a soil is greatly influenced by addition of organic matter and tillage practices (Franzluebbers et al., 2000; Shukla et al., 2003). Organic matter addition and decomposition added organic matter leads to alteration of pore size distribution which is directly related to water retention, storage, and transport within the soil. Although the volume of transmission pores has been reported to be decreased with time under organic farming primarily at 10-20 and 20-30 cm depths but there was only little variation in other physical properties related to soil structure (Ikemura et al., 2008) invalidating the hypothesis that manure application would show better soil structure in organic than conventional farming. Krol et al. (2013) compared the effect of organic and conventional management systems on various soil properties including total porosity, water and ethanol sorptivity, repellency index, and tensile strength of soil aggregates and found that infiltration and sorptivity of water in aggregates were greater under organic than conventional management practices. There were significant differences in soil bulk density, porosity and water content among soils from organic and conventional management systems (Liu et al., 2007). The physical properties such as saturated and unsaturated hydraulic conductivity, water retention capacity, bulk density, total porosity, pore size distribution, soil resistance to penetration, aggregation, and aggregate stability were improved in plots amended with sewage (Aggelides and Londra, 2000). Similarly, Williams et al. (2017) investigated the long term impacts of organic management on soil aggregate stability, bulk density, water infiltration, saturated hydraulic conductivity, and soil water retention characteristics. Results indicated that organically managed soils have more water-stable aggregates, greater ability to absorb irrigation water, and less compactable than conventionally farmed soils. Mean weight diameter of water-stable soil aggregates increased by fifty percent with the organic management. Sunita (2015) reported that plant available water content and water retention capacity showed increased values in organic soil, compared with conventionally farmed soil. The organic farming based on animal or green manure improved physical properties of soils by lowering its bulk density, increasing water-holding capacity and improves infiltration rates (Lee et al., 2006). The higher porosity at the macroscale in soil under conventional management was due to fewer larger pores while meso and micro scale porosity was found to be greater under organic management. Organically managed soils typically provided spatially well distributed pores of all sizes and of greater roughness compared to those

under conventional management. Malik et al. (2014) attempted to find difference in physical properties of soils under conventional and organic management. Data indicated that water retention was significantly higher (59.43%) at surface depth and (60.30%) value for subsurface depth under organic treatment. However, many benefits arise from increased organic additions to the soil (a practice common in organic agriculture) such as improvements in fertility and water holding capacity (Bhogal et al., 2009; Wortman et al., 2011), increase in soil resilience by reducing susceptibility to erosion, retaining soil moisture levels (water retention), and increasing the overall capability of the soil to maintain production (Shepherd et al., 2003). In the study conducted by Zeiger and Fohrer (2009), soil moisture content in the organic farm was relatively higher in comparison to conventional farm. Organic agriculture management promotes the maintenance of higher soil organic matter (Lampkin et al., 2011) and higher microbial biomass, larger fractions of mineralizable C and N, and greater microbial C and improvement inter aggregate stability (Reganold et al., 2010). Thus the physical properties of the soil can be used as indicators for making assessment of soil-quality and assessing sustainability of organic farming systems.

Adoption of organic farming was found to significantly influence the physical properties of soils (*Fig. 1*) and it can be concluded that conversion of land from conventional to organic farming system in long run have the potential to improve the soil physical properties and provide a prominent strategy for enhancing soil physical health while achieving the target of agricultural sustainability.

Soil chemical properties

pH, EC and CaCO₃

Organic farming system has been reported to increase the pH (Ikemura et al., 2008; Chin et al., 2010; Otero et al., 2010; Mendoza et al., 2011; Lee et al., 2014; Suja et al., 2017) and electrical conductivity (EC) (Ikemura et al., 2008; Mendoza et al., 2011) of acid soils and improve the availability of nutrients without exhausting the soil (Otero et al., 2010). The EC values mostly increased with increasing amount of time under organic farming. A comparative study of organic and conventional farming system at three different slope sections (Chong et al., 2008) showed that the soil pH increased in organics as compared to conventional farming plots. In his case study on chemical properties, microbial biomass, and activity between soils of organic and conventional horticultural systems under open field management. Ge et al. (2011) however observed highest pH (8.38) in conventionally managed plots followed by organic management (8.03). Herencia et al. (2007) and Abu-Zahra and Tahboub (2008), however reported no difference in soil pH, EC and calcium carbonate among plots managed organically as well as conventionally. On the other hand, Sihi et al. (2017) reported the enhanced availability of nutrients in organic fields due to favorable soil pH. Soil pH was 0.5 unit lower and EC was 26% lower in organic fields as compared to conventional fields due to excessive salts accumulations from chemical fertilizer usage (Velmourougane, 2016).

Soil organic carbon and its fractions

A large volume of literature is available which supports that long term organic farming increases the soil organic carbon (SOC) quite significantly over the conventional system under different crops/cropping systems (Liebig and Doran, 1999;

Marriott and Wander, 2006; Leifeld et al., 2009; Aher et al., 2015; Jadhav et al., 2016; Gajda et al., 2016; Maharjan et al., 2017) including integrated use of organic and fertilizers (Aher et al., 2015). The magnitude of increase in organic carbon was, however, observed to be higher in fields receiving farmyard manure (FYM), neem cake and vermicompost (Jadhav et al., 2016). It is largely reported that organic farming increases the content of particulate organic matter fraction in total organic matter.

Different fractions of soil organic carbon have been reported to respond differentially to land use and management (Degryze et al., 2004; Malhi et al., 2011; Benbi et al., 2012). Benbi et al. (2012, 2016) found significantly higher concentration of particulate organic carbon (POC) in organically amended plots under rice wheat system than the ones receiving fertilizer nitrogen only. The POC pools were lower, however, in subsurface than the surface soil. Addition of farmyard manure (FYM) alone or in combination with rice straw enlarged the light fraction organic carbon (LFOC) pool by 263 and 383%, and heavy fraction organic carbon (HFOC) pool by 62 and 127%, respectively, with insignificant effect on mineral associated organic carbon (MOC). Marriott and Wander (2006) investigated the veracity of common perceptions about soil organic matter quantity in organically and conventionally managed soils by evaluating the relative responsiveness to organic management of particulate organic matter (POM). The results revealed that organic management enriched the soil particulate organic carbon (POMC) by 30 to 40% relative to the conventional and this level of enrichment was two to four times greater than that in any other fraction. Similar results were earlier reported by Fortuna et al. (2003). Wander and Traina (1996) reported that organic systems had significantly higher quantities of carbon in its light fraction and heavy fraction than the conventionally managed soils.

In many studies, the SOC stocks under organic and conventional systems of farming have also been compared (Canqui et al., 2013; Leifeld and Fuhrer, 2010). Canqui et al. (2013) found the organic farming to increase SOC stocks, aggregate associated SOC and POC concentrations but only in surface soil depth. The SOC stock under organic cattle manure system was 19% greater than under conventional farming (33.1 Mg ha^{-1}). Leifeld and Fuhrer (2010) reported that higher SOC accumulation in organic systems is mainly due to the higher application of organic fertilizer compared with most conventional farming systems. Converting cropland to organic production may provide significant GHG reduction opportunities over the next few decades by increasing the soil organic carbon stocks (Kumar, 2012). Mohamad et al. (2016) reported that manure was the primary contributor to increased SOC in the organic system, resulting in a higher efficiency of carbon sequestration in the soil following the addition of soil organic matter. The contribution of the manure to increased SOC compensated for the higher carbon emission from the organic system, resulting in higher negative net carbon flux in the organic versus the conventional system.

Available N, P, K and micronutrients

Various studies have been reported that organic farming have potential to increase the level of total nitrogen, nitrate and available phosphorus in soil and prevent nutrients leaching (Hansen et al., 2001; Diepeningen et al., 2006) due to manure inputs and the use of cover crops. Herencia et al. (2007) conducted a study over a period of nine years in Spain and found that organic farming management resulted in higher soil organic carbon, N and available P, K, Fe and Zn. The available Mn and especially Cu values did not show significant differences. Liebig and Doran (1999) presented significantly higher

total soil nitrogen in the organic farm than in the conventional farm. Studies that compare organic and conventional farming practices in soils show higher organic matter and macronutrient contents under organic farming (Edmeades, 2003). Monokrousos et al. (2006) found significantly higher extractable soil phosphorus content in organic asparagus (*Asparagus officinalis*) field in comparison to conventional field. In contrast, Romanya and Rovira (2009) indicated significantly higher soil phosphorus content in conventional farm in comparison to organic farm. Andrist et al. (2007) compared soil potassium content between conventional farm and organic farm from 1987 to 2004 in Sweden and found non-significant difference. Lotter (2003) indicated that organic farm can either have significantly higher or no significant difference in soil potassium content than in conventional farm. A comparative study of commercial organic and conventional vegetable farming systems was carried out by Shrestha (2014) to find out impact of different farming systems on soil properties. Results showed that total soil nitrogen and available soil nitrogen content were significantly higher in comparison to the organic farm. Available soil potassium content was significantly higher in the organically managed soil than in the conventionally managed soil. Sudhakaran et al. (2013) found that soils from organic farms had improved soil chemical parameters (total elements and available nutrients) and higher level of total N, P, K, Ca, Mg, Fe, Cu, OC, NH₄-N, NO₃-N, SO₄-S and soluble sodium. A short term organic farming resulted in higher SOC, N and available P, K, Fe and Zn but not available Mn and Cu in soil. Smitha et al. (2015) carried out a study on soil and plant nutrient status as influenced by organic farming in Long pepper (*Piper longum*) and reported that the application of organic manures has a significant impact on plant and soil nutrient and increased the levels of available NPK and microbial population in the soil after three years of cropping. Sihi et al. (2012) and Askegaard and Eriksen (2007) observed a higher available (potentially mineralizable) N concentration in organic systems resulting from the substantial input of nitrogen from different organic manures which mainly include green manures and legumes that release nitrogen simultaneously with the plant demand and reduce nitrogen loss through leaching and volatilization. Likewise, organic farming with legumes and organic amendments (i.e., manure) often increases nutrient concentrations and biological activity (Pelosi et al., 2015). For example, in eastern Nebraska, organic matter, Ca, K, Mg, and Zn concentrations increased with organic farming (Wortman et al., 2011). Uddin et al. (2016) studied the impact of organic and conventional practices on physico-chemical properties and reported the significant increase in the health properties including pH, available organic matter, nitrogen, and P, K, Ca, and S increased significantly in the compost-amended soils compared to the conventional practices. Similarly, Aher et al. (2015) observed that available nitrogen (125 mg kg⁻¹) and P (49.7 mg kg⁻¹) were significantly higher in the plot managed organically while available K (320.1 mg kg⁻¹) was not significant with respect to chemical and integrated practices.

The long-term effects of organic versus conventional farming on soil properties were reviewed and from the literature it can be revealed that organic farming can be considered as an eco-friendly as compared to conventional farming in maintaining soil health. Shifting from conventional to organic farming enhanced the soil organic carbon and its fractions and overall carbon stocks in soils were observed to be higher in organic soils over the conventionally managed soils with higher available plant nutrients (Figure 2).

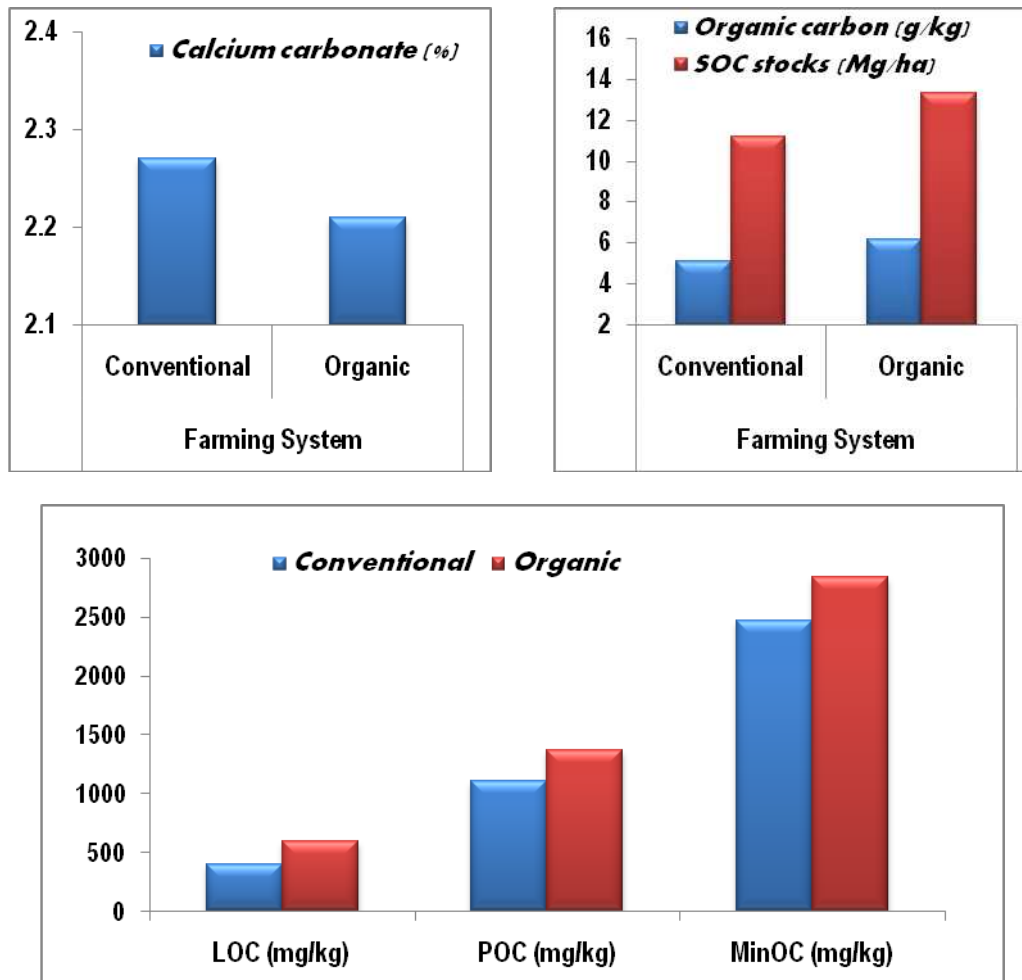


Figure 2. Some chemical properties of soils under organic and conventional farming system (Sheoran, 2018)

Soil biological properties

Microbial biomass carbon

Microbial biomass has been found to be higher in organically managed soils than in conventionally managed (Schjonning et al., 2002; Crecchio et al., 2004; Melero, 2006; Araujo et al., 2009; Amaral et al., 2011) due to the permanent input of organic residues with high C/N ratio. Liu et al. (2007) reported that soils under organic farming had higher microbial biomass carbon and nitrogen, and net mineralizable N. In addition, soil microbial respiration was higher in soils from organic than conventional farms indicating higher microbial activity and populations of Fungi and thermophiles (Thermophilic detected in this study were mainly Actinomycetes; which are indigenous soil bacteria which can be responsible for both the degradation of plant debris and inhibition of soil borne diseases) were also significantly higher in soils from organic than conventional managed fields. Similarly, Okur et al. (2009) reported that SOC and soil microbial biomass C, and protease, urease, alkaline phosphatase, and dehydrogenase activity were significantly higher in the organic farming system than the conventional system.

Stark (2008) evaluated the effect of two organic and conventionally managed sites on soil microbial biomass. The organic site has been managed under a low input six year rotation (*Lolium perenne*, *Medicago sativa* and *Trifolium repens*) and organic fertilization with compost or manures. The results showed positive effect of the management on soil microbial biomass. The influence of different farming systems on microbial community were analyzed using samples from long term field experiment in Switzerland by Esperschütz (2007). The experiment comprised organic and conventional farming systems as well as an unfertilized as control. They observed higher concentrations of phospholipids fatty acids in organic system, indicating a clear influence of the system on microbial biomass. Gajda et al. (2016) found higher activity of microorganisms as measured by fluorescein diacetate hydrolysis under organic farming. Maharjan et al. (2017) studied the effect of land use and management practices on microbial biomass and enzyme activities in subtropical top and sub-soils and found that organic C and N contents as well as microbial biomass were significantly higher in the organic farming topsoil as compared to conventional farming.

Microbial population and enzymatic activities

Benbi et al. (2016) studied the differences in soil organic carbon fractions and biological activity between organic and conventionally managed rice-wheat fields. Under both the systems of management, the highest population was of culturable Bacteria followed by Actinomycetes and the least in case of Fungi in terms of their population which is represented in numbers. The population of culturable Bacteria, Fungi and Actinomycetes were significantly higher under organic than conventional system of farming. Lopes et al. (2011) ascertained that both organically and conventionally farmed soils show temporal variations in the functional but not in the bacterial community structure. Use of an organic fertilizer instead of a synthetic fertilizer is reported to reduce groundwater contamination, improve microbial activity, recycle dairy/poultry wastes and improve soil physical and chemical properties (Pang and Letey, 2000; Poudel et al., 2002). In recent years, multiple studies comparing conventional and organic agriculture have reported differences in soil properties, higher microbial activity and diversity in organically managed soils, or distinct microbial profiles between the two systems (Wu et al., 2008). Bobulska et al. (2015) reported large differences between the organic and conventional sites in terms of microbiological properties, which are sensitive soil indicators of changes occurred under different farming systems. The study confirmed the positive influence and higher microbial activity indices of ecological farming (36% higher enzymatic activity, 65% higher soil respiration content, 60% higher soil microbial biomass carbon content) compared to conventional farming system. Moeskops et al. (2010) compared the effect of organic and conventional farming practices on soil microbial dynamics in West Java, Indonesia and concluded that based on the amounts of marker fatty acids, all microbial groups considered (Actinomycetes, Bacteria, AMF and Fungi) were significantly higher in organically managed soil than in soil from conventional farms ($P < 0.01$, except for Fungi: $P < 0.05$). Babu et al. (2014) conducted a field study to determine the vertical distribution of carbon, nitrogen and other soil properties in four representative soil profiles, one each from <3 years, 3-6 years and >6 years of organic farming practice and one profile representing conventional farming system. Results showed that the enzymatic activities (dehydrogenase and phosphatase) were consistently higher in the surface layer (Ap horizon) in all the four representative profiles studied and the activity

of dehydrogenase and phosphatase of soil increased significantly in the fields subjected to organic farming for three specified time periods irrespective of cropping systems evaluated over conventional farming, with maximum activity being in the profile where organic farming has been practiced for over six years. Ge et al. (2011) carried out a comparative study of organic and conventional arable farming systems and reported the extreme differences between organic and conventional management practices and were reflected in strong differences in microbial biomass and enzyme activities. Velmourougane in 2016 evaluated the long-term impacts of organic and conventional methods of coffee farming on soil physical, chemical, biological, and microbial diversity. Organic system was found to have higher macrofauna (31.4%), microbial population (34%), and microbial diversity indices compared to conventional system. Sudhakaran et al. (2013) investigated the effects of different farm management practices (conventional and organic) on soil biochemical and microbial populations and reported that microbial population (Bacteria, Fungi, Actinomycetes, *Beijerinckia*, *Azotobacter*, Bacteria, *Rhizobium*, bacillus (Bacillus is a genus of gram-positive, rod-shaped bacteria and a member of the phylum Firmicutes. Bacillus species can be obligate aerobes (oxygen depending), or facultative anaerobes (having the ability to be aerobic or anaerobic) and phosphobacteria) were higher in soils from organic farming than sustainable and conventional farms. Carine et al. (2009) also reported that the soil enzyme activities and microbial population are higher in organically managed farm compared to the counterpart's conventional farms. Uddin et al. (2016) studied the impact of organic and conventional practices on physico-chemical properties, behavior and persistence of plant growth promoting microorganisms including *Rhizobium*, *Azotobacter*, phosphate solubilizing Bacteria etc. and reported that population of beneficial soil microbes and health properties including pH, nitrogen content, organic matter, phosphorus, K, Ca, and S, increased significantly in the compost-amended soils compared to the conventional practices. Soil enzymatic activities, organic carbon and microbial population were assessed by Jadhav et al. (2016) and reported that higher population of Actinomycetes ($118 \times 10^5 \text{ g}^{-1} \text{ soil}$), fungal ($141 \times 10^4 \text{ g}^{-1} \text{ soil}$) and Bacteria ($159 \times 10^6 \text{ g}^{-1} \text{ soil}$) were observed with the application of organic materials. Moreover, dehydrogenase and phosphatase activities were increased also increased significantly. The incorporation of cover crops or other organic soil amendments significantly improve soil microbial properties under potato (*Solanum tuberosum*) (Ochiai et al., 2008). In an apple orchard, biological soil properties were improved in the organic compared to the conventional management, however, there were significant differences in soil properties between the conventional and organic farming practices (Glover et al., 2000). Most research suggests that organic farming practices have a positive, stimulating influence on the soil microbes by enhancing diversity and improving soil functions like nutrient cycling and antagonistic potential and it was clearly established that soil quality was higher in soils under organic farming (Girvan et al., 2003; Bending et al., 2004). In general, microbial biomass, enzyme activities, soil respiration, earthworm numbers and/or activity were observed to be higher in soils under organic practices than in those receiving synthetic inorganic fertilizers. Differences in microbial diversity between organically and conventionally managed soils were small (Shannon et al., 2002), although there is evidence for greater bacterial, Actinomycetes and fungal abundance and activity under organic management (Bulluck et al., 2002; Shannon et al., 2002). Mader et al. (2002) reported higher microbial biomass and enzyme activities in organics compared to conventional system of farming with and without farmyard

manure. In contrast, some studies failed to find significant differences in microbial properties of soil between organic and conventional systems or suggested a negative impact of organic practices (Cook and Lee, 1995) while Aher et al. (2015) reported that soil organic carbon (11.3 g kg^{-1}) and enzyme activities in soil viz., dehydrogenase (DHA) ($98.20 \mu \text{ grams TPF/g soil/24 h}$) and alkaline phosphatase ($178.2 \mu \text{ grams p-nitro phenol/g soil/h}$) were significantly higher in the plots managed with organic practices with respect to conventional practices.

From the review, it was observed that organic farming showed a positive stimulating influence on the microbial populations in the soil (*Rhizobium*, *Azotobacter* and *Azospirillum*, phosphate solubilizing bacteria etc.). Overall, soil microbial populations were higher in soils under organic farming, indicating higher microbial activity under organic farming (Figure 3).

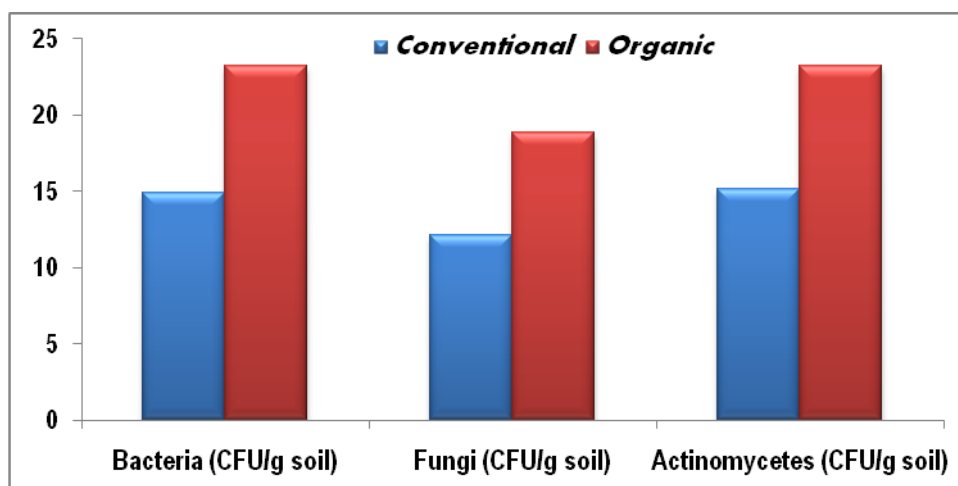


Figure 3. The bacteria, fungi and actinomycetes populations in soils under organic and conventional farming system (Sheoran, 2018)

Conclusion

The study concluded that conversion of land from conventional to organic farming found to have better soil quality in terms of physical, chemical and biological properties which is essential for enhancing soil productivity and other functions of soil in the given ecosystem. In the present agriculture scenario, organic farming may be adopted or promoted as an alternative to the conventional farming practices for sustainable use of natural resources, particularly, with respect to the impending global food safety coupled with climate change.

REFERENCES

- [1] Abu-Zahra, T. R., Tahboub, A. B. (2008): Effect of organic matter sources on chemical properties of the soil and yield of strawberry under organic farming conditions. – World Applied Sciences Journal 5(3): 383-388.
- [2] Aggelides, S. M., Londra, P. A. (2000): Effects of compost produced from town wastes and sewage sludge on the physical properties of a loamy and a clay soil. – Bioresource Technology 71: 253-259.

- [3] Aher, S. B., Lakaria, B. L., Kaleshananda, S., Singh, A. B., Ramana, S., Ramesh, K., Thakur, J. K. (2015): Effect of organic farming practices on soil and performance of soybean (*Glycine max*) under semi-arid tropical conditions in Central India. – *Journal of Applied and Natural Science* 7(1): 67-71.
- [4] Amaral, H. F., Ozinaldo, J., Sena, A., Regina, K., Schwan, E. F., Balota, E. L., Andrade, D. S. (2011): Soil chemical and microbial properties in vineyards under organic and conventional management in southern Brazil. – *Brazilian Journal of Soil Science* 35: 1517-1526.
- [5] Andrist, R. Y., Edwards, A., Hillier, S., Oborn, I. (2007): Long-term K dynamics in organic and conventional mixed cropping systems as related to management and soil properties. – *Agriculture, Ecosystems and Environment* 122: 413-426.
- [6] Araujo, A. S. F. (2009): Soil microbial activity in conventional and organic agricultural systems. – *Sustainability* 1: 268-276.
- [7] Askegaard, M., Eriksen, J. (2007): Growth of legume and non-legume catch crops and residual-N effects in spring barley on coarse sand. – *Journal of Plant Nutrition and Soil Science* 170: 773-780.
- [8] Babu, M. V. S., Ramakrishna, V. R., Parama, Prakash, S. S., Mohan, M., Reddy, V. S. (2014): Vertical distribution of soil total carbon and nitrogen stocks and other properties in profiles as influenced by organic and conventional farming systems under southern dry zone of Karnataka. – *Progressive Agriculture* 14(1): 10-16.
- [9] Benbi, D. K., Sharma, S., Toor, A. S., Brar, K., Sodhi, G. P. S., Garg, A. K. (2016): Differences in soil organic carbon pools and biological activity between organic and conventionally managed rice-wheat fields. – *Organic Agriculture* 16: 168-182.
- [10] Benbi, D. K., Toor, A. S., Kumar, S. (2012): Management of organic amendments in rice-wheat cropping system determines the pool where carbon is sequestered. – *Plant and Soil* 360(1): 145-162.
- [11] Bending, G. D., Turner, M. K., Rayns, F., Marx, M. C., Wood, M. (2004): Microbial and biochemical soil quality indicators and their potential for differentiating areas under contrasting agricultural management regimes. – *Soil Biology & Biochemistry* 36: 1785-1792.
- [12] Bhogal, A., Nicholson, F. A., Chambers, B. J. (2009): Organic carbon additions: Effects on soil bio-physical and physico-chemical properties. – *European Journal of Soil Science* 60: 276-286.
- [13] Bobulska, L., Fazekasova, D., Angelovicova, L., Kotorova, D. (2015): Impact of ecological and conventional farming systems on chemical and biological soil quality indices in a cold mountain climate in Slovakia. – *Biological Agriculture and Horticulture* 26: 2-17.
- [14] Brady, N. C., Weil, R. R. (2002). *The nature and properties of soils*. Upper Saddle River, N.J: Prentice Hall.
- [15] Bulluck, L. R., Brosius, M., Evanylo, G. K., Ristaino, J. B. (2002): Organic and synthetic fertility amendments influence soil microbial, physical and chemical properties on organic and conventional farms. – *Applied Soil Ecology* 19: 147-160.
- [16] Canqui, H. B., Charles, A., Francis, L., Tomie, D., Galusha (2013): Does organic farming accumulate carbon in deeper soil profiles in the long term? – *Geoderma* 288: 213-221.
- [17] Carine, F., Capowicz, Y., Criquet, S. (2009): Enzyme activities in apple orchard agroecosystems: How are they affected by management strategy and soil properties? – *Soil Biology & Biochemistry* 41: 61-68.
- [18] Chen, G., Wail, R. R. (2011): Root growth and yield of maize as affected by soil compaction and cover crops. – *Soil & Tillage Research* 117: 17-27.
- [19] Chin, F. S., Ho, Y. T., Khim, P. C., Jalloh, M. B., Wong, N. K. (2010): Organic versus conventional farming of Tea plantation. – *Borneo Science* 26: 19-26.

- [20] Chong, K. P., Ho, Y. T., Jalloh, M. B. (2008): Soil nitrogen phosphorus and tea leaf growth in organic and conventional farming of selected fields at Sabah Tea plantation slope. – *Journal of Sustainable Development* 1(3): 117-122.
- [21] Chung, J. B. (2007): Comparison of Soil Physical Properties in Conventional and Organic Farming Apple Orchards. – *Korean Journal of Environmental Agriculture* 26(4): 279-285.
- [22] Cook, H. F., Lee, H. C. (1995): Soil management in sustainable agriculture. – *Proceedings of the Third International Conference on Sustainable Agriculture*, Wye College, University of London, 31 August to 4 September 1993.
- [23] Crecchia, C., Gelsomino, A., Ambrosio, R., Minati, J. L., Ruggiero, R. (2004): Functional and molecular responses of soil microbial communities under differing soil management practices. – *Soil Biology & Biochemistry* 36: 1873-1883.
- [24] Das, S., Kumar, P. B., Rajib, M. B. (2015): Infiltration characteristics of tea soil under organic and conventional farming systems in North-East India. – *Journal of the Indian Society of Soil Science* 63(4): 449-453.
- [25] Degryze, S., Six, J., Paustian, K., Morris, S. J., Paul, E. A., Merckx, R. (2004): Soil organic carbon pool changes following land-use conversions. – *Global Change Biology* 10: 1120-1132.
- [26] Diepeningen, A. D., Vos, O. J., Korthals, G. W., Bruggen, A. H. C. (2006): Effects of organic versus conventional management on chemical and biological parameters in agricultural soils. – *Applied Soil Ecology* 31(2): 120-135.
- [27] Edmeades, D. C. (2003): The long-term effects of manures and fertilizers on soil productivity and quality: a review. – *Nutrient Cycling in Agroecosystems* 66: 165-180.
- [28] Esperschütz, J. (2007): Response of soil microbial biomass and community structures to conventional and organic farming systems under identical crop rotations. – *FEMS Microbiology Ecology* 61: 263-267.
- [29] Fließbach, A., Oberholzer, H., Gunst, L., Mader, P. (2007): Soil organic matter and biological soil quality indicators after 21 years of organic and conventional farming. – *Agriculture, Ecosystems & Environment* 118(1-4): 273-284.
- [30] Fortuna, A., Harwood, R. R., Paul, E. A. (2003): The effects of compost and crop rotations on carbon turnover and the particulate organic matter fraction. – *Soil Science* 168: 434-444.
- [31] Franzluebbers, A. J., Stuedemann, J. A., Schomberg, H. H., Wilkinson, S. R. (2000): Soil organic C and N pools under long-term pasture management in the Southern Piedmont USA. – *Soil Biology & Biochemistry* 32: 469-478.
- [32] Fueki, N., Jerzy, L., Jan, K., Urszula, K., Artur, N. (2012): Difference in infiltration and macropore between organic and conventional soil management. – *Soil Science and Plant Nutrition* 58: 65-69.
- [33] Gajda, A. M., Ewa, A. C., Dexter, A. R. (2016): Effects of long-term use of different farming systems on some physical, chemical and microbiological parameters of soil quality. – *International Agrophysics* 30: 165-172.
- [34] Ge, T., Nie, S., Wu, J., Shen, J., Xiao, H., Tong, C., Huang, D., Hong, Y., Iwasaki, K. (2011): Chemical properties, microbial biomass, and activity differ between soils of organic and conventional horticultural systems under greenhouse and open field management: A case study. – *Journal of Soils and Sediments* 11: 25-36.
- [35] Girvan, M. S., Bullimore, J., Pretty, J. N., Osborn, A. M., Ball, A. S. (2003): Soil type is the primary determinant of the composition of the total and active bacterial communities in arable soils. – *Applied & Environmental Microbiology* 69: 1800-1809.
- [36] Glover, J. D., Reganold, J. P., Andrews, P. K. (2000): Systematic method for rating soil quality of conventional, organic, and integrated apple orchards in Washington State. – *Agriculture, Ecosystems & Environment* 80: 29-45.
- [37] Gomiero, T., Pimentel, D., Paoletti, M. G. (2011): environmental impact of different agricultural management practices: conventional vs. organic agriculture. – *Critical Reviews in Plant Sciences* 30(1-2): 95-124.

- [38] Hansen, B. Alroe, H. F., Kristensen, E. S. (2001): Approaches to assess the environmental impacts of organic farming with particular regard to Denmark. – *Agriculture, Ecosystem and Environment* 83(1-2): 11-26.
- [39] Hati, K., Bandyopadhyay, K. (2011): Fertilizers (Mineral, Organic) Effect on Soil Physical Properties. – In: Gliński, J., Horabik, J., Lipiec, J. (eds.) *Encyclopedia of Agrophysics*. Springer, Dordrecht-Heidelberg-London-New York.
- [40] Herencia, J. F., Ruiz-porras, J. C., Melero, S., Garciagalavis, P. A., Morillo, E., Maqueda, C. (2007): Comparison between organic and mineral fertilization for soil fertility levels, crop macronutrient concentrations, and yield. – *Agronomy Journal* 99: 973-983.
- [41] Ikemura, Y., Shukla, M. K., Tahboub, M., Leinauer, B. (2008): Some physical and chemical properties of soil in organic and conventional farms for a semi-arid ecosystem of New Mexico. – *Journal of Sustainable Agriculture* 31: 149-170.
- [42] Jadhav, A. B., Kadlag, A. D., Amrutsagar, V. M. (2016): Soil enzyme activities, organic carbon and microbial population as influenced by integrated nitrogen management for Banana. – *Journal of the Indian Society of Soil Science* 64(1): 98-107.
- [43] Jenkins, L. J., Sakrabani, R., Pearce, B., Whitmore, A. P., Godwin, R. J. (2011): A comparison of soil and water properties in organic and conventional farming systems in England. – *Soil Use and Management* 27: 133-142.
- [44] Krol, A., Lipiec, J., Turski, M., Kuoe, J. (2013): Effects of organic and conventional management on physical properties of soil aggregates. – *International Agrophysics* 27: 15-21.
- [45] Kumar, V. (2012): Comparison of twelve organic and conventional farming systems: A life cycle greenhouse gas emissions perspective. – *Journal of Sustainable Agriculture* 36: 620-649.
- [46] Lampkin, N. H., Measures, M., Padel, S. (2011): *Organic Farm Management Handbook*. – 9th ed. Organic Research Centre, Newbury.
- [47] Lee, Y. H., Lee, S. M., Sung, J. K., Kim, Y. H., Choi, D. H., Ryu, G. H. (2006): The effects of applied organic materials for improving soil physico-chemical properties in paddy fields. – 18th World Congress of Soil Sci. Philadelphia, PA, USA.
- [48] Leifeld, J., Fuhrer, J. (2010): Organic farming and soil carbon sequestration: what do we really know about the benefits? – *Ambio* 39: 585-599.
- [49] Leifeld, J., Reiser, R., Oberholzer, H. R. (2009): Consequences of conventional versus organic farming on soil carbon: results from a 27-year field experiment. – *Agronomy Journal* 101(5): 204-1218.
- [50] Levick, M. (1992): A comparison of some aspects of two orchard plot management systems. – B. Holt (Tech) thesis. Dept. of Soil Science, Mavvey Univ., Palmerston North, New Zealand.
- [51] Liebig, M. A., Doran, J. W. (1999): Impact of organic production practices on soil quality indicators. – *Journal of Environmental Quality* 28: 1601-1609.
- [52] Liu, B., Tu, C., Hua, S., Gumpertz, M., Ristaino, J. B. (2007): Effect of organic, sustainable, and conventional management strategies in grower fields on soil physical, chemical, and biological factors and the incidence of Southern blight. – *Applied Soil Ecology* 37: 202-214.
- [53] Lopes, A. R., Faria, C., Prieto-Fernández, A., Trasar, C. C., Manaia, C. M., Nunes, O. C. (2011): Comparative study of the microbial diversity of bulk paddy soil of two rice fields subjected to organic and conventional farming. – *Soil Biology & Biochemistry* 43: 115-125.
- [54] Lotter, D. W. (2003): Organic agriculture. – *Journal of Sustainable Agriculture* 21: 59-128.
- [55] Mader, P., Fließbach, A., Dubois, D., Gunst, L., Fried, P., Niggli, U. (2002): Soil fertility and biodiversity in organic farming. – *Science* 296: 1694-1697.

- [56] Maharjan, M., Sanaullah, M., Bahar, S., Razavi, Kuzyakov, Y. (2017): Effect of land use and management practices on microbial biomass and enzyme activities in subtropical top- and sub-soils. – *Applied Soil Ecology* 113: 22-28.
- [57] Malhi, S. S., Nyborg, M., Solberg, E. D., McConkey, B., Dyck, M., Puurveen, D. (2011): Long-term straw management and N fertilizer rate effects on quantity and quality of organic C and N and some chemical properties in two contrasting soils in western Canada. – *Biology and Fertility of Soils* 47: 785-800.
- [58] Malik, S. S., Ramesh, C., Chauhan, J. S., Kapoor, T., Raashee, A., Sharma, N. (2014): Influence of organic and synthetic fertilizers on soil physical properties. – *International Journal of Current Microbiology and Applied Sciences* 3(8): 802-810.
- [59] Marriott, E. E., Wander, M. M. (2006): Total and labile soil organic matter in organic and conventional farming systems. – *Soil Science Society of America Journal* 70: 950-959.
- [60] Meleró, S. (2006): Chemical and biochemical properties in a silty loam soil under conventional and organic management. – *Soil & Tillage Research* 90: 162-170.
- [61] Mendoza, G. O., Shukla, M. K., John, G., Mexal, Vanleeuwen, D. M., Ikemura, Y. (2011): Assessment of properties of a Harkey soil under organic and conventional farming systems. – *Communications in Soil Science and Plant Analysis* 42: 1791-1808.
- [62] Moeskops, M. B., Sukristiyonubowo, B., Buchana, D., Sleutel, S., Herawaty, L., Husenb, E., Saraswati, R., Setyorini, D., De, N. S. (2010): Soil microbial communities and activities under intensive organic and conventional vegetable farming in West Java, Indonesia. – *Applied Soil Ecology* 45: 112-120.
- [63] Mohamad, R. S., Vincenzo, A. C., Verrastro, A., Bitar, A. L., Rocco, R. B., Michele, M. B., Chami, Z. A. (2016): Effect of different agricultural practices on carbon emission and carbon stock in organic and conventional olive systems. – *Soil Research* 10: 1071-80.
- [64] Monokrousos, N., Papatheodorou, E. M., Diamantopoulos, J. D., Stamou, G. P. (2006): Soil quality variables in organically and conventionally cultivated field sites. – *Soil Biology and Biochemistry* 38: 1282-1289.
- [65] Montgomery, D. R. (2007a): Soil erosion and agricultural sustainability. – *Proceedings of the National Academy of Sciences (PNAS)* 104: 13268-13272.
- [66] Ochiai, N., Powelson, M., Crowe, F., Dick, R. (2008): Green manure effects on soil quality in relation to suppression of *Verticillium wilt* of potatoes. – *Soil Biology and Biochemistry* 44: 1013-1023.
- [67] Okur, N., Ahmed, A., Muzaffer, C., Selçuk, G. N., Huseyin, H. K. (2009): Microbial biomass and enzyme activity in vineyard soils under organic and conventional farming systems. – *Turkish Journal of Agriculture and Forestry* 33: 413-423.
- [68] Otero, V., Barreal, M. E., Martínez, N. L., Gallego, P. P. (2010): Nutritional status of kiwifruit in organic and conventional farming systems. – *Proceedings VIth IS on Mineral Nutrition of Fruit Crops*, pp. 155-160.
- [69] Pang, X. P., Letey, J. (2000): Organic farming: Challenge of timing nitrogen availability to crop nitrogen requirements. – *Soil Science Society of America Journal* 64: 247-253.
- [70] Papadopoulos, A., Bird, N. R., Whitmore, A. P., Mooney, S. J. (2006): The effects of organic farming on the soil physical environment. – *Aspects of Applied Biology* 79: 263-267.
- [71] Pelosi, C., Bertrand, M., Thenard, J., Mougin, C. (2015): Earthworms in a 15 year agricultural trial. – *Applied Soil Ecology* 88: 1-8.
- [72] Petersen, S. O., Deboz, K., Schonning, P., Christensen, B. T., Elmholt, S. (1997): Phospholipid fatty acid profiles and C availability in wet-stable macro-aggregates from conventionally and organically farmed soils. – *Geoderma* 78: 181-196.
- [73] Pimentel, D., Edwards, C. A. (1982): Pesticide and ecosystem. – *BioScience* 32: 595-600.
- [74] Poudel, D. D., Ferris, H., Klonsky, H., Horwath, W. R., Scow, K. M., Van Brugen, A. H. C., Lanini, W. T., Mitchell, J. P., Temple, S. R. (2001): The sustainable agriculture farming system project in California's Sacramento Valley. – *Outlook on Agriculture* 30: 159-160.

- [75] Poudel, D. D., Horwath, W. R., Lanini, W. T., Temple, S. R., Bruggen, A. H. C. (2002): Comparison of soil N availability and leaching potential, crop yields and weeds in organic, low-input and conventional farming systems in northern California. – *Agriculture, Ecosystems and Environment* 90: 125-137.
- [76] Pulleman, M. M., Six, J., Breemen, N., Jongmans, A. G. (2004): Soil organic matter distribution and microaggregate characteristics as affected by agricultural management and earthworm activity. – *European Journal of Soil Science* 9: 759-772.
- [77] Quist, K., Strock, J. S., Mulla, D. J. (2006): Influence of alternative and conventional management practices on soil physical and hydraulic properties. – *Vadose Zone Journal* 5: 356-364.
- [78] Reganold, J. P., Andrews, P. K., Reeve, J. R., Boogs, C. L., Schadt, C. W., Alldredge, R., Ross, C. F., Davies, N. M., Zhou, J. (2010): Fruit and soil quality of organic and conventional strawberry agroecosystem. – *Plos One* 5(9): 123-146.
- [79] Romanya, J., Rovira, P. (2009): Organic and inorganic P reserves in rain-fed and irrigated calcareous soils under long-term organic and conventional agriculture. – *Geoderma* 151: 378-386.
- [80] Rothamsted Research (2005): Annual Report 2004-2005 World Class Science for Sustainable Land Management. – The Laws Trust, Rothamsted.
- [81] Schjonning, P., Elmholt, S., Munkholm, L. J., Debosz, K. (2002): Soil quality aspects of humid sandy loams as influenced by organic and conventional long-term management. – *Agriculture, Ecosystems & Environment* 88: 195-214.
- [82] Schnug, E., Haneklaus, S. (2002): Agricultural production techniques and infiltration significance of organic farming for preventive flood protection. – *Land Bauforsch Volkenrode* 52: 197-203.
- [83] Schnug, E., Rogasik, J., Panten, K., Paulsen, H. M., Haneklaus, S. (2004): Oekologischer Landbau erhoeht die Versickerungsleistung von Boeden - ein unverzichtbarer Beitrag zum vorbeugenden Hochwasserschutz. – *Oekologie & Landbau* 32(132): 53-55.
- [84] Shannon, D., Sen, A. M., Johnson, D. B. (2002): A comparative study of the microbiology of soils managed under organic and conventional regimes. – *Soil Use & Management* 18: 274-283.
- [85] Sheoran, H. S. (2018). Impact of organic and conventional farming practices on soil quality. Ph.D. Thesis. – Department of Soil Science, CCS Haryana Agricultural University, Hisar (India).
- [86] Shepherd, M. A., Harrison, R., Webb, J. (2002): Managing soil organic matter—implications for soil structure on organic farms. – *Soil Use & Management* 18: 284-292.
- [87] Shepherd, M., Pearce, B., Cormack, B., Phillipps, L., Cuttle, S., Bhogal, A., Costagin, P., Unwin, R. (2003): An assessment of the environmental impacts of organic farming. – <http://www.defra.gov.uk/science/> (accessed on 01/03/2005).
- [88] Shrestha, G. (2014): Soil properties and soil management practices in commercial organic and conventional vegetable farms in Kathmandu Valley. – *Nepal Journal of Science and Technology* 15(1): 13-22.
- [89] Shukla, M. K., Lal, R., Owens, L. B., Unkefer, P. (2003): Land use and management impacts on structure and infiltration characteristics of soils in the north Appalachian region of Ohio. – *Soil Science* 168: 167-177.
- [90] Siegrist, S. S., Pfiffner, D., Mader, P. (1998): Does organic agriculture reduce soil erodibility? The results of a long-term field trial study on loess in Switzerland. – *Agriculture, Ecosystems & Environment* 69: 253-264.
- [91] Sihi, D., Dari, B., Dinesh, K., Sharma, H. P., Nain, L., Sharma, O. P. (2017): Evaluation of soil health in organic vs. conventional farming of basmati rice in North India. – *Journal of Plant Nutrition and Soil Science* 2: 1-18.
- [92] Sihi, D., Sharma, D. K., Pathak, H., Singh, Y. V., Sharma, O. P., Nain, N., Chaudhary, A., Dari, B. (2012): Effect of organic farming on productivity and quality of basmati rice. – *Journal of Rice Research* 49: 24-29.

- [93] Smitha, G. R., Umesha, K., Sreeramu, B. S. (2015): Soil and plant nutrient status as influenced by organic farming in Long pepper. – *Journal of Medicinal and Aromatic Plants* 6(1): 21-28.
- [94] Stark, C. H. (2008): Are soil biological properties and microbial community structure altered by organic farm management? – *Proceedings of IFOAM Organic World Congress* 16, Modena, Italy, pp. 121-124.
- [95] Sudhakaran, M., Ramamoorthy, D., Kumar, R. S. (2013): Impacts of conventional, sustainable and organic farming system on soil microbial population and soil biochemical properties, Puducherry, India. – *International Journal of Environmental Sciences* 4: 28-41.
- [96] Suja, G., Byju, G., Jyothi, A. N., Veena, S. S., Sreekumar, J. (2017): Yield, quality and soil health under organic vs. conventional farming in Taro. – *Scientia Horticulturae* 218: 334-343.
- [97] Sunita (2015): Effect of organic farming on quality of soil under rice cultivation. – *Journal of Agroecology and Natural Resource Management* 2(5): 391-393.
- [98] Thuries, L., Feller, C., Herrmann, P., Remy, J. (2001): Kinetics of added organic matter decomposition in a Mediterranean sandy soil. – *Soil Biology & Biochemistry* 33(7-8): 997-1010.
- [99] Uddin, M. N., Siddiqy, M. A., Hossain, A. M., Islam, F., Halim, G. M. A., Bari, M. L. (2016): Impact of organic and conventional practices on, soil health and crop yield under tropical and subtropical environment of Bangladesh. – *International Journal of Environment & Agriculture Research* 2(12): 89-100.
- [100] Velmourougane, K. (2016): Impact of organic and conventional systems of coffee farming on soil properties and culturable microbial diversity. – *Scientifica*. <http://dx.doi.org/10.1155/2016/3604026>.
- [101] Wander, M. M., Traina, S. J. (1996): Organic matter fractions from organic and conventionally managed soils: carbon and nitrogen distribution. – *Soil Science Society of America Journal* 60: 1081-1087.
- [102] Willer, H., Lernoud, J. (2013): *The World of Organic Agriculture: The Results of the Latest Survey on Organic Agriculture Worldwide*. – Bio-Fach Congress, Nuremberg, Germany.
- [103] Williams, D. M., Canqui, H. B., Charles, A. F., Galusha, T. D. (2017): Organic farming and soil physical properties: an assessment after 40 years. – *Journal of Agronomy* 109: 600-609.
- [104] Wortman, S. E., Galusha, T. D., Mason, S. C., Francis, C. A. (2011): Soil fertility and crop yields in long-term organic and conventional cropping systems in eastern Nebraska. – *Renewable Agriculture and Food Systems* 27: 200-216.
- [105] Wu, T., Chellemi, D., Graham, J., Martin, K., Roskopf, E. (2008): Comparison of soil bacterial communities under diverse agricultural land management and crop production practices. – *Microbial Ecology* 55: 293-310.
- [106] Zeiger, M., Fohrer, N. (2009): Impact of organic farming systems on runoff formation processes - A long-term sequential rainfall experiment. – *Soil & Tillage Research* 102: 45-54.
- [107] Zhao, J., Chen, S., Hu, R., Li, Y. (2017): Aggregate stability and size distribution of red soils under different land uses integrally regulated by soil organic matter, and iron and aluminum oxides. – *Soil & Tillage Research* 167: 73-79.

EFFECT OF BIOCHAR ON CADMIUM, NICKEL AND LEAD UPTAKE AND TRANSLOCATION IN MAIZE IRRIGATED WITH HEAVY METAL CONTAMINATED WATER

SAYYADIAN, K.^{1,3} – MOEZZI, A.^{2*} – GHOLAMI, A.³ – PANAHPOUR, E.³ – MOHSENFAR, K.³

¹*Department of Soil Science, Khouzestan Science and Research Branch, Islamic Azad University, Ahvaz, Iran*

²*Department of Soil Science, Chamran University, Ahvaz, Iran*

³*Department of Soil Science, Ahvaz Branch, Islamic Azad University, Ahvaz, Iran*

**Corresponding author*

e-mail: abdulmirmoezzi@yahoo.com

(Received 25th Jul 2018; accepted 7th Nov 2018)

Abstract. This study was conducted to investigate the effect of biochar on bioavailability reduction of cadmium (Cd²⁺), nickel (Ni²⁺), and lead (Pb²⁺) and its subsequent effects on soil properties and maize plant growth in a soil which was irrigated by contaminated water with above heavy metals. Twelve different biochar were prepared under two temperatures of 500 °C and 700 °C by using six biomass including residuals of wheat (WB), chickpea (CB), maize (MB), reed (RB), olive (OB) and sugarbeet (SB). Physicochemical properties of biochar including product percentage, percentage volatile matter, ash, pH, electrical conductivity (EC), cation exchange capacity (CEC), specific surface, and organic carbon (OC) were studied as well. Subsequently, the effects of 3 biochar selected under 700 °C (MB₇₀₀, RB₇₀₀, WB₇₀₀) at the levels of 0%, 2%, and 4% were employed for pot experiments. The results showed that higher level of temperature significantly (P < 0.05) increased pH, EC, ash percentage, specific surface area, and OC content of soil however Cd, Ni, and both shoot and root dry biomass decreased. This study results indicated that high application of biochar significantly decreased leaf area, and also shoot and root biomass.

Keywords: *maize, contaminated water, volatile matter, heavy metal, biochar*

Introduction

Soils are increasingly become contaminated by accumulation of heavy metals through applying urban and industrial sewage sludge along with chemical fertilizers (Hejazizadeh et al., 2016). In developing countries due to expanding of population, food demand is driving up which in turn increases the resources application and subsequently resulted in rising accumulation of Cd, Ni, and Pb in soils. Long term application of sewage sludge even with low concentration of heavy metals can also result in accumulation of these metals in soils (Lu et al., 2015). Low availability of water due to population increment, climate change and climate pollution has been turned into one of the major environment problems (Yao et al., 2012). Accumulation of heavy metal in soils is not only a serious threat for plants but also is a potential danger to human health as well (Hejazizadeh et al., 2016). Heavy metal should be of more concern as in contrast to organic matters, they do not decompose (Ingole and Tale, 2016).

In recent decade, biochar has gained more attention as their capability of carbon sequestration mitigates global warming, enhances soil fertility and reduces both organic and inorganic pollutants of soil (Zheng et al., 2013). Biochar is a carbonaceous material product of organic waste under oxygen-limited or fully depleted oxygen condition

(Zhao et al., 2017; Lehmann, 2007). Physicochemical properties of biochar depend on starting material and applied temperature and by increasing temperature beyond 550 °C, specific surface area and aromatic components of biochar would increase (Elzobair, 2013). Biochar can also reduce the pollutants movement and thus prevent their uptake by crops (Yao et al., 2012). Different characters of biochar (due to feedstock or pyrolysis conditions) can enforce different impacts on soils fertility and crop production (Paneque et al., 2016). Various studies have indicated that biochar positive effects on environment and for crop production it depends on biochar feedstock and its production conditions (da Silva et al., 2017). Most of published results are originated from tropical, subtropical, and temperate regions but the impact of biochar in Mediterranean regions with hot and dry summers containing calcareous soils has not been fully realized yet (Paneque et al., 2016).

This study was conducted to investigate the effect of biochar on bioavailability reduction of cadmium (Cd^{+2}), nickel (Ni^{+2}), and lead (Pb^{+2}) and its subsequent effects on soil characteristics and corn plant growth in a soil which was irrigated by contaminated water with above heavy metals.

Materials and methods

This experiment was conducted as factorial based on complete random design with three replications in Anahita soil-plant-water analysis lab of Kermanshah state (Iran) in 2017. Twelve different biochars were prepared under two temperatures of 500 °C and 700 °C by using six starting biomass including residuals of wheat (WB₅₀₀, WB₇₀₀), chickpea (CB₅₀₀, CB₇₀₀), maize (MB₅₀₀, MB₇₀₀), reed (RB₅₀₀, RB₇₀₀), olive (OB₅₀₀, OB₇₀₀) and sugarbeet (SB₅₀₀, SB₇₀₀) to study the physicochemical properties of biochars. All feedstocks were dried in oven at 60 °C for 24 h and then were placed in electric furnace (Shimifan Model F. 47, Iran) for 2 h with warming rate of 8 °C min⁻¹ under oxygen-limited conditions. After pyrolysis, when materials temperature equals to room temperature, they were weighed and after grinding them for physicochemical experiments, they were passed through 0.5 mm mesh. The physicochemical properties included yield%, ash%, pH, EC, CEC, specific surface area, assimilated carbon%, volatile material% elements (CHNO) analysis, and molar ratio of H/C and O/C. The study results were analyzed using SAS 9.3 and means were compared based on LSD. Due to high importance of specific surface area, porosity and CEC in metal pollutants reductions (Komkiene and Baltrenaitis, 2016) three biochars with high specific surface area and high CEC and oxygen factor groups like carboxyl and hydroxyl groups were chosen for pot experiments. Biochars MB₇₀₀, WB₇₀₀, and RB₇₀₀ were final selections.

Pot experiment

In order to find the impacts different amounts of selected biochars (MB₇₀₀, WB₇₀₀, and RB₇₀₀) on soil physicochemical properties (pH, EC, OC, amount of cadmium, nickel, and lead in soil and plant materials) and plant properties (leaf area, root and shoot dry matter), a pot experiment was conducted in June 2017, as factorial based on complete random design with three replications in Mahidasht Research Center in Kermanshah (Iran). The study results were analyzed using SAS 9.3 and means were compared based on LSD.

About 82 kg soil, classified as fine mixed thermic typic calcixerepts, was used to fill the pots and a sample of soil was used to determine its physicochemical properties.

Each pot (250 mm height and 240 mm diameter) was filled by 3 kg soil. The selected three biochars at same level were added to pots. Preventing soil wash by irrigation, plastic nets were applied at the bottom of each pot. Three seeds corn (*Zea mays* L.) were planted at depth of 5 mm in each pot. All pots were irrigated up to field capacity by polluted water with Cd, Ni, and Pb at 1000, 2000, and 3000 microgram per liter, respectively, for two months. Ten days after emergence, two of seedlings were removed, and plants were harvested two months after sowing. At final harvest, leaf area was measured by leaf area meter (CID Bio-Science model CI-202, USA). After harvest, shoots and roots were separated, roots were washed by tap water and then by deionized water to remove soil and any remained biochar. Both shoots and roots were dried at 60 °C till to get a constant weight and then were grinded. Finally, a soil sample was taken from each pot.

Analysis of biochar physicochemical properties

Biochar production was obtained as (Sadaka et al., 2014; Zhao et al., 2017) the ratio of biochar weight to initial material weight (dried at 60 °C) and percentage of volatiles and ash were determined at two temperatures of 750 °C and 950 °C according to the procedure of American Society for Testing and Material (ASTM). To measure the pH, biochar was mixed with deionized water as ratio (W/V) of 1:20 then was on shaker for 1.5 h (Rajkovich et al., 2012) and finally samples were taken to determine pH by using pH meter (Metrohm model 691, Switzerland).

Biochar was mixed with deionized water as ratio of 1:10, was on shaker for 1 h and then by using conductivity meter (Jenway model 4010, UK) electrical conductivity was determined (Yang et al., 2015). Cation exchange capacity was determined by using NH₄OAC solution (Melo et al., 2013; Song and Guo, 2012) and specific surface area was determined based on Brunauer-Emmett-Teller (BET) method (Brunauer et al., 1937). Biochars functional group were studied using Fourier-transform infrared (FTIR) spectrometer (Bruker model vertex 70, Germany) at wavelengths of 500-4000 nm. Biochar elemental composition (CHN) was measured by elemental analyzer (Costech model ECS4010, Italy). Oxygen percentage was calculated as:

$$O (\%) = 100 - (C\% + H\% + N\% + Ash\%)$$

and molar element ratios, O/C and H/C were calculated as well. Nutrients of MB₇₀₀, RB₇₀₀, WB₇₀₀ samples including P, K, Ca, Mg, Zn, Fe, and trace elements (Pb, Ni, and Cd) were measured using peroxide hydrogen (H₂O₂ digestion) and sulfuric acid (H₂SO₄) (Wolf, 1982). All samples were tested by atomic absorption (Perkin Elmer Model 1100 D) while Na and K were tested by flame photometer (Jenway model PFP7, UK) and P by spectrometer (Apel Model PD303S, Japan).

Soil physicochemical properties analyses

Soil pH was determined by using paste saturation method (Metrohm 691, Switzerland pH meter) and EC were measured using EC meter (Jenway model 4010, UK). Phosphorous was measured according to Olsen method by using a spectrophotometer, (Apel model PD 303S, Japan) and potassium (ammonium acetate extract) was determined using a flame photometer (Jenway model PFP7, Japan). Organic carbon (wet ash method) and total neutralization value (TNV %) (CaCO₃) were measured using neutralization with

1N HCl. The bioavailable Cd, Ni and Pb content of soil were determined by DTPA method (0.005 mol L⁻¹ DTPA and 0.01 mol L⁻¹ CaCl₂ and 0.01 mol L⁻¹ triethylamine) (Lindsay and Norvell, 1978) using an atomic absorption spectrophotometer (Perkin-Elmer model 1100 D, USA).

Feedstock and maize plant analysis

All elements including the heavy metals of feedstock samples and maize plant shoots and roots were measured using dry ash and digest in HCl extraction methods by flame photometer and spectrophotometry and atomic absorption.

Results and discussion

Biochar properties

Biochar properties (*Table 1*) showed that with increasing temperature from 500 °C to 700 °C biochar production reduced but their ash increased. This is consistent with Rajkovich et al. (2012) study. Low production of biochar due to high temperature may be due to cracking of organic matter and gases drift (Zhang et al., 2015). In this study the highest production (34.17%) was for WB₅₀₀ and in the second rank was CB₅₀₀ by 33.93%. Results also showed that increasing temperature (pyrolysis temperature) significantly reduced volatile matter percentage (*Table 1*), which is consistent with Rajkovich et al. (2012). Reduction of volatile matter percentage can be due to water loss and organic material (cellulose, hemicellulose, and lignin) decomposition during pyrolysis (Sadaka et al., 2014). Increasing pyrolysis temperature significantly (P < 0.05) increased pH and EC as well (*Table 1*). Similarly, Jindo et al. (2014) reported that increasing temperature to 700 °C increased the biochar. Samples of pH and EC were 9.06-10.14 and 167.7-760 mS/m respectively. Increasing pH and EC may be due to increasing of ash (Wu et al., 2012; Paz-Ferreiro et al., 2014; da Silva et al., 2017; Novak et al., 2009).

Table 1. Physical and chemical characteristic of biochars (values are mean of three replications)

Biochar	Yield (%)		pH		Dry ash (%)		VM (%)		Fixed carbon (%)		EC (mS m ⁻¹)		BET (m ² g ⁻¹)		CEC (Cm kg ⁻¹)	
	500 °C	700 °C	500 °C	700 °C	500 °C	700 °C	500 °C	700 °C	500 °C	700 °C	500 °C	700 °C	500 °C	700 °C	500 °C	700 °C
WB	34.17 ^a	29.07 ^{cd}	9.39 ^{bcd}	10.13 ^a	25.86 ^b	29.91 ^a	40.57 ^c	32.28 ^c	33.57 ^g	38.05 ^f	410.0 ^e	578.3 ^c	4.14 ^g	142.2 ^b	16.17 ^f	20.52 ^{cd}
RB	27.80 ^d	25.70 ^e	9.06 ^d	9.74 ^{abc}	8.98 ^{gh}	12.48 ^f	43.97 ^b	36.05 ^d	47.05 ^{de}	51.47 ^c	410.3 ^e	462.3 ^d	3.29 ^g	241.1 ^a	12.86 ^g	19.77 ^{cd}
MB	29.53 ^{bcd}	25.17 ^e	9.35 ^{cd}	9.97 ^a	9.50 ^e	12.47 ^f	43.20 ^{bc}	24.84 ^{gh}	47.30 ^{de}	62.69 ^b	167.7 ^g	214.3 ^f	5.28 ^g	97.89 ^c	18.90 ^{de}	21.60 ^{bc}
CB	33.93 ^a	30.00 ^{bc}	9.41 ^{bcd}	10.14 ^a	15.70 ^e	22.16 ^c	47.90 ^a	27.48 ^{fg}	36.40 ^{fg}	50.36 ^{cd}	540.0 ^e	760.0 ^a	3.41 ^g	23.17 ^e	22.84 ^b	11.01 ^g
OB	29.70 ^{bc}	27.80 ^d	9.14 ^d	9.78 ^{ab}	7.47 ^h	9.75 ^e	28.20 ^f	21.70 ^h	64.33 ^b	68.55 ^a	206.0 ^{fg}	398.7 ^e	6.64 ^g	82.39 ^d	17.25 ^{ef}	11.47 ^g
SB	31.20 ^b	24.70 ^e	9.30 ^d	10.08 ^a	17.89 ^d	15.36 ^e	35.93 ^d	31.59 ^e	46.18 ^c	53.05 ^c	400.3 ^e	631.3 ^b	3.40 ^g	11.18 ^f	25.78 ^a	11.82 ^g
LSD (5%)	1.78		0.43		1.62		3.33		3.90		39.92		4.12		1.98	

Different letters indicate significant differences between treatments P < 0.05

BET and CEC results (*Table 1*) indicated that specific surface and CEC of biochars (WB, RB and MB) significantly increased as the temperature increased from 500 °C to 700 °C. Increase of biochar specific surface due to high temperature can be the result of organic matter degradation and developing pores and channels in biochar during pyrolysis (Zhao et al., 2017) and CEC increase can be due to change of negative charge

in relation to pH (da Silva et al., 2017) and specific surface area rise. Komkiene and Baltreinaite (2016) resulted that by increasing temperature from 450 °C to 700 °C specific surface area of two types of biochar increased from 9.6 to 10.4 and 5.92 to 7.17 m² g⁻¹ which is similar to this study results.

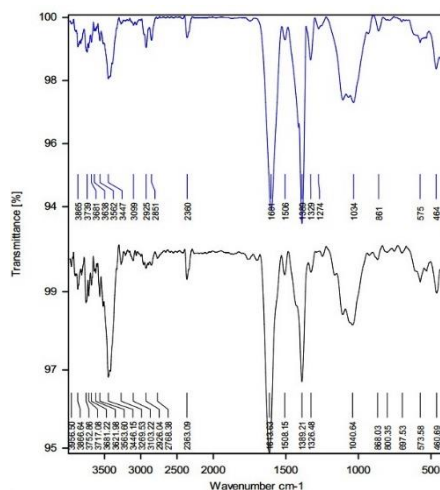
Elemental analysis and determination of ratios O/C and H/C are most important indices for realization of aromaticity and maturity of biochars (Schmidt and Noack, 2000; Nguyen and Lehmann, 2009). Results of analysis (Table 2) showed that by increasing pyrolysis temperature, carbon percentage of biochar samples increased while H, N, O and ratios H/C, O/C reduced. Reduction of O and H can be the result of removal of water and oxygen from hydroxyl and carboxyl agents (Wang et al., 2015). The highest (84.75%) and lowest (43.19%) carbon percentage were from OB₇₀₀ and SB₅₀₀ respectively. Melo et al. (2013) and Jindo et al. (2014) showed that by increasing pyrolysis temperature from 500 °C to 700 °C, carbon%, hydrogen%, N% and molar ratio of H/C and O/C of biochar increased as well which are also consistent with our results.

Table 2. Elemental analysis of biochars, H/C and O/C ratios (values are mean of three replications)

Biochar	N		C		H		O*		H/C		O/C	
	%											
	Molar ratio											
	500 °C	700 °C	500 °C	700 °C	500 °C	700 °C	500 °C	700 °C	500 °C	700 °C	500 °C	700 °C
WB	0.67 ^b	0.35 ^{def}	54.12 ^f	60.84 ^{de}	2.60 ^a	1.25 ^d	20.33 ^d	8.48 ^g	0.58 ^a	0.25 ^c	0.28 ^d	0.10 ^{gh}
RB	0.47 ^{cd}	0.28 ^f	55.11 ^f	75.80 ^b	2.60 ^a	1.39 ^d	33.42 ^b	10.82 ^f	0.56 ^a	0.22 ^{cd}	0.45 ^b	0.11 ^g
MB	0.82 ^a	0.41 ^{cde}	68.91 ^c	78.22 ^b	2.72 ^a	1.81 ^c	18.6 ^e	7.80 ^{gh}	0.47 ^b	0.28 ^c	0.20 ^f	0.07 ⁱ
CB	0.89 ^a	0.48 ^c	63.09 ^d	70.13 ^c	2.67 ^a	1.25 ^d	18.2 ^e	6.75 ^{hi}	0.51 ^{ab}	0.21 ^{cd}	0.22 ^e	0.07 ⁱ
OB	0.88 ^a	0.38 ^{cdef}	59.25 ^e	84.75 ^a	2.23 ^b	1.85 ^c	30.73 ^c	5.40 ⁱ	0.45 ^b	0.26 ^c	0.39 ^c	0.05 ^j
SB	0.79 ^{ab}	0.31 ^{ef}	43.19 ^g	75.33 ^b	1.82 ^c	1.06 ^d	36.89 ^a	8.70 ^g	0.51 ^{ab}	0.17 ^d	0.64 ^a	0.09 ^h
LSD (5%)	0.125		3.305		0.361		1.663		0.072		0.014	

*Determined by difference. Different letters indicate significant differences between treatments P < 0.05

FTIR spectrum of selected biochar at two different temperatures are presented in Figure 1.



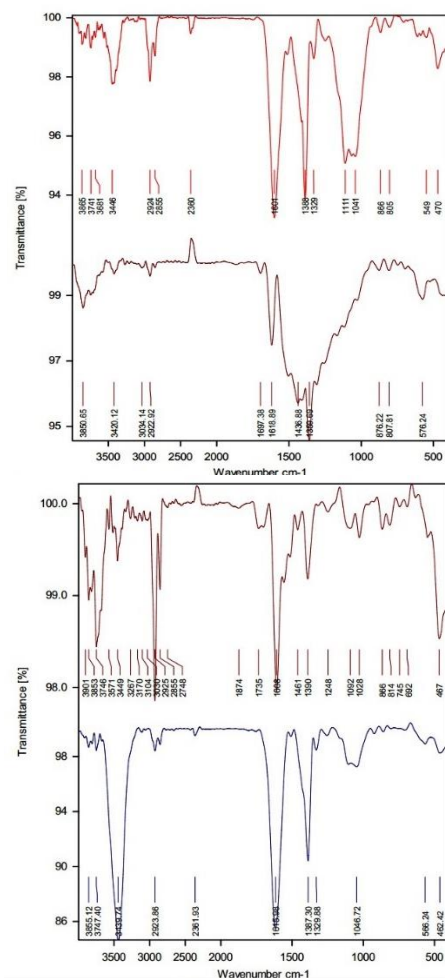


Figure 1. Biochar spectrum for MB, RB, and WB

As temperature increased a reduction of O-H stretching (3680 cm^{-1}) was observed within FTIR spectrum which may be due to dehydration of biomass and reduction of polarity during pyrolysis.

Effect of biochar on soil pH, EC and OC

The results indicated that the effect of biochar type (*Table 3*) and amount were significant on soil pH, OC and EC (*Fig. 2A, B, C*). Comparison of means showed that WB₇₀₀ was more effective in increasing soil pH compared to MB₇₀₀ or RB₇₀₀ (*Table 3*). WB₇₀₀ and MB₇₀₀ significantly ($P < 0.05$) increased soil EC and OC (*Table 3*). Although the effects of MB₇₀₀ and RB₇₀₀ on soil OC were similar, these biochars were more effective than WB₇₀₀. Similarly, there was no significant ($P < 0.05$) difference between WB₇₀₀ and RB₇₀₀ in terms of soil EC, but these biochars were more effective than MB₇₀₀. Results showed (*Tables 1 and 4*) that biochars pH were 10.13, 9.74, and 9.97 for WB₇₀₀, RB₇₀₀ and MB₇₀₀, respectively, whereas soil pH was 7.52. Therefore, it should be expected that soil pH may increase as a result of biochar application in soil. Albuquerque et al. (2011) and Xu (2012) showed that adding biochar to soil increased the pH. da Silva et al. (2017) showed that adding 3 biochar types at highest amount into

the soil not only increased pH by 0.76 to 1.68, but also soil organic carbon content also linearly increased. These results are consistent with this study results. Soil pH increase may be due to high biochar ash and its components. The ash product from pyrolysis contains oxide and hydroxide of alkali metals which are easily dissolve in water and are able to increase soil pH (da Silva et al., 2017). Further to ash, type of feedstock has also shown effects on pH and EC (Qayyum et al., 2015; Abdelhafez et al., 2014). Qayyum et al. (2015) showed that from 9 different biochars, 5 of them were able to increase soil EC, 3 of them increased soil pH and one did not show any significant ($P < 0.05$) effect on soil pH and EC. Biochars properties depend on factors such as feedstock type, feedstock size, pyrolysis temperature and retention time in oven (Paz-Ferreiro et al., 2014). In our study increasing biochar dose (Fig. 2A, B and C) led to increasing soil pH, EC and OC (except MB₇₀₀ for EC). Similarly, some studies have shown that increasing biochar dose would increase soil organic matter (Dume et al., 2016; da Silva et al., 2014) as well as soil EC (Abdelhafez et al., 2014; Yang et al., 2015).

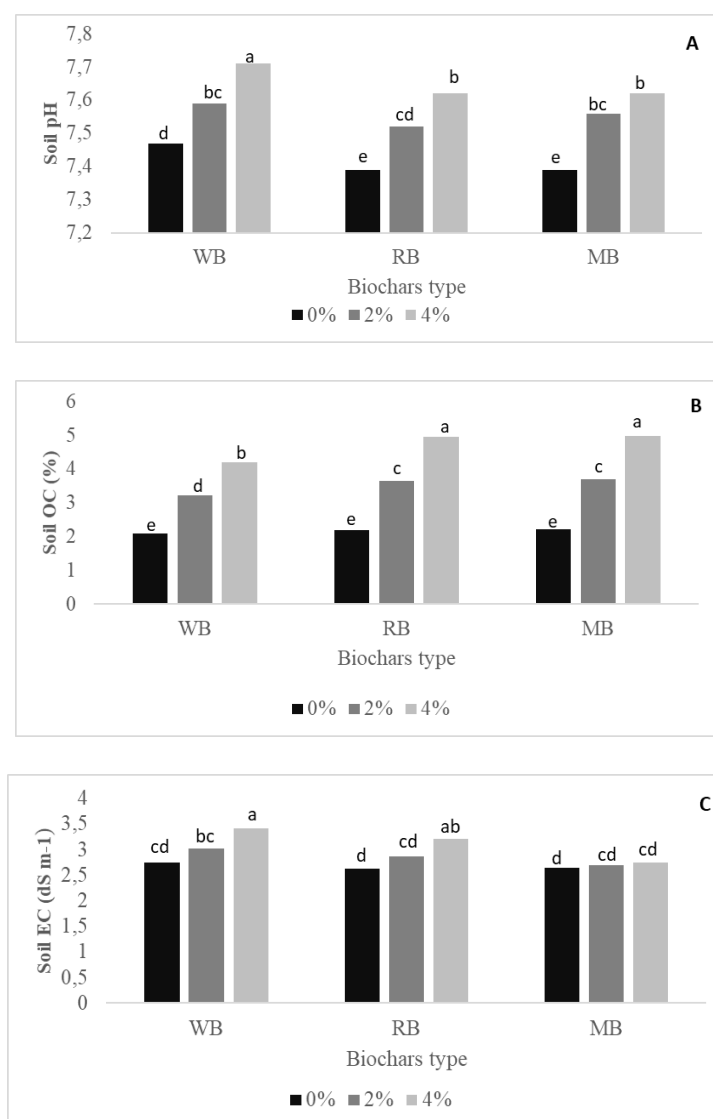


Figure 2. Effect of different rates of biochars on soil pH (A), OC (B) and EC (C)

Table 3. Effect of biochar types on shoot, root, soil properties, plant indices and translocation factor (values are mean of three replications)

Biochar types	Shoot			Root			Soil						Plant				TF value		
	Cd	Ni	Pb	Cd	Ni	Pb	Cd	Ni	Pb	pH	EC	OC	LA	Shoot	Root	R:S	TF _{Cd}	TF _{Ni}	TF _{Pb}
	mg kg ⁻¹									dS/m	%	cm ²	gr						
WB	0.56 ^b	1.22 ^a	3.35 ^a	2.26 ^a	3.61 ^a	6.24 ^a	0.41 ^a	2.41 ^c	2.38 ^a	7.58 ^a	3.06 ^a	3.17 ^b	294.7 ^a	7.04 ^b	1.71 ^c	4.11 ^a	0.24 ^b	0.34 ^a	0.53 ^a
RB	0.60 ^a	1.24 ^a	2.75 ^b	2.25 ^a	3.60 ^a	6.36 ^a	0.41 ^{ab}	2.81 ^a	2.33 ^a	7.50 ^b	2.89 ^a	3.59 ^a	322.6 ^b	7.34 ^a	1.85 ^b	3.96 ^b	0.27 ^a	0.34 ^a	0.41 ^b
MB	0.57 ^b	1.23 ^a	2.69 ^b	2.03 ^b	3.68 ^a	6.20 ^a	0.39 ^b	2.56 ^b	2.33 ^a	7.52 ^b	2.70 ^b	3.62 ^a	330.8 ^a	7.37 ^a	1.87 ^a	3.93 ^b	0.28 ^a	0.31 ^b	0.41 ^b
LSD (0.01)	0.02 2	0.072	0.091	0.045	0.112	0.234	0.013	0.064	0.125	0.045	0.187	0.182	4.342	0.078	0.018	0.045	0.012	0.018	0.012

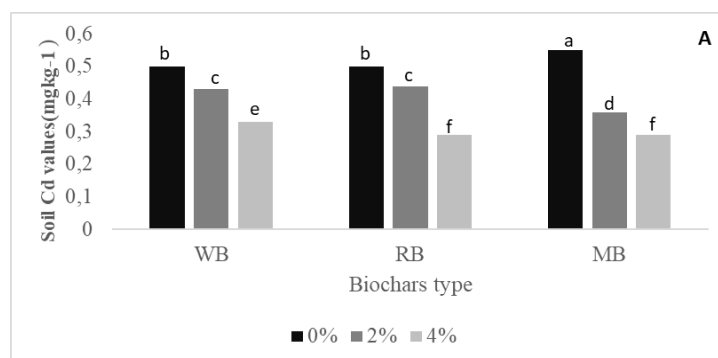
Different letters indicate significant differences between treatments P < 0.05

Table 4. Soil physicochemical analyses

pH	EC	TNV	OC	N	P	K	Mn	Fe	Zn	Cu	Cd	Ni	Pb
	dS/m	%			mg kg ⁻¹								
7.52	2.12	32.5	2.19	0.22	21	1120	23.4	11.40	4.12	2.34	0.31	1.51	2.1

Effect of biochar on bioavailability of Cd, Ni and Pb in soil

Mean comparison (Table 3) showed that biochar types differ in their reducing effect on Cd and Ni bioavailability, whereas there was no significant (P < 0.05) difference between them for effect on Pb. The amended soil with MB₇₀₀ showed less bioavailable Cd in comparison to WB₇₀₀ or RB₇₀₀. There was no significant (P < 0.05) difference between WB₇₀₀ and RB₇₀₀. The effect of WB₇₀₀ in reducing soil bioavailable Ni concentration was more pronounced compared to RB₇₀₀ or MB₇₀₀. Increasing biochar does significantly (P < 0.05) decreased bioavailable Cd, Ni, and Pb compared to control (0.00% application) (Fig. 3A, B and C). In comparison with control, application of 4% biochar decreased bioavailable Cd, Ni, and Pb by 58.8%, 46% and 76%, respectively. Increasing soil pH may lead to Cd precipitation as Cd (CO₃) (Mousavi et al., 2011) and lead to precipitation as pb5 (PO₄)₃Cl (Kopittke et al., 2008). In addition, increasing soil pH increases binding metal ions by pH dependent surface ligands (Uchimiya et al., 2011). The effect of biochar depends highly on the type of pollutant metal (Uchimiya et al., 2010). Lead in soil highly depends to organic matter and by increasing pH, lead stability (Karami et al., 2011) and also Cd and Ni stability (Yang et al., 2015) will increase. According to Park et al. (2011) and Fellet et al. (2011) adding biochar to soil decreases bioavailability of Cd and Pb of soil. Similar to this study results, Cui et al. (2011) also reported lower Cd of soil as biochar was added to soil.



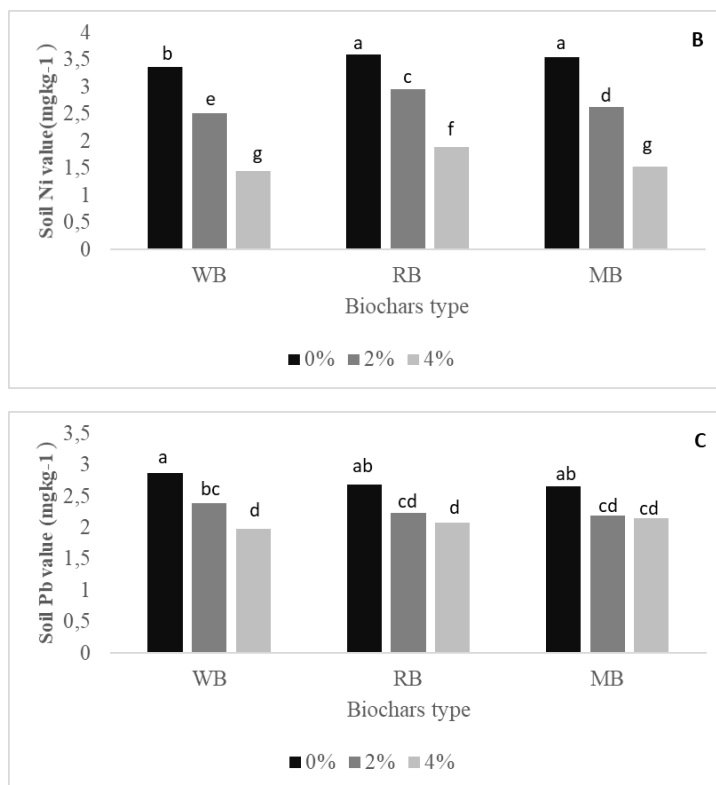


Figure 3. Effect of different rates of biochar different rates on soil bioavailable Cd (A), Ni (B) and Pb (C)

The feedstock and three types of biochar (WB₇₀₀, RB₇₀₀, and MB₇₀₀) analysis (Tables 5 and 6) indicated that P, Na, Ca, and Mg content in biochar are more compared to feedstocks. In addition, the soil Ca and P content were also high (Table 4). Increasing P availability due to biochar application plays a key role in Pb stabilization in water solution (Cao et al., 2009) and lead stabilization through precipitation or in complex with phosphate (Ahmad et al., 2014). Simultaneous release of elements Na, Ca, K, Mg, P, and S from soil and biochar can result in stability of heavy metals (Uchimiya et al., 2011). In this study, WB₇₀₀, RB₇₀₀, and MB₇₀₀, had O-containing functional groups (Fig. 1). These functional groups increase biochar effect (Yang et al., 2015; Ahmad et al., 2014) therefore they should be more effective for heavy metal stabilization especially in acidic soils with low CEC and organic matter (Uchimiya et al., 2011).

Table 5. Chemical analyses of three types of feedstocks

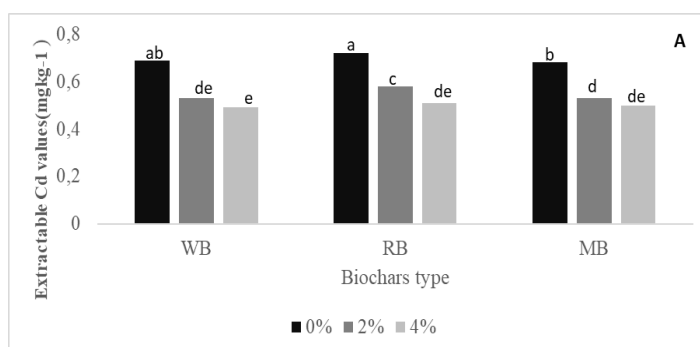
Feedstock	Cd	Ni	Pb	Cu	Zn	Fe	Mn	N	P	K	Ca	Mg
	mg kg ⁻¹							%				
Wheat residual	0.23	1.14	1.38	10.8	25	80	18	1.22	0.16	1.10	0.33	0.18
Reed (leave and stalk)	0.1	1.0	0.90	8.3	23	65	13	1.03	0.11	0.92	0.37	0.25
Maize residual	0.27	1.25	1.61	14.7	32	87	25	2.12	0.25	1.42	0.30	0.21

Table 6. Chemical composition of biochar

Biochar	Cd	Ni	Pb	Cu	Zn	Fe	Mn	P	K	Ca	Mg	Na
	mg kg ⁻¹							g kg ⁻¹				
WB700	0.63	2.2	2.1	20	85	360	156	3.6	29.7	8.2	6.5	6.8
RB700	0.27	1.1	1.3	17	73	310	148	3.0	18.8	10.4	7.8	5.7
MB700	0.71	2.6	2.7	27	89	395	175	4.2	38.0	9.0	6.9	4.9

Effect of biochar on Cd, Ni, and Pb uptake and translocation by maize

Means comparison (Table 3) indicated that there was no significant difference between MB₇₀₀ and WB₇₀₀ biochars for Cd reduction in maize shoots but their effect was higher than RB₇₀₀. In addition, this study results indicated that there was no significant difference between MB₇₀₀ and RB₇₀₀ for reducing Pb in maize shoots, however their effect was less than WB₇₀₀. For reduction of Ni in shoots, results showed no significant ($P < 0.05$) difference between biochars. This study revealed that Cd, Ni, and Pb concentrations significantly ($P < 0.05$) decreased in both shoot and root of maize as biochar application increased (Fig. 4A, B, C). Kacálková et al. (2014) reported that increasing heavy metal concentration in soil increased their uptake by plants (Komkiene and Baltreinaite, 2016) also found that application of adsorbent materials into the soil decrease heavy metal uptake by plants. Reduction of metal concentration in plants due to biochar application may be related to immobilization of bioavailable metals and dilution effects of increased biomass (Park et al., 2011). In this study highest uptake of Cd, Ni and Pb by corn plants was monitored when no biochar was applied into the soil while by adding 4% biochar the uptake of these metals was at minimum level. By increasing amount of biochar application, concentration of Cd, Ni and Pb in plants reduced (Fig. 4A, B, C). Similarly, Jatav et al. (2016) showed that maximum and minimum uptake of Cd, Ni and Pb were respectively obtained by only applying 30 t/ha of sewage sludge and 20 t/ha biochar plus 30 t/ha of sewage sludge. Increasing the amount of applied biochar reduced in heavy metal uptake. Al-Wabel et al. (2015) showed that 5% biochar application reduced heavy metal (Cu, Zn, Mn, and Cd) in corn plants.



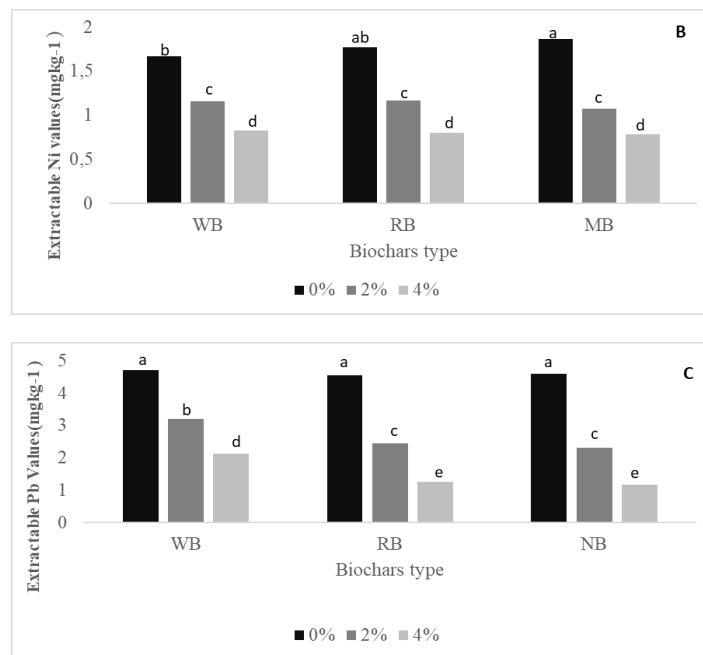


Figure 4. Effect of different rates of biochar different rates on shoot extractable Cd (A), Ni (B) and Pb (C)

Among higher plants, there are two groups of plants that can tolerate high concentrations of heavy metals: excluder plants and accumulator plants. The former is able to inhibit heavy metal transport into the plants whereas the later uptake heavy metals and accumulate them in different parts for example, roots or shoots (Lu et al., 2015). In this study, translocation factor (TF) was determined by using the ratio of heavy metal concentration in shoots to roots ($TF = C_{shoot} / C_{root}$) (Bu-Olayan and Thomas, 2009). Statistical analyses showed that TF value was affected by biochar type and amount (Table 3 and 7). The minimum TF_{Cd} (0.23) was related to $WB_{2\%}$ whereas the minimum TF_{Ni} (0.28) and TF_{Pb} (0.33) were related to $MB_{2\%}$ and $MB_{4\%}$ respectively. Accumulator plants can be identified by $TF > 1$ whereas excluders can be recognized by $TF < 1$ (Shumaker and Begonia, 2005). The results demonstrated that TF values for Cd, Ni and Pb were less than 1.

Table 7. Effect of different rates of biochars on shoot, root, soil properties, plant indices and translocation factor (values are mean of three replications)

Biochar	Rate	Shoot			Root			Soil					Plant				TF value			
		Cd	Ni	Pb	Cd	Ni	Pb	Cd	Ni	Pb	pH	EC	OC	LA	Shoot	Root	R:S	TF_{Cd}	TF_{Ni}	TF_{Pb}
		mg kg ⁻¹						dS/m		%		cm ²		gr						
WB	R ₀	0.69 ^{ab}	1.67 ^b	4.73 ^a	2.45 ^b	4.71 ^a	8.48 ^a	0.50 ^b	3.38 ^b	2.78 ^a	7.47 ^d	2.75 ^{cd}	2.10 ^f	326.7 ^d	7.35 ^b	1.82 ^c	4.03 ^b	0.28 ^a	0.35 ^{bc}	0.55 ^a
	R _{2%}	0.53 ^{de}	1.16 ^c	3.21 ^b	2.26 ^c	3.63 ^b	6.34 ^b	0.4 ^c	2.51 ^c	2.39 ^{bc}	7.59 ^{bc}	3.02 ^{bc}	3.23 ^d	294.8 ^{ef}	7.07 ^c	1.71 ^c	4.13 ^a	0.23 ^c	0.32 ^b	0.50 ^b
	R _{4%}	0.49 ^e	0.83 ^d	2.14 ^d	2.08 ^d	2.38 ^c	3.91 ^{cd}	0.33 ^c	1.44 ^d	1.98 ^d	7.71 ^a	3.42 ^a	4.19 ^b	262.7 ^g	6.73 ^d	1.61 ^d	4.19 ^a	0.24 ^{bc}	0.37 ^{ab}	0.55 ^a
RB	R ₀	0.72 ^a	1.77 ^{ab}	4.54 ^a	2.60 ^a	4.64 ^a	8.56 ^a	0.50 ^b	3.60 ^a	2.69 ^{ab}	7.39 ^c	2.62 ^d	2.20 ^f	349.8 ^b	7.46 ^{ab}	1.90 ^{ab}	3.92 ^{de}	0.28 ^a	0.37 ^{ab}	0.54 ^a
	R _{2%}	0.58 ^c	1.18 ^c	2.44 ^c	2.10 ^d	3.69 ^b	6.52 ^b	0.44 ^c	2.95 ^c	2.23 ^{cd}	7.52 ^{cd}	2.86 ^{cd}	3.64 ^c	329.9 ^{cd}	7.44 ^{ab}	1.88 ^b	3.97 ^{bcd}	0.28 ^a	0.32 ^c	0.38 ^c
	R _{4%}	0.51 ^{de}	0.80 ^d	1.26 ^d	2.05 ^d	2.47 ^c	3.99 ^c	0.29 ^d	1.89 ^d	2.08 ^d	7.62 ^b	3.21 ^{ab}	4.96 ^b	288.2 ^f	7.13 ^c	1.78 ^d	4.02 ^{bc}	0.25 ^b	0.33 ^c	0.33 ^c
MB	R ₀	0.68 ^b	1.86 ^a	4.57 ^a	2.38 ^b	4.71 ^a	8.59 ^a	0.55 ^c	3.54 ^a	2.65 ^{ab}	7.39 ^c	2.65 ^d	2.22 ^f	357.8 ^a	7.49 ^a	1.93 ^a	3.88 ^c	0.39 ^a	0.39 ^a	0.54 ^a
	R _{2%}	0.53 ^d	1.07 ^c	2.31 ^c	1.96 ^e	3.76 ^b	6.67 ^b	0.36 ^d	2.63 ^d	2.19 ^{cd}	7.56 ^{bc}	2.70 ^{cd}	3.70 ^c	337.2 ^c	7.48 ^{ab}	1.89 ^b	3.94 ^{de}	0.28 ^a	0.28 ^d	0.36 ^d
	R _{4%}	0.50 ^{de}	0.78 ^d	1.17 ^d	1.76 ^f	2.57 ^c	3.36 ^d	0.29 ^d	1.53 ^d	2.15 ^{cd}	7.62 ^b	2.75 ^{cd}	4.98 ^a	297.3 ^c	7.18 ^c	1.81 ^c	3.97 ^{bcd}	0.29 ^a	0.29 ^d	0.33 ^{de}
LSD (0.01)		0.035	0.098	0.138	0.098	0.240	0.285	0.036	0.196	0.219	0.069	0.346	0.219	16.82	0.208	0.03	0.170	0.069	0.020	0.033

Different letters indicate significant differences between treatments $P < 0.05$

Effect of biochar on leaf area, shoot and root biomass

This study results indicated that the effects of biochar type were significant ($P < 0.05$) on leaf area, shoot and root biomass (*Table 3*). Comparison of means showed that MB₇₀₀ caused the maximum leaf area (330.8 cm²), shoot (7.37 g), and root biomass (1.93 g), respectively. The minimum leaf area (294.7 cm²) and root biomass (1.61 g) were related to WB₇₀₀. This study results showed that leaf area, shoot and root biomass significantly decreased with increasing biochar application (*Table 7*). In current research, produced biochars showed different properties which resulted in different effects on soil (Paneque et al., 2016) and thus may result in different responses from plants (da Silva et al., 2017). Results analysis (*Table 6*) showed that Na concentration in biochars was 4900-6800 mg kg⁻¹. Increasing biochar dose can increase Na in soil. Rajkovich et al. (2011) reported that Na negatively (especially in low salty soil) affects maize growth, increases the soil osmotic potential and reduces the water uptake by plants. However, the liming effect of biochar is considered positive property for acidic soils but in soils with high pH, liming effect can have undesirable effects (Alburquerque et al., 2014). As well as Paneque et al. (2016) reported that large specific surface area of some biochars with high CEC and water holding capacity may have increased the competition for water which cuts down the potentially positive effect of biochar amendment.

Conclusion

Application of biochar in a semi-arid environment with high alkaline soil, high lime and rather low organic matter resulted in reduction of Cd, Ni, and Pb in both soil and plants however high level application of biochar, increased the pH and EC of the soil and reduced plants growth indices like leaf area and shoot and root biomass. Effects of MB₇₀₀ was less than effects of WB₇₀₀ and RB₇₀₀ on the mentioned growth indices. To reduce the translocation of heavy metals to plants and biochar effects on growth indices, application of 2% or less from MB₇₀₀ is recommended. Production of biochar with less EC and pH and suitable application dose in lime soils of semi-arid regions may be beneficial but requires more studies.

REFERENCES

- [1] Abdelhafez, A. A., Li, J., Abass, M. H. (2014): Feasibility of biochar manufactured from organic waste on stabilization of heavy metals in a metal smelter contaminated soil. – *Chemosphere* 117: 66-71.
- [2] Ahmad, M., Rajapaksha, A. U., Lim, J. E., Zhang, M., Bolan, N., Mohan, D., Vithanage, M., Lee, S. S., OK, Y. S. (2014): Biochar as a sorbent for contaminant management soil and water. – *Italian Chemosphere* 99: 19-33.
- [3] Alburquerque, J. A., Calero, J. M., Barron, V., Torrent, J., Del Campillo, M. C., Gallardo, A., Villar, R. (2014): Effect of biochars produced from different feedstocks on soil properties and sunflower growth. – *Journal of Plant Nutrition and Soil Science* 177(1): pp16-25.
- [4] ASTM International (2009): D5142 Standard Test Method for Proximate Analysis of the analysis Sample of Coal and Koke Instrumental Procedures. – American Society for Testing and Material (ASTM) International, USA.

- [5] Brunauer, S., Emmett, P. H., Teller, E. (1938): Adsorption of gases in multimolecular layers. – *Journal of American Chemical Society* 60(2): 309-319.
- [6] Bu-Olayan, A. H., Thomas, B. V. (2009): Translocation of trace metals in desert plants of Kuwait governorates. – *Research Journal of Environmental Sciences* 3(5): 581-587.
- [7] Cao, X., Ma, L., Gao, B., Haris, W. (2009): Dairy-manure derived biochar effectively sorbs lead and atrazine. – *Environ. Sci. Technol.* 43: 3285-3291.
- [8] da Silva, I. C. B., Basilo, J. J. N., Fernandes, L. A., Colen, F., Sampaio, R. A., Frazão, L. A. (2017): Biochip from different residues on soil properties and common bean production. – *Sci. Agric.* 74(5): 378-382.
- [9] Dume, B., Mosisa, T., Nebiyu, A. (2016): Effect of biochar on soil properties and lead (Pb) availability in military camp in south west Ethiopia. – *Afri. J. Envi. Sci. Tech.* 10(3): 77-85.
- [10] Elzobair, K. (2013): Biochar effects on soil microbial communities and resistance of enzymes to stress. – Thesis, Department of Soil and Crop Science, Colorado State University.
- [11] Hejazizadeh, A., Gholamizadeh Ahangar, A., Ghorbani, M. (2016): Effect of biochip on lead and cadmium from applied paper factory sewage sludge by sunflower (*heliantus annus* L.). – *Water and Soil Science University of Tabriz* 26(1/2): 259-271.
- [12] Ingole, S. P., Tale, S. S. (2016): Review on toxicity assessment for carcinogenic soil contaminants. – *The Pharmaceutical and Chemical Journal* 3(2): 139-144.
- [13] Kacálková, L., Tlustoš, P., Szakpvá, J. (2014): Chromium, nickel and lead accumulation in mize, sunflower, willow and poplar. – *Pol. J. Environ. Stud.* 23(3): 753-761.
- [14] Karami, N., Clemente, R., Moreno-Jimenez, E., Lepp, N. W., Beesley, L. (2011): Efficiency of green waste compost and biochar soil amendments for reducing lead and copper mobility and uptake to rygrass. – *Journal of Hazardous Materials* 191: 41-48.
- [15] Komkiene, J., Baltrenaite, E. (2016): Biochar as adsorbent for removal heavy metal ions cadmium (II), copper (II), lead (II), zinc (II) from aqueous phase. – *Int. J. Environ. Sci. Technol.* 13: 471-482.
- [16] Kopittke, P. M., Asher, C. J., Menzies, N. W. (2008): Prediction of Pb speciation in concentrated and dilute nutrient solutions. – *Environ. Pollut.* 153: 548-554.
- [17] Lehmann, J. (2007): A handful of carbon. – *Nature* 447(May): 10-11.
- [18] Lindsay, W. L., Norvell, W. A. (1978): Development of DTPA soil test for zinc, iron, manganese and copper. – *Soil Science Society of America Journal* 42(3): 421-428.
- [19] Lu, Y., Yao, H., Shan, D., Jiang, Y., Zhang, S., Yang, J. (2015): Heavy metal residues in soil and accumulation in maize at long- term wastewater irrigation area in Tongliao, China. – *Hindawi Journal of Chemistry*. <http://dx.doi.org/10.1155/2015/628280>.
- [20] Melo, L. C. A., Coscione, A. R., Albreu, C. A., Puga, A. P., Camargo, O. A. (2013): Influence of pyrolysis temperature on Cadmium and zinc sorption capacity of sugar cane straw- derived biochip. – *Bio Resources* 8(4): 4992-5004.
- [21] Mousavi, H. Z., Hosseinifar, A., Jahed, V. (2011): Removal of Cu^{II} from wastewater by waste tire rubber ash. – *J. Ser. Chem. Soc.* 75: 845-753.
- [22] Novak, J. M., Lima, I., Xing, B., Gaskin, J. W., Steiner, C., Das, K. C., Ahmendna, M., Rehra, D., Watts, D. W., Busscher, W. J., Schomberg, H. (2009): Characterization of designer biochar produced at different temperature and their effects on a loamy sand. – *Annals of Environmental Science* 2: 195-206.
- [23] Nguyen, B. T., Lehmann, J. (2009): Black carbon decomposition under varying water regimes. – *Org. Geochem.* 40: 846-835.
- [24] Paneque, M., De la Rosa, J. M., Franco-Navarro, J. D., Colmenero-Flores, J. M., Knicher, H. (2016): Effect of biochar amendment on morphology, productivity and water relations of sunflower plants under non- irrigation conditions. – *Catena* 147:280-287.
- [25] Park, J. H., Choppala, G. K., Bolan, N. S., Chaung, J. W., Chuasavathi, T. (2011): Biochar reduces the bioavailability and phytotoxicity of heavy metals. – *Plant Soil* 348: 439-451.

- [26] Paz-Ferreiro, J., Lu, H., Fu, S., Mendez, A., Gasco, G. (2014): Phytoremediation and biochar to remediate heavy metal polluted soils: a review. – *Solid Earth* 5: 65-75.
- [27] Qayyum, M. F., Abid, M., Danish, S., Saeed, M. K., Ali, M. A. (2015): Effect of various biochars on seed germination and carbon mineralization in an alkaline soil. – *Pak. J. Agri. Sci.* 51(4): 977-982.
- [28] Rajkovich, S., Enders, A., Hanley, K., Hyland, C., Zimmerman, A. R. (2011): Corn growth and nitrogen nutrition after additions of biochars with varying properties to temperate soil. – *Biol. Ferti. Soils.* 48: 271-284.
- [29] Rajkovich, S., Enders, A., Hanley, K., Haylands, C., Zimmerman, A. R., Lehmann, J. (2012): Corn Growth and nitrogen nutrition after additions of biochar with varying properties to temperate soil. – *Biology and Fertility of Soils* 47(3): 271-84.
- [30] Sadaka, S., Sharara, M. A., Ashworth, A., Keyser, P., Allen, F., Wright, A. (2014): Characterization of biochar from switchgrass carbonization. – *Energies* 7: 548-567.
- [31] Schmidt, M. W., Noack, A. G. (2000): Black carbon in soil and sediments: analysis, distribution, implications and current challenges. – *Glob Biogeochem Cycle* 14(3): 777-793.
- [32] Shumaker, K. L., Begonia, G. (2005): Heavy metal uptake, translocation and bioaccumulation studies of (*Triticum aestivum*) cultivated in contaminated dredged materials. – *Int. J. Environ. Res. Public Health.* 2(2): 293-298.
- [33] Song, W., Guo, M. (2012): Quality variations of poultry litter biochar generated at different pyrolysis temperature. – *J. Anal. Appl. Pyrolysis.* 94: 138-145.
- [34] Uchimiya, M., Lima, I. M., Classon, K. T., Chang, S., Wartelle, L. H., Rodgres, J. E. (2010): Immobilization of heavy metal ions (Cu^{II} , Cd^{II} , Ni^{II} and Pb^{II}) by broiler litter-derived biochars in water and soils. – *J. Agric. Food Chem.* 58: 5538-5544.
- [35] Uchimiya, M., Chang, S., Klasson, K. T. (2011): Screening biochars for heavy metal retention in soil: Role of Oxygen functional groups. – *Journal of Hazardous Materials* 190: 432-441.
- [36] Wang, S., Gao, B., Zimmerman, A. R., Li, Y., Ma, L., Harris, W. G., Migliaccio, K. W. (2015): Physiochemical and adsorptive properties of biochars derived from woody and herbaceous biomass. – *Chemosphere* 134: 257-262.
- [37] Wolf, B. (1982): The comprehensive system of lead analysis and its use for diagnosing crop nutrient status. – *Comm Soil Sci. Plant Anal.* 13: 1035-1059.
- [38] Wu, W., Yang, M., Feng, Q., McGrouter, K., Wang, H., Lu, H., Chen, Y. (2012): Chemical characterization of rice straw-derived biochar for soil amendment. – *Biomass Bioenerg.* 47: 268-276.
- [39] Yang, X., Liu, J., Mc Grother, K., Huang, H., Lu, K., Guo, X., He, L., Lin, X., Che, L., Ye, Z., Wang, H. (2015): Effect of biochar on extractability of heavy metals (Cd, Cu, Pb and Zn) and enzyme activity in soil. – *Environ Sci. Pollut Res.* 23: 974-984.
- [40] Yao, Y., Gao, B., Zhang, M., Inyang, M., Zimmerman, A. R. (2012): Effect of biochar amendment on sorption and leaching of nitrate ammonium and phosphate in a sandy soil. – *Chemosphere* 89: 1467-1471.
- [41] Zhang, J., Lu, F., Zhang, H., Shao, L., Chen, D., He, P. (2015): Multiscale visualization of the structural and characteristic changes of sewage sludge biochar oriented towards potential agronomic and environmental implication. – *Scientific Report* 5: 9406.
- [42] Zhao, S. X., Ta, N., Wang, X. D. (2017): Effect of temperature on the structural and physiochemical properties of biochar with apple tree branches as feedstock material. – *Energies* 10: 1293. DOI: 10.3390/en10091293.
- [43] Zheng, R., Chen, Z., Cai, C., Wang, X., Huang, Y., Xiao, B., Sun, G. (2013): Effect of biochars from rice husk, bran and straw on heavy metal uptake by post-grown wheat seedling in a historically contaminated soil. – *Biores.* 8: 5965-5982.

THREE NEW RECORDS FOR TURKISH MYCOBIOTA

KELES, A.

*Van Yüzüncü Yıl University, Education Faculty, Department of Science and Mathematics
Education, Van, Turkey
(e-mail: alikeles61@yahoo.com; phone: +90 432 225 17 01)*

(Received 16th Aug 2018; accepted 2nd Jan 2019)

Abstract. The study was based on three basidiomycetous macrocete samples, collected from Trabzon and Erzincan provinces between 2013-2014, and aims to make a contribution to the mycomycota of Turkey by adding new records. The ecological characteristics of the fruit bodies were recorded and macro photographs of them were taken at their natural habitats. Then they were transferred to the fungarium and necessary investigations were carried out. By comparing the obtained macroscopic and microscopic measuremental data with those in literature, they were identified as *Agaricus smithii* Kerrigan, *Coprinopsis goudensis* (Uljé) Redhead, Vilgalys & Moncalvo and *Suillus tomentosus* Singer. Tracing the current literature on macrofungi of Turkey, it is found that they were not reported from Turkey before. The taxa are described briefly and required data about their, habitat, ecology and geographical positions are provided together with macromorphological photographs and line drawings related to their micromorphologies.

Keywords: *biodiversity, Basidiomycota, Erzincan, Trabzon*

Introduction

Taxonomic studies on Turkish mycobiota had not a long history and has been accelerated especially in last three to four decades. Starting especially from 1970's numerous regional lists and new contributions were presented by many researchers, and the findings of these studies were prepared as checklists by Sesli and Denchev (2014) and Solak et al. (2015) with about 2,400 macrofungi species. Analysis of these checklist indicated that almost half of the current taxa were still reported from only 1 or two localities (Kaya, 2015). Contributory studies are still being carried out (Demirel et al., 2016; Keleş and Oruç, 2017; Uzun et al., 2017; Sadullahoğlu and Demirel, 2018; Sesli, 2018). But, considering the existence of about 15,000 macromycete taxa in Europe (Lukić, 2009) and the macrofungal diversity estimates of Mueller et al. (2007) regarding the plant/macrofungus ratios of temperate regions, we believe that, there is still much to be done to obtain the overall macrofungal data of Turkey (Kaya, 2009). Starting from this stand point, I usually perform field trips to observe and determine the macromycetes in our country. During such field trips three basidiomycetous macrofungi samples belonging to the families Agaricaceae, Psathyrellaceae and Suillaceae were collected from Erzincan and Trabzon provinces which fall in Irano-Turanian and Euro-Siberian phytogeographical regions respectively within the holarctic floral kingdom. As a result of necessary investigations, the samples were identified as *Agaricus smithii* Kerrigan, *Coprinopsis goudensis* (Uljé) Redhead, Vilgalys & Moncalvo and *Suillus tomentosus* Singer. Tracing the current checklists macrofungi of Turkey (Sesli and Denchev, 2014; Solak et al., 2015) and latest contributions (Allı et al., 2017; Işık and Türkekul, 2017; Kaşık et al., 2017; Uzun et al., 2018; Uzun and Kaya, 2019), it is found that 35 species *Agaricus* L., 18 species *Coprinopsis* P. Karst., and 11 species of *Suillus* Gray. have been reported from Turkey, and the above three taxa were not recorded before. The study aims to make a contribution to the Turkish mycobiota.

Materials and methods

Basidiomata of *Coprinus goudensis* were collected from İliç district of Erzincan province in 2013, and the basidiomata of *Agaricus smithii* and *Suillus tomentosus* were collected from Çamburnu district of Trabzon province in 2014 (Figure 1). During field studies, the ecological characteristics of the fruit bodies were recorded and macro photographs of them were taken at their natural habitats. Then the samples were transferred to the fungarium, dried in an air conditioned room, and prepared as fungarium materials. Dry materials were used for further investigations. Macroscopic measurements and micromorphologic investigations were carried out in fungarium. A Leica DM500 trinocular compound microscope was used for micromorphologic investigations. Microscopic features were portrayed with the CorelDRAW drawing program. The specimens were identified by comparing the obtained macroscopic and microscopic measuremental data with Smith and Thiers (1964), McKnight and McKnight (1987), Uljé and Bas (1993), Trudell and Ammirati (2009), Bessette et al. (2010), Desjardin et al. (2014), Gierczyk et al. (2014), Kuo and Methven (2014) and Kerrigan (2016). The samples are kept at the fungarium of Van Yüzüncü Yıl University in Van (VANF).



Figure 1. Collection locations of the determined macrofungi samples

Results

Brief descriptions, photograph of fruit bodies, and drawings of microcharacters are provided. The taxonomy of the taxa follows that of Kirk et al. (2008).

Agaricus smithii Kerrigan

Macroscopic and microscopic features

Pileus 8-12 cm wide, it grows from cylindrical to large convex. The edges not curved but sometimes can be slightly tasseled. The fibrillary is pale yellowish, brownish on a whitish ground color. Flesh thickness reaches up to 1.5 cm and does not change. Flavor and odour is like almonds. Lamellae not cramped, the color is pale, then turn into pinkish and becomes brown at maturity. Stipe 5-10 × 2-3 cm hairless, whitish to yellowish brown. Spores 7.1-9.2 × 4.7-5.7 µm elliptical, smooth, dark brown. Basidia 19-24 × 8.7-10 µm, clavate, 4-spored (Figure 2).

Specimen examined

Trabzon, Çamburnu, north of Maritime Faculty, on soil under mixed trees, 40°55'378" N, 40°12'613" E, 13 m., 21.10.2014, AK. 2941.

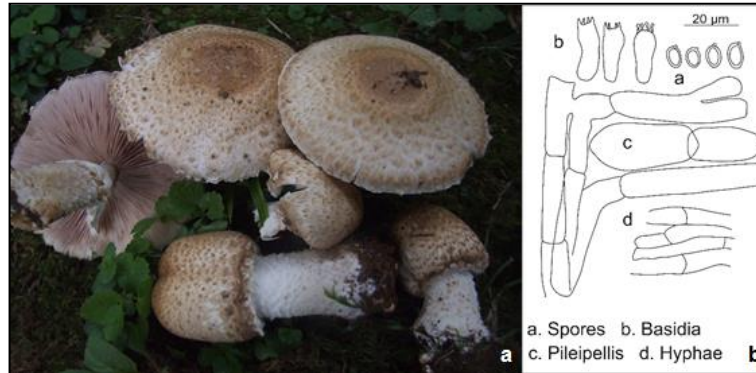


Figure 2. *Agaricus smithii* a) basidiocarps, b) microchaerecters

***Coprinopsis goudensis* (Uljé) Redhead, Vilgalys & Moncalvo (Syn: *Coprinus goudensis* Uljé)**

Macroscopic and microscopic features

Pileus 1-2.2 cm when young, up to 3 cm when broadened, ellipsoid when young, then ovoid or conical, greyish-brown when young, then whitish brown, finally greyish black-brown. Veil white, disintegrator in small, radial, hairy-fibrillose scales. Lamellae rather crowded, free, first white, then grey-brown to blackish. Stipe 2-5 × 0.1-0.2 cm, white, greyish white, slightly white floccose, especially clavate at the base. Spores 6.8-11 × 4.4-6.5 µm, ellipsoid or ovoid with rounded apex, sometimes oblong, rather pale red-brown and central, some with germpor. Basidia 22-38 × 7.5-10 µm, 4-spored. Cheilocystidia subglobose, ovoid, 33-70 × 25-52 µm. Pleurocystidia cylindrical to oblong, 50-105 × 32-55 µm. Elements of veil up to 13 µm widen and diverticulate (*Figure 3*).

Specimen examined

Erzincan, İliç, Kuruçay village, on decaying wood remnants, Erzincan, 39°36'744" N, 38°31'147" E, 999 m, 08.05.2013, AK. 2066.

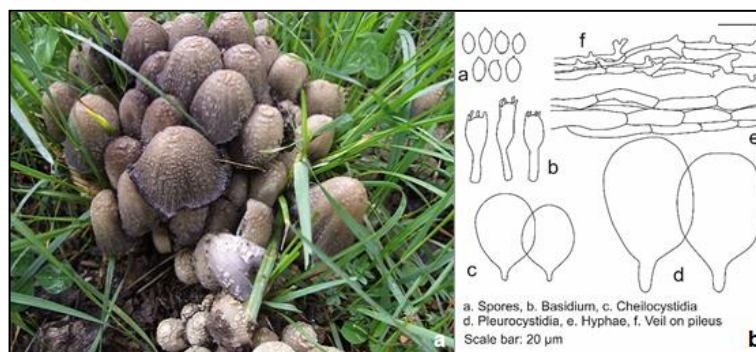


Figure 3. *Coprinopsis goudensis* a) basidiocarps, b) microchaerecters

Suillus tomentosus Singer

Macroscopic and microscopic features

Pileus 6-12 cm wide, convex when young, edges curved when matured, the curve disappear when moist, the surface sticky, color vary from pale yellow color to dirty skin color, stain characteristically vary from gray to olive greenish-gray. Flesh thick, soft, white to pale yellow, turns blue when damaged. Hymenophore tubes up to 1.5 cm long, pores approximately 1 mm thick, angled pale brown, when matures become dark yellow. Stipe 5-10 × 1.5-3 cm hard and sticky to the floor. While the upper part varies from yellowish to orange, the lower part varies from slightly reddish to brown. Spores 8-12 × 3-4.5 μm, narrow, ellipsoid, smooth, thick-walled, dark olive greenish-brown (Figure 4).

Specimen examined

Trabzon, Çamburnu, near Forestry Directorate Hotel, among needle-litter under pine trees, 40°55'379" N, 40°12'790" E, 93 m., 29.10.2014, AK. 2962.

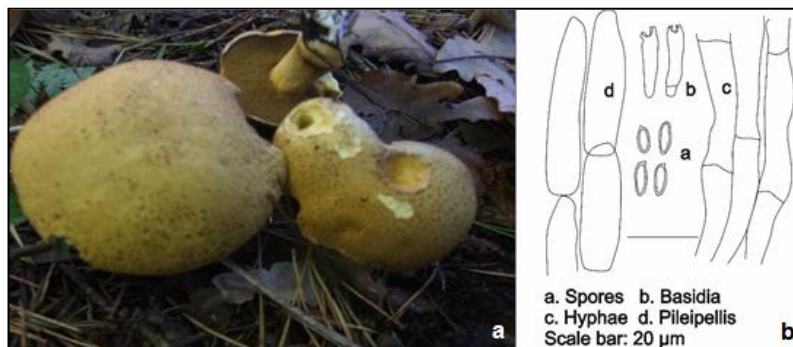


Figure 4. *Suillus tomentosus* a) basidiocarps, b) microcharacters

Discussion

With this study, the basidiomycete taxa *Agaricus smithii*, *Coprinopsis goudensis*, and *Suillus tomentosus* were given as new records from Turkey. The determined characteristics of the investigated samples conforms those given in literature.

Agaricus smithii is easily determined by the egg-shaped pileus when young, tawny to gold or orange cap colors, long stipe and amygdale odor. Young specimens of this species have similar morphology with *A. sylvicola* (Vittad.) Peck. But the appressed-fibrillose to fibrillose-scaly mature cap differs it from *A. sylvicola* which have a subglabrous to silky fibrillose cap at maturity (Desjardin et al., 2014). Shorter spores of *A. sylvicola* is another distinguishing feature between the two species (Kerrigan, 1986).

Coprinopsis goudensis can easily be recognized by the ellipsoid spores which in average are less than 10 μm long, having an average quotient of 1.6 or more, and the lignicolous habitat (Gierczyk et al., 2014). In terms of morphological similarity this species can be compared with *C. luteocephala* (Watling) Redhead, Vilgalys & Moncalvo, *C. neotropica* (Redhead & Pegler) Redhead, Vilgalys & Moncalvo, *C. stangliana* (Enderle, Bender & Gröger) Redhead, Vilgalys & Moncalvo and *C. urticicola* (Berk. & Broome) Redhead, Vilgalys & Moncalvo. Among them *C. luteocephala* differs with yellow veil, larger spore and substrate (dung), *C. neotropica*

differs with smaller and much broader spores, and trophical habitat, *C. stangliana* differs with much larger basidiocarps and spores, and habitat (soil), and *C. urticicola* differs in much smaller spores and basidiocarps (Ulje and Bas, 1993).

Suillus tomentosus is a very common species and is morphologically similar to *S. americanus*, *S. hirtellus*, *S. pictus* and *S. subaureus*, but any of the latter species present blue-staining reactions when cut or injured (Lincoff, 1981; McKnight and MacKnight, 1987; Trudell and Ammirati, 2009). Since all parts this edible species stains blue when bruised or cut, one should be sure while distinguishing it from other blue-staining *Suillus* species (McKnight and MacKnight, 1987).

Conclusion

Agaricus smithii, *Coprinopsis goudensis*, and *Suillus tomentosus* were given as new records from Turkey, increasing the current taxa numbers of the genera *Agaricus*, *Coprinopsis* and *Suillus*, in Turkey, to 36, 19 and 12, respectively.

REFERENCES

- [1] Allı, H., Çöl, B., Şen, İ. (2017): Macrofungi biodiversity of Kütahya (Turkey) province. – *Biological Diversity and Conservation* 10(1): 133-143.
- [2] Bessette, A. E., Roody, W. C., Bessette, A. R. (2010): *North American Boletes, A Color Guide to the Fleshy Pored Mushrooms*. – Syracuse: Syracuse University Press.
- [3] Demirel, K., Uzun, Y., Keleş, A., Akçay, M. E., Acar, İ. (2016): Macrofungi of Karagöl–Sahara National Park (Şavşat-Artvin/Turkey). – *Biological Diversity and Conservation* 10(2): 32-40.
- [4] Desjardin, D. E., Wood, M. G., Stevens, F. A. (2014): *California Mushrooms, The Comprehensive Identification Guide*. – London: Timber Press.
- [5] Gierczyk, B., Kujawa, A., Szczepkowski, A. (2014): New to Poland species of the broadly defined genus *Coprinus* (Basidiomycota, Agaricomycotina). – *Acta Mycol* 49(2): 159-188.
- [6] Işık, H., Türkekul, İ. (2017): A new record for Turkish mycota from Akdağmadeni (Yozgat) province: *Russula decolorans* (Fr.). – *Anatolian Journal of Botany* 1(1): 1-3.
- [7] Kaşık, G., Aktaş, S., Alkan, S., Öztürk, C. (2017): Additions to the Macrofungi of Selçuk University Alaeddin Keykubat Campus (Konya). – *The Journal of Fungus* 8(2): 129-136.
- [8] Kaya, A. (2009): Macrofungal diversity of Adıyaman Province (Turkey). – *Mycotaxon* 110: 43-46.
- [9] Kaya, A. (2015): Contributions to the macrofungal diversity of Atatürk Dam Lake basin. – *Turk J Bot* 39: 162-172.
- [10] Keleş, A., Oruç, Y. (2017): *Leucocoprinus brebissonii* (Godey) Locq, A New Record for Turkish Mycobiota. – *Anatolian Journal of Botany* 1(2): 49-51.
- [11] Kerrigan, R. W. (2016): *Agaricus of North America*. – New York Botanical Garden, New York, USA.
- [12] Kirk, P. F., Cannon, P. F., Minter, D. W., Stalpers, J. A. (2008): *Dictionary of the Fungi*. 10th ed. – Wallingford, UK: CAB International.
- [13] Kuo, M., Methven, S. A. (2014): *Mushrooms of the Midwest*. – University of Illinois Press. Urbana, Chicago and Springfield. USA.
- [14] Lincoff, G. H. (1981): *Field Guide to North American Mushrooms*. – New York: Alfred A. Knopf.
- [15] Lukić, N. (2009): The distribution and diversity of *Boletus* genus in central Serbia. – *Kragujevac J. Sci.* 31: 59-68.

- [16] McKnight, K. H., McKnight, V. B. (1987): A Field Guide to Mushrooms of North America. – New York: Houghton Mifflin Co.
- [17] Mueller, G. M., Schmit, J. P., Leacock, P. R., Buyck, B., Cifuentes, J., Desjardin, D. E., Halling, R. E., Hjortstam, K., Iturriaga, T., Larsson, K. H., Lodge, D. J., May, T. W., Minter, D., Rajchenberg, M., Redhead, S. A., Ryvarden, L., Trappe, J. M., Watling, R., Wu, Q. (2007): Global diversity and distribution of macrofungi. – *Biodiversity and Conservation* 16: 37-48.
- [18] Sadullahoğlu, C., Demirel, K. (2018): *Flammulina fennae* Bas, A New Record from Karz Mountain (Bitlis). – *Anatolian Journal of Botany* 2(1): 19-21.
- [19] Sesli, E. (2018): Cortinarius ve Lyophyllum Cinslerine Ait Yeni Kayıtlar. – *Mantar Dergisi* 9(1): 18-23.
- [20] Sesli, E., Denchev, C. M. (2014): Checklists of the myxomycetes, larger ascomycetes, and larger basidiomycetes in Turkey. 6th edn. Mycotaxon. – Checklists Online (<http://www.mycotaxon.com/resources/checklists/sesli-v106-checklist.pdf>): 1-136.
- [21] Smith, A. H., Thiers, H. D. (1964): A Contribution Toward a monograph of North American Species of Suillus. – Ann Arbor, Michigan, USA. 85.
- [22] Solak, M. H., Işıloğlu, M., Kalmış, E., Allı, H. (2015): Macrofungi of Turkey, Checklist, Volume- II. – Üniversiteliler Ofset, Bornova, İzmir.
- [23] Trudell, S., Ammirati, J. (2009): Mushrooms of the Pacific Northwest. – Oregon: Timber Press.
- [24] Uljé, C. B., Bas, C. (1993): Some new species of Coprinus from the Netherlands. – *Persoonia* 15(3): 357-368.
- [25] Uzun, Y., Acar, İ., Akçay, M. E., Kaya, A. (2017): Contributions to the macrofungi of Bingöl, Turkey. – *Turk J Bot* 41: 516-534.
- [26] Uzun, Y., Kaya, A. (2019): *Elaphomyces granulatus*, A New Hypogeous Ascomycete Record for Turkey. – *KSU J. Agric Nat* 22(1): 85-88.
- [27] Uzun, Y., Yakar, S., Karacan, İ. H., Kaya, A. (2018): New additions to the Turkish Pezizales. – *Turk J Bot* 42: 335-345.

LOW-CONCENTRATION SODIUM SELENITE APPLICATIONS IMPROVE OXIDATION RESISTANCE OF FILLING-STAGE RICE

HE, L. X.^{1,2#*} – ZHENG, A. X.^{1,2#} – DU, B.^{1,2#} – LUO, H. W.^{1,2} – LU, R. H.¹ – DU, P.³ – CHEN, Y. L.¹ – ZHANG, T. T.^{1,2} – LAI, R. F.^{1,2} – TANG, X. R.^{1,2*}

¹*Department of Crop Science and Technology, College of Agriculture
South China Agricultural University, 510642 Guangzhou, PR China*

²*Scientific Observing and Experimental Station of Crop Cultivation in South China
Ministry of Agriculture, 510642 Guangzhou, PR China*

³*Key Laboratory of Key Technology for South Agricultural Machine and Equipment
Ministry of Education, 510642 Guangzhou, PR China*

#These authors have contributed equally to this work.

**Corresponding author*

e-mail: tangxr@scau.edu.cn; phone/fax: +20-8528-0204-618

(Received 16th Aug 2018; accepted 2nd Jan 2019)

Abstract. Effects of sodium selenite treatments on rice were investigated using two known cultivars *Xiangyaxiangzhan* and *Meixiangzhan2* cultivated at two sites of Guangdong Province, China. Sodium selenite solutions at 10 (Se1), 30 (Se2) and 50 (Se3) $\mu\text{mol}\cdot\text{L}^{-1}$ were sprinkled to the rupturing-stage rice separately, with a control set with double distilled water instead. For *Xiangyaxiangzhan*, comparing with control, 6.91, 24.81 and 25.00% higher SOD, POD and CAT activity were recorded in Se1. For *Meixiangzhan2*, 2.10, 9.44 and 10.00% higher SOD, POD and CAT activity were recorded in Se1. Moreover, high-concentration sodium selenite (Se3) depressed the antioxidant enzyme activities and caused MDA over-production in *Xiangyaxiangzhan*. In conclusion, sodium selenite low-concentration applications could be an exogenous regulator to improve rice oxidation resistance in rice production.

Keywords: *sodium selenite, rice, yield, antioxidant enzymes, malondialdehyde*

Introduction

As a staple food in most Asian nations, rice contributes to 35%–75% of caloric intake for more than three billion people around the globe, which means rice production is an important part of the global food security system. The world population may increase to 10 billion, which intensifies the demand of rice in the next few decades (Krishnan et al., 2007). However, many uncertain factors could affect the rice yield and quality. Normally, rice is widely grown where the rainfall during the growing season is 50-3000 mm. Paddy fields are often under inundated condition for long time and produce abundant reduced toxic matter, such as ferrous ion and organic acids (XinLiu and Song, 2004), which could negatively affect rice growth. However, the concerns over the effects of global climate change and heavy metal pollution on crop growth and yield have been increased markedly (Krishnan et al., 2007). The stresses of environment pollution and climate changes would cause great loss in rice yield and quality, if the stress tolerance of rice plants cannot be strengthened. Hence, cultivation techniques should be improved in order to ensure the food security novel genetic approaches, of which exogenous regulators might be necessary in rice production.

Selenium (Se) is an essential element to humans, animals and plants. Se deficiency is associated with poor immune function, increased risk of mortality, and cognitive decline, while Se sufficiency or supplementation has antiviral effects and reduces the risk of autoimmune thyroid disease. Se could be a cancer-protective agent (Gladyshev et al., 1999). Moreover, the physiological response to Se varies considerably among plants because some plant species growing on seleniferous soils are tolerant and could accumulate abundant Se, but most plants are Se nonaccumulators and Se-sensitive (Terry et al., 2000). It has been proved that Se helps to resist toxic elements such as arsenic, antimony, mercury and copper (Gotsis, 1982; Srivastava et al., 2009). The study of Hu et al. (2014) showed that Se fertilizer significantly decreases the accumulation of cadmium and lead in rice tissues. Moreover, Proteomics analysis suggests Se treatment could highly affect the biological processes of rice seedlings, such as primary metabolism, photosynthesis and redox homeostasis (Wang et al., 2012). Thus, Se might be a potential exogenous regulator that helps to ensure the food security in rice production.

As is well-known, Se not only is a component element of glutathione peroxidase and thioredoxin reductase, but also is the key component of the catalyzing active center. Se could enhance the activity of glutathione peroxidase and hence the resisting oxidation, scavenge abundant free radicals and protect membranes from the injury of lipid peroxidation (Xin et al., 2004). Suitable Se supply promotes the growth of rice seedlings, but excessive Se injures rice plants and reduces biomass, especially in the roots (Liu et al., 2004).

Hence, this study was conducted in Guangdong (a major rice-producing province in South China) with the hypothesis that exogenous sodium selenite application in the rupturing stage could enhance the rice antioxidant capacity during the filling stage.

Materials and Methods

Plant materials and growing condition

Two rice cultivars, *Xiangyaxiangzhan* and *Meixiangzhan2* with a growth period of 111-114 days, which were planted widely in South China, were used as materials and planted at late season in both Guangzhou (23°16' N, 113°23' E) and Zengcheng (23°13' N, 113°81' E), Guangdong, China. Both experimental sites enjoyed a subtropical monsoon climate with mean annual air temperatures of 22.4°C and mean annual precipitation of 2680.9 mm. Before sowing, the seeds were soaked in water for 24 h, germinated in manual climatic boxes for another 24 h, and shade-dried, followed by sowing in polyvinyl chloride trays for nursery raising. Then the 20-day-old seedlings were transplanted to the fields at the planting distance of 30 × 12 cm². Rice seedlings were transplanted in July and harvested in October. The experimental soil in Guangzhou was sandy loam containing 25.65% organic matter, 1.360% total N, 0.956% total P, and 17.460% total K, while that in Zengcheng was sandy loam with 20.12% organic matter, 1.408% total N, 1.068% total P, and 15.767% total K.

Treatments and plant sampling

Four treatments were as set: Overhead sprinkle with 0, 10, 30 and 50 µmol·L⁻¹ sodium selenite at the rupturing stage of rice, which were marked as CK (double distilled water instead), Se1, Se2 and Se3, respectively. A special Knapsack Electric

sprayer (3WBD-Qianfeng Agricultural machinery, Yangjiang, Guangdong, China) with 0.2–0.5 mPa pressure and 16–18 L capacity fitted with a special windproof atomizing spray nozzle was used for sprinkle. The treatments were arranged in randomized complete block design (RCBD) in triplicate in each year with net plot size of 36 m². Fresh leaves were separated and collected from the rice plants after 15 days at the heading stage, washed with double distilled water and stored at -80°C for physio-biochemical analysis.

Yield and yield-related traits

At the maturity stage, the rice grains were harvested from six unit sampling areas (1.75 m²) in each plot and then threshed. The harvested grains were sun-dried and weighed in order to determine the grain yield. Twenty hills of rice from different locations in each plot were sampled for estimation of average effective panicle number per hill. At flowering, 30 panicles were randomly marked and then sampled from each treatment and weighed. Seed-setting rate was measured as: Panicle Weight₂– PanicleWeight₁/Time₂– Time₁ (Kong et al., 2017). Then representative plants from three hills were taken to estimate the yield-related traits.

Estimation of malondialdehyde (MDA) and anti-oxidant responses

The MDA content and activities of peroxidase (POD), superoxide (SOD) and catalase (CAT) were detected according to the methods of Kong et al. (2017). After MDA reacted with thiobarbituric acid, the absorbance was read at the 532, 600 and 450 nm. The MDA content in the reaction solution was calculated as: MDA content (μmol/L) = 6.45(OD₅₃₂ – OD₆₀₀) – 0.56OD₄₅₀, and finally expressed as μmol/g FW.

POD (EC 1.11.1.7) activity was estimated after the reaction in the solution including enzyme extract (50 μl), 1 ml of 0.3% H₂O₂, 0.95 ml of 0.2% guaiacol, and 1 ml of 50 mM·l⁻¹ sodium phosphate buffer (SPB, pH 7.0). One POD unit of enzyme activity was expressed as the absorbance increase by 0.01 (U/g FW) due to guaiacol oxidation. SOD (EC 1.15.1.1) activity was measured by using nitro blue tetrazolium (NBT). In brief, 0.05 ml of an enzyme extract was added into the reaction mixture which contained 1.75 ml of SPB (pH 7.8), 0.3 ml of 130 mM methionine buffer, 0.3 ml of 750 μmol·L⁻¹ NBT buffer, 0.3 ml of 100 μmol·L⁻¹ ethylene diamine tetraacetic acid (EDTA)-2Na buffer and 0.3 ml of 20 μmol·L⁻¹ lactoflavin. After the reaction, the absorbance was recorded at 560 nm. One unit of SOD activity was equal to the volume of the extract needed to cause 50% inhibition of the color reaction. CAT (EC 1.11.1.6) activity was estimated by adding an aliquot of enzyme extract (50 μl) to the reaction solution containing 1 ml of 0.3% H₂O₂ and 1.95 ml of SPB and then the absorbance was read at 240 nm. One CAT unit of enzyme activity was defined as the absorbance decrease by 0.01 (U/g FW).

Detection of Chlorophyll contents

The contents of total chlorophyll (total Chl), chlorophyll a (Chl a) and chlorophyll b (Chl b) were detected by the methods of Anjum (2016). A ground leaf sample (about 0.1 g) was placed in a 15 ml centrifuge tube along with 95% absolute ethyl alcohol (10 ml) and then kept at dark until the sample turned white. Then Chl a, Chl b and total Chl contents were estimated at 645, 652 and 663 nm respectively on an ultraviolet-visible spectrophotometer.

Statistical analysis

Data were analyzed on Statistix 8.1 (Analytical Software, Tallahassee, FL, USA) while differences among means were separated by using least significant difference (LSD) test at 5% probability level. Graphical representation was conducted via Sigma Plot 14.0 (Systat Software Inc., California, USA).

Results

MDA content

Sodium selenite applications significantly affected the MDA contents in rice leaves at the filling stage (Figure 1). For *Xiangyaxiangzhan* in both Guangzhou and Zengcheng, MDA contents under Se1 treatment were significantly lower compared with CK, Se2 or Se3, while the MDA contents increased with the increment of sodium selenite concentration. For *Meixiangzhan2*, MDA contents in Guangzhou were not remarkably different among CK, Se1 and Se3, but significantly decreased after the Se2 treatment. In Zengcheng, however, both Se1 and Se2 treatments lowered the MDA contents compared with CK and the trend was Se2 < Se1 < CK < Se3.

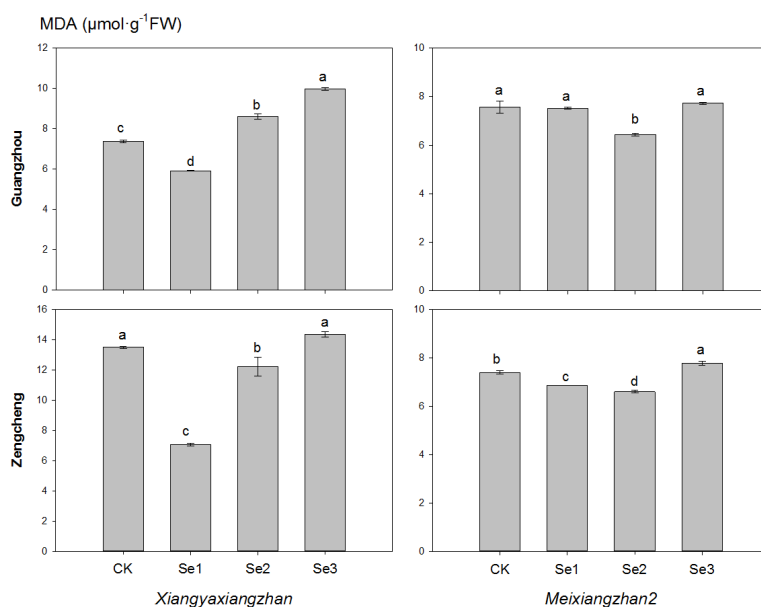


Figure 1. Effects of sodium selenite application on MDA contents. Means sharing a common letter don't differ significantly at ($P \leq 0.05$) according to least significant difference (LSD) test. The same as below

Anti-oxidant responses

Sodium selenite applications into *Xiangyaxiangzhan* regulated the anti-oxidant system in terms of POD, SOD and CAT activities and soluble protein contents (Figure 2). For example, POD activity was maximized in Se1 while did not significantly differ among CK, Se2 and Se3. For *Meixiangzhan2*, POD activity was the highest in Se2 and

changed in the trend of CK < Se3 < Se1 < Se2. SOD activity was significantly higher in Se1 treatment and was lowest in Se3 for *Xiangyaxiangzhan*. For *Meixiangzhan2*, SOD activity did not remarkably differ between CK and sodium selenite treatments in Guangzhou, but in Zengcheng, SOD activity under Se2 treatment was significantly higher than in CK, Se1 and Se3, which were 278.32, 229.13, 235.68 and 244.83 U g⁻¹min⁻¹ FW, respectively. Compared with CK, CAT activities under Se1 treatment in Guangzhou and Zengcheng were 1.24 and 1.08 fold higher for *Xiangyaxiangzhan*. For *Meixiangzhan2*, the CAT activity was improved by both Se1 and Se2, but was maximized in Se2 treatment in two locations. The effects of sodium selenite on soluble protein accumulation differed among treatments and between cultivars. For *Xiangyaxiangzhan*, the trend of soluble protein contents was Se3 < CK < Se2 < Se1 in Guangzhou, but did not significantly differ among treatments in Zengcheng. For *Meixiangzhan2*, the highest protein concentration in Guangzhou was recorded in Se1; the contents in Se1 and Se2 were significantly higher than CK and Se3 in Zengcheng.

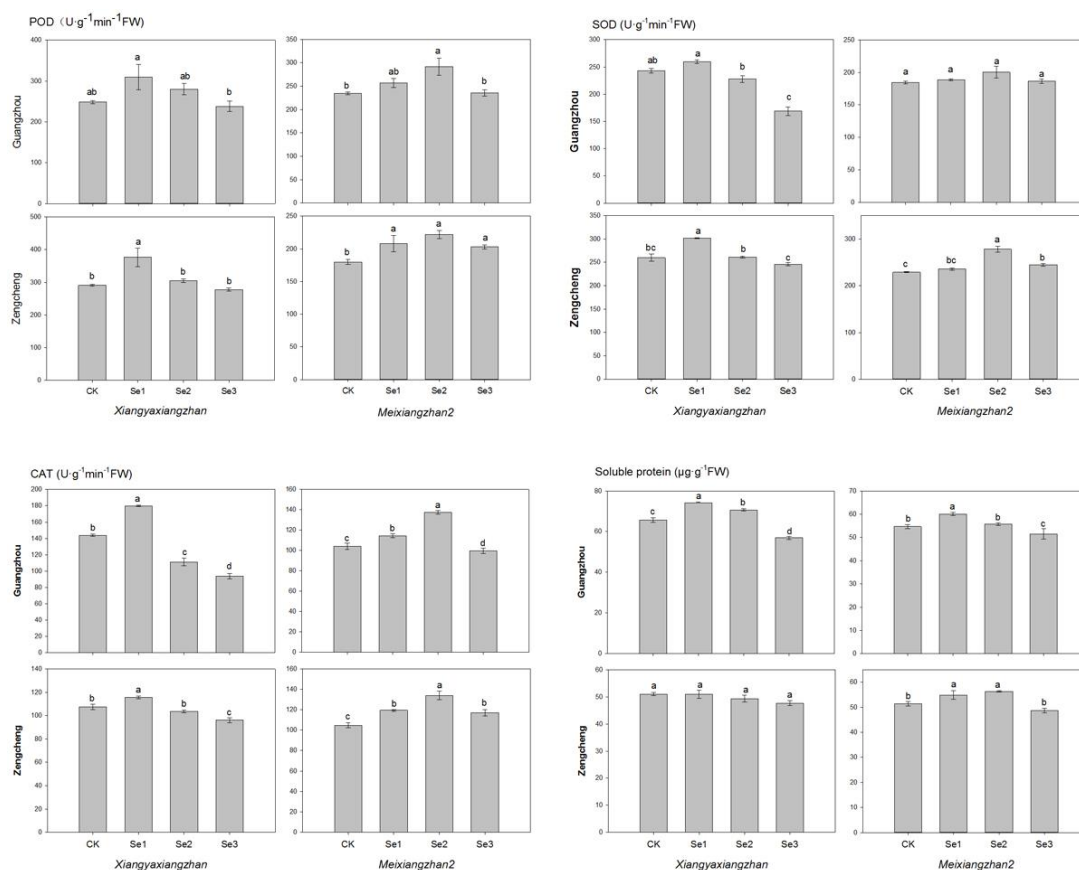


Figure 2. Effects of sodium selenite application on anti-oxidant responses

Chlorophyll

Chlorophyll contents were significantly affected by sodium selenite applications (Figure 3). For *Xiangyaxiangzhan*, the total Chl content maximized in Se1 and minimized in Se3 for both Guangzhou and Zengcheng, and a similar trend was found in Chl a contents. For *Meixiangzhan2* in Guangzhou, total Chl contents under Se1, Se2 and Se3 were 1.10, 1.18 and 1.06 fold higher than CK, respectively, and the trends of

both Chl a and Chl b were recorded as: CK < Se1 < Se3 < Se2. In Zengcheng, however, total Chl contents were not remarkably different between Se1 and Se2, but were both higher than CK and Se3, and similar trends were also found in both Chl a and Chl b.

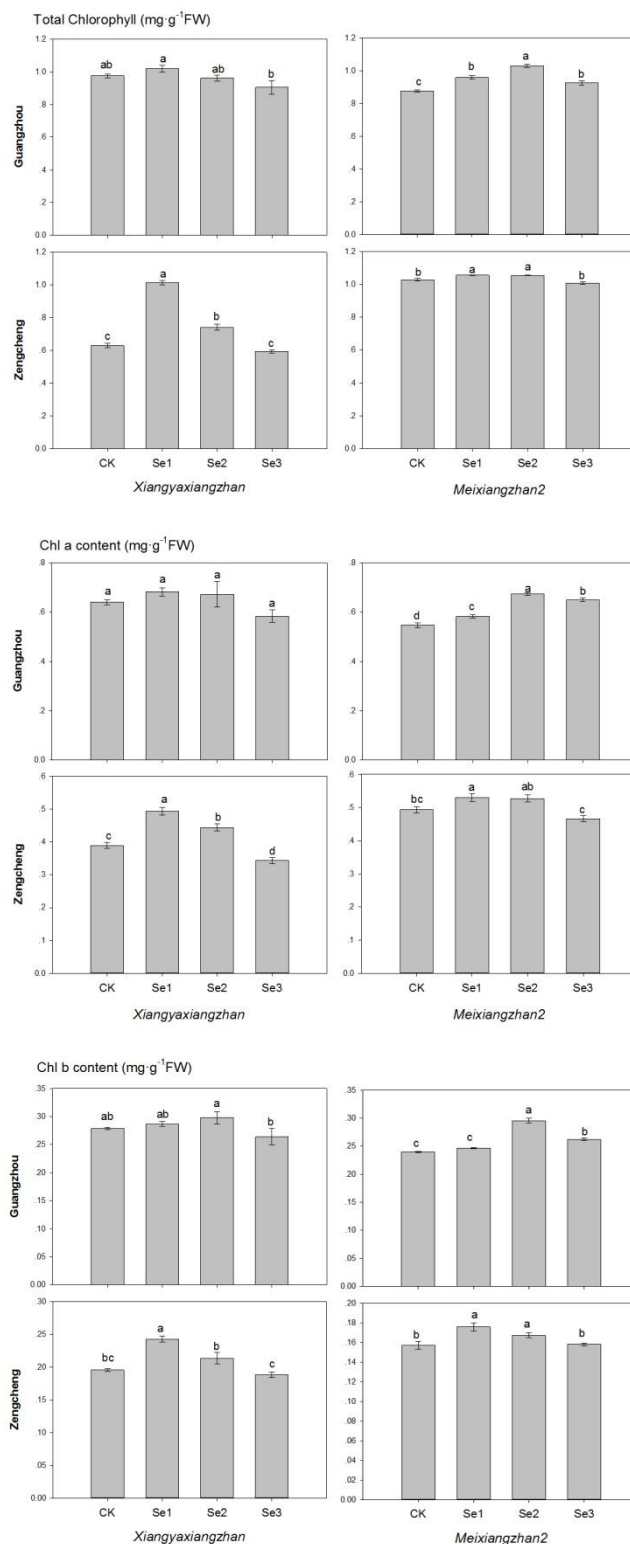


Figure 3. Effects of sodium selenite application on chlorophyll contents

Yield and yield-related traits

No significant difference among CK, Se1, Se2 and Se3 was found in panicle number per m² or grain number per panicle irrespective of locations or cultivars (*Table 1*). For *Xiangyaxiangzhan*, however, seed-setting rate of Se2 was higher than CK, Se1 and Se3 in Zengcheng, which were 78.85%, 70.81%, 66.53% and 71.43%, respectively. In Guangzhou, 1000-grain weights of Se1 and Se2 remained higher than CK and Se3. Furthermore, Se1 significantly improved grain yield compared with CK. For *Meixiangzhan2*, the sodium selenite treatments had no remarkable effect on seed-setting rate, grain weight or yield.

Discussion

As one of the important life elements, Se has many similar chemical properties as sulfur (S). The most important biofunction of Se in animals and humans is as a component of the glutathione peroxidase system (GSH-PX), which is involved in the REDOX reaction in the body, scavenging free radicals, and reducing the body peroxidation damage caused by biofilms (Qiang et al., 2011). Se could significantly enhance the antioxidant capacity of higher plants, such as wheat, corn, soybean and rape, and maintains the normal growth of plants (Wang et al., 1996; Nawaz et al., 2014). The mechanism is that Se can significantly improve the transcriptional levels of SOD and guaiacol peroxidase in plants, thus activating the antioxidant protection ability. The present study proves that sodium selenite treatments improved the activities of antioxidant enzymes, including POD, SOD and CAT. Furthermore, the sodium selenite applications also reduced oxidative damage by decreasing lipid per-oxidation (MDA concentration), while inducing dynamics in soluble proteins. Normally, the MDA production might be related to oxidation of polyunsaturated fatty acids (e.g., linoleic and linolenic acid) that play an important role in the arrangement of photosystem reaction centers. MDA could even react with free amino acids and cause ethylene over-production in cellular membranes (Rakwal et al., 2003). Thus, MDA content could be an important indicator of oxidative stress. We observed the treatments Se1 and Se2 reduced MDA concentration and enhanced the activities of POD, SOD and CAT. This finding indicates that low-rate sodium selenite applications at the rupturing stage could improve the antioxidant performance and strength of filling-stage rice under external environment stress. This study also agreed with (Ríos et al., 2009) that low-rate selenite application could enhance the activities of H₂O₂-detoxifying enzymes, especially glutathione (GSH), POD and SOD. Moreover, selenite treatment could regulate the accumulation of soluble proteins that help in maintaining cellular structures and functions when the antioxidant system quenches reactive oxygen species.

In our study, sodium selenite applications significantly affected the chlorophyll content, and the total Chl contents first increased and then decreased with the increase of sodium selenite concentration. This finding agrees with (Wu et al., 2000) that the electron transfer of chloroplast is accelerated at low Se concentration.

Interestingly, the sensitivity to sodium selenite was quite different between *Xiangyaxiangzhan* and *Meixiangzhan2*. As reported, different genotype cultivars responded differently to selenium fertilizers and differed in terms of selenium uptake and distribution. For *Xiangyaxiangzhan*, low concentration selenite applications such as Se1 significantly improved the activities of antioxidant enzymes, up-regulated the chlorophyll contents and increased the grain yields.

Table 1. Effects of sodium selenite application on yield and yield-related traits

Location	Cultivar	Treatment	Panicle number per m ²	Grains number per panicle	Seed-setting rate (%)	1000-grain weight (g)	Yield (t hm ⁻²)
Guangzhou	Xiangyaxiangzhan	CK	271.33±13.49a	105.51±11.56a	84.49±1.73a	18.26±0.36b	4.90±0.21b
		Se1	253.02±16.33a	87.47±11.05a	86.45±2.57a	19.49±0.06a	6.65±0.19a
		Se2	246.85±33.99a	111.59±8.15a	85.33±0.24a	19.78±0.13a	5.59±0.43ab
		Se3	286.17±29.17a	93.63±1.13a	86.58±1.57a	18.48±0.23b	5.64±0.66ab
	Meixiangzhan2	CK	227.40±28.23a	178.37±1.04a	79.26±1.95a	18.84±0.21a	5.33±0.72a
		Se1	219.66±14.76a	176.69±3.67a	80.52±0.35a	18.91±0.15a	5.18±0.29a
		Se2	250.6±9.66a	176.68±12.19a	81.75±2.59a	18.93±0.18a	7.51±0.11a
		Se3	202.64±13.75a	175.59±13.42a	78.58±4.19a	19.07±0.11a	5.64±1.06a
Zengcheng	Xiangyaxiangzhan	CK	292.1±11.45a	110.23±9.02a	70.81±3.36ab	20.27±0.35a	4.23±0.61a
		Se1	292.1±33.11a	104.62±2.95a	66.53±0.27b	20.55±0.12a	4.95±0.28a
		Se2	283.87±25.69a	117.19±7.37a	78.85±4.84a	20.36±0.11a	4.88±0.53a
		Se3	306.5±20.88a	106.12±6.34a	71.43±3.43ab	20.67±0.13a	3.72±0.22a
	Meixiangzhan2	CK	266.07±32.19a	138.56±2.25a	85.35±0.24a	18.07±0.39a	3.65±0.15a
		Se1	262.2±14.11a	116.14±3.17a	85.13±0.40a	18.18±0.14a	3.54±0.26a
		Se2	230.49±12.67a	120.63±7.73a	81.51±3.76a	18.41±0.07a	3.85±0.20a
		Se3	259.11±14.94a	124.54±6.62a	78.36±2.28a	18.00±0.02a	3.47±0.14a

However, high-concentration selenite application such as Se3 remarkably restricted the antioxidant system while inducing the over-production of MDA. For *Meixiangzhan2*, the best concentration of sodium selenite seemed to be Se2 with regard to the lowest MDA content and highest activities of POD, SOD and CAT, while antioxidant responses or chlorophyll contents were not significantly different among CK, Se1 and Se2. The result of our study indicated different rice cultivars had different sensibility to exogenous selenite and thus more study should be done in rice sensibility for Se.

Conclusions

Sodium selenite applications at low concentration could enhance the antioxidant system in term of POD, SOD and CAT, lower the MDA production and increase the chlorophyll contents. For *Meixiangzhan 2*, we considered that 30 $\mu\text{mol}\cdot\text{L}^{-1}$ was the most suitable concentration for application. For *Xiangyaxiangzhan*, we considered that 10 $\mu\text{mol}\cdot\text{L}^{-1}$ was the most suitable concentration for application. In the future, sodium selenite application could be used in the rice production to improve the rice oxidation resistance and prevent the yield loss caused by environmental stress.

Acknowledgements. This study was supported by National Natural Science Foundation of China (31271646), Student's Platform for Innovation and Entrepreneurship Training Program (201810564029), National Key R&D Program of China(2016YFD0700301), the World Bank Loan Agricultural Pollution Control Project in Guangdong (0724-1510A08N3684) and the Technology System of Modern Agricultural Industry in Guangdong (2017LM1098). The authors declare no conflicts of interest.

REFERENCES

- [1] Anjum, S. A. (2016): Chromium toxicity induced alterations in growth, photosynthesis, gas exchange attributes and yield formation in maize. – *Pakistan Journal of Agricultural Sciences* 53: 751-757.
- [2] El-Shintinawy, F. (2000): Structural and Functional Damage Caused by Boron Deficiency in Sunflower Leaves. – *Photosynthetica* 36: 565-573.
- [3] Gladyshev, V. N., Martín-Romero, F. J., Xu, X. M., Kumaraswamy, E., Carlson, B. A., Hatfield, D. L., Lee, B. J. (1999): Molecular biology of selenium and its role in cancer, AIDS and other human diseases. – *Recent Research Developments in Biochemistry*.
- [4] Gong, R., Ai, C., Zhang, B., Cheng, X. (2018): Effect of selenite on organic selenium speciation and selenium bioaccessibility in rice grains of two Se-enriched rice cultivars. – *Food Chemistry* 264: 443-448.
- [5] Gotsis, O. (1982): Combined effects of selenium/mercury and selenium/copper on the cell population of the alga *Dunaliella minuta*. – *Marine Biology* 71: 217-222.
- [6] Hu, Y., Norton, G. J., Duan, G., Huang, Y., Liu, Y. (2014): Effect of selenium fertilization on the accumulation of cadmium and lead in rice plants. – *Plant & Soil* 384: 131-140.
- [7] Kong, L., Ashraf, U., Cheng, S., Rao, G., Mo, Z., Tian, H., Pan, S., Tang, X. (2017): Short-term water management at early filling stage improves early-season rice performance under high temperature stress in South China. – *European Journal of Agronomy* 90: 117-126.
- [8] Liu, Q., Wang, D. J., Jiang, X. J., Cao, Z. H. (2004): Effects of the Interactions Between Selenium and Phosphorus on the Growth and Selenium Accumulation in Rice (*Oryza Sativa*). – *Environmental Geochemistry & Health* 26: 325-330.

- [9] Nawaz, F., Ashraf, M. Y., Ahmad, R., Waraich, E. A., Shabbir, R. N. (2014): Selenium (Se) Regulates Seedling Growth in Wheat under Drought Stress. – *Advances in Chemistry* (2014-7-22): 670-675.
- [10] Qiang, X., Shu, Y., Hai-Lei, A. Z. (2011): Effects of Exogenous Nitric Oxide Donor SNP on Lipid Peroxidation Caused by Selenium in Rice Seedlings. – *Acta Agronomica Sinica* 37: 177-181.
- [11] Rakwal, R., Agrawal, G. K., Kubo, A., Yonekura, M., Tamogami, S., Saji, H., Iwahashi, H. (2003): Defense/stress responses elicited in rice seedlings exposed to the gaseous air pollutant sulfur dioxide. – *Environmental & Experimental Botany* 49: 223-235.
- [12] Ríos, J. J., Blasco, B., Cervilla, L. M., Rosales, M. A., Sanchezrodriguez, E., Romero, L., Ruiz, J. M. (2009): Production and detoxification of H₂O₂ in lettuce plants exposed to selenium. – *Annals of Applied Biology* 154: 107-116.
- [13] Sairam, R. K., Srivastava, G. C., Saxena, D. C. (2000): Increased Antioxidant Activity under Elevated Temperatures: A Mechanism of Heat Stress Tolerance in Wheat Genotypes. – *Biologia Plantarum* 43: 245-251.
- [14] Srivastava, M., Ma, L. Q., Rathinasabapathi, B., Srivastava, P. (2009): Effects of selenium on arsenic uptake in arsenic hyperaccumulator *Pteris vittata* L. – *Bioresource Technology* 100:1115.
- [15] Terry, N., de Souza, M. P., Am, T. A. Z. (2000): Selenium in higher plants. – *Annual Review of Plant Physiology & Plant Molecular Biology* 51: 401-432.
- [16] Wang, Y. D., Wang, X., Wong, Y. S. (2012): Proteomics analysis reveals multiple regulatory mechanisms in response to selenium in rice. – *Journal of Proteomics* 75: 1849-1866.
- [17] Wang, Z., Xie, S., Peng, A. (1996): Distribution of Se in soybean samples with different Se concentration. – *Journal of Agricultural & Food Chemistry* 44: 2754-2759.
- [18] Wu, Y. Y., Lu, X. Y., Peng, Z. K., Luo, Z. M. (2000): Effect of Se on physiological and biochemical characters of paddy rice. – *Scientia Agricultura Sinica* 33(1): 100-103.

SEED TREATMENT WITH PACLOBUTRAZOL AFFECTS EARLY GROWTH, PHOTOSYNTHESIS, CHLOROPHYLL FLUORESCENCE AND PHYSIOLOGY OF RICE

HUANG, S.^{1,2#} – LUO, H.^{1,2#} – ASHRAF, U.^{1,2,3} – ABRAR, M.⁴ – HE, L.^{1,2} – ZHENG, A.¹ – WANG, Z.⁵
ZHANG, T.^{1,2} – TANG, X.^{1,2*}

¹*Department of Crop Science and Technology, College of Agriculture, South China Agricultural University, Guangzhou 510642, PR China*

²*Scientific Observing and Experimental Station of Crop Cultivation in South China, Ministry of Agriculture, Guangzhou 510642, PR China*

³*Department of Botany, University of Education (Lahore), Faisalabad-Campus, Faisalabad 38000, Pakistan*

⁴*State Key Lab. Grassland Argo-Ecosystem, School of Life Sciences, Lanzhou University, Lanzhou, Gansu 730000, PR China*

⁵*Key Laboratory of Key Technology for South Agricultural Machine and Equipment, Ministry of Education, Guangzhou 510642, PR China*

#These author have contributed equally to this work.

**Corresponding author
e-mail: tangxr@scau.edu.cn*

(Received 20th Aug 2018; accepted 29th Nov 2018)

Abstract. A pot experiment was conducted to investigate the effects of paclobutrazol seed treatment on early growth, photosynthesis and physio-biochemical attributes on rice. The seeds of two rice cultivars i.e., Basmati-385 and Xiangyaxiangzhan were treated with paclobutrazol at 40 mg per 5 kg of seeds (T) whilst non-treated seeds were taken as control (CK). Result showed that the seedling length of Basmati-385 and Xiangyaxiangzhan was reduced by 32.16 and 26.85% when seeds were treated with paclobutrazol, however, net photosynthetic rate, maximal efficiency of PSII photochemistry (F_v/F_m) and electron transport rate (ETR) were increased by 25.34 and 7.98%, 4.22 and 7.76% and 30.07 and 11.84% in Basmati-385 and Xiangyaxiangzhan, respectively. The malondialdehyde (MDA) contents were reduced up to 14% in both rice cultivars under paclobutrazol treatment. Furthermore, the activities of superoxide dismutase (SOD), peroxidase (POD), and catalase (CAT) were increased by 4.92 and 3.58%, 10.64 and 14.42%, 31.19 and 25.80% in paclobutrazol treated seeds than CK in both Basmati-385 and Xiangyaxiangzhan, respectively. In addition, dry weight per unit seedling length was significantly correlated with SPAD values, root length, surface area, diameter, and root volume, net photosynthetic rate, chlorophyll a, chlorophyll b, carotenoids, F_v/F_m , ETR , antioxidant enzymes, soluble sugar, and soluble protein of both rice cultivars. However, negative correlations were also recorded between dry weight per unit seedling length and intercellular CO₂, transpirational rates, non-photochemical quenching (NPQ) and malondialdehyde (MDA) contents in both Basmati-385 and Xiangyaxiangzhan. Hence, paclobutrazol seed treatment enhanced photosynthetic and gas exchange attributes, physio-biochemical attributes and root morphological characters in rice.
Keywords: *antioxidants; seed dressing agent; net photosynthetic rate; rice seedlings; root morphology*

Introduction

Paclobutrazol [(2RS, 3RS)-1-(4-chlorophenyl)-4, 4-dimethyl-2-(1, 2, 4-triazol -1-yl) pentan-3-ol] is a broad-spectrum gibberellin biosynthesis inhibitor which was developed by Imperial Chemical Industries (ICI) agrochemicals in 1986 (French et al., 1990).

Paclobutrazol being a triazole, regulates the plant growth by antagonizing the hormone gibberellin biosynthesis by inhibiting the ent-kaurene oxidase enzyme which catalyses the oxidation of ent-kaurene to ent-kaurenoic acid in the terpenoid pathway for the production of gibberellins through inactivation of cytochrome P450-dependent monooxygenases (Fletcher et al., 2000). Paclobutrazol hinders gibberellic acid (GA) and endogenous indole acetic acid (IAA), whilst enhances abscisic acid (ABA), cytokinin and ethylene production within the plants (Fletcher et al., 2000; Zhang et al., 1998). Roles of auxins and cytokinins to promote growth and development of lateral and adventitious roots have been well reported (Fletcher et al., 2000; Zhang et al., 1998). The previous work has shown ample effectiveness of paclobutrazol and certain other triazoles for improving proline and soluble proteins, lignin contents, decreasing transpirational rate through the partial closure of stomata in several crops (Gopi et al., 2006; Özmen et al., 2003; Wang et al., 2015; Kamran et al., 2018). It is being widely used in many crops, mainly for producing shorter plant canopies whilst its anti-gibberellic behaviour has been reported in numerous plants (Özmen et al., 2003; Kamran et al., 2018; Upreti et al., 2013). Commonly, paclobutrazol and triazole regulate various plant morpho-physiological functions such as root growth stimulation, reduction in shoot growth (Jaleel et al., 2007; Manivannan et al., 2008), enhancement of chlorophyll contents, net photosynthetic rate, and carbohydrate content (Fletcher et al., 2000; Zhang et al., 1998), reduction of free-radical induced damage, improving antioxidant efficacy (Fletcher et al., 2000; Zhang et al., 1998). It further regulates cytokinin production and hinders abscisic acid biosynthesis (Fletcher et al., 2000).

In rice production system, paclobutrazol has been used to develop semi-dwarf and/or dwarf plant varieties to reduce lodging and to improve rice yield (Street et al., 1986). Furthermore, paclobutrazol treatment improved chlorophyll contents, root morphology plant architectural characters (Yim et al., 1997). Foliar applied paclobutrazol-induced growth regulations has been previously reported (Xiang et al., 2017), however a little is known about the seed treatment with paclobutrazol-induced modulations in morpho-physiological and biochemical attributes of rice. Therefore, present study was conducted to investigate the effects of rice seed treatment with paclobutrazol on the morphological and physio-biochemical traits of rice.

Materials and methods

Experimental details

A pot experiment was conducted at Experimental Research Farm, College of Agriculture, South China Agricultural University, Guangzhou (23°09' N, 113°22' E and 11 m from mean sea level) China in September 2016. Seeds of two popularized aromatic rice cultivars i.e., Basmati-385 and Xiangyaxixangzhan were soaked in water for 12 h at room temperature and then put into the dark incubator at constant temperature (35 °C) for 12 h for germination. The following treatments were applied to germinated seed before sowing i.e., CK (no paclobutrazol treatment, taken as control) and T (paclobutrazol treatment (40 mg per 5 kg seeds). On 12th September, 2016, 50 seeds per pot were sown according to the layout (*Fig. 1*). The average temperature was 28.5 °C to 29.0 °C during experimental period, while the average humidity was about 68-70%. The experimental soil was collected from the paddy field and containing 1.14 g kg⁻¹ total N, 0.92 g kg⁻¹ total P, 16.65 g kg⁻¹ total K, 77.35 mg kg⁻¹ available N, 61.34 mg kg⁻¹ available P, 127.04 mg kg⁻¹ available K, and 23.34 g kg⁻¹ organic matter.

Before pot filling, the soil was kept under shade, air-dried, crushed and passed through 2 cm sieve.

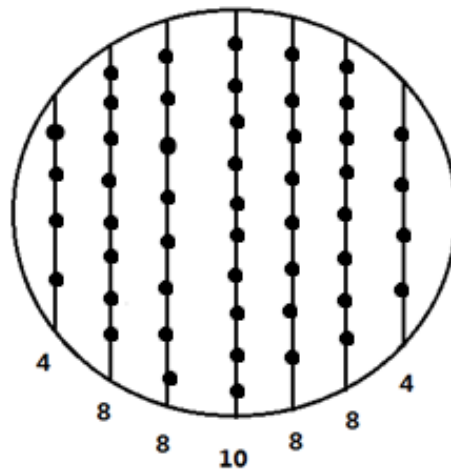


Figure 1. Layout of the sowing of seeds in pots

Seedling growth parameters

On 15th October, seedlings were collected for determination of seedling growth parameters and physio-biochemical indices. The samples were uprooted manually, washed with tap water to clean deposits in the roots. The morphological attributes i.e., seedling length, stem base width, roots morphology, SPAD values and dry weight per seedling were recorded. Leaf SPAD values were recorded with a SPAD meter “SPAD-502” and represented as relative chlorophyll contents. Roots morphology was determined by WinRHTZO Root System Analysis through scanning the roots of rice seedlings (Gu et al., 2010).

Photosynthesis and chlorophyll fluorescence

Photosynthesis and chlorophyll fluorescence were determined on the 32th day after emergence. Portable photosynthesis system (LI-6400, LI-COR, USA) was used to determine net photosynthetic rate and gas exchange attributes i.e., stomatal conductance, intercellular CO₂, and transpirational rates at 09:00–10:30 a.m. according to the standard method (Pan et al., 2015). Maximal efficiency of PSII photochemistry (F_v/F_m), the quantum yield of PSII, non-photochemical quenching (q_N), electron transport rate (ETR) were measured with an integrating fluorescence fluoro-meter (LI-6400–40 leaf chamber fluorometer, Li-Cor, USA) under dark conditions.

Physio-biochemical parameters

Fresh leaves were separated from the plant for each treatment, double washed with distilled water and stored at $-80\text{ }^{\circ}\text{C}$ till physio-biochemical analysis. The measurements were repeated in quadruplicate and mean values were calculated.

The photosynthetic pigments were determined by using 95% alcohol to extract contents (Lichtenthaler et al., 1987). The absorption was read at 665 nm, 652 nm, 649 nm and 470 nm.

The malondialdehyde (MDA) contents were measured by reacting with thiobarbituric acid (TBA) (Schmedes et al., 1989). The absorbance of the reaction solutions were recorded at 532 nm, 600 nm, and 450 nm. The reaction solutions were calculated as: MDA content ($\mu\text{mol}\cdot\text{L}^{-1}$) = $6.45 (\text{OD}_{532} - \text{OD}_{600}) - 0.56 \text{OD}_{450}$ and expressed as $\mu\text{mol}\cdot\text{g}^{-1}$ FW (fresh weight).

Nitro blue tetrazolium (NBT) method was used to measure the superoxide (SOD, EC 1.15.1.1) activity (Li, 2000). The reaction mixture contained 1.75 ml of buffer (pH 7.8), 0.3 ml of $130 \text{mM}\cdot\text{l}^{-1}$ methionine buffer, 0.3 ml of $750 \mu\text{mol}\cdot\text{l}^{-1}$ NBT buffer, 0.3 ml of $100 \mu\text{mol}\cdot\text{l}^{-1}$ EDTA- Na_2 buffer, 0.3 ml of $20 \mu\text{mol}\cdot\text{l}^{-1}$ lactoflavin and 0.05 ml of enzyme extract. After reaction, the change in color was measured at 560 nm. One unit of SOD activity is equal to the volume of extract needed to cause 50% inhibition of the color reaction.

The peroxidase (POD, EC 1.11.1.7) activity was measured by using enzyme extract. An aliquot of 50 μl of extract was added to the reaction solution containing 1 ml of 0.3% H_2O_2 , 0.95 ml of 0.2% guaiacol and 1 ml of $50 \text{mmol}\cdot\text{L}^{-1}$ buffer (pH 7.0). The absorbance change of the brown guaiacol was recorded at 470 nm to calculate POD activity. One POD unit of enzyme activity was defined as the absorbance increase due to guaiacol oxidation by 0.01 ($\text{U}\cdot\text{g}^{-1}$) (Luo et al., 2017). For catalase (CAT, EC 1.11.1.6) activity, an aliquot of 50 μl of enzyme extract was added to the reaction solution containing 1 ml of 0.3% H_2O_2 and 1.95 ml of H_2O . The change in absorbance was recorded at 240 nm. One unit of enzyme activity was defined as the absorbance decrease by 0.01 ($\text{U}\cdot\text{g}^{-1}$ FW) (Aebi et al., 1983).

The protein contents of leaves were estimated by using Coomassie Brilliant Blue G250 Reagent, and the absorbance was recorded at 595 nm and expressed as $\mu\text{g}\cdot\text{g}^{-1}$ of fresh weight (Bradford et al., 1976). The soluble sugar contents were determined by using anthrone-sulfuric acid method (Sun et al., 2010). The absorbance was recorded at 620 nm and expressed as $\text{mg}\cdot\text{g}^{-1}$ of fresh weight. Proline contents were estimated by using ninhydrin (Bates et al., 1973). The absorbance of the red chromophore in the toluene fraction was recorded at 520 nm and the amount of proline was estimated by comparing with a standard curve ($y = 0.0531 x - 0.0054$) and expressed as $\mu\text{g}\cdot\text{g}^{-1}$ FW.

Experimental design and statistical analyses

There were 10 pots per treatment and all pots were arranged in completely randomized design (CRD). Data were analysed by a statistical software “Statistix 8.1” (Analytical Software, Tallahassee, FL, USA) whilst treatment means were compared by using least significant difference (LSD) test at 5% probability level. Computer software “Origin 8.1” (Origin Lab Co., Northampton, MA, USA) was used for graphical representation.

Results

Seedling growth parameters

Seed treatment with paclobutrazol (T) significantly ($P \leq 0.05$) affected seedling length, base stem width, SPAD values and dry weight per unit seedling length (*Table 1*). Comparing T with CK, both Basmati-385 and Xiangyaxianzhan had lower seedling length whilst paclobutrazol enhanced SPAD values, base stem width and dry weight per unit seedling length. For example, 32.16 and 26.85% reduction in seedling length were

recorded in Basmati-385 and Xiangyaxianzhan, respectively, whereas an increase of 34.46 and 17.36% in base stem width, 25.59 and 16.41% in SPAD values, and 38.81 and 51.41% in dry weight per unit seedling length were recorded in paclobutrazol seed treatment in treated seeds than control for Basmati-385 and Xiangyaxianzhan, respectively. Negative correlations were recorded between dry weight per unit seedling length in Basmati-385 and Xiangyaxianzhan but significant positive correlations were observed between dry weight per unit seedling length and stem base width, SPAD values and root length (Table 2). The morphological appearance of treated and non-treated rice seedlings was presented in Figure 2.

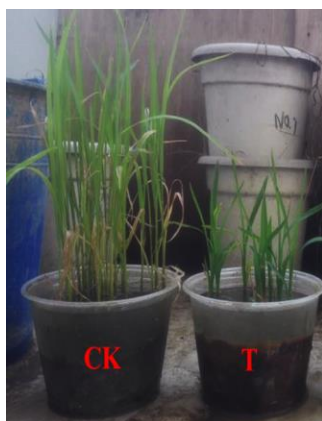


Figure 2. The physical appearance treated and non-treated rice seedlings. CK (non-treated); T (seed treatment with paclobutrazol at 40 mg per 5 kg seeds)

Paclobutrazol seed treatment also affected root morphology in terms of root length, surface area, diameter and volume (Table 1). Root length was 6.26 and 15.22% higher than CK in Basmati-385 and Xiangyaxianzhan, respectively. Seedlings of Basmati-385 and Xiangyaxianzhan in paclobutrazol seed treatment had 8.24 and 11.28% higher root diameter and 15.54 and 71.83% higher root volume, respectively than CK. Moreover, significant and positive correlations were observed between dry weight per unit seedling length, root surface area, root volume in response to paclobutrazol seed treatment (Table 2).

Table 1. Effect of seed dressing with paclobutrazol on rice seedling quality

		Shoot				Root			
		Height (cm)	Base stem width (mm)	SPAD values	Dry weight per unit seedling length (mg cm ⁻¹)	Length (cm)	Surface area (cm ²)	Diameter (mm)	Volume (cm ³)
Basmati	CK	20.93a	6.21b	20.07b	5.86b	228.66b	16.60b	0.23b	0.10b
	T	14.13b	8.44a	24.79a	7.84a	242.97a	18.48a	0.25a	0.12a
Xiangyaxianzhan	CK	17.90a	5.34b	17.53b	3.27b	142.26b	9.83b	0.23b	0.05b
	T	13.17b	6.14a	20.57a	4.97a	163.90a	13.77a	0.25a	0.10a

Values sharing a common letter within a column don't differ significantly at $P \leq 0.05$ according to least significant difference (LSD) test. CK (non-treated); T (seed treatment with paclobutrazol at 40 mg per 5 kg seeds)

Table 2. Correlation coefficients among dry weight per unit seedling length, height, stem base width, SPAD, length, surf area, average diameter and root volume

	Basmati	P value	Xiangyaxiangzhan	P value
Height	-0.9622	0.0021	-0.9865	0.0003
Stem base width	0.9923	0.0001	0.9500	0.0037
SPAD values	0.9877	0.0002	0.9487	0.0039
Length	0.9461	0.0043	0.9821	0.0005
Surf area	0.8870	0.0184	0.9741	0.0010
Average diameter	0.9479	0.0040	0.8414	0.0357
Root volume	0.7036	0.1187	0.9755	0.0009

Net photosynthesis, gas exchange and chlorophyll contents

Net photosynthetic rate and gas exchange attributes were substantially affected by paclobutrazol seed treatment. Both Basmati-385 and Xiangyaxiangzhan had 24.47 and 7.55% higher net photosynthetic rate (respectively) in paclobutrazol seed treatment compared with CK (Fig. 3a), whereas the both cultivars had decreased intercellular CO₂ concentration (6.60 and 6.69% reduction in Basmati and Xiangyaxiangzhan, respectively) in paclobutrazol seed treatment as compared with CK (Fig. 3c).

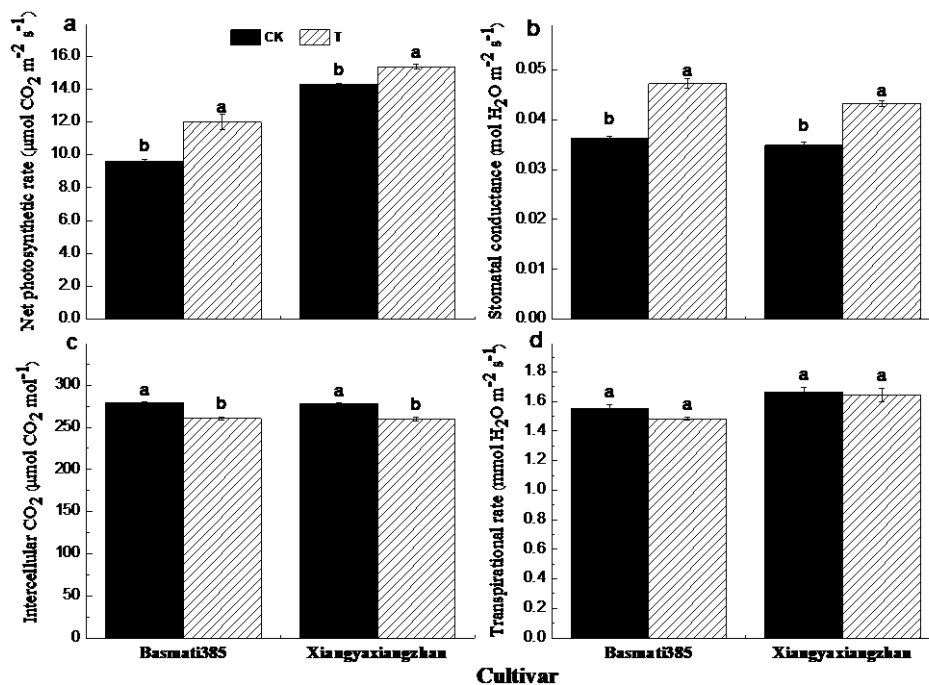


Figure 3. Effect of seed treatment with paclobutrazol on a) net photosynthesis, b) stomatal conductance, c) intercellular CO₂, d) transpirational rate. Capped bars represent S.E. of three replicates. Means sharing a common letter do not differ significantly at $P \leq 0.05$ according to least significant difference (LSD) test. CK (non-treated); T (seed treatment with paclobutrazol at 40 mg per 5 kg seeds)

However, there was no significant difference between T and CK for transpirational rates in both cultivars as shown in Figure 1d. In addition, the leaves of seedlings in

paclobutrazol seed treatment had higher contents of chlorophyll a, chlorophyll b and carotenoid. Compared with CK, paclobutrazol seed treatment increased 50.19 and 11.55% chl a, 47.22 and 12.23% chl b contents, 56.53 and 9.45% in carotenoids and 44.53 and 12.48% in total chl contents of Basmati and Xiangyaxiangzhan, respectively (Fig. 4a-d). Furthermore, significant positive correlations were recorded between dry weight per unit seedling length and net photosynthetic rate, stomatal conductance, chl a, chl b, carotenoids and total chl contents in both rice cultivars, however, negative correlations were found among dry weight per unit seedling length and intercellular CO₂ as well as transpiration rates in Basmati and Xiangyaxiangzhan (Table 3).

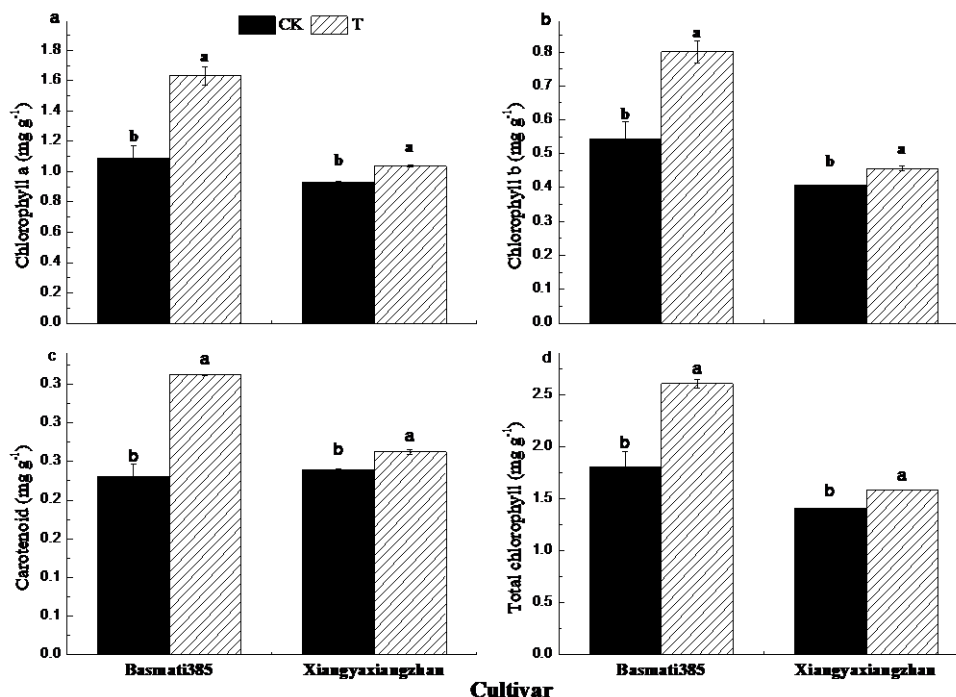


Figure 4. Effect of seed treatment with paclobutrazol on a) chlorophyll a, b) chlorophyll b, c) carotenoid, d) total chlorophyll. Capped bars represent S.E. of three replicates. Means sharing a common letter do not differ significantly at $P \leq 0.05$ according to least significant difference (LSD) test. CK (non-treated); T (seed treatment with paclobutrazol at 40 mg per 5 kg seeds)

Table 3. Correlation coefficients among dry weight per unit seedling length, net photosynthetic rate, stomatal conductance, intercellular CO₂, transpirational rates, chlorophyll a, chlorophyll b, carotenoids and total chlorophyll

	Basmati	P value	Xiangyaxiangzhan	P value
Net photosynthetic rate	0.9191	0.0096	0.9484	0.0039
Stomatal conductance	0.9936	0.0001	0.9712	0.0012
Intercellular CO ₂	-0.9722	0.0012	-0.9473	0.0041
Transpirational rates	-0.7883	0.0625	-0.1930	0.7141
Chlorophyll a	0.9126	0.0111	0.9826	0.0004
Chlorophyll b	0.8906	0.0173	0.9717	0.0012
Carotenoids	0.9343	0.0063	0.9558	0.0029
Total chlorophyll	0.9011	0.0142	0.9951	0.0000

Chlorophyll fluorescence

Significant differences in chlorophyll fluorescence parameters i.e., maximal efficiency of PSII photochemistry (F_v/F_m), photochemical quenching (qP), electron transport rate (ETR), F_0 and F_m . Compared with CK, an increase of 4.08 and 5.39% in F_v/F_m , 15.72 and 6.13% in qP , 21.76 and 31.36% in F_0 , 21.45 and 18.48% in F_m , 32.50 and 10.39% in ETR was recorded for both Basmati-385 and Xiangyaxiangzhan, respectively (Fig. 5a-f). Moreover, significant decrease was recorded in non-photochemical quenching (NPQ) with the application paclobutrazol as compared with CK (Fig. 5e). Additionally, positive correlations were observed between dry weight per unit seedling length and F_v/F_m , ETR , qP , F_0 and F_m whilst dry weight per unit seedling length was negatively associated with NPQ (Table 4).

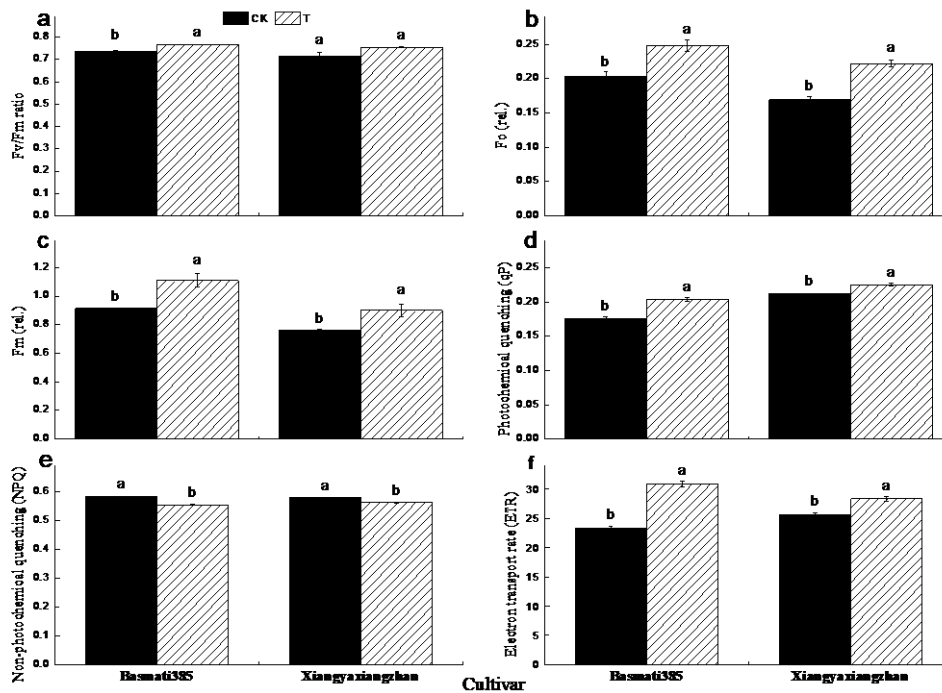


Figure 5. Effect of seed treatment with paclobutrazol on a) F_v/F_m , b) F_0 , c) F_m , d) photochemical quenching (qP), e) Non-photochemical quenching (NPQ), f) electron transport rate (ETR). Capped bars represent S.E. of three replicates. Means sharing a common letter do not differ significantly at $P \leq 0.05$ according to least significant difference (LSD) test. CK (non-treated); T (seed treatment with paclobutrazol at 40 mg per 5 kg seeds)

Table 4. Correlation coefficients among F_v/F_m , ETR , NPQ , qP , F_0 , F_m

Parameters	Basmati	P value	Xiangyaxiangzhan	P value
F_v/F_m	0.9695	0.0014	0.7341	0.0967
ETR	0.9832	0.0004	0.9244	0.0084
NPQ	-0.9511	0.0035	-0.9688	0.0014
qP	0.9618	0.0022	0.9477	0.004
F_0	0.8980	0.0151	0.9591	0.0025
F_m	0.8849	0.0191	0.8543	0.0303

Anti-oxidant responses, malodialdehyde, and soluble protein and sugar

Paclobutrazol regulated anti-oxidative enzymatic activities in terms of SOD, POD and CAT, but lowered lipid per-oxidation (in terms of MDA production) and also induced changes in both protein and sugar contents in both rice cultivars (*Fig. 6a-f*). The POD, SOD and CAT activities were enhanced by 10.79 and 15.71%, 4.44 and 3.57%, and 31.30 and 26.48% in both Basmati-385 and Xiangyaxiangzhan, respectively compared with CK. On the other hand, Basmati-385 and Xiangyaxiangzhan showed a decrease of 16.43 and 14.33% in MDA contents, respectively with the application of paclobutrazol as compared with CK. Paclobutrazol seed treatment led to substantial improvements in soluble protein and soluble sugar contents of both rice cultivars. For instance, an increase of 8.87 and 28.38% in soluble protein and 19.57 and 25.44% in soluble sugar contents was recorded for Basmati-385 and Xiangyaxianzhan, respectively with the application of paclobutrazol. Furthermore, positive correlations were recorded among dry weight per unit seedling length and CAT, SOD, POD, soluble protein, proline and soluble sugar. However, negative correlation was recorded between dry weight per unit seedling length and MDA contents (*Table 5*).

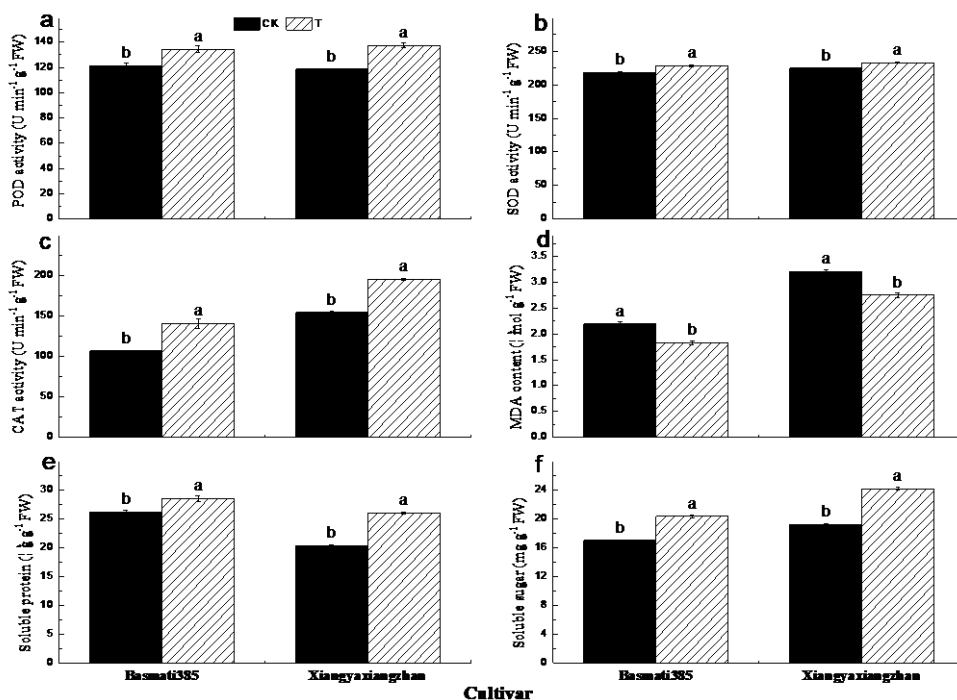


Figure 6. Effect of seed treatment with paclobutrazol on activity of a) POD, b) SOD, c) CAT, content of d) MDA, e) soluble protein, f) soluble sugar. Capped bars represent S.E. of three replicates. Means sharing a common letter do not differ significantly at $P \leq 0.05$ according to least significant difference (LSD) test

Discussion

Application of growth retardants modifies plant growth, development, root architecture, and physio-biochemical traits in crop plants. Previously, various triazoles have been studied as growth retardants and as anti-lodging agent of which paclobutrazole is a potential anti-gibberellic triazole (Peng et al., 2014). It inhibits the

biosynthesis of endogenous GA, hence can be used for canopy management in various crops. It also provides relief against various abiotic stresses by regulating photosynthetic process, osmolyte production and activities of various enzymatic and non-enzymatic antioxidants (Hu et al., 2016). In this study, it was observed that seed treatment with paclobutrazol (T) substantially reduced seedling length whilst improved base stem width, SPAD values and dry weight per unit seedling length and root morphology (Table 1). Moreover, significant and positive correlations were observed between dry weight per unit seedling length, root surface area, root volume in response to paclobutrazol seed treatment (Table 2). The result of reduction in seedling length and increase in the dry weight per unit seedling in paclobutrazol seed treatment are in agreement with Fletcher et al. (2000) who have indicated that paclobutrazol could induce semi-dwarf phenotype due to decreased production in growth promoting hormones which would help to reduce unnecessary vertical growth while promote productive growth. Previously, it was observed that semi-dwarf plants were able to avoid the serious grain losses from lodging. The roots help in the acquisition of plant nutrients from soil, so its morphological characteristics play an important role in plant growth (Yang et al., 2004). In present study, seed treatment with paclobutrazol stimulated root growth and thus improved the early growth of both rice cultivars. Increased root growth by paclobutrazol is associated with an increased level of endogenous cytokinin that promotes plant growth and development and delays senescence in plants (Fletcher et al., 2000). Seed treatment with paclobutrazol improved photosynthetic and gas exchange attributes and chlorophyll contents of both rice cultivars (Figs. 3 and 4), whereas dry weight per unit seedling length was positively correlated with net photosynthetic rate, stomatal conductance, chl a, chl b, carotenoids and total chl contents in both rice cultivars (Table 3). Photosynthesis is the process of converting light energy into chemical energy by synthesizing some organic compounds. Chlorophyll absorbs energy from the light, and energy is then used to convert carbon dioxide into carbohydrates (Connelly et al., 1997). The increased chl and carotenoid contents by paclobutrazol treatment may be due to improved root growth, which is the major site for cytokinin biosynthesis (Fletcher et al., 2000). They further reported that high levels of cytokinins may stimulate chlorophyll biosynthesis, and hence photosynthetic capacities of plants (Fletcher et al., 2000). Enhancement of photosynthetic pigment in plants by paclobutrazol has also been reported in barley (Özmen et al., 2003) and wheat (Hajihashemi et al., 2006). Trizole-induced modulations in leaf greenness, photosynthesis, chlorophyll biosynthesis and root morphological traits were noted in agronomic and horticultural crops (Hajihashemi et al., 2007).

Table 5. Correlation coefficients among dry weight per unit seedling length, CAT, MDA, POD, SOD, protein, proline and sugar

Parameters	Basmati	P value	Xiangyaxiangzhan	P value
POD	0.8576	0.0290	0.9802	0.0006
SOD	0.9500	0.0037	0.9651	0.0018
CAT	0.9581	0.0026	0.9968	0.0000
MDA	-0.9787	0.0007	-0.9698	0.0014
Soluble protein	0.8275	0.0421	0.9908	0.0001
Soluble sugar	0.9879	0.0002	0.9958	0.0000

Seed treatment with paclobutrazol enhanced *Fv/Fm*, *qP*, *F0*, *Fm* and *ETR* but decreased *NPQ* in both Basmati-385 and Xiangyaxuangzhan as compared to CK (Fig. 5). These parameters were also positively correlated with dry weight per unit seedling length except *NPQ* which showed negative relations (Table 4). The improvement of *Fv/Fm*, *ETR* and *qP* manifested that paclobutrazol treatment have improved the activity of PSII reaction center and enhanced the energy efficiency. The results are in agreement with Hajihashemi et al. (2006) who have reported that high levels of cytokinins may stimulate chlorophyll biosynthesis which may result in improved activity of PS-II reaction center.

Paclobutrazol seed treatment further improved the antioxidant enzyme activities i.e., POD, SOD and CAT, as well as soluble protein and soluble sugars whilst reduced MDA contents (Fig. 6). Furthermore, positive correlations were recorded among dry weight per unit seedling length and CAT, SOD, POD, soluble protein, proline and soluble sugar whereas negative correlation was recorded between dry weight per unit seedling length and MDA contents. MDA production is an important indicator of oxidative stress. Lower MDA contents in paclobutrazol treatment indicated that its application may reduce the rate of lipid peroxidation. The results are similar to the previous studies because it can react with free amino acids and produce ethylene in cellular membranes (Rakwal et al., 2003) whilst it could imparts the characteristics of cellular membranes and results in increased ion leakage through cell membranes (Dash et al., 2002). When plants are subjected to external stress, reactive oxygen species (ROS) will accumulate inside which may cause oxidative damage to cellular membranes and organelles. On this occasion, proteins and sugar would help to maintain cellular structures and functions whilst anti-oxidants help for quenching ROS. For instance, SOD scavenges superoxide radical whereas POD and CAT involve in scavenging H₂O₂ (Pan et al., 2013). Thus paclobutrazol induced regulations in protein and sugar accumulation and anti-oxidative defence responses. This indicated that application of paclobutrazol will increase resistance ability of seedlings against stress. The fundamental mechanism of paclobutrazol for improving antioxidant defence system has not been fully understood (Sankar et al., 2007). Possibly, paclobutrazol might increase antioxidant efficiency via enzymatic and non-enzymatic antioxidants and the results are similar to former reports that paclobutrazol enhances antioxidant defence system by increasing the activities of different anti-oxidant enzymes i.e., SOD, CAT, APX, and POX and the contents of ascorbate, glutathione, and α -tocopherol (Jaleel et al., 2007; Manivannan et al., 2008; Sankar et al., 2007). Enhancing antioxidant efficiency in plants by paclobutrazol has also been reported in *Catharanthus roseus* (Jaleel et al., 2007) and barley (Özmen et al., 2003). It is also possible that high antioxidant efficiency may result to prevent degradation of chlorophylls and carotenoids due to their higher ability to scavenge and trap ROS before damaging cells (Kong et al., 2017).

Conclusion

This study showed that seed treatment with paclobutrazol improved the shoot and root characters i.e., seedling length, base stem width, dry weight per unit seedling length, root length, root surface area, root diameter and root volume. Paclobutrazol treatment further modulated the photosynthetic and gas exchange traits, promoted the activities of antioxidants i.e., POD, SOD, and CAT whilst reduced MDA contents. Improved photosynthesis and anti-oxidant activities could lead to improved early

growth of both rice cultivars; nonetheless optimization of paclobutrazol concentration for seed treatment of different crops is needed in future.

Acknowledgements. This study was supported by National Natural Science Foundation of China (31271646), National Key R&D Program of China (2016YFD0700301), The World Bank Loan Agricultural Pollution Control Project in Guangdong (0724-1510A08N3684), The Technology System of Modern Agricultural Industry in Guangdong (2017LM1098) and Student's Platform for Innovation and Entrepreneurship Training Program (201810564029). The authors declare no conflicts of interest.

REFERENCES

- [1] Aebi, H. (1983): Catalase in vitro. – *Methods in Enzymology* 105(105): 121-126.
- [2] Bates, L. S., Waldren, R. P., Teare, I. D. (1973): Rapid determination of free proline for water-stress studies. – *Plant & Soil* 1(39): 205-207.
- [3] Bradford, M. M. (1976): A rapid and sensitive method for the quantitation of microgram quantities of protein utilizing the principle of protein-dye binding. – *Analytical Biochemistry* 72(2): 248-254.
- [4] Connelly, J. P., Müller, M. G., Bassi, R. et al. (1997): Femtosecond transient absorption study of carotenoid to chlorophyll energy transfer in the light-harvesting complex II of photosystem II. – *Biochemistry* 36(6): 281-287.
- [5] Dash, S., Mohanty, N. (2002): Response of seedlings to heat-stress in cultivars of wheat: Growth temperature-dependent differential modulation of photosystem I and II activity, and foliar antioxidant defense capacity. – *Journal of Plant Physiology* 159(1): 49-59.
- [6] Fletcher, R. A., Gilley, A., Sankhla, N., Davis, T. D. (2000) Triazoles as plant growth regulators and stress protectants. – *Horticultural Reviews* 24: 55-138.
- [7] French, P., Matsuyuki, H., Ueno, H. (1990): Paclobutrazol: control of lodging in Japanese paddy rice. Pest management in rice. – Conference held by the Society of Chemical Industry, London, UK, 4-7 June 1990, pp. 474-485.
- [8] Gopi, R., Lakshmanan, G. A., Panneerselvam, R. (2006): Triadimefon induced changes in the antioxidant metabolism and ajmalicine production in *Catharanthus roseus* (L.) G. Don. – *Plant Science* 211(2): 271-276.
- [9] Gu, D. X., Tang, L., Cao, W. X., Zhu, Y. (2010): Quantitative analysis on root morphological characteristics based on image analysis method in rice. – *Acta Agronomica Sinica* 36(8): 810-817.
- [10] Hajhashemi, S., Kiarostami, K., Enteshari, S., Saboora, A. (2006): The effects of salt stress and paclobutrazol on some physiological parameters of two salt-tolerant and salt-sensitive cultivars of wheat. – *Pakistan Journal of Biological Sciences* 9(7): 1370-1374.
- [11] Hajhashemi, S., Kiarostami, K., Saboora, A., Enteshari, S. (2007): Exogenously applied paclobutrazol modulates growth in salt-stressed wheat plants. – *Plant Growth Regulation* 53(2): 117-128.
- [12] Hu, Y., Yu, W., Liu, T. et al. (2016): Effects of paclobutrazol on cultivars of Chinese bayberry (*Myrica rubra*) under salinity stress. – *Photosynthetica* 54(1): 1-11.
- [13] Jaleel, C. A., Gopi, R., Manivannan, P., Panneerselvam, R. (2007): Responses of antioxidant defense system of *Catharanthus roseus* (L.) G. Don. to paclobutrazol treatment under salinity. – *Acta Physiologiae Plantarum* 37(2): 205-209.
- [14] Kamran, M., Cui, W., Ahmad, I. et al. (2018): Correction to: Effect of paclobutrazol, a potential growth regulator on stalk mechanical strength, lignin accumulation and its relation with lodging resistance of maize. – *Plant Growth Regulation* 84(1): 1-2.

- [15] Kong, L., Ashraf, U., Cheng, S. et al. (2017): Short-term water management at early filling stage improves early-season rice performance under high temperature stress in South China. – *European Journal of Agronomy* 90: 117-126.
- [16] Li, H. (2000): Principles and Techniques of Plant Physiology and Biochemistry Experiment. – Beijing Higher Education Press, Beijing, pp. 167-169.
- [17] Lichtenthaler, H. K. (1987): Chlorophylls and carotenoids: Pigments of photosynthetic biomembranes. – *Methods in Enzymology* 1(148): 350-382.
- [18] Luo, H., Zhong, Z., Nie, J., Tang, X. (2017): Effects of ultrasound on physiological characters, yield and quality of rice Yuejingsimiao. – *China Rice* 23(2): 64-67.
- [19] Manivannan, P., Jaleel, C. A., Kishorekumar, A., Sankar, B., Somasundaram, R., Panneerselvam, R. (2008): Protection of *Vigna unguiculata* (L.) Walp. plants from salt stress by paclobutrazol. – *Colloids & Surfaces B Biointerfaces* 2(61): 315-318.
- [20] Özmen, A. D., Özdemir, F., Türkan, I. (2003): Effects of paclobutrazol on response of two barley cultivars to salt stress. – *Biological Plantarum* 2(46): 263-268.
- [21] Pan, S., Rasul, F., Wu, L. et al. (2013): Roles of plant growth regulators on yield, grain qualities and antioxidant enzyme activities in super hybrid rice (*Oryza sativa* L.). – *Rice* 1(6): 9.
- [22] Pan, S., Wen, X., Mo, Z. et al. (2015): Effects of nitrogen application and shading on yields and some physiological characteristics in different rice genotypes. – *Rice Science* 29(2): 141-149.
- [23] Peng, D., Chen, X., Yin, Y. et al. (2014): Lodging resistance of winter wheat (*Triticum aestivum* L.): Lignin accumulation and its related enzymes activities due to the application of paclobutrazol or gibberellin acid. – *Field Crops Research* 2(157): 1-7.
- [24] Rakwal, R., Agrawal, G. K., Kubo, A. et al. (2003): Defense/stress responses elicited in rice seedlings exposed to the gaseous air pollutant sulfur dioxide. – *Environmental & Experimental Botany* 3(49): 223-235.
- [25] Sankar, B., Jaleel, C. A., Manivannan, P., Kishorekumar, A., Somasundaram, R., Panneerselvam, R. (2007): Effect of paclobutrazol on water stress amelioration through antioxidants and free radical scavenging enzymes in *Arachis hypogaea* L. – *Colloids & Surfaces B Biointerfaces* 2(60): 229-235.
- [26] Schmedes, A., Holmer, G. (1989): A new thiobarbituric acid (TBA) method for determining free malondialdehyde (MDA) and hydroperoxides selectively as a measure of lipid peroxidation. – *Journal of the American Oil Chemists Society* 6(66): 813-817.
- [27] Street, J. E., Jordan, J. H., Ebelhar, M. W., Boykin, D. L. (1986): Plant height and yield responses of rice to paclobutrazol. – *Agronomy Journal* 2(78): 288-291.
- [28] Sun, B., Zhang, W., Long, Z., Li, N., Wu, L., Gao, H. (2010): The sugar content analysis of codonopsis-astragalus root injection with anthrone-sulfuric acid method. – *Modern Chinese Medicine* 2(163): 284-295.
- [29] Upreti, K. K., Reddy, Y. T. N., Prasad, S. R. S., Bindu, G. V., Jayaram, H. L., Rajan, S. (2013): Hormonal changes in response to paclobutrazol induced early flowering in mango cv. Totapuri. – *Scientia Horticulturae* 2(150): 414-418.
- [30] Wang, C., Hu, D., Liu, X. et al. (2015): Effects of uniconazole on the lignin metabolism and lodging resistance of culm in common buckwheat (*Fagopyrum esculentum* M.). – *Field Crops Research* 180): 46-53.
- [31] Xiang, J., Wu, H., Zhang, Y. et al. (2017): Transcriptomic analysis of gibberellin- and paclobutrazol-treated rice seedlings under submergence. – *International Journal of Molecular Sciences* 10(18): 2225.
- [32] Yang, C., Yang, L., Yang, Y., Ouyang, Z. (2004): Rice root growth and nutrient uptake as influenced by organic manure in continuously and alternately flooded paddy soils. – *Agricultural Water Management* 1(70): 67-81.

- [33] Yim, K. O., Kwon, Y.W., Bayer, D. E. (1997): growth responses and allocation of assimilates of rice seedlings by paclobutrazol and gibberellin Treatment. – *Journal of Plant Growth Regulation* 1(16): 35-41.
- [34] Zhang, J., Sui, X., Li, B., Su, B., Li, J., Zhou, D. (1998): An improved water-use efficiency for winter wheat grown under reduced irrigation. – *Field Crops Research* 2(59): 91-98.